PNNL-18098, Rev. 1
WTP-RPT-182, Rev. 1

U.S. DEPARTMENT OF ENERGY

Prepared for the U.S. Department of Energy
under Contract DE-AC05-76RL01830

Pulse Jet Mixing Tests With Noncohesive Solids

PA Meyer
CW Enderlin
BE Wells
PA Scott
GL Smith
MS Greenwood
EBK Baer
M White
BG Amidan
JA Bamberger
JA Fort
SK Sundaram
MJ Minette
CA Burns
GP Morgen
SF Snyder
GF Piepel
A Heredia-Langner

February 2012

Pacific Northwest NATIONAL LABORATORY

Proudly Operated by Battelle Since 1965

DISCLAIMER

This report was prepared as an account of work sponsored by an agency of the United States Government. Neither the United States Government nor any agency thereof, nor Battelle Memorial Institute, nor any of their employees, makes **any warranty, express or implied, or assumes any legal liability or responsibility for the accuracy, completeness, or usefulness of any information, apparatus, product, or process disclosed, or represents that its use would not infringe privately owned rights**. Reference herein to any specific commercial product, process, or service by trade name, trademark, manufacturer, or otherwise does not necessarily constitute or imply its endorsement, recommendation, or favoring by the United States Government or any agency thereof, or Battelle Memorial Institute. The views and opinions of authors expressed herein do not necessarily state or reflect those of the United States Government or any agency thereof.

PACIFIC NORTHWEST NATIONAL LABORATORY
operated by
BATTELLE
for the
UNITED STATES DEPARTMENT OF ENERGY
under Contract DE-AC05-76RL01830

Printed in the United States of America

Available to DOE and DOE contractors from the
Office of Scientific and Technical Information,
P.O. Box 62, Oak Ridge, TN 37831-0062;
ph: (865) 576-8401
fax: (865) 576 5728
email: reports@adonis.osti.gov

Available to the public from the National Technical Information Service,
U.S. Department of Commerce, 5285 Port Royal Rd., Springfield, VA 22161
ph: (800) 553-6847
fax: (703) 605-6900
email: orders@ntis.fedworld.gov
online ordering: http://www.ntis.gov/ordering.htm

PNNL-18098, Rev. 1
WTP-RPT-182, Rev. 1

Pulse Jet Mixing Tests With Noncohesive Solids

PA Meyer
JA Fort
PA Scott
CA Burns
EBK Baer
GF Piepel
JA Bamberger
BE Wells
MJ Minette
MS Greenwood
SF Snyder
BG Amidan
CW Enderlin
SK Sundaram
GL Smith
GP Morgen
M White
A Heredia-Langner

Additional Authors:

SA Bailey
JC Bower
KM Denslow
DE Eakin
MR Elmore
PA Gauglitz
AD Guzman
BK Hatchell
DF Hopkins
DE Hurley
MD Johnson
LJ Kirihara
BD Lawler
JS Loveland
O D Mullen
MS Pekour
TJ Peters
PJ Robinson
MS Russcher
S Sande
CB Santoso
SV Shoemaker
SM Silva
DE Smith
Y Su
JJ Toth
JD Wiberg
X Yu
N Zuljevic

February 2012

Key WTP R&T References

Test Specification	24590-PTF-TSP-RT-06-007
Test Plan	TP-RPP-WTP-480
Test Exceptions	24590-WTP-TEF-RT-07-00013
	CCN 178425
	CNN 190723
R&T Focus Area	Pretreatment

Prepared for
the U.S. Department of Energy
under Contract DE-AC05-76RL01830

Pacific Northwest National Laboratory
Richland, Washington 99352

Completeness of Testing

This report describes the results of work and testing specified by Test Specification 24590-PTF-TSP-RT-06-007 and Test Plan TP-RPP-WTP-480. The work and any associated testing followed the quality assurance requirements outlined in the Test Specification 24590-PTF-TSP-RT-06-007 and Test Plan TP-RPP-WTP-480. The descriptions provided in this test report are an accurate account of both the conduct of the work and the data collected. Test plan results are reported. Also reported are any unusual or anomalous occurrences that are different from expected results. The test results and this report have been reviewed and verified.

Approved:

D E Kurath

Dean E. Kurath, Manager
RPP-WTP Support Program

2/16/12
Date

Revision History

Revision Number	Interim Change No.	Effective Date	Description of Change
0	0	5/5/2009	Initial issue.
1	0	2/16/2012	Revision History Document updated to show Rev 1. Publication Date Updated. Revision History Added Executive Summary reference list updated to identify references that are not publicly available. Section 1.5: Listed NCR OTS-00327. Table 6.3 updated values of Return Line Height, Outer Nozzles Operated, U2URMS, (Fall 2007), and U_{CS} based on Decreasing Velocity (2008, July 2007, and Fall 2007). Section 6.5: Concentration Profiles. Updated the following figures: 6.25, 6.26, 6.27, 6.28, 6.29, 6.30, 6.31, 6.32, and 6.33 to reflect updates to data set used to develop concentration profiles. Table 6.14. Changed heading to Elevation of Highest Positive Concentration Measurement. Updated columns to match elevations shown in Appendix C plots. Figure 6.24: Updated title to show "Solids Concentration by Volume Distribution Plots…" Updated figures to reflect refinements to data sets and add points at 0.05 H/D. Figures 7.22 and 7.23. Updated figures to reflect refinements to data sets and add points at 0.05 H/D. Section 7.8 Updates to Models Since Initial Document Release. Added references to models developed since completion of Rev. 0 to describe reciprocating (prototypic) PJM flow. Section 11 reference list updated to identify references that are not publicly available. Appendix B Table B.9. Added to show corrections to Table B.8. Appendix C. Updated Table C.1 to match Table 6.14. The following plots in Appendix C were updated: C.27, C.29, C.32, C.33, C.34, C.35, C.36, C.37, C.38, C.39, C.40, C.42, C.44, C.45, C.46, C.48-C.50, C.51-C.53, C.55-C.57, C.58, C.59-C.61, C.62-C.64, C.65, to reflect refinements to the data set. Appendix E. Table numbers were corrected. Appendix F: A non-cited reference was removed.

Abstract

This report summarizes results from pulse jet mixing (PJM) tests with noncohesive solids in Newtonian liquid. The tests were conducted during FY 2007 and 2008 to support the design of mixing systems for the Hanford Waste Treatment and Immobilization Plant (WTP). Tests were conducted at three geometric scales using noncohesive simulants, and the test data were used to develop models predicting two measures of mixing performance for full-scale WTP vessels. The models predict the *cloud height* (the height to which solids will be lifted by the PJM action) and the *critical suspension velocity* (the minimum velocity needed to ensure all solids are suspended off the floor, though not fully mixed). From the cloud height, the concentration of solids at the pump inlet can be estimated. The predicted critical suspension velocity for lifting all solids is not precisely the same as the mixing requirement for "disturbing" a sufficient volume of solids, but the values will be similar and closely related. These predictive models were successfully benchmarked against larger scale tests and compared well with results from computational fluid dynamics simulations.

The application of the models to assess mixing in WTP vessels is illustrated in examples for 13 distinct designs and selected operational conditions. The values selected for these examples are not final; thus, the estimates of performance should not be interpreted as final conclusions of design adequacy or inadequacy. However, this work does reveal that several vessels may require adjustments to design, operating features, or waste feed properties to ensure confidence in operation. The models described in this report will prove to be valuable engineering tools to evaluate options as designs are finalized for the WTP.

Revision 1 refines data sets used for model development and provides references to models developed since the completion of Revision 0.

Executive Summary

This report summarizes results from pulse jet mixing (PJM) tests with noncohesive solids in Newtonian liquid conducted during FY 2007 and 2008 to support the design of mixing systems for the Hanford Waste Treatment and Immobilization Plant (WTP). This report does not address mixing behaviors of cohesive solids. Tests were conducted at three geometric scales using noncohesive simulants. The test data were used to develop mixing models that would predict two measures of mixing performance for full-scale WTP vessels: the *cloud height* (the height to which solids will be lifted by the PJM action) and the *critical suspension velocity* (the minimum velocity needed to ensure that all solids are suspended off the floor, though not fully mixed). From the cloud height, the concentration of solids at the pump inlet was estimated. For noncohesive solids, the velocity needed to lift the solids is slightly more demanding than the current mixing requirement of "disturbing" a sufficient volume of solids, but the values will be similar and closely related. Because satisfying the former also satisfies the latter, we report the minimum velocity predicted to lift solids.

We applied the models to 13 WTP mixing vessel designs using two defined waste conditions to illustrate how the models predict mixing performance. The examples predict two performance parameters: the pump inlet concentration and the critical suspension velocity for each vessel. One of the wastes was defined by design limits (Olsen 2008a), and one was derived from Hanford waste characterization reports (Wells et al. 2007). These examples show that, for the assumed conditions, several vessels would not satisfy the two requirements addressed in this work. This result suggests that, to satisfy the requirements, WTP should consider changes to design, operating conditions, or inlet waste properties, and the mixing models provide a means to evaluate the benefit that could be expected from any of these changes. Conversely, the models can be used to estimate the waste properties that can be accommodated by the current designs.

The mixing models were successfully benchmarked against a limited set of larger-scale test results from prior tests that used prototypic PJM geometries and prototypic operations. These benchmarking results provide confidence that the models can predict prototypic performance at larger scale, but also revealed a need for additional data to guide the choice of model input values selected by the user. Specifically, because the value of the characteristic settling velocity has a strong effect on the predicted performance, more work is needed to select the appropriate value.

We also compared the model predictions to the results generated by computational fluid dynamic (CFD) codes. For vessel HLP-22, both of our models predict concentration profiles that are consistent with the profile from the CFD model. For the conditions selected, the models and CFD both predict that the PJMs will not satisfy the performance requirements. The PJMs would not be sufficient to lift all solids from the floor of HLP-22, and the solids would not be well distributed, resulting in concentrations near the pump inlet that would exceed the 20 wt% maximum.

An example of predicted performance was also developed for an alternative design for the HLP-22 vessel, which included increasing the pulse jet velocity from 8 m/s to 12 m/s, and increasing the jet nozzle diameter from 4 to 6 inches. This alternative configuration was predicted to improve performance, but, for the conditions evaluated, the models indicate it would not satisfy the suction inlet concentration or waste mobilization criteria. These results reflect a direct comparison of the predicted performance to the requirements, with no allowance for uncertainty in the model, performance of the mixing system, or waste properties. Appropriate margin should be added as required for the specific application. This example

demonstrates how the models can be used to predict mixing performance trends and improvements based on potential design and/or operational changes.

There were several analysis and application improvement opportunities that became apparent during the production period of this report. The practicalities of schedule constraints and extensive QA implementation requirements necessary to support the NQA-1 needs of this document did not permit the inclusion of these improvements into this report. These improvements are discussed in the conclusions section.

The effort to develop a generalized basis for predicting PJM mixing performance involved substantial review of more conventional mixing systems, both mechanically agitated and steady jet systems. Much of the work presented in this report shows that the physics involved in a PJM mixed system are consistent with other mixing systems. However, the feature that separates a PJM system from others is that the energy input is not steady (pulsed). That difference has profound implications on the ability of the system to suspend all solids and to distribute solids vertically.

Background

The WTP is being designed and built to pretreat and vitrify the waste from Hanford's 177 underground waste storage tanks. Several process vessels will hold waste at various stages in the WTP. Many of these vessels will have mixing systems with requirements to maintain the waste in a safe condition and within the specified operating limits of the equipment.

In October 2005, a team of experts from industry, national laboratories, and universities (referred to as the External Flowsheet Review Team, or EFRT) was assembled by Bechtel National, Inc. (BNI) to conduct a thorough and in-depth review of the process flowsheet for the design of the WTP. Among the findings, the EFRT identified potential inadequate mixing of the vessels using PJMs as a technical issue; this issue is referred to as M3–Inadequate Design of Mixing Systems–Pulse Jet Mixers (referred to subsequently as M3).

In response to M3, BNI issued Test Specification 24590-PTF-TSP-RT-06-007 (Smith 2007) defining a test program to resolve the PJM mixing issue. The objective of this test program has been to close issues related to mixing system designs that could result in insufficient mixing and/or extended mixing times. These issues included a design basis that discounted the effects of large particles and of rapidly settling Newtonian slurries.

The test specification calls for geometrically scaled tests to be performed with simulants for developing models to be used for confirming the PJM design basis applied to WTP vessels. As part of project No. 53023, PNNL generated Test Plan TP-RPP-WTP-480 (Elmore et al. 2007) for conducting scaled tests.

The initial phase of testing conducted in July 2007 focused on HLP-22, the tank design identified by the EFRT as the most likely to fail to meet mixing requirements. Testing focused on the HLP-22 base line design performance and the relative performance of design alternatives. Specific tests were conducted that evaluated mixing performance related to the nozzle diameter and discharge velocity. Testing was conducted in the mid-scale [nominal 0.86-m- (34-in.-) diameter] tank to provide a relative comparison of designs with respect to the critical suspension velocity and cloud height. In the fall of

2007, additional parametric testing was conducted in the mid-scale vessel to evaluate the effect of several additional parameters on mixing performance. The initial testing identified that the HLP-22 PJM systems will have significant challenges when mixing fast-settling solids.

Following the initial test campaigns conducted in July 2007 and fall 2007, BNI generated test Exception 24590-WTP-TEF-RT-07-00013 (Hazen 2007). Testing to TP-RPP-WTP-480 Rev 0, ICN 1 (Elmore et al. 2008) was conducted from March through July of 2008 in three test systems with nominal tank diameters of 0.38, 0.86, and 1.78 m (15, 34, and 70 in.), respectively. The test campaign focused on parametric testing using 12-tube arrays, representing the HLP-22 configuration, and supplemented these with limited tests of 4- and 8-tube configurations. The 2008 test campaign used five simulants with size distributions significantly narrower than those employed during 2007 testing.

BNI issued two additional modifications for testing, one via SCN 71 (Hazen 2008a) that canceled cohesive and confirmatory testing, and the second via letter CCN 190723 (Hazen 2008b) has assigned the responsibility of applying the test results to determine if mixing systems meet WTP requirements to WTP Mechanical and Process Engineering (M&PE) staff.

Test Objectives

The objectives of the M3 test program are presented in Table S.1 along with an explanation of how each objective was met. The objectives are quoted verbatim from Test Plan TP-RPP-WTP-480 (Elmore et al. 2007) and from Test Plan TP-RPP-WTP-480 R0.2 (Elmore et al. 2009). Because of their wording, Objectives 1 and 5 require additional explanation. Previous work indicated that the mixing performance of some WTP vessels may be inadequate at design conditions. The intent of Objectives 1 and 5 was to perform sufficient testing to assess mixing performance and provide strong evidence of inadequacy (if that was the conclusion). It was not the intent of these objectives to assume inadequate mixing and require strong experimental evidence to demonstrate adequate mixing.

Table S.1. M3 Test Program Objectives and Corresponding Discussion of Resolution

Test Objectives	Objective Met (Y/N)	Discussion
1. Determine through experimental results whether there is a high probability that, for Tank HLP-22, 0.10 m (4 in.) nozzles operating at 8 m/s discharge velocity (current baseline design) will not be adequate to resuspend settled solids.	Yes	Application of the developed models (Section 9.0) indicated that 0.10-m (4-in.) nozzles operating at 8 m/s for a pulse volume fraction of 0.05 would be insufficient to achieve full solids suspension. Also, solids concentration at tank bottom exceeded 20 wt% for a bulk tank concentration of 15.6 wt%.

Table S.1. (contd)

<table>
<tr><th>Test Objectives</th><th>Objective Met (Y/N)</th><th>Discussion</th></tr>
<tr><td>2. Provide experimental results from a scaled HLP-22 mixing system for constant volume discharges that provide the relative difference in performance with respect to off-bottom suspension for the following conditions:
• Full-scale conditions of 0.10 m (4-in.) diameter nozzles operating at 8 m/s.
• Full-scale conditions of 0.10 m (4-in.) diameter nozzles operating at 12 m/s.
• Full-scale conditions of 0.15 m (6-in.) diameter nozzles operating at 8 m/s.
• Full-scale conditions of 0.15 m (6-in.) diameter nozzles operating at 12 m/s.</td><td>Yes</td><td>Application of the developed models (Section 9.0) indicated that a 0.15-m (6-in.) nozzle operating with a pulse volume fraction of 0.05 and 22% duty cycle improved performance (relative to U_{CS}) over a 0.10-m (4-in.) nozzle with pulse volume fraction of 0.05 and 33% duty cycle. For the conditions evaluated, the models predicted that 0.15 m (6-in.) nozzles operating at 12 m/s would not achieve full solids suspension.
Following are magnitude-of-improvement comparisons from Table 9.55:
<table>
<tr><th>Vessel</th><th>Velocity m/s</th><th>Nozzle in.</th><th>U_{95} U/U_{CS}</th><th>Max Fill $0.2/W_0$*</th></tr>
<tr><td>HLP-22</td><td>8</td><td>4</td><td>0.48</td><td>0.03[(a)]</td></tr>
<tr><td>HLP-22</td><td>12</td><td>4</td><td>0.73</td><td>0.11[(a)]</td></tr>
<tr><td>HLP-22</td><td>8</td><td>6</td><td>0.64</td><td>0.07[(a)]</td></tr>
<tr><td>HLP-22</td><td>12</td><td>6</td><td>0.96</td><td>0.30</td></tr>
</table>
(a) Indicates waste is considered fully settled on the bottom for these conditions; the calculated ratio is shown to indicate the relative performance only and should not be construed to imply values of W_0* that are non-physically high.</td></tr>
<tr><td>3. Obtain measurements of U_{CS} over a range of test conditions in scaled vessels to evaluate the dependence of vessel performance on parameters associated with waste properties, equipment design, and process operations.</td><td>Yes</td><td>Testing was conducted at 3 test scales (Section 4.0). U_{CS} was evaluated over a range of test conditions that exercised:
• Geometric parameters: nozzle diameter, vessel diameter, number of operating nozzles.
• Operating parameters: drive time, cycle time, pulse discharge volume, duty cycle.
• Physical parameters: particle size, solids density, solids concentration (see Section 5.0 for the range of each parameter tested).</td></tr>
<tr><td>4. Obtain test results at multiple geometric scales to allow scaled test result to be used to predict vessel performance at full-scale.</td><td>Yes</td><td>Testing was conducted in three test tanks with nominal tank diameters of 0.38, 0.86, and 1.78 m (15, 34, and 70 in.).</td></tr>
<tr><td>5. Develop tools/models that will allow WTP M&PE staff to rate/evaluate/bin WTP tank designs at a coarse level and to determine with high confidence WTP vessels that will not meet minimum required performance levels.</td><td>Yes</td><td>Models were developed for U_{CS}, H_C, and solids concentration at the tank bottom to predict full-scale performance. Example applications of the models were provided for several vessels and waste conditions.</td></tr>
<tr><td>6. Obtain test results, observations, and experience that facilitate development of a focused/ reduced test matrix for M3 scaled tests.</td><td>Yes</td><td>Planning for future tests will be limited to the parameters with the strongest impact on vessel performance. The recommendations for extending applicability of the models are covered in Section 10.3 and include considerations for prototypic drive systems, adjusting operating fill levels, varying viscosities, and broad distribution simulant runs for both particle size and particle density.</td></tr>
</table>

Test Exceptions

One test exception (Hazen 2007) was generated during the course of the M3 test program. Interim change notice ICN-TP-RPP-WTP-480_R0.1 (Elmore et al. 2008) was generated in response to the test exception. Table S.2 lists the test exception and the corresponding scope of work. In addition to the formal test exception, letters of direction were issued by BNI that modified testing objectives, one via SCN-71 (Hazen 2008a) that cancelled cohesive and confirmatory testing, and the second via letter CCN 190723 (Hazen 2008b) that assigned the responsibility of applying the test results to determine if mixing systems meet WTP requirements to WTP Mechanical and Process Engineering (M&PE) staff. Consequently vessel evaluations in this document are to be considered as examples only.

Results and Performance Against Success Criteria

The success criteria were based on obtaining answers to several questions. The success criteria are listed in Table S.3 along with discussion of how the tests did (or did not) meet the success criteria. The success criteria are quoted verbatim from Test Plan TP-RPP-WTP-480 (Elmore et al. 2007) and from Test Plan TP-RPP-WTP-480 R0.2 (Elmore et al. 2009). Because of their wording, Success Criteria 1 and 6 require additional explanation. Previous work had indicated that the mixing performance of some WTP vessels may be inadequate at design conditions. The intent of Success Criteria 1 and 6 was to perform sufficient testing to assess mixing performance and provide strong evidence of inadequacy (if that was the conclusion). It was not the intent of these success criteria to assume inadequate mixing and require strong experimental evidence to demonstrate adequate mixing.

Table S.2. Test Exceptions Generated During the Test Program

List Test Exceptions	Describe Test Exceptions
24590-WTP-TEF-RT-07-00013 (Hazen 2007)	The test exception specified that the M3 parametric tests were to be conducted in available test platforms using the nonprototypic drive system to expedite the rating of all the plant vessels. The change in direction was due to the delay in receiving the new test platforms and challenges to develop a prototypic drive system for the smaller tanks in the expedited time frame. Expediting the test program was expected to shorten it once the three all-acrylic test vessels arrived. The test campaign outlined by the test exception consisted of: 1. Screening testing that • Provides mixing performance (ranking) for all plant vessels • Includes parametric tests over reduced ranges and values • Covers testing of cohesive and noncohesive simulants. 2. Blended simulant studies that • Aid interpretation/application of M3 results to complex Hanford wastes • Examine the effects of wastes with constituents of multiple sizes and densities • Examine the effects of particle size and density distribution width. 3. Geometry effects testing that • Provides technical basis of supporting enabling assumptions in response to reviewer comments • Improves logistical and a greatly focused/reduced test matrix for future M3 scaled testing. 4. Geometric scale-up testing that • Demonstrates whether exact geometric scaled testing of PJM mixing vessels is necessary to rate vessels. The objective of the parametric tests was to identify the variables that strongly affect performance and provide enough scaled information to support broad predictions of vessel performance.

Table S.3. Success Criteria for M3 Test Program

<table>
<tr><th>List Success Criteria</th><th>Explain How Tests Did or Did Not Meet Success Criteria</th></tr>
<tr><td>1. Do experimental results provide a strong indication that the current baseline design (0.10 m [4-in.] nozzles at 8 m/s discharge velocity) will not be adequate for resuspending settled solids in HLP-22 based on assessment using just-suspended velocity as the critical parameter?</td><td>Yes. Projected tank performances using current design and evaluating pulse jet velocities and nozzle sizes show:
<table>
<tr><th rowspan="2">Vessel</th><th rowspan="2">Velocity m/s</th><th rowspan="2">Nozzle in.</th><th colspan="2">U_{95} Max Fill</th></tr>
<tr><th>U/U_{CS}</th><th>$0.2/W_0$*</th></tr>
<tr><td>HLP-22</td><td>8</td><td>4</td><td>0.48</td><td>0.03[(a)]</td></tr>
<tr><td colspan="5">(a) Indicates waste is considered fully settled on the bottom for these conditions; the calculated ratio is shown to indicate the relative performance only and should not be construed to imply values of W_0* that are non-physically high.</td></tr>
</table>
These results indicate that the criterion for critical suspension velocity (U_{CS}) and pump inlet concentration will not be met for the U_{95} settling velocity particle at 8 m/s with a 4-in. nozzle.</td></tr>
<tr><td>2. Do experimental results indicate that, for a constant pulse volume, increasing discharge velocity to 12 m/s will improve mixing performance in HLP-22?</td><td>Yes. Based on the application of the models (as discussed in Section 9.0), performance does improve as nozzle velocity is increased to 12 m/s. This alternative configuration was an improvement, but for the conditions evaluated, the model predicted the results would not satisfy the suction inlet or waste mobilization criteria.
<table>
<tr><th rowspan="2">Vessel</th><th rowspan="2">Velocity m/s</th><th rowspan="2">Nozzle in.</th><th colspan="2">U_{95} Max Fill</th></tr>
<tr><th>U/U_{CS}</th><th>$0.2/W_0$*</th></tr>
<tr><td>HLP-22</td><td>12</td><td>4</td><td>0.73</td><td>0.11[(a)]</td></tr>
<tr><td colspan="5">(a) Indicates waste is considered fully settled on the bottom for these conditions; the calculated ratio is shown to indicate the relative performance only and should not be construed to imply values of W_0* that are non-physically high.</td></tr>
</table></td></tr>
<tr><td>3. Do experimental results indicate that, for a constant pulse volume, increasing the nozzle diameter and discharge velocity to 0.15 m (6 in.) and 12 m/s, respectively, will improve the mixing performance in HLP-22? An evaluation will also be made for nozzle diameter and discharge velocity of 0.15 m (6 in.) and 8 m/s, respectively.</td><td>Yes. Based on the application of the models (discussed in Section 9.0), performance does improve as nozzle size is increased to 6 inches. This alternative configuration was an improvement, but, for the conditions evaluated, the model predicted the results would not satisfy the suction inlet or waste mobilization criteria.
<table>
<tr><th rowspan="2">Vessel</th><th rowspan="2">Velocity m/s</th><th rowspan="2">Nozzle in.</th><th colspan="2">U_{95} Max Fill</th></tr>
<tr><th>U/U_{CS}</th><th>$0.2/W_0$*</th></tr>
<tr><td>HLP-22</td><td>8</td><td>6</td><td>0.64</td><td>0.07[(a)]</td></tr>
<tr><td>HLP-22</td><td>12</td><td>6</td><td>0.96</td><td>0.30</td></tr>
<tr><td colspan="5">(a) Indicates waste is considered fully settled on the bottom for these conditions; the calculated ratio is shown to indicate the relative performance only and should not be construed to imply values of W_0* that are non-physically high.</td></tr>
</table></td></tr>
<tr><td>4. Does the test apparatus and methodology being used provide results that are comparable to those predicted by the client's jet mixing correlation?</td><td>No longer applicable – Per direction of the WTP M3 Program Manager, the comparison of the testing models with the original jet mixing correlations is now WTP work scope.</td></tr>
</table>

Table S.3. (contd)

List Success Criteria	Explain How Tests Did or Did Not Meet Success Criteria
5. Do test results adequately support the project need for WTP M&PE staff to rate/evaluate/bin WTP tanks designs at a coarse level?	Yes. Predictive models for vessel performance were developed. Refer to Section 9.0 for examples of how the models can be applied to predict vessel performance with respect to criteria on U_{CS} concentration at the tank bottom (suction line inlet).
6. Are test result models and examples provided so WTP M&PE staff can provide recommendations on what operating conditions/configurations would bring the vessel into compliance?	Yes. Models are provided in Section 7.0 and the examples for vessels HLP-22, FRP-02 A/B/C/D, PWD-15/16, PWD-33, PWD-43, PWD-44, TCP-01, FEP-17 A/B, TLP-09 A/B, RLD-07, RLD-08, HOP-903/904, and UFP-01 A/B are provided in Section 9.0.
7. In addition, do the tests illustrate how PJM mixing performance is affected by a change in any one of several important variables in waste properties or equipment design and operation?	Yes. Refer to Section 7.0.
8. Does this testing and data evaluation allow for a focused/reduced test matrix for M3 scaled tests?	Yes. Success of benchmarking against previous results obtained for larger-scale systems indicates strong predictive power and identifies the parameters that have the greatest impact on performance. Future test matrices will not include investigations of low-value parameters.

Quality Requirements

Pacific Northwest National Laboratory (PNNL) is operated by Battelle for the U.S. Department of Energy. Battelle's Pacific Northwest Division (PNWD) has a Quality Assurance Program that is based on requirements defined in the U.S. Department of Energy (DOE) Order 414.1C, "Quality Assurance," and 10 CFR 830, "Energy/Nuclear Safety Management," Subpart A, "Quality Assurance Requirements." PNWD has chosen to implement the requirements of DOE Order 414.1C and 10 CFR 830 Subpart A by integrating them into the Laboratory's management systems and daily operating processes.

PNNL implements the River Protection Project (RPP)-WTP quality requirements by performing work in accordance with the River Protection Project – Waste Treatment Plant Support Program (RPP-WTP) Quality Assurance Plan (RPP-WTP-QA-001, QAP). Work is performed to the quality requirements of NQA-1-1989 Part I, "Basic and Supplementary Requirements," NQA-2a-1990 Part 2.7, and DOE/RW-0333P Rev. 13, Quality Assurance Requirements and Descriptions (QARD). These quality requirements are implemented through the River Protection Project – Waste Treatment Plant Support Program (RPP-WTP) Quality Assurance Manual (RPP-WTP-QA-003, QAM).

NCR OTS-00327 outlines bases for all changes in graphs and tables that are listed in Revision History. The NCR identifies CCPs associated with this update and provides a basis for data sets selected for inclusion in Revision 1 of this report.

Test Conditions

The R&T (research and technology) test conditions referred to in Table S.4 are summarized in Table 6.3 of Section 6.0.

Table S.4. R&T Test Conditions

List R&T Test Conditions	Were Test Conditions Followed?
1. See Section 6.0, Table 6.3	Yes

Simulant Use

The July and Fall 2007 test campaigns were conducted using Potter glass beads with a broad size distribution. The 2008 test campaign was conducted using five types of glass beads with significantly narrower size distributions than those used for the 2007 testing. The simulants are listed in Table S.5. The supernatant liquid for all testing was process water from the Applied Process Engineering Laboratory. The water was treated with Mt. Hood-480[1] biocide and periodically cleaned using a standard pool filter with diatomaceous earth.

Table S.5. M3 Simulants Used for 2007 and 2008 Test Campaigns[(a)]

Simulant Designation	Particle Size, d_{50} (μm)	Density (g/cm^3)	Test Campaign
p1d8	90	2.45	2007
p1d7	178	2.45	2007
p2d6	766	2.46	2007
s1d5	44	2.50	2008
s1d2	69	2.48	2008
s1d1	167	2.46	2008
s2d2	76	4.18	2008
s2d1	164	4.17	2008

(a) Particle size distributions for the simulants are shown in Table 3.6.

Discrepancies and Follow-on Tests

This section summarizes the discrepancies between the test systems and a fully scaled WTP vessel. These discrepancies are compromises that were made in the design of the test platforms in an attempt to meet the demands of the project schedule.

The successful benchmarking of models for mixing response variables against previous test results for large-scale systems using prototypic PJMs, prototypic operations, and complex simulants provide confidence that the compromises made in the geometric scaling and test system operation do not significantly affect the performance of the models. The main characteristics of the test system that differed from a perfectly scaled WTP vessel were the following:

- The test system used pulse tubes instead of PJMs. A pulse tube has a smaller diameter and volume than a PJM. This results in the open cross-sectional area of the test tank being greater than that of a scaled WTP vessel.
- The pulse tubes used straight-bore nozzles that were 10 diameters long while PJMs have conical-shaped nozzles. The straight bore tubes provide a more idealized flow and minimize swirl effects, which can cause asymmetrical flow patterns.

[1] Mt. Hood Chemical Corporation material safety data sheet, product name: Mt. Hood 480, Portland, Oregon.

- The pulse tubes were operated with intermittent flow compared with reciprocating flow in PJMs. The pulse tubes use suction lines located in the upper region of the tank. Therefore, the pulse tube cycle includes a quiescent period during the vent and refill portions of a PJM cycle.
- Testing was conducted using a 12-nozzle array constructed to represent that of the WTP HLP-22 vessel. The radial location of the nozzles in the scaled tanks was adjusted because of differing tank bottom contours to achieve an angle of incidence between the nozzle centerlines and the tank bottom similar to those in the full-scale HLP-22 vessel. After all the tests had been completed, a careful examination of the mid-sized test tank revealed that the bottom head contour was somewhat different than manufacturer's drawings. An evaluation of the data suggests that the models would likely fit the data somewhat more tightly if this discrepancy was fully accounted for. However, this work has not been pursued.

The relationships generated from the test data are expected to take the same form as those that would have been developed for data obtained using a prototypic drive system. A shift or offset in the relationship may exist between models developed from data using the two different drive systems. However, the shift is not expected to have a strong influence on the performance assessments presented in this report. The existence of the shift may affect predictions for full-scale vessel performance. To improve tank performance predictions, it is recommended that additional parametric testing with prototypic drive systems be conducted to establish an adjustment factor for full-cycle (reciprocating flow) operations. Additional testing is recommended to evaluate the effects of small cohesive particles with respect to correlation predictions.

References

Olsen J. 2008a. *Determination of Mixing Requirements for Pulse-Jet-Mixed Vessels in the Waste Treatment Plant.* 24590-WTP-ES-PT-08-002, Rev. 0. Bechtel National Incorporated, Richland, Washington.

Smith GL. January 2007. *Scaled Testing to Determine the Adequacy of the WTP Pulse Jet Mixer Designs*. 24590-PTF-TSP-RT-06-007, Bechtel National Inc., Richland Washington.

Wells BE, MA Knight, EC Buck, SK Cooley, RC Daniel, LA Mahoney, PA Meyer, AP Poloski, JM Tingey, WS Callaway III, GA Cooke, ME Johnson, MG Thien, DJ Washenfelder, JJ Davis, MN Hall, GL Smith, SL Thomson, and Y Onishi. 2007. *Estimate of Hanford Waste Insoluble Solid Particle Size and Density Distribution*. PNWD-3824, WTP-RPT-153 Rev. 0, Battelle – Pacific Northwest Division, Richland, Washington.

References Not Publically Available

Elmore MR, CW Enderlin, and PA Meyer. July 2007. *M3 Testing Approach in Support of Tank HLP-22 Issues*. TP-RPP-WTP-480, Pacific Northwest National Laboratory, Richland, Washington.

Elmore MR and CW Enderlin. January 2008. *M3 Testing Approach in Support of Tank HLP-22 Issues.* ICN-TP-RPP-WTP-480-R0.1, Pacific Northwest National Laboratory, Richland, Washington.

Elmore MR, CW Enderlin, and PA Meyer. January 2009. *M3 Testing Approach in Support of Tank HLP-22 Issues ICN 0.2*. TP-RPP-WTP-480 R0.2, Pacific Northwest National Laboratory, Richland, Washington.

Hazen H. October 2007. *Contract No. DE-AC27-01RV14136, Hanford Tank Waste Treatment and Immobilization Plant, Memorandum of Agreement (MOA), 24590-QL-HC9-WA49-00001, PNNL R&T Support, Subcontract Change Notice (SCN) No. 44 Additional Work Required by Test Exception Report 24590-WTP-TEF-RT-07-00013*. Bechtel National Inc., Richland, Washington.

Hazen H. 2008a. Letter CCN 178425. *Contract No. DE-AC27-01RV14136 – Hanford Tank Waste Treatment and Immobilization Plant, Memorandum of Agreement (MOA) 24590-QL-HC9-WA49-00001, PNNL R&T Support, Subcontract Change Notice (SCN) No. 71 for Work Authorization (WA) 08 Work Cancellations*. Bechtel National, Inc. , Richland, Washington.

Hazen H. 2008b. *Contract No. DE-AC27-01RV14136, Hanford Tank Waste Treatment and Immobilization Plant, Memorandum of Agreement (MOA), 24590-QL-HC9-WA49-00001, PNNL R&T Support, Direction for M3 WA2007-08 PJM Testing, Test Specification 24590-PTF-TSP-RT-06-006 Rev. 0.* CCN 190723, Bechtel National Inc., Richland, Washington.

Acknowledgments

The authors would like to thank Sheila Q. Bennett for valuable editorial support, Michael J. Parker and Mandi J. Oukrop for document production support, and William L. Kuhn and O. Dennis Mullen for their careful and thorough technical reviews and discussions. We appreciate and highly value their abilities to work flexibly and to put in the extra effort to support our M3 Mixing team to produce a well-thought-out and critically reviewed report summarizing all aspects of the project.

In addition to the authors, this work was supported by many dedicated staff involved in setting up experimental equipment and instrumentation, testing, data acquisition, data processing, and analysis. Crafts support was timely and helped us meet a demanding schedule. Engineering and administrative support occurred in a timely and effective manner when needed. These people are especially recognized for putting in extra effort to support the M3 Mixing Project.

Facility Operations and Engineering Support

CM Flaucher	JR Sapp	RL Meicenheimer	RC Brown
R Ewing	MR Townsend	GG Brodaczynski	TM Loftus
SP Panther	H Schulz	FB Knode	RM Jones
AM Sutherland	HR Shintaffer	DL Cravens	ER Langevin
RW Lucas	JL Allen	RL Gaston	CF Weems
JA Clark	RM Bechtol	JE Sandberg	DP Hebert
RN Blundon	MK Krouse	RL Mays	SB Saslow
ST Steer	DR Brawn	JJ Wodtli	D Bell
MH Hartzell	J Guajardo		

Engineering and Administrative Support

WB Taylor	BE Watson	JA Willett	AP Poloski
JM Tingey	BF Saffell	JH Sachs	WC Buchmiller
MR Zumhoff	SC Pratt	RD Daudt	DR Sisk
JK Young	EK Mercer	RL Johnson	JM Cuta
WF Mar	LK Angel	EC Golovich	BK Bragg
JA Bailey	RB Branton	CC Duncan	DS Curtis
RA Pappas	M Luna	JA Serkowski	MS Fountain
JB Lang	MM Watts	DS Sklarew	JC Tucker
JM Alzheimer	JM Billing	WR Park	ST Yokuda
CM Flynn	SK Franks	RD Stahl	SL Crowell
S Pilli	M Morra	J Larsen	RC Daniel
JT Munley	AI Thronas	DB Barnett	AJ Heieren
KD Nelson	F Nigl	TM Koehler	NK Karri
JB Sorensen	DJ Corbett	KJ Lessor	AM Casella
JC Follansbee	JD Adgerson	MD Wojcik	

Acronyms and Abbreviations

AEA	Atomic Energy Authority (UK)
APEL	Applied Process Engineering Laboratory
ASME	American Society of Mechanical Engineers
BDC	bottom dead center
BM	benchmark
BNFL	British Nuclear Fuels, Ltd.
BNI	Bechtel National, Incorporated
CDS	consolidated data spreadsheet
CFD	computational fluid dynamics
CI	confidence interval
DAS	data acquisition system
DBE	design basis event
DDE	dynamic data exchange
DOE	Department of Energy
EFRT	External Flowsheet Review Team
F&D	flange and dish
FIO	for information only
FY	fiscal year
HS	head shape
ID	inner diameter; case ID for test conditions (see Table 6.4 for Case ID coding)
JPP	jet pump pair
LS	lag storage
LRB	laboratory record book
M3	EFRT technical issue M3–Inadequate Design of Mixing Systems–Pulse Jet Mixers
MOA	memorandum of agreement
MOV	maximum operating volume
MR	multiple regression
MSS	master spread sheet
M&PE	Mechanical and Process Engineering
NCAW	neutralized current acid waste
NPT	National Pipe Thread
NQA	nuclear quality assurance
OD	outer diameter
OLS	ordinary least squares regression
PJM	pulse jet mixer (mixing)
PM	particle motion

PNNL	Pacific Northwest National Laboratory
PNWD	Pacific Northwest Division
%RSD	percent relative standard deviation
PSD	particle-size distribution
PSDD	particle-size and density distributions
PVC	polyvinyl chloride
PvM	predicted versus modeled
QA	quality assurance
QAM	Quality Assurance Manual
QAP	Quality Assurance Plan
QARD	Quality Assurance Requirements and Descriptions
R&T	Research and Technology
RMC	root mean cubed
RMS	root mean squared
RPP	River Protection Project
RSD	relative standard deviation
SEM	scanning electron microscopy
TCT	test condition transmittal
UCC	ultrasonic command and control
UDV	ultrasonic Doppler velocimetry
UFP	ultrafiltration process feed
UT	ultrasonic testing
UT-CDS	ultrasonic testing composite data spreadsheet
VFD	variable-frequency drive
WTP	Waste Treatment and Immobilization Plant
WV	working volume
8TA	eight-tube array jet configuration

Symbols

A1, A2, A3	coefficient determined by experimental data
B1, B2, B3	exponent determined by experimental data
C	concentration, solids volume concentration
C_F	average solids concentration at vessel fill height
CS	critical suspension
C(Z)	solids vertical distribution, concentration as a function of elevation
C_0	average solids concentration at the vessel bottom (at elevation 0)
C_0'	average solids concentration at the vessel bottom with finite fill level
D	diameter of tank
D*	nondimensional critical suspension defined by Eqs. (7.31 and 7.33)
D_I	diameter of impeller
D_{PT}	diameter of pulse tube
DC	duty cycle = t_D / t_C
d	diameter of jet nozzle
d_S	diameter of solids particle
d_{05}	diameter of fifth percentile particle
d_{50}	median particle diameter
d_{95}	diameter of 95th percentile particle
E	elliptical tank bottom
E_S	potential energy required to lift solids
E_V	jet energy imparted to tank during a pulse
F	flanged and dished tank bottom
F_C	Froude number based on cloud height
F_{CS}	Froude number at critical suspension
F_{CST}	Froude number at critical suspension based on terminal settling velocity
$F_{CS\ TH}$	Froude number at critical suspension based on hindered settling velocity
F_D	Froude number based on tank diameter (D)
F_{DT}	Froude based on tank diameter (D) and settling velocity (U_T)
F_{HcT}	Froude number based on cloud height (H_C) and settling velocity (U_T)
Fr	Froude number = U^2 / [gd(s-1)]
Fr_{JS}	Froude number at the just-suspended velocity
Fr_p	particle Froude number
F_S	densimetric Froude number
f	function
fct	functional relationship
Ga	Galileo number

Ga_p	particle Galileo number
Gr	gravity number = $(s-1)\ g\ d^2/(\nu\ U_T)$
g	gravitational constant
$g(y_i)$	mathematical transformation
H	fluid height, normal fill level
H_{bed}	solids bed height measured by ultrasonic Doppler velocimetry
H_C	average peak cloud height
H_C*	nondimensional cloud height defined by Eqs. (7.32) and (7.40)
$H_{CSpulsed}$	average peak cloud height at critical suspension for pulsed flow
$H_{CSsteady}$	average peak cloud height at critical suspension for steady flow
H_{CS}	average peak cloud height at critical suspension
H_{dish}	dish height
H_F	vessel fill height
Jet	type of jet either pulsed or steady
k	coefficient, constant for concentration profile
k_C	geometric constant for H_C for dish shape
k_D	nozzle discharge coefficient
k_U	geometric constant for U_{CS} for dish shape
k_I	impeller specific constant
k_J	jet mixer specific constant
k_P	pulse-jet mixer specific constant
m_S	relative mass of solids (difference between solid mass and liquid it displaces)
N	number of installed jets or pulse tubes
N_I	number of jets operating in the inner ring
N_J	number of operating jets/pulse tubes
N_{JS}	shaft speed for just-suspended condition (Zwietering-mechanical mixers)
N_O	number of jets operating in outer ring
N_S	settling number (ratio of useful jet energy imparted to the tank during a pulse to energy required to keep solids suspended during a pulse)
n	velocity exponent; 1, 2, 3 corresponds to mass (peak average), momentum, and energy-based average velocities
P_J	hydraulic power input at nozzles
P_V	effective jet hydraulic power
PM	particle motion
PPV	power per unit volume
PT	pulse tube configuration (e.g., HLP-22 or 8TA)
PT_{od}	pulse tube outer diameter
p	empirical constant

p_D	drive pressure
p_E	pressure head at nozzle exit
Q	volumetric flow rate
R	radial location of PJMs; tank radius
R^2	coefficient of determination, fraction of variation in response values accounted for by a model ($0 \leq R^2 \leq 1$)
Re	jet Reynolds number = Ud/ν
Re_{CS}	jet Reynolds number at critical suspension velocity = $U_{CS}d/\nu$
Re_D	tank diameter Reynolds number = UD/ν
Re_p	particle Reynolds number based on particle size and settling velocity = $U_T d_S/\nu$
R_I	radial PJM inner ring location
R_O	radial PJM outer ring location
Rtn	return line height
S	scale; spherical tank bottom
SF	scale factor
Sol	solids level
SP_I	solids bottom pattern in inner region of tank
SP_O	solids bottom pattern in outer region of tank
S_W	velocity increment increase or decrease
s	density ratio, ratio of particle density to liquid density = ρ_s/ρ_l
sod	nozzle stand-off distance
sxdx	simulant designator (density#particle#)
T	tank liquid temperature
TPA	thrust per unit area
t_C	cycle time
t_D	drive time, discharge time, pulse time, time at end of pressurization during pulse discharge
t_{DA}	time of actual drive
t_{DP}	time over which U_{PA} is measured
t_{FE}	time of end of flow
t_{FS}	time of the start of the flow
t_m	time of maximum velocity during pulse discharge
t_R	refill time
U	jet velocity
$\overline{U}$	volume-weighted average settling velocity (Ubar)
$\overline{U}_n$	cumulative volume-weighted average settling velocity for n% of fastest-settling particles
U_C	velocity required for complete suspension when the cloud height reaches the height of the fluid $H_C = H$

U_{CS}	critical suspension velocity, all solids suspended at the end of the pulse
U_{CS_D}	U_{CS} condition based on decreasing velocity
U_{CSM}	U_{CS} condition method of selection
$U_{CSpulsed}$	critical suspension velocity for pulsed flow
$U_{CSsteady}$	critical suspension velocity for steady flow
U_{CSR}	selected U_{CS} condition for test
U_{CS}cen	U_{CS} condition determined visually at the tank center
U_{CS}udv	U_{CS} condition determine using ultrasonic Doppler velocimetry at the tank center
U_{CS}vis	U_{CS} condition determined visually
U_{CS15}	critical suspension velocity in the small-scale vessel
U_{design}	vessel design velocity
U_{end}	velocity at the end of pressurization during discharge
U_{JS}	jet velocity for off-bottom suspension (jet mixers)
U_{max}	maximum jet discharge velocity during pulse
U_{PA}	peak average velocity
U_{pulsed}	pulse jet velocity
U_S	steady jet velocity
U_{steady}	steady jet velocity
$U(t)^n$	instantaneous velocity
U_T	unhindered terminal settling velocity
U_{TH}	hindered terminal settling velocity
U_{TH}'	modified hindered terminal settling velocity
U_{pa}	peak average velocity, which was either observed visually or computed
U_V	effective average vertical velocity
U_x	settling velocity of xth percentile of PSDD
U_0	average velocity
U1	mass-based average pulse velocity
U2	momentum-based average root mean square (RMS) pulse velocity
U3	energy-based average root mean cubed pulse velocity
U_{90}	settling velocity of 90th percentile of PSDD
U_{95}	settling velocity of 95th percentile of PSDD
$\overline{U}_{90}$, $Ubar_{90}$	volume weighted average settling velocity of 90th percentile and above settling velocity of PSDD (fastest settling 10% fraction)
V	nominal volume of tank
V_{dish}	dish volume
V_P	volume of pulse (per PJM)
V_{PT}	volume of pulse tube

V_{REF}	reference volume based on the volume of a right circular cylinder of diameter D where height equals diameter, $V_{REF} = (\pi D^3)/4$
V_S	volume of solid particulate
V_T	vessel volume
vf	void fraction
vol%	volume percent
W_{MP}	wt% solids at maximum packing fraction
W_0	wt% solids at bottom
W_0^*	wt% solids at bottom adjusted by a factor of 1.5 ($W_0^* = 1.5\ W_0$)
w_{Smax}%	insoluble solids concentration (in wt%) for the WTP vessels
wt%	weight percent
X	weight of solid per weight of liquid times 100 (percent); threshold velocity for distinguishing assumed zero flow from measured flow (comparator setpoint)
x_{ni}	predictor variables ($x_1, x_2, \ldots, x_n$)
y	response variable
Z	vertical elevation
z	distance that jet travels

Greek Symbols

α	scale-up exponent
α_1	ϕ_p coefficient to optimize U_{CS} and H_C
α_2	ϕ_J coefficient to optimize U_{CS} and H_C
α_j	sensitivity coefficient
ε_i	random error representing experimental and measurement uncertainty in the ith data
ε_{31}	pulse shape ratio
ΔE_S	energy required to keep solids suspended during a pulse
ΔH	level change in fluid height during pulse
ΔL	level change in pulse tube during discharge
Δt	time interval
Δt_n	primary discharge time, time interval over which the integration is performed
ν	kinematic viscosity = μ/ρ_l
μ	viscosity
ϕ	local solids fraction
ϕ_J	jet density = $N_J d^2/D^2$
ϕ_{max}	packing fraction
ϕ_p	pulse volume fraction = $N\ V_P\ /\ V_{REF}$

ϕ_{PT}	ratio of pulse tube to vessel cross-sectional area = $N\ D_{PT}^2/D^2$
ϕ_S	ratio of volume of solids particulate to reference volume = $V_S/V_{REF} = V_S/(\pi D^3/4)$
ϕ_{Smax}	solids volume fraction corresponding to maximum packing
ρ	slurry density
ρ_l	liquid density
ρ_s	solids density
θ	impingement angle
θ_I	inner impingement angle
θ_O	outer impingement angle

Contents

Revision History iii
Abstract v
Executive Summary vii
Acknowledgments xvii
Acronyms and Abbreviations xix
Symbols xxi
Greek Symbols xxv
1.0 Introduction 1.1
1.1 Background 1.1
1.2 Test Justification 1.3
1.3 Objectives 1.4
1.4 Overview of Testing and Modeling 1.5
1.4.1 Model Development Approaches 1.5
1.4.2 Phased Approach to Testing 1.6
1.4.3 Scaled Testing Approach 1.6
1.4.4 Three Tank Scales 1.7
1.4.5 Test Tank Sizing 1.7
1.4.6 Mixing System Configuration 1.8
1.4.7 Initial Testing to Define System Parameters that Meet Test Objectives 1.9
1.4.8 Scaled Testing and Model Development 1.9
1.5 Quality Requirements 1.9
1.6 Organization of Document 1.10
2.0 Technical Approach for Assessing WTP Mixing Systems 2.1
2.1 Mechanical Mixing 2.1
2.2 Jet Mixing 2.2
2.3 Pulse Jet Mixing 2.3
2.3.1 Pulse Jet Mixer Operation 2.3
2.3.2 Expected Solids Behavior During PJM Operation 2.6
2.3.3 Mixing Requirements 2.7
2.3.4 Synopsis of Prior PJM Mixing Studies 2.7
2.4 WTP Plant Vessels 2.8
2.5 Evaluating Mixing Systems 2.14
2.5.1 Mixing System Parameters 2.15
2.5.2 Just-Suspended Jet Velocity 2.18
2.5.3 Solids Vertical Distribution 2.19
2.6 Parametric Tests 2.19

2.7 Scale-up of Metrics 2.19
2.8 Test Design 2.20
2.8.1 Approach 2.20
2.8.2 Constraints 2.21
2.8.3 Plant Variable Ranges 2.21
3.0 Hanford Waste Properties and Simulant Selection 3.1
3.1 Hanford Waste Properties 3.1
3.2 Selection of Slurry Property Ranges 3.6
3.3 Characterization Techniques 3.8
3.3.1 Density Measurement Technique 3.8
3.3.2 Packing Fraction Measurement Technique 3.8
3.3.3 Particle Size Measurement Technique 3.8
3.3.4 Simulant Selection and Characterization 3.8
3.3.5 Simulant Scaling 3.14
3.4 Simulant Preparation 3.14
3.4.1 Water Addition and Removal 3.15
3.4.2 Solids Addition and Removal 3.15
4.0 Experimental Equipment 4.1
4.1 Modeling Tank HLP-22 Configuration 4.1
4.2 Small-Scale Test Stand 4.6
4.2.1 Components 4.6
4.2.2 Control Equipment 4.9
4.3 Mid-Scale Test Stand 4.10
4.3.1 Components 4.10
4.3.2 Control Equipment 4.13
4.4 Large-Scale Test Stand 4.14
4.4.1 Components 4.14
4.4.2 Control Equipment 4.19
4.5 Pulse Flow Operating Parameters 4.19
4.6 Instrumentation 4.20
4.7 Data Acquisition System 4.21
4.8 Tube Arrays and Nozzles 4.21
5.0 Experimental Procedures 5.1
5.1 Testing Overview 5.1
5.2 Observation Procedures 5.3
5.2.1 Observation Procedures Used in 2007 ..... 5.3
5.2.2 Observation Procedures Used in 2008 ..... 5.6
5.3 Data Acquisition System Calculations 5.11
5.4 Governing Documents 5.13

6.0 Mixing Experiments 6.1
6.1 Data Reporting Format 6.1
6.2 July 2007 Tests in Mid-Scale Tank with Spherical Head 6.6
6.3 Fall 2007 Tests in Mid-Scale Tank with Spherical Head 6.13
6.4 2008 Tests 6.20
6.4.1 Small-Scale Tank Tests with Elliptical Head 6.21
6.4.2 Mid-Scale Tests with Spherical Head 6.27
6.4.3 Large-Scale Tank Tests with Elliptical Head 6.30
6.4.4 Large-Scale Tank Tests with Flanged and Dished Head 6.35
6.4.5 Comparisons Among Tanks 6.37
6.4.6 Repeat and Replicate Tests 6.39
6.5 Concentration Profiles 6.43
6.5.1 Concentration Profile Measurements 6.43
6.5.2 Variation with Critical Suspension Velocity U_{CS} 6.49
6.5.3 Variation with Radial Location 6.49
6.5.4 Variation with Tank 6.52
6.5.5 Variation with Nozzle Diameter and Number of Pulse Tubes 6.52
6.5.6 Variation with Concentration 6.56
6.5.7 Variation with Duty Cycle 6.56
6.6 Transient Cloud Height Tests 6.60
7.0 Analysis and Modeling of Mixing Data 7.1
7.1 Analysis and Modeling Approach 7.1
7.1.1 Physical Approach 7.3
7.1.2 Statistical Multiple Regression Approach 7.4
7.2 Mixing Behavior 7.4
7.2.1 Parametric Sensitivity and Functional Form 7.5
7.2.2 Jet Velocity 7.6
7.2.3 Slurry Properties 7.8
7.2.4 Operational Parameters 7.13
7.2.5 Geometry 7.14
7.2.6 Scale 7.16
7.2.7 Pulse Shape 7.19
7.2.8 Aspects of Mixing Behavior Included in Model Development 7.20
7.3 Physical Model Results 7.20
7.3.1 Nondimensional Variables 7.21
7.3.2 Physical Models for Critical Suspension Velocity and Cloud Height Based on Nondimensional Variables 7.23
7.3.3 Solids Vertical Distribution 7.29
7.3.4 Summary of Physical Models 7.30

7.4 Dimensional and Dimensionally Consistent Models for U_{CS} and H_C Developed Using the Statistical MR Approach 7.32
7.4.1 Development of U_{CS} and H_C Dimensional Models Without Interaction Terms 7.33
7.4.2 U_{CS} and H_C Dimensionally Consistent (Generalized) Models 7.35
7.4.3 U_{CS} and H_C Dimensional Models with Interaction Terms 7.38
7.5 Comparing Physical, Dimensional, and Generalized Models for U_{CS} and H_C 7.38
7.6 Possible Model Improvements 7.39
7.6.1 Possible Improvements to Physical Models 7.40
7.6.2 Possible Improvements to Generalized Models 7.41
7.7 Conclusions Regarding Possible Model Improvements 7.41
7.8 Updates to Models Since Initial Document Release 7.42
8.0 Applicability and Benchmarking of Mixing Models 8.1
8.1 Accounting for Prototypic Conditions 8.1
8.1.1 Geometry and Operation 8.1
8.1.2 Accounting for Prototypic Fill Level 8.3
8.1.3 Accounting for Distributions of Particle Size and Density 8.4
8.2 Uncertainty and Applicability 8.5
8.2.1 Measurement Uncertainty 8.5
8.2.2 Experimental Uncertainty 8.8
8.2.3 Model Uncertainty 8.9
8.2.4 Uncertainty Associated with Applying Models to WTP Vessel Mixing 8.10
8.2.5 Margin for Vessel Performance Evaluations 8.11
8.3 Model Benchmarks 8.11
8.3.1 Mixing Tests with AZ-101/102 Filtration Waste Simulant 8.13
8.3.2 Mixing Tests with Glass Bead Simulants 8.21
8.3.3 Comparison with CFD Simulation 8.24
8.3.4 Benchmarking Summary 8.26
9.0 WTP Mixing Systems Performance Examples 9.1
9.1 Approach for Predicting Vessel Performance 9.1
9.1.1 Overview of Requirements 9.2
9.1.2 Assumptions and Limitations 9.2
9.1.3 Uncertainties Related to the Application of the Mixing Models 9.3
9.1.4 Proposed Evaluation Methodology 9.4
9.2 Input Parameters for Plant Vessels 9.6
9.2.1 Vessel Geometry and Operational Data 9.7
9.2.2 Waste Property Conditions 9.7
9.2.3 Dimensionless Variable Evaluation 9.9
9.2.4 Hanford Tank AZ-101 PSDD and Settling Velocity 9.13

9.3 Vessel Evaluation Examples Using the Physical Models and the Design Point Limits..... 9.17
9.3.1 FRP-02 A/B/C/D (Design Point) Physical Model 9.18
9.3.2 HLP-22 8 m/s, 4-in. Nozzles (Design Point) Physical Model 9.19
9.3.3 HLP-22 12 m/s, 4-in. Nozzles (Design Point) Physical Model 9.20
9.3.4 HLP-22 8 m/s, 6-in. Nozzles (Design Point) Physical Model 9.21
9.3.5 HLP-22 12 m/s, 6-in. Nozzles (Design Point) Physical Model 9.22
9.3.6 TCP-01 (Design Point) Physical Model 9.23
9.3.7 TLP-09 A/B (Design Point) Physical Model 9.24
9.3.8 PWD-33 (Design Point) Physical Model 9.25
9.3.9 PWD-43 (Design Point) Physical Model 9.26
9.3.10 PWD-44 (Design Point) Physical Model 9.27
9.3.11 FEP-17 A/B (Design Point) Physical Model 9.28
9.3.12 PWD-15/16 (Design Point) Physical Model 9.29
9.3.13 UFP-01 A/B (Design Point) Physical Model 9.30
9.3.14 RLD-07 (Design Point) Physical Model 9.31
9.3.15 RLD-08 (Design Point) Physical Model 9.32
9.3.16 HOP-903/904 (Design Point) Simple Calculation 9.33
9.4 Vessel Evaluation Examples with the Physical Models and the Hanford Waste Distribution 9.34
9.4.1 FRP-02 A/B/C/D (Hanford PSDD, ρ_l=1.1 g/cm^3, μ=1.5 cP Fluid) Physical Model 9.35
9.4.2 HLP-22 8 m/s, 4-in. (Hanford PSDD, ρ_l = 1.1 g/cm^3, μ = 1.5 cP Fluid) Physical Model 9.37
9.4.3 HLP-22 12 m/s, 4-in. (Hanford PSDD, ρ_l = 1.1 g/cm^3, μ = 1.5 cP Fluid) Physical Model 9.38
9.4.4 HLP-22 8 m/s, 6-in. (Hanford PSDD, ρ_l = 1.1 g/cm^3, μ = 1.5 cP Fluid) Physical Model 9.40
9.4.5 HLP-22 12 m/s, 6-in. (Hanford PSDD, ρ_l = 1.1 g/cm^3, μ = 1.5 cP Fluid) Physical Model 9.41
9.4.6 TCP-01 (Hanford PSDD, ρ_l = 1.1 g/cm^3, μ = 1.5 cP Fluid) Physical Model 9.42
9.4.7 TLP-09 A/B (Hanford PSDD, ρ_l = 1.1 g/cm^3, μ = 1.5 cP Fluid) Physical Model 9.43
9.4.8 PWD-33 (Hanford PSDD, ρ_l = 1.1 g/cm^3, μ = 1.5 cP Fluid) Physical Model 9.44
9.4.9 PWD-43 (Hanford PSDD, ρ_l = 1.1 g/cm^3, μ = 1.5 cP Fluid) Physical Model 9.46
9.4.10 PWD-44 (Hanford PSDD, ρ_l = 1.1 g/cm^3, μ = 1.5 cP Fluid) Physical Model 9.47
9.4.11 FEP-17 A/B (Hanford PSDD, ρ_l = 1.1 g/cm^3, μ = 1.5 cP Fluid) Physical Model 9.48
9.4.12 PWD-15/16 (Hanford PSDD, ρ_l = 1.1 g/cm^3, μ = 1.5 cP Fluid) Physical Model 9.49

9.4.13 UFP-01 A/B (Hanford PSDD, ρ_l = 1.1 g/cm^3, μ =1.5 cP Fluid) Physical Model 9.50
9.4.14 RLD-07 (Hanford PSDD, ρ_l = 1.1 g/cm^3, μ = 1.5 cP Fluid) Physical Model 9.51
9.4.15 RLD-08 (Hanford PSDD, ρ_l = 1.1 g/cm^3, μ = 1.5 cP Fluid) Physical Model 9.52
9.4.16 HOP-903/904 (Hanford PSDD, ρ_l=1.1 g/cm^3, μ=1.5 cP Fluid) Physical Model 9.53
9.5 Vessel Evaluation Examples Using the Generalized Models and the Hanford Waste Distribution 9.54
9.5.1 FRP-02 A/B/C/D (Hanford PSDD, ρ_l = 1.1 g/cm^3, μ = 1.5 cP Fluid) Generalized Model 9.55
9.5.2 HLP-22 8 m/s, 4-in. (Hanford PSDD, ρ_l = 1.1 g/cm^3, μ = 1.5 cP Fluid) Generalized Model 9.56
9.5.3 HLP-22 12 m/s, 4-in. (Hanford PSDD, ρ_l = 1.1 g/cm^3, μ = 1.5 cP Fluid) Generalized Model 9.57
9.5.4 HLP-22 8 m/s, 6-in. (Hanford PSDD, ρ_l = 1.1 g/cm^3, μ = 1.5 cP Fluid) Generalized Model 9.58
9.5.5 HLP-22 12 m/s, 6-in. (Hanford PSDD, ρ_l = 1.1 g/cm^3, μ = 1.5 cP Fluid) Generalized Model 9.59
9.5.6 TCP-01 (Hanford PSDD, ρ_l = 1.1 g/cm^3, μ = 1.5 cP Fluid) Generalized Model 9.60
9.5.7 TLP-09 A/B (Hanford PSDD, ρ_l = 1.1 g/cm^3, μ = 1.5 cP Fluid) Generalized Model 9.61
9.5.8 PWD-33 (Hanford PSDD, ρ_l = 1.1 g/cm^3, μ = 1.5 cP Fluid) Generalized Model 9.62
9.5.9 PWD-43 (Hanford PSDD, ρ_l = 1.1 g/cm^3, μ = 1.5 cP Fluid) Generalized Model 9.63
9.5.10 PWD-44 (Hanford PSDD, ρ_l = 1.1 g/cm^3, μ = 1.5 cP Fluid) Generalized Model 9.64
9.5.11 FEP-17 A/B (Hanford PSDD, ρ_l = 1.1 g/cm^3, μ = 1.5 cP Fluid) Generalized Model 9.65
9.5.12 PWD-15/16 (Hanford PSDD, ρ_l = 1.1 g/cm^3, μ = 1.5 cP Fluid) Generalized Model 9.66
9.5.13 UFP-01 A/B (Hanford PSDD, ρ_l = 1.1 g/cm^3, μ = 1.5 cP Fluid) Generalized Model 9.67
9.5.14 RLD-07 (Hanford PSDD, ρ_l = 1.1 g/cm^3, μ = 1.5 cP Fluid) Generalized Model 9.68
9.5.15 RLD-08 (Hanford PSDD, ρ_l = 1.1 g/cm^3, μ = 1.5 cP Fluid) Generalized Model 9.69
9.5.16 HOP-903/904 (Hanford PSDD, ρ_l = 1.1 g/cm^3, μ = 1.5 cP Fluid) Generalized Model 9.70
9.6 Summary of Vessel Performance Ratios 9.71
10.0 Conclusions 10.1

10.1 Model Development 10.1
10.1.1 Recommendations for Using the Models 10.2
10.1.2 Estimates of Confidence 10.2
10.2 WTP Vessel Performance Prediction Examples 10.3
10.3 Recommendations for Extending Applicability of the Models 10.4
10.4 Major Findings 10.6
11.0 References 11.1
Appendix A – Ultrasonic Instrumentation A.1
Appendix B – Mixing Data B.1
Appendix C – Concentration Profile Data C.1
Appendix D – Statistical Methods Used to Develop, Evaluate, and Validate Multiple Regression Models D.1
Appendix E – Data Assessment and Analysis to Support Developing Multiple Regression Models for Mixing Responses E.1
Appendix F – Multiple Regression Modeling of Mixing Data F.1

Figures

2.1. Illustration of a Typical PJM System in a WTP Vessel 2.4
2.2. Illustration of Nozzle Velocity Transient During PJM Discharge 2.5
2.3. Illustration of a Typical PJM System in a WTP Vessel. 2.6
2.4. Some Common Mixing Metrics Applied to the 18 Distinct WTP Vessel Configurations 2.14
2.5. Just-Suspended Speed as a Function of Fill Level for Mechanical Agitators 2.17
2.6. Effects of Fill Level on Cloud Height for Solids Suspension with Mechanical Agitators 2.18
3.1. Cumulative Undissolved Solid Volume Percent as Function of Settling Velocity for Case 3 PSDD 3.3
3.2. Cumulative Undissolved Solid Volume Percent as Function of Cumulative Volume Weighted Average Settling Velocity for Case 3 PSDD 3.5
3.3. Cumulative Volume Percent as a Function of Settling Velocity for Hanford PSDD Case 3 and Simulants 3.7
3.4. Cumulative Volume Percent as a Function of Cumulative Volume-Weighted Average for Hanford PSDD Case 3 and Simulants 3.7
3.5. XLSciTech As-Received Beads; s1d2, s2d2, s1d1, and s2d1 ..... 3.11
3.6. As-Received Beads; s1d5, #3 p2d6, #8 p1d7, and #12 p1d8 ..... 3.11
3.7. PSD Around the Mean Particle Size of XLSciTech Microspheres and Potters Beads 3.12
3.8. SEM Pictures of Reused s1d2 Beads Removed During Testing 3.13
3.9. SEM Images of XLSciTech Microspheres at the Completion of Testing 3.13
4.1. Schematic of Conceptual Arrangement of Test Tank and Drive System for HLP-22 Testing 4.2
4.2. Comparison of Profiles for F&D and 2:1 Semi-Elliptical Tank Heads 4.2
4.3. Illustration of Jet Impingement Angle, θ, Which is the Angle Between the Vertically Downward Jet and the Bottom of the Tank at the Point of Impingement 4.3
4.4. Illustration of the Change in Impingement Angles for Different Head Profiles. 4.4
4.5. Diagram of Small-Scale Test System Showing the HLP-22 12-Tube Array 4.7
4.6. Small-Scale Elliptical-Head Test Tank with Pulse Tubes Installed; Pulse Tubes Mounted in the Tank 4.8
4.7. Pump Skid with Pumps and Coriolis Flow Meter; Pump Control Panel 4.9
4.8. The Pneumatic Butterfly Control Valve Mounted Between Pump Skid and Tank Skid. 4.9
4.9. Diagram of Mid-Scale Test System 4.11
4.10. Mid-Scale Test Tank with Pulse Tubes Installed; View from Above with Upper Pulse Tube Support Rack and Static Pressure Tubes Visible 4.12
4.11. Pump Skid with Pumps, Bladder Tanks, Suction and Discharge Manifolds; Control Valve Assembly with Blue Pulse Control Valve, Air Control Valve, Control Valve Pressure Reservoir, and Micro Motion Coriolis Flow Meter 4.13
4.12. Diagram of Large-Scale Test System with the 8-Tube Array 4.15
4.13. Pulse Tube Assembly Before Installation in Tank; Close-up of Pulse Tube Nozzles 4.16
4.14. Large-Scale Vessel Flanged and Dished Head; 0.46-m Acrylic Viewing Port 4.17

4.15. Pump Assembly and Coriolis Meters with Test Tank in Background, Upper End of Pump System as it Enters the Manifold, Pump Assembly with Scaffolding, and the Large-Scale Test Stand with the 8-Tube Array and Elliptical Head 4.18
4.16. Plan View of 12-Tube HLP-22 F&D Orientation Between Inner and Outer Rings in the Large-Scale Tank. 4.23
4.17. Plan View of 12-Tube HLP-22 Elliptical Array Orientation Between Inner and Outer Rings in the Large-Scale Tank. 4.24
4.18. In-Tank Structural Support for the Tube Array in the Large-Scale Tank 4.25
4.19. Plan View of 8-Tube Array Orientation Between Inner and Outer Rings in Small-Scale Tank 4.25
4.20. HLP-22 12-Tube Tank Array; 8-Tube Array in Large-Scale Elliptical-Head Tank 4.27
5.1. Illustration of Relative Positions of Pulse Tubes and Nozzles in the Mid-Scale Test Tank in HLP-22 Configuration 5.3
5.2. Photograph of Particulate Cloud Near End of Pulse in Mid-Scale Tank Showing a Centrally Peaked Cloud and Measuring Tapes Used for Cloud Height Measurement. 5.5
5.3. Illustration of Nozzle Velocity as a Function of Time for Several Discharge Cycles. 5.8
6.1. View from the Bottom of the Tank Showing Pulse Tubes with No Simulant and Mixing at Some Suspension and BP3 Mixing State 6.8
6.2. Sequence of Photos Showing Growth of Mobilized Area and Solids Settling During Test 34S_6p1d8Yd_8 Conducted in the Mid-Scale Tank with 6-in. Full-Scale Nozzle, for Simulant p1d8, Solids Fraction for Constant Duty Cycle at Pulse Volume Fraction 6.9
6.3. Cloud Height as a Function of Velocity for Two Concentrations in the Mid-Scale Tank with Spherical Head for a Range of Pulse Volume Fractions: Solids Fraction $\phi_S = 0.005$ [Y], Solids Fraction $\phi_S = 0.016$ [X]. 6.11
6.4. Cloud Height as a Function of Velocity for Two Duty Cycles in the Mid-Scale Tank with Spherical Head for a Range of Pulse Volume Fractions: DC = 0.33 [c], DC = 0.18 [d] 6.12
6.5. Cloud Height as Function of Velocity for Simulants p1d7, p1d8, and p2d6 for Two Concentrations in the Mid-Scale Tank with Spherical Head: Linear, Log. 6-in. Full-Scale Nozzle at Solids Fraction, Constant Duty Cycle, and Pulse Volume Fraction 6.12
6.6. Cloud Height as Function of Velocity for Two Duty Cycles for PJM Combinations: DC = 0.18 [d], DC = 0.33 [c] 6.17
6.7. Cloud Height as Function of Velocity for Two Duty Cycles for PJM Combinations: DC = 0.18 [d], DC = 0.33 [c]. 6.18
6.8. Cloud Height as Function of Velocity for Two Fill Heights: H/D=0.7, Rtn/D=0.6, with a 6 in. Full-Scale Nozzle at Solids Fraction, for Constant Duty Cycle at Pulse Volume Fraction and Nozzle Combinations for Simulant p1d7 ..... 6.19
6.9. Cloud Height as Function of Velocity Comparing Results in July and Fall 2007 for Continuous Flow with a 0.4 in. Full-Scale, Solids Fraction for Constant DC for Simulant p1d7 and Data Sets Fall 2007 green, July 2007 orange and pink 6.19
6.10. Cloud Height as Function of Velocity for Seven Concentrations: all Concentrations and Five Concentrations. 6.25
6.11. Cloud Height as Function of Velocity for Two Solids Fractions: $\phi_S = 0.00155$ [Z] and $\phi_S = 0.005$ [Y]. 6.26

6.12. Cloud Height as Function of Velocity for Four Full-Scale Nozzle Diameters in Two Tank Configurations. 6.27
6.13. Cloud Height as Function of Velocity for Different Simulants 6.29
6.14. Cloud Height as a Function of Velocity for Three Simulants near 170 μm Median Diameter 6.30
6.15. Cloud Height as a Function of Velocity for Three Duty Cycles: Duty Cycle = 0.18 [d], Duty Cycle = 0.33 [c], and Duty Cycle = 0.66 [e]. 6.32
6.16. Cloud Height as Function of Velocity for Three Duty Cycles. 6.33
6.17. Cloud Height as a Function of Velocity for Two Tank Configurations, HLP-22 and 8TA 6.34
6.18. Cloud Height as Function of Velocity for Three Simulants: s1d2, s1d1, and s2d2. 6.35
6.19. Cloud Height as a Function of Velocity for Four Duty Cycles. 6.37
6.20. Comparison of Tank Heads at Large Scale: 70E with Elliptical and 70F with F&D Head. 6.38
6.21. Comparison of Small-, Mid-, Large-Scale: s2d2. 6.38
6.22. Comparison of Six Simulants in Four Tanks: Linear Scale and Log Scale. 6.39
6.23. Examples of Solids Concentration by Volume as a Function of Cycle Fraction at an Elevation of H/D = 0.2 and Radially Located at the Tank Center. 6.47
6.24. Solids Concentration by Volume Distribution Plots Showing Minimum, Average, Maximum, and Standard Deviation of Concentration Measured for All Data Points 6.48
6.25. Comparison of Dimensional Profiles Below, At, or Above U_{CS} 6.50
6.26. Comparison of Average Radial Concentration Profiles for Each Test at R=0, 0.5, and 0.9 for Large-Scale F&D and Elliptical Bottom Tanks at and Below U_{CS} for Pulse Volume Fraction 0.05 6.51
6.27. Comparison of Nondimensional Average Radial Concentration Profiles Across Tests at R=0, 0.5, 0.9 for the Large-Scale Flanged and Dished and Elliptical Bottomed Tanks at and Below U_{CS} for Pulse Volume Fraction of 0.05 6.52
6.28. Concentration Profiles at U_{CS} in the 15E, 34S, 70E, and 70F Tanks Segregated by Tank: Dimensional Plots and Nondimensional Plots 6.53
6.29. Comparison of Tank Head Shape for Small-Scale Elliptical, Mid-Scale Spherical, Large-Scale F&D, and Elliptical Bottom Tanks at U_{CS}. 6.54
6.30. Comparison of Dimensional and Nondimensional Plots of Pulse Tube Array, Number of Operating Pulse Tubes, and Nozzle Diameter for Small-Scale Elliptical, Large-Scale F&D, and Elliptical Bottom Tanks at U_{CS}. 6.55
6.31. Concentration Profiles for the Five Simulants in the HLP-22 Tank Configuration 6.57
6.32. Comparing Profiles for Simulants and Tanks at U_{CS} for HLP-22 Tank Configuration as Solids Concentration ϕ_S Increases from 0.00150 to 0.06 6.58
6.33. Concentration Profiles at Varying Duty Cycles 6.59
6.34. Cloud Height Transient Data Shown Dimensionally and Nondimensionally on Linear and Log Scales. 6.61
7.1. Illustration of the Physical Meaning of the Sensitivity Coefficient; Linear and Nonlinear Behavior, Interaction Between Variables 7.5
7.2. Examples of H_C Data as a Function of Jet Velocity; Linear Scale, Logarithmic Scale with U_{CS} Conditions Denoted by Black Center 7.6

7.3. Illustration of the Completely-Suspended Condition as an Energy Maxima with U_{CS} Conditions Denoted by Black Center 7.7
7.4. Behavior of H_C Relative to Critical Suspension Condition for $U \geq U_{CS}$ 7.8
7.5. Sensitivity Coefficients for Terminal Settling Velocity Given by Eq. (7.5a) with Simulant Designations Shown on Vertical Lines 7.9
7.6. Illustrating the Benefit of Using Setting Velocity to Model U_{CS} Data; Dimensional, Nondimensional 7.10
7.7. Illustration of the Benefit of Using Setting Velocity to Model Cloud Height Data: F_{CST} Plotted as a Function of $Ga(s-1)^{1/2}$, F_{CST} Plotted as a Function of U/U_T 7.11
7.8. Effect of Solids Loading on U_{CS} for Five Simulants in Small-Scale Tests: U_{CS}/U_T Plotted as a Function of ϕ_S, U_{CS}/U_{TH} Plotted as a Function of ϕ_S 7.11
7.9. Effect of Solids Loading on Cloud Height for Five Simulants in Small-Scale Tests: $1/F_{CST}$ Plotted as a Function of U_{CS}/U_T, $\phi_S/F_{CS\,TH}$ Plotted as a Function of U_{CS}/U_{TH} 7.12
7.10. Effect of Duty Cycle on Solids Suspension with Data from Small-Scale Vessel with Simulant s1d2 and $\phi_S = 0.015$; U_{CS} and Cloud Height 7.13
7.11. Effect of Pulse Volume Fraction (ϕ_p) on Solids Suspension: U_{CS}, H_C Data from 15-in. Vessel with Simulant s1d2 and $\phi_S = 0.015$ 7.14
7.12. Effect of Nozzle Diameter, Jet Diameter, and Number of Operating Pulse Tubes for Small-Scale Tank: U_{CS}/U_T as a Function of d, U_{CS}/U_T as a Function of ϕ_J 7.15
7.13. Scale Dependence of U_{CS}: U_{CS}/U_{CS15} Versus Tank Diameter with Fit of Scale-up Data Showing Scale-Up Exponent of 0.276 ..... 7.18
7.14. Scale-up Exponent for Average Cloud Parameters $(U^n/H_C)_{ave}$ as a Function of Velocity Exponent, n 7.18
7.15. Illustration of Nozzle Velocity Transient During PJM Discharge 7.19
7.16. Pulse Shape Ratio Versus Peak Average Velocity for Tests at Three Scales 7.20
7.17. Fit of U_{CS} Model to Experimental Data Using Nondimensional Variables U_{CS}/U_{TH} and $D^*/Ga^{0.5}$ 7.25
7.18. Fit of H_C Model to Experimental Data Using Nondimensional Variables $\ln(H_C^*)$ and U/U_{TH} 7.26
7.19. Fit of H_C Model to Experimental Data Using Nondimensional Variables H_C^* and U/U_{TH} 7.26
7.20. Log-Log Plot of Predicted Versus Measured U_{CS} (m/s) Values for the Nondimensional Model in Eq. (7.41) 7.28
7.21. Log-Log Plot of Predicted Versus Measured H_C (m) Values for the Nondimensional Model in Eq. (7.43) 7.28
7.22. Average Solids Vertical Distribution Data for All Tests; Concentration as a Function of Elevation, Normalized Profile for Estimating Concentration on Tank Bottom 7.29
7.23. Maximum Solids Vertical Distribution Data for all Tests; Concentration as a Function of Elevation, Normalized Profiles for Estimating Concentration on Tank Bottom 7.30
7.24. Log-Log Plot of Predicted Versus Measured U_{CS} (m/s) Values for the Nine-Term Dimensional Model in Eq. (7.52b) Fit to Full Data Set 7.34
7.25. Log-Log Plot of Predicted Versus Measured H_C for 11-Term Dimensional Model in Eq. (7.53b) Fit to Full Data Set 7.35

7.26. Log-Log Plot of PvM U_{CS} (m/s) Values for the Nine-Term Generalized Model in Eq. (7.54b) with Eight Coefficients Fit to Full Data Set 7.36

7.27. Log-Log Plot of PvM H_C (m) Values for the 11-Term Generalized Model in Eq. (7.55b) with 10 Coefficients Fit to the Full Data Set. 7.38

8.1. Effective Settling Velocity Associated with Vertical Entrainment from Pump Suction Returns 8.3

8.2. Illustration of How Finite Fill Level Affects Maximum Concentration 8.4

8.3. Illustration of How Stratification Results in Higher Effective Settling Velocities for Noncohesive Solids with a Broad Size Distribution: Settling Velocity for a Well-Mixed Slurry, Settling Velocity for a Stratified Slurry 8.5

8.4. Prototypic PJM Tank in 336 Building 8.12

8.5. Concentration Profiles for Case 1: 17.6 wt% and Maximum Drive Using the Physical Model and Generalized Model, with $U_T = U_{90}$ Optimized for the Physical Model 8.15

8.6. Concentration Profiles for Case 2: 17.6 wt% and 50% of Maximum Drive Using Physical Model and Generalized Model, with $U_T = U_{90}$ Optimized for the Physical Model 8.16

8.7. Concentration Profiles for Case 3: 17.6 wt%, 10% of Maximum Drive Case Using the Physical Model and the Generalized Model, with $U_T = U_{90}$ Optimized for the Physical Model 8.17

8.8. Concentration Profiles for Case 4: 28.3 wt% and Maximum Drive Using the Physical Model and the Generalized Model, with $U_T = U_{90}$ Optimized for the Physical Model 8.18

8.9. Concentration Profiles for Case 5: 28.3 wt% and 50% of Maximum Drive Using the Physical Model and the Generalized Model, with $U_T = U_{90}$ Optimized for the Physical Model 8.19

8.10. Concentration Profiles for Case 6: 28.3 wt% and 10% of Maximum Drive Using the Physical Model and the Generalized Model, with $U_T = U_{90}$ Optimized for the Physical Model 8.20

8.11. Concentration Profiles for Case 7: 10 wt% and 75-μm Glass Beads Using the Physical Model and the Generalized Model, with $U_T = U_{50}$ Optimized for the Physical Model 8.22

8.12. Concentration Profiles for Case 8: 20 wt% and 35-μm Glass Beads with 4 PJMs Operating Using the Physical Model and the Generalized Model, with $U_T = U_{60}$ Optimized for the Physical Model 8.23

8.13. Concentration Profiles for Case 9: 20 wt% and 35-μm Glass Beads with 2 PJMs Operating Using the Physical Model and the Generalized Model, with $U_T = U_{60}$ Optimized for the Physical Model 8.24

8.14. Velocity Profile (Drive Function) for HLP-22 ..... 8.25

8.15. Comparison of Model-Predicted Concentration Profiles with Predictions from CFD Simulation of HLP-22, 12 m/s, Normal Firing Case Using the Physical Model and the Generalized Model 8.26

9.1. Performance Ratio Example Using FEP-17 A/B. 9.6

9.2. Test Data and Application Range for $\frac{U}{U_{TH}}$ 9.10

9.3. Test Data and Application Range for $\frac{D^*}{Ga^{0.5}}$ 9.11

9.4. Test Data and Application Range for $\frac{d}{D}$ 9.11

9.5. Test Data and Application Range for $\frac{U_T}{U}$ 9.12

9.6. Test Data and Application Range for $\frac{(s-1)gD}{U^2}$ 9.12

9.7. Test Data and Application Range for $\frac{(s-1)gD}{U_T{}^2}$ 9.13

9.8. Cumulative Undissolved Solids Volume Fraction as a Function of Settling Velocity for AZ-101 ..... 9.16

9.9. Cumulative Undissolved Solids Volume Fraction as a Function of Cumulative Volume-Weighted Average Settling Velocity for AZ-101 ..... 9.16

9.10. Physical Model Predictions for FRP-02 A/B/C/D: Concentration Profile at Maximum Fill, Inlet Concentration and Suspension Ratio, Maximum Solids Concentration Versus Loading Design Conditions, U_{CS} Versus Vessel Loading 9.18

9.11. Physical Model Predictions for HLP-22: Concentration Profile at Max Fill, Inlet Concentration and Suspension Ratio, Maximum Solids Concentration Versus Loading Design Conditions, U_{CS} Versus Loading at 8 m/s, 4-in. Nozzles 9.19

9.12. Physical Model Predictions for HLP-22: Concentration Profile at Max Fill, Inlet Concentration and Suspension Ratio, Maximum Solids Concentration Versus Loading Design Conditions, U_{CS} Versus Loading at 12 m/s, 4-in. Nozzles 9.20

9.13. Physical Model Predictions for HLP-22: Concentration Profile at Max Fill, Inlet Concentration and Suspension Ratio, Maximum Solids Concentration Versus Loading Design Conditions, U_{CS} Versus Loading at 8 m/s, 6-in. Nozzles 9.21

9.14. Physical Model Predictions for HLP-22: Concentration Profile at Max Fill, Inlet Concentration and Suspension Ratio, Maximum Solids Concentration Versus Loading Design Conditions, U_{CS} Versus Loading at 12 m/s, 6-in. Nozzles 9.22

9.15. Physical Model Predictions for TCP-01: Concentration Profile at Max Fill, Inlet Concentration and Suspension Ratio, Maximum Solids Concentration Versus Loading Design Conditions, U_{CS} Versus Loading 9.23

9.16. Physical Model Predictions for TLP-09 A/B: Concentration Profile at Max Fill, Inlet Concentration and Suspension Ratio, Maximum Solids Concentration Versus Loading Design Conditions, U_{CS} Versus Loading 9.24

9.17. Physical Model Predictions for PWD-33: Concentration Profile at Max Fill, Inlet Concentration and Suspension Ratio, Maximum Solids Concentration Versus Loading Design Conditions, U_{CS} Versus Loading for PWD-33 ..... 9.25

9.18. Physical Model Predictions for PWD-43: Concentration Profile at Max Fill, Inlet Concentration and Suspension Ratio, Maximum Solids Concentration Versus Loading Design Conditions, U_{CS} Versus Loading 9.26

9.19. Physical Model Predictions for PWD-44: Concentration Profile at Max Fill, Inlet Concentration and Suspension Ratio, Maximum Solids Concentration Versus Loading Design Conditions, U_{CS} Versus Loading 9.27

9.20. Physical Model Predictions for FEP-17 A/B: Concentration Profile at Max Fill, Inlet Concentration and Suspension Ratio, Maximum Solids Concentration Versus Loading Design Conditions, U_{CS} Versus Loading 9.28
9.21. Physical Model Predictions for PWD-15/16: Concentration Profile at Max Fill, Inlet Concentration and Suspension Ratio, Maximum Solids Concentration Versus Loading Design Conditions, U_{CS} Versus Loading 9.29
9.22. Physical Model Predictions for UFP-01 A/B: Concentration Profile at Max Fill, Inlet Concentration and Suspension Ratio, Maximum Solids Concentration Versus Loading Design Conditions, U_{CS} Versus Loading 9.30
9.23. Physical Model Predictions for RLD-07: Concentration Profile at Max Fill, Inlet Concentration and Suspension Ratio, Maximum Solids Concentration Versus Loading Design Conditions, U_{CS} Versus Loading 9.31
9.24. Physical Model Predictions for RLD-08: Concentration Profile at Max Fill, Inlet Concentration and Suspension Ratio, Maximum Solids Concentration Versus Loading Design Conditions, U_{CS} Versus Loading 9.32
9.25. Physical Model Predictions for HOP-903/904: Concentration Profile at Max Fill, Inlet Concentration and Suspension Ratio, Maximum Solids Concentration Versus Loading Design Conditions, U_{CS} Versus Loading 9.33
9.26. Physical Model Predictions for FRP-02 A/B/C/D: Concentration Profile at Max Fill, Inlet Concentration and Suspension Ratio, Maximum Solids Concentration Versus Loading Design Conditions, U_{CS} Versus Loading 9.35
9.27. Physical Model Predictions for HLP-22: Concentration Profile at Max Fill, Inlet Concentration and Suspension Ratio, Maximum Solids Concentration Versus Loading Design Conditions, U_{CS} Versus Loading at 8 m/s, 4-in. Nozzle 9.37
9.28. Physical Model Predictions for HLP-22: Concentration Profile at Max Fill, Inlet Concentration and Suspension Ratio, Maximum Solids Concentration Versus Loading Design Conditions, U_{CS} Versus Loading at 12 m/s, 4-in. Nozzle 9.38
9.29. Physical Model Predictions for HLP-22: Concentration Profile at Max Fill, Inlet Concentration and Suspension Ratio, Maximum Solids Concentration Versus Loading Design Conditions, U_{CS} Versus Loading at 8 m/s, 6-in. Nozzle 9.40
9.30. Physical Model Predictions for HLP-22: Concentration Profile at Max Fill, Inlet Concentration and Suspension Ratio, Maximum Solids Concentration Versus Loading Design Conditions, U_{CS} Versus Loading at 12 m/s with a 6-in. Nozzle 9.41
9.31. Physical Model Predictions for TCP-01: Concentration Profile at Max Fill, Inlet Concentration and Suspension Ratio, Maximum Solids Concentration Versus Loading Design Conditions, U_{CS} Versus Loading 9.42
9.32. Physical Model Predictions for TLP-09 A/B: Concentration Profile at Max Fill, Inlet Concentration and Suspension Ratio, Maximum Solids Concentration Versus Loading Design Conditions, U_{CS} Versus Loading 9.43
9.33. Physical Model Predictions for PWD-33: Concentration Profile at Max Fill, Inlet Concentration and Suspension Ratio, Maximum Solids Concentration Versus Loading Design Conditions, U_{CS} Versus Loading 9.44
9.34. Physical Model Predictions for PWD-43: Concentration Profile at Max Fill, Inlet Concentration and Suspension Ratio, Maximum Solids Concentration Versus Loading Design Conditions, U_{CS} Versus Loading 9.46

9.35. Physical Model Predictions for PWD-44: Concentration Profile at Max Fill, Inlet Concentration and Suspension Ratio, Maximum Solids Concentration Versus Loading Design Conditions, U_{CS} Versus Loading 9.47

9.36. Physical Model Predictions for FEP-17 A/B: Concentration Profile at Max Fill, Inlet Concentration and Suspension Ratio, Maximum Solids Concentration Versus Loading Design Conditions, U_{CS} Versus Loading 9.48

9.37. Physical Model Predictions for PWD-15/16: Concentration Profile at Max Fill, Inlet Concentration and Suspension Ratio, Maximum Solids Concentration Versus Loading Design Conditions, U_{CS} Versus Loading 9.49

9.38. Physical Model Predictions for UFP-01 A/B: Concentration Profile at Max Fill, Inlet Concentration and Suspension Ratio, Maximum Solids Concentration Versus Loading Design Conditions, U_{CS} Versus Loading 9.50

9.39 Physical Model Predictions for RLD-07: Concentration Profile at Max Fill, Inlet Concentration and Suspension Ratio, Maximum Solids Concentration Versus Loading Design Conditions, U_{CS} Versus Loading 9.51

9.40. Physical Model Predictions for RLD-08: Concentration Profile at Max Fill, Inlet Concentration and Suspension Ratio, Maximum Solids Concentration Versus Loading Design Conditions, U_{CS} Versus Loading 9.52

9.41. Physical Model Predictions for HOP-903/904: Concentration Profile at Max Fill, Inlet Concentration and Suspension Ratio, Maximum Solids Concentration Versus Loading for Design Condition, U_{CS} Versus Loading 9.53

9.42. Generalized Model Predictions for FRP-02 A/B/C/D: Concentration Profile at Max Fill, Inlet Concentration and Suspension Ratio, Maximum Solids Concentration Versus Loading Design Conditions, U_{CS} Versus Loading 9.55

9.43. Generalized Model Predictions for HLP-22: Concentration Profile at Max Fill, Inlet Concentration and Suspension Ratio, Maximum Solids Concentration Versus Loading Design Conditions, U_{CS} Versus Loading 9.56

9.44. Generalized Model Predictions for HLP-22: Concentration Profile at Max Fill, Inlet Concentration and Suspension Ratio, Maximum Solids Concentration Versus Loading Design Conditions, U_{CS} Versus Loading 9.57

9.45. Generalized Model Predictions for HLP-22: Concentration Profile at Max Fill, Inlet Concentration and Suspension Ratio, Maximum Solids Concentration Versus Loading Design Conditions, U_{CS} Versus Loading 9.58

9.46. Generalized Model Predictions for HLP-22: Concentration Profile at Max Fill, Inlet Concentration and Suspension Ratio, Maximum Solids Concentration Versus Loading Design Conditions, U_{CS} Versus Loading 9.59

9.47. Generalized Model Predictions for TCP-01: Concentration Profile at Max Fill, Inlet Concentration and Suspension Ratio, Maximum Solids Concentration Versus Loading Design Conditions, U_{CS} Versus Loading 9.60

9.48. Generalized Model Predictions for TLP-09 A/B: Concentration Profile at Max Fill, Inlet Concentration and Suspension Ratio, Maximum Solids Concentration Versus Loading Design Conditions, U_{CS} Versus Loading 9.61

9.49. Generalized Model Predictions for PWD-33: Concentration Profile at Max Fill, Inlet Concentration and Suspension Ratio, Maximum Solids Concentration Versus Loading Design Conditions; U_{CS} Versus Loading 9.62

9.50. Generalized Model Predictions for PWD-43: Concentration Profile at Max Fill, Inlet Concentration and Suspension Ratio, Maximum Solids Concentration Versus Loading Design Conditions, U_{CS} Versus Loading 9.63

9.51. Generalized Model Predictions for PWD-44: Concentration Profile at Max Fill, Inlet Concentration and Suspension Ratio, Maximum Solids Concentration Versus Loading Design Conditions, U_{CS} Versus Loading 9.64

9.52. Generalized Model Predictions for FEP-17 A/B: Concentration Profile at Max Fill, Inlet Concentration and Suspension Ratio, Maximum Solids Concentration Versus Loading Design Conditions, U_{CS} Versus Loading 9.65

9.53. Generalized Model Predictions for PWD-15/16: Concentration Profile at Max Fill, Inlet Concentration and Suspension Ratio, Maximum Solids Concentration Versus Loading Design Conditions, U_{CS} Versus Loading 9.66

9.54. Generalized Model Predictions for UFP-01 A/B: Concentration Profile at Max Fill, Inlet Concentration and Suspension Ratio, Maximum Solids Concentration Versus Loading Design Conditions, U_{CS} Versus Loading 9.67

9.55. Generalized Model Predictions for RLD-07: Concentration Profile at Max Fill, Inlet Concentration and Suspension Ratio, Maximum Solids Concentration Versus Loading Design Conditions, U_{CS} Versus Loading 9.68

9.56. Generalized Model Predictions for RLD-08: Concentration Profile at Max Fill, Inlet Concentration and Suspension Ratio, Maximum Solids Concentration Versus Loading Design Conditions; U_{CS} Versus Loading 9.69

9.57. Generalized Model Predictions for HOP-903/904: Concentration Profile at Max Fill, Inlet Concentration and Suspension Ratio, Maximum Solids Concentration Versus Loading Design Conditions, U_{CS} Versus Loading 9.70

9.58. WTP Vessel Performance Ratio Summary Using U_{95} and $\overline{U}_{90}$ Settling Velocities from the Hanford Tank Waste PSDD (Case 3) Using the Physical Models for U_{CS} and C_0 from Sections 7.3.2 to 7.3.4 with C_0 modified to W_0^*, as Described in Section 9.1.4. ..... 9.71

9.59. WTP Vessel Performance Ratio Summary Using the Design-Limit Particle from Olsen (2008a) and the Physical Models for U_{CS} and C_0 from Section 7.3.2 to 7.3.4 Modified to W_0^* in Section 9.1.4. ..... 9.72

9.60. WTP Vessel Performance Ratio Summary Using U_{95} and $\overline{U}_{90}$ Settling Velocities from the Hanford Waste PSDD (Case 3) Using the Generalized Models for U_{CS} and C_0 from Section 7.4.2 with C_0 Modified to W_0^*, as Described in Section 8.1.4. ..... 9.72

9.61. WTP Vessel Performance Ratio Summary Using the Design Limit Particle from Olsen (2008a) and Generalized Models for U_{CS} and C_0 from Section 7.4.2 with C_0 Modified to W_0^*, as Described in Section 9.1.4. ..... 9.73

Tables

2.1. Description of Mixing States for Different Nozzle Velocities 2.7
2.2. Geometric and Operational Data for Solids-Containing Vessels in the WTP—Dimensional Data 2.9
2.3. Geometric and Operational Data for Solids-Containing Vessels in the WTP—Nondimensional Values 2.11
2.4. Primary Mixing System Physical Parameters 2.15
2.5. Mixing System Nondimensional Variables 2.16
2.6. Comparison of Scaled Test Approaches 2.20
2.7. Preliminary Bracketing Noncohesive Property Ranges for the WTP 2.22
3.1. Case 3 PSDD 3.2
3.2. Solid Phase Compound Density, Volume Fraction, and Numerical Identification for Case 3 PSDD 3.3
3.3. Hanford Insoluble Solid Settling Velocity Percentiles for Case 3 PSDD 3.5
3.4. Hanford Insoluble Solid Settling Velocity Quantiles: 1.1 g/mL and 1.5 cP Liquid Density and Viscosity, Case 3 PSDD 3.6
3.5. Bracketing Noncohesive Particle Test Ranges 3.6
3.6. Simulant Characterization: As-Received, Post-Test, and Average Values 3.10
4.1. Comparison of Planned Pulse Tube Radius for Equivalent Angle of Impingement in Tank Heads Formed with F&D and 2:1 Semi-Elliptical Heads 4.4
4.2. General PJM Configurations 4.5
4.3. Vessel Scaling Versus HLP-22 ..... 4.22
4.4. Tank and Pulse Tube Array Matrix 4.22
4.5. Measured HLP-22 12-Tube Array Positions 4.24
4.6. Measured 8-Tube Array Positions 4.26
4.7. HLP-22 12-Tube Array Nozzle and Pulse Tube Sizes 4.26
4.8. 8-Tube Array Nozzle and Pulse Tube Sizes 4.26
5.1. Mixing System Parameters 5.2
5.2. Particle Motion Descriptors 5.4
5.3. Solids Level Nomenclature 5.6
5.4. Pattern of Cleared Region Viewed from Beneath the Tank 5.7
5.5. Procedures for U_{CS} Observations 5.9
5.6. Particle Motion Descriptors for Visual Observations 5.10
5.7. Documents Governing the 2007 and 2008 Tests 5.13
6.1. Summary of Mixing Test General Conditions and Data 6.1
6.2. Test Parameter Description 6.2
6.3. Range of Test Conditions 6.4
6.4. Summary of Case ID Format 6.7
6.5. July 2007 Test Summary in Mid-Scale Tank with Spherical Head 6.10

6.6. Fall 2007 Test Summary in Mid-Scale Tank with Spherical Head 6.14
6.7. Summary of Fill Height and Return Line Height Test Conditions 6.17
6.8. 2008 Test Summary 6.20
6.9. 2008 Test Summary for Small-Scale Tank 6.22
6.10. 2008 Test Summary for Mid-Scale Tank 6.28
6.11. 2008 Test Summary for Large-Scale Tank with Elliptical Head 6.31
6.12. 2008 Test Summary for Large-Scale Tank with Flanged and Dished Head 6.36
6.13. Near-Replicate and Near-Repeat Tests at Critical Suspension Conditions 6.41
6.14. Summary of Concentration Profile Cases 6.45
7.1. As-Tested Dish Parameters and Geometric Coefficients for Various Dish Shapes 7.16
7.2. Direct Scale-up Data from Elliptical Tests: Ratios of Measured Variables at Large Versus Small Scales 7.16
7.3. Direct Scale-up Data from Elliptical Tests: Scale Exponents Based on Large-Versus Small-Scale Data 7.17
7.4. Basis for Comparing U_{CS} and H_C Models Fit to the Full Data Sets 7.39
8.1. Test Parameters and Associated Bounding Uncertainties 8.6
8.2. Solids Inventory in AZ-101/102 Filtration Simulant 8.13
8.3. Solids PSDD for AZ-101/102 Filtration Simulant 8.14
8.4. Model Inputs for Prototypic PJM 336-Building Tests with AZ-101/102 Filtration Simulant 8.14
8.5. PSD for 75-µm Glass Beads 8.21
8.6. Model Inputs for 336-Building Tests with 75-µm Glass Beads 8.22
8.7. Model Inputs for 336-Building Tests with 35-µm Glass Beads 8.23
8.8. Model Inputs to Compare with CFD Simulation of HLP-22, 12 m/s Normal Firing Case 8.25
9.1. Sources of Physical Mixing System Parameters for Plant Vessels 9.7
9.2. Vessel Geometry and Operations Data Used in WTP Vessel Assessments 9.7
9.3. Vessel Solids Loading Data Used in Design Point Assessments 9.8
9.4. Vessel Solids Loading Data Used in Hanford PSDD-Based Assessments 9.8
9.5. AZ-101 PSDD 9.15
9.6. AZ-101 Insoluble Solids Settling Velocity Quantiles 9.17
9.7. Physical Model Results for Design Point Conditions of FRP-02 ..... 9.18
9.8. Physical Model Results for Design Point Conditions for HLP-22 ..... 9.19
9.9. Physical Model Results for Design Point Conditions for HLP-22 ..... 9.20
9.10. Physical Model Results for Design Point Conditions for HLP-22 ..... 9.21
9.11. Physical Model Results for Design Point Conditions for HLP-22 ..... 9.22
9.12. Physical Model Results for Design Point Conditions for TCP-01 ..... 9.23
9.13. Physical Model Results for Design Point Conditions for TLP-09 ..... 9.24
9.14. Physical Model Results for Design Point Conditions for PWD-33 ..... 9.25
9.15. Physical Model Results for Design Point Conditions for PWD-43 ..... 9.26
9.16. Physical Model Results for Design Point Conditions for PWD-44 ..... 9.27

9.17. Physical Model Results for Design Point Conditions for FEP-17 ..... 9.28
9.18. Physical Model Results for Design Point Conditions for PWD-15/16 ..... 9.29
9.19. Physical Model Results for Design Point Conditions for UFP-01 ..... 9.30
9.20. Physical Model Results for Design Point Conditions for RLD-07 ..... 9.31
9.21. Physical Model Results for Design Point Conditions for RLD-08 ..... 9.32
9.22. Physical Model Results for Design Point Conditions for HOP-903/904 ..... 9.33
9.23. Physical Model Results for FRP-02 Using Hanford PSDD 9.35
9.24. Physical Model Results for HLP-22 Using Hanford PSDD 9.37
9.25. Physical Model Results for HLP-22 Using Hanford PSDD 9.38
9.26. Physical Model Results for HLP-22 Using Hanford PSDD 9.40
9.27. Physical Model Results for HLP-22 Using Hanford PSDD 9.41
9.28. Physical Model Results TCP-01 Using Hanford PSDD 9.42
9.29. Physical Model Results for TLP-09 Using Hanford PSDD 9.43
9.30. Physical Model Results for PWD-33 Using Hanford PSDD 9.44
9.31. Physical Model Results for PWD-43 Using Hanford PSDD 9.46
9.32. Physical Model Results for PWD-44 Using Hanford PSDD 9.47
9.33. Physical Model Results for FEP-17 Using Hanford PSDD 9.48
9.34. Physical Model Results for PWD-15/16 Using Hanford PSDD 9.49
9.35. Physical Model Results for UFP-01 Using Hanford PSDD 9.50
9.36. Physical Model Results for RLD-07 Using Hanford PSDD 9.51
9.37. Physical Model Results for RLD-08 Using Hanford PSDD 9.52
9.38. Physical Model Results for HOP-903/904 Using Hanford PSDD 9.53
9.39. Generalized Model Results for FRP-02 Using Hanford PSDD 9.55
9.40. Generalized Model Results for HLP-22 Using Hanford PSDD 9.56
9.41. Generalized Model Results for HLP-22 Using Hanford PSDD 9.57
9.42. Generalized Model Results for HLP-22 Using Hanford PSDD 9.58
9.43. Model Results for Design Conditions for HLP-22 ..... 9.59
9.44. Generalized Model Results for TCP-01 Using Hanford PSDD 9.60
9.45. Generalized Model Results for TLP-09 Using Hanford PSDD 9.61
9.46. Generalized Model Results for PWD-33 Using Hanford PSDD 9.62
9.47. Generalized Model Results for PWD-43 Using Hanford PSDD 9.63
9.48. Generalized Model Results for PWD-44 Using Hanford PSDD 9.64
9.49. Generalized Model Results for FEP-17 Using Hanford PSDD 9.65
9.50. Generalized Model Results for PWD-15/16 Using Hanford PSDD 9.66
9.51. Generalized Model Results for UFP-01 Using Hanford PSDD 9.67
9.52. Generalized Model Results for RLD-07 Using Hanford PSDD 9.68
9.53. Generalized Model Results for RLD-08 Using Hanford PSDD 9.69
9.54. Generalized Model Results for HOP-903/904 Using Hanford PSDD 9.70
9.55. Impact of HLP-22 Design Variations Using the Physical Models 9.73

1.0 Introduction

This report summarizes results from pulse jet mixing (PJM) tests for mixing noncohesive solids in Newtonian liquid. The tests were conducted during FY 2007 and 2008 to support the design of the mixing systems for the Hanford Waste Treatment and Immobilization Plant (WTP). Tests were conducted at three geometric scales using noncohesive simulants. The test data were used to develop new mixing models that can be used to predict the mixing performance of full-scale WTP vessels and to assess mixing system designs compared with performance requirements.

Section 1.1 describes the background associated with this project—the testing of PJM systems with noncohesive solids for evaluating the adequacy of WTP mixing. The justification supporting the tests performed is described in Section 1.2. Test objectives are listed in Section 1.3. An overview of the research is presented in Section 1.4; project Quality Assurance is described in Section 1.5; and the organization of the remainder of the document is listed in Section 1.6.

1.1 Background

The WTP at the Hanford Site is being designed and built to pretreat and vitrify a large portion of the waste stored in Hanford's 177 underground waste storage tanks. Several process vessels will hold the waste at various stages in the WTP. These vessels have the mixing[1] system requirements to maintain conditions in which hydrogen gas accumulation stays below acceptable limits and the mixing within the vessels is sufficient to ensure that pump transfer and normal operations occur reliably (Olsen 2008a).

Some of the WTP process streams are slurries of solid particles suspended in Newtonian fluids that may behave as non-Newtonian slurries. The effects of large particles and rapidly settling slurries may affect mixing and the ability of the slurry to maintain particles in suspension.

The WTP Project uses PJM technology for tank mixing applications requiring solids suspension, solids mixing, fluid blending, and release of hydrogen gas. PJMs are driven by jet pump pairs (JPPs) that use compressed air as the motive force. The suction phase draws process liquid into the PJM from the vessel. The drive phase pressurizes the PJMs via a JPP. This pressurization discharges the PJM liquid at high velocity into the vessel, causing mixing to occur. The drive phase is followed by the vent phase, which allows for depressurization of the PJM by venting through the JPP into the pulse jet vent system. These three phases (suction, drive, and vent) make up the mixing cycle.

The PJMs can be operated in a continuous pulsing mode (e.g., all PJMs on during normal operation) or can be turned off for a time and restarted in the pulsing mode [e.g., for some post-design basis event (DBE) scenarios, vessels that use the 50/50 mixing rack design will only have half their PJMs operational], depending on process requirements. In vessels that contain particulates, solids will settle to the bottom between mixing periods. When the PJMs restart, the settled solids must be resuspended.

[1] Mixing is the mobilization and subsequent suspension of undissolved solids within a vessel. Mixing can have varying results: 1) a fully mixed vessel where the solids concentration is uniform throughout the vessel, 2) a partially mixed vessel where there is a solids concentration gradient that is higher at the bottom of the vessel, or 3) a poorly mixed vessel where the solids are disturbed but remain on or near the bottom of the vessel.

Bechtel National, Inc. (BNI) has assessed the resuspension capabilities in the past using two available methods. One method used a BNI controlled proprietary correlation; the other method used an approach recommended by Atomic Energy Authority of United Kingdom (AEA) called the "Bathija Off-Bottom Method" (Bathija 1982). BNI has determined that the proprietary resuspension correlation is the best method available at this time to evaluate potential risks with current PJM mixing system designs.[1]

In October 2005, an External Flowsheet Review Team (EFRT) made up of experts from industry, national laboratories, and universities was assembled by BNI to conduct a thorough, in-depth review of the process flowsheet for the design of the WTP. The following issues from the critical review of the process flowsheet (Smith 2007) are considered relevant to the mixing process:

- Issue M1: Piping that transports slurries will plug unless it is properly designed to minimize this risk. This design approach has not been followed consistently, which will lead to frequent shutdowns due to line plugging.
- Issue M2: Large, dense particles will accelerate erosive wear in mixing vessels. The effects of such particles on vessel life must be reevaluated.
- Issue M3: Issues were identified related to mixing system designs that will result in insufficient mixing and/or extended mixing times. These issues include a design basis that discounts the effects of large particles and of rapidly settling Newtonian slurries. There is also insufficient testing of the selected designs.
- Issue M4: The WTP has not demonstrated that its design is sufficiently flexible to reliably process all of the Hanford tank farm wastes at design throughputs.
- Issue M6: Many of the process operating limits have not been defined. Further testing is required to define process limits for WTP unit operations. Without this more complete understanding of each process, it will be difficult or impossible to define a practical operating range for each unit operation.
- Issue M12: Neither the caustic leaching nor the oxidative leaching process has been demonstrated at greater than bench scale. The small-scale experiments are capable of defining the leaching chemistry; however, they are limited in their ability to predict the effectiveness of these processes without a scale-up demonstration.
- Issue P9: The sampling system has not been demonstrated and may not prove adequate for handling slurries. This system is critical to the success of WTP operation. The completion of the planned testing is necessary to ensure sampling system adequacy. The capabilities of the current baseline sampling equipment need to be confirmed.

In response to Issue M3, Inadequate Design of Mixing Systems–Pulse Jet Mixers, BNI issued Test Specification 24590-PTF-TSP-RT-06-007 (Smith 2007), defining a test program to resolve the PJM issue. The objective of this test program has been to close issues related to mixing system designs that could result in insufficient mixing and/or extended mixing times. These issues included a design basis that discounted the effects of large particles and of rapidly settling Newtonian slurries.

[1] The proprietary method is essentially a correlation of data from small-scale, steady jet mixing tests. While it represents the best available data for assessing PJM off-bottom suspension capability in solids-containing vessels, the correlation does not specifically account for the effects of pulsation or nozzle geometry. In addition, the correlation database does not cover the range of particle sizes in Hanford waste.

The test specification calls for performing geometrically scaled tests with simulants to generate data for developing models of vessel mixing performance. The models will be used to assess the PJM design basis for WTP vessels. As part of Project No. 53023, Pacific Northwest National Laboratory (PNNL) generated Test Plan TP-RPP-WTP-480 (Elmore et al. 2007) for conducting scaled tests.

Vessels with relatively lower solids concentrations have historically been termed "Newtonian vessels" to differentiate them from vessels containing slurries that exhibit bounding non-Newtonian rheology.[1] However, this terminology may be misleading because there is a continuum of rheological behavior between these Newtonian and non-Newtonian vessels. In fact, some of the Newtonian vessels may exhibit non-Newtonian behavior under certain conditions. Some vessels with lower concentrations may have a small but finite yield stress under normal mixing conditions. Even a yield stress of a few Pascals may affect mixing performance, particularly with regard to gas retention and release behavior. Other Newtonian vessels with slurries exhibiting Newtonian behavior under normal mixing conditions may in fact become non-Newtonian in the absence of mixing (e.g., during a mixing system shutdown) as solids concentrations increase due to settling.

To avoid confusion between vessel nomenclature and slurry rheology, vessels previously termed Newtonian will hereafter be termed "solids-containing" if they contain solids and "liquid-containing" if they have no solids or trace solids. Those vessels previously termed non-Newtonian will be termed "high solids-containing."

Under normal mixing operations, the process areas of concern are solids off-bottom suspension, solids vertical distribution (i.e., concentration profiles), solids accumulation on the vessel bottom, and mixing times. For off-normal mixing operations, the process areas of concern are solids resuspension and overcoming increased rheological properties associated with solids settling. During post-design basis event (DBE) operations vessels may be operated intermittently, with mixing systems idle for 12 hours or longer. Hence, solids settling will occur to varying degrees.

The design-basis particle characteristics for mixing have been documented in Wells et al. (2007). These results were used to develop noncohesive simulants for testing PJM vessel mixing.

1.2 Test Justification

When the EFRT conducted a thorough and in-depth review of the process flowsheet for the design of the Hanford WTP, one of the issues identified was M3 (Smith 2007, Saunders and Keuhlen 2008):

> Issues were identified related to mixing system designs that will result in insufficient mixing and/or extended mixing times. These issues include a design basis that discounts the effects of large particles and of rapidly settling Newtonian slurries. There is also insufficient test data to support the selected designs.

[1] Vessels historically termed "non-Newtonian" include UFP-VSL-00002A/2B ultrafiltration feed process vessels, HLP-VSL-00027A/B HLW lag storage vessels, and the HLP-VSL-00028 high-level waste blend vessel.

Under normal mixing operations, process areas of concern include:

- Solids off-bottom suspension
- Solids vertical distribution (concentration profile)
- Solids accumulation on the vessel bottom
- Mixing times.

For off-normal mixing operations, process areas of concern include:

- Solids resuspension
- Overcoming increased rheological properties associated with solids setting
- Ability to release hydrogen gas from settled solids following a DBE.

1.3 Objectives

The first two objectives for this work were provided by the client in Test Specification 24590-PTF-TSP-RT-06-007 (Smith 2007) and were incorporated in Test Plan TP-RPP-WTP-480 (Elmore et al. 2007). Objectives three through six for this work were provided by the client in SCN 71 (Hazen 2008a) and letter CCN 190723 (Hazen 2008b) and were incorporated into Test Plan TP-RPP-WTP-480 R0.2 (Elmore et al. 2009). Both test plans were approved by the client:

1. Determine through experimental results whether there is a high probability that for vessel HLP-22, 0.10 m (4-in.) nozzles operating at 8 m/s discharge velocity (current baseline design) will not be adequate for resuspending settled solids.
2. Provide experimental results from a scaled HLP-22 mixing system for constant volume discharges that provide the relative difference in performance with respect to off-bottom suspension for the following conditions:
   - Full-scale conditions of 0.10-m- (4-in.-) diameter nozzles operating at 8 m/s
   - Full-scale conditions of 0.10-m- (4-in.-) diameter nozzles operating at 12 m/s
   - Full-scale conditions of 0.15-m- (6-in.-) diameter nozzles operating at 8 m/s
   - Full-scale conditions of 0.15-m- (6-in.-) diameter nozzles operating at 12 m/s.
3. Obtain measurements of U_{CS}[1] over a range of test conditions in scaled vessels to evaluate the dependence of vessel mixing performance on parameters associated with waste properties, equipment design, and process operations.
4. Obtain test results at multiple geometric scales to allow scaled test results to be used to predict vessel mixing performance at full scale.

[1] U_{CS} is defined as the critical suspension velocity. At U_{CS} the solids are completely suspended off the vessel bottom at the end of the jet pulse.

5. Develop tools/models that will allow WTP Mechanical and Process Engineering (M&PE) staff to rate/evaluate/bin WTP vessels designs at a coarse level and to determine with high confidence any WTP vessels that will not meet minimum required performance levels.
6. Obtain test results, observations, and experience that facilitate development of a focused/reduced test matrix for M3 scaled tests.

1.4 Overview of Testing and Modeling

Scaled testing was selected as the most direct, accurate, and cost-effective approach to address and close the EFRT M3 issue. Parametric scaled testing of mixing systems was used to generate data from which mixing performance models were developed. These models were applied to assess all of the WTP solids-containing vessels. This scaled-testing approach was determined to be sufficient because it is commonly used in the mixing industry (Paul et al. 2004) and is technically appropriate.

1.4.1 Model Development Approaches

The development of mixing performance models naturally follows testing performed to generate data for model development. However, it is useful to discuss the model development approaches first so they can be referred to in subsequent sections.

Three approaches were used in this work to develop models for predicting mixing performance using data from scaled tests.

1. The *physical approach* involves fitting the data to functional forms derived from, or suggested by, a dimensionless analysis of the phenomena expected to affect mixing performance. The functional forms obtained through the physical approach provide similarity criteria for relating behavior observed during scaled tests to the behavior expected during corresponding full-scale operations, which enables predicting the performance of a full-scale system.
2. The *empirical approach* uses multiple regression (MR) methods to relate mixing performance variables to the test parameters. This approach provides for predicting the mixing performance as a function of system parameters. Because this approach includes the length scale (size) as a parameter, it also enables predicting the performance of a full-scale system.
3. The *semi-empirical approach* uses MR methods to relate mixing performance variables to nondimensional variables, which are functions of the test parameters. This approach is a combination of the first two approaches in that physical bases are still used in specifying the nondimensional variables but within a MR framework.

The empirical approach lacks a physical basis but provides a systematic evaluation of the dependence of the mixing performance on system parameters valid over the domain of the test data. The physical and semi-empirical approaches use physical reasoning to explain the effect of scale and other parameters on mixing performance. Hence, these two approaches increase the confidence in extrapolating results outside the domain of the test data. These two approaches also depend on the experience and subject knowledge of those proposing the functional forms for fitting the data. It is important to compare and reconcile the models resulting from the empirical and semi-empirical approaches with those from the physical approach. Used together, these three approaches provide technical reliability and credibility,

improve the accuracy of extrapolation of model results to full scale, and reduce the extrapolation uncertainty.

Parametric mixing models derived from scaled test results using the three approaches have the following benefits:

- They provide for assessing the performance of WTP mixing systems and design-basis waste properties.
- They are cost-effective because they greatly minimize the number of scaled vessel prototypes that would otherwise require testing.
- The models used to rate mixing system performance can be exercised to evaluate the effect of potential design changes, should they be required.

This parametric model-based scaled testing approach meets the WTP Project requirements for rating the design of the fluidic mixing systems in WTP vessels.

1.4.2 Phased Approach to Testing

Mixing studies to address EFRT Issue M3 will be conducted in phases to focus on differences in slurry physical properties. The distinction between vessels containing noncohesive and cohesive slurries has been based on anticipated solids concentrations of the waste in the vessels. Waste slurries containing a moderately low solids concentration can exhibit some non-Newtonian (cohesive) behavior, especially near the bottom of the vessel, during a planned or unplanned shutdown of mixing as solids settle. Conversely, some vessels contain slurries with a relatively high solids concentration that may still behave like Newtonian (noncohesive) slurries. Thus, both Newtonian and non-Newtonian slurries will be evaluated in the testing program and will account for variations in solids loading, solids properties, and rheology. The testing described in this report was conducted using noncohesive slurries. Tests to evaluate mixing performance with cohesive slurries are being considered for the future.

Given the different mixing system demands posed by noncohesive and cohesive slurry properties, as well as the need to determine flammable gas release capability for various conditions, the EFRT Issue M3 test program has been conducted based on simulant type. Tests described in this report address mixing system performance with noncohesive particulates, where solids suspension and settling are important. Some other solids mixing challenges that were <u>not</u> included in this phase of testing include evaluation of:

- Cohesive waste mixing, blending, and solids resuspension
- Gas retention and release behaviors in the solids-containing vessels.

The tests described in this report cover d_{50} particle diameters ranging from 44 to 766 μm. The 44-μm d_{50}-diameter solids did not reach the onset of cohesion or cohesive behavior. Therefore, the particle sizes and concentrations used in model development are in the Newtonian behavior regime.

1.4.3 Scaled Testing Approach

The approach for predicting the performance of full-scale systems based on tests in scaled systems is to maintain geometric similarity to the extent practicable (the mixing systems use cylindrical vessels with

dished bottoms, conical downward pointing nozzles, etc.), test slurries with properties spanning the range of those in the full-scale system to the extent practicable, and controlling operation to span conditions expected in the full-scale system. Practical constraints prevented perfect compliance with these principles, but compliance was sufficient to meet the test objectives.

In general, mixing system performance for the solids-containing vessels in the WTP depends on the physical and rheological properties of their contents, the number and size of PJMs, vessel size (diameter), and the relative fill level. In addition, mixing performance depends on PJM operating conditions such as jet velocity (U), drive time (t_D), and duty cycle (DC), which is drive time divided by the cycle time (t_C). The scaled testing approach included a series of tests in scaled vessels where these important parameters were varied and measured: relevant similarity criteria; critical suspension velocity (U_{CS}); cloud height (H_C), which is a visible interface above which the fluid is relatively quiescent; and solids vertical distribution C(Z). Mixing times and the distance along the tank bottom over which solids are mobilized by the PJM were not specifically determined.

The forms of *physical models* for the U_{CS} and H_C were based on similarity criteria and fitted to the test data. Models for the solids concentration at the bottom of a tank (C_0) and the solids vertical distribution [C(Z)] were developed from the H_C model. The forms of empirical and semi-empirical models for U_{CS} and H_C were generalized forms of the physical models for U_{CS} and H_C, which allow for possibly improving predictions as well as assessing the bases for the physical models. The physical models and semi-empirical models (semi-empirical models are subsequently referred to as *generalized models*) were used to evaluate the performance of the WTP project's mixing-system designs in the solids-containing vessels. These models may also be exercised to explore mixing performance sensitivity to waste properties.

1.4.4 Three Tank Scales

Three test scales were required to achieve the primary objective of rating the mixing systems in the largest solids-containing vessels in a timely and cost-effective manner. Mixing performance depends on vessel size (scale). It is necessary to vary vessel scale during testing to develop robust models. While some useful scale information can be achieved with only two tank sizes, using data from three tank sizes provides more-accurate models and enables assessing the predictive uncertainty of the models. This is especially important for applying the models to the largest of the WTP vessels. Not only are these vessels significantly larger than any practical test scale, they are also of the greatest concern regarding mixing.

There are additional benefits to testing at three scales as well. The test matrix was configured to perform more tests in the small-scale tank, thereby reducing the number of tests performed in the medium- and large-scale test tanks.

1.4.5 Test Tank Sizing

There was some latitude in the selection of the test tank sizes. Nominal sizes selected were small scale, 0.4 m (15 in.); mid scale, 0.9 m (34 in.); and large scale, 1.8 m (70 in) in diameter.[1] The smallest

[1] The scaled vessel size was approved by BNI via email transmittal, March 20, 2007, referencing *Recommended Test Vessel Scales for the M-3 Mixing Test Program,* from GL Smith to PA Scott, PA Meyer, and GH Beeman (PNNL). "Concurrence to Purchase Scaled Vessels for M3 PJM Mixing Systems Testing Program."

tank [0.4 m (15 in.)] is large enough to ensure that the transitional flow regime is avoided. This was accomplished by making sure the jet Reynolds number (based on jet velocity and nozzle diameter) was at least 5,000. There is no physically based, upper size limit for the largest test tank; rather, cost and testing duration were the practical constraints. The largest tank is large enough to exercise a reasonable range of scales to develop the models. These nominal sizes were selected based on practical considerations associated with fabrication and availability of "standard" tank diameters.

The solids-containing vessels in the WTP are expected to have relative fill levels (fill height-to-diameter ratios [H/D]) that range from 0.5 to 1.6. Given the parametric testing approach, it would be desirable to test values of H/D that span this range, but this one parameter could not be varied due to equipment limitations. For the small- and mid-scale test systems, the test tanks were normally operated at an H/D of around 2.4 and 2.0, respectively, during testing. For the large-scale test system, the tank (which was supplied from an earlier testing program) was operated at an H/D of around 1.3. Specific fill levels for each test are included in Appendix B.

The test specification references the tank bottom (head) shape as 2:1 elliptical. The scaled-tank heads were specified to match the WTP vessel specifications, which include 2:1 elliptical and flange-and-dish (F&D) head shapes. Tests were also conducted using a tank with a spherical head.

1.4.6 Mixing System Configuration

The test approach used PJM systems that are easily reconfigured to represent geometrically scaled versions of the solids-containing WTP vessels. By changing the configuration of the PJMs, any given test tank can be a geometric miniature of a given plant mixing system. Because the plant vessels vary widely in size, each test tank configuration represented a plant vessel reduced in size by the relative geometric scale factor, which depends not only on the size of the plant vessel but also on the size of the test tank (small, mid-sized, or large).

Reconfiguring the PJMs in the test tanks to replicate the prototypic mixing systems requires changing the number, size, and nozzle diameter of the pulse tubes, as well as the spatial arrangement of the pulse tube array. Hence, many pulse tubes of varying sizes would be required by this approach. Based on extensive previous testing experience (Bamberger et al. 2005), it is known that pulse tube reconfiguration is cumbersome and time-consuming. Adjusting operating parameters such as jet velocity, drive time, and duty cycle via the control system can also be time-consuming, especially when the fill level or simulant properties are changed. It is also challenging to accurately determine as-tested values for jet velocity and drive time, and typically significant post-processing and analysis are required. Given the need to test many different PJM configurations, as well as vary PJM operating parameters and simulant properties, using a simplified, flexible, and easily controllable intermittent jet mixing system alternative was required to complete testing in a reasonable time frame. This configuration was adequate to meet test objectives.

The external shape of pulse tubes (external form factor) has a minor effect on flow patterns within the tank. Geometric changes to the jet nozzles (such as modifying or eliminating the conical section) may have an effect on mixing. However, mixing effects due to nozzle geometry may well be handled by the application of simple geometric correction factors (similar to nozzle loss coefficients). PJM modeling was performed in a simplified geometry configuration using small-diameter pulse tubes (straight pipes). The effect of pulse tube shape on tank flow patterns was discussed but not evaluated during the parameter definition testing to determine whether inserts that model PJM shape were required. The number of tubes

and their radial spacing was configured experimentally using an adjustable series of pulse tubes. The potential effects or differences in geometry are discussed in Section 8.1.

1.4.7 Initial Testing to Define System Parameters that Meet Test Objectives

The experimental program was conducted in stages. In July 2007, initial tests were conducted to vary parameters such as nozzle size and waste particle size in the mid-scale tank, which had been used in previous WTP experiments while the smaller and larger tanks were being fabricated. The July 2007 tests were designed to give an early indication of HLP-22 adequacy. More tests were conducted in the fall of 2007 (Fall 2007) to evaluate the experimental test stand equipment and answer operational questions specific to the use of this test stand. Factors evaluated included the effect of fill height in the test tank and the impacts of elevation of the return line that are unique to the testing system. The original objective of this test program was to obtain scalable metrics for assessing PJM vessel performance over a range of geometric scales using fixed simulant properties (i.e., scale-up, not similarity, of phenomena). The fill height through the majority of the test program was maximized with the intent of:

- Minimizing solids entrainment into the pulse system
- Maximizing the range of pulse tube velocities that could be assessed
- Minimizing the particle density and diameter that could be evaluated
- Maximize the cloud height elevation that could be measured.

The investigation of fill height during the Fall 2007 test effort was only to assess the effect fill height had on the results obtained in the current test setup. No attempt was made or was part of the test scope to evaluate the effect of the design operating levels for each of the WTP vessel types. The WTP fill heights were not investigated for the same reason.

1.4.8 Scaled Testing and Model Development

When the scaled tanks and additional real-time diagnostic instrumentation to measure key parameters were available, parametric testing began. The parametric test matrix for 2008 testing included refinements made based on the results of the 2007 testing. The refinements included the need for more simulant variation, collecting concentration data at multiple locations in the tank, inclusion of ultrasonic Doppler velocimetry (UDV) to speed up testing, and the need for testing at additional tank scales. In addition, simulant properties were refined to provide a narrower, more monodisperse particle size distribution (PSD). Testing was conducted in the three scaled tanks to complete the parametric variations. The scaled-tank test data sets were then used to develop mixing performance models using the three approaches described in Section 1.4.1.

1.5 Quality Requirements

Pacific Northwest National Laboratory (PNNL) is operated by Battelle for the U.S. Department of Energy. Its Pacific Northwest Division (PNWD) has a Quality Assurance Program that is based upon the requirements as defined in the U.S. Department of Energy (DOE) Order 414.1C, “Quality Assurance,” and 10 CFR 830, “Energy/Nuclear Safety Management,” Subpart A, “Quality Assurance Requirements.” PNWD has chosen to implement the requirements of DOE Order 414.1C and 10 CFR 830 Subpart A by

integrating them into the Laboratory's management systems and daily operating processes. The procedures needed to implement the requirements are documented through the Laboratory's Standards-Based Management System.

PNNL implements the WTP River Protection Project (RPP) quality requirements by performing work in accordance with the River Protection Project – Waste Treatment Plant Support Program (RPP-WTP) Quality Assurance Plan (RPP-WTP-QA-001, QAP). Work is performed to the quality requirements of NQA-1-1989 Part I, "Basic and Supplementary Requirements," NQA-2a-1990 Part 2.7, and DOE/RW-0333P Rev. 13, Quality Assurance Requirements and Descriptions (QARD). These quality requirements are implemented through the RPP-WTP Quality Assurance Manual (RPP-WTP-QA-003, QAM). The analytical requirements are implemented through RPP-WTP's Statement of Work (RPP-WTP-QA-005) with the Radiochemical Processing Laboratory Analytical Service Operations.

Experiments that were not method-specific were performed in accordance with RPP-WTP's procedures QA-RPP-WTP-1101, "Scientific Investigations," and QA RPP WTP-1201, "Calibration and Control of Measuring and Testing Equipment." Properly calibrated measuring and test equipment was used to acquire sufficient data to produce quality results.

Additional equipment that may be used includes balances. Balances are calibrated annually by a certified contractor, QC Services, Portland, Oregon.

RPP-WTP addresses internal verification and validation activities by conducting an Independent Technical Review of the final data report in accordance with RPP-WTP's procedure QA-RPP-WTP-604. This review verifies that the reported results are traceable, that inferences and conclusions are soundly based, and the reported work satisfies the test plan objectives. This review procedure is part of PNNL's RPP-WTP Quality Assurance Manual.

NCR OTS-00327 outlines bases for all changes in graphs and tables that are listed in Revision History. The NCR identifies CCPs associated with this update and provides a basis for data sets selected for inclusion in Revision 1 of this report.

1.6 Organization of Document

Section 2.0 describes mixing of solid-liquid systems for both steady and pulsed mixing. Hanford waste properties and simulant selection are described in Section 3.0. Experimental equipment, procedures, and data are described in Sections 4.0, 5.0, and 6.0, respectively. Section 7.0 discusses the analysis and modeling of mixing data. Methodology and examples of WTP vessels are presented in Sections 8.0 and 9.0. Conclusions and recommendations are provided in Section 10.0, and cited references are listed in Section 11.0.

Appendixes provide additional data and analyses. Ultrasonic instrumentation is described in Appendix A, and mixing data and concentration profile data are presented in Appendixes B and C, respectively. Statistical methods, data analysis, and modeling are described in Appendixes D, E, and F, respectively.

2.0 Technical Approach for Assessing WTP Mixing Systems

Section 2.0 describes the technical approach used for assessing WTP mixing systems. This approach is the framework for the experiments and results presented in the remainder of the report. In Section 2.1 mechanical mixing is briefly discussed to provide a basis for the type of model used to describe agitator-based mechanical mixing. The adaptation of this model for application to steady jet mixing is discussed in Section 2.2. Section 2.3 describes how the model can be expanded to incorporate pulse jet mixing. To provide background for rating WTP mixing systems, the WTP plant vessel configurations and operating conditions are described in Section 2.4. In Section 2.5 the approach for assessing the solids-handling capability of mixing systems is outlined. The type of parametric testing required to develop models for mixing performance in terms of mixing parameters is described in Section 2.6. Section 2.7 describes the scale-up strategy for mixing results. This is followed by a summary of factors and consideration involved in experimental test design in Section 2.9.

2.1 Mechanical Mixing

Agitation equipment is a significant component of solid-liquid mixing systems. The agitation approach and the vessel shape both contribute to mixing system performance. Three types of mixing approaches for slurries are briefly described, leading to the pulse jet mixing system whose performance is being evaluated in these studies. Models for mechanical mixing system performance lay the framework for extension to jet mixing and pulse jet mixing.

Mechanical mixing systems are based on bladed mixers of varying designs. Industrial correlations for mixing performance for bladed mixers have been used for over 50 years. One of these correlations (Zwietering 1958, Eq. 7) can be written in the form:[1]

$$N_{JS} = k_I\,(g)^{0.45}\,(s-1)^{0.45}\,(d_S)^{0.2}\,(X)^{0.13}\,(D_I)^{-0.85}\,(\nu)^{0.1} \tag{2.1}$$

where

N_{JS} = shaft speed for just-suspended condition (Zwietering mechanical mixers) (rev/s)
k_I = impeller specific constant
g = gravitational constant (m/s^2)
s = ratio of particle density to liquid density (dimensionless)
d_S = diameter of particle (m)
X = weight of solid per weight of liquid times 100 (percent)
D_I = diameter of impeller (m)
ν = kinematic viscosity (m^2/s).

[1] The Zwietering correlation has no vessel diameter, so there must be an assumption of vessel diameter relative to agitator blade diameter.

This expression is dimensionally consistent, and as for all such expressions, can be put in an alternative form involving only dimensionless groups, such as:

$$N_{JS}\sqrt{\frac{D_I}{(s-1)g}} = k_I\left(\frac{d_S}{D_I}\right)^{0.35}\left(\frac{g(s-1)d_s^3}{\nu^2}\right)^{-0.05} \tag{2.2}$$

where the left-hand-side is the square root of the Froude number. See Section 7.4.2 for examples of invoking dimensionless forms for statistically developed empirical models describing the results of M3 testing.

2.2 Jet Mixing

Jet mixing differs from agitator-based, liquid-solid mixing; the driving force is hydraulic rather than mechanical. A mechanical agitator works by shearing the fluid and propelling it around the mixing vessel. A jet mixer uses a pump to force the fluid through nozzles within the tank, creating high-velocity jets that entrain other fluid. The result is shear and circulation that mix the tank contents efficiently. For steady jet mixing, a power law expression similar to Eq. (2.1) can be written for the velocity required to just suspend particles from the floor of the vessel.

$$U_{JS} = k_J\,(g)^{0.5}\,(s\text{-}1)^{\alpha}\,(d_S)^{\beta}\,(X)^{\gamma}\,(D)^{\delta}\,(d)^{\varepsilon}\,(H/D)^{\zeta} \tag{2.3}$$

Equation (2.3) can be expressed in general functional form

$$U_{JS} = f\,(g, (s\text{-}1), d_S, X, D, d, H/D) \tag{2.4}$$

where

U_{JS} = jet velocity for off-bottom suspension (jet mixers)
k_J = jet mixer specific constant
g = gravitational constant (m/s^2)
s = ratio of particle density to liquid density (dimensionless)
d_S = diameter of particle (m)
X = weight of solid per weight of liquid times 100 (percent)
D = diameter of vessel
d = diameter of jet nozzle
H = fluid height
f = general function.

The exponents of the correlation in Eq. (2.3) are denoted by Greek letters. The exponent of the gravitational term is chosen to provide dimensional consistency with respect to time within the equation. The terms in Eq. (2.3) correspond to the similarly positioned terms in Eq. (2.1). However, no viscosity term is shown in Eq. (2.3) because viscosity was not varied during the development of Eq. (2.1).

PNNL has conducted many studies evaluating the performance of jet mixing applied to waste stored at Hanford both with respect to sludge mobilization (Powell et al. 1995a, 1995b, 1997; Shekarriz et al. 1997) and maintaining slurry uniformity (Bamberger et al. 1990, Liljegren and Bamberger 1992, Fort et al. 1993, Bamberger and Meyer 2001, Bamberger and Greenwood 2004, Bamberger et al. 2007,

Fort et al. 2007). Jet mixing work was expanded to include understanding gas release events in Hanford double-shell tanks (Meyer and Wells 2000).

2.3 Pulse Jet Mixing

Pulse jet mixing differs significantly from steady jet mixing. This section describes the unique aspects of PJMs. In Section 2.3.1, PJM configuration and operation are described. In Section 2.3.2, the expected solids behavior during PJM operation is described. PJM mixing requirements are listed in Section 2.3.3, and previous pulse jet mixing studies are briefly described in Section 2.3.4.

2.3.1 Pulse Jet Mixer Operation

PJMs differ from mixers that sustain a steady jet to provide mixing. Jets are formed by alternating pressure and suction on fluid in pulse tubes coupled with jet nozzles, creating a pulsating flow. The nozzle end of the tube is immersed in the tank, while periodic pressure, vacuum, and venting are supplied to the opposite end. There are three operating modes for the pulse tube: 1) the drive mode, when pressure is applied to discharge the contents of the PJM tube at high velocity through the nozzle; 2) the refill mode, when vacuum is applied to refill the pulse tube; and 3) the vent mode, when the pressure is vented to atmosphere and the pulse tube and tank approach the same fill level. The PJM system uses these operating modes to produce a sequence of drive cycles that provide mixing in the vessel. In the right conditions, multiple pulse tubes, operating either in parallel or in sequence, can be used to effectively provide mixing in liquid/solid systems. The pulse tubes are oriented in rings one or two radii from the tank center. The PJMs are distributed uniformly around the vessel circumference.

A typical PJM system configuration in a vessel is shown schematically in Figure 2.1. The vessel shows diameter (D), volume (V), and fill level (H). There are N pulse jets in the vessel, each with pulse tube diameter ($D_{PT,}$) and volume (V_{PT}). Each PJM has a conical nozzle with diameter (d). The volume of fluid expelled during a pulse (V_P) is about 80% of the pulse tube volume to avoid the potential for a pressurized air overblow (i.e., blowing pressurized air from the PJM tubes into the vessel must be avoided). Typically, the total pulse volume ($N \times V_P$) is approximately 5 to 10% of the operating volume of the vessel. During the drive phase the tube is pressurized, and a volume of slurry is discharged. The level change in the tube during discharge is ΔL with a corresponding increase in waste level (ΔH), which is also about 5 to 10% of the operating level, H. Figure 2.1 illustrates a typical PJM system.

The discharge velocity during the drive phase is controlled by the drive pressure, the pressure head at the nozzle exit, and the nozzle loss coefficient. The average velocity (U_0) is given by

$$U_0 = \frac{4V_p}{\pi d^2 t_D} \tag{2.5}$$

where t_D is drive time. The drive pressure (p_D) required to produce the discharge velocity is approximated by

$$p_D = p_E + \frac{k_D}{2}\rho U_0^2 \tag{2.6}$$

where p_E is pressure head at the nozzle exit, k_D is nozzle discharge coefficient, and ρ is slurry density.

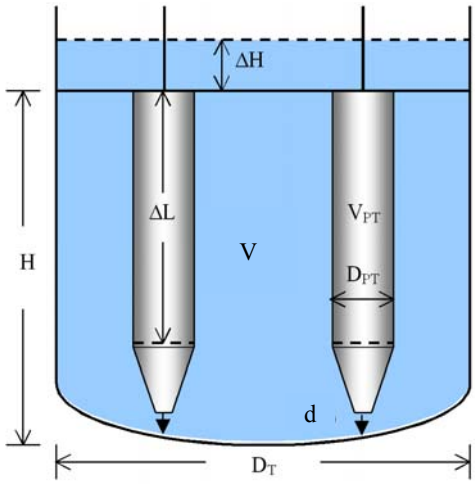

Figure 2.1. Illustration of a Typical PJM System in a WTP Vessel

Immediately after the drive phase, a vent is opened, and excess pressure is allowed to vent to atmosphere. During the suction phase, vacuum is applied to the pulse tube, which fills due to a combination of applied vacuum and difference in hydrostatic head between the fluid level and the level in the tube. The refill time (t_R) is the sum of the vent and suction times. The total cycle time for PJM operation is given by

$$t_C = t_D + t_R \tag{2.7}$$

The average drive velocity is averaged both spatially and temporally. Spatially, the velocity varies over the cross-section of the nozzle. Temporally, the velocity varies due to transients in the drive pressure and inertial effects. Figure 2.2 is an illustration of the temporal variation of velocity during one PJM cycle, referred to as a drive function. At the beginning of the drive phase, the fluid inside the PJM is stationary and must be accelerated. When the drive phase is over, some fluid continues to discharge due to the inertia of the moving column of fluid. The inertial effects depend on the physical size of the system. Pulse jet drive functions can vary considerably among mixing vessels in the WTP; mixing system scale, fill level, and slurry properties all have an effect. To compare PJM systems on a common basis, average velocities can be considered. These have the form:

$$U_n = \left(\frac{1}{\Delta t_n} \int U(t)^n \, dt \right)^{1/n} \qquad n = 1, 2, 3, \text{ and peak average with } n = 1,\ \Delta t_n = \text{primary discharge time} \tag{2.8}$$

where U(t) is instantaneous velocity, Δt is the time interval over which the integration is performed, and n is a specified exponent. The cases n = 1, 2, 3 correspond to mass, momentum, and energy-based average velocities.

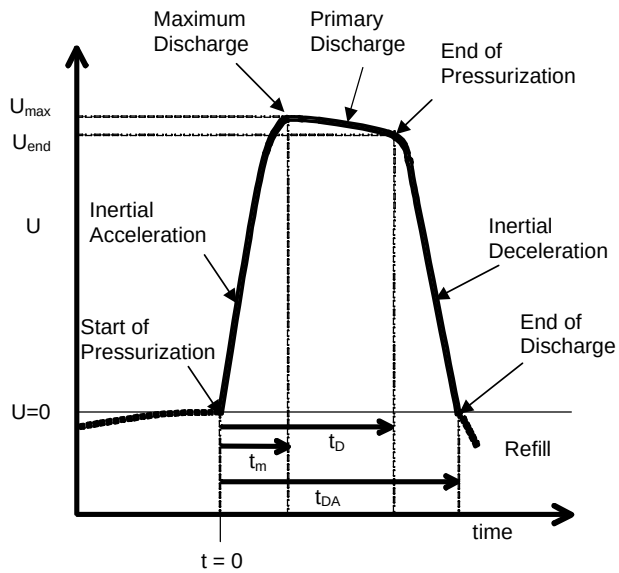

Figure 2.2. Illustration of Nozzle Velocity Transient During PJM Discharge

When the steady jet mixing correlation expressed by Eq. 2.3 is extended to pulse jet mixing, the correlation can be written in the expanded form:

$$U_{CS} = k_P\,(g)^{0.5}\,(s\text{-}1)^{\alpha}\,(d_S)^{\beta}\,(\phi_S)^{\gamma}\,(D)^{\delta}\,(d)^{\varepsilon}\,(DC)^{\zeta}\,(N)^{\eta}\,(\phi_p)^{\theta}\,(H/D)^{\kappa} \tag{2.9}$$

As before, Eq. (2.9) can be expressed in general functional form as

$$U_{CS} = f\,(g, (s\text{-}1), d_S, \phi_S, D, d, DC, N, \phi_p, DC, H/D) \tag{2.10}$$

where

U_{CS} = critical suspension velocity, all solids suspended at the end of the pulse
k_P = PJM specific constant
g = gravitational constant
s = ratio of particle density to liquid density = ρ_s/ρ_l
d_S = diameter of particle (m)
ϕ_S = solids volume fraction
D = diameter of vessel
d = diameter of jet nozzle
DC = duty cycle
N = number of tubes
ϕ_p = pulse volume fraction
H = fluid height
f = general function.

Again, the terms in Eq. (2.9) correspond to the similarly positioned terms in Eq. (2.3) with solids volume fraction substituted for the weight-based term. The duty cycle is added to account for the pulsating flow. This pulse jet model (Eq. 2.9) does not include the ratio of radius of PJM nozzles to tank radius, although nozzle diameter and tank diameter are factored in separately. For the tests performed and

discussed in this report, this parameter was matched either to that of HLP-22, with four inner and eight outer PJMs, or to an eight-tube array representing vessels with four inner and four outer PJMs.

2.3.2 Expected Solids Behavior During PJM Operation

During pulse jet mixing, fluid contained in pulse tubes submerged in the vessel is periodically expelled through the nozzles and into the vessel. This fluid mixes with fluid in the vessel, and solids entrained in the jet are mobilized. While the pulse tubes refill, solids suspended in the fluid may start to settle. This cyclic process is used to suspend, resuspend, and mix particulates contained in the vessel.

During the PJM cycle, process parameters affect the degree of mixing and solids motion that occurs. The jet velocity can be used to characterize the state of the solids within the vessel. There are four conditions of note:

1. The velocity at which the particles on the bottom of the tank are all in motion, complete solids suspension or critical suspension velocity (U_{CS}).
2. The cloud height (H_C) at each velocity, should one exist.
3. The jet velocity and pulse cycle for which the solids reach the liquid surface.
4. The PJM operating conditions under which the vertical concentration profile becomes uniform.

To illustrate the concepts of critical suspension velocity and cloud height that guided testing, Figure 2.3 shows the mixing conditions that may exist during gradual, sequential increases in pulse characteristics (duration and duty cycle) and jet velocity. Steady state is assumed to be achieved between each increase. The resulting mixing states are summarized in Table 2.1 and are related to these key characteristics.

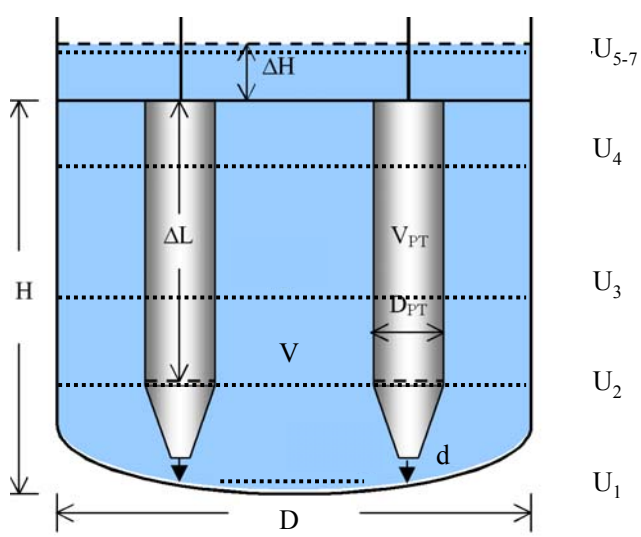

Figure 2.3. Illustration of a Typical PJM System in a WTP Vessel. Solids levels at U_1 can be significantly higher than shown.

Table 2.1. Description of Mixing States for Different Nozzle Velocities (U)

Condition	Characteristic	Description
U_1	$U = 0$	At this initial condition, solids are settled in the vessel, and PJMs are not operating.
U_2	$U < U_{CS}$	PJMs are now pulsing, and jet velocity is less than required to completely suspend particles at the end of the pulse.
U_3	$U = U_{CS}$	This is the velocity required to completely suspend the particles so that they are moving about the tank floor at the end of the pulse.
U_4	$U > U_{CS}$ $H_C < H$	The velocity is above the critical suspension velocity. A particle interface, the cloud height, may be visible below the maximum fluid fill height, H.
U_5	$H_C = H$, U_C	The height of the cloud has reached the maximum fluid fill height H. The velocity at this point is U_C, the velocity required for "complete suspension."
U_6	$U > U_C$	The velocity is greater than that required to sustain the cloud at the maximum fill height, H.
U_7	U_{max}	The maximum velocity obtainable in the test fixture has been reached. The solids concentration profile may be constant with elevation at this velocity, or perhaps significant concentration gradients may still exist.

2.3.3 Mixing Requirements

Mixing requirements for the WTP are described in BNI document 24590-WTP-ES-PT-08-002 Rev. 0, *Determination of Mixing Requirements for Pulse Jet-Mixed Vessels in the Waste Treatment Plant* (Olsen 2008a). We do not provide analysis of WTP vessels using values from later revisions of that document in this report.

2.3.4 Synopsis of Prior PJM Mixing Studies

PNNL staff have conducted significant experimental and analytical studies investigating PJM performance for mixing non-Newtonian slurries (Bamberger et al. 2005, Johnson et al. 2005, Meyer et al. 2005 and 2006, Kurath et al. 2007, Meyer and Etchells 2007, Bamberger et al. 2008) and conducted tests with neutralized current acid waste simulant (Bontha et al. 2000). The work with non-Newtonian slurries was expanded to determine the technical basis for scaling air sparging systems for mixing non-Newtonian slurries (Poloski et al. 2005, Guerrero and Restivo 2004). Experiments have been conducted to evaluate the performance of specific vessels, including the ultrafiltration feed process (UFP) and high-level waste lag storage (LS) vessels (Bates et al. 2003). These studies were expanded to define the technical bases for predicting mixing and flammable gas behavior in the ultrafiltration process feed (UFP) and lag storage (LS) vessels (Bontha et al. 2005). PJM controller and instrumentation performance were also evaluated (Bontha et al. 2007).

Prior to the scaled tests described in this report, PNNL conducted tests to demonstrate the ability to mix in a small-scale PJM test facility (Johnson et al. 2003), and scaling relationships were proposed by Bamberger and Meyer (2007).

2.4 WTP Plant Vessels

There are 32 different WTP solids-containing vessels with 18 unique geometries. All are planned to have PJM systems installed. Pertinent vessel design and operational conditions were supplied by the client and are shown in Tables 2.2[1] and 2.3.[2] Vessel volumes at normal operating fill levels vary from 22.7 to 1438 m^3 (6 to 380 kgal). Vessel diameters range from about 3 to 14.6 m (10 to 48 ft), and operating levels vary from 2.4 to 9.8 m (8 to 32 ft). About half the vessels have elliptical dish bottoms, and the rest have flanged and dish (F&D) heads. The number of PJMs varies from 1 to 12. All but the single-PJM designs involve single or double rings of pulse tubes. All of the baseline PJM designs have 0.10-m (4-in.) nozzles elevated 0.15 m (6 in.) off the bottom. These nozzles are designed to operate at approximately 8 m/s when the vessel is full. The volume of the pulse tubes varies significantly, with total pulse volume being about 5 to 10% of the vessel working volume. The drive times are related to the actual volume of the pulse tubes, and these also vary significantly, from 20 seconds to 4 minutes.

Various metrics can be applied to the WTP mixing systems to obtain an indication of relative mixing performance. Some are shown in Figure 2.4 along with the relative heights and diameters of the vessels. All parameters shown have been normalized by the largest value. For steady jet mixers, power per volume (PPV) is approximately $N\rho U^3 d^2/(D^2 H)$, where N is number of PJMs. Thrust per area (TPA) is given by $N\rho U^2 d^2/D^2$. The Froude number metric is given by $NU^2 d^2/(gHD^2)$. The range in these metrics illustrates some of the uncertainty on the adequacy of the mixing system designs and the wide range of conditions the M3 Test Program must consider. Design changes are being considered for some vessels due to relative ratings such as those shown in Figure 2.4.[3] The primary changes being considered involve increasing jet velocity up to 12 m/s and nozzle diameter up to 15 cm (6 in.).

[1] Data in the table are for information only (FIO). Email transmittal from GL Smith to PA Scott, PA Meyer et al., Feb. 23, 2007, 13:30:52. "PJM Mixing Systems Geometry: Documented in WTP Project Document CCN 146683," with attachment "WTP Project Memorandum CCN 146683_PJM Mixing Systems Geometry for M3 Testing_DRAFT_Feb20'07.pdf."
[2] Nondimensional data in the table are for information only (FIO).
[3] Figure 2.4 is provided FIO.

Table 2.2. Geometric and Operational Data for Solids-Containing Vessels in the WTP—Dimensional Data (FIO)

ID	Vessel	50/50 Vessel (Y,N)	Vessel Sparged (Y,N)	Max Operating Volume (MOV)	Working Volume (WV)	Max Operating Volume	Working Volume	Vessel Dia.	Vessel Bottom Head Type	Norm Vessel Waste Depth	Max Vessel Waste Depth	Min Vessel Waste Depth	Relative Scale	Nom H/D	Max H/D	Min H/D	PJM Vol	PJM Vol
-	-	-	-	gal	gal	ft^3	ft^3	ft	-	ft	ft	ft	-	-	-	-	gal	ft^3
1	FEP-17A/B	Y	N	71,292	56,223	9,530	7,516	22.0	2:1 elliptical	21.60	26.20	2.00	2.1	0.98	1.19	0.09	885	118.3
2	FRP-02A/B/C/D	N	N	406,800	379,891	54,381	50,784	47.0	F&D	30.60	34.11	1.00	1.0	0.65	0.73	0.02	1,614	215.8
3	HLP-22	N	N	234,500	203,927	31,348	27,261	38.0	F&D	26.56	30.27	7.63	1.2	0.70	0.80	0.20	1,693	226.3
4	HOP-903/904	N	N	8,199	5,808	1,096	776	12.0	2:1 elliptical	7.87	10.30	2.26	3.9	0.66	0.86	0.19	115	15.4
5	PWD-15/16	N	N	105,850	87,657	14,150	11,718	22.0	2:1 elliptical	32.68	39.08	4.17	2.1	1.49	1.78	0.19	540	72.2
6	PWD-33/43	Y	N	29,580	20,802	3,954	2,781	24.0	F&D	7.71	10.89	2.34	2.0	0.32	0.45	0.10	265	35.4
7	PWD-44	Y	N	88,631	74,147	11,848	9,912	23.0	2:1 elliptical	25.79	30.45	4.39	2.0	1.12	1.32	0.19	1,085	145.0
8	RDP-02A/B/C	N	N	12,688	7,508	1,696	1,004	12.0	2:1 elliptical	9.87	13.93	0.17	3.9	0.82	1.16	0.01	311	41.6
9	RLD-07	N	N	15,758	12,184	2,107	1,629	13.0	F&D	13.14	15.59	2.18	3.6	1.01	1.20	0.17	207	27.7
10	RLD-08	N	N	10,628	8,681	1,421	1,160	13.0	2:1 elliptical	9.87	11.79	2.19	3.6	0.76	0.91	0.17	214	28.6
11	TLP-09A/B	N	N	114,060	87,138	15,248	11,649	26.0	F&D	23.66	27.96	1.50	1.8	0.91	1.08	0.06	581	77.7
12	UFP-01A/B	Y	N	64,626	54,536	8,639	7,290	20.0	2:1 elliptical	24.87	29.05	2.00	2.4	1.24	1.45	0.10	693	92.6
13	UFP-62A/B/C	N	N	30,072	25,503	4,020	3,409	15.0	2:1 elliptical	20.54	24.00	2.21	3.1	1.37	1.60	0.15	251	33.6
14	CNP-03	N	N	18,750	15,350	2,507	2,052	14.0	F&D	14.67	17.21	2.20	3.4	1.05	1.23	0.16	198	26.5
15	CNP-04	N	N	10,065	7,853	1,345	1,050	9.5	F&D	19.61	15.44	2.13	4.9	2.06	1.63	0.22	129	17.2
16	CXP-04	N	N	9,393	7,840	1,256	1,048	10.5	F&D	12.76	14.15	2.15	4.5	1.22	1.35	0.20	470	62.8
17	CXP-26A/B/C	N	N	34,370	29,929	4,595	4,001	15.0	2:1 elliptical	23.86	26.81	2.47	3.1	1.59	1.79	0.16	243	32.5
18	TCP-01	N	N	129,963	103,200	17,374	13,796	26.5	F&D	26.78	33.25	2.00	1.8	1.01	1.25	0.08	1,625	217.2
-	UFP-02A/B	N	Y	36,561	26,778	4,887	3,580	14.0	2:1 elliptical	24.85	30.68	2.00	3.4	1.78	2.19	0.14	606	81.0
-	HLP-27A/B	N	Y	112,900	92,087	15,093	12,310	25.0	F&D	26.73	32.40	3.20	1.9	1.07	1.30	0.13	1,405	187.8
-	HLP-28	N	Y	125,430	97,012	16,768	12,969	26.5	F&D	25.27	32.65	2.00	1.8	0.95	1.23	0.08	1,555	207.9
-	CNP-01	N	N	108	108	15	15	4.0	F&D	1.60	1.60	0.00	11.8	0.40	0.40	0.00	N/A	N/A
-	CXP-01	N	N	92,850	85,038	12,412	11,368	23.0	F&D	28.69	31.39	1.50	2.0	1.25	1.36	0.07	N/A	N/A
-	CXP-05	N	N	883	486	118	65	5.0	F&D	3.64	6.33	1.00	9.4	0.73	1.27	0.20	N/A	N/A
-	FEP-05	N	N	4,144	60	554	413	8.0	F&D	6.68	9.46	1.50	5.9	0.84	1.18	0.19	N/A	N/A
-	PJV-02	N	N	7,408	6,141	990	821	10.0	2:1 elliptical	11.29	13.50	1.42	4.7	1.13	1.35	0.14	N/A	N/A
-	PVP-01	N	N	1,650	1,547	221	207	6.0	2:1 elliptical	7.81	8.31	1.50	7.8	1.30	1.39	0.25	N/A	N/A
-	TLP-02	N	N	1,916	45	256	157	6.0	F&D	5.95	8.46	1.50	7.8	0.99	1.41	0.25	N/A	N/A

Table 2.2. (contd)

PJM Dia.	PJM Length	Stroke Length	PJM Type	Total PJMs	PJM Vol Fraction of MOV @ 100% Stroke	PJM Vol Fraction of WV @ 80% Stroke	Number PJMs Inner Circle	Radius Inner Circle	Number PJMs Outer Circle	Radius Outer Circle	Nozzle Dia	Normal Nozzle Velocity	Norm Drive Time	Norm PJM Cycle Time	Norm Duty Cycle	Peak Nozzle Velocity	Min. Drive Time	Min. PJM Cycle Time	Min Duty Cycle	ID	Vessel
ft	ft	ft	-	-	-	-	-	in.	-	in.	in.	m/sec	sec	sec	-	m/sec	sec	sec	-	-	-
3.00	18.4	14.7	E	8	0.10	0.10	4.00	132.00	4.00	176.00	4.00	8	38	129	0.29	9.8	35	135	0.26	1	FEP-17A/B
4.50	16.4	13.1	J	12	0.05	0.04	4.00	158.00	8.00	394.00	4.00	8	80	217	0.37	12	40	266	0.15	2	FRP-02A/B/C/D
4.50	16.9	13.5	J	12	0.09	0.08	4.00	152.00	8.00	342.00	4.00	8	77	233	0.33	10.7	40	270	0.15	3	HLP-22
1.50	9.4	7.5	A	4	0.06	0.06	0.00	96.00	4.00	-	4.00	8	6	23	0.26	10.5	4	20	0.20	4	HOP-903/904
2.67	14.4	11.5	D	8	0.04	0.04	4.00	120.00	4.00	176.00	4.00	8	24	68	0.35	9	22	66	0.33	5	PWD-15/16
2.67	7.8	6.3	D	8	0.07	0.08	4.00	168.00	4.00	192.00	4.00	8	11	37	0.30	11	7	36	0.19	6	PWD-33/43
3.50	17.1	13.7	F	8	0.10	0.09	4.00	138.00	4.00	184.00	4.00	8	52	158	0.33	10.5	38	150	0.25	7	PWD-44
2.67	8.9	7.1	D	4	0.10	0.13	0.00	96.00	4.00	-	4.00	8	13	45	0.29	10.8	10	49	0.20	8	RDP-02A/B/C
2.00	9.8	7.9	B	4	0.05	0.05	0.00	104.00	4.00	-	4.00	8	9	33	0.27	10.6	7	33	0.21	9	RLD-07
2.00	10.2	8.1	B	4	0.08	0.08	0.00	104.00	4.00	-	4.00	8	9	31	0.29	11	7	35	0.20	10	RLD-08
3.50	10.1	8.1	F	8	0.04	0.04	4.00	148.00	4.00	208.00	4.00	8	23	76	0.30	10	20	76	0.26	11	TLP-09A/B
3.00	14.8	11.9	E	8	0.09	0.08	4.00	120.00	4.00	160.00	4.00	8	30	96	0.31	11.5	18	111	0.16	12	UFP-01A/B
2.00	11.8	9.4	B	6	0.05	0.05	3.00	90.00	3.00	128.00	4.00	8	14	45	0.31	9	10	37	0.27	13	UFP-62A/B/C
2.50	6.8	5.4	C	4	0.04	0.04	0.00	112.00	4.00	-	4.00	8	9	34	0.26	9.2	7	30	0.23	14	CNP-03
1.50	10.5	8.4	A	4	0.05	0.05	0.00	76.00	4.00	-	4.00	8	6	22	0.27	10	4	19	0.21	15	CNP-04
3.00	10.6	8.5	E	1	0.05	0.05	1.00	0.00	0.00	-	4.00	8	20	69	0.29	11	15	72	0.21	16	CXP-04
2.00	11.4	9.1	B	6	0.04	0.04	0.00	120.00	6.00	-	4.00	8	12	38	0.32	9	10	35	0.29	17	CXP-26A/B/C
4.33	17.3	13.9	H	8	0.10	0.10	4.00	150.00	4.00	212.00	4.00	8	76	227	0.33	9	74	230	0.32	18	TCP-01
2.67	14.6	11.7	D	6	0.10	0.11	1.00	-	5.00	37.00	4.00	12	15	91	0.16	12	15	91	0.16	-	UFP-02A/B
4.00	14.9	12.0	G	8	0.10	0.10	1.00	-	7.00	61.00	4.00	12	30	223	0.13	12	30	223	0.13	-	HLP-27A/B
4.33	14.1	11.3	H	8	0.10	0.10	1.00	-	7.00	65.50	4.00	12	30	222	0.14	6+	30	222	0.14	-	HLP-28
N/A	N/A	N/A	N/A	0	N/A	N/A	N/A	N/A	N/A	N/A	N/A	N/A	N/A	N/A	N/A	N/A	N/A	N/A	N/A	-	CNP-01
N/A	N/A	N/A	N/A	0	N/A	N/A	N/A	N/A	N/A	N/A	N/A	N/A	N/A	N/A	N/A	N/A	N/A	N/A	N/A	-	CXP-01
N/A	N/A	N/A	N/A	0	N/A	N/A	N/A	N/A	N/A	N/A	N/A	N/A	N/A	N/A	N/A	N/A	N/A	N/A	N/A	-	CXP-05
N/A	N/A	N/A	N/A	0	N/A	N/A	N/A	N/A	N/A	N/A	N/A	N/A	N/A	N/A	N/A	N/A	N/A	N/A	N/A	-	FEP-05
N/A	N/A	N/A	N/A	0	N/A	N/A	N/A	N/A	N/A	N/A	N/A	N/A	N/A	N/A	N/A	N/A	N/A	N/A	N/A	-	PJV-02
N/A	N/A	N/A	N/A	0	N/A	N/A	N/A	N/A	N/A	N/A	N/A	N/A	N/A	N/A	N/A	N/A	N/A	N/A	N/A	-	PVP-01
N/A	N/A	N/A	N/A	0	N/A	N/A	N/A	N/A	N/A	N/A	N/A	N/A	N/A	N/A	N/A	N/A	N/A	N/A	N/A	-	TLP-02

Table 2.3. Geometric and Operational Data for Solids-Containing Vessels in the WTP—Nondimensional Values (FIO)

Vessel	S	N			d/D			H/D		8/4in./1cP	8/4in./25cP	12/8in./1cP
	-	tot	in	out	4in.	6in.	8in.	norm	max	nom	min	max
FRP-02A/B/C/D	1	12	4	8	7.10E-03	1.10E-02	1.40E-02	6.50E-01	7.30E-01	8.10E+05	3.30E+04	3.40E+06
HLP-22	1.2	12	4	8	8.80E-03	1.30E-02	1.80E-02	7.00E-01	8.00E-01	8.10E+05	3.30E+04	3.40E+06
TCP-01	1.8	8	4	4	1.30E-02	1.90E-02	2.50E-02	1.00E+00	1.30E+00	8.10E+05	3.30E+04	3.40E+06
TLP-09A/B	1.8	8	4	4	1.30E-02	1.90E-02	2.60E-02	9.10E-01	1.10E+00	8.10E+05	3.30E+04	3.40E+06
PWD-33/43	2	8	4	4	1.40E-02	2.10E-02	2.80E-02	3.20E-01	4.50E-01	8.10E+05	3.30E+04	3.40E+06
PWD-44	2	8	4	4	1.40E-02	2.20E-02	2.90E-02	1.10E+00	1.30E+00	8.10E+05	3.30E+04	3.40E+06
FEP-17A/B	2.1	8	4	4	1.50E-02	2.30E-02	3.00E-02	9.80E-01	1.20E+00	8.10E+05	3.30E+04	3.40E+06
PWD-15/16	2.1	8	4	4	1.50E-02	2.30E-02	3.00E-02	1.50E+00	1.80E+00	8.10E+05	3.30E+04	3.40E+06
UFP-01A/B	2.4	8	4	4	1.70E-02	2.50E-02	3.30E-02	1.20E+00	1.50E+00	8.10E+05	3.30E+04	3.40E+06
UFP-62A/B/C	3.1	6	3	3	2.20E-02	3.30E-02	4.40E-02	1.40E+00	1.60E+00	8.10E+05	3.30E+04	3.40E+06
CXP-26A/B/C	3.1	6	6	-	2.20E-02	3.30E-02	4.40E-02	1.60E+00	1.80E+00	8.10E+05	3.30E+04	3.40E+06
CNP-03	3.4	4	4	-	2.40E-02	3.60E-02	4.80E-02	1.00E+00	1.20E+00	8.10E+05	3.30E+04	3.40E+06
RLD-07	3.6	4	4	-	2.60E-02	3.80E-02	5.10E-02	1.00E+00	1.20E+00	8.10E+05	3.30E+04	3.40E+06
RLD-08	3.6	4	4	-	2.60E-02	3.80E-02	5.10E-02	7.60E-01	9.10E-01	8.10E+05	3.30E+04	3.40E+06
HOP-903/904	3.9	4	4	-	2.80E-02	4.20E-02	5.60E-02	6.60E-01	8.60E-01	8.10E+05	3.30E+04	3.40E+06
RDP-02A/B/C	3.9	4	4	-	2.80E-02	4.20E-02	5.60E-02	8.20E-01	1.20E+00	8.10E+05	3.30E+04	3.40E+06
CXP-04	4.5	1	0	-	3.20E-02	4.80E-02	6.30E-02	1.20E+00	1.30E+00	8.10E+05	3.30E+04	3.40E+06
CNP-04	4.9	4	4	-	3.50E-02	5.30E-02	7.00E-02	2.10E+00	1.60E+00	8.10E+05	3.30E+04	3.40E+06
-	-	-	-	-	-	-	-	-	-	-	-	-
min	1	1	-	-	7.09E-03	1.06E-02	1.42E-02	3.21E-01	4.54E-01	8.13E+05	3.25E+04	3.41E+06
max	4.95	12	-	-	3.51E-02	5.26E-02	7.02E-02	2.06E+00	1.79E+00	8.13E+05	3.25E+04	3.41E+06
average	2.81	6.5	-	-	1.99E-02	2.99E-02	3.98E-02	1.05E+00	1.21E+00	8.13E+05	3.25E+04	3.41E+06
-	-	-	-	-	-	-	-	-	-	-	-	-
Recommended Min	-	1	4	4	0.007	-	-	0.3	-	3.25E+04	-	-
Recommended Max	-	12	4	8	0.04	-	-	2	-	3.40E+06	-	-

Table 2.3. (contd)

	Primary Nondimensional Variables									
	Density Ratio		Froude No.	Densimetric Froude No.		12m/s	12m/s	12m/s	% Pulse	Duty Cycle
	s	s	Fr	Fs	Fs	Fr	Fs	Fs	ϕ_p	DC
Vessel	min	max	norm	min	max	norm	min	max	norm	norm
FRP-02A/B/C/D	1.5	11	3.50E-01	3.50E-02	7.00E-01	7.90E-01	1.60E+00	7.90E-02	9.10E-02	3.50E-01
HLP-22	1.5	11	4.00E-01	4.00E-02	8.10E-01	9.10E-01	1.80E+00	9.10E-02	2.50E-02	3.40E-01
TCP-01	1.5	11	4.00E-01	4.00E-02	8.00E-01	9.00E-01	1.80E+00	9.00E-02	5.00E-02	3.30E-01
TLP-09A/B	1.5	11	4.50E-01	4.50E-02	9.00E-01	1.00E+00	2.00E+00	1.00E-01	3.60E-02	3.60E-01
PWD-33/43	1.5	11	1.40E+00	1.40E-01	2.80E+00	3.10E+00	6.20E+00	3.10E-01	5.50E-02	3.30E-01
PWD-44	1.5	11	4.10E-01	4.10E-02	8.30E-01	9.30E-01	1.90E+00	9.30E-02	2.10E-02	3.20E-01
FEP-17A/B	1.5	11	5.00E-01	5.00E-02	9.90E-01	1.10E+00	2.20E+00	1.10E-01	9.70E-02	3.20E-01
PWD-15/16	1.5	11	3.30E-01	3.30E-02	6.50E-01	7.40E-01	1.50E+00	7.40E-02	9.80E-02	3.70E-01
UFP-01A/B	1.5	11	4.30E-01	4.30E-02	8.60E-01	9.70E-01	1.90E+00	9.70E-02	5.10E-02	3.40E-01
UFP-62A/B/C	1.5	11	5.20E-01	5.20E-02	1.00E+00	1.20E+00	2.30E+00	1.20E-01	5.30E-02	2.60E-01
CXP-26A/B/C	1.5	11	4.50E-01	4.50E-02	9.00E-01	1.00E+00	2.00E+00	1.00E-01	3.60E-02	3.00E-01
CNP-03	1.5	11	7.30E-01	7.30E-02	1.50E+00	1.60E+00	3.30E+00	1.60E-01	9.40E-02	2.70E-01
RLD-07	1.5	11	8.10E-01	8.10E-02	1.60E+00	1.80E+00	3.70E+00	1.80E-01	6.10E-02	2.90E-01
RLD-08	1.5	11	1.10E+00	1.10E-01	2.20E+00	2.40E+00	4.90E+00	2.40E-01	3.90E-02	3.20E-01
HOP-903/904	1.5	11	1.40E+00	1.40E-01	2.70E+00	3.10E+00	6.10E+00	3.10E-01	8.20E-02	2.30E-01
RDP-02A/B/C	1.5	11	1.10E+00	1.10E-01	2.20E+00	2.40E+00	4.90E+00	2.40E-01	5.50E-02	3.20E-01
CXP-04	1.5	11	8.40E-01	8.40E-02	1.70E+00	1.90E+00	3.80E+00	1.90E-01	5.90E-02	3.20E-01
CNP-04	1.5	11	5.50E-01	5.50E-02	1.10E+00	1.20E+00	2.50E+00	1.20E-01	9.50E-02	2.70E-01
-	-	-	-	-	-	-	-	-	-	-
min	1.5	11	3.27E-01	3.27E-02	6.55E-01	7.37E-01	1.47E+00	7.37E-02	2.09E-02	2.34E-01
max	1.5	11	1.39E+00	1.39E-01	2.78E+00	3.12E+00	6.25E+00	3.12E-01	9.80E-02	3.71E-01
average	1.5	11	6.71E-01	6.71E-02	1.34E+00	1.51E+00	3.02E+00	1.51E-01	6.11E-02	3.14E-01
-	-	-	-	-	-	-	-	-	-	-
Recommended Min	1.5	-	-	1.00E-01	-	-	-	-	2.00E-02	2.00E-01
Recommended Max	11	-	-	6.00E+00	-	-	-	-	1.50E-01	4.00E-01

Table 2.3. (contd)

Primary Nondimensional Variables							
Particle Size Ratio				Jet Density			
d_S/d	d_S/d	d_S/d	d_S/d	$N^{1/2}d/D$	$N^{1/2}d/D$	$N^{1/2}d/D$	
min (4in.)	max (4in.)	min(8in.)	max(8in.)	4in.	6in.	8in.	Vessel
9.80E-05	9.80E-03	4.90E-05	4.90E-03	0.025	0.037	0.049	FRP-02A/B/C/D
9.80E-05	9.80E-03	4.90E-05	4.90E-03	0.030	0.046	0.061	HLP-22
9.80E-05	9.80E-03	4.90E-05	4.90E-03	0.036	0.053	0.071	TCP-01
9.80E-05	9.80E-03	4.90E-05	4.90E-03	0.036	0.054	0.073	TLP-09A/B
9.80E-05	9.80E-03	4.90E-05	4.90E-03	0.039	0.059	0.079	PWD-33/43
9.80E-05	9.80E-03	4.90E-05	4.90E-03	0.041	0.061	0.082	PWD-44
9.80E-05	9.80E-03	4.90E-05	4.90E-03	0.043	0.064	0.086	FEP-17A/B
9.80E-05	9.80E-03	4.90E-05	4.90E-03	0.043	0.064	0.086	PWD-15/16
9.80E-05	9.80E-03	4.90E-05	4.90E-03	0.047	0.071	0.094	UFP-01A/B
9.80E-05	9.80E-03	4.90E-05	4.90E-03	0.054	0.082	0.109	UFP-62A/B/C
9.80E-05	9.80E-03	4.90E-05	4.90E-03	0.054	0.082	0.109	CXP-26A/B/C
9.80E-05	9.80E-03	4.90E-05	4.90E-03	0.048	0.071	0.095	CNP-03
9.80E-05	9.80E-03	4.90E-05	4.90E-03	0.051	0.077	0.103	RLD-07
9.80E-05	9.80E-03	4.90E-05	4.90E-03	0.051	0.077	0.103	RLD-08
9.80E-05	9.80E-03	4.90E-05	4.90E-03	0.056	0.083	0.111	HOP-903/904
9.80E-05	9.80E-03	4.90E-05	4.90E-03	0.056	0.083	0.111	RDP-02A/B/C
9.80E-05	9.80E-03	4.90E-05	4.90E-03	0.032	0.048	0.063	CXP-04
9.80E-05	9.80E-03	4.90E-05	4.90E-03	0.070	0.105	0.140	CNP-04
-	-	-	-	-	-	-	-
9.84E-05	9.84E-03	4.92E-05	4.92E-03	0.025	0.037	0.049	min
9.84E-05	9.84E-03	4.92E-05	4.92E-03	0.070	0.105	0.140	max
9.84E-05	9.84E-03	4.92E-05	4.92E-03	0.045	0.068	0.090	average
-	-	-	-	-	-	-	-
1.00E-02	-	-	-	-	-	-	Recommended Min
1.00E-04	-	-	-	-	-	-	Recommended Max

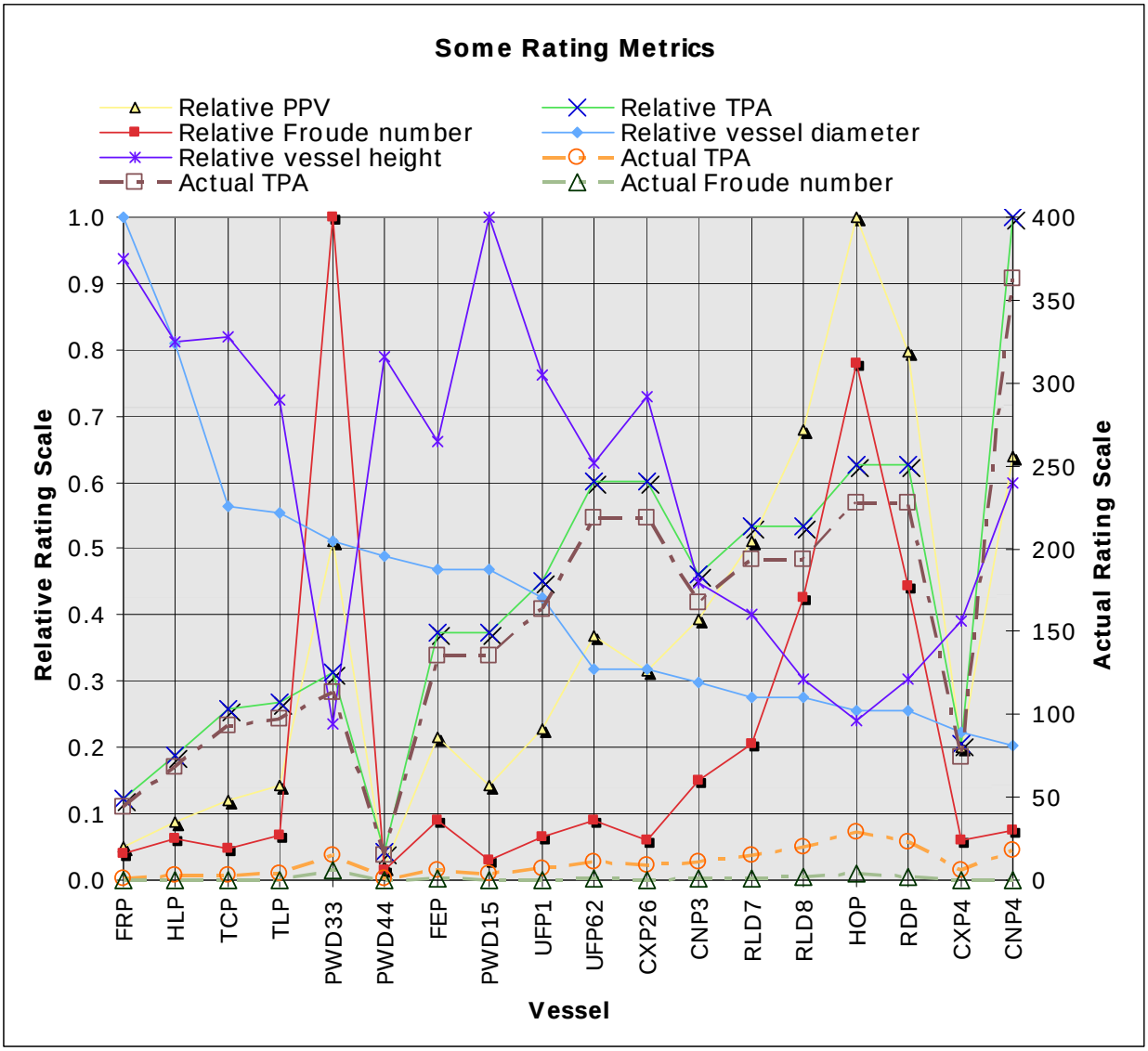

Figure 2.4. Some Common Mixing Metrics Applied to the 18 Distinct WTP Vessel Configurations (FIO)

2.5 Evaluating Mixing Systems

The general approach used to evaluate the solids-handling capability of the WTP mixing systems in solids-containing vessels is as follows:

- Develop simulants for noncohesive slurries with properties that bracket anticipated slurry properties in the WTP.
- Perform scaled tests with mixing systems that can be configured to span the geometric and operational parameter space of WTP mixing systems.
- Use well-established metrics to evaluate mixing performance over the testing parameter space.
- Use experimental data to develop models relating mixing performance to slurry properties, geometric parameters, and operational parameters.

- Apply the models to the plant mixing systems and determine the limiting solids properties the mixing system can handle.
- Assess the acceptability of the limiting solids properties by considering the specific requirements for a given vessel and the percentage of Hanford waste that exceeds the limit.

If limiting conditions were deemed unacceptable, the models could then be exercised to evaluate design modifications.

2.5.1 Mixing System Parameters

The primary mixing system parameters shown in Table 2.4 are slurry properties, mixing system geometric parameters, and operational parameters. Mixing performance in general will depend on the values of these parameters, which can be formed into an equivalent set of dimensionless groups.

Table 2.4. Primary[(a)] Mixing System Physical Parameters

Slurry Properties/Variables	Symbol	Units
Solids diameter	d_S	μm
Solids volume fraction	ϕ_S	[(b)]
Solids density	ρ_s	g/cm^3
Liquid density	ρ_l	g/cm^3
Liquid kinematic viscosity	$\nu = \mu/\rho_l$	m^2/s
Geometric Configuration	**Symbol**	**Units**
Vessel diameter	D	m (in.)
Nozzle (jet) diameter	d	m (in.)
Number PJMs[(c)]	N	each
Radial location of PJMs[(c)]	R	m (ft)
Operational Parameters	**Symbol**	**Units**
Fill level	H	m (in.)
Pulse volume	V_P	m^3
Drive time	t_D	s
Cycle time	t_C	s
Jet velocity	U	m/s

(a) Secondary variables such as settling velocity, U_T, (derived from primary measured variables such as particle size and particle density) are discussed in Sections 7.0, 8.0, and 9.0.
(b) Indicates the parameter is nondimensional.
(c) Includes single and double rings.

Dimensional analysis applied to the physical parameters in Table 2.4 results in 11 (13 parameters constrained by consistency in three units, mass, length, and time) nondimensional variables when considering single-ring PJM configurations.[1] Double-ring PJM configurations introduce up to two more variables (N_o and R_o/D). The primary nondimensional variables are shown in Table 2.5. These nondimensional variables are not unique; others can be selected that favor physical insight or specific

[1] This is true because all single-ring PJM configurations have the same relative radial positioning (R/D). Hence, R/D is not a variable with respect to the plant mixing system designs.

processes or provide better models of test data. However, they all can be expressed in terms of the physical parameters in Table 2.4.

Table 2.5. Mixing System Nondimensional Variables

Slurry Property	Nondimensional Variable
Density ratio	$s = \rho_s/\rho_l$
Solids volume fraction	$\phi_S = V_S/ V_{REF}$ where $V_{REF} =(\pi D^3)/4$
Particle diameter ratio	d_S/D
Geometric Properties	
Nozzle diameter ratio	d/D
Number of pulse tubes	N
Jet density	$\phi_J =N_J(d/D)^2$
PJM location	R/D
Ratio of pulse tube to vessel cross-sectional area	$\phi_{PT} =N(D_{PT}/D)^2$
Operational Parameters	
Fill level	H/D
Pulse volume fraction	$\phi_p = N V_P/ V_{REF}$ where $V_{REF} =(\pi D^3)/4$
Duty cycle	$DC = t_D / t_C$
Jet Reynolds number	$Re = U d / \nu$
Froude number	$Fr = U^2 /gd(s-1)$

Some examples of other potentially useful nondimensional variables and their relationships with the physical parameters in Table 2.4 are given here:

Ratio of pulse time to fluid transit time in vessel:

$$t_D U / D = \phi_p (D/d)^2 /N \tag{2.11}$$

Particle Reynolds number

$$Re_p = U_T d_S /\nu = (U_T/U) (d_S / D) (D/d) Re \tag{2.12}$$

Particle Froude number

$$F_p = U_T^2 /g d_S \tag{2.13}$$

Particle Galileo number

$$Ga_p = (s-1)g d_S^3 / \nu^2 = Re_p^2 / Fr_p \tag{2.14}$$

Settling velocity (U_T) ratio

$$U_T/U = f(Re_p, Fr_p) = g(U_T/U, d_S/D, d/D, Re, Fr) \tag{2.15}$$

Hindered settling velocity (U_{TH}) ratio

$$U_{TH} /U = f(U_T/U, \phi_S) \tag{2.16}$$

In much of the mixing literature the solids content is defined in terms of a solids loading where the solids volume (or mass) is divided by the slurry volume (or mass). However, there is a significant advantage to describing the solids content relative to a reference volume that is independent of the fill level in the vessel. Just-suspended velocity and solids cloud height are found to depend on fill level when the solids loading is held constant. However, they tend to be independent of fill level when the total mass in the system is held constant. This phenomenon has been demonstrated for solids suspensions using mechanical agitators.[1] Hicks and Myers measured just-suspended speed, N_{JS}, under two different conditions: keeping the solids loading constant while varying the liquid level and holding the solids mass constant while varying the liquid level. Some of their data are reproduced in Figure 2.5. When the solids loading was held constant, the data show that N_{JS} increases with the fill level; however, when the solids mass was held constant, N_{JS} was independent of fill level. These data make clear the benefit of basing ϕ_S on a reference volume instead of the slurry volume. By doing so, just-suspended velocity should be independent of fill level (H).

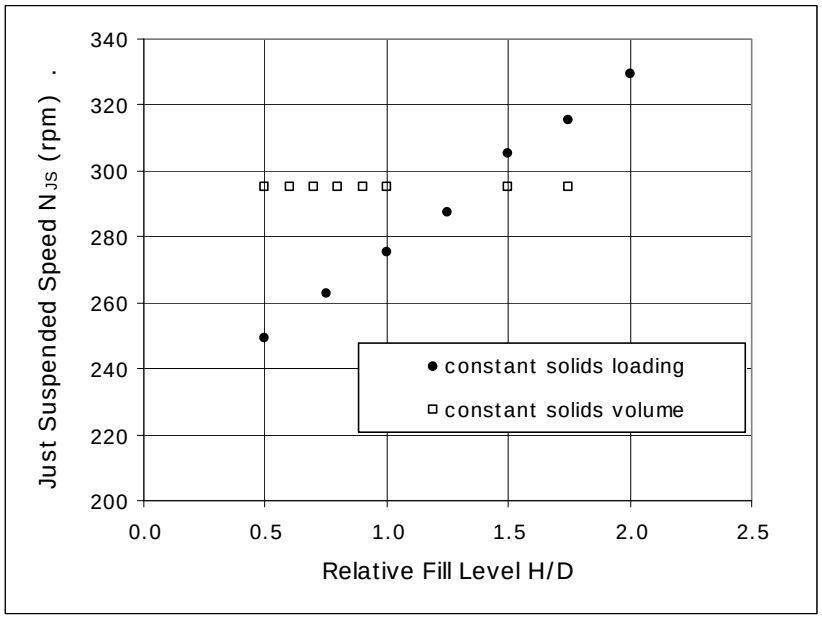

Figure 2.5. Just-Suspended Speed as a Function of Fill Level for Mechanical Agitators (data reproduced from Hicks and Myers)[1]

Hicks and Myers also looked at the effect of fill level on cloud height. They varied impeller speed and measured cloud height for two different fill levels. Some of those results are reproduced in Figure 2.6, where it is seen that fill level had negligible effect on cloud height.

In summary, when the solids fraction is based on reference volume, it is anticipated that test results for U_{CS} and H_C will be independent of fill level. It follows that solid vertical distribution will be independent of fill level as long as the cloud is less than the fill level. If the cloud reaches the liquid surface, the solids vertical distribution will depend on fill level.

[1] Hicks MT and KJ Myers. 1993. "Cloud Height, Fillet Volume, and the Effect of Multiple Impellers in Solids Suspension." MIXING XIV, Santa Barbara, Calif. Engineering Foundation, New York, and North American Mixing Forum.

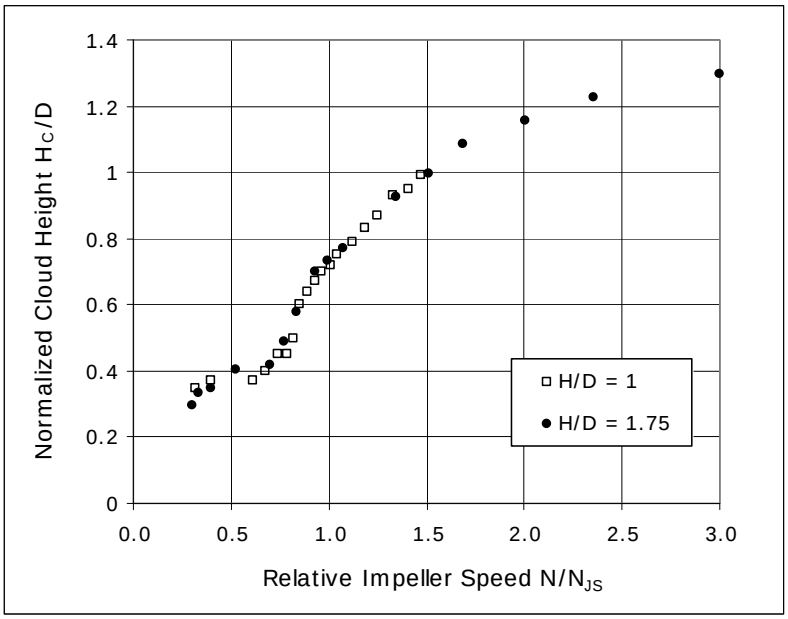

Figure 2.6. Effects of Fill Level on Cloud Height for Solids Suspension with Mechanical Agitators (data reproduced from Hicks and Myers)[1]

2.5.2 Just-Suspended Jet Velocity

The just-suspended jet velocity, U_{JS}, is defined for steady jet mixing as the discharge velocity required to completely suspend solids that are on the bottom of the vessel. For steady jet mixing, a commonly used criterion is that no solid particles are observed resting on the bottom for more than 1 to 2 seconds. For pulse jet mixing, a reasonable criterion would be that no solids remain on the bottom at the end of the pulse, or, alternatively, that all the solids that have settled during the refill period are completely resuspended during the subsequent pulse. For this study, the velocity to suspend all solids at the end of the pulse is defined as the critical suspension velocity (U_{CS}).

In general it can be expected that U_{CS} is a function of the important mixing parameters. This is expressed mathematically by

$$U_{CS} = f(d_S, \rho_s, \rho_l, \phi_S, \nu, D, d, N, V_P, R, H, t_D, t_C) \tag{2.17}$$

The critical suspension velocity can also be expressed in terms of the (dimensionless) Froude number as

$$F_{CS} = U_{CS}^2 / [gd(s-1)] = g(s, \phi_S, d_S/D, d/D, N, R/D, H/D, \phi_p, DC, Re_{CS}) \tag{2.18}$$

This Froude number can be interpreted as the ratio of jet kinetic energy to the potential energy required to suspend the mass of settled solids one particle diameter in elevation.

[1] Hicks MT and KJ Myers. 1993. "Cloud Height, Fillet Volume, and the Effect of Multiple Impellers in Solids Suspension." MIXING XIV, Santa Barbara, Calif. Engineering Foundation, New York, and North American Mixing Forum.

2.5.3 Solids Vertical Distribution

During mixing system operation, solids will become suspended off the bottom of the vessel. For continuous mixing, the solids fraction will achieve a stable distribution. With pulse jet mixing, changes in solids concentration may occur between pulses. By either assuming quasi-steady solids distributions or averaging over a drive cycle, the solids fraction vertical distribution can be expressed mathematically as

$$\phi / \phi_S (Z/D) = f(s, \phi_S, d_S/D, d/D, N, R/D, H/D, \phi_p, DC, Re, Fr) \quad (2.19)$$

where ϕ is the local solids fraction and Z/D is the normalized vertical elevation.

For some conditions a distinct interface, cloud height (H_C), forms at a certain vertical elevation, with no solids suspended above. Cloud height can also be expressed in terms of the mixing parameters.

A useful measure of the degree of homogeneity is the relative standard deviation (RSD) of the solids fraction. The RSD can also be expressed as a function of the various nondimensional variables. This can be considered in future analyses.

2.6 Parametric Tests

Parametric testing is required to develop functional expressions (models) for the rating metrics in terms of the pertinent mixing parameters. In this regard the parameters, either physical or nondimensional, are essentially test variables. The functional expressions are essentially models of the parametric data. To achieve accuracy in rating the plant mixing systems, it is important to obtain accurate models of the scaled test data. To this end, the testing approach focused initially on identifying the most sensitive parameters. Sufficient data were collected to capture the dependencies between various parameters. Also, the parametric ranges tested were selected to span the range of plant conditions insofar as it is possible to achieve them (see Section 2.8.3 for a comparison of test conditions to WTP vessel conditions).

2.7 Scale-up of Metrics

Mixing results obtained from parametric scaled tests must be applied at plant scale. This section describes four potential approaches and discusses their relative strengths and limitations. With this understanding, a scale-up strategy is presented.

Table 2.6 lists four approaches for performing scaled tests and their limitations or consequences. All of the approaches involve geometric similarity. The magnitude of the limitations and relative differences between approaches are reduced as the test scale is increased. Approach 1 was used for a limited number of tests to satisfy the test specification (Smith 2007) as well as to aid in isolating the jet Reynolds number effects, which may be larger than expected due to periodic flow conditions. Approach 2 was used extensively for developing the models but is not relied upon for scale-up information per se. Approach 3 is a relatively new concept that replaces particle size with settling velocity as a variable. It has the potential to isolate the effects of scale to a single variable, though it is not clear what other limitations may exist. This approach would require determination of a characteristic or representative settling velocity for all simulants. Approach 4 is the standard commonly used in industrial mixing, in which scale-up laws are determined by testing with the same simulants at various scales. Many test conditions

provide data that are applicable to some or all of the approaches, so using multiple approaches to scale up does not imply a big increase in test conditions.

Table 2.6. Comparison of Scaled Test Approaches

Scaled Test Approach	Description	Fundamental Limitation/Requirement	Consequence at Plant Scale	Common Name for Approach
1	Match all full-scale nondimensional variables at small scale	Forces s range higher and d_S range significantly lower (into cohesive regime)	Plant conditions outside range of mixing model, especially for small d_S	True similarity
2	Test over complete range of nondimensional variables	Does not capture all interactions and coupling	Plant conditions sometimes outside range of mixing model	Parametric approach
3	Match all nondimensional variables except Re	Replace with U_T/U	Extrapolate in Re	Relatively new approach
4	Keep all properties constant	Test at more than one scale	Extrapolate in scale	Industrial approach

2.8 Test Design

This section summarizes factors and considerations involved in the experimental test design.

2.8.1 Approach

The following test design approach was used to ensure that robust models for rating metrics would be achieved by the test program.

- The conditions tested bracketed plant parameter ranges to the extent practical.
- Testing occurred at three scales to establish scale-up.
- Test variable ranges were extended so that test results are applicable to evaluating design improvements (such as large nozzles, more pulse tubes, etc.).
- Sufficient data were collected to develop models for rating metrics that, when applied to plant vessels, have reasonable uncertainty.
- Jet discharge characteristics were the same at all scales.
- The same instrumentation and measurement methods were used at all scales.

Shortly after the M3 testing program was planned, WTP needs changed to emphasize the importance of vessel HLP-22. In response, the original test design to evaluate each parameter at all three scales was modified to focus on the specific characteristics of HLP-22. This change reduced testing for parameters such as the number of PJM jets, nozzle diameters, particle densities, broad particle distributions, and similar parameters. A more limited set of these parameters was strategically tested to provide information for each parameter used in the models.

2.8.2 Constraints

The following are constraints that were considered when designing and conducting tests. They fall into three categories: time, material hazards, and capacity of the test apparatus. For small-diameter simulants, the settling time may increase the time between conducting sequenced test runs, and solids may begin to exhibit cohesive behavior. Exotic simulants increase the cost for procurement; exotic fluids increase costs associated with handling, test apparatus cleaning, and disposal. The test apparatus operating space also constrains the tests conducted. The PJM valve response characteristics limit the pulse time. The capacity of the PJMs limits the pulse duration. Additional limitations include the following:

- Use of low-viscosity liquids was not pursued due to hazards associated with these fluids in the PNNL test fixtures.
- Maximum fluid jet velocity limits on larger vessels are in the range of 14 m/s.
- Specific constraints related to the vessel scale also exist. The scale of the vessel and ancillary piping limited the height of the fluid in the test vessel.
- PJM flow capacity is limited at the large test scale, so smaller WTP vessel conditions cannot be tested.
- When testing at small scale, Reynolds number requirements prevent matching Froude number at low velocities; this precludes testing of the largest plant vessels in the small test vessel.
- Drive function limitations associated with valve response time in the large vessel (large valves) may limit some pulse durations. However, the test conditions conducted for this report were not limited by the valve response times of the three test systems.

2.8.3 Plant Variable Ranges

Table 2.7 gives a summary of the ranges of nondimensional variables associated with WTP mixing systems. The test parameter ranges were designed to bracket these conditions. The extent to which these ranges were bracketed in the test data used for developing models is discussed in Section 9.2.3.

Table 2.7. Preliminary Bracketing Noncohesive Property Ranges for the WTP[(a)]

Property	Symbol	Units	Minimum Value	Maximum Value
Slurry Properties				
Solids diameter[(b)]	$\mathbf{d_S}$	μm	10	1000
Solids volume fraction	$\boldsymbol{\phi_S}$	fraction	0.001	0.15
Density ratio	$\mathbf{s = \rho_s / \rho_l}$	ratio	1.5	11
Solids density[(c)]	ρ_s	*g/cm³*	*2.2*	*11*
Liquid density	ρ_l	g/cm³	1	1.4
Slurry density	ρ	g/cm³	1	2.7
Viscosity	μ	*cP*	*1*	*25*
Kinematic viscosity	$\nu = \mu/\rho_l$	m²/s	7.10E-07	2.50E-05
Settling velocity	U_T	*m/s*	*1.10E-06*	*1.80E-01*
Galileo number	$Ga_p = (s-1) g\, d_S^3 / \nu^2$	number	7.80E-06	1.90E+05
Particle Reynolds number	$Re_p = U_T\, d_S / \nu$	number	4.40E-07	7.30E+02
Particle Froude number	$F_p = U_T^2 / (g\, d_S)$	number	2.40E-08	2.80E+00
Geometric Configuration				
Vessel diameter	**D**	ft	9.5	47
Nozzle diameter ratio	**d/D**	number	0.007	0.07
Number PJMs	**N**	number	1	12
Number of PJMs in inner ring	$\mathbf{N_I}$	number	0	4
Number of PJMs in outer ring	$\mathbf{N_O}$	number	0	8
Operational Parameters				
Fill level ratio	**H/D**	number	0.32	1.6
Drive time	t_D	s	5.4	79
Duty cycle	**DC**	fraction	0.23	0.37
Pulse volume fraction	$\boldsymbol{\phi_p}$	fraction	0.0039	0.13
Jet velocity	**U**	m/s	8	13
Reynolds number	$Re = U\, d / \nu$	number	3.30E+04	3.40E+06
Froude number	$Fr = U^2 / (2g\, d)$	number	0.3	2.3
Particle ratio	d_S / d	number	4.90E-05	9.80E-03

(a) Data in Table 2.7 provided for information only.
(b) **Bold** = Test variable.
(c) *Italics* = Secondary variable.

3.0 Hanford Waste Properties and Simulant Selection

Properties that affect the mixing of noncohesive solids in liquid include the undissolved solids density, particle size, liquid density, and viscosity. A brief discussion of these parameters for Hanford waste is provided in Section 3.1. Simulant selection, characterization, and preparation are presented in Sections 3.2, 3.3, and 3.4, respectively.

3.1 Hanford Waste Properties

Wells et al. (2007) presents particle size and density distributions (PSDDs) based on the combination of particle size distributions (PSDs) of 19 Hanford sludge (i.e., non-saltcake waste) tanks and the insoluble solid-phase compounds from all 177 Hanford tanks. The Case 3 PSDD of Wells et al. (2007), which uses "minimal disturbance" PSDs and the crystal density of the solid phase, was selected as the basis for solid particle size and density.

The PSDD of Case 3 from Wells et al. (2007) is recommended by WTP Project Memorandum CCN 186332, from AW Etchells, Dupont Technology Consulting, to SA Saunders, BNI, on January 29, 2007, "Comments on the Input Particle Size Report," as "...the most accurate and most conservative" approach. While the Case 4 PSDD more accurately represents the understanding of the system—that is, the larger particulate beyond the maximum observed primary particle size consists of agglomerates with interstitial liquid, which have a lower density than the primary particulate (crystal density)—the lack of data to model the fractal relation for individual solid-phase compounds, much less for their interactions, results in an estimate for the fractal dimension used for the Case 4 PSDD. Case 3 is selected over Case 1 because the PSD for Cases 1 and 2 was developed from "sonicated" data. Per WTP Project Memorandum CCN 186332, sonification "...is a very high energy and irreproducible process." Further, sonication "...is much more energy intensive than pumping or mixing for many hours and is similar to grinding or milling."

The Case 3 PSDD is provided by Wells et al. (2007) as a 3-dimensional matrix of volume-based probability of each solid-phase compound in a PSD "bin" and its density in that bin (Tables 3.1 and 3.2). The PSD bins represent the upper and lower size limit of the particles associated with a given bin. Thus, the volume fraction of insoluble solid particulate at a given size and density is specified for the Hanford waste volume. For example, in Tables 3.1 and 3.2, it can be seen that gibbsite, $Al(OH)_3$, composes 51.5% of the Hanford insoluble solid particulate by volume, and that gibbsite particles greater than 7.7 and less than or equal to 10 μm have a density of 2.42 g/mL and compose 4% of the solids by volume.

To select representative solid simulants for mixing analysis based on the PSDD, the particle size and density are used in the settling velocity equations in Section 7.0. These are used in conjunction with the respective volume fraction to produce the cumulative volume-based probability of the settling velocity of Hanford insoluble solids in water (liquid density 1 g/mL, liquid viscosity, 1 cP). This cumulative probability distribution for settling velocity is shown in Figure 3.1, where the median (50th percentile) and 95th percentile settling velocities by volume are approximately 4.6E-5 and 3.8E-3 m/s, respectively. The volume-weighted average settling velocity ($\overline{U}$) is determined by Eq. (3.1).

Table 3.1. Case 3 PSDD (Wells et al. 2007)

Particle Size	Solid-Phase Compound Volume Fraction (refer to Table 3.2 for compound identification)															
(μm)	1	2	3	4	5	6	7	8	9	10	11	12	13	14	15	16
0.22	1E-04	5E-05	3E-05	3E-05	1E-05	6E-06	5E-06	3E-06	2E-06	2E-06	2E-06	2E-06	7E-07	4E-07	3E-08	4E-09
0.28	3E-04	1E-04	6E-05	6E-05	2E-05	1E-05	9E-06	6E-06	5E-06	4E-06	3E-06	3E-06	1E-06	8E-07	5E-08	8E-09
0.36	6E-04	2E-04	1E-04	1E-04	5E-05	2E-05	2E-05	1E-05	1E-05	8E-06	7E-06	7E-06	3E-06	2E-06	1E-07	2E-08
0.46	5E-05	2E-05	1E-05	1E-05	4E-06	2E-06	2E-06	1E-06	9E-07	7E-07	6E-07	6E-07	2E-07	1E-07	1E-08	1E-09
0.60	2E-03	5E-04	3E-04	3E-04	1E-04	6E-05	5E-05	3E-05	2E-05	2E-05	2E-05	2E-05	7E-06	4E-06	3E-07	4E-08
0.77	8E-03	3E-03	2E-03	1E-03	6E-04	3E-04	2E-04	2E-04	1E-04	1E-04	8E-05	8E-05	3E-05	2E-05	1E-06	2E-07
1.0	2E-02	5E-03	3E-03	3E-03	1E-03	6E-04	5E-04	3E-04	2E-04	2E-04	2E-04	2E-04	7E-05	4E-05	3E-06	4E-07
1.3	2E-02	6E-03	4E-03	4E-03	2E-03	8E-04	6E-04	4E-04	3E-04	3E-04	2E-04	2E-04	9E-05	5E-05	4E-06	5E-07
1.7	3E-02	1E-02	7E-03	6E-03	3E-03	1E-03	1E-03	7E-04	5E-04	4E-04	4E-04	3E-04	1E-04	8E-05	6E-06	8E-07
2.2	1E-02	5E-03	3E-03	3E-03	1E-03	5E-04	4E-04	3E-04	2E-04	2E-04	1E-04	1E-04	6E-05	4E-05	3E-06	4E-07
2.8	4E-02	1E-02	7E-03	6E-03	3E-03	1E-03	1E-03	7E-04	6E-04	5E-04	4E-04	4E-04	2E-04	9E-05	6E-06	9E-07
3.6	5E-02	2E-02	1E-02	9E-03	4E-03	2E-03	1E-03	1E-03	7E-04	6E-04	5E-04	5E-04	2E-04	1E-04	9E-06	1E-06
4.6	3E-02	1E-02	6E-03	6E-03	3E-03	1E-03	1E-03	7E-04	5E-04	4E-04	3E-04	3E-04	1E-04	8E-05	6E-06	8E-07
6.0	4E-02	1E-02	9E-03	8E-03	3E-03	2E-03	1E-03	9E-04	7E-04	6E-04	5E-04	4E-04	2E-04	1E-04	8E-06	1E-06
7.7	5E-02	2E-02	1E-02	9E-03	4E-03	2E-03	2E-03	1E-03	8E-04	7E-04	5E-04	5E-04	2E-04	1E-04	9E-06	1E-06
10	4E-02	1E-02	8E-03	7E-03	3E-03	2E-03	1E-03	9E-04	6E-04	5E-04	4E-04	4E-04	2E-04	1E-04	7E-06	1E-06
13	4E-02	1E-02	8E-03	7E-03	3E-03	1E-03	1E-03	8E-04	6E-04	5E-04	4E-04	4E-04	2E-04	9E-05	7E-06	9E-07
17	4E-02	1E-02	8E-03	7E-03	3E-03	2E-03	1E-03	8E-04	6E-04	5E-04	4E-04	4E-04	2E-04	1E-04	7E-06	1E-06
22	3E-02	1E-02	6E-03	6E-03	2E-03	1E-03	9E-04	6E-04	5E-04	4E-04	3E-04	3E-04	1E-04	8E-05	5E-06	8E-07
28	1E-02	5E-03	3E-03	3E-03	1E-03	6E-04	4E-04	3E-04	2E-04	2E-04	2E-04	2E-04	6E-05	4E-05	3E-06	4E-07
36	2E-02	6E-03	4E-03	4E-03	2E-03	8E-04	6E-04	4E-04	3E-04	3E-04	2E-04	2E-04	9E-05	5E-05	4E-06	5E-07
46	7E-03	2E-03	1E-03	1E-03	6E-04	3E-04	2E-04	1E-04	1E-04	9E-05	7E-05	7E-05	3E-05	2E-05	1E-06	2E-07
60	5E-03	1E-03	9E-04	8E-04	4E-04	2E-04	1E-04	1E-04	7E-05	6E-05	5E-05	5E-05	2E-05	1E-05	8E-07	1E-07
77	4E-03	1E-03	9E-04	8E-04	3E-04	2E-04	1E-04	9E-05	7E-05	6E-05	5E-05	4E-05	2E-05	1E-05	8E-07	1E-07
100	3E-03	9E-04	5E-04	5E-04	2E-04	1E-04	8E-05	6E-05	4E-05	4E-05	3E-05	3E-05	1E-05	7E-06	5E-07	7E-08
129	2E-03	6E-04	4E-04	3E-04	1E-04	7E-05	5E-05	4E-05	3E-05	2E-05	2E-05	2E-05	8E-06	4E-06	3E-07	4E-08
167	7E-03	2E-03	1E-03	1E-03	5E-04	3E-04	2E-04	1E-04	1E-04	9E-05	7E-05	7E-05	3E-05	2E-05	1E-06	2E-07
215	4E-03	1E-03	7E-04	7E-04	3E-04	1E-04	1E-04	8E-05	6E-05	5E-05	4E-05	4E-05	2E-05	9E-06	7E-07	9E-08
278	2E-03	7E-04	4E-04	4E-04	2E-04	8E-05	6E-05	4E-05	3E-05	3E-05	2E-05	2E-05	9E-06	5E-06	4E-07	5E-08
359	3E-03	1E-03	6E-04	5E-04	2E-04	1E-04	9E-05	6E-05	5E-05	4E-05	3E-05	3E-05	1E-05	7E-06	5E-07	8E-08
464	6E-04	2E-04	1E-04	1E-04	5E-05	2E-05	2E-05	1E-05	1E-05	9E-06	7E-06	7E-06	3E-06	2E-06	1E-07	2E-08
599	4E-04	1E-04	8E-05	7E-05	3E-05	1E-05	1E-05	8E-06	6E-06	5E-06	4E-06	4E-06	2E-06	1E-06	7E-08	1E-08
774	4E-04	1E-04	9E-05	8E-05	3E-05	2E-05	1E-05	9E-06	7E-06	6E-06	4E-06	4E-06	2E-06	1E-06	8E-08	1E-08
1000	3E-05	9E-06	6E-06	5E-06	2E-06	1E-06	8E-07	6E-07	4E-07	4E-07	3E-07	3E-07	1E-07	7E-08	5E-09	7E-10

Table 3.2. Solid Phase Compound Density, Volume Fraction, and Numerical Identification for Case 3 PSDD (Wells et al. 2007)

Solid-Phase Compound	Crystal Density (g/mL)	Volume Fraction	Numerical Identification
$Al(OH)_3$, Gibbsite	2.42	0.515	1
$(NaAlSiO_4)_6 \bullet (NaNO_3)_{1.6} \bullet 2H_2O$	2.365	0.166	2
AlOOH, Boehmite	3.01	0.106	3
$NaAlCO_3(OH)_2$	2.42	0.095	4
Fe_2O_3	5.24	0.041	5
$Ca_5OH(PO_4)_3$	3.14	0.020	6
$Na_2U_2O_7$	5.617	0.016	7
ZrO_2	5.68	0.011	8
Bi_2O_3	8.9	0.0081	9
SiO_2	2.6	0.0069	10
$Ni(OH)_2$	4.1	0.0055	11
MnO_2	5.026	0.0054	12
CaF_2	3.18	0.0023	13
$LaPO_4 \bullet 2H_2O$	6.51	0.0013	14
Ag_2CO_3	6.077	0.000094	15
PuO_2	11.43	0.000013	16

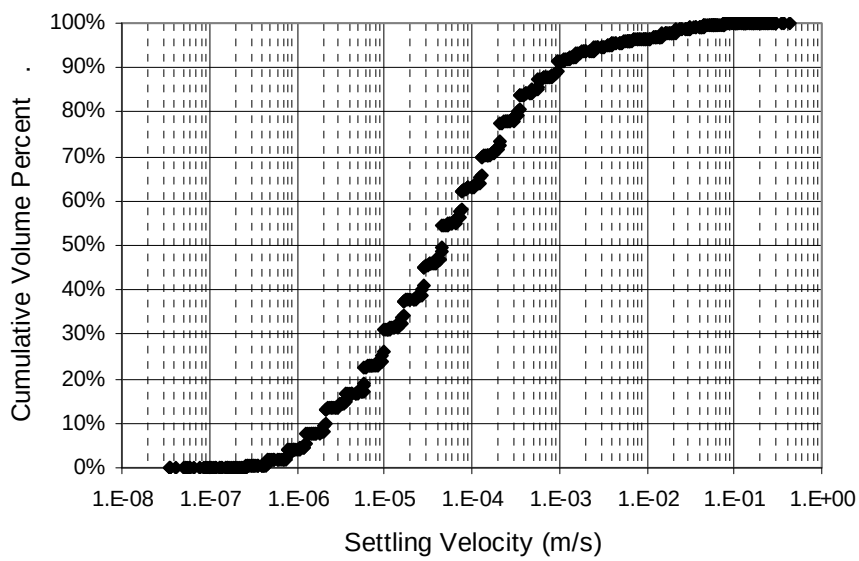

Figure 3.1. Cumulative Undissolved Solid Volume Percent as Function of Settling Velocity for Case 3 PSDD (Wells et al. 2007)

$$\bar{U} = \frac{\sum_{i=1}^{n} x_i U_i}{\sum_{i=1}^{n} x_i} \tag{3.1}$$

where x_i is the volume fraction of the ith solid relative to the total solid volume, U_i is the settling velocity of the ith solid, and n is the number of entries in the PSDD (particle size bins multiplied by the number of solid phase compounds).[1]

The volume-weighted average settling velocity is independent of the summation order (i.e., $\overline{U}$ may be computed by summation from either the minimum or maximum settling velocity). However, the volume-weighted average settling velocity of a specific volume fraction of the solid particles is dependent on the specific volume fraction. That is, one may consider the cumulative volume-weighted average settling velocity of, for example, 10% by volume of either the slowest- or fastest-settling solid particles. For the latter consideration, the volume-weighted average settling velocity is determined via Eq. (3.1) with *n* set such that the fastest settling 10% of the solid particles by volume are included in the summation.

The cumulative volume-weighted average settling velocity summed from the fastest-settling solid particulate is shown in Figure 3.2. The plot is interpreted as the volume-weighted average settling velocity of the indicated fraction of the solid particles. For example, to determine the cumulative volume-weighted average settling velocity for the fastest-settling 10% by volume of the solid particles, read the value corresponding to the curve at the 10% value for cumulative volume fraction. Necessarily, the summation over 100% of the solid particulate results in $\overline{U}$. The cumulative volume fraction of Figure 3.2 illustrates that the cumulative volume-weighted average settling velocity for the fastest-settling 10% by volume of the solid particles is the 90th percentile of the cumulative volume-weighted average settling velocity summed from the fastest-settling solid particulate. Thus, the cumulative volume-weighted average settling velocity of the fastest-settling 10% of the solid particulate by volume is denoted by $\overline{U}_{90}$.

From Figure 3.2, $\overline{U}_{90}$ is approximately 1.4E-2 m/s. Case 3 PSDD settling velocity percentiles from Figures 3.1 and 3.2 are listed in Table 3.3. Altering the base liquid from water to a fluid with 1.1 g/mL density and 1.5 cP viscosity reduces the Case 3 PSDD settling velocity for all percentiles (Table 3.4).

The cumulative volume-weighted average settling velocity is an important physical quantity. A homogenous polydispersed system of solids in a liquid will settle with volume flux ($\overline{U}C$), where C is the solids volume concentration. For the Hanford Case 3 PSDD, $\overline{U} > U_{90}$ (Table 3.4). Also if vertical segregation is present in a mixing vessel, the fastest settling particulate will be at lower vessel elevations. Thus, the characteristic settling velocity in that region of the vessel will exceed $\overline{U}$.

[1] The binning of the PSDD affects a volume-weighted average computed using Eq. (3.1). For example, if particle size is considered instead of settling velocity, and one bin represents the entire distribution, the volume-weighted average is the maximum particle size. If the PSDD is binned so each particle size has a specific bin, the volume-weighted average is at its minimum. Thus, to provide a representative volume-weighted average, a minimum number of bins are required. Caution must be taken in applying Eq. (3.1) to ensure that binning is appropriate.

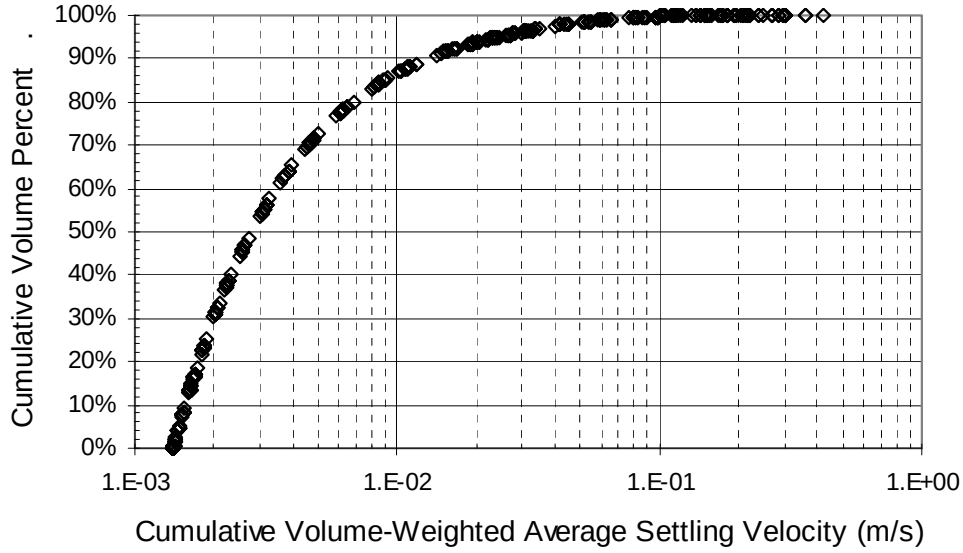

Figure 3.2. Cumulative Undissolved Solid Volume Percent as Function of Cumulative Volume Weighted Average Settling Velocity for Case 3 PSDD (Wells et al. 2007)

Table 3.3. Hanford Insoluble Solid Settling Velocity Percentiles for Case 3 PSDD (Wells et al. 2007)

Percentiles (%)	Settling Velocity (m/s)	Volume-Weighted Average Settling Velocity (m/s)[(a)]
5	1.2E-06	1.5E-03
10	2.2E-06	1.6E-03
25	9.5E-06	1.9E-03
50	4.6E-05	3.0E-03
55	6.4E-05	3.2E-03
60	7.7E-05	3.6E-03
65	1.2E-04	4.0E-03
70	1.3E-04	4.6E-03
75	2.1E-04	5.8E-03
80	3.4E-04	6.8E-03
85	5.0E-04	8.9E-03
90	9.5E-04	1.4E-02
95	3.8E-03	2.4E-02
99	4.1E-02	6.3E-02
Volume Weighted Average	1.4E-03	1.4E-03
Minimum	3.5E-08	1.4E-03
Maximum	4.2E-01	4.2E-01

(a) Summed from fastest-settling solid particulate.

Table 3.4. Hanford Insoluble Solid Settling Velocity Quantiles: 1.1 g/mL and 1.5 cP Liquid Density and Viscosity, Case 3 PSDD (Wells et al. 2007)

Percentiles (%)	Settling Velocity (m/s)	Volume-Weighted Average Settling Velocity (m/s)[a]
5	7.6E-07	1.1E-03
10	1.3E-06	1.2E-03
25	5.8E-06	1.4E-03
50	2.9E-05	2.2E-03
55	3.9E-05	2.3E-03
60	4.8E-05	2.6E-03
65	7.5E-05	2.9E-03
70	8.5E-05	3.4E-03
75	1.3E-04	4.3E-03
80	2.1E-04	5.0E-03
85	3.2E-04	6.5E-03
90	6.0E-04	1.0E-02
95	2.5E-03	1.8E-02
99	3.1E-02	4.9E-02
Volume-Weighted Average	1.0E-03	1.0E-03
Minimum	2.1E-08	1.0E-03
Maximum	3.8E-01	3.8E-01

(a) Summed from fastest-settling solid particulate.

3.2 Selection of Slurry Property Ranges

Solid particle simulants were selected to permit evaluation of mixing performance over a range of operating conditions. Physical properties of density and size distribution were considered. Initial particles selected were commercially available glass beads with a relatively broad size distribution. Tests in 2007 were conducted with these solids. To gain additional insight into the effect that the size distribution of the 2007 simulant on mixing parameters, particles with a much narrower size distribution were selected for the 2008 tests. The testing system limited the use of very small and low density particles because these particles would be removed from the testing tank by the pump inlet at the top of the tank. See Section 4.0 for system description. Section 8.1.3 discusses why the larger/heavier particles with faster settling velocities are the controlling waste characteristics when stratification is present.

The property ranges for these simulants are summarized in Table 3.5, where values bound the ranges used during testing with noncohesive simulants.

Table 3.5. Bracketing Noncohesive Particle Test Ranges

Property	Symbol	Units	Test Range Minimum Value	Test Range Maximum Value
Solids size (d_{50})	d_S	μm	44	766
Solids density	ρ_s	g/cm^3	2.45	4.18
Volume weighted average settling velocity (see Section 7.0 and Eq. 3.1)	U_T	m/s	0.0017	0.11

Testing identified settling velocity as a parameter with a significant effect on mixing performance. The settling velocity range of the particles used is compared with that of PSDD Case 3. Settling

velocities for the PSDD Case 3 and simulants used in this program are plotted in Figure 3.3 and the volume-weighted average settling velocities summed from the fastest-settling particulate for both in Figure 3.4. The volume-weighted average settling velocity of the particles used in testing spans the range expected in PSDD Case 3.

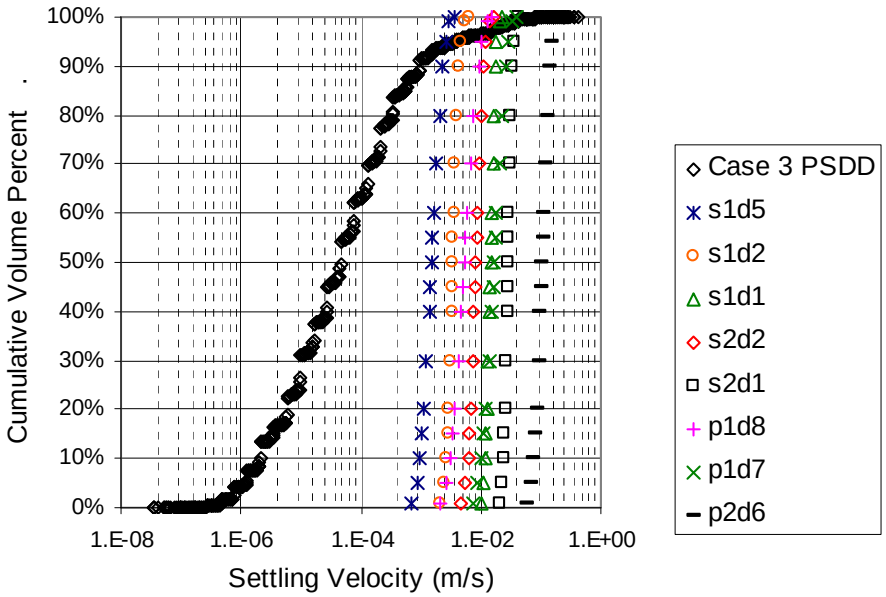

Figure 3.3. Cumulative Volume Percent as a Function of Settling Velocity for Hanford PSDD Case 3 and Simulants (see Table 3.6 for Simulant Identification)

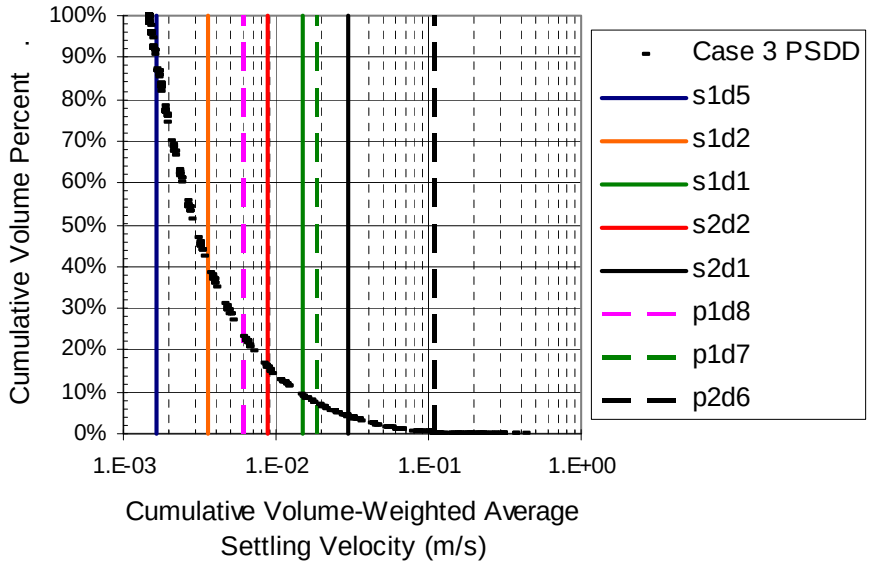

Figure 3.4. Cumulative Volume Percent as a Function of Cumulative Volume-Weighted Average for Hanford PSDD Case 3 and Simulants (see Table 3.6 for Simulant Identification)

3.3 Characterization Techniques

Standard procedures were used to characterize particle density, packing fraction, and particle size, as described in the following subsections. Uncertainties of the measured parameters are provided in Section 6.1.

3.3.1 Density Measurement Technique

Particle density was determined by water displacement using a calibrated pycnometer. The procedure involves adding a known mass of beads to a calibrated pycnometer and determining the volume of water displaced by the beads. From this, density is readily obtained.

3.3.2 Packing Fraction Measurement Technique

The packing fraction of the beads in water was determined by adding a known mass of beads to a measuring cylinder with a known volume of deionized water. The beads were allowed to settle for 72 hours, and the final volume was measured. The void fraction of the beads was calculated using the settling volume in deionized water from which the packing fraction was calculated. The packing fraction (ϕ_{max}) is defined as one minus the void fraction.

3.3.3 Particle Size Measurement Technique

PSDs were obtained using a Malvern[1] Mastersizer 2000 with a Hydro G dispersion unit, which uses laser diffraction to obtain the PSD. Six measurements were used to obtain the average PSDs used throughout this report. Optimum measuring conditions were investigated whereby the pump and stirrer speed as well as sonication level were manipulated to ensure that the beads were well dispersed and an accurate, reproducible PSD was obtained. Subsampling is very important when measuring PSD; special care was taken when handling the dry glass beads to obtain a representative sample for analysis in accordance with TPR-RPP-WTP-626 Rev. 0. See Section 5.0 for specific test instruction references.

3.3.4 Simulant Selection and Characterization

The simulant parameters used to characterize the solids used during the mixing tests were particle size (d_S) and particle density (ρ_s). Two materials were chosen based on density: soda-lime glass with a density of approximately 2.5 g/cm^3 (denoted as "s1") and a high-density glass with a density of 4.2 g/cm^3 (denoted as "s2"). Tests were conducted using two types of PSDs: a broad size distribution for tests conducted in 2007 and a narrow size distribution for tests conducted in 2008.

Three sizes of Potters[2] BALLOTINI™ impact beads,[3] (designation 3, 8, and 12 in Table 3.6), were used during the 2007 tests. Three sizes of particles were manufactured by XL Science and Technology[4] specifically for the tests conducted in 2008. These particles were made using the same manufacturing

[1] Malvern Instruments Ltd., Worcestershire, UK, www.malvern.com.
[2] Potters Industries Inc, www.pottersbeads.com.
[3] http://www.pottersbeads.com/Literature/HiIndex--BallotiniBeads.pdf.
[4] XL Science and Technology, Richland, Washington.

platform to obtain particles of different density and size with similar physical attributes such as PSD, particle shape, and surface properties. Given that commercially available beads have a specific industrial use in which particle size range is considered along with density, but the distribution of size is usually not a concern, the custom manufacturing of the beads enabled us to specify the consistency of the PSD. The shape (spherical nature) and surface properties of the particles were also considered when selecting the particles, along with the purity of the beads. To eliminate the mixing effects of irregularly shaped angular particles that can be present in low-grade beads, spherical particles free of surface irregularities and raw materials were chosen. The ability to reuse the beads was also a consideration when selecting the simulant composition.

3.3.4.1 As-Received

The as-received density and PSD were measured for all simulants before use, and samples were archived for future reference. Scanning electron microscopy (SEM) was also used to visually inspect the surface of the beads and identify any surface changes resulting from the drying and reuse of the beads during the course of testing. The as-received PSDs are given in Table 3.6 along with the density for both the XLSciTech and the Potters beads. In Table 3.6 and subsequently throughout the report, the solid particle simulants are designated by sxdx (where sx and dx are defined in Table 3.6). The nominal particle size as per the specifications provided by Potters Industries is also given in parentheses for all three Potters beads used previously.

Pictures obtained from SEM are shown in Figures 3.5 and 3.6 for both XLSciTech and Potters beads. The SEM images of the XLSciTech beads in Figure 3.5(a) through 3.5(d) show that the beads are free of dust and raw materials used during production. The shape and surface properties of these particles are well illustrated in Figure 3.5. The smaller soda-lime beads used in simulant s1d5 are shown in Figure 3.6(a). The presence of raw materials used to manufacture the beads (irregular, angular particles) is noted. These beads are of lower grade than the other beads used in this study that were manufactured by XLSciTech; they were manufactured with a broader PSD that was reduced by sieving through a 45 μm sieve. Unlike the beads in Figure 3.5(a) through (d), the s1d5 simulant has some surface irregularities, holes, and small particulate matter adhered to the surface of the beads. Figure 3.6(b) through (d) shows SEM images of the Potters beads used in the 2007 tests. These beads are inexpensive beads manufactured for the metal finishing industry. From SEM images of the Potters beads, we can see that the larger beads, shown in Figure 3.6(b), are free of raw material, particulate matter, and dust. The honeycomb surface that can be seen on one of the beads results from the formation of surface bubbles during bead manufacturing. The white coating visible on one of the beads is also a contamination resulting from raw materials used. The smaller Potters beads, shown in Figure 3.6(c) and (d), appear to have small dust particles on the surface and raw material particles are present in increasing amounts with decrease in bead size. Smaller microspheres are more difficult to manufacture; the presence of irregular particles and conjoined beads is typical of low-grade beads in this size range.

The volume percent passing has been plotted as a function of the particles size for a given volume percent d(vol%) normalized by the mean particle size (d_{50}) in Figure 3.7 for both XLSciTech and Potters beads. From this plot we are able to determine the PSD of the beads around the mean value. The four simulants, s1d1, s1d2, s2d1, and the s2d2, have narrower distributions around the particle mean size than the Potters beads and the s1d5 simulant.

Table 3.6. Simulant Characterization: As-Received, Post-Test, and Average Values

Simulant	Density g/cm^3	Packing Fraction	Condition	d(0.01) µm	d(0.05) µm	d(0.10) µm	d(0.20) µm	d(0.30) µm	d(0.40) µm	d(0.50) µm	d(0.60) µm	d(0.70) µm	d(0.80) µm	d(0.90) µm	d(0.95) µm	d(0.99) µm
s1d1	2.46	0.59	as received	134.8	142.8	147.7	153.8	158.3	162.4	166.4	170.6	175.2	180.7	188.7	195.1	205.7
XLSciTech			post test	132.6	140.0	145.6	153.6	158.6	162.8	166.8	171.0	175.6	181.1	189.0	195.5	208.2
XLSL150180			average	133.7	141.4	146.6	153.7	158.4	162.6	166.6	170.8	175.4	180.9	188.8	195.3	207.0
s1d2	2.48	0.63	as received	53.9	56.9	59.8	63.5	65.7	67.5	69.3	71.2	73.2	75.7	79.2	82.1	89.7
XLSciTech			post test	53.6	56.6	59.4	63.3	65.5	67.4	69.2	71.1	73.2	75.7	79.2	82.3	90.3
XLSL063075			average	53.7	56.7	59.6	63.4	65.6	67.5	69.3	71.1	73.2	75.7	79.2	82.2	90.0
s1d5	2.50	0.60	as received	30.2	32.8	35.0	37.6	39.8	41.8	43.9	46.0	48.2	51.0	55.5	58.5	62.6
XLSciTech			post test	30.2	32.9	35.2	37.8	40.1	42.2	44.4	46.7	49.2	52.2	56.3	59.5	64.6
XLSL038063			average	30.2	32.8	35.1	37.7	39.9	42.0	44.1	46.3	48.7	51.6	55.9	59.0	63.6
(sieved <45 µm)																
s2d1	4.17	0.60	as received	132.3	139.9	144.8	151.2	156.0	160.1	164.2	168.3	172.8	178.2	185.9	192.4	203.5
XLSciTech			post test	134.9	142.4	147.0	152.9	157.1	160.9	164.5	168.3	172.3	177.1	184.2	190.1	200.6
XLHD150180			average	133.6	141.1	145.9	152.0	156.5	160.5	164.4	168.3	172.5	177.6	185.1	191.3	202.0
s2d2	4.18	0.63	as received	55.7	60.9	64.1	67.6	70.4	73.0	75.6	78.2	81.1	84.6	89.3	93.1	102.1
XLSciTech			post test	56.0	61.6	64.6	68.1	70.9	73.6	76.2	78.8	81.8	85.2	89.9	93.7	103.4
XLHD067080			average	55.8	61.3	64.3	67.8	70.7	73.3	75.9	78.5	81.4	84.9	89.6	93.4	102.8
p1d8	2.45	0.57	as received	52.8	60.5	65.7	72.8	78.6	84.0	89.5	95.2	101.6	109.6	122.4	132.0	151.2
Potters			post test													
Ballotine - 12			average													
p1d7	2.45	0.57	as received	106.3	121.3	131.4	145.4	156.8	167.4	178.0	189.2	201.9	217.7	240.7	260.6	296.0
Potters			post test													
Ballotine - 8			average													
p2d6	2.46	0.59	as received	455.9	518.4	559.0	624.5	673.1	718.9	766.2	817.8	877.1	952.1	1067.8	1172.9	1376.9
Potters			post test													
Ballotine - 3			average													

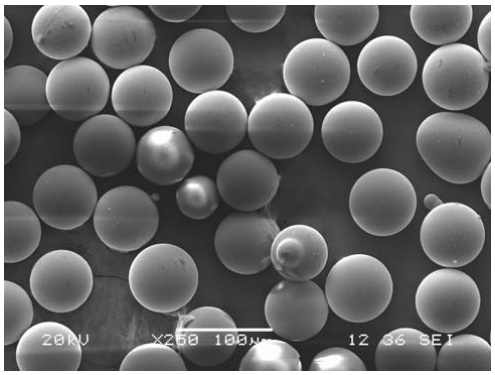

(a) s1d2 Soda-Lime Glass XLSciTech

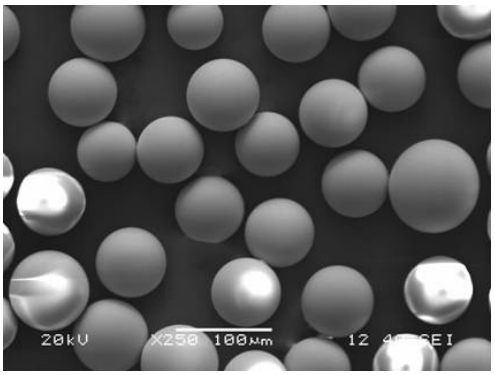

(b) s2d2 High-Density Glass XLSciTech

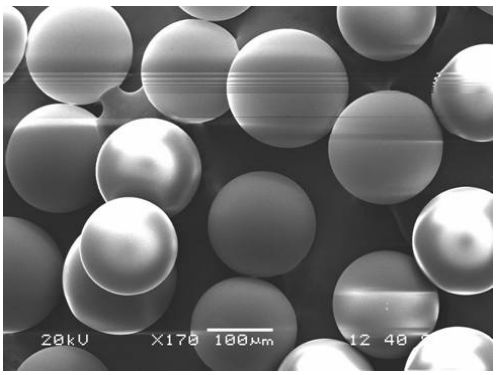

(c) s1d1 Soda-Lime Glass XLSciTech

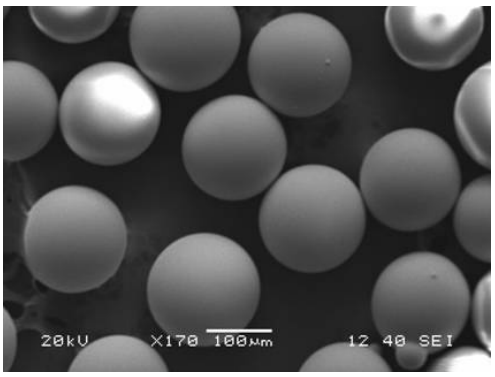

(d) s2d1 High-Density Glass XLSciTech

Figure 3.5. XLSciTech As-Received Beads; (a) s1d2, (b) s2d2, (c) s1d1, and (d) s2d1

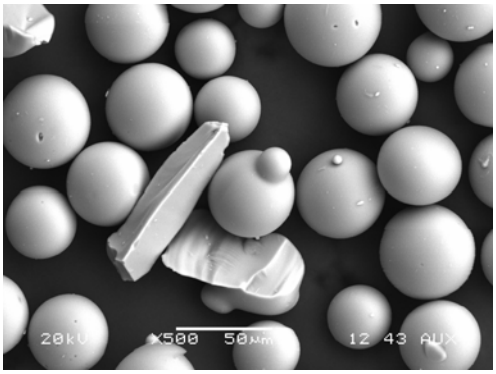

(a) s1d5 Soda-Lime Glass XLSciTech

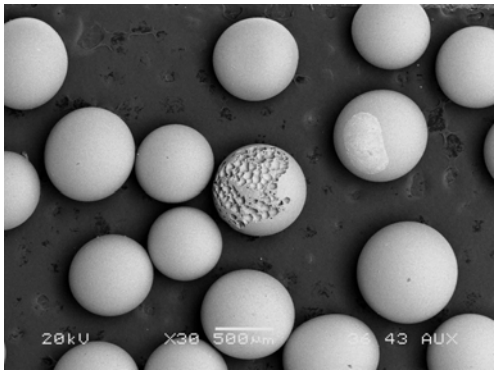

(b) p2d6 Potters #3 Soda-Lime Glass 600-850 µm

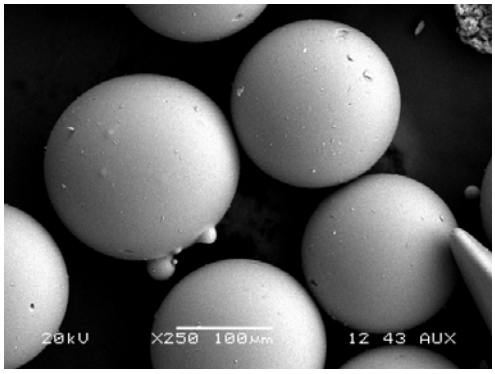

(c) p1d7 Potters # 8 Soda-Lime Glass 150-212 µm

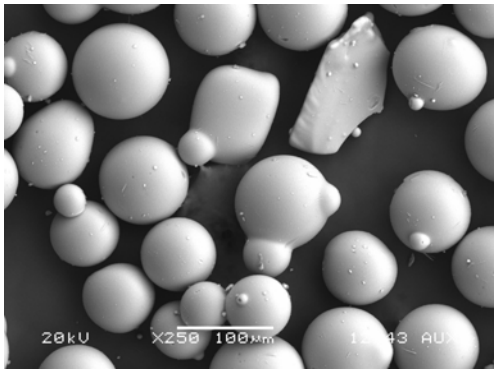

(d) p1d8 Potters #12 Soda-Lime Glass 63-106 µm

Figure 3.6. As-Received Beads; (a) s1d5, (b) #3 p2d6, (c) #8 p1d7, and (d) #12 p1d8

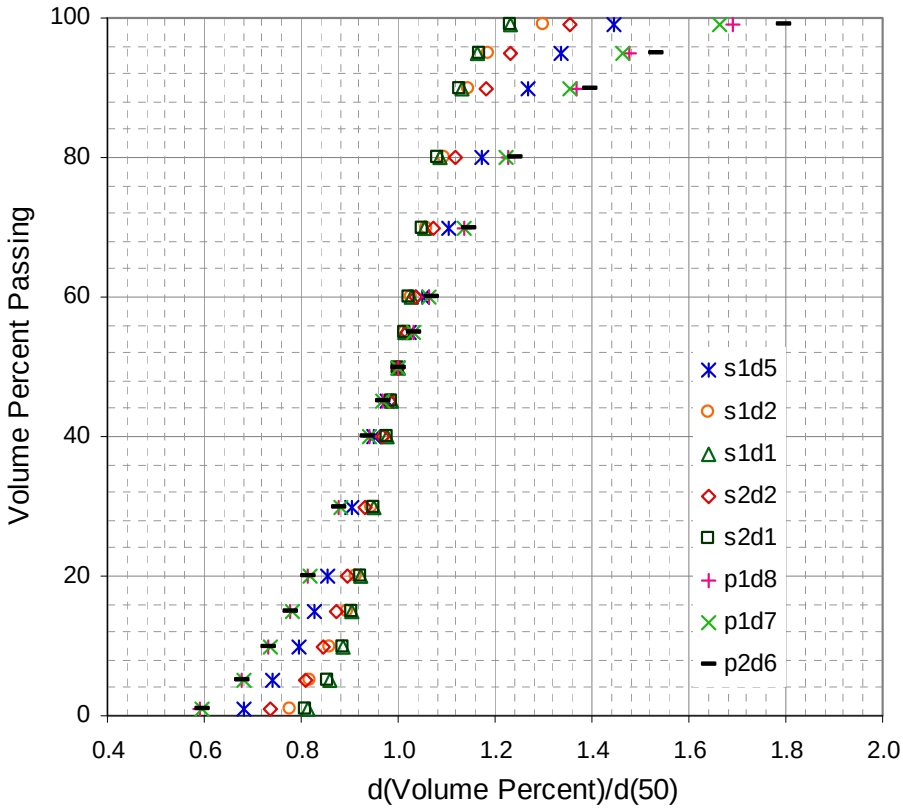

Figure 3.7. PSD Around the Mean Particle Size of XLSciTech Microspheres and Potters Beads

3.3.4.2 Post Test

Once simulants were removed from the tanks after testing, they were oven dried, and PSD measurements were performed before reusing the beads as a simple, quick technique to determine whether the beads were changing due to the test conditions or from the drying process. The acceptance criterion implemented for the PSD measurements of the used beads was based on the method used to verify the instrument performance check. If the d_5, d_{50}, and d_{95} values all fell within ± 10% of the as-received simulant values (Table 3.6), they were accepted for further use. The acceptance criterion for a check standard on the MS2000 using the Hydro G dispersion unit is ±5 (lower end) to 3% (upper end). The moisture content of the simulant was also measured to verify that the beads were dry and ready to be reused. The s1d2 beads were used and dried multiple times in all three test tanks. It was observed during testing in the large-scale [1.78 m (70 in.)] tank, that if the s1d2 simulant was left overnight to settle at higher concentrations (>1.43%) it was difficult to restart the PJMs the next day, and tubes were often plugged with beads. This phenomenon was not observed while testing in the mid-scale [0.864 m (34 in.)] tank. A SEM image of the s1d2 beads was taken during this test to ensure that the observations were not due to simulant fouling; at this point the simulant had been used and dried once. The SEM images obtained on the dried beads are given in Figure 3.8(a) through (d). Note the difference in observation scale to Figures 3.5 and 3.6. The SEM images revealed that there were some bead clumps present and that crystals had formed on some of the beads. Clumped beads were readily dispersed on wetting, which was confirmed by observing the wet beads under an optical microscope. The difficulty in restarting the PJMs was not due to the presence of bead clumps found on dried, reused particles because minimal energy was required to disperse the clumped beads.

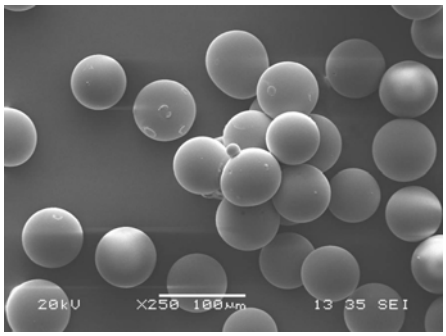

(a) s1d2 Beads Removed from Large-Scale Vessel During Testing

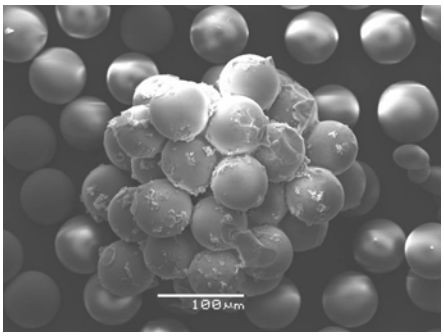

(b) s1d2 Beads After Testing in the Mid-Scale Vessel

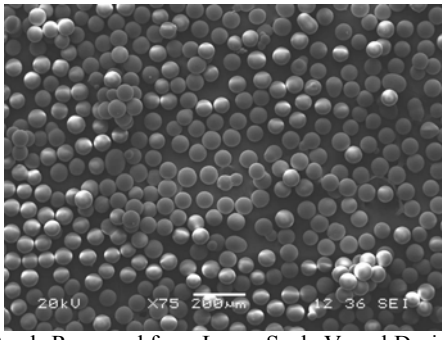

(c) s1d2 Beads Removed from Large-Scale Vessel During Testing

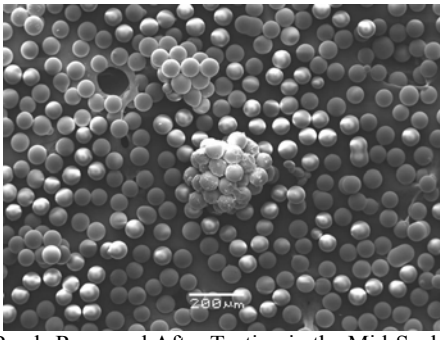

(d) s1d2 Beads Removed After Testing in the Mid-Scale Vessel

Figure 3.8. SEM Pictures of Reused s1d2 Beads Removed During Testing

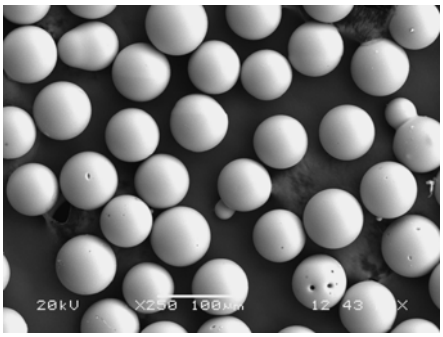

(a) s1d2 Soda-Lime Glass, XLSciTech

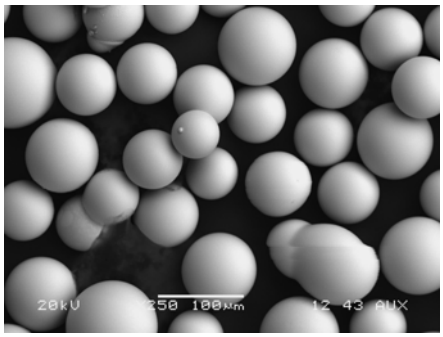

(b) s2d2 High-Density Glass, XLSciTech

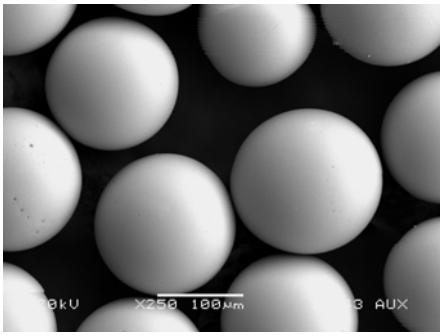

(c) s1d1 Soda-Lime Glass, XLSciTech

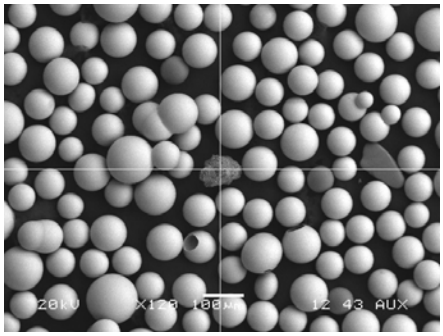

(d) s2d2 High-Density Glass, XLSciTech

Figure 3.9. SEM Images of XLSciTech Microspheres at the Completion of Testing

It is not clear whether the bead clumping was due to slight dissolution of the soda-lime glass and surface precipitation during drying or to the cleaning product used on the inside of the large-scale tank wall (before initial use) being removed by the beads during testing, forming a thin coating on some of the beads. The difficulty restarting the PJMs at high bead concentrations was not observed while testing in the mid-scale tank because of the dual-shift operation and short test times, as well as the fact that higher concentrations of beads were not left overnight as they were routinely for the large-scale system. Nor was this observed in the small-scale [nominal 0.38 m (15 in.)] tank due to changes in the startup process that were necessary to clear air out of the nozzles prior to testing; this process ran continuous flows through each nozzle individually to clear entrained air before testing. It was noted, however, that metal particles from the pumps used during testing, especially from the large-scale tank, were present and visible in the simulant when removed from the tank. These particles tended to concentrate at the surface of the beads in the drying pans and were removed where possible. The metal particles were clearly visible to the observers, who were able to distinguish the simulant from metal during testing. The quantity of metal in the simulant was minute compared to the amount of simulant in the tanks. SEM images were taken at the end of testing and are given in Figure 3.9. A foreign particle is observed in Figure 3.9(d). Energy dispersive spectroscopy of the material revealed aluminum as the major component with a small amount of iron. No calcium or sodium was detected. The post-testing SEM images reveal that the simulants remained intact after multiple drying cycles and tests. In Figure 3.9(a), the s1d2 simulant used the most during testing no longer has any clumps, as observed initially during testing in the large-scale tank. The only minor observation is that some of the particles appear to have small holes in the surface, most likely due to a small particle originally adhered to the surface wearing off during testing.

The post-test PSD data are given in Table 3.6. These values are the average of all the PSD analyses of the simulants as received and during testing, between tests after each drying cycle. If we consider the values for d_{05}, d_{50}, and d_{95} for all of the simulants, the difference between the as-received values obtained before testing and after testing all fall well within the limitations of reproducibility of the instrument, with the greatest difference less than 2%.

3.3.4.3 Recommended Values for Analysis

The recommended particle size values for use in analyzing the mixing test data are given in Table 3.6. No change in PSD was observed between the as-received and post-test simulants.

3.3.5 Simulant Scaling

Nondimensional plots of all simulants for comparison of PSDs are shown in Figure 3.7.

3.4 Simulant Preparation

Tests were conducted with water and commercially available particulate (spherical glass beads). The solids were used in their as-received state. No additional segregation or manipulation of particle size of the received materials was conducted. No drying or sieving of the materials was generally required for as-received materials.[1] Drying was used for reclaimed materials in the 2008 tests (24 hr at 100°C was typical). Drying was verified by taking a representative subsample following the drying period and

[1] One simulant, s1d5, was sieved to obtain the desired PSD (see Section 3.3.4.1).

verifying the moisture content. Drying was considered complete when a subsample moisture content reading of 1% or less had been obtained.

The inventory of simulant added to the test tank was recorded in the laboratory record book (LRB). During the test program, additions of solid simulant were made to the tank following previously executed test runs to increase the solids volume fraction. Water was added as needed to maintain the required fill level. The water used was from the Applied Process Engineering Laboratory (APEL) facility process or potable water lines and hence was chlorinated. Small amounts of biocide were added to the tanks during testing to prevent algae and bacteria. The addition of biocide was not considered quality effecting and was added to the tank systems as per the label directions provided by the manufacturer (Mt Hood Biocide[1]).

3.4.1 Water Addition and Removal

The supernatant is the liquid phase of the simulant in the tank; only water was used as the supernatant for testing described in this report. The liquid inventory was monitored by taking measurements of the water fill level of the tank. Water was added to the tank as needed to bring the total fluid level up to the specified level. The water used was from the APEL facility process or potable water lines.

3.4.2 Solids Addition and Removal

The following describes addition of solids to the test vessel. Any calculation of the solids volume fraction within the test tank assumes there is no holdup of solids within the drive system plumbing.

- The mass of solids prior to the addition was determined based on previous LRB entries and entered into the LRB, including the cross reference to the prior entry.
- The total mass of solids was determined after adding solids and the results entered in the LRB.

When it was necessary to remove solids before a test system change, such as changing to a different simulant, the majority of the water was decanted and the wet solids dispositioned, either dried and reclaimed or discarded as appropriate. Samples were obtained periodically for archive and post-test measurements.

[1] Mt. Hood Chemical Corporation material safety data sheet, product name: Mt. Hood 480, Portland, Oregon.

4.0 Experimental Equipment

The configuration of the equipment used during the scaled mixing tests is described in this section. Section 4.1 gives an overview of the multiscale test systems. This section also describes the approach used to compensate for impingement angle when the HLP-22 vessel has a different bottom shape than the test tank.

Design details for the small-scale test stand are described in Section 4.2, the mid-scale test stand in Section 4.3, and the large-scale test stand in Section 4.4. Key elements of the test stands are the vessel size, differences in the drive systems versus the PJMs, and the bottom shapes available with each test stand. The method to generate pulsating flow is described in Section 4.5. Instrumentation and data acquisition are described in Sections 4.6 and 4.7, respectively.

The configuration of the pulse jet arrays and nozzles tested is described in Section 4.8. Key elements in this discussion include the different nozzle array configurations and tube numbers used, different nozzle sizes used, and an illustration of the impingement angles of the jets for the different shaped heads (bottoms).

4.1 Modeling Tank HLP-22 Configuration

Figure 4.1 is a schematic of the conceptual arrangement of the test systems. Tests were conducted in three test systems (small-, mid-, and large-scale) using acrylic tanks with diameters of 0.367, 0.86, and 1.78 m (14-$^{7}/_{16}$, 34, and 70 in.), respectively. Four different test tank head[1] (bottom) profiles were prepared: flat, 100-to-6 F&D, semi-elliptical, and spherical.

The small-scale system includes three tanks that can be used one at a time. Each of the three small-scale tanks has a different bottom profile: one has a flat head, one has a 2:1 elliptical head, and one has a 100-to-6 F&D head. Only the 2:1 elliptical-headed small-scale tank was used during the tests described in this report.

The bottom of the mid-scale test vessel was understood to be a 2:1 elliptical head; however, post-test measurements and analysis of the tank more accurately characterized the head as a spherical segment (called spherical in this report) with a radius of curvature of approximately 0.51 m (20 in.) (FIO)[2] and a 0.229 m (9 in.) depth. Therefore, the mid-scale tank is not completely geometrically similar to the small-and large-scale tanks.

The large-scale tank system has two heads (elliptical and F&D) that can be exchanged using a flanged connection. Both heads are made of steel and modified with acrylic ports at bottom center for viewing. A visual comparison of the 100-to-6 F&D head and a 2:1 semi-elliptical head is provided in Figure 4.2.

[1] The tank "head" is the bottom surface of the tank. For the small- and mid-scale tanks, the head is integral to the tank. For the large-scale tank, the head is interchangeable by placing the 70-in. acrylic tube on the either the F&D or elliptical heads.
[2] FIO data are included for information only and do not necessarily meet NQA1 standards.

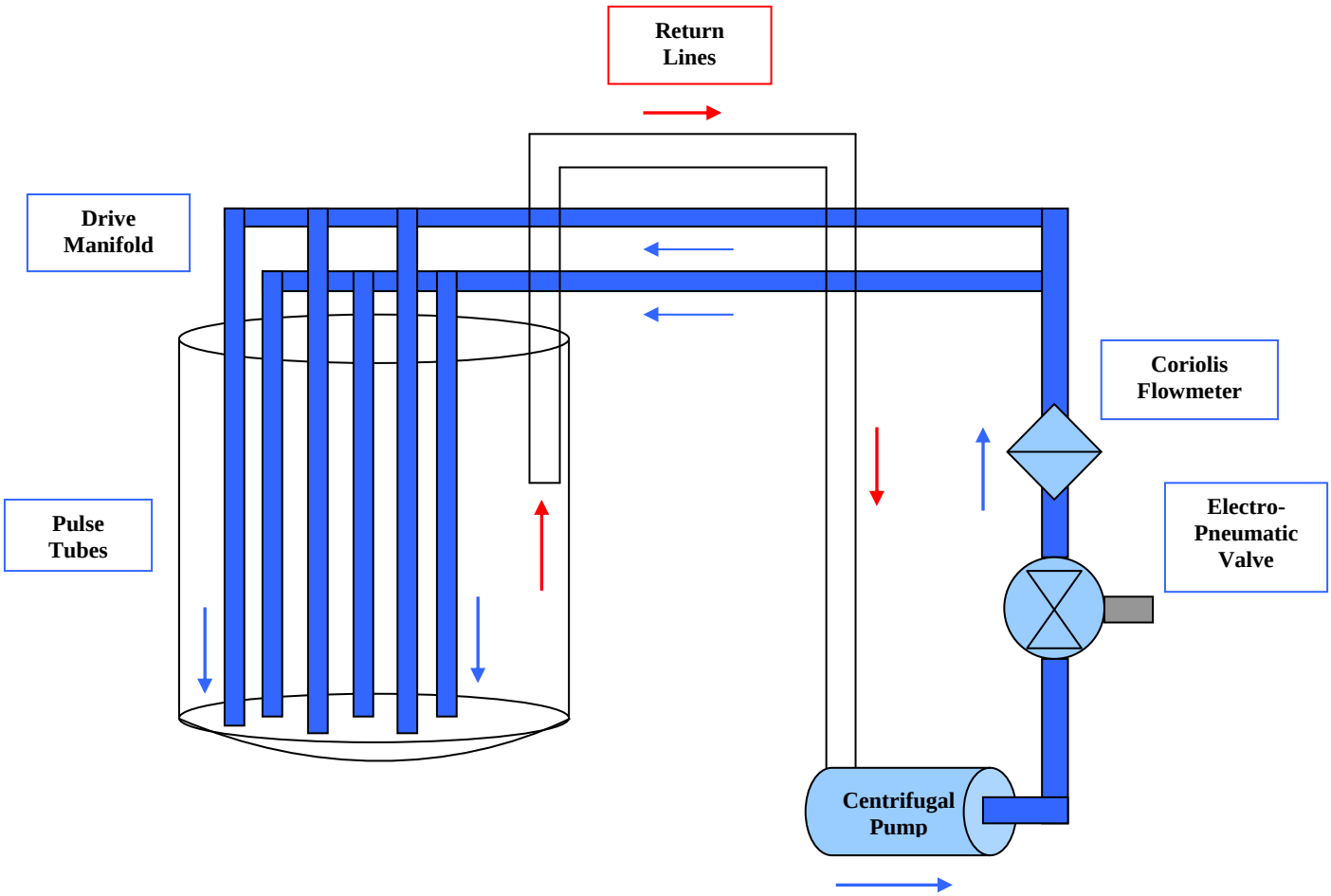

Figure 4.1. Schematic of Conceptual Arrangement of Test Tank and Drive System for HLP-22 Testing

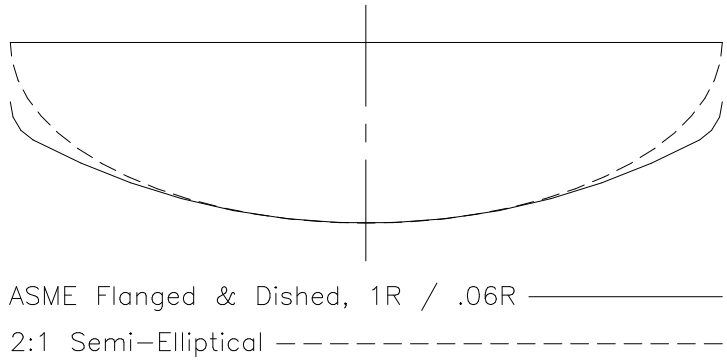

Figure 4.2. Comparison of Profiles for F&D and 2:1 Semi-Elliptical Tank Heads

The HLP-22 vessel has an F&D head (BNI 2007). The heads of scaled tanks used in the experiments are not all geometrically the same as the HLP-22 vessel, and the difference affects the flow geometry where PJM jets contact the head. This can be compensated for by slightly changing the radial locations of PJMs in the scaled systems to create geometrically similar jet impingement angles.

The differences in tank head profiles result in different impingement angles between the vertical jet and the tank head. For the outer ring of PJMs, the differences in tank head profiles result in significantly different impingement angles at the same radius from the center. Figure 4.3 illustrates the impingement angle of the jets. To duplicate the impingement angle of an F&D configuration (e.g., the HLP-22 vessel), the radial location of the outer PJM ring was changed to an elliptical configuration. Figure 4.4 illustrates the tank head elevation as a function of the nondimensional tank radius for F&D, 2:1 semi-elliptical, and spherical tank heads to show the differences in impingement angles at the same radial position. The actual adjustments for the radial position and the resulting impingement angles are shown in Table 4.1 for the tube arrays used in testing, including as-tested impingement angles (FIO).

The PJMs are made of standard pipe with changeable nozzles at the ends. Because the F&D head has shallower impingement angles than the semi-elliptical head, particularly at the outer tank radii, the distribution of flow toward the tank center and wall is altered. To achieve similar angles, the radial positions of the pulse tubes were adjusted based on the values provided in Table 4.1.

In the test planning, all three test systems were to operate with at least a 2:1 semi-elliptical head. The mid-scale system used a tank that had been supplied by other projects and was represented as a 2:1 semi-elliptical head. The other systems purchased at least one head as semi-elliptical and one head as F&D. Testing was completed in the mid-scale system first due to its availability. The mid-scale tank failed several months after its use in testing, which allowed for a post-test measurement of the tank head.

The post-test measurements of the mid-scale tank head more accurately characterized the tank as having a spherical segment head with a 0.511-m (20.1-in.) radius and a 22.9-cm (9-in.) depth. This results in different jet impingement angles in the mid-scale tank than planned. The resulting difference between the planned and as-tested jet impingement angles for the mid-scale are shown in Table 4.2.

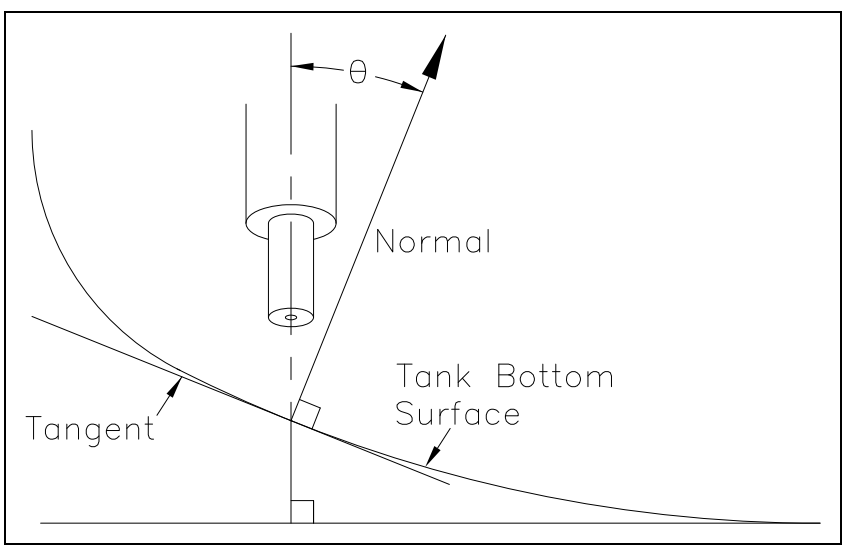

Figure 4.3. Illustration of Jet Impingement Angle, θ, Which is the Angle Between the Vertically Downward Jet and the Bottom of the Tank at the Point of Impingement. (This definition agrees with the definition of the angle of incidence used in optics.)

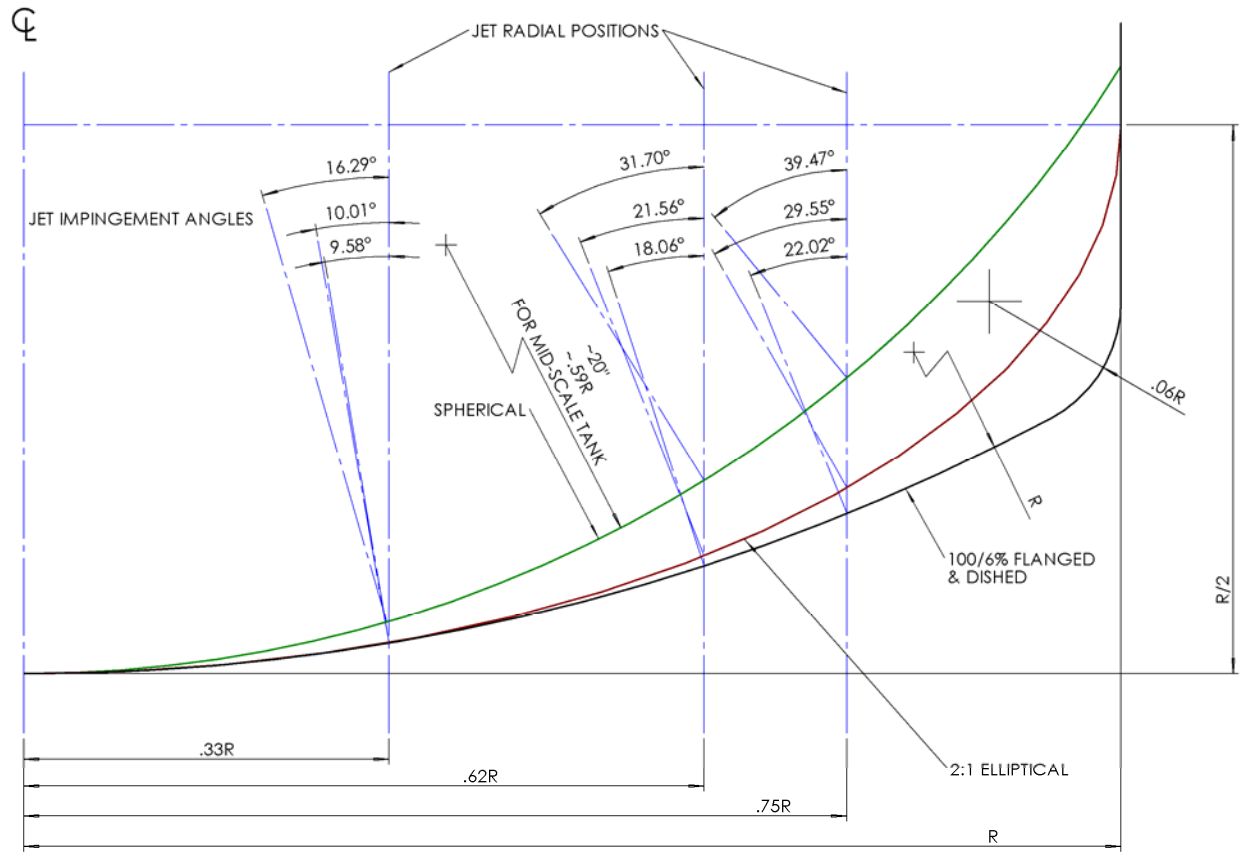

HEAD PROFILE COMPARISON, NORMALIZED TO TANK RADIUS

Figure 4.4. Illustration of the Change in Impingement Angles for Different Head Profiles.[1] This illustration shows the shape using nondimensional tank radius for F&D, spherical, and 2:1 semi-elliptical heads (FIO).

Table 4.1. Comparison of Planned Pulse Tube Radius for Equivalent Angle of Impingement in Tank Heads Formed with F&D and 2:1 Semi-Elliptical Heads

Parameter	Inner Ring of PJMs	Outer Ring of PJMs
Radial position of PJM centerlines in Tank HLP-22 design with F&D head for tank head	0.33R[(a)]	0.75R
Angle of impingement[(b)] of the tank head at the specified tank radius	9.6 degree	22.1 degree
Radial position of PJM centerline in a semi-elliptical tank head that matches the angle of impingement in the F&D tank head	0.33R	0.62R

(a) R = tank radius
(b) Figure 4.3 illustrates the angle of impingement.

[1] Actual impingement angles from the test are listed in Table 4.1. The illustration in Figure 4.4 is for information only.

Table 4.2. General PJM Configurations

Vessel Configuration	Ratio of Inner Ring Radius to Tank Radius R_I/R		Ratio of Outer Ring Radius to Tank Radius R_O/R		Inner PJM Impingement Angle θ_I (deg)		Outer PJM Impingement Angle θ_O (deg)	
	Planned	As-Tested	Planned	As-Tested	Planned	As-Tested (FIO)	Planned	As-Tested (FIO)
15E 12-tube	0.33	0.34	0.62	0.62	9.6	*10.1*[(a)]	22.1	*21.8*
34S 12-tube[(b)]	0.33	0.33	0.62	0.62	9.6	*16.1*	22.1	*30.8*
70E 12-tube	0.33	0.33	0.62	0.62	9.6	*10.5*	22.1	*20.3*
70F 12-tube	0.33	0.34	0.75	0.76	9.6	*9.7*	22.1	*22.4*
15E 8-tube	n/a	0.50	n/a	0.67	n/a	*16.0*	n/a	*24.4*
70E 8-tube	n/a	0.50	n/a	0.67	n/a	*16.1*	n/a	*21.9*

(a) Data in italics are for information only.
(b) Planned values indicated for the mid-scale tank are those for the semi-elliptical tank head. No spherical segment values are indicated in the test plan.

For straight-bore nozzles, the bore has a minimum length of 10 diameters for each nozzle size tested. The proximity (1.5 nozzle diameters)[1] of the nozzle discharge to the tank floor results in the core of the jet impacting the tank floor with minimal to no decrease in the centerline velocity of the jets. While not part of this testing program, computational fluid dynamics (CFD) modeling was performed by BNI to compare the applied shear stress on the tank floor produced from a conical nozzle with a 60-degree taper and a straight-bore nozzle. The straight-bore nozzle results agreed with literature values for floor shear stress (Beltaos and Rajaratnam 1977). The CFD results for a nozzle elevation of 1.5 nozzle diameters indicate that the conical nozzle results in a higher shear stress at the tank floor within approximately 10 nozzle diameters from the point of impact. The difference is greatly reduced between 10 and 20 diameters and appears negligible after 20 diameters.

For mobilization of solids on the tank floor (using CFD results), the straight-bore nozzles provide conservative results at lower discharge velocities in which the radial clearing of solids from the tank floor is less than that required for the critical suspension velocity to be achieved. As the discharge velocity is increased and solids mobilization is achieved at higher radial distances, the differences in solids mobilization obtained for conical and straight-bore nozzles are predicted by CFD analysis to become negligible.

To simplify and expedite the testing, the test apparatus was designed with a closed-loop, pumped-jet system with the pump return line near the liquid surface. Pulsation of the discharge flow was achieved by valve operation.

The test system for all three scales used centrifugal pumps to circulate water through the pulse tubes to simulate the pulse phase of the PJM system (the vacuum or suction refill phase is not simulated). The full-scale plant vessels contain PJMs that are much larger in diameter than the pulse tubes used in the test stands. A PJM is operated by applying an oscillating gas pressure to the headspace. During the high-pressure part of the cycle, fluid is discharged from the PJM. When the headspace pressure is

[1] In the small-scale vessel, 0.0049-m (0.193-in.) nozzles were tested at a standoff distance of 1.04 nozzle diameters.

reduced (by venting and/or vacuum), the PJM refills with fluid from the tank. A PJM can hold the entire volume of fluid that is discharged during the high-pressure portion of the cycle. The differences between the prototypic PJM system and the pulse tubes used in testing that are thought to be consequential include:

- The PJM system will pull both liquids and solids from the bottom of the vessel during the vacuum or suction refill phase. In the pulse tube system used in testing, the jets expel nearly pure water. This may increase the solids concentration that settles to the bottom of the tank. It may also result in a jet of lower bulk density and less premixing of the pulse volume and may lead to plugging of the PJM nozzles during discharge or between pulses, which is less likely in the PJM system. These conditions identify a benefit of conducting additional testing with a prototypic, full-cycle drive system.
- The diameters of the PJMs are much larger than the pulse tubes used in testing. The smaller diameters of the pulse tubes may result in less lifting of solids from the bottom to the upper regions of the tank as well as less alteration of radial and tangential circulation within a test tank (compared to a prototypic tank). This condition may identify a benefit of conducting additional testing with a prototypic PJM geometry.
- Flow within the pulse tubes is one-directional rather than reciprocating as in a PJM. During a pulse, liquid is suctioned from the top of the test vessel through the pump(s) outside the tank and returned to the tank through the pulse tubes. This imparts a circulatory flow through the ex-tank piping and a net upward flow through the constant tank fluid volume during the pulses.

In the test system that simulates PJM action, the pulse tubes are connected by a common manifold and activated using a centrifugal pump to generate the motive power. Pressure sensor ports on each pulse tube (after the manifold) allowed the flow to all the nozzles to be balanced or made uniform before testing starts. Cycling of the pump operation and the synchronized opening and closing of the control valve generate the periodic flow through the pulse tubes.

4.2 Small-Scale Test Stand

The small-scale test stand was located in the APEL high bay. The components of the small-scale test stand are described in Section 4.2.1, and the control equipment is described in Section 4.2.2.

4.2.1 Components

The small-scale test apparatus consists of several components, including three interchangeable transparent acrylic 0.367-m- ($14^{7}/_{16}$-in.-) diameter tanks, a pump skid, plumbing connecting the tank to the pump skid, a liquid drive system, instrumentation, and a data acquisition system (DAS). The three tanks have different head geometries, flat, elliptical, or F&D, but only the 2:1 elliptical-headed tank was selected for use during the tests described in this report because all three (small-, mid-, and large-scale) had elliptical heads. Thus the results from any of the three could be used to establish tank diameter scaling factors. (It was later determined that the shape of the mid-scale test stand was spherical, different than the elliptical shapes of the other two stands.) The test tanks, plumbing configuration, and pump skid discussed in this section are shown in Figure 4.5. The three test tanks in the small-scale apparatus are approximately 0.99-m ($38^{7}/_{8}$-in.) deep and open at the top.

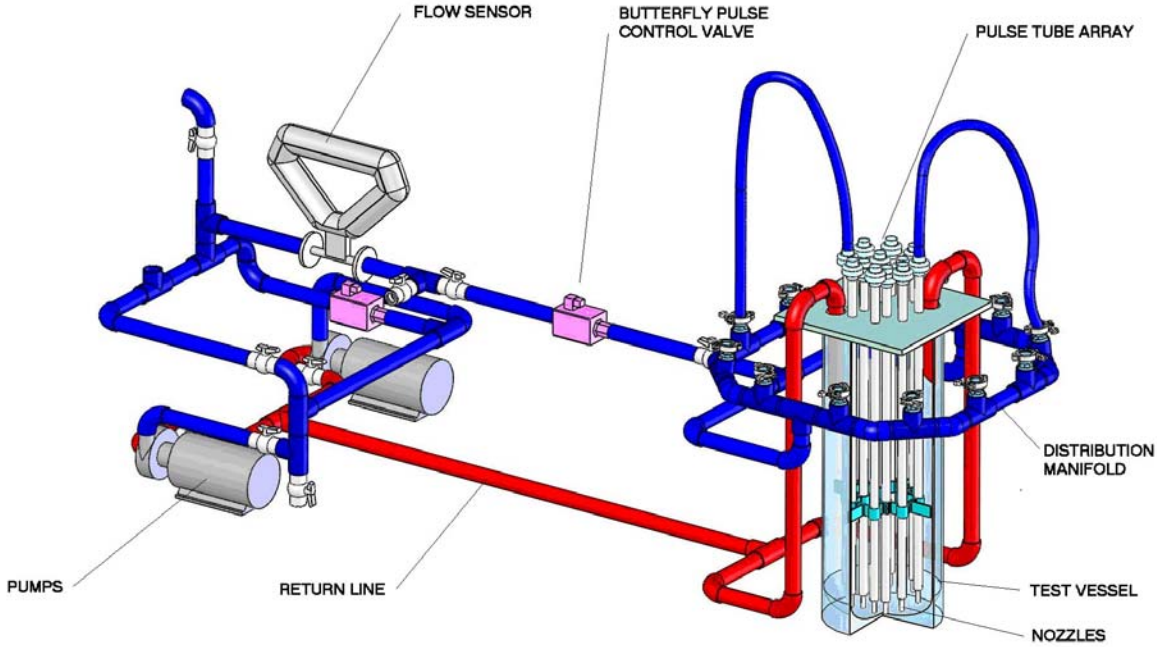

Figure 4.5. Diagram of Small-Scale Test System Showing the HLP-22 12-Tube Array (not to scale)

The elliptical-headed tank was mounted on the raised mobile test stand about 2 ft above the floor to allow visual observation from beneath the tank head. An array of pulse tube assemblies (12 tubes for the HLP-022 configuration) was positioned in the tank with radial locations of 0.33R and 0.62R (see Table 4.2) to match impingement angles. The tank and pulse tube array were connected to the pumps and instrumentation via PVC piping.

Each pulse tube assembly consists of a nozzle at the bottom, a pulse tube body, and fittings at the top to attach the assembly to the flexible supply hoses and to mount liquid pressure sensors in the tube. The pulse tube bodies are made of Schedule 40 PVC pipe with a precision-machined nozzle glued or threaded at the bottom. The larger nozzles used pulse tubes with female-threaded ends, and the male-threaded discharge nozzles were threaded onto the ends of the pulse tube bodies. Smaller nozzles were glued to the pulse tube bodies. The nozzles have straight bores that are at least 10 nozzle diameters in length. The pulse tube assemblies are supported in the tank by precision-machined PVC and/or metal-channel frames and clamped with split-collar clamps to fix their elevations. Nozzle elevation is adjustable and was set for each pulse tube assembly using a machined spacer temporarily inserted into the end of the nozzle.

Each pulse tube assembly had a fitting at the top through which water flowed into the tube. On the side of the tube was a ¼-in. fitting attached to a static pressure probe in the pulse tube. Pulse tube assemblies were connected to a common supply manifold via approximately 1.2-m- (4-ft-) long by 1-in.-diameter flexible hoses.[1] Figure 4.6 depicts the small-scale test tank assembly.

[1] Pipe, tubing and fitting sizes in Sections 4.2, 4.3, and 4.4 are nominal/commercial standard sizes, not measured values.

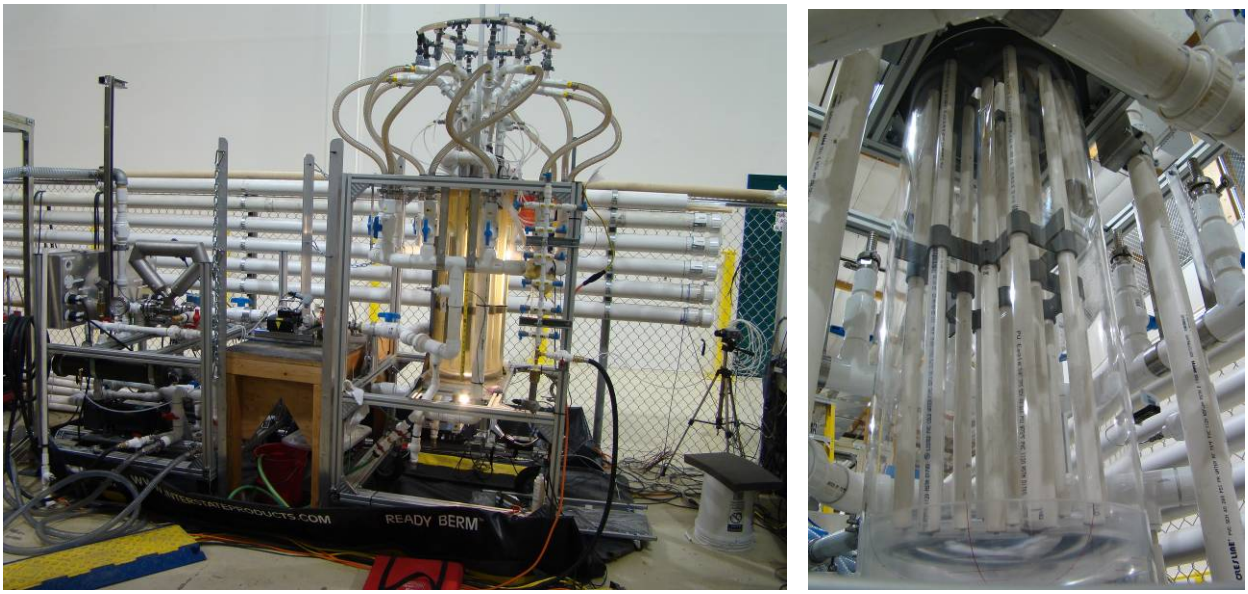

(a) (b)

Figure 4.6. (a) Small-Scale Elliptical-Head Test Tank with Pulse Tubes Installed; (b) Pulse Tubes Mounted in the Tank

The test tank also contained two nominal 2-in.-diameter PVC drop-tube suction lines. The elevation of the suction lines was fixed. The inlet of the suction pipes was made of 2-in. Schedule 40 PVC pipe with the inlet sliced at an angle to reduce intake velocity and thus reduce the lifting force on the solids during testing. The suction pipes were connected to a common manifold that returns liquid to the pumps through PVC pipe and a flex hose between the skids (total line length is about 2.7 m [9 ft]). The configuration connected both suction lines for use during pump operations.

The manifolds for both the discharge and suction lines were on the tank skid. The system was set up for closed-loop operation. The pump skid included two centrifugal pumps, one 0.373 kW (½ hp) and one 0.755 kW (1 hp), that supplied the motive power for circulating liquid through the tank. The pumps were plumbed in parallel and wired to separate variable-frequency drives (VFDs). Additional detail on pump controls is presented in Section 4.2.1. Figure 4.7 presents photographs of the pump skid and Coriolis mass flow meter as well as the pump control panel. The pneumatic valve is pictured in Figure 4.8.

To simulate PJM action in the test system, the pulse tubes were connected by a common manifold and activated using a centrifugal pump to generate the motive power. Pressure ports on each pulse tube (after the manifold) allowed the flow to all nozzles to be balanced or made uniform before testing began. Cycling of the pump operation and the synchronized opening and closing of the control valve generate the periodic flow through the pulse tubes. Flow within the pulse tubes was one-directional rather than reciprocating like a PJM. During a pulse, liquid was suctioned from the top of the test vessel through the pump(s) outside the tank and returned to the tank through the pulse tubes.

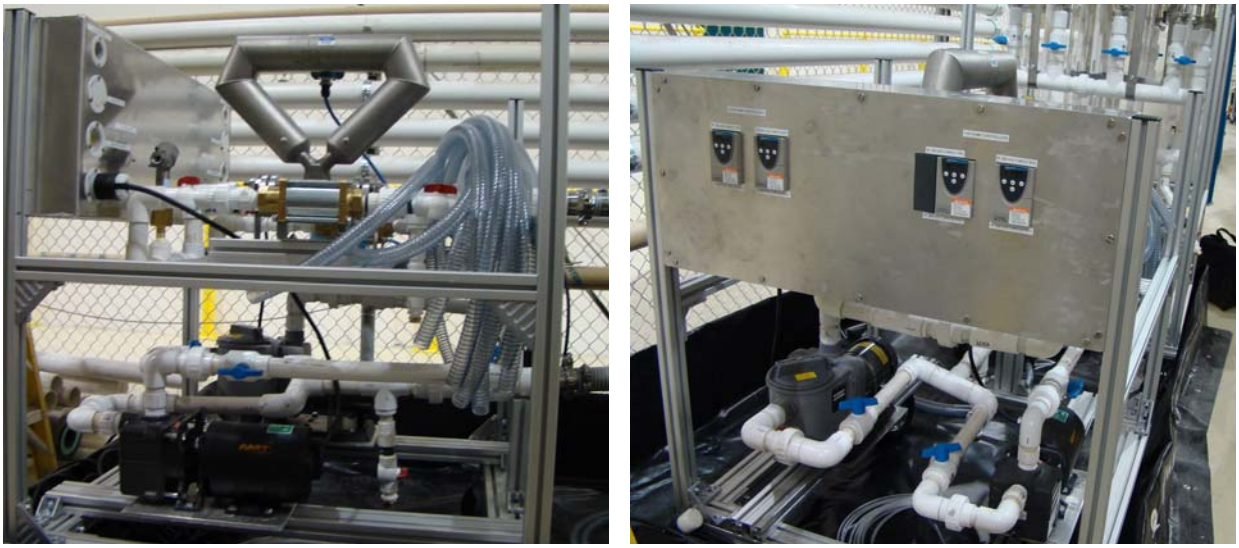

(a) (b)

Figure 4.7. **(**a) Pump Skid with Pumps and Coriolis Flow Meter; (b) Pump Control Panel

Figure 4.8. The Pneumatic Butterfly Control Valve Mounted Between Pump Skid and Tank Skid. The red throttle valve is also visible to the right of the butterfly valve.

4.2.2 Control Equipment

The following list presents an overview of the test equipment and controls for the small-scale test stand:

- The two centrifugal pumps were plumbed in parallel and driven by separate VFDs wired to dual set-point boxes with two potentiometers for controlling pump speed. The dual set-point boxes allowed pump frequency to be cycled between two operating frequencies. (The dual set-point feature was not used during testing in the small-scale tank.) The frequency output of the VFDs was controlled by potentiometers that were adjusted manually. The timing for alternating between the dual frequency setpoints was controlled by the DAS or ultrasonic command and control (UCC) computer based on values for the cycle time and duty cycle that are manually entered.

- A nominal 1½-in. ID pulse control valve was operated by a pneumatic actuator, which was controlled by an electric solenoid air control valve. An air reservoir was installed near the air control valve to minimize the response time of the pulse control valve. A throttle valve on the exhaust from the pneumatic actuator allowed for improved control of the wave shape. The pulse control valve was operated to pulse the discharge flow. An air regulator allowed the air pressure to the air control valve to be manually adjusted. The timing of a supply voltage provided by the DAS or UCC computer controlled the actuation of the pulse control valve. The potentiometers also controlled the pump frequency when the pulse control valve was not powered.
- Manual inputs for pulse cycle time and duty cycle are entered into either the DAS or the UCC system. These parameters controlled the timing of the supply voltage to the pump dual set-point boxes and the air control valve.

4.3 Mid-Scale Test Stand

The mid-scale test apparatus was located in the APEL high bay. The components of the mid-scale test stand are described in Section 4.3.1. The control equipment is described in Section 4.3.2.

4.3.1 Components

The mid-scale test apparatus consists of several components. The apparatus consisted of a transparent acrylic test tank, nominally 0.86 m (34 in.) in diameter, with a spherical segment head and integrated stand, a pump skid, plumbing connecting the test tank to the pump skid, a liquid drive system, instrumentation, and a DAS. The test tank, plumbing configuration, and pump skid are shown in the schematic in Figure 4.9.

The test tank was approximately 2.1-m (84-in.) deep with an open top. It was raised approximately 0.36 m (14 in.) above the floor to allow visual observations of the tank head. Moveable mirrors were installed under the tank to assist with visual observations of the tank head.

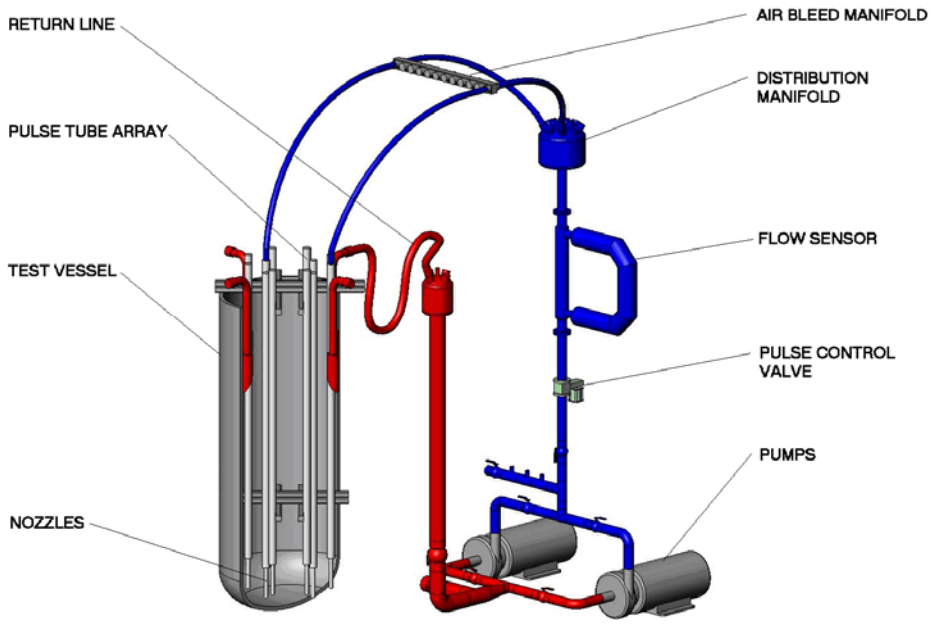

Figure 4.9. Diagram of Mid-Scale Test System (not to scale)

The tank was supported by an integral clear plastic skirt resting on the floor. The tank was surrounded by a steel frame which supported the pulse jet array (see Figure 4.10). An array of pulse tube assemblies (12 for the HLP-22 configuration) was suspended in the tank and centered with small standoffs. During the testing described in this report, a 2:1 elliptical head was assumed, so the inner tubes were located radially at 0.33R, while the radius of the outer tubes was adjusted inward to 0.62R to compensate for the different impingement angle. After testing was completed, careful measurements revealed that the tank bottom was spherical, not 2:1 semi-elliptical. Hence, the radial positioning of the outer tubes did not compensate to match the HLP-22 F&D bottom (see Table 4.2). The tank and pulse tube array were connected to the pumps and instrumentation via PVC piping.

The outer pulse tube radius was modified for the impingement angle when an elliptical head was used with the HLP-22 12-tube array. The pulse tubes were connected by a common manifold and were activated using one or both of the centrifugal pump(s) to push the liquid through the tubes. Pressure ports on each pulse tube (after the manifold) allowed the flow to all nozzles to be balanced or made uniform before testing started. Cycling of the pump operation and the synchronized opening and closing of the control valve generated the periodic flow through the pulse tubes, which was one-directional rather than reciprocating. During a pulse, liquid was suctioned from the top of the test vessel through the pump(s) outside the tank, and returned to the tank through the pulse tubes. Each pulse tube assembly consisted of a nozzle at the bottom, pulse tube body, and fittings at the top to attach the assembly to flexible supply hoses, to control liquid flow, and to measure liquid pressure in the tube. Pulse tube bodies were ¾ in. Schedule 40 PVC pipe with a bushing to nominal ¾ in. NPT (national pipe thread) female threads at the bottom. Various sizes of discharge nozzles were threaded to the bushings. The nozzles had straight bores at least 10 nozzle diameters long. The pulse tube assemblies were supported by an adjustable framework of metal channel, all-thread, and U-bolts. Nozzle elevation was adjustable and was set for each assembly using a machined spacer temporarily inserted into the end of the nozzle.

Each pulse tube assembly included a T-fitting at the top with the flow entering through the branch and discharging through the lower portion of the run. The top of the T-run was bushed to nominal ¼-in. NPT containing a compression fitting with a nominal ¼-in. tube configured to sense static pressure in the pulse tube. The tube assemblies were connected to a common manifold via flex hoses that were approximately 3.7 m (12 ft) long and 1½-in. inside diameter. Figure 4.10 shows photographs of the test tank assembly. Figure 4.10(b) was taken from above the tank and shows the upper pulse tube support rack, the red valve handles for operating the tube or balancing the tube flow across the array, and static pressure tubes.

The test tank also had four nominal 2-in.-diameter PVC drop-tube suction lines at its perimeter. The elevation of the suction lines was adjustable. The inlet of the suction pipes was 3-in. Schedule 40 PVC pipe cut at an angle to reduce inlet velocity, which reduced lifting force on the solids lifted during testing. The suction pipes were connected to a common manifold via flex hoses that were approximately 3.7-m (12-ft) long by 2 in. in diameter. An isolation valve was connected to each suction line to assist with air purging. The configuration allowed one to four suction lines to be used during pump operations.

The manifolds for the discharge and suction lines were on the pump skid shown in Figure 4.11(a). The system was configured for closed-loop operation. The pump skid contained two 3.7 kW (5-hp) centrifugal pumps that supplied the motive power for circulating liquid through the tank. The pumps were plumbed in parallel and wired to separate VFDs. The pump skid also had three 0.125-m^3 (33-gal) accumulator/bladder tanks plumbed to the discharge line of the pumps. These tanks could be valved on- or off-line to increase/decrease the hydraulic capacitance of the system. The air pressure in the bladder tanks could be adjusted to change the capacitance of the system. This feature was not used during testing.

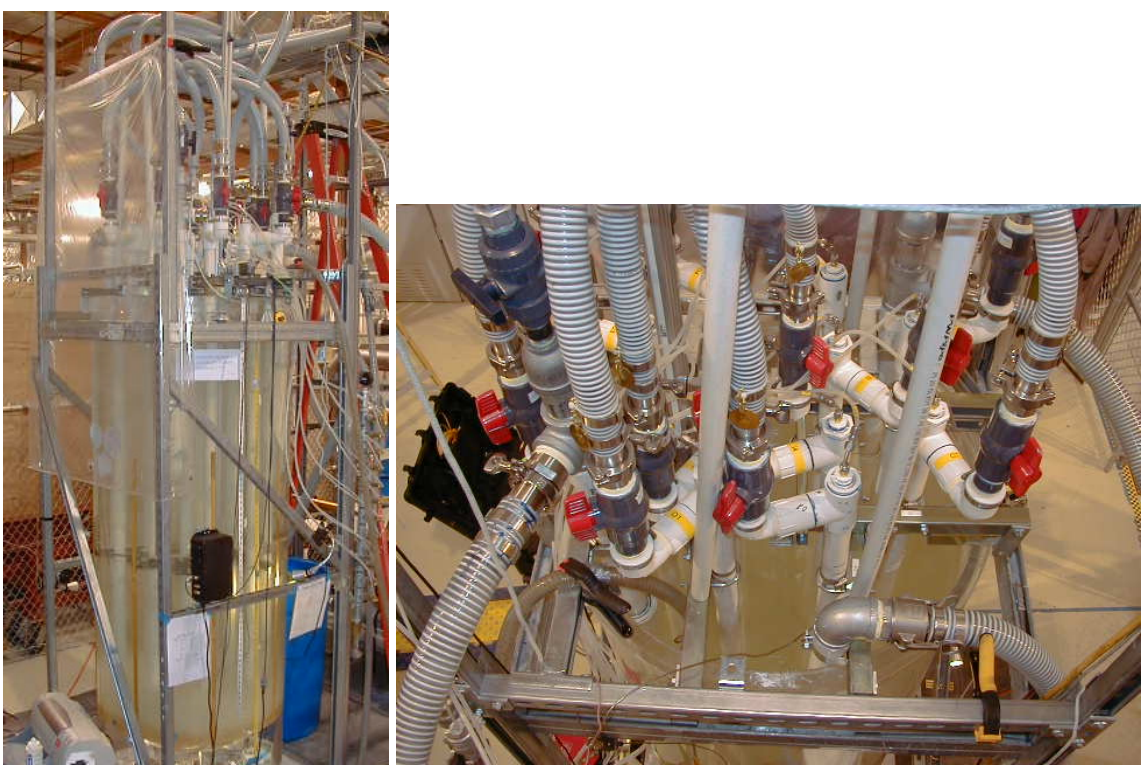

(a) (b)

Figure 4.10. (a) Mid-Scale Test Tank with Pulse Tubes Installed; (b) View from Above with Upper Pulse Tube Support Rack and Static Pressure Tubes Visible

(a) (b)

Figure 4.11. (a) Pump Skid with Pumps, Bladder Tanks, Suction and Discharge Manifolds; (b) Control Valve Assembly with Blue Pulse Control Valve, Air Control Valve (left of pulse control valve), Control Valve Pressure Reservoir, and Micro Motion Coriolis Flow Meter (behind reservoir)

A pulse control valve (butterfly, or in 2007 tests, a pinch valve) was installed in the pump discharge line to help generate the pulsed flow through the nozzles. The pulse control valve was pneumatically operated via an air-control valve. An air reservoir was close-coupled to the air control valve to minimize the response time. The valve assembly and Coriolis mass flow meter are shown in Figure 4.11(b).

4.3.2 Control Equipment

This section provides an overview of the test equipment and controls for the mid-scale test stand. The control equipment consisted of:

- Two 3.7 kW (5-hp) centrifugal pumps plumbed in parallel and driven by separate VFDs wired to dual set-point boxes with two potentiometers for controlling pump speed. The dual set-point boxes allowed pump frequency to be cycled between two operating frequencies. The frequency output of the VFDs was controlled by manually adjusted potentiometers. The timing for the setpoints was controlled by the DAS or UCC based on values entered manually into the DAS or UCC.
- Compressed air piped to the air chambers of the bladder tanks and the air control valve. The compressed air supply line included a regulator for adjusting the feed pressure.
  The liquid side of the three bladder tanks piped in common to a nominal 2-in. cross that connected to the discharge line of the pumps. An isolation ball valve allowed the bladder tanks to be isolated from the drive system flow. (Testing from 7/2007 through 12/2007 indicated that these bladder tanks were not needed to meet project objectives. The bladder tanks were also not needed in the 2008 testing.)
  The gas sides of the bladder tanks were connected using ¼-in. tubing. An air regulator allowed the bladder tank gas pressure to be adjusted.

- A nominal 3-in. pulse control valve operated pneumatically by pressurizing the air control valve via the air reservoir and venting the air control valve to room atmosphere. The pulse control valve was operated by a pneumatic actuator, which was controlled by an electric solenoid valve. An air reservoir near the air control valve minimized the response time of the pulse control valve. A throttle valve on the exhaust from the pneumatic actuator allowed for improved control of the wave shape. The pulse control valve enabled pulsing of the discharge flow with adequate control of the fluid velocity wave form. An air regulator allowed air pressure to the air control valve to be adjusted manually to improve valve opening response times if needed. The timing of supply voltage provided by the DAS controlled actuation of the pulse control valve. The potentiometers could also control pump frequency when the pulse control valve was not powered. The pulse wave was controlled primarily by opening the pulse control valve for a controlled period of time (the pump would run at a preset speed, dead-heading when the pulse control valve was closed).
- Pulse cycle time and duty cycle are manually entered into the DAS or UCC system. These parameters controlled the timing of the supply voltage to the dual set-point boxes and air control valve.
- Initial tests in July 2007 only used the DAS, but UCC control had been implemented by the fall testing.

4.4 Large-Scale Test Stand

The large-scale test apparatus was located in the APEL high bay. The large-scale test stand components are described in Section 4.4.1. The control equipment is described in Section 4.4.2.

4.4.1 Components

The large-scale test apparatus consists of several components. The large-scale test apparatus in the APEL high bay consisted of an acrylic 1.78-m- (70-in.-) diameter test tank, pump skid, plumbing connecting the test tank to the pump skid, a liquid drive system, instrumentation, and DAS. The tank had two interchangeable heads, an ASME 90-17 semi-elliptical and a 100-6 F&D. The tank, plumbing configuration, and skid are shown in Figure 4.12.

The open-topped test tank was 2.36-m (92¾-in.) deep with the F&D head and 2.52-m (99 1/8-in.) deep with the semi-elliptical head. The tank was raised above the floor to allow visual observation of the interior through a 0.46-m- (18-in.-) diameter acrylic viewing port in the center of the head. The tank contained an array of pulse tube assemblies (12 for the HLP-22 configuration, 8- and 4-tube arrays to approximate those tank configurations (See Section 4.8) with radial and azimuthal locations geometrically scaled to the corresponding WTP vessel. The test system circulated water through the pulse tubes to simulate the pulse phase of the PJM system (the vacuum portion is not simulated). Pressure ports on each pulse tube (after the manifold) allowed flow to the nozzles to be balanced or made uniform before testing began. As discussed in Section 4.2, full-scale plant vessels contain PJMs instead of pulse tubes.

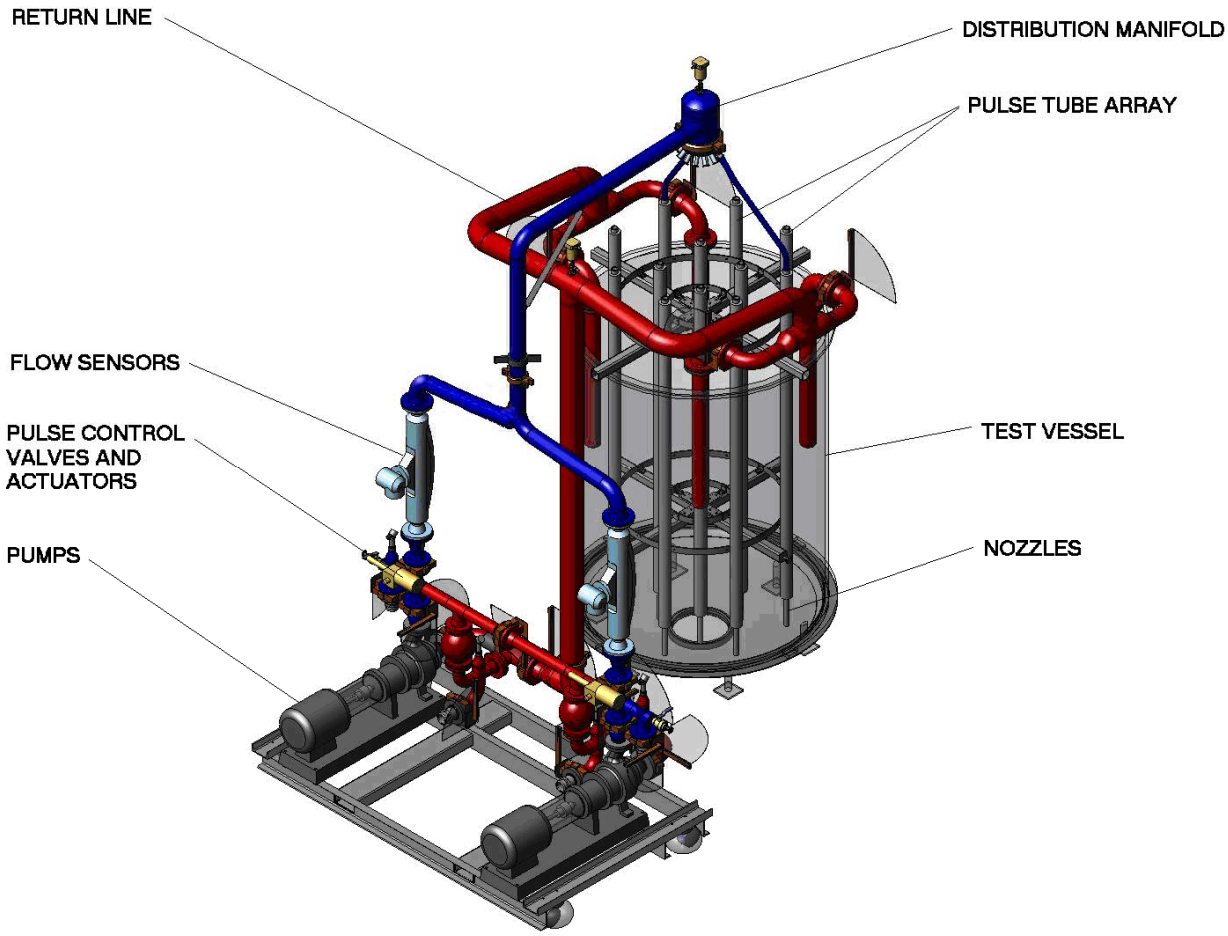

Figure 4.12. Diagram of Large-Scale Test System with the 8-Tube Array (not to scale)

The pulse tubes were connected to a distribution manifold and activated by a pair of 18.6-kW (25-hp) centrifugal pumps to generate the motive power, using an electrically synchronized control valve at each pump outlet to generate the periodic flow through the pulse tubes. Flow within the pulse tubes was one-directional rather than the reciprocating flow within a PJM. During a pulse, liquid was suctioned from the top of the test vessel through the pump(s) outside the tank and returned to the tank through the pulse tube.

Each pulse tube assembly consisted of a nozzle at the bottom, a pulse tube body, and fittings at the top to attach the assembly to the flexible supply hoses, control liquid flow, and measure static pressure in the tube. The pulse tube bodies were made of nominal 3-inch Schedule 40 PVC pipe with a bushing to nominal ¾ in. NPT female threads at the bottom. Various sizes of discharge nozzles are threaded into the bushings. The nozzles had straight bores at least 10 nozzle diameters long. The assemblies were supported by a retainer assembly of metal rings, unistrut channel, square tube stock, Delrin® spacers, and U-bolts. Nozzle elevation was adjusted by changing the pulse tube clamping position on the retainer assembly and was set for each nozzle diameter using a machined aluminum spacer temporarily inserted into the end of the nozzle. The pulse tube assembly and nozzles are shown in Figure 4.13.

(a) (b)

Figure 4.13. (a) Pulse Tube Assembly Before Installation in Tank; (b) Close-up of Pulse Tube Nozzles

Each pulse tube assembly contained a ball valve at the top through which the water flowed into the tube. The valves enabled any number of the tubes to be shut down and provided a way to balance the flow between the active tubes. Below the valve was a T-fitting that mounted a static pressure tube aligned in the center bore of the pulse tube connected to a tree-type pressure-sensor manifold to sense the static pressure in individual pulse tubes to indicate relative flow rates. Pulse tube assemblies were connected to the distribution manifold via approximately 2.1-m- (7-ft-) long by 1½-in.-diameter flex hoses mounted to the ball valves. Figure 4.14 presents photos of the F&D tank assembly.

(a) (b)

Figure 4.14. (a) Large-Scale Vessel Flanged and Dished Head; (b) 0.46-m (18-in.) Acrylic Viewing Port

The test tank also had four nominal 4-in.-diameter PVC drop-tube suction intakes at its perimeter. The suction intake pipes were nominal 4-in. PVC pipe with the submerged end cut off at an angle to reduce the fluid velocity around the inlet orifice. The placement of the suction intakes was intended to minimize the lifting of solids to the top of the tank. The suction intakes were connected to a return manifold via stainless steel pipes; full-flow ball valves on each suction intake allowed from one to four intakes to be used during pump operations.

Manifolds for both discharge and suction lines were supported over the tank by the pump skid. The system had a closed-loop configuration. The pump assembly is shown in Figure 4.15.

(a)

(b)

(c)

(d)

Figure 4.15. (a) Pump Assembly and Coriolis Meters with Test Tank in Background and (b) Upper End of Pump System as it Enters the Manifold (the blue hoses are not yet attached to the pulse tubes), (c) Pump Assembly with Scaffolding, and (d) the Large-Scale Test Stand with the 8-Tube Array and Elliptical Head

4.4.2 Control Equipment

This section provides an overview of the test equipment and controls for the large-scale test stand. The control equipment consists of:

- Two 18.6-kW (25-hp) centrifugal pumps plumbed in parallel. The pumps were powered through a remotely controlled VFD that allowed two manually set pump-speed setpoints to be activated by the DAS or UCC with timing for set-point changes based on cycle time and duty cycle. [Note: the dual set-point feature was not used during large-scale (1.78-m, 70–in.) tank testing.] The VFDs also controlled the pump speed when the pulse control valves were not powered. The pump speed/jet discharge velocity relationship was determined for each test setup so the pump speed could be set quickly and accurately to produce any required velocity during the tests.
- Two nominal 3-in. pulse control valves were actuated pneumatically in response to a control signal from the DAS. The pulse control valves made it possible to pulse the discharge flow with a velocity and wave form that met testing requirements. An air regulator allowed the air pressure to the valve actuator to be manually adjusted, thereby adjusting the rate of opening and the jet pulse velocity rise. A throttle valve on the actuator exhaust allowed for closing rate control. The valve actuator control signal provided by the DAS could also signal the VFDs to alternate the pump speed between the high and low setpoints if desired.
- The jet pulse period and duration were set with manual inputs for pulse cycle time and duty cycle entered into the DAS or UCC. These parameters controlled the timing of the supply voltage to the pump dual set-point boxes and air control valve.

4.5 Pulse Flow Operating Parameters

The drive system was designed to provide a continuous steady flow or a pulsed, periodic flow. The following methods were available to generate a pulsed flow:

- Set the cycle time and duty cycle on the DAS or UCC computer. (While earlier testing used the DAS to control the pulse, later testing used the UCC because of its improved control of the pulse echo, Doppler, and attenuation system data collection.) Open the pulse control (butterfly) valve. Set the high-point pump frequency to obtain the desired volumetric flow or nozzle discharge velocity. Set the low-point pump frequency to zero. Allow the flow rate through the system to be controlled by the cycling of the pump frequency.
- Set the low- and high-point pump frequencies to the same value. Set the cycle time and duty cycle on the DAS or the UCC computer. Set the air pressure on the pulse control valve pneumatic supply line as needed up to the pressure recommended by the valve manufacturer. The pump will run at a constant speed while the pulse control valve cycles the flow in the pump discharge line. (Testing note: While all the methods for generating the pulse were allowed during testing, this pump running at constant speed was the method used to generate the pulse for all testing conducted for this report.)
- Use a combination of the pulse control valve operation and cycling of the pump speed setpoints to generate the pulsed flow.

The physical limitations of the drive system components caused the velocity pulse to deviate from a square wave, especially at high velocities. The various controls described were used to tune the system

and provide some adjustment to the velocity pulse. The operating and control conditions required to achieve the desired pulsed flow were developed during the shakedown testing for each system.

4.6 Instrumentation

During the tests, several variables were monitored in the time domain and recorded to an electronic DAS file, including:

- Total volumetric flow rate to the nozzle array
- Specific gravity of the liquid downstream of the pump/s discharge
- Tank liquid temperature
- Pulse tube pressure, one tube monitored at a time (refer to description below).

Additionally, multiple ultrasonic devices were employed during the 2008 testing to monitor 1) the thickness of the settled solids layer on the bottom of the tank using UDV (described in Appendix A) and pulse echo techniques with external transducers attached to the bottom of the tank, and 2) the concentration of suspended solids at various depths in the tank during mixing using frequency attenuation (described in Appendix A) with horizontally oriented send-and-receive transducers. Signals from the ultrasonic instruments were recorded to the consolidated data sheet (CDS) file according to the test instruction. These signals were collected at discrete times and within the same time period that visual observations were recorded. No reportable ultrasonic data were collected during the 2007 tests in the mid-scale vessel, though some evaluation of the ultrasonic techniques was done in the Fall 2007 testing.

Several variables were monitored based on manual measurements or visual observations that were recorded to data sheets according to the test instruction. These variables were liquid level in the test tank, cloud height in the tank, and (as requested by the test engineer) observations of solids patterns and particle motion on the tank bottom. A Micro Motion Coriolis[1] flow meter provided the volumetric flow rate and the specific gravity of the liquid downstream of the pumps and upstream of the discharge manifold in the small- and mid-scale vessels. An Endress+Hauser Coriolis[2] meter provided the same measurements in the large-scale vessel. Air was removed from the high points in the system and instruments were oriented vertically (in the mid- and large systems) to avoid captured air from affecting the Coriolis meter signal. Type J thermocouples were installed to measure liquid temperatures.

The static pressure in the pulse tubes was measured using a common pressure transducer to balance the liquid flow through the discharge nozzles. Given identical geometries, identical flow rates produced similar pressure drops. The static pressure tubes installed in the top of each pulse tube are plumbed to a tree-type manifold with isolation valves to allow the static pressure in each tube to be measured.

Commercially available measuring equipment (tape measures, rulers, etc.) was used to obtain liquid levels, cloud heights, solid depths, and dimensions of observable patterns. The same type of equipment was used to obtain dimensions of the test configuration and place reference marks for test observations.

---

[1]Emerson Process Management, Micro Motion Americas Worldwide Headquarters, Boulder, Colorado.
[2]Endress+Hauser Inc., Greenwood, Indiana.

4.7 Data Acquisition System

Data were collected from flow system instruments (flow, temperature, and pressure data) with DASYLab[1] software on a desktop PC running Windows XP called the DAS computer. The data acquisition board was an analog input/digital input/output (I/O) board. The recommended frequency and time averaging for data logging and recording by the DAS was specified in the test instruction or test condition transmittal. For ultrasonic measurements, data were collected by the UCC computer, a PC running Windows XP. Requirements for ultrasonic data collection were specified by the test condition transmittal. Starting with the 2008 tests, additional test data files called the CDS and the ultrasonic (UT-CDS) were used.

A CDS was created for each DAS log file. The CDS contains values for parameters associated with the geometry and simulant that were listed in the master spreadsheet for post-test analysis. These values were obtained from the geometry and simulant configuration sheets. In addition, a single line of data associated with a single pulse cycle was written to the CDS by DASYLab worksheet via dynamic data exchange each time the program was manually triggered. The CDS file was printed and included in the data packages. Electronic copies of the DASYLab output file and the CDS were copied to the designated M3 server on the isolated M3 network after each test. Data from the electronic CDS were transferred to the master spreadsheet following the completion of a test.

A UT-CDS was also generated for each test in which data was obtained from the ultrasonic instrumentation. The UT-CDS data were also written to it for a single pulse cycle when manually triggered. The UT-CDS file was printed and included in the data packages. An electronic copy was placed on the designated M3 server on the isolated M3 network after each test. Data from the electronic UT-CDS was transferred to the master spreadsheet following the completion of a test.

4.8 Tube Arrays and Nozzles

The HLP-22 tube array configuration was used for all testing in the mid-scale vessel in 2007. Using this tube array, tests were conducted with 12 (8 outer and 4 inner), 8 (8 outer and no inner or 4 outer and 4 inner), 4 (4 outer and no inner or no outer and 4 inner) tubes.

During 2008 testing in all tanks was conducted with scaled tube arrays that included:

- A 12-tube array modeled from the F&D head HLP-22 vessel (HLP-22 12-tube F&D array)
- 12-tube arrays based on the HLP-22 vessel with the radius adjustment on the outer ring to standardize the impingement angle of the jets in tests using elliptical or spherical- head tanks (HLP-22 12-tube elliptical array)
- 8-tube arrays based on approximate radial positions for the grouping of 8-tube vessels,[2] including FEP-17A/B, PWD-15/16, PWD-33/43, PWD-44, TCP-01, TLP-09A/B and UFP-01A/B. This array was also used for the 4-tube tests by leaving the outer radial rings open and closing the tubes/nozzles on the inner ring or vice versa.

---

[1] Measurement Computing Corporation, Norton, Massachusetts.

[2] GL Smith (BNI), February 28, 2007. "Gary Smith's Action Items from: M3 PJM Mixing Program Status Meeting Held Tuesday Morning, February 27, 2007." Email to PA Scott (PNNL) and PA Meyer (PNNL) including Excel file, "WTP Project Memorandum CCN 146683_Revised M3 PJM Mixing Systems Basic Data Final1.xls."

Tube arrays were scaled by the inner diameter of the test tank being used. Scaling of HLP-22 is shown in Table 4.3. The tube arrays used during tests across the tanks scales are shown in the matrix in Table 4.4. The HLP-22 12-tube F&D and elliptical arrays were based on the 8 outer tube/4 inner tube orientations shown in Figure 4.16.

HLP-22 is an F&D vessel that is 11.6 m (38 ft) in diameter [radius of 5.79 m (19 ft or 228 in.)] with an inner ring of four nozzles at a radius of 1.93 m (76 in.) (0.33 R) and an outer ring of eight nozzles at a radius of 4.34 m (171 in.) (0.75 R) (BNI 2007). The spacing of the inner and outer rings for the large-scale F&D tank was scaled to 0.33 R and 0.75 R, respectively.

Table 4.3. Vessel Scaling Versus HLP-22

Vessel	Diameter (Inner)	Relative Scale	Scale Factor
HLP-22[(a)]	38 ft (11.58 m)	1	1
Small Scale (APEL15)	14 7/16 in. (0.367 m)	0.0317	31.58
Mid Scale (APEL34)	33. 7/8 in. (0.860 m) near top of dish	0.0743	13.46
Large Scale (APEL70) Elliptical Head	70 in. (1.78 m) at top of tank[(b)]	0.1535	6.514
Large Scale (APEL70) F&D Head	69.16 in. (1.76 m) at top of dish[(b)]	0.1517	6.593

(a) The data for HLP-22 were supplied by WTP in contractor CCN 146683; transmitted via email from GL Smith on 2/23/2007.
(b) Used for calculation of PJM radial locations and impingement angles.

Table 4.4. Tank and Pulse Tube Array Matrix

	HLP-22 12-Tube Flange and Dish Array	HLP-22 12-Tube Elliptical Array	8-Tube Array	8-Tube Array using only the 4 Inner or Outer Tubes
Small-Scale Elliptical	–	X	X	X
Mid-Scale Spherical[(a)]	–	X	–	–
Large-Scale F&D	X	–	–	–
Large-Scale Elliptical	–	X	X	X

(a) While the mid-scale tank is described as an elliptical headed tank throughout all the testing documents, post-test measurement and analysis of the tank more accurately characterized the tank as having a spherical segment head with a 0.511 m (20.1 in.) radius and a 22.9 cm (9 in.) depth.

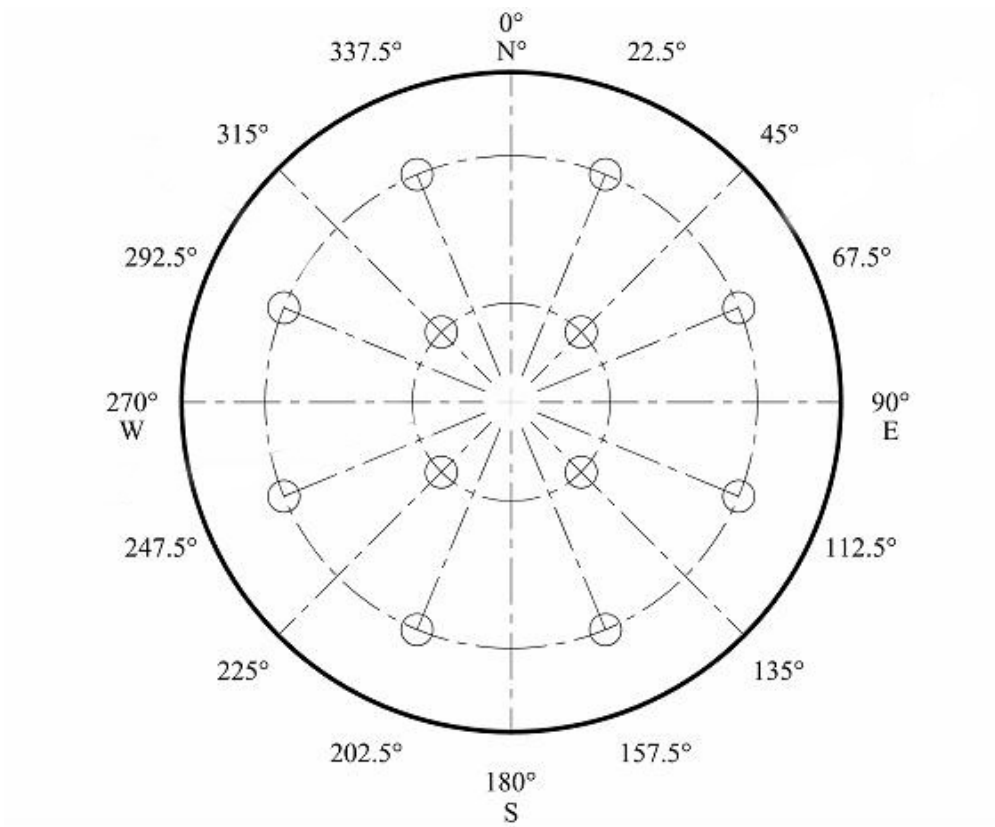

Figure 4.16. Plan View of 12-Tube HLP-22 F&D Orientation Between Inner and Outer Rings in the Large-Scale Tank. The as-tested inner-ring radius was 0.297 m (11.7 in.) and the as-tested outer-ring radius was 0.671 m (26.4 in.).

In the test tanks with elliptical heads, the HLP-22 12-tube elliptical arrays had the outer ring radial positioning reduced to 0.62 R. This adjusted for the difference in the nozzle impingement angle caused by the difference between F&D head and the elliptical head (see Figure 4.17). The planned pulse tube locations based on equivalent impingement angles are shown in Table 4.1. The measured positions of the 12-tube arrays in the tanks are presented in Table 4.5.

Structural supports for the tube arrays inside the test tanks were constructed to limit interference with the particle cloud in the center of the tank. An example of the large-scale tank structural component is shown in Figure 4.18. The 8-tube array was configured to model approximate radial positions for the 8-tube tanks in the WTP, including FEP-17A/B, PWD-15/16, PWD-33/43, PWD-44, TCP-01, TLP-09A/B and UFP-01A/B. This array was also used for the 4-tube tests by leaving the outer radial rings open and closing the tubes/nozzles on the inner ring. The inner ring of 4 tubes was tested at a radius of 0.5R and the outer ring of 4 at 0.67R. Figure 4.19 shows the orientation of the tubes during testing.

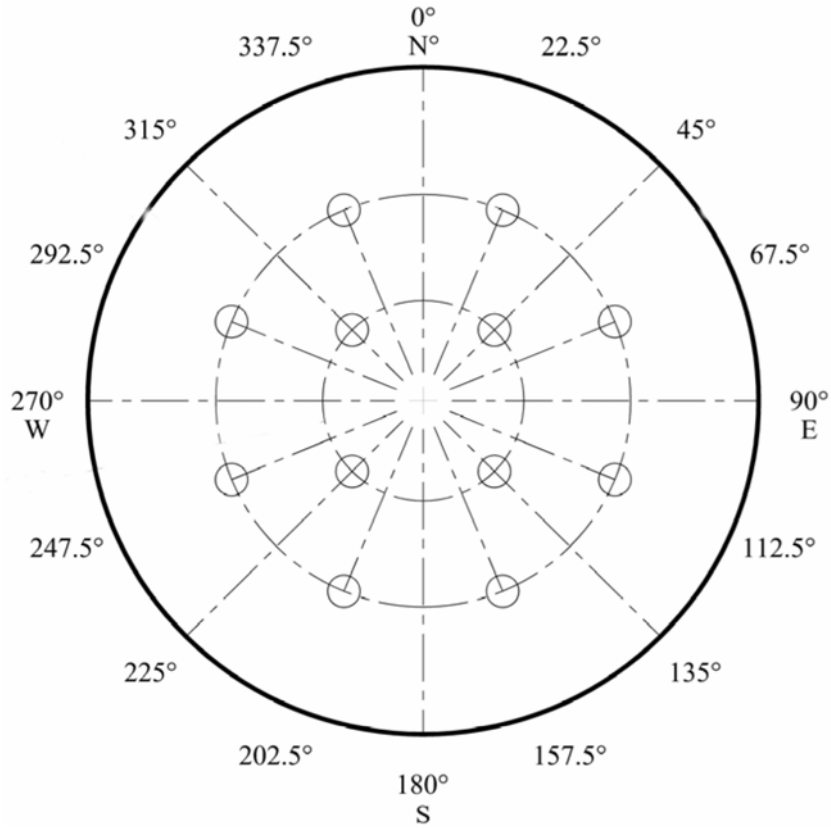

Figure 4.17. Plan View of 12-Tube HLP-22 Elliptical Array Orientation Between Inner and Outer Rings in the Large-Scale Tank. The as-tested outer ring radius was 0.555 m (21.85 in.); the inner ring radius was 0.292 m (11.5 in.).

Table 4.5. Measured HLP-22 12-Tube Array Positions

	Tank Diameter		Tank Radius		Inner Tube Radial Position R_i		Average Inner Tube Radial R_i/R	Outer Tube Radial Position R_o		Average Outer Tube Radial R_o/R
	in.	m	in.	m	in.	m		in.	m	
Small-Scale Elliptical	14.44	0.367	7.22	0.183	2.44	0.0620	0.34	4.5	0.114	0.62
Mid-Scale Spherical[(a)]	33.9	0.860	16.9	0.430	5.67	0.144	0.33	10.46	0.266	0.62
Large-Scale F&D	70.0	1.78	35.0	0.889	11.48	0.292	0.33	21.85	0.555	0.62
Large-Scale Elliptical	70.0[(a)]	1.78	34.6	0.878	11.68	0.297	0.34	26.40	0.671	0.76
-	69.16[(b)]	1.76	-	-	-	-	-	-	-	-

(a) Measurement at top of tank rim.
(b) Measurement at top of dish.

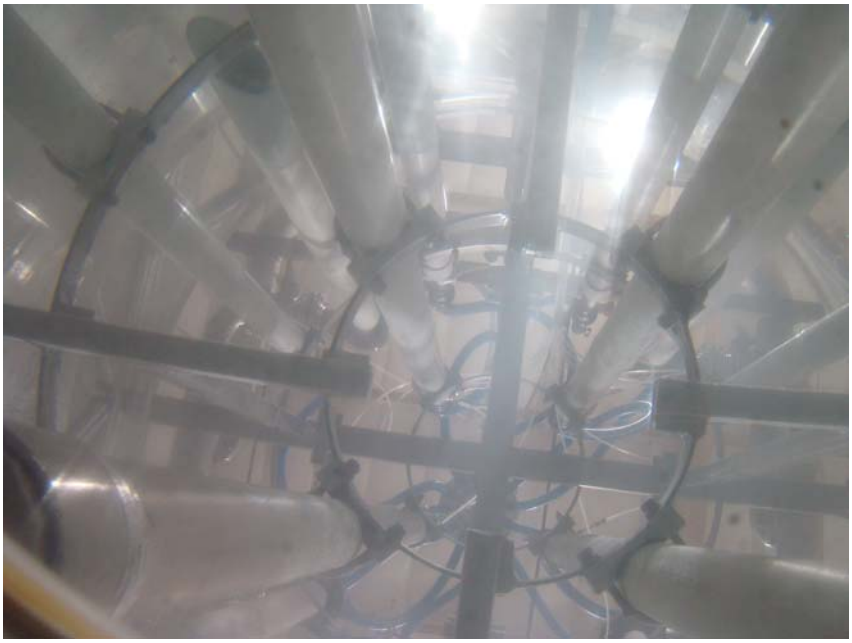

Figure 4.18. In-Tank Structural Support for the Tube Array in the Large-Scale Tank (as viewed from underneath the tank through the viewing window)

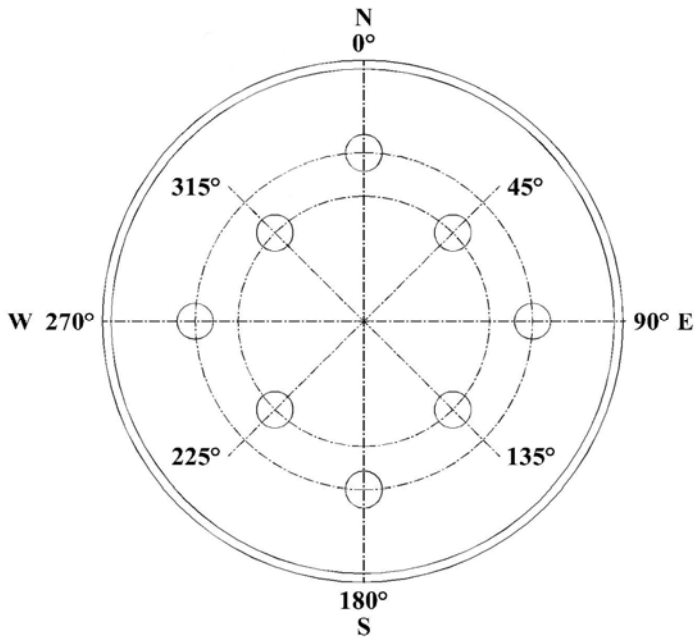

Figure 4.19. Plan View of 8-Tube Array Orientation Between Inner and Outer Rings in Small-Scale Tank

The positions of the 8-tube arrays in the tanks are listed in Table 4.6. Initial testing used two nozzle sets for each test stand. Nozzle diameters for the 12-tube arrays are shown in Table 4.7 and those for the 8-tube arrays in Table 4.8. The jet stand-off target for the nozzles was 1.5 jet nozzle diameters from the bottom of the tank. Additional nozzles were used in the 8-tube array tests to represent small, medium and large nozzle sizes in the 8-PJM tanks. Isometric views of the 8-tube array are shown in Figure 4.20.

Table 4.6. Measured 8-Tube Array Positions

	Tank Diameter		Tank Radius		Inner Tube Bottom		Inner Tube Radial as-Tested	Outer Tube Bottom		Outer Tube Radial as-Tested
	in.	m	in.	m	in.	m	R	in.	m	R
Small-Scale 8-Tube Small Nozzle	14-7/16	0.367	7.22	0.183	3.61	0.0917	0.50	4.85	0.123	0.67
Small-Scale 8-Tube Medium Nozzle	14-7/16	0.367	7.22	0.183	3.61	0.0917	0.50	4.85	0.123	0.67
Small-Scale 8-Tube Large Nozzle	14-7/16	0.367	7.22	0.183	3.61	0.0917	0.50	4.85	0.123	0.67
Large-Scale 8-Tube	70	1.78	35	0.89	17.5	0.44	0.50	23.5	0.60	0.67

Table 4.7. HLP-22 12-Tube Array Nozzle and Pulse Tube Sizes

	HLP-22 0.102 m (4-in.) Nominal Nozzle Equivalent		HLP-22 0.152 m (6-in.) Nominal Nozzle Equivalent		Pulse Tube (Nominal size for Schedule 40 PVC)[(a)]	Pulse Tube ID		Pulse Tube OD	
Vessel	in.	cm	in.	cm	in.	in.	cm	in.	cm
Small-Scale	0.126	0.320	0.191	0.485	3/4	0.824	(b)	1.05	(b)
Mid-Scale	0.297	0.75	0.446	1.13	1.5	1.61	(b)	1.9	(b)
Large-Scale	0.613	1.56	0.920	2.34	3	3.068	(b)	3.5	(b)

(a) All schedule 40 PVC pipe information is from the ASTM International Designation: D 1785-06 standard for PVC plastic pipe, Schedules 40, 80 and 120 American National Standard.
(b) The ASTM standard does not show metric values.

Table 4.8. 8-Tube Array Nozzle and Pulse Tube Sizes

		Nominal Nozzle Size		Pulse Tube (Nominal size for Sched 40 PVC)	Pulse Tube ID		Pulse Tube OD	
Vessel	Nozzle	in.	cm	in.	in.	cm	in.	cm
APEL15	Small	0.191	0.49	3/4	0.824	(a)	1.05	(a)
APEL15	Medium	0.268	0.68	3/4	0.824	(a)	1.05	(a)
APEL15	Large	0.375	0.95	3/4	0.824	(a)	1.05	(a)
APEL70	Small	0.920	2.34	3	3.068	(a)	3.5	(a)

(a) The ASTM standard does not show metric values.

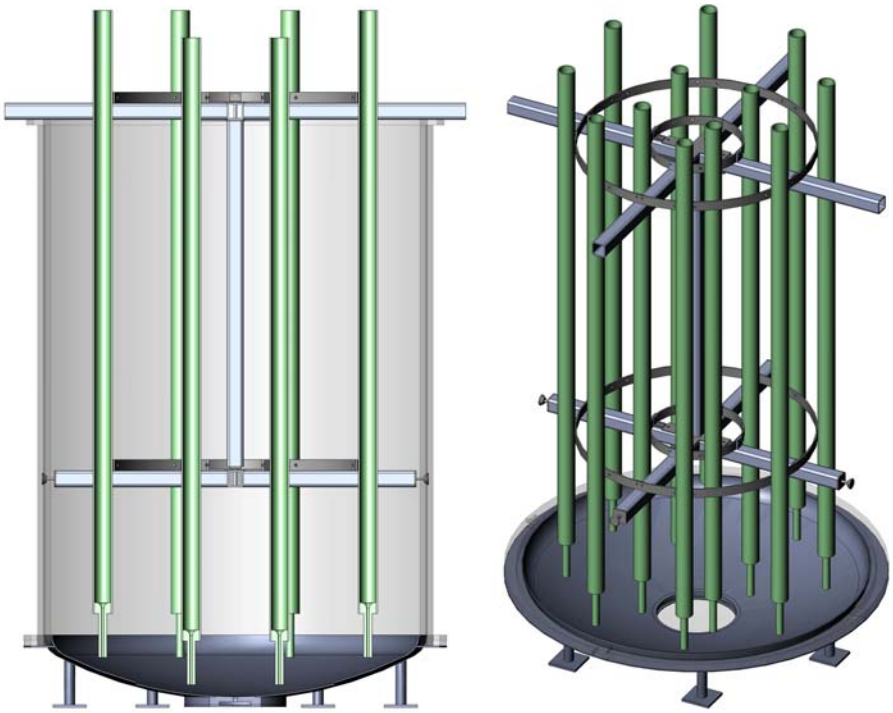

(a)

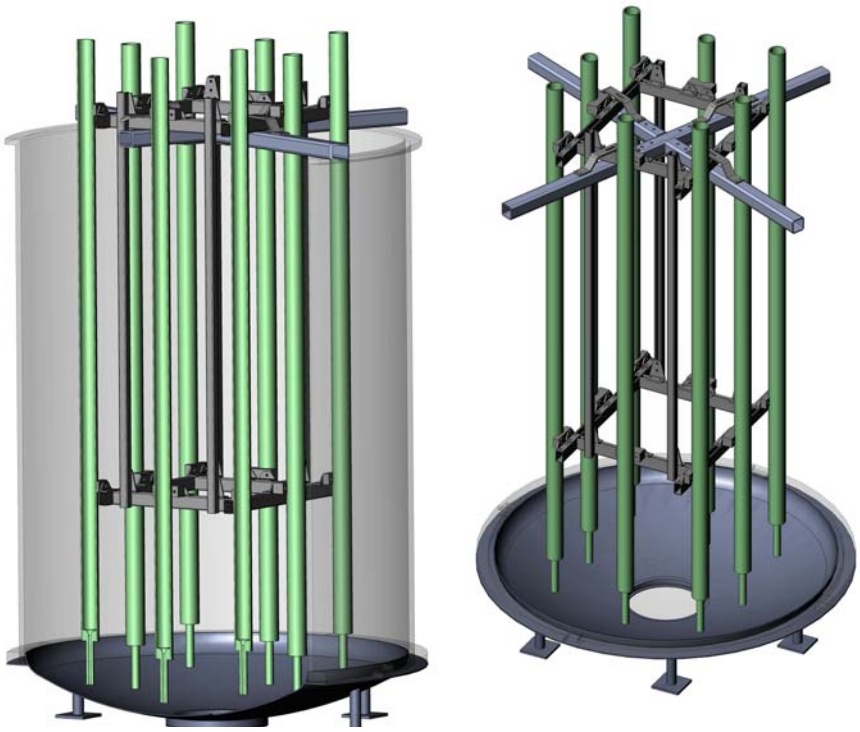

(b)

Figure 4.20. (a) HLP-22 12-Tube Tank Array (not to scale); (b) 8-Tube Array in Large-Scale Elliptical-Head Tank (not to scale)

5.0 Experimental Procedures

The experimental procedures used during the scaled mixing experiments are described in this section. The experiments were conducted in three test campaigns: July 2007, Fall 2007, and 2008. During each test campaign, improvements in testing protocol and instrumentation were implemented. However, the overall goal of the testing remained the same: to determine the U_{CS} for each test and to determine the cloud height at a range of velocities surrounding U_{CS}. Section 5.1 gives an overview of the tests performed in each campaign. In Section 5.2, key observation procedures related to performance criteria are described. Only the elements of the procedures relating to the performance criteria are covered. Calculations performed in the DAS are described in Section 5.3. The test procedures and other documents used during the experiments are listed in Section 5.4. The full details of the experimental procedures used are contained in the test documents listed in Table 5.7.

5.1 Testing Overview

The main test objective was to observe the influence of vertically downward-directed jets on noncohesive solids in a series of scaled tanks with several bottom shapes. As described in Section 4.0, the test tanks and bottom shapes included small-and large-scale tanks with elliptical bottoms, a mid-scale tank with a spherical bottom, and a large-scale tank with an F&D bottom. Program test objectives are discussed in Section 1.3. The test campaigns were conducted to address the objectives (using numbering shown in Table S.1 from Executive Summary) as follows:

- July 2007 tests using only the mid-scale system were used mainly to address the first two program objectives regarding the nozzle size and operating velocities to be used in HLP-22.
- Fall 2007 tests began to examine the effect of several geometric parameters (still using only the mid-scale system); this addressed part of the third objective. The effects of variations in the number of operating nozzles, tank fill level, and height of the return suction line were investigated in preparation for further parametric tests performed in 2008.
- 2008 tests continued to evaluate the effect of various parameters (waste properties, equipment design, and process operations), and included investigation of scale effects by testing in all three scaled test systems (covering Objectives 3 and 4).
- Results from all three test campaigns were used to develop the models and identify the key parameters for vessel mixing performance (Objectives 5 and 6).

During testing, the downward-directed jets were operated in either a steady flow condition or a pulsed (periodic) flow condition. The mobilization of the solids resulting from the jets was evaluated based on:

- The motion/agitation of the particulate on the tank floor.
- The elevation the solids reach within the tank; the height the solids material reaches in the tank is referred to as the cloud height (H_C).
- Other observations deemed significant to characterize the system performance relative to mobilization and/or suspension of solids, such as patterns and dimensions of the cleared regions of the tank floor where particulate had been swept away. In the 2008 tests, measurements of the solids concentration profile were collected using ultrasonic attenuation methods (described in Appendix A).

During testing in 2008, the client expressed significant interest in being able to predict waste concentrations at the suction pump inlet near the bottom of the HLP-22 vessel. Although not in the original test objectives, data collected during testing has been analyzed to provide understanding of solid concentrations near the tank bottom (see Sections 6.0 and 7.0 and Appendix C).

Testing was performed using water as the working fluid, and the temperature was recorded to determine the reference viscosity and density for post-test analysis. The test parameters of interest are listed in Table 5.1. Important operating parameters for a PJM vessel are jet velocity, duty cycle, drive time, cycle time, pulse volume fraction, solids volume fraction, and normalized fill level. The parameters that are important in tank design and the effect of tank design on material movement are tank diameter, nominal volume of tank, number of pulse tubes, radial PJM ring positions, nozzle diameter, and head shape. Parameters that reflect differences between test systems and a full-scale PJM vessel include return line height, impingement angle, scaling factors, and nozzle ratio.

Table 5.1. Mixing System Parameters

Parameter	Symbol
Dimensional	
Tank diameter	D
Normal fill level of tank	H
Reference volume of tank where $V_{REF}=\pi D^3/4$	V_{REF}
Number of pulse tubes	N
Number of operating jets	N_J
Number operating jets-(inner/outer)	N_I / N_O
Radial PJM ring position (inner/outer)	R_I / R_O
Impingement angle (inner/outer)	θ_I / θ_O
Nozzle diameter	d
Jet velocity	U
Drive time	t_D
Cycle time	t_C
Return line height	Rtn
Head shape	HS
Nondimensional	
Scale factor	S
Nozzle ratio	d/D
Normalized fill level	H/D
Solids volume fraction where $\phi_S = V_S/V_{REF}$	ϕ_S
Pulse volume fraction where $\phi_p = NV_P/V_{REF}$	ϕ_p
Duty cycle	DC
Jet density where $\phi_J = N_J d^2/D^2$	ϕ_J

For an individual test, jet velocity was varied while solids volume fraction and normalized fill level were held constant. For a pulsed flow test, pulse volume fraction and duty cycle were also held constant, while drive time and cycle time were adjusted to achieve the desired duty cycle. All other system parameters from Table 5.1 were also held constant. Most tests were performed by starting from an initial

condition at which settled solids were present on the tank floor (i.e., a starting velocity below U_{CS}) and incrementally increasing the velocity over the test. This type of test was called an upward velocity sweep. Critical suspension velocity determined from an upward sweep velocity is called U_{CS}. Downward velocity sweep tests were also performed by starting from a velocity above U_{CS} and incrementally decreasing the velocity over the test. When critical suspension velocity is determined from a downward sweep test, it is called U_{CS_D}. Observations were recorded at each velocity as described in Section 5.2.

5.2 Observation Procedures

Observation procedures were developed and applied during the July 2007 and Fall 2007 test campaigns and were refined for 2008 as additional ultrasonic instrumentation became available to measure the thickness of the settled solids layer and the concentration profiles inside the suspended cloud. Both of the ultrasonic techniques are described in Appendix A. Solids layer thickness was recorded at the end of the pulse, while concentration profiles were obtained as a function of time throughout each pulse.

To assist with observations, each pulse tube in the mid-scale tank was given a unique identification, as shown in Figure 5.1. North was considered zero degrees, with the angle increasing clockwise when viewed from above. The tubes were labeled with a letter indicating relative radial position of the pulse tube, I for inner ring, O for outer ring, and a number for designating each tube at a particular tank radius.

For the example of the HLP-22 (12-tube) configuration shown in Figure 5.1, consider the inner ring of four nozzles starting at 45°. The tubes and nozzles are labeled I1 through I4, corresponding to angles of 45°, 135°, 225°, and 315°, respectively. Likewise, the labeling for the outer ring of tubes/nozzles starts at 22.5° and increases sequentially in 45° increments starting with O1 through O8.

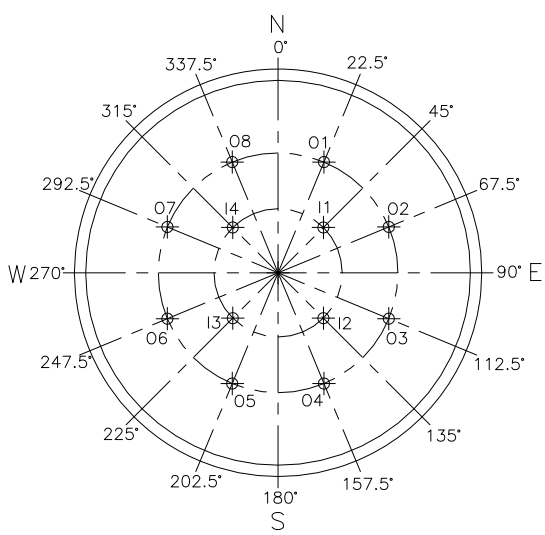

Figure 5.1. Illustration of Relative Positions of Pulse Tubes and Nozzles in the Mid-Scale Test Tank in HLP-22 (12-tube) Configuration

5.2.1 Observation Procedures Used in 2007

All observations were recorded when the motion in the tank appeared to have reached a steady-state condition (or a periodic condition that was considered a steady-state condition). The steady-state

condition was said to exist when no visually observed changes in the solids behavior and no significant changes in the operating conditions were occurring. The test engineer determined the duration of operation required to achieve a steady condition. Prior to the collection of cloud height data, the test system was pulsed or operated until the clouds were stable. After the clouds were stable, the test engineer opened an "observation window" (i.e., a limited time period during which data were recorded) for the collection of cloud height, U_{CS}, and other data. During the observation window, data were collected for a period of at least five pulses with no observable changes over the five pulses. If the cloud conditions changed over the observation window, the window was closed, the cloud was stabilized, and a new observation window was then opened. The suggested minimum durations to demonstrate steady-state conditions were three minutes for steady jet operation and five cycles for pulsing jets, with no observable change in solids behavior over the duration. This was based on experience from the initial tests conducted using a 5-minute period for steady jets and 25 cycles for pulsing jets.

Four categories of phenomena were selected for observation: particle motion, cloud height, solids level, and the pattern of cleared region on the tank floor. These categories are explained in Subsections 5.2.1.1 through 5.2.1.4. The categories were given scales, as discussed below. All but cloud height were observed through the transparent tank head by observers viewing directly or using mirrors placed on the floor under the tank—whichever method provided the best view in the circumstances.

5.2.1.1 Particle Motion

Particle motion was observed through the clear tank head and characterized using the two-letter abbreviations listed in Table 5.2.

Table 5.2. Particle Motion Descriptors[(a)]

Abbreviation/ Nomenclature	Meaning	Description
NM	No motion	No or very little movement of solids.
SM	Some mobilization	Some solids are moving but minimal or no observed suspension. Some regions appear to have no moving particles.
SS	Some suspension	Some particles appear to be becoming suspended. Some regions appear to have no moving particles remaining on the tank floor.
AM	All moving, mostly suspended	Essentially all solids are mobilized. No areas of non-moving solids.
CS	Critical suspension	Initial state of complete solids suspension (all moving off of bottom). For pulsing jets, this is defined as all particles moving at the end of a pulse cycle.
BC	Beyond critical suspension velocity	Discharge velocity is greater than U_{CS}.

(a) The critical observation for these tests was to determine U_{CS}, the velocity at which the transition to/from the state of complete solids suspension occurred for incremental increases/decreases in nozzle discharge velocity.

5.2.1.2 Particle Cloud Height

The particle cloud height was based on the upper height of the opaque cloud created by the suspension of solids, which may or may not be a well-defined boundary. The height was based on the cloud (see example in Figure 5.2), not the height of a few outlier particles. Measurements were taken with respect to a fixed reference point[1] and recorded to the nearest 0.5 in., including the range (fluctuation) of any oscillation. For example, if cloud heights oscillated between 20 and 24 in., 20 to 24 in. was recorded.

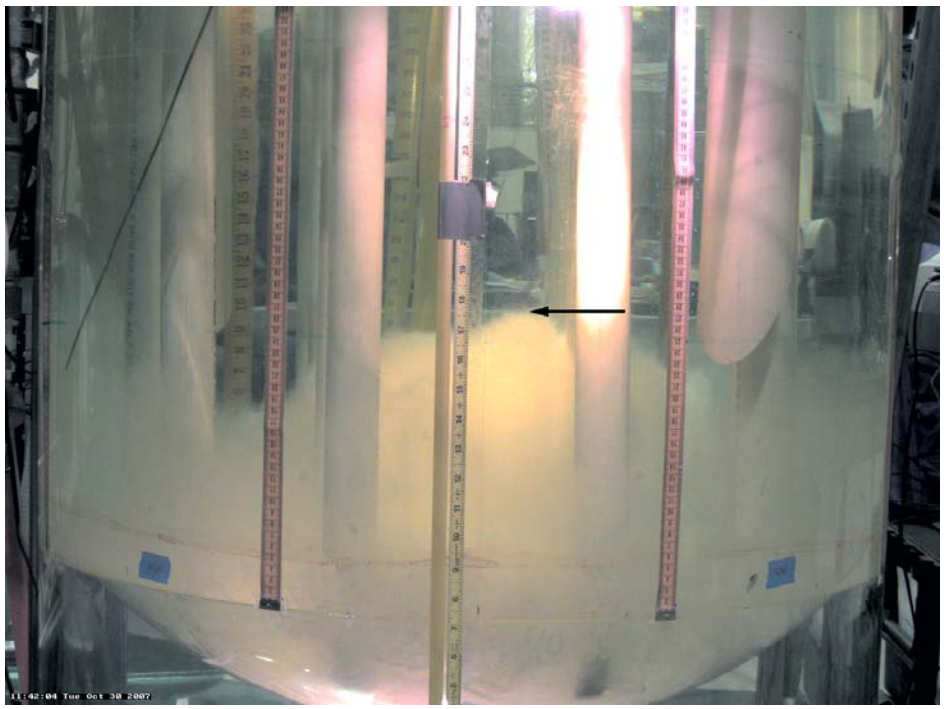

Figure 5.2. Photograph of Particulate Cloud Near End of Pulse in Mid-Scale Tank Showing a Centrally Peaked Cloud and Measuring Tapes Used for Cloud Height Measurement (for information only). Arrow indicates the peak portion of the cloud that is measured to get cloud height.

5.2.1.3 Solids Level

The solids level was defined as the upper edge of settled solids in the bottom of the tank. The solids level could fall entirely within the dished bottom of the tank or, at high solids volume fraction, reach the vertical side of the tank. The top surface of settled solids in the dished bottom was optically distorted due to the curvature of the dish, which made a true level measurement more uncertain. Thus, solids level below the cylinder/elliptical bottom junction was described relative to the pulse tube nozzle rings (e.g., solids level was just below the outer nozzle ring). If the solids level was above the cylinder/dish junction, the level was measured in a manner similar to cloud height. Solids level observations were described using the nomenclature shown in Table 5.3.

[1] During initial testing in 2007, cloud height was measured from the top surface of the tank rim (and converted to height from bottom center for data analysis), but by October 2007 cloud height was being measured with respect to the bottom center of the tank.

Table 5.3. Solids Level Nomenclature

Abbreviation/Nomenclature	Associated Observations
Record actual measurement	Solids level was above the lower seam of the cylindrical portion of the tank.
SON	Solids level was above the nozzle discharge of the outer ring of nozzles but below the lower seam of the cylindrical portion of the tank.
SIN	Solids level was above the nozzle discharge of the inner ring of nozzles but below the nozzle discharge of the outer ring of nozzles.
SCO	Settled solids observed in the center region of the tank but below the nozzle discharge of the inner ring of nozzles.
SOO	Solids observed only between outer nozzle ring and the end of tank.
NSS	No settled solids were observed.

5.2.1.4 Pattern of Cleared Region

The pattern of cleared region/settled solids column was described using the three-character nomenclature (two letters followed by a numeral) shown in Table 5.4. The settled solids may or may not have been moving.

5.2.2 Observation Procedures Used in 2008

All observations were recorded when the measured flow and the particle motion in the tank appeared to have reached steady state, and no observable change in solids behavior (e.g., transient behavior in cloud height) was detected over the observation period.

- Steady state for pulsed flow (a true periodic condition) was considered to exist when, for a period of 5 pulses, the charted instantaneous velocity, U(t), yielded a visually observed peak average velocity, U_{PA}, which appeared to remain constant to within ±5% (see Figure 5.3). U_{PA} was obtained by visually monitoring a DAS velocity chart screen that was scaled to display the range of target U_{PA} to ±5%.

- Steady state for steady flow conditions was said to exist when the steady jet velocity, U_S, was constant to within ±5% over 2 minutes. U_S was a running time-average of the instantaneous velocity, U(t), taken over a time interval sufficient to smooth out noise in the velocity signal. U_S was calculated by the DAS.

The time required to reach steady state may depend on the settling velocity of the simulant. Thus, observers needed to be cognizant of slow transients occurring in the mobilization of the solids.

Table 5.4. Pattern of Cleared Region Viewed from Beneath the Tank

Abbreviation/ Nomenclature	Description	Visual
BP0	No cleared region of the tank.	N/A
BP1	Some but not all nozzle locations have a cleared region.	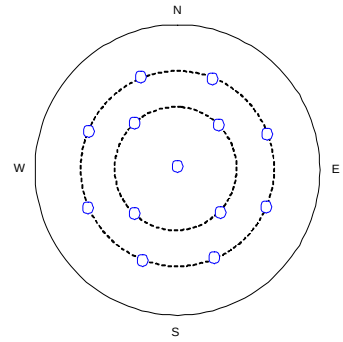
BP2	All nozzle locations have a small cleared region, no larger than about 2 in.	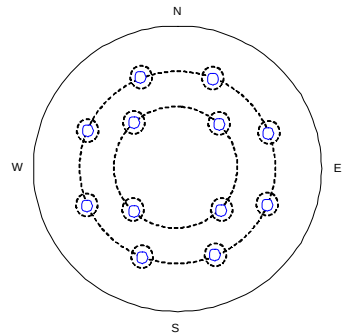
BP3	All nozzle locations have a cleared region greater than 2 in., but the regions are still separate with no merging of clear spaces.	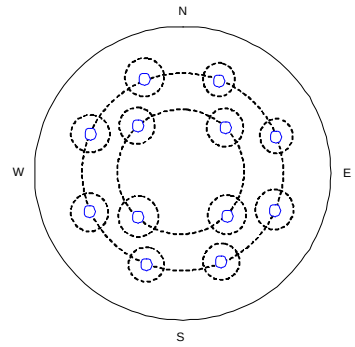
BP4	Cleared regions created by individual nozzles have merged.	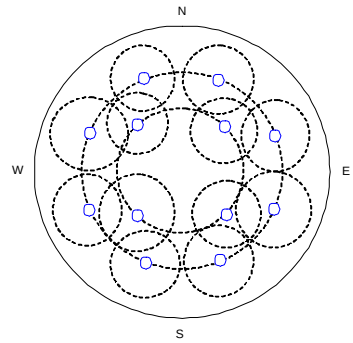
BP5	Settled solids only observed in center region and/or at the edges of the tank.	N/A
BP6	No observable pattern of settled solids.	N/A

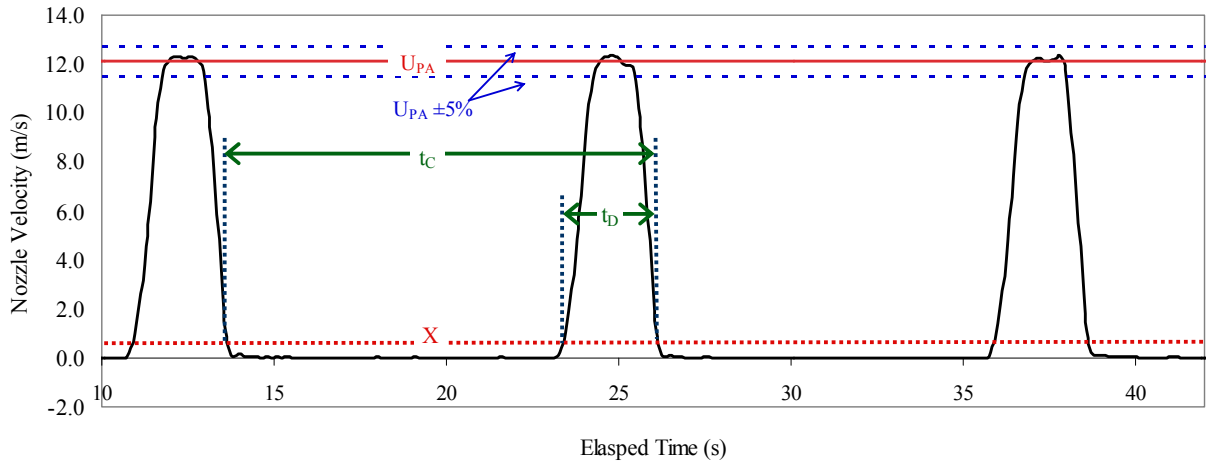

Figure 5.3. Illustration of Nozzle Velocity as a Function of Time for Several Discharge Cycles. X, the setpoint used by the DAS, is a threshold velocity for distinguishing assumed zero flow from the pulse flow. A pulse or discharge is the portion of the cycle for which the velocity (calculated from the mass flow rate signal) is greater than X. t_D is the discharge or pulse time. For this example assume target U_{PA}=12.1 m/s over the observation period.

Two phenomena were selected for visual observations of solids behavior: particle motion and particle cloud height, which are explained in Subsections 5.2.2.1 and 5.2.2.2. These two phenomena most directly related and correlated to measurements taken at different scales; the observation of settled solids level and clearing pattern were omitted from the 2008 procedures. Observations of particle motion and cloud heights were taken at each test condition unless specified otherwise by the test condition transmittal (TCT). When specified in the TCT, attenuation data for concentration profiles were also taken. The procedures used for the attenuation data are covered in Section A.2 (Appendix A) and Section 6.5. Attenuation data were collected at specified velocity conditions only, generally at or just beyond U_{CS}.

5.2.2.1 Particle Motion

Two methods were used to monitor solids suspension: visual observation and detection of solids layer thickness at the end of the pulse using UDV. Particle motion was observed visually from beneath the transparent tank bottom or through the window in the center of the bottom of the large-scale tank. Table 5.5 lists observation procedures; differences in procedures between tanks are shown in italics. Table 5.6 lists a scale of observations relative to the condition of visually determined U_{CS}. The numeric scale used to describe particle motion in the 2008 tests was slightly simplified from the abbreviations used in 2007 in that all conditions below U_{CS} were grouped together. The critical observation for these tests was to determine U_{CS}, the velocity at which the transition to/from the state of complete solids suspension occurred for incremental increases/decreases in nozzle discharge velocity. The test engineer decided whether sufficient resolution had been obtained for the increment between conditions.

Table 5.5. Procedures for U_{CS} Observations

Small-Scale Test Observations	Mid- and Large-Scale Test Observations
Detection of U_{CS} [by UDV] was based on the layer of settled solids monitored by the UDV transducer at tank center. U_{CS} was considered to exist between discharge velocities where the transducer sensed a solids layer from 0 to 4 mm *over at least 5 pulses.* When determining U_{CS}, the *minimum* resolution of nozzle discharge velocity is ± 0.2 m/s. To evaluate UDV results, the velocities to be determined are those that *over 5 pulses:*	Detection of U_{CS} [by UDV] was based on the layer of settled solids monitored by a UDV transducer at tank center. U_{CS} senses a solids layer from 0 to 4 mm *during the observation.* When determining U_{CS}, *target* resolution with respect to nozzle discharge velocity is ± 0.2 m/s. To evaluate UDV results, velocities to be determined are those that:
1) Yield a thin solids layer ideally between 4 and 10 mm (<U_{CS} corresponds to #1 from Table 5.6).	1) Yield a solids layer between 4 and 10 mm (<U_{CS}, corresponds to #1 from Table 5.6).
2) Yield a solids layer ranging from 0 to < 4 mm with at least one of the 5 values > 0 (this is considered the UDV U_{CS} value; may correspond to #2 from Table 5.6). These solids depths may be obtained over a range of velocities. If values from 0 to < 4 mm are obtained, the U_{CS} is the highest velocity that *yields values of 0 to less than 4 mm with at least one value in 5 greater than 0.* • If no measurements meet the *5-pulse criterion*, U_{CS} is the lowest velocity yielding all 0 values *that is within 0.2 m/s of the lowest velocity to yield a solids depth of 4 mm or more.*	2) Yield a solids layer ranging from 0 to less than 4 mm with at least one of the *observed* values greater than 0 (this is considered the UDV U_{CS} value; may correspond to #2 from Table 5.6) *These* depths may be obtained over a range of velocities. If values from 0 to less than 4 mm are obtained *at multiple velocities,* the U_{CS} is the highest velocity that *meets this criterion.* • If no measurements meet this criterion, U_{CS} is the lowest velocity yielding all 0 values.
3) Yield only 0 values for solids layer for a velocity no more than 0.2 m/s greater than that, which yielded a solids layer ranging from 0 to less than 4 mm (>U_{CS} verifies that UDV U_{CS} was obtained at previous step; may correspond to #3 from Table 5.6).	3) Yield only 0 values for solids layer; *ideally* for velocity no more than 0.2 m/s greater than what yielded a solids layer from 0 to less than 4 mm (> U_{CS} verifies that UDV U_{CS} obtained in #2 may correspond to #3 from Table 5.6).
At the discretion of the test engineer or the TCT, additional velocities can be evaluated that yield solids layers between 5 and 20 mm to help predict U_{CS} by curve fitting the data.	
It is expected that the visually observed detection of U_{CS} may differ from that detected by the UDV transducer. It is also expected that as particle size is reduced, greater ambiguity or disparity may exist in visually detecting U_{CS}. Neither condition creates problems because the goal is to define metrics that can predict full-scale vessel performance. If the detection of U_{CS} or the metric of choice (visual or UDV-detected U_{CS}) is consistent at the different geometric scales, the developed models will trend with scale. Test results over a range of particle diameters allow comparison of visually observed U_{CS} and UDV detected U_{CS}.	
UDV determination of U_{CS} takes precedent over visual measurements; thus the TCT may request only UDV detection be used. Otherwise, both methods are used. *Note (Particle Motion): For any U_{CS} determination (visual or UDV), velocity for reported U_{CS} values must be bracketed by observations at velocities no more than 0.2 m/s higher/lower (smaller increment acceptable).*	UDV determination of U_{CS} takes precedent over visual measurements; thus the TCT may request only UDV detection be used. Otherwise, both methods are used.

Table 5.6. Particle Motion Descriptors for Visual Observations

Number	Meaning	Description
1	Below critical suspension velocity $<U_{CS}$	Solids may be moving or partly suspended; regions of settled particles are apparent (settled particles may be moving).
2	Critical suspension, U_{CS} at tank center	Initial state of complete solids suspension (all moving off bottom) occurs at the center of the tank at the end of the fluid pulse while unsuspended particles exist elsewhere on tank bottom. This behavior is not observed for all combinations of simulants and geometries/tube arrays.
3	Overall critical suspension[(a)]	Initial state of complete solids suspension (all moving off bottom) occurs over entire tank. For pulsing jets, this is defined as all particles moving at the end of a pulse. For steady jets, any settling particles appear to lift off the bottom within 2 s of touching down. By definition this behavior only exists at a single velocity for a given set of operating, geometry, and physical conditions (not at multiple velocities for the same test conditions).
4	Beyond critical suspension velocity $>U_{CS}$	Discharge velocity is greater than U_{CS}. For pulsing jets, particles are fully suspended before the end of the pulse.

(a) In the large-scale systems, overall U_{CS} (condition 3) is not visually observable due to the steel heads (viewing ports only allow observation of the particulate at the bottom center). Only test conditions that yielded final solids suspension in the tank center in the 34- and 15-in. vessels were tested in the 70-in. system.

The center of the tank was selected as a readily scalable location to monitor the solids mobilization. Therefore, regardless of the test condition or potential pulse tube configuration, the solids mobilization at the tank center was monitored whether or not it was the final location on the tank bottom at which solids became mobilized. For this test program, the desire was to identify/determine metrics that could be used to evaluate trends over geometric scales. Without knowing what were the best metrics before testing, the decision was to monitor both the occurrence of a condition at a specific location as well as a defined condition regardless of location.

For the WTP test vessel configurations tested (e.g., HLP-22 and RDL-8), the center of the vessel was always the last location that the solids became mobilized. However, for other configurations evaluated to investigate the effects of pulse tube location, such as a four-tube configuration that consisted of only the inner ring of HLP-22 pulse tubes, the center region was not the last to mobilize. To accommodate the potential of having to monitor U_{CS} other than at tank center, observation conditions 2 and 3 were defined (see Table 5.6).

Condition 2 was noted by the test observers for a discharge velocity if the U_{CS} condition at the tank center was satisfied but solids elsewhere on the tank bottom were not fully suspended at the end of a pulse. This condition was never observed for the WTP configurations tested. This condition also could not be monitored in the 70-in. vessel due to the limited viewing port on the tank bottom. Therefore, testing in the 70-in. system was performed only for those configurations and conditions that yielded the location of final solids mobilization at the tank center. These conditions were later tested in the 15-in. system to confirm that final solids mobilization occurred at the tank center. It was assumed, based on

these results, that final mobilization occurred at the tank center for the conditions tested in the 70-in. vessel.

For those cases where the final mobilization of solids on the tank bottom coincided with the tank center, condition 3 (Table 5.6) was noted by the test observers for the corresponding discharge velocity and the location of final suspension was given as the tank center. This is the condition occurring for all of the WTP configurations that were tested.

5.2.2.2 Particle Cloud Height

The particle cloud height was based on the upper height of the opaque cloud created by the suspension of solids at the center of the tank, which may or may not have been a well-defined boundary. The height was based on the cloud, not on the height of a few outlier particles. Note that cloud heights were measured the same way in the 2008 tests as they had been in the 2007 tests. The cloud heights tended to vary within a range of values during an observation period. Thus, in 2008 the procedure was modified to specify recording the range of cloud heights as upper and lower bounds.

- For steady flow the cloud heights were reported as the upper and lower bounds observed over a 1-minute interval. If the cloud height appeared constant the same value was recorded for both observations.
- For pulsed flow, the cloud heights were reported as the upper and lower bounds of the peak height of the opaque cloud (only one value per pulse) observed over at least three pulses (i.e., of the observed cloud heights only the minimum and maximum values are reported as the bounds). If the cloud height appeared constant the same value was recorded for both observations.

The average cloud height was determined by averaging the recorded upper and lower bound values. Cloud height was generally measured from the bottom center of the tank and data was always evaluated with respect to the bottom dead center of the tank. Measurements were recorded to the nearest 0.5 in. Measuring tapes were attached to the tank to facilitate these measurements.

5.3 Data Acquisition System Calculations

The DAS receives mass flow rate and fluid density signals from the Coriolis meter and converts those signals to instantaneous nozzle velocity, U(t), and volumetric flow rate, Q (as a function of time). From these the DAS can also calculate other parameters of interest. For the Fall 2007 and 2008 tests, the DAS was used to calculate the following values for each pulse cycle:

the average pulse velocity

$$U1 = \frac{\int U(t)dt}{t_D} \tag{5.1}$$

the average root-mean-squared pulse velocity

$$U2 = \left(\frac{\int U(t)^2 \, dt}{t_D} \right)^{\frac{1}{2}} \tag{5.2}$$

the average root-mean-cubed pulse velocity

$$U3 = \left(\frac{\int U(t)^3 \, dt}{t_D} \right)^{\frac{1}{3}} \tag{5.3}$$

the pulse volume fraction

$$\phi_p = \frac{\int Q(t) dt}{V_{REF}} \tag{5.4}$$

and the duty cycle

$$DC = \frac{t_D}{t_C} \tag{5.5}$$

where t_D, the pulse or discharge time, is the time from start of flow (t_{FS}) to end of flow (t_{FE}): $t_D = t_{FE} - t_{FS}$, and t_C is the cycle time. $V_{REF} = (\pi/4)D^3$ is the reference volume based on the volume of a right circular cylinder of height and diameter D. Using a reference volume to model mixing performance is discussed further in Section 7.2.3.

The numerical integrations were performed over the duration of the pulse, from t_{FS} to t_{FE}. The specified calculation time periods are depicted in Figure 5.3. Also depicted is the parameter X (comparator setpoint), used in the DAS to determine the time periods. Parameter X is the velocity setpoint above which the system is judged to have flow and below which non-zero flow is assumed to be system variation and/or noise that is below the threshold velocity of interest for mobilization. Thus, X determines the start and end of flow used to determine t_D and t_C in Eq. (5.1) through (5.5).

For steady jet tests, the steady jet velocity, U_S, was calculated as a running time average of the instantaneous velocity, U(t), over a time interval sufficient to smooth out noise in the velocity signal.

Early testing conducted in July 2007 used the DAS to calculate the pulse volume fraction, ϕ_p, as shown in Eq. (5.4). However, the DAS performed the integration over the duration of the cycle (including the no-flow period prior to pulse), and the integration cycle was triggered by the valve drive voltage rather than nozzle velocity, U(t). The average velocities, U1, U2, and U3, were calculated similarly in post-test analysis. Several system improvements were made to the DAS after the July 2007 tests that allowed the additional calculations.

5.4 Governing Documents

The tests were conducted based on test plans, test procedures, and test instructions. The documents controlling each test are listed in Table 5.7. This table also includes test procedures applicable to the ultrasonic methods and particle size analysis described in Appendix A and Section 3.0, respectively.

Table 5.7. Documents Governing the 2007 and 2008 Tests

Document Type	Number	Title	Test
Test Plan	TP-RPP-WTP-480, Rev. 0	M3 Testing Approach in Support of Tank HLP-22	2007
Test Procedure	TPR-RPP-WTP-522, Rev. 0	Mobilization Experiments in 34-in. Test Tank	2007
Test Instruction	TI-RPP-WTP-523, Rev. 0	34-in. Test Tank Instructions for Obtaining V_{JS}[(a)]	2007
Test Instruction	TI-RPP-WTP-526, Rev. 0	Test instructions for Benchmarking V_{JS} Observers	2007
Test Plan	TP-RPP-WTP-480, Rev. 0.1	M3 Testing Approach in Support of Tank HLP-22	2008
Test Plan	TP-RPP-WTP-480, Rev. 0.2	M3 Testing Approach in Support of Tank HLP-22	2009
Test Procedure	TPR-RPP-WTP-595, Rev. 0	Mobilization Experiments in 34-in. Test Tank	2008
Test Procedure	TPR-RPP-WTP-596, Rev. 0.1	Mobilization Experiments in 15-in. Test Tank	2008
Test Procedure	TPR-RPP-WTP-597, Rev. 0.1	Mobilization Experiments in 70-in. Test Tank	2008
Test Instruction	TI-RPP-WTP-598, Rev. 0	34-in. Test Tank Instructions for Obtaining U_{CS}	2008
Test Instruction	TI-RPP-WTP-600, Rev. 0	70-in. Test Tank Instructions for Obtaining U_{CS}	2008
Test Instruction	TI-RPP-WTP-636, Rev. 0	15-in. Test Tank Instructions for Obtaining U_{CS}	2008
Test Procedure	TPR-RPP-WTP-608, Rev. 0	Calibration Procedure for Determining Velocity of Ultrasonic Energy in Simulants	2008
Test Procedure	TPR-RPP-WTP-626, Rev. 0	Particle Size Analysis Using Malvern MS2000	2008
Test Procedure	TPR-RPP-WTP-628, Rev. 0	Procedure for Correlation of Ultrasonic Attenuation and Slurry Concentration	2008
Test Procedure	TPR-RPP-WTP-628, Rev. 0.1	Procedure for Correlation of Ultrasonic Attenuation and Slurry Concentration	2008

(a) V_{JS} terminology was changed to U_{CS} as the project progressed.

6.0 Mixing Experiments

The mixing experiments and data obtained during the July 2007, Fall 2007, and 2008 mixing test campaigns are described in this section. In Section 6.1 the data reporting format is presented. In Sections 6.2, 6.3, and 6.4, the details of the three mixing test campaigns are summarized and cloud height results for specific tests are presented as functions of the nozzle velocity. Solids concentration by volume profile data are summarized in Section 6.5, and data from transient tests in which the cloud height at a constant nozzle velocity as a function of operation time from fully settled conditions are summarized in Section 6.6.

6.1 Data Reporting Format

The data from the mixing tests are summarized in Table 6.1 together with the general test conditions of tank scale (small, mid, or large) and head shape (elliptical, flanged and dished, or spherical). The first column of Table 6.1 lists the table number in Appendix B where the data is tabulated. The data are categorized by test campaigns denoted as tests conducted in 2008, July 2007, or Fall 2007. The tests conducted in 2008 used simulant from a different manufacturer than those conducted in 2007. The test details column shows the types of measurements used to determine the critical suspension velocity and the cloud height. The test data in Appendix B are listed chronologically based on increasing row number. The row number format based on the first several digits of the Appendix B row number are specified in the last column of Table 6.1. The tests conducted in 2008 in the elliptical or spherical head all start with the number 9 followed by the nominal tank diameter in inches. The tests conducted in 2008 using the flanged and dished head start with the nominal tank diameter in inches (70). The tests conducted in Fall 2007 start with 709, and the tests conducted in July 2007 start with 2007.

Table 6.1. Summary of Mixing Test General Conditions and Data

Table	Test Campaign	Tank Scale	Head Shape	Simulant Manufacturer	Test Details	Row Number Format
B.3	2008	Small (15)	Elliptical (E)	XLSciTech	Visual observation of cloud height H_C. Ultrasonic measurement of U_{CS} and concentration.	915XXXX
B.4	2008	Mid (34)	Spherical (S)	XLSciTech	Visual observation of cloud height H_C. Ultrasonic measurement of U_{CS} and concentration.	934XXXX
B.5	2008	Large (70)	Elliptical (E)	XLSciTech	Visual observation of cloud height H_C. Ultrasonic measurement of U_{CS} and concentration.	970XXXX
B.6	2008	Large (70)	Flanged and dished (F)	XLSciTech	Visual observation of cloud height H_C. Ultrasonic measurement of U_{CS} and concentration.	70XXXX
B.7	July 2007	Mid (34)	Spherical (S)	Potters	Visual observation of cloud height H_C. Visual observation of U_{CS}.	2007XXXX
B.8	Fall 2007	Mid (34)	Spherical (S)	Potters	Visual observation of cloud height H_C. Visual observation of U_{CS}.	709XXXX

X denotes numeral entry.

The test data parameters are described in Table 6.2 and the measurement uncertainties are provided. These data are tabulated in Appendix B. The data in the first three columns of Table 6.2 are presented in the first three rows of Appendix B.

Table 6.2. Test Parameter Description

Appendix B Column Heading	Units	Symbol	Bounding Uncertainty[(a)] All or small-/mid-/large-scale	Description
			Location in Appendix B	
Row 1	*Row 2*	*Row 3*	*Not included*	*Not included*
Row Number	text	MSS	N/A	numeric ID for data row
Test	text	M/DDX	N/A	notation for month, day and sequence of the test on that day
Case ID	text	ID	N/A	abbreviated test descriptor (see Table 6.4)
Tank Diameter (measured)	in.	D	±0.07/±0.5/±0.2	inner diameter of cylindrical section of tank
Head Shape	text	HS	N/A	shape (contour) of head for tank bottom
Dish Height (head depth)	in.	H_{dish}	±0.2/±0.5/±0.5	height of dish bottom interior measured from dish bottom center
Dish Volume (ideal shape)	$in.^3$	V_{dish}	4%/7%/4%	calculated volume of head (dish) assuming ideal contour
Tank Fill Height	in.	H	±0.3/±0.3/±0.5	height of liquid above bottom center of tank
Return Line Height (average)	in.	Rtn	±0.3/±0.3/±0.5	height of mid-line of return line opening above bottom center of tank (return line opening incline)
Nozzle Inner Diameter (average)	in.	d	±5E-4	average inner diameter for set of nozzles
Nozzle Stand-off Distance (average)	in.	sod	±0.08	average distance from the nozzle discharge to the tank floor at the nozzle center line
Pulse Tube Configuration	text	PT	N/A	number and placement of pulse tubes including radial and azimuthal coordinates
Installed Nozzles	number	N	0	number of installed pulse tubes
Outer Nozzles Operated	number	N_O	0	number of pulse tubes operated in the outer ring
Inner Nozzles Operated	number	N_I	0	number of pulse tubes operated in the inner ring
Pulse Tube Outer Diameter	in.	PT_{od}	±0.01	outer diameter of pulse tube
Outer PJM Radius (average)	in.	R_O	±0.03/±0.1/±0.2	calculated average distance from pulse-tube array centerline to nozzle centerlines in outer ring of pulse tubes
Inner PJM Radius (average)	in.	R_I	±0.03/±0.1/±0.2	calculated average distance from pulse-tube array centerline to nozzle centerlines in inner ring of pulse tubes
Outer PJM Impingement Angle	deg	θ_O	$\pm 1^0$	impingement angle between nozzle centerline, for pulse tubes in outer ring, and the tangent plane of the ideal head contour taken at the point directly below the nozzle centerline
Inner PJM Impingement Angle	deg	θ_I	$\pm 1^0$	impingement angle between nozzle centerline, for pulse tubes in inner ring, and the tangent plane of the ideal head contour taken at the point directly below the nozzle centerline
Ratio Outer PJM (average) to Tank Radius	nondim	R_O/R	±0.01	ratio of R_O to tank radius
Ratio Inner PJM (average) to Tank Radius	nondim	R_I/R	±0.01	ratio of R_I to tank radius

Table 6.2. (contd)

Appendix B Column Heading	Units	Symbol	Bounding Uncertainty[a] All or small-/mid-/large-scale	Description
			Location in Appendix B	
Row 1	*Row 2*	*Row 3*	*Not included*	*Not included*
Simulant	text	sxdx	N/A	symbol combines simulant density (sx or px) and particle diameter (dx)
Solids Density	g/cm^3	ρ_s	±0.02	solids simulant density
Particle Diameter d5	µm	d_5	±10% of measurement	5th percentile of particle diameter
Particle Diameter d50	µm	d_{50}	±10% of measurement	50th percentile of particle diameter
Particle Diameter d95	µm	d_{95}	±10% of measurement	95th percentile of particle diameter
Void Fraction	fraction	vf	±0.06	volume fraction of fluid in settled bed of solids
Tank Water Temperature	C	T	±2^0	temperature of water measured near tank wall at mid-fill height
Water Density	g/cm^3	ρ_l	±0.006	density of water in tank obtained from correlating measured tank temperature with water density from published source
Solids Fraction (relative to reference volume)	fraction	ϕ_S	±0.0004 /±0.0008 /±0.0006	calculated solids fraction relative to reference volume of a right circular cylinder with diameter and height equal to the nominal tank diameter (14.5 in., 34 in, or 70 in.)
Pulse Volume Fraction	fraction	ϕ_p	±0.001 /±0.003 /±0.002	ratio of the volume of the total discharge pulse (sum of all nozzles) to the volume of a right circular cylinder with diameter and height equal to the measured tank diameter (14-7/16 in.) or nominal tank diameter (70 in. and 34 in.)
Duty Cycle	fraction	DC	±0.003 /±0.002 /±0.0004	fraction of the fluid discharge pulse cycle with fluid flowing out the nozzles at a flow rate greater than the Setpoint X
Cycle Time	s	t_C	±0.01	period of the fluid discharge pulse cycle
Pulsed or Steady Jet	text	Jet	N/A	indication of pulsed or steady flow in the tank
Us Steady Jet (discharge velocity averaged)	m/s	U_S	±0.06 /±0.03/ ±0.01	steady jet velocity calculated by the DAS from volume flow rate measurements
U1 Pulsing Jet	m/s	U1	±0.07 /±0.03/ ±0.02	average pulse velocity calculated by DAS from volume flow rate measurements [see Eq. (5.1)]
U2 URMS	m/s	U2	±0.07 /±0.03/ ±0.02	average RMS (root mean squared) pulse velocity calculated by DAS [see Eq. (5.2)]
U3 URM3	m/s	U3	±0.07 /±0.03/ ±0.02	average RMC (root mean cubed) pulse velocity calculated by DAS [see Eq. (5.3)]
Discharge Velocity	m/s	U	±0.9 /±0.5/ ±0.3	velocity obtained by visually averaging charted real-time signal on DAS screen (U_{PA}) and manually recording values for individual discharge pulses with an acceptable variation on the target velocity of ± 5%. Visual averaging done for steady portion of discharge pulse following any initial overshoot.
Critical Suspension Velocity	m/s	U_{CS}	±0.9[b] /±0.5[b,c]/ ±0.4[b]	critical suspension velocity for the test conditions
Average Peak Cloud Height	in.	H_C	±0.005	average peak cloud height measured from dish center
U_{CS} Condition	m/s	U_{CSR}	±0.9[b] /±0.5[b,c]/ ±0.4[b]	cell used to select the critical suspension velocity, upon data analyst review of test data
U_{CS} Method	text	U_{CSM}	N/A	U_{cs} condition based on method indicated: Udv measurements, visual observations (tankwide), or visual observations (tank center)

Table 6.2. (contd)

Appendix B Column Heading	Units	Symbol	Bounding Uncertainty[a] All or small-/mid-/large-scale	Description
			Location in Appendix B	
Row 1	*Row 2*	*Row 3*	*Not included*	*Not included*
U_{CS} Flag	text	U_{CS}vis	N/A	flag for U_{CS} determined visually at current test condition
U_{CS} Center Flag	text	U_{CS}cen	N/A	flag for U_{CS} determined visually at center of tank at current test condition
U_{CS} UDV Flag	text	U_{CS}udv	N/A	flag for U_{CS} determined using ultrasonic Doppler velocimeter at center of tank at current test condition
U_{CS} Based on Decreasing Velocity	m/s	U_{CS}_D	±0.9[b] /±0.5[b,c]/ ±0.4[b]	flag for U_{CS} determined after a decrease in velocity at current test condition
Sweep Increase / Decrease	text	S_W	N/A	increase (I) or decrease (D) from last change. A "(null)" is indicated as no change (start of day velocity) or if recent history is indeterminant
UDV Height Bed	mm	H_{bed}	±2	indicated depth of settled solids determined by ultrasonic Doppler velocimetry
Particle Motion	text	PM	N/A	particle motion descriptor based (see Table 5.2 for 2007 tests and Table 5.7 for 2008 tests)
Solids Level	text	Sol	N/A	visually determined solids level descriptor (see Table 5.3)
Outer Bottom Pattern	text	SP_O	N/A	visually determined outer cleared region viewed from beneath the tank (see Table 5.4)
Inner Bottom Pattern	text	SP_I	N/A	visually determined inner cleared region viewed from beneath the tank (see Table 5.4)
TDP	text	N/A	N/A	Test Data Package number where original test data recorded

(a) Uncertainties indicated are bounding values for the entire test program and range of configurations tested. For many test conditions/configurations, the uncertainties are significantly lower.
(b) Does not apply to the test cases listed in Appendix B with the following MSS row numbers 700223, 700224, 700324, 700237, 700356, 700374, 700380, 700387, 9700003, 9700060, 9700068, 9700095, 9700119, 9700121, 9700126, 9700144, 9740232, 9740233, 9740234, and 9700313. The listed cases were not fully bounded by the ±0.2 m/s surrounding (sequential) observations.
(c) Does not apply to test cases run in 2007.

The parameter ranges and test count of the test campaigns are listed in Table 6.3. Note that during the Fall 2007 test campaign, broad ranges are shown for tank fill height and return line height. As stated in Section 1.4.7, these parameters were only varied to determine the limits of the test fixture performance.

Table 6.3. Range of Test Conditions

Appendix B Column Heading	Units	Test Campaign (Campaign – Nominal Tank Diameter – Head Shape Indicator)					
		2008 15E	2008 34S	2008 70E	2008 70F	July 2007 34S	Fall 2007 34S
Row Number	text	9150001-9150793	9340001-9340234	9700001-9700338	700204-700446	20070019-20071401	7090002-7091423
Test	text	62	19	37	27	30	81
Case ID	text	52	19	27	23	24	45
Tank Diameter	in.	14-7/16	33-7/8	70	70	33-7/8	33-7/8
Head Shape	text	E	S	E	FD	S	S
Dish Height	in.	3.25	9	19	12.7	9	9

Table 6.3. (contd)

Appendix B Column Heading	Units	Test Campaign (Campaign – Nominal Tank Diameter – Head shape Indicator)					
		2008 15E	2008 34S	2008 70E	2008 70F	July 2007 34S	Fall 2007 34S
Dish Volume	in.^{3}	354.8	4437.4	49770.7	30569	4437.4	4437.4
Tank Fill Height	in.	33.5–36	69–72	91–94	87.5–90.5	65.8–76.1	23.7–67.8
Return Line Height	in.	29–30	66	80	83-5/8	62	21.7–61-3/4
Nozzle Inner Diameter	in.	0.126–0.375	0.297	0.613, 0.92	0.613, 0.92	0.297, 0.446	0.297, 0.446
Nozzle Standoff Distance	in.	0.19–0.56	0.45	0.92, 1.38	0.92, 1.38	0.45, 0.67	0.45, 0.67
Pulse Tube Configuration	text	HLP-22, 8TA	HLP-22	HLP-22, 8TA	HLP-22	HLP-22	HLP-22
Installed Nozzles	number	8,12	12	8,12	12	12	12
Outer Nozzles Operated	number	4,8	8	4,8	8	8	0,4,8
Inner Nozzles Operated	number	0,4	4	0,4	4	4	0,4
Nozzle Combinations (outer/inner)	number/ number	8/4 (HLP 22) 4/4, 4/0 (8TA)	8/4	8/4 (HLP 22) 4/4, 4/0 (8TA)	8/4	8/4	4/0, 8/0, 4/4, 8/4, 0/4
Pulse Tube Outer Diameter	in.	1.05	1.9	3.5	3.5	1.9	1.9
Outer PJM Radius	in.	4.5, 4.85	10.46	21.85, 23.5	26.4	10.46	10.46
Inner PJM Radius	in.	2.44, 3.61	5.67	11.48, 17.48	11.68	5.67	5.67
FIO Outer PJM Impingement Angle	deg	21.8, 24.4	30.8	20.3, 21.9	22.4	30.8	30.8
FIO Inner PJM Impingement Angle	deg	10.1, 16	16.1	10.5, 16.1	9.7	16.1	16.1
Ratio Outer PJM to Tank Radius	nondim	0.62, 0.67	0.62	0.62, 0.67	0.75	0.62	0.62
Ratio Inner PJM to Tank Radius	nondim	0.34, 0.5	0.33	0.33, 0.5	0.33	0.33	0.33
Simulant	text	s1d1, s1d2, s1d5, s2d1, s2d2	s1d1, s1d2, s2d1, s2d2	s1d1, s1d2, s2d2	s1d1, s1d2, s2d2	p1d7, p1d8, p2d6	p1d7, p1d8
Solids Density	g/cm^3	2.46–4.18	2.46–4.18	2.46–4.18	2.46–4.18	2.45–2.46	2.45
Particle Diameter d5	µm	32.8–142.8	56.9–142.8	56.9–142.8	56.9–142.8	60.5–518.4	60.5, 121.3
Particle Diameter d50	µm	43.9–166.4	69.3–166.4	69.3–166.4	69.3–166.4	89.5–766.2	89.5, 178.0
Particle Diameter d95	µm	58.5–195.1	82.1–195.1	82.1–195.1	82.1–195.1	132.0–1172.9	132.0, 260.6
Void Fraction	fraction	0.37–0.41	0.37–0.41	0.37–0.41	0.37–0.41	0.41–0.43	0.43
Tank Water Temp.	C	20.4–34.2	12.6–23.8	17.3–27.1	20.4–25.1	22.0–30	20.5–24.0
Water Density	g/cm^3	0.997–1	0.997–1	0.993–0.996	0.994–0.996	0.997–0.999	0.995–0.999
Solids Fraction	fraction	0.0005–0.06	0.00015–0.015	0.00155–0.015	0.00155–0.0143	0.00485–0.01592	0.00487
Pulse Volume Fraction	fraction	0.050.15	0.050.1	0.05–0.15	0.05–0.15	0.025–0.1	0.04–0.06
Duty Cycle[(a)]	fraction	0.17–1	0.18–0.5	0.17–1	0.14–0.67	0.18–1	0.18–1
Cycle Time (pulsed tests)	s	4.2–90.6	10–75	22.6–285	18.4–252	1–82	12–190
Pulsed or Steady Jet	text	P, S	P	P,S	P	P,S	P,S
Us Steady Jet	m/s	2–3.2	N/A	3.5	N/A	1.5–9.1	2–13.1
U1 Pulsing Jet	m/s	0.8–14	2.2–12.8	2.9–14.7	4.2–11.6	1.8–11.4	2.3–15.9
U2 URMS	m/s	0.8–14.7	2.2–13.2	2.9–15.1	4.2–11.9	1.8–12.8	2.4–16.3
U3 URM3	m/s	0.8–15	2.2–13.4	2.9–15.4	4.3–12	1.9–13.5	2.4–16.8
Discharge Velocity	m/s	0.8–15	2.2–14	3–16.1	3.8–12.5	1.5–15.2	2–15

Table 6.3. (contd)

Appendix B Column Heading	Units	Test Campaign (Campaign – Nominal Tank Diameter – Head shape Indicator)					
		2008 15E	2008 34S	2008 70E	2008 70F	July 2007 34S	Fall 2007 34S
Critical Suspension Velocity	m/s	1.3–11.8	2.75–10.4	4.3–14	4.4–11.4	2–8.5	2.6–14
Average Peak Cloud Height	in.	3.25–27	9.25–53.5	21.5–88	18.5–51.5	8.6–42.1	8.5–51
U_{CS} Condition	m/s	1.3–11.8	2.75–10.4	4.3–14	4.4–11.4	3.3–8.5	3–14
U_{CS} based on Decreasing Velocity	m/s	6.2-7.2	5–10.1	N/A	6.6	2-8.25	3.7-9.5
UDV Height Bed	mm	0–30.7	0–41.6	0–36.8	0–40.2	N/A	N/A

(a) Typical, nominal duty cycles were 0.18, 0.33, 0.5, 0.66, and 1.0.

A Case ID was assigned to each test that provided a concise summary of specific test parameters. The Case IDs are defined in Table 6.4. This notation is used to identify test conditions throughout the report. The first two digits (DD) of the Case ID show the tank diameter in inches (15, 34, or 70). The next digit (B) shows the head shape (E for elliptical, F for flanged and dished, and S for spherical). In some cases the head shape is shown as E8, which denotes tests conducted configured as an 8 tube array instead of a 12-tube array. The next digit (L) shows the full-scale nozzle diameter in inches (4, 6, M for 8.5 in., and L for 11.8 in.). The next 4-digit sequence (MMNN) is the simulant code with MM showing the density and NN showing the nominal particle size. The next digit (O, an upper case letter) shows the solids volume fraction. The next digit (P, a lower case letter) shows the nominal duty cycle. The last digit (Q) shows the nominal pulse volume fraction. For pulsating flow, Q is shown as an underscore followed by a number (such as _1). For steady flow with a reduced number of pulse tubes in operation, Q is shown as a dash followed by the number of outer nozzles in operation followed by the number of inner nozzles in operation (such as -80, 8 outer nozzles operating and 0 inner nozzles operating). Additional details are provided in Table 6.4.

6.2 July 2007 Tests in Mid-Scale Tank with Spherical Head

The July 2007 mixing test campaign was the first group of tests conducted at PNNL in response to Issue M3, Inadequate Design of Mixing Systems–Pulse Jet Mixers to evaluate noncohesive solids suspension using PJMs. During the initial tests, significant time was spent visually observing the flow patterns of the solid particulate on the tank bottom during operation of the PJMs to determine when U_{CS}, the critical suspension velocity, occurred. The visual observations were made from below the tank. An example of the view from beneath the mid-scale tank is shown in Figure 6.1. In Figure 6.1(a) no solids are in the vessel; in each of the white pulse tubes the black plastic jet nozzle is visible. The four inner pulse tubes are visible as a square pattern. Around the tank perimeter the eight outer pulse tubes are visible. The four larger-diameter tubes with angled ends are the return lines. In the center of the tank bottom, an access plug is visible. In Figure 6.1(b) solids are in the vessel and the pulse tubes are operating; circular patterns in the settled solid particulate from the jets are visible; the black nozzles of the four inner jets may be observed. Blue taped cross patterns, placed on the bottom of the tank to indicate the size of the mobilized area, are visible in two of the inner jet rings. The cleared patterns from the ring of outer nozzles are also visible around the perimeter of the vessel.

Table 6.4. Summary of Case ID Format

Case ID Format: DDB_LMMNNOPQQ

DD		B		L			MMNN			O		P		QQ (optional)		
Code	Tank	Code	Head Shape	Code	Nozzle		Code	Simulant		Code	Solids Concentration	Code	Nominal Duty Cycle	Code	Pulsing Flow	
Nom. Diam (in.)	Scale		Tank bottom		Full-scale[a] nozzle diam.		Simulant	density (g/cm^3)	d50 (μm)	Upper case letter	(fraction)	Lower case letter	(fraction)		Nominal Pulse Volume Fraction	Outer/Inner nozzles
					in.	m										
15	**Small**	**E**	elliptical 15E and 70E (HLP-22 config.)	**4**	4	0.10	**s1d5**	2.5	44	**U**	0.00015	**a**[b]	1.0	**_0**	0.05	4/4
34	**Mid**	**E8**	elliptical 15E and 70E (8-tube array config.)	**6**	6	0.15	**s1d2**	2.48	69	**T**	0.0005	**e**	0.66	**_1**[b]	0.05	8/4 or 4/4[c]
70	**Large**	**F**	F&D 70F (HLP-22 config.)	**M**[d]	8.5	0.22	**s1d1**	2.46	166	**S**	0.0015	**b**	0.50	**_2**	0.1	8/4 or 4/4[c]
		S	spherical 34S (HLP-22 config.)	**L**[d]	11.8	0.30	**s2d2**	4.18	76	**Z**	0.00155	**c**	0.33	**_3**	0.025	8/4
							s2d1	4.17	164	**Y**	0.005 (0.00485–0.005)	**i**	0.28*	**_4**	0.15	8/4
							p1d8[e]	2.45	90	**R**	0.01	**f**	0.25*	**_5**	0.05	8/0
							p1d7[e]	2.45	178	**V**	0.0143	**h**	0.24*	**_6**	0.05	4/0
							p2d6[e]	2.46	766	**X**	0.015 (0.0146–0.0159)	**m**	0.21*	**_7**	0.1	4/0
										Q	0.03	**d**	0.18	**_8**	0.048	8/4
Test		**MSS Row Format**								**W**	0.045[d]	**k**	0.14*	**_9**	0.05	0/4
15E or 15E8		915XXXX								**P**	0.06[d]		* = limited tests			
34S		934XXXX													**Steady flow with reduced number of jets operated**	
70E or 70E8		970XXXX												Code[f]	Pulse Vol. Fraction	Outer/Inner nozzles
70F		70XXXX												**-80**	undefined	8 / 0
Fall 2007		709XXXX												**-44**	undefined	4 / 4
July 2007		2007XXXX												**-40**	undefined	4 / 0
														-04	undefined	0 / 4

(a) Scaled to HLP-22 sized tank of diameter 38 ft.
(b) Limited set of _1_FM01 observations; 70F tests with flow meter averaging set at 0.1 sec instead of 0.01 sec.
(c) Full tube array operated (8/4 for HLP-22 tests and 4/4 for 8-tube array tests) for cases with P=a and QQ=<blank>; and cases with QQ= _1 or _2.
(d) Tested only in the small-scale tank with 8-tube array. Scaled nozzle dimension provides reference for size relative to HLP-22.
(e) 34-inch tank only: p1d8=MIL-12; p1d7=MIL-8; p2d6=MIL-3.
(f) Tested only in mid-scale tank.

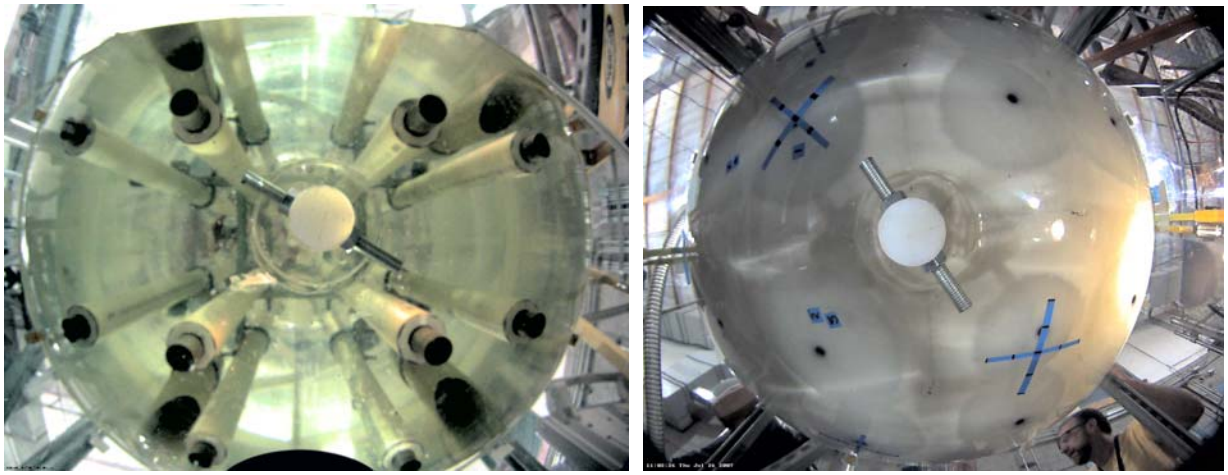

(a) (b)

Figure 6.1. View from the Bottom of the Tank Showing (a) Pulse Tubes with No Simulant and (b) Mixing at Some Suspension and BP3 Mixing State

A 15-second sequence of the growth of the mobilized area in the settled solid particulate taken during the end of the drive portion of the pulse cycle is shown in Figure 6.2. During the drive portion of the pulse (the first seven photos during the sequence) fluid is exiting the nozzles and the black nozzle ends are visible. When the flow stops (between the 7th and 8th photos) the nozzles are not visible and the cleared area rapidly disappears (shown in the last three photos of the sequence) as the solids settle. In the last two photos of the sequence the solids appear to be fully settled.

All of the July 2007 tests were conducted in the mid-scale tank with a spherical head geometry using the HLP-22 pulse tube configuration with all tubes (8 outer and 4 inner [8/4]) operating and a liquid fill height of ~2H/D and a return line height of 1.8 H/D. The nozzle stand-off distance was 1.5 d.

The test conditions varied three simulants with solids density (ρ_s = 2.45 and 2.46 g/cm^3) and particle diameters (d_S = 89, 178, and 766 μm) identified as p1d7 (ρ_s = 2.45 g/cm^3, d_{50} = 178 μm), p1d8 (ρ_s = 2.45 g/cm^3, d_{50} = 90 μm), and p2d6 (ρ_s = 2.46 g/cm^3, d_{50} = 766 μm); two nozzle diameters (d = 0.297 [4 in. full scale] and 0.446 in.[6 in. full scale]); two solids fractions (ϕ_S = 0.005 [Y] and 0.016 [X]); a series of duty cycles (0.18 [d], 0.33 [c], 0.50 [b], 1.00–continuous flow [a]); and several pulse volume fractions (ϕ_p = 0.025 [_3], 0.048 [_8], 0.1 [_2], and infinite–continuous flow). The test combinations are listed chronologically in Table 6.5. Data pairs of nozzle exit velocity (U) and cloud height (H_C) were observed at a series of velocities starting below the U_{CS}, increasing above U_{CS}, and then ramping down. At times the velocity produced a cloud height that was below the straight section of the tank. The fact that the cloud height was in the tank head volume was noted, but the associated cloud height was not recorded.

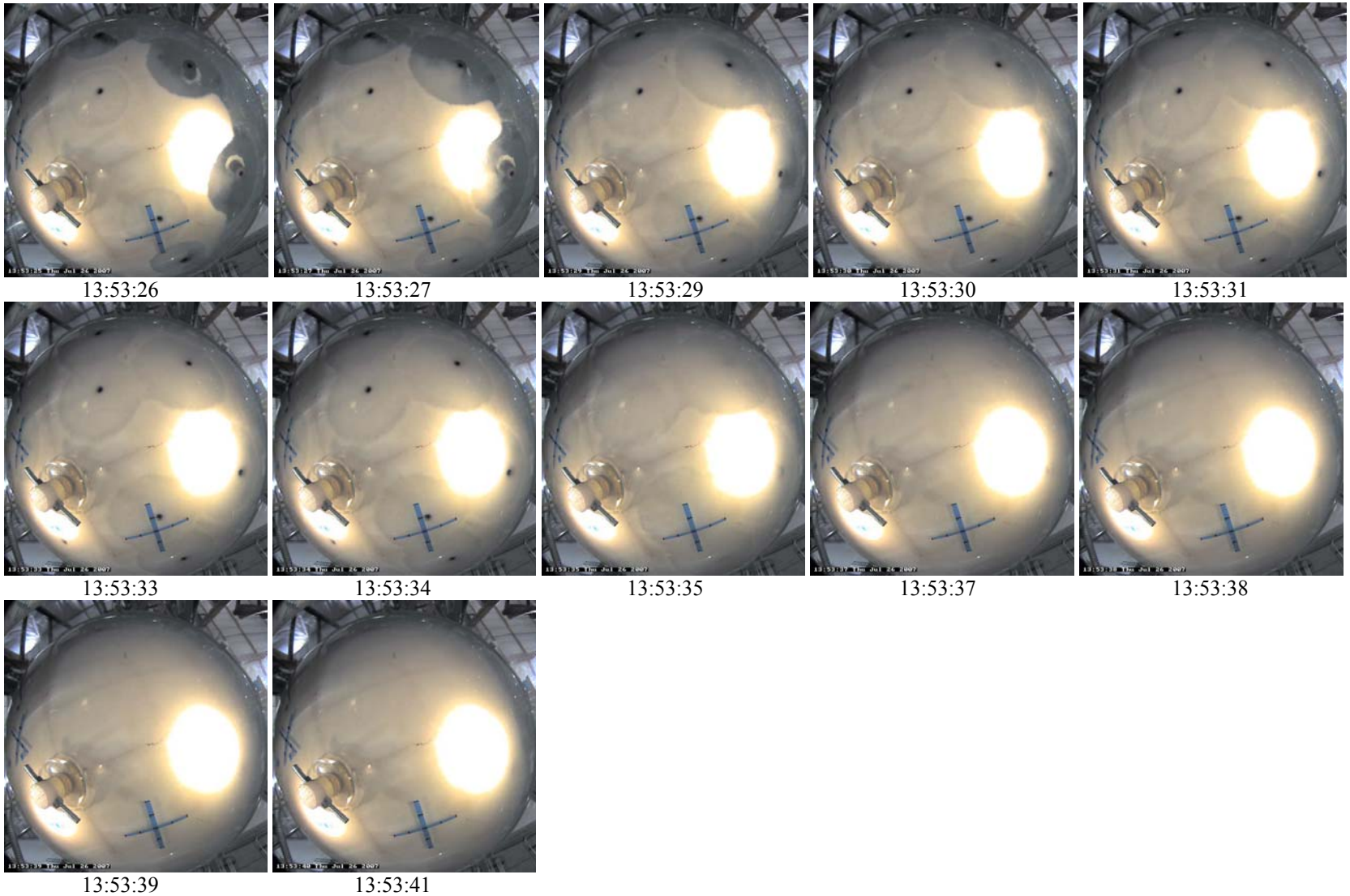

Figure 6.2. Sequence of Photos Showing Growth of Mobilized Area (first 7 photos) and Solids Settling (last 5 photos) During Test 34S_6p1d8Yd_8 Conducted in the Mid-Scale Tank with 6-in. Full-Scale Nozzle, for Simulant p1d8 (ρ_s = 2.45 g/cm^3, d_{50} = 90 μm), Solids Fraction (ϕ_S = 0.005 [Y]) for Constant Duty Cycle (DC = 0.18 [d]) at Pulse Volume Fraction (ϕ_p = 0.048 [_8])

Table 6.5. July 2007 Test Summary in Mid-Scale Tank with Spherical Head

Test	Case ID	Tank Fill Height	Return Line Height	Nozzle Inner Diameter	Nozzle Standoff Distance	Pulse Tube Configuration	Installed Nozzles	Outer Nozzles Operated	Inner Nozzles Operated	Simulant	Solids Density	Particle Diameter d50	Solids Fraction	Pulse Volume Fraction	Duty Cycle	Pulsed or Steady Jet	Fill Height to Diameter	Return Line Height to Diameter
text	text	in.	in.	in.	in.	text	number	number	number	text	g/cm^3	m	fraction	fraction	fraction	text	ratio	ratio
M/DDX	ID	H	Rtn	d	sod	PT	N	N_O	N_I	sxdx	ρ_S	d_{50}	ϕ_S	ϕ_p	DC	Jet	H/D	Rtn/D
7/16 A1	34S_4p1d7Ya	71.1	62	0.297	0.446	HLP-22	12	8	4	p1d7	2.45	0.000178	0.005	undefined	1.00	S	2.1	1.8
7/16 A2	34S_4p1d7Yc_8	71.1	62	0.297	0.446	HLP-22	12	8	4	p1d7	2.45	0.000178	0.005	0.050	0.33	P	2.1	1.8
7/17 A1	34S_4p1d7Xa	66.1	62	0.297	0.446	HLP-22	12	8	4	p1d7	2.45	0.000178	0.016	undefined	1.00	S	2.0	1.8
7/17 A2	34S_4p1d7Xc_8	66.1	62	0.297	0.446	HLP-22	12	8	4	p1d7	2.45	0.000178	0.016	0.048	0.33	P	2.0	1.8
7/18 A1	34S_4p1d7Xc_8	76.1	62	0.297	0.446	HLP-22	12	8	4	p1d7	2.45	0.000178	0.016	0.048	0.33	P	2.2	1.8
7/18 A2	34S_4p1d7Xc_2	76.1	62	0.297	0.446	HLP-22	12	8	4	p1d7	2.45	0.000178	0.016	0.100	0.33	P	2.2	1.8
7/19 A1	34S_4p1d7Yc_8	67.6	62	0.297	0.446	HLP-22	12	8	4	p1d7	2.45	0.000178	0.005	0.048	0.33	P	2.0	1.8
7/19 A2	34S_4p1d7Ya	67.6	62	0.297	0.446	HLP-22	12	8	4	p1d7	2.45	0.000178	0.005	undefined	1.00	S	2.0	1.8
7/19 A3	34S_4p1d7Yc_2	67.6	62	0.297	0.446	HLP-22	12	8	4	p1d7	2.45	0.000178	0.005	0.100	0.33	P	2.0	1.8
7/19 A4	34S_4p1d7Yd_8	67.6	62	0.297	0.446	HLP-22	12	8	4	p1d7	2.45	0.000178	0.005	0.048	0.18	P	2.0	1.8
7/20 A1	34S_4p1d7Yb_8	67.6	62	0.297	0.446	HLP-22	12	8	4	p1d7	2.45	0.000178	0.005	0.048	0.50	P	2.0	1.8
7/20 A2	34S_4p1d7Yc_3	67.6	62	0.297	0.446	HLP-22	12	8	4	p1d7	2.45	0.000178	0.005	0.025	0.33	P	2.0	1.8
7/21 A1	34S_6p1d7Ya	68.4	62	0.446	0.669	HLP-22	12	8	4	p1d7	2.45	0.000178	0.005	undefined	1.00	S	2.0	1.8
7/21 A2	34S_6p1d7Yc_8	68.4	62	0.446	0.669	HLP-22	12	8	4	p1d7	2.45	0.000178	0.005	0.048	0.33	P	2.0	1.8
7/23 A1	34S_6p1d7Yd_8	67.9	62	0.446	0.669	HLP-22	12	8	4	p1d7	2.45	0.000178	0.005	0.048	0.18	P	2.0	1.8
7/23 A2	34S_6p1d7Yd_2	67.9	62	0.446	0.669	HLP-22	12	8	4	p1d7	2.45	0.000178	0.005	0.100	0.18	P	2.0	1.8
7/23 A3	34S_6p1d7Yc_2	67.9	62	0.446	0.669	HLP-22	12	8	4	p1d7	2.45	0.000178	0.005	0.100	0.33	P	2.0	1.8
7/23 A4	34S_6p1d7Yc_3	67.9	62	0.446	0.669	HLP-22	12	8	4	p1d7	2.45	0.000178	0.005	0.025	0.33	P	2.0	1.8
7/23 A5	34S_6p1d7Yb_8	67.9	62	0.446	0.669	HLP-22	12	8	4	p1d7	2.45	0.000178	0.005	0.048	0.50	P	2.0	1.8
7/24 A1	34S_6p1d7Xa	67.9	62	0.446	0.669	HLP-22	12	8	4	p1d7	2.45	0.000178	0.016	undefined	1.00	S	2.0	1.8
7/24 B1	34S_6p1d7Xd_8	67.9	62	0.446	0.669	HLP-22	12	8	4	p1d7	2.45	0.000178	0.016	0.048	0.18	P	2.0	1.8
7/25 A1	34S_6p2d6Ya	68.1	62	0.446	0.669	HLP-22	12	8	4	p2d6	2.46	0.000766	0.005	undefined	1.00	S	2.0	1.8
7/25 B1	34S_6p2d6Yd_8	68.1	62	0.446	0.669	HLP-22	12	8	4	p2d6	2.46	0.000766	0.005	0.048	0.18	P	2.0	1.8
7/26 A1	34S_6p1d8Ya	68.9	62	0.446	0.669	HLP-22	12	8	4	p1d8	2.45	0.000089	0.005	undefined	1.00	S	2.0	1.8
7/26 B1	34S_6p1d8Yd_8	68.9	62	0.446	0.669	HLP-22	12	8	4	p1d8	2.45	0.000089	0.005	0.048	0.18	P	2.0	1.8
7/27 A1	34S_6p1d8Yd_8	68.9	62	0.446	0.669	HLP-22	12	8	4	p1d8	2.45	0.000089	0.005	0.048	0.18	P	2.0	1.8
7/27 B1	34S_6p1d8Yc_8	68.9	62	0.446	0.669	HLP-22	12	8	4	p1d8	2.45	0.000089	0.005	0.048	0.33	P	2.0	1.8
7/27 C1	34S_6p2d6Yd_8	68.1	62	0.446	0.669	HLP-22	12	8	4	p2d6	2.46	0.000766	0.005	0.048	0.18	P	2.0	1.8
7/27 D1	34S_6p2d6Yc_8	68.1	62	0.446	0.669	HLP-22	12	8	4	p2d6	2.46	0.000766	0.005	0.048	0.33	P	2.0	1.8
7/27 B2	34S_6p2d6Ya	68.1	62	0.446	0.669	HLP-22	12	8	4	p2d6	2.46	0.000766	0.005	undefined	1.00	S	2.0	1.8

Selected July 2007 cloud height data are plotted as a function of velocity in Figures 6.3, 6.4, and 6.5. When identified, the U_{CS} velocity is shown as the darkened symbol in the legend beneath the test; the method used to determine U_{CS} is also shown. For example, in the legend for Figure 6.3(a) each Case ID shows the U_{CS} condition beneath it. The first Case ID (34S_4p1d7Yc_8) symbol is a green X, the corresponding U_{CS} condition symbol is shown as a green X with a black background. The next three U_{CS} condition symbols are shown as colored diamonds with black centers. The description to the right of the U_{CS} condition shows the method used to determine U_{CS}, which is either "vis" or "vis dec." Vis means that the U_{CS} condition was determined visually after an increase in velocity. Vis dec means that the U_{CS} condition was determined visually after a decrease in velocity. In Figure 6.3, two concentrations are compared; in Figure 6.4, two duty cycles are compared; and in Figure 6.5, three simulants are compared.

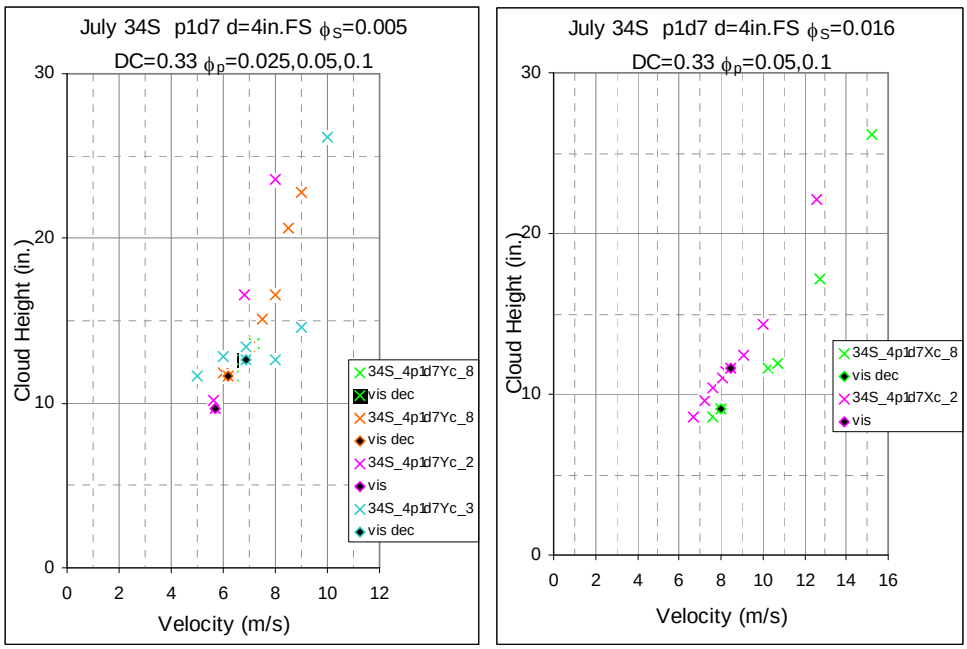

(a) (b)

Figure 6.3. Cloud Height as a Function of Velocity for Two Concentrations in the Mid-Scale Tank with Spherical Head for a Range of Pulse Volume Fractions: (a) Solids Fraction $\phi_S = 0.005$ [Y], (b) Solids Fraction $\phi_S = 0.016$ [X]. Both use 4-in. full-scale nozzle for constant duty cycle (DC = 0.33 [c]) and three pulse volume fractions ($\phi_p = 0.025$[_3], 0.048 [_8], 0.1 [_2]) for simulant p1d7 ($\rho_s = 2.45$ g/cm^3, $d_{50} = 178$ μm).

In Figure 6.4(b) the data shown in pink have a higher solids fraction ($\phi_S = 0.016$ [X, see Table 6.4]) than the other two sets of data with solids fraction ($\phi_S = 0.005$ [Y]). Compared with the data shown in green with the same pulse volume fraction, the U_{CS} condition occurs at an increased velocity. In Figure 6.5 the data shown in green have a higher solids fraction ($\phi_S = 0.016$ [X]) and therefore higher U_{CS} velocity than the other three sets of data with solids fraction ($\phi_S = 0.005$ [Y]).

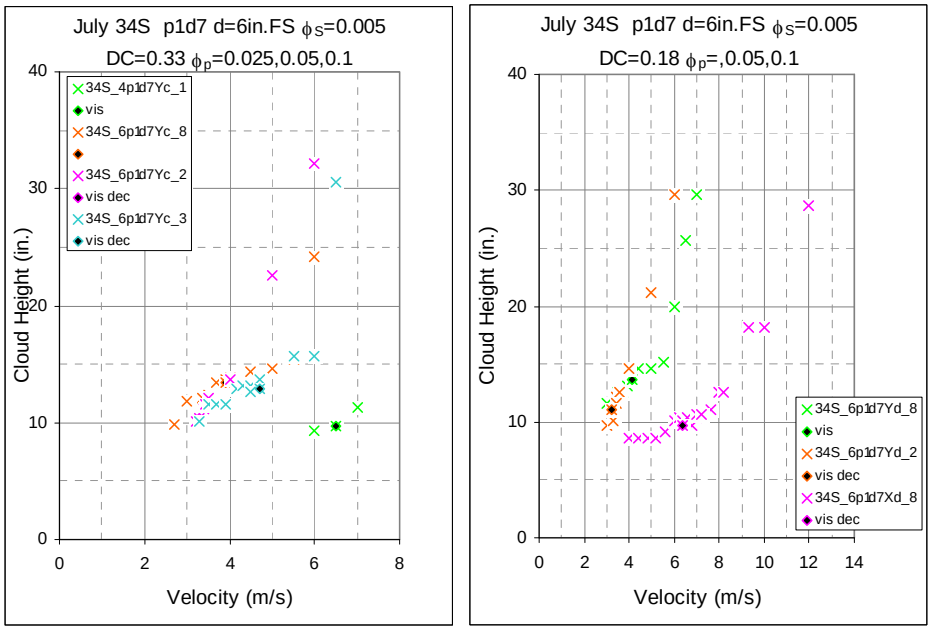

(a) (b)

Figure 6.4. Cloud Height as a Function of Velocity for Two Duty Cycles in the Mid-Scale Tank with Spherical Head for a Range of Pulse Volume Fractions: (a) DC = 0.33 [c], (b) DC = 0.18 [d]. Both use 6 in. full-scale nozzles for constant solids fraction (ϕ_S = 0.005 [Y], 0.016 [X]) and two or four pulse volume fractions (ϕ_p = 0.025 [_3], 0.048 [_8], 0.05 [_1], 0.1 [_2]) for simulant p1d7 (ρ_s = 2.45 g/cm^3, d_{50} = 178 μm).

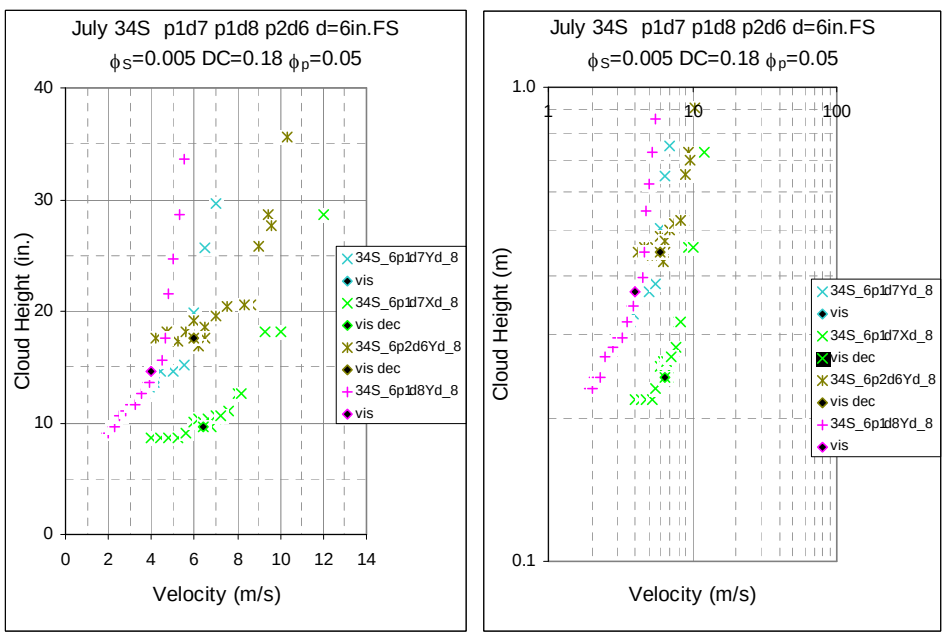

(a) (b)

Figure 6.5. Cloud Height as Function of Velocity for Simulants p1d7 (ρ_s = 2.45 g/cm^3, d_{50} = 178 μm), p1d8 (ρ_s = 2.45 g/cm^3, d_{50} = 90 μm), and p2d6 (ρ_s = 2.46 g/cm^3, d_{50} = 766 μm) for Two Concentrations in the Mid-Scale Tank with Spherical Head: (a) Linear, (b) Log. 6-in. Full-Scale Nozzle at Solids Fraction (ϕ_S = 0.005 [Y], 0.016 [X])), Constant Duty Cycle (DC = 0.18 [d]), and Pulse Volume Fraction (ϕ_p = 0.048 [_8])

6.3 Fall 2007 Tests in Mid-Scale Tank with Spherical Head

The Fall 2007 tests were conducted to evaluate the experimental test stand equipment performance and address operational questions specific to the use of this test stand. Factors evaluated included the effect of liquid fill height in the test tank and the impacts of elevation of the return line. The investigation of fill height during the Fall 2007 test effort was only to assess the effect fill height had on the results obtained in the current test setup. No attempt was made or was part of the test scope to evaluate the impact of the design operating levels for each of the WTP vessel types.

The Fall 2007 test campaign followed the same procedures used during the July 2007 tests. The Fall 2007 tests were conducted with two simulants with differing particle size: p1d7 (ρ_s = 2.45 g/cm^3, d_{50} = 178 μm) and p1d8 (ρ_s = 2.45 g/cm^3, d_{50} = 90 μm), two nozzle diameters (d = 0.297 [4 in. full scale] and 0.446 in. [6 in. full scale]), one solids fraction (ϕ_S = 0.004872 [Y]), and a series of duty cycles (DC = 0.018 [d], 0.33 [c] and 1.00–continuous flow [a]). Test conditions are listed chronologically in Table 6.6. The test parameters listed in Table 6.6 are the same as those presented for the July 2007 tests.

During the Fall 2007 test campaign, broad ranges are shown for tank fill height (H) and return line elevation (Rtn). As stated in Section 1.4.7, these parameters were only varied to determine the limits of the test fixture performance. The nondimensional representations of these variable H/D and Rtn/D combinations are summarized in Table 6.7. The tests conducted at H/D of 2.0 and Rtn/D of 1.8 are within the standard range for these test parameters for tests conducted in the mid-scale tank. Tests conducted with H/D and Rtn/D values less than these were conducted to evaluate the test fixture performance.

Tests were conducted during the Fall 2007 test campaign, with combinations of the number of outer and inner pulse tubes in operation. The number of pulse tubes in operation can be determined from the last digit in the Case ID. These combinations included all tubes in operation with 8 outer and 4 inner (8/4) [shown as _1 in the Case ID], operating only the outer pulse tubes (8/0) [shown as _5 in the Case ID], operating 4 outer and 4 inner pulse tubes (4/4) [shown as _0 in the Case ID], operating four outer pulse tubes (4/0) [shown as _6 in the Case ID], and operating four inner pulse tubes (0/4) [shown as _9 in the Case ID]. Examples of the effects of operating with these pulse tube combinations are shown in Figures 6.6 through 6.8. When identified, the U_{CS} velocity is shown as the darkened symbol in the legend beneath the test, and the method used to determine U_{CS} is also shown. For example, in the legend for Figure 6.6(a) each test Case ID shows the U_{CS} condition beneath it. The first Case ID (34S_4p1d7Yd_1) symbol is a pink X, the corresponding U_{CS} condition symbol is shown as a pink outline around a black diamond. The next remaining U_{CS} condition symbols are also shown as colored diamonds with black centers. The description to the right of the U_{CS} condition shows the method used to determine U_{CS}, which is either "vis" or "vis dec." Vis means that the U_{CS} condition was determined visually after an increase in velocity. Vis dec means that the U_{CS} condition was determined visually after a decrease in velocity.

Figure 6.6 shows data for simulant p1d7 (ρ_s = 2.45 g/cm^3, d_{50} = 178 μm) with a 4 in. full-scale nozzle. Figure 6.7 shows data for simulant p1d8 (ρ_s = 2.45 g/cm^3, d_{50} = 90 μm) with a 4 in- full-scale nozzle. Figure 6.8 shows data for simulant p1d7 with a 6 in. full-scale nozzle. Duty cycles of 0.18 [d] are shown in Figure 6.6(a), 6.7(a) and 6.8. Duty cycles of 0.33 [c] are shown in Figure 6.6(b) and 6.7(b).

Table 6.6. Fall 2007 Test Summary in Mid-Scale Tank with Spherical Head

Test	Case ID	Tank Fill Height	Return Line Height	Nozzle Inner Diameter	Nozzle Standoff Distance	Pulse Tube Configuration	Installed Nozzles	Outer Nozzles Operated	Inner Nozzles Operated	Simulant	Solids Density	Particle Diameter d50	Solids Fraction	Pulse Volume Fraction	Duty Cycle	Pulsed or Steady Jet	Fill Height to Diameter	Return Line Height to Diameter
text	text	in.	in.	in.	in.	text	number	number	number	text	g/cm^3	m	fraction	fraction	fraction	text	ratio	ratio
M/DDX	ID	H	Rtn	d	sod	PT	N	N_O	N_I	sxdx	ρ_S	d_{50}	ϕ_S	ϕ_p	DC	Jet	H/D	Rtn/D
10/17A1	34S_6p1d7Ya-80	67.8	61.8	0.446	0.669	HLP-22	12	8	0	p1d7	2.45	0.000178	0.004872	undefined	1	S	2	1.8
10/17A2	34S_6p1d7Yd_5	67.8	61.8	0.446	0.669	HLP-22	12	8	0	p1d7	2.45	0.000178	0.004872	0.05	0.18	P	2	1.8
10/18A1	34S_6p1d7Ya-44	67.8	61.8	0.446	0.669	HLP-22	12	4	4	p1d7	2.45	0.000178	0.004872	undefined	1	S	2	1.8
10/18A2	34S_6p1d7Yd_0	67.8	61.8	0.446	0.669	HLP-22	12	4	4	p1d7	2.45	0.000178	0.004872	0.05	0.18	P	2	1.8
10/18B1	34S_6p1d7Ya-40	67.8	61.8	0.446	0.669	HLP-22	12	4	0	p1d7	2.45	0.000178	0.004872	undefined	1	S	2	1.8
10/18B2	34S_6p1d7Yd_6	67.8	61.8	0.446	0.669	HLP-22	12	4	0	p1d7	2.45	0.000178	0.004872	0.04	0.18	P	2	1.8
10/19A1	34S_6p1d7Ya-04	67.8	61.8	0.446	0.669	HLP-22	12	0	4	p1d7	2.45	0.000178	0.004872	undefined	1	S	2	1.8
10/19A2	34S_6p1d7Yd_9	67.8	61.8	0.446	0.669	HLP-22	12	0	4	p1d7	2.45	0.000178	0.004872	0.05	0.18	P	2	1.8
10/26A1	34S_6p1d7Ya	67.8	65.8	0.446	0.669	HLP-22	12	8	4	p1d7	2.45	0.000178	0.004872	undefined	1	S	2	0.9
10/26A2	34S_6p1d7Yd_1	67.8	65.8	0.446	0.669	HLP-22	12	8	4	p1d7	2.45	0.000178	0.004872	0.05	0.18	P	2	0.9
10/26B1	34S_6p1d7Ya-44	67.8	65.8	0.446	0.669	HLP-22	12	4	4	p1d7	2.45	0.000178	0.004872	undefined	1	S	2	0.9
10/26B2	34S_6p1d7Yd_0	67.8	65.8	0.446	0.669	HLP-22	12	4	4	p1d7	2.45	0.000178	0.004872	0.05	0.18	P	2	0.9
10/29A1	34S_6p1d7Ya-04	67.8	65.8	0.446	0.669	HLP-22	12	0	4	p1d7	2.45	0.000178	0.004872	undefined	1	S	2	0.9
10/29A2	34S_6p1d7Ym_9	67.8	65.8	0.446	0.669	HLP-22	12	0	4	p1d7	2.45	0.000178	0.004872	0.05	0.196	P	2	0.9
10/29B1	34S_6p1d7Ya-40	67.8	65.8	0.446	0.669	HLP-22	12	4	0	p1d7	2.45	0.000178	0.004872	undefined	1	S	2	0.9
10/29B2	34S_6p1d7Yd_6	67.8	65.8	0.446	0.669	HLP-22	12	4	0	p1d7	2.45	0.000178	0.004872	0.05	0.18	P	2	0.6
10/30A1	34S_6p1d7Ya	67.8	65.8	0.446	0.669	HLP-22	12	8	4	p1d7	2.45	0.000178	0.004872	undefined	1	S	2	0.6
10/30A2	34S_6p1d7Yd_1	67.8	65.8	0.446	0.669	HLP-22	12	8	4	p1d7	2.45	0.000178	0.004872	0.04	0.18	P	2	0.6
10/30C1	34S_6p1d7Ya-04	67.8	65.8	0.446	0.669	HLP-22	12	0	4	p1d7	2.45	0.000178	0.004872	undefined	1	S	2	0.6
10/30C2	34S_6p1d7Yd_9	67.8	65.8	0.446	0.669	HLP-22	12	0	4	p1d7	2.45	0.000178	0.004872	0.05	0.18	P	2	0.6
10/31A1	34S_6p1d7Ya	33.9	31.9	0.446	0.669	HLP-22	12	8	4	p1d7	2.45	0.000178	0.004872	undefined	1	S	1	0.9
10/31A2	34S_6p1d7Yd_1	33.9	31.9	0.446	0.669	HLP-22	12	8	4	p1d7	2.45	0.000178	0.004872	0.05	0.18	P	1	0.9
11/2A1	34S_6p1d7Ya-80	33.9	31.9	0.446	0.669	HLP-22	12	8	0	p1d7	2.45	0.000178	0.004872	undefined	1	S	1	0.9
11/2A2	34S_6p1d7Yd_5	33.9	31.9	0.446	0.669	HLP-22	12	8	0	p1d7	2.45	0.000178	0.004872	0.05	0.18	P	1	0.9
11/5A1	34S_6p1d7Ya-44	33.9	31.9	0.446	0.669	HLP-22	12	4	4	p1d7	2.45	0.000178	0.004872	undefined	1	S	1	0.9
11/5A2	34S_6p1d7Yd_0	33.9	31.9	0.446	0.669	HLP-22	12	4	4	p1d7	2.45	0.000178	0.004872	0.05	0.18	P	1	0.9
11/5B1	34S_6p1d7Ya-04	33.9	31.9	0.446	0.669	HLP-22	12	0	4	p1d7	2.45	0.000178	0.004872	undefined	1	S	1	0.9
11/5B2	34S_6p1d7Yd_9	33.9	31.9	0.446	0.669	HLP-22	12	0	4	p1d7	2.45	0.000178	0.004872	0.05	0.18	P	1	0.9
11/6A1	34S_6p1d7Ya-40	33.9	31.9	0.446	0.669	HLP-22	12	4	0	p1d7	2.45	0.000178	0.004872	undefined	1	S	1	0.9
11/6A2	34S_6p1d7Yd_6	33.9	31.9	0.446	0.669	HLP-22	12	4	0	p1d7	2.45	0.000178	0.004872	0.05	0.18	P	1	0.9
11/7A1	34S_6p1d7Ya	23.7	21.7	0.446	0.669	HLP-22	12	8	4	p1d7	2.45	0.000178	0.004872	undefined	1	S	0.7	0.6
11/7A2	34S_6p1d7Yd_1	23.7	21.7	0.446	0.669	HLP-22	12	8	4	p1d7	2.45	0.000178	0.004872	0.05	0.18	P	0.7	0.6

Table 6.6. (contd)

Test	Case ID	Tank Fill Height	Return Line Height	Nozzle Inner Diameter	Nozzle Standoff Distance	Pulse Tube Configuration	Installed Nozzles	Outer Nozzles Operated	Inner Nozzles Operated	Simulant	Solids Density	Particle Diameter d50	Solids Fraction	Pulse Volume Fraction	Duty Cycle	Pulsed or Steady Jet	Fill Height to Diameter	Return Line Height to Diameter
text	text	in.	in.	in.	in.	text	number	number	number	text	g/cm^3	m	fraction	fraction	fraction	text	ratio	ratio
M/DDX	ID	H	Rtn	d	sod	PT	N	N_O	N_I	sxdx	ρ_S	d_{50}	ϕ_Σ	ϕ_p	DC	Jet	H/D	Rtn/D
11/7B1	34S_6p1d7Ya-44	23.7	21.7	0.446	0.669	HLP-22	12	4	4	p1d7	2.45	0.000178	0.004872	undefined	1	S	0.7	0.6
11/7B2	34S_6p1d7Yd_0	23.7	21.7	0.446	0.669	HLP-22	12	4	4	p1d7	2.45	0.000178	0.004872	0.05	0.18	P	0.7	0.6
11/8A2	34S_6p1d7Yd_9	23.7	21.7	0.446	0.669	HLP-22	12	0	4	p1d7	2.45	0.000178	0.004872	0.05	0.18	P	0.7	0.6
11/8C1	34S_6p1d7Ya	33.9	31.9	0.446	0.669	HLP-22	12	8	4	p1d7	2.45	0.000178	0.004872	undefined	1	S	1	0.6
11/8C2	34S_6p1d7Yd_1	33.9	31.9	0.446	0.669	HLP-22	12	8	4	p1d7	2.45	0.000178	0.004872	0.05	0.18	P	1	0.6
11/8D2	34S_6p1d7Yd_0	33.9	31.9	0.446	0.669	HLP-22	12	4	4	p1d7	2.45	0.000178	0.004872	0.05	0.18	P	1	0.6
11/9A1	34S_6p1d7Ya-04	33.9	31.9	0.446	0.669	HLP-22	12	0	4	p1d7	2.45	0.000178	0.004872	undefined	1	S	1	0.6
11/9A2	34S_6p1d7Yd_9	33.9	31.9	0.446	0.669	HLP-22	12	0	4	p1d7	2.45	0.000178	0.004872	0.05	0.18	P	1	0.6
11/14A1	34S_6p1d7Ya-44	67.8	65.8	0.446	0.669	HLP-22	12	4	4	p1d7	2.45	0.000178	0.004872	undefined	1	S	2	0.6
11/14A2	34S_6p1d7Yd_0	67.8	65.8	0.446	0.669	HLP-22	12	4	4	p1d7	2.45	0.000178	0.004872	0.05	0.18	P	2	0.6
11/14B1	34S_6p1d7Ya-44	67.8	61.8	0.446	0.669	HLP-22	12	4	4	p1d7	2.45	0.000178	0.004872	undefined	1	S	2	1.8
11/14B2	34S_6p1d7Yd_0	67.8	61.8	0.446	0.669	HLP-22	12	4	4	p1d7	2.45	0.000178	0.004872	0.05	0.18	P	2	1.8
11/14C1	34S_6p1d7Ya-04	67.8	61.8	0.446	0.669	HLP-22	12	0	4	p1d7	2.45	0.000178	0.004872	undefined	1	S	2	1.8
11/14C2	34S_6p1d7Yd_9	67.8	61.8	0.446	0.669	HLP-22	12	0	4	p1d7	2.45	0.000178	0.004872	0.05	0.18	P	2	1.8
11/14D1	34S_6p1d7Yc_1	67.8	61.8	0.446	0.669	HLP-22	12	8	4	p1d7	2.45	0.000178	0.004872	0.05	0.33	P	2	1.8
11/15A1	34S_6p1d7Yc_0	67.8	61.8	0.446	0.669	HLP-22	12	4	4	p1d7	2.45	0.000178	0.004872	0.05	0.33	P	2	1.8
11/15B1	34S_6p1d7Yc_9	67.8	61.8	0.446	0.669	HLP-22	12	0	4	p1d7	2.45	0.000178	0.004872	0.05	0.33	P	2	1.8
11/15C1	34S_6p1d7Yc_6	67.8	61.8	0.446	0.669	HLP-22	12	4	0	p1d7	2.45	0.000178	0.004872	0.05	0.33	P	2	1.8
11/19A1	34S_4p1d7Ya	67.8	61.8	0.297	0.4455	HLP-22	12	8	4	p1d7	2.45	0.000178	0.004872	undefined	1	S	2	1.8
11/19A2	34S_4p1d7Yd_1	67.8	61.8	0.297	0.4455	HLP-22	12	8	4	p1d7	2.45	0.000178	0.004872	0.05	0.18	P	2	1.8
11/20A1	34S_4p1d7Ya-44	67.8	61.8	0.297	0.4455	HLP-22	12	4	4	p1d7	2.45	0.000178	0.004872	undefined	1	S	2	1.8
11/20A2	34S_4p1d7Yd_0	67.8	61.8	0.297	0.4455	HLP-22	12	4	4	p1d7	2.45	0.000178	0.004872	0.05	0.18	P	2	1.8
11/20B1	34S_4p1d7Ya-04	67.8	61.8	0.297	0.4455	HLP-22	12	0	4	p1d7	2.45	0.000178	0.004872	undefined	1	S	2	1.8
11/20B2	34S_4p1d7Yd_9	67.8	61.8	0.297	0.4455	HLP-22	12	0	4	p1d7	2.45	0.000178	0.004872	0.05	0.18	P	2	1.8
11/26A1	34S_4p1d7Ya-40	67.8	61.8	0.297	0.4455	HLP-22	12	4	0	p1d7	2.45	0.000178	0.004872	undefined	1	S	2	1.8
11/26A2	34S_4p1d7Yd_6	67.8	61.8	0.297	0.4455	HLP-22	12	4	0	p1d7	2.45	0.000178	0.004872	0.05	0.18	P	2	1.8
11/26B1	34S_4p1d7Yc_1	67.8	61.8	0.297	0.4455	HLP-22	12	8	4	p1d7	2.45	0.000178	0.004872	0.05	0.33	P	2	1.8
11/26C1	34S_4p1d7Yc_0	67.8	61.8	0.297	0.4455	HLP-22	12	4	4	p1d7	2.45	0.000178	0.004872	0.05	0.33	P	2	1.8
11/26D1	34S_4p1d7Yd_9	67.8	61.8	0.297	0.4455	HLP-22	12	0	4	p1d7	2.45	0.000178	0.004872	0.06	0.18	P	2	1.8
11/26D2	34S_4p1d7Yc_9	67.8	61.8	0.297	0.4455	HLP-22	12	0	4	p1d7	2.45	0.000178	0.004872	0.05	0.33	P	2	1.8
11/27A1	34S_4p1d7Yc_6	67.8	61.8	0.297	0.4455	HLP-22	12	4	0	p1d7	2.45	0.000178	0.004872	0.05	0.33	P	2	1.8

Table 6.6. (contd)

Test	Case ID	Tank Fill Height	Return Line Height	Nozzle Inner Diameter	Nozzle Standoff Distance	Pulse Tube Configuration	Installed Nozzles	Outer Nozzles Operated	Inner Nozzles Operated	Simulant	Solids Density	Particle Diameter d50	Solids Fraction	Pulse Volume Fraction	Duty Cycle	Pulsed or Steady Jet	Fill Height to Diameter	Return Line Height to Diameter
text	text	in.	in.	in.	in.	text	number	number	number	text	g/cm^3	m	fraction	fraction	fraction	text	ratio	ratio
M/DDX	ID	H	Rtn	d	sod	PT	N	N_O	N_I	sxdx	ρ_S	d_{50}	ϕ_Σ	ϕ_p	DC	Jet	H/D	Rtn/D
11/27B1	34S_4p1d7Ya-80	67.8	61.8	0.297	0.4455	HLP-22	12	8	0	p1d7	2.45	0.000178	0.004872	undefined	1	S	2	1.8
11/27B2	34S_4p1d7Yd_5	67.8	61.8	0.297	0.4455	HLP-22	12	8	0	p1d7	2.45	0.000178	0.004872	0.05	0.18	P	2	1.8
11/27B3	34S_4p1d7Yc_5	67.8	61.8	0.297	0.4455	HLP-22	12	8	0	p1d7	2.45	0.000178	0.004872	0.05	0.33	P	2	1.8
11/30A1	34S_4p1d8Ya	67.8	61.8	0.297	0.4455	HLP-22	12	8	4	p1d8	2.45	8.95E-05	0.004872	undefined	1	S	2	1.8
11/30A2	34S_4p1d8Yd_1	67.8	61.8	0.297	0.4455	HLP-22	12	8	4	p1d8	2.45	8.95E-05	0.004872	0.05	0.18	P	2	1.8
11/30B1	34S_4p1d8Yc_1	67.8	61.8	0.297	0.4455	HLP-22	12	8	4	p1d8	2.45	8.95E-05	0.004872	0.05	0.33	P	2	1.8
11/30C1	34S_4p1d8Ya-44	67.8	61.8	0.297	0.4455	HLP-22	12	4	4	p1d8	2.45	8.95E-05	0.004872	undefined	1	S	2	1.8
11/30C2	34S_4p1d8Yd_0	67.8	61.8	0.297	0.4455	HLP-22	12	4	4	p1d8	2.45	8.95E-05	0.004872	0.05	0.18	P	2	1.8
12/3A1	34S_4p1d8Yc_0	67.8	61.8	0.297	0.4455	HLP-22	12	4	4	p1d8	2.45	8.95E-05	0.004872	0.05	0.33	P	2	1.8
12/3B1	34S_4p1d8Ya-04	67.8	61.8	0.297	0.4455	HLP-22	12	0	4	p1d8	2.45	8.95E-05	0.004872	undefined	1	S	2	1.8
12/3B2	34S_4p1d8Yd_9	67.8	61.8	0.297	0.4455	HLP-22	12	0	4	p1d8	2.45	8.95E-05	0.004872	0.05	0.18	P	2	1.8
12/3C1	34S_4p1d8Yc_9	67.8	61.8	0.297	0.4455	HLP-22	12	0	4	p1d8	2.45	8.95E-05	0.004872	0.05	0.33	P	2	1.8
12/4A1	34S_4p1d8Ya-40	67.8	61.8	0.297	0.4455	HLP-22	12	4	0	p1d8	2.45	8.95E-05	0.004872	undefined	1	S	2	1.8
12/4A2	34S_4p1d8Yd_6	67.8	61.8	0.297	0.4455	HLP-22	12	4	0	p1d8	2.45	8.95E-05	0.004872	0.05	0.18	P	2	1.8
12/4B1	34S_4p1d8Yc_6	67.8	61.8	0.297	0.4455	HLP-22	12	4	0	p1d8	2.45	8.95E-05	0.004872	0.05	0.33	P	2	1.8
12/4C1	34S_4p1d8Ya-80	67.8	61.8	0.297	0.4455	HLP-22	12	8	0	p1d8	2.45	8.95E-05	0.004872	undefined	1	S	2	1.8
12/4C2	34S_4p1d8Yd_5	67.8	61.8	0.297	0.4455	HLP-22	12	8	0	p1d8	2.45	8.95E-05	0.004872	0.05	0.18	P	2	1.8
12/4D1	34S_4p1d8Yc_5	67.8	61.8	0.297	0.4455	HLP-22	12	8	0	p1d8	2.45	8.95E-05	0.004872	0.05	0.33	P	2	1.8

Table 6.7. Summary of Fill Height and Return Line Height Test Conditions

Test Campaign		2008	2008	2008	2008	July 2007	Fall 2007
Tank and Head		15E	34S	70E	70F	34S	34S
H/D	Rtn/D	Number of Tests at Condition					
0.7	0.6	-	-	-	-	-	5
1.0	0.6	-	-	-	-	-	5
1.0	0.9	-	-	-	-	-	10
1.3	1.1	-	-	37	-	-	-
1.3	1.2	-	-	-	27	-	-
2.0	0.6	-	-	-	-	-	6
2.0	0.9	-	-	-	-	-	8
2.0	1.8	-	-	-	-	26	47
2.0	1.9	-	7	-	-	-	-
2.1	1.8	-	-	-	-	2	-
2.1	1.9	-	12	-	-	-	-
2.2	1.8	-	-	-	-	2	-
2.3	2.1	1	-	-	-	-	-
2.4	2.0	4	-	-	-	-	-
2.4	2.1	40	-	-	-	-	-
2.5	2.1	17	-	-	-	-	-

- indicates that no tests were conducted at this condition.

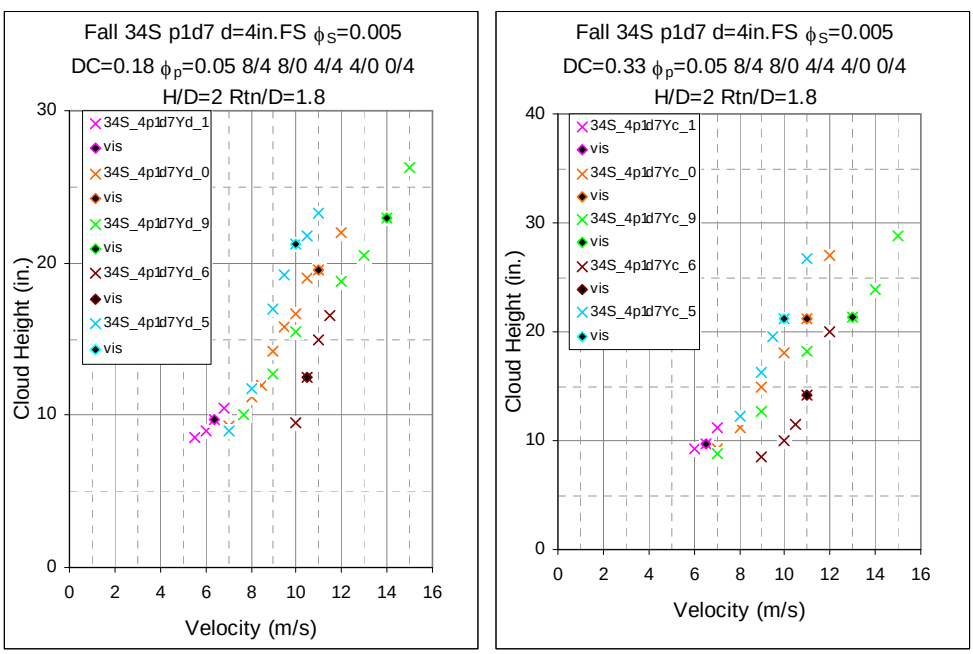

(a) (b)

Figure 6.6. Cloud Height as Function of Velocity for Two Duty Cycles for PJM Combinations: (a) DC = 0.18 [d], (b) DC = 0.33 [c]. Both use 4 in. full-scale nozzle at solids fraction (ϕ_S = 0.005 [Y]), pulse volume fraction (ϕ_p = 0.05), and nozzle combinations (N_O/N_I = 8/4 [_1] pink, 8/0 [_5] aqua, 4/4 [_0] orange, 4/0 [_6] brown, 0/4 [_9] green) at fill level (H/D = 2) for simulant p1d7 (ρ_s = 2.45 g/cm^3, d_{50} = 178 µm)

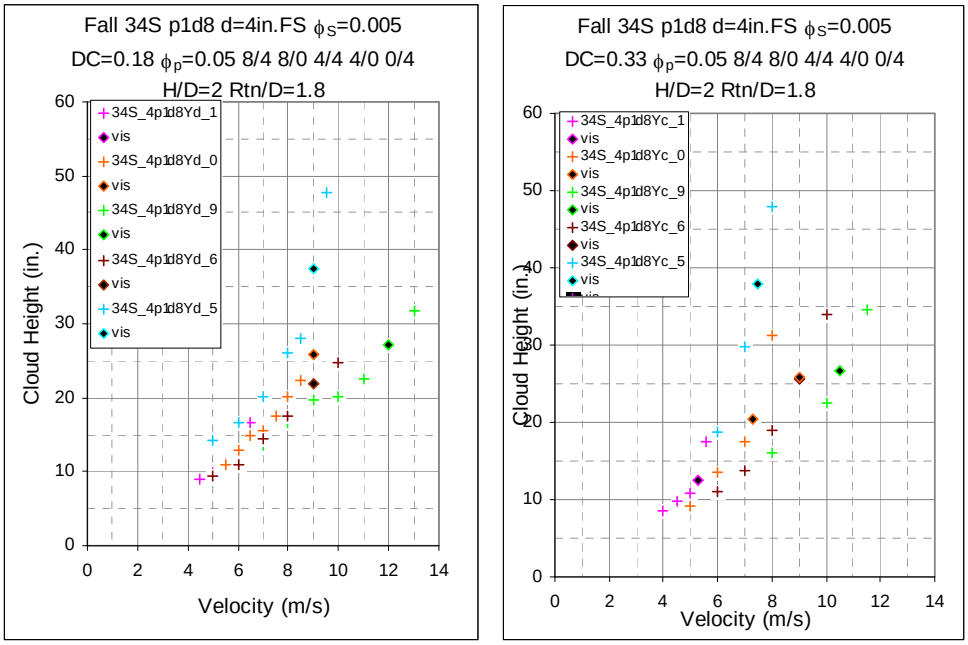

(a) (b)

Figure 6.7. Cloud Height as Function of Velocity for Two Duty Cycles for PJM Combinations: (a) DC = 0.18 [d], (b) DC = 0.33 [c]. Both use 4 in. full-scale nozzle at solids fraction (ϕ_S = 0.005 [Y]), pulse volume fraction (ϕ_p = 0.05), and nozzle combinations (N_O/N_I = 8/4 [_1] pink, 8/0 [_5] aqua, 4/4 [_0] orange, 4/0 [_6] brown, 0/4 [_9] green) at fill level (H/D = 2) for simulant p1d8 (ρ_s = 2.45 g/cm^3, d_{50} = 90 μm).

In Figures 6.6 and 6.7, when the number of nozzles in operation is compared, the results follow this pattern: 12 nozzles [8/4] in operation produced the lowest critical suspension velocity. The critical suspension velocity increased when eight nozzles were operated; however, eight outer nozzles in operation [8/0] produced a lower critical suspension velocity than the [4/4] combination of four inner and four outer nozzles in operation. This is similar to what occurs when four nozzles are in operation. The critical suspension velocity increased when four nozzles were operated; however, four outer nozzles [4/0] in operation produced a lower critical suspension velocity than four inner nozzles in operation [0/4]. This trend in increase in critical suspension was observed for both duty cycles (DC = 0.18 and 0.33).

In Figure 6.8 the test conditions are similar to those shown in Figure 6.7(a) with two exceptions: 1) the full-scale nozzle size increased from 4 in. to 6 in. and 2) the tests were conducted at reduced fluid fill level with H/D = 0.7 and Rtn/D = 0.6. The data show the same trend with decrease in the number of PJMs, as shown in Figures 6.6 and 6.7. Due to the decrease in fill height, no cloud height data were obtained above the critical suspension velocity.

Several of the July 2007 tests were replicated during the Fall 2007 tests. Test conditions replicated in the July and Fall 2007 tests are plotted in Figure 6.9. These tests were conducted at continuous flow with a duty cycle of 1 instead of pulsating flow. The Fall 2007 data are shown in green, and the July 2007 data sets are shown in orange and pink. The data show that cloud height is essentially constant.

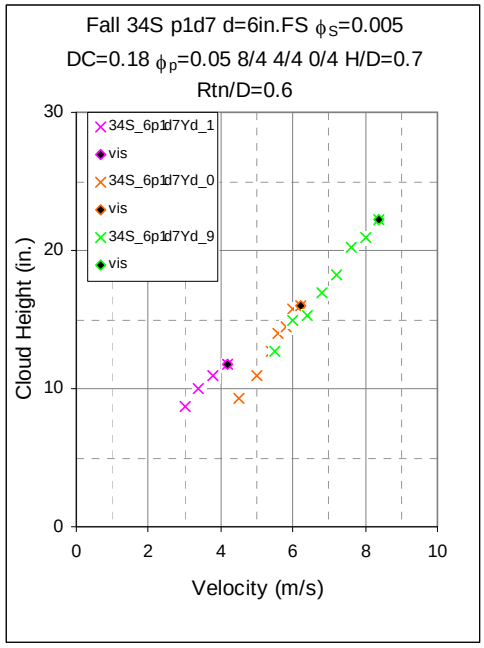

Figure 6.8. Cloud Height as Function of Velocity for Two Fill Heights: H/D=0.7, Rtn/D=0.6, with a 6 in. Full-Scale Nozzle at Solids Fraction (ϕ_S = 0.005 [Y]), for Constant Duty Cycle (DC = 0.18 [d]) at Pulse Volume Fraction (ϕ_p = 0.05) and Nozzle Combinations (N_O/N_I = 8/4 [_1] pink, 4/4 [_0] orange, 0/4 [_9] green) for Simulant p1d7 (ρ_s = 2.45 g/cm^3, d_{50} = 178 μm)

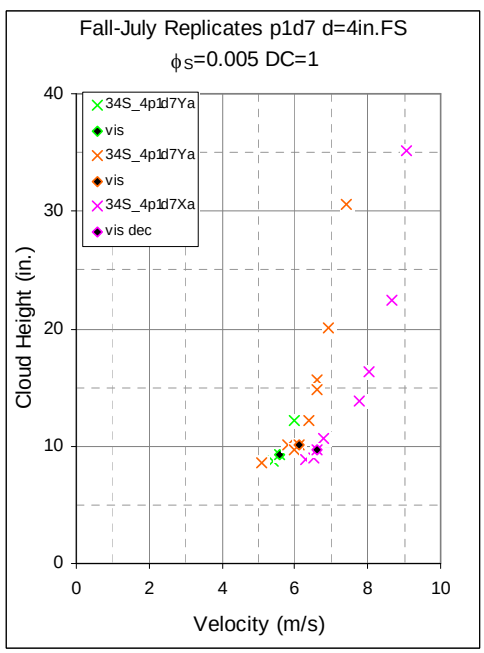

Figure 6.9. Cloud Height as Function of Velocity Comparing Results in July and Fall 2007 for Continuous Flow with a 0.4 in. Full-Scale, Solids Fraction (ϕ_S = 0.005 [Y]) for Constant DC (1–continuous flow) for Simulant p1d7 (ρ_s = 2.45 g/cm^3, d_{50} = 178 μm) and Data Sets Fall 2007 green, July 2007 orange and pink

6.4 2008 Tests

The 2008 mixing test campaign was conducted using a new series of particles with narrower size distributions than the simulants of the prior test series (see Table 3.6). The tests were conducted with five simulants (three with lower density, two with higher density), as described in Section 3.0. Concentration varied extensively compared with the prior test series from 0.00015 to 0.06 solids fraction. Test condition ranges are listed in Table 6.3. The tests were conducted in three scaled tanks, small, mid and large. The large-scale tank tests were conducted with two head shapes, elliptical [E] and flanged and dished [F]; the small-scale tank tests were conducted with an elliptical head [E]; and the mid-scale tank tests were conducted with a spherical head [S]. A brief summary of test conditions grouped by tank is provided in Table 6.8. Test conditions for the tests in these four tanks are summarized in Tables 6.9 (small-scale), 6.10 (mid-scale), 6.11 (large-scale elliptical head), and 6.12 (large-scale flanged and dished head). The majority of the variations in test conditions were conducted in the small-scale tank.

Table 6.8. 2008 Test Summary

Test Tank	Small-Scale with Elliptical Head	Mid-Scale with Spherical Head	Large-Scale with Elliptical Head	Large-Scale with Flanged and Dished Head
Full-scale nozzle diameter, d	4	4	4	4
	6	-	6	6
	8.5 [M]	-	-	-
	11.8 [L]	-	-	-
Simulants, sxdx	s1d5	-	-	-
	s1d1	s1d1	s1d1	s1d1
	s1d2	s1d2	s1d2	s1d2
	s2d1	s2d1	-	-
	s2d2	s2d2	s2d2	s2d2
Solids volume fraction, ϕ_S	0.0005 [T]	0.0005 [T]	-	-
	0.00155 [Z]	0.00155 [Z]	0.00155 [Z]	0.00155 [Z]
	0.005 [Y]	0.005 [Y]	0.005 [Y]	0.005 [Y]
	0.01 [R]	-	0.01 [R]	0.01 [R]
	0.0143 [V]	-	0.0143 [V]	0.0143 [V]
	0.015 [X]	0.015 [X]	0.015 [X]	-
	0.03 [Q]	-	-	-
	0.045 [W]	-	-	-
	0.060 [P]	-	-	-
Duty Cycle, DC	0.18 [d]	0.18 [d]	0.18 [d]	0.18 [d]
	0.33 [c]	0.33 [c]	0.33 [c]	0.33 [c]
	-	0.50 [b]	-	-
	0.66 [e]	0.66 [e]	0.66 [e]	0.66 [e]
	1.0 – continuous flow [a]	-	1.0 – continuous flow [a]	-
Pulse volume fraction, ϕ_p	0.05 [_1]	0.05 [_1]	0.05 [_1]	0.05 [_1]
	0.1 [_2]	0.1 [_2]	0.1 [_2]	0.1 [_2]
	0.15 [_4]	-	0.15 [_4]	0.15 [_4]
PJM Array Configuration	HLP-22 [8/4]	HLP-22 [8/4]	HLP-22 [8/4]	HLP-22 [8/4]
	8TA [4/4]	-	8TA [4/4]	-
	8TA [4/0]	-	8TA [4/0]	-

6.4.1 Small-Scale Tank Tests with Elliptical Head

The test conditions that were varied during the 2008 tests in the small-scale tank included five simulants: s1d5 (ρ_s = 2.5 g/cm^3, d_{50} = 44 μm), s1d2 (ρ_s = 2.48 g/cm^3, d_{50} = 69 μm), s1d1 (ρ_s = 2.46 g/cm^3, d_{50} = 166 μm), s2d2 (ρ_s = 4.18 g/cm^3, d_{50} = 76 μm), and s2d1 (ρ_s = 4.17 g/cm^3, d_{50} = 164 μm); four full-scale nozzle diameters (d = 4, 6, 8.5 [M] and 11.8 [L] in. full scale); a series of solids fractions (ϕ_S = 0.0005 [T, see Table 6.4], 0.00155 [Z], 0.005 [Y], 0.01 [R], 0.0143 [V], 0.015 [X], 0.03 [Q], 0.045 [W], 0.060 [P]); a series of duty cycles (DC = 0.18 [d], 0.33 [c], 0.66 [e], 1.0–continuous flow [a]); and several pulse volume fractions (ϕ_p = 0.05 [_1], 0.1 [_2], 0.15 [_4]). These tests were conducted with two pulse tube configurations described by number of outer pulse tubes/number of inner pulse tubes: HLP-22 (8 outer and 4 inner pulse tubes with all pulse tubes in operation) and 8TA (4 outer and 4 inner pulse tube in operating combinations of 4/4 and 4/0). The pulse tube combinations are described in Table 6.4 designator QQ, which is part of the Case ID for each test. The test combinations are listed in Table 6.9.

Data for cloud height as a function of velocity from the small-scale tests are shown in Figures 6.10 through 6.12. The plot legend presents the Case ID followed by the U_{CS} velocity if it was measured for that case. When identified, the U_{CS} velocity is shown as the darkened symbol in the legend beneath the test and the method used to determine U_{CS} is also shown. For example, in the legend for Figure 6.10(a) each test Case ID shows the U_{CS} condition beneath it. The first Case ID (34S_4s1d2Zc_1) symbol is a red circle with black outline; the corresponding U_{CS} condition symbol is shown as a black circle with a red outline. The remaining U_{CS} condition symbols are shown as colored symbols with black centers. The color matches the corresponding Case ID above it. The description to the right of the U_{CS} condition shows the method used to determine U_{CS} which is either "udv" or "vis dec." Udv means that the U_{CS} condition was determined ultrasonically after an increase in velocity. Vis dec means that the U_{CS} condition was determined visually after a decrease in velocity.

In Figure 6.10 the effects of concentration are observed with all parameters held constant except for solids volume fraction. Figure 6.10(a) shows all concentrations in the series; 6.10(b) shows the lowest five concentrations in the series. The concentration is color coded to increase as the rainbow from red to green. In Figure 6.10(b) as concentration increases from 0.00155 to 0.03, the velocity increases with concentration as seen from red, orange, gold, and yellow data points. In Figure 6.10(a) the higher concentration points are also shown with lime and green shown on top of the other cases, especially at velocities below critical suspension velocity.

Table 6.9. 2008 Test Summary for Small-Scale Tank

Test	Case ID	Tank Fill Height	Return Line Height	Nozzle Inner Diameter	Nozzle Standoff Distance	Pulse Tube Configuration	Installed Nozzles	Outer Nozzles Operated	Inner Nozzles Operated	Simulant	Solids Density	Particle Diameter d50	Solids Fraction	Pulse Volume Fraction	Duty Cycle	Pulsed or Steady Jet	Fill Height to Diameter	Return Line Height to Diameter
text	text	in.	in.	in.	in.	text	number	number	number	text	g/cm^3	m	fraction	fraction	fraction	text	ratio	ratio
M/DDX	ID	H	Rtn	d	sod	PT	N	N_O	N_I	sxdx	ρ_S	d_{50}	ϕ_S	ϕ_p	DC	Jet	H/D	Rtn/D
6/6A	15E_4s1d2Zc_1	35	29	0.126	0.189	HLP-22	12	8	4	s1d2	2.48	0.000069	0.00155	0.05	0.33	P	2.4	2.0
6/6B	15E_4s1d2Zd_1	35	29	0.126	0.189	HLP-22	12	8	4	s1d2	2.48	0.000069	0.00155	0.05	0.18	P	2.4	2.0
6/9A	15E_4s1d2Yc_1	35	29	0.126	0.189	HLP-22	12	8	4	s1d2	2.48	0.000069	0.005	0.05	0.33	P	2.4	2.0
6/9B	15E_4s1d2Rc_1	35	29	0.126	0.189	HLP-22	12	8	4	s1d2	2.48	0.000069	0.01	0.05	0.33	P	2.4	2.0
6/10A	15E_4s1d2Rc_1	35	30	0.126	0.189	HLP-22	12	8	4	s1d2	2.48	0.000069	0.01	0.05	0.33	P	2.4	2.1
6/10B	15E_4s1d2Xc_1	35	30	0.126	0.189	HLP-22	12	8	4	s1d2	2.48	0.000069	0.015	0.05	0.33	P	2.4	2.1
6/11A	15E_4s1d2Xd_1	34.5	30	0.126	0.189	HLP-22	12	8	4	s1d2	2.48	0.000069	0.015	0.05	0.18	P	2.4	2.1
6/11B	15E_4s1d2Xa	34.5	30	0.126	0.189	HLP-22	12	8	4	s1d2	2.48	0.000069	0.015	undefined	1.00	S	2.4	2.1
6/11C	15E_4s1d2Xc_1	34.5	30	0.126	0.189	HLP-22	12	8	4	s1d2	2.48	0.000069	0.015	0.05	0.33	P	2.4	2.1
6/12A	15E_4s1d2Xe_1	34.75	30	0.126	0.189	HLP-22	12	8	4	s1d2	2.48	0.000069	0.015	0.05	0.66	P	2.4	2.1
6/12B	15E_4s1d2Xc_2	34.75	30	0.126	0.189	HLP-22	12	8	4	s1d2	2.48	0.000069	0.015	0.10	0.33	P	2.4	2.1
6/12C	15E_4s1d2Xd_2	34.75	30	0.126	0.189	HLP-22	12	8	4	s1d2	2.48	0.000069	0.015	0.10	0.18	P	2.4	2.1
6/12D	15E_4s1d2Xe_2	34.75	30	0.126	0.189	HLP-22	12	8	4	s1d2	2.48	0.000069	0.015	0.10	0.66	P	2.4	2.1
6/12E	15E_4s1d2Xc_4	34.75	30	0.126	0.189	HLP-22	12	8	4	s1d2	2.48	0.000069	0.015	0.15	0.32	P	2.4	2.1
6/13A	15E_4s1d2Xd_4	35	30	0.126	0.189	HLP-22	12	8	4	s1d2	2.48	0.000069	0.015	0.15	0.18	P	2.4	2.1
6/13B	15E_4s1d2Xe_4	35	30	0.126	0.189	HLP-22	12	8	4	s1d2	2.48	0.000069	0.015	0.15	0.66	P	2.4	2.1
6/13C	15E_4s1d2Xd_1	35	30	0.126	0.189	HLP-22	12	8	4	s1d2	2.48	0.000069	0.015	0.05	0.17	P	2.4	2.1
6/16A	15E_4s1d2Qc_1	35	30	0.126	0.189	HLP-22	12	8	4	s1d2	2.48	0.000069	0.03	0.05	0.33	P	2.4	2.1
6/16B	15E_4s1d2Wc_1	34.75	30	0.126	0.189	HLP-22	12	8	4	s1d2	2.48	0.000069	0.045	0.05	0.33	P	2.4	2.1
6/17A	15E_4s1d2Wd_1	34.5	30	0.126	0.189	HLP-22	12	8	4	s1d2	2.48	0.000069	0.045	0.05	0.18	P	2.4	2.1
6/17B	15E_4s1d2Wa	34.5	30	0.126	0.189	HLP-22	12	8	4	s1d2	2.48	0.000069	0.045	undefined	1.00	S	2.4	2.1
6/17C	15E_4s1d2Wc_1	34.5	30	0.126	0.189	HLP-22	12	8	4	s1d2	2.48	0.000069	0.045	0.05	0.34	P	2.4	2.1
6/18A	15E_4s1d2Pc_1	34.5	30	0.126	0.189	HLP-22	12	8	4	s1d2	2.48	0.000069	0.06	0.05	0.33	P	2.4	2.1
6/18B	15E_4s2d2Zc_1	35	30	0.126	0.189	HLP-22	12	8	4	s2d2	4.18	0.000076	0.00155	0.05	0.33	P	2.4	2.1

Table 6.9. (contd)

Test	Case ID	Tank Fill Height	Return Line Height	Nozzle Inner Diameter	Nozzle Standoff Distance	Pulse Tube Configuration	Installed Nozzles	Outer Nozzles Operated	Inner Nozzles Operated	Simulant	Solids Density	Particle Diameter d50	Solids Fraction	Pulse Volume Fraction	Duty Cycle	Pulsed or Steady Jet	Fill Height to Diameter	Return Line Height to Diameter
text	text	in.	in.	in.	in.	text	number	number	number	text	g/cm^3	m	fraction	fraction	fraction	text	ratio	ratio
M/DDX	ID	H	Rtn	d	sod	PT	N	N_O	N_I	sxdx	ρ_S	d_{50}	ϕ_S	ϕ_p	DC	Jet	H/D	Rtn/D
6/19A	15E_4s2d2Zc_1	35	30	0.126	0.189	HLP-22	12	8	4	s2d2	4.18	0.000076	0.00155	0.05	0.33	P	2.4	2.1
6/19B	15E_4s2d2Zd_1	35	30	0.126	0.189	HLP-22	12	8	4	s2d2	4.18	0.000076	0.00155	0.05	0.18	P	2.4	2.1
6/19C	15E_4s2d2Yc_1	35	30	0.126	0.189	HLP-22	12	8	4	s2d2	4.18	0.000076	0.005	0.05	0.34	P	2.4	2.1
6/20A	15E_4s2d2Yc_1	35	30	0.126	0.189	HLP-22	12	8	4	s2d2	4.18	0.000076	0.005	0.05	0.33	P	2.4	2.1
6/20B	15E_4s2d2Xc_1	35	30	0.126	0.189	HLP-22	12	8	4	s2d2	4.18	0.000076	0.015	0.05	0.33	P	2.4	2.1
6/23A	15E_4s2d2Xd_1	33.5	30	0.126	0.189	HLP-22	12	8	4	s2d2	4.18	0.000076	0.015	0.05	0.19	P	2.3	2.1
6/24A	15E_4s2d2Xd_1	35.25	30	0.126	0.189	HLP-22	12	8	4	s2d2	4.18	0.000076	0.015	0.05	0.18	P	2.4	2.1
6/24B	15E_4s2d2Wc_1	35.75	30	0.126	0.189	HLP-22	12	8	4	s2d2	4.18	0.000076	0.045	0.05	0.33	P	2.5	2.1
6/25A	15E_4s2d2Wc	34.5	30	0.126	0.189	HLP-22	12	8	4	s2d2	4.18	0.000076	0.045	0.05	0.33	P	2.4	2.1
6/25B	15E_4s2d2Pc_1	34.5	30	0.126	0.189	HLP-22	12	8	4	s2d2	4.18	0.000076	0.06	0.05	0.33	P	2.4	2.1
6/26A	15E_4s1d1Zc_1	34.75	30	0.126	0.189	HLP-22	12	8	4	s1d1	2.46	0.000166	0.00155	0.05	0.33	P	2.4	2.1
6/26B	15E_4s1d1Zd_1	34.75	30	0.126	0.189	HLP-22	12	8	4	s1d1	2.46	0.000166	0.00155	0.05	0.18	P	2.4	2.1
6/27A	15E_4s1d1Yc_1	34.75	30	0.126	0.189	HLP-22	12	8	4	s1d1	2.46	0.000166	0.005	0.05	0.33	P	2.4	2.1
6/27B	15E_4s1d1Yd_1	34.75	30	0.126	0.189	HLP-22	12	8	4	s1d1	2.46	0.000166	0.005	0.05	0.19	P	2.4	2.1
6/27C	15E_4s1d1Xc_1	35.5	30	0.126	0.189	HLP-22	12	8	4	s1d1	2.46	0.000166	0.015	0.05	0.33	P	2.5	2.1
6/30A	15E_4s1d1Xc_1	35	30	0.126	0.189	HLP-22	12	8	4	s1d1	2.46	0.000166	0.015	0.05	0.33	P	2.4	2.1
6/30B	15E_4s1d5Zc_1	35	30	0.126	0.189	HLP-22	12	8	4	s1d5	2.5	0.000044	0.00155	0.05	0.33	P	2.4	2.1
7/1A	15E_4s1d5Zc_1	35	30	0.126	0.189	HLP-22	12	8	4	s1d5	2.5	0.000044	0.00155	0.05	0.33	P	2.4	2.1
7/1B	15E_4s1d5Yc_1	35	30	0.126	0.189	HLP-22	12	8	4	s1d5	2.5	0.000044	0.005	0.05	0.33	P	2.4	2.1
7/2A	15E_4s2d1Tc_1	36	30	0.126	0.189	HLP-22	12	8	4	s2d1	4.17	0.000164	0.0005	0.05	0.33	P	2.5	2.1
7/2B	15E_4s2d1Zc_1	36	30	0.126	0.189	HLP-22	12	8	4	s2d1	4.17	0.000164	0.00155	0.05	0.33	P	2.5	2.1
7/3A	15E_4s2d1Yc_1	35.5	30	0.126	0.189	HLP-22	12	8	4	s2d1	4.17	0.000164	0.005	0.05	0.33	P	2.5	2.1
7/3B	15E_4s2d1Xc_1	35.5	30	0.126	0.189	HLP-22	12	8	4	s2d1	4.17	0.000164	0.015	0.05	0.33	P	2.5	2.1
7/8A	15E8_6s1d2Zc_1	35	30	0.191	0.20246	8TA	8	4	4	s1d2	2.48	0.000069	0.00155	0.05	0.33	P	2.4	2.1
7/8B	15E8_6s1d2Zc_2	35	30	0.191	0.20246	8TA	8	4	4	s1d2	2.48	0.000069	0.00155	0.10	0.33	P	2.4	2.1
7/8C	15E8_6s1d2Vc_1	36	30	0.191	0.20246	8TA	8	4	4	s1d2	2.48	0.000069	0.0143	0.05	0.34	P	2.5	2.1
7/9A	15E8_6s1d2Vc_2	36	30	0.191	0.2865	8TA	8	4	4	s1d2	2.48	0.000069	0.0143	0.10	0.33	P	2.5	2.1
7/9B	15E8_6s1d2Xc_1	36	30	0.191	0.2865	8TA	8	4	4	s1d2	2.48	0.000069	0.015	0.05	0.33	P	2.5	2.1

Table 6.9. (contd)

Test	Case ID	Tank Fill Height	Return Line Height	Nozzle Inner Diameter	Nozzle Standoff Distance	Pulse Tube Configuration	Installed Nozzles	Outer Nozzles Operated	Inner Nozzles Operated	Simulant	Solids Density	Particle Diameter d50	Solids Fraction	Pulse Volume Fraction	Duty Cycle	Pulsed or Steady Jet	Fill Height to Diameter	Return Line Height to Diameter
text	text	in.	in.	in.	in.	text	number	number	number	text	g/cm^3	m	fraction	fraction	fraction	text	ratio	ratio
M/DDX	ID	H	Rtn	d	sod	PT	N	N_O	N_I	sxdx	ρ_S	d_{50}	ϕ_S	ϕ_p	DC	Jet	H/D	Rtn/D
7/9C	15E8_6s1d2Xc_2	36	30	0.191	0.2865	8TA	8	4	4	s1d2	2.48	0.000069	0.015	0.10	0.33	P	2.5	2.1
7/10A	15E8_Ms1d2Zc_1	35.5	30	0.268	0.402	8TA	8	4	4	s1d2	2.48	0.000069	0.00155	0.05	0.33	P	2.5	2.1
7/10B	15E8_Ms1d2Zc_2	35.5	30	0.268	0.402	8TA	8	4	4	s1d2	2.48	0.000069	0.00155	0.10	0.33	P	2.5	2.1
7/11A	15E8_Ms1d2Vc_1	35	30	0.268	0.402	8TA	8	4	4	s1d2	2.48	0.000069	0.0143	0.05	0.33	P	2.4	2.1
7/11B	15E8_Ms1d2Vc_2	35	30	0.268	0.402	8TA	8	4	4	s1d2	2.48	0.000069	0.0143	0.10	0.33	P	2.4	2.1
7/14A	15E8_Ls1d2Zc_1	36	30	0.375	0.5625	8TA	8	4	4	s1d2	2.48	0.000069	0.00155	0.05	0.33	P	2.5	2.1
7/14B	15E8_Ls1d2Vc_1	36	30	0.375	0.5625	8TA	8	4	4	s1d2	2.48	0.000069	0.0143	0.05	0.34	P	2.5	2.1
7/15A	15E8_Ls1d2Vc_7	35.5	30	0.375	0.5625	8TA	8	4	0	s1d2	2.48	0.000069	0.0143	0.10	0.33	P	2.5	2.1
7/15B	15E8_Ls1d2Vc_2	35.5	30	0.375	0.5625	8TA	8	4	4	s1d2	2.48	0.000069	0.0143	0.10	0.33	P	2.5	2.1
7/15C	15E8_Ls1d2Vc_6	35.5	30	0.375	0.5625	8TA	8	4	0	s1d2	2.48	0.000069	0.0143	0.05	0.33	P	2.5	2.1

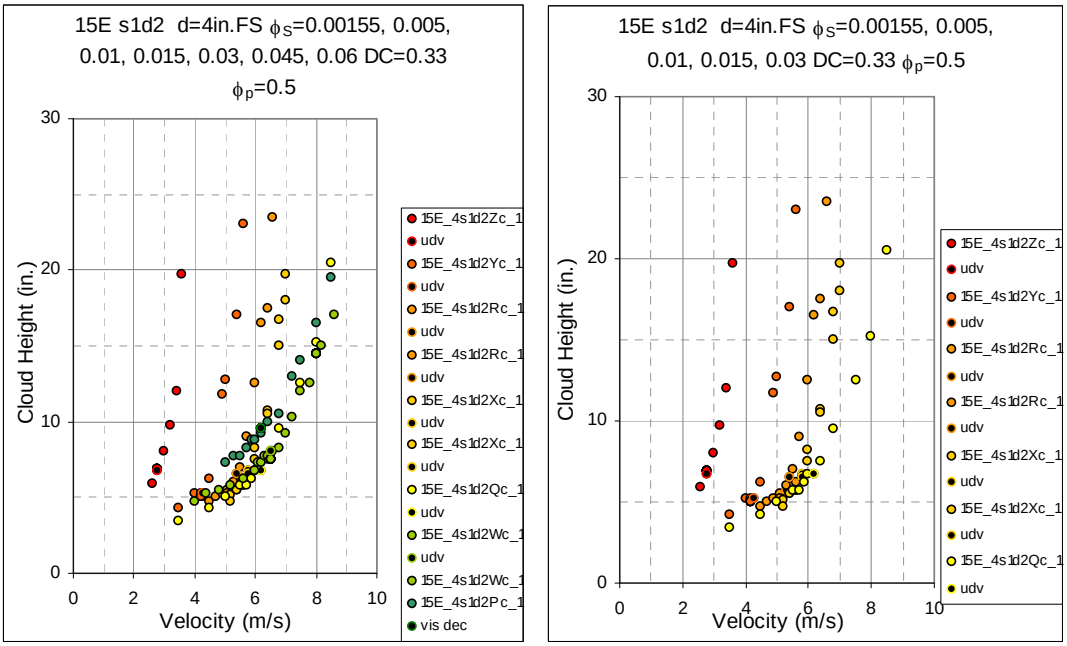

(a) (b)

Figure 6.10. Cloud Height as Function of Velocity for Seven Concentrations: (a) all Concentrations, (b) Five Concentrations. Test conditions are solids fractions (ϕ_S = 0.00155 [Z] red, 0.005 [Y] red-orange, 0.01 [R] light orange, 0.015 [X] gold, 0.03 [Q] yellow, 0.045 [W] lime, 0.06 [P] green), simulant s1d2 (ρ_s = 2.48 g/cm^3, d_{50} = 69 μm), 4 in. full-scale nozzle for duty cycle (DC = 0.33) and pulse volume fraction (ϕ_p = 0.05).

In Figure 6.11 simulant is varied while other parameters are constant for two solids fractions. In Figure 6.11(a) the solids fraction is 0.00155 [Z]; in Figure 6.11(b) the solids fraction is 0.005 [Y]. In both (a) and (b) when the simulant density is held constant and the particle size increases, the critical suspension velocity increases as the settling velocity of the simulants increases. When the simulant particle size is held constant and the simulant density increases, the critical suspension velocity also increases as does the settling velocity. The simulant settling velocities are plotted in Figures 3.3 and 3.4.

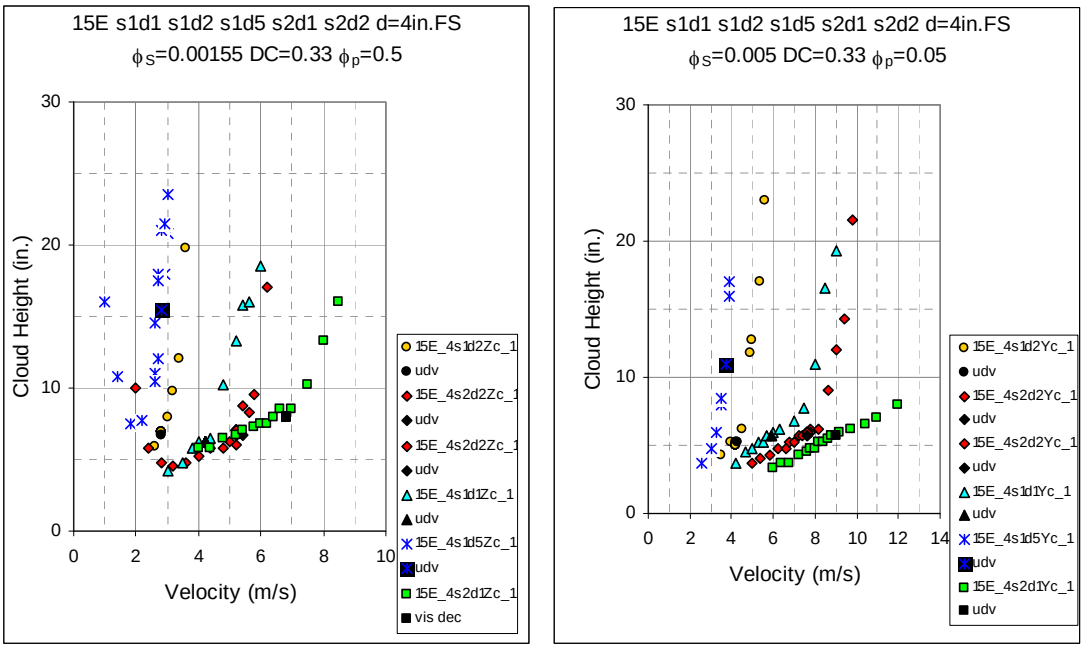

(a) (b)

Figure 6.11. Cloud Height as Function of Velocity for Two Solids Fractions: (a) $\phi_S = 0.00155$ [Z] and (b) $\phi_S = 0.005$ [Y]. Both use five simulants: s1d5 ($\rho_s = 2.5$ g/cm^3, $d_{50} = 44$ µm) blue asterisk, s1d2 ($\rho_s = 2.48$ g/cm^3, $d_{50} = 69$ µm) gold circle, s1d1 ($\rho_s = 2.46$ g/cm^3, $d_{50} = 166$ µm) aqua triangle, s2d2 ($\rho_s = 4.18$ g/cm^3, $d_{50} = 76$ µm) red diamond, and s2d1 ($\rho_s = 4.17$ g/cm^3, $d_{50} = 164$ µm) green square , 4 in. full-scale nozzle, duty cycle (DC = 0.33 [c]), and pulse volume fraction ($\phi_p = 0.05$).

In Figure 6.12 the effect of varying nozzle diameter is shown for two tank pulse tube configurations, HLP-22 and 8TA (an eight tube array). The data suggest that the larger the nozzle diameter, the lower the critical suspension velocity.

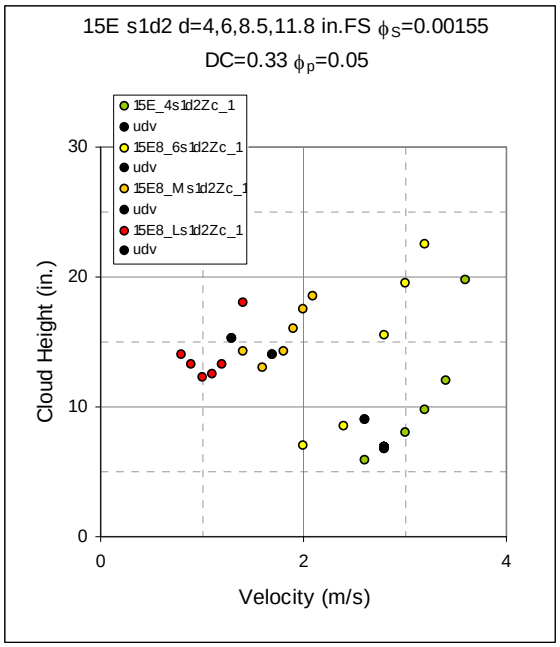

Figure 6.12. Cloud Height as Function of Velocity for Four Full-Scale Nozzle Diameters in Two Tank Configurations. Test conditions are simulant s1d2 (ρ_s = 2.48 g/cm^3, d_{50} = 69 μm) at solids fraction (ϕ_S = 0.00155 [Z]) for constant duty cycle (DC = 0.33 [c]) and pulse volume fraction (ϕ_p = 0.05) with full-scale nozzle diameters of 4 in. (green circles [o] HLP-22 [8/4 pulse tubes]), 6 in. (yellow circles [o] 8TA [4/4 pulse tubes]), 8.5 in. ([M] gold circles [o] 8TA [4/4 pulse tubes]), 11.8 in. ([L] red circles [o] 8TA [4/4 pulse tubes]).

6.4.2 Mid-Scale Tests with Spherical Head

The test conditions that were varied during the 2008 tests in the mid-scale tank included four simulants: s1d2 (ρ_s = 2.48 g/cm^3, d_{50} = 69 μm), s2d2 (ρ_s = 4.18 g/cm^3, d_{50} = 76 μm), s1d1 (ρ_s = 2.46 g/cm^3, d_{50} = 166 μm), and s2d1 (ρ_s = 4.17 g/cm^3, d_{50} = 164 μm); one nozzle diameter (d = 4 in. full scale); a series of solids fractions (ϕ_S = 0.0005 [T, see Table 6.4], 0.00155 [Z], 0.005 [Y], 0.0150 [X]); a series of duty cycles (DC = 0.18 [d], 0.33 [c], 0.50 [b], 0.66 [e]); and two pulse volume fractions (ϕ_p = 0.05 [_1], 0.1 [_2]). These tests were conducted with pulse tube configuration of HLP-22, 8 outer pulse tubes and 4 inner pulse tubes [8/4] with all pulse tubes in operation. The test combinations are listed in Table 6.10.

Table 6.10. 2008 Test Summary for Mid-Scale Tank

Test	Case ID	Tank Fill Height	Return Line Height	Nozzle Inner Diameter	Nozzle Standoff Distance	Pulse Tube Configuration	Installed Nozzles	Outer Nozzles Operated	Inner Nozzles Operated	Simulant	Solids Density	Particle Diameter d50	Solids Fraction	Pulse Volume Fraction	Duty Cycle	Pulsed or Steady Jet	Fill Height to Diameter	Return Line Height to Diameter
text	text	in.	in.	in.	in.	text	number	number	number	text	g/cm^3	m	fraction	fraction	fraction	text	ratio	ratio
M/DDX	ID	H	Rtn	d	sod	PT	N	N_O	N_I	sxdx	ρ_S	d_{50}	ϕ_S	ϕ_p	DC	Jet	H/D	Rtn/D
3/5A	34S_4s1d1Zc_1	69	66	0.297	0.446	HLP-22	12	8	4	s1d1	2.46	0.000166	0.00155	0.05	0.34	P	2.0	1.9
3/5B	34S_4s1d1Zd_1	69	66	0.297	0.446	HLP-22	12	8	4	s1d1	2.46	0.000166	0.00155	0.05	0.18	P	2.0	1.9
3/5C	34S_4s1d1Zc_2	69	66	0.297	0.446	HLP-22	12	8	4	s1d1	2.46	0.000166	0.00155	0.10	0.33	P	2.0	1.9
3/6A	34S_4s1d1Yc_1	69	66	0.297	0.446	HLP-22	12	8	4	s1d1	2.46	0.000166	0.005	0.05	0.34	P	2.0	1.9
3/6B	34S_4s1d1Yd_1	69	66	0.297	0.446	HLP-22	12	8	4	s1d1	2.46	0.000166	0.005	0.05	0.19	P	2.0	1.9
3/6C	34S_4s1d1Xc_1	69	66	0.297	0.446	HLP-22	12	8	4	s1d1	2.46	0.000166	0.015	0.05	0.34	P	2.0	1.9
3/7A	34S_4s1d2Uc_1	69	66	0.297	0.446	HLP-22	12	8	4	s1d2	2.48	0.000069	0.00015	0.05	0.33	P	2.0	1.9
3/7B	34S_4s1d2Tc_1	70	66	0.297	0.446	HLP-22	12	8	4	s1d2	2.48	0.000069	0.0005	0.05	0.33	P	2.1	1.9
3/7C	34S_4s1d2Sc_1	70	66	0.297	0.446	HLP-22	12	8	4	s1d2	2.48	0.000069	0.0015	0.05	0.34	P	2.1	1.9
3/9A	34S_4s1d2Yc_1	70	66	0.297	0.446	HLP-22	12	8	4	s1d2	2.48	0.000069	0.005	0.05	0.34	P	2.1	1.9
3/9B	34S_4s1d2Yd_1	70	66	0.297	0.446	HLP-22	12	8	4	s1d2	2.48	0.000069	0.005	0.05	0.19	P	2.1	1.9
3/11A	34S_4s2d2Tc_1	72	66	0.297	0.446	HLP-22	12	8	4	s2d2	4.18	0.000076	0.0005	0.05	0.33	P	2.1	1.9
3/11B	34S_4s2d2Zc_1	72	66	0.297	0.446	HLP-22	12	8	4	s2d2	4.18	0.000076	0.00155	0.05	0.33	P	2.1	1.9
3/11C	34S_4s2d2Yd_1	72	66	0.297	0.446	HLP-22	12	8	4	s2d2	4.18	0.000076	0.005	0.05	0.19	P	2.1	1.9
3/12A	34S_4s2d2Yc_1	72	66	0.297	0.446	HLP-22	12	8	4	s2d2	4.18	0.000076	0.005	0.05	0.34	P	2.1	1.9
3/12C	34S_4s2d2Xc_1	72	66	0.297	0.446	HLP-22	12	8	4	s2d2	4.18	0.000076	0.015	0.05	0.35	P	2.1	1.9
3/12D	34S_4s2d2Xc_2	72	66	0.297	0.446	HLP-22	12	8	4	s2d2	4.18	0.000076	0.015	0.10	0.33	P	2.1	1.9
3/12E	34S_4s2d2Xb_1	72	66	0.297	0.446	HLP-22	12	8	4	s2d2	4.18	0.000076	0.015	0.05	0.50	P	2.1	1.9
3/12F	34S_4s2d1Yc_1	70	66	0.297	0.446	HLP-22	12	8	4	s2d1	4.17	0.000164	0.005	0.05	0.34	P	2.1	1.9

Data from selected tests in the mid-scale vessel are shown in Figures 6.13 and 6.14. The plot legend presents the Case ID followed by the U_{CS} velocity if it was measured for that case. When identified, the U_{CS} velocity is shown as the darkened symbol in the legend beneath the test and the method used to determine U_{CS} is also shown. For example, in the legend for Figure 6.13(a) each test Case ID shows the U_{CS} condition beneath it. The first Case ID (34S_4s1d1Yc_1) symbol is an aqua triangle, the corresponding U_{CS} condition symbol is shown as a black triangle. The next three U_{CS} condition symbols are shown as either black symbols or colored symbols with black centers where the color matches that of the Case ID listed above it. The description to the right of the U_{CS} condition shows the method used to determine U_{CS} which is either "udv" or "vis dec." Udv means that the U_{CS} condition was determined ultrasonically after an increase in velocity. Vis dec means that the U_{CS} condition was determined visually after a decrease in velocity.

The four sxdx simulants are compared in Figure 6.13(a) at the same solids fraction. In Figure 6.13(b) two simulants are compared at three solids fractions. In both (a) and (b), when the simulant density is held constant and the particle size increases, the critical suspension velocity increases as the settling velocity of the simulants increases. When the simulant particle size is held constant and the simulant density increases, the critical suspension velocity also increases as does the settling velocity. The simulant settling velocities are plotted in Figures 3.3 and 3.4. In Figure 6.13(b) the data are grouped based on solids fraction; the lowest solids fraction is shown by the circles, the mid solids fraction by the diamonds, and the largest solids fraction by squares. Within these groupings the critical suspension velocity increases with increasing settling velocity.

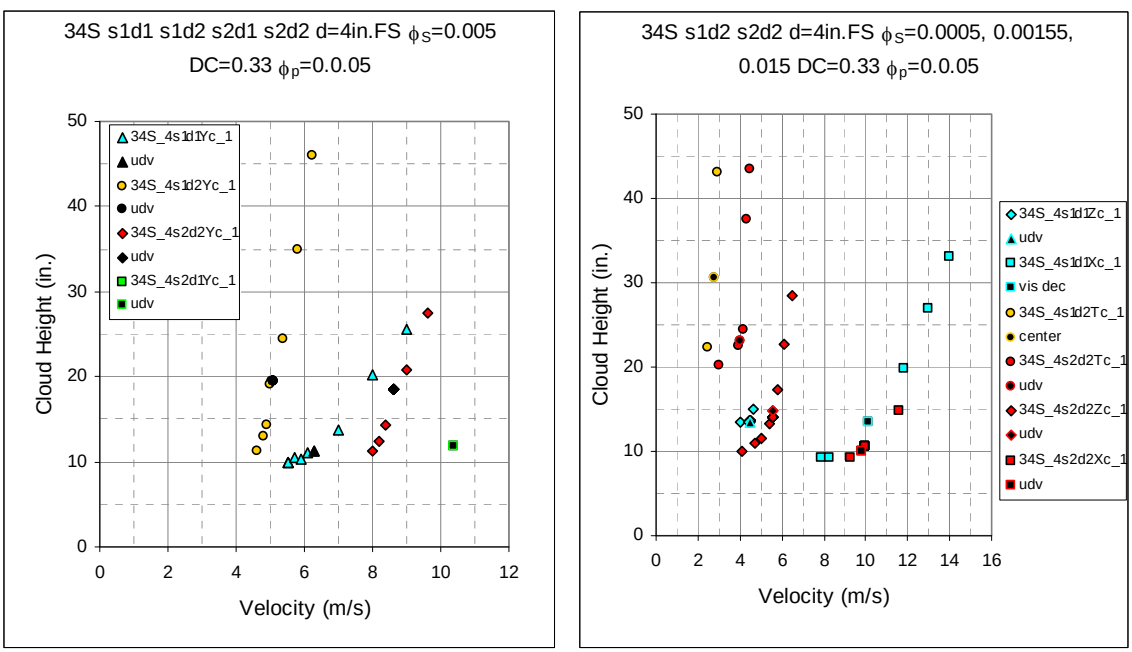

(a) (b)

Figure 6.13. Cloud Height as Function of Velocity for Different Simulants. (a) Four simulants at solids fraction (ϕ_S = 0.005 [Y]), (b) two simulants at three solids fractions (ϕ_S = 0.0005 [T] circle, 0.00155 [Z] diamond, 0.015 [X] square) using a 4 in. full-scale nozzle with duty cycle (DC = 0.33 [c]) and pulse volume fraction (ϕ_p = 0.05). Simulants are s1d2 (ρ_s = 2.48 g/cm^3, d_{50} = 69 μm) gold [o], s1d1 (ρ_s = 2.46 g/cm^3, d_{50} = 166 μm) aqua [o], s2d2 (ρ_s = 4.18 g/cm^3, d_{50} = 76 μm) red [o], and s2d1 (ρ_s = 4.17 g/cm^3, d_{50} = 164 μm) green [o].

In Figure 6.14, the three simulants with median solids diameters near 170 μm are compared. The simulant densities range from ~ 2.5 to 4.17 g/cm^3. Again the critical suspension velocity is shown to increase with density and with settling velocity.

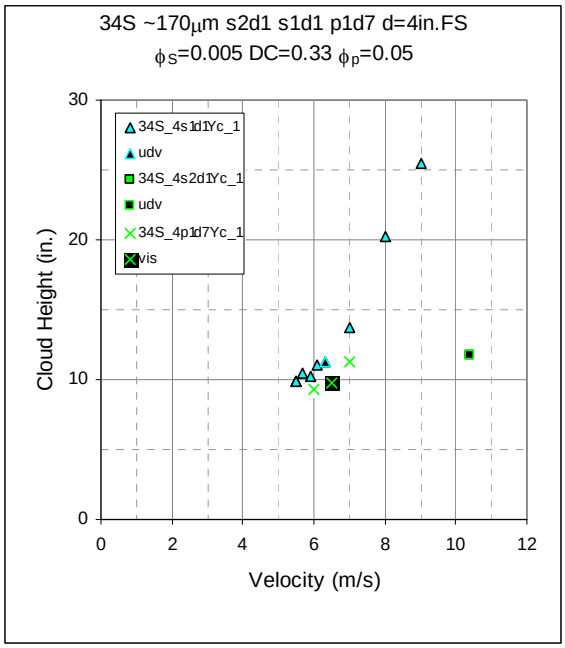

Figure 6.14. Cloud Height as a Function of Velocity for Three Simulants near 170 μm Median Diameter. Test conditions are simulants: p1d7 (ρ_s = 2.45 g/cm^3, d_{50} = 178 μm) green X symbol, s1d1 (ρ_s = 2.46 g/cm^3, d_{50} = 166 μm) aqua triangle, s2d1 (ρ_s = 4.17 g/cm^3, d_{50} = 164 μm) green square with solids fraction (ϕ_S = 0.005 [Y]) using 4 in. full-scale nozzle with duty cycle (DC = 0.33 [c]) and pulse volume fraction (ϕ_p = 0.05**).**

6.4.3 Large-Scale Tank Tests with Elliptical Head

The test conditions that were varied during the 2008 tests in the large-scale tank with the elliptical head included three simulants: s1d2 (ρ_s = 2.48 g/cm^3, d_{50} = 69 μm), s1d1 (ρ_s = 2.46 g/cm^3, d_{50} = 166 μm), and s2d2 (ρ_s = 4.18 g/cm^3, d_{50} = 76 μm); two nozzle diameters (d = 4, 6 in. full scale); a series of solids fractions (ϕ_S = 0.00155 [Z, see Table 6.4], 0.005 [Y], 0.01 [R], 0.0143 [V], and 0.015 [X]); a series of duty cycles (DC = 0.18 [d], 0.33 [c], 0.66 [e], 1.0–continuous[a]); and several pulse volume fractions (ϕ_p = 0.05 [_1], 0.1 [_2], 0.15 [_4]). These tests were conducted with two pulse tube configurations, HLP-22 (8 outer and 4 inner pulse tubes with all in operation [8/4]) and 8TA (4 outer pulse tubes and 4 inner pulse tube in combinations of 4/4 [4/4] and 4/0 [4/0]). The test combinations are listed in Table 6.11.

Data from selected tests in the large-scale vessel with the elliptical head are shown in Figures 6.15 through 6.18.

Table 6.11. 2008 Test Summary for Large-Scale Tank with Elliptical Head

Test	Case ID	Tank Fill Height	Return Line Height	Nozzle Inner Diameter	Nozzle Standoff Distance	Pulse Tube Configuration	Installed Nozzles	Outer Nozzles Operated	Inner Nozzles Operated	Simulant	Solids Density	Particle Diameter d50	Solids Fraction	Pulse Volume Fraction	Duty Cycle	Pulsed or Steady Jet	Fill Height to Diameter	Return Line Height to Diameter
text	text	in.	in.	in.	in.	text	number	number	number	text	g/cm^3	m	fraction	fraction	fraction	text	ratio	ratio
M/DDX	ID	H	Rtn	d	sod	PT	N	N_O	N_I	sxdx	ρ_S	d_{50}	ϕ_S	ϕ_p	DC	Jet	H/D	Rtn/D
5/8A	70E_4s1d2Zc_1	93	80	0.613	0.92	HLP-22	12	8	4	s1d2	2.48	0.000069	0.00155	0.05	0.33	P	1.3	1.1
5/9A	70E_4s1d2Zc_1	93	80	0.613	0.92	HLP-22	12	8	4	s1d2	2.48	0.000069	0.00155	0.05	0.34	P	1.3	1.1
5/9B	70E_4s1d2Zd_1	93	80	0.613	0.92	HLP-22	12	8	4	s1d2	2.48	0.000069	0.00155	0.05	0.18	P	1.3	1.1
5/12A	70E_4s1d2Yc_1	93	80	0.613	0.92	HLP-22	12	8	4	s1d2	2.48	0.000069	0.005	0.05	0.33	P	1.3	1.1
5/12B	70E_4s1d2Rc_1	93	80	0.613	0.92	HLP-22	12	8	4	s1d2	2.48	0.000069	0.01	0.05	0.33	P	1.3	1.1
5/13A	70E_4s1d2Rc_1	92.5	80	0.613	0.92	HLP-22	12	8	4	s1d2	2.48	0.000069	0.01	0.05	0.34	P	1.3	1.1
5/13B	70E_4s1d2Rd_1	92.5	80	0.613	0.92	HLP-22	12	8	4	s1d2	2.48	0.000069	0.01	0.05	0.18	P	1.3	1.1
5/13C	70E_4s1d2Vc_1	92.5	80	0.613	0.92	HLP-22	12	8	4	s1d2	2.48	0.000069	0.0143	0.05	0.33	P	1.3	1.1
5/14A	70E_4s1d2Vc_1	92.5	80	0.613	0.92	HLP-22	12	8	4	s1d2	2.48	0.000069	0.0143	0.05	0.33	P	1.3	1.1
5/14B	70E_4s1d2Vd_1	92.5	80	0.613	0.92	HLP-22	12	8	4	s1d2	2.48	0.000069	0.0143	0.05	0.18	P	1.3	1.1
5/15A	70E_4s1d2Vd_1	92.5	80	0.613	0.92	HLP-22	12	8	4	s1d2	2.48	0.000069	0.0143	0.05	0.19	P	1.3	1.1
5/15B	70E_4s1d2Ve_1	92.5	80	0.613	0.92	HLP-22	12	8	4	s1d2	2.48	0.000069	0.0143	0.05	0.66	P	1.3	1.1
5/15C	70E_4s1d2Vc_2	92.5	80	0.613	0.92	HLP-22	12	8	4	s1d2	2.48	0.000069	0.0143	0.10	0.33	P	1.3	1.1
5/15D	70E_4s1d2Vd_2	92.5	80	0.613	0.92	HLP-22	12	8	4	s1d2	2.48	0.000069	0.0143	0.10	0.17	P	1.3	1.1
5/16A	70E_4s1d2Ve_2	92.5	80	0.613	0.92	HLP-22	12	8	4	s1d2	2.48	0.000069	0.0143	0.10	0.66	P	1.3	1.1
5/16B	70E_4s1d2Vc_4	92.5	80	0.613	0.92	HLP-22	12	8	4	s1d2	2.48	0.000069	0.0143	0.15	0.33	P	1.3	1.1
5/16C	70E_4s1d2Vd_4	92.5	80	0.613	0.92	HLP-22	12	8	4	s1d2	2.48	0.000069	0.0143	0.15	0.18	P	1.3	1.1
5/19A	70E_4s1d2Vd_4	91.5	80	0.613	0.92	HLP-22	12	8	4	s1d2	2.48	0.000069	0.0143	0.15	0.18	P	1.3	1.1
5/19B	70E_4s1d2Ve_4	91.5	80	0.613	0.92	HLP-22	12	8	4	s1d2	2.48	0.000069	0.0143	0.15	0.66	P	1.3	1.1
5/19C	70E_4s1d2Xc_1	91.5	80	0.613	0.92	HLP-22	12	8	4	s1d2	2.48	0.000069	0.015	0.05	0.33	P	1.3	1.1
5/20A	70E_4s1d2Xc_1	91.5	80	0.613	0.92	HLP-22	12	8	4	s1d2	2.48	0.000069	0.015	0.05	0.33	P	1.3	1.1
5/20B	70E_4s1d2Xd_1	91.5	80	0.613	0.92	HLP-22	12	8	4	s1d2	2.48	0.000069	0.015	0.05	0.19	P	1.3	1.1
5/21A	70E_4s1d2Xd_1	91	80	0.613	0.92	HLP-22	12	8	4	s1d2	2.48	0.000069	0.015	0.05	0.19	P	1.3	1.1
5/21B	70E_4s1d2Xa	91	80	0.613	0.92	HLP-22	12	8	4	s1d2	2.48	0.000069	0.015	undefined	1.00	S	1.3	1.1
5/22A	70E_4s2d2Zc_1	92.5	80	0.613	0.92	HLP-22	12	8	4	s2d2	4.18	0.000076	0.00155	0.05	0.33	P	1.3	1.1
5/27A	70E_4s2d2Zc_1	92	80	0.613	0.92	HLP-22	12	8	4	s2d2	4.18	0.000076	0.00155	0.05	0.34	P	1.3	1.1
5/27B	70E_4s2d2Yd_1	92	80	0.613	0.92	HLP-22	12	8	4	s2d2	4.18	0.000076	0.005	0.05	0.18	P	1.3	1.1
5/27C	70E_4s2d2Yc_1	92	80	0.613	0.92	HLP-22	12	8	4	s2d2	4.18	0.000076	0.005	0.05	0.34	P	1.3	1.1
5/28A	70E_4s2d2Yc_1	92	80	0.613	0.92	HLP-22	12	8	4	s2d2	4.18	0.000076	0.005	0.05	0.33	P	1.3	1.1
5/29A	70E_4s1d1Zd_1	92	80	0.613	0.92	HLP-22	12	8	4	s1d1	2.46	0.000166	0.00155	0.05	0.18	P	1.3	1.1
5/29B	70E_4s1d1Zc_1	92	80	0.613	0.92	HLP-22	12	8	4	s1d1	2.46	0.000166	0.00155	0.05	0.33	P	1.3	1.1
5/30A	70E_4s1d1Zc_1	92	80	0.613	0.92	HLP-22	12	8	4	s1d1	2.46	0.000166	0.00155	0.05	0.33	P	1.3	1.1
7/17A	70E8_6s1d2Zc_1	93	80	0.92	1.38	8TA	8	4	4	s1d2	2.48	0.000069	0.00155	0.05	0.33	P	1.3	1.1

Table 6.11. (contd)

Test	Case ID	Tank Fill Height	Return Line Height	Nozzle Inner Diameter	Nozzle Standoff Distance	Pulse Tube Configuration	Installed Nozzles	Outer Nozzles Operated	Inner Nozzles Operated	Simulant	Solids Density	Particle Diameter d50	Solids Fraction	Pulse Volume Fraction	Duty Cycle	Pulsed or Steady Jet	Fill Height to Diameter	Return Line Height to Diameter
text	text	in.	in.	in.	in.	text	number	number	number	text	g/cm^3	m	fraction	fraction	fraction	text	ratio	ratio
M/DDX	ID	H	Rtn	d	sod	PT	N	N_O	N_I	sxdx	ρ_S	d_{50}	ϕ_S	ϕ_p	DC	Jet	H/D	Rtn/D
7/17B	70E8_6s1d2Zc_2	93	80	0.92	1.38	8TA	8	4	4	s1d2	2.48	0.000069	0.00155	0.10	0.33	P	1.3	1.1
7/18A	70E8_6s1d2Vc_1	94	80	0.92	1.38	8TA	8	4	4	s1d2	2.48	0.000069	0.0143	0.05	0.34	P	1.3	1.1
7/18B	70E8_6s1d2Vc_2	94	80	0.92	1.38	8TA	8	4	4	s1d2	2.48	0.000069	0.0143	0.10	0.33	P	1.3	1.1
7/18C	70E8_6s1d2Vc_7	94	80	0.92	1.38	8TA	8	4	0	s1d2	2.48	0.000069	0.0143	0.10	0.32	P	1.3	1.1

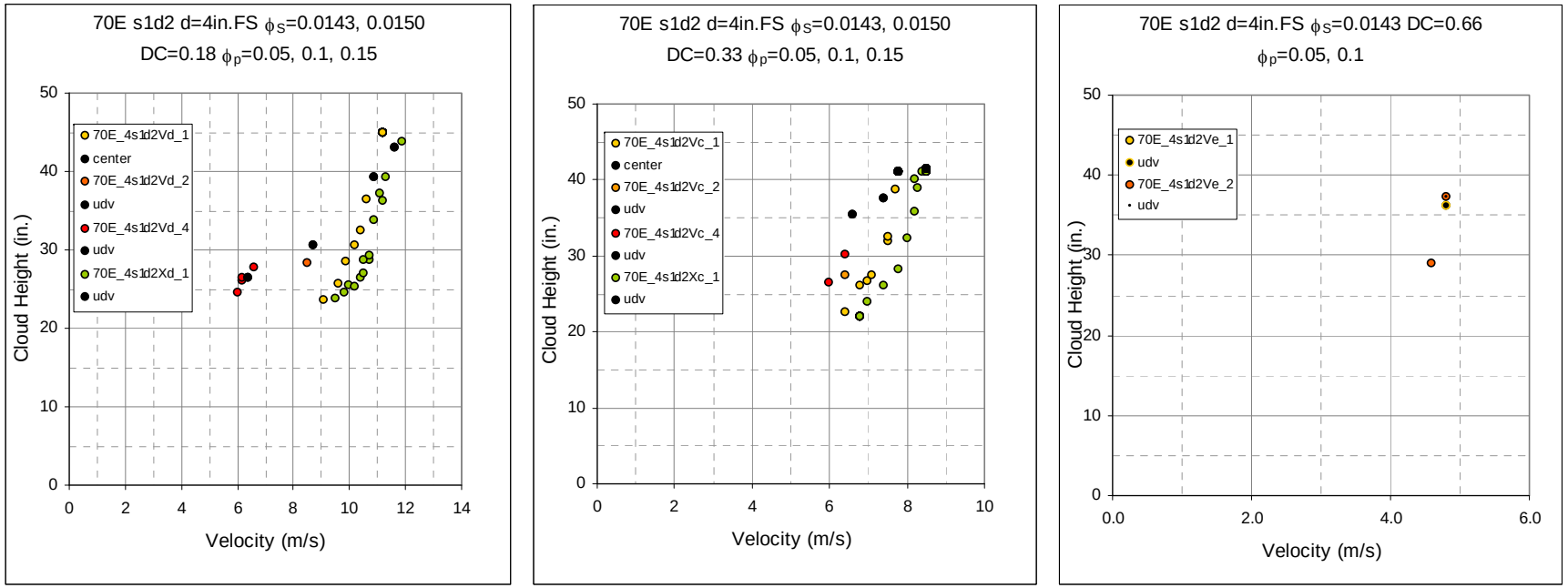

(a) (b) (c)

Figure 6.15. Cloud Height as a Function of Velocity for Three Duty Cycles: (a) Duty Cycle = 0.18 [d], (b) Duty Cycle = 0.33 [c], and (c) Duty Cycle = 0.66 [e]. All use 4 in. full-scale nozzle with simulant s1d2 (ρ_s = 2.48 g/cm^3, d_{50} = 69 μm) at solids fraction (ϕ_S = 0.0143 [V]) at pulse volume fractions (ϕ_p = 0.05 [_1] gold [o], 0.1 [_2] orange [o], 0.15 [_4] red [o]) and at solids fraction (ϕ_S = 0.015 [X]) at pulse volume fractions (ϕ_p = 0.05 [_1] lime green [o].

The plot legend presents the Case ID followed by the U_{CS} velocity if it was measured for that case. When identified, the U_{CS} velocity is shown as the darkened symbol in the legend beneath the test and the method used to determine U_{CS} is also shown. For example, in the legend for Figure 6.15(a) each test Case ID shows the U_{CS} condition beneath it. The first Case ID (70E_4s1d2Vd_1) symbol is a gold circle with a black border, the corresponding U_{CS} condition symbol is shown as a black circle. The next three U_{CS} condition symbols are shown as black symbols. In some cases the U_{CS} symbols are shown as colored symbols with black centers where the color matches that of the Case ID listed above it. The description to the right of the U_{CS} condition shows the method used to determine U_{CS} which is either "udv" or "center." Udv means that the U_{CS} condition was determined ultrasonically after an increase in velocity. Center means that the U_{CS} condition was determined visually through the viewing window in the center of the bottom of the test tank.

In Figure 6.15(a), (b), and (c), three duty cycles are compared for up to three pulse volume fractions. The data are at two solids fractions, (ϕ_S = 0.0143 [V] and 0.015 [X]. The critical suspension velocity decreases with increasing pulse volume fraction. The critical suspension velocity for the higher solids fraction case (ϕ_S = 0.015) is higher than that for the lower solids fraction case (ϕ_S = 0.0143).

In Figure 6.16 the three duty cycles 0.18 [d], 0.33 [c] and 0.66 [e] are compared while other conditions are held constant. This plot shows that the lower the duty cycle, the higher the critical suspension velocity.

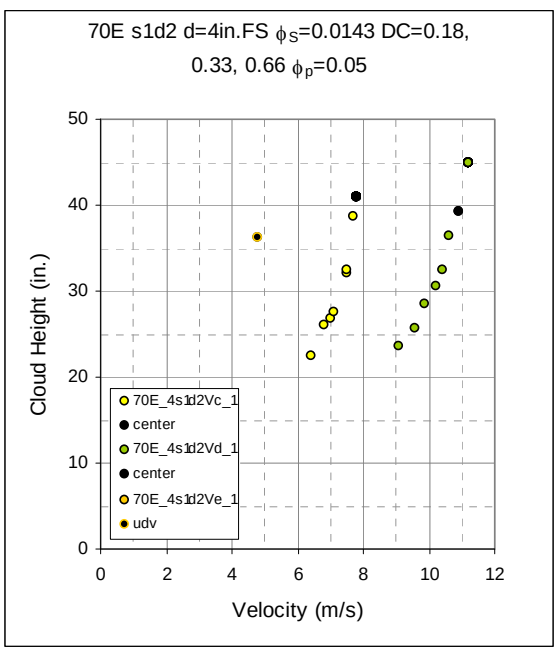

Figure 6.16. Cloud Height as Function of Velocity for Three Duty Cycles (DC = 0.18 [d] gold [o], 0.33 [c] yellow [o], 0.66 [e] lime green [o]). Test conditions are simulant s1d2 (ρ_s = 2.48 g/cm^3, d_{50} = 69 μm) at solids fraction (ϕ_S = 0.0143 [V]) using 4 in. full-scale nozzle with pulse volume fraction (ϕ_p = 0.05).

In Figure 6.17 differences between the HLP-22 (12-tube array with 8 outer and four inner nozzles with 4 in. diameter full-scale nozzle) and 8TA (8-tube array configuration 4 outer and 4 inner nozzles with 6 in. full-scale nozzles) can be observed. The 8-tube array configuration is shown in the Case ID by

the E8 after the vessel diameter. The 8TA configuration has a lower critical suspension velocity than the HLP-22 configuration, and when comparing the two 8TA cases the lower pulse volume fraction has a higher critical suspension velocity.

In Figure 6.18 three simulants are compared with other conditions held constant. When simulant density is held constant, the smaller diameter particle (s1d2) has the lower critical suspension velocity than the larger diameter particle (s1d1). When the particle size is held constant, the lower density particle (s1d2) has the lower critical suspension velocity than the higher density particle (s2d2).

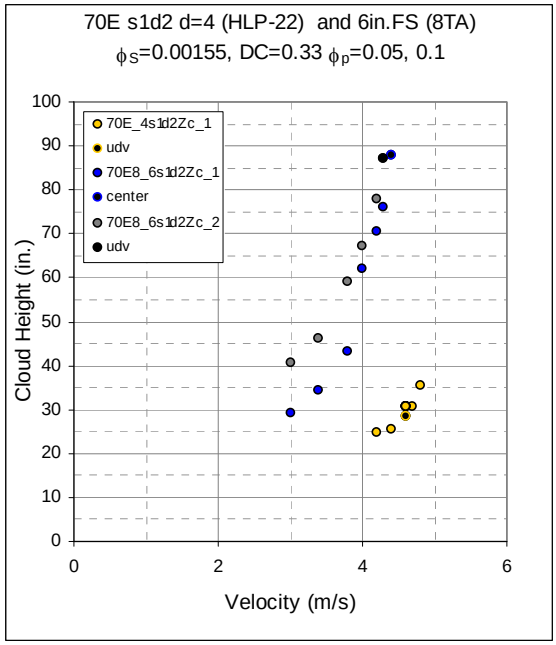

Figure 6.17. Cloud Height as a Function of Velocity for Two Tank Configurations, HLP-22 (70E 4-in. full-scale nozzle 12 pulse tube array gold [o]) and 8TA (70E8 6-in. full-scale nozzle eight pulse tube array). Test conditions are simulant s1d2 (ρ_s = 2.48 g/cm^3, d_{50} = 69 μm) at solids fraction (ϕ_S = 0.00155 [Z]) with duty cycle (DC = 0.33 [c]) and pulse volume fractions (ϕ_p = 0.05 [_1] blue [o], 0.1 [_2] gray [o]).

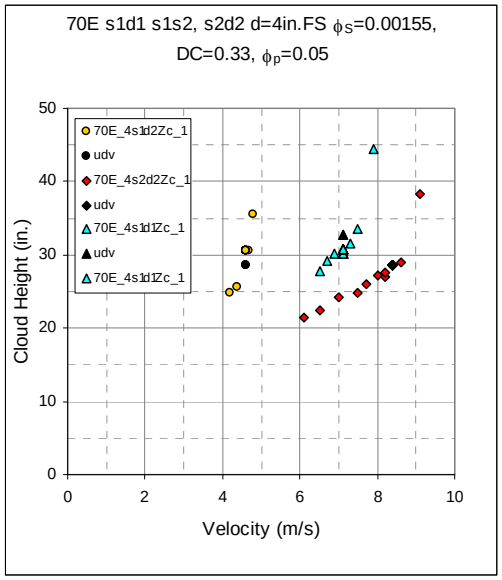

Figure 6.18. Cloud Height as Function of Velocity for Three Simulants: s1d2 (ρ_s = 2.48 g/cm^3, d_{50} = 69 µm) gold [o], s1d1 (ρ_s = 2.46 g/cm^3, d_{50} = 166 µm) aqua triangle, and s2d2 (ρ_s = 4.18 g/cm^3, d_{50} = 76 µm) red diamond. Test conditions are solids fraction (ϕ_S = 0.00155 [Z]) using 4 in. full-scale nozzle with duty cycle (DC = 0.33 [c]) and pulse volume fraction (ϕ_p = 0.05 [_1]).

6.4.4 Large-Scale Tank Tests with Flanged and Dished Head

The test conditions that were varied during the 2008 tests in the large-scale tank with the flanged and dished head included three simulants: s1d2 (ρ_s = 2.48 g/cm^3 d_{50} = 69 µm), s1d1 (ρ_s = 2.46 g/cm^3, d_{50} = 166 µm), and s2d2 (ρ_s = 4.18 g/cm^3, d_{50} = 76 µm); two nozzle diameters (d = 4 and 6 in. full scale); a series of solids fractions (ϕ_S = 0.00155 [Z, see Table 6.4], 0.005 [Y], 0.01 [R], 0.0143 [V]); a series of duty cycles (DC = 0.18 [d], 0.33 [c], 0.66 [e] with a few limited tests at other values); and several pulse volume fractions (ϕ_p = 0.05 [_1], 0.1 [_2], 0.15 [_4]). These tests were conducted with one pulse tube configuration, HLP-22 (8 outer pulse tubes and 4 inner pulse tubes with all pulse tubes in operation). The test combinations are listed in Table 6.12.

Data from selected tests in the large-scale tank with the flanged and dished head are shown in Figure 6.19. The plot legend presents the Case ID followed by the U_{CS} velocity if it was measured for that case. When identified, the U_{CS} velocity is shown as the darkened symbol in the legend beneath the test and the method used to determine U_{CS} is also shown. For example, in the legend for Figure 6.19 each Case ID shows the U_{CS} condition beneath it. The first Case ID (70F_4s1d2Vc_1) symbol is an orange circle with a black border; the corresponding U_{CS} condition symbol is shown as a black circle with an orange border. The next five U_{CS} condition symbols are shown as black symbols with colored borders where the color matches that of the Case ID listed above it. The description to the right of the U_{CS} condition shows the method used to determine U_{CS}; udv means that the U_{CS} condition was determined ultrasonically after an increase in velocity. Four duty cycles (DC = 0.18 [d], 0.25 [f], 0.33 [c], and 0.66 [e]) are compared while other conditions are constant. Repeat test identifications in Figure 6.19 are either repeat tests or additional data at that Case ID condition taken at a different time. The critical suspension velocity increases with decreasing duty cycle.

Table 6.12. 2008 Test Summary for Large-Scale Tank with Flanged and Dished Head

Test	Case ID	Tank Fill Height	Return Line Height	Nozzle Inner Diameter	Nozzle Standoff Distance	Pulse Tube Configuration	Installed Nozzles	Outer Nozzles Operated	Inner Nozzles Operated	Simulant	Solids Density	Particle Diameter d50	Solids Fraction	Pulse Volume Fraction	Duty Cycle	Pulsed or Steady Jet	Fill Height to Diameter	Return Line Height to Diameter
text	text	in.	in.	in.	in.	text	number	number	number	text	g/cm3	m	fraction	fraction	fraction	text	ratio	ratio
M/DDX	ID	H	Rtn	d	sod	PT	N	N_O	N_I	sxdx	ρ_S	d_{50}	ϕ_S	ϕ_p	DC	Jet	H/D	Rtn/D
4/7A	70F_6s2d2Yc_1_FM01	88	83.6	0.92	1.38	HLP-22	12	8	4	s2d2	4.18	0.000076	0.005	0.05	0.33	P	1.3	1.2
4/8A	70F_6s2d2Yh_1	89	83.6	0.92	1.38	HLP-22	12	8	4	s2d2	4.18	0.000076	0.005	0.05	0.24	P	1.3	1.2
4/10A	70F_4s2d2Yi_1	90.5	83.6	0.613	0.92	HLP-22	12	8	4	s2d2	4.18	0.000076	0.005	0.05	0.28	P	1.3	1.2
4/10B	70F_4s2d2Yk_1	90.5	83.6	0.613	0.92	HLP-22	12	8	4	s2d2	4.18	0.000076	0.005	0.05	0.14	P	1.3	1.2
4/10C	70F_4s2d2Yc_1	90.5	83.6	0.613	0.92	HLP-22	12	8	4	s2d2	4.18	0.000076	0.005	0.05	0.34	P	1.3	1.2
4/14A	70F_4s1d1Zc_1	89	83.6	0.613	0.92	HLP-22	12	8	4	s1d1	2.46	0.000166	0.00155	0.05	0.32	P	1.3	1.2
4/15A	70F_4s1d1Zc_2	88	83.6	0.613	0.92	HLP-22	12	8	4	s1d1	2.46	0.000166	0.00155	0.10	0.33	P	1.3	1.2
4/15B	70F_4s1d1Zc_4	88.5	83.6	0.613	0.92	HLP-22	12	8	4	s1d1	2.46	0.000166	0.00155	0.15	0.33	P	1.3	1.2
4/15C	70F_4s1d1Zc_2	88.5	83.6	0.613	0.92	HLP-22	12	8	4	s1d1	2.46	0.000166	0.00155	0.10	0.33	P	1.3	1.2
4/16A	70F_4s1d2Zc_1	88.5	83.6	0.613	0.92	HLP-22	12	8	4	s1d2	2.48	0.000069	0.00155	0.05	0.33	P	1.3	1.2
4/17A	70F_4s1d2Zc_1	87.5	83.6	0.613	0.92	HLP-22	12	8	4	s1d2	2.48	0.000069	0.00155	0.05	0.34	P	1.3	1.2
4/18A	70F_4s1d2Yc_1	87.5	83.6	0.613	0.92	HLP-22	12	8	4	s1d2	2.48	0.000069	0.005	0.05	0.33	P	1.3	1.2
4/18B	70F_4s1d2Rc_1	87.5	83.6	0.613	0.92	HLP-22	12	8	4	s1d2	2.48	0.000069	0.01	0.05	0.34	P	1.3	1.2
4/21A	70F_4s1d2Vc_1	87.5	83.6	0.613	0.92	HLP-22	12	8	4	s1d2	2.48	0.000069	0.0143	0.05	0.33	P	1.3	1.2
4/22A	70F_4s1d2Vd_1	88	83.6	0.613	0.92	HLP-22	12	8	4	s1d2	2.48	0.000069	0.0143	0.05	0.18	P	1.3	1.2
4/22B	70F_4s1d2Vc_2	87.5	83.6	0.613	0.92	HLP-22	12	8	4	s1d2	2.48	0.000069	0.0143	0.10	0.33	P	1.3	1.2
4/23A	70F_4s1d2Ve_1	87.5	83.6	0.613	0.92	HLP-22	12	8	4	s1d2	2.48	0.000069	0.0143	0.05	0.67	P	1.3	1.2
4/23B	70F_4s1d2Ve_2	87.5	83.6	0.613	0.92	HLP-22	12	8	4	s1d2	2.48	0.000069	0.0143	0.10	0.66	P	1.3	1.2
4/23C	70F_4s1d2Ve_4	88	83.6	0.613	0.92	HLP-22	12	8	4	s1d2	2.48	0.000069	0.0143	0.15	0.66	P	1.3	1.2
4/24A	70F_4s1d2Vc_4	88	83.6	0.613	0.92	HLP-22	12	8	4	s1d2	2.48	0.000069	0.0143	0.15	0.33	P	1.3	1.2
4/24B	70F_4s1d2Vd_2	88	83.6	0.613	0.92	HLP-22	12	8	4	s1d2	2.48	0.000069	0.0143	0.10	0.19	P	1.3	1.2
4/25A	70F_4s1d2Vd_4	87.5	83.6	0.613	0.92	HLP-22	12	8	4	s1d2	2.48	0.000069	0.0143	0.15	0.18	P	1.3	1.2
4/25B	70F_4s1d2Ve_1	87.5	83.6	0.613	0.92	HLP-22	12	8	4	s1d2	2.48	0.000069	0.0143	0.05	0.67	P	1.3	1.2
4/25C	70F_4s1d2Vc_2	87.5	83.6	0.613	0.92	HLP-22	12	8	4	s1d2	2.48	0.000069	0.0143	0.10	0.33	P	1.3	1.2
4/28A	70F_4s1d2Vd_1	89.5	83.6	0.613	0.92	HLP-22	12	8	4	s1d2	2.48	0.000069	0.0143	0.05	0.18	P	1.3	1.2
4/29A	70F_4s1d2Vc_1	89	83.6	0.613	0.92	HLP-22	12	8	4	s1d2	2.48	0.000069	0.0143	0.05	0.33	P	1.3	1.2
4/29B	70F_4s1d2Vf_1	89	83.6	0.613	0.92	HLP-22	12	8	4	s1d2	2.48	0.000069	0.0143	0.05	0.25	P	1.3	1.2

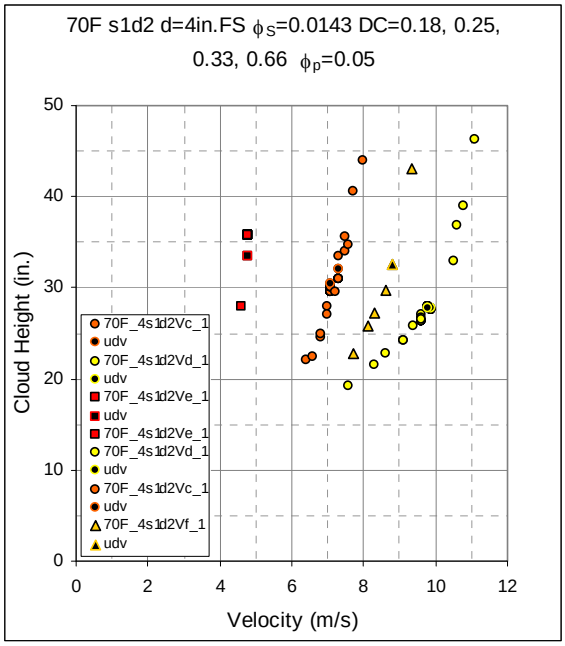

Figure 6.19. Cloud Height as a Function of Velocity for Four Duty Cycles (DC = 0.18 [d] yellow [o], 0.25 [f] gold triangle [o], 0.33 [c] orange [o], 0.66 [e] red square). Test conditions are simulant s1d2 (ρ_s = 2.48 g/cm^3, d_{50} = 69 μm), at solids fraction (ϕ_S = 0.0143 [V]) using with 4 in. full-scale nozzle and pulse volume fraction (ϕ_p = 0.05).

6.4.5 Comparisons Among Tanks

Several tests were directly comparable among the four tanks. Plots of these data are shown in Figures 6.20 through 6.22. The plot legend presents the Case ID followed by the U_{CS} velocity if it was measured for that case. When identified, the U_{CS} velocity is shown as the darkened symbol in the legend beneath the test and the method used to determine U_{CS} is also shown. For example, in the legend for Figure 6.20 each test Case ID shows the U_{CS} condition beneath it. The first Case ID (70F_4s1d2Yc_1) symbol is a green circle with black outline, the corresponding U_{CS} condition symbol is shown as a black circle with a green outline. Other U_{CS} condition symbols are shown as colored symbols with black centers. The color matches the corresponding Case ID above it. The description to the right of the U_{CS} condition shows the method used to determine U_{CS} which is either "udv" or "vis." Udv means that the U_{CS} condition was determined ultrasonically after an increase in velocity. Vis means that the U_{CS} condition was determined visually after an increase in velocity.

In Figure 6.20, data obtained in the large-scale tanks with the elliptical and flanged and dished heads are compared. The data are similar and overlap at velocities greater than the critical suspension velocity.

In Figure 6.21, data from simulant s1d2 (ρ_s = 2.48 g/cm^3, d_{50} = 69 μm) and s2d2 (ρ_s = 4.18 g/cm^3, d_{50} = 76 μm) are shown, with tank diameter and head shape the only condition varied. Figure 6.21(a) shows data for simulant s2d2. The elliptical head at the small- and large-scale produce data that seem to fall along the same line at velocities above 8 m/s, with the mid-scale spherical head slightly offset but parallel to the elliptical head data. Figure 6.21(b) shows data for simulant s1d2 and p1d8, which have similar densities and mean diameters.

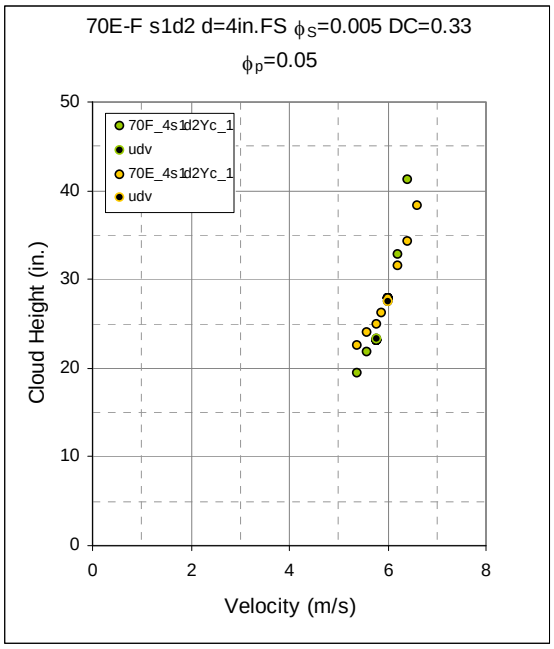

Figure 6.20. Comparison of Tank Heads at Large Scale: 70E with Elliptical and 70F with F&D Head. Test conditions are simulant s1d2 (ρ_s = 2.48 g/cm^3, d_{50} = 69 μm) at solids fraction (ϕ_S = 0.005 [Y]) using 4 in. full-scale nozzle with duty cycle (DC = 0.33 [c]) and pulse volume fraction (ϕ_p = 0.05).

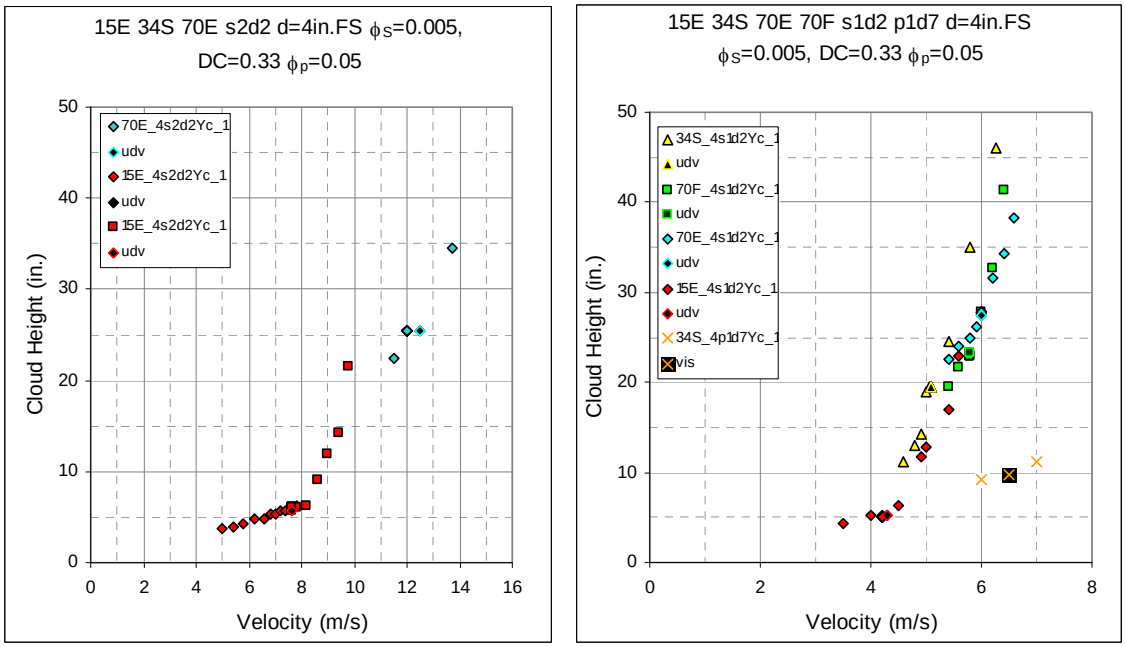

(a) (b)

Figure 6.21. Comparison of Small-, Mid-, Large-Scale: (a) s2d2 (ρ_s = 4.18 g/cm^3, d_{50} = 76 μm). Shown at 15E and 70E with Elliptical, and 70F with Flanged and Dished Head; (b) s1d2 (ρ_s = 2.48 g/cm^3, d_{50} = 69 μm) and p1d8 (ρ_s = 2.45 g/cm^3, d_{50} = 90 μm) in all vessels. Both are at solids fraction (ϕ_S = 0.005 [Y]) using 4 in. full-scale nozzle with duty cycle (DC = 0.33 [c]) and pulse volume fraction (ϕ_p = 0.05).

In Figure 6.22, selected data from five simulants are compared, with simulant and tank the only conditions varied. In both the plots the simulant listing in the heading is in terms of increasing settling velocity, as shown in Figures 3.3 and 3.4. A linear plot shown in Figure 6.22(a), and a log plot is provided in Figure 6.22(b). Simulant s1d5 is shown by the blue asterisks, followed by s1d2 with gold filled symbols. Next is the p1d8 shown by magenta cross symbols; s2d2 is shown by red-filled diamond symbols; s1d1 is shown by aqua triangle symbols; p1d7 is shown by green x symbols; s2d1 is shown by green-filled square symbols. For the tests conducted in 2008, the mid-scale test symbols are outlined in red; the small-scale test symbols are outlined in black; the large-scale test with elliptical head symbols are outlined in blue; and the large-scale test with flanged and dished head symbols are outlined in green. Tests with the 2007 simulants and s1d5 symbols are not outlined.

In both 6.22(a) and (b), when the simulant density is held constant and the particle size increases, the critical suspension velocity increases as the settling velocity of the simulants increases. When the simulant particle size is held constant and the simulant density increases, the critical suspension velocity also increases as does the settling velocity. The simulant settling velocities are plotted in Figures 3.3 and 3.4.

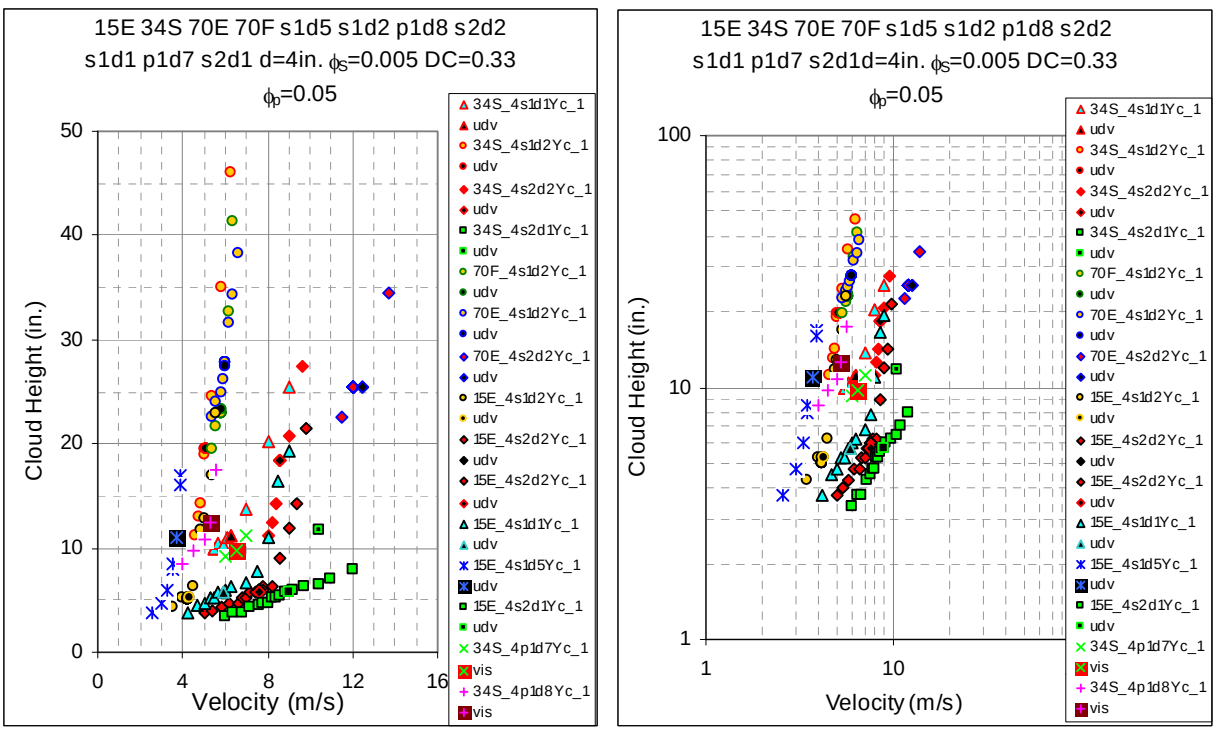

(a) (b)

Figure 6.22. Comparison of Six Simulants in Four Tanks: (a) Linear Scale and (b) Log Scale. All simulants at solids fraction (ϕ_S = 0.005 [Y]) using 4 in. full-scale nozzle with duty cycle (DC = 0.33 [c]) and pulse volume fraction (ϕ_p = 0.05).

6.4.6 Repeat and Replicate Tests

During test campaigns tests with the same Case ID were often performed over multiple days. At times tests were conducted at similar or near similar conditions. These tests were called *repeat tests*,

which were defined as tests performed at the same conditions one after another (or close in time), without a change of simulant. In addition, some tests were conducted during more than one test campaign or after a significant change such as a change of simulant. These tests were called *replicate tests*, which were defined as tests performed at the same set of conditions but at different times, with tests at other sets of conditions intervening. Only limited replicate tests involving the July 2007 and Fall 2007 test campaigns were performed. In addition to replicate tests, some repeat testing was performed within the July 2007, Fall 2007 and 2008 test campaigns. Table 6.13 lists the test conditions investigated with near-replicate and near-repeat testing. The terms *near-replicate* and *near-repeat* are used because the test conditions are close but not exactly the same for some test variables. The replicate and repeat data are discussed in Appendix E, Section E.3.

Table 6.13. Near-Replicate and Near-Repeat Tests at Critical Suspension Conditions

Row Number	Case ID	Test	Tank Diameter	Solids Density	Solids Fraction	Particle Size	Duty Cycle	Pulse Volume Fraction	Installed Tubes	Operating Tubes	Outer Tubes	Inner Tubes	Nozzle Inner Diameter	Head Shape	Discharge Velocity	Near-Repeat Set	Near-Replicate Set
text	text	text	in	g/cm^3	fraction	m	fraction	fraction	Number	Number	Number	Number	in	text	m/s		
MSS	ID	M/DDX	D	S	ϕ_S	d_{50} (d_S)	DC	ϕ_P	N	N_J	N_O	N_I	d	HS	U		
9150506	15E_4s1d1Xc_1	6/27C	14.4375	2.46	0.015	0.00017	0.334	0.050	12	12	8	4	0.126	E	8.2	1	–[a]
9150516	15E_4s1d1Xc_1	6/30A	14.4375	2.46	0.015	0.00017	0.335	0.050	12	12	8	4	0.126	E	8.6	1	–
9150048	15E_4s1d2Rc_1	6/9B	14.4375	2.48	0.01	6.9E-05	0.338	0.050	12	12	8	4	0.126	E	5.3	2	–
9150053	15E_4s1d2Rc_1	6/10A	14.4375	2.48	0.01	6.9E-05	0.331	0.050	12	12	8	4	0.126	E	5.4	2	–
9150063	15E_4s1d2Xc_1	6/10B	14.4375	2.48	0.015	6.9E-05	0.331	0.050	12	12	8	4	0.126	E	5.8	3	–
9150108	15E_4s1d2Xc_1	6/11C	14.4375	2.48	0.015	6.9E-05	0.333	0.050	12	12	8	4	0.126	E	5.8	3	–
9150083	15E_4s1d2Xd_1	6/11A	14.4375	2.48	0.015	6.9E-05	0.184	0.050	12	12	8	4	0.126	E	7.2	4	–
9150174	15E_4s1d2Xd_1	6/13C	14.4375	2.48	0.015	6.9E-05	0.186	0.050	12	12	8	4	0.126	E	7.4	4	–
9150412	15E_4s2d2Wc_1	6/24B	14.4375	4.18	0.045	7.6E-05	0.333	0.050	12	12	8	4	0.126	E	11.5	5	–
9150419	15E_4s2d2Wc_1	6/25A	14.4375	4.18	0.045	7.6E-05	0.332	0.050	12	12	8	4	0.126	E	11.5	5	–
9150345	15E_4s2d2Yc_1	6/19C	14.4375	4.18	0.005	7.6E-05	0.335	0.050	12	12	8	4	0.126	E	7.6	6	–
9150347	15E_4s2d2Yc_1	6/20A	14.4375	4.18	0.005	7.6E-05	0.334	0.050	12	12	8	4	0.126	E	7.6	6	–
9150307	15E_4s2d2Zc_1	6/18B	14.4375	4.18	0.00155	7.6E-05	0.337	0.050	12	12	8	4	0.126	E	5.4	7	–
9150312	15E_4s2d2Zc_1	6/19A	14.4375	4.18	0.00155	7.6E-05	0.334	0.050	12	12	8	4	0.126	E	5.2	7	–
7091025	34S_4p1d7Yc_1	11/26B1	33.875	2.45	0.00487	0.00018	0.330	0.05105	12	12	8	4	0.297	S	6.5	–	1
20070105	34S_4p1d7Yc_8	7/16 A2	33.875	2.45	0.00487	0.00018	0.330	0.05	12	12	8	4	0.297	S	6.4	–	1
20070387	34S_4p1d7Yc_8	7/19 A1	33.875	2.45	0.00487	0.00018	0.330	0.048	12	12	8	4	0.297	S	6.2	–	1
7090875	34S_4p1d7Yd_1	11/19A2	33.875	2.45	0.00487	0.00018	0.180	0.05325	12	12	8	4	0.297	S	6.4	–	2
20070441	34S_4p1d7Yd_8	7/19 A4	33.875	2.45	0.00487	0.00018	0.180	0.048	12	12	8	4	0.297	S	6.4	–	2
7090779	34S_6p1d7Yc_1	11/14D1	33.875	2.45	0.00487	0.00018	0.330	0.05109	12	12	8	4	0.446	S	4.5	–	3
20070627	34S_6p1d7Yc_8	7/21 A2	33.875	2.45	0.00487	0.00018	0.330	0.048	12	12	8	4	0.446	S	4.0	–	3
7090095	34S_6p1d7Yd_0	10/18A2	33.875	2.45	0.00487	0.00018	0.180	0.052	12	8	4	4	0.446	S	6.1	8	–
7090244	34S_6p1d7Yd_0	10/26B2	33.875	2.45	0.00487	0.00018	0.180	0.050	12	8	4	4	0.446	S	6.1	8	–
7090758	34S_6p1d7Yd_0	11/14A2	33.875	2.45	0.00487	0.00018	0.180	0.050	12	8	4	4	0.446	S	7.0	8	–
7090136	34S_6p1d7Yd_6	10/18B2	33.875	2.45	0.00487	0.00018	0.180	0.051	12	4	4	0	0.446	S	6.4	9	–
7090298	34S_6p1d7Yd_6	10/29B2	33.875	2.45	0.00487	0.00018	0.180	0.050	12	4	4	0	0.446	S	6.2	9	–

Table 6.13. (contd)

Row Number	Case ID	Test	Tank Diameter	Solids Density	Solids Fraction	Particle Size	Duty Cycle	Pulse Volume Fraction	Installed Tubes	Operating Tubes	Outer Tubes	Inner Tubes	Nozzle Inner Diameter	Head Shape	Discharge Velocity	Near-Repeat Set	Near-Replicate Set
text	text	text	in	g/cm^3	fraction	m	fraction	fraction	Number	Number	Number	Number	in	text	m/s		
MSS	ID	M/DDX	D	S	ϕ_S	d_{50} (d_S)	DC	ϕ_p	N	N_J	N_O	N_I	d	HS	U		
7090208	34S_6p1d7Yd_1	10/26A2	33.875	2.45	0.00487	0.00018	0.180	0.051	12	12	8	4	0.446	S	4.0	10	4a
7090328	34S_6p1d7Yd_1	10/30A2	33.875	2.45	0.00487	0.00018	0.180	0.051	12	12	8	4	0.446	S	3.6	10	4b
20070750	34S_6p1d7Yd_8	7/23 A1	33.875	2.45	0.00487	0.00018	0.180	0.048	12	12	8	4	0.446	S	4.1	–	4a, 4b
7090184	34S_6p1d7Yd_9	10/19A2	33.875	2.45	0.00487	0.00018	0.180	0.050	12	4	0	4	0.446	S	8.5	11	–
7090360	34S_6p1d7Yd_9	10/30C2	33.875	2.45	0.00487	0.00018	0.180	0.050	12	4	0	4	0.446	S	6.7	11	–
700319	70F_4s1d2Vc_1	4/21A	70	2.48	0.0143	6.9E-05	0.336	0.050	12	12	8	4	0.613	FD	7.1	12	–
700430	70F_4s1d2Vc_1	4/29A	70	2.48	0.0143	6.9E-05	0.336	0.050	12	12	8	4	0.613	FD	7.3	12	–
700356	70F_4s1d2Vd_1	4/22A	70	2.48	0.0143	6.9E-05	0.185	0.050	12	12	8	4	0.613	FD	9.9	13	–
700415	70F_4s1d2Vd_1	4/28A	70	2.48	0.0143	6.9E-05	0.187	0.050	12	12	8	4	0.613	FD	9.8	13	–

(a) A dash (–) indicates the test condition is not included in a near-replicate or near-repeat set.

6.5 Concentration Profiles

During selected tests and at specific test conditions, the ultrasonic concentration probe described in Appendix A was used to measure the concentration of solids by volume in the cloud during a pulse cycle. The procedure for this measurement, the range of tests conducted, and a summary of the transient and averaged data are presented in Section 6.5.1. In Sections 6.5.2 through 6.5.7, the concentration profiles are compared to provide insight regarding variations of concentration profiles with critical suspension velocity, radial location, tank, nozzle diameter, concentration and duty cycle.

6.5.1 Concentration Profile Measurements

The concentration probe was suspended in the tank at a specified elevation and radial location. The most frequent radial location was in the tank center. Data from a series of up to five cycles at steady state conditions (see Section 6.5.1, Figure 6.23) were averaged to determine the average solids concentration by volume during a cycle at the probe location. The data in the cycles were averaged at specified time steps in the cycle to provide transient data of solids concentration by volume during a cycle. Examples of these individual cycle data for all the test tanks are shown in Figure 6.23. The same test conditions and nondimensional probe location are shown for the four tanks: the small- and large-scale tanks with elliptical heads, the mid-scale tank with spherical head, and the large-scale tank with flanged and dished head.

For each tank the sequence of five cycles of transient solids concentration by volume measurements at that location are very similar in shape. Just after the start of the cycle an increase in concentration is visible when the pulse from the PJM mobilizes solids to the elevation of the probe. After the pulse stops the concentration decays. Near the end of the cycle some small fluctuations are observed due to solids settling back to the floor and rebounding in a “sloshing” manner. This sequence, an increase in concentration after pulse start followed by a decrease in concentration after pulse end, is observed when comparing the data for the three tanks.

The tests with concentration profile data are listed in Table 6.14. The table shows the test parameters and radial position of the probe. The first column lists the figure number where the data is found in Appendix C. The second column lists the test Case ID. This is followed by the operating parameters for that test. The measurements were taken at elevations within the cloud. For some tests in the large-scale tank, profiles were obtained at three radial locations: tank center [0R], halfway between the center and the wall [0.5R], and near the wall [0.9R], where R is the tank radius. Table 6.14 lists the “highest concentration test measurement location.” This is the nondimensional elevation within the cloud where a measurement was taken. Above this location the cloud was not visually observable. These measurements are provided at the three radial measurement locations. This information is followed by the velocity, the critical suspension velocity, and the cloud height. The last column lists the test that shows the date of the measurement followed by the sequence during the day. If the data in the velocity column are shown in italics, the profile was taken at a velocity below U_{CS}; if the data in the velocity column are shown in bold, the profile was taken at a velocity above U_{CS}. All other entries were taken at the U_{CS} condition.

The minimum, average, and maximum solids concentration by volume for each profile location and the standard deviation at that location were calculated based on up to five-cycle averages. This information is shown in Figure 6.24. For comparison the data are plotted dimensionally and

nondimensionally. The dimensional plots show elevation (Z), on the y axis to provide a physical relationship with the elevation in the test tank. Concentration [C(Z)] is plotted on the x axis. Two data sets are shown in the dimensional plot: the entire concentration profile data set and the cases limited to the critical suspension condition. Linear fits are provided for each data set. The dimensional plots show that most concentration profile measurements occurred at the U_{CS} condition. The nondimensional plots show elevation (Z) normalized with respect to cloud height (H_C) on the y axis and concentration, C(Z) divided by solids loading (ϕ_S) normalized with respect to the ratio of cloud height to tank diameter (H_C/D). The dimensional plots provide comparison between tanks; the nondimensional plots provide comparison between the clouds within the tanks.

Table 6.14. Summary of Concentration Profile Cases

Figure Number	Case ID	Tank Diameter	Head Shape	Nozzle Diameter	Number of Nozzles Operated: Outer	Number of Nozzles Operated: Inner	Density	Particle Diameter: d50	Concentration	Duty Cycle	Pulse Volume	Elevation of Highest Positive Concentration Measurement: at 0 R	Elevation of Highest Positive Concentration Measurement: at 0.5 R	Elevation of Highest Positive Concentration Measurement: at 0.9 R	Velocity	Velocity at U_{CS}	Cloud Height	Test
text	text	in.	text	in.	integer	integer	g/cm^3	µm	volume fraction	fraction	fraction	Z/D	Z/D	Z/D	m/s	m/s	In.	text
C.1	15E_4s1d2Zc_1	14 7/16	E	0.126	8	4	2.48	69.3	0.00155	0.33	0.05	0.5	n/a	n/a	2.8	2.8	6.88	6/6A
C.2	15E_4s1d2Yc_1	14 7/16	E	0.126	8	4	2.48	69.3	0.005	0.33	0.05	0.4	n/a	n/a	*4.2*[(a)]	4.3	5	6/9A
C.3	15E_4s1d2Xd_1	14 7/16	E	0.126	8	4	2.48	69.3	0.015	0.18	0.05	0.4	n/a	n/a	7.2	7.2	5.75	6/11A
C.4	15E_4s1d2Xc_1	14 7/16	E	0.126	8	4	2.48	69.3	0.015	0.33	0.05	0.45	n/a	n/a	5.8	5.8	6.62	6/10B
C.5	15E_4s1d2Xe_1	14 7/16	E	0.126	8	4	2.48	69.3	0.015	0.67	0.05	0.55	n/a	n/a	3.9	3.9	7.25	6/12A
C.6	15E_4s1d2Wd_1	14 7/16	E	0.126	8	4	2.48	69.3	0.045	0.19	0.05	0.45	n/a	n/a	7.2	7.2	5.75	6/17A
C.7	15E_4s1d2Wc_1	14 7/16	E	0.126	8	4	2.48	69.3	0.045	0.33	0.05	0.55	n/a	n/a	6.5	6.5	7.5	6/16B
C.8	15E_4s1d2Wa	14 7/16	E	0.126	8	4	2.48	69.3	0.045	1.00	undefined	1.1	n/a	n/a	3	3	14.5	6/17B
C.9	15E_4s1d2Wc_1	14 7/16	E	0.126	8	4	2.48	69.3	0.045	0.34	0.05	1	n/a	n/a	**8**[(a)]	6.5	14.5	6/17C
C.10	15E_4s1d2Pc_1	14 7/16	E	0.126	8	4	2.48	69.3	0.06	0.34	0.05	0.7	n/a	n/a	6.2	6.2	9.5	6/18A
C.11	15E_4s2d2Zc_1	14 7/16	E	0.126	8	4	4.18	75.6	0.00155	0.34	0.05	0.4	n/a	n/a	5.2	5.2	7	6/19A
C.12	15E_4s2d2Xc_1	14 7/16	E	0.126	8	4	4.18	75.6	0.015	0.33	0.05	0.35	n/a	n/a	11.8	11.8	6	6/20B
C.13	15E_4s2d2Yc_1	14 7/16	E	0.126	8	4	4.18	75.6	0.005	0.33	0.05	0.4	n/a	n/a	7.6	7.6	6	6/20A
C.14	15E_4s1d1Zc_1	14 7/16	E	0.126	8	4	2.46	166.4	0.00155	0.33	0.05	0.45	n/a	n/a	4.2	4.2	6.25	6/26A
C.15	15E_4s1d1Xc_1	14 7/16	E	0.126	8	4	2.46	166.4	0.015	0.34	0.05	0.3	n/a	n/a	8.6	8.6	5.5	6/30A
C.16	15E_4s1d5Yc_1	14 7/16	E	0.126	8	4	2.5	43.9	0.005	0.33	0.05	0.6	n/a	n/a	*3.5*	3.7	8.5	7/1B
C.17	15E_4s2d1Zc_1	14 7/16	E	0.126	8	4	4.17	164.2	0.00155	0.33	0.05	0.6	n/a	n/a	6.8	6.8	8	7/2B
C.18	15E_6s1d2Vc_1	14 7/16	E	0.191	4	4	2.48	69.3	0.0143	0.33	0.05	0.7	n/a	n/a	4.8	4.8	9.5	7/8C
C.19	15E_6s1d2Xc_1	14 7/16	E	0.191	4	4	2.48	69.3	0.015	0.33	0.05	0.6	n/a	n/a	4.6	4.6	8.5	7/9B
C.20	15E_6s1d2Xc_2	14 7/16	E	0.191	4	4	2.48	69.3	0.015	0.33	0.10	0.7	n/a	n/a	4.4	4.4	8.5	7/9C
C.21	15E_Ms1d2Vc_1	14 7/16	E	0.268	4	4	2.48	69.3	0.0143	0.33	0.05	0.8	n/a	n/a	2.9	2.9	8.5	7/11A
C.22	15E_Ls1d2Vc_1	14 7/16	E	0.375	4	4	2.48	69.3	0.0143	0.34	0.05	0.7	n/a	n/a	1.9	1.9	9.5	7/14B
C.23	15E_Ls1d2Vc_2	14 7/16	E	0.375	4	4	2.48	69.3	0.0143	0.33	0.10	0.9	n/a	n/a	1.9	1.9	11.5	7/15B
C.24	15E_Ls1d2Vc_7	14 7/16	E	0.375	4	0	2.48	69.3	0.0143	0.34	0.10	0.9	n/a	n/a	2.5	2.5	11.5	7/15A
C.25	34S_4s1d1Zc_1	33 7/8	S	0.297	8	4	2.46	166.4	0.00155	0.34	0.05	0.4	n/a	n/a	4.5	4.5	13.75	3/5A
C.26	34S_4s1d2Sc_1	33 7/8	S	0.297	8	4	2.48	69.3	0.0015	0.34	0.05	0.6	n/a	n/a	3.7	3.7	19.75	3/7C
C.27	34S_4s1d2Yc_1	33 7/8	S	0.297	8	4	2.48	69.3	0.005	0.34	0.05	0.7	n/a	n/a	5.1	5.1	19.5	3/9A
C.28	34S_4s1d2Yd_1	33 7/8	S	0.297	8	4	2.48	69.3	0.005	0.19	0.05	0.5	n/a	n/a	**6.2**	6	21	3/9B
C.29	34S_4s2d2Zc_1	33 7/8	S	0.297	8	4	4.18	75.6	0.00155	0.33	0.05	0.4	n/a	n/a	5.6	5.6	14	3/11B
C.30	34S_4s2d2Xc_1	33 7/8	S	0.297	8	4	4.18	75.6	0.015	0.34	0.05	0.35	n/a	n/a	**10**	9.8	10.5	3/12C
C.31	34S_4s2d2Yc_1	33 7/8	S	0.297	8	4	4.18	75.6	0.005	0.34	0.05	0.5	n/a	n/a	8.6	8.6	18.5	3/12A

Table 6.14. (contd)

Figure Number	Case ID	Tank Diameter	Head Shape	Nozzle Diameter	Number of Nozzles Operated		Density	Particle Diameter	Concentration	Duty Cycle	Pulse Volume	Elevation of Highest Positive Concentration Measurement			Velocity	Velocity at U_{CS}	Cloud Height	Test
					Outer	Inner		d50				at 0 R	at 0.5 R	at 0.9 R				
text	text	in.	text	in.	integer	integer	g/cm^3	µm	volume fraction	fraction	fraction	Z/D	Z/D	Z/D	m/s	m/s	m	text
C.32	70F_4s1d1Zc_1	70	FD	0.613	8	4	2.46	166.4	0.00155	0.33	0.05	0.4	n/a	n/a	6.7	6.7	25.5	4/14A
C.33	70F_4s1d1Zc_2	70	FD	0.613	8	4	2.46	166.4	0.00155	0.33	0.10	0.5	n/a	n/a	5.8	5.8	26	4/15C
C.34	70F_4s1d2Zc_1	70	FD	0.613	8	4	2.48	69.3	0.00155	0.34	0.05	0.45	n/a	n/a	4.4	4.4	28.25	4/17A
C.35	70F_4s1d2Rc_1	70	FD	0.613	8	4	2.48	69.3	0.01	0.34	0.05	0.4	n/a	n/a	6.6	6.6	23	4/18B
C.36	70F_4s1d2Yc_1	70	FD	0.613	8	4	2.48	69.3	0.005	0.33	0.05	0.35	n/a	n/a	5.8	5.8	23	4/18A
C.37	70F_4s1d2Vc_1	70	FD	0.613	8	4	2.48	69.3	0.0143	0.34	0.05	0.45	n/a	n/a	7.1	7.1	30	4/21A
C.38	70F_4s1d2Vc_1	70	FD	0.613	8	4	2.48	69.3	0.0143	0.34	0.05	n/a	0.35	n/a	7.1	7.1	30	4/21A
C.39	70F_4s1d2Vc_1	70	FD	0.613	8	4	2.48	69.3	0.0143	0.34	0.05	n/a	n/a	0.35	7.1	7.1	30	4/21A
C.40	70F_4s1d2Vd_1	70	FD	0.613	8	4	2.48	69.3	0.0143	0.19	0.05	0.4	n/a	n/a	*9.6*	9.8	26.25	4/28A
C.41	70F_4s1d2Vd_1	70	FD	0.613	8	4	2.48	69.3	0.0143	0.19	0.05	0.4	n/a	n/a	9.8	9.8	28	4/28A
C.42	70F_4s1d2Vd_1	70	FD	0.613	8	4	2.48	69.3	0.0143	0.19	0.05	0.45	n/a	n/a	9.9	9.9	27.5	4/22A
C.43	70F_4s1d2Vc_1	70	FD	0.613	8	4	2.48	69.3	0.0143	0.34	0.05	0.45	n/a	n/a	7.3	7.3	31	4/29A
C.44	70F_4s1d2Ve_1	70	FD	0.613	8	4	2.48	69.3	0.0143	0.67	0.05	0.6	n/a	n/a	4.8	4.8	35.75	4/25B
C.45	70F_4s1d2Vc_2	70	FD	0.613	8	4	2.48	69.3	0.0143	0.33	0.10	0.45	n/a	n/a	6.6	6.6	28.5	4/25C
C.46	70E_4s1d2Zc_1	70	E	0.613	8	4	2.48	69.3	0.00155	0.34	0.05	0.45	n/a	n/a	4.6	4.6	30.5	5/9A
C.47	70E_4s1d2Yc_1	70	E	0.613	8	4	2.48	69.3	0.005	0.34	0.05	0.45	n/a	n/a	6	6	27.75	5/12A
C.48	70E_4s1d2Vd_1	70	E	0.613	8	4	2.48	69.3	0.0143	0.19	0.05	0.6	n/a	n/a	**11.2**	10.9	45	5/15A
C.49	70E_4s1d2Vd_1	70	E	0.613	8	4	2.48	69.3	0.0143	0.19	0.05	n/a	0.6	n/a	**11.2**	10.9	45	5/15A
C.50	70E_4s1d2Vd_1	70	E	0.613	8	4	2.48	69.3	0.0143	0.19	0.05	n/a	n/a	0.6	**11.2**	10.9	45	5/15A
C.51	70E_4s1d2Vc_1	70	E	0.613	8	4	2.48	69.3	0.0143	0.33	0.05	0.6	n/a	n/a	7.8	7.8	41	5/14A
C.52	70E_4s1d2Vc_1	70	E	0.613	8	4	2.48	69.3	0.0143	0.33	0.05	n/a	0.6	n/a	7.8	7.8	41	5/14A
C.53	70E_4s1d2Vc_1	70	E	0.613	8	4	2.48	69.3	0.0143	0.33	0.05	n/a	n/a	0.6	7.8	7.8	41	5/14A
C.54	70E_4s1d2Xc_1	70	E	0.613	8	4	2.48	69.3	0.015	0.33	0.05	0.35	n/a	n/a	*6.8*	8.5	22	5/20A
C.55	70E_4s1d2Xc_1	70	E	0.613	8	4	2.48	69.3	0.015	0.34	0.05	0.7	n/a	n/a	8.5	8.5	41	5/20A
C.56	70E_4s1d2Xc_1	70	E	0.613	8	4	2.48	69.3	0.015	0.34	0.05	n/a	0.7	n/a	8.5	8.5	41	5/20A
C.57	70E_4s1d2Xc_1	70	E	0.613	8	4	2.48	69.3	0.015	0.34	0.05	n/a	n/a	0.7	8.5	8.5	41	5/20A
C.58	70E_4s2d2Zc_1	70	E	0.613	8	4	4.18	75.6	0.00155	0.34	0.05	0.5	n/a	n/a	8.4	8.4	28.5	5/27A
C.59	70E_4s2d2Yc_1	70	E	0.613	8	4	4.18	75.6	0.005	0.33	0.05	0.35	n/a	n/a	*12*	12.5	25.5	5/28A
C.60	70E_4s2d2Yc_1	70	E	0.613	8	4	4.18	75.6	0.005	0.33	0.05	n/a	0.35	n/a	*12*	12.5	25.5	5/28A
C.61	70E_4s2d2Yc_1	70	E	0.613	8	4	4.18	75.6	0.005	0.33	0.05	n/a	n/a	0.35	*12*	12.5	25.5	5/28A
C.62	70E_4s1d1Zc_1	70	E	0.613	8	4	2.46	166.4	0.00155	0.33	0.05	0.4	n/a	n/a	7.1	7.1	30.75	5/30A
C.63	70E_4s1d1Zc_1	70	E	0.613	8	4	2.46	166.4	0.00155	0.33	0.05	n/a	0.35	n/a	7.1	7.1	30.75	5/30A
C.64	70E_4s1d1Zc_1	70	E	0.613	8	4	2.46	166.4	0.00155	0.33	0.05	n/a	n/a	0.35	7.1	7.1	30.75	5/30A
C.65	70E_6s1d2Vc_1	70	E	0.92	4	4	2.48	69.3	0.0143	0.34	0.05	1.0	n/a	n/a	6.8	6.8	70	7/18A
C.66	70E_6s1d2Vc_2	70	E	0.92	4	4	2.48	69.3	0.0143	0.33	0.10	0.8	n/a	n/a	6.4	6.4	63	7/18B

(a) If the data in the velocity column are shown in italics, the profile was taken at a velocity below U_{CS}; if the data in the velocity column are shown in bold, the profile was taken at a velocity above U_{CS}. All other entries were taken at the U_{CS} condition.

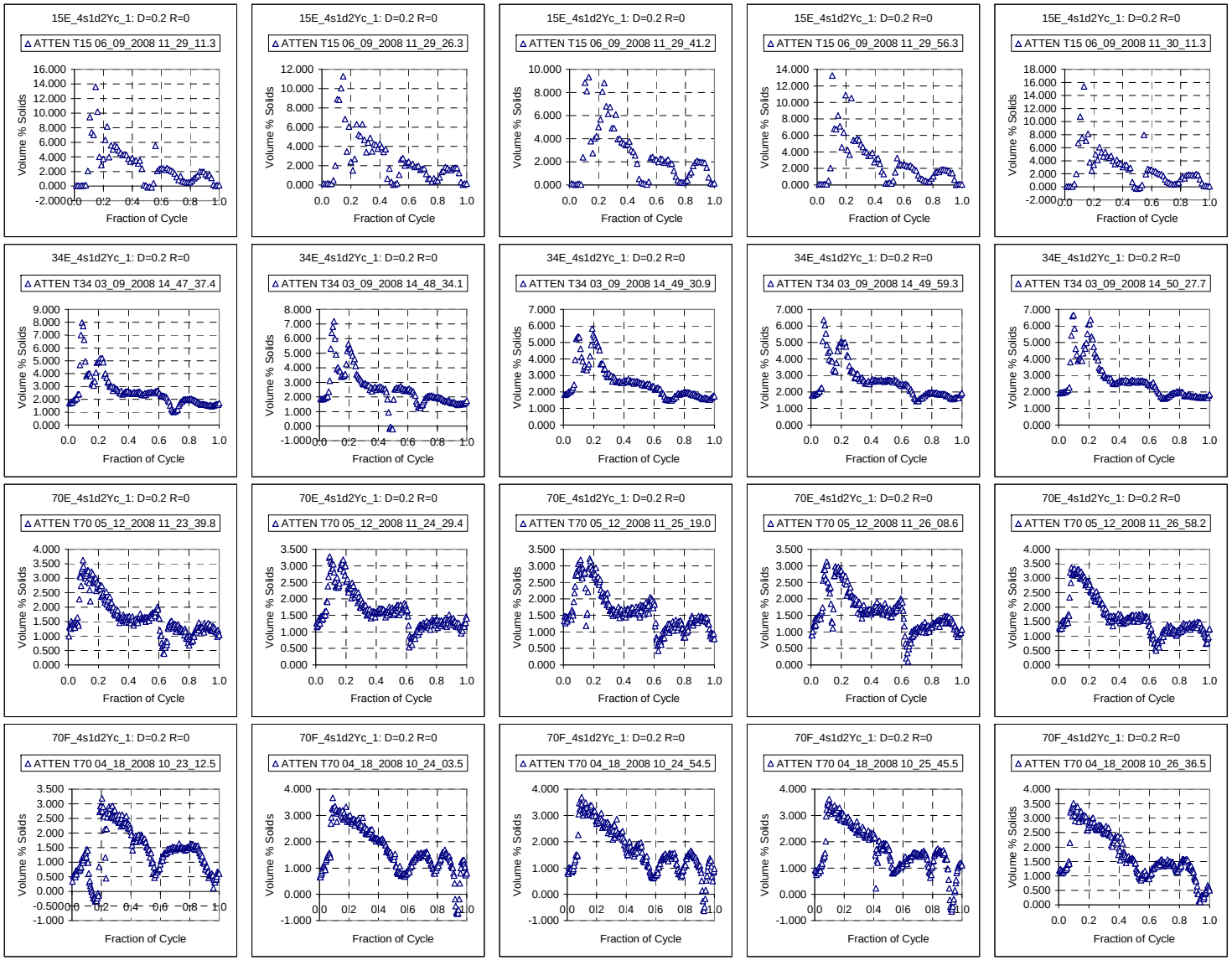

Figure 6.23. Examples of Solids Concentration by Volume as a Function of Cycle Fraction at an Elevation of H/D = 0.2 and Radially Located at the Tank Center. Test conditions are simulant s1d2 (ρ_s = 2.48 g/cm^3 and d_{50} = 69.2 μm) at solids fraction of (ϕ_S = 0.005), duty cycle (DC = 0.33), and pulse volume fraction (ϕ_p = 0.05) for small- and large-scale tanks with elliptical heads, mid-scale tank with spherical head and large-scale tank with flanged and dished head.

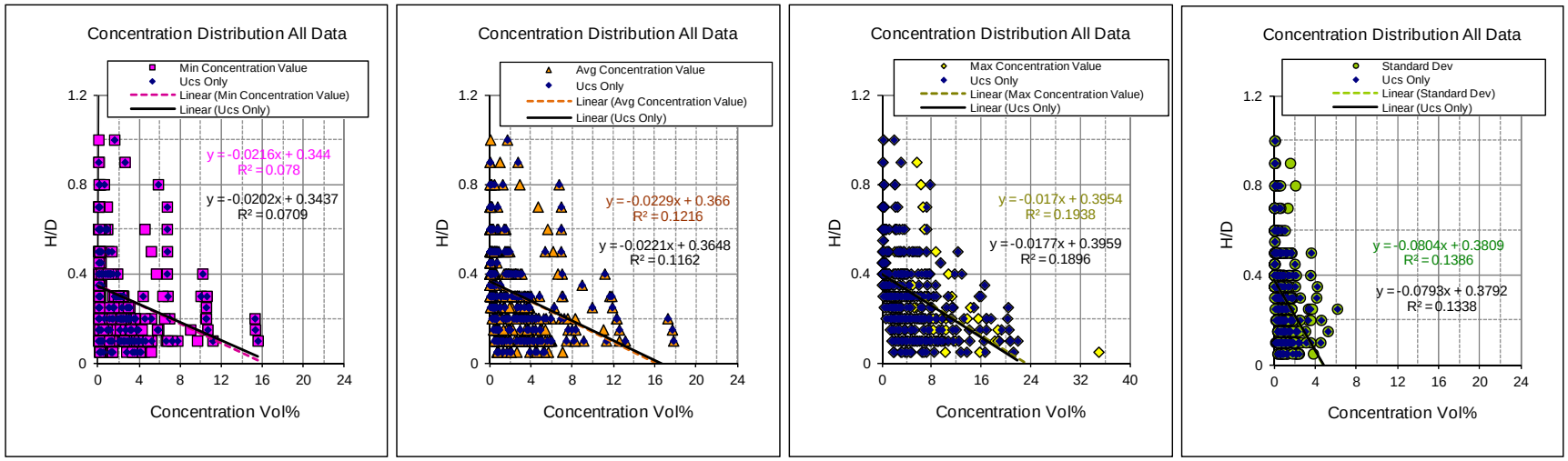

Dimensional Plots Showing All Data and Correlation in Color and UCS Data and Correlation in Blue

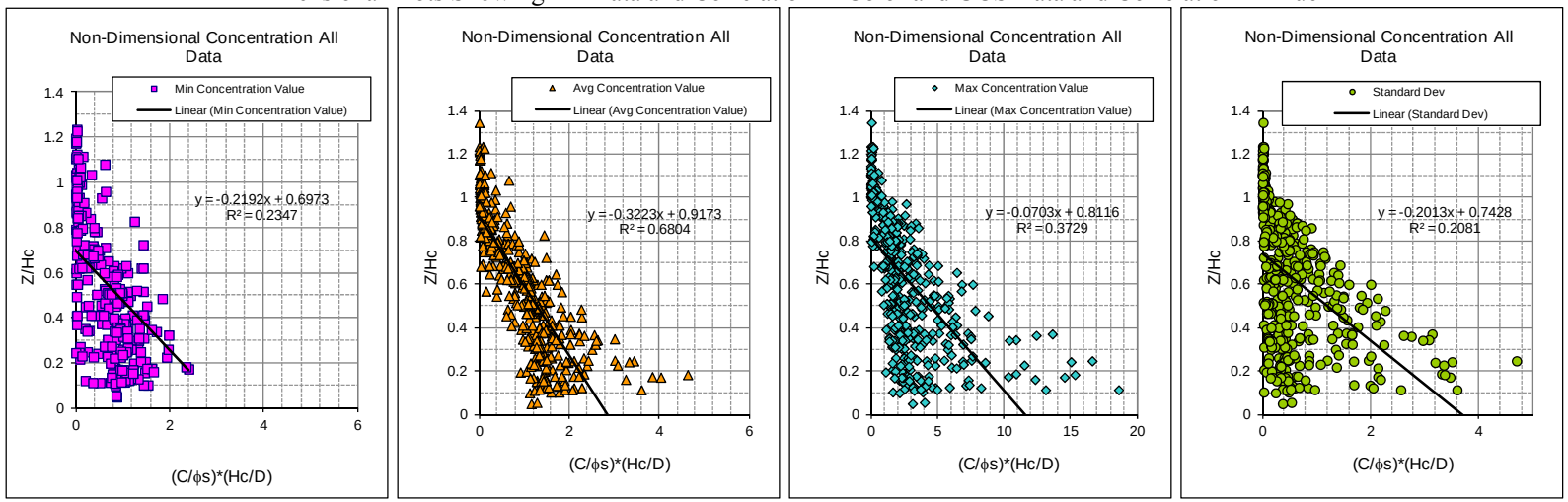

Nondimensional Plots Showing All Data and Correlations

Figure 6.24. Solids Concentration by Volume Distribution Plots Showing Minimum, Average, Maximum, and Standard Deviation of Concentration Measured for All Data Points

6.5.2 Variation with Critical Suspension Velocity U_{CS}

The data in Table 6.14 show that solids concentration by volume profiles were taken at three U_{CS} conditions: $<U_{CS}$, at U_{CS}, and $> U_{CS}$. The data obtained at these three U_{CS} cases are plotted together and presented in Figure 6.25. These figures show the minimum (left column of plots), average (center column of plots), and maximum (right column of plots) solids concentration at each elevation based on an average of five cycles. Four concentration profiles were obtained at velocities above the critical suspension velocity. These data were obtained at four solids fractions with two simulants and in three tanks. When viewing the concentration profiles it is useful to keep in mind that a fully mixed concentration profile would be represented by a constant concentration over the range of elevations within the cloud.

The data in the small-scale vessel (15E_4s1d2Wc_1) show that solids were suspended to a height equal to the tank diameter. These data provide a more vertical profile up to an elevation of 0.6Z/D, showing that this portion of the vessel is mixed more than that above this elevation. The next series of plots at U_{CS} shows that many profiles were obtained at this condition. One of the plots in the All Profiles at U_{CS} Avg (15E_4s1d2Wa) shows an almost vertical, fully mixed profile. This test was a continuous flow test, without jet pulsation. Five concentration profiles were obtained at concentrations below the critical suspension velocity. These data show significantly lower cloud heights than the other two conditions.

6.5.3 Variation with Radial Location

During six tests, solids concentration by volume profiles were obtained at three radial locations: 0R, the tank center (shown by diamond symbol on plots), 0.5R, halfway between the tank center and the tank wall (shown by triangle symbol on plots), and 0.9R, near the tank wall (shown by square symbol on plots). These data are plotted in Figure 6.26. Having data at three radial locations shows the interaction between the jets and solids throughout the tank and shows the uniformity or lack of radial uniformity in the concentration profiles at these locations. For the vessel to be fully mixed, the concentration profiles at these radial locations would be equal. Three simulants were tested: s1d2 ($\rho_s = 2.48$ g/cm^3, $d_{50} = 69.2$ μm), shown in (a-d); s1d1 ($\rho_s = 2.46$ g/cm^3, $d_{50} = 166$ μm), shown in (e); and s2d2 ($\rho_s = 4.18$ g/cm^3, $d_{50} = 76$ μm), shown in (f).

Figures 6.26(a) and (b) compare the difference between the flanged and dished (a) and elliptical (b) heads. Figures 6.26(b) and (c) compare the effect of duty cycle, 0.33 in (b) and 0.18 in (c). The profiles are very similar, but (b) was taken at U_{CS} and (c) was taken above U_{CS}. Increasing concentrations are compared in (b) and (d). As expected, U_{CS} is higher at higher concentration; however, the concentration profiles are very similar. Figures 6.26(a–d) with s1d2 ($\rho_s = 2.48$ g/cm^3, $d_{50} = 69$ μm) all show that for a specific elevation the concentration at the three radial locations is similar with the concentration slightly higher at R = 0 the tank center line. This trend changes when simulants s1d1 ($\rho_s = 2.46$ g/cm^3, $d_{50} = 166$ μm), shown in (e), and s2d2 ($\rho_s = 4.18$ g/cm^3, $d_{50} = 76$ μm), shown in (f), profiles are examined. Profiles (e) with larger particle diameter and (f) denser simulant show a marked increase in the concentration at R = 0, the vertical tank centerline, at elevations up to 0.2 Z/D; profile (f) was measured slightly below U_{CS}.

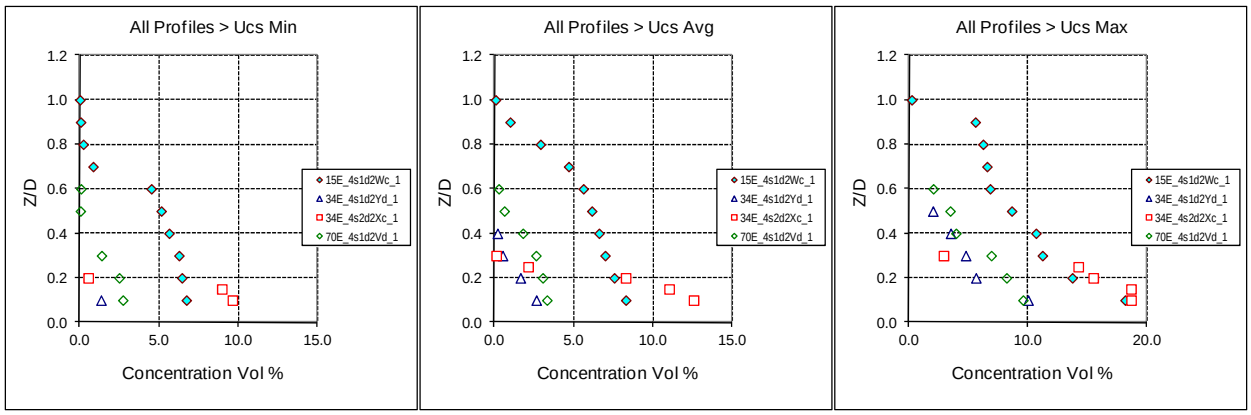

Velocities > U_{CS}

(a) (b) (c)

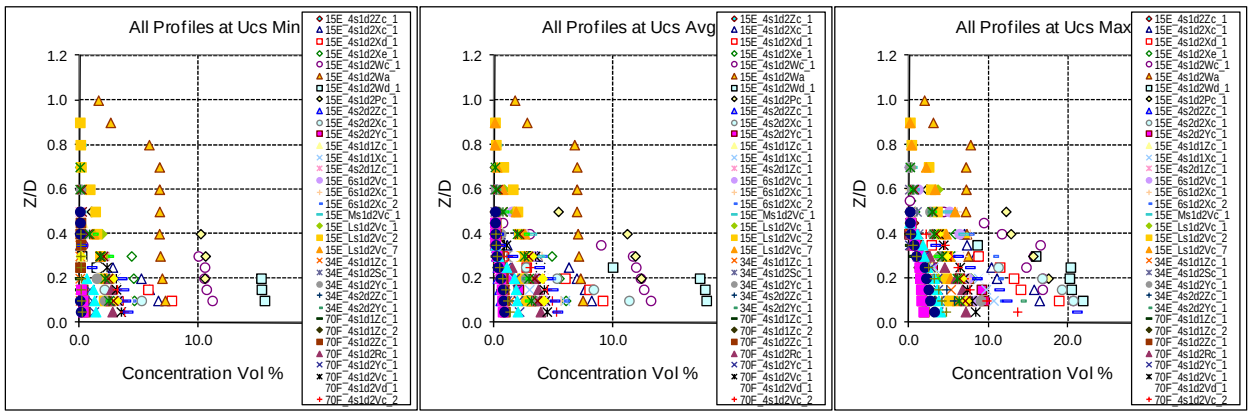

Velocity at U_{CS}

(d) (e) (f)

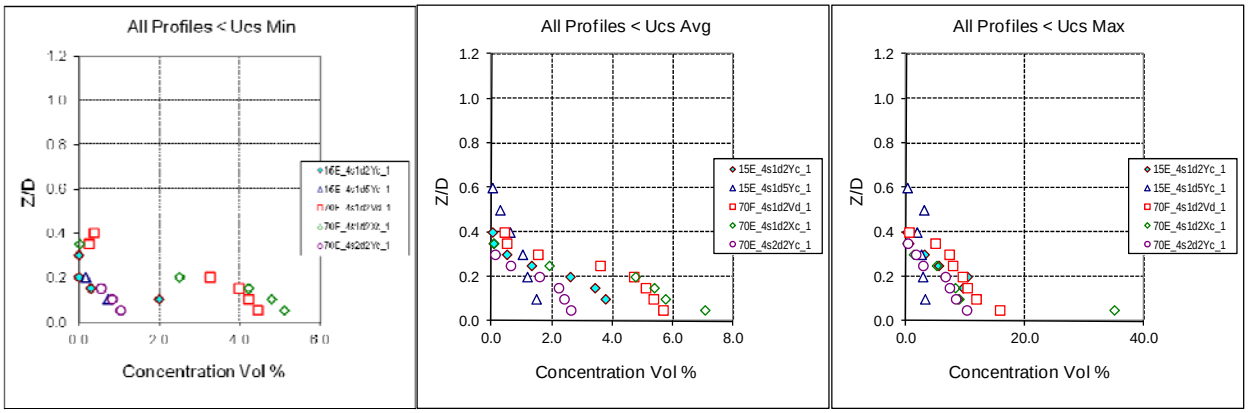

Velocity < U_{CS}

(g) (h) (i)

Figure 6.25. Comparison of Dimensional Profiles Below, At, or Above U_{CS}

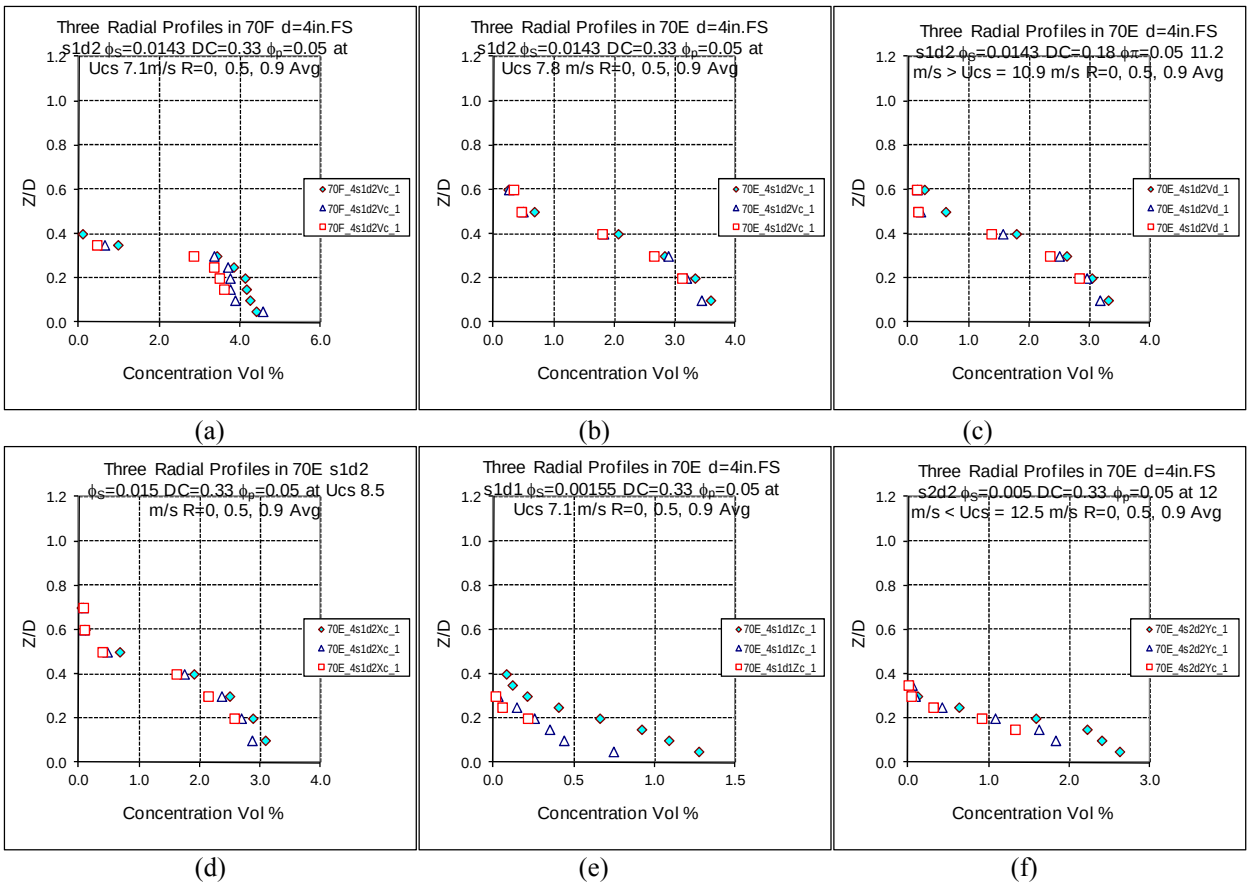

Figure 6.26. Comparison of Average Radial Concentration Profiles for Each Test at R=0 (diamond symbol), 0.5 (triangle symbol), and 0.9 (square symbol) for Large-Scale F&D and Elliptical Bottom Tanks at and Below U_{CS} for Pulse Volume Fraction 0.05

In Figure 6.27, the nondimensional average profiles are compared between tests at each radial position. At R = 0 all of the profiles appear relatively similar except for the s1d1 (ρ_s = 2.46 g/cm^3, d_{50} = 166 μm) simulant (yellow triangle symbol), where higher concentrations are observed up to height Z/H_C = 0.4. However, this is balanced by lower concentrations at R = 0.5 and R = 0.9.

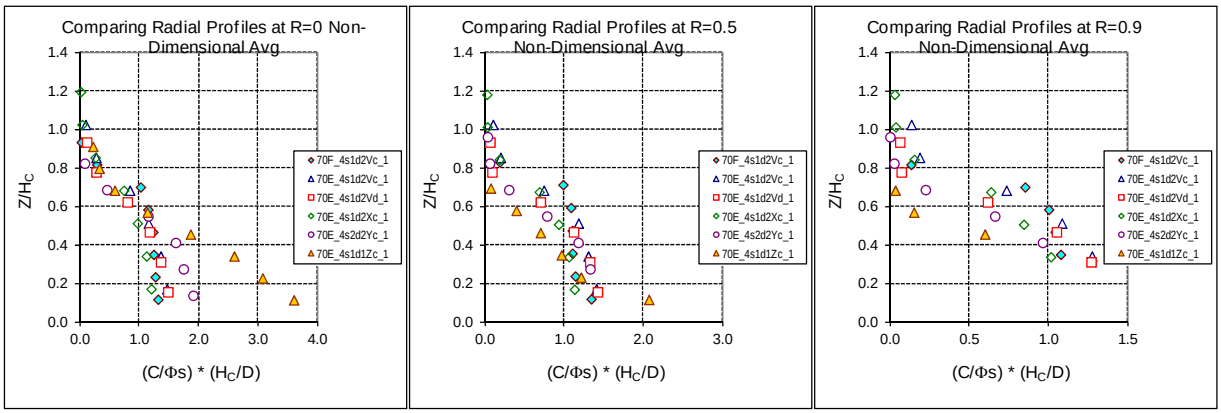

(a) (b) (d)

Figure 6.27. Comparison of Nondimensional Average Radial Concentration Profiles Across Tests at R=0, 0.5, 0.9 for the Large-Scale Flanged and Dished and Elliptical Bottomed Tanks At and Below U_{CS} (purple circle $<U_{CS}$) for Pulse Volume Fraction of 0.05

6.5.4 Variation with Tank

All solids concentration by volume profiles taken in the four tank configurations at U_{CS} are plotted in Figure 6.28. Dimensional plots for small-, mid-, large-elliptical, and large flanged-and-dished are shown in (a-d), and corresponding nondimensional plots (e-h) are shown beneath. For an individual tank, at elevations above 0.4 Z/H_C the data on the nondimensional plots tend to collapse onto one line. This can be observed in plots (f) and (g), where fewer tests were plotted.

Head shape is compared in Figure 6.29(a-d) in four tanks for simulant s1d1 ($\rho_s = 2.46$ g/cm^3, $d_{50} = 166$ μm) and in Figure 6.29(e-h) in three tanks for simulant s2d2 ($\rho_s = 4.18$ g/cm^3, $d_{50} = 76$ μm). For the average concentration profile both the dimensional and nondimensional figures are provided. For both simulants the maximum elevation with a measured solids concentration was ~0.4 Z/D for all tests. Only one flanged-and-dished test that matched the other conditions was available for the s1d1 ($\rho_s = 2.46$ g/cm^3, $d_{50} = 166$ μm) simulant. This profile shows a slightly lower concentration at each elevation than the other head shapes.

6.5.5 Variation with Nozzle Diameter and Number of Pulse Tubes

Concentration profiles were measured using four nozzle diameters that scaled to 4, 6, 8.5, and 11.8 in. in the full-scale HLP-22 vessel. These tests also included evaluation of two pulse-tube configurations: HLP-22 (12 pulse tube array) and 8TA, which is an abbreviation for an eight pulse tube array. All of the concentration profiles obtained using the HLP-22 configuration were conducted with all pulse tubes (8 outer and 4 inner) operating. The concentration profiles obtained using the 6, 8.5, and 11.8 in. HLP-22 full-scale nozzle diameters using the 8TA configuration were conducted with all pulse tubes (4 outer and 4 inner) operating. In addition one profile was obtained with the 11.8 in. HLP-22 full scale nozzle, with 4 outer and no inner pulse tubes operating. These data are shown in Figure 6.30.

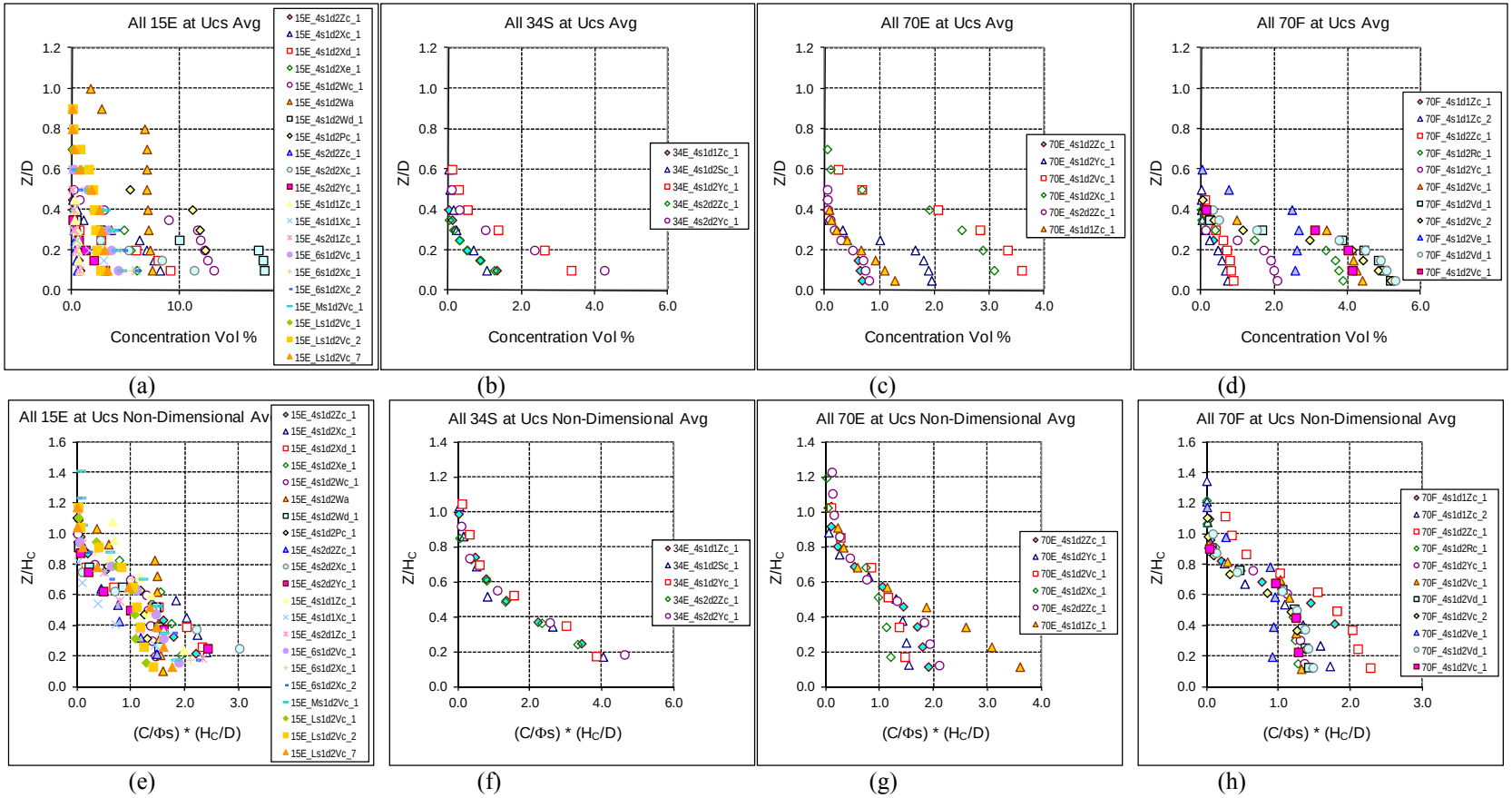

Figure 6.28. Concentration Profiles at U_{CS} in the 15E, 34S, 70E, and 70F Tanks Segregated by Tank: (a–d) Dimensional Plots and (e–h) Nondimensional Plots

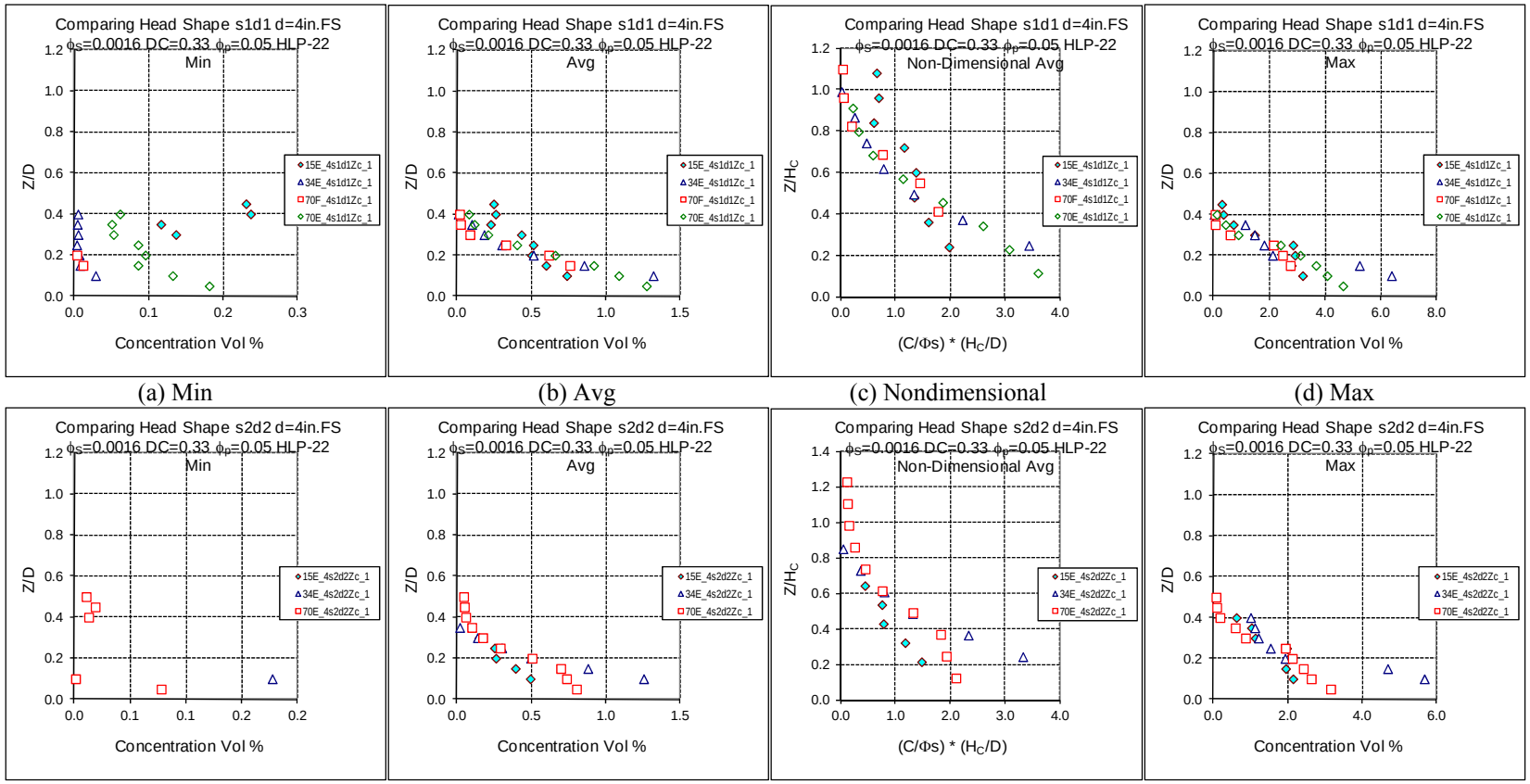

(a) Min (b) Avg (c) Nondimensional (d) Max

(e) Min (f) Avg (g) Nondimensional (h) Max

Figure 6.29. Comparison of Tank Head Shape for Small-Scale Elliptical (15E, aqua diamonds), Mid-Scale Spherical (shown as 34E, dark blue triangles), Large-Scale F&D (70E red squares), and Elliptical (70E green diamonds) Bottom Tanks at U_{CS}. Test conditions are simulants s1d1 (ρ_s = 2.46 g/cm^3, d_{50} = 166 μm) and s2d2 (ρ_s = 4.18 g/cm^3, d_{50} = 76 μm), solids fraction (ϕ_S = 0.016), duty cycle (DC = 0.33), and pulse volume fraction (ϕ_p = 0.05).

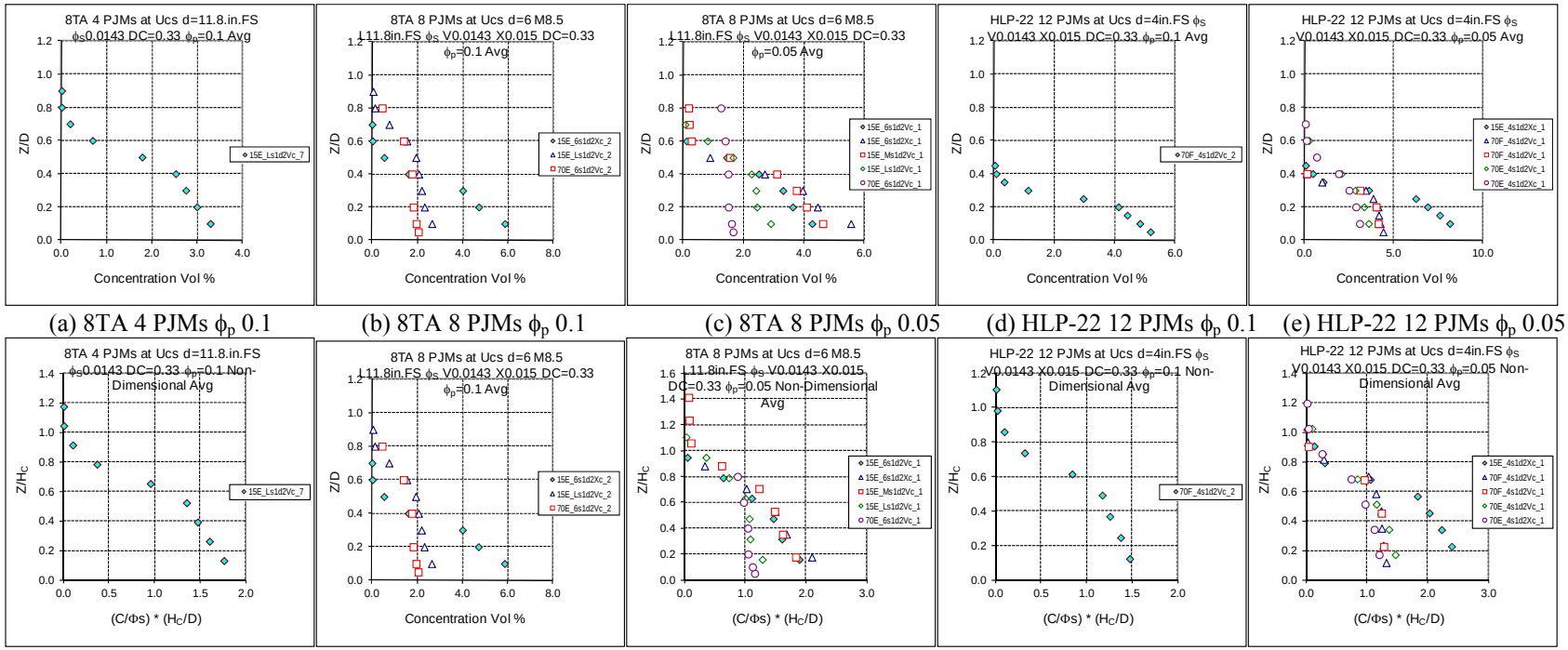

(a) 8TA 4 PJMs ϕ_p 0.1 (b) 8TA 8 PJMs ϕ_p 0.1 (c) 8TA 8 PJMs ϕ_p 0.05 (d) HLP-22 12 PJMs ϕ_p 0.1 (e) HLP-22 12 PJMs ϕ_p 0.05

(f) 8TA 4 PJMs ϕ_p 0.1 (g) 8TA 8 PJMs ϕ_p 0.1 (h) 8TA 8 PJMs ϕ_p 0.05 (i) HLP-22 12 PJMs ϕ_p 0.1 (j) HLP-22 12 PJMs ϕ_p 0.05

Figure 6.30. Comparison of Dimensional and Nondimensional Plots of Pulse Tube Array (HLP-22 or 8TA), Number of Operating Pulse Tubes (4, 8, or 12), and Nozzle Diameter (4, 6, 8.5 [M] and 11.8 [L]in. Full Scale) for Small-Scale Elliptical (15E), Large-Scale F&D (70F), and Elliptical (70E) Bottom Tanks at U_{CS}. Test conditions are simulant s1d2 (ρ_s = 2.48 g/cm^3, d_{50} = 69 μm), solids fraction (ϕ_S = 0.0143 [V], 0.015 [X]), duty cycle (DC = 0.33 [c]), pulse volume fraction (ϕ_p = 0.1 [_2], 0.05 [_1]).

6.5.6 Variation with Concentration

Solids concentration by volume profiles taken with five simulants over a range of bulk solids concentrations are plotted in Figure 6.31. All profiles were taken at U_{CS} except with stimulant s1d5 ($\rho_s = 2.5$ g/cm^3, $d_{50} = 44$ μm) where the velocity was 5% lower than U_{CS}. The two highest concentrations are shown in Figure 6.31(b) red squares (0.06 solids fraction) and green diamonds (0.045 solids fraction) and the average profile shows a relatively high concentration from 0.1 to 0.4 Z/D.

Concentration profiles taken with several simulants in different tanks are plotted in Figure 6.32. All profiles were taken at U_{CS} with 4 in. full-scale nozzles at a duty cycle of 0.33 and pulse volume fraction of 0.05. Solids fraction varies between plots.

6.5.7 Variation with Duty Cycle

Duty cycle is the fraction of time during the cycle that the fluid is discharging from the pulse tube. Tests were conducted over a range of duty cycles, including 0.18, 0.33, 0.66, and 1.0 (a steady jet). Solids concentration by volume profiles obtained for these conditions are shown in Figure 6.33(a-d). In (e) and (f), duty cycle is varied while other properties except tank diameter are held constant. The concentration profile for the steady jet (blue triangles) shown in (f) is constant to an elevation of 0.8 Z/D and reduced above that point. In (f), the duty cycle of 0.33 shows that the concentration in the tank is relatively constant to an elevation of 0.3 Z/D, and the duty cycle of 0.18 shows that the concentration is relatively constant to an elevation of 0.2 Z/D.

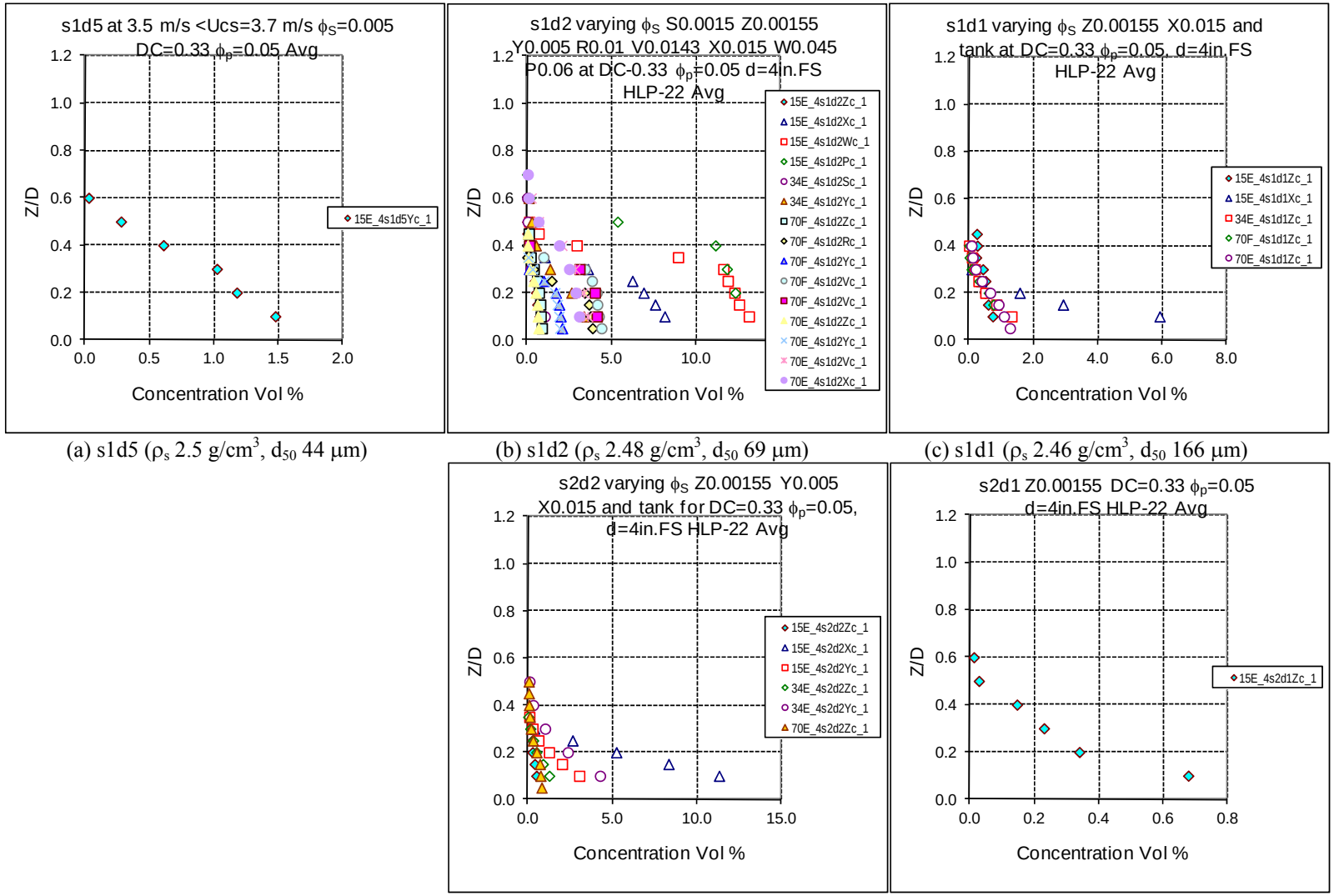

(a) s1d5 (ρ_s 2.5 g/cm^3, d_{50} 44 μm) (b) s1d2 (ρ_s 2.48 g/cm^3, d_{50} 69 μm) (c) s1d1 (ρ_s 2.46 g/cm^3, d_{50} 166 μm)

(d) s2d2 (ρ_s 4.18 g/cm^3, d_{50} 76 μm) (e) s2d1 (ρ_s 4.17 g/cm^3, d_{50} 164 μm)

Figure 6.31. Concentration Profiles for the Five Simulants in the HLP-22 Tank Configuration. Test conditions are solids volume fraction (ϕ_S = 0.0015 [S], 0.00155 [Z], 0.005 [Y], 0.01 [R], 0.0143 [V], 0.015 [X], 0.045 [W], 0.06 [P]), nozzle diameter d = 4 in. full-scale, duty cycle (DC = 0.33 [c]), pulse volume fraction (ϕ_p = 0.05 [_1]).

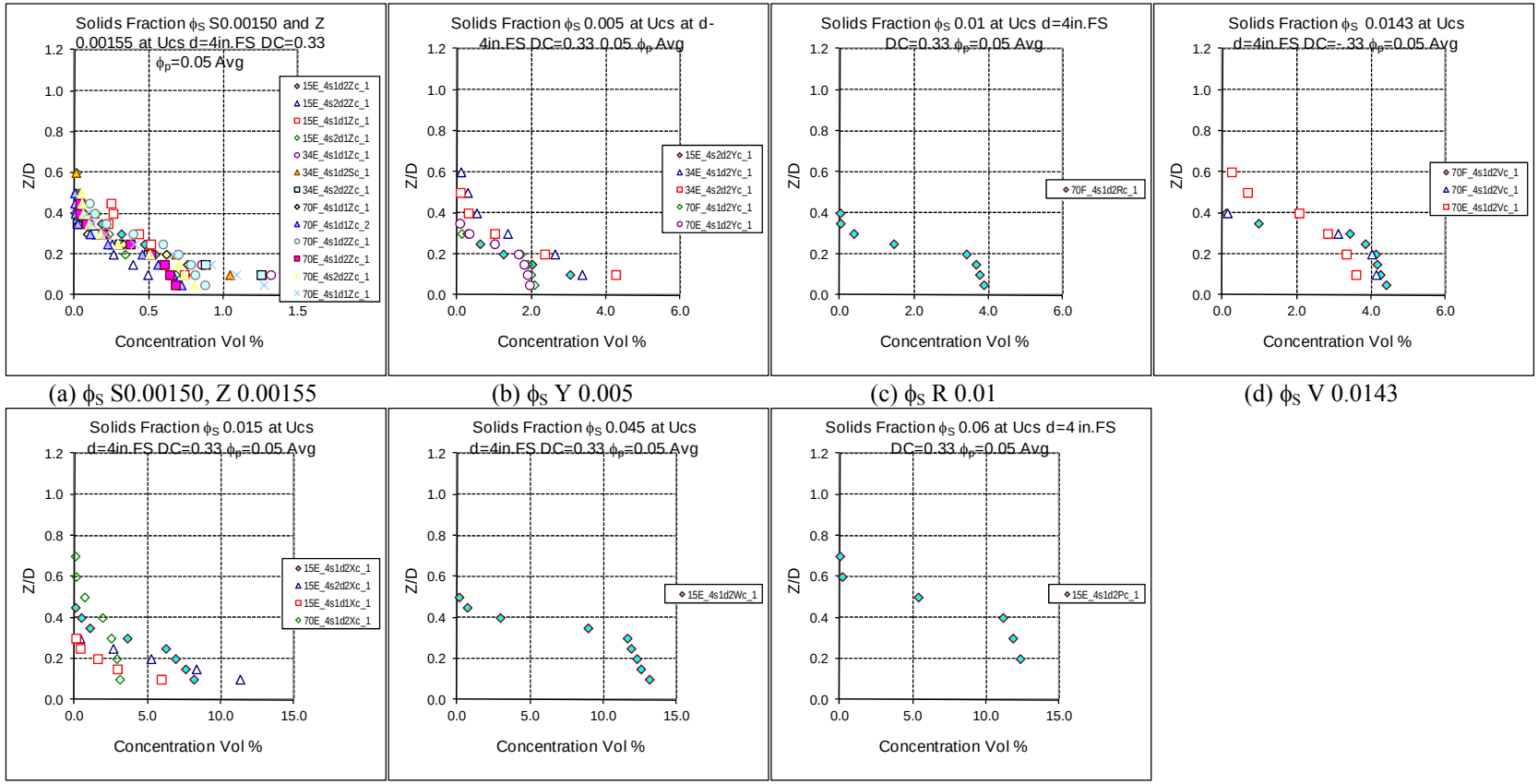

(a) ϕ_S S0.00150, Z 0.00155 (b) ϕ_S Y 0.005 (c) ϕ_S R 0.01 (d) ϕ_S V 0.0143

(e) ϕ_S X 0.015 (f) ϕ_S W 0.045 (g) ϕ_S P 0.06

Figure 6.32. Comparing Profiles for Simulants and Tanks at U_{CS} for HLP-22 Tank Configuration as Solids Concentration ϕ_S Increases from 0.00150 to 0.06. Test conditions are nozzle diameter d = 4 in. full-scale, solids volume fraction (ϕ_S = 0.00155 [Z], 0.005 [Y], 0.01 [R], 0.0143 [V], 0.015 [X], 0.045 [W], 0.06 [P])duty cycle (DC = 0.33 [c]), pulse volume fraction (ϕ_p = 0.05 [_1]).

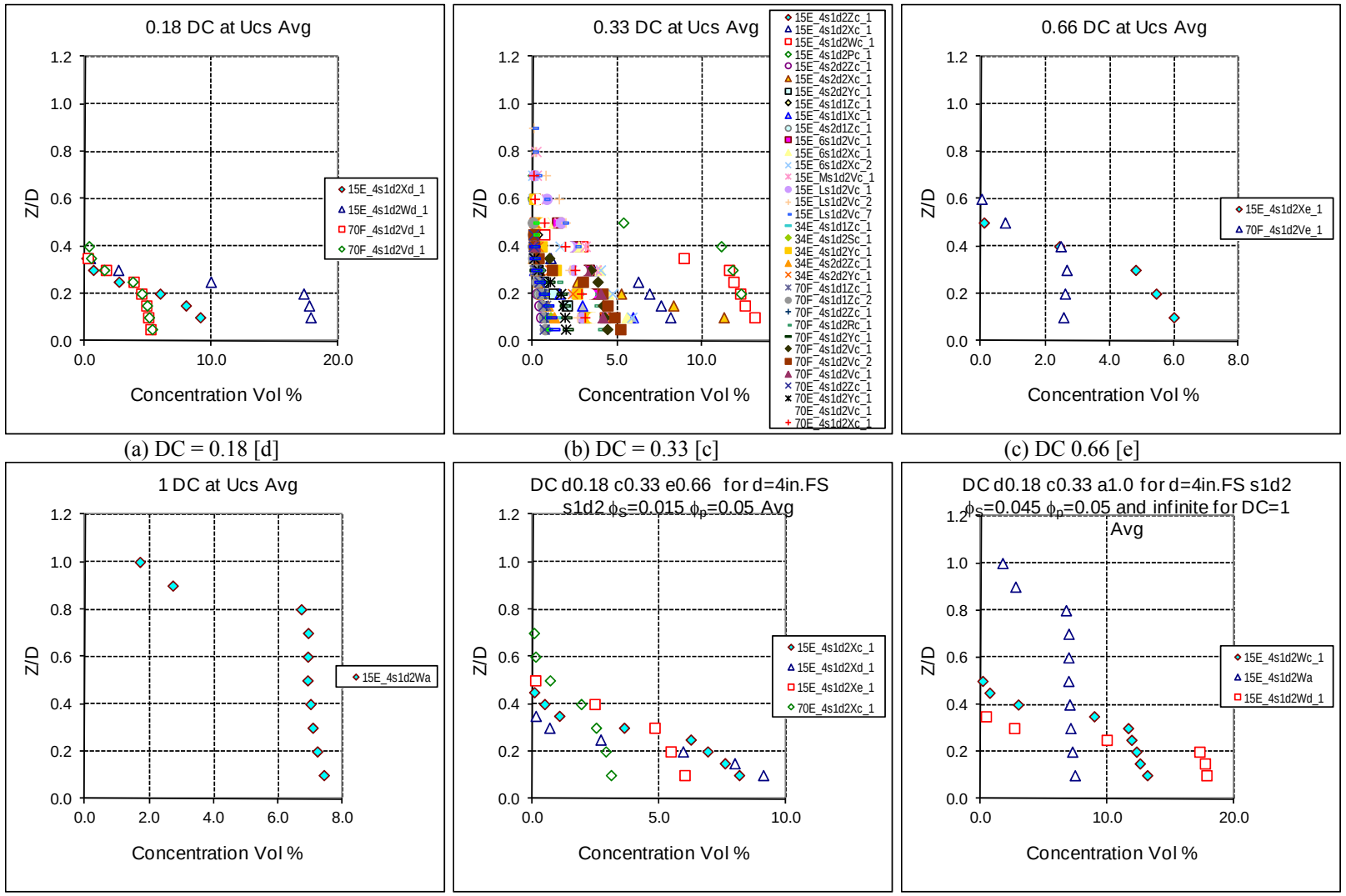

(a) DC = 0.18 [d] (b) DC = 0.33 [c] (c) DC 0.66 [e]

(d) DC =1.0 [a] (e) DC = 0.18 [d], 0.33 [c], 0.66 [e] (f) DC = 0.18 [d], 0.33 [c], 1.0 [a]

Figure 6.33. Concentration Profiles at Varying Duty Cycles

6.6 Transient Cloud Height Tests

Several transient tests cloud height were conducted. Prior to the start of these tests, the solids in the tank were allowed to fully settle. For transient tests the target velocity and operating conditions were set at the start of the test to those of a previously obtained U_{CS} condition and held constant for the duration of the test. Cloud height measurements were taken every pulse as the test proceeded. The test continued until no growth trend was observed in the peak cloud height for approximately 10 cycles or more. These transient tests were conducted in four tanks using combinations of two simulants and three concentrations. The transient test cloud height data are plotted dimensionally and nondimensionally in Figure 6.34 and show that steady state was attained at approximately 10 pulse cycles, apparent in the flattening of trends in the semi-log plot of H_C/H_{CS}. Comparison of the transient test cloud heights to that reported for equivalent U_{CS} conditions demonstrates that the testing methodology, incremental nozzle velocity increase, and reported cloud height measurements at each velocity (see Section 5.0), produced cloud height results that were independent of cycle count at the nozzle exit velocity condition. Data shown with FM1 at the end of the Case ID are shown for information only.

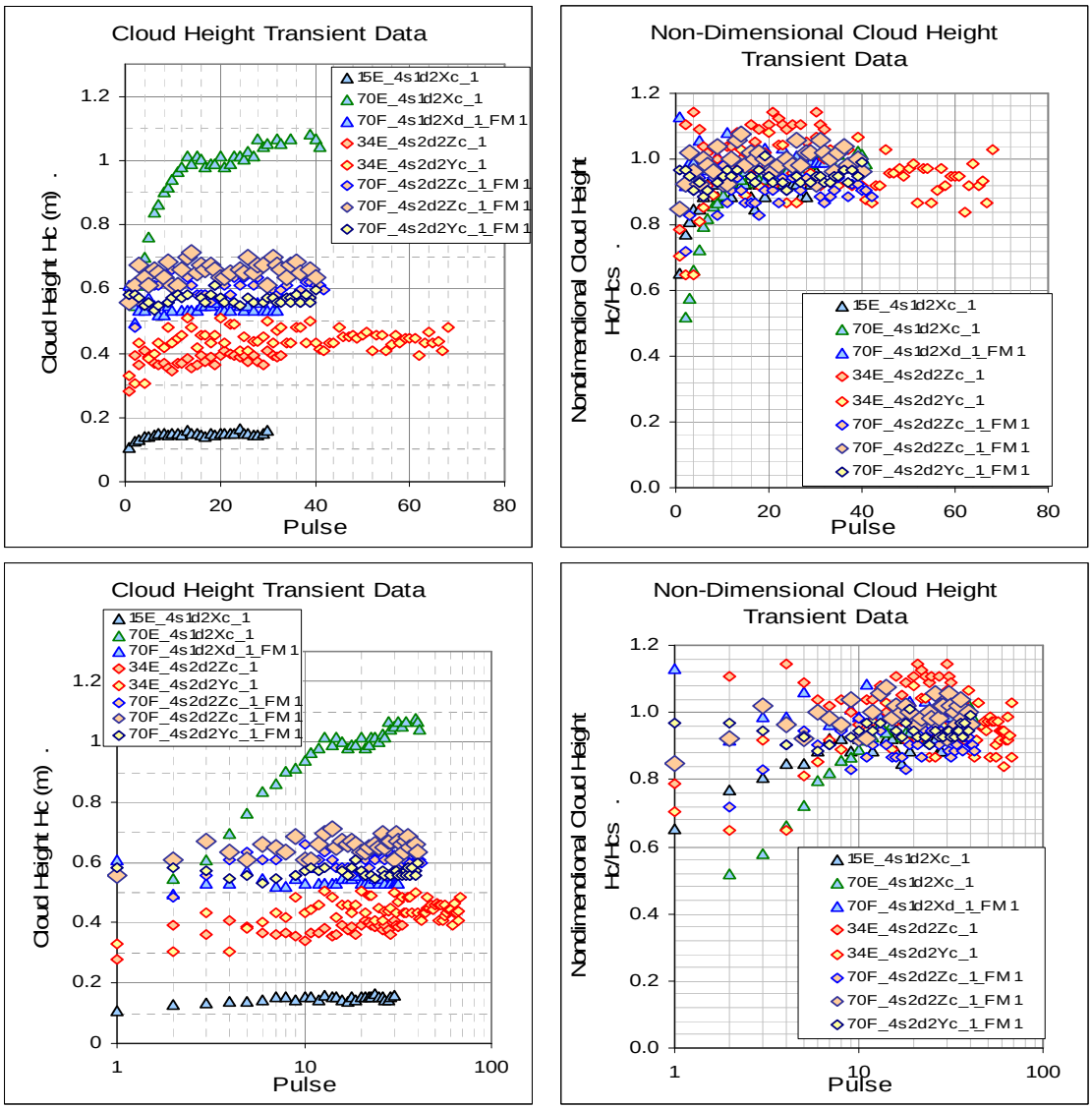

Figure 6.34. Cloud Height Transient Data Shown Dimensionally and Nondimensionally on Linear and Log Scales. Test conditions are simulant s1d2 (ρ_s = 2.48 g/cm^3, d_{50} = 69 μm) and s2d2 (ρ_s = 4.18 g/cm^3, d_{50} = 76 μm), solids fraction (ϕ_S = 0.015 [X], 0.00155 [Z], 0.005 [Y]) duty cycle (DC = 0.18 [d], 0.33 [c]) pulse volume fraction (ϕ_p = 0.05).

7.0 Analysis and Modeling of Mixing Data

This section presents an analysis of the mixing data, including critical suspension velocity (U_{CS}), average peak cloud height (H_C), and vertical solids distribution [C(Z)]. Predictive models were developed for U_{CS}, H_C, and average solids concentration at the vessel bottom (C_0). In Section 8.0, the models are benchmarked by applying them to previous testing results in prototypic pulse jet mixer (PJM) systems as well as computational fluid dynamics (CFD) simulations. In Section 9.0, the models are used to evaluate the mixing performance of the WTP vessels with Hanford waste conditions. The models presented in this section are believed to be sufficient for evaluating (rating) the WTP vessels. However, given the design of the data set and the complexity of the mixing phenomena, improved models may be obtainable with additional analysis.

In Section 7.1, the approaches taken to develop models for the experimental data are described. In Section 7.2, the observed physical behavior and the various forms of test parameter functionality are discussed. In Section 7.3, the data for off-bottom suspension and vertical solids distribution are analyzed. In addition, models are presented for U_{CS}, H_C, C(Z), and C_0 developed using a physical approach. The results of a statistical approach to develop U_{CS} and H_C models are summarized in Section 7.4, with more detailed discussion in Appendix F. The differences in model performance obtained using the two approaches are summarized in Section 7.5. Possible model improvements are discussed in Section 7.6.

7.1 Analysis and Modeling Approach

Experimental data sets can be analyzed in more than one way. We used graphical methods as well as modeling methods to analyze the M3 mixing experimental data. The goal of modeling is to develop mathematical equations for predicting mixing response variables as functions of relevant variables. Two approaches were used to analyze the mixing data and develop models:

- a physical approach based on hydrodynamic behavior
- a statistical approach involving multiple regression (MR) analysis of the data.

In very general terms, the hydrodynamic behavior observed in a scaled system is related to the behavior that would be observed in the full-scale system because the behavior in both systems is controlled by the same physical laws. So, for both systems we have the same general relationship:

[behavior controlling the performance] = f [the system and conditions imposed on it]

where “f” is some comprehensive function; “behavior” means the transient spatial distribution of velocity, solids, and settling rate; and “the system and conditions imposed on it” means location and history of momentum added by the PJMs, the physical boundary, and material properties.

The system conditions cannot be represented by a single parameter. Rather, several parameters are required. The geometry, choice of materials, and operational scheme of the experiment can be represented by parameters such as the ratio of total volume of solids to total volume of liquid and the velocity at an entrance nozzle averaged over the peak pulse period. The mixing performance can be represented by measurements of response variables such as U_{CS}, H_C, C(Z), and C_0. These performance variables are then measured for test combinations of parameters defining the system (e.g., scale, solids loading) and the conditions imposed on it (e.g., jet velocity).

It is known a priori that the functional relationship (f) depends on the physical laws controlling the behavior, namely, the conservation of momentum for hydrodynamic systems. Unfortunately, the resulting behavior is too complex to be predicted directly from this. But, from the dimensionless forms of physical laws, dimensionless groups that represent "behavior" and "conditions imposed" can be identified. These dimensionless groups in turn identify how the data can be reduced to their simplest and most instructive form before seeking the form of f. A classic example is the stream-wise pressure drop due to flow of fluid in a pipe, where the physical laws dictate that the pressure drop (in the form of a dimensionless group, the friction factor) depends on only the Reynolds number (a dimensionless group). Although f cannot be derived theoretically, plotting the data reduced to these dimensionless groups essentially "draws" f.

For the goal of developing mixing models applicable to WTP use, there is a substantial benefit to following this philosophy. If dimensionless groups related by the physical laws can be identified, the effect of length scale can be subsumed into one or more groups. Then, models developed from experimental data over the ranges of the controlling dimensionless groups expected in the full-scale system can be interpreted as interpolating the data over the ranges of dimensionless groups rather than extrapolating over scale. Predictive models are generally more accurate and thus subject to less uncertainty when interpolating than when extrapolating.

Obviously, and unfortunately, the system of interest is too complicated to surrender to direct analysis based on physical laws. The attempt can be made, however, to correlate the data or parts of it based on dimensionless groups suggested by the physical laws using trial functional forms that can be derived or rationalized from the physical laws.

The above physical approach cannot be relied upon solely. It must be complemented with a general approach wherein the data are analyzed without presuming physically based relationships. This general approach involves fitting functional relationships to the data using MR tools. This approach is discussed in Appendix D. In Appendix E the nature of the data obtained and their internal structure are discussed. The resulting MR models are presented and discussed in Appendix F. The MR models were developed using a power-law relationship between the response variable and predictor variables. The basis for using power-law relationships is discussed in Appendix F.

The physically based functions developed in Sections 7.2 and 7.3 result in power-law model forms, with some variations. This form often is found when making physical laws dimensionless and is consistent (as described in Section 2.0) with scaling approaches traditionally used for other types of mixing systems. Model forms obtained using the general approach without considering dimensional analysis or the controlling physical laws can be put into dimensionless forms. This serves both to confirm dimensional consistency and to facilitate comparisons with the inherently dimensionless model forms obtained based on physical reasoning.

The physical and statistical MR approaches are described in Sections 7.1.1 and 7.1.2, respectively. The results of the physical approach are presented in Sections 7.2 and 7.3.1 to 7.3.4. The results of the statistical approach are summarized in Section 7.4, with more detailed discussion in Appendix F. The differences in model performance obtained using the two approaches (stemming in part from their underlying assumptions, limitations, and developmental histories) are summarized in Section 7.5.

7.1.1 Physical Approach

Using the physical approach we consider the data from the perspective of the physical processes underlying the observed behavior. This approach is based on the understanding that hydrodynamic behavior is governed by underlying physical laws—conservation of mass, momentum, and energy--applied to the liquid and solid phases and subject to the appropriate geometric and temporal boundary conditions of the mixing apparatus. Using this approach, the fundamental variables governing mixing behavior are nondimensional (for example, ratios of generalized forces, velocities, or diffusivities), based on presumed underlying physical laws. Actual mixing behavior is complex, with solids concentration varying spatially and temporally. An enormous amount of high-quality data would be required to fully describe this behavior. However, the observable behavior (i.e., averaged over space and time) are governed by the same underlying physical laws. Examples of observable behavior are U_{CS} and H_C. The goal of the physical approach is thus to identify the relationships based on physical laws that describe the behavior of U_{CS} and H_C. The physical approach to analyzing and modeling the data involves the following steps:

- *Identify the underlying physical laws that likely govern mixing performance and the fundamental dimensionless groups associated with them.* The goal is to identify the most dominant dimensionless groups. The choice of dimensionless groups is not unique; experience, physical insight, or trial and error can all be used in choosing them.
- *Find relationships among dimensionless groups.* Plotting one group as a function of another while holding others constant reveals relationships among the groups. The power of this approach is that it reveals the form of the fundamental relationship regardless of its complexity.
- *Find physically reasonable functions that describe the relationships.* Many alternative functional forms can be fit to data. The goal is to find the simplest, physically reasonable functions that represent the observed behavior. The limiting forms of the functions when variables are extrapolated to small or large values should give physically sensible results. When a specific relationship between measured parameters and characteristics known to influence the behavior of the system is understood, substituting the calculated characteristic for the measurements used to calculate it removes the complexity of the known relationship from the overall relationship (e.g., f) being determined. This simplifies correlating performance variables in terms of remaining properties. The principal example of this is limiting behavior in the particle settling velocity relative to the fluid in which it is embedded. This is illustrated in Section 7.2.3, where slurry properties are discussed. In that section, knowledge of the relationship between the particle settling velocity and slurry properties is used to introduce settling velocity as a composite representative property.

The relationships developed from this type of approach are then incorporated into a model that can be applied to WTP conditions for evaluating mixing performance. Statistical methods to evaluate uncertainty and goodness of fit to the data can in principle be applied (although more complicated methods than those associated with the statistical MR approach discussed in Appendix D may be required). The value of the physical approach is that the resulting models have a physical basis in addition to a numerical basis, thereby increasing confidence in their applicability.

7.1.2 Statistical Multiple Regression Approach

As noted in Section 7.1, physical models must be complemented with more general models developed without assuming specific physical relationships. This provides an independent check on the assumptions on which the physical models are based. The greater the agreement between the resulting models, the greater the confidence in both.

The statistical MR approach applies statistical methods for MR to the experimental data to develop, evaluate, and validate empirical or semi-empirical models and to take advantage of systematic methods for quantifying their uncertainties. An MR model expresses the relationship in the experimental data between a response variable (y) and multiple predictor variables (x_1, x_2, …, x_n):

$$g(y_i) = f(x_{1i}, x_{2i}, \ldots, x_{ni}) + \varepsilon_i \tag{7.1}$$

In this general expression, $g(y_i)$ is an appropriate mathematical transformation of the response variable y for the ith data point; $f(x_{1i}, x_{2i}, \ldots, x_{ni})$ denotes a function of the predictor variable values $x_{1i}, x_{2i}, \ldots, x_{ni}$ for the ith data point; and ε_i is a random error representing experimental and measurement uncertainty in the ith data point. To satisfy the requirements for ordinary least squares (OLS) regression, the random errors ε_i must be statistically independent and come from the same probability distribution (and thus have the same standard deviation). The functional relationship $f(x_{1i}, x_{2i}, \ldots, x_{ni})$ may be completely empirical or also include subject matter knowledge and experience (semi-empirical). The mixing response variables (y) modeled using the MR approach were U_{CS} and H_C. The approach discussed in Section 7.3.3 to obtain a model for C_0 from the model for H_C may also be applied to statistically developed MR models. The predictor variables x_i in Eq. (7.1) are generally test variables or functions of test variables (e.g., dimensionless groups).

The statistical MR approach can also be applied to dimensionless groups formed systematically as products or ratios of subsets of dimensional variables. This ensures dimensional consistency of the resulting model, as discussed later in Section 7.4. In what is subsequently referred to as the *generalized approach*, the dimensionless groups are formed as functions of the dimensional variables. This can always be done based on the dimensions alone, without presuming specific physical relationships as a basis for the grouping. However, as for any dimensional analysis of hydrodynamic systems, the resulting groups can be given physical interpretations after the model is constructed. Thus, this approach also facilitates comparing the results of the physical and generalized approaches.

The statistical MR methods and formulas that were applied are discussed in Appendix D. Appendix E contains assessments of the experimental data that are useful in guiding the development of MR models and assessing their reasonableness. Section 7.4 summarizes the U_{CS} and H_C models developed using the statistical MR approach, where the model forms used are generalizations of those developed subsequently using the physical approach discussed in Section 7.1.1. The statistical MR models summarized in Section 7.4 are discussed in more detail in Appendix F.

7.2 Mixing Behavior

This section presents an overview of the observed physical behavior for critical suspension velocity (U_{CS}) and average peak cloud height (H_C). The functional dependence of U_{CS} and H_C on the test parameters is discussed, and the basis for various functional forms for modeling important trends and

behaviors is developed. The data presented in this section represent a small sample of the complete data set selected to illustrate the important relationships.

7.2.1 Parametric Sensitivity and Functional Form

In general, we expect the mixing metrics (U_{CS}, H_C) to be functions of the various geometric, operational, and physical parameters. Expressed mathematically, $y = f(x_1, x_2, ..., x_n)$, where y is any variable, dimensional or nondimensional, and x_i (i = 1 to n) is all the other parameters on which y may depend. The sensitivity coefficient, α_j, is a useful way to quantify the dependence of one variable on another. It is defined as

$$\alpha_j = \frac{x_i}{f(x_1, x_2, ..., x_n)} \frac{\partial f(x_1, x_2, ..., x_n)}{\partial x_j} = \frac{\partial \ln(y)}{\partial \ln(x_j)} \tag{7.2}$$

The derivative in Eq. (7.2) is the partial derivative, meaning all other variables ($x_{i \neq j}$) are held constant when the derivative is carried out.

If ln(y) is plotted versus ln(x_j), α_j is the local slope, as illustrated in Figure 7.1. If α_j is constant, the functional form is a power law:

$$y = k(x_{i \neq j}) x_j^{\alpha_j} \tag{7.3}$$

Here the coefficient, k, is a constant with respect to x_j, but it can depend on the other variables. This is illustrated by the two parallel lines in Figure 7.1.

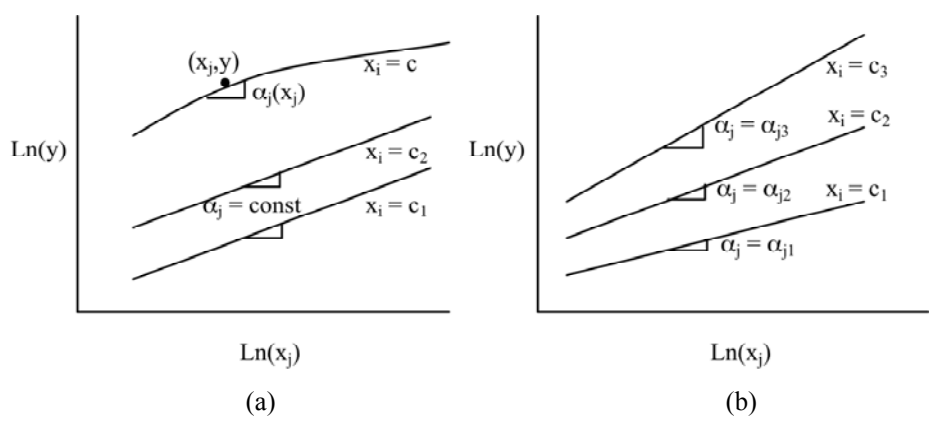

Figure 7.1. Illustration of the Physical Meaning of the Sensitivity Coefficient; (a) Linear and Nonlinear Behavior, (b) Interaction Between Variables

When α_j is not a constant, the data plotted on a ln(y) versus ln(x_j) may be curved or have different slopes depending on other variables. When the relationship is curved it is referred to as nonlinear behavior; it is understood that this means nonlinear with respect to a logarithmic scale. When $\alpha_j = f(x_i)$, there is an apparent coupling or interaction between two or more variables. This can result either from some actual physical interaction beyond that represented by the power-law form or potentially from a different functional relationship. The power law implies that the effects of all parameters are

multiplicative. But, if two parameters affect the performance in some additive fashion, where the effect of one does not depend on the other, the true functional form would involve a sum, rather than a product, of terms. In this case, forcing the data into the power-law form would result in sensitivity coefficients that are not constant. The case of interactions (apparent or actual) is illustrated in Figure 7.1(b).

7.2.2 Jet Velocity

The majority of the testing performed involved varying the jet velocity, starting below U_{CS} and increasing it until equipment limitations (such as either solids entrainment into the pump returns or flow rate limits) were approached. Figure 7.2 shows several examples of H_C plotted versus the corresponding velocity, U. Also shown in the plots by the symbols with black centers are the critical suspension conditions, U_{CS} and H_{CS}. For most test conditions H_C was an increasing function of velocity. However, under certain circumstances H_C initially decreased, went through a minimum, and then increased at higher velocities. This behavior was visible in the small-scale tank. This phenomenon may have occurred in the larger tanks as well, but, if so, it was not detectable because the clouds were below the dish bottom knuckle and thus not visible. This appears to be because only a small fraction of the solids were suspended at lower velocities, which allowed the solids plume to rise higher. As the velocity was increased, more of the settled solids were suspended, resulting in a higher solid loading in the plume and thus a lower cloud height. When most or all of the solids were suspended, increasing the velocity increased cloud height. The Case ID shown in the figure legend is described in Table 6.4.

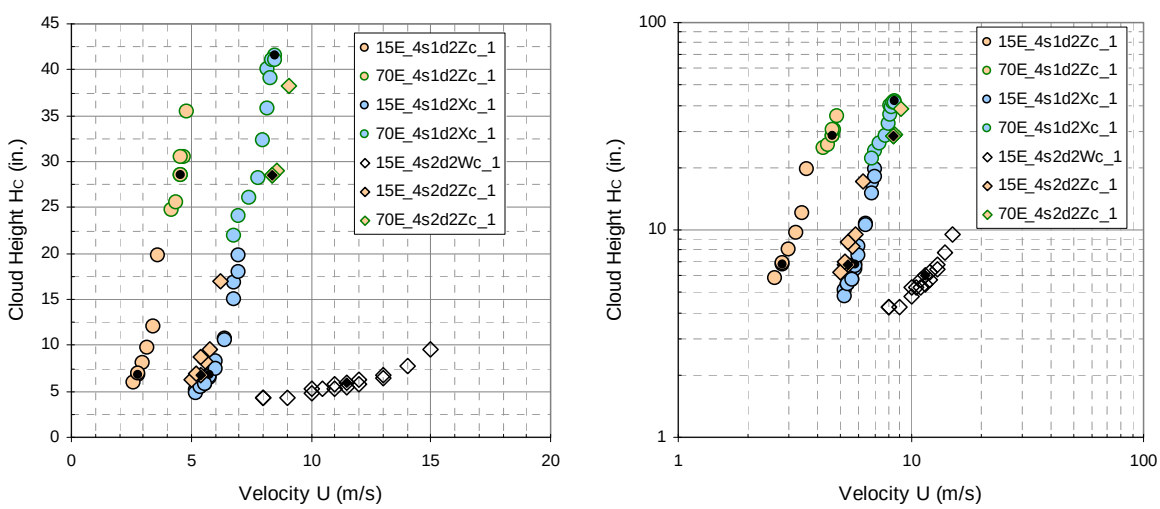

Figure 7.2. Examples of H_C Data as a Function of Jet Velocity; (a) Linear Scale, (b) Logarithmic Scale with U_{CS} Conditions Denoted by Black Center

The velocity exponent tends to increase with H_C, which can be seen from the $\ln(H_C)$ versus $\ln(U)$ plot in Figure 7.2. The exponent generally is about 2 for velocities just above U_{CS} and approaches 3 or 4 as U is increased. Cloud height is generally expected to be nonlinear in jet velocity, and the power-law form may be insufficient to accurately describe the function. However, it may provide an adequate approximation for $U \geq U_{CS}$.

An interesting feature of the H_C behavior is shown in Figure 7.3. Here the Froude number based on cloud height (F_C) is plotted versus jet velocity:

$$F_C = \frac{U^2}{(s-1)gH_C} \tag{7.4}$$

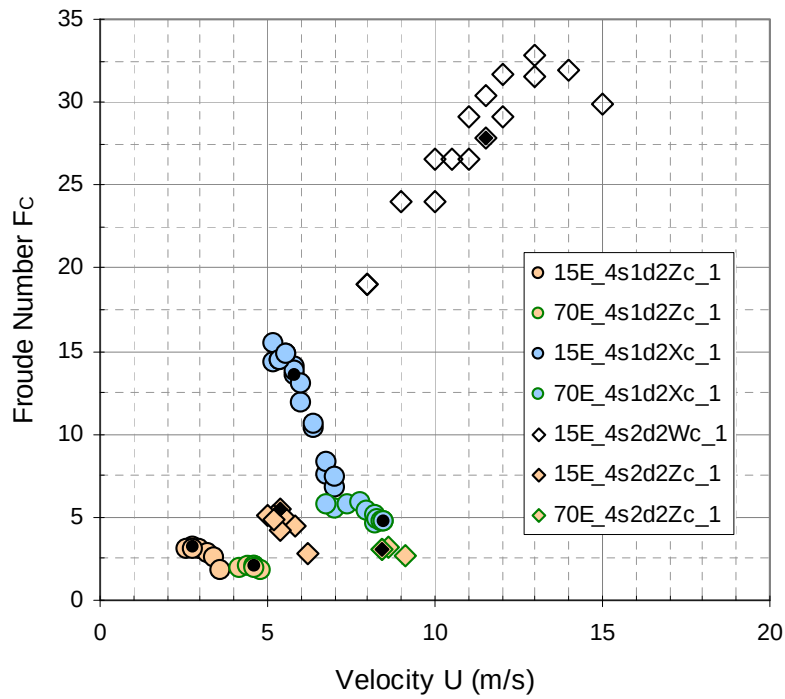

Figure 7.3. Illustration of the Completely-Suspended Condition as an Energy Maxima with U_{CS} Conditions Denoted by Black Center

A maximum in F_C occurs near the U_{CS} condition, giving some insight into the processes of off-bottom suspension and vertical distribution. F_C can be interpreted as the ratio of jet kinetic energy to solids potential energy. Below U_{CS} much of the jet energy apparently goes into the erosion process of mobilizing solids off the tank bottom. Once all of the solids are suspended, F_C decreases with increasing velocity, implying the additional energy goes into lifting the solids cloud.

Given the apparent transition in physical behavior that occurs at the critical suspension (CS) condition, one might suspect that cloud height behavior relative to CS condition (H_C/H_{CS}) is independent of other parameters. That is, it seems reasonable that the CS condition may be independent of other parameters and may contain most or all of the important functionality. Figure 7.4 shows H_C/H_{CS} plotted versus U/U_{CS} for the data set where $U/U_{CS} \geq 1$. There is some correlation between the two variables, though there is clearly significant scatter. However, the result shows that, on average, $H_C/H_{CS} \sim (U/U_{CS})^2$, meaning that over the entire range of test conditions F_C is on average approximately equal to F_{CS}, the Froude number at critical suspension. The deviation from this average condition is evidently dependent on the other test parameters.

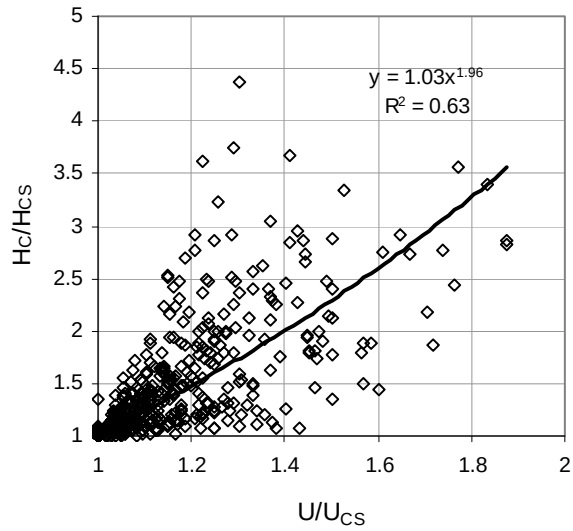

Figure 7.4. Behavior of H_C Relative to Critical Suspension Condition for $U \geq U_{CS}$ (all test conditions shown)

7.2.3 Slurry Properties

It is common practice to attempt correlations for off-bottom suspension and vertical solids distribution using density ratio (s), solids diameter (d_S), and kinematic viscosity (ν). An alternative approach is to introduce the unhindered terminal settling velocity (U_T). For monodisperse spherical particles, a useful relation for calculating U_T is given by Camenen (2007) in terms of the Galileo number (Ga):

$$U_T = \frac{\nu}{d_S}\left(\sqrt{15+\sqrt{Ga/0.3}} - \sqrt{15}\right)^2 \tag{7.5a}$$

which may be written as

$$Re_p^{1/2} = \sqrt{\frac{d_S U_T}{\nu}} = \sqrt{15+\sqrt{Ga/0.3}} - \sqrt{15} \tag{7.5b}$$

where

$$Ga = \frac{(s-1)g d_S^3}{\nu^2} \tag{7.6}$$

The square of the left side of Eq. (7.5b) is the (dimensionless) Reynolds number based on the particle size and settling velocity (Re_p), which a priori from hydrodynamic principles is a function of only the (dimensionless) Galileo number, as specified in this equation. This is an example of using knowledge of the underlying physical laws to obtain a behavior = f(conditions) relationship, as addressed in Section 7.1. Using values of U_T calculated with Eq. (7.5a) as a modeling parameter (instead of the value of d_S it represents through the Galileo number) avoids adding the complexity of this relationship to the complexity of either a physical model or a generalized model. This is apparent in Figure 7.5 and explained below the figure, which is shown for information only.

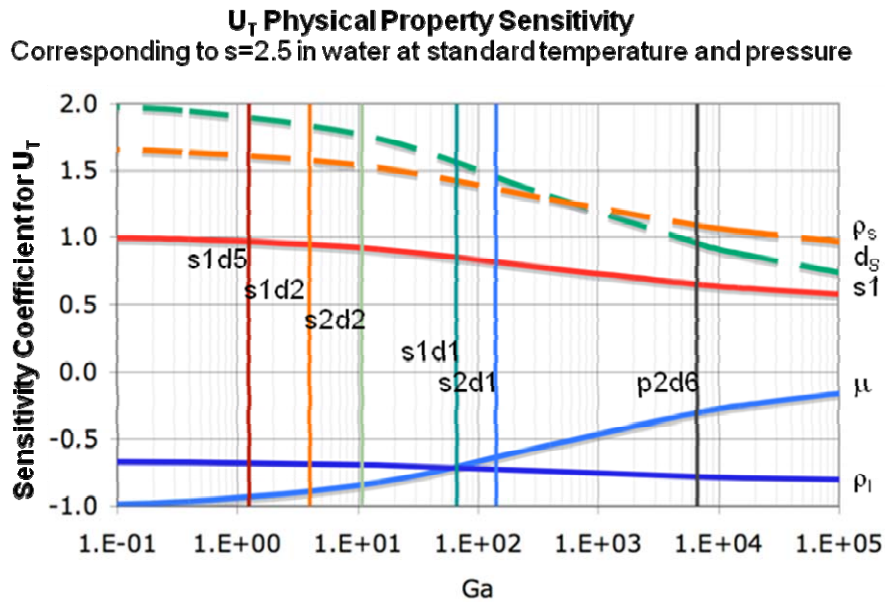

Figure 7.5. Sensitivity Coefficients (effective power-law exponents) for Terminal Settling Velocity Given by Eq. (7.5a) with Simulant Designations Shown on Vertical (constant Ga) Lines (FIO)

There are several reasons to expect that this approach may be superior to simple power-law expressions. First, even though U_T may not be representative of the overall process occurring in the tank, functionally it is a characteristic scale for many complex processes occurring in the slurry. Local settling rates within the tank vary spatially and temporally. Solid particle interactions, especially at higher local concentrations, affect the settling rate. Turbulent transport processes also compete with gravitational settling. Solids off-bottom suspension is a complex balance between erosion and deposition behavior. In these complex processes, the unhindered settling velocity is pertinent at the scale of individual particles, no matter how complex the flow field around them. For example, hindered settling rates tend to be proportional to U_T, and local unsteady force and energy interactions between the liquid and solid phases depend on various scales involving U_T.

Second, when expressed as a function of s, d_S, and ν, U_T is a more complex function than can be expressed by typical power-law terms. In general, one can express

$$U_T \propto (s-1)^{a_1} d_S^{a_2} \nu^{a_3} \tag{7.7}$$

only for a limited range of conditions. For example, Eq. (7.5a) has the form

$$U_T = \frac{\nu}{d_S} f(Ga) \tag{7.8}$$

For small and large Ga, the limiting results are, respectively,

$$Ga << 1 \quad Re_P \approx Ga \quad U_T \approx \nu d_S^{-1} Ga = (s-1) g \nu^{-1} d_S^2 \tag{7.9}$$

and

$$Ga >> 1 \quad Re_P \approx Ga^{0.5} \quad U_T \approx \nu d_S^{-1} Ga^{0.5} = (s-1)^{0.5} g^{0.5} d_S^{0.5} \tag{7.10}$$

For all other values of Ga, the exponents on s, d_S, and ν are functions of Ga, as shown in Figure 7.5. The values of Ga for several simulants used in the M3 testing are shown as vertical bars in Figure 7.5.

The third benefit of introducing U_T as a parameter in mixing models is that it relates mixing solids with a broad particle size distribution. An average settling velocity has greater physical meaning than an average particle size. The average settling velocity is the volume-weighted sum of the individual particle settling velocities and is the rate at which the distribution settles insofar as it is well-mixed. The average particle size, on the other hand, is purely a geometric average, with little meaning in terms of the physical process.

Figure 7.6 illustrates the benefit of using U_T to correlate off-bottom suspension data from tests with five different simulants in the small-scale tank configured with HLP-22 geometry and operational conditions. When the U_{CS} data are plotted dimensionally versus d_S in Figure 7.6(a), there is not a simple relationship. The exponent on d_S depends on the density ratio and has a value of 0.35 for s = 2.5 and 0.22 for s = 4.2. However, when U_{CS} is normalized by U_T and plotted versus Ga in Figure 7.6(b), a good model is observed with $U_{CS}/U_T \sim Ga^{-0.43}$.

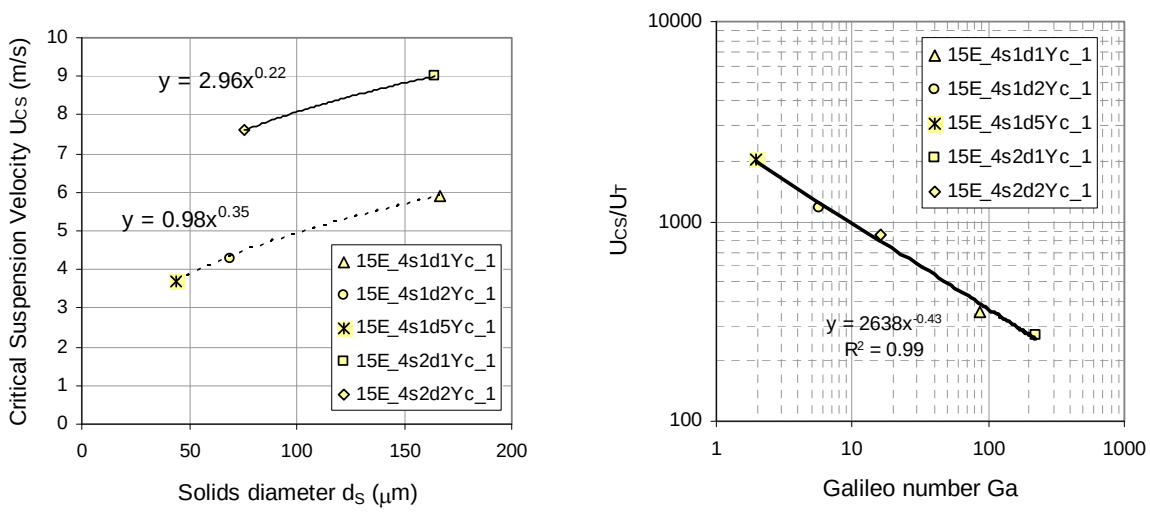

(a) (b)

Figure 7.6. Illustrating the Benefit of Using Setting Velocity to Model U_{CS} Data; (a) Dimensional, (b) Nondimensional

Figure 7.7 illustrates the use of U_T in modeling cloud height data. Figure 7.7(a) shows that when the critical suspension Froude number based on H_{CS} and U_T (F_{CST}) is used, it correlates well with a function of Ga and (s-1). In Figure 7.7(b), the Froude number (in Eq. 7.4) based on H_C and U_T is plotted versus U/U_T. Also shown is the nondimensional cloud height data for $U/U_{CS} \geq 1$.

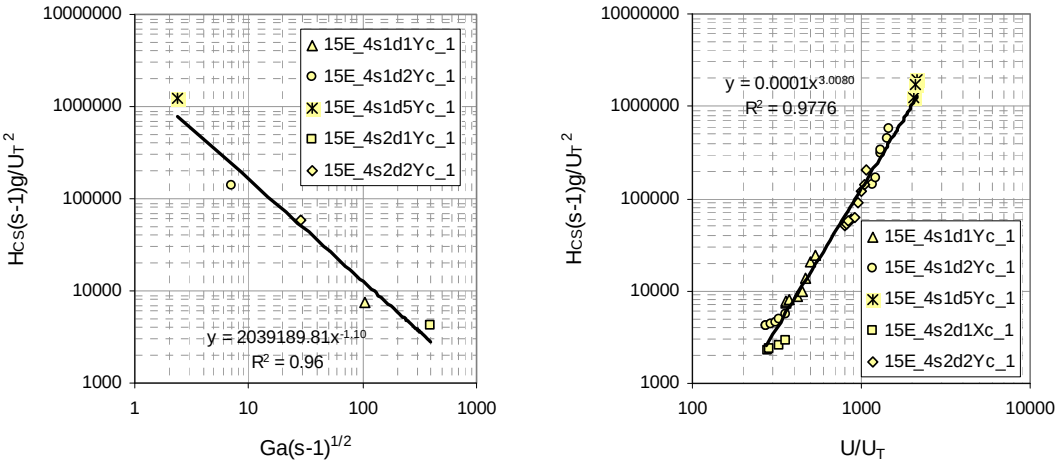

(a) (b)

Figure 7.7. Illustration of the Benefit of Using Setting Velocity to Model Cloud Height Data: (a) F_{CST} Plotted as a Function of $Ga(s-1)^{1/2}$, (b) F_{CST} Plotted as a Function of U/U_T

The effect of solids volume fraction (ϕ_S) on U_{CS} is illustrated in Figure 7.8(a), where data for all simulants in the small-scale tank are shown. At low concentration, the exponent on ϕ_S is about 0.3. As solids loading is increased the exponent is reduced, becoming equal to zero when ϕ_S is about 0.03–0.04. Further increases in solids loading result in decreased U_{CS}. This behavior is consistent with the phenomenon of hindered settling. At higher solids loading the clouds are low, and the local concentration near the bottom of the tank becomes very high. The concentration where the maximum occurs is clearly a function of the particle properties; hence, the nonlinear interaction is complicated.

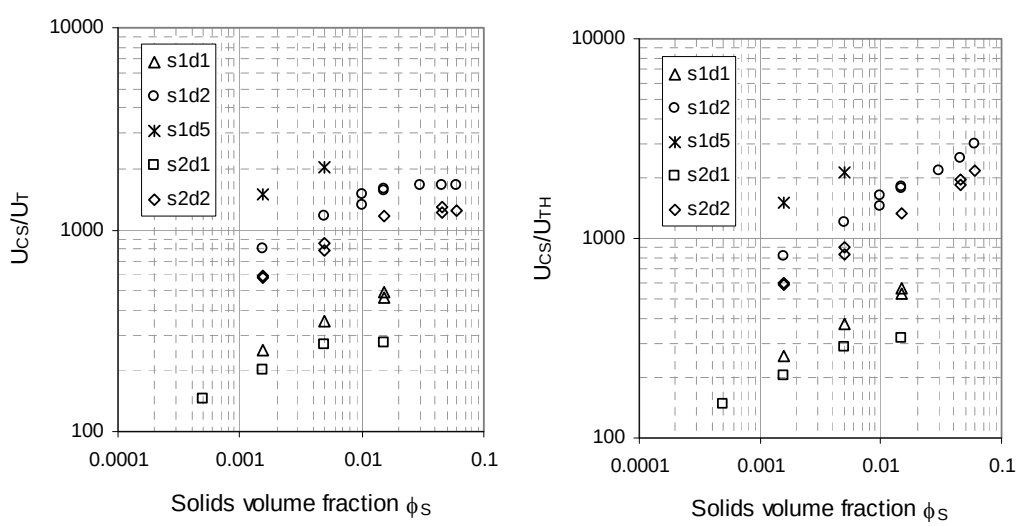

(a) (b)

Figure 7.8. Effect of Solids Loading on U_{CS} for Five Simulants in Small-Scale Tests: (a) U_{CS}/U_T Plotted as a Function of ϕ_S, (b) U_{CS}/U_{TH} Plotted as a Function of ϕ_S

As a first-order means of accounting for the observed behavior, we introduce a modified settling velocity (U_{TH}) that is analogous in form to models for hindered settling:

$$U_{TH} = U_T (1 - \phi_S / \phi_{Smax})^p \tag{7.11}$$

Subsequently, U_{TH} is referred to as the terminal hindered settling velocity. Thus, for a specific test condition, since ϕ_S is constant, the hindered settling velocity of Eq. (7.11) is constant for that test.

In Eq. (7.11), the term ϕ_{Smax} is the solids fraction corresponding to maximum packing, and p is an empirical constant. For our simulants, ϕ_{Smax} ranged from about 0.57 to 0.63 with an average of about 0.60 (Table 3.6). Figure 7.8b shows the same data with U_{CS}/U_{TH} plotted versus ϕ_S, where $\phi_{Smax} = 0.5$ was used (as noted above with regards to Eq. (7.11), ϕ_S is the solid volume fraction for the reference volume (V_{REF}), thus $\phi_{Smax} = 0.5$ has essentially no effect on the results). With the addition of the term for hindered terminal settling velocity, the slopes for the different particles are now approximately constant.

The effect of solids loading on cloud height is demonstrated in Figure 7.9. Here inverse Froude number based on H_{CS} and U_T is shown versus U_{CS}/U_T in Figure 7.9(a). Figure 7.9(b) accounts for the hindered settling effect by using U_{TH} in both the Froude number and the velocity ratio. Also, the inverse Froude number is multiplied by ϕ_S, which accounts for the difference in solids loadings.

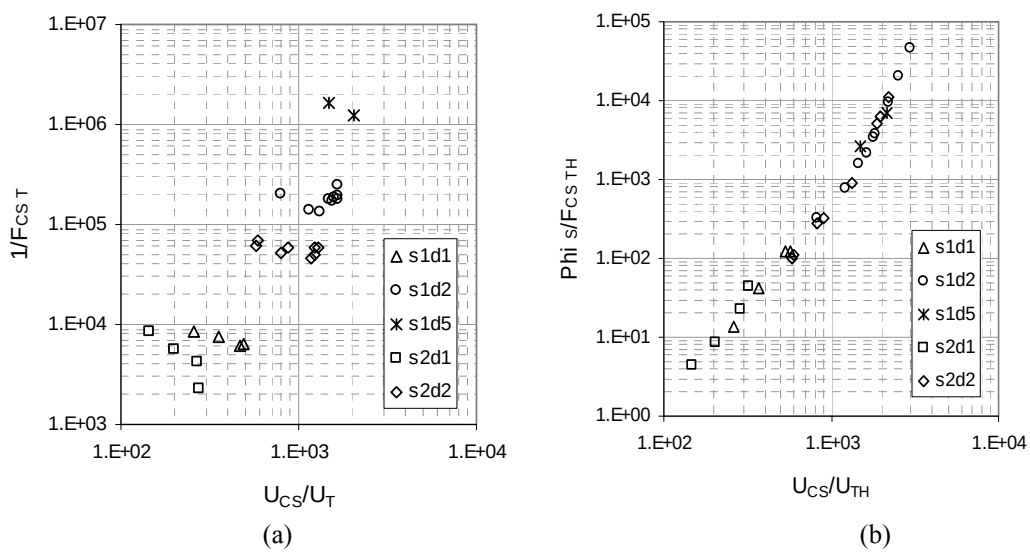

Figure 7.9. Effect of Solids Loading on Cloud Height for Five Simulants in Small-Scale Tests: (a) $1/F_{CST}$ Plotted as a Function of U_{CS}/U_T, (b) $\phi_S/F_{CS\ TH}$ (Phi $_S/F_{CS\ TH}$) Plotted as a Function of U_{CS}/U_{TH}

Viscosity was not one of the variables in the test data. While a recommendation of this report is to include viscosity effects in limited follow-on experiments, the effect of viscosity is included implicitly in the particle settling velocity. Testing will help assess whether the influence of viscosity extends beyond particle settling.

7.2.4 Operational Parameters

The primary operational parameters are duty cycle (DC) and pulse volume fraction (ϕ_p). These two terms describe the unsteady jet mixing effects. In the WTP vessel mixing designs, duty cycle ranges from about 0.18 to 0.35. Tests at higher duty cycle were included to obtain some insight into the potential benefit of sequential operation and to compare the data with steady jet mixing results. In the WTP vessel mixing design, ϕ_p ranges from about 0.04 to 0.1. Testing was performed for ϕ_p up to 0.15 to gain some understanding of the performance of large pulse tubes. Values for these parameters are found in Appendix B, in columns 4 and 5 of the data tables for each test. Figure 7.10 shows the effects of duty cycle on U_{CS} and H_{CS}. Data are from the small-scale tank with $\phi_S = 0.015$ for values of pulse volume fraction. The sensitivity of duty cycle on U_{CS} depends on pulse volume fraction. For small values of ϕ_p, $U_{CS} \sim DC^{-1/2}$. For larger values of ϕ_p and smaller values of duty cycle, U_{CS} is relatively insensitive to duty cycle. Figure 7.10(b) shows H_{CS} is a strong function of DC. In Figure 7.11 the same data are plotted versus ϕ_p for families of constant DC.

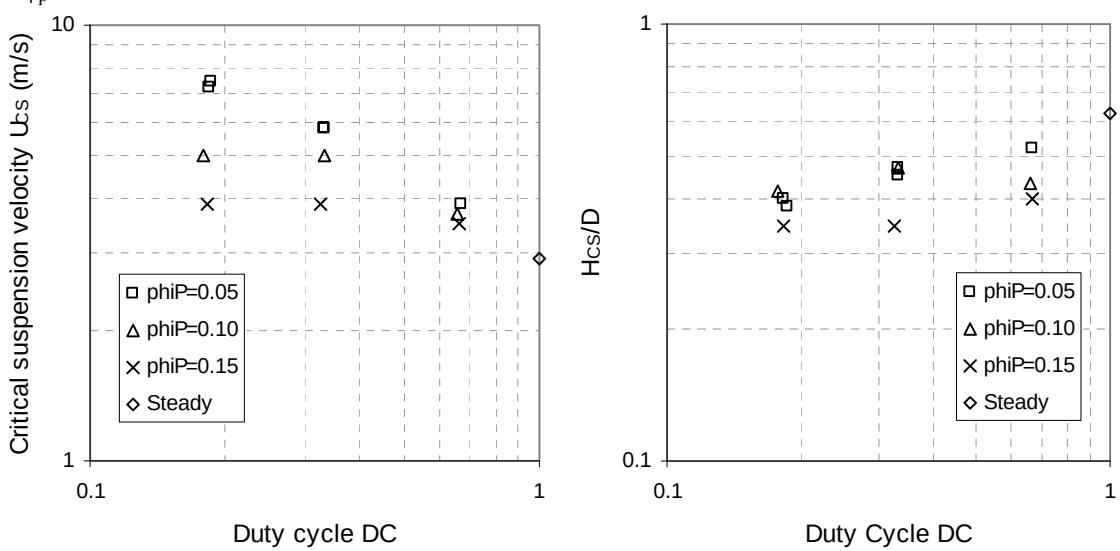

(a) (b)

Figure 7.10. Effect of Duty Cycle on Solids Suspension with Data from Small-Scale Vessel with Simulant s1d2 and $\phi_S = 0.015$; (a) U_{CS}, and (b) Cloud Height

From the U_{CS} and H_{CS} data shown in Figure 7.10, one can obtain a sense for the difference between pulse jet mixing (DC < 1) and steady jet mixing (DC = 1). For $\phi_p = 0.05$ and DC = 0.18, $U_{CSpulsed}/U_{CSsteady}$ is approximately 2.5 and $H_{CSpulsed}/H_{CSsteady}$ is approximately 0.6. Using the approximate relationship from Section 7.2.2, $H_C/H_{CS} \sim (U/U_{CS})^2$, for the same cloud height (equivalent vertical distribution) we find $U_{pulsed}/U_{steady} = 0.6^{-1/2}*2.5 = 3.2$. Hence, the pulse jet velocity must be about 3 times larger than the steady jet velocity for equivalent cloud height. Because the hydraulic mixing power is proportional to U^3 (see Section 7.3.1), it follows that the pulse jet requires 27 times more power for the same cloud height. This is instantaneous jet power; for average power the duty cycle must be factored in. Hence, for this example, DC = 0.18 and average pulse jet power is 0.18*27 = 4.9. Even after factoring in duty cycle, about five times more total energy is required for pulse jets. The difference between pulse jet and steady jet mixing is greatly reduced as DC is increased. For example, if DC = 0.5, as used in the previous example, the instantaneous power required for equivalent mixing is about 5X, and the average power is about 2.5X.

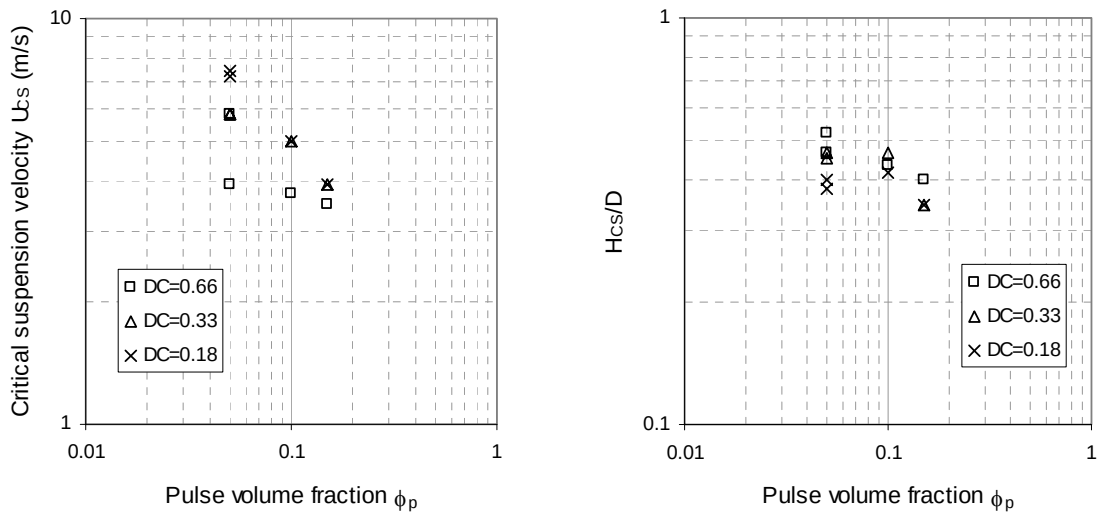

(a) (b)

Figure 7.11. Effect of Pulse Volume Fraction (ϕ_p) on Solids Suspension: (a) U_{CS}, (b) H_C Data from 15-in. Vessel with Simulant s1d2 and $\phi_S = 0.015$

7.2.5 Geometry

The primary geometric variables include number of jets (N), jet diameter (d), and tank diameter (D). Also important is the dished bottom, the radial arrangement of PJMs, and the impingement angle of the jets on the bottom. Other geometric variables include PJM outer diameter and nozzle shape and standoff.

Figure 7.12 demonstrates the value of the jet density (ϕ_J) where

$$\phi_J = N_J (d/D)^2 \tag{7.12}$$

for multiple jet systems. Figure 7.12(a) shows U_{CS}/U_T versus nozzle diameter for N = 4, 8, and 12; Figure 7.12(b) shows the same data plotted versus ϕ_J. The result indicates

$$U_{CS} \sim N_J^{1/2} d \tag{7.13}$$

which is the nozzle diameter for the total jet discharge area.

Several different dish bottom geometries were tested, with relevant parameters shown in Table 7.1 (FIO). The effect of geometry can be explored by introducing leading geometric constants (k_U and k_C) for U_{CS} and H_C, respectively[1]. Best-fit values for these were determined for the 70F and 34S tanks; the constants for 15E and 70E are defined to be 1. When less than 12 operating jets were tested in any of the geometries, the dish constant was not adjusted even if the radial position was adjusted. Any geometric effects associated with different impingement angles were not accounted for in the constants shown in Table 7.1. The constants for the F&D head in the large-scale tank were found to be 0.94 and 1.04 for U_{CS} and H_C, respectively.

[1] The geometric constants are multipliers on the right side of a correlation for U_{CS} and H_C. For example $U_{CS} = k_U$ x f(test variables), where k_U is only a function of dish shape.

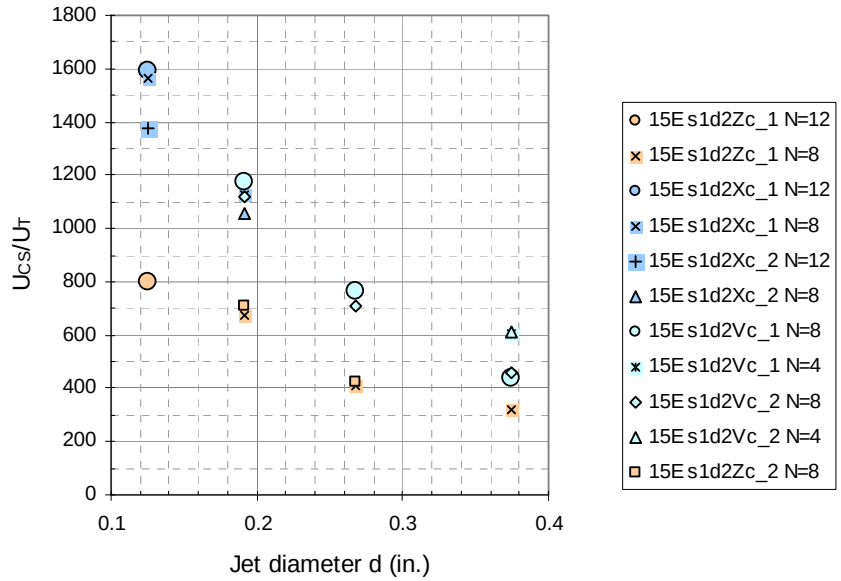

(a)

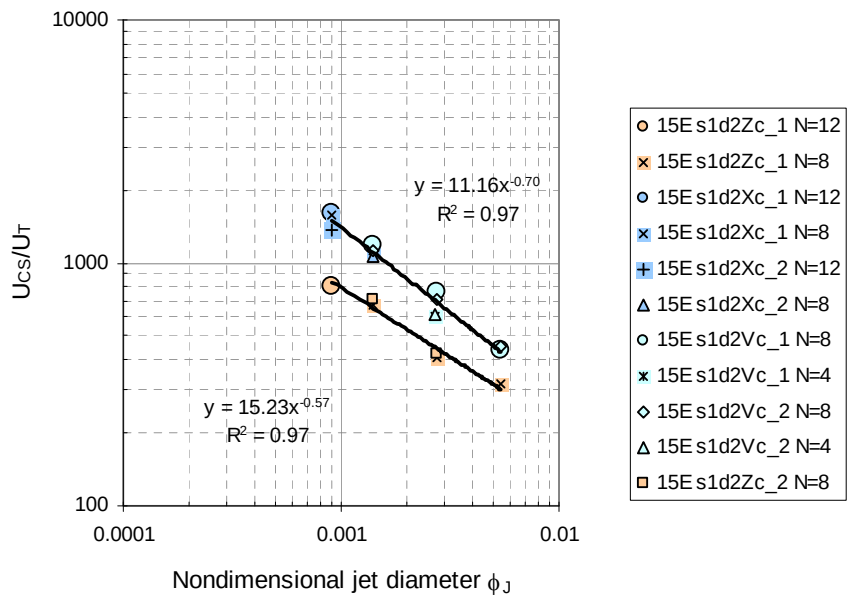

(b)

Figure 7.12. Effect of Nozzle Diameter, Jet Diameter, and Number of Operating Pulse Tubes for Small-Scale Tank: (a) U_{CS}/U_T as a Function of d, (b) U_{CS}/U_T as a Function of ϕ_J

In principle, we could model the geometric constants in terms of ring radius and impingement angle. Because of the limited number of combinations tested, this was considered to add little value over a simple dish constant. The values obtained for the dish constants are reasonable when considering the likely geometric effect on the bulk flow in the tank.

Table 7.1. As-Tested Dish Parameters and Geometric Coefficients for Various Dish Shapes (FIO)

Tank and PJM Configuration	Dish Type	Inner Ring Radius/Tank Radius	Outer Ring Radius/Tank Radius	Inner Ring Impingement Angle	Outer Ring Impingement Angle	Geometric Constant for U_{CS}	Geometric Constant for H_C
Tank		R_I/R	R_O/R	θ_I	θ_O	k_U	k_C
15E 4/8-tube	2:1 Elliptical	0.50	0.67	16.0°	24.4°	NA	NA
15E 12-tube	2:1 Elliptical	0.34	0.62	10.1°	21.8°	1	1
70E 4/8-tube	2:1 Elliptical	0.50	0.67	16.1°	21.9°	NA	NA
70E 12-tube	2:1 Elliptical	0.33	0.62	10.5°	20.3°	1	1
70F 12-tube	F&D	0.34	0.76	9.7°	22.4°	0.94	1.04
34S 12-tube	Spherical	0.33	0.62	16.1°	30.8°	0.85	1.35

7.2.6 Scale

Direct scale-up data were obtained for the 14 different test conditions evaluated in the 15E and 70E tanks; these conditions are shown in Table 7.2. The exponent on tank scale (referred to as the scale-up exponent, α) is given by

$$\alpha = \frac{\ln(y_{70}/y_{15})}{\ln(SF_{70-15})} \tag{7.14}$$

where y_{70} and y_{15} are measured variables (U_{CS} or H_{CS}) in the large- and small-scale tanks, respectively, and the scale factor (SF) is $SF_{70-15} = D_{70}/D_{15} = 70/14.44 = 4.85$.

Table 7.2. Direct Scale-up Data from Elliptical Tests: Ratios of Measured Variables at Large Versus Small Scales

Test Conditions					Critical Suspension Conditions				Average Cloud Data for $U \geq U_{CS}$		
d	Simulant	ϕ_S	DC	ϕ_p	U_{CS}	H_{CS}	U^2_{CS}/H_{CS}	U^3_{CS}/H_{CS}	(U^2/H_C)avg	(U^3/H_C)avg	(U^4/H_C)avg
4	s1d1	0.00155	0.18	0.05	1.58	4.52	0.55	0.87	0.65	1.14	1.94
4	s1d1	0.00155	0.33	0.05	1.69	5.24	0.55	0.92	0.72	1.17	1.89
4	s1d2	0.00155	0.18	0.05	1.59	3.85	0.65	1.04	0.75	1.15	1.75
4	s1d2	0.015	0.18	0.05	1.61	7.48	0.35	0.56	0.38	0.55	0.80
4	s1d2	0.00155	0.34	0.05	1.64	4.22	0.64	1.05	0.70	1.05	1.57
4	s1d2	0.005	0.34	0.05	1.40	5.24	0.37	0.52	0.54	0.73	0.99
4	s1d2	0.01	0.34	0.05	1.36	6.22	0.30	0.40	0.43	0.57	0.75
4	s1d2	0.015	0.34	0.05	1.47	6.38	0.34	0.49	0.45	0.57	0.73
4	s2d2	0.00155	0.34	0.05	1.62	4.22	0.62	1.00	0.66	1.08	1.75
4	s2d2	0.005	0.34	0.05	1.64	4.43	0.61	1.00	0.57	0.89	1.38
6	s1d2	0.0143	0.33	0.05	1.42	7.33	0.27	0.39	0.30	0.42	0.57
6	s1d2	0.00155	0.33	0.05	1.69	9.78	0.29	0.50	0.40	0.63	0.96
6	s1d2	0.0143	0.33	0.05	1.45	6.45	0.33	0.48	0.50	0.73	1.07
6	s1d2	0.00155	0.33	0.05	1.54	5.35	0.44	0.68	0.35	0.47	0.64
Average					**1.55**	**5.77**	**0.45**	**0.71**	**0.53**	**0.80**	**1.20**
Standard Deviation					**0.11**	**1.64**	**0.15**	**0.26**	**0.15**	**0.27**	**0.50**

Table 7.2 shows values of the ratios y_{70}/y_{15} for $y = U_{CS}$ and H_{CS}, as well as other variables. The quantity U^2_{CS}/H_{CS} is the simplified Froude number, and U^3_{CS}/H_{CS} is a power-type number. The other terms required for dimensional consistency [density ratio (s), gravitational constant (g), etc.] are neglected because they will cancel out in the ratios. The average ratios in Table 7.2 for H_C data with $U \geq U_{CS}$ were

obtained by averaging the indicated variables for each test. This was necessary because, in general, values of H_C and U were not the same for tests at both scales. The scale-up exponents derived from the ratios are shown in Table 7.3.

Table 7.3. Direct Scale-up Data from Elliptical Tests: Scale Exponents Based on Large-Versus Small-Scale Data

Test Conditions					Critical Suspension Conditions				Average Cloud Data for $U \geq U_{CS}$		
d	Simulant	ϕ_S	DC	ϕ_p	U_{CS}	H_{CS}	U^2_{CS}/H_{CS}	U^3_{CS}/H_{CS}	(U^2/H_C)avg	(U^3/H_C)avg	(U^4/H_C)avg
4	s1d1	0.00155	0.18	0.05	0.29	0.96	-0.38	-0.09	-0.27	0.08	0.42
4	s1d1	0.00155	0.33	0.05	0.33	1.05	-0.38	-0.05	-0.21	0.10	0.40
4	s1d2	0.00155	0.18	0.05	0.29	0.85	-0.27	0.02	-0.18	0.09	0.35
4	s1d2	0.015	0.18	0.05	0.30	1.27	-0.67	-0.37	-0.61	-0.37	-0.14
4	s1d2	0.00155	0.34	0.05	0.31	0.91	-0.28	0.03	-0.23	0.03	0.29
4	s1d2	0.005	0.34	0.05	0.21	1.05	-0.63	-0.42	-0.39	-0.20	-0.01
4	s1d2	0.01	0.34	0.05	0.19	1.16	-0.77	-0.58	-0.53	-0.36	-0.18
4	s1d2	0.015	0.34	0.05	0.24	1.17	-0.69	-0.45	-0.51	-0.35	-0.20
4	s2d2	0.00155	0.34	0.05	0.30	0.91	-0.30	0.00	-0.26	0.05	0.36
4	s2d2	0.005	0.34	0.05	0.32	0.94	-0.31	0.00	-0.36	-0.08	0.21
6	s1d2	0.0143	0.33	0.05	0.22	1.26	-0.82	-0.60	-0.77	-0.56	-0.35
6	s1d2	0.00155	0.33	0.05	0.33	1.44	-0.78	-0.44	-0.57	-0.30	-0.02
6	s1d2	0.0143	0.33	0.05	0.24	1.18	-0.71	-0.47	-0.44	-0.20	0.04
6	s1d2	0.00155	0.33	0.05	0.27	1.06	-0.52	-0.25	-0.67	-0.47	-0.28
Average					**0.28**	**1.09**	**-0.54**	**-0.26**	**-0.43**	**-0.18**	**0.06**
Standard Deviation					**0.05**	**0.17**	**0.21**	**0.24**	**0.19**	**0.23**	**0.27**

Some examples of the scale-up data for U_{CS} are shown in Figure 7.13. The upper plot shows the U_{CS}/U_{CS15}, and the lower plot shows a best fit of scale-up data. The average scale-up exponent for U_{CS} based on the data is 0.28 ± 0.05. The scale-up data for H_C equal to and above U_{CS} indicates non-power-law behavior since the scale-up exponents for the averaged variables U^n/H_C show a dependence on the velocity exponent n. Figure 7.14 shows the scale-up exponent versus n for the average cloud data. For tests at a given scale it turns out that $H_C \sim U^3$ is a reasonable approximation of cloud behavior (see Figure 7.7). Based on this we would expect an average cloud height scale-up exponent of about 0.2.

Studies of the complete data set yield cloud scale-up exponent values ranging from 0.1 to 0.4, depending on the details of the fitting approach and which data are included. Gravitational work-energy arguments alone suggest H_C is independent of scale. However, if ϕ_s is held constant as scale is increased (in which case the volume of solids increases with the cube of the scale), the average solids concentration in clouds of constant height will increase proportional to scale (because the volume of the cloud would increase only as the square of the scale). Hence, the settling velocity would be reduced because of the hindering effect, and the cloud height could not be constant, but would have to increase slightly. If the same energy arguments are applied to the change in cloud position due to a single pulse, scale comes into play from the presence of concentration gradients. Scale also can contribute through the jet Reynolds number. While all testing occurred at conditions above the turbulent transition for free jets, there still can be a weak Reynolds number effect. For example, the floor shear stress in a turbulent boundary layer is proportional to $Re^{-1/5}$ (Schlichting 1979). It is not known exactly how the shear stress Re dependence directly translates to the impinging jet and associated slurry flow, but it is reasonable that it would be would be on the order of 0.1. Thus, a scale-up on the order of 0.2–0.4 due to the combined effects mentioned here is reasonable.

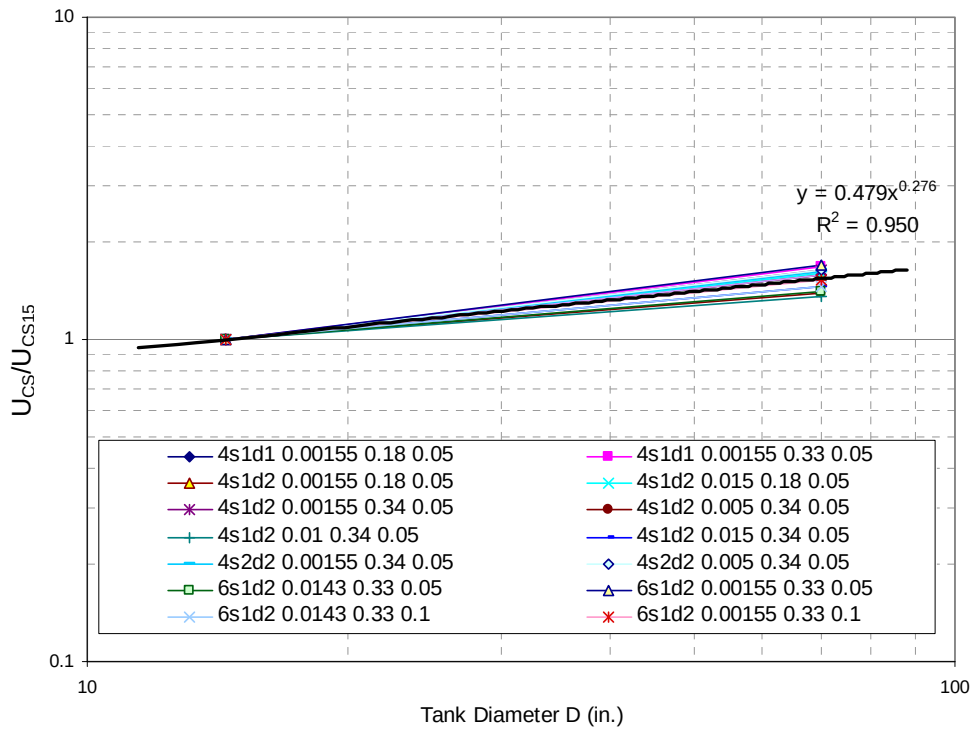

Figure 7.13. Scale Dependence of U_{CS}: U_{CS}/U_{CS15} Versus Tank Diameter with Fit of Scale-up Data Showing Scale-Up Exponent of 0.276

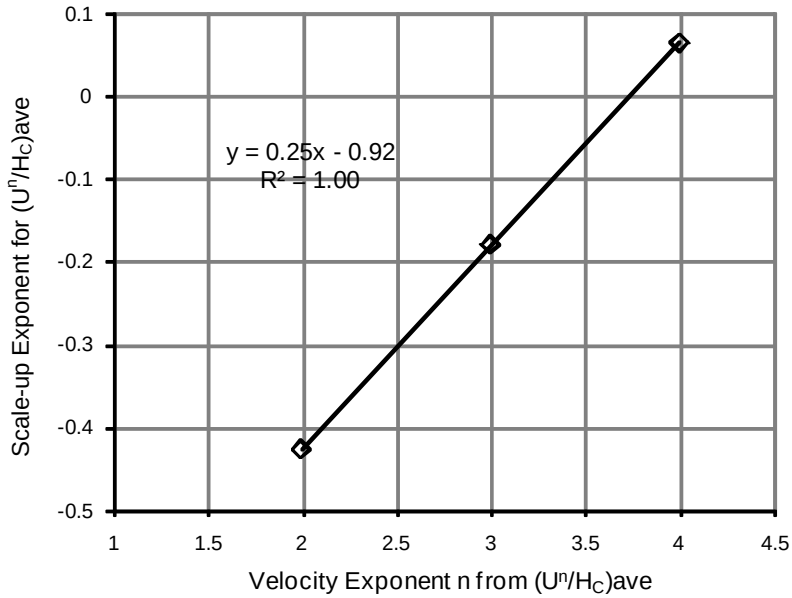

Figure 7.14. Scale-up Exponent for Average Cloud Parameters $(U^n/H_C)_{ave}$ as a Function of Velocity Exponent, n

7.2.7 Pulse Shape

This section addresses the effects of pulse shape on U_{CS} and H_C. Pulse shape varied during testing as a function of average jet velocity and test scale. A generic drive function is shown in Figure 7.15. To account for these variations, four different velocity integrals were computed from the test data. These all have the form:

$$U_n = \left(\frac{1}{\Delta t_n} \int U(t)^n \, dt \right)^{1/n} \qquad n = 1, 2, 3, \text{ and peak average with } n = 1,\ \Delta t_n = \text{primary discharge time} \qquad (7.15)$$

where U(t) is instantaneous velocity, and Δt_n is the time interval over which the integration is performed. The velocities U_1, U_2, and U_3 correspond to mass, momentum, and energy-based average velocities, respectively, where $\Delta t \approx t_{DA}$. The velocity, U_{PA}, corresponds to the peak average velocity, which was observed visually or computed. The time interval for U_{PA} is $\Delta t \sim t_m - t_D$, times associated within U_{max} and U_{end}.

In analyzing the test data, the peak average velocity was used with the pulse shape ratio ε_{31}:

$$\varepsilon_{31} = U_3/U_1 - 1 \qquad (7.16)$$

The pulse shape ratio is equal to 0 for a square wave and may be as high as 0.4–0.5 for prototypic PJMs at plant scale. During testing, ε_{31} varied from ~ 0.01–0.3, as shown in Figure 7.16. Analysis of the data indicates that $U_{CS} \sim (1+\varepsilon_{31})^{0.4}$ and $H_C \sim (1+\varepsilon_{31})^{-0.35}$ (FIO).

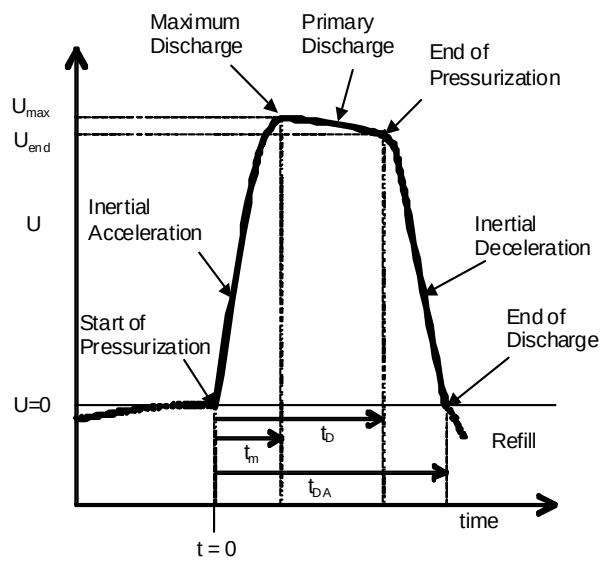

Figure 7.15. Illustration of Nozzle Velocity Transient During PJM Discharge

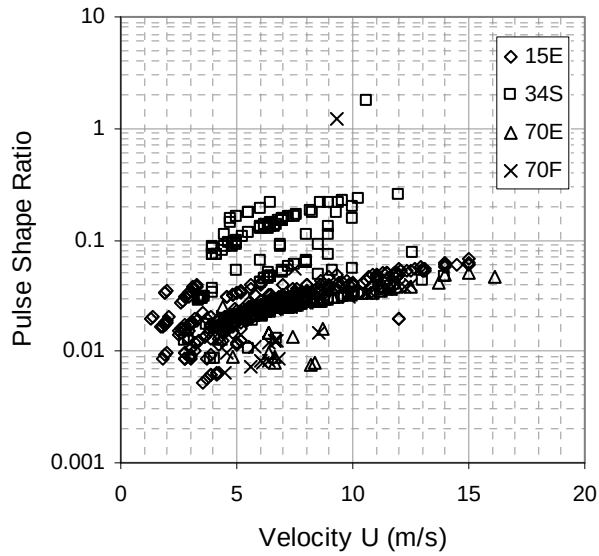

Figure 7.16. Pulse Shape Ratio Versus Peak Average Velocity for Tests at Three Scales

7.2.8 Aspects of Mixing Behavior Included in Model Development

Not all of the mixing behavior aspects addressed in the previous Subsections were included in limited model development efforts discussed subsequently in Sections 7.3 and 7.4. Specifically, experimental data were used that met the criteria

- DC < 0.7 (no steady jet data were included)
- $U/U_{CS} \geq 1$ for the H_C model[1]
- Ratio of the return line height to the tank diameter ≥ 1.

Additionally, the following variables were not included in the models:

- Dish geometric constants k_U and k_C. The effects of dish geometry were not included in the models.
- Pulse shape parameter ε_{31}.

7.3 Physical Model Results

The nondimensional variables and models developed using the physical approach are described in Sections 7.3.1 to 7.3.4. Section 7.3.1 presents the nondimensional variables used to develop mixing models for U_{CS}, H_C, C(Z), and C_0. Section 7.3.2 discusses the models developed for U_{CS} and H_C using the physical approach described in Section 7.1.1. Section 7.3.3 presents the models for solids vertical distribution [C(Z)] and C_0 developed using the physical approach. Section 7.3.4 summarizes the physical model equations and coefficients for U_{CS}, H_C, C(Z), and C_0.

[1] It is reasonable to exclude data below U_{CS} for modeling H_C because below U_{CS} the quantity of the solids that are fully suspended is unknown.

7.3.1 Nondimensional Variables

The analyses presented in Section 7.2 indicate that using nondimensional variables to describe the data works reasonably well. Hence, we envision a model for U_{CS} of the form

$$U_{CS}/U_T = k_U f(F_{DT}, s, Ga, \phi_S, \phi_J, \phi_p, DC, \varepsilon_{31}, Re) \tag{7.17}$$

where the Froude number (F_{DT}) is based on U_T and tank diameter:

$$F_{DT} = \frac{U_T^2}{(s-1)gD} \tag{7.18}$$

The leading constant, k_U, in Eq. (7.17) accounts for the different dish geometries. Similarly, we envision a model for H_C of the form

$$F_{H_CT} = k_C f(U/U_T, s, Ga, \phi_S, \phi_J, \phi_p, DC, \varepsilon_{31}, Re) \tag{7.19}$$

where the Froude number (F_{H_cT}) based on H_C and U_T is

$$F_{H_cT} = \frac{U_T^2}{(s\text{-}1)gH_C} \tag{7.20}$$

Again, the leading constant, k_C, in Eq. (7.19) accounts for dish geometry.

Additional physical insight and simplification can be obtained by considering a nondimensional settling number (N_S). Bamberger et al. (1990) and Liljegren and Bamberger (1992) introduced this parameter for correlating solids vertical distribution when mixing with submerged rotating jets. They interpreted the settling number as the ratio of "jet hydraulic power to the viscous dissipation rate due to settling." As it turns out, the dissipation rate is equivalent to the rate at which potential energy increased lifting the solids cloud during a pulse.

The flow field resulting from a pulse jet behaves essentially like a steady jet if the drive time is large compared with the flow establishment time. The ratio of these two time scales is ϕ_p/ϕ_J, which, in general, was much greater than 1 for the test conditions as well as plant conditions. The value of ϕ_p/ϕ_J for the plant vessels varies from ~12 (HOP-903/904) to ~75 (TCP-01). The range of ϕ_p/ϕ_J covered during testing was approximately 9 to 170.

The hydraulic power input at the nozzles (P_J) is

$$P_J = \frac{1}{2}\rho U_2^2 U_1 \frac{\pi N d^2}{4} \tag{7.21}$$

Jet power is dissipated as the jets spread out and entrain fluid. Rajaratnam (1976) shows that the jet energy at a distance z from the nozzle is reduced by ~ d/z. Because the jet velocity is reduced in the same manner, the jet power is reduced by ~ $(d/z)^2$. If we take the characteristic distance the jet travels[1] as

[1] The characteristic length scale over which the jet travels depends only on geometry for a Newtonian impinging jet. The choice of length scale is somewhat arbitrary. One length scale is the vessel diameter, another is the cube root of vessel volume, and a third could be cloud height. The expression used is a reasonable choice for characteristic length scale because it accounts for the reduced work a single jet must do when multiple jets are present. It is similar to the concept of the geometric zone of influence of a single jet.

$$z \sim D/\sqrt{N} \tag{7.22}$$

then the effective jet hydraulic power (P_V) is

$$P_V = cP_J\phi_J \tag{7.23}$$

where c is a constant. Substituting for P_J we obtain

$$P_V = c\frac{\pi}{4}\rho U_2^2 U_1 \phi_J^2 D^2 \tag{7.24}$$

The useful jet energy (E_V) imparted to the tank during a pulse is

$$E_V = P_V t_D \tag{7.25}$$

During each cycle, the solids settle proportional to the settling distance, $t_C U_T$, where t_C is the cycle time. The relative mass of solids (m_S) (difference between solid mass and the mass of the liquid it displaces) is

$$m_S = (\rho_s - \rho_l)\phi_S \frac{\pi}{4} D^3 \tag{7.26}$$

Hence the energy required to keep the solids suspended during a pulse (ΔE_S) is

$$\Delta E_S = m_S g(t_C U_T) = \left(\frac{\pi}{4} D^3 \phi_S (s-1)\rho_l\right) g\left(t_C U_T\right) \tag{7.27}$$

The settling number N_S is given by the ratio

$$N_S = E_V / \Delta E_S = \frac{U}{U_T}\frac{U^2\phi_J^2 DC}{(s-1)g\phi_S D} f(\varepsilon_{31}) \tag{7.28}$$

We made the assumption that

$$U_1 U_2^2 = U^3 f(\varepsilon_{31}) \tag{7.29}$$

which allows using the average peak velocity in developing and applying any mixing model. The function $f(\varepsilon_{31})$ is easily approximated by a power-law term.

N_S given by Eq. (7.28) has all the main variables with the exception of H_C and ϕ_p. The following relations are also useful:

Settling number
$$N_S = \left(\frac{U}{U_T}\right)^3 F_{DT}\frac{\phi_J^2 DC}{\phi_S} f(\varepsilon_{31}) \tag{7.30}$$

Nondimensional critical suspension
$$D^* = \frac{1}{F_{DT}}\frac{\phi_S}{\phi_J^2 DC} f(\varepsilon_{31}) = \frac{1}{N_S}\left(\frac{U}{U_T}\right)^3 \tag{7.31}$$

Nondimensional cloud height $H_C^* = \frac{1}{F_{H_C T}} \frac{\phi_S}{\phi_J^2 DC} f(\varepsilon_{31}) = \frac{H_C / D}{N_S} \left(\frac{U}{U_T} \right)^3$ (7.32)

These nondimensional variables are used to construct models for mixing response variables in Section 7.3.2.

7.3.2 Physical Models for Critical Suspension Velocity and Cloud Height Based on Nondimensional Variables

This section presents models for U_{CS} and H_C developed using the physical approach described in Section 7.1.1. Hence, these models are subsequently referred to as the *physical models*. The physical models were developed using nondimensional variables presented in Section 7.3.1.

The nondimensional critical suspension variable D* in Eq. (7.31) may be rewritten by 1) using the hindered terminal settling velocity (U_{TH}) in place of the terminal settling velocity (U_T), 2) including the pulse volume fraction (ϕ_p) in the relationship, and 3) allowing the exponent of ϕ_J to be determined by the experimental data. These changes give

$$D^* = \frac{D(s-1)g\phi_S}{DC\, U_{TH}^2 \phi_p^{\alpha_1} \phi_J^{\alpha_2}} \tag{7.33}$$

where α_1 and α_2 are coefficients to capture the effects of ϕ_p and ϕ_J (which were varied in testing). The α_1 and α_2 coefficients were determined (by methods for fitting models to data) to optimize the U_{CS} and H_C model fits to the data set. U_{TH} is the modified hindered-settling velocity introduced in Section 7.2.3 and rewritten as

$$U_{TH} = U_T (1 - \phi_S / 0.5)^{4.5} \tag{7.34}$$

The value of the exponent p in Eq. (7.11) equal to 4.5 was found to give a reasonable fit.

The nondimensional model form for U_{CS} is expressed in terms of the nondimensional critical suspension variable D* as

$$\frac{U_{CS}}{U_{TH}} = A1 (D^* Ga^{-0.5})^{B1} \tag{7.35}$$

where A1 and B1 are coefficients to be estimated from the experimental data.

As discussed in Section 7.3.1 regarding the settling number (N_S), the ratio U_{CS}/U_T is related to the ratio of viscous power dissipated by suspending the particles to the power of the PJMs. Because the mass of suspended particles is constant, the power required to suspend them depends on their dissipation power per mass. For small particles, viscous stresses dominate inertial stresses attending their settling such that the settling velocity occurs when viscous and gravitational stresses balance; that is, when the gravity number (Gr) is unity where

$$Gr = \frac{(s-1)gd^2}{\nu U_T} \tag{7.36}$$

Also, the gravity number, Reynolds, Froude, and Galileo numbers are related by

$$Ga = \frac{Re^2}{Fr} = ReGr \tag{7.37}$$

Hence, for small particles, Gr ~ 1 and Ga is small, and Ga ~ Re, consistent with Eq. (7.9). For large particles, inertial stresses dominate viscous stresses, such that the settling velocity occurs when inertial and gravitational stresses balance; that is, when the Froude number (Fr) is unity. Hence, for large particles, Re ~ 1 and Ga is large, and Ga ~ Re^2, consistent with Eq. (7.10). The rate of dissipation of power of settling particles per mass of particles is simply $(s\text{-}1)gU_T$. Then the ratio of the power per mass dissipated by small particles to the power per mass dissipated by large particles is

$$\frac{(U_T)_{Gr=1}}{(U_T)_{Fr=1}} = \frac{\frac{(s-1)gd^2}{\nu}}{\sqrt{(s-1)gd}} = \sqrt{\frac{(s-1)gd^3}{\nu^2}} = \sqrt{Ga} \tag{7.38}$$

Hence, the appearance of $\sqrt{Ga}$ in Eq. (7.36) helps describe the power required to suspend the particles. This is physically reasonable because Eq. (7.36) is related (see Eq. 7.30) to the fraction of PJM power required to suspend the particles. This relationship also helps explain Figure 7.6.

The nondimensional model form for H_C is expressed as

$$\ln\left(H_C^*\right) = A2\left(\frac{U}{U_{TH}}\right)^{B2} \tag{7.39}$$

where A2 and B2 are coefficients to be estimated from the experimental data and

$$H_C^* = \frac{H_C}{D} D^* = \frac{H_C (s-1) g \phi_S}{DC\, U_{TH}^2 \phi_p^{\alpha 1} \phi_J^{\alpha 2}} \tag{7.40}$$

All other variables in both models are as previously defined.

The nondimensional model forms for U_{CS} and H_C, given in Eq. (7.38) and (7.39), respectively, were linearized as

$$\ln\left(\frac{U_{CS}}{U_{TH}}\right) = \ln(A1) + B1 \ln(D * Ga^{-0.5}) \tag{7.41}$$

and

$$\ln\left[\ln\left(H_C^*\right)\right] = \ln(A2) + B2 \ln\left(\frac{U}{U_{TH}}\right) \tag{7.42}$$

Eq. (7.41) and (7.42) were fit to the experimental data set using the ordinary least squares (OLS) regression capability of Excel®. The summation of the R^2 values from the OLS regression for Eq. (7.41)

and (7.42) was maximized using the Excel® Solver by adjusting the coefficients α_1 and α_2 of D* in Eq. (7.33). This resulted in $\alpha_1 = 0.698$ and $\alpha_2 = 1.714$.

With $\alpha_1 = 0.698$ and $\alpha_2 = 1.714$, the OLS regression provided A1 = 2.220, B1 = 0.284, A2 = 8.847, and B2 = 0.131. The resulting nondimensional models for U_{CS} and H_C are thus

$$\frac{U_{CS}}{U_{TH}} = 2.220(D^* Ga^{-0.5})^{0.284} \tag{7.43}$$

and

$$\ln\left(H_C^*\right) = 8.847\left(\frac{U}{U_{TH}}\right)^{0.131} \tag{7.44}$$

Figures 7.17 and 7.18 show the fits of the nondimensional U_{CS} and H_C models, respectively, to the experimental data using the nondimensional variables appearing on the left (y-axis) and right (x-axis) sides of each model.

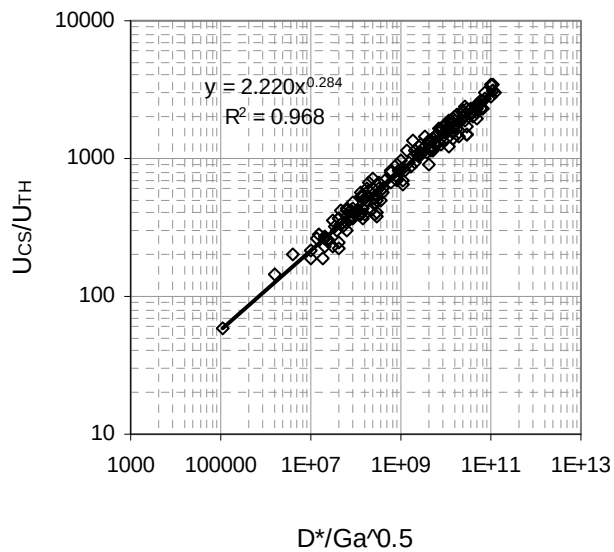

Figure 7.17. Fit of U_{CS} Model to Experimental Data Using Nondimensional Variables U_{CS}/U_{TH} and $D^*/Ga^{0.5}$

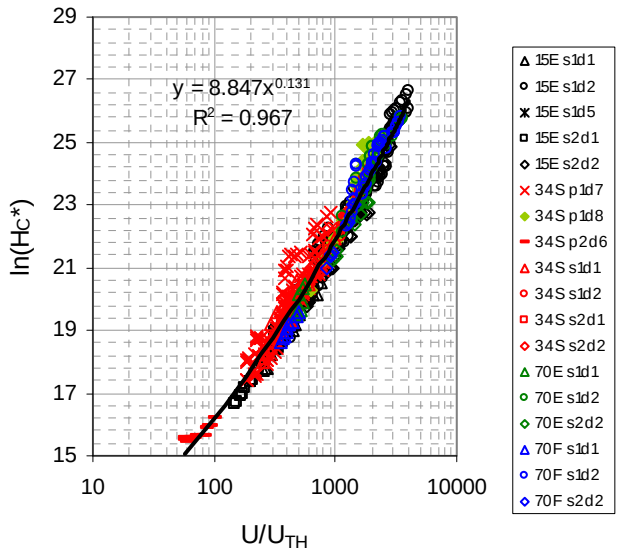

Figure 7.18. Fit of H_C Model to Experimental Data Using Nondimensional Variables $\ln(H_C^*)$ and U/U_{TH}

Figure 7.19 shows the fit of the following nondimensional model form for H_C:

$$H_C^* = A3\left(\frac{U}{U_{TH}}\right)^{B3} \tag{7.45}$$

to the cloud height data, where A3 and B3 are coefficients estimated from the data. This nondimensional model for H_C is similar to Eq. (7.39) but without the natural logarithm of H_C^* on the left side. Fitting Eq. (7.45) to the same data discussed earlier yields A3 = 17.780 and B3 = 2.775. An B3 exponent of 3 would correspond to N_S = constant. Hence the behavior is very close to constant N_S.

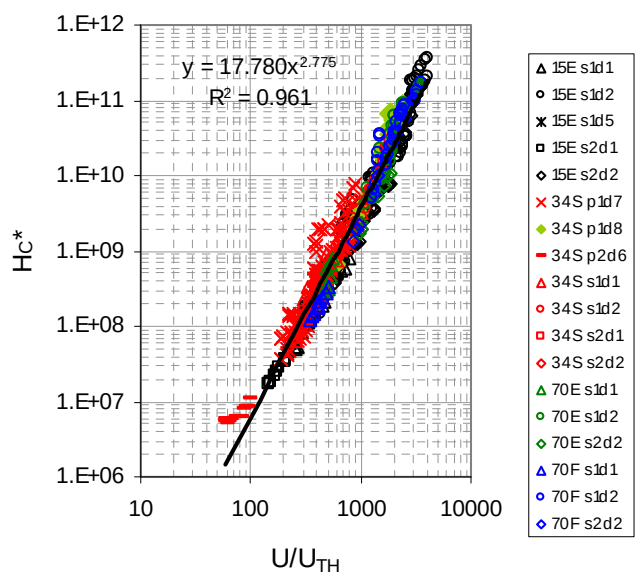

Figure 7.19. Fit of H_C Model to Experimental Data Using Nondimensional Variables H_C^* and U/U_{TH}

The nondimensional variables used in the U_{CS} model of Eq. (7.43) and the H_C model of Eq. (7.44) include some of the same variables on each side of the model. This can cause spurious correlation (see Section D.1.3 of Appendix D), which results in higher R^2 values and tighter fits than exist for the dimensional response variables (U_{CS} and H_C). The goodness of fits of the U_{CS} and H_C models to the data using predicted versus measured plots (see Section D.3.2 of Appendix D) are shown in Figures F.8 and F.15 of Appendix F. For convenience, these plots are reproduced here as Figures 7.20 (U_{CS}) and 7.21 (H_C), respectively. The R^2 values in Figures 7.17 and 7.18 are calculated using predicted and actual values of $\ln(U_{CS}/U_{TH})$ and $\ln[\ln(H_C^*)]$, respectively. On the other hand, the R^2 values in Figures 7.20 and 7.21 are calculated using predicted and measured values of $\ln(U_{CS})$ and $\ln(H_C)$, respectively. Hence, the R^2 values in Figures 7.17 and 7.18 are calculated in different units than those in Figures 7.20 and 7.21 and thus are not directly comparable; still, they may be compared as indicators of the degree of spurious correlation.

The effect of spurious correlation in the physical models for U_{CS} and H_C can be assessed by comparing Figure 7.17 with Figure 7.20 (U_{CS}) and Figure 7.18 with Figure 7.21 (H_C). Figures 7.20 and 7.21 look directly at how well U_{CS} and H_C are predicted for the physical models and thus are not affected by spurious correlation like Figures 7.17 and 7.18 are. For the U_{CS} physical model, the broader scatter and smaller $R^2 = 0.896$ in Figure 7.20 compared with the tighter scatter and larger $R^2 = 0.966$ in Figure 7.17 indicates the physical model is subject to relatively low spurious correlation, but even the smaller R^2 value is reasonably large. However, the much broader scatter and smaller $R^2 = 0.493$ in Figure 7.21 compared with the substantially tighter scatter and larger $R^2 = 0.967$ in Figure 7.18 indicates the physical model for H_C is subject to substantial spurious correlation. Also, Figure 7.21 shows that the physical model for H_C tends to significantly underpredict H_C for much of the data from the Fall 2007 testing, particularly those tests with 4 PJMs in operation. Improved results can be obtained by including the dish geometry constant as well as additional functionality for tube number (N) in the model; however, this was not done given higher priorities and time constraints.

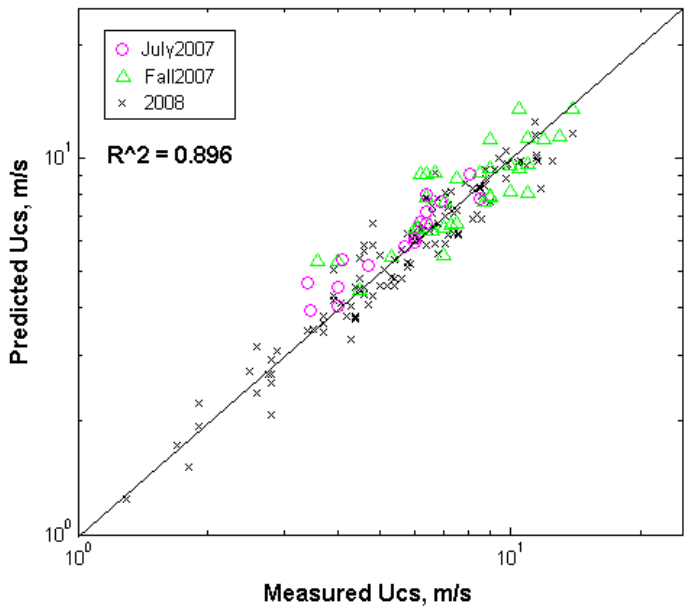

Figure 7.20. Log-Log Plot of Predicted Versus Measured U_{CS} (m/s) Values for the Nondimensional Model in Eq. (7.41). The 45-degree line represents perfect prediction where predicted U_{CS} values equal measured U_{CS} values.

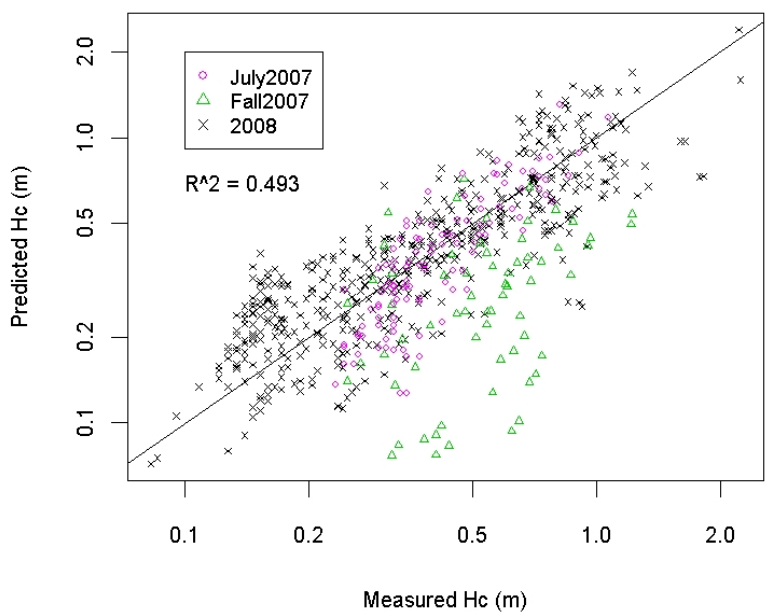

Figure 7.21. Log-Log Plot of Predicted Versus Measured H_C (m) Values for the Nondimensional Model in Eq. (7.43). The 45-degree line represents perfect prediction where predicted H_C values equal measured H_C values.

The statistical MR approach to modeling (described in Section 7.1.2) was also investigated as a way to develop models not affected by spurious correlations. The results from that approach are summarized in Section 7.4 and discussed in more detail in Appendix F.

7.3.3 Solids Vertical Distribution

Solids vertical concentration data (determined as described in Section 6.5) are shown in Figure 7.22. Profiles were taken at tank center. The data are from approximately 64 tests in all three scales, where for each test the solids vertical concentration data were averaged over five pulses. Also shown is the normalized average concentration at the tank bottom, $(C_0/\phi_S)(H_C/D)$, which is plotted as a function of Z/H_C. C_0 is the average concentration on the tank bottom, and Z is the elevation within the cloud.

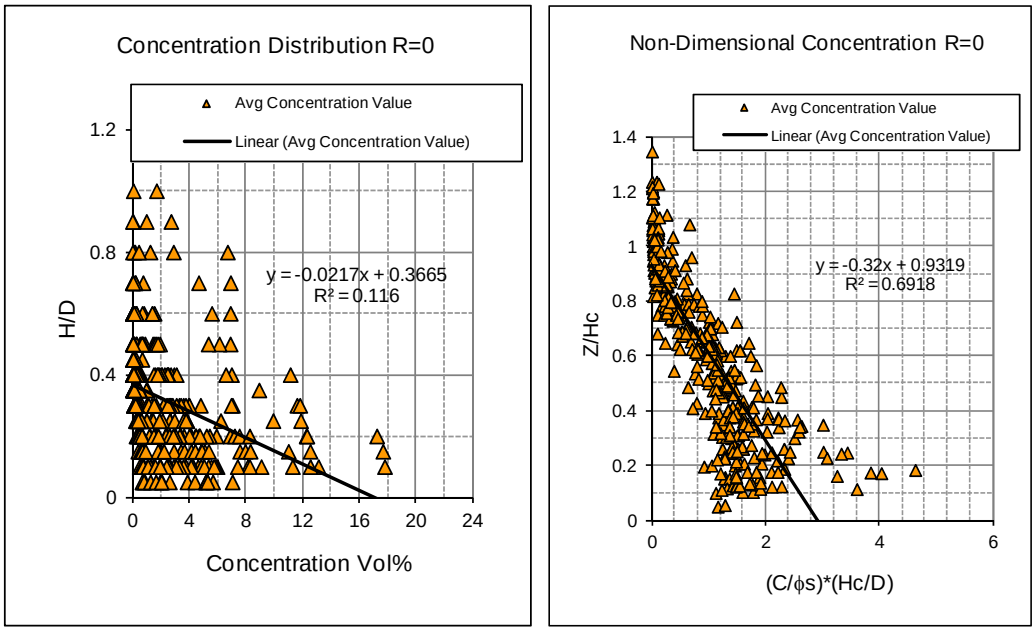

(a) (b)

Figure 7.22. Average Solids Vertical Distribution Data for All Tests; (a) Concentration as a Function of Elevation, (b) Normalized Profile for Estimating Concentration on Tank Bottom

If the area under a concentration profile is less than that of a linear curve, solids are either near or on the tank bottom or higher concentrations exist at other radial locations. Conversely, if the area is larger, the concentration is lower at larger radius. Actual radial variations in the concentration and departures from linear profiles over height are described and discussed in Section 6.0. Because such departures are complex and have not been estimated by separate models, here we assume a linear profile with height and a uniform radial profile throughout a cloud. Then the average concentration on the tank bottom is

$$C_0 = k\phi_S(H_C/D)^{-1} \tag{7.46}$$

where C_0 is in volume percent. For a fully homogenously mixed system with $C_0/\phi_S = H_C/D = 1$, k = 2 satisfies mass conservation for a linear profile from $C_0/\phi_S = 0$ at $H_C/D = 1$ to $C_0/\phi_S = 2$ at $H_C/D = 0$. The linear curve fit of the data, shown in Figure 7.22(b), gives k = 3 (linear curve fit intersects the abscissa, $Z/H_C = 0$, at approximately 3). The average maximum concentration data, as shown in Figure 7.23, indicate that the maximum concentration is significantly larger than the average concentration. This suggests the concentration on the bottom may be quite a bit higher than indicated by k = 3. Therefore, in applying Eq. (7.46), the concentration at the tank floor is estimated with k = 2.

Because we used a linear concentration profile with zero concentration at the elevation of H_C to determine C_0, we estimate the concentration at any elevation Z within the cloud to be

$$\begin{aligned} C(Z) &= C_0\,(1 - Z/H_C) \\ &= k\,\phi_S\,(H_C/D)^{-1}[1 - Z/H_C] \end{aligned} \tag{7.47}$$

where k = 2 was chosen as described above.

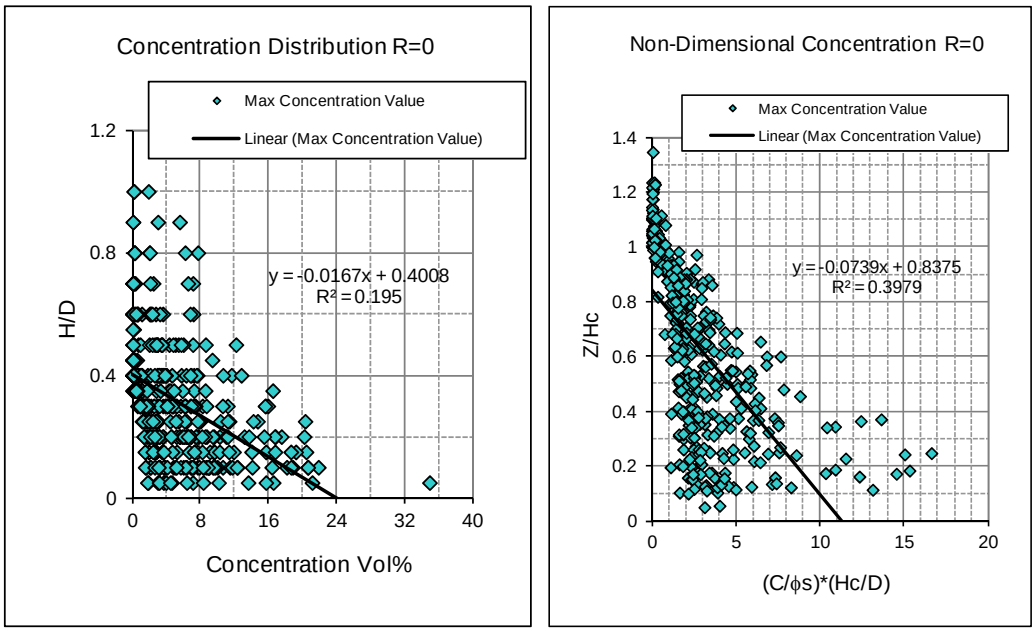

(a) (b)

Figure 7.23. Maximum Solids Vertical Distribution Data for all Tests; (a) Concentration as a Function of Elevation, (b) Normalized Profiles for Estimating Concentration on Tank Bottom

7.3.4 Summary of Physical Models

This section summarizes the physical models for U_{CS}, H_C, C_0, and C(Z) from Sections 7.3.2 and 7.3.3. For U_{CS}, expanding Eq. (7.43) and using Eq. (7.33) yields

$$U_{CS} = 2.220\,U_{TH}\left(\frac{D(s-1)g}{U_{TH}^{\,2}}\right)^{0.284}\phi_J^{\,-0.487}DC^{-0.284}\phi_S^{\,0.284}\phi_p^{\,-0.198}Ga^{-0.142} \tag{7.48}$$

Similarly for H_C, expanding Eq. (7.44) and using Eq. (7.40) yields

$$H_C = \frac{DC\cdot U_{TH}^{\,2}\phi_p^{\,0.698}\phi_J^{\,1.714}}{(s-1)g\phi_S}\cdot\exp\left[8.847\left(\frac{U}{U_{TH}}\right)^{0.131}\right] \tag{7.49}$$

The model for solids concentration on the vessel floor is obtained by substituting Eq. (7.49) into Eq. (7.46) with k = 2, which yields

$$C_0 = \frac{2D(s-1)g\phi_S{}^2}{DC \cdot U_{TH}{}^2 \phi_p{}^{0.698} \phi_J{}^{1.714}} \cdot \frac{1}{\exp\left[8.847\left(\frac{U}{U_{TH}}\right)^{0.131}\right]} . \tag{7.50}$$

Finally, the model for the solids concentration at height Z (m) assuming a linear profile is obtained by substituting Eq. (7.49) into Eq. (7.47) with k = 2, which gives

$$C(Z) = 2\phi_S \left\{ \frac{DC \cdot U_{TH}{}^2 \phi_p{}^{0.698} \phi_J{}^{1.714}}{D(s-1)g\phi_S} \cdot \exp\left[8.847\left(\frac{U}{U_{TH}}\right)^{0.131}\right] \right\}^{-1} \bullet \left[1 - \frac{Z}{\frac{DC \cdot U_{TH}{}^2 \phi_p{}^{0.698} \phi_J{}^{1.714}}{(s-1)g\phi_S} \cdot \exp\left[8.847\left(\frac{U}{U_{TH}}\right)^{0.131}\right]} \right] \tag{7.51}$$

The models for U_{CS} and H_C were obtained using plots of nondimensional variables, as described in Section 7.3.2. Better fitting models for U_{CS} and H_C [hence C_0 and C(Z)] are readily attainable by allowing the exponents on the terms involving (s−1), DC, ϕ_S, and Ga to be estimated from the experimental data. (The statistical MR models summarized in Section 7.4 and discussed in more detail in Appendix F are generally based on such generalizations of the physical models.) Additionally, a scale-up term for H_C can be added. It was these types of generalizations of the physical model that were investigated in Appendix F using the MR modeling approach.

The effects of dish geometry could also be included to improve the models, although the M3 testing data provide a limited basis for doing so (as discussed at the end of Section F.2.2 in Appendix F). Improvements to models could also be made by breaking the data set into subgroups. For example, the majority of M3 testing was performed with 12-tube arrays, and only a limited number of tests used 4- and 8-tube arrays. Further, functionality plots (Figures E.7 and E.23 in Appendix E) show that the dependence of U_{CS} and H_{CS} (and presumably also H_C) on the number of operating pulse tubes is not exactly a power-law relationship. Hence, a 12-tube-only data group could be used to develop models tailored for application to vessels HLP-22 and FRP-02 only. Such models would be expected to be better predictors for these 12-tube vessels because they were developed using these data only. Models for a subset of the data that eliminated subranges of some variables are discussed in Appendix F. However, that work did not consider the 12-tube-only subset.

Potential improvements to the models are discussed in more detail in Section 7.6.

7.4 Dimensional and Dimensionally Consistent Models for U_{CS} and H_C Developed Using the Statistical MR Approach

To provide direction for developing models for U_{CS} and H_C using the MR approach, functional dependencies of mixing response variables on test variables were investigated graphically, as described in Sections F.2.1 (U_{CS}) and F.3.1 (H_C) of Appendix F. The investigations concluded that functional dependencies for several test variables are well approximated by a power-law relationship. For a few test variables, a power-law relationship did not provide the best approximation but was adequate as a first-order approximation. Even in those cases the power-law relationship was adequate over most of the ranges of variables studied in M3 testing. There was not sufficient time or budget to develop the complicated models that would result from different forms of dependence of mixing response variables on test variables. Hence, model forms based on the power-law form were pursued.

As discussed in Section 7.1.2, statistical MR methods were used to develop and fit U_{CS} and H_C models to the experimental data. The statistical MR methods used are discussed in Appendix D. The results of graphically assessing the experimental data prior to developing MR models are presented in Appendix E. Appendix F contains a discussion of the approaches and results of fitting three kinds of models to the experimental data using MR:

- dimensional models without interaction terms
- dimensionally consistent models without interaction terms, subsequently referred to as generalized models
- dimensional models with two variable interaction terms.

The term interaction is used in the following way: Two variables interact if the effect on the response variable (e.g., U_{CS} or H_C) of one variable depends on the value of the second variable. Each of the three types of models listed in the bullets is further discussed for U_{CS} and H_C in the following subsections.

All three kinds of models (for each of U_{CS} and H_C) were fit by MR to two data sets, referred to as the full data set and the trimmed data set. These two data sets are discussed in Appendix F, Section F.1.1. The full data set included all relevant data points (173 test conditions) for U_{CS} and H_C as discussed in Section 7.3.2. Only data with $U \geq U_{CS}$ were used to model H_C. The trimmed data set excludes data with DC > 0.41 (which eliminates 11 of 173 test conditions), $\phi_S > 0.016$ (which eliminates 7 of 173 test conditions), and d_S (d_{50}) > 1.8E-04 (which eliminates 1 of 173 test conditions). The functional dependence of U_{CS} and/or H_C on these three predictor variables was observed to change within the excluded ranges. It was expected that more accurate models with less uncertainty could be obtained over the trimmed data set; however, models over the full data set (the one used to develop the physical models in Sections 7.3.2 to 7.3.4) are of primary interest. Thus, only the models fit to the full data set are discussed in the remainder of Section 7.4. Models fit to the trimmed data set are discussed in Appendix F.

The U_{CS} and H_C models developed using the full data set with the statistical MR approach are described in Sections 7.4.1 to 7.4.3. Although it was not done for this report, any of the statistical MR models for H_C could be used with the approach discussed in Section 7.3.3 for modeling C(Z) and C_0.

7.4.1 Development of U_{CS} and H_C Dimensional Models Without Interaction Terms

The dimensional models for U_{CS} and H_C were developed as follows. The nondimensional variables on both sides of the U_{CS} and H_C nondimensional models of Section 7.3.2 to 7.3.4 were expressed in terms of their separate component test variables. These model forms were next rewritten with only the response variable (U_{CS} or H_C) on the left side of the model and the predictor variables on the right. Then the terms for each test variable were collected, and each collected term was assigned a coefficient to be estimated from the data using MR. By assigning a separate coefficient for each predictor variable, we obtained a generalized form of the physical model on which it was based. The results from fitting the resulting model forms to the experimental data are summarized here with references to Appendix F, where more detail can be found.

7.4.1.1 U_{CS} Dimensional Models without Interaction Terms

The dimensional model forms without interaction terms for U_{CS} are listed as Eq. (F.8a) and (F.8b) in Appendix F. Sections F.2.2 and F.2.4.1 discuss how these U_{CS} model forms were developed. In addition, Section F.3.1 contains an explanation of why MR software was used to fit Eq. (F.8b) instead of Eq. (F.8a) to experimental data. The results of fitting Eq. (F.8b) to the full data set are given in Table F.1 and discussed in Section F.2.4.2. The predicted-versus-measured (PvM) plot (Section D.3.2 of Appendix D) showing the goodness of fit of the U_{CS} dimensional model form without interactions to the full data set is presented as Figure F.2.

The resulting U_{CS} dimensional models without interaction terms for the full data set, in Eq. (F.11a) and (F.11b) in Appendix F, are

$$\begin{aligned} U_{CS} &= 0.309\,(D)^{1.321}(s-1)^{0.471}(\phi_S)^{0.222}(U_T)^{0.148}(DC)^{-0.247}(\phi_p)^{-0.211} \\ &\quad \times (N_J)^{-0.525}(d)^{-1.072} \end{aligned} \tag{7.52a}$$

and

$$\begin{aligned} \ln(U_{CS}) &= -1.173 + 1.321\ln(D) + 0.471\ln(s-1) + 0.222\ln(\phi_S) + 0.148\ln(U_T) \\ &\quad - 0.247\ln(DC) - 0.211\ln(\phi_p) - 0.525\ln(N_J) - 1.072\ln(d)\,. \end{aligned} \tag{7.52b}$$

The U_{CS} dimensional model was fit to the full data set in the form of Eq. (7.52b) and also used to calculate model prediction uncertainties. It is also useful to view the U_{CS} model in the Eq. (7.52a) form. The PvM plot for these models from Figure F.2 is reproduced in Figure 7.24. The $R^2 = 0.913$ value indicates that the model accounts for 91.3% of the variation in the $\ln(U_{CS})$ values for the full data set.

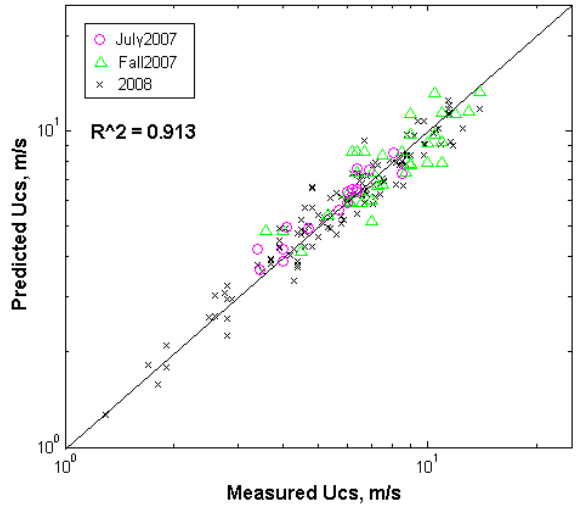

Figure 7.24. Log-Log Plot of Predicted Versus Measured U_{CS} (m/s) Values for the Nine-Term Dimensional Model in Eq. (7.52b) Fit to Full Data Set. The 45-degree line represents perfect prediction where predicted equal measured U_{CS} values. The R^2 value was calculated using predicted and measured values of $\ln(U_{CS})$.

The exponents in Eq. (7.52a) for the U_{CS} dimensional model agree qualitatively with those in Eq. (7.30) for the U_{CS} physical model if the settling number is assumed to be constant.

7.4.1.2 H_C Dimensional Models Without Interaction Terms

The dimensional model forms without interaction terms for H_C are listed as Eq. (F.21a) and (F.21b) in Appendix F. Sections F.3.2 and F.3.4.1 discuss how these H_C model forms were developed. The results of fitting Eq. (F.22b) to the full data set are given in Table F.8 and discussed in Section F.3.4.2 of Appendix F. The PvM plots showing the goodness of fit of the H_C dimensional model form without interactions to the full data set is given in Figure F.9.

The resulting H_C dimensional models without interaction terms for the full data set, listed in Eq. (F.24a) and (F.24b) in Appendix F, are

$$\begin{aligned} H_C &= 1.079\,(D)^{-1.191}(s-1)^{-0.836}(\phi_S)^{-0.623}(1-\phi_S)^{-17.502}(U_T)^{-0.412}(DC)^{0.371} \\ &\quad \times (\phi_p)^{0.218}(N_J)^{0.330}(d)^{1.722}(U)^{1.378} \end{aligned} \tag{7.53a}$$

and

$$\begin{aligned} \ln(H_C) &= 0.076 - 1.191\ln(D) - 0.836\ln(s-1) - 0.623\ln(\phi_S) - 17.502\ln(1-\phi_S) \\ &\quad - 0.412\ln(U_T) + 0.371\ln(DC) + 0.218\ln(\phi_p) + 0.330\ln(N_J) + 1.722\ln(d) \\ &\quad + 1.378\ln(U)\,. \end{aligned} \tag{7.53b}$$

The H_C dimensional model was fit to the full data set in the form of Eq. (7.53b) and also used to calculate model prediction uncertainties. It is also useful to view the H_C dimensional model in the Eq. (7.53a) form. The PvM plot for these models from Figure F.9 is reproduced in Figure 7.25. The $R^2 = 0.830$ value indicates the model accounts for 83% of the variation in the $\ln(H_C)$ values for the full data set.

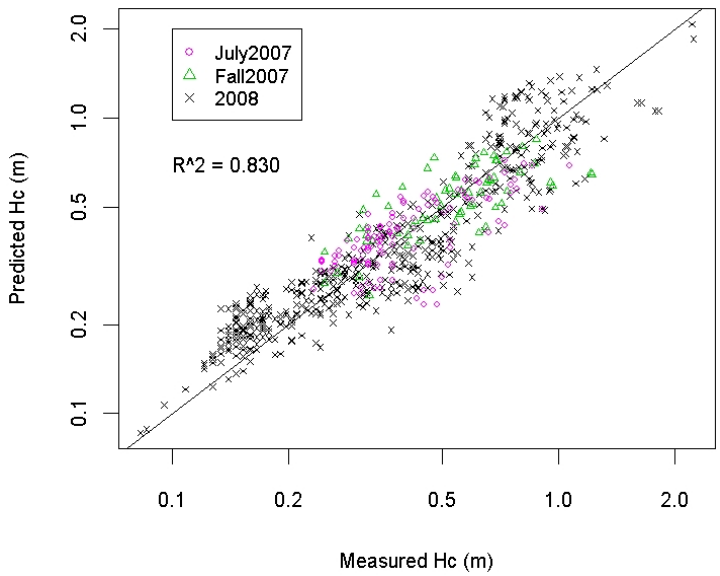

Figure 7.25. Log-Log Plot of Predicted Versus Measured H_C for 11-Term Dimensional Model in Eq. (7.53b) Fit to Full Data Set. The 45-degree line represents perfect prediction where predicted equal measured H_C; R^2 was calculated using predicted and measured $\ln(H_C)$.

The large negative coefficient of -17.502 on the $(1-\phi_S)$ term in Eq. (7.53a) and (7.53b) requires some explanation because it stands out from other coefficients. As seen in Table F.8 of Appendix F, this term in the H_C models is highly statistically significant. Having both ϕ_S and $(1-\phi_S)$ terms in Eq. (7.53a) and (7.53b) serves to model the curvature effect of ϕ_S on H_C. This curvature can be seen in the functionality plot of ϕ_S for H_{CS} in Figure E.28 of Appendix E. A model like Eq. (7.53b), but fit without the $(1-\phi_S)$ term, show biased predictions of H_C for $\phi_S > 0.015$. Finally, when the coefficient -17.502 is combined with $(1-\phi_S)$ values in the M3 test data set (ranging from 0.94 to 0.9995), the range of contributions of this term to model predictions is smaller than for several other model terms. Hence, the $(1-\phi_S)^{-17.502}$ and $-17.502(1-\phi_S)$ terms in Eq. (7.53a) and (7.53b) are appropriate for the range of ϕ_S studied in M3 testing. However, caution is advised if these H_C models need to be extrapolated to ϕ_S values outside the range of M3 testing.

7.4.2 U_{CS} and H_C Dimensionally Consistent (Generalized) Models

The dimensional model forms for U_{CS} and H_C in Eq. (F.46a) and (F.47a), respectively, may be dimensionally consistent only through attaching the correct units to the constant term. Dimensionally consistent models with a dimensionless constant term may be preferred. Hence, dimensionally consistent versions of the dimensional models for U_{CS} and H_C were developed. The intent was to achieve dimensional consistency while maintaining, to the extent possible, the generalizations of the U_{CS} and H_C dimensional models compared to the nondimensional models in Sections 7.3.2 to 7.3.4. This was accomplished by grouping the dimensional predictor variables to form dimensionless predictor variables so that the model constant is dimensionless. For ease of subsequent discussion, the dimensionally consistent models without interaction terms are henceforth referred to as the *generalized models*.

7.4.2.1 U_{CS} Generalized Models

The generalized model forms for U_{CS} are listed as Eq. (F.9a) and (F.9b) in Section F.2.4.1 of Appendix F. That section discusses how these U_{CS} model forms were developed. The results of fitting Eq. (F.9b) to the full data set are given in Table F.3 and discussed in Section F.2.4.3. The predicted versus modeled (PvM) plot showing the goodness of fit of the U_{CS} generalized model form to the full data set is given in Figure F.4.

The resulting U_{CS} generalized models for the full data set, listed in Eq. (F.13a) and (F.13b) of Appendix F, are

$$U_{CS} = 0.273\, U_T \left(\frac{D(s-1)g}{U_T^2}\right)^{0.397} \left(\frac{d}{D}\right)^{-0.991} (s-1)^{0.086}\, DC^{-0.205}\, \phi_S^{0.243}\, \phi_p^{-0.221}\, N_J^{-0.511} \tag{7.54a}$$

and

$$\ln(U_{CS}) = -1.297 + \ln(U_T) + 0.397 \ln\left(\frac{D(s-1)g}{U_T^2}\right) - 0.991 \ln\left(\frac{d}{D}\right) + 0.086 \ln(s-1) \tag{7.54b}$$
$$- 0.205 \ln(DC) + 0.243 \ln(\phi_S) - 0.221 \ln(\phi_p) - 0.511 \ln(N_J)$$

The U_{CS} generalized model was fit to the full data set in the form of Eq. (7.54b). However, it is also useful to view the U_{CS} model in the Eq. (7.54a) form. The PvM plot for these models from Figure F.4 is reproduced in Figure 7.26 for convenience. The $R^2 = 0.867$ value indicates that the generalized model accounts for 86.7% of the variation in the $\ln(U_{CS})$ values for the full data set. This is somewhat less than the 91.3% accounted for by the U_{CS} dimensional model without interaction terms. As discussed in Section F.2.4, this suggests that the generalized model form may not represent the dependence of U_{CS} on U_T as well as the dimensional model without interaction terms. However, the advantage of Eq. (7.54a) and (7.54b) being based on physically interpretable, nondimensional variables may be considered an advantage for extrapolative application of the model.

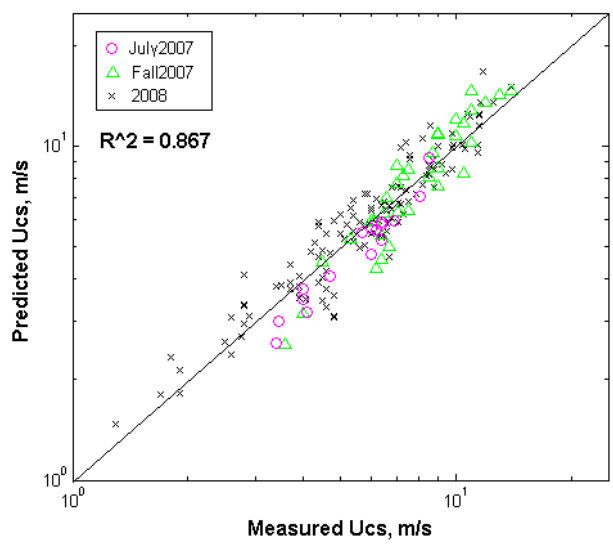

Figure 7.26. Log-Log Plot of PvM U_{CS} (m/s) Values for the Nine-Term Generalized Model in Eq. (7.54b) with Eight Coefficients Fit to Full Data Set. The 45-degree line represents perfect prediction where predicted and measured U_{CS} values are equal. The R^2 value was calculated using predicted and measured values of $\ln(U_{CS})$.

7.4.2.2 H_C Generalized Models

The generalized model forms for H_C are listed as Eq. (F.22a) and (F.22b) in Appendix F. Section F.3.4.1 discusses how these H_C model forms were developed. The results of fitting Eq. (F.22b) to the full data set are given in Table F.10 and discussed in Section F.3.4.3 of Appendix F. The PvM plot showing the goodness of fit of the H_C generalized model form to the full data set is given in Figure F.11.

The resulting H_C generalized models for the full data set, listed in Eq. (F.26a) and (F.26b) in Appendix F, are

$$H_C = 3.040\, D \left(\frac{U^2}{D(s-1)g}\right)^{0.473} \left(\frac{d}{D}\right)^{1.693} (s-1)^{-0.356} \left(\frac{U_T}{U}\right)^{-0.410} DC^{0.364} \times \phi_S^{-0.616} (1-\phi_s)^{-17.206}\, \phi_p^{0.213}\, N_J^{0.320} \tag{7.55a}$$

and

$$\ln(H_C) = 1.112 + \ln(D) + 0.473 \ln\left(\frac{U^2}{D(s-1)g}\right) + 1.693 \ln\left(\frac{d}{D}\right) - 0.356 \ln(s-1) - 0.410 \ln\left(\frac{U_T}{U}\right) + 0.364 \ln(DC) - 0.616 \ln(\phi_S) - 17.206 \ln(1-\phi_S) + 0.213 \ln(\phi_p) + 0.320 \ln(N_J) \tag{7.55b}$$

The H_C generalized model was fit to the full data set in Eq. (7.55b). However, it is also useful to view the H_C dimensionally consistent model in the Eq. (7.55a) form. The PvM plot for these models from Figure F.11 is reproduced in Figure 7.27. The $R^2 = 0.830$ value indicates the H_C generalized model accounts for 83% of the variation in the $\ln(H_C)$ values for the full data set. This matches the H_C dimensional model without interactions, which is nearly dimensionally consistent, as discussed in Section F.3.4.3.

The large negative coefficient of -17.206 on the $(1-\phi_S)$ term in Eq. (7.55a) and (7.55b) requires some explanation because it stands out from other coefficients. As seen in Table F.10 of Appendix F, this term in the H_C models is highly statistically significant. Other justification for this term is similar to that discussed at the end of Section 7.4.1.2.

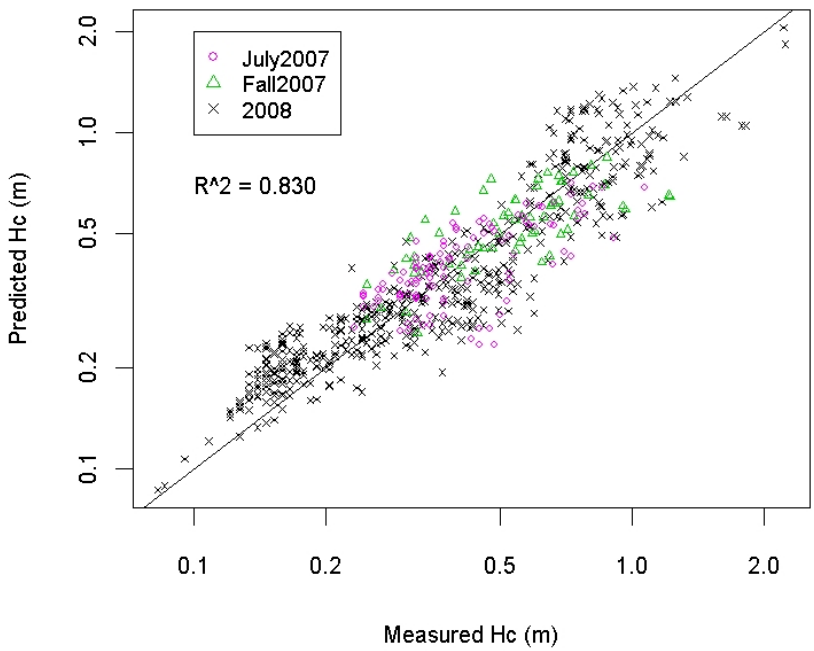

Figure 7.27. Log-Log Plot of PvM H_C (m) Values for the 11-Term Generalized Model in Eq. (7.55b) with 10 Coefficients Fit to the Full Data Set. The 45-degree line represents perfect prediction where predicted equal measured H_C values. The R^2 value was calculated using predicted and measured values of $\ln(H_C)$.

7.4.3 U_{CS} and H_C Dimensional Models with Interaction Terms

The method used to add interactions to the U_{CS} and H_C dimensional model forms and the results of fitting these model forms to the full and trimmed data sets are discussed in Sections F.2.5 and F.3.5 of Appendix F. Adding interaction terms moderately improved the interpolative prediction performance of the dimensional models without interaction terms. However, extrapolative use of models with interaction terms can yield significantly inaccurate predictions. Hence, it is recommended the dimensional models with interaction terms be limited to interpolative use within the region of conditions covered during experimental testing (see Section F.5 of Appendix F).

7.5 Comparing Physical, Dimensional, and Generalized Models for U_{CS} and H_C

The abilities of the U_{CS} and H_C models (physical, dimensional without interactions, generalized, and dimensional with interactions) to predict the U_{CS} and H_C full data sets are now assessed by comparing the model R^2 values and PvM plots. Recall that the full data sets for U_{CS} and H_C were used to develop and fit the models; thus, using the same data to assess their performance consists of model evaluation rather than model validation. Leave-one-out cross-validation of the dimensional models without and with interactions using the full data set was performed via the R_P^2 statistic [see Appendix F, Sections F.2.4.2 and F.2.5 (U_{CS}) and Sections F.3.4.2 and F.3.5 (H_C)]. Validation (benchmarking) of the physical and generalized models is discussed in Section 8.0.

Table 7.4 lists the R^2 values and locations of the PvM plots for each of the U_{CS} and H_C models fit to the full data sets for U_{CS} and H_C (described in Section 7.3.2 and Section F.1.1 of Appendix F). Table 7.4 shows that the U_{CS} and H_C dimensional models with interactions have the highest R^2 values. However, as noted in Section 7.4.3, and discussed more in Sections F.2.5 and F.3.5 of Appendix F, models with interaction terms should only be used for extrapolative predictions after substantial extrapolative validation. Because such validation work has not been performed, the dimensional models with interaction terms should only be used for interpolative predictions inside the test-variable region experimentally investigated during M3 testing.

Table 7.4. Basis for Comparing U_{CS} and H_C Models Fit to the Full Data Sets

Model Type	U_{CS} Model		H_C Model	
	R^2	PvM Plot(a)	R^2	PvM Plot
Physical	0.896	Figure 7.20 Figure F.8	0.493	Figure 7.21 Figure F.15
Dimensional without interactions	0.913	Figure 7.24 Figure F.2	0.830	Figure 7.25 Figure F.9
Generalized (dimensionally consistent without interactions)	0.867	Figure 7.26 Figure F.4	0.830	Figure 7.27 Figure F.11
Dimensional with interactions	0.939	Figure F.6	0.861	Figure F.13

For U_{CS}, the dimensional model without interactions fits the full data set the best, followed by the physical model, and finally the generalized model. A choice among these models should depend on their performance in benchmarking (validation) work, as well as subject matter knowledge and expectations regarding how appropriate each model is for extrapolative prediction.

For H_C, the dimensional model without interaction terms and the generalized model are essentially equivalent, because the former is nearly dimensionally consistent without restricting the model to be so. Hence, either one of these models could be used. The physical model for H_C does not predict the full data set as well as the other two models.

The benchmarking performance of the physical and generalized models for each of U_{CS} and H_C are compared in Section 8.0. These models were selected for additional investigation because they both use nondimensional variables as predictor variables and thus each have a physical basis for interpretation.

7.6 Possible Model Improvements

Possible improvements to the physical and generalized models are discussed in Sections 7.6.1 and 7.6.2, respectively. Section 7.6.3 makes some concluding remarks regarding possible model improvements.

7.6.1 Possible Improvements to Physical Models

The physical models for U_{CS} and H_C were obtained by plotting basic nondimensional variables with fewer coefficients estimated from the data (using model fitting methods) than the MR models. Various additional physical models were explored. These are briefly described and discussed here.

Better parameter fits: By allowing the exponents on (s-1), DC, ϕ_S, and Ga to vary, better-fitting models were achieved. The models were improved further by introducing additional terms such as (1-DC) and $(1-\phi_p)$.

Including dish geometry: When different dish geometries are accounted for by an adjustable leading constant, improvement in the model fits is achieved. This is particularly true for data points from testing in the mid-scale (34-in.) tank.

Limited data sets and parameter ranges: Improvements could also be made by breaking the data set into subgroups and fitting separate models for each. For example, a 12-tube-only data group (which makes up the vast majority of M3 testing data) and models could be developed for application to the HLP-22 and FRP-02 vessels. Further improvements could be achieved by limiting some of the variable ranges such as DC < 0.4 and $\phi_S \leq 0.015$.

Including scale term for cloud height: Several different approaches to introducing the effect of scale into the cloud height model were explored. These include Reynolds number based jet diameter, Re, Reynolds number based on tank diameter (Re_D), nondimensional critical suspension parameter D*, and Froude number based on tank diameter (F_D). The best model fit to the data is achieved when both D* and Re are used. This is reasonable because Re is not so much a scale-up term as a way of capturing the effect of the jet turbulence level. We expect some jet Reynolds number effect to be present in the data taken from the small-scale (15-in.) tank. Hence it is reasonable that the model fit would be improved by inclusion of the term. However, we also expect there to be little or no Re effect for large-scale vessels. So while inclusion of Re provides a better data fit, it probably does not provide more accurate predictions at large scale.

Accounting for vertical solids entrainment: The slight curvature seen in the cloud height data in Figures 7.19 and 7.20 is likely due to the vertical entrainment effect of the closed loop pump returns. When the settling velocity is small, U/U_{TH} becomes large and the potential for entrainment is high. This is consistent with the slight upward curvature observed when H_C* is plotted versus U/U_{TH}.

Prototypic PJMs induce a periodic bulk vertical motion, which on average has zero velocity, so the average level remains stationary. The test apparatus used a closed-loop pump system where the drive phase was achieved by opening a valve, and refill was modeled by simply closing the valve. The absence of the refill contribution results in a net upward vertical displacement of the bulk fluid during each drive cycle. The effective average vertical velocity induced (U_V) is

$$U_V = \phi_J \, DC \, U \tag{7.56}$$

which will affect the test results if it is comparable to the settling velocity. To account for this effect, we introduce the modified setting velocity, U'_{TH}:

$$U'_{TH} = U_{TH} - U_v \tag{7.57}$$

given by

$$\frac{U}{U'_{TH}} = \frac{U}{U_{TH}(1 - \phi_J DC \frac{U}{U_{TH}})} \tag{7.58}$$

Very good data fits were achieved for both H_C and U_{CS} when the effective settling velocity was used instead of U_{TH}, and the effect of scale was included through D* and Re. The model fits to the data had an R^2 of 0.97 for U_{CS} and 0.93 for H_C. While this approach gives very good fits to the test data, it produces some unrealistic results when applied at plant scale, where the effective settling velocity is replaced with the regular settling velocity. This suggests that not all of the curvature in the cloud height data is due to the vertical entrainment effect. It is therefore not possible to know the exact magnitude of the vertical entrainment without performing tests with prototypic drive systems.

7.6.2 Possible Improvements to Generalized Models

As discussed in Sections F.2.1 and F.3.1 of Appendix F, a power-law relationship was deemed best or adequate (for a first-order approximation) for statistically modeling the dependence of U_{CS} and H_C on the primary M3 test variables. However, that discussion also indicated that improvements to statistical MR models (as well as physical models) are possible by considering relationship forms other than the power-law for different test variables.

Based on the functionality plots for U_{CS} in Figures E.6 to E.16, test variables for which non-power-law relationships may be beneficial are N_J (the number of operating jets), DC > 0.33 for some conditions, and $\phi_S > 0.015$. Based on the functionality plots in Figures E.17 to E.32 for H_{CS}, test variables for which non-power-law relationships may be beneficial are N_J (the number of operating jets), $\phi_S > 0.015$, and the smallest and largest values of d_S and U_T (for which very few tests were performed).

Other improvements discussed in Section 7.6.1, such including a dish geometry term, fitting models to subgroups of the data, and accounting for vertical solids entrainment, are also possibilities for improving statistical MR models.

Finally, a response surface methodology approach to developing polynomial-type models was investigated for U_{CS} and H_C, but it did not lead to improved models. See Sections F.2.1 and F.3.1 of Appendix F for additional discussion of this topic.

7.7 Conclusions Regarding Possible Model Improvements

All of the improvements discussed in Sections 7.6.1 and 7.6.2 would result in better-fitting models. The physical approach used to develop the models discussed in Section 7.3 was based on the philosophy that the simplest explanation consistent with data supersedes any more complicated explanation. Given the overall uncertainty and the primary desire of the WTP project to rate and evaluate all of the plant

vessels, it is not clear whether the predictive capability of a better-fitting model would be an improvement. As the complexity of a model form is increased to improve the fit when interpolating, there may be less confidence the form remains valid when extrapolating. However, some model improvements could improve model extrapolation as well as interpolation performance. For example, this appears to be the case for the H_C model developed by the generalized approach, which significantly improves on the H_C model developed by the physical approach (compare Figures 7.21 and 7.27). Ultimately, it was decided to investigate both the physical and generalized models for U_{CS} and H_C in Sections 8.0 and 9.0.

It is envisioned that there are ways to improve the models (as discussed in Section 7.6) that would be beneficial for interpolative as well as extrapolative prediction performance. However, per direction from the WTP project, no model improvement efforts were to be conducted as part of revising the report to address formal comments. Such model-improvement efforts are left to future work if it is determined improved models are needed for WTP applications.

7.8 Updates to Models Since Initial Document Release

Work on refinements to the PJM models continued after publication of Rev. 0 of this document. These have focused on the physical model, however, consideration should be given to similar refinements in other models in future work. These model refinements were published in Fort et al. (2010), Meyer et al. (2010), and Bamberger et al. (2011). Note that in Bamberger et al (2011) there is an error in the cloud height correlation: the exponent on ϕ_p should be corrected from 0.539 to 0.898.

8.0 Applicability and Benchmarking of Mixing Models

This section addresses the applicability of the mixing models presented in Section 7.0 to the WTP mixing systems. Section 8.1 addresses how the work accounted for prototypic geometries, operation, and slurry properties. Section 8.2 discusses the sources of uncertainty, bias, and margin. Finally, Section 8.3 provides the results of some benchmarking exercises where the mixing models were applied and the results compared to data from previous testing in prototypic PJM systems and as well as calculations from some CFD simulations.

8.1 Accounting for Prototypic Conditions

The testing equipment used to produce the data for this report had some features that were not prototypic of PJM mixing designs, and some of the differences would be expected to affect the data. This section discusses how the departures from prototypic designs would be manifested in the data and what accommodations or adjustments were made.

8.1.1 Geometry and Operation

The geometry and operational aspects of the M3 test program that were different from prototypic PJM operation are discussed in the following:

- *Jet slurry density*: The jet slurry density during discharge will be higher with prototypic PJMs than with the pulse tubes tested, which discharged liquid only. Actual densities will be 5 to 10% higher with slurry being discharged from the PJM, as long as the designs are able to suspend solids.[1] To estimate the effect of higher jet density, we can examine the effect of increased liquid density on U_{CS} and H_C. For typical conditions, a 5% increase in density increases U_{CS} by about 1% and decreases H_C by about 3%; hence, the effect of applying the models to prototypic systems which discharge slurries should be minor.
- *Suction effects*: The flow field resulting from suction during the PJM refill has little effect on the mixing within the vessel. The induced velocity during suction at some distance (z) from the nozzle (with diameter, d) decreases away from the nozzle in proportion to $(d/z)^2$, whereas during discharge the velocity decreases by (d/z). When the relationship between drive and refill flow rates are considered, the ratio of the suction velocity to the jet velocity is approximately $[DC/(1-DC)](d/z)^2$, where DC is the duty cycle. For a 10.2-cm (4-in.) nozzle and a 33% DC, the ratio is 0.02 at 50.8 cm (20 in.) from the nozzle. The suction-induced flow field becomes larger closer to the nozzle. However, the area closest to the nozzle is also the area most impacted by the jet flow. Thus, the effect should be negligible of disregarding the suction-induced flow field in applying the models to prototypic systems which have refill suction.
- *Nozzle geometry*: Prototypic PJMs have conical nozzles, unlike the straight nozzles used for testing. The effect of nozzle geometry was explored by BNI using the FLUENT[2] CFD model. Floor shear

[1] Actual jet density may be much higher for designs that are unable to suspend solids well. Hence high densities would be associated with inadequate designs and the effect of higher jet densities would only exacerbate problems in those vessels. For vessels that mix well, the impact of this approximation would be relatively small.
[2] http://www.fluent.com/.

stress profiles were computed for both nozzle types. While there was some difference near the nozzle, far from the nozzle the differences were negligible. This finding is consistent with the well-accepted observation that the detail of nozzle cross-section geometry is lost far from the orifice, with the hydraulic diameter being the controlling parameter. The effect of applying the models to prototypic systems that have conical nozzles should thus be negligible.

- *Pulse Tube Outer Diameter*: Prototypic pulse tubes have much larger diameters than the straight pipes used during testing. There are two potential effects of this simplification to consider, flow-field effects and volumetric displacement effects. The effect of pulse tube diameter on the overall flow-field in the vessel should be negligible. For off-bottom suspension, the primary flow is at the vessel bottom, beneath the nozzles, and is therefore unaffected by pulse tube diameter. For solids vertical distribution, the upwelling flow is important. The primary vertical flow occurs at the center of the vessel, with lesser upwells occurring between adjacent pulse tubes, particularly for the 12-tube designs. A useful parameter to consider is

$$\phi_{PT} = N(D_{PT}/D)^2, \tag{8.1}$$

  the ratio of total pulse tube cross-sectional area to the vessel cross-sectional area. For the plant vessels, this ratio varies from 0.063 for HOP-903/904 to 0.214 for TCP-01. For HLP-22 the value is 0.168. If the upwelling flow was uniform and confined by the vessel diameter, the effect of an area reduction equivalent to this ratio would result in velocities increased by $(1- \phi_{PT})^{-1}$, corresponding to a velocity increase of about 20% for HLP-22. However, the upwell flows are not uniform over the vessel diameter. The width of the upwell flows scale with nozzle diameter and are therefore much smaller than the vessel diameter. Hence, it is expected that actual increased upwell velocity associated with prototypic pulse tube outer diameters is much smaller than $(1- \phi_{PT})^{-1}$.

  The potential magnitude of the displacement effect associated with pulse tube diameter can be estimated by the derivation leading to the definition of H_C^* given by Eq. (7.32). When considering the displaced volume associated with pulse tube diameter, the slurry mass in Eq. (7.26) is multiplied by $(1- \phi_{PT})$. This results in the nondimensional cloud height parameter H_C^* given by Eq. (7.32) being multiplied by $(1- \phi_{PT})$ and suggests actual clouds could be increased by a factor of $(1- \phi_{PT})^{-1}$ due to the displacement effect of pulse tube outer diameter.

- *Solids vertical entrainment*: The vertical entrainment effect associated with the closed loop operation of the test apparatus was discussed in Section 7.6 and pictured in Figure 8.1. The effect suggests that predicted cloud height for plant vessels will be lower than that predicted by the correlations, which were based on data from tests with entrainment. The modified settling velocity introduced in Section 7.6 can be used to estimate the magnitude of the potential effect in terms of an effective settling velocity. The term $(1-\phi_J DCU/U_{TH})$ in Eq. (7.58) can be interpreted as the correction factor required to apply to the prototypic settling velocity to account for the entrainment effect. For example, for conditions corresponding to HLP-22 and taking U_{TH} to be 1 cm/s, the correction factor is ~0.63, implying that the predicted result would be relevant for a slurry with settling velocity of 0.63 cm/s. Conversely, a settling velocity of 1.57 cm/s would be used in the correlation to predict the cloud height for a slurry with an actual settling velocity of 1 cm/s.

In summary, the effects of vertical entrainment associated with the nonprototypic drive system can be accounted for by modifying the settling velocity in the rating equations according to Eq. (7.58).

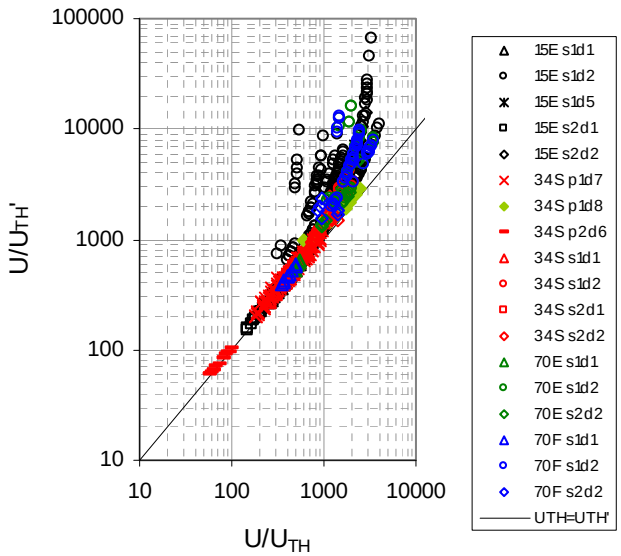

Figure 8.1. Effective Settling Velocity Associated with Vertical Entrainment from Pump Suction Returns (FIO)

8.1.2 Accounting for Prototypic Fill Level

The results of Hicks, which were discussed in Section 2.0, demonstrated that U_{CS} is insensitive to fill level when the solids loading is based on a reference volume and not the slurry volume. Similarly, cloud height is also insensitive to fill level as long as the cloud is below the fill level. It follows therefore that solids vertical distribution is also independent of fill level as long as the cloud is below the fill level. However, once the cloud reaches the fill level, the solids vertical distribution will depend on the fill level.

The cloud height models (physical and generalized) developed from the test data can be accurately used to predict cloud height. If the model produces a cloud height that exceeds the fill level, this application is obviously not physical. In this case the predicted cloud height is simply the fill level. However, the concentration profile will not be accurately predicted by the model and an adjustment is required.

We handle the effect of fill level (H_F)on solids concentration in the following way:

- When using a physical or generalized model to determine H_C, if $H_C \leq H_F$ the result is valid, and the concentration at the floor, C_0, is estimated by the linear concentration profile model, C(Z) (Eq. 7.47), as developed in Section 7.3.3:

$$\frac{C_0}{\phi_S} = \frac{k}{H_C / D} \tag{8.2}$$

- For predicted $H_C > H_F$, we set $H_C = H_F$, the fill height, as shown in Figure 8.2. Then a corrected C_0 is determined from this value of H_C by matching both the total mass and the concentration gradient.

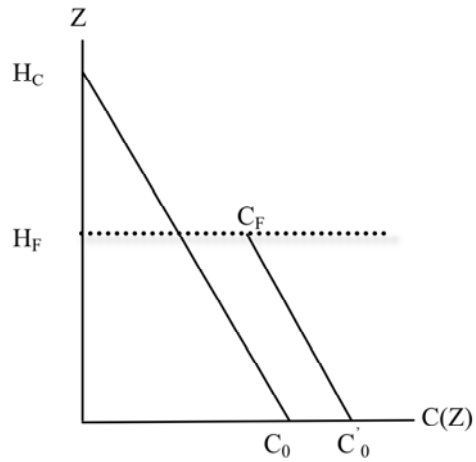

Figure 8.2. Illustration of How Finite Fill Level Affects Maximum Concentration

- Using k = 2 for a linear distribution that conserves mass (Section 7.3.3), the equation for the corrected average solids concentration at the floor ($C_0^{'}$) is given by

$$\frac{C_0^{'}}{\phi_S} = \frac{1}{H_F / D} + \frac{1}{4}\left(\frac{C_0}{\phi_S}\right)^2 \frac{H_F}{D} \tag{8.3}$$

- The associated equation for average concentration at the fill height (C_F) is given by

$$\frac{C_F}{\phi_S} = \frac{1}{H_F / D} - \frac{1}{4}\left(\frac{C_0}{\phi_S}\right)^2 \frac{H_F}{D} \tag{8.4}$$

In both Eq. (8.3) and Eq. (8.4), C_0 is the concentration at the floor given by Eq. (8.2) using the initial prediction of cloud height.

8.1.3 Accounting for Distributions of Particle Size and Density

One of the advantages of using the settling velocity in the mixing models is that it has a consistent physical meaning regardless of the size distribution of the solids. For a slurry that is well mixed such that no stratification in particle size or density exists, the volume-weighted average settling velocity ($\overline{U}$) is a good representation of the actual settling. (See Section 3.0 for a discussion of volume-weighted averages and terminology). This well-mixed condition is illustrated in Figure 8.3(a). Also shown in Figure 8.3(b) is the same slurry with some degree of stratification. The average settling velocity near the bottom of the vessel will be much higher than that near the top if significant stratification is present. Because of this, we expect that the characteristic settling velocity that best represents mixing performance is one that describes the faster settling part of the size distribution ($U_T > \overline{U}$, e.g., U_{90}, U_{95}, etc.). Therefore, for slurries with particle size distributions, the appropriate settling velocity for evaluating the sufficiency of a PJM operating with certain system parameters must be significantly larger than the nominal volume-fraction-averaged settling velocity, which itself is significantly larger than the median settling velocity. (For example, see

Table 9.6, comparing the 50th percentile velocity to the volume-weighted average.) This is reasonable given the physical process involved and is consistent with some industrial experience.

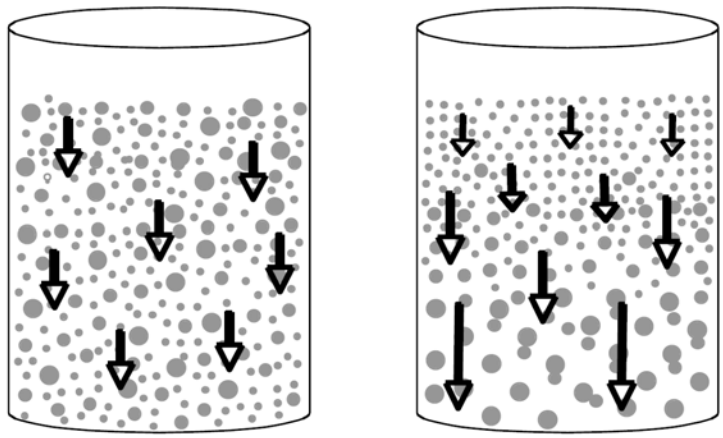

Figure 8.3. Illustration of How Stratification Results in Higher Effective Settling Velocities for Noncohesive Solids with a Broad Size Distribution: (a) Settling Velocity for a Well-Mixed Slurry, (b) Settling Velocity for a Stratified Slurry

8.2 Uncertainty and Applicability

Sections 8.2.1 to 8.2.4 discuss several types of uncertainty associated with the experimental data, models developed from the data, and applying the models to predict mixing performance of WTP vessels.

8.2.1 Measurement Uncertainty

Measurement uncertainties were associated with four categories of parameters: geometric, operational, physical (simulant parameters), and performance (U_{CS}, H_C, C_0, and C(Z)). Each category is discussed below.

8.2.1.1 Geometric Parameters

Geometric parameters are those associated with the geometric configuration of the test setup. Most were measured before and after a test as part of the configuration management of the test setup. The geometric parameters include tank diameter, nozzle diameter, nozzle standoff distance, nozzle radial position, nozzle azimuthal location, profile of tank bottom contour, suction line elevation, suction line position, and liquid elevation. For some parameters such as nozzle diameter, measurements were made and recorded for each individual component. The average values of these measurements were used for developing the models and post-test analysis. The uncertainties for the geometric parameters are listed in Table 8.1.

Table 8.1. Test Parameters and Associated Bounding Uncertainties

Parameter Symbol or Abbreviation	Parameter Description	Bounding Uncertainty (The listed uncertainties are the bounding values for the entire test program and range of configurations tested. For many test condition/configurations, the uncertainties are significantly lower) Value (all or small-/mid-/large-scale tank)	Units
D	Measured tank diameter small-/mid-/ large-scale tank	±2 /±13[(a)] /±3	mm
d	average nozzle inner diameter	±0.02	mm
sod	average nozzle stand-off distance	±2 /±2 /±1	mm
R_0, R_I	average nozzle radial position	±1 /±3 /±5	mm
N/A	nozzle azimuthal location	±6 /±6 /±3	degrees
Rtn	average suction line elevation	±6 /±6 /±13	mm
N/A	suction line radial position	±6 /±13 /±25	mm
N/A	suction line azimuthal location	±3	degrees
H	liquid fill level	±6 /±6 /±13	mm
N/A	contour profile	+1.25 % of D outward -1% of D inward	N/A
t_D	drive time	±0.01	s
t_C	cycle time	±0.01	s
DC	duty cycle	±0.003 /±0.002 /±0.0004	fraction
ϕ_p	pulse volume fraction	±0.001 /±0.003 /±0.002	fraction
U_S	discharge velocity–steady flow	±0.06 /±0.03/ ±0.01	m/s
U	discharge velocity–pulsed flow (single pulse)	±0.9 / ±0.5 / ±0.3	m/s
ρ_s	solids density	±0.02	g/cm^3
d_{05}, d_{50}, d_{95}	5th, 50th, and 95th percentiles of the particle size distribution	10% of measurement	N/A
N/A	particle sphericity	assumed spheres	N/A
ϕ_S	relative solids volume fraction = $V_S/(\pi D^3_{nom}/4)$	±0.0004 /±0.0008 /±0.0006	vol. fraction
ρ_l	liquid density	±0.006	g/cm^3
T	tank liquid temperature	±2.2	^0C
U_{CS}	critical suspension velocity, the discharge velocity at which complete suspension occurs	±0.9[(c)] /±0.5[(b), (c)] /±0.4[(c)]	m/s
H_C	average peak cloud height	±13 / ±13 /±25	mm
C_0	concentration on the vessel bottom (concentration at elevation 0)	Simulant / Range / Uncertainty S1d1 / 1 – 11 / 0.1 – 0.3 S1d2 / 1 – 22 / 0.3 – 0.7 S1d5 / 1 – 3.2 / 0.8 – 0.9 S1d1 / 1 – 4 / 0.2 – 0.4 S2d2 / 1 – 21 / 1.1 – 1.9	volume %

(a) Manufacturing techniques for the mid-sized tank resulted in a higher variability in roundness.
(b) Does not apply to test cases run in 2007.
(c) Does not apply to the test cases listed in Appendix B with the following MSS row numbers 700223, 700224, 700324, 700237, 700356, 700374, 700380, 700387, 9700003, 9700060, 9700068, 9700095, 9700119, 9700121, 9700126, 9700144, 9740232, 9740233, 9740234, and 9700313. Listed cases not fully bounded by ±0.2 m/s surrounding (sequential) observations.

The contour of the tank bottom is an important geometrical parameter, and no single measurement is sufficient to characterize it. Instead, specifications for head shapes such as elliptical, F&D, and spherical are used to characterize the tank bottom contour. The heads were profiled along diametric lines to assess how well the tank bottom complied with the specified head shapes. The manufacturing process influenced the uniformity/variability of the head shape (e.g., the small-scale tank heads were small enough that acrylic stock was machined to the prescribed contours). The mid-scale tank was an existing tank with a molded acrylic bottom. As described in Section 4.1 and Table 4.2, tests were planned assuming the mid-scale vessel had a 2:1 semi-elliptical head, but it was discovered and verified afterward to be spherical. For the mid-scale tank the uncertainties in Table 8.1 apply to the as-tested, not planned, measurements. The large-scale tank used standard commercial steel heads that were cut, welded, and ground to insert acrylic windows and add flanges to mate to the acrylic cylinder section. Based on the prescribed fabrication tolerances and profile measurement, the bottom contours for each test tank matched the specified shapes (e.g., 100-6 F&D) to within ±1%[1] of the test tank diameter.

8.2.1.2 Operational Parameters

Operational parameters were used to control and define the pulse cycle. Measurements or calculations based on direct measurements were used to evaluate all of the operational parameters as opposed to relying on calibrated control inputs. The operational parameters included drive time, cycle time, duty cycle, pulse volume fraction (i.e., discharge volume), and discharge velocity (both for steady state and pulsed-flow conditions). The time parameters associated with the pulse cycle were determined by analyzing, in real time, the fluid flow pulse from the Coriolis flow meter. The fluid-flow pulse is geometrically squared in real time using a DAS comparator module to facilitate pulse signal analysis. These real-time calculations were compared with the timing obtained from the pulse tube pressure measurements to check for anomalies. Because of the intermittent drive system that was used, the pulse volume fraction and discharge velocity were obtained from volumetric flow measurements using Coriolis mass flow meters that measured the total flow rate for all of the nozzles. The discharge velocity was calculated using the nozzle diameter and the number of tubes being operated. To verify balanced flow through the nozzles, the pressure drop across the nozzles was periodically measured using a single pressure transmitter. The pressure check was performed for conditions exceeding complete suspension (the condition of unsuspended solids can cause an imbalance in flow through the tubes due to varying flow restrictions for each nozzle). The acceptable variation in the measured pressure drop for all of the nozzles was 0.2 psi (1.4 kPa). The uncertainties for the operational parameters are listed in Table 8.1.

8.2.1.3 Physical Parameters

The physical parameters consist mainly of the simulant properties and include the solids density, particle size distribution, particle sphericity, relative solids loading, liquid density, and liquid temperature. All of these simulant properties were well characterized within a relatively small degree of uncertainty that is not expected to contribute significantly to the overall uncertainty of the correlated models. The uncertainties for the listed physical parameters are listed in Table 8.1.

[1] For information only.

8.2.1.4 Performance Parameters

The parameters measured to evaluate the mixing performance of a tank for a given configuration included the discharge velocity required for complete suspension (U_{CS}), the average peak elevation of the opaque solids cloud (H_C), and the solids concentration as a function of elevation, C(Z).

Measured values of U_{CS} obtained in the tanks were typically distinguishable within approximately 0.2 m/s and repeatable to within approximately 0.3 m/s. In the mid-scale tank some instances of replicate conditions yielded differences of 0.5 m/s for U_{CS}.

The visual measurements of H_C were obtained by capturing the peak elevation of the opaque cloud. The variability of cloud height was high due to the transient and turbulent nature of the rising plumes. The interface between the plume of suspended solids and the clear supernatant liquid was very dynamic with the clear interface in solids concentration creating a nonuniform (wavy) interface. These variations in cloud height depend on tank scale as well as operational and simulant properties. Therefore, the cloud heights were measured and recorded over a prescribed number of pulses for a given test condition, and the average value of the recorded cloud heights was used as the representative cloud height. Because the measurement of clouds involved sampling a fluctuating quantity, the overall fit of H_C models to data is likely accurate. This is not unlike the ability to measure sea level fairly accurately even when the wave-height fluctuations far exceed the desired resolution of the measurement. As such, the average values are considered more representative and meaningful than any single measurement.

8.2.2 Experimental Uncertainty

Replicate and repeated tests are needed to identify systematic errors introduced inadvertently during testing and to quantify random errors (uncertainty) in testing. Highly prescriptive testing and measuring procedures, and the mechanical aspect of the measurements, were used to reduce the likelihood of any significant random or systematic error. However, random uncertainties cannot be completely avoided in experimental work. A limited number of near-replicate tests were performed, and a relatively small number of tests were conducted with near-repeat conditions.[1] Section E.3 of Appendix E presents the results of using the results from limited near-replicate tests and near-repeat conditions to quantify experimental and measurement uncertainties in U_{CS} and H_C. Based on the limited near-replicate test results, estimates of experimental uncertainties are %RSD[2] = 5.3 for U_{CS} and %RSD = 13.3 for H_{CS} and H_C. These results indicate that the relative experimental uncertainties in determining H_{CS} and H_C are notably larger than in determining U_{CS}.

Some features of the experimental setup were not prototypic of the WTP designs and could contribute to systematic or random uncertainties, as discussed below.

---

[1] Replicate tests are tests using the same set of test conditions at different times with tests at other conditions in between. Repeat tests involve performing tests with the same set of test conditions at successive times, with no change of simulant intervening. Repeat tests are shown by a different test date. In some cases, during a test with a given Case ID, researchers returned to a test condition. This was called a repeat condition, not a repeat test. Variability in test results is typically much greater for replicate tests than repeat tests or repeat conditions. In situations where test conditions are close but not exactly the same, the terminology of near-replicate and near-repeat tests or conditions is used.

[2] %RSD = percent relative standard deviation.

- *Solids vertical entrainment due to pump return*: The design of the testing systems included pump suction inlets at the top of the testing tanks that were necessary for system operation. This upward draw of liquids in the tank creates an upward flow that results in higher clouds. The effect of this is negligible on U_{CS}. For H_C, the effect is that the model will over predict cloud heights in proportion to the modified settling velocity discussed in Section 8.1.
- *Tank liquid levels*: The fill level for liquids in the testing tanks, relative to tank diameter, ranged from 1.1 to 2.0, whereas the relative fill height for HLP-22 is 0.7. Little bias is introduced on cloud height for cases where the clouds are predicted to be very low or where very good mixing in the tank is projected. The effect of relative fill levels for cloud heights in the marginal regime is less certain.

8.2.3 Model Uncertainty

This section discusses various contributions to model uncertainty, that is, uncertainty in predictions made with models for the mixing response variables. Model uncertainty could be systematic (causing predictions to be biased) or random (predictions generally accurate, but imprecise).

- *Model form*: The mathematical forms of models must provide for adequately approximating the true, unknown relationships between the mixing responses and the test variables. Within the region of test variable combinations, the adequacy of a model form (with respect to systematic and random uncertainties) can be assessed by goodness-of-fit statistics and graphical methods. For extrapolative use of the models, model forms must be defensible based on physical considerations and previous modeling work. Of particular interest is uncertainty with respect to the scale effect. The model forms in this report are based on a power-law dependency for the scale effect, which are expected to provide for unbiased extrapolation of scale effects.
- *Model fit*: There is uncertainty in the models associated with imperfect mathematical fits to the data. The models presented in Sections 7.3.2 to 7.3.4 emphasized establishing reasonable physical models over seeking better numerical fits, because the former is essential when extrapolating to capture the relevant physics of the system. Generalizations and expansions of physical-based models for U_{CS} and H_C were investigated using the MR approach are discussed in Appendix F. The MR models for U_{CS} and H_C are summarized in Section 7.4.
- *Ranges of variables*: Limited ranges of some of variables were tested. We explored a broad range of particle sizes, including those comparable to the largest expected in the Hanford waste. We expect extrapolation to smaller particles should be acceptable insofar as cohesive effects are avoided. No tests were conducted with multiple sizes of particles. Density was tested over a fairly narrow range (2.5 to 4.3 g/cm^3), and no tests were conducted with multiple-density particles. Hanford waste encompasses a range of viscosity and of non-Newtonian rheology, neither of which was evaluated in this program. Finally, most of the testing was conducted with a 12-tube configuration, representing the HLP-22 design. Relatively few data were generated on 4- and 8-tube configurations.
- *Interactive effects of variables*: A statistically designed test matrix[1] was not used to specify the test combinations in the M3 mixing study; thus there were gaps in the coverage of test variable

[1] A statistically developed test matrix was generated as a part of the test plan (TP-RPP-WTP-491, "Test Plan for Scaled Testing to Determine Adequacy of the WTP Pulse Jet Mixer Designs – Phase 1," May 2007) developed during the initial stages of the M3 Mixing program. This statistically developed test approach was tabled in favor of the testing presented in this report. The change was made to address changing client considerations. The information learned while developing the prior test plan was used to guide simulant and other variable range selections for these tests.

combinations over the region of interest. Thus, the experimental data may provide limited or no basis for understanding and quantifying interactive effects of some test variables, and test variable interactions identified as significant in the MR modeling (Appendix F) will only include interactions with sufficient data to assess them. Also, the M3 mixing testing focused on certain combinations of some test variables (design values), so that the coverage of the test variable space was focused in some subregions and less focused in others. This means that the uncertainties of model predictions of the mixing responses will tend to be higher where there are limited or no data and smaller where there are more data. Within the region of test variable combinations investigated, the effects of uneven distribution of test combinations are accounted for by statistical methods for quantifying uncertainties of model predictions. However, care should be taken when applying the models to explore operational scenarios outside the test region of variables or for combinations within the region but not tested. One such case is large duty cycle, high ϕ_S, small d_S, and large density ratio (s).

- *Cloud height scaling factor*: Examinations of cloud height test results from the small- and large-scale elliptical tank tests indicate that a tank scaling factor for the cloud height model may be appropriate. A tank-size scaling factor was not included in the physical model for H_C but was included in the generalized model for H_C. A sensitivity check for H_C scaling factors shows that for HLP-22 the inclusion of scale-up factor exponents of 0.1, 0.2, and 0.3 would result in an H_C increase (C_0 decrease) of factors of 1.2, 1.45, and 1.75, respectively. A sensitivity check for H_C scaling factors (using the physical model) shows that, for a 20-ft- (6.1-m-) diameter tank, the inclusion of scale-up factors exponent of 0.1, 0.2, and 0.3 would result in an H_C increase (C_0 decrease) by factors of 1.13, 1.27, and 1.43, respectively. The impact would continue to be reduced for tank diameters less than 20 ft (6.1 m).[1]

8.2.4 Uncertainty Associated with Applying Models to WTP Vessel Mixing

Using the models to evaluate designs or operational options will require additional judgment on the part of the user. The models assume perfect knowledge of the waste properties, including the assumption that the wastes are uniform and will behave consistently within the mixing system. The experimental data do not include investigations on the effects of broad size or density distributions, and, at this time, allowance should be made for potential interactive effects of variables that were not experimentally investigated.

- *Nonprototypic factors*: As previously discussed, there were several nonprototypic aspects to the testing, including imperfect geometric similitude as well as operational differences such as refill operation and level change. We believe that most of these differences are secondary effects and do not contribute to performance differences significant enough to change a performance category (discussed in Section 9.0). This assertion is mainly based on the requirement for sufficient energy to perform mixing functions. If there is insufficient energy to achieve good solids suspension by a significant margin, geometric differences cannot reasonably make up for that deficit. Alternatively, we recognize that nonprototypic geometry at one scale could make a significant difference in the full-scale prediction. This position is supported by relative accuracy of the models in predicting results of larger-scale tests done by others (Bontha et al. 2000; 2003a, b) (see Section 8.3).

[1] This cloud height scaling factor discussion is FIO.

- *Hanford waste*: There are many dimensions of uncertainty and variability associated with Hanford waste. Further, the PSDD has implicit and explicit uncertainties that are very difficult to quantify given the inherent limitations of accurately characterizing radioactive waste. Even if we assume the PSDD is highly accurate, it represents average properties for the entire inventory, and on a batch basis there could be significant variability. For example, this could mean the U_{95} for a given batch is significantly higher than the Hanford bulk average value. The uncertainty associated with waste properties will become important when applying the models (such as in the vessel example evaluations in Section 9.0). However, it does not introduce uncertainty into the model itself.
- *Operational alternatives*: The models provide insight to parameters that could be manipulated to achieve improvements in mixing performance, such as reducing the solids concentration or lowering the fill height of the vessel. These relationships are inferred from the model form, but more work would be needed to demonstrate how well the model can predict these options.

8.2.5 Margin for Vessel Performance Evaluations

Although margins should certainly be applied to compensate for the uncertainties in applying the models, we have not addressed the appropriate value to use for design confidence or to address operational risk. The example performance evaluations of WTP vessels in Section 9.0 include no margin.

8.3 Model Benchmarks

Results of comparing model predictions against experimental results are shown in this section for several experiments conducted in the 336 Building large-scale test facility at PNNL. This section also discusses the comparison between model predictions and predictions made for a full-scale vessel (HLP-22) using a CFD model. These benchmarks investigate whether the models give reasonable results for prototypic conditions prior to using them in application examples for the full-scale WTP vessels. Further, the comparison of predicted results with independent experiments and CFD calculations provides support for selecting a characteristic settling rate for a known particle size distribution such that one defined particle can be used to represent the behavior of the material in a mixing system.

The benchmark experiments performed in the 336 Building used actual PJMs and JPPs and were therefore prototypic of full-scale WTP vessels. The 12.75-ft-(3.9-m-) diameter tank and 4-PJM arrangement (pictured with 8-PJM array in Figure 8.4) is actually very close to a full-scale model of the WTP vessel RLD-8. Two of the experiments conducted in this prototypic system used glass beads in water, similar to what was used for M3 model development. However, another experiment conducted in this prototypic system used a complex physical simulant with a wide range of particle sizes and densities. This test was a closer approximation to what will be seen with Hanford waste in the WTP vessels. The 336-Building experiments are an intermediate step between the highly idealized experiments upon which the models in this report are based and the full complexity of the conditions in the actual WTP vessels.

Figure 8.4. Prototypic PJM Tank in 336 Building (shown here with 8-PJM shrouded PJM cluster)

In all of the experiments used as benchmarks, the objectives did not require assessing U_{CS}. Indeed, that determination would be very difficult in a steel tank with a 2-in.-thick wall. Hence, only the cloud height and vertical solids concentration profiles can be compared. In fact, the cloud height was not explicitly measured but inferred from the concentration profile that was constructed from point concentration measurements. The concentration measurements consisted of slurry density measurements from flow loops with inlets at various depths and lateral positions. Thus, the techniques used to measure cloud height and concentration profile were different for the benchmark and current tests. In each benchmark case, we applied both the physical and generalized models for U_{CS} and H_C, as well as the linear concentration profile model based on the models for H_C. The physical models for U_{CS} and H_C are presented in Sections 7.3.3 and 7.3.5, while the generalized models are presented in Section 7.4. The linear concentration profile model is presented in Sections 7.3.4 and 8.1.2.[1] Lacking measurements for comparison, the model-predicted U_{CS} is reported for each benchmark case for information. One qualitative comparison that can be made for U_{CS} is the solids inventory represented in the concentration profile versus what may still be on the floor.

The approach used in each benchmark was to use model inputs that were consistent with the experimental conditions. The one exception was particle-settling velocity, which was varied within the range of the PSDD to determine what value produced a best match between the cloud height and concentration profile predicted by the models and the concentration profile established in the experiment. This optimization was done with the physical cloud height model and the results are shown here. The generalized model was run with settling velocities identical to those developed based on the physical

[1] Because both cloud height models (physical and generalized) were always applied in concert with the concentration profile model from Section 7.3.4, subsequent reference to physical or generalized cloud height models also includes the concentration profile model.

cloud height model. Comments are included with each benchmark about differences observed when optimizing particle settling velocity for the generalized model. U_{CS} models were always run with the particle settling velocity that was selected for use with the respective cloud height model.

8.3.1 Mixing Tests with AZ-101/102 Filtration Waste Simulant

The AZ-101/102 Filtration Waste Simulant tests are described in Bontha et al. (2000) and continue to be referenced frequently as PJM mixing tests with a broad size and density distribution of settling solids. The simulant recipe was initially developed to physically represent the AZ-101/102 solids for cross-flow ultrafiltration equipment tests. To simulate the washed solids, the aqueous liquid phase was water with 0.01 M NaOH. The recipe is described in full in Golcar et al. (2000), and the solids inventory is shown in Table 8.2. The solid particulate PSDD is listed in Table 8.3.

In an application of the H_C and C(Z) models, a key parameter choice is particle settling velocity. A range of particle-settling velocities were investigated to determine the best match between the experimentally measured concentration profile and that predicted by the physical model for C(Z). The optimal particle-settling velocity was determined in this fashion for each of the six separate benchmark cases considered (three different duty cycles at two different solids loadings). As an example at the lower end of the settling velocity range, using U_{50} does not provide realistic results. The physical models for H_C and C(Z) predict in all cases that the slurry would be uniformly mixed to the fill height, which is clearly not borne out in the measured data. As an example at the upper end of the settling-velocity range, U_{95} gave results that were not as representative as U_{90} (which was selected for use with the physical model). Later work to optimize particle settling velocity for the H_C and C(Z) generalized models showed that they gave equally representative results using the U_{90} and U_{95} settling velocities.

Table 8.2. Solids Inventory in AZ-101/102 Filtration Simulant (reproduced from Golcar et al. 2000)

Compounds Bearing	Total wt%	Mineral Phase	Powder Grade	Mean Volume PSDD	Component wt%
Iron	58	Hematite	Iron oxide No: 07-5001	22 μm	17.4
			Red iron oxide No: 07-3752	2–3 μm	29.0
			Synthetic red iron oxide No: 07-2568	0.6 μm	11.6
Aluminum	24	Boehmite[(a)]	HiQ-10 alumina	50 μm[(b)]	7.2
		Gibbsite[(a)]	C-231 ground white hydrate	14 μm (broad)	8.4
			SpaceRite S-23 alumina	7.5 μm (broad)	5.04
			SpaceRite S-11 alumina	0.25μm (narrow)	3.36
Zirconium	13	Zirconium hydroxide	Zirconium hydroxide; product code: FZO922/01	15 μm	13.0
Silicon	5	Nepheline	Spectrum A 400 nepheline syenite	10 μm	5.0

(a) Gibbsite/Boehmite ratio = 2.33.
(b) This value is corrected from Table S.1 in Golcar et al. (2000). The corrected value is d_{50}, from the manufacturer's MSDS, which is also included in the Golcar report.

Table 8.3. Solids PSDD for AZ-101/102 Filtration Simulant

Particle Size (μm)	Volume Fraction	Undissolved Solids Density (g/cm^3)
0.25	0.05	2.42
0.6	0.10	5.00
2.5	0.21	5.00
7.5	0.07	2.42
10	0.07	2.66
14	0.12	2.42
15	0.15	3.25
22	0.12	5.00
50	0.10	3.01

This section compares measured H_C and C(Z) results versus model-predicted results using both the physical and generalized models, with the settling velocity optimized for the physical model. This settling velocity (U_{90}) is shown in Table 8.4 along with other input parameters used in the models. Work to optimize the settling velocity for the generalized models was performed in some cases, and the results are mentioned in those cases. Plotted concentration profile results for the six separate cases are shown consecutively in Figures 8.5 to 8.16.

Table 8.4. Model Inputs for Prototypic PJM 336-Building Tests with AZ-101/102 Filtration Simulant ($U_T = U_{90}$)

Case #	% Max Drive	wt% Solids	ϕ_S	DC[(a)]	ϕ_p	ϕ_J	H/D	U (m/s)	U_T (mm/s)
1	100%	17.6	0.044	0.22	0.077	0.0027	0.82	8	0.99
2	50%	17.6	0.044	0.11	0.077	0.0027	0.82	8	0.99
3	10%	17.6	0.044	0.022	0.077	0.0027	0.82	8	0.99
4	100%	28.3	0.082	0.22	0.077	0.0027	0.86	8	0.99
5	50%	28.3	0.082	0.11	0.077	0.0027	0.86	8	0.99
6	10%	28.3	0.082	0.022	0.077	0.0027	0.86	8	0.99

(a) The physical and generalized models for H_C and C(Z) used data over the approximate range $0.14 \leq DC \leq 0.67$. Hence, 4 of the 6 cases require extrapolating the H_C and C(Z) models with respect to DC.

8.3.1.1 Case 1

The maximum drive case at the lower solids loading (17.6 wt%) is shown for the physical and generalized models in Figure 8.5. The solids loading for a uniform state is shown as the red line, and the experimental measurements can be compared with this to check mass balance. The data in this case show a significant degree of stratification in the upper ~25% of the tank; however, concentrations over the rest of the tank are not increased over the fully mixed value (17.6 wt%). The difference may be explained by an increase in wt% at the bottom, higher concentrations in other parts of the tank, or measurement uncertainty. The physical and generalized models predicted U_{CS} = 7.2 and 9.3 m/s, respectively, which are both near the experimental drive velocity of 8 m/s. These values suggest that the solids should be suspended or nearly suspended, and this is consistent with observations during the experiment for all cases tested where a settled solids layer could not be detected on the floor.[1]

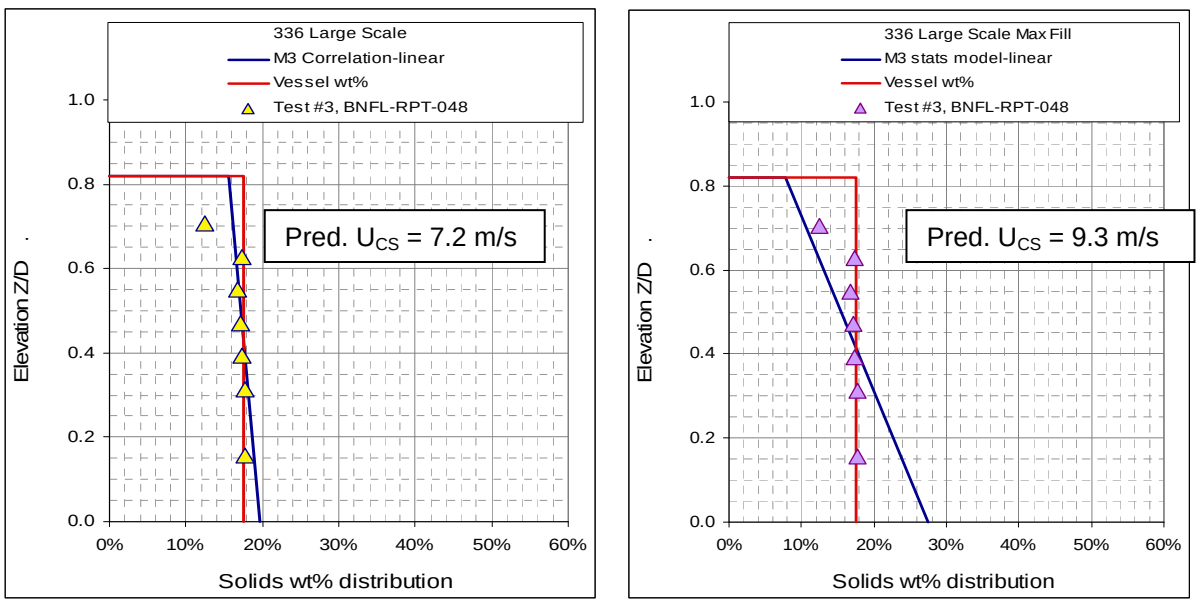

(a) (b)

Figure 8.5. Concentration Profiles for Case 1: 17.6 wt% and Maximum Drive Using the (a) Physical Model and (b) Generalized Model, with $U_T = U_{90}$ Optimized for the Physical Model

The cloud height model is used to predict a solids concentration distribution using a linear fit (blue line), as given by Eq. (7.47) in Section 7.3.3. The predicted variation from both physical and generalized cloud height models matches the data at mid-height but does not capture the curvature at the top. However, this is reasonable agreement for the linear solids distribution model being used. In this case, a key part of that distribution model is to redistribute the solids while matching the initial predicted gradient for cloud heights that are predicted above the fill height (H_F) (see Eq. 8.4 and 8.5). Using the generalized model for H_C in Eqs. (8.3), (8.4) and (8.5) predicts a smaller initial cloud height and a not-as-steep gradient in the concentration profile, shown in Figure 8.5(b), compared with the results for the physical model, shown in Figure 8.5(a).

[1] Jagan Bontha, personal communication to James Fort (PNNL).

8.3.1.2 Case 2

Results for the 50% max drive case at the lower solids concentration (17.6 wt%) are shown in Figure 8.6. The physical and generalized models predicted U_{CS} = 8.8 and 10.7 m/s, respectively, which are both higher than the experimental drive velocity of 8 m/s. The amount of suspended solids suggested by the measured concentration profile depends on the interpretation of the curve above and below the measurement points; it could be equal to or somewhat less than Case 1. The stratification is more pronounced than in Case 1 with wt% values exceeding the uniformly mixed value below 40% of the fill height (H/D = 0.4). In Figure 8.6, the straight-line distributions from both models show a reasonable slope change from Case 1, shown in Figure 8.5. The physical model, shown in Figure 8.6(a), more closely approximates the data near the tank bottom and the generalized model, shown in Figure 8.6(b), agrees better at the top.

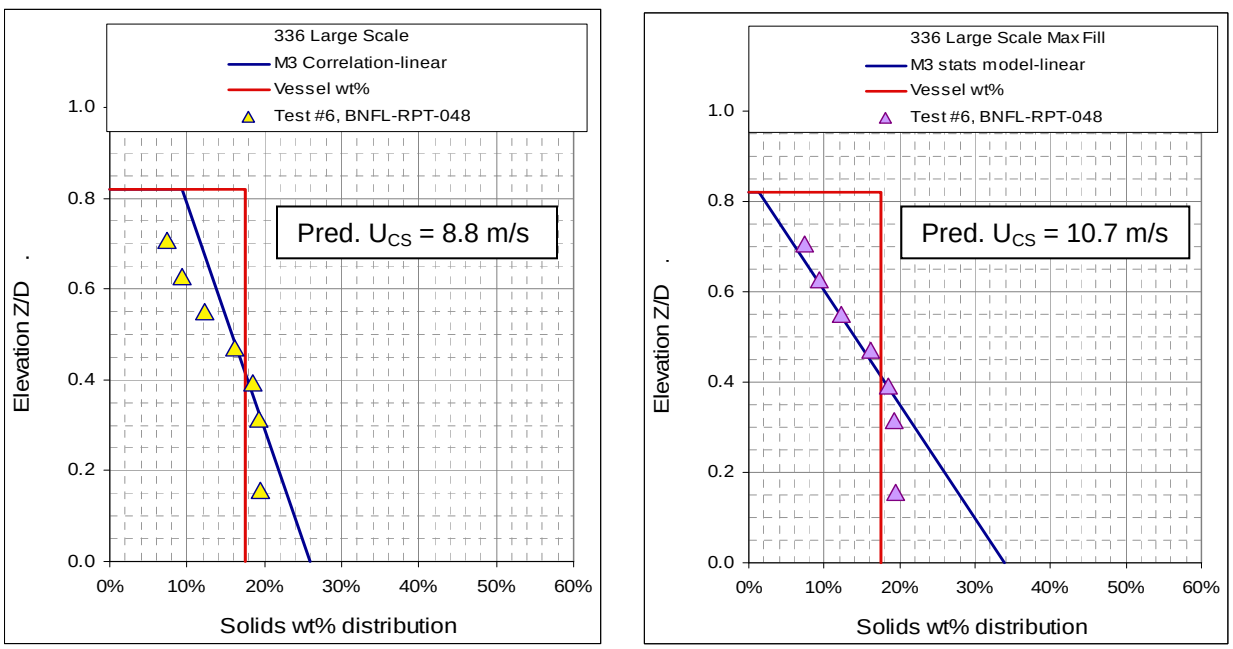

(a) (b)

Figure 8.6. Concentration Profiles for Case 2: 17.6 wt% and 50% of Maximum Drive Using (a) Physical Model and (b) Generalized Model, with $U_T = U_{90}$ Optimized for the Physical Model

8.3.1.3 Case 3

Results for the 10% max drive case at the lower solids concentration (17.6 wt%) are shown in Figure 8.7. The physical and generalized models predicted U_{CS} = 13.8 and 14.9 m/s, respectively, which are both well above the experimental drive velocity of 8 m/s. Again, the amount of suspended solids indicated by the concentration measurements depends on the interpretation of the curve beyond these points. But one could argue that the same amount of solids is suspended as in Case 2. The stratification is much more pronounced for this case with the cloud height below the fill level and measured wt% significantly exceeding the uniformly mixed value below 35% of the fill height (H/D = 0.35). The physical model significantly underpredicts cloud height for this case, and consequently the resulting concentration distributions are not close to the slope in the experimental data. The generalized model also underpredicts the cloud height, but the average slope is a closer approximation to the data.

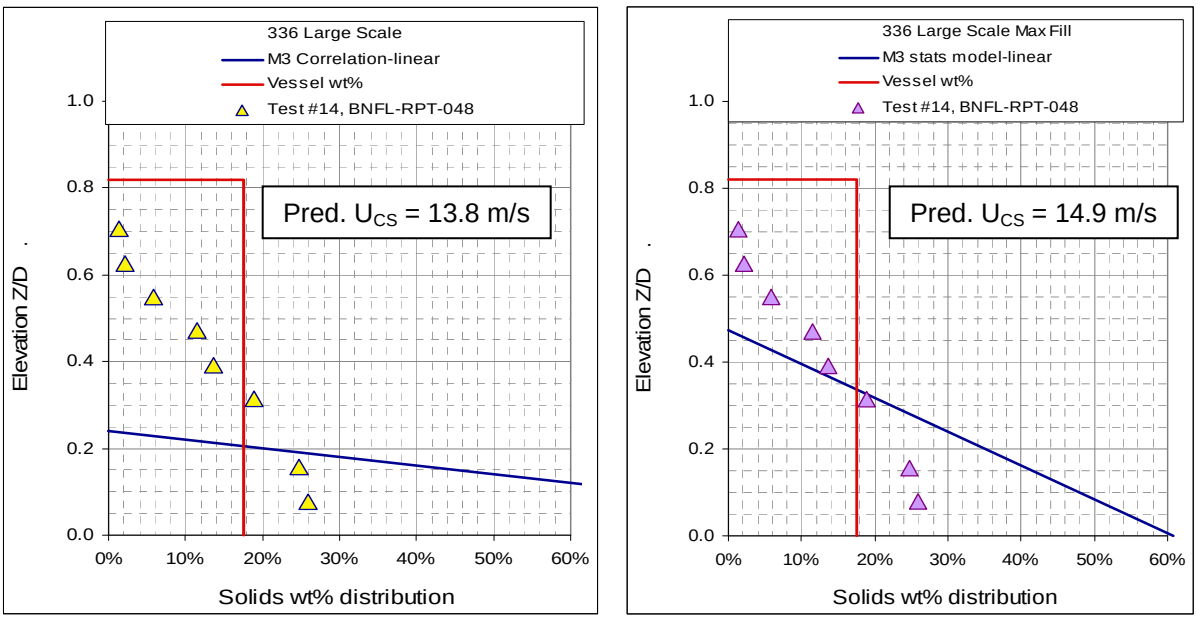

(a) (b)

Figure 8.7. Concentration Profiles for Case 3: 17.6 wt%, 10% of Maximum Drive Case Using (a) the Physical Model and (b) the Generalized Model, with $U_T = U_{90}$ Optimized for the Physical Model

8.3.1.4 Case 4

Results for the 100% max drive case at the higher solids concentration (28.3 wt%) are shown in Figure 8.8. The physical and generalized models predicted U_{CS} = 7.2 and 10.8 m/s, respectively, compared with the experimental drive velocity of 8 m/s. The appearance of the measured concentration data is of a uniformly mixed system at approximately 27 wt%. The behavior at the top and bottom of the tank cannot be determined from these measurements. However, their magnitude and uniformity suggest a well-mixed state with solids suspended off the floor. This is consistent with the physical model prediction of U_{CS}, but is not consistent with the higher value predicted by the generalized model. The predicted concentration profile using the physical model is consistent with the measurements, while the concentration profile predicted using the generalized model is not as good in this case.

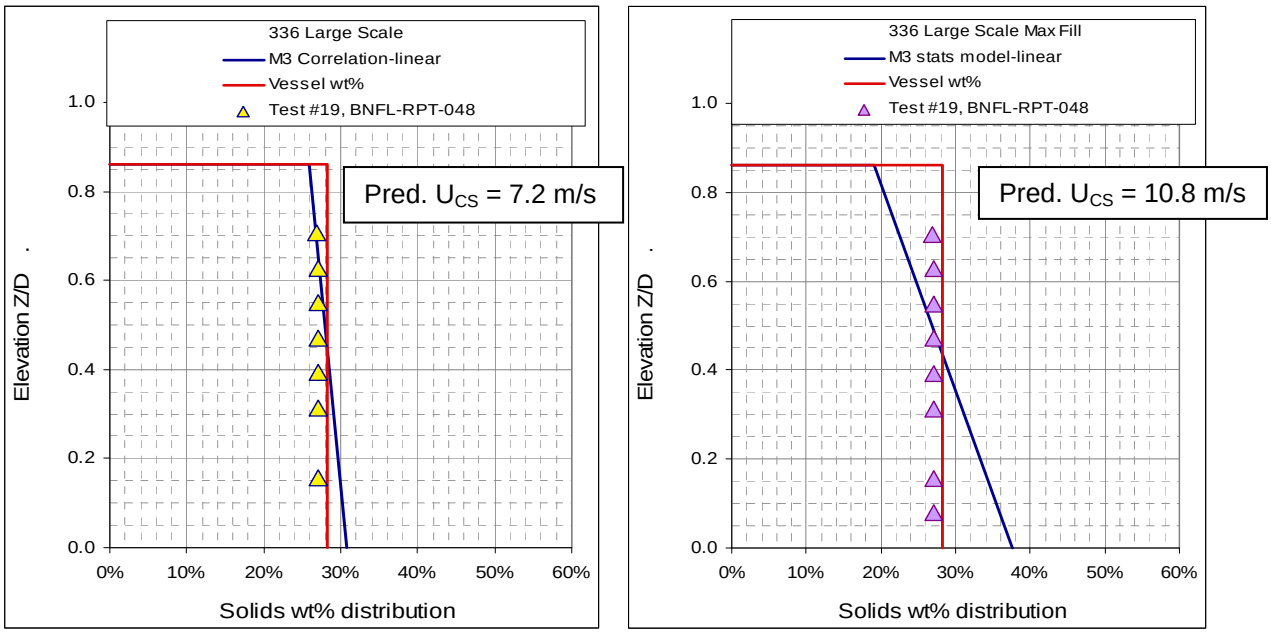

(a) (b)

Figure 8.8. Concentration Profiles for Case 4: 28.3 wt% and Maximum Drive Using (a) the Physical Model and (b) the Generalized Model, with $U_T = U_{90}$ Optimized for the Physical Model

8.3.1.5 Case 5

Results for the 50% max drive case at the higher solids concentration (28.3 wt%) are shown in Figure 8.9. The physical and generalized models predicted U_{CS} = 8.8 and 12.4 m/s, respectively, compared with the experimental drive velocity of 8 m/s. The shape of the concentration profile shown by the measured data is very similar to Case 1, the 100% drive case at the lower solids loading. Again, depending on the actual shape of this profile above the uppermost measurement point, there could be a high solids concentration near the floor. For this case, arguing which of the U_{CS} predictions is more reasonable requires more information than can be provided by these measurements. The qualitative comparisons of the measurements and the predicted concentration profiles using the physical model, shown in Figure 8.9(a), and the generalized model, shown in Figure 8.9(b), are similar. Both predictions are plausible representations of the measured data.

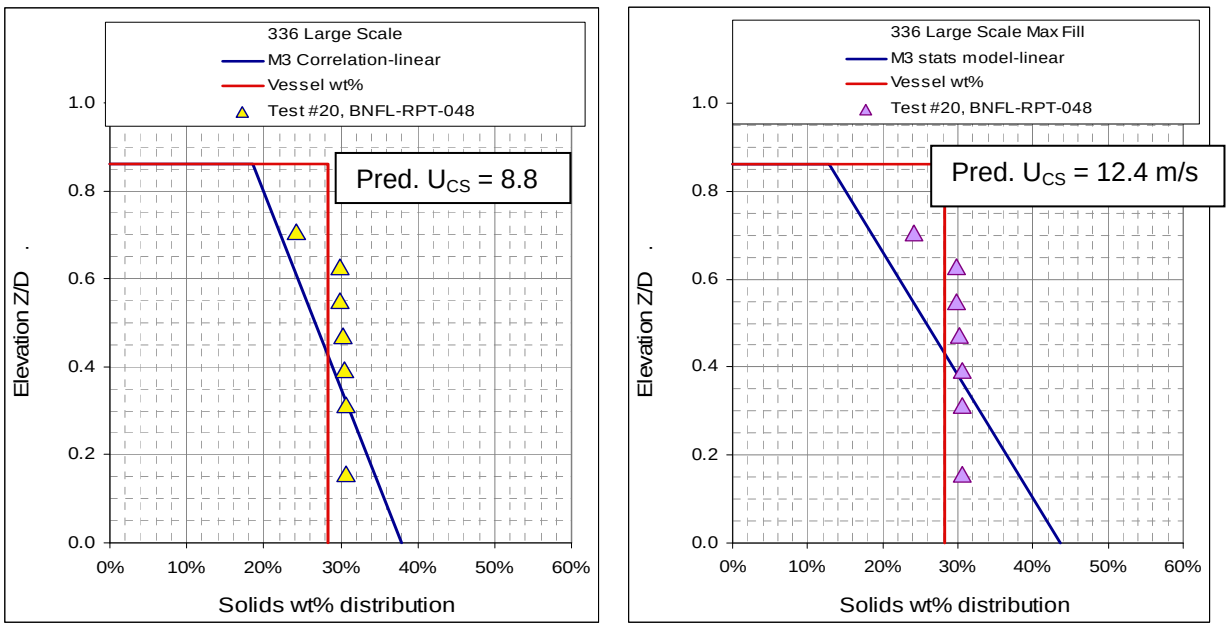

(a) (b)

Figure 8.9. Concentration Profiles for Case 5: 28.3 wt% and 50% of Maximum Drive Using (a) the Physical Model and (b) the Generalized Model, with $U_T = U_{90}$ Optimized for the Physical Model

8.3.1.6 Case 6

Results for the 10% max drive case at the higher solids concentration (28.3 wt%) are shown in Figure 8.10. The physical and generalized models predicted U_{CS} = 13.9 and 17.3 m/s, respectively, which are both significantly greater than the experimental drive velocity of 8 m/s. This is consistent with the solids inventory indicated by the measured concentration profile being significantly less than the total solids loading.

The qualitative comparisons of the concentration profiles using the physical and generalized models are similar to what was observed in Figures 8.9 and 8.10 for Case 3. The generalized model prediction is best in both Case 3 and Case 6, but the assumed linear concentration profile is not very satisfying for either model. The vessel slurry is stratified with the bulk of the solids below Z/D = 0.5. The measured concentrations indicate a large amount of solids are below the lowest measurement point.

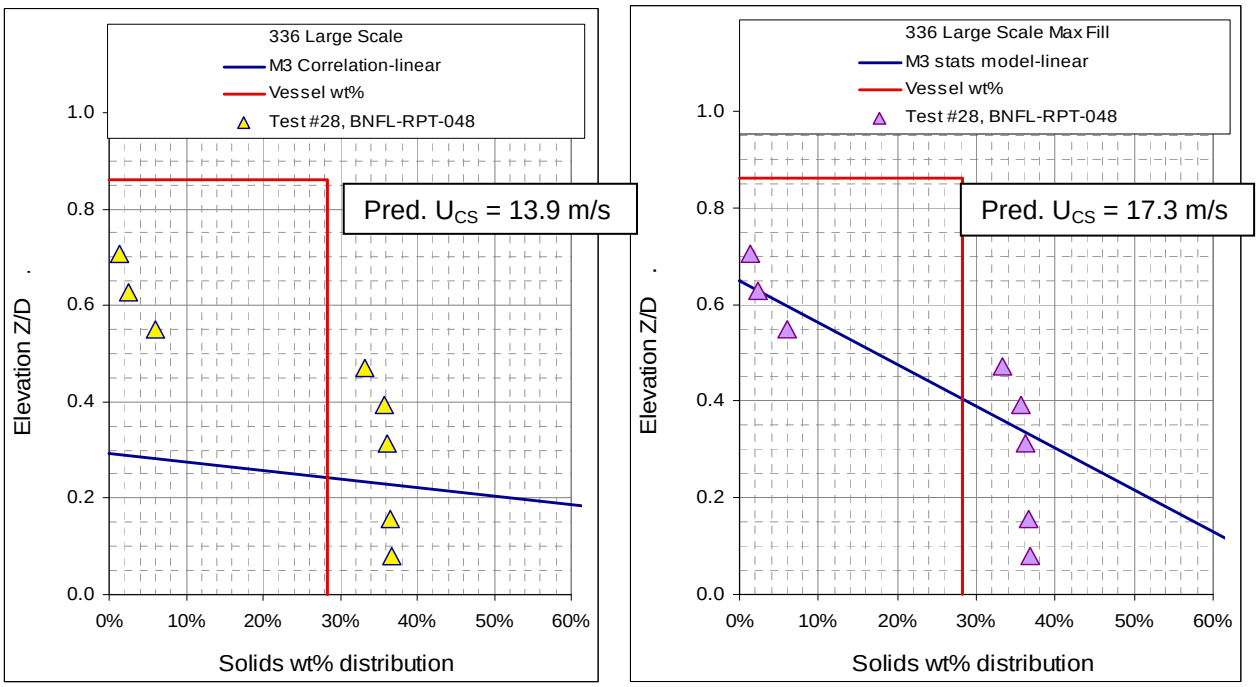

(a) (b)

Figure 8.10. Concentration Profiles for Case 6: 28.3 wt% and 10% of Maximum Drive Using (a) the Physical Model and (b) the Generalized Model, with $U_T = U_{90}$ Optimized for the Physical Model

8.3.1.7 Discussion of Results

Note from Table 8.4 that DC = 0.022 in Cases 3 and 6, which is well outside the DC > 0.18 range tested and used to develop the models. This may be the reason the physical and generalized models for C(Z) performed the worst for Cases 3 and 6. For Cases 2 and 5, DC = 0.11, which is also outside this range. Although the physical and generalized models performed better for these cases, there still was a noticeable difference in model-predicted versus measured concentration profile. Finally, Cases 1 and 4 had DC = 0.22, which was inside the range tested. The physical and generalized models performed the

best for these cases. This suggests that the physical and generalized models for H_C, C_0, and C(Z) should not be extrapolated to duty cycle values much lower than the lowest value tested (0.14).

8.3.2 Mixing Tests with Glass Bead Simulants

Two additional sets of experiments were performed in the 4-PJM, 12.75-ft (3.9-m) tank in the 336 Building during the 2001 to 2003 time period. Both of these sets of experiments were for CFD code validation. Comparisons of model-predicted and measured concentration profiles from those two sets of experiments are provided in Subsections 8.3.2.1 and 8.3.2.2.

8.3.2.1 Tests with 75-μm Glass Beads

The first test used 75-μm glass beads as the solids. This experiment and results are described in Bontha et al. (2003a). These tests used a single loading of 10 wt% solids in water. This particle had a relatively high settling rate and was selected for this test to give incomplete suspension under normal PJM operations.

The distribution of particle sizes was typical of industrial-grade glass beads. The PSD from Bontha et al. (2003a, Appendix E) is reproduced in Table 8.5. Of the particle settling velocities that were tested with the physical model, the best agreement with the measured concentration profile was given with U_{50}. This is a settling rate of 4.05 mm/s. Model input parameters for this benchmark are shown in Table 8.6.

Table 8.5. PSD for 75-μm Glass Beads (from Bontha et al. 2003a, p. E.2)

Particle Size Distribution of Potter Chemical C.2530 Glass Beads	
Particle Size (μm)	vol%
37.00	0.00
40.35	0.15
44.00	0.35
47.98	0.71
52.33	1.86
57.06	4.18
62.23	7.88
67.86	13.68
74.00	16.88
80.70	17.54
88.00	15.20
95.96	9.87
104.65	5.99
114.12	3.11
124.45	1.48
135.71	0.78
148.00	0.34
161.39	0.00

Table 8.6. Model Inputs for 336-Building Tests with 75-µm Glass Beads ($U_T = U_{50}$)

Case #	Case	wt% Solids	ϕ_S	DC	ϕ_p	ϕ_J	H/D	U (m/s)	U_T (mm/s)
7	4 PJMs	10	0.042	0.14	0.056	0.0027	0.99	6.8	4.05

Model results for this case are compared with the experimental data in Figure 8.11. The U_{CS} predictions are 9.3 m/s for the physical model and 10.7 m/s for the generalized model. These values are both well above the 6.8 m/s experimental drive velocity. The integrated area under the measured concentrations is comparable to the average solids loading. Again, we have no data to compare with this prediction, but if correct it would suggest that some part of the solids inventory may not have been mobilized.

As for the model predictions for the cloud height and concentration profile, the physical model underpredicts the cloud height and consequently the concentration profile is too shallow. The generalized model overpredicts the cloud height, which results in a concentration profile that is steeper than that associated with the experimental concentration measurements. Later tests that optimized the settling velocity for the generalized model showed best agreement with this case using the U_{95} particle-settling velocity. Hence, the predicted concentration profile for the generalized model using $U_T = U_{95}$ would agree more closely with the measured profile, shown in Figure 8.11(b).

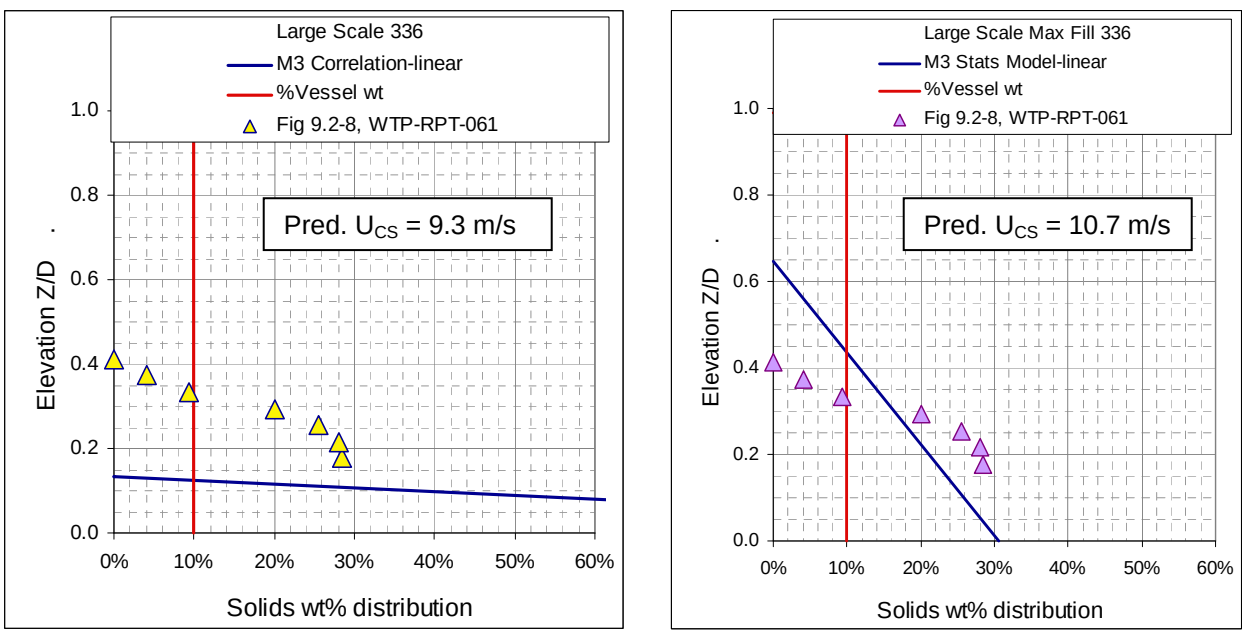

(a) (b)

Figure 8.11. Concentration Profiles for Case 7: 10 wt% and 75-µm Glass Beads Using (a) the Physical Model and (b) the Generalized Model, with $U_T = U_{50}$ Optimized for the Physical Model

8.3.2.2 Mixing Tests with 35-µm Glass Beads

The second set of experiments used 35-µm glass beads as the solids, and water was again used as the liquid phase. This test is described in Bontha et al. (2003b). The relative distribution of the 35-µm

particle size was broader than that of the 75-µm particle described in Subsection 8.3.2.1. Like the benchmark with the larger glass beads, the best agreement between the physical model and measured concentration profile was found near the middle of the particle size range, at d_{60} (37 µm). Because the particle density is constant, this is U_{60}, which in water corresponds to a settling rate of 1.06 mm/s.

Two test cases from this experiment were selected for comparison with the physical and generalized models. Both are for the 20 wt% solids: one with 4 PJMs operating and the other at a reduced power level reflected by running just 2 PJMs. The input parameters for the model applied to these two benchmarks are shown in Table 8.7.

Table 8.7. Model Inputs for 336-Building Tests with 35-µm Glass Beads ($U_T = U_{60}$)

Case #	Case	wt% Solids	ϕ_S	DC	ϕ_p	ϕ_J	H/D	U (m/s)	U_T (mm/s)
8	4 PJMs	20	0.085	0.22	0.070	0.0027	0.93	8.3	1.06
9	2 PJMs	20	0.085	0.22	0.036	0.0014	0.93	8.0	1.06

Model results for Case 8 (4 PJMs) are compared with the experimental data, shown in Figure 8.12, and Case 9 (2 PJMs) is shown in Figure 8.13. In the 4-PJM test (Case 8), Figure 8.12 shows that the integrated profile associated with the concentration measurements agrees with the total solids inventory, and this is consistent with predicted U_{CS} values (6.0 m/s for the physical model and 8.4 m/s for the generalized model) being less than or equal to the experimental drive velocity (8.3 m/s). The predicted concentration profiles for the 4-PJM case are reasonable approximations of the data for both the physical and generalized models.

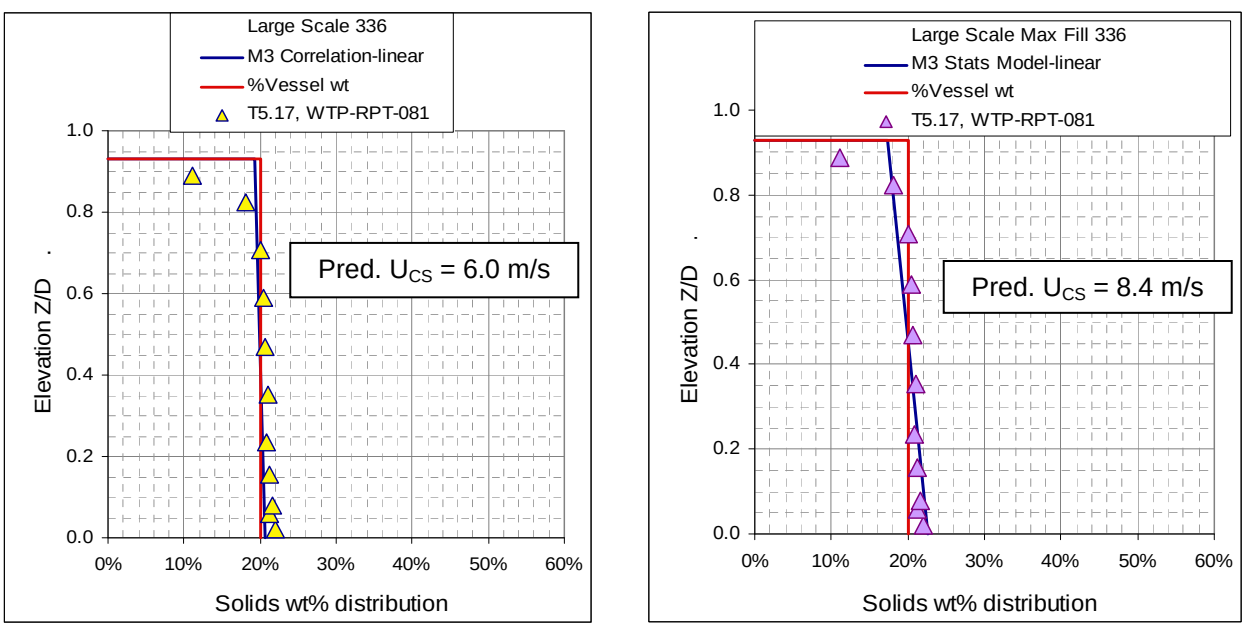

(a) (b)

Figure 8.12. Concentration Profiles for Case 8: 20 wt% and 35-µm Glass Beads with 4 PJMs Operating Using (a) the Physical Model and (b) the Generalized Model, with $U_T = U_{60}$ Optimized for the Physical Model

For the 2-PJM test (Case 9), the measured concentration data, shown in Figure 8.13, show significant stratification. The measured profile is nearly symmetric vertically about the fully mixed concentration line at 20 wt%, and roughly accounts for the total solids inventory. Concentration measurements were not available near the bottom for this test, so it is difficult to rule out a higher concentration zone near the floor. The presence of incompletely suspended solids would be consistent with the predicted U_{CS} values of 9.6 and 13.9 m/s using the physical and generalized models, which are well in excess of the 8 m/s experimental drive velocity. For the predicted concentration profiles, the physical model somewhat overpredicts the cloud in the 2-PJM case, but the trend is approximately correct. The generalized model significantly overpredicts the cloud height with this settling velocity ($U_T = U_{60}$). Later investigations with particle settling velocity optimized for the generalized model showed best agreement with the measured concentration profile using the U_{95} particle settling velocity. Hence, the predicted concentration profile for the generalized model using $U_T = U_{95}$ would agree more closely with the measured profile shown in Figure 8.13(b).

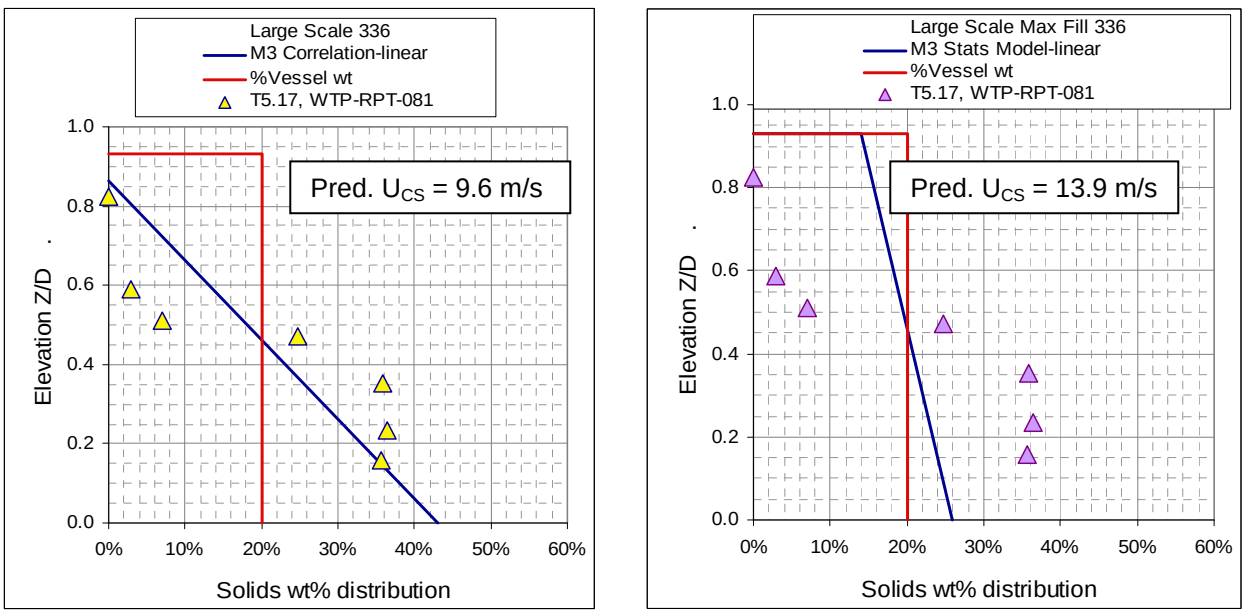

(a) (b)

Figure 8.13. Concentration Profiles for Case 9: 20 wt% and 35-µm Glass Beads with 2 PJMs Operating Using (a) the Physical Model and (b) the Generalized Model, with $U_T = U_{60}$ Optimized for the Physical Model

8.3.3 Comparison with CFD Simulation

CFD simulations have been used routinely by BNI to predict vessel mixing behavior for the WTP vessels. These simulations have been repeated as CFD models improve and as best-estimate conditions for the vessels change. As a supplement to the benchmarking experiments, predictions made with the physical and generalized models were compared with recent CFD model predictions for vessel HLP-22. Satisfactory agreement in this case demonstrates consistency between the experiment-based models and the CFD model.

The model input parameters for conditions of the CFD simulation are shown in Table 8.8. These inputs were taken from the list of CFD model inputs, with the exception of the drive velocity and duty

cycle, which were obtained from the PJM velocity profile, shown in Figure 8.14, and particle settling velocity, which was calculated with Eq. (7.5) using the 60-μm particle diameter used in the simulation and particle density and fluid properties in Table 8.8.

Table 8.8. Model Inputs to Compare with CFD Simulation of HLP-22, 12 m/s Normal Firing Case[(a)]

ρ_l (kg/m^3)	μ_l (cP)	wt% Solids	ρ_s (kg/m^3)	ϕ_S	DC	ϕ_p	ϕ_J	H/D	U (m/s)	U_T (mm/s)
1.13	2.2	8.1	2.9	0.026	0.33	0.05	0.00092	0.8	12	1.49

(a) B. Rosendall, "Update on HLP22." HLP22_Results_082708_BMR.ppt. BNI.

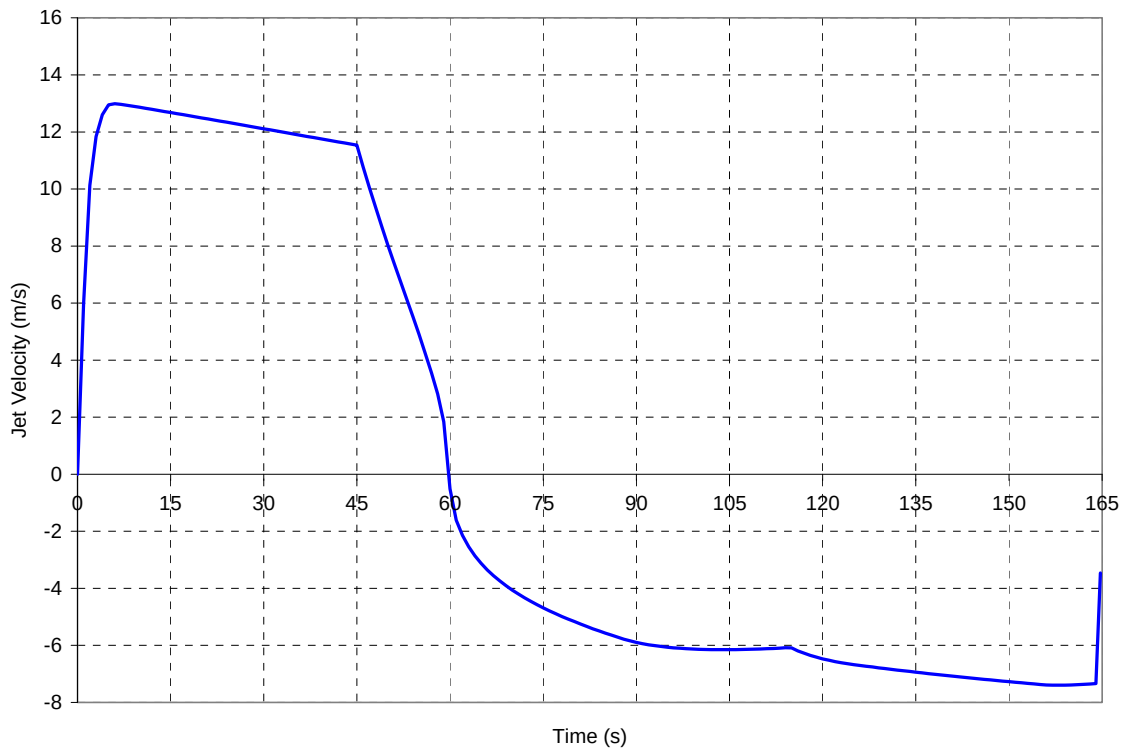

Figure 8.14. Velocity Profile (Drive Function) for HLP-22 (FIO)

Initial model applications for C(Z) and U_{CS} were made with the average velocity during the 60-sec PJM discharge, approximately 11 m/s. The associated duty cycle was 0.36 (60/165). The final model applications shown here were made with the 12 m/s average velocity over the 45-second drive portion of the cycle, and the associated duty cycle was 0.33 (45/165). Both give approximately the same cloud height, which suggests that the increased velocity compensates for the reduction in duty cycle.

Cloud height and concentration profile model results for this case are compared with CFD results for the physical model, shown in Figure 8.15(a), and the generalized model, shown in Figure 8.15(b). The solids concentration from the CFD model is the average over the final cycle in the simulation at the centerline of the vessel. The simulation was not yet at steady state but seems close. The physical model overpredicts the concentration profile, but the generalized model concentration profile agrees well with

that of the CFD model. Note that no optimization can be done for either model in terms of particle settling velocity because this is a monodisperse system, and therefore has a prescribed settling velocity. Both show a highly stratified system. The integrated mass fraction for the CFD model is 0.064 (6.4 wt%), so much of the solids are still on the tank bottom. This is consistent with the drive velocity (12 m/s) being significantly below predicted values of U_{CS} (14.1 m/s for physical model and 17.9 m/s for the generalized model).

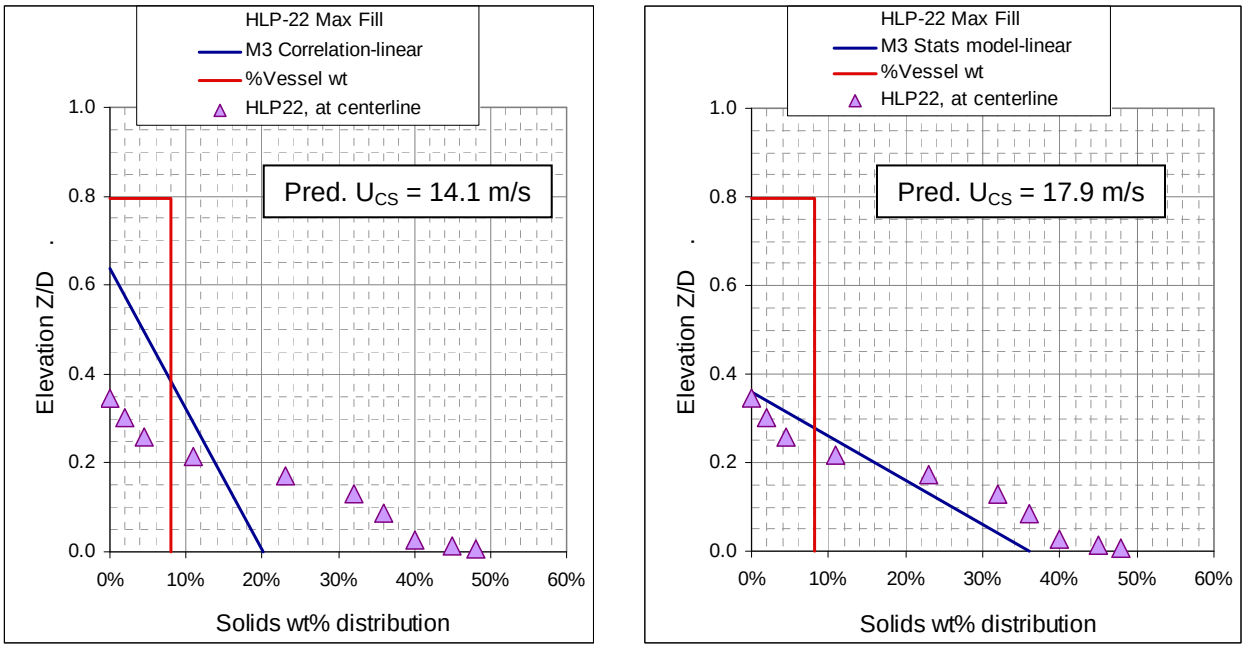

(a) (b)

Figure 8.15. Comparison of Model-Predicted Concentration Profiles with Predictions from CFD Simulation of HLP-22, 12 m/s, Normal Firing Case Using (a) the Physical Model and (b) the Generalized Model

8.3.4 Benchmarking Summary

Predictions using the U_{CS}, H_C, and C(Z) models presented in Sections 7.3 and 7.4, with C(Z) corrections for fill level presented in Section 8.1.2, were compared with experimental results for the available set of larger-scale experiments that mixed particle suspensions with PJMs. These benchmarks spanned a wide range of noncohesive simulants and degrees of mixing. The objectives of these experiments did not require the identification of U_{CS}, so that parameter was not available for evaluation.

Benchmark comparisons in cloud height/concentration profiles and critical suspension velocities showed the following:

- Settling velocities representing various fractions of the simulant PSDD were evaluated to find one providing the best agreement with the experimentally measured concentration profiles.
  - For the physical model, a characteristic particle settling velocity on the high end of PSDD (U_{90}) gave the best match in the benchmarks of neutralized current acid waste (NCAW) filtration simulants. This same model required a settling velocity in the middle of the particle size range

(U_{50} or U_{60}) to match the measured concentration profiles in the benchmarks against the glass bead simulants.

  - For the generalized model, a characteristic particle settling velocity of either U_{90} or U_{95} gave equally good results for the NCAW filtration simulants, but in contrast to the physical model, the generalized model also gave best fit with the glass simulants with U_{95}.

- For settling velocities indicated above, cloud heights were in reasonably good agreement with benchmark measurements as long as duty cycle was in the range of the test data upon which the models were based. The associated concentration profiles were qualitatively correct, at least to the extent that a linear model could reproduce often complicated concentration profiles. In the cases for the NCAW filtration simulant, where the duty cycle was well below that used in the current experiments, cloud heights and associated concentration profiles were not consistent with the benchmark measurements. This indicates that models should not be used to extrapolate outside of the test duty cycle range and in general suggests that model predictions based on extrapolation of other test variables may not be correct.

- Geometric and operational simplifications made in the experiments apparently did not adversely affect the development of models that can be applied to prototypic equipment.

- Although measured values of critical suspension velocity were not obtained in the benchmark experiments, physical and generalized model predictions of critical suspension velocity were usually consistent with solids suspension in measured concentration profiles. The values of U_{CS} predicted by the generalized model were always larger than those predicted by the physical model.

In summary, the benchmark results allow us to move ahead to vessel assessment examples in Section 9.0 with confidence that, if used with an appropriate settling velocity and with system operating parameters that are within the range of the test data, model predictions will be consistent with observed physical responses. This is in light of the intended use of the models to identify WTP vessel mixing designs that are adequate or inadequate, and not as precise predictors of system performance. Based in particular on the results for the NCAW filtration simulant, these benchmarks support use of a U_{95} particle setting velocity when representing the Hanford waste in the WTP vessel assessments.

9.0 WTP Mixing Systems Performance Examples

This section presents examples of the application of the developed models to assess two of the established WTP vessel mixing performance metrics: off-bottom suspension and concentration near the pump suction inlet. Model predictions of the concentration near the vessel bottom (C_0) may be compared to the vessel performance requirement for concentration at the suction pump inlet. Model predictions of critical suspension velocity (U_{CS})[1] are a close indicator of the current requirement to disturb all settled solids in the vessel. Assessing other performance requirements related to mixing (such as gas retention and release, or blending times) are not within the scope of the work.

Evaluation of WTP vessel performance was made using two sets of assumed waste conditions. One set of conditions was defined for each vessel by the WTP mixing requirements document (Olsen 2008a), and these are referred to as the "design point" conditions in this section. The second set was extracted from the Hanford PSDD and is provided for comparison. In both cases the results from the models show how predicted performance for the assumed conditions would relate to the requirements. This is a useful illustration of applying the models, but it is not sufficient for design decisions and not intended to be used without considering other uncertainties and risks. Design margin must be applied to account for uncertainties in the waste properties that will be received and any discrepancy between actual PJM performance and the design value, in addition to the uncertainties inherent in the models. Determining whether mixing systems for solids-containing WTP vessels meet WTP project mixing flowsheet requirements had originally been in the scope of the work documented in this report, but that responsibility was reassigned to the WTP M&PE group (Hazen 2008b).

Section 9.1 provides an overview of the approach used to predict vessel performance for the examples. Section 9.2 describes the input parameters for the evaluation. Section 9.3 gives the specific vessel performance examples at the design point conditions supplied by WTP using the physical models for U_{CS}, H_C, and C_0 from Sections 7.3.2 to 7.3.4. Section 9.4 presents predictions of vessel performance using the same models with the waste conditions extracted from the Hanford PSDD. Section 9.5 presents predictions of vessel performance for the same waste conditions as Section 9.4 but uses the generalized models discussed in Section 7.4. Section 9.6 summarizes the results.

9.1 Approach for Predicting Vessel Performance

Evaluating the mixing system design for a particular WTP vessel involves comparing the predicted performance with the required performance. For the WTP vessels, the mixing requirements (Olsen 2008a) and the vessel and PJM mixing system design parameters (BNI 2007)[2] were provided by the client. The predicted performance can be calculated using the models with these inputs and assumed waste properties. The evaluation then becomes a direct comparison of predictions with requirements, with no allowance for uncertainty or design margin. This is not to imply that uncertainties and design margins aren't important, just that they were not included in the examples considered. For the different waste or design limit conditions, the physical and generalized models were used to predict 1) the velocity

[1] U_{CS} is the velocity at which all solids are suspended at the end of the drive cycle of the PJM pulse. U_{CS} velocity is not the velocity required to fully mix the solids in the tank. During testing, simulant clouds would often remain near the bottom of the tank when the U_{CS} velocity had been achieved.
[2] Email communication from GL Smith to PA Scott, February 23, 2007 regarding CCN 51865.

needed for off-bottom suspension (U_{CS}) and 2) the average solids concentration at the floor of the vessel (C_0). The requirements and the use of these variables to evaluate these requirements are discussed in Section 9.1.1.

9.1.1 Overview of Requirements

The WTP has established nine performance criteria that apply to the various mixing systems. Not all of these criteria apply to all WTP vessels. For the solids-containing WTP PJM vessels, the developed models allow for evaluating the following two criteria:

- Maintain the solids concentration at the pump suction lower than 20 wt% to prevent line plugging
- Ensure that the solids (above a minimal fraction) are disturbed to release flammable gas.

The first criterion is related to the solids concentrations at the pump inlet of the vessel. The models presented in this report predict the solids concentration near the floor of the vessel rather than precisely at the pump suction inlet. The difference in elevation is negligible, and the predicted value is expected to be within the uncertainty of the prediction. The second criterion for disturbing the solids is not quite the same as the U_{CS} predicted by the models. A predicted U_{CS} value represents the condition under which all of the solids have just barely been suspended at the end of the pulse, and thus represents a minimal condition or satisfying the solids disturbance requirement.

9.1.2 Assumptions and Limitations

Testing requires controllable conditions, measurable results, and some compromises. In this program, testing was conducted using noncohesive simulants of tightly controlled single-size distribution, single-density spherical particulate in a water medium (distribution and density ranges of each simulant are discussed in Section 3.0). These physical properties are not identical to actual wastes, of course, but the settling velocities that were investigated covered the range of interest for Hanford waste (see Figure 3.4). In addition, the test equipment used was not prototypic in geometry (size of tank and relative size of tank internals) or performance (full cycle PJMs), and some compromises and assumptions were required. As such, there are some caveats to the conclusions. Important assumptions and limitations follow:

- The Hanford PSDD (Wells et al. 2007) Case 3 is assumed to represent reasonable and actual waste conditions entering the WTP. The waste characterizations in Hanford PSDD examine the full suite of Hanford tank wastes. The individual treatment batches of waste that will be delivered to the WTP will be subsets of the total Hanford waste. The characteristics of an individual batch will vary from those characterized in the Hanford PSDD.
- The mixing performance models were developed for noncohesive solids. As such they do not apply to wastes exhibiting cohesive properties. Cohesive wastes have an additional interparticle bonding force that must be overcome to mobilize them in a vessel; the force can change mixing behavior in the vessel.
- Testing for this report was conducted using simulants with very narrow PSDD. The results from the tight distribution testing were used to create models that were compared with benchmark tests that had broader distributions and/or multiple particle sizes and densities (Section 8.0). The models were applied assuming that a single settling velocity can be used to represent a broader particle size and

are adequately accounted for in the models using settling velocity terms. Results for the NCAW filtration simulant benchmark support use of a U_{95} particle settling velocity in the vessel ratings.

- The test systems did not use a prototypic (reciprocating) pulsing action but a drive (recirculating) action. This resulted in a net upward velocity in the vessel that would not be present in a prototypic system and would tend to increase the height of a cloud. In that sense, the system used for testing was nonconservative. On the other hand, the recirculating pulse did not withdraw solids into a PJM, and that results in a pulse consisting only of water rather than the more dense slurry that would result from a prototypic system. This difference would likely result in a higher velocity being needed for off-bottom suspension than would be needed in a prototypic system.
- The PJMs in the test system were straight pipes of a much smaller diameter than geometrically scaled PJMs and did not have the same nozzle shape. These differences were assumed to be of second order in terms of variables that would affect performance.
- The preponderant test data were collected for a PJM configuration that was scaled down from HLP-22, which has 12 PJMs. This tends to favor predictions of similar configurations. The limited 8- and 4-tube tests indicate that the mixing models can be applied to those configurations as well, but the results may have more uncertainty or some bias.

The comparisons of model predictions with mixing results for benchmark experiments (in larger-scale vessels with actual PJM and representative PSDDs) discussed in Section 8.0 indicate the ability of models to predict mixing performance in actual WTP vessels. Although good comparisons could not be achieved for all benchmark cases, the results allow us to proceed to assessing vessel mixing performance with confidence that model predictions are reasonably consistent with observed physical responses. This is sufficient in light of the intended use of the models to identify adequacy or inadequacy of mixing system designs, but not for close prediction of performance to assess design margins.

9.1.3 Uncertainties Related to the Application of the Mixing Models

Several types of uncertainty related to testing and development of the mixing models were discussed in Section 8.2.4. When applying the models to specific cases, additional assumptions are required related to the waste properties and the actual performance of the design. If the models were considered perfect predictors, performance uncertainty would be related to the selection of the appropriate settling velocity and any deviation of the pulse jets from design values. Of these two, the waste properties likely introduce the greater uncertainty. This is due to the variations in waste properties for individual treatment batches from the total Hanford wastes described in the PSDD (Wells et al. 2007).

The models can be used to predict the mixing performance at defined conditions and then exercised to determine the sensitivity of a WTP vessel mixing design to changes in conditions. Such sensitivity analyses have not been conducted, but would provide insight to alternatives or modifications that could improve mixing performance. The sensitivity can be used to determine how design and operating margins should be selected and where they should be applied. For example, a change in design will affect the margin for all waste streams but may not be needed for most of them. Alternatively, a change in feed characteristics, such as volume percent solids, may be implemented only on problematic wastes streams to achieve sufficient margin.

9.1.4 Proposed Evaluation Methodology

In the following examples, the WTP vessels were grouped into similar design and operational types, and performance metrics were evaluated for the vessel types. Additional assessments for HLP-22 were conducted to provide key information for design modification options. The assessment of the vessel types is based on two performance metrics:

- *Solids concentration metric*: This metric is the predicted concentration at the floor relative to 20 wt%. The value of 20 wt% is the client-supplied upper concentration limit at the pump inlet (normally at the bottom of the vessel, within 1 ft of the floor). The model given by Eq. (7.50) gives the floor concentration in terms of volume fraction C_0. In evaluating plant vessels it is useful to express the solids concentration as the weight fraction (W_0) [or as shown in the tables for the examples as a wt% where W_0 is multiplied by 100], which is related to the volume fraction by

$$W_0 = \frac{sC_0}{(s-1)C_0 + 1} \tag{9.1}$$

To compensate for observed underprediction of the concentration at the floor (as discussed in Section 7.3.3), the model-predicted W_0 is multiplied by 1.5. Therefore the metric is

$$\text{Concentration Metric} = \frac{0.20}{W_0^*} \tag{9.2}$$

where, $W_0^* = 1.5W_0$. Hence when $0.20/W_0^* > 1$ the concentration on the floor is predicted to be less than 20 wt%. This criterion, however, does not necessarily imply a well-mixed vessel with good vertical solids distribution. For that to be achieved, the value of C_0 needs to approach the average solids loading in the vessel.

- *Solids suspension metric*: This metric compares the vessel's design velocity with the model-predicted U_{CS}. While achieving U_{CS} in general may not provide sufficient mixing in a vessel, it is generally considered to be a minimum requirement for a robust mixing system. The suspension metric is given by

$$\text{Suspension Metric} = \frac{U_{design}}{U_{CS}} \tag{9.3}$$

where $U_{design}/U_{CS} > 1$ implies the design is sufficient to just suspend the all solids off the floor by the end of the PJM drive pulse.

The example assessments were conducted using three sets of waste properties. The waste properties used in the evaluation included:

- U_{95}: This is the 95th percentile of the particle settling velocity distribution, based on the Hanford tank waste PSDD Case 3. Use of the 95th percentile is supported by the results of the model benchmarking (Section 8.0).
- $\overline{U}_{90}$: This is the volume-weighted average settling velocity for the fastest settling 10% of the Hanford tank waste.
- *Design limit particle*: For assessing the vessel types, WTP provided *Determination of Mixing Requirements for Pulse-Jet-Mixed Vessels in the Waste Treatment Plant* (Olsen 2008a). This

requirements document identified the upper limit for waste concentrations and particle characteristics for each vessel. While upper limits were specified, the PSDDs were not identified. The vessels were also assessed using the design-limit particle.

The U_{95} and $\overline{U}_{90}$ settling velocities and the design limit particle are used to establish an evaluation range for assessing the vessel types.

The examples provided can be used by the WTP M&PE group for assessing the mixing designs of WTP vessels. The examples show a combined assessment of the two criteria (concentration at the pump inlet using W_0^* and off-bottom solids suspension using U_{CS}) that can be used to evaluate a vessel type. The performance ratios for U_{CS} (U_{design}/U_{CS} = design velocity/U_{CS} predicted) and for suction inlet concentration ($0.20/W_0^* = 20\%/W_0^*$) can be compared to 1.0 to assess whether the criteria are met. The WTP M&PE group could use these ratios to assess whether mixing designs for WTP vessels meet plant needs. However, the ratios would need to be adjusted upward by proper engineering margins. These engineering design margins must take into consideration waste feed variations, operating variations, uncertainties in the models, design sensitivities, and other engineering concerns.

Figure 9.1(b) shows an example of vessel type FEP-17 A/B using the U_{95} and $\overline{U}_{90}$ settling velocity from the Hanford waste tanks (Hanford PSDD Case 3). In this example, the U_{design}/U_{CS} value is less than 1 for wastes with U_{95} and $\overline{U}_{90}$ settling velocities. Hence, the suspension of solids is predicted to be less than the requirement for both settling velocities. The second criterion for the pump inlet concentration assessment uses the $0.20/W_0^*$ ratio. For wastes with U_{95} (U95) and $\overline{U}_{90}$ (Ubar90) settling velocities, the vessel type would not satisfy the requirement. If the WTP M&PE group used the assessment basis above for this example, vessel-type FEP-17 A/B would not meet plant needs using the combined (suspension of solids and waste concentration at the pump inlet) performance ratios.

The vessel performance examples include other important figures to support the WTP M&PE assessments of the vessel types for the conditions evaluated. These figures (which may contain curves for one or more waste conditions) include:

- A plot of U_{CS} velocities, shown in Figure 9.1(d), necessary to maintain a concentration of 20 wt% at the suction inlet ($\sim W_0^*$) for different bulk solids concentrations in the vessel listed as average (wt%) solids concentration in the vessel. This can be used as a quick performance sensitivity check for a vessel; the procedure matches current or alternative design velocities to operationally acceptable vessel solids loadings. Engineering design margins would need to be added to these figures by WTP M&PE.
- Vessel concentration distributions at the design velocity plotted for each example (or set of conditions) shown in Figure 9.1(a). For a given vessel solids loading, the elevation of the waste cloud divided by the diameter of the vessel (Z/D) is compared to the wt% solids (solids wt% distribution). An idealized curve for a fully mixed (homogenous) vessel (at the given solids loading or bulk solids wt% in the vessel) is also provided. The closer the design performance curve is to the idealized curve, the better mixed the vessel is at the design velocity. Conversely, a lower solids distribution curve indicates the waste cloud will remain near the bottom of the vessel, thereby increasing concentrations at the suction inlet.

- A graph of the maximum solids concentration on the tank bottom (W_0^*) compared with average (bulk wt%) solids concentration in the vessel, shown in Figure 9.1(c). This plot is based at the vessel's design velocity and can be used as a quick performance sensitivity check for the tank to match current or alternative vessel solids loading options to meet pump inlet concentration requirements.

These plots are based on the maximum operating fill height from Olsen (2008a). Engineering design margins would need to be added to these figures by WTP M&PE.

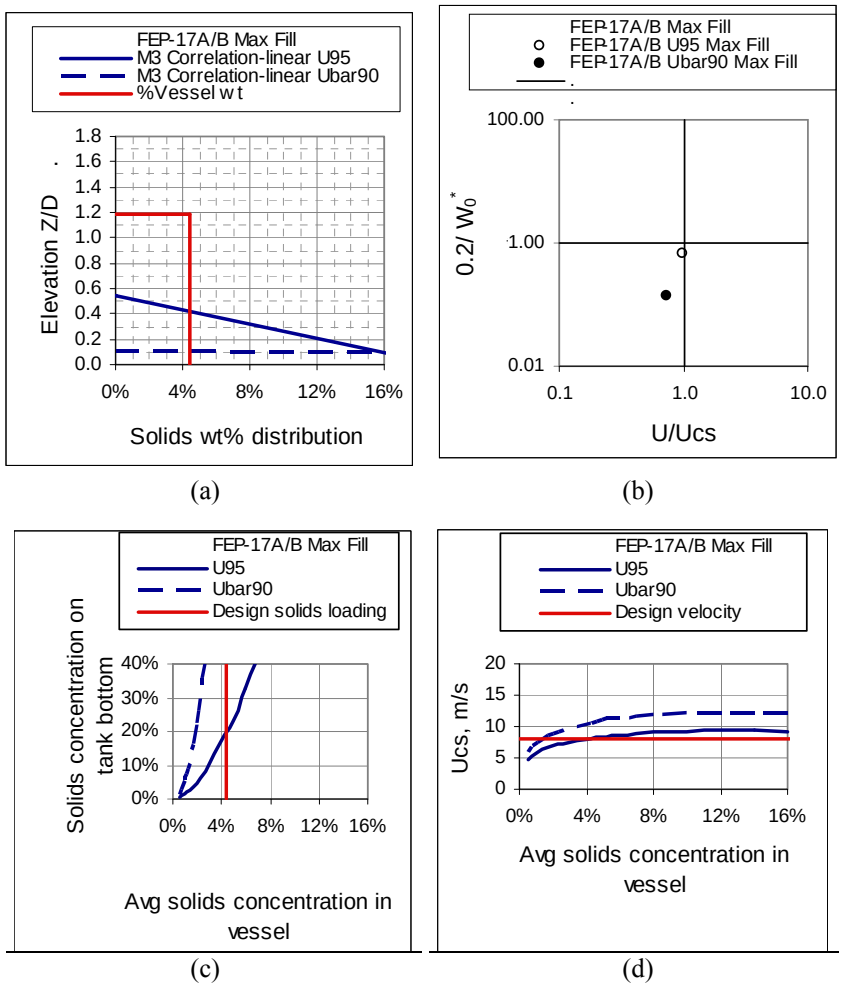

Figure 9.1. Performance Ratio Example Using FEP-17 A/B. Engineering margins would need to be added to the design ratio acceptance range by WTP M&PE. (a) Concentration distribution at design velocity, (b) FEP-17 A/B using the U_{95} and $\overline{U}_{90}$ settling velocities, (c) maximum solids concentration on the tank bottom (W_0^*) compared with average (bulk wt%) solids concentration in the vessel, (d) U_{CS} velocities to maintain 20 wt% at the suction inlet.

9.2 Input Parameters for Plant Vessels

Input parameters for the example vessel assessments came from two sources, as shown in Table 9.1. Vessel geometry and operations data tables were taken from CCN151865 (BNI 2007), and solids loading data were found in mixing requirements (Olsen 2008a, Table 6).

Table 9.1. Sources of Physical Mixing System Parameters for Plant Vessels

Information Type	WTP Source of Information
Vessel sizes, PJM number, nozzle size, duty cycle, pulse volume fractions, maximum liquid operating levels	CCN 151865 (BNI 2007)
Operational information such as limits for bulk solids loading, particle size, average particle density, liquid density, and liquid rheology	Olsen (2008a)

9.2.1 Vessel Geometry and Operational Data

The vessel geometry and operations data were converted to model-specific parameters as required. The reference volume (V_{REF}) for each WTP vessel was calculated using the vessel diameter. Other parameters (ϕ_p and ϕ_J) were computed from vessel geometry for an 80% PJM stroke. The vessel geometry and operations data that were used as model inputs are shown in Table 9.2. Fill levels (expressed as H/D) are for maximum fill conditions. Duty cycles for the 4-in. cases were used as listed, with the assumption that the new jet pump pairs (JPPs) would operate at the recently proposed 12 m/s. For the 6-in. cases, suction time was assumed to remain the same as the 4-in. cases, and the drive time was assumed to scale with increased flow area. This reduced the duty cycle for the 6-in. cases from 0.33 to 0.22.

Table 9.2. Vessel Geometry and Operations Data Used in WTP Vessel Assessments

Vessel	w_{Smax}%[(a)]	V_{REF} (ft^3)[(b)]	N	D (ft)[(b)]	d (in.)[(b)]	ϕ_p	ϕ_J	H/D	U (m/s)	DC
FRP-02A/B/C/D	0.049	81542	12	47.0	4.0	0.025	0.00060	0.73	8	0.37
HLP-22 (4in,8m/s)	0.154	43096	12	38.0	4.0	0.050	0.00092	0.80	8	0.33
HLP-22 (4in,12m/s)	0.154	43096	12	38.0	4.0	0.050	0.00092	0.80	12	0.33
HLP-22 (6in,8m/s)	0.154	43096	12	38.0	6.0	0.050	0.00208	0.80	8	0.22
HLP-22 (6in,12m/s)	0.154	43096	12	38.0	6.0	0.050	0.00208	0.80	12	0.22
TCP-01	0.027	14616	8	26.5	4.0	0.095	0.00127	1.25	8	0.33
TLP-09A/B	0.003	13804	8	26.0	4.0	0.036	0.00131	1.08	8	0.30
PWD-33	0.081	10857	8	24.0	4.0	0.021	0.00154	0.45	8	0.30
PWD-43	0.002	10857	8	24.0	4.0	0.021	0.00154	0.45	8	0.30
PWD-44	0.081	9556	8	23.0	4.0	0.097	0.00168	1.32	8	0.33
FEP-17A/B	0.044	8363	8	22.0	4.0	0.091	0.00184	1.19	8	0.29
PWD-15/16	0.03	8363	8	22.0	4.0	0.055	0.00184	1.78	8	0.35
UFP-01A/B	0.038	6283	8	20.0	4.0	0.094	0.00222	1.45	8	0.31
RLD-07	0.022	1726	4	13.0	4.0	0.051	0.00263	1.20	8	0.27
RLD-08	0.022	1726	4	13.0	4.0	0.053	0.00263	0.91	8	0.29
HOP-903/904	0.01	1357	4	12.0	4.0	0.036	0.00309	0.86	8	0.26

(a) w_{Smax}% is the designed insoluble solids concentration (in wt%) for the WTP vessels.
(b) Units need to be converted from English to metric before being used in the physical and generalized models.

9.2.2 Waste Property Conditions

Waste conditions that were used in the vessel assessments are summarized in Tables 9.3 and 9.4. Table 9.3 shows inputs used in the design point cases; Table 9.4 shows corresponding inputs used in the Hanford PSDD-based cases.

Table 9.3. Vessel Solids Loading Data Used in Design Point Assessments

Vessel	Solids Loading (wt%)	Particle Size (μm)	Particle Density (g/cm^3)	Liquid Density (g/cm^3)	Liquid Viscosity (cP)	Unhindered Terminal Settling Velocity (U_T) (m/s)
FRP-02A/B/C/D	4.9	50	2.18	1.1	1.5	9.36E-4
HLP-22	15.4	210	2.18	1.1	1.5	1.25E-2
TCP-01	2.7	164	3.60	1.2	2.0	1.33E-2
TLP-09A/B	0.3	164	3.60	1.1	1.5	1.74E-2
PWD-33	8.1	210	2.18	1.0	1.0	1.81E-2
PWD-43	0.2	210	2.18	1.0	1.0	1.81E-2
PWD-44	8.1	210	2.18	1.0	1.0	1.81E-2
FEP-17A/B	4.4	50	2.18	1.1	1.5	9.36E-4
PWD-15/16	3.0	210	2.18	1.0	1.0	1.81E-2
UFP-01A/B	3.8	210	2.18	1.1	1.5	1.25E-2
RLD-07	2.2	210	2.18	1.0	1.0	1.81E-2
RLD-08	2.2	210	2.18	1.0	1.0	1.81E-2
HOP-903/904	1.0	210	2.18	1.0	1.0	1.81E-2

Table 9.4. Vessel Solids Loading Data Used in Hanford PSDD-Based Assessments

Vessel	Solids Loading (wt%)	Particle Density (g/cm^3)	Liquid Density (g/cm^3)	Liquid Viscosity (cP)	Particle Settling Velocity U_{95} (m/s)	Particle Settling Velocity $\overline{U}_{90}$ (m/s)
FRP-02A/B/C/D	4.9	2.78	1.1	1.5	2.50E-3	1.04E-2
HLP-22	15.4	2.78	1.1	1.5	2.50E-3	1.04E-2
TCP-01	2.7	2.78	1.1	1.5	2.50E-3	1.04E-2
TLP-09A/B	0.3	2.78	1.1	1.5	2.50E-3	1.04E-2
PWD-33	8.1	2.78	1.1	1.5	2.50E-3	1.04E-2
PWD-43	0.2	2.78	1.1	1.5	2.50E-3	1.04E-2
PWD-44	8.1	2.78	1.1	1.5	2.50E-3	1.04E-2
FEP-17A/B	4.4	2.78	1.1	1.5	2.50E-3	1.04E-2
PWD-15/16	3.0	2.78	1.1	1.5	2.50E-3	1.04E-2
UFP-01A/B	3.8	2.78	1.1	1.5	2.50E-3	1.04E-2
RLD-07	2.2	2.78	1.1	1.5	2.50E-3	1.04E-2
RLD-08	2.2	2.78	1.1	1.5	2.50E-3	1.04E-2
HOP-903/904	1.0	2.78	1.1	1.5	2.50E-3	1.04E-2

The solids loading data is the maximum concentration from the mixing requirements (Olsen 2008a). Solids and liquid properties depended on whether the design cases (Table 9.3) or Hanford PSDD (Table 9.4) were being evaluated. Olsen (2008a) included liquid density but did not specify liquid viscosity. For the design point examples in Section 9.3, where density was specified as 1 g/cm^3, the viscosity of water was used (1 cP). If the density was specified as 1.1 g/cm^3, a viscosity of 1.5 cP was used. For the single vessel with a liquid density of 1.2 g/cm^3 specified, a viscosity of 2 cP was used. The fluid viscosities were based on measurements of Hanford waste with the specified densities (Wells et al. 2007). The settling velocities in Table 9.3 were calculated from the liquid and particulate properties shown for each vessel (as per Section 7.0).

A uniform liquid density of 1.1 g/cm^3 was used in the Hanford PSDD cases with a fluid viscosity of 1.5 cP. The settling velocities in Table 9.4 were calculated from the Hanford PSDD as presented in Table 3.4 and were assigned the same for all vessels evaluated.

9.2.3 Dimensionless Variable Evaluation

The U_{CS} and H_C physical models presented in Sections 7.3.2 and 7.3.4, and the generalized models presented in Section 7.4, are functions of dimensionless variables. The values of these dimensionless variables were evaluated for the WTP vessel mixing systems, relative to the ranges of the variables for the test data and benchmark cases in Section 8.0. The dimensionless variables from the physical models for U_{CS} and H_C include:

Ratio of jet velocity to hindered terminal settling velocity

$$\frac{U}{U_{TH}} \tag{9.4}$$

Ratio of D* to square root of the Galileo number

$$\frac{D^*}{Ga^{0.5}} \tag{9.5}$$

The dimensionless variables from the generalized models for U_{CS} and H_C include:

Ratio of jet diameter to tank diameter

$$\frac{d}{D} \tag{9.6}$$

Ratio of unhindered terminal settling velocity to jet velocity

$$\frac{U_T}{U} \tag{9.7}$$

Froude number based on jet velocity and tank diameter

$$\frac{(s-1)gD}{U^2} \tag{9.8}$$

Froude number based on unhindered terminal settling velocity and tank diameter

$$\frac{(s-1)gD}{U_T{}^2} \tag{9.9}$$

The test data set is the same as that described in Section 7.3.2 (the complete data set is listed in Appendix B). The benchmark and WTP vessel parameters are taken from Section 8.0 and Tables 9.2 and 9.4. The dimensionless variables for the test data are presented in Figures 9.2 through 9.7 as cumulative probability distributions (M3 tests). Thus, for example, from Figure 9.2, 10% of the test data had U/U_{TH} less than approximately 3E2 and 90% greater than 3E2. In Figures 9.2 to 9.7, the WTP vessels are designated by name, and the benchmarks are denoted by "BM."

For dimensionless variables with a terminal or hindered settling velocity (Eq. 9.3, 9.4, 9.6, and 9.8), the vertical location of the WTP vessel and benchmark data points represent the quantiles (also known as percentiles) of the settling velocities used in application. For the WTP vessels, 0.95 denotes U_{95}, and 0.9 denotes $\overline{U}_{90}$. The 90th, 60th, and 50th percentiles are the settling velocities used for the respective benchmarks (see Section 8.0). For the dimensionless variables of Eq. (9.5) and (9.7), the vertical location of the WTP vessel and benchmark data points at 0.5 is arbitrary.

In general, the WTP vessel and benchmark data points are within or close to the test data range. However, some extrapolation does occur for four of the six nondimensional variables. Thus, application of the U_{CS} and H_C models is via interpolation or minor to moderate extrapolation.

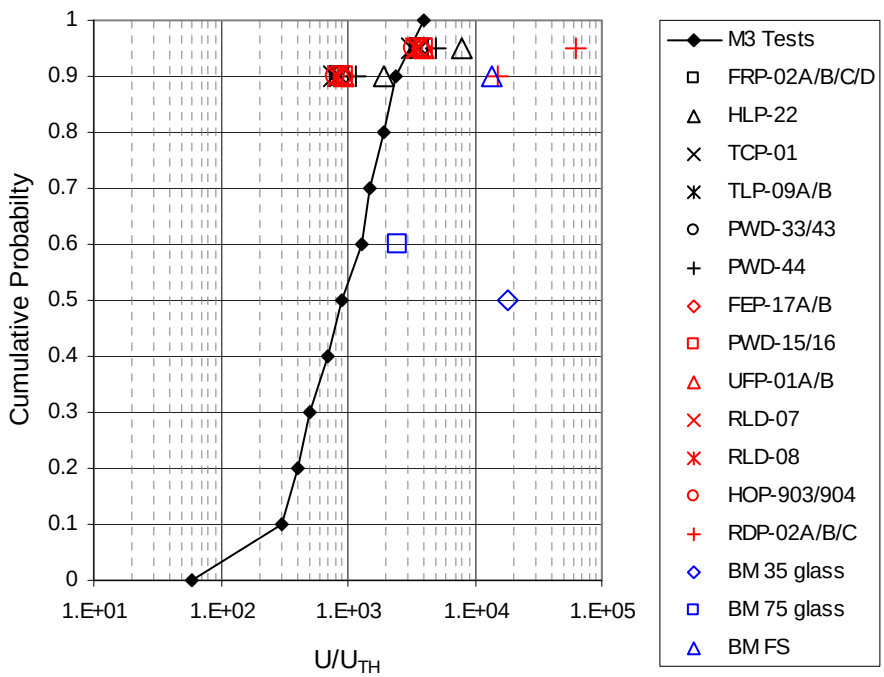

Figure 9.2. Test Data and Application Range for $\frac{U}{U_{TH}}$

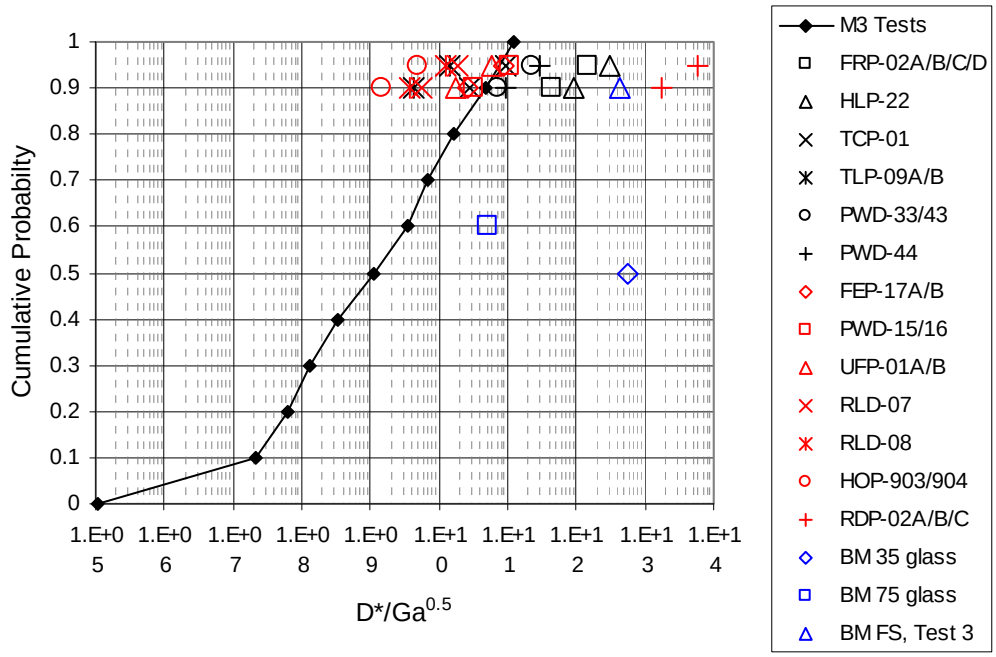

Figure 9.3. Test Data and Application Range for $\frac{D^*}{Ga^{0.5}}$

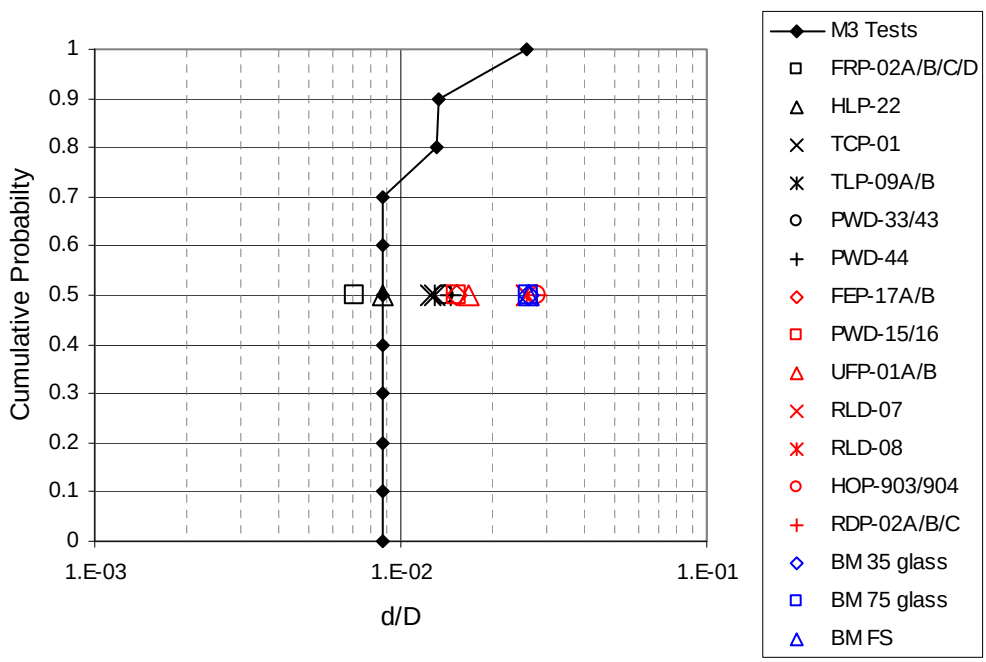

Figure 9.4. Test Data and Application Range for $\frac{d}{D}$

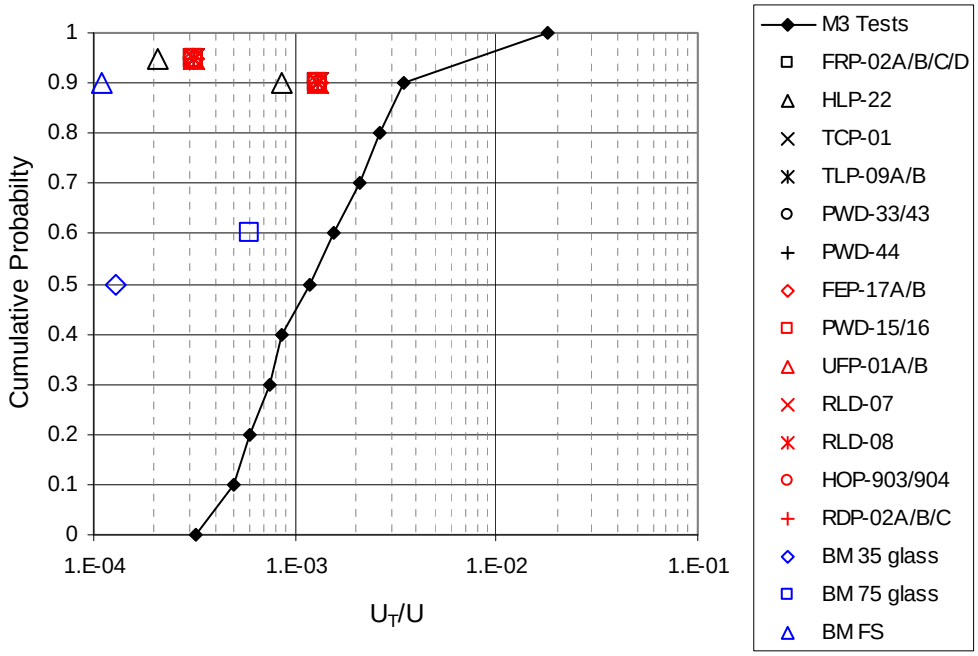

Figure 9.5. Test Data and Application Range for $\frac{U_T}{U}$

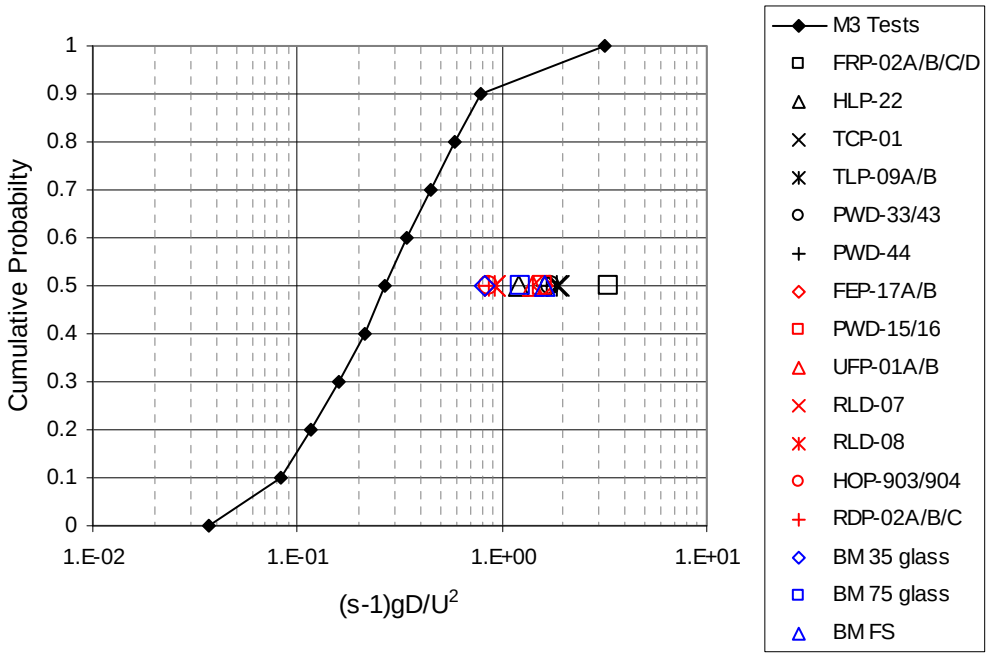

Figure 9.6. Test Data and Application Range for $\frac{(s-1)gD}{U^2}$

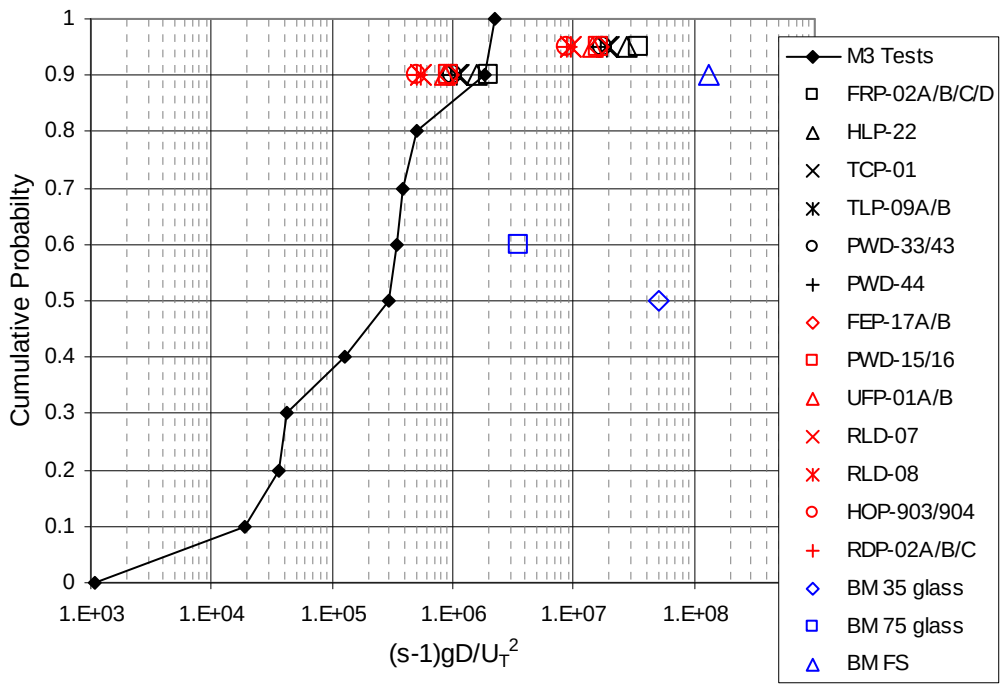

Figure 9.7. Test Data and Application Range for $\frac{(s-1)gD}{U_T^2}$

9.2.4 Hanford Tank AZ-101 PSDD and Settling Velocity

The in situ settling velocity for AZ-101 is compared with a PSDD-based settling velocity to investigate the applicability of the settling velocity approach for systems with distributions of solid size and density.

Two 300-hp mixer pumps were used to mobilize the sediment layer in AZ-101 from April to May 2000 (Carlson et al. 2001). The capability of the mixer pumps to mobilize the sediment was tracked with the following:

- thermocouples located throughout the waste and in the tank floor
- a gamma monitoring system (detects radionuclides)
- a suspended-solids profiler (uses light reflectance to determine turbidity)
- an ultrasonic interface level analyzer.

Carlson et al. (2001) report that, for the oscillatory operation of both mixer pumps, the AZ-101 thermocouple data indicated that the majority of the sediment was mobilized. The gamma monitoring system, suspended-solids profiler, and ultrasonic interface level analyzer data indicated that 1) significant settling occurs as soon as mixer pump operations are concluded and 2) significant settling occurs in the first 8 to 12 hours. The unhindered settling rate was determined as 2.2 m/hr (6E-4 m/s). In consideration of the "...high unhindered settling rate determined from the test data," Carlson et al. (2001) recommended "...that mixer pumps be operated to maintain solids in suspension during future deliveries of waste from

this tank (AZ-101) to the WTP. This will maintain the solid phase in a more uniform concentration during batch deliveries that are expected to last approximately 20 hours each."

An AZ-101 PSDD was created according to the Case 3 approach of Wells et al. (2007). The Case 3 PSDD is provided in Section 3.1. The AZ-101 minimal disturbance PSD was combined with the insoluble solid-phase compounds, volume fractions thereof, and crystal densities (Wells et al. 2007, Table A.4 and Section 3.2). The resulting PSDD is provided in Table 9.5. Like the PSDDs of Wells et al. (2007), the AZ-101 PSDD in Table 9.5 is a 3-dimensional matrix of volume-based probability of each solid-phase compound in a PSD bin and its density in that bin. The PSDD bins represent the upper and lower size limit of the particles in each bin. For example, in Table 9.5 it can be seen that gibbsite [$Al(OH)_3$] makes up 75% of the solid particulate by volume, and gibbsite particles > 7.74 μm and less than or equal to 10 μm have a density of 2.42 g/cm^3 and make up 3.6% of the solids by volume.

The particle size and density of the AZ-101 PSDD are used in the settling velocity equations in Section 7.0 in conjunction with the volume fraction to produce the cumulative volume-based probability of the settling velocity of the AZ-101 insoluble solids (Figure 9.2) as per Section 3.1. In Figure 9.2, the 50th (median) and 95th percentiles by volume of settling velocity are approximately 6.4E-6 and 2.3E-4 m/s, respectively.

As in Section 3.1, a volume-weighted average of a specified fraction of the solids by volume may be determined, resulting in the cumulative average settling velocity of Figure 9.3. In the figure, the volume-weighted average settling velocity of the fastest 10% by volume is 4.8E-5 m/s.

The percentiles of settling velocity for the AZ-101 PSDD from Figures 9.8 and 9.9 are provided in Table 9.6. In the table it can be seen that the unhindered settling rate of Carlson et al. (2001), 6E-4 m/s, is greater than both the 99th percentile by volume of the settling velocity and the volume-weighted average of the fastest 1%.

Comparing the AZ-101 unhindered settling rate from Carlson et al. (2001), 6E-4 m/s, with the settling velocities of the Hanford PSDD (Table 3.3) indicates the AZ-101 settling rate is between the 85th to 90th percentiles of the settling velocity distribution from the Hanford PSDD. This suggests that 10 to 15% of the Hanford insoluble solids by volume may be expected to settle at a rate equal to or greater than that indicated by the in situ settling data for AZ-101.

Table 9.5. AZ-101 PSDD

Particle Size (μm)	Solid Phase Compounds and Density (g/cm^3)								
	$Al(OH)_3$ 2.42	Fe_2O_3 5.24	ZrO_2 5.68	$Ca_5OH(PO_4)_3$ 3.14	$Ni(OH)_2$ 4.1	$Na_2U_2O_7$ 5.617	MnO_2 5.026	$LaPO_4 \cdot 2H_2O$ 6.51	PuO_2 11.43
	Solid Volume Fraction								
0.22	3.8E-04	7.7E-05	2.4E-05	6.9E-06	6.7E-06	4.9E-06	1.1E-06	3.7E-06	2.5E-08
0.28	9.1E-03	1.9E-03	5.7E-04	1.7E-04	1.6E-04	1.2E-04	2.7E-05	9.0E-05	6.0E-07
0.36	1.0E-02	2.1E-03	6.4E-04	1.9E-04	1.8E-04	1.3E-04	3.1E-05	1.0E-04	6.8E-07
0.46	1.3E-02	2.7E-03	8.4E-04	2.5E-04	2.4E-04	1.7E-04	4.0E-05	1.3E-04	8.8E-07
0.60	1.8E-02	3.6E-03	1.1E-03	3.2E-04	3.1E-04	2.3E-04	5.3E-05	1.7E-04	1.2E-06
0.77	2.2E-02	4.5E-03	1.4E-03	4.0E-04	3.9E-04	2.9E-04	6.5E-05	2.2E-04	1.4E-06
1.00	5.4E-02	1.1E-02	3.4E-03	9.9E-04	9.6E-04	7.0E-04	1.6E-04	5.3E-04	3.6E-06
1.29	5.1E-02	1.0E-02	3.2E-03	9.3E-04	9.0E-04	6.6E-04	1.5E-04	5.0E-04	3.4E-06
1.67	4.6E-02	9.4E-03	2.9E-03	8.5E-04	8.2E-04	6.0E-04	1.4E-04	4.6E-04	3.0E-06
2.15	6.1E-02	1.2E-02	3.8E-03	1.1E-03	1.1E-03	7.9E-04	1.8E-04	6.0E-04	4.0E-06
2.78	5.6E-02	1.1E-02	3.5E-03	1.0E-03	1.0E-03	7.3E-04	1.7E-04	5.6E-04	3.7E-06
3.59	6.0E-02	1.2E-02	3.8E-03	1.1E-03	1.1E-03	7.9E-04	1.8E-04	6.0E-04	4.0E-06
4.64	6.8E-02	1.4E-02	4.3E-03	1.3E-03	1.2E-03	8.9E-04	2.0E-04	6.8E-04	4.5E-06
5.99	6.2E-02	1.3E-02	3.9E-03	1.1E-03	1.1E-03	8.1E-04	1.8E-04	6.1E-04	4.1E-06
7.74	6.3E-02	1.3E-02	4.0E-03	1.2E-03	1.1E-03	8.3E-04	1.9E-04	6.3E-04	4.2E-06
10.00	3.6E-02	7.3E-03	2.2E-03	6.6E-04	6.3E-04	4.7E-04	1.1E-04	3.5E-04	2.4E-06
12.92	3.5E-02	7.2E-03	2.2E-03	6.5E-04	6.2E-04	4.6E-04	1.0E-04	3.5E-04	2.3E-06
16.68	3.2E-02	6.6E-03	2.0E-03	6.0E-04	5.8E-04	4.2E-04	9.7E-05	3.2E-04	2.1E-06
21.54	2.8E-02	5.7E-03	1.8E-03	5.2E-04	5.0E-04	3.7E-04	8.4E-05	2.8E-04	1.8E-06
27.83	2.3E-02	4.7E-03	1.5E-03	4.3E-04	4.1E-04	3.0E-04	6.9E-05	2.3E-04	1.5E-06
35.94	4.7E-03	9.5E-04	2.9E-04	8.6E-05	8.3E-05	6.1E-05	1.4E-05	4.6E-05	3.1E-07
Total Solid-Phase Volume Fraction	0.75	0.15	0.047	0.014	0.013	0.010	0.002	0.007	0.00005

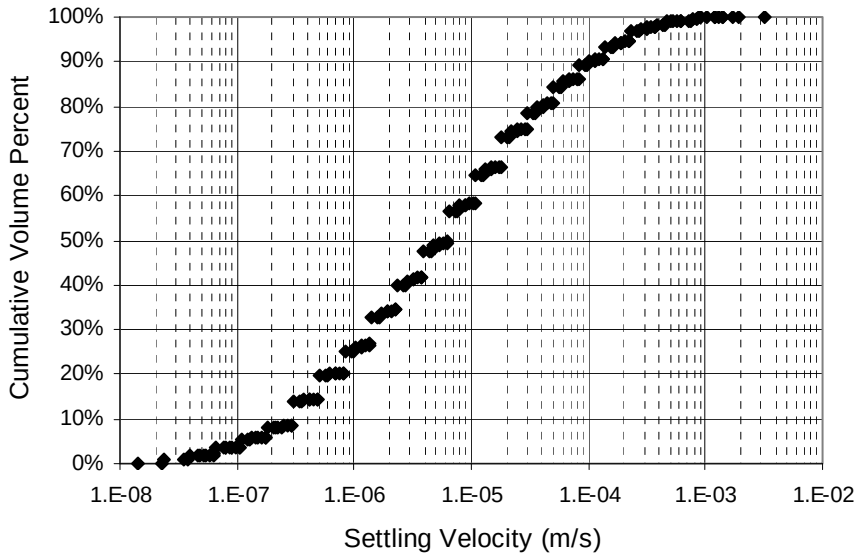

Figure 9.8. Cumulative Undissolved Solids Volume Fraction as a Function of Settling Velocity for AZ-101

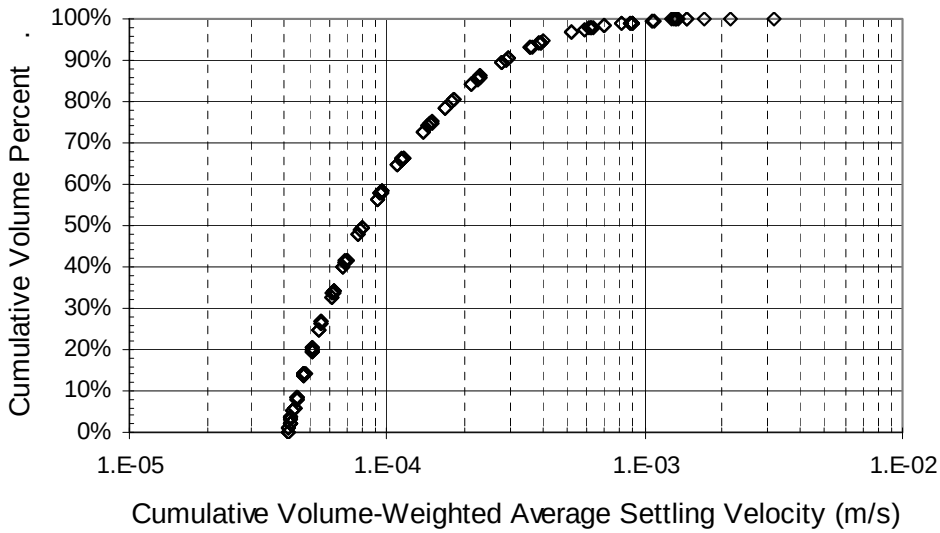

Figure 9.9. Cumulative Undissolved Solids Volume Fraction as a Function of Cumulative Volume-Weighted Average Settling Velocity for AZ-101

Table 9.6. AZ-101 Insoluble Solids Settling Velocity Quantiles (see Section 3.1 for discussion of volume-weighted averaging and summations)

Percentiles (%)	Settling Velocity (m/s)	Volume-Weighted Average Settling Velocity (m/s)[(a)]
5	1.1E-07	4.3E-05
10	3.0E-07	4.8E-05
25	9.8E-07	5.5E-05
50	6.4E-06	9.1E-05
55	6.4E-06	9.1E-05
60	1.1E-05	1.1E-04
65	1.3E-05	1.1E-04
70	1.8E-05	1.4E-04
75	2.9E-05	1.5E-04
80	3.7E-05	1.8E-04
85	5.9E-05	2.2E-04
90	9.8E-05	2.9E-04
95	2.3E-04	5.2E-04
99	5.2E-04	8.7E-04
Volume Weighted Average	4.1E-05	4.1E-05
Minimum	1.4E-08	4.1E-05
Maximum	3.2E-03	3.2E-03

(a) Summed from fastest-settling solid particulate.

9.3 Vessel Evaluation Examples Using the Physical Models and the Design Point Limits

This section includes examples of assessing mixing performance of WTP vessels at the design point limits from Olsen (2008a). Since particle distributions are not specified in Olsen (2008a), the particles specified in the design limit section were used for these model inputs. Many of the vessel evaluations show two points labeled "design" and "design2." Design denotes a solids density of 2.18 g/cm^3 established in Olsen (2008a, Table 6), and design 2 denotes a solids density of 2.78 g/cm^3 (which is believed to better represent the solids density). This information is presented in the tables and figures that make up Sections 9.3.1 through 9.3.16.

The evaluation in this section used the physical models for U_{CS}, H_C and C_0 from Section 7.3.4 with C_0 modified to W_0^* as described in Section 9.1.4. The vessel geometry and operating conditions used are listed in Table 9.2 with vessel loading shown in Table 9.3.

These examples are for the vessel conditions that were provided in Olsen (2008a). This document has recently been revised to Olsen (2008b); however, these examples are based on Olsen (2008a). The examples are provided for the specific set of conditions described above. The analysis of the vessels used in the examples has been reassigned to the WTP M&PE group per Hazen (2008b).

Note that Tables 9.7 through 9.22 display only a few significant figures. The calculations are not based on this reduced number of digits. Therefore, small calculation differences are observed when using the displayed rounded numbers for calculations.

9.3.1 FRP-02 A/B/C/D (Design Point) Physical Model

Table 9.7 presents the results of the physical model for design point conditions of FRP-02 A/B/C/D. Figure 9.10 shows the physical model predictions at maximum fill for FRP-02 A/B/C/D.

Table 9.7. Physical Model Results for Design Point Conditions of FRP-02

FRP-02A/B/C/D Design Max Fill			FRP-02A/B/C/D Design2 Max Fill		
U (m/s)	U_{CS} (m/s)	U/U_{CS}	U (m/s)	U_{CS} (m/s)	U/U_{CS}
8	14.3	0.56	8	17.4	0.46
H/D	H_C/D	H_C/H	H/D	H_C/D	H_C/H
0.73	0.17	0.24	0.73	0.06	0.08
W (wt%)	W_0^* (wt%)	$0.2/W_0^*$	W (wt%)	W_0^* (wt%)	$0.2/W_0^*$
4.9	62.2	0.32	4.9	$> W_{MP}$ [(a)]	0.11

(a) Calculated value exceeds maximum packing fraction.

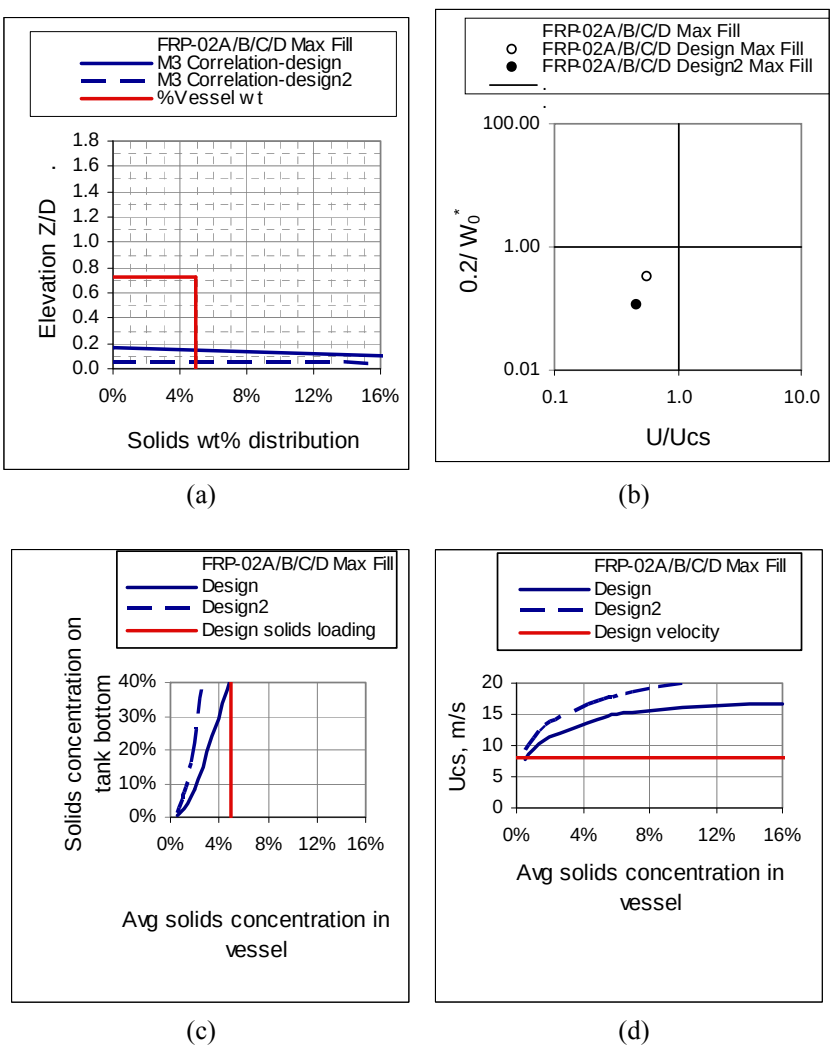

Figure 9.10. Physical Model Predictions for FRP-02 A/B/C/D: (a) Concentration Profile at Maximum Fill, (b) Inlet Concentration and Suspension Ratio, (c) Maximum Solids Concentration Versus Loading Design Conditions, (d) U_{CS} Versus Vessel Loading

9.3.2 HLP-22 8 m/s, 4-in. Nozzles (Design Point) Physical Model

Table 9.8 presents the physical model results for design point conditions for HLP-22, and Figure 9.11 depicts the physical model predictions for HLP-22 for 8 m/s with 4-in. nozzles.

Table 9.8. Physical Model Results for Design Point Conditions for HLP-22

HLP-22 Design Max Fill			HLP-22 Design2 Max Fill		
U (m/s)	U_{CS} (m/s)	U/U_{CS}	U (m/s)	U_{CS} (m/s)	U/U_{CS}
8	19.1	0.42	8	23.9	0.33
H/D	H_C/D	H_C/H	H/D	H_C/D	H_C/H
0.80	0.01	0.01	0.80	0.01	0.01
W (wt%)	W_0^* (wt%)	$0.2/W_0^*$	W (wt%)	W_0^* (wt%)	$0.2/W_0^*$
15.4	$> W_{MP}$[(a)]	0.005	15.4	$> W_{MP}$[(a)]	0.002

(a) Calculated value exceeds maximum packing fraction.

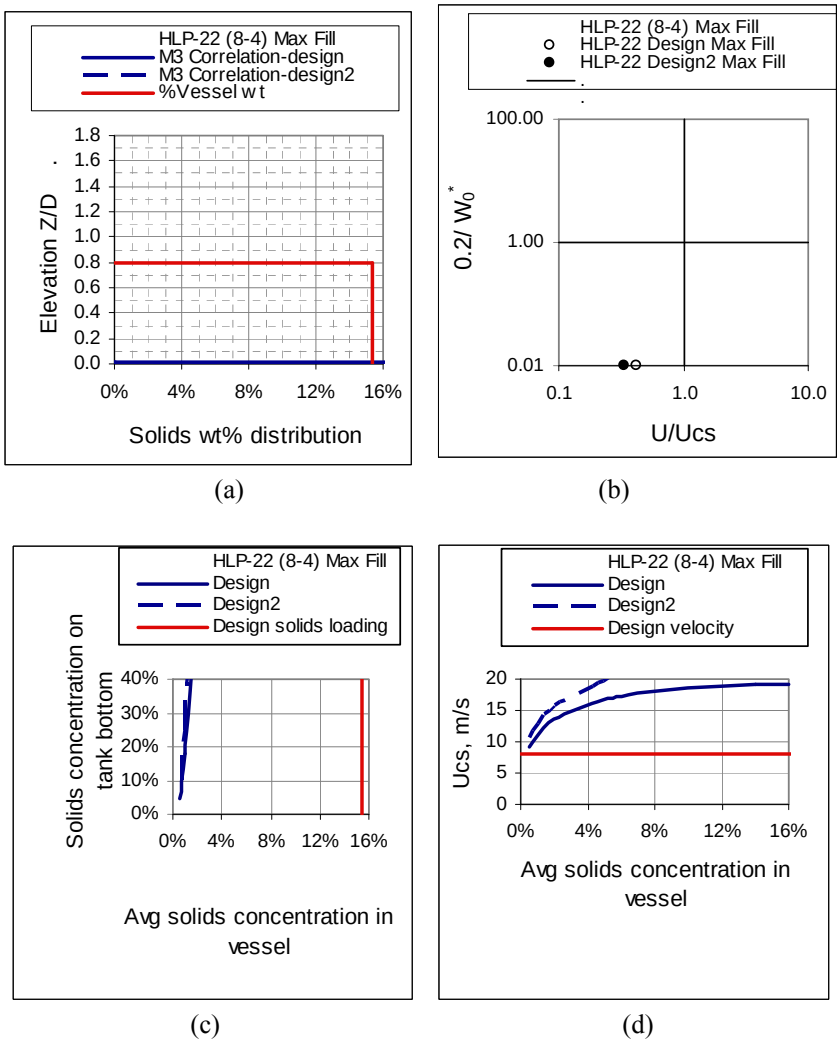

Figure 9.11. Physical Model Predictions for HLP-22: (a) Concentration Profile at Max Fill, (b) Inlet Concentration and Suspension Ratio, (c) Maximum Solids Concentration Versus Loading Design Conditions, (d) U_{CS} Versus Loading at 8 m/s, 4-in. Nozzles (design point)

9.3.3 HLP-22 12 m/s, 4-in. Nozzles (Design Point) Physical Model

Table 9.9 presents the physical model results for design point conditions for HLP-22, and Figure 9.12 depicts the physical model predictions for HLP-22 with 4-in. nozzles.

Table 9.9. Physical Model Results for Design Point Conditions for HLP-22

HLP-22 Design Max Fill			HLP-22 Design2 Max Fill		
U (m/s)	U_{CS} (m/s)	U/U_{CS}	U (m/s)	U_{CS} (m/s)	U/U_{CS}
12	19.1	0.63	12	23.9	0.50
H/D	H_C/D	H_C/H	H/D	H_C/D	H_C/H
0.80	0.03	0.04	0.80	0.02	0.02
W (wt%)	W_0^* (wt%)	$0.2/W_0^*$	W (wt%)	W_0^* (wt%)	$0.2/W_0^*$
15.4	$> W_{MP}$[(a)]	0.02	15.4	$> W_{MP}$[(a)]	0.01

(a) Calculated value exceeds maximum packing fraction.

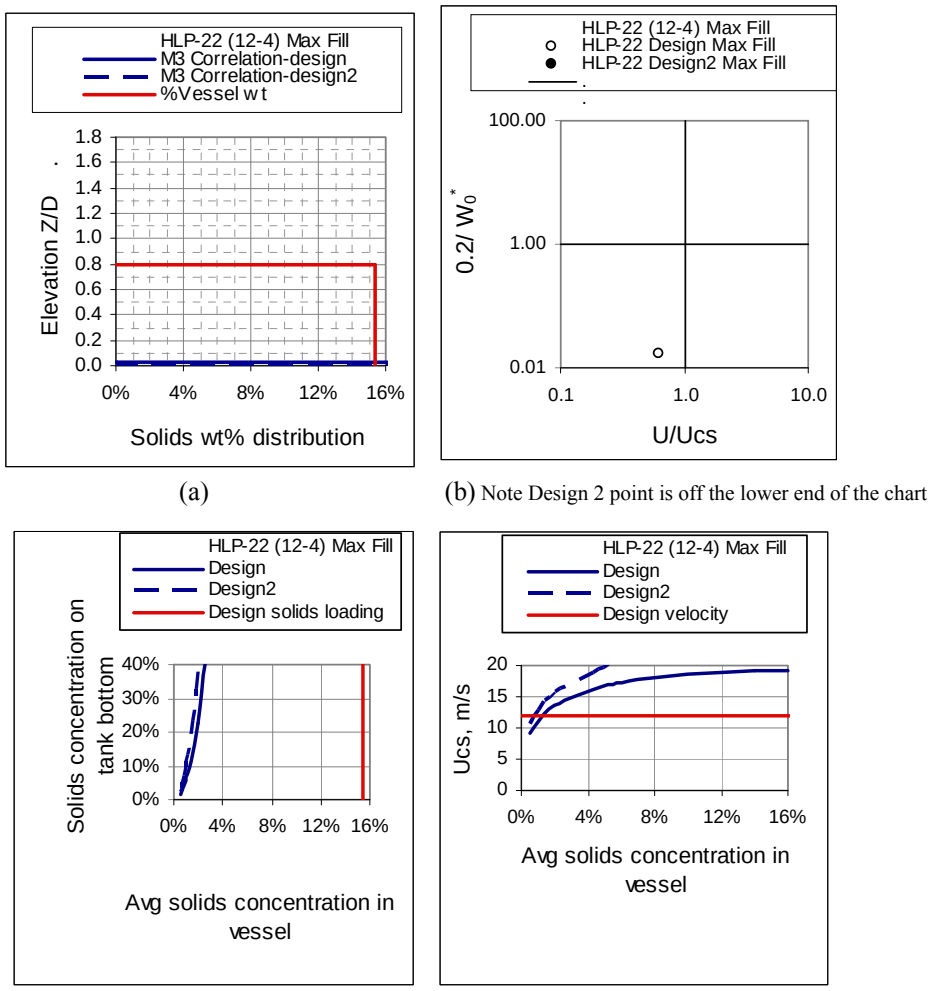

Figure 9.12. Physical Model Predictions for HLP-22: (a) Concentration Profile at Max Fill, (b) Inlet Concentration and Suspension Ratio, (c) Maximum Solids Concentration Versus Loading Design Conditions, (d) U_{CS} Versus Loading at 12 m/s, 4-in. Nozzles (design point)

9.3.4 HLP-22 8 m/s, 6-in. Nozzles (Design Point) Physical Model

Table 9.10 lists the physical model results for design point conditions for HLP-22, and Figure 9.13 shows the physical model predictions at max fill for HLP-22 for 8 m/s with 6-in. nozzles.

Table 9.10. Physical Model Results for Design Point Conditions for HLP-22

HLP-22 Design Max Fill			HLP-22 Design2 Max Fill		
U (m/s)	U_{CS} (m/s)	U/U_{CS}	U (m/s)	U_{CS} (m/s)	U/U_{CS}
8	14.5	0.55	8	18.1	0.44
H/D	H_C/D	H_C/H	H/D	H_C/D	H_C/H
0.80	0.02	0.03	0.80	0.01	0.02
W (wt%)	W_0^* (wt%)	$0.2/W_0^*$	W (wt%)	W_0^* (wt%)	$0.2/W_0^*$
15.4	$> W_{MP}$ [(a)]	0.013	15.4	$> W_{MP}$ [(a)]	0.007

(a) Calculated value exceeds maximum packing fraction.

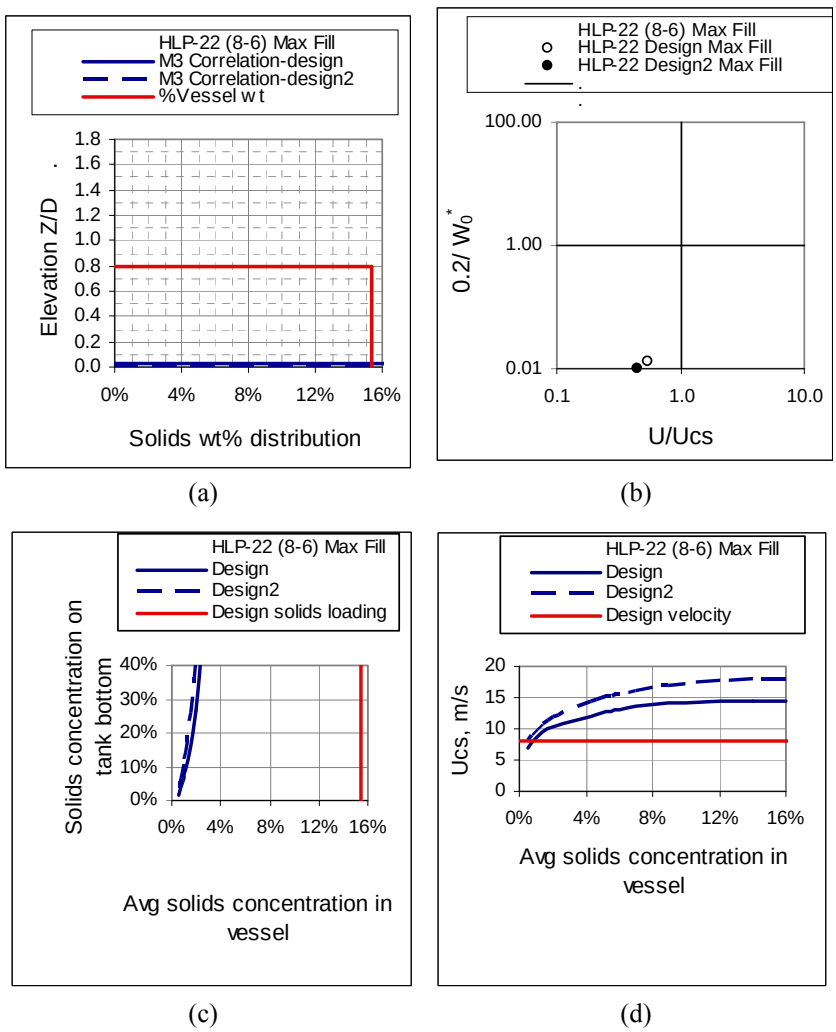

Figure 9.13. Physical Model Predictions for HLP-22: (a) Concentration Profile at Max Fill, (b) Inlet Concentration and Suspension Ratio, (c) Maximum Solids Concentration Versus Loading Design Conditions, (d) U_{CS} Versus Loading at 8 m/s, 6-in. Nozzles (design point)

9.3.5 HLP-22 12 m/s, 6-in. Nozzles (Design Point) Physical Model

Table 9.11 contains the results for the physical model for design point conditions for HLP-22, and Figure 9.14 presents physical model predictions for HLP-22 for 12 m/s with 6-in. nozzles.

Table 9.11. Physical Model Results for Design Point Conditions for HLP-22

HLP-22 Design Max Fill			HLP-22 Design2 Max Fill		
U (m/s)	U_{CS} (m/s)	U/U_{CS}	U (m/s)	U_{CS} (m/s)	U/U_{CS}
12	14.5	0.83	12	18.1	0.66
H/D	H_C/D	H_C/H	H/D	H_C/D	H_C/H
0.80	0.08	0.10	0.80	0.04	0.05
W (wt%)	W_0^* (wt%)	$0.2/W_0^*$	W (wt%)	W_0^* (wt%)	$0.2/W_0^*$
15.4	$> W_{MP}$ [(a)]	0.044	15.4	$> W_{MP}$ [(a)]	0.021

(a) Calculated value exceeds maximum packing fraction.

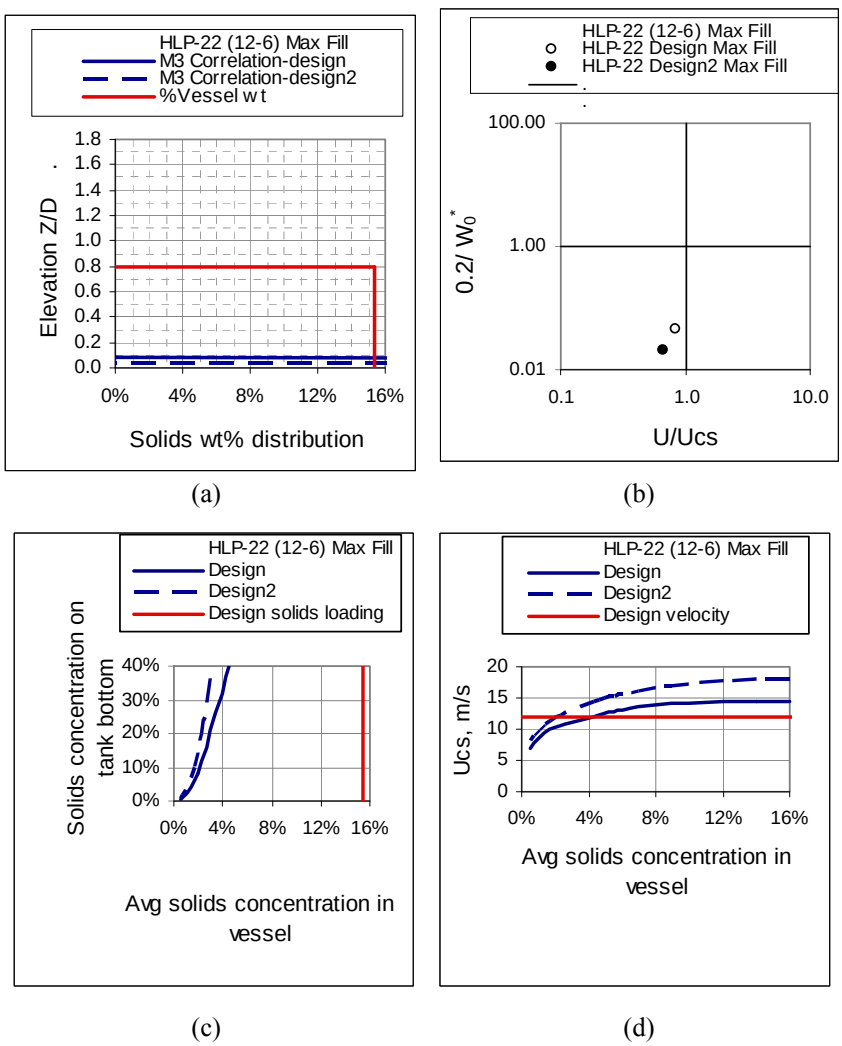

Figure 9.14. Physical Model Predictions for HLP-22: (a) Concentration Profile at Max Fill, (b) Inlet Concentration and Suspension Ratio, (c) Maximum Solids Concentration Versus Loading Design Conditions, (d) U_{CS} Versus Loading at 12 m/s, 6-in. Nozzles (design point)

9.3.6 TCP-01 (Design Point) Physical Model

Table 9.12 lists the physical model results for design point conditions for TCP-01, and Figure 9.15 depicts the physical model predictions for TCP-01.

Table 9.12. Physical Model Results for Design Point Conditions for TCP-01

TCP-01 Design Max Fill		
U (m/s)	U_{CS} (m/s)	U/U_{CS}
8	13.4	0.60
H/D	H_C/D	H_C/H
1.25	0.06	0.05
W (wt%)	W_0^* (wt%)	$0.2/W_0^*$
2.7	$> W_{MP}$ [(a)]	0.12

(a) Calculated value exceeds maximum packing fraction.

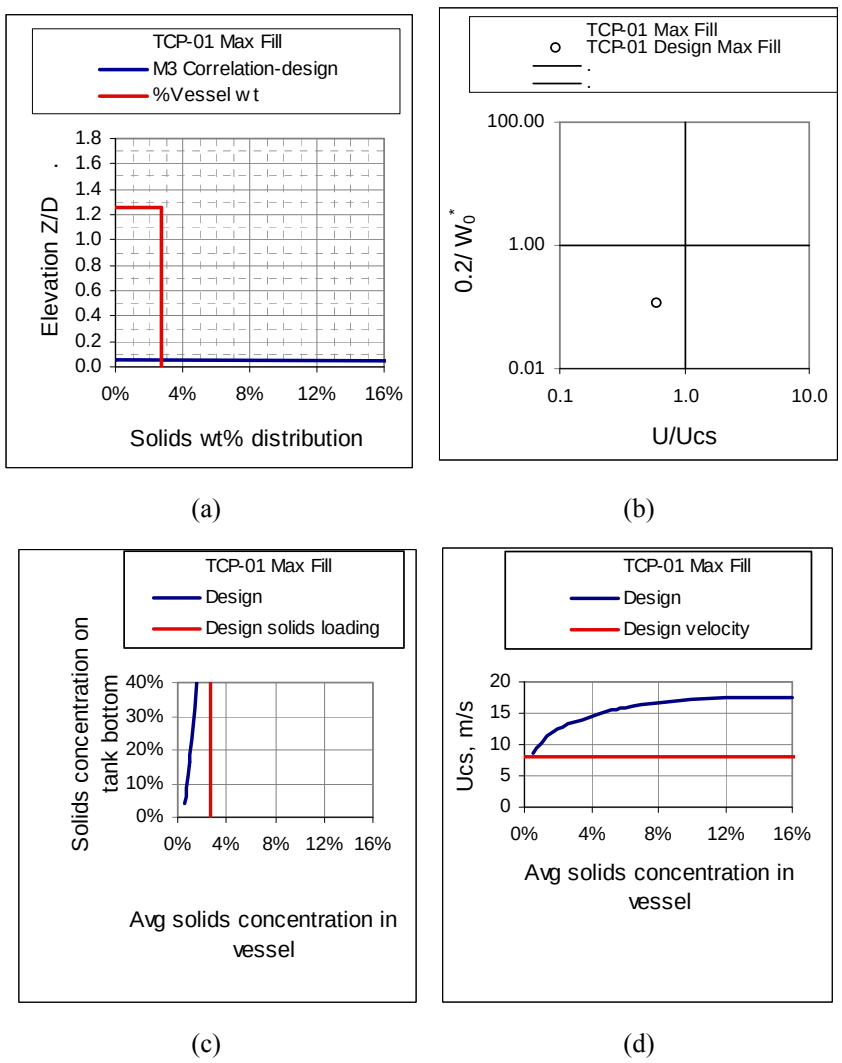

Figure 9.15. Physical Model Predictions for TCP-01: (a) Concentration Profile at Max Fill, (b) Inlet Concentration and Suspension Ratio, (c) Maximum Solids Concentration Versus Loading Design Conditions, (d) U_{CS} Versus Loading (design point)

9.3.7 TLP-09 A/B (Design Point) Physical Model

Table 9.13 lists the physical model results for design point conditions for TLP-09 A/B, and Figure 9.16 depicts the physical model predictions for TLP-09 A/B.

Table 9.13. Physical Model Results for Design Point Conditions for TLP-09

TLP-09A/B Design Max Fill		
U (m/s)	U_{CS} (m/s)	U/U_{CS}
8	9.1	0.88
H/D	H_C/D	H_C/H
1.08	0.24	0.22
W (wt%)	W_0^* (wt%)	$0.2/W_0^*$
0.3	4.1	4.92

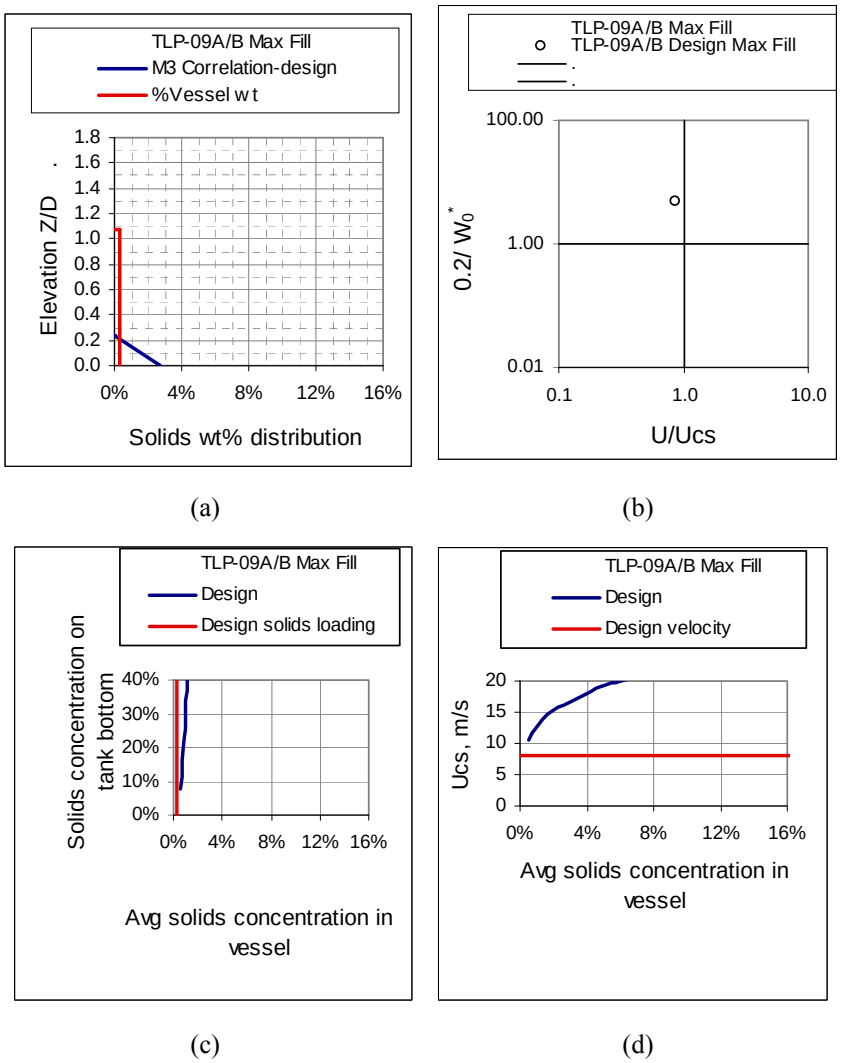

Figure 9.16. Physical Model Predictions for TLP-09 A/B: (a) Concentration Profile at Max Fill, (b) Inlet Concentration and Suspension Ratio, (c) Maximum Solids Concentration Versus Loading Design Conditions, (d) U_{CS} Versus Loading (design point)

9.3.8 PWD-33 (Design Point) Physical Model

Table 9.14 lists the physical model results for design point conditions for PWD-33, and Figure 9.17 depicts the physical model predictions for PWD-33.

Table 9.14. Physical Model Results for Design Point Conditions for PWD-33

PWD-33 Design Max Fill			PWD-33 Design2 Max Fill		
U (m/s)	U_{CS} (m/s)	U/U_{CS}	U (m/s)	U_{CS} (m/s)	U/U_{CS}
8	15.0	0.53	8	17.5	0.46
H/D	H_C/D	H_C/H	H/D	H_C/D	H_C/H
0.45	0.03	0.06	0.45	0.02	0.04
W (wt%)	W_0^* (wt%)	$0.2/W_0^*$	W (wt%)	W_0^* (wt%)	$0.2/W_0^*$
8.1	$> W_{MP}$[(a)]	0.05	8.1	$> W_{MP}$[(a)]	0.03

(a) Calculated value exceeds maximum packing fraction.

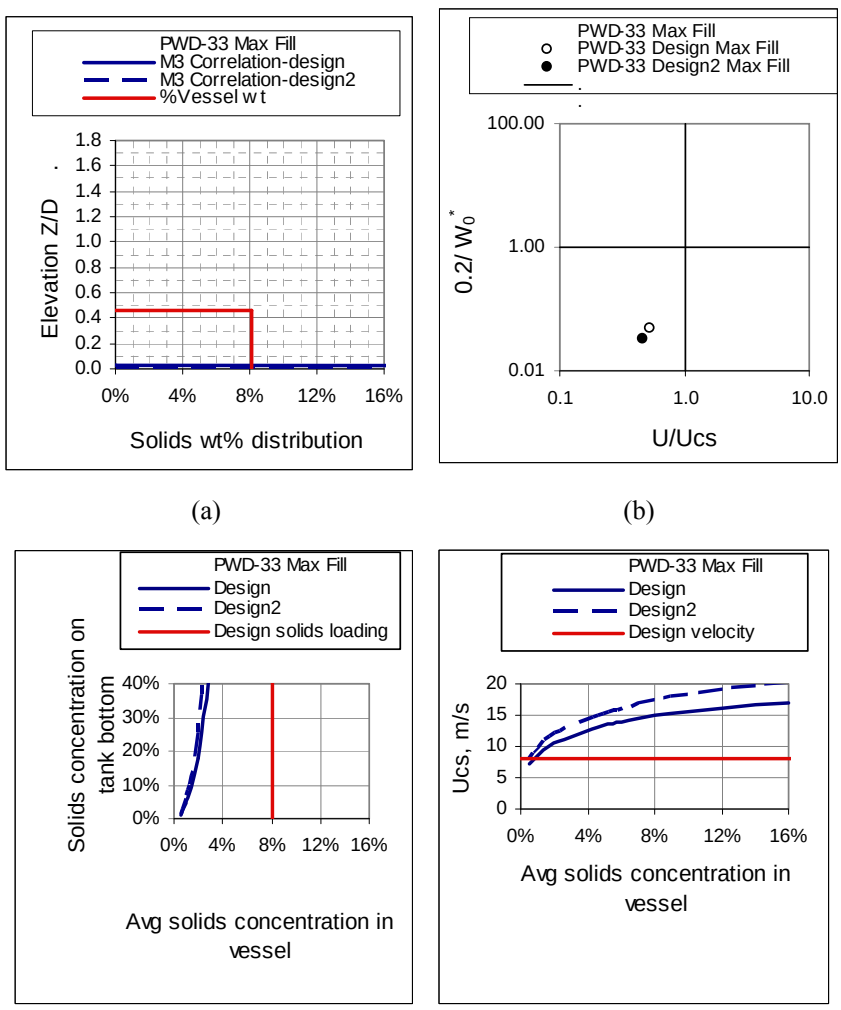

Figure 9.17. Physical Model Predictions for PWD-33: (a) Concentration Profile at Max Fill, (b) Inlet Concentration and Suspension Ratio, (c) Maximum Solids Concentration Versus Loading Design Conditions, (d) U_{CS} Versus Loading for PWD-33 (design point)

9.3.9 PWD-43 (Design Point) Physical Model

Table 9.15 lists the physical model results for design point conditions for PWD-43, and Figure 9.18 depicts the physical model predictions for PWD-43.

Table 9.15. Physical Model Results for Design Point Conditions for PWD-43

PWD-43 Design Max Fill			PWD-43 Design2 Max Fill		
U (m/s)	U_{CS} (m/s)	U/U_{CS}	U (m/s)	U_{CS} (m/s)	U/U_{CS}
8	5.5	1.44	8	6.3	1.26
H/D	H_C/D	H_C/H	H/D	H_C/D	H_C/H
0.45	1.01	2.23	0.45	0.71	1.57
W (wt%)	W_0^* (wt%)	$0.2/W_0^*$	W (wt%)	W_0^* (wt%)	$0.2/W_0^*$
0.2	0.4	55.47	0.2	0.4	47.45

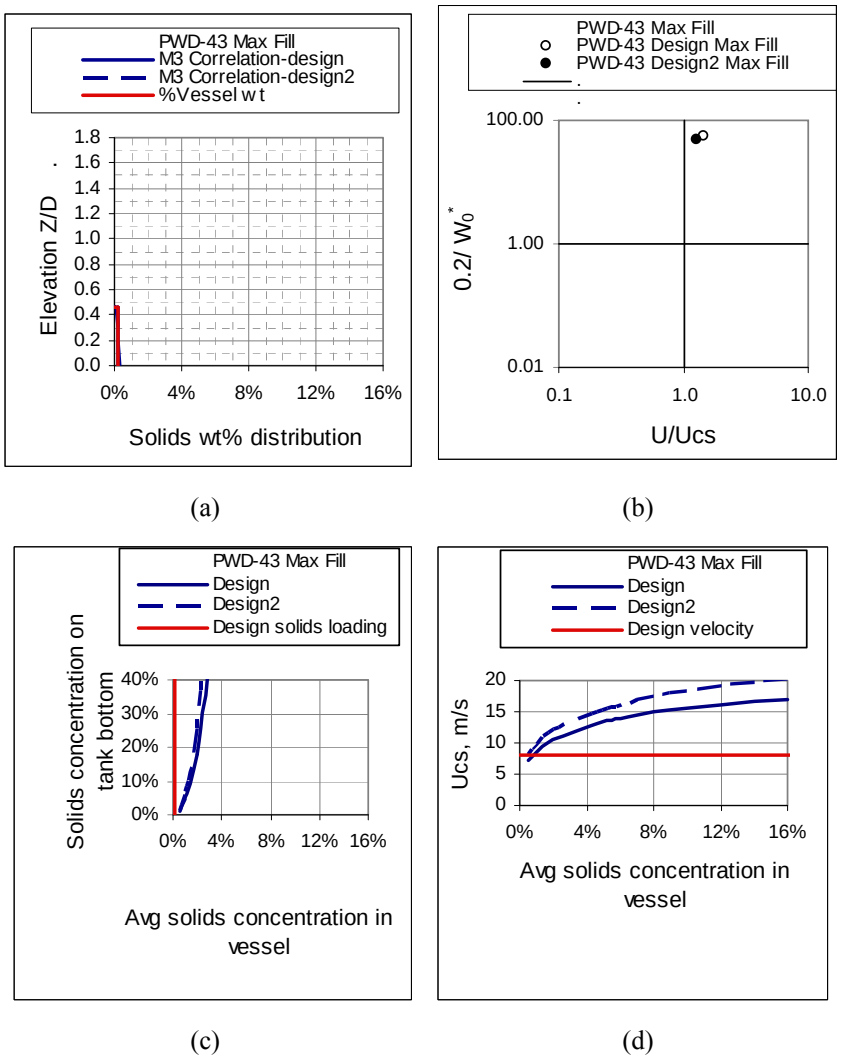

Figure 9.18. Physical Model Predictions for PWD-43: (a) Concentration Profile at Max Fill, (b) Inlet Concentration and Suspension Ratio, (c) Maximum Solids Concentration Versus Loading Design Conditions, (d) U_{CS} Versus Loading (design point)

9.3.10 PWD-44 (Design Point) Physical Model

Table 9.16 presents the physical model results for design point conditions for PWD-44, and Figure 9.19 shows the physical model predictions for PWD-44.

Table 9.16. Physical Model Results for Design Point Conditions for PWD-44

PWD-44 Design Max Fill			PWD-44 Design2 Max Fill		
U (m/s)	U_{CS} (m/s)	U/U_{CS}	U (m/s)	U_{CS} (m/s)	U/U_{CS}
8	12.0	0.67	8	14.4	0.56
H/D	H_C/D	H_C/H	H/D	H_C/D	H_C/H
1.32	0.04	0.03	1.32	0.03	0.02
W (wt%)	W_0^* (wt%)	$0.2/W_0^*$	W (wt%)	W_0^* (wt%)	$0.2/W_0^*$
8.1	$> W_{MP}$[(a)]	0.03	8.1	$> W_{MP}$[(a)]	0.02

(a) Calculated value exceeds maximum packing fraction.

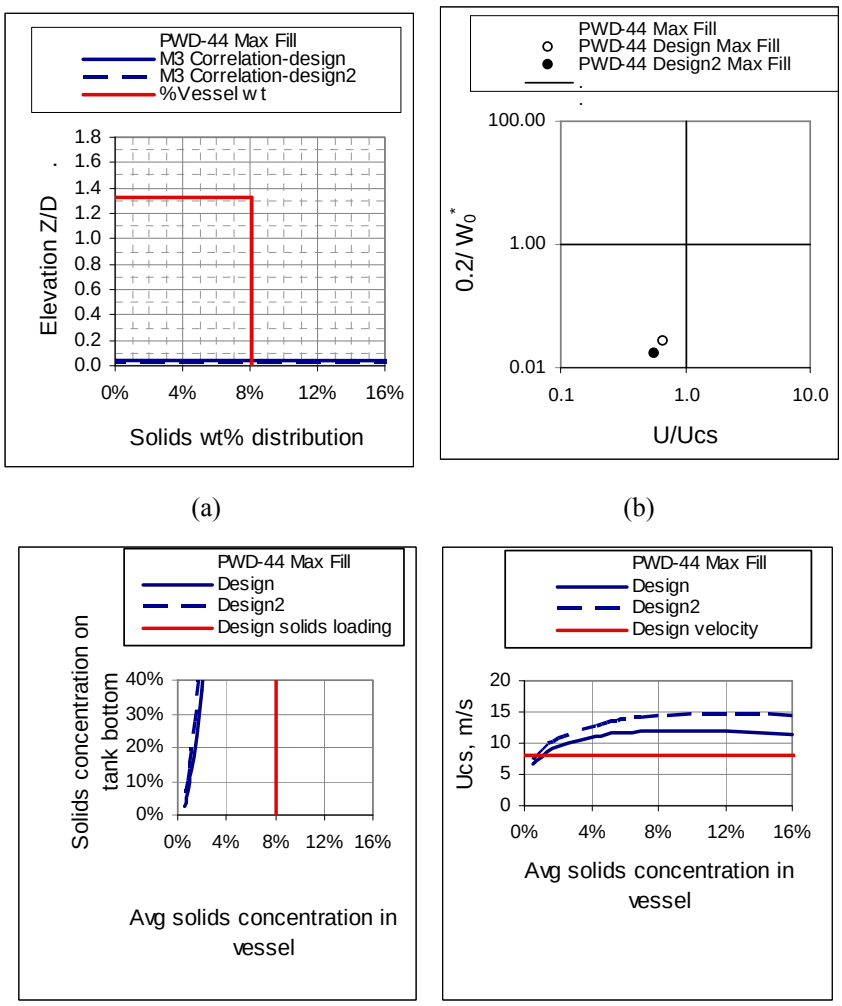

Figure 9.19. Physical Model Predictions for PWD-44: (a) Concentration Profile at Max Fill, (b) Inlet Concentration and Suspension Ratio, (c) Maximum Solids Concentration Versus Loading Design Conditions, (d) U_{CS} Versus Loading (design point)

9.3.11 FEP-17 A/B (Design Point) Physical Model

Table 9.17 lists the physical model results for design point conditions for FEP-17 A/B, and Figure 9.20 depicts the physical model predictions for FEP-17 A/B.

Table 9.17. Physical Model Results for Design Point Conditions for FEP-17

FEP-17A/B Design Max Fill			FEP-17A/B Design2 Max Fill		
U (m/s)	U_{CS} (m/s)	U/U_{CS}	U (m/s)	U_{CS} (m/s)	U/U_{CS}
8	6.0	1.34	8	7.3	1.09
H/D	H_C/D	H_C/H	H/D	H_C/D	H_C/H
1.19	3.81	3.20	1.19	1.28	1.08
W (wt%)	W_0^* (wt%)	$0.2/W_0^*$	W (wt%)	W_0^* (wt%)	$0.2/W_0^*$
4.4	7.2	2.76	4.4	12.3	1.63

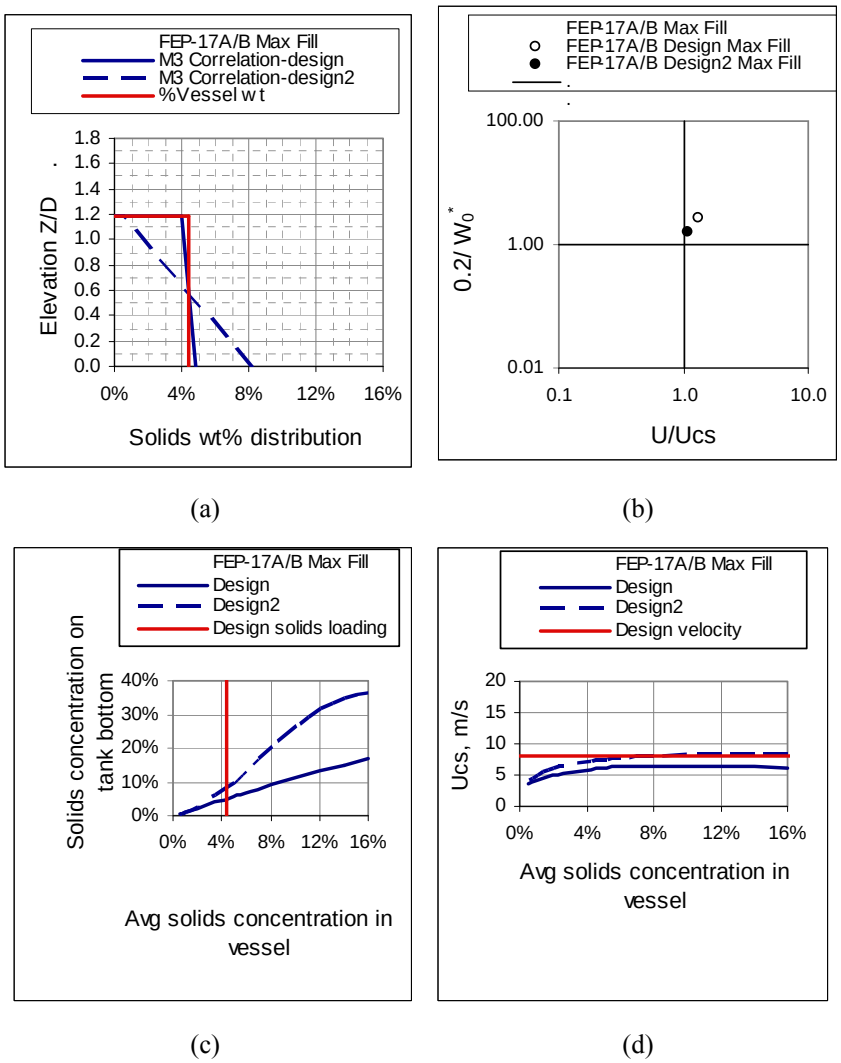

Figure 9.20. Physical Model Predictions for FEP-17 A/B: (a) Concentration Profile at Max Fill, (b) Inlet Concentration and Suspension Ratio, (c) Maximum Solids Concentration Versus Loading Design Conditions, (d) U_{CS} Versus Loading (design point)

9.3.12 PWD-15/16 (Design Point) Physical Model

Table 9.18 lists the physical model results for design point conditions for PWD-15/16, and Figure 9.21 depicts the physical model predictions for PWD-15/16.

Table 9.18. Physical Model Results for Design Point Conditions for PWD-15/16

PWD-15/16 Design Max Fill			PWD-15/16 Design2 Max Fill		
U (m/s)	U_{CS} (m/s)	U/U_{CS}	U (m/s)	U_{CS} (m/s)	U/U_{CS}
8	11.3	0.71	8	13.2	0.61
H/D	H_C/D	H_C/H	H/D	H_C/D	H_C/H
1.78	0.07	0.04	1.78	0.05	0.03
W (wt%)	W_0^* (wt%)	$0.2/W_0^*$	W (wt%)	W_0^* (wt%)	$0.2/W_0^*$
3	$> W_{MP}$[(a)]	0.08	3	$> W_{MP}$[(a)]	0.06

(a) Calculated value exceeds maximum packing fraction.

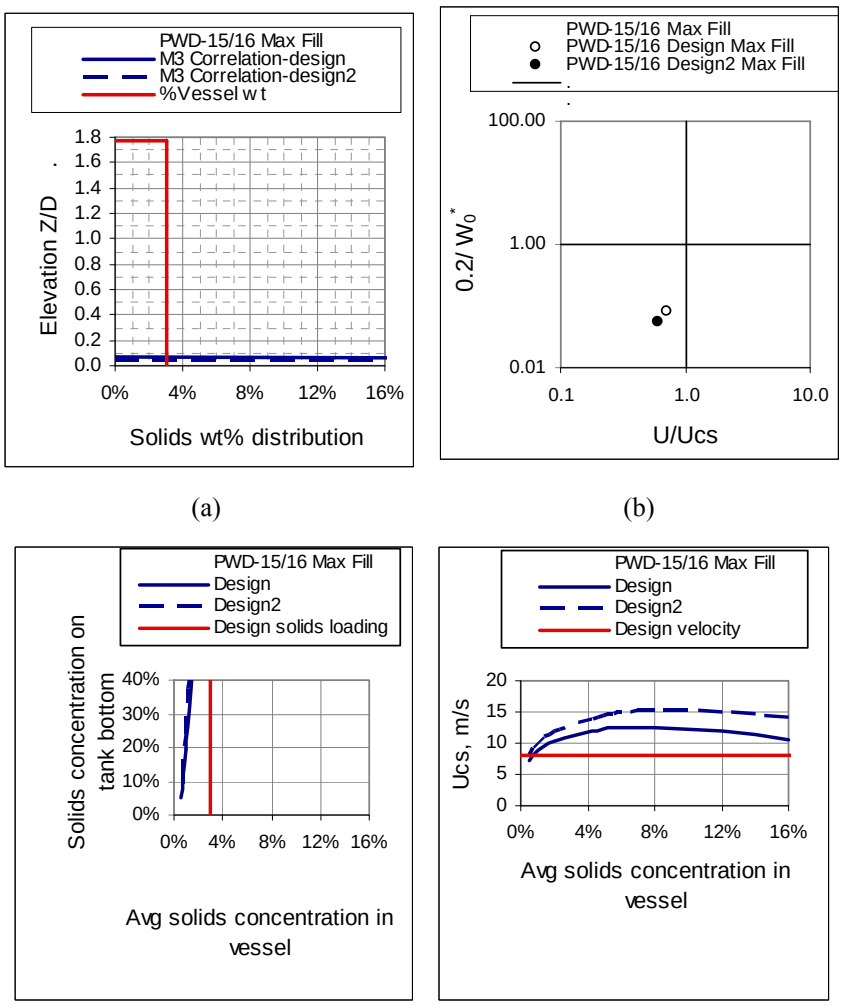

Figure 9.21. Physical Model Predictions for PWD-15/16: (a) Concentration Profile at Max Fill, (b) Inlet Concentration and Suspension Ratio, (c) Maximum Solids Concentration Versus Loading Design Conditions, (d) U_{CS} Versus Loading (design point)

9.3.13 UFP-01 A/B (Design Point) Physical Model

Table 9.19 lists the physical model results for design point conditions for UFP-01 A/B, and Figure 9.22 depicts the physical model predictions for UFP-01 A/B.

Table 9.19. Physical Model Results for Design Point Conditions for UFP-01

UFP-01A/B Design Max Fill			UFP-01A/B Design2 Max Fill		
U (m/s)	U_{CS} (m/s)	U/U_{CS}	U (m/s)	U_{CS} (m/s)	U/U_{CS}
8	8.6	0.93	8	10.4	0.77
H/D	H_C/D	H_C/H	H/D	H_C/D	H_C/H
1.45	0.19	0.13	1.45	0.11	0.08
W (wt%)	W_0^* (wt%)	$0.2/W_0^*$	W (wt%)	W_0^* (wt%)	$0.2/W_0^*$
3.8	$> W_{MP}$ [(a)]	0.23	3.8	$> W_{MP}$ [(a)]	0.13

(a) Calculated value exceeds maximum packing fraction.

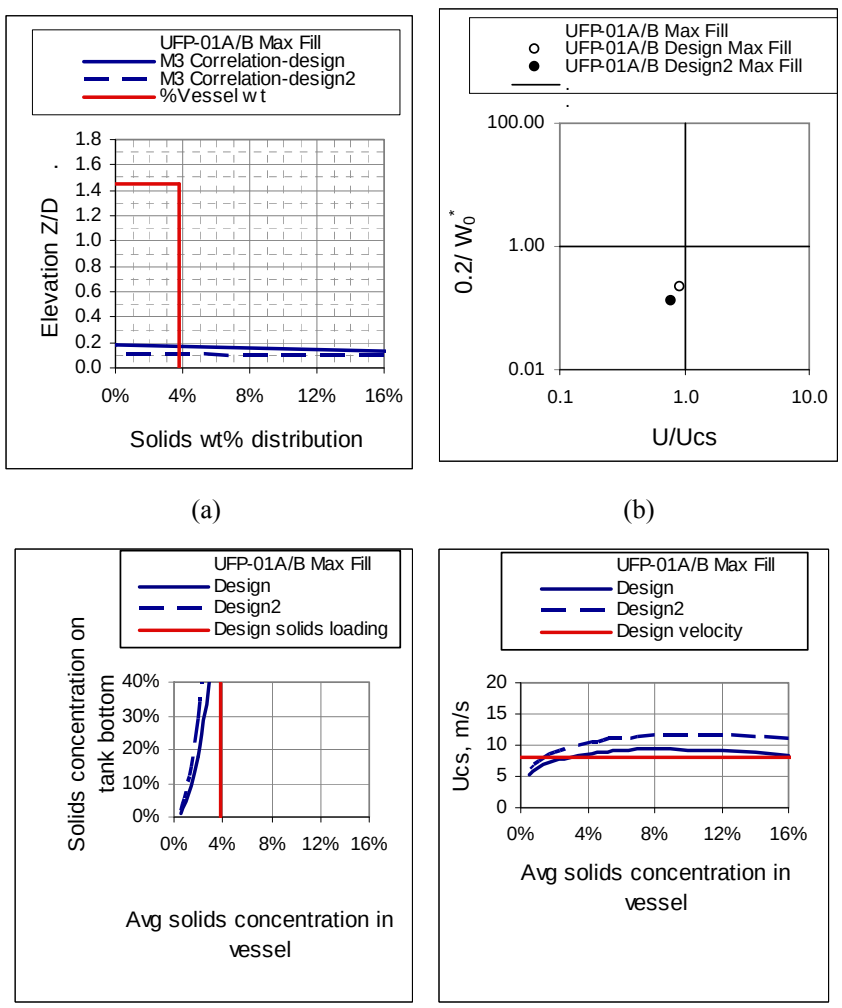

Figure 9.22. Physical Model Predictions for UFP-01 A/B: (a) Concentration Profile at Max Fill, (b) Inlet Concentration and Suspension Ratio, (c) Maximum Solids Concentration Versus Loading Design Conditions, (d) U_{CS} Versus Loading (design point)

9.3.14 RLD-07 (Design Point) Physical Model

Table 9.20 lists the physical model results for design point conditions for RLD-07, and Figure 9.23 presents the physical model predictions for RLD-07.

Table 9.20. Physical Model Results for Design Point Conditions for RLD-07

RLD-07 Design Max Fill			RLD-07 Design2 Max Fill		
U (m/s)	U_{CS} (m/s)	U/U_{CS}	U (m/s)	U_{CS} (m/s)	U/U_{CS}
8	7.7	1.04	8	8.9	0.90
H/D	H_C/D	H_C/H	H/D	H_C/D	H_C/H
1.20	0.29	0.24	1.20	0.20	0.17
W (wt%)	W_0^* (wt%)	$0.2/W_0^*$	W (wt%)	W_0^* (wt%)	$0.2/W_0^*$
2.2	27.3	0.73	2.2	39.7	0.50

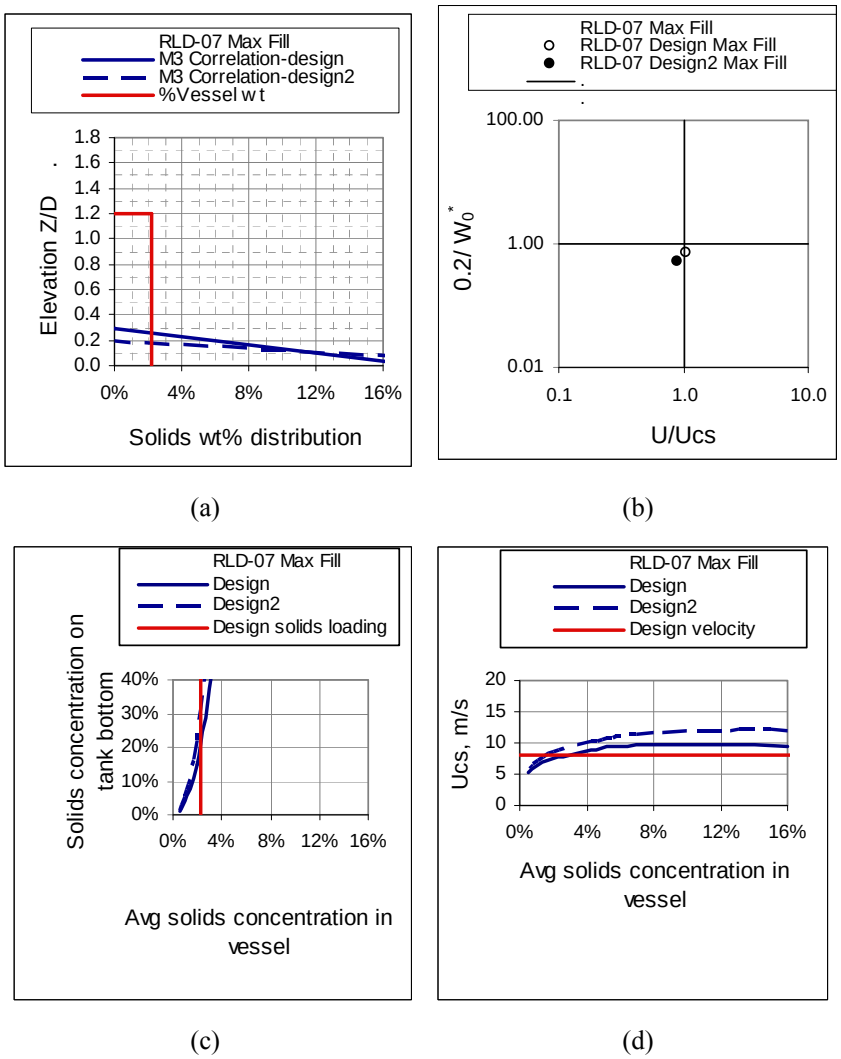

Figure 9.23. Physical Model Predictions for RLD-07: (a) Concentration Profile at Max Fill, (b) Inlet Concentration and Suspension Ratio, (c) Maximum Solids Concentration Versus Loading Design Conditions, (d) U_{CS} Versus Loading (design point)

9.3.15 RLD-08 (Design Point) Physical Model

Table 9.21 presents the physical model results for design point conditions for RLD-08, and Figure 9.24 depicts the physical model predictions for RLD-08.

Table 9.21. Physical Model Results for Design Point Conditions for RLD-08

RLD-08 Design Max Fill			RLD-08 Design2 Max Fill		
U (m/s)	U_{CS} (m/s)	U/U_{CS}	U (m/s)	U_{CS} (m/s)	U/U_{CS}
8	7.0	1.14	8	8.1	0.99
H/D	H_C/D	H_C/H	H/D	H_C/D	H_C/H
0.91	0.41	0.45	0.91	0.28	0.31
W (wt%)	W_0^* (wt%)	$0.2/W_0^*$	W (wt%)	W_0^* (wt%)	$0.2/W_0^*$
2.2	14.6	1.37	2.2	21.0	0.95

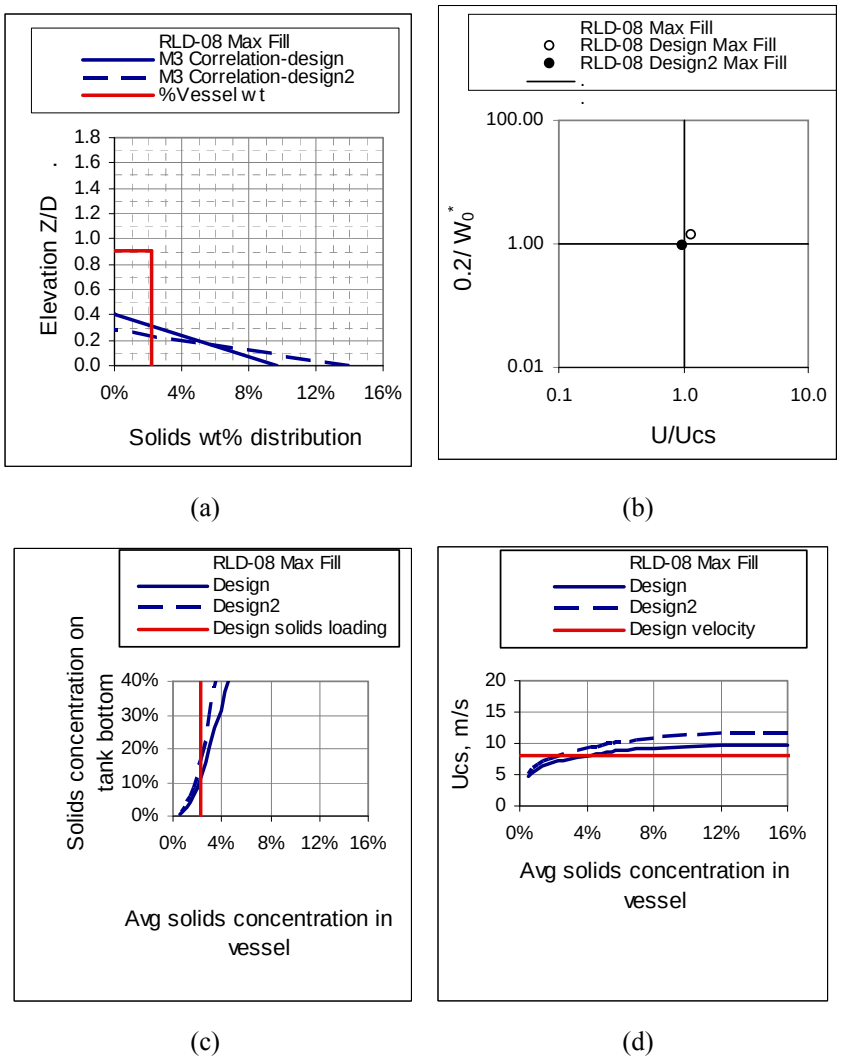

Figure 9.24. Physical Model Predictions for RLD-08: (a) Concentration Profile at Max Fill, (b) Inlet Concentration and Suspension Ratio, (c) Maximum Solids Concentration Versus Loading Design Conditions, (d) U_{CS} Versus Loading (design point)

9.3.16 HOP-903/904 (Design Point) Simple Calculation

Table 9.22 lists the physical model results for design point conditions for HOP-903/904, and Figure 9.25 depicts the physical model predictions for HOP-903/904.

Table 9.22. Physical Model Results for Design Point Conditions for HOP-903/904

HOP-903/904 Design Max Fill			HOP-903/904 Design2 Max Fill		
U (m/s)	U_{CS} (m/s)	U/U_{CS}	U (m/s)	U_{CS} (m/s)	U/U_{CS}
8	5.6	1.42	8	6.5	1.23
H/D	H_C/D	H_C/H	H/D	H_C/D	H_C/H
0.86	0.92	1.07	0.86	0.64	0.75
W (wt%)	W_0^* (wt%)	$0.2/W_0^*$	W (wt%)	W_0^* (wt%)	$0.2/W_0^*$
1	2.8	7.11	1	4.0	4.99

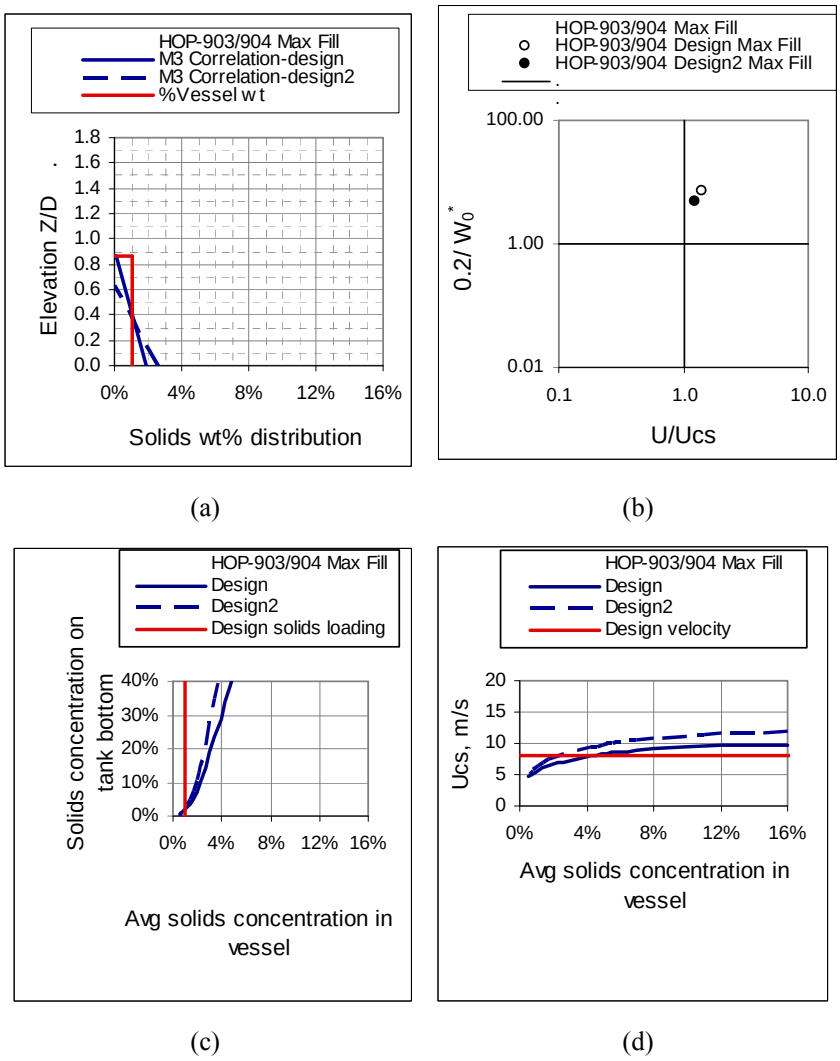

Figure 9.25. Physical Model Predictions for HOP-903/904: (a) Concentration Profile at Max Fill, (b) Inlet Concentration and Suspension Ratio, (c) Maximum Solids Concentration Versus Loading Design Conditions, (d) U_{CS} Versus Loading (design point)

9.4 Vessel Evaluation Examples with the Physical Models and the Hanford Waste Distribution

Mixing performance of WTP vessels was evaluated based on the Hanford waste distribution using the physical models for U_{CS}, H_C, and C_0, as described in Sections 7.3.2 to 7.3.4 with C_0 modified to W_0^*, as described in Section 9.1.4. The results of the evaluations are presented in Sections 9.4.1 through 9.4.16.

The Hanford waste settling properties used in the examples in this section include the following:

- U_{95}: This is the 95th percentile of the particle-settling velocity distribution based on the Hanford tank waste PSDD (Case 3). The use of the 95th percentile is supported by the results of the model benchmarking and is similar to common industry practice of using the 95th percentile of particle size when designing slurry handling equipment.
- $\overline{U}_{90}$: This is the average settling velocity for the fastest settling 10% of the Hanford tank waste.

  The U_{95} and $\overline{U}_{90}$ are used to establish the primary range for assessing the vessel types.
- A uniform liquid density of 1.15 g/cm^3; this was used in the Hanford PSDD cases with a fluid viscosity of 1.5 cP.

The vessel geometry and operating conditions are listed in Table 9.2 with vessel loading shown in Table 9.4.

These examples are for the vessel conditions that were provided in Olsen (2008a). This document has recently been revised to Rev. 1 (Olsen 2008b) ; however, these examples are based on Rev. 0 (Olsen 2008a). The examples are provided for the specific set of conditions described above. The analysis of the vessels used in the examples has been reassigned to the WTP M&PE group (Hazen 2008b).

Note that Tables 9.23 through 9.38 display only a few significant figures. The calculations are not based on this reduced number of digits. Therefore, small calculation differences are observed when using the displayed rounded numbers for calculations.

9.4.1 FRP-02 A/B/C/D (Hanford PSDD, ρ_l=1.1 g/cm^3, μ=1.5 cP Fluid) Physical Model

Table 9.23 lists the physical model results for FRP-02 A/B/C/D using the Hanford PSDD, and Figure 9.26 shows the physical model predictions for FRP-02 A/B/C/D based on the Hanford waste distribution.

Table 9.23. Physical Model Results for FRP-02 Using Hanford PSDD

FRP-02A/B/C/D U_{95} Max Fill			FRP-02A/B/C/D $\bar{U}_{90}$ Max Fill		
U (m/s)	U_{CS} (m/s)	U/U_{CS}	U (m/s)	U_{CS} (m/s)	U/U_{CS}
8	19.4	0.41	8	25.6	0.31
H/D	H_C/D	H_C/H	H/D	H_C/D	H_C/H
0.73	0.03	0.04	0.73	0.01	0.01
W (wt%)	W_0^* (wt%)	$0.2/W_0^*$	W (wt%)	W_0^* (wt%)	$0.2/W_0^*$
4.9	> W_{MP}[(a)]	0.05	4.9	> W_{MP}[(a)]	0.01

(a) Calculated value exceeds maximum packing fraction.

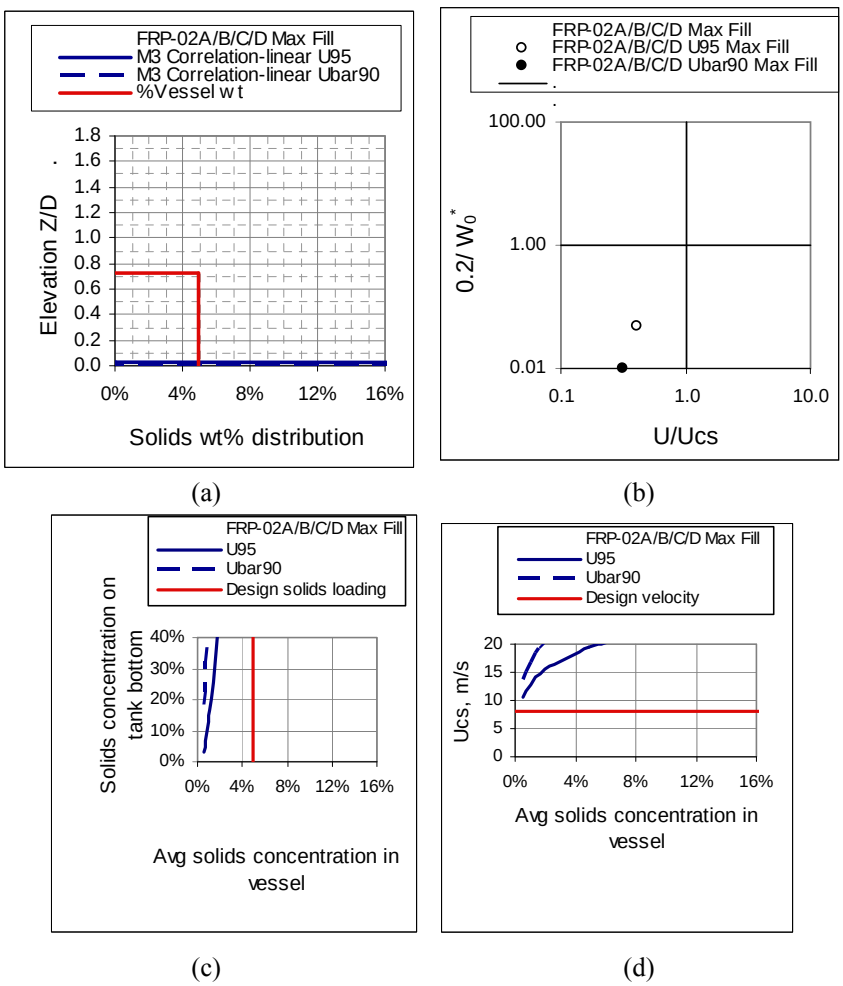

Figure 9.26. Physical Model Predictions for FRP-02 A/B/C/D: (a) Concentration Profile at Max Fill, (b) Inlet Concentration and Suspension Ratio, (c) Maximum Solids Concentration Versus Loading Design Conditions, (d) U_{CS} Versus Loading (Hanford PSDD, ρ_l = 1.1 g/cm^3, μ= 1.5 cP fluid)

The characteristic settling rate selected for a vessel assessment affects the predictions of U_{CS}. To illustrate the sensitivity of this input value, another calculation for FRP-02 is provided assuming conditions that are likely bounding in a non-conservative direction (i.e., the actual performance would likely be worse than these predicted values). The bounding condition for calculating U_{CS} uses a particle settling rate, U_T, which is the average of the entire distribution of the Hanford PSDD. This particle settling rate is 1.02E-3 m/s, and corresponds to a particle diameter d of 42 μm with a specific gravity of 2.78. Under these conditions, the U_{CS} is predicted to be 16.1 m/s.

Similarly, the solids concentration at the bottom of the vessel is sensitive to the gradient of the solids concentration within the cloud. Observations and attenuation (concentration) measurements taken during testing identified much higher concentrations of solids near the bottom of the test vessels than at the peak of the recorded cloud. A non-conservatively bounding condition for calculating the concentration at the pump suction is based on an assumption that the suspension of solids would be perfectly (homogeneously) mixed up to the peak of the cloud. In this example, the cloud height is calculated using the U_{95} particle settling velocity, and the cloud height that corresponds to a pump suction concentration of 20 wt% is 8.4 ft. Using the physical model, the jet velocity U required to lift solids to 8.4 ft would need to be 13.8 m/s.

9.4.2 HLP-22 8 m/s, 4-in. (Hanford PSDD, ρ_l = 1.1 g/cm^3, μ = 1.5 cP Fluid) Physical Model

Table 9.24 lists physical model results for HLP-22, and Figure 9.27 shows the physical model predictions for HLP-22 at 8 m/s with a 4-in. nozzle based on the Hanford waste distribution.

Table 9.24. Physical Model Results for HLP-22 Using Hanford PSDD

HLP-22 U_{95} Max Fill			HLP-22 $\bar{U}_{90}$ Max Fill		
U (m/s)	U_{CS} (m/s)	U/U_{CS}	U (m/s)	U_{CS} (m/s)	U/U_{CS}
8	16.5	0.48	8	21.7	0.37
H/D	H_C/D	H_C/H	H/D	H_C/D	H_C/H
0.80	0.05	0.06	0.80	0.01	0.01
W (wt%)	W_0^* (wt%)	$0.2/W_0^*$	W (wt%)	W_0^* (wt%)	$0.2/W_0^*$
15.4	> W_{MP}[(a)]	0.03	15.4	> W_{MP}[(a)]	0.004

(a) Calculated value exceeds maximum packing fraction.

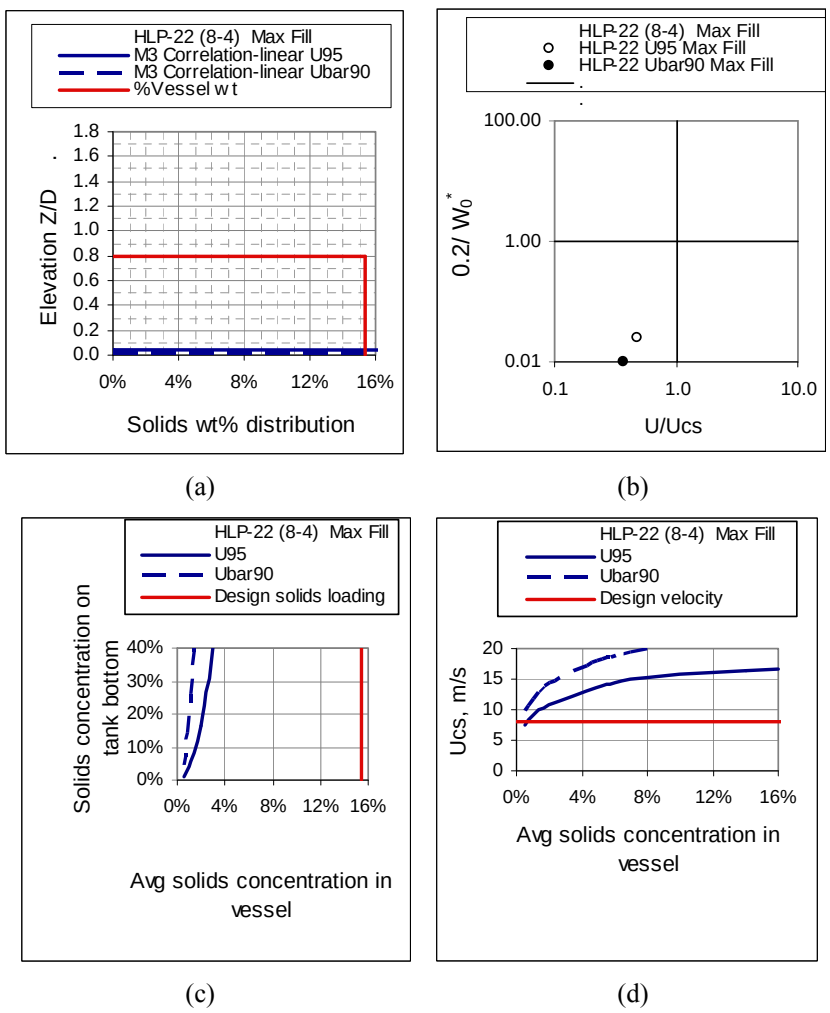

Figure 9.27. Physical Model Predictions for HLP-22: (a) Concentration Profile at Max Fill, (b) Inlet Concentration and Suspension Ratio, (c) Maximum Solids Concentration Versus Loading Design Conditions, (d) U_{CS} Versus Loading at 8 m/s, 4-in. Nozzle (Hanford PSDD, ρ_l = 1.1 g/cm^3, μ = 1.5 cP fluid)

9.4.3 HLP-22 12 m/s, 4-in. (Hanford PSDD, ρ_l = 1.1 g/cm^3, μ = 1.5 cP Fluid) Physical Model

Table 9.25 presents the physical model results for HLP-22, and Figure 9.28 shows the physical model predictions for HLP-22 at 12 m/s with a 4-in. nozzle using the Hanford PSDD.

Table 9.25. Physical Model Results for HLP-22 Using Hanford PSDD

HLP-22 U_{95} Max Fill			HLP-22 $\bar{U}_{90}$ Max Fill		
U (m/s)	U_{CS} (m/s)	U/U_{CS}	U (m/s)	U_{CS}(m/s)	U/U_{CS}
12	16.5	0.73	12	21.7	0.55
H/D	H_C/D	H_C/H	H/D	H_C/D	H_C/H
0.80	0.21	0.26	0.80	0.03	0.03
W (wt%)	W_0^* (wt%)	$0.2/W_0^*$	W (wt%)	W_0^* (wt%)	$0.2/W_0^*$
15.4	> W_{MP}[(a)]	0.11	15.4	> W_{MP}[(a)]	0.01

(a) Calculated value exceeds maximum packing fraction.

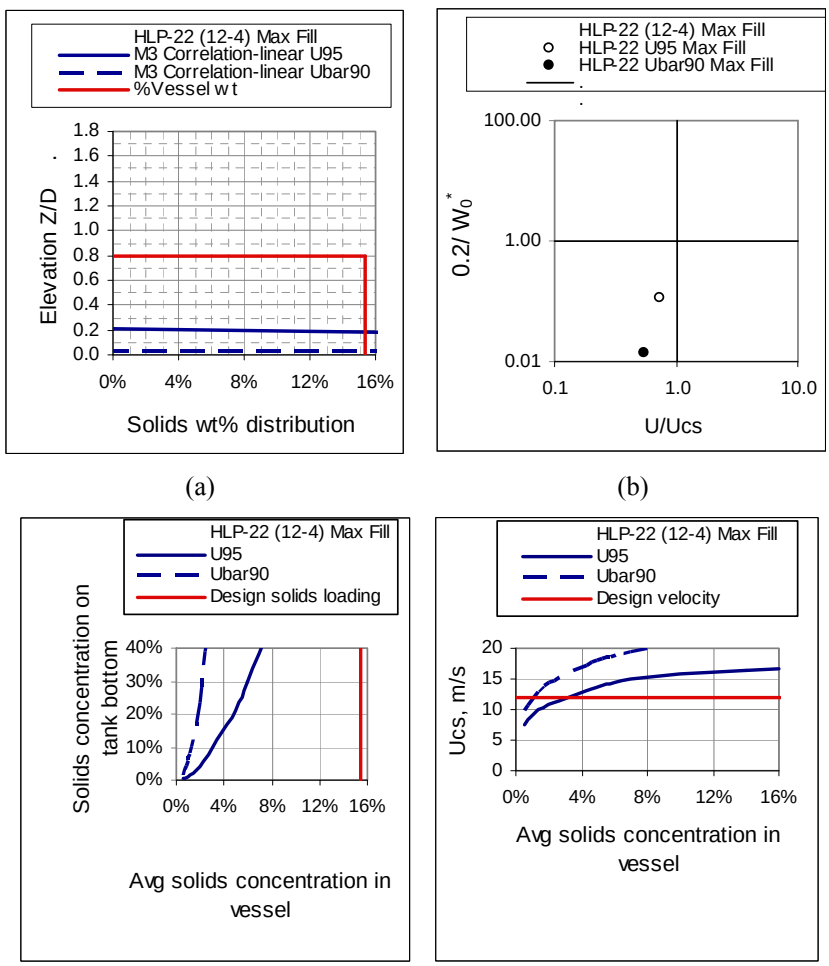

Figure 9.28. Physical Model Predictions for HLP-22: (a) Concentration Profile at Max Fill, (b) Inlet Concentration and Suspension Ratio, (c) Maximum Solids Concentration Versus Loading Design Conditions, (d) U_{CS} Versus Loading at 12 m/s, 4-in. Nozzle (Hanford PSDD, ρ_l = 1.1 g/cm^3, μ = 1.5 cP fluid)

The characteristic settling rate selected for a vessel assessment affects the predictions of U_{CS}. To illustrate the sensitivity of this input value, another calculation for HLP-22 (12 m/s, 4 inch nozzles) is provided assuming conditions that are likely bounding in a non-conservative direction (i.e., the actual performance would likely be worse than these predicted values). The bounding condition for calculating U_{CS} uses a particle settling rate, U_T, which is the average of the entire distribution of the Hanford PSDD. This particle settling rate is 1.02E-3 m/s, and corresponds to a particle diameter d of 42 μm with a specific gravity of 2.78. Under these conditions, the U_{CS} is predicted to be 13.7 m/s.

Similarly, the solids concentration at the bottom of the vessel is sensitive to the gradient of the solids concentration within the cloud. Observations and attenuation (concentration) measurements taken during testing identified much higher concentrations of solids near the bottom of the test vessels than at the peak of the recorded cloud. A non-conservatively bounding condition for calculating the concentration at the pump suction is based on an assumption that the suspension of solids would be perfectly (homogeneously) mixed up to the peak of the cloud. In this example, the cloud height is calculated using the U_{95} particle settling velocity, and the cloud height that corresponds to a pump suction concentration of 20 wt% is 23.3 ft. Using the physical model, the jet velocity U required to lift solids to 23.3 ft would need to be 15.9 m/s.

9.4.4 HLP-22 8 m/s, 6-in. (Hanford PSDD, ρ_l = 1.1 g/cm^3, μ = 1.5 cP Fluid) Physical Model

Table 9.26 lists the physical model results for HLP-22, and Figure 9.29 presents the physical model predictions for HLP-22 at 8 m/s, a 6-in. nozzle, and using the Hanford PSDD.

Table 9.26. Physical Model Results for HLP-22 Using Hanford PSDD

HLP-22 U_{95} Max Fill			HLP-22 $\bar{U}_{90}$ Max Fill		
U (m/s)	U_{CS} (m/s)	U/U_{CS}	U (m/s)	U_{CS} (m/s)	U/U_{CS}
8	12.5	0.64	8	16.4	0.49
H/D	H_C/D	H_C/H	H/D	H_C/D	H_C/H
0.80	0.12	0.15	0.80	0.02	0.03
W (wt%)	W_0^* (wt%)	$0.2/W_0^*$	W (wt%)	W_0^* (wt%)	$0.2/W_0^*$
15.4	> W_{MP}[(a)]	0.07	15.4	> W_{MP}[(a)]	0.011

(a) Calculated value exceeds maximum packing fraction.

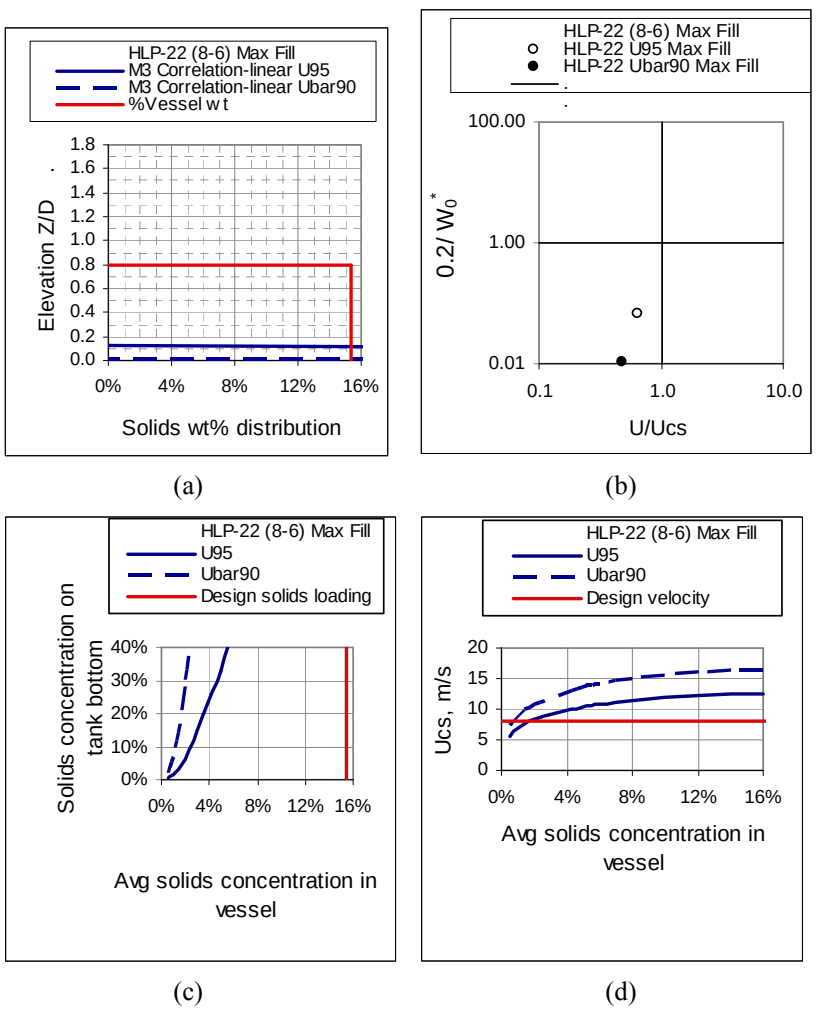

Figure 9.29. Physical Model Predictions for HLP-22: (a) Concentration Profile at Max Fill, (b) Inlet Concentration and Suspension Ratio, (c) Maximum Solids Concentration Versus Loading Design Conditions, (d) U_{CS} Versus Loading at 8 m/s, 6-in. Nozzle, Hanford PSDD

9.4.5 HLP-22 12 m/s, 6-in. (Hanford PSDD, ρ_l = 1.1 g/cm^3, μ = 1.5 cP Fluid) Physical Model

Table 9.27 lists the physical model results for HLP-22, and Figure 9.30 presents the physical model predictions for HLP-22 at 12 m/s with a 6-in. nozzle using the Hanford PSDD.

Table 9.27. Physical Model Results for HLP-22 Using Hanford PSDD

HLP-22 U_{95} Max Fill			HLP-22 $\bar{U}_{90}$ Max Fill		
U (m/s)	U_{CS} (m/s)	U/U_{CS}	U (m/s)	U_{CS} (m/s)	U/U_{CS}
12	12.5	0.96	12	16.4	0.73
H/D	H_C/D	H_C/H	H/D	H_C/D	H_C/H
0.80	0.55	0.69	0.80	0.07	0.09
W (wt%)	W_0^* (wt%)	$0.2/W_0^*$	W (wt%)	W_0^* (wt%)	$0.2/W_0^*$
15.4	67.2	0.30	15.4	> W_{MP}[(a)]	0.038

(a) Calculated value exceeds maximum packing fraction.

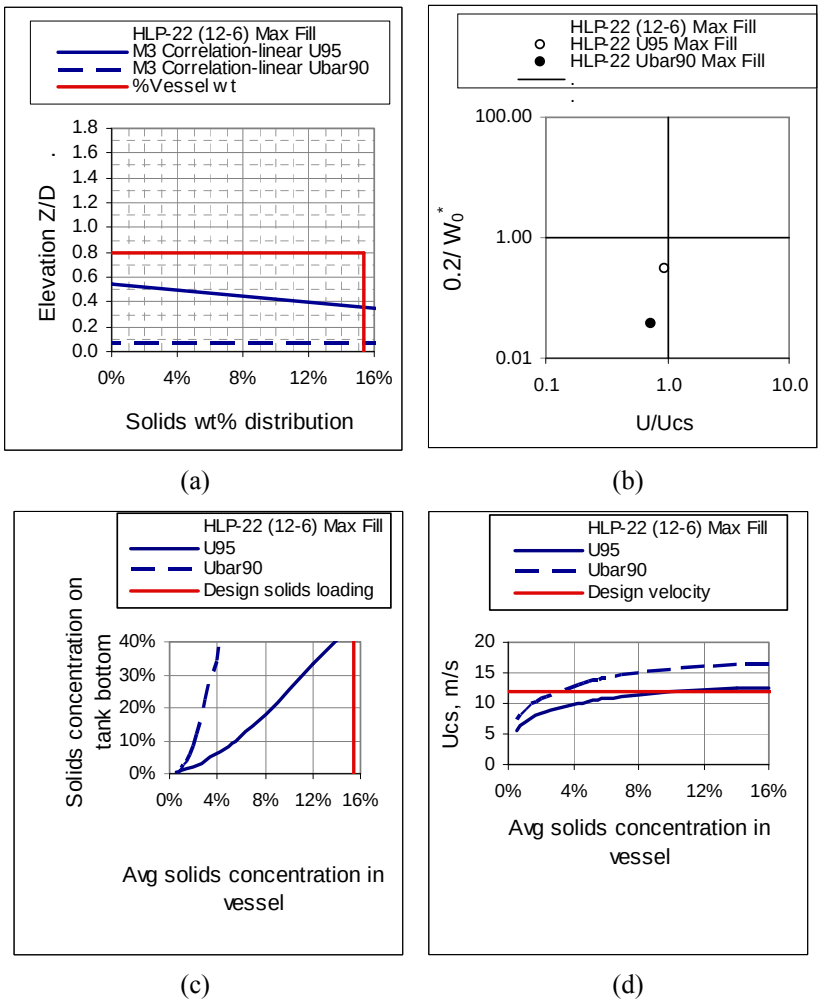

Figure 9.30. Physical Model Predictions for HLP-22: (a) Concentration Profile at Max Fill, (b) Inlet Concentration and Suspension Ratio, (c) Maximum Solids Concentration Versus Loading Design Conditions, (d) U_{CS} Versus Loading at 12 m/s with a 6-in. Nozzle (Hanford PSDD, ρ_l = 1.1 g/cm^3, μ = 1.5 cP fluid)

9.4.6 TCP-01 (Hanford PSDD, ρ_l = 1.1 g/cm^3, μ = 1.5 cP Fluid) Physical Model

Table 9.28 presents the physical model results for TCP-01 using the Hanford PSDD, and Figure 9.31 shows the physical model predictions for TCP-01 using the Hanford PSDD.

Table 9.28. Physical Model Results TCP-01 Using Hanford PSDD

TCP-01 U_{95} Max Fill			TCP-01 $\bar{U}_{90}$ Max Fill		
U (m/s)	U_{CS} (m/s)	U/U_{CS}	U (m/s)	U_{CS} (m/s)	U/U_{CS}
8	9.0	0.89	8	11.8	0.68
H/D	H_C/D	H_C/H	H/D	H_C/D	H_C/H
1.25	0.39	0.31	1.25	0.08	0.06
W (wt%)	W_0^* (wt%)	$0.2/W_0^*$	W (wt%)	W_0^* (wt%)	$0.2/W_0^*$
2.7	25.8	0.77	2.7	> W_{MP}[(a)]	0.16

(a) Calculated value exceeds maximum packing fraction.

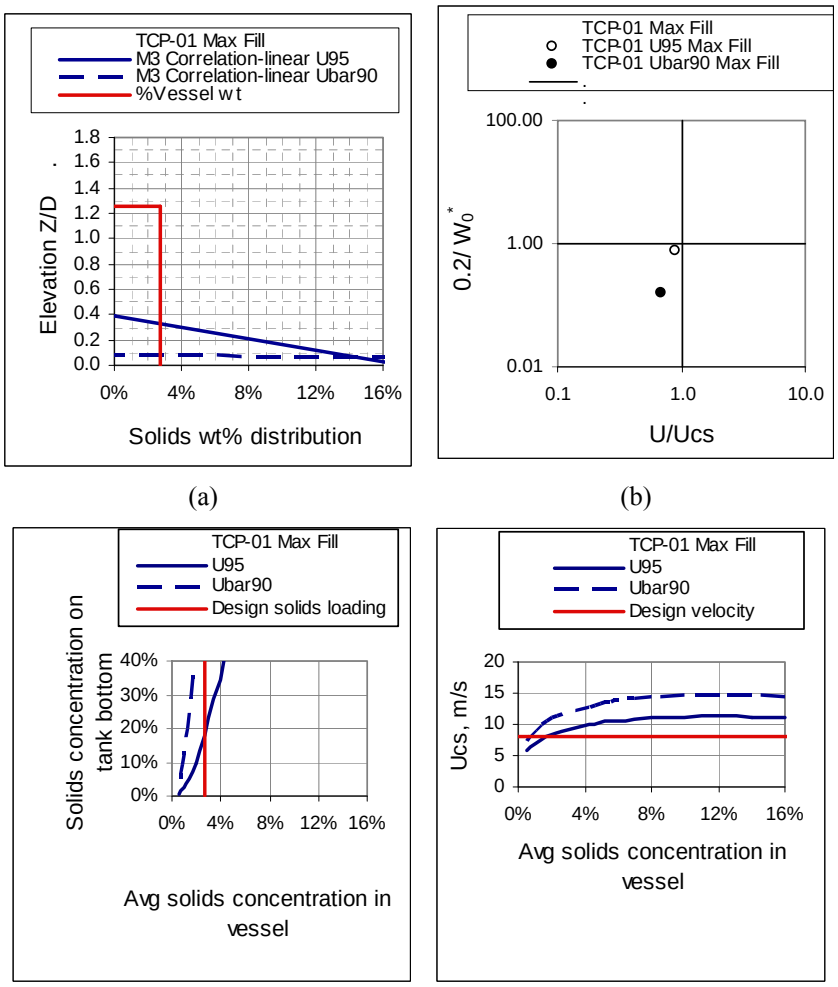

Figure 9.31. Physical Model Predictions for TCP-01: (a) Concentration Profile at Max Fill, (b) Inlet Concentration and Suspension Ratio, (c) Maximum Solids Concentration Versus Loading Design Conditions, (d) U_{CS} Versus Loading (Hanford PSDD, ρ_l = 1.1 g/cm^3, μ = 1.5 cP fluid)

9.4.7 TLP-09 A/B (Hanford PSDD, ρ_l = 1.1 g/cm^3, μ = 1.5 cP Fluid) Physical Model

Table 9.29 lists the physical model results for TLP-09 A/B, and Figure 9.32 depicts the physical model predictions for TLP-09 A/B using the Hanford PSDD.

Table 9.29. Physical Model Results for TLP-09 Using Hanford PSDD

TLP-09A/B U_{95} Max Fill			TLP-09A/B $\bar{U}_{90}$ Max Fill		
U (m/s)	U_{CS} (m/s)	U/U_{CS}	U (m/s)	U_{CS} (m/s)	U/U_{CS}
8	5.9	1.36	8	7.7	1.03
H/D	H_C/D	H_C/H	H/D	H_C/D	H_C/H
1.08	1.79	1.66	1.08	0.39	0.36
W (wt%)	W_0^* (wt%)	$0.2/W_0^*$	W (wt%)	W_0^* (wt%)	$0.2/W_0^*$
0.3	0.6	32.65	0.3	2.5	8.10

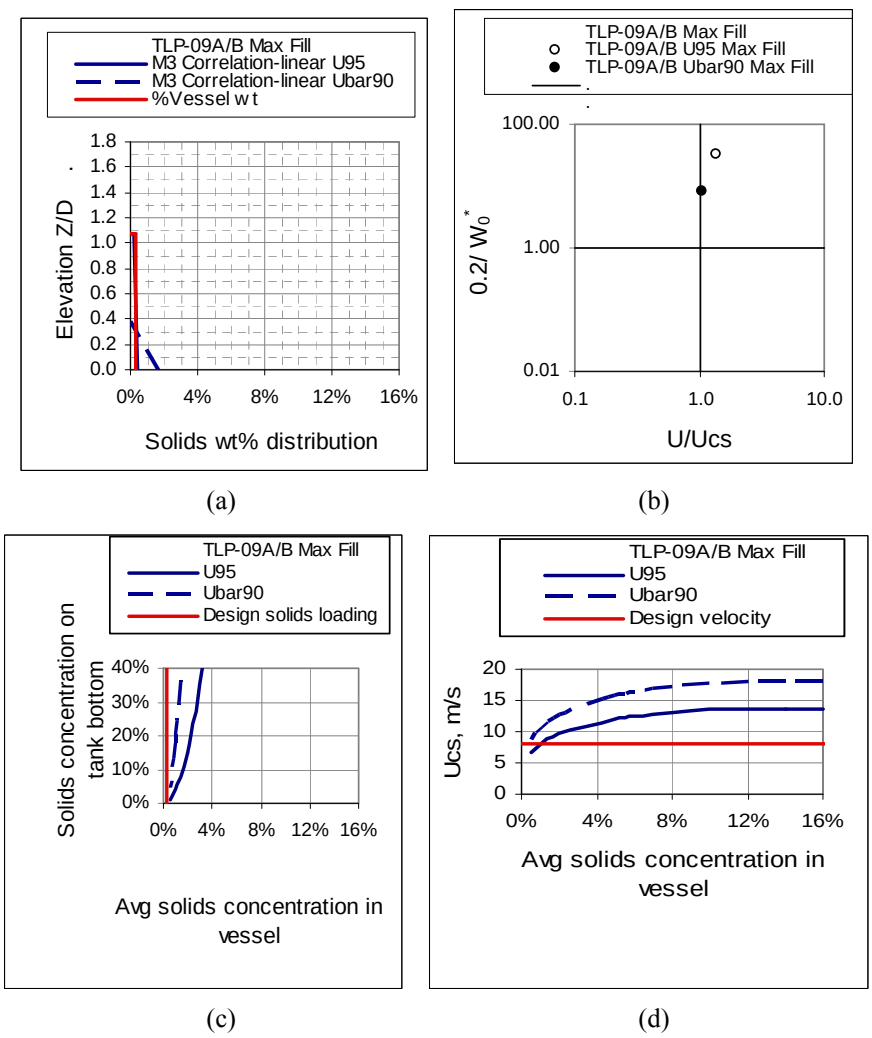

Figure 9.32. Physical Model Predictions for TLP-09 A/B: (a) Concentration Profile at Max Fill, (b) Inlet Concentration and Suspension Ratio, (c) Maximum Solids Concentration Versus Loading Design Conditions, (d) U_{CS} Versus Loading (Hanford PSDD, ρ_l = 1.1 g/cm^3, μ = 1.5 cP fluid)

9.4.8 PWD-33 (Hanford PSDD, ρ_l = 1.1 g/cm^3, μ = 1.5 cP Fluid) Physical Model

Table 9.30 presents physical model results for PWD-33, and Figure 9.33 shows the physical model predictions for PWD-33 using the Hanford PSDD.

Table 9.30. Physical Model Results for PWD-33 Using Hanford PSDD

PWD-33 U_{95} Max Fill			PWD-33 $\bar{U}_{90}$ Max Fill		
U (m/s)	U_{CS} (m/s)	U/ U_{CS}	U (m/s)	U_{CS} (m/s)	U/ U_{CS}
8	11.4	0.70	8	15.0	0.53
H/D	H_C/D	H_C/H	H/D	H_C/D	H_C/H
0.45	0.17	0.38	0.45	0.04	0.08
W (wt%)	W_0^* (wt%)	0.2/W_0^*	W (wt%)	W_0^* (wt%)	0.2/W_0^*
8.1	64.4	0.31	8.1	> W_{MP}[(a)]	0.06

(a) Calculated value exceeds maximum packing fraction.

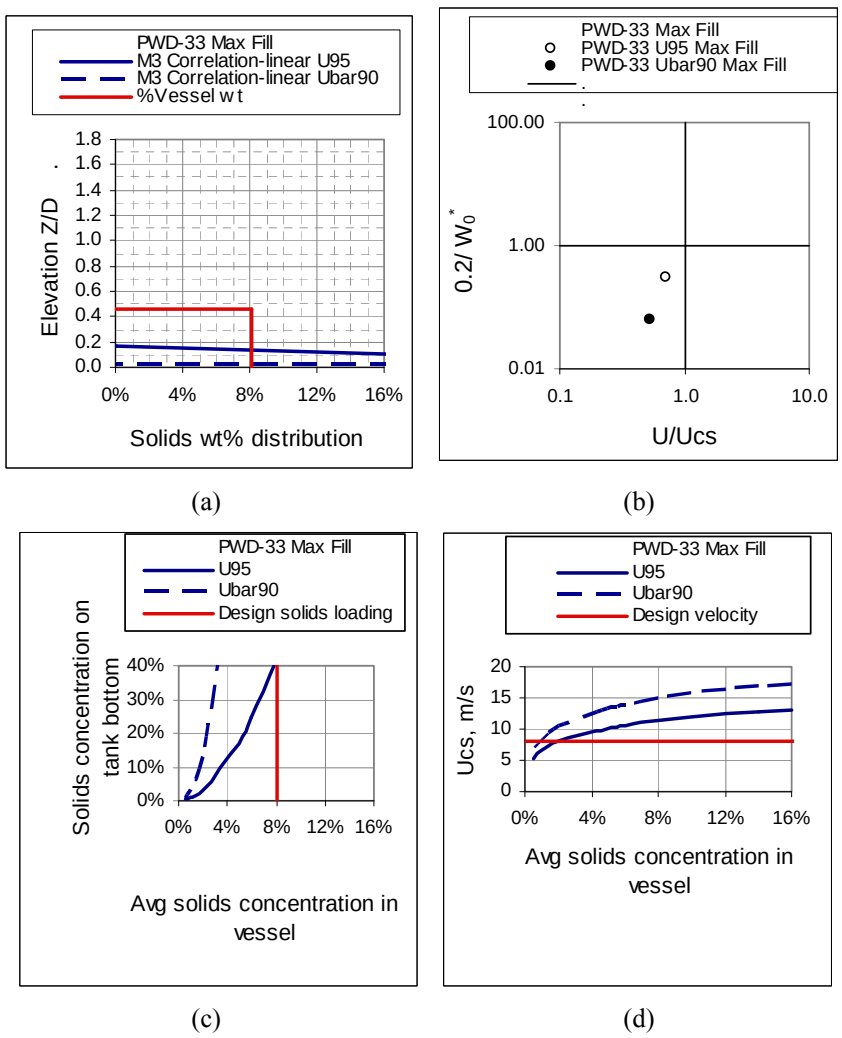

Figure 9.33. Physical Model Predictions for PWD-33: (a) Concentration Profile at Max Fill, (b) Inlet Concentration and Suspension Ratio, (c) Maximum Solids Concentration Versus Loading Design Conditions, (d) U_{CS} Versus Loading (Hanford PSDD, ρ_l = 1.1 g/cm^3, μ = 1.5 cP fluid)

The characteristic settling rate selected for a vessel assessment affects the predictions of U_{CS}. To illustrate the sensitivity of this input value, another calculation for PWD-33 is provided assuming conditions that are likely bounding in a non-conservative direction (i.e., the actual performance would likely be worse than these predicted values). The bounding condition for calculating U_{CS} uses a particle settling rate, U_T, which is the average of the entire distribution of the Hanford PSDD. This particle settling rate is 1.02E-3 m/s, and corresponds to a particle diameter d of 42 μm with a specific gravity of 2.78. Under these conditions, the U_{CS} is predicted to be 9.4 m/s.

Similarly, the solids concentration at the bottom of the vessel is sensitive to the gradient of the solids concentration within the cloud. Observations and attenuation (concentration) measurements taken during testing identified much higher concentrations of solids near the bottom of the test vessels than at the peak of the recorded cloud. A non-conservatively bounding condition for calculating the concentration at the pump suction is based on an assumption that the suspension of solids would be perfectly (homogeneously) mixed up to the peak of the cloud. In this example, the cloud height is calculated using the U_{95} particle settling velocity, and the cloud height that corresponds to a pump suction concentration of 20 wt% is 4.4 ft. Using the physical model, the jet velocity U required to lift solids to 4.4 ft would need to be 8.1 m/s.

9.4.9 PWD-43 (Hanford PSDD, ρ_l = 1.1 g/cm^3, μ = 1.5 cP Fluid) Physical Model

Table 9.31 presents physical model results for PWD-43, and Figure 9.34 depicts the physical model predictions for PWD-43 using the Hanford PSDD.

Table 9.31. Physical Model Results for PWD-43 Using Hanford PSDD

PWD-43 U_{95} Max Fill			PWD-43 $\bar{U}_{90}$ Max Fill		
U (m/s)	U_{CS} (m/s)	U/ U_{CS}	U (m/s)	U_{CS} (m/s)	U/ U_{CS}
8	4.2	1.92	8	5.5	1.46
H/D	H_C/D	H_C/H	H/D	H_C/D	H_C/H
0.45	6.02	13.27	0.45	1.33	2.92
W (wt%)	W_0^* (wt%)	0.2/W_0^*	W (wt%)	W_0^* (wt%)	0.2/W_0^*
0.2	0.3	66.29	0.2	0.3	59.67

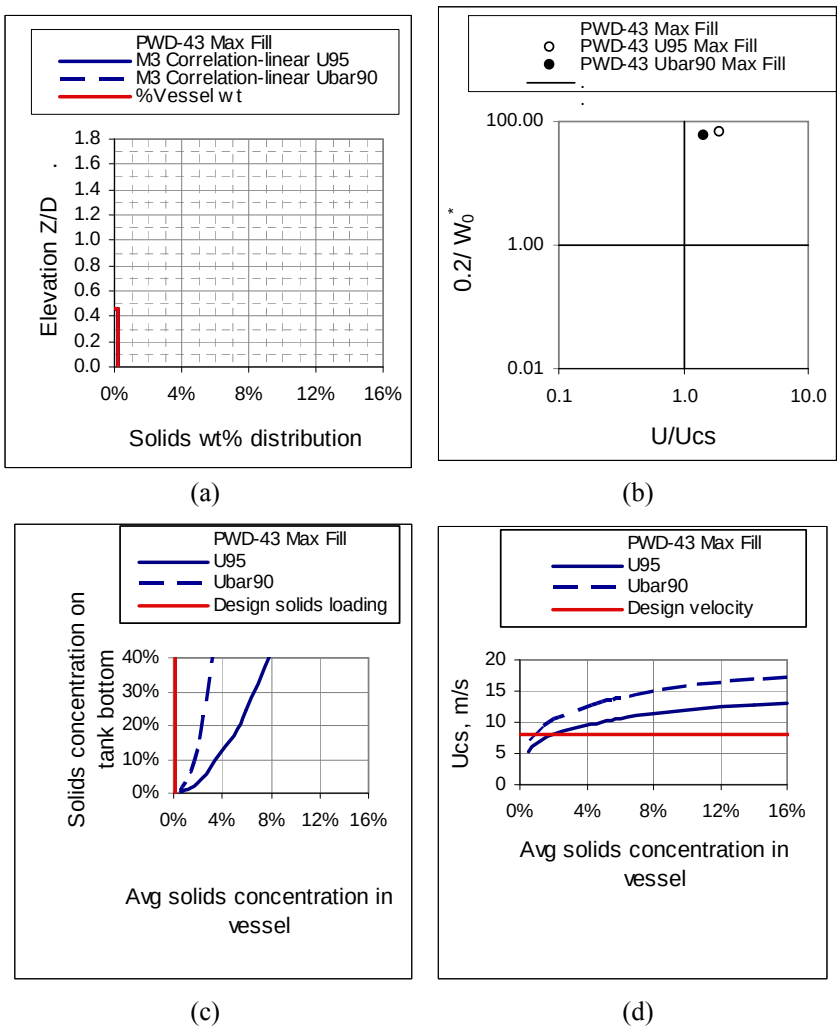

Figure 9.34. Physical Model Predictions for PWD-43: (a) Concentration Profile at Max Fill, (b) Inlet Concentration and Suspension Ratio, (c) Maximum Solids Concentration Versus Loading Design Conditions, (d) U_{CS} Versus Loading (Hanford PSDD, ρ_l = 1.1 g/cm^3, μ = 1.5 cP fluid)

9.4.10 PWD-44 (Hanford PSDD, ρ_l = 1.1 g/cm^3, μ = 1.5 cP Fluid) Physical Model

Table 9.32 presents physical model results for PWD-44 using the Hanford PSDD, and Figure 9.35 depicts the physical model predictions for PWD-44 using the Hanford PSDD.

Table 9.32. Physical Model Results for PWD-44 Using Hanford PSDD

PWD-44 U_{95} Max Fill			PWD-44 $\bar{U}_{90}$ Max Fill		
U (m/s)	U_{CS} (m/s)	U/U_{CS}	U (m/s)	U_{CS} (m/s)	U/U_{CS}
8	9.3	0.86	8	12.2	0.66
H/D	H_C/D	H_C/H	H/D	H_C/D	H_C/H
1.32	0.35	0.26	1.32	0.06	0.05
W (wt%)	W_0^* (wt%)	$0.2/W_0^*$	W (wt%)	W_0^* (wt%)	$0.2/W_0^*$
8.1	> W_{MP}[(a)]	0.22	8.1	> W_{MP}[(a)]	0.04

(a) Calculated value exceeds maximum packing fraction.

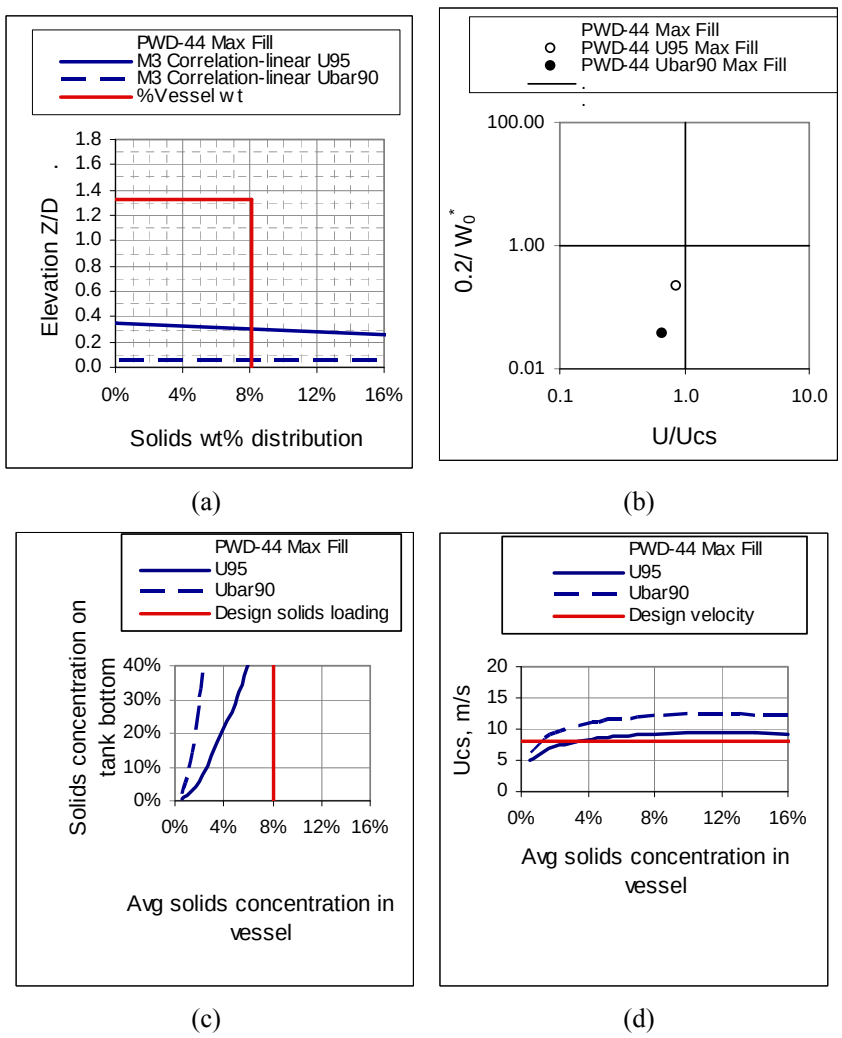

Figure 9.35. Physical Model Predictions for PWD-44: (a) Concentration Profile at Max Fill, (b) Inlet Concentration and Suspension Ratio, (c) Maximum Solids Concentration Versus Loading Design Conditions, (d) U_{CS} Versus Loading (Hanford PSDD, ρ_l = 1.1 g/cm^3, μ = 1.5 cP fluid)

9.4.11 FEP-17 A/B (Hanford PSDD, ρ_l = 1.1 g/cm^3, μ = 1.5 cP Fluid) Physical Model

Table 9.33 presents physical model results for FEP-17 A/B using the Hanford PSDD, and Figure 9.36 depicts the physical model predictions for FEP-17 A/B using the Hanford PSDD.

Table 9.33. Physical Model Results for FEP-17 Using Hanford PSDD

FEP-17A/B U_{95} Max Fill			FEP-17A/B $\bar{U}_{90}$ Max Fill		
U (m/s)	U_{CS} (m/s)	U/U_{CS}	U (m/s)	U_{CS} (m/s)	U/U_{CS}
8	8.2	0.98	8	10.8	0.74
H/D	H_C/D	H_C/H	H/D	H_C/D	H_C/H
1.19	0.54	0.45	1.19	0.11	0.09
W (wt%)	W_0^* (wt%)	$0.2/W_0^*$	W (wt%)	W_0^* (wt%)	$0.2/W_0^*$
4.4	29.1	0.69	4.4	> W_{MP}[(a)]	0.14

(a) Calculated value exceeds maximum packing fraction.

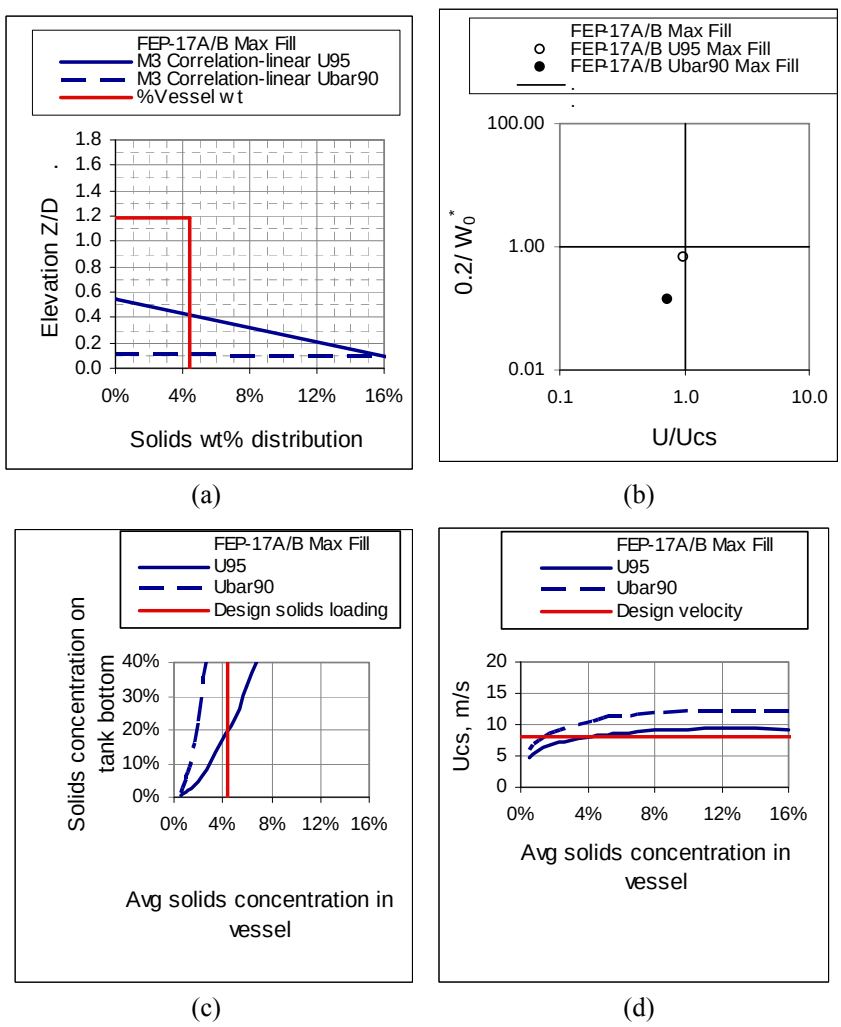

Figure 9.36. Physical Model Predictions for FEP-17 A/B: (a) Concentration Profile at Max Fill, (b) Inlet Concentration and Suspension Ratio, (c) Maximum Solids Concentration Versus Loading Design Conditions, (d) U_{CS} Versus Loading (Hanford PSDD, ρ_l = 1.1 g/cm^3, μ = 1.5 cP fluid)

9.4.12 PWD-15/16 (Hanford PSDD, ρ_l = 1.1 g/cm^3, μ = 1.5 cP Fluid) Physical Model

Table 9.34 lists physical model results for PWD-15/16 using the Hanford PSDD, and Figure 9.37 presents the physical model predictions for PWD-15/16 using the Hanford PSDD.

Table 9.34. Physical Model Results for PWD-15/16 Using Hanford PSDD

PWD-15/16 U_{95} Max Fill			PWD-15/16 $\bar{U}_{90}$ Max Fill		
U (m/s)	U_{CS} (m/s)	U/U_{CS}	U (m/s)	U_{CS} (m/s)	U/U_{CS}
8	8.6	0.93	8	11.3	0.71
H/D	H_C/D	H_C/H	H/D	H_C/D	H_C/H
1.78	0.46	0.26	1.78	0.09	0.05
W (wt%)	W_0^* (wt%)	$0.2/W_0^*$	W (wt%)	W_0^* (wt%)	$0.2/W_0^*$
3	35.1	0.57	3	> W_{MP}[(a)]	0.11

(a) Calculated value exceeds maximum packing fraction.

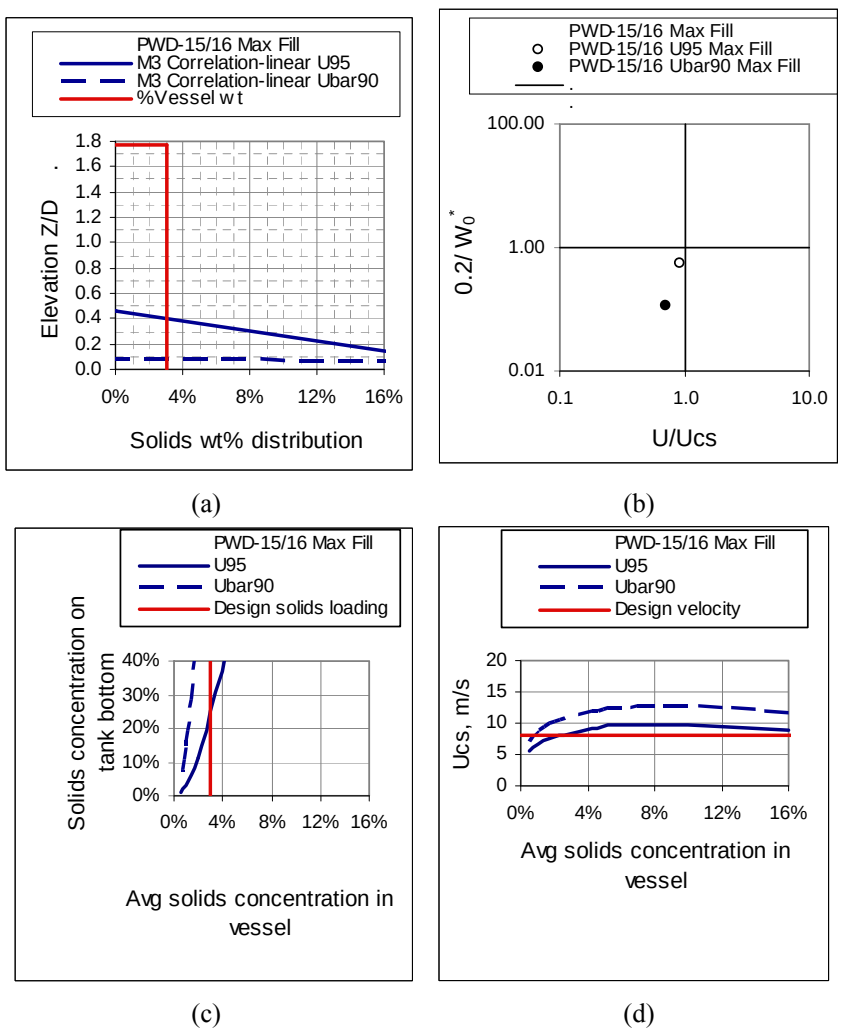

Figure 9.37. Physical Model Predictions for PWD-15/16: (a) Concentration Profile at Max Fill, (b) Inlet Concentration and Suspension Ratio, (c) Maximum Solids Concentration Versus Loading Design Conditions, (d) U_{CS} Versus Loading (Hanford PSDD, ρ_l = 1.1 g/cm^3, μ = 1.5 cP fluid)

9.4.13 UFP-01 A/B (Hanford PSDD, ρ_l = 1.1 g/cm^3, μ =1.5 cP Fluid) Physical Model

Table 9.35 presents physical model results for UFP-01 A/B, and Figure 9.38 presents the physical model predictions for UFP-01 A/B using the Hanford PSDD.

Table 9.35. Physical Model Results for UFP-01 Using Hanford PSDD

UFP-01A/B U_{95} Max Fill			UFP-01A/B $\bar{U}_{90}$ Max Fill		
U (m/s)	U_{CS} (m/s)	U/U_{CS}	U (m/s)	U_{CS} (m/s)	U/U_{CS}
8	7.2	1.12	8	9.4	0.85
H/D	H_C/D	H_C/H	H/D	H_C/D	H_C/H
1.45	0.87	0.60	1.45	0.17	0.12
W (wt%)	W_0^* (wt%)	$0.2/W_0^*$	W (wt%)	W_0^* (wt%)	$0.2/W_0^*$
3.8	19.0	1.05	3.8	> W_{MP}[(a)]	0.21

(a) Calculated value exceeds maximum packing fraction.

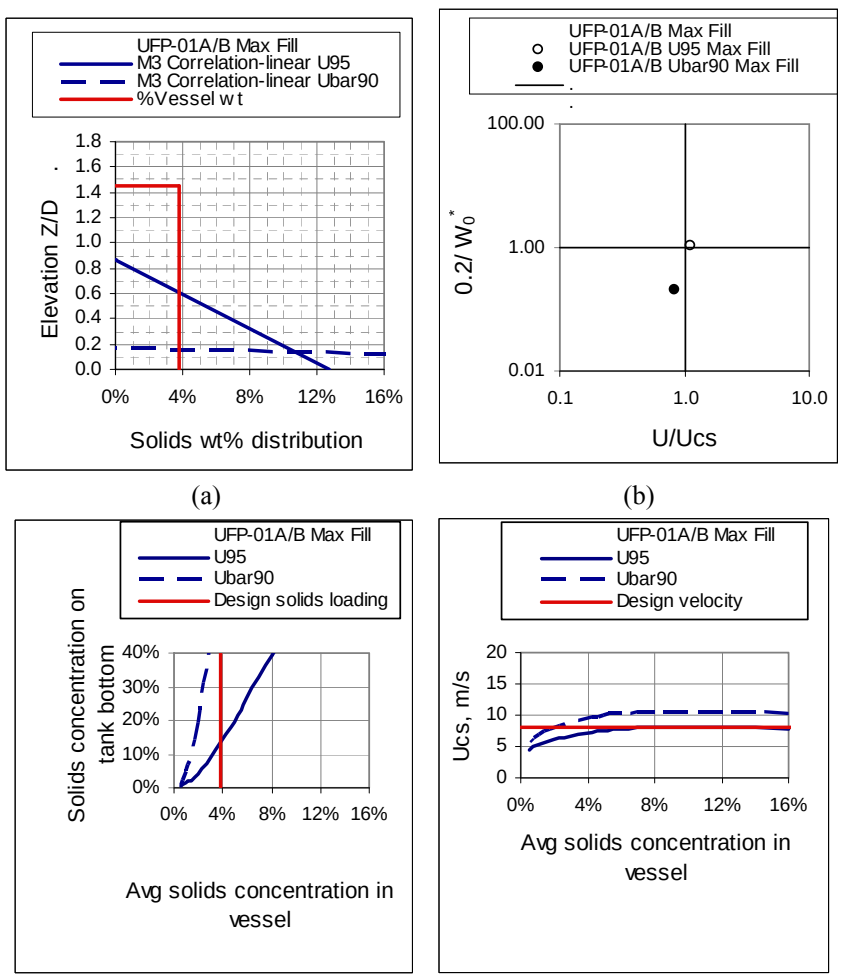

Figure 9.38. Physical Model Predictions for UFP-01 A/B: (a) Concentration Profile at Max Fill, (b) Inlet Concentration and Suspension Ratio, (c) Maximum Solids Concentration Versus Loading Design Conditions, (d) U_{CS} Versus Loading (Hanford PSDD, ρ_l = 1.1 g/cm^3, μ = 1.5 cP fluid)

9.4.14 RLD-07 (Hanford PSDD, ρ_l = 1.1 g/cm^3, μ = 1.5 cP Fluid) Physical Model

Table 9.36 presents physical model results for RLD-07, and Figure 9.39 shows the physical model predictions for RLD-07 using the Hanford PSDD.

Table 9.36. Physical Model Results for RLD-07 Using Hanford PSDD

RLD-07 U_{95} Max Fill			RLD-07 $\bar{U}_{90}$ Max Fill		
U (m/s)	U_{CS} (m/s)	U/ U_{CS}	U (m/s)	U_{CS} (m/s)	U/ U_{CS}
8	5.8	1.38	8	7.6	1.05
H/D	H_C/D	H_C/H	H/D	H_C/D	H_C/H
1.20	1.84	1.54	1.20	0.38	0.32
W (wt%)	W_0^* (wt%)	0.2/W_0^*	W (wt%)	W_0^* (wt%)	0.2/W_0^*
2.2	4.7	4.26	2.2	20.6	0.97

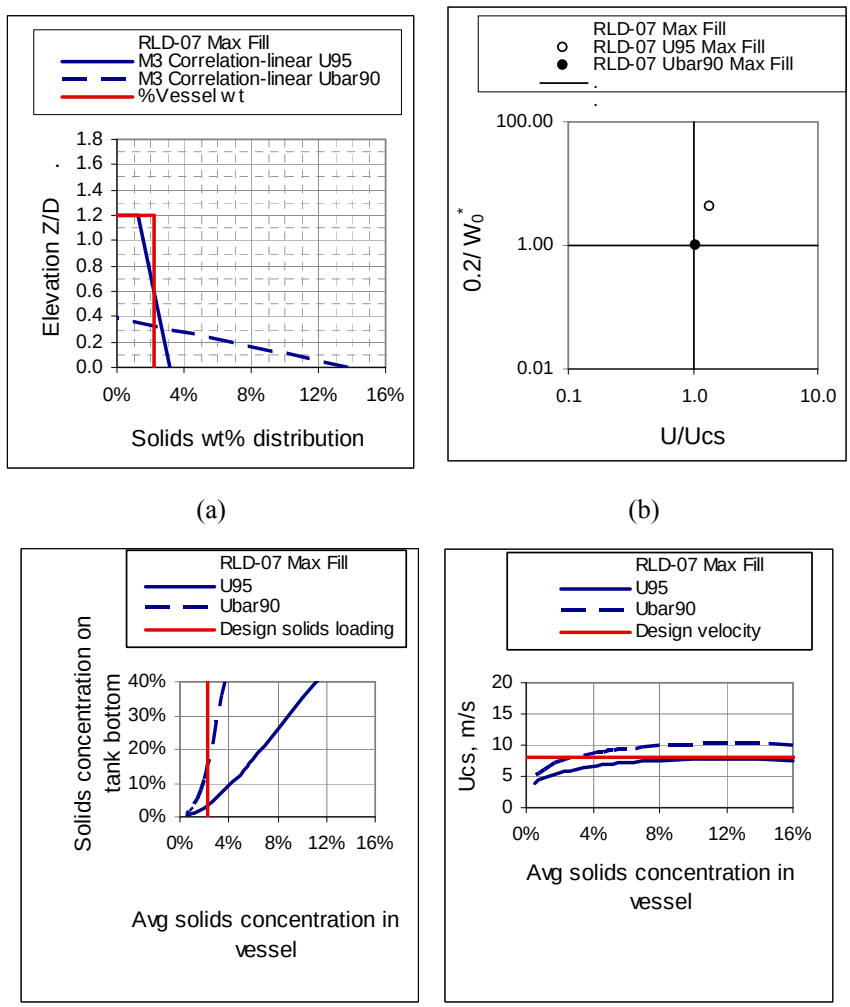

Figure 9.39 Physical Model Predictions for RLD-07: (a) Concentration Profile at Max Fill, (b) Inlet Concentration and Suspension Ratio, (c) Maximum Solids Concentration Versus Loading Design Conditions, (d) U_{CS} Versus Loading (Hanford PSDD, ρ_l = 1.1 g/cm^3, μ = 1.5 cP fluid)

9.4.15 RLD-08 (Hanford PSDD, ρ_l = 1.1 g/cm^3, μ = 1.5 cP Fluid) Physical Model

Table 9.37 lists physical model results for RLD-08, and Figure 9.40 shows physical model predictions for RLD-08 using the Hanford PSDD.

Table 9.37. Physical Model Results for RLD-08 Using Hanford PSDD

RLD-08 U_{95} Max Fill			RLD-08 $\bar{U}_{90}$ Max Fill		
U (m/s)	U_{CS} (m/s)	U/ U_{CS}	U (m/s)	U_{CS} (m/s)	U/ U_{CS}
8	5.3	1.51	8	7.0	1.15
H/D	H_C/D	H_C/H	H/D	H_C/D	H_C/H
0.91	2.57	2.83	0.91	0.54	0.60
W (wt%)	W_0^* (wt%)	0.2/W_0^*	W (wt%)	W_0^* (wt%)	0.2/W_0^*
2.2	3.7	5.39	2.2	11.0	1.81

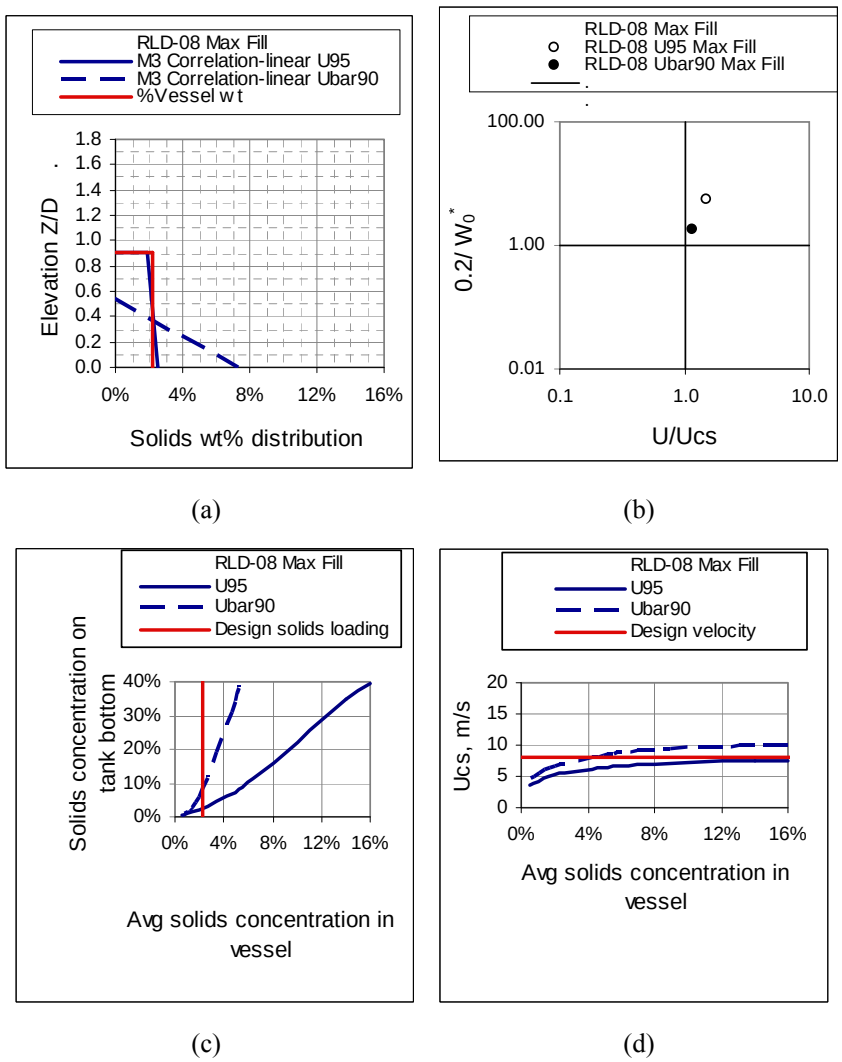

Figure 9.40. Physical Model Predictions for RLD-08: (a) Concentration Profile at Max Fill, (b) Inlet Concentration and Suspension Ratio, (c) Maximum Solids Concentration Versus Loading Design Conditions, (d) U_{CS} Versus Loading (Hanford PSDD, ρ_l = 1.1 g/cm^3, μ = 1.5 cP fluid)

9.4.16 HOP-903/904 (Hanford PSDD, ρ_l=1.1 g/cm^3, μ=1.5 cP Fluid) Physical Model

Table 9.38 lists physical model results for HOP-903/904, and Figure 9.41 depicts physical model predictions for HOP-903/904 using the Hanford PSDD.

Table 9.38. Physical Model Results for HOP-903/904 Using Hanford PSDD

HOP-903/904 U_{95} Max Fill			HOP-903/904 $\bar{U}_{90}$ Max Fill		
U (m/s)	U_{CS} (m/s)	U/U_{CS}	U (m/s)	U_{CS} (m/s)	U/U_{CS}
8	4.1	1.96	8	5.6	1.43
H/D	H_C/D	H_C/H	H/D	H_C/D	H_C/H
0.86	5.57	6.49	0.86	1.21	1.41
W (wt%)	W_0^* (wt%)	$0.2/W_0^*$	W (wt%)	W_0^* (wt%)	$0.2/W_0^*$
1	1.5	13.02	1	2.3	8.85

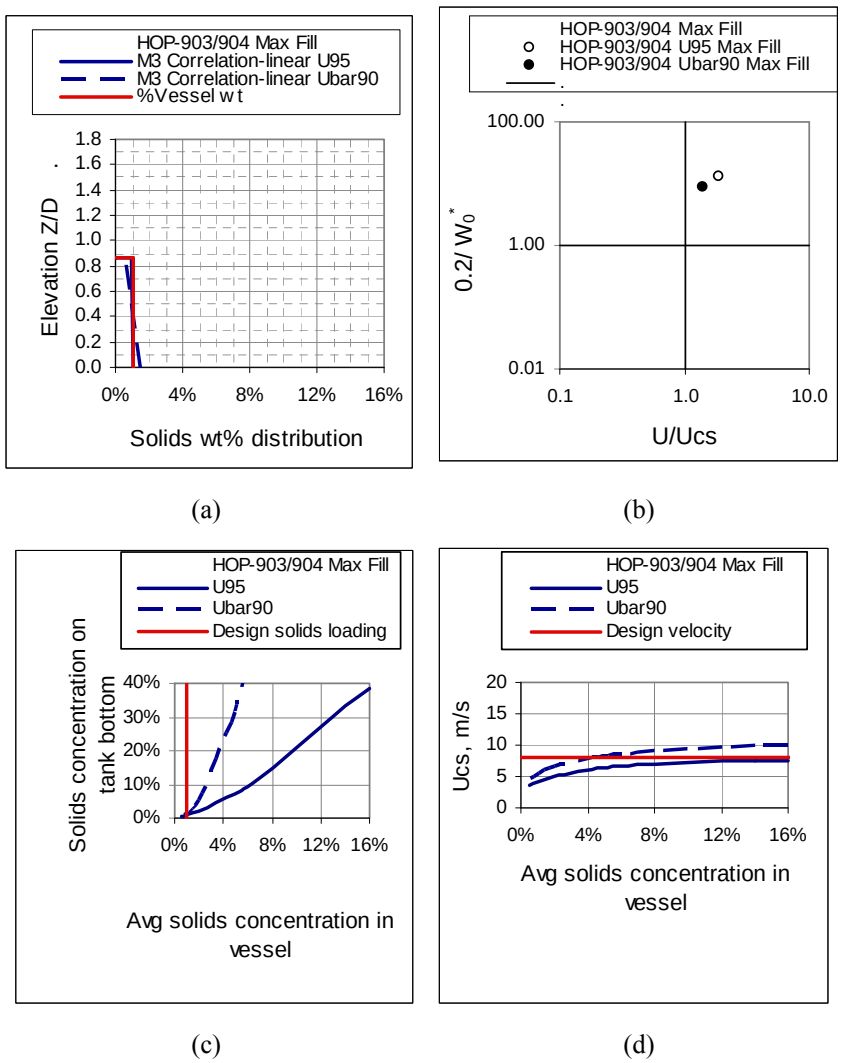

Figure 9.41. Physical Model Predictions for HOP-903/904: (a) Concentration Profile at Max Fill, (b) Inlet Concentration and Suspension Ratio, (c) Maximum Solids Concentration Versus Loading for Design Condition, (d) U_{CS} Versus Loading (Hanford PSDD, ρ_l = 1.1 g/cm^3, μ = 1.5 cP fluid)

9.5 Vessel Evaluation Examples Using the Generalized Models and the Hanford Waste Distribution

Mixing performance of WTP vessels was evaluated based on the Hanford waste distribution using the generalized models for U_{CS} and H_C statistically developed in Appendix F and summarized in Section 7.4. The H_C generalized model was substituted in the C_0 model discussed in Sections 7.3.3 and 7.3.4, with C_0 Model modified to W_0^*, as described in Section 9.1.4. The results of the evaluations are presented in Sections 9.5.1 through 9.5.16.

The Hanford waste settling properties and particle characteristics used in the examples are the same as those used in Section 9.4. The vessel geometry and operating conditions are listed in Table 9.2, and vessel loading is shown in Table 9.4. These examples are for the vessel conditions that were provided in Olsen (2008a).

Note that Tables 9.39 through 9.54 display only a few significant figures. The calculations are not based on this reduced number of digits. Therefore, small calculation differences are observed when using the displayed rounded numbers for calculations.

9.5.1 FRP-02 A/B/C/D (Hanford PSDD, ρ_l = 1.1 g/cm^3, μ = 1.5 cP Fluid) Generalized Model

Table 9.39 lists generalized model results for FRP-02 A/B/C/D using the Hanford PSDD. Figure 9.42 presents the generalized model predictions for FRP-02 A/B/C/D using the Hanford PSDD.

Table 9.39. Generalized Model Results for FRP-02 Using Hanford PSDD

FRP-02A/B/C/D U_{95} Max Fill			FRP-02A/B/C/D $\bar{U}_{90}$ Max Fill		
U (m/s)	U_{CS} (m/s)	U/ U_{CS}	U (m/s)	U_{CS} (m/s)	U/ U_{CS}
8	26.0	0.31	8	34.8	0.23
H/D	H_C/D	H_C/H	H/D	H_C/D	H_C/H
0.73	0.11	0.16	0.73	0.06	0.09
W (wt%)	W_0^* (wt%)	0.2/W_0^*	W (wt%)	W_0^* (wt%)	0.2/W_0^*
4.9	> W_{MP}[(a)]	0.21	4.9	> W_{MP}[(a)]	0.12

(a) Calculated value exceeds maximum packing fraction.

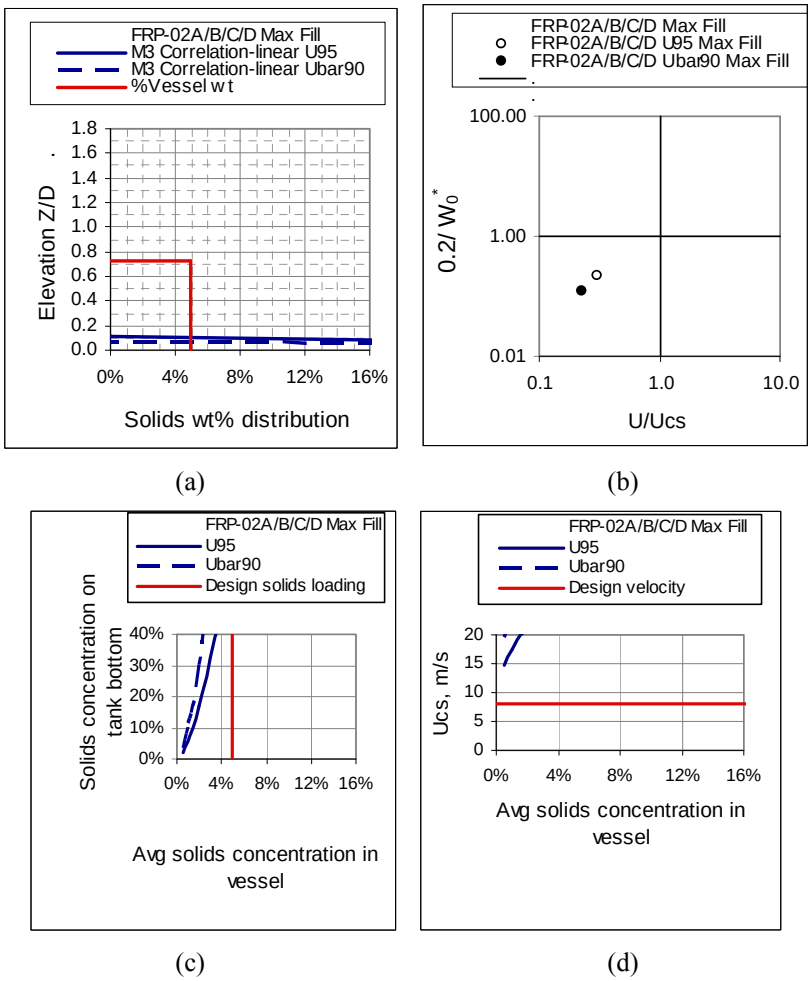

Figure 9.42. Generalized Model Predictions for FRP-02 A/B/C/D: (a) Concentration Profile at Max Fill, (b) Inlet Concentration and Suspension Ratio, (c) Maximum Solids Concentration Versus Loading Design Conditions, (d) U_{CS} Versus Loading (Hanford PSDD, ρ_l = 1.1 g/cm^3, μ = 1.5 cP fluid)

9.5.2 HLP-22 8 m/s, 4-in. (Hanford PSDD, ρ_l = 1.1 g/cm^3, μ = 1.5 cP Fluid) Generalized Model

Table 9.40 presents the generalized model results for HLP-22 using Hanford PSDD. Figure 9.43 presents the generalized model predictions for HLP-22 using the Hanford PSDD.

Table 9.40. Generalized Model Results for HLP-22 Using Hanford PSDD

HLP-22 U_{95} Max Fill			HLP-22 $\bar{U}_{90}$ Max Fill		
U (m/s)	U_{CS} (m/s)	U/ U_{CS}	U (m/s)	U_{CS} (m/s)	U/ U_{CS}
8	23.3	0.34	8	31.3	0.26
H/D	H_C/D	H_C/H	H/D	H_C/D	H_C/H
0.80	0.18	0.23	0.80	0.10	0.13
W (wt%)	W_0^* (wt%)	$0.2/W_0^*$	W (wt%)	W_0^* (wt%)	$0.2/W_0^*$
15.4	> W_{MP}[(a)]	0.10	15.4	> W_{MP}[(a)]	0.05

(a) Calculated value exceeds maximum packing fraction.

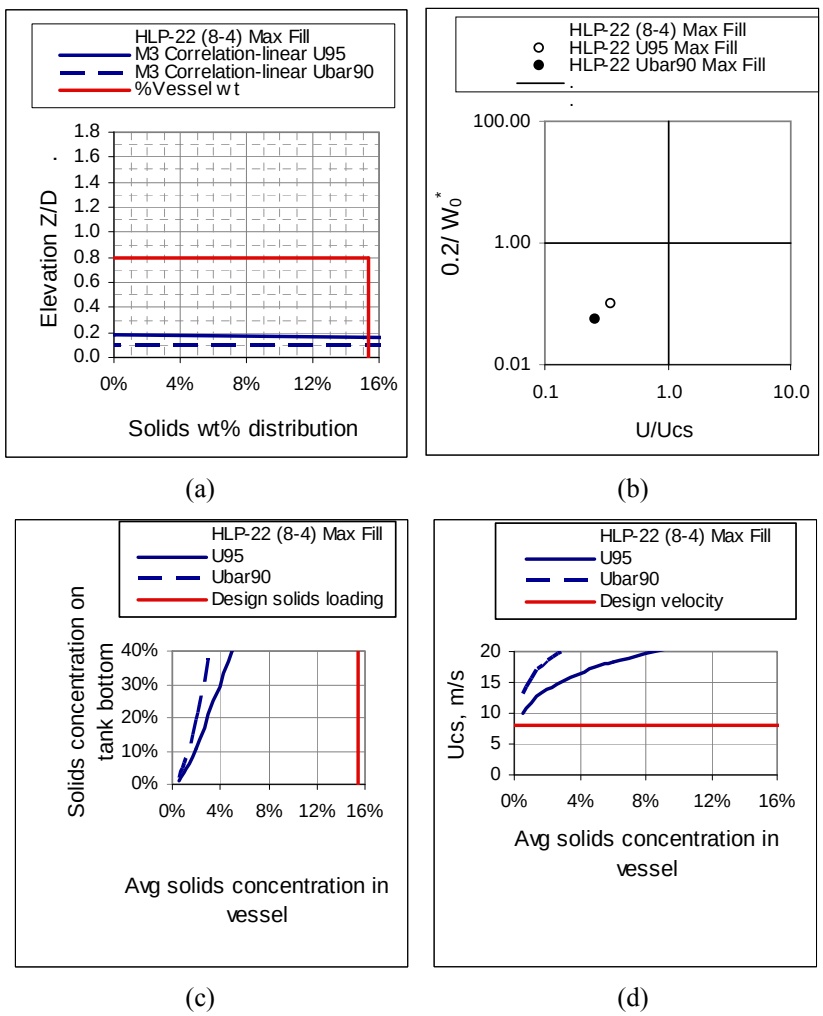

Figure 9.43. Generalized Model Predictions for HLP-22: (a) Concentration Profile at Max Fill, (b) Inlet Concentration and Suspension Ratio, (c) Maximum Solids Concentration Versus Loading Design Conditions, (d) U_{CS} Versus Loading (8 m/s, 4-in. nozzles, Hanford PSDD)

9.5.3 HLP-22 12 m/s, 4-in. (Hanford PSDD, ρ_l = 1.1 g/cm^3, μ = 1.5 cP Fluid) Generalized Model

Table 9.41 lists generalized model results for HLP-22 using the Hanford PSDD. Figure 9.44 presents the generalized model predictions for HLP-22 using the Hanford PSDD.

Table 9.41. Generalized Model Results for HLP-22 Using Hanford PSDD

HLP-22 U_{95} Max Fill			HLP-22 $\bar{U}_{90}$ Max Fill		
U (m/s)	U_{CS} (m/s)	U/U_{CS}	U (m/s)	U_{CS} (m/s)	U/U_{CS}
12	23.3	0.51	12	31.3	0.38
H/D	H_C/D	H_C/H	H/D	H_C/D	H_C/H
0.80	0.31	0.39	0.80	0.18	0.22
W (wt%)	W_0^* (wt%)	$0.2/W_0^*$	W (wt%)	W_0^* (wt%)	$0.2/W_0^*$
15.4	> W_{MP}[(a)]	0.17	15.4	> W_{MP}[(a)]	0.09

(a) Calculated value exceeds maximum packing fraction.

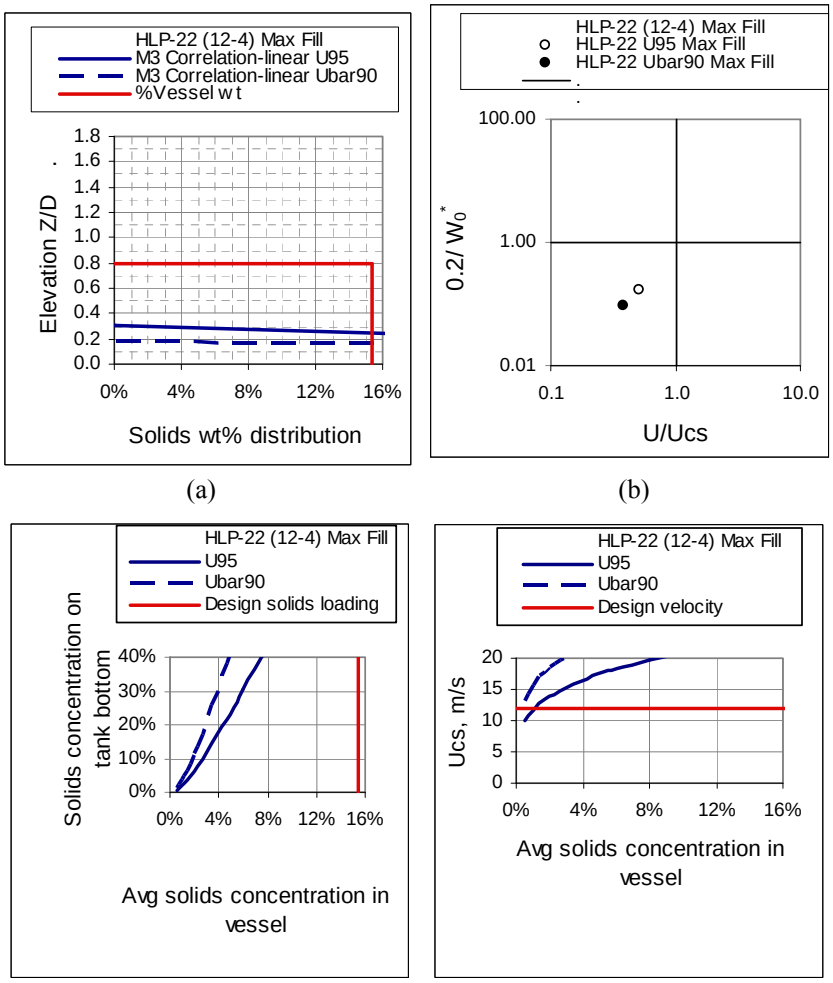

Figure 9.44. Generalized Model Predictions for HLP-22: (a) Concentration Profile at Max Fill, (b) Inlet Concentration and Suspension Ratio, (c) Maximum Solids Concentration Versus Loading Design Conditions, (d) U_{CS} Versus Loading (12 m/s, 4-in. nozzles, Hanford PSDD)

9.5.4 HLP-22 8 m/s, 6-in. (Hanford PSDD, ρ_l = 1.1 g/cm^3, μ = 1.5 cP Fluid) Generalized Model

Table 9.42 presents generalized model results for HLP-22 using the Hanford PSDD. Figure 9.45 shows the generalized model predictions for HLP-22 8 m/s, 6-in. (8 m/s, 6-in. nozzle).

Table 9.42. Generalized Model Results for HLP-22 Using Hanford PSDD

HLP-22 U_{95} Max Fill			HLP-22 $\bar{U}_{90}$ Max Fill		
U (m/s)	U_{CS} (m/s)	U/ U_{CS}	U (m/s)	U_{CS} (m/s)	U/ U_{CS}
8	17.0	0.47	8	22.8	0.35
H/D	H_C/D	H_C/H	H/D	H_C/D	H_C/H
0.80	0.31	0.39	0.80	0.17	0.22
W (wt%)	W_0^* (wt%)	0.2/W_0^*	W (wt%)	W_0^* (wt%)	0.2/W_0^*
15.4	> W_{MP}[(a)]	0.17	15.4	> W_{MP}[(a)]	0.09

(a) Calculated value exceeds maximum packing fraction.

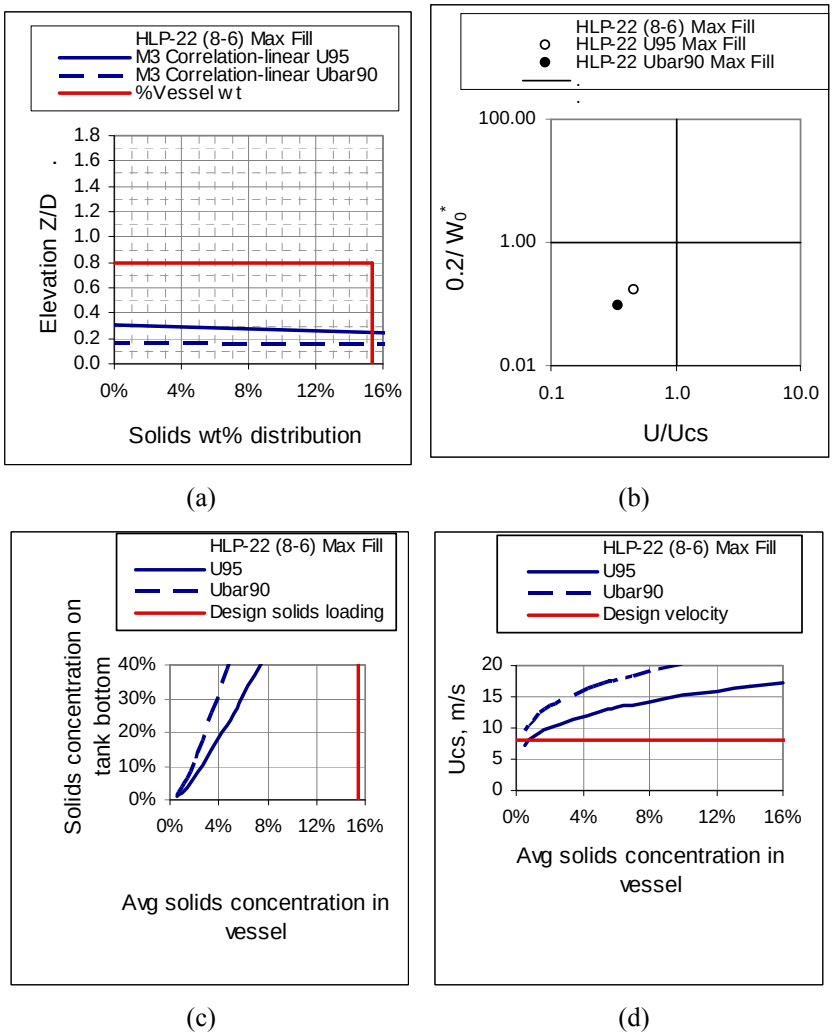

Figure 9.45. Generalized Model Predictions for HLP-22: (a) Concentration Profile at Max Fill, (b) Inlet Concentration and Suspension Ratio, (c) Maximum Solids Concentration Versus Loading Design Conditions, (d) U_{CS} Versus Loading (Hanford PSDD, 8 m/s, 6-in. nozzles)

9.5.5 HLP-22 12 m/s, 6-in. (Hanford PSDD, ρ_l = 1.1 g/cm^3, μ = 1.5 cP Fluid) Generalized Model

Table 9.43 contains generalized model results for HLP-22 using the Hanford PSDD. Figure 9.46 presents the generalized model predictions for HLP-22 (Hanford PSDD, 12 m/s, 6-in. nozzle).

Table 9.43. Model Results for Design Conditions for HLP-22

HLP-22 U_{95} Max Fill			HLP-22 $\bar{U}_{90}$ Max Fill		
U (m/s)	U_{CS} (m/s)	U/ U_{CS}	U (m/s)	U_{CS} (m/s)	U/ U_{CS}
12	17.0	0.71	12	22.8	0.53
H/D	H_C/D	H_C/H	H/D	H_C/D	H_C/H
0.80	0.54	0.67	0.80	0.30	0.38
W (wt%)	W_0^* (wt%)	0.2/W_0^*	W (wt%)	W_0^* (wt%)	0.2/W_0^*
15.4	68.6	0.29	15.4	> W_{MP}[(a)]	0.16

(a) Calculated value exceeds maximum packing fraction.

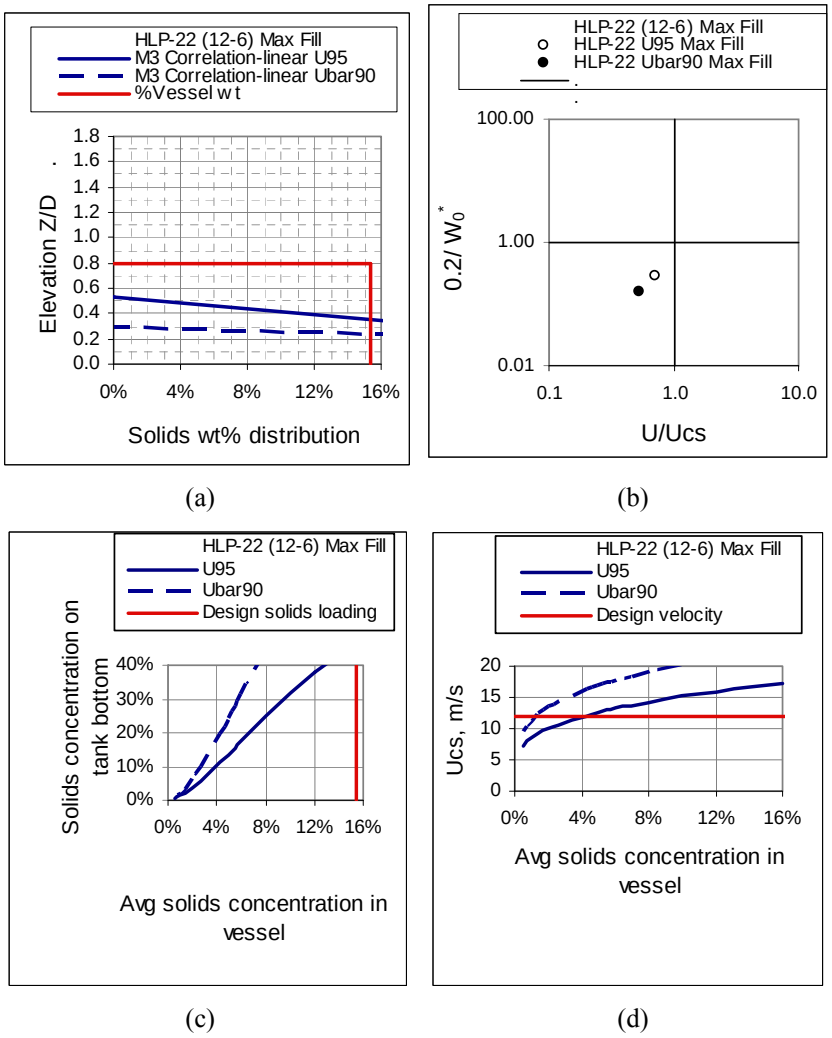

Figure 9.46. Generalized Model Predictions for HLP-22: (a) Concentration Profile at Max Fill, (b) Inlet Concentration and Suspension Ratio, (c) Maximum Solids Concentration Versus Loading Design Conditions, (d) U_{CS} Versus Loading (Hanford PSDD, 12 m/s, 6-in. nozzles)

9.5.6 TCP-01 (Hanford PSDD, ρ_l = 1.1 g/cm^3, μ = 1.5 cP Fluid) Generalized Model

Table 9.44 shows generalized model results for TCP-01 using the Hanford PSDD, and Figure 9.47 presents the generalized model predictions for TCP-01 (Hanford PSDD, ρ_l = 1.1 g/cm^3, μ = 1.5 cP fluid).

Table 9.44. Generalized Model Results for TCP-01 Using Hanford PSDD

TCP-01 U_{95} Max Fill			TCP-01 $\bar{U}_{90}$ Max Fill		
U (m/s)	U_{CS} (m/s)	U/ U_{CS}	U (m/s)	U_{CS} (m/s)	U/ U_{CS}
8	10.8	0.74	8	14.5	0.55
H/D	H_C/D	H_C/H	H/D	H_C/D	H_C/H
1.25	0.45	0.36	1.25	0.25	0.20
W (wt%)	W_0^* (wt%)	0.2/W_0^*	W (wt%)	W_0^* (wt%)	0.2/W_0^*
2.7	22.4	0.89	2.7	40.1	0.50

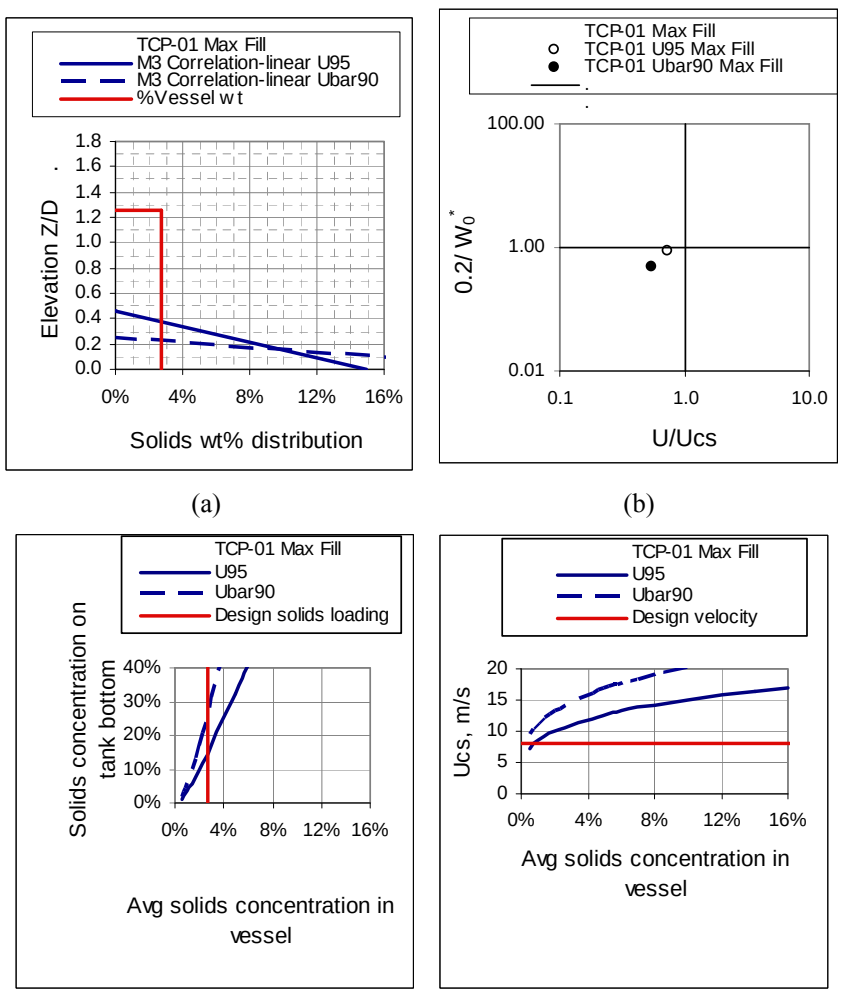

Figure 9.47. Generalized Model Predictions for TCP-01: (a) Concentration Profile at Max Fill, (b) Inlet Concentration and Suspension Ratio, (c) Maximum Solids Concentration Versus Loading Design Conditions, (d) U_{CS} Versus Loading (Hanford PSDD, ρ_l = 1.1 g/cm^3, μ = 1.5 cP fluid)

9.5.7 TLP-09 A/B (Hanford PSDD, ρ_l = 1.1 g/cm^3, μ = 1.5 cP Fluid) Generalized Model

Table 9.45 lists generalized model results for TLP-09 A/B using the Hanford PSDD, and Figure 9.48 presents the generalized model predictions for TLP-09 A/B (Hanford PSDD, ρ_l = 1.1 g/cm^3, μ = 1.5 cP fluid).

Table 9.45. Generalized Model Results for TLP-09 Using Hanford PSDD

TLP-09A/B U_{95} Max Fill			TLP-09A/B $\bar{U}_{90}$ Max Fill		
U (m/s)	U_{CS} (m/s)	U/ U_{CS}	U (m/s)	U_{CS} (m/s)	U/ U_{CS}
8	7.5	1.07	8	10.1	0.80
H/D	H_C/D	H_C/H	H/D	H_C/D	H_C/H
1.08	1.29	1.20	1.08	0.72	0.67
W (wt%)	W_0^* (wt%)	0.2/W_0^*	W (wt%)	W_0^* (wt%)	0.2/W_0^*
0.3	0.8	26.16	0.3	1.3	14.82

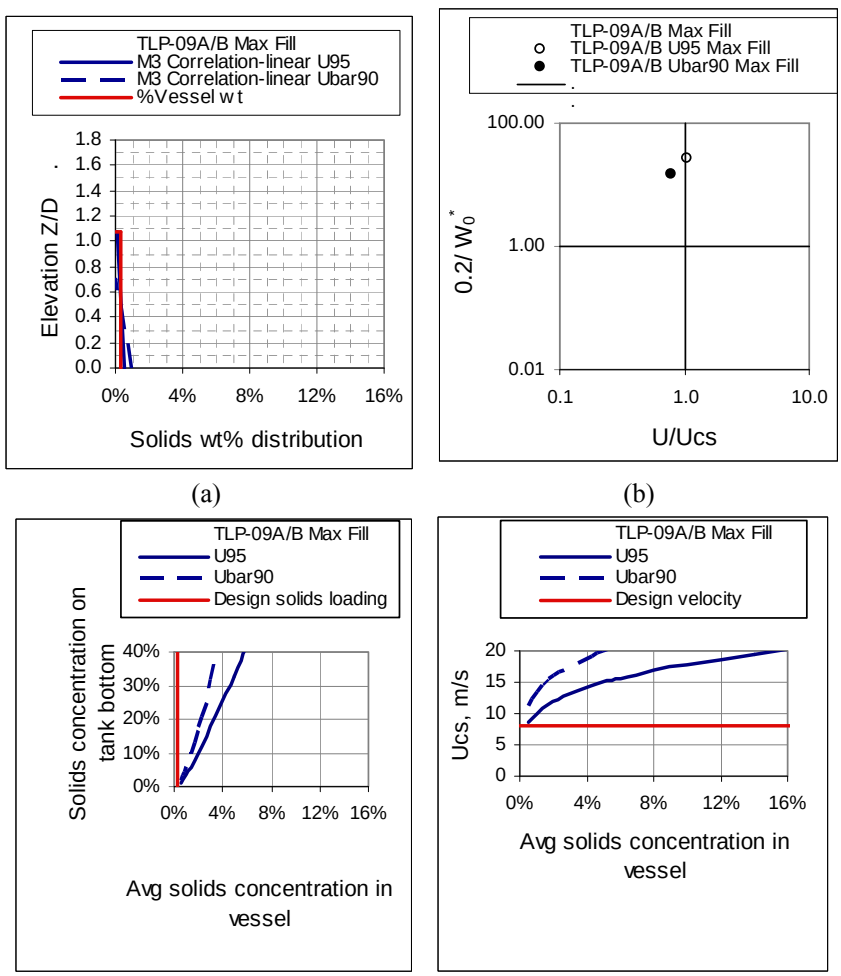

Figure 9.48. Generalized Model Predictions for TLP-09 A/B: (a) Concentration Profile at Max Fill, (b) Inlet Concentration and Suspension Ratio, (c) Maximum Solids Concentration Versus Loading Design Conditions, (d) U_{CS} Versus Loading (Hanford PSDD, ρ_l = 1.1 g/cm^3, μ = 1.5 cP fluid)

9.5.8 PWD-33 (Hanford PSDD, ρ_l = 1.1 g/cm^3, μ = 1.5 cP Fluid) Generalized Model

Table 9.46 contains generalized model results for PWD-33 using the Hanford PSDD, and Figure 9.49 shows generalized model predictions for PWD-33 (Hanford PSDD, ρ_l = 1.1 g/cm^3, μ = 1.5 cP fluid).

Table 9.46. Generalized Model Results for PWD-33 Using Hanford PSDD

PWD-33 U_{95} Max Fill			PWD-33 $\bar{U}_{90}$ Max Fill		
U (m/s)	U_{CS} (m/s)	U/ U_{CS}	U (m/s)	U_{CS} (m/s)	U/ U_{CS}
8	13.9	0.58	8	18.6	0.43
H/D	H_C/D	H_C/H	H/D	H_C/D	H_C/H
0.45	0.37	0.83	0.45	0.21	0.46
W (wt%)	W_0^* (wt%)	0.2/W_0^*	W (wt%)	W_0^* (wt%)	0.2/W_0^*
8.1	29.5	0.68	8.1	52.8	0.38

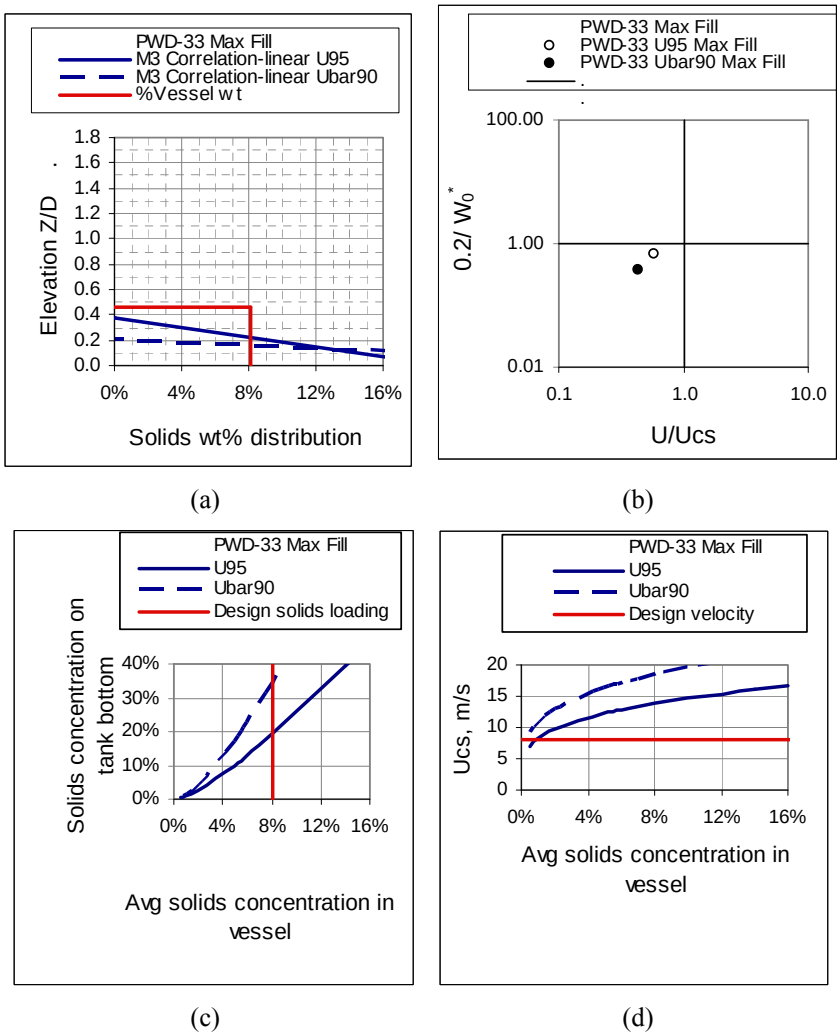

Figure 9.49. Generalized Model Predictions for PWD-33: (a) Concentration Profile at Max Fill, (b) Inlet Concentration and Suspension Ratio, (c) Maximum Solids Concentration Versus Loading Design Conditions; (d) U_{CS} Versus Loading (Hanford PSDD, ρ_l = 1.1 g/cm^3, μ = 1.5 cP fluid)

9.5.9 PWD-43 (Hanford PSDD, ρ_l = 1.1 g/cm^3, μ = 1.5 cP Fluid) Generalized Model

Table 9.47 presents generalized model results for PWD-43 using the Hanford PSDD. Figure 9.50 shows generalized model predictions for PWD-43 (Hanford PSDD, ρ_l = 1.1 g/cm^3, μ = 1.5 cP fluid).

Table 9.47. Generalized Model Results for PWD-43 Using Hanford PSDD

PWD-43 U_{95} Max Fill			PWD-43 $\bar{U}_{90}$ Max Fill		
U (m/s)	U_{CS} (m/s)	U/ U_{CS}	U (m/s)	U_{CS} (m/s)	U/ U_{CS}
8	5.6	1.43	8	7.5	1.07
H/D	H_C/D	H_C/H	H/D	H_C/D	H_C/H
0.45	2.91	6.41	0.45	1.62	3.58
W (wt%)	W_0^* (wt%)	0.2/W_0^*	W (wt%)	W_0^* (wt%)	0.2/W_0^*
0.2	0.3	65.08	0.2	0.3	61.83

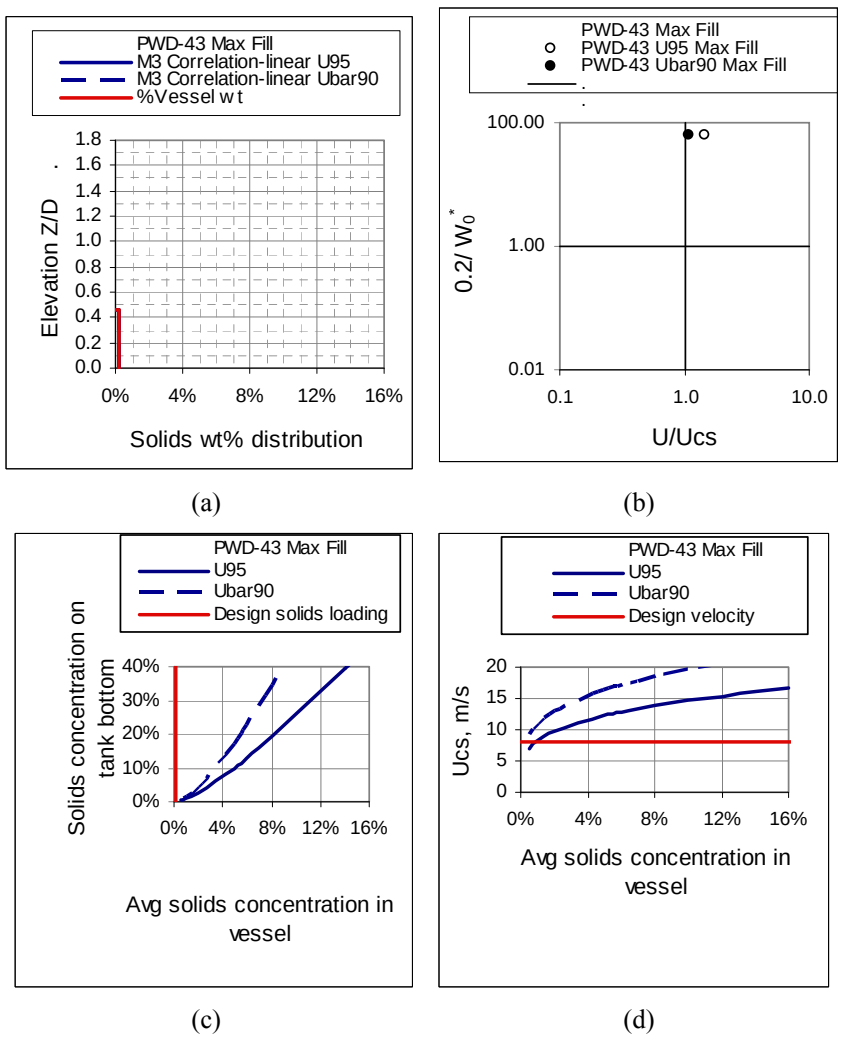

Figure 9.50. Generalized Model Predictions for PWD-43: (a) Concentration Profile at Max Fill, (b) Inlet Concentration and Suspension Ratio, (c) Maximum Solids Concentration Versus Loading Design Conditions, (d) U_{CS} Versus Loading (Hanford PSDD, ρ_l = 1.1 g/cm^3, μ = 1, 1.5 cP fluid)

9.5.10 PWD-44 (Hanford PSDD, ρ_l = 1.1 g/cm^3, μ = 1.5 cP Fluid) Generalized Model

Table 9.48 lists generalized model results for PWD-44 using the Hanford PSDD. Figure 9.51 shows generalized model predictions for PWD-44 (Hanford PSDD, ρ_l = 1.1 g/cm^3, μ = 1.5 cP fluid).

Table 9.48. Generalized Model Results for PWD-44 Using Hanford PSDD

PWD-44 U_{95} Max Fill			PWD-44 $\bar{U}_{90}$ Max Fill		
U (m/s)	U_{CS} (m/s)	U/ U_{CS}	U (m/s)	U_{CS} (m/s)	U/ U_{CS}
8	11.8	0.68	8	15.9	0.50
H/D	H_C/D	H_C/H	H/D	H_C/D	H_C/H
1.32	0.51	0.39	1.32	0.29	0.22
W (wt%)	W_0^* (wt%)	0.2/W_0^*	W (wt%)	W_0^* (wt%)	0.2/W_0^*
8.1	62.5	0.32	8.1	112.1	0.18

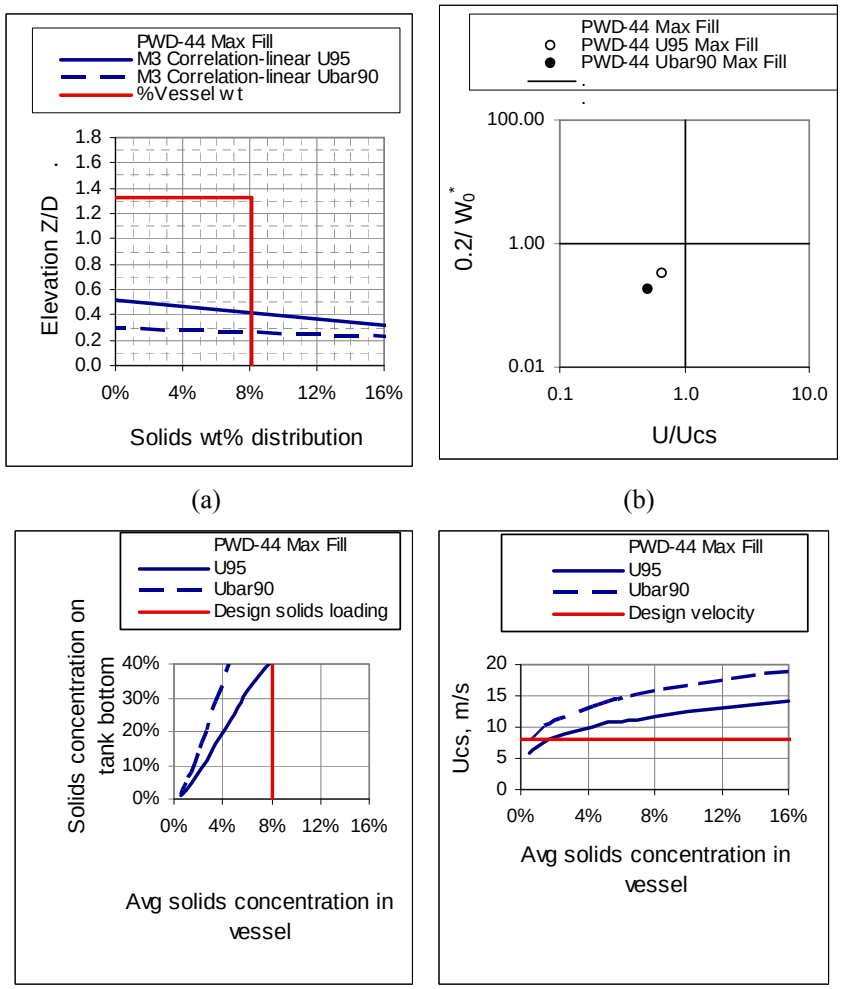

Figure 9.51. Generalized Model Predictions for PWD-44: (a) Concentration Profile at Max Fill, (b) Inlet Concentration and Suspension Ratio, (c) Maximum Solids Concentration Versus Loading Design Conditions, (d) U_{CS} Versus Loading (Hanford PSDD, ρ_l = 1.1 g/cm^3, μ = 1.5 cP fluid)

9.5.11 FEP-17 A/B (Hanford PSDD, ρ_l = 1.1 g/cm^3, μ = 1.5 cP Fluid) Generalized Model

Table 9.49 presents generalized model results for FEP-17 A/B using the Hanford PSDD. Figure 9.52 depicts generalized model predictions for FEP-17 A/B (Hanford PSDD, ρ_l = 1.1 g/cm^3, μ = 1.5 cP fluid).

Table 9.49. Generalized Model Results for FEP-17 Using Hanford PSDD

FEP-17A/B U_{95} Max Fill			FEP-17A/B $\bar{U}_{90}$ Max Fill		
U (m/s)	U_{CS} (m/s)	U/ U_{CS}	U (m/s)	U_{CS} (m/s)	U/ U_{CS}
8	9.7	0.83	8	13.0	0.62
H/D	H_C/D	H_C/H	H/D	H_C/D	H_C/H
1.19	0.56	0.47	1.19	0.31	0.26
W (wt%)	W_0^* (wt%)	0.2/W_0^*	W (wt%)	W_0^* (wt%)	0.2/W_0^*
4.4	28.2	0.71	4.4	50.5	0.40

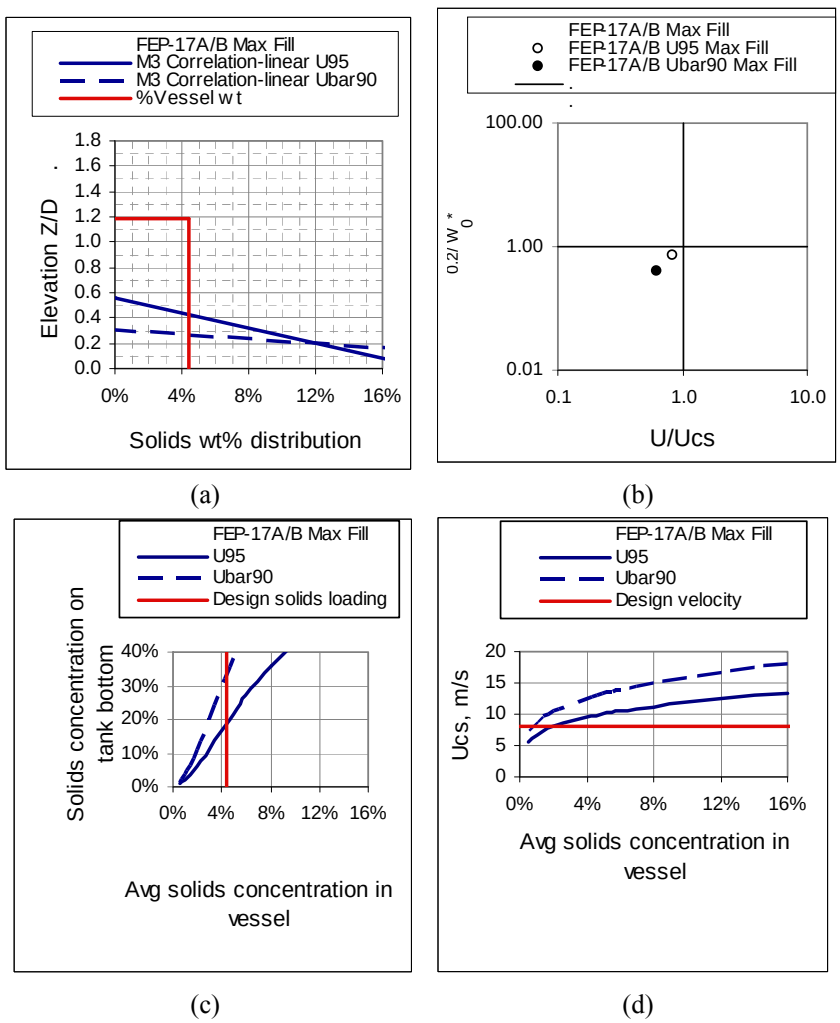

Figure 9.52. Generalized Model Predictions for FEP-17 A/B: (a) Concentration Profile at Max Fill, (b) Inlet Concentration and Suspension Ratio, (c) Maximum Solids Concentration Versus Loading Design Conditions, (d) U_{CS} Versus Loading (Hanford PSDD, ρ_l = 1.1 g/cm^3, μ = 1.5 cP fluid)

9.5.12 PWD-15/16 (Hanford PSDD, ρ_l = 1.1 g/cm^3, μ = 1.5 cP Fluid) Generalized Model

Table 9.50 contains generalized model results for PWD-15/16 using the Hanford PSDD. Figure 9.53 presents generalized model predictions for PWD-15/16 (Hanford PSDD, ρ_l = 1.1 g/cm^3, μ = 1.5 cP fluid).

Table 9.50. Generalized Model Results for PWD-15/16 Using Hanford PSDD

PWD-15/16 U_{95} Max Fill			PWD-15/16 $\bar{U}_{90}$ Max Fill		
U (m/s)	U_{CS} (m/s)	U/ U_{CS}	U (m/s)	U_{CS} (m/s)	U/ U_{CS}
8	10.4	0.77	8	14.0	0.57
H/D	H_C/D	H_C/H	H/D	H_C/D	H_C/H
1.78	0.54	0.30	1.78	0.30	0.17
W (wt%)	W_0^* (wt%)	0.2/W_0^*	W (wt%)	W_0^* (wt%)	0.2/W_0^*
3	29.9	0.67	3	53.6	0.37

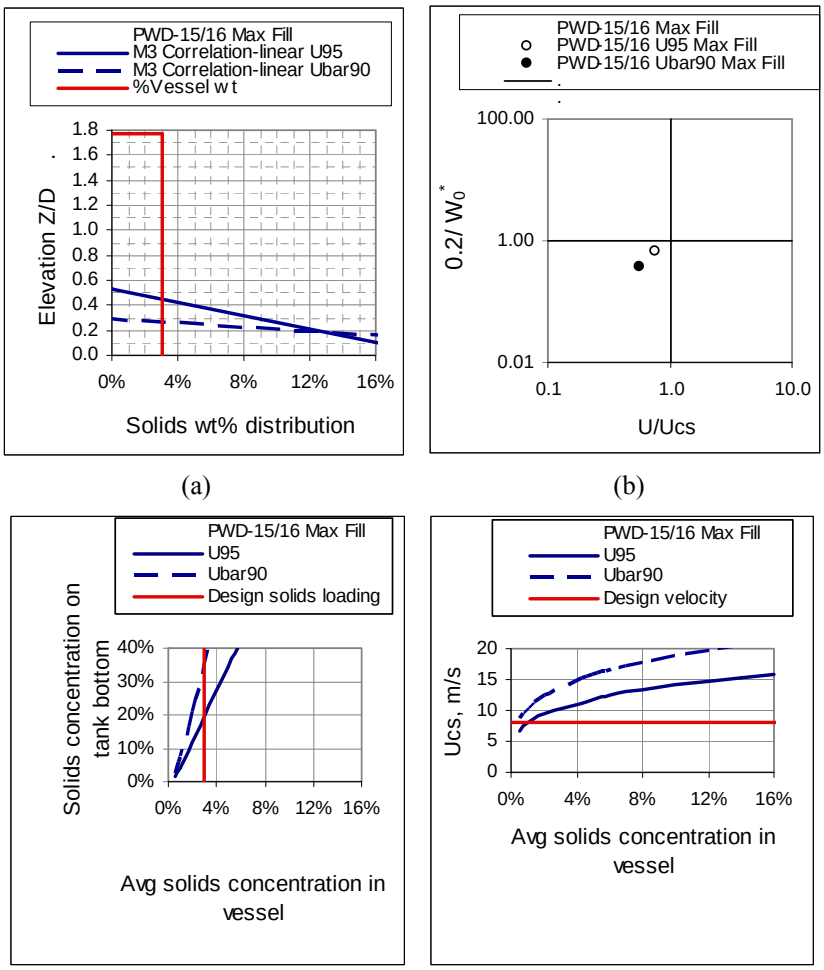

Figure 9.53. Generalized Model Predictions for PWD-15/16: (a) Concentration Profile at Max Fill, (b) Inlet Concentration and Suspension Ratio, (c) Maximum Solids Concentration Versus Loading Design Conditions, (d) U_{CS} Versus Loading (Hanford PSDD, ρ_l = 1.1 g/cm3, μ = 1.5 cP fluid)

9.5.13 UFP-01 A/B (Hanford PSDD, ρ_l = 1.1 g/cm^3, μ = 1.5 cP Fluid) Generalized Model

Table 9.51 presents generalized model results for UFP-01 A/B using the Hanford PSDD. Figure 9.54 shows generalized model predictions for UFP-01 A/B (Hanford PSDD, ρ_l = 1.1 g/cm^3, μ = 1.5 cP fluid).

Table 9.51. Generalized Model Results for UFP-01 Using Hanford PSDD

UFP-01A/B U_{95} Max Fill			UFP-01A/B $\bar{U}_{90}$ Max Fill		
U (m/s)	U_{CS} (m/s)	U/ U_{CS}	U (m/s)	U_{CS} (m/s)	U/ U_{CS}
8	8.4	0.95	8	11.2	0.71
H/D	H_C/D	H_C/H	H/D	H_C/D	H_C/H
1.45	0.70	0.48	1.45	0.39	0.27
W (wt%)	W_0^* (wt%)	0.2/W_0^*	W (wt%)	W_0^* (wt%)	0.2/W_0^*
3.8	23.7	0.84	3.8	42.5	0.47

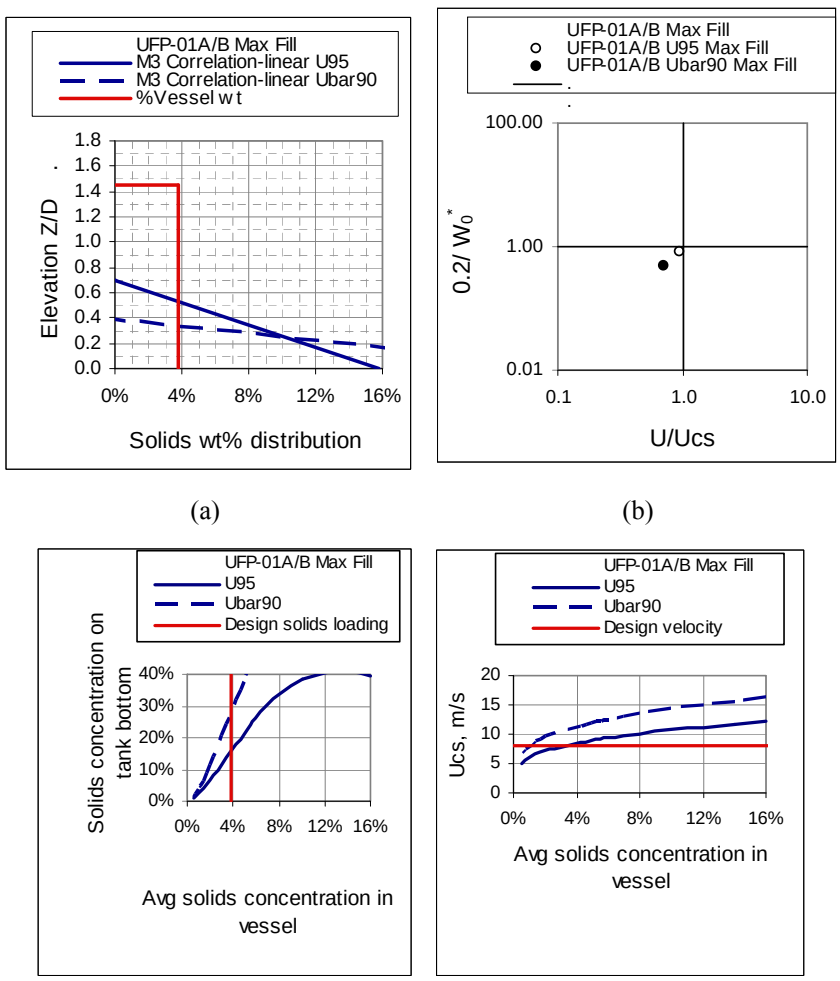

Figure 9.54. Generalized Model Predictions for UFP-01 A/B: (a) Concentration Profile at Max Fill, (b) Inlet Concentration and Suspension Ratio, (c) Maximum Solids Concentration Versus Loading Design Conditions, (d) U_{CS} Versus Loading (Hanford PSDD, ρ_l = 1.1 g/cm^3, μ = 1.5 cP fluid)

9.5.14 RLD-07 (Hanford PSDD, ρ_l = 1.1 g/cm^3, μ = 1.5 cP Fluid) Generalized Model

Table 9.52 contains generalized model results for RLD-07 using the Hanford PSDD. Figure 9.55 presents generalized model predictions for RLD-07 (Hanford PSDD, ρ_l = 1.1 g/cm^3, μ = 1.5 cP fluid).

Table 9.52. Generalized Model Results for RLD-07 Using Hanford PSDD

RLD-07 U_{95} Max Fill			RLD-07 $\bar{U}_{90}$ Max Fill		
U (m/s)	U_{CS} (m/s)	U/ U_{CS}	U (m/s)	U_{CS} (m/s)	U/ U_{CS}
8	6.4	1.24	8	8.6	0.93
H/D	H_C/D	H_C/H	H/D	H_C/D	H_C/H
1.20	1.54	1.28	1.20	0.86	0.71
W (wt%)	W_0^* (wt%)	0.2/W_0^*	W (wt%)	W_0^* (wt%)	0.2/W_0^*
2.2	5.3	3.76	2.2	9.2	2.16

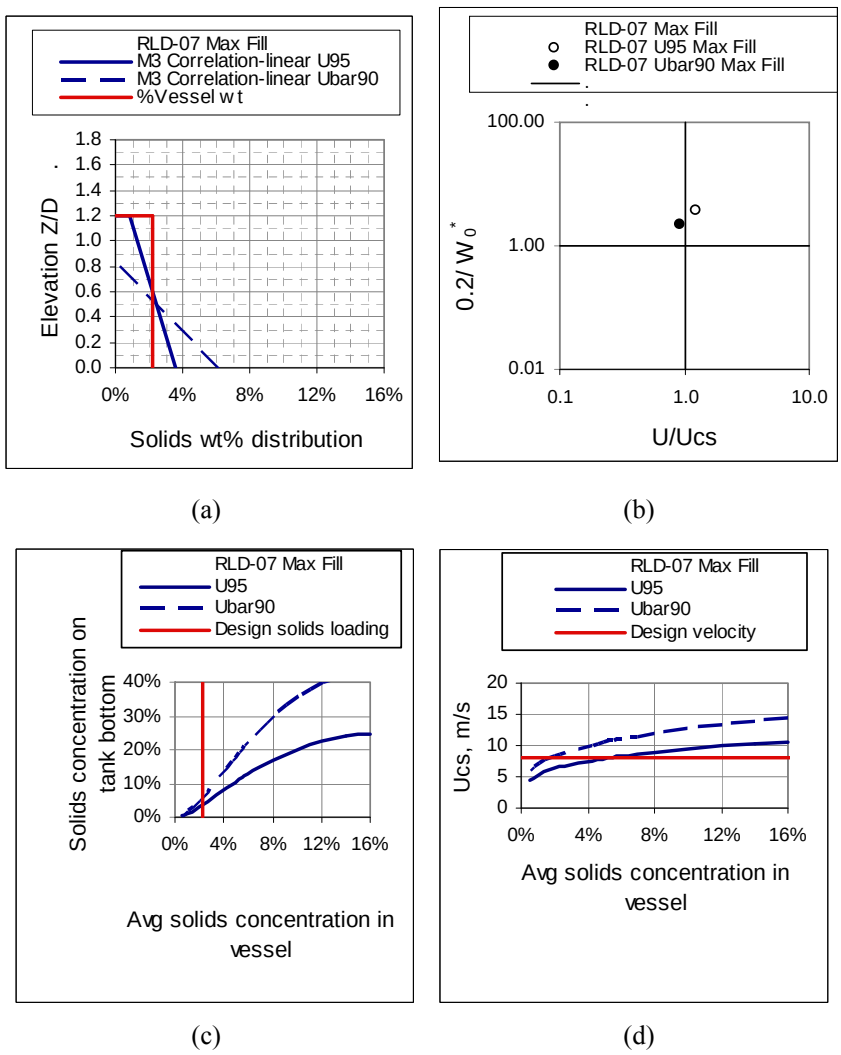

Figure 9.55. Generalized Model Predictions for RLD-07: (a) Concentration Profile at Max Fill, (b) Inlet Concentration and Suspension Ratio, (c) Maximum Solids Concentration Versus Loading Design Conditions, (d) U_{CS} Versus Loading (Hanford PSDD, ρ_l = 1.1 g/cm^3, μ = 1.5 cP fluid)

9.5.15 RLD-08 (Hanford PSDD, ρ_l = 1.1 g/cm^3, μ = 1.5 cP Fluid) Generalized Model

Table 9.53 lists generalized model results for RLD-08 using the Hanford PSDD. Figure 9.56 presents generalized model predictions for RLD-08 (Hanford PSDD, ρ_l = 1.1 g/cm^3, μ = 1.5 cP fluid).

Table 9.53. Generalized Model Results for RLD-08 Using Hanford PSDD

RLD-08 U_{95} Max Fill			RLD-08 $\bar{U}_{90}$ Max Fill		
U (m/s)	U_{CS} (m/s)	U/ U_{CS}	U (m/s)	U_{CS} (m/s)	U/ U_{CS}
8	5.9	1.36	8	7.9	1.01
H/D	H_C/D	H_C/H	H/D	H_C/D	H_C/H
0.91	1.80	1.98	0.91	1.00	1.10
W (wt%)	W_0^* (wt%)	0.2/W_0^*	W (wt%)	W_0^* (wt%)	0.2/W_0^*
2.2	4.1	4.83	2.2	6.0	3.33

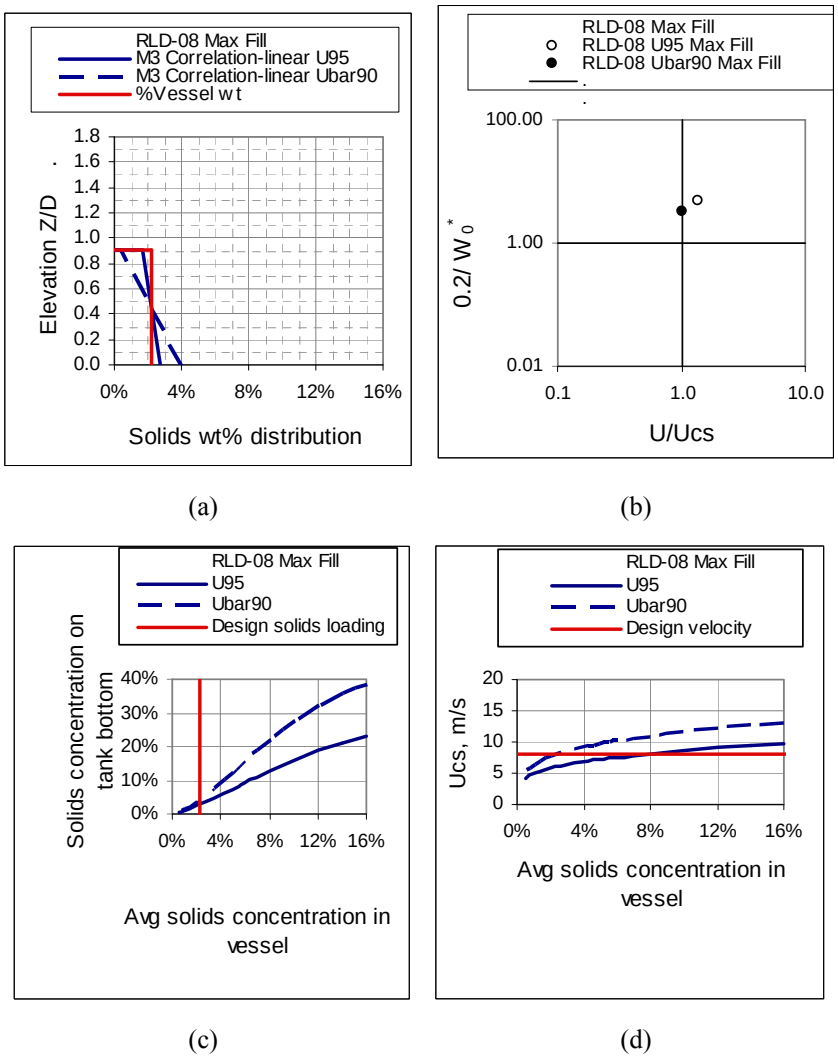

Figure 9.56. Generalized Model Predictions for RLD-08: (a) Concentration Profile at Max Fill, (b) Inlet Concentration and Suspension Ratio, (c) Maximum Solids Concentration Versus Loading Design Conditions; (d) U_{CS} Versus Loading (Hanford PSDD, ρ_l = 1.1 g/cm^3, μ = 1.5 cP fluid)

9.5.16 HOP-903/904 (Hanford PSDD, ρ_l = 1.1 g/cm^3, μ = 1.5 cP Fluid) Generalized Model

Table 9.54 lists generalized model results for HOP-903/904 using the Hanford PSDD. Figure 9.57 shows generalized model predictions for HOP-903/904 (Hanford PSDD, ρ_l = 1.1 g/cm^3, μ = 1.5 cP fluid).

Table 9.54. Generalized Model Results for HOP-903/904 Using Hanford PSDD

HOP-903/904 U_{95} Max Fill			HOP-903/904 $\bar{U}_{90}$ Max Fill		
U (m/s)	U_{CS} (m/s)	U/ U_{CS}	U (m/s)	U_{CS} (m/s)	U/ U_{CS}
8	4.8	1.67	8	6.4	1.25
H/D	H_C/D	H_C/H	H/D	H_C/D	H_C/H
0.86	2.96	3.44	0.86	1.65	1.92
W (wt%)	W_0^* (wt%)	0.2/W_0^*	W (wt%)	W_0^* (wt%)	0.2/W_0^*
1	1.6	12.30	1	1.9	10.49

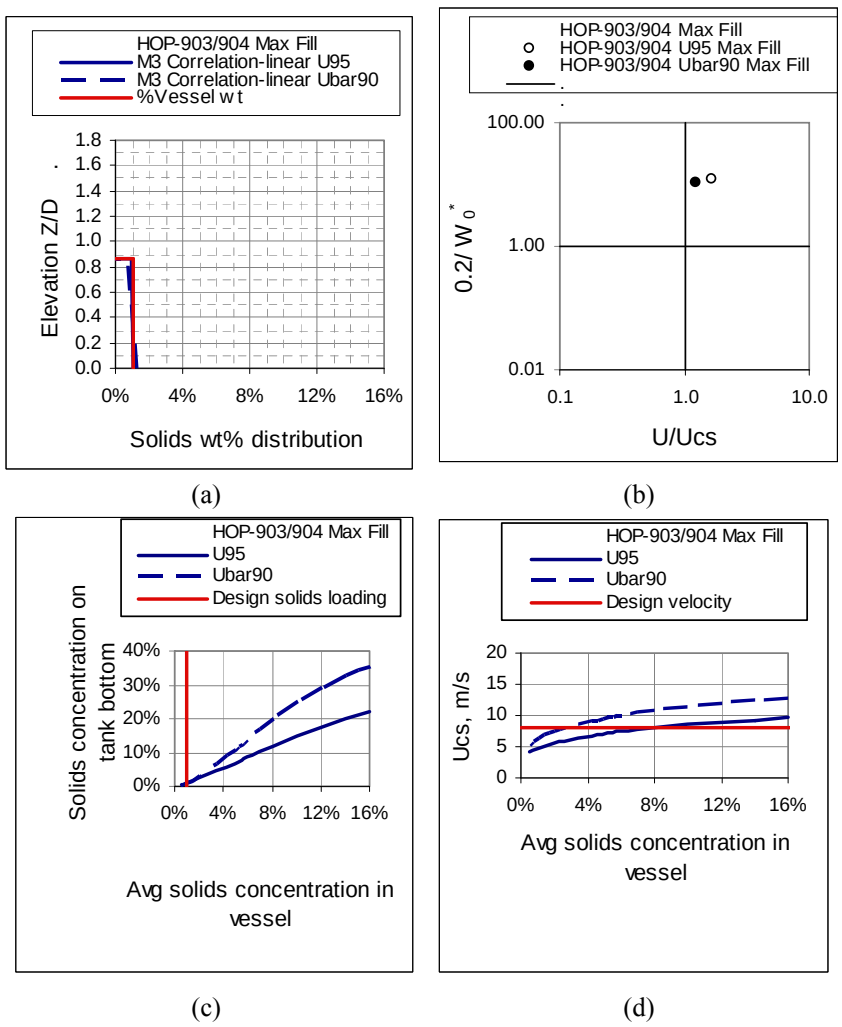

Figure 9.57. Generalized Model Predictions for HOP-903/904: (a) Concentration Profile at Max Fill, (b) Inlet Concentration and Suspension Ratio, (c) Maximum Solids Concentration Versus Loading Design Conditions, (d) U_{CS} Versus Loading (Hanford PSDD, ρ_l = 1.1 g/cm^3, μ = 1.5 cP fluid)

9.6 Summary of Vessel Performance Ratios

The vessel examples, including performance predictions, are provided using both physical and generalized models. These examples are for the vessel conditions provided in Olsen (2008a) and illustrate how the models can be used to predict vessel performance for the specific set of conditions described in Sections 9.1 through 9.5. The analysis of the vessels used in the examples has now been reassigned to the WTP M&PE group (Hazen 2008b).

Figure 9.58 shows the summary of the predicted vessel performance ratios using the representative U_{95} and $\overline{U}_{90}$ settling velocities from the Hanford tank waste PSDD (Case 3) with the physical models for U_{CS} and C_0 from Sections 7.3.2 to 7.3.4. Figure 9.59 presents a summary of the predicted vessel performance ratios using the design-limit particles specified in Olsen (2008a) with the physical models for U_{CS} and C_0 from Sections 7.3.2 to 7.3.4.

For Figures 9.58 through 9.61:

- Using the performance ratios for U_{CS} (U_{design}/U_{CS}) and suction inlet concentration ($0.20/W_0^*$), vessels can be assessed as satisfying these two requirements when both ratios are above 1.0. Design margin applied by the WTP M&PE group will increase the required performance ratio.
- The lowest solids concentration metric values shown are below a condition that would result in a fully settled layer of waste in the bottom of the vessel. The concentration performance ratios have not been adjusted to the maximum packing factor limit (for these cases a fully settled bed is predicted) and are shown as calculated to indicate relative performance.

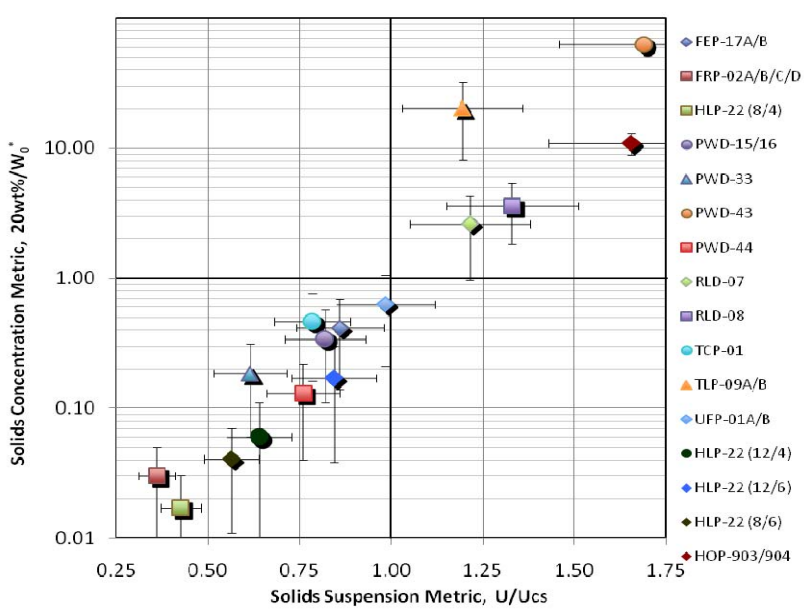

Figure 9.58. WTP Vessel Performance Ratio Summary Using U_{95} and $\overline{U}_{90}$ Settling Velocities from the Hanford Tank Waste PSDD (Case 3) Using the Physical Models for U_{CS} and C_0 from Sections 7.3.2 to 7.3.4 with C_0 modified to W_0^*, as Described in Section 9.1.4. The boundary bars shown are for the U_{95} and $\overline{U}_{90}$ particle ranges evaluated.

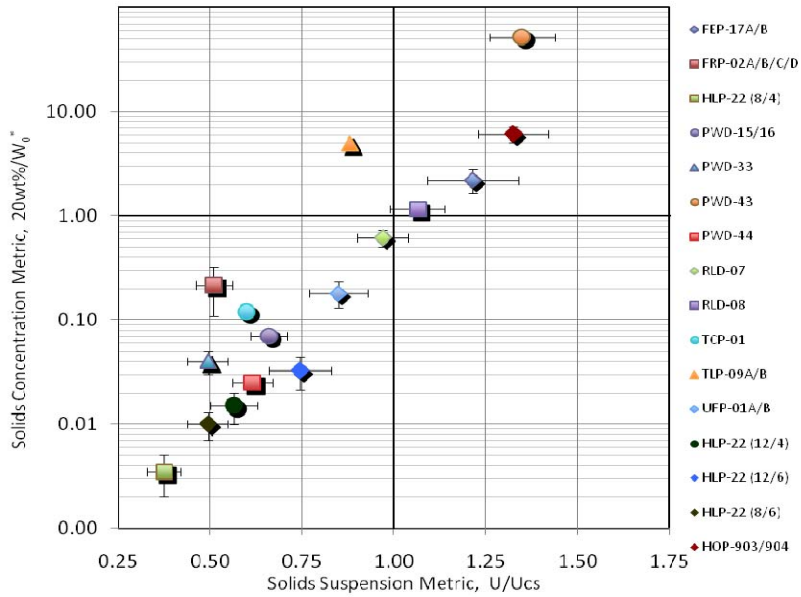

Figure 9.59. WTP Vessel Performance Ratio Summary Using the Design-Limit Particle from Olsen (2008a) and the Physical Models for U_{CS} and C_0 from Section 7.3.2 to 7.3.4 Modified to W_0^* in Section 9.1.4. The boundary bars shown are for the particle density range evaluated.

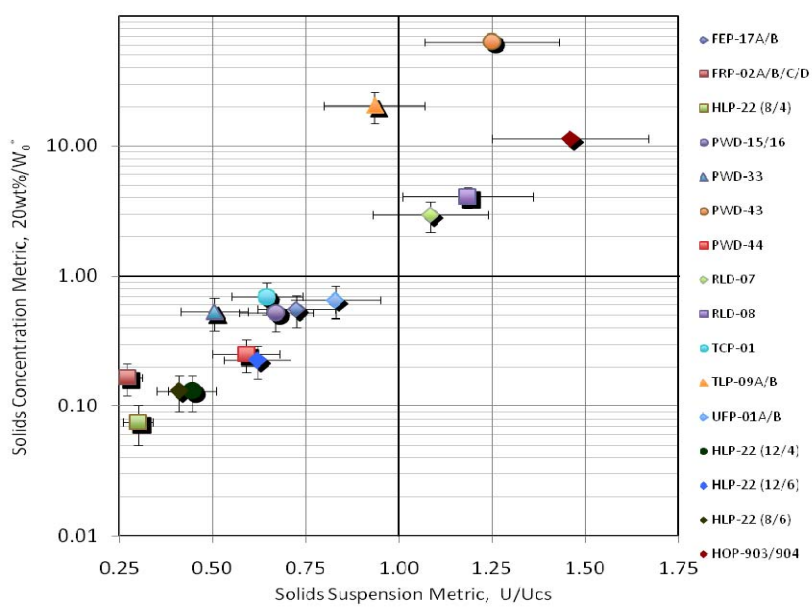

Figure 9.60. WTP Vessel Performance Ratio Summary Using U_{95} and $\overline{U}_{90}$ Settling Velocities from the Hanford Waste PSDD (Case 3) Using the Generalized Models for U_{CS} and C_0 from Section 7.4.2 with C_0 Modified to W_0^*, as Described in Section 8.1.4. The boundary bars shown are for the U_{95} and $\overline{U}_{90}$ particle ranges evaluated.

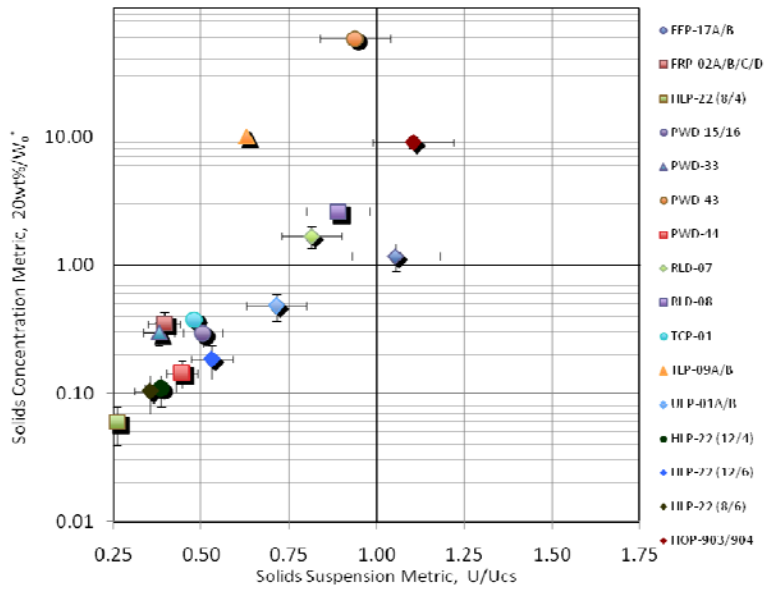

Figure 9.61. WTP Vessel Performance Ratio Summary Using the Design Limit Particle from Olsen (2008a) and Generalized Models for U_{CS} and C_0 from Section 7.4.2 with C_0 Modified to W_0^*, as Described in Section 9.1.4. The boundary bars shown are for the particle density range evaluated.

The HLP-22 vessel was also evaluated using 12 m/s pulse jet velocity with 6-in. nozzles. This alternative configuration was an improvement over the 8 m/s pulse jet velocity with 4-in. nozzles (in Olsen 2008a), but for the conditions evaluated, the physical models for U_{CS} and W_0^* predicted the results would not satisfy the suction inlet or waste mobilization criteria. Other HLP-22 vessel configurations were also evaluated (from Criteria 2 and 3 in Table S.1). The performance predicted for all HLP-22 vessel configurations is summarized in Table 9.55. The HLP-22 design with 6-in. nozzle and DC reduced from 33 to 22% for 4-in. nozzles provided improved performance for vessel mixing performance with respect to solids mobilization. That assessment is summarized in Table 9.55.

Performance ratios for the WTP vessels were also predicted using design limit particles and the settling characteristic from the Hanford waste tanks as described in the Hanford PSDD Case 3 (Wells et al. 2007). The results from using the physical models and the generalized models are relatively consistent, with slight variations when evaluated using the waste characteristics listed in Tables 9.3 and 9.4. The differences are that the generalized model normally predicts a higher U_{CS} velocity requirement and a lower concentration on the vessel floor.

Table 9.55. Impact of HLP-22 Design Variations Using the Physical Models

Vessel	Nozzle Velocity (m/s)	Nozzle Diameter (in.)	U_{95} Max Fill			$\overline{U}_{90}$ Max Fill		
			U/U_{CS}	H_C/H	$0.2/W_0^*$	U/U_{CS}	H_C/H	$0.2/W_0^*$
HLP-22	8	4	0.48	0.06[(a)]	0.03[(a)]	0.37	0.01[(a)]	0.004[(a)]
HLP-22	12	4	0.73	0.26	0.11[(a)]	0.55	0.03[(a)]	0.01[(a)]
HLP-22	8	6	0.64	0.15	0.07[(a)]	0.49	0.03[(a)]	0.01[(a)]
HLP-22	12	6	0.96	0.69	0.30	0.73	0.09[(a)]	0.04[(a)]

(a) Indicates that the waste is considered fully settled on the bottom of the vessel for these conditions; the calculated ratio is shown to indicate relative performance only, and should not be construed to imply values of W_0^* that are non-physically high.

10.0 Conclusions

This section summarizes the significant conclusions and insights resulting from this work. The development of the predictive models is discussed in Section 10.1, followed in Section 10.2 by examples of the application of the models to predict performance of the WTP designs that satisfy two criteria. In Section 10.3 we present a brief list of opportunities to extend and improve the models. Section 10.4 contains a list of observations and accomplishments.

10.1 Model Development

Data from hundreds of scaled experiments were analyzed to develop models that can predict the performance of PJM systems for mixing noncohesive solids in Newtonian liquids. The models were developed using two independent approaches. The first, or physical approach, involved fitting the data to functional forms derived from (or suggested by) a dimensionless analysis of the phenomena expected to affect the performance variables. Models resulting from this approach are referred to as *physical models*. The second approach used multiple-regression methods to develop empirical models relating specified performance variables to the test parameters. The empirical models were re-expressed in terms of dimensionless variables that are physically interpretable. Models resulting from this approach are referred to as *generalized models*. The combination of these two approaches provides technical reliability and credibility, improves the accuracy of extrapolating model results to full scale, and reduces the extrapolation uncertainty.

For given waste characteristics and vessel design, the physical and generalized models provide predictions of the maximum height that solids will be lifted (the cloud height, H_C) and the minimum velocity required to suspend all of the solids (the critical-suspension velocity, U_{CS}). From the cloud height, a solids concentration can be estimated at any elevation in the vessel.

Confidence in these models has been established by benchmarking predictions for PJM mixing experiments that were conducted on a larger scale using a range of simulant properties. As a part of the benchmarking exercise, we determined that the most reliable and accurate indicator for the mixing behavior of a waste with a broad particle size and density distribution was to select a particle at the 95th percentile of the particle settling velocity distribution. The benchmarking results (while limited to a single waste distribution) show strong qualitative agreement between the predictions and the measured values.

Confidence in applying the models to WTP vessels was gained by comparing the experimental ranges of dimensionless variables used to build the models to the values expected in full-scale WTP operations. These comparisons, illustrated in Section 9.2.3, show that for most applications the ranges of dimensionless variables covered by testing encompass the values of those variables for WTP vessels. That outcome greatly reduces the risks that can result from model extrapolation.

Another indicator of accuracy was provided by CFD. Model predictions were compared with CFD model predictions for Tank HLP-22. The models predicted cloud heights that were consistent with the solids concentration profiles from the CFD model. For the conditions selected, all predictions show a highly stratified system, which is expected when the design drive velocity (Olsen 2008a) is significantly below U_{CS}.

The physical and generalized models produce slightly different predictions. Until more opportunities for benchmarking are available, we recommend both models be used as a means of checking for sensitivities.

10.1.1 Recommendations for Using the Models

The predictions from any model will be no better than the quality of the inputs, of course, and we emphasize the importance of using the appropriate waste properties. The benchmarking exercise revealed that selecting the U_{95} setting velocity may generate a slightly conservative prediction. The user must also apply appropriate margins to account for possible inaccuracies and uncertainties in the model predictions, as well as other uncertainties in PJM performance or waste properties. At the current level of development, we consider the models appropriate for determining 1) the conditions that would challenge a given design or, conversely, 2) the minimum PJM operating parameters needed to achieve the two performance criteria for a given vessel-waste combination. In either case, the predictions of conditions that "just meet" the requirements are also conditions that are not well mixed (per Olsen 2008a, the WTP vessels do not have a requirement to be well mixed). The uncertainties inherent in these mixing systems suggest that a design margin is needed to ensure that vessel performance will always be sufficient in a specific system.

10.1.2 Estimates of Confidence

One benefit of using statistical methods to develop a model is that statistical intervals (e.g., a 95% confidence interval) can be explicitly calculated for a model prediction at a defined set of parameters. Formulas for statistical intervals are presented in Appendix D for dimensional models. Formulas could be developed for the dimensionless-variable (generalized) models, but were not because of additional complications and time/budget constraints. Instead, as shown in Appendix F, the dimensional and generalized models are very close to the same form and provide nearly the same results. Hence, the uncertainties for the generalized models are expected to be similar to those obtained for the dimensional models because the forms and fits are similar.

This suggests that it is reasonable to apply the confidence intervals for dimensional models to the generalized models. The example shown in Appendix F for a 1.778-m (70-in.) tank yields a 95% confidence interval (95% CI) for U_{CS} of approximately 1.8 to 2.1 m/s, or roughly ±7% of the predicted value. For H_C, the 95% CI is from 0.70 to 0.82 m, which, for illustration, is about ±8% of the predicted value. A similar calculation for a hypothetical 10-m (32.7-ft) tank diameter yields values of about ±11% for U_{CS} and about ±13% for H_C.

Note that the statistical methods for calculating uncertainties of model predictions assume that the mathematical form of the model well approximates the true underlying relationship. While the U_{CS} models fit the experimental data better than the H_C models, predictions for both mixing responses will likely have some inaccuracy. Appropriate margins are needed to account for the fact that no model will perfectly represent the true underlying relationship.

For a full-scale application the actual waste properties must be known, and the degree to which they are measured or inaccurately estimated will contribute to prediction error. It is possible to statistically

combine uncertainties from the model itself and from model inputs. However, for this report we have assumed perfect knowledge of the physical and rheological properties.

10.2 WTP Vessel Performance Prediction Examples

The WTP vessels were grouped into 13 distinct design and operational vessel types in Section 9.0, and performance predictions were developed for these vessels using the operating conditions discussed in Section 9.0. Additional performance predictions for HLP-22 were conducted to provide information for specific design modification options. The models provide performance metrics relative to requirements:

- Achieve complete suspension of solids (while this is not the specific WTP performance requirement for disturbing solids above a de minimis quantity, the two conditions are expected to be very close in value)
- Maintain suspended solids concentration at the pump suction at less than 20 wt%.

The example performance predictions were conducted using both the physical models and the generalized models. Performance was calculated for each vessel using two different assumed conditions for the waste properties. One condition is defined as the Hanford PSDD Case #3, and second set of waste properties was specified by WTP (Olsen 2008a). Performance predictions were developed assuming particle settling velocities described by the 95th percentile (U_{95}) and the fastest settling 10% fraction ($\overline{U}_{90}$)for the Hanford PSDD and used the limiting particle size and density to establish the settling rate for the WTP design conditions. This use of a characteristic single settling rate to represent a broad waste distribution was developed in the benchmarking in Section 8.0.

The example predications for the WTP vessel designs indicate a broad range of mixing performance. These calculated values provide a technically sound basis to identify those vessels that easily satisfy the requirements and those that fall quite short. Vessels predicted to fall close to the requirements should be evaluated further using additional methods. Final assessment of design adequacy will be made by the WTP M&PE Group (Hazen 2008b).

We applied both the physical models and the generalized models to all 13 distinct design types, and the results were nearly identical. That is, both models identified the same vessels predicted to easily satisfy requirements and were similarly consistent in identifying the group of vessels predicted to be seriously deficient.

The HLP-22 vessel performance was also predicted using 12 m/s pulse jet velocity with 6-in. nozzles. While this alternative configuration is predicted to improve performance, the models also show that the performance would not satisfy the suction inlet or waste mobilization criteria for the conditions evaluated (Sections 9.3, 9.4, and 9.5).

The sensitivity of predicted performance to the selection of input values was illustrated by developing two favorably bounding scenarios: one for the characteristic settling rate that affects the prediction of U_{CS}, and one for the solids concentration profile, which affects W_0. Benchmarking comparisons suggest the use of a settling rate that is faster than the average (e.g. U_{95} or $\overline{U}_{90}$), but the most appropriate value has not been well-established. The sensitivity of this input value is illustrated by assuming conditions that are likely bounding in a non-conservative direction (i.e., the actual performance would likely be worse than

these predicted values). A bounding calculation (Section 9.4.1) for U_{CS} based on a particle settling rate that is the average of the entire distribution of the Hanford PSD shows that the U_{CS} for the FRP-02 vessel is predicted to be 13.1 m/s, compared to a prediction based on the U_{95} particle settling rate of 19.4 m/s. Additional testing would help refine the best value to use.

Similarly, the prediction of solids concentration at the bottom of the vessel is sensitive to the assumed gradient of the solids concentration within the cloud. Observations and attenuation (concentration) measurements taken during testing indicated higher concentrations of solids near the bottom of the test vessels than at the peak of the recorded cloud, but the concentration profile was not well defined. A non-conservatively bounding condition for calculating the concentration at the pump suction was based on an assumption that the suspension of solids would be perfectly (homogeneously) mixed up to the peak of the cloud. Again using the FRP-02 example, the cloud height that corresponds to a uniform concentration of 20 wt% is 8.4 feet. Using the physical model and the U_{95} particle settling velocity to calculate cloud height, the jet velocity U required to lift solids to 8.4 ft would need to be 13.8 m/s. Tests with distributions of solids coupled with measurements of solids concentrations near the vessel floor would help narrow the range of predicted concentrations at the pump suction. Actual performance is not expected to be this favorable.

10.3 Recommendations for Extending Applicability of the Models

The experimental program involved three scales of test vessels, state-of-the-art instrumentation and control equipment, and several high-quality simulants to conduct tests on a complex and transient fluid system. The goal was to develop general models that would capture the relevant geometric, operational, and waste properties to generate accurate predictions. The testing program was limited in scope to Newtonian fluids operating with noncohesive solids, and not all of the parameters that could affect performance were investigated.

Extending the capability of the models should consider the following opportunities:

- Testing with prototypic drive systems is needed to evaluate effects of small cohesive particles and to establish an adjustment factor for full-cycle (reciprocating flow) operations. In addition, testing at different fill levels could be evaluated to assess limits for solids loading.
- Performance for mixtures of solids (sizes and densities) has been predicted but has not been tested or confirmed. Some limited investigation should be conducted so that interactions among these physical properties can be evaluated.
- Most of the testing was conducted with the 12-tube configuration, and relatively few data were collected for 4- and 8-tube designs. Hence, the models favor the 12-PJM designs, but the degree to which adjustments are needed for other configurations is uncertain.
- Testing did not evaluate the effect of viscosity, although we have included its effect in the models. The influence of viscosity on both fluid flow and particle settling rate has been studied by others, and we do not expect that PJM mixing systems will behave differently than conventional mechanical systems relative to this parameter, so only limited testing should be needed.
- Benchmarking against larger scaled tests was considered successful, but more data from other relevant experiments would help build confidence in the models and assess sensitivity of results to input values.

- Methods for quantifying and combining all uncertainties associated with mixing response models should be pursued. Statistical uncertainty intervals for quantifying model fitting uncertainty are presented in Appendix D, Section D.6 for the generalized model, and illustrated in Appendix F, Section F.4. However, such methods need to be extended for application to the other model forms. Further, statistical intervals should be developed that combine model-fitting uncertainty with the uncertainty from propagating uncertainties in the predictor variables of a model. Methods for quantifying possible inaccuracies or uncertainties associated with the form of the model should also be investigated.

Additionally, there were several analysis and application improvement opportunities that became apparent during the production period of this report. The practicalities of schedule constraints and extensive QA implementation requirements necessary to support the NQA-1 needs of this document did not permit the inclusion of these improvements into this report. The improvement opportunities are[1]:

- **Adding a tube number term to the physical model** – The physical model was originally developed using a data set that excluded the Fall 2007 test data. The Fall 2007 data set included a substantial number of tests with 4 and 8 jets. When the additional data were included, the cloud height model was found to underpredict much of the 4- and 8-tube results. It was determined that the fit of cloud height (H_C) model to the complete data set was significantly improved by simply introducing into the H_C physical model the number of operating tubes as an unconstrained correlating parameter in the model. While this change to the H_C physical model is small, the ramifications to the benchmarking and model application are likely to be significant, as described below.

- **Benchmarking approach –** The initial benchmarking of the models against previous test data from a large-scale prototypic testing was somewhat qualitative. Consequently, the selection of U_{95} as the settling velocity that best characterizes mixing when the model is applied to slurries with a broad particle size distribution (PSD) lacked a rigorous basis. A better approach was to systematically determine the best-fit value of U_T for each benchmark case. This was briefly explored for two meaningful cases: a favorably conservative bound, and a best estimate. The favorably conservative bound involved assuming the maximum concentration measured in each of the benchmark test cases was the value that was at the floor of the test tank. The best-estimate method involved estimating the concentration at the floor by applying mass conservation.

- **Benchmarking results –** The benchmarking approach described above can be systematically applied to the benchmark test cases using the improved physical model mentioned previously. The resulting best-fit values for settling velocity where approximately $\overline{U}_{40}$ for the favorably conservative bound and approximately $\overline{U}_{60}$ for the best estimate. When these values are translated to the Hanford PSDD, they correspond to approximately U_{94} and U_{96}, respectively. It turns out that the U_{95} value recommended in this report is bounded by these more systematically determined values, and a more rigorous treatment of the benchmarking data would provide a clear technical basis for this choice.

- **Vessel evaluation methodology** – There are two improvements to the vessel evaluations that will be significant. First, based on the benchmarking approach mentioned above, the settling velocity values

[1] The information on the potential model improvements has not been reviewed through the quality assurance (QA) process, the discussions above are "For Information Only."

of U_{95} and $\overline{U}_{90}$ can be replaced with the systematically determined values (approximately $\overline{U}_{40}$ and $\overline{U}_{60}$, and approximately U_{94} and U_{96}, respectively). The results in much tighter range of predicted performance in the plant vessels.

The second improvement relates to the concentration performance metric. The approach used to predict the concentration on the floor of a prototypic vessel involved several assumptions. First, it was assumed the solids vertical distributions are linear. While this is indeed correct to first order for the average of all data, it is clear that in many cases it was not the case. Also it was assumed that the value of concentration on the floor could be linearly extrapolated from the profiles. Finally, a method was used to translate concentration profiles from predicted high clouds that exceeded actual fill levels into concentration profiles within the finite fill level. In the absence of actual measurements of concentration near the floor of vessels, the above-mentioned assumptions result in unquantifiable uncertainty for the calculated concentration at the floor of the vessel. In light of this uncertainty, an alternative performance metric that is more closely and directly tied to the actual test data is the jet velocity required to achieve a solids cloud that reaches the fill level in the prototypic vessel. The magnitude of this velocity relative to the design velocity is an important indicator of a given design's ability to vertically distribute solids. Floor concentrations can still be inferred from this approach by assuming uniform or linear concentration profiles.

10.4 Major Findings

The effort to develop a generalized basis for predicting PJM mixing performance involved substantial review of more conventional mixing systems, both mechanically agitated and with steady jets. Much of the work presented in this report shows that the physics involved in a PJM mixed system are consistent with other systems. However, the feature that separates a PJM system from others is that the energy input is unsteady (pulsed). That difference has profound implications on the ability of the system to achieve specific functions, as summarized below.

Off-bottom suspension. The test results indicate that the off-bottom suspension characteristics of PJMs are similar to those of steady jet mixers and mechanical agitators. The dependence of U_{CS} on solids loading, particle characteristics, nozzle diameter, and vessel scale are similar to the dependencies found for other mixing systems. The pulsation effects are readily accounted for by the inclusion of additional parameters such as the duty cycle and pulse volume fraction. However an important feature unique to pulsed jet mixing is that off-bottom suspension is intrinsically cyclical. At the U_{CS} condition, the solids are completely off the bottom of the vessel only for a moment at the end of the pulse. Even when the pulse velocity is operated above the U_{CS}, solids will settle on the vessel floor during the time the PJM is refilling.

Solids vertical distribution. The test results indicate that the ability of PJMs to vertically distribute solids is significantly diminished compared with steady jets mixers and mechanical agitators. There is a significant penalty associated the refill period of the pulse cycle. Evidently, during the refill period the upward momentum of the primary flow created from the previous pulse is lost. Hence, the steady-state concentration distribution that would be attained for continuous mixing is not achieved for solid-liquid systems with pulsed jets. This effect is not simply due to particle settling during the refill period, as it is observed for small and large particles alike. Rather, it appears to be dominated by gravitational dynamics of the stratified bulk slurry. Another consequence of the pulsation is that significant temporal variation in

concentration occurs during the discharge period, particularly near the bottom of the vessel. The ramifications of these transients to mixing and transfer requirements deserve a careful assessment.

Settling velocity. The inclusion of settling velocity as a correlating parameter was found to be beneficial for monodisperse simulants. It also provides a physically meaningful way to characterize mixing in slurries with a broad size and density distribution. It was argued that a settling velocity greater than the volume-weighted mean is the appropriate choice. While more data are required to fully establish this, the results of benchmarking clearly support the finding and suggest that the appropriate settling velocity is greatly influenced by the fastest-settling particles.

11.0 References

Bamberger JA and MS Greenwood. 2004. "Using Ultrasonic Attenuation to Monitor Slurry Mixing in Real Time." *Ultrasonics* 42(1-9):145-148.

Bamberger JA and PA Meyer. 2001. "Using Oscillating Jets to Maintain Solids in Suspension - An Integrated Experimental and Computational Investigation." PNNL-SA-34149, Pacific Northwest National Laboratory, Richland, Washington.

Bamberger JA and PA Meyer. 2007. "Characterizing Pulsating Mixing of Slurries." *Proceedings of FEDSM2007 5th Joint ASME/JSME Fluids Engineering Conference* 2 (FEDSM2007-37666):201-205. American Society of Mechanical Engineers, New York.

Bamberger JA, PS Lowery, and LM Liljegren. 1990. *Strategy Plan A Methodology to Predict the Uniformity of Double-Shell Tank Waste Slurries Based on Mixing Pump Operation.* PNL-7665, Pacific Northwest Laboratory, Richland, Washington.

Bamberger JA, LM Liljegren, CW Enderlin, PA Meyer, MS Greenwood, PA Titzler, and G Terrones. 2007. *Final Report One-Twelfth-Scale Mixing Experiments to Characterize Double-Shell Tank Slurry Uniformity*. PNNL-16859, Pacific Northwest National Laboratory, Richland, Washington.

Bamberger JA, PA Meyer, JR Bontha, CW Enderlin, DA Wilson, AP Poloski, JA Fort, ST Yokuda, HD Smith, F Nigl, MA Friedrich, DE Kurath, GL Smith, JM Bates, and MA Gerber. 2005. *Technical Basis for Testing Scaled Pulse Jet Mixing Systems for Non-Newtonian Slurries.* PNWD-3551, WTP-RPT-113 Rev. 0, Battelle – Pacific Northwest Division, Richland, Washington.

Bamberger JA, PA Meyer, JR Bontha, JA Fort, F Nigl, JM Bates, CW Enderlin, ST Yokuda, DE Kurath, AP Poloski, HD Smith, GL Smith, and MA Gerber. 2008. "Evaluating Pulse Jet Mixing with Non-Newtonian Slurries." *Proceedings of IMECE2007 2007 ASME International Mechanical Engineering Congress and Exposition*, 8 (IMECE2007-42223):1909-1930. American Society of Mechanical Engineers, New York.

Bamberger JA, MJ Minette, PA Meyer, JA Fort, and EBK Baer. 2011. "Assessment of Prototypic and Closed Loop Operation During Pulse Jet Mixer Tests with Non-Cohesive Solids to Develop Scale-Up Relationships." Proceedings of the *ASME 2011 International Mechanical Engineering Congress & Exposition (IMECE2011-63793)*. American Society of Mechanical Engineers, New York.

Bates JM, JW Brothers, JM Alzheimer, DE Wallace, and PA Meyer. 2003. *Test Results for Pulse Jet Mixers in Prototypic Ultrafiltration Feed Process and High-Level Waste Lag Storage Vessels.* PNWD-3496, WTP-RPT-110 Rev. 0, Battelle – Pacific Northwest Division, Richland, Washington.

Bathija PR. 1982. *Jet Mixing Design and Applications. Chemical Engineering*. 13 Dec., 89(25):89-94.

Beltaos S and N Rajaratnam. 1977. "Impingement of Axisymmetric Developing Jets." *J. Hydraulic Research* 15(4):311-326.

Bontha JR, GR Golcar, and N Hannigan. 2000. *Demonstration and Optimization of BNFL's Pulsed Jet Mixing and RFD Sampling Systems Performance Using NCAW Simulant*. PNWD-3054, BNFL-RPT-048 Rev. 0, Battelle – Pacific Northwest Division, Richland, Washington.

Bontha JR, TE Michener, DS Trent, JM Bates, and MD Johnson. 2003a. *Development and Assessment of the TEMPEST CFD Model of the Pulsed Jet Mixing Systems*. PNWD-3261, WTP-RPT-061 Rev. 0, Battelle – Pacific Northwest Division, Richland, Washington.

Bontha JR, JM Bates, CW Enderlin, and MG Dodson. 2003b. *Large Tank Experimental Data for Validation of the FLUENT CFD Model of Pulsed Jet Mixers*. PNWD-3303, WTP-RPT-081 Rev. 0, Battelle – Pacific Northwest Division, Richland, Washington.

Bontha JR, CW Stewart, DE Kurath, PA Meyer, ST Arm, CE Guzman-Leong, MS Fountain, M Friedrich, SA Hartley, LK Jagoda, CD Johnson, KS Koschik, DL Lessor, F Nigl, RL Russell, GL Smith, W Yantasee, and ST Yokuda. 2005. *Technical Basis for Predicting Mixing and Flammable Gas Behavior in the Ultrafiltration Feed Process and High-Level Waste Lag Storage Vessels with Non-Newtonian Slurries*. PNWD-3676, WTP-RPT-132 Rev. 0, Battelle – Pacific Northwest Division, Richland, Washington.

Bontha JR, DE Kurath, AP Poloski, WC Buchmiller, WH Combs, ED Johnson, HC Webber, and KL Herman. 2007. *Pulse Jet Mixer Controller and Instrumentation Testing*. PNWD-3828, WTP-RPT-146 Rev. 0, Battelle – Pacific Northwest Division, Richland, Washington.

Camenen B. 2007. "Simple and General Formula for the Settling Velocity of Particles." *Journal of Hydraulic Engineering – ASCE* 133(2):229-233.

Carlson AB, PJ Certa, TM Hohl, JR Bellomy, TW Crawford, DC Hedengren, AM Templeton, HS Fisher, SJ Geelhood, DG Douglas, and WJ Ulbricht. 2001. *Test Report, 241-AZ-101 Mixer Pump Test*. RPP-6548 Rev. 1, CH2MHill Hanford Group, Inc., Richland, Washington.

Fort JA, JA Bamberger, JM Bates, CW Enderlin, and MR Elmore. 1993. *1/12-Scale Physical Modeling Experiments in Support of 241-SY-101 Hydrogen Mitigation*. PNL-8476, Pacific Northwest Laboratory, Richland, Washington.

Fort JA, JA Bamberger, PA Meyer, and CW Stewart. 2007. *Initial Investigation of Waste Feed Delivery Tank Mixing and Sampling Issues*. PNNL-17043, Pacific Northwest National Laboratory, Richland, Washington.

Fort JA, PA Meyer, JA Bamberger, CW Enderlin, PA Scott, MJ Minette, and PA Gauglitz. 2010. "Scaled Testing to Evaluate Pulse Jet Mixer Performance in Waste Treatment Plant Mixing Vessels" - 10487. In *Proceedings of WM2010 Conference*, March 7-10, 2010, Phoenix, Arizona.

Golcar GR, NG Colton, JG Darab, and HD Smith. 2000. *Hanford Tank Waste Simulant Specification and Their Applicability for the Retrieval, Pretreatment, and Vitrification Processes*. PNWD-2455, Battelle - Pacific Northwest Division, Richland, Washington.

Guerrero HA and M Restivo. 2004. *Final Report UFP Restart and Sparger Testing*. WSRC-TR-2004-00488, Rev. 0, SRNL-RPP-2004-00066 Rev. 0, Westinghouse Savannah River Company, Aiken, South Carolina.

Johnson MD, JR Bontha, and JM Bates. 2003. *Demonstration of Ability to Mix in a Small-Scale Pulsed-Jet Mixer Test Facility.* PNWD-3273, WTP-RPT-077 Rev. 0, Battelle – Pacific Northwest Division, Richland, Washington.

Johnson MD, MA Gerber, JR Bontha, AP Poloski, RT Hallen, SK Sundaram, and DE Wallace. 2005. *Hybrid Mixing System Test Results for Prototype Ultrafiltration Feed Process and High-Level Waste Lag Storage Vessels.* PNWD-3586, WTP-RPT-128 Rev. 0, Battelle – Pacific Northwest Division, Richland, Washington.

Kurath DE, PA Meyer, JR Bontha, AP Poloski, JA Fort, WH Combs, WC Buchmiller, ID Welch, and MD Bleich. 2007. *Assessment of Pulse Tube Mixing for Vessels Containing Non-Newtonian Slurries.* PNWD-3827, WTP-RPT-155 Rev. 0, Battelle - Pacific Northwest Division, Richland, Washington.

Liljegren LM and JA Bamberger. 1992. "A Methodology to Predict the Uniformity of Double-Shell Waste Slurries Based on Mixer Pump Operation." PNL-SA-20281, Pacific Northwest Laboratory, Richland, Washington.

Meyer PA and AW Etchells. 2007. "Mixing with Intermittent Jets with Application in Handling Radioactive Waste Sludges." *Chemical Engineering Research and Design* 85(5):691-696.

Meyer PA and BE Wells. 2000. "Understanding Gas Release Events in Hanford Double Shell Tanks." PNNL-SA-32640, Pacific Northwest National Laboratory, Richland, Washington.

Meyer PA, DE Kurath, and CW Stewart. 2005. *Overview of the Non-Newtonian Pulse Jet Mixer Test Program*. PNWD-3677, WTP-RPT-127 Rev. 0, Battelle - Pacific Northwest Division, Richland, Washington.

Meyer PA, DE Kurath, JA Bamberger, AW Etchells, and SM Barnes. 2006. "Scaling Laws for Reduced-Scale Tests of Pulse Jet Mixing Systems in Non-Newtonian Slurries: Mixing Cavern Behavior." 2006 *Waste Management Symposium*, Tucson, Arizona, WM Symposia, Inc. Available online at http://www.wmsym.org/abstracts/2006/index.html.

Meyer PA, EBK Baer, JA Bamberger, JA Fort, and MJ Minette. 2010. *Assessment of Differences in Phase 1 and Phase 2 Test Observations for Waste Treatment Plant Pulse Jet Mixer Tests with Non-Cohesive Solids*. PNNL-19085, WTP-RPT-208 Rev. 0, Pacific Northwest National Laboratory, Richland, Washington.

Olsen J. 2008a. *Determination of Mixing Requirements for Pulse-Jet-Mixed Vessels in the Waste Treatment Plant*. 24590-WTP-ES-PT-08-002, Rev. 0, Bechtel National Incorporated, Richland, Washington.

Olsen J. 2008b. *Determination of Mixing Requirements for Pulse-Jet-Mixed Vessels in the Waste Treatment Plant.* 24590-WTP-ES-PT-08-002, Rev. 1, Bechtel National Incorporated, Richland, Washington.

Paul EL, VA Atiemo-Obeng, and SM Kresta (Eds.). 2004. *Handbook of Industrial Mixing*. John Wiley & Sons, Inc., Hoboken, New Jersey.

Poloski AP, ST Arm, JA Bamberger, DB Barnett, RS Brown, BJ Cook, CW Enderlin, MS Fountain, M Friedrich, BG Fritz, RP Mueller, F Nigl, Y Onishi, LA Schienbein, LA Snow, S Tzemos, M White, and JA Vucelick. 2005. *Technical Basis for Scaling of Air Sparging Systems for Mixing in Non Newtonian Slurries*. PNWD-3541, Battelle - Pacific Northwest Division, Richland, Washington.

Powell MR, CM Gates, CR Hymas, MA Sprecher, and NJ Morter. 1995a. *Fiscal Year 1994 1/25th-Scale Sludge Mobilization Testing.* PNL-10582, Pacific Northwest Laboratory, Richland, Washington.

Powell MR, GR Golcar, CR Hymas, and RL McKay. 1995b. *Fiscal Year 1993 1/25th-Scale Sludge Mobilization Testing.* PNL-10464, Pacific Northwest Laboratory, Richland, Washington.

Powell MR, Y Onishi, and R Shekarriz. 1997. *Research on Jet Mixing of Settled Sludges in Nuclear Waste Tanks at Hanford and Other DOE Sites: A Historical Perspective.* PNNL-11686, Pacific Northwest National Laboratory, Richland, Washington.

Rajaratnam N. 1976. *Turbulent Jets.* Elsevier Science Publishers, New York.

Saunders SA and PJ Keuhlen. 2008. Issue Response Plan for Implementation of External Flowsheet Review Team (EFRT) Recommendations – M3, Inadequate Mixing System Design, 24950-WTP-PL-ENG-06-0013, Rev. 3, Bechtel National Inc., Richland Washington.

Schlichting, H. 1979. *Boundary-layer theory*. McGraw-Hill, New York.

Shekarriz A, KJ Hammad, MR Powell. 1997. *Evaluation of Scaling Correlations for Mobilization of Double-Shell Tank Waste*. PNNL-11737, Pacific Northwest National Laboratory, Richland, Washington.

Smith GL. January 2007. *Scaled Testing to Determine the Adequacy of the WTP Pulse Jet Mixer Designs*. 24590-PTF-TSP-RT-06-007, Bechtel National Inc., Richland, Washington.

Urie MW, GM Mong, PR Bredt, AP Poloski, JA Campbell, RD Scheele, OT Farmer, CZ Soderquist, SK Fiskum, RG Swoboda, LR Greenwood, MP Thomas, EW Hoppe, JJ Wagner, and LK Jagoda. 2002. *Chemical Analysis and Physical Property Testing of 241-AZ-101 Tank Waste—Supernatant and Centrifuged Solids*. PNWD-3215, WTP-RPT-048 Rev. 0, Battelle – Pacific Northwest Division, Richland, Washington.

Wells BE, MA Knight, EC Buck, SK Cooley, RC Daniel, LA Mahoney, PA Meyer, AP Poloski, JM Tingey, WS Callaway III, GA Cooke, ME Johnson, MG Thien, DJ Washenfelder, JJ Davis, MN Hall, GL Smith, SL Thomson, and Y Onishi. 2007. *Estimate of Hanford Waste Insoluble Solid Particle Size and Density Distribution.* PNWD-3824, WTP-RPT-153 Rev. 0, Battelle – Pacific Northwest Division, Richland, Washington.

Zwietering TN. 1958. "Suspending of Solid Particles in Liquid by Agitators." *Chemical Engineering Science* 8:244-253.

References Not Publically Available

BNI. 2007. WTP Project Memorandum CCN 151865. Contractor Change Notice for the *Waste Treatment Plant Vessel PJM Data Table*. Bechtel National Incorporated, Richland, Washington.

Elmore MR, CW Enderlin, and PA Meyer. July 2007. "M3 Testing Approach in Support of Tank HLP-22 Issues." TP-RPP-WTP-480, Pacific Northwest National Laboratory, Richland, Washington.

Elmore MR, CW Enderlin, and PA Meyer. February 2008. "M3 Testing Approach in Support of Tank HLP-22 Issues." TP-RPP-WTP-480 Rev. 0, ICN 1, Pacific Northwest National Laboratory, Richland, Washington.

Elmore MR, CW Enderlin, and PA Meyer. January 2009. *M3 Testing Approach in Support of Tank HLP-22 Issues ICN 0.2*. TP-RPP-WTP-480 R0.2, Pacific Northwest National Laboratory, Richland, Washington.

Hazen H. 2008a. Contract No. DE-AC27-01RV14136, Hanford Tank Waste Treatment and Immobilization Plant, Memorandum of Agreement (MOA), 24590-QL-HC9-WA49-00001, PNNL R&T Support, Direction for M3 WA2007-08 PJM Testing, Test Specification 24590-PTF-TSP-RT-06-006 Rev. 0. CCN 190723, Bechtel National Inc., Richland, Washington.

Hazen H. 2008b. Letter CCN 178425. Contract No. DE-AC27-01RV14136 – Hanford Tank Waste Treatment and Immobilization Plant, Memorandum of Agreement (MOA) 24590-QL-HC9-WA49-00001, PNNL R&T Support, Subcontract Change Notice (SCN) No. 71 for Work Authorization (WA) 08 Work Cancellations. Bechtel National, Inc., Richland, Washington.

Appendix A

Ultrasonic Instrumentation

MS Greenwood
GP Morgen

Appendix A

Contents

A.1 Ultrasonic Doppler Velocimetry A.1
A.1.1 Theory of Operation A.1
A.1.2 Measuing Slurry Bed Thickness A.4
A.1.3 UDV System Components A.6
A.2 Ultrasonic Concentration Probe A.7
A.2.1 Data Acquisition System and Measurement of Attenuation A.9
A.2.2 Calculation of Attenuation A.10
A.2.3 Relationship Between Concentration and Attenuation A.12
A.3 References A.16

Figures

A.1 Schematic of Typical UDV Application A.2
A.2 UDV Applied to the Measurement of a Settled Bed in a Mixing Tank A.4
A.3 Ultrasonic Transducers Mounted to the Small-Scale Tank Bottom A.5
A.4 UDV Component Diagram A.6
A.5 Photograph of the Concentration Sensor Near the Bottom of the Small-Scale Tank A.8
A.6 Concentration Sensor Configuration A.8
A.7 Schematic Diagram of the DAS A.10
A.8 Voltage Versus Time Signal in Top Panel and the FFT of Each Signal in the Bottom Panel A.11
A.9 Example of Attenuation Versus Frequency for Slurry of s1d2 Particulate Using 3.5 MHz Transducers A.12
A.10 Mixer and Baffle Unit for Laboratory Measurements of Attenuation and Slurry Concentration A.13
A.11 Concentration and Attenuation Measurements for Slurries s1d1, s1d2, and s1d5 for Determination of the Slope of the Straight Line Through the Data Points A.15
A.12 Concentration and Attenuation Measurements for Slurries s2d1 and s2d2 for Determination of the Slope of the Straight Line Through the Data Points A.15

Tables

A.1 Values of CONC for Five Simulants and Seven Frequencies A.16

Acronyms and Abbreviations

Atten	attenuation
CONC	concentration
DAS	data acquisition system
FFT	fast Fourier transform
PC	personal computer
PNNL	Pacific Northwest National Laboratory
UCC	ultrasonic command and control (computer)
UDV	ultrasonic Doppler velocimeter

Symbols

A	fast Fourier transform amplitude
B	frequency bandwidth
c	speed of sound in the fluid
D	distance between transducer faces
D_{max}	maximum distance
f	ultrasonic frequency
f_D	Doppler frequency shift
k	angular wave number, $2\pi/\lambda$
N	number of cycles
R	repetition rate time
t	time
v	particle velocity
V_{max}	maximum velocity
V_F	volume fraction
$V_{particles}$	volume occupied by particles in sample
V_{liquid}	volume of liquid in the sample
x	distance

Greek Symbols

Δ_R	range resolution
λ	wavelength
θ	angle of transducer with respect to pipe centerline
ρ_{slurry}	density of the slurry
ρ_{part}	density of the particulate
ρ_{wtr}	density of the liquid
φ	phase
ω	angular frequency, $2\pi f$

Appendix A

Ultrasonic Instrumentation

Two ultrasonic instruments are used to characterize solids suspension during mixing. The ultrasonic Doppler velocimeter (UDV), which is described in Section A.1, was adapted to determine the thickness of the nonmoving settled layer of solids in the vessel by detecting vertical movement of the particles at the interface with the settled solids. The ultrasonic concentration probe, which is described in Section A.2, was used to measure the suspended solids concentration at a desired location in the vessel.

The UDV and the ultrasonic concentration probe (classified as category-2 measurement equipment) evaluate the desired metrics based on relative measurements. The relative measurements are correlated with results obtained from a series of working standards. A series of working standards is created for each simulant used in the test platform, and the correlations developed are specific to each simulant.

For the UDV instrument, the working standards are gravity-settled beds of varying depth for which the time of flight of the ultrasonic signal is measured. A linear least squares fit is used to correlate the depth of the working standard as a function of the measured time of flight. The slope of this relationship provides the speed of sound through the settled bed. The determined speed of sound is used during the experiments to calculate the range (distance increments) at which the interface between nonmoving and moving particles is found, reported as the thickness of the settled bed.

For the concentration probe, the ultrasonic attenuation, relative to the attenuation through the carrier liquid (supernatant liquid), over a known distance is measured for a series of working standards varying in volume concentration. Working standards are created for each simulant used. The ultrasonic attenuation is measured over a frequency spectrum, and from the data set the volume percent solids can be correlated as a function of the ultrasonic attenuation for a given frequency. By comparing the attenuation for a given simulant to the baseline attenuation for the carrier liquid, optimum frequencies can be selected (based on sensitivity of attenuation of signal at the specific frequency) for monitoring solids concentration during testing.

A.1 Ultrasonic Doppler Velocimetry

The UDV theory of operation is described in Section A.1.1. The method for measuring the slurry bed thickness is described in Section A.1.2. The components of the UDV system for detecting the interface between the settled and moving particles are listed in Section A.1.3.

A.1.1 Theory of Operation

An advanced UDV method that provides nondisruptive measurements of a flowing fluid or slurry has been developed by Pacific Northwest National Laboratory (PNNL). The method is based on integration of spatially resolved ultrasonic Doppler backscatter measurements and forward-scatter attenuation measurements. The method provides a flow velocity profile and shear stress values across the diameter of the process pipe for both Newtonian and non-Newtonian fluids. The device is designed for use on a large

variety of products, including food products, consumer products, and polymer process streams. A complete description of UDV can be found in U.S. Patent No. 6,871,148 B2 (Morgen et al. 2002).

This Doppler-based system operates by generating a tone burst, a specific number of cycles of a sinusoidal waveform (N sinewave cycles) at a specific repetition rate. Depending on the application and material properties of the test medium, the frequency of the sinusoidal waveform is typically 200 kHz to 10 MHz. The tone burst signal is applied to an ultrasonic transducer that transmits ultrasound into the material being monitored. The repetition rate is the frequency (rate) at which the tone burst signal is applied to the transducer. After the tone burst (ultrasound) is transmitted into the test material, the same transducer is used to receive ultrasound echoes from scattering particles in the test material. The transducer converts the ultrasound echoes into an electronic signal that is amplified and analyzed.

The UDV system relies on measurement of the Doppler frequency shift of moving particles within the material flowing in the pipe, as shown in Figure A.1. Using a short ultrasonic pulse system, the cross-sectional velocity profile can be obtained from the Doppler shift at each differential range point. The Doppler frequency shift (f_D) is given by Eq. (A.1):

$$f_D = \frac{2v\cos\theta}{c} f \tag{A.1}$$

where v is the particle velocity, c is the speed of sound in the fluid, f is the ultrasonic frequency, and θ is the angle of the transducer with respect to the pipe centerline. For example, the Doppler shift for a particle moving with velocity of 1 m/s in water with speed of sound equal to 1500 m/s, a transducer angle of 45°, and an ultrasonic frequency of 5 MHz is 4.714 kHz.

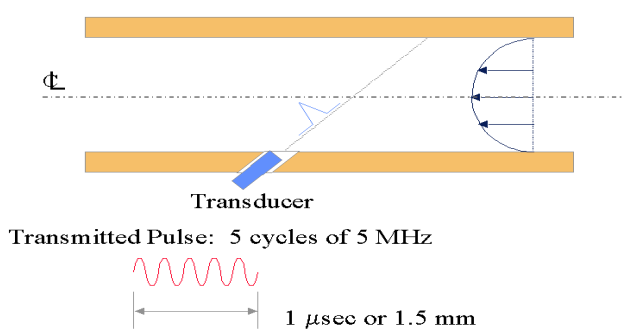

Figure A.1. Schematic of Typical UDV Application

To obtain good range resolution, it is essential to transmit a short ultrasonic pulse. The range resolution is approximately equal to one-half of the spatial width of the pulse. For N sine-wave cycles of wavelength λ, the range resolution Δ_R is approximately

$$\Delta_R = N\frac{\lambda}{2} \tag{A.2}$$

For example, 5 cycles of 5 MHz (0.3-mm wavelength for speed of sound of water) results in a range resolution of approximately 0.75 mm.

Obtaining good resolution creates a problem for the measurement of the Doppler frequency shift, which is typically in the 1- to 10-kHz frequency range. A gated sinewave (tone burst) of frequency f and N cycles has a relatively wide frequency bandwidth, B, of approximately

$$B=\frac{f}{N} \tag{A.3}$$

For a tone burst signal of 5 cycles of 5 MHz, the bandwidth (B) is 1 MHz. The Doppler shift needs to be on the order of or larger than B to be distinguishably measurable from the frequency spectrum of the signal scattered from the particles. Doppler shifts this large would only be expected if the fluid velocity were on the same order as the speed of sound in the fluid. Velocities of interest in pipe flow problems are much lower than the speed of sound. A fixed operating frequency, f, is used, so reducing the bandwidth by increasing N would allow for good Doppler velocity resolution, but it results in directly degrading the range resolution per Eq. (A.2). To resolve this conflict, data from multiple transmit and receive sequences occurring at the repetition rate are acquired over a long time interval (1 to 20 sec) to obtain a number of data points from each differential range section in the flowing material. The repetition rate may vary from 100 Hz to 20 kHz.

This measurement method has several limitations. One is an aliasing artifact introduced by the repetition rate that causes incorrect velocity measurements. This is a Nyquist limitation associated with the discrete sampling of Doppler frequency. The aliasing artifact occurs when the Doppler-induced frequency shift exceeds one-half the repetition rate. Using R to denote the repetition rate, in equation form this becomes

$$f_D \leq \frac{R}{2} \tag{A.4}$$

Substituting Eq. (A.1) with the angle equal to 0 gives

$$v \leq \frac{cR}{4f} \tag{A.5}$$

or

$$V_{max} = \frac{cR}{4f} \tag{A.6}$$

Increasing the repetition rate for a given speed of sound and transducer frequency increases the maximum particle velocity (V_{max}) that can be measured.

Another limitation of this measurement method is the distance that can be measured, or the range of UDV. The repetition rate is limited by the round-trip time for the ultrasound to travel from the transducer to a particle and back. Using the form distance = velocity × time, where distance is $2D_{max}$ (round-trip distance), velocity is c (speed of sound), and time is 1/R (repetition rate) results in the equation

$$D_{max} = \frac{c}{2R} \tag{A.7}$$

Combining Eqs. (A.6) and (A.7) links the maximum velocity, V_{max}, and the maximum distance, D_{max}, parameters by the following equation:

$$D_{max} V_{max} = \frac{c^2}{8f} \tag{A.8}$$

A.1.2 Measuring Slurry Bed Thickness

To support testing, the operation of the UDV system was adapted to identify the boundary between moving slurry with suspended particles and a settled bed of particles (see Figure A.2). This boundary, if present, indicates that the particles are not fully suspended. The depth of this boundary corresponds to the depth of the settled bed.

As depicted in Figure A.2, the UDV ultrasonic transducer is mounted on the bottom of the mixing tank at an angle of 0 degrees relative to the centerline of the pipe shown in Figure A.1. In actual practice, a mounting ring with a 7-degree angle was used to mount the transducer to the tank; this reduced the multipath return signals between the transducer and the inside tank wall. Figure A.3 is a picture of the UDV transducer mounted to the bottom of the small-scale (15-in.) tank.

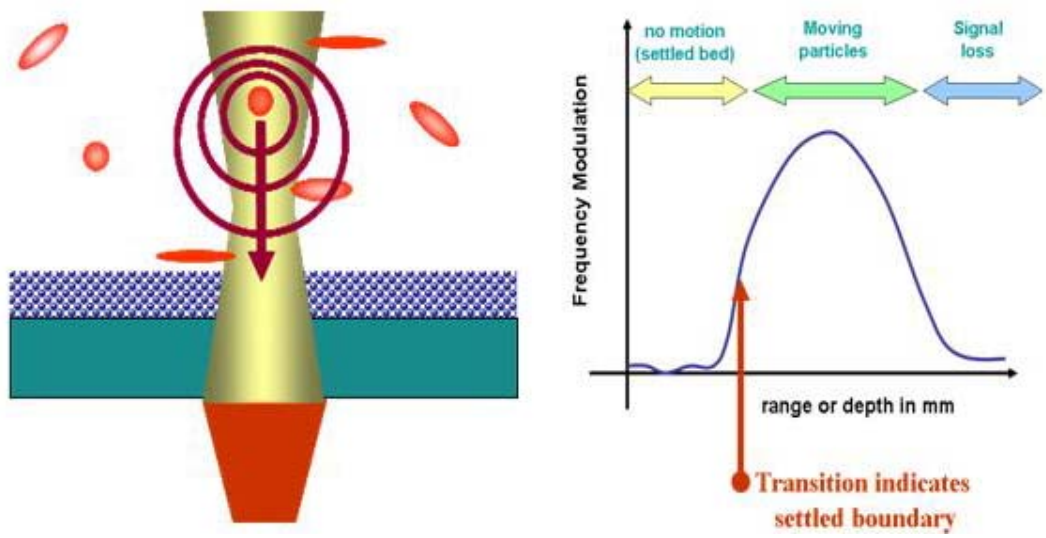

Figure A.2. UDV Applied to the Measurement of a Settled Bed in a Mixing Tank

The ultrasound transmit tone burst used for all testing was 4 cycles of 2.25 MHz, which results in a range resolution of approximately 1.33 mm (Eq. A.2) based on the speed of sound in water, 1500 m/s. The speed of sound in the simulants used in testing ranged from about 1400 to 1700 m/s, resulting in range resolutions of 1.24 to 1.51 mm. To support this calculation and the ranging calculations used to generate the velocity profile plots, the speed of sound was measured for each simulant using *Calibration Procedure for Determining Velocity of Ultrasonic Energy in Simulants* (TPR-RPP-WTP-608).

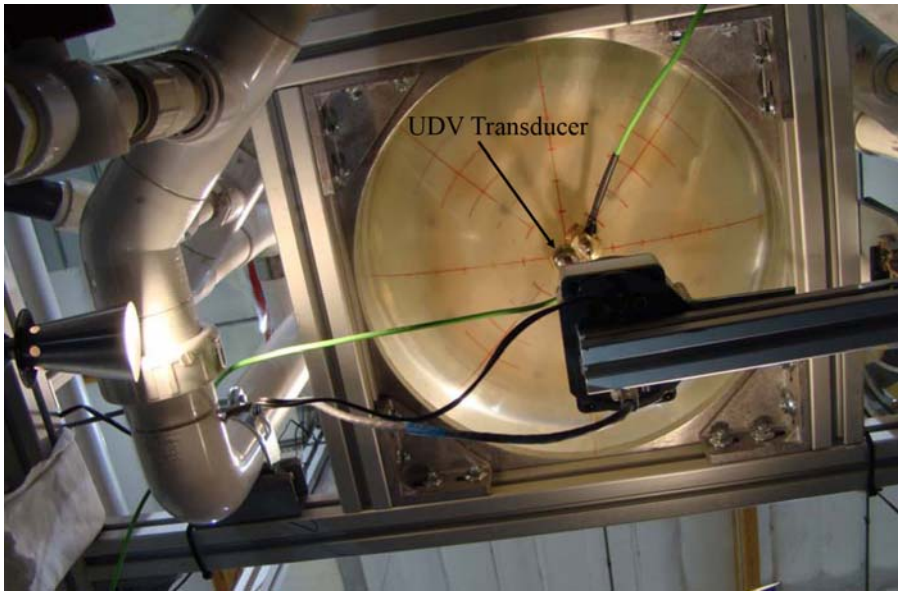

Figure A.3. Ultrasonic Transducers Mounted to the Small-Scale Tank Bottom

The repetition rate used for most of the testing was in the 5- to 5.5-kHz range. Operating procedures allowed the repetition rate to be varied from 1 to 10 kHz. Small adjustments to the repetition rate were occasionally required to eliminate extraneous ultrasound signals from fixed objects in the tank, or even the surface of the water in the tank, that could occur during the actual sampling of the Doppler signal. For a nominal 5 kHz repetition rate and the speed of sound range previously listed for the simulants tested, equation (A.7) indicates the maximum range varies from 14 to 17 cm. The calculated maximum range distances are larger than the actual measurement range of 4 cm used during testing, and this was not a factor during UDV measurements. Using the same conditions and applying equation (A.6) indicates the maximum particle velocity varies from 77 to 94 cm/s before aliasing would be a factor. Aliasing was not a factor during UDV measurements.

The UDV data acquisition is triggered by a pulse signal generated from the ultrasonic command and control (UCC) computer. The UDV trigger signal is set up to occur at the end of the valve open time, when the depth of the settled bed should be at a minimum. The standard UDV analysis was conducted to generate a velocity profile plot. These data are then analyzed to determine the range where there is a transition from stationary to moving particles. The range value is reported as the settled bed depth. A block diagram of the UDV system as used during testing is illustrated in Figure A.4.

The transmitted tone burst, 4 cycles of 2.25 MHz, is output through a diplexer to the transducer. The ultrasound travels into the tank and is scattered by particles. Some of the ultrasound returns to the transducer, which generates a receive signal that is routed by the Diplexer to an external 40-dB wideband amplifier. The output of the amplifier goes directly into the R#1 input on UDV. For M3 operations, the UCC system sends a trigger signal to UDV that controls when data are acquired and analyzed to determine the bed layer depth. The UDV trigger was set to occur 0.4 to 0.0 seconds before the closure of the valve that controls flow into the tank. After calculating the bed layer depth, UDV transmits the depth data and a time stamp to the UCC via the network connection. All data files logged during data acquisition are downloaded to the M3 server.

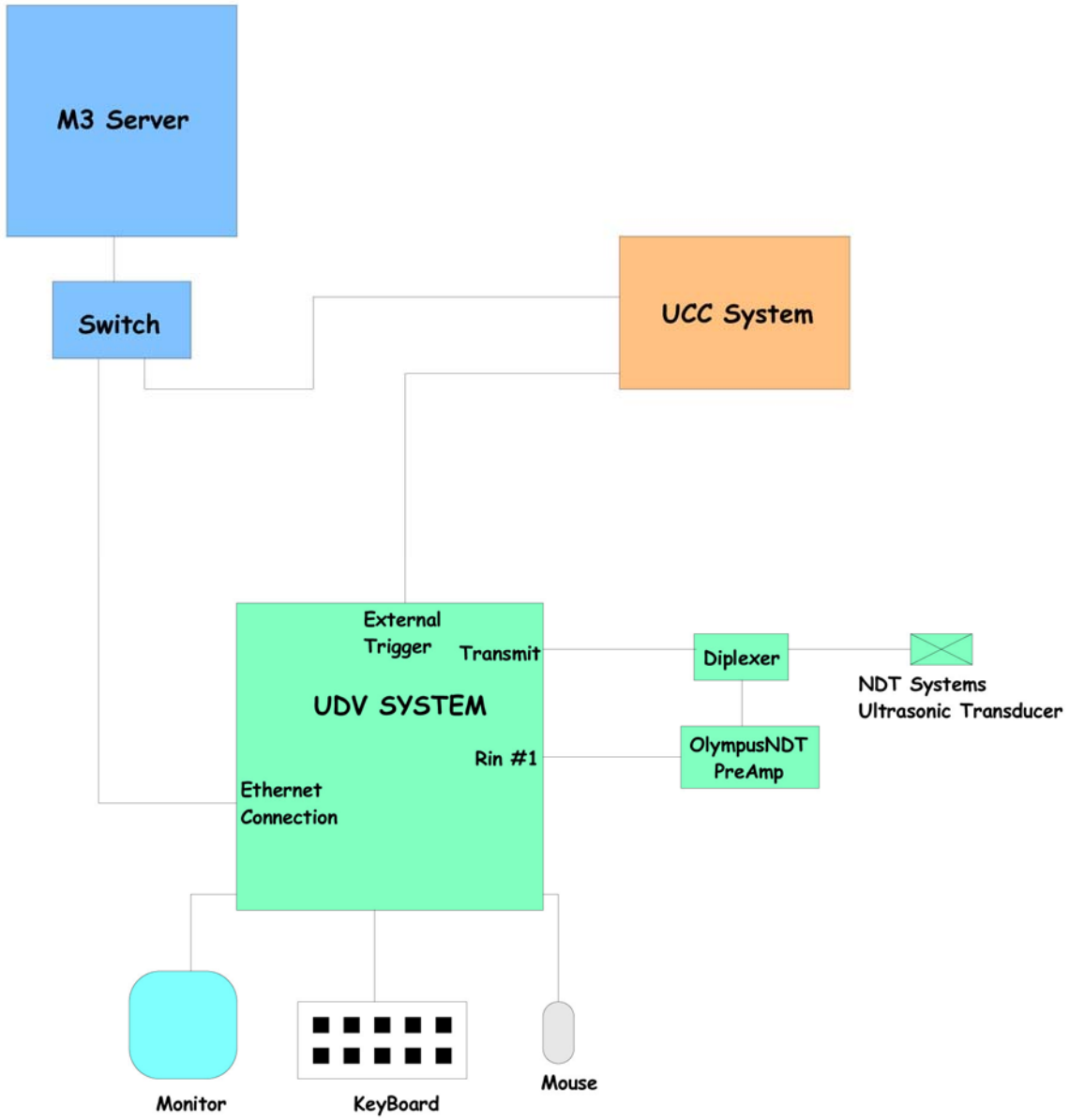

Figure A.4. UDV Component Diagram

A.1.3 UDV System Components

The UDV system hardware is based around the Arcom Olympus EBX single-board personal computer (PC). The UDV system has a monitor, keyboard, and mouse that are used to select operating parameters and display results. Following is a listing of the major components of the UDV system.

Arcom Olympus EBX Single-Board Computer

1 GHz Pentium III
256 MB / 512 MB RAM
Standard PC I/O (comm, parallel, IDE, video, keyboard and mouse, USB)

1 PCI expansion slot
PC104 expansion bus

CyberResearch PCIDAQ 2012

4-channel 12-bit simultaneous sampling
20 MSamples/second max rate on all channels

PNNL-Developed Analog Circuit Board

PC 104 bus
Signal conditioning – filter/gain/time variable gain
Mixer/down converter – I/Q Doppler frequency signal

PNNL-Developed Digital Circuit Board

PC104 bus
Generates fundamental transducer operating frequency
Generates transmit "tone burst"
Generates repetition rate
Synchronizes transmit – receive – data acquisition timing.

A.2 Ultrasonic Concentration Probe

The ultrasonic concentration probe operates by determining the attenuation of an ultrasonic pulse over a frequency spectrum when it passes through fluid or slurry from the transmit transducer to the receive transducer. The concentration is determined by comparing the attenuation for a given simulant to the baseline attenuation for the carrier liquid and by using a correlation developed for that simulant using a reference standard for the volume percent solids as a function of the ultrasonic attenuation for a given frequency.

Figure A.5 is a photograph of the ultrasonic concentration probe sensor in the small-scale tank for the mixing studies, and Figure A.6 illustrates the concentration sensor hardware. The two ultrasonic sensors are shown as black discs on the mounting hardware. A voltage pulse is sent to the transmit transducer, causing the piezoelectric crystal to vibrate and emit ultrasound. The ultrasound reaches the receive transducer, causing the piezoelectric crystal to vibrate, and this in turn produces a voltage signal. As the ultrasound travels through the slurry, its intensity is attenuated based on interaction with particles in the slurry, and the receive transducer measures a smaller voltage signal than it would for water. Thus, there is a direct correspondence between the attenuation of the signal and the concentration of the slurry. The attenuation is also dependent on the type and size of the particulate. In the mixing tests, the attenuation of the ultrasound was measured. Laboratory measurements are required to relate the measured attenuation to the concentration. This relationship has the following form for slurry concentration in units of volume percentage:

$$\text{Volume Percentage} = \text{CONC} \times \text{Attenuation} \tag{A.9}$$

Laboratory measurements were required to obtain the concentration constant (CONC) for each type of particulate and for each ultrasonic frequency used in the tests. (These laboratory measurements are discussed in more detail in the next section.) During laboratory measurements, slurry is placed in a

mixing vessel with a mechanical stirrer to keep it suspended. The two transducers mounted in the wall of the vessel are separated by 5 cm, which is the same distance as used in the tests.

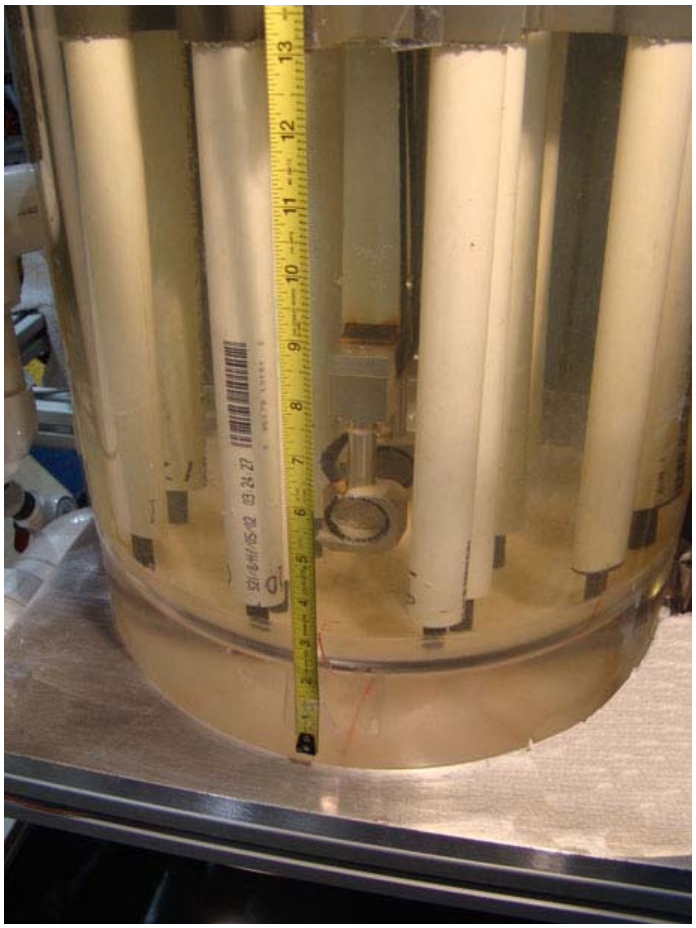

Figure A.5. Photograph of the Concentration Sensor Near the Bottom of the Small-Scale Tank. The transducer faces are separated by 5.08 cm (2 in.).

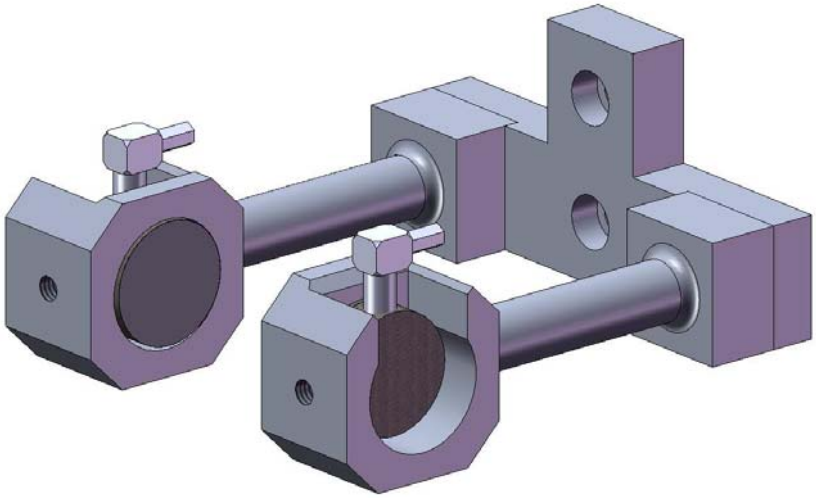

Figure A.6. Concentration Sensor Configuration

The data acquisition system (DAS) is used to measure the attenuation. Using a pipette, a sample of the slurry between the transducer faces is extracted, and the density of the sample is determined using a pycnometer to measure mass and volume. The density is used to determine the volume percentage of the slurry. Plotting the volume percentage on the vertical axis of a graph and the attenuation (at a specified frequency) on horizontal axis yields a straight line, confirming the validity of linear Eq. (A.9). The slope of this line is equal to the concentration constant in Eq. (A.9). The values of the concentration constant can then be used to analyze the attenuation data and obtain the concentration in volume percentage for many different locations within the tank.

A.2.1 Data Acquisition System and Measurement of Attenuation

The DAS developed at PNNL has been used for many years for investigations of physical properties of liquids and slurries, such as density, viscosity, attenuation measurements, and velocity of sound (Greenwood and Bamberger 2002, 2004; Bamberger and Greenwood 2004; Greenwood 2004). A schematic diagram of the DAS, shown in Figure A.7, consists of a computer-controlled pulser-receiver, a computer with a digitizer card, and a multiplexer to switch the electronics from the current transducer pair to another pair. The maximum number of transducer pairs is six. The DAS for the M3 mixing experiments used only one transducer pair, while measurements with a second DAS, for determining the value of concentration in Eq. (A.9), used two transducer pairs. The pulser-receiver sends a short voltage pulse to the transmit transducer and amplifies the signal obtained by the receive transducer. The analog signal, produced at the output of the pulser-receiver, is sent to a digitizer in the computer. The 12-bit digitizer analyzes the voltage into 2^{12} (or 4096) bins for high accuracy. The data acquisition code, written in the MATLAB language, is completely automated and has the following functions: 1) sets the parameters for the digitizer, pulser-receiver, and the multiplexer; 2) performs the desired calculations using the digitized voltage-versus-time signal; and 3) stores information in a file.

This DAS was modified to determine the attenuation for this project. The pulser-receiver sends out a pulse at the pulser connection each time it receives a trigger signal. This trigger signal can be generated internally in the pulser-receiver at a specified pulse-repetition rate or can be externally triggered. Because the timing of events in the tank is very important, an external trigger signal from the UCC computer was sent to the trigger input on the pulser-receiver, as shown in Figure A.7, at 5 signals per second. With each trigger signal, the pulser-receiver sends a short voltage pulse to the transmit transducer. For a 3.5-MHz transmit transducer, this signal consisted of a negative voltage of several hundred volts (depending upon the value in the setup code) for a time of about 143 nanoseconds. This caused the piezoelectric crystal to vibrate and produce a pulse similar to that shown in Figure A.8. The frequency content of the signal is determined using a fast Fourier transform (FFT), as shown in Figure A.8. The signal from the receive transducer was analyzed to determine the attenuation at 5 values per second. Each attenuation value was sent to the UCC computer. At this high rate, no signal averaging was used and the gain was not changed during the data acquisition. Thus, the slurry concentration between the transducer faces could be captured every 0.2 seconds.

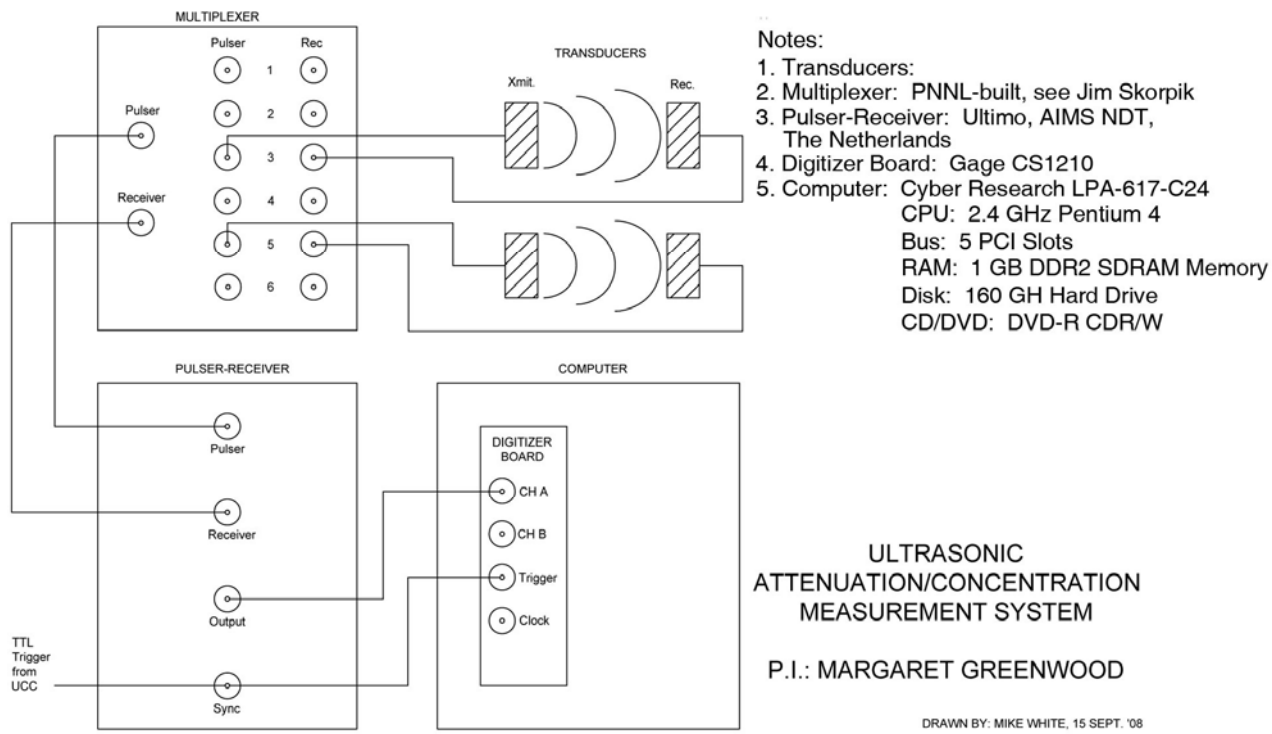

Figure A.7. Schematic Diagram of the DAS

A.2.2 Calculation of Attenuation

The top section of Figure A.8 shows the voltage signal as a function of time (hereafter called the time signal) for water, a slurry, and a highly concentrated slurry (very highly attenuative) and demonstrates the attenuation of the signal resulting from different concentrations of the slurry. Each time signal is analyzed by obtaining the FFT of the time signal, and the results are shown in the bottom panel. The results of the FFT show that the time signal contains many frequencies, which peak at 5 MHz in this example. These effects are due to the bandwidth of the transducers.

Conceptually, the short time signal can be viewed as a superposition of many plane waves of different frequencies. That is, all of the plane waves added together yield the short time signal. A plane wave traveling in the x-direction has a form given by $A\sin(kx - \omega t + \varphi)$, where $k = 2\pi/\lambda$ and $\omega = 2\pi f$. The FFT analysis provides the FFT amplitude, A, and the phase, φ, for a large range of frequencies. Thus, the short time signal is viewed as composed of plane waves of many different frequencies and phases. Because the attenuation of a plane wave passing through a slurry depends on frequency, the information contained in the FFT can be used to calculate the attenuation for a range of frequencies. The attenuation relative to water is defined as

$$\text{Attenuation} = (-20/D)\ \log10\ (\text{FFT amplitude for slurry}/\text{FFT amplitude for water}) \qquad (A.10)$$

The units of attenuation are decibels (dB) per the length unit used for the distance D between the transducer faces.

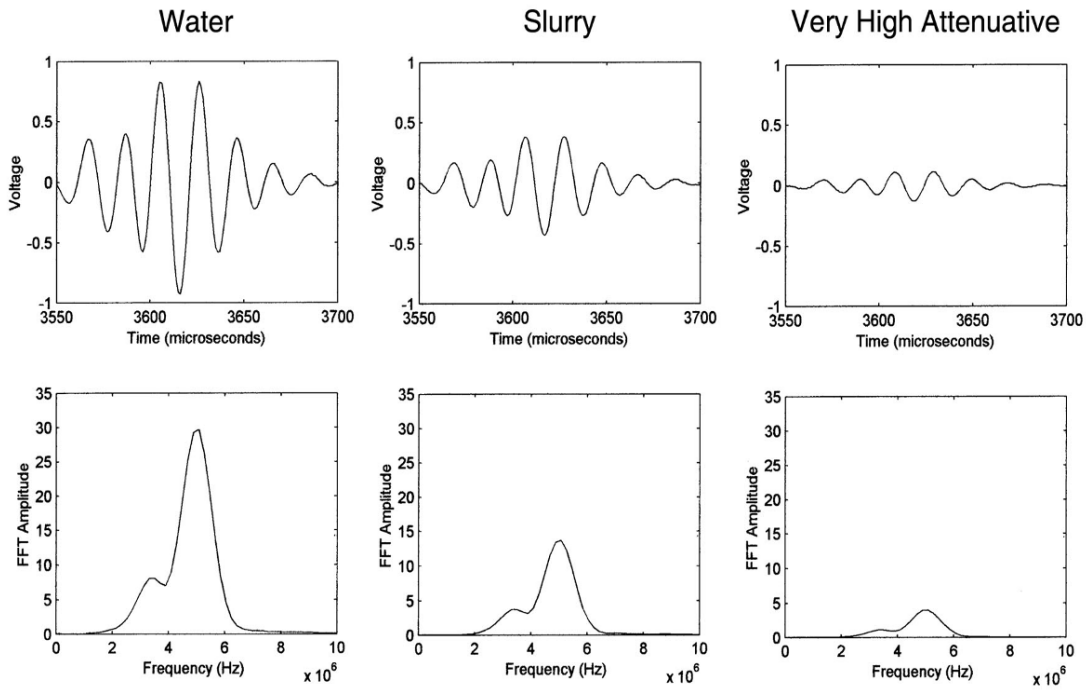

Figure A.8. Voltage Versus Time Signal in Top Panel and the FFT of Each Signal in the Bottom Panel

As an example, the attenuation of the slurry in the middle panel of Figure A.8 can be easily calculated for the peak, which occurs at 5 MHz. The peak for water has an FFT amplitude of 29.5 units, while that for the slurry has an amplitude of 13.5 units. If the distance between the two transducers faces is 5 cm, the attenuation is equal to 1.36 dB/cm. In this plot, similar calculations can be carried out for frequencies ranging from about 2.5 to 6 MHz.

The data acquisition code for this application used the procedure described above for calculating the attenuation. The first step was to obtain the frequency spectrum for water, similar to the left bottom panel in Figure A.8, which resulted in values of the FFT amplitude as a function of frequency being stored in a file. This water calibration was carried out at least once every two hours during testing, with the sensor moved to the top of the tank and the pulse jet mixers not operating so the calibration was performed in clear water.

During data acquisition, a frequency spectrum similar to that shown in the lower middle panel of Figure A.8 was obtained every 0.2 seconds. The code calculated attenuation over a range of frequencies and an example is shown in Figure A.9. The attenuation at one frequency value was sent to the UCC, and the attenuation for five frequency values was saved to a file in the DAS computer. Because the attenuation of ultrasound increases with the frequency, the objective is to choose a frequency for the UCC that is not too attenuative but large enough that changes in attenuation and the resulting slurry concentration can be observed.

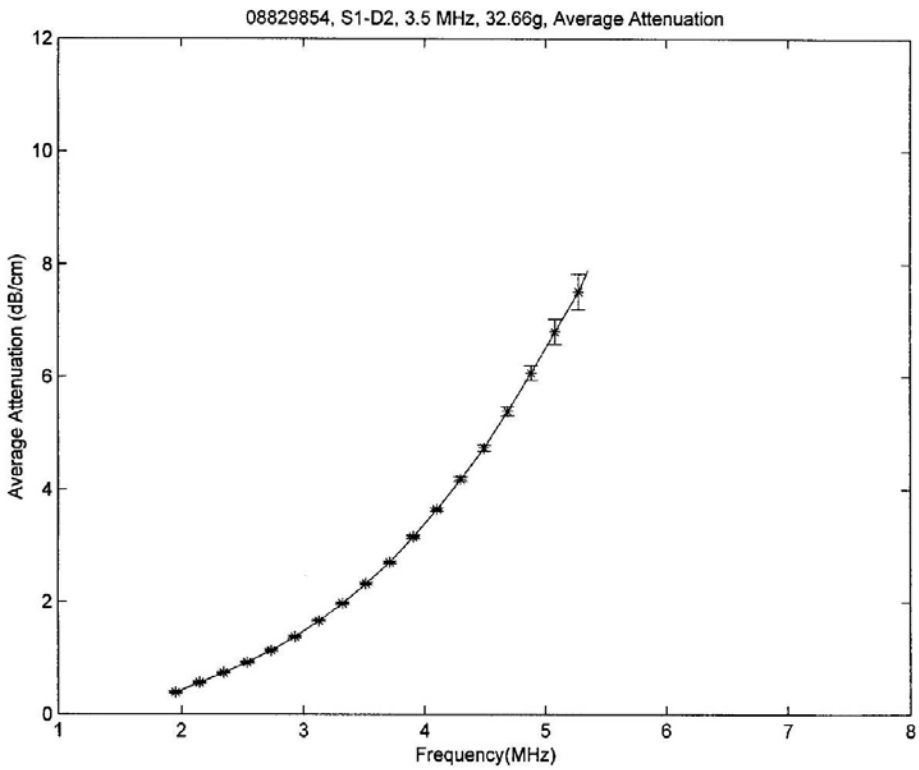

Figure A.9. Example of Attenuation Versus Frequency for Slurry of s1d2 Particulate Using 3.5 MHz Transducers

A.2.3 Relationship Between Concentration and Attenuation

The experimental apparatus shown in Figure A.10 consists of a vessel that has a 5 × 5-cm cross-section of with rounded corners and is 7.5-cm high. Four transducers are mounted in the wall, which permits the attenuation to be measured for two pairs of transducers with different center frequencies, using the multiplexer to switch the electronics to the desired pair. The simulant is kept in uniform suspension by a variable-speed vertical axis propeller mixer at the bottom of the test vessel. A baffle unit is placed in the vessel to reduce the vortex caused by the stirrer and to provide a more uniform suspension. A second DAS, identical to the first, was used to obtain data at a laboratory in the 2400 Stevens Building.

A slurry sample was extracted between the two transducer faces using a pipette or a syringe. The sample was placed in a pycnometer, and the density of the sample was determined. The slurry concentration was specified by the density ρ_{slurry}, the volume fraction (V_F), or the volume percentage. The basic definition of the V_F is the volume of the particles divided by total volume of the sample:

$$V_F = V_{particles} / (V_{particles} + V_{liquid}) \tag{A.11}$$

where $V_{particles}$ is the volume occupied by the particles in the sample, and V_{liquid} is the volume of the liquid in the sample, which is usually water.

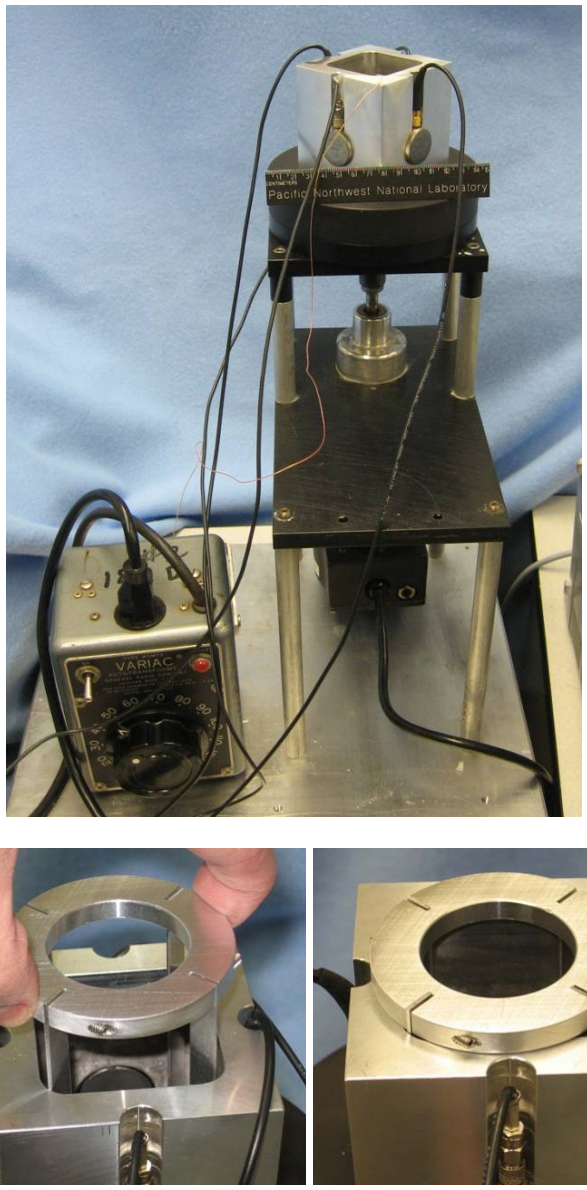

Figure A.10. Mixer and Baffle Unit for Laboratory Measurements of Attenuation and Slurry Concentration

The volume fraction is related to the density of the slurry, ρ_{slurry}, the density of the particulate, ρ_{part}, and the density of the liquid, ρ_{wtr}:

$$V_F = (\rho_{slurry} - \rho_{wtr}) / (\rho_{part} - \rho_{wtr}) \quad \text{(A.12)}$$

The volume percentage is related to the volume fraction in the usual manner:

$$\text{Volume Percentage} = 100\ (V_F) \quad \text{(A.13)}$$

The attenuation measurements were obtained using a DAS that is very similar to that used for the M3 mixing tests. The attenuation measurement tests were conducted in the 2400 Stevens Building. The code to measure the attenuation is similar to that used for M3 tests, except that the output has been modified to

record the values of the attenuation for a larger number of frequencies, obtain an average attenuation over 1000 runs, and obtain the standard deviation. The slurry sample is extracted between the transducer faces while the slurry is being stirred. Usually three samples were extracted for each concentration of slurry.

Data were obtained for the five types of particulate used in the mixing tests: s1d5, s1d1, s1d2, s2d1, and s2d2. The simulant properties are described in Section 3.0. A data input file was generated that contains the attenuation and the corresponding density measurements for several concentrations of slurry. A MATLAB code named attentoconc.m read the input file. For each simulant sample taken during a run, the density was converted to a volume percentage, and the average volume percentage value and its standard deviation for each run were obtained. Also, for each simulant concentration tested, the average attenuation and its standard deviation were obtained for several runs of 1000 data points (measurements). The data for each simulant were plotted with the attenuation along the horizontal axis and the volume percentage along the vertical axis. Each data point contains an uncertainty in the attenuation and an uncertainty in the volume percentage. The code uses a weighted total least-squares-straight-line fit to the data for each simulant using uncertainties in both the attenuation and the volume percentage and determines CONC, the slope of the straight line. Theory (Eq. A.9) predicts a straight line passing through the origin, and this is confirmed by the results of these experiments.

It is assumed that each particle in the slurry contributes to the attenuation in the same manner. Thus, if the volume percentage of the slurry is, for example, doubled, then the number of particles in the slurry is doubled. The attenuation is also expected to double in this example. Thus, the attenuation and volume percentage are related linearly, as shown in Eq. (A.9). In these experiments, the attenuation relative to water is measured, as shown by Eq. (A.10). This means that the attenuation of water is identically zero. That is, if the slurry is taken to be water, then the numerator and denominator in Eq. (A.10) are the same, and the attenuation is equal to zero. Thus, in Figures A.11 and A.12 (and similar figures), the data point for water is at the origin. The slope of the line is calculated by finding the best fit through the data points, with uncertainties in attenuation and uncertainties in volume percentage included in the calculation. In this calculation, the attenuation for water has an uncertainty of 0.02 dB/cm and an uncertainty of 0.02% for volume percentage, so the intercept is a very small number.

The data for slurries for three particulates, s1d1, s1d2, and s1d5, are shown in Figure A.11 for an ultrasonic frequency of 3.125 MHz. Similar data are presented in Figure A.12 for slurries of s2d1 and s2d2. A straight line passing through the origin has the form given by Eq. (A.9), where the value of CONC is the slope of the straight line on a graph of volume percentage (vertical axis) versus the attenuation (horizontal axis).

In Figure A.11, data are shown for three simulants. Simulant s1d1 shows fairly large error bars for the three smallest volume percentages, but the data points are within two standard deviations of the straight line. The error bars for attenuation at these small volume percentages are large because the slurry is so granular for these large-diameter particles. Note that the error bars in attenuation decrease for the smaller diameter particles, such as simulants s1d5 and s1d2, because the slurry is more uniform. The two data points for the higher volume percentages have small uncertainties and are very close to the straight line for s1d1.

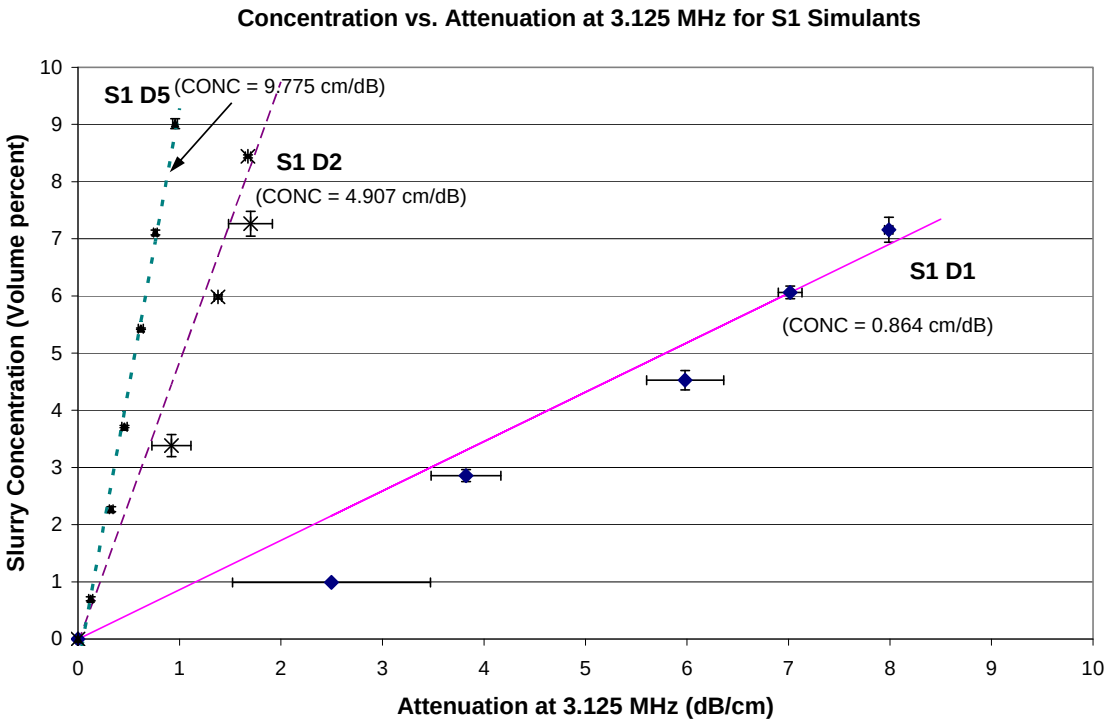

Figure A.11. Concentration and Attenuation Measurements for Slurries s1d1, s1d2, and s1d5 for Determination of the Slope of the Straight Line Through the Data Points

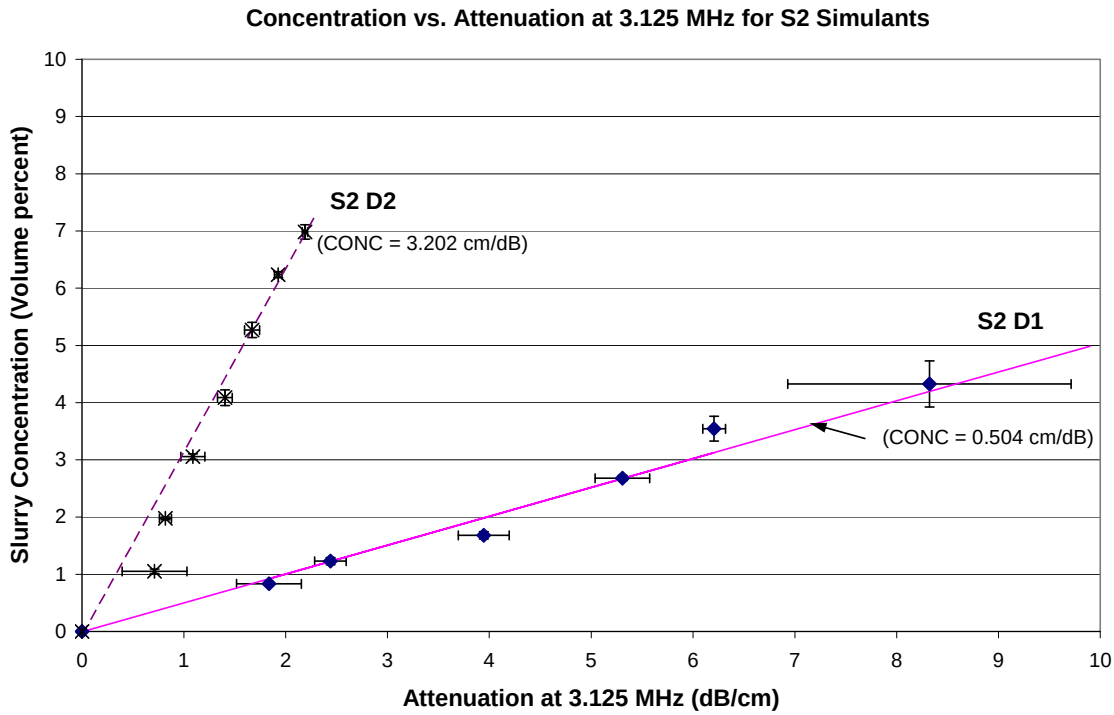

Figure A.12. Concentration and Attenuation Measurements for Slurries s2d1 and s2d2 for Determining the Slope of the Straight Line Through the Data Points

In Figure A.12, the data point for s2d1 for the greatest concentration has large uncertainties. The calculation for the slope was repeated excluding this data point and yielded a slope of 0.506 cm/dB, a negligible change. This shows the validity of the original calculation because the slope is determined essentially by the five data points with smaller uncertainties and water.

The two graphs show the effects of particle diameter and density on attenuation value. Eq. (A.9) shows that attenuation is given by volume percentage divided by concentration constant (CONC). Figure A.11 for simulant s1 and Figure A.12 for s2 considers a constant slurry concentration of 4%. In both figures, attenuation increases as CONC decreases. Therefore, for each simulant, the attenuation increases as particle size increases. However, density also has an effect when both simulants are considered. For simulant pairs s1d1/s2d1 and s1d2/s2d2, both members of the pair have similar particle diameters, either d1 or d2. For each pair, the attenuation is greater for the denser stimulant, s2. By arranging the values of CONC in Table A.1 for a single frequency from the largest value of CONC to the smallest, we find the following order for increasing attenuation at the same slurry concentration: s1d5 (lowest), s1d2, s2d2, s1d1, and s2d1 (highest).

For the five simulants and the frequencies used in the M3 tests, Table A.1 provides the values of the constant CONC. To analyze the data from the M3 tests, the attenuation at the specified frequency is multiplied by the appropriate value of CONC to yield the slurry concentration in volume percentage.

Table A.1. Values of CONC for Five Simulants and Seven Frequencies

UCC Frequency, MHz	s1d2, CONC, cm/dB	s1d1, CONC, cm/dB	s1d5, CONC, cm/dB	s2d1, CONC, cm/dB	s2d2, CONC, cm/dB
3.906	2.602	0.530	5.765	0.323	1.645
3.125	4.907	0.864	9.775	0.504	3.202
2.930	5.888	1.017	11.236	0.588	3.890
2.734	7.130	1.221	13.138	0.701	4.785
2.539	8.768	1.503	15.470	0.858	5.943
2.344	10.009	1.806	21.812	1.086	7.836
1.953	14.187	3.175	26.917	1.928	12.648

A.3 References

Bamberger JA and MS Greenwood. 2004. "Measuring fluid and slurry density and solids concentration non-invasively." *Ultrasonics* 42:563-567.

Greenwood MS. 2004. "Self-Calibrating System and Technique for Ultrasonic Determination of Fluid Properties." U.S. Patent 6,763,698.

Greenwood MS and JA Bamberger. 2002. "Measurement of Viscosity and Shear Wave Velocity of a Liquid or Slurry for On-line Process Control." *Ultrasonics* 39:623-630.

Greenwood MS and JA Bamberger. 2004. "Self-calibrating sensor for measuring density through stainless steel pipeline wall." *Journal of Fluids Engineering-Transactions of the ASME* 126:189-192.

Morgen GP, RA Pappas, DM Pfund, WC Weimer, DM Sheen, and BJ Burghard. 2002. "Ultrasonic system and technique for fluid characterization." U.S. Patent 6,871,148.

Appendix B

Mixing Data

Tables

B.1 Summary of Mixing Test General Conditions and Data B.1
B.2 Key for Case IDs and MSS Row Numbers.....B.3
B.3 Data from 2008 Tests in Small-Scale Vessel with Elliptical Head A.1.....B.4
B.4 Data from 2008 Tests in Mid-Scale Vessel with Spherical Head A.1 .....B.48
B.5 Data from 2008 Tests in Large-Scale Vessel with Elliptical Head A.1.....B.56
B.6 Data from 2008 in Large-Scale Vessel with Flanged and Dished Head A.1 .....B.78
B.7 Data from July 2007 Tests in Mid-Scale Vessel with Spherical Head A1 .....B.92
B.8 Data from Fall 2007 Tests in Mid-Scale Vessel with Spherical Head A.1.....B.108
B.9 Updated Data from Fall 2007 Tests in Mid-Scale Vessel with Spherical Head A.1 .....B.132

Appendix B

Mixing Data

Mixing data from tests conducted in several scaled tanks are listed in Appendix B. The data from the mixing tests are summarized in Table B.1 together with the general test conditions of tank scale (small, mid, or large) and head shape (elliptical, flanged and dished, or spherical). The first column of Table B.1 lists the table number in Appendix B where the data is tabulated. The data is categorized by test campaigns denoted as tests conducted in 2008, July 2007, or Fall 2007. The tests conducted in 2008 used simulant from a different manufacturer than those tests conducted in 2007. The test details column shows the types of measurements used to determine the critical suspension velocity and the cloud height for each test. The test data in Tables B.3 through B.8 is listed chronologically based on increasing row number. The first several digits of the Appendix B row number are specified in the last column of Table B.1. The tests conducted in 2008 in the elliptical or spherical head all start with the number 9 followed by the nominal tank diameter in inches. The tests conducted in 2008 using the flanged and dished head start with the nominal tank diameter in inches (70).

Table B.1. Summary of Mixing Test General Conditions and Data

Table	Test Campaign	Tank Scale (nominal diameter in.)	Head Shape (abbreviation)	Simulant Manufacturer	Test Details	Row Number Format
B.3	2008	Small (15)	Elliptical (E)	XLSciTech	Visual observation of cloud height H_C. Ultrasonic measurement of U_{CS} and concentration.	915XXXX
B.4	2008	Mid (34)	Spherical (S)	XLSciTech	Visual observation of cloud height H_C. Ultrasonic measurement of U_{CS} and concentration.	934XXXX
B.5	2008	Large (70)	Elliptical (E)	XLSciTech	Visual observation of cloud height H_C. Ultrasonic measurement of U_{CS} and concentration.	970XXXX
B.6	2008	Large (70)	Flanged and dished (F)	XLSciTech	Visual observation of cloud height H_C. Ultrasonic measurement of U_{CS} and concentration.	70XXXX
B.7	July 2007	Mid (34)	Spherical (S)	Potters	Visual observation of cloud height H_C. Visual observation of U_{CS}.	2007XXXX
B.8	Fall 2007	Mid (34)	Spherical (S)	Potters	Visual observation of cloud height H_C. Visual observation of U_{CS}.	709XXXX

X denotes numeral entry.

A Case ID was assigned to each test that provided a concise summary of specific test parameters. The Case IDs are defined in Table B.2. This notation is used to identify test conditions throughout the report. The first two digits (DD) of the Case ID show the nominal tank diameter in inches (15, 34, or 70). The next digit (B) shows the head shape (E for elliptical, F for flanged and dished, and S for spherical).

In some cases the head shape is shown as E8. This denotes when tests were conducted with an 8 tube array instead of a 12 tube array. The next digit (L) shows the full-scale nozzle diameter in inches (4, 6, M for 8.5, and L for 11.8). The next 4 digit sequence (MMNN) is the simulant code with MM showing the density and NN showing the nominal particle size. The next digit (O, an upper case letter) shows the solids volume fraction. The next digit (P, a lower case letter) shows the nominal duty cycle. The last digit (Q) shows the nominal pulse volume fraction. For pulsating flow Q is shown as an underscore followed by a number (such as _1). For steady flow with a reduced number of pulse tubes in operation Q is shown as a dash followed by the number of outer nozzles in operation followed by the number of inner nozzles in operation (such as -80, 8 outer nozzles operating and 0 inner nozzles operating). Additional details are provided in Table B.2.

The test data are listed in Tables B.3 through B.8. The test data parameters tabulated in Appendix B Tables B.3 through B.8 are described in Table 6.2 and the measurement uncertainties are also provided. The data in the first three rows of Appendix B are presented in the first three columns of Table 6.2. The data in Tables B.3 through B.8 is presented on two sheets to be viewed side by side. The Row is the first column heading of the left part of the table (shown in the caption as A.X) and the last column heading of the right part of the table (shown in the caption as B.X).

The row number listed as the first column of Tables B.3 through B.8 may have either an M or MX listed to the right of the number. M signifies that the row of data was used for development of the critical suspension and cloud height models. X signifies that the row of data was included in the model, however, the test was conducted at a return line height that was lower than listed and the row should have been excluded from the model data set. Rows affected are 7090186-7090366 and 7090616-7090759. Only ten rows in this range were included in the model H_C model, of these seven rows were used in the U_{CS} model. Rows with Case IDs 10/26A1 through 10/29B2 have return line heights of 31.875 in. Rows with Case IDs 10/31A1 through 10/30C2 and 11/8C1 through 11/14A2 have return line heights of 21.7125 in.

Table B.9, an update of Table B.8, was added to this appendix as a part of Rev. 1. Table B.9 corrects return line height data described in the prior paragraph.

Table B.2. Key for Case IDs and MSS Row Numbers

Case ID Format: DDB_LMMNNOPQQ

DD		B		L			MMNN			O		P		QQ (optional)		
Code	Tank	Code	Head Shape	Code	Nozzle		Code	Simulant		Code	Solids Concentration	Code	Nominal Duty Cycle	Code	Pulsing Flow	
Nom. Diam (in.)	Scale		Tank bottom		Full-scale[a] nozzle diam. in.	m	Simulant	density (g/cm^3)	d50 (μm)	Upper case letter	(fraction)	Lower case letter	(fraction)		Nominal Pulse Volume Fraction	Outer/Inner nozzles
15	**Small**	**E**	elliptical 15E and 70E (HLP-22 config.)	**4**	4	0.10	**s1d5**	2.5	44	**U**	0.00015	**a**[b]	1.0	**_0**	0.05	4/4
34	**Mid**	**E8**	elliptical 15E and 70E (8-tube array config.)	**6**	6	0.15	**s1d2**	2.48	69	**T**	0.0005	**e**	0.66	**_1**[b]	0.05	8/4 or 4/4[c]
70	**Large**	**F**	F&D 70F (HLP-22 config.)	**M**[d]	8.5	0.22	**s1d1**	2.46	166	**S**	0.0015	**b**	0.50	**_2**	0.1	8/4 or 4/4[c]
		S	spherical 34S (HLP-22 config.)	**L**[d]	11.8	0.30	**s2d2**	4.18	76	**Z**	0.00155	**c**	0.33	**_3**	0.025	8/4
							s2d1	4.17	164	**Y**	0.005 (0.00485–0.005)	**i**	0.28*	**_4**	0.15	8/4
							p1d8[e]	2.45	90	**R**	0.01	**f**	0.25*	**_5**	0.05	8/0
							p1d7[e]	2.45	178	**V**	0.0143	**h**	0.24*	**_6**	0.05	4/0
							p2d6[e]	2.46	766	**X**	0.015 (0.0146–0.0159)	**m**	0.21*	**_7**	0.1	4/0
										Q	0.03	**d**	0.18	**_8**	0.048	8/4
Test		**MSS Row Format**								**W**	0.045[d]	**k**	0.14*	**_9**	0.05	0/4
15E or 15E8		915XXXX								**P**	0.06[d]		* = limited tests			
34S		934XXXX													**Steady flow with reduced number of jets operated**	
70E or 70E8		970XXXX												Code[f]	Pulse Vol. Fraction	Outer/Inner nozzles
70F		70XXXX												**-80**	undefined	8 / 0
Fall 2007		709XXXX												**-44**	undefined	4 / 4
July 2007		2007XXXX												**-40**	undefined	4 / 0
														-04	undefined	0 / 4

(a) Scaled to HLP-22 sized tank of diameter 38 ft.
(b) Limited set of _1_FM01 observations; 70F tests with flow meter averaging set at 0.1 sec instead of 0.01 sec.
(c) Full tube array operated (8/4 for HLP-22 tests and 4/4 for 8-tube array tests) for cases with P=a and QQ=<blank>; and cases with QQ= _1 or _2.
(d) Tested only in the small-scale tank with 8-tube array. Scaled nozzle dimension provides reference for size relative to HLP-22.
(e) 34-inch tank only: p1d8=MIL-12; p1d7=MIL-8; p2d6=MIL-3.
(f) Tested only in mid-scale tank.

Table B.3. Data from 2008 Tests in Small-Scale Vessel with Elliptical Head A.1

Row Number	Test	Case ID	Tank Diameter	Head Shape	Dish Height	Dish Volume	Tank Fill Height	Return Line Height	Nozzle Inner Diameter	Nozzle Stand-off Distance	Pulse Tube Configuration	Installed Nozzles	Outer Nozzles Operated	Inner Nozzles Operated	Pulse Tube Outer Diameter	Outer PJM Radius	Inner PJM Radius	"FIO" Outer PJM Impingement Angle	"FIO" Inner PJM Impingement Angle	Ratio Outer PJM to Tank Radius	Ratio Inner PJM to Tank Radius	Simulant	Solids Density	Particle Diameter d5	Particle Diameter d50	Particle Diameter d95	Void Fraction
text	text	text	in.	text	in.	in. ^{3}	in.	in.	in.	in.	text	number	number	number	in.	in.	in.	deg	deg	nondim	nondim	text	g/cm^3	m	m	m	fraction
MSS	M/DDX	ID	D	HS	H_{dish}	V_{dish}	H	Rtn	d	sod	PT	N	N_O	N_I	PT_{od}	R_O	R_I	θ_O	θ_I	R_O/R	R_I/R	sxdx	ρ_s	d_5	d_{50}	d_{95}	vf
9150001	6/6A	15E_4s1d2Zc_1	14 7/16	E	3.25	354.8	35	29	0.126	0.189	HLP-22	12	8	4	1.05	4.5	2.4	21.8	10.1	0.62	0.34	s1d2	2.48	0.0000569	0.0000693	0.0000821	0.3750
9150002M	6/6A	15E_4s1d2Zc_1	14 7/16	E	3.25	354.8	35	29	0.126	0.189	HLP-22	12	8	4	1.05	4.5	2.4	21.8	10.1	0.62	0.34	s1d2	2.48	0.0000569	0.0000693	0.0000821	0.3750
9150003M	6/6A	15E_4s1d2Zc_1	14 7/16	E	3.25	354.8	35	29	0.126	0.189	HLP-22	12	8	4	1.05	4.5	2.4	21.8	10.1	0.62	0.34	s1d2	2.48	0.0000569	0.0000693	0.0000821	0.3750
9150004M	6/6A	15E_4s1d2Zc_1	14 7/16	E	3.25	354.8	35	29	0.126	0.189	HLP-22	12	8	4	1.05	4.5	2.4	21.8	10.1	0.62	0.34	s1d2	2.48	0.0000569	0.0000693	0.0000821	0.3750
9150005M	6/6A	15E_4s1d2Zc_1	14 7/16	E	3.25	354.8	35	29	0.126	0.189	HLP-22	12	8	4	1.05	4.5	2.4	21.8	10.1	0.62	0.34	s1d2	2.48	0.0000569	0.0000693	0.0000821	0.3750
9150006M	6/6A	15E_4s1d2Zc_1	14 7/16	E	3.25	354.8	35	29	0.126	0.189	HLP-22	12	8	4	1.05	4.5	2.4	21.8	10.1	0.62	0.34	s1d2	2.48	0.0000569	0.0000693	0.0000821	0.3750
9150007M	6/6A	15E_4s1d2Zc_1	14 7/16	E	3.25	354.8	35	29	0.126	0.189	HLP-22	12	8	4	1.05	4.5	2.4	21.8	10.1	0.62	0.34	s1d2	2.48	0.0000569	0.0000693	0.0000821	0.3750
9150008	6/6A	15E_4s1d2Zc_1	14 7/16	E	3.25	354.8	35	29	0.126	0.189	HLP-22	12	8	4	1.05	4.5	2.4	21.8	10.1	0.62	0.34	s1d2	2.48	0.0000569	0.0000693	0.0000821	0.3750
9150009	6/6A	15E_4s1d2Zc_1	14 7/16	E	3.25	354.8	35	29	0.126	0.189	HLP-22	12	8	4	1.05	4.5	2.4	21.8	10.1	0.62	0.34	s1d2	2.48	0.0000569	0.0000693	0.0000821	0.3750
9150010	6/6A	15E_4s1d2Zc_1	14 7/16	E	3.25	354.8	35	29	0.126	0.189	HLP-22	12	8	4	1.05	4.5	2.4	21.8	10.1	0.62	0.34	s1d2	2.48	0.0000569	0.0000693	0.0000821	0.3750
9150011	6/6A	15E_4s1d2Zc_1	14 7/16	E	3.25	354.8	35	29	0.126	0.189	HLP-22	12	8	4	1.05	4.5	2.4	21.8	10.1	0.62	0.34	s1d2	2.48	0.0000569	0.0000693	0.0000821	0.3750
9150012	6/6A	15E_4s1d2Zc_1	14 7/16	E	3.25	354.8	35	29	0.126	0.189	HLP-22	12	8	4	1.05	4.5	2.4	21.8	10.1	0.62	0.34	s1d2	2.48	0.0000569	0.0000693	0.0000821	0.3750
9150013	6/6A	15E_4s1d2Zc_1	14 7/16	E	3.25	354.8	35	29	0.126	0.189	HLP-22	12	8	4	1.05	4.5	2.4	21.8	10.1	0.62	0.34	s1d2	2.48	0.0000569	0.0000693	0.0000821	0.3750
9150014	6/6A	15E_4s1d2Zc_1	14 7/16	E	3.25	354.8	35	29	0.126	0.189	HLP-22	12	8	4	1.05	4.5	2.4	21.8	10.1	0.62	0.34	s1d2	2.48	0.0000569	0.0000693	0.0000821	0.3750
9150015	6/6A	15E_4s1d2Zc_1	14 7/16	E	3.25	354.8	35	29	0.126	0.189	HLP-22	12	8	4	1.05	4.5	2.4	21.8	10.1	0.62	0.34	s1d2	2.48	0.0000569	0.0000693	0.0000821	0.3750
9150016	6/6A	15E_4s1d2Zc_1	14 7/16	E	3.25	354.8	35	29	0.126	0.189	HLP-22	12	8	4	1.05	4.5	2.4	21.8	10.1	0.62	0.34	s1d2	2.48	0.0000569	0.0000693	0.0000821	0.3750
9150017	6/6B	15E_4s1d2Zd_1	14 7/16	E	3.25	354.8	35	29	0.126	0.189	HLP-22	12	8	4	1.05	4.5	2.4	21.8	10.1	0.62	0.34	s1d2	2.48	0.0000569	0.0000693	0.0000821	0.3750
9150018	6/6B	15E_4s1d2Zd_1	14 7/16	E	3.25	354.8	35	29	0.126	0.189	HLP-22	12	8	4	1.05	4.5	2.4	21.8	10.1	0.62	0.34	s1d2	2.48	0.0000569	0.0000693	0.0000821	0.3750
9150019M	6/6B	15E_4s1d2Zd_1	14 7/16	E	3.25	354.8	35	29	0.126	0.189	HLP-22	12	8	4	1.05	4.5	2.4	21.8	10.1	0.62	0.34	s1d2	2.48	0.0000569	0.0000693	0.0000821	0.3750
9150020M	6/6B	15E_4s1d2Zd_1	14 7/16	E	3.25	354.8	35	29	0.126	0.189	HLP-22	12	8	4	1.05	4.5	2.4	21.8	10.1	0.62	0.34	s1d2	2.48	0.0000569	0.0000693	0.0000821	0.3750
9150021M	6/6B	15E_4s1d2Zd_1	14 7/16	E	3.25	354.8	35	29	0.126	0.189	HLP-22	12	8	4	1.05	4.5	2.4	21.8	10.1	0.62	0.34	s1d2	2.48	0.0000569	0.0000693	0.0000821	0.3750
9150022M	6/6B	15E_4s1d2Zd_1	14 7/16	E	3.25	354.8	35	29	0.126	0.189	HLP-22	12	8	4	1.05	4.5	2.4	21.8	10.1	0.62	0.34	s1d2	2.48	0.0000569	0.0000693	0.0000821	0.3750
9150023M	6/6B	15E_4s1d2Zd_1	14 7/16	E	3.25	354.8	35	29	0.126	0.189	HLP-22	12	8	4	1.05	4.5	2.4	21.8	10.1	0.62	0.34	s1d2	2.48	0.0000569	0.0000693	0.0000821	0.3750
9150024M	6/6B	15E_4s1d2Zd_1	14 7/16	E	3.25	354.8	35	29	0.126	0.189	HLP-22	12	8	4	1.05	4.5	2.4	21.8	10.1	0.62	0.34	s1d2	2.48	0.0000569	0.0000693	0.0000821	0.3750
9150025M	6/6B	15E_4s1d2Zd_1	14 7/16	E	3.25	354.8	35	29	0.126	0.189	HLP-22	12	8	4	1.05	4.5	2.4	21.8	10.1	0.62	0.34	s1d2	2.48	0.0000569	0.0000693	0.0000821	0.3750
9150026M	6/6B	15E_4s1d2Zd_1	14 7/16	E	3.25	354.8	35	29	0.126	0.189	HLP-22	12	8	4	1.05	4.5	2.4	21.8	10.1	0.62	0.34	s1d2	2.48	0.0000569	0.0000693	0.0000821	0.3750
9150027	6/9A	15E_4s1d2Yc_1	14 7/16	E	3.25	354.8	35	29	0.126	0.189	HLP-22	12	8	4	1.05	4.5	2.4	21.8	10.1	0.62	0.34	s1d2	2.48	0.0000569	0.0000693	0.0000821	0.3750
9150028	6/9A	15E_4s1d2Yc_1	14 7/16	E	3.25	354.8	35	29	0.126	0.189	HLP-22	12	8	4	1.05	4.5	2.4	21.8	10.1	0.62	0.34	s1d2	2.48	0.0000569	0.0000693	0.0000821	0.3750
9150029	6/9A	15E_4s1d2Yc_1	14 7/16	E	3.25	354.8	35	29	0.126	0.189	HLP-22	12	8	4	1.05	4.5	2.4	21.8	10.1	0.62	0.34	s1d2	2.48	0.0000569	0.0000693	0.0000821	0.3750
9150030M	6/9A	15E_4s1d2Yc_1	14 7/16	E	3.25	354.8	35	29	0.126	0.189	HLP-22	12	8	4	1.05	4.5	2.4	21.8	10.1	0.62	0.34	s1d2	2.48	0.0000569	0.0000693	0.0000821	0.3750
9150031M	6/9A	15E_4s1d2Yc_1	14 7/16	E	3.25	354.8	35	29	0.126	0.189	HLP-22	12	8	4	1.05	4.5	2.4	21.8	10.1	0.62	0.34	s1d2	2.48	0.0000569	0.0000693	0.0000821	0.3750
9150032M	6/9A	15E_4s1d2Yc_1	14 7/16	E	3.25	354.8	35	29	0.126	0.189	HLP-22	12	8	4	1.05	4.5	2.4	21.8	10.1	0.62	0.34	s1d2	2.48	0.0000569	0.0000693	0.0000821	0.3750
9150033M	6/9A	15E_4s1d2Yc_1	14 7/16	E	3.25	354.8	35	29	0.126	0.189	HLP-22	12	8	4	1.05	4.5	2.4	21.8	10.1	0.62	0.34	s1d2	2.48	0.0000569	0.0000693	0.0000821	0.3750
9150034M	6/9A	15E_4s1d2Yc_1	14 7/16	E	3.25	354.8	35	29	0.126	0.189	HLP-22	12	8	4	1.05	4.5	2.4	21.8	10.1	0.62	0.34	s1d2	2.48	0.0000569	0.0000693	0.0000821	0.3750
9150035M	6/9A	15E_4s1d2Yc_1	14 7/16	E	3.25	354.8	35	29	0.126	0.189	HLP-22	12	8	4	1.05	4.5	2.4	21.8	10.1	0.62	0.34	s1d2	2.48	0.0000569	0.0000693	0.0000821	0.3750
9150035.1	6/9A	15E_4s1d2Yc_1	14 7/16	E	3.25	354.8	35	29	0.126	0.189	HLP-22	12	8	4	1.05	4.5	2.4	21.8	10.1	0.62	0.34	s1d2	2.48	0.0000569	0.0000693	0.0000821	0.3750
9150035.2	6/9A	15E_4s1d2Yc_1	14 7/16	E	3.25	354.8	35	29	0.126	0.189	HLP-22	12	8	4	1.05	4.5	2.4	21.8	10.1	0.62	0.34	s1d2	2.48	0.0000569	0.0000693	0.0000821	0.3750
9150035.3	6/9A	15E_4s1d2Yc_1	14 7/16	E	3.25	354.8	35	29	0.126	0.189	HLP-22	12	8	4	1.05	4.5	2.4	21.8	10.1	0.62	0.34	s1d2	2.48	0.0000569	0.0000693	0.0000821	0.3750
9150035.4	6/9A	15E_4s1d2Yc_1	14 7/16	E	3.25	354.8	35	29	0.126	0.189	HLP-22	12	8	4	1.05	4.5	2.4	21.8	10.1	0.62	0.34	s1d2	2.48	0.0000569	0.0000693	0.0000821	0.3750
9150035.5	6/9A	15E_4s1d2Yc_1	14 7/16	E	3.25	354.8	35	29	0.126	0.189	HLP-22	12	8	4	1.05	4.5	2.4	21.8	10.1	0.62	0.34	s1d2	2.48	0.0000569	0.0000693	0.0000821	0.3750
9150035.6	6/9A	15E_4s1d2Yc_1	14 7/16	E	3.25	354.8	35	29	0.126	0.189	HLP-22	12	8	4	1.05	4.5	2.4	21.8	10.1	0.62	0.34	s1d2	2.48	0.0000569	0.0000693	0.0000821	0.3750

Table B.3. Data from 2008 Tests in Small-Scale Vessel with Elliptical Head B.1

Tank Water Temperature	Water Density	Solids Fraction	Pulse Volume Fraction	Duty Cycle	Cycle Time	Pulsed or Steady Jet	Us Steady Jet	U1 Pulsing Jet	U2 URMS	U3 URM3	Discharge Velocity	Critical Suspension Velocity	Average Peak Cloud Height	UCS Condition	UCS Method	UCS Flag	UCS Center Flag	UCS udv Flag	UCS based on Decreasing Velocity	Sweep Increase / Decrease	UDV Height Bed	Particle Motion	Solids Level	Outer Bottom Pattern	Inner Bottom Pattern	Case ID	Test	TDP	Row Number
C	g/cm³	fraction	fraction	fraction	s	text	m/s	m/s	m/s	m/s	m/s	m/s	in.	m/s	text	text	text	text	m/s	text	mm	text	text	text	text	text	text	text	text
T	ρ_l	ϕ_S	ϕ_P	DC	t_C	Jet	U_S	U1	U2	U3	U	U_{CS}	H_C	U_{CSR}	U_{CSM}	U_{CS}vis	U_{CS}cen	U_{CS}udv	U_{CS}_D	S_W	H_{bed}	PM	Sol	SP_O	SP_I	ID	M/DDX	TDP	MSS
20.8	1.000	0.00155	0.050	0.329	23.8	P	N/A	2.56	2.57	2.58	2.60	2.80	5.88	N/A	N/A	N/A	N/A	N/A	N/A	(null)	4.1	1	N/A	N/A	N/A	15E_4s1d2Zc_1	6/6A	TDP-172	9150001
21.0	1.000	0.00155	0.050	0.331	22.0	P	N/A	2.74	2.76	2.77	2.80	2.80	6.75	2.80	udv	N/A	N/A	UCSudv	N/A	I	2.3	1	N/A	N/A	N/A	15E_4s1d2Zc_1	6/6A	TDP-172	9150002
21.3	1.000	0.00155	0.050	0.333	20.6	P	N/A	2.94	2.96	2.97	3.00	2.80	8.00	N/A	N/A	N/A	UCScen	N/A	N/A	I	0.0	2	N/A	N/A	N/A	15E_4s1d2Zc_1	6/6A	TDP-172	9150003
21.5	1.000	0.00155	0.050	0.334	19.2	P	N/A	3.12	3.15	3.16	3.20	2.80	9.75	N/A	N/A	UCSvis	N/A	N/A	N/A	I	0.0	3	N/A	N/A	N/A	15E_4s1d2Zc_1	6/6A	TDP-172	9150004
21.7	1.000	0.00155	0.050	0.336	18.0	P	N/A	3.32	3.35	3.36	3.40	2.80	12.00	N/A	N/A	N/A	N/A	N/A	N/A	I	0.0	4	N/A	N/A	N/A	15E_4s1d2Zc_1	6/6A	TDP-172	9150005
21.9	1.000	0.00155	0.050	0.337	17.0	P	N/A	3.52	3.55	3.56	3.60	2.80	19.75	N/A	N/A	N/A	N/A	N/A	N/A	I	1.5	4	N/A	N/A	N/A	15E_4s1d2Zc_1	6/6A	TDP-172	9150006
22.4	0.999	0.00155	0.050	0.332	22.0	P	N/A	2.74	2.76	2.77	2.80	2.80	6.88	N/A	N/A	N/A	N/A	N/A	N/A	D	2.7	1	N/A	N/A	N/A	15E_4s1d2Zc_1	6/6A	TDP-172	9150007
22.4	0.999	0.00155	0.050	0.332	22.0	P	N/A	2.74	2.76	2.77	2.80	2.80	6.88	N/A	N/A	N/A	N/A	N/A	N/A	N/A	3.4	N/A	N/A	N/A	N/A	15E_4s1d2Zc_1	6/6A	TDP-172	9150008
22.4	0.999	0.00155	0.050	0.332	22.0	P	N/A	2.74	2.76	2.77	2.80	2.80	6.88	N/A	N/A	N/A	N/A	N/A	N/A	N/A	2.9	N/A	N/A	N/A	N/A	15E_4s1d2Zc_1	6/6A	TDP-172	9150009
22.4	0.999	0.00155	0.050	0.332	22.0	P	N/A	2.74	2.76	2.77	2.80	2.80	6.88	N/A	N/A	N/A	N/A	N/A	N/A	N/A	2.4	N/A	N/A	N/A	N/A	15E_4s1d2Zc_1	6/6A	TDP-172	9150010
22.4	0.999	0.00155	0.050	0.332	22.0	P	N/A	2.74	2.76	2.77	2.80	2.80	6.88	N/A	N/A	N/A	N/A	N/A	N/A	N/A	8.6	N/A	N/A	N/A	N/A	15E_4s1d2Zc_1	6/6A	TDP-172	9150011
22.4	0.999	0.00155	0.050	0.332	22.0	P	N/A	2.74	2.76	2.77	2.80	2.80	6.88	N/A	N/A	N/A	N/A	N/A	N/A	N/A	3.6	N/A	N/A	N/A	N/A	15E_4s1d2Zc_1	6/6A	TDP-172	9150012
22.4	0.999	0.00155	0.050	0.332	22.0	P	N/A	2.74	2.76	2.77	2.80	2.80	6.88	N/A	N/A	N/A	N/A	N/A	N/A	N/A	0.7	N/A	N/A	N/A	N/A	15E_4s1d2Zc_1	6/6A	TDP-172	9150013
22.4	0.999	0.00155	0.050	0.332	22.0	P	N/A	2.74	2.76	2.77	2.80	2.80	6.88	N/A	N/A	N/A	N/A	N/A	N/A	N/A	20.2	N/A	N/A	N/A	N/A	15E_4s1d2Zc_1	6/6A	TDP-172	9150014
22.4	0.999	0.00155	0.050	0.332	22.0	P	N/A	2.74	2.76	2.77	2.80	2.80	6.88	N/A	N/A	N/A	N/A	N/A	N/A	N/A	4.2	N/A	N/A	N/A	N/A	15E_4s1d2Zc_1	6/6A	TDP-172	9150015
22.4	0.999	0.00155	0.050	0.332	22.0	P	N/A	2.74	2.76	2.77	2.80	2.80	6.88	N/A	N/A	N/A	N/A	N/A	N/A	N/A	4.1	N/A	N/A	N/A	N/A	15E_4s1d2Zc_1	6/6A	TDP-172	9150016
22.9	0.999	0.00155	0.050	0.179	40.6	P	N/A	2.74	2.76	2.77	2.80	3.40	5.63	N/A	N/A	N/A	N/A	N/A	N/A	(null)	4.2	1	N/A	N/A	N/A	15E_4s1d2Zd_1	6/6B	TDP-172	9150017
23.1	0.999	0.00155	0.050	0.181	35.4	P	N/A	3.11	3.14	3.15	3.20	3.40	6.50	N/A	N/A	N/A	N/A	N/A	N/A	I	3.8	1	N/A	N/A	N/A	15E_4s1d2Zd_1	6/6B	TDP-172	9150018
23.2	1.000	0.00155	0.050	0.182	33.2	P	N/A	3.32	3.35	3.36	3.40	3.40	6.88	3.40	udv	UCSvis	N/A	UCSudv	N/A	I	0.0	3	N/A	N/A	N/A	15E_4s1d2Zd_1	6/6B	TDP-172	9150019
23.6	1.000	0.00155	0.050	0.182	31.4	P	N/A	3.49	3.53	3.54	3.60	3.40	8.50	N/A	N/A	N/A	N/A	N/A	N/A	I	0.0	4	N/A	N/A	N/A	15E_4s1d2Zd_1	6/6B	TDP-172	9150020
24.3	0.999	0.00155	0.050	0.183	29.6	P	N/A	3.70	3.74	3.75	3.80	3.40	9.75	N/A	N/A	N/A	N/A	N/A	N/A	I	0.0	4	N/A	N/A	N/A	15E_4s1d2Zd_1	6/6B	TDP-172	9150021
24.5	0.999	0.00155	0.050	0.184	28.0	P	N/A	3.88	3.92	3.94	4.00	3.40	13.00	N/A	N/A	N/A	N/A	N/A	N/A	I	0.0	4	N/A	N/A	N/A	15E_4s1d2Zd_1	6/6B	TDP-172	9150022
24.7	0.999	0.00155	0.050	0.185	26.6	P	N/A	4.08	4.12	4.15	4.20	3.40	14.25	N/A	N/A	N/A	N/A	N/A	N/A	I	0.0	4	N/A	N/A	N/A	15E_4s1d2Zd_1	6/6B	TDP-172	9150023
24.9	0.999	0.00155	0.050	0.186	25.4	P	N/A	4.25	4.30	4.33	4.40	3.40	17.00	N/A	N/A	N/A	N/A	N/A	N/A	I	0.0	4	N/A	N/A	N/A	15E_4s1d2Zd_1	6/6B	TDP-172	9150024
25.0	0.999	0.00155	0.050	0.187	24.2	P	N/A	4.46	4.52	4.54	4.60	3.40	18.00	N/A	N/A	N/A	N/A	N/A	N/A	I	0.0	4	N/A	N/A	N/A	15E_4s1d2Zd_1	6/6B	TDP-172	9150025
25.3	0.999	0.00155	0.050	0.188	23.2	P	N/A	4.60	4.66	4.69	4.80	3.40	25.25	N/A	N/A	N/A	N/A	N/A	N/A	I	0.0	4	N/A	N/A	N/A	15E_4s1d2Zd_1	6/6B	TDP-172	9150026
22.9	1.000	0.00500	0.050	0.333	17.6	P	N/A	3.40	3.43	3.44	3.50	4.30	4.25	N/A	N/A	N/A	N/A	N/A	N/A	I	9.5	1	N/A	N/A	N/A	15E_4s1d2Yc_1	6/9A	TDP-173	9150027
23.1	0.999	0.00500	0.050	0.336	15.4	P	N/A	3.88	3.92	3.94	4.00	4.30	5.25	N/A	N/A	N/A	N/A	N/A	N/A	I	3.7	1	N/A	N/A	N/A	15E_4s1d2Yc_1	6/9A	TDP-173	9150028
23.5	0.999	0.00500	0.050	0.329	15.0	P	N/A	4.06	4.10	4.12	4.20	4.30	5.25	N/A	N/A	UCSvis	N/A	N/A	N/A	I	3.7	3	N/A	N/A	N/A	15E_4s1d2Yc_1	6/9A	TDP-173	9150029
24.0	0.999	0.00500	0.050	0.329	14.6	P	N/A	4.15	4.20	4.23	4.30	4.30	5.25	4.30	udv	N/A	N/A	UCSudv	N/A	I	2.5	4	N/A	N/A	N/A	15E_4s1d2Yc_1	6/9A	TDP-173	9150030
24.4	0.999	0.00500	0.050	0.330	13.8	P	N/A	4.36	4.41	4.44	4.50	4.30	6.25	N/A	N/A	N/A	N/A	N/A	N/A	I	0.0	4	N/A	N/A	N/A	15E_4s1d2Yc_1	6/9A	TDP-173	9150031
24.7	0.999	0.00500	0.050	0.334	12.8	P	N/A	4.68	4.76	4.79	4.90	4.30	11.75	N/A	N/A	N/A	N/A	N/A	N/A	I	0.0	4	N/A	N/A	N/A	15E_4s1d2Yc_1	6/9A	TDP-173	9150032
25.1	0.999	0.00500	0.050	0.333	12.6	P	N/A	4.81	4.88	4.91	5.00	4.30	12.75	N/A	N/A	N/A	N/A	N/A	N/A	I	0.0	4	N/A	N/A	N/A	15E_4s1d2Yc_1	6/9A	TDP-173	9150033
25.3	0.999	0.00500	0.050	0.338	11.6	P	N/A	5.15	5.23	5.27	5.40	4.30	17.00	N/A	N/A	N/A	N/A	N/A	N/A	I	0.0	4	N/A	N/A	N/A	15E_4s1d2Yc_1	6/9A	TDP-173	9150034
25.7	0.999	0.00500	0.050	0.335	11.2	P	N/A	5.34	5.43	5.47	5.60	4.30	23.00	N/A	N/A	N/A	N/A	N/A	N/A	I	0.0	4	N/A	N/A	N/A	15E_4s1d2Yc_1	6/9A	TDP-173	9150035
26.9	0.999	0.00500	0.050	0.330	15.0	P	N/A	4.07	4.11	4.13	4.20	4.30	5.00	N/A	N/A	N/A	N/A	N/A	N/A	N/A	n/a	N/A	N/A	N/A	N/A	15E_4s1d2Yc_1	6/9A	TDP-173	9150035.1
26.9	0.999	0.00500	0.050	0.330	15.0	P	N/A	4.07	4.11	4.13	4.20	4.30	5.00	N/A	N/A	N/A	N/A	N/A	N/A	N/A	n/a	N/A	N/A	N/A	N/A	15E_4s1d2Yc_1	6/9A	TDP-173	9150035.2
26.9	0.999	0.00500	0.050	0.330	15.0	P	N/A	4.07	4.11	4.13	4.20	4.30	5.00	N/A	N/A	N/A	N/A	N/A	N/A	N/A	n/a	N/A	N/A	N/A	N/A	15E_4s1d2Yc_1	6/9A	TDP-173	9150035.3
26.9	0.999	0.00500	0.050	0.330	15.0	P	N/A	4.07	4.11	4.13	4.20	4.30	5.00	N/A	N/A	N/A	N/A	N/A	N/A	N/A	n/a	N/A	N/A	N/A	N/A	15E_4s1d2Yc_1	6/9A	TDP-173	9150035.4
26.9	0.999	0.00500	0.050	0.330	15.0	P	N/A	4.07	4.11	4.13	4.20	4.30	5.00	N/A	N/A	N/A	N/A	N/A	N/A	N/A	n/a	N/A	N/A	N/A	N/A	15E_4s1d2Yc_1	6/9A	TDP-173	9150035.5
26.9	0.999	0.00500	0.050	0.330	15.0	P	N/A	4.07	4.11	4.13	4.20	4.30	5.00	N/A	N/A	N/A	N/A	N/A	N/A	N/A	n/a	N/A	N/A	N/A	N/A	15E_4s1d2Yc_1	6/9A	TDP-173	9150035.6

Table B.3. Data from 2008 Tests in Small-Scale Vessel with Elliptical Head A.2

Row Number	Test	Case ID	Tank Diameter	Head Shape	Dish Height	Dish Volume	Tank Fill Height	Return Line Height	Nozzle Inner Diameter	Nozzle Stand-off Distance	Pulse Tube Configuration	Installed Nozzles	Outer Nozzles Operated	Inner Nozzles Operated	Pulse Tube Outer Diameter	Outer PJM Radius	Inner PJM Radius	"FIO" Outer PJM Impingement Angle	"FIO" Inner PJM Impingement Angle	Ratio Outer PJM to Tank Radius	Ratio Inner PJM to Tank Radius	Simulant	Solids Density	Particle Diameter d5	Particle Diameter d50	Particle Diameter d95	Void Fraction
text	text	text	in.	text	in.	in. ^{3}	in.	in.	in.	in.	text	number	number	number	in.	in.	in.	deg	deg	nondim	nondim	text	g/cm^3	m	m	m	fraction
MSS	M/DDX	ID	D	HS	H_{dish}	V_{dish}	H	Rtn	d	sod	PT	N	N_O	N_I	PT_{od}	R_O	R_I	θ_O	θ_I	R_O/R	R_I/R	sxdx	ρ_s	d_5	d_{50}	d_{95}	vf
9150035.7	6/9A	15E_4s1d2Yc_1	14 7/16	E	3.25	354.8	35	29	0.126	0.189	HLP-22	12	8	4	1.05	4.5	2.4	21.8	10.1	0.62	0.34	s1d2	2.48	0.0000569	0.0000693	0.0000821	0.3750
9150036	6/9A	15E_4s1d2Yc_1	14 7/16	E	3.25	354.8	35	29	0.126	0.189	HLP-22	12	8	4	1.05	4.5	2.4	21.8	10.1	0.62	0.34	s1d2	2.48	0.0000569	0.0000693	0.0000821	0.3750
9150037	6/9A	15E_4s1d2Yc_1	14 7/16	E	3.25	354.8	35	29	0.126	0.189	HLP-22	12	8	4	1.05	4.5	2.4	21.8	10.1	0.62	0.34	s1d2	2.48	0.0000569	0.0000693	0.0000821	0.3750
9150038	6/9A	15E_4s1d2Yc_1	14 7/16	E	3.25	354.8	35	29	0.126	0.189	HLP-22	12	8	4	1.05	4.5	2.4	21.8	10.1	0.62	0.34	s1d2	2.48	0.0000569	0.0000693	0.0000821	0.3750
9150039	6/9A	15E_4s1d2Yc_1	14 7/16	E	3.25	354.8	35	29	0.126	0.189	HLP-22	12	8	4	1.05	4.5	2.4	21.8	10.1	0.62	0.34	s1d2	2.48	0.0000569	0.0000693	0.0000821	0.3750
9150040	6/9A	15E_4s1d2Yc_1	14 7/16	E	3.25	354.8	35	29	0.126	0.189	HLP-22	12	8	4	1.05	4.5	2.4	21.8	10.1	0.62	0.34	s1d2	2.48	0.0000569	0.0000693	0.0000821	0.3750
9150041	6/9A	15E_4s1d2Yc_1	14 7/16	E	3.25	354.8	35	29	0.126	0.189	HLP-22	12	8	4	1.05	4.5	2.4	21.8	10.1	0.62	0.34	s1d2	2.48	0.0000569	0.0000693	0.0000821	0.3750
9150042	6/9A	15E_4s1d2Yc_1	14 7/16	E	3.25	354.8	35	29	0.126	0.189	HLP-22	12	8	4	1.05	4.5	2.4	21.8	10.1	0.62	0.34	s1d2	2.48	0.0000569	0.0000693	0.0000821	0.3750
9150043	6/9A	15E_4s1d2Yc_1	14 7/16	E	3.25	354.8	35	29	0.126	0.189	HLP-22	12	8	4	1.05	4.5	2.4	21.8	10.1	0.62	0.34	s1d2	2.48	0.0000569	0.0000693	0.0000821	0.3750
9150044	6/9B	15E_4s1d2Rc_1	14 7/16	E	3.25	354.8	35	29	0.126	0.189	HLP-22	12	8	4	1.05	4.5	2.4	21.8	10.1	0.62	0.34	s1d2	2.48	0.0000569	0.0000693	0.0000821	0.3750
9150045	6/9B	15E_4s1d2Rc_1	14 7/16	E	3.25	354.8	35	29	0.126	0.189	HLP-22	12	8	4	1.05	4.5	2.4	21.8	10.1	0.62	0.34	s1d2	2.48	0.0000569	0.0000693	0.0000821	0.3750
9150046	6/9B	15E_4s1d2Rc_1	14 7/16	E	3.25	354.8	35	29	0.126	0.189	HLP-22	12	8	4	1.05	4.5	2.4	21.8	10.1	0.62	0.34	s1d2	2.48	0.0000569	0.0000693	0.0000821	0.3750
9150047	6/9B	15E_4s1d2Rc_1	14 7/16	E	3.25	354.8	35	29	0.126	0.189	HLP-22	12	8	4	1.05	4.5	2.4	21.8	10.1	0.62	0.34	s1d2	2.48	0.0000569	0.0000693	0.0000821	0.3750
9150048M	6/9B	15E_4s1d2Rc_1	14 7/16	E	3.25	354.8	35	29	0.126	0.189	HLP-22	12	8	4	1.05	4.5	2.4	21.8	10.1	0.62	0.34	s1d2	2.48	0.0000569	0.0000693	0.0000821	0.3750
9150049M	6/9B	15E_4s1d2Rc_1	14 7/16	E	3.25	354.8	35	29	0.126	0.189	HLP-22	12	8	4	1.05	4.5	2.4	21.8	10.1	0.62	0.34	s1d2	2.48	0.0000569	0.0000693	0.0000821	0.3750
9150050M	6/9B	15E_4s1d2Rc_1	14 7/16	E	3.25	354.8	35	29	0.126	0.189	HLP-22	12	8	4	1.05	4.5	2.4	21.8	10.1	0.62	0.34	s1d2	2.48	0.0000569	0.0000693	0.0000821	0.3750
9150051	6/10A	15E_4s1d2Rc_1	14 7/16	E	3.25	354.8	35	30	0.126	0.189	HLP-22	12	8	4	1.05	4.5	2.4	21.8	10.1	0.62	0.34	s1d2	2.48	0.0000569	0.0000693	0.0000821	0.3750
9150052	6/10A	15E_4s1d2Rc_1	14 7/16	E	3.25	354.8	35	30	0.126	0.189	HLP-22	12	8	4	1.05	4.5	2.4	21.8	10.1	0.62	0.34	s1d2	2.48	0.0000569	0.0000693	0.0000821	0.3750
9150053M	6/10A	15E_4s1d2Rc_1	14 7/16	E	3.25	354.8	35	30	0.126	0.189	HLP-22	12	8	4	1.05	4.5	2.4	21.8	10.1	0.62	0.34	s1d2	2.48	0.0000569	0.0000693	0.0000821	0.3750
9150054M	6/10A	15E_4s1d2Rc_1	14 7/16	E	3.25	354.8	35	30	0.126	0.189	HLP-22	12	8	4	1.05	4.5	2.4	21.8	10.1	0.62	0.34	s1d2	2.48	0.0000569	0.0000693	0.0000821	0.3750
9150055M	6/10A	15E_4s1d2Rc_1	14 7/16	E	3.25	354.8	35	30	0.126	0.189	HLP-22	12	8	4	1.05	4.5	2.4	21.8	10.1	0.62	0.34	s1d2	2.48	0.0000569	0.0000693	0.0000821	0.3750
9150056M	6/10A	15E_4s1d2Rc_1	14 7/16	E	3.25	354.8	35	30	0.126	0.189	HLP-22	12	8	4	1.05	4.5	2.4	21.8	10.1	0.62	0.34	s1d2	2.48	0.0000569	0.0000693	0.0000821	0.3750
9150057M	6/10A	15E_4s1d2Rc_1	14 7/16	E	3.25	354.8	35	30	0.126	0.189	HLP-22	12	8	4	1.05	4.5	2.4	21.8	10.1	0.62	0.34	s1d2	2.48	0.0000569	0.0000693	0.0000821	0.3750
9150058M	6/10A	15E_4s1d2Rc_1	14 7/16	E	3.25	354.8	35	30	0.126	0.189	HLP-22	12	8	4	1.05	4.5	2.4	21.8	10.1	0.62	0.34	s1d2	2.48	0.0000569	0.0000693	0.0000821	0.3750
9150059M	6/10A	15E_4s1d2Rc_1	14 7/16	E	3.25	354.8	35	30	0.126	0.189	HLP-22	12	8	4	1.05	4.5	2.4	21.8	10.1	0.62	0.34	s1d2	2.48	0.0000569	0.0000693	0.0000821	0.3750
9150060	6/10B	15E_4s1d2Xc_1	14 7/16	E	3.25	354.8	35	30	0.126	0.189	HLP-22	12	8	4	1.05	4.5	2.4	21.8	10.1	0.62	0.34	s1d2	2.48	0.0000569	0.0000693	0.0000821	0.3750
9150061	6/10B	15E_4s1d2Xc_1	14 7/16	E	3.25	354.8	35	30	0.126	0.189	HLP-22	12	8	4	1.05	4.5	2.4	21.8	10.1	0.62	0.34	s1d2	2.48	0.0000569	0.0000693	0.0000821	0.3750
9150062	6/10B	15E_4s1d2Xc_1	14 7/16	E	3.25	354.8	35	30	0.126	0.189	HLP-22	12	8	4	1.05	4.5	2.4	21.8	10.1	0.62	0.34	s1d2	2.48	0.0000569	0.0000693	0.0000821	0.3750
9150063M	6/10B	15E_4s1d2Xc_1	14 7/16	E	3.25	354.8	35	30	0.126	0.189	HLP-22	12	8	4	1.05	4.5	2.4	21.8	10.1	0.62	0.34	s1d2	2.48	0.0000569	0.0000693	0.0000821	0.3750
9150064M	6/10B	15E_4s1d2Xc_1	14 7/16	E	3.25	354.8	35	30	0.126	0.189	HLP-22	12	8	4	1.05	4.5	2.4	21.8	10.1	0.62	0.34	s1d2	2.48	0.0000569	0.0000693	0.0000821	0.3750
9150065M	6/10B	15E_4s1d2Xc_1	14 7/16	E	3.25	354.8	35	30	0.126	0.189	HLP-22	12	8	4	1.05	4.5	2.4	21.8	10.1	0.62	0.34	s1d2	2.48	0.0000569	0.0000693	0.0000821	0.3750
9150066M	6/10B	15E_4s1d2Xc_1	14 7/16	E	3.25	354.8	35	30	0.126	0.189	HLP-22	12	8	4	1.05	4.5	2.4	21.8	10.1	0.62	0.34	s1d2	2.48	0.0000569	0.0000693	0.0000821	0.3750
9150067M	6/10B	15E_4s1d2Xc_1	14 7/16	E	3.25	354.8	35	30	0.126	0.189	HLP-22	12	8	4	1.05	4.5	2.4	21.8	10.1	0.62	0.34	s1d2	2.48	0.0000569	0.0000693	0.0000821	0.3750
9150067.1	6/10B	15E_4s1d2Xc_1	14 7/16	E	3.25	354.8	35	30	0.126	0.189	HLP-22	12	8	4	1.05	4.5	2.4	21.8	10.1	0.62	0.34	s1d2	2.48	0.0000569	0.0000693	0.0000821	0.3750
9150067.2	6/10B	15E_4s1d2Xc_1	14 7/16	E	3.25	354.8	35	30	0.126	0.189	HLP-22	12	8	4	1.05	4.5	2.4	21.8	10.1	0.62	0.34	s1d2	2.48	0.0000569	0.0000693	0.0000821	0.3750
9150067.3	6/10B	15E_4s1d2Xc_1	14 7/16	E	3.25	354.8	35	30	0.126	0.189	HLP-22	12	8	4	1.05	4.5	2.4	21.8	10.1	0.62	0.34	s1d2	2.48	0.0000569	0.0000693	0.0000821	0.3750
9150067.4	6/10B	15E_4s1d2Xc_1	14 7/16	E	3.25	354.8	35	30	0.126	0.189	HLP-22	12	8	4	1.05	4.5	2.4	21.8	10.1	0.62	0.34	s1d2	2.48	0.0000569	0.0000693	0.0000821	0.3750
9150067.5	6/10B	15E_4s1d2Xc_1	14 7/16	E	3.25	354.8	35	30	0.126	0.189	HLP-22	12	8	4	1.05	4.5	2.4	21.8	10.1	0.62	0.34	s1d2	2.48	0.0000569	0.0000693	0.0000821	0.3750
9150068M	6/10B	15E_4s1d2Xc_1	14 7/16	E	3.25	354.8	35	30	0.126	0.189	HLP-22	12	8	4	1.05	4.5	2.4	21.8	10.1	0.62	0.34	s1d2	2.48	0.0000569	0.0000693	0.0000821	0.3750
9150069	6/10B	15E_4s1d2Xc_1	14 7/16	E	3.25	354.8	35	30	0.126	0.189	HLP-22	12	8	4	1.05	4.5	2.4	21.8	10.1	0.62	0.34	s1d2	2.48	0.0000569	0.0000693	0.0000821	0.3750
9150070	6/10B	15E_4s1d2Xc_1	14 7/16	E	3.25	354.8	35	30	0.126	0.189	HLP-22	12	8	4	1.05	4.5	2.4	21.8	10.1	0.62	0.34	s1d2	2.48	0.0000569	0.0000693	0.0000821	0.3750

Table B.3. Data from 2008 Tests in Small-Scale Vessel with Elliptical Head B.2

Tank Water Temperature	Water Density	Solids Fraction	Pulse Volume Fraction	Duty Cycle	Cycle Time	Pulsed or Steady Jet	Us Steady Jet	U1 Pulsing Jet	U2 URMS	U3 URM3	Discharge Velocity	Critical Suspension Velocity	Average Peak Cloud Height	UCS Condition	UCS Method	UCS Flag	UCS Center Flag	UCS udv Flag	UCS based on Decreasing Velocity	Sweep Increase / Decrease	UDV Height Bed	Particle Motion	Solids Level	Outer Bottom Pattern	Inner Bottom Pattern	Case ID	Test	TDP	Row Number
C	g/cm^3	fraction	fraction	fraction	s	text	m/s	m/s	m/s	m/s	m/s	m/s	in.	m/s	text	text	text	text	m/s	text	mm	text	text	text	text	text	text	text	text
T	ρ_c	ϕ_S	ϕ_P	DC	t_C	Jet	U_S	U1	U2	U3	U	U_{CS}	H_C	U_{CSR}	U_{CSM}	U_{CS}vis	U_{CS}cen	U_{CS}udv	U_{CS}_D	S_W	H_{bed}	PM	Sol	SP_O	SP_I	ID	M/DDX	TDP	MSS
26.9	0.999	0.00500	0.050	0.330	15.0	P	N/A	4.07	4.11	4.13	4.20	4.30	5.00	N/A	N/A	N/A	N/A	N/A	N/A	N/A	n/a	N/A	N/A	N/A	N/A	15E_4s1d2Yc_1	6/9A	TDP-173	9150035.7
26.9	0.999	0.00500	0.050	0.330	15.0	P	N/A	4.07	4.11	4.13	4.20	4.30	5.00	N/A	N/A	UCSvis	N/A	N/A	N/A	(null)	3.9	3	N/A	N/A	N/A	15E_4s1d2Yc_1	6/9A	TDP-173	9150036
26.9	0.999	0.00500	0.050	0.330	15.0	P	N/A	4.07	4.11	4.13	4.20	4.30	5.00	N/A	N/A	N/A	N/A	N/A	N/A	N/A	3.9	N/A	N/A	N/A	N/A	15E_4s1d2Yc_1	6/9A	TDP-173	9150037
26.9	0.999	0.00500	0.050	0.330	15.0	P	N/A	4.07	4.11	4.13	4.20	4.30	5.00	N/A	N/A	N/A	N/A	N/A	N/A	N/A	3.8	N/A	N/A	N/A	N/A	15E_4s1d2Yc_1	6/9A	TDP-173	9150038
26.9	0.999	0.00500	0.050	0.330	15.0	P	N/A	4.07	4.11	4.13	4.20	4.30	5.00	N/A	N/A	N/A	N/A	N/A	N/A	N/A	4.4	N/A	N/A	N/A	N/A	15E_4s1d2Yc_1	6/9A	TDP-173	9150039
26.9	0.999	0.00500	0.050	0.330	15.0	P	N/A	4.07	4.11	4.13	4.20	4.30	5.00	N/A	N/A	N/A	N/A	N/A	N/A	N/A	3.8	N/A	N/A	N/A	N/A	15E_4s1d2Yc_1	6/9A	TDP-173	9150040
26.9	0.999	0.00500	0.050	0.330	15.0	P	N/A	4.07	4.11	4.13	4.20	4.30	5.00	N/A	N/A	N/A	N/A	N/A	N/A	N/A	7.0	N/A	N/A	N/A	N/A	15E_4s1d2Yc_1	6/9A	TDP-173	9150041
26.9	0.999	0.00500	0.050	0.330	15.0	P	N/A	4.07	4.11	4.13	4.20	4.30	5.00	N/A	N/A	N/A	N/A	N/A	N/A	N/A	4.0	N/A	N/A	N/A	N/A	15E_4s1d2Yc_1	6/9A	TDP-173	9150042
26.9	0.999	0.00500	0.050	0.330	15.0	P	N/A	4.07	4.11	4.13	4.20	4.30	5.00	N/A	N/A	N/A	N/A	N/A	N/A	N/A	4.1	N/A	N/A	N/A	N/A	15E_4s1d2Yc_1	6/9A	TDP-173	9150043
27.2	0.998	0.01000	0.050	0.331	14.0	P	N/A	4.34	4.40	4.42	4.50	5.30	4.75	N/A	N/A	N/A	N/A	N/A	N/A	I	8.4	1	N/A	N/A	N/A	15E_4s1d2Rc_1	6/9B	TDP-174	9150044
27.5	0.998	0.01000	0.050	0.332	13.4	P	N/A	4.53	4.59	4.61	4.70	5.30	5.00	N/A	N/A	N/A	N/A	N/A	N/A	I	7.6	1	N/A	N/A	N/A	15E_4s1d2Rc_1	6/9B	TDP-174	9150045
27.6	0.998	0.01000	0.050	0.333	12.8	P	N/A	4.71	4.77	4.80	4.90	5.30	5.25	N/A	N/A	N/A	N/A	N/A	N/A	I	6.8	1	N/A	N/A	N/A	15E_4s1d2Rc_1	6/9B	TDP-174	9150046
28.0	0.998	0.01000	0.050	0.335	12.2	P	N/A	4.88	4.95	4.98	5.10	5.30	5.50	N/A	N/A	N/A	N/A	N/A	N/A	I	4.8	1	N/A	N/A	N/A	15E_4s1d2Rc_1	6/9B	TDP-174	9150047
28.3	0.998	0.01000	0.050	0.338	11.6	P	N/A	5.07	5.15	5.18	5.30	5.30	5.75	5.30	udv	N/A	N/A	UCSudv	N/A	I	3.7	1	N/A	N/A	N/A	15E_4s1d2Rc_1	6/9B	TDP-174	9150048
28.6	0.998	0.01000	0.050	0.330	11.6	P	N/A	5.24	5.33	5.37	5.50	5.30	6.00	N/A	N/A	UCSvis	N/A	N/A	N/A	I	0.6	3	N/A	N/A	N/A	15E_4s1d2Rc_1	6/9B	TDP-174	9150049
29.4	0.998	0.01000	0.050	0.330	11.2	P	N/A	5.39	5.47	5.51	5.60	5.30	6.25	N/A	N/A	N/A	N/A	N/A	N/A	I	0.0	4	N/A	N/A	N/A	15E_4s1d2Rc_1	6/9B	TDP-174	9150050
22.7	0.999	0.01000	0.050	0.329	12.4	P	N/A	4.89	4.96	4.99	5.10	5.40	5.25	N/A	N/A	N/A	N/A	N/A	N/A	D	3.7	1	N/A	N/A	N/A	15E_4s1d2Rc_1	6/10A	TDP-175	9150051
22.9	0.999	0.01000	0.050	0.330	12.0	P	N/A	5.07	5.15	5.18	5.30	5.40	6.00	N/A	N/A	N/A	N/A	N/A	N/A	I	3.7	1	N/A	N/A	N/A	15E_4s1d2Rc_1	6/10A	TDP-175	9150052
23.1	0.999	0.01000	0.050	0.331	11.8	P	N/A	5.16	5.24	5.28	5.40	5.40	6.50	5.40	udv	UCSvis	N/A	UCSudv	N/A	I	2.9	3	N/A	N/A	N/A	15E_4s1d2Rc_1	6/10A	TDP-175	9150053
23.3	0.999	0.01000	0.050	0.331	11.6	P	N/A	5.25	5.33	5.37	5.50	5.40	7.00	N/A	N/A	N/A	N/A	N/A	N/A	I	0.0	4	N/A	N/A	N/A	15E_4s1d2Rc_1	6/10A	TDP-175	9150054
23.4	0.999	0.01000	0.050	0.333	11.0	P	N/A	5.43	5.52	5.56	5.70	5.40	9.00	N/A	N/A	N/A	N/A	N/A	N/A	I	0.0	4	N/A	N/A	N/A	15E_4s1d2Rc_1	6/10A	TDP-175	9150055
23.6	0.999	0.01000	0.050	0.335	10.4	P	N/A	5.70	5.80	5.84	6.00	5.40	12.50	N/A	N/A	N/A	N/A	N/A	N/A	I	0.0	4	N/A	N/A	N/A	15E_4s1d2Rc_1	6/10A	TDP-175	9150056
24.0	0.999	0.01000	0.050	0.337	10.0	P	N/A	5.90	6.00	6.05	6.20	5.40	16.50	N/A	N/A	N/A	N/A	N/A	N/A	I	0.0	4	N/A	N/A	N/A	15E_4s1d2Rc_1	6/10A	TDP-175	9150057
24.2	0.999	0.01000	0.050	0.336	9.8	P	N/A	6.08	6.19	6.24	6.40	5.40	17.50	N/A	N/A	N/A	N/A	N/A	N/A	I	0.0	4	N/A	N/A	N/A	15E_4s1d2Rc_1	6/10A	TDP-175	9150058
24.5	0.999	0.01000	0.050	0.334	9.6	P	N/A	6.25	6.37	6.43	6.60	5.40	23.50	N/A	N/A	N/A	N/A	N/A	N/A	I	0.0	4	N/A	N/A	N/A	15E_4s1d2Rc_1	6/10A	TDP-175	9150059
22.8	0.999	0.01500	0.050	0.328	12.2	P	N/A	4.96	5.04	5.08	5.20	5.80	5.13	N/A	N/A	N/A	N/A	N/A	N/A	(null)	7.6	1	N/A	N/A	N/A	15E_4s1d2Xc_1	6/10B	TDP-176	9150060
22.9	1.000	0.01500	0.050	0.329	11.8	P	N/A	5.14	5.23	5.27	5.40	5.80	5.50	N/A	N/A	N/A	N/A	N/A	N/A	I	4.2	1	N/A	N/A	N/A	15E_4s1d2Xc_1	6/10B	TDP-176	9150061
22.9	1.000	0.01500	0.050	0.330	11.4	P	N/A	5.35	5.44	5.48	5.60	5.80	5.75	N/A	N/A	N/A	N/A	N/A	N/A	I	3.8	1	N/A	N/A	N/A	15E_4s1d2Xc_1	6/10B	TDP-176	9150062
23.0	1.000	0.01500	0.050	0.331	11.0	P	N/A	5.52	5.61	5.66	5.80	5.80	6.75	5.80	udv	UCSvis	N/A	UCSudv	N/A	I	1.5	3	N/A	N/A	N/A	15E_4s1d2Xc_1	6/10B	TDP-176	9150063
23.1	1.000	0.01500	0.050	0.332	10.6	P	N/A	5.70	5.80	5.84	6.00	5.80	8.25	N/A	N/A	N/A	N/A	N/A	N/A	I	0.0	4	N/A	N/A	N/A	15E_4s1d2Xc_1	6/10B	TDP-176	9150064
23.1	0.999	0.01500	0.050	0.335	9.8	P	N/A	6.07	6.17	6.23	6.40	5.80	10.75	N/A	N/A	N/A	N/A	N/A	N/A	I	0.0	4	N/A	N/A	N/A	15E_4s1d2Xc_1	6/10B	TDP-176	9150065
23.3	0.999	0.01500	0.050	0.338	9.2	P	N/A	6.42	6.54	6.60	6.80	5.80	16.75	N/A	N/A	N/A	N/A	N/A	N/A	I	0.0	4	N/A	N/A	N/A	15E_4s1d2Xc_1	6/10B	TDP-176	9150066
23.4	0.999	0.01500	0.050	0.335	9.0	P	N/A	6.60	6.73	6.80	7.00	5.80	19.75	N/A	N/A	N/A	N/A	N/A	N/A	I	0.0	4	N/A	N/A	N/A	15E_4s1d2Xc_1	6/10B	TDP-176	9150067
23.7	0.999	0.01500	0.050	0.330	11.0	P	N/A	5.53	5.62	5.67	5.80	5.80	6.63	N/A	N/A	N/A	N/A	N/A	N/A	N/A	n/a	N/A	N/A	N/A	N/A	15E_4s1d2Xc_1	6/10B	TDP-176	9150067.1
23.7	0.999	0.01500	0.050	0.330	11.0	P	N/A	5.53	5.62	5.67	5.80	5.80	6.63	N/A	N/A	N/A	N/A	N/A	N/A	N/A	n/a	N/A	N/A	N/A	N/A	15E_4s1d2Xc_1	6/10B	TDP-176	9150067.2
23.7	0.999	0.01500	0.050	0.330	11.0	P	N/A	5.53	5.62	5.67	5.80	5.80	6.63	N/A	N/A	N/A	N/A	N/A	N/A	N/A	n/a	N/A	N/A	N/A	N/A	15E_4s1d2Xc_1	6/10B	TDP-176	9150067.3
23.7	0.999	0.01500	0.050	0.330	11.0	P	N/A	5.53	5.62	5.67	5.80	5.80	6.63	N/A	N/A	N/A	N/A	N/A	N/A	N/A	n/a	N/A	N/A	N/A	N/A	15E_4s1d2Xc_1	6/10B	TDP-176	9150067.4
23.7	0.999	0.01500	0.050	0.330	11.0	P	N/A	5.53	5.62	5.67	5.80	5.80	6.63	N/A	N/A	N/A	N/A	N/A	N/A	N/A	n/a	N/A	N/A	N/A	N/A	15E_4s1d2Xc_1	6/10B	TDP-176	9150067.5
23.7	0.999	0.01500	0.050	0.330	11.0	P	N/A	5.53	5.62	5.67	5.80	5.80	6.63	N/A	N/A	UCSvis	N/A	N/A	N/A	I	3.7	3	N/A	N/A	N/A	15E_4s1d2Xc_1	6/10B	TDP-176	9150068
23.7	0.999	0.01500	0.050	0.330	11.0	P	N/A	5.53	5.62	5.67	5.80	5.80	6.63	N/A	N/A	N/A	N/A	N/A	N/A	N/A	2.2	N/A	N/A	N/A	N/A	15E_4s1d2Xc_1	6/10B	TDP-176	9150069
23.7	0.999	0.01500	0.050	0.330	11.0	P	N/A	5.53	5.62	5.67	5.80	5.80	6.63	N/A	N/A	N/A	N/A	N/A	N/A	N/A	2.9	N/A	N/A	N/A	N/A	15E_4s1d2Xc_1	6/10B	TDP-176	9150070

Table B.3. Data from 2008 Tests in Small-Scale Vessel with Elliptical Head A.3

Row Number	Test	Case ID	Tank Diameter	Head Shape	Dish Height	Dish Volume	Tank Fill Height	Return Line Height	Nozzle Inner Diameter	Nozzle Stand-off Distance	Pulse Tube Configuration	Installed Nozzles	Outer Nozzles Operated	Inner Nozzles Operated	Pulse Tube Outer Diameter	Outer PJM Radius	Inner PJM Radius	"FIO" Outer PJM Impingement Angle	"FIO" Inner PJM Impingement Angle	Ratio Outer PJM to Tank Radius	Ratio Inner PJM to Tank Radius	Simulant	Solids Density	Particle Diameter d5	Particle Diameter d50	Particle Diameter d95	Void Fraction
text	text	text	in.	text	in.	in. ^{3}	in.	in.	in.	in.	text	number	number	number	in.	in.	in.	deg	deg	nondim	nondim	text	g/cm^3	m	m	m	fraction
MSS	M/DDX	ID	D	HS	H_{dish}	V_{dish}	H	Rtn	d	sod	PT	N	N_O	N_I	PT_{od}	R_O	R_I	θ_O	θ_I	R_O/R	R_I/R	sxdx	ρ_s	d_5	d_{50}	d_{95}	vf
9150071	6/10B	15E_4s1d2Xc_1	14 7/16	E	3.25	354.8	35	30	0.126	0.189	HLP-22	12	8	4	1.05	4.5	2.4	21.8	10.1	0.62	0.34	s1d2	2.48	0.0000569	0.0000693	0.0000821	0.3750
9150072	6/10B	15E_4s1d2Xc_1	14 7/16	E	3.25	354.8	35	30	0.126	0.189	HLP-22	12	8	4	1.05	4.5	2.4	21.8	10.1	0.62	0.34	s1d2	2.48	0.0000569	0.0000693	0.0000821	0.3750
9150073	6/10B	15E_4s1d2Xc_1	14 7/16	E	3.25	354.8	35	30	0.126	0.189	HLP-22	12	8	4	1.05	4.5	2.4	21.8	10.1	0.62	0.34	s1d2	2.48	0.0000569	0.0000693	0.0000821	0.3750
9150074	6/10B	15E_4s1d2Xc_1	14 7/16	E	3.25	354.8	35	30	0.126	0.189	HLP-22	12	8	4	1.05	4.5	2.4	21.8	10.1	0.62	0.34	s1d2	2.48	0.0000569	0.0000693	0.0000821	0.3750
9150075	6/10B	15E_4s1d2Xc_1	14 7/16	E	3.25	354.8	35	30	0.126	0.189	HLP-22	12	8	4	1.05	4.5	2.4	21.8	10.1	0.62	0.34	s1d2	2.48	0.0000569	0.0000693	0.0000821	0.3750
9150076	6/10B	15E_4s1d2Xc_1	14 7/16	E	3.25	354.8	35	30	0.126	0.189	HLP-22	12	8	4	1.05	4.5	2.4	21.8	10.1	0.62	0.34	s1d2	2.48	0.0000569	0.0000693	0.0000821	0.3750
9150077	6/10B	15E_4s1d2Xc_1	14 7/16	E	3.25	354.8	35	30	0.126	0.189	HLP-22	12	8	4	1.05	4.5	2.4	21.8	10.1	0.62	0.34	s1d2	2.48	0.0000569	0.0000693	0.0000821	0.3750
9150078	6/11A	15E_4s1d2Xd_1	14 7/16	E	3.25	354.8	34 1/2	30	0.126	0.189	HLP-22	12	8	4	1.05	4.5	2.4	21.8	10.1	0.62	0.34	s1d2	2.48	0.0000569	0.0000693	0.0000821	0.3750
9150079	6/11A	15E_4s1d2Xd_1	14 7/16	E	3.25	354.8	34 1/2	30	0.126	0.189	HLP-22	12	8	4	1.05	4.5	2.4	21.8	10.1	0.62	0.34	s1d2	2.48	0.0000569	0.0000693	0.0000821	0.3750
9150080	6/11A	15E_4s1d2Xd_1	14 7/16	E	3.25	354.8	34 1/2	30	0.126	0.189	HLP-22	12	8	4	1.05	4.5	2.4	21.8	10.1	0.62	0.34	s1d2	2.48	0.0000569	0.0000693	0.0000821	0.3750
9150081	6/11A	15E_4s1d2Xd_1	14 7/16	E	3.25	354.8	34 1/2	30	0.126	0.189	HLP-22	12	8	4	1.05	4.5	2.4	21.8	10.1	0.62	0.34	s1d2	2.48	0.0000569	0.0000693	0.0000821	0.3750
9150082	6/11A	15E_4s1d2Xd_1	14 7/16	E	3.25	354.8	34 1/2	30	0.126	0.189	HLP-22	12	8	4	1.05	4.5	2.4	21.8	10.1	0.62	0.34	s1d2	2.48	0.0000569	0.0000693	0.0000821	0.3750
9150083M	6/11A	15E_4s1d2Xd_1	14 7/16	E	3.25	354.8	34 1/2	30	0.126	0.189	HLP-22	12	8	4	1.05	4.5	2.4	21.8	10.1	0.62	0.34	s1d2	2.48	0.0000569	0.0000693	0.0000821	0.3750
9150084M	6/11A	15E_4s1d2Xd_1	14 7/16	E	3.25	354.8	34 1/2	30	0.126	0.189	HLP-22	12	8	4	1.05	4.5	2.4	21.8	10.1	0.62	0.34	s1d2	2.48	0.0000569	0.0000693	0.0000821	0.3750
9150085M	6/11A	15E_4s1d2Xd_1	14 7/16	E	3.25	354.8	34 1/2	30	0.126	0.189	HLP-22	12	8	4	1.05	4.5	2.4	21.8	10.1	0.62	0.34	s1d2	2.48	0.0000569	0.0000693	0.0000821	0.3750
9150086M	6/11A	15E_4s1d2Xd_1	14 7/16	E	3.25	354.8	34 1/2	30	0.126	0.189	HLP-22	12	8	4	1.05	4.5	2.4	21.8	10.1	0.62	0.34	s1d2	2.48	0.0000569	0.0000693	0.0000821	0.3750
9150087M	6/11A	15E_4s1d2Xd_1	14 7/16	E	3.25	354.8	34 1/2	30	0.126	0.189	HLP-22	12	8	4	1.05	4.5	2.4	21.8	10.1	0.62	0.34	s1d2	2.48	0.0000569	0.0000693	0.0000821	0.3750
9150087.1	6/11A	15E_4s1d2Xd_1	14 7/16	E	3.25	354.8	34 1/2	30	0.126	0.189	HLP-22	12	8	4	1.05	4.5	2.4	21.8	10.1	0.62	0.34	s1d2	2.48	0.0000569	0.0000693	0.0000821	0.3750
9150087.2	6/11A	15E_4s1d2Xd_1	14 7/16	E	3.25	354.8	34 1/2	30	0.126	0.189	HLP-22	12	8	4	1.05	4.5	2.4	21.8	10.1	0.62	0.34	s1d2	2.48	0.0000569	0.0000693	0.0000821	0.3750
9150087.3	6/11A	15E_4s1d2Xd_1	14 7/16	E	3.25	354.8	34 1/2	30	0.126	0.189	HLP-22	12	8	4	1.05	4.5	2.4	21.8	10.1	0.62	0.34	s1d2	2.48	0.0000569	0.0000693	0.0000821	0.3750
9150087.4	6/11A	15E_4s1d2Xd_1	14 7/16	E	3.25	354.8	34 1/2	30	0.126	0.189	HLP-22	12	8	4	1.05	4.5	2.4	21.8	10.1	0.62	0.34	s1d2	2.48	0.0000569	0.0000693	0.0000821	0.3750
9150087.5	6/11A	15E_4s1d2Xd_1	14 7/16	E	3.25	354.8	34 1/2	30	0.126	0.189	HLP-22	12	8	4	1.05	4.5	2.4	21.8	10.1	0.62	0.34	s1d2	2.48	0.0000569	0.0000693	0.0000821	0.3750
9150088M	6/11A	15E_4s1d2Xd_1	14 7/16	E	3.25	354.8	34 1/2	30	0.126	0.189	HLP-22	12	8	4	1.05	4.5	2.4	21.8	10.1	0.62	0.34	s1d2	2.48	0.0000569	0.0000693	0.0000821	0.3750
9150089	6/11A	15E_4s1d2Xd_1	14 7/16	E	3.25	354.8	34 1/2	30	0.126	0.189	HLP-22	12	8	4	1.05	4.5	2.4	21.8	10.1	0.62	0.34	s1d2	2.48	0.0000569	0.0000693	0.0000821	0.3750
9150090	6/11A	15E_4s1d2Xd_1	14 7/16	E	3.25	354.8	34 1/2	30	0.126	0.189	HLP-22	12	8	4	1.05	4.5	2.4	21.8	10.1	0.62	0.34	s1d2	2.48	0.0000569	0.0000693	0.0000821	0.3750
9150091	6/11A	15E_4s1d2Xd_1	14 7/16	E	3.25	354.8	34 1/2	30	0.126	0.189	HLP-22	12	8	4	1.05	4.5	2.4	21.8	10.1	0.62	0.34	s1d2	2.48	0.0000569	0.0000693	0.0000821	0.3750
9150092	6/11A	15E_4s1d2Xd_1	14 7/16	E	3.25	354.8	34 1/2	30	0.126	0.189	HLP-22	12	8	4	1.05	4.5	2.4	21.8	10.1	0.62	0.34	s1d2	2.48	0.0000569	0.0000693	0.0000821	0.3750
9150093	6/11A	15E_4s1d2Xd_1	14 7/16	E	3.25	354.8	34 1/2	30	0.126	0.189	HLP-22	12	8	4	1.05	4.5	2.4	21.8	10.1	0.62	0.34	s1d2	2.48	0.0000569	0.0000693	0.0000821	0.3750
9150094	6/11A	15E_4s1d2Xd_1	14 7/16	E	3.25	354.8	34 1/2	30	0.126	0.189	HLP-22	12	8	4	1.05	4.5	2.4	21.8	10.1	0.62	0.34	s1d2	2.48	0.0000569	0.0000693	0.0000821	0.3750
9150095	6/11A	15E_4s1d2Xd_1	14 7/16	E	3.25	354.8	34 1/2	30	0.126	0.189	HLP-22	12	8	4	1.05	4.5	2.4	21.8	10.1	0.62	0.34	s1d2	2.48	0.0000569	0.0000693	0.0000821	0.3750
9150096	6/11A	15E_4s1d2Xd_1	14 7/16	E	3.25	354.8	34 1/2	30	0.126	0.189	HLP-22	12	8	4	1.05	4.5	2.4	21.8	10.1	0.62	0.34	s1d2	2.48	0.0000569	0.0000693	0.0000821	0.3750
9150097	6/11B	15E_4s1d2Xa	14 7/16	E	3.25	354.8	34 1/2	30	0.126	0.189	HLP-22	12	8	4	1.05	4.5	2.4	21.8	10.1	0.62	0.34	s1d2	2.48	0.0000569	0.0000693	0.0000821	0.3750
9150098	6/11B	15E_4s1d2Xa	14 7/16	E	3.25	354.8	34 1/2	30	0.126	0.189	HLP-22	12	8	4	1.05	4.5	2.4	21.8	10.1	0.62	0.34	s1d2	2.48	0.0000569	0.0000693	0.0000821	0.3750
9150099	6/11B	15E_4s1d2Xa	14 7/16	E	3.25	354.8	34 1/2	30	0.126	0.189	HLP-22	12	8	4	1.05	4.5	2.4	21.8	10.1	0.62	0.34	s1d2	2.48	0.0000569	0.0000693	0.0000821	0.3750
9150100	6/11B	15E_4s1d2Xa	14 7/16	E	3.25	354.8	34 1/2	30	0.126	0.189	HLP-22	12	8	4	1.05	4.5	2.4	21.8	10.1	0.62	0.34	s1d2	2.48	0.0000569	0.0000693	0.0000821	0.3750
9150101	6/11B	15E_4s1d2Xa	14 7/16	E	3.25	354.8	34 1/2	30	0.126	0.189	HLP-22	12	8	4	1.05	4.5	2.4	21.8	10.1	0.62	0.34	s1d2	2.48	0.0000569	0.0000693	0.0000821	0.3750
9150102	6/11B	15E_4s1d2Xa	14 7/16	E	3.25	354.8	34 1/2	30	0.126	0.189	HLP-22	12	8	4	1.05	4.5	2.4	21.8	10.1	0.62	0.34	s1d2	2.48	0.0000569	0.0000693	0.0000821	0.3750
9150103	6/11B	15E_4s1d2Xa	14 7/16	E	3.25	354.8	34 1/2	30	0.126	0.189	HLP-22	12	8	4	1.05	4.5	2.4	21.8	10.1	0.62	0.34	s1d2	2.48	0.0000569	0.0000693	0.0000821	0.3750
9150104	6/11B	15E_4s1d2Xa	14 7/16	E	3.25	354.8	34 1/2	30	0.126	0.189	HLP-22	12	8	4	1.05	4.5	2.4	21.8	10.1	0.62	0.34	s1d2	2.48	0.0000569	0.0000693	0.0000821	0.3750
9150105	6/11C	15E_4s1d2Xc_1	14 7/16	E	3.25	354.8	34 1/2	30	0.126	0.189	HLP-22	12	8	4	1.05	4.5	2.4	21.8	10.1	0.62	0.34	s1d2	2.48	0.0000569	0.0000693	0.0000821	0.3750
9150106	6/11C	15E_4s1d2Xc_1	14 7/16	E	3.25	354.8	34 1/2	30	0.126	0.189	HLP-22	12	8	4	1.05	4.5	2.4	21.8	10.1	0.62	0.34	s1d2	2.48	0.0000569	0.0000693	0.0000821	0.3750

Table B.3. Data from 2008 Tests in Small-Scale Vessel with Elliptical Head B.3

Tank Water Temperature	Water Density	Solids Fraction	Pulse Volume Fraction	Duty Cycle	Cycle Time	Pulsed or Steady Jet	Us Steady Jet	U1 Pulsing Jet	U2 URMS	U3 URM3	Discharge Velocity	Critical Suspension Velocity	Average Peak Cloud Height	UCS Condition	UCS Method	UCS Flag	UCS Center Flag	UCS udv Flag	UCS based on Decreasing Velocity	Sweep Increase / Decrease	UDV Height Bed	Particle Motion	Solids Level	Outer Bottom Pattern	Inner Bottom Pattern	Case ID	Test	TDP	Row Number
C	g/cm³	fraction	fraction	fraction	s	text	m/s	m/s	m/s	m/s	m/s	m/s	in.	m/s	text	text	text	text	m/s	text	mm	text	text	text	text	text	text	text	text
T	ρ_l	ϕ_S	ϕ_P	DC	t_C	Jet	U_S	U1	U2	U3	U	U_{CS}	H_C	U_{CSR}	U_{CSM}	U_{CS}vis	U_{CS}cen	U_{CS}udv	U_{CS}_D	S_W	H_{bed}	PM	Sol	SP_O	SP_I	ID	M/DDX	TDP	MSS
23.7	0.999	0.01500	0.050	0.330	11.0	P	N/A	5.53	5.62	5.67	5.80	5.80	6.63	N/A	N/A	N/A	N/A	N/A	N/A	N/A	3.7	N/A	N/A	N/A	N/A	15E_4s1d2Xc_1	6/10B	TDP-176	9150071
23.7	0.999	0.01500	0.050	0.330	11.0	P	N/A	5.53	5.62	5.67	5.80	5.80	6.63	N/A	N/A	N/A	N/A	N/A	N/A	N/A	1.5	N/A	N/A	N/A	N/A	15E_4s1d2Xc_1	6/10B	TDP-176	9150072
23.7	0.999	0.01500	0.050	0.330	11.0	P	N/A	5.53	5.62	5.67	5.80	5.80	6.63	N/A	N/A	N/A	N/A	N/A	N/A	N/A	1.5	N/A	N/A	N/A	N/A	15E_4s1d2Xc_1	6/10B	TDP-176	9150073
23.7	0.999	0.01500	0.050	0.330	11.0	P	N/A	5.53	5.62	5.67	5.80	5.80	6.63	N/A	N/A	N/A	N/A	N/A	N/A	N/A	3.7	N/A	N/A	N/A	N/A	15E_4s1d2Xc_1	6/10B	TDP-176	9150074
23.7	0.999	0.01500	0.050	0.330	11.0	P	N/A	5.53	5.62	5.67	5.80	5.80	6.63	N/A	N/A	N/A	N/A	N/A	N/A	N/A	2.9	N/A	N/A	N/A	N/A	15E_4s1d2Xc_1	6/10B	TDP-176	9150075
23.7	0.999	0.01500	0.050	0.330	11.0	P	N/A	5.53	5.62	5.67	5.80	5.80	6.63	N/A	N/A	N/A	N/A	N/A	N/A	N/A	4.0	N/A	N/A	N/A	N/A	15E_4s1d2Xc_1	6/10B	TDP-176	9150076
23.7	0.999	0.01500	0.050	0.330	11.0	P	N/A	5.53	5.62	5.67	5.80	5.80	6.63	N/A	N/A	N/A	N/A	N/A	N/A	N/A	2.2	N/A	N/A	N/A	N/A	15E_4s1d2Xc_1	6/10B	TDP-176	9150077
20.4	1.000	0.01500	0.050	0.180	18.8	P	N/A	5.88	5.99	6.04	6.20	7.20	4.75	N/A	N/A	N/A	N/A	N/A	N/A	(null)	7.6	1	N/A	N/A	N/A	15E_4s1d2Xd_1	6/11A	TDP-177	9150078
20.5	1.000	0.01500	0.050	0.181	18.2	P	N/A	6.06	6.18	6.23	6.40	7.20	5.00	N/A	N/A	N/A	N/A	N/A	N/A	I	5.8	1	N/A	N/A	N/A	15E_4s1d2Xd_1	6/11A	TDP-177	9150079
20.7	1.000	0.01500	0.050	0.182	17.6	P	N/A	6.24	6.36	6.42	6.60	7.20	5.25	N/A	N/A	N/A	N/A	N/A	N/A	I	4.3	1	N/A	N/A	N/A	15E_4s1d2Xd_1	6/11A	TDP-177	9150080
20.9	1.000	0.01500	0.050	0.182	17.0	P	N/A	6.41	6.54	6.60	6.80	7.20	5.25	N/A	N/A	N/A	N/A	N/A	N/A	I	3.7	1	N/A	N/A	N/A	15E_4s1d2Xd_1	6/11A	TDP-177	9150081
21.1	1.000	0.01500	0.050	0.183	16.6	P	N/A	6.60	6.73	6.80	7.00	7.20	5.75	N/A	N/A	N/A	N/A	N/A	N/A	I	3.7	1	N/A	N/A	N/A	15E_4s1d2Xd_1	6/11A	TDP-177	9150082
21.3	1.000	0.01500	0.050	0.184	16.0	P	N/A	6.77	6.91	6.98	7.20	7.20	5.75	7.20	udv	UCSvis	N/A	UCSudv	N/A	I	3.7	3	N/A	N/A	N/A	15E_4s1d2Xd_1	6/11A	TDP-177	9150083
21.6	1.000	0.01500	0.050	0.185	15.6	P	N/A	6.94	7.09	7.16	7.40	7.20	6.25	N/A	N/A	N/A	N/A	N/A	N/A	I	0.0	4	N/A	N/A	N/A	15E_4s1d2Xd_1	6/11A	TDP-177	9150084
21.9	1.000	0.01500	0.050	0.182	14.6	P	N/A	7.49	7.65	7.73	8.00	7.20	8.00	N/A	N/A	N/A	N/A	N/A	N/A	I	0.0	4	N/A	N/A	N/A	15E_4s1d2Xd_1	6/11A	TDP-177	9150085
22.2	0.999	0.01500	0.050	0.184	13.6	P	N/A	8.00	8.19	8.28	8.60	7.20	12.50	N/A	N/A	N/A	N/A	N/A	N/A	I	0.0	4	N/A	N/A	N/A	15E_4s1d2Xd_1	6/11A	TDP-177	9150086
22.4	1.000	0.01500	0.050	0.185	13.0	P	N/A	8.36	8.57	8.68	9.00	7.20	16.50	N/A	N/A	N/A	N/A	N/A	N/A	I	0.0	4	N/A	N/A	N/A	15E_4s1d2Xd_1	6/11A	TDP-177	9150087
23.2	1.000	0.01500	0.050	0.184	16.0	P	N/A	6.80	6.93	7.00	7.20	7.20	5.75	N/A	N/A	N/A	N/A	N/A	N/A	N/A	n/a	N/A	N/A	N/A	N/A	15E_4s1d2Xd_1	6/11A	TDP-177	9150087.1
23.2	1.000	0.01500	0.050	0.184	16.0	P	N/A	6.80	6.93	7.00	7.20	7.20	5.75	N/A	N/A	N/A	N/A	N/A	N/A	N/A	n/a	N/A	N/A	N/A	N/A	15E_4s1d2Xd_1	6/11A	TDP-177	9150087.2
23.2	1.000	0.01500	0.050	0.184	16.0	P	N/A	6.80	6.93	7.00	7.20	7.20	5.75	N/A	N/A	N/A	N/A	N/A	N/A	N/A	n/a	N/A	N/A	N/A	N/A	15E_4s1d2Xd_1	6/11A	TDP-177	9150087.3
23.2	1.000	0.01500	0.050	0.184	16.0	P	N/A	6.80	6.93	7.00	7.20	7.20	5.75	N/A	N/A	N/A	N/A	N/A	N/A	N/A	n/a	N/A	N/A	N/A	N/A	15E_4s1d2Xd_1	6/11A	TDP-177	9150087.4
23.2	1.000	0.01500	0.050	0.184	16.0	P	N/A	6.80	6.93	7.00	7.20	7.20	5.75	N/A	N/A	N/A	N/A	N/A	N/A	N/A	n/a	N/A	N/A	N/A	N/A	15E_4s1d2Xd_1	6/11A	TDP-177	9150087.5
23.2	1.000	0.01500	0.050	0.184	16.0	P	N/A	6.80	6.93	7.00	7.20	7.20	5.75	N/A	vis dec	UCSvis	N/A	N/A	7.20	D	3.7	3	N/A	N/A	N/A	15E_4s1d2Xd_1	6/11A	TDP-177	9150088
23.2	1.000	0.01500	0.050	0.184	16.0	P	N/A	6.80	6.93	7.00	7.20	7.20	5.75	N/A	N/A	N/A	N/A	N/A	N/A	N/A	3.7	N/A	N/A	N/A	N/A	15E_4s1d2Xd_1	6/11A	TDP-177	9150089
23.2	1.000	0.01500	0.050	0.184	16.0	P	N/A	6.80	6.93	7.00	7.20	7.20	5.75	N/A	N/A	N/A	N/A	N/A	N/A	N/A	3.7	N/A	N/A	N/A	N/A	15E_4s1d2Xd_1	6/11A	TDP-177	9150090
23.2	1.000	0.01500	0.050	0.184	16.0	P	N/A	6.80	6.93	7.00	7.20	7.20	5.75	N/A	N/A	N/A	N/A	N/A	N/A	N/A	3.7	N/A	N/A	N/A	N/A	15E_4s1d2Xd_1	6/11A	TDP-177	9150091
23.2	1.000	0.01500	0.050	0.184	16.0	P	N/A	6.80	6.93	7.00	7.20	7.20	5.75	N/A	N/A	N/A	N/A	N/A	N/A	N/A	3.7	N/A	N/A	N/A	N/A	15E_4s1d2Xd_1	6/11A	TDP-177	9150092
23.2	1.000	0.01500	0.050	0.184	16.0	P	N/A	6.80	6.93	7.00	7.20	7.20	5.75	N/A	N/A	N/A	N/A	N/A	N/A	N/A	3.7	N/A	N/A	N/A	N/A	15E_4s1d2Xd_1	6/11A	TDP-177	9150093
23.2	1.000	0.01500	0.050	0.184	16.0	P	N/A	6.80	6.93	7.00	7.20	7.20	5.75	N/A	N/A	N/A	N/A	N/A	N/A	N/A	3.7	N/A	N/A	N/A	N/A	15E_4s1d2Xd_1	6/11A	TDP-177	9150094
23.2	1.000	0.01500	0.050	0.184	16.0	P	N/A	6.80	6.93	7.00	7.20	7.20	5.75	N/A	N/A	N/A	N/A	N/A	N/A	N/A	3.8	N/A	N/A	N/A	N/A	15E_4s1d2Xd_1	6/11A	TDP-177	9150095
23.2	1.000	0.01500	0.050	0.184	16.0	P	N/A	6.80	6.93	7.00	7.20	7.20	5.75	N/A	N/A	N/A	N/A	N/A	N/A	N/A	0.7	N/A	N/A	N/A	N/A	15E_4s1d2Xd_1	6/11A	TDP-177	9150096
23.8	0.999	0.01500	undefined	1.000	infinite	S	2.51	n/a	n/a	n/a	2.50	2.90	4.38	N/A	N/A	N/A	N/A	N/A	N/A	(null)	9.4	1	N/A	N/A	N/A	15E_4s1d2Xa	6/11B	TDP-177	9150097
23.8	0.999	0.01500	undefined	1.000	infinite	S	2.70	n/a	n/a	n/a	2.70	2.90	5.75	N/A	N/A	N/A	N/A	N/A	N/A	I	7.0	1	N/A	N/A	N/A	15E_4s1d2Xa	6/11B	TDP-177	9150098
23.8	0.999	0.01500	undefined	1.000	infinite	S	2.71	n/a	n/a	n/a	2.70	2.90	5.75	N/A	N/A	N/A	N/A	N/A	N/A	D	6.0	1	N/A	N/A	N/A	15E_4s1d2Xa	6/11B	TDP-177	9150099
23.9	0.999	0.01500	undefined	1.000	infinite	S	2.80	n/a	n/a	n/a	2.80	2.90	7.25	N/A	N/A	N/A	N/A	N/A	N/A	I	3.0	1	N/A	N/A	N/A	15E_4s1d2Xa	6/11B	TDP-177	9150100
23.8	0.999	0.01500	undefined	1.000	infinite	S	2.90	n/a	n/a	n/a	2.90	2.90	9.00	2.90	udv	UCSvis	N/A	UCSudv	N/A	I	0.0	3	N/A	N/A	N/A	15E_4s1d2Xa	6/11B	TDP-177	9150101
23.9	0.999	0.01500	undefined	1.000	infinite	S	3.01	n/a	n/a	n/a	3.00	2.90	11.00	N/A	N/A	N/A	N/A	N/A	N/A	I	0.0	4	N/A	N/A	N/A	15E_4s1d2Xa	6/11B	TDP-177	9150102
23.9	0.999	0.01500	undefined	1.000	infinite	S	3.11	n/a	n/a	n/a	3.10	2.90	13.50	N/A	N/A	N/A	N/A	N/A	N/A	I	0.0	4	N/A	N/A	N/A	15E_4s1d2Xa	6/11B	TDP-177	9150103
23.9	0.999	0.01500	undefined	1.000	infinite	S	3.21	n/a	n/a	n/a	3.20	2.90	16.50	N/A	N/A	N/A	N/A	N/A	N/A	I	0.0	4	N/A	N/A	N/A	15E_4s1d2Xa	6/11B	TDP-177	9150104
24.0	0.999	0.01500	0.050	0.329	12.2	P	N/A	4.96	5.04	5.08	5.20	5.80	4.75	N/A	N/A	N/A	N/A	N/A	N/A	(null)	6.1	1	N/A	N/A	N/A	15E_4s1d2Xc_1	6/11C	TDP-177	9150105
24.2	0.999	0.01500	0.050	0.330	11.8	P	N/A	5.14	5.23	5.27	5.40	5.80	5.50	N/A	N/A	N/A	N/A	N/A	N/A	I	5.0	1	N/A	N/A	N/A	15E_4s1d2Xc_1	6/11C	TDP-177	9150106

Table B.3. Data from 2008 Tests in Small-Scale Vessel with Elliptical Head A.4

Row Number	Test	Case ID	Tank Diameter	Head Shape	Dish Height	Dish Volume	Tank Fill Height	Return Line Height	Nozzle Inner Diameter	Nozzle Stand-off Distance	Pulse Tube Configuration	Installed Nozzles	Outer Nozzles Operated	Inner Nozzles Operated	Pulse Tube Outer Diameter	Outer PJM Radius	Inner PJM Radius	"FIO" Outer PJM Impingement Angle	"FIO" Inner PJM Impingement Angle	Ratio Outer PJM to Tank Radius	Ratio Inner PJM to Tank Radius	Simulant	Solids Density	Particle Diameter d5	Particle Diameter d50	Particle Diameter d95	Void Fraction
text	text	text	in.	text	in.	in. ^{3}	in.	in.	in.	in.	text	number	number	number	in.	in.	in.	deg	deg	nondim	nondim	text	g/cm^3	m	m	m	fraction
MSS	M/DDX	ID	D	HS	H_{dish}	V_{dish}	H	Rtn	d	sod	PT	N	N_O	N_I	PT_{od}	R_O	R_I	θ_O	θ_I	R_O/R	R_I/R	sxdx	ρ_s	d_5	d_{50}	d_{95}	vf
9150107	6/11C	15E_4s1d2Xc_1	14 7/16	E	3.25	354.8	34 1/2	30	0.126	0.189	HLP-22	12	8	4	1.05	4.5	2.4	21.8	10.1	0.62	0.34	s1d2	2.48	0.0000569	0.0000693	0.0000821	0.3750
9150108M	6/11C	15E_4s1d2Xc_1	14 7/16	E	3.25	354.8	34 1/2	30	0.126	0.189	HLP-22	12	8	4	1.05	4.5	2.4	21.8	10.1	0.62	0.34	s1d2	2.48	0.0000569	0.0000693	0.0000821	0.3750
9150109M	6/11C	15E_4s1d2Xc_1	14 7/16	E	3.25	354.8	34 1/2	30	0.126	0.189	HLP-22	12	8	4	1.05	4.5	2.4	21.8	10.1	0.62	0.34	s1d2	2.48	0.0000569	0.0000693	0.0000821	0.3750
9150110M	6/11C	15E_4s1d2Xc_1	14 7/16	E	3.25	354.8	34 1/2	30	0.126	0.189	HLP-22	12	8	4	1.05	4.5	2.4	21.8	10.1	0.62	0.34	s1d2	2.48	0.0000569	0.0000693	0.0000821	0.3750
9150111M	6/11C	15E_4s1d2Xc_1	14 7/16	E	3.25	354.8	34 1/2	30	0.126	0.189	HLP-22	12	8	4	1.05	4.5	2.4	21.8	10.1	0.62	0.34	s1d2	2.48	0.0000569	0.0000693	0.0000821	0.3750
9150112M	6/11C	15E_4s1d2Xc_1	14 7/16	E	3.25	354.8	34 1/2	30	0.126	0.189	HLP-22	12	8	4	1.05	4.5	2.4	21.8	10.1	0.62	0.34	s1d2	2.48	0.0000569	0.0000693	0.0000821	0.3750
9150113	6/11C	15E_4s1d2Xc_1	14 7/16	E	3.25	354.8	34 1/2	30	0.126	0.189	HLP-22	12	8	4	1.05	4.5	2.4	21.8	10.1	0.62	0.34	s1d2	2.48	0.0000569	0.0000693	0.0000821	0.3750
9150114	6/11C	15E_4s1d2Xc_1	14 7/16	E	3.25	354.8	34 1/2	30	0.126	0.189	HLP-22	12	8	4	1.05	4.5	2.4	21.8	10.1	0.62	0.34	s1d2	2.48	0.0000569	0.0000693	0.0000821	0.3750
9150115	6/11C	15E_4s1d2Xc_1	14 7/16	E	3.25	354.8	34 1/2	30	0.126	0.189	HLP-22	12	8	4	1.05	4.5	2.4	21.8	10.1	0.62	0.34	s1d2	2.48	0.0000569	0.0000693	0.0000821	0.3750
9150116	6/11C	15E_4s1d2Xc_1	14 7/16	E	3.25	354.8	34 1/2	30	0.126	0.189	HLP-22	12	8	4	1.05	4.5	2.4	21.8	10.1	0.62	0.34	s1d2	2.48	0.0000569	0.0000693	0.0000821	0.3750
9150117	6/11C	15E_4s1d2Xc_1	14 7/16	E	3.25	354.8	34 1/2	30	0.126	0.189	HLP-22	12	8	4	1.05	4.5	2.4	21.8	10.1	0.62	0.34	s1d2	2.48	0.0000569	0.0000693	0.0000821	0.3750
9150118	6/11C	15E_4s1d2Xc_1	14 7/16	E	3.25	354.8	34 1/2	30	0.126	0.189	HLP-22	12	8	4	1.05	4.5	2.4	21.8	10.1	0.62	0.34	s1d2	2.48	0.0000569	0.0000693	0.0000821	0.3750
9150119	6/11C	15E_4s1d2Xc_1	14 7/16	E	3.25	354.8	34 1/2	30	0.126	0.189	HLP-22	12	8	4	1.05	4.5	2.4	21.8	10.1	0.62	0.34	s1d2	2.48	0.0000569	0.0000693	0.0000821	0.3750
9150120	6/11C	15E_4s1d2Xc_1	14 7/16	E	3.25	354.8	34 1/2	30	0.126	0.189	HLP-22	12	8	4	1.05	4.5	2.4	21.8	10.1	0.62	0.34	s1d2	2.48	0.0000569	0.0000693	0.0000821	0.3750
9150121	6/11C	15E_4s1d2Xc_1	14 7/16	E	3.25	354.8	34 1/2	30	0.126	0.189	HLP-22	12	8	4	1.05	4.5	2.4	21.8	10.1	0.62	0.34	s1d2	2.48	0.0000569	0.0000693	0.0000821	0.3750
9150122	6/11C	15E_4s1d2Xc_1	14 7/16	E	3.25	354.8	34 1/2	30	0.126	0.189	HLP-22	12	8	4	1.05	4.5	2.4	21.8	10.1	0.62	0.34	s1d2	2.48	0.0000569	0.0000693	0.0000821	0.3750
9150123	6/11C	15E_4s1d2Xc_1	14 7/16	E	3.25	354.8	34 1/2	30	0.126	0.189	HLP-22	12	8	4	1.05	4.5	2.4	21.8	10.1	0.62	0.34	s1d2	2.48	0.0000569	0.0000693	0.0000821	0.3750
9150124	6/11C	15E_4s1d2Xc_1	14 7/16	E	3.25	354.8	34 1/2	30	0.126	0.189	HLP-22	12	8	4	1.05	4.5	2.4	21.8	10.1	0.62	0.34	s1d2	2.48	0.0000569	0.0000693	0.0000821	0.3750
9150125	6/11C	15E_4s1d2Xc_1	14 7/16	E	3.25	354.8	34 1/2	30	0.126	0.189	HLP-22	12	8	4	1.05	4.5	2.4	21.8	10.1	0.62	0.34	s1d2	2.48	0.0000569	0.0000693	0.0000821	0.3750
9150126	6/11C	15E_4s1d2Xc_1	14 7/16	E	3.25	354.8	34 1/2	30	0.126	0.189	HLP-22	12	8	4	1.05	4.5	2.4	21.8	10.1	0.62	0.34	s1d2	2.48	0.0000569	0.0000693	0.0000821	0.3750
9150127	6/11C	15E_4s1d2Xc_1	14 7/16	E	3.25	354.8	34 1/2	30	0.126	0.189	HLP-22	12	8	4	1.05	4.5	2.4	21.8	10.1	0.62	0.34	s1d2	2.48	0.0000569	0.0000693	0.0000821	0.3750
9150128	6/11C	15E_4s1d2Xc_1	14 7/16	E	3.25	354.8	34 1/2	30	0.126	0.189	HLP-22	12	8	4	1.05	4.5	2.4	21.8	10.1	0.62	0.34	s1d2	2.48	0.0000569	0.0000693	0.0000821	0.3750
9150129	6/11C	15E_4s1d2Xc_1	14 7/16	E	3.25	354.8	34 1/2	30	0.126	0.189	HLP-22	12	8	4	1.05	4.5	2.4	21.8	10.1	0.62	0.34	s1d2	2.48	0.0000569	0.0000693	0.0000821	0.3750
9150130	6/11C	15E_4s1d2Xc_1	14 7/16	E	3.25	354.8	34 1/2	30	0.126	0.189	HLP-22	12	8	4	1.05	4.5	2.4	21.8	10.1	0.62	0.34	s1d2	2.48	0.0000569	0.0000693	0.0000821	0.3750
9150131	6/11C	15E_4s1d2Xc_1	14 7/16	E	3.25	354.8	34 1/2	30	0.126	0.189	HLP-22	12	8	4	1.05	4.5	2.4	21.8	10.1	0.62	0.34	s1d2	2.48	0.0000569	0.0000693	0.0000821	0.3750
9150132	6/12A	15E_4s1d2Xe_1	14 7/16	E	3.25	354.8	34 3/4	30	0.126	0.189	HLP-22	12	8	4	1.05	4.5	2.4	21.8	10.1	0.62	0.34	s1d2	2.48	0.0000569	0.0000693	0.0000821	0.3750
9150133	6/12A	15E_4s1d2Xe_1	14 7/16	E	3.25	354.8	34 3/4	30	0.126	0.189	HLP-22	12	8	4	1.05	4.5	2.4	21.8	10.1	0.62	0.34	s1d2	2.48	0.0000569	0.0000693	0.0000821	0.3750
9150134	6/12A	15E_4s1d2Xe_1	14 7/16	E	3.25	354.8	34 3/4	30	0.126	0.189	HLP-22	12	8	4	1.05	4.5	2.4	21.8	10.1	0.62	0.34	s1d2	2.48	0.0000569	0.0000693	0.0000821	0.3750
9150135M	6/12A	15E_4s1d2Xe_1	14 7/16	E	3.25	354.8	34 3/4	30	0.126	0.189	HLP-22	12	8	4	1.05	4.5	2.4	21.8	10.1	0.62	0.34	s1d2	2.48	0.0000569	0.0000693	0.0000821	0.3750
9150136M	6/12A	15E_4s1d2Xe_1	14 7/16	E	3.25	354.8	34 3/4	30	0.126	0.189	HLP-22	12	8	4	1.05	4.5	2.4	21.8	10.1	0.62	0.34	s1d2	2.48	0.0000569	0.0000693	0.0000821	0.3750
9150137M	6/12A	15E_4s1d2Xe_1	14 7/16	E	3.25	354.8	34 3/4	30	0.126	0.189	HLP-22	12	8	4	1.05	4.5	2.4	21.8	10.1	0.62	0.34	s1d2	2.48	0.0000569	0.0000693	0.0000821	0.3750
9150137.1	6/12A	15E_4s1d2Xe_1	14 7/16	E	3.25	354.8	34 3/4	30	0.126	0.189	HLP-22	12	8	4	1.05	4.5	2.4	21.8	10.1	0.62	0.34	s1d2	2.48	0.0000569	0.0000693	0.0000821	0.3750
9150137.2	6/12A	15E_4s1d2Xe_1	14 7/16	E	3.25	354.8	34 3/4	30	0.126	0.189	HLP-22	12	8	4	1.05	4.5	2.4	21.8	10.1	0.62	0.34	s1d2	2.48	0.0000569	0.0000693	0.0000821	0.3750
9150137.3	6/12A	15E_4s1d2Xe_1	14 7/16	E	3.25	354.8	34 3/4	30	0.126	0.189	HLP-22	12	8	4	1.05	4.5	2.4	21.8	10.1	0.62	0.34	s1d2	2.48	0.0000569	0.0000693	0.0000821	0.3750
9150137.4	6/12A	15E_4s1d2Xe_1	14 7/16	E	3.25	354.8	34 3/4	30	0.126	0.189	HLP-22	12	8	4	1.05	4.5	2.4	21.8	10.1	0.62	0.34	s1d2	2.48	0.0000569	0.0000693	0.0000821	0.3750
9150137.5	6/12A	15E_4s1d2Xe_1	14 7/16	E	3.25	354.8	34 3/4	30	0.126	0.189	HLP-22	12	8	4	1.05	4.5	2.4	21.8	10.1	0.62	0.34	s1d2	2.48	0.0000569	0.0000693	0.0000821	0.3750
9150138M	6/12A	15E_4s1d2Xe_1	14 7/16	E	3.25	354.8	34 3/4	30	0.126	0.189	HLP-22	12	8	4	1.05	4.5	2.4	21.8	10.1	0.62	0.34	s1d2	2.48	0.0000569	0.0000693	0.0000821	0.3750
9150139	6/12A	15E_4s1d2Xe_1	14 7/16	E	3.25	354.8	34 3/4	30	0.126	0.189	HLP-22	12	8	4	1.05	4.5	2.4	21.8	10.1	0.62	0.34	s1d2	2.48	0.0000569	0.0000693	0.0000821	0.3750
9150139.1	6/12A	15E_4s1d2Xe_1	14 7/16	E	3.25	354.8	34 3/4	30	0.126	0.189	HLP-22	12	8	4	1.05	4.5	2.4	21.8	10.1	0.62	0.34	s1d2	2.48	0.0000569	0.0000693	0.0000821	0.3750
9150140	6/12A	15E_4s1d2Xe_1	14 7/16	E	3.25	354.8	34 3/4	30	0.126	0.189	HLP-22	12	8	4	1.05	4.5	2.4	21.8	10.1	0.62	0.34	s1d2	2.48	0.0000569	0.0000693	0.0000821	0.3750
9150140.1	6/12A	15E_4s1d2Xe_1	14 7/16	E	3.25	354.8	34 3/4	30	0.126	0.189	HLP-22	12	8	4	1.05	4.5	2.4	21.8	10.1	0.62	0.34	s1d2	2.48	0.0000569	0.0000693	0.0000821	0.3750

Table B.3. Data from 2008 Tests in Small-Scale Vessel with Elliptical Head B.4

Tank Water Temperature	Water Density	Solids Fraction	Pulse Volume Fraction	Duty Cycle	Cycle Time	Pulsed or Steady Jet	Us Steady Jet	U1 Pulsing Jet	U2 URMS	U3 URM3	Discharge Velocity	Critical Suspension Velocity	Average Peak Cloud Height	UCS Condition	UCS Method	UCS Flag	UCS Center Flag	UCS udv Flag	UCS based on Decreasing Velocity	Sweep Increase / Decrease	UDV Height Bed	Particle Motion	Solids Level	Outer Bottom Pattern	Inner Bottom Pattern	Case ID	Test	TDP	Row Number
C	g/cm^3	fraction	fraction	fraction	s	text	m/s	m/s	m/s	m/s	m/s	m/s	in.	m/s	text	text	text	text	m/s	text	mm	text	text	text	text	text	text	text	text
T	ρ_c	ϕ_S	ϕ_P	DC	t_C	Jet	U_S	U1	U2	U3	U	U_{CS}	H_C	U_{CSR}	U_{CSM}	U_{CS}vis	U_{CS}cen	U_{CS}udv	U_{CS}_D	S_W	H_{bed}	PM	Sol	SP_O	SP_I	ID	M/DDX	TDP	MSS
24.3	0.999	0.01500	0.050	0.331	11.4	P	N/A	5.33	5.41	5.46	5.60	5.80	5.75	N/A	N/A	N/A	N/A	N/A	N/A	I	3.8	1	N/A	N/A	N/A	15E_4s1d2Xc_1	6/11C	TDP-177	9150107
24.4	0.999	0.01500	0.050	0.333	11.0	P	N/A	5.47	5.59	5.64	5.80	5.80	6.50	5.80	udv	UCSvis	N/A	UCSudv	N/A	I	0.7	3	N/A	N/A	N/A	15E_4s1d2Xc_1	6/11C	TDP-177	9150108
24.5	0.999	0.01500	0.050	0.334	10.6	P	N/A	5.67	5.78	5.82	6.00	5.80	7.50	N/A	N/A	N/A	N/A	N/A	N/A	I	0.0	4	N/A	N/A	N/A	15E_4s1d2Xc_1	6/11C	TDP-177	9150109
24.7	0.999	0.01500	0.050	0.332	10.0	P	N/A	6.06	6.17	6.23	6.40	5.80	10.50	N/A	N/A	N/A	N/A	N/A	N/A	I	0.0	4	N/A	N/A	N/A	15E_4s1d2Xc_1	6/11C	TDP-177	9150110
24.9	0.999	0.01500	0.050	0.332	9.4	P	N/A	6.44	6.56	6.62	6.80	5.80	15.00	N/A	N/A	N/A	N/A	N/A	N/A	I	N/A	4	N/A	N/A	N/A	15E_4s1d2Xc_1	6/11C	TDP-177	9150111
25.1	0.999	0.01500	0.050	0.334	9.0	P	N/A	6.60	6.73	6.80	7.00	5.80	18.00	N/A	N/A	N/A	N/A	N/A	N/A	I	0.0	4	N/A	N/A	N/A	15E_4s1d2Xc_1	6/11C	TDP-177	9150112
25.4	0.999	0.01500	0.050	0.333	11.0	P	N/A	5.50	5.59	5.64	5.80	5.80	N/A	N/A	N/A	N/A	N/A	N/A	N/A	I	15.4	n/a	N/A	N/A	N/A	15E_4s1d2Xc_1	6/11C	TDP-177	9150113
25.4	0.999	0.01500	0.050	0.333	11.0	P	N/A	5.50	5.59	5.64	5.80	5.80	N/A	N/A	N/A	N/A	N/A	N/A	N/A	N/A	12.6	N/A	N/A	N/A	N/A	15E_4s1d2Xc_1	6/11C	TDP-177	9150114
25.4	0.999	0.01500	0.050	0.333	11.0	P	N/A	5.50	5.59	5.64	5.80	5.80	N/A	N/A	N/A	N/A	N/A	N/A	N/A	N/A	3.7	N/A	N/A	N/A	N/A	15E_4s1d2Xc_1	6/11C	TDP-177	9150115
25.4	0.999	0.01500	0.050	0.333	11.0	P	N/A	5.50	5.59	5.64	5.80	5.80	N/A	N/A	N/A	N/A	N/A	N/A	N/A	N/A	3.7	N/A	N/A	N/A	N/A	15E_4s1d2Xc_1	6/11C	TDP-177	9150116
25.4	0.999	0.01500	0.050	0.333	11.0	P	N/A	5.50	5.59	5.64	5.80	5.80	N/A	N/A	N/A	N/A	N/A	N/A	N/A	N/A	3.7	N/A	N/A	N/A	N/A	15E_4s1d2Xc_1	6/11C	TDP-177	9150117
25.4	0.999	0.01500	0.050	0.333	11.0	P	N/A	5.50	5.59	5.64	5.80	5.80	N/A	N/A	N/A	N/A	N/A	N/A	N/A	N/A	3.7	N/A	N/A	N/A	N/A	15E_4s1d2Xc_1	6/11C	TDP-177	9150118
25.4	0.999	0.01500	0.050	0.333	11.0	P	N/A	5.50	5.59	5.64	5.80	5.80	N/A	N/A	N/A	N/A	N/A	N/A	N/A	N/A	0.0	N/A	N/A	N/A	N/A	15E_4s1d2Xc_1	6/11C	TDP-177	9150119
25.4	0.999	0.01500	0.050	0.333	11.0	P	N/A	5.50	5.59	5.64	5.80	5.80	N/A	N/A	N/A	N/A	N/A	N/A	N/A	N/A	0.0	N/A	N/A	N/A	N/A	15E_4s1d2Xc_1	6/11C	TDP-177	9150120
25.4	0.999	0.01500	0.050	0.333	11.0	P	N/A	5.50	5.59	5.64	5.80	5.80	N/A	N/A	N/A	N/A	N/A	N/A	N/A	N/A	3.7	N/A	N/A	N/A	N/A	15E_4s1d2Xc_1	6/11C	TDP-177	9150121
25.4	0.999	0.01500	0.050	0.333	11.0	P	N/A	5.50	5.60	5.64	5.80	5.80	N/A	N/A	N/A	N/A	N/A	N/A	N/A	N/A	0.0	n/a	N/A	N/A	N/A	15E_4s1d2Xc_1	6/11C	TDP-177	9150122
25.4	0.999	0.01500	0.050	0.333	11.0	P	N/A	5.50	5.60	5.64	5.80	5.80	N/A	N/A	N/A	N/A	N/A	N/A	N/A	N/A	3.7	N/A	N/A	N/A	N/A	15E_4s1d2Xc_1	6/11C	TDP-177	9150123
25.4	0.999	0.01500	0.050	0.333	11.0	P	N/A	5.50	5.60	5.64	5.80	5.80	N/A	N/A	N/A	N/A	N/A	N/A	N/A	N/A	0.0	N/A	N/A	N/A	N/A	15E_4s1d2Xc_1	6/11C	TDP-177	9150124
25.4	0.999	0.01500	0.050	0.333	11.0	P	N/A	5.50	5.60	5.64	5.80	5.80	N/A	N/A	N/A	N/A	N/A	N/A	N/A	N/A	3.7	N/A	N/A	N/A	N/A	15E_4s1d2Xc_1	6/11C	TDP-177	9150125
25.4	0.999	0.01500	0.050	0.333	11.0	P	N/A	5.50	5.60	5.64	5.80	5.80	N/A	N/A	N/A	N/A	N/A	N/A	N/A	N/A	3.7	N/A	N/A	N/A	N/A	15E_4s1d2Xc_1	6/11C	TDP-177	9150126
25.4	0.999	0.01500	0.050	0.333	11.0	P	N/A	5.50	5.60	5.64	5.80	5.80	N/A	N/A	N/A	N/A	N/A	N/A	N/A	N/A	0.0	N/A	N/A	N/A	N/A	15E_4s1d2Xc_1	6/11C	TDP-177	9150127
25.4	1.000	0.01500	0.050	0.333	11.0	P	N/A	5.50	5.59	5.64	5.80	5.80	N/A	N/A	N/A	N/A	N/A	N/A	N/A	N/A	3.7	n/a	N/A	N/A	N/A	15E_4s1d2Xc_1	6/11C	TDP-177	9150128
25.4	1.000	0.01500	0.050	0.333	11.0	P	N/A	5.50	5.59	5.64	5.80	5.80	N/A	N/A	N/A	N/A	N/A	N/A	N/A	N/A	3.7	N/A	N/A	N/A	N/A	15E_4s1d2Xc_1	6/11C	TDP-177	9150129
25.4	0.999	0.01500	0.050	0.333	11.0	P	N/A	5.50	5.59	5.64	5.80	5.80	N/A	N/A	N/A	N/A	N/A	N/A	N/A	N/A	3.7	n/a	N/A	N/A	N/A	15E_4s1d2Xc_1	6/11C	TDP-177	9150130
25.5	0.999	0.01500	0.050	0.332	11.0	P	N/A	5.51	5.60	5.64	5.80	5.80	N/A	N/A	N/A	N/A	N/A	N/A	N/A	N/A	0.0	n/a	N/A	N/A	N/A	15E_4s1d2Xc_1	6/11C	TDP-177	9150131
21.1	1.000	0.01500	0.050	0.661	9.0	P	N/A	3.38	3.42	3.44	3.50	3.90	5.13	N/A	N/A	N/A	N/A	N/A	N/A	(null)	6.1	1	N/A	N/A	N/A	15E_4s1d2Xe_1	6/12A	TDP-178	9150132
21.1	1.000	0.01500	0.050	0.664	8.4	P	N/A	3.57	3.61	3.63	3.70	3.90	6.25	N/A	N/A	N/A	N/A	N/A	N/A	I	2.5	1	N/A	N/A	N/A	15E_4s1d2Xe_1	6/12A	TDP-178	9150133
21.4	1.000	0.01500	0.050	0.665	8.4	P	N/A	3.57	3.61	3.63	3.70	3.90	6.25	N/A	N/A	N/A	N/A	N/A	N/A	D	3.8	1	N/A	N/A	N/A	15E_4s1d2Xe_1	6/12A	TDP-178	9150134
21.3	1.000	0.01500	0.050	0.668	8.0	P	N/A	3.75	3.79	3.82	3.90	3.90	7.50	3.90	udv	UCSvis	N/A	UCSudv	N/A	I	0.0	3	N/A	N/A	N/A	15E_4s1d2Xe_1	6/12A	TDP-178	9150135
21.6	1.000	0.01500	0.050	0.660	7.6	P	N/A	3.95	4.00	4.03	4.10	3.90	9.50	N/A	N/A	N/A	N/A	N/A	N/A	I	0.0	4	N/A	N/A	N/A	15E_4s1d2Xe_1	6/12A	TDP-178	9150136
21.6	1.000	0.01500	0.050	0.665	7.0	P	N/A	4.30	4.36	4.39	4.50	3.90	14.50	N/A	N/A	N/A	N/A	N/A	N/A	I	0.0	4	N/A	N/A	N/A	15E_4s1d2Xe_1	6/12A	TDP-178	9150137
22.0	1.000	0.01500	0.050	0.667	8.0	P	N/A	3.75	3.80	3.82	3.90	3.90	7.25	N/A	N/A	N/A	N/A	N/A	N/A	N/A	n/a	N/A	N/A	N/A	N/A	15E_4s1d2Xe_1	6/12A	TDP-178	9150137.1
22.0	1.000	0.01500	0.050	0.667	8.0	P	N/A	3.75	3.80	3.82	3.90	3.90	7.25	N/A	N/A	N/A	N/A	N/A	N/A	N/A	n/a	N/A	N/A	N/A	N/A	15E_4s1d2Xe_1	6/12A	TDP-178	9150137.2
22.0	1.000	0.01500	0.050	0.667	8.0	P	N/A	3.75	3.80	3.82	3.90	3.90	7.25	N/A	N/A	N/A	N/A	N/A	N/A	N/A	n/a	N/A	N/A	N/A	N/A	15E_4s1d2Xe_1	6/12A	TDP-178	9150137.3
22.0	1.000	0.01500	0.050	0.667	8.0	P	N/A	3.75	3.80	3.82	3.90	3.90	7.25	N/A	N/A	N/A	N/A	N/A	N/A	N/A	n/a	N/A	N/A	N/A	N/A	15E_4s1d2Xe_1	6/12A	TDP-178	9150137.4
22.0	1.000	0.01500	0.050	0.667	8.0	P	N/A	3.75	3.80	3.82	3.90	3.90	7.25	N/A	N/A	N/A	N/A	N/A	N/A	N/A	n/a	N/A	N/A	N/A	N/A	15E_4s1d2Xe_1	6/12A	TDP-178	9150137.5
22.0	1.000	0.01500	0.050	0.667	8.0	P	N/A	3.75	3.80	3.82	3.90	3.90	7.25	N/A	N/A	UCSvis	N/A	N/A	N/A	I	0.0	3	N/A	N/A	N/A	15E_4s1d2Xe_1	6/12A	TDP-178	9150138
22.0	1.000	0.01500	0.050	0.667	8.0	P	N/A	3.75	3.80	3.82	3.90	3.90	7.25	N/A	N/A	N/A	N/A	N/A	N/A	N/A	0.0	N/A	N/A	N/A	N/A	15E_4s1d2Xe_1	6/12A	TDP-178	9150139
22.0	1.000	0.01500	0.050	0.667	8.0	P	N/A	3.75	3.80	3.82	3.90	3.90	7.25	N/A	N/A	N/A	N/A	N/A	N/A	N/A	n/a	N/A	N/A	N/A	N/A	15E_4s1d2Xe_1	6/12A	TDP-178	9150139.1
22.0	1.000	0.01500	0.050	0.667	8.0	P	N/A	3.75	3.80	3.82	3.90	3.90	7.25	N/A	N/A	N/A	N/A	N/A	N/A	N/A	0.0	N/A	N/A	N/A	N/A	15E_4s1d2Xe_1	6/12A	TDP-178	9150140
22.0	1.000	0.01500	0.050	0.667	8.0	P	N/A	3.75	3.80	3.82	3.90	3.90	7.25	N/A	N/A	N/A	N/A	N/A	N/A	N/A	n/a	N/A	N/A	N/A	N/A	15E_4s1d2Xe_1	6/12A	TDP-178	9150140.1

Table B.3. Data from 2008 Tests in Small-Scale Vessel with Elliptical Head A.5

Row Number	Test	Case ID	Tank Diameter	Head Shape	Dish Height	Dish Volume	Tank Fill Height	Return Line Height	Nozzle Inner Diameter	Nozzle Stand-off Distance	Pulse Tube Configuration	Installed Nozzles	Outer Nozzles Operated	Inner Nozzles Operated	Pulse Tube Outer Diameter	Outer PJM Radius	Inner PJM Radius	"FIO" Outer PJM Impingement Angle	"FIO" Inner PJM Impingement Angle	Ratio Outer PJM to Tank Radius	Ratio Inner PJM to Tank Radius	Simulant	Solids Density	Particle Diameter d5	Particle Diameter d50	Particle Diameter d95	Void Fraction
text	text	text	in.	text	in.	in. ^{3}	in.	in.	in.	in.	text	number	number	number	in.	in.	in.	deg	deg	nondim	nondim	text	g/cm^3	m	m	m	fraction
MSS	M/DDX	ID	D	HS	H_{dish}	V_{dish}	H	Rtn	d	sod	PT	N	N_O	N_I	PT_{od}	R_O	R_I	θ_O	θ_I	R_O/R	R_I/R	sxdx	ρ_s	d_5	d_{50}	d_{95}	vf
9150141	6/12A	15E_4s1d2Xe_1	14 7/16	E	3.25	354.8	34 3/4	30	0.126	0.189	HLP-22	12	8	4	1.05	4.5	2.4	21.8	10.1	0.62	0.34	s1d2	2.48	0.0000569	0.0000693	0.0000821	0.3750
9150141.1	6/12A	15E_4s1d2Xe_1	14 7/16	E	3.25	354.8	34 3/4	30	0.126	0.189	HLP-22	12	8	4	1.05	4.5	2.4	21.8	10.1	0.62	0.34	s1d2	2.48	0.0000569	0.0000693	0.0000821	0.3750
9150142	6/12A	15E_4s1d2Xe_1	14 7/16	E	3.25	354.8	34 3/4	30	0.126	0.189	HLP-22	12	8	4	1.05	4.5	2.4	21.8	10.1	0.62	0.34	s1d2	2.48	0.0000569	0.0000693	0.0000821	0.3750
9150142.1	6/12A	15E_4s1d2Xe_1	14 7/16	E	3.25	354.8	34 3/4	30	0.126	0.189	HLP-22	12	8	4	1.05	4.5	2.4	21.8	10.1	0.62	0.34	s1d2	2.48	0.0000569	0.0000693	0.0000821	0.3750
9150143	6/12A	15E_4s1d2Xe_1	14 7/16	E	3.25	354.8	34 3/4	30	0.126	0.189	HLP-22	12	8	4	1.05	4.5	2.4	21.8	10.1	0.62	0.34	s1d2	2.48	0.0000569	0.0000693	0.0000821	0.3750
9150144	6/12B	15E_4s1d2Xc_2	14 7/16	E	3.25	354.8	34 3/4	30	0.126	0.189	HLP-22	12	8	4	1.05	4.5	2.4	21.8	10.1	0.62	0.34	s1d2	2.48	0.0000569	0.0000693	0.0000821	0.3750
9150145	6/12B	15E_4s1d2Xc_2	14 7/16	E	3.25	354.8	34 3/4	30	0.126	0.189	HLP-22	12	8	4	1.05	4.5	2.4	21.8	10.1	0.62	0.34	s1d2	2.48	0.0000569	0.0000693	0.0000821	0.3750
9150146	6/12B	15E_4s1d2Xc_2	14 7/16	E	3.25	354.8	34 3/4	30	0.126	0.189	HLP-22	12	8	4	1.05	4.5	2.4	21.8	10.1	0.62	0.34	s1d2	2.48	0.0000569	0.0000693	0.0000821	0.3750
9150147	6/12B	15E_4s1d2Xc_2	14 7/16	E	3.25	354.8	34 3/4	30	0.126	0.189	HLP-22	12	8	4	1.05	4.5	2.4	21.8	10.1	0.62	0.34	s1d2	2.48	0.0000569	0.0000693	0.0000821	0.3750
9150148	6/12B	15E_4s1d2Xc_2	14 7/16	E	3.25	354.8	34 3/4	30	0.126	0.189	HLP-22	12	8	4	1.05	4.5	2.4	21.8	10.1	0.62	0.34	s1d2	2.48	0.0000569	0.0000693	0.0000821	0.3750
9150149M	6/12B	15E_4s1d2Xc_2	14 7/16	E	3.25	354.8	34 3/4	30	0.126	0.189	HLP-22	12	8	4	1.05	4.5	2.4	21.8	10.1	0.62	0.34	s1d2	2.48	0.0000569	0.0000693	0.0000821	0.3750
9150150M	6/12B	15E_4s1d2Xc_2	14 7/16	E	3.25	354.8	34 3/4	30	0.126	0.189	HLP-22	12	8	4	1.05	4.5	2.4	21.8	10.1	0.62	0.34	s1d2	2.48	0.0000569	0.0000693	0.0000821	0.3750
9150151	6/12C	15E_4s1d2Xd_2	14 7/16	E	3.25	354.8	34 3/4	30	0.126	0.189	HLP-22	12	8	4	1.05	4.5	2.4	21.8	10.1	0.62	0.34	s1d2	2.48	0.0000569	0.0000693	0.0000821	0.3750
9150152M	6/12C	15E_4s1d2Xd_2	14 7/16	E	3.25	354.8	34 3/4	30	0.126	0.189	HLP-22	12	8	4	1.05	4.5	2.4	21.8	10.1	0.62	0.34	s1d2	2.48	0.0000569	0.0000693	0.0000821	0.3750
9150153M	6/12C	15E_4s1d2Xd_2	14 7/16	E	3.25	354.8	34 3/4	30	0.126	0.189	HLP-22	12	8	4	1.05	4.5	2.4	21.8	10.1	0.62	0.34	s1d2	2.48	0.0000569	0.0000693	0.0000821	0.3750
9150154	6/12D	15E_4s1d2Xe_2	14 7/16	E	3.25	354.8	34 3/4	30	0.126	0.189	HLP-22	12	8	4	1.05	4.5	2.4	21.8	10.1	0.62	0.34	s1d2	2.48	0.0000569	0.0000693	0.0000821	0.3750
9150155M	6/12D	15E_4s1d2Xe_2	14 7/16	E	3.25	354.8	34 3/4	30	0.126	0.189	HLP-22	12	8	4	1.05	4.5	2.4	21.8	10.1	0.62	0.34	s1d2	2.48	0.0000569	0.0000693	0.0000821	0.3750
9150156M	6/12D	15E_4s1d2Xe_2	14 7/16	E	3.25	354.8	34 3/4	30	0.126	0.189	HLP-22	12	8	4	1.05	4.5	2.4	21.8	10.1	0.62	0.34	s1d2	2.48	0.0000569	0.0000693	0.0000821	0.3750
9150157	6/12E	15E_4s1d2Xc_4	14 7/16	E	3.25	354.8	34 3/4	30	0.126	0.189	HLP-22	12	8	4	1.05	4.5	2.4	21.8	10.1	0.62	0.34	s1d2	2.48	0.0000569	0.0000693	0.0000821	0.3750
9150158M	6/12E	15E_4s1d2Xc_4	14 7/16	E	3.25	354.8	34 3/4	30	0.126	0.189	HLP-22	12	8	4	1.05	4.5	2.4	21.8	10.1	0.62	0.34	s1d2	2.48	0.0000569	0.0000693	0.0000821	0.3750
9150159M	6/12E	15E_4s1d2Xc_4	14 7/16	E	3.25	354.8	34 3/4	30	0.126	0.189	HLP-22	12	8	4	1.05	4.5	2.4	21.8	10.1	0.62	0.34	s1d2	2.48	0.0000569	0.0000693	0.0000821	0.3750
9150160	6/13A	15E_4s1d2Xd_4	14 7/16	E	3.25	354.8	35	30	0.126	0.189	HLP-22	12	8	4	1.05	4.5	2.4	21.8	10.1	0.62	0.34	s1d2	2.48	0.0000569	0.0000693	0.0000821	0.3750
9150161M	6/13A	15E_4s1d2Xd_4	14 7/16	E	3.25	354.8	35	30	0.126	0.189	HLP-22	12	8	4	1.05	4.5	2.4	21.8	10.1	0.62	0.34	s1d2	2.48	0.0000569	0.0000693	0.0000821	0.3750
9150162M	6/13A	15E_4s1d2Xd_4	14 7/16	E	3.25	354.8	35	30	0.126	0.189	HLP-22	12	8	4	1.05	4.5	2.4	21.8	10.1	0.62	0.34	s1d2	2.48	0.0000569	0.0000693	0.0000821	0.3750
9150163	6/13B	15E_4s1d2Xe_4	14 7/16	E	3.25	354.8	35	30	0.126	0.189	HLP-22	12	8	4	1.05	4.5	2.4	21.8	10.1	0.62	0.34	s1d2	2.48	0.0000569	0.0000693	0.0000821	0.3750
9150164	6/13B	15E_4s1d2Xe_4	14 7/16	E	3.25	354.8	35	30	0.126	0.189	HLP-22	12	8	4	1.05	4.5	2.4	21.8	10.1	0.62	0.34	s1d2	2.48	0.0000569	0.0000693	0.0000821	0.3750
9150165M	6/13B	15E_4s1d2Xe_4	14 7/16	E	3.25	354.8	35	30	0.126	0.189	HLP-22	12	8	4	1.05	4.5	2.4	21.8	10.1	0.62	0.34	s1d2	2.48	0.0000569	0.0000693	0.0000821	0.3750
9150166M	6/13B	15E_4s1d2Xe_4	14 7/16	E	3.25	354.8	35	30	0.126	0.189	HLP-22	12	8	4	1.05	4.5	2.4	21.8	10.1	0.62	0.34	s1d2	2.48	0.0000569	0.0000693	0.0000821	0.3750
9150167	6/13C	15E_4s1d2Xd_1	14 7/16	E	3.25	354.8	35	30	0.126	0.189	HLP-22	12	8	4	1.05	4.5	2.4	21.8	10.1	0.62	0.34	s1d2	2.48	0.0000569	0.0000693	0.0000821	0.3750
9150168	6/13C	15E_4s1d2Xd_1	14 7/16	E	3.25	354.8	35	30	0.126	0.189	HLP-22	12	8	4	1.05	4.5	2.4	21.8	10.1	0.62	0.34	s1d2	2.48	0.0000569	0.0000693	0.0000821	0.3750
9150169	6/13C	15E_4s1d2Xd_1	14 7/16	E	3.25	354.8	35	30	0.126	0.189	HLP-22	12	8	4	1.05	4.5	2.4	21.8	10.1	0.62	0.34	s1d2	2.48	0.0000569	0.0000693	0.0000821	0.3750
9150170	6/13C	15E_4s1d2Xd_1	14 7/16	E	3.25	354.8	35	30	0.126	0.189	HLP-22	12	8	4	1.05	4.5	2.4	21.8	10.1	0.62	0.34	s1d2	2.48	0.0000569	0.0000693	0.0000821	0.3750
9150171	6/13C	15E_4s1d2Xd_1	14 7/16	E	3.25	354.8	35	30	0.126	0.189	HLP-22	12	8	4	1.05	4.5	2.4	21.8	10.1	0.62	0.34	s1d2	2.48	0.0000569	0.0000693	0.0000821	0.3750
9150172	6/13C	15E_4s1d2Xd_1	14 7/16	E	3.25	354.8	35	30	0.126	0.189	HLP-22	12	8	4	1.05	4.5	2.4	21.8	10.1	0.62	0.34	s1d2	2.48	0.0000569	0.0000693	0.0000821	0.3750
9150173	6/13C	15E_4s1d2Xd_1	14 7/16	E	3.25	354.8	35	30	0.126	0.189	HLP-22	12	8	4	1.05	4.5	2.4	21.8	10.1	0.62	0.34	s1d2	2.48	0.0000569	0.0000693	0.0000821	0.3750
9150174M	6/13C	15E_4s1d2Xd_1	14 7/16	E	3.25	354.8	35	30	0.126	0.189	HLP-22	12	8	4	1.05	4.5	2.4	21.8	10.1	0.62	0.34	s1d2	2.48	0.0000569	0.0000693	0.0000821	0.3750
9150175M	6/13C	15E_4s1d2Xd_1	14 7/16	E	3.25	354.8	35	30	0.126	0.189	HLP-22	12	8	4	1.05	4.5	2.4	21.8	10.1	0.62	0.34	s1d2	2.48	0.0000569	0.0000693	0.0000821	0.3750
9150176M	6/13C	15E_4s1d2Xd_1	14 7/16	E	3.25	354.8	35	30	0.126	0.189	HLP-22	12	8	4	1.05	4.5	2.4	21.8	10.1	0.62	0.34	s1d2	2.48	0.0000569	0.0000693	0.0000821	0.3750
9150177M	6/13C	15E_4s1d2Xd_1	14 7/16	E	3.25	354.8	35	30	0.126	0.189	HLP-22	12	8	4	1.05	4.5	2.4	21.8	10.1	0.62	0.34	s1d2	2.48	0.0000569	0.0000693	0.0000821	0.3750
9150178M	6/13C	15E_4s1d2Xd_1	14 7/16	E	3.25	354.8	35	30	0.126	0.189	HLP-22	12	8	4	1.05	4.5	2.4	21.8	10.1	0.62	0.34	s1d2	2.48	0.0000569	0.0000693	0.0000821	0.3750
9150179M	6/13C	15E_4s1d2Xd_1	14 7/16	E	3.25	354.8	35	30	0.126	0.189	HLP-22	12	8	4	1.05	4.5	2.4	21.8	10.1	0.62	0.34	s1d2	2.48	0.0000569	0.0000693	0.0000821	0.3750

Table B.3. Data from 2008 Tests in Small-Scale Vessel with Elliptical Head B.5

Tank Water Temperature	Water Density	Solids Fraction	Pulse Volume Fraction	Duty Cycle	Cycle Time	Pulsed or Steady Jet	Us Steady Jet	U1 Pulsing Jet	U2 URMS	U3 URM3	Discharge Velocity	Critical Suspension Velocity	Average Peak Cloud Height	UCS Condition	UCS Method	UCS Flag	UCS Center Flag	UCS udv Flag	UCS based on Decreasing Velocity	Sweep Increase / Decrease	UDV Height Bed	Particle Motion	Solids Level	Outer Bottom Pattern	Inner Bottom Pattern	Case ID	Test	TDP	Row Number
C	g/cm³	fraction	fraction	fraction	s	text	m/s	m/s	m/s	m/s	m/s	m/s	in.	m/s	text	text	text	text	m/s	text	mm	text	text	text	text	text	text	text	text
T	ρ_c	ϕ_S	ϕ_P	DC	t_C	Jet	U_S	U1	U2	U3	U	U_{CS}	H_C	U_{CSR}	U_{CSM}	U_{CS}vis	U_{CS}cen	U_{CS}udv	U_{CS}_D	S_W	H_{bed}	PM	Sol	SP_O	SP_I	ID	M/DDX	TDP	MSS
22.0	1.000	0.01500	0.050	0.667	8.0	P	N/A	3.75	3.80	3.82	3.90	3.90	7.25	N/A	N/A	N/A	N/A	N/A	N/A	N/A	0.0	N/A	N/A	N/A	N/A	15E_4s1d2Xe_1	6/12A	TDP-178	9150141
22.0	1.000	0.01500	0.050	0.667	8.0	P	N/A	3.75	3.80	3.82	3.90	3.90	7.25	N/A	N/A	N/A	N/A	N/A	N/A	N/A	n/a	N/A	N/A	N/A	N/A	15E_4s1d2Xe_1	6/12A	TDP-178	9150141.1
22.0	1.000	0.01500	0.050	0.667	8.0	P	N/A	3.75	3.80	3.82	3.90	3.90	7.25	N/A	N/A	N/A	N/A	N/A	N/A	N/A	17.6	N/A	N/A	N/A	N/A	15E_4s1d2Xe_1	6/12A	TDP-178	9150142
22.0	1.000	0.01500	0.050	0.667	8.0	P	N/A	3.75	3.80	3.82	3.90	3.90	7.25	N/A	N/A	N/A	N/A	N/A	N/A	N/A	n/a	N/A	N/A	N/A	N/A	15E_4s1d2Xe_1	6/12A	TDP-178	9150142.1
22.0	1.000	0.01500	0.050	0.667	8.0	P	N/A	3.75	3.80	3.82	3.90	3.90	7.25	N/A	N/A	N/A	N/A	N/A	N/A	N/A	3.7	N/A	N/A	N/A	N/A	15E_4s1d2Xe_1	6/12A	TDP-178	9150143
22.6	1.000	0.01500	0.100	0.329	32.2	P	N/A	3.80	3.82	3.83	3.90	5.00	N/A	N/A	N/A	N/A	N/A	N/A	N/A	I	11.0	1	N/A	N/A	N/A	15E_4s1d2Xc_2	6/12B	TDP-178	9150144
22.8	0.999	0.01500	0.101	0.330	29.6	P	N/A	4.12	4.14	4.16	4.20	5.00	N/A	N/A	N/A	N/A	N/A	N/A	N/A	I	4.3	1	N/A	N/A	N/A	15E_4s1d2Xc_2	6/12B	TDP-178	9150145
22.9	0.999	0.01500	0.100	0.331	28.2	P	N/A	4.31	4.34	4.35	4.40	5.00	N/A	N/A	N/A	N/A	N/A	N/A	N/A	I	4.0	1	N/A	N/A	N/A	15E_4s1d2Xc_2	6/12B	TDP-178	9150146
23.0	0.999	0.01500	0.100	0.332	27.0	P	N/A	4.49	4.52	4.54	4.60	5.00	N/A	N/A	N/A	N/A	N/A	N/A	N/A	I	4.0	1	N/A	N/A	N/A	15E_4s1d2Xc_2	6/12B	TDP-178	9150147
23.1	1.000	0.01500	0.101	0.332	25.8	P	N/A	4.70	4.73	4.75	4.80	5.00	6.00	N/A	N/A	UCSvis	N/A	N/A	N/A	I	2.8	3	N/A	N/A	N/A	15E_4s1d2Xc_2	6/12B	TDP-178	9150148
23.3	1.000	0.01500	0.101	0.333	24.8	P	N/A	4.88	4.92	4.94	5.00	5.00	6.75	5.00	N/A	N/A	N/A	UCSudv	N/A	I	0.0	4	N/A	N/A	N/A	15E_4s1d2Xc_2	6/12B	TDP-178	9150149
23.4	1.000	0.01500	0.101	0.334	23.8	P	N/A	5.07	5.11	5.13	5.20	5.00	7.25	N/A	N/A	N/A	N/A	N/A	N/A	I	0.0	4	N/A	N/A	N/A	15E_4s1d2Xc_2	6/12B	TDP-178	9150150
24.3	0.999	0.01500	0.100	0.178	48.0	P	N/A	4.68	4.71	4.73	4.80	5.00	5.75	N/A	N/A	N/A	N/A	N/A	N/A	D	3.7	1	N/A	N/A	N/A	15E_4s1d2Xd_2	6/12C	TDP-178	9150151
24.5	0.999	0.01500	0.100	0.179	46.0	P	N/A	4.88	4.92	4.94	5.00	5.00	6.00	5.00	N/A	UCSvis	N/A	UCSudv	N/A	I	0.7	3	N/A	N/A	N/A	15E_4s1d2Xd_2	6/12C	TDP-178	9150152
24.6	0.999	0.01500	0.100	0.179	44.2	P	N/A	5.07	5.11	5.13	5.20	5.00	6.25	N/A	N/A	N/A	N/A	N/A	N/A	I	0.0	4	N/A	N/A	N/A	15E_4s1d2Xd_2	6/12C	TDP-178	9150153
24.9	0.999	0.01500	0.100	0.657	18.0	P	N/A	3.40	3.41	3.42	3.50	3.70	5.00	N/A	N/A	N/A	N/A	N/A	N/A	I	3.8	1	N/A	N/A	N/A	15E_4s1d2Xe_2	6/12D	TDP-178	9150154
25.1	0.999	0.01500	0.100	0.659	16.8	P	N/A	3.63	3.65	3.66	3.70	3.70	6.25	3.70	udv	UCSvis	N/A	UCSudv	N/A	I	0.6	3	N/A	N/A	N/A	15E_4s1d2Xe_2	6/12D	TDP-178	9150155
25.3	0.999	0.01500	0.100	0.660	15.8	P	N/A	3.82	3.85	3.86	3.90	3.70	7.25	N/A	N/A	N/A	N/A	N/A	N/A	I	0.0	4	N/A	N/A	N/A	15E_4s1d2Xe_2	6/12D	TDP-178	9150156
25.5	0.999	0.01500	0.149	0.324	50.6	P	N/A	3.64	3.65	3.66	3.70	3.90	4.75	N/A	N/A	N/A	N/A	N/A	N/A	D	4.1	1	N/A	N/A	N/A	15E_4s1d2Xc_4	6/12E	TDP-178	9150157
25.7	0.999	0.01500	0.150	0.325	48.0	P	N/A	3.85	3.87	3.87	3.90	3.90	5.00	3.90	udv	UCSvis	N/A	UCSudv	N/A	I	2.9	3	N/A	N/A	N/A	15E_4s1d2Xc_4	6/12E	TDP-178	9150158
25.8	0.999	0.01500	0.150	0.326	45.6	P	N/A	4.04	4.06	4.06	4.10	3.90	5.25	N/A	N/A	N/A	N/A	N/A	N/A	I	0.0	4	N/A	N/A	N/A	15E_4s1d2Xc_4	6/12E	TDP-178	9150159
23.2	0.999	0.01500	0.151	0.182	90.6	P	N/A	3.66	3.67	3.68	3.70	3.90	4.75	N/A	N/A	N/A	N/A	N/A	N/A	(null)	3.7	1	N/A	N/A	N/A	15E_4s1d2Xd_4	6/13A	TDP-179	9150160
23.5	0.999	0.01500	0.151	0.182	86.0	P	N/A	3.85	3.86	3.87	3.90	3.90	5.00	3.90	udv	UCSvis	N/A	UCSudv	N/A	I	2.2	3	N/A	N/A	N/A	15E_4s1d2Xd_4	6/13A	TDP-179	9150161
23.7	0.999	0.01500	0.151	0.183	81.8	P	N/A	4.04	4.06	4.07	4.10	3.90	5.50	N/A	N/A	N/A	N/A	N/A	N/A	I	0.0	4	N/A	N/A	N/A	15E_4s1d2Xd_4	6/13A	TDP-179	9150162
24.4	0.999	0.01500	0.151	0.663	28.8	P	N/A	3.16	3.17	3.17	3.20	3.50	4.25	N/A	N/A	N/A	N/A	N/A	N/A	I	5.3	1	N/A	N/A	N/A	15E_4s1d2Xe_4	6/13B	TDP-179	9150163
24.6	0.999	0.01500	0.151	0.664	27.2	P	N/A	3.35	3.37	3.37	3.40	3.50	5.25	N/A	N/A	N/A	N/A	N/A	N/A	I	2.9	1	N/A	N/A	N/A	15E_4s1d2Xe_4	6/13B	TDP-179	9150164
24.9	0.999	0.01500	0.151	0.664	26.4	P	N/A	3.45	3.46	3.47	3.50	3.50	5.75	3.50	udv	UCSvis	N/A	UCSudv	N/A	I	2.2	3	N/A	N/A	N/A	15E_4s1d2Xe_4	6/13B	TDP-179	9150165
25.1	0.999	0.01500	0.151	0.665	24.8	P	N/A	3.66	3.67	3.68	3.70	3.50	6.50	N/A	N/A	N/A	N/A	N/A	N/A	I	0.0	4	N/A	N/A	N/A	15E_4s1d2Xe_4	6/13B	TDP-179	9150166
25.6	0.999	0.01500	0.050	0.175	26.0	P	N/A	4.38	4.44	4.47	4.60	7.40	3.38	N/A	N/A	N/A	N/A	N/A	N/A	(null)	15.2	1	N/A	N/A	N/A	15E_4s1d2Xd_1	6/13C	TDP-179	9150167
26.0	0.999	0.01500	0.050	0.181	19.0	P	N/A	5.84	5.96	6.01	6.20	7.40	4.75	N/A	N/A	N/A	N/A	N/A	N/A	I	5.8	1	N/A	N/A	N/A	15E_4s1d2Xd_1	6/13C	TDP-179	9150168
26.2	0.999	0.01500	0.050	0.182	18.4	P	N/A	6.00	6.13	6.19	6.40	7.40	4.75	N/A	N/A	N/A	N/A	N/A	N/A	I	5.1	1	N/A	N/A	N/A	15E_4s1d2Xd_1	6/13C	TDP-179	9150169
26.4	0.999	0.01500	0.050	0.183	17.6	P	N/A	6.20	6.33	6.40	6.60	7.40	5.00	N/A	N/A	N/A	N/A	N/A	N/A	I	3.7	1	N/A	N/A	N/A	15E_4s1d2Xd_1	6/13C	TDP-179	9150170
26.6	0.999	0.01500	0.050	0.184	17.0	P	N/A	6.38	6.53	6.59	6.80	7.40	5.25	N/A	N/A	N/A	N/A	N/A	N/A	I	4.0	1	N/A	N/A	N/A	15E_4s1d2Xd_1	6/13C	TDP-179	9150171
26.9	0.999	0.01500	0.050	0.185	16.6	P	N/A	6.57	6.72	6.79	7.00	7.40	5.50	N/A	N/A	UCSvis	N/A	N/A	N/A	I	3.7	3	N/A	N/A	N/A	15E_4s1d2Xd_1	6/13C	TDP-179	9150172
27.0	0.999	0.01500	0.050	0.186	16.0	P	N/A	6.73	6.89	6.97	7.20	7.40	5.50	N/A	N/A	N/A	N/A	N/A	N/A	I	3.7	4	N/A	N/A	N/A	15E_4s1d2Xd_1	6/13C	TDP-179	9150173
27.8	0.998	0.01500	0.050	0.186	15.6	P	N/A	6.92	7.09	7.17	7.40	7.40	5.50	7.40	udv	N/A	N/A	UCSudv	N/A	I	0.7	4	N/A	N/A	N/A	15E_4s1d2Xd_1	6/13C	TDP-179	9150174
28.1	0.998	0.01500	0.050	0.187	15.2	P	N/A	7.09	7.27	7.35	7.60	7.40	5.75	N/A	N/A	N/A	N/A	N/A	N/A	I	0.0	4	N/A	N/A	N/A	15E_4s1d2Xd_1	6/13C	TDP-179	9150175
28.4	0.998	0.01500	0.050	0.185	14.6	P	N/A	7.42	7.62	7.71	8.00	7.40	6.25	N/A	N/A	N/A	N/A	N/A	N/A	I	0.0	4	N/A	N/A	N/A	15E_4s1d2Xd_1	6/13C	TDP-179	9150176
28.8	0.998	0.01500	0.050	0.188	13.4	P	N/A	7.95	8.18	8.30	8.60	7.40	8.50	N/A	N/A	N/A	N/A	N/A	N/A	I	0.0	4	N/A	N/A	N/A	15E_4s1d2Xd_1	6/13C	TDP-179	9150177
29.0	0.998	0.01500	0.050	0.188	12.8	P	N/A	8.26	8.53	8.66	9.00	7.40	11.00	N/A	N/A	N/A	N/A	N/A	N/A	I	0.0	4	N/A	N/A	N/A	15E_4s1d2Xd_1	6/13C	TDP-179	9150178
29.5	0.998	0.01500	0.050	0.184	12.8	P	N/A	8.50	8.78	8.91	9.30	7.40	11.00	N/A	N/A	N/A	N/A	N/A	N/A	I	0.0	4	N/A	N/A	N/A	15E_4s1d2Xd_1	6/13C	TDP-179	9150179

Table B.3. Data from 2008 Tests in Small-Scale Vessel with Elliptical Head A.6

Row Number	Test	Case ID	Tank Diameter	Head Shape	Dish Height	Dish Volume	Tank Fill Height	Return Line Height	Nozzle Inner Diameter	Nozzle Stand-off Distance	Pulse Tube Configuration	Installed Nozzles	Outer Nozzles Operated	Inner Nozzles Operated	Pulse Tube Outer Diameter	Outer PJM Radius	Inner PJM Radius	"FIO" Outer PJM Impingement Angle	"FIO" Inner PJM Impingement Angle	Ratio Outer PJM to Tank Radius	Ratio Inner PJM to Tank Radius	Simulant	Solids Density	Particle Diameter d5	Particle Diameter d50	Particle Diameter d95	Void Fraction
text	text	text	in.	text	in.	in. ^{3}	in.	in.	in.	in.	text	number	number	number	in.	in.	in.	deg	deg	nondim	nondim	text	g/cm^3	m	m	m	fraction
MSS	M/DDX	ID	D	HS	H_{dish}	V_{dish}	H	Rtn	d	sod	PT	N	N_O	N_I	PT_{od}	R_O	R_I	θ_O	θ_I	R_O/R	R_I/R	sxdx	ρ_s	d_5	d_{50}	d_{95}	vf
9150180	6/16A	15E_4s1d2Qc_1	14 7/16	E	3.25	354.8	35	30	0.126	0.189	HLP-22	12	8	4	1.05	4.5	2.4	21.8	10.1	0.62	0.34	s1d2	2.48	0.0000569	0.0000693	0.0000821	0.3750
9150181	6/16A	15E_4s1d2Qc_1	14 7/16	E	3.25	354.8	35	30	0.126	0.189	HLP-22	12	8	4	1.05	4.5	2.4	21.8	10.1	0.62	0.34	s1d2	2.48	0.0000569	0.0000693	0.0000821	0.3750
9150182	6/16A	15E_4s1d2Qc_1	14 7/16	E	3.25	354.8	35	30	0.126	0.189	HLP-22	12	8	4	1.05	4.5	2.4	21.8	10.1	0.62	0.34	s1d2	2.48	0.0000569	0.0000693	0.0000821	0.3750
9150183	6/16A	15E_4s1d2Qc_1	14 7/16	E	3.25	354.8	35	30	0.126	0.189	HLP-22	12	8	4	1.05	4.5	2.4	21.8	10.1	0.62	0.34	s1d2	2.48	0.0000569	0.0000693	0.0000821	0.3750
9150184	6/16A	15E_4s1d2Qc_1	14 7/16	E	3.25	354.8	35	30	0.126	0.189	HLP-22	12	8	4	1.05	4.5	2.4	21.8	10.1	0.62	0.34	s1d2	2.48	0.0000569	0.0000693	0.0000821	0.3750
9150185	6/16A	15E_4s1d2Qc_1	14 7/16	E	3.25	354.8	35	30	0.126	0.189	HLP-22	12	8	4	1.05	4.5	2.4	21.8	10.1	0.62	0.34	s1d2	2.48	0.0000569	0.0000693	0.0000821	0.3750
9150186	6/16A	15E_4s1d2Qc_1	14 7/16	E	3.25	354.8	35	30	0.126	0.189	HLP-22	12	8	4	1.05	4.5	2.4	21.8	10.1	0.62	0.34	s1d2	2.48	0.0000569	0.0000693	0.0000821	0.3750
9150187M	6/16A	15E_4s1d2Qc_1	14 7/16	E	3.25	354.8	35	30	0.126	0.189	HLP-22	12	8	4	1.05	4.5	2.4	21.8	10.1	0.62	0.34	s1d2	2.48	0.0000569	0.0000693	0.0000821	0.3750
9150188M	6/16A	15E_4s1d2Qc_1	14 7/16	E	3.25	354.8	35	30	0.126	0.189	HLP-22	12	8	4	1.05	4.5	2.4	21.8	10.1	0.62	0.34	s1d2	2.48	0.0000569	0.0000693	0.0000821	0.3750
9150189M	6/16A	15E_4s1d2Qc_1	14 7/16	E	3.25	354.8	35	30	0.126	0.189	HLP-22	12	8	4	1.05	4.5	2.4	21.8	10.1	0.62	0.34	s1d2	2.48	0.0000569	0.0000693	0.0000821	0.3750
9150191M	6/16A	15E_4s1d2Qc_1	14 7/16	E	3.25	354.8	35	30	0.126	0.189	HLP-22	12	8	4	1.05	4.5	2.4	21.8	10.1	0.62	0.34	s1d2	2.48	0.0000569	0.0000693	0.0000821	0.3750
9150192M	6/16A	15E_4s1d2Qc_1	14 7/16	E	3.25	354.8	35	30	0.126	0.189	HLP-22	12	8	4	1.05	4.5	2.4	21.8	10.1	0.62	0.34	s1d2	2.48	0.0000569	0.0000693	0.0000821	0.3750
9150193M	6/16A	15E_4s1d2Qc_1	14 7/16	E	3.25	354.8	35	30	0.126	0.189	HLP-22	12	8	4	1.05	4.5	2.4	21.8	10.1	0.62	0.34	s1d2	2.48	0.0000569	0.0000693	0.0000821	0.3750
9150194	6/16B	15E_4s1d2Wc_1	14 7/16	E	3.25	354.8	34 3/4	30	0.126	0.189	HLP-22	12	8	4	1.05	4.5	2.4	21.8	10.1	0.62	0.34	s1d2	2.48	0.0000569	0.0000693	0.0000821	0.3750
9150195	6/16B	15E_4s1d2Wc_1	14 7/16	E	3.25	354.8	34 3/4	30	0.126	0.189	HLP-22	12	8	4	1.05	4.5	2.4	21.8	10.1	0.62	0.34	s1d2	2.48	0.0000569	0.0000693	0.0000821	0.3750
9150196	6/16B	15E_4s1d2Wc_1	14 7/16	E	3.25	354.8	34 3/4	30	0.126	0.189	HLP-22	12	8	4	1.05	4.5	2.4	21.8	10.1	0.62	0.34	s1d2	2.48	0.0000569	0.0000693	0.0000821	0.3750
9150197	6/16B	15E_4s1d2Wc_1	14 7/16	E	3.25	354.8	34 3/4	30	0.126	0.189	HLP-22	12	8	4	1.05	4.5	2.4	21.8	10.1	0.62	0.34	s1d2	2.48	0.0000569	0.0000693	0.0000821	0.3750
9150198	6/16B	15E_4s1d2Wc_1	14 7/16	E	3.25	354.8	34 3/4	30	0.126	0.189	HLP-22	12	8	4	1.05	4.5	2.4	21.8	10.1	0.62	0.34	s1d2	2.48	0.0000569	0.0000693	0.0000821	0.3750
9150199	6/16B	15E_4s1d2Wc_1	14 7/16	E	3.25	354.8	34 3/4	30	0.126	0.189	HLP-22	12	8	4	1.05	4.5	2.4	21.8	10.1	0.62	0.34	s1d2	2.48	0.0000569	0.0000693	0.0000821	0.3750
9150200	6/16B	15E_4s1d2Wc_1	14 7/16	E	3.25	354.8	34 3/4	30	0.126	0.189	HLP-22	12	8	4	1.05	4.5	2.4	21.8	10.1	0.62	0.34	s1d2	2.48	0.0000569	0.0000693	0.0000821	0.3750
9150201	6/16B	15E_4s1d2Wc_1	14 7/16	E	3.25	354.8	34 3/4	30	0.126	0.189	HLP-22	12	8	4	1.05	4.5	2.4	21.8	10.1	0.62	0.34	s1d2	2.48	0.0000569	0.0000693	0.0000821	0.3750
9150202	6/16B	15E_4s1d2Wc_1	14 7/16	E	3.25	354.8	34 3/4	30	0.126	0.189	HLP-22	12	8	4	1.05	4.5	2.4	21.8	10.1	0.62	0.34	s1d2	2.48	0.0000569	0.0000693	0.0000821	0.3750
9150203	6/16B	15E_4s1d2Wc_1	14 7/16	E	3.25	354.8	34 3/4	30	0.126	0.189	HLP-22	12	8	4	1.05	4.5	2.4	21.8	10.1	0.62	0.34	s1d2	2.48	0.0000569	0.0000693	0.0000821	0.3750
9150204M	6/16B	15E_4s1d2Wc_1	14 7/16	E	3.25	354.8	34 3/4	30	0.126	0.189	HLP-22	12	8	4	1.05	4.5	2.4	21.8	10.1	0.62	0.34	s1d2	2.48	0.0000569	0.0000693	0.0000821	0.3750
9150205M	6/16B	15E_4s1d2Wc_1	14 7/16	E	3.25	354.8	34 3/4	30	0.126	0.189	HLP-22	12	8	4	1.05	4.5	2.4	21.8	10.1	0.62	0.34	s1d2	2.48	0.0000569	0.0000693	0.0000821	0.3750
9150206M	6/16B	15E_4s1d2Wc_1	14 7/16	E	3.25	354.8	34 3/4	30	0.126	0.189	HLP-22	12	8	4	1.05	4.5	2.4	21.8	10.1	0.62	0.34	s1d2	2.48	0.0000569	0.0000693	0.0000821	0.3750
9150207M	6/16B	15E_4s1d2Wc_1	14 7/16	E	3.25	354.8	34 3/4	30	0.126	0.189	HLP-22	12	8	4	1.05	4.5	2.4	21.8	10.1	0.62	0.34	s1d2	2.48	0.0000569	0.0000693	0.0000821	0.3750
9150208M	6/16B	15E_4s1d2Wc_1	14 7/16	E	3.25	354.8	34 3/4	30	0.126	0.189	HLP-22	12	8	4	1.05	4.5	2.4	21.8	10.1	0.62	0.34	s1d2	2.48	0.0000569	0.0000693	0.0000821	0.3750
9150209M	6/16B	15E_4s1d2Wc_1	14 7/16	E	3.25	354.8	34 3/4	30	0.126	0.189	HLP-22	12	8	4	1.05	4.5	2.4	21.8	10.1	0.62	0.34	s1d2	2.48	0.0000569	0.0000693	0.0000821	0.3750
9150210M	6/16B	15E_4s1d2Wc_1	14 7/16	E	3.25	354.8	34 3/4	30	0.126	0.189	HLP-22	12	8	4	1.05	4.5	2.4	21.8	10.1	0.62	0.34	s1d2	2.48	0.0000569	0.0000693	0.0000821	0.3750
9150211M	6/16B	15E_4s1d2Wc_1	14 7/16	E	3.25	354.8	34 3/4	30	0.126	0.189	HLP-22	12	8	4	1.05	4.5	2.4	21.8	10.1	0.62	0.34	s1d2	2.48	0.0000569	0.0000693	0.0000821	0.3750
9150212M	6/16B	15E_4s1d2Wc_1	14 7/16	E	3.25	354.8	34 3/4	30	0.126	0.189	HLP-22	12	8	4	1.05	4.5	2.4	21.8	10.1	0.62	0.34	s1d2	2.48	0.0000569	0.0000693	0.0000821	0.3750
9150212.1	6/16B	15E_4s1d2Wc_1	14 7/16	E	3.25	354.8	34 3/4	30	0.126	0.189	HLP-22	12	8	4	1.05	4.5	2.4	21.8	10.1	0.62	0.34	s1d2	2.48	0.0000569	0.0000693	0.0000821	0.3750
9150212.2	6/16B	15E_4s1d2Wc_1	14 7/16	E	3.25	354.8	34 3/4	30	0.126	0.189	HLP-22	12	8	4	1.05	4.5	2.4	21.8	10.1	0.62	0.34	s1d2	2.48	0.0000569	0.0000693	0.0000821	0.3750
9150212.3	6/16B	15E_4s1d2Wc_1	14 7/16	E	3.25	354.8	34 3/4	30	0.126	0.189	HLP-22	12	8	4	1.05	4.5	2.4	21.8	10.1	0.62	0.34	s1d2	2.48	0.0000569	0.0000693	0.0000821	0.3750
9150212.4	6/16B	15E_4s1d2Wc_1	14 7/16	E	3.25	354.8	34 3/4	30	0.126	0.189	HLP-22	12	8	4	1.05	4.5	2.4	21.8	10.1	0.62	0.34	s1d2	2.48	0.0000569	0.0000693	0.0000821	0.3750
9150213M	6/16B	15E_4s1d2Wc_1	14 7/16	E	3.25	354.8	34 3/4	30	0.126	0.189	HLP-22	12	8	4	1.05	4.5	2.4	21.8	10.1	0.62	0.34	s1d2	2.48	0.0000569	0.0000693	0.0000821	0.3750
9150214	6/16B	15E_4s1d2Wc_1	14 7/16	E	3.25	354.8	34 3/4	30	0.126	0.189	HLP-22	12	8	4	1.05	4.5	2.4	21.8	10.1	0.62	0.34	s1d2	2.48	0.0000569	0.0000693	0.0000821	0.3750
9150215	6/16B	15E_4s1d2Wc_1	14 7/16	E	3.25	354.8	34 3/4	30	0.126	0.189	HLP-22	12	8	4	1.05	4.5	2.4	21.8	10.1	0.62	0.34	s1d2	2.48	0.0000569	0.0000693	0.0000821	0.3750
9150216	6/16B	15E_4s1d2Wc_1	14 7/16	E	3.25	354.8	34 3/4	30	0.126	0.189	HLP-22	12	8	4	1.05	4.5	2.4	21.8	10.1	0.62	0.34	s1d2	2.48	0.0000569	0.0000693	0.0000821	0.3750
9150217	6/16B	15E_4s1d2Wc_1	14 7/16	E	3.25	354.8	34 3/4	30	0.126	0.189	HLP-22	12	8	4	1.05	4.5	2.4	21.8	10.1	0.62	0.34	s1d2	2.48	0.0000569	0.0000693	0.0000821	0.3750

Table B.3. Data from 2008 Tests in Small-Scale Vessel with Elliptical Head B.6

Tank Water Temperature	Water Density	Solids Fraction	Pulse Volume Fraction	Duty Cycle	Cycle Time	Pulsed or Steady Jet	Us Steady Jet	U1 Pulsing Jet	U2 URMS	U3 URM3	Discharge Velocity	Critical Suspension Velocity	Average Peak Cloud Height	UCS Condition	UCS Method	UCS Flag	UCS Center Flag	UCS udv Flag	UCS based on Decreasing Velocity	Sweep Increase / Decrease	UDV Height Bed	Particle Motion	Solids Level	Outer Bottom Pattern	Inner Bottom Pattern	Case ID	Test	TDP	Row Number
C	g/cm³	fraction	fraction	fraction	s	text	m/s	m/s	m/s	m/s	m/s	m/s	in.	m/s	text	text	text	text	m/s	text	mm	text	text	text	text	text	text	text	text
T	ρ_l	ϕ_S	ϕ_P	DC	t_C	Jet	U_S	U1	U2	U3	U	U_{CS}	H_C	U_{CSR}	U_{CSM}	U_{CS}vis	U_{CS}cen	U_{CS}udv	U_{CS_D}	S_W	H_{bed}	PM	Sol	SP_O	SP_I	ID	M/DDX	TDP	MSS
23.4	0.999	0.03000	0.050	0.335	18.0	P	N/A	3.35	3.38	3.40	3.50	6.20	3.38	N/A	N/A	N/A	N/A	N/A	N/A	(null)	22.0	1	N/A	N/A	N/A	15E_4s1d2Qc_1	6/16A	TDP-180	9150180
23.4	0.999	0.03000	0.050	0.332	14.0	P	N/A	4.31	4.37	4.40	4.50	6.20	4.25	N/A	N/A	N/A	N/A	N/A	N/A	I	10.7	1	N/A	N/A	N/A	15E_4s1d2Qc_1	6/16A	TDP-180	9150181
23.4	1.000	0.03000	0.050	0.336	12.6	P	N/A	4.75	4.82	4.86	5.00	6.20	5.00	N/A	N/A	N/A	N/A	N/A	N/A	I	10.9	1	N/A	N/A	N/A	15E_4s1d2Qc_1	6/16A	TDP-180	9150182
23.5	0.999	0.03000	0.050	0.339	11.4	P	N/A	5.21	5.30	5.34	5.50	6.20	5.75	N/A	N/A	N/A	N/A	N/A	N/A	I	4.5	1	N/A	N/A	N/A	15E_4s1d2Qc_1	6/16A	TDP-180	9150183
23.7	0.999	0.03000	0.050	0.336	11.0	P	N/A	5.39	5.49	5.53	5.70	6.20	5.75	N/A	N/A	N/A	N/A	N/A	N/A	I	4.2	1	N/A	N/A	N/A	15E_4s1d2Qc_1	6/16A	TDP-180	9150184
23.8	1.000	0.03000	0.050	0.336	10.6	P	N/A	5.58	5.68	5.73	5.90	6.20	6.25	N/A	N/A	N/A	N/A	N/A	N/A	I	3.8	1	N/A	N/A	N/A	15E_4s1d2Qc_1	6/16A	TDP-180	9150185
23.9	0.999	0.03000	0.050	0.337	10.4	P	N/A	5.69	5.80	5.85	6.00	6.20	6.75	N/A	N/A	UCSvis	N/A	N/A	N/A	I	3.7	3	N/A	N/A	N/A	15E_4s1d2Qc_1	6/16A	TDP-180	9150186
24.1	0.999	0.03000	0.050	0.328	10.4	P	N/A	5.85	5.96	6.02	6.20	6.20	6.75	6.20	udv	N/A	N/A	UCSudv	N/A	I	3.7	4	N/A	N/A	N/A	15E_4s1d2Qc_1	6/16A	TDP-180	9150187
24.2	0.999	0.03000	0.050	0.329	10.0	P	N/A	6.05	6.17	6.23	6.40	6.20	7.50	N/A	N/A	N/A	N/A	N/A	N/A	I	0.0	4	N/A	N/A	N/A	15E_4s1d2Qc_1	6/16A	TDP-180	9150188
24.3	0.999	0.03000	0.050	0.332	9.4	P	N/A	6.43	6.55	6.62	6.80	6.20	9.50	N/A	N/A	N/A	N/A	N/A	N/A	I	0.0	4	N/A	N/A	N/A	15E_4s1d2Qc_1	6/16A	TDP-180	9150189
24.7	0.999	0.03000	0.050	0.337	8.4	P	N/A	7.03	7.19	7.27	7.50	6.20	12.50	N/A	N/A	N/A	N/A	N/A	N/A	I	0.0	4	N/A	N/A	N/A	15E_4s1d2Qc_1	6/16A	TDP-180	9150191
24.9	0.999	0.03000	0.050	0.328	8.1	P	N/A	7.49	7.66	7.74	8.00	6.20	15.25	N/A	N/A	N/A	N/A	N/A	N/A	I	0.0	4	N/A	N/A	N/A	15E_4s1d2Qc_1	6/16A	TDP-180	9150192
25.1	0.999	0.03000	0.050	0.332	7.6	P	N/A	7.92	8.11	8.20	8.50	6.20	20.50	N/A	N/A	N/A	N/A	N/A	N/A	I	0.0	4	N/A	N/A	N/A	15E_4s1d2Qc_1	6/16A	TDP-180	9150193
25.7	0.999	0.04500	0.050	0.331	15.9	P	N/A	3.81	3.87	3.89	4.00	6.50	4.75	N/A	N/A	N/A	N/A	N/A	N/A	(null)	17.1	1	N/A	N/A	N/A	15E_4s1d2Wc_1	6/16B	TDP-181	9150194
25.8	0.999	0.04500	0.050	0.333	14.4	P	N/A	4.20	4.26	4.29	4.40	6.50	5.25	N/A	N/A	N/A	N/A	N/A	N/A	I	16.1	1	N/A	N/A	N/A	15E_4s1d2Wc_1	6/16B	TDP-181	9150195
25.8	0.999	0.04500	0.050	0.332	13.2	P	N/A	4.57	4.64	4.68	4.80	6.50	5.50	N/A	N/A	N/A	N/A	N/A	N/A	I	12.6	1	N/A	N/A	N/A	15E_4s1d2Wc_1	6/16B	TDP-181	9150196
25.9	0.999	0.04500	0.050	0.334	12.2	P	N/A	4.93	5.00	5.04	5.20	6.50	5.75	N/A	N/A	N/A	N/A	N/A	N/A	I	8.6	1	N/A	N/A	N/A	15E_4s1d2Wc_1	6/16B	TDP-181	9150197
26.1	0.999	0.04500	0.050	0.332	11.4	P	N/A	5.30	5.38	5.43	5.60	6.50	6.25	N/A	N/A	N/A	N/A	N/A	N/A	I	5.8	1	N/A	N/A	N/A	15E_4s1d2Wc_1	6/16B	TDP-181	9150198
26.2	0.999	0.04500	0.050	0.335	10.6	P	N/A	5.67	5.77	5.82	6.00	6.50	6.75	N/A	N/A	N/A	N/A	N/A	N/A	I	3.7	1	N/A	N/A	N/A	15E_4s1d2Wc_1	6/16B	TDP-181	9150199
26.2	0.999	0.04500	0.050	0.336	10.4	P	N/A	5.76	5.87	5.92	6.10	6.50	7.25	N/A	N/A	N/A	N/A	N/A	N/A	I	3.7	1	N/A	N/A	N/A	15E_4s1d2Wc_1	6/16B	TDP-181	9150200
26.6	0.999	0.04500	0.050	0.332	10.4	P	N/A	5.83	5.95	6.00	6.20	6.50	7.25	N/A	N/A	N/A	N/A	N/A	N/A	I	2.9	1	N/A	N/A	N/A	15E_4s1d2Wc_1	6/16B	TDP-181	9150201
26.7	0.999	0.04500	0.050	0.333	10.0	P	N/A	5.96	6.07	6.12	6.30	6.50	7.75	N/A	N/A	UCSvis	N/A	N/A	N/A	I	0.7	3	N/A	N/A	N/A	15E_4s1d2Wc_1	6/16B	TDP-181	9150202
26.9	0.999	0.04500	0.050	0.330	10.0	P	N/A	6.04	6.15	6.21	6.40	6.50	7.75	N/A	N/A	N/A	N/A	N/A	N/A	I	0.6	4	N/A	N/A	N/A	15E_4s1d2Wc_1	6/16B	TDP-181	9150203
27.1	0.999	0.04500	0.050	0.332	9.8	P	N/A	6.13	6.25	6.31	6.50	6.50	8.00	6.50	udv	N/A	N/A	UCSudv	N/A	I	1.2	4	N/A	N/A	N/A	15E_4s1d2Wc_1	6/16B	TDP-181	9150204
27.3	0.998	0.04500	0.050	0.329	9.8	P	N/A	6.22	6.34	6.40	6.60	6.50	8.00	N/A	N/A	N/A	N/A	N/A	N/A	I	0.0	4	N/A	N/A	N/A	15E_4s1d2Wc_1	6/16B	TDP-181	9150205
27.5	0.999	0.04500	0.050	0.331	9.4	P	N/A	6.40	6.53	6.59	6.80	6.50	8.25	N/A	N/A	N/A	N/A	N/A	N/A	I	0.0	4	N/A	N/A	N/A	15E_4s1d2Wc_1	6/16B	TDP-181	9150206
27.7	0.999	0.04500	0.050	0.335	9.0	P	N/A	6.59	6.72	6.78	7.00	6.50	9.25	N/A	N/A	N/A	N/A	N/A	N/A	I	0.0	4	N/A	N/A	N/A	15E_4s1d2Wc_1	6/16B	TDP-181	9150207
27.8	0.999	0.04500	0.050	0.336	8.8	P	N/A	6.77	6.91	6.98	7.20	6.50	10.25	N/A	N/A	N/A	N/A	N/A	N/A	I	0.0	4	N/A	N/A	N/A	15E_4s1d2Wc_1	6/16B	TDP-181	9150208
28.2	0.998	0.04500	0.050	0.337	8.4	P	N/A	7.07	7.22	7.29	7.50	6.50	12.00	N/A	N/A	N/A	N/A	N/A	N/A	I	0.0	4	N/A	N/A	N/A	15E_4s1d2Wc_1	6/16B	TDP-181	9150209
28.3	0.998	0.04500	0.050	0.334	8.2	P	N/A	7.34	7.49	7.57	7.80	6.50	12.50	N/A	N/A	N/A	N/A	N/A	N/A	I	0.0	4	N/A	N/A	N/A	15E_4s1d2Wc_1	6/16B	TDP-181	9150210
28.6	0.998	0.04500	0.050	0.335	7.8	P	N/A	7.69	7.86	7.95	8.20	6.50	15.00	N/A	N/A	N/A	N/A	N/A	N/A	I	0.0	4	N/A	N/A	N/A	15E_4s1d2Wc_1	6/16B	TDP-181	9150211
28.8	0.998	0.04500	0.050	0.338	7.4	P	N/A	8.04	8.23	8.32	8.60	6.50	17.00	N/A	N/A	N/A	N/A	N/A	N/A	I	0.0	4	N/A	N/A	N/A	15E_4s1d2Wc_1	6/16B	TDP-181	9150212
29.2	0.998	0.04500	0.050	0.332	9.8	P	N/A	6.14	6.26	6.32	6.50	6.50	7.50	N/A	N/A	N/A	N/A	N/A	N/A	N/A	n/a	N/A	N/A	N/A	N/A	15E_4s1d2Wc_1	6/16B	TDP-181	9150212.1
29.2	0.998	0.04500	0.050	0.332	9.8	P	N/A	6.14	6.26	6.32	6.50	6.50	7.50	N/A	N/A	N/A	N/A	N/A	N/A	N/A	n/a	N/A	N/A	N/A	N/A	15E_4s1d2Wc_1	6/16B	TDP-181	9150212.2
29.2	0.998	0.04500	0.050	0.332	9.8	P	N/A	6.14	6.26	6.32	6.50	6.50	7.50	N/A	N/A	N/A	N/A	N/A	N/A	N/A	n/a	N/A	N/A	N/A	N/A	15E_4s1d2Wc_1	6/16B	TDP-181	9150212.3
29.2	0.998	0.04500	0.050	0.332	9.8	P	N/A	6.14	6.26	6.32	6.50	6.50	7.50	N/A	N/A	N/A	N/A	N/A	N/A	N/A	n/a	N/A	N/A	N/A	N/A	15E_4s1d2Wc_1	6/16B	TDP-181	9150212.4
29.2	0.998	0.04500	0.050	0.332	9.8	P	N/A	6.14	6.26	6.32	6.50	6.50	7.50	N/A	N/A	N/A	N/A	N/A	N/A	I	2.5	4	N/A	N/A	N/A	15E_4s1d2Wc_1	6/16B	TDP-181	9150213
29.2	0.998	0.04500	0.050	0.332	9.8	P	N/A	6.14	6.26	6.32	6.50	6.50	7.50	N/A	N/A	N/A	N/A	N/A	N/A	N/A	1.9	N/A	N/A	N/A	N/A	15E_4s1d2Wc_1	6/16B	TDP-181	9150214
29.2	0.998	0.04500	0.050	0.332	9.8	P	N/A	6.14	6.26	6.32	6.50	6.50	7.50	N/A	N/A	N/A	N/A	N/A	N/A	N/A	2.5	N/A	N/A	N/A	N/A	15E_4s1d2Wc_1	6/16B	TDP-181	9150215
29.2	0.998	0.04500	0.050	0.332	9.8	P	N/A	6.14	6.26	6.32	6.50	6.50	7.50	N/A	N/A	N/A	N/A	N/A	N/A	N/A	1.2	N/A	N/A	N/A	N/A	15E_4s1d2Wc_1	6/16B	TDP-181	9150216
29.2	0.998	0.04500	0.050	0.332	9.8	P	N/A	6.14	6.26	6.32	6.50	6.50	7.50	N/A	N/A	N/A	N/A	N/A	N/A	N/A	0.6	N/A	N/A	N/A	N/A	15E_4s1d2Wc_1	6/16B	TDP-181	9150217

Table B.3. Data from 2008 Tests in Small-Scale Vessel with Elliptical Head A.7

Row Number	Test	Case ID	Tank Diameter	Head Shape	Dish Height	Dish Volume	Tank Fill Height	Return Line Height	Nozzle Inner Diameter	Nozzle Stand-off Distance	Pulse Tube Configuration	Installed Nozzles	Outer Nozzles Operated	Inner Nozzles Operated	Pulse Tube Outer Diameter	Outer PJM Radius	Inner PJM Radius	"FIO" Outer PJM Impingement Angle	"FIO" Inner PJM Impingement Angle	Ratio Outer PJM to Tank Radius	Ratio Inner PJM to Tank Radius	Simulant	Solids Density	Particle Diameter d5	Particle Diameter d50	Particle Diameter d95	Void Fraction
text	text	text	in.	text	in.	in. ^{3}	in.	in.	in.	in.	text	number	number	number	in.	in.	in.	deg	deg	nondim	nondim	text	g/cm^3	m	m	m	fraction
MSS	M/DDX	ID	D	HS	H_{dish}	V_{dish}	H	Rtn	d	sod	PT	N	N_O	N_I	PT_{od}	R_O	R_I	θ_O	θ_I	R_O/R	R_I/R	sxdx	ρ_s	d_5	d_{50}	d_{95}	vf
9150218	6/16B	15E_4s1d2Wc_1	14 7/16	E	3.25	354.8	34 3/4	30	0.126	0.189	HLP-22	12	8	4	1.05	4.5	2.4	21.8	10.1	0.62	0.34	s1d2	2.48	0.0000569	0.0000693	0.0000821	0.3750
9150219	6/16B	15E_4s1d2Wc_1	14 7/16	E	3.25	354.8	34 3/4	30	0.126	0.189	HLP-22	12	8	4	1.05	4.5	2.4	21.8	10.1	0.62	0.34	s1d2	2.48	0.0000569	0.0000693	0.0000821	0.3750
9150220	6/16B	15E_4s1d2Wc_1	14 7/16	E	3.25	354.8	34 3/4	30	0.126	0.189	HLP-22	12	8	4	1.05	4.5	2.4	21.8	10.1	0.62	0.34	s1d2	2.48	0.0000569	0.0000693	0.0000821	0.3750
9150221	6/16B	15E_4s1d2Wc_1	14 7/16	E	3.25	354.8	34 3/4	30	0.126	0.189	HLP-22	12	8	4	1.05	4.5	2.4	21.8	10.1	0.62	0.34	s1d2	2.48	0.0000569	0.0000693	0.0000821	0.3750
9150222	6/16B	15E_4s1d2Wc_1	14 7/16	E	3.25	354.8	34 3/4	30	0.126	0.189	HLP-22	12	8	4	1.05	4.5	2.4	21.8	10.1	0.62	0.34	s1d2	2.48	0.0000569	0.0000693	0.0000821	0.3750
9150223	6/16B	15E_4s1d2Wc_1	14 7/16	E	3.25	354.8	34 3/4	30	0.126	0.189	HLP-22	12	8	4	1.05	4.5	2.4	21.8	10.1	0.62	0.34	s1d2	2.48	0.0000569	0.0000693	0.0000821	0.3750
9150224	6/17A	15E_4s1d2Wd_1	14 7/16	E	3.25	354.8	34 1/2	30	0.126	0.189	HLP-22	12	8	4	1.05	4.5	2.4	21.8	10.1	0.62	0.34	s1d2	2.48	0.0000569	0.0000693	0.0000821	0.3750
9150225	6/17A	15E_4s1d2Wd_1	14 7/16	E	3.25	354.8	34 1/2	30	0.126	0.189	HLP-22	12	8	4	1.05	4.5	2.4	21.8	10.1	0.62	0.34	s1d2	2.48	0.0000569	0.0000693	0.0000821	0.3750
9150226	6/17A	15E_4s1d2Wd_1	14 7/16	E	3.25	354.8	34 1/2	30	0.126	0.189	HLP-22	12	8	4	1.05	4.5	2.4	21.8	10.1	0.62	0.34	s1d2	2.48	0.0000569	0.0000693	0.0000821	0.3750
9150227	6/17A	15E_4s1d2Wd_1	14 7/16	E	3.25	354.8	34 1/2	30	0.126	0.189	HLP-22	12	8	4	1.05	4.5	2.4	21.8	10.1	0.62	0.34	s1d2	2.48	0.0000569	0.0000693	0.0000821	0.3750
9150228	6/17A	15E_4s1d2Wd_1	14 7/16	E	3.25	354.8	34 1/2	30	0.126	0.189	HLP-22	12	8	4	1.05	4.5	2.4	21.8	10.1	0.62	0.34	s1d2	2.48	0.0000569	0.0000693	0.0000821	0.3750
9150229	6/17A	15E_4s1d2Wd_1	14 7/16	E	3.25	354.8	34 1/2	30	0.126	0.189	HLP-22	12	8	4	1.05	4.5	2.4	21.8	10.1	0.62	0.34	s1d2	2.48	0.0000569	0.0000693	0.0000821	0.3750
9150230	6/17A	15E_4s1d2Wd_1	14 7/16	E	3.25	354.8	34 1/2	30	0.126	0.189	HLP-22	12	8	4	1.05	4.5	2.4	21.8	10.1	0.62	0.34	s1d2	2.48	0.0000569	0.0000693	0.0000821	0.3750
9150231	6/17A	15E_4s1d2Wd_1	14 7/16	E	3.25	354.8	34 1/2	30	0.126	0.189	HLP-22	12	8	4	1.05	4.5	2.4	21.8	10.1	0.62	0.34	s1d2	2.48	0.0000569	0.0000693	0.0000821	0.3750
9150232	6/17A	15E_4s1d2Wd_1	14 7/16	E	3.25	354.8	34 1/2	30	0.126	0.189	HLP-22	12	8	4	1.05	4.5	2.4	21.8	10.1	0.62	0.34	s1d2	2.48	0.0000569	0.0000693	0.0000821	0.3750
9150233M	6/17A	15E_4s1d2Wd_1	14 7/16	E	3.25	354.8	34 1/2	30	0.126	0.189	HLP-22	12	8	4	1.05	4.5	2.4	21.8	10.1	0.62	0.34	s1d2	2.48	0.0000569	0.0000693	0.0000821	0.3750
9150234M	6/17A	15E_4s1d2Wd_1	14 7/16	E	3.25	354.8	34 1/2	30	0.126	0.189	HLP-22	12	8	4	1.05	4.5	2.4	21.8	10.1	0.62	0.34	s1d2	2.48	0.0000569	0.0000693	0.0000821	0.3750
9150235M	6/17A	15E_4s1d2Wd_1	14 7/16	E	3.25	354.8	34 1/2	30	0.126	0.189	HLP-22	12	8	4	1.05	4.5	2.4	21.8	10.1	0.62	0.34	s1d2	2.48	0.0000569	0.0000693	0.0000821	0.3750
9150236M	6/17A	15E_4s1d2Wd_1	14 7/16	E	3.25	354.8	34 1/2	30	0.126	0.189	HLP-22	12	8	4	1.05	4.5	2.4	21.8	10.1	0.62	0.34	s1d2	2.48	0.0000569	0.0000693	0.0000821	0.3750
9150237M	6/17A	15E_4s1d2Wd_1	14 7/16	E	3.25	354.8	34 1/2	30	0.126	0.189	HLP-22	12	8	4	1.05	4.5	2.4	21.8	10.1	0.62	0.34	s1d2	2.48	0.0000569	0.0000693	0.0000821	0.3750
9150238M	6/17A	15E_4s1d2Wd_1	14 7/16	E	3.25	354.8	34 1/2	30	0.126	0.189	HLP-22	12	8	4	1.05	4.5	2.4	21.8	10.1	0.62	0.34	s1d2	2.48	0.0000569	0.0000693	0.0000821	0.3750
9150239M	6/17A	15E_4s1d2Wd_1	14 7/16	E	3.25	354.8	34 1/2	30	0.126	0.189	HLP-22	12	8	4	1.05	4.5	2.4	21.8	10.1	0.62	0.34	s1d2	2.48	0.0000569	0.0000693	0.0000821	0.3750
9150240M	6/17A	15E_4s1d2Wd_1	14 7/16	E	3.25	354.8	34 1/2	30	0.126	0.189	HLP-22	12	8	4	1.05	4.5	2.4	21.8	10.1	0.62	0.34	s1d2	2.48	0.0000569	0.0000693	0.0000821	0.3750
9150240.1	6/17A	15E_4s1d2Wd_1	14 7/16	E	3.25	354.8	34 1/2	30	0.126	0.189	HLP-22	12	8	4	1.05	4.5	2.4	21.8	10.1	0.62	0.34	s1d2	2.48	0.0000569	0.0000693	0.0000821	0.3750
9150240.2	6/17A	15E_4s1d2Wd_1	14 7/16	E	3.25	354.8	34 1/2	30	0.126	0.189	HLP-22	12	8	4	1.05	4.5	2.4	21.8	10.1	0.62	0.34	s1d2	2.48	0.0000569	0.0000693	0.0000821	0.3750
9150240.3	6/17A	15E_4s1d2Wd_1	14 7/16	E	3.25	354.8	34 1/2	30	0.126	0.189	HLP-22	12	8	4	1.05	4.5	2.4	21.8	10.1	0.62	0.34	s1d2	2.48	0.0000569	0.0000693	0.0000821	0.3750
9150240.4	6/17A	15E_4s1d2Wd_1	14 7/16	E	3.25	354.8	34 1/2	30	0.126	0.189	HLP-22	12	8	4	1.05	4.5	2.4	21.8	10.1	0.62	0.34	s1d2	2.48	0.0000569	0.0000693	0.0000821	0.3750
9150240.5	6/17A	15E_4s1d2Wd_1	14 7/16	E	3.25	354.8	34 1/2	30	0.126	0.189	HLP-22	12	8	4	1.05	4.5	2.4	21.8	10.1	0.62	0.34	s1d2	2.48	0.0000569	0.0000693	0.0000821	0.3750
9150240.6	6/17A	15E_4s1d2Wd_1	14 7/16	E	3.25	354.8	34 1/2	30	0.126	0.189	HLP-22	12	8	4	1.05	4.5	2.4	21.8	10.1	0.62	0.34	s1d2	2.48	0.0000569	0.0000693	0.0000821	0.3750
9150240.7	6/17A	15E_4s1d2Wd_1	14 7/16	E	3.25	354.8	34 1/2	30	0.126	0.189	HLP-22	12	8	4	1.05	4.5	2.4	21.8	10.1	0.62	0.34	s1d2	2.48	0.0000569	0.0000693	0.0000821	0.3750
9150241M	6/17A	15E_4s1d2Wd_1	14 7/16	E	3.25	354.8	34 1/2	30	0.126	0.189	HLP-22	12	8	4	1.05	4.5	2.4	21.8	10.1	0.62	0.34	s1d2	2.48	0.0000569	0.0000693	0.0000821	0.3750
9150242	6/17A	15E_4s1d2Wd_1	14 7/16	E	3.25	354.8	34 1/2	30	0.126	0.189	HLP-22	12	8	4	1.05	4.5	2.4	21.8	10.1	0.62	0.34	s1d2	2.48	0.0000569	0.0000693	0.0000821	0.3750
9150243	6/17A	15E_4s1d2Wd_1	14 7/16	E	3.25	354.8	34 1/2	30	0.126	0.189	HLP-22	12	8	4	1.05	4.5	2.4	21.8	10.1	0.62	0.34	s1d2	2.48	0.0000569	0.0000693	0.0000821	0.3750
9150244	6/17A	15E_4s1d2Wd_1	14 7/16	E	3.25	354.8	34 1/2	30	0.126	0.189	HLP-22	12	8	4	1.05	4.5	2.4	21.8	10.1	0.62	0.34	s1d2	2.48	0.0000569	0.0000693	0.0000821	0.3750
9150245	6/17A	15E_4s1d2Wd_1	14 7/16	E	3.25	354.8	34 1/2	30	0.126	0.189	HLP-22	12	8	4	1.05	4.5	2.4	21.8	10.1	0.62	0.34	s1d2	2.48	0.0000569	0.0000693	0.0000821	0.3750
9150246	6/17A	15E_4s1d2Wd_1	14 7/16	E	3.25	354.8	34 1/2	30	0.126	0.189	HLP-22	12	8	4	1.05	4.5	2.4	21.8	10.1	0.62	0.34	s1d2	2.48	0.0000569	0.0000693	0.0000821	0.3750
9150247	6/17A	15E_4s1d2Wd_1	14 7/16	E	3.25	354.8	34 1/2	30	0.126	0.189	HLP-22	12	8	4	1.05	4.5	2.4	21.8	10.1	0.62	0.34	s1d2	2.48	0.0000569	0.0000693	0.0000821	0.3750
9150248	6/17A	15E_4s1d2Wd_1	14 7/16	E	3.25	354.8	34 1/2	30	0.126	0.189	HLP-22	12	8	4	1.05	4.5	2.4	21.8	10.1	0.62	0.34	s1d2	2.48	0.0000569	0.0000693	0.0000821	0.3750
9150249	6/17B	15E_4s1d2Wa	14 7/16	E	3.25	354.8	34 1/2	30	0.126	0.189	HLP-22	12	8	4	1.05	4.5	2.4	21.8	10.1	0.62	0.34	s1d2	2.48	0.0000569	0.0000693	0.0000821	0.3750
9150250	6/17B	15E_4s1d2Wa	14 7/16	E	3.25	354.8	34 1/2	30	0.126	0.189	HLP-22	12	8	4	1.05	4.5	2.4	21.8	10.1	0.62	0.34	s1d2	2.48	0.0000569	0.0000693	0.0000821	0.3750
9150251	6/17B	15E_4s1d2Wa	14 7/16	E	3.25	354.8	34 1/2	30	0.126	0.189	HLP-22	12	8	4	1.05	4.5	2.4	21.8	10.1	0.62	0.34	s1d2	2.48	0.0000569	0.0000693	0.0000821	0.3750

Table B.3. Data from 2008 Tests in Small-Scale Vessel with Elliptical Head B.7

Tank Water Temperature	Water Density	Solids Fraction	Pulse Volume Fraction	Duty Cycle	Cycle Time	Pulsed or Steady Jet	Us Steady Jet	U1 Pulsing Jet	U2 URMS	U3 URM3	Discharge Velocity	Critical Suspension Velocity	Average Peak Cloud Height	UCS Condition	UCS Method	UCS Flag	UCS Center Flag	UCS udv Flag	UCS based on Decreasing Velocity	Sweep Increase / Decrease	UDV Height Bed	Particle Motion	Solids Level	Outer Bottom Pattern	Inner Bottom Pattern	Case ID	Test	TDP	Row Number
C	g/cm3	fraction	fraction	fraction	s	text	m/s	m/s	m/s	m/s	m/s	m/s	in.	m/s	text	text	text	text	m/s	text	mm	text	text	text	text	text	text	text	text
T	ρ_l	ϕ_S	ϕ_P	DC	t_C	Jet	U_S	U1	U2	U3	U	U_{CS}	H_C	U_{CSR}	U_{CSM}	U_{CS}vis	U_{CS}cen	U_{CS}udv	U_{CS}_D	S_W	H_{bed}	PM	Sol	SP_O	SP_I	ID	M/DDX	TDP	MSS
29.2	0.998	0.04500	0.050	0.332	9.8	P	N/A	6.14	6.26	6.32	6.50	6.50	7.50	N/A	N/A	N/A	N/A	N/A	N/A	N/A	1.2	N/A	N/A	N/A	N/A	15E_4s1d2Wc_1	6/16B	TDP-181	9150218
29.2	0.998	0.04500	0.050	0.332	9.8	P	N/A	6.14	6.26	6.32	6.50	6.50	7.50	N/A	N/A	N/A	N/A	N/A	N/A	N/A	0.0	N/A	N/A	N/A	N/A	15E_4s1d2Wc_1	6/16B	TDP-181	9150219
29.2	0.998	0.04500	0.050	0.332	9.8	P	N/A	6.14	6.26	6.32	6.50	6.50	7.50	N/A	N/A	N/A	N/A	N/A	N/A	N/A	3.1	N/A	N/A	N/A	N/A	15E_4s1d2Wc_1	6/16B	TDP-181	9150220
29.2	0.998	0.04500	0.050	0.332	9.8	P	N/A	6.14	6.26	6.32	6.50	6.50	7.50	N/A	N/A	N/A	N/A	N/A	N/A	N/A	0.0	N/A	N/A	N/A	N/A	15E_4s1d2Wc_1	6/16B	TDP-181	9150221
29.2	0.998	0.04500	0.050	0.332	9.8	P	N/A	6.14	6.26	6.32	6.50	6.50	7.50	N/A	N/A	N/A	N/A	N/A	N/A	N/A	3.1	N/A	N/A	N/A	N/A	15E_4s1d2Wc_1	6/16B	TDP-181	9150222
29.2	0.998	0.04500	0.050	0.332	9.8	P	N/A	6.14	6.26	6.32	6.50	6.50	7.50	N/A	N/A	N/A	N/A	N/A	N/A	N/A	2.5	N/A	N/A	N/A	N/A	15E_4s1d2Wc_1	6/16B	TDP-181	9150223
24.5	0.999	0.04500	0.050	0.183	29.0	P	N/A	3.79	3.84	3.87	4.00	7.20	3.50	N/A	N/A	N/A	N/A	N/A	N/A	(null)	22.0	1	N/A	N/A	N/A	15E_4s1d2Wd_1	6/17A	TDP-182	9150224
24.5	0.999	0.04500	0.050	0.184	26.2	P	N/A	4.17	4.23	4.26	4.40	7.20	3.75	N/A	N/A	N/A	N/A	N/A	N/A	I	18.8	1	N/A	N/A	N/A	15E_4s1d2Wd_1	6/17A	TDP-182	9150225
24.7	0.999	0.04500	0.050	0.184	24.0	P	N/A	4.54	4.61	4.64	4.80	7.20	4.25	N/A	N/A	N/A	N/A	N/A	N/A	I	16.4	1	N/A	N/A	N/A	15E_4s1d2Wd_1	6/17A	TDP-182	9150226
24.7	0.999	0.04500	0.050	0.185	22.0	P	N/A	4.91	4.99	5.03	5.20	7.20	4.50	N/A	N/A	N/A	N/A	N/A	N/A	I	13.5	1	N/A	N/A	N/A	15E_4s1d2Wd_1	6/17A	TDP-182	9150227
24.8	0.999	0.04500	0.050	0.186	19.0	P	N/A	5.65	5.75	5.80	6.00	7.20	5.25	N/A	N/A	N/A	N/A	N/A	N/A	I	6.5	1	N/A	N/A	N/A	15E_4s1d2Wd_1	6/17A	TDP-182	9150228
25.0	0.999	0.04500	0.050	0.187	17.8	P	N/A	6.03	6.14	6.20	6.40	7.20	5.50	N/A	N/A	N/A	N/A	N/A	N/A	I	3.9	1	N/A	N/A	N/A	15E_4s1d2Wd_1	6/17A	TDP-182	9150229
25.1	0.999	0.04500	0.050	0.188	17.2	P	N/A	6.21	6.33	6.39	6.60	7.20	5.75	N/A	N/A	N/A	N/A	N/A	N/A	I	3.8	1	N/A	N/A	N/A	15E_4s1d2Wd_1	6/17A	TDP-182	9150230
25.2	0.999	0.04500	0.050	0.189	16.6	P	N/A	6.41	6.53	6.60	6.80	7.20	5.75	N/A	N/A	N/A	N/A	N/A	N/A	I	3.8	1	N/A	N/A	N/A	15E_4s1d2Wd_1	6/17A	TDP-182	9150231
25.4	0.999	0.04500	0.050	0.187	16.2	P	N/A	6.58	6.71	6.78	7.00	7.20	6.00	N/A	N/A	N/A	N/A	N/A	N/A	I	3.8	1	N/A	N/A	N/A	15E_4s1d2Wd_1	6/17A	TDP-182	9150232
25.6	0.999	0.04500	0.050	0.188	15.8	P	N/A	6.78	6.91	6.98	7.20	7.20	6.00	7.20	udv	N/A	N/A	UCSudv	N/A	I	2.5	1	N/A	N/A	N/A	15E_4s1d2Wd_1	6/17A	TDP-182	9150233
25.8	0.999	0.04500	0.050	0.187	15.4	P	N/A	6.95	7.10	7.17	7.40	7.20	6.25	N/A	N/A	UCSvis	N/A	N/A	N/A	I	0.0	3	N/A	N/A	N/A	15E_4s1d2Wd_1	6/17A	TDP-182	9150234
25.9	0.999	0.04500	0.050	0.187	15.0	P	N/A	7.13	7.28	7.36	7.60	7.20	6.75	N/A	N/A	N/A	N/A	N/A	N/A	I	0.0	4	N/A	N/A	N/A	15E_4s1d2Wd_1	6/17A	TDP-182	9150235
26.3	0.999	0.04500	0.050	0.189	14.2	P	N/A	7.49	7.65	7.73	8.00	7.20	7.00	N/A	N/A	N/A	N/A	N/A	N/A	I	0.0	4	N/A	N/A	N/A	15E_4s1d2Wd_1	6/17A	TDP-182	9150236
26.5	0.999	0.04500	0.050	0.187	13.0	P	N/A	8.18	8.38	8.48	8.80	7.20	8.25	N/A	N/A	N/A	N/A	N/A	N/A	I	0.0	4	N/A	N/A	N/A	15E_4s1d2Wd_1	6/17A	TDP-182	9150237
26.9	0.999	0.04500	0.050	0.187	12.2	P	N/A	8.70	8.92	9.04	9.40	7.20	9.25	N/A	N/A	N/A	N/A	N/A	N/A	I	0.0	4	N/A	N/A	N/A	15E_4s1d2Wd_1	6/17A	TDP-182	9150238
27.2	0.999	0.04500	0.050	0.189	11.4	P	N/A	9.26	9.50	9.63	10.00	7.20	10.50	N/A	N/A	N/A	N/A	N/A	N/A	I	0.0	4	N/A	N/A	N/A	15E_4s1d2Wd_1	6/17A	TDP-182	9150239
27.9	0.998	0.04500	0.050	0.185	11.0	P	N/A	9.77	###	10.18	10.60	7.20	12.00	N/A	N/A	N/A	N/A	N/A	N/A	I	0.0	4	N/A	N/A	N/A	15E_4s1d2Wd_1	6/17A	TDP-182	9150240
28.3	0.998	0.04500	0.050	0.188	15.8	P	N/A	6.77	6.91	6.98	7.20	7.20	5.75	N/A	N/A	N/A	N/A	N/A	N/A	N/A	n/a	N/A	N/A	N/A	N/A	15E_4s1d2Wd_1	6/17A	TDP-182	9150240.1
28.3	0.998	0.04500	0.050	0.188	15.8	P	N/A	6.77	6.91	6.98	7.20	7.20	5.75	N/A	N/A	N/A	N/A	N/A	N/A	N/A	n/a	N/A	N/A	N/A	N/A	15E_4s1d2Wd_1	6/17A	TDP-182	9150240.2
28.3	0.998	0.04500	0.050	0.188	15.8	P	N/A	6.77	6.91	6.98	7.20	7.20	5.75	N/A	N/A	N/A	N/A	N/A	N/A	N/A	n/a	N/A	N/A	N/A	N/A	15E_4s1d2Wd_1	6/17A	TDP-182	9150240.3
28.3	0.998	0.04500	0.050	0.188	15.8	P	N/A	6.77	6.91	6.98	7.20	7.20	5.75	N/A	N/A	N/A	N/A	N/A	N/A	N/A	n/a	N/A	N/A	N/A	N/A	15E_4s1d2Wd_1	6/17A	TDP-182	9150240.4
28.3	0.998	0.04500	0.050	0.188	15.8	P	N/A	6.77	6.91	6.98	7.20	7.20	5.75	N/A	N/A	N/A	N/A	N/A	N/A	N/A	n/a	N/A	N/A	N/A	N/A	15E_4s1d2Wd_1	6/17A	TDP-182	9150240.5
28.3	0.998	0.04500	0.050	0.188	15.8	P	N/A	6.77	6.91	6.98	7.20	7.20	5.75	N/A	N/A	N/A	N/A	N/A	N/A	I	n/a	N/A	N/A	N/A	N/A	15E_4s1d2Wd_1	6/17A	TDP-182	9150240.6
28.3	0.998	0.04500	0.050	0.188	15.8	P	N/A	6.77	6.91	6.98	7.20	7.20	5.75	N/A	N/A	N/A	N/A	N/A	N/A	N/A	n/a	N/A	N/A	N/A	N/A	15E_4s1d2Wd_1	6/17A	TDP-182	9150240.7
28.3	0.998	0.04500	0.050	0.188	15.8	P	N/A	6.77	6.91	6.98	7.20	7.20	5.75	N/A	N/A	N/A	N/A	N/A	N/A	N/A	3.7	1	N/A	N/A	N/A	15E_4s1d2Wd_1	6/17A	TDP-182	9150241
28.3	0.998	0.04500	0.050	0.188	15.8	P	N/A	6.77	6.91	6.98	7.20	7.20	5.75	N/A	N/A	N/A	N/A	N/A	N/A	N/A	1.5	N/A	N/A	N/A	N/A	15E_4s1d2Wd_1	6/17A	TDP-182	9150242
28.3	0.998	0.04500	0.050	0.188	15.8	P	N/A	6.77	6.91	6.98	7.20	7.20	5.75	N/A	N/A	N/A	N/A	N/A	N/A	N/A	0.7	N/A	N/A	N/A	N/A	15E_4s1d2Wd_1	6/17A	TDP-182	9150243
28.3	0.998	0.04500	0.050	0.188	15.8	P	N/A	6.77	6.91	6.98	7.20	7.20	5.75	N/A	N/A	N/A	N/A	N/A	N/A	N/A	2.2	N/A	N/A	N/A	N/A	15E_4s1d2Wd_1	6/17A	TDP-182	9150244
28.3	0.998	0.04500	0.050	0.188	15.8	P	N/A	6.77	6.91	6.98	7.20	7.20	5.75	N/A	N/A	N/A	N/A	N/A	N/A	N/A	2.1	N/A	N/A	N/A	N/A	15E_4s1d2Wd_1	6/17A	TDP-182	9150245
28.3	0.998	0.04500	0.050	0.188	15.8	P	N/A	6.77	6.91	6.98	7.20	7.20	5.75	N/A	N/A	N/A	N/A	N/A	N/A	N/A	2.2	N/A	N/A	N/A	N/A	15E_4s1d2Wd_1	6/17A	TDP-182	9150246
28.3	0.998	0.04500	0.050	0.188	15.8	P	N/A	6.77	6.91	6.98	7.20	7.20	5.75	N/A	N/A	N/A	N/A	N/A	N/A	N/A	2.2	N/A	N/A	N/A	N/A	15E_4s1d2Wd_1	6/17A	TDP-182	9150247
28.3	0.998	0.04500	0.050	0.188	15.8	P	N/A	6.77	6.91	6.98	7.20	7.20	5.75	N/A	N/A	N/A	N/A	N/A	N/A	N/A	3.1	N/A	N/A	N/A	N/A	15E_4s1d2Wd_1	6/17A	TDP-182	9150248
27.1	0.999	0.04500	undefined	1.000	infinite	S	2.00	n/a	n/a	n/a	2.00	3.00	5.63	N/A	N/A	N/A	N/A	N/A	N/A	(null)	20.4	1	N/A	N/A	N/A	15E_4s1d2Wa	6/17B	TDP-182	9150249
27.1	0.999	0.04500	undefined	1.000	infinite	S	2.41	n/a	n/a	n/a	2.40	3.00	7.88	N/A	N/A	N/A	N/A	N/A	N/A	I	7.5	1	N/A	N/A	N/A	15E_4s1d2Wa	6/17B	TDP-182	9150250
27.2	0.998	0.04500	undefined	1.000	infinite	S	2.79	n/a	n/a	n/a	2.80	3.00	11.50	N/A	N/A	N/A	N/A	N/A	N/A	I	4.2	1	N/A	N/A	N/A	15E_4s1d2Wa	6/17B	TDP-182	9150251

Table B.3. Data from 2008 Tests in Small-Scale Vessel with Elliptical Head A.8

Row Number	Test	Case ID	Tank Diameter	Head Shape	Dish Height	Dish Volume	Tank Fill Height	Return Line Height	Nozzle Inner Diameter	Nozzle Stand-off Distance	Pulse Tube Configuration	Installed Nozzles	Outer Nozzles Operated	Inner Nozzles Operated	Pulse Tube Outer Diameter	Outer PJM Radius	Inner PJM Radius	"FIO" Outer PJM Impingement Angle	"FIO" Inner PJM Impingement Angle	Ratio Outer PJM to Tank Radius	Ratio Inner PJM to Tank Radius	Simulant	Solids Density	Particle Diameter d5	Particle Diameter d50	Particle Diameter d95	Void Fraction
text	text	text	in.	text	in.	in. ^{3}	in.	in.	in.	in.	text	number	number	number	in.	in.	in.	deg	deg	nondim	nondim	text	g/cm^3	m	m	m	fraction
MSS	M/DDX	ID	D	HS	H_{dish}	V_{dish}	H	Rtn	d	sod	PT	N	N_O	N_I	PT_{od}	R_O	R_I	θ_O	θ_I	R_O/R	R_I/R	sxdx	ρ_s	d_5	d_{50}	d_{95}	vf
9150252	6/17B	15E_4s1d2Wa	14 7/16	E	3.25	354.8	34 1/2	30	0.126	0.189	HLP-22	12	8	4	1.05	4.5	2.4	21.8	10.1	0.62	0.34	s1d2	2.48	0.0000569	0.0000693	0.0000821	0.3750
9150253	6/17B	15E_4s1d2Wa	14 7/16	E	3.25	354.8	34 1/2	30	0.126	0.189	HLP-22	12	8	4	1.05	4.5	2.4	21.8	10.1	0.62	0.34	s1d2	2.48	0.0000569	0.0000693	0.0000821	0.3750
9150254	6/17B	15E_4s1d2Wa	14 7/16	E	3.25	354.8	34 1/2	30	0.126	0.189	HLP-22	12	8	4	1.05	4.5	2.4	21.8	10.1	0.62	0.34	s1d2	2.48	0.0000569	0.0000693	0.0000821	0.3750
9150255	6/17B	15E_4s1d2Wa	14 7/16	E	3.25	354.8	34 1/2	30	0.126	0.189	HLP-22	12	8	4	1.05	4.5	2.4	21.8	10.1	0.62	0.34	s1d2	2.48	0.0000569	0.0000693	0.0000821	0.3750
9150256	6/17B	15E_4s1d2Wa	14 7/16	E	3.25	354.8	34 1/2	30	0.126	0.189	HLP-22	12	8	4	1.05	4.5	2.4	21.8	10.1	0.62	0.34	s1d2	2.48	0.0000569	0.0000693	0.0000821	0.3750
9150257	6/17B	15E_4s1d2Wa	14 7/16	E	3.25	354.8	34 1/2	30	0.126	0.189	HLP-22	12	8	4	1.05	4.5	2.4	21.8	10.1	0.62	0.34	s1d2	2.48	0.0000569	0.0000693	0.0000821	0.3750
9150258	6/17B	15E_4s1d2Wa	14 7/16	E	3.25	354.8	34 1/2	30	0.126	0.189	HLP-22	12	8	4	1.05	4.5	2.4	21.8	10.1	0.62	0.34	s1d2	2.48	0.0000569	0.0000693	0.0000821	0.3750
9150259	6/17B	15E_4s1d2Wa	14 7/16	E	3.25	354.8	34 1/2	30	0.126	0.189	HLP-22	12	8	4	1.05	4.5	2.4	21.8	10.1	0.62	0.34	s1d2	2.48	0.0000569	0.0000693	0.0000821	0.3750
9150260	6/17B	15E_4s1d2Wa	14 7/16	E	3.25	354.8	34 1/2	30	0.126	0.189	HLP-22	12	8	4	1.05	4.5	2.4	21.8	10.1	0.62	0.34	s1d2	2.48	0.0000569	0.0000693	0.0000821	0.3750
9150261	6/17B	15E_4s1d2Wa	14 7/16	E	3.25	354.8	34 1/2	30	0.126	0.189	HLP-22	12	8	4	1.05	4.5	2.4	21.8	10.1	0.62	0.34	s1d2	2.48	0.0000569	0.0000693	0.0000821	0.3750
9150262	6/17B	15E_4s1d2Wa	14 7/16	E	3.25	354.8	34 1/2	30	0.126	0.189	HLP-22	12	8	4	1.05	4.5	2.4	21.8	10.1	0.62	0.34	s1d2	2.48	0.0000569	0.0000693	0.0000821	0.3750
9150263	6/17B	15E_4s1d2Wa	14 7/16	E	3.25	354.8	34 1/2	30	0.126	0.189	HLP-22	12	8	4	1.05	4.5	2.4	21.8	10.1	0.62	0.34	s1d2	2.48	0.0000569	0.0000693	0.0000821	0.3750
9150264	6/17B	15E_4s1d2Wa	14 7/16	E	3.25	354.8	34 1/2	30	0.126	0.189	HLP-22	12	8	4	1.05	4.5	2.4	21.8	10.1	0.62	0.34	s1d2	2.48	0.0000569	0.0000693	0.0000821	0.3750
9150265	6/17B	15E_4s1d2Wa	14 7/16	E	3.25	354.8	34 1/2	30	0.126	0.189	HLP-22	12	8	4	1.05	4.5	2.4	21.8	10.1	0.62	0.34	s1d2	2.48	0.0000569	0.0000693	0.0000821	0.3750
9150266M	6/17C	15E_4s1d2Wc_1	14 7/16	E	3.25	354.8	34 1/2	30	0.126	0.189	HLP-22	12	8	4	1.05	4.5	2.4	21.8	10.1	0.62	0.34	s1d2	2.48	0.0000569	0.0000693	0.0000821	0.3750
9150267	6/17C	15E_4s1d2Wc_1	14 7/16	E	3.25	354.8	34 1/2	30	0.126	0.189	HLP-22	12	8	4	1.05	4.5	2.4	21.8	10.1	0.62	0.34	s1d2	2.48	0.0000569	0.0000693	0.0000821	0.3750
9150268	6/17C	15E_4s1d2Wc_1	14 7/16	E	3.25	354.8	34 1/2	30	0.126	0.189	HLP-22	12	8	4	1.05	4.5	2.4	21.8	10.1	0.62	0.34	s1d2	2.48	0.0000569	0.0000693	0.0000821	0.3750
9150269	6/17C	15E_4s1d2Wc_1	14 7/16	E	3.25	354.8	34 1/2	30	0.126	0.189	HLP-22	12	8	4	1.05	4.5	2.4	21.8	10.1	0.62	0.34	s1d2	2.48	0.0000569	0.0000693	0.0000821	0.3750
9150270	6/17C	15E_4s1d2Wc_1	14 7/16	E	3.25	354.8	34 1/2	30	0.126	0.189	HLP-22	12	8	4	1.05	4.5	2.4	21.8	10.1	0.62	0.34	s1d2	2.48	0.0000569	0.0000693	0.0000821	0.3750
9150271	6/17C	15E_4s1d2Wc_1	14 7/16	E	3.25	354.8	34 1/2	30	0.126	0.189	HLP-22	12	8	4	1.05	4.5	2.4	21.8	10.1	0.62	0.34	s1d2	2.48	0.0000569	0.0000693	0.0000821	0.3750
9150272	6/17C	15E_4s1d2Wc_1	14 7/16	E	3.25	354.8	34 1/2	30	0.126	0.189	HLP-22	12	8	4	1.05	4.5	2.4	21.8	10.1	0.62	0.34	s1d2	2.48	0.0000569	0.0000693	0.0000821	0.3750
9150273	6/17C	15E_4s1d2Wc_1	14 7/16	E	3.25	354.8	34 1/2	30	0.126	0.189	HLP-22	12	8	4	1.05	4.5	2.4	21.8	10.1	0.62	0.34	s1d2	2.48	0.0000569	0.0000693	0.0000821	0.3750
9150274	6/17C	15E_4s1d2Wc_1	14 7/16	E	3.25	354.8	34 1/2	30	0.126	0.189	HLP-22	12	8	4	1.05	4.5	2.4	21.8	10.1	0.62	0.34	s1d2	2.48	0.0000569	0.0000693	0.0000821	0.3750
9150275	6/17C	15E_4s1d2Wc_1	14 7/16	E	3.25	354.8	34 1/2	30	0.126	0.189	HLP-22	12	8	4	1.05	4.5	2.4	21.8	10.1	0.62	0.34	s1d2	2.48	0.0000569	0.0000693	0.0000821	0.3750
9150276	6/17C	15E_4s1d2Wc_1	14 7/16	E	3.25	354.8	34 1/2	30	0.126	0.189	HLP-22	12	8	4	1.05	4.5	2.4	21.8	10.1	0.62	0.34	s1d2	2.48	0.0000569	0.0000693	0.0000821	0.3750
9150277	6/17C	15E_4s1d2Wc_1	14 7/16	E	3.25	354.8	34 1/2	30	0.126	0.189	HLP-22	12	8	4	1.05	4.5	2.4	21.8	10.1	0.62	0.34	s1d2	2.48	0.0000569	0.0000693	0.0000821	0.3750
9150278	6/18A	15E_4s1d2Pc_1	14 7/16	E	3.25	354.8	34 1/2	30	0.126	0.189	HLP-22	12	8	4	1.05	4.5	2.4	21.8	10.1	0.62	0.34	s1d2	2.48	0.0000569	0.0000693	0.0000821	0.3750
9150279	6/18A	15E_4s1d2Pc_1	14 7/16	E	3.25	354.8	34 1/2	30	0.126	0.189	HLP-22	12	8	4	1.05	4.5	2.4	21.8	10.1	0.62	0.34	s1d2	2.48	0.0000569	0.0000693	0.0000821	0.3750
9150280	6/18A	15E_4s1d2Pc_1	14 7/16	E	3.25	354.8	34 1/2	30	0.126	0.189	HLP-22	12	8	4	1.05	4.5	2.4	21.8	10.1	0.62	0.34	s1d2	2.48	0.0000569	0.0000693	0.0000821	0.3750
9150281	6/18A	15E_4s1d2Pc_1	14 7/16	E	3.25	354.8	34 1/2	30	0.126	0.189	HLP-22	12	8	4	1.05	4.5	2.4	21.8	10.1	0.62	0.34	s1d2	2.48	0.0000569	0.0000693	0.0000821	0.3750
9150282	6/18A	15E_4s1d2Pc_1	14 7/16	E	3.25	354.8	34 1/2	30	0.126	0.189	HLP-22	12	8	4	1.05	4.5	2.4	21.8	10.1	0.62	0.34	s1d2	2.48	0.0000569	0.0000693	0.0000821	0.3750
9150283	6/18A	15E_4s1d2Pc_1	14 7/16	E	3.25	354.8	34 1/2	30	0.126	0.189	HLP-22	12	8	4	1.05	4.5	2.4	21.8	10.1	0.62	0.34	s1d2	2.48	0.0000569	0.0000693	0.0000821	0.3750
9150284M	6/18A	15E_4s1d2Pc_1	14 7/16	E	3.25	354.8	34 1/2	30	0.126	0.189	HLP-22	12	8	4	1.05	4.5	2.4	21.8	10.1	0.62	0.34	s1d2	2.48	0.0000569	0.0000693	0.0000821	0.3750
9150285M	6/18A	15E_4s1d2Pc_1	14 7/16	E	3.25	354.8	34 1/2	30	0.126	0.189	HLP-22	12	8	4	1.05	4.5	2.4	21.8	10.1	0.62	0.34	s1d2	2.48	0.0000569	0.0000693	0.0000821	0.3750
9150286M	6/18A	15E_4s1d2Pc_1	14 7/16	E	3.25	354.8	34 1/2	30	0.126	0.189	HLP-22	12	8	4	1.05	4.5	2.4	21.8	10.1	0.62	0.34	s1d2	2.48	0.0000569	0.0000693	0.0000821	0.3750
9150287M	6/18A	15E_4s1d2Pc_1	14 7/16	E	3.25	354.8	34 1/2	30	0.126	0.189	HLP-22	12	8	4	1.05	4.5	2.4	21.8	10.1	0.62	0.34	s1d2	2.48	0.0000569	0.0000693	0.0000821	0.3750
9150288M	6/18A	15E_4s1d2Pc_1	14 7/16	E	3.25	354.8	34 1/2	30	0.126	0.189	HLP-22	12	8	4	1.05	4.5	2.4	21.8	10.1	0.62	0.34	s1d2	2.48	0.0000569	0.0000693	0.0000821	0.3750
9150289M	6/18A	15E_4s1d2Pc_1	14 7/16	E	3.25	354.8	34 1/2	30	0.126	0.189	HLP-22	12	8	4	1.05	4.5	2.4	21.8	10.1	0.62	0.34	s1d2	2.48	0.0000569	0.0000693	0.0000821	0.3750
9150290M	6/18A	15E_4s1d2Pc_1	14 7/16	E	3.25	354.8	34 1/2	30	0.126	0.189	HLP-22	12	8	4	1.05	4.5	2.4	21.8	10.1	0.62	0.34	s1d2	2.48	0.0000569	0.0000693	0.0000821	0.3750
9150290.1	6/18A	15E_4s1d2Pc_1	14 7/16	E	3.25	354.8	34 1/2	30	0.126	0.189	HLP-22	12	8	4	1.05	4.5	2.4	21.8	10.1	0.62	0.34	s1d2	2.48	0.0000569	0.0000693	0.0000821	0.3750
9150290.2	6/18A	15E_4s1d2Pc_1	14 7/16	E	3.25	354.8	34 1/2	30	0.126	0.189	HLP-22	12	8	4	1.05	4.5	2.4	21.8	10.1	0.62	0.34	s1d2	2.48	0.0000569	0.0000693	0.0000821	0.3750

Table B.3. Data from 2008 Tests in Small-Scale Vessel with Elliptical Head B.8

Tank Water Temperature	Water Density	Solids Fraction	Pulse Volume Fraction	Duty Cycle	Cycle Time	Pulsed or Steady Jet	Us Steady Jet	U1 Pulsing Jet	U2 URMS	U3 URM3	Discharge Velocity	Critical Suspension Velocity	Average Peak Cloud Height	UCS Condition	UCS Method	UCS Flag	UCS Center Flag	UCS udv Flag	UCS based on Decreasing Velocity	Sweep Increase / Decrease	UDV Height Bed	Particle Motion	Solids Level	Outer Bottom Pattern	Inner Bottom Pattern	Case ID	Test	TDP	Row Number
C	g/cm³	fraction	fraction	fraction	s	text	m/s	m/s	m/s	m/s	m/s	m/s	in.	m/s	text	text	text	text	m/s	text	mm	text	text	text	text	text	text	text	text
T	ρ_l	ϕ_S	ϕ_P	DC	t_C	Jet	U_S	U1	U2	U3	U	U_{CS}	H_C	U_{CSR}	U_{CSM}	U_{CS}vis	U_{CS}cen	U_{CS}udv	U_{CS_D}	S_W	H_{bed}	PM	Sol	SP_O	SP_I	ID	M/DDX	TDP	MSS
27.3	0.999	0.04500	undefined	1.000	infinite	S	2.99	n/a	n/a	n/a	3.00	3.00	14.50	3.00	udv	UCSvis	N/A	UCSudv	N/A	I	0.0	3	N/A	N/A	N/A	15E_4s1d2Wa	6/17B	TDP-182	9150252
27.4	0.998	0.04500	undefined	1.000	infinite	S	2.99	n/a	n/a	n/a	3.00	3.00	14.50	N/A	N/A	UCSvis	N/A	N/A	N/A	(null)	0.0	3	N/A	N/A	N/A	15E_4s1d2Wa	6/17B	TDP-182	9150253
27.4	0.998	0.04500	undefined	1.000	infinite	S	2.99	n/a	n/a	n/a	3.00	3.00	14.50	N/A	N/A	N/A	N/A	N/A	N/A	N/A	0.0	N/A	N/A	N/A	N/A	15E_4s1d2Wa	6/17B	TDP-182	9150254
27.4	0.998	0.04500	undefined	1.000	infinite	S	2.99	n/a	n/a	n/a	3.00	3.00	14.50	N/A	N/A	N/A	N/A	N/A	N/A	N/A	0.7	N/A	N/A	N/A	N/A	15E_4s1d2Wa	6/17B	TDP-182	9150255
27.4	0.998	0.04500	undefined	1.000	infinite	S	2.99	n/a	n/a	n/a	3.00	3.00	14.50	N/A	N/A	N/A	N/A	N/A	N/A	N/A	0.0	N/A	N/A	N/A	N/A	15E_4s1d2Wa	6/17B	TDP-182	9150256
27.4	0.998	0.04500	undefined	1.000	infinite	S	2.99	n/a	n/a	n/a	3.00	3.00	14.50	N/A	N/A	N/A	N/A	N/A	N/A	N/A	0.0	N/A	N/A	N/A	N/A	15E_4s1d2Wa	6/17B	TDP-182	9150257
27.4	0.998	0.04500	undefined	1.000	infinite	S	2.99	n/a	n/a	n/a	3.00	3.00	14.50	N/A	N/A	N/A	N/A	N/A	N/A	N/A	0.0	N/A	N/A	N/A	N/A	15E_4s1d2Wa	6/17B	TDP-182	9150258
27.4	0.998	0.04500	undefined	1.000	infinite	S	2.99	n/a	n/a	n/a	3.00	3.00	14.50	N/A	N/A	N/A	N/A	N/A	N/A	N/A	0.0	N/A	N/A	N/A	N/A	15E_4s1d2Wa	6/17B	TDP-182	9150259
27.4	0.998	0.04500	undefined	1.000	infinite	S	2.99	n/a	n/a	n/a	3.00	3.00	14.50	N/A	N/A	N/A	N/A	N/A	N/A	N/A	0.0	N/A	N/A	N/A	N/A	15E_4s1d2Wa	6/17B	TDP-182	9150260
27.4	0.998	0.04500	undefined	1.000	infinite	S	2.99	n/a	n/a	n/a	3.00	3.00	14.50	N/A	N/A	N/A	N/A	N/A	N/A	N/A	0.0	N/A	N/A	N/A	N/A	15E_4s1d2Wa	6/17B	TDP-182	9150261
27.4	0.998	0.04500	undefined	1.000	infinite	S	2.99	n/a	n/a	n/a	3.00	3.00	14.50	N/A	N/A	N/A	N/A	N/A	N/A	N/A	0.8	N/A	N/A	N/A	N/A	15E_4s1d2Wa	6/17B	TDP-182	9150262
27.4	0.998	0.04500	undefined	1.000	infinite	S	2.99	n/a	n/a	n/a	3.00	3.00	14.50	N/A	N/A	N/A	N/A	N/A	N/A	N/A	0.0	N/A	N/A	N/A	N/A	15E_4s1d2Wa	6/17B	TDP-182	9150263
27.4	0.998	0.04500	undefined	1.000	infinite	S	2.99	n/a	n/a	n/a	3.00	3.00	14.50	N/A	N/A	N/A	N/A	N/A	N/A	N/A	5.2	N/A	N/A	N/A	N/A	15E_4s1d2Wa	6/17B	TDP-182	9150264
27.7	0.998	0.04500	undefined	1.000	infinite	S	3.12	n/a	n/a	n/a	3.10	3.00	16.00	N/A	N/A	N/A	N/A	N/A	N/A	N/A	0.0	4	N/A	N/A	N/A	15E_4s1d2Wa	6/17B	TDP-182	9150265
28.0	0.998	0.04500	0.050	0.337	8.0	P	N/A	7.40	7.59	7.69	8.00	6.50	14.50	N/A	N/A	N/A	N/A	N/A	N/A	(null)	0.0	4	N/A	N/A	N/A	15E_4s1d2Wc_1	6/17C	TDP-182	9150266
28.0	0.998	0.04500	0.050	0.337	8.0	P	N/A	7.40	7.59	7.69	8.00	6.50	14.50	N/A	N/A	N/A	N/A	N/A	N/A	N/A	0.0	N/A	N/A	N/A	N/A	15E_4s1d2Wc_1	6/17C	TDP-182	9150267
28.0	0.998	0.04500	0.050	0.337	8.0	P	N/A	7.40	7.59	7.69	8.00	6.50	14.50	N/A	N/A	N/A	N/A	N/A	N/A	N/A	0.0	N/A	N/A	N/A	N/A	15E_4s1d2Wc_1	6/17C	TDP-182	9150268
28.0	0.998	0.04500	0.050	0.337	8.0	P	N/A	7.40	7.59	7.69	8.00	6.50	14.50	N/A	N/A	N/A	N/A	N/A	N/A	N/A	0.0	N/A	N/A	N/A	N/A	15E_4s1d2Wc_1	6/17C	TDP-182	9150269
28.0	0.998	0.04500	0.050	0.337	8.0	P	N/A	7.40	7.59	7.69	8.00	6.50	14.50	N/A	N/A	N/A	N/A	N/A	N/A	N/A	0.0	N/A	N/A	N/A	N/A	15E_4s1d2Wc_1	6/17C	TDP-182	9150270
28.0	0.998	0.04500	0.050	0.337	8.0	P	N/A	7.40	7.59	7.69	8.00	6.50	14.50	N/A	N/A	N/A	N/A	N/A	N/A	N/A	0.0	N/A	N/A	N/A	N/A	15E_4s1d2Wc_1	6/17C	TDP-182	9150271
28.0	0.998	0.04500	0.050	0.337	8.0	P	N/A	7.40	7.59	7.69	8.00	6.50	14.50	N/A	N/A	N/A	N/A	N/A	N/A	N/A	0.0	N/A	N/A	N/A	N/A	15E_4s1d2Wc_1	6/17C	TDP-182	9150272
28.0	0.998	0.04500	0.050	0.337	8.0	P	N/A	7.40	7.59	7.69	8.00	6.50	14.50	N/A	N/A	N/A	N/A	N/A	N/A	N/A	0.0	N/A	N/A	N/A	N/A	15E_4s1d2Wc_1	6/17C	TDP-182	9150273
28.0	0.998	0.04500	0.050	0.337	8.0	P	N/A	7.40	7.59	7.69	8.00	6.50	14.50	N/A	N/A	N/A	N/A	N/A	N/A	N/A	0.0	N/A	N/A	N/A	N/A	15E_4s1d2Wc_1	6/17C	TDP-182	9150274
28.0	0.998	0.04500	0.050	0.337	8.0	P	N/A	7.40	7.59	7.69	8.00	6.50	14.50	N/A	N/A	N/A	N/A	N/A	N/A	N/A	0.0	N/A	N/A	N/A	N/A	15E_4s1d2Wc_1	6/17C	TDP-182	9150275
28.0	0.998	0.04500	0.050	0.337	8.0	P	N/A	7.40	7.59	7.69	8.00	6.50	14.50	N/A	N/A	N/A	N/A	N/A	N/A	N/A	0.0	N/A	N/A	N/A	N/A	15E_4s1d2Wc_1	6/17C	TDP-182	9150276
28.0	0.998	0.04500	0.050	0.337	8.0	P	N/A	7.40	7.59	7.69	8.00	6.50	14.50	N/A	N/A	N/A	N/A	N/A	N/A	N/A	0.0	N/A	N/A	N/A	N/A	15E_4s1d2Wc_1	6/17C	TDP-182	9150277
23.3	1.000	0.06000	0.050	0.329	12.8	P	N/A	4.74	4.82	4.86	5.00	6.20	7.25	N/A	N/A	N/A	N/A	N/A	N/A	(null)	9.9	1	N/A	N/A	N/A	15E_4s1d2Pc_1	6/18A	TDP-183	9150278
23.3	1.000	0.06000	0.050	0.331	12.0	P	N/A	5.00	5.09	5.13	5.30	6.20	7.75	N/A	N/A	N/A	N/A	N/A	N/A	I	7.6	1	N/A	N/A	N/A	15E_4s1d2Pc_1	6/18A	TDP-183	9150279
23.5	0.999	0.06000	0.050	0.333	11.6	P	N/A	5.18	5.27	5.32	5.50	6.20	7.75	N/A	N/A	N/A	N/A	N/A	N/A	I	5.4	1	N/A	N/A	N/A	15E_4s1d2Pc_1	6/18A	TDP-183	9150280
23.5	0.999	0.06000	0.050	0.332	11.2	P	N/A	5.39	5.48	5.53	5.70	6.20	8.25	N/A	N/A	N/A	N/A	N/A	N/A	I	4.5	1	N/A	N/A	N/A	15E_4s1d2Pc_1	6/18A	TDP-183	9150281
23.7	0.999	0.06000	0.050	0.333	10.8	P	N/A	5.57	5.67	5.72	5.90	6.20	8.75	N/A	N/A	N/A	N/A	N/A	N/A	I	3.7	1	N/A	N/A	N/A	15E_4s1d2Pc_1	6/18A	TDP-183	9150282
23.7	1.000	0.06000	0.050	0.334	10.6	P	N/A	5.67	5.77	5.82	6.00	6.20	8.75	N/A	N/A	N/A	N/A	N/A	N/A	I	3.7	1	N/A	N/A	N/A	15E_4s1d2Pc_1	6/18A	TDP-183	9150283
23.8	1.000	0.06000	0.050	0.335	10.2	P	N/A	5.86	5.97	6.03	6.20	6.20	9.25	6.20	udv	UCSvis	N/A	UCSudv	N/A	I	2.5	3	N/A	N/A	N/A	15E_4s1d2Pc_1	6/18A	TDP-183	9150284
24.0	0.999	0.06000	0.050	0.337	9.8	P	N/A	6.05	6.16	6.22	6.40	6.20	10.00	N/A	N/A	N/A	N/A	N/A	N/A	I	0.0	4	N/A	N/A	N/A	15E_4s1d2Pc_1	6/18A	TDP-183	9150285
24.1	0.999	0.06000	0.050	0.339	9.2	P	N/A	6.40	6.53	6.60	6.80	6.20	10.50	N/A	N/A	N/A	N/A	N/A	N/A	I	0.0	4	N/A	N/A	N/A	15E_4s1d2Pc_1	6/18A	TDP-183	9150286
24.2	0.999	0.06000	0.050	0.336	8.8	P	N/A	6.77	6.90	6.97	7.20	6.20	13.00	N/A	N/A	N/A	N/A	N/A	N/A	I	0.0	4	N/A	N/A	N/A	15E_4s1d2Pc_1	6/18A	TDP-183	9150287
24.3	0.999	0.06000	0.050	0.338	8.4	P	N/A	7.00	7.15	7.23	7.50	6.20	14.00	N/A	N/A	N/A	N/A	N/A	N/A	I	0.0	4	N/A	N/A	N/A	15E_4s1d2Pc_1	6/18A	TDP-183	9150288
24.5	0.999	0.06000	0.050	0.330	8.1	P	N/A	7.46	7.63	7.71	8.00	6.20	16.50	N/A	N/A	N/A	N/A	N/A	N/A	I	0.0	4	N/A	N/A	N/A	15E_4s1d2Pc_1	6/18A	TDP-183	9150289
24.7	0.999	0.06000	0.050	0.333	7.6	P	N/A	7.94	8.13	8.22	8.50	6.20	19.50	N/A	N/A	N/A	N/A	N/A	N/A	I	0.0	4	N/A	N/A	N/A	15E_4s1d2Pc_1	6/18A	TDP-183	9150290
25.0	0.999	0.06000	0.050	0.336	10.2	P	N/A	5.87	5.97	6.03	6.20	6.20	9.50	N/A	N/A	N/A	N/A	N/A	N/A	N/A	n/a	N/A	N/A	N/A	N/A	15E_4s1d2Pc_1	6/18A	TDP-183	9150290.1
25.0	0.999	0.06000	0.050	0.336	10.2	P	N/A	5.87	5.97	6.03	6.20	6.20	9.50	N/A	N/A	N/A	N/A	N/A	N/A	N/A	n/a	N/A	N/A	N/A	N/A	15E_4s1d2Pc_1	6/18A	TDP-183	9150290.2

Table B.3. Data from 2008 Tests in Small-Scale Vessel with Elliptical Head A.9

Row Number	Test	Case ID	Tank Diameter	Head Shape	Dish Height	Dish Volume	Tank Fill Height	Return Line Height	Nozzle Inner Diameter	Nozzle Stand-off Distance	Pulse Tube Configuration	Installed Nozzles	Outer Nozzles Operated	Inner Nozzles Operated	Pulse Tube Outer Diameter	Outer PJM Radius	Inner PJM Radius	"FIO" Outer PJM Impingement Angle	"FIO" Inner PJM Impingement Angle	Ratio Outer PJM to Tank Radius	Ratio Inner PJM to Tank Radius	Simulant	Solids Density	Particle Diameter d5	Particle Diameter d50	Particle Diameter d95	Void Fraction
text	text	text	in.	text	in.	in. ^{3}	in.	in.	in.	in.	text	number	number	number	in.	in.	in.	deg	deg	nondim	nondim	text	g/cm^3	m	m	m	fraction
MSS	M/DDX	ID	D	HS	H_{dish}	V_{dish}	H	Rtn	d	sod	PT	N	N_O	N_I	PT_{od}	R_O	R_I	θ_O	θ_I	R_O/R	R_I/R	sxdx	ρ_s	d_5	d_{50}	d_{95}	vf
9150290.3	6/18A	15E_4s1d2Pc_1	14 7/16	E	3.25	354.8	34 1/2	30	0.126	0.189	HLP-22	12	8	4	1.05	4.5	2.4	21.8	10.1	0.62	0.34	s1d2	2.48	0.0000569	0.0000693	0.0000821	0.3750
9150291M	6/18A	15E_4s1d2Pc_1	14 7/16	E	3.25	354.8	34 1/2	30	0.126	0.189	HLP-22	12	8	4	1.05	4.5	2.4	21.8	10.1	0.62	0.34	s1d2	2.48	0.0000569	0.0000693	0.0000821	0.3750
9150291M	6/18A	15E_4s1d2Pc_1	14 7/16	E	3.25	354.8	34 1/2	30	0.126	0.189	HLP-22	12	8	4	1.05	4.5	2.4	21.8	10.1	0.62	0.34	s1d2	2.48	0.0000569	0.0000693	0.0000821	0.3750
9150292	6/18A	15E_4s1d2Pc_1	14 7/16	E	3.25	354.8	34 1/2	30	0.126	0.189	HLP-22	12	8	4	1.05	4.5	2.4	21.8	10.1	0.62	0.34	s1d2	2.48	0.0000569	0.0000693	0.0000821	0.3750
9150293	6/18A	15E_4s1d2Pc_1	14 7/16	E	3.25	354.8	34 1/2	30	0.126	0.189	HLP-22	12	8	4	1.05	4.5	2.4	21.8	10.1	0.62	0.34	s1d2	2.48	0.0000569	0.0000693	0.0000821	0.3750
9150293.1	6/18A	15E_4s1d2Pc_1	14 7/16	E	3.25	354.8	34 1/2	30	0.126	0.189	HLP-22	12	8	4	1.05	4.5	2.4	21.8	10.1	0.62	0.34	s1d2	2.48	0.0000569	0.0000693	0.0000821	0.3750
9150294	6/18A	15E_4s1d2Pc_1	14 7/16	E	3.25	354.8	34 1/2	30	0.126	0.189	HLP-22	12	8	4	1.05	4.5	2.4	21.8	10.1	0.62	0.34	s1d2	2.48	0.0000569	0.0000693	0.0000821	0.3750
9150294.1	6/18A	15E_4s1d2Pc_1	14 7/16	E	3.25	354.8	34 1/2	30	0.126	0.189	HLP-22	12	8	4	1.05	4.5	2.4	21.8	10.1	0.62	0.34	s1d2	2.48	0.0000569	0.0000693	0.0000821	0.3750
9150295	6/18A	15E_4s1d2Pc_1	14 7/16	E	3.25	354.8	34 1/2	30	0.126	0.189	HLP-22	12	8	4	1.05	4.5	2.4	21.8	10.1	0.62	0.34	s1d2	2.48	0.0000569	0.0000693	0.0000821	0.3750
9150295.1	6/18A	15E_4s1d2Pc_1	14 7/16	E	3.25	354.8	34 1/2	30	0.126	0.189	HLP-22	12	8	4	1.05	4.5	2.4	21.8	10.1	0.62	0.34	s1d2	2.48	0.0000569	0.0000693	0.0000821	0.3750
9150296	6/18A	15E_4s1d2Pc_1	14 7/16	E	3.25	354.8	34 1/2	30	0.126	0.189	HLP-22	12	8	4	1.05	4.5	2.4	21.8	10.1	0.62	0.34	s1d2	2.48	0.0000569	0.0000693	0.0000821	0.3750
9150296.1	6/18A	15E_4s1d2Pc_1	14 7/16	E	3.25	354.8	34 1/2	30	0.126	0.189	HLP-22	12	8	4	1.05	4.5	2.4	21.8	10.1	0.62	0.34	s1d2	2.48	0.0000569	0.0000693	0.0000821	0.3750
9150297	6/18A	15E_4s1d2Pc_1	14 7/16	E	3.25	354.8	34 1/2	30	0.126	0.189	HLP-22	12	8	4	1.05	4.5	2.4	21.8	10.1	0.62	0.34	s1d2	2.48	0.0000569	0.0000693	0.0000821	0.3750
9150298	6/18B	15E_4s2d2Zc_1	14 7/16	E	3.25	354.8	35	30	0.126	0.189	HLP-22	12	8	4	1.05	4.5	2.4	21.8	10.1	0.62	0.34	s2d2	4.18	0.0000609	0.0000756	0.0000931	0.3684
9150299	6/18B	15E_4s2d2Zc_1	14 7/16	E	3.25	354.8	35	30	0.126	0.189	HLP-22	12	8	4	1.05	4.5	2.4	21.8	10.1	0.62	0.34	s2d2	4.18	0.0000609	0.0000756	0.0000931	0.3684
9150300	6/18B	15E_4s2d2Zc_1	14 7/16	E	3.25	354.8	35	30	0.126	0.189	HLP-22	12	8	4	1.05	4.5	2.4	21.8	10.1	0.62	0.34	s2d2	4.18	0.0000609	0.0000756	0.0000931	0.3684
9150301	6/18B	15E_4s2d2Zc_1	14 7/16	E	3.25	354.8	35	30	0.126	0.189	HLP-22	12	8	4	1.05	4.5	2.4	21.8	10.1	0.62	0.34	s2d2	4.18	0.0000609	0.0000756	0.0000931	0.3684
9150302	6/18B	15E_4s2d2Zc_1	14 7/16	E	3.25	354.8	35	30	0.126	0.189	HLP-22	12	8	4	1.05	4.5	2.4	21.8	10.1	0.62	0.34	s2d2	4.18	0.0000609	0.0000756	0.0000931	0.3684
9150303	6/18B	15E_4s2d2Zc_1	14 7/16	E	3.25	354.8	35	30	0.126	0.189	HLP-22	12	8	4	1.05	4.5	2.4	21.8	10.1	0.62	0.34	s2d2	4.18	0.0000609	0.0000756	0.0000931	0.3684
9150304	6/18B	15E_4s2d2Zc_1	14 7/16	E	3.25	354.8	35	30	0.126	0.189	HLP-22	12	8	4	1.05	4.5	2.4	21.8	10.1	0.62	0.34	s2d2	4.18	0.0000609	0.0000756	0.0000931	0.3684
9150305	6/18B	15E_4s2d2Zc_1	14 7/16	E	3.25	354.8	35	30	0.126	0.189	HLP-22	12	8	4	1.05	4.5	2.4	21.8	10.1	0.62	0.34	s2d2	4.18	0.0000609	0.0000756	0.0000931	0.3684
9150306	6/18B	15E_4s2d2Zc_1	14 7/16	E	3.25	354.8	35	30	0.126	0.189	HLP-22	12	8	4	1.05	4.5	2.4	21.8	10.1	0.62	0.34	s2d2	4.18	0.0000609	0.0000756	0.0000931	0.3684
9150307M	6/18B	15E_4s2d2Zc_1	14 7/16	E	3.25	354.8	35	30	0.126	0.189	HLP-22	12	8	4	1.05	4.5	2.4	21.8	10.1	0.62	0.34	s2d2	4.18	0.0000609	0.0000756	0.0000931	0.3684
9150308M	6/18B	15E_4s2d2Zc_1	14 7/16	E	3.25	354.8	35	30	0.126	0.189	HLP-22	12	8	4	1.05	4.5	2.4	21.8	10.1	0.62	0.34	s2d2	4.18	0.0000609	0.0000756	0.0000931	0.3684
9150309M	6/18B	15E_4s2d2Zc_1	14 7/16	E	3.25	354.8	35	30	0.126	0.189	HLP-22	12	8	4	1.05	4.5	2.4	21.8	10.1	0.62	0.34	s2d2	4.18	0.0000609	0.0000756	0.0000931	0.3684
9150310M	6/18B	15E_4s2d2Zc_1	14 7/16	E	3.25	354.8	35	30	0.126	0.189	HLP-22	12	8	4	1.05	4.5	2.4	21.8	10.1	0.62	0.34	s2d2	4.18	0.0000609	0.0000756	0.0000931	0.3684
9150311	6/19A	15E_4s2d2Zc_1	14 7/16	E	3.25	354.8	35	30	0.126	0.189	HLP-22	12	8	4	1.05	4.5	2.4	21.8	10.1	0.62	0.34	s2d2	4.18	0.0000609	0.0000756	0.0000931	0.3684
9150312M	6/19A	15E_4s2d2Zc_1	14 7/16	E	3.25	354.8	35	30	0.126	0.189	HLP-22	12	8	4	1.05	4.5	2.4	21.8	10.1	0.62	0.34	s2d2	4.18	0.0000609	0.0000756	0.0000931	0.3684
9150313M	6/19A	15E_4s2d2Zc_1	14 7/16	E	3.25	354.8	35	30	0.126	0.189	HLP-22	12	8	4	1.05	4.5	2.4	21.8	10.1	0.62	0.34	s2d2	4.18	0.0000609	0.0000756	0.0000931	0.3684
9150313.1	6/19A	15E_4s2d2Zc_1	14 7/16	E	3.25	354.8	35	30	0.126	0.189	HLP-22	12	8	4	1.05	4.5	2.4	21.8	10.1	0.62	0.34	s2d2	4.18	0.0000609	0.0000756	0.0000931	0.3684
9150313.2	6/19A	15E_4s2d2Zc_1	14 7/16	E	3.25	354.8	35	30	0.126	0.189	HLP-22	12	8	4	1.05	4.5	2.4	21.8	10.1	0.62	0.34	s2d2	4.18	0.0000609	0.0000756	0.0000931	0.3684
9150313.3	6/19A	15E_4s2d2Zc_1	14 7/16	E	3.25	354.8	35	30	0.126	0.189	HLP-22	12	8	4	1.05	4.5	2.4	21.8	10.1	0.62	0.34	s2d2	4.18	0.0000609	0.0000756	0.0000931	0.3684
9150313.4	6/19A	15E_4s2d2Zc_1	14 7/16	E	3.25	354.8	35	30	0.126	0.189	HLP-22	12	8	4	1.05	4.5	2.4	21.8	10.1	0.62	0.34	s2d2	4.18	0.0000609	0.0000756	0.0000931	0.3684
9150313.5	6/19A	15E_4s2d2Zc_1	14 7/16	E	3.25	354.8	35	30	0.126	0.189	HLP-22	12	8	4	1.05	4.5	2.4	21.8	10.1	0.62	0.34	s2d2	4.18	0.0000609	0.0000756	0.0000931	0.3684
9150314M	6/19A	15E_4s2d2Zc_1	14 7/16	E	3.25	354.8	35	30	0.126	0.189	HLP-22	12	8	4	1.05	4.5	2.4	21.8	10.1	0.62	0.34	s2d2	4.18	0.0000609	0.0000756	0.0000931	0.3684
9150315	6/19A	15E_4s2d2Zc_1	14 7/16	E	3.25	354.8	35	30	0.126	0.189	HLP-22	12	8	4	1.05	4.5	2.4	21.8	10.1	0.62	0.34	s2d2	4.18	0.0000609	0.0000756	0.0000931	0.3684
9150316	6/19A	15E_4s2d2Zc_1	14 7/16	E	3.25	354.8	35	30	0.126	0.189	HLP-22	12	8	4	1.05	4.5	2.4	21.8	10.1	0.62	0.34	s2d2	4.18	0.0000609	0.0000756	0.0000931	0.3684
9150317	6/19A	15E_4s2d2Zc_1	14 7/16	E	3.25	354.8	35	30	0.126	0.189	HLP-22	12	8	4	1.05	4.5	2.4	21.8	10.1	0.62	0.34	s2d2	4.18	0.0000609	0.0000756	0.0000931	0.3684
9150318	6/19A	15E_4s2d2Zc_1	14 7/16	E	3.25	354.8	35	30	0.126	0.189	HLP-22	12	8	4	1.05	4.5	2.4	21.8	10.1	0.62	0.34	s2d2	4.18	0.0000609	0.0000756	0.0000931	0.3684
9150319	6/19A	15E_4s2d2Zc_1	14 7/16	E	3.25	354.8	35	30	0.126	0.189	HLP-22	12	8	4	1.05	4.5	2.4	21.8	10.1	0.62	0.34	s2d2	4.18	0.0000609	0.0000756	0.0000931	0.3684
9150320	6/19A	15E_4s2d2Zc_1	14 7/16	E	3.25	354.8	35	30	0.126	0.189	HLP-22	12	8	4	1.05	4.5	2.4	21.8	10.1	0.62	0.34	s2d2	4.18	0.0000609	0.0000756	0.0000931	0.3684

Table B.3. Data from 2008 Tests in Small-Scale Vessel with Elliptical Head B.9

Tank Water Temperature	Water Density	Solids Fraction	Pulse Volume Fraction	Duty Cycle	Cycle Time	Pulsed or Steady Jet	Us Steady Jet	U1 Pulsing Jet	U2 URMS	U3 URM3	Discharge Velocity	Critical Suspension Velocity	Average Peak Cloud Height	UCS Condition	UCS Method	UCS Flag	UCS Center Flag	UCS udv Flag	UCS based on Decreasing Velocity	Sweep Increase / Decrease	UDV Height Bed	Particle Motion	Solids Level	Outer Bottom Pattern	Inner Bottom Pattern	Case ID	Test	TDP	Row Number
C	g/cm³	fraction	fraction	fraction	s	text	m/s	m/s	m/s	m/s	m/s	m/s	in.	m/s	text	text	text	text	m/s	text	mm	text	text	text	text	text	text	text	text
T	ρ_l	ϕ_S	ϕ_P	DC	t_C	Jet	U_S	U1	U2	U3	U	U_{CS}	H_C	U_{CSR}	U_{CSM}	U_{CS}vis	U_{CS}cen	U_{CS}udv	U_{CS_D}	S_W	H_{bed}	PM	Sol	SP_O	SP_I	ID	M/DDX	TDP	MSS
25.0	0.999	0.06000	0.050	0.336	10.2	P	N/A	5.87	5.97	6.03	6.20	6.20	9.50	N/A	N/A	N/A	N/A	N/A	N/A	N/A	n/a	N/A	N/A	N/A	N/A	15E_4s1d2Pc_1	6/18A	TDP-183	9150290.3
25.0	0.999	0.06000	0.050	0.336	10.2	P	N/A	5.87	5.97	6.03	6.20	6.20	9.50	N/A	vis dec	UCSvis	N/A	N/A	6.20	D	3.7	3	N/A	N/A	N/A	15E_4s1d2Pc_1	6/18A	TDP-183	9150291
25.0	0.999	0.06000	0.050	0.336	10.2	P	N/A	5.87	5.97	6.03	6.20	6.20	9.50	N/A	N/A	N/A	N/A	N/A	N/A	N/A	n/a	N/A	N/A	N/A	N/A	15E_4s1d2Pc_1	6/18A	TDP-183	9150291
25.0	0.999	0.06000	0.050	0.336	10.2	P	N/A	5.87	5.97	6.03	6.20	6.20	9.50	N/A	N/A	N/A	N/A	N/A	N/A	N/A	3.6	N/A	N/A	N/A	N/A	15E_4s1d2Pc_1	6/18A	TDP-183	9150292
25.0	0.999	0.06000	0.050	0.336	10.2	P	N/A	5.87	5.97	6.03	6.20	6.20	9.50	N/A	N/A	N/A	N/A	N/A	N/A	N/A	3.7	N/A	N/A	N/A	N/A	15E_4s1d2Pc_1	6/18A	TDP-183	9150293
25.0	0.999	0.06000	0.050	0.336	10.2	P	N/A	5.87	5.97	6.03	6.20	6.20	9.50	N/A	N/A	N/A	N/A	N/A	N/A	N/A	n/a	N/A	N/A	N/A	N/A	15E_4s1d2Pc_1	6/18A	TDP-183	9150293.1
25.0	0.999	0.06000	0.050	0.336	10.2	P	N/A	5.87	5.97	6.03	6.20	6.20	9.50	N/A	N/A	N/A	N/A	N/A	N/A	N/A	3.7	N/A	N/A	N/A	N/A	15E_4s1d2Pc_1	6/18A	TDP-183	9150294
25.0	0.999	0.06000	0.050	0.336	10.2	P	N/A	5.87	5.97	6.03	6.20	6.20	9.50	N/A	N/A	N/A	N/A	N/A	N/A	N/A	n/a	N/A	N/A	N/A	N/A	15E_4s1d2Pc_1	6/18A	TDP-183	9150294.1
25.0	0.999	0.06000	0.050	0.336	10.2	P	N/A	5.87	5.97	6.03	6.20	6.20	9.50	N/A	N/A	N/A	N/A	N/A	N/A	N/A	3.7	N/A	N/A	N/A	N/A	15E_4s1d2Pc_1	6/18A	TDP-183	9150295
25.0	0.999	0.06000	0.050	0.336	10.2	P	N/A	5.87	5.97	6.03	6.20	6.20	9.50	N/A	N/A	N/A	N/A	N/A	N/A	N/A	n/a	N/A	N/A	N/A	N/A	15E_4s1d2Pc_1	6/18A	TDP-183	9150295.1
25.0	0.999	0.06000	0.050	0.336	10.2	P	N/A	5.87	5.97	6.03	6.20	6.20	9.50	N/A	N/A	N/A	N/A	N/A	N/A	N/A	3.7	N/A	N/A	N/A	N/A	15E_4s1d2Pc_1	6/18A	TDP-183	9150296
25.0	0.999	0.06000	0.050	0.336	10.2	P	N/A	5.87	5.97	6.03	6.20	6.20	9.50	N/A	N/A	N/A	N/A	N/A	N/A	N/A	n/a	N/A	N/A	N/A	N/A	15E_4s1d2Pc_1	6/18A	TDP-183	9150296.1
25.0	0.999	0.06000	0.050	0.336	10.2	P	N/A	5.87	5.97	6.03	6.20	6.20	9.50	N/A	N/A	N/A	N/A	N/A	N/A	N/A	3.7	N/A	N/A	N/A	N/A	15E_4s1d2Pc_1	6/18A	TDP-183	9150297
24.5	0.999	0.00155	0.050	0.331	31.0	P	N/A	1.96	1.97	1.98	2.00	5.40	10.00	N/A	N/A	N/A	N/A	N/A	N/A	(null)	14.9	1	N/A	N/A	N/A	15E_4s2d2Zc_1	6/18B	TDP-184	9150298
24.7	0.999	0.00155	0.050	0.331	25.6	P	N/A	2.37	2.38	2.38	2.40	5.40	5.75	N/A	N/A	N/A	N/A	N/A	N/A	I	13.9	1	N/A	N/A	N/A	15E_4s2d2Zc_1	6/18B	TDP-184	9150299
24.8	0.999	0.00155	0.050	0.335	21.9	P	N/A	2.75	2.76	2.77	2.80	5.40	4.75	N/A	N/A	N/A	N/A	N/A	N/A	I	14.1	1	N/A	N/A	N/A	15E_4s2d2Zc_1	6/18B	TDP-184	9150300
25.1	0.999	0.00155	0.050	0.335	19.2	P	N/A	3.13	3.15	3.16	3.20	5.40	4.50	N/A	N/A	N/A	N/A	N/A	N/A	I	13.7	1	N/A	N/A	N/A	15E_4s2d2Zc_1	6/18B	TDP-184	9150301
25.3	0.999	0.00155	0.050	0.335	17.1	P	N/A	3.51	3.54	3.56	3.60	5.40	4.75	N/A	N/A	N/A	N/A	N/A	N/A	I	13.1	1	N/A	N/A	N/A	15E_4s2d2Zc_1	6/18B	TDP-184	9150302
25.5	0.999	0.00155	0.050	0.337	15.4	P	N/A	3.88	3.92	3.94	4.00	5.40	5.25	N/A	N/A	N/A	N/A	N/A	N/A	I	11.1	1	N/A	N/A	N/A	15E_4s2d2Zc_1	6/18B	TDP-184	9150303
25.8	0.999	0.00155	0.050	0.338	14.0	P	N/A	4.26	4.31	4.33	4.40	5.40	5.75	N/A	N/A	N/A	N/A	N/A	N/A	I	8.5	1	N/A	N/A	N/A	15E_4s2d2Zc_1	6/18B	TDP-184	9150304
26.0	0.999	0.00155	0.050	0.337	12.8	P	N/A	4.62	4.68	4.71	4.80	5.40	5.75	N/A	N/A	N/A	N/A	N/A	N/A	I	6.5	1	N/A	N/A	N/A	15E_4s2d2Zc_1	6/18B	TDP-184	9150305
26.3	0.999	0.00155	0.050	0.335	11.9	P	N/A	4.99	5.07	5.10	5.20	5.40	6.00	N/A	N/A	N/A	N/A	N/A	N/A	I	4.2	1	N/A	N/A	N/A	15E_4s2d2Zc_1	6/18B	TDP-184	9150306
26.5	0.999	0.00155	0.050	0.337	11.5	P	N/A	5.18	5.26	5.30	5.40	5.40	6.75	5.40	udv	N/A	N/A	UCSudv	N/A	I	2.7	1	N/A	N/A	N/A	15E_4s2d2Zc_1	6/18B	TDP-184	9150307
26.9	0.999	0.00155	0.050	0.338	11.1	P	N/A	5.37	5.45	5.49	5.60	5.40	8.25	N/A	N/A	UCSvis	N/A	N/A	N/A	I	0.0	3	N/A	N/A	N/A	15E_4s2d2Zc_1	6/18B	TDP-184	9150308
27.3	0.998	0.00155	0.050	0.339	10.7	P	N/A	5.54	5.64	5.69	5.80	5.40	9.50	N/A	N/A	N/A	N/A	N/A	N/A	I	0.0	4	N/A	N/A	N/A	15E_4s2d2Zc_1	6/18B	TDP-184	9150309
27.7	0.998	0.00155	0.050	0.336	10.0	P	N/A	5.90	6.01	6.06	6.20	5.40	17.00	N/A	N/A	N/A	N/A	N/A	N/A	I	0.0	4	N/A	N/A	N/A	15E_4s2d2Zc_1	6/18B	TDP-184	9150310
23.6	0.999	0.00155	0.050	0.334	12.4	P	N/A	4.79	4.87	4.90	5.00	5.20	6.25	N/A	N/A	N/A	N/A	N/A	N/A	I	3.2	1	N/A	N/A	N/A	15E_4s2d2Zc_1	6/19A	TDP-185	9150311
23.7	0.999	0.00155	0.050	0.334	12.0	P	N/A	4.98	5.06	5.10	5.20	5.20	6.75	5.20	udv	N/A	N/A	UCSudv	N/A	I	0.5	1	N/A	N/A	N/A	15E_4s2d2Zc_1	6/19A	TDP-185	9150312
23.9	0.999	0.00155	0.050	0.335	11.5	P	N/A	5.17	5.25	5.29	5.40	5.20	8.75	N/A	N/A	UCSvis	N/A	N/A	N/A	I	0.0	3	N/A	N/A	N/A	15E_4s2d2Zc_1	6/19A	TDP-185	9150313
24.2	0.999	0.00155	0.050	0.335	12.0	P	N/A	4.98	5.06	5.10	5.20	5.20	7.00	N/A	N/A	N/A	N/A	N/A	N/A	N/A	n/a	N/A	N/A	N/A	N/A	15E_4s2d2Zc_1	6/19A	TDP-185	9150313.1
24.2	0.999	0.00155	0.050	0.335	12.0	P	N/A	4.98	5.06	5.10	5.20	5.20	7.00	N/A	N/A	N/A	N/A	N/A	N/A	N/A	n/a	N/A	N/A	N/A	N/A	15E_4s2d2Zc_1	6/19A	TDP-185	9150313.2
24.2	0.999	0.00155	0.050	0.335	12.0	P	N/A	4.98	5.06	5.10	5.20	5.20	7.00	N/A	N/A	N/A	N/A	N/A	N/A	N/A	n/a	N/A	N/A	N/A	N/A	15E_4s2d2Zc_1	6/19A	TDP-185	9150313.3
24.2	0.999	0.00155	0.050	0.335	12.0	P	N/A	4.98	5.06	5.10	5.20	5.20	7.00	N/A	N/A	N/A	N/A	N/A	N/A	N/A	n/a	N/A	N/A	N/A	N/A	15E_4s2d2Zc_1	6/19A	TDP-185	9150313.4
24.2	0.999	0.00155	0.050	0.335	12.0	P	N/A	4.98	5.06	5.10	5.20	5.20	7.00	N/A	N/A	N/A	N/A	N/A	N/A	N/A	n/a	N/A	N/A	N/A	N/A	15E_4s2d2Zc_1	6/19A	TDP-185	9150313.5
24.2	0.999	0.00155	0.050	0.335	12.0	P	N/A	4.98	5.06	5.10	5.20	5.20	7.00	N/A	N/A	N/A	N/A	N/A	N/A	I	1.6	1	N/A	N/A	N/A	15E_4s2d2Zc_1	6/19A	TDP-185	9150314
24.2	0.999	0.00155	0.050	0.335	12.0	P	N/A	4.98	5.06	5.10	5.20	5.20	7.00	N/A	N/A	N/A	N/A	N/A	N/A	N/A	1.3	N/A	N/A	N/A	N/A	15E_4s2d2Zc_1	6/19A	TDP-185	9150315
24.2	0.999	0.00155	0.050	0.335	12.0	P	N/A	4.98	5.06	5.10	5.20	5.20	7.00	N/A	N/A	N/A	N/A	N/A	N/A	N/A	1.9	N/A	N/A	N/A	N/A	15E_4s2d2Zc_1	6/19A	TDP-185	9150316
24.2	0.999	0.00155	0.050	0.335	12.0	P	N/A	4.98	5.06	5.10	5.20	5.20	7.00	N/A	N/A	N/A	N/A	N/A	N/A	N/A	1.9	N/A	N/A	N/A	N/A	15E_4s2d2Zc_1	6/19A	TDP-185	9150317
24.2	0.999	0.00155	0.050	0.335	12.0	P	N/A	4.98	5.06	5.10	5.20	5.20	7.00	N/A	N/A	N/A	N/A	N/A	N/A	N/A	1.9	N/A	N/A	N/A	N/A	15E_4s2d2Zc_1	6/19A	TDP-185	9150318
24.2	0.999	0.00155	0.050	0.335	12.0	P	N/A	4.98	5.06	5.10	5.20	5.20	7.00	N/A	N/A	N/A	N/A	N/A	N/A	N/A	0.6	N/A	N/A	N/A	N/A	15E_4s2d2Zc_1	6/19A	TDP-185	9150319
24.2	0.999	0.00155	0.050	0.335	12.0	P	N/A	4.98	5.06	5.10	5.20	5.20	7.00	N/A	N/A	N/A	N/A	N/A	N/A	N/A	0.0	N/A	N/A	N/A	N/A	15E_4s2d2Zc_1	6/19A	TDP-185	9150320

Table B.3. Data from 2008 Tests in Small-Scale Vessel with Elliptical Head A.10

Row Number	Test	Case ID	Tank Diameter	Head Shape	Dish Height	Dish Volume	Tank Fill Height	Return Line Height	Nozzle Inner Diameter	Nozzle Stand-off Distance	Pulse Tube Configuration	Installed Nozzles	Outer Nozzles Operated	Inner Nozzles Operated	Pulse Tube Outer Diameter	Outer PJM Radius	Inner PJM Radius	"FIO" Outer PJM Impingement Angle	"FIO" Inner PJM Impingement Angle	Ratio Outer PJM to Tank Radius	Ratio Inner PJM to Tank Radius	Simulant	Solids Density	Particle Diameter d5	Particle Diameter d50	Particle Diameter d95	Void Fraction
text	text	text	in.	text	in.	in. ^{3}	in.	in.	in.	in.	text	number	number	number	in.	in.	in.	deg	deg	nondim	nondim	text	g/cm^3	m	m	m	fraction
MSS	M/DDX	ID	D	HS	H_{dish}	V_{dish}	H	Rtn	d	sod	PT	N	N_O	N_I	PT_{od}	R_O	R_I	θ_O	θ_I	R_O/R	R_I/R	sxdx	ρ_s	d_5	d_{50}	d_{95}	vf
9150321	6/19A	15E_4s2d2Zc_1	14 7/16	E	3.25	354.8	35	30	0.126	0.189	HLP-22	12	8	4	1.05	4.5	2.4	21.8	10.1	0.62	0.34	s2d2	4.18	0.0000609	0.0000756	0.0000931	0.3684
9150322	6/19A	15E_4s2d2Zc_1	14 7/16	E	3.25	354.8	35	30	0.126	0.189	HLP-22	12	8	4	1.05	4.5	2.4	21.8	10.1	0.62	0.34	s2d2	4.18	0.0000609	0.0000756	0.0000931	0.3684
9150323	6/19A	15E_4s2d2Zc_1	14 7/16	E	3.25	354.8	35	30	0.126	0.189	HLP-22	12	8	4	1.05	4.5	2.4	21.8	10.1	0.62	0.34	s2d2	4.18	0.0000609	0.0000756	0.0000931	0.3684
9150324	6/19B	15E_4s2d2Zd_1	14 7/16	E	3.25	354.8	35	30	0.126	0.189	HLP-22	12	8	4	1.05	4.5	2.4	21.8	10.1	0.62	0.34	s2d2	4.18	0.0000609	0.0000756	0.0000931	0.3684
9150325	6/19B	15E_4s2d2Zd_1	14 7/16	E	3.25	354.8	35	30	0.126	0.189	HLP-22	12	8	4	1.05	4.5	2.4	21.8	10.1	0.62	0.34	s2d2	4.18	0.0000609	0.0000756	0.0000931	0.3684
9150326	6/19B	15E_4s2d2Zd_1	14 7/16	E	3.25	354.8	35	30	0.126	0.189	HLP-22	12	8	4	1.05	4.5	2.4	21.8	10.1	0.62	0.34	s2d2	4.18	0.0000609	0.0000756	0.0000931	0.3684
9150327	6/19B	15E_4s2d2Zd_1	14 7/16	E	3.25	354.8	35	30	0.126	0.189	HLP-22	12	8	4	1.05	4.5	2.4	21.8	10.1	0.62	0.34	s2d2	4.18	0.0000609	0.0000756	0.0000931	0.3684
9150328M	6/19B	15E_4s2d2Zd_1	14 7/16	E	3.25	354.8	35	30	0.126	0.189	HLP-22	12	8	4	1.05	4.5	2.4	21.8	10.1	0.62	0.34	s2d2	4.18	0.0000609	0.0000756	0.0000931	0.3684
9150329M	6/19B	15E_4s2d2Zd_1	14 7/16	E	3.25	354.8	35	30	0.126	0.189	HLP-22	12	8	4	1.05	4.5	2.4	21.8	10.1	0.62	0.34	s2d2	4.18	0.0000609	0.0000756	0.0000931	0.3684
9150330M	6/19B	15E_4s2d2Zd_1	14 7/16	E	3.25	354.8	35	30	0.126	0.189	HLP-22	12	8	4	1.05	4.5	2.4	21.8	10.1	0.62	0.34	s2d2	4.18	0.0000609	0.0000756	0.0000931	0.3684
9150331M	6/19B	15E_4s2d2Zd_1	14 7/16	E	3.25	354.8	35	30	0.126	0.189	HLP-22	12	8	4	1.05	4.5	2.4	21.8	10.1	0.62	0.34	s2d2	4.18	0.0000609	0.0000756	0.0000931	0.3684
9150332M	6/19B	15E_4s2d2Zd_1	14 7/16	E	3.25	354.8	35	30	0.126	0.189	HLP-22	12	8	4	1.05	4.5	2.4	21.8	10.1	0.62	0.34	s2d2	4.18	0.0000609	0.0000756	0.0000931	0.3684
9150333M	6/19B	15E_4s2d2Zd_1	14 7/16	E	3.25	354.8	35	30	0.126	0.189	HLP-22	12	8	4	1.05	4.5	2.4	21.8	10.1	0.62	0.34	s2d2	4.18	0.0000609	0.0000756	0.0000931	0.3684
9150334M	6/19B	15E_4s2d2Zd_1	14 7/16	E	3.25	354.8	35	30	0.126	0.189	HLP-22	12	8	4	1.05	4.5	2.4	21.8	10.1	0.62	0.34	s2d2	4.18	0.0000609	0.0000756	0.0000931	0.3684
9150335M	6/19B	15E_4s2d2Zd_1	14 7/16	E	3.25	354.8	35	30	0.126	0.189	HLP-22	12	8	4	1.05	4.5	2.4	21.8	10.1	0.62	0.34	s2d2	4.18	0.0000609	0.0000756	0.0000931	0.3684
9150336	6/19C	15E_4s2d2Yc_1	14 7/16	E	3.25	354.8	35	30	0.126	0.189	HLP-22	12	8	4	1.05	4.5	2.4	21.8	10.1	0.62	0.34	s2d2	4.18	0.0000609	0.0000756	0.0000931	0.3684
9150337	6/19C	15E_4s2d2Yc_1	14 7/16	E	3.25	354.8	35	30	0.126	0.189	HLP-22	12	8	4	1.05	4.5	2.4	21.8	10.1	0.62	0.34	s2d2	4.18	0.0000609	0.0000756	0.0000931	0.3684
9150338	6/19C	15E_4s2d2Yc_1	14 7/16	E	3.25	354.8	35	30	0.126	0.189	HLP-22	12	8	4	1.05	4.5	2.4	21.8	10.1	0.62	0.34	s2d2	4.18	0.0000609	0.0000756	0.0000931	0.3684
9150339	6/19C	15E_4s2d2Yc_1	14 7/16	E	3.25	354.8	35	30	0.126	0.189	HLP-22	12	8	4	1.05	4.5	2.4	21.8	10.1	0.62	0.34	s2d2	4.18	0.0000609	0.0000756	0.0000931	0.3684
9150340	6/19C	15E_4s2d2Yc_1	14 7/16	E	3.25	354.8	35	30	0.126	0.189	HLP-22	12	8	4	1.05	4.5	2.4	21.8	10.1	0.62	0.34	s2d2	4.18	0.0000609	0.0000756	0.0000931	0.3684
9150341	6/19C	15E_4s2d2Yc_1	14 7/16	E	3.25	354.8	35	30	0.126	0.189	HLP-22	12	8	4	1.05	4.5	2.4	21.8	10.1	0.62	0.34	s2d2	4.18	0.0000609	0.0000756	0.0000931	0.3684
9150342	6/19C	15E_4s2d2Yc_1	14 7/16	E	3.25	354.8	35	30	0.126	0.189	HLP-22	12	8	4	1.05	4.5	2.4	21.8	10.1	0.62	0.34	s2d2	4.18	0.0000609	0.0000756	0.0000931	0.3684
9150343	6/19C	15E_4s2d2Yc_1	14 7/16	E	3.25	354.8	35	30	0.126	0.189	HLP-22	12	8	4	1.05	4.5	2.4	21.8	10.1	0.62	0.34	s2d2	4.18	0.0000609	0.0000756	0.0000931	0.3684
9150344	6/19C	15E_4s2d2Yc_1	14 7/16	E	3.25	354.8	35	30	0.126	0.189	HLP-22	12	8	4	1.05	4.5	2.4	21.8	10.1	0.62	0.34	s2d2	4.18	0.0000609	0.0000756	0.0000931	0.3684
9150345M	6/19C	15E_4s2d2Yc_1	14 7/16	E	3.25	354.8	35	30	0.126	0.189	HLP-22	12	8	4	1.05	4.5	2.4	21.8	10.1	0.62	0.34	s2d2	4.18	0.0000609	0.0000756	0.0000931	0.3684
9150346M	6/19C	15E_4s2d2Yc_1	14 7/16	E	3.25	354.8	35	30	0.126	0.189	HLP-22	12	8	4	1.05	4.5	2.4	21.8	10.1	0.62	0.34	s2d2	4.18	0.0000609	0.0000756	0.0000931	0.3684
9150347M	6/20A	15E_4s2d2Yc_1	14 7/16	E	3.25	354.8	35	30	0.126	0.189	HLP-22	12	8	4	1.05	4.5	2.4	21.8	10.1	0.62	0.34	s2d2	4.18	0.0000609	0.0000756	0.0000931	0.3684
9150348M	6/20A	15E_4s2d2Yc_1	14 7/16	E	3.25	354.8	35	30	0.126	0.189	HLP-22	12	8	4	1.05	4.5	2.4	21.8	10.1	0.62	0.34	s2d2	4.18	0.0000609	0.0000756	0.0000931	0.3684
9150349M	6/20A	15E_4s2d2Yc_1	14 7/16	E	3.25	354.8	35	30	0.126	0.189	HLP-22	12	8	4	1.05	4.5	2.4	21.8	10.1	0.62	0.34	s2d2	4.18	0.0000609	0.0000756	0.0000931	0.3684
9150350M	6/20A	15E_4s2d2Yc_1	14 7/16	E	3.25	354.8	35	30	0.126	0.189	HLP-22	12	8	4	1.05	4.5	2.4	21.8	10.1	0.62	0.34	s2d2	4.18	0.0000609	0.0000756	0.0000931	0.3684
9150351M	6/20A	15E_4s2d2Yc_1	14 7/16	E	3.25	354.8	35	30	0.126	0.189	HLP-22	12	8	4	1.05	4.5	2.4	21.8	10.1	0.62	0.34	s2d2	4.18	0.0000609	0.0000756	0.0000931	0.3684
9150352M	6/20A	15E_4s2d2Yc_1	14 7/16	E	3.25	354.8	35	30	0.126	0.189	HLP-22	12	8	4	1.05	4.5	2.4	21.8	10.1	0.62	0.34	s2d2	4.18	0.0000609	0.0000756	0.0000931	0.3684
9150353M	6/20A	15E_4s2d2Yc_1	14 7/16	E	3.25	354.8	35	30	0.126	0.189	HLP-22	12	8	4	1.05	4.5	2.4	21.8	10.1	0.62	0.34	s2d2	4.18	0.0000609	0.0000756	0.0000931	0.3684
9150353.1	6/20A	15E_4s2d2Yc_1	14 7/16	E	3.25	354.8	35	30	0.126	0.189	HLP-22	12	8	4	1.05	4.5	2.4	21.8	10.1	0.62	0.34	s2d2	4.18	0.0000609	0.0000756	0.0000931	0.3684
9150353.2	6/20A	15E_4s2d2Yc_1	14 7/16	E	3.25	354.8	35	30	0.126	0.189	HLP-22	12	8	4	1.05	4.5	2.4	21.8	10.1	0.62	0.34	s2d2	4.18	0.0000609	0.0000756	0.0000931	0.3684
9150353.3	6/20A	15E_4s2d2Yc_1	14 7/16	E	3.25	354.8	35	30	0.126	0.189	HLP-22	12	8	4	1.05	4.5	2.4	21.8	10.1	0.62	0.34	s2d2	4.18	0.0000609	0.0000756	0.0000931	0.3684
9150353.4	6/20A	15E_4s2d2Yc_1	14 7/16	E	3.25	354.8	35	30	0.126	0.189	HLP-22	12	8	4	1.05	4.5	2.4	21.8	10.1	0.62	0.34	s2d2	4.18	0.0000609	0.0000756	0.0000931	0.3684
9150353.5	6/20A	15E_4s2d2Yc_1	14 7/16	E	3.25	354.8	35	30	0.126	0.189	HLP-22	12	8	4	1.05	4.5	2.4	21.8	10.1	0.62	0.34	s2d2	4.18	0.0000609	0.0000756	0.0000931	0.3684
9150354M	6/20A	15E_4s2d2Yc_1	14 7/16	E	3.25	354.8	35	30	0.126	0.189	HLP-22	12	8	4	1.05	4.5	2.4	21.8	10.1	0.62	0.34	s2d2	4.18	0.0000609	0.0000756	0.0000931	0.3684
9150355	6/20A	15E_4s2d2Yc_1	14 7/16	E	3.25	354.8	35	30	0.126	0.189	HLP-22	12	8	4	1.05	4.5	2.4	21.8	10.1	0.62	0.34	s2d2	4.18	0.0000609	0.0000756	0.0000931	0.3684
9150356	6/20A	15E_4s2d2Yc_1	14 7/16	E	3.25	354.8	35	30	0.126	0.189	HLP-22	12	8	4	1.05	4.5	2.4	21.8	10.1	0.62	0.34	s2d2	4.18	0.0000609	0.0000756	0.0000931	0.3684

Table B.3. Data from 2008 Tests in Small-Scale Vessel with Elliptical Head B.10

Tank Water Temperature	Water Density	Solids Fraction	Pulse Volume Fraction	Duty Cycle	Cycle Time	Pulsed or Steady Jet	Us Steady Jet	U1 Pulsing Jet	U2 URMS	U3 URM3	Discharge Velocity	Critical Suspension Velocity	Average Peak Cloud Height	UCS Condition	UCS Method	UCS Flag	UCS Center Flag	UCS udv Flag	UCS based on Decreasing Velocity	Sweep Increase / Decrease	UDV Height Bed	Particle Motion	Solids Level	Outer Bottom Pattern	Inner Bottom Pattern	Case ID	Test	TDP	Row Number
C	g/cm³	fraction	fraction	fraction	s	text	m/s	m/s	m/s	m/s	m/s	m/s	in.	m/s	text	text	text	text	m/s	text	mm	text	text	text	text	text	text	text	text
T	ρ_l	ϕ_S	ϕ_P	DC	t_C	Jet	U_S	U1	U2	U3	U	U_{CS}	H_C	U_{CSR}	U_{CSM}	U_{CS}vis	U_{CS}cen	U_{CS}udv	U_{CS_D}	S_W	H_{bed}	PM	Sol	SP_O	SP_I	ID	M/DDX	TDP	MSS
24.2	0.999	0.00155	0.050	0.335	12.0	P	N/A	4.98	5.06	5.10	5.20	5.20	7.00	N/A	N/A	N/A	N/A	N/A	N/A	N/A	1.9	N/A	N/A	N/A	N/A	15E_4s2d2Zc_1	6/19A	TDP-185	9150321
24.2	0.999	0.00155	0.050	0.335	12.0	P	N/A	4.98	5.06	5.10	5.20	5.20	7.00	N/A	N/A	N/A	N/A	N/A	N/A	N/A	1.3	N/A	N/A	N/A	N/A	15E_4s2d2Zc_1	6/19A	TDP-185	9150322
24.2	0.999	0.00155	0.050	0.335	12.0	P	N/A	4.98	5.06	5.10	5.20	5.20	7.00	N/A	N/A	N/A	N/A	N/A	N/A	N/A	3.2	N/A	N/A	N/A	N/A	15E_4s2d2Zc_1	6/19A	TDP-185	9150323
24.6	0.999	0.00155	0.050	0.183	28.4	P	N/A	3.86	3.90	3.93	4.00	5.40	5.25	N/A	N/A	N/A	N/A	N/A	N/A	(null)	7.9	1	N/A	N/A	N/A	15E_4s2d2Zd_1	6/19B	TDP-185	9150324
24.7	0.999	0.00155	0.050	0.185	25.6	P	N/A	4.25	4.30	4.32	4.40	5.40	5.75	N/A	N/A	N/A	N/A	N/A	N/A	I	6.0	1	N/A	N/A	N/A	15E_4s2d2Zd_1	6/19B	TDP-185	9150325
24.8	0.999	0.00155	0.050	0.186	23.4	P	N/A	4.62	4.69	4.72	4.80	5.40	6.25	N/A	N/A	N/A	N/A	N/A	N/A	I	4.5	1	N/A	N/A	N/A	15E_4s2d2Zd_1	6/19B	TDP-185	9150326
25.0	0.999	0.00155	0.050	0.186	21.6	P	N/A	4.98	5.06	5.09	5.20	5.40	6.75	N/A	N/A	N/A	N/A	N/A	N/A	I	3.3	1	N/A	N/A	N/A	15E_4s2d2Zd_1	6/19B	TDP-185	9150327
25.1	0.999	0.00155	0.050	0.187	20.8	P	N/A	5.17	5.25	5.29	5.40	5.40	6.75	5.40	udv	N/A	N/A	UCSudv	N/A	I	1.6	1	N/A	N/A	N/A	15E_4s2d2Zd_1	6/19B	TDP-185	9150328
25.5	0.999	0.00155	0.050	0.185	20.1	P	N/A	5.37	5.45	5.49	5.60	5.40	7.00	N/A	N/A	UCSvis	N/A	N/A	N/A	I	0.0	3	N/A	N/A	N/A	15E_4s2d2Zd_1	6/19B	TDP-185	9150329
25.6	0.999	0.00155	0.050	0.185	19.4	P	N/A	5.56	5.65	5.70	5.80	5.40	7.75	N/A	N/A	N/A	N/A	N/A	N/A	I	0.0	4	N/A	N/A	N/A	15E_4s2d2Zd_1	6/19B	TDP-185	9150330
25.8	0.999	0.00155	0.050	0.187	18.1	P	N/A	5.93	6.03	6.08	6.20	5.40	10.25	N/A	N/A	N/A	N/A	N/A	N/A	I	0.0	4	N/A	N/A	N/A	15E_4s2d2Zd_1	6/19B	TDP-185	9150331
25.9	0.998	0.00155	0.050	0.187	17.0	P	N/A	6.29	6.40	6.46	6.60	5.40	12.50	N/A	N/A	N/A	N/A	N/A	N/A	I	0.0	4	N/A	N/A	N/A	15E_4s2d2Zd_1	6/19B	TDP-185	9150332
26.3	0.999	0.00155	0.050	0.188	16.0	P	N/A	6.66	6.79	6.85	7.00	5.40	13.75	N/A	N/A	N/A	N/A	N/A	N/A	I	0.0	4	N/A	N/A	N/A	15E_4s2d2Zd_1	6/19B	TDP-185	9150333
26.5	0.998	0.00155	0.050	0.188	15.2	P	N/A	7.04	7.18	7.25	7.40	5.40	15.75	N/A	N/A	N/A	N/A	N/A	N/A	I	0.0	4	N/A	N/A	N/A	15E_4s2d2Zd_1	6/19B	TDP-185	9150334
26.9	0.999	0.00155	0.050	0.189	14.4	P	N/A	7.40	7.56	7.64	7.80	5.40	18.00	N/A	N/A	N/A	N/A	N/A	N/A	I	0.6	4	N/A	N/A	N/A	15E_4s2d2Zd_1	6/19B	TDP-185	9150335
27.7	0.999	0.00500	0.050	0.337	12.4	P	N/A	4.76	4.83	4.87	5.00	7.60	3.75	N/A	N/A	N/A	N/A	N/A	N/A	(null)	11.4	1	N/A	N/A	N/A	15E_4s2d2Yc_1	6/19C	TDP-186	9150336
27.7	0.998	0.00500	0.050	0.334	11.7	P	N/A	5.12	5.20	5.25	5.40	7.60	4.00	N/A	N/A	N/A	N/A	N/A	N/A	I	10.2	1	N/A	N/A	N/A	15E_4s2d2Yc_1	6/19C	TDP-186	9150337
27.8	0.998	0.00500	0.050	0.335	10.9	P	N/A	5.50	5.60	5.65	5.80	7.60	4.25	N/A	N/A	N/A	N/A	N/A	N/A	I	7.7	1	N/A	N/A	N/A	15E_4s2d2Yc_1	6/19C	TDP-186	9150338
27.9	0.999	0.00500	0.050	0.335	10.2	P	N/A	5.89	6.00	6.05	6.20	7.60	4.75	N/A	N/A	N/A	N/A	N/A	N/A	I	6.0	1	N/A	N/A	N/A	15E_4s2d2Yc_1	6/19C	TDP-186	9150339
28.0	0.999	0.00500	0.050	0.335	9.6	P	N/A	6.25	6.37	6.43	6.60	7.60	4.75	N/A	N/A	N/A	N/A	N/A	N/A	I	3.3	1	N/A	N/A	N/A	15E_4s2d2Yc_1	6/19C	TDP-186	9150340
28.1	0.998	0.00500	0.050	0.336	9.3	P	N/A	6.43	6.55	6.61	6.80	7.60	5.25	N/A	N/A	N/A	N/A	N/A	N/A	I	3.8	1	N/A	N/A	N/A	15E_4s2d2Yc_1	6/19C	TDP-186	9150341
28.3	0.998	0.00500	0.050	0.338	9.0	P	N/A	6.63	6.76	6.82	7.00	7.60	5.25	N/A	N/A	N/A	N/A	N/A	N/A	I	3.2	1	N/A	N/A	N/A	15E_4s2d2Yc_1	6/19C	TDP-186	9150342
28.4	0.998	0.00500	0.050	0.337	8.8	P	N/A	6.80	6.94	7.01	7.20	7.60	5.75	N/A	N/A	UCSvis	N/A	N/A	N/A	I	3.2	3	N/A	N/A	N/A	15E_4s2d2Yc_1	6/19C	TDP-186	9150343
28.5	0.998	0.00500	0.050	0.334	8.6	P	N/A	6.99	7.13	7.20	7.40	7.60	5.75	N/A	N/A	N/A	N/A	N/A	N/A	I	3.2	4	N/A	N/A	N/A	15E_4s2d2Yc_1	6/19C	TDP-186	9150344
28.7	0.998	0.00500	0.050	0.335	8.4	P	N/A	7.15	7.30	7.38	7.60	7.60	6.00	7.60	udv	N/A	N/A	UCSudv	N/A	I	2.6	4	N/A	N/A	N/A	15E_4s2d2Yc_1	6/19C	TDP-186	9150345
28.8	0.998	0.00500	0.050	0.334	8.2	P	N/A	7.34	7.50	7.58	7.80	7.60	6.25	N/A	N/A	N/A	N/A	N/A	N/A	I	0.0	4	N/A	N/A	N/A	15E_4s2d2Yc_1	6/19C	TDP-186	9150346
24.3	0.999	0.00500	0.050	0.334	8.4	P	N/A	7.17	7.32	7.40	7.60	7.60	5.75	7.60	udv	N/A	N/A	UCSudv	N/A	(null)	1.3	4	N/A	N/A	N/A	15E_4s2d2Yc_1	6/20A	TDP-187	9150347
24.5	0.999	0.00500	0.050	0.335	8.2	P	N/A	7.32	7.48	7.56	7.80	7.60	6.00	N/A	N/A	N/A	N/A	N/A	N/A	I	0.0	4	N/A	N/A	N/A	15E_4s2d2Yc_1	6/20A	TDP-187	9150348
24.8	0.999	0.00500	0.050	0.335	7.8	P	N/A	7.72	7.89	7.97	8.20	7.60	6.25	N/A	N/A	N/A	N/A	N/A	N/A	I	0.0	4	N/A	N/A	N/A	15E_4s2d2Yc_1	6/20A	TDP-187	9150349
24.9	0.999	0.00500	0.050	0.336	7.4	P	N/A	8.08	8.27	8.36	8.60	7.60	9.00	N/A	N/A	N/A	N/A	N/A	N/A	I	0.0	4	N/A	N/A	N/A	15E_4s2d2Yc_1	6/20A	TDP-187	9150350
25.2	0.999	0.00500	0.050	0.337	7.1	P	N/A	8.43	8.63	8.73	9.00	7.60	12.00	N/A	N/A	N/A	N/A	N/A	N/A	I	0.0	4	N/A	N/A	N/A	15E_4s2d2Yc_1	6/20A	TDP-187	9150351
25.5	0.999	0.00500	0.050	0.334	6.8	P	N/A	8.77	8.99	9.10	9.40	7.60	14.25	N/A	N/A	N/A	N/A	N/A	N/A	I	0.0	4	N/A	N/A	N/A	15E_4s2d2Yc_1	6/20A	TDP-187	9150352
25.7	0.999	0.00500	0.050	0.336	6.5	P	N/A	9.14	9.38	9.50	9.80	7.60	21.50	N/A	N/A	N/A	N/A	N/A	N/A	I	0.0	4	N/A	N/A	N/A	15E_4s2d2Yc_1	6/20A	TDP-187	9150353
26.0	0.999	0.00500	0.050	0.334	8.4	P	N/A	7.16	7.31	7.39	7.60	7.60	6.00	N/A	N/A	N/A	N/A	N/A	N/A	N/A	n/a	N/A	N/A	N/A	N/A	15E_4s2d2Yc_1	6/20A	TDP-187	9150353.1
26.0	0.999	0.00500	0.050	0.334	8.4	P	N/A	7.16	7.31	7.39	7.60	7.60	6.00	N/A	N/A	N/A	N/A	N/A	N/A	N/A	n/a	N/A	N/A	N/A	N/A	15E_4s2d2Yc_1	6/20A	TDP-187	9150353.2
26.0	0.999	0.00500	0.050	0.334	8.4	P	N/A	7.16	7.31	7.39	7.60	7.60	6.00	N/A	N/A	N/A	N/A	N/A	N/A	N/A	n/a	N/A	N/A	N/A	N/A	15E_4s2d2Yc_1	6/20A	TDP-187	9150353.3
26.0	0.999	0.00500	0.050	0.334	8.4	P	N/A	7.16	7.31	7.39	7.60	7.60	6.00	N/A	N/A	N/A	N/A	N/A	N/A	N/A	n/a	N/A	N/A	N/A	N/A	15E_4s2d2Yc_1	6/20A	TDP-187	9150353.4
26.0	0.999	0.00500	0.050	0.334	8.4	P	N/A	7.16	7.31	7.39	7.60	7.60	6.00	N/A	N/A	N/A	N/A	N/A	N/A	N/A	n/a	N/A	N/A	N/A	N/A	15E_4s2d2Yc_1	6/20A	TDP-187	9150353.5
26.0	0.999	0.00500	0.050	0.334	8.4	P	N/A	7.16	7.31	7.39	7.60	7.60	6.00	N/A	N/A	N/A	N/A	N/A	N/A	I	2.6	4	N/A	N/A	N/A	15E_4s2d2Yc_1	6/20A	TDP-187	9150354
26.0	0.999	0.00500	0.050	0.334	8.4	P	N/A	7.16	7.31	7.39	7.60	7.60	6.00	N/A	N/A	N/A	N/A	N/A	N/A	N/A	2.6	N/A	N/A	N/A	N/A	15E_4s2d2Yc_1	6/20A	TDP-187	9150355
26.0	0.999	0.00500	0.050	0.334	8.4	P	N/A	7.16	7.31	7.39	7.60	7.60	6.00	N/A	N/A	N/A	N/A	N/A	N/A	N/A	2.0	N/A	N/A	N/A	N/A	15E_4s2d2Yc_1	6/20A	TDP-187	9150356

Table B.3. Data from 2008 Tests in Small-Scale Vessel with Elliptical Head A.11

Row Number	Test	Case ID	Tank Diameter	Head Shape	Dish Height	Dish Volume	Tank Fill Height	Return Line Height	Nozzle Inner Diameter	Nozzle Stand-off Distance	Pulse Tube Configuration	Installed Nozzles	Outer Nozzles Operated	Inner Nozzles Operated	Pulse Tube Outer Diameter	Outer PJM Radius	Inner PJM Radius	"FIO" Outer PJM Impingement Angle	"FIO" Inner PJM Impingement Angle	Ratio Outer PJM to Tank Radius	Ratio Inner PJM to Tank Radius	Simulant	Solids Density	Particle Diameter d5	Particle Diameter d50	Particle Diameter d95	Void Fraction
text	text	text	in.	text	in.	in. ^{3}	in.	in.	in.	in.	text	number	number	number	in.	in.	in.	deg	deg	nondim	nondim	text	g/cm^3	m	m	m	fraction
MSS	M/DDX	ID	D	HS	H_{dish}	V_{dish}	H	Rtn	d	sod	PT	N	N_O	N_I	PT_{od}	R_O	R_I	θ_O	θ_I	R_O/R	R_I/R	sxdx	ρ_s	d_5	d_{50}	d_{95}	vf
9150357	6/20A	15E_4s2d2Yc_1	14 7/16	E	3.25	354.8	35	30	0.126	0.189	HLP-22	12	8	4	1.05	4.5	2.4	21.8	10.1	0.62	0.34	s2d2	4.18	0.0000609	0.0000756	0.0000931	0.3684
9150358	6/20A	15E_4s2d2Yc_1	14 7/16	E	3.25	354.8	35	30	0.126	0.189	HLP-22	12	8	4	1.05	4.5	2.4	21.8	10.1	0.62	0.34	s2d2	4.18	0.0000609	0.0000756	0.0000931	0.3684
9150359	6/20A	15E_4s2d2Yc_1	14 7/16	E	3.25	354.8	35	30	0.126	0.189	HLP-22	12	8	4	1.05	4.5	2.4	21.8	10.1	0.62	0.34	s2d2	4.18	0.0000609	0.0000756	0.0000931	0.3684
9150360	6/20A	15E_4s2d2Yc_1	14 7/16	E	3.25	354.8	35	30	0.126	0.189	HLP-22	12	8	4	1.05	4.5	2.4	21.8	10.1	0.62	0.34	s2d2	4.18	0.0000609	0.0000756	0.0000931	0.3684
9150361	6/20A	15E_4s2d2Yc_1	14 7/16	E	3.25	354.8	35	30	0.126	0.189	HLP-22	12	8	4	1.05	4.5	2.4	21.8	10.1	0.62	0.34	s2d2	4.18	0.0000609	0.0000756	0.0000931	0.3684
9150362	6/20A	15E_4s2d2Yc_1	14 7/16	E	3.25	354.8	35	30	0.126	0.189	HLP-22	12	8	4	1.05	4.5	2.4	21.8	10.1	0.62	0.34	s2d2	4.18	0.0000609	0.0000756	0.0000931	0.3684
9150363	6/20B	15E_4s2d2Xc_1	14 7/16	E	3.25	354.8	35	30	0.126	0.189	HLP-22	12	8	4	1.05	4.5	2.4	21.8	10.1	0.62	0.34	s2d2	4.18	0.0000609	0.0000756	0.0000931	0.3684
9150364	6/20B	15E_4s2d2Xc_1	14 7/16	E	3.25	354.8	35	30	0.126	0.189	HLP-22	12	8	4	1.05	4.5	2.4	21.8	10.1	0.62	0.34	s2d2	4.18	0.0000609	0.0000756	0.0000931	0.3684
9150365	6/20B	15E_4s2d2Xc_1	14 7/16	E	3.25	354.8	35	30	0.126	0.189	HLP-22	12	8	4	1.05	4.5	2.4	21.8	10.1	0.62	0.34	s2d2	4.18	0.0000609	0.0000756	0.0000931	0.3684
9150366	6/20B	15E_4s2d2Xc_1	14 7/16	E	3.25	354.8	35	30	0.126	0.189	HLP-22	12	8	4	1.05	4.5	2.4	21.8	10.1	0.62	0.34	s2d2	4.18	0.0000609	0.0000756	0.0000931	0.3684
9150367	6/20B	15E_4s2d2Xc_1	14 7/16	E	3.25	354.8	35	30	0.126	0.189	HLP-22	12	8	4	1.05	4.5	2.4	21.8	10.1	0.62	0.34	s2d2	4.18	0.0000609	0.0000756	0.0000931	0.3684
9150368	6/20B	15E_4s2d2Xc_1	14 7/16	E	3.25	354.8	35	30	0.126	0.189	HLP-22	12	8	4	1.05	4.5	2.4	21.8	10.1	0.62	0.34	s2d2	4.18	0.0000609	0.0000756	0.0000931	0.3684
9150369	6/20B	15E_4s2d2Xc_1	14 7/16	E	3.25	354.8	35	30	0.126	0.189	HLP-22	12	8	4	1.05	4.5	2.4	21.8	10.1	0.62	0.34	s2d2	4.18	0.0000609	0.0000756	0.0000931	0.3684
9150370	6/20B	15E_4s2d2Xc_1	14 7/16	E	3.25	354.8	35	30	0.126	0.189	HLP-22	12	8	4	1.05	4.5	2.4	21.8	10.1	0.62	0.34	s2d2	4.18	0.0000609	0.0000756	0.0000931	0.3684
9150371	6/20B	15E_4s2d2Xc_1	14 7/16	E	3.25	354.8	35	30	0.126	0.189	HLP-22	12	8	4	1.05	4.5	2.4	21.8	10.1	0.62	0.34	s2d2	4.18	0.0000609	0.0000756	0.0000931	0.3684
9150372	6/20B	15E_4s2d2Xc_1	14 7/16	E	3.25	354.8	35	30	0.126	0.189	HLP-22	12	8	4	1.05	4.5	2.4	21.8	10.1	0.62	0.34	s2d2	4.18	0.0000609	0.0000756	0.0000931	0.3684
9150373	6/20B	15E_4s2d2Xc_1	14 7/16	E	3.25	354.8	35	30	0.126	0.189	HLP-22	12	8	4	1.05	4.5	2.4	21.8	10.1	0.62	0.34	s2d2	4.18	0.0000609	0.0000756	0.0000931	0.3684
9150374	6/20B	15E_4s2d2Xc_1	14 7/16	E	3.25	354.8	35	30	0.126	0.189	HLP-22	12	8	4	1.05	4.5	2.4	21.8	10.1	0.62	0.34	s2d2	4.18	0.0000609	0.0000756	0.0000931	0.3684
9150375	6/20B	15E_4s2d2Xc_1	14 7/16	E	3.25	354.8	35	30	0.126	0.189	HLP-22	12	8	4	1.05	4.5	2.4	21.8	10.1	0.62	0.34	s2d2	4.18	0.0000609	0.0000756	0.0000931	0.3684
9150376	6/20B	15E_4s2d2Xc_1	14 7/16	E	3.25	354.8	35	30	0.126	0.189	HLP-22	12	8	4	1.05	4.5	2.4	21.8	10.1	0.62	0.34	s2d2	4.18	0.0000609	0.0000756	0.0000931	0.3684
9150377M	6/20B	15E_4s2d2Xc_1	14 7/16	E	3.25	354.8	35	30	0.126	0.189	HLP-22	12	8	4	1.05	4.5	2.4	21.8	10.1	0.62	0.34	s2d2	4.18	0.0000609	0.0000756	0.0000931	0.3684
9150378M	6/20B	15E_4s2d2Xc_1	14 7/16	E	3.25	354.8	35	30	0.126	0.189	HLP-22	12	8	4	1.05	4.5	2.4	21.8	10.1	0.62	0.34	s2d2	4.18	0.0000609	0.0000756	0.0000931	0.3684
9150378.1	6/20B	15E_4s2d2Xc_1	14 7/16	E	3.25	354.8	35	30	0.126	0.189	HLP-22	12	8	4	1.05	4.5	2.4	21.8	10.1	0.62	0.34	s2d2	4.18	0.0000609	0.0000756	0.0000931	0.3684
9150378.2	6/20B	15E_4s2d2Xc_1	14 7/16	E	3.25	354.8	35	30	0.126	0.189	HLP-22	12	8	4	1.05	4.5	2.4	21.8	10.1	0.62	0.34	s2d2	4.18	0.0000609	0.0000756	0.0000931	0.3684
9150378.3	6/20B	15E_4s2d2Xc_1	14 7/16	E	3.25	354.8	35	30	0.126	0.189	HLP-22	12	8	4	1.05	4.5	2.4	21.8	10.1	0.62	0.34	s2d2	4.18	0.0000609	0.0000756	0.0000931	0.3684
9150378.4	6/20B	15E_4s2d2Xc_1	14 7/16	E	3.25	354.8	35	30	0.126	0.189	HLP-22	12	8	4	1.05	4.5	2.4	21.8	10.1	0.62	0.34	s2d2	4.18	0.0000609	0.0000756	0.0000931	0.3684
9150378.5	6/20B	15E_4s2d2Xc_1	14 7/16	E	3.25	354.8	35	30	0.126	0.189	HLP-22	12	8	4	1.05	4.5	2.4	21.8	10.1	0.62	0.34	s2d2	4.18	0.0000609	0.0000756	0.0000931	0.3684
9150379M	6/20B	15E_4s2d2Xc_1	14 7/16	E	3.25	354.8	35	30	0.126	0.189	HLP-22	12	8	4	1.05	4.5	2.4	21.8	10.1	0.62	0.34	s2d2	4.18	0.0000609	0.0000756	0.0000931	0.3684
9150380	6/20B	15E_4s2d2Xc_1	14 7/16	E	3.25	354.8	35	30	0.126	0.189	HLP-22	12	8	4	1.05	4.5	2.4	21.8	10.1	0.62	0.34	s2d2	4.18	0.0000609	0.0000756	0.0000931	0.3684
9150381	6/20B	15E_4s2d2Xc_1	14 7/16	E	3.25	354.8	35	30	0.126	0.189	HLP-22	12	8	4	1.05	4.5	2.4	21.8	10.1	0.62	0.34	s2d2	4.18	0.0000609	0.0000756	0.0000931	0.3684
9150382	6/20B	15E_4s2d2Xc_1	14 7/16	E	3.25	354.8	35	30	0.126	0.189	HLP-22	12	8	4	1.05	4.5	2.4	21.8	10.1	0.62	0.34	s2d2	4.18	0.0000609	0.0000756	0.0000931	0.3684
9150383	6/20B	15E_4s2d2Xc_1	14 7/16	E	3.25	354.8	35	30	0.126	0.189	HLP-22	12	8	4	1.05	4.5	2.4	21.8	10.1	0.62	0.34	s2d2	4.18	0.0000609	0.0000756	0.0000931	0.3684
9150384	6/20B	15E_4s2d2Xc_1	14 7/16	E	3.25	354.8	35	30	0.126	0.189	HLP-22	12	8	4	1.05	4.5	2.4	21.8	10.1	0.62	0.34	s2d2	4.18	0.0000609	0.0000756	0.0000931	0.3684
9150385	6/20B	15E_4s2d2Xc_1	14 7/16	E	3.25	354.8	35	30	0.126	0.189	HLP-22	12	8	4	1.05	4.5	2.4	21.8	10.1	0.62	0.34	s2d2	4.18	0.0000609	0.0000756	0.0000931	0.3684
9150386	6/20B	15E_4s2d2Xc_1	14 7/16	E	3.25	354.8	35	30	0.126	0.189	HLP-22	12	8	4	1.05	4.5	2.4	21.8	10.1	0.62	0.34	s2d2	4.18	0.0000609	0.0000756	0.0000931	0.3684
9150387	6/20B	15E_4s2d2Xc_1	14 7/16	E	3.25	354.8	35	30	0.126	0.189	HLP-22	12	8	4	1.05	4.5	2.4	21.8	10.1	0.62	0.34	s2d2	4.18	0.0000609	0.0000756	0.0000931	0.3684
9150388	6/23A	15E_4s2d2Xd_1	14 7/16	E	3.25	354.8	33 1/2	30	0.126	0.189	HLP-22	12	8	4	1.05	4.5	2.4	21.8	10.1	0.62	0.34	s2d2	4.18	0.0000609	0.0000756	0.0000931	0.3684
9150389M	6/23A	15E_4s2d2Xd_1	14 7/16	E	3.25	354.8	33 1/2	30	0.126	0.189	HLP-22	12	8	4	1.05	4.5	2.4	21.8	10.1	0.62	0.34	s2d2	4.18	0.0000609	0.0000756	0.0000931	0.3684
9150390	6/23A	15E_4s2d2Xd_1	14 7/16	E	3.25	354.8	33 1/2	30	0.126	0.189	HLP-22	12	8	4	1.05	4.5	2.4	21.8	10.1	0.62	0.34	s2d2	4.18	0.0000609	0.0000756	0.0000931	0.3684
9150391M	6/23A	15E_4s2d2Xd_1	14 7/16	E	3.25	354.8	33 1/2	30	0.126	0.189	HLP-22	12	8	4	1.05	4.5	2.4	21.8	10.1	0.62	0.34	s2d2	4.18	0.0000609	0.0000756	0.0000931	0.3684
9150392M	6/23A	15E_4s2d2Xd_1	14 7/16	E	3.25	354.8	33 1/2	30	0.126	0.189	HLP-22	12	8	4	1.05	4.5	2.4	21.8	10.1	0.62	0.34	s2d2	4.18	0.0000609	0.0000756	0.0000931	0.3684

Table B.3. Data from 2008 Tests in Small-Scale Vessel with Elliptical Head B.11

Tank Water Temperature	Water Density	Solids Fraction	Pulse Volume Fraction	Duty Cycle	Cycle Time	Pulsed or Steady Jet	Us Steady Jet	U1 Pulsing Jet	U2 URMS	U3 URM3	Discharge Velocity	Critical Suspension Velocity	Average Peak Cloud Height	UCS Condition	UCS Method	UCS Flag	UCS Center Flag	UCS udv Flag	UCS based on Decreasing Velocity	Sweep Increase / Decrease	UDV Height Bed	Particle Motion	Solids Level	Outer Bottom Pattern	Inner Bottom Pattern	Case ID	Test	TDP	Row Number
C	g/cm3	fraction	fraction	fraction	s	text	m/s	m/s	m/s	m/s	m/s	m/s	in.	m/s	text	text	text	text	m/s	text	mm	text	text	text	text	text	text	text	text
T	ρ_l	ϕ_S	ϕ_P	DC	t_C	Jet	U_S	U1	U2	U3	U	U_{CS}	H_C	U_{CSR}	U_{CSM}	U_{CS}vis	U_{CS}cen	U_{CS}udv	U_{CS_D}	S_W	H_{bed}	PM	Sol	SP_O	SP_I	ID	M/DDX	TDP	MSS
26.0	0.999	0.00500	0.050	0.334	8.4	P	N/A	7.16	7.31	7.39	7.60	7.60	6.00	N/A	N/A	N/A	N/A	N/A	N/A	N/A	1.9	N/A	N/A	N/A	N/A	15E_4s2d2Yc_1	6/20A	TDP-187	9150357
26.0	0.999	0.00500	0.050	0.334	8.4	P	N/A	7.16	7.31	7.39	7.60	7.60	6.00	N/A	N/A	N/A	N/A	N/A	N/A	N/A	2.6	N/A	N/A	N/A	N/A	15E_4s2d2Yc_1	6/20A	TDP-187	9150358
26.0	0.999	0.00500	0.050	0.334	8.4	P	N/A	7.16	7.31	7.39	7.60	7.60	6.00	N/A	N/A	N/A	N/A	N/A	N/A	N/A	3.2	N/A	N/A	N/A	N/A	15E_4s2d2Yc_1	6/20A	TDP-187	9150359
26.0	0.999	0.00500	0.050	0.334	8.4	P	N/A	7.16	7.31	7.39	7.60	7.60	6.00	N/A	N/A	N/A	N/A	N/A	N/A	N/A	2.6	N/A	N/A	N/A	N/A	15E_4s2d2Yc_1	6/20A	TDP-187	9150360
26.0	0.999	0.00500	0.050	0.334	8.4	P	N/A	7.16	7.31	7.39	7.60	7.60	6.00	N/A	N/A	N/A	N/A	N/A	N/A	N/A	3.2	N/A	N/A	N/A	N/A	15E_4s2d2Yc_1	6/20A	TDP-187	9150361
26.0	0.999	0.00500	0.050	0.334	8.4	P	N/A	7.16	7.31	7.39	7.60	7.60	6.00	N/A	N/A	N/A	N/A	N/A	N/A	N/A	1.9	N/A	N/A	N/A	N/A	15E_4s2d2Yc_1	6/20A	TDP-187	9150362
26.6	0.999	0.01500	0.050	0.333	8.0	P	N/A	7.50	7.67	7.75	8.00	11.80	3.75	N/A	N/A	N/A	N/A	N/A	N/A	(null)	11.1	1	N/A	N/A	N/A	15E_4s2d2Xc_1	6/20B	TDP-188	9150363
27.2	0.999	0.01500	0.050	0.334	7.6	P	N/A	7.88	8.06	8.14	8.40	11.80	4.00	N/A	N/A	N/A	N/A	N/A	N/A	I	10.2	1	N/A	N/A	N/A	15E_4s2d2Xc_1	6/20B	TDP-188	9150364
27.4	0.998	0.01500	0.050	0.335	7.4	P	N/A	8.08	8.27	8.36	8.60	11.80	4.25	N/A	N/A	N/A	N/A	N/A	N/A	I	9.0	1	N/A	N/A	N/A	15E_4s2d2Xc_1	6/20B	TDP-188	9150365
27.8	0.999	0.01500	0.050	0.335	7.1	P	N/A	8.39	8.60	8.71	9.00	11.80	4.25	N/A	N/A	N/A	N/A	N/A	N/A	I	6.6	1	N/A	N/A	N/A	15E_4s2d2Xc_1	6/20B	TDP-188	9150366
28.0	0.999	0.01500	0.050	0.336	6.8	P	N/A	8.78	9.01	9.12	9.40	11.80	4.75	N/A	N/A	N/A	N/A	N/A	N/A	I	6.1	1	N/A	N/A	N/A	15E_4s2d2Xc_1	6/20B	TDP-188	9150367
27.8	0.998	0.01500	0.050	0.334	6.4	P	N/A	9.32	9.57	9.69	10.00	11.80	5.00	N/A	N/A	N/A	N/A	N/A	N/A	(null)	3.4	1	N/A	N/A	N/A	15E_4s2d2Xc_1	6/20B	TDP-188	9150368
28.1	0.998	0.01500	0.050	0.336	6.3	P	N/A	9.47	9.74	9.88	10.20	11.80	5.00	N/A	N/A	N/A	N/A	N/A	N/A	I	3.6	1	N/A	N/A	N/A	15E_4s2d2Xc_1	6/20B	TDP-188	9150369
29.2	0.998	0.01500	0.050	0.334	6.2	P	N/A	9.61	9.88	10.02	10.40	11.80	5.00	N/A	N/A	UCSvis	N/A	N/A	N/A	I	3.2	3	N/A	N/A	N/A	15E_4s2d2Xc_1	6/20B	TDP-188	9150370
29.5	0.998	0.01500	0.050	0.334	6.1	P	N/A	9.77	10.06	10.21	10.60	11.80	5.25	N/A	N/A	N/A	N/A	N/A	N/A	I	3.2	4	N/A	N/A	N/A	15E_4s2d2Xc_1	6/20B	TDP-188	9150371
29.7	0.998	0.01500	0.050	0.334	6.0	P	N/A	9.97	10.26	10.40	10.80	11.80	5.25	N/A	N/A	N/A	N/A	N/A	N/A	I	3.2	4	N/A	N/A	N/A	15E_4s2d2Xc_1	6/20B	TDP-188	9150372
29.9	0.998	0.01500	0.050	0.335	5.9	P	N/A	10.16	10.45	10.60	11.00	11.80	5.50	N/A	N/A	N/A	N/A	N/A	N/A	I	2.1	4	N/A	N/A	N/A	15E_4s2d2Xc_1	6/20B	TDP-188	9150373
30.2	0.998	0.01500	0.050	0.335	5.8	P	N/A	10.35	10.64	10.79	11.20	11.80	6.00	N/A	N/A	N/A	N/A	N/A	N/A	I	2.2	4	N/A	N/A	N/A	15E_4s2d2Xc_1	6/20B	TDP-188	9150374
30.6	0.998	0.01500	0.050	0.334	5.7	P	N/A	10.48	10.80	10.97	11.40	11.80	5.75	N/A	N/A	N/A	N/A	N/A	N/A	I	1.1	4	N/A	N/A	N/A	15E_4s2d2Xc_1	6/20B	TDP-188	9150375
31.2	0.998	0.01500	0.050	0.336	5.6	P	N/A	10.65	10.99	11.16	11.60	11.80	5.75	N/A	N/A	N/A	N/A	N/A	N/A	I	1.4	4	N/A	N/A	N/A	15E_4s2d2Xc_1	6/20B	TDP-188	9150376
32.1	0.998	0.01500	0.050	0.334	5.5	P	N/A	10.89	11.25	11.43	11.80	11.80	6.00	11.80	udv	N/A	N/A	UCSudv	N/A	I	1.9	4	N/A	N/A	N/A	15E_4s2d2Xc_1	6/20B	TDP-188	9150377
32.7	0.997	0.01500	0.050	0.334	5.4	P	N/A	11.09	11.44	11.63	12.00	11.80	6.25	N/A	N/A	N/A	N/A	N/A	N/A	I	0.0	4	N/A	N/A	N/A	15E_4s2d2Xc_1	6/20B	TDP-188	9150378
33.4	0.997	0.01500	0.050	0.334	5.5	P	N/A	10.85	11.21	11.39	11.80	11.80	6.00	N/A	N/A	N/A	N/A	N/A	N/A	N/A	n/a	N/A	N/A	N/A	N/A	15E_4s2d2Xc_1	6/20B	TDP-188	9150378.1
33.4	0.997	0.01500	0.050	0.334	5.5	P	N/A	10.85	11.21	11.39	11.80	11.80	6.00	N/A	N/A	N/A	N/A	N/A	N/A	N/A	n/a	N/A	N/A	N/A	N/A	15E_4s2d2Xc_1	6/20B	TDP-188	9150378.2
33.4	0.997	0.01500	0.050	0.334	5.5	P	N/A	10.85	11.21	11.39	11.80	11.80	6.00	N/A	N/A	N/A	N/A	N/A	N/A	N/A	n/a	N/A	N/A	N/A	N/A	15E_4s2d2Xc_1	6/20B	TDP-188	9150378.3
33.4	0.997	0.01500	0.050	0.334	5.5	P	N/A	10.85	11.21	11.39	11.80	11.80	6.00	N/A	N/A	N/A	N/A	N/A	N/A	N/A	n/a	N/A	N/A	N/A	N/A	15E_4s2d2Xc_1	6/20B	TDP-188	9150378.4
33.4	0.997	0.01500	0.050	0.334	5.5	P	N/A	10.85	11.21	11.39	11.80	11.80	6.00	N/A	N/A	N/A	N/A	N/A	N/A	N/A	n/a	N/A	N/A	N/A	N/A	15E_4s2d2Xc_1	6/20B	TDP-188	9150378.5
33.4	0.997	0.01500	0.050	0.334	5.5	P	N/A	10.85	11.21	11.39	11.80	11.80	6.00	N/A	N/A	N/A	N/A	N/A	N/A	I	3.4	4	N/A	N/A	N/A	15E_4s2d2Xc_1	6/20B	TDP-188	9150379
33.4	0.997	0.01500	0.050	0.334	5.5	P	N/A	10.85	11.21	11.39	11.80	11.80	6.00	N/A	N/A	N/A	N/A	N/A	N/A	N/A	3.3	N/A	N/A	N/A	N/A	15E_4s2d2Xc_1	6/20B	TDP-188	9150380
33.4	0.997	0.01500	0.050	0.334	5.5	P	N/A	10.85	11.21	11.39	11.80	11.80	6.00	N/A	N/A	N/A	N/A	N/A	N/A	N/A	4.0	N/A	N/A	N/A	N/A	15E_4s2d2Xc_1	6/20B	TDP-188	9150381
33.4	0.997	0.01500	0.050	0.334	5.5	P	N/A	10.85	11.21	11.39	11.80	11.80	6.00	N/A	N/A	N/A	N/A	N/A	N/A	N/A	3.6	N/A	N/A	N/A	N/A	15E_4s2d2Xc_1	6/20B	TDP-188	9150382
33.4	0.997	0.01500	0.050	0.334	5.5	P	N/A	10.85	11.21	11.39	11.80	11.80	6.00	N/A	N/A	N/A	N/A	N/A	N/A	N/A	3.7	N/A	N/A	N/A	N/A	15E_4s2d2Xc_1	6/20B	TDP-188	9150383
33.4	0.997	0.01500	0.050	0.334	5.5	P	N/A	10.85	11.21	11.39	11.80	11.80	6.00	N/A	N/A	N/A	N/A	N/A	N/A	N/A	3.6	N/A	N/A	N/A	N/A	15E_4s2d2Xc_1	6/20B	TDP-188	9150384
33.4	0.997	0.01500	0.050	0.334	5.5	P	N/A	10.85	11.21	11.39	11.80	11.80	6.00	N/A	N/A	N/A	N/A	N/A	N/A	N/A	3.4	N/A	N/A	N/A	N/A	15E_4s2d2Xc_1	6/20B	TDP-188	9150385
33.4	0.997	0.01500	0.050	0.334	5.5	P	N/A	10.85	11.21	11.39	11.80	11.80	6.00	N/A	N/A	N/A	N/A	N/A	N/A	N/A	3.4	N/A	N/A	N/A	N/A	15E_4s2d2Xc_1	6/20B	TDP-188	9150386
33.4	0.997	0.01500	0.050	0.334	5.5	P	N/A	10.85	11.21	11.39	11.80	11.80	6.00	N/A	N/A	N/A	N/A	N/A	N/A	N/A	3.7	N/A	N/A	N/A	N/A	15E_4s2d2Xc_1	6/20B	TDP-188	9150387
24.8	0.999	0.01500	0.050	0.186	11.2	P	N/A	9.66	9.95	10.11	10.50	10.70	4.25	N/A	N/A	N/A	N/A	N/A	N/A	(null)	4.5	1	N/A	N/A	N/A	15E_4s2d2Xd_1	6/23A	TDP-189	9150388
25.2	0.999	0.01500	0.050	0.188	10.6	P	N/A	10.02	10.34	10.51	11.00	10.70	5.25	N/A	N/A	N/A	N/A	N/A	N/A	I	4.5	4	N/A	N/A	N/A	15E_4s2d2Xd_1	6/23A	TDP-189	9150389
25.8	0.999	0.01500	0.050	0.186	11.2	P	N/A	9.68	9.97	10.13	10.50	10.70	4.25	N/A	N/A	N/A	N/A	N/A	N/A	D	4.7	1	N/A	N/A	N/A	15E_4s2d2Xd_1	6/23A	TDP-189	9150390
26.1	0.999	0.01500	0.050	0.186	10.8	P	N/A	9.90	10.21	10.37	10.70	10.70	4.75	10.70	vis	UCSvis	N/A	N/A	N/A	I	5.0	3	N/A	N/A	N/A	15E_4s2d2Xd_1	6/23A	TDP-189	9150391
26.3	0.999	0.01500	0.050	0.187	10.6	P	N/A	10.11	10.43	10.60	10.90	10.70	4.75	N/A	N/A	N/A	N/A	N/A	N/A	I	4.2	4	N/A	N/A	N/A	15E_4s2d2Xd_1	6/23A	TDP-189	9150392

Table B.3. Data from 2008 Tests in Small-Scale Vessel with Elliptical Head A.12

Row Number	Test	Case ID	Tank Diameter	Head Shape	Dish Height	Dish Volume	Tank Fill Height	Return Line Height	Nozzle Inner Diameter	Nozzle Stand-off Distance	Pulse Tube Configuration	Installed Nozzles	Outer Nozzles Operated	Inner Nozzles Operated	Pulse Tube Outer Diameter	Outer PJM Radius	Inner PJM Radius	"FIO" Outer PJM Impingement Angle	"FIO" Inner PJM Impingement Angle	Ratio Outer PJM to Tank Radius	Ratio Inner PJM to Tank Radius	Simulant	Solids Density	Particle Diameter d5	Particle Diameter d50	Particle Diameter d95	Void Fraction
text	text	text	in.	text	in.	in. ^{3}	in.	in.	in.	in.	text	number	number	number	in.	in.	in.	deg	deg	nondim	nondim	text	g/cm^3	m	m	m	fraction
MSS	M/DDX	ID	D	HS	H_{dish}	V_{dish}	H	Rtn	d	sod	PT	N	N_O	N_I	PT_{od}	R_O	R_I	θ_O	θ_I	R_O/R	R_I/R	sxdx	ρ_s	d_5	d_{50}	d_{95}	vf
9150393M	6/23A	15E_4s2d2Xd_1	14 7/16	E	3.25	354.8	33 1/2	30	0.126	0.189	HLP-22	12	8	4	1.05	4.5	2.4	21.8	10.1	0.62	0.34	s2d2	4.18	0.0000609	0.0000756	0.0000931	0.3684
9150394M	6/23A	15E_4s2d2Xd_1	14 7/16	E	3.25	354.8	33 1/2	30	0.126	0.189	HLP-22	12	8	4	1.05	4.5	2.4	21.8	10.1	0.62	0.34	s2d2	4.18	0.0000609	0.0000756	0.0000931	0.3684
9150395M	6/23A	15E_4s2d2Xd_1	14 7/16	E	3.25	354.8	33 1/2	30	0.126	0.189	HLP-22	12	8	4	1.05	4.5	2.4	21.8	10.1	0.62	0.34	s2d2	4.18	0.0000609	0.0000756	0.0000931	0.3684
9150396M	6/23A	15E_4s2d2Xd_1	14 7/16	E	3.25	354.8	33 1/2	30	0.126	0.189	HLP-22	12	8	4	1.05	4.5	2.4	21.8	10.1	0.62	0.34	s2d2	4.18	0.0000609	0.0000756	0.0000931	0.3684
9150397M	6/23A	15E_4s2d2Xd_1	14 7/16	E	3.25	354.8	33 1/2	30	0.126	0.189	HLP-22	12	8	4	1.05	4.5	2.4	21.8	10.1	0.62	0.34	s2d2	4.18	0.0000609	0.0000756	0.0000931	0.3684
9150398M	6/23A	15E_4s2d2Xd_1	14 7/16	E	3.25	354.8	33 1/2	30	0.126	0.189	HLP-22	12	8	4	1.05	4.5	2.4	21.8	10.1	0.62	0.34	s2d2	4.18	0.0000609	0.0000756	0.0000931	0.3684
9150399M	6/23A	15E_4s2d2Xd_1	14 7/16	E	3.25	354.8	33 1/2	30	0.126	0.189	HLP-22	12	8	4	1.05	4.5	2.4	21.8	10.1	0.62	0.34	s2d2	4.18	0.0000609	0.0000756	0.0000931	0.3684
9150400M	6/23A	15E_4s2d2Xd_1	14 7/16	E	3.25	354.8	33 1/2	30	0.126	0.189	HLP-22	12	8	4	1.05	4.5	2.4	21.8	10.1	0.62	0.34	s2d2	4.18	0.0000609	0.0000756	0.0000931	0.3684
9150401M	6/23A	15E_4s2d2Xd_1	14 7/16	E	3.25	354.8	33 1/2	30	0.126	0.189	HLP-22	12	8	4	1.05	4.5	2.4	21.8	10.1	0.62	0.34	s2d2	4.18	0.0000609	0.0000756	0.0000931	0.3684
9150402M	6/23A	15E_4s2d2Xd_1	14 7/16	E	3.25	354.8	33 1/2	30	0.126	0.189	HLP-22	12	8	4	1.05	4.5	2.4	21.8	10.1	0.62	0.34	s2d2	4.18	0.0000609	0.0000756	0.0000931	0.3684
9150403M	6/23A	15E_4s2d2Xd_1	14 7/16	E	3.25	354.8	33 1/2	30	0.126	0.189	HLP-22	12	8	4	1.05	4.5	2.4	21.8	10.1	0.62	0.34	s2d2	4.18	0.0000609	0.0000756	0.0000931	0.3684
9150404M	6/24A	15E_4s2d2Xd_1	14 7/16	E	3.25	354.8	35 1/4	30	0.126	0.189	HLP-22	12	8	4	1.05	4.5	2.4	21.8	10.1	0.62	0.34	s2d2	4.18	0.0000609	0.0000756	0.0000931	0.3684
9150405M	6/24A	15E_4s2d2Xd_1	14 7/16	E	3.25	354.8	35 1/4	30	0.126	0.189	HLP-22	12	8	4	1.05	4.5	2.4	21.8	10.1	0.62	0.34	s2d2	4.18	0.0000609	0.0000756	0.0000931	0.3684
9150406M	6/24A	15E_4s2d2Xd_1	14 7/16	E	3.25	354.8	35 1/4	30	0.126	0.189	HLP-22	12	8	4	1.05	4.5	2.4	21.8	10.1	0.62	0.34	s2d2	4.18	0.0000609	0.0000756	0.0000931	0.3684
9150407M	6/24A	15E_4s2d2Xd_1	14 7/16	E	3.25	354.8	35 1/4	30	0.126	0.189	HLP-22	12	8	4	1.05	4.5	2.4	21.8	10.1	0.62	0.34	s2d2	4.18	0.0000609	0.0000756	0.0000931	0.3684
9150408	6/24B	15E_4s2d2Wc_1	14 7/16	E	3.25	354.8	35 3/4	30	0.126	0.189	HLP-22	12	8	4	1.05	4.5	2.4	21.8	10.1	0.62	0.34	s2d2	4.18	0.0000609	0.0000756	0.0000931	0.3684
9150409	6/24B	15E_4s2d2Wc_1	14 7/16	E	3.25	354.8	35 3/4	30	0.126	0.189	HLP-22	12	8	4	1.05	4.5	2.4	21.8	10.1	0.62	0.34	s2d2	4.18	0.0000609	0.0000756	0.0000931	0.3684
9150410	6/24B	15E_4s2d2Wc_1	14 7/16	E	3.25	354.8	35 3/4	30	0.126	0.189	HLP-22	12	8	4	1.05	4.5	2.4	21.8	10.1	0.62	0.34	s2d2	4.18	0.0000609	0.0000756	0.0000931	0.3684
9150411	6/24B	15E_4s2d2Wc_1	14 7/16	E	3.25	354.8	35 3/4	30	0.126	0.189	HLP-22	12	8	4	1.05	4.5	2.4	21.8	10.1	0.62	0.34	s2d2	4.18	0.0000609	0.0000756	0.0000931	0.3684
9150412M	6/24B	15E_4s2d2Wc_1	14 7/16	E	3.25	354.8	35 3/4	30	0.126	0.189	HLP-22	12	8	4	1.05	4.5	2.4	21.8	10.1	0.62	0.34	s2d2	4.18	0.0000609	0.0000756	0.0000931	0.3684
9150413M	6/24B	15E_4s2d2Wc_1	14 7/16	E	3.25	354.8	35 3/4	30	0.126	0.189	HLP-22	12	8	4	1.05	4.5	2.4	21.8	10.1	0.62	0.34	s2d2	4.18	0.0000609	0.0000756	0.0000931	0.3684
9150414M	6/24B	15E_4s2d2Wc_1	14 7/16	E	3.25	354.8	35 3/4	30	0.126	0.189	HLP-22	12	8	4	1.05	4.5	2.4	21.8	10.1	0.62	0.34	s2d2	4.18	0.0000609	0.0000756	0.0000931	0.3684
9150415	6/25A	15E_4s2d2Wc_1	14 7/16	E	3.25	354.8	34 1/2	30	0.126	0.189	HLP-22	12	8	4	1.05	4.5	2.4	21.8	10.1	0.62	0.34	s2d2	4.18	0.0000609	0.0000756	0.0000931	0.3684
9150416	6/25A	15E_4s2d2Wc_1	14 7/16	E	3.25	354.8	34 1/2	30	0.126	0.189	HLP-22	12	8	4	1.05	4.5	2.4	21.8	10.1	0.62	0.34	s2d2	4.18	0.0000609	0.0000756	0.0000931	0.3684
9150417	6/25A	15E_4s2d2Wc_1	14 7/16	E	3.25	354.8	34 1/2	30	0.126	0.189	HLP-22	12	8	4	1.05	4.5	2.4	21.8	10.1	0.62	0.34	s2d2	4.18	0.0000609	0.0000756	0.0000931	0.3684
9150418	6/25A	15E_4s2d2Wc_1	14 7/16	E	3.25	354.8	34 1/2	30	0.126	0.189	HLP-22	12	8	4	1.05	4.5	2.4	21.8	10.1	0.62	0.34	s2d2	4.18	0.0000609	0.0000756	0.0000931	0.3684
9150419M	6/25A	15E_4s2d2Wc_1	14 7/16	E	3.25	354.8	34 1/2	30	0.126	0.189	HLP-22	12	8	4	1.05	4.5	2.4	21.8	10.1	0.62	0.34	s2d2	4.18	0.0000609	0.0000756	0.0000931	0.3684
9150420M	6/25A	15E_4s2d2Wc_1	14 7/16	E	3.25	354.8	34 1/2	30	0.126	0.189	HLP-22	12	8	4	1.05	4.5	2.4	21.8	10.1	0.62	0.34	s2d2	4.18	0.0000609	0.0000756	0.0000931	0.3684
9150421M	6/25A	15E_4s2d2Wc_1	14 7/16	E	3.25	354.8	34 1/2	30	0.126	0.189	HLP-22	12	8	4	1.05	4.5	2.4	21.8	10.1	0.62	0.34	s2d2	4.18	0.0000609	0.0000756	0.0000931	0.3684
9150422M	6/25A	15E_4s2d2Wc_1	14 7/16	E	3.25	354.8	34 1/2	30	0.126	0.189	HLP-22	12	8	4	1.05	4.5	2.4	21.8	10.1	0.62	0.34	s2d2	4.18	0.0000609	0.0000756	0.0000931	0.3684
9150423M	6/25A	15E_4s2d2Wc_1	14 7/16	E	3.25	354.8	34 1/2	30	0.126	0.189	HLP-22	12	8	4	1.05	4.5	2.4	21.8	10.1	0.62	0.34	s2d2	4.18	0.0000609	0.0000756	0.0000931	0.3684
9150424	6/25B	15E_4s2d2Pc_1	14 7/16	E	3.25	354.8	34 1/2	30	0.126	0.189	HLP-22	12	8	4	1.05	4.5	2.4	21.8	10.1	0.62	0.34	s2d2	4.18	0.0000609	0.0000756	0.0000931	0.3684
9150425	6/25B	15E_4s2d2Pc_1	14 7/16	E	3.25	354.8	34 1/2	30	0.126	0.189	HLP-22	12	8	4	1.05	4.5	2.4	21.8	10.1	0.62	0.34	s2d2	4.18	0.0000609	0.0000756	0.0000931	0.3684
9150426	6/25B	15E_4s2d2Pc_1	14 7/16	E	3.25	354.8	34 1/2	30	0.126	0.189	HLP-22	12	8	4	1.05	4.5	2.4	21.8	10.1	0.62	0.34	s2d2	4.18	0.0000609	0.0000756	0.0000931	0.3684
9150427	6/25B	15E_4s2d2Pc_1	14 7/16	E	3.25	354.8	34 1/2	30	0.126	0.189	HLP-22	12	8	4	1.05	4.5	2.4	21.8	10.1	0.62	0.34	s2d2	4.18	0.0000609	0.0000756	0.0000931	0.3684
9150428	6/25B	15E_4s2d2Pc_1	14 7/16	E	3.25	354.8	34 1/2	30	0.126	0.189	HLP-22	12	8	4	1.05	4.5	2.4	21.8	10.1	0.62	0.34	s2d2	4.18	0.0000609	0.0000756	0.0000931	0.3684
9150429M	6/25B	15E_4s2d2Pc_1	14 7/16	E	3.25	354.8	34 1/2	30	0.126	0.189	HLP-22	12	8	4	1.05	4.5	2.4	21.8	10.1	0.62	0.34	s2d2	4.18	0.0000609	0.0000756	0.0000931	0.3684
9150430M	6/25B	15E_4s2d2Pc_1	14 7/16	E	3.25	354.8	34 1/2	30	0.126	0.189	HLP-22	12	8	4	1.05	4.5	2.4	21.8	10.1	0.62	0.34	s2d2	4.18	0.0000609	0.0000756	0.0000931	0.3684
9150431M	6/25B	15E_4s2d2Pc_1	14 7/16	E	3.25	354.8	34 1/2	30	0.126	0.189	HLP-22	12	8	4	1.05	4.5	2.4	21.8	10.1	0.62	0.34	s2d2	4.18	0.0000609	0.0000756	0.0000931	0.3684
9150432M	6/25B	15E_4s2d2Pc_1	14 7/16	E	3.25	354.8	34 1/2	30	0.126	0.189	HLP-22	12	8	4	1.05	4.5	2.4	21.8	10.1	0.62	0.34	s2d2	4.18	0.0000609	0.0000756	0.0000931	0.3684
9150433M	6/25B	15E_4s2d2Pc_1	14 7/16	E	3.25	354.8	34 1/2	30	0.126	0.189	HLP-22	12	8	4	1.05	4.5	2.4	21.8	10.1	0.62	0.34	s2d2	4.18	0.0000609	0.0000756	0.0000931	0.3684

Table B.3. Data from 2008 Tests in Small-Scale Vessel with Elliptical Head B.12

Tank Water Temperature	Water Density	Solids Fraction	Pulse Volume Fraction	Duty Cycle	Cycle Time	Pulsed or Steady Jet	Us Steady Jet	U1 Pulsing Jet	U2 URMS	U3 URM3	Discharge Velocity	Critical Suspension Velocity	Average Peak Cloud Height	UCS Condition	UCS Method	UCS Flag	UCS Center Flag	UCS udv Flag	UCS based on Decreasing Velocity	Sweep Increase / Decrease	UDV Height Bed	Particle Motion	Solids Level	Outer Bottom Pattern	Inner Bottom Pattern	Case ID	Test	TDP	Row Number
C	g/cm³	fraction	fraction	fraction	s	text	m/s	m/s	m/s	m/s	m/s	m/s	in.	m/s	text	text	text	text	m/s	text	mm	text	text	text	text	text	text	text	text
T	ρ_l	ϕ_S	ϕ_P	DC	t_C	Jet	U_S	U1	U2	U3	U	U_{CS}	H_C	U_{CSR}	U_{CSM}	U_{CS}vis	U_{CS}cen	U_{CS}udv	U_{CS_D}	S_W	H_{bed}	PM	Sol	SP_O	SP_I	ID	M/DDX	TDP	MSS
26.7	0.999	0.01500	0.050	0.187	10.4	P	N/A	10.31	10.62	10.79	11.10	10.70	4.75	N/A	N/A	N/A	N/A	N/A	N/A	I	4.0	4	N/A	N/A	N/A	15E_4s2d2Xd_1	6/23A	TDP-189	9150393
27.0	0.999	0.01500	0.050	0.188	10.2	P	N/A	10.45	10.79	10.97	11.30	10.70	5.00	N/A	N/A	N/A	N/A	N/A	N/A	I	3.6	4	N/A	N/A	N/A	15E_4s2d2Xd_1	6/23A	TDP-189	9150394
27.3	0.999	0.01500	0.050	0.189	10.0	P	N/A	10.63	10.97	11.16	11.50	10.70	5.00	N/A	N/A	N/A	N/A	N/A	N/A	I	3.5	4	N/A	N/A	N/A	15E_4s2d2Xd_1	6/23A	TDP-189	9150395
27.6	0.999	0.01500	0.050	0.189	9.8	P	N/A	10.85	11.19	11.37	11.70	10.70	5.00	N/A	N/A	N/A	N/A	N/A	N/A	I	3.4	4	N/A	N/A	N/A	15E_4s2d2Xd_1	6/23A	TDP-189	9150396
28.0	0.999	0.01500	0.050	0.178	10.2	P	N/A	11.07	11.44	11.64	11.90	10.70	5.25	N/A	N/A	N/A	N/A	N/A	N/A	I	3.6	4	N/A	N/A	N/A	15E_4s2d2Xd_1	6/23A	TDP-189	9150397
28.3	0.998	0.01500	0.050	0.180	10.0	P	N/A	11.17	11.55	11.75	12.10	10.70	5.50	N/A	N/A	N/A	N/A	N/A	N/A	I	3.3	4	N/A	N/A	N/A	15E_4s2d2Xd_1	6/23A	TDP-189	9150398
28.5	0.998	0.01500	0.050	0.180	9.8	P	N/A	11.35	11.73	11.94	12.30	10.70	5.25	N/A	N/A	N/A	N/A	N/A	N/A	I	3.5	4	N/A	N/A	N/A	15E_4s2d2Xd_1	6/23A	TDP-189	9150399
28.8	0.998	0.01500	0.050	0.180	9.6	P	N/A	11.50	11.89	12.10	12.50	10.70	5.25	N/A	N/A	N/A	N/A	N/A	N/A	I	1.9	4	N/A	N/A	N/A	15E_4s2d2Xd_1	6/23A	TDP-189	9150400
29.2	0.998	0.01500	0.050	0.182	9.4	P	N/A	11.67	12.08	12.30	12.70	10.70	5.50	N/A	N/A	N/A	N/A	N/A	N/A	I	3.4	4	N/A	N/A	N/A	15E_4s2d2Xd_1	6/23A	TDP-189	9150401
29.6	0.998	0.01500	0.050	0.184	9.2	P	N/A	11.78	12.22	12.45	12.90	10.70	5.50	N/A	N/A	N/A	N/A	N/A	N/A	I	2.6	4	N/A	N/A	N/A	15E_4s2d2Xd_1	6/23A	TDP-189	9150402
29.9	0.998	0.01500	0.050	0.182	9.2	P	N/A	12.03	12.46	12.69	13.10	10.70	5.75	N/A	N/A	N/A	N/A	N/A	N/A	I	1.7	4	N/A	N/A	N/A	15E_4s2d2Xd_1	6/23A	TDP-189	9150403
25.7	0.998	0.01500	0.050	0.179	9.2	P	N/A	12.21	12.63	12.86	13.10	10.70	5.50	N/A	N/A	N/A	N/A	N/A	N/A	(null)	3.3	4	N/A	N/A	N/A	15E_4s2d2Xd_1	6/24A	TDP-190	9150404
26.2	0.998	0.01500	0.050	0.184	8.4	P	N/A	13.03	13.53	13.81	14.00	10.70	5.75	N/A	N/A	N/A	N/A	N/A	N/A	I	1.8	4	N/A	N/A	N/A	15E_4s2d2Xd_1	6/24A	TDP-190	9150405
26.6	0.999	0.01500	0.050	0.185	8.0	P	N/A	13.54	14.07	14.36	14.50	10.70	5.75	N/A	N/A	N/A	N/A	N/A	N/A	I	1.0	4	N/A	N/A	N/A	15E_4s2d2Xd_1	6/24A	TDP-190	9150406
27.1	0.998	0.01500	0.050	0.186	7.8	P	N/A	13.80	14.34	14.64	15.00	10.70	6.00	N/A	N/A	N/A	N/A	N/A	N/A	I	0.6	4	N/A	N/A	N/A	15E_4s2d2Xd_1	6/24A	TDP-190	9150407
26.6	0.998	0.04500	0.050	0.326	8.0	P	N/A	7.70	7.83	7.91	8.00	11.50	4.25	N/A	N/A	N/A	N/A	N/A	N/A	(null)	13.1	1	N/A	N/A	N/A	15E_4s2d2Wc_1	6/24B	TDP-191	9150408
27.0	0.999	0.04500	0.050	0.336	7.1	P	N/A	8.40	8.61	8.72	9.00	11.50	4.25	N/A	N/A	N/A	N/A	N/A	N/A	I	9.1	1	N/A	N/A	N/A	15E_4s2d2Wc_1	6/24B	TDP-191	9150409
27.1	0.999	0.04500	0.050	0.339	6.4	P	N/A	9.24	9.50	9.64	10.00	11.50	4.75	N/A	N/A	N/A	N/A	N/A	N/A	I	7.9	1	N/A	N/A	N/A	15E_4s2d2Wc_1	6/24B	TDP-191	9150410
27.4	0.999	0.04500	0.050	0.337	5.8	P	N/A	10.20	10.51	10.67	11.00	11.50	5.25	N/A	N/A	N/A	N/A	N/A	N/A	I	3.6	1	N/A	N/A	N/A	15E_4s2d2Wc_1	6/24B	TDP-191	9150411
27.8	0.998	0.04500	0.050	0.333	5.7	P	N/A	10.61	10.93	11.09	11.50	11.50	5.50	11.50	udv	N/A	N/A	UCSudv	N/A	I	1.1	4	N/A	N/A	N/A	15E_4s2d2Wc_1	6/24B	TDP-191	9150412
28.5	0.998	0.04500	0.050	0.337	5.3	P	N/A	11.10	11.46	11.65	12.00	11.50	5.75	N/A	N/A	N/A	N/A	N/A	N/A	I	0.0	4	N/A	N/A	N/A	15E_4s2d2Wc_1	6/24B	TDP-191	9150413
29.1	0.998	0.04500	0.050	0.337	4.9	P	N/A	12.03	12.46	12.68	13.00	11.50	6.50	N/A	N/A	N/A	N/A	N/A	N/A	I	0.0	4	N/A	N/A	N/A	15E_4s2d2Wc_1	6/24B	TDP-191	9150414
24.2	0.999	0.04500	0.050	0.329	8.0	P	N/A	7.61	7.78	7.87	8.00	11.50	4.25	N/A	N/A	N/A	N/A	N/A	N/A	(null)	8.5	1	N/A	N/A	N/A	15E_4s2d2Wc_1	6/25A	TDP-192	9150415
24.2	1.000	0.04500	0.050	0.331	6.4	P	N/A	9.38	9.64	9.77	10.00	11.50	5.25	N/A	N/A	N/A	N/A	N/A	N/A	I	3.2	1	N/A	N/A	N/A	15E_4s2d2Wc_1	6/25A	TDP-192	9150416
24.4	0.999	0.04500	0.050	0.336	6.0	P	N/A	9.88	10.16	10.31	10.50	11.50	5.25	N/A	N/A	UCSvis	N/A	N/A	N/A	I	3.2	3	N/A	N/A	N/A	15E_4s2d2Wc_1	6/25A	TDP-192	9150417
24.7	0.999	0.04500	0.050	0.333	5.8	P	N/A	10.43	10.76	10.93	11.00	11.50	5.75	N/A	N/A	N/A	N/A	N/A	N/A	I	1.9	4	N/A	N/A	N/A	15E_4s2d2Wc_1	6/25A	TDP-192	9150418
24.9	0.999	0.04500	0.050	0.332	5.6	P	N/A	10.80	11.16	11.34	11.50	11.50	6.00	11.50	udv	N/A	N/A	UCSudv	N/A	I	0.6	4	N/A	N/A	N/A	15E_4s2d2Wc_1	6/25A	TDP-192	9150419
25.2	0.999	0.04500	0.050	0.331	5.4	P	N/A	11.17	11.56	11.77	12.00	11.50	6.25	N/A	N/A	N/A	N/A	N/A	N/A	I	0.0	4	N/A	N/A	N/A	15E_4s2d2Wc_1	6/25A	TDP-192	9150420
25.6	0.999	0.04500	0.050	0.328	5.0	P	N/A	12.21	12.65	12.88	13.00	11.50	6.75	N/A	N/A	N/A	N/A	N/A	N/A	I	0.0	4	N/A	N/A	N/A	15E_4s2d2Wc_1	6/25A	TDP-192	9150421
25.9	0.999	0.04500	0.050	0.336	4.6	P	N/A	13.00	13.53	13.81	14.00	11.50	7.75	N/A	N/A	N/A	N/A	N/A	N/A	I	0.0	4	N/A	N/A	N/A	15E_4s2d2Wc_1	6/25A	TDP-192	9150422
26.3	0.999	0.04500	0.050	0.338	4.2	P	N/A	14.04	14.67	15.01	15.00	11.50	9.50	N/A	N/A	N/A	N/A	N/A	N/A	I	0.0	4	N/A	N/A	N/A	15E_4s2d2Wc_1	6/25A	TDP-192	9150423
26.4	0.999	0.06000	0.050	0.330	8.1	P	N/A	7.50	7.68	7.78	8.00	11.50	5.25	N/A	N/A	N/A	N/A	N/A	N/A	(null)	11.0	1	N/A	N/A	N/A	15E_4s2d2Pc_1	6/25B	TDP-193	9150424
26.4	0.999	0.06000	0.050	0.335	7.2	P	N/A	8.34	8.55	8.66	9.00	11.50	5.25	N/A	N/A	N/A	N/A	N/A	N/A	I	7.3	1	N/A	N/A	N/A	15E_4s2d2Pc_1	6/25B	TDP-193	9150425
26.5	0.999	0.06000	0.050	0.335	6.5	P	N/A	9.26	9.53	9.66	10.00	11.50	5.75	N/A	N/A	N/A	N/A	N/A	N/A	I	3.2	1	N/A	N/A	N/A	15E_4s2d2Pc_1	6/25B	TDP-193	9150426
26.7	0.999	0.06000	0.050	0.334	6.2	P	N/A	9.73	9.99	10.13	10.50	11.50	6.00	N/A	N/A	UCSvis	N/A	N/A	N/A	I	3.2	3	N/A	N/A	N/A	15E_4s2d2Pc_1	6/25B	TDP-193	9150427
26.9	0.999	0.06000	0.050	0.333	5.9	P	N/A	10.23	10.54	10.70	11.00	11.50	6.25	N/A	N/A	N/A	N/A	N/A	N/A	I	1.0	4	N/A	N/A	N/A	15E_4s2d2Pc_1	6/25B	TDP-193	9150428
27.1	0.999	0.06000	0.050	0.333	5.6	P	N/A	10.66	11.02	11.20	11.50	11.50	6.25	11.50	udv	N/A	N/A	UCSudv	N/A	I	0.5	4	N/A	N/A	N/A	15E_4s2d2Pc_1	6/25B	TDP-193	9150429
27.3	0.999	0.06000	0.050	0.334	5.2	P	N/A	11.53	11.67	11.76	12.00	11.50	6.75	N/A	N/A	N/A	N/A	N/A	N/A	I	0.0	4	N/A	N/A	N/A	15E_4s2d2Pc_1	6/25B	TDP-193	9150430
27.7	0.999	0.06000	0.050	0.333	5.0	P	N/A	12.01	12.43	12.64	13.00	11.50	7.75	N/A	N/A	N/A	N/A	N/A	N/A	I	0.0	4	N/A	N/A	N/A	15E_4s2d2Pc_1	6/25B	TDP-193	9150431
27.9	0.998	0.06000	0.050	0.339	4.6	P	N/A	12.88	13.36	13.61	14.00	11.50	8.75	N/A	N/A	N/A	N/A	N/A	N/A	I	0.0	4	N/A	N/A	N/A	15E_4s2d2Pc_1	6/25B	TDP-193	9150432
28.3	0.999	0.06000	0.050	0.337	4.3	P	N/A	13.80	14.37	14.66	15.00	11.50	9.50	N/A	N/A	N/A	N/A	N/A	N/A	I	0.0	4	N/A	N/A	N/A	15E_4s2d2Pc_1	6/25B	TDP-193	9150433

Table B.3. Data from 2008 Tests in Small-Scale Vessel with Elliptical Head A.13

Row Number	Test	Case ID	Tank Diameter	Head Shape	Dish Height	Dish Volume	Tank Fill Height	Return Line Height	Nozzle Inner Diameter	Nozzle Stand-off Distance	Pulse Tube Configuration	Installed Nozzles	Outer Nozzles Operated	Inner Nozzles Operated	Pulse Tube Outer Diameter	Outer PJM Radius	Inner PJM Radius	"FIO" Outer PJM Impingement Angle	"FIO" Inner PJM Impingement Angle	Ratio Outer PJM to Tank Radius	Ratio Inner PJM to Tank Radius	Simulant	Solids Density	Particle Diameter d5	Particle Diameter d50	Particle Diameter d95	Void Fraction
text	text	text	in.	text	in.	in. ^{3}	in.	in.	in.	in.	text	number	number	number	in.	in.	in.	deg	deg	nondim	nondim	text	g/cm^3	m	m	m	fraction
MSS	M/DDX	ID	D	HS	H_{dish}	V_{dish}	H	Rtn	d	sod	PT	N	N_O	N_I	PT_{od}	R_O	R_I	θ_O	θ_I	R_O/R	R_I/R	sxdx	ρ_s	d_5	d_{50}	d_{95}	vf
9150434	6/26A	15E_4s1d1Zc_1	14 7/16	E	3.25	354.8	34 3/4	30	0.126	0.189	HLP-22	12	8	4	1.05	4.5	2.4	21.8	10.1	0.62	0.34	s1d1	2.46	0.0001428	0.0001664	0.0001951	0.4118
9150435	6/26A	15E_4s1d1Zc_1	14 7/16	E	3.25	354.8	34 3/4	30	0.126	0.189	HLP-22	12	8	4	1.05	4.5	2.4	21.8	10.1	0.62	0.34	s1d1	2.46	0.0001428	0.0001664	0.0001951	0.4118
9150436	6/26A	15E_4s1d1Zc_1	14 7/16	E	3.25	354.8	34 3/4	30	0.126	0.189	HLP-22	12	8	4	1.05	4.5	2.4	21.8	10.1	0.62	0.34	s1d1	2.46	0.0001428	0.0001664	0.0001951	0.4118
9150437	6/26A	15E_4s1d1Zc_1	14 7/16	E	3.25	354.8	34 3/4	30	0.126	0.189	HLP-22	12	8	4	1.05	4.5	2.4	21.8	10.1	0.62	0.34	s1d1	2.46	0.0001428	0.0001664	0.0001951	0.4118
9150438M	6/26A	15E_4s1d1Zc_1	14 7/16	E	3.25	354.8	34 3/4	30	0.126	0.189	HLP-22	12	8	4	1.05	4.5	2.4	21.8	10.1	0.62	0.34	s1d1	2.46	0.0001428	0.0001664	0.0001951	0.4118
9150439M	6/26A	15E_4s1d1Zc_1	14 7/16	E	3.25	354.8	34 3/4	30	0.126	0.189	HLP-22	12	8	4	1.05	4.5	2.4	21.8	10.1	0.62	0.34	s1d1	2.46	0.0001428	0.0001664	0.0001951	0.4118
9150440M	6/26A	15E_4s1d1Zc_1	14 7/16	E	3.25	354.8	34 3/4	30	0.126	0.189	HLP-22	12	8	4	1.05	4.5	2.4	21.8	10.1	0.62	0.34	s1d1	2.46	0.0001428	0.0001664	0.0001951	0.4118
9150441M	6/26A	15E_4s1d1Zc_1	14 7/16	E	3.25	354.8	34 3/4	30	0.126	0.189	HLP-22	12	8	4	1.05	4.5	2.4	21.8	10.1	0.62	0.34	s1d1	2.46	0.0001428	0.0001664	0.0001951	0.4118
9150442M	6/26A	15E_4s1d1Zc_1	14 7/16	E	3.25	354.8	34 3/4	30	0.126	0.189	HLP-22	12	8	4	1.05	4.5	2.4	21.8	10.1	0.62	0.34	s1d1	2.46	0.0001428	0.0001664	0.0001951	0.4118
9150443M	6/26A	15E_4s1d1Zc_1	14 7/16	E	3.25	354.8	34 3/4	30	0.126	0.189	HLP-22	12	8	4	1.05	4.5	2.4	21.8	10.1	0.62	0.34	s1d1	2.46	0.0001428	0.0001664	0.0001951	0.4118
9150444M	6/26A	15E_4s1d1Zc_1	14 7/16	E	3.25	354.8	34 3/4	30	0.126	0.189	HLP-22	12	8	4	1.05	4.5	2.4	21.8	10.1	0.62	0.34	s1d1	2.46	0.0001428	0.0001664	0.0001951	0.4118
9150445M	6/26A	15E_4s1d1Zc_1	14 7/16	E	3.25	354.8	34 3/4	30	0.126	0.189	HLP-22	12	8	4	1.05	4.5	2.4	21.8	10.1	0.62	0.34	s1d1	2.46	0.0001428	0.0001664	0.0001951	0.4118
9150446	6/26A	15E_4s1d1Zc_1	14 7/16	E	3.25	354.8	34 3/4	30	0.126	0.189	HLP-22	12	8	4	1.05	4.5	2.4	21.8	10.1	0.62	0.34	s1d1	2.46	0.0001428	0.0001664	0.0001951	0.4118
9150447	6/26A	15E_4s1d1Zc_1	14 7/16	E	3.25	354.8	34 3/4	30	0.126	0.189	HLP-22	12	8	4	1.05	4.5	2.4	21.8	10.1	0.62	0.34	s1d1	2.46	0.0001428	0.0001664	0.0001951	0.4118
9150448	6/26A	15E_4s1d1Zc_1	14 7/16	E	3.25	354.8	34 3/4	30	0.126	0.189	HLP-22	12	8	4	1.05	4.5	2.4	21.8	10.1	0.62	0.34	s1d1	2.46	0.0001428	0.0001664	0.0001951	0.4118
9150449	6/26A	15E_4s1d1Zc_1	14 7/16	E	3.25	354.8	34 3/4	30	0.126	0.189	HLP-22	12	8	4	1.05	4.5	2.4	21.8	10.1	0.62	0.34	s1d1	2.46	0.0001428	0.0001664	0.0001951	0.4118
9150450	6/26A	15E_4s1d1Zc_1	14 7/16	E	3.25	354.8	34 3/4	30	0.126	0.189	HLP-22	12	8	4	1.05	4.5	2.4	21.8	10.1	0.62	0.34	s1d1	2.46	0.0001428	0.0001664	0.0001951	0.4118
9150451	6/26A	15E_4s1d1Zc_1	14 7/16	E	3.25	354.8	34 3/4	30	0.126	0.189	HLP-22	12	8	4	1.05	4.5	2.4	21.8	10.1	0.62	0.34	s1d1	2.46	0.0001428	0.0001664	0.0001951	0.4118
9150452	6/26A	15E_4s1d1Zc_1	14 7/16	E	3.25	354.8	34 3/4	30	0.126	0.189	HLP-22	12	8	4	1.05	4.5	2.4	21.8	10.1	0.62	0.34	s1d1	2.46	0.0001428	0.0001664	0.0001951	0.4118
9150453	6/26B	15E_4s1d1Zd_1	14 7/16	E	3.25	354.8	34 3/4	30	0.126	0.189	HLP-22	12	8	4	1.05	4.5	2.4	21.8	10.1	0.62	0.34	s1d1	2.46	0.0001428	0.0001664	0.0001951	0.4118
9150454	6/26B	15E_4s1d1Zd_1	14 7/16	E	3.25	354.8	34 3/4	30	0.126	0.189	HLP-22	12	8	4	1.05	4.5	2.4	21.8	10.1	0.62	0.34	s1d1	2.46	0.0001428	0.0001664	0.0001951	0.4118
9150455	6/26B	15E_4s1d1Zd_1	14 7/16	E	3.25	354.8	34 3/4	30	0.126	0.189	HLP-22	12	8	4	1.05	4.5	2.4	21.8	10.1	0.62	0.34	s1d1	2.46	0.0001428	0.0001664	0.0001951	0.4118
9150456	6/26B	15E_4s1d1Zd_1	14 7/16	E	3.25	354.8	34 3/4	30	0.126	0.189	HLP-22	12	8	4	1.05	4.5	2.4	21.8	10.1	0.62	0.34	s1d1	2.46	0.0001428	0.0001664	0.0001951	0.4118
9150457	6/26B	15E_4s1d1Zd_1	14 7/16	E	3.25	354.8	34 3/4	30	0.126	0.189	HLP-22	12	8	4	1.05	4.5	2.4	21.8	10.1	0.62	0.34	s1d1	2.46	0.0001428	0.0001664	0.0001951	0.4118
9150458	6/26B	15E_4s1d1Zd_1	14 7/16	E	3.25	354.8	34 3/4	30	0.126	0.189	HLP-22	12	8	4	1.05	4.5	2.4	21.8	10.1	0.62	0.34	s1d1	2.46	0.0001428	0.0001664	0.0001951	0.4118
9150459	6/26B	15E_4s1d1Zd_1	14 7/16	E	3.25	354.8	34 3/4	30	0.126	0.189	HLP-22	12	8	4	1.05	4.5	2.4	21.8	10.1	0.62	0.34	s1d1	2.46	0.0001428	0.0001664	0.0001951	0.4118
9150460M	6/26B	15E_4s1d1Zd_1	14 7/16	E	3.25	354.8	34 3/4	30	0.126	0.189	HLP-22	12	8	4	1.05	4.5	2.4	21.8	10.1	0.62	0.34	s1d1	2.46	0.0001428	0.0001664	0.0001951	0.4118
9150461M	6/26B	15E_4s1d1Zd_1	14 7/16	E	3.25	354.8	34 3/4	30	0.126	0.189	HLP-22	12	8	4	1.05	4.5	2.4	21.8	10.1	0.62	0.34	s1d1	2.46	0.0001428	0.0001664	0.0001951	0.4118
9150462M	6/26B	15E_4s1d1Zd_1	14 7/16	E	3.25	354.8	34 3/4	30	0.126	0.189	HLP-22	12	8	4	1.05	4.5	2.4	21.8	10.1	0.62	0.34	s1d1	2.46	0.0001428	0.0001664	0.0001951	0.4118
9150463M	6/26B	15E_4s1d1Zd_1	14 7/16	E	3.25	354.8	34 3/4	30	0.126	0.189	HLP-22	12	8	4	1.05	4.5	2.4	21.8	10.1	0.62	0.34	s1d1	2.46	0.0001428	0.0001664	0.0001951	0.4118
9150464M	6/26B	15E_4s1d1Zd_1	14 7/16	E	3.25	354.8	34 3/4	30	0.126	0.189	HLP-22	12	8	4	1.05	4.5	2.4	21.8	10.1	0.62	0.34	s1d1	2.46	0.0001428	0.0001664	0.0001951	0.4118
9150465M	6/26B	15E_4s1d1Zd_1	14 7/16	E	3.25	354.8	34 3/4	30	0.126	0.189	HLP-22	12	8	4	1.05	4.5	2.4	21.8	10.1	0.62	0.34	s1d1	2.46	0.0001428	0.0001664	0.0001951	0.4118
9150466	6/27A	15E_4s1d1Yc_1	14 7/16	E	3.25	354.8	34 3/4	30	0.126	0.189	HLP-22	12	8	4	1.05	4.5	2.4	21.8	10.1	0.62	0.34	s1d1	2.46	0.0001428	0.0001664	0.0001951	0.4118
9150467	6/27A	15E_4s1d1Yc_1	14 7/16	E	3.25	354.8	34 3/4	30	0.126	0.189	HLP-22	12	8	4	1.05	4.5	2.4	21.8	10.1	0.62	0.34	s1d1	2.46	0.0001428	0.0001664	0.0001951	0.4118
9150468	6/27A	15E_4s1d1Yc_1	14 7/16	E	3.25	354.8	34 3/4	30	0.126	0.189	HLP-22	12	8	4	1.05	4.5	2.4	21.8	10.1	0.62	0.34	s1d1	2.46	0.0001428	0.0001664	0.0001951	0.4118
9150469	6/27A	15E_4s1d1Yc_1	14 7/16	E	3.25	354.8	34 3/4	30	0.126	0.189	HLP-22	12	8	4	1.05	4.5	2.4	21.8	10.1	0.62	0.34	s1d1	2.46	0.0001428	0.0001664	0.0001951	0.4118
9150470	6/27A	15E_4s1d1Yc_1	14 7/16	E	3.25	354.8	34 3/4	30	0.126	0.189	HLP-22	12	8	4	1.05	4.5	2.4	21.8	10.1	0.62	0.34	s1d1	2.46	0.0001428	0.0001664	0.0001951	0.4118
9150471	6/27A	15E_4s1d1Yc_1	14 7/16	E	3.25	354.8	34 3/4	30	0.126	0.189	HLP-22	12	8	4	1.05	4.5	2.4	21.8	10.1	0.62	0.34	s1d1	2.46	0.0001428	0.0001664	0.0001951	0.4118
9150472M	6/27A	15E_4s1d1Yc_1	14 7/16	E	3.25	354.8	34 3/4	30	0.126	0.189	HLP-22	12	8	4	1.05	4.5	2.4	21.8	10.1	0.62	0.34	s1d1	2.46	0.0001428	0.0001664	0.0001951	0.4118
9150473M	6/27A	15E_4s1d1Yc_1	14 7/16	E	3.25	354.8	34 3/4	30	0.126	0.189	HLP-22	12	8	4	1.05	4.5	2.4	21.8	10.1	0.62	0.34	s1d1	2.46	0.0001428	0.0001664	0.0001951	0.4118
9150474M	6/27A	15E_4s1d1Yc_1	14 7/16	E	3.25	354.8	34 3/4	30	0.126	0.189	HLP-22	12	8	4	1.05	4.5	2.4	21.8	10.1	0.62	0.34	s1d1	2.46	0.0001428	0.0001664	0.0001951	0.4118

Table B.3. Data from 2008 Tests in Small-Scale Vessel with Elliptical Head B.13

Tank Water Temperature	Water Density	Solids Fraction	Pulse Volume Fraction	Duty Cycle	Cycle Time	Pulsed or Steady Jet	Us Steady Jet	U1 Pulsing Jet	U2 URMS	U3 URM3	Discharge Velocity	Critical Suspension Velocity	Average Peak Cloud Height	UCS Condition	UCS Method	UCS Flag	UCS Center Flag	UCS udv Flag	UCS based on Decreasing Velocity	Sweep Increase / Decrease	UDV Height Bed	Particle Motion	Solids Level	Outer Bottom Pattern	Inner Bottom Pattern	Case ID	Test	TDP	Row Number
C	g/cm³	fraction	fraction	fraction	s	text	m/s	m/s	m/s	m/s	m/s	m/s	in.	m/s	text	text	text	text	m/s	text	mm	text	text	text	text	text	text	text	text
T	ρ_l	ϕ_S	ϕ_P	DC	t_C	Jet	U_S	U1	U2	U3	U	U_{CS}	H_C	U_{CSR}	U_{CSM}	U_{CS}vis	U_{CS}cen	U_{CS}udv	U_{CS_D}	S_W	H_{bed}	PM	Sol	SP_O	SP_I	ID	M/DDX	TDP	MSS
24.8	0.999	0.00155	0.050	0.327	20.8	P	N/A	2.94	2.95	2.96	3.00	4.20	4.25	N/A	N/A	N/A	N/A	N/A	N/A	(null)	11.6	1	N/A	N/A	N/A	15E_4s1d1Zc_1	6/26A	TDP-194	9150434
24.9	0.999	0.00155	0.050	0.331	17.8	P	N/A	3.42	3.44	3.45	3.50	4.20	4.75	N/A	N/A	N/A	N/A	N/A	N/A	I	8.6	1	N/A	N/A	N/A	15E_4s1d1Zc_1	6/26A	TDP-194	9150435
25.1	0.999	0.00155	0.050	0.332	16.4	P	N/A	3.70	3.72	3.73	3.80	4.20	5.75	N/A	N/A	N/A	N/A	N/A	N/A	I	4.8	1	N/A	N/A	N/A	15E_4s1d1Zc_1	6/26A	TDP-194	9150436
25.2	0.999	0.00155	0.050	0.332	15.6	P	N/A	3.90	3.92	3.94	4.00	4.20	6.25	N/A	N/A	N/A	N/A	N/A	N/A	I	3.5	1	N/A	N/A	N/A	15E_4s1d1Zc_1	6/26A	TDP-194	9150437
25.2	0.999	0.00155	0.050	0.334	14.6	P	N/A	4.10	4.13	4.15	4.20	4.20	6.25	4.20	udv	UCSvis	N/A	UCSudv	N/A	I	2.8	3	N/A	N/A	N/A	15E_4s1d1Zc_1	6/26A	TDP-194	9150438
25.4	0.999	0.00155	0.050	0.335	14.0	P	N/A	4.28	4.31	4.33	4.40	4.20	6.50	N/A	N/A	N/A	N/A	N/A	N/A	I	0.0	4	N/A	N/A	N/A	15E_4s1d1Zc_1	6/26A	TDP-194	9150439
25.5	0.999	0.00155	0.050	0.338	12.8	P	N/A	4.65	4.70	4.72	4.80	4.20	10.25	N/A	N/A	N/A	N/A	N/A	N/A	I	0.0	4	N/A	N/A	N/A	15E_4s1d1Zc_1	6/26A	TDP-194	9150440
25.8	0.999	0.00155	0.050	0.335	11.8	P	N/A	5.03	5.08	5.11	5.20	4.20	13.25	N/A	N/A	N/A	N/A	N/A	N/A	I	0.0	4	N/A	N/A	N/A	15E_4s1d1Zc_1	6/26A	TDP-194	9150441
25.9	0.999	0.00155	0.050	0.339	11.4	P	N/A	5.19	5.26	5.30	5.40	4.20	15.75	N/A	N/A	N/A	N/A	N/A	N/A	I	0.0	4	N/A	N/A	N/A	15E_4s1d1Zc_1	6/26A	TDP-194	9150442
26.3	0.999	0.00155	0.050	0.333	11.2	P	N/A	5.37	5.44	5.48	5.60	4.20	16.00	N/A	N/A	N/A	N/A	N/A	N/A	I	0.0	4	N/A	N/A	N/A	15E_4s1d1Zc_1	6/26A	TDP-194	9150443
26.5	0.999	0.00155	0.050	0.338	10.4	P	N/A	5.71	5.80	5.85	6.00	4.20	18.50	N/A	N/A	N/A	N/A	N/A	N/A	I	0.0	4	N/A	N/A	N/A	15E_4s1d1Zc_1	6/26A	TDP-194	9150444
26.9	0.999	0.00155	0.050	0.334	14.6	P	N/A	4.10	4.13	4.15	4.20	4.20	6.25	N/A	N/A	UCSvis	N/A	N/A	N/A	I	2.8	3	N/A	N/A	N/A	15E_4s1d1Zc_1	6/26A	TDP-194	9150445
26.9	0.999	0.00155	0.050	0.334	14.6	P	N/A	4.10	4.13	4.15	4.20	4.20	6.25	N/A	N/A	N/A	N/A	N/A	N/A	N/A	2.9	N/A	N/A	N/A	N/A	15E_4s1d1Zc_1	6/26A	TDP-194	9150446
26.9	0.999	0.00155	0.050	0.334	14.6	P	N/A	4.10	4.13	4.15	4.20	4.20	6.25	N/A	N/A	N/A	N/A	N/A	N/A	N/A	1.4	N/A	N/A	N/A	N/A	15E_4s1d1Zc_1	6/26A	TDP-194	9150447
26.9	0.999	0.00155	0.050	0.334	14.6	P	N/A	4.10	4.13	4.15	4.20	4.20	6.25	N/A	N/A	N/A	N/A	N/A	N/A	N/A	2.1	N/A	N/A	N/A	N/A	15E_4s1d1Zc_1	6/26A	TDP-194	9150448
26.9	0.999	0.00155	0.050	0.334	14.6	P	N/A	4.10	4.13	4.15	4.20	4.20	6.25	N/A	N/A	N/A	N/A	N/A	N/A	N/A	2.1	N/A	N/A	N/A	N/A	15E_4s1d1Zc_1	6/26A	TDP-194	9150449
26.9	0.999	0.00155	0.050	0.334	14.6	P	N/A	4.10	4.13	4.15	4.20	4.20	6.25	N/A	N/A	N/A	N/A	N/A	N/A	N/A	1.4	N/A	N/A	N/A	N/A	15E_4s1d1Zc_1	6/26A	TDP-194	9150450
26.9	0.999	0.00155	0.050	0.334	14.6	P	N/A	4.10	4.13	4.15	4.20	4.20	6.25	N/A	N/A	N/A	N/A	N/A	N/A	N/A	2.8	N/A	N/A	N/A	N/A	15E_4s1d1Zc_1	6/26A	TDP-194	9150451
26.9	0.999	0.00155	0.050	0.334	14.6	P	N/A	4.10	4.13	4.15	4.20	4.20	6.25	N/A	N/A	N/A	N/A	N/A	N/A	N/A	1.4	N/A	N/A	N/A	N/A	15E_4s1d1Zc_1	6/26A	TDP-194	9150452
27.6	0.999	0.00155	0.050	0.179	35.6	P	N/A	3.15	3.17	3.18	3.20	4.50	4.25	N/A	N/A	N/A	N/A	N/A	N/A	(null)	8.7	1	N/A	N/A	N/A	15E_4s1d1Zd_1	6/26B	TDP-194	9150453
27.7	0.998	0.00155	0.050	0.181	31.6	P	N/A	3.52	3.55	3.56	3.60	4.50	5.25	N/A	N/A	N/A	N/A	N/A	N/A	I	7.1	1	N/A	N/A	N/A	15E_4s1d1Zd_1	6/26B	TDP-194	9150454
27.9	0.999	0.00155	0.050	0.182	30.0	P	N/A	3.70	3.72	3.74	3.80	4.50	5.50	N/A	N/A	N/A	N/A	N/A	N/A	I	4.8	1	N/A	N/A	N/A	15E_4s1d1Zd_1	6/26B	TDP-194	9150455
28.1	0.998	0.00155	0.050	0.183	28.2	P	N/A	3.89	3.93	3.95	4.00	4.50	6.25	N/A	N/A	N/A	N/A	N/A	N/A	I	4.1	1	N/A	N/A	N/A	15E_4s1d1Zd_1	6/26B	TDP-194	9150456
28.2	0.998	0.00155	0.050	0.183	26.8	P	N/A	4.07	4.11	4.13	4.20	4.50	6.50	N/A	N/A	N/A	N/A	N/A	N/A	I	3.6	1	N/A	N/A	N/A	15E_4s1d1Zd_1	6/26B	TDP-194	9150457
28.5	0.998	0.00155	0.050	0.184	25.6	P	N/A	4.26	4.31	4.33	4.40	4.50	6.50	N/A	N/A	UCSvis	N/A	N/A	N/A	I	1.4	3	N/A	N/A	N/A	15E_4s1d1Zd_1	6/26B	TDP-194	9150458
28.9	0.998	0.00155	0.050	0.185	25.6	P	N/A	4.26	4.31	4.33	4.40	4.50	6.75	N/A	N/A	UCSvis	N/A	N/A	N/A	I	2.2	3	N/A	N/A	N/A	15E_4s1d1Zd_1	6/26B	TDP-194	9150459
29.1	0.998	0.00155	0.050	0.185	25.0	P	N/A	4.35	4.40	4.43	4.50	4.50	6.75	4.50	udv	N/A	N/A	UCSudv	N/A	I	0.7	4	N/A	N/A	N/A	15E_4s1d1Zd_1	6/26B	TDP-194	9150460
29.3	0.998	0.00155	0.050	0.184	24.0	P	N/A	4.52	4.59	4.62	4.70	4.50	7.50	N/A	N/A	N/A	N/A	N/A	N/A	I	0.0	4	N/A	N/A	N/A	15E_4s1d1Zd_1	6/26B	TDP-194	9150461
29.4	0.998	0.00155	0.050	0.185	22.6	P	N/A	4.81	4.87	4.90	5.00	4.50	9.75	N/A	N/A	N/A	N/A	N/A	N/A	I	0.0	4	N/A	N/A	N/A	15E_4s1d1Zd_1	6/26B	TDP-194	9150462
29.7	0.998	0.00155	0.050	0.186	20.6	P	N/A	5.25	5.34	5.39	5.50	4.50	13.75	N/A	N/A	N/A	N/A	N/A	N/A	I	0.0	4	N/A	N/A	N/A	15E_4s1d1Zd_1	6/26B	TDP-194	9150463
29.9	0.998	0.00155	0.050	0.188	18.8	P	N/A	5.70	5.81	5.86	6.00	4.50	16.25	N/A	N/A	N/A	N/A	N/A	N/A	I	0.0	4	N/A	N/A	N/A	15E_4s1d1Zd_1	6/26B	TDP-194	9150464
30.1	0.998	0.00155	0.050	0.187	17.4	P	N/A	6.14	6.27	6.33	6.50	4.50	18.50	N/A	N/A	N/A	N/A	N/A	N/A	I	0.0	4	N/A	N/A	N/A	15E_4s1d1Zd_1	6/26B	TDP-194	9150465
24.3	0.999	0.00500	0.050	0.333	14.8	P	N/A	4.07	4.11	4.13	4.20	5.90	3.75	N/A	N/A	N/A	N/A	N/A	N/A	(null)	9.5	1	N/A	N/A	N/A	15E_4s1d1Yc_1	6/27A	TDP-195	9150466
24.6	0.999	0.00500	0.050	0.333	13.3	P	N/A	4.53	4.59	4.62	4.70	5.90	4.50	N/A	N/A	N/A	N/A	N/A	N/A	I	5.5	1	N/A	N/A	N/A	15E_4s1d1Yc_1	6/27A	TDP-195	9150467
24.7	0.999	0.00500	0.050	0.338	12.5	P	N/A	4.76	4.85	4.89	5.00	5.90	4.75	N/A	N/A	N/A	N/A	N/A	N/A	I	4.8	1	N/A	N/A	N/A	15E_4s1d1Yc_1	6/27A	TDP-195	9150468
25.0	0.999	0.00500	0.050	0.338	11.8	P	N/A	5.05	5.15	5.19	5.30	5.90	5.25	N/A	N/A	N/A	N/A	N/A	N/A	I	4.2	1	N/A	N/A	N/A	15E_4s1d1Yc_1	6/27A	TDP-195	9150469
25.2	0.999	0.00500	0.050	0.337	11.4	P	N/A	5.24	5.34	5.38	5.50	5.90	5.25	N/A	N/A	N/A	N/A	N/A	N/A	I	3.6	1	N/A	N/A	N/A	15E_4s1d1Yc_1	6/27A	TDP-195	9150470
25.5	0.999	0.00500	0.050	0.333	11.0	P	N/A	5.47	5.55	5.60	5.70	5.90	5.75	N/A	N/A	UCSvis	N/A	N/A	N/A	I	2.9	3	N/A	N/A	N/A	15E_4s1d1Yc_1	6/27A	TDP-195	9150471
25.7	0.999	0.00500	0.050	0.335	10.6	P	N/A	5.64	5.74	5.78	5.90	5.90	5.75	5.90	udv	N/A	N/A	UCSudv	N/A	I	0.6	4	N/A	N/A	N/A	15E_4s1d1Yc_1	6/27A	TDP-195	9150472
25.8	0.999	0.00500	0.050	0.338	10.4	P	N/A	5.70	5.81	5.86	6.00	5.90	6.00	N/A	N/A	N/A	N/A	N/A	N/A	I	0.0	4	N/A	N/A	N/A	15E_4s1d1Yc_1	6/27A	TDP-195	9150473
26.1	0.999	0.00500	0.050	0.331	10.1	P	N/A	6.02	6.11	6.16	6.30	5.90	6.25	N/A	N/A	N/A	N/A	N/A	N/A	I	0.0	4	N/A	N/A	N/A	15E_4s1d1Yc_1	6/27A	TDP-195	9150474

Table B.3. Data from 2008 Tests in Small-Scale Vessel with Elliptical Head A.14

Row Number	Test	Case ID	Tank Diameter	Head Shape	Dish Height	Dish Volume	Tank Fill Height	Return Line Height	Nozzle Inner Diameter	Nozzle Stand-off Distance	Pulse Tube Configuration	Installed Nozzles	Outer Nozzles Operated	Inner Nozzles Operated	Pulse Tube Outer Diameter	Outer PJM Radius	Inner PJM Radius	"FIO" Outer PJM Impingement Angle	"FIO" Inner PJM Impingement Angle	Ratio Outer PJM to Tank Radius	Ratio Inner PJM to Tank Radius	Simulant	Solids Density	Particle Diameter d5	Particle Diameter d50	Particle Diameter d95	Void Fraction
text	text	text	in.	text	in.	in. ^{3}	in.	in.	in.	in.	text	number	number	number	in.	in.	in.	deg	deg	nondim	nondim	text	g/cm^3	m	m	m	fraction
MSS	M/DDX	ID	D	HS	H_{dish}	V_{dish}	H	Rtn	d	sod	PT	N	N_O	N_I	PT_{od}	R_O	R_I	θ_O	θ_I	R_O/R	R_I/R	sxdx	ρ_s	d_5	d_{50}	d_{95}	vf
9150475M	6/27A	15E_4s1d1Yc_1	14 7/16	E	3.25	354.8	34 3/4	30	0.126	0.189	HLP-22	12	8	4	1.05	4.5	2.4	21.8	10.1	0.62	0.34	s1d1	2.46	0.0001428	0.0001664	0.0001951	0.4118
9150476M	6/27A	15E_4s1d1Yc_1	14 7/16	E	3.25	354.8	34 3/4	30	0.126	0.189	HLP-22	12	8	4	1.05	4.5	2.4	21.8	10.1	0.62	0.34	s1d1	2.46	0.0001428	0.0001664	0.0001951	0.4118
9150477M	6/27A	15E_4s1d1Yc_1	14 7/16	E	3.25	354.8	34 3/4	30	0.126	0.189	HLP-22	12	8	4	1.05	4.5	2.4	21.8	10.1	0.62	0.34	s1d1	2.46	0.0001428	0.0001664	0.0001951	0.4118
9150478M	6/27A	15E_4s1d1Yc_1	14 7/16	E	3.25	354.8	34 3/4	30	0.126	0.189	HLP-22	12	8	4	1.05	4.5	2.4	21.8	10.1	0.62	0.34	s1d1	2.46	0.0001428	0.0001664	0.0001951	0.4118
9150479M	6/27A	15E_4s1d1Yc_1	14 7/16	E	3.25	354.8	34 3/4	30	0.126	0.189	HLP-22	12	8	4	1.05	4.5	2.4	21.8	10.1	0.62	0.34	s1d1	2.46	0.0001428	0.0001664	0.0001951	0.4118
9150480	6/27B	15E_4s1d1Yd_1	14 7/16	E	3.25	354.8	34 3/4	30	0.126	0.189	HLP-22	12	8	4	1.05	4.5	2.4	21.8	10.1	0.62	0.34	s1d1	2.46	0.0001428	0.0001664	0.0001951	0.4118
9150481	6/27B	15E_4s1d1Yd_1	14 7/16	E	3.25	354.8	34 3/4	30	0.126	0.189	HLP-22	12	8	4	1.05	4.5	2.4	21.8	10.1	0.62	0.34	s1d1	2.46	0.0001428	0.0001664	0.0001951	0.4118
9150482	6/27B	15E_4s1d1Yd_1	14 7/16	E	3.25	354.8	34 3/4	30	0.126	0.189	HLP-22	12	8	4	1.05	4.5	2.4	21.8	10.1	0.62	0.34	s1d1	2.46	0.0001428	0.0001664	0.0001951	0.4118
9150483	6/27B	15E_4s1d1Yd_1	14 7/16	E	3.25	354.8	34 3/4	30	0.126	0.189	HLP-22	12	8	4	1.05	4.5	2.4	21.8	10.1	0.62	0.34	s1d1	2.46	0.0001428	0.0001664	0.0001951	0.4118
9150484	6/27B	15E_4s1d1Yd_1	14 7/16	E	3.25	354.8	34 3/4	30	0.126	0.189	HLP-22	12	8	4	1.05	4.5	2.4	21.8	10.1	0.62	0.34	s1d1	2.46	0.0001428	0.0001664	0.0001951	0.4118
9150485	6/27B	15E_4s1d1Yd_1	14 7/16	E	3.25	354.8	34 3/4	30	0.126	0.189	HLP-22	12	8	4	1.05	4.5	2.4	21.8	10.1	0.62	0.34	s1d1	2.46	0.0001428	0.0001664	0.0001951	0.4118
9150486M	6/27B	15E_4s1d1Yd_1	14 7/16	E	3.25	354.8	34 3/4	30	0.126	0.189	HLP-22	12	8	4	1.05	4.5	2.4	21.8	10.1	0.62	0.34	s1d1	2.46	0.0001428	0.0001664	0.0001951	0.4118
9150487M	6/27B	15E_4s1d1Yd_1	14 7/16	E	3.25	354.8	34 3/4	30	0.126	0.189	HLP-22	12	8	4	1.05	4.5	2.4	21.8	10.1	0.62	0.34	s1d1	2.46	0.0001428	0.0001664	0.0001951	0.4118
9150488M	6/27B	15E_4s1d1Yd_1	14 7/16	E	3.25	354.8	34 3/4	30	0.126	0.189	HLP-22	12	8	4	1.05	4.5	2.4	21.8	10.1	0.62	0.34	s1d1	2.46	0.0001428	0.0001664	0.0001951	0.4118
9150489M	6/27B	15E_4s1d1Yd_1	14 7/16	E	3.25	354.8	34 3/4	30	0.126	0.189	HLP-22	12	8	4	1.05	4.5	2.4	21.8	10.1	0.62	0.34	s1d1	2.46	0.0001428	0.0001664	0.0001951	0.4118
9150490M	6/27B	15E_4s1d1Yd_1	14 7/16	E	3.25	354.8	34 3/4	30	0.126	0.189	HLP-22	12	8	4	1.05	4.5	2.4	21.8	10.1	0.62	0.34	s1d1	2.46	0.0001428	0.0001664	0.0001951	0.4118
9150491M	6/27B	15E_4s1d1Yd_1	14 7/16	E	3.25	354.8	34 3/4	30	0.126	0.189	HLP-22	12	8	4	1.05	4.5	2.4	21.8	10.1	0.62	0.34	s1d1	2.46	0.0001428	0.0001664	0.0001951	0.4118
9150492M	6/27B	15E_4s1d1Yd_1	14 7/16	E	3.25	354.8	34 3/4	30	0.126	0.189	HLP-22	12	8	4	1.05	4.5	2.4	21.8	10.1	0.62	0.34	s1d1	2.46	0.0001428	0.0001664	0.0001951	0.4118
9150493M	6/27B	15E_4s1d1Yd_1	14 7/16	E	3.25	354.8	34 3/4	30	0.126	0.189	HLP-22	12	8	4	1.05	4.5	2.4	21.8	10.1	0.62	0.34	s1d1	2.46	0.0001428	0.0001664	0.0001951	0.4118
9150494M	6/27B	15E_4s1d1Yd_1	14 7/16	E	3.25	354.8	34 3/4	30	0.126	0.189	HLP-22	12	8	4	1.05	4.5	2.4	21.8	10.1	0.62	0.34	s1d1	2.46	0.0001428	0.0001664	0.0001951	0.4118
9150497	6/27C	15E_4s1d1Xc_1	14 7/16	E	3.25	354.8	35 1/2	30	0.126	0.189	HLP-22	12	8	4	1.05	4.5	2.4	21.8	10.1	0.62	0.34	s1d1	2.46	0.0001428	0.0001664	0.0001951	0.4118
9150498	6/27C	15E_4s1d1Xc_1	14 7/16	E	3.25	354.8	35 1/2	30	0.126	0.189	HLP-22	12	8	4	1.05	4.5	2.4	21.8	10.1	0.62	0.34	s1d1	2.46	0.0001428	0.0001664	0.0001951	0.4118
9150499	6/27C	15E_4s1d1Xc_1	14 7/16	E	3.25	354.8	35 1/2	30	0.126	0.189	HLP-22	12	8	4	1.05	4.5	2.4	21.8	10.1	0.62	0.34	s1d1	2.46	0.0001428	0.0001664	0.0001951	0.4118
9150500	6/27C	15E_4s1d1Xc_1	14 7/16	E	3.25	354.8	35 1/2	30	0.126	0.189	HLP-22	12	8	4	1.05	4.5	2.4	21.8	10.1	0.62	0.34	s1d1	2.46	0.0001428	0.0001664	0.0001951	0.4118
9150501	6/27C	15E_4s1d1Xc_1	14 7/16	E	3.25	354.8	35 1/2	30	0.126	0.189	HLP-22	12	8	4	1.05	4.5	2.4	21.8	10.1	0.62	0.34	s1d1	2.46	0.0001428	0.0001664	0.0001951	0.4118
9150502	6/27C	15E_4s1d1Xc_1	14 7/16	E	3.25	354.8	35 1/2	30	0.126	0.189	HLP-22	12	8	4	1.05	4.5	2.4	21.8	10.1	0.62	0.34	s1d1	2.46	0.0001428	0.0001664	0.0001951	0.4118
9150503	6/27C	15E_4s1d1Xc_1	14 7/16	E	3.25	354.8	35 1/2	30	0.126	0.189	HLP-22	12	8	4	1.05	4.5	2.4	21.8	10.1	0.62	0.34	s1d1	2.46	0.0001428	0.0001664	0.0001951	0.4118
9150504	6/27C	15E_4s1d1Xc_1	14 7/16	E	3.25	354.8	35 1/2	30	0.126	0.189	HLP-22	12	8	4	1.05	4.5	2.4	21.8	10.1	0.62	0.34	s1d1	2.46	0.0001428	0.0001664	0.0001951	0.4118
9150505	6/27C	15E_4s1d1Xc_1	14 7/16	E	3.25	354.8	35 1/2	30	0.126	0.189	HLP-22	12	8	4	1.05	4.5	2.4	21.8	10.1	0.62	0.34	s1d1	2.46	0.0001428	0.0001664	0.0001951	0.4118
9150506M	6/27C	15E_4s1d1Xc_1	14 7/16	E	3.25	354.8	35 1/2	30	0.126	0.189	HLP-22	12	8	4	1.05	4.5	2.4	21.8	10.1	0.62	0.34	s1d1	2.46	0.0001428	0.0001664	0.0001951	0.4118
9150507M	6/27C	15E_4s1d1Xc_1	14 7/16	E	3.25	354.8	35 1/2	30	0.126	0.189	HLP-22	12	8	4	1.05	4.5	2.4	21.8	10.1	0.62	0.34	s1d1	2.46	0.0001428	0.0001664	0.0001951	0.4118
9150508M	6/27C	15E_4s1d1Xc_1	14 7/16	E	3.25	354.8	35 1/2	30	0.126	0.189	HLP-22	12	8	4	1.05	4.5	2.4	21.8	10.1	0.62	0.34	s1d1	2.46	0.0001428	0.0001664	0.0001951	0.4118
9150509M	6/27C	15E_4s1d1Xc_1	14 7/16	E	3.25	354.8	35 1/2	30	0.126	0.189	HLP-22	12	8	4	1.05	4.5	2.4	21.8	10.1	0.62	0.34	s1d1	2.46	0.0001428	0.0001664	0.0001951	0.4118
9150510M	6/27C	15E_4s1d1Xc_1	14 7/16	E	3.25	354.8	35 1/2	30	0.126	0.189	HLP-22	12	8	4	1.05	4.5	2.4	21.8	10.1	0.62	0.34	s1d1	2.46	0.0001428	0.0001664	0.0001951	0.4118
9150512M	6/27C	15E_4s1d1Xc_1	14 7/16	E	3.25	354.8	35 1/2	30	0.126	0.189	HLP-22	12	8	4	1.05	4.5	2.4	21.8	10.1	0.62	0.34	s1d1	2.46	0.0001428	0.0001664	0.0001951	0.4118
9150513	6/30A	15E_4s1d1Xc_1	14 7/16	E	3.25	354.8	35	30	0.126	0.189	HLP-22	12	8	4	1.05	4.5	2.4	21.8	10.1	0.62	0.34	s1d1	2.46	0.0001428	0.0001664	0.0001951	0.4118
9150514	6/30A	15E_4s1d1Xc_1	14 7/16	E	3.25	354.8	35	30	0.126	0.189	HLP-22	12	8	4	1.05	4.5	2.4	21.8	10.1	0.62	0.34	s1d1	2.46	0.0001428	0.0001664	0.0001951	0.4118
9150515	6/30A	15E_4s1d1Xc_1	14 7/16	E	3.25	354.8	35	30	0.126	0.189	HLP-22	12	8	4	1.05	4.5	2.4	21.8	10.1	0.62	0.34	s1d1	2.46	0.0001428	0.0001664	0.0001951	0.4118
9150516M	6/30A	15E_4s1d1Xc_1	14 7/16	E	3.25	354.8	35	30	0.126	0.189	HLP-22	12	8	4	1.05	4.5	2.4	21.8	10.1	0.62	0.34	s1d1	2.46	0.0001428	0.0001664	0.0001951	0.4118
9150517M	6/30A	15E_4s1d1Xc_1	14 7/16	E	3.25	354.8	35	30	0.126	0.189	HLP-22	12	8	4	1.05	4.5	2.4	21.8	10.1	0.62	0.34	s1d1	2.46	0.0001428	0.0001664	0.0001951	0.4118
9150518M	6/30A	15E_4s1d1Xc_1	14 7/16	E	3.25	354.8	35	30	0.126	0.189	HLP-22	12	8	4	1.05	4.5	2.4	21.8	10.1	0.62	0.34	s1d1	2.46	0.0001428	0.0001664	0.0001951	0.4118

Table B.3. Data from 2008 Tests in Small-Scale Vessel with Elliptical Head B.14

Tank Water Temperature	Water Density	Solids Fraction	Pulse Volume Fraction	Duty Cycle	Cycle Time	Pulsed or Steady Jet	Us Steady Jet	U1 Pulsing Jet	U2 URMS	U3 URM3	Discharge Velocity	Critical Suspension Velocity	Average Peak Cloud Height	UCS Condition	UCS Method	UCS Flag	UCS Center Flag	UCS udv Flag	UCS based on Decreasing Velocity	Sweep Increase / Decrease	UDV Height Bed	Particle Motion	Solids Level	Outer Bottom Pattern	Inner Bottom Pattern	Case ID	Test	TDP	Row Number
C	g/cm³	fraction	fraction	fraction	s	text	m/s	m/s	m/s	m/s	m/s	m/s	in.	m/s	text	text	text	text	m/s	text	mm	text	text	text	text	text	text	text	text
T	$\rho_\pm$	ϕ_S	ϕ_P	DC	t_C	Jet	U_S	U1	U2	U3	U	U_{CS}	H_C	U_{CSR}	U_{CSM}	U_{CS}vis	U_{CS}cen	U_{CS}udv	U_{CS}_D	S_W	H_{bed}	PM	Sol	SP_O	SP_I	ID	M/DDX	TDP	MSS
26.4	0.999	0.00500	0.050	0.338	9.1	P	N/A	6.55	6.73	6.81	7.00	5.90	6.75	N/A	N/A	N/A	N/A	N/A	N/A	I	0.0	4	N/A	N/A	N/A	15E_4s1d1Yc_1	6/27A	TDP-195	9150475
26.6	0.999	0.00500	0.050	0.333	8.0	P	N/A	7.51	7.69	7.78	8.00	5.90	11.00	N/A	N/A	N/A	N/A	N/A	N/A	I	0.0	4	N/A	N/A	N/A	15E_4s1d1Yc_1	6/27A	TDP-195	9150476
26.9	0.999	0.00500	0.050	0.337	7.5	P	N/A	7.97	8.17	8.27	8.50	5.90	16.50	N/A	N/A	N/A	N/A	N/A	N/A	I	0.0	4	N/A	N/A	N/A	15E_4s1d1Yc_1	6/27A	TDP-195	9150477
27.2	0.999	0.00500	0.050	0.337	7.1	P	N/A	8.41	8.63	8.74	9.00	5.90	19.25	N/A	N/A	N/A	N/A	N/A	N/A	I	0.0	4	N/A	N/A	N/A	15E_4s1d1Yc_1	6/27A	TDP-195	9150478
27.4	0.999	0.00500	0.050	0.330	8.5	P	N/A	7.09	7.24	7.32	7.50	5.90	7.75	N/A	N/A	N/A	N/A	N/A	N/A	I	0.0	4	N/A	N/A	N/A	15E_4s1d1Yc_1	6/27A	TDP-195	9150479
27.8	0.999	0.00500	0.050	0.186	25.0	P	N/A	4.28	4.36	4.40	4.50	6.00	3.75	N/A	N/A	N/A	N/A	N/A	N/A	(null)	7.3	1	N/A	N/A	N/A	15E_4s1d1Yd_1	6/27B	TDP-195	9150480
27.6	0.999	0.00500	0.050	0.188	22.5	P	N/A	4.74	4.83	4.88	5.00	6.00	4.75	N/A	N/A	N/A	N/A	N/A	N/A	I	4.3	1	N/A	N/A	N/A	15E_4s1d1Yd_1	6/27B	TDP-195	9150481
27.7	0.999	0.00500	0.050	0.187	20.5	P	N/A	5.18	5.30	5.36	5.50	6.00	5.25	N/A	N/A	N/A	N/A	N/A	N/A	I	4.3	1	N/A	N/A	N/A	15E_4s1d1Yd_1	6/27B	TDP-195	9150482
27.8	0.999	0.00500	0.050	0.188	19.4	P	N/A	5.45	5.59	5.65	5.80	6.00	5.50	N/A	N/A	UCSvis	N/A	N/A	N/A	I	2.1	3	N/A	N/A	N/A	15E_4s1d1Yd_1	6/27B	TDP-195	9150483
27.8	0.999	0.00500	0.050	0.186	20.1	P	N/A	5.35	5.44	5.48	5.60	6.00	5.00	N/A	N/A	N/A	N/A	N/A	N/A	I	3.6	1	N/A	N/A	N/A	15E_4s1d1Yd_1	6/27B	TDP-195	9150484
27.9	0.998	0.00500	0.050	0.186	19.4	P	N/A	5.55	5.64	5.68	5.80	6.00	5.50	N/A	N/A	UCSvis	N/A	N/A	N/A	I	2.8	3	N/A	N/A	N/A	15E_4s1d1Yd_1	6/27B	TDP-195	9150485
27.9	0.999	0.00500	0.050	0.186	18.8	P	N/A	5.73	5.82	5.87	6.00	6.00	5.75	6.00	udv	N/A	N/A	UCSudv	N/A	I	0.7	4	N/A	N/A	N/A	15E_4s1d1Yd_1	6/27B	TDP-195	9150486
28.1	0.999	0.00500	0.050	0.187	18.2	P	N/A	5.93	6.03	6.08	6.20	6.00	6.00	N/A	N/A	N/A	N/A	N/A	N/A	I	0.0	4	N/A	N/A	N/A	15E_4s1d1Yd_1	6/27B	TDP-195	9150487
28.2	0.998	0.00500	0.050	0.188	17.6	P	N/A	6.06	6.19	6.25	6.40	6.00	6.50	N/A	N/A	N/A	N/A	N/A	N/A	I	0.0	4	N/A	N/A	N/A	15E_4s1d1Yd_1	6/27B	TDP-195	9150488
28.3	0.999	0.00500	0.050	0.188	16.1	P	N/A	6.62	6.76	6.83	7.00	6.00	7.00	N/A	N/A	N/A	N/A	N/A	N/A	I	0.0	4	N/A	N/A	N/A	15E_4s1d1Yd_1	6/27B	TDP-195	9150489
28.4	0.998	0.00500	0.050	0.187	15.2	P	N/A	7.02	7.16	7.23	7.40	6.00	7.50	N/A	N/A	N/A	N/A	N/A	N/A	I	0.0	4	N/A	N/A	N/A	15E_4s1d1Yd_1	6/27B	TDP-195	9150490
28.5	0.998	0.00500	0.050	0.186	14.1	P	N/A	7.56	7.72	7.80	8.00	6.00	8.50	N/A	N/A	N/A	N/A	N/A	N/A	I	0.0	4	N/A	N/A	N/A	15E_4s1d1Yd_1	6/27B	TDP-195	9150491
28.6	0.998	0.00500	0.050	0.188	12.5	P	N/A	8.45	8.65	8.75	9.00	6.00	12.25	N/A	N/A	N/A	N/A	N/A	N/A	I	0.0	4	N/A	N/A	N/A	15E_4s1d1Yd_1	6/27B	TDP-195	9150492
29.1	0.998	0.00500	0.050	0.186	11.5	P	N/A	9.36	9.61	9.74	10.00	6.00	15.75	N/A	N/A	N/A	N/A	N/A	N/A	I	0.0	4	N/A	N/A	N/A	15E_4s1d1Yd_1	6/27B	TDP-195	9150493
29.3	0.998	0.00500	0.050	0.189	10.5	P	N/A	10.07	10.41	10.57	11.00	6.00	19.50	N/A	N/A	N/A	N/A	N/A	N/A	I	0.0	4	N/A	N/A	N/A	15E_4s1d1Yd_1	6/27B	TDP-195	9150494
28.9	0.998	0.01500	0.050	0.334	11.7	P	N/A	5.17	5.28	5.34	5.50	8.20	3.38	N/A	N/A	N/A	N/A	N/A	N/A	(null)	11.0	1	N/A	N/A	N/A	15E_4s1d1Xc_1	6/27C	TDP-196	9150497
28.9	0.998	0.01500	0.050	0.336	10.5	P	N/A	5.67	5.79	5.84	6.00	8.20	3.75	N/A	N/A	N/A	N/A	N/A	N/A	I	8.8	1	N/A	N/A	N/A	15E_4s1d1Xc_1	6/27C	TDP-196	9150498
28.9	0.998	0.01500	0.050	0.337	9.7	P	N/A	6.09	6.24	6.31	6.50	8.20	4.25	N/A	N/A	N/A	N/A	N/A	N/A	I	7.3	1	N/A	N/A	N/A	15E_4s1d1Xc_1	6/27C	TDP-196	9150499
29.0	0.998	0.01500	0.050	0.336	9.0	P	N/A	6.63	6.77	6.84	7.00	8.20	4.50	N/A	N/A	N/A	N/A	N/A	N/A	I	4.6	1	N/A	N/A	N/A	15E_4s1d1Xc_1	6/27C	TDP-196	9150500
29.1	0.998	0.01500	0.050	0.332	8.8	P	N/A	6.83	6.97	7.03	7.20	8.20	4.75	N/A	N/A	N/A	N/A	N/A	N/A	I	5.0	1	N/A	N/A	N/A	15E_4s1d1Xc_1	6/27C	TDP-196	9150501
29.2	0.998	0.01500	0.050	0.338	8.6	P	N/A	6.92	7.09	7.18	7.40	8.20	4.75	N/A	N/A	UCSvis	N/A	N/A	N/A	I	4.6	3	N/A	N/A	N/A	15E_4s1d1Xc_1	6/27C	TDP-196	9150502
29.3	0.998	0.01500	0.050	0.333	8.4	P	N/A	7.16	7.32	7.40	7.60	8.20	4.75	N/A	N/A	N/A	N/A	N/A	N/A	I	4.1	4	N/A	N/A	N/A	15E_4s1d1Xc_1	6/27C	TDP-196	9150503
29.4	0.998	0.01500	0.050	0.337	8.2	P	N/A	7.29	7.47	7.56	7.80	8.20	5.00	N/A	N/A	N/A	N/A	N/A	N/A	I	1.4	4	N/A	N/A	N/A	15E_4s1d1Xc_1	6/27C	TDP-196	9150504
29.5	0.998	0.01500	0.050	0.337	8.0	P	N/A	7.47	7.67	7.76	8.00	8.20	5.25	N/A	N/A	N/A	N/A	N/A	N/A	I	2.9	4	N/A	N/A	N/A	15E_4s1d1Xc_1	6/27C	TDP-196	9150505
29.6	0.998	0.01500	0.050	0.334	7.8	P	N/A	7.71	7.88	7.97	8.20	8.20	5.25	8.20	udv	N/A	N/A	UCSudv	N/A	I	0.4	4	N/A	N/A	N/A	15E_4s1d1Xc_1	6/27C	TDP-196	9150506
29.7	0.998	0.01500	0.050	0.336	7.6	P	N/A	7.89	8.08	8.17	8.40	8.20	5.50	N/A	N/A	N/A	N/A	N/A	N/A	I	0.0	4	N/A	N/A	N/A	15E_4s1d1Xc_1	6/27C	TDP-196	9150507
29.9	0.998	0.01500	0.050	0.335	7.1	P	N/A	8.45	8.66	8.77	9.00	8.20	5.75	N/A	N/A	N/A	N/A	N/A	N/A	I	0.0	4	N/A	N/A	N/A	15E_4s1d1Xc_1	6/27C	TDP-196	9150508
30.1	0.998	0.01500	0.050	0.336	6.4	P	N/A	9.35	9.59	9.71	10.00	8.20	6.25	N/A	N/A	N/A	N/A	N/A	N/A	I	0.0	4	N/A	N/A	N/A	15E_4s1d1Xc_1	6/27C	TDP-196	9150509
30.2	0.998	0.01500	0.050	0.337	5.8	P	N/A	10.23	10.52	10.67	11.00	8.20	6.50	N/A	N/A	N/A	N/A	N/A	N/A	I	0.0	4	N/A	N/A	N/A	15E_4s1d1Xc_1	6/27C	TDP-196	9150510
30.7	0.998	0.01500	0.050	0.337	5.4	P	N/A	11.07	11.44	11.62	12.00	8.20	9.50	N/A	N/A	N/A	N/A	N/A	N/A	I	0.8	4	N/A	N/A	N/A	15E_4s1d1Xc_1	6/27C	TDP-196	9150512
28.6	0.998	0.01500	0.050	0.329	8.1	P	N/A	7.52	7.69	7.78	8.00	8.60	5.00	N/A	N/A	N/A	N/A	N/A	N/A	I	1.4	4	N/A	N/A	N/A	15E_4s1d1Xc_1	6/30A	TDP-197	9150513
28.8	0.998	0.01500	0.050	0.333	7.8	P	N/A	7.65	7.84	7.94	8.20	8.60	5.25	N/A	N/A	N/A	N/A	N/A	N/A	I	2.9	4	N/A	N/A	N/A	15E_4s1d1Xc_1	6/30A	TDP-197	9150514
29.0	0.998	0.01500	0.050	0.334	7.6	P	N/A	7.83	8.03	8.14	8.40	8.60	5.25	N/A	N/A	N/A	N/A	N/A	N/A	I	0.6	4	N/A	N/A	N/A	15E_4s1d1Xc_1	6/30A	TDP-197	9150515
29.1	0.998	0.01500	0.050	0.335	7.4	P	N/A	8.01	8.23	8.33	8.60	8.60	5.25	8.60	udv	N/A	N/A	UCSudv	N/A	I	1.4	4	N/A	N/A	N/A	15E_4s1d1Xc_1	6/30A	TDP-197	9150516
29.3	0.998	0.01500	0.050	0.333	7.3	P	N/A	8.23	8.44	8.55	8.80	8.60	5.50	N/A	N/A	N/A	N/A	N/A	N/A	I	0.0	4	N/A	N/A	N/A	15E_4s1d1Xc_1	6/30A	TDP-197	9150517
29.6	0.998	0.01500	0.050	0.335	7.4	P	N/A	8.03	8.24	8.34	8.60	8.60	5.50	N/A	N/A	N/A	N/A	N/A	N/A	D	0.0	4	N/A	N/A	N/A	15E_4s1d1Xc_1	6/30A	TDP-197	9150518

Table B.3. Data from 2008 Tests in Small-Scale Vessel with Elliptical Head A.15

Row Number	Test	Case ID	Tank Diameter	Head Shape	Dish Height	Dish Volume	Tank Fill Height	Return Line Height	Nozzle Inner Diameter	Nozzle Stand-off Distance	Pulse Tube Configuration	Installed Nozzles	Outer Nozzles Operated	Inner Nozzles Operated	Pulse Tube Outer Diameter	Outer PJM Radius	Inner PJM Radius	"FIO" Outer PJM Impingement Angle	"FIO" Inner PJM Impingement Angle	Ratio Outer PJM to Tank Radius	Ratio Inner PJM to Tank Radius	Simulant	Solids Density	Particle Diameter d5	Particle Diameter d50	Particle Diameter d95	Void Fraction
text	text	text	in.	text	in.	in. ^{3}	in.	in.	in.	in.	text	number	number	number	in.	in.	in.	deg	deg	nondim	nondim	text	g/cm^3	m	m	m	fraction
MSS	M/DDX	ID	D	HS	H_{dish}	V_{dish}	H	Rtn	d	sod	PT	N	N_O	N_I	PT_{od}	R_O	R_I	θ_O	θ_I	R_O/R	R_I/R	sxdx	ρ_s	d_5	d_{50}	d_{95}	vf
9150519	6/30A	15E_4s1d1Xc_1	14 7/16	E	3.25	354.8	35	30	0.126	0.189	HLP-22	12	8	4	1.05	4.5	2.4	21.8	10.1	0.62	0.34	s1d1	2.46	0.0001428	0.0001664	0.0001951	0.4118
9150520	6/30A	15E_4s1d1Xc_1	14 7/16	E	3.25	354.8	35	30	0.126	0.189	HLP-22	12	8	4	1.05	4.5	2.4	21.8	10.1	0.62	0.34	s1d1	2.46	0.0001428	0.0001664	0.0001951	0.4118
9150521	6/30A	15E_4s1d1Xc_1	14 7/16	E	3.25	354.8	35	30	0.126	0.189	HLP-22	12	8	4	1.05	4.5	2.4	21.8	10.1	0.62	0.34	s1d1	2.46	0.0001428	0.0001664	0.0001951	0.4118
9150522	6/30A	15E_4s1d1Xc_1	14 7/16	E	3.25	354.8	35	30	0.126	0.189	HLP-22	12	8	4	1.05	4.5	2.4	21.8	10.1	0.62	0.34	s1d1	2.46	0.0001428	0.0001664	0.0001951	0.4118
9150523	6/30A	15E_4s1d1Xc_1	14 7/16	E	3.25	354.8	35	30	0.126	0.189	HLP-22	12	8	4	1.05	4.5	2.4	21.8	10.1	0.62	0.34	s1d1	2.46	0.0001428	0.0001664	0.0001951	0.4118
9150524	6/30A	15E_4s1d1Xc_1	14 7/16	E	3.25	354.8	35	30	0.126	0.189	HLP-22	12	8	4	1.05	4.5	2.4	21.8	10.1	0.62	0.34	s1d1	2.46	0.0001428	0.0001664	0.0001951	0.4118
9150525	6/30A	15E_4s1d1Xc_1	14 7/16	E	3.25	354.8	35	30	0.126	0.189	HLP-22	12	8	4	1.05	4.5	2.4	21.8	10.1	0.62	0.34	s1d1	2.46	0.0001428	0.0001664	0.0001951	0.4118
9150526	6/30B	15E_4s1d5Zc_1	14 7/16	E	3.25	354.8	35	30	0.126	0.189	HLP-22	12	8	4	1.05	4.5	2.4	21.8	10.1	0.62	0.34	s1d5	2.5	0.0000328	0.0000439	0.0000585	0.4012
9150527	6/30B	15E_4s1d5Zc_1	14 7/16	E	3.25	354.8	35	30	0.126	0.189	HLP-22	12	8	4	1.05	4.5	2.4	21.8	10.1	0.62	0.34	s1d5	2.5	0.0000328	0.0000439	0.0000585	0.4012
9150528	6/30B	15E_4s1d5Zc_1	14 7/16	E	3.25	354.8	35	30	0.126	0.189	HLP-22	12	8	4	1.05	4.5	2.4	21.8	10.1	0.62	0.34	s1d5	2.5	0.0000328	0.0000439	0.0000585	0.4012
9150529	6/30B	15E_4s1d5Zc_1	14 7/16	E	3.25	354.8	35	30	0.126	0.189	HLP-22	12	8	4	1.05	4.5	2.4	21.8	10.1	0.62	0.34	s1d5	2.5	0.0000328	0.0000439	0.0000585	0.4012
9150530	6/30B	15E_4s1d5Zc_1	14 7/16	E	3.25	354.8	35	30	0.126	0.189	HLP-22	12	8	4	1.05	4.5	2.4	21.8	10.1	0.62	0.34	s1d5	2.5	0.0000328	0.0000439	0.0000585	0.4012
9150531	6/30B	15E_4s1d5Zc_1	14 7/16	E	3.25	354.8	35	30	0.126	0.189	HLP-22	12	8	4	1.05	4.5	2.4	21.8	10.1	0.62	0.34	s1d5	2.5	0.0000328	0.0000439	0.0000585	0.4012
9150532	6/30B	15E_4s1d5Zc_1	14 7/16	E	3.25	354.8	35	30	0.126	0.189	HLP-22	12	8	4	1.05	4.5	2.4	21.8	10.1	0.62	0.34	s1d5	2.5	0.0000328	0.0000439	0.0000585	0.4012
9150533M	6/30B	15E_4s1d5Zc_1	14 7/16	E	3.25	354.8	35	30	0.126	0.189	HLP-22	12	8	4	1.05	4.5	2.4	21.8	10.1	0.62	0.34	s1d5	2.5	0.0000328	0.0000439	0.0000585	0.4012
9150534M	6/30B	15E_4s1d5Zc_1	14 7/16	E	3.25	354.8	35	30	0.126	0.189	HLP-22	12	8	4	1.05	4.5	2.4	21.8	10.1	0.62	0.34	s1d5	2.5	0.0000328	0.0000439	0.0000585	0.4012
9150535M	6/30B	15E_4s1d5Zc_1	14 7/16	E	3.25	354.8	35	30	0.126	0.189	HLP-22	12	8	4	1.05	4.5	2.4	21.8	10.1	0.62	0.34	s1d5	2.5	0.0000328	0.0000439	0.0000585	0.4012
9150536M	7/1A	15E_4s1d5Zc_1	14 7/16	E	3.25	354.8	35	30	0.126	0.189	HLP-22	12	8	4	1.05	4.5	2.4	21.8	10.1	0.62	0.34	s1d5	2.5	0.0000328	0.0000439	0.0000585	0.4012
9150537M	7/1A	15E_4s1d5Zc_1	14 7/16	E	3.25	354.8	35	30	0.126	0.189	HLP-22	12	8	4	1.05	4.5	2.4	21.8	10.1	0.62	0.34	s1d5	2.5	0.0000328	0.0000439	0.0000585	0.4012
9150538M	7/1A	15E_4s1d5Zc_1	14 7/16	E	3.25	354.8	35	30	0.126	0.189	HLP-22	12	8	4	1.05	4.5	2.4	21.8	10.1	0.62	0.34	s1d5	2.5	0.0000328	0.0000439	0.0000585	0.4012
9150539	7/1A	15E_4s1d5Zc_1	14 7/16	E	3.25	354.8	35	30	0.126	0.189	HLP-22	12	8	4	1.05	4.5	2.4	21.8	10.1	0.62	0.34	s1d5	2.5	0.0000328	0.0000439	0.0000585	0.4012
9150540	7/1A	15E_4s1d5Zc_1	14 7/16	E	3.25	354.8	35	30	0.126	0.189	HLP-22	12	8	4	1.05	4.5	2.4	21.8	10.1	0.62	0.34	s1d5	2.5	0.0000328	0.0000439	0.0000585	0.4012
9150541	7/1A	15E_4s1d5Zc_1	14 7/16	E	3.25	354.8	35	30	0.126	0.189	HLP-22	12	8	4	1.05	4.5	2.4	21.8	10.1	0.62	0.34	s1d5	2.5	0.0000328	0.0000439	0.0000585	0.4012
9150542	7/1A	15E_4s1d5Zc_1	14 7/16	E	3.25	354.8	35	30	0.126	0.189	HLP-22	12	8	4	1.05	4.5	2.4	21.8	10.1	0.62	0.34	s1d5	2.5	0.0000328	0.0000439	0.0000585	0.4012
9150543	7/1A	15E_4s1d5Zc_1	14 7/16	E	3.25	354.8	35	30	0.126	0.189	HLP-22	12	8	4	1.05	4.5	2.4	21.8	10.1	0.62	0.34	s1d5	2.5	0.0000328	0.0000439	0.0000585	0.4012
9150544	7/1A	15E_4s1d5Zc_1	14 7/16	E	3.25	354.8	35	30	0.126	0.189	HLP-22	12	8	4	1.05	4.5	2.4	21.8	10.1	0.62	0.34	s1d5	2.5	0.0000328	0.0000439	0.0000585	0.4012
9150545	7/1A	15E_4s1d5Zc_1	14 7/16	E	3.25	354.8	35	30	0.126	0.189	HLP-22	12	8	4	1.05	4.5	2.4	21.8	10.1	0.62	0.34	s1d5	2.5	0.0000328	0.0000439	0.0000585	0.4012
9150546	7/1A	15E_4s1d5Zc_1	14 7/16	E	3.25	354.8	35	30	0.126	0.189	HLP-22	12	8	4	1.05	4.5	2.4	21.8	10.1	0.62	0.34	s1d5	2.5	0.0000328	0.0000439	0.0000585	0.4012
9150547	7/1A	15E_4s1d5Zc_1	14 7/16	E	3.25	354.8	35	30	0.126	0.189	HLP-22	12	8	4	1.05	4.5	2.4	21.8	10.1	0.62	0.34	s1d5	2.5	0.0000328	0.0000439	0.0000585	0.4012
9150548	7/1A	15E_4s1d5Zc_1	14 7/16	E	3.25	354.8	35	30	0.126	0.189	HLP-22	12	8	4	1.05	4.5	2.4	21.8	10.1	0.62	0.34	s1d5	2.5	0.0000328	0.0000439	0.0000585	0.4012
9150549	7/1A	15E_4s1d5Zc_1	14 7/16	E	3.25	354.8	35	30	0.126	0.189	HLP-22	12	8	4	1.05	4.5	2.4	21.8	10.1	0.62	0.34	s1d5	2.5	0.0000328	0.0000439	0.0000585	0.4012
9150550	7/1A	15E_4s1d5Zc_1	14 7/16	E	3.25	354.8	35	30	0.126	0.189	HLP-22	12	8	4	1.05	4.5	2.4	21.8	10.1	0.62	0.34	s1d5	2.5	0.0000328	0.0000439	0.0000585	0.4012
9150551	7/1A	15E_4s1d5Zc_1	14 7/16	E	3.25	354.8	35	30	0.126	0.189	HLP-22	12	8	4	1.05	4.5	2.4	21.8	10.1	0.62	0.34	s1d5	2.5	0.0000328	0.0000439	0.0000585	0.4012
9150552	7/1A	15E_4s1d5Zc_1	14 7/16	E	3.25	354.8	35	30	0.126	0.189	HLP-22	12	8	4	1.05	4.5	2.4	21.8	10.1	0.62	0.34	s1d5	2.5	0.0000328	0.0000439	0.0000585	0.4012
9150553	7/1A	15E_4s1d5Zc_1	14 7/16	E	3.25	354.8	35	30	0.126	0.189	HLP-22	12	8	4	1.05	4.5	2.4	21.8	10.1	0.62	0.34	s1d5	2.5	0.0000328	0.0000439	0.0000585	0.4012
9150554	7/1A	15E_4s1d5Zc_1	14 7/16	E	3.25	354.8	35	30	0.126	0.189	HLP-22	12	8	4	1.05	4.5	2.4	21.8	10.1	0.62	0.34	s1d5	2.5	0.0000328	0.0000439	0.0000585	0.4012
9150555	7/1B	15E_4s1d5Yc_1	14 7/16	E	3.25	354.8	35	30	0.126	0.189	HLP-22	12	8	4	1.05	4.5	2.4	21.8	10.1	0.62	0.34	s1d5	2.5	0.0000328	0.0000439	0.0000585	0.4012
9150556	7/1B	15E_4s1d5Yc_1	14 7/16	E	3.25	354.8	35	30	0.126	0.189	HLP-22	12	8	4	1.05	4.5	2.4	21.8	10.1	0.62	0.34	s1d5	2.5	0.0000328	0.0000439	0.0000585	0.4012
9150557	7/1B	15E_4s1d5Yc_1	14 7/16	E	3.25	354.8	35	30	0.126	0.189	HLP-22	12	8	4	1.05	4.5	2.4	21.8	10.1	0.62	0.34	s1d5	2.5	0.0000328	0.0000439	0.0000585	0.4012
9150558	7/1B	15E_4s1d5Yc_1	14 7/16	E	3.25	354.8	35	30	0.126	0.189	HLP-22	12	8	4	1.05	4.5	2.4	21.8	10.1	0.62	0.34	s1d5	2.5	0.0000328	0.0000439	0.0000585	0.4012
9150559M	7/1B	15E_4s1d5Yc_1	14 7/16	E	3.25	354.8	35	30	0.126	0.189	HLP-22	12	8	4	1.05	4.5	2.4	21.8	10.1	0.62	0.34	s1d5	2.5	0.0000328	0.0000439	0.0000585	0.4012

Table B.3. Data from 2008 Tests in Small-Scale Vessel with Elliptical Head B.15

Tank Water Temperature	Water Density	Solids Fraction	Pulse Volume Fraction	Duty Cycle	Cycle Time	Pulsed or Steady Jet	Us Steady Jet	U1 Pulsing Jet	U2 URMS	U3 URM3	Discharge Velocity	Critical Suspension Velocity	Average Peak Cloud Height	UCS Condition	UCS Method	UCS Flag	UCS Center Flag	UCS udv Flag	UCS based on Decreasing Velocity	Sweep Increase / Decrease	UDV Height Bed	Particle Motion	Solids Level	Outer Bottom Pattern	Inner Bottom Pattern	Case ID	Test	TDP	Row Number
C	g/cm³	fraction	fraction	fraction	s	text	m/s	m/s	m/s	m/s	m/s	m/s	in.	m/s	text	text	text	text	m/s	text	mm	text	text	text	text	text	text	text	text
T	ρ_l	ϕ_S	ϕ_P	DC	t_C	Jet	U_S	U1	U2	U3	U	U_{CS}	H_C	U_{CSR}	U_{CSM}	U_{CS}vis	U_{CS}cen	U_{CS}udv	U_{CS}_D	S_W	H_{bed}	PM	Sol	SP_O	SP_I	ID	M/DDX	TDP	MSS
29.6	0.998	0.01500	0.050	0.335	7.4	P	N/A	8.03	8.24	8.34	8.60	8.60	5.50	N/A	N/A	N/A	N/A	N/A	N/A	N/A	0.0	N/A	N/A	N/A	N/A	15E_4s1d1Xc_1	6/30A	TDP-197	9150519
29.6	0.998	0.01500	0.050	0.335	7.4	P	N/A	8.03	8.24	8.34	8.60	8.60	5.50	N/A	N/A	N/A	N/A	N/A	N/A	N/A	0.0	N/A	N/A	N/A	N/A	15E_4s1d1Xc_1	6/30A	TDP-197	9150520
29.6	0.998	0.01500	0.050	0.335	7.4	P	N/A	8.03	8.24	8.34	8.60	8.60	5.50	N/A	N/A	N/A	N/A	N/A	N/A	N/A	0.0	N/A	N/A	N/A	N/A	15E_4s1d1Xc_1	6/30A	TDP-197	9150521
29.6	0.998	0.01500	0.050	0.335	7.4	P	N/A	8.03	8.24	8.34	8.60	8.60	5.50	N/A	N/A	N/A	N/A	N/A	N/A	N/A	0.7	N/A	N/A	N/A	N/A	15E_4s1d1Xc_1	6/30A	TDP-197	9150522
29.6	0.998	0.01500	0.050	0.335	7.4	P	N/A	8.03	8.24	8.34	8.60	8.60	5.50	N/A	N/A	N/A	N/A	N/A	N/A	N/A	0.0	N/A	N/A	N/A	N/A	15E_4s1d1Xc_1	6/30A	TDP-197	9150523
29.6	0.998	0.01500	0.050	0.335	7.4	P	N/A	8.03	8.24	8.34	8.60	8.60	5.50	N/A	N/A	N/A	N/A	N/A	N/A	N/A	0.0	N/A	N/A	N/A	N/A	15E_4s1d1Xc_1	6/30A	TDP-197	9150524
29.6	0.998	0.01500	0.050	0.335	7.4	P	N/A	8.03	8.24	8.34	8.60	8.60	5.50	N/A	N/A	N/A	N/A	N/A	N/A	N/A	0.7	N/A	N/A	N/A	N/A	15E_4s1d1Xc_1	6/30A	TDP-197	9150525
30.3	0.998	0.00155	0.050	0.328	61.4	P	N/A	1.00	1.00	1.00	1.00	2.80	16.00	N/A	N/A	N/A	N/A	N/A	N/A	(null)	14.7	1	N/A	N/A	N/A	15E_4s1d5Zc_1	6/30B	TDP-198	9150526
30.4	0.998	0.00155	0.050	0.330	43.8	P	N/A	1.39	1.39	1.39	1.40	2.80	10.75	N/A	N/A	N/A	N/A	N/A	N/A	I	8.7	1	N/A	N/A	N/A	15E_4s1d5Zc_1	6/30B	TDP-198	9150527
30.6	0.998	0.00155	0.050	0.333	34.0	P	N/A	1.78	1.79	1.79	1.80	2.80	7.50	N/A	N/A	N/A	N/A	N/A	N/A	I	11.2	1	N/A	N/A	N/A	15E_4s1d5Zc_1	6/30B	TDP-198	9150528
30.9	0.998	0.00155	0.050	0.333	27.8	P	N/A	2.17	2.17	2.18	2.20	2.80	7.75	N/A	N/A	N/A	N/A	N/A	N/A	I	6.2	1	N/A	N/A	N/A	15E_4s1d5Zc_1	6/30B	TDP-198	9150529
31.0	0.998	0.00155	0.050	0.335	23.4	P	N/A	2.56	2.57	2.58	2.60	2.80	11.00	N/A	N/A	N/A	N/A	N/A	N/A	I	5.0	1	N/A	N/A	N/A	15E_4s1d5Zc_1	6/30B	TDP-198	9150530
31.5	0.998	0.00155	0.050	0.336	23.4	P	N/A	2.55	2.57	2.57	2.60	2.80	10.50	N/A	N/A	N/A	N/A	N/A	N/A	I	4.5	1	N/A	N/A	N/A	15E_4s1d5Zc_1	6/30B	TDP-198	9150531
31.7	0.997	0.00155	0.050	0.336	22.4	P	N/A	2.66	2.68	2.68	2.70	2.80	12.00	N/A	N/A	N/A	N/A	N/A	N/A	I	3.7	1	N/A	N/A	N/A	15E_4s1d5Zc_1	6/30B	TDP-198	9150532
31.9	0.997	0.00155	0.050	0.337	21.6	P	N/A	2.76	2.77	2.78	2.80	2.80	15.50	2.80	udv	UCSvis	N/A	UCSudv	N/A	I	0.7	3	N/A	N/A	N/A	15E_4s1d5Zc_1	6/30B	TDP-198	9150533
32.1	0.997	0.00155	0.050	0.338	20.8	P	N/A	2.82	2.84	2.85	2.90	2.80	18.00	N/A	N/A	N/A	N/A	N/A	N/A	I	0.0	4	N/A	N/A	N/A	15E_4s1d5Zc_1	6/30B	TDP-198	9150534
32.2	0.997	0.00155	0.050	0.333	20.4	P	N/A	2.94	2.95	2.96	3.00	2.80	20.75	N/A	N/A	N/A	N/A	N/A	N/A	I	0.0	4	N/A	N/A	N/A	15E_4s1d5Zc_1	6/30B	TDP-198	9150535
28.5	0.999	0.00155	0.050	0.334	21.7	P	N/A	2.76	2.77	2.78	2.80	2.80	21.00	N/A	N/A	UCSvis	N/A	N/A	N/A	(null)	3.6	3	N/A	N/A	N/A	15E_4s1d5Zc_1	7/1A	TDP-199	9150536
28.4	0.998	0.00155	0.050	0.337	21.0	P	N/A	2.81	2.84	2.86	2.90	2.80	21.50	N/A	N/A	N/A	N/A	N/A	N/A	I	0.8	4	N/A	N/A	N/A	15E_4s1d5Zc_1	7/1A	TDP-199	9150537
28.5	0.999	0.00155	0.050	0.333	20.4	P	N/A	2.94	2.96	2.96	3.00	2.80	23.50	N/A	N/A	N/A	N/A	N/A	N/A	I	3.1	4	N/A	N/A	N/A	15E_4s1d5Zc_1	7/1A	TDP-199	9150538
28.5	0.998	0.00155	0.050	0.331	23.6	P	N/A	2.55	2.57	2.57	2.60	2.80	14.50	N/A	N/A	N/A	N/A	N/A	N/A	I	6.4	1	N/A	N/A	N/A	15E_4s1d5Zc_1	7/1A	TDP-199	9150539
28.6	0.998	0.00155	0.050	0.331	22.8	P	N/A	2.66	2.67	2.68	2.70	2.80	18.00	N/A	N/A	N/A	UCScen	N/A	N/A	I	4.5	2	N/A	N/A	N/A	15E_4s1d5Zc_1	7/1A	TDP-199	9150540
28.9	0.998	0.00155	0.050	0.332	22.8	P	N/A	2.64	2.66	2.67	2.70	2.80	17.50	N/A	N/A	N/A	UCScen	N/A	N/A	(null)	4.3	2	N/A	N/A	N/A	15E_4s1d5Zc_1	7/1A	TDP-199	9150541
28.9	0.998	0.00155	0.050	0.332	22.8	P	N/A	2.64	2.66	2.67	2.70	2.80	17.50	N/A	N/A	N/A	N/A	N/A	N/A	N/A	6.3	N/A	N/A	N/A	N/A	15E_4s1d5Zc_1	7/1A	TDP-199	9150542
28.9	0.998	0.00155	0.050	0.332	22.8	P	N/A	2.64	2.66	2.67	2.70	2.80	17.50	N/A	N/A	N/A	N/A	N/A	N/A	N/A	3.1	N/A	N/A	N/A	N/A	15E_4s1d5Zc_1	7/1A	TDP-199	9150543
28.9	0.998	0.00155	0.050	0.332	22.8	P	N/A	2.64	2.66	2.67	2.70	2.80	17.50	N/A	N/A	N/A	N/A	N/A	N/A	N/A	2.2	N/A	N/A	N/A	N/A	15E_4s1d5Zc_1	7/1A	TDP-199	9150544
28.9	0.998	0.00155	0.050	0.332	22.8	P	N/A	2.64	2.66	2.67	2.70	2.80	17.50	N/A	N/A	N/A	N/A	N/A	N/A	N/A	3.0	N/A	N/A	N/A	N/A	15E_4s1d5Zc_1	7/1A	TDP-199	9150545
28.9	0.998	0.00155	0.050	0.332	22.8	P	N/A	2.64	2.66	2.67	2.70	2.80	17.50	N/A	N/A	N/A	N/A	N/A	N/A	N/A	6.8	N/A	N/A	N/A	N/A	15E_4s1d5Zc_1	7/1A	TDP-199	9150546
28.9	0.998	0.00155	0.050	0.332	22.8	P	N/A	2.64	2.66	2.67	2.70	2.80	17.50	N/A	N/A	N/A	N/A	N/A	N/A	N/A	4.0	N/A	N/A	N/A	N/A	15E_4s1d5Zc_1	7/1A	TDP-199	9150547
28.9	0.998	0.00155	0.050	0.332	22.8	P	N/A	2.64	2.66	2.67	2.70	2.80	17.50	N/A	N/A	N/A	N/A	N/A	N/A	N/A	2.3	N/A	N/A	N/A	N/A	15E_4s1d5Zc_1	7/1A	TDP-199	9150548
28.9	0.998	0.00155	0.050	0.332	22.8	P	N/A	2.64	2.66	2.67	2.70	2.80	17.50	N/A	N/A	N/A	N/A	N/A	N/A	N/A	2.5	N/A	N/A	N/A	N/A	15E_4s1d5Zc_1	7/1A	TDP-199	9150549
28.9	0.998	0.00155	0.050	0.332	22.8	P	N/A	2.64	2.66	2.67	2.70	2.80	17.50	N/A	N/A	N/A	N/A	N/A	N/A	N/A	2.2	N/A	N/A	N/A	N/A	15E_4s1d5Zc_1	7/1A	TDP-199	9150550
28.9	0.998	0.00155	0.050	0.332	22.8	P	N/A	2.64	2.66	2.67	2.70	2.80	17.50	N/A	N/A	N/A	N/A	N/A	N/A	N/A	3.8	N/A	N/A	N/A	N/A	15E_4s1d5Zc_1	7/1A	TDP-199	9150551
28.9	0.998	0.00155	0.050	0.332	22.8	P	N/A	2.64	2.66	2.67	2.70	2.80	17.50	N/A	N/A	N/A	N/A	N/A	N/A	N/A	1.5	N/A	N/A	N/A	N/A	15E_4s1d5Zc_1	7/1A	TDP-199	9150552
28.9	0.998	0.00155	0.050	0.332	22.8	P	N/A	2.64	2.66	2.67	2.70	2.80	17.50	N/A	N/A	N/A	N/A	N/A	N/A	N/A	14.7	N/A	N/A	N/A	N/A	15E_4s1d5Zc_1	7/1A	TDP-199	9150553
28.9	0.998	0.00155	0.050	0.332	22.8	P	N/A	2.64	2.66	2.67	2.70	2.80	17.50	N/A	N/A	N/A	N/A	N/A	N/A	N/A	13.6	N/A	N/A	N/A	N/A	15E_4s1d5Zc_1	7/1A	TDP-199	9150554
29.4	0.998	0.00500	0.050	0.331	23.6	P	N/A	2.56	2.57	2.58	2.60	3.70	3.75	N/A	N/A	N/A	N/A	N/A	N/A	(null)	13.4	1	N/A	N/A	N/A	15E_4s1d5Yc_1	7/1B	TDP-200	9150555
29.5	0.998	0.00500	0.050	0.338	20.4	P	N/A	2.88	2.92	2.94	3.00	3.70	4.75	N/A	N/A	N/A	N/A	N/A	N/A	I	9.3	1	N/A	N/A	N/A	15E_4s1d5Yc_1	7/1B	TDP-200	9150556
29.6	0.998	0.00500	0.050	0.333	18.6	P	N/A	3.23	3.25	3.26	3.30	3.70	6.00	N/A	N/A	N/A	N/A	N/A	N/A	I	4.5	1	N/A	N/A	N/A	15E_4s1d5Yc_1	7/1B	TDP-200	9150557
29.7	0.998	0.00500	0.050	0.334	17.6	P	N/A	3.42	3.45	3.46	3.50	3.70	8.00	N/A	N/A	N/A	UCScen	N/A	N/A	I	2.3	2	N/A	N/A	N/A	15E_4s1d5Yc_1	7/1B	TDP-200	9150558
29.9	0.998	0.00500	0.050	0.339	16.6	P	N/A	3.56	3.61	3.63	3.70	3.70	11.00	3.70	udv	UCSvis	N/A	UCSudv	N/A	I	0.7	3	N/A	N/A	N/A	15E_4s1d5Yc_1	7/1B	TDP-200	9150559

Table B.3. Data from 2008 Tests in Small-Scale Vessel with Elliptical Head A.16

Row Number	Test	Case ID	Tank Diameter	Head Shape	Dish Height	Dish Volume	Tank Fill Height	Return Line Height	Nozzle Inner Diameter	Nozzle Stand-off Distance	Pulse Tube Configuration	Installed Nozzles	Outer Nozzles Operated	Inner Nozzles Operated	Pulse Tube Outer Diameter	Outer PJM Radius	Inner PJM Radius	"FIO" Outer PJM Impingement Angle	"FIO" Inner PJM Impingement Angle	Ratio Outer PJM to Tank Radius	Ratio Inner PJM to Tank Radius	Simulant	Solids Density	Particle Diameter d5	Particle Diameter d50	Particle Diameter d95	Void Fraction
text	text	text	in.	text	in.	in. ^{3}	in.	in.	in.	in.	text	number	number	number	in.	in.	in.	deg	deg	nondim	nondim	text	g/cm^3	m	m	m	fraction
MSS	M/DDX	ID	D	HS	H_{dish}	V_{dish}	H	Rtn	d	sod	PT	N	N_O	N_I	PT_{od}	R_O	R_I	θ_O	θ_I	R_O/R	R_I/R	sxdx	ρ_s	d_5	d_{50}	d_{95}	vf
9150560M	7/1B	15E_4s1d5Yc_1	14 7/16	E	3.25	354.8	35	30	0.126	0.189	HLP-22	12	8	4	1.05	4.5	2.4	21.8	10.1	0.62	0.34	s1d5	2.5	0.0000328	0.0000439	0.0000585	0.4012
9150561	7/1B	15E_4s1d5Yc_1	14 7/16	E	3.25	354.8	35	30	0.126	0.189	HLP-22	12	8	4	1.05	4.5	2.4	21.8	10.1	0.62	0.34	s1d5	2.5	0.0000328	0.0000439	0.0000585	0.4012
9150562	7/1B	15E_4s1d5Yc_1	14 7/16	E	3.25	354.8	35	30	0.126	0.189	HLP-22	12	8	4	1.05	4.5	2.4	21.8	10.1	0.62	0.34	s1d5	2.5	0.0000328	0.0000439	0.0000585	0.4012
9150563	7/1B	15E_4s1d5Yc_1	14 7/16	E	3.25	354.8	35	30	0.126	0.189	HLP-22	12	8	4	1.05	4.5	2.4	21.8	10.1	0.62	0.34	s1d5	2.5	0.0000328	0.0000439	0.0000585	0.4012
9150564	7/1B	15E_4s1d5Yc_1	14 7/16	E	3.25	354.8	35	30	0.126	0.189	HLP-22	12	8	4	1.05	4.5	2.4	21.8	10.1	0.62	0.34	s1d5	2.5	0.0000328	0.0000439	0.0000585	0.4012
9150565	7/1B	15E_4s1d5Yc_1	14 7/16	E	3.25	354.8	35	30	0.126	0.189	HLP-22	12	8	4	1.05	4.5	2.4	21.8	10.1	0.62	0.34	s1d5	2.5	0.0000328	0.0000439	0.0000585	0.4012
9150566	7/1B	15E_4s1d5Yc_1	14 7/16	E	3.25	354.8	35	30	0.126	0.189	HLP-22	12	8	4	1.05	4.5	2.4	21.8	10.1	0.62	0.34	s1d5	2.5	0.0000328	0.0000439	0.0000585	0.4012
9150567	7/1B	15E_4s1d5Yc_1	14 7/16	E	3.25	354.8	35	30	0.126	0.189	HLP-22	12	8	4	1.05	4.5	2.4	21.8	10.1	0.62	0.34	s1d5	2.5	0.0000328	0.0000439	0.0000585	0.4012
9150568M	7/1B	15E_4s1d5Yc_1	14 7/16	E	3.25	354.8	35	30	0.126	0.189	HLP-22	12	8	4	1.05	4.5	2.4	21.8	10.1	0.62	0.34	s1d5	2.5	0.0000328	0.0000439	0.0000585	0.4012
9150569	7/2A	15E_4s2d1Tc_1	14 7/16	E	3.25	354.8	36	30	0.126	0.189	HLP-22	12	8	4	1.05	4.5	2.4	21.8	10.1	0.62	0.34	s2d1	4.17	0.0001399	0.0001642	0.0001924	0.4000
9150570	7/2A	15E_4s2d1Tc_1	14 7/16	E	3.25	354.8	36	30	0.126	0.189	HLP-22	12	8	4	1.05	4.5	2.4	21.8	10.1	0.62	0.34	s2d1	4.17	0.0001399	0.0001642	0.0001924	0.4000
9150571	7/2A	15E_4s2d1Tc_1	14 7/16	E	3.25	354.8	36	30	0.126	0.189	HLP-22	12	8	4	1.05	4.5	2.4	21.8	10.1	0.62	0.34	s2d1	4.17	0.0001399	0.0001642	0.0001924	0.4000
9150572	7/2A	15E_4s2d1Tc_1	14 7/16	E	3.25	354.8	36	30	0.126	0.189	HLP-22	12	8	4	1.05	4.5	2.4	21.8	10.1	0.62	0.34	s2d1	4.17	0.0001399	0.0001642	0.0001924	0.4000
9150573M	7/2A	15E_4s2d1Tc_1	14 7/16	E	3.25	354.8	36	30	0.126	0.189	HLP-22	12	8	4	1.05	4.5	2.4	21.8	10.1	0.62	0.34	s2d1	4.17	0.0001399	0.0001642	0.0001924	0.4000
9150574M	7/2A	15E_4s2d1Tc_1	14 7/16	E	3.25	354.8	36	30	0.126	0.189	HLP-22	12	8	4	1.05	4.5	2.4	21.8	10.1	0.62	0.34	s2d1	4.17	0.0001399	0.0001642	0.0001924	0.4000
9150575M	7/2A	15E_4s2d1Tc_1	14 7/16	E	3.25	354.8	36	30	0.126	0.189	HLP-22	12	8	4	1.05	4.5	2.4	21.8	10.1	0.62	0.34	s2d1	4.17	0.0001399	0.0001642	0.0001924	0.4000
9150576M	7/2A	15E_4s2d1Tc_1	14 7/16	E	3.25	354.8	36	30	0.126	0.189	HLP-22	12	8	4	1.05	4.5	2.4	21.8	10.1	0.62	0.34	s2d1	4.17	0.0001399	0.0001642	0.0001924	0.4000
9150577M	7/2A	15E_4s2d1Tc_1	14 7/16	E	3.25	354.8	36	30	0.126	0.189	HLP-22	12	8	4	1.05	4.5	2.4	21.8	10.1	0.62	0.34	s2d1	4.17	0.0001399	0.0001642	0.0001924	0.4000
9150578	7/2B	15E_4s2d1Zc_1	14 7/16	E	3.25	354.8	36	30	0.126	0.189	HLP-22	12	8	4	1.05	4.5	2.4	21.8	10.1	0.62	0.34	s2d1	4.17	0.0001399	0.0001642	0.0001924	0.4000
9150579	7/2B	15E_4s2d1Zc_1	14 7/16	E	3.25	354.8	36	30	0.126	0.189	HLP-22	12	8	4	1.05	4.5	2.4	21.8	10.1	0.62	0.34	s2d1	4.17	0.0001399	0.0001642	0.0001924	0.4000
9150580	7/2B	15E_4s2d1Zc_1	14 7/16	E	3.25	354.8	36	30	0.126	0.189	HLP-22	12	8	4	1.05	4.5	2.4	21.8	10.1	0.62	0.34	s2d1	4.17	0.0001399	0.0001642	0.0001924	0.4000
9150581	7/2B	15E_4s2d1Zc_1	14 7/16	E	3.25	354.8	36	30	0.126	0.189	HLP-22	12	8	4	1.05	4.5	2.4	21.8	10.1	0.62	0.34	s2d1	4.17	0.0001399	0.0001642	0.0001924	0.4000
9150582	7/2B	15E_4s2d1Zc_1	14 7/16	E	3.25	354.8	36	30	0.126	0.189	HLP-22	12	8	4	1.05	4.5	2.4	21.8	10.1	0.62	0.34	s2d1	4.17	0.0001399	0.0001642	0.0001924	0.4000
9150583	7/2B	15E_4s2d1Zc_1	14 7/16	E	3.25	354.8	36	30	0.126	0.189	HLP-22	12	8	4	1.05	4.5	2.4	21.8	10.1	0.62	0.34	s2d1	4.17	0.0001399	0.0001642	0.0001924	0.4000
9150584	7/2B	15E_4s2d1Zc_1	14 7/16	E	3.25	354.8	36	30	0.126	0.189	HLP-22	12	8	4	1.05	4.5	2.4	21.8	10.1	0.62	0.34	s2d1	4.17	0.0001399	0.0001642	0.0001924	0.4000
9150585	7/2B	15E_4s2d1Zc_1	14 7/16	E	3.25	354.8	36	30	0.126	0.189	HLP-22	12	8	4	1.05	4.5	2.4	21.8	10.1	0.62	0.34	s2d1	4.17	0.0001399	0.0001642	0.0001924	0.4000
9150586	7/2B	15E_4s2d1Zc_1	14 7/16	E	3.25	354.8	36	30	0.126	0.189	HLP-22	12	8	4	1.05	4.5	2.4	21.8	10.1	0.62	0.34	s2d1	4.17	0.0001399	0.0001642	0.0001924	0.4000
9150587	7/2B	15E_4s2d1Zc_1	14 7/16	E	3.25	354.8	36	30	0.126	0.189	HLP-22	12	8	4	1.05	4.5	2.4	21.8	10.1	0.62	0.34	s2d1	4.17	0.0001399	0.0001642	0.0001924	0.4000
9150588M	7/2B	15E_4s2d1Zc_1	14 7/16	E	3.25	354.8	36	30	0.126	0.189	HLP-22	12	8	4	1.05	4.5	2.4	21.8	10.1	0.62	0.34	s2d1	4.17	0.0001399	0.0001642	0.0001924	0.4000
9150589M	7/2B	15E_4s2d1Zc_1	14 7/16	E	3.25	354.8	36	30	0.126	0.189	HLP-22	12	8	4	1.05	4.5	2.4	21.8	10.1	0.62	0.34	s2d1	4.17	0.0001399	0.0001642	0.0001924	0.4000
9150590M	7/2B	15E_4s2d1Zc_1	14 7/16	E	3.25	354.8	36	30	0.126	0.189	HLP-22	12	8	4	1.05	4.5	2.4	21.8	10.1	0.62	0.34	s2d1	4.17	0.0001399	0.0001642	0.0001924	0.4000
9150591M	7/2B	15E_4s2d1Zc_1	14 7/16	E	3.25	354.8	36	30	0.126	0.189	HLP-22	12	8	4	1.05	4.5	2.4	21.8	10.1	0.62	0.34	s2d1	4.17	0.0001399	0.0001642	0.0001924	0.4000
9150592M	7/2B	15E_4s2d1Zc_1	14 7/16	E	3.25	354.8	36	30	0.126	0.189	HLP-22	12	8	4	1.05	4.5	2.4	21.8	10.1	0.62	0.34	s2d1	4.17	0.0001399	0.0001642	0.0001924	0.4000
9150592.1	7/2B	15E_4s2d1Zc_1	14 7/16	E	3.25	354.8	36	30	0.126	0.189	HLP-22	12	8	4	1.05	4.5	2.4	21.8	10.1	0.62	0.34	s2d1	4.17	0.0001399	0.0001642	0.0001924	0.4000
9150592.2	7/2B	15E_4s2d1Zc_1	14 7/16	E	3.25	354.8	36	30	0.126	0.189	HLP-22	12	8	4	1.05	4.5	2.4	21.8	10.1	0.62	0.34	s2d1	4.17	0.0001399	0.0001642	0.0001924	0.4000
9150592.3	7/2B	15E_4s2d1Zc_1	14 7/16	E	3.25	354.8	36	30	0.126	0.189	HLP-22	12	8	4	1.05	4.5	2.4	21.8	10.1	0.62	0.34	s2d1	4.17	0.0001399	0.0001642	0.0001924	0.4000
9150592.4	7/2B	15E_4s2d1Zc_1	14 7/16	E	3.25	354.8	36	30	0.126	0.189	HLP-22	12	8	4	1.05	4.5	2.4	21.8	10.1	0.62	0.34	s2d1	4.17	0.0001399	0.0001642	0.0001924	0.4000
9150593M	7/2B	15E_4s2d1Zc_1	14 7/16	E	3.25	354.8	36	30	0.126	0.189	HLP-22	12	8	4	1.05	4.5	2.4	21.8	10.1	0.62	0.34	s2d1	4.17	0.0001399	0.0001642	0.0001924	0.4000
9150594	7/2B	15E_4s2d1Zc_1	14 7/16	E	3.25	354.8	36	30	0.126	0.189	HLP-22	12	8	4	1.05	4.5	2.4	21.8	10.1	0.62	0.34	s2d1	4.17	0.0001399	0.0001642	0.0001924	0.4000
9150594.1	7/2B	15E_4s2d1Zc_1	14 7/16	E	3.25	354.8	36	30	0.126	0.189	HLP-22	12	8	4	1.05	4.5	2.4	21.8	10.1	0.62	0.34	s2d1	4.17	0.0001399	0.0001642	0.0001924	0.4000
9150595	7/2B	15E_4s2d1Zc_1	14 7/16	E	3.25	354.8	36	30	0.126	0.189	HLP-22	12	8	4	1.05	4.5	2.4	21.8	10.1	0.62	0.34	s2d1	4.17	0.0001399	0.0001642	0.0001924	0.4000

Table B.3. Data from 2008 Tests in Small-Scale Vessel with Elliptical Head B.16

Tank Water Temperature	Water Density	Solids Fraction	Pulse Volume Fraction	Duty Cycle	Cycle Time	Pulsed or Steady Jet	Us Steady Jet	U1 Pulsing Jet	U2 URMS	U3 URM3	Discharge Velocity	Critical Suspension Velocity	Average Peak Cloud Height	UCS Condition	UCS Method	UCS Flag	UCS Center Flag	UCS udv Flag	UCS based on Decreasing Velocity	Sweep Increase / Decrease	UDV Height Bed	Particle Motion	Solids Level	Outer Bottom Pattern	Inner Bottom Pattern	Case ID	Test	TDP	Row Number
C	g/cm³	fraction	fraction	fraction	s	text	m/s	m/s	m/s	m/s	m/s	m/s	in.	m/s	text	text	text	text	m/s	text	mm	text	text	text	text	text	text	text	text
T	ρ_l	ϕ_S	ϕ_P	DC	t_C	Jet	U_S	U1	U2	U3	U	U_{CS}	H_C	U_{CSR}	U_{CSM}	U_{CS}vis	U_{CS}cen	U_{CS}udv	U_{CS_D}	S_W	H_{bed}	PM	Sol	SP_O	SP_I	ID	M/DDX	TDP	MSS
30.1	0.998	0.00500	0.050	0.339	15.8	P	N/A	3.76	3.81	3.83	3.90	3.70	17.00	N/A	N/A	N/A	N/A	N/A	N/A	I	4.5	4	N/A	N/A	N/A	15E_4s1d5Yc_1	7/1B	TDP-200	9150560
30.4	0.998	0.00500	0.050	0.332	17.6	P	N/A	3.43	3.45	3.47	3.50	3.70	8.50	N/A	N/A	N/A	UCScen	N/A	N/A	(null)	0.0	2	N/A	N/A	N/A	15E_4s1d5Yc_1	7/1B	TDP-200	9150561
30.4	0.998	0.00500	0.050	0.332	17.6	P	N/A	3.43	3.45	3.47	3.50	3.70	8.50	N/A	N/A	N/A	N/A	N/A	N/A	N/A	0.0	N/A	N/A	N/A	N/A	15E_4s1d5Yc_1	7/1B	TDP-200	9150562
30.4	0.998	0.00500	0.050	0.332	17.6	P	N/A	3.43	3.45	3.47	3.50	3.70	8.50	N/A	N/A	N/A	N/A	N/A	N/A	N/A	0.0	N/A	N/A	N/A	N/A	15E_4s1d5Yc_1	7/1B	TDP-200	9150563
30.4	0.998	0.00500	0.050	0.332	17.6	P	N/A	3.43	3.45	3.47	3.50	3.70	8.50	N/A	N/A	N/A	N/A	N/A	N/A	N/A	0.0	N/A	N/A	N/A	N/A	15E_4s1d5Yc_1	7/1B	TDP-200	9150564
30.4	0.998	0.00500	0.050	0.332	17.6	P	N/A	3.43	3.45	3.47	3.50	3.70	8.50	N/A	N/A	N/A	N/A	N/A	N/A	N/A	0.0	N/A	N/A	N/A	N/A	15E_4s1d5Yc_1	7/1B	TDP-200	9150565
30.4	0.998	0.00500	0.050	0.332	17.6	P	N/A	3.43	3.45	3.47	3.50	3.70	8.50	N/A	N/A	N/A	N/A	N/A	N/A	N/A	0.8	N/A	N/A	N/A	N/A	15E_4s1d5Yc_1	7/1B	TDP-200	9150566
30.4	0.998	0.00500	0.050	0.332	17.6	P	N/A	3.43	3.45	3.47	3.50	3.70	8.50	N/A	N/A	N/A	N/A	N/A	N/A	N/A	0.0	N/A	N/A	N/A	N/A	15E_4s1d5Yc_1	7/1B	TDP-200	9150567
30.7	0.998	0.00500	0.050	0.334	15.8	P	N/A	3.78	3.81	3.83	3.90	3.70	16.00	N/A	N/A	N/A	N/A	N/A	N/A	I	0.0	4	N/A	N/A	N/A	15E_4s1d5Yc_1	7/1B	TDP-200	9150568
27.7	0.998	0.00050	0.050	0.327	20.9	P	N/A	2.94	2.97	2.98	3.00	4.70	10.00	N/A	N/A	N/A	N/A	N/A	N/A	D	5.9	1	N/A	N/A	N/A	15E_4s2d1Tc_1	7/2A	TDP-201	9150569
27.9	0.998	0.00050	0.050	0.330	17.8	P	N/A	3.42	3.45	3.46	3.50	4.70	10.50	N/A	N/A	N/A	N/A	N/A	N/A	I	7.2	1	N/A	N/A	N/A	15E_4s2d1Tc_1	7/2A	TDP-201	9150570
28.0	0.998	0.00050	0.050	0.336	15.4	P	N/A	3.87	3.92	3.94	4.00	4.70	9.00	N/A	N/A	N/A	N/A	N/A	N/A	I	7.4	1	N/A	N/A	N/A	15E_4s2d1Tc_1	7/2A	TDP-201	9150571
28.2	0.998	0.00050	0.050	0.337	13.6	P	N/A	4.36	4.41	4.43	4.50	4.70	10.00	N/A	N/A	N/A	N/A	N/A	N/A	I	2.6	1	N/A	N/A	N/A	15E_4s2d1Tc_1	7/2A	TDP-201	9150572
28.6	0.998	0.00050	0.050	0.330	13.4	P	N/A	4.52	4.59	4.62	4.70	4.70	11.25	4.70	udv	UCSvis	N/A	UCSudv	N/A	I	0.6	3	N/A	N/A	N/A	15E_4s2d1Tc_1	7/2A	TDP-201	9150573
28.9	0.998	0.00050	0.050	0.331	12.8	P	N/A	4.72	4.78	4.82	4.90	4.70	12.25	N/A	N/A	N/A	N/A	N/A	N/A	I	0.0	4	N/A	N/A	N/A	15E_4s2d1Tc_1	7/2A	TDP-201	9150574
29.4	0.998	0.00050	0.050	0.335	11.8	P	N/A	5.06	5.14	5.18	5.30	4.70	14.50	N/A	N/A	N/A	N/A	N/A	N/A	I	0.0	4	N/A	N/A	N/A	15E_4s2d1Tc_1	7/2A	TDP-201	9150575
29.7	0.998	0.00050	0.050	0.335	11.2	P	N/A	5.36	5.45	5.49	5.60	4.70	16.75	N/A	N/A	N/A	N/A	N/A	N/A	I	0.0	4	N/A	N/A	N/A	15E_4s2d1Tc_1	7/2A	TDP-201	9150576
29.8	0.998	0.00050	0.050	0.337	10.6	P	N/A	5.63	5.72	5.77	5.90	4.70	19.50	N/A	N/A	N/A	N/A	N/A	N/A	I	0.0	4	N/A	N/A	N/A	15E_4s2d1Tc_1	7/2A	TDP-201	9150577
30.1	0.998	0.00155	0.050	0.329	15.6	P	N/A	3.91	3.94	3.96	4.00	6.80	5.75	N/A	N/A	N/A	N/A	N/A	N/A	(null)	14.5	1	N/A	N/A	N/A	15E_4s2d1Zc_1	7/2B	TDP-202	9150578
30.4	0.998	0.00155	0.050	0.334	14.2	P	N/A	4.25	4.30	4.33	4.40	6.80	5.75	N/A	N/A	N/A	N/A	N/A	N/A	I	14.8	1	N/A	N/A	N/A	15E_4s2d1Zc_1	7/2B	TDP-202	9150579
30.5	0.998	0.00155	0.050	0.335	13.0	P	N/A	4.62	4.69	4.72	4.80	6.80	6.50	N/A	N/A	N/A	N/A	N/A	N/A	I	13.9	1	N/A	N/A	N/A	15E_4s2d1Zc_1	7/2B	TDP-202	9150580
31.4	0.998	0.00155	0.050	0.338	12.0	P	N/A	4.98	5.06	5.10	5.20	6.80	6.75	N/A	N/A	N/A	N/A	N/A	N/A	I	N/A	1	N/A	N/A	N/A	15E_4s2d1Zc_1	7/2B	TDP-202	9150581
31.8	0.997	0.00155	0.050	0.334	11.6	P	N/A	5.18	5.26	5.30	5.40	6.80	7.00	N/A	N/A	N/A	N/A	N/A	N/A	I	8.5	1	N/A	N/A	N/A	15E_4s2d1Zc_1	7/2B	TDP-202	9150582
32.1	0.997	0.00155	0.050	0.336	10.8	P	N/A	5.54	5.63	5.67	5.80	6.80	7.25	N/A	N/A	N/A	N/A	N/A	N/A	I	6.3	1	N/A	N/A	N/A	15E_4s2d1Zc_1	7/2B	TDP-202	9150583
32.4	0.997	0.00155	0.050	0.339	10.4	P	N/A	5.72	5.82	5.86	6.00	6.80	7.50	N/A	N/A	N/A	N/A	N/A	N/A	I	5.1	1	N/A	N/A	N/A	15E_4s2d1Zc_1	7/2B	TDP-202	9150584
32.7	0.997	0.00155	0.050	0.337	10.0	P	N/A	5.91	6.01	6.06	6.20	6.80	7.50	N/A	N/A	N/A	N/A	N/A	N/A	I	4.1	1	N/A	N/A	N/A	15E_4s2d1Zc_1	7/2B	TDP-202	9150585
32.9	0.997	0.00155	0.050	0.333	9.8	P	N/A	6.09	6.20	6.25	6.40	6.80	8.00	N/A	N/A	N/A	N/A	N/A	N/A	I	4.6	1	N/A	N/A	N/A	15E_4s2d1Zc_1	7/2B	TDP-202	9150586
33.1	0.997	0.00155	0.050	0.335	9.5	P	N/A	6.29	6.40	6.45	6.60	6.80	8.50	N/A	N/A	N/A	N/A	N/A	N/A	I	3.5	1	N/A	N/A	N/A	15E_4s2d1Zc_1	7/2B	TDP-202	9150587
33.5	0.997	0.00155	0.050	0.327	9.4	P	N/A	6.49	6.60	6.66	6.80	6.80	8.00	6.80	udv	UCSvis	N/A	UCSudv	N/A	I	0.4	3	N/A	N/A	N/A	15E_4s2d1Zc_1	7/2B	TDP-202	9150588
33.6	0.997	0.00155	0.050	0.330	9.1	P	N/A	6.64	6.77	6.84	7.00	6.80	8.50	N/A	N/A	N/A	N/A	N/A	N/A	I	0.0	4	N/A	N/A	N/A	15E_4s2d1Zc_1	7/2B	TDP-202	9150589
33.6	0.997	0.00155	0.050	0.333	8.4	P	N/A	7.12	7.27	7.34	7.50	6.80	10.25	N/A	N/A	N/A	N/A	N/A	N/A	I	0.0	4	N/A	N/A	N/A	15E_4s2d1Zc_1	7/2B	TDP-202	9150590
33.8	0.997	0.00155	0.050	0.338	7.8	P	N/A	7.55	7.71	7.80	8.00	6.80	13.25	N/A	N/A	N/A	N/A	N/A	N/A	I	0.0	4	N/A	N/A	N/A	15E_4s2d1Zc_1	7/2B	TDP-202	9150591
34.0	0.997	0.00155	0.050	0.335	7.5	P	N/A	7.97	8.16	8.25	8.50	6.80	16.00	N/A	N/A	N/A	N/A	N/A	N/A	I	0.0	4	N/A	N/A	N/A	15E_4s2d1Zc_1	7/2B	TDP-202	9150592
34.2	0.997	0.00155	0.050	0.328	9.4	P	N/A	6.46	6.58	6.64	6.80	6.80	8.00	N/A	N/A	N/A	N/A	N/A	N/A	N/A	n/a	N/A	N/A	N/A	N/A	15E_4s2d1Zc_1	7/2B	TDP-202	9150592.1
34.2	0.997	0.00155	0.050	0.328	9.4	P	N/A	6.46	6.58	6.64	6.80	6.80	8.00	N/A	N/A	N/A	N/A	N/A	N/A	N/A	n/a	N/A	N/A	N/A	N/A	15E_4s2d1Zc_1	7/2B	TDP-202	9150592.2
34.2	0.997	0.00155	0.050	0.328	9.4	P	N/A	6.46	6.58	6.64	6.80	6.80	8.00	N/A	N/A	N/A	N/A	N/A	N/A	N/A	n/a	N/A	N/A	N/A	N/A	15E_4s2d1Zc_1	7/2B	TDP-202	9150592.3
34.2	0.997	0.00155	0.050	0.328	9.4	P	N/A	6.46	6.58	6.64	6.80	6.80	8.00	N/A	N/A	N/A	N/A	N/A	N/A	N/A	n/a	N/A	N/A	N/A	N/A	15E_4s2d1Zc_1	7/2B	TDP-202	9150592.4
34.2	0.997	0.00155	0.050	0.328	9.4	P	N/A	6.46	6.58	6.64	6.80	6.80	8.00	N/A	vis dec	UCSvis	N/A	N/A	6.80	D	1.1	3	N/A	N/A	N/A	15E_4s2d1Zc_1	7/2B	TDP-202	9150593
34.2	0.997	0.00155	0.050	0.328	9.4	P	N/A	6.46	6.58	6.64	6.80	6.80	8.00	N/A	N/A	N/A	N/A	N/A	N/A	N/A	1.2	N/A	N/A	N/A	N/A	15E_4s2d1Zc_1	7/2B	TDP-202	9150594
34.2	0.997	0.00155	0.050	0.328	9.4	P	N/A	6.46	6.58	6.64	6.80	6.80	8.00	N/A	N/A	N/A	N/A	N/A	N/A	N/A	n/a	N/A	N/A	N/A	N/A	15E_4s2d1Zc_1	7/2B	TDP-202	9150594.1
34.2	0.997	0.00155	0.050	0.328	9.4	P	N/A	6.46	6.58	6.64	6.80	6.80	8.00	N/A	N/A	N/A	N/A	N/A	N/A	N/A	0.0	N/A	N/A	N/A	N/A	15E_4s2d1Zc_1	7/2B	TDP-202	9150595

Table B.3. Data from 2008 Tests in Small-Scale Vessel with Elliptical Head A.17

Row Number	Test	Case ID	Tank Diameter	Head Shape	Dish Height	Dish Volume	Tank Fill Height	Return Line Height	Nozzle Inner Diameter	Nozzle Stand-off Distance	Pulse Tube Configuration	Installed Nozzles	Outer Nozzles Operated	Inner Nozzles Operated	Pulse Tube Outer Diameter	Outer PJM Radius	Inner PJM Radius	"FIO" Outer PJM Impingement Angle	"FIO" Inner PJM Impingement Angle	Ratio Outer PJM to Tank Radius	Ratio Inner PJM to Tank Radius	Simulant	Solids Density	Particle Diameter d5	Particle Diameter d50	Particle Diameter d95	Void Fraction
text	text	text	in.	text	in.	in. ^{3}	in.	in.	in.	in.	text	number	number	number	in.	in.	in.	deg	deg	nondim	nondim	text	g/cm^3	m	m	m	fraction
MSS	M/DDX	ID	D	HS	H_{dish}	V_{dish}	H	Rtn	d	sod	PT	N	N_O	N_I	PT_{od}	R_O	R_I	θ_O	θ_I	R_O/R	R_I/R	sxdx	ρ_s	d_5	d_{50}	d_{95}	vf
9150595.1	7/2B	15E_4s2d1Zc_1	14 7/16	E	3.25	354.8	36	30	0.126	0.189	HLP-22	12	8	4	1.05	4.5	2.4	21.8	10.1	0.62	0.34	s2d1	4.17	0.0001399	0.0001642	0.0001924	0.4000
9150596	7/2B	15E_4s2d1Zc_1	14 7/16	E	3.25	354.8	36	30	0.126	0.189	HLP-22	12	8	4	1.05	4.5	2.4	21.8	10.1	0.62	0.34	s2d1	4.17	0.0001399	0.0001642	0.0001924	0.4000
9150596.1	7/2B	15E_4s2d1Zc_1	14 7/16	E	3.25	354.8	36	30	0.126	0.189	HLP-22	12	8	4	1.05	4.5	2.4	21.8	10.1	0.62	0.34	s2d1	4.17	0.0001399	0.0001642	0.0001924	0.4000
9150597	7/2B	15E_4s2d1Zc_1	14 7/16	E	3.25	354.8	36	30	0.126	0.189	HLP-22	12	8	4	1.05	4.5	2.4	21.8	10.1	0.62	0.34	s2d1	4.17	0.0001399	0.0001642	0.0001924	0.4000
9150597.1	7/2B	15E_4s2d1Zc_1	14 7/16	E	3.25	354.8	36	30	0.126	0.189	HLP-22	12	8	4	1.05	4.5	2.4	21.8	10.1	0.62	0.34	s2d1	4.17	0.0001399	0.0001642	0.0001924	0.4000
9150598	7/2B	15E_4s2d1Zc_1	14 7/16	E	3.25	354.8	36	30	0.126	0.189	HLP-22	12	8	4	1.05	4.5	2.4	21.8	10.1	0.62	0.34	s2d1	4.17	0.0001399	0.0001642	0.0001924	0.4000
9150599	7/3A	15E_4s2d1Yc_1	14 7/16	E	3.25	354.8	35 1/2	30	0.126	0.189	HLP-22	12	8	4	1.05	4.5	2.4	21.8	10.1	0.62	0.34	s2d1	4.17	0.0001399	0.0001642	0.0001924	0.4000
9150600	7/3A	15E_4s2d1Yc_1	14 7/16	E	3.25	354.8	35 1/2	30	0.126	0.189	HLP-22	12	8	4	1.05	4.5	2.4	21.8	10.1	0.62	0.34	s2d1	4.17	0.0001399	0.0001642	0.0001924	0.4000
9150601	7/3A	15E_4s2d1Yc_1	14 7/16	E	3.25	354.8	35 1/2	30	0.126	0.189	HLP-22	12	8	4	1.05	4.5	2.4	21.8	10.1	0.62	0.34	s2d1	4.17	0.0001399	0.0001642	0.0001924	0.4000
9150602	7/3A	15E_4s2d1Yc_1	14 7/16	E	3.25	354.8	35 1/2	30	0.126	0.189	HLP-22	12	8	4	1.05	4.5	2.4	21.8	10.1	0.62	0.34	s2d1	4.17	0.0001399	0.0001642	0.0001924	0.4000
9150603	7/3A	15E_4s2d1Yc_1	14 7/16	E	3.25	354.8	35 1/2	30	0.126	0.189	HLP-22	12	8	4	1.05	4.5	2.4	21.8	10.1	0.62	0.34	s2d1	4.17	0.0001399	0.0001642	0.0001924	0.4000
9150604	7/3A	15E_4s2d1Yc_1	14 7/16	E	3.25	354.8	35 1/2	30	0.126	0.189	HLP-22	12	8	4	1.05	4.5	2.4	21.8	10.1	0.62	0.34	s2d1	4.17	0.0001399	0.0001642	0.0001924	0.4000
9150605	7/3A	15E_4s2d1Yc_1	14 7/16	E	3.25	354.8	35 1/2	30	0.126	0.189	HLP-22	12	8	4	1.05	4.5	2.4	21.8	10.1	0.62	0.34	s2d1	4.17	0.0001399	0.0001642	0.0001924	0.4000
9150606	7/3A	15E_4s2d1Yc_1	14 7/16	E	3.25	354.8	35 1/2	30	0.126	0.189	HLP-22	12	8	4	1.05	4.5	2.4	21.8	10.1	0.62	0.34	s2d1	4.17	0.0001399	0.0001642	0.0001924	0.4000
9150607	7/3A	15E_4s2d1Yc_1	14 7/16	E	3.25	354.8	35 1/2	30	0.126	0.189	HLP-22	12	8	4	1.05	4.5	2.4	21.8	10.1	0.62	0.34	s2d1	4.17	0.0001399	0.0001642	0.0001924	0.4000
9150608	7/3A	15E_4s2d1Yc_1	14 7/16	E	3.25	354.8	35 1/2	30	0.126	0.189	HLP-22	12	8	4	1.05	4.5	2.4	21.8	10.1	0.62	0.34	s2d1	4.17	0.0001399	0.0001642	0.0001924	0.4000
9150609	7/3A	15E_4s2d1Yc_1	14 7/16	E	3.25	354.8	35 1/2	30	0.126	0.189	HLP-22	12	8	4	1.05	4.5	2.4	21.8	10.1	0.62	0.34	s2d1	4.17	0.0001399	0.0001642	0.0001924	0.4000
9150610M	7/3A	15E_4s2d1Yc_1	14 7/16	E	3.25	354.8	35 1/2	30	0.126	0.189	HLP-22	12	8	4	1.05	4.5	2.4	21.8	10.1	0.62	0.34	s2d1	4.17	0.0001399	0.0001642	0.0001924	0.4000
9150611M	7/3A	15E_4s2d1Yc_1	14 7/16	E	3.25	354.8	35 1/2	30	0.126	0.189	HLP-22	12	8	4	1.05	4.5	2.4	21.8	10.1	0.62	0.34	s2d1	4.17	0.0001399	0.0001642	0.0001924	0.4000
9150612M	7/3A	15E_4s2d1Yc_1	14 7/16	E	3.25	354.8	35 1/2	30	0.126	0.189	HLP-22	12	8	4	1.05	4.5	2.4	21.8	10.1	0.62	0.34	s2d1	4.17	0.0001399	0.0001642	0.0001924	0.4000
9150613M	7/3A	15E_4s2d1Yc_1	14 7/16	E	3.25	354.8	35 1/2	30	0.126	0.189	HLP-22	12	8	4	1.05	4.5	2.4	21.8	10.1	0.62	0.34	s2d1	4.17	0.0001399	0.0001642	0.0001924	0.4000
9150614M	7/3A	15E_4s2d1Yc_1	14 7/16	E	3.25	354.8	35 1/2	30	0.126	0.189	HLP-22	12	8	4	1.05	4.5	2.4	21.8	10.1	0.62	0.34	s2d1	4.17	0.0001399	0.0001642	0.0001924	0.4000
9150615M	7/3A	15E_4s2d1Yc_1	14 7/16	E	3.25	354.8	35 1/2	30	0.126	0.189	HLP-22	12	8	4	1.05	4.5	2.4	21.8	10.1	0.62	0.34	s2d1	4.17	0.0001399	0.0001642	0.0001924	0.4000
9150616	7/3B	15E_4s2d1Xc_1	14 7/16	E	3.25	354.8	35 1/2	30	0.126	0.189	HLP-22	12	8	4	1.05	4.5	2.4	21.8	10.1	0.62	0.34	s2d1	4.17	0.0001399	0.0001642	0.0001924	0.4000
9150617	7/3B	15E_4s2d1Xc_1	14 7/16	E	3.25	354.8	35 1/2	30	0.126	0.189	HLP-22	12	8	4	1.05	4.5	2.4	21.8	10.1	0.62	0.34	s2d1	4.17	0.0001399	0.0001642	0.0001924	0.4000
9150618M	7/3B	15E_4s2d1Xc_1	14 7/16	E	3.25	354.8	35 1/2	30	0.126	0.189	HLP-22	12	8	4	1.05	4.5	2.4	21.8	10.1	0.62	0.34	s2d1	4.17	0.0001399	0.0001642	0.0001924	0.4000
9150619M	7/3B	15E_4s2d1Xc_1	14 7/16	E	3.25	354.8	35 1/2	30	0.126	0.189	HLP-22	12	8	4	1.05	4.5	2.4	21.8	10.1	0.62	0.34	s2d1	4.17	0.0001399	0.0001642	0.0001924	0.4000
9150620M	7/3B	15E_4s2d1Xc_1	14 7/16	E	3.25	354.8	35 1/2	30	0.126	0.189	HLP-22	12	8	4	1.05	4.5	2.4	21.8	10.1	0.62	0.34	s2d1	4.17	0.0001399	0.0001642	0.0001924	0.4000
9150621M	7/3B	15E_4s2d1Xc_1	14 7/16	E	3.25	354.8	35 1/2	30	0.126	0.189	HLP-22	12	8	4	1.05	4.5	2.4	21.8	10.1	0.62	0.34	s2d1	4.17	0.0001399	0.0001642	0.0001924	0.4000
9150622	7/8A	15E8_6s1d2Zc_1	14 7/16	E	3.25	354.8	35	30	0.191	0.202	8TA	8	4	4	1.05	4.9	3.6	24.4	16	0.67	0.50	s1d2	2.48	0.0000569	0.0000693	0.0000821	0.3750
9150623	7/8A	15E8_6s1d2Zc_1	14 7/16	E	3.25	354.8	35	30	0.191	0.202	8TA	8	4	4	1.05	4.9	3.6	24.4	16	0.67	0.50	s1d2	2.48	0.0000569	0.0000693	0.0000821	0.3750
9150624M	7/8A	15E8_6s1d2Zc_1	14 7/16	E	3.25	354.8	35	30	0.191	0.202	8TA	8	4	4	1.05	4.9	3.6	24.4	16	0.67	0.50	s1d2	2.48	0.0000569	0.0000693	0.0000821	0.3750
9150625M	7/8A	15E8_6s1d2Zc_1	14 7/16	E	3.25	354.8	35	30	0.191	0.202	8TA	8	4	4	1.05	4.9	3.6	24.4	16	0.67	0.50	s1d2	2.48	0.0000569	0.0000693	0.0000821	0.3750
9150626M	7/8A	15E8_6s1d2Zc_1	14 7/16	E	3.25	354.8	35	30	0.191	0.202	8TA	8	4	4	1.05	4.9	3.6	24.4	16	0.67	0.50	s1d2	2.48	0.0000569	0.0000693	0.0000821	0.3750
9150627M	7/8A	15E8_6s1d2Zc_1	14 7/16	E	3.25	354.8	35	30	0.191	0.202	8TA	8	4	4	1.05	4.9	3.6	24.4	16	0.67	0.50	s1d2	2.48	0.0000569	0.0000693	0.0000821	0.3750
9150628	7/8B	15E8_6s1d2Zc_2	14 7/16	E	3.25	354.8	35	30	0.191	0.202	8TA	8	4	4	1.05	4.9	3.6	24.4	16	0.67	0.50	s1d2	2.48	0.0000569	0.0000693	0.0000821	0.3750
9150629	7/8B	15E8_6s1d2Zc_2	14 7/16	E	3.25	354.8	35	30	0.191	0.202	8TA	8	4	4	1.05	4.9	3.6	24.4	16	0.67	0.50	s1d2	2.48	0.0000569	0.0000693	0.0000821	0.3750
9150630	7/8B	15E8_6s1d2Zc_2	14 7/16	E	3.25	354.8	35	30	0.191	0.202	8TA	8	4	4	1.05	4.9	3.6	24.4	16	0.67	0.50	s1d2	2.48	0.0000569	0.0000693	0.0000821	0.3750
9150631	7/8B	15E8_6s1d2Zc_2	14 7/16	E	3.25	354.8	35	30	0.191	0.202	8TA	8	4	4	1.05	4.9	3.6	24.4	16	0.67	0.50	s1d2	2.48	0.0000569	0.0000693	0.0000821	0.3750
9150632M	7/8B	15E8_6s1d2Zc_2	14 7/16	E	3.25	354.8	35	30	0.191	0.202	8TA	8	4	4	1.05	4.9	3.6	24.4	16	0.67	0.50	s1d2	2.48	0.0000569	0.0000693	0.0000821	0.3750
9150633M	7/8B	15E8_6s1d2Zc_2	14 7/16	E	3.25	354.8	35	30	0.191	0.202	8TA	8	4	4	1.05	4.9	3.6	24.4	16	0.67	0.50	s1d2	2.48	0.0000569	0.0000693	0.0000821	0.3750

Table B.3. Data from 2008 Tests in Small-Scale Vessel with Elliptical Head B.17

Tank Water Temperature	Water Density	Solids Fraction	Pulse Volume Fraction	Duty Cycle	Cycle Time	Pulsed or Steady Jet	Us Steady Jet	U1 Pulsing Jet	U2 URMS	U3 URM3	Discharge Velocity	Critical Suspension Velocity	Average Peak Cloud Height	UCS Condition	UCS Method	UCS Flag	UCS Center Flag	UCS udv Flag	UCS based on Decreasing Velocity	Sweep Increase / Decrease	UDV Height Bed	Particle Motion	Solids Level	Outer Bottom Pattern	Inner Bottom Pattern	Case ID	Test	TDP	Row Number
C	g/cm³	fraction	fraction	fraction	s	text	m/s	m/s	m/s	m/s	m/s	m/s	in.	m/s	text	text	text	text	m/s	text	mm	text	text	text	text	text	text	text	text
T	ρ_c	ϕ_S	ϕ_p	DC	t_C	Jet	U_S	U1	U2	U3	U	U_{CS}	H_C	U_{CSR}	U_{CSM}	U_{CS}vis	U_{CS}cen	U_{CS}udv	U_{CS}_D	S_W	H_{bed}	PM	Sol	SP_O	SP_I	ID	M/DDX	TDP	MSS
34.2	0.997	0.00155	0.050	0.328	9.4	P	N/A	6.46	6.58	6.64	6.80	6.80	8.00	N/A	N/A	N/A	N/A	N/A	N/A	N/A	n/a	N/A	N/A	N/A	N/A	15E_4s2d1Zc_1	7/2B	TDP-202	9150595.1
34.2	0.997	0.00155	0.050	0.328	9.4	P	N/A	6.46	6.58	6.64	6.80	6.80	8.00	N/A	N/A	N/A	N/A	N/A	N/A	N/A	0.6	N/A	N/A	N/A	N/A	15E_4s2d1Zc_1	7/2B	TDP-202	9150596
34.2	0.997	0.00155	0.050	0.328	9.4	P	N/A	6.46	6.58	6.64	6.80	6.80	8.00	N/A	N/A	N/A	N/A	N/A	N/A	N/A	n/a	N/A	N/A	N/A	N/A	15E_4s2d1Zc_1	7/2B	TDP-202	9150596.1
34.2	0.997	0.00155	0.050	0.328	9.4	P	N/A	6.46	6.58	6.64	6.80	6.80	8.00	N/A	N/A	N/A	N/A	N/A	N/A	N/A	1.9	N/A	N/A	N/A	N/A	15E_4s2d1Zc_1	7/2B	TDP-202	9150597
34.2	0.997	0.00155	0.050	0.328	9.4	P	N/A	6.46	6.58	6.64	6.80	6.80	8.00	N/A	N/A	N/A	N/A	N/A	N/A	N/A	n/a	N/A	N/A	N/A	N/A	15E_4s2d1Zc_1	7/2B	TDP-202	9150597.1
34.2	0.997	0.00155	0.050	0.328	9.4	P	N/A	6.46	6.58	6.64	6.80	6.80	8.00	N/A	N/A	N/A	N/A	N/A	N/A	N/A	0.0	N/A	N/A	N/A	N/A	15E_4s2d1Zc_1	7/2B	TDP-202	9150598
29.1	0.998	0.00500	0.050	0.331	10.6	P	N/A	5.67	5.78	5.84	6.00	9.00	3.38	N/A	N/A	N/A	N/A	N/A	N/A	(null)	16.2	1	N/A	N/A	N/A	15E_4s2d1Yc_1	7/3A	TDP-203	9150599
29.2	0.998	0.00500	0.050	0.332	10.0	P	N/A	6.06	6.17	6.22	6.40	9.00	3.75	N/A	N/A	N/A	N/A	N/A	N/A	I	14.2	1	N/A	N/A	N/A	15E_4s2d1Yc_1	7/3A	TDP-203	9150600
29.3	0.998	0.00500	0.050	0.333	9.4	P	N/A	6.44	6.56	6.62	6.80	9.00	3.75	N/A	N/A	N/A	N/A	N/A	N/A	I	9.7	1	N/A	N/A	N/A	15E_4s2d1Yc_1	7/3A	TDP-203	9150601
29.5	0.998	0.00500	0.050	0.332	8.9	P	N/A	6.83	6.96	7.03	7.20	9.00	4.25	N/A	N/A	N/A	N/A	N/A	N/A	I	6.7	1	N/A	N/A	N/A	15E_4s2d1Yc_1	7/3A	TDP-203	9150602
29.6	0.998	0.00500	0.050	0.333	8.4	P	N/A	7.19	7.34	7.41	7.60	9.00	4.50	N/A	N/A	N/A	N/A	N/A	N/A	I	5.2	1	N/A	N/A	N/A	15E_4s2d1Yc_1	7/3A	TDP-203	9150603
29.9	0.998	0.00500	0.050	0.335	8.2	P	N/A	7.33	7.49	7.57	7.80	9.00	4.75	N/A	N/A	N/A	N/A	N/A	N/A	I	3.9	1	N/A	N/A	N/A	15E_4s2d1Yc_1	7/3A	TDP-203	9150604
30.0	0.998	0.00500	0.050	0.335	8.0	P	N/A	7.51	7.68	7.76	8.00	9.00	4.75	N/A	N/A	N/A	N/A	N/A	N/A	I	3.5	1	N/A	N/A	N/A	15E_4s2d1Yc_1	7/3A	TDP-203	9150605
30.2	0.998	0.00500	0.050	0.335	7.8	P	N/A	7.70	7.87	7.96	8.20	9.00	5.25	N/A	N/A	N/A	N/A	N/A	N/A	I	3.6	1	N/A	N/A	N/A	15E_4s2d1Yc_1	7/3A	TDP-203	9150606
30.4	0.998	0.00500	0.050	0.336	7.6	P	N/A	7.90	8.08	8.17	8.40	9.00	5.25	N/A	N/A	N/A	N/A	N/A	N/A	I	2.9	1	N/A	N/A	N/A	15E_4s2d1Yc_1	7/3A	TDP-203	9150607
30.6	0.998	0.00500	0.050	0.335	7.4	P	N/A	8.07	8.27	8.36	8.60	9.00	5.50	N/A	N/A	N/A	N/A	N/A	N/A	I	3.1	1	N/A	N/A	N/A	15E_4s2d1Yc_1	7/3A	TDP-203	9150608
30.9	0.998	0.00500	0.050	0.338	7.2	P	N/A	8.26	8.46	8.55	8.80	9.00	5.75	N/A	N/A	UCSvis	N/A	N/A	N/A	I	1.3	3	N/A	N/A	N/A	15E_4s2d1Yc_1	7/3A	TDP-203	9150609
31.3	0.998	0.00500	0.050	0.339	7.0	P	N/A	8.39	8.60	8.71	9.00	9.00	5.75	9.00	udv	N/A	N/A	UCSudv	N/A	I	0.7	4	N/A	N/A	N/A	15E_4s2d1Yc_1	7/3A	TDP-203	9150610
31.5	0.998	0.00500	0.050	0.334	7.0	P	N/A	8.59	8.79	8.89	9.20	9.00	6.00	N/A	N/A	N/A	N/A	N/A	N/A	I	0.0	4	N/A	N/A	N/A	15E_4s2d1Yc_1	7/3A	TDP-203	9150611
31.7	0.998	0.00500	0.050	0.337	6.6	P	N/A	9.04	9.30	9.43	9.70	9.00	6.25	N/A	N/A	N/A	N/A	N/A	N/A	I	0.0	4	N/A	N/A	N/A	15E_4s2d1Yc_1	7/3A	TDP-203	9150612
32.1	0.997	0.00500	0.050	0.333	6.2	P	N/A	9.73	10.00	10.13	10.40	9.00	6.50	N/A	N/A	N/A	N/A	N/A	N/A	I	0.0	4	N/A	N/A	N/A	15E_4s2d1Yc_1	7/3A	TDP-203	9150613
32.3	0.997	0.00500	0.050	0.335	5.9	P	N/A	10.21	10.53	10.69	11.00	9.00	7.00	N/A	N/A	N/A	N/A	N/A	N/A	I	0.0	4	N/A	N/A	N/A	15E_4s2d1Yc_1	7/3A	TDP-203	9150614
32.5	0.998	0.00500	0.050	0.321	5.4	P	N/A	11.60	11.74	11.83	12.00	9.00	8.00	N/A	N/A	N/A	N/A	N/A	N/A	I	0.0	4	N/A	N/A	N/A	15E_4s2d1Yc_1	7/3A	TDP-203	9150615
32.4	0.997	0.01500	0.050	0.334	7.1	P	N/A	8.38	8.61	8.73	9.00	9.40	N/A	N/A	N/A	N/A	N/A	N/A	N/A	(null)	3.2	1	N/A	N/A	N/A	15E_4s2d1Xc_1	7/3B	TDP-204	9150616
32.5	0.997	0.01500	0.050	0.333	7.0	P	N/A	8.59	8.83	8.94	9.20	9.40	N/A	N/A	N/A	N/A	N/A	N/A	N/A	I	2.9	1	N/A	N/A	N/A	15E_4s2d1Xc_1	7/3B	TDP-204	9150617
32.7	0.997	0.01500	0.050	0.336	6.8	P	N/A	8.79	9.04	9.16	9.40	9.40	3.25	9.40	udv	UCSvis	N/A	UCSudv	N/A	I	0.4	3	N/A	N/A	N/A	15E_4s2d1Xc_1	7/3B	TDP-204	9150618
32.7	0.997	0.01500	0.050	0.336	6.6	P	N/A	8.97	9.22	9.34	9.60	9.40	3.38	N/A	N/A	N/A	N/A	N/A	N/A	I	0.0	4	N/A	N/A	N/A	15E_4s2d1Xc_1	7/3B	TDP-204	9150619
33.0	0.997	0.01500	0.050	0.333	5.9	P	N/A	10.23	10.54	10.69	11.00	9.40	3.75	N/A	N/A	N/A	N/A	N/A	N/A	I	0.0	4	N/A	N/A	N/A	15E_4s2d1Xc_1	7/3B	TDP-204	9150620
33.2	0.997	0.01500	0.050	0.337	5.4	P	N/A	11.06	11.42	11.60	12.00	9.40	4.25	N/A	N/A	N/A	N/A	N/A	N/A	I	0.0	4	N/A	N/A	N/A	15E_4s2d1Xc_1	7/3B	TDP-204	9150621
26.4	0.999	0.00155	0.050	0.330	20.8	P	N/A	1.93	1.95	1.96	2.00	2.60	7.00	N/A	N/A	N/A	N/A	N/A	N/A	(null)	10.0	1	N/A	N/A	N/A	15E8_6s1d2Zc_1	7/8A	TDP-205	9150622
26.3	0.999	0.00155	0.050	0.333	17.3	P	N/A	2.32	2.34	2.35	2.40	2.60	8.50	N/A	N/A	N/A	N/A	N/A	N/A	I	5.6	1	N/A	N/A	N/A	15E8_6s1d2Zc_1	7/8A	TDP-205	9150623
26.3	0.999	0.00155	0.050	0.335	16.0	P	N/A	2.49	2.52	2.53	2.60	2.60	9.00	2.60	udv	N/A	N/A	UCSudv	N/A	I	0.0	1	N/A	N/A	N/A	15E8_6s1d2Zc_1	7/8A	TDP-205	9150624
26.4	0.999	0.00155	0.050	0.333	14.9	P	N/A	2.68	2.71	2.72	2.80	2.60	15.50	N/A	N/A	UCSvis	N/A	N/A	N/A	I	0.0	3	N/A	N/A	N/A	15E8_6s1d2Zc_1	7/8A	TDP-205	9150625
26.5	0.999	0.00155	0.050	0.335	13.9	P	N/A	2.87	2.91	2.92	3.00	2.60	19.50	N/A	N/A	N/A	N/A	N/A	N/A	I	0.0	4	N/A	N/A	N/A	15E8_6s1d2Zc_1	7/8A	TDP-205	9150626
26.5	0.999	0.00155	0.050	0.335	13.0	P	N/A	3.06	3.10	3.12	3.20	2.60	22.50	N/A	N/A	N/A	N/A	N/A	N/A	I	0.7	4	N/A	N/A	N/A	15E8_6s1d2Zc_1	7/8A	TDP-205	9150627
26.7	0.999	0.00155	0.100	0.328	41.2	P	N/A	1.97	1.98	1.98	2.00	2.80	11.00	N/A	N/A	N/A	N/A	N/A	N/A	(null)	6.2	1	N/A	N/A	N/A	15E8_6s1d2Zc_2	7/8B	TDP-205	9150628
26.8	0.999	0.00155	0.101	0.329	37.5	P	N/A	2.16	2.17	2.18	2.20	2.80	11.00	N/A	N/A	N/A	N/A	N/A	N/A	I	9.5	1	N/A	N/A	N/A	15E8_6s1d2Zc_2	7/8B	TDP-205	9150629
26.8	0.999	0.00155	0.101	0.330	34.3	P	N/A	2.36	2.37	2.37	2.40	2.80	13.00	N/A	N/A	N/A	N/A	N/A	N/A	I	6.9	1	N/A	N/A	N/A	15E8_6s1d2Zc_2	7/8B	TDP-205	9150630
26.8	0.999	0.00155	0.101	0.331	31.7	P	N/A	2.54	2.56	2.57	2.60	2.80	13.50	N/A	N/A	N/A	N/A	N/A	N/A	I	3.8	1	N/A	N/A	N/A	15E8_6s1d2Zc_2	7/8B	TDP-205	9150631
26.9	0.999	0.00155	0.100	0.332	29.2	P	N/A	2.74	2.76	2.77	2.80	2.80	16.25	2.80	vis	UCSvis	N/A	N/A	N/A	I	1.5	3	N/A	N/A	N/A	15E8_6s1d2Zc_2	7/8B	TDP-205	9150632
27.1	0.999	0.00155	0.100	0.333	27.3	P	N/A	2.93	2.95	2.96	3.00	2.80	21.50	N/A	N/A	N/A	N/A	N/A	N/A	I	0.8	4	N/A	N/A	N/A	15E8_6s1d2Zc_2	7/8B	TDP-205	9150633

Table B.3. Data from 2008 Tests in Small-Scale Vessel with Elliptical Head A.18

Row Number	Test	Case ID	Tank Diameter	Head Shape	Dish Height	Dish Volume	Tank Fill Height	Return Line Height	Nozzle Inner Diameter	Nozzle Stand-off Distance	Pulse Tube Configuration	Installed Nozzles	Outer Nozzles Operated	Inner Nozzles Operated	Pulse Tube Outer Diameter	Outer PJM Radius	Inner PJM Radius	"FIO" Outer PJM Impingement Angle	"FIO" Inner PJM Impingement Angle	Ratio Outer PJM to Tank Radius	Ratio Inner PJM to Tank Radius	Simulant	Solids Density	Particle Diameter d5	Particle Diameter d50	Particle Diameter d95	Void Fraction
text	text	text	in.	text	in.	in. ^{3}	in.	in.	in.	in.	text	number	number	number	in.	in.	in.	deg	deg	nondim	nondim	text	g/cm^3	m	m	m	fraction
MSS	M/DDX	ID	D	HS	H_{dish}	V_{dish}	H	Rtn	d	sod	PT	N	N_O	N_I	PT_{od}	R_O	R_I	θ_O	θ_I	R_O/R	R_I/R	sxdx	ρ_s	d_5	d_{50}	d_{95}	vf
9150634M	7/8B	15E8_6s1d2Zc_2	14 7/16	E	3.25	354.8	35	30	0.191	0.202	8TA	8	4	4	1.05	4.9	3.6	24.4	16	0.67	0.50	s1d2	2.48	0.0000569	0.0000693	0.0000821	0.3750
9150635	7/8C	15E8_6s1d2Vc_1	14 7/16	E	3.25	354.8	36	30	0.191	0.202	8TA	8	4	4	1.05	4.9	3.6	24.4	16	0.67	0.50	s1d2	2.48	0.0000569	0.0000693	0.0000821	0.3750
9150636	7/8C	15E8_6s1d2Vc_1	14 7/16	E	3.25	354.8	36	30	0.191	0.202	8TA	8	4	4	1.05	4.9	3.6	24.4	16	0.67	0.50	s1d2	2.48	0.0000569	0.0000693	0.0000821	0.3750
9150637	7/8C	15E8_6s1d2Vc_1	14 7/16	E	3.25	354.8	36	30	0.191	0.202	8TA	8	4	4	1.05	4.9	3.6	24.4	16	0.67	0.50	s1d2	2.48	0.0000569	0.0000693	0.0000821	0.3750
9150638M	7/8C	15E8_6s1d2Vc_1	14 7/16	E	3.25	354.8	36	30	0.191	0.202	8TA	8	4	4	1.05	4.9	3.6	24.4	16	0.67	0.50	s1d2	2.48	0.0000569	0.0000693	0.0000821	0.3750
9150639M	7/8C	15E8_6s1d2Vc_1	14 7/16	E	3.25	354.8	36	30	0.191	0.202	8TA	8	4	4	1.05	4.9	3.6	24.4	16	0.67	0.50	s1d2	2.48	0.0000569	0.0000693	0.0000821	0.3750
9150640M	7/8C	15E8_6s1d2Vc_1	14 7/16	E	3.25	354.8	36	30	0.191	0.202	8TA	8	4	4	1.05	4.9	3.6	24.4	16	0.67	0.50	s1d2	2.48	0.0000569	0.0000693	0.0000821	0.3750
9150641M	7/8C	15E8_6s1d2Vc_1	14 7/16	E	3.25	354.8	36	30	0.191	0.202	8TA	8	4	4	1.05	4.9	3.6	24.4	16	0.67	0.50	s1d2	2.48	0.0000569	0.0000693	0.0000821	0.3750
9150642M	7/8C	15E8_6s1d2Vc_1	14 7/16	E	3.25	354.8	36	30	0.191	0.202	8TA	8	4	4	1.05	4.9	3.6	24.4	16	0.67	0.50	s1d2	2.48	0.0000569	0.0000693	0.0000821	0.3750
9150642.1	7/8C	15E8_6s1d2Vc_1	14 7/16	E	3.25	354.8	36	30	0.191	0.202	8TA	8	4	4	1.05	4.9	3.6	24.4	16	0.67	0.50	s1d2	2.48	0.0000569	0.0000693	0.0000821	0.3750
9150642.2	7/8C	15E8_6s1d2Vc_1	14 7/16	E	3.25	354.8	36	30	0.191	0.202	8TA	8	4	4	1.05	4.9	3.6	24.4	16	0.67	0.50	s1d2	2.48	0.0000569	0.0000693	0.0000821	0.3750
9150643M	7/8C	15E8_6s1d2Vc_1	14 7/16	E	3.25	354.8	36	30	0.191	0.202	8TA	8	4	4	1.05	4.9	3.6	24.4	16	0.67	0.50	s1d2	2.48	0.0000569	0.0000693	0.0000821	0.3750
9150644	7/8C	15E8_6s1d2Vc_1	14 7/16	E	3.25	354.8	36	30	0.191	0.202	8TA	8	4	4	1.05	4.9	3.6	24.4	16	0.67	0.50	s1d2	2.48	0.0000569	0.0000693	0.0000821	0.3750
9150645	7/8C	15E8_6s1d2Vc_1	14 7/16	E	3.25	354.8	36	30	0.191	0.202	8TA	8	4	4	1.05	4.9	3.6	24.4	16	0.67	0.50	s1d2	2.48	0.0000569	0.0000693	0.0000821	0.3750
9150646	7/8C	15E8_6s1d2Vc_1	14 7/16	E	3.25	354.8	36	30	0.191	0.202	8TA	8	4	4	1.05	4.9	3.6	24.4	16	0.67	0.50	s1d2	2.48	0.0000569	0.0000693	0.0000821	0.3750
9150646.1	7/8C	15E8_6s1d2Vc_1	14 7/16	E	3.25	354.8	36	30	0.191	0.202	8TA	8	4	4	1.05	4.9	3.6	24.4	16	0.67	0.50	s1d2	2.48	0.0000569	0.0000693	0.0000821	0.3750
9150647	7/8C	15E8_6s1d2Vc_1	14 7/16	E	3.25	354.8	36	30	0.191	0.202	8TA	8	4	4	1.05	4.9	3.6	24.4	16	0.67	0.50	s1d2	2.48	0.0000569	0.0000693	0.0000821	0.3750
9150647.1	7/8C	15E8_6s1d2Vc_1	14 7/16	E	3.25	354.8	36	30	0.191	0.202	8TA	8	4	4	1.05	4.9	3.6	24.4	16	0.67	0.50	s1d2	2.48	0.0000569	0.0000693	0.0000821	0.3750
9150648	7/8C	15E8_6s1d2Vc_1	14 7/16	E	3.25	354.8	36	30	0.191	0.202	8TA	8	4	4	1.05	4.9	3.6	24.4	16	0.67	0.50	s1d2	2.48	0.0000569	0.0000693	0.0000821	0.3750
9150648.1	7/8C	15E8_6s1d2Vc_1	14 7/16	E	3.25	354.8	36	30	0.191	0.202	8TA	8	4	4	1.05	4.9	3.6	24.4	16	0.67	0.50	s1d2	2.48	0.0000569	0.0000693	0.0000821	0.3750
9150649	7/8C	15E8_6s1d2Vc_1	14 7/16	E	3.25	354.8	36	30	0.191	0.202	8TA	8	4	4	1.05	4.9	3.6	24.4	16	0.67	0.50	s1d2	2.48	0.0000569	0.0000693	0.0000821	0.3750
9150649.1	7/8C	15E8_6s1d2Vc_1	14 7/16	E	3.25	354.8	36	30	0.191	0.202	8TA	8	4	4	1.05	4.9	3.6	24.4	16	0.67	0.50	s1d2	2.48	0.0000569	0.0000693	0.0000821	0.3750
9150650	7/8C	15E8_6s1d2Vc_1	14 7/16	E	3.25	354.8	36	30	0.191	0.202	8TA	8	4	4	1.05	4.9	3.6	24.4	16	0.67	0.50	s1d2	2.48	0.0000569	0.0000693	0.0000821	0.3750
9150651	7/9A	15E8_6s1d2Vc_2	14 7/16	E	3.25	354.8	36	30	0.191	0.287	8TA	8	4	4	1.05	4.9	3.6	24.4	16	0.67	0.50	s1d2	2.48	0.0000569	0.0000693	0.0000821	0.3750
9150652	7/9A	15E8_6s1d2Vc_2	14 7/16	E	3.25	354.8	36	30	0.191	0.287	8TA	8	4	4	1.05	4.9	3.6	24.4	16	0.67	0.50	s1d2	2.48	0.0000569	0.0000693	0.0000821	0.3750
9150653M	7/9A	15E8_6s1d2Vc_2	14 7/16	E	3.25	354.8	36	30	0.191	0.287	8TA	8	4	4	1.05	4.9	3.6	24.4	16	0.67	0.50	s1d2	2.48	0.0000569	0.0000693	0.0000821	0.3750
9150654M	7/9A	15E8_6s1d2Vc_2	14 7/16	E	3.25	354.8	36	30	0.191	0.287	8TA	8	4	4	1.05	4.9	3.6	24.4	16	0.67	0.50	s1d2	2.48	0.0000569	0.0000693	0.0000821	0.3750
9150655M	7/9A	15E8_6s1d2Vc_2	14 7/16	E	3.25	354.8	36	30	0.191	0.287	8TA	8	4	4	1.05	4.9	3.6	24.4	16	0.67	0.50	s1d2	2.48	0.0000569	0.0000693	0.0000821	0.3750
9150656M	7/9A	15E8_6s1d2Vc_2	14 7/16	E	3.25	354.8	36	30	0.191	0.287	8TA	8	4	4	1.05	4.9	3.6	24.4	16	0.67	0.50	s1d2	2.48	0.0000569	0.0000693	0.0000821	0.3750
9150657M	7/9A	15E8_6s1d2Vc_2	14 7/16	E	3.25	354.8	36	30	0.191	0.287	8TA	8	4	4	1.05	4.9	3.6	24.4	16	0.67	0.50	s1d2	2.48	0.0000569	0.0000693	0.0000821	0.3750
9150658	7/9B	15E8_6s1d2Xc_1	14 7/16	E	3.25	354.8	36	30	0.191	0.287	8TA	8	4	4	1.05	4.9	3.6	24.4	16	0.67	0.50	s1d2	2.48	0.0000569	0.0000693	0.0000821	0.3750
9150659	7/9B	15E8_6s1d2Xc_1	14 7/16	E	3.25	354.8	36	30	0.191	0.287	8TA	8	4	4	1.05	4.9	3.6	24.4	16	0.67	0.50	s1d2	2.48	0.0000569	0.0000693	0.0000821	0.3750
9150660M	7/9B	15E8_6s1d2Xc_1	14 7/16	E	3.25	354.8	36	30	0.191	0.287	8TA	8	4	4	1.05	4.9	3.6	24.4	16	0.67	0.50	s1d2	2.48	0.0000569	0.0000693	0.0000821	0.3750
9150661M	7/9B	15E8_6s1d2Xc_1	14 7/16	E	3.25	354.8	36	30	0.191	0.287	8TA	8	4	4	1.05	4.9	3.6	24.4	16	0.67	0.50	s1d2	2.48	0.0000569	0.0000693	0.0000821	0.3750
9150662M	7/9B	15E8_6s1d2Xc_1	14 7/16	E	3.25	354.8	36	30	0.191	0.287	8TA	8	4	4	1.05	4.9	3.6	24.4	16	0.67	0.50	s1d2	2.48	0.0000569	0.0000693	0.0000821	0.3750
9150663M	7/9B	15E8_6s1d2Xc_1	14 7/16	E	3.25	354.8	36	30	0.191	0.287	8TA	8	4	4	1.05	4.9	3.6	24.4	16	0.67	0.50	s1d2	2.48	0.0000569	0.0000693	0.0000821	0.3750
9150664M	7/9B	15E8_6s1d2Xc_1	14 7/16	E	3.25	354.8	36	30	0.191	0.287	8TA	8	4	4	1.05	4.9	3.6	24.4	16	0.67	0.50	s1d2	2.48	0.0000569	0.0000693	0.0000821	0.3750
9150665M	7/9B	15E8_6s1d2Xc_1	14 7/16	E	3.25	354.8	36	30	0.191	0.287	8TA	8	4	4	1.05	4.9	3.6	24.4	16	0.67	0.50	s1d2	2.48	0.0000569	0.0000693	0.0000821	0.3750
9150665.1	7/9B	15E8_6s1d2Xc_1	14 7/16	E	3.25	354.8	36	30	0.191	0.287	8TA	8	4	4	1.05	4.9	3.6	24.4	16	0.67	0.50	s1d2	2.48	0.0000569	0.0000693	0.0000821	0.3750
9150665.2	7/9B	15E8_6s1d2Xc_1	14 7/16	E	3.25	354.8	36	30	0.191	0.287	8TA	8	4	4	1.05	4.9	3.6	24.4	16	0.67	0.50	s1d2	2.48	0.0000569	0.0000693	0.0000821	0.3750
9150665.3	7/9B	15E8_6s1d2Xc_1	14 7/16	E	3.25	354.8	36	30	0.191	0.287	8TA	8	4	4	1.05	4.9	3.6	24.4	16	0.67	0.50	s1d2	2.48	0.0000569	0.0000693	0.0000821	0.3750

Table B.3. Data from 2008 Tests in Small-Scale Vessel with Elliptical Head B.18

Tank Water Temperature	Water Density	Solids Fraction	Pulse Volume Fraction	Duty Cycle	Cycle Time	Pulsed or Steady Jet	Us Steady Jet	U1 Pulsing Jet	U2 URMS	U3 URM3	Discharge Velocity	Critical Suspension Velocity	Average Peak Cloud Height	UCS Condition	UCS Method	UCS Flag	UCS Center Flag	UCS udv Flag	UCS based on Decreasing Velocity	Sweep Increase / Decrease	UDV Height Bed	Particle Motion	Solids Level	Outer Bottom Pattern	Inner Bottom Pattern	Case ID	Test	TDP	Row Number
C	g/cm³	fraction	fraction	fraction	s	text	m/s	m/s	m/s	m/s	m/s	m/s	in.	m/s	text	text	text	text	m/s	text	mm	text	text	text	text	text	text	text	text
T	ρ_c	ϕ_S	ϕ_p	DC	t_C	Jet	U_S	U1	U2	U3	U	U_{CS}	H_C	U_{CSR}	U_{CSM}	U_{CS}vis	U_{CS}cen	U_{CS}udv	U_{CS}_D	S_W	H_{bed}	PM	Sol	SP_O	SP_I	ID	M/DDX	TDP	MSS
27.2	0.999	0.00155	0.100	0.332	25.6	P	N/A	3.13	3.15	3.16	3.20	2.80	27.00	N/A	N/A	N/A	N/A	N/A	N/A	I	2.2	4	N/A	N/A	N/A	15E8_6s1d2Zc_2	7/8B	TDP-205	9150634
28.1	0.999	0.01430	0.050	0.337	10.4	P	N/A	3.78	3.85	3.88	4.00	4.80	6.00	N/A	N/A	N/A	N/A	N/A	N/A	(null)	15.6	1	N/A	N/A	N/A	15E8_6s1d2Vc_1	7/8C	TDP-206	9150635
28.4	0.999	0.01430	0.050	0.329	9.8	P	N/A	4.14	4.22	4.26	4.40	4.80	8.25	N/A	N/A	N/A	N/A	N/A	N/A	I	3.8	1	N/A	N/A	N/A	15E8_6s1d2Vc_1	7/8C	TDP-206	9150636
28.6	0.998	0.01430	0.050	0.332	9.2	P	N/A	4.31	4.40	4.45	4.60	4.80	8.75	N/A	N/A	N/A	N/A	N/A	N/A	I	3.6	1	N/A	N/A	N/A	15E8_6s1d2Vc_1	7/8C	TDP-206	9150637
28.7	0.998	0.01430	0.050	0.334	8.8	P	N/A	4.49	4.59	4.63	4.80	4.80	9.75	4.80	udv	N/A	N/A	UCSudv	N/A	I	0.8	1	N/A	N/A	N/A	15E8_6s1d2Vc_1	7/8C	TDP-206	9150638
29.0	0.999	0.01430	0.050	0.332	8.6	P	N/A	4.67	4.78	4.83	5.00	4.80	11.00	N/A	N/A	UCSvis	N/A	N/A	N/A	I	0.0	3	N/A	N/A	N/A	15E8_6s1d2Vc_1	7/8C	TDP-206	9150639
29.2	0.998	0.01430	0.050	0.331	8.3	P	N/A	4.85	4.96	5.01	5.20	4.80	13.00	N/A	N/A	N/A	N/A	N/A	N/A	I	0.0	4	N/A	N/A	N/A	15E8_6s1d2Vc_1	7/8C	TDP-206	9150640
29.4	0.998	0.01430	0.050	0.328	7.8	P	N/A	5.21	5.33	5.39	5.60	4.80	15.25	N/A	N/A	N/A	N/A	N/A	N/A	I	0.0	4	N/A	N/A	N/A	15E8_6s1d2Vc_1	7/8C	TDP-206	9150641
29.7	0.998	0.01430	0.050	0.332	7.2	P	N/A	5.54	5.70	5.77	6.00	4.80	18.50	N/A	N/A	N/A	N/A	N/A	N/A	I	0.0	4	N/A	N/A	N/A	15E8_6s1d2Vc_1	7/8C	TDP-206	9150642
30.0	0.998	0.01430	0.050	0.333	8.8	P	N/A	4.49	4.59	4.64	4.80	4.80	9.50	N/A	N/A	N/A	N/A	N/A	N/A	N/A	n/a	N/A	N/A	N/A	N/A	15E8_6s1d2Vc_1	7/8C	TDP-206	9150642.1
30.0	0.998	0.01430	0.050	0.333	8.8	P	N/A	4.49	4.59	4.64	4.80	4.80	9.50	N/A	N/A	N/A	N/A	N/A	N/A	N/A	n/a	N/A	N/A	N/A	N/A	15E8_6s1d2Vc_1	7/8C	TDP-206	9150642.2
30.0	0.998	0.01430	0.050	0.333	8.8	P	N/A	4.49	4.59	4.64	4.80	4.80	9.50	N/A	N/A	N/A	N/A	N/A	N/A	I	0.0	1	N/A	N/A	N/A	15E8_6s1d2Vc_1	7/8C	TDP-206	9150643
30.0	0.998	0.01430	0.050	0.333	8.8	P	N/A	4.49	4.59	4.64	4.80	4.80	9.50	N/A	N/A	N/A	N/A	N/A	N/A	N/A	0.0	N/A	N/A	N/A	N/A	15E8_6s1d2Vc_1	7/8C	TDP-206	9150644
30.0	0.998	0.01430	0.050	0.333	8.8	P	N/A	4.49	4.59	4.64	4.80	4.80	9.50	N/A	N/A	N/A	N/A	N/A	N/A	N/A	0.7	N/A	N/A	N/A	N/A	15E8_6s1d2Vc_1	7/8C	TDP-206	9150645
30.0	0.998	0.01430	0.050	0.333	8.8	P	N/A	4.49	4.59	4.64	4.80	4.80	9.50	N/A	N/A	N/A	N/A	N/A	N/A	N/A	0.7	N/A	N/A	N/A	N/A	15E8_6s1d2Vc_1	7/8C	TDP-206	9150646
30.0	0.998	0.01430	0.050	0.333	8.8	P	N/A	4.49	4.59	4.64	4.80	4.80	9.50	N/A	N/A	N/A	N/A	N/A	N/A	N/A	n/a	N/A	N/A	N/A	N/A	15E8_6s1d2Vc_1	7/8C	TDP-206	9150646.1
30.0	0.998	0.01430	0.050	0.333	8.8	P	N/A	4.49	4.59	4.64	4.80	4.80	9.50	N/A	N/A	N/A	N/A	N/A	N/A	N/A	1.6	N/A	N/A	N/A	N/A	15E8_6s1d2Vc_1	7/8C	TDP-206	9150647
30.0	0.998	0.01430	0.050	0.333	8.8	P	N/A	4.49	4.59	4.64	4.80	4.80	9.50	N/A	N/A	N/A	N/A	N/A	N/A	N/A	n/a	N/A	N/A	N/A	N/A	15E8_6s1d2Vc_1	7/8C	TDP-206	9150647.1
30.0	0.998	0.01430	0.050	0.333	8.8	P	N/A	4.49	4.59	4.64	4.80	4.80	9.50	N/A	N/A	N/A	N/A	N/A	N/A	N/A	0.7	N/A	N/A	N/A	N/A	15E8_6s1d2Vc_1	7/8C	TDP-206	9150648
30.0	0.998	0.01430	0.050	0.333	8.8	P	N/A	4.49	4.59	4.64	4.80	4.80	9.50	N/A	N/A	N/A	N/A	N/A	N/A	N/A	n/a	N/A	N/A	N/A	N/A	15E8_6s1d2Vc_1	7/8C	TDP-206	9150648.1
30.0	0.998	0.01430	0.050	0.333	8.8	P	N/A	4.49	4.59	4.64	4.80	4.80	9.50	N/A	N/A	N/A	N/A	N/A	N/A	N/A	2.0	N/A	N/A	N/A	N/A	15E8_6s1d2Vc_1	7/8C	TDP-206	9150649
30.0	0.998	0.01430	0.050	0.333	8.8	P	N/A	4.49	4.59	4.64	4.80	4.80	9.50	N/A	N/A	N/A	N/A	N/A	N/A	N/A	n/a	N/A	N/A	N/A	N/A	15E8_6s1d2Vc_1	7/8C	TDP-206	9150649.1
30.0	0.998	0.01430	0.050	0.333	8.8	P	N/A	4.49	4.59	4.64	4.80	4.80	9.50	N/A	N/A	N/A	N/A	N/A	N/A	N/A	3.0	N/A	N/A	N/A	N/A	15E8_6s1d2Vc_1	7/8C	TDP-206	9150650
27.2	0.999	0.01430	0.099	0.328	20.7	P	N/A	3.89	3.92	3.94	4.00	4.40	7.50	N/A	N/A	N/A	N/A	N/A	N/A	D	7.5	1	N/A	N/A	N/A	15E8_6s1d2Vc_2	7/9A	TDP-207	9150651
27.3	0.999	0.01430	0.099	0.329	19.7	P	N/A	4.07	4.11	4.13	4.20	4.40	8.50	N/A	N/A	N/A	N/A	N/A	N/A	I	1.5	1	N/A	N/A	N/A	15E8_6s1d2Vc_2	7/9A	TDP-207	9150652
27.4	0.999	0.01430	0.100	0.331	18.8	P	N/A	4.26	4.31	4.33	4.40	4.40	10.00	4.40	udv	N/A	N/A	UCSudv	N/A	I	0.8	1	N/A	N/A	N/A	15E8_6s1d2Vc_2	7/9A	TDP-207	9150653
27.6	0.999	0.01430	0.100	0.332	18.0	P	N/A	4.45	4.50	4.52	4.60	4.40	11.00	N/A	N/A	UCSvis	N/A	N/A	N/A	I	0.0	3	N/A	N/A	N/A	15E8_6s1d2Vc_2	7/9A	TDP-207	9150654
27.7	0.999	0.01430	0.100	0.331	17.3	P	N/A	4.64	4.69	4.72	4.80	4.40	12.00	N/A	N/A	N/A	N/A	N/A	N/A	I	0.0	4	N/A	N/A	N/A	15E8_6s1d2Vc_2	7/9A	TDP-207	9150655
27.8	0.999	0.01430	0.100	0.333	16.0	P	N/A	5.01	5.07	5.10	5.20	4.40	14.75	N/A	N/A	N/A	N/A	N/A	N/A	I	0.0	4	N/A	N/A	N/A	15E8_6s1d2Vc_2	7/9A	TDP-207	9150656
28.2	0.998	0.01430	0.100	0.331	14.9	P	N/A	5.39	5.47	5.50	5.60	4.40	20.00	N/A	N/A	N/A	N/A	N/A	N/A	I	0.0	4	N/A	N/A	N/A	15E8_6s1d2Vc_2	7/9A	TDP-207	9150657
28.4	0.999	0.01500	0.050	0.328	10.7	P	N/A	3.78	3.85	3.88	4.00	4.60	5.75	N/A	N/A	N/A	N/A	N/A	N/A	(null)	16.2	1	N/A	N/A	N/A	15E8_6s1d2Xc_1	7/9B	TDP-208	9150658
28.7	0.998	0.01500	0.050	0.333	9.7	P	N/A	4.13	4.22	4.26	4.40	4.60	7.75	N/A	N/A	N/A	N/A	N/A	N/A	I	10.3	1	N/A	N/A	N/A	15E8_6s1d2Xc_1	7/9B	TDP-208	9150659
28.8	0.998	0.01500	0.050	0.333	9.3	P	N/A	4.32	4.41	4.45	4.60	4.60	8.25	4.60	udv	N/A	N/A	UCSudv	N/A	I	0.5	1	N/A	N/A	N/A	15E8_6s1d2Xc_1	7/9B	TDP-208	9150660
28.9	0.999	0.01500	0.050	0.333	8.9	P	N/A	4.49	4.59	4.64	4.80	4.60	9.50	N/A	N/A	N/A	N/A	N/A	N/A	I	0.0	1	N/A	N/A	N/A	15E8_6s1d2Xc_1	7/9B	TDP-208	9150661
29.0	0.998	0.01500	0.050	0.335	8.5	P	N/A	4.68	4.78	4.83	5.00	4.60	10.25	N/A	N/A	UCSvis	N/A	N/A	N/A	I	0.0	3	N/A	N/A	N/A	15E8_6s1d2Xc_1	7/9B	TDP-208	9150662
29.1	0.998	0.01500	0.050	0.335	8.2	P	N/A	4.85	4.96	5.01	5.20	4.60	11.75	N/A	N/A	N/A	N/A	N/A	N/A	I	0.0	4	N/A	N/A	N/A	15E8_6s1d2Xc_1	7/9B	TDP-208	9150663
29.3	0.998	0.01500	0.050	0.337	7.6	P	N/A	5.18	5.32	5.38	5.60	4.60	15.50	N/A	N/A	N/A	N/A	N/A	N/A	I	0.0	4	N/A	N/A	N/A	15E8_6s1d2Xc_1	7/9B	TDP-208	9150664
29.4	0.998	0.01500	0.050	0.336	7.1	P	N/A	5.56	5.70	5.77	6.00	4.60	19.50	N/A	N/A	N/A	N/A	N/A	N/A	I	0.0	4	N/A	N/A	N/A	15E8_6s1d2Xc_1	7/9B	TDP-208	9150665
29.8	0.998	0.01500	0.050	0.333	9.3	P	N/A	4.32	4.41	4.46	4.60	4.60	8.50	N/A	N/A	N/A	N/A	N/A	N/A	N/A	n/a	N/A	N/A	N/A	N/A	15E8_6s1d2Xc_1	7/9B	TDP-208	9150665.1
29.8	0.998	0.01500	0.050	0.333	9.3	P	N/A	4.32	4.41	4.46	4.60	4.60	8.50	N/A	N/A	N/A	N/A	N/A	N/A	N/A	n/a	N/A	N/A	N/A	N/A	15E8_6s1d2Xc_1	7/9B	TDP-208	9150665.2
29.8	0.998	0.01500	0.050	0.333	9.3	P	N/A	4.32	4.41	4.46	4.60	4.60	8.50	N/A	N/A	N/A	N/A	N/A	N/A	N/A	n/a	N/A	N/A	N/A	N/A	15E8_6s1d2Xc_1	7/9B	TDP-208	9150665.3

Table B.3. Data from 2008 Tests in Small-Scale Vessel with Elliptical Head A.19

Row Number	Test	Case ID	Tank Diameter	Head Shape	Dish Height	Dish Volume	Tank Fill Height	Return Line Height	Nozzle Inner Diameter	Nozzle Stand-off Distance	Pulse Tube Configuration	Installed Nozzles	Outer Nozzles Operated	Inner Nozzles Operated	Pulse Tube Outer Diameter	Outer PJM Radius	Inner PJM Radius	"FIO" Outer PJM Impingement Angle	"FIO" Inner PJM Impingement Angle	Ratio Outer PJM to Tank Radius	Ratio Inner PJM to Tank Radius	Simulant	Solids Density	Particle Diameter d5	Particle Diameter d50	Particle Diameter d95	Void Fraction
text	text	text	in.	text	in.	in. ^{3}	in.	in.	in.	in.	text	number	number	number	in.	in.	in.	deg	deg	nondim	nondim	text	g/cm^3	m	m	m	fraction
MSS	M/DDX	ID	D	HS	H_{dish}	V_{dish}	H	Rtn	d	sod	PT	N	N_O	N_I	PT_{od}	R_O	R_I	θ_O	θ_I	R_O/R	R_I/R	sxdx	ρ_s	d_5	d_{50}	d_{95}	vf
9150665.4	7/9B	15E8_6s1d2Xc_1	14 7/16	E	3.25	354.8	36	30	0.191	0.287	8TA	8	4	4	1.05	4.9	3.6	24.4	16	0.67	0.50	s1d2	2.48	0.0000569	0.0000693	0.0000821	0.3750
9150666M	7/9B	15E8_6s1d2Xc_1	14 7/16	E	3.25	354.8	36	30	0.191	0.287	8TA	8	4	4	1.05	4.9	3.6	24.4	16	0.67	0.50	s1d2	2.48	0.0000569	0.0000693	0.0000821	0.3750
9150667	7/9B	15E8_6s1d2Xc_1	14 7/16	E	3.25	354.8	36	30	0.191	0.287	8TA	8	4	4	1.05	4.9	3.6	24.4	16	0.67	0.50	s1d2	2.48	0.0000569	0.0000693	0.0000821	0.3750
9150668	7/9B	15E8_6s1d2Xc_1	14 7/16	E	3.25	354.8	36	30	0.191	0.287	8TA	8	4	4	1.05	4.9	3.6	24.4	16	0.67	0.50	s1d2	2.48	0.0000569	0.0000693	0.0000821	0.3750
9150668.1	7/9B	15E8_6s1d2Xc_1	14 7/16	E	3.25	354.8	36	30	0.191	0.287	8TA	8	4	4	1.05	4.9	3.6	24.4	16	0.67	0.50	s1d2	2.48	0.0000569	0.0000693	0.0000821	0.3750
9150669	7/9B	15E8_6s1d2Xc_1	14 7/16	E	3.25	354.8	36	30	0.191	0.287	8TA	8	4	4	1.05	4.9	3.6	24.4	16	0.67	0.50	s1d2	2.48	0.0000569	0.0000693	0.0000821	0.3750
9150669.1	7/9B	15E8_6s1d2Xc_1	14 7/16	E	3.25	354.8	36	30	0.191	0.287	8TA	8	4	4	1.05	4.9	3.6	24.4	16	0.67	0.50	s1d2	2.48	0.0000569	0.0000693	0.0000821	0.3750
9150670	7/9B	15E8_6s1d2Xc_1	14 7/16	E	3.25	354.8	36	30	0.191	0.287	8TA	8	4	4	1.05	4.9	3.6	24.4	16	0.67	0.50	s1d2	2.48	0.0000569	0.0000693	0.0000821	0.3750
9150670.1	7/9B	15E8_6s1d2Xc_1	14 7/16	E	3.25	354.8	36	30	0.191	0.287	8TA	8	4	4	1.05	4.9	3.6	24.4	16	0.67	0.50	s1d2	2.48	0.0000569	0.0000693	0.0000821	0.3750
9150671	7/9B	15E8_6s1d2Xc_1	14 7/16	E	3.25	354.8	36	30	0.191	0.287	8TA	8	4	4	1.05	4.9	3.6	24.4	16	0.67	0.50	s1d2	2.48	0.0000569	0.0000693	0.0000821	0.3750
9150671.1	7/9B	15E8_6s1d2Xc_1	14 7/16	E	3.25	354.8	36	30	0.191	0.287	8TA	8	4	4	1.05	4.9	3.6	24.4	16	0.67	0.50	s1d2	2.48	0.0000569	0.0000693	0.0000821	0.3750
9150672	7/9B	15E8_6s1d2Xc_1	14 7/16	E	3.25	354.8	36	30	0.191	0.287	8TA	8	4	4	1.05	4.9	3.6	24.4	16	0.67	0.50	s1d2	2.48	0.0000569	0.0000693	0.0000821	0.3750
9150673	7/9C	15E8_6s1d2Xc_2	14 7/16	E	3.25	354.8	36	30	0.191	0.287	8TA	8	4	4	1.05	4.9	3.6	24.4	16	0.67	0.50	s1d2	2.48	0.0000569	0.0000693	0.0000821	0.3750
9150674	7/9C	15E8_6s1d2Xc_2	14 7/16	E	3.25	354.8	36	30	0.191	0.287	8TA	8	4	4	1.05	4.9	3.6	24.4	16	0.67	0.50	s1d2	2.48	0.0000569	0.0000693	0.0000821	0.3750
9150675M	7/9C	15E8_6s1d2Xc_2	14 7/16	E	3.25	354.8	36	30	0.191	0.287	8TA	8	4	4	1.05	4.9	3.6	24.4	16	0.67	0.50	s1d2	2.48	0.0000569	0.0000693	0.0000821	0.3750
9150676M	7/9C	15E8_6s1d2Xc_2	14 7/16	E	3.25	354.8	36	30	0.191	0.287	8TA	8	4	4	1.05	4.9	3.6	24.4	16	0.67	0.50	s1d2	2.48	0.0000569	0.0000693	0.0000821	0.3750
9150677M	7/9C	15E8_6s1d2Xc_2	14 7/16	E	3.25	354.8	36	30	0.191	0.287	8TA	8	4	4	1.05	4.9	3.6	24.4	16	0.67	0.50	s1d2	2.48	0.0000569	0.0000693	0.0000821	0.3750
9150678M	7/9C	15E8_6s1d2Xc_2	14 7/16	E	3.25	354.8	36	30	0.191	0.287	8TA	8	4	4	1.05	4.9	3.6	24.4	16	0.67	0.50	s1d2	2.48	0.0000569	0.0000693	0.0000821	0.3750
9150679M	7/9C	15E8_6s1d2Xc_2	14 7/16	E	3.25	354.8	36	30	0.191	0.287	8TA	8	4	4	1.05	4.9	3.6	24.4	16	0.67	0.50	s1d2	2.48	0.0000569	0.0000693	0.0000821	0.3750
9150680M	7/9C	15E8_6s1d2Xc_2	14 7/16	E	3.25	354.8	36	30	0.191	0.287	8TA	8	4	4	1.05	4.9	3.6	24.4	16	0.67	0.50	s1d2	2.48	0.0000569	0.0000693	0.0000821	0.3750
9150681M	7/9C	15E8_6s1d2Xc_2	14 7/16	E	3.25	354.8	36	30	0.191	0.287	8TA	8	4	4	1.05	4.9	3.6	24.4	16	0.67	0.50	s1d2	2.48	0.0000569	0.0000693	0.0000821	0.3750
9150681.1	7/9C	15E8_6s1d2Xc_2	14 7/16	E	3.25	354.8	36	30	0.191	0.287	8TA	8	4	4	1.05	4.9	3.6	24.4	16	0.67	0.50	s1d2	2.48	0.0000569	0.0000693	0.0000821	0.3750
9150681.2	7/9C	15E8_6s1d2Xc_2	14 7/16	E	3.25	354.8	36	30	0.191	0.287	8TA	8	4	4	1.05	4.9	3.6	24.4	16	0.67	0.50	s1d2	2.48	0.0000569	0.0000693	0.0000821	0.3750
9150681.3	7/9C	15E8_6s1d2Xc_2	14 7/16	E	3.25	354.8	36	30	0.191	0.287	8TA	8	4	4	1.05	4.9	3.6	24.4	16	0.67	0.50	s1d2	2.48	0.0000569	0.0000693	0.0000821	0.3750
9150682M	7/9C	15E8_6s1d2Xc_2	14 7/16	E	3.25	354.8	36	30	0.191	0.287	8TA	8	4	4	1.05	4.9	3.6	24.4	16	0.67	0.50	s1d2	2.48	0.0000569	0.0000693	0.0000821	0.3750
9150683	7/9C	15E8_6s1d2Xc_2	14 7/16	E	3.25	354.8	36	30	0.191	0.287	8TA	8	4	4	1.05	4.9	3.6	24.4	16	0.67	0.50	s1d2	2.48	0.0000569	0.0000693	0.0000821	0.3750
9150684	7/9C	15E8_6s1d2Xc_2	14 7/16	E	3.25	354.8	36	30	0.191	0.287	8TA	8	4	4	1.05	4.9	3.6	24.4	16	0.67	0.50	s1d2	2.48	0.0000569	0.0000693	0.0000821	0.3750
9150684.1	7/9C	15E8_6s1d2Xc_2	14 7/16	E	3.25	354.8	36	30	0.191	0.287	8TA	8	4	4	1.05	4.9	3.6	24.4	16	0.67	0.50	s1d2	2.48	0.0000569	0.0000693	0.0000821	0.3750
9150685	7/9C	15E8_6s1d2Xc_2	14 7/16	E	3.25	354.8	36	30	0.191	0.287	8TA	8	4	4	1.05	4.9	3.6	24.4	16	0.67	0.50	s1d2	2.48	0.0000569	0.0000693	0.0000821	0.3750
9150685.1	7/9C	15E8_6s1d2Xc_2	14 7/16	E	3.25	354.8	36	30	0.191	0.287	8TA	8	4	4	1.05	4.9	3.6	24.4	16	0.67	0.50	s1d2	2.48	0.0000569	0.0000693	0.0000821	0.3750
9150686	7/9C	15E8_6s1d2Xc_2	14 7/16	E	3.25	354.8	36	30	0.191	0.287	8TA	8	4	4	1.05	4.9	3.6	24.4	16	0.67	0.50	s1d2	2.48	0.0000569	0.0000693	0.0000821	0.3750
9150686.1	7/9C	15E8_6s1d2Xc_2	14 7/16	E	3.25	354.8	36	30	0.191	0.287	8TA	8	4	4	1.05	4.9	3.6	24.4	16	0.67	0.50	s1d2	2.48	0.0000569	0.0000693	0.0000821	0.3750
9150687	7/9C	15E8_6s1d2Xc_2	14 7/16	E	3.25	354.8	36	30	0.191	0.287	8TA	8	4	4	1.05	4.9	3.6	24.4	16	0.67	0.50	s1d2	2.48	0.0000569	0.0000693	0.0000821	0.3750
9150687.1	7/9C	15E8_6s1d2Xc_2	14 7/16	E	3.25	354.8	36	30	0.191	0.287	8TA	8	4	4	1.05	4.9	3.6	24.4	16	0.67	0.50	s1d2	2.48	0.0000569	0.0000693	0.0000821	0.3750
9150688	7/9C	15E8_6s1d2Xc_2	14 7/16	E	3.25	354.8	36	30	0.191	0.287	8TA	8	4	4	1.05	4.9	3.6	24.4	16	0.67	0.50	s1d2	2.48	0.0000569	0.0000693	0.0000821	0.3750
9150689	7/10A	15E8_Ms1d2Zc_1	14 7/16	E	3.25	354.8	35 1/2	30	0.268	0.402	8TA	8	4	4	1.05	4.9	3.6	24.4	16	0.67	0.50	s1d2	2.48	0.0000569	0.0000693	0.0000821	0.3750
9150690	7/10A	15E8_Ms1d2Zc_1	14 7/16	E	3.25	354.8	35 1/2	30	0.268	0.402	8TA	8	4	4	1.05	4.9	3.6	24.4	16	0.67	0.50	s1d2	2.48	0.0000569	0.0000693	0.0000821	0.3750
9150691M	7/10A	15E8_Ms1d2Zc_1	14 7/16	E	3.25	354.8	35 1/2	30	0.268	0.402	8TA	8	4	4	1.05	4.9	3.6	24.4	16	0.67	0.50	s1d2	2.48	0.0000569	0.0000693	0.0000821	0.3750
9150692M	7/10A	15E8_Ms1d2Zc_1	14 7/16	E	3.25	354.8	35 1/2	30	0.268	0.402	8TA	8	4	4	1.05	4.9	3.6	24.4	16	0.67	0.50	s1d2	2.48	0.0000569	0.0000693	0.0000821	0.3750
9150693M	7/10A	15E8_Ms1d2Zc_1	14 7/16	E	3.25	354.8	35 1/2	30	0.268	0.402	8TA	8	4	4	1.05	4.9	3.6	24.4	16	0.67	0.50	s1d2	2.48	0.0000569	0.0000693	0.0000821	0.3750
9150694M	7/10A	15E8_Ms1d2Zc_1	14 7/16	E	3.25	354.8	35 1/2	30	0.268	0.402	8TA	8	4	4	1.05	4.9	3.6	24.4	16	0.67	0.50	s1d2	2.48	0.0000569	0.0000693	0.0000821	0.3750

Table B.3. Data from 2008 Tests in Small-Scale Vessel with Elliptical Head B.19

Tank Water Temperature	Water Density	Solids Fraction	Pulse Volume Fraction	Duty Cycle	Cycle Time	Pulsed or Steady Jet	Us Steady Jet	U1 Pulsing Jet	U2 URMS	U3 URM3	Discharge Velocity	Critical Suspension Velocity	Average Peak Cloud Height	UCS Condition	UCS Method	UCS Flag	UCS Center Flag	UCS udv Flag	UCS based on Decreasing Velocity	Sweep Increase / Decrease	UDV Height Bed	Particle Motion	Solids Level	Outer Bottom Pattern	Inner Bottom Pattern	Case ID	Test	TDP	Row Number
C	g/cm³	fraction	fraction	fraction	s	text	m/s	m/s	m/s	m/s	m/s	m/s	in.	m/s	text	text	text	text	m/s	text	mm	text	text	text	text	text	text	text	text
T	ρ_c	ϕ_S	ϕ_p	DC	t_C	Jet	U_S	U1	U2	U3	U	U_{CS}	H_C	U_{CSR}	U_{CSM}	U_{CS}vis	U_{CS}cen	U_{CS}udv	U_{CS_D}	S_W	H_{bed}	PM	Sol	SP_O	SP_I	ID	M/DDX	TDP	MSS
29.8	0.998	0.01500	0.050	0.333	9.3	P	N/A	4.32	4.41	4.46	4.60	4.60	8.50	N/A	N/A	N/A	N/A	N/A	N/A	N/A	n/a	N/A	N/A	N/A	N/A	15E8_6s1d2Xc_1	7/9B	TDP-208	9150665.4
29.8	0.998	0.01500	0.050	0.333	9.3	P	N/A	4.32	4.41	4.46	4.60	4.60	8.50	N/A	N/A	N/A	N/A	N/A	N/A	I	3.3	1	N/A	N/A	N/A	15E8_6s1d2Xc_1	7/9B	TDP-208	9150666
29.8	0.998	0.01500	0.050	0.333	9.3	P	N/A	4.32	4.41	4.46	4.60	4.60	8.50	N/A	N/A	N/A	N/A	N/A	N/A	N/A	3.3	N/A	N/A	N/A	N/A	15E8_6s1d2Xc_1	7/9B	TDP-208	9150667
29.8	0.998	0.01500	0.050	0.333	9.3	P	N/A	4.32	4.41	4.46	4.60	4.60	8.50	N/A	N/A	N/A	N/A	N/A	N/A	N/A	3.1	N/A	N/A	N/A	N/A	15E8_6s1d2Xc_1	7/9B	TDP-208	9150668
29.8	0.998	0.01500	0.050	0.333	9.3	P	N/A	4.32	4.41	4.46	4.60	4.60	8.50	N/A	N/A	N/A	N/A	N/A	N/A	N/A	n/a	N/A	N/A	N/A	N/A	15E8_6s1d2Xc_1	7/9B	TDP-208	9150668.1
29.8	0.998	0.01500	0.050	0.333	9.3	P	N/A	4.32	4.41	4.46	4.60	4.60	8.50	N/A	N/A	N/A	N/A	N/A	N/A	N/A	3.3	N/A	N/A	N/A	N/A	15E8_6s1d2Xc_1	7/9B	TDP-208	9150669
29.8	0.998	0.01500	0.050	0.333	9.3	P	N/A	4.32	4.41	4.46	4.60	4.60	8.50	N/A	N/A	N/A	N/A	N/A	N/A	N/A	n/a	N/A	N/A	N/A	N/A	15E8_6s1d2Xc_1	7/9B	TDP-208	9150669.1
29.8	0.998	0.01500	0.050	0.333	9.3	P	N/A	4.32	4.41	4.46	4.60	4.60	8.50	N/A	N/A	N/A	N/A	N/A	N/A	N/A	3.4	N/A	N/A	N/A	N/A	15E8_6s1d2Xc_1	7/9B	TDP-208	9150670
29.8	0.998	0.01500	0.050	0.333	9.3	P	N/A	4.32	4.41	4.46	4.60	4.60	8.50	N/A	N/A	N/A	N/A	N/A	N/A	N/A	n/a	N/A	N/A	N/A	N/A	15E8_6s1d2Xc_1	7/9B	TDP-208	9150670.1
29.8	0.998	0.01500	0.050	0.333	9.3	P	N/A	4.32	4.41	4.46	4.60	4.60	8.50	N/A	N/A	N/A	N/A	N/A	N/A	N/A	4.5	N/A	N/A	N/A	N/A	15E8_6s1d2Xc_1	7/9B	TDP-208	9150671
29.8	0.998	0.01500	0.050	0.333	9.3	P	N/A	4.32	4.41	4.46	4.60	4.60	8.50	N/A	N/A	N/A	N/A	N/A	N/A	N/A	n/a	N/A	N/A	N/A	N/A	15E8_6s1d2Xc_1	7/9B	TDP-208	9150671.1
29.8	0.998	0.01500	0.050	0.333	9.3	P	N/A	4.32	4.41	4.46	4.60	4.60	8.50	N/A	N/A	N/A	N/A	N/A	N/A	N/A	4.7	N/A	N/A	N/A	N/A	15E8_6s1d2Xc_1	7/9B	TDP-208	9150672
30.3	0.998	0.01500	0.099	0.329	20.6	P	N/A	3.89	3.92	3.94	4.00	4.40	7.00	N/A	N/A	N/A	N/A	N/A	N/A	(null)	7.4	1	N/A	N/A	N/A	15E8_6s1d2Xc_2	7/9C	TDP-208	9150673
30.3	0.998	0.01500	0.099	0.330	19.6	P	N/A	4.08	4.12	4.14	4.20	4.40	8.00	N/A	N/A	N/A	N/A	N/A	N/A	I	5.4	1	N/A	N/A	N/A	15E8_6s1d2Xc_2	7/9C	TDP-208	9150674
30.4	0.998	0.01500	0.099	0.329	18.8	P	N/A	4.27	4.31	4.33	4.40	4.40	8.75	4.40	udv	N/A	N/A	UCSudv	N/A	I	0.0	1	N/A	N/A	N/A	15E8_6s1d2Xc_2	7/9C	TDP-208	9150675
30.4	0.998	0.01500	0.100	0.330	18.0	P	N/A	4.45	4.50	4.52	4.60	4.40	9.50	N/A	N/A	N/A	N/A	N/A	N/A	I	0.0	1	N/A	N/A	N/A	15E8_6s1d2Xc_2	7/9C	TDP-208	9150676
30.6	0.998	0.01500	0.100	0.332	17.2	P	N/A	4.64	4.69	4.71	4.80	4.40	10.75	N/A	N/A	UCSvis	N/A	N/A	N/A	I	0.0	3	N/A	N/A	N/A	15E8_6s1d2Xc_2	7/9C	TDP-208	9150677
30.8	0.998	0.01500	0.100	0.332	16.6	P	N/A	4.82	4.88	4.91	5.00	4.40	12.25	N/A	N/A	N/A	N/A	N/A	N/A	I	0.0	4	N/A	N/A	N/A	15E8_6s1d2Xc_2	7/9C	TDP-208	9150678
31.0	0.998	0.01500	0.100	0.332	15.4	P	N/A	5.19	5.26	5.29	5.40	4.40	15.25	N/A	N/A	N/A	N/A	N/A	N/A	I	0.0	4	N/A	N/A	N/A	15E8_6s1d2Xc_2	7/9C	TDP-208	9150679
31.2	0.998	0.01500	0.100	0.333	14.8	P	N/A	5.38	5.45	5.49	5.60	4.40	17.25	N/A	N/A	N/A	N/A	N/A	N/A	I	0.0	4	N/A	N/A	N/A	15E8_6s1d2Xc_2	7/9C	TDP-208	9150680
31.4	0.998	0.01500	0.100	0.336	13.8	P	N/A	5.75	5.83	5.87	6.00	4.40	21.00	N/A	N/A	N/A	N/A	N/A	N/A	I	0.7	4	N/A	N/A	N/A	15E8_6s1d2Xc_2	7/9C	TDP-208	9150681
31.7	0.998	0.01500	0.100	0.329	18.8	P	N/A	4.27	4.31	4.33	4.40	4.40	8.50	N/A	N/A	N/A	N/A	N/A	N/A	N/A	n/a	N/A	N/A	N/A	N/A	15E8_6s1d2Xc_2	7/9C	TDP-208	9150681.1
31.7	0.998	0.01500	0.100	0.329	18.8	P	N/A	4.27	4.31	4.33	4.40	4.40	8.50	N/A	N/A	N/A	N/A	N/A	N/A	N/A	n/a	N/A	N/A	N/A	N/A	15E8_6s1d2Xc_2	7/9C	TDP-208	9150681.2
31.7	0.998	0.01500	0.100	0.329	18.8	P	N/A	4.27	4.31	4.33	4.40	4.40	8.50	N/A	N/A	N/A	N/A	N/A	N/A	N/A	n/a	N/A	N/A	N/A	N/A	15E8_6s1d2Xc_2	7/9C	TDP-208	9150681.3
31.7	0.998	0.01500	0.100	0.329	18.8	P	N/A	4.27	4.31	4.33	4.40	4.40	8.50	N/A	N/A	N/A	N/A	N/A	N/A	I	0.7	1	N/A	N/A	N/A	15E8_6s1d2Xc_2	7/9C	TDP-208	9150682
31.7	0.998	0.01500	0.100	0.329	18.8	P	N/A	4.27	4.31	4.33	4.40	4.40	8.50	N/A	N/A	N/A	N/A	N/A	N/A	N/A	0.6	N/A	N/A	N/A	N/A	15E8_6s1d2Xc_2	7/9C	TDP-208	9150683
31.7	0.998	0.01500	0.100	0.329	18.8	P	N/A	4.27	4.31	4.33	4.40	4.40	8.50	N/A	N/A	N/A	N/A	N/A	N/A	N/A	4.8	N/A	N/A	N/A	N/A	15E8_6s1d2Xc_2	7/9C	TDP-208	9150684
31.7	0.998	0.01500	0.100	0.329	18.8	P	N/A	4.27	4.31	4.33	4.40	4.40	8.50	N/A	N/A	N/A	N/A	N/A	N/A	N/A	n/a	N/A	N/A	N/A	N/A	15E8_6s1d2Xc_2	7/9C	TDP-208	9150684.1
31.7	0.998	0.01500	0.100	0.329	18.8	P	N/A	4.27	4.31	4.33	4.40	4.40	8.50	N/A	N/A	N/A	N/A	N/A	N/A	N/A	2.4	N/A	N/A	N/A	N/A	15E8_6s1d2Xc_2	7/9C	TDP-208	9150685
31.7	0.998	0.01500	0.100	0.329	18.8	P	N/A	4.27	4.31	4.33	4.40	4.40	8.50	N/A	N/A	N/A	N/A	N/A	N/A	N/A	n/a	N/A	N/A	N/A	N/A	15E8_6s1d2Xc_2	7/9C	TDP-208	9150685.1
31.7	0.998	0.01500	0.100	0.329	18.8	P	N/A	4.27	4.31	4.33	4.40	4.40	8.50	N/A	N/A	N/A	N/A	N/A	N/A	N/A	2.1	N/A	N/A	N/A	N/A	15E8_6s1d2Xc_2	7/9C	TDP-208	9150686
31.7	0.998	0.01500	0.100	0.329	18.8	P	N/A	4.27	4.31	4.33	4.40	4.40	8.50	N/A	N/A	N/A	N/A	N/A	N/A	N/A	n/a	N/A	N/A	N/A	N/A	15E8_6s1d2Xc_2	7/9C	TDP-208	9150686.1
31.7	0.998	0.01500	0.100	0.329	18.8	P	N/A	4.27	4.31	4.33	4.40	4.40	8.50	N/A	N/A	N/A	N/A	N/A	N/A	N/A	0.7	N/A	N/A	N/A	N/A	15E8_6s1d2Xc_2	7/9C	TDP-208	9150687
31.7	0.998	0.01500	0.100	0.329	18.8	P	N/A	4.27	4.31	4.33	4.40	4.40	8.50	N/A	N/A	N/A	N/A	N/A	N/A	N/A	n/a	N/A	N/A	N/A	N/A	15E8_6s1d2Xc_2	7/9C	TDP-208	9150687.1
31.7	0.998	0.01500	0.100	0.329	18.8	P	N/A	4.27	4.31	4.33	4.40	4.40	8.50	N/A	N/A	N/A	N/A	N/A	N/A	N/A	5.6	N/A	N/A	N/A	N/A	15E8_6s1d2Xc_2	7/9C	TDP-208	9150688
30.2	0.998	0.00155	0.050	0.331	15.0	P	N/A	1.35	1.36	1.36	1.40	1.70	14.25	N/A	N/A	N/A	N/A	N/A	N/A	(null)	9.2	1	N/A	N/A	N/A	15E8_Ms1d2Zc_1	7/10A	TDP-209	9150689
30.3	0.998	0.00155	0.050	0.335	13.0	P	N/A	1.54	1.55	1.56	1.60	1.70	13.00	N/A	N/A	N/A	N/A	N/A	N/A	I	4.3	1	N/A	N/A	N/A	15E8_Ms1d2Zc_1	7/10A	TDP-209	9150690
30.5	0.998	0.00155	0.050	0.335	12.4	P	N/A	1.62	1.64	1.65	1.70	1.70	14.00	1.70	udv	N/A	N/A	UCSudv	N/A	I	0.0	1	N/A	N/A	N/A	15E8_Ms1d2Zc_1	7/10A	TDP-209	9150691
30.6	0.998	0.00155	0.050	0.335	11.6	P	N/A	1.72	1.74	1.75	1.80	1.70	14.25	N/A	N/A	N/A	N/A	N/A	N/A	I	0.0	1	N/A	N/A	N/A	15E8_Ms1d2Zc_1	7/10A	TDP-209	9150692
30.7	0.998	0.00155	0.050	0.337	11.0	P	N/A	1.82	1.84	1.85	1.90	1.70	16.00	N/A	N/A	UCSvis	N/A	N/A	N/A	I	0.0	3	N/A	N/A	N/A	15E8_Ms1d2Zc_1	7/10A	TDP-209	9150693
30.7	0.998	0.00155	0.050	0.338	10.4	P	N/A	1.91	1.94	1.95	2.00	1.70	17.50	N/A	N/A	N/A	N/A	N/A	N/A	I	0.0	4	N/A	N/A	N/A	15E8_Ms1d2Zc_1	7/10A	TDP-209	9150694

Table B.3. Data from 2008 Tests in Small-Scale Vessel with Elliptical Head A.20

Row Number	Test	Case ID	Tank Diameter	Head Shape	Dish Height	Dish Volume	Tank Fill Height	Return Line Height	Nozzle Inner Diameter	Nozzle Stand-off Distance	Pulse Tube Configuration	Installed Nozzles	Outer Nozzles Operated	Inner Nozzles Operated	Pulse Tube Outer Diameter	Outer PJM Radius	Inner PJM Radius	"FIO" Outer PJM Impingement Angle	"FIO" Inner PJM Impingement Angle	Ratio Outer PJM to Tank Radius	Ratio Inner PJM to Tank Radius	Simulant	Solids Density	Particle Diameter d5	Particle Diameter d50	Particle Diameter d95	Void Fraction
text	text	text	in.	text	in.	in. ^{3}	in.	in.	in.	in.	text	number	number	number	in.	in.	in.	deg	deg	nondim	nondim	text	g/cm^3	m	m	m	fraction
MSS	M/DDX	ID	D	HS	H_{dish}	V_{dish}	H	Rtn	d	sod	PT	N	N_O	N_I	PT_{od}	R_O	R_I	θ_O	θ_I	R_O/R	R_I/R	sxdx	ρ_s	d_5	d_{50}	d_{95}	vf
9150695M	7/10A	15E8_Ms1d2Zc_1	14 7/16	E	3.25	354.8	35 1/2	30	0.268	0.402	8TA	8	4	4	1.05	4.9	3.6	24.4	16	0.67	0.50	s1d2	2.48	0.0000569	0.0000693	0.0000821	0.3750
9150696	7/10B	15E8_Ms1d2Zc_2	14 7/16	E	3.25	354.8	35 1/2	30	0.268	0.402	8TA	8	4	4	1.05	4.9	3.6	24.4	16	0.67	0.50	s1d2	2.48	0.0000569	0.0000693	0.0000821	0.3750
9150697	7/10B	15E8_Ms1d2Zc_2	14 7/16	E	3.25	354.8	35 1/2	30	0.268	0.402	8TA	8	4	4	1.05	4.9	3.6	24.4	16	0.67	0.50	s1d2	2.48	0.0000569	0.0000693	0.0000821	0.3750
9150698	7/10B	15E8_Ms1d2Zc_2	14 7/16	E	3.25	354.8	35 1/2	30	0.268	0.402	8TA	8	4	4	1.05	4.9	3.6	24.4	16	0.67	0.50	s1d2	2.48	0.0000569	0.0000693	0.0000821	0.3750
9150699	7/10B	15E8_Ms1d2Zc_2	14 7/16	E	3.25	354.8	35 1/2	30	0.268	0.402	8TA	8	4	4	1.05	4.9	3.6	24.4	16	0.67	0.50	s1d2	2.48	0.0000569	0.0000693	0.0000821	0.3750
9150700M	7/10B	15E8_Ms1d2Zc_2	14 7/16	E	3.25	354.8	35 1/2	30	0.268	0.402	8TA	8	4	4	1.05	4.9	3.6	24.4	16	0.67	0.50	s1d2	2.48	0.0000569	0.0000693	0.0000821	0.3750
9150701M	7/10B	15E8_Ms1d2Zc_2	14 7/16	E	3.25	354.8	35 1/2	30	0.268	0.402	8TA	8	4	4	1.05	4.9	3.6	24.4	16	0.67	0.50	s1d2	2.48	0.0000569	0.0000693	0.0000821	0.3750
9150702M	7/10B	15E8_Ms1d2Zc_2	14 7/16	E	3.25	354.8	35 1/2	30	0.268	0.402	8TA	8	4	4	1.05	4.9	3.6	24.4	16	0.67	0.50	s1d2	2.48	0.0000569	0.0000693	0.0000821	0.3750
9150703	7/11A	15E8_Ms1d2Vc_1	14 7/16	E	3.25	354.8	35	30	0.268	0.402	8TA	8	4	4	1.05	4.9	3.6	24.4	16	0.67	0.50	s1d2	2.48	0.0000569	0.0000693	0.0000821	0.3750
9150704M	7/11A	15E8_Ms1d2Vc_1	14 7/16	E	3.25	354.8	35	30	0.268	0.402	8TA	8	4	4	1.05	4.9	3.6	24.4	16	0.67	0.50	s1d2	2.48	0.0000569	0.0000693	0.0000821	0.3750
9150705M	7/11A	15E8_Ms1d2Vc_1	14 7/16	E	3.25	354.8	35	30	0.268	0.402	8TA	8	4	4	1.05	4.9	3.6	24.4	16	0.67	0.50	s1d2	2.48	0.0000569	0.0000693	0.0000821	0.3750
9150706M	7/11A	15E8_Ms1d2Vc_1	14 7/16	E	3.25	354.8	35	30	0.268	0.402	8TA	8	4	4	1.05	4.9	3.6	24.4	16	0.67	0.50	s1d2	2.48	0.0000569	0.0000693	0.0000821	0.3750
9150707M	7/11A	15E8_Ms1d2Vc_1	14 7/16	E	3.25	354.8	35	30	0.268	0.402	8TA	8	4	4	1.05	4.9	3.6	24.4	16	0.67	0.50	s1d2	2.48	0.0000569	0.0000693	0.0000821	0.3750
9150707.1	7/11A	15E8_Ms1d2Vc_1	14 7/16	E	3.25	354.8	35	30	0.268	0.402	8TA	8	4	4	1.05	4.9	3.6	24.4	16	0.67	0.50	s1d2	2.48	0.0000569	0.0000693	0.0000821	0.3750
9150707.2	7/11A	15E8_Ms1d2Vc_1	14 7/16	E	3.25	354.8	35	30	0.268	0.402	8TA	8	4	4	1.05	4.9	3.6	24.4	16	0.67	0.50	s1d2	2.48	0.0000569	0.0000693	0.0000821	0.3750
9150708M	7/11A	15E8_Ms1d2Vc_1	14 7/16	E	3.25	354.8	35	30	0.268	0.402	8TA	8	4	4	1.05	4.9	3.6	24.4	16	0.67	0.50	s1d2	2.48	0.0000569	0.0000693	0.0000821	0.3750
9150709	7/11A	15E8_Ms1d2Vc_1	14 7/16	E	3.25	354.8	35	30	0.268	0.402	8TA	8	4	4	1.05	4.9	3.6	24.4	16	0.67	0.50	s1d2	2.48	0.0000569	0.0000693	0.0000821	0.3750
9150710	7/11A	15E8_Ms1d2Vc_1	14 7/16	E	3.25	354.8	35	30	0.268	0.402	8TA	8	4	4	1.05	4.9	3.6	24.4	16	0.67	0.50	s1d2	2.48	0.0000569	0.0000693	0.0000821	0.3750
9150711	7/11A	15E8_Ms1d2Vc_1	14 7/16	E	3.25	354.8	35	30	0.268	0.402	8TA	8	4	4	1.05	4.9	3.6	24.4	16	0.67	0.50	s1d2	2.48	0.0000569	0.0000693	0.0000821	0.3750
9150711.1	7/11A	15E8_Ms1d2Vc_1	14 7/16	E	3.25	354.8	35	30	0.268	0.402	8TA	8	4	4	1.05	4.9	3.6	24.4	16	0.67	0.50	s1d2	2.48	0.0000569	0.0000693	0.0000821	0.3750
9150712	7/11A	15E8_Ms1d2Vc_1	14 7/16	E	3.25	354.8	35	30	0.268	0.402	8TA	8	4	4	1.05	4.9	3.6	24.4	16	0.67	0.50	s1d2	2.48	0.0000569	0.0000693	0.0000821	0.3750
9150712.1	7/11A	15E8_Ms1d2Vc_1	14 7/16	E	3.25	354.8	35	30	0.268	0.402	8TA	8	4	4	1.05	4.9	3.6	24.4	16	0.67	0.50	s1d2	2.48	0.0000569	0.0000693	0.0000821	0.3750
9150713	7/11A	15E8_Ms1d2Vc_1	14 7/16	E	3.25	354.8	35	30	0.268	0.402	8TA	8	4	4	1.05	4.9	3.6	24.4	16	0.67	0.50	s1d2	2.48	0.0000569	0.0000693	0.0000821	0.3750
9150713.1	7/11A	15E8_Ms1d2Vc_1	14 7/16	E	3.25	354.8	35	30	0.268	0.402	8TA	8	4	4	1.05	4.9	3.6	24.4	16	0.67	0.50	s1d2	2.48	0.0000569	0.0000693	0.0000821	0.3750
9150714	7/11A	15E8_Ms1d2Vc_1	14 7/16	E	3.25	354.8	35	30	0.268	0.402	8TA	8	4	4	1.05	4.9	3.6	24.4	16	0.67	0.50	s1d2	2.48	0.0000569	0.0000693	0.0000821	0.3750
9150714.1	7/11A	15E8_Ms1d2Vc_1	14 7/16	E	3.25	354.8	35	30	0.268	0.402	8TA	8	4	4	1.05	4.9	3.6	24.4	16	0.67	0.50	s1d2	2.48	0.0000569	0.0000693	0.0000821	0.3750
9150715	7/11A	15E8_Ms1d2Vc_1	14 7/16	E	3.25	354.8	35	30	0.268	0.402	8TA	8	4	4	1.05	4.9	3.6	24.4	16	0.67	0.50	s1d2	2.48	0.0000569	0.0000693	0.0000821	0.3750
9150716	7/11B	15E8_Ms1d2Vc_2	14 7/16	E	3.25	354.8	35	30	0.268	0.402	8TA	8	4	4	1.05	4.9	3.6	24.4	16	0.67	0.50	s1d2	2.48	0.0000569	0.0000693	0.0000821	0.3750
9150717	7/11B	15E8_Ms1d2Vc_2	14 7/16	E	3.25	354.8	35	30	0.268	0.402	8TA	8	4	4	1.05	4.9	3.6	24.4	16	0.67	0.50	s1d2	2.48	0.0000569	0.0000693	0.0000821	0.3750
9150718	7/11B	15E8_Ms1d2Vc_2	14 7/16	E	3.25	354.8	35	30	0.268	0.402	8TA	8	4	4	1.05	4.9	3.6	24.4	16	0.67	0.50	s1d2	2.48	0.0000569	0.0000693	0.0000821	0.3750
9150719M	7/11B	15E8_Ms1d2Vc_2	14 7/16	E	3.25	354.8	35	30	0.268	0.402	8TA	8	4	4	1.05	4.9	3.6	24.4	16	0.67	0.50	s1d2	2.48	0.0000569	0.0000693	0.0000821	0.3750
9150720M	7/11B	15E8_Ms1d2Vc_2	14 7/16	E	3.25	354.8	35	30	0.268	0.402	8TA	8	4	4	1.05	4.9	3.6	24.4	16	0.67	0.50	s1d2	2.48	0.0000569	0.0000693	0.0000821	0.3750
9150721M	7/11B	15E8_Ms1d2Vc_2	14 7/16	E	3.25	354.8	35	30	0.268	0.402	8TA	8	4	4	1.05	4.9	3.6	24.4	16	0.67	0.50	s1d2	2.48	0.0000569	0.0000693	0.0000821	0.3750
9150722M	7/11B	15E8_Ms1d2Vc_2	14 7/16	E	3.25	354.8	35	30	0.268	0.402	8TA	8	4	4	1.05	4.9	3.6	24.4	16	0.67	0.50	s1d2	2.48	0.0000569	0.0000693	0.0000821	0.3750
9150723M	7/11B	15E8_Ms1d2Vc_2	14 7/16	E	3.25	354.8	35	30	0.268	0.402	8TA	8	4	4	1.05	4.9	3.6	24.4	16	0.67	0.50	s1d2	2.48	0.0000569	0.0000693	0.0000821	0.3750
9150724M	7/11B	15E8_Ms1d2Vc_2	14 7/16	E	3.25	354.8	35	30	0.268	0.402	8TA	8	4	4	1.05	4.9	3.6	24.4	16	0.67	0.50	s1d2	2.48	0.0000569	0.0000693	0.0000821	0.3750
9150725	7/14A	15E8_Ls1d2Zc_1	14 7/16	E	3.25	354.8	36	30	0.375	0.563	8TA	8	4	4	1.05	4.9	3.6	24.4	16	0.67	0.50	s1d2	2.48	0.0000569	0.0000693	0.0000821	0.3750
9150726	7/14A	15E8_Ls1d2Zc_1	14 7/16	E	3.25	354.8	36	30	0.375	0.563	8TA	8	4	4	1.05	4.9	3.6	24.4	16	0.67	0.50	s1d2	2.48	0.0000569	0.0000693	0.0000821	0.3750
9150727	7/14A	15E8_Ls1d2Zc_1	14 7/16	E	3.25	354.8	36	30	0.375	0.563	8TA	8	4	4	1.05	4.9	3.6	24.4	16	0.67	0.50	s1d2	2.48	0.0000569	0.0000693	0.0000821	0.3750
9150728	7/14A	15E8_Ls1d2Zc_1	14 7/16	E	3.25	354.8	36	30	0.375	0.563	8TA	8	4	4	1.05	4.9	3.6	24.4	16	0.67	0.50	s1d2	2.48	0.0000569	0.0000693	0.0000821	0.3750
9150729	7/14A	15E8_Ls1d2Zc_1	14 7/16	E	3.25	354.8	36	30	0.375	0.563	8TA	8	4	4	1.05	4.9	3.6	24.4	16	0.67	0.50	s1d2	2.48	0.0000569	0.0000693	0.0000821	0.3750

Table B.3. Data from 2008 Tests in Small-Scale Vessel with Elliptical Head B.20

Tank Water Temperature	Water Density	Solids Fraction	Pulse Volume Fraction	Duty Cycle	Cycle Time	Pulsed or Steady Jet	Us Steady Jet	U1 Pulsing Jet	U2 URMS	U3 URM3	Discharge Velocity	Critical Suspension Velocity	Average Peak Cloud Height	UCS Condition	UCS Method	UCS Flag	UCS Center Flag	UCS udv Flag	UCS based on Decreasing Velocity	Sweep Increase / Decrease	UDV Height Bed	Particle Motion	Solids Level	Outer Bottom Pattern	Inner Bottom Pattern	Case ID	Test	TDP	Row Number
C	g/cm³	fraction	fraction	fraction	s	text	m/s	m/s	m/s	m/s	m/s	m/s	in.	m/s	text	text	text	text	m/s	text	mm	text	text	text	text	text	text	text	text
T	ρ_c	ϕ_S	ϕ_p	DC	t_C	Jet	U_S	U1	U2	U3	U	U_{CS}	H_C	U_{CSR}	U_{CSM}	U_{CS}vis	U_{CS}cen	U_{CS}udv	$U_{CS_}D$	S_W	H_{bed}	PM	Sol	SP_O	SP_I	ID	M/DDX	TDP	MSS
30.9	0.998	0.00155	0.050	0.337	10.0	P	N/A	2.00	2.03	2.04	2.10	1.70	18.50	N/A	N/A	N/A	N/A	N/A	N/A	I	0.0	4	N/A	N/A	N/A	15E8_Ms1d2Zc_1	7/10A	TDP-209	9150695
31.1	0.998	0.00155	0.099	0.330	29.6	P	N/A	1.37	1.38	1.38	1.40	1.80	10.50	N/A	N/A	N/A	N/A	N/A	N/A	(null)	4.4	1	N/A	N/A	N/A	15E8_Ms1d2Zc_2	7/10B	TDP-209	9150696
31.4	0.998	0.00155	0.100	0.331	27.6	P	N/A	1.47	1.48	1.48	1.50	1.80	11.00	N/A	N/A	N/A	N/A	N/A	N/A	I	6.3	1	N/A	N/A	N/A	15E8_Ms1d2Zc_2	7/10B	TDP-209	9150697
31.2	0.998	0.00155	0.100	0.332	25.8	P	N/A	1.57	1.58	1.58	1.60	1.80	11.00	N/A	N/A	N/A	N/A	N/A	N/A	I	3.6	1	N/A	N/A	N/A	15E8_Ms1d2Zc_2	7/10B	TDP-209	9150698
31.3	0.998	0.00155	0.099	0.333	24.2	P	N/A	1.66	1.67	1.67	1.70	1.80	11.50	N/A	N/A	N/A	N/A	N/A	N/A	I	5.1	1	N/A	N/A	N/A	15E8_Ms1d2Zc_2	7/10B	TDP-209	9150699
31.4	0.998	0.00155	0.099	0.334	22.8	P	N/A	1.76	1.77	1.78	1.80	1.80	12.00	1.80	udv	N/A	N/A	UCSudv	N/A	I	0.8	1	N/A	N/A	N/A	15E8_Ms1d2Zc_2	7/10B	TDP-209	9150700
31.4	0.998	0.00155	0.099	0.335	21.6	P	N/A	1.85	1.87	1.87	1.90	1.80	16.50	N/A	N/A	UCSvis	N/A	N/A	N/A	I	0.0	3	N/A	N/A	N/A	15E8_Ms1d2Zc_2	7/10B	TDP-209	9150701
31.8	0.998	0.00155	0.100	0.336	20.6	P	N/A	1.95	1.96	1.97	2.00	1.80	20.50	N/A	N/A	N/A	N/A	N/A	N/A	I	0.0	4	N/A	N/A	N/A	15E8_Ms1d2Zc_2	7/10B	TDP-209	9150702
24.5	0.999	0.01430	0.050	0.332	7.8	P	N/A	2.61	2.66	2.69	2.80	2.90	8.50	N/A	N/A	N/A	N/A	N/A	N/A	(null)	2.9	1	N/A	N/A	N/A	15E8_Ms1d2Vc_1	7/11A	TDP-210	9150703
24.8	0.999	0.01430	0.050	0.329	7.6	P	N/A	2.70	2.76	2.79	2.90	2.90	9.00	2.90	udv	N/A	N/A	UCSudv	N/A	I	0.6	1	N/A	N/A	N/A	15E8_Ms1d2Vc_1	7/11A	TDP-210	9150704
25.1	0.999	0.01430	0.050	0.330	7.4	P	N/A	2.78	2.84	2.87	3.00	2.90	10.25	N/A	N/A	UCSvis	N/A	N/A	N/A	I	0.0	3	N/A	N/A	N/A	15E8_Ms1d2Vc_1	7/11A	TDP-210	9150705
25.5	0.999	0.01430	0.050	0.328	7.2	P	N/A	2.86	2.93	2.96	3.10	2.90	11.75	N/A	N/A	N/A	N/A	N/A	N/A	I	0.0	4	N/A	N/A	N/A	15E8_Ms1d2Vc_1	7/11A	TDP-210	9150706
25.7	0.999	0.01430	0.050	0.335	6.6	P	N/A	3.03	3.11	3.15	3.30	2.90	14.50	N/A	N/A	N/A	N/A	N/A	N/A	I	0.0	4	N/A	N/A	N/A	15E8_Ms1d2Vc_1	7/11A	TDP-210	9150707
26.2	0.999	0.01430	0.050	0.330	7.6	P	N/A	2.70	2.76	2.79	2.90	2.90	8.50	N/A	N/A	N/A	N/A	N/A	N/A	N/A	n/a	N/A	N/A	N/A	N/A	15E8_Ms1d2Vc_1	7/11A	TDP-210	9150707.1
26.2	0.999	0.01430	0.050	0.330	7.6	P	N/A	2.70	2.76	2.79	2.90	2.90	8.50	N/A	N/A	N/A	N/A	N/A	N/A	N/A	n/a	N/A	N/A	N/A	N/A	15E8_Ms1d2Vc_1	7/11A	TDP-210	9150707.2
26.2	0.999	0.01430	0.050	0.330	7.6	P	N/A	2.70	2.76	2.79	2.90	2.90	8.50	N/A	N/A	N/A	N/A	N/A	N/A	I	0.6	1	N/A	N/A	N/A	15E8_Ms1d2Vc_1	7/11A	TDP-210	9150708
26.2	0.999	0.01430	0.050	0.330	7.6	P	N/A	2.70	2.76	2.79	2.90	2.90	8.50	N/A	N/A	N/A	N/A	N/A	N/A	N/A	0.6	N/A	N/A	N/A	N/A	15E8_Ms1d2Vc_1	7/11A	TDP-210	9150709
26.2	0.999	0.01430	0.050	0.330	7.6	P	N/A	2.70	2.76	2.79	2.90	2.90	8.50	N/A	N/A	N/A	N/A	N/A	N/A	N/A	0.6	N/A	N/A	N/A	N/A	15E8_Ms1d2Vc_1	7/11A	TDP-210	9150710
26.2	0.999	0.01430	0.050	0.330	7.6	P	N/A	2.70	2.76	2.79	2.90	2.90	8.50	N/A	N/A	N/A	N/A	N/A	N/A	N/A	0.0	N/A	N/A	N/A	N/A	15E8_Ms1d2Vc_1	7/11A	TDP-210	9150711
26.2	0.999	0.01430	0.050	0.330	7.6	P	N/A	2.70	2.76	2.79	2.90	2.90	8.50	N/A	N/A	N/A	N/A	N/A	N/A	N/A	n/a	N/A	N/A	N/A	N/A	15E8_Ms1d2Vc_1	7/11A	TDP-210	9150711.1
26.2	0.999	0.01430	0.050	0.330	7.6	P	N/A	2.70	2.76	2.79	2.90	2.90	8.50	N/A	N/A	N/A	N/A	N/A	N/A	N/A	0.0	N/A	N/A	N/A	N/A	15E8_Ms1d2Vc_1	7/11A	TDP-210	9150712
26.2	0.999	0.01430	0.050	0.330	7.6	P	N/A	2.70	2.76	2.79	2.90	2.90	8.50	N/A	N/A	N/A	N/A	N/A	N/A	N/A	n/a	N/A	N/A	N/A	N/A	15E8_Ms1d2Vc_1	7/11A	TDP-210	9150712.1
26.2	0.999	0.01430	0.050	0.330	7.6	P	N/A	2.70	2.76	2.79	2.90	2.90	8.50	N/A	N/A	N/A	N/A	N/A	N/A	N/A	1.5	N/A	N/A	N/A	N/A	15E8_Ms1d2Vc_1	7/11A	TDP-210	9150713
26.2	0.999	0.01430	0.050	0.330	7.6	P	N/A	2.70	2.76	2.79	2.90	2.90	8.50	N/A	N/A	N/A	N/A	N/A	N/A	N/A	n/a	N/A	N/A	N/A	N/A	15E8_Ms1d2Vc_1	7/11A	TDP-210	9150713.1
26.2	0.999	0.01430	0.050	0.330	7.6	P	N/A	2.70	2.76	2.79	2.90	2.90	8.50	N/A	N/A	N/A	N/A	N/A	N/A	N/A	0.0	N/A	N/A	N/A	N/A	15E8_Ms1d2Vc_1	7/11A	TDP-210	9150714
26.2	0.999	0.01430	0.050	0.330	7.6	P	N/A	2.70	2.76	2.79	2.90	2.90	8.50	N/A	N/A	N/A	N/A	N/A	N/A	N/A	n/a	N/A	N/A	N/A	N/A	15E8_Ms1d2Vc_1	7/11A	TDP-210	9150714.1
26.2	0.999	0.01430	0.050	0.330	7.6	P	N/A	2.70	2.76	2.79	2.90	2.90	8.50	N/A	N/A	N/A	N/A	N/A	N/A	N/A	0.0	N/A	N/A	N/A	N/A	15E8_Ms1d2Vc_1	7/11A	TDP-210	9150715
26.4	0.999	0.01430	0.100	0.333	17.4	P	N/A	2.33	2.35	2.36	2.40	2.80	6.50	N/A	N/A	N/A	N/A	N/A	N/A	(null)	18.9	1	N/A	N/A	N/A	15E8_Ms1d2Vc_2	7/11B	TDP-210	9150716
26.5	0.999	0.01430	0.100	0.335	16.0	P	N/A	2.52	2.54	2.55	2.60	2.80	8.50	N/A	N/A	N/A	N/A	N/A	N/A	I	3.0	1	N/A	N/A	N/A	15E8_Ms1d2Vc_2	7/11B	TDP-210	9150717
26.6	0.999	0.01430	0.100	0.336	15.4	P	N/A	2.61	2.63	2.65	2.70	2.80	9.00	N/A	N/A	N/A	N/A	N/A	N/A	I	2.7	1	N/A	N/A	N/A	15E8_Ms1d2Vc_2	7/11B	TDP-210	9150718
26.8	0.999	0.01430	0.100	0.337	14.8	P	N/A	2.71	2.73	2.75	2.80	2.80	10.00	2.80	udv	N/A	N/A	UCSudv	N/A	I	0.0	1	N/A	N/A	N/A	15E8_Ms1d2Vc_2	7/11B	TDP-210	9150719
26.9	0.999	0.01430	0.100	0.339	14.2	P	N/A	2.80	2.83	2.85	2.90	2.80	10.75	N/A	N/A	N/A	N/A	N/A	N/A	I	0.0	1	N/A	N/A	N/A	15E8_Ms1d2Vc_2	7/11B	TDP-210	9150720
27.1	0.999	0.01430	0.100	0.335	14.0	P	N/A	2.88	2.91	2.93	3.00	2.80	11.25	N/A	N/A	UCSvis	N/A	N/A	N/A	I	0.0	3	N/A	N/A	N/A	15E8_Ms1d2Vc_2	7/11B	TDP-210	9150721
27.4	0.998	0.01430	0.100	0.333	13.6	P	N/A	2.98	3.01	3.03	3.10	2.80	12.50	N/A	N/A	N/A	N/A	N/A	N/A	I	0.0	4	N/A	N/A	N/A	15E8_Ms1d2Vc_2	7/11B	TDP-210	9150722
27.6	0.999	0.01430	0.101	0.335	12.8	P	N/A	3.16	3.20	3.22	3.30	2.80	14.75	N/A	N/A	N/A	N/A	N/A	N/A	I	0.0	4	N/A	N/A	N/A	15E8_Ms1d2Vc_2	7/11B	TDP-210	9150723
27.8	0.999	0.01430	0.100	0.338	12.0	P	N/A	3.33	3.38	3.41	3.50	2.80	19.25	N/A	N/A	N/A	N/A	N/A	N/A	I	0.0	4	N/A	N/A	N/A	15E8_Ms1d2Vc_2	7/11B	TDP-210	9150724
28.1	0.998	0.00155	0.050	0.334	13.2	P	N/A	0.78	0.78	0.78	0.80	1.30	14.00	N/A	N/A	N/A	N/A	N/A	N/A	(null)	11.5	1	N/A	N/A	N/A	15E8_Ls1d2Zc_1	7/14A	TDP-211	9150725
28.1	0.999	0.00155	0.050	0.337	11.8	P	N/A	0.87	0.88	0.88	0.90	1.30	13.25	N/A	N/A	N/A	N/A	N/A	N/A	I	7.3	1	N/A	N/A	N/A	15E8_Ls1d2Zc_1	7/14A	TDP-211	9150726
28.3	0.999	0.00155	0.050	0.335	10.6	P	N/A	0.96	0.97	0.98	1.00	1.30	12.25	N/A	N/A	N/A	N/A	N/A	N/A	I	5.6	1	N/A	N/A	N/A	15E8_Ls1d2Zc_1	7/14A	TDP-211	9150727
28.5	0.998	0.00155	0.050	0.339	9.6	P	N/A	1.06	1.07	1.07	1.10	1.30	12.50	N/A	N/A	N/A	N/A	N/A	N/A	I	4.2	1	N/A	N/A	N/A	15E8_Ls1d2Zc_1	7/14A	TDP-211	9150728
28.7	0.998	0.00155	0.050	0.334	9.0	P	N/A	1.15	1.16	1.17	1.20	1.30	13.25	N/A	N/A	N/A	N/A	N/A	N/A	I	2.3	1	N/A	N/A	N/A	15E8_Ls1d2Zc_1	7/14A	TDP-211	9150729

Table B.3. Data from 2008 Tests in Small-Scale Vessel with Elliptical Head A.21

Row Number	Test	Case ID	Tank Diameter	Head Shape	Dish Height	Dish Volume	Tank Fill Height	Return Line Height	Nozzle Inner Diameter	Nozzle Stand-off Distance	Pulse Tube Configuration	Installed Nozzles	Outer Nozzles Operated	Inner Nozzles Operated	Pulse Tube Outer Diameter	Outer PJM Radius	Inner PJM Radius	"FIO" Outer PJM Impingement Angle	"FIO" Inner PJM Impingement Angle	Ratio Outer PJM to Tank Radius	Ratio Inner PJM to Tank Radius	Simulant	Solids Density	Particle Diameter d5	Particle Diameter d50	Particle Diameter d95	Void Fraction
text	text	text	in.	text	in.	in. ^{3}	in.	in.	in.	in.	text	number	number	number	in.	in.	in.	deg	deg	nondim	nondim	text	g/cm^3	m	m	m	fraction
MSS	M/DDX	ID	D	HS	H_{dish}	V_{dish}	H	Rtn	d	sod	PT	N	N_O	N_I	PT_{od}	R_O	R_I	θ_O	θ_I	R_O/R	R_I/R	sxdx	ρ_s	d_5	d_{50}	d_{95}	vf
9150730M	7/14A	15E8_Ls1d2Zc_1	14 7/16	E	3.25	354.8	36	30	0.375	0.563	8TA	8	4	4	1.05	4.9	3.6	24.4	16	0.67	0.50	s1d2	2.48	0.0000569	0.0000693	0.0000821	0.3750
9150731M	7/14A	15E8_Ls1d2Zc_1	14 7/16	E	3.25	354.8	36	30	0.375	0.563	8TA	8	4	4	1.05	4.9	3.6	24.4	16	0.67	0.50	s1d2	2.48	0.0000569	0.0000693	0.0000821	0.3750
9150732	7/14B	15E8_Ls1d2Vc_1	14 7/16	E	3.25	354.8	36	30	0.375	0.563	8TA	8	4	4	1.05	4.9	3.6	24.4	16	0.67	0.50	s1d2	2.48	0.0000569	0.0000693	0.0000821	0.3750
9150733	7/14B	15E8_Ls1d2Vc_1	14 7/16	E	3.25	354.8	36	30	0.375	0.563	8TA	8	4	4	1.05	4.9	3.6	24.4	16	0.67	0.50	s1d2	2.48	0.0000569	0.0000693	0.0000821	0.3750
9150734	7/14B	15E8_Ls1d2Vc_1	14 7/16	E	3.25	354.8	36	30	0.375	0.563	8TA	8	4	4	1.05	4.9	3.6	24.4	16	0.67	0.50	s1d2	2.48	0.0000569	0.0000693	0.0000821	0.3750
9150735	7/14B	15E8_Ls1d2Vc_1	14 7/16	E	3.25	354.8	36	30	0.375	0.563	8TA	8	4	4	1.05	4.9	3.6	24.4	16	0.67	0.50	s1d2	2.48	0.0000569	0.0000693	0.0000821	0.3750
9150736	7/14B	15E8_Ls1d2Vc_1	14 7/16	E	3.25	354.8	36	30	0.375	0.563	8TA	8	4	4	1.05	4.9	3.6	24.4	16	0.67	0.50	s1d2	2.48	0.0000569	0.0000693	0.0000821	0.3750
9150737M	7/14B	15E8_Ls1d2Vc_1	14 7/16	E	3.25	354.8	36	30	0.375	0.563	8TA	8	4	4	1.05	4.9	3.6	24.4	16	0.67	0.50	s1d2	2.48	0.0000569	0.0000693	0.0000821	0.3750
9150738M	7/14B	15E8_Ls1d2Vc_1	14 7/16	E	3.25	354.8	36	30	0.375	0.563	8TA	8	4	4	1.05	4.9	3.6	24.4	16	0.67	0.50	s1d2	2.48	0.0000569	0.0000693	0.0000821	0.3750
9150738.1	7/14B	15E8_Ls1d2Vc_1	14 7/16	E	3.25	354.8	36	30	0.375	0.563	8TA	8	4	4	1.05	4.9	3.6	24.4	16	0.67	0.50	s1d2	2.48	0.0000569	0.0000693	0.0000821	0.3750
9150738.2	7/14B	15E8_Ls1d2Vc_1	14 7/16	E	3.25	354.8	36	30	0.375	0.563	8TA	8	4	4	1.05	4.9	3.6	24.4	16	0.67	0.50	s1d2	2.48	0.0000569	0.0000693	0.0000821	0.3750
9150739M	7/14B	15E8_Ls1d2Vc_1	14 7/16	E	3.25	354.8	36	30	0.375	0.563	8TA	8	4	4	1.05	4.9	3.6	24.4	16	0.67	0.50	s1d2	2.48	0.0000569	0.0000693	0.0000821	0.3750
9150740	7/14B	15E8_Ls1d2Vc_1	14 7/16	E	3.25	354.8	36	30	0.375	0.563	8TA	8	4	4	1.05	4.9	3.6	24.4	16	0.67	0.50	s1d2	2.48	0.0000569	0.0000693	0.0000821	0.3750
9150741	7/14B	15E8_Ls1d2Vc_1	14 7/16	E	3.25	354.8	36	30	0.375	0.563	8TA	8	4	4	1.05	4.9	3.6	24.4	16	0.67	0.50	s1d2	2.48	0.0000569	0.0000693	0.0000821	0.3750
9150742	7/14B	15E8_Ls1d2Vc_1	14 7/16	E	3.25	354.8	36	30	0.375	0.563	8TA	8	4	4	1.05	4.9	3.6	24.4	16	0.67	0.50	s1d2	2.48	0.0000569	0.0000693	0.0000821	0.3750
9150742.1	7/14B	15E8_Ls1d2Vc_1	14 7/16	E	3.25	354.8	36	30	0.375	0.563	8TA	8	4	4	1.05	4.9	3.6	24.4	16	0.67	0.50	s1d2	2.48	0.0000569	0.0000693	0.0000821	0.3750
9150743	7/14B	15E8_Ls1d2Vc_1	14 7/16	E	3.25	354.8	36	30	0.375	0.563	8TA	8	4	4	1.05	4.9	3.6	24.4	16	0.67	0.50	s1d2	2.48	0.0000569	0.0000693	0.0000821	0.3750
9150743.1	7/14B	15E8_Ls1d2Vc_1	14 7/16	E	3.25	354.8	36	30	0.375	0.563	8TA	8	4	4	1.05	4.9	3.6	24.4	16	0.67	0.50	s1d2	2.48	0.0000569	0.0000693	0.0000821	0.3750
9150744	7/14B	15E8_Ls1d2Vc_1	14 7/16	E	3.25	354.8	36	30	0.375	0.563	8TA	8	4	4	1.05	4.9	3.6	24.4	16	0.67	0.50	s1d2	2.48	0.0000569	0.0000693	0.0000821	0.3750
9150744.1	7/14B	15E8_Ls1d2Vc_1	14 7/16	E	3.25	354.8	36	30	0.375	0.563	8TA	8	4	4	1.05	4.9	3.6	24.4	16	0.67	0.50	s1d2	2.48	0.0000569	0.0000693	0.0000821	0.3750
9150745	7/14B	15E8_Ls1d2Vc_1	14 7/16	E	3.25	354.8	36	30	0.375	0.563	8TA	8	4	4	1.05	4.9	3.6	24.4	16	0.67	0.50	s1d2	2.48	0.0000569	0.0000693	0.0000821	0.3750
9150745.1	7/14B	15E8_Ls1d2Vc_1	14 7/16	E	3.25	354.8	36	30	0.375	0.563	8TA	8	4	4	1.05	4.9	3.6	24.4	16	0.67	0.50	s1d2	2.48	0.0000569	0.0000693	0.0000821	0.3750
9150746	7/14B	15E8_Ls1d2Vc_1	14 7/16	E	3.25	354.8	36	30	0.375	0.563	8TA	8	4	4	1.05	4.9	3.6	24.4	16	0.67	0.50	s1d2	2.48	0.0000569	0.0000693	0.0000821	0.3750
9150747	7/15A	15E8_Ls1d2Vc_7	14 7/16	E	3.25	354.8	35 1/2	30	0.375	0.563	8TA	8	4	0	1.05	4.9	3.6	24.4	16	0.67	0.50	s1d2	2.48	0.0000569	0.0000693	0.0000821	0.3750
9150748	7/15A	15E8_Ls1d2Vc_7	14 7/16	E	3.25	354.8	35 1/2	30	0.375	0.563	8TA	8	4	0	1.05	4.9	3.6	24.4	16	0.67	0.50	s1d2	2.48	0.0000569	0.0000693	0.0000821	0.3750
9150749	7/15A	15E8_Ls1d2Vc_7	14 7/16	E	3.25	354.8	35 1/2	30	0.375	0.563	8TA	8	4	0	1.05	4.9	3.6	24.4	16	0.67	0.50	s1d2	2.48	0.0000569	0.0000693	0.0000821	0.3750
9150750	7/15A	15E8_Ls1d2Vc_7	14 7/16	E	3.25	354.8	35 1/2	30	0.375	0.563	8TA	8	4	0	1.05	4.9	3.6	24.4	16	0.67	0.50	s1d2	2.48	0.0000569	0.0000693	0.0000821	0.3750
9150751	7/15A	15E8_Ls1d2Vc_7	14 7/16	E	3.25	354.8	35 1/2	30	0.375	0.563	8TA	8	4	0	1.05	4.9	3.6	24.4	16	0.67	0.50	s1d2	2.48	0.0000569	0.0000693	0.0000821	0.3750
9150752	7/15A	15E8_Ls1d2Vc_7	14 7/16	E	3.25	354.8	35 1/2	30	0.375	0.563	8TA	8	4	0	1.05	4.9	3.6	24.4	16	0.67	0.50	s1d2	2.48	0.0000569	0.0000693	0.0000821	0.3750
9150753	7/15A	15E8_Ls1d2Vc_7	14 7/16	E	3.25	354.8	35 1/2	30	0.375	0.563	8TA	8	4	0	1.05	4.9	3.6	24.4	16	0.67	0.50	s1d2	2.48	0.0000569	0.0000693	0.0000821	0.3750
9150754M	7/15A	15E8_Ls1d2Vc_7	14 7/16	E	3.25	354.8	35 1/2	30	0.375	0.563	8TA	8	4	0	1.05	4.9	3.6	24.4	16	0.67	0.50	s1d2	2.48	0.0000569	0.0000693	0.0000821	0.3750
9150755M	7/15A	15E8_Ls1d2Vc_7	14 7/16	E	3.25	354.8	35 1/2	30	0.375	0.563	8TA	8	4	0	1.05	4.9	3.6	24.4	16	0.67	0.50	s1d2	2.48	0.0000569	0.0000693	0.0000821	0.3750
9150756M	7/15A	15E8_Ls1d2Vc_7	14 7/16	E	3.25	354.8	35 1/2	30	0.375	0.563	8TA	8	4	0	1.05	4.9	3.6	24.4	16	0.67	0.50	s1d2	2.48	0.0000569	0.0000693	0.0000821	0.3750
9150757M	7/15A	15E8_Ls1d2Vc_7	14 7/16	E	3.25	354.8	35 1/2	30	0.375	0.563	8TA	8	4	0	1.05	4.9	3.6	24.4	16	0.67	0.50	s1d2	2.48	0.0000569	0.0000693	0.0000821	0.3750
9150758M	7/15A	15E8_Ls1d2Vc_7	14 7/16	E	3.25	354.8	35 1/2	30	0.375	0.563	8TA	8	4	0	1.05	4.9	3.6	24.4	16	0.67	0.50	s1d2	2.48	0.0000569	0.0000693	0.0000821	0.3750
9150758.1	7/15A	15E8_Ls1d2Vc_7	14 7/16	E	3.25	354.8	35 1/2	30	0.375	0.563	8TA	8	4	0	1.05	4.9	3.6	24.4	16	0.67	0.50	s1d2	2.48	0.0000569	0.0000693	0.0000821	0.3750
9150759M	7/15A	15E8_Ls1d2Vc_7	14 7/16	E	3.25	354.8	35 1/2	30	0.375	0.563	8TA	8	4	0	1.05	4.9	3.6	24.4	16	0.67	0.50	s1d2	2.48	0.0000569	0.0000693	0.0000821	0.3750
9150760	7/15A	15E8_Ls1d2Vc_7	14 7/16	E	3.25	354.8	35 1/2	30	0.375	0.563	8TA	8	4	0	1.05	4.9	3.6	24.4	16	0.67	0.50	s1d2	2.48	0.0000569	0.0000693	0.0000821	0.3750
9150761	7/15A	15E8_Ls1d2Vc_7	14 7/16	E	3.25	354.8	35 1/2	30	0.375	0.563	8TA	8	4	0	1.05	4.9	3.6	24.4	16	0.67	0.50	s1d2	2.48	0.0000569	0.0000693	0.0000821	0.3750
9150762	7/15A	15E8_Ls1d2Vc_7	14 7/16	E	3.25	354.8	35 1/2	30	0.375	0.563	8TA	8	4	0	1.05	4.9	3.6	24.4	16	0.67	0.50	s1d2	2.48	0.0000569	0.0000693	0.0000821	0.3750
9150763	7/15A	15E8_Ls1d2Vc_7	14 7/16	E	3.25	354.8	35 1/2	30	0.375	0.563	8TA	8	4	0	1.05	4.9	3.6	24.4	16	0.67	0.50	s1d2	2.48	0.0000569	0.0000693	0.0000821	0.3750

Table B.3. Data from 2008 Tests in Small-Scale Vessel with Elliptical Head B.21

Tank Water Temperature	Water Density	Solids Fraction	Pulse Volume Fraction	Duty Cycle	Cycle Time	Pulsed or Steady Jet	Us Steady Jet	U1 Pulsing Jet	U2 URMS	U3 URM3	Discharge Velocity	Critical Suspension Velocity	Average Peak Cloud Height	UCS Condition	UCS Method	UCS Flag	UCS Center Flag	UCS udv Flag	UCS based on Decreasing Velocity	Sweep Increase / Decrease	UDV Height Bed	Particle Motion	Solids Level	Outer Bottom Pattern	Inner Bottom Pattern	Case ID	Test	TDP	Row Number
C	g/cm³	fraction	fraction	fraction	s	text	m/s	m/s	m/s	m/s	m/s	m/s	in.	m/s	text	text	text	text	m/s	text	mm	text	text	text	text	text	text	text	text
T	ρ_c	ϕ_S	ϕ_p	DC	t_C	Jet	U_S	U1	U2	U3	U	U_{CS}	H_C	U_{CSR}	U_{CSM}	U_{CS}vis	U_{CS}cen	U_{CS}udv	U_{CS}_D	S_W	H_{bed}	PM	Sol	SP_O	SP_I	ID	M/DDX	TDP	MSS
28.8	0.998	0.00155	0.050	0.337	8.2	P	N/A	1.24	1.25	1.26	1.30	1.30	15.25	1.30	udv	UCSvis	N/A	UCSudv	N/A	I	0.0	3	N/A	N/A	N/A	15E8_Ls1d2Zc_1	7/14A	TDP-211	9150730
29.2	0.998	0.00155	0.050	0.333	7.8	P	N/A	1.32	1.34	1.35	1.40	1.30	18.00	N/A	N/A	N/A	N/A	N/A	N/A	I	0.0	4	N/A	N/A	N/A	15E8_Ls1d2Zc_1	7/14A	TDP-211	9150731
30.1	0.998	0.01430	0.050	0.338	6.8	P	N/A	1.50	1.52	1.54	1.60	1.90	5.50	N/A	N/A	N/A	N/A	N/A	N/A	(null)	16.8	1	N/A	N/A	N/A	15E8_Ls1d2Vc_1	7/14B	TDP-212	9150732
30.6	0.998	0.01430	0.050	0.332	6.2	P	N/A	1.67	1.71	1.73	1.80	1.90	8.50	N/A	N/A	N/A	N/A	N/A	N/A	I	3.6	1	N/A	N/A	N/A	15E8_Ls1d2Vc_1	7/14B	TDP-212	9150733
31.1	0.997	0.01430	0.050	0.329	7.0	P	N/A	1.50	1.52	1.54	1.60	1.90	5.00	N/A	N/A	N/A	N/A	N/A	N/A	I	18.6	1	N/A	N/A	N/A	15E8_Ls1d2Vc_1	7/14B	TDP-212	9150734
31.4	0.997	0.01430	0.050	0.332	6.6	P	N/A	1.58	1.61	1.62	1.70	1.90	6.50	N/A	N/A	N/A	N/A	N/A	N/A	I	13.1	1	N/A	N/A	N/A	15E8_Ls1d2Vc_1	7/14B	TDP-212	9150735
31.6	0.997	0.01430	0.050	0.333	6.2	P	N/A	1.67	1.70	1.72	1.80	1.90	8.00	N/A	N/A	N/A	N/A	N/A	N/A	I	1.1	1	N/A	N/A	N/A	15E8_Ls1d2Vc_1	7/14B	TDP-212	9150736
31.8	0.997	0.01430	0.050	0.338	5.8	P	N/A	1.75	1.79	1.81	1.90	1.90	9.75	1.90	udv	UCSvis	N/A	UCSudv	N/A	I	0.0	3	N/A	N/A	N/A	15E8_Ls1d2Vc_1	7/14B	TDP-212	9150737
32.2	0.998	0.01430	0.050	0.330	5.7	P	N/A	1.84	1.88	1.90	2.00	1.90	10.50	N/A	N/A	N/A	N/A	N/A	N/A	I	0.0	4	N/A	N/A	N/A	15E8_Ls1d2Vc_1	7/14B	TDP-212	9150738
32.6	0.997	0.01430	0.050	0.337	5.8	P	N/A	1.75	1.79	1.81	1.90	1.90	9.50	N/A	N/A	N/A	N/A	N/A	N/A	N/A	n/a	N/A	N/A	N/A	N/A	15E8_Ls1d2Vc_1	7/14B	TDP-212	9150738.1
32.6	0.997	0.01430	0.050	0.337	5.8	P	N/A	1.75	1.79	1.81	1.90	1.90	9.50	N/A	N/A	N/A	N/A	N/A	N/A	N/A	n/a	N/A	N/A	N/A	N/A	15E8_Ls1d2Vc_1	7/14B	TDP-212	9150738.2
32.6	0.997	0.01430	0.050	0.337	5.8	P	N/A	1.75	1.79	1.81	1.90	1.90	9.50	N/A	N/A	UCSvis	N/A	N/A	N/A	I	0.0	3	N/A	N/A	N/A	15E8_Ls1d2Vc_1	7/14B	TDP-212	9150739
32.6	0.997	0.01430	0.050	0.337	5.8	P	N/A	1.75	1.79	1.81	1.90	1.90	9.50	N/A	N/A	N/A	N/A	N/A	N/A	N/A	0.0	N/A	N/A	N/A	N/A	15E8_Ls1d2Vc_1	7/14B	TDP-212	9150740
32.6	0.997	0.01430	0.050	0.337	5.8	P	N/A	1.75	1.79	1.81	1.90	1.90	9.50	N/A	N/A	N/A	N/A	N/A	N/A	N/A	0.0	N/A	N/A	N/A	N/A	15E8_Ls1d2Vc_1	7/14B	TDP-212	9150741
32.6	0.997	0.01430	0.050	0.337	5.8	P	N/A	1.75	1.79	1.81	1.90	1.90	9.50	N/A	N/A	N/A	N/A	N/A	N/A	N/A	0.0	N/A	N/A	N/A	N/A	15E8_Ls1d2Vc_1	7/14B	TDP-212	9150742
32.6	0.997	0.01430	0.050	0.337	5.8	P	N/A	1.75	1.79	1.81	1.90	1.90	9.50	N/A	N/A	N/A	N/A	N/A	N/A	N/A	n/a	N/A	N/A	N/A	N/A	15E8_Ls1d2Vc_1	7/14B	TDP-212	9150742.1
32.6	0.997	0.01430	0.050	0.337	5.8	P	N/A	1.75	1.79	1.81	1.90	1.90	9.50	N/A	N/A	N/A	N/A	N/A	N/A	N/A	0.0	N/A	N/A	N/A	N/A	15E8_Ls1d2Vc_1	7/14B	TDP-212	9150743
32.6	0.997	0.01430	0.050	0.337	5.8	P	N/A	1.75	1.79	1.81	1.90	1.90	9.50	N/A	N/A	N/A	N/A	N/A	N/A	N/A	n/a	N/A	N/A	N/A	N/A	15E8_Ls1d2Vc_1	7/14B	TDP-212	9150743.1
32.6	0.997	0.01430	0.050	0.337	5.8	P	N/A	1.75	1.79	1.81	1.90	1.90	9.50	N/A	N/A	N/A	N/A	N/A	N/A	N/A	0.0	N/A	N/A	N/A	N/A	15E8_Ls1d2Vc_1	7/14B	TDP-212	9150744
32.6	0.997	0.01430	0.050	0.337	5.8	P	N/A	1.75	1.79	1.81	1.90	1.90	9.50	N/A	N/A	N/A	N/A	N/A	N/A	N/A	n/a	N/A	N/A	N/A	N/A	15E8_Ls1d2Vc_1	7/14B	TDP-212	9150744.1
32.6	0.997	0.01430	0.050	0.337	5.8	P	N/A	1.75	1.79	1.81	1.90	1.90	9.50	N/A	N/A	N/A	N/A	N/A	N/A	N/A	0.0	N/A	N/A	N/A	N/A	15E8_Ls1d2Vc_1	7/14B	TDP-212	9150745
32.6	0.997	0.01430	0.050	0.337	5.8	P	N/A	1.75	1.79	1.81	1.90	1.90	9.50	N/A	N/A	N/A	N/A	N/A	N/A	N/A	n/a	N/A	N/A	N/A	N/A	15E8_Ls1d2Vc_1	7/14B	TDP-212	9150745.1
32.6	0.997	0.01430	0.050	0.337	5.8	P	N/A	1.75	1.79	1.81	1.90	1.90	9.50	N/A	N/A	N/A	N/A	N/A	N/A	N/A	0.0	N/A	N/A	N/A	N/A	15E8_Ls1d2Vc_1	7/14B	TDP-212	9150746
27.9	0.998	0.01430	0.100	0.329	26.8	P	N/A	1.56	1.57	1.58	1.60	2.50	4.50	N/A	N/A	N/A	N/A	N/A	N/A	(null)	14.6	1	N/A	N/A	N/A	15E8_Ls1d2Vc_7	7/15A	TDP-213	9150747
27.9	0.998	0.01430	0.100	0.331	23.8	P	N/A	1.75	1.76	1.77	1.80	2.50	4.75	N/A	N/A	N/A	N/A	N/A	N/A	I	11.3	1	N/A	N/A	N/A	15E8_Ls1d2Vc_7	7/15A	TDP-213	9150748
28.1	0.998	0.01430	0.100	0.331	21.4	P	N/A	1.95	1.96	1.97	2.00	2.50	5.75	N/A	N/A	N/A	N/A	N/A	N/A	D	17.6	1	N/A	N/A	N/A	15E8_Ls1d2Vc_7	7/15A	TDP-213	9150749
28.2	0.999	0.01430	0.100	0.333	20.2	P	N/A	2.04	2.06	2.07	2.10	2.50	6.75	N/A	N/A	N/A	N/A	N/A	N/A	I	11.8	1	N/A	N/A	N/A	15E8_Ls1d2Vc_7	7/15A	TDP-213	9150750
28.3	0.998	0.01430	0.100	0.334	19.2	P	N/A	2.14	2.16	2.17	2.20	2.50	8.50	N/A	N/A	N/A	N/A	N/A	N/A	I	0.0	1	N/A	N/A	N/A	15E8_Ls1d2Vc_7	7/15A	TDP-213	9150751
28.5	0.998	0.01430	0.100	0.332	18.6	P	N/A	2.23	2.24	2.25	2.30	2.50	9.50	N/A	N/A	N/A	N/A	N/A	N/A	I	4.0	1	N/A	N/A	N/A	15E8_Ls1d2Vc_7	7/15A	TDP-213	9150752
28.6	0.998	0.01430	0.100	0.333	17.8	P	N/A	2.32	2.34	2.35	2.40	2.50	10.75	N/A	N/A	N/A	N/A	N/A	N/A	I	2.8	1	N/A	N/A	N/A	15E8_Ls1d2Vc_7	7/15A	TDP-213	9150753
28.7	0.998	0.01430	0.100	0.335	17.0	P	N/A	2.41	2.43	2.45	2.50	2.50	11.00	2.50	udv	N/A	N/A	UCSudv	N/A	I	0.0	1	N/A	N/A	N/A	15E8_Ls1d2Vc_7	7/15A	TDP-213	9150754
28.9	0.998	0.01430	0.101	0.334	16.6	P	N/A	2.50	2.53	2.54	2.60	2.50	12.25	N/A	N/A	UCSvis	N/A	N/A	N/A	I	0.0	3	N/A	N/A	N/A	15E8_Ls1d2Vc_7	7/15A	TDP-213	9150755
29.0	0.998	0.01430	0.100	0.333	16.0	P	N/A	2.59	2.62	2.63	2.70	2.50	13.00	N/A	N/A	N/A	N/A	N/A	N/A	I	0.0	4	N/A	N/A	N/A	15E8_Ls1d2Vc_7	7/15A	TDP-213	9150756
29.1	0.998	0.01430	0.100	0.336	14.8	P	N/A	2.78	2.81	2.83	2.90	2.50	15.25	N/A	N/A	N/A	N/A	N/A	N/A	I	0.0	4	N/A	N/A	N/A	15E8_Ls1d2Vc_7	7/15A	TDP-213	9150757
29.3	0.998	0.01430	0.100	0.335	13.8	P	N/A	2.98	3.01	3.03	3.10	2.50	18.75	N/A	N/A	N/A	N/A	N/A	N/A	I	0.0	4	N/A	N/A	N/A	15E8_Ls1d2Vc_7	7/15A	TDP-213	9150758
29.5	0.998	0.01430	0.100	0.335	17.0	P	N/A	2.41	2.43	2.45	2.50	2.50	11.50	N/A	N/A	N/A	N/A	N/A	N/A	N/A	n/a	N/A	N/A	N/A	N/A	15E8_Ls1d2Vc_7	7/15A	TDP-213	9150758.1
29.5	0.998	0.01430	0.100	0.335	17.0	P	N/A	2.41	2.43	2.45	2.50	2.50	11.50	N/A	N/A	N/A	N/A	N/A	N/A	I	1.8	1	N/A	N/A	N/A	15E8_Ls1d2Vc_7	7/15A	TDP-213	9150759
29.5	0.998	0.01430	0.100	0.335	17.0	P	N/A	2.41	2.43	2.45	2.50	2.50	11.50	N/A	N/A	N/A	N/A	N/A	N/A	N/A	0.0	N/A	N/A	N/A	N/A	15E8_Ls1d2Vc_7	7/15A	TDP-213	9150760
29.5	0.998	0.01430	0.100	0.335	17.0	P	N/A	2.41	2.43	2.45	2.50	2.50	11.50	N/A	N/A	N/A	N/A	N/A	N/A	N/A	0.0	N/A	N/A	N/A	N/A	15E8_Ls1d2Vc_7	7/15A	TDP-213	9150761
29.5	0.998	0.01430	0.100	0.335	17.0	P	N/A	2.41	2.43	2.45	2.50	2.50	11.50	N/A	N/A	N/A	N/A	N/A	N/A	N/A	0.0	N/A	N/A	N/A	N/A	15E8_Ls1d2Vc_7	7/15A	TDP-213	9150762
29.5	0.998	0.01430	0.100	0.335	17.0	P	N/A	2.41	2.43	2.45	2.50	2.50	11.50	N/A	N/A	N/A	N/A	N/A	N/A	N/A	0.0	N/A	N/A	N/A	N/A	15E8_Ls1d2Vc_7	7/15A	TDP-213	9150763

Table B.3. Data from 2008 Tests in Small-Scale Vessel with Elliptical Head A.22

Row Number	Test	Case ID	Tank Diameter	Head Shape	Dish Height	Dish Volume	Tank Fill Height	Return Line Height	Nozzle Inner Diameter	Nozzle Stand-off Distance	Pulse Tube Configuration	Installed Nozzles	Outer Nozzles Operated	Inner Nozzles Operated	Pulse Tube Outer Diameter	Outer PJM Radius	Inner PJM Radius	"FIO" Outer PJM Impingement Angle	"FIO" Inner PJM Impingement Angle	Ratio Outer PJM to Tank Radius	Ratio Inner PJM to Tank Radius	Simulant	Solids Density	Particle Diameter d5	Particle Diameter d50	Particle Diameter d95	Void Fraction
text	text	text	in.	text	in.	in. ^{3}	in.	in.	in.	in.	text	number	number	number	in.	in.	in.	deg	deg	nondim	nondim	text	g/cm^3	m	m	m	fraction
MSS	M/DDX	ID	D	HS	H_{dish}	V_{dish}	H	Rtn	d	sod	PT	N	N_O	N_I	PT_{od}	R_O	R_I	θ_O	θ_I	R_O/R	R_I/R	sxdx	ρ_s	d_5	d_{50}	d_{95}	vf
9150763.1	7/15A	15E8_Ls1d2Vc_7	14 7/16	E	3.25	354.8	35 1/2	30	0.375	0.563	8TA	8	4	0	1.05	4.9	3.6	24.4	16	0.67	0.50	s1d2	2.48	0.0000569	0.0000693	0.0000821	0.3750
9150764	7/15A	15E8_Ls1d2Vc_7	14 7/16	E	3.25	354.8	35 1/2	30	0.375	0.563	8TA	8	4	0	1.05	4.9	3.6	24.4	16	0.67	0.50	s1d2	2.48	0.0000569	0.0000693	0.0000821	0.3750
9150764.1	7/15A	15E8_Ls1d2Vc_7	14 7/16	E	3.25	354.8	35 1/2	30	0.375	0.563	8TA	8	4	0	1.05	4.9	3.6	24.4	16	0.67	0.50	s1d2	2.48	0.0000569	0.0000693	0.0000821	0.3750
9150765	7/15A	15E8_Ls1d2Vc_7	14 7/16	E	3.25	354.8	35 1/2	30	0.375	0.563	8TA	8	4	0	1.05	4.9	3.6	24.4	16	0.67	0.50	s1d2	2.48	0.0000569	0.0000693	0.0000821	0.3750
9150765.1	7/15A	15E8_Ls1d2Vc_7	14 7/16	E	3.25	354.8	35 1/2	30	0.375	0.563	8TA	8	4	0	1.05	4.9	3.6	24.4	16	0.67	0.50	s1d2	2.48	0.0000569	0.0000693	0.0000821	0.3750
9150766	7/15A	15E8_Ls1d2Vc_7	14 7/16	E	3.25	354.8	35 1/2	30	0.375	0.563	8TA	8	4	0	1.05	4.9	3.6	24.4	16	0.67	0.50	s1d2	2.48	0.0000569	0.0000693	0.0000821	0.3750
9150766.1	7/15A	15E8_Ls1d2Vc_7	14 7/16	E	3.25	354.8	35 1/2	30	0.375	0.563	8TA	8	4	0	1.05	4.9	3.6	24.4	16	0.67	0.50	s1d2	2.48	0.0000569	0.0000693	0.0000821	0.3750
9150767	7/15A	15E8_Ls1d2Vc_7	14 7/16	E	3.25	354.8	35 1/2	30	0.375	0.563	8TA	8	4	0	1.05	4.9	3.6	24.4	16	0.67	0.50	s1d2	2.48	0.0000569	0.0000693	0.0000821	0.3750
9150768	7/15B	15E8_Ls1d2Vc_2	14 7/16	E	3.25	354.8	35 1/2	30	0.375	0.563	8TA	8	4	4	1.05	4.9	3.6	24.4	16	0.67	0.50	s1d2	2.48	0.0000569	0.0000693	0.0000821	0.3750
9150769	7/15B	15E8_Ls1d2Vc_2	14 7/16	E	3.25	354.8	35 1/2	30	0.375	0.563	8TA	8	4	4	1.05	4.9	3.6	24.4	16	0.67	0.50	s1d2	2.48	0.0000569	0.0000693	0.0000821	0.3750
9150770	7/15B	15E8_Ls1d2Vc_2	14 7/16	E	3.25	354.8	35 1/2	30	0.375	0.563	8TA	8	4	4	1.05	4.9	3.6	24.4	16	0.67	0.50	s1d2	2.48	0.0000569	0.0000693	0.0000821	0.3750
9150771M	7/15B	15E8_Ls1d2Vc_2	14 7/16	E	3.25	354.8	35 1/2	30	0.375	0.563	8TA	8	4	4	1.05	4.9	3.6	24.4	16	0.67	0.50	s1d2	2.48	0.0000569	0.0000693	0.0000821	0.3750
9150772M	7/15B	15E8_Ls1d2Vc_2	14 7/16	E	3.25	354.8	35 1/2	30	0.375	0.563	8TA	8	4	4	1.05	4.9	3.6	24.4	16	0.67	0.50	s1d2	2.48	0.0000569	0.0000693	0.0000821	0.3750
9150773M	7/15B	15E8_Ls1d2Vc_2	14 7/16	E	3.25	354.8	35 1/2	30	0.375	0.563	8TA	8	4	4	1.05	4.9	3.6	24.4	16	0.67	0.50	s1d2	2.48	0.0000569	0.0000693	0.0000821	0.3750
9150774	7/15B	15E8_Ls1d2Vc_2	14 7/16	E	3.25	354.8	35 1/2	30	0.375	0.563	8TA	8	4	4	1.05	4.9	3.6	24.4	16	0.67	0.50	s1d2	2.48	0.0000569	0.0000693	0.0000821	0.3750
9150775	7/15B	15E8_Ls1d2Vc_2	14 7/16	E	3.25	354.8	35 1/2	30	0.375	0.563	8TA	8	4	4	1.05	4.9	3.6	24.4	16	0.67	0.50	s1d2	2.48	0.0000569	0.0000693	0.0000821	0.3750
9150776	7/15B	15E8_Ls1d2Vc_2	14 7/16	E	3.25	354.8	35 1/2	30	0.375	0.563	8TA	8	4	4	1.05	4.9	3.6	24.4	16	0.67	0.50	s1d2	2.48	0.0000569	0.0000693	0.0000821	0.3750
9150777	7/15B	15E8_Ls1d2Vc_2	14 7/16	E	3.25	354.8	35 1/2	30	0.375	0.563	8TA	8	4	4	1.05	4.9	3.6	24.4	16	0.67	0.50	s1d2	2.48	0.0000569	0.0000693	0.0000821	0.3750
9150778	7/15B	15E8_Ls1d2Vc_2	14 7/16	E	3.25	354.8	35 1/2	30	0.375	0.563	8TA	8	4	4	1.05	4.9	3.6	24.4	16	0.67	0.50	s1d2	2.48	0.0000569	0.0000693	0.0000821	0.3750
9150778.1	7/15B	15E8_Ls1d2Vc_2	14 7/16	E	3.25	354.8	35 1/2	30	0.375	0.563	8TA	8	4	4	1.05	4.9	3.6	24.4	16	0.67	0.50	s1d2	2.48	0.0000569	0.0000693	0.0000821	0.3750
9150779	7/15B	15E8_Ls1d2Vc_2	14 7/16	E	3.25	354.8	35 1/2	30	0.375	0.563	8TA	8	4	4	1.05	4.9	3.6	24.4	16	0.67	0.50	s1d2	2.48	0.0000569	0.0000693	0.0000821	0.3750
9150779.1	7/15B	15E8_Ls1d2Vc_2	14 7/16	E	3.25	354.8	35 1/2	30	0.375	0.563	8TA	8	4	4	1.05	4.9	3.6	24.4	16	0.67	0.50	s1d2	2.48	0.0000569	0.0000693	0.0000821	0.3750
9150780	7/15B	15E8_Ls1d2Vc_2	14 7/16	E	3.25	354.8	35 1/2	30	0.375	0.563	8TA	8	4	4	1.05	4.9	3.6	24.4	16	0.67	0.50	s1d2	2.48	0.0000569	0.0000693	0.0000821	0.3750
9150780.1	7/15B	15E8_Ls1d2Vc_2	14 7/16	E	3.25	354.8	35 1/2	30	0.375	0.563	8TA	8	4	4	1.05	4.9	3.6	24.4	16	0.67	0.50	s1d2	2.48	0.0000569	0.0000693	0.0000821	0.3750
9150781	7/15B	15E8_Ls1d2Vc_2	14 7/16	E	3.25	354.8	35 1/2	30	0.375	0.563	8TA	8	4	4	1.05	4.9	3.6	24.4	16	0.67	0.50	s1d2	2.48	0.0000569	0.0000693	0.0000821	0.3750
9150781.1	7/15B	15E8_Ls1d2Vc_2	14 7/16	E	3.25	354.8	35 1/2	30	0.375	0.563	8TA	8	4	4	1.05	4.9	3.6	24.4	16	0.67	0.50	s1d2	2.48	0.0000569	0.0000693	0.0000821	0.3750
9150782	7/15B	15E8_Ls1d2Vc_2	14 7/16	E	3.25	354.8	35 1/2	30	0.375	0.563	8TA	8	4	4	1.05	4.9	3.6	24.4	16	0.67	0.50	s1d2	2.48	0.0000569	0.0000693	0.0000821	0.3750
9150783	7/15C	15E8_Ls1d2Vc_6	14 7/16	E	3.25	354.8	35 1/2	30	0.375	0.563	8TA	8	4	0	1.05	4.9	3.6	24.4	16	0.67	0.50	s1d2	2.48	0.0000569	0.0000693	0.0000821	0.3750
9150784	7/15C	15E8_Ls1d2Vc_6	14 7/16	E	3.25	354.8	35 1/2	30	0.375	0.563	8TA	8	4	0	1.05	4.9	3.6	24.4	16	0.67	0.50	s1d2	2.48	0.0000569	0.0000693	0.0000821	0.3750
9150785	7/15C	15E8_Ls1d2Vc_6	14 7/16	E	3.25	354.8	35 1/2	30	0.375	0.563	8TA	8	4	0	1.05	4.9	3.6	24.4	16	0.67	0.50	s1d2	2.48	0.0000569	0.0000693	0.0000821	0.3750
9150786	7/15C	15E8_Ls1d2Vc_6	14 7/16	E	3.25	354.8	35 1/2	30	0.375	0.563	8TA	8	4	0	1.05	4.9	3.6	24.4	16	0.67	0.50	s1d2	2.48	0.0000569	0.0000693	0.0000821	0.3750
9150787	7/15C	15E8_Ls1d2Vc_6	14 7/16	E	3.25	354.8	35 1/2	30	0.375	0.563	8TA	8	4	0	1.05	4.9	3.6	24.4	16	0.67	0.50	s1d2	2.48	0.0000569	0.0000693	0.0000821	0.3750
9150788M	7/15C	15E8_Ls1d2Vc_6	14 7/16	E	3.25	354.8	35 1/2	30	0.375	0.563	8TA	8	4	0	1.05	4.9	3.6	24.4	16	0.67	0.50	s1d2	2.48	0.0000569	0.0000693	0.0000821	0.3750
9150789M	7/15C	15E8_Ls1d2Vc_6	14 7/16	E	3.25	354.8	35 1/2	30	0.375	0.563	8TA	8	4	0	1.05	4.9	3.6	24.4	16	0.67	0.50	s1d2	2.48	0.0000569	0.0000693	0.0000821	0.3750
9150790M	7/15C	15E8_Ls1d2Vc_6	14 7/16	E	3.25	354.8	35 1/2	30	0.375	0.563	8TA	8	4	0	1.05	4.9	3.6	24.4	16	0.67	0.50	s1d2	2.48	0.0000569	0.0000693	0.0000821	0.3750
9150791M	7/15C	15E8_Ls1d2Vc_6	14 7/16	E	3.25	354.8	35 1/2	30	0.375	0.563	8TA	8	4	0	1.05	4.9	3.6	24.4	16	0.67	0.50	s1d2	2.48	0.0000569	0.0000693	0.0000821	0.3750
9150792M	7/15C	15E8_Ls1d2Vc_6	14 7/16	E	3.25	354.8	35 1/2	30	0.375	0.563	8TA	8	4	0	1.05	4.9	3.6	24.4	16	0.67	0.50	s1d2	2.48	0.0000569	0.0000693	0.0000821	0.3750
9150793M	7/15C	15E8_Ls1d2Vc_6	14 7/16	E	3.25	354.8	35 1/2	30	0.375	0.563	8TA	8	4	0	1.05	4.9	3.6	24.4	16	0.67	0.50	s1d2	2.48	0.0000569	0.0000693	0.0000821	0.3750

Table B.3. Data from 2008 Tests in Small-Scale Vessel with Elliptical Head B.22

Tank Water Temperature	Water Density	Solids Fraction	Pulse Volume Fraction	Duty Cycle	Cycle Time	Pulsed or Steady Jet	Us Steady Jet	U1 Pulsing Jet	U2 URMS	U3 URM3	Discharge Velocity	Critical Suspension Velocity	Average Peak Cloud Height	UCS Condition	UCS Method	UCS Flag	UCS Center Flag	UCS udv Flag	UCS based on Decreasing Velocity	Sweep Increase / Decrease	UDV Height Bed	Particle Motion	Solids Level	Outer Bottom Pattern	Inner Bottom Pattern	Case ID	Test	TDP	Row Number
C	g/cm³	fraction	fraction	fraction	s	text	m/s	m/s	m/s	m/s	m/s	m/s	in.	m/s	text	text	text	text	m/s	text	mm	text	text	text	text	text	text	text	text
T	ρ_c	ϕ_S	ϕ_p	DC	t_C	Jet	U_S	U1	U2	U3	U	U_{CS}	H_C	U_{CSR}	U_{CSM}	U_{CS}vis	U_{CS}cen	U_{CS}udv	$U_{CS_}D$	S_W	H_{bed}	PM	Sol	SP_O	SP_I	ID	M/DDX	TDP	MSS
29.5	0.998	0.01430	0.100	0.335	17.0	P	N/A	2.41	2.43	2.45	2.50	2.50	11.50	N/A	N/A	N/A	N/A	N/A	N/A	N/A	n/a	N/A	N/A	N/A	N/A	15E8_Ls1d2Vc_7	7/15A	TDP-213	9150763.1
29.5	0.998	0.01430	0.100	0.335	17.0	P	N/A	2.41	2.43	2.45	2.50	2.50	11.50	N/A	N/A	N/A	N/A	N/A	N/A	N/A	0.0	N/A	N/A	N/A	N/A	15E8_Ls1d2Vc_7	7/15A	TDP-213	9150764
29.5	0.998	0.01430	0.100	0.335	17.0	P	N/A	2.41	2.43	2.45	2.50	2.50	11.50	N/A	N/A	N/A	N/A	N/A	N/A	N/A	n/a	N/A	N/A	N/A	N/A	15E8_Ls1d2Vc_7	7/15A	TDP-213	9150764.1
29.5	0.998	0.01430	0.100	0.335	17.0	P	N/A	2.41	2.43	2.45	2.50	2.50	11.50	N/A	N/A	N/A	N/A	N/A	N/A	N/A	0.7	N/A	N/A	N/A	N/A	15E8_Ls1d2Vc_7	7/15A	TDP-213	9150765
29.5	0.998	0.01430	0.100	0.335	17.0	P	N/A	2.41	2.43	2.45	2.50	2.50	11.50	N/A	N/A	N/A	N/A	N/A	N/A	N/A	n/a	N/A	N/A	N/A	N/A	15E8_Ls1d2Vc_7	7/15A	TDP-213	9150765.1
29.5	0.998	0.01430	0.100	0.335	17.0	P	N/A	2.41	2.43	2.45	2.50	2.50	11.50	N/A	N/A	N/A	N/A	N/A	N/A	N/A	2.2	N/A	N/A	N/A	N/A	15E8_Ls1d2Vc_7	7/15A	TDP-213	9150766
29.5	0.998	0.01430	0.100	0.335	17.0	P	N/A	2.41	2.43	2.45	2.50	2.50	11.50	N/A	N/A	N/A	N/A	N/A	N/A	N/A	n/a	N/A	N/A	N/A	N/A	15E8_Ls1d2Vc_7	7/15A	TDP-213	9150766.1
29.5	0.998	0.01430	0.100	0.335	17.0	P	N/A	2.41	2.43	2.45	2.50	2.50	11.50	N/A	N/A	N/A	N/A	N/A	N/A	N/A	3.7	N/A	N/A	N/A	N/A	15E8_Ls1d2Vc_7	7/15A	TDP-213	9150767
29.5	0.998	0.01430	0.101	0.326	15.6	P	N/A	1.36	1.37	1.38	1.40	1.90	5.25	N/A	N/A	N/A	N/A	N/A	N/A	(null)	24.1	1	N/A	N/A	N/A	15E8_Ls1d2Vc_2	7/15B	TDP-213	9150768
29.6	0.998	0.01430	0.101	0.330	13.6	P	N/A	1.55	1.56	1.57	1.60	1.90	7.75	N/A	N/A	N/A	N/A	N/A	N/A	I	13.7	1	N/A	N/A	N/A	15E8_Ls1d2Vc_2	7/15B	TDP-213	9150769
29.8	0.998	0.01430	0.100	0.332	12.0	P	N/A	1.73	1.75	1.76	1.80	1.90	10.50	N/A	N/A	N/A	N/A	N/A	N/A	I	3.3	1	N/A	N/A	N/A	15E8_Ls1d2Vc_2	7/15B	TDP-213	9150770
30.0	0.998	0.01430	0.101	0.334	11.4	P	N/A	1.82	1.84	1.85	1.90	1.90	12.00	1.90	udv	UCSvis	N/A	UCSudv	N/A	I	0.0	3	N/A	N/A	N/A	15E8_Ls1d2Vc_2	7/15B	TDP-213	9150771
30.3	0.998	0.01430	0.100	0.335	10.8	P	N/A	1.91	1.94	1.95	2.00	1.90	15.25	N/A	N/A	N/A	N/A	N/A	N/A	I	0.0	4	N/A	N/A	N/A	15E8_Ls1d2Vc_2	7/15B	TDP-213	9150772
30.8	0.998	0.01430	0.101	0.335	11.4	P	N/A	1.82	1.84	1.85	1.90	1.90	11.50	N/A	N/A	UCSvis	N/A	N/A	N/A	I	0.0	3	N/A	N/A	N/A	15E8_Ls1d2Vc_2	7/15B	TDP-213	9150773
30.8	0.998	0.01430	0.101	0.335	11.4	P	N/A	1.82	1.84	1.85	1.90	1.90	11.50	N/A	N/A	N/A	N/A	N/A	N/A	N/A	0.0	N/A	N/A	N/A	N/A	15E8_Ls1d2Vc_2	7/15B	TDP-213	9150774
30.8	0.998	0.01430	0.101	0.335	11.4	P	N/A	1.82	1.84	1.85	1.90	1.90	11.50	N/A	N/A	N/A	N/A	N/A	N/A	N/A	0.0	N/A	N/A	N/A	N/A	15E8_Ls1d2Vc_2	7/15B	TDP-213	9150775
30.8	0.998	0.01430	0.101	0.335	11.4	P	N/A	1.82	1.84	1.85	1.90	1.90	11.50	N/A	N/A	N/A	N/A	N/A	N/A	N/A	0.0	N/A	N/A	N/A	N/A	15E8_Ls1d2Vc_2	7/15B	TDP-213	9150776
30.8	0.998	0.01430	0.101	0.335	11.4	P	N/A	1.82	1.84	1.85	1.90	1.90	11.50	N/A	N/A	N/A	N/A	N/A	N/A	N/A	0.0	N/A	N/A	N/A	N/A	15E8_Ls1d2Vc_2	7/15B	TDP-213	9150777
30.8	0.998	0.01430	0.101	0.335	11.4	P	N/A	1.82	1.84	1.85	1.90	1.90	11.50	N/A	N/A	N/A	N/A	N/A	N/A	N/A	0.0	N/A	N/A	N/A	N/A	15E8_Ls1d2Vc_2	7/15B	TDP-213	9150778
30.8	0.998	0.01430	0.101	0.335	11.4	P	N/A	1.82	1.84	1.85	1.90	1.90	11.50	N/A	N/A	N/A	N/A	N/A	N/A	N/A	n/a	N/A	N/A	N/A	N/A	15E8_Ls1d2Vc_2	7/15B	TDP-213	9150778.1
30.8	0.998	0.01430	0.101	0.335	11.4	P	N/A	1.82	1.84	1.85	1.90	1.90	11.50	N/A	N/A	N/A	N/A	N/A	N/A	N/A	0.0	N/A	N/A	N/A	N/A	15E8_Ls1d2Vc_2	7/15B	TDP-213	9150779
30.8	0.998	0.01430	0.101	0.335	11.4	P	N/A	1.82	1.84	1.85	1.90	1.90	11.50	N/A	N/A	N/A	N/A	N/A	N/A	N/A	n/a	N/A	N/A	N/A	N/A	15E8_Ls1d2Vc_2	7/15B	TDP-213	9150779.1
30.8	0.998	0.01430	0.101	0.335	11.4	P	N/A	1.82	1.84	1.85	1.90	1.90	11.50	N/A	N/A	N/A	N/A	N/A	N/A	N/A	0.0	N/A	N/A	N/A	N/A	15E8_Ls1d2Vc_2	7/15B	TDP-213	9150780
30.8	0.998	0.01430	0.101	0.335	11.4	P	N/A	1.82	1.84	1.85	1.90	1.90	11.50	N/A	N/A	N/A	N/A	N/A	N/A	N/A	n/a	N/A	N/A	N/A	N/A	15E8_Ls1d2Vc_2	7/15B	TDP-213	9150780.1
30.8	0.998	0.01430	0.101	0.335	11.4	P	N/A	1.82	1.84	1.85	1.90	1.90	11.50	N/A	N/A	N/A	N/A	N/A	N/A	N/A	0.0	N/A	N/A	N/A	N/A	15E8_Ls1d2Vc_2	7/15B	TDP-213	9150781
30.8	0.998	0.01430	0.101	0.335	11.4	P	N/A	1.82	1.84	1.85	1.90	1.90	11.50	N/A	N/A	N/A	N/A	N/A	N/A	N/A	n/a	N/A	N/A	N/A	N/A	15E8_Ls1d2Vc_2	7/15B	TDP-213	9150781.1
30.8	0.998	0.01430	0.101	0.335	11.4	P	N/A	1.82	1.84	1.85	1.90	1.90	11.50	N/A	N/A	N/A	N/A	N/A	N/A	N/A	0.0	N/A	N/A	N/A	N/A	15E8_Ls1d2Vc_2	7/15B	TDP-213	9150782
31.2	0.998	0.01430	0.050	0.330	12.2	P	N/A	1.71	1.73	1.74	1.80	2.60	4.25	N/A	N/A	N/A	N/A	N/A	N/A	D	30.7	1	N/A	N/A	N/A	15E8_Ls1d2Vc_6	7/15C	TDP-213	9150783
31.3	0.997	0.01430	0.050	0.332	11.0	P	N/A	1.90	1.92	1.94	2.00	2.60	4.75	N/A	N/A	N/A	N/A	N/A	N/A	I	25.4	1	N/A	N/A	N/A	15E8_Ls1d2Vc_6	7/15C	TDP-213	9150784
31.3	0.997	0.01430	0.050	0.334	10.0	P	N/A	2.07	2.10	2.12	2.20	2.60	5.50	N/A	N/A	N/A	N/A	N/A	N/A	I	19.2	1	N/A	N/A	N/A	15E8_Ls1d2Vc_6	7/15C	TDP-213	9150785
31.4	0.997	0.01430	0.050	0.329	9.4	P	N/A	2.24	2.28	2.30	2.40	2.60	7.25	N/A	N/A	N/A	N/A	N/A	N/A	I	6.9	1	N/A	N/A	N/A	15E8_Ls1d2Vc_6	7/15C	TDP-213	9150786
31.4	0.998	0.01430	0.050	0.329	9.0	P	N/A	2.35	2.39	2.41	2.50	2.60	8.50	N/A	N/A	N/A	N/A	N/A	N/A	I	4.0	1	N/A	N/A	N/A	15E8_Ls1d2Vc_6	7/15C	TDP-213	9150787
31.5	0.997	0.01430	0.050	0.330	8.6	P	N/A	2.43	2.47	2.50	2.60	2.60	9.75	2.60	udv	N/A	N/A	UCSudv	N/A	I	0.0	1	N/A	N/A	N/A	15E8_Ls1d2Vc_6	7/15C	TDP-213	9150788
31.7	0.998	0.01430	0.050	0.325	8.4	P	N/A	2.52	2.56	2.59	2.70	2.60	10.25	N/A	N/A	N/A	N/A	N/A	N/A	I	0.0	1	N/A	N/A	N/A	15E8_Ls1d2Vc_6	7/15C	TDP-213	9150789
31.8	0.997	0.01430	0.050	0.328	8.0	P	N/A	2.60	2.65	2.68	2.80	2.60	12.00	N/A	N/A	UCSvis	N/A	N/A	N/A	I	0.0	3	N/A	N/A	N/A	15E8_Ls1d2Vc_6	7/15C	TDP-213	9150790
31.9	0.998	0.01430	0.050	0.332	7.8	P	N/A	2.67	2.73	2.76	2.90	2.60	13.50	N/A	N/A	N/A	N/A	N/A	N/A	I	0.0	4	N/A	N/A	N/A	15E8_Ls1d2Vc_6	7/15C	TDP-213	9150791
32.0	0.998	0.01430	0.050	0.336	7.2	P	N/A	2.85	2.92	2.96	3.10	2.60	15.75	N/A	N/A	N/A	N/A	N/A	N/A	I	0.0	4	N/A	N/A	N/A	15E8_Ls1d2Vc_6	7/15C	TDP-213	9150792
32.1	0.998	0.01430	0.050	0.335	6.8	P	N/A	3.03	3.11	3.15	3.30	2.60	21.00	N/A	N/A	N/A	N/A	N/A	N/A	I	0.0	4	N/A	N/A	N/A	15E8_Ls1d2Vc_6	7/15C	TDP-213	9150793

Table B.4. Data from 2008 Tests in Mid-Scale Vessel with Spherical Head A.1

Row Number	Test	Case ID	Tank Diameter	Head Shape	Dish Height	Dish Volume	Tank Fill Height	Return Line Height	Nozzle Inner Diameter	Nozzle Stand-off Distance	Pulse Tube Configuration	Installed Nozzles	Outer Nozzles Operated	Inner Nozzles Operated	Pulse Tube Outer Diameter	Outer PJM Radius	Inner PJM Radius	"FIO" Outer PJM Impingement Angle	"FIO" Inner PJM Impingement Angle	Ratio Outer PJM to Tank Radius	Ratio Inner PJM to Tank Radius	Simulant	Solids Density	Particle Diameter d5	Particle Diameter d50	Particle Diameter d95	Void Fraction
text	text	text	in.	text	in.	in. ^{3}	in.	in.	in.	in.	text	number	number	number	in.	in.	in.	deg	deg	nondim	nondim	text	g/cm^3	m	m	m	fraction
MSS	M/DDX	ID	D	HS	H_{dish}	V_{dish}	H	Rtn	d	sod	PT	N	N_O	N_I	PT_{od}	R_O	R_I	θ_O	θ_I	R_O/R	R_I/R	sxdx	ρ_s	d_5	d_{50}	d_{95}	vf
9340001	3/5A	34S_4s1d1Zc_1	33 7/8	S	9	4437.4	69	66	0.297	0.446	HLP-22	12	8	4	1.9	10.5	5.7	30.8	16.1	0.62	0.33	s1d1	2.46	0.0001428	0.0001664	0.0001951	0.4118
9340002M	3/5A	34S_4s1d1Zc_1	33 7/8	S	9	4437.4	69	66	0.297	0.446	HLP-22	12	8	4	1.9	10.5	5.7	30.8	16.1	0.62	0.33	s1d1	2.46	0.0001428	0.0001664	0.0001951	0.4118
9340003M	3/5A	34S_4s1d1Zc_1	33 7/8	S	9	4437.4	69	66	0.297	0.446	HLP-22	12	8	4	1.9	10.5	5.7	30.8	16.1	0.62	0.33	s1d1	2.46	0.0001428	0.0001664	0.0001951	0.4118
9340004	3/5A	34S_4s1d1Zc_1	33 7/8	S	9	4437.4	69	66	0.297	0.446	HLP-22	12	8	4	1.9	10.5	5.7	30.8	16.1	0.62	0.33	s1d1	2.46	0.0001428	0.0001664	0.0001951	0.4118
9340005	3/5A	34S_4s1d1Zc_1	33 7/8	S	9	4437.4	69	66	0.297	0.446	HLP-22	12	8	4	1.9	10.5	5.7	30.8	16.1	0.62	0.33	s1d1	2.46	0.0001428	0.0001664	0.0001951	0.4118
9340006	3/5A	34S_4s1d1Zc_1	33 7/8	S	9	4437.4	69	66	0.297	0.446	HLP-22	12	8	4	1.9	10.5	5.7	30.8	16.1	0.62	0.33	s1d1	2.46	0.0001428	0.0001664	0.0001951	0.4118
9340007	3/5A	34S_4s1d1Zc_1	33 7/8	S	9	4437.4	69	66	0.297	0.446	HLP-22	12	8	4	1.9	10.5	5.7	30.8	16.1	0.62	0.33	s1d1	2.46	0.0001428	0.0001664	0.0001951	0.4118
9340008	3/5A	34S_4s1d1Zc_1	33 7/8	S	9	4437.4	69	66	0.297	0.446	HLP-22	12	8	4	1.9	10.5	5.7	30.8	16.1	0.62	0.33	s1d1	2.46	0.0001428	0.0001664	0.0001951	0.4118
9340009	3/5A	34S_4s1d1Zc_1	33 7/8	S	9	4437.4	69	66	0.297	0.446	HLP-22	12	8	4	1.9	10.5	5.7	30.8	16.1	0.62	0.33	s1d1	2.46	0.0001428	0.0001664	0.0001951	0.4118
9340010	3/5A	34S_4s1d1Zc_1	33 7/8	S	9	4437.4	69	66	0.297	0.446	HLP-22	12	8	4	1.9	10.5	5.7	30.8	16.1	0.62	0.33	s1d1	2.46	0.0001428	0.0001664	0.0001951	0.4118
9340011	3/5A	34S_4s1d1Zc_1	33 7/8	S	9	4437.4	69	66	0.297	0.446	HLP-22	12	8	4	1.9	10.5	5.7	30.8	16.1	0.62	0.33	s1d1	2.46	0.0001428	0.0001664	0.0001951	0.4118
9340012M	3/5A	34S_4s1d1Zc_1	33 7/8	S	9	4437.4	69	66	0.297	0.446	HLP-22	12	8	4	1.9	10.5	5.7	30.8	16.1	0.62	0.33	s1d1	2.46	0.0001428	0.0001664	0.0001951	0.4118
9340013	3/5B	34S_4s1d1Zd_1	33 7/8	S	9	4437.4	69	66	0.297	0.446	HLP-22	12	8	4	1.9	10.5	5.7	30.8	16.1	0.62	0.33	s1d1	2.46	0.0001428	0.0001664	0.0001951	0.4118
9340014	3/5B	34S_4s1d1Zd_1	33 7/8	S	9	4437.4	69	66	0.297	0.446	HLP-22	12	8	4	1.9	10.5	5.7	30.8	16.1	0.62	0.33	s1d1	2.46	0.0001428	0.0001664	0.0001951	0.4118
9340015M	3/5B	34S_4s1d1Zd_1	33 7/8	S	9	4437.4	69	66	0.297	0.446	HLP-22	12	8	4	1.9	10.5	5.7	30.8	16.1	0.62	0.33	s1d1	2.46	0.0001428	0.0001664	0.0001951	0.4118
9340016M	3/5B	34S_4s1d1Zd_1	33 7/8	S	9	4437.4	69	66	0.297	0.446	HLP-22	12	8	4	1.9	10.5	5.7	30.8	16.1	0.62	0.33	s1d1	2.46	0.0001428	0.0001664	0.0001951	0.4118
9340017M	3/5B	34S_4s1d1Zd_1	33 7/8	S	9	4437.4	69	66	0.297	0.446	HLP-22	12	8	4	1.9	10.5	5.7	30.8	16.1	0.62	0.33	s1d1	2.46	0.0001428	0.0001664	0.0001951	0.4118
9340018M	3/5B	34S_4s1d1Zd_1	33 7/8	S	9	4437.4	69	66	0.297	0.446	HLP-22	12	8	4	1.9	10.5	5.7	30.8	16.1	0.62	0.33	s1d1	2.46	0.0001428	0.0001664	0.0001951	0.4118
9340019	3/5C	34S_4s1d1Zc_2	33 7/8	S	9	4437.4	69	66	0.297	0.446	HLP-22	12	8	4	1.9	10.5	5.7	30.8	16.1	0.62	0.33	s1d1	2.46	0.0001428	0.0001664	0.0001951	0.4118
9340021M	3/5C	34S_4s1d1Zc_2	33 7/8	S	9	4437.4	69	66	0.297	0.446	HLP-22	12	8	4	1.9	10.5	5.7	30.8	16.1	0.62	0.33	s1d1	2.46	0.0001428	0.0001664	0.0001951	0.4118
9340022M	3/5C	34S_4s1d1Zc_2	33 7/8	S	9	4437.4	69	66	0.297	0.446	HLP-22	12	8	4	1.9	10.5	5.7	30.8	16.1	0.62	0.33	s1d1	2.46	0.0001428	0.0001664	0.0001951	0.4118
9340023M	3/5C	34S_4s1d1Zc_2	33 7/8	S	9	4437.4	69	66	0.297	0.446	HLP-22	12	8	4	1.9	10.5	5.7	30.8	16.1	0.62	0.33	s1d1	2.46	0.0001428	0.0001664	0.0001951	0.4118
9340024	3/6A	34S_4s1d1Yc_1	33 7/8	S	9	4437.4	69	66	0.297	0.446	HLP-22	12	8	4	1.9	10.5	5.7	30.8	16.1	0.62	0.33	s1d1	2.46	0.0001428	0.0001664	0.0001951	0.4118
9340025	3/6A	34S_4s1d1Yc_1	33 7/8	S	9	4437.4	69	66	0.297	0.446	HLP-22	12	8	4	1.9	10.5	5.7	30.8	16.1	0.62	0.33	s1d1	2.46	0.0001428	0.0001664	0.0001951	0.4118
9340026	3/6A	34S_4s1d1Yc_1	33 7/8	S	9	4437.4	69	66	0.297	0.446	HLP-22	12	8	4	1.9	10.5	5.7	30.8	16.1	0.62	0.33	s1d1	2.46	0.0001428	0.0001664	0.0001951	0.4118
9340027	3/6A	34S_4s1d1Yc_1	33 7/8	S	9	4437.4	69	66	0.297	0.446	HLP-22	12	8	4	1.9	10.5	5.7	30.8	16.1	0.62	0.33	s1d1	2.46	0.0001428	0.0001664	0.0001951	0.4118
9340028	3/6A	34S_4s1d1Yc_1	33 7/8	S	9	4437.4	69	66	0.297	0.446	HLP-22	12	8	4	1.9	10.5	5.7	30.8	16.1	0.62	0.33	s1d1	2.46	0.0001428	0.0001664	0.0001951	0.4118
9340029	3/6A	34S_4s1d1Yc_1	33 7/8	S	9	4437.4	69	66	0.297	0.446	HLP-22	12	8	4	1.9	10.5	5.7	30.8	16.1	0.62	0.33	s1d1	2.46	0.0001428	0.0001664	0.0001951	0.4118
9340030M	3/6A	34S_4s1d1Yc_1	33 7/8	S	9	4437.4	69	66	0.297	0.446	HLP-22	12	8	4	1.9	10.5	5.7	30.8	16.1	0.62	0.33	s1d1	2.46	0.0001428	0.0001664	0.0001951	0.4118
9340031M	3/6A	34S_4s1d1Yc_1	33 7/8	S	9	4437.4	69	66	0.297	0.446	HLP-22	12	8	4	1.9	10.5	5.7	30.8	16.1	0.62	0.33	s1d1	2.46	0.0001428	0.0001664	0.0001951	0.4118
9340032M	3/6A	34S_4s1d1Yc_1	33 7/8	S	9	4437.4	69	66	0.297	0.446	HLP-22	12	8	4	1.9	10.5	5.7	30.8	16.1	0.62	0.33	s1d1	2.46	0.0001428	0.0001664	0.0001951	0.4118
9340033M	3/6A	34S_4s1d1Yc_1	33 7/8	S	9	4437.4	69	66	0.297	0.446	HLP-22	12	8	4	1.9	10.5	5.7	30.8	16.1	0.62	0.33	s1d1	2.46	0.0001428	0.0001664	0.0001951	0.4118
9340034	3/6B	34S_4s1d1Yd_1	33 7/8	S	9	4437.4	69	66	0.297	0.446	HLP-22	12	8	4	1.9	10.5	5.7	30.8	16.1	0.62	0.33	s1d1	2.46	0.0001428	0.0001664	0.0001951	0.4118
9340035	3/6B	34S_4s1d1Yd_1	33 7/8	S	9	4437.4	69	66	0.297	0.446	HLP-22	12	8	4	1.9	10.5	5.7	30.8	16.1	0.62	0.33	s1d1	2.46	0.0001428	0.0001664	0.0001951	0.4118
9340036M	3/6B	34S_4s1d1Yd_1	33 7/8	S	9	4437.4	69	66	0.297	0.446	HLP-22	12	8	4	1.9	10.5	5.7	30.8	16.1	0.62	0.33	s1d1	2.46	0.0001428	0.0001664	0.0001951	0.4118
9340037M	3/6B	34S_4s1d1Yd_1	33 7/8	S	9	4437.4	69	66	0.297	0.446	HLP-22	12	8	4	1.9	10.5	5.7	30.8	16.1	0.62	0.33	s1d1	2.46	0.0001428	0.0001664	0.0001951	0.4118
9340038M	3/6B	34S_4s1d1Yd_1	33 7/8	S	9	4437.4	69	66	0.297	0.446	HLP-22	12	8	4	1.9	10.5	5.7	30.8	16.1	0.62	0.33	s1d1	2.46	0.0001428	0.0001664	0.0001951	0.4118
9340039	3/6C	34S_4s1d1Xc_1	33 7/8	S	9	4437.4	69	66	0.297	0.446	HLP-22	12	8	4	1.9	10.5	5.7	30.8	16.1	0.62	0.33	s1d1	2.46	0.0001428	0.0001664	0.0001951	0.4118
9340040	3/6C	34S_4s1d1Xc_1	33 7/8	S	9	4437.4	69	66	0.297	0.446	HLP-22	12	8	4	1.9	10.5	5.7	30.8	16.1	0.62	0.33	s1d1	2.46	0.0001428	0.0001664	0.0001951	0.4118
9340041M	3/6C	34S_4s1d1Xc_1	33 7/8	S	9	4437.4	69	66	0.297	0.446	HLP-22	12	8	4	1.9	10.5	5.7	30.8	16.1	0.62	0.33	s1d1	2.46	0.0001428	0.0001664	0.0001951	0.4118
9340042M	3/6C	34S_4s1d1Xc_1	33 7/8	S	9	4437.4	69	66	0.297	0.446	HLP-22	12	8	4	1.9	10.5	5.7	30.8	16.1	0.62	0.33	s1d1	2.46	0.0001428	0.0001664	0.0001951	0.4118

Table B.4. Data from 2008 Tests in Mid-Scale Vessel with Spherical Head B.1

Tank Water Temperature	Water Density	Solids Fraction	Pulse Volume Fraction	Duty Cycle	Cycle Time	Pulsed or Steady Jet	Us Steady Jet	U1 Pulsing Jet	U2 URMS	U3 URM3	Discharge Velocity	Critical Suspension Velocity	Average Peak Cloud Height	UCS Condition	UCS Method	UCS Flag	UCS Center Flag	UCS udv Flag	UCS based on Decreasing Velocity	Sweep Increase / Decrease	UDV Height Bed	Particle Motion	Solids Level	Outer Bottom Pattern	Inner Bottom Pattern	Case ID	Test	TDP	Row Number
C	g/cm³	fraction	fraction	fraction	s	text	m/s	m/s	m/s	m/s	m/s	m/s	in.	m/s	text	text	text	text	m/s	text	mm	text	text	text	text	text	text	text	text
T	ρ_l	ϕ_S	ϕ_p	DC	t_C	Jet	U_S	U1	U2	U3	U	U_{CS}	H_C	U_{CSR}	U_{CSM}	U_{CS}vis	U_{CS}cen	U_{CS}udv	U_{CS}_D	S_W	H_{bed}	PM	Sol	SP_O	SP_I	ID	M/DDX	TDP	MSS
21.5	0.998	0.00155	0.050	0.337	36.0	P	N/A	3.84	3.89	3.91	4.00	4.50	13.50	N/A	N/A	N/A	N/A	N/A	N/A	I	15.8	1	N/A	N/A	N/A	34S_4s1d1Zc_1	3/5A	TDP-100	9340001
21.4	0.998	0.00155	0.050	0.338	32.0	P	N/A	4.34	4.39	4.42	4.50	4.50	13.50	4.50	udv	UCSvis	N/A	UCSudv	N/A	I	2.4	3	N/A	N/A	N/A	34S_4s1d1Zc_1	3/5A	TDP-100	9340002
21.6	0.998	0.00155	0.050	0.338	32.0	P	N/A	4.35	4.40	4.43	4.50	4.50	13.75	N/A	N/A	N/A	N/A	N/A	N/A	I	N/A	4	N/A	N/A	N/A	34S_4s1d1Zc_1	3/5A	TDP-100	9340003
21.0	0.998	0.00155	0.050	0.338	32.0	P	N/A	N/A	N/A	N/A	4.50	4.50	13.75	N/A	N/A	N/A	N/A	N/A	N/A	N/A	3.1	N/A	N/A	N/A	N/A	34S_4s1d1Zc_1	3/5A	TDP-100	9340004
21.0	0.998	0.00155	0.050	0.338	32.0	P	N/A	N/A	N/A	N/A	4.50	4.50	13.75	N/A	N/A	N/A	N/A	N/A	N/A	N/A	2.9	N/A	N/A	N/A	N/A	34S_4s1d1Zc_1	3/5A	TDP-100	9340005
21.0	0.998	0.00155	0.050	0.338	32.0	P	N/A	N/A	N/A	N/A	4.50	4.50	13.75	N/A	N/A	N/A	N/A	N/A	N/A	N/A	3.6	N/A	N/A	N/A	N/A	34S_4s1d1Zc_1	3/5A	TDP-100	9340006
21.0	0.998	0.00155	0.050	0.338	32.0	P	N/A	N/A	N/A	N/A	4.50	4.50	13.75	N/A	N/A	N/A	N/A	N/A	N/A	N/A	2.7	N/A	N/A	N/A	N/A	34S_4s1d1Zc_1	3/5A	TDP-100	9340007
21.0	0.998	0.00155	0.050	0.338	32.0	P	N/A	N/A	N/A	N/A	4.50	4.50	13.75	N/A	N/A	N/A	N/A	N/A	N/A	N/A	2.7	N/A	N/A	N/A	N/A	34S_4s1d1Zc_1	3/5A	TDP-100	9340008
21.0	0.998	0.00155	0.050	0.338	32.0	P	N/A	N/A	N/A	N/A	4.50	4.50	13.75	N/A	N/A	N/A	N/A	N/A	N/A	N/A	1.5	N/A	N/A	N/A	N/A	34S_4s1d1Zc_1	3/5A	TDP-100	9340009
21.0	0.998	0.00155	0.050	0.338	32.0	P	N/A	N/A	N/A	N/A	4.50	4.50	13.75	N/A	N/A	N/A	N/A	N/A	N/A	N/A	0.9	N/A	N/A	N/A	N/A	34S_4s1d1Zc_1	3/5A	TDP-100	9340010
21.9	0.998	0.00155	0.050	0.338	33.0	P	N/A	4.23	4.28	4.30	4.40	4.50	13.50	N/A	N/A	N/A	N/A	N/A	N/A	I	4.0	1	N/A	N/A	N/A	34S_4s1d1Zc_1	3/5A	TDP-100	9340011
21.9	0.998	0.00155	0.050	0.339	31.0	P	N/A	4.42	4.48	4.50	4.60	4.50	15.00	N/A	N/A	N/A	N/A	N/A	N/A	I	0.0	4	N/A	N/A	N/A	34S_4s1d1Zc_1	3/5A	TDP-100	9340012
21.9	0.998	0.00155	0.050	0.184	63.0	P	N/A	4.05	4.09	4.12	4.20	4.60	11.75	N/A	N/A	N/A	N/A	N/A	N/A	D	7.1	1	N/A	N/A	N/A	34S_4s1d1Zd_1	3/5B	TDP-101	9340013
21.8	0.998	0.00155	0.050	0.184	60.0	P	N/A	4.24	4.29	4.31	4.40	4.60	N/A	N/A	N/A	N/A	N/A	N/A	N/A	I	N/A	1	N/A	N/A	N/A	34S_4s1d1Zd_1	3/5B	TDP-101	9340014
21.9	0.998	0.00155	0.050	0.184	58.0	P	N/A	4.40	4.46	4.48	4.60	4.60	13.50	4.60	vis	UCSvis	N/A	N/A	N/A	I	0.0	3	N/A	N/A	N/A	34S_4s1d1Zd_1	3/5B	TDP-101	9340015
22.0	0.998	0.00155	0.050	0.185	52.0	P	N/A	4.84	4.90	4.94	5.00	4.60	19.50	N/A	N/A	N/A	N/A	N/A	N/A	I	3.6	4	N/A	N/A	N/A	34S_4s1d1Zd_1	3/5B	TDP-101	9340016
21.9	0.998	0.00155	0.050	0.186	47.0	P	N/A	5.42	5.50	5.53	5.70	4.60	24.25	N/A	N/A	N/A	N/A	N/A	N/A	I	0.0	4	N/A	N/A	N/A	34S_4s1d1Zd_1	3/5B	TDP-101	9340017
22.0	0.999	0.00155	0.050	0.187	38.0	P	N/A	6.56	6.66	6.72	6.85	4.60	33.50	N/A	N/A	N/A	N/A	N/A	N/A	I	0.0	4	N/A	N/A	N/A	34S_4s1d1Zd_1	3/5B	TDP-101	9340018
22.0	0.998	0.00155	0.100	0.333	75.0	P	N/A	3.76	3.78	3.79	3.80	3.90	11.25	N/A	N/A	N/A	N/A	N/A	N/A	I	N/A	1	N/A	N/A	N/A	34S_4s1d1Zc_2	3/5C	TDP-101	9340019
22.0	0.998	0.00155	0.100	0.333	73.0	P	N/A	3.83	3.85	3.87	3.90	3.90	11.25	3.90	vis	UCSvis	N/A	N/A	N/A	I	2.9	3	N/A	N/A	N/A	34S_4s1d1Zc_2	3/5C	TDP-101	9340021
22.0	0.998	0.00155	0.101	0.334	71.0	P	N/A	3.99	4.01	4.03	4.05	3.90	13.25	N/A	N/A	N/A	N/A	N/A	N/A	I	0.0	4	N/A	N/A	N/A	34S_4s1d1Zc_2	3/5C	TDP-101	9340022
22.1	0.998	0.00155	0.100	0.335	52.0	P	N/A	5.40	5.44	5.46	5.50	3.90	32.00	N/A	N/A	N/A	N/A	N/A	N/A	I	0.0	4	N/A	N/A	N/A	34S_4s1d1Zc_2	3/5C	TDP-101	9340023
21.5	0.998	0.00500	0.050	0.341	26.0	P	N/A	5.25	5.33	5.37	5.50	6.30	9.88	N/A	N/A	N/A	N/A	N/A	N/A	(null)	14.3	1	N/A	N/A	N/A	34S_4s1d1Yc_1	3/6A	TDP-102	9340024
21.6	0.998	0.00500	0.050	0.341	26.0	P	N/A	5.25	5.33	5.37	5.50	6.30	9.88	N/A	N/A	N/A	N/A	N/A	N/A	(null)	N/A	1	N/A	N/A	N/A	34S_4s1d1Yc_1	3/6A	TDP-102	9340025
21.6	0.998	0.00500	0.050	0.340	26.0	P	N/A	5.26	5.33	5.37	5.50	6.30	9.88	N/A	N/A	N/A	N/A	N/A	N/A	(null)	17.2	1	N/A	N/A	N/A	34S_4s1d1Yc_1	3/6A	TDP-102	9340026
21.6	0.998	0.00500	0.050	0.340	25.0	P	N/A	5.46	5.53	5.57	5.70	6.30	10.50	N/A	N/A	N/A	N/A	N/A	N/A	I	11.0	1	N/A	N/A	N/A	34S_4s1d1Yc_1	3/6A	TDP-102	9340027
21.7	0.998	0.00500	0.050	0.341	24.2	P	N/A	5.65	5.73	5.77	5.90	6.30	10.25	N/A	N/A	N/A	N/A	N/A	N/A	I	7.3	1	N/A	N/A	N/A	34S_4s1d1Yc_1	3/6A	TDP-102	9340028
21.7	0.998	0.00500	0.050	0.341	23.4	P	N/A	5.83	5.91	5.95	6.10	6.30	11.00	N/A	N/A	UCSvis	N/A	N/A	N/A	I	3.9	3	N/A	N/A	N/A	34S_4s1d1Yc_1	3/6A	TDP-102	9340029
21.8	0.998	0.00500	0.050	0.342	22.6	P	N/A	6.05	6.13	6.18	6.30	6.30	11.25	6.30	udv	UCSvis	N/A	UCSudv	N/A	I	0.7	3	N/A	N/A	N/A	34S_4s1d1Yc_1	3/6A	TDP-102	9340030
22.0	0.998	0.00500	0.050	0.343	20.4	P	N/A	6.67	6.77	6.82	7.00	6.30	13.75	N/A	N/A	N/A	N/A	N/A	N/A	(null)	0.0	4	N/A	N/A	N/A	34S_4s1d1Yc_1	3/6A	TDP-102	9340031
22.0	0.998	0.00500	0.050	0.346	18.0	P	N/A	7.57	7.71	7.78	8.00	6.30	20.25	N/A	N/A	N/A	N/A	N/A	N/A	I	0.8	4	N/A	N/A	N/A	34S_4s1d1Yc_1	3/6A	TDP-102	9340032
22.1	0.998	0.00500	0.050	0.347	16.0	P	N/A	8.48	8.64	8.72	9.00	6.30	25.50	N/A	N/A	N/A	N/A	N/A	N/A	I	1.1	4	N/A	N/A	N/A	34S_4s1d1Yc_1	3/6A	TDP-102	9340033
23.0	0.998	0.00500	0.050	0.186	44.0	P	N/A	5.71	5.80	5.84	6.00	6.40	9.75	N/A	N/A	N/A	N/A	N/A	N/A	(null)	6.6	1	N/A	N/A	N/A	34S_4s1d1Yd_1	3/6B	TDP-103	9340034
23.0	0.998	0.00500	0.050	0.186	42.0	P	N/A	5.99	6.08	6.13	6.30	6.40	10.75	N/A	N/A	N/A	N/A	N/A	N/A	I	3.6	1	N/A	N/A	N/A	34S_4s1d1Yd_1	3/6B	TDP-103	9340035
22.9	0.998	0.00500	0.050	0.186	41.0	P	N/A	6.11	6.20	6.24	6.40	6.40	10.75	6.40	vis	UCSvis	N/A	N/A	N/A	I	0.0	3	N/A	N/A	N/A	34S_4s1d1Yd_1	3/6B	TDP-103	9340036
22.8	0.998	0.00500	0.049	0.188	35.0	P	N/A	7.04	7.17	7.23	7.40	6.40	16.50	N/A	N/A	N/A	N/A	N/A	N/A	I	0.0	4	N/A	N/A	N/A	34S_4s1d1Yd_1	3/6B	TDP-103	9340037
23.1	0.998	0.00500	0.050	0.191	25.0	P	N/A	9.77	9.98	10.09	10.30	6.40	29.50	N/A	N/A	N/A	N/A	N/A	N/A	(null)	N/A	4	N/A	N/A	N/A	34S_4s1d1Yd_1	3/6B	TDP-103	9340038
23.0	0.998	0.01500	0.050	0.342	22.0	P	N/A	6.18	6.28	6.33	6.50	7.90	N/A	N/A	N/A	N/A	N/A	N/A	N/A	I	19.6	1	N/A	N/A	N/A	34S_4s1d1Xc_1	3/6C	TDP-104	9340039
22.9	0.998	0.01500	0.050	0.344	20.0	P	N/A	6.84	6.95	7.01	7.20	7.90	N/A	N/A	N/A	N/A	N/A	N/A	N/A	I	7.1	1	N/A	N/A	N/A	34S_4s1d1Xc_1	3/6C	TDP-104	9340040
23.0	0.998	0.01500	0.050	0.346	18.0	P	N/A	7.49	7.63	7.71	7.90	7.90	9.25	7.90	udv	N/A	UCScen	UCSudv	N/A	I	2.9	2	N/A	N/A	N/A	34S_4s1d1Xc_1	3/6C	TDP-104	9340041
23.1	0.998	0.01500	0.050	0.346	17.0	P	N/A	7.91	8.05	8.13	8.30	7.90	9.25	N/A	N/A	N/A	UCScen	N/A	N/A	(null)	0.0	2	N/A	N/A	N/A	34S_4s1d1Xc_1	3/6C	TDP-104	9340042

Table B.4. Data from 2008 Tests in Mid-Scale Vessel with Spherical Head A.2

Row Number	Test	Case ID	Tank Diameter	Head Shape	Dish Height	Dish Volume	Tank Fill Height	Return Line Height	Nozzle Inner Diameter	Nozzle Stand-off Distance	Pulse Tube Configuration	Installed Nozzles	Outer Nozzles Operated	Inner Nozzles Operated	Pulse Tube Outer Diameter	Outer PJM Radius	Inner PJM Radius	"FIO" Outer PJM Impingement Angle	"FIO" Inner PJM Impingement Angle	Ratio Outer PJM to Tank Radius	Ratio Inner PJM to Tank Radius	Simulant	Solids Density	Particle Diameter d5	Particle Diameter d50	Particle Diameter d95	Void Fraction
text	text	text	in.	text	in.	in. ^{3}	in.	in.	in.	in.	text	number	number	number	in.	in.	in.	deg	deg	nondim	nondim	text	g/cm^3	m	m	m	fraction
MSS	M/DDX	ID	D	HS	H_{dish}	V_{dish}	H	Rtn	d	sod	PT	N	N_O	N_I	PT_{od}	R_O	R_I	θ_O	θ_I	R_O/R	R_I/R	sxdx	ρ_s	d_5	d_{50}	d_{95}	vf
9340043M	3/5A	34S_4s1d1Zc_1	33 7/8	S	9	4437.4	69	66	0.297	0.446	HLP-22	12	8	4	1.9	10.5	5.7	30.8	16.1	0.62	0.33	s1d1	2.46	0.0001428	0.0001664	0.0001951	0.4118
9340044M	3/5A	34S_4s1d1Zc_1	33 7/8	S	9	4437.4	69	66	0.297	0.446	HLP-22	12	8	4	1.9	10.5	5.7	30.8	16.1	0.62	0.33	s1d1	2.46	0.0001428	0.0001664	0.0001951	0.4118
9340045M	3/5A	34S_4s1d1Zc_1	33 7/8	S	9	4437.4	69	66	0.297	0.446	HLP-22	12	8	4	1.9	10.5	5.7	30.8	16.1	0.62	0.33	s1d1	2.46	0.0001428	0.0001664	0.0001951	0.4118
9340046M	3/5A	34S_4s1d1Zc_1	33 7/8	S	9	4437.4	69	66	0.297	0.446	HLP-22	12	8	4	1.9	10.5	5.7	30.8	16.1	0.62	0.33	s1d1	2.46	0.0001428	0.0001664	0.0001951	0.4118
9340047	3/5A	34S_4s1d1Zc_1	33 7/8	S	9	4437.4	69	66	0.297	0.446	HLP-22	12	8	4	1.9	10.5	5.7	30.8	16.1	0.62	0.33	s1d1	2.46	0.0001428	0.0001664	0.0001951	0.4118
9340048	3/5A	34S_4s1d1Zc_1	33 7/8	S	9	4437.4	69	66	0.297	0.446	HLP-22	12	8	4	1.9	10.5	5.7	30.8	16.1	0.62	0.33	s1d1	2.46	0.0001428	0.0001664	0.0001951	0.4118
9340049	3/5A	34S_4s1d1Zc_1	33 7/8	S	9	4437.4	69	66	0.297	0.446	HLP-22	12	8	4	1.9	10.5	5.7	30.8	16.1	0.62	0.33	s1d1	2.46	0.0001428	0.0001664	0.0001951	0.4118
9340050M	3/5A	34S_4s1d1Zc_1	33 7/8	S	9	4437.4	69	66	0.297	0.446	HLP-22	12	8	4	1.9	10.5	5.7	30.8	16.1	0.62	0.33	s1d1	2.46	0.0001428	0.0001664	0.0001951	0.4118
9340051M	3/5A	34S_4s1d1Zc_1	33 7/8	S	9	4437.4	69	66	0.297	0.446	HLP-22	12	8	4	1.9	10.5	5.7	30.8	16.1	0.62	0.33	s1d1	2.46	0.0001428	0.0001664	0.0001951	0.4118
9340052	3/5A	34S_4s1d1Zc_1	33 7/8	S	9	4437.4	69	66	0.297	0.446	HLP-22	12	8	4	1.9	10.5	5.7	30.8	16.1	0.62	0.33	s1d1	2.46	0.0001428	0.0001664	0.0001951	0.4118
9340053	3/5A	34S_4s1d1Zc_1	33 7/8	S	9	4437.4	69	66	0.297	0.446	HLP-22	12	8	4	1.9	10.5	5.7	30.8	16.1	0.62	0.33	s1d1	2.46	0.0001428	0.0001664	0.0001951	0.4118
9340054	3/5A	34S_4s1d1Zc_1	33 7/8	S	9	4437.4	69	66	0.297	0.446	HLP-22	12	8	4	1.9	10.5	5.7	30.8	16.1	0.62	0.33	s1d1	2.46	0.0001428	0.0001664	0.0001951	0.4118
9340055M	3/5B	34S_4s1d1Zd_1	33 7/8	S	9	4437.4	69	66	0.297	0.446	HLP-22	12	8	4	1.9	10.5	5.7	30.8	16.1	0.62	0.33	s1d1	2.46	0.0001428	0.0001664	0.0001951	0.4118
9340056M	3/5B	34S_4s1d1Zd_1	33 7/8	S	9	4437.4	69	66	0.297	0.446	HLP-22	12	8	4	1.9	10.5	5.7	30.8	16.1	0.62	0.33	s1d1	2.46	0.0001428	0.0001664	0.0001951	0.4118
9340057	3/5B	34S_4s1d1Zd_1	33 7/8	S	9	4437.4	69	66	0.297	0.446	HLP-22	12	8	4	1.9	10.5	5.7	30.8	16.1	0.62	0.33	s1d1	2.46	0.0001428	0.0001664	0.0001951	0.4118
9340058	3/5B	34S_4s1d1Zd_1	33 7/8	S	9	4437.4	69	66	0.297	0.446	HLP-22	12	8	4	1.9	10.5	5.7	30.8	16.1	0.62	0.33	s1d1	2.46	0.0001428	0.0001664	0.0001951	0.4118
9340059	3/5B	34S_4s1d1Zd_1	33 7/8	S	9	4437.4	69	66	0.297	0.446	HLP-22	12	8	4	1.9	10.5	5.7	30.8	16.1	0.62	0.33	s1d1	2.46	0.0001428	0.0001664	0.0001951	0.4118
9340060	3/5B	34S_4s1d1Zd_1	33 7/8	S	9	4437.4	69	66	0.297	0.446	HLP-22	12	8	4	1.9	10.5	5.7	30.8	16.1	0.62	0.33	s1d1	2.46	0.0001428	0.0001664	0.0001951	0.4118
9340061	3/5C	34S_4s1d1Zc_2	33 7/8	S	9	4437.4	69	66	0.297	0.446	HLP-22	12	8	4	1.9	10.5	5.7	30.8	16.1	0.62	0.33	s1d1	2.46	0.0001428	0.0001664	0.0001951	0.4118
9340062	3/5C	34S_4s1d1Zc_2	33 7/8	S	9	4437.4	69	66	0.297	0.446	HLP-22	12	8	4	1.9	10.5	5.7	30.8	16.1	0.62	0.33	s1d1	2.46	0.0001428	0.0001664	0.0001951	0.4118
9340063	3/5C	34S_4s1d1Zc_2	33 7/8	S	9	4437.4	69	66	0.297	0.446	HLP-22	12	8	4	1.9	10.5	5.7	30.8	16.1	0.62	0.33	s1d1	2.46	0.0001428	0.0001664	0.0001951	0.4118
9340064	3/5C	34S_4s1d1Zc_2	33 7/8	S	9	4437.4	69	66	0.297	0.446	HLP-22	12	8	4	1.9	10.5	5.7	30.8	16.1	0.62	0.33	s1d1	2.46	0.0001428	0.0001664	0.0001951	0.4118
9340065	3/6A	34S_4s1d1Yc_1	33 7/8	S	9	4437.4	69	66	0.297	0.446	HLP-22	12	8	4	1.9	10.5	5.7	30.8	16.1	0.62	0.33	s1d1	2.46	0.0001428	0.0001664	0.0001951	0.4118
9340066	3/6A	34S_4s1d1Yc_1	33 7/8	S	9	4437.4	69	66	0.297	0.446	HLP-22	12	8	4	1.9	10.5	5.7	30.8	16.1	0.62	0.33	s1d1	2.46	0.0001428	0.0001664	0.0001951	0.4118
9340067M	3/6A	34S_4s1d1Yc_1	33 7/8	S	9	4437.4	69	66	0.297	0.446	HLP-22	12	8	4	1.9	10.5	5.7	30.8	16.1	0.62	0.33	s1d1	2.46	0.0001428	0.0001664	0.0001951	0.4118
9340068	3/6A	34S_4s1d1Yc_1	33 7/8	S	9	4437.4	69	66	0.297	0.446	HLP-22	12	8	4	1.9	10.5	5.7	30.8	16.1	0.62	0.33	s1d1	2.46	0.0001428	0.0001664	0.0001951	0.4118
9340069M	3/6A	34S_4s1d1Yc_1	33 7/8	S	9	4437.4	69	66	0.297	0.446	HLP-22	12	8	4	1.9	10.5	5.7	30.8	16.1	0.62	0.33	s1d1	2.46	0.0001428	0.0001664	0.0001951	0.4118
9340070M	3/6A	34S_4s1d1Yc_1	33 7/8	S	9	4437.4	69	66	0.297	0.446	HLP-22	12	8	4	1.9	10.5	5.7	30.8	16.1	0.62	0.33	s1d1	2.46	0.0001428	0.0001664	0.0001951	0.4118
9340071M	3/6A	34S_4s1d1Yc_1	33 7/8	S	9	4437.4	69	66	0.297	0.446	HLP-22	12	8	4	1.9	10.5	5.7	30.8	16.1	0.62	0.33	s1d1	2.46	0.0001428	0.0001664	0.0001951	0.4118
9340072	3/6A	34S_4s1d1Yc_1	33 7/8	S	9	4437.4	69	66	0.297	0.446	HLP-22	12	8	4	1.9	10.5	5.7	30.8	16.1	0.62	0.33	s1d1	2.46	0.0001428	0.0001664	0.0001951	0.4118
9340073	3/6A	34S_4s1d1Yc_1	33 7/8	S	9	4437.4	69	66	0.297	0.446	HLP-22	12	8	4	1.9	10.5	5.7	30.8	16.1	0.62	0.33	s1d1	2.46	0.0001428	0.0001664	0.0001951	0.4118
9340074M	3/6A	34S_4s1d1Yc_1	33 7/8	S	9	4437.4	69	66	0.297	0.446	HLP-22	12	8	4	1.9	10.5	5.7	30.8	16.1	0.62	0.33	s1d1	2.46	0.0001428	0.0001664	0.0001951	0.4118
9340075	3/6B	34S_4s1d1Yd_1	33 7/8	S	9	4437.4	69	66	0.297	0.446	HLP-22	12	8	4	1.9	10.5	5.7	30.8	16.1	0.62	0.33	s1d1	2.46	0.0001428	0.0001664	0.0001951	0.4118
9340076	3/6B	34S_4s1d1Yd_1	33 7/8	S	9	4437.4	69	66	0.297	0.446	HLP-22	12	8	4	1.9	10.5	5.7	30.8	16.1	0.62	0.33	s1d1	2.46	0.0001428	0.0001664	0.0001951	0.4118
9340077	3/6B	34S_4s1d1Yd_1	33 7/8	S	9	4437.4	69	66	0.297	0.446	HLP-22	12	8	4	1.9	10.5	5.7	30.8	16.1	0.62	0.33	s1d1	2.46	0.0001428	0.0001664	0.0001951	0.4118
9340078	3/6B	34S_4s1d1Yd_1	33 7/8	S	9	4437.4	69	66	0.297	0.446	HLP-22	12	8	4	1.9	10.5	5.7	30.8	16.1	0.62	0.33	s1d1	2.46	0.0001428	0.0001664	0.0001951	0.4118
9340079	3/6B	34S_4s1d1Yd_1	33 7/8	S	9	4437.4	69	66	0.297	0.446	HLP-22	12	8	4	1.9	10.5	5.7	30.8	16.1	0.62	0.33	s1d1	2.46	0.0001428	0.0001664	0.0001951	0.4118
9340080	3/6C	34S_4s1d1Xc_1	33 7/8	S	9	4437.4	69	66	0.297	0.446	HLP-22	12	8	4	1.9	10.5	5.7	30.8	16.1	0.62	0.33	s1d1	2.46	0.0001428	0.0001664	0.0001951	0.4118
9340081	3/6C	34S_4s1d1Xc_1	33 7/8	S	9	4437.4	69	66	0.297	0.446	HLP-22	12	8	4	1.9	10.5	5.7	30.8	16.1	0.62	0.33	s1d1	2.46	0.0001428	0.0001664	0.0001951	0.4118
9340082	3/6C	34S_4s1d1Xc_1	33 7/8	S	9	4437.4	69	66	0.297	0.446	HLP-22	12	8	4	1.9	10.5	5.7	30.8	16.1	0.62	0.33	s1d1	2.46	0.0001428	0.0001664	0.0001951	0.4118
9340083	3/6C	34S_4s1d1Xc_1	33 7/8	S	9	4437.4	69	66	0.297	0.446	HLP-22	12	8	4	1.9	10.5	5.7	30.8	16.1	0.62	0.33	s1d1	2.46	0.0001428	0.0001664	0.0001951	0.4118

Table B.4. Data from 2008 Tests in Mid-Scale Vessel with Spherical Head B.2

Tank Water Temperature	Water Density	Solids Fraction	Pulse Volume Fraction	Duty Cycle	Cycle Time	Pulsed or Steady Jet	Us Steady Jet	U1 Pulsing Jet	U2 URMS	U3 URM3	Discharge Velocity	Critical Suspension Velocity	Average Peak Cloud Height	UCS Condition	UCS Method	UCS Flag	UCS Center Flag	UCS udv Flag	UCS based on Decreasing Velocity	Sweep Increase / Decrease	UDV Height Bed	Particle Motion	Solids Level	Outer Bottom Pattern	Inner Bottom Pattern	Case ID	Test	TDP	Row Number
C	g/cm³	fraction	fraction	fraction	s	text	m/s	m/s	m/s	m/s	m/s	m/s	in.	m/s	text	text	text	text	m/s	text	mm	text	text	text	text	text	text	text	text
T	$\rho_\pm$	ϕ_S	ϕ_P	DC	t_C	Jet	U_S	U1	U2	U3	U	U_{CS}	H_C	U_{CSR}	U_{CSM}	U_{CS}vis	U_{CS}cen	U_{CS}udv	U_{CS}_D	S_W	H_{bed}	PM	Sol	SP_O	SP_I	ID	M/DDX	TDP	MSS
23.4	0.998	0.01500	0.050	0.354	12.0	P	N/A	11.02	11.31	11.45	11.80	7.90	19.75	N/A	N/A	N/A	N/A	N/A	N/A	(null)	N/A	4	N/A	N/A	N/A	34S_4s1d1Xc_1	3/6C	TDP-104	9340043
23.6	0.997	0.01500	0.050	0.357	11.0	P	N/A	11.99	12.33	12.50	13.00	7.90	27.00	N/A	N/A	N/A	N/A	N/A	N/A	I	N/A	4	N/A	N/A	N/A	34S_4s1d1Xc_1	3/6C	TDP-104	9340044
23.8	0.998	0.01500	0.049	0.360	10.0	P	N/A	12.84	13.24	13.44	14.00	7.90	33.00	N/A	N/A	N/A	N/A	N/A	N/A	I	N/A	4	N/A	N/A	N/A	34S_4s1d1Xc_1	3/6C	TDP-104	9340045
23.6	0.998	0.01500	0.050	0.350	14.0	P	N/A	9.52	9.73	9.84	10.10	7.90	13.50	N/A	vis dec	UCSvis	N/A	N/A	10.10	D	N/A	3	N/A	N/A	N/A	34S_4s1d1Xc_1	3/6C	TDP-104	9340046
18.6	0.999	0.00015	0.050	0.333	65.0	P	N/A	2.16	2.18	2.18	2.20	N/A	53.50	N/A	N/A	UCSvis	N/A	N/A	N/A	(null)	28.4	3	N/A	N/A	N/A	34S_4s1d2Uc_1	3/7A	TDP-105	9340047
18.5	0.999	0.00015	0.050	0.333	65.0	P	N/A	2.16	2.18	2.18	2.20	N/A	53.50	N/A	N/A	UCSvis	N/A	N/A	N/A	(null)	29.7	3	N/A	N/A	N/A	34S_4s1d2Uc_1	3/7A	TDP-105	9340048
19.3	0.999	0.00050	0.050	0.333	58.0	P	N/A	2.42	2.44	2.45	2.50	2.75	22.25	N/A	N/A	N/A	N/A	N/A	N/A	(null)	3.7	1	N/A	N/A	N/A	34S_4s1d2Tc_1	3/7B	TDP-106	9340049
19.6	0.999	0.00050	0.050	0.334	52.6	P	N/A	2.69	2.71	2.73	2.75	2.75	30.50	2.75	center	N/A	UCScen	N/A	N/A	I	3.7	2	N/A	N/A	N/A	34S_4s1d2Tc_1	3/7B	TDP-106	9340050
19.7	0.999	0.00050	0.050	0.334	49.0	P	N/A	2.88	2.90	2.92	2.95	2.75	43.00	N/A	N/A	N/A	N/A	N/A	N/A	I	N/A	4	N/A	N/A	N/A	34S_4s1d2Tc_1	3/7B	TDP-106	9340051
N/A	N/A	0.00050	0.049	0.332	65.0	P	N/A	N/A	N/A	N/A	2.20	2.75	N/A	N/A	N/A	N/A	N/A	N/A	N/A	N/A	37.6	N/A	N/A	N/A	N/A	34S_4s1d2Tc_1	3/7B	TDP-106	9340052
N/A	N/A	0.00150	0.050	0.336	40.0	P	N/A	N/A	N/A	N/A	3.60	3.70	N/A	N/A	N/A	N/A	N/A	N/A	N/A	N/A	0.0	N/A	N/A	N/A	N/A	34S_4s1d2Sc_1	3/7C	TDP-107	9340053
20.2	0.999	0.00150	0.050	0.336	40.0	P	N/A	3.47	3.50	3.52	3.55	3.70	17.50	N/A	N/A	N/A	N/A	N/A	N/A	D	N/A	1	N/A	N/A	N/A	34S_4s1d2Sc_1	3/7C	TDP-107	9340054
20.2	0.999	0.00150	0.050	0.337	39.0	P	N/A	3.57	3.61	3.63	3.70	3.70	19.75	3.70	center	N/A	UCScen	N/A	N/A	I	0.0	2	N/A	N/A	N/A	34S_4s1d2Sc_1	3/7C	TDP-107	9340055
20.4	0.999	0.00150	0.049	0.336	36.0	P	N/A	3.82	3.86	3.88	3.90	3.70	25.50	N/A	N/A	N/A	N/A	N/A	N/A	I	N/A	4	N/A	N/A	N/A	34S_4s1d2Sc_1	3/7C	TDP-107	9340056
20.6	0.999	0.00150	0.050	0.335	47.0	P	N/A	2.96	2.99	3.00	3.00	3.70	10.75	N/A	N/A	N/A	N/A	N/A	N/A	D	N/A	1	N/A	N/A	N/A	34S_4s1d2Sc_1	3/7C	TDP-107	9340057
20.5	0.999	0.00150	0.050	0.336	43.0	P	N/A	3.22	3.25	3.27	3.30	3.70	12.25	N/A	N/A	N/A	N/A	N/A	N/A	I	N/A	1	N/A	N/A	N/A	34S_4s1d2Sc_1	3/7C	TDP-107	9340058
20.5	0.999	0.00150	0.050	0.336	39.0	P	N/A	3.57	3.61	3.63	3.70	3.70	19.75	N/A	N/A	N/A	UCScen	N/A	N/A	I	0.7	2	N/A	N/A	N/A	34S_4s1d2Sc_1	3/7C	TDP-107	9340059
20.5	0.999	0.00150	0.050	0.336	39.0	P	N/A	N/A	N/A	N/A	3.70	3.70	19.75	N/A	N/A	N/A	N/A	N/A	N/A	N/A	0.0	N/A	N/A	N/A	N/A	34S_4s1d2Sc_1	3/7C	TDP-107	9340060
20.5	0.999	0.00150	0.050	0.336	39.0	P	N/A	N/A	N/A	N/A	3.70	3.70	19.75	N/A	N/A	N/A	N/A	N/A	N/A	N/A	0.0	N/A	N/A	N/A	N/A	34S_4s1d2Sc_1	3/7C	TDP-107	9340061
20.5	0.999	0.00150	0.050	0.336	39.0	P	N/A	N/A	N/A	N/A	3.70	3.70	19.75	N/A	N/A	N/A	N/A	N/A	N/A	N/A	0.0	N/A	N/A	N/A	N/A	34S_4s1d2Sc_1	3/7C	TDP-107	9340062
20.5	0.999	0.00150	0.050	0.336	39.0	P	N/A	N/A	N/A	N/A	3.70	3.70	19.75	N/A	N/A	N/A	N/A	N/A	N/A	N/A	0.0	N/A	N/A	N/A	N/A	34S_4s1d2Sc_1	3/7C	TDP-107	9340063
20.5	0.999	0.00150	0.050	0.336	39.0	P	N/A	N/A	N/A	N/A	3.70	3.70	19.75	N/A	N/A	N/A	N/A	N/A	N/A	N/A	0.0	N/A	N/A	N/A	N/A	34S_4s1d2Sc_1	3/7C	TDP-107	9340064
21.1	0.998	0.00500	0.050	0.339	28.0	P	N/A	4.91	4.97	5.01	5.05	5.10	19.50	N/A	N/A	N/A	UCScen	N/A	N/A	I	0.0	2	N/A	N/A	N/A	34S_4s1d2Yc_1	3/9A	TDP-108	9340065
21.1	0.998	0.00500	0.050	0.338	29.0	P	N/A	4.78	4.84	4.87	4.90	5.10	14.25	N/A	N/A	N/A	N/A	N/A	N/A	I	21.1	1	N/A	N/A	N/A	34S_4s1d2Yc_1	3/9A	TDP-108	9340066
21.3	0.998	0.00500	0.050	0.339	28.0	P	N/A	4.96	5.02	5.05	5.10	5.10	19.50	N/A	N/A	UCSvis	N/A	N/A	N/A	I	0.0	3	N/A	N/A	N/A	34S_4s1d2Yc_1	3/9A	TDP-108	9340067
21.2	0.998	0.00500	0.050	0.339	28.4	P	N/A	4.88	4.94	4.97	5.00	5.10	19.00	N/A	udv dec	UCSvis	N/A	UCSudv	5.00	D	0.0	3	N/A	N/A	N/A	34S_4s1d2Yc_1	3/9A	TDP-108	9340068
21.5	0.999	0.00500	0.050	0.336	23.0	P	N/A	6.03	6.12	6.17	6.25	5.10	46.00	N/A	N/A	N/A	N/A	N/A	N/A	I	0.0	N/A	N/A	N/A	N/A	34S_4s1d2Yc_1	3/9A	TDP-108	9340069
21.3	0.998	0.00500	0.050	0.335	25.0	P	N/A	5.58	5.66	5.70	5.80	5.10	35.00	N/A	N/A	N/A	N/A	N/A	N/A	D	19.4	N/A	N/A	N/A	N/A	34S_4s1d2Yc_1	3/9A	TDP-108	9340070
21.3	0.999	0.00500	0.050	0.334	27.0	P	N/A	5.23	5.29	5.33	5.40	5.10	24.50	N/A	N/A	N/A	N/A	N/A	N/A	D	0.0	N/A	N/A	N/A	N/A	34S_4s1d2Yc_1	3/9A	TDP-108	9340071
21.4	0.998	0.00500	0.050	0.338	31.0	P	N/A	4.47	4.52	4.55	4.60	5.10	11.25	N/A	N/A	N/A	N/A	N/A	N/A	D	16.7	N/A	N/A	N/A	N/A	34S_4s1d2Yc_1	3/9A	TDP-108	9340072
21.6	0.998	0.00500	0.050	0.335	30.0	P	N/A	4.66	4.72	4.75	4.80	5.10	13.00	N/A	N/A	N/A	N/A	N/A	N/A	I	23.2	N/A	N/A	N/A	N/A	34S_4s1d2Yc_1	3/9A	TDP-108	9340073
21.4	0.998	0.00500	0.050	0.336	28.4	P	N/A	4.89	4.96	4.99	5.10	5.10	19.50	5.10	udv	UCSvis	N/A	UCSudv	N/A	I	0.0	3	N/A	N/A	N/A	34S_4s1d2Yc_1	3/9A	TDP-108	9340074
21.4	0.998	0.00500	0.050	0.336	28.4	P	N/A	N/A	N/A	N/A	5.10	5.10	19.50	N/A	N/A	N/A	N/A	N/A	N/A	N/A	0.0	N/A	N/A	N/A	N/A	34S_4s1d2Yc_1	3/9A	TDP-108	9340075
21.4	0.998	0.00500	0.050	0.336	28.4	P	N/A	N/A	N/A	N/A	5.10	5.10	19.50	N/A	N/A	N/A	N/A	N/A	N/A	N/A	0.0	N/A	N/A	N/A	N/A	34S_4s1d2Yc_1	3/9A	TDP-108	9340076
21.4	0.998	0.00500	0.050	0.336	28.4	P	N/A	N/A	N/A	N/A	5.10	5.10	19.50	N/A	N/A	N/A	N/A	N/A	N/A	N/A	0.0	N/A	N/A	N/A	N/A	34S_4s1d2Yc_1	3/9A	TDP-108	9340077
21.4	0.998	0.00500	0.050	0.336	28.4	P	N/A	N/A	N/A	N/A	5.10	5.10	19.50	N/A	N/A	N/A	N/A	N/A	N/A	N/A	0.0	N/A	N/A	N/A	N/A	34S_4s1d2Yc_1	3/9A	TDP-108	9340078
21.4	0.998	0.00500	0.050	0.336	28.4	P	N/A	N/A	N/A	N/A	5.10	5.10	19.50	N/A	N/A	N/A	N/A	N/A	N/A	N/A	0.7	N/A	N/A	N/A	N/A	34S_4s1d2Yc_1	3/9A	TDP-108	9340079
21.4	0.998	0.00500	0.050	0.336	28.4	P	N/A	N/A	N/A	N/A	5.10	5.10	19.50	N/A	N/A	N/A	N/A	N/A	N/A	N/A	3.7	N/A	N/A	N/A	N/A	34S_4s1d2Yc_1	3/9A	TDP-108	9340080
21.7	0.999	0.00500	0.050	0.186	47.0	P	N/A	5.33	5.40	5.44	5.50	6.00	13.00	N/A	N/A	N/A	N/A	N/A	N/A	I	41.6	1	N/A	N/A	N/A	34S_4s1d2Yd_1	3/9B	TDP-108	9340081
21.8	0.998	0.00500	0.050	0.186	45.4	P	N/A	5.57	5.65	5.69	5.80	6.00	15.25	N/A	N/A	N/A	N/A	N/A	N/A	I	19.9	1	N/A	N/A	N/A	34S_4s1d2Yd_1	3/9B	TDP-108	9340082
21.9	0.998	0.00500	0.050	0.186	44.4	P	N/A	5.68	5.76	5.80	5.90	6.00	16.75	N/A	N/A	UCSvis	N/A	N/A	N/A	I	3.6	3	N/A	N/A	N/A	34S_4s1d2Yd_1	3/9B	TDP-108	9340083

Table B.4. Data from 2008 Tests in Mid-Scale Vessel with Spherical Head A.3

Row Number	Test	Case ID	Tank Diameter	Head Shape	Dish Height	Dish Volume	Tank Fill Height	Return Line Height	Nozzle Inner Diameter	Nozzle Stand-off Distance	Pulse Tube Configuration	Installed Nozzles	Outer Nozzles Operated	Inner Nozzles Operated	Pulse Tube Outer Diameter	Outer PJM Radius	Inner PJM Radius	"FIO" Outer PJM Impingement Angle	"FIO" Inner PJM Impingement Angle	Ratio Outer PJM to Tank Radius	Ratio Inner PJM to Tank Radius	Simulant	Solids Density	Particle Diameter d5	Particle Diameter d50	Particle Diameter d95	Void Fraction
text	text	text	in.	text	in.	in. ^{3}	in.	in.	in.	in.	text	number	number	number	in.	in.	in.	deg	deg	nondim	nondim	text	g/cm^3	m	m	m	fraction
MSS	M/DDX	ID	D	HS	H_{dish}	V_{dish}	H	Rtn	d	sod	PT	N	N_O	N_I	PT_{od}	R_O	R_I	θ_O	θ_I	R_O/R	R_I/R	sxdx	ρ_s	d_5	d_{50}	d_{95}	vf
9340084M	3/9B	34S_4s1d2Yd_1	33 7/8	S	9	4437.4	70	66	0.297	0.446	HLP-22	12	8	4	1.9	10.5	5.7	30.8	16.1	0.62	0.33	s1d2	2.48	0.0000569	0.0000693	0.0000821	0.3750
9340085M	3/9B	34S_4s1d2Yd_1	33 7/8	S	9	4437.4	70	66	0.297	0.446	HLP-22	12	8	4	1.9	10.5	5.7	30.8	16.1	0.62	0.33	s1d2	2.48	0.0000569	0.0000693	0.0000821	0.3750
9340086	3/9B	34S_4s1d2Yd_1	33 7/8	S	9	4437.4	70	66	0.297	0.446	HLP-22	12	8	4	1.9	10.5	5.7	30.8	16.1	0.62	0.33	s1d2	2.48	0.0000569	0.0000693	0.0000821	0.3750
9340087	3/9B	34S_4s1d2Yd_1	33 7/8	S	9	4437.4	70	66	0.297	0.446	HLP-22	12	8	4	1.9	10.5	5.7	30.8	16.1	0.62	0.33	s1d2	2.48	0.0000569	0.0000693	0.0000821	0.3750
9340088	3/9B	34S_4s1d2Yd_1	33 7/8	S	9	4437.4	70	66	0.297	0.446	HLP-22	12	8	4	1.9	10.5	5.7	30.8	16.1	0.62	0.33	s1d2	2.48	0.0000569	0.0000693	0.0000821	0.3750
9340089	3/9B	34S_4s1d2Yd_1	33 7/8	S	9	4437.4	70	66	0.297	0.446	HLP-22	12	8	4	1.9	10.5	5.7	30.8	16.1	0.62	0.33	s1d2	2.48	0.0000569	0.0000693	0.0000821	0.3750
9340090	3/9B	34S_4s1d2Yd_1	33 7/8	S	9	4437.4	70	66	0.297	0.446	HLP-22	12	8	4	1.9	10.5	5.7	30.8	16.1	0.62	0.33	s1d2	2.48	0.0000569	0.0000693	0.0000821	0.3750
9340091	3/9B	34S_4s1d2Yd_1	33 7/8	S	9	4437.4	70	66	0.297	0.446	HLP-22	12	8	4	1.9	10.5	5.7	30.8	16.1	0.62	0.33	s1d2	2.48	0.0000569	0.0000693	0.0000821	0.3750
9340092M	3/9B	34S_4s1d2Yd_1	33 7/8	S	9	4437.4	70	66	0.297	0.446	HLP-22	12	8	4	1.9	10.5	5.7	30.8	16.1	0.62	0.33	s1d2	2.48	0.0000569	0.0000693	0.0000821	0.3750
9340093M	3/9B	34S_4s1d2Yd_1	33 7/8	S	9	4437.4	70	66	0.297	0.446	HLP-22	12	8	4	1.9	10.5	5.7	30.8	16.1	0.62	0.33	s1d2	2.48	0.0000569	0.0000693	0.0000821	0.3750
9340094M	3/9B	34S_4s1d2Yd_1	33 7/8	S	9	4437.4	70	66	0.297	0.446	HLP-22	12	8	4	1.9	10.5	5.7	30.8	16.1	0.62	0.33	s1d2	2.48	0.0000569	0.0000693	0.0000821	0.3750
9340176	3/11A	34S_4s2d2Tc_1	33 7/8	S	9	4437.4	72	66	0.297	0.446	HLP-22	12	8	4	1.9	10.5	5.7	30.8	16.1	0.62	0.33	s2d2	4.18	0.0000609	0.0000756	0.0000931	0.3684
9340177M	3/11A	34S_4s2d2Tc_1	33 7/8	S	9	4437.4	72	66	0.297	0.446	HLP-22	12	8	4	1.9	10.5	5.7	30.8	16.1	0.62	0.33	s2d2	4.18	0.0000609	0.0000756	0.0000931	0.3684
9340178M	3/11A	34S_4s2d2Tc_1	33 7/8	S	9	4437.4	72	66	0.297	0.446	HLP-22	12	8	4	1.9	10.5	5.7	30.8	16.1	0.62	0.33	s2d2	4.18	0.0000609	0.0000756	0.0000931	0.3684
9340179	3/11A	34S_4s2d2Tc_1	33 7/8	S	9	4437.4	72	66	0.297	0.446	HLP-22	12	8	4	1.9	10.5	5.7	30.8	16.1	0.62	0.33	s2d2	4.18	0.0000609	0.0000756	0.0000931	0.3684
9340180M	3/11A	34S_4s2d2Tc_1	33 7/8	S	9	4437.4	72	66	0.297	0.446	HLP-22	12	8	4	1.9	10.5	5.7	30.8	16.1	0.62	0.33	s2d2	4.18	0.0000609	0.0000756	0.0000931	0.3684
9340181M	3/11A	34S_4s2d2Tc_1	33 7/8	S	9	4437.4	72	66	0.297	0.446	HLP-22	12	8	4	1.9	10.5	5.7	30.8	16.1	0.62	0.33	s2d2	4.18	0.0000609	0.0000756	0.0000931	0.3684
9340182	3/11B	34S_4s2d2Zc_1	33 7/8	S	9	4437.4	72	66	0.297	0.446	HLP-22	12	8	4	1.9	10.5	5.7	30.8	16.1	0.62	0.33	s2d2	4.18	0.0000609	0.0000756	0.0000931	0.3684
9340183	3/11B	34S_4s2d2Zc_1	33 7/8	S	9	4437.4	72	66	0.297	0.446	HLP-22	12	8	4	1.9	10.5	5.7	30.8	16.1	0.62	0.33	s2d2	4.18	0.0000609	0.0000756	0.0000931	0.3684
9340184	3/11B	34S_4s2d2Zc_1	33 7/8	S	9	4437.4	72	66	0.297	0.446	HLP-22	12	8	4	1.9	10.5	5.7	30.8	16.1	0.62	0.33	s2d2	4.18	0.0000609	0.0000756	0.0000931	0.3684
9340185M	3/11B	34S_4s2d2Zc_1	33 7/8	S	9	4437.4	72	66	0.297	0.446	HLP-22	12	8	4	1.9	10.5	5.7	30.8	16.1	0.62	0.33	s2d2	4.18	0.0000609	0.0000756	0.0000931	0.3684
9340186M	3/11B	34S_4s2d2Zc_1	33 7/8	S	9	4437.4	72	66	0.297	0.446	HLP-22	12	8	4	1.9	10.5	5.7	30.8	16.1	0.62	0.33	s2d2	4.18	0.0000609	0.0000756	0.0000931	0.3684
9340187	3/11B	34S_4s2d2Zc_1	33 7/8	S	9	4437.4	72	66	0.297	0.446	HLP-22	12	8	4	1.9	10.5	5.7	30.8	16.1	0.62	0.33	s2d2	4.18	0.0000609	0.0000756	0.0000931	0.3684
9340188M	3/11B	34S_4s2d2Zc_1	33 7/8	S	9	4437.4	72	66	0.297	0.446	HLP-22	12	8	4	1.9	10.5	5.7	30.8	16.1	0.62	0.33	s2d2	4.18	0.0000609	0.0000756	0.0000931	0.3684
9340189M	3/11B	34S_4s2d2Zc_1	33 7/8	S	9	4437.4	72	66	0.297	0.446	HLP-22	12	8	4	1.9	10.5	5.7	30.8	16.1	0.62	0.33	s2d2	4.18	0.0000609	0.0000756	0.0000931	0.3684
9340190	3/11B	34S_4s2d2Zc_1	33 7/8	S	9	4437.4	72	66	0.297	0.446	HLP-22	12	8	4	1.9	10.5	5.7	30.8	16.1	0.62	0.33	s2d2	4.18	0.0000609	0.0000756	0.0000931	0.3684
9340191	3/11B	34S_4s2d2Zc_1	33 7/8	S	9	4437.4	72	66	0.297	0.446	HLP-22	12	8	4	1.9	10.5	5.7	30.8	16.1	0.62	0.33	s2d2	4.18	0.0000609	0.0000756	0.0000931	0.3684
9340192	3/11B	34S_4s2d2Zc_1	33 7/8	S	9	4437.4	72	66	0.297	0.446	HLP-22	12	8	4	1.9	10.5	5.7	30.8	16.1	0.62	0.33	s2d2	4.18	0.0000609	0.0000756	0.0000931	0.3684
9340193	3/11B	34S_4s2d2Zc_1	33 7/8	S	9	4437.4	72	66	0.297	0.446	HLP-22	12	8	4	1.9	10.5	5.7	30.8	16.1	0.62	0.33	s2d2	4.18	0.0000609	0.0000756	0.0000931	0.3684
9340194	3/11B	34S_4s2d2Zc_1	33 7/8	S	9	4437.4	72	66	0.297	0.446	HLP-22	12	8	4	1.9	10.5	5.7	30.8	16.1	0.62	0.33	s2d2	4.18	0.0000609	0.0000756	0.0000931	0.3684
9340195	3/11B	34S_4s2d2Zc_1	33 7/8	S	9	4437.4	72	66	0.297	0.446	HLP-22	12	8	4	1.9	10.5	5.7	30.8	16.1	0.62	0.33	s2d2	4.18	0.0000609	0.0000756	0.0000931	0.3684
9340196	3/11B	34S_4s2d2Zc_1	33 7/8	S	9	4437.4	72	66	0.297	0.446	HLP-22	12	8	4	1.9	10.5	5.7	30.8	16.1	0.62	0.33	s2d2	4.18	0.0000609	0.0000756	0.0000931	0.3684
9340197	3/11B	34S_4s2d2Zc_1	33 7/8	S	9	4437.4	72	66	0.297	0.446	HLP-22	12	8	4	1.9	10.5	5.7	30.8	16.1	0.62	0.33	s2d2	4.18	0.0000609	0.0000756	0.0000931	0.3684
9340198M	3/11B	34S_4s2d2Zc_1	33 7/8	S	9	4437.4	72	66	0.297	0.446	HLP-22	12	8	4	1.9	10.5	5.7	30.8	16.1	0.62	0.33	s2d2	4.18	0.0000609	0.0000756	0.0000931	0.3684
9340199M	3/11B	34S_4s2d2Zc_1	33 7/8	S	9	4437.4	72	66	0.297	0.446	HLP-22	12	8	4	1.9	10.5	5.7	30.8	16.1	0.62	0.33	s2d2	4.18	0.0000609	0.0000756	0.0000931	0.3684
9340200	3/11B	34S_4s2d2Zc_1	33 7/8	S	9	4437.4	72	66	0.297	0.446	HLP-22	12	8	4	1.9	10.5	5.7	30.8	16.1	0.62	0.33	s2d2	4.18	0.0000609	0.0000756	0.0000931	0.3684
9340201	3/11C	34S_4s2d2Yd_1	33 7/8	S	9	4437.4	72	66	0.297	0.446	HLP-22	12	8	4	1.9	10.5	5.7	30.8	16.1	0.62	0.33	s2d2	4.18	0.0000609	0.0000756	0.0000931	0.3684
9340202	3/11C	34S_4s2d2Yd_1	33 7/8	S	9	4437.4	72	66	0.297	0.446	HLP-22	12	8	4	1.9	10.5	5.7	30.8	16.1	0.62	0.33	s2d2	4.18	0.0000609	0.0000756	0.0000931	0.3684
9340203M	3/11C	34S_4s2d2Yd_1	33 7/8	S	9	4437.4	72	66	0.297	0.446	HLP-22	12	8	4	1.9	10.5	5.7	30.8	16.1	0.62	0.33	s2d2	4.18	0.0000609	0.0000756	0.0000931	0.3684
9340204M	3/11C	34S_4s2d2Yd_1	33 7/8	S	9	4437.4	72	66	0.297	0.446	HLP-22	12	8	4	1.9	10.5	5.7	30.8	16.1	0.62	0.33	s2d2	4.18	0.0000609	0.0000756	0.0000931	0.3684
9340205M	3/11C	34S_4s2d2Yd_1	33 7/8	S	9	4437.4	72	66	0.297	0.446	HLP-22	12	8	4	1.9	10.5	5.7	30.8	16.1	0.62	0.33	s2d2	4.18	0.0000609	0.0000756	0.0000931	0.3684

Table B.4. Data from 2008 Tests in Mid-Scale Vessel with Spherical Head B.3

Tank Water Temperature	Water Density	Solids Fraction	Pulse Volume Fraction	Duty Cycle	Cycle Time	Pulsed or Steady Jet	Us Steady Jet	U1 Pulsing Jet	U2 URMS	U3 URM3	Discharge Velocity	Critical Suspension Velocity	Average Peak Cloud Height	UCS Condition	UCS Method	UCS Flag	UCS Center Flag	UCS udv Flag	UCS based on Decreasing Velocity	Sweep Increase / Decrease	UDV Height Bed	Particle Motion	Solids Level	Outer Bottom Pattern	Inner Bottom Pattern	Case ID	Test	TDP	Row Number
C	g/cm³	fraction	fraction	fraction	s	text	m/s	m/s	m/s	m/s	m/s	m/s	in.	m/s	text	text	text	text	m/s	text	mm	text	text	text	text	text	text	text	text
T	ρ_c	ϕ_S	ϕ_P	DC	t_C	Jet	U_S	U1	U2	U3	U	U_{CS}	H_C	U_{CSR}	U_{CSM}	U_{CS}vis	U_{CS}cen	U_{CS}udv	U_{CS}_D	S_W	H_{bed}	PM	Sol	SP_O	SP_I	ID	M/DDX	TDP	MSS
21.8	0.998	0.00500	0.050	0.186	43.4	P	N/A	5.80	5.89	5.93	6.00	6.00	20.25	6.00	udv	N/A	N/A	UCSudv	N/A	I	2.2	4	N/A	N/A	N/A	34S_4s1d2Yd_1	3/9B	TDP-108	9340084
21.8	0.998	0.00500	0.050	0.186	42.4	P	N/A	5.94	6.03	6.08	6.20	6.00	21.00	N/A	N/A	N/A	N/A	N/A	N/A	I	0.0	4	N/A	N/A	N/A	34S_4s1d2Yd_1	3/9B	TDP-108	9340085
21.8	0.998	0.00500	0.050	0.186	42.4	P	N/A	N/A	N/A	N/A	6.20	6.00	21.00	N/A	N/A	N/A	N/A	N/A	N/A	N/A	0.0	N/A	N/A	N/A	N/A	34S_4s1d2Yd_1	3/9B	TDP-108	9340086
21.8	0.998	0.00500	0.050	0.186	42.4	P	N/A	N/A	N/A	N/A	6.20	6.00	21.00	N/A	N/A	N/A	N/A	N/A	N/A	N/A	0.0	N/A	N/A	N/A	N/A	34S_4s1d2Yd_1	3/9B	TDP-108	9340087
21.8	0.998	0.00500	0.050	0.186	42.4	P	N/A	N/A	N/A	N/A	6.20	6.00	21.00	N/A	N/A	N/A	N/A	N/A	N/A	N/A	0.0	N/A	N/A	N/A	N/A	34S_4s1d2Yd_1	3/9B	TDP-108	9340088
21.8	0.998	0.00500	0.050	0.186	42.4	P	N/A	N/A	N/A	N/A	6.20	6.00	21.00	N/A	N/A	N/A	N/A	N/A	N/A	N/A	0.0	N/A	N/A	N/A	N/A	34S_4s1d2Yd_1	3/9B	TDP-108	9340089
21.8	0.998	0.00500	0.050	0.186	42.4	P	N/A	N/A	N/A	N/A	6.20	6.00	21.00	N/A	N/A	N/A	N/A	N/A	N/A	N/A	0.0	N/A	N/A	N/A	N/A	34S_4s1d2Yd_1	3/9B	TDP-108	9340090
21.8	0.998	0.00500	0.050	0.186	42.4	P	N/A	N/A	N/A	N/A	6.20	6.00	21.00	N/A	N/A	N/A	N/A	N/A	N/A	N/A	0.7	N/A	N/A	N/A	N/A	34S_4s1d2Yd_1	3/9B	TDP-108	9340091
21.9	0.998	0.00500	0.050	0.186	40.0	P	N/A	6.25	6.34	6.39	6.50	6.00	23.00	N/A	N/A	N/A	N/A	N/A	N/A	I	0.0	4	N/A	N/A	N/A	34S_4s1d2Yd_1	3/9B	TDP-108	9340092
21.9	0.999	0.00500	0.050	0.187	37.6	P	N/A	6.63	6.74	6.79	6.90	6.00	30.50	N/A	N/A	N/A	N/A	N/A	N/A	I	0.0	N/A	N/A	N/A	N/A	34S_4s1d2Yd_1	3/9B	TDP-108	9340093
21.9	0.998	0.00500	0.050	0.185	36.4	P	N/A	6.91	7.02	7.08	7.25	6.00	33.25	N/A	N/A	N/A	N/A	N/A	N/A	I	0.0	N/A	N/A	N/A	N/A	34S_4s1d2Yd_1	3/9B	TDP-108	9340094
12.6	1.000	0.00050	0.050	0.331	35.8	P	N/A	3.82	3.86	3.88	3.95	4.05	22.50	N/A	N/A	N/A	N/A	N/A	N/A	D	4.6	1	N/A	N/A	N/A	34S_4s2d2Tc_1	3/11A	TDP-112	9340176
12.8	1.000	0.00050	0.050	0.332	35.0	P	N/A	4.03	4.08	4.10	4.20	4.05	24.50	N/A	N/A	N/A	UCScen	N/A	N/A	I	0.0	2	N/A	N/A	N/A	34S_4s2d2Tc_1	3/11A	TDP-112	9340177
13.1	1.000	0.00050	0.050	0.332	36.0	P	N/A	3.93	3.97	3.99	4.05	4.05	23.00	4.05	udv	N/A	N/A	UCSudv	N/A	I	0.7	1	N/A	N/A	N/A	34S_4s2d2Tc_1	3/11A	TDP-112	9340178
14.0	1.000	0.00050	0.050	0.330	49.0	P	N/A	2.90	2.92	2.94	3.00	4.05	20.25	N/A	N/A	N/A	N/A	N/A	N/A	(null)	N/A	NR	N/A	N/A	N/A	34S_4s2d2Tc_1	3/11A	TDP-112	9340179
14.0	1.000	0.00050	0.050	0.333	32.4	P	N/A	4.35	4.40	4.42	4.50	4.05	43.50	N/A	N/A	N/A	N/A	N/A	N/A	I	N/A	NR	N/A	N/A	N/A	34S_4s2d2Tc_1	3/11A	TDP-112	9340180
14.0	1.000	0.00050	0.050	0.332	32.6	P	N/A	4.20	4.24	4.26	4.35	4.05	37.50	N/A	N/A	N/A	N/A	N/A	N/A	D	N/A	NR	N/A	N/A	N/A	34S_4s2d2Tc_1	3/11A	TDP-112	9340181
15.2	1.000	0.00155	0.050	0.332	36.0	P	N/A	3.91	3.96	3.98	4.10	5.60	10.00	N/A	N/A	N/A	N/A	N/A	N/A	(null)	N/A	1	N/A	N/A	N/A	34S_4s2d2Zc_1	3/11B	TDP-111	9340182
15.2	1.000	0.00155	0.050	0.333	31.0	P	N/A	4.54	4.60	4.63	4.70	5.60	11.00	N/A	N/A	N/A	N/A	N/A	N/A	I	N/A	1	N/A	N/A	N/A	34S_4s2d2Zc_1	3/11B	TDP-111	9340183
15.5	1.000	0.00155	0.050	0.334	29.0	P	N/A	4.83	4.89	4.92	5.00	5.60	11.50	N/A	N/A	N/A	N/A	N/A	N/A	I	11.8	1	N/A	N/A	N/A	34S_4s2d2Zc_1	3/11B	TDP-111	9340184
16.0	1.000	0.00155	0.050	0.335	25.0	P	N/A	5.58	5.65	5.69	5.80	5.60	17.25	N/A	N/A	N/A	N/A	N/A	N/A	I	0.0	1	N/A	N/A	N/A	34S_4s2d2Zc_1	3/11B	TDP-111	9340185
16.2	1.000	0.00155	0.050	0.336	26.2	P	N/A	5.32	5.39	5.43	5.60	5.60	14.00	N/A	N/A	N/A	N/A	N/A	N/A	I	3.5	1	N/A	N/A	N/A	34S_4s2d2Zc_1	3/11B	TDP-111	9340186
16.4	1.000	0.00155	0.050	0.335	26.6	P	N/A	5.23	5.31	5.34	5.40	5.60	13.25	N/A	N/A	N/A	N/A	N/A	N/A	I	3.5	1	N/A	N/A	N/A	34S_4s2d2Zc_1	3/11B	TDP-111	9340187
16.6	1.000	0.00155	0.050	0.335	26.2	P	N/A	5.37	5.44	5.48	5.60	5.60	14.75	5.60	udv	N/A	N/A	UCSudv	N/A	I	1.7	1	N/A	N/A	N/A	34S_4s2d2Zc_1	3/11B	TDP-111	9340188
17.0	1.000	0.00155	0.050	0.335	24.9	P	N/A	5.37	5.45	5.48	5.60	5.60	14.00	N/A	N/A	N/A	N/A	UCSudv	N/A	(null)	2.0	1	N/A	N/A	N/A	34S_4s2d2Zc_1	3/11B	TDP-111	9340189
17.0	1.000	0.00155	0.050	0.335	24.9	P	N/A	5.37	5.45	5.48	5.60	5.60	14.00	N/A	N/A	N/A	N/A	N/A	N/A	N/A	1.3	N/A	N/A	N/A	N/A	34S_4s2d2Zc_1	3/11B	TDP-111	9340190
17.0	1.000	0.00155	0.050	0.335	24.9	P	N/A	5.37	5.45	5.48	5.60	5.60	14.00	N/A	N/A	N/A	N/A	N/A	N/A	N/A	1.4	N/A	N/A	N/A	N/A	34S_4s2d2Zc_1	3/11B	TDP-111	9340191
17.0	1.000	0.00155	0.050	0.335	24.9	P	N/A	5.37	5.45	5.48	5.60	5.60	14.00	N/A	N/A	N/A	N/A	N/A	N/A	N/A	1.3	N/A	N/A	N/A	N/A	34S_4s2d2Zc_1	3/11B	TDP-111	9340192
17.0	1.000	0.00155	0.050	0.335	24.9	P	N/A	5.37	5.45	5.48	5.60	5.60	14.00	N/A	N/A	N/A	N/A	N/A	N/A	N/A	0.0	N/A	N/A	N/A	N/A	34S_4s2d2Zc_1	3/11B	TDP-111	9340193
17.0	1.000	0.00155	0.050	0.335	24.9	P	N/A	5.37	5.45	5.48	5.60	5.60	14.00	N/A	N/A	N/A	N/A	N/A	N/A	N/A	1.9	N/A	N/A	N/A	N/A	34S_4s2d2Zc_1	3/11B	TDP-111	9340194
17.0	1.000	0.00155	0.050	0.335	24.9	P	N/A	5.37	5.45	5.48	5.60	5.60	14.00	N/A	N/A	N/A	N/A	N/A	N/A	N/A	1.3	N/A	N/A	N/A	N/A	34S_4s2d2Zc_1	3/11B	TDP-111	9340195
17.0	1.000	0.00155	0.050	0.335	24.9	P	N/A	5.37	5.45	5.48	5.60	5.60	14.00	N/A	N/A	N/A	N/A	N/A	N/A	N/A	2.0	N/A	N/A	N/A	N/A	34S_4s2d2Zc_1	3/11B	TDP-111	9340196
17.0	1.000	0.00155	0.050	0.335	24.9	P	N/A	5.37	5.45	5.48	5.60	5.60	14.00	N/A	N/A	N/A	N/A	N/A	N/A	N/A	0.0	N/A	N/A	N/A	N/A	34S_4s2d2Zc_1	3/11B	TDP-111	9340197
17.3	0.999	0.00155	0.050	0.335	23.6	P	N/A	5.92	6.00	6.04	6.10	5.60	22.75	N/A	N/A	N/A	N/A	N/A	N/A	D	0.0	4	N/A	N/A	N/A	34S_4s2d2Zc_1	3/11B	TDP-111	9340198
17.3	0.999	0.00155	0.050	0.337	22.4	P	N/A	6.20	6.29	6.34	6.50	5.60	28.50	N/A	N/A	N/A	N/A	N/A	N/A	I	0.0	4	N/A	N/A	N/A	34S_4s2d2Zc_1	3/11B	TDP-111	9340199
17.9	0.999	0.00155	0.050	0.335	28.1	P	N/A	5.36	5.43	5.47	5.60	5.60	N/A	N/A	N/A	N/A	N/A	N/A	N/A	(null)	0.0	N/A	N/A	N/A	N/A	34S_4s2d2Zc_1	3/11B	TDP-111	9340200
18.7	0.999	0.00500	0.050	0.189	30.4	P	N/A	8.21	8.36	8.44	8.60	9.20	12.25	N/A	N/A	N/A	N/A	N/A	N/A	I	7.8	1	N/A	N/A	N/A	34S_4s2d2Yd_1	3/11C	TDP-113	9340201
19.0	0.999	0.00500	0.050	0.189	29.6	P	N/A	8.36	8.52	8.60	8.80	9.20	12.25	N/A	N/A	N/A	N/A	N/A	N/A	I	4.3	1	N/A	N/A	N/A	34S_4s2d2Yd_1	3/11C	TDP-113	9340202
19.2	0.999	0.00500	0.050	0.185	28.8	P	N/A	8.75	8.92	9.01	9.20	9.20	13.00	9.20	udv	N/A	N/A	UCSudv	N/A	I	0.7	1	N/A	N/A	N/A	34S_4s2d2Yd_1	3/11C	TDP-113	9340203
19.2	0.999	0.00500	0.050	0.185	28.0	P	N/A	8.97	9.15	9.24	9.40	9.20	13.00	N/A	N/A	UCSvis	N/A	N/A	N/A	I	0.0	3	N/A	N/A	N/A	34S_4s2d2Yd_1	3/11C	TDP-113	9340204
19.4	0.999	0.00500	0.050	0.187	25.0	P	N/A	10.01	10.24	10.36	10.60	9.20	20.50	N/A	N/A	N/A	N/A	N/A	N/A	I	0.0	4	N/A	N/A	N/A	34S_4s2d2Yd_1	3/11C	TDP-113	9340205

Table B.4. Data from 2008 Tests in Mid-Scale Vessel with Spherical Head A.4

Row Number	Test	Case ID	Tank Diameter	Head Shape	Dish Height	Dish Volume	Tank Fill Height	Return Line Height	Nozzle Inner Diameter	Nozzle Stand-off Distance	Pulse Tube Configuration	Installed Nozzles	Outer Nozzles Operated	Inner Nozzles Operated	Pulse Tube Outer Diameter	Outer PJM Radius	Inner PJM Radius	"FIO" Outer PJM Impingement Angle	"FIO" Inner PJM Impingement Angle	Ratio Outer PJM to Tank Radius	Ratio Inner PJM to Tank Radius	Simulant	Solids Density	Particle Diameter d5	Particle Diameter d50	Particle Diameter d95	Void Fraction
text	text	text	in.	text	in.	in. ^{3}	in.	in.	in.	in.	text	number	number	number	in.	in.	in.	deg	deg	nondim	nondim	text	g/cm^3	m	m	m	fraction
MSS	M/DDX	ID	D	HS	H_{dish}	V_{dish}	H	Rtn	d	sod	PT	N	N_O	N_I	PT_{od}	R_O	R_I	θ_O	θ_I	R_O/R	R_I/R	sxdx	ρ_s	d_5	d_{50}	d_{95}	vf
9340206M	3/11C	34S_4s2d2Yd_1	33 7/8	S	9	4437.4	72	66	0.297	0.446	HLP-22	12	8	4	1.9	10.5	5.7	30.8	16.1	0.62	0.33	s2d2	4.18	0.0000609	0.0000756	0.0000931	0.3684
9340207	3/12A	34S_4s2d2Yc_1	33 7/8	S	9	4437.4	72	66	0.297	0.446	HLP-22	12	8	4	1.9	10.5	5.7	30.8	16.1	0.62	0.33	s2d2	4.18	0.0000609	0.0000756	0.0000931	0.3684
9340208	3/12A	34S_4s2d2Yc_1	33 7/8	S	9	4437.4	72	66	0.297	0.446	HLP-22	12	8	4	1.9	10.5	5.7	30.8	16.1	0.62	0.33	s2d2	4.18	0.0000609	0.0000756	0.0000931	0.3684
9340209	3/12A	34S_4s2d2Yc_1	33 7/8	S	9	4437.4	72	66	0.297	0.446	HLP-22	12	8	4	1.9	10.5	5.7	30.8	16.1	0.62	0.33	s2d2	4.18	0.0000609	0.0000756	0.0000931	0.3684
9340210M	3/12A	34S_4s2d2Yc_1	33 7/8	S	9	4437.4	72	66	0.297	0.446	HLP-22	12	8	4	1.9	10.5	5.7	30.8	16.1	0.62	0.33	s2d2	4.18	0.0000609	0.0000756	0.0000931	0.3684
9340211	3/12A	34S_4s2d2Yc_1	33 7/8	S	9	4437.4	72	66	0.297	0.446	HLP-22	12	8	4	1.9	10.5	5.7	30.8	16.1	0.62	0.33	s2d2	4.18	0.0000609	0.0000756	0.0000931	0.3684
9340212	3/12A	34S_4s2d2Yc_1	33 7/8	S	9	4437.4	72	66	0.297	0.446	HLP-22	12	8	4	1.9	10.5	5.7	30.8	16.1	0.62	0.33	s2d2	4.18	0.0000609	0.0000756	0.0000931	0.3684
9340213	3/12A	34S_4s2d2Yc_1	33 7/8	S	9	4437.4	72	66	0.297	0.446	HLP-22	12	8	4	1.9	10.5	5.7	30.8	16.1	0.62	0.33	s2d2	4.18	0.0000609	0.0000756	0.0000931	0.3684
9340214	3/12A	34S_4s2d2Yc_1	33 7/8	S	9	4437.4	72	66	0.297	0.446	HLP-22	12	8	4	1.9	10.5	5.7	30.8	16.1	0.62	0.33	s2d2	4.18	0.0000609	0.0000756	0.0000931	0.3684
9340215	3/12A	34S_4s2d2Yc_1	33 7/8	S	9	4437.4	72	66	0.297	0.446	HLP-22	12	8	4	1.9	10.5	5.7	30.8	16.1	0.62	0.33	s2d2	4.18	0.0000609	0.0000756	0.0000931	0.3684
9340216	3/12A	34S_4s2d2Yc_1	33 7/8	S	9	4437.4	72	66	0.297	0.446	HLP-22	12	8	4	1.9	10.5	5.7	30.8	16.1	0.62	0.33	s2d2	4.18	0.0000609	0.0000756	0.0000931	0.3684
9340217M	3/12A	34S_4s2d2Yc_1	33 7/8	S	9	4437.4	72	66	0.297	0.446	HLP-22	12	8	4	1.9	10.5	5.7	30.8	16.1	0.62	0.33	s2d2	4.18	0.0000609	0.0000756	0.0000931	0.3684
9340218M	3/12A	34S_4s2d2Yc_1	33 7/8	S	9	4437.4	72	66	0.297	0.446	HLP-22	12	8	4	1.9	10.5	5.7	30.8	16.1	0.62	0.33	s2d2	4.18	0.0000609	0.0000756	0.0000931	0.3684
9340219	3/12C	34S_4s2d2Xc_1	33 7/8	S	9	4437.4	72	66	0.297	0.446	HLP-22	12	8	4	1.9	10.5	5.7	30.8	16.1	0.62	0.33	s2d2	4.18	0.0000609	0.0000756	0.0000931	0.3684
9340220M	3/12C	34S_4s2d2Xc_1	33 7/8	S	9	4437.4	72	66	0.297	0.446	HLP-22	12	8	4	1.9	10.5	5.7	30.8	16.1	0.62	0.33	s2d2	4.18	0.0000609	0.0000756	0.0000931	0.3684
9340221	3/12C	34S_4s2d2Xc_1	33 7/8	S	9	4437.4	72	66	0.297	0.446	HLP-22	12	8	4	1.9	10.5	5.7	30.8	16.1	0.62	0.33	s2d2	4.18	0.0000609	0.0000756	0.0000931	0.3684
9340222	3/12C	34S_4s2d2Xc_1	33 7/8	S	9	4437.4	72	66	0.297	0.446	HLP-22	12	8	4	1.9	10.5	5.7	30.8	16.1	0.62	0.33	s2d2	4.18	0.0000609	0.0000756	0.0000931	0.3684
9340223	3/12C	34S_4s2d2Xc_1	33 7/8	S	9	4437.4	72	66	0.297	0.446	HLP-22	12	8	4	1.9	10.5	5.7	30.8	16.1	0.62	0.33	s2d2	4.18	0.0000609	0.0000756	0.0000931	0.3684
9340224	3/12C	34S_4s2d2Xc_1	33 7/8	S	9	4437.4	72	66	0.297	0.446	HLP-22	12	8	4	1.9	10.5	5.7	30.8	16.1	0.62	0.33	s2d2	4.18	0.0000609	0.0000756	0.0000931	0.3684
9340225	3/12C	34S_4s2d2Xc_1	33 7/8	S	9	4437.4	72	66	0.297	0.446	HLP-22	12	8	4	1.9	10.5	5.7	30.8	16.1	0.62	0.33	s2d2	4.18	0.0000609	0.0000756	0.0000931	0.3684
9340226	3/12C	34S_4s2d2Xc_1	33 7/8	S	9	4437.4	72	66	0.297	0.446	HLP-22	12	8	4	1.9	10.5	5.7	30.8	16.1	0.62	0.33	s2d2	4.18	0.0000609	0.0000756	0.0000931	0.3684
9340227	3/12C	34S_4s2d2Xc_1	33 7/8	S	9	4437.4	72	66	0.297	0.446	HLP-22	12	8	4	1.9	10.5	5.7	30.8	16.1	0.62	0.33	s2d2	4.18	0.0000609	0.0000756	0.0000931	0.3684
9340228M	3/12C	34S_4s2d2Xc_1	33 7/8	S	9	4437.4	72	66	0.297	0.446	HLP-22	12	8	4	1.9	10.5	5.7	30.8	16.1	0.62	0.33	s2d2	4.18	0.0000609	0.0000756	0.0000931	0.3684
9340229	3/12C	34S_4s2d2Xc_1	33 7/8	S	9	4437.4	72	66	0.297	0.446	HLP-22	12	8	4	1.9	10.5	5.7	30.8	16.1	0.62	0.33	s2d2	4.18	0.0000609	0.0000756	0.0000931	0.3684
9340230M	3/12C	34S_4s2d2Xc_1	33 7/8	S	9	4437.4	72	66	0.297	0.446	HLP-22	12	8	4	1.9	10.5	5.7	30.8	16.1	0.62	0.33	s2d2	4.18	0.0000609	0.0000756	0.0000931	0.3684
9340231	3/12D	34S_4s2d2Xc_2	33 7/8	S	9	4437.4	72	66	0.297	0.446	HLP-22	12	8	4	1.9	10.5	5.7	30.8	16.1	0.62	0.33	s2d2	4.18	0.0000609	0.0000756	0.0000931	0.3684
9340232M	3/12D	34S_4s2d2Xc_2	33 7/8	S	9	4437.4	72	66	0.297	0.446	HLP-22	12	8	4	1.9	10.5	5.7	30.8	16.1	0.62	0.33	s2d2	4.18	0.0000609	0.0000756	0.0000931	0.3684
9340233M	3/12E	34S_4s2d2Xb_1	33 7/8	S	9	4437.4	72	66	0.297	0.446	HLP-22	12	8	4	1.9	10.5	5.7	30.8	16.1	0.62	0.33	s2d2	4.18	0.0000609	0.0000756	0.0000931	0.3684
9340234M	3/12F	34S_4s2d1Yc_1	33 7/8	S	9	4437.4	70	66	0.297	0.446	HLP-22	12	8	4	1.9	10.5	5.7	30.8	16.1	0.62	0.33	s2d1	4.17	0.0001399	0.0001642	0.0001924	0.4000

Table B.4. Data from 2008 Tests in Mid-Scale Vessel with Spherical Head B.4

Tank Water Temperature	Water Density	Solids Fraction	Pulse Volume Fraction	Duty Cycle	Cycle Time	Pulsed or Steady Jet	Us Steady Jet	U1 Pulsing Jet	U2 URMS	U3 URM3	Discharge Velocity	Critical Suspension Velocity	Average Peak Cloud Height	UCS Condition	UCS Method	UCS Flag	UCS Center Flag	UCS udv Flag	UCS based on Decreasing Velocity	Sweep Increase / Decrease	UDV Height Bed	Particle Motion	Solids Level	Outer Bottom Pattern	Inner Bottom Pattern	Case ID	Test	TDP	Row Number
C	g/cm³	fraction	fraction	fraction	s	text	m/s	m/s	m/s	m/s	m/s	m/s	in.	m/s	text	text	text	text	m/s	text	mm	text	text	text	text	text	text	text	text
T	ρ_l	ϕ_S	ϕ_P	DC	t_C	Jet	U_S	U1	U2	U3	U	U_{CS}	H_C	U_{CSR}	U_{CSM}	U_{CS}vis	U_{CS}cen	U_{CS}udv	U_{CS}_D	S_W	H_{bed}	PM	Sol	SP_O	SP_I	ID	M/DDX	TDP	MSS
19.5	0.999	0.00500	0.050	0.186	26.6	P	N/A	9.41	9.62	9.72	10.00	9.20	17.75	N/A	N/A	N/A	N/A	N/A	N/A	D	0.0	4	N/A	N/A	N/A	34S_4s2d2Yd_1	3/11C	TDP-113	9340206
19.9	0.999	0.00500	0.050	0.336	18.1	P	N/A	7.59	7.74	7.81	8.00	8.60	11.25	N/A	N/A	N/A	N/A	N/A	N/A	(null)	N/A	1	N/A	N/A	N/A	34S_4s2d2Yc_1	3/12A	TDP-114	9340207
20.1	0.999	0.00500	0.050	0.335	18.0	P	N/A	7.82	7.96	8.03	8.20	8.60	12.50	N/A	N/A	N/A	N/A	N/A	N/A	I	5.1	1	N/A	N/A	N/A	34S_4s2d2Yc_1	3/12A	TDP-114	9340208
20.1	0.998	0.00500	0.050	0.335	17.6	P	N/A	7.98	8.13	8.21	8.40	8.60	14.25	N/A	N/A	N/A	N/A	N/A	N/A	I	4.1	1	N/A	N/A	N/A	34S_4s2d2Yc_1	3/12A	TDP-114	9340209
20.8	0.999	0.00500	0.050	0.336	17.0	P	N/A	8.17	8.33	8.41	8.60	8.60	18.50	8.60	udv	UCSvis	N/A	UCSudv	N/A	(null)	0.0	3	N/A	N/A	N/A	34S_4s2d2Yc_1	3/12A	TDP-114	9340210
20.8	0.999	0.00500	0.050	0.336	17.0	P	N/A	8.17	8.33	8.41	8.60	8.60	18.50	N/A	N/A	N/A	N/A	N/A	N/A	N/A	0.0	N/A	N/A	N/A	N/A	34S_4s2d2Yc_1	3/12A	TDP-114	9340211
20.8	0.999	0.00500	0.050	0.336	17.0	P	N/A	8.17	8.33	8.41	8.60	8.60	18.50	N/A	N/A	N/A	N/A	N/A	N/A	N/A	0.0	N/A	N/A	N/A	N/A	34S_4s2d2Yc_1	3/12A	TDP-114	9340212
20.8	0.999	0.00500	0.050	0.336	17.0	P	N/A	8.17	8.33	8.41	8.60	8.60	18.50	N/A	N/A	N/A	N/A	N/A	N/A	N/A	0.0	N/A	N/A	N/A	N/A	34S_4s2d2Yc_1	3/12A	TDP-114	9340213
20.8	0.999	0.00500	0.050	0.336	17.0	P	N/A	8.17	8.33	8.41	8.60	8.60	18.50	N/A	N/A	N/A	N/A	N/A	N/A	N/A	0.0	N/A	N/A	N/A	N/A	34S_4s2d2Yc_1	3/12A	TDP-114	9340214
20.8	0.999	0.00500	0.050	0.336	17.0	P	N/A	8.17	8.33	8.41	8.60	8.60	18.50	N/A	N/A	N/A	N/A	N/A	N/A	N/A	0.0	N/A	N/A	N/A	N/A	34S_4s2d2Yc_1	3/12A	TDP-114	9340215
20.8	0.999	0.00500	0.050	0.336	17.0	P	N/A	8.17	8.33	8.41	8.60	8.60	18.50	N/A	N/A	N/A	N/A	N/A	N/A	N/A	0.0	N/A	N/A	N/A	N/A	34S_4s2d2Yc_1	3/12A	TDP-114	9340216
21.0	0.999	0.00500	0.050	0.337	16.4	P	N/A	8.53	8.70	8.78	9.00	8.60	20.75	N/A	N/A	N/A	N/A	N/A	N/A	I	0.0	4	N/A	N/A	N/A	34S_4s2d2Yc_1	3/12A	TDP-114	9340217
21.1	0.999	0.00500	0.050	0.338	15.4	P	N/A	9.06	9.24	9.34	9.60	8.60	27.50	N/A	N/A	N/A	N/A	N/A	N/A	I	0.0	4	N/A	N/A	N/A	34S_4s2d2Yc_1	3/12A	TDP-114	9340218
21.5	0.999	0.01500	0.051	0.349	15.2	P	N/A	N/A	N/A	N/A	9.80	9.80	N/A	N/A	N/A	N/A	N/A	UCSudv	N/A	N/A	1.3	N/A	N/A	N/A	N/A	34S_4s2d2Xc_1	3/12C	TDP-115	9340219
21.8	0.998	0.01500	0.050	0.339	14.8	P	N/A	9.41	9.62	9.72	10.00	9.80	10.50	N/A	N/A	N/A	N/A	N/A	N/A	I	0.0	4	N/A	N/A	N/A	34S_4s2d2Xc_1	3/12C	TDP-115	9340220
21.8	0.998	0.01500	0.050	0.339	14.8	P	N/A	9.41	9.62	9.72	10.00	9.80	10.50	N/A	N/A	N/A	N/A	N/A	N/A	N/A	0.0	N/A	N/A	N/A	N/A	34S_4s2d2Xc_1	3/12C	TDP-115	9340221
21.8	0.998	0.01500	0.050	0.339	14.8	P	N/A	9.41	9.62	9.72	10.00	9.80	10.50	N/A	N/A	N/A	N/A	N/A	N/A	N/A	0.6	N/A	N/A	N/A	N/A	34S_4s2d2Xc_1	3/12C	TDP-115	9340222
21.8	0.998	0.01500	0.050	0.339	14.8	P	N/A	9.41	9.62	9.72	10.00	9.80	10.50	N/A	N/A	N/A	N/A	N/A	N/A	N/A	0.0	N/A	N/A	N/A	N/A	34S_4s2d2Xc_1	3/12C	TDP-115	9340223
21.8	0.998	0.01500	0.050	0.339	14.8	P	N/A	9.41	9.62	9.72	10.00	9.80	10.50	N/A	N/A	N/A	N/A	N/A	N/A	N/A	0.6	N/A	N/A	N/A	N/A	34S_4s2d2Xc_1	3/12C	TDP-115	9340224
21.8	0.998	0.01500	0.050	0.339	14.8	P	N/A	9.41	9.62	9.72	10.00	9.80	10.50	N/A	N/A	N/A	N/A	N/A	N/A	N/A	0.8	N/A	N/A	N/A	N/A	34S_4s2d2Xc_1	3/12C	TDP-115	9340225
21.8	0.998	0.01500	0.050	0.339	14.8	P	N/A	9.41	9.62	9.72	10.00	9.80	10.50	N/A	N/A	N/A	N/A	N/A	N/A	N/A	0.5	N/A	N/A	N/A	N/A	34S_4s2d2Xc_1	3/12C	TDP-115	9340226
21.8	0.998	0.01500	0.050	0.339	14.8	P	N/A	9.41	9.62	9.72	10.00	9.80	10.50	N/A	N/A	N/A	N/A	N/A	N/A	N/A	0.0	N/A	N/A	N/A	N/A	34S_4s2d2Xc_1	3/12C	TDP-115	9340227
22.7	0.999	0.01500	0.050	0.337	12.8	P	N/A	10.80	11.06	11.20	11.60	9.80	14.75	N/A	N/A	N/A	N/A	N/A	N/A	I	N/A	4	N/A	N/A	N/A	34S_4s2d2Xc_1	3/12C	TDP-115	9340228
22.5	0.998	0.01500	0.050	0.332	16.0	P	N/A	8.81	8.99	9.08	9.30	9.80	9.25	N/A	N/A	N/A	N/A	N/A	N/A	D	4.0	1	N/A	N/A	N/A	34S_4s2d2Xc_1	3/12C	TDP-115	9340229
22.6	0.998	0.01500	0.050	0.333	15.2	P	N/A	9.23	9.43	9.53	9.80	9.80	10.00	9.80	udv	UCSvis	N/A	UCSudv	N/A	I	2.1	3	N/A	N/A	N/A	34S_4s2d2Xc_1	3/12C	TDP-115	9340230
22.6	0.998	0.01500	0.100	0.330	45.0	P	N/A	6.30	6.35	6.38	6.50	6.70	9.25	N/A	N/A	N/A	N/A	N/A	N/A	I	3.7	1	N/A	N/A	N/A	34S_4s2d2Xc_2	3/12D	TDP-115	9340231
22.7	0.998	0.01500	0.101	0.331	44.0	P	N/A	6.48	6.54	6.57	6.70	6.70	9.25	6.70	udv	N/A	N/A	UCSudv	N/A	I	0.6	1	N/A	N/A	N/A	34S_4s2d2Xc_2	3/12D	TDP-115	9340232
22.7	0.998	0.01500	0.050	0.504	11.0	P	N/A	8.42	8.58	8.66	8.80	8.80	12.25	8.80	udv	N/A	N/A	UCSudv	N/A	I	1.3	1	N/A	N/A	N/A	34S_4s2d2Xb_1	3/12E	TDP-115	9340233
13.4	1.000	0.00500	0.050	0.340	14.0	P	N/A	9.83	10.04	10.15	10.40	10.40	11.75	10.40	udv	UCSvis	N/A	UCSudv	N/A	I	0.0	3	N/A	N/A	N/A	34S_4s2d1Yc_1	3/12F	TDP-116	9340234

Table B.5. Data from 2008 Tests in Large-Scale Vessel with Elliptical Head A.1

Row Number	Test	Case ID	Tank Diameter	Head Shape	Dish Height	Dish Volume	Tank Fill Height	Return Line Height	Nozzle Inner Diameter	Nozzle Stand-off Distance	Pulse Tube Configuration	Installed Nozzles	Outer Nozzles Operated	Inner Nozzles Operated	Pulse Tube Outer Diameter	Outer PJM Radius	Inner PJM Radius	"FIO" Outer PJM Impingement Angle	"FIO" Inner PJM Impingement Angle	Ratio Outer PJM to Tank Radius	Ratio Inner PJM to Tank Radius	Simulant	Solids Density	Particle Diameter d5	Particle Diameter d50	Particle Diameter d95	Void Fraction
text	text	text	in.	text	in.	in. ^{3}	in.	in.	in.	in.	text	number	number	number	in.	in.	in.	deg	deg	nondim	nondim	text	g/cm^3	m	m	m	fraction
MSS	M/DDX	ID	D	HS	H_{dish}	V_{dish}	H	Rtn	d	sod	PT	N	N_O	N_I	PT_{od}	R_O	R_I	θ_O	θ_I	R_O/R	R_I/R	sxdx	ρ_s	d_5	d_{50}	d_{95}	vf
9700001	5/8A	70E_4s1d2Zc_1	70	E	19	49770.7	93	80	0.613	0.920	HLP-22	12	8	4	3.5	21.9	11.5	20.3	10.5	0.62	0.33	s1d2	2.48	0.0000569	0.0000693	0.0000821	0.3750
9700002	5/8A	70E_4s1d2Zc_1	70	E	19	49770.7	93	80	0.613	0.920	HLP-22	12	8	4	3.5	21.9	11.5	20.3	10.5	0.62	0.33	s1d2	2.48	0.0000569	0.0000693	0.0000821	0.3750
9700003M	5/8A	70E_4s1d2Zc_1	70	E	19	49770.7	93	80	0.613	0.920	HLP-22	12	8	4	3.5	21.9	11.5	20.3	10.5	0.62	0.33	s1d2	2.48	0.0000569	0.0000693	0.0000821	0.3750
9700004M	5/8A	70E_4s1d2Zc_1	70	E	19	49770.7	93	80	0.613	0.920	HLP-22	12	8	4	3.5	21.9	11.5	20.3	10.5	0.62	0.33	s1d2	2.48	0.0000569	0.0000693	0.0000821	0.3750
9700013M	5/8A	70E_4s1d2Zc_1	70	E	19	49770.7	93	80	0.613	0.920	HLP-22	12	8	4	3.5	21.9	11.5	20.3	10.5	0.62	0.33	s1d2	2.48	0.0000569	0.0000693	0.0000821	0.3750
9700014M	5/8A	70E_4s1d2Zc_1	70	E	19	49770.7	93	80	0.613	0.920	HLP-22	12	8	4	3.5	21.9	11.5	20.3	10.5	0.62	0.33	s1d2	2.48	0.0000569	0.0000693	0.0000821	0.3750
9700014.1	5/9A	70E_4s1d2Zc_1	70	E	19	49770.7	93	80	0.613	0.920	HLP-22	12	8	4	3.5	21.9	11.5	20.3	10.5	0.62	0.33	s1d2	2.48	0.0000569	0.0000693	0.0000821	0.3750
9700015M	5/9A	70E_4s1d2Zc_1	70	E	19	49770.7	93	80	0.613	0.920	HLP-22	12	8	4	3.5	21.9	11.5	20.3	10.5	0.62	0.33	s1d2	2.48	0.0000569	0.0000693	0.0000821	0.3750
9700016	5/9A	70E_4s1d2Zc_1	70	E	19	49770.7	93	80	0.613	0.920	HLP-22	12	8	4	3.5	21.9	11.5	20.3	10.5	0.62	0.33	s1d2	2.48	0.0000569	0.0000693	0.0000821	0.3750
9700017	5/9A	70E_4s1d2Zc_1	70	E	19	49770.7	93	80	0.613	0.920	HLP-22	12	8	4	3.5	21.9	11.5	20.3	10.5	0.62	0.33	s1d2	2.48	0.0000569	0.0000693	0.0000821	0.3750
9700018	5/9A	70E_4s1d2Zc_1	70	E	19	49770.7	93	80	0.613	0.920	HLP-22	12	8	4	3.5	21.9	11.5	20.3	10.5	0.62	0.33	s1d2	2.48	0.0000569	0.0000693	0.0000821	0.3750
9700019	5/9A	70E_4s1d2Zc_1	70	E	19	49770.7	93	80	0.613	0.920	HLP-22	12	8	4	3.5	21.9	11.5	20.3	10.5	0.62	0.33	s1d2	2.48	0.0000569	0.0000693	0.0000821	0.3750
9700020	5/9A	70E_4s1d2Zc_1	70	E	19	49770.7	93	80	0.613	0.920	HLP-22	12	8	4	3.5	21.9	11.5	20.3	10.5	0.62	0.33	s1d2	2.48	0.0000569	0.0000693	0.0000821	0.3750
9700021	5/9A	70E_4s1d2Zc_1	70	E	19	49770.7	93	80	0.613	0.920	HLP-22	12	8	4	3.5	21.9	11.5	20.3	10.5	0.62	0.33	s1d2	2.48	0.0000569	0.0000693	0.0000821	0.3750
9700022	5/9A	70E_4s1d2Zc_1	70	E	19	49770.7	93	80	0.613	0.920	HLP-22	12	8	4	3.5	21.9	11.5	20.3	10.5	0.62	0.33	s1d2	2.48	0.0000569	0.0000693	0.0000821	0.3750
9700023	5/9A	70E_4s1d2Zc_1	70	E	19	49770.7	93	80	0.613	0.920	HLP-22	12	8	4	3.5	21.9	11.5	20.3	10.5	0.62	0.33	s1d2	2.48	0.0000569	0.0000693	0.0000821	0.3750
9700024	5/9B	70E_4s1d2Zd_1	70	E	19	49770.7	93	80	0.613	0.920	HLP-22	12	8	4	3.5	21.9	11.5	20.3	10.5	0.62	0.33	s1d2	2.48	0.0000569	0.0000693	0.0000821	0.3750
9700025	5/9B	70E_4s1d2Zd_1	70	E	19	49770.7	93	80	0.613	0.920	HLP-22	12	8	4	3.5	21.9	11.5	20.3	10.5	0.62	0.33	s1d2	2.48	0.0000569	0.0000693	0.0000821	0.3750
9700026	5/9B	70E_4s1d2Zd_1	70	E	19	49770.7	93	80	0.613	0.920	HLP-22	12	8	4	3.5	21.9	11.5	20.3	10.5	0.62	0.33	s1d2	2.48	0.0000569	0.0000693	0.0000821	0.3750
9700027M	5/9B	70E_4s1d2Zd_1	70	E	19	49770.7	93	80	0.613	0.920	HLP-22	12	8	4	3.5	21.9	11.5	20.3	10.5	0.62	0.33	s1d2	2.48	0.0000569	0.0000693	0.0000821	0.3750
9700028M	5/9B	70E_4s1d2Zd_1	70	E	19	49770.7	93	80	0.613	0.920	HLP-22	12	8	4	3.5	21.9	11.5	20.3	10.5	0.62	0.33	s1d2	2.48	0.0000569	0.0000693	0.0000821	0.3750
9700029M	5/9B	70E_4s1d2Zd_1	70	E	19	49770.7	93	80	0.613	0.920	HLP-22	12	8	4	3.5	21.9	11.5	20.3	10.5	0.62	0.33	s1d2	2.48	0.0000569	0.0000693	0.0000821	0.3750
9700030M	5/9B	70E_4s1d2Zd_1	70	E	19	49770.7	93	80	0.613	0.920	HLP-22	12	8	4	3.5	21.9	11.5	20.3	10.5	0.62	0.33	s1d2	2.48	0.0000569	0.0000693	0.0000821	0.3750
9700031	5/12A	70E_4s1d2Yc_1	70	E	19	49770.7	93	80	0.613	0.920	HLP-22	12	8	4	3.5	21.9	11.5	20.3	10.5	0.62	0.33	s1d2	2.48	0.0000569	0.0000693	0.0000821	0.3750
9700032	5/12A	70E_4s1d2Yc_1	70	E	19	49770.7	93	80	0.613	0.920	HLP-22	12	8	4	3.5	21.9	11.5	20.3	10.5	0.62	0.33	s1d2	2.48	0.0000569	0.0000693	0.0000821	0.3750
9700033	5/12A	70E_4s1d2Yc_1	70	E	19	49770.7	93	80	0.613	0.920	HLP-22	12	8	4	3.5	21.9	11.5	20.3	10.5	0.62	0.33	s1d2	2.48	0.0000569	0.0000693	0.0000821	0.3750
9700034	5/12A	70E_4s1d2Yc_1	70	E	19	49770.7	93	80	0.613	0.920	HLP-22	12	8	4	3.5	21.9	11.5	20.3	10.5	0.62	0.33	s1d2	2.48	0.0000569	0.0000693	0.0000821	0.3750
9700035M	5/12A	70E_4s1d2Yc_1	70	E	19	49770.7	93	80	0.613	0.920	HLP-22	12	8	4	3.5	21.9	11.5	20.3	10.5	0.62	0.33	s1d2	2.48	0.0000569	0.0000693	0.0000821	0.3750
9700035.1	5/12A	70E_4s1d2Yc_1	70	E	19	49770.7	93	80	0.613	0.920	HLP-22	12	8	4	3.5	21.9	11.5	20.3	10.5	0.62	0.33	s1d2	2.48	0.0000569	0.0000693	0.0000821	0.3750
9700036M	5/12A	70E_4s1d2Yc_1	70	E	19	49770.7	93	80	0.613	0.920	HLP-22	12	8	4	3.5	21.9	11.5	20.3	10.5	0.62	0.33	s1d2	2.48	0.0000569	0.0000693	0.0000821	0.3750
9700037	5/12A	70E_4s1d2Yc_1	70	E	19	49770.7	93	80	0.613	0.920	HLP-22	12	8	4	3.5	21.9	11.5	20.3	10.5	0.62	0.33	s1d2	2.48	0.0000569	0.0000693	0.0000821	0.3750
9700038	5/12A	70E_4s1d2Yc_1	70	E	19	49770.7	93	80	0.613	0.920	HLP-22	12	8	4	3.5	21.9	11.5	20.3	10.5	0.62	0.33	s1d2	2.48	0.0000569	0.0000693	0.0000821	0.3750
9700039	5/12A	70E_4s1d2Yc_1	70	E	19	49770.7	93	80	0.613	0.920	HLP-22	12	8	4	3.5	21.9	11.5	20.3	10.5	0.62	0.33	s1d2	2.48	0.0000569	0.0000693	0.0000821	0.3750
9700040	5/12A	70E_4s1d2Yc_1	70	E	19	49770.7	93	80	0.613	0.920	HLP-22	12	8	4	3.5	21.9	11.5	20.3	10.5	0.62	0.33	s1d2	2.48	0.0000569	0.0000693	0.0000821	0.3750
9700041	5/12A	70E_4s1d2Yc_1	70	E	19	49770.7	93	80	0.613	0.920	HLP-22	12	8	4	3.5	21.9	11.5	20.3	10.5	0.62	0.33	s1d2	2.48	0.0000569	0.0000693	0.0000821	0.3750
9700042	5/12A	70E_4s1d2Yc_1	70	E	19	49770.7	93	80	0.613	0.920	HLP-22	12	8	4	3.5	21.9	11.5	20.3	10.5	0.62	0.33	s1d2	2.48	0.0000569	0.0000693	0.0000821	0.3750
9700043	5/12A	70E_4s1d2Yc_1	70	E	19	49770.7	93	80	0.613	0.920	HLP-22	12	8	4	3.5	21.9	11.5	20.3	10.5	0.62	0.33	s1d2	2.48	0.0000569	0.0000693	0.0000821	0.3750
9700044	5/12A	70E_4s1d2Yc_1	70	E	19	49770.7	93	80	0.613	0.920	HLP-22	12	8	4	3.5	21.9	11.5	20.3	10.5	0.62	0.33	s1d2	2.48	0.0000569	0.0000693	0.0000821	0.3750
9700045M	5/12A	70E_4s1d2Yc_1	70	E	19	49770.7	93	80	0.613	0.920	HLP-22	12	8	4	3.5	21.9	11.5	20.3	10.5	0.62	0.33	s1d2	2.48	0.0000569	0.0000693	0.0000821	0.3750
9700046M	5/12A	70E_4s1d2Yc_1	70	E	19	49770.7	93	80	0.613	0.920	HLP-22	12	8	4	3.5	21.9	11.5	20.3	10.5	0.62	0.33	s1d2	2.48	0.0000569	0.0000693	0.0000821	0.3750
9700047M	5/12A	70E_4s1d2Yc_1	70	E	19	49770.7	93	80	0.613	0.920	HLP-22	12	8	4	3.5	21.9	11.5	20.3	10.5	0.62	0.33	s1d2	2.48	0.0000569	0.0000693	0.0000821	0.3750

Table B.5. Data from 2008 Tests in Large-Scale Vessel with Elliptical Head B.1

Tank Water Temperature	Water Density	Solids Fraction	Pulse Volume Fraction	Duty Cycle	Cycle Time	Pulsed or Steady Jet	Us Steady Jet	U1 Pulsing Jet	U2 URMS	U3 URM3	Discharge Velocity	Critical Suspension Velocity	Average Peak Cloud Height	UCS Condition	UCS Method	UCS Flag	UCS Center Flag	UCS udv Flag	UCS based on Decreasing Velocity	Sweep Increase / Decrease	UDV Height Bed	Particle Motion	Solids Level	Outer Bottom Pattern	Inner Bottom Pattern	Case ID	Test	TDP	Row Number
C	g/cm³	fraction	fraction	fraction	s	text	m/s	m/s	m/s	m/s	m/s	m/s	in.	m/s	text	text	text	text	m/s	text	mm	text	text	text	text	text	text	text	text
T	ρ_c	ϕ_S	ϕ_p	DC	t_C	Jet	U_S	U1	U2	U3	U	U_{CS}	H_C	U_{CSR}	U_{CSM}	U_{CS}vis	U_{CS}cen	U_{CS}udv	U_{CS_D}	S_W	H_{bed}	PM	Sol	SP_O	SP_I	ID	M/DDX	TDP	MSS
21.8	0.995	0.00155	0.050	0.335	69.4	P	N/A	4.06	4.10	4.13	4.20	4.60	24.75	N/A	N/A	N/A	N/A	N/A	N/A	I	6.9	1	N/A	N/A	N/A	70E_4s1d2Zc_1	5/8A	TDP-149	9700001
21.6	0.994	0.00155	0.050	0.335	66.2	P	N/A	4.26	4.31	4.33	4.40	4.60	25.50	N/A	N/A	N/A	N/A	N/A	N/A	I	3.9	1	N/A	N/A	N/A	70E_4s1d2Zc_1	5/8A	TDP-149	9700002
21.9	0.995	0.00155	0.050	0.336	63.2	P	N/A	4.44	4.49	4.51	4.60	4.60	28.50	4.60	udv	N/A	UCScen	UCSudv	N/A	I	0.0	2	N/A	N/A	N/A	70E_4s1d2Zc_1	5/8A	TDP-149	9700003
21.8	0.995	0.00155	0.050	0.335	63.4	P	N/A	4.44	4.49	4.52	4.60	4.60	28.50	N/A	N/A	N/A	UCScen	N/A	N/A	I	N/A	2	N/A	N/A	N/A	70E_4s1d2Zc_1	5/8A	TDP-149	9700004
22.0	0.995	0.00155	0.050	0.337	62.0	P	N/A	4.52	4.57	4.60	4.70	4.60	30.50	N/A	N/A	N/A	N/A	N/A	N/A	I	N/A	4	N/A	N/A	N/A	70E_4s1d2Zc_1	5/8A	TDP-149	9700013
22.0	0.995	0.00155	0.050	0.338	60.8	P	N/A	4.60	4.66	4.69	4.80	4.60	35.50	N/A	N/A	N/A	N/A	N/A	N/A	I	N/A	4	N/A	N/A	N/A	70E_4s1d2Zc_1	5/8A	TDP-149	9700014
19.8	0.995	0.00155	0.050	0.337	63.6	P	N/A	4.41	4.46	4.49	4.60	4.60	30.50	N/A	N/A	N/A	N/A	N/A	N/A	N/A	n/a	N/A	N/A	N/A	N/A	70E_4s1d2Zc_1	5/9A	TDP-150	9700014.1
19.8	0.995	0.00155	0.050	0.337	63.6	P	N/A	4.41	4.46	4.49	4.60	4.60	30.50	N/A	N/A	N/A	UCScen	N/A	N/A	I	0.0	2	N/A	N/A	N/A	70E_4s1d2Zc_1	5/9A	TDP-150	9700015
19.8	0.995	0.00155	0.050	0.337	63.6	P	N/A	4.41	4.46	4.49	4.60	4.60	30.50	N/A	N/A	N/A	N/A	N/A	N/A	N/A	0.0	N/A	N/A	N/A	N/A	70E_4s1d2Zc_1	5/9A	TDP-150	9700016
19.8	0.995	0.00155	0.050	0.337	63.6	P	N/A	4.41	4.46	4.49	4.60	4.60	30.50	N/A	N/A	N/A	N/A	N/A	N/A	N/A	0.0	N/A	N/A	N/A	N/A	70E_4s1d2Zc_1	5/9A	TDP-150	9700017
19.8	0.995	0.00155	0.050	0.337	63.6	P	N/A	4.41	4.46	4.49	4.60	4.60	30.50	N/A	N/A	N/A	N/A	N/A	N/A	N/A	0.0	N/A	N/A	N/A	N/A	70E_4s1d2Zc_1	5/9A	TDP-150	9700018
19.8	0.995	0.00155	0.050	0.337	63.6	P	N/A	4.41	4.46	4.49	4.60	4.60	30.50	N/A	N/A	N/A	N/A	N/A	N/A	N/A	0.0	N/A	N/A	N/A	N/A	70E_4s1d2Zc_1	5/9A	TDP-150	9700019
19.8	0.995	0.00155	0.050	0.337	63.6	P	N/A	4.41	4.46	4.49	4.60	4.60	30.50	N/A	N/A	N/A	N/A	N/A	N/A	N/A	0.0	N/A	N/A	N/A	N/A	70E_4s1d2Zc_1	5/9A	TDP-150	9700020
19.8	0.995	0.00155	0.050	0.337	63.6	P	N/A	4.41	4.46	4.49	4.60	4.60	30.50	N/A	N/A	N/A	N/A	N/A	N/A	N/A	0.0	N/A	N/A	N/A	N/A	70E_4s1d2Zc_1	5/9A	TDP-150	9700021
19.8	0.995	0.00155	0.050	0.337	63.6	P	N/A	4.41	4.46	4.49	4.60	4.60	30.50	N/A	N/A	N/A	N/A	N/A	N/A	N/A	0.0	N/A	N/A	N/A	N/A	70E_4s1d2Zc_1	5/9A	TDP-150	9700022
19.8	0.995	0.00155	0.050	0.337	63.6	P	N/A	4.41	4.46	4.49	4.60	4.60	30.50	N/A	N/A	N/A	N/A	N/A	N/A	N/A	0.0	N/A	N/A	N/A	N/A	70E_4s1d2Zc_1	5/9A	TDP-150	9700023
20.6	0.995	0.00155	0.050	0.178	132.0	P	N/A	4.05	4.09	4.11	4.20	5.40	21.75	N/A	N/A	N/A	N/A	N/A	N/A	(null)	33.9	1	N/A	N/A	N/A	70E_4s1d2Zd_1	5/9B	TDP-150	9700024
20.9	0.995	0.00155	0.050	0.181	110.0	P	N/A	4.78	4.85	4.88	5.00	5.40	25.25	N/A	N/A	N/A	N/A	N/A	N/A	I	7.1	1	N/A	N/A	N/A	70E_4s1d2Zd_1	5/9B	TDP-150	9700025
21.0	0.995	0.00155	0.050	0.181	105.8	P	N/A	4.99	5.05	5.08	5.20	5.40	26.00	N/A	N/A	N/A	N/A	N/A	N/A	I	6.8	1	N/A	N/A	N/A	70E_4s1d2Zd_1	5/9B	TDP-150	9700026
21.3	0.995	0.00155	0.050	0.182	101.8	P	N/A	5.17	5.24	5.28	5.40	5.40	26.50	5.40	udv	N/A	N/A	UCSudv	N/A	I	1.8	1	N/A	N/A	N/A	70E_4s1d2Zd_1	5/9B	TDP-150	9700027
21.4	0.995	0.00155	0.050	0.182	97.6	P	N/A	5.38	5.45	5.49	5.60	5.40	31.50	N/A	N/A	N/A	UCScen	N/A	N/A	I	0.0	2	N/A	N/A	N/A	70E_4s1d2Zd_1	5/9B	TDP-150	9700028
21.5	0.995	0.00155	0.050	0.183	91.0	P	N/A	5.74	5.83	5.87	6.00	5.40	37.50	N/A	N/A	N/A	N/A	N/A	N/A	I	0.0	4	N/A	N/A	N/A	70E_4s1d2Zd_1	5/9B	TDP-150	9700029
21.6	0.995	0.00155	0.050	0.185	84.2	P	N/A	6.12	6.22	6.27	6.40	5.40	49.25	N/A	N/A	N/A	N/A	N/A	N/A	I	0.0	4	N/A	N/A	N/A	70E_4s1d2Zd_1	5/9B	TDP-150	9700030
19.7	0.995	0.00500	0.050	0.332	55.0	P	N/A	5.20	5.26	5.30	5.40	6.00	22.50	N/A	N/A	N/A	N/A	N/A	N/A	I	28.9	1	N/A	N/A	N/A	70E_4s1d2Yc_1	5/12A	TDP-151	9700031
20.1	0.995	0.00500	0.050	0.333	53.0	P	N/A	5.38	5.46	5.50	5.60	6.00	24.00	N/A	N/A	N/A	N/A	N/A	N/A	I	13.5	1	N/A	N/A	N/A	70E_4s1d2Yc_1	5/12A	TDP-151	9700032
20.2	0.995	0.00500	0.050	0.334	51.2	P	N/A	5.55	5.64	5.68	5.80	6.00	25.00	N/A	N/A	N/A	N/A	N/A	N/A	I	5.6	1	N/A	N/A	N/A	70E_4s1d2Yc_1	5/12A	TDP-151	9700033
20.2	0.995	0.00500	0.050	0.335	50.4	P	N/A	5.64	5.73	5.77	5.90	6.00	26.25	N/A	N/A	N/A	UCScen	N/A	N/A	I	8.5	2	N/A	N/A	N/A	70E_4s1d2Yc_1	5/12A	TDP-151	9700034
20.5	0.995	0.00500	0.050	0.335	49.6	P	N/A	5.72	5.81	5.85	6.00	6.00	27.50	6.00	udv	N/A	N/A	UCSudv	N/A	I	0.8	4	N/A	N/A	N/A	70E_4s1d2Yc_1	5/12A	TDP-151	9700035
20.5	0.995	0.00500	0.050	0.335	49.6	P	N/A	5.72	5.81	5.85	6.00	6.00	27.75	N/A	N/A	N/A	N/A	UCSudv	N/A	N/A	n/a	N/A	N/A	N/A	N/A	70E_4s1d2Yc_1	5/12A	TDP-151	9700035.1
20.5	0.995	0.00500	0.050	0.335	49.6	P	N/A	5.72	5.81	5.85	6.00	6.00	27.75	N/A	N/A	N/A	N/A	N/A	N/A	(null)	0.0	4	N/A	N/A	N/A	70E_4s1d2Yc_1	5/12A	TDP-151	9700036
20.5	0.995	0.00500	0.050	0.335	49.6	P	N/A	5.72	5.81	5.85	6.00	6.00	27.75	N/A	N/A	N/A	N/A	N/A	N/A	N/A	0.0	N/A	N/A	N/A	N/A	70E_4s1d2Yc_1	5/12A	TDP-151	9700037
20.5	0.995	0.00500	0.050	0.335	49.6	P	N/A	5.72	5.81	5.85	6.00	6.00	27.75	N/A	N/A	N/A	N/A	N/A	N/A	N/A	0.0	N/A	N/A	N/A	N/A	70E_4s1d2Yc_1	5/12A	TDP-151	9700038
20.5	0.995	0.00500	0.050	0.335	49.6	P	N/A	5.72	5.81	5.85	6.00	6.00	27.75	N/A	N/A	N/A	N/A	N/A	N/A	N/A	0.0	N/A	N/A	N/A	N/A	70E_4s1d2Yc_1	5/12A	TDP-151	9700039
20.5	0.995	0.00500	0.050	0.335	49.6	P	N/A	5.72	5.81	5.85	6.00	6.00	27.75	N/A	N/A	N/A	N/A	N/A	N/A	N/A	0.0	N/A	N/A	N/A	N/A	70E_4s1d2Yc_1	5/12A	TDP-151	9700040
20.5	0.995	0.00500	0.050	0.335	49.6	P	N/A	5.72	5.81	5.85	6.00	6.00	27.75	N/A	N/A	N/A	N/A	N/A	N/A	N/A	0.9	N/A	N/A	N/A	N/A	70E_4s1d2Yc_1	5/12A	TDP-151	9700041
20.5	0.995	0.00500	0.050	0.335	49.6	P	N/A	5.72	5.81	5.85	6.00	6.00	27.75	N/A	N/A	N/A	N/A	N/A	N/A	N/A	3.1	N/A	N/A	N/A	N/A	70E_4s1d2Yc_1	5/12A	TDP-151	9700042
20.5	0.995	0.00500	0.050	0.335	49.6	P	N/A	5.72	5.81	5.85	6.00	6.00	27.75	N/A	N/A	N/A	N/A	N/A	N/A	N/A	0.0	N/A	N/A	N/A	N/A	70E_4s1d2Yc_1	5/12A	TDP-151	9700043
20.5	0.995	0.00500	0.050	0.335	49.6	P	N/A	5.72	5.81	5.85	6.00	6.00	27.75	N/A	N/A	N/A	N/A	N/A	N/A	N/A	0.0	N/A	N/A	N/A	N/A	70E_4s1d2Yc_1	5/12A	TDP-151	9700044
21.0	0.995	0.00500	0.050	0.336	47.8	P	N/A	5.90	5.99	6.04	6.20	6.00	31.50	N/A	N/A	N/A	N/A	N/A	N/A	(null)	0.0	4	N/A	N/A	N/A	70E_4s1d2Yc_1	5/12A	TDP-151	9700045
20.7	0.995	0.00500	0.050	0.337	46.4	P	N/A	6.09	6.19	6.23	6.40	6.00	34.25	N/A	N/A	N/A	N/A	N/A	N/A	I	0.0	4	N/A	N/A	N/A	70E_4s1d2Yc_1	5/12A	TDP-151	9700046
21.2	0.995	0.00500	0.050	0.339	45.0	P	N/A	6.26	6.36	6.42	6.60	6.00	38.25	N/A	N/A	N/A	N/A	N/A	N/A	I	0.0	4	N/A	N/A	N/A	70E_4s1d2Yc_1	5/12A	TDP-151	9700047

Table B.5. Data from 2008 Tests in Large-Scale Vessel with Elliptical Head A.2

Row Number	Test	Case ID	Tank Diameter	Head Shape	Dish Height	Dish Volume	Tank Fill Height	Return Line Height	Nozzle Inner Diameter	Nozzle Stand-off Distance	Pulse Tube Configuration	Installed Nozzles	Outer Nozzles Operated	Inner Nozzles Operated	Pulse Tube Outer Diameter	Outer PJM Radius	Inner PJM Radius	"FIO" Outer PJM Impingement Angle	"FIO" Inner PJM Impingement Angle	Ratio Outer PJM to Tank Radius	Ratio Inner PJM to Tank Radius	Simulant	Solids Density	Particle Diameter d5	Particle Diameter d50	Particle Diameter d95	Void Fraction
text	text	text	in.	text	in.	in. ^{3}	in.	in.	in.	in.	text	number	number	number	in.	in.	in.	deg	deg	nondim	nondim	text	g/cm^3	m	m	m	fraction
MSS	M/DDX	ID	D	HS	H_{dish}	V_{dish}	H	Rtn	d	sod	PT	N	N_O	N_I	PT_{od}	R_O	R_I	θ_O	θ_I	R_O/R	R_I/R	sxdx	ρ_s	d_5	d_{50}	d_{95}	vf
9700048	5/12B	70E_4s1d2Rc_1	70	E	19	49770.7	93	80	0.613	0.920	HLP-22	12	8	4	3.5	21.9	11.5	20.3	10.5	0.62	0.33	s1d2	2.48	0.0000569	0.0000693	0.0000821	0.3750
9700049	5/12B	70E_4s1d2Rc_1	70	E	19	49770.7	93	80	0.613	0.920	HLP-22	12	8	4	3.5	21.9	11.5	20.3	10.5	0.62	0.33	s1d2	2.48	0.0000569	0.0000693	0.0000821	0.3750
9700050	5/12B	70E_4s1d2Rc_1	70	E	19	49770.7	93	80	0.613	0.920	HLP-22	12	8	4	3.5	21.9	11.5	20.3	10.5	0.62	0.33	s1d2	2.48	0.0000569	0.0000693	0.0000821	0.3750
9700051M	5/12B	70E_4s1d2Rc_1	70	E	19	49770.7	93	80	0.613	0.920	HLP-22	12	8	4	3.5	21.9	11.5	20.3	10.5	0.62	0.33	s1d2	2.48	0.0000569	0.0000693	0.0000821	0.3750
9700052M	5/13A	70E_4s1d2Rc_1	70	E	19	49770.7	92 1/2	80	0.613	0.920	HLP-22	12	8	4	3.5	21.9	11.5	20.3	10.5	0.62	0.33	s1d2	2.48	0.0000569	0.0000693	0.0000821	0.3750
9700053M	5/13A	70E_4s1d2Rc_1	70	E	19	49770.7	92 1/2	80	0.613	0.920	HLP-22	12	8	4	3.5	21.9	11.5	20.3	10.5	0.62	0.33	s1d2	2.48	0.0000569	0.0000693	0.0000821	0.3750
9700054	5/13A	70E_4s1d2Rc_1	70	E	19	49770.7	92 1/2	80	0.613	0.920	HLP-22	12	8	4	3.5	21.9	11.5	20.3	10.5	0.62	0.33	s1d2	2.48	0.0000569	0.0000693	0.0000821	0.3750
9700055	5/13B	70E_4s1d2Rd_1	70	E	19	49770.7	92 1/2	80	0.613	0.920	HLP-22	12	8	4	3.5	21.9	11.5	20.3	10.5	0.62	0.33	s1d2	2.48	0.0000569	0.0000693	0.0000821	0.3750
9700056	5/13B	70E_4s1d2Rd_1	70	E	19	49770.7	92 1/2	80	0.613	0.920	HLP-22	12	8	4	3.5	21.9	11.5	20.3	10.5	0.62	0.33	s1d2	2.48	0.0000569	0.0000693	0.0000821	0.3750
9700057	5/13B	70E_4s1d2Rd_1	70	E	19	49770.7	92 1/2	80	0.613	0.920	HLP-22	12	8	4	3.5	21.9	11.5	20.3	10.5	0.62	0.33	s1d2	2.48	0.0000569	0.0000693	0.0000821	0.3750
9700058	5/13B	70E_4s1d2Rd_1	70	E	19	49770.7	92 1/2	80	0.613	0.920	HLP-22	12	8	4	3.5	21.9	11.5	20.3	10.5	0.62	0.33	s1d2	2.48	0.0000569	0.0000693	0.0000821	0.3750
9700059	5/13B	70E_4s1d2Rd_1	70	E	19	49770.7	92 1/2	80	0.613	0.920	HLP-22	12	8	4	3.5	21.9	11.5	20.3	10.5	0.62	0.33	s1d2	2.48	0.0000569	0.0000693	0.0000821	0.3750
9700060M	5/13B	70E_4s1d2Rd_1	70	E	19	49770.7	92 1/2	80	0.613	0.920	HLP-22	12	8	4	3.5	21.9	11.5	20.3	10.5	0.62	0.33	s1d2	2.48	0.0000569	0.0000693	0.0000821	0.3750
9700061	5/13C	70E_4s1d2Vc_1	70	E	19	49770.7	92 1/2	80	0.613	0.920	HLP-22	12	8	4	3.5	21.9	11.5	20.3	10.5	0.62	0.33	s1d2	2.48	0.0000569	0.0000693	0.0000821	0.3750
9700062	5/13C	70E_4s1d2Vc_1	70	E	19	49770.7	92 1/2	80	0.613	0.920	HLP-22	12	8	4	3.5	21.9	11.5	20.3	10.5	0.62	0.33	s1d2	2.48	0.0000569	0.0000693	0.0000821	0.3750
9700063	5/13C	70E_4s1d2Vc_1	70	E	19	49770.7	92 1/2	80	0.613	0.920	HLP-22	12	8	4	3.5	21.9	11.5	20.3	10.5	0.62	0.33	s1d2	2.48	0.0000569	0.0000693	0.0000821	0.3750
9700064	5/13C	70E_4s1d2Vc_1	70	E	19	49770.7	92 1/2	80	0.613	0.920	HLP-22	12	8	4	3.5	21.9	11.5	20.3	10.5	0.62	0.33	s1d2	2.48	0.0000569	0.0000693	0.0000821	0.3750
9700065	5/13C	70E_4s1d2Vc_1	70	E	19	49770.7	92 1/2	80	0.613	0.920	HLP-22	12	8	4	3.5	21.9	11.5	20.3	10.5	0.62	0.33	s1d2	2.48	0.0000569	0.0000693	0.0000821	0.3750
9700066	5/14A	70E_4s1d2Vc_1	70	E	19	49770.7	92 1/2	80	0.613	0.920	HLP-22	12	8	4	3.5	21.9	11.5	20.3	10.5	0.62	0.33	s1d2	2.48	0.0000569	0.0000693	0.0000821	0.3750
9700067	5/14A	70E_4s1d2Vc_1	70	E	19	49770.7	92 1/2	80	0.613	0.920	HLP-22	12	8	4	3.5	21.9	11.5	20.3	10.5	0.62	0.33	s1d2	2.48	0.0000569	0.0000693	0.0000821	0.3750
9700068M	5/14A	70E_4s1d2Vc_1	70	E	19	49770.7	92 1/2	80	0.613	0.920	HLP-22	12	8	4	3.5	21.9	11.5	20.3	10.5	0.62	0.33	s1d2	2.48	0.0000569	0.0000693	0.0000821	0.3750
9700069	5/14A	70E_4s1d2Vc_1	70	E	19	49770.7	92 1/2	80	0.613	0.920	HLP-22	12	8	4	3.5	21.9	11.5	20.3	10.5	0.62	0.33	s1d2	2.48	0.0000569	0.0000693	0.0000821	0.3750
9700070	5/14A	70E_4s1d2Vc_1	70	E	19	49770.7	92 1/2	80	0.613	0.920	HLP-22	12	8	4	3.5	21.9	11.5	20.3	10.5	0.62	0.33	s1d2	2.48	0.0000569	0.0000693	0.0000821	0.3750
9700070.1	5/14A	70E_4s1d2Vc_1	70	E	19	49770.7	92 1/2	80	0.613	0.920	HLP-22	12	8	4	3.5	21.9	11.5	20.3	10.5	0.62	0.33	s1d2	2.48	0.0000569	0.0000693	0.0000821	0.3750
9700071	5/14A	70E_4s1d2Vc_1	70	E	19	49770.7	92 1/2	80	0.613	0.920	HLP-22	12	8	4	3.5	21.9	11.5	20.3	10.5	0.62	0.33	s1d2	2.48	0.0000569	0.0000693	0.0000821	0.3750
9700071.1	5/14A	70E_4s1d2Vc_1	70	E	19	49770.7	92 1/2	80	0.613	0.920	HLP-22	12	8	4	3.5	21.9	11.5	20.3	10.5	0.62	0.33	s1d2	2.48	0.0000569	0.0000693	0.0000821	0.3750
9700072	5/14A	70E_4s1d2Vc_1	70	E	19	49770.7	92 1/2	80	0.613	0.920	HLP-22	12	8	4	3.5	21.9	11.5	20.3	10.5	0.62	0.33	s1d2	2.48	0.0000569	0.0000693	0.0000821	0.3750
9700072.1	5/14A	70E_4s1d2Vc_1	70	E	19	49770.7	92 1/2	80	0.613	0.920	HLP-22	12	8	4	3.5	21.9	11.5	20.3	10.5	0.62	0.33	s1d2	2.48	0.0000569	0.0000693	0.0000821	0.3750
9700073	5/14A	70E_4s1d2Vc_1	70	E	19	49770.7	92 1/2	80	0.613	0.920	HLP-22	12	8	4	3.5	21.9	11.5	20.3	10.5	0.62	0.33	s1d2	2.48	0.0000569	0.0000693	0.0000821	0.3750
9700073.1	5/14A	70E_4s1d2Vc_1	70	E	19	49770.7	92 1/2	80	0.613	0.920	HLP-22	12	8	4	3.5	21.9	11.5	20.3	10.5	0.62	0.33	s1d2	2.48	0.0000569	0.0000693	0.0000821	0.3750
9700074	5/14A	70E_4s1d2Vc_1	70	E	19	49770.7	92 1/2	80	0.613	0.920	HLP-22	12	8	4	3.5	21.9	11.5	20.3	10.5	0.62	0.33	s1d2	2.48	0.0000569	0.0000693	0.0000821	0.3750
9700074.1	5/14A	70E_4s1d2Vc_1	70	E	19	49770.7	92 1/2	80	0.613	0.920	HLP-22	12	8	4	3.5	21.9	11.5	20.3	10.5	0.62	0.33	s1d2	2.48	0.0000569	0.0000693	0.0000821	0.3750
9700075	5/14A	70E_4s1d2Vc_1	70	E	19	49770.7	92 1/2	80	0.613	0.920	HLP-22	12	8	4	3.5	21.9	11.5	20.3	10.5	0.62	0.33	s1d2	2.48	0.0000569	0.0000693	0.0000821	0.3750
9700076	5/14A	70E_4s1d2Vc_1	70	E	19	49770.7	92 1/2	80	0.613	0.920	HLP-22	12	8	4	3.5	21.9	11.5	20.3	10.5	0.62	0.33	s1d2	2.48	0.0000569	0.0000693	0.0000821	0.3750
9700076.1	5/14A	70E_4s1d2Vc_1	70	E	19	49770.7	92 1/2	80	0.613	0.920	HLP-22	12	8	4	3.5	21.9	11.5	20.3	10.5	0.62	0.33	s1d2	2.48	0.0000569	0.0000693	0.0000821	0.3750
9700077	5/14A	70E_4s1d2Vc_1	70	E	19	49770.7	92 1/2	80	0.613	0.920	HLP-22	12	8	4	3.5	21.9	11.5	20.3	10.5	0.62	0.33	s1d2	2.48	0.0000569	0.0000693	0.0000821	0.3750
9700077.1	5/14A	70E_4s1d2Vc_1	70	E	19	49770.7	92 1/2	80	0.613	0.920	HLP-22	12	8	4	3.5	21.9	11.5	20.3	10.5	0.62	0.33	s1d2	2.48	0.0000569	0.0000693	0.0000821	0.3750
9700078	5/14A	70E_4s1d2Vc_1	70	E	19	49770.7	92 1/2	80	0.613	0.920	HLP-22	12	8	4	3.5	21.9	11.5	20.3	10.5	0.62	0.33	s1d2	2.48	0.0000569	0.0000693	0.0000821	0.3750
9700078.1	5/14A	70E_4s1d2Vc_1	70	E	19	49770.7	92 1/2	80	0.613	0.920	HLP-22	12	8	4	3.5	21.9	11.5	20.3	10.5	0.62	0.33	s1d2	2.48	0.0000569	0.0000693	0.0000821	0.3750
9700079	5/14A	70E_4s1d2Vc_1	70	E	19	49770.7	92 1/2	80	0.613	0.920	HLP-22	12	8	4	3.5	21.9	11.5	20.3	10.5	0.62	0.33	s1d2	2.48	0.0000569	0.0000693	0.0000821	0.3750
9700079.1	5/14A	70E_4s1d2Vc_1	70	E	19	49770.7	92 1/2	80	0.613	0.920	HLP-22	12	8	4	3.5	21.9	11.5	20.3	10.5	0.62	0.33	s1d2	2.48	0.0000569	0.0000693	0.0000821	0.3750

Table B.5. Data from 2008 Tests in Large-Scale Vessel with Elliptical Head B.2

Tank Water Temperature	Water Density	Solids Fraction	Pulse Volume Fraction	Duty Cycle	Cycle Time	Pulsed or Steady Jet	Us Steady Jet	U1 Pulsing Jet	U2 URMS	U3 URM3	Discharge Velocity	Critical Suspension Velocity	Average Peak Cloud Height	UCS Condition	UCS Method	UCS Flag	UCS Center Flag	UCS udv Flag	UCS based on Decreasing Velocity	Sweep Increase / Decrease	UDV Height Bed	Particle Motion	Solids Level	Outer Bottom Pattern	Inner Bottom Pattern	Case ID	Test	TDP	Row Number
C	g/cm³	fraction	fraction	fraction	s	text	m/s	m/s	m/s	m/s	m/s	m/s	in.	m/s	text	text	text	text	m/s	text	mm	text	text	text	text	text	text	text	text
T	ρ_L	ϕ_S	ϕ_P	DC	t_C	Jet	U_S	U1	U2	U3	U	U_{CS}	H_C	U_{CSR}	U_{CSM}	U_{CS}vis	U_{CS}cen	U_{CS}udv	U_{CS}_D	S_W	H_{bed}	PM	Sol	SP_O	SP_I	ID	M/DDX	TDP	MSS
21.9	0.995	0.01000	0.050	0.331	47.0	P	N/A	6.09	6.19	6.24	6.40	7.00	24.00	N/A	N/A	N/A	N/A	N/A	N/A	(null)	23.6	1	N/A	N/A	N/A	70E_4s1d2Rc_1	5/12B	TDP-152	9700048
21.9	0.995	0.01000	0.050	0.332	45.6	P	N/A	6.29	6.38	6.43	6.60	7.00	25.50	N/A	N/A	N/A	N/A	N/A	N/A	I	19.7	1	N/A	N/A	N/A	70E_4s1d2Rc_1	5/12B	TDP-152	9700049
22.2	0.995	0.01000	0.050	0.333	44.2	P	N/A	6.46	6.57	6.62	6.80	7.00	27.00	N/A	N/A	N/A	N/A	N/A	N/A	I	35.5	1	N/A	N/A	N/A	70E_4s1d2Rc_1	5/12B	TDP-152	9700050
22.3	0.995	0.01000	0.050	0.334	42.8	P	N/A	6.64	6.75	6.81	7.00	7.00	31.50	N/A	N/A	N/A	N/A	N/A	N/A	I	9.3	1	N/A	N/A	N/A	70E_4s1d2Rc_1	5/12B	TDP-152	9700051
20.3	0.995	0.01000	0.050	0.335	41.6	P	N/A	6.83	6.94	7.00	7.20	7.20	35.75	7.20	udv	N/A	N/A	UCSudv	N/A	I	0.0	4	N/A	N/A	N/A	70E_4s1d2Rc_1	5/13A	TDP-153	9700052
20.5	0.995	0.01000	0.050	0.337	39.6	P	N/A	7.11	7.23	7.30	7.50	7.20	42.50	N/A	N/A	N/A	N/A	N/A	N/A	I	0.0	4	N/A	N/A	N/A	70E_4s1d2Rc_1	5/13A	TDP-153	9700053
20.6	0.995	0.01000	0.050	0.334	43.0	P	N/A	6.64	6.75	6.81	7.00	7.20	33.25	N/A	N/A	N/A	UCScen	N/A	N/A	I	2.4	2	N/A	N/A	N/A	70E_4s1d2Rc_1	5/13A	TDP-153	9700054
21.3	0.995	0.01000	0.050	0.184	70.0	P	N/A	7.37	7.51	7.58	7.80	9.80	22.00	N/A	N/A	N/A	N/A	N/A	N/A	I	30.4	1	N/A	N/A	N/A	70E_4s1d2Rd_1	5/13B	TDP-153	9700055
21.5	0.995	0.01000	0.050	0.185	65.0	P	N/A	7.91	8.06	8.14	8.40	9.80	24.00	N/A	N/A	N/A	N/A	N/A	N/A	I	31.2	1	N/A	N/A	N/A	70E_4s1d2Rd_1	5/13B	TDP-153	9700056
21.8	0.996	0.01000	0.050	0.186	62.0	P	N/A	8.29	8.46	8.54	8.80	9.80	25.75	N/A	N/A	N/A	N/A	N/A	N/A	I	24.1	1	N/A	N/A	N/A	70E_4s1d2Rd_1	5/13B	TDP-153	9700057
21.8	0.996	0.01000	0.050	0.183	59.0	P	N/A	8.84	9.02	9.11	9.40	9.80	31.00	N/A	N/A	N/A	N/A	N/A	N/A	I	28.5	1	N/A	N/A	N/A	70E_4s1d2Rd_1	5/13B	TDP-153	9700058
21.9	0.995	0.01000	0.050	0.184	57.8	P	N/A	9.01	9.20	9.30	9.60	9.80	35.50	N/A	N/A	N/A	UCScen	N/A	N/A	I	8.1	2	N/A	N/A	N/A	70E_4s1d2Rd_1	5/13B	TDP-153	9700059
22.0	0.995	0.01000	0.050	0.184	56.6	P	N/A	9.20	9.39	9.49	9.80	9.80	36.50	9.80	udv	N/A	N/A	UCSudv	N/A	I	1.2	4	N/A	N/A	N/A	70E_4s1d2Rd_1	5/13B	TDP-153	9700060
22.0	0.995	0.01430	0.050	0.329	47.4	P	N/A	6.12	6.20	6.25	6.40	7.80	22.50	N/A	N/A	N/A	N/A	N/A	N/A	(null)	28.7	1	N/A	N/A	N/A	70E_4s1d2Vc_1	5/13C	TDP-154	9700061
22.1	0.994	0.01430	0.050	0.332	44.6	P	N/A	6.46	6.56	6.61	6.80	7.80	26.00	N/A	N/A	N/A	N/A	N/A	N/A	I	23.8	1	N/A	N/A	N/A	70E_4s1d2Vc_1	5/13C	TDP-154	9700062
21.3	0.995	0.01430	0.050	0.334	42.8	P	N/A	6.66	6.77	6.82	7.00	7.80	26.75	N/A	N/A	N/A	N/A	N/A	N/A	I	27.3	1	N/A	N/A	N/A	70E_4s1d2Vc_1	5/13C	TDP-154	9700063
21.3	0.995	0.01430	0.050	0.334	42.6	P	N/A	6.74	6.85	6.91	7.10	7.80	27.50	N/A	N/A	N/A	N/A	N/A	N/A	I	19.2	1	N/A	N/A	N/A	70E_4s1d2Vc_1	5/13C	TDP-154	9700064
21.3	0.995	0.01430	0.050	0.337	39.8	P	N/A	7.10	7.23	7.29	7.50	7.80	32.00	N/A	N/A	N/A	N/A	N/A	N/A	I	32.7	1	N/A	N/A	N/A	70E_4s1d2Vc_1	5/13C	TDP-154	9700065
21.0	0.995	0.01430	0.050	0.332	40.4	P	N/A	7.11	7.24	7.30	7.50	7.80	32.50	N/A	N/A	N/A	N/A	N/A	N/A	(null)	35.1	1	N/A	N/A	N/A	70E_4s1d2Vc_1	5/14A	TDP-155	9700066
20.9	0.995	0.01430	0.050	0.333	39.4	P	N/A	7.30	7.43	7.49	7.70	7.80	38.75	N/A	N/A	N/A	N/A	N/A	N/A	I	25.9	1	N/A	N/A	N/A	70E_4s1d2Vc_1	5/14A	TDP-155	9700067
21.0	0.995	0.01430	0.050	0.333	38.8	P	N/A	7.39	7.52	7.59	7.80	7.80	41.00	N/A	N/A	N/A	UCScen	N/A	N/A	I	2.6	2	N/A	N/A	N/A	70E_4s1d2Vc_1	5/14A	TDP-155	9700068
20.9	0.995	0.01430	0.050	0.333	38.8	P	N/A	7.39	7.52	7.59	7.80	7.80	41.00	7.80	center	N/A	UCScen	N/A	N/A	(null)	0.8	2	N/A	N/A	N/A	70E_4s1d2Vc_1	5/14A	TDP-155	9700069
20.9	0.995	0.01430	0.050	0.333	38.8	P	N/A	7.39	7.52	7.59	7.80	7.80	41.00	N/A	N/A	N/A	N/A	N/A	N/A	N/A	0.0	N/A	N/A	N/A	N/A	70E_4s1d2Vc_1	5/14A	TDP-155	9700070
20.9	0.995	0.01430	0.050	0.333	38.8	P	N/A	7.39	7.52	7.59	7.80	7.80	41.00	N/A	N/A	N/A	N/A	N/A	N/A	N/A	n/a	N/A	N/A	N/A	N/A	70E_4s1d2Vc_1	5/14A	TDP-155	9700070.1
20.9	0.995	0.01430	0.050	0.333	38.8	P	N/A	7.39	7.52	7.59	7.80	7.80	41.00	N/A	N/A	N/A	N/A	N/A	N/A	N/A	0.8	N/A	N/A	N/A	N/A	70E_4s1d2Vc_1	5/14A	TDP-155	9700071
20.9	0.995	0.01430	0.050	0.333	38.8	P	N/A	7.39	7.52	7.59	7.80	7.80	41.00	N/A	N/A	N/A	N/A	N/A	N/A	N/A	n/a	N/A	N/A	N/A	N/A	70E_4s1d2Vc_1	5/14A	TDP-155	9700071.1
20.9	0.995	0.01430	0.050	0.333	38.8	P	N/A	7.39	7.52	7.59	7.80	7.80	41.00	N/A	N/A	N/A	N/A	N/A	N/A	N/A	0.0	N/A	N/A	N/A	N/A	70E_4s1d2Vc_1	5/14A	TDP-155	9700072
20.9	0.995	0.01430	0.050	0.333	38.8	P	N/A	7.39	7.52	7.59	7.80	7.80	41.00	N/A	N/A	N/A	N/A	N/A	N/A	N/A	n/a	N/A	N/A	N/A	N/A	70E_4s1d2Vc_1	5/14A	TDP-155	9700072.1
20.9	0.995	0.01430	0.050	0.333	38.8	P	N/A	7.39	7.52	7.59	7.80	7.80	41.00	N/A	N/A	N/A	N/A	N/A	N/A	N/A	1.0	N/A	N/A	N/A	N/A	70E_4s1d2Vc_1	5/14A	TDP-155	9700073
20.9	0.995	0.01430	0.050	0.333	38.8	P	N/A	7.39	7.52	7.59	7.80	7.80	41.00	N/A	N/A	N/A	N/A	N/A	N/A	N/A	n/a	N/A	N/A	N/A	N/A	70E_4s1d2Vc_1	5/14A	TDP-155	9700073.1
20.9	0.995	0.01430	0.050	0.333	38.8	P	N/A	7.39	7.52	7.59	7.80	7.80	41.00	N/A	N/A	N/A	N/A	N/A	N/A	N/A	0.0	N/A	N/A	N/A	N/A	70E_4s1d2Vc_1	5/14A	TDP-155	9700074
20.9	0.995	0.01430	0.050	0.333	38.8	P	N/A	7.39	7.52	7.59	7.80	7.80	41.00	N/A	N/A	N/A	N/A	N/A	N/A	N/A	n/a	N/A	N/A	N/A	N/A	70E_4s1d2Vc_1	5/14A	TDP-155	9700074.1
21.0	0.995	0.01430	0.050	0.334	38.8	P	N/A	7.39	7.52	7.59	7.80	7.80	41.00	N/A	N/A	N/A	UCScen	N/A	N/A	(null)	5.5	2	N/A	N/A	N/A	70E_4s1d2Vc_1	5/14A	TDP-155	9700075
21.0	0.995	0.01430	0.050	0.334	38.8	P	N/A	7.39	7.52	7.59	7.80	7.80	41.00	N/A	N/A	N/A	N/A	N/A	N/A	N/A	11.5	N/A	N/A	N/A	N/A	70E_4s1d2Vc_1	5/14A	TDP-155	9700076
21.0	0.995	0.01430	0.050	0.334	38.8	P	N/A	7.39	7.52	7.59	7.80	7.80	41.00	N/A	N/A	N/A	N/A	N/A	N/A	N/A	n/a	N/A	N/A	N/A	N/A	70E_4s1d2Vc_1	5/14A	TDP-155	9700076.1
21.0	0.995	0.01430	0.050	0.334	38.8	P	N/A	7.39	7.52	7.59	7.80	7.80	41.00	N/A	N/A	N/A	N/A	N/A	N/A	N/A	4.4	N/A	N/A	N/A	N/A	70E_4s1d2Vc_1	5/14A	TDP-155	9700077
21.0	0.995	0.01430	0.050	0.334	38.8	P	N/A	7.39	7.52	7.59	7.80	7.80	41.00	N/A	N/A	N/A	N/A	N/A	N/A	N/A	n/a	N/A	N/A	N/A	N/A	70E_4s1d2Vc_1	5/14A	TDP-155	9700077.1
21.0	0.995	0.01430	0.050	0.334	38.8	P	N/A	7.39	7.52	7.59	7.80	7.80	41.00	N/A	N/A	N/A	N/A	N/A	N/A	N/A	1.0	N/A	N/A	N/A	N/A	70E_4s1d2Vc_1	5/14A	TDP-155	9700078
21.0	0.995	0.01430	0.050	0.334	38.8	P	N/A	7.39	7.52	7.59	7.80	7.80	41.00	N/A	N/A	N/A	N/A	N/A	N/A	N/A	n/a	N/A	N/A	N/A	N/A	70E_4s1d2Vc_1	5/14A	TDP-155	9700078.1
21.0	0.995	0.01430	0.050	0.334	38.8	P	N/A	7.39	7.52	7.59	7.80	7.80	41.00	N/A	N/A	N/A	N/A	N/A	N/A	N/A	3.5	N/A	N/A	N/A	N/A	70E_4s1d2Vc_1	5/14A	TDP-155	9700079
21.0	0.995	0.01430	0.050	0.334	38.8	P	N/A	7.39	7.52	7.59	7.80	7.80	41.00	N/A	N/A	N/A	N/A	N/A	N/A	N/A	n/a	N/A	N/A	N/A	N/A	70E_4s1d2Vc_1	5/14A	TDP-155	9700079.1

Table B.5. Data from 2008 Tests in Large-Scale Vessel with Elliptical Head A.3

Row Number	Test	Case ID	Tank Diameter	Head Shape	Dish Height	Dish Volume	Tank Fill Height	Return Line Height	Nozzle Inner Diameter	Nozzle Stand-off Distance	Pulse Tube Configuration	Installed Nozzles	Outer Nozzles Operated	Inner Nozzles Operated	Pulse Tube Outer Diameter	Outer PJM Radius	Inner PJM Radius	"FIO" Outer PJM Impingement Angle	"FIO" Inner PJM Impingement Angle	Ratio Outer PJM to Tank Radius	Ratio Inner PJM to Tank Radius	Simulant	Solids Density	Particle Diameter d5	Particle Diameter d50	Particle Diameter d95	Void Fraction
text	text	text	in.	text	in.	in. ^{3}	in.	in.	in.	in.	text	number	number	number	in.	in.	in.	deg	deg	nondim	nondim	text	g/cm^3	m	m	m	fraction
MSS	M/DDX	ID	D	HS	H_{dish}	V_{dish}	H	Rtn	d	sod	PT	N	N_O	N_I	PT_{od}	R_O	R_I	θ_O	θ_I	R_O/R	R_I/R	sxdx	ρ_s	d_5	d_{50}	d_{95}	vf
9700080	5/14A	70E_4s1d2Vc_1	70	E	19	49770.7	92 1/2	80	0.613	0.920	HLP-22	12	8	4	3.5	21.9	11.5	20.3	10.5	0.62	0.33	s1d2	2.48	0.0000569	0.0000693	0.0000821	0.3750
9700080.1	5/14A	70E_4s1d2Vc_1	70	E	19	49770.7	92 1/2	80	0.613	0.920	HLP-22	12	8	4	3.5	21.9	11.5	20.3	10.5	0.62	0.33	s1d2	2.48	0.0000569	0.0000693	0.0000821	0.3750
9700081	5/14A	70E_4s1d2Vc_1	70	E	19	49770.7	92 1/2	80	0.613	0.920	HLP-22	12	8	4	3.5	21.9	11.5	20.3	10.5	0.62	0.33	s1d2	2.48	0.0000569	0.0000693	0.0000821	0.3750
9700082	5/14A	70E_4s1d2Vc_1	70	E	19	49770.7	92 1/2	80	0.613	0.920	HLP-22	12	8	4	3.5	21.9	11.5	20.3	10.5	0.62	0.33	s1d2	2.48	0.0000569	0.0000693	0.0000821	0.3750
9700082.1	5/14A	70E_4s1d2Vc_1	70	E	19	49770.7	92 1/2	80	0.613	0.920	HLP-22	12	8	4	3.5	21.9	11.5	20.3	10.5	0.62	0.33	s1d2	2.48	0.0000569	0.0000693	0.0000821	0.3750
9700083	5/14A	70E_4s1d2Vc_1	70	E	19	49770.7	92 1/2	80	0.613	0.920	HLP-22	12	8	4	3.5	21.9	11.5	20.3	10.5	0.62	0.33	s1d2	2.48	0.0000569	0.0000693	0.0000821	0.3750
9700083.1	5/14A	70E_4s1d2Vc_1	70	E	19	49770.7	92 1/2	80	0.613	0.920	HLP-22	12	8	4	3.5	21.9	11.5	20.3	10.5	0.62	0.33	s1d2	2.48	0.0000569	0.0000693	0.0000821	0.3750
9700084	5/14A	70E_4s1d2Vc_1	70	E	19	49770.7	92 1/2	80	0.613	0.920	HLP-22	12	8	4	3.5	21.9	11.5	20.3	10.5	0.62	0.33	s1d2	2.48	0.0000569	0.0000693	0.0000821	0.3750
9700084.1	5/14A	70E_4s1d2Vc_1	70	E	19	49770.7	92 1/2	80	0.613	0.920	HLP-22	12	8	4	3.5	21.9	11.5	20.3	10.5	0.62	0.33	s1d2	2.48	0.0000569	0.0000693	0.0000821	0.3750
9700085	5/14A	70E_4s1d2Vc_1	70	E	19	49770.7	92 1/2	80	0.613	0.920	HLP-22	12	8	4	3.5	21.9	11.5	20.3	10.5	0.62	0.33	s1d2	2.48	0.0000569	0.0000693	0.0000821	0.3750
9700085.1	5/14A	70E_4s1d2Vc_1	70	E	19	49770.7	92 1/2	80	0.613	0.920	HLP-22	12	8	4	3.5	21.9	11.5	20.3	10.5	0.62	0.33	s1d2	2.48	0.0000569	0.0000693	0.0000821	0.3750
9700085.2	5/14A	70E_4s1d2Vc_1	70	E	19	49770.7	92 1/2	80	0.613	0.920	HLP-22	12	8	4	3.5	21.9	11.5	20.3	10.5	0.62	0.33	s1d2	2.48	0.0000569	0.0000693	0.0000821	0.3750
9700085.3	5/14A	70E_4s1d2Vc_1	70	E	19	49770.7	92 1/2	80	0.613	0.920	HLP-22	12	8	4	3.5	21.9	11.5	20.3	10.5	0.62	0.33	s1d2	2.48	0.0000569	0.0000693	0.0000821	0.3750
9700086	5/14B	70E_4s1d2Vd_1	70	E	19	49770.7	92 1/2	80	0.613	0.920	HLP-22	12	8	4	3.5	21.9	11.5	20.3	10.5	0.62	0.33	s1d2	2.48	0.0000569	0.0000693	0.0000821	0.3750
9700087	5/14B	70E_4s1d2Vd_1	70	E	19	49770.7	92 1/2	80	0.613	0.920	HLP-22	12	8	4	3.5	21.9	11.5	20.3	10.5	0.62	0.33	s1d2	2.48	0.0000569	0.0000693	0.0000821	0.3750
9700088	5/14B	70E_4s1d2Vd_1	70	E	19	49770.7	92 1/2	80	0.613	0.920	HLP-22	12	8	4	3.5	21.9	11.5	20.3	10.5	0.62	0.33	s1d2	2.48	0.0000569	0.0000693	0.0000821	0.3750
9700089	5/14B	70E_4s1d2Vd_1	70	E	19	49770.7	92 1/2	80	0.613	0.920	HLP-22	12	8	4	3.5	21.9	11.5	20.3	10.5	0.62	0.33	s1d2	2.48	0.0000569	0.0000693	0.0000821	0.3750
9700090	5/14B	70E_4s1d2Vd_1	70	E	19	49770.7	92 1/2	80	0.613	0.920	HLP-22	12	8	4	3.5	21.9	11.5	20.3	10.5	0.62	0.33	s1d2	2.48	0.0000569	0.0000693	0.0000821	0.3750
9700091	5/14B	70E_4s1d2Vd_1	70	E	19	49770.7	92 1/2	80	0.613	0.920	HLP-22	12	8	4	3.5	21.9	11.5	20.3	10.5	0.62	0.33	s1d2	2.48	0.0000569	0.0000693	0.0000821	0.3750
9700092	5/14B	70E_4s1d2Vd_1	70	E	19	49770.7	92 1/2	80	0.613	0.920	HLP-22	12	8	4	3.5	21.9	11.5	20.3	10.5	0.62	0.33	s1d2	2.48	0.0000569	0.0000693	0.0000821	0.3750
9700093	5/14B	70E_4s1d2Vd_1	70	E	19	49770.7	92 1/2	80	0.613	0.920	HLP-22	12	8	4	3.5	21.9	11.5	20.3	10.5	0.62	0.33	s1d2	2.48	0.0000569	0.0000693	0.0000821	0.3750
9700094M	5/14B	70E_4s1d2Vd_1	70	E	19	49770.7	92 1/2	80	0.613	0.920	HLP-22	12	8	4	3.5	21.9	11.5	20.3	10.5	0.62	0.33	s1d2	2.48	0.0000569	0.0000693	0.0000821	0.3750
9700095M	5/14B	70E_4s1d2Vd_1	70	E	19	49770.7	92 1/2	80	0.613	0.920	HLP-22	12	8	4	3.5	21.9	11.5	20.3	10.5	0.62	0.33	s1d2	2.48	0.0000569	0.0000693	0.0000821	0.3750
9700096M	5/15A	70E_4s1d2Vd_1	70	E	19	49770.7	92 1/2	80	0.613	0.920	HLP-22	12	8	4	3.5	21.9	11.5	20.3	10.5	0.62	0.33	s1d2	2.48	0.0000569	0.0000693	0.0000821	0.3750
9700097	5/15A	70E_4s1d2Vd_1	70	E	19	49770.7	92 1/2	80	0.613	0.920	HLP-22	12	8	4	3.5	21.9	11.5	20.3	10.5	0.62	0.33	s1d2	2.48	0.0000569	0.0000693	0.0000821	0.3750
9700098	5/15A	70E_4s1d2Vd_1	70	E	19	49770.7	92 1/2	80	0.613	0.920	HLP-22	12	8	4	3.5	21.9	11.5	20.3	10.5	0.62	0.33	s1d2	2.48	0.0000569	0.0000693	0.0000821	0.3750
9700098.1	5/15A	70E_4s1d2Vd_1	70	E	19	49770.7	92 1/2	80	0.613	0.920	HLP-22	12	8	4	3.5	21.9	11.5	20.3	10.5	0.62	0.33	s1d2	2.48	0.0000569	0.0000693	0.0000821	0.3750
9700099	5/15A	70E_4s1d2Vd_1	70	E	19	49770.7	92 1/2	80	0.613	0.920	HLP-22	12	8	4	3.5	21.9	11.5	20.3	10.5	0.62	0.33	s1d2	2.48	0.0000569	0.0000693	0.0000821	0.3750
9700099.1	5/15A	70E_4s1d2Vd_1	70	E	19	49770.7	92 1/2	80	0.613	0.920	HLP-22	12	8	4	3.5	21.9	11.5	20.3	10.5	0.62	0.33	s1d2	2.48	0.0000569	0.0000693	0.0000821	0.3750
9700100	5/15A	70E_4s1d2Vd_1	70	E	19	49770.7	92 1/2	80	0.613	0.920	HLP-22	12	8	4	3.5	21.9	11.5	20.3	10.5	0.62	0.33	s1d2	2.48	0.0000569	0.0000693	0.0000821	0.3750
9700100.1	5/15A	70E_4s1d2Vd_1	70	E	19	49770.7	92 1/2	80	0.613	0.920	HLP-22	12	8	4	3.5	21.9	11.5	20.3	10.5	0.62	0.33	s1d2	2.48	0.0000569	0.0000693	0.0000821	0.3750
9700101	5/15A	70E_4s1d2Vd_1	70	E	19	49770.7	92 1/2	80	0.613	0.920	HLP-22	12	8	4	3.5	21.9	11.5	20.3	10.5	0.62	0.33	s1d2	2.48	0.0000569	0.0000693	0.0000821	0.3750
9700101.1	5/15A	70E_4s1d2Vd_1	70	E	19	49770.7	92 1/2	80	0.613	0.920	HLP-22	12	8	4	3.5	21.9	11.5	20.3	10.5	0.62	0.33	s1d2	2.48	0.0000569	0.0000693	0.0000821	0.3750
9700102	5/15A	70E_4s1d2Vd_1	70	E	19	49770.7	92 1/2	80	0.613	0.920	HLP-22	12	8	4	3.5	21.9	11.5	20.3	10.5	0.62	0.33	s1d2	2.48	0.0000569	0.0000693	0.0000821	0.3750
9700102.1	5/15A	70E_4s1d2Vd_1	70	E	19	49770.7	92 1/2	80	0.613	0.920	HLP-22	12	8	4	3.5	21.9	11.5	20.3	10.5	0.62	0.33	s1d2	2.48	0.0000569	0.0000693	0.0000821	0.3750
9700103M	5/15A	70E_4s1d2Vd_1	70	E	19	49770.7	92 1/2	80	0.613	0.920	HLP-22	12	8	4	3.5	21.9	11.5	20.3	10.5	0.62	0.33	s1d2	2.48	0.0000569	0.0000693	0.0000821	0.3750
9700104	5/15A	70E_4s1d2Vd_1	70	E	19	49770.7	92 1/2	80	0.613	0.920	HLP-22	12	8	4	3.5	21.9	11.5	20.3	10.5	0.62	0.33	s1d2	2.48	0.0000569	0.0000693	0.0000821	0.3750
9700105	5/15A	70E_4s1d2Vd_1	70	E	19	49770.7	92 1/2	80	0.613	0.920	HLP-22	12	8	4	3.5	21.9	11.5	20.3	10.5	0.62	0.33	s1d2	2.48	0.0000569	0.0000693	0.0000821	0.3750
9700105.1	5/15A	70E_4s1d2Vd_1	70	E	19	49770.7	92 1/2	80	0.613	0.920	HLP-22	12	8	4	3.5	21.9	11.5	20.3	10.5	0.62	0.33	s1d2	2.48	0.0000569	0.0000693	0.0000821	0.3750
9700106	5/15A	70E_4s1d2Vd_1	70	E	19	49770.7	92 1/2	80	0.613	0.920	HLP-22	12	8	4	3.5	21.9	11.5	20.3	10.5	0.62	0.33	s1d2	2.48	0.0000569	0.0000693	0.0000821	0.3750
9700106.1	5/15A	70E_4s1d2Vd_1	70	E	19	49770.7	92 1/2	80	0.613	0.920	HLP-22	12	8	4	3.5	21.9	11.5	20.3	10.5	0.62	0.33	s1d2	2.48	0.0000569	0.0000693	0.0000821	0.3750

Table B.5. Data from 2008 Tests in Large-Scale Vessel with Elliptical Head B.3

Tank Water Temperature	Water Density	Solids Fraction	Pulse Volume Fraction	Duty Cycle	Cycle Time	Pulsed or Steady Jet	Us Steady Jet	U1 Pulsing Jet	U2 URMS	U3 URM3	Discharge Velocity	Critical Suspension Velocity	Average Peak Cloud Height	UCS Condition	UCS Method	UCS Flag	UCS Center Flag	UCS udv Flag	UCS based on Decreasing Velocity	Sweep Increase / Decrease	UDV Height Bed	Particle Motion	Solids Level	Outer Bottom Pattern	Inner Bottom Pattern	Case ID	Test	TDP	Row Number
C	g/cm³	fraction	fraction	fraction	s	text	m/s	m/s	m/s	m/s	m/s	m/s	in.	m/s	text	text	text	text	m/s	text	mm	text	text	text	text	text	text	text	text
T	ρ_c	ϕ_S	ϕ_p	DC	t_C	Jet	U_S	U1	U2	U3	U	U_{CS}	H_C	U_{CSR}	U_{CSM}	U_{CS}vis	U_{CS}cen	U_{CS}udv	U_{CS}_D	S_W	H_{bed}	PM	Sol	SP_O	SP_I	ID	M/DDX	TDP	MSS
21.0	0.995	0.01430	0.050	0.334	38.8	P	N/A	7.39	7.52	7.59	7.80	7.80	41.00	N/A	N/A	N/A	N/A	N/A	N/A	N/A	4.1	N/A	N/A	N/A	N/A	70E_4s1d2Vc_1	5/14A	TDP-155	9700080
21.0	0.995	0.01430	0.050	0.334	38.8	P	N/A	7.39	7.52	7.59	7.80	7.80	41.00	N/A	N/A	N/A	N/A	N/A	N/A	N/A	n/a	N/A	N/A	N/A	N/A	70E_4s1d2Vc_1	5/14A	TDP-155	9700080.1
21.2	0.995	0.01430	0.050	0.334	38.8	P	N/A	7.39	7.52	7.59	7.80	7.80	41.00	N/A	N/A	N/A	UCScen	N/A	N/A	(null)	3.9	2	N/A	N/A	N/A	70E_4s1d2Vc_1	5/14A	TDP-155	9700081
21.2	0.995	0.01430	0.050	0.334	38.8	P	N/A	7.39	7.52	7.59	7.80	7.80	41.00	N/A	N/A	N/A	N/A	N/A	N/A	N/A	3.8	N/A	N/A	N/A	N/A	70E_4s1d2Vc_1	5/14A	TDP-155	9700082
21.2	0.995	0.01430	0.050	0.334	38.8	P	N/A	7.39	7.52	7.59	7.80	7.80	41.00	N/A	N/A	N/A	N/A	N/A	N/A	N/A	n/a	N/A	N/A	N/A	N/A	70E_4s1d2Vc_1	5/14A	TDP-155	9700082.1
21.2	0.995	0.01430	0.050	0.334	38.8	P	N/A	7.39	7.52	7.59	7.80	7.80	41.00	N/A	N/A	N/A	N/A	N/A	N/A	N/A	1.2	N/A	N/A	N/A	N/A	70E_4s1d2Vc_1	5/14A	TDP-155	9700083
21.2	0.995	0.01430	0.050	0.334	38.8	P	N/A	7.39	7.52	7.59	7.80	7.80	41.00	N/A	N/A	N/A	N/A	N/A	N/A	N/A	n/a	N/A	N/A	N/A	N/A	70E_4s1d2Vc_1	5/14A	TDP-155	9700083.1
21.2	0.995	0.01430	0.050	0.334	38.8	P	N/A	7.39	7.52	7.59	7.80	7.80	41.00	N/A	N/A	N/A	N/A	N/A	N/A	N/A	3.7	N/A	N/A	N/A	N/A	70E_4s1d2Vc_1	5/14A	TDP-155	9700084
21.2	0.995	0.01430	0.050	0.334	38.8	P	N/A	7.39	7.52	7.59	7.80	7.80	41.00	N/A	N/A	N/A	N/A	N/A	N/A	N/A	n/a	N/A	N/A	N/A	N/A	70E_4s1d2Vc_1	5/14A	TDP-155	9700084.1
21.2	0.995	0.01430	0.050	0.334	38.8	P	N/A	7.39	7.52	7.59	7.80	7.80	41.00	N/A	N/A	N/A	N/A	N/A	N/A	N/A	2.5	N/A	N/A	N/A	N/A	70E_4s1d2Vc_1	5/14A	TDP-155	9700085
21.2	0.995	0.01430	0.050	0.334	38.8	P	N/A	7.39	7.52	7.59	7.80	7.80	41.00	N/A	N/A	N/A	N/A	N/A	N/A	N/A	n/a	N/A	N/A	N/A	N/A	70E_4s1d2Vc_1	5/14A	TDP-155	9700085.1
21.2	0.995	0.01430	0.050	0.334	38.8	P	N/A	7.39	7.52	7.59	7.80	7.80	41.00	N/A	N/A	N/A	N/A	N/A	N/A	N/A	n/a	N/A	N/A	N/A	N/A	70E_4s1d2Vc_1	5/14A	TDP-155	9700085.2
21.2	0.995	0.01430	0.050	0.334	38.8	P	N/A	7.39	7.52	7.59	7.80	7.80	41.00	N/A	N/A	N/A	N/A	N/A	N/A	N/A	n/a	N/A	N/A	N/A	N/A	70E_4s1d2Vc_1	5/14A	TDP-155	9700085.3
21.8	0.995	0.01430	0.050	0.181	67.8	P	N/A	7.83	7.98	8.06	8.30	10.90	N/A	N/A	N/A	N/A	N/A	N/A	N/A	I	25.5	1	N/A	N/A	N/A	70E_4s1d2Vd_1	5/14B	TDP-155	9700086
21.8	0.995	0.01430	0.050	0.182	65.2	P	N/A	8.08	8.25	8.34	8.60	10.90	N/A	N/A	N/A	N/A	N/A	N/A	N/A	I	18.0	1	N/A	N/A	N/A	70E_4s1d2Vd_1	5/14B	TDP-155	9700087
22.0	0.995	0.01430	0.050	0.183	61.0	P	N/A	8.56	8.74	8.83	9.10	10.90	23.50	N/A	N/A	N/A	N/A	N/A	N/A	I	36.8	1	N/A	N/A	N/A	70E_4s1d2Vd_1	5/14B	TDP-155	9700088
22.0	0.995	0.01430	0.050	0.184	57.6	P	N/A	9.00	9.19	9.29	9.60	10.90	25.75	N/A	N/A	N/A	N/A	N/A	N/A	I	28.2	1	N/A	N/A	N/A	70E_4s1d2Vd_1	5/14B	TDP-155	9700089
22.1	0.995	0.01430	0.050	0.185	55.8	P	N/A	9.29	9.49	9.59	9.90	10.90	28.50	N/A	N/A	N/A	N/A	N/A	N/A	I	25.3	1	N/A	N/A	N/A	70E_4s1d2Vd_1	5/14B	TDP-155	9700090
22.5	0.994	0.01430	0.051	0.185	54.2	P	N/A	9.57	9.77	9.87	10.20	10.90	30.50	N/A	N/A	N/A	N/A	N/A	N/A	I	20.8	1	N/A	N/A	N/A	70E_4s1d2Vd_1	5/14B	TDP-155	9700091
22.1	0.995	0.01430	0.050	0.186	52.4	P	N/A	9.74	9.95	10.05	10.40	10.90	32.50	N/A	N/A	N/A	N/A	N/A	N/A	I	14.8	1	N/A	N/A	N/A	70E_4s1d2Vd_1	5/14B	TDP-155	9700092
22.4	0.995	0.01430	0.050	0.187	51.4	P	N/A	9.93	10.14	10.26	10.60	10.90	36.50	N/A	N/A	N/A	N/A	N/A	N/A	I	9.9	1	N/A	N/A	N/A	70E_4s1d2Vd_1	5/14B	TDP-155	9700093
22.5	0.995	0.01430	0.050	0.187	50.4	P	N/A	10.10	10.33	10.45	10.90	10.90	39.25	10.90	center	N/A	UCScen	N/A	N/A	I	11.2	2	N/A	N/A	N/A	70E_4s1d2Vd_1	5/14B	TDP-155	9700094
22.8	0.995	0.01430	0.050	0.188	48.6	P	N/A	10.44	10.68	10.80	11.20	10.90	45.00	N/A	N/A	N/A	N/A	N/A	N/A	I	3.0	4	N/A	N/A	N/A	70E_4s1d2Vd_1	5/14B	TDP-155	9700095
22.9	0.995	0.01430	0.050	0.189	48.6	P	N/A	10.38	10.65	10.78	11.20	10.90	45.00	N/A	N/A	N/A	N/A	N/A	N/A	(null)	6.3	4	N/A	N/A	N/A	70E_4s1d2Vd_1	5/15A	TDP-156	9700096
22.9	0.995	0.01430	0.050	0.189	48.6	P	N/A	10.38	10.65	10.78	11.20	10.90	45.00	N/A	N/A	N/A	N/A	N/A	N/A	N/A	8.3	N/A	N/A	N/A	N/A	70E_4s1d2Vd_1	5/15A	TDP-156	9700097
22.9	0.995	0.01430	0.050	0.189	48.6	P	N/A	10.38	10.65	10.78	11.20	10.90	45.00	N/A	N/A	N/A	N/A	N/A	N/A	N/A	11.5	N/A	N/A	N/A	N/A	70E_4s1d2Vd_1	5/15A	TDP-156	9700098
22.9	0.995	0.01430	0.050	0.189	48.6	P	N/A	10.38	10.65	10.78	11.20	10.90	45.00	N/A	N/A	N/A	N/A	N/A	N/A	N/A	n/a	N/A	N/A	N/A	N/A	70E_4s1d2Vd_1	5/15A	TDP-156	9700098.1
22.9	0.995	0.01430	0.050	0.189	48.6	P	N/A	10.38	10.65	10.78	11.20	10.90	45.00	N/A	N/A	N/A	N/A	N/A	N/A	N/A	0.0	N/A	N/A	N/A	N/A	70E_4s1d2Vd_1	5/15A	TDP-156	9700099
22.9	0.995	0.01430	0.050	0.189	48.6	P	N/A	10.38	10.65	10.78	11.20	10.90	45.00	N/A	N/A	N/A	N/A	N/A	N/A	N/A	n/a	N/A	N/A	N/A	N/A	70E_4s1d2Vd_1	5/15A	TDP-156	9700099.1
22.9	0.995	0.01430	0.050	0.189	48.6	P	N/A	10.38	10.65	10.78	11.20	10.90	45.00	N/A	N/A	N/A	N/A	N/A	N/A	N/A	0.0	N/A	N/A	N/A	N/A	70E_4s1d2Vd_1	5/15A	TDP-156	9700100
22.9	0.995	0.01430	0.050	0.189	48.6	P	N/A	10.38	10.65	10.78	11.20	10.90	45.00	N/A	N/A	N/A	N/A	N/A	N/A	N/A	n/a	N/A	N/A	N/A	N/A	70E_4s1d2Vd_1	5/15A	TDP-156	9700100.1
22.9	0.995	0.01430	0.050	0.189	48.6	P	N/A	10.38	10.65	10.78	11.20	10.90	45.00	N/A	N/A	N/A	N/A	N/A	N/A	N/A	0.0	N/A	N/A	N/A	N/A	70E_4s1d2Vd_1	5/15A	TDP-156	9700101
22.9	0.995	0.01430	0.050	0.189	48.6	P	N/A	10.38	10.65	10.78	11.20	10.90	45.00	N/A	N/A	N/A	N/A	N/A	N/A	N/A	n/a	N/A	N/A	N/A	N/A	70E_4s1d2Vd_1	5/15A	TDP-156	9700101.1
22.9	0.995	0.01430	0.050	0.189	48.6	P	N/A	10.38	10.65	10.78	11.20	10.90	45.00	N/A	N/A	N/A	N/A	N/A	N/A	N/A	0.0	N/A	N/A	N/A	N/A	70E_4s1d2Vd_1	5/15A	TDP-156	9700102
22.9	0.995	0.01430	0.050	0.189	48.6	P	N/A	10.38	10.65	10.78	11.20	10.90	45.00	N/A	N/A	N/A	N/A	N/A	N/A	N/A	n/a	N/A	N/A	N/A	N/A	70E_4s1d2Vd_1	5/15A	TDP-156	9700102.1
23.0	0.995	0.01430	0.050	0.189	48.6	P	N/A	10.39	10.65	10.79	11.20	10.90	45.00	N/A	N/A	N/A	N/A	N/A	N/A	(null)	0.0	4	N/A	N/A	N/A	70E_4s1d2Vd_1	5/15A	TDP-156	9700103
23.0	0.995	0.01430	0.050	0.189	48.6	P	N/A	10.39	10.65	10.79	11.20	10.90	45.00	N/A	N/A	N/A	N/A	N/A	N/A	N/A	0.0	N/A	N/A	N/A	N/A	70E_4s1d2Vd_1	5/15A	TDP-156	9700104
23.0	0.995	0.01430	0.050	0.189	48.6	P	N/A	10.39	10.65	10.79	11.20	10.90	45.00	N/A	N/A	N/A	N/A	N/A	N/A	N/A	0.0	N/A	N/A	N/A	N/A	70E_4s1d2Vd_1	5/15A	TDP-156	9700105
23.0	0.995	0.01430	0.050	0.189	48.6	P	N/A	10.39	10.65	10.79	11.20	10.90	45.00	N/A	N/A	N/A	N/A	N/A	N/A	N/A	n/a	N/A	N/A	N/A	N/A	70E_4s1d2Vd_1	5/15A	TDP-156	9700105.1
23.0	0.995	0.01430	0.050	0.189	48.6	P	N/A	10.39	10.65	10.79	11.20	10.90	45.00	N/A	N/A	N/A	N/A	N/A	N/A	N/A	0.0	N/A	N/A	N/A	N/A	70E_4s1d2Vd_1	5/15A	TDP-156	9700106
23.0	0.995	0.01430	0.050	0.189	48.6	P	N/A	10.39	10.65	10.79	11.20	10.90	45.00	N/A	N/A	N/A	N/A	N/A	N/A	N/A	n/a	N/A	N/A	N/A	N/A	70E_4s1d2Vd_1	5/15A	TDP-156	9700106.1

Table B.5. Data from 2008 Tests in Large-Scale Vessel with Elliptical Head A.4

Row Number	Test	Case ID	Tank Diameter	Head Shape	Dish Height	Dish Volume	Tank Fill Height	Return Line Height	Nozzle Inner Diameter	Nozzle Stand-off Distance	Pulse Tube Configuration	Installed Nozzles	Outer Nozzles Operated	Inner Nozzles Operated	Pulse Tube Outer Diameter	Outer PJM Radius	Inner PJM Radius	"FIO" Outer PJM Impingement Angle	"FIO" Inner PJM Impingement Angle	Ratio Outer PJM to Tank Radius	Ratio Inner PJM to Tank Radius	Simulant	Solids Density	Particle Diameter d5	Particle Diameter d50	Particle Diameter d95	Void Fraction
text	text	text	in.	text	in.	in. ^{3}	in.	in.	in.	in.	text	number	number	number	in.	in.	in.	deg	deg	nondim	nondim	text	g/cm^3	m	m	m	fraction
MSS	M/DDX	ID	D	HS	H_{dish}	V_{dish}	H	Rtn	d	sod	PT	N	N_O	N_I	PT_{od}	R_O	R_I	θ_O	θ_I	R_O/R	R_I/R	sxdx	ρ_s	d_5	d_{50}	d_{95}	vf
9700107	5/15A	70E_4s1d2Vd_1	70	E	19	49770.7	92 1/2	80	0.613	0.920	HLP-22	12	8	4	3.5	21.9	11.5	20.3	10.5	0.62	0.33	s1d2	2.48	0.0000569	0.0000693	0.0000821	0.3750
9700107.1	5/15A	70E_4s1d2Vd_1	70	E	19	49770.7	92 1/2	80	0.613	0.920	HLP-22	12	8	4	3.5	21.9	11.5	20.3	10.5	0.62	0.33	s1d2	2.48	0.0000569	0.0000693	0.0000821	0.3750
9700108	5/15A	70E_4s1d2Vd_1	70	E	19	49770.7	92 1/2	80	0.613	0.920	HLP-22	12	8	4	3.5	21.9	11.5	20.3	10.5	0.62	0.33	s1d2	2.48	0.0000569	0.0000693	0.0000821	0.3750
9700108.1	5/15A	70E_4s1d2Vd_1	70	E	19	49770.7	92 1/2	80	0.613	0.920	HLP-22	12	8	4	3.5	21.9	11.5	20.3	10.5	0.62	0.33	s1d2	2.48	0.0000569	0.0000693	0.0000821	0.3750
9700109	5/15A	70E_4s1d2Vd_1	70	E	19	49770.7	92 1/2	80	0.613	0.920	HLP-22	12	8	4	3.5	21.9	11.5	20.3	10.5	0.62	0.33	s1d2	2.48	0.0000569	0.0000693	0.0000821	0.3750
9700109.1	5/15A	70E_4s1d2Vd_1	70	E	19	49770.7	92 1/2	80	0.613	0.920	HLP-22	12	8	4	3.5	21.9	11.5	20.3	10.5	0.62	0.33	s1d2	2.48	0.0000569	0.0000693	0.0000821	0.3750
9700110M	5/15A	70E_4s1d2Vd_1	70	E	19	49770.7	92 1/2	80	0.613	0.920	HLP-22	12	8	4	3.5	21.9	11.5	20.3	10.5	0.62	0.33	s1d2	2.48	0.0000569	0.0000693	0.0000821	0.3750
9700111	5/15A	70E_4s1d2Vd_1	70	E	19	49770.7	92 1/2	80	0.613	0.920	HLP-22	12	8	4	3.5	21.9	11.5	20.3	10.5	0.62	0.33	s1d2	2.48	0.0000569	0.0000693	0.0000821	0.3750
9700112	5/15A	70E_4s1d2Vd_1	70	E	19	49770.7	92 1/2	80	0.613	0.920	HLP-22	12	8	4	3.5	21.9	11.5	20.3	10.5	0.62	0.33	s1d2	2.48	0.0000569	0.0000693	0.0000821	0.3750
9700112.1	5/15A	70E_4s1d2Vd_1	70	E	19	49770.7	92 1/2	80	0.613	0.920	HLP-22	12	8	4	3.5	21.9	11.5	20.3	10.5	0.62	0.33	s1d2	2.48	0.0000569	0.0000693	0.0000821	0.3750
9700113	5/15A	70E_4s1d2Vd_1	70	E	19	49770.7	92 1/2	80	0.613	0.920	HLP-22	12	8	4	3.5	21.9	11.5	20.3	10.5	0.62	0.33	s1d2	2.48	0.0000569	0.0000693	0.0000821	0.3750
9700113.1	5/15A	70E_4s1d2Vd_1	70	E	19	49770.7	92 1/2	80	0.613	0.920	HLP-22	12	8	4	3.5	21.9	11.5	20.3	10.5	0.62	0.33	s1d2	2.48	0.0000569	0.0000693	0.0000821	0.3750
9700114	5/15A	70E_4s1d2Vd_1	70	E	19	49770.7	92 1/2	80	0.613	0.920	HLP-22	12	8	4	3.5	21.9	11.5	20.3	10.5	0.62	0.33	s1d2	2.48	0.0000569	0.0000693	0.0000821	0.3750
9700114.1	5/15A	70E_4s1d2Vd_1	70	E	19	49770.7	92 1/2	80	0.613	0.920	HLP-22	12	8	4	3.5	21.9	11.5	20.3	10.5	0.62	0.33	s1d2	2.48	0.0000569	0.0000693	0.0000821	0.3750
9700115	5/15A	70E_4s1d2Vd_1	70	E	19	49770.7	92 1/2	80	0.613	0.920	HLP-22	12	8	4	3.5	21.9	11.5	20.3	10.5	0.62	0.33	s1d2	2.48	0.0000569	0.0000693	0.0000821	0.3750
9700115.1	5/15A	70E_4s1d2Vd_1	70	E	19	49770.7	92 1/2	80	0.613	0.920	HLP-22	12	8	4	3.5	21.9	11.5	20.3	10.5	0.62	0.33	s1d2	2.48	0.0000569	0.0000693	0.0000821	0.3750
9700115.2	5/15A	70E_4s1d2Vd_1	70	E	19	49770.7	92 1/2	80	0.613	0.920	HLP-22	12	8	4	3.5	21.9	11.5	20.3	10.5	0.62	0.33	s1d2	2.48	0.0000569	0.0000693	0.0000821	0.3750
9700115.3	5/15A	70E_4s1d2Vd_1	70	E	19	49770.7	92 1/2	80	0.613	0.920	HLP-22	12	8	4	3.5	21.9	11.5	20.3	10.5	0.62	0.33	s1d2	2.48	0.0000569	0.0000693	0.0000821	0.3750
9700116	5/15B	70E_4s1d2Ve_1	70	E	19	49770.7	92 1/2	80	0.613	0.920	HLP-22	12	8	4	3.5	21.9	11.5	20.3	10.5	0.62	0.33	s1d2	2.48	0.0000569	0.0000693	0.0000821	0.3750
9700117M	5/15B	70E_4s1d2Ve_1	70	E	19	49770.7	92 1/2	80	0.613	0.920	HLP-22	12	8	4	3.5	21.9	11.5	20.3	10.5	0.62	0.33	s1d2	2.48	0.0000569	0.0000693	0.0000821	0.3750
9700118	5/15C	70E_4s1d2Vc_2	70	E	19	49770.7	92 1/2	80	0.613	0.920	HLP-22	12	8	4	3.5	21.9	11.5	20.3	10.5	0.62	0.33	s1d2	2.48	0.0000569	0.0000693	0.0000821	0.3750
9700119M	5/15C	70E_4s1d2Vc_2	70	E	19	49770.7	92 1/2	80	0.613	0.920	HLP-22	12	8	4	3.5	21.9	11.5	20.3	10.5	0.62	0.33	s1d2	2.48	0.0000569	0.0000693	0.0000821	0.3750
9700120	5/15D	70E_4s1d2Vd_2	70	E	19	49770.7	92 1/2	80	0.613	0.920	HLP-22	12	8	4	3.5	21.9	11.5	20.3	10.5	0.62	0.33	s1d2	2.48	0.0000569	0.0000693	0.0000821	0.3750
9700121M	5/15D	70E_4s1d2Vd_2	70	E	19	49770.7	92 1/2	80	0.613	0.920	HLP-22	12	8	4	3.5	21.9	11.5	20.3	10.5	0.62	0.33	s1d2	2.48	0.0000569	0.0000693	0.0000821	0.3750
9700122	5/16A	70E_4s1d2Ve_2	70	E	19	49770.7	92 1/2	80	0.613	0.920	HLP-22	12	8	4	3.5	21.9	11.5	20.3	10.5	0.62	0.33	s1d2	2.48	0.0000569	0.0000693	0.0000821	0.3750
9700123M	5/16A	70E_4s1d2Ve_2	70	E	19	49770.7	92 1/2	80	0.613	0.920	HLP-22	12	8	4	3.5	21.9	11.5	20.3	10.5	0.62	0.33	s1d2	2.48	0.0000569	0.0000693	0.0000821	0.3750
9700124	5/16B	70E_4s1d2Vc_4	70	E	19	49770.7	92 1/2	80	0.613	0.920	HLP-22	12	8	4	3.5	21.9	11.5	20.3	10.5	0.62	0.33	s1d2	2.48	0.0000569	0.0000693	0.0000821	0.3750
9700125	5/16B	70E_4s1d2Vc_4	70	E	19	49770.7	92 1/2	80	0.613	0.920	HLP-22	12	8	4	3.5	21.9	11.5	20.3	10.5	0.62	0.33	s1d2	2.48	0.0000569	0.0000693	0.0000821	0.3750
9700126M	5/16B	70E_4s1d2Vc_4	70	E	19	49770.7	92 1/2	80	0.613	0.920	HLP-22	12	8	4	3.5	21.9	11.5	20.3	10.5	0.62	0.33	s1d2	2.48	0.0000569	0.0000693	0.0000821	0.3750
9700127	5/16C	70E_4s1d2Vd_4	70	E	19	49770.7	92 1/2	80	0.613	0.920	HLP-22	12	8	4	3.5	21.9	11.5	20.3	10.5	0.62	0.33	s1d2	2.48	0.0000569	0.0000693	0.0000821	0.3750
9700128	5/16C	70E_4s1d2Vd_4	70	E	19	49770.7	92 1/2	80	0.613	0.920	HLP-22	12	8	4	3.5	21.9	11.5	20.3	10.5	0.62	0.33	s1d2	2.48	0.0000569	0.0000693	0.0000821	0.3750
9700129	5/19A	70E_4s1d2Vd_4	70	E	19	49770.7	91 1/2	80	0.613	0.920	HLP-22	12	8	4	3.5	21.9	11.5	20.3	10.5	0.62	0.33	s1d2	2.48	0.0000569	0.0000693	0.0000821	0.3750
9700130M	5/19A	70E_4s1d2Vd_4	70	E	19	49770.7	91 1/2	80	0.613	0.920	HLP-22	12	8	4	3.5	21.9	11.5	20.3	10.5	0.62	0.33	s1d2	2.48	0.0000569	0.0000693	0.0000821	0.3750
9700131M	5/19A	70E_4s1d2Vd_4	70	E	19	49770.7	91 1/2	80	0.613	0.920	HLP-22	12	8	4	3.5	21.9	11.5	20.3	10.5	0.62	0.33	s1d2	2.48	0.0000569	0.0000693	0.0000821	0.3750
9700132	5/19B	70E_4s1d2Ve_4	70	E	19	49770.7	91 1/2	80	0.613	0.920	HLP-22	12	8	4	3.5	21.9	11.5	20.3	10.5	0.62	0.33	s1d2	2.48	0.0000569	0.0000693	0.0000821	0.3750
9700133	5/19B	70E_4s1d2Ve_4	70	E	19	49770.7	91 1/2	80	0.613	0.920	HLP-22	12	8	4	3.5	21.9	11.5	20.3	10.5	0.62	0.33	s1d2	2.48	0.0000569	0.0000693	0.0000821	0.3750
9700134	5/19B	70E_4s1d2Ve_4	70	E	19	49770.7	91 1/2	80	0.613	0.920	HLP-22	12	8	4	3.5	21.9	11.5	20.3	10.5	0.62	0.33	s1d2	2.48	0.0000569	0.0000693	0.0000821	0.3750
9700135	5/19C	70E_4s1d2Xc_1	70	E	19	49770.7	91 1/2	80	0.613	0.920	HLP-22	12	8	4	3.5	21.9	11.5	20.3	10.5	0.62	0.33	s1d2	2.48	0.0000569	0.0000693	0.0000821	0.3750
9700136	5/19C	70E_4s1d2Xc_1	70	E	19	49770.7	91 1/2	80	0.613	0.920	HLP-22	12	8	4	3.5	21.9	11.5	20.3	10.5	0.62	0.33	s1d2	2.48	0.0000569	0.0000693	0.0000821	0.3750
9700137	5/19C	70E_4s1d2Xc_1	70	E	19	49770.7	91 1/2	80	0.613	0.920	HLP-22	12	8	4	3.5	21.9	11.5	20.3	10.5	0.62	0.33	s1d2	2.48	0.0000569	0.0000693	0.0000821	0.3750
9700138	5/19C	70E_4s1d2Xc_1	70	E	19	49770.7	91 1/2	80	0.613	0.920	HLP-22	12	8	4	3.5	21.9	11.5	20.3	10.5	0.62	0.33	s1d2	2.48	0.0000569	0.0000693	0.0000821	0.3750

Table B.5. Data from 2008 Tests in Large-Scale Vessel with Elliptical Head B.4

Tank Water Temperature	Water Density	Solids Fraction	Pulse Volume Fraction	Duty Cycle	Cycle Time	Pulsed or Steady Jet	Us Steady Jet	U1 Pulsing Jet	U2 URMS	U3 URM3	Discharge Velocity	Critical Suspension Velocity	Average Peak Cloud Height	UCS Condition	UCS Method	UCS Flag	UCS Center Flag	UCS udv Flag	UCS based on Decreasing Velocity	Sweep Increase / Decrease	UDV Height Bed	Particle Motion	Solids Level	Outer Bottom Pattern	Inner Bottom Pattern	Case ID	Test	TDP	Row Number
C	g/cm³	fraction	fraction	fraction	s	text	m/s	m/s	m/s	m/s	m/s	m/s	in.	m/s	text	text	text	text	m/s	text	mm	text	text	text	text	text	text	text	text
T	ρ_c	ϕ_S	ϕ_p	DC	t_C	Jet	U_S	U1	U2	U3	U	U_{CS}	H_C	U_{CSR}	U_{CSM}	U_{CS}vis	U_{CS}cen	U_{CS}udv	$U_{CS_}D$	S_W	H_{bed}	PM	Sol	SP_O	SP_I	ID	M/DDX	TDP	MSS
23.0	0.995	0.01430	0.050	0.189	48.6	P	N/A	10.39	10.65	10.79	11.20	10.90	45.00	N/A	N/A	N/A	N/A	N/A	N/A	N/A	6.0	N/A	N/A	N/A	N/A	70E_4s1d2Vd_1	5/15A	TDP-156	9700107
23.0	0.995	0.01430	0.050	0.189	48.6	P	N/A	10.39	10.65	10.79	11.20	10.90	45.00	N/A	N/A	N/A	N/A	N/A	N/A	N/A	n/a	N/A	N/A	N/A	N/A	70E_4s1d2Vd_1	5/15A	TDP-156	9700107.1
23.0	0.995	0.01430	0.050	0.189	48.6	P	N/A	10.39	10.65	10.79	11.20	10.90	45.00	N/A	N/A	N/A	N/A	N/A	N/A	N/A	0.0	N/A	N/A	N/A	N/A	70E_4s1d2Vd_1	5/15A	TDP-156	9700108
23.0	0.995	0.01430	0.050	0.189	48.6	P	N/A	10.39	10.65	10.79	11.20	10.90	45.00	N/A	N/A	N/A	N/A	N/A	N/A	N/A	n/a	N/A	N/A	N/A	N/A	70E_4s1d2Vd_1	5/15A	TDP-156	9700108.1
23.0	0.995	0.01430	0.050	0.189	48.6	P	N/A	10.39	10.65	10.79	11.20	10.90	45.00	N/A	N/A	N/A	N/A	N/A	N/A	N/A	4.3	N/A	N/A	N/A	N/A	70E_4s1d2Vd_1	5/15A	TDP-156	9700109
23.0	0.995	0.01430	0.050	0.189	48.6	P	N/A	10.39	10.65	10.79	11.20	10.90	45.00	N/A	N/A	N/A	N/A	N/A	N/A	N/A	n/a	N/A	N/A	N/A	N/A	70E_4s1d2Vd_1	5/15A	TDP-156	9700109.1
23.3	0.995	0.01430	0.050	0.189	48.6	P	N/A	10.38	10.65	10.78	11.20	10.90	45.00	N/A	N/A	N/A	N/A	N/A	N/A	(null)	0.0	4	N/A	N/A	N/A	70E_4s1d2Vd_1	5/15A	TDP-156	9700110
23.3	0.995	0.01430	0.050	0.189	48.6	P	N/A	10.38	10.65	10.78	11.20	10.90	45.00	N/A	N/A	N/A	N/A	N/A	N/A	N/A	0.2	N/A	N/A	N/A	N/A	70E_4s1d2Vd_1	5/15A	TDP-156	9700111
23.3	0.995	0.01430	0.050	0.189	48.6	P	N/A	10.38	10.65	10.78	11.20	10.90	45.00	N/A	N/A	N/A	N/A	N/A	N/A	N/A	0.0	N/A	N/A	N/A	N/A	70E_4s1d2Vd_1	5/15A	TDP-156	9700112
23.3	0.995	0.01430	0.050	0.189	48.6	P	N/A	10.38	10.65	10.78	11.20	10.90	45.00	N/A	N/A	N/A	N/A	N/A	N/A	N/A	n/a	N/A	N/A	N/A	N/A	70E_4s1d2Vd_1	5/15A	TDP-156	9700112.1
23.3	0.995	0.01430	0.050	0.189	48.6	P	N/A	10.38	10.65	10.78	11.20	10.90	45.00	N/A	N/A	N/A	N/A	N/A	N/A	N/A	8.8	N/A	N/A	N/A	N/A	70E_4s1d2Vd_1	5/15A	TDP-156	9700113
23.3	0.995	0.01430	0.050	0.189	48.6	P	N/A	10.38	10.65	10.78	11.20	10.90	45.00	N/A	N/A	N/A	N/A	N/A	N/A	N/A	n/a	N/A	N/A	N/A	N/A	70E_4s1d2Vd_1	5/15A	TDP-156	9700113.1
23.3	0.995	0.01430	0.050	0.189	48.6	P	N/A	10.38	10.65	10.78	11.20	10.90	45.00	N/A	N/A	N/A	N/A	N/A	N/A	N/A	0.0	N/A	N/A	N/A	N/A	70E_4s1d2Vd_1	5/15A	TDP-156	9700114
23.3	0.995	0.01430	0.050	0.189	48.6	P	N/A	10.38	10.65	10.78	11.20	10.90	45.00	N/A	N/A	N/A	N/A	N/A	N/A	N/A	n/a	N/A	N/A	N/A	N/A	70E_4s1d2Vd_1	5/15A	TDP-156	9700114.1
23.3	0.995	0.01430	0.050	0.189	48.6	P	N/A	10.38	10.65	10.78	11.20	10.90	45.00	N/A	N/A	N/A	N/A	N/A	N/A	N/A	2.3	N/A	N/A	N/A	N/A	70E_4s1d2Vd_1	5/15A	TDP-156	9700115
23.3	0.995	0.01430	0.050	0.189	48.6	P	N/A	10.38	10.65	10.78	11.20	10.90	45.00	N/A	N/A	N/A	N/A	N/A	N/A	N/A	n/a	N/A	N/A	N/A	N/A	70E_4s1d2Vd_1	5/15A	TDP-156	9700115.1
23.3	0.995	0.01430	0.050	0.189	48.6	P	N/A	10.38	10.65	10.78	11.20	10.90	45.00	N/A	N/A	N/A	N/A	N/A	N/A	N/A	n/a	N/A	N/A	N/A	N/A	70E_4s1d2Vd_1	5/15A	TDP-156	9700115.2
23.3	0.995	0.01430	0.050	0.189	48.6	P	N/A	10.38	10.65	10.78	11.20	10.90	45.00	N/A	N/A	N/A	N/A	N/A	N/A	N/A	n/a	N/A	N/A	N/A	N/A	70E_4s1d2Vd_1	5/15A	TDP-156	9700115.3
23.7	0.994	0.01430	0.050	0.656	32.4	P	N/A	4.43	4.48	4.50	4.60	4.80	N/A	N/A	N/A	N/A	N/A	N/A	N/A	D	26.7	1	N/A	N/A	N/A	70E_4s1d2Ve_1	5/15B	TDP-156	9700116
23.7	0.994	0.01430	0.050	0.662	31.0	P	N/A	4.62	4.68	4.71	4.80	4.80	36.25	4.80	udv	N/A	UCScen	UCSudv	N/A	I	0.0	2	N/A	N/A	N/A	70E_4s1d2Ve_1	5/15B	TDP-156	9700117
24.2	0.994	0.01430	0.100	0.330	92.4	P	N/A	6.24	6.29	6.32	6.40	7.40	27.50	N/A	N/A	N/A	N/A	N/A	N/A	I	25.6	1	N/A	N/A	N/A	70E_4s1d2Vc_2	5/15C	TDP-156	9700118
24.1	0.995	0.01430	0.101	0.332	80.0	P	N/A	7.19	7.26	7.29	7.40	7.40	37.50	7.40	udv	N/A	UCScen	UCSudv	N/A	I	0.0	2	N/A	N/A	N/A	70E_4s1d2Vc_2	5/15C	TDP-156	9700119
24.3	0.994	0.01430	0.100	0.170	136.0	P	N/A	8.22	8.31	8.35	8.50	8.70	28.25	N/A	N/A	N/A	UCScen	N/A	N/A	(null)	5.1	2	N/A	N/A	N/A	70E_4s1d2Vd_2	5/15D	TDP-156	9700120
24.5	0.994	0.01430	0.101	0.182	125.0	P	N/A	8.44	8.52	8.57	8.70	8.70	30.50	8.70	udv	N/A	N/A	UCSudv	N/A	(null)	0.7	4	N/A	N/A	N/A	70E_4s1d2Vd_2	5/15D	TDP-156	9700121
24.1	0.994	0.01430	0.101	0.660	64.0	P	N/A	4.53	4.55	4.56	4.60	4.80	29.00	N/A	N/A	N/A	N/A	N/A	N/A	(null)	7.8	1	N/A	N/A	N/A	70E_4s1d2Ve_2	5/16A	TDP-157	9700122
24.2	0.994	0.01430	0.100	0.663	60.6	P	N/A	4.72	4.75	4.76	4.80	4.80	37.25	4.80	udv	N/A	UCScen	UCSudv	N/A	I	0.0	2	N/A	N/A	N/A	70E_4s1d2Ve_2	5/16A	TDP-157	9700123
24.1	0.994	0.01430	0.150	0.330	146.6	P	N/A	5.88	5.91	5.93	6.00	6.60	26.50	N/A	N/A	N/A	N/A	N/A	N/A	(null)	12.4	1	N/A	N/A	N/A	70E_4s1d2Vc_4	5/16B	TDP-157	9700124
24.3	0.994	0.01430	0.150	0.331	137.4	P	N/A	6.29	6.33	6.35	6.40	6.60	30.25	N/A	N/A	N/A	UCScen	N/A	N/A	(null)	6.6	2	N/A	N/A	N/A	70E_4s1d2Vc_4	5/16B	TDP-157	9700125
24.4	0.995	0.01430	0.151	0.331	133.2	P	N/A	6.50	6.53	6.55	6.60	6.60	35.50	6.60	udv	N/A	N/A	UCSudv	N/A	I	0.0	4	N/A	N/A	N/A	70E_4s1d2Vc_4	5/16B	TDP-157	9700126
25.0	0.995	0.01430	0.152	0.175	285.0	P	N/A	5.78	5.82	5.85	6.00	6.40	24.50	N/A	N/A	N/A	N/A	N/A	N/A	(null)	19.4	1	N/A	N/A	N/A	70E_4s1d2Vd_4	5/16C	TDP-157	9700127
25.3	0.994	0.01430	0.150	0.175	271.0	P	N/A	6.00	6.04	6.06	6.20	6.40	26.00	N/A	N/A	N/A	N/A	N/A	N/A	(null)	12.8	1	N/A	N/A	N/A	70E_4s1d2Vd_4	5/16C	TDP-157	9700128
24.4	0.995	0.01430	0.152	0.175	271.0	P	N/A	6.10	6.13	6.15	6.20	6.40	26.50	N/A	N/A	N/A	N/A	N/A	N/A	(null)	5.9	1	N/A	N/A	N/A	70E_4s1d2Vd_4	5/19A	TDP-158	9700129
24.4	0.995	0.01430	0.152	0.176	262.4	P	N/A	6.27	6.31	6.33	6.40	6.40	26.50	6.40	udv	N/A	UCScen	UCSudv	N/A	I	0.9	2	N/A	N/A	N/A	70E_4s1d2Vd_4	5/19A	TDP-158	9700130
24.6	0.994	0.01430	0.152	0.176	254.4	P	N/A	6.48	6.52	6.54	6.60	6.40	27.75	N/A	N/A	N/A	N/A	N/A	N/A	I	0.0	4	N/A	N/A	N/A	70E_4s1d2Vd_4	5/19A	TDP-158	9700131
24.9	0.995	0.01430	0.151	0.658	100.4	P	N/A	4.34	4.36	4.37	4.40	4.50	N/A	N/A	N/A	N/A	N/A	N/A	N/A	(null)	7.4	1	N/A	N/A	N/A	70E_4s1d2Ve_4	5/19B	TDP-158	9700132
24.8	0.994	0.01430	0.151	0.659	98.2	P	N/A	4.44	4.46	4.47	4.50	4.50	N/A	4.50	udv	N/A	UCScen	UCSudv	N/A	I	1.8	2	N/A	N/A	N/A	70E_4s1d2Ve_4	5/19B	TDP-158	9700133
24.9	0.994	0.01430	0.151	0.660	94.0	P	N/A	4.64	4.65	4.67	4.70	4.50	N/A	N/A	N/A	N/A	N/A	N/A	N/A	I	0.0	4	N/A	N/A	N/A	70E_4s1d2Ve_4	5/19B	TDP-158	9700134
25.1	0.995	0.01500	0.050	0.330	43.2	P	N/A	6.64	6.76	6.81	7.00	8.50	24.00	N/A	N/A	N/A	N/A	N/A	N/A	(null)	17.2	1	N/A	N/A	N/A	70E_4s1d2Xc_1	5/19C	TDP-159	9700135
25.1	0.994	0.01500	0.050	0.331	40.8	P	N/A	7.01	7.13	7.19	7.40	8.50	26.00	N/A	N/A	N/A	N/A	N/A	N/A	I	26.2	1	N/A	N/A	N/A	70E_4s1d2Xc_1	5/19C	TDP-159	9700136
25.2	0.994	0.01500	0.050	0.333	38.8	P	N/A	7.39	7.52	7.59	7.80	8.50	28.25	N/A	N/A	N/A	N/A	N/A	N/A	I	30.9	1	N/A	N/A	N/A	70E_4s1d2Xc_1	5/19C	TDP-159	9700137
25.3	0.995	0.01500	0.050	0.334	37.8	P	N/A	7.58	7.71	7.78	8.00	8.50	32.25	N/A	N/A	N/A	N/A	N/A	N/A	I	28.2	1	N/A	N/A	N/A	70E_4s1d2Xc_1	5/19C	TDP-159	9700138

Table B.5. Data from 2008 Tests in Large-Scale Vessel with Elliptical Head A.5

Row Number	Test	Case ID	Tank Diameter	Head Shape	Dish Height	Dish Volume	Tank Fill Height	Return Line Height	Nozzle Inner Diameter	Nozzle Stand-off Distance	Pulse Tube Configuration	Installed Nozzles	Outer Nozzles Operated	Inner Nozzles Operated	Pulse Tube Outer Diameter	Outer PJM Radius	Inner PJM Radius	"FIO" Outer PJM Impingement Angle	"FIO" Inner PJM Impingement Angle	Ratio Outer PJM to Tank Radius	Ratio Inner PJM to Tank Radius	Simulant	Solids Density	Particle Diameter d5	Particle Diameter d50	Particle Diameter d95	Void Fraction
text	text	text	in.	text	in.	in. ^{3}	in.	in.	in.	in.	text	number	number	number	in.	in.	in.	deg	deg	nondim	nondim	text	g/cm^3	m	m	m	fraction
MSS	M/DDX	ID	D	HS	H_{dish}	V_{dish}	H	Rtn	d	sod	PT	N	N_O	N_I	PT_{od}	R_O	R_I	θ_O	θ_I	R_O/R	R_I/R	sxdx	ρ_s	d_5	d_{50}	d_{95}	vf
9700139	5/19C	70E_4s1d2Xc_1	70	E	19	49770.7	91 1/2	80	0.613	0.920	HLP-22	12	8	4	3.5	21.9	11.5	20.3	10.5	0.62	0.33	s1d2	2.48	0.0000569	0.0000693	0.0000821	0.3750
9700140	5/19C	70E_4s1d2Xc_1	70	E	19	49770.7	91 1/2	80	0.613	0.920	HLP-22	12	8	4	3.5	21.9	11.5	20.3	10.5	0.62	0.33	s1d2	2.48	0.0000569	0.0000693	0.0000821	0.3750
9700141	5/20A	70E_4s1d2Xc_1	70	E	19	49770.7	91 1/2	80	0.613	0.920	HLP-22	12	8	4	3.5	21.9	11.5	20.3	10.5	0.62	0.33	s1d2	2.48	0.0000569	0.0000693	0.0000821	0.3750
9700142	5/20A	70E_4s1d2Xc_1	70	E	19	49770.7	91 1/2	80	0.613	0.920	HLP-22	12	8	4	3.5	21.9	11.5	20.3	10.5	0.62	0.33	s1d2	2.48	0.0000569	0.0000693	0.0000821	0.3750
9700143	5/20A	70E_4s1d2Xc_1	70	E	19	49770.7	91 1/2	80	0.613	0.920	HLP-22	12	8	4	3.5	21.9	11.5	20.3	10.5	0.62	0.33	s1d2	2.48	0.0000569	0.0000693	0.0000821	0.3750
9700144M	5/20A	70E_4s1d2Xc_1	70	E	19	49770.7	91 1/2	80	0.613	0.920	HLP-22	12	8	4	3.5	21.9	11.5	20.3	10.5	0.62	0.33	s1d2	2.48	0.0000569	0.0000693	0.0000821	0.3750
9700145M	5/20A	70E_4s1d2Xc_1	70	E	19	49770.7	91 1/2	80	0.613	0.920	HLP-22	12	8	4	3.5	21.9	11.5	20.3	10.5	0.62	0.33	s1d2	2.48	0.0000569	0.0000693	0.0000821	0.3750
9700146	5/20A	70E_4s1d2Xc_1	70	E	19	49770.7	91 1/2	80	0.613	0.920	HLP-22	12	8	4	3.5	21.9	11.5	20.3	10.5	0.62	0.33	s1d2	2.48	0.0000569	0.0000693	0.0000821	0.3750
9700147	5/20A	70E_4s1d2Xc_1	70	E	19	49770.7	91 1/2	80	0.613	0.920	HLP-22	12	8	4	3.5	21.9	11.5	20.3	10.5	0.62	0.33	s1d2	2.48	0.0000569	0.0000693	0.0000821	0.3750
9700147.1	5/20A	70E_4s1d2Xc_1	70	E	19	49770.7	91 1/2	80	0.613	0.920	HLP-22	12	8	4	3.5	21.9	11.5	20.3	10.5	0.62	0.33	s1d2	2.48	0.0000569	0.0000693	0.0000821	0.3750
9700148	5/20A	70E_4s1d2Xc_1	70	E	19	49770.7	91 1/2	80	0.613	0.920	HLP-22	12	8	4	3.5	21.9	11.5	20.3	10.5	0.62	0.33	s1d2	2.48	0.0000569	0.0000693	0.0000821	0.3750
9700148.1	5/20A	70E_4s1d2Xc_1	70	E	19	49770.7	91 1/2	80	0.613	0.920	HLP-22	12	8	4	3.5	21.9	11.5	20.3	10.5	0.62	0.33	s1d2	2.48	0.0000569	0.0000693	0.0000821	0.3750
9700149	5/20A	70E_4s1d2Xc_1	70	E	19	49770.7	91 1/2	80	0.613	0.920	HLP-22	12	8	4	3.5	21.9	11.5	20.3	10.5	0.62	0.33	s1d2	2.48	0.0000569	0.0000693	0.0000821	0.3750
9700149.1	5/20A	70E_4s1d2Xc_1	70	E	19	49770.7	91 1/2	80	0.613	0.920	HLP-22	12	8	4	3.5	21.9	11.5	20.3	10.5	0.62	0.33	s1d2	2.48	0.0000569	0.0000693	0.0000821	0.3750
9700150	5/20A	70E_4s1d2Xc_1	70	E	19	49770.7	91 1/2	80	0.613	0.920	HLP-22	12	8	4	3.5	21.9	11.5	20.3	10.5	0.62	0.33	s1d2	2.48	0.0000569	0.0000693	0.0000821	0.3750
9700150.1	5/20A	70E_4s1d2Xc_1	70	E	19	49770.7	91 1/2	80	0.613	0.920	HLP-22	12	8	4	3.5	21.9	11.5	20.3	10.5	0.62	0.33	s1d2	2.48	0.0000569	0.0000693	0.0000821	0.3750
9700151	5/20A	70E_4s1d2Xc_1	70	E	19	49770.7	91 1/2	80	0.613	0.920	HLP-22	12	8	4	3.5	21.9	11.5	20.3	10.5	0.62	0.33	s1d2	2.48	0.0000569	0.0000693	0.0000821	0.3750
9700151.1	5/20A	70E_4s1d2Xc_1	70	E	19	49770.7	91 1/2	80	0.613	0.920	HLP-22	12	8	4	3.5	21.9	11.5	20.3	10.5	0.62	0.33	s1d2	2.48	0.0000569	0.0000693	0.0000821	0.3750
9700152	5/20A	70E_4s1d2Xc_1	70	E	19	49770.7	91 1/2	80	0.613	0.920	HLP-22	12	8	4	3.5	21.9	11.5	20.3	10.5	0.62	0.33	s1d2	2.48	0.0000569	0.0000693	0.0000821	0.3750
9700153	5/20A	70E_4s1d2Xc_1	70	E	19	49770.7	91 1/2	80	0.613	0.920	HLP-22	12	8	4	3.5	21.9	11.5	20.3	10.5	0.62	0.33	s1d2	2.48	0.0000569	0.0000693	0.0000821	0.3750
9700154	5/20A	70E_4s1d2Xc_1	70	E	19	49770.7	91 1/2	80	0.613	0.920	HLP-22	12	8	4	3.5	21.9	11.5	20.3	10.5	0.62	0.33	s1d2	2.48	0.0000569	0.0000693	0.0000821	0.3750
9700154.1	5/20A	70E_4s1d2Xc_1	70	E	19	49770.7	91 1/2	80	0.613	0.920	HLP-22	12	8	4	3.5	21.9	11.5	20.3	10.5	0.62	0.33	s1d2	2.48	0.0000569	0.0000693	0.0000821	0.3750
9700155	5/20A	70E_4s1d2Xc_1	70	E	19	49770.7	91 1/2	80	0.613	0.920	HLP-22	12	8	4	3.5	21.9	11.5	20.3	10.5	0.62	0.33	s1d2	2.48	0.0000569	0.0000693	0.0000821	0.3750
9700155.1	5/20A	70E_4s1d2Xc_1	70	E	19	49770.7	91 1/2	80	0.613	0.920	HLP-22	12	8	4	3.5	21.9	11.5	20.3	10.5	0.62	0.33	s1d2	2.48	0.0000569	0.0000693	0.0000821	0.3750
9700156	5/20A	70E_4s1d2Xc_1	70	E	19	49770.7	91 1/2	80	0.613	0.920	HLP-22	12	8	4	3.5	21.9	11.5	20.3	10.5	0.62	0.33	s1d2	2.48	0.0000569	0.0000693	0.0000821	0.3750
9700156.1	5/20A	70E_4s1d2Xc_1	70	E	19	49770.7	91 1/2	80	0.613	0.920	HLP-22	12	8	4	3.5	21.9	11.5	20.3	10.5	0.62	0.33	s1d2	2.48	0.0000569	0.0000693	0.0000821	0.3750
9700157	5/20A	70E_4s1d2Xc_1	70	E	19	49770.7	91 1/2	80	0.613	0.920	HLP-22	12	8	4	3.5	21.9	11.5	20.3	10.5	0.62	0.33	s1d2	2.48	0.0000569	0.0000693	0.0000821	0.3750
9700157.1	5/20A	70E_4s1d2Xc_1	70	E	19	49770.7	91 1/2	80	0.613	0.920	HLP-22	12	8	4	3.5	21.9	11.5	20.3	10.5	0.62	0.33	s1d2	2.48	0.0000569	0.0000693	0.0000821	0.3750
9700158	5/20A	70E_4s1d2Xc_1	70	E	19	49770.7	91 1/2	80	0.613	0.920	HLP-22	12	8	4	3.5	21.9	11.5	20.3	10.5	0.62	0.33	s1d2	2.48	0.0000569	0.0000693	0.0000821	0.3750
9700158.1	5/20A	70E_4s1d2Xc_1	70	E	19	49770.7	91 1/2	80	0.613	0.920	HLP-22	12	8	4	3.5	21.9	11.5	20.3	10.5	0.62	0.33	s1d2	2.48	0.0000569	0.0000693	0.0000821	0.3750
9700159	5/20A	70E_4s1d2Xc_1	70	E	19	49770.7	91 1/2	80	0.613	0.920	HLP-22	12	8	4	3.5	21.9	11.5	20.3	10.5	0.62	0.33	s1d2	2.48	0.0000569	0.0000693	0.0000821	0.3750
9700160	5/20A	70E_4s1d2Xc_1	70	E	19	49770.7	91 1/2	80	0.613	0.920	HLP-22	12	8	4	3.5	21.9	11.5	20.3	10.5	0.62	0.33	s1d2	2.48	0.0000569	0.0000693	0.0000821	0.3750
9700161	5/20A	70E_4s1d2Xc_1	70	E	19	49770.7	91 1/2	80	0.613	0.920	HLP-22	12	8	4	3.5	21.9	11.5	20.3	10.5	0.62	0.33	s1d2	2.48	0.0000569	0.0000693	0.0000821	0.3750
9700161.1	5/20A	70E_4s1d2Xc_1	70	E	19	49770.7	91 1/2	80	0.613	0.920	HLP-22	12	8	4	3.5	21.9	11.5	20.3	10.5	0.62	0.33	s1d2	2.48	0.0000569	0.0000693	0.0000821	0.3750
9700162	5/20A	70E_4s1d2Xc_1	70	E	19	49770.7	91 1/2	80	0.613	0.920	HLP-22	12	8	4	3.5	21.9	11.5	20.3	10.5	0.62	0.33	s1d2	2.48	0.0000569	0.0000693	0.0000821	0.3750
9700162.1	5/20A	70E_4s1d2Xc_1	70	E	19	49770.7	91 1/2	80	0.613	0.920	HLP-22	12	8	4	3.5	21.9	11.5	20.3	10.5	0.62	0.33	s1d2	2.48	0.0000569	0.0000693	0.0000821	0.3750
9700163	5/20A	70E_4s1d2Xc_1	70	E	19	49770.7	91 1/2	80	0.613	0.920	HLP-22	12	8	4	3.5	21.9	11.5	20.3	10.5	0.62	0.33	s1d2	2.48	0.0000569	0.0000693	0.0000821	0.3750
9700163.1	5/20A	70E_4s1d2Xc_1	70	E	19	49770.7	91 1/2	80	0.613	0.920	HLP-22	12	8	4	3.5	21.9	11.5	20.3	10.5	0.62	0.33	s1d2	2.48	0.0000569	0.0000693	0.0000821	0.3750
9700164	5/20A	70E_4s1d2Xc_1	70	E	19	49770.7	91 1/2	80	0.613	0.920	HLP-22	12	8	4	3.5	21.9	11.5	20.3	10.5	0.62	0.33	s1d2	2.48	0.0000569	0.0000693	0.0000821	0.3750
9700164.1	5/20A	70E_4s1d2Xc_1	70	E	19	49770.7	91 1/2	80	0.613	0.920	HLP-22	12	8	4	3.5	21.9	11.5	20.3	10.5	0.62	0.33	s1d2	2.48	0.0000569	0.0000693	0.0000821	0.3750
9700164.2	5/20A	70E_4s1d2Xc_1	70	E	19	49770.7	91 1/2	80	0.613	0.920	HLP-22	12	8	4	3.5	21.9	11.5	20.3	10.5	0.62	0.33	s1d2	2.48	0.0000569	0.0000693	0.0000821	0.3750

Table B.5. Data from 2008 Tests in Large-Scale Vessel with Elliptical Head B.5

Tank Water Temperature	Water Density	Solids Fraction	Pulse Volume Fraction	Duty Cycle	Cycle Time	Pulsed or Steady Jet	Us Steady Jet	U1 Pulsing Jet	U2 URMS	U3 URM3	Discharge Velocity	Critical Suspension Velocity	Average Peak Cloud Height	UCS Condition	UCS Method	UCS Flag	UCS Center Flag	UCS udv Flag	UCS based on Decreasing Velocity	Sweep Increase / Decrease	UDV Height Bed	Particle Motion	Solids Level	Outer Bottom Pattern	Inner Bottom Pattern	Case ID	Test	TDP	Row Number
C	g/cm³	fraction	fraction	fraction	s	text	m/s	m/s	m/s	m/s	m/s	m/s	in.	m/s	text	text	text	text	m/s	text	mm	text	text	text	text	text	text	text	text
T	ρ_c	ϕ_S	ϕ_p	DC	t_C	Jet	U_S	U1	U2	U3	U	U_{CS}	H_C	U_{CSR}	U_{CSM}	U_{CS}vis	U_{CS}cen	U_{CS}udv	$U_{CS_}D$	S_W	H_{bed}	PM	Sol	SP_O	SP_I	ID	M/DDX	TDP	MSS
25.3	0.994	0.01500	0.050	0.335	36.8	P	N/A	7.75	7.89	7.97	8.20	8.50	40.00	N/A	N/A	N/A	N/A	N/A	N/A	I	9.4	1	N/A	N/A	N/A	70E_4s1d2Xc_1	5/19C	TDP-159	9700139
25.5	0.994	0.01500	0.051	0.336	36.0	P	N/A	7.94	8.09	8.17	8.40	8.50	N/A	N/A	N/A	N/A	N/A	N/A	N/A	I	0.0	4	N/A	N/A	N/A	70E_4s1d2Xc_1	5/19C	TDP-159	9700140
26.5	0.994	0.01500	0.050	0.335	36.8	P	N/A	7.76	7.90	7.97	8.20	8.50	35.75	N/A	N/A	N/A	N/A	N/A	N/A	(null)	25.5	1	N/A	N/A	N/A	70E_4s1d2Xc_1	5/20A	TDP-160	9700141
26.7	0.994	0.01500	0.050	0.336	36.4	P	N/A	7.85	8.00	8.07	8.30	8.50	39.00	N/A	N/A	N/A	N/A	N/A	N/A	I	16.2	1	N/A	N/A	N/A	70E_4s1d2Xc_1	5/20A	TDP-160	9700142
26.7	0.994	0.01500	0.050	0.336	35.8	P	N/A	7.94	8.09	8.17	8.40	8.50	41.00	N/A	N/A	N/A	UCScen	N/A	N/A	I	3.5	2	N/A	N/A	N/A	70E_4s1d2Xc_1	5/20A	TDP-160	9700143
26.7	0.994	0.01500	0.050	0.337	35.4	P	N/A	8.03	8.18	8.26	8.50	8.50	41.50	8.50	udv	N/A	N/A	UCSudv	N/A	I	1.0	4	N/A	N/A	N/A	70E_4s1d2Xc_1	5/20A	TDP-160	9700144
26.6	0.994	0.01500	0.050	0.337	35.4	P	N/A	8.03	8.18	8.26	8.50	8.50	41.00	N/A	N/A	N/A	N/A	N/A	N/A	I	0.0	4	N/A	N/A	N/A	70E_4s1d2Xc_1	5/20A	TDP-160	9700145
26.6	0.994	0.01500	0.050	0.337	35.4	P	N/A	8.03	8.18	8.26	8.50	8.50	41.00	N/A	N/A	N/A	N/A	N/A	N/A	N/A	0.0	N/A	N/A	N/A	N/A	70E_4s1d2Xc_1	5/20A	TDP-160	9700146
26.6	0.994	0.01500	0.050	0.337	35.4	P	N/A	8.03	8.18	8.26	8.50	8.50	41.00	N/A	N/A	N/A	N/A	N/A	N/A	N/A	0.0	N/A	N/A	N/A	N/A	70E_4s1d2Xc_1	5/20A	TDP-160	9700147
26.6	0.994	0.01500	0.050	0.337	35.4	P	N/A	8.03	8.18	8.26	8.50	8.50	41.00	N/A	N/A	N/A	N/A	N/A	N/A	N/A	n/a	N/A	N/A	N/A	N/A	70E_4s1d2Xc_1	5/20A	TDP-160	9700147.1
26.6	0.994	0.01500	0.050	0.337	35.4	P	N/A	8.03	8.18	8.26	8.50	8.50	41.00	N/A	N/A	N/A	N/A	N/A	N/A	N/A	0.0	N/A	N/A	N/A	N/A	70E_4s1d2Xc_1	5/20A	TDP-160	9700148
26.6	0.994	0.01500	0.050	0.337	35.4	P	N/A	8.03	8.18	8.26	8.50	8.50	41.00	N/A	N/A	N/A	N/A	N/A	N/A	N/A	n/a	N/A	N/A	N/A	N/A	70E_4s1d2Xc_1	5/20A	TDP-160	9700148.1
26.6	0.994	0.01500	0.050	0.337	35.4	P	N/A	8.03	8.18	8.26	8.50	8.50	41.00	N/A	N/A	N/A	N/A	N/A	N/A	N/A	0.0	N/A	N/A	N/A	N/A	70E_4s1d2Xc_1	5/20A	TDP-160	9700149
26.6	0.994	0.01500	0.050	0.337	35.4	P	N/A	8.03	8.18	8.26	8.50	8.50	41.00	N/A	N/A	N/A	N/A	N/A	N/A	N/A	n/a	N/A	N/A	N/A	N/A	70E_4s1d2Xc_1	5/20A	TDP-160	9700149.1
26.6	0.994	0.01500	0.050	0.337	35.4	P	N/A	8.03	8.18	8.26	8.50	8.50	41.00	N/A	N/A	N/A	N/A	N/A	N/A	N/A	0.0	N/A	N/A	N/A	N/A	70E_4s1d2Xc_1	5/20A	TDP-160	9700150
26.6	0.994	0.01500	0.050	0.337	35.4	P	N/A	8.03	8.18	8.26	8.50	8.50	41.00	N/A	N/A	N/A	N/A	N/A	N/A	N/A	n/a	N/A	N/A	N/A	N/A	70E_4s1d2Xc_1	5/20A	TDP-160	9700150.1
26.6	0.994	0.01500	0.050	0.337	35.4	P	N/A	8.03	8.18	8.26	8.50	8.50	41.00	N/A	N/A	N/A	N/A	N/A	N/A	N/A	0.0	N/A	N/A	N/A	N/A	70E_4s1d2Xc_1	5/20A	TDP-160	9700151
26.6	0.994	0.01500	0.050	0.337	35.4	P	N/A	8.03	8.18	8.26	8.50	8.50	41.00	N/A	N/A	N/A	N/A	N/A	N/A	N/A	n/a	N/A	N/A	N/A	N/A	70E_4s1d2Xc_1	5/20A	TDP-160	9700151.1
26.6	0.994	0.01500	0.050	0.337	35.4	P	N/A	8.03	8.18	8.25	8.50	8.50	41.50	N/A	N/A	N/A	N/A	N/A	N/A	(null)	0.0	4	N/A	N/A	N/A	70E_4s1d2Xc_1	5/20A	TDP-160	9700152
26.6	0.994	0.01500	0.050	0.337	35.4	P	N/A	8.03	8.18	8.25	8.50	8.50	41.50	N/A	N/A	N/A	N/A	N/A	N/A	N/A	0.0	N/A	N/A	N/A	N/A	70E_4s1d2Xc_1	5/20A	TDP-160	9700153
26.6	0.994	0.01500	0.050	0.337	35.4	P	N/A	8.03	8.18	8.25	8.50	8.50	41.50	N/A	N/A	N/A	N/A	N/A	N/A	N/A	0.0	N/A	N/A	N/A	N/A	70E_4s1d2Xc_1	5/20A	TDP-160	9700154
26.6	0.994	0.01500	0.050	0.337	35.4	P	N/A	8.03	8.18	8.25	8.50	8.50	41.50	N/A	N/A	N/A	N/A	N/A	N/A	N/A	n/a	N/A	N/A	N/A	N/A	70E_4s1d2Xc_1	5/20A	TDP-160	9700154.1
26.6	0.994	0.01500	0.050	0.337	35.4	P	N/A	8.03	8.18	8.25	8.50	8.50	41.50	N/A	N/A	N/A	N/A	N/A	N/A	N/A	0.0	N/A	N/A	N/A	N/A	70E_4s1d2Xc_1	5/20A	TDP-160	9700155
26.6	0.994	0.01500	0.050	0.337	35.4	P	N/A	8.03	8.18	8.25	8.50	8.50	41.50	N/A	N/A	N/A	N/A	N/A	N/A	N/A	n/a	N/A	N/A	N/A	N/A	70E_4s1d2Xc_1	5/20A	TDP-160	9700155.1
26.6	0.994	0.01500	0.050	0.337	35.4	P	N/A	8.03	8.18	8.25	8.50	8.50	41.50	N/A	N/A	N/A	N/A	N/A	N/A	N/A	0.0	N/A	N/A	N/A	N/A	70E_4s1d2Xc_1	5/20A	TDP-160	9700156
26.6	0.994	0.01500	0.050	0.337	35.4	P	N/A	8.03	8.18	8.25	8.50	8.50	41.50	N/A	N/A	N/A	N/A	N/A	N/A	N/A	n/a	N/A	N/A	N/A	N/A	70E_4s1d2Xc_1	5/20A	TDP-160	9700156.1
26.6	0.994	0.01500	0.050	0.337	35.4	P	N/A	8.03	8.18	8.25	8.50	8.50	41.50	N/A	N/A	N/A	N/A	N/A	N/A	N/A	0.0	N/A	N/A	N/A	N/A	70E_4s1d2Xc_1	5/20A	TDP-160	9700157
26.6	0.994	0.01500	0.050	0.337	35.4	P	N/A	8.03	8.18	8.25	8.50	8.50	41.50	N/A	N/A	N/A	N/A	N/A	N/A	N/A	n/a	N/A	N/A	N/A	N/A	70E_4s1d2Xc_1	5/20A	TDP-160	9700157.1
26.6	0.994	0.01500	0.050	0.337	35.4	P	N/A	8.03	8.18	8.25	8.50	8.50	41.50	N/A	N/A	N/A	N/A	N/A	N/A	N/A	0.0	N/A	N/A	N/A	N/A	70E_4s1d2Xc_1	5/20A	TDP-160	9700158
26.6	0.994	0.01500	0.050	0.337	35.4	P	N/A	8.03	8.18	8.25	8.50	8.50	41.50	N/A	N/A	N/A	N/A	N/A	N/A	N/A	n/a	N/A	N/A	N/A	N/A	70E_4s1d2Xc_1	5/20A	TDP-160	9700158.1
26.7	0.994	0.01500	0.050	0.337	35.4	P	N/A	8.04	8.19	8.26	8.50	8.50	41.50	N/A	N/A	N/A	N/A	N/A	N/A	(null)	0.0	4	N/A	N/A	N/A	70E_4s1d2Xc_1	5/20A	TDP-160	9700159
26.7	0.994	0.01500	0.050	0.337	35.4	P	N/A	8.04	8.19	8.26	8.50	8.50	41.50	N/A	N/A	N/A	N/A	N/A	N/A	N/A	0.0	N/A	N/A	N/A	N/A	70E_4s1d2Xc_1	5/20A	TDP-160	9700160
26.7	0.994	0.01500	0.050	0.337	35.4	P	N/A	8.04	8.19	8.26	8.50	8.50	41.50	N/A	N/A	N/A	N/A	N/A	N/A	N/A	0.0	N/A	N/A	N/A	N/A	70E_4s1d2Xc_1	5/20A	TDP-160	9700161
26.7	0.994	0.01500	0.050	0.337	35.4	P	N/A	8.04	8.19	8.26	8.50	8.50	41.50	N/A	N/A	N/A	N/A	N/A	N/A	N/A	n/a	N/A	N/A	N/A	N/A	70E_4s1d2Xc_1	5/20A	TDP-160	9700161.1
26.7	0.994	0.01500	0.050	0.337	35.4	P	N/A	8.04	8.19	8.26	8.50	8.50	41.50	N/A	N/A	N/A	N/A	N/A	N/A	N/A	2.8	N/A	N/A	N/A	N/A	70E_4s1d2Xc_1	5/20A	TDP-160	9700162
26.7	0.994	0.01500	0.050	0.337	35.4	P	N/A	8.04	8.19	8.26	8.50	8.50	41.50	N/A	N/A	N/A	N/A	N/A	N/A	N/A	n/a	N/A	N/A	N/A	N/A	70E_4s1d2Xc_1	5/20A	TDP-160	9700162.1
26.7	0.994	0.01500	0.050	0.337	35.4	P	N/A	8.04	8.19	8.26	8.50	8.50	41.50	N/A	N/A	N/A	N/A	N/A	N/A	N/A	0.0	N/A	N/A	N/A	N/A	70E_4s1d2Xc_1	5/20A	TDP-160	9700163
26.7	0.994	0.01500	0.050	0.337	35.4	P	N/A	8.04	8.19	8.26	8.50	8.50	41.50	N/A	N/A	N/A	N/A	N/A	N/A	N/A	n/a	N/A	N/A	N/A	N/A	70E_4s1d2Xc_1	5/20A	TDP-160	9700163.1
26.7	0.994	0.01500	0.050	0.337	35.4	P	N/A	8.04	8.19	8.26	8.50	8.50	41.50	N/A	N/A	N/A	N/A	N/A	N/A	N/A	0.0	N/A	N/A	N/A	N/A	70E_4s1d2Xc_1	5/20A	TDP-160	9700164
26.7	0.994	0.01500	0.050	0.337	35.4	P	N/A	8.04	8.19	8.26	8.50	8.50	41.50	N/A	N/A	N/A	N/A	N/A	N/A	N/A	n/a	N/A	N/A	N/A	N/A	70E_4s1d2Xc_1	5/20A	TDP-160	9700164.1
26.7	0.994	0.01500	0.050	0.337	35.4	P	N/A	8.04	8.19	8.26	8.50	8.50	41.50	N/A	N/A	N/A	N/A	N/A	N/A	N/A	n/a	N/A	N/A	N/A	N/A	70E_4s1d2Xc_1	5/20A	TDP-160	9700164.2

Table B.5. Data from 2008 Tests in Large-Scale Vessel with Elliptical Head A.6

Row Number	Test	Case ID	Tank Diameter	Head Shape	Dish Height	Dish Volume	Tank Fill Height	Return Line Height	Nozzle Inner Diameter	Nozzle Stand-off Distance	Pulse Tube Configuration	Installed Nozzles	Outer Nozzles Operated	Inner Nozzles Operated	Pulse Tube Outer Diameter	Outer PJM Radius	Inner PJM Radius	"FIO" Outer PJM Impingement Angle	"FIO" Inner PJM Impingement Angle	Ratio Outer PJM to Tank Radius	Ratio Inner PJM to Tank Radius	Simulant	Solids Density	Particle Diameter d5	Particle Diameter d50	Particle Diameter d95	Void Fraction
text	text	text	in.	text	in.	in. ^{3}	in.	in.	in.	in.	text	number	number	number	in.	in.	in.	deg	deg	nondim	nondim	text	g/cm^3	m	m	m	fraction
MSS	M/DDX	ID	D	HS	H_{dish}	V_{dish}	H	Rtn	d	sod	PT	N	N_O	N_I	PT_{od}	R_O	R_I	θ_O	θ_I	R_O/R	R_I/R	sxdx	ρ_s	d_5	d_{50}	d_{95}	vf
9700164.3	5/20A	70E_4s1d2Xc_1	70	E	19	49770.7	91 1/2	80	0.613	0.920	HLP-22	12	8	4	3.5	21.9	11.5	20.3	10.5	0.62	0.33	s1d2	2.48	0.0000569	0.0000693	0.0000821	0.3750
9700165	5/20A	70E_4s1d2Xc_1	70	E	19	49770.7	91 1/2	80	0.613	0.920	HLP-22	12	8	4	3.5	21.9	11.5	20.3	10.5	0.62	0.33	s1d2	2.48	0.0000569	0.0000693	0.0000821	0.3750
9700166	5/20A	70E_4s1d2Xc_1	70	E	19	49770.7	91 1/2	80	0.613	0.920	HLP-22	12	8	4	3.5	21.9	11.5	20.3	10.5	0.62	0.33	s1d2	2.48	0.0000569	0.0000693	0.0000821	0.3750
9700167	5/20A	70E_4s1d2Xc_1	70	E	19	49770.7	91 1/2	80	0.613	0.920	HLP-22	12	8	4	3.5	21.9	11.5	20.3	10.5	0.62	0.33	s1d2	2.48	0.0000569	0.0000693	0.0000821	0.3750
9700168	5/20A	70E_4s1d2Xc_1	70	E	19	49770.7	91 1/2	80	0.613	0.920	HLP-22	12	8	4	3.5	21.9	11.5	20.3	10.5	0.62	0.33	s1d2	2.48	0.0000569	0.0000693	0.0000821	0.3750
9700169	5/20A	70E_4s1d2Xc_1	70	E	19	49770.7	91 1/2	80	0.613	0.920	HLP-22	12	8	4	3.5	21.9	11.5	20.3	10.5	0.62	0.33	s1d2	2.48	0.0000569	0.0000693	0.0000821	0.3750
9700170	5/20A	70E_4s1d2Xc_1	70	E	19	49770.7	91 1/2	80	0.613	0.920	HLP-22	12	8	4	3.5	21.9	11.5	20.3	10.5	0.62	0.33	s1d2	2.48	0.0000569	0.0000693	0.0000821	0.3750
9700171	5/20A	70E_4s1d2Xc_1	70	E	19	49770.7	91 1/2	80	0.613	0.920	HLP-22	12	8	4	3.5	21.9	11.5	20.3	10.5	0.62	0.33	s1d2	2.48	0.0000569	0.0000693	0.0000821	0.3750
9700172	5/20A	70E_4s1d2Xc_1	70	E	19	49770.7	91 1/2	80	0.613	0.920	HLP-22	12	8	4	3.5	21.9	11.5	20.3	10.5	0.62	0.33	s1d2	2.48	0.0000569	0.0000693	0.0000821	0.3750
9700173	5/20A	70E_4s1d2Xc_1	70	E	19	49770.7	91 1/2	80	0.613	0.920	HLP-22	12	8	4	3.5	21.9	11.5	20.3	10.5	0.62	0.33	s1d2	2.48	0.0000569	0.0000693	0.0000821	0.3750
9700174	5/20A	70E_4s1d2Xc_1	70	E	19	49770.7	91 1/2	80	0.613	0.920	HLP-22	12	8	4	3.5	21.9	11.5	20.3	10.5	0.62	0.33	s1d2	2.48	0.0000569	0.0000693	0.0000821	0.3750
9700174.1	5/20A	70E_4s1d2Xc_1	70	E	19	49770.7	91 1/2	80	0.613	0.920	HLP-22	12	8	4	3.5	21.9	11.5	20.3	10.5	0.62	0.33	s1d2	2.48	0.0000569	0.0000693	0.0000821	0.3750
9700174.2	5/20A	70E_4s1d2Xc_1	70	E	19	49770.7	91 1/2	80	0.613	0.920	HLP-22	12	8	4	3.5	21.9	11.5	20.3	10.5	0.62	0.33	s1d2	2.48	0.0000569	0.0000693	0.0000821	0.3750
9700174.3	5/20A	70E_4s1d2Xc_1	70	E	19	49770.7	91 1/2	80	0.613	0.920	HLP-22	12	8	4	3.5	21.9	11.5	20.3	10.5	0.62	0.33	s1d2	2.48	0.0000569	0.0000693	0.0000821	0.3750
9700174.4	5/20A	70E_4s1d2Xc_1	70	E	19	49770.7	91 1/2	80	0.613	0.920	HLP-22	12	8	4	3.5	21.9	11.5	20.3	10.5	0.62	0.33	s1d2	2.48	0.0000569	0.0000693	0.0000821	0.3750
9700174.5	5/20A	70E_4s1d2Xc_1	70	E	19	49770.7	91 1/2	80	0.613	0.920	HLP-22	12	8	4	3.5	21.9	11.5	20.3	10.5	0.62	0.33	s1d2	2.48	0.0000569	0.0000693	0.0000821	0.3750
9700175	5/20A	70E_4s1d2Xc_1	70	E	19	49770.7	91 1/2	80	0.613	0.920	HLP-22	12	8	4	3.5	21.9	11.5	20.3	10.5	0.62	0.33	s1d2	2.48	0.0000569	0.0000693	0.0000821	0.3750
9700176	5/20A	70E_4s1d2Xc_1	70	E	19	49770.7	91 1/2	80	0.613	0.920	HLP-22	12	8	4	3.5	21.9	11.5	20.3	10.5	0.62	0.33	s1d2	2.48	0.0000569	0.0000693	0.0000821	0.3750
9700177	5/20A	70E_4s1d2Xc_1	70	E	19	49770.7	91 1/2	80	0.613	0.920	HLP-22	12	8	4	3.5	21.9	11.5	20.3	10.5	0.62	0.33	s1d2	2.48	0.0000569	0.0000693	0.0000821	0.3750
9700178	5/20A	70E_4s1d2Xc_1	70	E	19	49770.7	91 1/2	80	0.613	0.920	HLP-22	12	8	4	3.5	21.9	11.5	20.3	10.5	0.62	0.33	s1d2	2.48	0.0000569	0.0000693	0.0000821	0.3750
9700179	5/20A	70E_4s1d2Xc_1	70	E	19	49770.7	91 1/2	80	0.613	0.920	HLP-22	12	8	4	3.5	21.9	11.5	20.3	10.5	0.62	0.33	s1d2	2.48	0.0000569	0.0000693	0.0000821	0.3750
9700180	5/20A	70E_4s1d2Xc_1	70	E	19	49770.7	91 1/2	80	0.613	0.920	HLP-22	12	8	4	3.5	21.9	11.5	20.3	10.5	0.62	0.33	s1d2	2.48	0.0000569	0.0000693	0.0000821	0.3750
9700181	5/20A	70E_4s1d2Xc_1	70	E	19	49770.7	91 1/2	80	0.613	0.920	HLP-22	12	8	4	3.5	21.9	11.5	20.3	10.5	0.62	0.33	s1d2	2.48	0.0000569	0.0000693	0.0000821	0.3750
9700182	5/20B	70E_4s1d2Xd_1	70	E	19	49770.7	91 1/2	80	0.613	0.920	HLP-22	12	8	4	3.5	21.9	11.5	20.3	10.5	0.62	0.33	s1d2	2.48	0.0000569	0.0000693	0.0000821	0.3750
9700183	5/20B	70E_4s1d2Xd_1	70	E	19	49770.7	91 1/2	80	0.613	0.920	HLP-22	12	8	4	3.5	21.9	11.5	20.3	10.5	0.62	0.33	s1d2	2.48	0.0000569	0.0000693	0.0000821	0.3750
9700184	5/20B	70E_4s1d2Xd_1	70	E	19	49770.7	91 1/2	80	0.613	0.920	HLP-22	12	8	4	3.5	21.9	11.5	20.3	10.5	0.62	0.33	s1d2	2.48	0.0000569	0.0000693	0.0000821	0.3750
9700185	5/20B	70E_4s1d2Xd_1	70	E	19	49770.7	91 1/2	80	0.613	0.920	HLP-22	12	8	4	3.5	21.9	11.5	20.3	10.5	0.62	0.33	s1d2	2.48	0.0000569	0.0000693	0.0000821	0.3750
9700186	5/20B	70E_4s1d2Xd_1	70	E	19	49770.7	91 1/2	80	0.613	0.920	HLP-22	12	8	4	3.5	21.9	11.5	20.3	10.5	0.62	0.33	s1d2	2.48	0.0000569	0.0000693	0.0000821	0.3750
9700187	5/20B	70E_4s1d2Xd_1	70	E	19	49770.7	91 1/2	80	0.613	0.920	HLP-22	12	8	4	3.5	21.9	11.5	20.3	10.5	0.62	0.33	s1d2	2.48	0.0000569	0.0000693	0.0000821	0.3750
9700188	5/20B	70E_4s1d2Xd_1	70	E	19	49770.7	91 1/2	80	0.613	0.920	HLP-22	12	8	4	3.5	21.9	11.5	20.3	10.5	0.62	0.33	s1d2	2.48	0.0000569	0.0000693	0.0000821	0.3750
9700189	5/20B	70E_4s1d2Xd_1	70	E	19	49770.7	91 1/2	80	0.613	0.920	HLP-22	12	8	4	3.5	21.9	11.5	20.3	10.5	0.62	0.33	s1d2	2.48	0.0000569	0.0000693	0.0000821	0.3750
9700190	5/21A	70E_4s1d2Xd_1	70	E	19	49770.7	91	80	0.613	0.920	HLP-22	12	8	4	3.5	21.9	11.5	20.3	10.5	0.62	0.33	s1d2	2.48	0.0000569	0.0000693	0.0000821	0.3750
9700191	5/21A	70E_4s1d2Xd_1	70	E	19	49770.7	91	80	0.613	0.920	HLP-22	12	8	4	3.5	21.9	11.5	20.3	10.5	0.62	0.33	s1d2	2.48	0.0000569	0.0000693	0.0000821	0.3750
9700192	5/21A	70E_4s1d2Xd_1	70	E	19	49770.7	91	80	0.613	0.920	HLP-22	12	8	4	3.5	21.9	11.5	20.3	10.5	0.62	0.33	s1d2	2.48	0.0000569	0.0000693	0.0000821	0.3750
9700193	5/21A	70E_4s1d2Xd_1	70	E	19	49770.7	91	80	0.613	0.920	HLP-22	12	8	4	3.5	21.9	11.5	20.3	10.5	0.62	0.33	s1d2	2.48	0.0000569	0.0000693	0.0000821	0.3750
9700194	5/21A	70E_4s1d2Xd_1	70	E	19	49770.7	91	80	0.613	0.920	HLP-22	12	8	4	3.5	21.9	11.5	20.3	10.5	0.62	0.33	s1d2	2.48	0.0000569	0.0000693	0.0000821	0.3750
9700195M	5/21A	70E_4s1d2Xd_1	70	E	19	49770.7	91	80	0.613	0.920	HLP-22	12	8	4	3.5	21.9	11.5	20.3	10.5	0.62	0.33	s1d2	2.48	0.0000569	0.0000693	0.0000821	0.3750
9700196M	5/21A	70E_4s1d2Xd_1	70	E	19	49770.7	91	80	0.613	0.920	HLP-22	12	8	4	3.5	21.9	11.5	20.3	10.5	0.62	0.33	s1d2	2.48	0.0000569	0.0000693	0.0000821	0.3750
9700197	5/21B	70E_4s1d2Xa	70	E	19	49770.7	91	80	0.613	0.920	HLP-22	12	8	4	3.5	21.9	11.5	20.3	10.5	0.62	0.33	s1d2	2.48	0.0000569	0.0000693	0.0000821	0.3750
9700198	5/22A	70E_4s2d2Zc_1	70	E	19	49770.7	92 1/2	80	0.613	0.920	HLP-22	12	8	4	3.5	21.9	11.5	20.3	10.5	0.62	0.33	s2d2	4.18	0.0000609	0.0000756	0.0000931	0.3684
9700199	5/22A	70E_4s2d2Zc_1	70	E	19	49770.7	92 1/2	80	0.613	0.920	HLP-22	12	8	4	3.5	21.9	11.5	20.3	10.5	0.62	0.33	s2d2	4.18	0.0000609	0.0000756	0.0000931	0.3684

Table B.5. Data from 2008 Tests in Large-Scale Vessel with Elliptical Head B.6

Tank Water Temperature	Water Density	Solids Fraction	Pulse Volume Fraction	Duty Cycle	Cycle Time	Pulsed or Steady Jet	Us Steady Jet	U1 Pulsing Jet	U2 URMS	U3 URM3	Discharge Velocity	Critical Suspension Velocity	Average Peak Cloud Height	UCS Condition	UCS Method	UCS Flag	UCS Center Flag	UCS udv Flag	UCS based on Decreasing Velocity	Sweep Increase / Decrease	UDV Height Bed	Particle Motion	Solids Level	Outer Bottom Pattern	Inner Bottom Pattern	Case ID	Test	TDP	Row Number
C	g/cm³	fraction	fraction	fraction	s	text	m/s	m/s	m/s	m/s	m/s	m/s	in.	m/s	text	text	text	text	m/s	text	mm	text	text	text	text	text	text	text	text
T	ρ_L	ϕ_S	ϕ_P	DC	t_C	Jet	U_S	U1	U2	U3	U	U_{CS}	H_C	U_{CSR}	U_{CSM}	U_{CS}vis	U_{CS}cen	U_{CS}udv	U_{CS}_D	S_W	H_{bed}	PM	Sol	SP_O	SP_I	ID	M/DDX	TDP	MSS
26.7	0.994	0.01500	0.050	0.337	35.4	P	N/A	8.04	8.19	8.26	8.50	8.50	41.50	N/A	N/A	N/A	N/A	N/A	N/A	N/A	n/a	N/A	N/A	N/A	N/A	70E_4s1d2Xc_1	5/20A	TDP-160	9700164.3
27.1	0.994	0.01500	0.050	0.336	35.4	P	N/A	8.04	8.19	8.26	8.50	8.50	N/A	N/A	N/A	N/A	N/A	N/A	N/A	I	30.9	n/a	N/A	N/A	N/A	70E_4s1d2Xc_1	5/20A	TDP-160	9700165
26.8	0.994	0.01500	0.050	0.337	35.4	P	N/A	8.03	8.18	8.25	8.50	8.50	N/A	N/A	N/A	N/A	N/A	N/A	N/A	I	20.6	n/a	N/A	N/A	N/A	70E_4s1d2Xc_1	5/20A	TDP-160	9700166
27.0	0.994	0.01500	0.050	0.337	35.4	P	N/A	8.04	8.19	8.27	8.50	8.50	N/A	N/A	N/A	N/A	N/A	N/A	N/A	I	N/A	n/a	N/A	N/A	N/A	70E_4s1d2Xc_1	5/20A	TDP-160	9700167
26.7	0.994	0.01500	0.050	0.337	35.4	P	N/A	8.03	8.19	8.26	8.50	8.50	N/A	N/A	N/A	N/A	N/A	N/A	N/A	I	21.1	n/a	N/A	N/A	N/A	70E_4s1d2Xc_1	5/20A	TDP-160	9700168
26.7	0.994	0.01500	0.050	0.337	35.4	P	N/A	8.02	8.17	8.25	8.50	8.50	N/A	N/A	N/A	N/A	N/A	N/A	N/A	I	7.0	n/a	N/A	N/A	N/A	70E_4s1d2Xc_1	5/20A	TDP-160	9700169
26.8	0.994	0.01500	0.050	0.337	35.4	P	N/A	8.04	8.19	8.27	8.50	8.50	N/A	N/A	N/A	N/A	N/A	N/A	N/A	I	3.8	n/a	N/A	N/A	N/A	70E_4s1d2Xc_1	5/20A	TDP-160	9700170
27.0	0.994	0.01500	0.050	0.337	35.4	P	N/A	8.02	8.18	8.25	8.50	8.50	N/A	N/A	N/A	N/A	N/A	N/A	N/A	I	0.0	n/a	N/A	N/A	N/A	70E_4s1d2Xc_1	5/20A	TDP-160	9700171
26.9	0.994	0.01500	0.050	0.337	35.4	P	N/A	8.03	8.19	8.27	8.50	8.50	N/A	N/A	N/A	N/A	N/A	N/A	N/A	I	0.0	n/a	N/A	N/A	N/A	70E_4s1d2Xc_1	5/20A	TDP-160	9700172
26.9	0.994	0.01500	0.050	0.337	35.4	P	N/A	8.03	8.18	8.26	8.50	8.50	N/A	N/A	N/A	N/A	N/A	N/A	N/A	I	0.0	n/a	N/A	N/A	N/A	70E_4s1d2Xc_1	5/20A	TDP-160	9700173
26.9	0.994	0.01500	0.050	0.337	35.4	P	N/A	8.04	8.19	8.27	8.50	8.50	N/A	N/A	N/A	N/A	N/A	N/A	N/A	I	N/A	n/a	N/A	N/A	N/A	70E_4s1d2Xc_1	5/20A	TDP-160	9700174
26.7	0.994	0.01500	0.050	0.329	44.6	P	N/A	6.46	6.57	6.62	6.80	8.50	22.00	N/A	N/A	N/A	N/A	N/A	N/A	N/A	n/a	N/A	N/A	N/A	N/A	70E_4s1d2Xc_1	5/20A	TDP-160	9700174.1
26.7	0.994	0.01500	0.050	0.329	44.6	P	N/A	6.46	6.57	6.62	6.80	8.50	22.00	N/A	N/A	N/A	N/A	N/A	N/A	N/A	n/a	N/A	N/A	N/A	N/A	70E_4s1d2Xc_1	5/20A	TDP-160	9700174.2
26.7	0.994	0.01500	0.050	0.329	44.6	P	N/A	6.46	6.57	6.62	6.80	8.50	22.00	N/A	N/A	N/A	N/A	N/A	N/A	N/A	n/a	N/A	N/A	N/A	N/A	70E_4s1d2Xc_1	5/20A	TDP-160	9700174.3
26.7	0.994	0.01500	0.050	0.329	44.6	P	N/A	6.46	6.57	6.62	6.80	8.50	22.00	N/A	N/A	N/A	N/A	N/A	N/A	N/A	n/a	N/A	N/A	N/A	N/A	70E_4s1d2Xc_1	5/20A	TDP-160	9700174.4
26.7	0.994	0.01500	0.050	0.329	44.6	P	N/A	6.46	6.57	6.62	6.80	8.50	22.00	N/A	N/A	N/A	N/A	N/A	N/A	N/A	n/a	N/A	N/A	N/A	N/A	70E_4s1d2Xc_1	5/20A	TDP-160	9700174.5
26.7	0.994	0.01500	0.050	0.329	44.6	P	N/A	6.46	6.57	6.62	6.80	8.50	22.00	N/A	N/A	N/A	N/A	N/A	N/A	(null)	30.3	1	N/A	N/A	N/A	70E_4s1d2Xc_1	5/20A	TDP-160	9700175
26.7	0.994	0.01500	0.050	0.329	44.6	P	N/A	6.46	6.57	6.62	6.80	8.50	22.00	N/A	N/A	N/A	N/A	N/A	N/A	N/A	35.5	N/A	N/A	N/A	N/A	70E_4s1d2Xc_1	5/20A	TDP-160	9700176
26.7	0.994	0.01500	0.050	0.329	44.6	P	N/A	6.46	6.57	6.62	6.80	8.50	22.00	N/A	N/A	N/A	N/A	N/A	N/A	N/A	26.4	N/A	N/A	N/A	N/A	70E_4s1d2Xc_1	5/20A	TDP-160	9700177
26.7	0.994	0.01500	0.050	0.329	44.6	P	N/A	6.46	6.57	6.62	6.80	8.50	22.00	N/A	N/A	N/A	N/A	N/A	N/A	N/A	21.4	N/A	N/A	N/A	N/A	70E_4s1d2Xc_1	5/20A	TDP-160	9700178
26.7	0.994	0.01500	0.050	0.329	44.6	P	N/A	6.46	6.57	6.62	6.80	8.50	22.00	N/A	N/A	N/A	N/A	N/A	N/A	N/A	25.3	N/A	N/A	N/A	N/A	70E_4s1d2Xc_1	5/20A	TDP-160	9700179
26.7	0.994	0.01500	0.050	0.329	44.6	P	N/A	6.46	6.57	6.62	6.80	8.50	22.00	N/A	N/A	N/A	N/A	N/A	N/A	N/A	27.8	N/A	N/A	N/A	N/A	70E_4s1d2Xc_1	5/20A	TDP-160	9700180
26.7	0.994	0.01500	0.050	0.329	44.6	P	N/A	6.46	6.57	6.62	6.80	8.50	22.00	N/A	N/A	N/A	N/A	N/A	N/A	N/A	31.3	N/A	N/A	N/A	N/A	70E_4s1d2Xc_1	5/20A	TDP-160	9700181
26.7	0.994	0.01500	0.050	0.187	57.4	P	N/A	8.90	9.09	9.18	9.50	11.60	23.75	N/A	N/A	N/A	N/A	N/A	N/A	I	32.6	1	N/A	N/A	N/A	70E_4s1d2Xd_1	5/20B	TDP-160	9700182
26.6	0.994	0.01500	0.050	0.183	56.0	P	N/A	9.17	9.37	9.47	9.80	11.60	24.50	N/A	N/A	N/A	N/A	N/A	N/A	I	28.9	1	N/A	N/A	N/A	70E_4s1d2Xd_1	5/20B	TDP-160	9700183
26.8	0.994	0.01500	0.050	0.184	54.8	P	N/A	9.37	9.57	9.68	10.00	11.60	25.50	N/A	N/A	N/A	N/A	N/A	N/A	I	25.5	1	N/A	N/A	N/A	70E_4s1d2Xd_1	5/20B	TDP-160	9700184
27.1	0.994	0.01500	0.050	0.185	53.6	P	N/A	9.54	9.76	9.87	10.20	11.60	25.25	N/A	N/A	N/A	N/A	N/A	N/A	I	21.1	1	N/A	N/A	N/A	70E_4s1d2Xd_1	5/20B	TDP-160	9700185
26.9	0.994	0.01500	0.050	0.185	52.6	P	N/A	9.74	9.95	10.06	10.40	11.60	26.50	N/A	N/A	N/A	N/A	N/A	N/A	I	18.9	1	N/A	N/A	N/A	70E_4s1d2Xd_1	5/20B	TDP-160	9700186
26.8	0.994	0.01500	0.050	0.185	52.0	P	N/A	9.83	10.05	10.16	10.50	11.60	27.00	N/A	N/A	N/A	UCScen	N/A	N/A	I	16.5	2	N/A	N/A	N/A	70E_4s1d2Xd_1	5/20B	TDP-160	9700187
27.0	0.993	0.01500	0.050	0.186	51.0	P	N/A	10.00	10.23	10.35	10.70	11.60	28.75	N/A	N/A	N/A	N/A	N/A	N/A	I	13.5	4	N/A	N/A	N/A	70E_4s1d2Xd_1	5/20B	TDP-160	9700188
27.1	0.994	0.01500	0.050	0.187	49.0	P	N/A	10.45	10.70	10.82	11.20	11.60	36.25	N/A	N/A	N/A	N/A	N/A	N/A	I	4.3	4	N/A	N/A	N/A	70E_4s1d2Xd_1	5/20B	TDP-160	9700189
25.4	0.994	0.01500	0.050	0.185	52.6	P	N/A	9.82	10.04	10.15	10.50	11.60	28.75	N/A	N/A	N/A	N/A	N/A	N/A	(null)	12.1	1	N/A	N/A	N/A	70E_4s1d2Xd_1	5/21A	TDP-161	9700190
25.4	0.994	0.01500	0.050	0.185	51.6	P	N/A	9.99	10.21	10.33	10.70	11.60	29.25	N/A	N/A	N/A	UCScen	N/A	N/A	I	7.6	2	N/A	N/A	N/A	70E_4s1d2Xd_1	5/21A	TDP-161	9700191
25.5	0.993	0.01500	0.050	0.186	50.6	P	N/A	10.14	10.38	10.50	10.90	11.60	33.75	N/A	N/A	N/A	N/A	N/A	N/A	I	5.2	4	N/A	N/A	N/A	70E_4s1d2Xd_1	5/21A	TDP-161	9700192
25.5	0.994	0.01500	0.050	0.186	49.6	P	N/A	10.36	10.60	10.72	11.10	11.60	37.25	N/A	N/A	N/A	N/A	N/A	N/A	I	4.7	4	N/A	N/A	N/A	70E_4s1d2Xd_1	5/21A	TDP-161	9700193
25.6	0.994	0.01500	0.050	0.187	48.6	P	N/A	10.53	10.78	10.90	11.30	11.60	39.25	N/A	N/A	N/A	N/A	N/A	N/A	I	4.3	4	N/A	N/A	N/A	70E_4s1d2Xd_1	5/21A	TDP-161	9700194
25.7	0.994	0.01500	0.050	0.184	47.8	P	N/A	10.81	11.07	11.20	11.60	11.60	43.00	11.60	udv	N/A	N/A	UCSudv	N/A	I	0.8	4	N/A	N/A	N/A	70E_4s1d2Xd_1	5/21A	TDP-161	9700195
25.6	0.994	0.01500	0.050	0.184	46.6	P	N/A	11.04	11.31	11.45	11.90	11.60	43.75	N/A	N/A	N/A	N/A	N/A	N/A	I	0.0	4	N/A	N/A	N/A	70E_4s1d2Xd_1	5/21A	TDP-161	9700196
25.3	0.994	0.01500	undefined	1.000	infinite	S	3.49	n/a	n/a	n/a	3.50	N/A	N/A	N/A	N/A	N/A	N/A	N/A	N/A	(null)	0.0	1	N/A	N/A	N/A	70E_4s1d2Xa	5/21B	TDP-161	9700197
24.4	0.994	0.00155	0.050	0.330	53.8	P	N/A	5.38	5.44	5.48	5.60	8.40	N/A	N/A	N/A	N/A	N/A	N/A	N/A	(null)	25.7	1	N/A	N/A	N/A	70E_4s2d2Zc_1	5/22A	TDP-162	9700198
24.7	0.994	0.00155	0.050	0.334	49.4	P	N/A	5.82	5.91	5.95	6.10	8.40	21.50	N/A	N/A	N/A	N/A	N/A	N/A	(null)	16.9	1	N/A	N/A	N/A	70E_4s2d2Zc_1	5/22A	TDP-162	9700199

Table B.5. Data from 2008 Tests in Large-Scale Vessel with Elliptical Head A.7

Row Number	Test	Case ID	Tank Diameter	Head Shape	Dish Height	Dish Volume	Tank Fill Height	Return Line Height	Nozzle Inner Diameter	Nozzle Stand-off Distance	Pulse Tube Configuration	Installed Nozzles	Outer Nozzles Operated	Inner Nozzles Operated	Pulse Tube Outer Diameter	Outer PJM Radius	Inner PJM Radius	"FIO" Outer PJM Impingement Angle	"FIO" Inner PJM Impingement Angle	Ratio Outer PJM to Tank Radius	Ratio Inner PJM to Tank Radius	Simulant	Solids Density	Particle Diameter d5	Particle Diameter d50	Particle Diameter d95	Void Fraction
text	text	text	in.	text	in.	in. ^{3}	in.	in.	in.	in.	text	number	number	number	in.	in.	in.	deg	deg	nondim	nondim	text	g/cm^3	m	m	m	fraction
MSS	M/DDX	ID	D	HS	H_{dish}	V_{dish}	H	Rtn	d	sod	PT	N	N_O	N_I	PT_{od}	R_O	R_I	θ_O	θ_I	R_O/R	R_I/R	sxdx	ρ_s	d_5	d_{50}	d_{95}	vf
9700200	5/22A	70E_4s2d2Zc_1	70	E	19	49770.7	92 1/2	80	0.613	0.920	HLP-22	12	8	4	3.5	21.9	11.5	20.3	10.5	0.62	0.33	s2d2	4.18	0.0000609	0.0000756	0.0000931	0.3684
9700201	5/22A	70E_4s2d2Zc_1	70	E	19	49770.7	92 1/2	80	0.613	0.920	HLP-22	12	8	4	3.5	21.9	11.5	20.3	10.5	0.62	0.33	s2d2	4.18	0.0000609	0.0000756	0.0000931	0.3684
9700202	5/22A	70E_4s2d2Zc_1	70	E	19	49770.7	92 1/2	80	0.613	0.920	HLP-22	12	8	4	3.5	21.9	11.5	20.3	10.5	0.62	0.33	s2d2	4.18	0.0000609	0.0000756	0.0000931	0.3684
9700203	5/22A	70E_4s2d2Zc_1	70	E	19	49770.7	92 1/2	80	0.613	0.920	HLP-22	12	8	4	3.5	21.9	11.5	20.3	10.5	0.62	0.33	s2d2	4.18	0.0000609	0.0000756	0.0000931	0.3684
9700204	5/22A	70E_4s2d2Zc_1	70	E	19	49770.7	92 1/2	80	0.613	0.920	HLP-22	12	8	4	3.5	21.9	11.5	20.3	10.5	0.62	0.33	s2d2	4.18	0.0000609	0.0000756	0.0000931	0.3684
9700205	5/22A	70E_4s2d2Zc_1	70	E	19	49770.7	92 1/2	80	0.613	0.920	HLP-22	12	8	4	3.5	21.9	11.5	20.3	10.5	0.62	0.33	s2d2	4.18	0.0000609	0.0000756	0.0000931	0.3684
9700206M	5/22A	70E_4s2d2Zc_1	70	E	19	49770.7	92 1/2	80	0.613	0.920	HLP-22	12	8	4	3.5	21.9	11.5	20.3	10.5	0.62	0.33	s2d2	4.18	0.0000609	0.0000756	0.0000931	0.3684
9700207M	5/22A	70E_4s2d2Zc_1	70	E	19	49770.7	92 1/2	80	0.613	0.920	HLP-22	12	8	4	3.5	21.9	11.5	20.3	10.5	0.62	0.33	s2d2	4.18	0.0000609	0.0000756	0.0000931	0.3684
9700208M	5/22A	70E_4s2d2Zc_1	70	E	19	49770.7	92 1/2	80	0.613	0.920	HLP-22	12	8	4	3.5	21.9	11.5	20.3	10.5	0.62	0.33	s2d2	4.18	0.0000609	0.0000756	0.0000931	0.3684
9700208.1	5/27A	70E_4s2d2Zc_1	70	E	19	49770.7	92	80	0.613	0.920	HLP-22	12	8	4	3.5	21.9	11.5	20.3	10.5	0.62	0.33	s2d2	4.18	0.0000609	0.0000756	0.0000931	0.3684
9700208.2	5/27A	70E_4s2d2Zc_1	70	E	19	49770.7	92	80	0.613	0.920	HLP-22	12	8	4	3.5	21.9	11.5	20.3	10.5	0.62	0.33	s2d2	4.18	0.0000609	0.0000756	0.0000931	0.3684
9700209	5/27A	70E_4s2d2Zc_1	70	E	19	49770.7	92	80	0.613	0.920	HLP-22	12	8	4	3.5	21.9	11.5	20.3	10.5	0.62	0.33	s2d2	4.18	0.0000609	0.0000756	0.0000931	0.3684
9700210M	5/27A	70E_4s2d2Zc_1	70	E	19	49770.7	92	80	0.613	0.920	HLP-22	12	8	4	3.5	21.9	11.5	20.3	10.5	0.62	0.33	s2d2	4.18	0.0000609	0.0000756	0.0000931	0.3684
9700211	5/27A	70E_4s2d2Zc_1	70	E	19	49770.7	92	80	0.613	0.920	HLP-22	12	8	4	3.5	21.9	11.5	20.3	10.5	0.62	0.33	s2d2	4.18	0.0000609	0.0000756	0.0000931	0.3684
9700212	5/27A	70E_4s2d2Zc_1	70	E	19	49770.7	92	80	0.613	0.920	HLP-22	12	8	4	3.5	21.9	11.5	20.3	10.5	0.62	0.33	s2d2	4.18	0.0000609	0.0000756	0.0000931	0.3684
9700213	5/27A	70E_4s2d2Zc_1	70	E	19	49770.7	92	80	0.613	0.920	HLP-22	12	8	4	3.5	21.9	11.5	20.3	10.5	0.62	0.33	s2d2	4.18	0.0000609	0.0000756	0.0000931	0.3684
9700214	5/27A	70E_4s2d2Zc_1	70	E	19	49770.7	92	80	0.613	0.920	HLP-22	12	8	4	3.5	21.9	11.5	20.3	10.5	0.62	0.33	s2d2	4.18	0.0000609	0.0000756	0.0000931	0.3684
9700215	5/27A	70E_4s2d2Zc_1	70	E	19	49770.7	92	80	0.613	0.920	HLP-22	12	8	4	3.5	21.9	11.5	20.3	10.5	0.62	0.33	s2d2	4.18	0.0000609	0.0000756	0.0000931	0.3684
9700216	5/27A	70E_4s2d2Zc_1	70	E	19	49770.7	92	80	0.613	0.920	HLP-22	12	8	4	3.5	21.9	11.5	20.3	10.5	0.62	0.33	s2d2	4.18	0.0000609	0.0000756	0.0000931	0.3684
9700217	5/27A	70E_4s2d2Zc_1	70	E	19	49770.7	92	80	0.613	0.920	HLP-22	12	8	4	3.5	21.9	11.5	20.3	10.5	0.62	0.33	s2d2	4.18	0.0000609	0.0000756	0.0000931	0.3684
9700218	5/27A	70E_4s2d2Zc_1	70	E	19	49770.7	92	80	0.613	0.920	HLP-22	12	8	4	3.5	21.9	11.5	20.3	10.5	0.62	0.33	s2d2	4.18	0.0000609	0.0000756	0.0000931	0.3684
9700219	5/27A	70E_4s2d2Zc_1	70	E	19	49770.7	92	80	0.613	0.920	HLP-22	12	8	4	3.5	21.9	11.5	20.3	10.5	0.62	0.33	s2d2	4.18	0.0000609	0.0000756	0.0000931	0.3684
9700220	5/27B	70E_4s2d2Yd_1	70	E	19	49770.7	92	80	0.613	0.920	HLP-22	12	8	4	3.5	21.9	11.5	20.3	10.5	0.62	0.33	s2d2	4.18	0.0000609	0.0000756	0.0000931	0.3684
9700221	5/27B	70E_4s2d2Yd_1	70	E	19	49770.7	92	80	0.613	0.920	HLP-22	12	8	4	3.5	21.9	11.5	20.3	10.5	0.62	0.33	s2d2	4.18	0.0000609	0.0000756	0.0000931	0.3684
9700222	5/27B	70E_4s2d2Yd_1	70	E	19	49770.7	92	80	0.613	0.920	HLP-22	12	8	4	3.5	21.9	11.5	20.3	10.5	0.62	0.33	s2d2	4.18	0.0000609	0.0000756	0.0000931	0.3684
9700223	5/27B	70E_4s2d2Yd_1	70	E	19	49770.7	92	80	0.613	0.920	HLP-22	12	8	4	3.5	21.9	11.5	20.3	10.5	0.62	0.33	s2d2	4.18	0.0000609	0.0000756	0.0000931	0.3684
9700224M	5/27B	70E_4s2d2Yd_1	70	E	19	49770.7	92	80	0.613	0.920	HLP-22	12	8	4	3.5	21.9	11.5	20.3	10.5	0.62	0.33	s2d2	4.18	0.0000609	0.0000756	0.0000931	0.3684
9700225M	5/27B	70E_4s2d2Yd_1	70	E	19	49770.7	92	80	0.613	0.920	HLP-22	12	8	4	3.5	21.9	11.5	20.3	10.5	0.62	0.33	s2d2	4.18	0.0000609	0.0000756	0.0000931	0.3684
9700226M	5/27B	70E_4s2d2Yd_1	70	E	19	49770.7	92	80	0.613	0.920	HLP-22	12	8	4	3.5	21.9	11.5	20.3	10.5	0.62	0.33	s2d2	4.18	0.0000609	0.0000756	0.0000931	0.3684
9700227	5/27C	70E_4s2d2Yc_1	70	E	19	49770.7	92	80	0.613	0.920	HLP-22	12	8	4	3.5	21.9	11.5	20.3	10.5	0.62	0.33	s2d2	4.18	0.0000609	0.0000756	0.0000931	0.3684
9700228	5/27C	70E_4s2d2Yc_1	70	E	19	49770.7	92	80	0.613	0.920	HLP-22	12	8	4	3.5	21.9	11.5	20.3	10.5	0.62	0.33	s2d2	4.18	0.0000609	0.0000756	0.0000931	0.3684
9700229M	5/27C	70E_4s2d2Yc_1	70	E	19	49770.7	92	80	0.613	0.920	HLP-22	12	8	4	3.5	21.9	11.5	20.3	10.5	0.62	0.33	s2d2	4.18	0.0000609	0.0000756	0.0000931	0.3684
9700230M	5/27C	70E_4s2d2Yc_1	70	E	19	49770.7	92	80	0.613	0.920	HLP-22	12	8	4	3.5	21.9	11.5	20.3	10.5	0.62	0.33	s2d2	4.18	0.0000609	0.0000756	0.0000931	0.3684
9700230.1	5/28A	70E_4s2d2Yc_1	70	E	19	49770.7	92	80	0.613	0.920	HLP-22	12	8	4	3.5	21.9	11.5	20.3	10.5	0.62	0.33	s2d2	4.18	0.0000609	0.0000756	0.0000931	0.3684
9700230.2	5/28A	70E_4s2d2Yc_1	70	E	19	49770.7	92	80	0.613	0.920	HLP-22	12	8	4	3.5	21.9	11.5	20.3	10.5	0.62	0.33	s2d2	4.18	0.0000609	0.0000756	0.0000931	0.3684
9700230.3	5/28A	70E_4s2d2Yc_1	70	E	19	49770.7	92	80	0.613	0.920	HLP-22	12	8	4	3.5	21.9	11.5	20.3	10.5	0.62	0.33	s2d2	4.18	0.0000609	0.0000756	0.0000931	0.3684
9700231	5/28A	70E_4s2d2Yc_1	70	E	19	49770.7	92	80	0.613	0.920	HLP-22	12	8	4	3.5	21.9	11.5	20.3	10.5	0.62	0.33	s2d2	4.18	0.0000609	0.0000756	0.0000931	0.3684
9700232	5/28A	70E_4s2d2Yc_1	70	E	19	49770.7	92	80	0.613	0.920	HLP-22	12	8	4	3.5	21.9	11.5	20.3	10.5	0.62	0.33	s2d2	4.18	0.0000609	0.0000756	0.0000931	0.3684
9700233	5/28A	70E_4s2d2Yc_1	70	E	19	49770.7	92	80	0.613	0.920	HLP-22	12	8	4	3.5	21.9	11.5	20.3	10.5	0.62	0.33	s2d2	4.18	0.0000609	0.0000756	0.0000931	0.3684
9700234	5/28A	70E_4s2d2Yc_1	70	E	19	49770.7	92	80	0.613	0.920	HLP-22	12	8	4	3.5	21.9	11.5	20.3	10.5	0.62	0.33	s2d2	4.18	0.0000609	0.0000756	0.0000931	0.3684
9700235	5/28A	70E_4s2d2Yc_1	70	E	19	49770.7	92	80	0.613	0.920	HLP-22	12	8	4	3.5	21.9	11.5	20.3	10.5	0.62	0.33	s2d2	4.18	0.0000609	0.0000756	0.0000931	0.3684

Table B.5. Data from 2008 Tests in Large-Scale Vessel with Elliptical Head B.7

Tank Water Temperature	Water Density	Solids Fraction	Pulse Volume Fraction	Duty Cycle	Cycle Time	Pulsed or Steady Jet	Us Steady Jet	U1 Pulsing Jet	U2 URMS	U3 URM3	Discharge Velocity	Critical Suspension Velocity	Average Peak Cloud Height	UCS Condition	UCS Method	UCS Flag	UCS Center Flag	UCS udv Flag	UCS based on Decreasing Velocity	Sweep Increase / Decrease	UDV Height Bed	Particle Motion	Solids Level	Outer Bottom Pattern	Inner Bottom Pattern	Case ID	Test	TDP	Row Number
C	g/cm³	fraction	fraction	fraction	s	text	m/s	m/s	m/s	m/s	m/s	m/s	in.	m/s	text	text	text	text	m/s	text	mm	text	text	text	text	text	text	text	text
T	ρ_c	ϕ_S	ϕ_p	DC	t_C	Jet	U_S	U1	U2	U3	U	U_{CS}	H_C	U_{CSR}	U_{CSM}	U_{CS}vis	U_{CS}cen	U_{CS}udv	U_{CS}_D	S_W	H_{bed}	PM	Sol	SP_O	SP_I	ID	M/DDX	TDP	MSS
24.5	0.995	0.00155	0.050	0.336	46.0	P	N/A	6.19	6.28	6.33	6.50	8.40	22.50	N/A	N/A	N/A	N/A	N/A	N/A	I	34.1	1	N/A	N/A	N/A	70E_4s2d2Zc_1	5/22A	TDP-162	9700200
24.6	0.994	0.00155	0.050	0.338	42.6	P	N/A	6.64	6.75	6.81	7.00	8.40	24.25	N/A	N/A	N/A	N/A	N/A	N/A	I	23.7	1	N/A	N/A	N/A	70E_4s2d2Zc_1	5/22A	TDP-162	9700201
24.8	0.994	0.00155	0.050	0.335	39.8	P	N/A	7.09	7.21	7.28	7.50	8.40	24.75	N/A	N/A	N/A	N/A	N/A	N/A	I	16.6	1	N/A	N/A	N/A	70E_4s2d2Zc_1	5/22A	TDP-162	9700202
24.5	0.994	0.00155	0.050	0.335	38.8	P	N/A	7.29	7.41	7.48	7.70	8.40	26.00	N/A	N/A	N/A	N/A	N/A	N/A	I	11.5	1	N/A	N/A	N/A	70E_4s2d2Zc_1	5/22A	TDP-162	9700203
24.8	0.994	0.00155	0.051	0.337	37.4	P	N/A	7.63	7.77	7.84	8.00	8.40	27.25	N/A	N/A	N/A	N/A	N/A	N/A	I	7.3	1	N/A	N/A	N/A	70E_4s2d2Zc_1	5/22A	TDP-162	9700204
24.8	0.994	0.00155	0.050	0.338	36.4	P	N/A	7.79	7.93	8.00	8.20	8.40	27.00	N/A	N/A	N/A	N/A	N/A	N/A	I	2.1	1	N/A	N/A	N/A	70E_4s2d2Zc_1	5/22A	TDP-162	9700205
24.8	0.994	0.00155	0.050	0.339	35.4	P	N/A	7.94	8.09	8.17	8.40	8.40	28.50	8.40	udv	N/A	UCScen	UCSudv	N/A	I	0.0	2	N/A	N/A	N/A	70E_4s2d2Zc_1	5/22A	TDP-162	9700206
24.9	0.994	0.00155	0.050	0.340	34.6	P	N/A	8.12	8.27	8.35	8.60	8.40	29.00	N/A	N/A	N/A	N/A	N/A	N/A	I	0.0	4	N/A	N/A	N/A	70E_4s2d2Zc_1	5/22A	TDP-162	9700207
24.6	0.994	0.00155	0.049	0.331	33.2	P	N/A	8.55	8.72	8.81	9.10	8.40	38.25	N/A	N/A	N/A	N/A	N/A	N/A	D	0.0	4	N/A	N/A	N/A	70E_4s2d2Zc_1	5/22A	TDP-162	9700208
21.8	0.995	0.00155	0.050	0.339	35.6	P	N/A	7.95	8.10	8.17	8.40	8.40	28.50	N/A	N/A	N/A	N/A	N/A	N/A	N/A	n/a	N/A	N/A	N/A	N/A	70E_4s2d2Zc_1	5/27A	TDP-163	9700208.1
21.8	0.995	0.00155	0.050	0.339	35.6	P	N/A	7.95	8.10	8.17	8.40	8.40	28.50	N/A	N/A	N/A	N/A	N/A	N/A	N/A	n/a	N/A	N/A	N/A	N/A	70E_4s2d2Zc_1	5/27A	TDP-163	9700208.2
22.0	0.995	0.00155	0.050	0.338	36.4	P	N/A	7.76	7.90	7.97	8.20	8.40	27.50	N/A	N/A	N/A	UCScen	N/A	N/A	(null)	0.0	2	N/A	N/A	N/A	70E_4s2d2Zc_1	5/27A	TDP-163	9700209
21.8	0.995	0.00155	0.050	0.339	35.6	P	N/A	7.95	8.10	8.17	8.40	8.40	28.50	N/A	N/A	N/A	N/A	N/A	N/A	I	0.0	4	N/A	N/A	N/A	70E_4s2d2Zc_1	5/27A	TDP-163	9700210
21.8	0.995	0.00155	0.050	0.339	35.6	P	N/A	7.95	8.10	8.17	8.40	8.40	28.50	N/A	N/A	N/A	N/A	N/A	N/A	N/A	0.0	N/A	N/A	N/A	N/A	70E_4s2d2Zc_1	5/27A	TDP-163	9700211
21.8	0.995	0.00155	0.050	0.339	35.6	P	N/A	7.95	8.10	8.17	8.40	8.40	28.50	N/A	N/A	N/A	N/A	N/A	N/A	N/A	3.7	N/A	N/A	N/A	N/A	70E_4s2d2Zc_1	5/27A	TDP-163	9700212
21.8	0.995	0.00155	0.050	0.339	35.6	P	N/A	7.95	8.10	8.17	8.40	8.40	28.50	N/A	N/A	N/A	N/A	N/A	N/A	N/A	0.0	N/A	N/A	N/A	N/A	70E_4s2d2Zc_1	5/27A	TDP-163	9700213
21.8	0.995	0.00155	0.050	0.339	35.6	P	N/A	7.95	8.10	8.17	8.40	8.40	28.50	N/A	N/A	N/A	N/A	N/A	N/A	N/A	0.0	N/A	N/A	N/A	N/A	70E_4s2d2Zc_1	5/27A	TDP-163	9700214
21.8	0.995	0.00155	0.050	0.339	35.6	P	N/A	7.95	8.10	8.17	8.40	8.40	28.50	N/A	N/A	N/A	N/A	N/A	N/A	N/A	0.0	N/A	N/A	N/A	N/A	70E_4s2d2Zc_1	5/27A	TDP-163	9700215
21.8	0.995	0.00155	0.050	0.339	35.6	P	N/A	7.95	8.10	8.17	8.40	8.40	28.50	N/A	N/A	N/A	N/A	N/A	N/A	N/A	1.0	N/A	N/A	N/A	N/A	70E_4s2d2Zc_1	5/27A	TDP-163	9700216
21.8	0.995	0.00155	0.050	0.339	35.6	P	N/A	7.95	8.10	8.17	8.40	8.40	28.50	N/A	N/A	N/A	N/A	N/A	N/A	N/A	0.0	N/A	N/A	N/A	N/A	70E_4s2d2Zc_1	5/27A	TDP-163	9700217
21.8	0.995	0.00155	0.050	0.339	35.6	P	N/A	7.95	8.10	8.17	8.40	8.40	28.50	N/A	N/A	N/A	N/A	N/A	N/A	N/A	0.0	N/A	N/A	N/A	N/A	70E_4s2d2Zc_1	5/27A	TDP-163	9700218
21.8	0.995	0.00155	0.050	0.339	35.6	P	N/A	7.95	8.10	8.17	8.40	8.40	28.50	N/A	N/A	N/A	N/A	N/A	N/A	N/A	0.0	N/A	N/A	N/A	N/A	70E_4s2d2Zc_1	5/27A	TDP-163	9700219
23.8	0.994	0.00500	0.050	0.184	47.2	P	N/A	10.97	11.27	11.42	11.90	14.00	22.00	N/A	N/A	N/A	N/A	N/A	N/A	I	24.0	1	N/A	N/A	N/A	70E_4s2d2Yd_1	5/27B	TDP-163	9700220
23.7	0.995	0.00500	0.050	0.186	45.0	P	N/A	11.38	11.71	11.87	12.40	14.00	22.50	N/A	N/A	N/A	N/A	N/A	N/A	I	17.0	1	N/A	N/A	N/A	70E_4s2d2Yd_1	5/27B	TDP-163	9700221
24.3	0.995	0.00500	0.050	0.187	43.0	P	N/A	11.82	12.17	12.34	12.90	14.00	23.50	N/A	N/A	N/A	N/A	N/A	N/A	I	13.1	1	N/A	N/A	N/A	70E_4s2d2Yd_1	5/27B	TDP-163	9700222
24.2	0.995	0.00500	0.050	0.184	41.2	P	N/A	12.49	12.88	13.08	13.70	14.00	25.50	N/A	N/A	N/A	UCScen	N/A	N/A	I	1.8	2	N/A	N/A	N/A	70E_4s2d2Yd_1	5/27B	TDP-163	9700223
24.4	0.994	0.00500	0.050	0.184	40.4	P	N/A	12.76	13.16	13.37	14.00	14.00	26.25	14.00	udv	N/A	N/A	UCSudv	N/A	I	0.9	4	N/A	N/A	N/A	70E_4s2d2Yd_1	5/27B	TDP-163	9700224
24.4	0.995	0.00500	0.049	0.186	37.2	P	N/A	13.57	14.03	14.26	15.00	14.00	26.00	N/A	N/A	N/A	N/A	N/A	N/A	I	N/A	4	N/A	N/A	N/A	70E_4s2d2Yd_1	5/27B	TDP-163	9700225
24.5	0.995	0.00500	0.050	0.188	34.6	P	N/A	14.68	15.13	15.36	16.10	14.00	28.50	N/A	N/A	N/A	N/A	N/A	N/A	I	0.0	4	N/A	N/A	N/A	70E_4s2d2Yd_1	5/27B	TDP-163	9700226
24.9	0.994	0.00500	0.050	0.336	26.2	P	N/A	10.74	10.97	11.09	11.50	12.50	22.50	N/A	N/A	N/A	N/A	N/A	N/A	I	10.3	1	N/A	N/A	N/A	70E_4s2d2Yc_1	5/27C	TDP-163	9700227
25.1	0.995	0.00500	0.050	0.340	25.0	P	N/A	11.13	11.40	11.54	12.00	12.50	25.50	N/A	N/A	N/A	UCScen	N/A	N/A	I	3.2	2	N/A	N/A	N/A	70E_4s2d2Yc_1	5/27C	TDP-163	9700228
25.2	0.994	0.00500	0.050	0.336	24.4	P	N/A	11.56	11.86	12.01	12.50	12.50	25.50	12.50	udv	N/A	N/A	UCSudv	N/A	I	0.0	4	N/A	N/A	N/A	70E_4s2d2Yc_1	5/27C	TDP-163	9700229
25.4	0.995	0.00500	0.050	0.333	22.6	P	N/A	12.59	12.94	13.12	13.70	12.50	34.50	N/A	N/A	N/A	N/A	N/A	N/A	I	0.3	4	N/A	N/A	N/A	70E_4s2d2Yc_1	5/27C	TDP-163	9700230
23.5	0.994	0.00500	0.050	0.328	26.0	P	N/A	11.16	11.43	11.57	12.00	12.50	25.50	N/A	N/A	N/A	N/A	N/A	N/A	N/A	n/a	N/A	N/A	N/A	N/A	70E_4s2d2Yc_1	5/28A	TDP-164	9700230.1
23.5	0.994	0.00500	0.050	0.328	26.0	P	N/A	11.16	11.43	11.57	12.00	12.50	25.50	N/A	N/A	N/A	N/A	N/A	N/A	N/A	n/a	N/A	N/A	N/A	N/A	70E_4s2d2Yc_1	5/28A	TDP-164	9700230.2
23.5	0.994	0.00500	0.050	0.328	26.0	P	N/A	11.16	11.43	11.57	12.00	12.50	25.50	N/A	N/A	N/A	N/A	N/A	N/A	N/A	n/a	N/A	N/A	N/A	N/A	70E_4s2d2Yc_1	5/28A	TDP-164	9700230.3
23.5	0.994	0.00500	0.050	0.328	26.0	P	N/A	11.16	11.43	11.57	12.00	12.50	25.50	N/A	N/A	N/A	UCScen	N/A	N/A	(null)	0.0	2	N/A	N/A	N/A	70E_4s2d2Yc_1	5/28A	TDP-164	9700231
23.5	0.994	0.00500	0.050	0.328	26.0	P	N/A	11.16	11.43	11.57	12.00	12.50	25.50	N/A	N/A	N/A	N/A	N/A	N/A	N/A	0.0	N/A	N/A	N/A	N/A	70E_4s2d2Yc_1	5/28A	TDP-164	9700232
23.5	0.994	0.00500	0.050	0.328	26.0	P	N/A	11.16	11.43	11.57	12.00	12.50	25.50	N/A	N/A	N/A	N/A	N/A	N/A	N/A	0.0	N/A	N/A	N/A	N/A	70E_4s2d2Yc_1	5/28A	TDP-164	9700233
23.5	0.994	0.00500	0.050	0.328	26.0	P	N/A	11.16	11.43	11.57	12.00	12.50	25.50	N/A	N/A	N/A	N/A	N/A	N/A	N/A	0.0	N/A	N/A	N/A	N/A	70E_4s2d2Yc_1	5/28A	TDP-164	9700234
23.5	0.994	0.00500	0.050	0.328	26.0	P	N/A	11.16	11.43	11.57	12.00	12.50	25.50	N/A	N/A	N/A	N/A	N/A	N/A	N/A	0.0	N/A	N/A	N/A	N/A	70E_4s2d2Yc_1	5/28A	TDP-164	9700235

Table B.5. Data from 2008 Tests in Large-Scale Vessel with Elliptical Head A.8

Row Number	Test	Case ID	Tank Diameter	Head Shape	Dish Height	Dish Volume	Tank Fill Height	Return Line Height	Nozzle Inner Diameter	Nozzle Stand-off Distance	Pulse Tube Configuration	Installed Nozzles	Outer Nozzles Operated	Inner Nozzles Operated	Pulse Tube Outer Diameter	Outer PJM Radius	Inner PJM Radius	"FIO" Outer PJM Impingement Angle	"FIO" Inner PJM Impingement Angle	Ratio Outer PJM to Tank Radius	Ratio Inner PJM to Tank Radius	Simulant	Solids Density	Particle Diameter d5	Particle Diameter d50	Particle Diameter d95	Void Fraction
text	text	text	in.	text	in.	in. ^{3}	in.	in.	in.	in.	text	number	number	number	in.	in.	in.	deg	deg	nondim	nondim	text	g/cm^3	m	m	m	fraction
MSS	M/DDX	ID	D	HS	H_{dish}	V_{dish}	H	Rtn	d	sod	PT	N	N_O	N_I	PT_{od}	R_O	R_I	θ_O	θ_I	R_O/R	R_I/R	sxdx	ρ_s	d_5	d_{50}	d_{95}	vf
9700236	5/28A	70E_4s2d2Yc_1	70	E	19	49770.7	92	80	0.613	0.920	HLP-22	12	8	4	3.5	21.9	11.5	20.3	10.5	0.62	0.33	s2d2	4.18	0.0000609	0.0000756	0.0000931	0.3684
9700237	5/28A	70E_4s2d2Yc_1	70	E	19	49770.7	92	80	0.613	0.920	HLP-22	12	8	4	3.5	21.9	11.5	20.3	10.5	0.62	0.33	s2d2	4.18	0.0000609	0.0000756	0.0000931	0.3684
9700238	5/28A	70E_4s2d2Yc_1	70	E	19	49770.7	92	80	0.613	0.920	HLP-22	12	8	4	3.5	21.9	11.5	20.3	10.5	0.62	0.33	s2d2	4.18	0.0000609	0.0000756	0.0000931	0.3684
9700239	5/28A	70E_4s2d2Yc_1	70	E	19	49770.7	92	80	0.613	0.920	HLP-22	12	8	4	3.5	21.9	11.5	20.3	10.5	0.62	0.33	s2d2	4.18	0.0000609	0.0000756	0.0000931	0.3684
9700239.1	5/28A	70E_4s2d2Yc_1	70	E	19	49770.7	92	80	0.613	0.920	HLP-22	12	8	4	3.5	21.9	11.5	20.3	10.5	0.62	0.33	s2d2	4.18	0.0000609	0.0000756	0.0000931	0.3684
9700239.2	5/28A	70E_4s2d2Yc_1	70	E	19	49770.7	92	80	0.613	0.920	HLP-22	12	8	4	3.5	21.9	11.5	20.3	10.5	0.62	0.33	s2d2	4.18	0.0000609	0.0000756	0.0000931	0.3684
9700239.3	5/28A	70E_4s2d2Yc_1	70	E	19	49770.7	92	80	0.613	0.920	HLP-22	12	8	4	3.5	21.9	11.5	20.3	10.5	0.62	0.33	s2d2	4.18	0.0000609	0.0000756	0.0000931	0.3684
9700240	5/28A	70E_4s2d2Yc_1	70	E	19	49770.7	92	80	0.613	0.920	HLP-22	12	8	4	3.5	21.9	11.5	20.3	10.5	0.62	0.33	s2d2	4.18	0.0000609	0.0000756	0.0000931	0.3684
9700241	5/28A	70E_4s2d2Yc_1	70	E	19	49770.7	92	80	0.613	0.920	HLP-22	12	8	4	3.5	21.9	11.5	20.3	10.5	0.62	0.33	s2d2	4.18	0.0000609	0.0000756	0.0000931	0.3684
9700242	5/28A	70E_4s2d2Yc_1	70	E	19	49770.7	92	80	0.613	0.920	HLP-22	12	8	4	3.5	21.9	11.5	20.3	10.5	0.62	0.33	s2d2	4.18	0.0000609	0.0000756	0.0000931	0.3684
9700243	5/28A	70E_4s2d2Yc_1	70	E	19	49770.7	92	80	0.613	0.920	HLP-22	12	8	4	3.5	21.9	11.5	20.3	10.5	0.62	0.33	s2d2	4.18	0.0000609	0.0000756	0.0000931	0.3684
9700244	5/28A	70E_4s2d2Yc_1	70	E	19	49770.7	92	80	0.613	0.920	HLP-22	12	8	4	3.5	21.9	11.5	20.3	10.5	0.62	0.33	s2d2	4.18	0.0000609	0.0000756	0.0000931	0.3684
9700245	5/28A	70E_4s2d2Yc_1	70	E	19	49770.7	92	80	0.613	0.920	HLP-22	12	8	4	3.5	21.9	11.5	20.3	10.5	0.62	0.33	s2d2	4.18	0.0000609	0.0000756	0.0000931	0.3684
9700246	5/28A	70E_4s2d2Yc_1	70	E	19	49770.7	92	80	0.613	0.920	HLP-22	12	8	4	3.5	21.9	11.5	20.3	10.5	0.62	0.33	s2d2	4.18	0.0000609	0.0000756	0.0000931	0.3684
9700247	5/28A	70E_4s2d2Yc_1	70	E	19	49770.7	92	80	0.613	0.920	HLP-22	12	8	4	3.5	21.9	11.5	20.3	10.5	0.62	0.33	s2d2	4.18	0.0000609	0.0000756	0.0000931	0.3684
9700247.1	5/28A	70E_4s2d2Yc_1	70	E	19	49770.7	92	80	0.613	0.920	HLP-22	12	8	4	3.5	21.9	11.5	20.3	10.5	0.62	0.33	s2d2	4.18	0.0000609	0.0000756	0.0000931	0.3684
9700247.2	5/28A	70E_4s2d2Yc_1	70	E	19	49770.7	92	80	0.613	0.920	HLP-22	12	8	4	3.5	21.9	11.5	20.3	10.5	0.62	0.33	s2d2	4.18	0.0000609	0.0000756	0.0000931	0.3684
9700247.3	5/28A	70E_4s2d2Yc_1	70	E	19	49770.7	92	80	0.613	0.920	HLP-22	12	8	4	3.5	21.9	11.5	20.3	10.5	0.62	0.33	s2d2	4.18	0.0000609	0.0000756	0.0000931	0.3684
9700247.4	5/28A	70E_4s2d2Yc_1	70	E	19	49770.7	92	80	0.613	0.920	HLP-22	12	8	4	3.5	21.9	11.5	20.3	10.5	0.62	0.33	s2d2	4.18	0.0000609	0.0000756	0.0000931	0.3684
9700248	5/28A	70E_4s2d2Yc_1	70	E	19	49770.7	92	80	0.613	0.920	HLP-22	12	8	4	3.5	21.9	11.5	20.3	10.5	0.62	0.33	s2d2	4.18	0.0000609	0.0000756	0.0000931	0.3684
9700249	5/28A	70E_4s2d2Yc_1	70	E	19	49770.7	92	80	0.613	0.920	HLP-22	12	8	4	3.5	21.9	11.5	20.3	10.5	0.62	0.33	s2d2	4.18	0.0000609	0.0000756	0.0000931	0.3684
9700250	5/28A	70E_4s2d2Yc_1	70	E	19	49770.7	92	80	0.613	0.920	HLP-22	12	8	4	3.5	21.9	11.5	20.3	10.5	0.62	0.33	s2d2	4.18	0.0000609	0.0000756	0.0000931	0.3684
9700251	5/28A	70E_4s2d2Yc_1	70	E	19	49770.7	92	80	0.613	0.920	HLP-22	12	8	4	3.5	21.9	11.5	20.3	10.5	0.62	0.33	s2d2	4.18	0.0000609	0.0000756	0.0000931	0.3684
9700252	5/28A	70E_4s2d2Yc_1	70	E	19	49770.7	92	80	0.613	0.920	HLP-22	12	8	4	3.5	21.9	11.5	20.3	10.5	0.62	0.33	s2d2	4.18	0.0000609	0.0000756	0.0000931	0.3684
9700253	5/28A	70E_4s2d2Yc_1	70	E	19	49770.7	92	80	0.613	0.920	HLP-22	12	8	4	3.5	21.9	11.5	20.3	10.5	0.62	0.33	s2d2	4.18	0.0000609	0.0000756	0.0000931	0.3684
9700254	5/28A	70E_4s2d2Yc_1	70	E	19	49770.7	92	80	0.613	0.920	HLP-22	12	8	4	3.5	21.9	11.5	20.3	10.5	0.62	0.33	s2d2	4.18	0.0000609	0.0000756	0.0000931	0.3684
9700254.1	5/28A	70E_4s2d2Yc_1	70	E	19	49770.7	92	80	0.613	0.920	HLP-22	12	8	4	3.5	21.9	11.5	20.3	10.5	0.62	0.33	s2d2	4.18	0.0000609	0.0000756	0.0000931	0.3684
9700254.2	5/28A	70E_4s2d2Yc_1	70	E	19	49770.7	92	80	0.613	0.920	HLP-22	12	8	4	3.5	21.9	11.5	20.3	10.5	0.62	0.33	s2d2	4.18	0.0000609	0.0000756	0.0000931	0.3684
9700255	5/29A	70E_4s1d1Zd_1	70	E	19	49770.7	92	80	0.613	0.920	HLP-22	12	8	4	3.5	21.9	11.5	20.3	10.5	0.62	0.33	s1d1	2.46	0.0001428	0.0001664	0.0001951	0.4118
9700256	5/29A	70E_4s1d1Zd_1	70	E	19	49770.7	92	80	0.613	0.920	HLP-22	12	8	4	3.5	21.9	11.5	20.3	10.5	0.62	0.33	s1d1	2.46	0.0001428	0.0001664	0.0001951	0.4118
9700257	5/29A	70E_4s1d1Zd_1	70	E	19	49770.7	92	80	0.613	0.920	HLP-22	12	8	4	3.5	21.9	11.5	20.3	10.5	0.62	0.33	s1d1	2.46	0.0001428	0.0001664	0.0001951	0.4118
9700258	5/29A	70E_4s1d1Zd_1	70	E	19	49770.7	92	80	0.613	0.920	HLP-22	12	8	4	3.5	21.9	11.5	20.3	10.5	0.62	0.33	s1d1	2.46	0.0001428	0.0001664	0.0001951	0.4118
9700259M	5/29A	70E_4s1d1Zd_1	70	E	19	49770.7	92	80	0.613	0.920	HLP-22	12	8	4	3.5	21.9	11.5	20.3	10.5	0.62	0.33	s1d1	2.46	0.0001428	0.0001664	0.0001951	0.4118
9700260M	5/29A	70E_4s1d1Zd_1	70	E	19	49770.7	92	80	0.613	0.920	HLP-22	12	8	4	3.5	21.9	11.5	20.3	10.5	0.62	0.33	s1d1	2.46	0.0001428	0.0001664	0.0001951	0.4118
9700261M	5/29A	70E_4s1d1Zd_1	70	E	19	49770.7	92	80	0.613	0.920	HLP-22	12	8	4	3.5	21.9	11.5	20.3	10.5	0.62	0.33	s1d1	2.46	0.0001428	0.0001664	0.0001951	0.4118
9700262	5/29B	70E_4s1d1Zc_1	70	E	19	49770.7	92	80	0.613	0.920	HLP-22	12	8	4	3.5	21.9	11.5	20.3	10.5	0.62	0.33	s1d1	2.46	0.0001428	0.0001664	0.0001951	0.4118
9700263	5/29B	70E_4s1d1Zc_1	70	E	19	49770.7	92	80	0.613	0.920	HLP-22	12	8	4	3.5	21.9	11.5	20.3	10.5	0.62	0.33	s1d1	2.46	0.0001428	0.0001664	0.0001951	0.4118
9700264M	5/29B	70E_4s1d1Zc_1	70	E	19	49770.7	92	80	0.613	0.920	HLP-22	12	8	4	3.5	21.9	11.5	20.3	10.5	0.62	0.33	s1d1	2.46	0.0001428	0.0001664	0.0001951	0.4118
9700265M	5/29B	70E_4s1d1Zc_1	70	E	19	49770.7	92	80	0.613	0.920	HLP-22	12	8	4	3.5	21.9	11.5	20.3	10.5	0.62	0.33	s1d1	2.46	0.0001428	0.0001664	0.0001951	0.4118
9700266M	5/29B	70E_4s1d1Zc_1	70	E	19	49770.7	92	80	0.613	0.920	HLP-22	12	8	4	3.5	21.9	11.5	20.3	10.5	0.62	0.33	s1d1	2.46	0.0001428	0.0001664	0.0001951	0.4118
9700267M	5/29B	70E_4s1d1Zc_1	70	E	19	49770.7	92	80	0.613	0.920	HLP-22	12	8	4	3.5	21.9	11.5	20.3	10.5	0.62	0.33	s1d1	2.46	0.0001428	0.0001664	0.0001951	0.4118

Table B.5. Data from 2008 Tests in Large-Scale Vessel with Elliptical Head B.8

Tank Water Temperature	Water Density	Solids Fraction	Pulse Volume Fraction	Duty Cycle	Cycle Time	Pulsed or Steady Jet	Us Steady Jet	U1 Pulsing Jet	U2 URMS	U3 URM3	Discharge Velocity	Critical Suspension Velocity	Average Peak Cloud Height	UCS Condition	UCS Method	UCS Flag	UCS Center Flag	UCS udv Flag	UCS based on Decreasing Velocity	Sweep Increase / Decrease	UDV Height Bed	Particle Motion	Solids Level	Outer Bottom Pattern	Inner Bottom Pattern	Case ID	Test	TDP	Row Number
C	g/cm³	fraction	fraction	fraction	s	text	m/s	m/s	m/s	m/s	m/s	m/s	in.	m/s	text	text	text	text	m/s	text	mm	text	text	text	text	text	text	text	text
T	ρ_c	ϕ_S	ϕ_p	DC	t_C	Jet	U_S	U1	U2	U3	U	U_{CS}	H_C	U_{CSR}	U_{CSM}	U_{CS}vis	U_{CS}cen	U_{CS}udv	$U_{CS_}D$	S_W	H_{bed}	PM	Sol	SP_O	SP_I	ID	M/DDX	TDP	MSS
23.5	0.994	0.00500	0.050	0.328	26.0	P	N/A	11.16	11.43	11.57	12.00	12.50	25.50	N/A	N/A	N/A	N/A	N/A	N/A	N/A	0.0	N/A	N/A	N/A	N/A	70E_4s2d2Yc_1	5/28A	TDP-164	9700236
23.5	0.994	0.00500	0.050	0.328	26.0	P	N/A	11.16	11.43	11.57	12.00	12.50	25.50	N/A	N/A	N/A	N/A	N/A	N/A	N/A	0.0	N/A	N/A	N/A	N/A	70E_4s2d2Yc_1	5/28A	TDP-164	9700237
23.5	0.994	0.00500	0.050	0.328	26.0	P	N/A	11.16	11.43	11.57	12.00	12.50	25.50	N/A	N/A	N/A	N/A	N/A	N/A	N/A	0.0	N/A	N/A	N/A	N/A	70E_4s2d2Yc_1	5/28A	TDP-164	9700238
23.5	0.994	0.00500	0.050	0.328	26.0	P	N/A	11.16	11.43	11.57	12.00	12.50	25.50	N/A	N/A	N/A	N/A	N/A	N/A	N/A	0.0	N/A	N/A	N/A	N/A	70E_4s2d2Yc_1	5/28A	TDP-164	9700239
23.8	0.994	0.00500	0.050	0.328	26.0	P	N/A	11.16	11.43	11.56	12.00	12.50	25.50	N/A	N/A	N/A	N/A	N/A	N/A	N/A	n/a	N/A	N/A	N/A	N/A	70E_4s2d2Yc_1	5/28A	TDP-164	9700239.1
23.8	0.994	0.00500	0.050	0.328	26.0	P	N/A	11.16	11.43	11.56	12.00	12.50	25.50	N/A	N/A	N/A	N/A	N/A	N/A	N/A	n/a	N/A	N/A	N/A	N/A	70E_4s2d2Yc_1	5/28A	TDP-164	9700239.2
23.8	0.994	0.00500	0.050	0.328	26.0	P	N/A	11.16	11.43	11.56	12.00	12.50	25.50	N/A	N/A	N/A	N/A	N/A	N/A	N/A	n/a	N/A	N/A	N/A	N/A	70E_4s2d2Yc_1	5/28A	TDP-164	9700239.3
23.8	0.994	0.00500	0.050	0.328	26.0	P	N/A	11.16	11.43	11.56	12.00	12.50	25.50	N/A	N/A	N/A	UCScen	N/A	N/A	(null)	0.0	2	N/A	N/A	N/A	70E_4s2d2Yc_1	5/28A	TDP-164	9700240
23.8	0.994	0.00500	0.050	0.328	26.0	P	N/A	11.16	11.43	11.56	12.00	12.50	25.50	N/A	N/A	N/A	N/A	N/A	N/A	N/A	0.0	N/A	N/A	N/A	N/A	70E_4s2d2Yc_1	5/28A	TDP-164	9700241
23.8	0.994	0.00500	0.050	0.328	26.0	P	N/A	11.16	11.43	11.56	12.00	12.50	25.50	N/A	N/A	N/A	N/A	N/A	N/A	N/A	0.0	N/A	N/A	N/A	N/A	70E_4s2d2Yc_1	5/28A	TDP-164	9700242
23.8	0.994	0.00500	0.050	0.328	26.0	P	N/A	11.16	11.43	11.56	12.00	12.50	25.50	N/A	N/A	N/A	N/A	N/A	N/A	N/A	0.0	N/A	N/A	N/A	N/A	70E_4s2d2Yc_1	5/28A	TDP-164	9700243
23.8	0.994	0.00500	0.050	0.328	26.0	P	N/A	11.16	11.43	11.56	12.00	12.50	25.50	N/A	N/A	N/A	N/A	N/A	N/A	N/A	0.0	N/A	N/A	N/A	N/A	70E_4s2d2Yc_1	5/28A	TDP-164	9700244
23.8	0.994	0.00500	0.050	0.328	26.0	P	N/A	11.16	11.43	11.56	12.00	12.50	25.50	N/A	N/A	N/A	N/A	N/A	N/A	N/A	0.0	N/A	N/A	N/A	N/A	70E_4s2d2Yc_1	5/28A	TDP-164	9700245
23.8	0.994	0.00500	0.050	0.328	26.0	P	N/A	11.16	11.43	11.56	12.00	12.50	25.50	N/A	N/A	N/A	N/A	N/A	N/A	N/A	0.0	N/A	N/A	N/A	N/A	70E_4s2d2Yc_1	5/28A	TDP-164	9700246
23.8	0.994	0.00500	0.050	0.328	26.0	P	N/A	11.16	11.43	11.56	12.00	12.50	25.50	N/A	N/A	N/A	N/A	N/A	N/A	N/A	0.0	N/A	N/A	N/A	N/A	70E_4s2d2Yc_1	5/28A	TDP-164	9700247
23.8	0.994	0.00500	0.050	0.328	26.0	P	N/A	11.16	11.43	11.56	12.00	12.50	25.50	N/A	N/A	N/A	N/A	N/A	N/A	N/A	n/a	N/A	N/A	N/A	N/A	70E_4s2d2Yc_1	5/28A	TDP-164	9700247.1
23.9	0.994	0.00500	0.050	0.328	26.0	P	N/A	11.15	11.42	11.56	12.00	12.50	25.50	N/A	N/A	N/A	N/A	N/A	N/A	N/A	n/a	N/A	N/A	N/A	N/A	70E_4s2d2Yc_1	5/28A	TDP-164	9700247.2
23.9	0.994	0.00500	0.050	0.328	26.0	P	N/A	11.15	11.42	11.56	12.00	12.50	25.50	N/A	N/A	N/A	N/A	N/A	N/A	N/A	n/a	N/A	N/A	N/A	N/A	70E_4s2d2Yc_1	5/28A	TDP-164	9700247.3
23.9	0.994	0.00500	0.050	0.328	26.0	P	N/A	11.15	11.42	11.56	12.00	12.50	25.50	N/A	N/A	N/A	N/A	N/A	N/A	N/A	n/a	N/A	N/A	N/A	N/A	70E_4s2d2Yc_1	5/28A	TDP-164	9700247.4
23.9	0.994	0.00500	0.050	0.328	26.0	P	N/A	11.15	11.42	11.56	12.00	12.50	25.50	N/A	N/A	N/A	UCScen	N/A	N/A	(null)	0.0	2	N/A	N/A	N/A	70E_4s2d2Yc_1	5/28A	TDP-164	9700248
23.9	0.994	0.00500	0.050	0.328	26.0	P	N/A	11.15	11.42	11.56	12.00	12.50	25.50	N/A	N/A	N/A	N/A	N/A	N/A	N/A	0.0	N/A	N/A	N/A	N/A	70E_4s2d2Yc_1	5/28A	TDP-164	9700249
23.9	0.994	0.00500	0.050	0.328	26.0	P	N/A	11.15	11.42	11.56	12.00	12.50	25.50	N/A	N/A	N/A	N/A	N/A	N/A	N/A	0.0	N/A	N/A	N/A	N/A	70E_4s2d2Yc_1	5/28A	TDP-164	9700250
23.9	0.994	0.00500	0.050	0.328	26.0	P	N/A	11.15	11.42	11.56	12.00	12.50	25.50	N/A	N/A	N/A	N/A	N/A	N/A	N/A	0.0	N/A	N/A	N/A	N/A	70E_4s2d2Yc_1	5/28A	TDP-164	9700251
23.9	0.994	0.00500	0.050	0.328	26.0	P	N/A	11.15	11.42	11.56	12.00	12.50	25.50	N/A	N/A	N/A	N/A	N/A	N/A	N/A	0.0	N/A	N/A	N/A	N/A	70E_4s2d2Yc_1	5/28A	TDP-164	9700252
23.9	0.994	0.00500	0.050	0.328	26.0	P	N/A	11.15	11.42	11.56	12.00	12.50	25.50	N/A	N/A	N/A	N/A	N/A	N/A	N/A	0.0	N/A	N/A	N/A	N/A	70E_4s2d2Yc_1	5/28A	TDP-164	9700253
23.9	0.994	0.00500	0.050	0.328	26.0	P	N/A	11.15	11.42	11.56	12.00	12.50	25.50	N/A	N/A	N/A	N/A	N/A	N/A	N/A	0.0	N/A	N/A	N/A	N/A	70E_4s2d2Yc_1	5/28A	TDP-164	9700254
23.9	0.994	0.00500	0.050	0.328	26.0	P	N/A	11.15	11.42	11.56	12.00	12.50	25.50	N/A	N/A	N/A	N/A	N/A	N/A	N/A	n/a	N/A	N/A	N/A	N/A	70E_4s2d2Yc_1	5/28A	TDP-164	9700254.1
23.9	0.994	0.00500	0.050	0.328	26.0	P	N/A	11.15	11.42	11.56	12.00	12.50	25.50	N/A	N/A	N/A	N/A	N/A	N/A	N/A	n/a	N/A	N/A	N/A	N/A	70E_4s2d2Yc_1	5/28A	TDP-164	9700254.2
17.3	0.996	0.00155	0.050	0.181	97.6	P	N/A	5.42	5.50	5.55	5.70	7.10	24.00	N/A	N/A	N/A	N/A	N/A	N/A	I	31.8	1	N/A	N/A	N/A	70E_4s1d1Zd_1	5/29A	TDP-165	9700255
17.6	0.996	0.00155	0.050	0.183	85.6	P	N/A	6.09	6.19	6.24	6.40	7.10	28.00	N/A	N/A	N/A	N/A	N/A	N/A	I	18.0	1	N/A	N/A	N/A	70E_4s1d1Zd_1	5/29A	TDP-165	9700256
17.6	0.996	0.00155	0.050	0.184	80.4	P	N/A	6.48	6.58	6.64	6.80	7.10	27.75	N/A	N/A	N/A	N/A	N/A	N/A	I	7.4	1	N/A	N/A	N/A	70E_4s1d1Zd_1	5/29A	TDP-165	9700257
17.9	0.995	0.00155	0.050	0.185	78.0	P	N/A	6.64	6.75	6.81	7.00	7.10	29.50	N/A	N/A	N/A	UCScen	N/A	N/A	I	5.7	2	N/A	N/A	N/A	70E_4s1d1Zd_1	5/29A	TDP-165	9700258
18.3	0.996	0.00155	0.050	0.185	76.8	P	N/A	6.72	6.84	6.90	7.10	7.10	30.50	7.10	udv	N/A	N/A	UCSudv	N/A	I	2.0	4	N/A	N/A	N/A	70E_4s1d1Zd_1	5/29A	TDP-165	9700259
18.4	0.996	0.00155	0.050	0.182	68.0	P	N/A	7.65	7.80	7.87	8.10	7.10	40.50	N/A	N/A	N/A	N/A	N/A	N/A	I	0.0	4	N/A	N/A	N/A	70E_4s1d1Zd_1	5/29A	TDP-165	9700260
18.5	0.996	0.00155	0.050	0.181	72.4	P	N/A	7.30	7.43	7.50	7.70	7.10	34.75	N/A	N/A	N/A	N/A	N/A	N/A	D	0.0	4	N/A	N/A	N/A	70E_4s1d1Zd_1	5/29A	TDP-165	9700261
18.7	0.996	0.00155	0.050	0.331	46.6	P	N/A	6.18	6.28	6.33	6.50	7.10	27.75	N/A	N/A	N/A	N/A	N/A	N/A	D	13.9	1	N/A	N/A	N/A	70E_4s1d1Zc_1	5/29B	TDP-165	9700262
18.9	0.996	0.00155	0.050	0.333	43.8	P	N/A	6.54	6.65	6.71	6.90	7.10	30.25	N/A	N/A	N/A	UCScen	N/A	N/A	I	5.4	2	N/A	N/A	N/A	70E_4s1d1Zc_1	5/29B	TDP-165	9700263
18.9	0.996	0.00155	0.050	0.334	42.6	P	N/A	6.74	6.85	6.91	7.10	7.10	32.75	7.10	udv	N/A	N/A	UCSudv	N/A	I	0.7	4	N/A	N/A	N/A	70E_4s1d1Zc_1	5/29B	TDP-165	9700264
19.0	0.996	0.00155	0.050	0.337	39.8	P	N/A	7.12	7.25	7.31	7.50	7.10	33.50	N/A	N/A	N/A	N/A	N/A	N/A	I	0.0	4	N/A	N/A	N/A	70E_4s1d1Zc_1	5/29B	TDP-165	9700265
19.0	0.996	0.00155	0.050	0.340	37.2	P	N/A	7.48	7.62	7.69	7.90	7.10	44.50	N/A	N/A	N/A	N/A	N/A	N/A	D	0.0	4	N/A	N/A	N/A	70E_4s1d1Zc_1	5/29B	TDP-165	9700266
19.3	0.996	0.00155	0.050	0.336	40.8	P	N/A	6.92	7.04	7.10	7.30	7.10	31.50	N/A	N/A	N/A	N/A	N/A	N/A	D	0.0	4	N/A	N/A	N/A	70E_4s1d1Zc_1	5/29B	TDP-165	9700267

Table B.5. Data from 2008 Tests in Large-Scale Vessel with Elliptical Head A.9

Row Number	Test	Case ID	Tank Diameter	Head Shape	Dish Height	Dish Volume	Tank Fill Height	Return Line Height	Nozzle Inner Diameter	Nozzle Stand-off Distance	Pulse Tube Configuration	Installed Nozzles	Outer Nozzles Operated	Inner Nozzles Operated	Pulse Tube Outer Diameter	Outer PJM Radius	Inner PJM Radius	"FIO" Outer PJM Impingement Angle	"FIO" Inner PJM Impingement Angle	Ratio Outer PJM to Tank Radius	Ratio Inner PJM to Tank Radius	Simulant	Solids Density	Particle Diameter d5	Particle Diameter d50	Particle Diameter d95	Void Fraction
text	text	text	in.	text	in.	in. ^{3}	in.	in.	in.	in.	text	number	number	number	in.	in.	in.	deg	deg	nondim	nondim	text	g/cm^3	m	m	m	fraction
MSS	M/DDX	ID	D	HS	H_{dish}	V_{dish}	H	Rtn	d	sod	PT	N	N_O	N_I	PT_{od}	R_O	R_I	θ_O	θ_I	R_O/R	R_I/R	sxdx	ρ_s	d_5	d_{50}	d_{95}	vf
9700268	5/29B	70E_4s1d1Zc_1	70	E	19	49770.7	92	80	0.613	0.920	HLP-22	12	8	4	3.5	21.9	11.5	20.3	10.5	0.62	0.33	s1d1	2.46	0.0001428	0.0001664	0.0001951	0.4118
9700268.1	5/30A	70E_4s1d1Zc_1	70	E	19	49770.7	92	80	0.613	0.920	HLP-22	12	8	4	3.5	21.9	11.5	20.3	10.5	0.62	0.33	s1d1	2.46	0.0001428	0.0001664	0.0001951	0.4118
9700268.2	5/30A	70E_4s1d1Zc_1	70	E	19	49770.7	92	80	0.613	0.920	HLP-22	12	8	4	3.5	21.9	11.5	20.3	10.5	0.62	0.33	s1d1	2.46	0.0001428	0.0001664	0.0001951	0.4118
9700269M	5/30A	70E_4s1d1Zc_1	70	E	19	49770.7	92	80	0.613	0.920	HLP-22	12	8	4	3.5	21.9	11.5	20.3	10.5	0.62	0.33	s1d1	2.46	0.0001428	0.0001664	0.0001951	0.4118
9700270	5/30A	70E_4s1d1Zc_1	70	E	19	49770.7	92	80	0.613	0.920	HLP-22	12	8	4	3.5	21.9	11.5	20.3	10.5	0.62	0.33	s1d1	2.46	0.0001428	0.0001664	0.0001951	0.4118
9700271	5/30A	70E_4s1d1Zc_1	70	E	19	49770.7	92	80	0.613	0.920	HLP-22	12	8	4	3.5	21.9	11.5	20.3	10.5	0.62	0.33	s1d1	2.46	0.0001428	0.0001664	0.0001951	0.4118
9700272	5/30A	70E_4s1d1Zc_1	70	E	19	49770.7	92	80	0.613	0.920	HLP-22	12	8	4	3.5	21.9	11.5	20.3	10.5	0.62	0.33	s1d1	2.46	0.0001428	0.0001664	0.0001951	0.4118
9700273	5/30A	70E_4s1d1Zc_1	70	E	19	49770.7	92	80	0.613	0.920	HLP-22	12	8	4	3.5	21.9	11.5	20.3	10.5	0.62	0.33	s1d1	2.46	0.0001428	0.0001664	0.0001951	0.4118
9700274	5/30A	70E_4s1d1Zc_1	70	E	19	49770.7	92	80	0.613	0.920	HLP-22	12	8	4	3.5	21.9	11.5	20.3	10.5	0.62	0.33	s1d1	2.46	0.0001428	0.0001664	0.0001951	0.4118
9700275	5/30A	70E_4s1d1Zc_1	70	E	19	49770.7	92	80	0.613	0.920	HLP-22	12	8	4	3.5	21.9	11.5	20.3	10.5	0.62	0.33	s1d1	2.46	0.0001428	0.0001664	0.0001951	0.4118
9700276	5/30A	70E_4s1d1Zc_1	70	E	19	49770.7	92	80	0.613	0.920	HLP-22	12	8	4	3.5	21.9	11.5	20.3	10.5	0.62	0.33	s1d1	2.46	0.0001428	0.0001664	0.0001951	0.4118
9700277	5/30A	70E_4s1d1Zc_1	70	E	19	49770.7	92	80	0.613	0.920	HLP-22	12	8	4	3.5	21.9	11.5	20.3	10.5	0.62	0.33	s1d1	2.46	0.0001428	0.0001664	0.0001951	0.4118
9700278	5/30A	70E_4s1d1Zc_1	70	E	19	49770.7	92	80	0.613	0.920	HLP-22	12	8	4	3.5	21.9	11.5	20.3	10.5	0.62	0.33	s1d1	2.46	0.0001428	0.0001664	0.0001951	0.4118
9700278.1	5/30A	70E_4s1d1Zc_1	70	E	19	49770.7	92	80	0.613	0.920	HLP-22	12	8	4	3.5	21.9	11.5	20.3	10.5	0.62	0.33	s1d1	2.46	0.0001428	0.0001664	0.0001951	0.4118
9700278.2	5/30A	70E_4s1d1Zc_1	70	E	19	49770.7	92	80	0.613	0.920	HLP-22	12	8	4	3.5	21.9	11.5	20.3	10.5	0.62	0.33	s1d1	2.46	0.0001428	0.0001664	0.0001951	0.4118
9700279M	5/30A	70E_4s1d1Zc_1	70	E	19	49770.7	92	80	0.613	0.920	HLP-22	12	8	4	3.5	21.9	11.5	20.3	10.5	0.62	0.33	s1d1	2.46	0.0001428	0.0001664	0.0001951	0.4118
9700280	5/30A	70E_4s1d1Zc_1	70	E	19	49770.7	92	80	0.613	0.920	HLP-22	12	8	4	3.5	21.9	11.5	20.3	10.5	0.62	0.33	s1d1	2.46	0.0001428	0.0001664	0.0001951	0.4118
9700281	5/30A	70E_4s1d1Zc_1	70	E	19	49770.7	92	80	0.613	0.920	HLP-22	12	8	4	3.5	21.9	11.5	20.3	10.5	0.62	0.33	s1d1	2.46	0.0001428	0.0001664	0.0001951	0.4118
9700282	5/30A	70E_4s1d1Zc_1	70	E	19	49770.7	92	80	0.613	0.920	HLP-22	12	8	4	3.5	21.9	11.5	20.3	10.5	0.62	0.33	s1d1	2.46	0.0001428	0.0001664	0.0001951	0.4118
9700283	5/30A	70E_4s1d1Zc_1	70	E	19	49770.7	92	80	0.613	0.920	HLP-22	12	8	4	3.5	21.9	11.5	20.3	10.5	0.62	0.33	s1d1	2.46	0.0001428	0.0001664	0.0001951	0.4118
9700284	5/30A	70E_4s1d1Zc_1	70	E	19	49770.7	92	80	0.613	0.920	HLP-22	12	8	4	3.5	21.9	11.5	20.3	10.5	0.62	0.33	s1d1	2.46	0.0001428	0.0001664	0.0001951	0.4118
9700285	5/30A	70E_4s1d1Zc_1	70	E	19	49770.7	92	80	0.613	0.920	HLP-22	12	8	4	3.5	21.9	11.5	20.3	10.5	0.62	0.33	s1d1	2.46	0.0001428	0.0001664	0.0001951	0.4118
9700286	5/30A	70E_4s1d1Zc_1	70	E	19	49770.7	92	80	0.613	0.920	HLP-22	12	8	4	3.5	21.9	11.5	20.3	10.5	0.62	0.33	s1d1	2.46	0.0001428	0.0001664	0.0001951	0.4118
9700287	5/30A	70E_4s1d1Zc_1	70	E	19	49770.7	92	80	0.613	0.920	HLP-22	12	8	4	3.5	21.9	11.5	20.3	10.5	0.62	0.33	s1d1	2.46	0.0001428	0.0001664	0.0001951	0.4118
9700288	5/30A	70E_4s1d1Zc_1	70	E	19	49770.7	92	80	0.613	0.920	HLP-22	12	8	4	3.5	21.9	11.5	20.3	10.5	0.62	0.33	s1d1	2.46	0.0001428	0.0001664	0.0001951	0.4118
9700288.1	5/30A	70E_4s1d1Zc_1	70	E	19	49770.7	92	80	0.613	0.920	HLP-22	12	8	4	3.5	21.9	11.5	20.3	10.5	0.62	0.33	s1d1	2.46	0.0001428	0.0001664	0.0001951	0.4118
9700288.2	5/30A	70E_4s1d1Zc_1	70	E	19	49770.7	92	80	0.613	0.920	HLP-22	12	8	4	3.5	21.9	11.5	20.3	10.5	0.62	0.33	s1d1	2.46	0.0001428	0.0001664	0.0001951	0.4118
9700289M	5/30A	70E_4s1d1Zc_1	70	E	19	49770.7	92	80	0.613	0.920	HLP-22	12	8	4	3.5	21.9	11.5	20.3	10.5	0.62	0.33	s1d1	2.46	0.0001428	0.0001664	0.0001951	0.4118
9700290	5/30A	70E_4s1d1Zc_1	70	E	19	49770.7	92	80	0.613	0.920	HLP-22	12	8	4	3.5	21.9	11.5	20.3	10.5	0.62	0.33	s1d1	2.46	0.0001428	0.0001664	0.0001951	0.4118
9700291	5/30A	70E_4s1d1Zc_1	70	E	19	49770.7	92	80	0.613	0.920	HLP-22	12	8	4	3.5	21.9	11.5	20.3	10.5	0.62	0.33	s1d1	2.46	0.0001428	0.0001664	0.0001951	0.4118
9700292	5/30A	70E_4s1d1Zc_1	70	E	19	49770.7	92	80	0.613	0.920	HLP-22	12	8	4	3.5	21.9	11.5	20.3	10.5	0.62	0.33	s1d1	2.46	0.0001428	0.0001664	0.0001951	0.4118
9700293	5/30A	70E_4s1d1Zc_1	70	E	19	49770.7	92	80	0.613	0.920	HLP-22	12	8	4	3.5	21.9	11.5	20.3	10.5	0.62	0.33	s1d1	2.46	0.0001428	0.0001664	0.0001951	0.4118
9700294	5/30A	70E_4s1d1Zc_1	70	E	19	49770.7	92	80	0.613	0.920	HLP-22	12	8	4	3.5	21.9	11.5	20.3	10.5	0.62	0.33	s1d1	2.46	0.0001428	0.0001664	0.0001951	0.4118
9700295	5/30A	70E_4s1d1Zc_1	70	E	19	49770.7	92	80	0.613	0.920	HLP-22	12	8	4	3.5	21.9	11.5	20.3	10.5	0.62	0.33	s1d1	2.46	0.0001428	0.0001664	0.0001951	0.4118
9700295.1	5/30A	70E_4s1d1Zc_1	70	E	19	49770.7	92	80	0.613	0.920	HLP-22	12	8	4	3.5	21.9	11.5	20.3	10.5	0.62	0.33	s1d1	2.46	0.0001428	0.0001664	0.0001951	0.4118
9700295.2	5/30A	70E_4s1d1Zc_1	70	E	19	49770.7	92	80	0.613	0.920	HLP-22	12	8	4	3.5	21.9	11.5	20.3	10.5	0.62	0.33	s1d1	2.46	0.0001428	0.0001664	0.0001951	0.4118
9700295.3	5/30A	70E_4s1d1Zc_1	70	E	19	49770.7	92	80	0.613	0.920	HLP-22	12	8	4	3.5	21.9	11.5	20.3	10.5	0.62	0.33	s1d1	2.46	0.0001428	0.0001664	0.0001951	0.4118
9700296	7/17A	70E8_6s1d2Zc_1	70	E	19	49770.7	93	80	0.92	1.380	8TA	8	4	4	3.5	23.5	17.5	21.9	16.1	0.67	0.50	s1d2	2.48	0.0000569	0.0000693	0.0000821	0.3750
9700297	7/17A	70E8_6s1d2Zc_1	70	E	19	49770.7	93	80	0.92	1.380	8TA	8	4	4	3.5	23.5	17.5	21.9	16.1	0.67	0.50	s1d2	2.48	0.0000569	0.0000693	0.0000821	0.3750
9700298	7/17A	70E8_6s1d2Zc_1	70	E	19	49770.7	93	80	0.92	1.380	8TA	8	4	4	3.5	23.5	17.5	21.9	16.1	0.67	0.50	s1d2	2.48	0.0000569	0.0000693	0.0000821	0.3750
9700299	7/17A	70E8_6s1d2Zc_1	70	E	19	49770.7	93	80	0.92	1.380	8TA	8	4	4	3.5	23.5	17.5	21.9	16.1	0.67	0.50	s1d2	2.48	0.0000569	0.0000693	0.0000821	0.3750

Table B.5. Data from 2008 Tests in Large-Scale Vessel with Elliptical Head B.9

Tank Water Temperature	Water Density	Solids Fraction	Pulse Volume Fraction	Duty Cycle	Cycle Time	Pulsed or Steady Jet	Us Steady Jet	U1 Pulsing Jet	U2 URMS	U3 URM3	Discharge Velocity	Critical Suspension Velocity	Average Peak Cloud Height	UCS Condition	UCS Method	UCS Flag	UCS Center Flag	UCS udv Flag	UCS based on Decreasing Velocity	Sweep Increase / Decrease	UDV Height Bed	Particle Motion	Solids Level	Outer Bottom Pattern	Inner Bottom Pattern	Case ID	Test	TDP	Row Number
C	g/cm³	fraction	fraction	fraction	s	text	m/s	m/s	m/s	m/s	m/s	m/s	in.	m/s	text	text	text	text	m/s	text	mm	text	text	text	text	text	text	text	text
T	ρ_c	ϕ_S	ϕ_p	DC	t_C	Jet	U_S	U1	U2	U3	U	U_{CS}	H_C	U_{CSR}	U_{CSM}	U_{CS}vis	U_{CS}cen	U_{CS}udv	$U_{CS_}D$	S_W	H_{bed}	PM	Sol	SP_O	SP_I	ID	M/DDX	TDP	MSS
19.2	0.996	0.00155	0.050	0.332	45.0	P	N/A	6.37	6.47	6.52	6.70	7.10	29.25	N/A	N/A	N/A	N/A	N/A	N/A	D	8.8	1	N/A	N/A	N/A	70E_4s1d1Zc_1	5/29B	TDP-165	9700268
19.8	0.995	0.00155	0.050	0.334	42.6	P	N/A	6.72	6.84	6.89	7.10	7.10	30.75	N/A	N/A	N/A	N/A	N/A	N/A	N/A	n/a	N/A	N/A	N/A	N/A	70E_4s1d1Zc_1	5/30A	TDP-166	9700268.1
19.8	0.995	0.00155	0.050	0.334	42.6	P	N/A	6.72	6.84	6.89	7.10	7.10	30.75	N/A	N/A	N/A	N/A	N/A	N/A	N/A	n/a	N/A	N/A	N/A	N/A	70E_4s1d1Zc_1	5/30A	TDP-166	9700268.2
19.8	0.995	0.00155	0.050	0.334	42.6	P	N/A	6.72	6.84	6.89	7.10	7.10	30.75	N/A	N/A	N/A	N/A	N/A	N/A	(null)	0.0	4	N/A	N/A	N/A	70E_4s1d1Zc_1	5/30A	TDP-166	9700269
19.8	0.995	0.00155	0.050	0.334	42.6	P	N/A	6.72	6.84	6.89	7.10	7.10	30.75	N/A	N/A	N/A	N/A	N/A	N/A	N/A	0.0	N/A	N/A	N/A	N/A	70E_4s1d1Zc_1	5/30A	TDP-166	9700270
19.8	0.995	0.00155	0.050	0.334	42.6	P	N/A	6.72	6.84	6.89	7.10	7.10	30.75	N/A	N/A	N/A	N/A	N/A	N/A	N/A	0.0	N/A	N/A	N/A	N/A	70E_4s1d1Zc_1	5/30A	TDP-166	9700271
19.8	0.995	0.00155	0.050	0.334	42.6	P	N/A	6.72	6.84	6.89	7.10	7.10	30.75	N/A	N/A	N/A	N/A	N/A	N/A	N/A	1.4	N/A	N/A	N/A	N/A	70E_4s1d1Zc_1	5/30A	TDP-166	9700272
19.8	0.995	0.00155	0.050	0.334	42.6	P	N/A	6.72	6.84	6.89	7.10	7.10	30.75	N/A	N/A	N/A	N/A	N/A	N/A	N/A	0.0	N/A	N/A	N/A	N/A	70E_4s1d1Zc_1	5/30A	TDP-166	9700273
19.8	0.995	0.00155	0.050	0.334	42.6	P	N/A	6.72	6.84	6.89	7.10	7.10	30.75	N/A	N/A	N/A	N/A	N/A	N/A	N/A	0.7	N/A	N/A	N/A	N/A	70E_4s1d1Zc_1	5/30A	TDP-166	9700274
19.8	0.995	0.00155	0.050	0.334	42.6	P	N/A	6.72	6.84	6.89	7.10	7.10	30.75	N/A	N/A	N/A	N/A	N/A	N/A	N/A	0.7	N/A	N/A	N/A	N/A	70E_4s1d1Zc_1	5/30A	TDP-166	9700275
19.8	0.995	0.00155	0.050	0.334	42.6	P	N/A	6.72	6.84	6.89	7.10	7.10	30.75	N/A	N/A	N/A	N/A	N/A	N/A	N/A	0.7	N/A	N/A	N/A	N/A	70E_4s1d1Zc_1	5/30A	TDP-166	9700276
19.8	0.995	0.00155	0.050	0.334	42.6	P	N/A	6.72	6.84	6.89	7.10	7.10	30.75	N/A	N/A	N/A	N/A	N/A	N/A	N/A	0.7	N/A	N/A	N/A	N/A	70E_4s1d1Zc_1	5/30A	TDP-166	9700277
19.8	0.995	0.00155	0.050	0.334	42.6	P	N/A	6.72	6.84	6.89	7.10	7.10	30.75	N/A	N/A	N/A	N/A	N/A	N/A	N/A	1.6	N/A	N/A	N/A	N/A	70E_4s1d1Zc_1	5/30A	TDP-166	9700278
20.1	0.995	0.00155	0.050	0.334	42.6	P	N/A	6.72	6.83	6.89	7.10	7.10	30.75	N/A	N/A	N/A	N/A	N/A	N/A	N/A	n/a	N/A	N/A	N/A	N/A	70E_4s1d1Zc_1	5/30A	TDP-166	9700278.1
20.1	0.995	0.00155	0.050	0.334	42.6	P	N/A	6.72	6.83	6.89	7.10	7.10	30.75	N/A	N/A	N/A	N/A	N/A	N/A	N/A	n/a	N/A	N/A	N/A	N/A	70E_4s1d1Zc_1	5/30A	TDP-166	9700278.2
20.1	0.995	0.00155	0.050	0.334	42.6	P	N/A	6.72	6.83	6.89	7.10	7.10	30.25	N/A	N/A	N/A	N/A	N/A	N/A	(null)	0.9	4	N/A	N/A	N/A	70E_4s1d1Zc_1	5/30A	TDP-166	9700279
20.1	0.995	0.00155	0.050	0.334	42.6	P	N/A	6.72	6.83	6.89	7.10	7.10	30.25	N/A	N/A	N/A	N/A	N/A	N/A	N/A	1.8	N/A	N/A	N/A	N/A	70E_4s1d1Zc_1	5/30A	TDP-166	9700280
20.1	0.995	0.00155	0.050	0.334	42.6	P	N/A	6.72	6.83	6.89	7.10	7.10	30.25	N/A	N/A	N/A	N/A	N/A	N/A	N/A	0.0	N/A	N/A	N/A	N/A	70E_4s1d1Zc_1	5/30A	TDP-166	9700281
20.1	0.995	0.00155	0.050	0.334	42.6	P	N/A	6.72	6.83	6.89	7.10	7.10	30.25	N/A	N/A	N/A	N/A	N/A	N/A	N/A	0.0	N/A	N/A	N/A	N/A	70E_4s1d1Zc_1	5/30A	TDP-166	9700282
20.1	0.995	0.00155	0.050	0.334	42.6	P	N/A	6.72	6.83	6.89	7.10	7.10	30.25	N/A	N/A	N/A	N/A	N/A	N/A	N/A	1.8	N/A	N/A	N/A	N/A	70E_4s1d1Zc_1	5/30A	TDP-166	9700283
20.1	0.995	0.00155	0.050	0.334	42.6	P	N/A	6.72	6.83	6.89	7.10	7.10	30.25	N/A	N/A	N/A	N/A	N/A	N/A	N/A	0.8	N/A	N/A	N/A	N/A	70E_4s1d1Zc_1	5/30A	TDP-166	9700284
20.1	0.995	0.00155	0.050	0.334	42.6	P	N/A	6.72	6.83	6.89	7.10	7.10	30.25	N/A	N/A	N/A	N/A	N/A	N/A	N/A	0.0	N/A	N/A	N/A	N/A	70E_4s1d1Zc_1	5/30A	TDP-166	9700285
20.1	0.995	0.00155	0.050	0.334	42.6	P	N/A	6.72	6.83	6.89	7.10	7.10	30.25	N/A	N/A	N/A	N/A	N/A	N/A	N/A	1.4	N/A	N/A	N/A	N/A	70E_4s1d1Zc_1	5/30A	TDP-166	9700286
20.1	0.995	0.00155	0.050	0.334	42.6	P	N/A	6.72	6.83	6.89	7.10	7.10	30.25	N/A	N/A	N/A	N/A	N/A	N/A	N/A	0.7	N/A	N/A	N/A	N/A	70E_4s1d1Zc_1	5/30A	TDP-166	9700287
20.1	0.995	0.00155	0.050	0.334	42.6	P	N/A	6.72	6.83	6.89	7.10	7.10	30.25	N/A	N/A	N/A	N/A	N/A	N/A	N/A	1.6	N/A	N/A	N/A	N/A	70E_4s1d1Zc_1	5/30A	TDP-166	9700288
20.2	0.995	0.00155	0.050	0.334	42.6	P	N/A	6.72	6.83	6.89	7.10	7.10	30.25	N/A	N/A	N/A	N/A	N/A	N/A	N/A	n/a	N/A	N/A	N/A	N/A	70E_4s1d1Zc_1	5/30A	TDP-166	9700288.1
20.2	0.995	0.00155	0.050	0.334	42.6	P	N/A	6.72	6.83	6.89	7.10	7.10	30.25	N/A	N/A	N/A	N/A	N/A	N/A	N/A	n/a	N/A	N/A	N/A	N/A	70E_4s1d1Zc_1	5/30A	TDP-166	9700288.2
20.2	0.995	0.00155	0.050	0.334	42.6	P	N/A	6.72	6.83	6.89	7.10	7.10	30.75	N/A	N/A	N/A	N/A	N/A	N/A	(null)	1.6	4	N/A	N/A	N/A	70E_4s1d1Zc_1	5/30A	TDP-166	9700289
20.2	0.995	0.00155	0.050	0.334	42.6	P	N/A	6.72	6.83	6.89	7.10	7.10	30.75	N/A	N/A	N/A	N/A	N/A	N/A	N/A	0.8	N/A	N/A	N/A	N/A	70E_4s1d1Zc_1	5/30A	TDP-166	9700290
20.2	0.995	0.00155	0.050	0.334	42.6	P	N/A	6.72	6.83	6.89	7.10	7.10	30.75	N/A	N/A	N/A	N/A	N/A	N/A	N/A	0.9	N/A	N/A	N/A	N/A	70E_4s1d1Zc_1	5/30A	TDP-166	9700291
20.2	0.995	0.00155	0.050	0.334	42.6	P	N/A	6.72	6.83	6.89	7.10	7.10	30.75	N/A	N/A	N/A	N/A	N/A	N/A	N/A	1.9	N/A	N/A	N/A	N/A	70E_4s1d1Zc_1	5/30A	TDP-166	9700292
20.2	0.995	0.00155	0.050	0.334	42.6	P	N/A	6.72	6.83	6.89	7.10	7.10	30.75	N/A	N/A	N/A	N/A	N/A	N/A	N/A	0.0	N/A	N/A	N/A	N/A	70E_4s1d1Zc_1	5/30A	TDP-166	9700293
20.2	0.995	0.00155	0.050	0.334	42.6	P	N/A	6.72	6.83	6.89	7.10	7.10	30.75	N/A	N/A	N/A	N/A	N/A	N/A	N/A	1.9	N/A	N/A	N/A	N/A	70E_4s1d1Zc_1	5/30A	TDP-166	9700294
20.2	0.995	0.00155	0.050	0.334	42.6	P	N/A	6.72	6.83	6.89	7.10	7.10	30.75	N/A	N/A	N/A	N/A	N/A	N/A	N/A	0.7	N/A	N/A	N/A	N/A	70E_4s1d1Zc_1	5/30A	TDP-166	9700295
20.2	0.995	0.00155	0.050	0.334	42.6	P	N/A	6.72	6.83	6.89	7.10	7.10	30.75	N/A	N/A	N/A	N/A	N/A	N/A	N/A	n/a	N/A	N/A	N/A	N/A	70E_4s1d1Zc_1	5/30A	TDP-166	9700295.1
20.2	0.995	0.00155	0.050	0.334	42.6	P	N/A	6.72	6.83	6.89	7.10	7.10	30.75	N/A	N/A	N/A	N/A	N/A	N/A	N/A	n/a	N/A	N/A	N/A	N/A	70E_4s1d1Zc_1	5/30A	TDP-166	9700295.2
20.2	0.995	0.00155	0.050	0.334	42.6	P	N/A	6.72	6.83	6.89	7.10	7.10	30.75	N/A	N/A	N/A	N/A	N/A	N/A	N/A	n/a	N/A	N/A	N/A	N/A	70E_4s1d1Zc_1	5/30A	TDP-166	9700295.3
25.6	0.994	0.00155	0.050	0.332	67.0	P	N/A	2.85	2.90	2.92	3.00	4.40	29.00	N/A	N/A	N/A	N/A	N/A	N/A	(null)	16.7	1	N/A	N/A	N/A	70E8_6s1d2Zc_1	7/17A	TDP-168	9700296
25.7	0.994	0.00155	0.050	0.332	59.2	P	N/A	3.24	3.29	3.31	3.40	4.40	34.25	N/A	N/A	N/A	N/A	N/A	N/A	I	16.6	1	N/A	N/A	N/A	70E8_6s1d2Zc_1	7/17A	TDP-168	9700297
25.8	0.994	0.00155	0.050	0.335	53.0	P	N/A	3.57	3.63	3.66	3.80	4.40	43.25	N/A	N/A	N/A	N/A	N/A	N/A	I	16.5	1	N/A	N/A	N/A	70E8_6s1d2Zc_1	7/17A	TDP-168	9700298
25.8	0.994	0.00155	0.050	0.334	50.4	P	N/A	3.78	3.84	3.88	4.00	4.40	62.00	N/A	N/A	N/A	N/A	N/A	N/A	I	20.9	1	N/A	N/A	N/A	70E8_6s1d2Zc_1	7/17A	TDP-168	9700299

Table B.5. Data from 2008 Tests in Large-Scale Vessel with Elliptical Head A.10

Row Number	Test	Case ID	Tank Diameter	Head Shape	Dish Height	Dish Volume	Tank Fill Height	Return Line Height	Nozzle Inner Diameter	Nozzle Stand-off Distance	Pulse Tube Configuration	Installed Nozzles	Outer Nozzles Operated	Inner Nozzles Operated	Pulse Tube Outer Diameter	Outer PJM Radius	Inner PJM Radius	"FIO" Outer PJM Impingement Angle	"FIO" Inner PJM Impingement Angle	Ratio Outer PJM to Tank Radius	Ratio Inner PJM to Tank Radius	Simulant	Solids Density	Particle Diameter d5	Particle Diameter d50	Particle Diameter d95	Void Fraction
text	text	text	in.	text	in.	in. ^{3}	in.	in.	in.	in.	text	number	number	number	in.	in.	in.	deg	deg	nondim	nondim	text	g/cm^3	m	m	m	fraction
MSS	M/DDX	ID	D	HS	H_{dish}	V_{dish}	H	Rtn	d	sod	PT	N	N_O	N_I	PT_{od}	R_O	R_I	θ_O	θ_I	R_O/R	R_I/R	sxdx	ρ_s	d_5	d_{50}	d_{95}	vf
9700300	7/17A	70E8_6s1d2Zc_1	70	E	19	49770.7	93	80	0.92	1.380	8TA	8	4	4	3.5	23.5	17.5	21.9	16.1	0.67	0.50	s1d2	2.48	0.0000569	0.0000693	0.0000821	0.3750
9700301	7/17A	70E8_6s1d2Zc_1	70	E	19	49770.7	93	80	0.92	1.380	8TA	8	4	4	3.5	23.5	17.5	21.9	16.1	0.67	0.50	s1d2	2.48	0.0000569	0.0000693	0.0000821	0.3750
9700302M	7/17A	70E8_6s1d2Zc_1	70	E	19	49770.7	93	80	0.92	1.380	8TA	8	4	4	3.5	23.5	17.5	21.9	16.1	0.67	0.50	s1d2	2.48	0.0000569	0.0000693	0.0000821	0.3750
9700303	7/17B	70E8_6s1d2Zc_2	70	E	19	49770.7	93	80	0.92	1.380	8TA	8	4	4	3.5	23.5	17.5	21.9	16.1	0.67	0.50	s1d2	2.48	0.0000569	0.0000693	0.0000821	0.3750
9700304	7/17B	70E8_6s1d2Zc_2	70	E	19	49770.7	93	80	0.92	1.380	8TA	8	4	4	3.5	23.5	17.5	21.9	16.1	0.67	0.50	s1d2	2.48	0.0000569	0.0000693	0.0000821	0.3750
9700305	7/17B	70E8_6s1d2Zc_2	70	E	19	49770.7	93	80	0.92	1.380	8TA	8	4	4	3.5	23.5	17.5	21.9	16.1	0.67	0.50	s1d2	2.48	0.0000569	0.0000693	0.0000821	0.3750
9700306	7/17B	70E8_6s1d2Zc_2	70	E	19	49770.7	93	80	0.92	1.380	8TA	8	4	4	3.5	23.5	17.5	21.9	16.1	0.67	0.50	s1d2	2.48	0.0000569	0.0000693	0.0000821	0.3750
9700307	7/17B	70E8_6s1d2Zc_2	70	E	19	49770.7	93	80	0.92	1.380	8TA	8	4	4	3.5	23.5	17.5	21.9	16.1	0.67	0.50	s1d2	2.48	0.0000569	0.0000693	0.0000821	0.3750
9700308M	7/17B	70E8_6s1d2Zc_2	70	E	19	49770.7	93	80	0.92	1.380	8TA	8	4	4	3.5	23.5	17.5	21.9	16.1	0.67	0.50	s1d2	2.48	0.0000569	0.0000693	0.0000821	0.3750
9700309	7/18A	70E8_6s1d2Vc_1	70	E	19	49770.7	94	80	0.92	1.380	8TA	8	4	4	3.5	23.5	17.5	21.9	16.1	0.67	0.50	s1d2	2.48	0.0000569	0.0000693	0.0000821	0.3750
9700310	7/18A	70E8_6s1d2Vc_1	70	E	19	49770.7	94	80	0.92	1.380	8TA	8	4	4	3.5	23.5	17.5	21.9	16.1	0.67	0.50	s1d2	2.48	0.0000569	0.0000693	0.0000821	0.3750
9700311	7/18A	70E8_6s1d2Vc_1	70	E	19	49770.7	94	80	0.92	1.380	8TA	8	4	4	3.5	23.5	17.5	21.9	16.1	0.67	0.50	s1d2	2.48	0.0000569	0.0000693	0.0000821	0.3750
9700312	7/18A	70E8_6s1d2Vc_1	70	E	19	49770.7	94	80	0.92	1.380	8TA	8	4	4	3.5	23.5	17.5	21.9	16.1	0.67	0.50	s1d2	2.48	0.0000569	0.0000693	0.0000821	0.3750
9700313M	7/18A	70E8_6s1d2Vc_1	70	E	19	49770.7	94	80	0.92	1.380	8TA	8	4	4	3.5	23.5	17.5	21.9	16.1	0.67	0.50	s1d2	2.48	0.0000569	0.0000693	0.0000821	0.3750
9700314M	7/18A	70E8_6s1d2Vc_1	70	E	19	49770.7	94	80	0.92	1.380	8TA	8	4	4	3.5	23.5	17.5	21.9	16.1	0.67	0.50	s1d2	2.48	0.0000569	0.0000693	0.0000821	0.3750
9700315	7/18A	70E8_6s1d2Vc_1	70	E	19	49770.7	94	80	0.92	1.380	8TA	8	4	4	3.5	23.5	17.5	21.9	16.1	0.67	0.50	s1d2	2.48	0.0000569	0.0000693	0.0000821	0.3750
9700315.1	7/18A	70E8_6s1d2Vc_1	70	E	19	49770.7	94	80	0.92	1.380	8TA	8	4	4	3.5	23.5	17.5	21.9	16.1	0.67	0.50	s1d2	2.48	0.0000569	0.0000693	0.0000821	0.3750
9700316	7/18A	70E8_6s1d2Vc_1	70	E	19	49770.7	94	80	0.92	1.380	8TA	8	4	4	3.5	23.5	17.5	21.9	16.1	0.67	0.50	s1d2	2.48	0.0000569	0.0000693	0.0000821	0.3750
9700316.1	7/18A	70E8_6s1d2Vc_1	70	E	19	49770.7	94	80	0.92	1.380	8TA	8	4	4	3.5	23.5	17.5	21.9	16.1	0.67	0.50	s1d2	2.48	0.0000569	0.0000693	0.0000821	0.3750
9700316.2	7/18A	70E8_6s1d2Vc_1	70	E	19	49770.7	94	80	0.92	1.380	8TA	8	4	4	3.5	23.5	17.5	21.9	16.1	0.67	0.50	s1d2	2.48	0.0000569	0.0000693	0.0000821	0.3750
9700317	7/18A	70E8_6s1d2Vc_1	70	E	19	49770.7	94	80	0.92	1.380	8TA	8	4	4	3.5	23.5	17.5	21.9	16.1	0.67	0.50	s1d2	2.48	0.0000569	0.0000693	0.0000821	0.3750
9700317.1	7/18A	70E8_6s1d2Vc_1	70	E	19	49770.7	94	80	0.92	1.380	8TA	8	4	4	3.5	23.5	17.5	21.9	16.1	0.67	0.50	s1d2	2.48	0.0000569	0.0000693	0.0000821	0.3750
9700317.2	7/18A	70E8_6s1d2Vc_1	70	E	19	49770.7	94	80	0.92	1.380	8TA	8	4	4	3.5	23.5	17.5	21.9	16.1	0.67	0.50	s1d2	2.48	0.0000569	0.0000693	0.0000821	0.3750
9700317.3	7/18A	70E8_6s1d2Vc_1	70	E	19	49770.7	94	80	0.92	1.380	8TA	8	4	4	3.5	23.5	17.5	21.9	16.1	0.67	0.50	s1d2	2.48	0.0000569	0.0000693	0.0000821	0.3750
9700318	7/18A	70E8_6s1d2Vc_1	70	E	19	49770.7	94	80	0.92	1.380	8TA	8	4	4	3.5	23.5	17.5	21.9	16.1	0.67	0.50	s1d2	2.48	0.0000569	0.0000693	0.0000821	0.3750
9700318.1	7/18A	70E8_6s1d2Vc_1	70	E	19	49770.7	94	80	0.92	1.380	8TA	8	4	4	3.5	23.5	17.5	21.9	16.1	0.67	0.50	s1d2	2.48	0.0000569	0.0000693	0.0000821	0.3750
9700319	7/18A	70E8_6s1d2Vc_1	70	E	19	49770.7	94	80	0.92	1.380	8TA	8	4	4	3.5	23.5	17.5	21.9	16.1	0.67	0.50	s1d2	2.48	0.0000569	0.0000693	0.0000821	0.3750
9700320	7/18A	70E8_6s1d2Vc_1	70	E	19	49770.7	94	80	0.92	1.380	8TA	8	4	4	3.5	23.5	17.5	21.9	16.1	0.67	0.50	s1d2	2.48	0.0000569	0.0000693	0.0000821	0.3750
9700321	7/18B	70E8_6s1d2Vc_2	70	E	19	49770.7	94	80	0.92	1.380	8TA	8	4	4	3.5	23.5	17.5	21.9	16.1	0.67	0.50	s1d2	2.48	0.0000569	0.0000693	0.0000821	0.3750
9700322	7/18B	70E8_6s1d2Vc_2	70	E	19	49770.7	94	80	0.92	1.380	8TA	8	4	4	3.5	23.5	17.5	21.9	16.1	0.67	0.50	s1d2	2.48	0.0000569	0.0000693	0.0000821	0.3750
9700323	7/18B	70E8_6s1d2Vc_2	70	E	19	49770.7	94	80	0.92	1.380	8TA	8	4	4	3.5	23.5	17.5	21.9	16.1	0.67	0.50	s1d2	2.48	0.0000569	0.0000693	0.0000821	0.3750
9700324M	7/18B	70E8_6s1d2Vc_2	70	E	19	49770.7	94	80	0.92	1.380	8TA	8	4	4	3.5	23.5	17.5	21.9	16.1	0.67	0.50	s1d2	2.48	0.0000569	0.0000693	0.0000821	0.3750
9700325M	7/18B	70E8_6s1d2Vc_2	70	E	19	49770.7	94	80	0.92	1.380	8TA	8	4	4	3.5	23.5	17.5	21.9	16.1	0.67	0.50	s1d2	2.48	0.0000569	0.0000693	0.0000821	0.3750
9700326	7/18B	70E8_6s1d2Vc_2	70	E	19	49770.7	94	80	0.92	1.380	8TA	8	4	4	3.5	23.5	17.5	21.9	16.1	0.67	0.50	s1d2	2.48	0.0000569	0.0000693	0.0000821	0.3750
9700326.1	7/18B	70E8_6s1d2Vc_2	70	E	19	49770.7	94	80	0.92	1.380	8TA	8	4	4	3.5	23.5	17.5	21.9	16.1	0.67	0.50	s1d2	2.48	0.0000569	0.0000693	0.0000821	0.3750
9700327	7/18B	70E8_6s1d2Vc_2	70	E	19	49770.7	94	80	0.92	1.380	8TA	8	4	4	3.5	23.5	17.5	21.9	16.1	0.67	0.50	s1d2	2.48	0.0000569	0.0000693	0.0000821	0.3750
9700327.1	7/18B	70E8_6s1d2Vc_2	70	E	19	49770.7	94	80	0.92	1.380	8TA	8	4	4	3.5	23.5	17.5	21.9	16.1	0.67	0.50	s1d2	2.48	0.0000569	0.0000693	0.0000821	0.3750
9700327.2	7/18B	70E8_6s1d2Vc_2	70	E	19	49770.7	94	80	0.92	1.380	8TA	8	4	4	3.5	23.5	17.5	21.9	16.1	0.67	0.50	s1d2	2.48	0.0000569	0.0000693	0.0000821	0.3750
9700328	7/18B	70E8_6s1d2Vc_2	70	E	19	49770.7	94	80	0.92	1.380	8TA	8	4	4	3.5	23.5	17.5	21.9	16.1	0.67	0.50	s1d2	2.48	0.0000569	0.0000693	0.0000821	0.3750
9700328.1	7/18B	70E8_6s1d2Vc_2	70	E	19	49770.7	94	80	0.92	1.380	8TA	8	4	4	3.5	23.5	17.5	21.9	16.1	0.67	0.50	s1d2	2.48	0.0000569	0.0000693	0.0000821	0.3750
9700328.2	7/18B	70E8_6s1d2Vc_2	70	E	19	49770.7	94	80	0.92	1.380	8TA	8	4	4	3.5	23.5	17.5	21.9	16.1	0.67	0.50	s1d2	2.48	0.0000569	0.0000693	0.0000821	0.3750

Table B.5. Data from 2008 Tests in Large-Scale Vessel with Elliptical Head B.10

Tank Water Temperature	Water Density	Solids Fraction	Pulse Volume Fraction	Duty Cycle	Cycle Time	Pulsed or Steady Jet	Us Steady Jet	U1 Pulsing Jet	U2 URMS	U3 URM3	Discharge Velocity	Critical Suspension Velocity	Average Peak Cloud Height	UCS Condition	UCS Method	UCS Flag	UCS Center Flag	UCS udv Flag	UCS based on Decreasing Velocity	Sweep Increase / Decrease	UDV Height Bed	Particle Motion	Solids Level	Outer Bottom Pattern	Inner Bottom Pattern	Case ID	Test	TDP	Row Number
C	g/cm³	fraction	fraction	fraction	s	text	m/s	m/s	m/s	m/s	m/s	m/s	in.	m/s	text	text	text	text	m/s	text	mm	text	text	text	text	text	text	text	text
T	ρ_c	ϕ_S	ϕ_p	DC	t_C	Jet	U_S	U1	U2	U3	U	U_{CS}	H_C	U_{CSR}	U_{CSM}	U_{CS}vis	U_{CS}cen	U_{CS}udv	U_{CS}_D	S_W	H_{bed}	PM	Sol	SP_O	SP_I	ID	M/DDX	TDP	MSS
25.8	0.994	0.00155	0.050	0.333	48.0	P	N/A	3.96	4.03	4.07	4.20	4.40	70.50	N/A	N/A	N/A	N/A	N/A	N/A	I	11.4	1	N/A	N/A	N/A	70E8_6s1d2Zc_1	7/17A	TDP-168	9700300
25.8	0.994	0.00155	0.050	0.334	46.8	P	N/A	4.05	4.13	4.16	4.30	4.40	76.00	N/A	N/A	N/A	N/A	N/A	N/A	I	3.7	1	N/A	N/A	N/A	70E8_6s1d2Zc_1	7/17A	TDP-168	9700301
25.8	0.995	0.00155	0.050	0.333	45.8	P	N/A	4.17	4.23	4.27	4.40	4.40	88.00	4.40	center	N/A	UCScen	N/A	N/A	I	2.2	2	N/A	N/A	N/A	70E8_6s1d2Zc_1	7/17A	TDP-168	9700302
26.1	0.994	0.00155	0.100	0.327	131.0	P	N/A	2.94	2.96	2.97	3.00	4.30	40.50	N/A	N/A	N/A	N/A	N/A	N/A	(null)	17.0	1	N/A	N/A	N/A	70E8_6s1d2Zc_2	7/17B	TDP-168	9700303
26.1	0.994	0.00155	0.099	0.328	115.2	P	N/A	3.32	3.35	3.36	3.40	4.30	46.00	N/A	N/A	N/A	N/A	N/A	N/A	I	15.7	1	N/A	N/A	N/A	70E8_6s1d2Zc_2	7/17B	TDP-168	9700304
26.1	0.994	0.00155	0.100	0.329	103.0	P	N/A	3.71	3.74	3.76	3.80	4.30	59.00	N/A	N/A	N/A	N/A	N/A	N/A	I	20.3	1	N/A	N/A	N/A	70E8_6s1d2Zc_2	7/17B	TDP-168	9700305
26.1	0.994	0.00155	0.099	0.330	97.8	P	N/A	3.89	3.92	3.94	4.00	4.30	67.00	N/A	N/A	N/A	N/A	N/A	N/A	I	9.9	1	N/A	N/A	N/A	70E8_6s1d2Zc_2	7/17B	TDP-168	9700306
26.2	0.994	0.00155	0.100	0.331	93.2	P	N/A	4.08	4.12	4.14	4.20	4.30	78.00	N/A	N/A	N/A	UCScen	N/A	N/A	I	5.0	2	N/A	N/A	N/A	70E8_6s1d2Zc_2	7/17B	TDP-168	9700307
26.2	0.995	0.00155	0.100	0.331	91.0	P	N/A	4.18	4.22	4.24	4.30	4.30	87.00	4.30	udv	N/A	N/A	UCSudv	N/A	I	0.0	4	N/A	N/A	N/A	70E8_6s1d2Zc_2	7/17B	TDP-168	9700308
25.7	0.994	0.01430	0.050	0.335	36.6	P	N/A	5.20	5.28	5.33	5.50	6.80	28.25	N/A	N/A	N/A	N/A	N/A	N/A	I	16.9	1	N/A	N/A	N/A	70E8_6s1d2Vc_1	7/18A	TDP-169	9700309
25.7	0.994	0.01430	0.050	0.334	33.6	P	N/A	5.65	5.75	5.81	6.00	6.80	40.50	N/A	N/A	N/A	N/A	N/A	N/A	I	10.2	1	N/A	N/A	N/A	70E8_6s1d2Vc_1	7/18A	TDP-169	9700310
25.6	0.994	0.01430	0.050	0.333	31.6	P	N/A	6.02	6.13	6.19	6.40	6.80	54.00	N/A	N/A	N/A	N/A	N/A	N/A	I	9.5	1	N/A	N/A	N/A	70E8_6s1d2Vc_1	7/18A	TDP-169	9700311
25.8	0.994	0.01430	0.050	0.334	30.6	P	N/A	6.20	6.31	6.37	6.60	6.80	62.00	N/A	N/A	N/A	N/A	N/A	N/A	I	5.6	1	N/A	N/A	N/A	70E8_6s1d2Vc_1	7/18A	TDP-169	9700312
25.8	0.994	0.01430	0.050	0.335	29.6	P	N/A	6.40	6.52	6.58	6.80	6.80	71.50	6.80	udv	N/A	UCScen	UCSudv	N/A	I	2.2	2	N/A	N/A	N/A	70E8_6s1d2Vc_1	7/18A	TDP-169	9700313
25.9	0.994	0.01430	0.050	0.335	29.6	P	N/A	6.39	6.51	6.58	6.80	6.80	70.00	N/A	N/A	N/A	UCScen	N/A	N/A	I	0.0	2	N/A	N/A	N/A	70E8_6s1d2Vc_1	7/18A	TDP-169	9700314
25.9	0.994	0.01430	0.050	0.335	29.6	P	N/A	6.39	6.51	6.58	6.80	6.80	70.00	N/A	N/A	N/A	N/A	N/A	N/A	N/A	0.0	N/A	N/A	N/A	N/A	70E8_6s1d2Vc_1	7/18A	TDP-169	9700315
25.9	0.994	0.01430	0.050	0.335	29.6	P	N/A	6.39	6.51	6.58	6.80	6.80	70.00	N/A	N/A	N/A	N/A	N/A	N/A	N/A	n/a	N/A	N/A	N/A	N/A	70E8_6s1d2Vc_1	7/18A	TDP-169	9700315.1
25.9	0.994	0.01430	0.050	0.335	29.6	P	N/A	6.39	6.51	6.58	6.80	6.80	70.00	N/A	N/A	N/A	N/A	N/A	N/A	N/A	0.0	N/A	N/A	N/A	N/A	70E8_6s1d2Vc_1	7/18A	TDP-169	9700316
25.9	0.994	0.01430	0.050	0.335	29.6	P	N/A	6.39	6.51	6.58	6.80	6.80	70.00	N/A	N/A	N/A	N/A	N/A	N/A	N/A	n/a	N/A	N/A	N/A	N/A	70E8_6s1d2Vc_1	7/18A	TDP-169	9700316.1
25.9	0.994	0.01430	0.050	0.335	29.6	P	N/A	6.39	6.51	6.58	6.80	6.80	70.00	N/A	N/A	N/A	N/A	N/A	N/A	N/A	n/a	N/A	N/A	N/A	N/A	70E8_6s1d2Vc_1	7/18A	TDP-169	9700316.2
25.9	0.994	0.01430	0.050	0.335	29.6	P	N/A	6.39	6.51	6.58	6.80	6.80	70.00	N/A	N/A	N/A	N/A	N/A	N/A	N/A	0.0	N/A	N/A	N/A	N/A	70E8_6s1d2Vc_1	7/18A	TDP-169	9700317
25.9	0.994	0.01430	0.050	0.335	29.6	P	N/A	6.39	6.51	6.58	6.80	6.80	70.00	N/A	N/A	N/A	N/A	N/A	N/A	N/A	n/a	N/A	N/A	N/A	N/A	70E8_6s1d2Vc_1	7/18A	TDP-169	9700317.1
25.9	0.994	0.01430	0.050	0.335	29.6	P	N/A	6.39	6.51	6.58	6.80	6.80	70.00	N/A	N/A	N/A	N/A	N/A	N/A	N/A	n/a	N/A	N/A	N/A	N/A	70E8_6s1d2Vc_1	7/18A	TDP-169	9700317.2
25.9	0.994	0.01430	0.050	0.335	29.6	P	N/A	6.39	6.51	6.58	6.80	6.80	70.00	N/A	N/A	N/A	N/A	N/A	N/A	N/A	n/a	N/A	N/A	N/A	N/A	70E8_6s1d2Vc_1	7/18A	TDP-169	9700317.3
25.9	0.994	0.01430	0.050	0.335	29.6	P	N/A	6.39	6.51	6.58	6.80	6.80	70.00	N/A	N/A	N/A	N/A	N/A	N/A	N/A	0.0	N/A	N/A	N/A	N/A	70E8_6s1d2Vc_1	7/18A	TDP-169	9700318
25.9	0.994	0.01430	0.050	0.335	29.6	P	N/A	6.39	6.51	6.58	6.80	6.80	70.00	N/A	N/A	N/A	N/A	N/A	N/A	N/A	n/a	N/A	N/A	N/A	N/A	70E8_6s1d2Vc_1	7/18A	TDP-169	9700318.1
25.9	0.994	0.01430	0.050	0.335	29.6	P	N/A	6.39	6.51	6.58	6.80	6.80	70.00	N/A	N/A	N/A	N/A	N/A	N/A	N/A	0.0	N/A	N/A	N/A	N/A	70E8_6s1d2Vc_1	7/18A	TDP-169	9700319
25.9	0.994	0.01430	0.050	0.335	29.6	P	N/A	6.39	6.51	6.58	6.80	6.80	70.00	N/A	N/A	N/A	N/A	N/A	N/A	N/A	0.2	N/A	N/A	N/A	N/A	70E8_6s1d2Vc_1	7/18A	TDP-169	9700320
25.9	0.994	0.01430	0.100	0.329	72.0	P	N/A	5.34	5.39	5.41	5.50	6.40	40.00	N/A	N/A	N/A	N/A	N/A	N/A	D	13.2	1	N/A	N/A	N/A	70E8_6s1d2Vc_2	7/18B	TDP-169	9700321
26.1	0.994	0.01430	0.100	0.330	66.0	P	N/A	5.82	5.88	5.90	6.00	6.40	50.00	N/A	N/A	N/A	N/A	N/A	N/A	I	19.9	1	N/A	N/A	N/A	70E8_6s1d2Vc_2	7/18B	TDP-169	9700322
26.1	0.994	0.01430	0.100	0.331	63.8	P	N/A	6.01	6.07	6.10	6.20	6.40	57.50	N/A	N/A	N/A	N/A	N/A	N/A	I	4.2	1	N/A	N/A	N/A	70E8_6s1d2Vc_2	7/18B	TDP-169	9700323
26.2	0.995	0.01430	0.100	0.331	61.8	P	N/A	6.20	6.26	6.29	6.40	6.40	64.50	6.40	udv	N/A	UCScen	UCSudv	N/A	I	0.7	2	N/A	N/A	N/A	70E8_6s1d2Vc_2	7/18B	TDP-169	9700324
26.3	0.994	0.01430	0.100	0.331	61.8	P	N/A	6.20	6.26	6.29	6.40	6.40	63.00	N/A	N/A	N/A	UCScen	N/A	N/A	I	2.8	2	N/A	N/A	N/A	70E8_6s1d2Vc_2	7/18B	TDP-169	9700325
26.3	0.994	0.01430	0.100	0.331	61.8	P	N/A	6.20	6.26	6.29	6.40	6.40	63.00	N/A	N/A	N/A	N/A	N/A	N/A	N/A	0.7	N/A	N/A	N/A	N/A	70E8_6s1d2Vc_2	7/18B	TDP-169	9700326
26.3	0.994	0.01430	0.100	0.331	61.8	P	N/A	6.20	6.26	6.29	6.40	6.40	63.00	N/A	N/A	N/A	N/A	N/A	N/A	N/A	n/a	N/A	N/A	N/A	N/A	70E8_6s1d2Vc_2	7/18B	TDP-169	9700326.1
26.3	0.994	0.01430	0.100	0.331	61.8	P	N/A	6.20	6.26	6.29	6.40	6.40	63.00	N/A	N/A	N/A	N/A	N/A	N/A	N/A	0.7	N/A	N/A	N/A	N/A	70E8_6s1d2Vc_2	7/18B	TDP-169	9700327
26.3	0.994	0.01430	0.100	0.331	61.8	P	N/A	6.20	6.26	6.29	6.40	6.40	63.00	N/A	N/A	N/A	N/A	N/A	N/A	N/A	n/a	N/A	N/A	N/A	N/A	70E8_6s1d2Vc_2	7/18B	TDP-169	9700327.1
26.3	0.994	0.01430	0.100	0.331	61.8	P	N/A	6.20	6.26	6.29	6.40	6.40	63.00	N/A	N/A	N/A	N/A	N/A	N/A	N/A	n/a	N/A	N/A	N/A	N/A	70E8_6s1d2Vc_2	7/18B	TDP-169	9700327.2
26.3	0.994	0.01430	0.100	0.331	61.8	P	N/A	6.20	6.26	6.29	6.40	6.40	63.00	N/A	N/A	N/A	N/A	N/A	N/A	N/A	0.0	N/A	N/A	N/A	N/A	70E8_6s1d2Vc_2	7/18B	TDP-169	9700328
26.3	0.994	0.01430	0.100	0.331	61.8	P	N/A	6.20	6.26	6.29	6.40	6.40	63.00	N/A	N/A	N/A	N/A	N/A	N/A	N/A	n/a	N/A	N/A	N/A	N/A	70E8_6s1d2Vc_2	7/18B	TDP-169	9700328.1
26.3	0.994	0.01430	0.100	0.331	61.8	P	N/A	6.20	6.26	6.29	6.40	6.40	63.00	N/A	N/A	N/A	N/A	N/A	N/A	N/A	n/a	N/A	N/A	N/A	N/A	70E8_6s1d2Vc_2	7/18B	TDP-169	9700328.2

Table B.5. Data from 2008 Tests in Large-Scale Vessel with Elliptical Head A.11

Row Number	Test	Case ID	Tank Diameter	Head Shape	Dish Height	Dish Volume	Tank Fill Height	Return Line Height	Nozzle Inner Diameter	Nozzle Stand-off Distance	Pulse Tube Configuration	Installed Nozzles	Outer Nozzles Operated	Inner Nozzles Operated	Pulse Tube Outer Diameter	Outer PJM Radius	Inner PJM Radius	"FIO" Outer PJM Impingement Angle	"FIO" Inner PJM Impingement Angle	Ratio Outer PJM to Tank Radius	Ratio Inner PJM to Tank Radius	Simulant	Solids Density	Particle Diameter d5	Particle Diameter d50	Particle Diameter d95	Void Fraction
text	text	text	in.	text	in.	in. ^{3}	in.	in.	in.	in.	text	number	number	number	in.	in.	in.	deg	deg	nondim	nondim	text	g/cm^3	m	m	m	fraction
MSS	M/DDX	ID	D	HS	H_{dish}	V_{dish}	H	Rtn	d	sod	PT	N	N_O	N_I	PT_{od}	R_O	R_I	θ_O	θ_I	R_O/R	R_I/R	sxdx	ρ_s	d_5	d_{50}	d_{95}	vf
9700328.3	7/18B	70E8_6s1d2Vc_2	70	E	19	49770.7	94	80	0.92	1.380	8TA	8	4	4	3.5	23.5	17.5	21.9	16.1	0.67	0.50	s1d2	2.48	0.0000569	0.0000693	0.0000821	0.3750
9700329	7/18B	70E8_6s1d2Vc_2	70	E	19	49770.7	94	80	0.92	1.380	8TA	8	4	4	3.5	23.5	17.5	21.9	16.1	0.67	0.50	s1d2	2.48	0.0000569	0.0000693	0.0000821	0.3750
9700329.1	7/18B	70E8_6s1d2Vc_2	70	E	19	49770.7	94	80	0.92	1.380	8TA	8	4	4	3.5	23.5	17.5	21.9	16.1	0.67	0.50	s1d2	2.48	0.0000569	0.0000693	0.0000821	0.3750
9700330	7/18B	70E8_6s1d2Vc_2	70	E	19	49770.7	94	80	0.92	1.380	8TA	8	4	4	3.5	23.5	17.5	21.9	16.1	0.67	0.50	s1d2	2.48	0.0000569	0.0000693	0.0000821	0.3750
9700331	7/18B	70E8_6s1d2Vc_2	70	E	19	49770.7	94	80	0.92	1.380	8TA	8	4	4	3.5	23.5	17.5	21.9	16.1	0.67	0.50	s1d2	2.48	0.0000569	0.0000693	0.0000821	0.3750
9700332	7/18C	70E8_6s1d2Vc_7	70	E	19	49770.7	94	80	0.92	1.380	8TA	8	4	0	3.5	23.5	17.5	21.9	16.1	0.67	0.50	s1d2	2.48	0.0000569	0.0000693	0.0000821	0.3750
9700333	7/18C	70E8_6s1d2Vc_7	70	E	19	49770.7	94	80	0.92	1.380	8TA	8	4	0	3.5	23.5	17.5	21.9	16.1	0.67	0.50	s1d2	2.48	0.0000569	0.0000693	0.0000821	0.3750
9700334	7/18C	70E8_6s1d2Vc_7	70	E	19	49770.7	94	80	0.92	1.380	8TA	8	4	0	3.5	23.5	17.5	21.9	16.1	0.67	0.50	s1d2	2.48	0.0000569	0.0000693	0.0000821	0.3750
9700335	7/18C	70E8_6s1d2Vc_7	70	E	19	49770.7	94	80	0.92	1.380	8TA	8	4	0	3.5	23.5	17.5	21.9	16.1	0.67	0.50	s1d2	2.48	0.0000569	0.0000693	0.0000821	0.3750
9700336	7/18C	70E8_6s1d2Vc_7	70	E	19	49770.7	94	80	0.92	1.380	8TA	8	4	0	3.5	23.5	17.5	21.9	16.1	0.67	0.50	s1d2	2.48	0.0000569	0.0000693	0.0000821	0.3750
9700337M	7/18C	70E8_6s1d2Vc_7	70	E	19	49770.7	94	80	0.92	1.380	8TA	8	4	0	3.5	23.5	17.5	21.9	16.1	0.67	0.50	s1d2	2.48	0.0000569	0.0000693	0.0000821	0.3750
9700338M	7/18C	70E8_6s1d2Vc_7	70	E	19	49770.7	94	80	0.92	1.380	8TA	8	4	0	3.5	23.5	17.5	21.9	16.1	0.67	0.50	s1d2	2.48	0.0000569	0.0000693	0.0000821	0.3750

Table B.5. Data from 2008 Tests in Large-Scale Vessel with Elliptical Head B.11

Tank Water Temperature	Water Density	Solids Fraction	Pulse Volume Fraction	Duty Cycle	Cycle Time	Pulsed or Steady Jet	Us Steady Jet	U1 Pulsing Jet	U2 URMS	U3 URM3	Discharge Velocity	Critical Suspension Velocity	Average Peak Cloud Height	UCS Condition	UCS Method	UCS Flag	UCS Center Flag	UCS udv Flag	UCS based on Decreasing Velocity	Sweep Increase / Decrease	UDV Height Bed	Particle Motion	Solids Level	Outer Bottom Pattern	Inner Bottom Pattern	Case ID	Test	TDP	Row Number
C	g/cm³	fraction	fraction	fraction	s	text	m/s	m/s	m/s	m/s	m/s	m/s	in.	m/s	text	text	text	text	m/s	text	mm	text	text	text	text	text	text	text	text
T	ρ_ℓ	ϕ_S	ϕ_p	DC	t_C	Jet	U_S	U1	U2	U3	U	U_{CS}	H_C	U_{CSR}	U_{CSM}	U_{CS}vis	U_{CS}cen	U_{CS}udv	$U_{CS_}D$	S_W	H_{bed}	PM	Sol	SP_O	SP_I	ID	M/DDX	TDP	MSS
26.3	0.994	0.01430	0.100	0.331	61.8	P	N/A	6.20	6.26	6.29	6.40	6.40	63.00	N/A	N/A	N/A	N/A	N/A	N/A	N/A	n/a	N/A	N/A	N/A	N/A	70E8_6s1d2Vc_2	7/18B	TDP-169	9700328.3
26.3	0.994	0.01430	0.100	0.331	61.8	P	N/A	6.20	6.26	6.29	6.40	6.40	63.00	N/A	N/A	N/A	N/A	N/A	N/A	N/A	0.0	N/A	N/A	N/A	N/A	70E8_6s1d2Vc_2	7/18B	TDP-169	9700329
26.3	0.994	0.01430	0.100	0.331	61.8	P	N/A	6.20	6.26	6.29	6.40	6.40	63.00	N/A	N/A	N/A	N/A	N/A	N/A	N/A	n/a	N/A	N/A	N/A	N/A	70E8_6s1d2Vc_2	7/18B	TDP-169	9700329.1
26.3	0.994	0.01430	0.100	0.331	61.8	P	N/A	6.20	6.26	6.29	6.40	6.40	63.00	N/A	N/A	N/A	N/A	N/A	N/A	N/A	0.9	N/A	N/A	N/A	N/A	70E8_6s1d2Vc_2	7/18B	TDP-169	9700330
26.3	0.994	0.01430	0.100	0.331	61.8	P	N/A	6.20	6.26	6.29	6.40	6.40	63.00	N/A	N/A	N/A	N/A	N/A	N/A	N/A	0.0	N/A	N/A	N/A	N/A	70E8_6s1d2Vc_2	7/18B	TDP-169	9700331
26.6	0.994	0.01430	0.100	0.324	132.0	P	N/A	5.93	5.95	5.97	6.00	8.20	23.00	N/A	N/A	N/A	N/A	N/A	N/A	D	12.2	1	N/A	N/A	N/A	70E8_6s1d2Vc_7	7/18C	TDP-169	9700332
26.5	0.994	0.01430	0.100	0.325	113.0	P	N/A	6.88	6.91	6.93	7.00	8.20	29.75	N/A	N/A	N/A	N/A	N/A	N/A	I	10.5	1	N/A	N/A	N/A	70E8_6s1d2Vc_7	7/18C	TDP-169	9700333
26.6	0.994	0.01430	0.100	0.325	105.6	P	N/A	7.37	7.41	7.43	7.50	8.20	40.50	N/A	N/A	N/A	N/A	N/A	N/A	I	10.2	1	N/A	N/A	N/A	70E8_6s1d2Vc_7	7/18C	TDP-169	9700334
26.6	0.994	0.01430	0.100	0.326	99.0	P	N/A	7.87	7.91	7.93	8.00	8.20	45.50	N/A	N/A	N/A	N/A	N/A	N/A	I	9.7	1	N/A	N/A	N/A	70E8_6s1d2Vc_7	7/18C	TDP-169	9700335
26.8	0.994	0.01430	0.100	0.326	99.0	P	N/A	7.87	7.90	7.93	8.00	8.20	47.00	N/A	N/A	N/A	N/A	N/A	N/A	D	5.3	1	N/A	N/A	N/A	70E8_6s1d2Vc_7	7/18C	TDP-169	9700336
26.7	0.994	0.01430	0.101	0.326	96.6	P	N/A	8.08	8.12	8.14	8.20	8.20	49.50	8.20	udv	N/A	N/A	UCSudv	N/A	I	0.0	1	N/A	N/A	N/A	70E8_6s1d2Vc_7	7/18C	TDP-169	9700337
26.8	0.994	0.01430	0.101	0.327	94.2	P	N/A	8.27	8.32	8.34	8.40	8.20	52.50	N/A	N/A	N/A	UCScen	N/A	N/A	I	0.0	2	N/A	N/A	N/A	70E8_6s1d2Vc_7	7/18C	TDP-169	9700338

Table B.6. Data from 2008 in Large-Scale Vessel with Flanged and Dished Head A.1

Row Number	Test	Case ID	Tank Diameter	Head Shape	Dish Height	Dish Volume	Tank Fill Height	Return Line Height	Nozzle Inner Diameter	Nozzle Stand-off Distance	Pulse Tube Configuration	Installed Nozzles	Outer Nozzles Operated	Inner Nozzles Operated	Pulse Tube Outer Diameter	Outer PJM Radius	Inner PJM Radius	"FIO" Outer PJM Impingement Angle	"FIO" Inner PJM Impingement Angle	Ratio Outer PJM to Tank Radius	Ratio Inner PJM to Tank Radius	Simulant	Solids Density	Particle Diameter d5	Particle Diameter d50	Particle Diameter d95	Void Fraction
text	text	text	in.	text	in.	in. ^{3}	in.	in.	in.	in.	text	number	number	number	in.	in.	in.	deg	deg	nondim	nondim	text	g/cm^3	m	m	m	fraction
MSS	M/DDX	ID	D	HS	H_{dish}	V_{dish}	H	Rtn	d	sod	PT	N	N_O	N_I	PT_{od}	R_O	R_I	θ_O	θ_I	R_O/R	R_I/R	sxdx	ρ_s	d_5	d_{50}	d_{95}	vf
700204	4/7A	70F_6s2d2Yc_1_FM01[1]	70	FD	12.7	30569.0	88	83 5/8	0.92	1.380	HLP-22	12	8	4	3.5	26.4	11.7	22.4	9.7	0.75	0.33	s2d2	4.18	0.0000609	0.0000756	0.0000931	0.3684
700205	4/7A	70F_6s2d2Yc_1_FM01	70	FD	12.7	30569.0	88	83 5/8	0.92	1.380	HLP-22	12	8	4	3.5	26.4	11.7	22.4	9.7	0.75	0.33	s2d2	4.18	0.0000609	0.0000756	0.0000931	0.3684
700206	4/7A	70F_6s2d2Yc_1_FM01	70	FD	12.7	30569.0	88	83 5/8	0.92	1.380	HLP-22	12	8	4	3.5	26.4	11.7	22.4	9.7	0.75	0.33	s2d2	4.18	0.0000609	0.0000756	0.0000931	0.3684
700207	4/7A	70F_6s2d2Yc_1_FM01	70	FD	12.7	30569.0	88	83 5/8	0.92	1.380	HLP-22	12	8	4	3.5	26.4	11.7	22.4	9.7	0.75	0.33	s2d2	4.18	0.0000609	0.0000756	0.0000931	0.3684
700208M	4/7A	70F_6s2d2Yc_1_FM01	70	FD	12.7	30569.0	88	83 5/8	0.92	1.380	HLP-22	12	8	4	3.5	26.4	11.7	22.4	9.7	0.75	0.33	s2d2	4.18	0.0000609	0.0000756	0.0000931	0.3684
700208.1	4/7A	70F_6s2d2Yc_1_FM01	70	FD	12.7	30569.0	88	83 5/8	0.92	1.380	HLP-22	12	8	4	3.5	26.4	11.7	22.4	9.7	0.75	0.33	s2d2	4.18	0.0000609	0.0000756	0.0000931	0.3684
700208.2	4/7A	70F_6s2d2Yc_1_FM01	70	FD	12.7	30569.0	88	83 5/8	0.92	1.380	HLP-22	12	8	4	3.5	26.4	11.7	22.4	9.7	0.75	0.33	s2d2	4.18	0.0000609	0.0000756	0.0000931	0.3684
700209	4/7A	70F_6s2d2Yc_1_FM01	70	FD	12.7	30569.0	88	83 5/8	0.92	1.380	HLP-22	12	8	4	3.5	26.4	11.7	22.4	9.7	0.75	0.33	s2d2	4.18	0.0000609	0.0000756	0.0000931	0.3684
700210	4/7A	70F_6s2d2Yc_1_FM01	70	FD	12.7	30569.0	88	83 5/8	0.92	1.380	HLP-22	12	8	4	3.5	26.4	11.7	22.4	9.7	0.75	0.33	s2d2	4.18	0.0000609	0.0000756	0.0000931	0.3684
700211	4/7A	70F_6s2d2Yc_1_FM01	70	FD	12.7	30569.0	88	83 5/8	0.92	1.380	HLP-22	12	8	4	3.5	26.4	11.7	22.4	9.7	0.75	0.33	s2d2	4.18	0.0000609	0.0000756	0.0000931	0.3684
700211.1	4/7A	70F_6s2d2Yc_1_FM01	70	FD	12.7	30569.0	88	83 5/8	0.92	1.380	HLP-22	12	8	4	3.5	26.4	11.7	22.4	9.7	0.75	0.33	s2d2	4.18	0.0000609	0.0000756	0.0000931	0.3684
700212	4/7A	70F_6s2d2Yc_1_FM01	70	FD	12.7	30569.0	88	83 5/8	0.92	1.380	HLP-22	12	8	4	3.5	26.4	11.7	22.4	9.7	0.75	0.33	s2d2	4.18	0.0000609	0.0000756	0.0000931	0.3684
700212.1	4/7A	70F_6s2d2Yc_1_FM01	70	FD	12.7	30569.0	88	83 5/8	0.92	1.380	HLP-22	12	8	4	3.5	26.4	11.7	22.4	9.7	0.75	0.33	s2d2	4.18	0.0000609	0.0000756	0.0000931	0.3684
700213	4/7A	70F_6s2d2Yc_1_FM01	70	FD	12.7	30569.0	88	83 5/8	0.92	1.380	HLP-22	12	8	4	3.5	26.4	11.7	22.4	9.7	0.75	0.33	s2d2	4.18	0.0000609	0.0000756	0.0000931	0.3684
700214	4/7A	70F_6s2d2Yc_1_FM01	70	FD	12.7	30569.0	88	83 5/8	0.92	1.380	HLP-22	12	8	4	3.5	26.4	11.7	22.4	9.7	0.75	0.33	s2d2	4.18	0.0000609	0.0000756	0.0000931	0.3684
700215M	4/7A	70F_6s2d2Yc_1_FM01	70	FD	12.7	30569.0	88	83 5/8	0.92	1.380	HLP-22	12	8	4	3.5	26.4	11.7	22.4	9.7	0.75	0.33	s2d2	4.18	0.0000609	0.0000756	0.0000931	0.3684
700216M	4/7A	70F_6s2d2Yc_1_FM01	70	FD	12.7	30569.0	88	83 5/8	0.92	1.380	HLP-22	12	8	4	3.5	26.4	11.7	22.4	9.7	0.75	0.33	s2d2	4.18	0.0000609	0.0000756	0.0000931	0.3684
700218M	4/8A	70F_6s2d2Yh_1	70	FD	12.7	30569.0	89	83 5/8	0.92	1.380	HLP-22	12	8	4	3.5	26.4	11.7	22.4	9.7	0.75	0.33	s2d2	4.18	0.0000609	0.0000756	0.0000931	0.3684
700220	4/8A	70F_6s2d2Yg_1	70	FD	12.7	30569.0	89	83 5/8	0.92	1.380	HLP-22	12	8	4	3.5	26.4	11.7	22.4	9.7	0.75	0.33	s2d2	4.18	0.0000609	0.0000756	0.0000931	0.3684
700223	4/10A	70F_4s2d2Yi_1	70	FD	12.7	30569.0	90 1/2	83 5/8	0.613	0.920	HLP-22	12	8	4	3.5	26.4	11.7	22.4	9.7	0.75	0.33	s2d2	4.18	0.0000609	0.0000756	0.0000931	0.3684
700224M	4/10A	70F_4s2d2Yc_1	70	FD	12.7	30569.0	90 1/2	83 5/8	0.613	0.920	HLP-22	12	8	4	3.5	26.4	11.7	22.4	9.7	0.75	0.33	s2d2	4.18	0.0000609	0.0000756	0.0000931	0.3684
700227M	4/10B	70F_4s2d2Yk_1	70	FD	12.7	30569.0	90 1/2	83 5/8	0.613	0.920	HLP-22	12	8	4	3.5	26.4	11.7	22.4	9.7	0.75	0.33	s2d2	4.18	0.0000609	0.0000756	0.0000931	0.3684
700228M	4/10B	70F_4s2d2Yd_1	70	FD	12.7	30569.0	90 1/2	83 5/8	0.613	0.920	HLP-22	12	8	4	3.5	26.4	11.7	22.4	9.7	0.75	0.33	s2d2	4.18	0.0000609	0.0000756	0.0000931	0.3684
700229M	4/10B	70F_4s2d2Yd_1	70	FD	12.7	30569.0	90 1/2	83 5/8	0.613	0.920	HLP-22	12	8	4	3.5	26.4	11.7	22.4	9.7	0.75	0.33	s2d2	4.18	0.0000609	0.0000756	0.0000931	0.3684
700230	4/10C	70F_4s2d2Yc_1	70	FD	12.7	30569.0	90 1/2	83 5/8	0.613	0.920	HLP-22	12	8	4	3.5	26.4	11.7	22.4	9.7	0.75	0.33	s2d2	4.18	0.0000609	0.0000756	0.0000931	0.3684
700231	4/10C	70F_4s2d2Yc_1	70	FD	12.7	30569.0	90 1/2	83 5/8	0.613	0.920	HLP-22	12	8	4	3.5	26.4	11.7	22.4	9.7	0.75	0.33	s2d2	4.18	0.0000609	0.0000756	0.0000931	0.3684
700232	4/10C	70F_4s2d2Yc_1	70	FD	12.7	30569.0	90 1/2	83 5/8	0.613	0.920	HLP-22	12	8	4	3.5	26.4	11.7	22.4	9.7	0.75	0.33	s2d2	4.18	0.0000609	0.0000756	0.0000931	0.3684
700233	4/10C	70F_4s2d2Yc_1	70	FD	12.7	30569.0	90 1/2	83 5/8	0.613	0.920	HLP-22	12	8	4	3.5	26.4	11.7	22.4	9.7	0.75	0.33	s2d2	4.18	0.0000609	0.0000756	0.0000931	0.3684
700234	4/14A	70F_4s1d1Zc_1	70	FD	12.7	30569.0	89	83 5/8	0.613	0.920	HLP-22	12	8	4	3.5	26.4	11.7	22.4	9.7	0.75	0.33	s1d1	2.46	0.0001428	0.0001664	0.0001951	0.4118
700235	4/14A	70F_4s1d1Zc_1	70	FD	12.7	30569.0	89	83 5/8	0.613	0.920	HLP-22	12	8	4	3.5	26.4	11.7	22.4	9.7	0.75	0.33	s1d1	2.46	0.0001428	0.0001664	0.0001951	0.4118
700236	4/14A	70F_4s1d1Zc_1	70	FD	12.7	30569.0	89	83 5/8	0.613	0.920	HLP-22	12	8	4	3.5	26.4	11.7	22.4	9.7	0.75	0.33	s1d1	2.46	0.0001428	0.0001664	0.0001951	0.4118
700237M	4/14A	70F_4s1d1Zc_1	70	FD	12.7	30569.0	89	83 5/8	0.613	0.920	HLP-22	12	8	4	3.5	26.4	11.7	22.4	9.7	0.75	0.33	s1d1	2.46	0.0001428	0.0001664	0.0001951	0.4118
700238	4/14A	70F_4s1d1Zc_1	70	FD	12.7	30569.0	89	83 5/8	0.613	0.920	HLP-22	12	8	4	3.5	26.4	11.7	22.4	9.7	0.75	0.33	s1d1	2.46	0.0001428	0.0001664	0.0001951	0.4118
700239	4/14A	70F_4s1d1Zc_1	70	FD	12.7	30569.0	89	83 5/8	0.613	0.920	HLP-22	12	8	4	3.5	26.4	11.7	22.4	9.7	0.75	0.33	s1d1	2.46	0.0001428	0.0001664	0.0001951	0.4118
700240	4/14A	70F_4s1d1Zc_1	70	FD	12.7	30569.0	89	83 5/8	0.613	0.920	HLP-22	12	8	4	3.5	26.4	11.7	22.4	9.7	0.75	0.33	s1d1	2.46	0.0001428	0.0001664	0.0001951	0.4118
700241	4/14A	70F_4s1d1Zc_1	70	FD	12.7	30569.0	89	83 5/8	0.613	0.920	HLP-22	12	8	4	3.5	26.4	11.7	22.4	9.7	0.75	0.33	s1d1	2.46	0.0001428	0.0001664	0.0001951	0.4118
700242	4/14A	70F_4s1d1Zc_1	70	FD	12.7	30569.0	89	83 5/8	0.613	0.920	HLP-22	12	8	4	3.5	26.4	11.7	22.4	9.7	0.75	0.33	s1d1	2.46	0.0001428	0.0001664	0.0001951	0.4118
700243	4/14A	70F_4s1d1Zc_1	70	FD	12.7	30569.0	89	83 5/8	0.613	0.920	HLP-22	12	8	4	3.5	26.4	11.7	22.4	9.7	0.75	0.33	s1d1	2.46	0.0001428	0.0001664	0.0001951	0.4118
700244	4/14A	70F_4s1d1Zc_1	70	FD	12.7	30569.0	89	83 5/8	0.613	0.920	HLP-22	12	8	4	3.5	26.4	11.7	22.4	9.7	0.75	0.33	s1d1	2.46	0.0001428	0.0001664	0.0001951	0.4118
700244.1	4/14A	70F_4s1d1Zc_1	70	FD	12.7	30569.0	89	83 5/8	0.613	0.920	HLP-22	12	8	4	3.5	26.4	11.7	22.4	9.7	0.75	0.33	s1d1	2.46	0.0001428	0.0001664	0.0001951	0.4118
700244.2	4/14A	70F_4s1d1Zc_1	70	FD	12.7	30569.0	89	83 5/8	0.613	0.920	HLP-22	12	8	4	3.5	26.4	11.7	22.4	9.7	0.75	0.33	s1d1	2.46	0.0001428	0.0001664	0.0001951	0.4118

[1] FM01 indicates flow meter time constant of 0.1 instead of 0.01.

Table B.6. Data from 2008 in Large-Scale Vessel with Flanged and Dished Head B.1

Tank Water Temperature	Water Density	Solids Fraction	Pulse Volume Fraction	Duty Cycle	Cycle Time	Pulsed or Steady Jet	Us Steady Jet	U1 Pulsing Jet	U2 URMS	U3 URM3	Discharge Velocity	Critical Suspension Velocity	Average Peak Cloud Height	UCS Condition	UCS Method	UCS Flag	UCS Center Flag	UCS udv Flag	UCS based on Decreasing Velocity	Sweep Increase / Decrease	UDV Height Bed	Particle Motion	Solids Level	Outer Bottom Pattern	Inner Bottom Pattern	Case ID	Test	TDP	Row Number
C	g/cm³	fraction	fraction	fraction	s	text	m/s	m/s	m/s	m/s	m/s	m/s	in.	m/s	text	text	text	text	m/s	text	mm	text	text	text	text	text	text	text	text
T	ρ_l	ϕ_S	ϕ_P	DC	t_C	Jet	U_S	U1	U2	U3	U	U_{CS}	H_C	U_{CSR}	U_{CSM}	U_{CS}vis	U_{CS}cen	U_{CS}udv	U_{CS}_D	S_W	H_{bed}	PM	Sol	SP_O	SP_I	ID	M/DDX	TDP	MSS
20.8	0.995	0.00500	0.049	0.332	22.5	P	N/A	5.56	5.75	5.85	6.20	6.70	N/A	N/A	N/A	N/A	N/A	N/A	N/A	I	9.4	1	N/A	N/A	N/A	70F_6s2d2Yc_1_FM01	4/7A	TDP-133	700204
20.6	0.995	0.00500	0.050	0.338	21.7	P	N/A	5.74	5.92	6.01	6.40	6.70	N/A	N/A	N/A	N/A	N/A	N/A	N/A	I	5.4	1	N/A	N/A	N/A	70F_6s2d2Yc_1_FM01	4/7A	TDP-133	700205
20.7	0.995	0.00500	0.050	0.341	20.8	P	N/A	5.95	6.13	6.24	6.60	6.70	N/A	N/A	N/A	N/A	N/A	N/A	N/A	I	3.2	1	N/A	N/A	N/A	70F_6s2d2Yc_1_FM01	4/7A	TDP-133	700206
20.7	0.995	0.00500	0.050	0.336	21.2	P	N/A	5.94	6.13	6.23	6.60	6.70	22.00	N/A	N/A	N/A	N/A	N/A	N/A	I	4.0	1	N/A	N/A	N/A	70F_6s2d2Yc_1_FM01	4/7A	TDP-133	700207
20.7	0.995	0.00500	0.050	0.338	20.6	P	N/A	6.06	6.25	6.36	6.70	6.70	22.00	6.70	udv	N/A	UCScen	UCSudv	N/A	I	0.0	2	N/A	N/A	N/A	70F_6s2d2Yc_1_FM01	4/7A	TDP-133	700208
20.7	0.995	0.00500	0.050	0.338	20.6	P	N/A	6.06	6.25	6.36	6.70	6.70	N/A	N/A	N/A	N/A	N/A	N/A	N/A	N/A	n/a	N/A	N/A	N/A	N/A	70F_6s2d2Yc_1_FM01	4/7A	TDP-133	700208.1
20.7	0.995	0.00500	0.050	0.338	20.6	P	N/A	6.06	6.25	6.36	6.70	6.70	N/A	N/A	N/A	N/A	N/A	N/A	N/A	N/A	n/a	N/A	N/A	N/A	N/A	70F_6s2d2Yc_1_FM01	4/7A	TDP-133	700208.2
20.7	0.995	0.00500	0.050	0.338	20.6	P	N/A	6.06	6.25	6.36	6.70	6.70	N/A	N/A	N/A	N/A	N/A	N/A	N/A	I	0.0	NA	N/A	N/A	N/A	70F_6s2d2Yc_1_FM01	4/7A	TDP-133	700209
20.7	0.995	0.00500	0.050	0.338	20.6	P	N/A	6.06	6.25	6.36	6.70	6.70	N/A	N/A	N/A	N/A	N/A	N/A	N/A	N/A	0.6	N/A	N/A	N/A	N/A	70F_6s2d2Yc_1_FM01	4/7A	TDP-133	700210
20.7	0.995	0.00500	0.050	0.338	20.6	P	N/A	6.06	6.25	6.36	6.70	6.70	N/A	N/A	N/A	N/A	N/A	N/A	N/A	N/A	0.0	N/A	N/A	N/A	N/A	70F_6s2d2Yc_1_FM01	4/7A	TDP-133	700211
20.7	0.995	0.00500	0.050	0.338	20.6	P	N/A	6.06	6.25	6.36	6.70	6.70	N/A	N/A	N/A	N/A	N/A	N/A	N/A	N/A	n/a	N/A	N/A	N/A	N/A	70F_6s2d2Yc_1_FM01	4/7A	TDP-133	700211.1
20.7	0.995	0.00500	0.050	0.338	20.6	P	N/A	6.06	6.25	6.36	6.70	6.70	N/A	N/A	N/A	N/A	N/A	N/A	N/A	N/A	1.3	N/A	N/A	N/A	N/A	70F_6s2d2Yc_1_FM01	4/7A	TDP-133	700212
20.7	0.995	0.00500	0.050	0.338	20.6	P	N/A	6.06	6.25	6.36	6.70	6.70	N/A	N/A	N/A	N/A	N/A	N/A	N/A	N/A	n/a	N/A	N/A	N/A	N/A	70F_6s2d2Yc_1_FM01	4/7A	TDP-133	700212.1
20.7	0.995	0.00500	0.050	0.338	20.6	P	N/A	6.06	6.25	6.36	6.70	6.70	N/A	N/A	N/A	N/A	N/A	N/A	N/A	N/A	2.5	N/A	N/A	N/A	N/A	70F_6s2d2Yc_1_FM01	4/7A	TDP-133	700213
20.7	0.995	0.00500	0.050	0.338	20.6	P	N/A	6.06	6.25	6.36	6.70	6.70	N/A	N/A	N/A	N/A	N/A	N/A	N/A	N/A	1.9	N/A	N/A	N/A	N/A	70F_6s2d2Yc_1_FM01	4/7A	TDP-133	700214
21.0	0.995	0.00500	0.050	0.339	18.4	P	N/A	6.73	6.97	7.10	7.60	6.70	36.00	N/A	N/A	N/A	N/A	N/A	N/A	I	0.0	4	N/A	N/A	N/A	70F_6s2d2Yc_1_FM01	4/7A	TDP-133	700215
20.8	0.995	0.00500	0.049	0.315	20.2	P	N/A	6.57	6.76	6.86	7.20	6.70	29.50	N/A	N/A	N/A	N/A	N/A	N/A	D	0.0	4	N/A	N/A	N/A	70F_6s2d2Yc_1_FM01	4/7A	TDP-133	700216
22.5	0.995	0.00500	0.050	0.237	26.6	P	N/A	6.70	6.94	7.07	7.50	7.50	24.00	7.50	center	N/A	UCScen	N/A	N/A	(null)	4.1	2	N/A	N/A	N/A	70F_6s2d2Yh_1	4/8A	TDP-134	700218
22.8	0.996	0.00500	0.050	0.220	24.0	P	N/A	7.95	8.29	8.48	9.10	N/A	30.25	N/A	N/A	N/A	N/A	N/A	N/A	I	1.0	4	N/A	N/A	N/A	70F_6s2d2Yg_1	4/8A	TDP-134	700220
21.4	0.995	0.00500	0.054	0.278	37.0	P	N/A	10.02	10.22	10.32	10.60	N/A	23.25	N/A	N/A	N/A	N/A	N/A	N/A	(null)	0.6	1	N/A	N/A	N/A	70F_4s2d2Yi_1	4/10A	TDP-135	700223
21.5	0.995	0.00500	0.050	0.334	28.4	P	N/A	9.95	10.17	10.28	10.60	10.60	23.50	10.60	udv	N/A	UCScen	UCSudv	N/A	(null)	1.7	2	N/A	N/A	N/A	70F_4s2d2Yc_1	4/10A	TDP-135	700224
21.8	0.995	0.00500	0.050	0.143	62.0	P	N/A	10.67	10.92	11.05	11.40	11.40	22.50	11.40	udv	N/A	N/A	UCSudv	N/A	(null)	9.8	1	N/A	N/A	N/A	70F_4s2d2Yk_1	4/10B	TDP-135	700227
21.9	0.995	0.00500	0.050	0.183	49.0	P	N/A	10.67	10.92	11.05	11.40	11.40	23.00	11.40	udv	N/A	N/A	UCSudv	N/A	(null)	3.5	1	N/A	N/A	N/A	70F_4s2d2Yd_1	4/10B	TDP-135	700228
22.1	0.995	0.00500	0.050	0.184	48.0	P	N/A	10.84	11.10	11.23	11.60	11.40	23.00	N/A	N/A	N/A	UCScen	N/A	N/A	I	2.0	2	N/A	N/A	N/A	70F_4s2d2Yd_1	4/10B	TDP-135	700229
22.3	0.995	0.00500	0.050	0.338	26.4	P	N/A	10.70	10.95	11.08	11.50	N/A	28.00	N/A	N/A	N/A	N/A	N/A	N/A	D	N/A	4	N/A	N/A	N/A	70F_4s2d2Yc_1	4/10C	TDP-135	700230
22.4	0.995	0.00500	0.050	0.337	25.4	P	N/A	11.13	11.40	11.54	12.00	N/A	29.75	N/A	N/A	N/A	N/A	N/A	N/A	I	N/A	4	N/A	N/A	N/A	70F_4s2d2Yc_1	4/10C	TDP-135	700231
22.5	0.994	0.00500	0.050	0.335	24.4	P	N/A	11.59	11.89	12.04	12.50	N/A	45.75	N/A	N/A	N/A	N/A	N/A	N/A	I	N/A	4	N/A	N/A	N/A	70F_4s2d2Yc_1	4/10C	TDP-135	700232
22.4	0.995	0.00500	0.050	0.333	25.4	P	N/A	11.28	11.56	11.71	12.20	N/A	32.00	N/A	N/A	N/A	N/A	N/A	N/A	D	N/A	4	N/A	N/A	N/A	70F_4s2d2Yc_1	4/10C	TDP-135	700233
25.0	0.994	0.00155	0.050	0.321	70.0	P	N/A	N/A	N/A	N/A	4.40	6.70	21.50	N/A	N/A	N/A	N/A	N/A	N/A	(null)	0.0	1	N/A	N/A	N/A	70F_4s1d1Zc_1	4/14A	TDP-136	700234
25.1	0.994	0.00155	0.050	0.327	53.0	P	N/A	5.45	5.53	5.57	5.70	6.70	22.50	N/A	N/A	N/A	N/A	N/A	N/A	I	16.3	1	N/A	N/A	N/A	70F_4s1d1Zc_1	4/14A	TDP-136	700235
25.0	0.994	0.00155	0.051	0.331	47.0	P	N/A	6.17	6.27	6.32	6.50	6.70	25.25	N/A	N/A	N/A	UCScen	N/A	N/A	I	2.5	2	N/A	N/A	N/A	70F_4s1d1Zc_1	4/14A	TDP-136	700236
24.6	0.994	0.00155	0.050	0.332	45.4	P	N/A	6.35	6.45	6.51	6.70	6.70	25.50	6.70	udv	N/A	UCScen	UCSudv	N/A	I	1.5	2	N/A	N/A	N/A	70F_4s1d1Zc_1	4/14A	TDP-136	700237
24.6	0.994	0.00155	0.050	0.332	45.4	P	N/A	6.35	6.45	6.51	6.70	6.70	25.50	N/A	N/A	N/A	N/A	N/A	N/A	N/A	1.3	N/A	N/A	N/A	N/A	70F_4s1d1Zc_1	4/14A	TDP-136	700238
24.6	0.994	0.00155	0.050	0.332	45.4	P	N/A	6.35	6.45	6.51	6.70	6.70	25.50	N/A	N/A	N/A	N/A	N/A	N/A	N/A	0.0	N/A	N/A	N/A	N/A	70F_4s1d1Zc_1	4/14A	TDP-136	700239
24.6	0.994	0.00155	0.050	0.332	45.4	P	N/A	6.35	6.45	6.51	6.70	6.70	25.50	N/A	N/A	N/A	N/A	N/A	N/A	N/A	0.0	N/A	N/A	N/A	N/A	70F_4s1d1Zc_1	4/14A	TDP-136	700240
24.6	0.994	0.00155	0.050	0.332	45.4	P	N/A	6.35	6.45	6.51	6.70	6.70	25.50	N/A	N/A	N/A	N/A	N/A	N/A	N/A	0.0	N/A	N/A	N/A	N/A	70F_4s1d1Zc_1	4/14A	TDP-136	700241
24.6	0.994	0.00155	0.050	0.332	45.4	P	N/A	6.35	6.45	6.51	6.70	6.70	25.50	N/A	N/A	N/A	N/A	N/A	N/A	N/A	0.6	N/A	N/A	N/A	N/A	70F_4s1d1Zc_1	4/14A	TDP-136	700242
24.6	0.994	0.00155	0.050	0.332	45.4	P	N/A	6.35	6.45	6.51	6.70	6.70	25.50	N/A	N/A	N/A	N/A	N/A	N/A	N/A	0.0	N/A	N/A	N/A	N/A	70F_4s1d1Zc_1	4/14A	TDP-136	700243
24.6	0.994	0.00155	0.050	0.332	45.4	P	N/A	6.35	6.45	6.51	6.70	6.70	25.50	N/A	N/A	N/A	N/A	N/A	N/A	N/A	0.6	N/A	N/A	N/A	N/A	70F_4s1d1Zc_1	4/14A	TDP-136	700244
24.6	0.994	0.00155	0.050	0.332	45.4	P	N/A	6.35	6.45	6.51	6.70	6.70	25.50	N/A	N/A	N/A	N/A	N/A	N/A	N/A	n/a	N/A	N/A	N/A	N/A	70F_4s1d1Zc_1	4/14A	TDP-136	700244.1
24.6	0.994	0.00155	0.050	0.332	45.4	P	N/A	6.35	6.45	6.51	6.70	6.70	25.50	N/A	N/A	N/A	N/A	N/A	N/A	N/A	n/a	N/A	N/A	N/A	N/A	70F_4s1d1Zc_1	4/14A	TDP-136	700244.2

Table B.6. Data from 2008 in Large-Scale Vessel with Flanged and Dished Head A.2

Row Number	Test	Case ID	Tank Diameter	Head Shape	Dish Height	Dish Volume	Tank Fill Height	Return Line Height	Nozzle Inner Diameter	Nozzle Stand-off Distance	Pulse Tube Configuration	Installed Nozzles	Outer Nozzles Operated	Inner Nozzles Operated	Pulse Tube Outer Diameter	Outer PJM Radius	Inner PJM Radius	"FIO" Outer PJM Impingement Angle	"FIO" Inner PJM Impingement Angle	Ratio Outer PJM to Tank Radius	Ratio Inner PJM to Tank Radius	Simulant	Solids Density	Particle Diameter d5	Particle Diameter d50	Particle Diameter d95	Void Fraction
text	text	text	in.	text	in.	in. ^{3}	in.	in.	in.	in.	text	number	number	number	in.	in.	in.	deg	deg	nondim	nondim	text	g/cm^3	m	m	m	fraction
MSS	M/DDX	ID	D	HS	H_{dish}	V_{dish}	H	Rtn	d	sod	PT	N	N_O	N_I	PT_{od}	R_O	R_I	θ_O	θ_I	R_O/R	R_I/R	sxdx	ρ_s	d_5	d_{50}	d_{95}	vf
700245M	4/14A	70F_4s1d1Zc_1	70	FD	12.7	30569.0	89	83 5/8	0.613	0.920	HLP-22	12	8	4	3.5	26.4	11.7	22.4	9.7	0.75	0.33	s1d1	2.46	0.0001428	0.0001664	0.0001951	0.4118
700246M	4/14A	70F_4s1d1Zc_1	70	FD	12.7	30569.0	89	83 5/8	0.613	0.920	HLP-22	12	8	4	3.5	26.4	11.7	22.4	9.7	0.75	0.33	s1d1	2.46	0.0001428	0.0001664	0.0001951	0.4118
700247M	4/14A	70F_4s1d1Zc_1	70	FD	12.7	30569.0	89	83 5/8	0.613	0.920	HLP-22	12	8	4	3.5	26.4	11.7	22.4	9.7	0.75	0.33	s1d1	2.46	0.0001428	0.0001664	0.0001951	0.4118
700248	4/15A	70F_4s1d1Zc_2	70	FD	12.7	30569.0	88	83 5/8	0.613	0.920	HLP-22	12	8	4	3.5	26.4	11.7	22.4	9.7	0.75	0.33	s1d1	2.46	0.0001428	0.0001664	0.0001951	0.4118
700249	4/15A	70F_4s1d1Zc_2	70	FD	12.7	30569.0	88	83 5/8	0.613	0.920	HLP-22	12	8	4	3.5	26.4	11.7	22.4	9.7	0.75	0.33	s1d1	2.46	0.0001428	0.0001664	0.0001951	0.4118
700250	4/15A	70F_4s1d1Zc_2	70	FD	12.7	30569.0	88	83 5/8	0.613	0.920	HLP-22	12	8	4	3.5	26.4	11.7	22.4	9.7	0.75	0.33	s1d1	2.46	0.0001428	0.0001664	0.0001951	0.4118
700251	4/15A	70F_4s1d1Zc_2	70	FD	12.7	30569.0	88	83 5/8	0.613	0.920	HLP-22	12	8	4	3.5	26.4	11.7	22.4	9.7	0.75	0.33	s1d1	2.46	0.0001428	0.0001664	0.0001951	0.4118
700252M	4/15A	70F_4s1d1Zc_2	70	FD	12.7	30569.0	88	83 5/8	0.613	0.920	HLP-22	12	8	4	3.5	26.4	11.7	22.4	9.7	0.75	0.33	s1d1	2.46	0.0001428	0.0001664	0.0001951	0.4118
700253M	4/15A	70F_4s1d1Zc_2	70	FD	12.7	30569.0	88	83 5/8	0.613	0.920	HLP-22	12	8	4	3.5	26.4	11.7	22.4	9.7	0.75	0.33	s1d1	2.46	0.0001428	0.0001664	0.0001951	0.4118
700254M	4/15A	70F_4s1d1Zc_2	70	FD	12.7	30569.0	88	83 5/8	0.613	0.920	HLP-22	12	8	4	3.5	26.4	11.7	22.4	9.7	0.75	0.33	s1d1	2.46	0.0001428	0.0001664	0.0001951	0.4118
700255	4/15B	70F_4s1d1Zc_4	70	FD	12.7	30569.0	88 1/2	83 5/8	0.613	0.920	HLP-22	12	8	4	3.5	26.4	11.7	22.4	9.7	0.75	0.33	s1d1	2.46	0.0001428	0.0001664	0.0001951	0.4118
700256	4/15B	70F_4s1d1Zc_4	70	FD	12.7	30569.0	88 1/2	83 5/8	0.613	0.920	HLP-22	12	8	4	3.5	26.4	11.7	22.4	9.7	0.75	0.33	s1d1	2.46	0.0001428	0.0001664	0.0001951	0.4118
700257	4/15B	70F_4s1d1Zc_4	70	FD	12.7	30569.0	88 1/2	83 5/8	0.613	0.920	HLP-22	12	8	4	3.5	26.4	11.7	22.4	9.7	0.75	0.33	s1d1	2.46	0.0001428	0.0001664	0.0001951	0.4118
700258	4/15B	70F_4s1d1Zc_4	70	FD	12.7	30569.0	88 1/2	83 5/8	0.613	0.920	HLP-22	12	8	4	3.5	26.4	11.7	22.4	9.7	0.75	0.33	s1d1	2.46	0.0001428	0.0001664	0.0001951	0.4118
700259M	4/15B	70F_4s1d1Zc_4	70	FD	12.7	30569.0	88 1/2	83 5/8	0.613	0.920	HLP-22	12	8	4	3.5	26.4	11.7	22.4	9.7	0.75	0.33	s1d1	2.46	0.0001428	0.0001664	0.0001951	0.4118
700260M	4/15B	70F_4s1d1Zc_4	70	FD	12.7	30569.0	88 1/2	83 5/8	0.613	0.920	HLP-22	12	8	4	3.5	26.4	11.7	22.4	9.7	0.75	0.33	s1d1	2.46	0.0001428	0.0001664	0.0001951	0.4118
700261M	4/15B	70F_4s1d1Zc_4	70	FD	12.7	30569.0	88 1/2	83 5/8	0.613	0.920	HLP-22	12	8	4	3.5	26.4	11.7	22.4	9.7	0.75	0.33	s1d1	2.46	0.0001428	0.0001664	0.0001951	0.4118
700262	4/15C	70F_4s1d1Zc_2	70	FD	12.7	30569.0	88 1/2	83 5/8	0.613	0.920	HLP-22	12	8	4	3.5	26.4	11.7	22.4	9.7	0.75	0.33	s1d1	2.46	0.0001428	0.0001664	0.0001951	0.4118
700263	4/15C	70F_4s1d1Zc_2	70	FD	12.7	30569.0	88 1/2	83 5/8	0.613	0.920	HLP-22	12	8	4	3.5	26.4	11.7	22.4	9.7	0.75	0.33	s1d1	2.46	0.0001428	0.0001664	0.0001951	0.4118
700264	4/15C	70F_4s1d1Zc_2	70	FD	12.7	30569.0	88 1/2	83 5/8	0.613	0.920	HLP-22	12	8	4	3.5	26.4	11.7	22.4	9.7	0.75	0.33	s1d1	2.46	0.0001428	0.0001664	0.0001951	0.4118
700265	4/15C	70F_4s1d1Zc_2	70	FD	12.7	30569.0	88 1/2	83 5/8	0.613	0.920	HLP-22	12	8	4	3.5	26.4	11.7	22.4	9.7	0.75	0.33	s1d1	2.46	0.0001428	0.0001664	0.0001951	0.4118
700266	4/15C	70F_4s1d1Zc_2	70	FD	12.7	30569.0	88 1/2	83 5/8	0.613	0.920	HLP-22	12	8	4	3.5	26.4	11.7	22.4	9.7	0.75	0.33	s1d1	2.46	0.0001428	0.0001664	0.0001951	0.4118
700267	4/15C	70F_4s1d1Zc_2	70	FD	12.7	30569.0	88 1/2	83 5/8	0.613	0.920	HLP-22	12	8	4	3.5	26.4	11.7	22.4	9.7	0.75	0.33	s1d1	2.46	0.0001428	0.0001664	0.0001951	0.4118
700268	4/15C	70F_4s1d1Zc_2	70	FD	12.7	30569.0	88 1/2	83 5/8	0.613	0.920	HLP-22	12	8	4	3.5	26.4	11.7	22.4	9.7	0.75	0.33	s1d1	2.46	0.0001428	0.0001664	0.0001951	0.4118
700269	4/15C	70F_4s1d1Zc_2	70	FD	12.7	30569.0	88 1/2	83 5/8	0.613	0.920	HLP-22	12	8	4	3.5	26.4	11.7	22.4	9.7	0.75	0.33	s1d1	2.46	0.0001428	0.0001664	0.0001951	0.4118
700270	4/15C	70F_4s1d1Zc_2	70	FD	12.7	30569.0	88 1/2	83 5/8	0.613	0.920	HLP-22	12	8	4	3.5	26.4	11.7	22.4	9.7	0.75	0.33	s1d1	2.46	0.0001428	0.0001664	0.0001951	0.4118
700271	4/15C	70F_4s1d1Zc_2	70	FD	12.7	30569.0	88 1/2	83 5/8	0.613	0.920	HLP-22	12	8	4	3.5	26.4	11.7	22.4	9.7	0.75	0.33	s1d1	2.46	0.0001428	0.0001664	0.0001951	0.4118
700272	4/16A	70F_4s1d2Zc_1	70	FD	12.7	30569.0	88 1/2	83 5/8	0.613	0.920	HLP-22	12	8	4	3.5	26.4	11.7	22.4	9.7	0.75	0.33	s1d2	2.48	0.0000569	0.0000693	0.0000821	0.3750
700273M	4/16A	70F_4s1d2Zc_1	70	FD	12.7	30569.0	88 1/2	83 5/8	0.613	0.920	HLP-22	12	8	4	3.5	26.4	11.7	22.4	9.7	0.75	0.33	s1d2	2.48	0.0000569	0.0000693	0.0000821	0.3750
700274M	4/16A	70F_4s1d2Zc_1	70	FD	12.7	30569.0	88 1/2	83 5/8	0.613	0.920	HLP-22	12	8	4	3.5	26.4	11.7	22.4	9.7	0.75	0.33	s1d2	2.48	0.0000569	0.0000693	0.0000821	0.3750
700275	4/16A	70F_4s1d2Zc_1	70	FD	12.7	30569.0	88 1/2	83 5/8	0.613	0.920	HLP-22	12	8	4	3.5	26.4	11.7	22.4	9.7	0.75	0.33	s1d2	2.48	0.0000569	0.0000693	0.0000821	0.3750
700276M	4/16A	70F_4s1d2Zc_1	70	FD	12.7	30569.0	88 1/2	83 5/8	0.613	0.920	HLP-22	12	8	4	3.5	26.4	11.7	22.4	9.7	0.75	0.33	s1d2	2.48	0.0000569	0.0000693	0.0000821	0.3750
700276.1	4/17A	70F_4s1d2Zc_1	70	FD	12.7	30569.0	87 1/2	83 5/8	0.613	0.920	HLP-22	12	8	4	3.5	26.4	11.7	22.4	9.7	0.75	0.33	s1d2	2.48	0.0000569	0.0000693	0.0000821	0.3750
700277M	4/17A	70F_4s1d2Zc_1	70	FD	12.7	30569.0	87 1/2	83 5/8	0.613	0.920	HLP-22	12	8	4	3.5	26.4	11.7	22.4	9.7	0.75	0.33	s1d2	2.48	0.0000569	0.0000693	0.0000821	0.3750
700278	4/17A	70F_4s1d2Zc_1	70	FD	12.7	30569.0	87 1/2	83 5/8	0.613	0.920	HLP-22	12	8	4	3.5	26.4	11.7	22.4	9.7	0.75	0.33	s1d2	2.48	0.0000569	0.0000693	0.0000821	0.3750
700279	4/17A	70F_4s1d2Zc_1	70	FD	12.7	30569.0	87 1/2	83 5/8	0.613	0.920	HLP-22	12	8	4	3.5	26.4	11.7	22.4	9.7	0.75	0.33	s1d2	2.48	0.0000569	0.0000693	0.0000821	0.3750
700280	4/17A	70F_4s1d2Zc_1	70	FD	12.7	30569.0	87 1/2	83 5/8	0.613	0.920	HLP-22	12	8	4	3.5	26.4	11.7	22.4	9.7	0.75	0.33	s1d2	2.48	0.0000569	0.0000693	0.0000821	0.3750
700281	4/17A	70F_4s1d2Zc_1	70	FD	12.7	30569.0	87 1/2	83 5/8	0.613	0.920	HLP-22	12	8	4	3.5	26.4	11.7	22.4	9.7	0.75	0.33	s1d2	2.48	0.0000569	0.0000693	0.0000821	0.3750
700282	4/17A	70F_4s1d2Zc_1	70	FD	12.7	30569.0	87 1/2	83 5/8	0.613	0.920	HLP-22	12	8	4	3.5	26.4	11.7	22.4	9.7	0.75	0.33	s1d2	2.48	0.0000569	0.0000693	0.0000821	0.3750
700283	4/17A	70F_4s1d2Zc_1	70	FD	12.7	30569.0	87 1/2	83 5/8	0.613	0.920	HLP-22	12	8	4	3.5	26.4	11.7	22.4	9.7	0.75	0.33	s1d2	2.48	0.0000569	0.0000693	0.0000821	0.3750
700284	4/17A	70F_4s1d2Zc_1	70	FD	12.7	30569.0	87 1/2	83 5/8	0.613	0.920	HLP-22	12	8	4	3.5	26.4	11.7	22.4	9.7	0.75	0.33	s1d2	2.48	0.0000569	0.0000693	0.0000821	0.3750

Table B.6. Data from 2008 in Large-Scale Vessel with Flanged and Dished Head B.2

Tank Water Temperature	Water Density	Solids Fraction	Pulse Volume Fraction	Duty Cycle	Cycle Time	Pulsed or Steady Jet	Us Steady Jet	U1 Pulsing Jet	U2 URMS	U3 URM3	Discharge Velocity	Critical Suspension Velocity	Average Peak Cloud Height	UCS Condition	UCS Method	UCS Flag	UCS Center Flag	UCS udv Flag	UCS based on Decreasing Velocity	Sweep Increase / Decrease	UDV Height Bed	Particle Motion	Solids Level	Outer Bottom Pattern	Inner Bottom Pattern	Case ID	Test	TDP	Row Number
C	g/cm³	fraction	fraction	fraction	s	text	m/s	m/s	m/s	m/s	m/s	m/s	in.	m/s	text	text	text	text	m/s	text	mm	text	text	text	text	text	text	text	text
T	ρ_L	ϕ_S	ϕ_P	DC	t_C	Jet	U_S	U1	U2	U3	U	U_{CS}	H_C	U_{CSR}	U_{CSM}	U_{CS}vis	U_{CS}cen	U_{CS}udv	U_{CS_D}	S_W	H_{bed}	PM	Sol	SP_O	SP_I	ID	M/DDX	TDP	MSS
24.7	0.994	0.00155	0.050	0.336	41.0	P	N/A	6.93	7.05	7.11	7.30	6.70	28.50	N/A	N/A	N/A	N/A	N/A	N/A	I	N/A	4	N/A	N/A	N/A	70F_4s1d1Zc_1	4/14A	TDP-136	700245
24.8	0.994	0.00155	0.050	0.335	38.0	P	N/A	7.49	7.62	7.69	7.90	6.70	33.00	N/A	N/A	N/A	N/A	N/A	N/A	I	N/A	4	N/A	N/A	N/A	70F_4s1d1Zc_1	4/14A	TDP-136	700246
24.8	0.995	0.00155	0.050	0.336	36.6	P	N/A	7.72	7.86	7.94	8.20	6.70	39.50	N/A	N/A	N/A	N/A	N/A	N/A	I	N/A	4	N/A	N/A	N/A	70F_4s1d1Zc_1	4/14A	TDP-136	700247
24.3	0.994	0.00155	0.100	0.332	127.0	P	N/A	4.51	4.54	4.56	4.60	5.80	20.00	N/A	N/A	N/A	N/A	N/A	N/A	I	34.9	1	N/A	N/A	N/A	70F_4s1d1Zc_2	4/15A	TDP-137	700248
24.0	0.995	0.00155	0.100	0.333	116.8	P	N/A	4.90	4.94	4.95	5.00	5.80	22.50	N/A	N/A	N/A	N/A	N/A	N/A	I	21.4	1	N/A	N/A	N/A	70F_4s1d1Zc_2	4/15A	TDP-137	700249
24.0	0.994	0.00155	0.101	0.334	108.2	P	N/A	5.30	5.34	5.36	5.40	5.80	24.50	N/A	N/A	N/A	N/A	N/A	N/A	I	11.3	1	N/A	N/A	N/A	70F_4s1d1Zc_2	4/15A	TDP-137	700250
24.1	0.994	0.00155	0.100	0.334	104.4	P	N/A	5.47	5.51	5.53	5.60	5.80	25.50	N/A	N/A	N/A	N/A	N/A	N/A	I	6.1	1	N/A	N/A	N/A	70F_4s1d1Zc_2	4/15A	TDP-137	700251
24.0	0.994	0.00155	0.101	0.334	100.8	P	N/A	5.67	5.71	5.73	5.80	5.80	26.00	5.80	udv	N/A	UCScen	UCSudv	N/A	I	0.0	2	N/A	N/A	N/A	70F_4s1d1Zc_2	4/15A	TDP-137	700252
24.0	0.994	0.00155	0.101	0.336	91.2	P	N/A	6.26	6.31	6.34	6.40	5.80	33.00	N/A	N/A	N/A	N/A	N/A	N/A	I	0.0	4	N/A	N/A	N/A	70F_4s1d1Zc_2	4/15A	TDP-137	700253
23.8	0.994	0.00155	0.100	0.333	87.2	P	N/A	6.53	6.59	6.62	6.70	5.80	40.00	N/A	N/A	N/A	N/A	N/A	N/A	I	0.0	4	N/A	N/A	N/A	70F_4s1d1Zc_2	4/15A	TDP-137	700254
23.8	0.994	0.00155	0.150	0.328	191.0	P	N/A	4.55	4.57	4.58	4.60	5.60	21.50	N/A	N/A	N/A	N/A	N/A	N/A	(null)	28.4	1	N/A	N/A	N/A	70F_4s1d1Zc_4	4/15B	TDP-137	700255
23.9	0.994	0.00155	0.151	0.329	175.8	P	N/A	4.96	4.99	5.00	5.00	5.60	26.00	N/A	N/A	N/A	N/A	N/A	N/A	I	15.1	1	N/A	N/A	N/A	70F_4s1d1Zc_4	4/15B	TDP-137	700256
23.8	0.995	0.00155	0.150	0.329	169.0	P	N/A	5.15	5.17	5.19	5.20	5.60	26.75	N/A	N/A	N/A	N/A	N/A	N/A	I	10.2	1	N/A	N/A	N/A	70F_4s1d1Zc_4	4/15B	TDP-137	700257
23.7	0.994	0.00155	0.150	0.329	162.8	P	N/A	5.33	5.35	5.36	5.40	5.60	28.00	N/A	N/A	N/A	N/A	N/A	N/A	I	7.1	1	N/A	N/A	N/A	70F_4s1d1Zc_4	4/15B	TDP-137	700258
23.7	0.994	0.00155	0.150	0.329	157.0	P	N/A	5.51	5.54	5.55	5.60	5.60	29.75	5.60	udv	N/A	UCScen	UCSudv	N/A	I	0.0	2	N/A	N/A	N/A	70F_4s1d1Zc_4	4/15B	TDP-137	700259
23.7	0.994	0.00155	0.151	0.330	146.6	P	N/A	5.92	5.95	5.97	6.00	5.60	36.75	N/A	N/A	N/A	N/A	N/A	N/A	I	0.0	4	N/A	N/A	N/A	70F_4s1d1Zc_4	4/15B	TDP-137	700260
23.8	0.994	0.00155	0.151	0.331	137.4	P	N/A	6.30	6.34	6.36	6.40	5.60	48.00	N/A	N/A	N/A	N/A	N/A	N/A	I	0.0	4	N/A	N/A	N/A	70F_4s1d1Zc_4	4/15B	TDP-137	700261
23.7	0.994	0.00155	0.101	0.335	100.8	P	N/A	5.67	5.71	5.73	5.80	5.80	26.00	N/A	N/A	N/A	N/A	N/A	N/A	(null)	0.6	N/A	N/A	N/A	N/A	70F_4s1d1Zc_2	4/15C	TDP-137	700262
23.7	0.994	0.00155	0.101	0.335	100.8	P	N/A	5.67	5.71	5.73	5.80	5.80	26.00	N/A	N/A	N/A	N/A	N/A	N/A	N/A	0.7	N/A	N/A	N/A	N/A	70F_4s1d1Zc_2	4/15C	TDP-137	700263
23.7	0.994	0.00155	0.101	0.335	100.8	P	N/A	5.67	5.71	5.73	5.80	5.80	26.00	N/A	N/A	N/A	N/A	N/A	N/A	N/A	2.4	N/A	N/A	N/A	N/A	70F_4s1d1Zc_2	4/15C	TDP-137	700264
23.7	0.994	0.00155	0.101	0.335	100.8	P	N/A	5.67	5.71	5.73	5.80	5.80	26.00	N/A	N/A	N/A	N/A	N/A	N/A	N/A	1.2	N/A	N/A	N/A	N/A	70F_4s1d1Zc_2	4/15C	TDP-137	700265
23.7	0.994	0.00155	0.101	0.335	100.8	P	N/A	5.67	5.71	5.73	5.80	5.80	26.00	N/A	N/A	N/A	N/A	N/A	N/A	N/A	0.0	N/A	N/A	N/A	N/A	70F_4s1d1Zc_2	4/15C	TDP-137	700266
23.7	0.994	0.00155	0.101	0.335	100.8	P	N/A	5.67	5.71	5.73	5.80	5.80	26.00	N/A	N/A	N/A	N/A	N/A	N/A	N/A	0.7	N/A	N/A	N/A	N/A	70F_4s1d1Zc_2	4/15C	TDP-137	700267
23.7	0.994	0.00155	0.101	0.335	100.8	P	N/A	5.67	5.71	5.73	5.80	5.80	26.00	N/A	N/A	N/A	N/A	N/A	N/A	N/A	0.7	N/A	N/A	N/A	N/A	70F_4s1d1Zc_2	4/15C	TDP-137	700268
23.7	0.994	0.00155	0.101	0.335	100.8	P	N/A	5.67	5.71	5.73	5.80	5.80	26.00	N/A	N/A	N/A	N/A	N/A	N/A	N/A	0.0	N/A	N/A	N/A	N/A	70F_4s1d1Zc_2	4/15C	TDP-137	700269
23.7	0.994	0.00155	0.101	0.335	100.8	P	N/A	5.67	5.71	5.73	5.80	5.80	26.00	N/A	N/A	N/A	N/A	N/A	N/A	N/A	0.7	N/A	N/A	N/A	N/A	70F_4s1d1Zc_2	4/15C	TDP-137	700270
23.7	0.994	0.00155	0.101	0.335	100.8	P	N/A	5.67	5.71	5.73	5.80	5.80	26.00	N/A	N/A	N/A	N/A	N/A	N/A	N/A	1.5	N/A	N/A	N/A	N/A	70F_4s1d1Zc_2	4/15C	TDP-137	700271
21.3	0.995	0.00155	0.050	0.333	77.0	P	N/A	n/a	n/a	n/a	3.80	4.40	21.75	N/A	N/A	N/A	N/A	N/A	N/A	D	17.7	1	N/A	N/A	N/A	70F_4s1d2Zc_1	4/16A	TDP-138	700272
21.4	0.995	0.00155	0.050	0.336	68.0	P	N/A	4.18	4.23	4.26	4.40	4.40	27.75	4.40	udv	N/A	UCScen	UCSudv	N/A	I	1.9	2	N/A	N/A	N/A	70F_4s1d2Zc_1	4/16A	TDP-138	700273
21.6	0.995	0.00155	0.050	0.335	63.6	P	N/A	4.50	4.56	4.59	4.70	4.40	36.50	N/A	N/A	N/A	N/A	N/A	N/A	I	0.0	4	N/A	N/A	N/A	70F_4s1d2Zc_1	4/16A	TDP-138	700274
21.6	0.995	0.00155	0.050	0.331	71.2	P	N/A	n/a	n/a	n/a	4.20	4.40	25.75	N/A	N/A	N/A	N/A	N/A	N/A	D	3.5	1	N/A	N/A	N/A	70F_4s1d2Zc_1	4/16A	TDP-138	700275
21.4	0.995	0.00155	0.050	0.334	62.4	P	N/A	4.60	4.66	4.69	4.80	4.40	42.50	N/A	N/A	N/A	N/A	N/A	N/A	I	0.0	4	N/A	N/A	N/A	70F_4s1d2Zc_1	4/16A	TDP-138	700276
22.3	0.995	0.00155	0.050	0.336	67.4	P	N/A	4.21	4.27	4.30	4.40	4.40	28.25	N/A	N/A	N/A	N/A	N/A	N/A	N/A	n/a	N/A	N/A	N/A	N/A	70F_4s1d2Zc_1	4/17A	TDP-139	700276.1
22.3	0.995	0.00155	0.050	0.336	67.4	P	N/A	4.21	4.27	4.30	4.40	4.40	28.25	N/A	N/A	N/A	N/A	N/A	N/A	(null)	0.0	4	N/A	N/A	N/A	70F_4s1d2Zc_1	4/17A	TDP-139	700277
22.3	0.995	0.00155	0.050	0.336	67.4	P	N/A	4.21	4.27	4.30	4.40	4.40	28.25	N/A	N/A	N/A	N/A	N/A	N/A	N/A	0.0	N/A	N/A	N/A	N/A	70F_4s1d2Zc_1	4/17A	TDP-139	700278
22.3	0.995	0.00155	0.050	0.336	67.4	P	N/A	4.21	4.27	4.30	4.40	4.40	28.25	N/A	N/A	N/A	N/A	N/A	N/A	N/A	0.0	N/A	N/A	N/A	N/A	70F_4s1d2Zc_1	4/17A	TDP-139	700279
22.3	0.995	0.00155	0.050	0.336	67.4	P	N/A	4.21	4.27	4.30	4.40	4.40	28.25	N/A	N/A	N/A	N/A	N/A	N/A	N/A	0.0	N/A	N/A	N/A	N/A	70F_4s1d2Zc_1	4/17A	TDP-139	700280
22.3	0.995	0.00155	0.050	0.336	67.4	P	N/A	4.21	4.27	4.30	4.40	4.40	28.25	N/A	N/A	N/A	N/A	N/A	N/A	N/A	0.0	N/A	N/A	N/A	N/A	70F_4s1d2Zc_1	4/17A	TDP-139	700281
22.3	0.995	0.00155	0.050	0.336	67.4	P	N/A	4.21	4.27	4.30	4.40	4.40	28.25	N/A	N/A	N/A	N/A	N/A	N/A	N/A	0.0	N/A	N/A	N/A	N/A	70F_4s1d2Zc_1	4/17A	TDP-139	700282
22.3	0.995	0.00155	0.050	0.336	67.4	P	N/A	4.21	4.27	4.30	4.40	4.40	28.25	N/A	N/A	N/A	N/A	N/A	N/A	N/A	0.0	N/A	N/A	N/A	N/A	70F_4s1d2Zc_1	4/17A	TDP-139	700283
22.3	0.995	0.00155	0.050	0.336	67.4	P	N/A	4.21	4.27	4.30	4.40	4.40	28.25	N/A	N/A	N/A	N/A	N/A	N/A	N/A	0.0	N/A	N/A	N/A	N/A	70F_4s1d2Zc_1	4/17A	TDP-139	700284

Table B.6. Data from 2008 in Large-Scale Vessel with Flanged and Dished Head A.3

Row Number	Test	Case ID	Tank Diameter	Head Shape	Dish Height	Dish Volume	Tank Fill Height	Return Line Height	Nozzle Inner Diameter	Nozzle Stand-off Distance	Pulse Tube Configuration	Installed Nozzles	Outer Nozzles Operated	Inner Nozzles Operated	Pulse Tube Outer Diameter	Outer PJM Radius	Inner PJM Radius	"FIO" Outer PJM Impingement Angle	"FIO" Inner PJM Impingement Angle	Ratio Outer PJM to Tank Radius	Ratio Inner PJM to Tank Radius	Simulant	Solids Density	Particle Diameter d5	Particle Diameter d50	Particle Diameter d95	Void Fraction
text	text	text	in.	text	in.	in. ^{3}	in.	in.	in.	in.	text	number	number	number	in.	in.	in.	deg	deg	nondim	nondim	text	g/cm^3	m	m	m	fraction
MSS	M/DDX	ID	D	HS	H_{dish}	V_{dish}	H	Rtn	d	sod	PT	N	N_O	N_I	PT_{od}	R_O	R_I	θ_O	θ_I	R_O/R	R_I/R	sxdx	ρ_s	d_5	d_{50}	d_{95}	vf
700285	4/17A	70F_4s1d2Zc_1	70	FD	12.7	30569.0	87 1/2	83 5/8	0.613	0.920	HLP-22	12	8	4	3.5	26.4	11.7	22.4	9.7	0.75	0.33	s1d2	2.48	0.0000569	0.0000693	0.0000821	0.3750
700286	4/18A	70F_4s1d2Yc_1	70	FD	12.7	30569.0	87 1/2	83 5/8	0.613	0.920	HLP-22	12	8	4	3.5	26.4	11.7	22.4	9.7	0.75	0.33	s1d2	2.48	0.0000569	0.0000693	0.0000821	0.3750
700287	4/18A	70F_4s1d2Yc_1	70	FD	12.7	30569.0	87 1/2	83 5/8	0.613	0.920	HLP-22	12	8	4	3.5	26.4	11.7	22.4	9.7	0.75	0.33	s1d2	2.48	0.0000569	0.0000693	0.0000821	0.3750
700288M	4/18A	70F_4s1d2Yc_1	70	FD	12.7	30569.0	87 1/2	83 5/8	0.613	0.920	HLP-22	12	8	4	3.5	26.4	11.7	22.4	9.7	0.75	0.33	s1d2	2.48	0.0000569	0.0000693	0.0000821	0.3750
700288.1	4/18A	70F_4s1d2Yc_1	70	FD	12.7	30569.0	87 1/2	83 5/8	0.613	0.920	HLP-22	12	8	4	3.5	26.4	11.7	22.4	9.7	0.75	0.33	s1d2	2.48	0.0000569	0.0000693	0.0000821	0.3750
700288.2	4/18A	70F_4s1d2Yc_1	70	FD	12.7	30569.0	87 1/2	83 5/8	0.613	0.920	HLP-22	12	8	4	3.5	26.4	11.7	22.4	9.7	0.75	0.33	s1d2	2.48	0.0000569	0.0000693	0.0000821	0.3750
700289M	4/18A	70F_4s1d2Yc_1	70	FD	12.7	30569.0	87 1/2	83 5/8	0.613	0.920	HLP-22	12	8	4	3.5	26.4	11.7	22.4	9.7	0.75	0.33	s1d2	2.48	0.0000569	0.0000693	0.0000821	0.3750
700290	4/18A	70F_4s1d2Yc_1	70	FD	12.7	30569.0	87 1/2	83 5/8	0.613	0.920	HLP-22	12	8	4	3.5	26.4	11.7	22.4	9.7	0.75	0.33	s1d2	2.48	0.0000569	0.0000693	0.0000821	0.3750
700291	4/18A	70F_4s1d2Yc_1	70	FD	12.7	30569.0	87 1/2	83 5/8	0.613	0.920	HLP-22	12	8	4	3.5	26.4	11.7	22.4	9.7	0.75	0.33	s1d2	2.48	0.0000569	0.0000693	0.0000821	0.3750
700292	4/18A	70F_4s1d2Yc_1	70	FD	12.7	30569.0	87 1/2	83 5/8	0.613	0.920	HLP-22	12	8	4	3.5	26.4	11.7	22.4	9.7	0.75	0.33	s1d2	2.48	0.0000569	0.0000693	0.0000821	0.3750
700293	4/18A	70F_4s1d2Yc_1	70	FD	12.7	30569.0	87 1/2	83 5/8	0.613	0.920	HLP-22	12	8	4	3.5	26.4	11.7	22.4	9.7	0.75	0.33	s1d2	2.48	0.0000569	0.0000693	0.0000821	0.3750
700294	4/18A	70F_4s1d2Yc_1	70	FD	12.7	30569.0	87 1/2	83 5/8	0.613	0.920	HLP-22	12	8	4	3.5	26.4	11.7	22.4	9.7	0.75	0.33	s1d2	2.48	0.0000569	0.0000693	0.0000821	0.3750
700295	4/18A	70F_4s1d2Yc_1	70	FD	12.7	30569.0	87 1/2	83 5/8	0.613	0.920	HLP-22	12	8	4	3.5	26.4	11.7	22.4	9.7	0.75	0.33	s1d2	2.48	0.0000569	0.0000693	0.0000821	0.3750
700296	4/18A	70F_4s1d2Yc_1	70	FD	12.7	30569.0	87 1/2	83 5/8	0.613	0.920	HLP-22	12	8	4	3.5	26.4	11.7	22.4	9.7	0.75	0.33	s1d2	2.48	0.0000569	0.0000693	0.0000821	0.3750
700297M	4/18A	70F_4s1d2Yc_1	70	FD	12.7	30569.0	87 1/2	83 5/8	0.613	0.920	HLP-22	12	8	4	3.5	26.4	11.7	22.4	9.7	0.75	0.33	s1d2	2.48	0.0000569	0.0000693	0.0000821	0.3750
700298M	4/18A	70F_4s1d2Yc_1	70	FD	12.7	30569.0	87 1/2	83 5/8	0.613	0.920	HLP-22	12	8	4	3.5	26.4	11.7	22.4	9.7	0.75	0.33	s1d2	2.48	0.0000569	0.0000693	0.0000821	0.3750
700299M	4/18A	70F_4s1d2Yc_1	70	FD	12.7	30569.0	87 1/2	83 5/8	0.613	0.920	HLP-22	12	8	4	3.5	26.4	11.7	22.4	9.7	0.75	0.33	s1d2	2.48	0.0000569	0.0000693	0.0000821	0.3750
700300	4/18B	70F_4s1d2Rc_1	70	FD	12.7	30569.0	87 1/2	83 5/8	0.613	0.920	HLP-22	12	8	4	3.5	26.4	11.7	22.4	9.7	0.75	0.33	s1d2	2.48	0.0000569	0.0000693	0.0000821	0.3750
700301M	4/18B	70F_4s1d2Rc_1	70	FD	12.7	30569.0	87 1/2	83 5/8	0.613	0.920	HLP-22	12	8	4	3.5	26.4	11.7	22.4	9.7	0.75	0.33	s1d2	2.48	0.0000569	0.0000693	0.0000821	0.3750
700301.1	4/18B	70F_4s1d2Rc_1	70	FD	12.7	30569.0	87 1/2	83 5/8	0.613	0.920	HLP-22	12	8	4	3.5	26.4	11.7	22.4	9.7	0.75	0.33	s1d2	2.48	0.0000569	0.0000693	0.0000821	0.3750
700301.2	4/18B	70F_4s1d2Rc_1	70	FD	12.7	30569.0	87 1/2	83 5/8	0.613	0.920	HLP-22	12	8	4	3.5	26.4	11.7	22.4	9.7	0.75	0.33	s1d2	2.48	0.0000569	0.0000693	0.0000821	0.3750
700302M	4/18B	70F_4s1d2Rc_1	70	FD	12.7	30569.0	87 1/2	83 5/8	0.613	0.920	HLP-22	12	8	4	3.5	26.4	11.7	22.4	9.7	0.75	0.33	s1d2	2.48	0.0000569	0.0000693	0.0000821	0.3750
700303	4/18B	70F_4s1d2Rc_1	70	FD	12.7	30569.0	87 1/2	83 5/8	0.613	0.920	HLP-22	12	8	4	3.5	26.4	11.7	22.4	9.7	0.75	0.33	s1d2	2.48	0.0000569	0.0000693	0.0000821	0.3750
700304	4/18B	70F_4s1d2Rc_1	70	FD	12.7	30569.0	87 1/2	83 5/8	0.613	0.920	HLP-22	12	8	4	3.5	26.4	11.7	22.4	9.7	0.75	0.33	s1d2	2.48	0.0000569	0.0000693	0.0000821	0.3750
700305	4/18B	70F_4s1d2Rc_1	70	FD	12.7	30569.0	87 1/2	83 5/8	0.613	0.920	HLP-22	12	8	4	3.5	26.4	11.7	22.4	9.7	0.75	0.33	s1d2	2.48	0.0000569	0.0000693	0.0000821	0.3750
700306	4/18B	70F_4s1d2Rc_1	70	FD	12.7	30569.0	87 1/2	83 5/8	0.613	0.920	HLP-22	12	8	4	3.5	26.4	11.7	22.4	9.7	0.75	0.33	s1d2	2.48	0.0000569	0.0000693	0.0000821	0.3750
700307	4/18B	70F_4s1d2Rc_1	70	FD	12.7	30569.0	87 1/2	83 5/8	0.613	0.920	HLP-22	12	8	4	3.5	26.4	11.7	22.4	9.7	0.75	0.33	s1d2	2.48	0.0000569	0.0000693	0.0000821	0.3750
700308	4/18B	70F_4s1d2Rc_1	70	FD	12.7	30569.0	87 1/2	83 5/8	0.613	0.920	HLP-22	12	8	4	3.5	26.4	11.7	22.4	9.7	0.75	0.33	s1d2	2.48	0.0000569	0.0000693	0.0000821	0.3750
700309	4/18B	70F_4s1d2Rc_1	70	FD	12.7	30569.0	87 1/2	83 5/8	0.613	0.920	HLP-22	12	8	4	3.5	26.4	11.7	22.4	9.7	0.75	0.33	s1d2	2.48	0.0000569	0.0000693	0.0000821	0.3750
700310M	4/18B	70F_4s1d2Rc_1	70	FD	12.7	30569.0	87 1/2	83 5/8	0.613	0.920	HLP-22	12	8	4	3.5	26.4	11.7	22.4	9.7	0.75	0.33	s1d2	2.48	0.0000569	0.0000693	0.0000821	0.3750
700311M	4/18B	70F_4s1d2Rc_1	70	FD	12.7	30569.0	87 1/2	83 5/8	0.613	0.920	HLP-22	12	8	4	3.5	26.4	11.7	22.4	9.7	0.75	0.33	s1d2	2.48	0.0000569	0.0000693	0.0000821	0.3750
700312M	4/18B	70F_4s1d2Rc_1	70	FD	12.7	30569.0	87 1/2	83 5/8	0.613	0.920	HLP-22	12	8	4	3.5	26.4	11.7	22.4	9.7	0.75	0.33	s1d2	2.48	0.0000569	0.0000693	0.0000821	0.3750
700313M	4/18B	70F_4s1d2Rc_1	70	FD	12.7	30569.0	87 1/2	83 5/8	0.613	0.920	HLP-22	12	8	4	3.5	26.4	11.7	22.4	9.7	0.75	0.33	s1d2	2.48	0.0000569	0.0000693	0.0000821	0.3750
700314M	4/18B	70F_4s1d2Rc_1	70	FD	12.7	30569.0	87 1/2	83 5/8	0.613	0.920	HLP-22	12	8	4	3.5	26.4	11.7	22.4	9.7	0.75	0.33	s1d2	2.48	0.0000569	0.0000693	0.0000821	0.3750
700315	4/21A	70F_4s1d2Vc_1	70	FD	12.7	30569.0	87 1/2	83 5/8	0.613	0.920	HLP-22	12	8	4	3.5	26.4	11.7	22.4	9.7	0.75	0.33	s1d2	2.48	0.0000569	0.0000693	0.0000821	0.3750
700316	4/21A	70F_4s1d2Vc_1	70	FD	12.7	30569.0	87 1/2	83 5/8	0.613	0.920	HLP-22	12	8	4	3.5	26.4	11.7	22.4	9.7	0.75	0.33	s1d2	2.48	0.0000569	0.0000693	0.0000821	0.3750
700317	4/21A	70F_4s1d2Vc_1	70	FD	12.7	30569.0	87 1/2	83 5/8	0.613	0.920	HLP-22	12	8	4	3.5	26.4	11.7	22.4	9.7	0.75	0.33	s1d2	2.48	0.0000569	0.0000693	0.0000821	0.3750
700318	4/21A	70F_4s1d2Vc_1	70	FD	12.7	30569.0	87 1/2	83 5/8	0.613	0.920	HLP-22	12	8	4	3.5	26.4	11.7	22.4	9.7	0.75	0.33	s1d2	2.48	0.0000569	0.0000693	0.0000821	0.3750
700319M	4/21A	70F_4s1d2Vc_1	70	FD	12.7	30569.0	87 1/2	83 5/8	0.613	0.920	HLP-22	12	8	4	3.5	26.4	11.7	22.4	9.7	0.75	0.33	s1d2	2.48	0.0000569	0.0000693	0.0000821	0.3750
700320M	4/21A	70F_4s1d2Vc_1	70	FD	12.7	30569.0	87 1/2	83 5/8	0.613	0.920	HLP-22	12	8	4	3.5	26.4	11.7	22.4	9.7	0.75	0.33	s1d2	2.48	0.0000569	0.0000693	0.0000821	0.3750
700321	4/21A	70F_4s1d2Vc_1	70	FD	12.7	30569.0	87 1/2	83 5/8	0.613	0.920	HLP-22	12	8	4	3.5	26.4	11.7	22.4	9.7	0.75	0.33	s1d2	2.48	0.0000569	0.0000693	0.0000821	0.3750

Table B.6. Data from 2008 in Large-Scale Vessel with Flanged and Dished Head B.3

Tank Water Temperature	Water Density	Solids Fraction	Pulse Volume Fraction	Duty Cycle	Cycle Time	Pulsed or Steady Jet	Us Steady Jet	U1 Pulsing Jet	U2 URMS	U3 URM3	Discharge Velocity	Critical Suspension Velocity	Average Peak Cloud Height	UCS Condition	UCS Method	UCS Flag	UCS Center Flag	UCS udv Flag	UCS based on Decreasing Velocity	Sweep Increase / Decrease	UDV Height Bed	Particle Motion	Solids Level	Outer Bottom Pattern	Inner Bottom Pattern	Case ID	Test	TDP	Row Number
C	g/cm³	fraction	fraction	fraction	s	text	m/s	m/s	m/s	m/s	m/s	m/s	in.	m/s	text	text	text	text	m/s	text	mm	text	text	text	text	text	text	text	text
T	ρ_L	ϕ_S	ϕ_P	DC	t_C	Jet	U_S	U1	U2	U3	U	U_{CS}	H_C	U_{CSR}	U_{CSM}	U_{CS}vis	U_{CS}cen	U_{CS}udv	U_{CS}_D	S_W	H_{bed}	PM	Sol	SP_O	SP_I	ID	M/DDX	TDP	MSS
22.3	0.995	0.00155	0.050	0.336	67.4	P	N/A	4.21	4.27	4.30	4.40	4.40	28.25	N/A	N/A	N/A	N/A	N/A	N/A	N/A	1.0	N/A	N/A	N/A	N/A	70F_4s1d2Zc_1	4/17A	TDP-139	700285
23.0	0.994	0.00500	0.050	0.332	55.0	P	N/A	5.16	5.24	5.28	5.40	5.80	19.50	N/A	N/A	N/A	N/A	N/A	N/A	I	9.0	1	N/A	N/A	N/A	70F_4s1d2Yc_1	4/18A	TDP-140	700286
22.8	0.994	0.00500	0.050	0.333	53.0	P	N/A	5.38	5.46	5.50	5.60	5.80	21.75	N/A	N/A	N/A	N/A	N/A	N/A	I	3.8	1	N/A	N/A	N/A	70F_4s1d2Yc_1	4/18A	TDP-140	700287
22.8	0.995	0.00500	0.050	0.334	51.0	P	N/A	5.54	5.62	5.66	5.80	5.80	23.25	5.80	udv	N/A	UCScen	UCSudv	N/A	I	0.0	2	N/A	N/A	N/A	70F_4s1d2Yc_1	4/18A	TDP-140	700288
22.9	0.994	0.00500	0.050	0.335	51.0	P	N/A	5.53	5.62	5.66	5.80	5.80	23.00	N/A	N/A	N/A	N/A	N/A	N/A	N/A	n/a	N/A	N/A	N/A	N/A	70F_4s1d2Yc_1	4/18A	TDP-140	700288.1
22.9	0.994	0.00500	0.050	0.335	51.0	P	N/A	5.53	5.62	5.66	5.80	5.80	23.00	N/A	N/A	N/A	N/A	N/A	N/A	N/A	n/a	N/A	N/A	N/A	N/A	70F_4s1d2Yc_1	4/18A	TDP-140	700288.2
22.9	0.994	0.00500	0.050	0.335	51.0	P	N/A	5.53	5.62	5.66	5.80	5.80	23.00	N/A	N/A	N/A	UCScen	N/A	N/A	I	0.0	2	N/A	N/A	N/A	70F_4s1d2Yc_1	4/18A	TDP-140	700289
22.9	0.994	0.00500	0.050	0.335	51.0	P	N/A	5.53	5.62	5.66	5.80	5.80	23.00	N/A	N/A	N/A	N/A	N/A	N/A	N/A	0.0	N/A	N/A	N/A	N/A	70F_4s1d2Yc_1	4/18A	TDP-140	700290
22.9	0.994	0.00500	0.050	0.335	51.0	P	N/A	5.53	5.62	5.66	5.80	5.80	23.00	N/A	N/A	N/A	N/A	N/A	N/A	N/A	0.0	N/A	N/A	N/A	N/A	70F_4s1d2Yc_1	4/18A	TDP-140	700291
22.9	0.994	0.00500	0.050	0.335	51.0	P	N/A	5.53	5.62	5.66	5.80	5.80	23.00	N/A	N/A	N/A	N/A	N/A	N/A	N/A	0.0	N/A	N/A	N/A	N/A	70F_4s1d2Yc_1	4/18A	TDP-140	700292
22.9	0.994	0.00500	0.050	0.335	51.0	P	N/A	5.53	5.62	5.66	5.80	5.80	23.00	N/A	N/A	N/A	N/A	N/A	N/A	N/A	0.0	N/A	N/A	N/A	N/A	70F_4s1d2Yc_1	4/18A	TDP-140	700293
22.9	0.994	0.00500	0.050	0.335	51.0	P	N/A	5.53	5.62	5.66	5.80	5.80	23.00	N/A	N/A	N/A	N/A	N/A	N/A	N/A	0.0	N/A	N/A	N/A	N/A	70F_4s1d2Yc_1	4/18A	TDP-140	700294
22.9	0.994	0.00500	0.050	0.335	51.0	P	N/A	5.53	5.62	5.66	5.80	5.80	23.00	N/A	N/A	N/A	N/A	N/A	N/A	N/A	0.0	N/A	N/A	N/A	N/A	70F_4s1d2Yc_1	4/18A	TDP-140	700295
22.9	0.994	0.00500	0.050	0.335	51.0	P	N/A	5.53	5.62	5.66	5.80	5.80	23.00	N/A	N/A	N/A	N/A	N/A	N/A	N/A	0.0	N/A	N/A	N/A	N/A	70F_4s1d2Yc_1	4/18A	TDP-140	700296
22.9	0.994	0.00500	0.050	0.337	47.6	P	N/A	5.91	6.00	6.05	6.20	5.80	32.75	N/A	N/A	N/A	N/A	N/A	N/A	(null)	0.0	4	N/A	N/A	N/A	70F_4s1d2Yc_1	4/18A	TDP-140	700297
23.0	0.995	0.00500	0.050	0.338	46.0	P	N/A	6.10	6.19	6.24	6.40	5.80	41.25	N/A	N/A	N/A	N/A	N/A	N/A	I	0.0	4	N/A	N/A	N/A	70F_4s1d2Yc_1	4/18A	TDP-140	700298
22.8	0.994	0.00500	0.050	0.335	49.0	P	N/A	5.75	5.83	5.87	6.00	5.80	27.75	N/A	N/A	N/A	N/A	N/A	N/A	D	0.0	4	N/A	N/A	N/A	70F_4s1d2Yc_1	4/18A	TDP-140	700299
22.9	0.995	0.01000	0.050	0.338	46.0	P	N/A	6.11	6.21	6.26	6.40	6.60	22.50	N/A	N/A	N/A	N/A	N/A	N/A	I	10.1	1	N/A	N/A	N/A	70F_4s1d2Rc_1	4/18B	TDP-141	700300
22.9	0.994	0.01000	0.050	0.339	44.6	P	N/A	6.28	6.38	6.44	6.60	6.60	23.00	6.60	udv	N/A	UCScen	UCSudv	N/A	I	0.0	2	N/A	N/A	N/A	70F_4s1d2Rc_1	4/18B	TDP-141	700301
22.9	0.995	0.01000	0.050	0.339	44.6	P	N/A	6.29	6.39	6.44	6.60	6.60	23.00	N/A	N/A	N/A	N/A	N/A	N/A	N/A	n/a	N/A	N/A	N/A	N/A	70F_4s1d2Rc_1	4/18B	TDP-141	700301.1
22.9	0.995	0.01000	0.050	0.339	44.6	P	N/A	6.29	6.39	6.44	6.60	6.60	23.00	N/A	N/A	N/A	N/A	N/A	N/A	N/A	n/a	N/A	N/A	N/A	N/A	70F_4s1d2Rc_1	4/18B	TDP-141	700301.2
22.9	0.995	0.01000	0.050	0.339	44.6	P	N/A	6.29	6.39	6.44	6.60	6.60	23.00	N/A	N/A	N/A	UCScen	N/A	N/A	(null)	1.9	2	N/A	N/A	N/A	70F_4s1d2Rc_1	4/18B	TDP-141	700302
22.9	0.995	0.01000	0.050	0.339	44.6	P	N/A	6.29	6.39	6.44	6.60	6.60	23.00	N/A	N/A	N/A	N/A	N/A	N/A	N/A	0.0	N/A	N/A	N/A	N/A	70F_4s1d2Rc_1	4/18B	TDP-141	700303
22.9	0.995	0.01000	0.050	0.339	44.6	P	N/A	6.29	6.39	6.44	6.60	6.60	23.00	N/A	N/A	N/A	N/A	N/A	N/A	N/A	0.0	N/A	N/A	N/A	N/A	70F_4s1d2Rc_1	4/18B	TDP-141	700304
22.9	0.995	0.01000	0.050	0.339	44.6	P	N/A	6.29	6.39	6.44	6.60	6.60	23.00	N/A	N/A	N/A	N/A	N/A	N/A	N/A	8.2	N/A	N/A	N/A	N/A	70F_4s1d2Rc_1	4/18B	TDP-141	700305
22.9	0.995	0.01000	0.050	0.339	44.6	P	N/A	6.29	6.39	6.44	6.60	6.60	23.00	N/A	N/A	N/A	N/A	N/A	N/A	N/A	2.9	N/A	N/A	N/A	N/A	70F_4s1d2Rc_1	4/18B	TDP-141	700306
22.9	0.995	0.01000	0.050	0.339	44.6	P	N/A	6.29	6.39	6.44	6.60	6.60	23.00	N/A	N/A	N/A	N/A	N/A	N/A	N/A	0.0	N/A	N/A	N/A	N/A	70F_4s1d2Rc_1	4/18B	TDP-141	700307
22.9	0.995	0.01000	0.050	0.339	44.6	P	N/A	6.29	6.39	6.44	6.60	6.60	23.00	N/A	N/A	N/A	N/A	N/A	N/A	N/A	0.0	N/A	N/A	N/A	N/A	70F_4s1d2Rc_1	4/18B	TDP-141	700308
22.9	0.995	0.01000	0.050	0.339	44.6	P	N/A	6.29	6.39	6.44	6.60	6.60	23.00	N/A	N/A	N/A	N/A	N/A	N/A	N/A	0.7	N/A	N/A	N/A	N/A	70F_4s1d2Rc_1	4/18B	TDP-141	700309
22.7	0.995	0.01000	0.050	0.340	43.2	P	N/A	6.47	6.58	6.63	6.80	6.60	27.50	N/A	N/A	N/A	N/A	N/A	N/A	(null)	0.0	4	N/A	N/A	N/A	70F_4s1d2Rc_1	4/18B	TDP-141	700310
22.9	0.995	0.01000	0.050	0.334	43.2	P	N/A	6.63	6.74	6.80	7.00	6.60	27.75	N/A	N/A	N/A	N/A	N/A	N/A	I	0.0	4	N/A	N/A	N/A	70F_4s1d2Rc_1	4/18B	TDP-141	700311
23.0	0.994	0.01000	0.050	0.335	42.0	P	N/A	6.81	6.92	6.98	7.20	6.60	30.25	N/A	N/A	N/A	N/A	N/A	N/A	I	0.0	4	N/A	N/A	N/A	70F_4s1d2Rc_1	4/18B	TDP-141	700312
23.0	0.994	0.01000	0.050	0.336	40.0	P	N/A	7.10	7.23	7.29	7.50	6.60	38.00	N/A	N/A	N/A	N/A	N/A	N/A	I	0.0	4	N/A	N/A	N/A	70F_4s1d2Rc_1	4/18B	TDP-141	700313
23.2	0.994	0.01000	0.050	0.338	38.6	P	N/A	7.27	7.40	7.47	7.70	6.60	51.50	N/A	N/A	N/A	N/A	N/A	N/A	I	0.0	4	N/A	N/A	N/A	70F_4s1d2Rc_1	4/18B	TDP-141	700314
20.4	0.995	0.01430	0.050	0.332	47.4	P	N/A	6.10	6.20	6.25	6.40	7.10	22.00	N/A	N/A	N/A	N/A	N/A	N/A	I	32.9	1	N/A	N/A	N/A	70F_4s1d2Vc_1	4/21A	TDP-142	700315
20.4	0.995	0.01430	0.050	0.334	44.4	P	N/A	6.48	6.58	6.63	6.80	7.10	24.50	N/A	N/A	N/A	N/A	N/A	N/A	I	10.5	1	N/A	N/A	N/A	70F_4s1d2Vc_1	4/21A	TDP-142	700316
21.0	0.995	0.01430	0.050	0.334	44.4	P	N/A	6.47	6.57	6.63	6.80	7.10	25.00	N/A	N/A	N/A	N/A	N/A	N/A	(null)	16.2	1	N/A	N/A	N/A	70F_4s1d2Vc_1	4/21A	TDP-142	700317
21.2	0.995	0.01430	0.050	0.335	43.0	P	N/A	6.64	6.75	6.81	7.00	7.10	28.00	N/A	N/A	N/A	N/A	N/A	N/A	I	4.1	1	N/A	N/A	N/A	70F_4s1d2Vc_1	4/21A	TDP-142	700318
21.1	0.995	0.01430	0.050	0.336	42.2	P	N/A	6.75	6.86	6.92	7.10	7.10	30.50	7.10	udv	N/A	UCScen	UCSudv	N/A	I	0.0	2	N/A	N/A	N/A	70F_4s1d2Vc_1	4/21A	TDP-142	700319
21.0	0.995	0.01430	0.050	0.336	42.2	P	N/A	6.74	6.86	6.91	7.10	7.10	30.00	N/A	N/A	N/A	UCScen	N/A	N/A	I	0.0	2	N/A	N/A	N/A	70F_4s1d2Vc_1	4/21A	TDP-142	700320
21.0	0.995	0.01430	0.050	0.336	42.2	P	N/A	6.74	6.86	6.91	7.10	7.10	30.00	N/A	N/A	N/A	N/A	N/A	N/A	N/A	1.5	N/A	N/A	N/A	N/A	70F_4s1d2Vc_1	4/21A	TDP-142	700321

Table B.6. Data from 2008 in Large-Scale Vessel with Flanged and Dished Head A.4

Row Number	Test	Case ID	Tank Diameter	Head Shape	Dish Height	Dish Volume	Tank Fill Height	Return Line Height	Nozzle Inner Diameter	Nozzle Stand-off Distance	Pulse Tube Configuration	Installed Nozzles	Outer Nozzles Operated	Inner Nozzles Operated	Pulse Tube Outer Diameter	Outer PJM Radius	Inner PJM Radius	"FIO" Outer PJM Impingement Angle	"FIO" Inner PJM Impingement Angle	Ratio Outer PJM to Tank Radius	Ratio Inner PJM to Tank Radius	Simulant	Solids Density	Particle Diameter d5	Particle Diameter d50	Particle Diameter d95	Void Fraction
text	text	text	in.	text	in.	in. ^{3}	in.	in.	in.	in.	text	number	number	number	in.	in.	in.	deg	deg	nondim	nondim	text	g/cm^3	m	m	m	fraction
MSS	M/DDX	ID	D	HS	H_{dish}	V_{dish}	H	Rtn	d	sod	PT	N	N_O	N_I	PT_{od}	R_O	R_I	θ_O	θ_I	R_O/R	R_I/R	sxdx	ρ_s	d_5	d_{50}	d_{95}	vf
700322	4/21A	70F_4s1d2Vc_1	70	FD	12.7	30569.0	87 1/2	83 5/8	0.613	0.920	HLP-22	12	8	4	3.5	26.4	11.7	22.4	9.7	0.75	0.33	s1d2	2.48	0.0000569	0.0000693	0.0000821	0.3750
700323	4/21A	70F_4s1d2Vc_1	70	FD	12.7	30569.0	87 1/2	83 5/8	0.613	0.920	HLP-22	12	8	4	3.5	26.4	11.7	22.4	9.7	0.75	0.33	s1d2	2.48	0.0000569	0.0000693	0.0000821	0.3750
700324	4/21A	70F_4s1d2Vc_1	70	FD	12.7	30569.0	87 1/2	83 5/8	0.613	0.920	HLP-22	12	8	4	3.5	26.4	11.7	22.4	9.7	0.75	0.33	s1d2	2.48	0.0000569	0.0000693	0.0000821	0.3750
700325	4/21A	70F_4s1d2Vc_1	70	FD	12.7	30569.0	87 1/2	83 5/8	0.613	0.920	HLP-22	12	8	4	3.5	26.4	11.7	22.4	9.7	0.75	0.33	s1d2	2.48	0.0000569	0.0000693	0.0000821	0.3750
700326	4/21A	70F_4s1d2Vc_1	70	FD	12.7	30569.0	87 1/2	83 5/8	0.613	0.920	HLP-22	12	8	4	3.5	26.4	11.7	22.4	9.7	0.75	0.33	s1d2	2.48	0.0000569	0.0000693	0.0000821	0.3750
700327	4/21A	70F_4s1d2Vc_1	70	FD	12.7	30569.0	87 1/2	83 5/8	0.613	0.920	HLP-22	12	8	4	3.5	26.4	11.7	22.4	9.7	0.75	0.33	s1d2	2.48	0.0000569	0.0000693	0.0000821	0.3750
700328	4/21A	70F_4s1d2Vc_1	70	FD	12.7	30569.0	87 1/2	83 5/8	0.613	0.920	HLP-22	12	8	4	3.5	26.4	11.7	22.4	9.7	0.75	0.33	s1d2	2.48	0.0000569	0.0000693	0.0000821	0.3750
700329	4/21A	70F_4s1d2Vc_1	70	FD	12.7	30569.0	87 1/2	83 5/8	0.613	0.920	HLP-22	12	8	4	3.5	26.4	11.7	22.4	9.7	0.75	0.33	s1d2	2.48	0.0000569	0.0000693	0.0000821	0.3750
700330M	4/21A	70F_4s1d2Vc_1	70	FD	12.7	30569.0	87 1/2	83 5/8	0.613	0.920	HLP-22	12	8	4	3.5	26.4	11.7	22.4	9.7	0.75	0.33	s1d2	2.48	0.0000569	0.0000693	0.0000821	0.3750
700331	4/21A	70F_4s1d2Vc_1	70	FD	12.7	30569.0	87 1/2	83 5/8	0.613	0.920	HLP-22	12	8	4	3.5	26.4	11.7	22.4	9.7	0.75	0.33	s1d2	2.48	0.0000569	0.0000693	0.0000821	0.3750
700332	4/21A	70F_4s1d2Vc_1	70	FD	12.7	30569.0	87 1/2	83 5/8	0.613	0.920	HLP-22	12	8	4	3.5	26.4	11.7	22.4	9.7	0.75	0.33	s1d2	2.48	0.0000569	0.0000693	0.0000821	0.3750
700333	4/21A	70F_4s1d2Vc_1	70	FD	12.7	30569.0	87 1/2	83 5/8	0.613	0.920	HLP-22	12	8	4	3.5	26.4	11.7	22.4	9.7	0.75	0.33	s1d2	2.48	0.0000569	0.0000693	0.0000821	0.3750
700334	4/21A	70F_4s1d2Vc_1	70	FD	12.7	30569.0	87 1/2	83 5/8	0.613	0.920	HLP-22	12	8	4	3.5	26.4	11.7	22.4	9.7	0.75	0.33	s1d2	2.48	0.0000569	0.0000693	0.0000821	0.3750
700335	4/21A	70F_4s1d2Vc_1	70	FD	12.7	30569.0	87 1/2	83 5/8	0.613	0.920	HLP-22	12	8	4	3.5	26.4	11.7	22.4	9.7	0.75	0.33	s1d2	2.48	0.0000569	0.0000693	0.0000821	0.3750
700336	4/21A	70F_4s1d2Vc_1	70	FD	12.7	30569.0	87 1/2	83 5/8	0.613	0.920	HLP-22	12	8	4	3.5	26.4	11.7	22.4	9.7	0.75	0.33	s1d2	2.48	0.0000569	0.0000693	0.0000821	0.3750
700337	4/21A	70F_4s1d2Vc_1	70	FD	12.7	30569.0	87 1/2	83 5/8	0.613	0.920	HLP-22	12	8	4	3.5	26.4	11.7	22.4	9.7	0.75	0.33	s1d2	2.48	0.0000569	0.0000693	0.0000821	0.3750
700338	4/21A	70F_4s1d2Vc_1	70	FD	12.7	30569.0	87 1/2	83 5/8	0.613	0.920	HLP-22	12	8	4	3.5	26.4	11.7	22.4	9.7	0.75	0.33	s1d2	2.48	0.0000569	0.0000693	0.0000821	0.3750
700339	4/21A	70F_4s1d2Vc_1	70	FD	12.7	30569.0	87 1/2	83 5/8	0.613	0.920	HLP-22	12	8	4	3.5	26.4	11.7	22.4	9.7	0.75	0.33	s1d2	2.48	0.0000569	0.0000693	0.0000821	0.3750
700340M	4/21A	70F_4s1d2Vc_1	70	FD	12.7	30569.0	87 1/2	83 5/8	0.613	0.920	HLP-22	12	8	4	3.5	26.4	11.7	22.4	9.7	0.75	0.33	s1d2	2.48	0.0000569	0.0000693	0.0000821	0.3750
700341	4/21A	70F_4s1d2Vc_1	70	FD	12.7	30569.0	87 1/2	83 5/8	0.613	0.920	HLP-22	12	8	4	3.5	26.4	11.7	22.4	9.7	0.75	0.33	s1d2	2.48	0.0000569	0.0000693	0.0000821	0.3750
700342	4/21A	70F_4s1d2Vc_1	70	FD	12.7	30569.0	87 1/2	83 5/8	0.613	0.920	HLP-22	12	8	4	3.5	26.4	11.7	22.4	9.7	0.75	0.33	s1d2	2.48	0.0000569	0.0000693	0.0000821	0.3750
700343	4/21A	70F_4s1d2Vc_1	70	FD	12.7	30569.0	87 1/2	83 5/8	0.613	0.920	HLP-22	12	8	4	3.5	26.4	11.7	22.4	9.7	0.75	0.33	s1d2	2.48	0.0000569	0.0000693	0.0000821	0.3750
700344	4/21A	70F_4s1d2Vc_1	70	FD	12.7	30569.0	87 1/2	83 5/8	0.613	0.920	HLP-22	12	8	4	3.5	26.4	11.7	22.4	9.7	0.75	0.33	s1d2	2.48	0.0000569	0.0000693	0.0000821	0.3750
700345	4/21A	70F_4s1d2Vc_1	70	FD	12.7	30569.0	87 1/2	83 5/8	0.613	0.920	HLP-22	12	8	4	3.5	26.4	11.7	22.4	9.7	0.75	0.33	s1d2	2.48	0.0000569	0.0000693	0.0000821	0.3750
700346	4/21A	70F_4s1d2Vc_1	70	FD	12.7	30569.0	87 1/2	83 5/8	0.613	0.920	HLP-22	12	8	4	3.5	26.4	11.7	22.4	9.7	0.75	0.33	s1d2	2.48	0.0000569	0.0000693	0.0000821	0.3750
700347	4/21A	70F_4s1d2Vc_1	70	FD	12.7	30569.0	87 1/2	83 5/8	0.613	0.920	HLP-22	12	8	4	3.5	26.4	11.7	22.4	9.7	0.75	0.33	s1d2	2.48	0.0000569	0.0000693	0.0000821	0.3750
700347.1	4/21A	70F_4s1d2Vc_1	70	FD	12.7	30569.0	87 1/2	83 5/8	0.613	0.920	HLP-22	12	8	4	3.5	26.4	11.7	22.4	9.7	0.75	0.33	s1d2	2.48	0.0000569	0.0000693	0.0000821	0.3750
700347.2	4/21A	70F_4s1d2Vc_1	70	FD	12.7	30569.0	87 1/2	83 5/8	0.613	0.920	HLP-22	12	8	4	3.5	26.4	11.7	22.4	9.7	0.75	0.33	s1d2	2.48	0.0000569	0.0000693	0.0000821	0.3750
700348M	4/21A	70F_4s1d2Vc_1	70	FD	12.7	30569.0	87 1/2	83 5/8	0.613	0.920	HLP-22	12	8	4	3.5	26.4	11.7	22.4	9.7	0.75	0.33	s1d2	2.48	0.0000569	0.0000693	0.0000821	0.3750
700349M	4/21A	70F_4s1d2Vc_1	70	FD	12.7	30569.0	87 1/2	83 5/8	0.613	0.920	HLP-22	12	8	4	3.5	26.4	11.7	22.4	9.7	0.75	0.33	s1d2	2.48	0.0000569	0.0000693	0.0000821	0.3750
700350M	4/21A	70F_4s1d2Vc_1	70	FD	12.7	30569.0	87 1/2	83 5/8	0.613	0.920	HLP-22	12	8	4	3.5	26.4	11.7	22.4	9.7	0.75	0.33	s1d2	2.48	0.0000569	0.0000693	0.0000821	0.3750
700351	4/22A	70F_4s1d2Vd_1	70	FD	12.7	30569.0	88	83 5/8	0.613	0.920	HLP-22	12	8	4	3.5	26.4	11.7	22.4	9.7	0.75	0.33	s1d2	2.48	0.0000569	0.0000693	0.0000821	0.3750
700352	4/22A	70F_4s1d2Vd_1	70	FD	12.7	30569.0	88	83 5/8	0.613	0.920	HLP-22	12	8	4	3.5	26.4	11.7	22.4	9.7	0.75	0.33	s1d2	2.48	0.0000569	0.0000693	0.0000821	0.3750
700353	4/22A	70F_4s1d2Vd_1	70	FD	12.7	30569.0	88	83 5/8	0.613	0.920	HLP-22	12	8	4	3.5	26.4	11.7	22.4	9.7	0.75	0.33	s1d2	2.48	0.0000569	0.0000693	0.0000821	0.3750
700354	4/22A	70F_4s1d2Vd_1	70	FD	12.7	30569.0	88	83 5/8	0.613	0.920	HLP-22	12	8	4	3.5	26.4	11.7	22.4	9.7	0.75	0.33	s1d2	2.48	0.0000569	0.0000693	0.0000821	0.3750
700355	4/22A	70F_4s1d2Vd_1	70	FD	12.7	30569.0	88	83 5/8	0.613	0.920	HLP-22	12	8	4	3.5	26.4	11.7	22.4	9.7	0.75	0.33	s1d2	2.48	0.0000569	0.0000693	0.0000821	0.3750
700356M	4/22A	70F_4s1d2Vd_1	70	FD	12.7	30569.0	88	83 5/8	0.613	0.920	HLP-22	12	8	4	3.5	26.4	11.7	22.4	9.7	0.75	0.33	s1d2	2.48	0.0000569	0.0000693	0.0000821	0.3750
700356.1	4/22A	70F_4s1d2Vd_1	70	FD	12.7	30569.0	88	83 5/8	0.613	0.920	HLP-22	12	8	4	3.5	26.4	11.7	22.4	9.7	0.75	0.33	s1d2	2.48	0.0000569	0.0000693	0.0000821	0.3750
700357M	4/22A	70F_4s1d2Vd_1	70	FD	12.7	30569.0	88	83 5/8	0.613	0.920	HLP-22	12	8	4	3.5	26.4	11.7	22.4	9.7	0.75	0.33	s1d2	2.48	0.0000569	0.0000693	0.0000821	0.3750
700358	4/22A	70F_4s1d2Vd_1	70	FD	12.7	30569.0	88	83 5/8	0.613	0.920	HLP-22	12	8	4	3.5	26.4	11.7	22.4	9.7	0.75	0.33	s1d2	2.48	0.0000569	0.0000693	0.0000821	0.3750
700359	4/22A	70F_4s1d2Vd_1	70	FD	12.7	30569.0	88	83 5/8	0.613	0.920	HLP-22	12	8	4	3.5	26.4	11.7	22.4	9.7	0.75	0.33	s1d2	2.48	0.0000569	0.0000693	0.0000821	0.3750

Table B.6. Data from 2008 in Large-Scale Vessel with Flanged and Dished Head B.4

Tank Water Temperature	Water Density	Solids Fraction	Pulse Volume Fraction	Duty Cycle	Cycle Time	Pulsed or Steady Jet	Us Steady Jet	U1 Pulsing Jet	U2 URMS	U3 URM3	Discharge Velocity	Critical Suspension Velocity	Average Peak Cloud Height	UCS Condition	UCS Method	UCS Flag	UCS Center Flag	UCS udv Flag	UCS based on Decreasing Velocity	Sweep Increase / Decrease	UDV Height Bed	Particle Motion	Solids Level	Outer Bottom Pattern	Inner Bottom Pattern	Case ID	Test	TDP	Row Number
C	g/cm³	fraction	fraction	fraction	s	text	m/s	m/s	m/s	m/s	m/s	m/s	in.	m/s	text	text	text	text	m/s	text	mm	text	text	text	text	text	text	text	text
T	ρ_L	ϕ_S	ϕ_P	DC	t_C	Jet	U_S	U1	U2	U3	U	U_{CS}	H_C	U_{CSR}	U_{CSM}	U_{CS}vis	U_{CS}cen	U_{CS}udv	U_{CS}_D	S_W	H_{bed}	PM	Sol	SP_O	SP_I	ID	M/DDX	TDP	MSS
21.0	0.995	0.01430	0.050	0.336	42.2	P	N/A	6.74	6.86	6.91	7.10	7.10	30.00	N/A	N/A	N/A	N/A	N/A	N/A	N/A	0.0	N/A	N/A	N/A	N/A	70F_4s1d2Vc_1	4/21A	TDP-142	700322
21.0	0.995	0.01430	0.050	0.336	42.2	P	N/A	6.74	6.86	6.91	7.10	7.10	30.00	N/A	N/A	N/A	N/A	N/A	N/A	N/A	0.6	N/A	N/A	N/A	N/A	70F_4s1d2Vc_1	4/21A	TDP-142	700323
21.0	0.995	0.01430	0.050	0.336	42.2	P	N/A	6.74	6.86	6.91	7.10	7.10	30.00	N/A	N/A	N/A	N/A	N/A	N/A	N/A	0.0	N/A	N/A	N/A	N/A	70F_4s1d2Vc_1	4/21A	TDP-142	700324
21.0	0.995	0.01430	0.050	0.336	42.2	P	N/A	6.74	6.86	6.91	7.10	7.10	30.00	N/A	N/A	N/A	N/A	N/A	N/A	N/A	0.0	N/A	N/A	N/A	N/A	70F_4s1d2Vc_1	4/21A	TDP-142	700325
21.0	0.995	0.01430	0.050	0.336	42.2	P	N/A	6.74	6.86	6.91	7.10	7.10	30.00	N/A	N/A	N/A	N/A	N/A	N/A	N/A	0.0	N/A	N/A	N/A	N/A	70F_4s1d2Vc_1	4/21A	TDP-142	700326
21.0	0.995	0.01430	0.050	0.336	42.2	P	N/A	6.74	6.86	6.91	7.10	7.10	30.00	N/A	N/A	N/A	N/A	N/A	N/A	N/A	0.0	N/A	N/A	N/A	N/A	70F_4s1d2Vc_1	4/21A	TDP-142	700327
21.0	0.995	0.01430	0.050	0.336	42.2	P	N/A	6.74	6.86	6.91	7.10	7.10	30.00	N/A	N/A	N/A	N/A	N/A	N/A	N/A	0.0	N/A	N/A	N/A	N/A	70F_4s1d2Vc_1	4/21A	TDP-142	700328
21.0	0.995	0.01430	0.050	0.336	42.2	P	N/A	6.74	6.86	6.91	7.10	7.10	30.00	N/A	N/A	N/A	N/A	N/A	N/A	N/A	0.0	N/A	N/A	N/A	N/A	70F_4s1d2Vc_1	4/21A	TDP-142	700329
21.1	0.995	0.01430	0.050	0.336	42.2	P	N/A	6.75	6.86	6.92	7.10	7.10	29.50	N/A	N/A	N/A	UCScen	N/A	N/A	(null)	0.0	2	N/A	N/A	N/A	70F_4s1d2Vc_1	4/21A	TDP-142	700330
21.1	0.995	0.01430	0.050	0.336	42.2	P	N/A	6.75	6.86	6.92	7.10	7.10	29.50	N/A	N/A	N/A	N/A	N/A	N/A	N/A	0.0	N/A	N/A	N/A	N/A	70F_4s1d2Vc_1	4/21A	TDP-142	700331
21.1	0.995	0.01430	0.050	0.336	42.2	P	N/A	6.75	6.86	6.92	7.10	7.10	29.50	N/A	N/A	N/A	N/A	N/A	N/A	N/A	0.0	N/A	N/A	N/A	N/A	70F_4s1d2Vc_1	4/21A	TDP-142	700332
21.1	0.995	0.01430	0.050	0.336	42.2	P	N/A	6.75	6.86	6.92	7.10	7.10	29.50	N/A	N/A	N/A	N/A	N/A	N/A	N/A	0.0	N/A	N/A	N/A	N/A	70F_4s1d2Vc_1	4/21A	TDP-142	700333
21.1	0.995	0.01430	0.050	0.336	42.2	P	N/A	6.75	6.86	6.92	7.10	7.10	29.50	N/A	N/A	N/A	N/A	N/A	N/A	N/A	0.0	N/A	N/A	N/A	N/A	70F_4s1d2Vc_1	4/21A	TDP-142	700334
21.1	0.995	0.01430	0.050	0.336	42.2	P	N/A	6.75	6.86	6.92	7.10	7.10	29.50	N/A	N/A	N/A	N/A	N/A	N/A	N/A	0.0	N/A	N/A	N/A	N/A	70F_4s1d2Vc_1	4/21A	TDP-142	700335
21.1	0.995	0.01430	0.050	0.336	42.2	P	N/A	6.75	6.86	6.92	7.10	7.10	29.50	N/A	N/A	N/A	N/A	N/A	N/A	N/A	0.0	N/A	N/A	N/A	N/A	70F_4s1d2Vc_1	4/21A	TDP-142	700336
21.1	0.995	0.01430	0.050	0.336	42.2	P	N/A	6.75	6.86	6.92	7.10	7.10	29.50	N/A	N/A	N/A	N/A	N/A	N/A	N/A	0.0	N/A	N/A	N/A	N/A	70F_4s1d2Vc_1	4/21A	TDP-142	700337
21.1	0.995	0.01430	0.050	0.336	42.2	P	N/A	6.75	6.86	6.92	7.10	7.10	29.50	N/A	N/A	N/A	N/A	N/A	N/A	N/A	0.0	N/A	N/A	N/A	N/A	70F_4s1d2Vc_1	4/21A	TDP-142	700338
21.1	0.995	0.01430	0.050	0.336	42.2	P	N/A	6.75	6.86	6.92	7.10	7.10	29.50	N/A	N/A	N/A	N/A	N/A	N/A	N/A	0.0	N/A	N/A	N/A	N/A	70F_4s1d2Vc_1	4/21A	TDP-142	700339
21.2	0.995	0.01430	0.050	0.336	42.2	P	N/A	6.75	6.86	6.92	7.10	7.10	30.00	N/A	N/A	N/A	UCScen	N/A	N/A	(null)	1.5	2	N/A	N/A	N/A	70F_4s1d2Vc_1	4/21A	TDP-142	700340
21.2	0.995	0.01430	0.050	0.336	42.2	P	N/A	6.75	6.86	6.92	7.10	7.10	30.00	N/A	N/A	N/A	N/A	N/A	N/A	N/A	3.3	N/A	N/A	N/A	N/A	70F_4s1d2Vc_1	4/21A	TDP-142	700341
21.2	0.995	0.01430	0.050	0.336	42.2	P	N/A	6.75	6.86	6.92	7.10	7.10	30.00	N/A	N/A	N/A	N/A	N/A	N/A	N/A	0.0	N/A	N/A	N/A	N/A	70F_4s1d2Vc_1	4/21A	TDP-142	700342
21.2	0.995	0.01430	0.050	0.336	42.2	P	N/A	6.75	6.86	6.92	7.10	7.10	30.00	N/A	N/A	N/A	N/A	N/A	N/A	N/A	0.0	N/A	N/A	N/A	N/A	70F_4s1d2Vc_1	4/21A	TDP-142	700343
21.2	0.995	0.01430	0.050	0.336	42.2	P	N/A	6.75	6.86	6.92	7.10	7.10	30.00	N/A	N/A	N/A	N/A	N/A	N/A	N/A	0.0	N/A	N/A	N/A	N/A	70F_4s1d2Vc_1	4/21A	TDP-142	700344
21.2	0.995	0.01430	0.050	0.336	42.2	P	N/A	6.75	6.86	6.92	7.10	7.10	30.00	N/A	N/A	N/A	N/A	N/A	N/A	N/A	0.0	N/A	N/A	N/A	N/A	70F_4s1d2Vc_1	4/21A	TDP-142	700345
21.2	0.995	0.01430	0.050	0.336	42.2	P	N/A	6.75	6.86	6.92	7.10	7.10	30.00	N/A	N/A	N/A	N/A	N/A	N/A	N/A	0.0	N/A	N/A	N/A	N/A	70F_4s1d2Vc_1	4/21A	TDP-142	700346
21.2	0.995	0.01430	0.050	0.336	42.2	P	N/A	6.75	6.86	6.92	7.10	7.10	30.00	N/A	N/A	N/A	N/A	N/A	N/A	N/A	0.7	N/A	N/A	N/A	N/A	70F_4s1d2Vc_1	4/21A	TDP-142	700347
21.2	0.995	0.01430	0.050	0.336	42.2	P	N/A	6.75	6.86	6.92	7.10	7.10	30.00	N/A	N/A	N/A	N/A	N/A	N/A	N/A	n/a	N/A	N/A	N/A	N/A	70F_4s1d2Vc_1	4/21A	TDP-142	700347.1
21.2	0.995	0.01430	0.050	0.336	42.2	P	N/A	6.75	6.86	6.92	7.10	7.10	30.00	N/A	N/A	N/A	N/A	N/A	N/A	N/A	n/a	N/A	N/A	N/A	N/A	70F_4s1d2Vc_1	4/21A	TDP-142	700347.2
21.3	0.994	0.01430	0.050	0.336	41.0	P	N/A	6.93	7.05	7.11	7.30	7.10	33.50	N/A	N/A	N/A	N/A	N/A	N/A	(null)	0.0	4	N/A	N/A	N/A	70F_4s1d2Vc_1	4/21A	TDP-142	700348
21.2	0.995	0.01430	0.050	0.338	39.6	P	N/A	7.10	7.22	7.29	7.50	7.10	35.50	N/A	N/A	N/A	N/A	N/A	N/A	I	0.0	4	N/A	N/A	N/A	70F_4s1d2Vc_1	4/21A	TDP-142	700349
21.3	0.995	0.01430	0.050	0.339	38.4	P	N/A	7.28	7.42	7.48	7.70	7.10	40.50	N/A	N/A	N/A	N/A	N/A	N/A	I	0.0	4	N/A	N/A	N/A	70F_4s1d2Vc_1	4/21A	TDP-142	700350
21.9	0.995	0.01430	0.050	0.183	72.8	P	N/A	7.20	7.33	7.40	7.60	9.90	19.25	N/A	N/A	N/A	N/A	N/A	N/A	I	N/A	1	N/A	N/A	N/A	70F_4s1d2Vd_1	4/22A	TDP-143	700351
22.1	0.995	0.01430	0.050	0.185	65.8	P	N/A	7.87	8.02	8.10	8.30	9.90	21.50	N/A	N/A	N/A	N/A	N/A	N/A	I	22.1	1	N/A	N/A	N/A	70F_4s1d2Vd_1	4/22A	TDP-143	700352
22.3	0.995	0.01430	0.050	0.184	63.4	P	N/A	8.13	8.29	8.37	8.60	9.90	22.75	N/A	N/A	N/A	N/A	N/A	N/A	I	19.9	1	N/A	N/A	N/A	70F_4s1d2Vd_1	4/22A	TDP-143	700353
22.4	0.995	0.01430	0.050	0.185	59.8	P	N/A	8.58	8.75	8.84	9.10	9.90	24.25	N/A	N/A	N/A	N/A	N/A	N/A	I	18.6	1	N/A	N/A	N/A	70F_4s1d2Vd_1	4/22A	TDP-143	700354
22.5	0.994	0.01430	0.050	0.186	56.6	P	N/A	9.00	9.19	9.29	9.60	9.90	27.00	N/A	N/A	N/A	UCScen	N/A	N/A	I	12.3	2	N/A	N/A	N/A	70F_4s1d2Vd_1	4/22A	TDP-143	700355
22.7	0.994	0.01430	0.050	0.185	54.8	P	N/A	9.30	9.50	9.60	9.90	9.90	27.75	9.90	udv	N/A	N/A	UCSudv	N/A	I	0.7	4	N/A	N/A	N/A	70F_4s1d2Vd_1	4/22A	TDP-143	700356
22.6	0.995	0.01430	0.050	0.185	54.8	P	N/A	9.29	9.49	9.59	9.90	9.90	27.50	N/A	N/A	N/A	N/A	N/A	N/A	N/A	n/a	N/A	N/A	N/A	N/A	70F_4s1d2Vd_1	4/22A	TDP-143	700356.1
22.6	0.995	0.01430	0.050	0.185	54.8	P	N/A	9.29	9.49	9.59	9.90	9.90	27.50	N/A	N/A	N/A	N/A	N/A	N/A	(null)	4.5	4	N/A	N/A	N/A	70F_4s1d2Vd_1	4/22A	TDP-143	700357
22.6	0.995	0.01430	0.050	0.185	54.8	P	N/A	9.29	9.49	9.59	9.90	9.90	27.50	N/A	N/A	N/A	N/A	N/A	N/A	N/A	0.0	N/A	N/A	N/A	N/A	70F_4s1d2Vd_1	4/22A	TDP-143	700358
22.6	0.995	0.01430	0.050	0.185	54.8	P	N/A	9.29	9.49	9.59	9.90	9.90	27.50	N/A	N/A	N/A	N/A	N/A	N/A	N/A	0.0	N/A	N/A	N/A	N/A	70F_4s1d2Vd_1	4/22A	TDP-143	700359

Table B.6. Data from 2008 in Large-Scale Vessel with Flanged and Dished Head A.5

Row Number	Test	Case ID	Tank Diameter	Head Shape	Dish Height	Dish Volume	Tank Fill Height	Return Line Height	Nozzle Inner Diameter	Nozzle Stand-off Distance	Pulse Tube Configuration	Installed Nozzles	Outer Nozzles Operated	Inner Nozzles Operated	Pulse Tube Outer Diameter	Outer PJM Radius	Inner PJM Radius	"FIO" Outer PJM Impingement Angle	"FIO" Inner PJM Impingement Angle	Ratio Outer PJM to Tank Radius	Ratio Inner PJM to Tank Radius	Simulant	Solids Density	Particle Diameter d5	Particle Diameter d50	Particle Diameter d95	Void Fraction
text	text	text	in.	text	in.	in. ^{3}	in.	in.	in.	in.	text	number	number	number	in.	in.	in.	deg	deg	nondim	nondim	text	g/cm^3	m	m	m	fraction
MSS	M/DDX	ID	D	HS	H_{dish}	V_{dish}	H	Rtn	d	sod	PT	N	N_O	N_I	PT_{od}	R_O	R_I	θ_O	θ_I	R_O/R	R_I/R	sxdx	ρ_s	d_5	d_{50}	d_{95}	vf
700360	4/22A	70F_4s1d2Vd_1	70	FD	12.7	30569.0	88	83 5/8	0.613	0.920	HLP-22	12	8	4	3.5	26.4	11.7	22.4	9.7	0.75	0.33	s1d2	2.48	0.0000569	0.0000693	0.0000821	0.3750
700361	4/22A	70F_4s1d2Vd_1	70	FD	12.7	30569.0	88	83 5/8	0.613	0.920	HLP-22	12	8	4	3.5	26.4	11.7	22.4	9.7	0.75	0.33	s1d2	2.48	0.0000569	0.0000693	0.0000821	0.3750
700362	4/22A	70F_4s1d2Vd_1	70	FD	12.7	30569.0	88	83 5/8	0.613	0.920	HLP-22	12	8	4	3.5	26.4	11.7	22.4	9.7	0.75	0.33	s1d2	2.48	0.0000569	0.0000693	0.0000821	0.3750
700363	4/22A	70F_4s1d2Vd_1	70	FD	12.7	30569.0	88	83 5/8	0.613	0.920	HLP-22	12	8	4	3.5	26.4	11.7	22.4	9.7	0.75	0.33	s1d2	2.48	0.0000569	0.0000693	0.0000821	0.3750
700364	4/22A	70F_4s1d2Vd_1	70	FD	12.7	30569.0	88	83 5/8	0.613	0.920	HLP-22	12	8	4	3.5	26.4	11.7	22.4	9.7	0.75	0.33	s1d2	2.48	0.0000569	0.0000693	0.0000821	0.3750
700365	4/22A	70F_4s1d2Vd_1	70	FD	12.7	30569.0	88	83 5/8	0.613	0.920	HLP-22	12	8	4	3.5	26.4	11.7	22.4	9.7	0.75	0.33	s1d2	2.48	0.0000569	0.0000693	0.0000821	0.3750
700366M	4/22A	70F_4s1d2Vd_1	70	FD	12.7	30569.0	88	83 5/8	0.613	0.920	HLP-22	12	8	4	3.5	26.4	11.7	22.4	9.7	0.75	0.33	s1d2	2.48	0.0000569	0.0000693	0.0000821	0.3750
700367M	4/22A	70F_4s1d2Vd_1	70	FD	12.7	30569.0	88	83 5/8	0.613	0.920	HLP-22	12	8	4	3.5	26.4	11.7	22.4	9.7	0.75	0.33	s1d2	2.48	0.0000569	0.0000693	0.0000821	0.3750
700368M	4/22B	70F_4s1d2Vc_2	70	FD	12.7	30569.0	87 1/2	83 5/8	0.613	0.920	HLP-22	12	8	4	3.5	26.4	11.7	22.4	9.7	0.75	0.33	s1d2	2.48	0.0000569	0.0000693	0.0000821	0.3750
700369	4/23A	70F_4s1d2Ve_1	70	FD	12.7	30569.0	87 1/2	83 5/8	0.613	0.920	HLP-22	12	8	4	3.5	26.4	11.7	22.4	9.7	0.75	0.33	s1d2	2.48	0.0000569	0.0000693	0.0000821	0.3750
700370M	4/23A	70F_4s1d2Ve_1	70	FD	12.7	30569.0	87 1/2	83 5/8	0.613	0.920	HLP-22	12	8	4	3.5	26.4	11.7	22.4	9.7	0.75	0.33	s1d2	2.48	0.0000569	0.0000693	0.0000821	0.3750
700371	4/23B	70F_4s1d2Ve_2	70	FD	12.7	30569.0	87 1/2	83 5/8	0.613	0.920	HLP-22	12	8	4	3.5	26.4	11.7	22.4	9.7	0.75	0.33	s1d2	2.48	0.0000569	0.0000693	0.0000821	0.3750
700372M	4/23B	70F_4s1d2Ve_2	70	FD	12.7	30569.0	87 1/2	83 5/8	0.613	0.920	HLP-22	12	8	4	3.5	26.4	11.7	22.4	9.7	0.75	0.33	s1d2	2.48	0.0000569	0.0000693	0.0000821	0.3750
700373	4/23C	70F_4s1d2Ve_4	70	FD	12.7	30569.0	88	83 5/8	0.613	0.920	HLP-22	12	8	4	3.5	26.4	11.7	22.4	9.7	0.75	0.33	s1d2	2.48	0.0000569	0.0000693	0.0000821	0.3750
700374M	4/23C	70F_4s1d2Ve_4	70	FD	12.7	30569.0	88	83 5/8	0.613	0.920	HLP-22	12	8	4	3.5	26.4	11.7	22.4	9.7	0.75	0.33	s1d2	2.48	0.0000569	0.0000693	0.0000821	0.3750
700375	4/24A	70F_4s1d2Vc_4	70	FD	12.7	30569.0	88	83 5/8	0.613	0.920	HLP-22	12	8	4	3.5	26.4	11.7	22.4	9.7	0.75	0.33	s1d2	2.48	0.0000569	0.0000693	0.0000821	0.3750
700376	4/24A	70F_4s1d2Vc_4	70	FD	12.7	30569.0	88	83 5/8	0.613	0.920	HLP-22	12	8	4	3.5	26.4	11.7	22.4	9.7	0.75	0.33	s1d2	2.48	0.0000569	0.0000693	0.0000821	0.3750
700377	4/24A	70F_4s1d2Vc_4	70	FD	12.7	30569.0	88	83 5/8	0.613	0.920	HLP-22	12	8	4	3.5	26.4	11.7	22.4	9.7	0.75	0.33	s1d2	2.48	0.0000569	0.0000693	0.0000821	0.3750
700378	4/24A	70F_4s1d2Vc_4	70	FD	12.7	30569.0	88	83 5/8	0.613	0.920	HLP-22	12	8	4	3.5	26.4	11.7	22.4	9.7	0.75	0.33	s1d2	2.48	0.0000569	0.0000693	0.0000821	0.3750
700379	4/24A	70F_4s1d2Vc_4	70	FD	12.7	30569.0	88	83 5/8	0.613	0.920	HLP-22	12	8	4	3.5	26.4	11.7	22.4	9.7	0.75	0.33	s1d2	2.48	0.0000569	0.0000693	0.0000821	0.3750
700380M	4/24A	70F_4s1d2Vc_4	70	FD	12.7	30569.0	88	83 5/8	0.613	0.920	HLP-22	12	8	4	3.5	26.4	11.7	22.4	9.7	0.75	0.33	s1d2	2.48	0.0000569	0.0000693	0.0000821	0.3750
700381	4/24B	70F_4s1d2Vd_2	70	FD	12.7	30569.0	88	83 5/8	0.613	0.920	HLP-22	12	8	4	3.5	26.4	11.7	22.4	9.7	0.75	0.33	s1d2	2.48	0.0000569	0.0000693	0.0000821	0.3750
700382	4/24B	70F_4s1d2Vd_2	70	FD	12.7	30569.0	88	83 5/8	0.613	0.920	HLP-22	12	8	4	3.5	26.4	11.7	22.4	9.7	0.75	0.33	s1d2	2.48	0.0000569	0.0000693	0.0000821	0.3750
700383	4/24B	70F_4s1d2Vd_2	70	FD	12.7	30569.0	88	83 5/8	0.613	0.920	HLP-22	12	8	4	3.5	26.4	11.7	22.4	9.7	0.75	0.33	s1d2	2.48	0.0000569	0.0000693	0.0000821	0.3750
700384M	4/24B	70F_4s1d2Vd_2	70	FD	12.7	30569.0	88	83 5/8	0.613	0.920	HLP-22	12	8	4	3.5	26.4	11.7	22.4	9.7	0.75	0.33	s1d2	2.48	0.0000569	0.0000693	0.0000821	0.3750
700385	4/25A	70F_4s1d2Vd_4	70	FD	12.7	30569.0	87 1/2	83 5/8	0.613	0.920	HLP-22	12	8	4	3.5	26.4	11.7	22.4	9.7	0.75	0.33	s1d2	2.48	0.0000569	0.0000693	0.0000821	0.3750
700386	4/25A	70F_4s1d2Vd_4	70	FD	12.7	30569.0	87 1/2	83 5/8	0.613	0.920	HLP-22	12	8	4	3.5	26.4	11.7	22.4	9.7	0.75	0.33	s1d2	2.48	0.0000569	0.0000693	0.0000821	0.3750
700387M	4/25A	70F_4s1d2Vd_4	70	FD	12.7	30569.0	87 1/2	83 5/8	0.613	0.920	HLP-22	12	8	4	3.5	26.4	11.7	22.4	9.7	0.75	0.33	s1d2	2.48	0.0000569	0.0000693	0.0000821	0.3750
700388M	4/25B	70F_4s1d2Ve_1	70	FD	12.7	30569.0	87 1/2	83 5/8	0.613	0.920	HLP-22	12	8	4	3.5	26.4	11.7	22.4	9.7	0.75	0.33	s1d2	2.48	0.0000569	0.0000693	0.0000821	0.3750
700389	4/25B	70F_4s1d2Ve_1	70	FD	12.7	30569.0	87 1/2	83 5/8	0.613	0.920	HLP-22	12	8	4	3.5	26.4	11.7	22.4	9.7	0.75	0.33	s1d2	2.48	0.0000569	0.0000693	0.0000821	0.3750
700389.1	4/25B	70F_4s1d2Ve_1	70	FD	12.7	30569.0	87 1/2	83 5/8	0.613	0.920	HLP-22	12	8	4	3.5	26.4	11.7	22.4	9.7	0.75	0.33	s1d2	2.48	0.0000569	0.0000693	0.0000821	0.3750
700390	4/25B	70F_4s1d2Ve_1	70	FD	12.7	30569.0	87 1/2	83 5/8	0.613	0.920	HLP-22	12	8	4	3.5	26.4	11.7	22.4	9.7	0.75	0.33	s1d2	2.48	0.0000569	0.0000693	0.0000821	0.3750
700390.1	4/25B	70F_4s1d2Ve_1	70	FD	12.7	30569.0	87 1/2	83 5/8	0.613	0.920	HLP-22	12	8	4	3.5	26.4	11.7	22.4	9.7	0.75	0.33	s1d2	2.48	0.0000569	0.0000693	0.0000821	0.3750
700391	4/25B	70F_4s1d2Ve_1	70	FD	12.7	30569.0	87 1/2	83 5/8	0.613	0.920	HLP-22	12	8	4	3.5	26.4	11.7	22.4	9.7	0.75	0.33	s1d2	2.48	0.0000569	0.0000693	0.0000821	0.3750
700391.1	4/25B	70F_4s1d2Ve_1	70	FD	12.7	30569.0	87 1/2	83 5/8	0.613	0.920	HLP-22	12	8	4	3.5	26.4	11.7	22.4	9.7	0.75	0.33	s1d2	2.48	0.0000569	0.0000693	0.0000821	0.3750
700392	4/25B	70F_4s1d2Ve_1	70	FD	12.7	30569.0	87 1/2	83 5/8	0.613	0.920	HLP-22	12	8	4	3.5	26.4	11.7	22.4	9.7	0.75	0.33	s1d2	2.48	0.0000569	0.0000693	0.0000821	0.3750
700392.1	4/25B	70F_4s1d2Ve_1	70	FD	12.7	30569.0	87 1/2	83 5/8	0.613	0.920	HLP-22	12	8	4	3.5	26.4	11.7	22.4	9.7	0.75	0.33	s1d2	2.48	0.0000569	0.0000693	0.0000821	0.3750
700393	4/25B	70F_4s1d2Ve_1	70	FD	12.7	30569.0	87 1/2	83 5/8	0.613	0.920	HLP-22	12	8	4	3.5	26.4	11.7	22.4	9.7	0.75	0.33	s1d2	2.48	0.0000569	0.0000693	0.0000821	0.3750
700393.1	4/25B	70F_4s1d2Ve_1	70	FD	12.7	30569.0	87 1/2	83 5/8	0.613	0.920	HLP-22	12	8	4	3.5	26.4	11.7	22.4	9.7	0.75	0.33	s1d2	2.48	0.0000569	0.0000693	0.0000821	0.3750
700393.2	4/25C	70F_4s1d2Vc_2	70	FD	12.7	30569.0	87 1/2	83 5/8	0.613	0.920	HLP-22	12	8	4	3.5	26.4	11.7	22.4	9.7	0.75	0.33	s1d2	2.48	0.0000569	0.0000693	0.0000821	0.3750
700394M	4/25C	70F_4s1d2Vc_2	70	FD	12.7	30569.0	87 1/2	83 5/8	0.613	0.920	HLP-22	12	8	4	3.5	26.4	11.7	22.4	9.7	0.75	0.33	s1d2	2.48	0.0000569	0.0000693	0.0000821	0.3750

Table B.6. Data from 2008 in Large-Scale Vessel with Flanged and Dished Head B.5

Tank Water Temperature	Water Density	Solids Fraction	Pulse Volume Fraction	Duty Cycle	Cycle Time	Pulsed or Steady Jet	Us Steady Jet	U1 Pulsing Jet	U2 URMS	U3 URM3	Discharge Velocity	Critical Suspension Velocity	Average Peak Cloud Height	UCS Condition	UCS Method	UCS Flag	UCS Center Flag	UCS udv Flag	UCS based on Decreasing Velocity	Sweep Increase / Decrease	UDV Height Bed	Particle Motion	Solids Level	Outer Bottom Pattern	Inner Bottom Pattern	Case ID	Test	TDP	Row Number
C	g/cm³	fraction	fraction	fraction	s	text	m/s	m/s	m/s	m/s	m/s	m/s	in.	m/s	text	text	text	text	m/s	text	mm	text	text	text	text	text	text	text	text
T	ρ_L	ϕ_S	ϕ_P	DC	t_C	Jet	U_S	U1	U2	U3	U	U_{CS}	H_C	U_{CSR}	U_{CSM}	U_{CS}vis	U_{CS}cen	U_{CS}udv	U_{CS}_D	S_W	H_{bed}	PM	Sol	SP_O	SP_I	ID	M/DDX	TDP	MSS
22.6	0.995	0.01430	0.050	0.185	54.8	P	N/A	9.29	9.49	9.59	9.90	9.90	27.50	N/A	N/A	N/A	N/A	N/A	N/A	N/A	0.2	N/A	N/A	N/A	N/A	70F_4s1d2Vd_1	4/22A	TDP-143	700360
22.6	0.995	0.01430	0.050	0.185	54.8	P	N/A	9.29	9.49	9.59	9.90	9.90	27.50	N/A	N/A	N/A	N/A	N/A	N/A	N/A	0.0	N/A	N/A	N/A	N/A	70F_4s1d2Vd_1	4/22A	TDP-143	700361
22.6	0.995	0.01430	0.050	0.185	54.8	P	N/A	9.29	9.49	9.59	9.90	9.90	27.50	N/A	N/A	N/A	N/A	N/A	N/A	N/A	0.0	N/A	N/A	N/A	N/A	70F_4s1d2Vd_1	4/22A	TDP-143	700362
22.6	0.995	0.01430	0.050	0.185	54.8	P	N/A	9.29	9.49	9.59	9.90	9.90	27.50	N/A	N/A	N/A	N/A	N/A	N/A	N/A	0.0	N/A	N/A	N/A	N/A	70F_4s1d2Vd_1	4/22A	TDP-143	700363
22.6	0.995	0.01430	0.050	0.185	54.8	P	N/A	9.29	9.49	9.59	9.90	9.90	27.50	N/A	N/A	N/A	N/A	N/A	N/A	N/A	0.0	N/A	N/A	N/A	N/A	70F_4s1d2Vd_1	4/22A	TDP-143	700364
22.6	0.995	0.01430	0.050	0.185	54.8	P	N/A	9.29	9.49	9.59	9.90	9.90	27.50	N/A	N/A	N/A	N/A	N/A	N/A	N/A	0.0	N/A	N/A	N/A	N/A	70F_4s1d2Vd_1	4/22A	TDP-143	700365
22.8	0.995	0.01430	0.050	0.184	52.0	P	N/A	9.91	10.13	10.24	10.60	9.90	36.75	N/A	N/A	N/A	N/A	N/A	N/A	I	N/A	4	N/A	N/A	N/A	70F_4s1d2Vd_1	4/22A	TDP-143	700366
23.0	0.995	0.01430	0.050	0.186	49.0	P	N/A	10.38	10.62	10.74	11.10	9.90	46.25	N/A	N/A	N/A	N/A	N/A	N/A	I	N/A	4	N/A	N/A	N/A	70F_4s1d2Vd_1	4/22A	TDP-143	700367
23.1	0.994	0.01430	0.099	0.327	90.0	P	N/A	6.42	6.47	6.50	6.60	6.60	29.00	N/A	center dec	N/A	UCScen	N/A	6.60	D	4.7	2	N/A	N/A	N/A	70F_4s1d2Vc_2	4/22B	TDP-143	700368
23.3	0.994	0.01430	0.050	0.666	32.6	P	N/A	4.40	4.45	4.48	4.60	4.80	28.00	N/A	N/A	N/A	N/A	N/A	N/A	D	12.8	1	N/A	N/A	N/A	70F_4s1d2Ve_1	4/23A	TDP-144	700369
23.4	0.994	0.01430	0.050	0.669	31.2	P	N/A	4.59	4.65	4.68	4.80	4.80	33.50	4.80	udv	N/A	UCScen	UCSudv	N/A	I	0.0	2	N/A	N/A	N/A	70F_4s1d2Ve_1	4/23A	TDP-144	700370
23.6	0.994	0.01430	0.100	0.660	67.0	P	N/A	4.31	4.34	4.35	4.40	4.60	26.00	N/A	N/A	N/A	N/A	N/A	N/A	(null)	13.8	1	N/A	N/A	N/A	70F_4s1d2Ve_2	4/23B	TDP-144	700371
23.4	0.994	0.01430	0.100	0.661	64.0	P	N/A	4.50	4.53	4.54	4.60	4.60	32.50	4.60	udv	N/A	UCScen	UCSudv	N/A	(null)	0.0	2	N/A	N/A	N/A	70F_4s1d2Ve_2	4/23B	TDP-144	700372
23.3	0.995	0.01430	0.150	0.662	101.0	P	N/A	4.25	4.27	4.27	4.30	4.50	27.00	N/A	N/A	N/A	N/A	N/A	N/A	I	6.9	1	N/A	N/A	N/A	70F_4s1d2Ve_4	4/23C	TDP-144	700373
23.3	0.995	0.01430	0.149	0.664	96.0	P	N/A	4.43	4.45	4.46	4.50	4.50	33.75	4.50	center	N/A	UCScen	N/A	N/A	I	2.3	2	N/A	N/A	N/A	70F_4s1d2Ve_4	4/23C	TDP-144	700374
23.0	0.994	0.01430	0.150	0.331	194.0	P	N/A	4.44	4.46	4.47	4.50	6.10	18.50	N/A	N/A	N/A	N/A	N/A	N/A	(null)	39.3	1	N/A	N/A	N/A	70F_4s1d2Vc_4	4/24A	TDP-145	700375
23.2	0.994	0.01430	0.150	0.332	185.6	P	N/A	4.64	4.66	4.67	4.70	6.10	19.50	N/A	N/A	N/A	N/A	N/A	N/A	(null)	37.6	1	N/A	N/A	N/A	70F_4s1d2Vc_4	4/24A	TDP-145	700376
23.2	0.995	0.01430	0.150	0.333	171.0	P	N/A	5.02	5.05	5.06	5.10	6.10	21.50	N/A	N/A	N/A	N/A	N/A	N/A	(null)	27.3	1	N/A	N/A	N/A	70F_4s1d2Vc_4	4/24A	TDP-145	700377
23.2	0.994	0.01430	0.150	0.333	158.6	P	N/A	5.41	5.44	5.45	5.50	6.10	24.00	N/A	N/A	N/A	N/A	N/A	N/A	I	20.1	1	N/A	N/A	N/A	70F_4s1d2Vc_4	4/24A	TDP-145	700378
23.1	0.994	0.01430	0.150	0.334	147.8	P	N/A	5.78	5.81	5.83	5.90	6.10	26.25	N/A	N/A	N/A	N/A	N/A	N/A	I	15.4	1	N/A	N/A	N/A	70F_4s1d2Vc_4	4/24A	TDP-145	700379
23.1	0.995	0.01430	0.151	0.334	143.0	P	N/A	5.99	6.02	6.04	6.10	6.10	28.25	6.10	udv	N/A	UCScen	UCSudv	N/A	I	2.5	2	N/A	N/A	N/A	70F_4s1d2Vc_4	4/24A	TDP-145	700380
23.0	0.994	0.01430	0.100	0.185	154.0	P	N/A	6.69	6.75	6.79	6.90	8.50	20.25	N/A	N/A	N/A	N/A	N/A	N/A	I	16.7	1	N/A	N/A	N/A	70F_4s1d2Vd_2	4/24B	TDP-145	700381
23.2	0.994	0.01430	0.100	0.186	145.0	P	N/A	7.09	7.15	7.18	7.30	8.50	21.00	N/A	N/A	N/A	N/A	N/A	N/A	I	12.8	1	N/A	N/A	N/A	70F_4s1d2Vd_2	4/24B	TDP-145	700382
23.2	0.994	0.01430	0.101	0.186	141.0	P	N/A	7.30	7.36	7.40	7.50	8.50	22.25	N/A	N/A	N/A	N/A	N/A	N/A	I	10.0	1	N/A	N/A	N/A	70F_4s1d2Vd_2	4/24B	TDP-145	700383
23.1	0.995	0.01430	0.100	0.188	123.0	P	N/A	8.26	8.34	8.38	8.50	8.50	27.25	8.50	udv	N/A	UCScen	UCSudv	N/A	I	0.0	2	N/A	N/A	N/A	70F_4s1d2Vd_2	4/24B	TDP-145	700384
23.3	0.994	0.01430	0.150	0.182	252.0	P	N/A	6.21	6.24	6.26	6.30	6.80	27.00	N/A	N/A	N/A	N/A	N/A	N/A	D	10.0	1	N/A	N/A	N/A	70F_4s1d2Vd_4	4/25A	TDP-146	700385
23.2	0.995	0.01430	0.149	0.182	244.0	P	N/A	6.40	6.44	6.45	6.50	6.80	27.75	N/A	N/A	N/A	UCScen	N/A	N/A	I	7.3	2	N/A	N/A	N/A	70F_4s1d2Vd_4	4/25A	TDP-146	700386
23.2	0.995	0.01430	0.150	0.182	234.0	P	N/A	6.69	6.73	6.75	6.80	6.80	29.50	6.80	udv	N/A	N/A	UCSudv	N/A	I	0.7	4	N/A	N/A	N/A	70F_4s1d2Vd_4	4/25A	TDP-146	700387
23.2	0.994	0.01430	0.050	0.666	31.2	P	N/A	4.59	4.64	4.67	4.80	4.80	35.75	N/A	N/A	N/A	UCScen	N/A	N/A	(null)	0.0	2	N/A	N/A	N/A	70F_4s1d2Ve_1	4/25B	TDP-146	700388
23.2	0.994	0.01430	0.050	0.666	31.2	P	N/A	4.59	4.64	4.67	4.80	4.80	35.75	N/A	N/A	N/A	N/A	N/A	N/A	N/A	0.0	N/A	N/A	N/A	N/A	70F_4s1d2Ve_1	4/25B	TDP-146	700389
23.2	0.994	0.01430	0.050	0.666	31.2	P	N/A	4.59	4.64	4.67	4.80	4.80	35.75	N/A	N/A	N/A	N/A	N/A	N/A	N/A	n/a	N/A	N/A	N/A	N/A	70F_4s1d2Ve_1	4/25B	TDP-146	700389.1
23.2	0.994	0.01430	0.050	0.666	31.2	P	N/A	4.59	4.64	4.67	4.80	4.80	35.75	N/A	N/A	N/A	N/A	N/A	N/A	N/A	0.0	N/A	N/A	N/A	N/A	70F_4s1d2Ve_1	4/25B	TDP-146	700390
23.2	0.994	0.01430	0.050	0.666	31.2	P	N/A	4.59	4.64	4.67	4.80	4.80	35.75	N/A	N/A	N/A	N/A	N/A	N/A	N/A	n/a	N/A	N/A	N/A	N/A	70F_4s1d2Ve_1	4/25B	TDP-146	700390.1
23.2	0.994	0.01430	0.050	0.666	31.2	P	N/A	4.59	4.64	4.67	4.80	4.80	35.75	N/A	N/A	N/A	N/A	N/A	N/A	N/A	0.0	N/A	N/A	N/A	N/A	70F_4s1d2Ve_1	4/25B	TDP-146	700391
23.2	0.994	0.01430	0.050	0.666	31.2	P	N/A	4.59	4.64	4.67	4.80	4.80	35.75	N/A	N/A	N/A	N/A	N/A	N/A	N/A	n/a	N/A	N/A	N/A	N/A	70F_4s1d2Ve_1	4/25B	TDP-146	700391.1
23.2	0.994	0.01430	0.050	0.666	31.2	P	N/A	4.59	4.64	4.67	4.80	4.80	35.75	N/A	N/A	N/A	N/A	N/A	N/A	N/A	0.0	N/A	N/A	N/A	N/A	70F_4s1d2Ve_1	4/25B	TDP-146	700392
23.2	0.994	0.01430	0.050	0.666	31.2	P	N/A	4.59	4.64	4.67	4.80	4.80	35.75	N/A	N/A	N/A	N/A	N/A	N/A	N/A	n/a	N/A	N/A	N/A	N/A	70F_4s1d2Ve_1	4/25B	TDP-146	700392.1
23.2	0.994	0.01430	0.050	0.666	31.2	P	N/A	4.59	4.64	4.67	4.80	4.80	35.75	N/A	N/A	N/A	N/A	N/A	N/A	N/A	0.0	N/A	N/A	N/A	N/A	70F_4s1d2Ve_1	4/25B	TDP-146	700393
23.2	0.994	0.01430	0.050	0.666	31.2	P	N/A	4.59	4.64	4.67	4.80	4.80	35.75	N/A	N/A	N/A	N/A	N/A	N/A	N/A	n/a	N/A	N/A	N/A	N/A	70F_4s1d2Ve_1	4/25B	TDP-146	700393.1
23.1	0.995	0.01430	0.100	0.327	90.0	P	N/A	6.46	6.51	6.54	6.60	6.60	28.50	N/A	N/A	N/A	N/A	N/A	N/A	N/A	n/a	N/A	N/A	N/A	N/A	70F_4s1d2Vc_2	4/25C	TDP-146	700393.2
23.1	0.995	0.01430	0.100	0.327	90.0	P	N/A	6.46	6.51	6.54	6.60	6.60	28.50	6.60	center	N/A	UCScen	N/A	N/A	(null)	7.8	2	N/A	N/A	N/A	70F_4s1d2Vc_2	4/25C	TDP-146	700394

Table B.6. Data from 2008 in Large-Scale Vessel with Flanged and Dished Head A.6

Row Number	Test	Case ID	Tank Diameter	Head Shape	Dish Height	Dish Volume	Tank Fill Height	Return Line Height	Nozzle Inner Diameter	Nozzle Stand-off Distance	Pulse Tube Configuration	Installed Nozzles	Outer Nozzles Operated	Inner Nozzles Operated	Pulse Tube Outer Diameter	Outer PJM Radius	Inner PJM Radius	"FIO" Outer PJM Impingement Angle	"FIO" Inner PJM Impingement Angle	Ratio Outer PJM to Tank Radius	Ratio Inner PJM to Tank Radius	Simulant	Solids Density	Particle Diameter d5	Particle Diameter d50	Particle Diameter d95	Void Fraction
text	text	text	in.	text	in.	in. ^{3}	in.	in.	in.	in.	text	number	number	number	in.	in.	in.	deg	deg	nondim	nondim	text	g/cm^3	m	m	m	fraction
MSS	M/DDX	ID	D	HS	H_{dish}	V_{dish}	H	Rtn	d	sod	PT	N	N_O	N_I	PT_{od}	R_O	R_I	θ_O	θ_I	R_O/R	R_I/R	sxdx	ρ_s	d_5	d_{50}	d_{95}	vf
700395	4/25C	70F_4s1d2Vc_2	70	FD	12.7	30569.0	87 1/2	83 5/8	0.613	0.920	HLP-22	12	8	4	3.5	26.4	11.7	22.4	9.7	0.75	0.33	s1d2	2.48	0.0000569	0.0000693	0.0000821	0.3750
700396	4/25C	70F_4s1d2Vc_2	70	FD	12.7	30569.0	87 1/2	83 5/8	0.613	0.920	HLP-22	12	8	4	3.5	26.4	11.7	22.4	9.7	0.75	0.33	s1d2	2.48	0.0000569	0.0000693	0.0000821	0.3750
700397	4/25C	70F_4s1d2Vc_2	70	FD	12.7	30569.0	87 1/2	83 5/8	0.613	0.920	HLP-22	12	8	4	3.5	26.4	11.7	22.4	9.7	0.75	0.33	s1d2	2.48	0.0000569	0.0000693	0.0000821	0.3750
700398	4/25C	70F_4s1d2Vc_2	70	FD	12.7	30569.0	87 1/2	83 5/8	0.613	0.920	HLP-22	12	8	4	3.5	26.4	11.7	22.4	9.7	0.75	0.33	s1d2	2.48	0.0000569	0.0000693	0.0000821	0.3750
700399	4/25C	70F_4s1d2Vc_2	70	FD	12.7	30569.0	87 1/2	83 5/8	0.613	0.920	HLP-22	12	8	4	3.5	26.4	11.7	22.4	9.7	0.75	0.33	s1d2	2.48	0.0000569	0.0000693	0.0000821	0.3750
700400	4/25C	70F_4s1d2Vc_2	70	FD	12.7	30569.0	87 1/2	83 5/8	0.613	0.920	HLP-22	12	8	4	3.5	26.4	11.7	22.4	9.7	0.75	0.33	s1d2	2.48	0.0000569	0.0000693	0.0000821	0.3750
700401	4/25C	70F_4s1d2Vc_2	70	FD	12.7	30569.0	87 1/2	83 5/8	0.613	0.920	HLP-22	12	8	4	3.5	26.4	11.7	22.4	9.7	0.75	0.33	s1d2	2.48	0.0000569	0.0000693	0.0000821	0.3750
700402	4/25C	70F_4s1d2Vc_2	70	FD	12.7	30569.0	87 1/2	83 5/8	0.613	0.920	HLP-22	12	8	4	3.5	26.4	11.7	22.4	9.7	0.75	0.33	s1d2	2.48	0.0000569	0.0000693	0.0000821	0.3750
700403	4/28A	70F_4s1d2Vd_1	70	FD	12.7	30569.0	89 1/2	83 5/8	0.613	0.920	HLP-22	12	8	4	3.5	26.4	11.7	22.4	9.7	0.75	0.33	s1d2	2.48	0.0000569	0.0000693	0.0000821	0.3750
700404	4/28A	70F_4s1d2Vd_1	70	FD	12.7	30569.0	89 1/2	83 5/8	0.613	0.920	HLP-22	12	8	4	3.5	26.4	11.7	22.4	9.7	0.75	0.33	s1d2	2.48	0.0000569	0.0000693	0.0000821	0.3750
700405	4/28A	70F_4s1d2Vd_1	70	FD	12.7	30569.0	89 1/2	83 5/8	0.613	0.920	HLP-22	12	8	4	3.5	26.4	11.7	22.4	9.7	0.75	0.33	s1d2	2.48	0.0000569	0.0000693	0.0000821	0.3750
700405.1	4/28A	70F_4s1d2Vd_1	70	FD	12.7	30569.0	89 1/2	83 5/8	0.613	0.920	HLP-22	12	8	4	3.5	26.4	11.7	22.4	9.7	0.75	0.33	s1d2	2.48	0.0000569	0.0000693	0.0000821	0.3750
700405.2	4/28A	70F_4s1d2Vd_1	70	FD	12.7	30569.0	89 1/2	83 5/8	0.613	0.920	HLP-22	12	8	4	3.5	26.4	11.7	22.4	9.7	0.75	0.33	s1d2	2.48	0.0000569	0.0000693	0.0000821	0.3750
700406	4/28A	70F_4s1d2Vd_1	70	FD	12.7	30569.0	89 1/2	83 5/8	0.613	0.920	HLP-22	12	8	4	3.5	26.4	11.7	22.4	9.7	0.75	0.33	s1d2	2.48	0.0000569	0.0000693	0.0000821	0.3750
700407	4/28A	70F_4s1d2Vd_1	70	FD	12.7	30569.0	89 1/2	83 5/8	0.613	0.920	HLP-22	12	8	4	3.5	26.4	11.7	22.4	9.7	0.75	0.33	s1d2	2.48	0.0000569	0.0000693	0.0000821	0.3750
700408	4/28A	70F_4s1d2Vd_1	70	FD	12.7	30569.0	89 1/2	83 5/8	0.613	0.920	HLP-22	12	8	4	3.5	26.4	11.7	22.4	9.7	0.75	0.33	s1d2	2.48	0.0000569	0.0000693	0.0000821	0.3750
700409	4/28A	70F_4s1d2Vd_1	70	FD	12.7	30569.0	89 1/2	83 5/8	0.613	0.920	HLP-22	12	8	4	3.5	26.4	11.7	22.4	9.7	0.75	0.33	s1d2	2.48	0.0000569	0.0000693	0.0000821	0.3750
700410	4/28A	70F_4s1d2Vd_1	70	FD	12.7	30569.0	89 1/2	83 5/8	0.613	0.920	HLP-22	12	8	4	3.5	26.4	11.7	22.4	9.7	0.75	0.33	s1d2	2.48	0.0000569	0.0000693	0.0000821	0.3750
700411	4/28A	70F_4s1d2Vd_1	70	FD	12.7	30569.0	89 1/2	83 5/8	0.613	0.920	HLP-22	12	8	4	3.5	26.4	11.7	22.4	9.7	0.75	0.33	s1d2	2.48	0.0000569	0.0000693	0.0000821	0.3750
700412	4/28A	70F_4s1d2Vd_1	70	FD	12.7	30569.0	89 1/2	83 5/8	0.613	0.920	HLP-22	12	8	4	3.5	26.4	11.7	22.4	9.7	0.75	0.33	s1d2	2.48	0.0000569	0.0000693	0.0000821	0.3750
700413	4/28A	70F_4s1d2Vd_1	70	FD	12.7	30569.0	89 1/2	83 5/8	0.613	0.920	HLP-22	12	8	4	3.5	26.4	11.7	22.4	9.7	0.75	0.33	s1d2	2.48	0.0000569	0.0000693	0.0000821	0.3750
700414	4/28A	70F_4s1d2Vd_1	70	FD	12.7	30569.0	89 1/2	83 5/8	0.613	0.920	HLP-22	12	8	4	3.5	26.4	11.7	22.4	9.7	0.75	0.33	s1d2	2.48	0.0000569	0.0000693	0.0000821	0.3750
700415M	4/28A	70F_4s1d2Vd_1	70	FD	12.7	30569.0	89 1/2	83 5/8	0.613	0.920	HLP-22	12	8	4	3.5	26.4	11.7	22.4	9.7	0.75	0.33	s1d2	2.48	0.0000569	0.0000693	0.0000821	0.3750
700415.1	4/28A	70F_4s1d2Vd_1	70	FD	12.7	30569.0	89 1/2	83 5/8	0.613	0.920	HLP-22	12	8	4	3.5	26.4	11.7	22.4	9.7	0.75	0.33	s1d2	2.48	0.0000569	0.0000693	0.0000821	0.3750
700416M	4/28A	70F_4s1d2Vd_1	70	FD	12.7	30569.0	89 1/2	83 5/8	0.613	0.920	HLP-22	12	8	4	3.5	26.4	11.7	22.4	9.7	0.75	0.33	s1d2	2.48	0.0000569	0.0000693	0.0000821	0.3750
700417	4/28A	70F_4s1d2Vd_1	70	FD	12.7	30569.0	89 1/2	83 5/8	0.613	0.920	HLP-22	12	8	4	3.5	26.4	11.7	22.4	9.7	0.75	0.33	s1d2	2.48	0.0000569	0.0000693	0.0000821	0.3750
700418	4/28A	70F_4s1d2Vd_1	70	FD	12.7	30569.0	89 1/2	83 5/8	0.613	0.920	HLP-22	12	8	4	3.5	26.4	11.7	22.4	9.7	0.75	0.33	s1d2	2.48	0.0000569	0.0000693	0.0000821	0.3750
700419	4/28A	70F_4s1d2Vd_1	70	FD	12.7	30569.0	89 1/2	83 5/8	0.613	0.920	HLP-22	12	8	4	3.5	26.4	11.7	22.4	9.7	0.75	0.33	s1d2	2.48	0.0000569	0.0000693	0.0000821	0.3750
700420	4/28A	70F_4s1d2Vd_1	70	FD	12.7	30569.0	89 1/2	83 5/8	0.613	0.920	HLP-22	12	8	4	3.5	26.4	11.7	22.4	9.7	0.75	0.33	s1d2	2.48	0.0000569	0.0000693	0.0000821	0.3750
700421	4/28A	70F_4s1d2Vd_1	70	FD	12.7	30569.0	89 1/2	83 5/8	0.613	0.920	HLP-22	12	8	4	3.5	26.4	11.7	22.4	9.7	0.75	0.33	s1d2	2.48	0.0000569	0.0000693	0.0000821	0.3750
700422	4/28A	70F_4s1d2Vd_1	70	FD	12.7	30569.0	89 1/2	83 5/8	0.613	0.920	HLP-22	12	8	4	3.5	26.4	11.7	22.4	9.7	0.75	0.33	s1d2	2.48	0.0000569	0.0000693	0.0000821	0.3750
700423	4/28A	70F_4s1d2Vd_1	70	FD	12.7	30569.0	89 1/2	83 5/8	0.613	0.920	HLP-22	12	8	4	3.5	26.4	11.7	22.4	9.7	0.75	0.33	s1d2	2.48	0.0000569	0.0000693	0.0000821	0.3750
700424	4/28A	70F_4s1d2Vd_1	70	FD	12.7	30569.0	89 1/2	83 5/8	0.613	0.920	HLP-22	12	8	4	3.5	26.4	11.7	22.4	9.7	0.75	0.33	s1d2	2.48	0.0000569	0.0000693	0.0000821	0.3750
700425M	4/28A	70F_4s1d2Vd_1	70	FD	12.7	30569.0	89 1/2	83 5/8	0.613	0.920	HLP-22	12	8	4	3.5	26.4	11.7	22.4	9.7	0.75	0.33	s1d2	2.48	0.0000569	0.0000693	0.0000821	0.3750
700426M	4/28A	70F_4s1d2Vd_1	70	FD	12.7	30569.0	89 1/2	83 5/8	0.613	0.920	HLP-22	12	8	4	3.5	26.4	11.7	22.4	9.7	0.75	0.33	s1d2	2.48	0.0000569	0.0000693	0.0000821	0.3750
700427	4/29A	70F_4s1d2Vc_1	70	FD	12.7	30569.0	89	83 5/8	0.613	0.920	HLP-22	12	8	4	3.5	26.4	11.7	22.4	9.7	0.75	0.33	s1d2	2.48	0.0000569	0.0000693	0.0000821	0.3750
700428	4/29A	70F_4s1d2Vc_1	70	FD	12.7	30569.0	89	83 5/8	0.613	0.920	HLP-22	12	8	4	3.5	26.4	11.7	22.4	9.7	0.75	0.33	s1d2	2.48	0.0000569	0.0000693	0.0000821	0.3750
700429	4/29A	70F_4s1d2Vc_1	70	FD	12.7	30569.0	89	83 5/8	0.613	0.920	HLP-22	12	8	4	3.5	26.4	11.7	22.4	9.7	0.75	0.33	s1d2	2.48	0.0000569	0.0000693	0.0000821	0.3750
700430M	4/29A	70F_4s1d2Vc_1	70	FD	12.7	30569.0	89	83 5/8	0.613	0.920	HLP-22	12	8	4	3.5	26.4	11.7	22.4	9.7	0.75	0.33	s1d2	2.48	0.0000569	0.0000693	0.0000821	0.3750
700431M	4/29A	70F_4s1d2Vc_1	70	FD	12.7	30569.0	89	83 5/8	0.613	0.920	HLP-22	12	8	4	3.5	26.4	11.7	22.4	9.7	0.75	0.33	s1d2	2.48	0.0000569	0.0000693	0.0000821	0.3750
700432M	4/29A	70F_4s1d2Vc_1	70	FD	12.7	30569.0	89	83 5/8	0.613	0.920	HLP-22	12	8	4	3.5	26.4	11.7	22.4	9.7	0.75	0.33	s1d2	2.48	0.0000569	0.0000693	0.0000821	0.3750

Table B.6. Data from 2008 in Large-Scale Vessel with Flanged and Dished Head B.6

Tank Water Temperature	Water Density	Solids Fraction	Pulse Volume Fraction	Duty Cycle	Cycle Time	Pulsed or Steady Jet	Us Steady Jet	U1 Pulsing Jet	U2 URMS	U3 URM3	Discharge Velocity	Critical Suspension Velocity	Average Peak Cloud Height	UCS Condition	UCS Method	UCS Flag	UCS Center Flag	UCS udv Flag	UCS based on Decreasing Velocity	Sweep Increase / Decrease	UDV Height Bed	Particle Motion	Solids Level	Outer Bottom Pattern	Inner Bottom Pattern	Case ID	Test	TDP	Row Number
C	g/cm³	fraction	fraction	fraction	s	text	m/s	m/s	m/s	m/s	m/s	m/s	in.	m/s	text	text	text	text	m/s	text	mm	text	text	text	text	text	text	text	text
T	ρ_l	ϕ_S	ϕ_P	DC	t_C	Jet	U_S	U1	U2	U3	U	U_{CS}	H_C	U_{CSR}	U_{CSM}	U_{CS}vis	U_{CS}cen	U_{CS}udv	U_{CS}_D	S_W	H_{bed}	PM	Sol	SP_O	SP_I	ID	M/DDX	TDP	MSS
23.1	0.995	0.01430	0.100	0.327	90.0	P	N/A	6.46	6.51	6.54	6.60	6.60	28.50	N/A	N/A	N/A	N/A	N/A	N/A	N/A	8.0	N/A	N/A	N/A	N/A	70F_4s1d2Vc_2	4/25C	TDP-146	700395
23.1	0.995	0.01430	0.100	0.327	90.0	P	N/A	6.46	6.51	6.54	6.60	6.60	28.50	N/A	N/A	N/A	N/A	N/A	N/A	N/A	8.0	N/A	N/A	N/A	N/A	70F_4s1d2Vc_2	4/25C	TDP-146	700396
23.1	0.995	0.01430	0.100	0.327	90.0	P	N/A	6.46	6.51	6.54	6.60	6.60	28.50	N/A	N/A	N/A	N/A	N/A	N/A	N/A	7.8	N/A	N/A	N/A	N/A	70F_4s1d2Vc_2	4/25C	TDP-146	700397
23.1	0.995	0.01430	0.100	0.327	90.0	P	N/A	6.46	6.51	6.54	6.60	6.60	28.50	N/A	N/A	N/A	N/A	N/A	N/A	N/A	7.5	N/A	N/A	N/A	N/A	70F_4s1d2Vc_2	4/25C	TDP-146	700398
23.1	0.995	0.01430	0.100	0.327	90.0	P	N/A	6.46	6.51	6.54	6.60	6.60	28.50	N/A	N/A	N/A	N/A	N/A	N/A	N/A	6.7	N/A	N/A	N/A	N/A	70F_4s1d2Vc_2	4/25C	TDP-146	700399
23.1	0.995	0.01430	0.100	0.327	90.0	P	N/A	6.46	6.51	6.54	6.60	6.60	28.50	N/A	N/A	N/A	N/A	N/A	N/A	N/A	6.4	N/A	N/A	N/A	N/A	70F_4s1d2Vc_2	4/25C	TDP-146	700400
23.1	0.995	0.01430	0.100	0.327	90.0	P	N/A	6.46	6.51	6.54	6.60	6.60	28.50	N/A	N/A	N/A	N/A	N/A	N/A	N/A	8.4	N/A	N/A	N/A	N/A	70F_4s1d2Vc_2	4/25C	TDP-146	700401
23.1	0.995	0.01430	0.100	0.327	90.0	P	N/A	6.46	6.51	6.54	6.60	6.60	28.50	N/A	N/A	N/A	N/A	N/A	N/A	N/A	8.7	N/A	N/A	N/A	N/A	70F_4s1d2Vc_2	4/25C	TDP-146	700402
22.5	0.995	0.01430	0.050	0.185	60.4	P	N/A	8.57	8.73	8.82	9.10	9.80	24.25	N/A	N/A	N/A	N/A	N/A	N/A	(null)	28.7	1	N/A	N/A	N/A	70F_4s1d2Vd_1	4/28A	TDP-147	700403
22.6	0.995	0.01430	0.050	0.186	58.0	P	N/A	8.87	9.04	9.13	9.40	9.80	25.75	N/A	N/A	N/A	N/A	N/A	N/A	I	20.8	1	N/A	N/A	N/A	70F_4s1d2Vd_1	4/28A	TDP-147	700404
22.7	0.995	0.01430	0.050	0.187	56.4	P	N/A	9.06	9.24	9.33	9.60	9.80	26.75	N/A	N/A	N/A	UCScen	N/A	N/A	I	2.8	2	N/A	N/A	N/A	70F_4s1d2Vd_1	4/28A	TDP-147	700405
22.9	0.994	0.01430	0.050	0.187	56.4	P	N/A	9.05	9.23	9.32	9.60	9.80	26.25	N/A	N/A	N/A	N/A	N/A	N/A	N/A	n/a	N/A	N/A	N/A	N/A	70F_4s1d2Vd_1	4/28A	TDP-147	700405
22.9	0.994	0.01430	0.050	0.187	56.4	P	N/A	9.05	9.23	9.32	9.60	9.80	26.25	N/A	N/A	N/A	N/A	N/A	N/A	N/A	n/a	N/A	N/A	N/A	N/A	70F_4s1d2Vd_1	4/28A	TDP-147	700405
22.9	0.994	0.01430	0.050	0.187	56.4	P	N/A	9.05	9.23	9.32	9.60	9.80	26.25	N/A	N/A	N/A	UCScen	N/A	N/A	(null)	19.7	2	N/A	N/A	N/A	70F_4s1d2Vd_1	4/28A	TDP-147	700406
22.9	0.994	0.01430	0.050	0.187	56.4	P	N/A	9.05	9.23	9.32	9.60	9.80	26.25	N/A	N/A	N/A	N/A	N/A	N/A	N/A	13.5	N/A	N/A	N/A	N/A	70F_4s1d2Vd_1	4/28A	TDP-147	700407
22.9	0.994	0.01430	0.050	0.187	56.4	P	N/A	9.05	9.23	9.32	9.60	9.80	26.25	N/A	N/A	N/A	N/A	N/A	N/A	N/A	11.0	N/A	N/A	N/A	N/A	70F_4s1d2Vd_1	4/28A	TDP-147	700408
22.9	0.994	0.01430	0.050	0.187	56.4	P	N/A	9.05	9.23	9.32	9.60	9.80	26.25	N/A	N/A	N/A	N/A	N/A	N/A	N/A	14.2	N/A	N/A	N/A	N/A	70F_4s1d2Vd_1	4/28A	TDP-147	700409
22.9	0.994	0.01430	0.050	0.187	56.4	P	N/A	9.05	9.23	9.32	9.60	9.80	26.25	N/A	N/A	N/A	N/A	N/A	N/A	N/A	14.4	N/A	N/A	N/A	N/A	70F_4s1d2Vd_1	4/28A	TDP-147	700410
22.9	0.994	0.01430	0.050	0.187	56.4	P	N/A	9.05	9.23	9.32	9.60	9.80	26.25	N/A	N/A	N/A	N/A	N/A	N/A	N/A	17.2	N/A	N/A	N/A	N/A	70F_4s1d2Vd_1	4/28A	TDP-147	700411
22.9	0.994	0.01430	0.050	0.187	56.4	P	N/A	9.05	9.23	9.32	9.60	9.80	26.25	N/A	N/A	N/A	N/A	N/A	N/A	N/A	15.0	N/A	N/A	N/A	N/A	70F_4s1d2Vd_1	4/28A	TDP-147	700412
22.9	0.994	0.01430	0.050	0.187	56.4	P	N/A	9.05	9.23	9.32	9.60	9.80	26.25	N/A	N/A	N/A	N/A	N/A	N/A	N/A	19.0	N/A	N/A	N/A	N/A	70F_4s1d2Vd_1	4/28A	TDP-147	700413
23.3	0.995	0.01430	0.050	0.186	56.8	P	N/A	9.04	9.22	9.32	9.60	9.80	26.50	N/A	N/A	N/A	UCScen	N/A	N/A	I	13.8	2	N/A	N/A	N/A	70F_4s1d2Vd_1	4/28A	TDP-147	700414
23.5	0.995	0.01430	0.050	0.187	55.6	P	N/A	9.21	9.40	9.50	9.80	9.80	27.75	9.80	udv	N/A	UCScen	UCSudv	N/A	I	3.7	2	N/A	N/A	N/A	70F_4s1d2Vd_1	4/28A	TDP-147	700415
23.7	0.995	0.01430	0.050	0.187	55.6	P	N/A	9.20	9.39	9.49	9.80	9.80	28.00	N/A	N/A	N/A	N/A	N/A	N/A	N/A	n/a	N/A	N/A	N/A	N/A	70F_4s1d2Vd_1	4/28A	TDP-147	700415
23.7	0.995	0.01430	0.050	0.187	55.6	P	N/A	9.20	9.39	9.49	9.80	9.80	28.00	N/A	N/A	N/A	UCScen	N/A	N/A	I	0.7	2	N/A	N/A	N/A	70F_4s1d2Vd_1	4/28A	TDP-147	700416
23.7	0.995	0.01430	0.050	0.187	55.6	P	N/A	9.20	9.39	9.49	9.80	9.80	28.00	N/A	N/A	N/A	N/A	N/A	N/A	N/A	0.7	N/A	N/A	N/A	N/A	70F_4s1d2Vd_1	4/28A	TDP-147	700417
23.7	0.995	0.01430	0.050	0.187	55.6	P	N/A	9.20	9.39	9.49	9.80	9.80	28.00	N/A	N/A	N/A	N/A	N/A	N/A	N/A	3.0	N/A	N/A	N/A	N/A	70F_4s1d2Vd_1	4/28A	TDP-147	700418
23.7	0.995	0.01430	0.050	0.187	55.6	P	N/A	9.20	9.39	9.49	9.80	9.80	28.00	N/A	N/A	N/A	N/A	N/A	N/A	N/A	3.7	N/A	N/A	N/A	N/A	70F_4s1d2Vd_1	4/28A	TDP-147	700419
23.7	0.995	0.01430	0.050	0.187	55.6	P	N/A	9.20	9.39	9.49	9.80	9.80	28.00	N/A	N/A	N/A	N/A	N/A	N/A	N/A	3.0	N/A	N/A	N/A	N/A	70F_4s1d2Vd_1	4/28A	TDP-147	700420
23.7	0.995	0.01430	0.050	0.187	55.6	P	N/A	9.20	9.39	9.49	9.80	9.80	28.00	N/A	N/A	N/A	N/A	N/A	N/A	N/A	3.2	N/A	N/A	N/A	N/A	70F_4s1d2Vd_1	4/28A	TDP-147	700421
23.7	0.995	0.01430	0.050	0.187	55.6	P	N/A	9.20	9.39	9.49	9.80	9.80	28.00	N/A	N/A	N/A	N/A	N/A	N/A	N/A	3.9	N/A	N/A	N/A	N/A	70F_4s1d2Vd_1	4/28A	TDP-147	700422
23.7	0.995	0.01430	0.050	0.187	55.6	P	N/A	9.20	9.39	9.49	9.80	9.80	28.00	N/A	N/A	N/A	N/A	N/A	N/A	N/A	3.0	N/A	N/A	N/A	N/A	70F_4s1d2Vd_1	4/28A	TDP-147	700423
23.7	0.995	0.01430	0.050	0.187	55.6	P	N/A	9.20	9.39	9.49	9.80	9.80	28.00	N/A	N/A	N/A	N/A	N/A	N/A	N/A	3.1	N/A	N/A	N/A	N/A	70F_4s1d2Vd_1	4/28A	TDP-147	700424
24.0	0.994	0.01430	0.050	0.183	53.0	P	N/A	9.84	10.05	10.17	10.50	9.80	33.00	N/A	N/A	N/A	N/A	N/A	N/A	I	0.0	4	N/A	N/A	N/A	70F_4s1d2Vd_1	4/28A	TDP-147	700425
24.1	0.995	0.01430	0.050	0.184	51.0	P	N/A	10.13	10.36	10.47	10.80	9.80	39.00	N/A	N/A	N/A	N/A	N/A	N/A	I	0.0	4	N/A	N/A	N/A	70F_4s1d2Vd_1	4/28A	TDP-147	700426
23.2	0.994	0.01430	0.050	0.333	45.4	P	N/A	6.29	6.39	6.44	6.60	7.30	22.50	N/A	N/A	N/A	N/A	N/A	N/A	I	40.2	1	N/A	N/A	N/A	70F_4s1d2Vc_1	4/29A	TDP-148	700427
23.0	0.995	0.01430	0.050	0.335	42.8	P	N/A	6.65	6.76	6.82	7.00	7.30	27.00	N/A	N/A	N/A	N/A	N/A	N/A	I	10.8	1	N/A	N/A	N/A	70F_4s1d2Vc_1	4/29A	TDP-148	700428
23.2	0.995	0.01430	0.050	0.336	41.6	P	N/A	6.83	6.95	7.01	7.20	7.30	29.50	N/A	N/A	N/A	N/A	N/A	N/A	I	2.6	1	N/A	N/A	N/A	70F_4s1d2Vc_1	4/29A	TDP-148	700429
23.2	0.995	0.01430	0.050	0.336	41.2	P	N/A	6.92	7.03	7.09	7.30	7.30	32.00	7.30	udv	N/A	UCScen	UCSudv	N/A	(null)	3.0	2	N/A	N/A	N/A	70F_4s1d2Vc_1	4/29A	TDP-148	700430
23.1	0.995	0.01430	0.050	0.335	40.0	P	N/A	7.11	7.24	7.30	7.50	7.30	34.00	N/A	N/A	N/A	N/A	N/A	N/A	I	0.0	4	N/A	N/A	N/A	70F_4s1d2Vc_1	4/29A	TDP-148	700431
23.3	0.995	0.01430	0.050	0.335	37.6	P	N/A	7.58	7.71	7.78	8.00	7.30	44.00	N/A	N/A	N/A	N/A	N/A	N/A	I	0.0	4	N/A	N/A	N/A	70F_4s1d2Vc_1	4/29A	TDP-148	700432

Table B.6. Data from 2008 in Large-Scale Vessel with Flanged and Dished Head A.7

Row Number	Test	Case ID	Tank Diameter	Head Shape	Dish Height	Dish Volume	Tank Fill Height	Return Line Height	Nozzle Inner Diameter	Nozzle Stand-off Distance	Pulse Tube Configuration	Installed Nozzles	Outer Nozzles Operated	Inner Nozzles Operated	Pulse Tube Outer Diameter	Outer PJM Radius	Inner PJM Radius	"FIO" Outer PJM Impingement Angle	"FIO" Inner PJM Impingement Angle	Ratio Outer PJM to Tank Radius	Ratio Inner PJM to Tank Radius	Simulant	Solids Density	Particle Diameter d5	Particle Diameter d50	Particle Diameter d95	Void Fraction
text	text	text	in.	text	in.	in. ^{3}	in.	in.	in.	in.	text	number	number	number	in.	in.	in.	deg	deg	nondim	nondim	text	g/cm^3	m	m	m	fraction
MSS	M/DDX	ID	D	HS	H_{dish}	V_{dish}	H	Rtn	d	sod	PT	N	N_O	N_I	PT_{od}	R_O	R_I	θ_O	θ_I	R_O/R	R_I/R	sxdx	ρ_s	d_5	d_{50}	d_{95}	vf
700433M	4/29A	70F_4s1d2Vc_1	70	FD	12.7	30569.0	89	83 5/8	0.613	0.920	HLP-22	12	8	4	3.5	26.4	11.7	22.4	9.7	0.75	0.33	s1d2	2.48	0.0000569	0.0000693	0.0000821	0.3750
700434	4/29A	70F_4s1d2Vc_1	70	FD	12.7	30569.0	89	83 5/8	0.613	0.920	HLP-22	12	8	4	3.5	26.4	11.7	22.4	9.7	0.75	0.33	s1d2	2.48	0.0000569	0.0000693	0.0000821	0.3750
700435	4/29A	70F_4s1d2Vc_1	70	FD	12.7	30569.0	89	83 5/8	0.613	0.920	HLP-22	12	8	4	3.5	26.4	11.7	22.4	9.7	0.75	0.33	s1d2	2.48	0.0000569	0.0000693	0.0000821	0.3750
700436	4/29A	70F_4s1d2Vc_1	70	FD	12.7	30569.0	89	83 5/8	0.613	0.920	HLP-22	12	8	4	3.5	26.4	11.7	22.4	9.7	0.75	0.33	s1d2	2.48	0.0000569	0.0000693	0.0000821	0.3750
700437	4/29A	70F_4s1d2Vc_1	70	FD	12.7	30569.0	89	83 5/8	0.613	0.920	HLP-22	12	8	4	3.5	26.4	11.7	22.4	9.7	0.75	0.33	s1d2	2.48	0.0000569	0.0000693	0.0000821	0.3750
700438	4/29A	70F_4s1d2Vc_1	70	FD	12.7	30569.0	89	83 5/8	0.613	0.920	HLP-22	12	8	4	3.5	26.4	11.7	22.4	9.7	0.75	0.33	s1d2	2.48	0.0000569	0.0000693	0.0000821	0.3750
700439M	4/29A	70F_4s1d2Vc_1	70	FD	12.7	30569.0	89	83 5/8	0.613	0.920	HLP-22	12	8	4	3.5	26.4	11.7	22.4	9.7	0.75	0.33	s1d2	2.48	0.0000569	0.0000693	0.0000821	0.3750
700440	4/29B	70F_4s1d2Vf_1	70	FD	12.7	30569.0	89	83 5/8	0.613	0.920	HLP-22	12	8	4	3.5	26.4	11.7	22.4	9.7	0.75	0.33	s1d2	2.48	0.0000569	0.0000693	0.0000821	0.3750
700441	4/29B	70F_4s1d2Vf_1	70	FD	12.7	30569.0	89	83 5/8	0.613	0.920	HLP-22	12	8	4	3.5	26.4	11.7	22.4	9.7	0.75	0.33	s1d2	2.48	0.0000569	0.0000693	0.0000821	0.3750
700442	4/29B	70F_4s1d2Vf_1	70	FD	12.7	30569.0	89	83 5/8	0.613	0.920	HLP-22	12	8	4	3.5	26.4	11.7	22.4	9.7	0.75	0.33	s1d2	2.48	0.0000569	0.0000693	0.0000821	0.3750
700444	4/29B	70F_4s1d2Vf_1	70	FD	12.7	30569.0	89	83 5/8	0.613	0.920	HLP-22	12	8	4	3.5	26.4	11.7	22.4	9.7	0.75	0.33	s1d2	2.48	0.0000569	0.0000693	0.0000821	0.3750
700445M	4/29B	70F_4s1d2Vf_1	70	FD	12.7	30569.0	89	83 5/8	0.613	0.920	HLP-22	12	8	4	3.5	26.4	11.7	22.4	9.7	0.75	0.33	s1d2	2.48	0.0000569	0.0000693	0.0000821	0.3750
700446M	4/29B	70F_4s1d2Vf_1	70	FD	12.7	30569.0	89	83 5/8	0.613	0.920	HLP-22	12	8	4	3.5	26.4	11.7	22.4	9.7	0.75	0.33	s1d2	2.48	0.0000569	0.0000693	0.0000821	0.3750

Table B.6. Data from 2008 in Large-Scale Vessel with Flanged and Dished Head B.7

Tank Water Temperature	Water Density	Solids Fraction	Pulse Volume Fraction	Duty Cycle	Cycle Time	Pulsed or Steady Jet	Us Steady Jet	U1 Pulsing Jet	U2 URMS	U3 URM3	Discharge Velocity	Critical Suspension Velocity	Average Peak Cloud Height	UCS Condition	UCS Method	UCS Flag	UCS Center Flag	UCS udv Flag	UCS based on Decreasing Velocity	Sweep Increase / Decrease	UDV Height Bed	Particle Motion	Solids Level	Outer Bottom Pattern	Inner Bottom Pattern	Case ID	Test	TDP	Row Number
C	g/cm³	fraction	fraction	fraction	s	text	m/s	m/s	m/s	m/s	m/s	m/s	in.	m/s	text	text	text	text	m/s	text	mm	text	text	text	text	text	text	text	text
T	ρ_L	ϕ_S	ϕ_P	DC	t_C	Jet	U_S	U1	U2	U3	U	U_{CS}	H_C	U_{CSR}	U_{CSM}	U_{CS}vis	U_{CS}cen	U_{CS}udv	U_{CS}_D	S_W	H_{bed}	PM	Sol	SP_O	SP_I	ID	M/DDX	TDP	MSS
23.3	0.994	0.01430	0.050	0.336	41.2	P	N/A	6.91	7.03	7.09	7.30	7.30	31.00	N/A	N/A	N/A	UCScen	N/A	N/A	(null)	3.7	2	N/A	N/A	N/A	70F_4s1d2Vc_1	4/29A	TDP-148	700433
23.3	0.994	0.01430	0.050	0.336	41.2	P	N/A	6.91	7.03	7.09	7.30	7.30	31.00	N/A	N/A	N/A	N/A	N/A	N/A	N/A	2.3	N/A	N/A	N/A	N/A	70F_4s1d2Vc_1	4/29A	TDP-148	700434
23.3	0.994	0.01430	0.050	0.336	41.2	P	N/A	6.91	7.03	7.09	7.30	7.30	31.00	N/A	N/A	N/A	N/A	N/A	N/A	N/A	4.0	N/A	N/A	N/A	N/A	70F_4s1d2Vc_1	4/29A	TDP-148	700435
23.3	0.994	0.01430	0.050	0.336	41.2	P	N/A	6.91	7.03	7.09	7.30	7.30	31.00	N/A	N/A	N/A	N/A	N/A	N/A	N/A	3.8	N/A	N/A	N/A	N/A	70F_4s1d2Vc_1	4/29A	TDP-148	700436
23.3	0.994	0.01430	0.050	0.336	41.2	P	N/A	6.91	7.03	7.09	7.30	7.30	31.00	N/A	N/A	N/A	N/A	N/A	N/A	N/A	1.5	N/A	N/A	N/A	N/A	70F_4s1d2Vc_1	4/29A	TDP-148	700437
23.3	0.994	0.01430	0.050	0.336	41.2	P	N/A	6.91	7.03	7.09	7.30	7.30	31.00	N/A	N/A	N/A	N/A	N/A	N/A	N/A	3.2	N/A	N/A	N/A	N/A	70F_4s1d2Vc_1	4/29A	TDP-148	700438
23.8	0.995	0.01430	0.050	0.336	39.4	P	N/A	7.23	7.35	7.42	7.60	7.30	34.75	N/A	N/A	N/A	N/A	N/A	N/A	D	0.0	4	N/A	N/A	N/A	70F_4s1d2Vc_1	4/29A	TDP-148	700439
23.6	0.994	0.01430	0.050	0.252	51.6	P	N/A	7.30	7.44	7.50	7.70	8.80	22.75	N/A	N/A	N/A	N/A	N/A	N/A	I	29.2	1	N/A	N/A	N/A	70F_4s1d2Vf_1	4/29B	TDP-148	700440
23.7	0.995	0.01430	0.050	0.254	49.0	P	N/A	7.66	7.80	7.87	8.10	8.80	25.75	N/A	N/A	N/A	N/A	N/A	N/A	I	26.5	1	N/A	N/A	N/A	70F_4s1d2Vf_1	4/29B	TDP-148	700441
23.7	0.994	0.01430	0.050	0.254	47.8	P	N/A	7.86	8.00	8.08	8.30	8.80	27.25	N/A	N/A	N/A	N/A	N/A	N/A	I	10.0	1	N/A	N/A	N/A	70F_4s1d2Vf_1	4/29B	TDP-148	700442
23.7	0.995	0.01430	0.050	0.255	46.2	P	N/A	8.13	8.28	8.36	8.60	8.80	29.75	N/A	N/A	N/A	UCScen	N/A	N/A	I	2.5	2	N/A	N/A	N/A	70F_4s1d2Vf_1	4/29B	TDP-148	700444
23.8	0.994	0.01430	0.050	0.256	45.2	P	N/A	8.29	8.45	8.53	8.80	8.80	32.50	8.80	udv	N/A	UCScen	UCSudv	N/A	I	0.7	2	N/A	N/A	N/A	70F_4s1d2Vf_1	4/29B	TDP-148	700445
23.9	0.994	0.01430	0.050	0.256	42.2	P	N/A	8.78	8.96	9.05	9.35	8.80	43.00	N/A	N/A	N/A	N/A	N/A	N/A	I	0.0	4	N/A	N/A	N/A	70F_4s1d2Vf_1	4/29B	TDP-148	700446

Table B.7. Data from July 2007 Tests in Mid-Scale Vessel with Spherical Head A1

Row Number	Test	Case ID	Tank Diameter	Head Shape	Dish Height	Dish Volume	Tank Fill Height	Return Line Height	Nozzle Inner Diameter	Nozzle Stand-off Distance	Pulse Tube Configuration	Installed Nozzles	Outer Nozzles Operated	Inner Nozzles Operated	Pulse Tube Outer Diameter	Outer PJM Radius	Inner PJM Radius	"FIO" Outer PJM Impingement Angle	"FIO" Inner PJM Impingement Angle	Ratio Outer PJM to Tank Radius	Ratio Inner PJM to Tank Radius	Simulant	Solids Density	Particle Diameter d5	Particle Diameter d50	Particle Diameter d95	Void Fraction
text	text	text	in.	text	in.	in. ^{3}	in.	in.	in.	in.	text	number	number	number	in.	in.	in.	deg	deg	nondim	nondim	text	g/cm^3	m	m	m	fraction
MSS	M/DDX	ID	D	HS	H_{dish}	V_{dish}	H	Rtn	d	sod	PT	N	N_O	N_I	PT_{od}	R_O	R_I	θ_O	θ_I	R_O/R	R_I/R	sxdx	ρ_s	d_5	d_{50}	d_{95}	vf
20070019	7/16 A1	34S_4p1d7Ya	33 7/8	S	9	4437.4	71 1/8	62	0.297	0.446	HLP-22	12	8	4	1.9	10.5	5.7	30.8	16.1	0.62	0.33	p1d7	2.45	0.0001213	0.0001780	0.0002606	0.4277
20070027	7/16 A1	34S_4p1d7Ya	33 7/8	S	9	4437.4	71 1/8	62	0.297	0.446	HLP-22	12	8	4	1.9	10.5	5.7	30.8	16.1	0.62	0.33	p1d7	2.45	0.0001213	0.0001780	0.0002606	0.4277
20070031	7/16 A1	34S_4p1d7Ya	33 7/8	S	9	4437.4	71 1/8	62	0.297	0.446	HLP-22	12	8	4	1.9	10.5	5.7	30.8	16.1	0.62	0.33	p1d7	2.45	0.0001213	0.0001780	0.0002606	0.4277
20070038	7/16 A1	34S_4p1d7Ya	33 7/8	S	9	4437.4	71 1/8	62	0.297	0.446	HLP-22	12	8	4	1.9	10.5	5.7	30.8	16.1	0.62	0.33	p1d7	2.45	0.0001213	0.0001780	0.0002606	0.4277
20070042	7/16 A1	34S_4p1d7Ya	33 7/8	S	9	4437.4	71 1/8	62	0.297	0.446	HLP-22	12	8	4	1.9	10.5	5.7	30.8	16.1	0.62	0.33	p1d7	2.45	0.0001213	0.0001780	0.0002606	0.4277
20070048	7/16 A1	34S_4p1d7Ya	33 7/8	S	9	4437.4	71 1/8	62	0.297	0.446	HLP-22	12	8	4	1.9	10.5	5.7	30.8	16.1	0.62	0.33	p1d7	2.45	0.0001213	0.0001780	0.0002606	0.4277
20070051	7/16 A1	34S_4p1d7Ya	33 7/8	S	9	4437.4	71 1/8	62	0.297	0.446	HLP-22	12	8	4	1.9	10.5	5.7	30.8	16.1	0.62	0.33	p1d7	2.45	0.0001213	0.0001780	0.0002606	0.4277
20070057	7/16 A1	34S_4p1d7Ya	33 7/8	S	9	4437.4	71 1/8	62	0.297	0.446	HLP-22	12	8	4	1.9	10.5	5.7	30.8	16.1	0.62	0.33	p1d7	2.45	0.0001213	0.0001780	0.0002606	0.4277
20070059	7/16 A1	34S_4p1d7Ya	33 7/8	S	9	4437.4	71 1/8	62	0.297	0.446	HLP-22	12	8	4	1.9	10.5	5.7	30.8	16.1	0.62	0.33	p1d7	2.45	0.0001213	0.0001780	0.0002606	0.4277
20070061	7/16 A1	34S_4p1d7Ya	33 7/8	S	9	4437.4	71 1/8	62	0.297	0.446	HLP-22	12	8	4	1.9	10.5	5.7	30.8	16.1	0.62	0.33	p1d7	2.45	0.0001213	0.0001780	0.0002606	0.4277
20070063	7/16 A1	34S_4p1d7Ya	33 7/8	S	9	4437.4	71 1/8	62	0.297	0.446	HLP-22	12	8	4	1.9	10.5	5.7	30.8	16.1	0.62	0.33	p1d7	2.45	0.0001213	0.0001780	0.0002606	0.4277
20070065	7/16 A1	34S_4p1d7Ya	33 7/8	S	9	4437.4	71 1/8	62	0.297	0.446	HLP-22	12	8	4	1.9	10.5	5.7	30.8	16.1	0.62	0.33	p1d7	2.45	0.0001213	0.0001780	0.0002606	0.4277
20070068	7/16 A1	34S_4p1d7Ya	33 7/8	S	9	4437.4	71 1/8	62	0.297	0.446	HLP-22	12	8	4	1.9	10.5	5.7	30.8	16.1	0.62	0.33	p1d7	2.45	0.0001213	0.0001780	0.0002606	0.4277
20070073	7/16 A1	34S_4p1d7Ya	33 7/8	S	9	4437.4	71 1/8	62	0.297	0.446	HLP-22	12	8	4	1.9	10.5	5.7	30.8	16.1	0.62	0.33	p1d7	2.45	0.0001213	0.0001780	0.0002606	0.4277
20070081	7/16 A2	34S_4p1d7Yc_8	33 7/8	S	9	4437.4	71 1/8	62	0.297	0.446	HLP-22	12	8	4	1.9	10.5	5.7	30.8	16.1	0.62	0.33	p1d7	2.45	0.0001213	0.0001780	0.0002606	0.4277
20070089	7/16 A2	34S_4p1d7Yc_8	33 7/8	S	9	4437.4	71 1/8	62	0.297	0.446	HLP-22	12	8	4	1.9	10.5	5.7	30.8	16.1	0.62	0.33	p1d7	2.45	0.0001213	0.0001780	0.0002606	0.4277
20070097	7/16 A2	34S_4p1d7Yc_8	33 7/8	S	9	4437.4	71 1/8	62	0.297	0.446	HLP-22	12	8	4	1.9	10.5	5.7	30.8	16.1	0.62	0.33	p1d7	2.45	0.0001213	0.0001780	0.0002606	0.4277
20070105M	7/16 A2	34S_4p1d7Yc_8	33 7/8	S	9	4437.4	71 1/8	62	0.297	0.446	HLP-22	12	8	4	1.9	10.5	5.7	30.8	16.1	0.62	0.33	p1d7	2.45	0.0001213	0.0001780	0.0002606	0.4277
20070109M	7/16 A2	34S_4p1d7Yc_8	33 7/8	S	9	4437.4	71 1/8	62	0.297	0.446	HLP-22	12	8	4	1.9	10.5	5.7	30.8	16.1	0.62	0.33	p1d7	2.45	0.0001213	0.0001780	0.0002606	0.4277
20070114M	7/16 A2	34S_4p1d7Yc_8	33 7/8	S	9	4437.4	71 1/8	62	0.297	0.446	HLP-22	12	8	4	1.9	10.5	5.7	30.8	16.1	0.62	0.33	p1d7	2.45	0.0001213	0.0001780	0.0002606	0.4277
20070127	7/17 A1	34S_4p1d7Xa	33 7/8	S	9	4437.4	66 1/8	62	0.297	0.446	HLP-22	12	8	4	1.9	10.5	5.7	30.8	16.1	0.62	0.33	p1d7	2.45	0.0001213	0.0001780	0.0002606	0.4277
20070131	7/17 A1	34S_4p1d7Xa	33 7/8	S	9	4437.4	66 1/8	62	0.297	0.446	HLP-22	12	8	4	1.9	10.5	5.7	30.8	16.1	0.62	0.33	p1d7	2.45	0.0001213	0.0001780	0.0002606	0.4277
20070135	7/17 A1	34S_4p1d7Xa	33 7/8	S	9	4437.4	66 1/8	62	0.297	0.446	HLP-22	12	8	4	1.9	10.5	5.7	30.8	16.1	0.62	0.33	p1d7	2.45	0.0001213	0.0001780	0.0002606	0.4277
20070142	7/17 A1	34S_4p1d7Xa	33 7/8	S	9	4437.4	66 1/8	62	0.297	0.446	HLP-22	12	8	4	1.9	10.5	5.7	30.8	16.1	0.62	0.33	p1d7	2.45	0.0001213	0.0001780	0.0002606	0.4277
20070146	7/17 A1	34S_4p1d7Xa	33 7/8	S	9	4437.4	66 1/8	62	0.297	0.446	HLP-22	12	8	4	1.9	10.5	5.7	30.8	16.1	0.62	0.33	p1d7	2.45	0.0001213	0.0001780	0.0002606	0.4277
20070151	7/17 A1	34S_4p1d7Xa	33 7/8	S	9	4437.4	66 1/8	62	0.297	0.446	HLP-22	12	8	4	1.9	10.5	5.7	30.8	16.1	0.62	0.33	p1d7	2.45	0.0001213	0.0001780	0.0002606	0.4277
20070155	7/17 A1	34S_4p1d7Xa	33 7/8	S	9	4437.4	66 1/8	62	0.297	0.446	HLP-22	12	8	4	1.9	10.5	5.7	30.8	16.1	0.62	0.33	p1d7	2.45	0.0001213	0.0001780	0.0002606	0.4277
20070161	7/17 A1	34S_4p1d7Xa	33 7/8	S	9	4437.4	66 1/8	62	0.297	0.446	HLP-22	12	8	4	1.9	10.5	5.7	30.8	16.1	0.62	0.33	p1d7	2.45	0.0001213	0.0001780	0.0002606	0.4277
20070168	7/17 A1	34S_4p1d7Xa	33 7/8	S	9	4437.4	66 1/8	62	0.297	0.446	HLP-22	12	8	4	1.9	10.5	5.7	30.8	16.1	0.62	0.33	p1d7	2.45	0.0001213	0.0001780	0.0002606	0.4277
20070171	7/17 A1	34S_4p1d7Xa	33 7/8	S	9	4437.4	66 1/8	62	0.297	0.446	HLP-22	12	8	4	1.9	10.5	5.7	30.8	16.1	0.62	0.33	p1d7	2.45	0.0001213	0.0001780	0.0002606	0.4277
20070174	7/17 A1	34S_4p1d7Xa	33 7/8	S	9	4437.4	66 1/8	62	0.297	0.446	HLP-22	12	8	4	1.9	10.5	5.7	30.8	16.1	0.62	0.33	p1d7	2.45	0.0001213	0.0001780	0.0002606	0.4277
20070179	7/17 A1	34S_4p1d7Xa	33 7/8	S	9	4437.4	66 1/8	62	0.297	0.446	HLP-22	12	8	4	1.9	10.5	5.7	30.8	16.1	0.62	0.33	p1d7	2.45	0.0001213	0.0001780	0.0002606	0.4277
20070183	7/17 A1	34S_4p1d7Xa	33 7/8	S	9	4437.4	66 1/8	62	0.297	0.446	HLP-22	12	8	4	1.9	10.5	5.7	30.8	16.1	0.62	0.33	p1d7	2.45	0.0001213	0.0001780	0.0002606	0.4277
20070200	7/17 A2	34S_4p1d7Xc_8	33 7/8	S	9	4437.4	66 1/8	62	0.297	0.446	HLP-22	12	8	4	1.9	10.5	5.7	30.8	16.1	0.62	0.33	p1d7	2.45	0.0001213	0.0001780	0.0002606	0.4277
20070206	7/17 A2	34S_4p1d7Xc_8	33 7/8	S	9	4437.4	66 1/8	62	0.297	0.446	HLP-22	12	8	4	1.9	10.5	5.7	30.8	16.1	0.62	0.33	p1d7	2.45	0.0001213	0.0001780	0.0002606	0.4277
20070211	7/17 A2	34S_4p1d7Xc_8	33 7/8	S	9	4437.4	66 1/8	62	0.297	0.446	HLP-22	12	8	4	1.9	10.5	5.7	30.8	16.1	0.62	0.33	p1d7	2.45	0.0001213	0.0001780	0.0002606	0.4277
20070217	7/17 A2	34S_4p1d7Xc_8	33 7/8	S	9	4437.4	66 1/8	62	0.297	0.446	HLP-22	12	8	4	1.9	10.5	5.7	30.8	16.1	0.62	0.33	p1d7	2.45	0.0001213	0.0001780	0.0002606	0.4277
20070228	7/17 A2	34S_4p1d7Xc_8	33 7/8	S	9	4437.4	66 1/8	62	0.297	0.446	HLP-22	12	8	4	1.9	10.5	5.7	30.8	16.1	0.62	0.33	p1d7	2.45	0.0001213	0.0001780	0.0002606	0.4277
20070233	7/17 A2	34S_4p1d7Xc_8	33 7/8	S	9	4437.4	66 1/8	62	0.297	0.446	HLP-22	12	8	4	1.9	10.5	5.7	30.8	16.1	0.62	0.33	p1d7	2.45	0.0001213	0.0001780	0.0002606	0.4277
20070234M	7/17 A2	34S_4p1d7Xc_8	33 7/8	S	9	4437.4	66 1/8	62	0.297	0.446	HLP-22	12	8	4	1.9	10.5	5.7	30.8	16.1	0.62	0.33	p1d7	2.45	0.0001213	0.0001780	0.0002606	0.4277
20070236M	7/17 A2	34S_4p1d7Xc_8	33 7/8	S	9	4437.4	66 1/8	62	0.297	0.446	HLP-22	12	8	4	1.9	10.5	5.7	30.8	16.1	0.62	0.33	p1d7	2.45	0.0001213	0.0001780	0.0002606	0.4277

Table B.7. Data from July 2007 Tests in Mid-Scale Vessel with Spherical Head B.1

Tank Water Temperature	Water Density	Solids Fraction	Pulse Volume Fraction	Duty Cycle	Cycle Time	Pulsed or Steady Jet	Us Steady Jet	U1 Pulsing Jet	U2 URMS	U3 URM3	Discharge Velocity	Critical Suspension Velocity	Average Peak Cloud Height	UCS Condition	UCS Method	UCS Flag	UCS Center Flag	UCS udv Flag	UCS based on Decreasing Velocity	Sweep Increase / Decrease	UDV Height Bed	Particle Motion	Solids Level	Outer Bottom Pattern	Inner Bottom Pattern	Case ID	Test	TDP	Row Number
C	g/cm³	fraction	fraction	fraction	s	text	m/s	m/s	m/s	m/s	m/s	m/s	in.	m/s	text	text	text	text	m/s	text	mm	text	text	text	text	text	text	text	text
T	ρ_ℓ	ϕ_S	ϕ_p	DC	t_C	Jet	U_S	U1	U2	U3	U	U_{CS}	H_C	U_{CSR}	U_{CSM}	U_{CS}vis	U_{CS}cen	U_{CS}udv	U_{CS}_D	S_W	H_{bed}	PM	Sol	SP_O	SP_I	ID	M/DDX	TDP	MSS
N/A	N/A	0.00487	undefined	1.000	infinite	S	N/A	N/A	N/A	N/A	3.00	6.10	N/A	N/A	N/A	N/A	N/A	N/A	N/A	N/A	N/A	SS	SON	BP3	BP2	34S_4p1d7Ya	7/16 A1	TDP-WTP-002	20070019
N/A	N/A	0.00487	undefined	1.000	infinite	S	N/A	N/A	N/A	N/A	3.40	6.10	N/A	N/A	N/A	N/A	N/A	N/A	N/A	N/A	N/A	SS	SON	BP3	N/A	34S_4p1d7Ya	7/16 A1	TDP-WTP-002	20070027
N/A	N/A	0.00487	undefined	1.000	infinite	S	N/A	N/A	N/A	N/A	4.40	6.10	N/A	N/A	N/A	N/A	N/A	N/A	N/A	N/A	N/A	SS	SON	BP3+	BP4	34S_4p1d7Ya	7/16 A1	TDP-WTP-002	20070031
28.2	0.997	0.00487	undefined	1.000	infinite	S	5.15	N/A	N/A	N/A	5.10	6.10	8.63	N/A	N/A	N/A	N/A	N/A	N/A	N/A	N/A	AM	SCO	BP5	N/A	34S_4p1d7Ya	7/16 A1	TDP-WTP-002	20070038
28.3	0.997	0.00487	undefined	1.000	infinite	S	5.84	N/A	N/A	N/A	5.80	6.10	10.13	N/A	N/A	UCSvis	N/A	N/A	N/A	I	N/A	AM	NSS	BP5/6	N/A	34S_4p1d7Ya	7/16 A1	TDP-WTP-002	20070042
28.3	0.997	0.00487	undefined	1.000	infinite	S	6.12	N/A	N/A	N/A	6.10	6.10	10.13	6.10	vis	UCSvis	N/A	N/A	N/A	I	N/A	CS	NSS	BP5/6	N/A	34S_4p1d7Ya	7/16 A1	TDP-WTP-002	20070048
28.4	0.997	0.00487	undefined	1.000	infinite	S	6.65	N/A	N/A	N/A	6.60	6.10	15.63	N/A	N/A	N/A	N/A	N/A	N/A	N/A	N/A	BC	NSS	BP6	N/A	34S_4p1d7Ya	7/16 A1	TDP-WTP-002	20070051
28.6	0.997	0.00487	undefined	1.000	infinite	S	7.44	N/A	N/A	N/A	7.40	6.10	30.63	N/A	N/A	N/A	N/A	N/A	N/A	N/A	N/A	BC	NSS	BP5/6	N/A	34S_4p1d7Ya	7/16 A1	TDP-WTP-002	20070057
28.6	0.997	0.00487	undefined	1.000	infinite	S	6.65	N/A	N/A	N/A	6.60	6.10	14.88	N/A	N/A	N/A	N/A	N/A	N/A	N/A	N/A	N/A	N/A	N/A	N/A	34S_4p1d7Ya	7/16 A1	TDP-WTP-002	20070059
28.7	0.997	0.00487	undefined	1.000	infinite	S	6.50	N/A	N/A	N/A	6.40	6.10	12.13	N/A	N/A	N/A	N/A	N/A	N/A	N/A	N/A	N/A	N/A	N/A	N/A	34S_4p1d7Ya	7/16 A1	TDP-WTP-002	20070061
28.6	0.997	0.00487	undefined	1.000	infinite	S	6.91	N/A	N/A	N/A	6.90	6.10	20.13	N/A	N/A	N/A	N/A	N/A	N/A	N/A	N/A	N/A	N/A	N/A	N/A	34S_4p1d7Ya	7/16 A1	TDP-WTP-002	20070063
28.7	0.997	0.00487	undefined	1.000	infinite	S	6.06	N/A	N/A	N/A	6.00	6.10	9.63	N/A	N/A	N/A	N/A	N/A	N/A	N/A	N/A	N/A	N/A	N/A	N/A	34S_4p1d7Ya	7/16 A1	TDP-WTP-002	20070065
N/A	N/A	0.00487	undefined	1.000	infinite	S	N/A	N/A	N/A	N/A	5.40	6.10	N/A	N/A	N/A	N/A	N/A	N/A	N/A	N/A	N/A	CS	NSS?	BP5/6	N/A	34S_4p1d7Ya	7/16 A1	TDP-WTP-002	20070068
N/A	N/A	0.00487	undefined	1.000	infinite	S	N/A	N/A	N/A	N/A	5.10	6.10	N/A	N/A	N/A	N/A	N/A	N/A	N/A	N/A	N/A	AM	SCO	BP5/6	N/A	34S_4p1d7Ya	7/16 A1	TDP-WTP-002	20070073
N/A	N/A	0.00487	0.050	0.330	54.3	P	N/A	N/A	N/A	N/A	2.10	6.40	N/A	N/A	N/A	N/A	N/A	N/A	N/A	N/A	N/A	SS	SON/SIN	BP1	N/A	34S_4p1d7Yc_8	7/16 A2	TDP-WTP-002	20070081
N/A	N/A	0.00487	0.050	0.330	41.7	P	N/A	N/A	N/A	N/A	3.40	6.40	N/A	N/A	N/A	N/A	N/A	N/A	N/A	N/A	N/A	SS	SON	BP3	N/A	34S_4p1d7Yc_8	7/16 A2	TDP-WTP-002	20070089
N/A	N/A	0.00487	0.050	0.330	27.8	P	N/A	N/A	N/A	N/A	5.10	6.40	N/A	N/A	N/A	N/A	N/A	N/A	N/A	N/A	N/A	SS	SON	BP3	N/A	34S_4p1d7Yc_8	7/16 A2	TDP-WTP-002	20070097
29.0	0.997	0.00487	0.050	0.330	22.1	P	N/A	5.94	6.14	6.24	6.40	6.40	11.63	6.40	vis	UCSvis	N/A	N/A	N/A	I	N/A	AM/CS	NSS	BP6	N/A	34S_4p1d7Yc_8	7/16 A2	TDP-WTP-002	20070105
29.0	0.997	0.00487	0.050	0.330	20.0	P	N/A	6.61	6.86	6.98	7.20	6.40	13.63	N/A	N/A	N/A	N/A	N/A	N/A	N/A	N/A	BC	NSS	BP6	N/A	34S_4p1d7Yc_8	7/16 A2	TDP-WTP-002	20070109
29.0	0.997	0.00487	0.050	0.330	22.1	P	N/A	5.92	6.11	6.20	6.40	6.40	12.63	N/A	vis dec	UCSvis	N/A	N/A	6.40	D	N/A	CS	NSS	BP6	N/A	34S_4p1d7Yc_8	7/16 A2	TDP-WTP-002	20070114
N/A	N/A	0.01592	undefined	1.000	infinite	S	N/A	N/A	N/A	N/A	3.00	6.80	N/A	N/A	N/A	N/A	N/A	N/A	N/A	N/A	N/A	SM	SON	BP3	BP0	34S_4p1d7Xa	7/17 A1	TDP-WTP-004	20070127
N/A	N/A	0.01592	undefined	1.000	infinite	S	N/A	N/A	N/A	N/A	3.40	6.80	N/A	N/A	N/A	N/A	N/A	N/A	N/A	N/A	N/A	SM	SON	BP3	BP0	34S_4p1d7Xa	7/17 A1	TDP-WTP-004	20070131
N/A	N/A	0.01592	undefined	1.000	infinite	S	N/A	N/A	N/A	N/A	4.35	6.80	N/A	N/A	N/A	N/A	N/A	N/A	N/A	N/A	N/A	SS	SON	BP3	BP2	34S_4p1d7Xa	7/17 A1	TDP-WTP-004	20070135
N/A	N/A	0.01592	undefined	1.000	infinite	S	N/A	N/A	N/A	N/A	5.10	6.80	N/A	N/A	N/A	N/A	N/A	N/A	N/A	N/A	N/A	SS	SON	BP3	BP2	34S_4p1d7Xa	7/17 A1	TDP-WTP-004	20070142
N/A	N/A	0.01592	undefined	1.000	infinite	S	N/A	N/A	N/A	N/A	6.00	6.80	N/A	N/A	N/A	N/A	N/A	N/A	N/A	N/A	N/A	SS	SCO	BP4	N/A	34S_4p1d7Xa	7/17 A1	TDP-WTP-004	20070146
n/a	n/a	0.01592	undefined	1.000	infinite	S	6.30	N/A	N/A	N/A	6.30	6.80	8.88	N/A	N/A	N/A	N/A	N/A	N/A	N/A	N/A	AM	SCO	BP5	N/A	34S_4p1d7Xa	7/17 A1	TDP-WTP-004	20070151
n/a	n/a	0.01592	undefined	1.000	infinite	S	6.80	N/A	N/A	N/A	6.80	6.80	10.63	6.80	vis	UCSvis	N/A	N/A	N/A	I	N/A	CS	NSS	BP5	N/A	34S_4p1d7Xa	7/17 A1	TDP-WTP-004	20070155
n/a	n/a	0.01592	undefined	1.000	infinite	S	7.80	N/A	N/A	N/A	7.75	6.80	13.88	N/A	N/A	N/A	N/A	N/A	N/A	N/A	N/A	N/A	N/A	N/A	N/A	34S_4p1d7Xa	7/17 A1	TDP-WTP-004	20070161
n/a	n/a	0.01592	undefined	1.000	infinite	S	8.10	N/A	N/A	N/A	8.05	6.80	16.38	N/A	N/A	N/A	N/A	N/A	N/A	N/A	N/A	N/A	N/A	N/A	N/A	34S_4p1d7Xa	7/17 A1	TDP-WTP-004	20070168
n/a	n/a	0.01592	undefined	1.000	infinite	S	8.70	N/A	N/A	N/A	8.65	6.80	22.38	N/A	N/A	N/A	N/A	N/A	N/A	N/A	N/A	N/A	N/A	N/A	N/A	34S_4p1d7Xa	7/17 A1	TDP-WTP-004	20070171
n/a	n/a	0.01592	undefined	1.000	infinite	S	9.10	N/A	N/A	N/A	9.05	6.80	35.13	N/A	N/A	N/A	N/A	N/A	N/A	N/A	N/A	N/A	N/A	N/A	N/A	34S_4p1d7Xa	7/17 A1	TDP-WTP-004	20070174
n/a	n/a	0.01592	undefined	1.000	infinite	S	6.50	N/A	N/A	N/A	6.50	6.80	9.00	N/A	N/A	N/A	N/A	N/A	N/A	N/A	N/A	AM	SCO	BP5	N/A	34S_4p1d7Xa	7/17 A1	TDP-WTP-004	20070179
n/a	n/a	0.01592	undefined	1.000	infinite	S	6.60	N/A	N/A	N/A	6.60	6.80	9.75	N/A	vis dec	UCSvis	N/A	N/A	6.60	D	N/A	CS	NSS	BP5+	N/A	34S_4p1d7Xa	7/17 A1	TDP-WTP-004	20070183
N/A	N/A	0.01592	0.048	0.330	50.0	P	N/A	N/A	N/A	N/A	2.80	8.20	N/A	N/A	N/A	N/A	N/A	N/A	N/A	N/A	N/A	SM	SON	BP3	BP1	34S_4p1d7Xc_8	7/17 A2	TDP-WTP-004	20070200
N/A	N/A	0.01592	0.048	0.330	40.5	P	N/A	N/A	N/A	N/A	3.20	8.20	N/A	N/A	N/A	N/A	N/A	N/A	N/A	N/A	N/A	SM	SON	BP3	BP0	34S_4p1d7Xc_8	7/17 A2	TDP-WTP-004	20070206
N/A	N/A	0.01592	0.048	0.330	28.6	P	N/A	N/A	N/A	N/A	4.90	8.20	N/A	N/A	N/A	N/A	N/A	N/A	N/A	N/A	N/A	SS	SON/SIN	BP3	BP1	34S_4p1d7Xc_8	7/17 A2	TDP-WTP-004	20070211
N/A	N/A	0.01592	0.048	0.330	27.5	P	N/A	N/A	N/A	N/A	5.10	8.20	N/A	N/A	N/A	N/A	N/A	N/A	N/A	N/A	N/A	SS	SON/SIN	BP3	BP2	34S_4p1d7Xc_8	7/17 A2	TDP-WTP-004	20070217
N/A	N/A	0.01592	0.048	0.330	19.0	P	N/A	N/A	N/A	N/A	7.60	8.20	N/A	N/A	N/A	N/A	N/A	N/A	N/A	N/A	N/A	AM	N/A	N/A	N/A	34S_4p1d7Xc_8	7/17 A2	TDP-WTP-004	20070228
29.0	0.997	0.01592	0.048	0.330	18.1	P	N/A	7.44	7.76	7.91	8.20	8.20	N/A	8.20	vis	UCSvis	N/A	N/A	N/A	I	N/A	CS	NSS	BP5+	N/A	34S_4p1d7Xc_8	7/17 A2	TDP-WTP-004	20070233
29.0	0.997	0.01592	0.048	0.330	14.8	P	N/A	8.45	8.93	9.15	9.50	8.20	10.38	N/A	N/A	N/A	N/A	N/A	N/A	N/A	N/A	N/A	N/A	N/A	N/A	34S_4p1d7Xc_8	7/17 A2	TDP-WTP-004	20070234
29.0	0.997	0.01592	0.048	0.330	12.3	P	N/A	9.71	10.47	10.83	11.60	8.20	13.63	N/A	N/A	N/A	N/A	N/A	N/A	N/A	N/A	N/A	N/A	N/A	N/A	34S_4p1d7Xc_8	7/17 A2	TDP-WTP-004	20070236

Table B.7. Data from July 2007 Tests in Mid-Scale Vessel with Spherical Head A.2

Row Number	Test	Case ID	Tank Diameter	Head Shape	Dish Height	Dish Volume	Tank Fill Height	Return Line Height	Nozzle Inner Diameter	Nozzle Stand-off Distance	Pulse Tube Configuration	Installed Nozzles	Outer Nozzles Operated	Inner Nozzles Operated	Pulse Tube Outer Diameter	Outer PJM Radius	Inner PJM Radius	"FIO" Outer PJM Impingement Angle	"FIO" Inner PJM Impingement Angle	Ratio Outer PJM to Tank Radius	Ratio Inner PJM to Tank Radius	Simulant	Solids Density	Particle Diameter d5	Particle Diameter d50	Particle Diameter d95	Void Fraction
text	text	text	in.	text	in.	in. ^{3}	in.	in.	in.	in.	text	number	number	number	in.	in.	in.	deg	deg	nondim	nondim	text	g/cm^3	m	m	m	fraction
MSS	M/DDX	ID	D	HS	H_{dish}	V_{dish}	H	Rtn	d	sod	PT	N	N_O	N_I	PT_{od}	R_O	R_I	θ_O	θ_I	R_O/R	R_I/R	sxdx	ρ_s	d_5	d_{50}	d_{95}	vf
20070238M	7/17 A2	34S_4p1d7Xc_8	33 7/8	S	9	4437.4	66 1/8	62	0.297	0.446	HLP-22	12	8	4	1.9	10.5	5.7	30.8	16.1	0.62	0.33	p1d7	2.45	0.0001213	0.0001780	0.0002606	0.4277
20070241M	7/17 A2	34S_4p1d7Xc_8	33 7/8	S	9	4437.4	66 1/8	62	0.297	0.446	HLP-22	12	8	4	1.9	10.5	5.7	30.8	16.1	0.62	0.33	p1d7	2.45	0.0001213	0.0001780	0.0002606	0.4277
20070245	7/17 A2	34S_4p1d7Xc_8	33 7/8	S	9	4437.4	66 1/8	62	0.297	0.446	HLP-22	12	8	4	1.9	10.5	5.7	30.8	16.1	0.62	0.33	p1d7	2.45	0.0001213	0.0001780	0.0002606	0.4277
20070253	7/17 A2	34S_4p1d7Xc_8	33 7/8	S	9	4437.4	65 5/6	62	0.297	0.446	HLP-22	12	8	4	1.9	10.5	5.7	30.8	16.1	0.62	0.33	p1d7	2.45	0.0001213	0.0001780	0.0002606	0.4277
20070255	7/17 A2	34S_4p1d7Xc_8	33 7/8	S	9	4437.4	65 5/6	62	0.297	0.446	HLP-22	12	8	4	1.9	10.5	5.7	30.8	16.1	0.62	0.33	p1d7	2.45	0.0001213	0.0001780	0.0002606	0.4277
20070257	7/17 A2	34S_4p1d7Xc_8	33 7/8	S	9	4437.4	65 5/6	62	0.297	0.446	HLP-22	12	8	4	1.9	10.5	5.7	30.8	16.1	0.62	0.33	p1d7	2.45	0.0001213	0.0001780	0.0002606	0.4277
20070258	7/17 A2	34S_4p1d7Xc_8	33 7/8	S	9	4437.4	65 5/6	62	0.297	0.446	HLP-22	12	8	4	1.9	10.5	5.7	30.8	16.1	0.62	0.33	p1d7	2.45	0.0001213	0.0001780	0.0002606	0.4277
20070283	7/18 A1	34S_4p1d7Xc_8	33 7/8	S	9	4437.4	76 1/8	62	0.297	0.446	HLP-22	12	8	4	1.9	10.5	5.7	30.8	16.1	0.62	0.33	p1d7	2.45	0.0001213	0.0001780	0.0002606	0.4277
20070286M	7/18 A1	34S_4p1d7Xc_8	33 7/8	S	9	4437.4	76 1/8	62	0.297	0.446	HLP-22	12	8	4	1.9	10.5	5.7	30.8	16.1	0.62	0.33	p1d7	2.45	0.0001213	0.0001780	0.0002606	0.4277
20070291M	7/18 A1	34S_4p1d7Xc_8	33 7/8	S	9	4437.4	76 1/8	62	0.297	0.446	HLP-22	12	8	4	1.9	10.5	5.7	30.8	16.1	0.62	0.33	p1d7	2.45	0.0001213	0.0001780	0.0002606	0.4277
20070293M	7/18 A1	34S_4p1d7Xc_8	33 7/8	S	9	4437.4	76 1/8	62	0.297	0.446	HLP-22	12	8	4	1.9	10.5	5.7	30.8	16.1	0.62	0.33	p1d7	2.45	0.0001213	0.0001780	0.0002606	0.4277
20070296M	7/18 A1	34S_4p1d7Xc_8	33 7/8	S	9	4437.4	76 1/8	62	0.297	0.446	HLP-22	12	8	4	1.9	10.5	5.7	30.8	16.1	0.62	0.33	p1d7	2.45	0.0001213	0.0001780	0.0002606	0.4277
20070299M	7/18 A1	34S_4p1d7Xc_8	33 7/8	S	9	4437.4	76 1/8	62	0.297	0.446	HLP-22	12	8	4	1.9	10.5	5.7	30.8	16.1	0.62	0.33	p1d7	2.45	0.0001213	0.0001780	0.0002606	0.4277
20070309	7/18 A1	34S_4p1d7Xc_8	33 7/8	S	9	4437.4	76 1/8	62	0.297	0.446	HLP-22	12	8	4	1.9	10.5	5.7	30.8	16.1	0.62	0.33	p1d7	2.45	0.0001213	0.0001780	0.0002606	0.4277
20070314	7/18 A1	34S_4p1d7Xc_8	33 7/8	S	9	4437.4	76 1/8	62	0.297	0.446	HLP-22	12	8	4	1.9	10.5	5.7	30.8	16.1	0.62	0.33	p1d7	2.45	0.0001213	0.0001780	0.0002606	0.4277
20070335M	7/18 A2	34S_4p1d7Xc_2	33 7/8	S	9	4437.4	76 1/8	62	0.297	0.446	HLP-22	12	8	4	1.9	10.5	5.7	30.8	16.1	0.62	0.33	p1d7	2.45	0.0001213	0.0001780	0.0002606	0.4277
20070339	7/18 A2	34S_4p1d7Xc_2	33 7/8	S	9	4437.4	76 1/8	62	0.297	0.446	HLP-22	12	8	4	1.9	10.5	5.7	30.8	16.1	0.62	0.33	p1d7	2.45	0.0001213	0.0001780	0.0002606	0.4277
20070344	7/18 A2	34S_4p1d7Xc_2	33 7/8	S	9	4437.4	76 1/8	62	0.297	0.446	HLP-22	12	8	4	1.9	10.5	5.7	30.8	16.1	0.62	0.33	p1d7	2.45	0.0001213	0.0001780	0.0002606	0.4277
20070347	7/18 A2	34S_4p1d7Xc_2	33 7/8	S	9	4437.4	76 1/8	62	0.297	0.446	HLP-22	12	8	4	1.9	10.5	5.7	30.8	16.1	0.62	0.33	p1d7	2.45	0.0001213	0.0001780	0.0002606	0.4277
20070352	7/18 A2	34S_4p1d7Xc_2	33 7/8	S	9	4437.4	76 1/8	62	0.297	0.446	HLP-22	12	8	4	1.9	10.5	5.7	30.8	16.1	0.62	0.33	p1d7	2.45	0.0001213	0.0001780	0.0002606	0.4277
20070357	7/18 A2	34S_4p1d7Xc_2	33 7/8	S	9	4437.4	76 1/8	62	0.297	0.446	HLP-22	12	8	4	1.9	10.5	5.7	30.8	16.1	0.62	0.33	p1d7	2.45	0.0001213	0.0001780	0.0002606	0.4277
20070362M	7/18 A2	34S_4p1d7Xc_2	33 7/8	S	9	4437.4	76 1/8	62	0.297	0.446	HLP-22	12	8	4	1.9	10.5	5.7	30.8	16.1	0.62	0.33	p1d7	2.45	0.0001213	0.0001780	0.0002606	0.4277
20070369M	7/18 A2	34S_4p1d7Xc_2	33 7/8	S	9	4437.4	76 1/8	62	0.297	0.446	HLP-22	12	8	4	1.9	10.5	5.7	30.8	16.1	0.62	0.33	p1d7	2.45	0.0001213	0.0001780	0.0002606	0.4277
20070372M	7/18 A2	34S_4p1d7Xc_2	33 7/8	S	9	4437.4	76 1/8	62	0.297	0.446	HLP-22	12	8	4	1.9	10.5	5.7	30.8	16.1	0.62	0.33	p1d7	2.45	0.0001213	0.0001780	0.0002606	0.4277
20070384	7/19 A1	34S_4p1d7Yc_8	33 7/8	S	9	4437.4	67 5/8	62	0.297	0.446	HLP-22	12	8	4	1.9	10.5	5.7	30.8	16.1	0.62	0.33	p1d7	2.45	0.0001213	0.0001780	0.0002606	0.4277
20070387M	7/19 A1	34S_4p1d7Yc_8	33 7/8	S	9	4437.4	67 5/8	62	0.297	0.446	HLP-22	12	8	4	1.9	10.5	5.7	30.8	16.1	0.62	0.33	p1d7	2.45	0.0001213	0.0001780	0.0002606	0.4277
20070392M	7/19 A1	34S_4p1d7Yc_8	33 7/8	S	9	4437.4	67 5/8	62	0.297	0.446	HLP-22	12	8	4	1.9	10.5	5.7	30.8	16.1	0.62	0.33	p1d7	2.45	0.0001213	0.0001780	0.0002606	0.4277
20070395M	7/19 A1	34S_4p1d7Yc_8	33 7/8	S	9	4437.4	67 5/8	62	0.297	0.446	HLP-22	12	8	4	1.9	10.5	5.7	30.8	16.1	0.62	0.33	p1d7	2.45	0.0001213	0.0001780	0.0002606	0.4277
20070398M	7/19 A1	34S_4p1d7Yc_8	33 7/8	S	9	4437.4	67 5/8	62	0.297	0.446	HLP-22	12	8	4	1.9	10.5	5.7	30.8	16.1	0.62	0.33	p1d7	2.45	0.0001213	0.0001780	0.0002606	0.4277
20070401M	7/19 A1	34S_4p1d7Yc_8	33 7/8	S	9	4437.4	67 5/8	62	0.297	0.446	HLP-22	12	8	4	1.9	10.5	5.7	30.8	16.1	0.62	0.33	p1d7	2.45	0.0001213	0.0001780	0.0002606	0.4277
20070403M	7/19 A1	34S_4p1d7Yc_8	33 7/8	S	9	4437.4	67 5/8	62	0.297	0.446	HLP-22	12	8	4	1.9	10.5	5.7	30.8	16.1	0.62	0.33	p1d7	2.45	0.0001213	0.0001780	0.0002606	0.4277
20070411M	7/19 A1	34S_4p1d7Yc_8	33 7/8	S	9	4437.4	67 5/8	62	0.297	0.446	HLP-22	12	8	4	1.9	10.5	5.7	30.8	16.1	0.62	0.33	p1d7	2.45	0.0001213	0.0001780	0.0002606	0.4277
20070417	7/19 A2	34S_4p1d7Ya	33 7/8	S	9	4437.4	67 5/8	62	0.297	0.446	HLP-22	12	8	4	1.9	10.5	5.7	30.8	16.1	0.62	0.33	p1d7	2.45	0.0001213	0.0001780	0.0002606	0.4277
20070423M	7/19 A3	34S_4p1d7Yc_2	33 7/8	S	9	4437.4	67 5/8	62	0.297	0.446	HLP-22	12	8	4	1.9	10.5	5.7	30.8	16.1	0.62	0.33	p1d7	2.45	0.0001213	0.0001780	0.0002606	0.4277
20070426M	7/19 A3	34S_4p1d7Yc_2	33 7/8	S	9	4437.4	67 5/8	62	0.297	0.446	HLP-22	12	8	4	1.9	10.5	5.7	30.8	16.1	0.62	0.33	p1d7	2.45	0.0001213	0.0001780	0.0002606	0.4277
20070428M	7/19 A3	34S_4p1d7Yc_2	33 7/8	S	9	4437.4	67 5/8	62	0.297	0.446	HLP-22	12	8	4	1.9	10.5	5.7	30.8	16.1	0.62	0.33	p1d7	2.45	0.0001213	0.0001780	0.0002606	0.4277
20070432M	7/19 A3	34S_4p1d7Yc_2	33 7/8	S	9	4437.4	67 5/8	62	0.297	0.446	HLP-22	12	8	4	1.9	10.5	5.7	30.8	16.1	0.62	0.33	p1d7	2.45	0.0001213	0.0001780	0.0002606	0.4277
20070434	7/19 A3	34S_4p1d7Yc_2	33 7/8	S	9	4437.4	67 5/8	62	0.297	0.446	HLP-22	12	8	4	1.9	10.5	5.7	30.8	16.1	0.62	0.33	p1d7	2.45	0.0001213	0.0001780	0.0002606	0.4277
20070438	7/19 A4	34S_4p1d7Yd_8	33 7/8	S	9	4437.4	67 5/8	62	0.297	0.446	HLP-22	12	8	4	1.9	10.5	5.7	30.8	16.1	0.62	0.33	p1d7	2.45	0.0001213	0.0001780	0.0002606	0.4277
20070441M	7/19 A4	34S_4p1d7Yd_8	33 7/8	S	9	4437.4	67 5/8	62	0.297	0.446	HLP-22	12	8	4	1.9	10.5	5.7	30.8	16.1	0.62	0.33	p1d7	2.45	0.0001213	0.0001780	0.0002606	0.4277
20070445M	7/19 A4	34S_4p1d7Yd_8	33 7/8	S	9	4437.4	67 5/8	62	0.297	0.446	HLP-22	12	8	4	1.9	10.5	5.7	30.8	16.1	0.62	0.33	p1d7	2.45	0.0001213	0.0001780	0.0002606	0.4277

Table B.7. Data from July 2007 Tests in Mid-Scale Vessel with Spherical Head B.2

Tank Water Temperature	Water Density	Solids Fraction	Pulse Volume Fraction	Duty Cycle	Cycle Time	Pulsed or Steady Jet	Us Steady Jet	U1 Pulsing Jet	U2 URMS	U3 URM3	Discharge Velocity	Critical Suspension Velocity	Average Peak Cloud Height	UCS Condition	UCS Method	UCS Flag	UCS Center Flag	UCS udv Flag	UCS based on Decreasing Velocity	Sweep Increase / Decrease	UDV Height Bed	Particle Motion	Solids Level	Outer Bottom Pattern	Inner Bottom Pattern	Case ID	Test	TDP	Row Number
C	g/cm³	fraction	fraction	fraction	s	text	m/s	m/s	m/s	m/s	m/s	m/s	in.	m/s	text	text	text	text	m/s	text	mm	text	text	text	text	text	text	text	text
T	ρ_l	ϕ_S	ϕ_P	DC	t_C	Jet	U_S	U1	U2	U3	U	U_{CS}	H_C	U_{CSR}	U_{CSM}	U_{CS}vis	U_{CS}cen	U_{CS}udv	U_{CS}_D	S_W	H_{bed}	PM	Sol	SP_O	SP_I	ID	M/DDX	TDP	MSS
29.0	0.997	0.01592	0.048	0.330	1.0	P	N/A	10.76	11.92	12.48	15.20	8.20	22.63	N/A	N/A	N/A	N/A	N/A	N/A	N/A	N/A	N/A	N/A	N/A	N/A	34S_4p1d7Xc_8	7/17 A2	TDP-WTP-004	20070238
29.0	0.997	0.01592	0.048	0.330	1.1	P	N/A	10.95	11.86	12.29	13.30	8.20	19.13	N/A	N/A	N/A	N/A	N/A	N/A	N/A	N/A	N/A	N/A	N/A	N/A	34S_4p1d7Xc_8	7/17 A2	TDP-WTP-004	20070241
N/A	N/A	0.01592	0.048	0.330	16.7	P	N/A	N/A	N/A	N/A	8.60	8.20	N/A	N/A	N/A	N/A	N/A	N/A	N/A	N/A	N/A	N/A	N/A	N/A	N/A	34S_4p1d7Xc_8	7/17 A2	TDP-WTP-004	20070245
N/A	N/A	0.01592	0.048	0.330	33.3	P	N/A	N/A	N/A	N/A	9.40	8.20	N/A	N/A	N/A	N/A	N/A	N/A	N/A	N/A	N/A	N/A	N/A	N/A	N/A	34S_4p1d7Xc_8	7/17 A2	TDP-WTP-005	20070253
N/A	N/A	0.01592	0.048	0.330	29.2	P	N/A	N/A	N/A	N/A	10.25	8.20	N/A	N/A	N/A	N/A	N/A	N/A	N/A	N/A	N/A	N/A	N/A	N/A	N/A	34S_4p1d7Xc_8	7/17 A2	TDP-WTP-005	20070255
N/A	N/A	0.01592	0.048	0.330	29.5	P	N/A	N/A	N/A	N/A	11.45	8.20	N/A	N/A	N/A	N/A	N/A	N/A	N/A	N/A	N/A	N/A	N/A	N/A	N/A	34S_4p1d7Xc_8	7/17 A2	TDP-WTP-005	20070257
N/A	N/A	0.01592	0.048	0.330	23.6	P	N/A	N/A	N/A	N/A	13.55	8.20	N/A	N/A	N/A	N/A	N/A	N/A	N/A	N/A	N/A	N/A	N/A	N/A	N/A	34S_4p1d7Xc_8	7/17 A2	TDP-WTP-005	20070258
27.0	0.998	0.01592	0.048	0.330	19.3	P	N/A	7.08	7.34	7.47	7.65	8.10	8.63	N/A	N/A	N/A	N/A	N/A	N/A	N/A	N/A	AM/CS	NSS	BP6	N/A	34S_4p1d7Xc_8	7/18 A1	TDP-WTP-006	20070283
27.0	0.998	0.01592	0.048	0.330	18.1	P	N/A	7.50	7.81	7.95	8.10	8.10	9.13	8.10	vis	UCSvis	N/A	N/A	N/A	I	N/A	CS	NSS	BP6	N/A	34S_4p1d7Xc_8	7/18 A1	TDP-WTP-006	20070286
27.0	0.998	0.01592	0.048	0.330	13.4	P	N/A	8.25	9.02	9.36	10.24	8.10	11.63	N/A	N/A	N/A	N/A	N/A	N/A	N/A	N/A	N/A	N/A	N/A	N/A	34S_4p1d7Xc_8	7/18 A1	TDP-WTP-006	20070291
27.0	0.998	0.01592	0.048	0.330	13.4	P	N/A	8.72	9.49	9.84	10.70	8.10	11.88	N/A	N/A	N/A	N/A	N/A	N/A	N/A	N/A	BC	NSS	BP6	N/A	34S_4p1d7Xc_8	7/18 A1	TDP-WTP-006	20070293
27.0	0.998	0.01592	0.048	0.330	11.1	P	N/A	11.43	12.81	13.48	15.20	8.10	26.13	N/A	N/A	N/A	N/A	N/A	N/A	N/A	N/A	N/A	N/A	N/A	N/A	34S_4p1d7Xc_8	7/18 A1	TDP-WTP-006	20070296
27.0	0.998	0.01592	0.048	0.330	11.8	P	N/A	10.12	11.14	11.62	12.70	8.10	17.13	N/A	N/A	N/A	N/A	N/A	N/A	N/A	N/A	N/A	N/A	N/A	N/A	34S_4p1d7Xc_8	7/18 A1	TDP-WTP-006	20070299
27.0	0.998	0.01592	0.048	0.330	18.3	P	N/A	7.00	7.43	7.61	8.00	8.10	9.13	N/A	vis dec	UCSvis	N/A	N/A	8.00	D	N/A	CS	NSS	BP6	N/A	34S_4p1d7Xc_8	7/18 A1	TDP-WTP-006	20070309
N/A	N/A	0.01592	0.048	0.330	18.6	P	N/A	N/A	N/A	N/A	7.90	8.10	N/A	N/A	N/A	N/A	N/A	N/A	N/A	N/A	N/A	AM	SOO	BP5/6	N/A	34S_4p1d7Xc_8	7/18 A1	TDP-WTP-006	20070314
27.0	0.998	0.01592	0.100	0.330	33.3	P	N/A	8.39	8.70	8.83	9.10	8.50	12.38	N/A	N/A	N/A	N/A	N/A	N/A	N/A	N/A	CS	NSS	BP6	N/A	34S_4p1d7Xc_2	7/18 A2	TDP-WTP-007	20070335
27.0	0.998	0.01592	0.100	0.330	35.6	P	N/A	7.69	7.94	8.05	8.25	8.50	11.38	N/A	vis dec	UCSvis	N/A	N/A	8.25	D	N/A	CS	NSS	BP6	N/A	34S_4p1d7Xc_2	7/18 A2	TDP-WTP-007	20070339
27.0	0.998	0.01592	0.100	0.330	43.5	P	N/A	6.45	6.55	6.59	6.70	8.50	8.63	N/A	N/A	N/A	N/A	N/A	N/A	N/A	N/A	AM	SOO	BP5	N/A	34S_4p1d7Xc_2	7/18 A2	TDP-WTP-007	20070344
27.0	0.998	0.01592	0.100	0.330	40.8	P	N/A	6.99	7.11	7.17	7.25	8.50	9.63	N/A	N/A	N/A	N/A	N/A	N/A	N/A	N/A	AM	SOO	BP5	N/A	34S_4p1d7Xc_2	7/18 A2	TDP-WTP-007	20070347
27.0	0.998	0.01592	0.100	0.330	39.4	P	N/A	7.36	7.49	7.55	7.60	8.50	10.38	N/A	N/A	N/A	N/A	N/A	N/A	N/A	N/A	AM	SOO	BP5/6	N/A	34S_4p1d7Xc_2	7/18 A2	TDP-WTP-007	20070352
27.0	0.998	0.01592	0.100	0.330	37.7	P	N/A	7.57	7.80	7.89	8.10	8.50	11.00	N/A	N/A	N/A	N/A	N/A	N/A	N/A	N/A	AM	SOO	BP5	N/A	34S_4p1d7Xc_2	7/18 A2	TDP-WTP-007	20070357
27.0	0.998	0.01592	0.100	0.330	36.1	P	N/A	7.93	8.20	8.31	8.50	8.50	11.63	8.50	vis	UCSvis	N/A	N/A	N/A	I	N/A	CS	NSS	BP6	N/A	34S_4p1d7Xc_2	7/18 A2	TDP-WTP-007	20070362
27.0	0.998	0.01592	0.100	0.330	30.3	P	N/A	9.13	9.48	9.64	10.00	8.50	14.38	N/A	N/A	N/A	N/A	N/A	N/A	N/A	N/A	N/A	N/A	N/A	N/A	34S_4p1d7Xc_2	7/18 A2	TDP-WTP-007	20070369
27.0	0.998	0.01592	0.100	0.330	22.7	P	N/A	11.19	11.79	12.06	12.60	8.50	22.13	N/A	N/A	N/A	N/A	N/A	N/A	N/A	N/A	N/A	N/A	N/A	N/A	34S_4p1d7Xc_2	7/18 A2	TDP-WTP-007	20070372
23.0	0.999	0.00487	0.048	0.330	24.3	P	N/A	5.60	5.77	5.84	6.00	6.20	11.88	N/A	N/A	N/A	N/A	N/A	N/A	N/A	N/A	AM	N/A	BP5	N/A	34S_4p1d7Yc_8	7/19 A1	TDP-WTP-008	20070384
23.0	0.999	0.00487	0.048	0.330	24.3	P	N/A	5.80	5.98	6.06	6.20	6.20	12.63	6.20	vis	UCSvis	N/A	N/A	N/A	I	N/A	CS	N/A	BP6	N/A	34S_4p1d7Yc_8	7/19 A1	TDP-WTP-008	20070387
23.0	0.999	0.00487	0.048	0.330	21.1	P	N/A	6.45	6.68	6.78	7.00	6.20	13.38	N/A	N/A	N/A	N/A	N/A	N/A	N/A	N/A	BC	N/A	BP6	N/A	34S_4p1d7Yc_8	7/19 A1	TDP-WTP-008	20070392
23.0	0.999	0.00487	0.048	0.330	18.3	P	N/A	7.23	7.54	7.68	8.00	6.20	16.63	N/A	N/A	N/A	N/A	N/A	N/A	N/A	N/A	BC	N/A	N/A	N/A	34S_4p1d7Yc_8	7/19 A1	TDP-WTP-008	20070395
23.0	0.999	0.00487	0.048	0.330	16.1	P	N/A	7.56	8.14	8.40	9.00	6.20	22.79	N/A	N/A	N/A	N/A	N/A	N/A	N/A	N/A	BC	N/A	N/A	N/A	34S_4p1d7Yc_8	7/19 A1	TDP-WTP-008	20070398
23.0	0.999	0.00487	0.048	0.330	17.1	P	N/A	7.38	7.84	8.05	8.50	6.20	20.63	N/A	N/A	N/A	N/A	N/A	N/A	N/A	N/A	BC	N/A	BP6	N/A	34S_4p1d7Yc_8	7/19 A1	TDP-WTP-008	20070401
23.0	0.999	0.00487	0.048	0.330	19.2	P	N/A	6.80	7.08	7.21	7.50	6.20	15.13	N/A	N/A	N/A	N/A	N/A	N/A	N/A	N/A	BC	N/A	BP6	N/A	34S_4p1d7Yc_8	7/19 A1	TDP-WTP-008	20070403
23.0	0.999	0.00487	0.048	0.330	22.7	P	N/A	5.77	5.95	6.03	6.20	6.20	11.63	N/A	vis dec	UCSvis	N/A	N/A	6.20	D	N/A	CS	N/A	BP5	N/A	34S_4p1d7Yc_8	7/19 A1	TDP-WTP-008	20070411
24.1	0.998	0.00487	undefined	1.000	infinite	S	7.09	N/A	N/A	N/A	7.00	N/A	38.63	N/A	N/A	N/A	N/A	N/A	N/A	N/A	N/A	N/A	N/A	N/A	N/A	34S_4p1d7Ya	7/19 A2	TDP-WTP-008	20070417
25.0	0.998	0.00487	0.100	0.330	N/A	P	N/A	5.48	5.55	5.58	5.70	5.70	9.63	5.70	vis	UCSvis	N/A	N/A	N/A	I	N/A	CS	N/A	N/A	N/A	34S_4p1d7Yc_2	7/19 A3	TDP-WTP-008	20070423
25.0	0.998	0.00487	0.100	0.330	48.8	P	N/A	5.95	6.04	6.08	6.10	5.70	12.63	N/A	N/A	N/A	N/A	N/A	N/A	N/A	N/A	BC	N/A	N/A	N/A	34S_4p1d7Yc_2	7/19 A3	TDP-WTP-008	20070426
25.0	0.998	0.00487	0.100	0.330	35.8	P	N/A	7.67	7.84	7.92	8.00	5.70	23.63	N/A	N/A	N/A	N/A	N/A	N/A	N/A	N/A	BC	N/A	N/A	N/A	34S_4p1d7Yc_2	7/19 A3	TDP-WTP-008	20070428
25.0	0.998	0.00487	0.100	0.330	42.2	P	N/A	6.54	6.66	6.71	6.80	5.70	16.63	N/A	N/A	N/A	N/A	N/A	N/A	N/A	N/A	BC	N/A	N/A	N/A	34S_4p1d7Yc_2	7/19 A3	TDP-WTP-008	20070432
25.0	0.998	0.00487	0.100	0.330	51.0	P	N/A	5.38	5.46	5.49	5.60	5.70	10.13	N/A	N/A	N/A	N/A	N/A	N/A	N/A	N/A	AM	N/A	N/A	N/A	34S_4p1d7Yc_2	7/19 A3	TDP-WTP-008	20070434
25.0	0.998	0.00487	0.048	0.180	41.7	P	N/A	5.83	6.01	6.09	6.30	6.40	11.88	N/A	N/A	N/A	N/A	N/A	N/A	N/A	N/A	AM	N/A	N/A	N/A	34S_4p1d7Yd_8	7/19 A4	TDP-WTP-008	20070438
25.0	0.998	0.00487	0.048	0.180	40.0	P	N/A	5.96	6.15	6.23	6.40	6.40	13.63	6.40	vis	UCSvis	N/A	N/A	N/A	I	N/A	CS	N/A	N/A	N/A	34S_4p1d7Yd_8	7/19 A4	TDP-WTP-008	20070441
25.0	0.998	0.00487	0.048	0.180	32.8	P	N/A	7.25	7.56	7.71	8.00	6.40	16.63	N/A	N/A	N/A	N/A	N/A	N/A	N/A	N/A	BC	N/A	N/A	N/A	34S_4p1d7Yd_8	7/19 A4	TDP-WTP-008	20070445

Table B.7. Data from July 2007 Tests in Mid-Scale Vessel with Spherical Head A.3

Row Number	Test	Case ID	Tank Diameter	Head Shape	Dish Height	Dish Volume	Tank Fill Height	Return Line Height	Nozzle Inner Diameter	Nozzle Stand-off Distance	Pulse Tube Configuration	Installed Nozzles	Outer Nozzles Operated	Inner Nozzles Operated	Pulse Tube Outer Diameter	Outer PJM Radius	Inner PJM Radius	"FIO" Outer PJM Impingement Angle	"FIO" Inner PJM Impingement Angle	Ratio Outer PJM to Tank Radius	Ratio Inner PJM to Tank Radius	Simulant	Solids Density	Particle Diameter d5	Particle Diameter d50	Particle Diameter d95	Void Fraction
text	text	text	in.	text	in.	in. ^{3}	in.	in.	in.	in.	text	number	number	number	in.	in.	in.	deg	deg	nondim	nondim	text	g/cm^3	m	m	m	fraction
MSS	M/DDX	ID	D	HS	H_{dish}	V_{dish}	H	Rtn	d	sod	PT	N	N_O	N_I	PT_{od}	R_O	R_I	θ_O	θ_I	R_O/R	R_I/R	sxdx	ρ_s	d_5	d_{50}	d_{95}	vf
20070449M	7/19 A4	34S_4p1d7Yd_8	33 7/8	S	9	4437.4	67 5/8	62	0.297	0.446	HLP-22	12	8	4	1.9	10.5	5.7	30.8	16.1	0.62	0.33	p1d7	2.45	0.0001213	0.0001780	0.0002606	0.4277
20070453	7/19 A4	34S_4p1d7Yd_8	33 7/8	S	9	4437.4	67 5/8	62	0.297	0.446	HLP-22	12	8	4	1.9	10.5	5.7	30.8	16.1	0.62	0.33	p1d7	2.45	0.0001213	0.0001780	0.0002606	0.4277
20070471	7/20 A1	34S_4p1d7Yb_8	33 7/8	S	9	4437.4	67 5/8	62	0.297	0.446	HLP-22	12	8	4	1.9	10.5	5.7	30.8	16.1	0.62	0.33	p1d7	2.45	0.0001213	0.0001780	0.0002606	0.4277
20070478	7/20 A1	34S_4p1d7Yb_8	33 7/8	S	9	4437.4	67 5/8	62	0.297	0.446	HLP-22	12	8	4	1.9	10.5	5.7	30.8	16.1	0.62	0.33	p1d7	2.45	0.0001213	0.0001780	0.0002606	0.4277
20070482	7/20 A1	34S_4p1d7Yb_8	33 7/8	S	9	4437.4	67 5/8	62	0.297	0.446	HLP-22	12	8	4	1.9	10.5	5.7	30.8	16.1	0.62	0.33	p1d7	2.45	0.0001213	0.0001780	0.0002606	0.4277
20070484	7/20 A1	34S_4p1d7Yb_8	33 7/8	S	9	4437.4	67 5/8	62	0.297	0.446	HLP-22	12	8	4	1.9	10.5	5.7	30.8	16.1	0.62	0.33	p1d7	2.45	0.0001213	0.0001780	0.0002606	0.4277
20070489M	7/20 A1	34S_4p1d7Yb_8	33 7/8	S	9	4437.4	67 5/8	62	0.297	0.446	HLP-22	12	8	4	1.9	10.5	5.7	30.8	16.1	0.62	0.33	p1d7	2.45	0.0001213	0.0001780	0.0002606	0.4277
20070495M	7/20 A1	34S_4p1d7Yb_8	33 7/8	S	9	4437.4	67 5/8	62	0.297	0.446	HLP-22	12	8	4	1.9	10.5	5.7	30.8	16.1	0.62	0.33	p1d7	2.45	0.0001213	0.0001780	0.0002606	0.4277
20070497M	7/20 A1	34S_4p1d7Yb_8	33 7/8	S	9	4437.4	67 5/8	62	0.297	0.446	HLP-22	12	8	4	1.9	10.5	5.7	30.8	16.1	0.62	0.33	p1d7	2.45	0.0001213	0.0001780	0.0002606	0.4277
20070502M	7/20 A1	34S_4p1d7Yb_8	33 7/8	S	9	4437.4	67 5/8	62	0.297	0.446	HLP-22	12	8	4	1.9	10.5	5.7	30.8	16.1	0.62	0.33	p1d7	2.45	0.0001213	0.0001780	0.0002606	0.4277
20070508M	7/20 A1	34S_4p1d7Yb_8	33 7/8	S	9	4437.4	67 5/8	62	0.297	0.446	HLP-22	12	8	4	1.9	10.5	5.7	30.8	16.1	0.62	0.33	p1d7	2.45	0.0001213	0.0001780	0.0002606	0.4277
20070512M	7/20 A1	34S_4p1d7Yb_8	33 7/8	S	9	4437.4	67 5/8	62	0.297	0.446	HLP-22	12	8	4	1.9	10.5	5.7	30.8	16.1	0.62	0.33	p1d7	2.45	0.0001213	0.0001780	0.0002606	0.4277
20070519M	7/20 A1	34S_4p1d7Yb_8	33 7/8	S	9	4437.4	67 5/8	62	0.297	0.446	HLP-22	12	8	4	1.9	10.5	5.7	30.8	16.1	0.62	0.33	p1d7	2.45	0.0001213	0.0001780	0.0002606	0.4277
20070524M	7/20 A1	34S_4p1d7Yb_8	33 7/8	S	9	4437.4	67 5/8	62	0.297	0.446	HLP-22	12	8	4	1.9	10.5	5.7	30.8	16.1	0.62	0.33	p1d7	2.45	0.0001213	0.0001780	0.0002606	0.4277
20070535	7/20 A2	34S_4p1d7Yc_3	33 7/8	S	9	4437.4	67 5/8	62	0.297	0.446	HLP-22	12	8	4	1.9	10.5	5.7	30.8	16.1	0.62	0.33	p1d7	2.45	0.0001213	0.0001780	0.0002606	0.4277
20070539	7/20 A2	34S_4p1d7Yc_3	33 7/8	S	9	4437.4	67 5/8	62	0.297	0.446	HLP-22	12	8	4	1.9	10.5	5.7	30.8	16.1	0.62	0.33	p1d7	2.45	0.0001213	0.0001780	0.0002606	0.4277
20070547M	7/20 A2	34S_4p1d7Yc_3	33 7/8	S	9	4437.4	67 5/8	62	0.297	0.446	HLP-22	12	8	4	1.9	10.5	5.7	30.8	16.1	0.62	0.33	p1d7	2.45	0.0001213	0.0001780	0.0002606	0.4277
20070552M	7/20 A2	34S_4p1d7Yc_3	33 7/8	S	9	4437.4	67 5/8	62	0.297	0.446	HLP-22	12	8	4	1.9	10.5	5.7	30.8	16.1	0.62	0.33	p1d7	2.45	0.0001213	0.0001780	0.0002606	0.4277
20070557M	7/20 A2	34S_4p1d7Yc_3	33 7/8	S	9	4437.4	67 5/8	62	0.297	0.446	HLP-22	12	8	4	1.9	10.5	5.7	30.8	16.1	0.62	0.33	p1d7	2.45	0.0001213	0.0001780	0.0002606	0.4277
20070562M	7/20 A2	34S_4p1d7Yc_3	33 7/8	S	9	4437.4	67 5/8	62	0.297	0.446	HLP-22	12	8	4	1.9	10.5	5.7	30.8	16.1	0.62	0.33	p1d7	2.45	0.0001213	0.0001780	0.0002606	0.4277
20070571M	7/20 A2	34S_4p1d7Yc_3	33 7/8	S	9	4437.4	67 5/8	62	0.297	0.446	HLP-22	12	8	4	1.9	10.5	5.7	30.8	16.1	0.62	0.33	p1d7	2.45	0.0001213	0.0001780	0.0002606	0.4277
20070584	7/21 A1	34S_6p1d7Ya	33 7/8	S	9	4437.4	68 3/8	62	0.446	0.669	HLP-22	12	8	4	1.9	10.5	5.7	30.8	16.1	0.62	0.33	p1d7	2.45	0.0001213	0.0001780	0.0002606	0.4277
20070587	7/21 A1	34S_6p1d7Ya	33 7/8	S	9	4437.4	68 3/8	62	0.446	0.669	HLP-22	12	8	4	1.9	10.5	5.7	30.8	16.1	0.62	0.33	p1d7	2.45	0.0001213	0.0001780	0.0002606	0.4277
20070591	7/21 A1	34S_6p1d7Ya	33 7/8	S	9	4437.4	68 3/8	62	0.446	0.669	HLP-22	12	8	4	1.9	10.5	5.7	30.8	16.1	0.62	0.33	p1d7	2.45	0.0001213	0.0001780	0.0002606	0.4277
20070593	7/21 A1	34S_6p1d7Ya	33 7/8	S	9	4437.4	68 3/8	62	0.446	0.669	HLP-22	12	8	4	1.9	10.5	5.7	30.8	16.1	0.62	0.33	p1d7	2.45	0.0001213	0.0001780	0.0002606	0.4277
20070598	7/21 A1	34S_6p1d7Ya	33 7/8	S	9	4437.4	68 3/8	62	0.446	0.669	HLP-22	12	8	4	1.9	10.5	5.7	30.8	16.1	0.62	0.33	p1d7	2.45	0.0001213	0.0001780	0.0002606	0.4277
20070601	7/21 A1	34S_6p1d7Ya	33 7/8	S	9	4437.4	68 3/8	62	0.446	0.669	HLP-22	12	8	4	1.9	10.5	5.7	30.8	16.1	0.62	0.33	p1d7	2.45	0.0001213	0.0001780	0.0002606	0.4277
20070605	7/21 A1	34S_6p1d7Ya	33 7/8	S	9	4437.4	68 3/8	62	0.446	0.669	HLP-22	12	8	4	1.9	10.5	5.7	30.8	16.1	0.62	0.33	p1d7	2.45	0.0001213	0.0001780	0.0002606	0.4277
20070609	7/21 A2	34S_6p1d7Yc_8	33 7/8	S	9	4437.4	68 3/8	62	0.446	0.669	HLP-22	12	8	4	1.9	10.5	5.7	30.8	16.1	0.62	0.33	p1d7	2.45	0.0001213	0.0001780	0.0002606	0.4277
20070613	7/21 A2	34S_6p1d7Yc_8	33 7/8	S	9	4437.4	68 3/8	62	0.446	0.669	HLP-22	12	8	4	1.9	10.5	5.7	30.8	16.1	0.62	0.33	p1d7	2.45	0.0001213	0.0001780	0.0002606	0.4277
20070615	7/21 A2	34S_6p1d7Yc_8	33 7/8	S	9	4437.4	68 3/8	62	0.446	0.669	HLP-22	12	8	4	1.9	10.5	5.7	30.8	16.1	0.62	0.33	p1d7	2.45	0.0001213	0.0001780	0.0002606	0.4277
20070617	7/21 A2	34S_6p1d7Yc_8	33 7/8	S	9	4437.4	68 3/8	62	0.446	0.669	HLP-22	12	8	4	1.9	10.5	5.7	30.8	16.1	0.62	0.33	p1d7	2.45	0.0001213	0.0001780	0.0002606	0.4277
20070620	7/21 A2	34S_6p1d7Yc_8	33 7/8	S	9	4437.4	68 3/8	62	0.446	0.669	HLP-22	12	8	4	1.9	10.5	5.7	30.8	16.1	0.62	0.33	p1d7	2.45	0.0001213	0.0001780	0.0002606	0.4277
20070625	7/21 A2	34S_6p1d7Yc_8	33 7/8	S	9	4437.4	68 3/8	62	0.446	0.669	HLP-22	12	8	4	1.9	10.5	5.7	30.8	16.1	0.62	0.33	p1d7	2.45	0.0001213	0.0001780	0.0002606	0.4277
20070627M	7/21 A2	34S_6p1d7Yc_8	33 7/8	S	9	4437.4	68 3/8	62	0.446	0.669	HLP-22	12	8	4	1.9	10.5	5.7	30.8	16.1	0.62	0.33	p1d7	2.45	0.0001213	0.0001780	0.0002606	0.4277
20070633M	7/21 A2	34S_6p1d7Yc_8	33 7/8	S	9	4437.4	68 3/8	62	0.446	0.669	HLP-22	12	8	4	1.9	10.5	5.7	30.8	16.1	0.62	0.33	p1d7	2.45	0.0001213	0.0001780	0.0002606	0.4277
20070636M	7/21 A2	34S_6p1d7Yc_8	33 7/8	S	9	4437.4	68 3/8	62	0.446	0.669	HLP-22	12	8	4	1.9	10.5	5.7	30.8	16.1	0.62	0.33	p1d7	2.45	0.0001213	0.0001780	0.0002606	0.4277
20070639M	7/21 A2	34S_6p1d7Yc_8	33 7/8	S	9	4437.4	68 3/8	62	0.446	0.669	HLP-22	12	8	4	1.9	10.5	5.7	30.8	16.1	0.62	0.33	p1d7	2.45	0.0001213	0.0001780	0.0002606	0.4277
20070641M	7/21 A2	34S_6p1d7Yc_8	33 7/8	S	9	4437.4	68 3/8	62	0.446	0.669	HLP-22	12	8	4	1.9	10.5	5.7	30.8	16.1	0.62	0.33	p1d7	2.45	0.0001213	0.0001780	0.0002606	0.4277
20070645M	7/21 A2	34S_6p1d7Yc_8	33 7/8	S	9	4437.4	68 3/8	62	0.446	0.669	HLP-22	12	8	4	1.9	10.5	5.7	30.8	16.1	0.62	0.33	p1d7	2.45	0.0001213	0.0001780	0.0002606	0.4277
20070648	7/21 A2	34S_6p1d7Yc_8	33 7/8	S	9	4437.4	68 3/8	62	0.446	0.669	HLP-22	12	8	4	1.9	10.5	5.7	30.8	16.1	0.62	0.33	p1d7	2.45	0.0001213	0.0001780	0.0002606	0.4277

Table B.7. Data from July 2007 Tests in Mid-Scale Vessel with Spherical Head B.3

Tank Water Temperature	Water Density	Solids Fraction	Pulse Volume Fraction	Duty Cycle	Cycle Time	Pulsed or Steady Jet	Us Steady Jet	U1 Pulsing Jet	U2 URMS	U3 URM3	Discharge Velocity	Critical Suspension Velocity	Average Peak Cloud Height	UCS Condition	UCS Method	UCS Flag	UCS Center Flag	UCS udv Flag	UCS based on Decreasing Velocity	Sweep Increase / Decrease	UDV Height Bed	Particle Motion	Solids Level	Outer Bottom Pattern	Inner Bottom Pattern	Case ID	Test	TDP	Row Number
C	g/cm³	fraction	fraction	fraction	s	text	m/s	m/s	m/s	m/s	m/s	m/s	in.	m/s	text	text	text	text	m/s	text	mm	text	text	text	text	text	text	text	text
T	ρ_l	ϕ_s	ϕ_p	DC	t_C	Jet	U_S	U1	U2	U3	U	U_{CS}	H_C	U_{CSR}	U_{CSM}	U_{CS}vis	U_{CS}cen	U_{CS}udv	U_{CS}_D	S_W	H_{bed}	PM	Sol	SP_O	SP_I	ID	M/DDX	TDP	MSS
25.0	0.998	0.00487	0.048	0.180	40.8	P	N/A	5.97	6.16	6.24	6.40	6.40	13.13	N/A	vis dec	UCSvis	N/A	N/A	6.40	D	N/A	CS	N/A	N/A	N/A	34S_4p1d7Yd_8	7/19 A4	TDP-WTP-008	20070449
25.0	0.998	0.00487	0.048	0.180	43.5	P	N/A	5.62	5.79	5.87	6.00	6.40	10.13	N/A	N/A	N/A	N/A	N/A	N/A	N/A	N/A	AM	N/A	N/A	N/A	34S_4p1d7Yd_8	7/19 A4	TDP-WTP-008	20070453
25.0	0.998	0.00487	0.048	0.500	19.0	P	N/A	4.79	4.89	4.94	5.00	6.00	11.13	N/A	N/A	N/A	N/A	N/A	N/A	N/A	N/A	AM	N/A	N/A	N/A	34S_4p1d7Yb_8	7/20 A1	TDP-WTP-010	20070471
25.0	0.998	0.00487	0.048	0.500	17.4	P	N/A	5.31	5.45	5.51	5.50	6.00	12.46	N/A	N/A	N/A	N/A	N/A	N/A	N/A	N/A	AM+	N/A	N/A	N/A	34S_4p1d7Yb_8	7/20 A1	TDP-WTP-010	20070478
25.0	0.998	0.00487	0.048	0.500	16.7	P	N/A	5.53	5.68	5.75	5.80	6.00	12.29	N/A	N/A	N/A	N/A	N/A	N/A	N/A	N/A	AM	N/A	N/A	N/A	34S_4p1d7Yb_8	7/20 A1	TDP-WTP-010	20070482
25.0	0.998	0.00487	0.048	0.500	16.7	P	N/A	5.53	5.68	5.75	5.80	6.00	12.29	N/A	N/A	N/A	N/A	N/A	N/A	N/A	N/A	CS-	N/A	N/A	N/A	34S_4p1d7Yb_8	7/20 A1	TDP-WTP-010	20070484
25.0	0.998	0.00487	0.048	0.500	15.9	P	N/A	5.66	5.82	5.90	6.00	6.00	12.63	6.00	vis	UCSvis	N/A	N/A	N/A	I	N/A	CS	N/A	N/A	N/A	34S_4p1d7Yb_8	7/20 A1	TDP-WTP-010	20070489
25.0	0.998	0.00487	0.048	0.500	14.7	P	N/A	6.07	6.27	6.36	6.50	6.00	13.79	N/A	N/A	N/A	N/A	N/A	N/A	N/A	N/A	BC	N/A	N/A	N/A	34S_4p1d7Yb_8	7/20 A1	TDP-WTP-010	20070495
25.0	0.998	0.00487	0.048	0.500	14.7	P	N/A	6.07	6.27	6.36	6.50	6.00	13.79	N/A	N/A	N/A	N/A	N/A	N/A	N/A	N/A	CS	N/A	N/A	N/A	34S_4p1d7Yb_8	7/20 A1	TDP-WTP-010	20070497
25.0	0.998	0.00487	0.048	0.500	13.7	P	N/A	6.52	6.75	6.85	7.00	6.00	14.38	N/A	N/A	N/A	N/A	N/A	N/A	N/A	N/A	BC	N/A	N/A	N/A	34S_4p1d7Yb_8	7/20 A1	TDP-WTP-010	20070502
25.0	0.998	0.00487	0.048	0.500	12.1	P	N/A	7.32	7.63	7.77	8.00	6.00	18.88	N/A	N/A	N/A	N/A	N/A	N/A	N/A	N/A	BC	N/A	N/A	N/A	34S_4p1d7Yb_8	7/20 A1	TDP-WTP-010	20070508
25.0	0.998	0.00487	0.048	0.500	11.2	P	N/A	8.11	8.51	8.70	9.00	6.00	30.38	N/A	N/A	N/A	N/A	N/A	N/A	N/A	N/A	BC	N/A	N/A	N/A	34S_4p1d7Yb_8	7/20 A1	TDP-WTP-010	20070512
25.0	0.998	0.00487	0.048	0.500	14.7	P	N/A	6.11	6.30	6.39	6.50	6.00	12.63	N/A	N/A	N/A	N/A	N/A	N/A	N/A	N/A	N/A	N/A	N/A	N/A	34S_4p1d7Yb_8	7/20 A1	TDP-WTP-010	20070519
25.0	0.998	0.00487	0.048	0.500	15.9	P	N/A	5.70	5.87	5.94	6.00	6.00	12.13	N/A	vis dec	UCSvis	N/A	N/A	6.00	D	N/A	N/A	N/A	N/A	N/A	34S_4p1d7Yb_8	7/20 A1	TDP-WTP-010	20070524
25.0	0.998	0.00487	0.025	0.330	15.2	P	N/A	4.59	4.78	4.87	5.00	6.90	11.63	N/A	N/A	N/A	N/A	N/A	N/A	N/A	N/A	AM-	N/A	N/A	N/A	34S_4p1d7Yc_3	7/20 A2	TDP-WTP-010	20070535
25.0	0.998	0.00487	0.025	0.330	13.3	P	N/A	5.41	5.68	5.81	6.00	6.90	12.88	N/A	N/A	N/A	N/A	N/A	N/A	N/A	N/A	AM	N/A	N/A	N/A	34S_4p1d7Yc_3	7/20 A2	TDP-WTP-010	20070539
25.0	0.998	0.00487	0.025	0.330	12.0	P	N/A	6.10	6.47	6.65	6.90	6.90	13.38	6.90	vis	UCSvis	N/A	N/A	N/A	I	N/A	CS	N/A	N/A	N/A	34S_4p1d7Yc_3	7/20 A2	TDP-WTP-010	20070547
25.0	0.998	0.00487	0.025	0.330	10.3	P	N/A	6.83	7.35	7.59	8.00	6.90	12.63	N/A	N/A	N/A	N/A	N/A	N/A	N/A	N/A	N/A	N/A	N/A	N/A	34S_4p1d7Yc_3	7/20 A2	TDP-WTP-010	20070552
25.0	0.998	0.00487	0.025	0.330	9.5	P	N/A	7.48	8.13	8.45	9.00	6.90	14.63	N/A	N/A	N/A	N/A	N/A	N/A	N/A	N/A	N/A	N/A	N/A	N/A	34S_4p1d7Yc_3	7/20 A2	TDP-WTP-010	20070557
25.0	0.998	0.00487	0.025	0.330	8.4	P	N/A	7.75	8.56	8.96	10.00	6.90	26.13	N/A	N/A	N/A	N/A	N/A	N/A	N/A	N/A	N/A	N/A	N/A	N/A	34S_4p1d7Yc_3	7/20 A2	TDP-WTP-010	20070562
25.0	0.998	0.00487	0.025	0.330	12.0	P	N/A	6.10	6.46	6.63	6.90	6.90	12.63	N/A	vis dec	UCSvis	N/A	N/A	6.90	D	N/A	CS	N/A	N/A	N/A	34S_4p1d7Yc_3	7/20 A2	TDP-WTP-010	20070571
N/A	N/A	0.00487	undefined	1.000	infinite	S	N/A	N/A	N/A	N/A	2.70	3.30	N/A	N/A	N/A	N/A	N/A	N/A	N/A	N/A	N/A	SS	N/A	N/A	N/A	34S_6p1d7Ya	7/21 A1	TDP-WTP-011	20070584
25.2	0.998	0.00487	undefined	1.000	infinite	S	3.02	N/A	N/A	N/A	3.00	3.30	9.13	N/A	N/A	N/A	N/A	N/A	N/A	N/A	N/A	AM	N/A	N/A	N/A	34S_6p1d7Ya	7/21 A1	TDP-WTP-011	20070587
25.2	0.998	0.00487	undefined	1.000	infinite	S	3.20	N/A	N/A	N/A	3.20	3.30	10.13	N/A	N/A	N/A	N/A	N/A	N/A	N/A	N/A	AM	N/A	N/A	N/A	34S_6p1d7Ya	7/21 A1	TDP-WTP-011	20070591
25.2	0.998	0.00487	undefined	1.000	infinite	S	3.32	N/A	N/A	N/A	3.30	3.30	10.38	3.30	vis	UCSvis	N/A	N/A	N/A	I	N/A	CS	N/A	N/A	N/A	34S_6p1d7Ya	7/21 A1	TDP-WTP-011	20070593
25.2	0.998	0.00487	undefined	1.000	infinite	S	3.99	N/A	N/A	N/A	4.00	3.30	28.13	N/A	N/A	N/A	N/A	N/A	N/A	N/A	N/A	BC	N/A	N/A	N/A	34S_6p1d7Ya	7/21 A1	TDP-WTP-011	20070598
25.3	0.998	0.00487	undefined	1.000	infinite	S	3.51	N/A	N/A	N/A	3.50	3.30	11.63	N/A	N/A	N/A	N/A	N/A	N/A	N/A	N/A	BC	N/A	N/A	N/A	34S_6p1d7Ya	7/21 A1	TDP-WTP-011	20070601
25.3	0.998	0.00487	undefined	1.000	infinite	S	3.71	N/A	N/A	N/A	3.70	3.30	16.63	N/A	N/A	N/A	N/A	N/A	N/A	N/A	N/A	BC	N/A	N/A	N/A	34S_6p1d7Ya	7/21 A1	TDP-WTP-011	20070605
25.0	0.998	0.00487	0.048	0.330	22.7	P	N/A	2.44	2.52	2.56	2.70	4.00	9.88	N/A	N/A	N/A	N/A	N/A	N/A	N/A	N/A	SS	N/A	N/A	N/A	34S_6p1d7Yc_8	7/21 A2	TDP-WTP-011	20070609
25.0	0.998	0.00487	0.048	0.330	20.8	P	N/A	2.68	2.78	2.82	3.00	4.00	11.88	N/A	N/A	N/A	N/A	N/A	N/A	N/A	N/A	SS	N/A	N/A	N/A	34S_6p1d7Yc_8	7/21 A2	TDP-WTP-011	20070613
25.0	0.998	0.00487	0.048	0.330	18.9	P	N/A	2.92	3.05	3.11	3.35	4.00	12.13	N/A	N/A	N/A	N/A	N/A	N/A	N/A	N/A	AM	N/A	N/A	N/A	34S_6p1d7Yc_8	7/21 A2	TDP-WTP-011	20070615
25.0	0.998	0.00487	0.048	0.330	18.2	P	N/A	3.03	3.19	3.26	3.50	4.00	12.38	N/A	N/A	N/A	N/A	N/A	N/A	N/A	N/A	AM	N/A	N/A	N/A	34S_6p1d7Yc_8	7/21 A2	TDP-WTP-011	20070617
25.0	0.998	0.00487	0.048	0.330	17.7	P	N/A	3.18	3.34	3.41	3.70	4.00	13.38	N/A	N/A	N/A	N/A	N/A	N/A	N/A	N/A	AM++	N/A	N/A	N/A	34S_6p1d7Yc_8	7/21 A2	TDP-WTP-011	20070620
25.0	0.998	0.00487	0.048	0.330	16.9	P	N/A	3.35	3.52	3.60	3.90	4.00	13.63	N/A	N/A	N/A	N/A	N/A	N/A	N/A	N/A	AM	N/A	N/A	N/A	34S_6p1d7Yc_8	7/21 A2	TDP-WTP-011	20070625
25.0	0.998	0.00487	0.048	0.330	16.5	P	N/A	3.42	3.62	3.71	4.00	4.00	13.63	4.00	vis	UCSvis	N/A	N/A	N/A	I	N/A	CS	N/A	N/A	N/A	34S_6p1d7Yc_8	7/21 A2	TDP-WTP-011	20070627
25.0	0.998	0.00487	0.048	0.330	14.6	P	N/A	3.69	3.97	4.09	4.50	4.00	14.38	N/A	N/A	N/A	N/A	N/A	N/A	N/A	N/A	BC	N/A	N/A	N/A	34S_6p1d7Yc_8	7/21 A2	TDP-WTP-011	20070633
25.0	0.998	0.00487	0.048	0.330	13.2	P	N/A	3.81	4.23	4.41	5.00	4.00	14.63	N/A	N/A	N/A	N/A	N/A	N/A	N/A	N/A	BC	N/A	N/A	N/A	34S_6p1d7Yc_8	7/21 A2	TDP-WTP-011	20070636
25.0	0.998	0.00487	0.048	0.330	12.3	P	N/A	4.14	4.63	4.85	5.50	4.00	15.38	N/A	N/A	N/A	N/A	N/A	N/A	N/A	N/A	BC	N/A	N/A	N/A	34S_6p1d7Yc_8	7/21 A2	TDP-WTP-011	20070639
25.0	0.998	0.00487	0.048	0.330	11.3	P	N/A	4.42	5.00	5.26	6.00	4.00	24.13	N/A	N/A	N/A	N/A	N/A	N/A	N/A	N/A	BC	N/A	N/A	N/A	34S_6p1d7Yc_8	7/21 A2	TDP-WTP-011	20070641
25.0	0.998	0.00487	0.048	0.330	16.3	P	N/A	3.41	3.61	3.70	4.00	4.00	13.88	N/A	vis dec	UCSvis	N/A	N/A	4.00	D	N/A	CS	N/A	N/A	N/A	34S_6p1d7Yc_8	7/21 A2	TDP-WTP-011	20070645
25.0	0.998	0.00487	0.048	0.330	16.9	P	N/A	3.35	3.52	3.60	3.90	4.00	13.38	3.90	N/A	UCSvis	N/A	N/A	N/A	D	N/A	AM	N/A	N/A	N/A	34S_6p1d7Yc_8	7/21 A2	TDP-WTP-011	20070648

Table B.7. Data from July 2007 Tests in Mid-Scale Vessel with Spherical Head A.4

Row Number	Test	Case ID	Tank Diameter	Head Shape	Dish Height	Dish Volume	Tank Fill Height	Return Line Height	Nozzle Inner Diameter	Nozzle Stand-off Distance	Pulse Tube Configuration	Installed Nozzles	Outer Nozzles Operated	Inner Nozzles Operated	Pulse Tube Outer Diameter	Outer PJM Radius	Inner PJM Radius	"FIO" Outer PJM Impingement Angle	"FIO" Inner PJM Impingement Angle	Ratio Outer PJM to Tank Radius	Ratio Inner PJM to Tank Radius	Simulant	Solids Density	Particle Diameter d5	Particle Diameter d50	Particle Diameter d95	Void Fraction
text	text	text	in.	text	in.	in. ^{3}	in.	in.	in.	in.	text	number	number	number	in.	in.	in.	deg	deg	nondim	nondim	text	g/cm^3	m	m	m	fraction
MSS	M/DDX	ID	D	HS	H_{dish}	V_{dish}	H	Rtn	d	sod	PT	N	N_O	N_I	PT_{od}	R_O	R_I	θ_O	θ_I	R_O/R	R_I/R	sxdx	ρ_s	d_5	d_{50}	d_{95}	vf
20070655	7/23 A1	34S_6p1d7Yd_8	33 7/8	S	9	4437.4	67 7/8	62	0.446	0.669	HLP-22	12	8	4	1.9	10.5	5.7	30.8	16.1	0.62	0.33	p1d7	2.45	0.0001213	0.0001780	0.0002606	0.4277
20070658	7/23 A1	34S_6p1d7Yd_8	33 7/8	S	9	4437.4	67 7/8	62	0.446	0.669	HLP-22	12	8	4	1.9	10.5	5.7	30.8	16.1	0.62	0.33	p1d7	2.45	0.0001213	0.0001780	0.0002606	0.4277
20070662	7/23 A1	34S_6p1d7Yd_8	33 7/8	S	9	4437.4	67 7/8	62	0.446	0.669	HLP-22	12	8	4	1.9	10.5	5.7	30.8	16.1	0.62	0.33	p1d7	2.45	0.0001213	0.0001780	0.0002606	0.4277
20070668	7/23 A1	34S_6p1d7Yd_8	33 7/8	S	9	4437.4	67 7/8	62	0.446	0.669	HLP-22	12	8	4	1.9	10.5	5.7	30.8	16.1	0.62	0.33	p1d7	2.45	0.0001213	0.0001780	0.0002606	0.4277
20070672	7/23 A1	34S_6p1d7Yd_8	33 7/8	S	9	4437.4	67 7/8	62	0.446	0.669	HLP-22	12	8	4	1.9	10.5	5.7	30.8	16.1	0.62	0.33	p1d7	2.45	0.0001213	0.0001780	0.0002606	0.4277
20070677M	7/23 A1	34S_6p1d7Yd_8	33 7/8	S	9	4437.4	67 7/8	62	0.446	0.669	HLP-22	12	8	4	1.9	10.5	5.7	30.8	16.1	0.62	0.33	p1d7	2.45	0.0001213	0.0001780	0.0002606	0.4277
20070683	7/23 A1	34S_6p1d7Yd_8	33 7/8	S	9	4437.4	67 7/8	62	0.446	0.669	HLP-22	12	8	4	1.9	10.5	5.7	30.8	16.1	0.62	0.33	p1d7	2.45	0.0001213	0.0001780	0.0002606	0.4277
20070686M	7/23 A1	34S_6p1d7Yd_8	33 7/8	S	9	4437.4	67 7/8	62	0.446	0.669	HLP-22	12	8	4	1.9	10.5	5.7	30.8	16.1	0.62	0.33	p1d7	2.45	0.0001213	0.0001780	0.0002606	0.4277
20070690M	7/23 A1	34S_6p1d7Yd_8	33 7/8	S	9	4437.4	67 7/8	62	0.446	0.669	HLP-22	12	8	4	1.9	10.5	5.7	30.8	16.1	0.62	0.33	p1d7	2.45	0.0001213	0.0001780	0.0002606	0.4277
20070695M	7/23 A1	34S_6p1d7Yd_8	33 7/8	S	9	4437.4	67 7/8	62	0.446	0.669	HLP-22	12	8	4	1.9	10.5	5.7	30.8	16.1	0.62	0.33	p1d7	2.45	0.0001213	0.0001780	0.0002606	0.4277
20070699M	7/23 A1	34S_6p1d7Yd_8	33 7/8	S	9	4437.4	67 7/8	62	0.446	0.669	HLP-22	12	8	4	1.9	10.5	5.7	30.8	16.1	0.62	0.33	p1d7	2.45	0.0001213	0.0001780	0.0002606	0.4277
20070704M	7/23 A1	34S_6p1d7Yd_8	33 7/8	S	9	4437.4	67 7/8	62	0.446	0.669	HLP-22	12	8	4	1.9	10.5	5.7	30.8	16.1	0.62	0.33	p1d7	2.45	0.0001213	0.0001780	0.0002606	0.4277
20070709M	7/23 A1	34S_6p1d7Yd_8	33 7/8	S	9	4437.4	67 7/8	62	0.446	0.669	HLP-22	12	8	4	1.9	10.5	5.7	30.8	16.1	0.62	0.33	p1d7	2.45	0.0001213	0.0001780	0.0002606	0.4277
20070714	7/23 A1	34S_6p1d7Yd_8	33 7/8	S	9	4437.4	67 7/8	62	0.446	0.669	HLP-22	12	8	4	1.9	10.5	5.7	30.8	16.1	0.62	0.33	p1d7	2.45	0.0001213	0.0001780	0.0002606	0.4277
20070718	7/23 A1	34S_6p1d7Yd_8	33 7/8	S	9	4437.4	67 7/8	62	0.446	0.669	HLP-22	12	8	4	1.9	10.5	5.7	30.8	16.1	0.62	0.33	p1d7	2.45	0.0001213	0.0001780	0.0002606	0.4277
20070724	7/23 A1	34S_6p1d7Yd_8	33 7/8	S	9	4437.4	67 7/8	62	0.446	0.669	HLP-22	12	8	4	1.9	10.5	5.7	30.8	16.1	0.62	0.33	p1d7	2.45	0.0001213	0.0001780	0.0002606	0.4277
20070729	7/23 A1	34S_6p1d7Yd_8	33 7/8	S	9	4437.4	67 7/8	62	0.446	0.669	HLP-22	12	8	4	1.9	10.5	5.7	30.8	16.1	0.62	0.33	p1d7	2.45	0.0001213	0.0001780	0.0002606	0.4277
20070736	7/23 A1	34S_6p1d7Yd_8	33 7/8	S	9	4437.4	67 7/8	62	0.446	0.669	HLP-22	12	8	4	1.9	10.5	5.7	30.8	16.1	0.62	0.33	p1d7	2.45	0.0001213	0.0001780	0.0002606	0.4277
20070742	7/23 A1	34S_6p1d7Yd_8	33 7/8	S	9	4437.4	67 7/8	62	0.446	0.669	HLP-22	12	8	4	1.9	10.5	5.7	30.8	16.1	0.62	0.33	p1d7	2.45	0.0001213	0.0001780	0.0002606	0.4277
20070747	7/23 A1	34S_6p1d7Yd_8	33 7/8	S	9	4437.4	67 7/8	62	0.446	0.669	HLP-22	12	8	4	1.9	10.5	5.7	30.8	16.1	0.62	0.33	p1d7	2.45	0.0001213	0.0001780	0.0002606	0.4277
20070750M	7/23 A1	34S_6p1d7Yd_8	33 7/8	S	9	4437.4	67 7/8	62	0.446	0.669	HLP-22	12	8	4	1.9	10.5	5.7	30.8	16.1	0.62	0.33	p1d7	2.45	0.0001213	0.0001780	0.0002606	0.4277
20070760M	7/23 A2	34S_6p1d7Yd_2	33 7/8	S	9	4437.4	67 7/8	62	0.446	0.669	HLP-22	12	8	4	1.9	10.5	5.7	30.8	16.1	0.62	0.33	p1d7	2.45	0.0001213	0.0001780	0.0002606	0.4277
20070765	7/23 A2	34S_6p1d7Yd_2	33 7/8	S	9	4437.4	67 7/8	62	0.446	0.669	HLP-22	12	8	4	1.9	10.5	5.7	30.8	16.1	0.62	0.33	p1d7	2.45	0.0001213	0.0001780	0.0002606	0.4277
20070769	7/23 A2	34S_6p1d7Yd_2	33 7/8	S	9	4437.4	67 7/8	62	0.446	0.669	HLP-22	12	8	4	1.9	10.5	5.7	30.8	16.1	0.62	0.33	p1d7	2.45	0.0001213	0.0001780	0.0002606	0.4277
20070770M	7/23 A2	34S_6p1d7Yd_2	33 7/8	S	9	4437.4	67 7/8	62	0.446	0.669	HLP-22	12	8	4	1.9	10.5	5.7	30.8	16.1	0.62	0.33	p1d7	2.45	0.0001213	0.0001780	0.0002606	0.4277
20070774M	7/23 A2	34S_6p1d7Yd_2	33 7/8	S	9	4437.4	67 7/8	62	0.446	0.669	HLP-22	12	8	4	1.9	10.5	5.7	30.8	16.1	0.62	0.33	p1d7	2.45	0.0001213	0.0001780	0.0002606	0.4277
20070778M	7/23 A2	34S_6p1d7Yd_2	33 7/8	S	9	4437.4	67 7/8	62	0.446	0.669	HLP-22	12	8	4	1.9	10.5	5.7	30.8	16.1	0.62	0.33	p1d7	2.45	0.0001213	0.0001780	0.0002606	0.4277
20070782M	7/23 A2	34S_6p1d7Yd_2	33 7/8	S	9	4437.4	67 7/8	62	0.446	0.669	HLP-22	12	8	4	1.9	10.5	5.7	30.8	16.1	0.62	0.33	p1d7	2.45	0.0001213	0.0001780	0.0002606	0.4277
20070787M	7/23 A2	34S_6p1d7Yd_2	33 7/8	S	9	4437.4	67 7/8	62	0.446	0.669	HLP-22	12	8	4	1.9	10.5	5.7	30.8	16.1	0.62	0.33	p1d7	2.45	0.0001213	0.0001780	0.0002606	0.4277
20070791M	7/23 A2	34S_6p1d7Yd_2	33 7/8	S	9	4437.4	67 7/8	62	0.446	0.669	HLP-22	12	8	4	1.9	10.5	5.7	30.8	16.1	0.62	0.33	p1d7	2.45	0.0001213	0.0001780	0.0002606	0.4277
20070794	7/23 A2	34S_6p1d7Yd_2	33 7/8	S	9	4437.4	67 7/8	62	0.446	0.669	HLP-22	12	8	4	1.9	10.5	5.7	30.8	16.1	0.62	0.33	p1d7	2.45	0.0001213	0.0001780	0.0002606	0.4277
20070800	7/23 A3	34S_6p1d7Yc_2	33 7/8	S	9	4437.4	67 7/8	62	0.446	0.669	HLP-22	12	8	4	1.9	10.5	5.7	30.8	16.1	0.62	0.33	p1d7	2.45	0.0001213	0.0001780	0.0002606	0.4277
20070803	7/23 A3	34S_6p1d7Yc_2	33 7/8	S	9	4437.4	67 7/8	62	0.446	0.669	HLP-22	12	8	4	1.9	10.5	5.7	30.8	16.1	0.62	0.33	p1d7	2.45	0.0001213	0.0001780	0.0002606	0.4277
20070807M	7/23 A3	34S_6p1d7Yc_2	33 7/8	S	9	4437.4	67 7/8	62	0.446	0.669	HLP-22	12	8	4	1.9	10.5	5.7	30.8	16.1	0.62	0.33	p1d7	2.45	0.0001213	0.0001780	0.0002606	0.4277
20070812M	7/23 A3	34S_6p1d7Yc_2	33 7/8	S	9	4437.4	67 7/8	62	0.446	0.669	HLP-22	12	8	4	1.9	10.5	5.7	30.8	16.1	0.62	0.33	p1d7	2.45	0.0001213	0.0001780	0.0002606	0.4277
20070816M	7/23 A3	34S_6p1d7Yc_2	33 7/8	S	9	4437.4	67 7/8	62	0.446	0.669	HLP-22	12	8	4	1.9	10.5	5.7	30.8	16.1	0.62	0.33	p1d7	2.45	0.0001213	0.0001780	0.0002606	0.4277
20070820M	7/23 A3	34S_6p1d7Yc_2	33 7/8	S	9	4437.4	67 7/8	62	0.446	0.669	HLP-22	12	8	4	1.9	10.5	5.7	30.8	16.1	0.62	0.33	p1d7	2.45	0.0001213	0.0001780	0.0002606	0.4277
20070823M	7/23 A3	34S_6p1d7Yc_2	33 7/8	S	9	4437.4	67 7/8	62	0.446	0.669	HLP-22	12	8	4	1.9	10.5	5.7	30.8	16.1	0.62	0.33	p1d7	2.45	0.0001213	0.0001780	0.0002606	0.4277
20070827	7/23 A3	34S_6p1d7Yc_2	33 7/8	S	9	4437.4	67 7/8	62	0.446	0.669	HLP-22	12	8	4	1.9	10.5	5.7	30.8	16.1	0.62	0.33	p1d7	2.45	0.0001213	0.0001780	0.0002606	0.4277
20070833	7/23 A4	34S_6p1d7Yc_3	33 7/8	S	9	4437.4	67 7/8	62	0.446	0.669	HLP-22	12	8	4	1.9	10.5	5.7	30.8	16.1	0.62	0.33	p1d7	2.45	0.0001213	0.0001780	0.0002606	0.4277
20070837	7/23 A4	34S_6p1d7Yc_3	33 7/8	S	9	4437.4	67 7/8	62	0.446	0.669	HLP-22	12	8	4	1.9	10.5	5.7	30.8	16.1	0.62	0.33	p1d7	2.45	0.0001213	0.0001780	0.0002606	0.4277

Table B.7. Data from July 2007 Tests in Mid-Scale Vessel with Spherical Head B.4

Tank Water Temperature	Water Density	Solids Fraction	Pulse Volume Fraction	Duty Cycle	Cycle Time	Pulsed or Steady Jet	Us Steady Jet	U1 Pulsing Jet	U2 URMS	U3 URM3	Discharge Velocity	Critical Suspension Velocity	Average Peak Cloud Height	UCS Condition	UCS Method	UCS Flag	UCS Center Flag	UCS udv Flag	UCS based on Decreasing Velocity	Sweep Increase / Decrease	UDV Height Bed	Particle Motion	Solids Level	Outer Bottom Pattern	Inner Bottom Pattern	Case ID	Test	TDP	Row Number
C	g/cm^3	fraction	fraction	fraction	s	text	m/s	m/s	m/s	m/s	m/s	m/s	in.	m/s	text	text	text	text	m/s	text	mm	text	text	text	text	text	text	text	text
T	ρ_c	ϕ_S	ϕ_P	DC	t_C	Jet	U_S	U1	U2	U3	U	U_{CS}	H_C	U_{CSR}	U_{CSM}	U_{CS}vis	U_{CS}cen	U_{CS}udv	U_{CS}_D	S_W	H_{bed}	PM	Sol	SP_O	SP_I	ID	M/DDX	TDP	MSS
N/A	N/A	0.00487	0.048	0.180	33.3	P	N/A	N/A	N/A	N/A	3.60	4.10	N/A	N/A	N/A	N/A	N/A	N/A	N/A	N/A	N/A	AM-	N/A	N/A	N/A	34S_6p1d7Yd_8	7/23 A1	TDP-WTP-012	20070655
N/A	N/A	0.00487	0.048	0.180	29.4	P	N/A	N/A	N/A	N/A	4.10	4.10	N/A	N/A	N/A	N/A	N/A	N/A	N/A	N/A	N/A	AM-	N/A	N/A	N/A	34S_6p1d7Yd_8	7/23 A1	TDP-WTP-012	20070658
N/A	N/A	0.00487	0.048	0.180	27.0	P	N/A	N/A	N/A	N/A	4.60	4.10	N/A	N/A	N/A	N/A	N/A	N/A	N/A	N/A	N/A	AM-	N/A	N/A	N/A	34S_6p1d7Yd_8	7/23 A1	TDP-WTP-012	20070662
N/A	N/A	0.00487	0.048	0.180	35.7	P	N/A	N/A	N/A	N/A	3.50	4.10	N/A	N/A	N/A	N/A	N/A	N/A	N/A	N/A	N/A	AM-	N/A	N/A	N/A	34S_6p1d7Yd_8	7/23 A1	TDP-WTP-012	20070668
N/A	N/A	0.00487	0.048	0.180	30.8	P	N/A	N/A	N/A	N/A	4.00	4.10	N/A	N/A	N/A	N/A	N/A	N/A	N/A	N/A	N/A	AM	N/A	N/A	N/A	34S_6p1d7Yd_8	7/23 A1	TDP-WTP-012	20070672
28.0	0.998	0.00487	0.048	0.180	29.8	P	N/A	3.61	3.79	3.87	4.10	4.10	14.63	N/A	N/A	UCSvis	N/A	N/A	N/A	I	N/A	CS-	N/A	N/A	N/A	34S_6p1d7Yd_8	7/23 A1	TDP-WTP-012	20070677
N/A	N/A	0.00487	0.048	0.180	29.0	P	N/A	N/A	N/A	N/A	4.25	4.10	N/A	N/A	N/A	N/A	N/A	N/A	N/A	N/A	N/A	CS-	N/A	N/A	N/A	34S_6p1d7Yd_8	7/23 A1	TDP-WTP-012	20070683
28.0	0.998	0.00487	0.048	0.180	27.8	P	N/A	3.80	4.01	4.11	4.40	4.10	14.63	N/A	N/A	N/A	N/A	N/A	N/A	N/A	N/A	BC	N/A	N/A	N/A	34S_6p1d7Yd_8	7/23 A1	TDP-WTP-012	20070686
28.0	0.998	0.00487	0.048	0.180	24.5	P	N/A	4.23	4.49	4.61	5.00	4.10	14.63	N/A	N/A	N/A	N/A	N/A	N/A	N/A	N/A	N/A	N/A	N/A	N/A	34S_6p1d7Yd_8	7/23 A1	TDP-WTP-012	20070690
28.0	0.998	0.00487	0.048	0.180	22.5	P	N/A	4.49	4.83	4.99	5.50	4.10	15.13	N/A	N/A	N/A	N/A	N/A	N/A	N/A	N/A	N/A	N/A	N/A	N/A	34S_6p1d7Yd_8	7/23 A1	TDP-WTP-012	20070695
28.0	0.998	0.00487	0.048	0.180	20.4	P	N/A	4.81	5.23	5.43	6.00	4.10	19.88	N/A	N/A	N/A	N/A	N/A	N/A	N/A	N/A	N/A	N/A	N/A	N/A	34S_6p1d7Yd_8	7/23 A1	TDP-WTP-012	20070699
28.0	0.998	0.00487	0.048	0.180	19.4	P	N/A	5.15	5.63	5.87	6.50	4.10	25.63	N/A	N/A	N/A	N/A	N/A	N/A	N/A	N/A	N/A	N/A	N/A	N/A	34S_6p1d7Yd_8	7/23 A1	TDP-WTP-012	20070704
28.0	0.998	0.00487	0.048	0.180	18.2	P	N/A	5.39	5.95	6.22	7.00	4.10	29.63	N/A	N/A	N/A	N/A	N/A	N/A	N/A	N/A	N/A	N/A	N/A	N/A	34S_6p1d7Yd_8	7/23 A1	TDP-WTP-012	20070709
28.0	0.998	0.00487	0.048	0.180	30.8	P	N/A	3.52	3.69	3.77	4.00	4.10	14.63	N/A	vis dec	UCSvis	N/A	N/A	4.00	D	N/A	CS	N/A	N/A	N/A	34S_6p1d7Yd_8	7/23 A1	TDP-WTP-012	20070714
N/A	N/A	0.00487	0.048	0.180	35.7	P	N/A	N/A	N/A	N/A	3.50	4.10	12.63	N/A	N/A	N/A	N/A	N/A	N/A	N/A	N/A	AM-	N/A	N/A	N/A	34S_6p1d7Yd_8	7/23 A1	TDP-WTP-012	20070718
28.0	0.998	0.00487	0.048	0.180	37.0	P	N/A	2.95	3.06	3.12	3.25	4.10	11.63	N/A	N/A	N/A	N/A	N/A	N/A	N/A	N/A	AM-	N/A	N/A	N/A	34S_6p1d7Yd_8	7/23 A1	TDP-WTP-012	20070724
28.0	0.998	0.00487	0.048	0.180	40.0	P	N/A	2.70	2.79	2.83	3.00	4.10	11.63	N/A	N/A	N/A	N/A	N/A	N/A	N/A	N/A	AM-	N/A	N/A	N/A	34S_6p1d7Yd_8	7/23 A1	TDP-WTP-012	20070729
28.0	0.998	0.00487	0.048	0.180	30.8	P	N/A	3.27	3.42	3.49	3.70	4.10	12.63	N/A	N/A	N/A	N/A	N/A	N/A	N/A	N/A	AM+	N/A	N/A	N/A	34S_6p1d7Yd_8	7/23 A1	TDP-WTP-012	20070736
28.0	0.998	0.00487	0.048	0.180	31.3	P	N/A	3.43	3.59	3.67	3.90	4.10	13.13	N/A	N/A	N/A	N/A	N/A	N/A	N/A	N/A	AM++	N/A	N/A	N/A	34S_6p1d7Yd_8	7/23 A1	TDP-WTP-012	20070742
28.0	0.998	0.00487	0.048	0.180	31.3	P	N/A	3.51	3.68	3.76	4.00	4.10	N/A	N/A	N/A	UCSvis	N/A	N/A	N/A	I	N/A	CS--	N/A	N/A	N/A	34S_6p1d7Yd_8	7/23 A1	TDP-WTP-012	20070747
28.0	0.998	0.00487	0.048	0.180	29.9	P	N/A	3.61	3.78	3.87	4.10	4.10	13.63	4.10	vis	UCSvis	N/A	N/A	N/A	I	N/A	CS	N/A	N/A	N/A	34S_6p1d7Yd_8	7/23 A1	TDP-WTP-012	20070750
28.0	0.998	0.00487	0.100	0.180	71.4	P	N/A	3.31	3.38	3.41	3.50	3.40	12.13	N/A	vis dec	UCSvis	N/A	N/A	3.50	D	N/A	CS	N/A	N/A	N/A	34S_6p1d7Yd_2	7/23 A2	TDP-WTP-012	20070760
29.0	0.997	0.00487	0.100	0.180	82.0	P	N/A	2.84	2.88	2.91	3.00	3.40	9.63	N/A	N/A	N/A	N/A	N/A	N/A	N/A	N/A	AM-	N/A	N/A	N/A	34S_6p1d7Yd_2	7/23 A2	TDP-WTP-012	20070765
29.0	0.997	0.00487	0.100	0.180	77.0	P	N/A	3.12	3.18	3.21	3.30	3.40	10.13	3.30	N/A	UCSvis	N/A	N/A	N/A	I	N/A	CS-	N/A	N/A	N/A	34S_6p1d7Yd_2	7/23 A2	TDP-WTP-012	20070769
29.0	0.997	0.00487	0.100	0.180	72.5	P	N/A	3.22	3.28	3.31	3.40	3.40	12.13	3.40	vis	UCSvis	N/A	N/A	N/A	I	N/A	CS	N/A	N/A	N/A	34S_6p1d7Yd_2	7/23 A2	TDP-WTP-012	20070770
29.0	0.997	0.00487	0.100	0.180	61.7	P	N/A	3.80	3.90	3.94	4.00	3.40	14.63	N/A	N/A	N/A	N/A	N/A	N/A	N/A	N/A	N/A	N/A	N/A	N/A	34S_6p1d7Yd_2	7/23 A2	TDP-WTP-012	20070774
29.0	0.997	0.00487	0.100	0.180	47.6	P	N/A	4.56	4.72	4.80	5.00	3.40	21.13	N/A	N/A	N/A	N/A	N/A	N/A	N/A	N/A	N/A	N/A	N/A	N/A	34S_6p1d7Yd_2	7/23 A2	TDP-WTP-012	20070778
29.0	0.997	0.00487	0.100	0.180	40.0	P	N/A	5.41	5.65	5.75	6.00	3.40	29.63	N/A	N/A	N/A	N/A	N/A	N/A	N/A	N/A	N/A	N/A	N/A	N/A	34S_6p1d7Yd_2	7/23 A2	TDP-WTP-012	20070782
29.0	0.997	0.00487	0.100	0.180	66.7	P	N/A	3.42	3.49	3.52	3.60	3.40	12.63	N/A	N/A	N/A	N/A	N/A	N/A	N/A	N/A	N/A	N/A	N/A	N/A	34S_6p1d7Yd_2	7/23 A2	TDP-WTP-012	20070787
29.0	0.997	0.00487	0.100	0.180	71.4	P	N/A	3.22	3.28	3.31	3.40	3.40	11.63	N/A	vis dec	UCSvis	N/A	N/A	3.40	D	N/A	N/A	N/A	N/A	N/A	34S_6p1d7Yd_2	7/23 A2	TDP-WTP-012	20070791
29.0	0.997	0.00487	0.100	0.180	74.1	P	N/A	3.07	3.12	3.15	3.20	3.40	11.13	N/A	vis dec	UCSvis	N/A	N/A	3.20	D	N/A	CS-	N/A	N/A	N/A	34S_6p1d7Yd_2	7/23 A2	TDP-WTP-012	20070794
29.0	0.997	0.00487	0.100	0.330	41.7	P	N/A	3.07	3.13	3.16	3.20	3.45	10.13	N/A	N/A	N/A	N/A	N/A	N/A	N/A	N/A	AM+	N/A	N/A	N/A	34S_6p1d7Yc_2	7/23 A3	TDP-WTP-012	20070800
29.0	0.997	0.00487	0.100	0.330	39.1	P	N/A	3.20	3.27	3.30	3.40	3.45	11.13	N/A	N/A	N/A	N/A	N/A	N/A	N/A	N/A	CS-	N/A	N/A	N/A	34S_6p1d7Yc_2	7/23 A3	TDP-WTP-012	20070803
29.0	0.997	0.00487	0.100	0.330	38.5	P	N/A	3.27	3.33	3.36	3.45	3.45	11.63	3.45	vis	UCSvis	N/A	N/A	N/A	I	N/A	CS	N/A	N/A	N/A	34S_6p1d7Yc_2	7/23 A3	TDP-WTP-012	20070807
29.0	0.997	0.00487	0.100	0.330	32.3	P	N/A	3.50	3.58	3.62	4.00	3.45	13.63	N/A	N/A	N/A	N/A	N/A	N/A	N/A	N/A	N/A	N/A	N/A	N/A	34S_6p1d7Yc_2	7/23 A3	TDP-WTP-012	20070812
29.0	0.997	0.00487	0.100	0.330	26.3	P	N/A	4.56	4.73	4.80	5.00	3.45	22.63	N/A	N/A	N/A	N/A	N/A	N/A	N/A	N/A	N/A	N/A	N/A	N/A	34S_6p1d7Yc_2	7/23 A3	TDP-WTP-012	20070816
29.0	0.997	0.00487	0.100	0.330	22.0	P	N/A	5.42	5.66	5.77	6.00	3.45	32.13	N/A	N/A	N/A	N/A	N/A	N/A	N/A	N/A	N/A	N/A	N/A	N/A	34S_6p1d7Yc_2	7/23 A3	TDP-WTP-012	20070820
30.0	0.997	0.00487	0.100	0.330	37.7	P	N/A	3.31	3.38	3.41	3.50	3.45	12.13	N/A	vis dec	UCSvis	N/A	N/A	3.50	D	N/A	CS+	N/A	N/A	N/A	34S_6p1d7Yc_2	7/23 A3	TDP-WTP-012	20070823
30.0	0.997	0.00487	0.100	0.330	41.7	P	N/A	3.13	3.18	3.21	3.30	3.45	10.38	N/A	vis dec	UCSvis	N/A	N/A	3.30	D	N/A	CS-	N/A	N/A	N/A	34S_6p1d7Yc_2	7/23 A3	TDP-WTP-012	20070827
30.0	0.997	0.00487	0.025	0.330	11.1	P	N/A	2.72	2.90	2.99	3.30	4.70	10.13	N/A	N/A	N/A	N/A	N/A	N/A	N/A	N/A	AM-	N/A	N/A	N/A	34S_6p1d7Yc_3	7/23 A4	TDP-WTP-012	20070833
30.0	0.997	0.00487	0.025	0.330	10.3	P	N/A	2.85	3.06	3.16	3.50	4.70	11.63	N/A	N/A	N/A	N/A	N/A	N/A	N/A	N/A	AM	N/A	N/A	N/A	34S_6p1d7Yc_3	7/23 A4	TDP-WTP-012	20070837

Table B.7. Data from July 2007 Tests in Mid-Scale Vessel with Spherical Head A.5

Row Number	Test	Case ID	Tank Diameter	Head Shape	Dish Height	Dish Volume	Tank Fill Height	Return Line Height	Nozzle Inner Diameter	Nozzle Stand-off Distance	Pulse Tube Configuration	Installed Nozzles	Outer Nozzles Operated	Inner Nozzles Operated	Pulse Tube Outer Diameter	Outer PJM Radius	Inner PJM Radius	"FIO" Outer PJM Impingement Angle	"FIO" Inner PJM Impingement Angle	Ratio Outer PJM to Tank Radius	Ratio Inner PJM to Tank Radius	Simulant	Solids Density	Particle Diameter d5	Particle Diameter d50	Particle Diameter d95	Void Fraction
text	text	text	in.	text	in.	in. ^{3}	in.	in.	in.	in.	text	number	number	number	in.	in.	in.	deg	deg	nondim	nondim	text	g/cm^3	m	m	m	fraction
MSS	M/DDX	ID	D	HS	H_{dish}	V_{dish}	H	Rtn	d	sod	PT	N	N_O	N_I	PT_{od}	R_O	R_I	θ_O	θ_I	R_O/R	R_I/R	sxdx	ρ_s	d_5	d_{50}	d_{95}	vf
20070841	7/23 A4	34S_6p1d7Yc_3	33 7/8	S	9	4437.4	67 7/8	62	0.446	0.669	HLP-22	12	8	4	1.9	10.5	5.7	30.8	16.1	0.62	0.33	p1d7	2.45	0.0001213	0.0001780	0.0002606	0.4277
20070846	7/23 A4	34S_6p1d7Yc_3	33 7/8	S	9	4437.4	67 7/8	62	0.446	0.669	HLP-22	12	8	4	1.9	10.5	5.7	30.8	16.1	0.62	0.33	p1d7	2.45	0.0001213	0.0001780	0.0002606	0.4277
20070850	7/23 A4	34S_6p1d7Yc_3	33 7/8	S	9	4437.4	67 7/8	62	0.446	0.669	HLP-22	12	8	4	1.9	10.5	5.7	30.8	16.1	0.62	0.33	p1d7	2.45	0.0001213	0.0001780	0.0002606	0.4277
20070855	7/23 A4	34S_6p1d7Yc_3	33 7/8	S	9	4437.4	67 7/8	62	0.446	0.669	HLP-22	12	8	4	1.9	10.5	5.7	30.8	16.1	0.62	0.33	p1d7	2.45	0.0001213	0.0001780	0.0002606	0.4277
20070860	7/23 A4	34S_6p1d7Yc_3	33 7/8	S	9	4437.4	67 7/8	62	0.446	0.669	HLP-22	12	8	4	1.9	10.5	5.7	30.8	16.1	0.62	0.33	p1d7	2.45	0.0001213	0.0001780	0.0002606	0.4277
20070864M	7/23 A4	34S_6p1d7Yc_3	33 7/8	S	9	4437.4	67 7/8	62	0.446	0.669	HLP-22	12	8	4	1.9	10.5	5.7	30.8	16.1	0.62	0.33	p1d7	2.45	0.0001213	0.0001780	0.0002606	0.4277
20070868M	7/23 A4	34S_6p1d7Yc_3	33 7/8	S	9	4437.4	67 7/8	62	0.446	0.669	HLP-22	12	8	4	1.9	10.5	5.7	30.8	16.1	0.62	0.33	p1d7	2.45	0.0001213	0.0001780	0.0002606	0.4277
20070872M	7/23 A4	34S_6p1d7Yc_3	33 7/8	S	9	4437.4	67 7/8	62	0.446	0.669	HLP-22	12	8	4	1.9	10.5	5.7	30.8	16.1	0.62	0.33	p1d7	2.45	0.0001213	0.0001780	0.0002606	0.4277
20070877M	7/23 A4	34S_6p1d7Yc_3	33 7/8	S	9	4437.4	67 7/8	62	0.446	0.669	HLP-22	12	8	4	1.9	10.5	5.7	30.8	16.1	0.62	0.33	p1d7	2.45	0.0001213	0.0001780	0.0002606	0.4277
20070882M	7/23 A4	34S_6p1d7Yc_3	33 7/8	S	9	4437.4	67 7/8	62	0.446	0.669	HLP-22	12	8	4	1.9	10.5	5.7	30.8	16.1	0.62	0.33	p1d7	2.45	0.0001213	0.0001780	0.0002606	0.4277
20070886	7/23 A4	34S_6p1d7Yc_3	33 7/8	S	9	4437.4	67 7/8	62	0.446	0.669	HLP-22	12	8	4	1.9	10.5	5.7	30.8	16.1	0.62	0.33	p1d7	2.45	0.0001213	0.0001780	0.0002606	0.4277
20070891	7/23 A5	34S_6p1d7Yb_8	33 7/8	S	9	4437.4	67 7/8	62	0.446	0.669	HLP-22	12	8	4	1.9	10.5	5.7	30.8	16.1	0.62	0.33	p1d7	2.45	0.0001213	0.0001780	0.0002606	0.4277
20070896	7/23 A5	34S_6p1d7Yb_8	33 7/8	S	9	4437.4	67 7/8	62	0.446	0.669	HLP-22	12	8	4	1.9	10.5	5.7	30.8	16.1	0.62	0.33	p1d7	2.45	0.0001213	0.0001780	0.0002606	0.4277
20070899	7/23 A5	34S_6p1d7Yb_8	33 7/8	S	9	4437.4	67 7/8	62	0.446	0.669	HLP-22	12	8	4	1.9	10.5	5.7	30.8	16.1	0.62	0.33	p1d7	2.45	0.0001213	0.0001780	0.0002606	0.4277
20070904M	7/23 A5	34S_6p1d7Yb_8	33 7/8	S	9	4437.4	67 7/8	62	0.446	0.669	HLP-22	12	8	4	1.9	10.5	5.7	30.8	16.1	0.62	0.33	p1d7	2.45	0.0001213	0.0001780	0.0002606	0.4277
20070909M	7/23 A5	34S_6p1d7Yb_8	33 7/8	S	9	4437.4	67 7/8	62	0.446	0.669	HLP-22	12	8	4	1.9	10.5	5.7	30.8	16.1	0.62	0.33	p1d7	2.45	0.0001213	0.0001780	0.0002606	0.4277
20070912M	7/23 A5	34S_6p1d7Yb_8	33 7/8	S	9	4437.4	67 7/8	62	0.446	0.669	HLP-22	12	8	4	1.9	10.5	5.7	30.8	16.1	0.62	0.33	p1d7	2.45	0.0001213	0.0001780	0.0002606	0.4277
20070916M	7/23 A5	34S_6p1d7Yb_8	33 7/8	S	9	4437.4	67 7/8	62	0.446	0.669	HLP-22	12	8	4	1.9	10.5	5.7	30.8	16.1	0.62	0.33	p1d7	2.45	0.0001213	0.0001780	0.0002606	0.4277
20070920M	7/23 A5	34S_6p1d7Yb_8	33 7/8	S	9	4437.4	67 7/8	62	0.446	0.669	HLP-22	12	8	4	1.9	10.5	5.7	30.8	16.1	0.62	0.33	p1d7	2.45	0.0001213	0.0001780	0.0002606	0.4277
20070924	7/23 A5	34S_6p1d7Yb_8	33 7/8	S	9	4437.4	67 7/8	62	0.446	0.669	HLP-22	12	8	4	1.9	10.5	5.7	30.8	16.1	0.62	0.33	p1d7	2.45	0.0001213	0.0001780	0.0002606	0.4277
20070932	7/24 A1	34S_6p1d7Xa	33 7/8	S	9	4437.4	67 7/8	62	0.446	0.669	HLP-22	12	8	4	1.9	10.5	5.7	30.8	16.1	0.62	0.33	p1d7	2.45	0.0001213	0.0001780	0.0002606	0.4277
20070935	7/24 A1	34S_6p1d7Xa	33 7/8	S	9	4437.4	67 7/8	62	0.446	0.669	HLP-22	12	8	4	1.9	10.5	5.7	30.8	16.1	0.62	0.33	p1d7	2.45	0.0001213	0.0001780	0.0002606	0.4277
20070936	7/24 A1	34S_6p1d7Xa	33 7/8	S	9	4437.4	67 7/8	62	0.446	0.669	HLP-22	12	8	4	1.9	10.5	5.7	30.8	16.1	0.62	0.33	p1d7	2.45	0.0001213	0.0001780	0.0002606	0.4277
20070938	7/24 A1	34S_6p1d7Xa	33 7/8	S	9	4437.4	67 7/8	62	0.446	0.669	HLP-22	12	8	4	1.9	10.5	5.7	30.8	16.1	0.62	0.33	p1d7	2.45	0.0001213	0.0001780	0.0002606	0.4277
20070940	7/24 A1	34S_6p1d7Xa	33 7/8	S	9	4437.4	67 7/8	62	0.446	0.669	HLP-22	12	8	4	1.9	10.5	5.7	30.8	16.1	0.62	0.33	p1d7	2.45	0.0001213	0.0001780	0.0002606	0.4277
20070941	7/24 A1	34S_6p1d7Xa	33 7/8	S	9	4437.4	67 7/8	62	0.446	0.669	HLP-22	12	8	4	1.9	10.5	5.7	30.8	16.1	0.62	0.33	p1d7	2.45	0.0001213	0.0001780	0.0002606	0.4277
20070944	7/24 A1	34S_6p1d7Xa	33 7/8	S	9	4437.4	67 7/8	62	0.446	0.669	HLP-22	12	8	4	1.9	10.5	5.7	30.8	16.1	0.62	0.33	p1d7	2.45	0.0001213	0.0001780	0.0002606	0.4277
20070947	7/24 A1	34S_6p1d7Xa	33 7/8	S	9	4437.4	67 7/8	62	0.446	0.669	HLP-22	12	8	4	1.9	10.5	5.7	30.8	16.1	0.62	0.33	p1d7	2.45	0.0001213	0.0001780	0.0002606	0.4277
20070948	7/24 A1	34S_6p1d7Xa	33 7/8	S	9	4437.4	67 7/8	62	0.446	0.669	HLP-22	12	8	4	1.9	10.5	5.7	30.8	16.1	0.62	0.33	p1d7	2.45	0.0001213	0.0001780	0.0002606	0.4277
20070951	7/24 A1	34S_6p1d7Xa	33 7/8	S	9	4437.4	67 7/8	62	0.446	0.669	HLP-22	12	8	4	1.9	10.5	5.7	30.8	16.1	0.62	0.33	p1d7	2.45	0.0001213	0.0001780	0.0002606	0.4277
20070956	7/24 A1	34S_6p1d7Xa	33 7/8	S	9	4437.4	67 7/8	62	0.446	0.669	HLP-22	12	8	4	1.9	10.5	5.7	30.8	16.1	0.62	0.33	p1d7	2.45	0.0001213	0.0001780	0.0002606	0.4277
20070959	7/24 A1	34S_6p1d7Xa	33 7/8	S	9	4437.4	67 7/8	62	0.446	0.669	HLP-22	12	8	4	1.9	10.5	5.7	30.8	16.1	0.62	0.33	p1d7	2.45	0.0001213	0.0001780	0.0002606	0.4277
20070961	7/24 A1	34S_6p1d7Xa	33 7/8	S	9	4437.4	67 7/8	62	0.446	0.669	HLP-22	12	8	4	1.9	10.5	5.7	30.8	16.1	0.62	0.33	p1d7	2.45	0.0001213	0.0001780	0.0002606	0.4277
20070964	7/24 A1	34S_6p1d7Xa	33 7/8	S	9	4437.4	67 7/8	62	0.446	0.669	HLP-22	12	8	4	1.9	10.5	5.7	30.8	16.1	0.62	0.33	p1d7	2.45	0.0001213	0.0001780	0.0002606	0.4277
20070967	7/24 A1	34S_6p1d7Xa	33 7/8	S	9	4437.4	67 7/8	62	0.446	0.669	HLP-22	12	8	4	1.9	10.5	5.7	30.8	16.1	0.62	0.33	p1d7	2.45	0.0001213	0.0001780	0.0002606	0.4277
20070970	7/24 A1	34S_6p1d7Xa	33 7/8	S	9	4437.4	67 7/8	62	0.446	0.669	HLP-22	12	8	4	1.9	10.5	5.7	30.8	16.1	0.62	0.33	p1d7	2.45	0.0001213	0.0001780	0.0002606	0.4277
20070974	7/24 B1	34S_6p1d7Xd_8	33 7/8	S	9	4437.4	67 7/8	62	0.446	0.669	HLP-22	12	8	4	1.9	10.5	5.7	30.8	16.1	0.62	0.33	p1d7	2.45	0.0001213	0.0001780	0.0002606	0.4277
20070977	7/24 B1	34S_6p1d7Xd_8	33 7/8	S	9	4437.4	67 7/8	62	0.446	0.669	HLP-22	12	8	4	1.9	10.5	5.7	30.8	16.1	0.62	0.33	p1d7	2.45	0.0001213	0.0001780	0.0002606	0.4277
20070979	7/24 B1	34S_6p1d7Xd_8	33 7/8	S	9	4437.4	67 7/8	62	0.446	0.669	HLP-22	12	8	4	1.9	10.5	5.7	30.8	16.1	0.62	0.33	p1d7	2.45	0.0001213	0.0001780	0.0002606	0.4277
20070982	7/24 B1	34S_6p1d7Xd_8	33 7/8	S	9	4437.4	67 7/8	62	0.446	0.669	HLP-22	12	8	4	1.9	10.5	5.7	30.8	16.1	0.62	0.33	p1d7	2.45	0.0001213	0.0001780	0.0002606	0.4277
20070986	7/24 B1	34S_6p1d7Xd_8	33 7/8	S	9	4437.4	67 7/8	62	0.446	0.669	HLP-22	12	8	4	1.9	10.5	5.7	30.8	16.1	0.62	0.33	p1d7	2.45	0.0001213	0.0001780	0.0002606	0.4277

Table B.7. Data from July 2007 Tests in Mid-Scale Vessel with Spherical Head B.5

Tank Water Temperature	Water Density	Solids Fraction	Pulse Volume Fraction	Duty Cycle	Cycle Time	Pulsed or Steady Jet	Us Steady Jet	U1 Pulsing Jet	U2 URMS	U3 URM3	Discharge Velocity	Critical Suspension Velocity	Average Peak Cloud Height	UCS Condition	UCS Method	UCS Flag	UCS Center Flag	UCS udv Flag	UCS based on Decreasing Velocity	Sweep Increase / Decrease	UDV Height Bed	Particle Motion	Solids Level	Outer Bottom Pattern	Inner Bottom Pattern	Case ID	Test	TDP	Row Number
C	g/cm³	fraction	fraction	fraction	s	text	m/s	m/s	m/s	m/s	m/s	m/s	in.	m/s	text	text	text	text	m/s	text	mm	text	text	text	text	text	text	text	text
T	ρ_L	ϕ_S	ϕ_P	DC	t_C	Jet	U_S	U1	U2	U3	U	U_{CS}	H_C	U_{CSR}	U_{CSM}	U_{CS}vis	U_{CS}cen	U_{CS}udv	U_{CS}_D	S_W	H_{bed}	PM	Sol	SP_O	SP_I	ID	M/DDX	TDP	MSS
30.0	0.997	0.00487	0.025	0.330	10.0	P	N/A	3.00	3.23	3.35	3.70	4.70	11.63	N/A	N/A	N/A	N/A	N/A	N/A	N/A	N/A	AM	N/A	N/A	N/A	34S_6p1d7Yc_3	7/23 A4	TDP-WTP-012	20070841
30.0	0.997	0.00487	0.025	0.330	9.6	P	N/A	3.13	3.39	3.52	3.90	4.70	11.63	N/A	N/A	N/A	N/A	N/A	N/A	N/A	N/A	AM	N/A	N/A	N/A	34S_6p1d7Yc_3	7/23 A4	TDP-WTP-012	20070846
30.0	0.997	0.00487	0.025	0.330	9.5	P	N/A	3.30	3.58	3.72	4.15	4.70	12.88	N/A	N/A	N/A	N/A	N/A	N/A	N/A	N/A	AM+	N/A	N/A	N/A	34S_6p1d7Yc_3	7/23 A4	TDP-WTP-012	20070850
30.0	0.997	0.00487	0.025	0.330	9.3	P	N/A	3.42	3.73	3.88	4.30	4.70	13.13	N/A	N/A	N/A	N/A	N/A	N/A	N/A	N/A	AM++	N/A	N/A	N/A	34S_6p1d7Yc_3	7/23 A4	TDP-WTP-012	20070855
30.0	0.997	0.00487	0.025	0.330	8.9	P	N/A	3.51	3.83	3.99	4.50	4.70	13.13	N/A	N/A	N/A	N/A	N/A	N/A	N/A	N/A	AM++	N/A	N/A	N/A	34S_6p1d7Yc_3	7/23 A4	TDP-WTP-012	20070860
30.0	0.997	0.00487	0.025	0.330	8.5	P	N/A	3.59	3.94	4.11	4.70	4.70	13.63	4.70	vis	UCSvis	N/A	N/A	N/A	I	N/A	CS	N/A	N/A	N/A	34S_6p1d7Yc_3	7/23 A4	TDP-WTP-012	20070864
30.0	0.997	0.00487	0.025	0.330	7.7	P	N/A	4.06	4.52	4.75	5.50	4.70	15.63	N/A	N/A	N/A	N/A	N/A	N/A	N/A	N/A	N/A	N/A	N/A	N/A	34S_6p1d7Yc_3	7/23 A4	TDP-WTP-012	20070868
30.0	0.997	0.00487	0.025	0.330	6.5	P	N/A	4.48	5.12	5.45	6.50	4.70	30.63	N/A	N/A	N/A	N/A	N/A	N/A	N/A	N/A	N/A	N/A	N/A	N/A	34S_6p1d7Yc_3	7/23 A4	TDP-WTP-012	20070872
30.0	0.997	0.00487	0.025	0.330	6.9	P	N/A	4.29	4.85	5.14	6.00	4.70	15.63	N/A	N/A	N/A	N/A	N/A	N/A	N/A	N/A	N/A	N/A	N/A	N/A	34S_6p1d7Yc_3	7/23 A4	TDP-WTP-012	20070877
30.0	0.997	0.00487	0.025	0.330	6.1	P	N/A	3.55	3.91	4.09	4.70	4.70	12.88	N/A	vis dec	UCSvis	N/A	N/A	4.70	D	N/A	CS	N/A	N/A	N/A	34S_6p1d7Yc_3	7/23 A4	TDP-WTP-012	20070882
30.0	0.997	0.00487	0.025	0.330	8.2	P	N/A	3.43	3.78	3.94	4.50	4.70	12.63	N/A	N/A	N/A	N/A	N/A	N/A	N/A	N/A	AM+	N/A	N/A	N/A	34S_6p1d7Yc_3	7/23 A4	TDP-WTP-012	20070886
30.0	0.997	0.00487	0.048	0.500	14.8	P	N/A	2.73	2.82	2.86	3.00	4.00	10.63	N/A	N/A	N/A	N/A	N/A	N/A	N/A	N/A	below AM	N/A	N/A	N/A	34S_6p1d7Yb_8	7/23 A5	TDP-WTP-012	20070891
30.0	0.997	0.00487	0.048	0.500	11.6	P	N/A	3.13	3.26	3.32	3.50	4.00	11.63	N/A	N/A	N/A	N/A	N/A	N/A	N/A	N/A	AM	N/A	N/A	N/A	34S_6p1d7Yb_8	7/23 A5	TDP-WTP-012	20070896
30.0	0.997	0.00487	0.048	0.500	1.2	P	N/A	3.33	3.49	3.56	3.75	4.00	14.13	N/A	N/A	N/A	N/A	N/A	N/A	N/A	N/A	AM+	N/A	N/A	N/A	34S_6p1d7Yb_8	7/23 A5	TDP-WTP-012	20070899
30.0	0.997	0.00487	0.048	0.500	1.1	P	N/A	3.52	3.70	3.79	4.00	4.00	14.63	4.00	vis	UCSvis	N/A	N/A	N/A	I	N/A	CS	N/A	N/A	N/A	34S_6p1d7Yb_8	7/23 A5	TDP-WTP-012	20070904
30.0	0.997	0.00487	0.048	0.500	8.9	P	N/A	4.28	4.56	4.69	5.00	4.00	18.63	N/A	N/A	N/A	N/A	N/A	N/A	N/A	N/A	N/A	N/A	N/A	N/A	34S_6p1d7Yb_8	7/23 A5	TDP-WTP-012	20070909
30.0	0.997	0.00487	0.048	0.500	7.7	P	N/A	4.91	5.31	5.50	6.00	4.00	42.13	N/A	N/A	N/A	N/A	N/A	N/A	N/A	N/A	N/A	N/A	N/A	N/A	34S_6p1d7Yb_8	7/23 A5	TDP-WTP-012	20070912
30.0	0.997	0.00487	0.048	0.500	10.6	P	N/A	3.70	3.88	3.97	4.25	4.00	13.63	N/A	N/A	N/A	N/A	N/A	N/A	N/A	N/A	N/A	N/A	N/A	N/A	34S_6p1d7Yb_8	7/23 A5	TDP-WTP-012	20070916
30.0	0.997	0.00487	0.048	0.500	11.1	P	N/A	3.53	3.70	3.78	4.00	4.00	13.13	N/A	N/A	N/A	N/A	N/A	N/A	N/A	N/A	BC	N/A	N/A	N/A	34S_6p1d7Yb_8	7/23 A5	TDP-WTP-012	20070920
30.0	0.997	0.00487	0.048	0.500	11.4	P	N/A	3.34	3.50	3.57	3.80	4.00	12.63	N/A	N/A	UCSvis	N/A	N/A	N/A	D	N/A	AM+	N/A	N/A	N/A	34S_6p1d7Yb_8	7/23 A5	TDP-WTP-012	20070924
N/A	N/A	0.01592	undefined	1.000	infinite	S	N/A	N/A	N/A	N/A	3.00	4.40	N/A	N/A	N/A	N/A	N/A	N/A	N/A	N/A	N/A	SS	SIN	BP3/4	N/A	34S_6p1d7Xa	7/24 A1	TDP-WTP-013	20070932
N/A	N/A	0.01592	undefined	1.000	infinite	S	N/A	N/A	N/A	N/A	3.20	4.40	N/A	N/A	N/A	N/A	N/A	N/A	N/A	N/A	N/A	AM	SIN	BP4/5	N/A	34S_6p1d7Xa	7/24 A1	TDP-WTP-013	20070935
28.3	0.997	0.01592	undefined	1.000	infinite	S	3.40	N/A	N/A	N/A	3.40	4.40	9.13	N/A	N/A	N/A	N/A	N/A	N/A	N/A	N/A	N/A	N/A	N/A	N/A	34S_6p1d7Xa	7/24 A1	TDP-WTP-013	20070936
N/A	N/A	0.01592	undefined	1.000	infinite	S	N/A	N/A	N/A	N/A	3.40	4.40	N/A	N/A	N/A	N/A	N/A	N/A	N/A	N/A	N/A	AM	SIN	BP4/5	N/A	34S_6p1d7Xa	7/24 A1	TDP-WTP-013	20070938
28.4	0.997	0.01592	undefined	1.000	infinite	S	3.54	N/A	N/A	N/A	3.50	4.40	8.63	N/A	N/A	N/A	N/A	N/A	N/A	N/A	N/A	N/A	SOO	N/A	N/A	34S_6p1d7Xa	7/24 A1	TDP-WTP-013	20070940
N/A	N/A	0.01592	undefined	1.000	infinite	S	N/A	N/A	N/A	N/A	3.50	4.40	N/A	N/A	N/A	N/A	N/A	N/A	N/A	N/A	N/A	AM	SOO	BP5	N/A	34S_6p1d7Xa	7/24 A1	TDP-WTP-013	20070941
28.4	0.998	0.01592	undefined	1.000	infinite	S	3.71	N/A	N/A	N/A	3.60	4.40	8.63	N/A	N/A	N/A	N/A	N/A	N/A	N/A	N/A	AM	N/A	BP5	N/A	34S_6p1d7Xa	7/24 A1	TDP-WTP-013	20070944
28.4	0.997	0.01592	undefined	1.000	infinite	S	3.81	N/A	N/A	N/A	3.80	4.40	9.88	N/A	N/A	N/A	N/A	N/A	N/A	N/A	N/A	AM	N/A	BP5	N/A	34S_6p1d7Xa	7/24 A1	TDP-WTP-013	20070947
28.4	0.997	0.01592	undefined	1.000	infinite	S	4.21	N/A	N/A	N/A	4.20	4.40	11.63	N/A	N/A	N/A	N/A	N/A	N/A	N/A	N/A	AM	N/A	BP5	N/A	34S_6p1d7Xa	7/24 A1	TDP-WTP-013	20070948
28.5	0.997	0.01592	undefined	1.000	infinite	N/A	4.44	N/A	N/A	N/A	4.40	4.40	14.13	4.40	vis	UCSvis	N/A	N/A	N/A	I	N/A	CS	N/A	N/A	N/A	34S_6p1d7Xa	7/24 A1	TDP-WTP-013	20070951
28.5	0.997	0.01592	undefined	1.000	infinite	S	4.76	N/A	N/A	N/A	4.75	4.40	18.88	N/A	N/A	N/A	N/A	N/A	N/A	N/A	N/A	BC	N/A	N/A	N/A	34S_6p1d7Xa	7/24 A1	TDP-WTP-013	20070956
28.6	0.997	0.01592	undefined	1.000	infinite	S	5.24	N/A	N/A	N/A	5.20	4.40	27.13	N/A	N/A	N/A	N/A	N/A	N/A	N/A	N/A	BC	N/A	N/A	N/A	34S_6p1d7Xa	7/24 A1	TDP-WTP-013	20070959
28.6	0.997	0.01592	undefined	1.000	infinite	S	4.44	N/A	N/A	N/A	4.40	4.40	13.13	N/A	N/A	N/A	N/A	N/A	N/A	N/A	N/A	BC	N/A	BP6	N/A	34S_6p1d7Xa	7/24 A1	TDP-WTP-013	20070961
28.6	0.997	0.01592	undefined	1.000	infinite	S	4.34	N/A	N/A	N/A	4.40	4.40	12.88	N/A	N/A	N/A	N/A	N/A	N/A	N/A	N/A	N/A	N/A	N/A	N/A	34S_6p1d7Xa	7/24 A1	TDP-WTP-013	20070964
28.6	0.997	0.01592	undefined	1.000	infinite	S	4.35	N/A	N/A	N/A	4.30	4.40	12.50	N/A	N/A	N/A	N/A	N/A	N/A	N/A	N/A	CS	N/A	N/A	N/A	34S_6p1d7Xa	7/24 A1	TDP-WTP-013	20070967
28.7	0.997	0.01592	undefined	1.000	infinite	S	4.22	N/A	N/A	N/A	4.20	4.40	10.63	N/A	N/A	N/A	N/A	N/A	N/A	N/A	N/A	CS	N/A	N/A	N/A	34S_6p1d7Xa	7/24 A1	TDP-WTP-013	20070970
29.0	0.997	0.01592	0.048	0.180	31.3	P	N/A	3.55	3.70	3.78	4.00	6.40	8.63	N/A	N/A	N/A	N/A	N/A	N/A	N/A	N/A	SS	N/A	BP3/4	N/A	34S_6p1d7Xd_8	7/24 B1	TDP-WTP-013	20070974
29.0	0.997	0.01592	0.048	0.180	27.8	P	N/A	3.82	4.02	4.12	4.40	6.40	8.63	N/A	N/A	N/A	N/A	N/A	N/A	N/A	N/A	SS	N/A	BP3/4	N/A	34S_6p1d7Xd_8	7/24 B1	TDP-WTP-013	20070977
29.0	0.997	0.01592	0.048	0.180	25.8	P	N/A	4.08	4.33	4.45	4.80	6.40	8.63	N/A	N/A	N/A	N/A	N/A	N/A	N/A	N/A	SS	N/A	BP3/4	N/A	34S_6p1d7Xd_8	7/24 B1	TDP-WTP-013	20070979
N/A	N/A	0.01592	0.048	0.180	23.8	P	N/A	N/A	N/A	N/A	5.20	6.40	8.63	N/A	N/A	N/A	N/A	N/A	N/A	N/A	N/A	AM	N/A	N/A	N/A	34S_6p1d7Xd_8	7/24 B1	TDP-WTP-013	20070982
29.0	0.997	0.01592	0.048	0.180	22.7	P	N/A	4.63	4.98	5.14	5.60	6.40	9.13	N/A	N/A	N/A	N/A	N/A	N/A	N/A	N/A	AM	N/A	N/A	N/A	34S_6p1d7Xd_8	7/24 B1	TDP-WTP-013	20070986

Table B.7. Data from July 2007 Tests in Mid-Scale Vessel with Spherical Head A.6

Row Number	Test	Case ID	Tank Diameter	Head Shape	Dish Height	Dish Volume	Tank Fill Height	Return Line Height	Nozzle Inner Diameter	Nozzle Stand-off Distance	Pulse Tube Configuration	Installed Nozzles	Outer Nozzles Operated	Inner Nozzles Operated	Pulse Tube Outer Diameter	Outer PJM Radius	Inner PJM Radius	"FIO" Outer PJM Impingement Angle	"FIO" Inner PJM Impingement Angle	Ratio Outer PJM to Tank Radius	Ratio Inner PJM to Tank Radius	Simulant	Solids Density	Particle Diameter d5	Particle Diameter d50	Particle Diameter d95	Void Fraction
text	text	text	in.	text	in.	in. ^{3}	in.	in.	in.	in.	text	number	number	number	in.	in.	in.	deg	deg	nondim	nondim	text	g/cm^3	m	m	m	fraction
MSS	M/DDX	ID	D	HS	H_{dish}	V_{dish}	H	Rtn	d	sod	PT	N	N_O	N_I	PT_{od}	R_O	R_I	θ_O	θ_I	R_O/R	R_I/R	sxdx	ρ_s	d_5	d_{50}	d_{95}	vf
20070989	7/24 B1	34S_6p1d7Xd_8	33 7/8	S	9	4437.4	67 7/8	62	0.446	0.669	HLP-22	12	8	4	1.9	10.5	5.7	30.8	16.1	0.62	0.33	p1d7	2.45	0.0001213	0.0001780	0.0002606	0.4277
20070993	7/24 B1	34S_6p1d7Xd_8	33 7/8	S	9	4437.4	67 7/8	62	0.446	0.669	HLP-22	12	8	4	1.9	10.5	5.7	30.8	16.1	0.62	0.33	p1d7	2.45	0.0001213	0.0001780	0.0002606	0.4277
20070995M	7/24 B1	34S_6p1d7Xd_8	33 7/8	S	9	4437.4	67 7/8	62	0.446	0.669	HLP-22	12	8	4	1.9	10.5	5.7	30.8	16.1	0.62	0.33	p1d7	2.45	0.0001213	0.0001780	0.0002606	0.4277
20070998M	7/24 B1	34S_6p1d7Xd_8	33 7/8	S	9	4437.4	67 7/8	62	0.446	0.669	HLP-22	12	8	4	1.9	10.5	5.7	30.8	16.1	0.62	0.33	p1d7	2.45	0.0001213	0.0001780	0.0002606	0.4277
20071001M	7/24 B1	34S_6p1d7Xd_8	33 7/8	S	9	4437.4	67 7/8	62	0.446	0.669	HLP-22	12	8	4	1.9	10.5	5.7	30.8	16.1	0.62	0.33	p1d7	2.45	0.0001213	0.0001780	0.0002606	0.4277
20071005M	7/24 B1	34S_6p1d7Xd_8	33 7/8	S	9	4437.4	67 7/8	62	0.446	0.669	HLP-22	12	8	4	1.9	10.5	5.7	30.8	16.1	0.62	0.33	p1d7	2.45	0.0001213	0.0001780	0.0002606	0.4277
20071010M	7/24 B1	34S_6p1d7Xd_8	33 7/8	S	9	4437.4	67 7/8	62	0.446	0.669	HLP-22	12	8	4	1.9	10.5	5.7	30.8	16.1	0.62	0.33	p1d7	2.45	0.0001213	0.0001780	0.0002606	0.4277
20071014M	7/24 B1	34S_6p1d7Xd_8	33 7/8	S	9	4437.4	67 7/8	62	0.446	0.669	HLP-22	12	8	4	1.9	10.5	5.7	30.8	16.1	0.62	0.33	p1d7	2.45	0.0001213	0.0001780	0.0002606	0.4277
20071016M	7/24 B1	34S_6p1d7Xd_8	33 7/8	S	9	4437.4	67 7/8	62	0.446	0.669	HLP-22	12	8	4	1.9	10.5	5.7	30.8	16.1	0.62	0.33	p1d7	2.45	0.0001213	0.0001780	0.0002606	0.4277
20071020M	7/24 B1	34S_6p1d7Xd_8	33 7/8	S	9	4437.4	67 7/8	62	0.446	0.669	HLP-22	12	8	4	1.9	10.5	5.7	30.8	16.1	0.62	0.33	p1d7	2.45	0.0001213	0.0001780	0.0002606	0.4277
20071025M	7/24 B1	34S_6p1d7Xd_8	33 7/8	S	9	4437.4	67 7/8	62	0.446	0.669	HLP-22	12	8	4	1.9	10.5	5.7	30.8	16.1	0.62	0.33	p1d7	2.45	0.0001213	0.0001780	0.0002606	0.4277
20071028M	7/24 B1	34S_6p1d7Xd_8	33 7/8	S	9	4437.4	67 7/8	62	0.446	0.669	HLP-22	12	8	4	1.9	10.5	5.7	30.8	16.1	0.62	0.33	p1d7	2.45	0.0001213	0.0001780	0.0002606	0.4277
20071032M	7/24 B1	34S_6p1d7Xd_8	33 7/8	S	9	4437.4	67 7/8	62	0.446	0.669	HLP-22	12	8	4	1.9	10.5	5.7	30.8	16.1	0.62	0.33	p1d7	2.45	0.0001213	0.0001780	0.0002606	0.4277
20071036M	7/24 B1	34S_6p1d7Xd_8	33 7/8	S	9	4437.4	67 7/8	62	0.446	0.669	HLP-22	12	8	4	1.9	10.5	5.7	30.8	16.1	0.62	0.33	p1d7	2.45	0.0001213	0.0001780	0.0002606	0.4277
20071038	7/24 B1	34S_6p1d7Xd_8	33 7/8	S	9	4437.4	67 7/8	62	0.446	0.669	HLP-22	12	8	4	1.9	10.5	5.7	30.8	16.1	0.62	0.33	p1d7	2.45	0.0001213	0.0001780	0.0002606	0.4277
20071042M	7/24 B1	34S_6p1d7Xd_8	33 7/8	S	9	4437.4	67 7/8	62	0.446	0.669	HLP-22	12	8	4	1.9	10.5	5.7	30.8	16.1	0.62	0.33	p1d7	2.45	0.0001213	0.0001780	0.0002606	0.4277
20071067	7/24 B1	34S_6p1d7Xd_8	33 7/8	S	9	4437.4	67 7/8	62	0.446	0.669	HLP-22	12	8	4	1.9	10.5	5.7	30.8	16.1	0.62	0.33	p1d7	2.45	0.0001213	0.0001780	0.0002606	0.4277
20071070M	7/24 B1	34S_6p1d7Xd_8	33 7/8	S	9	4437.4	67 7/8	62	0.446	0.669	HLP-22	12	8	4	1.9	10.5	5.7	30.8	16.1	0.62	0.33	p1d7	2.45	0.0001213	0.0001780	0.0002606	0.4277
20071074	7/25 A1	34S_6p2d6Ya	33 7/8	S	9	4437.4	68 1/8	62	0.446	0.669	HLP-22	12	8	4	1.9	10.5	5.7	30.8	16.1	0.62	0.33	p2d6	2.46	0.0005184	0.0007662	0.0011729	0.4080
20071075	7/25 A1	34S_6p2d6Ya	33 7/8	S	9	4437.4	68 1/8	62	0.446	0.669	HLP-22	12	8	4	1.9	10.5	5.7	30.8	16.1	0.62	0.33	p2d6	2.46	0.0005184	0.0007662	0.0011729	0.4080
20071076	7/25 A1	34S_6p2d6Ya	33 7/8	S	9	4437.4	68 1/8	62	0.446	0.669	HLP-22	12	8	4	1.9	10.5	5.7	30.8	16.1	0.62	0.33	p2d6	2.46	0.0005184	0.0007662	0.0011729	0.4080
20071080	7/25 A1	34S_6p2d6Ya	33 7/8	S	9	4437.4	68 1/8	62	0.446	0.669	HLP-22	12	8	4	1.9	10.5	5.7	30.8	16.1	0.62	0.33	p2d6	2.46	0.0005184	0.0007662	0.0011729	0.4080
20071085	7/25 A1	34S_6p2d6Ya	33 7/8	S	9	4437.4	68 1/8	62	0.446	0.669	HLP-22	12	8	4	1.9	10.5	5.7	30.8	16.1	0.62	0.33	p2d6	2.46	0.0005184	0.0007662	0.0011729	0.4080
20071088	7/25 A1	34S_6p2d6Ya	33 7/8	S	9	4437.4	68 1/8	62	0.446	0.669	HLP-22	12	8	4	1.9	10.5	5.7	30.8	16.1	0.62	0.33	p2d6	2.46	0.0005184	0.0007662	0.0011729	0.4080
20071092	7/25 A1	34S_6p2d6Ya	33 7/8	S	9	4437.4	68 1/8	62	0.446	0.669	HLP-22	12	8	4	1.9	10.5	5.7	30.8	16.1	0.62	0.33	p2d6	2.46	0.0005184	0.0007662	0.0011729	0.4080
20071095	7/25 A1	34S_6p2d6Ya	33 7/8	S	9	4437.4	68 1/8	62	0.446	0.669	HLP-22	12	8	4	1.9	10.5	5.7	30.8	16.1	0.62	0.33	p2d6	2.46	0.0005184	0.0007662	0.0011729	0.4080
20071101	7/25 A1	34S_6p2d6Ya	33 7/8	S	9	4437.4	68 1/8	62	0.446	0.669	HLP-22	12	8	4	1.9	10.5	5.7	30.8	16.1	0.62	0.33	p2d6	2.46	0.0005184	0.0007662	0.0011729	0.4080
20071104	7/25 A1	34S_6p2d6Ya	33 7/8	S	9	4437.4	68 1/8	62	0.446	0.669	HLP-22	12	8	4	1.9	10.5	5.7	30.8	16.1	0.62	0.33	p2d6	2.46	0.0005184	0.0007662	0.0011729	0.4080
20071108	7/25 A1	34S_6p2d6Ya	33 7/8	S	9	4437.4	68 1/8	62	0.446	0.669	HLP-22	12	8	4	1.9	10.5	5.7	30.8	16.1	0.62	0.33	p2d6	2.46	0.0005184	0.0007662	0.0011729	0.4080
20071112	7/25 A1	34S_6p2d6Ya	33 7/8	S	9	4437.4	68 1/8	62	0.446	0.669	HLP-22	12	8	4	1.9	10.5	5.7	30.8	16.1	0.62	0.33	p2d6	2.46	0.0005184	0.0007662	0.0011729	0.4080
20071115	7/25 A1	34S_6p2d6Ya	33 7/8	S	9	4437.4	68 1/8	62	0.446	0.669	HLP-22	12	8	4	1.9	10.5	5.7	30.8	16.1	0.62	0.33	p2d6	2.46	0.0005184	0.0007662	0.0011729	0.4080
20071121	7/25 A1	34S_6p2d6Ya	33 7/8	S	9	4437.4	68 1/8	62	0.446	0.669	HLP-22	12	8	4	1.9	10.5	5.7	30.8	16.1	0.62	0.33	p2d6	2.46	0.0005184	0.0007662	0.0011729	0.4080
20071123	7/25 A1	34S_6p2d6Ya	33 7/8	S	9	4437.4	68 1/8	62	0.446	0.669	HLP-22	12	8	4	1.9	10.5	5.7	30.8	16.1	0.62	0.33	p2d6	2.46	0.0005184	0.0007662	0.0011729	0.4080
20071129	7/25 A1	34S_6p2d6Ya	33 7/8	S	9	4437.4	68 1/8	62	0.446	0.669	HLP-22	12	8	4	1.9	10.5	5.7	30.8	16.1	0.62	0.33	p2d6	2.46	0.0005184	0.0007662	0.0011729	0.4080
20071133	7/25 A1	34S_6p2d6Ya	33 7/8	S	9	4437.4	68 1/8	62	0.446	0.669	HLP-22	12	8	4	1.9	10.5	5.7	30.8	16.1	0.62	0.33	p2d6	2.46	0.0005184	0.0007662	0.0011729	0.4080
20071139	7/25 B1	34S_6p2d6Yd_8	33 7/8	S	9	4437.4	68 1/8	62	0.446	0.669	HLP-22	12	8	4	1.9	10.5	5.7	30.8	16.1	0.62	0.33	p2d6	2.46	0.0005184	0.0007662	0.0011729	0.4080
20071142	7/25 B1	34S_6p2d6Yd_8	33 7/8	S	9	4437.4	68 1/8	62	0.446	0.669	HLP-22	12	8	4	1.9	10.5	5.7	30.8	16.1	0.62	0.33	p2d6	2.46	0.0005184	0.0007662	0.0011729	0.4080
20071143	7/25 B1	34S_6p2d6Yd_8	33 7/8	S	9	4437.4	68 1/8	62	0.446	0.669	HLP-22	12	8	4	1.9	10.5	5.7	30.8	16.1	0.62	0.33	p2d6	2.46	0.0005184	0.0007662	0.0011729	0.4080
20071146	7/25 B1	34S_6p2d6Yd_8	33 7/8	S	9	4437.4	68 1/8	62	0.446	0.669	HLP-22	12	8	4	1.9	10.5	5.7	30.8	16.1	0.62	0.33	p2d6	2.46	0.0005184	0.0007662	0.0011729	0.4080
20071148	7/25 B1	34S_6p2d6Yd_8	33 7/8	S	9	4437.4	68 1/8	62	0.446	0.669	HLP-22	12	8	4	1.9	10.5	5.7	30.8	16.1	0.62	0.33	p2d6	2.46	0.0005184	0.0007662	0.0011729	0.4080
20071150M	7/25 B1	34S_6p2d6Yd_8	33 7/8	S	9	4437.4	68 1/8	62	0.446	0.669	HLP-22	12	8	4	1.9	10.5	5.7	30.8	16.1	0.62	0.33	p2d6	2.46	0.0005184	0.0007662	0.0011729	0.4080

Table B.7. Data from July 2007 Tests in Mid-Scale Vessel with Spherical Head B.6

Tank Water Temperature	Water Density	Solids Fraction	Pulse Volume Fraction	Duty Cycle	Cycle Time	Pulsed or Steady Jet	Us Steady Jet	U1 Pulsing Jet	U2 URMS	U3 URM3	Discharge Velocity	Critical Suspension Velocity	Average Peak Cloud Height	UCS Condition	UCS Method	UCS Flag	UCS Center Flag	UCS udv Flag	UCS based on Decreasing Velocity	Sweep Increase / Decrease	UDV Height Bed	Particle Motion	Solids Level	Outer Bottom Pattern	Inner Bottom Pattern	Case ID	Test	TDP	Row Number
C	g/cm³	fraction	fraction	fraction	s	text	m/s	m/s	m/s	m/s	m/s	m/s	in.	m/s	text	text	text	text	m/s	text	mm	text	text	text	text	text	text	text	text
T	ρ_l	ϕ_s	ϕ_p	DC	t_C	Jet	U_S	U1	U2	U3	U	U_{CS}	H_C	U_{CSR}	U_{CSM}	U_{CS}vis	U_{CS}cen	U_{CS}udv	U_{CS}_D	S_W	H_{bed}	PM	Sol	SP_O	SP_I	ID	M/DDX	TDP	MSS
29.0	0.997	0.01592	0.048	0.180	20.8	P	N/A	4.86	5.27	5.46	6.00	6.40	10.13	N/A	N/A	N/A	N/A	N/A	N/A	N/A	N/A	AM	N/A	N/A	N/A	34S_6p1d7Xd_8	7/24 B1	TDP-WTP-013	20070989
29.0	0.997	0.01592	0.048	0.180	21.3	P	N/A	5.03	5.45	5.65	6.20	6.40	10.38	N/A	N/A	N/A	N/A	N/A	N/A	N/A	N/A	CS- -	N/A	N/A	N/A	34S_6p1d7Xd_8	7/24 B1	TDP-WTP-013	20070993
29.0	0.997	0.01592	0.048	0.180	20.2	P	N/A	5.15	5.59	5.81	6.40	6.40	10.13	6.40	vis	UCSvis	N/A	N/A	N/A	I	N/A	CS	N/A	N/A	N/A	34S_6p1d7Xd_8	7/24 B1	TDP-WTP-013	20070995
29.0	0.997	0.01592	0.048	0.180	18.9	P	N/A	5.31	5.80	6.04	6.75	6.40	9.63	N/A	N/A	N/A	N/A	N/A	N/A	N/A	N/A	BC	N/A	N/A	N/A	34S_6p1d7Xd_8	7/24 B1	TDP-WTP-013	20070998
29.0	0.997	0.01592	0.048	0.180	18.1	P	N/A	5.42	5.97	6.24	7.00	6.40	10.38	N/A	N/A	N/A	N/A	N/A	N/A	N/A	N/A	BC	N/A	N/A	N/A	34S_6p1d7Xd_8	7/24 B1	TDP-WTP-013	20071001
29.0	0.997	0.01592	0.048	0.180	17.4	P	N/A	5.64	6.29	6.60	7.60	6.40	11.13	N/A	N/A	N/A	N/A	N/A	N/A	N/A	N/A	BC	N/A	N/A	N/A	34S_6p1d7Xd_8	7/24 B1	TDP-WTP-013	20071005
29.0	0.997	0.01592	0.048	0.180	16.7	P	N/A	5.93	6.62	6.97	8.00	6.40	12.63	N/A	N/A	N/A	N/A	N/A	N/A	N/A	N/A	N/A	N/A	N/A	N/A	34S_6p1d7Xd_8	7/24 B1	TDP-WTP-013	20071010
29.0	0.997	0.01592	0.048	0.180	16.7	P	N/A	6.83	7.62	8.03	9.30	6.40	18.13	N/A	N/A	N/A	N/A	N/A	N/A	N/A	N/A	BC	N/A	N/A	N/A	34S_6p1d7Xd_8	7/24 B1	TDP-WTP-013	20071014
29.0	0.997	0.01592	0.048	0.180	15.2	P	N/A	7.01	7.92	8.39	10.00	6.40	18.13	N/A	N/A	N/A	N/A	N/A	N/A	N/A	N/A	BC	N/A	N/A	N/A	34S_6p1d7Xd_8	7/24 B1	TDP-WTP-013	20071016
29.0	0.997	0.01592	0.048	0.180	12.5	P	N/A	7.70	9.00	9.69	12.00	6.40	28.63	N/A	N/A	N/A	N/A	N/A	N/A	N/A	N/A	BC	N/A	N/A	N/A	34S_6p1d7Xd_8	7/24 B1	TDP-WTP-013	20071020
29.0	0.997	0.01592	0.048	0.180	19.6	P	N/A	5.19	5.66	5.88	6.60	6.40	10.38	N/A	N/A	N/A	N/A	N/A	N/A	N/A	N/A	CS	N/A	N/A	N/A	34S_6p1d7Xd_8	7/24 B1	TDP-WTP-013	20071025
29.0	0.997	0.01592	0.048	0.180	18.5	P	N/A	5.30	5.82	6.08	6.80	6.40	9.63	N/A	N/A	N/A	N/A	N/A	N/A	N/A	N/A	AM	N/A	N/A	N/A	34S_6p1d7Xd_8	7/24 B1	TDP-WTP-013	20071028
29.0	0.997	0.01592	0.048	0.180	1.8	P	N/A	5.42	5.97	6.24	7.00	6.40	10.63	N/A	N/A	N/A	N/A	N/A	N/A	N/A	N/A	AM	N/A	N/A	N/A	34S_6p1d7Xd_8	7/24 B1	TDP-WTP-013	20071032
29.0	0.997	0.01592	0.048	0.180	17.2	P	N/A	5.47	6.05	6.33	7.20	6.40	10.63	N/A	N/A	N/A	N/A	N/A	N/A	N/A	N/A	AM	N/A	N/A	N/A	34S_6p1d7Xd_8	7/24 B1	TDP-WTP-013	20071036
N/A	N/A	0.01592	0.048	0.180	16.3	P	N/A	N/A	N/A	N/A	8.00	6.40	N/A	N/A	N/A	N/A	N/A	N/A	N/A	N/A	N/A	AM	N/A	N/A	N/A	34S_6p1d7Xd_8	7/24 B1	TDP-WTP-013	20071038
29.0	0.997	0.01592	0.048	0.180	16.1	P	N/A	6.08	6.81	7.18	8.20	6.40	12.63	N/A	N/A	N/A	N/A	N/A	N/A	N/A	N/A	AM	N/A	N/A	N/A	34S_6p1d7Xd_8	7/24 B1	TDP-WTP-013	20071042
N/A	N/A	0.01592	0.048	0.180	19.4	P	N/A	N/A	N/A	N/A	6.60	6.40	N/A	N/A	N/A	N/A	N/A	N/A	N/A	N/A	N/A	CS+	N/A	N/A	N/A	34S_6p1d7Xd_8	7/24 B1	TDP-WTP-013	20071067
29.0	0.997	0.01592	0.048	0.180	20.0	P	N/A	5.02	5.45	5.66	6.40	6.40	9.63	N/A	vis dec	UCSvis	N/A	N/A	6.40	D	N/A	CS-	N/A	N/A	N/A	34S_6p1d7Xd_8	7/24 B1	TDP-WTP-013	20071070
N/A	N/A	0.00485	undefined	1.000	infinite	S	N/A	N/A	N/A	N/A	4.00	6.30	N/A	N/A	N/A	N/A	N/A	N/A	N/A	N/A	N/A	below AM	N/A	N/A	N/A	34S_6p2d6Ya	7/25 A1	TDP-WTP-014	20071074
N/A	N/A	0.00485	undefined	1.000	infinite	S	N/A	N/A	N/A	N/A	4.60	6.30	11.13	N/A	N/A	N/A	N/A	N/A	N/A	N/A	N/A	AM	N/A	N/A	N/A	34S_6p2d6Ya	7/25 A1	TDP-WTP-014	20071075
26.4	0.998	0.00485	undefined	1.000	infinite	S	4.61	N/A	N/A	N/A	4.58	6.30	11.13	N/A	N/A	N/A	N/A	N/A	N/A	N/A	N/A	AM-	SIN	BP4	N/A	34S_6p2d6Ya	7/25 A1	TDP-WTP-014	20071076
26.4	0.998	0.00485	undefined	1.000	infinite	S	6.33	N/A	N/A	N/A	6.30	6.30	13.21	6.30	vis	UCSvis	N/A	N/A	N/A	I	N/A	CS	N/A	N/A	N/A	34S_6p2d6Ya	7/25 A1	TDP-WTP-014	20071080
26.5	0.998	0.00485	undefined	1.000	infinite	S	6.02	N/A	N/A	N/A	6.00	6.30	11.96	N/A	vis dec	UCSvis	N/A	N/A	6.00	D	N/A	CS	N/A	N/A	N/A	34S_6p2d6Ya	7/25 A1	TDP-WTP-014	20071085
N/A	N/A	0.00485	undefined	1.000	infinite	S	N/A	N/A	N/A	N/A	5.60	6.30	N/A	N/A	N/A	N/A	N/A	N/A	N/A	N/A	N/A	AM	N/A	N/A	N/A	34S_6p2d6Ya	7/25 A1	TDP-WTP-014	20071088
26.6	0.998	0.00485	undefined	1.000	infinite	S	7.12	N/A	N/A	N/A	7.00	6.30	23.63	N/A	N/A	N/A	N/A	N/A	N/A	N/A	N/A	BC	N/A	N/A	N/A	34S_6p2d6Ya	7/25 A1	TDP-WTP-014	20071092
26.7	0.998	0.00485	undefined	1.000	infinite	S	7.54	N/A	N/A	N/A	7.50	6.30	31.96	N/A	N/A	N/A	N/A	N/A	N/A	N/A	N/A	BC	N/A	N/A	N/A	34S_6p2d6Ya	7/25 A1	TDP-WTP-014	20071095
26.9	0.998	0.00485	undefined	1.000	infinite	S	7.24	N/A	N/A	N/A	7.20	6.30	26.63	N/A	N/A	N/A	N/A	N/A	N/A	N/A	N/A	BC	N/A	N/A	N/A	34S_6p2d6Ya	7/25 A1	TDP-WTP-014	20071101
27.1	0.998	0.00485	undefined	1.000	infinite	S	6.73	N/A	N/A	N/A	6.70	6.30	17.96	N/A	N/A	N/A	N/A	N/A	N/A	N/A	N/A	BC	N/A	N/A	N/A	34S_6p2d6Ya	7/25 A1	TDP-WTP-014	20071104
27.2	0.998	0.00485	undefined	1.000	infinite	S	6.53	N/A	N/A	N/A	6.50	6.30	13.63	N/A	N/A	N/A	N/A	N/A	N/A	N/A	N/A	BC	N/A	N/A	N/A	34S_6p2d6Ya	7/25 A1	TDP-WTP-014	20071108
N/A	N/A	0.00485	undefined	1.000	infinite	S	N/A	N/A	N/A	N/A	6.30	6.30	N/A	N/A	N/A	N/A	N/A	N/A	N/A	N/A	N/A	BC	N/A	N/A	N/A	34S_6p2d6Ya	7/25 A1	TDP-WTP-014	20071112
27.3	0.998	0.00485	undefined	1.000	infinite	S	6.04	N/A	N/A	N/A	6.00	6.30	N/A	N/A	vis dec	UCSvis	N/A	N/A	6.00	D	N/A	CS	N/A	N/A	N/A	34S_6p2d6Ya	7/25 A1	TDP-WTP-014	20071115
N/A	N/A	0.00485	undefined	1.000	infinite	S	N/A	N/A	N/A	N/A	5.80	6.30	N/A	N/A	N/A	N/A	N/A	N/A	N/A	N/A	N/A	CS-	N/A	N/A	N/A	34S_6p2d6Ya	7/25 A1	TDP-WTP-014	20071121
27.5	0.998	0.00485	undefined	1.000	infinite	S	5.82	N/A	N/A	N/A	5.80	6.30	12.13	N/A	vis dec	UCSvis	N/A	N/A	5.80	D	N/A	CS	N/A	N/A	N/A	34S_6p2d6Ya	7/25 A1	TDP-WTP-014	20071123
N/A	N/A	0.00485	undefined	1.000	infinite	S	N/A	N/A	N/A	N/A	5.70	6.30	N/A	N/A	N/A	N/A	N/A	N/A	N/A	N/A	N/A	AM	N/A	N/A	N/A	34S_6p2d6Ya	7/25 A1	TDP-WTP-014	20071129
28.0	0.998	0.00485	undefined	1.000	infinite	S	4.22	N/A	N/A	N/A	4.20	6.30	8.63	N/A	N/A	N/A	N/A	N/A	N/A	N/A	N/A	SS+	N/A	N/A	N/A	34S_6p2d6Ya	7/25 A1	TDP-WTP-014	20071133
28.0	0.998	0.00485	0.048	0.180	29.9	P	N/A	3.63	3.83	3.93	4.20	6.00	17.63	N/A	N/A	N/A	N/A	N/A	N/A	N/A	N/A	SS	N/A	N/A	N/A	34S_6p2d6Yd_8	7/25 B1	TDP-WTP-014	20071139
28.0	0.998	0.00485	0.048	0.180	26.3	P	N/A	4.00	4.25	4.37	4.70	6.00	18.13	N/A	N/A	N/A	N/A	N/A	N/A	N/A	N/A	SS+	SIN	BP4	N/A	34S_6p2d6Yd_8	7/25 B1	TDP-WTP-014	20071142
28.0	0.998	0.00485	0.048	0.180	26.3	P	N/A	4.00	4.25	4.37	4.70	6.00	17.63	N/A	N/A	N/A	N/A	N/A	N/A	N/A	N/A	AM	N/A	N/A	N/A	34S_6p2d6Yd_8	7/25 B1	TDP-WTP-014	20071143
28.0	0.998	0.00485	0.048	0.180	24.4	P	N/A	4.35	4.64	4.79	5.20	6.00	17.38	N/A	N/A	N/A	N/A	N/A	N/A	N/A	N/A	AM	N/A	N/A	N/A	34S_6p2d6Yd_8	7/25 B1	TDP-WTP-014	20071146
28.0	0.998	0.00485	0.048	0.180	22.2	P	N/A	4.59	4.94	5.11	5.60	6.00	18.13	N/A	N/A	N/A	N/A	N/A	N/A	N/A	N/A	AM	N/A	N/A	N/A	34S_6p2d6Yd_8	7/25 B1	TDP-WTP-014	20071148
28.0	0.998	0.00485	0.048	0.180	20.8	P	N/A	4.82	5.24	5.44	6.00	6.00	19.13	6.00	vis	UCSvis	N/A	N/A	N/A	I	N/A	CS	N/A	N/A	N/A	34S_6p2d6Yd_8	7/25 B1	TDP-WTP-014	20071150

Table B.7. Data from July 2007 Tests in Mid-Scale Vessel with Spherical Head A.7

Row Number	Test	Case ID	Tank Diameter	Head Shape	Dish Height	Dish Volume	Tank Fill Height	Return Line Height	Nozzle Inner Diameter	Nozzle Stand-off Distance	Pulse Tube Configuration	Installed Nozzles	Outer Nozzles Operated	Inner Nozzles Operated	Pulse Tube Outer Diameter	Outer PJM Radius	Inner PJM Radius	"FIO" Outer PJM Impingement Angle	"FIO" Inner PJM Impingement Angle	Ratio Outer PJM to Tank Radius	Ratio Inner PJM to Tank Radius	Simulant	Solids Density	Particle Diameter d5	Particle Diameter d50	Particle Diameter d95	Void Fraction
text	text	text	in.	text	in.	in. ^{3}	in.	in.	in.	in.	text	number	number	number	in.	in.	in.	deg	deg	nondim	nondim	text	g/cm^3	m	m	m	fraction
MSS	M/DDX	ID	D	HS	H_{dish}	V_{dish}	H	Rtn	d	sod	PT	N	N_O	N_I	PT_{od}	R_O	R_I	θ_O	θ_I	R_O/R	R_I/R	sxdx	ρ_s	d_5	d_{50}	d_{95}	vf
20071155M	7/25 B1	34S_6p2d6Yd_8	33 7/8	S	9	4437.4	68 1/8	62	0.446	0.669	HLP-22	12	8	4	1.9	10.5	5.7	30.8	16.1	0.62	0.33	p2d6	2.46	0.0005184	0.0007662	0.0011729	0.4080
20071159M	7/25 B1	34S_6p2d6Yd_8	33 7/8	S	9	4437.4	68 1/8	62	0.446	0.669	HLP-22	12	8	4	1.9	10.5	5.7	30.8	16.1	0.62	0.33	p2d6	2.46	0.0005184	0.0007662	0.0011729	0.4080
20071160M	7/25 B1	34S_6p2d6Yd_8	33 7/8	S	9	4437.4	68 1/8	62	0.446	0.669	HLP-22	12	8	4	1.9	10.5	5.7	30.8	16.1	0.62	0.33	p2d6	2.46	0.0005184	0.0007662	0.0011729	0.4080
20071165M	7/25 B1	34S_6p2d6Yd_8	33 7/8	S	9	4437.4	68 1/8	62	0.446	0.669	HLP-22	12	8	4	1.9	10.5	5.7	30.8	16.1	0.62	0.33	p2d6	2.46	0.0005184	0.0007662	0.0011729	0.4080
20071168M	7/25 B1	34S_6p2d6Yd_8	33 7/8	S	9	4437.4	68 1/8	62	0.446	0.669	HLP-22	12	8	4	1.9	10.5	5.7	30.8	16.1	0.62	0.33	p2d6	2.46	0.0005184	0.0007662	0.0011729	0.4080
20071171M	7/25 B1	34S_6p2d6Yd_8	33 7/8	S	9	4437.4	68 1/8	62	0.446	0.669	HLP-22	12	8	4	1.9	10.5	5.7	30.8	16.1	0.62	0.33	p2d6	2.46	0.0005184	0.0007662	0.0011729	0.4080
20071176M	7/25 B1	34S_6p2d6Yd_8	33 7/8	S	9	4437.4	68 1/8	62	0.446	0.669	HLP-22	12	8	4	1.9	10.5	5.7	30.8	16.1	0.62	0.33	p2d6	2.46	0.0005184	0.0007662	0.0011729	0.4080
20071180M	7/25 B1	34S_6p2d6Yd_8	33 7/8	S	9	4437.4	68 1/8	62	0.446	0.669	HLP-22	12	8	4	1.9	10.5	5.7	30.8	16.1	0.62	0.33	p2d6	2.46	0.0005184	0.0007662	0.0011729	0.4080
20071182M	7/25 B1	34S_6p2d6Yd_8	33 7/8	S	9	4437.4	68 1/8	62	0.446	0.669	HLP-22	12	8	4	1.9	10.5	5.7	30.8	16.1	0.62	0.33	p2d6	2.46	0.0005184	0.0007662	0.0011729	0.4080
20071185M	7/25 B1	34S_6p2d6Yd_8	33 7/8	S	9	4437.4	68 1/8	62	0.446	0.669	HLP-22	12	8	4	1.9	10.5	5.7	30.8	16.1	0.62	0.33	p2d6	2.46	0.0005184	0.0007662	0.0011729	0.4080
20071187M	7/25 B1	34S_6p2d6Yd_8	33 7/8	S	9	4437.4	68 1/8	62	0.446	0.669	HLP-22	12	8	4	1.9	10.5	5.7	30.8	16.1	0.62	0.33	p2d6	2.46	0.0005184	0.0007662	0.0011729	0.4080
20071193M	7/25 B1	34S_6p2d6Yd_8	33 7/8	S	9	4437.4	68 1/8	62	0.446	0.669	HLP-22	12	8	4	1.9	10.5	5.7	30.8	16.1	0.62	0.33	p2d6	2.46	0.0005184	0.0007662	0.0011729	0.4080
20071200	7/26 A1	34S_6p1d8Ya	33 7/8	S	9	4437.4	68 7/8	62	0.446	0.669	HLP-22	12	8	4	1.9	10.5	5.7	30.8	16.1	0.62	0.33	p1d8	2.45	0.0000605	0.0000895	0.0001320	0.4269
20071203	7/26 A1	34S_6p1d8Ya	33 7/8	S	9	4437.4	68 7/8	62	0.446	0.669	HLP-22	12	8	4	1.9	10.5	5.7	30.8	16.1	0.62	0.33	p1d8	2.45	0.0000605	0.0000895	0.0001320	0.4269
20071205	7/26 A1	34S_6p1d8Ya	33 7/8	S	9	4437.4	68 7/8	62	0.446	0.669	HLP-22	12	8	4	1.9	10.5	5.7	30.8	16.1	0.62	0.33	p1d8	2.45	0.0000605	0.0000895	0.0001320	0.4269
20071209	7/26 A1	34S_6p1d8Ya	33 7/8	S	9	4437.4	68 7/8	62	0.446	0.669	HLP-22	12	8	4	1.9	10.5	5.7	30.8	16.1	0.62	0.33	p1d8	2.45	0.0000605	0.0000895	0.0001320	0.4269
20071212	7/26 A1	34S_6p1d8Ya	33 7/8	S	9	4437.4	68 7/8	62	0.446	0.669	HLP-22	12	8	4	1.9	10.5	5.7	30.8	16.1	0.62	0.33	p1d8	2.45	0.0000605	0.0000895	0.0001320	0.4269
20071213	7/26 A1	34S_6p1d8Ya	33 7/8	S	9	4437.4	68 7/8	62	0.446	0.669	HLP-22	12	8	4	1.9	10.5	5.7	30.8	16.1	0.62	0.33	p1d8	2.45	0.0000605	0.0000895	0.0001320	0.4269
20071216	7/26 A1	34S_6p1d8Ya	33 7/8	S	9	4437.4	68 7/8	62	0.446	0.669	HLP-22	12	8	4	1.9	10.5	5.7	30.8	16.1	0.62	0.33	p1d8	2.45	0.0000605	0.0000895	0.0001320	0.4269
20071219	7/26 A1	34S_6p1d8Ya	33 7/8	S	9	4437.4	68 7/8	62	0.446	0.669	HLP-22	12	8	4	1.9	10.5	5.7	30.8	16.1	0.62	0.33	p1d8	2.45	0.0000605	0.0000895	0.0001320	0.4269
20071222	7/26 A1	34S_6p1d8Ya	33 7/8	S	9	4437.4	68 7/8	62	0.446	0.669	HLP-22	12	8	4	1.9	10.5	5.7	30.8	16.1	0.62	0.33	p1d8	2.45	0.0000605	0.0000895	0.0001320	0.4269
20071225	7/26 A1	34S_6p1d8Ya	33 7/8	S	9	4437.4	68 7/8	62	0.446	0.669	HLP-22	12	8	4	1.9	10.5	5.7	30.8	16.1	0.62	0.33	p1d8	2.45	0.0000605	0.0000895	0.0001320	0.4269
20071229	7/26 B1	34S_6p1d8Yd_8	33 7/8	S	9	4437.4	68 7/8	62	0.446	0.669	HLP-22	12	8	4	1.9	10.5	5.7	30.8	16.1	0.62	0.33	p1d8	2.45	0.0000605	0.0000895	0.0001320	0.4269
20071235	7/26 B1	34S_6p1d8Yd_8	33 7/8	S	9	4437.4	68 7/8	62	0.446	0.669	HLP-22	12	8	4	1.9	10.5	5.7	30.8	16.1	0.62	0.33	p1d8	2.45	0.0000605	0.0000895	0.0001320	0.4269
20071238	7/26 B1	34S_6p1d8Yd_8	33 7/8	S	9	4437.4	68 7/8	62	0.446	0.669	HLP-22	12	8	4	1.9	10.5	5.7	30.8	16.1	0.62	0.33	p1d8	2.45	0.0000605	0.0000895	0.0001320	0.4269
20071241	7/26 B1	34S_6p1d8Yd_8	33 7/8	S	9	4437.4	68 7/8	62	0.446	0.669	HLP-22	12	8	4	1.9	10.5	5.7	30.8	16.1	0.62	0.33	p1d8	2.45	0.0000605	0.0000895	0.0001320	0.4269
20071244	7/26 B1	34S_6p1d8Yd_8	33 7/8	S	9	4437.4	68 7/8	62	0.446	0.669	HLP-22	12	8	4	1.9	10.5	5.7	30.8	16.1	0.62	0.33	p1d8	2.45	0.0000605	0.0000895	0.0001320	0.4269
20071246	7/26 B1	34S_6p1d8Yd_8	33 7/8	S	9	4437.4	68 7/8	62	0.446	0.669	HLP-22	12	8	4	1.9	10.5	5.7	30.8	16.1	0.62	0.33	p1d8	2.45	0.0000605	0.0000895	0.0001320	0.4269
20071248	7/26 B1	34S_6p1d8Yd_8	33 7/8	S	9	4437.4	68 7/8	62	0.446	0.669	HLP-22	12	8	4	1.9	10.5	5.7	30.8	16.1	0.62	0.33	p1d8	2.45	0.0000605	0.0000895	0.0001320	0.4269
20071250	7/26 B1	34S_6p1d8Yd_8	33 7/8	S	9	4437.4	68 7/8	62	0.446	0.669	HLP-22	12	8	4	1.9	10.5	5.7	30.8	16.1	0.62	0.33	p1d8	2.45	0.0000605	0.0000895	0.0001320	0.4269
20071253	7/26 B1	34S_6p1d8Yd_8	33 7/8	S	9	4437.4	68 7/8	62	0.446	0.669	HLP-22	12	8	4	1.9	10.5	5.7	30.8	16.1	0.62	0.33	p1d8	2.45	0.0000605	0.0000895	0.0001320	0.4269
20071256	7/26 B1	34S_6p1d8Yd_8	33 7/8	S	9	4437.4	68 7/8	62	0.446	0.669	HLP-22	12	8	4	1.9	10.5	5.7	30.8	16.1	0.62	0.33	p1d8	2.45	0.0000605	0.0000895	0.0001320	0.4269
20071261	7/26 B1	34S_6p1d8Yd_8	33 7/8	S	9	4437.4	68 7/8	62	0.446	0.669	HLP-22	12	8	4	1.9	10.5	5.7	30.8	16.1	0.62	0.33	p1d8	2.45	0.0000605	0.0000895	0.0001320	0.4269
20071264	7/26 B1	34S_6p1d8Yd_8	33 7/8	S	9	4437.4	68 7/8	62	0.446	0.669	HLP-22	12	8	4	1.9	10.5	5.7	30.8	16.1	0.62	0.33	p1d8	2.45	0.0000605	0.0000895	0.0001320	0.4269
20071267	7/26 B1	34S_6p1d8Yd_8	33 7/8	S	9	4437.4	68 7/8	62	0.446	0.669	HLP-22	12	8	4	1.9	10.5	5.7	30.8	16.1	0.62	0.33	p1d8	2.45	0.0000605	0.0000895	0.0001320	0.4269
20071270	7/26 B1	34S_6p1d8Yd_8	33 7/8	S	9	4437.4	68 7/8	62	0.446	0.669	HLP-22	12	8	4	1.9	10.5	5.7	30.8	16.1	0.62	0.33	p1d8	2.45	0.0000605	0.0000895	0.0001320	0.4269
20071272M	7/26 B1	34S_6p1d8Yd_8	33 7/8	S	9	4437.4	68 7/8	62	0.446	0.669	HLP-22	12	8	4	1.9	10.5	5.7	30.8	16.1	0.62	0.33	p1d8	2.45	0.0000605	0.0000895	0.0001320	0.4269
20071275M	7/26 B1	34S_6p1d8Yd_8	33 7/8	S	9	4437.4	68 7/8	62	0.446	0.669	HLP-22	12	8	4	1.9	10.5	5.7	30.8	16.1	0.62	0.33	p1d8	2.45	0.0000605	0.0000895	0.0001320	0.4269
20071276M	7/26 B1	34S_6p1d8Yd_8	33 7/8	S	9	4437.4	68 7/8	62	0.446	0.669	HLP-22	12	8	4	1.9	10.5	5.7	30.8	16.1	0.62	0.33	p1d8	2.45	0.0000605	0.0000895	0.0001320	0.4269
20071279M	7/26 B1	34S_6p1d8Yd_8	33 7/8	S	9	4437.4	68 7/8	62	0.446	0.669	HLP-22	12	8	4	1.9	10.5	5.7	30.8	16.1	0.62	0.33	p1d8	2.45	0.0000605	0.0000895	0.0001320	0.4269
20071280M	7/26 B1	34S_6p1d8Yd_8	33 7/8	S	9	4437.4	68 7/8	62	0.446	0.669	HLP-22	12	8	4	1.9	10.5	5.7	30.8	16.1	0.62	0.33	p1d8	2.45	0.0000605	0.0000895	0.0001320	0.4269

Table B.7. Data from July 2007 Tests in Mid-Scale Vessel with Spherical Head B.7

Tank Water Temperature	Water Density	Solids Fraction	Pulse Volume Fraction	Duty Cycle	Cycle Time	Pulsed or Steady Jet	Us Steady Jet	U1 Pulsing Jet	U2 URMS	U3 URM3	Discharge Velocity	Critical Suspension Velocity	Average Peak Cloud Height	UCS Condition	UCS Method	UCS Flag	UCS Center Flag	UCS udv Flag	UCS based on Decreasing Velocity	Sweep Increase / Decrease	UDV Height Bed	Particle Motion	Solids Level	Outer Bottom Pattern	Inner Bottom Pattern	Case ID	Test	TDP	Row Number
C	g/cm^3	fraction	fraction	fraction	s	text	m/s	m/s	m/s	m/s	m/s	m/s	in.	m/s	text	text	text	text	m/s	text	mm	text	text	text	text	text	text	text	text
T	ρ_l	ϕ_s	ϕ_p	DC	t_C	Jet	U_S	U1	U2	U3	U	U_{CS}	H_C	U_{CSR}	U_{CSM}	U_{CS}vis	U_{CS}cen	U_{CS}udv	U_{CS}_D	S_W	H_{bed}	PM	Sol	SP_O	SP_I	ID	M/DDX	TDP	MSS
28.0	0.998	0.00485	0.048	0.180	20.3	P	N/A	5.21	5.67	5.88	6.50	6.00	18.63	N/A	N/A	N/A	N/A	N/A	N/A	N/A	N/A	BC	N/A	N/A	N/A	34S_6p2d6Yd_8	7/25 B1	TDP-WTP-014	20071155
28.0	0.998	0.00485	0.048	0.180	18.2	P	N/A	5.40	5.95	6.22	7.00	6.00	19.63	N/A	N/A	N/A	N/A	N/A	N/A	N/A	N/A	BC	N/A	N/A	N/A	34S_6p2d6Yd_8	7/25 B1	TDP-WTP-014	20071159
28.0	0.998	0.00485	0.048	0.180	17.2	P	N/A	5.61	6.22	6.53	7.50	6.00	20.38	N/A	N/A	N/A	N/A	N/A	N/A	N/A	N/A	BC	N/A	N/A	N/A	34S_6p2d6Yd_8	7/25 B1	TDP-WTP-014	20071160
28.0	0.998	0.00485	0.048	0.180	19.4	P	N/A	5.10	5.58	5.82	6.50	6.00	17.63	N/A	N/A	N/A	N/A	N/A	N/A	N/A	N/A	BC	N/A	N/A	N/A	34S_6p2d6Yd_8	7/25 B1	TDP-WTP-014	20071165
28.0	0.998	0.00485	0.048	0.180	20.4	P	N/A	4.87	5.32	5.53	6.20	6.00	16.88	N/A	N/A	N/A	N/A	N/A	N/A	N/A	N/A	BC	N/A	N/A	N/A	34S_6p2d6Yd_8	7/25 B1	TDP-WTP-014	20071168
28.0	0.998	0.00485	0.048	0.180	20.4	P	N/A	4.83	5.25	5.45	6.00	6.00	17.63	N/A	vis dec	UCSvis	N/A	N/A	6.00	D	N/A	CS	N/A	N/A	N/A	34S_6p2d6Yd_8	7/25 B1	TDP-WTP-014	20071171
28.0	0.998	0.00485	0.048	0.180	14.3	P	N/A	5.95	6.79	7.22	8.60	6.00	20.63	N/A	N/A	N/A	N/A	N/A	N/A	N/A	N/A	BC	N/A	N/A	N/A	34S_6p2d6Yd_8	7/25 B1	TDP-WTP-014	20071176
28.0	0.998	0.00485	0.048	0.180	13.8	P	N/A	6.23	7.12	7.59	9.40	6.00	28.63	N/A	N/A	N/A	N/A	N/A	N/A	N/A	N/A	BC	N/A	N/A	N/A	34S_6p2d6Yd_8	7/25 B1	TDP-WTP-014	20071180
28.0	0.998	0.00485	0.048	0.180	13.8	P	N/A	6.20	7.08	7.54	9.00	6.00	25.88	N/A	N/A	N/A	N/A	N/A	N/A	N/A	N/A	BC	N/A	N/A	N/A	34S_6p2d6Yd_8	7/25 B1	TDP-WTP-014	20071182
28.0	0.998	0.00485	0.048	0.180	N/A	P	N/A	6.38	7.30	7.79	9.60	6.00	27.63	N/A	N/A	N/A	N/A	N/A	N/A	N/A	N/A	BC	N/A	N/A	N/A	34S_6p2d6Yd_8	7/25 B1	TDP-WTP-014	20071185
28.0	0.998	0.00485	0.048	0.180	13.1	P	N/A	6.81	7.85	8.39	10.30	6.00	35.63	N/A	N/A	N/A	N/A	N/A	N/A	N/A	N/A	BC	N/A	N/A	N/A	34S_6p2d6Yd_8	7/25 B1	TDP-WTP-014	20071187
28.0	0.998	0.00485	0.048	0.180	16.3	P	N/A	6.05	6.75	7.10	8.30	6.00	20.63	N/A	N/A	N/A	N/A	N/A	N/A	N/A	N/A	BC	N/A	N/A	N/A	34S_6p2d6Yd_8	7/25 B1	TDP-WTP-014	20071193
22.0	0.999	0.00487	undefined	1.000	infinite	S	1.90	N/A	N/A	N/A	1.90	2.00	13.63	N/A	N/A	N/A	N/A	N/A	N/A	N/A	N/A	AM	N/A	N/A	N/A	34S_6p1d8Ya	7/26 A1	TDP-WTP-015	20071200
22.1	0.999	0.00487	undefined	1.000	infinite	S	2.04	N/A	N/A	N/A	2.00	2.00	25.63	N/A	N/A	N/A	N/A	N/A	N/A	N/A	N/A	AM	N/A	N/A	N/A	34S_6p1d8Ya	7/26 A1	TDP-WTP-015	20071203
22.3	0.999	0.00487	undefined	1.000	infinite	S	2.20	N/A	N/A	N/A	2.20	2.00	32.63	N/A	N/A	N/A	N/A	N/A	N/A	N/A	N/A	AM	N/A	N/A	N/A	34S_6p1d8Ya	7/26 A1	TDP-WTP-015	20071205
22.4	0.999	0.00487	undefined	1.000	infinite	S	1.50	N/A	N/A	N/A	1.50	2.00	8.63	N/A	N/A	N/A	N/A	N/A	N/A	N/A	N/A	SS	N/A	N/A	N/A	34S_6p1d8Ya	7/26 A1	TDP-WTP-015	20071209
22.7	0.999	0.00487	undefined	1.000	infinite	S	1.68	N/A	N/A	N/A	1.70	2.00	9.63	N/A	N/A	N/A	N/A	N/A	N/A	N/A	N/A	SS	N/A	N/A	N/A	34S_6p1d8Ya	7/26 A1	TDP-WTP-015	20071212
22.8	0.999	0.00487	undefined	1.000	infinite	S	1.96	N/A	N/A	N/A	1.95	2.00	18.63	N/A	N/A	N/A	N/A	N/A	N/A	N/A	N/A	AM	N/A	N/A	N/A	34S_6p1d8Ya	7/26 A1	TDP-WTP-015	20071213
23.1	0.999	0.00487	undefined	1.000	infinite	S	2.07	N/A	N/A	N/A	2.05	2.00	27.63	N/A	N/A	N/A	N/A	N/A	N/A	N/A	N/A	AM	N/A	N/A	N/A	34S_6p1d8Ya	7/26 A1	TDP-WTP-015	20071216
23.4	0.998	0.00487	undefined	1.000	infinite	S	2.10	N/A	N/A	N/A	2.08	2.00	26.63	N/A	N/A	N/A	N/A	N/A	N/A	N/A	N/A	AM	N/A	N/A	N/A	34S_6p1d8Ya	7/26 A1	TDP-WTP-015	20071219
N/A	N/A	0.00487	undefined	1.000	infinite	S	N/A	N/A	N/A	N/A	2.90	2.00	N/A	N/A	N/A	N/A	N/A	N/A	N/A	N/A	N/A	AM	N/A	N/A	N/A	34S_6p1d8Ya	7/26 A1	TDP-WTP-015	20071222
23.9	0.998	0.00487	undefined	1.000	infinite	S	2.06	N/A	N/A	N/A	2.00	2.00	26.63	N/A	vis dec	UCSvis	N/A	N/A	2.00	D	N/A	CS	N/A	N/A	N/A	34S_6p1d8Ya	7/26 A1	TDP-WTP-015	20071225
25.0	0.998	0.00487	0.048	0.180	62.5	P	N/A	1.80	1.83	1.85	1.90	4.00	9.13	N/A	N/A	N/A	N/A	N/A	N/A	N/A	N/A	SS	N/A	N/A	N/A	34S_6p1d8Yd_8	7/26 B1	TDP-WTP-015	20071229
25.0	0.998	0.00487	0.048	0.180	58.8	P	N/A	1.92	1.96	1.98	2.00	4.00	9.13	N/A	N/A	N/A	N/A	N/A	N/A	N/A	N/A	SS	N/A	N/A	N/A	34S_6p1d8Yd_8	7/26 B1	TDP-WTP-015	20071235
25.0	0.998	0.00487	0.048	0.180	54.9	P	N/A	2.00	2.04	2.06	2.10	4.00	9.63	N/A	N/A	N/A	N/A	N/A	N/A	N/A	N/A	SS	N/A	N/A	N/A	34S_6p1d8Yd_8	7/26 B1	TDP-WTP-015	20071238
25.0	0.998	0.00487	0.048	0.180	54.1	P	N/A	2.07	2.11	2.13	2.20	4.00	9.63	N/A	N/A	N/A	N/A	N/A	N/A	N/A	N/A	SS	N/A	N/A	N/A	34S_6p1d8Yd_8	7/26 B1	TDP-WTP-015	20071241
25.0	0.998	0.00487	0.048	0.180	51.3	P	N/A	2.17	2.22	2.25	2.32	4.00	9.63	N/A	N/A	N/A	N/A	N/A	N/A	N/A	N/A	SS	N/A	N/A	N/A	34S_6p1d8Yd_8	7/26 B1	TDP-WTP-015	20071244
25.0	0.998	0.00487	0.048	0.180	47.6	P	N/A	2.37	2.44	2.47	2.55	4.00	10.63	N/A	N/A	N/A	N/A	N/A	N/A	N/A	N/A	SS	N/A	N/A	N/A	34S_6p1d8Yd_8	7/26 B1	TDP-WTP-015	20071246
N/A	N/A	0.00487	0.048	0.180	47.6	P	N/A	N/A	N/A	N/A	2.50	4.00	10.63	N/A	N/A	N/A	N/A	N/A	N/A	N/A	N/A	N/A	N/A	N/A	N/A	34S_6p1d8Yd_8	7/26 B1	TDP-WTP-015	20071248
25.0	0.998	0.00487	0.048	0.180	43.5	P	N/A	2.59	2.67	2.71	2.80	4.00	11.13	N/A	N/A	N/A	N/A	N/A	N/A	N/A	N/A	SS	N/A	N/A	N/A	34S_6p1d8Yd_8	7/26 B1	TDP-WTP-015	20071250
25.0	0.998	0.00487	0.048	0.180	41.7	P	N/A	2.71	2.80	2.84	3.00	4.00	11.63	N/A	N/A	N/A	N/A	N/A	N/A	N/A	N/A	SS	N/A	N/A	N/A	34S_6p1d8Yd_8	7/26 B1	TDP-WTP-015	20071253
N/A	N/A	0.00487	0.048	0.180	37.0	P	N/A	N/A	N/A	N/A	3.25	4.00	11.63	N/A	N/A	N/A	N/A	N/A	N/A	N/A	N/A	SS	N/A	N/A	N/A	34S_6p1d8Yd_8	7/26 B1	TDP-WTP-015	20071256
N/A	N/A	0.00487	0.048	0.180	35.1	P	N/A	N/A	N/A	N/A	3.50	4.00	12.63	N/A	N/A	N/A	N/A	N/A	N/A	N/A	N/A	SS	N/A	N/A	N/A	34S_6p1d8Yd_8	7/26 B1	TDP-WTP-015	20071261
25.0	0.998	0.00487	0.048	0.180	32.8	P	N/A	3.34	3.50	3.58	3.80	4.00	13.63	N/A	N/A	N/A	N/A	N/A	N/A	N/A	N/A	AM	N/A	N/A	N/A	34S_6p1d8Yd_8	7/26 B1	TDP-WTP-015	20071264
N/A	N/A	0.00487	0.048	0.180	31.3	P	N/A	N/A	N/A	N/A	3.90	4.00	13.63	N/A	N/A	N/A	N/A	N/A	N/A	N/A	N/A	AM	N/A	N/A	N/A	34S_6p1d8Yd_8	7/26 B1	TDP-WTP-015	20071267
25.0	0.998	0.00487	0.048	0.180	30.5	P	N/A	3.50	3.68	3.76	4.00	4.00	14.63	4.00	vis	UCSvis	N/A	N/A	N/A	I	N/A	CS	N/A	N/A	N/A	34S_6p1d8Yd_8	7/26 B1	TDP-WTP-015	20071270
25.0	0.998	0.00487	0.048	0.180	26.2	P	N/A	3.92	4.15	4.26	4.50	4.00	15.63	N/A	N/A	N/A	N/A	N/A	N/A	N/A	N/A	BC	N/A	N/A	N/A	34S_6p1d8Yd_8	7/26 B1	TDP-WTP-015	20071272
25.0	0.998	0.00487	0.048	0.180	25.6	P	N/A	4.20	4.48	4.61	5.00	4.00	24.63	N/A	N/A	N/A	N/A	N/A	N/A	N/A	N/A	BC	N/A	N/A	N/A	34S_6p1d8Yd_8	7/26 B1	TDP-WTP-015	20071275
25.0	0.998	0.00487	0.048	0.180	26.3	P	N/A	4.13	4.37	4.49	4.80	4.00	21.63	N/A	N/A	N/A	N/A	N/A	N/A	N/A	N/A	BC	N/A	N/A	N/A	34S_6p1d8Yd_8	7/26 B1	TDP-WTP-015	20071276
25.0	0.998	0.00487	0.048	0.180	23.8	P	N/A	4.40	4.72	4.87	5.30	4.00	28.63	N/A	N/A	N/A	N/A	N/A	N/A	N/A	N/A	BC	N/A	N/A	N/A	34S_6p1d8Yd_8	7/26 B1	TDP-WTP-015	20071279
25.0	0.998	0.00487	0.048	0.180	26.0	P	N/A	3.92	4.16	4.28	4.63	4.00	17.63	N/A	N/A	N/A	N/A	N/A	N/A	N/A	N/A	BC	N/A	N/A	N/A	34S_6p1d8Yd_8	7/26 B1	TDP-WTP-015	20071280

Table B.7. Data from July 2007 Tests in Mid-Scale Vessel with Spherical Head A.8

Row Number	Test	Case ID	Tank Diameter	Head Shape	Dish Height	Dish Volume	Tank Fill Height	Return Line Height	Nozzle Inner Diameter	Nozzle Stand-off Distance	Pulse Tube Configuration	Installed Nozzles	Outer Nozzles Operated	Inner Nozzles Operated	Pulse Tube Outer Diameter	Outer PJM Radius	Inner PJM Radius	"FIO" Outer PJM Impingement Angle	"FIO" Inner PJM Impingement Angle	Ratio Outer PJM to Tank Radius	Ratio Inner PJM to Tank Radius	Simulant	Solids Density	Particle Diameter d5	Particle Diameter d50	Particle Diameter d95	Void Fraction
text	text	text	in.	text	in.	in. ^{3}	in.	in.	in.	in.	text	number	number	number	in.	in.	in.	deg	deg	nondim	nondim	text	g/cm^3	m	m	m	fraction
MSS	M/DDX	ID	D	HS	H_{dish}	V_{dish}	H	Rtn	d	sod	PT	N	N_O	N_I	PT_{od}	R_O	R_I	θ_O	θ_I	R_O/R	R_I/R	sxdx	ρ_s	d_5	d_{50}	d_{95}	vf
20071283M	7/26 B1	34S_6p1d8Yd_8	33 7/8	S	9	4437.4	68 7/8	62	0.446	0.669	HLP-22	12	8	4	1.9	10.5	5.7	30.8	16.1	0.62	0.33	p1d8	2.45	0.0000605	0.0000895	0.0001320	0.4269
20071285	7/26 B1	34S_6p1d8Yd_8	33 7/8	S	9	4437.4	68 7/8	62	0.446	0.669	HLP-22	12	8	4	1.9	10.5	5.7	30.8	16.1	0.62	0.33	p1d8	2.45	0.0000605	0.0000895	0.0001320	0.4269
20071288	7/26 B1	34S_6p1d8Yd_8	33 7/8	S	9	4437.4	68 7/8	62	0.446	0.669	HLP-22	12	8	4	1.9	10.5	5.7	30.8	16.1	0.62	0.33	p1d8	2.45	0.0000605	0.0000895	0.0001320	0.4269
20071291	7/26 B1	34S_6p1d8Yd_8	33 7/8	S	9	4437.4	68 7/8	62	0.446	0.669	HLP-22	12	8	4	1.9	10.5	5.7	30.8	16.1	0.62	0.33	p1d8	2.45	0.0000605	0.0000895	0.0001320	0.4269
20071302	7/27 A1	34S_6p1d8Yd_8	33 7/8	S	9	4437.4	68 7/8	62	0.446	0.669	HLP-22	12	8	4	1.9	10.5	5.7	30.8	16.1	0.62	0.33	p1d8	2.45	0.0000605	0.0000895	0.0001320	0.4269
20071305	7/27 A1	34S_6p1d8Yd_8	33 7/8	S	9	4437.4	68 7/8	62	0.446	0.669	HLP-22	12	8	4	1.9	10.5	5.7	30.8	16.1	0.62	0.33	p1d8	2.45	0.0000605	0.0000895	0.0001320	0.4269
20071308	7/27 A1	34S_6p1d8Yd_8	33 7/8	S	9	4437.4	68 7/8	62	0.446	0.669	HLP-22	12	8	4	1.9	10.5	5.7	30.8	16.1	0.62	0.33	p1d8	2.45	0.0000605	0.0000895	0.0001320	0.4269
20071311	7/27 A1	34S_6p1d8Yd_8	33 7/8	S	9	4437.4	68 7/8	62	0.446	0.669	HLP-22	12	8	4	1.9	10.5	5.7	30.8	16.1	0.62	0.33	p1d8	2.45	0.0000605	0.0000895	0.0001320	0.4269
20071313	7/27 B1	34S_6p1d8Yc_8	33 7/8	S	9	4437.4	68 7/8	62	0.446	0.669	HLP-22	12	8	4	1.9	10.5	5.7	30.8	16.1	0.62	0.33	p1d8	2.45	0.0000605	0.0000895	0.0001320	0.4269
20071315	7/27 B1	34S_6p1d8Yc_8	33 7/8	S	9	4437.4	68 7/8	62	0.446	0.669	HLP-22	12	8	4	1.9	10.5	5.7	30.8	16.1	0.62	0.33	p1d8	2.45	0.0000605	0.0000895	0.0001320	0.4269
20071318	7/27 B1	34S_6p1d8Yc_8	33 7/8	S	9	4437.4	68 7/8	62	0.446	0.669	HLP-22	12	8	4	1.9	10.5	5.7	30.8	16.1	0.62	0.33	p1d8	2.45	0.0000605	0.0000895	0.0001320	0.4269
20071321	7/27 B1	34S_6p1d8Yc_8	33 7/8	S	9	4437.4	68 7/8	62	0.446	0.669	HLP-22	12	8	4	1.9	10.5	5.7	30.8	16.1	0.62	0.33	p1d8	2.45	0.0000605	0.0000895	0.0001320	0.4269
20071323	7/27 B1	34S_6p1d8Yc_8	33 7/8	S	9	4437.4	68 7/8	62	0.446	0.669	HLP-22	12	8	4	1.9	10.5	5.7	30.8	16.1	0.62	0.33	p1d8	2.45	0.0000605	0.0000895	0.0001320	0.4269
20071325	7/27 B1	34S_6p1d8Yc_8	33 7/8	S	9	4437.4	68 7/8	62	0.446	0.669	HLP-22	12	8	4	1.9	10.5	5.7	30.8	16.1	0.62	0.33	p1d8	2.45	0.0000605	0.0000895	0.0001320	0.4269
20071327M	7/27 B1	34S_6p1d8Yc_8	33 7/8	S	9	4437.4	68 7/8	62	0.446	0.669	HLP-22	12	8	4	1.9	10.5	5.7	30.8	16.1	0.62	0.33	p1d8	2.45	0.0000605	0.0000895	0.0001320	0.4269
20071331	7/27 C1	34S_6p2d6Yd_8	33 7/8	S	9	4437.4	68 1/8	62	0.446	0.669	HLP-22	12	8	4	1.9	10.5	5.7	30.8	16.1	0.62	0.33	p2d6	2.46	0.0005184	0.0007662	0.0011729	0.4080
20071335	7/27 C1	34S_6p2d6Yd_8	33 7/8	S	9	4437.4	68 1/8	62	0.446	0.669	HLP-22	12	8	4	1.9	10.5	5.7	30.8	16.1	0.62	0.33	p2d6	2.46	0.0005184	0.0007662	0.0011729	0.4080
20071338	7/27 C1	34S_6p2d6Yd_8	33 7/8	S	9	4437.4	68 1/8	62	0.446	0.669	HLP-22	12	8	4	1.9	10.5	5.7	30.8	16.1	0.62	0.33	p2d6	2.46	0.0005184	0.0007662	0.0011729	0.4080
20071343	7/27 C1	34S_6p2d6Yd_8	33 7/8	S	9	4437.4	68 1/8	62	0.446	0.669	HLP-22	12	8	4	1.9	10.5	5.7	30.8	16.1	0.62	0.33	p2d6	2.46	0.0005184	0.0007662	0.0011729	0.4080
20071344	7/27 C1	34S_6p2d6Yd_8	33 7/8	S	9	4437.4	68 1/8	62	0.446	0.669	HLP-22	12	8	4	1.9	10.5	5.7	30.8	16.1	0.62	0.33	p2d6	2.46	0.0005184	0.0007662	0.0011729	0.4080
20071347	7/27 C1	34S_6p2d6Yd_8	33 7/8	S	9	4437.4	68 1/8	62	0.446	0.669	HLP-22	12	8	4	1.9	10.5	5.7	30.8	16.1	0.62	0.33	p2d6	2.46	0.0005184	0.0007662	0.0011729	0.4080
20071350	7/27 C1	34S_6p2d6Yd_8	33 7/8	S	9	4437.4	68 1/8	62	0.446	0.669	HLP-22	12	8	4	1.9	10.5	5.7	30.8	16.1	0.62	0.33	p2d6	2.46	0.0005184	0.0007662	0.0011729	0.4080
20071353	7/27 C1	34S_6p2d6Yd_8	33 7/8	S	9	4437.4	68 1/8	62	0.446	0.669	HLP-22	12	8	4	1.9	10.5	5.7	30.8	16.1	0.62	0.33	p2d6	2.46	0.0005184	0.0007662	0.0011729	0.4080
20071356	7/27 D1	34S_6p2d6Yc_8	33 7/8	S	9	4437.4	68 1/8	62	0.446	0.669	HLP-22	12	8	4	1.9	10.5	5.7	30.8	16.1	0.62	0.33	p2d6	2.46	0.0005184	0.0007662	0.0011729	0.4080
20071358	7/27 D1	34S_6p2d6Yc_8	33 7/8	S	9	4437.4	68 1/8	62	0.446	0.669	HLP-22	12	8	4	1.9	10.5	5.7	30.8	16.1	0.62	0.33	p2d6	2.46	0.0005184	0.0007662	0.0011729	0.4080
20071360	7/27 D1	34S_6p2d6Yc_8	33 7/8	S	9	4437.4	68 1/8	62	0.446	0.669	HLP-22	12	8	4	1.9	10.5	5.7	30.8	16.1	0.62	0.33	p2d6	2.46	0.0005184	0.0007662	0.0011729	0.4080
20071362	7/27 D1	34S_6p2d6Yc_8	33 7/8	S	9	4437.4	68 1/8	62	0.446	0.669	HLP-22	12	8	4	1.9	10.5	5.7	30.8	16.1	0.62	0.33	p2d6	2.46	0.0005184	0.0007662	0.0011729	0.4080
20071367	7/27 D1	34S_6p2d6Yc_8	33 7/8	S	9	4437.4	68 1/8	62	0.446	0.669	HLP-22	12	8	4	1.9	10.5	5.7	30.8	16.1	0.62	0.33	p2d6	2.46	0.0005184	0.0007662	0.0011729	0.4080
20071369	7/27 D1	34S_6p2d6Yc_8	33 7/8	S	9	4437.4	68 1/8	62	0.446	0.669	HLP-22	12	8	4	1.9	10.5	5.7	30.8	16.1	0.62	0.33	p2d6	2.46	0.0005184	0.0007662	0.0011729	0.4080
20071371	7/27 D1	34S_6p2d6Yc_8	33 7/8	S	9	4437.4	68 1/8	62	0.446	0.669	HLP-22	12	8	4	1.9	10.5	5.7	30.8	16.1	0.62	0.33	p2d6	2.46	0.0005184	0.0007662	0.0011729	0.4080
20071374	7/27 D1	34S_6p2d6Yc_8	33 7/8	S	9	4437.4	68 1/8	62	0.446	0.669	HLP-22	12	8	4	1.9	10.5	5.7	30.8	16.1	0.62	0.33	p2d6	2.46	0.0005184	0.0007662	0.0011729	0.4080
20071377	7/27 D1	34S_6p2d6Yc_8	33 7/8	S	9	4437.4	68 1/8	62	0.446	0.669	HLP-22	12	8	4	1.9	10.5	5.7	30.8	16.1	0.62	0.33	p2d6	2.46	0.0005184	0.0007662	0.0011729	0.4080
20071381	7/27 D1	34S_6p2d6Yc_8	33 7/8	S	9	4437.4	68 1/8	62	0.446	0.669	HLP-22	12	8	4	1.9	10.5	5.7	30.8	16.1	0.62	0.33	p2d6	2.46	0.0005184	0.0007662	0.0011729	0.4080
20071382	7/27 D1	34S_6p2d6Yc_8	33 7/8	S	9	4437.4	68 1/8	62	0.446	0.669	HLP-22	12	8	4	1.9	10.5	5.7	30.8	16.1	0.62	0.33	p2d6	2.46	0.0005184	0.0007662	0.0011729	0.4080
20071383	7/27 D1	34S_6p2d6Yc_8	33 7/8	S	9	4437.4	68 1/8	62	0.446	0.669	HLP-22	12	8	4	1.9	10.5	5.7	30.8	16.1	0.62	0.33	p2d6	2.46	0.0005184	0.0007662	0.0011729	0.4080
20071387	7/27 B2	34S_6p2d6Ya	33 7/8	S	9	4437.4	68 1/8	62	0.446	0.669	HLP-22	12	8	4	1.9	10.5	5.7	30.8	16.1	0.62	0.33	p2d6	2.46	0.0005184	0.0007662	0.0011729	0.4080
20071389	7/27 B2	34S_6p2d6Ya	33 7/8	S	9	4437.4	68 1/8	62	0.446	0.669	HLP-22	12	8	4	1.9	10.5	5.7	30.8	16.1	0.62	0.33	p2d6	2.46	0.0005184	0.0007662	0.0011729	0.4080
20071390	7/27 B2	34S_6p2d6Ya	33 7/8	S	9	4437.4	68 1/8	62	0.446	0.669	HLP-22	12	8	4	1.9	10.5	5.7	30.8	16.1	0.62	0.33	p2d6	2.46	0.0005184	0.0007662	0.0011729	0.4080
20071394	7/27 B2	34S_6p2d6Ya	33 7/8	S	9	4437.4	68 1/8	62	0.446	0.669	HLP-22	12	8	4	1.9	10.5	5.7	30.8	16.1	0.62	0.33	p2d6	2.46	0.0005184	0.0007662	0.0011729	0.4080
20071397	7/27 B2	34S_6p2d6Ya	33 7/8	S	9	4437.4	68 1/8	62	0.446	0.669	HLP-22	12	8	4	1.9	10.5	5.7	30.8	16.1	0.62	0.33	p2d6	2.46	0.0005184	0.0007662	0.0011729	0.4080
20071401	7/27 B2	34S_6p2d6Ya	33 7/8	S	9	4437.4	68 1/8	62	0.446	0.669	HLP-22	12	8	4	1.9	10.5	5.7	30.8	16.1	0.62	0.33	p2d6	2.46	0.0005184	0.0007662	0.0011729	0.4080

Table B.7. Data from July 2007 Tests in Mid-Scale Vessel with Spherical Head B.8

Tank Water Temperature	Water Density	Solids Fraction	Pulse Volume Fraction	Duty Cycle	Cycle Time	Pulsed or Steady Jet	Us Steady Jet	U1 Pulsing Jet	U2 URMS	U3 URM3	Discharge Velocity	Critical Suspension Velocity	Average Peak Cloud Height	UCS Condition	UCS Method	UCS Flag	UCS Center Flag	UCS udv Flag	UCS based on Decreasing Velocity	Sweep Increase / Decrease	UDV Height Bed	Particle Motion	Solids Level	Outer Bottom Pattern	Inner Bottom Pattern	Case ID	Test	TDP	Row Number
C	g/cm³	fraction	fraction	fraction	s	text	m/s	m/s	m/s	m/s	m/s	m/s	in.	m/s	text	text	text	text	m/s	text	mm	text	text	text	text	text	text	text	text
T	ρ_l	ϕ_s	ϕ_p	DC	t_C	Jet	U_S	U1	U2	U3	U	U_{CS}	H_C	U_{CSR}	U_{CSM}	U_{CS}vis	U_{CS}cen	U_{CS}udv	U_{CS}_D	S_W	H_{bed}	PM	Sol	SP_O	SP_I	ID	M/DDX	TDP	MSS
25.0	0.998	0.00487	0.048	0.180	21.9	P	N/A	4.52	4.87	5.04	5.50	4.00	33.63	N/A	N/A	N/A	N/A	N/A	N/A	N/A	N/A	BC	N/A	N/A	N/A	34S_6p1d8Yd_8	7/26 B1	TDP-WTP-015	20071283
N/A	N/A	0.00487	0.048	0.180	27.8	P	N/A	N/A	N/A	N/A	4.50	4.00	N/A	N/A	N/A	N/A	N/A	N/A	N/A	N/A	N/A	BC	N/A	N/A	N/A	34S_6p1d8Yd_8	7/26 B1	TDP-WTP-015	20071285
N/A	N/A	0.00487	0.048	0.180	N/A	P	N/A	N/A	N/A	N/A	4.10	4.00	N/A	N/A	N/A	N/A	N/A	N/A	N/A	N/A	N/A	BC	N/A	N/A	N/A	34S_6p1d8Yd_8	7/26 B1	TDP-WTP-015	20071288
25.0	0.998	0.00487	0.048	0.180	29.4	P	N/A	3.51	3.68	3.76	4.00	4.00	N/A	N/A	vis dec	UCSvis	N/A	N/A	4.00	D	N/A	CS	N/A	N/A	N/A	34S_6p1d8Yd_8	7/26 B1	TDP-WTP-015	20071291
27.0	0.998	0.00487	0.048	0.180	30.6	P	N/A	3.51	3.68	3.77	4.00	4.00	N/A	4.00	vis	UCSvis	N/A	N/A	N/A	I	N/A	CS	N/A	N/A	N/A	34S_6p1d8Yd_8	7/27 A1	TDP-WTP-016	20071302
N/A	N/A	0.00487	0.048	0.180	32.8	P	N/A	N/A	N/A	N/A	3.80	4.00	N/A	N/A	N/A	N/A	N/A	N/A	N/A	N/A	N/A	SS/AM	N/A	N/A	N/A	34S_6p1d8Yd_8	7/27 A1	TDP-WTP-016	20071305
N/A	N/A	0.00487	0.048	0.180	N/A	P	N/A	N/A	N/A	N/A	4.50	4.00	N/A	N/A	N/A	N/A	N/A	N/A	N/A	N/A	N/A	BC	N/A	N/A	N/A	34S_6p1d8Yd_8	7/27 A1	TDP-WTP-016	20071308
27.0	0.998	0.00487	0.048	0.180	31.3	P	N/A	3.51	3.69	3.78	4.00	4.00	N/A	N/A	vis dec	UCSvis	N/A	N/A	4.00	D	N/A	CS	N/A	N/A	N/A	34S_6p1d8Yd_8	7/27 A1	TDP-WTP-016	20071311
N/A	N/A	0.00487	0.048	0.330	21.0	P	N/A	N/A	N/A	N/A	3.20	3.60	N/A	N/A	N/A	N/A	N/A	N/A	N/A	N/A	N/A	AM	N/A	N/A	N/A	34S_6p1d8Yc_8	7/27 B1	TDP-WTP-016	20071313
N/A	N/A	0.00487	0.048	0.330	19.2	P	N/A	N/A	N/A	N/A	3.50	3.60	N/A	N/A	N/A	N/A	N/A	N/A	N/A	N/A	N/A	AM	N/A	N/A	N/A	34S_6p1d8Yc_8	7/27 B1	TDP-WTP-016	20071315
27.0	0.998	0.00487	0.048	0.330	18.5	P	N/A	3.19	3.32	3.39	3.60	3.60	N/A	3.60	vis	UCSvis	N/A	N/A	N/A	I	N/A	CS	N/A	N/A	N/A	34S_6p1d8Yc_8	7/27 B1	TDP-WTP-016	20071318
N/A	N/A	0.00487	0.048	0.330	16.1	P	N/A	N/A	N/A	N/A	4.50	3.60	N/A	N/A	N/A	N/A	N/A	N/A	N/A	N/A	N/A	N/A	N/A	N/A	N/A	34S_6p1d8Yc_8	7/27 B1	TDP-WTP-016	20071321
N/A	N/A	0.00487	0.048	0.330	16.1	P	N/A	N/A	N/A	N/A	4.45	3.60	N/A	N/A	N/A	N/A	N/A	N/A	N/A	N/A	N/A	BC	N/A	N/A	N/A	34S_6p1d8Yc_8	7/27 B1	TDP-WTP-016	20071323
N/A	N/A	0.00487	0.048	0.330	17.4	P	N/A	N/A	N/A	N/A	3.80	3.60	N/A	N/A	N/A	N/A	N/A	N/A	N/A	N/A	N/A	BC	N/A	N/A	N/A	34S_6p1d8Yc_8	7/27 B1	TDP-WTP-016	20071325
27.0	0.998	0.00487	0.048	0.330	18.7	P	N/A	3.18	3.33	3.39	3.60	3.60	12.63	N/A	vis dec	UCSvis	N/A	N/A	3.60	D	N/A	CS	N/A	N/A	N/A	34S_6p1d8Yc_8	7/27 B1	TDP-WTP-016	20071327
N/A	N/A	0.00485	0.048	0.180	22.2	P	N/A	N/A	N/A	N/A	5.50	6.00	N/A	N/A	N/A	N/A	N/A	N/A	N/A	N/A	N/A	AM	N/A	N/A	N/A	34S_6p2d6Yd_8	7/27 C1	TDP-WTP-017	20071331
N/A	N/A	0.00485	0.048	0.180	21.5	P	N/A	N/A	N/A	N/A	5.70	6.00	N/A	N/A	N/A	N/A	N/A	N/A	N/A	N/A	N/A	AM	N/A	N/A	N/A	34S_6p2d6Yd_8	7/27 C1	TDP-WTP-017	20071335
23.0	0.999	0.00485	0.048	0.180	20.8	P	N/A	4.75	5.17	5.37	6.00	6.00	N/A	6.00	vis	UCSvis	N/A	N/A	N/A	I	N/A	CS	N/A	N/A	N/A	34S_6p2d6Yd_8	7/27 C1	TDP-WTP-017	20071338
N/A	N/A	0.00485	0.048	0.180	19.7	P	N/A	N/A	N/A	N/A	6.58	6.00	N/A	N/A	N/A	N/A	N/A	N/A	N/A	N/A	N/A	BC	N/A	N/A	N/A	34S_6p2d6Yd_8	7/27 C1	TDP-WTP-017	20071343
N/A	N/A	0.00485	0.048	0.180	19.7	P	N/A	N/A	N/A	N/A	6.60	6.00	N/A	N/A	N/A	N/A	N/A	N/A	N/A	N/A	N/A	BC	N/A	N/A	N/A	34S_6p2d6Yd_8	7/27 C1	TDP-WTP-017	20071344
N/A	N/A	0.00485	0.048	0.180	20.8	P	N/A	N/A	N/A	N/A	6.35	6.00	N/A	N/A	N/A	N/A	N/A	N/A	N/A	N/A	N/A	BC	N/A	N/A	N/A	34S_6p2d6Yd_8	7/27 C1	TDP-WTP-017	20071347
N/A	N/A	0.00485	0.048	0.180	20.8	P	N/A	N/A	N/A	N/A	6.10	6.00	N/A	N/A	N/A	N/A	N/A	N/A	N/A	N/A	N/A	BC	N/A	N/A	N/A	34S_6p2d6Yd_8	7/27 C1	TDP-WTP-017	20071350
23.0	0.999	0.00485	0.048	0.180	21.1	P	N/A	4.79	5.20	5.39	6.00	6.00	N/A	N/A	vis dec	UCSvis	N/A	N/A	6.00	D	N/A	CS	N/A	N/A	N/A	34S_6p2d6Yd_8	7/27 C1	TDP-WTP-017	20071353
N/A	N/A	0.00485	0.048	0.330	14.9	P	N/A	N/A	N/A	N/A	4.35	6.00	N/A	N/A	N/A	N/A	N/A	N/A	N/A	N/A	N/A	SS	N/A	N/A	N/A	34S_6p2d6Yc_8	7/27 D1	TDP-WTP-017	20071356
N/A	N/A	0.00485	0.048	0.330	N/A	P	N/A	N/A	N/A	N/A	4.10	6.00	N/A	N/A	N/A	N/A	N/A	N/A	N/A	N/A	N/A	SS	N/A	N/A	N/A	34S_6p2d6Yc_8	7/27 D1	TDP-WTP-017	20071358
N/A	N/A	0.00485	0.048	0.330	N/A	P	N/A	N/A	N/A	N/A	5.00	6.00	N/A	N/A	N/A	N/A	N/A	N/A	N/A	N/A	N/A	SS	N/A	N/A	N/A	34S_6p2d6Yc_8	7/27 D1	TDP-WTP-017	20071360
N/A	N/A	0.00485	0.048	0.330	12.6	P	N/A	N/A	N/A	N/A	5.50	6.00	N/A	N/A	N/A	N/A	N/A	N/A	N/A	N/A	N/A	AM	N/A	N/A	N/A	34S_6p2d6Yc_8	7/27 D1	TDP-WTP-017	20071362
N/A	N/A	0.00485	0.048	0.330	12.1	P	N/A	N/A	N/A	N/A	5.75	6.00	N/A	N/A	N/A	N/A	N/A	N/A	N/A	N/A	N/A	AM	N/A	N/A	N/A	34S_6p2d6Yc_8	7/27 D1	TDP-WTP-017	20071367
23.0	0.999	0.00485	0.048	0.330	11.6	P	N/A	4.74	5.17	5.37	6.00	6.00	N/A	6.00	vis	UCSvis	N/A	N/A	N/A	I	N/A	CS	N/A	N/A	N/A	34S_6p2d6Yc_8	7/27 D1	TDP-WTP-017	20071369
N/A	N/A	0.00485	0.048	0.330	10.6	P	N/A	N/A	N/A	N/A	6.60	6.00	N/A	N/A	N/A	N/A	N/A	N/A	N/A	N/A	N/A	BC	N/A	N/A	N/A	34S_6p2d6Yc_8	7/27 D1	TDP-WTP-017	20071371
N/A	N/A	0.00485	0.048	0.330	10.7	P	N/A	N/A	N/A	N/A	6.10	6.00	N/A	N/A	N/A	N/A	N/A	N/A	N/A	N/A	N/A	BC	N/A	N/A	N/A	34S_6p2d6Yc_8	7/27 D1	TDP-WTP-017	20071374
23.0	0.999	0.00485	0.048	0.330	11.6	P	N/A	4.72	5.16	5.36	6.00	6.00	N/A	N/A	vis dec	UCSvis	N/A	N/A	6.00	D	N/A	CS	N/A	N/A	N/A	34S_6p2d6Yc_8	7/27 D1	TDP-WTP-017	20071377
N/A	N/A	0.00485	0.048	0.330	11.7	P	N/A	N/A	N/A	N/A	5.80	6.00	N/A	N/A	N/A	N/A	N/A	N/A	N/A	N/A	N/A	AM	N/A	N/A	N/A	34S_6p2d6Yc_8	7/27 D1	TDP-WTP-017	20071381
N/A	N/A	0.00485	0.048	0.330	11.7	P	N/A	N/A	N/A	N/A	5.85	6.00	N/A	N/A	N/A	N/A	N/A	N/A	N/A	N/A	N/A	AM	N/A	N/A	N/A	34S_6p2d6Yc_8	7/27 D1	TDP-WTP-017	20071382
N/A	N/A	0.00485	0.048	0.330	N/A	P	N/A	N/A	N/A	N/A	1.55	6.00	N/A	N/A	N/A	N/A	N/A	N/A	N/A	N/A	N/A	N/A	N/A	N/A	N/A	34S_6p2d6Yc_8	7/27 D1	TDP-WTP-017	20071383
N/A	N/A	0.00485	undefined	1.000	infinite	S	N/A	N/A	N/A	N/A	4.06	5.75	N/A	N/A	N/A	N/A	N/A	N/A	N/A	N/A	N/A	SS	N/A	N/A	N/A	34S_6p2d6Ya	7/27 B2	TDP-WTP-017	20071387
N/A	N/A	0.00485	undefined	1.000	infinite	S	N/A	N/A	N/A	N/A	4.00	5.75	N/A	N/A	N/A	N/A	N/A	N/A	N/A	N/A	N/A	SS	N/A	N/A	N/A	34S_6p2d6Ya	7/27 B2	TDP-WTP-017	20071389
N/A	N/A	0.00485	undefined	1.000	infinite	S	N/A	N/A	N/A	N/A	5.00	5.75	N/A	N/A	N/A	N/A	N/A	N/A	N/A	N/A	N/A	SS	N/A	N/A	N/A	34S_6p2d6Ya	7/27 B2	TDP-WTP-017	20071390
N/A	N/A	0.00485	undefined	1.000	infinite	S	N/A	N/A	N/A	N/A	5.50	5.75	N/A	N/A	N/A	N/A	N/A	N/A	N/A	N/A	N/A	AM	N/A	N/A	N/A	34S_6p2d6Ya	7/27 B2	TDP-WTP-017	20071394
24.7	0.998	0.00485	undefined	1.000	infinite	S	5.75	N/A	N/A	N/A	5.75	5.75	N/A	5.75	vis	UCSvis	N/A	N/A	N/A	N/A	N/A	CS	N/A	N/A	N/A	34S_6p2d6Ya	7/27 B2	TDP-WTP-017	20071397
24.8	0.998	0.00485	undefined	1.000	infinite	S	5.53	N/A	N/A	N/A	5.50	5.75	N/A	N/A	N/A	N/A	N/A	N/A	N/A	N/A	N/A	AM	N/A	N/A	N/A	34S_6p2d6Ya	7/27 B2	TDP-WTP-017	20071401

Table B.8. Data from Fall 2007 Tests in Mid-Scale Vessel with Spherical Head A.1

Row Number	Test	Case ID	Tank Diameter	Head Shape	Dish Height	Dish Volume	Tank Fill Height	Return Line Height	Nozzle Inner Diameter	Nozzle Stand-off Distance	Pulse Tube Configuration	Installed Nozzles	Outer Nozzles Operated	Inner Nozzles Operated	Pulse Tube Outer Diameter	Outer PJM Radius	Inner PJM Radius	"FIO" Outer PJM Impingement Angle	"FIO" Inner PJM Impingement Angle	Ratio Outer PJM to Tank Radius	Ratio Inner PJM to Tank Radius	Simulant	Solids Density	Particle Diameter d5	Particle Diameter d50	Particle Diameter d95	Void Fraction
text	text	text	in.	text	in.	in. ^{3}	in.	in.	in.	in.	text	number	number	number	in.	in.	in.	deg	deg	nondim	nondim	text	g/cm^3	m	m	m	fraction
MSS	M/DDX	ID	D	HS	H_{dish}	V_{dish}	H	Rtn	d	sod	PT	N	N_O	N_I	PT_{od}	R_O	R_I	θ_O	θ_I	R_O/R	R_I/R	sxdx	ρ_s	d_5	d_{50}	d_{95}	vf
7090002	10/17A1	34S_6p1d7Ya-80	33 7/8	S	9	4437.4	67 3/4	61 3/4	0.446	0.669	HLP-22	12	8	0	1.9	10.5	5.7	30.8	16.1	0.62	0.33	p1d7	2.45	0.0001213	0.0001780	0.0002606	0.4277
7090004	10/17A1	34S_6p1d7Ya-80	33 7/8	S	9	4437.4	67 3/4	61 3/4	0.446	0.669	HLP-22	12	8	0	1.9	10.5	5.7	30.8	16.1	0.62	0.33	p1d7	2.45	0.0001213	0.0001780	0.0002606	0.4277
7090006	10/17A1	34S_6p1d7Ya-80	33 7/8	S	9	4437.4	67 3/4	61 3/4	0.446	0.669	HLP-22	12	8	0	1.9	10.5	5.7	30.8	16.1	0.62	0.33	p1d7	2.45	0.0001213	0.0001780	0.0002606	0.4277
7090008	10/17A1	34S_6p1d7Ya-80	33 7/8	S	9	4437.4	67 3/4	61 3/4	0.446	0.669	HLP-22	12	8	0	1.9	10.5	5.7	30.8	16.1	0.62	0.33	p1d7	2.45	0.0001213	0.0001780	0.0002606	0.4277
7090012	10/17A1	34S_6p1d7Ya-80	33 7/8	S	9	4437.4	67 3/4	61 3/4	0.446	0.669	HLP-22	12	8	0	1.9	10.5	5.7	30.8	16.1	0.62	0.33	p1d7	2.45	0.0001213	0.0001780	0.0002606	0.4277
7090015	10/17A1	34S_6p1d7Ya-80	33 7/8	S	9	4437.4	67 3/4	61 3/4	0.446	0.669	HLP-22	12	8	0	1.9	10.5	5.7	30.8	16.1	0.62	0.33	p1d7	2.45	0.0001213	0.0001780	0.0002606	0.4277
7090019	10/17A1	34S_6p1d7Ya-80	33 7/8	S	9	4437.4	67 3/4	61 3/4	0.446	0.669	HLP-22	12	8	0	1.9	10.5	5.7	30.8	16.1	0.62	0.33	p1d7	2.45	0.0001213	0.0001780	0.0002606	0.4277
7090023	10/17A2	34S_6p1d7Yd_5	33 7/8	S	9	4437.4	67 3/4	61 3/4	0.446	0.669	HLP-22	12	8	0	1.9	10.5	5.7	30.8	16.1	0.62	0.33	p1d7	2.45	0.0001213	0.0001780	0.0002606	0.4277
7090026	10/17A2	34S_6p1d7Yd_5	33 7/8	S	9	4437.4	67 3/4	61 3/4	0.446	0.669	HLP-22	12	8	0	1.9	10.5	5.7	30.8	16.1	0.62	0.33	p1d7	2.45	0.0001213	0.0001780	0.0002606	0.4277
7090029	10/17A2	34S_6p1d7Yd_5	33 7/8	S	9	4437.4	67 3/4	61 3/4	0.446	0.669	HLP-22	12	8	0	1.9	10.5	5.7	30.8	16.1	0.62	0.33	p1d7	2.45	0.0001213	0.0001780	0.0002606	0.4277
7090032	10/17A2	34S_6p1d7Yd_5	33 7/8	S	9	4437.4	67 3/4	61 3/4	0.446	0.669	HLP-22	12	8	0	1.9	10.5	5.7	30.8	16.1	0.62	0.33	p1d7	2.45	0.0001213	0.0001780	0.0002606	0.4277
7090035	10/17A2	34S_6p1d7Yd_5	33 7/8	S	9	4437.4	67 3/4	61 3/4	0.446	0.669	HLP-22	12	8	0	1.9	10.5	5.7	30.8	16.1	0.62	0.33	p1d7	2.45	0.0001213	0.0001780	0.0002606	0.4277
7090038	10/17A2	34S_6p1d7Yd_5	33 7/8	S	9	4437.4	67 3/4	61 3/4	0.446	0.669	HLP-22	12	8	0	1.9	10.5	5.7	30.8	16.1	0.62	0.33	p1d7	2.45	0.0001213	0.0001780	0.0002606	0.4277
7090040	10/17A2	34S_6p1d7Yd_5	33 7/8	S	9	4437.4	67 3/4	61 3/4	0.446	0.669	HLP-22	12	8	0	1.9	10.5	5.7	30.8	16.1	0.62	0.33	p1d7	2.45	0.0001213	0.0001780	0.0002606	0.4277
7090043	10/17A2	34S_6p1d7Yd_5	33 7/8	S	9	4437.4	67 3/4	61 3/4	0.446	0.669	HLP-22	12	8	0	1.9	10.5	5.7	30.8	16.1	0.62	0.33	p1d7	2.45	0.0001213	0.0001780	0.0002606	0.4277
7090046	10/17A2	34S_6p1d7Yd_5	33 7/8	S	9	4437.4	67 3/4	61 3/4	0.446	0.669	HLP-22	12	8	0	1.9	10.5	5.7	30.8	16.1	0.62	0.33	p1d7	2.45	0.0001213	0.0001780	0.0002606	0.4277
7090048	10/17A2	34S_6p1d7Yd_5	33 7/8	S	9	4437.4	67 3/4	61 3/4	0.446	0.669	HLP-22	12	8	0	1.9	10.5	5.7	30.8	16.1	0.62	0.33	p1d7	2.45	0.0001213	0.0001780	0.0002606	0.4277
7090052	10/17A2	34S_6p1d7Yd_5	33 7/8	S	9	4437.4	67 3/4	61 3/4	0.446	0.669	HLP-22	12	8	0	1.9	10.5	5.7	30.8	16.1	0.62	0.33	p1d7	2.45	0.0001213	0.0001780	0.0002606	0.4277
7090054M	10/17A2	34S_6p1d7Yd_5	33 7/8	S	9	4437.4	67 3/4	61 3/4	0.446	0.669	HLP-22	12	8	0	1.9	10.5	5.7	30.8	16.1	0.62	0.33	p1d7	2.45	0.0001213	0.0001780	0.0002606	0.4277
7090056	10/18A1	34S_6p1d7Ya-44	33 7/8	S	9	4437.4	67 3/4	61 3/4	0.446	0.669	HLP-22	12	4	4	1.9	10.5	5.7	30.8	16.1	0.62	0.33	p1d7	2.45	0.0001213	0.0001780	0.0002606	0.4277
7090059	10/18A1	34S_6p1d7Ya-44	33 7/8	S	9	4437.4	67 3/4	61 3/4	0.446	0.669	HLP-22	12	4	4	1.9	10.5	5.7	30.8	16.1	0.62	0.33	p1d7	2.45	0.0001213	0.0001780	0.0002606	0.4277
7090063	10/18A1	34S_6p1d7Ya-44	33 7/8	S	9	4437.4	67 3/4	61 3/4	0.446	0.669	HLP-22	12	4	4	1.9	10.5	5.7	30.8	16.1	0.62	0.33	p1d7	2.45	0.0001213	0.0001780	0.0002606	0.4277
7090066	10/18A1	34S_6p1d7Ya-44	33 7/8	S	9	4437.4	67 3/4	61 3/4	0.446	0.669	HLP-22	12	4	4	1.9	10.5	5.7	30.8	16.1	0.62	0.33	p1d7	2.45	0.0001213	0.0001780	0.0002606	0.4277
7090068	10/18A1	34S_6p1d7Ya-44	33 7/8	S	9	4437.4	67 3/4	61 3/4	0.446	0.669	HLP-22	12	4	4	1.9	10.5	5.7	30.8	16.1	0.62	0.33	p1d7	2.45	0.0001213	0.0001780	0.0002606	0.4277
7090071	10/18A2	34S_6p1d7Yd_0	33 7/8	S	9	4437.4	67 3/4	61 3/4	0.446	0.669	HLP-22	12	4	4	1.9	10.5	5.7	30.8	16.1	0.62	0.33	p1d7	2.45	0.0001213	0.0001780	0.0002606	0.4277
7090074	10/18A2	34S_6p1d7Yd_0	33 7/8	S	9	4437.4	67 3/4	61 3/4	0.446	0.669	HLP-22	12	4	4	1.9	10.5	5.7	30.8	16.1	0.62	0.33	p1d7	2.45	0.0001213	0.0001780	0.0002606	0.4277
7090077	10/18A2	34S_6p1d7Yd_0	33 7/8	S	9	4437.4	67 3/4	61 3/4	0.446	0.669	HLP-22	12	4	4	1.9	10.5	5.7	30.8	16.1	0.62	0.33	p1d7	2.45	0.0001213	0.0001780	0.0002606	0.4277
7090081	10/18A2	34S_6p1d7Yd_0	33 7/8	S	9	4437.4	67 3/4	61 3/4	0.446	0.669	HLP-22	12	4	4	1.9	10.5	5.7	30.8	16.1	0.62	0.33	p1d7	2.45	0.0001213	0.0001780	0.0002606	0.4277
7090085	10/18A2	34S_6p1d7Yd_0	33 7/8	S	9	4437.4	67 3/4	61 3/4	0.446	0.669	HLP-22	12	4	4	1.9	10.5	5.7	30.8	16.1	0.62	0.33	p1d7	2.45	0.0001213	0.0001780	0.0002606	0.4277
7090089	10/18A2	34S_6p1d7Yd_0	33 7/8	S	9	4437.4	67 3/4	61 3/4	0.446	0.669	HLP-22	12	4	4	1.9	10.5	5.7	30.8	16.1	0.62	0.33	p1d7	2.45	0.0001213	0.0001780	0.0002606	0.4277
7090095M	10/18A2	34S_6p1d7Yd_0	33 7/8	S	9	4437.4	67 3/4	61 3/4	0.446	0.669	HLP-22	12	4	4	1.9	10.5	5.7	30.8	16.1	0.62	0.33	p1d7	2.45	0.0001213	0.0001780	0.0002606	0.4277
7090097	10/18B1	34S_6p1d7Ya-40	33 7/8	S	9	4437.4	67 3/4	61 3/4	0.446	0.669	HLP-22	12	4	0	1.9	10.5	5.7	30.8	16.1	0.62	0.33	p1d7	2.45	0.0001213	0.0001780	0.0002606	0.4277
7090101	10/18B1	34S_6p1d7Ya-40	33 7/8	S	9	4437.4	67 3/4	61 3/4	0.446	0.669	HLP-22	12	4	0	1.9	10.5	5.7	30.8	16.1	0.62	0.33	p1d7	2.45	0.0001213	0.0001780	0.0002606	0.4277
7090105	10/18B1	34S_6p1d7Ya-40	33 7/8	S	9	4437.4	67 3/4	61 3/4	0.446	0.669	HLP-22	12	4	0	1.9	10.5	5.7	30.8	16.1	0.62	0.33	p1d7	2.45	0.0001213	0.0001780	0.0002606	0.4277
7090111	10/18B1	34S_6p1d7Ya-40	33 7/8	S	9	4437.4	67 3/4	61 3/4	0.446	0.669	HLP-22	12	4	0	1.9	10.5	5.7	30.8	16.1	0.62	0.33	p1d7	2.45	0.0001213	0.0001780	0.0002606	0.4277
7090113	10/18B2	34S_6p1d7Yd_6	33 7/8	S	9	4437.4	67 3/4	61 3/4	0.446	0.669	HLP-22	12	4	0	1.9	10.5	5.7	30.8	16.1	0.62	0.33	p1d7	2.45	0.0001213	0.0001780	0.0002606	0.4277
7090116	10/18B2	34S_6p1d7Yd_6	33 7/8	S	9	4437.4	67 3/4	61 3/4	0.446	0.669	HLP-22	12	4	0	1.9	10.5	5.7	30.8	16.1	0.62	0.33	p1d7	2.45	0.0001213	0.0001780	0.0002606	0.4277
7090119	10/18B2	34S_6p1d7Yd_6	33 7/8	S	9	4437.4	67 3/4	61 3/4	0.446	0.669	HLP-22	12	4	0	1.9	10.5	5.7	30.8	16.1	0.62	0.33	p1d7	2.45	0.0001213	0.0001780	0.0002606	0.4277
7090122	10/18B2	34S_6p1d7Yd_6	33 7/8	S	9	4437.4	67 3/4	61 3/4	0.446	0.669	HLP-22	12	4	0	1.9	10.5	5.7	30.8	16.1	0.62	0.33	p1d7	2.45	0.0001213	0.0001780	0.0002606	0.4277
7090126	10/18B2	34S_6p1d7Yd_6	33 7/8	S	9	4437.4	67 3/4	61 3/4	0.446	0.669	HLP-22	12	4	0	1.9	10.5	5.7	30.8	16.1	0.62	0.33	p1d7	2.45	0.0001213	0.0001780	0.0002606	0.4277
7090130	10/18B2	34S_6p1d7Yd_6	33 7/8	S	9	4437.4	67 3/4	61 3/4	0.446	0.669	HLP-22	12	4	0	1.9	10.5	5.7	30.8	16.1	0.62	0.33	p1d7	2.45	0.0001213	0.0001780	0.0002606	0.4277

Table B.8. Data from Fall 2007 Tests in Mid-Scale Vessel with Spherical Head B.1

Tank Water Temperature	Water Density	Solids Fraction	Pulse Volume Fraction	Duty Cycle	Cycle Time	Pulsed or Steady Jet	Us Steady Jet	U1 Pulsing Jet	U2 URMS	U3 URM3	Discharge Velocity	Critical Suspension Velocity	Average Peak Cloud Height	UCS Condition	UCS Method	UCS Flag	UCS Center Flag	UCS udv Flag	UCS based on Decreasing Velocity	Sweep Increase / Decrease	UDV Height Bed	Particle Motion	Solids Level	Outer Bottom Pattern	Inner Bottom Pattern	Case ID	Test	TDP	Row Number
C	g/cm³	fraction	fraction	fraction	s	text	m/s	m/s	m/s	m/s	m/s	m/s	in.	m/s	text	text	text	text	m/s	text	mm	text	text	text	text	text	text	text	text
T	ρ_l	ϕ_S	ϕ_P	DC	t_C	Jet	U_S	U1	U2	U3	U	U_{CS}	H_C	U_{CSR}	U_{CSM}	U_{CS}vis	U_{CS}cen	U_{CS}udv	U_{CS}_D	S_W	H_{bed}	PM	Sol	SP_O	SP_I	ID	M/DDX	TDP	MSS
21.2	0.999	0.00487	undefined	1.000	infinite	S	3.04	N/A	N/A	N/A	3.00	4.50	8.63	N/A	N/A	N/A	N/A	N/A	N/A	I	N/A	SS	N/A	N/A	N/A	34S_6p1d7Ya-80	10/17A1	TDP-WTP-033	7090002
21.3	0.999	0.00487	undefined	1.000	infinite	S	3.30	N/A	N/A	N/A	3.30	4.50	9.13	N/A	N/A	N/A	N/A	N/A	N/A	I	N/A	SS	N/A	N/A	N/A	34S_6p1d7Ya-80	10/17A1	TDP-WTP-033	7090004
21.2	0.999	0.00487	undefined	1.000	infinite	S	3.74	N/A	N/A	N/A	3.70	4.50	10.13	N/A	N/A	N/A	N/A	N/A	N/A	I	N/A	SS	N/A	N/A	N/A	34S_6p1d7Ya-80	10/17A1	TDP-WTP-033	7090006
21.3	0.999	0.00487	undefined	1.000	infinite	S	4.14	N/A	N/A	N/A	4.10	4.50	19.63	N/A	N/A	N/A	N/A	N/A	N/A	I	N/A	SS	SCO	BP5	N/A	34S_6p1d7Ya-80	10/17A1	TDP-WTP-033	7090008
21.3	0.999	0.00487	undefined	1.000	infinite	S	4.33	N/A	N/A	N/A	4.30	4.50	24.29	N/A	N/A	N/A	N/A	N/A	N/A	I	N/A	AM	SOO	BP6	N/A	34S_6p1d7Ya-80	10/17A1	TDP-WTP-033	7090012
21.3	0.999	0.00487	undefined	1.000	infinite	S	4.46	N/A	N/A	N/A	4.50	4.50	31.29	4.50	vis	UCSvis	N/A	N/A	N/A	I	N/A	CS	NSS	BP6	N/A	34S_6p1d7Ya-80	10/17A1	TDP-WTP-033	7090015
21.3	0.999	0.00487	undefined	1.000	infinite	S	4.40	N/A	N/A	N/A	4.40	4.50	28.29	N/A	vis dec	UCSvis	N/A	N/A	4.40	D	N/A	CS	NSS	BP6	N/A	34S_6p1d7Ya-80	10/17A1	TDP-WTP-033	7090019
21.0	0.999	0.00487	0.053	0.180	62.5	P	N/A	2.91	2.95	2.96	3.00	6.60	9.46	N/A	N/A	N/A	N/A	N/A	N/A	D	N/A	SS	N/A	N/A	N/A	34S_6p1d7Yd_5	10/17A2	TDP-WTP-033	7090023
21.0	0.999	0.00487	0.060	0.180	57.1	P	N/A	3.41	3.45	3.48	3.50	6.60	9.96	N/A	N/A	N/A	N/A	N/A	N/A	I	N/A	SS	N/A	N/A	N/A	34S_6p1d7Yd_5	10/17A2	TDP-WTP-033	7090026
21.0	0.999	0.00487	0.057	0.180	48.8	P	N/A	3.60	3.79	3.87	4.00	6.60	11.63	N/A	N/A	N/A	N/A	N/A	N/A	I	N/A	SS	N/A	N/A	N/A	34S_6p1d7Yd_5	10/17A2	TDP-WTP-033	7090029
21.0	0.999	0.00487	0.056	0.180	40.0	P	N/A	3.89	4.15	4.26	4.50	6.60	11.96	N/A	N/A	N/A	N/A	N/A	N/A	I	N/A	SS	N/A	N/A	N/A	34S_6p1d7Yd_5	10/17A2	TDP-WTP-033	7090032
21.0	0.999	0.00487	0.052	0.180	35.7	P	N/A	4.10	4.47	4.63	5.00	6.60	12.96	N/A	N/A	N/A	N/A	N/A	N/A	I	N/A	SS	N/A	N/A	N/A	34S_6p1d7Yd_5	10/17A2	TDP-WTP-033	7090035
21.0	0.999	0.00487	0.053	0.180	32.3	P	N/A	4.24	4.75	4.97	5.50	6.60	14.63	N/A	N/A	N/A	N/A	N/A	N/A	I	N/A	SS	N/A	N/A	N/A	34S_6p1d7Yd_5	10/17A2	TDP-WTP-033	7090038
21.0	0.999	0.00487	0.051	0.180	30.2	P	N/A	4.19	4.82	5.10	5.80	6.60	17.13	N/A	N/A	N/A	N/A	N/A	N/A	I	N/A	SS+	SCO	BP5	N/A	34S_6p1d7Yd_5	10/17A2	TDP-WTP-033	7090040
21.0	0.999	0.00487	0.051	0.180	29.1	P	N/A	4.18	4.88	5.20	6.00	6.60	19.13	N/A	N/A	N/A	N/A	N/A	N/A	I	N/A	AM	SCO	BP5	N/A	34S_6p1d7Yd_5	10/17A2	TDP-WTP-033	7090043
21.0	0.999	0.00487	0.053	0.180	28.7	P	N/A	4.12	4.93	5.30	6.20	6.60	21.63	N/A	N/A	N/A	N/A	N/A	N/A	I	N/A	AM	SCO	BP5	N/A	34S_6p1d7Yd_5	10/17A2	TDP-WTP-033	7090046
21.0	0.999	0.00487	0.051	0.180	27.0	P	N/A	3.97	4.88	5.30	6.40	6.60	21.63	N/A	N/A	N/A	N/A	N/A	N/A	I	N/A	AM+	SCO	BP5	N/A	34S_6p1d7Yd_5	10/17A2	TDP-WTP-033	7090048
21.0	0.999	0.00487	0.052	0.180	27.0	P	N/A	3.88	4.86	5.31	6.50	6.60	22.63	N/A	N/A	N/A	N/A	N/A	N/A	I	N/A	AM	SCO	BP5	N/A	34S_6p1d7Yd_5	10/17A2	TDP-WTP-033	7090052
21.0	0.999	0.00487	0.053	0.180	27.0	P	N/A	4.24	5.14	5.55	6.60	6.60	23.63	6.60	vis	UCSvis	N/A	N/A	N/A	I	N/A	CS	NSS	BP6	N/A	34S_6p1d7Yd_5	10/17A2	TDP-WTP-033	7090054
21.4	0.999	0.00487	undefined	1.000	infinite	S	3.52	N/A	N/A	N/A	3.50	5.50	N/A	N/A	N/A	N/A	N/A	N/A	N/A	I	N/A	SS	N/A	N/A	N/A	34S_6p1d7Ya-44	10/18A1	TDP-WTP-038	7090056
21.4	0.999	0.00487	undefined	1.000	infinite	S	4.02	N/A	N/A	N/A	4.00	5.50	10.00	N/A	N/A	N/A	N/A	N/A	N/A	I	N/A	AM	N/A	N/A	N/A	34S_6p1d7Ya-44	10/18A1	TDP-WTP-038	7090059
21.5	0.999	0.00487	undefined	1.000	infinite	S	4.51	N/A	N/A	N/A	4.50	5.50	16.00	N/A	N/A	N/A	N/A	N/A	N/A	I	N/A	AM	N/A	N/A	N/A	34S_6p1d7Ya-44	10/18A1	TDP-WTP-038	7090063
21.5	0.999	0.00487	undefined	1.000	infinite	S	5.01	N/A	N/A	N/A	5.00	5.50	31.00	N/A	N/A	N/A	N/A	N/A	N/A	I	N/A	AM	N/A	N/A	N/A	34S_6p1d7Ya-44	10/18A1	TDP-WTP-038	7090066
21.5	0.999	0.00487	undefined	1.000	infinite	S	5.52	N/A	N/A	N/A	5.50	5.50	47.50	5.50	vis	UCSvis	N/A	N/A	N/A	I	N/A	CS	N/A	N/A	N/A	34S_6p1d7Ya-44	10/18A1	TDP-WTP-038	7090068
22.0	0.999	0.00487	0.053	0.180	48.8	P	N/A	3.73	3.85	3.90	4.00	6.10	9.00	N/A	N/A	N/A	N/A	N/A	N/A	N/A	N/A	SS	N/A	N/A	N/A	34S_6p1d7Yd_0	10/18A2	TDP-WTP-038	7090071
22.0	0.999	0.00487	0.052	0.180	40.0	P	N/A	3.99	4.20	4.29	4.50	6.10	10.50	N/A	N/A	N/A	N/A	N/A	N/A	I	N/A	AM	N/A	N/A	N/A	34S_6p1d7Yd_0	10/18A2	TDP-WTP-038	7090074
22.0	0.999	0.00487	0.054	0.180	36.4	P	N/A	4.24	4.57	4.70	5.00	6.10	13.83	N/A	N/A	N/A	N/A	N/A	N/A	I	N/A	AM	N/A	N/A	N/A	34S_6p1d7Yd_0	10/18A2	TDP-WTP-038	7090077
22.0	0.999	0.00487	0.054	0.180	33.3	P	N/A	4.36	4.82	5.01	5.50	6.10	15.67	N/A	N/A	N/A	N/A	N/A	N/A	I	N/A	AM	N/A	N/A	N/A	34S_6p1d7Yd_0	10/18A2	TDP-WTP-038	7090081
22.0	0.999	0.00487	0.051	0.180	30.8	P	N/A	4.43	4.93	5.15	5.70	6.10	16.67	N/A	N/A	N/A	N/A	N/A	N/A	I	N/A	AM	N/A	N/A	N/A	34S_6p1d7Yd_0	10/18A2	TDP-WTP-038	7090085
22.0	0.999	0.00487	0.052	0.180	30.3	P	N/A	4.43	5.02	5.27	5.90	6.10	17.33	N/A	N/A	N/A	N/A	N/A	N/A	I	N/A	AM	N/A	N/A	N/A	34S_6p1d7Yd_0	10/18A2	TDP-WTP-038	7090089
22.0	0.999	0.00487	0.052	0.180	29.4	P	N/A	4.46	5.11	5.39	6.10	6.10	18.83	6.10	vis	UCSvis	N/A	N/A	N/A	I	N/A	CS	N/A	N/A	N/A	34S_6p1d7Yd_0	10/18A2	TDP-WTP-038	7090095
21.7	0.999	0.00487	undefined	1.000	infinite	S	5.05	N/A	N/A	N/A	5.00	5.90	11.00	N/A	N/A	N/A	N/A	N/A	N/A	I	N/A	SS	N/A	N/A	N/A	34S_6p1d7Ya-40	10/18B1	TDP-WTP-038	7090097
21.8	0.999	0.00487	undefined	1.000	infinite	S	5.52	N/A	N/A	N/A	5.50	5.90	13.17	N/A	N/A	N/A	N/A	N/A	N/A	I	N/A	AM	N/A	N/A	N/A	34S_6p1d7Ya-40	10/18B1	TDP-WTP-038	7090101
21.8	0.999	0.00487	undefined	1.000	infinite	S	5.72	N/A	N/A	N/A	5.70	5.90	20.33	N/A	N/A	N/A	N/A	N/A	N/A	I	N/A	AM+	N/A	N/A	N/A	34S_6p1d7Ya-40	10/18B1	TDP-WTP-038	7090105
21.8	0.999	0.00487	undefined	1.000	infinite	S	5.93	N/A	N/A	N/A	5.90	5.90	23.33	5.90	vis	UCSvis	N/A	N/A	N/A	I	N/A	CS	N/A	N/A	N/A	34S_6p1d7Ya-40	10/18B1	TDP-WTP-038	7090111
22.0	0.999	0.00487	0.037	0.180	87.0	P	N/A	3.98	4.04	4.07	4.00	6.40	9.17	N/A	N/A	N/A	N/A	N/A	N/A	D	N/A	SS	N/A	N/A	N/A	34S_6p1d7Yd_6	10/18B2	TDP-WTP-038	7090113
22.0	0.999	0.00487	0.054	0.180	80.0	P	N/A	4.41	4.45	4.47	4.50	6.40	9.33	N/A	N/A	N/A	N/A	N/A	N/A	I	N/A	SS	N/A	N/A	N/A	34S_6p1d7Yd_6	10/18B2	TDP-WTP-038	7090116
22.0	0.999	0.00487	0.054	0.180	71.4	P	N/A	4.92	4.97	4.99	5.00	6.40	9.50	N/A	N/A	N/A	N/A	N/A	N/A	I	N/A	SS	N/A	N/A	N/A	34S_6p1d7Yd_6	10/18B2	TDP-WTP-038	7090119
22.0	0.999	0.00487	0.051	0.180	64.5	P	N/A	5.38	5.44	5.46	5.50	6.40	10.33	N/A	N/A	N/A	N/A	N/A	N/A	I	N/A	SS	N/A	N/A	N/A	34S_6p1d7Yd_6	10/18B2	TDP-WTP-038	7090122
22.0	0.999	0.00487	0.052	0.180	58.8	P	N/A	5.84	5.91	5.95	6.00	6.40	11.33	N/A	N/A	N/A	N/A	N/A	N/A	I	N/A	AM	N/A	N/A	N/A	34S_6p1d7Yd_6	10/18B2	TDP-WTP-038	7090126
22.0	0.999	0.00487	0.051	0.180	57.1	P	N/A	6.01	6.09	6.13	6.20	6.40	12.00	N/A	N/A	N/A	N/A	N/A	N/A	I	N/A	AM	N/A	N/A	N/A	34S_6p1d7Yd_6	10/18B2	TDP-WTP-038	7090130

Table B.8. Data from Fall 2007 Tests in Mid-Scale Vessel with Spherical Head A.2

Row Number	Test	Case ID	Tank Diameter	Head Shape	Dish Height	Dish Volume	Tank Fill Height	Return Line Height	Nozzle Inner Diameter	Nozzle Stand-off Distance	Pulse Tube Configuration	Installed Nozzles	Outer Nozzles Operated	Inner Nozzles Operated	Pulse Tube Outer Diameter	Outer PJM Radius	Inner PJM Radius	"FIO" Outer PJM Impingement Angle	"FIO" Inner PJM Impingement Angle	Ratio Outer PJM to Tank Radius	Ratio Inner PJM to Tank Radius	Simulant	Solids Density	Particle Diameter d5	Particle Diameter d50	Particle Diameter d95	Void Fraction
text	text	text	in.	text	in.	in. ^{3}	in.	in.	in.	in.	text	number	number	number	in.	in.	in.	deg	deg	nondim	nondim	text	g/cm^3	m	m	m	fraction
MSS	M/DDX	ID	D	HS	H_{dish}	V_{dish}	H	Rtn	d	sod	PT	N	N_O	N_I	PT_{od}	R_O	R_I	θ_O	θ_I	R_O/R	R_I/R	sxdx	ρ_s	d_5	d_{50}	d_{95}	vf
7090136M	10/18B2	34S_6p1d7Yd_6	33 7/8	S	9	4437.4	67 3/4	61 3/4	0.446	0.669	HLP-22	12	4	0	1.9	10.5	5.7	30.8	16.1	0.62	0.33	p1d7	2.45	0.0001213	0.0001780	0.0002606	0.4277
7090138M	10/18B2	34S_6p1d7Yd_6	33 7/8	S	9	4437.4	67 3/4	61 3/4	0.446	0.669	HLP-22	12	4	0	1.9	10.5	5.7	30.8	16.1	0.62	0.33	p1d7	2.45	0.0001213	0.0001780	0.0002606	0.4277
7090142	10/19A1	34S_6p1d7Ya-04	33 7/8	S	9	4437.4	67 3/4	61 3/4	0.446	0.669	HLP-22	12	0	4	1.9	10.5	5.7	30.8	16.1	0.62	0.33	p1d7	2.45	0.0001213	0.0001780	0.0002606	0.4277
7090144	10/19A1	34S_6p1d7Ya-04	33 7/8	S	9	4437.4	67 3/4	61 3/4	0.446	0.669	HLP-22	12	0	4	1.9	10.5	5.7	30.8	16.1	0.62	0.33	p1d7	2.45	0.0001213	0.0001780	0.0002606	0.4277
7090146	10/19A1	34S_6p1d7Ya-04	33 7/8	S	9	4437.4	67 3/4	61 3/4	0.446	0.669	HLP-22	12	0	4	1.9	10.5	5.7	30.8	16.1	0.62	0.33	p1d7	2.45	0.0001213	0.0001780	0.0002606	0.4277
7090149	10/19A1	34S_6p1d7Ya-04	33 7/8	S	9	4437.4	67 3/4	61 3/4	0.446	0.669	HLP-22	12	0	4	1.9	10.5	5.7	30.8	16.1	0.62	0.33	p1d7	2.45	0.0001213	0.0001780	0.0002606	0.4277
7090152	10/19A1	34S_6p1d7Ya-04	33 7/8	S	9	4437.4	67 3/4	61 3/4	0.446	0.669	HLP-22	12	0	4	1.9	10.5	5.7	30.8	16.1	0.62	0.33	p1d7	2.45	0.0001213	0.0001780	0.0002606	0.4277
7090156	10/19A1	34S_6p1d7Ya-04	33 7/8	S	9	4437.4	67 3/4	61 3/4	0.446	0.669	HLP-22	12	0	4	1.9	10.5	5.7	30.8	16.1	0.62	0.33	p1d7	2.45	0.0001213	0.0001780	0.0002606	0.4277
7090158	10/19A1	34S_6p1d7Ya-04	33 7/8	S	9	4437.4	67 3/4	61 3/4	0.446	0.669	HLP-22	12	0	4	1.9	10.5	5.7	30.8	16.1	0.62	0.33	p1d7	2.45	0.0001213	0.0001780	0.0002606	0.4277
7090161	10/19A1	34S_6p1d7Ya-04	33 7/8	S	9	4437.4	67 3/4	61 3/4	0.446	0.669	HLP-22	12	0	4	1.9	10.5	5.7	30.8	16.1	0.62	0.33	p1d7	2.45	0.0001213	0.0001780	0.0002606	0.4277
7090165	10/19A1	34S_6p1d7Ya-04	33 7/8	S	9	4437.4	67 3/4	61 3/4	0.446	0.669	HLP-22	12	0	4	1.9	10.5	5.7	30.8	16.1	0.62	0.33	p1d7	2.45	0.0001213	0.0001780	0.0002606	0.4277
7090167	10/19A2	34S_6p1d7Yd_9	33 7/8	S	9	4437.4	67 3/4	61 3/4	0.446	0.669	HLP-22	12	0	4	1.9	10.5	5.7	30.8	16.1	0.62	0.33	p1d7	2.45	0.0001213	0.0001780	0.0002606	0.4277
7090169	10/19A2	34S_6p1d7Yd_9	33 7/8	S	9	4437.4	67 3/4	61 3/4	0.446	0.669	HLP-22	12	0	4	1.9	10.5	5.7	30.8	16.1	0.62	0.33	p1d7	2.45	0.0001213	0.0001780	0.0002606	0.4277
7090172	10/19A2	34S_6p1d7Yd_9	33 7/8	S	9	4437.4	67 3/4	61 3/4	0.446	0.669	HLP-22	12	0	4	1.9	10.5	5.7	30.8	16.1	0.62	0.33	p1d7	2.45	0.0001213	0.0001780	0.0002606	0.4277
7090174	10/19A2	34S_6p1d7Yd_9	33 7/8	S	9	4437.4	67 3/4	61 3/4	0.446	0.669	HLP-22	12	0	4	1.9	10.5	5.7	30.8	16.1	0.62	0.33	p1d7	2.45	0.0001213	0.0001780	0.0002606	0.4277
7090177	10/19A2	34S_6p1d7Yd_9	33 7/8	S	9	4437.4	67 3/4	61 3/4	0.446	0.669	HLP-22	12	0	4	1.9	10.5	5.7	30.8	16.1	0.62	0.33	p1d7	2.45	0.0001213	0.0001780	0.0002606	0.4277
7090180	10/19A2	34S_6p1d7Yd_9	33 7/8	S	9	4437.4	67 3/4	61 3/4	0.446	0.669	HLP-22	12	0	4	1.9	10.5	5.7	30.8	16.1	0.62	0.33	p1d7	2.45	0.0001213	0.0001780	0.0002606	0.4277
7090184M	10/19A2	34S_6p1d7Yd_9	33 7/8	S	9	4437.4	67 3/4	61 3/4	0.446	0.669	HLP-22	12	0	4	1.9	10.5	5.7	30.8	16.1	0.62	0.33	p1d7	2.45	0.0001213	0.0001780	0.0002606	0.4277
7090186	10/26A1	34S_6p1d7Ya	33 7/8	S	9	4437.4	67 3/4	65 3/4	0.446	0.669	HLP-22	12	8	4	1.9	10.5	5.7	30.8	16.1	0.62	0.33	p1d7	2.45	0.0001213	0.0001780	0.0002606	0.4277
7090189	10/26A1	34S_6p1d7Ya	33 7/8	S	9	4437.4	67 3/4	65 3/4	0.446	0.669	HLP-22	12	8	4	1.9	10.5	5.7	30.8	16.1	0.62	0.33	p1d7	2.45	0.0001213	0.0001780	0.0002606	0.4277
7090193	10/26A1	34S_6p1d7Ya	33 7/8	S	9	4437.4	67 3/4	65 3/4	0.446	0.669	HLP-22	12	8	4	1.9	10.5	5.7	30.8	16.1	0.62	0.33	p1d7	2.45	0.0001213	0.0001780	0.0002606	0.4277
7090195	10/26A2	34S_6p1d7Yd_1	33 7/8	S	9	4437.4	67 3/4	65 3/4	0.446	0.669	HLP-22	12	8	4	1.9	10.5	5.7	30.8	16.1	0.62	0.33	p1d7	2.45	0.0001213	0.0001780	0.0002606	0.4277
7090198	10/26A2	34S_6p1d7Yd_1	33 7/8	S	9	4437.4	67 3/4	65 3/4	0.446	0.669	HLP-22	12	8	4	1.9	10.5	5.7	30.8	16.1	0.62	0.33	p1d7	2.45	0.0001213	0.0001780	0.0002606	0.4277
7090201	10/26A2	34S_6p1d7Yd_1	33 7/8	S	9	4437.4	67 3/4	65 3/4	0.446	0.669	HLP-22	12	8	4	1.9	10.5	5.7	30.8	16.1	0.62	0.33	p1d7	2.45	0.0001213	0.0001780	0.0002606	0.4277
7090204	10/26A2	34S_6p1d7Yd_1	33 7/8	S	9	4437.4	67 3/4	65 3/4	0.446	0.669	HLP-22	12	8	4	1.9	10.5	5.7	30.8	16.1	0.62	0.33	p1d7	2.45	0.0001213	0.0001780	0.0002606	0.4277
7090208MX	10/26A2	34S_6p1d7Yd_1	33 7/8	S	9	4437.4	67 3/4	65 3/4	0.446	0.669	HLP-22	12	8	4	1.9	10.5	5.7	30.8	16.1	0.62	0.33	p1d7	2.45	0.0001213	0.0001780	0.0002606	0.4277
7090210	10/26B1	34S_6p1d7Ya-44	33 7/8	S	9	4437.4	67 3/4	65 3/4	0.446	0.669	HLP-22	12	4	4	1.9	10.5	5.7	30.8	16.1	0.62	0.33	p1d7	2.45	0.0001213	0.0001780	0.0002606	0.4277
7090213	10/26B1	34S_6p1d7Ya-44	33 7/8	S	9	4437.4	67 3/4	65 3/4	0.446	0.669	HLP-22	12	4	4	1.9	10.5	5.7	30.8	16.1	0.62	0.33	p1d7	2.45	0.0001213	0.0001780	0.0002606	0.4277
7090217	10/26B1	34S_6p1d7Ya-44	33 7/8	S	9	4437.4	67 3/4	65 3/4	0.446	0.669	HLP-22	12	4	4	1.9	10.5	5.7	30.8	16.1	0.62	0.33	p1d7	2.45	0.0001213	0.0001780	0.0002606	0.4277
7090219	10/26B1	34S_6p1d7Ya-44	33 7/8	S	9	4437.4	67 3/4	65 3/4	0.446	0.669	HLP-22	12	4	4	1.9	10.5	5.7	30.8	16.1	0.62	0.33	p1d7	2.45	0.0001213	0.0001780	0.0002606	0.4277
7090223	10/26B1	34S_6p1d7Ya-44	33 7/8	S	9	4437.4	67 3/4	65 3/4	0.446	0.669	HLP-22	12	4	4	1.9	10.5	5.7	30.8	16.1	0.62	0.33	p1d7	2.45	0.0001213	0.0001780	0.0002606	0.4277
7090225	10/26B2	34S_6p1d7Yd_0	33 7/8	S	9	4437.4	67 3/4	65 3/4	0.446	0.669	HLP-22	12	4	4	1.9	10.5	5.7	30.8	16.1	0.62	0.33	p1d7	2.45	0.0001213	0.0001780	0.0002606	0.4277
7090228	10/26B2	34S_6p1d7Yd_0	33 7/8	S	9	4437.4	67 3/4	65 3/4	0.446	0.669	HLP-22	12	4	4	1.9	10.5	5.7	30.8	16.1	0.62	0.33	p1d7	2.45	0.0001213	0.0001780	0.0002606	0.4277
7090231	10/26B2	34S_6p1d7Yd_0	33 7/8	S	9	4437.4	67 3/4	65 3/4	0.446	0.669	HLP-22	12	4	4	1.9	10.5	5.7	30.8	16.1	0.62	0.33	p1d7	2.45	0.0001213	0.0001780	0.0002606	0.4277
7090234	10/26B2	34S_6p1d7Yd_0	33 7/8	S	9	4437.4	67 3/4	65 3/4	0.446	0.669	HLP-22	12	4	4	1.9	10.5	5.7	30.8	16.1	0.62	0.33	p1d7	2.45	0.0001213	0.0001780	0.0002606	0.4277
7090237	10/26B2	34S_6p1d7Yd_0	33 7/8	S	9	4437.4	67 3/4	65 3/4	0.446	0.669	HLP-22	12	4	4	1.9	10.5	5.7	30.8	16.1	0.62	0.33	p1d7	2.45	0.0001213	0.0001780	0.0002606	0.4277
7090240	10/26B2	34S_6p1d7Yd_0	33 7/8	S	9	4437.4	67 3/4	65 3/4	0.446	0.669	HLP-22	12	4	4	1.9	10.5	5.7	30.8	16.1	0.62	0.33	p1d7	2.45	0.0001213	0.0001780	0.0002606	0.4277
7090244MX	10/26B2	34S_6p1d7Yd_0	33 7/8	S	9	4437.4	67 3/4	65 3/4	0.446	0.669	HLP-22	12	4	4	1.9	10.5	5.7	30.8	16.1	0.62	0.33	p1d7	2.45	0.0001213	0.0001780	0.0002606	0.4277
7090247	10/29A1	34S_6p1d7Ya-04	33 7/8	S	9	4437.4	67 3/4	65 3/4	0.446	0.669	HLP-22	12	0	4	1.9	10.5	5.7	30.8	16.1	0.62	0.33	p1d7	2.45	0.0001213	0.0001780	0.0002606	0.4277
7090250	10/29A1	34S_6p1d7Ya-04	33 7/8	S	9	4437.4	67 3/4	65 3/4	0.446	0.669	HLP-22	12	0	4	1.9	10.5	5.7	30.8	16.1	0.62	0.33	p1d7	2.45	0.0001213	0.0001780	0.0002606	0.4277
7090252	10/29A1	34S_6p1d7Ya-04	33 7/8	S	9	4437.4	67 3/4	65 3/4	0.446	0.669	HLP-22	12	0	4	1.9	10.5	5.7	30.8	16.1	0.62	0.33	p1d7	2.45	0.0001213	0.0001780	0.0002606	0.4277

Table B.8. Data from Fall 2007 Tests in Mid-Scale Vessel with Spherical Head B.2

Tank Water Temperature	Water Density	Solids Fraction	Pulse Volume Fraction	Duty Cycle	Cycle Time	Pulsed or Steady Jet	Us Steady Jet	U1 Pulsing Jet	U2 URMS	U3 URM3	Discharge Velocity	Critical Suspension Velocity	Average Peak Cloud Height	UCS Condition	UCS Method	UCS Flag	UCS Center Flag	UCS udv Flag	UCS based on Decreasing Velocity	Sweep Increase / Decrease	UDV Height Bed	Particle Motion	Solids Level	Outer Bottom Pattern	Inner Bottom Pattern	Case ID	Test	TDP	Row Number
C	g/cm^3	fraction	fraction	fraction	s	text	m/s	m/s	m/s	m/s	m/s	m/s	in.	m/s	text	text	text	text	m/s	text	mm	text	text	text	text	text	text	text	text
T	ρ_l	ϕ_S	ϕ_P	DC	t_C	Jet	U_S	U1	U2	U3	U	U_{CS}	H_C	U_{CSR}	U_{CSM}	U_{CS}vis	U_{CS}cen	U_{CS}udv	U_{CS}_D	S_W	H_{bed}	PM	Sol	SP_O	SP_I	ID	M/DDX	TDP	MSS
22.0	0.999	0.00487	0.051	0.180	54.9	P	N/A	6.22	6.31	6.35	6.40	6.40	13.00	6.40	vis	UCSvis	N/A	N/A	N/A	I	N/A	CS	N/A	N/A	N/A	34S_6p1d7Yd_6	10/18B2	TDP-WTP-038	7090136
22.0	0.999	0.00487	0.051	0.180	54.1	P	N/A	6.41	6.50	6.55	6.60	6.40	16.00	N/A	N/A	N/A	N/A	N/A	N/A	I	N/A	BC	N/A	N/A	N/A	34S_6p1d7Yd_6	10/18B2	TDP-WTP-038	7090138
21.8	0.999	0.00487	undefined	1.000	infinite	S	4.06	N/A	N/A	N/A	4.00	8.00	9.00	N/A	N/A	N/A	N/A	N/A	N/A	I	N/A	SS	N/A	N/A	N/A	34S_6p1d7Ya-04	10/19A1	TDP-WTP-034	7090142
21.7	0.999	0.00487	undefined	1.000	infinite	S	4.52	N/A	N/A	N/A	4.50	8.00	10.00	N/A	N/A	N/A	N/A	N/A	N/A	I	N/A	SS	N/A	N/A	N/A	34S_6p1d7Ya-04	10/19A1	TDP-WTP-034	7090144
21.8	0.999	0.00487	undefined	1.000	infinite	S	5.02	N/A	N/A	N/A	5.00	8.00	12.00	N/A	N/A	N/A	N/A	N/A	N/A	I	N/A	SS	N/A	BP5	N/A	34S_6p1d7Ya-04	10/19A1	TDP-WTP-034	7090146
21.8	0.999	0.00487	undefined	1.000	infinite	S	5.11	N/A	N/A	N/A	5.50	8.00	15.50	N/A	N/A	N/A	N/A	N/A	N/A	I	N/A	AM	N/A	BP5	N/A	34S_6p1d7Ya-04	10/19A1	TDP-WTP-034	7090149
21.8	0.999	0.00487	undefined	1.000	infinite	S	6.01	N/A	N/A	N/A	6.00	8.00	18.50	N/A	N/A	N/A	N/A	N/A	N/A	I	N/A	AM	N/A	BP5	N/A	34S_6p1d7Ya-04	10/19A1	TDP-WTP-034	7090152
21.8	0.999	0.00487	undefined	1.000	infinite	S	6.55	N/A	N/A	N/A	6.50	8.00	24.00	N/A	N/A	N/A	N/A	N/A	N/A	I	N/A	AM	N/A	BP5	N/A	34S_6p1d7Ya-04	10/19A1	TDP-WTP-034	7090156
21.8	0.999	0.00487	undefined	1.000	infinite	S	7.01	N/A	N/A	N/A	7.00	8.00	33.00	N/A	N/A	N/A	N/A	N/A	N/A	I	N/A	AM+	N/A	BP5	N/A	34S_6p1d7Ya-04	10/19A1	TDP-WTP-034	7090158
21.9	0.999	0.00487	undefined	1.000	infinite	S	7.51	N/A	N/A	N/A	7.50	8.00	40.00	N/A	N/A	N/A	N/A	N/A	N/A	I	N/A	AM+	N/A	BP5	N/A	34S_6p1d7Ya-04	10/19A1	TDP-WTP-034	7090161
21.9	0.999	0.00487	undefined	1.000	infinite	S	8.02	N/A	N/A	N/A	8.00	8.00	50.00	8.00	vis	UCSvis	N/A	N/A	N/A	I	N/A	CS	N/A	BP6	N/A	34S_6p1d7Ya-04	10/19A1	TDP-WTP-034	7090165
22.0	0.999	0.00487	0.049	0.180	87.0	P	N/A	4.09	4.13	4.15	4.00	8.50	9.00	N/A	N/A	N/A	N/A	N/A	N/A	I	N/A	SS	N/A	N/A	N/A	34S_6p1d7Yd_9	10/19A2	TDP-WTP-034	7090167
22.0	0.999	0.00487	0.052	0.180	71.4	P	N/A	4.95	5.00	5.02	5.00	8.50	12.50	N/A	N/A	N/A	N/A	N/A	N/A	I	N/A	SS	N/A	N/A	N/A	34S_6p1d7Yd_9	10/19A2	TDP-WTP-034	7090169
22.0	0.999	0.00487	0.053	0.180	58.8	P	N/A	5.85	5.92	5.96	6.00	8.50	16.00	N/A	N/A	N/A	N/A	N/A	N/A	I	N/A	SS	N/A	BP4	N/A	34S_6p1d7Yd_9	10/19A2	TDP-WTP-034	7090172
22.0	0.999	0.00487	0.054	0.180	51.3	P	N/A	6.23	6.58	6.72	7.00	8.50	19.50	N/A	N/A	N/A	N/A	N/A	N/A	I	N/A	AM	N/A	BP5	N/A	34S_6p1d7Yd_9	10/19A2	TDP-WTP-034	7090174
22.0	0.999	0.00487	0.051	0.180	46.5	P	N/A	6.32	6.83	7.04	7.50	8.50	23.00	N/A	N/A	N/A	N/A	N/A	N/A	I	N/A	AM+	N/A	BP5	N/A	34S_6p1d7Yd_9	10/19A2	TDP-WTP-034	7090177
22.0	0.999	0.00487	0.052	0.180	43.5	P	N/A	6.72	7.29	7.52	8.00	8.50	25.50	N/A	N/A	N/A	N/A	N/A	N/A	I	N/A	AM+	N/A	BP6	N/A	34S_6p1d7Yd_9	10/19A2	TDP-WTP-034	7090180
22.0	0.999	0.00487	0.050	0.180	40.0	P	N/A	6.76	7.51	7.83	8.50	8.50	29.00	8.50	vis	UCSvis	N/A	N/A	N/A	I	N/A	CS	N/A	BP6	N/A	34S_6p1d7Yd_9	10/19A2	TDP-WTP-034	7090184
20.8	0.999	0.00487	undefined	1.000	infinite	S	2.51	N/A	N/A	N/A	2.50	3.20	8.50	N/A	N/A	N/A	N/A	N/A	N/A	I	N/A	SS+	N/A	N/A	N/A	34S_6p1d7Ya	10/26A1	TDP-WTP-039	7090186
20.7	0.999	0.00487	undefined	1.000	infinite	S	3.02	N/A	N/A	N/A	3.00	3.20	10.00	N/A	N/A	N/A	N/A	N/A	N/A	I	N/A	AM+	N/A	N/A	N/A	34S_6p1d7Ya	10/26A1	TDP-WTP-039	7090189
20.7	0.999	0.00487	undefined	1.000	infinite	S	3.21	N/A	N/A	N/A	3.20	3.20	10.75	3.20	vis	UCSvis	N/A	N/A	N/A	I	N/A	CS	N/A	N/A	N/A	34S_6p1d7Ya	10/26A1	TDP-WTP-039	7090193
21.0	0.999	0.00487	0.045	0.180	40.0	P	N/A	2.74	2.85	2.90	3.00	4.00	9.75	N/A	N/A	N/A	N/A	N/A	N/A	D	N/A	AM	N/A	N/A	N/A	34S_6p1d7Yd_1	10/26A2	TDP-WTP-039	7090195
21.0	0.999	0.00487	0.050	0.180	37.0	P	N/A	2.92	3.02	3.07	3.20	4.00	11.00	N/A	N/A	N/A	N/A	N/A	N/A	I	N/A	AM	N/A	N/A	N/A	34S_6p1d7Yd_1	10/26A2	TDP-WTP-039	7090198
21.0	0.999	0.00487	0.051	0.180	35.5	P	N/A	3.02	3.15	3.22	3.40	4.00	11.00	N/A	N/A	N/A	N/A	N/A	N/A	I	N/A	AM+	N/A	N/A	N/A	34S_6p1d7Yd_1	10/26A2	TDP-WTP-039	7090201
21.0	0.999	0.00487	0.052	0.180	33.0	P	N/A	3.06	3.27	3.36	3.60	4.00	11.00	N/A	N/A	N/A	N/A	N/A	N/A	I	N/A	AM+	N/A	N/A	N/A	34S_6p1d7Yd_1	10/26A2	TDP-WTP-039	7090204
21.0	0.999	0.00487	0.051	0.180	29.5	P	N/A	3.23	3.53	3.67	4.00	4.00	12.00	4.00	vis	UCSvis	N/A	N/A	N/A	I	N/A	CS	N/A	N/A	N/A	34S_6p1d7Yd_1	10/26A2	TDP-WTP-039	7090208
20.8	0.999	0.00487	undefined	1.000	infinite	S	3.40	N/A	N/A	N/A	3.40	4.60	N/A	N/A	N/A	N/A	N/A	N/A	N/A	I	N/A	SS	N/A	N/A	N/A	34S_6p1d7Ya-44	10/26B1	TDP-WTP-039	7090210
20.8	0.999	0.00487	undefined	1.000	infinite	S	3.82	N/A	N/A	N/A	3.80	4.60	9.00	N/A	N/A	N/A	N/A	N/A	N/A	I	N/A	AM	N/A	N/A	N/A	34S_6p1d7Ya-44	10/26B1	TDP-WTP-039	7090213
20.8	0.999	0.00487	undefined	1.000	infinite	S	4.22	N/A	N/A	N/A	4.20	4.60	12.00	N/A	N/A	N/A	UCScen	N/A	N/A	I	N/A	AM	N/A	N/A	N/A	34S_6p1d7Ya-44	10/26B1	TDP-WTP-039	7090217
20.8	0.999	0.00487	undefined	1.000	infinite	S	4.42	N/A	N/A	N/A	4.40	4.60	17.00	N/A	N/A	N/A	N/A	N/A	N/A	I	N/A	AM+	N/A	N/A	N/A	34S_6p1d7Ya-44	10/26B1	TDP-WTP-039	7090219
20.9	0.999	0.00487	undefined	1.000	infinite	S	4.61	N/A	N/A	N/A	4.60	4.60	21.00	4.60	vis	UCSvis	N/A	N/A	N/A	I	N/A	CS	N/A	N/A	N/A	34S_6p1d7Ya-44	10/26B1	TDP-WTP-039	7090223
21.0	0.999	0.00487	0.045	0.180	45.0	P	N/A	3.69	3.79	3.84	4.00	6.10	9.00	N/A	N/A	N/A	N/A	N/A	N/A	D	N/A	SS+	N/A	N/A	N/A	34S_6p1d7Yd_0	10/26B2	TDP-WTP-039	7090225
21.0	0.999	0.00487	0.051	0.180	40.5	P	N/A	4.04	4.18	4.24	4.40	6.10	10.00	N/A	N/A	N/A	N/A	N/A	N/A	I	N/A	SS+	N/A	N/A	N/A	34S_6p1d7Yd_0	10/26B2	TDP-WTP-039	7090228
21.0	0.999	0.00487	0.051	0.180	37.5	P	N/A	4.14	4.40	4.51	4.80	6.10	12.50	N/A	N/A	N/A	N/A	N/A	N/A	I	N/A	AM	N/A	N/A	N/A	34S_6p1d7Yd_0	10/26B2	TDP-WTP-039	7090231
21.0	0.999	0.00487	0.050	0.180	34.0	P	N/A	4.41	4.72	4.86	5.20	6.10	14.00	N/A	N/A	N/A	N/A	N/A	N/A	I	N/A	AM	N/A	N/A	N/A	34S_6p1d7Yd_0	10/26B2	TDP-WTP-039	7090234
21.0	0.999	0.00487	0.050	0.180	31.5	P	N/A	4.52	4.94	5.12	5.60	6.10	14.75	N/A	N/A	N/A	N/A	N/A	N/A	I	N/A	AM+	N/A	N/A	N/A	34S_6p1d7Yd_0	10/26B2	TDP-WTP-039	7090237
21.0	0.999	0.00487	0.050	0.180	29.0	P	N/A	4.64	5.19	5.43	6.00	6.10	16.50	N/A	N/A	N/A	N/A	N/A	N/A	I	N/A	CS-	N/A	N/A	N/A	34S_6p1d7Yd_0	10/26B2	TDP-WTP-039	7090240
21.0	0.999	0.00487	0.050	0.180	28.5	P	N/A	4.66	5.23	5.47	6.10	6.10	18.00	6.10	vis	UCSvis	N/A	N/A	N/A	I	N/A	CS	N/A	N/A	N/A	34S_6p1d7Yd_0	10/26B2	TDP-WTP-039	7090244
20.9	0.999	0.00487	undefined	1.000	infinite	S	4.01	N/A	N/A	N/A	4.00	6.00	10.75	N/A	N/A	N/A	N/A	N/A	N/A	I	N/A	SS	N/A	N/A	N/A	34S_6p1d7Ya-04	10/29A1	TDP-WTP-040	7090247
20.9	0.999	0.00487	undefined	1.000	infinite	S	4.50	N/A	N/A	N/A	4.50	6.00	13.50	N/A	N/A	N/A	N/A	N/A	N/A	I	N/A	SS	N/A	N/A	N/A	34S_6p1d7Ya-04	10/29A1	TDP-WTP-040	7090250
20.9	0.999	0.00487	undefined	1.000	infinite	S	5.00	N/A	N/A	N/A	5.00	6.00	16.75	N/A	N/A	N/A	N/A	N/A	N/A	I	N/A	AM	N/A	N/A	N/A	34S_6p1d7Ya-04	10/29A1	TDP-WTP-040	7090252

Table B.8. Data from Fall 2007 Tests in Mid-Scale Vessel with Spherical Head A.3

Row Number	Test	Case ID	Tank Diameter	Head Shape	Dish Height	Dish Volume	Tank Fill Height	Return Line Height	Nozzle Inner Diameter	Nozzle Stand-off Distance	Pulse Tube Configuration	Installed Nozzles	Outer Nozzles Operated	Inner Nozzles Operated	Pulse Tube Outer Diameter	Outer PJM Radius	Inner PJM Radius	"FIO" Outer PJM Impingement Angle	"FIO" Inner PJM Impingement Angle	Ratio Outer PJM to Tank Radius	Ratio Inner PJM to Tank Radius	Simulant	Solids Density	Particle Diameter d5	Particle Diameter d50	Particle Diameter d95	Void Fraction
text	text	text	in.	text	in.	in. ^{3}	in.	in.	in.	in.	text	number	number	number	in.	in.	in.	deg	deg	nondim	nondim	text	g/cm^3	m	m	m	fraction
MSS	M/DDX	ID	D	HS	H_{dish}	V_{dish}	H	Rtn	d	sod	PT	N	N_O	N_I	PT_{od}	R_O	R_I	θ_O	θ_I	R_O/R	R_I/R	sxdx	ρ_s	d_5	d_{50}	d_{95}	vf
7090256	10/29A1	34S_6p1d7Ya-04	33 7/8	S	9	4437.4	67 3/4	65 3/4	0.446	0.669	HLP-22	12	0	4	1.9	10.5	5.7	30.8	16.1	0.62	0.33	p1d7	2.45	0.0001213	0.0001780	0.0002606	0.4277
7090258	10/29A1	34S_6p1d7Ya-04	33 7/8	S	9	4437.4	67 3/4	65 3/4	0.446	0.669	HLP-22	12	0	4	1.9	10.5	5.7	30.8	16.1	0.62	0.33	p1d7	2.45	0.0001213	0.0001780	0.0002606	0.4277
7090261	10/29A1	34S_6p1d7Ya-04	33 7/8	S	9	4437.4	67 3/4	65 3/4	0.446	0.669	HLP-22	12	0	4	1.9	10.5	5.7	30.8	16.1	0.62	0.33	p1d7	2.45	0.0001213	0.0001780	0.0002606	0.4277
7090265	10/29A1	34S_6p1d7Ya-04	33 7/8	S	9	4437.4	67 3/4	65 3/4	0.446	0.669	HLP-22	12	0	4	1.9	10.5	5.7	30.8	16.1	0.62	0.33	p1d7	2.45	0.0001213	0.0001780	0.0002606	0.4277
7090268	10/29A2	34S_6p1d7Ym_9	33 7/8	S	9	4437.4	67 3/4	65 3/4	0.446	0.669	HLP-22	12	0	4	1.9	10.5	5.7	30.8	16.1	0.62	0.33	p1d7	2.45	0.0001213	0.0001780	0.0002606	0.4277
7090271MX	10/29A2	34S_6p1d7Ym_9	33 7/8	S	9	4437.4	67 3/4	65 3/4	0.446	0.669	HLP-22	12	0	4	1.9	10.5	5.7	30.8	16.1	0.62	0.33	p1d7	2.45	0.0001213	0.0001780	0.0002606	0.4277
7090274MX	10/29A2	34S_6p1d7Ym_9	33 7/8	S	9	4437.4	67 3/4	65 3/4	0.446	0.669	HLP-22	12	0	4	1.9	10.5	5.7	30.8	16.1	0.62	0.33	p1d7	2.45	0.0001213	0.0001780	0.0002606	0.4277
7090276	10/29B1	34S_6p1d7Ya-40	33 7/8	S	9	4437.4	67 3/4	65 3/4	0.446	0.669	HLP-22	12	4	0	1.9	10.5	5.7	30.8	16.1	0.62	0.33	p1d7	2.45	0.0001213	0.0001780	0.0002606	0.4277
7090279	10/29B1	34S_6p1d7Ya-40	33 7/8	S	9	4437.4	67 3/4	65 3/4	0.446	0.669	HLP-22	12	4	0	1.9	10.5	5.7	30.8	16.1	0.62	0.33	p1d7	2.45	0.0001213	0.0001780	0.0002606	0.4277
7090283	10/29B1	34S_6p1d7Ya-40	33 7/8	S	9	4437.4	67 3/4	65 3/4	0.446	0.669	HLP-22	12	4	0	1.9	10.5	5.7	30.8	16.1	0.62	0.33	p1d7	2.45	0.0001213	0.0001780	0.0002606	0.4277
7090285	10/29B1	34S_6p1d7Ya-40	33 7/8	S	9	4437.4	67 3/4	65 3/4	0.446	0.669	HLP-22	12	4	0	1.9	10.5	5.7	30.8	16.1	0.62	0.33	p1d7	2.45	0.0001213	0.0001780	0.0002606	0.4277
7090288	10/29B2	34S_6p1d7Yd_6	33 7/8	S	9	4437.4	67 3/4	65 3/4	0.446	0.669	HLP-22	12	4	0	1.9	10.5	5.7	30.8	16.1	0.62	0.33	p1d7	2.45	0.0001213	0.0001780	0.0002606	0.4277
7090291	10/29B2	34S_6p1d7Yd_6	33 7/8	S	9	4437.4	67 3/4	65 3/4	0.446	0.669	HLP-22	12	4	0	1.9	10.5	5.7	30.8	16.1	0.62	0.33	p1d7	2.45	0.0001213	0.0001780	0.0002606	0.4277
7090294	10/29B2	34S_6p1d7Yd_6	33 7/8	S	9	4437.4	67 3/4	65 3/4	0.446	0.669	HLP-22	12	4	0	1.9	10.5	5.7	30.8	16.1	0.62	0.33	p1d7	2.45	0.0001213	0.0001780	0.0002606	0.4277
7090298MX	10/29B2	34S_6p1d7Yd_6	33 7/8	S	9	4437.4	67 3/4	65 3/4	0.446	0.669	HLP-22	12	4	0	1.9	10.5	5.7	30.8	16.1	0.62	0.33	p1d7	2.45	0.0001213	0.0001780	0.0002606	0.4277
7090300MX	10/29B2	34S_6p1d7Yd_6	33 7/8	S	9	4437.4	67 3/4	65 3/4	0.446	0.669	HLP-22	12	4	0	1.9	10.5	5.7	30.8	16.1	0.62	0.33	p1d7	2.45	0.0001213	0.0001780	0.0002606	0.4277
7090303	10/30A1	34S_6p1d7Ya	33 7/8	S	9	4437.4	67 3/4	65 3/4	0.446	0.669	HLP-22	12	8	4	1.9	10.5	5.7	30.8	16.1	0.62	0.33	p1d7	2.45	0.0001213	0.0001780	0.0002606	0.4277
7090306	10/30A1	34S_6p1d7Ya	33 7/8	S	9	4437.4	67 3/4	65 3/4	0.446	0.669	HLP-22	12	8	4	1.9	10.5	5.7	30.8	16.1	0.62	0.33	p1d7	2.45	0.0001213	0.0001780	0.0002606	0.4277
7090310	10/30A1	34S_6p1d7Ya	33 7/8	S	9	4437.4	67 3/4	65 3/4	0.446	0.669	HLP-22	12	8	4	1.9	10.5	5.7	30.8	16.1	0.62	0.33	p1d7	2.45	0.0001213	0.0001780	0.0002606	0.4277
7090313	10/30A1	34S_6p1d7Ya	33 7/8	S	9	4437.4	67 3/4	65 3/4	0.446	0.669	HLP-22	12	8	4	1.9	10.5	5.7	30.8	16.1	0.62	0.33	p1d7	2.45	0.0001213	0.0001780	0.0002606	0.4277
7090315	10/30A2	34S_6p1d7Yd_1	33 7/8	S	9	4437.4	67 3/4	65 3/4	0.446	0.669	HLP-22	12	8	4	1.9	10.5	5.7	30.8	16.1	0.62	0.33	p1d7	2.45	0.0001213	0.0001780	0.0002606	0.4277
7090318	10/30A2	34S_6p1d7Yd_1	33 7/8	S	9	4437.4	67 3/4	65 3/4	0.446	0.669	HLP-22	12	8	4	1.9	10.5	5.7	30.8	16.1	0.62	0.33	p1d7	2.45	0.0001213	0.0001780	0.0002606	0.4277
7090321	10/30A2	34S_6p1d7Yd_1	33 7/8	S	9	4437.4	67 3/4	65 3/4	0.446	0.669	HLP-22	12	8	4	1.9	10.5	5.7	30.8	16.1	0.62	0.33	p1d7	2.45	0.0001213	0.0001780	0.0002606	0.4277
7090324	10/30A2	34S_6p1d7Yd_1	33 7/8	S	9	4437.4	67 3/4	65 3/4	0.446	0.669	HLP-22	12	8	4	1.9	10.5	5.7	30.8	16.1	0.62	0.33	p1d7	2.45	0.0001213	0.0001780	0.0002606	0.4277
7090328MX	10/30A2	34S_6p1d7Yd_1	33 7/8	S	9	4437.4	67 3/4	65 3/4	0.446	0.669	HLP-22	12	8	4	1.9	10.5	5.7	30.8	16.1	0.62	0.33	p1d7	2.45	0.0001213	0.0001780	0.0002606	0.4277
7090333	10/30C1	34S_6p1d7Ya-04	33 7/8	S	9	4437.4	67 3/4	65 3/4	0.446	0.669	HLP-22	12	0	4	1.9	10.5	5.7	30.8	16.1	0.62	0.33	p1d7	2.45	0.0001213	0.0001780	0.0002606	0.4277
7090335	10/30C1	34S_6p1d7Ya-04	33 7/8	S	9	4437.4	67 3/4	65 3/4	0.446	0.669	HLP-22	12	0	4	1.9	10.5	5.7	30.8	16.1	0.62	0.33	p1d7	2.45	0.0001213	0.0001780	0.0002606	0.4277
7090338	10/30C1	34S_6p1d7Ya-04	33 7/8	S	9	4437.4	67 3/4	65 3/4	0.446	0.669	HLP-22	12	0	4	1.9	10.5	5.7	30.8	16.1	0.62	0.33	p1d7	2.45	0.0001213	0.0001780	0.0002606	0.4277
7090341	10/30C1	34S_6p1d7Ya-04	33 7/8	S	9	4437.4	67 3/4	65 3/4	0.446	0.669	HLP-22	12	0	4	1.9	10.5	5.7	30.8	16.1	0.62	0.33	p1d7	2.45	0.0001213	0.0001780	0.0002606	0.4277
7090344	10/30C1	34S_6p1d7Ya-04	33 7/8	S	9	4437.4	67 3/4	65 3/4	0.446	0.669	HLP-22	12	0	4	1.9	10.5	5.7	30.8	16.1	0.62	0.33	p1d7	2.45	0.0001213	0.0001780	0.0002606	0.4277
7090348	10/30C2	34S_6p1d7Yd_9	33 7/8	S	9	4437.4	67 3/4	65 3/4	0.446	0.669	HLP-22	12	0	4	1.9	10.5	5.7	30.8	16.1	0.62	0.33	p1d7	2.45	0.0001213	0.0001780	0.0002606	0.4277
7090350	10/30C2	34S_6p1d7Yd_9	33 7/8	S	9	4437.4	67 3/4	65 3/4	0.446	0.669	HLP-22	12	0	4	1.9	10.5	5.7	30.8	16.1	0.62	0.33	p1d7	2.45	0.0001213	0.0001780	0.0002606	0.4277
7090353	10/30C2	34S_6p1d7Yd_9	33 7/8	S	9	4437.4	67 3/4	65 3/4	0.446	0.669	HLP-22	12	0	4	1.9	10.5	5.7	30.8	16.1	0.62	0.33	p1d7	2.45	0.0001213	0.0001780	0.0002606	0.4277
7090357	10/30C2	34S_6p1d7Yd_9	33 7/8	S	9	4437.4	67 3/4	65 3/4	0.446	0.669	HLP-22	12	0	4	1.9	10.5	5.7	30.8	16.1	0.62	0.33	p1d7	2.45	0.0001213	0.0001780	0.0002606	0.4277
7090360MX	10/30C2	34S_6p1d7Yd_9	33 7/8	S	9	4437.4	67 3/4	65 3/4	0.446	0.669	HLP-22	12	0	4	1.9	10.5	5.7	30.8	16.1	0.62	0.33	p1d7	2.45	0.0001213	0.0001780	0.0002606	0.4277
7090362MX	10/30C2	34S_6p1d7Yd_9	33 7/8	S	9	4437.4	67 3/4	65 3/4	0.446	0.669	HLP-22	12	0	4	1.9	10.5	5.7	30.8	16.1	0.62	0.33	p1d7	2.45	0.0001213	0.0001780	0.0002606	0.4277
7090368	10/31A1	34S_6p1d7Ya	33 7/8	S	9	4437.4	33 7/8	31 7/8	0.446	0.669	HLP-22	12	8	4	1.9	10.5	5.7	30.8	16.1	0.62	0.33	p1d7	2.45	0.0001213	0.0001780	0.0002606	0.4277
7090371	10/31A1	34S_6p1d7Ya	33 7/8	S	9	4437.4	33 7/8	31 7/8	0.446	0.669	HLP-22	12	8	4	1.9	10.5	5.7	30.8	16.1	0.62	0.33	p1d7	2.45	0.0001213	0.0001780	0.0002606	0.4277
7090374	10/31A1	34S_6p1d7Ya	33 7/8	S	9	4437.4	33 7/8	31 7/8	0.446	0.669	HLP-22	12	8	4	1.9	10.5	5.7	30.8	16.1	0.62	0.33	p1d7	2.45	0.0001213	0.0001780	0.0002606	0.4277
7090376	10/31A1	34S_6p1d7Ya	33 7/8	S	9	4437.4	33 7/8	31 7/8	0.446	0.669	HLP-22	12	8	4	1.9	10.5	5.7	30.8	16.1	0.62	0.33	p1d7	2.45	0.0001213	0.0001780	0.0002606	0.4277
7090379	10/31A2	34S_6p1d7Yd_1	33 7/8	S	9	4437.4	33 7/8	31 7/8	0.446	0.669	HLP-22	12	8	4	1.9	10.5	5.7	30.8	16.1	0.62	0.33	p1d7	2.45	0.0001213	0.0001780	0.0002606	0.4277

Table B.8. Data from Fall 2007 Tests in Mid-Scale Vessel with Spherical Head B.3

Tank Water Temperature	Water Density	Solids Fraction	Pulse Volume Fraction	Duty Cycle	Cycle Time	Pulsed or Steady Jet	Us Steady Jet	U1 Pulsing Jet	U2 URMS	U3 URM3	Discharge Velocity	Critical Suspension Velocity	Average Peak Cloud Height	UCS Condition	UCS Method	UCS Flag	UCS Center Flag	UCS udv Flag	UCS based on Decreasing Velocity	Sweep Increase / Decrease	UDV Height Bed	Particle Motion	Solids Level	Outer Bottom Pattern	Inner Bottom Pattern	Case ID	Test	TDP	Row Number
C	g/cm³	fraction	fraction	fraction	s	text	m/s	m/s	m/s	m/s	m/s	m/s	in.	m/s	text	text	text	text	m/s	text	mm	text	text	text	text	text	text	text	text
T	ρ_l	ϕ_S	ϕ_P	DC	t_C	Jet	U_S	U1	U2	U3	U	U_{CS}	H_C	U_{CSR}	U_{CSM}	U_{CS}vis	U_{CS}cen	U_{CS}udv	U_{CS}_D	S_W	H_{bed}	PM	Sol	SP_O	SP_I	ID	M/DDX	TDP	MSS
20.9	0.999	0.00487	undefined	1.000	infinite	S	5.40	N/A	N/A	N/A	5.40	6.00	19.50	N/A	N/A	N/A	N/A	N/A	N/A	I	N/A	AM	N/A	N/A	N/A	34S_6p1d7Ya-04	10/29A1	TDP-WTP-040	7090256
20.9	0.999	0.00487	undefined	1.000	infinite	S	5.60	N/A	N/A	N/A	5.60	6.00	21.50	N/A	N/A	N/A	N/A	N/A	N/A	I	N/A	AM+	N/A	N/A	N/A	34S_6p1d7Ya-04	10/29A1	TDP-WTP-040	7090258
20.9	0.999	0.00487	undefined	1.000	infinite	S	5.80	N/A	N/A	N/A	5.80	6.00	23.00	N/A	N/A	N/A	N/A	N/A	N/A	I	N/A	CS-	N/A	N/A	N/A	34S_6p1d7Ya-04	10/29A1	TDP-WTP-040	7090261
20.9	0.999	0.00487	undefined	1.000	infinite	S	5.99	N/A	N/A	N/A	6.00	6.00	24.50	6.00	vis	UCSvis	N/A	N/A	N/A	I	N/A	CS	N/A	N/A	N/A	34S_6p1d7Ya-04	10/29A1	TDP-WTP-040	7090265
21.0	0.999	0.00487	0.046	0.196	45.0	P	N/A	6.11	6.53	6.70	7.00	7.50	24.50	N/A	N/A	N/A	N/A	N/A	N/A	I	N/A	AM	N/A	N/A	N/A	34S_6p1d7Ym_9	10/29A2	TDP-WTP-040	7090268
21.0	0.999	0.00487	0.049	0.203	45.0	P	N/A	6.44	6.92	7.12	7.50	7.50	27.00	7.50	vis	UCSvis	N/A	N/A	N/A	I	N/A	CS	N/A	N/A	N/A	34S_6p1d7Ym_9	10/29A2	TDP-WTP-040	7090271
21.0	0.999	0.00487	0.051	0.198	45.0	P	N/A	6.62	7.10	7.30	7.70	7.50	28.00	N/A	N/A	N/A	N/A	N/A	N/A	I	N/A	BC	N/A	N/A	N/A	34S_6p1d7Ym_9	10/29A2	TDP-WTP-040	7090274
21.0	0.999	0.00487	undefined	1.000	infinite	S	4.49	N/A	N/A	N/A	4.50	5.50	10.00	N/A	N/A	N/A	N/A	N/A	N/A	I	N/A	SS	N/A	N/A	N/A	34S_6p1d7Ya-40	10/29B1	TDP-WTP-040	7090276
21.0	0.999	0.00487	undefined	1.000	infinite	S	4.99	N/A	N/A	N/A	5.00	5.50	11.50	N/A	N/A	N/A	N/A	N/A	N/A	I	N/A	AM-	N/A	N/A	N/A	34S_6p1d7Ya-40	10/29B1	TDP-WTP-040	7090279
21.1	0.999	0.00487	undefined	1.000	infinite	S	5.50	N/A	N/A	N/A	5.50	5.50	21.25	5.50	vis	UCSvis	N/A	N/A	N/A	I	N/A	CS	N/A	N/A	N/A	34S_6p1d7Ya-40	10/29B1	TDP-WTP-040	7090283
21.0	0.999	0.00487	undefined	1.000	infinite	S	5.70	N/A	N/A	N/A	5.70	5.50	25.00	N/A	N/A	N/A	N/A	N/A	N/A	I	N/A	BC	N/A	N/A	N/A	34S_6p1d7Ya-40	10/29B1	TDP-WTP-040	7090285
21.0	0.999	0.00487	0.050	0.180	70.0	P	N/A	4.90	4.95	4.98	5.00	6.20	9.75	N/A	N/A	N/A	N/A	N/A	N/A	D	N/A	SS	N/A	N/A	N/A	34S_6p1d7Yd_6	10/29B2	TDP-WTP-040	7090288
21.0	0.999	0.00487	0.050	0.180	63.0	P	N/A	5.39	5.45	5.48	5.50	6.20	11.50	N/A	N/A	N/A	N/A	N/A	N/A	I	N/A	SS+	N/A	N/A	N/A	34S_6p1d7Yd_6	10/29B2	TDP-WTP-040	7090291
21.0	0.999	0.00487	0.055	0.180	58.0	P	N/A	5.83	5.90	5.93	6.00	6.20	14.00	N/A	N/A	N/A	N/A	N/A	N/A	I	N/A	AM+	N/A	N/A	N/A	34S_6p1d7Yd_6	10/29B2	TDP-WTP-040	7090294
21.0	0.999	0.00487	0.050	0.180	56.0	P	N/A	6.06	6.14	6.17	6.20	6.20	16.00	6.20	vis	UCSvis	N/A	N/A	N/A	I	N/A	CS	N/A	N/A	N/A	34S_6p1d7Yd_6	10/29B2	TDP-WTP-040	7090298
21.0	0.999	0.00487	0.050	0.180	53.0	P	N/A	6.23	6.32	6.37	6.40	6.20	17.25	N/A	N/A	N/A	N/A	N/A	N/A	I	N/A	BC	N/A	N/A	N/A	34S_6p1d7Yd_6	10/29B2	TDP-WTP-040	7090300
21.1	0.999	0.00487	undefined	1.000	infinite	S	2.02	N/A	N/A	N/A	2.00	3.20	N/A	N/A	N/A	N/A	N/A	N/A	N/A	N/A	N/A	SS	N/A	N/A	N/A	34S_6p1d7Ya	10/30A1	TDP-WTP-041	7090303
21.1	0.999	0.00487	undefined	1.000	infinite	S	2.50	N/A	N/A	N/A	2.50	3.20	9.00	N/A	N/A	N/A	N/A	N/A	N/A	I	N/A	SS+	N/A	N/A	N/A	34S_6p1d7Ya	10/30A1	TDP-WTP-041	7090306
21.1	0.999	0.00487	undefined	1.000	infinite	S	3.01	N/A	N/A	N/A	3.00	3.20	10.25	N/A	N/A	N/A	N/A	N/A	N/A	I	N/A	AM	N/A	N/A	N/A	34S_6p1d7Ya	10/30A1	TDP-WTP-041	7090310
21.1	0.999	0.00487	undefined	1.000	infinite	S	3.23	N/A	N/A	N/A	3.20	3.20	17.75	3.20	vis	UCSvis	N/A	N/A	N/A	I	N/A	CS	N/A	N/A	N/A	34S_6p1d7Ya	10/30A1	TDP-WTP-041	7090313
21.0	0.999	0.00487	0.043	0.180	48.0	P	N/A	2.30	2.36	2.39	2.50	3.60	9.50	N/A	N/A	N/A	N/A	N/A	N/A	I	N/A	SS	N/A	N/A	N/A	34S_6p1d7Yd_1	10/30A2	TDP-WTP-041	7090315
21.0	0.999	0.00487	0.050	0.180	39.5	P	N/A	2.78	2.86	2.90	3.00	3.60	11.00	N/A	N/A	N/A	N/A	N/A	N/A	I	N/A	SS+	N/A	N/A	N/A	34S_6p1d7Yd_1	10/30A2	TDP-WTP-041	7090318
21.0	0.999	0.00487	0.051	0.180	37.0	P	N/A	2.94	3.04	3.09	3.20	3.60	11.75	N/A	N/A	N/A	N/A	N/A	N/A	I	N/A	AM	N/A	N/A	N/A	34S_6p1d7Yd_1	10/30A2	TDP-WTP-041	7090321
21.0	0.999	0.00487	0.051	0.180	35.0	P	N/A	3.06	3.18	3.24	3.40	3.60	12.50	N/A	N/A	N/A	N/A	N/A	N/A	I	N/A	AM+	N/A	N/A	N/A	34S_6p1d7Yd_1	10/30A2	TDP-WTP-041	7090324
21.0	0.999	0.00487	0.051	0.180	33.0	P	N/A	3.09	3.25	3.33	3.60	3.60	12.75	3.60	vis	UCSvis	N/A	N/A	N/A	I	N/A	CS	N/A	N/A	N/A	34S_6p1d7Yd_1	10/30A2	TDP-WTP-041	7090328
21.3	0.999	0.00487	undefined	1.000	infinite	S	4.02	N/A	N/A	N/A	4.00	N/A	11.25	N/A	N/A	N/A	N/A	N/A	N/A	I	N/A	SS	N/A	N/A	N/A	34S_6p1d7Ya-04	10/30C1	TDP-WTP-041	7090333
21.3	0.999	0.00487	undefined	1.000	infinite	S	4.51	N/A	N/A	N/A	4.50	N/A	14.00	N/A	N/A	N/A	N/A	N/A	N/A	I	N/A	AM	N/A	N/A	N/A	34S_6p1d7Ya-04	10/30C1	TDP-WTP-041	7090335
21.3	0.999	0.00487	undefined	1.000	infinite	S	5.02	N/A	N/A	N/A	5.00	N/A	16.75	N/A	N/A	N/A	N/A	N/A	N/A	I	N/A	AM	N/A	N/A	N/A	34S_6p1d7Ya-04	10/30C1	TDP-WTP-041	7090338
21.4	0.999	0.00487	undefined	1.000	infinite	S	5.52	N/A	N/A	N/A	5.50	N/A	20.50	N/A	N/A	N/A	N/A	N/A	N/A	I	N/A	AM+	N/A	N/A	N/A	34S_6p1d7Ya-04	10/30C1	TDP-WTP-041	7090341
21.4	0.999	0.00487	undefined	1.000	infinite	S	5.74	N/A	N/A	N/A	5.70	N/A	23.50	N/A	N/A	N/A	N/A	N/A	N/A	I	N/A	CS-	N/A	N/A	N/A	34S_6p1d7Ya-04	10/30C1	TDP-WTP-041	7090344
21.0	0.999	0.00487	0.046	0.180	70.0	P	N/A	4.87	4.93	4.96	5.00	6.70	15.50	N/A	N/A	N/A	N/A	N/A	N/A	D	N/A	SS+	N/A	N/A	N/A	34S_6p1d7Yd_9	10/30C2	TDP-WTP-041	7090348
21.0	0.999	0.00487	0.050	0.180	63.5	P	N/A	5.37	5.44	5.48	5.50	6.70	18.25	N/A	N/A	N/A	N/A	N/A	N/A	I	N/A	AM	N/A	N/A	N/A	34S_6p1d7Yd_9	10/30C2	TDP-WTP-041	7090350
21.0	0.999	0.00487	0.050	0.180	57.5	P	N/A	5.86	5.95	5.99	6.00	6.70	20.50	N/A	N/A	N/A	N/A	N/A	N/A	I	N/A	AM	N/A	N/A	N/A	34S_6p1d7Yd_9	10/30C2	TDP-WTP-041	7090353
21.0	0.999	0.00487	0.051	0.180	54.0	P	N/A	6.25	6.38	6.44	6.50	6.70	22.25	N/A	N/A	N/A	N/A	N/A	N/A	I	N/A	AM+	N/A	N/A	N/A	34S_6p1d7Yd_9	10/30C2	TDP-WTP-041	7090357
21.0	0.999	0.00487	0.050	0.180	51.5	P	N/A	6.37	6.54	6.62	6.70	6.70	24.50	6.70	vis	UCSvis	N/A	N/A	N/A	I	N/A	CS	N/A	N/A	N/A	34S_6p1d7Yd_9	10/30C2	TDP-WTP-041	7090360
21.0	0.999	0.00487	0.051	0.180	50.5	P	N/A	6.12	6.49	6.64	6.90	6.70	25.50	N/A	N/A	N/A	N/A	N/A	N/A	I	N/A	BC	N/A	N/A	N/A	34S_6p1d7Yd_9	10/30C2	TDP-WTP-041	7090362
21.5	0.999	0.00487	undefined	1.000	infinite	S	2.81	N/A	N/A	N/A	2.80	3.00	10.50	N/A	N/A	N/A	N/A	N/A	N/A	I	N/A	AM	N/A	N/A	N/A	34S_6p1d7Ya	10/31A1	TDP-WTP-042	7090368
21.4	0.999	0.00487	undefined	1.000	infinite	S	2.42	N/A	N/A	N/A	2.40	3.00	9.50	N/A	N/A	N/A	N/A	N/A	N/A	D	N/A	SS	N/A	N/A	N/A	34S_6p1d7Ya	10/31A1	TDP-WTP-042	7090371
21.4	0.999	0.00487	undefined	1.000	infinite	S	3.01	N/A	N/A	N/A	3.00	3.00	16.50	3.00	vis	UCSvis	N/A	N/A	N/A	I	N/A	CS	N/A	N/A	N/A	34S_6p1d7Ya	10/31A1	TDP-WTP-042	7090374
21.4	0.999	0.00487	undefined	1.000	infinite	S	3.22	N/A	N/A	N/A	3.20	3.00	26.00	N/A	N/A	N/A	N/A	N/A	N/A	I	N/A	BC	N/A	N/A	N/A	34S_6p1d7Ya	10/31A1	TDP-WTP-042	7090376
21.0	0.999	0.00487	0.050	0.180	48.0	P	N/A	2.35	2.39	2.41	2.50	3.40	11.00	N/A	N/A	N/A	N/A	N/A	N/A	D	N/A	SS	N/A	N/A	N/A	34S_6p1d7Yd_1	10/31A2	TDP-WTP-042	7090379

Table B.8. Data from Fall 2007 Tests in Mid-Scale Vessel with Spherical Head A.4

Row Number	Test	Case ID	Tank Diameter	Head Shape	Dish Height	Dish Volume	Tank Fill Height	Return Line Height	Nozzle Inner Diameter	Nozzle Stand-off Distance	Pulse Tube Configuration	Installed Nozzles	Outer Nozzles Operated	Inner Nozzles Operated	Pulse Tube Outer Diameter	Outer PJM Radius	Inner PJM Radius	"FIO" Outer PJM Impingement Angle	"FIO" Inner PJM Impingement Angle	Ratio Outer PJM to Tank Radius	Ratio Inner PJM to Tank Radius	Simulant	Solids Density	Particle Diameter d5	Particle Diameter d50	Particle Diameter d95	Void Fraction
text	text	text	in.	text	in.	in. ^{3}	in.	in.	in.	in.	text	number	number	number	in.	in.	in.	deg	deg	nondim	nondim	text	g/cm^3	m	m	m	fraction
MSS	M/DDX	ID	D	HS	H_{dish}	V_{dish}	H	Rtn	d	sod	PT	N	N_O	N_I	PT_{od}	R_O	R_I	θ_O	θ_I	R_O/R	R_I/R	sxdx	ρ_s	d_5	d_{50}	d_{95}	vf
7090382	10/31A2	34S_6p1d7Yd_1	33 7/8	S	9	4437.4	33 7/8	31 7/8	0.446	0.669	HLP-22	12	8	4	1.9	10.5	5.7	30.8	16.1	0.62	0.33	p1d7	2.45	0.0001213	0.0001780	0.0002606	0.4277
7090385	10/31A2	34S_6p1d7Yd_1	33 7/8	S	9	4437.4	33 7/8	31 7/8	0.446	0.669	HLP-22	12	8	4	1.9	10.5	5.7	30.8	16.1	0.62	0.33	p1d7	2.45	0.0001213	0.0001780	0.0002606	0.4277
7090389	10/31A2	34S_6p1d7Yd_1	33 7/8	S	9	4437.4	33 7/8	31 7/8	0.446	0.669	HLP-22	12	8	4	1.9	10.5	5.7	30.8	16.1	0.62	0.33	p1d7	2.45	0.0001213	0.0001780	0.0002606	0.4277
7090391	10/31A2	34S_6p1d7Yd_1	33 7/8	S	9	4437.4	33 7/8	31 7/8	0.446	0.669	HLP-22	12	8	4	1.9	10.5	5.7	30.8	16.1	0.62	0.33	p1d7	2.45	0.0001213	0.0001780	0.0002606	0.4277
7090395	11/2A1	34S_6p1d7Ya-80	33 7/8	S	9	4437.4	33 7/8	31 7/8	0.446	0.669	HLP-22	12	8	0	1.9	10.5	5.7	30.8	16.1	0.62	0.33	p1d7	2.45	0.0001213	0.0001780	0.0002606	0.4277
7090398	11/2A1	34S_6p1d7Ya-80	33 7/8	S	9	4437.4	33 7/8	31 7/8	0.446	0.669	HLP-22	12	8	0	1.9	10.5	5.7	30.8	16.1	0.62	0.33	p1d7	2.45	0.0001213	0.0001780	0.0002606	0.4277
7090401	11/2A2	34S_6p1d7Yd_5	33 7/8	S	9	4437.4	33 7/8	31 7/8	0.446	0.669	HLP-22	12	8	0	1.9	10.5	5.7	30.8	16.1	0.62	0.33	p1d7	2.45	0.0001213	0.0001780	0.0002606	0.4277
7090403	11/2A2	34S_6p1d7Yd_5	33 7/8	S	9	4437.4	33 7/8	31 7/8	0.446	0.669	HLP-22	12	8	0	1.9	10.5	5.7	30.8	16.1	0.62	0.33	p1d7	2.45	0.0001213	0.0001780	0.0002606	0.4277
7090406	11/2A2	34S_6p1d7Yd_5	33 7/8	S	9	4437.4	33 7/8	31 7/8	0.446	0.669	HLP-22	12	8	0	1.9	10.5	5.7	30.8	16.1	0.62	0.33	p1d7	2.45	0.0001213	0.0001780	0.0002606	0.4277
7090409	11/2A2	34S_6p1d7Yd_5	33 7/8	S	9	4437.4	33 7/8	31 7/8	0.446	0.669	HLP-22	12	8	0	1.9	10.5	5.7	30.8	16.1	0.62	0.33	p1d7	2.45	0.0001213	0.0001780	0.0002606	0.4277
7090413	11/2A2	34S_6p1d7Yd_5	33 7/8	S	9	4437.4	33 7/8	31 7/8	0.446	0.669	HLP-22	12	8	0	1.9	10.5	5.7	30.8	16.1	0.62	0.33	p1d7	2.45	0.0001213	0.0001780	0.0002606	0.4277
7090416	11/5A1	34S_6p1d7Ya-44	33 7/8	S	9	4437.4	33 7/8	31 7/8	0.446	0.669	HLP-22	12	4	4	1.9	10.5	5.7	30.8	16.1	0.62	0.33	p1d7	2.45	0.0001213	0.0001780	0.0002606	0.4277
7090419	11/5A1	34S_6p1d7Ya-44	33 7/8	S	9	4437.4	33 7/8	31 7/8	0.446	0.669	HLP-22	12	4	4	1.9	10.5	5.7	30.8	16.1	0.62	0.33	p1d7	2.45	0.0001213	0.0001780	0.0002606	0.4277
7090421	11/5A1	34S_6p1d7Ya-44	33 7/8	S	9	4437.4	33 7/8	31 7/8	0.446	0.669	HLP-22	12	4	4	1.9	10.5	5.7	30.8	16.1	0.62	0.33	p1d7	2.45	0.0001213	0.0001780	0.0002606	0.4277
7090424	11/5A1	34S_6p1d7Ya-44	33 7/8	S	9	4437.4	33 7/8	31 7/8	0.446	0.669	HLP-22	12	4	4	1.9	10.5	5.7	30.8	16.1	0.62	0.33	p1d7	2.45	0.0001213	0.0001780	0.0002606	0.4277
7090428	11/5A1	34S_6p1d7Ya-44	33 7/8	S	9	4437.4	33 7/8	31 7/8	0.446	0.669	HLP-22	12	4	4	1.9	10.5	5.7	30.8	16.1	0.62	0.33	p1d7	2.45	0.0001213	0.0001780	0.0002606	0.4277
7090430	11/5A1	34S_6p1d7Ya-44	33 7/8	S	9	4437.4	33 7/8	31 7/8	0.446	0.669	HLP-22	12	4	4	1.9	10.5	5.7	30.8	16.1	0.62	0.33	p1d7	2.45	0.0001213	0.0001780	0.0002606	0.4277
7090434	11/5A2	34S_6p1d7Yd_0	33 7/8	S	9	4437.4	33 7/8	31 7/8	0.446	0.669	HLP-22	12	4	4	1.9	10.5	5.7	30.8	16.1	0.62	0.33	p1d7	2.45	0.0001213	0.0001780	0.0002606	0.4277
7090436	11/5A2	34S_6p1d7Yd_0	33 7/8	S	9	4437.4	33 7/8	31 7/8	0.446	0.669	HLP-22	12	4	4	1.9	10.5	5.7	30.8	16.1	0.62	0.33	p1d7	2.45	0.0001213	0.0001780	0.0002606	0.4277
7090439	11/5A2	34S_6p1d7Yd_0	33 7/8	S	9	4437.4	33 7/8	31 7/8	0.446	0.669	HLP-22	12	4	4	1.9	10.5	5.7	30.8	16.1	0.62	0.33	p1d7	2.45	0.0001213	0.0001780	0.0002606	0.4277
7090443	11/5A2	34S_6p1d7Yd_0	33 7/8	S	9	4437.4	33 7/8	31 7/8	0.446	0.669	HLP-22	12	4	4	1.9	10.5	5.7	30.8	16.1	0.62	0.33	p1d7	2.45	0.0001213	0.0001780	0.0002606	0.4277
7090445	11/5A2	34S_6p1d7Yd_0	33 7/8	S	9	4437.4	33 7/8	31 7/8	0.446	0.669	HLP-22	12	4	4	1.9	10.5	5.7	30.8	16.1	0.62	0.33	p1d7	2.45	0.0001213	0.0001780	0.0002606	0.4277
7090448	11/5A2	34S_6p1d7Yd_0	33 7/8	S	9	4437.4	33 7/8	31 7/8	0.446	0.669	HLP-22	12	4	4	1.9	10.5	5.7	30.8	16.1	0.62	0.33	p1d7	2.45	0.0001213	0.0001780	0.0002606	0.4277
7090451	11/5A2	34S_6p1d7Yd_0	33 7/8	S	9	4437.4	33 7/8	31 7/8	0.446	0.669	HLP-22	12	4	4	1.9	10.5	5.7	30.8	16.1	0.62	0.33	p1d7	2.45	0.0001213	0.0001780	0.0002606	0.4277
7090454	11/5A2	34S_6p1d7Yd_0	33 7/8	S	9	4437.4	33 7/8	31 7/8	0.446	0.669	HLP-22	12	4	4	1.9	10.5	5.7	30.8	16.1	0.62	0.33	p1d7	2.45	0.0001213	0.0001780	0.0002606	0.4277
7090458	11/5A2	34S_6p1d7Yd_0	33 7/8	S	9	4437.4	33 7/8	31 7/8	0.446	0.669	HLP-22	12	4	4	1.9	10.5	5.7	30.8	16.1	0.62	0.33	p1d7	2.45	0.0001213	0.0001780	0.0002606	0.4277
7090461	11/5B1	34S_6p1d7Ya-04	33 7/8	S	9	4437.4	33 7/8	31 7/8	0.446	0.669	HLP-22	12	0	4	1.9	10.5	5.7	30.8	16.1	0.62	0.33	p1d7	2.45	0.0001213	0.0001780	0.0002606	0.4277
7090464	11/5B1	34S_6p1d7Ya-04	33 7/8	S	9	4437.4	33 7/8	31 7/8	0.446	0.669	HLP-22	12	0	4	1.9	10.5	5.7	30.8	16.1	0.62	0.33	p1d7	2.45	0.0001213	0.0001780	0.0002606	0.4277
7090466	11/5B1	34S_6p1d7Ya-04	33 7/8	S	9	4437.4	33 7/8	31 7/8	0.446	0.669	HLP-22	12	0	4	1.9	10.5	5.7	30.8	16.1	0.62	0.33	p1d7	2.45	0.0001213	0.0001780	0.0002606	0.4277
7090469	11/5B1	34S_6p1d7Ya-04	33 7/8	S	9	4437.4	33 7/8	31 7/8	0.446	0.669	HLP-22	12	0	4	1.9	10.5	5.7	30.8	16.1	0.62	0.33	p1d7	2.45	0.0001213	0.0001780	0.0002606	0.4277
7090473	11/5B1	34S_6p1d7Ya-04	33 7/8	S	9	4437.4	33 7/8	31 7/8	0.446	0.669	HLP-22	12	0	4	1.9	10.5	5.7	30.8	16.1	0.62	0.33	p1d7	2.45	0.0001213	0.0001780	0.0002606	0.4277
7090476	11/5B2	34S_6p1d7Yd_9	33 7/8	S	9	4437.4	33 7/8	31 7/8	0.446	0.669	HLP-22	12	0	4	1.9	10.5	5.7	30.8	16.1	0.62	0.33	p1d7	2.45	0.0001213	0.0001780	0.0002606	0.4277
7090479	11/5B2	34S_6p1d7Yd_9	33 7/8	S	9	4437.4	33 7/8	31 7/8	0.446	0.669	HLP-22	12	0	4	1.9	10.5	5.7	30.8	16.1	0.62	0.33	p1d7	2.45	0.0001213	0.0001780	0.0002606	0.4277
7090481	11/5B2	34S_6p1d7Yd_9	33 7/8	S	9	4437.4	33 7/8	31 7/8	0.446	0.669	HLP-22	12	0	4	1.9	10.5	5.7	30.8	16.1	0.62	0.33	p1d7	2.45	0.0001213	0.0001780	0.0002606	0.4277
7090484	11/5B2	34S_6p1d7Yd_9	33 7/8	S	9	4437.4	33 7/8	31 7/8	0.446	0.669	HLP-22	12	0	4	1.9	10.5	5.7	30.8	16.1	0.62	0.33	p1d7	2.45	0.0001213	0.0001780	0.0002606	0.4277
7090487	11/5B2	34S_6p1d7Yd_9	33 7/8	S	9	4437.4	33 7/8	31 7/8	0.446	0.669	HLP-22	12	0	4	1.9	10.5	5.7	30.8	16.1	0.62	0.33	p1d7	2.45	0.0001213	0.0001780	0.0002606	0.4277
7090491	11/5B2	34S_6p1d7Yd_9	33 7/8	S	9	4437.4	33 7/8	31 7/8	0.446	0.669	HLP-22	12	0	4	1.9	10.5	5.7	30.8	16.1	0.62	0.33	p1d7	2.45	0.0001213	0.0001780	0.0002606	0.4277
7090493	11/6A1	34S_6p1d7Ya-40	33 7/8	S	9	4437.4	33 7/8	31 7/8	0.446	0.669	HLP-22	12	4	0	1.9	10.5	5.7	30.8	16.1	0.62	0.33	p1d7	2.45	0.0001213	0.0001780	0.0002606	0.4277
7090496	11/6A1	34S_6p1d7Ya-40	33 7/8	S	9	4437.4	33 7/8	31 7/8	0.446	0.669	HLP-22	12	4	0	1.9	10.5	5.7	30.8	16.1	0.62	0.33	p1d7	2.45	0.0001213	0.0001780	0.0002606	0.4277
7090499	11/6A1	34S_6p1d7Ya-40	33 7/8	S	9	4437.4	33 7/8	31 7/8	0.446	0.669	HLP-22	12	4	0	1.9	10.5	5.7	30.8	16.1	0.62	0.33	p1d7	2.45	0.0001213	0.0001780	0.0002606	0.4277
7090503	11/6A1	34S_6p1d7Ya-40	33 7/8	S	9	4437.4	33 7/8	31 7/8	0.446	0.669	HLP-22	12	4	0	1.9	10.5	5.7	30.8	16.1	0.62	0.33	p1d7	2.45	0.0001213	0.0001780	0.0002606	0.4277

Table B.8. Data from Fall 2007 Tests in Mid-Scale Vessel with Spherical Head B.4

Tank Water Temperature	Water Density	Solids Fraction	Pulse Volume Fraction	Duty Cycle	Cycle Time	Pulsed or Steady Jet	Us Steady Jet	U1 Pulsing Jet	U2 URMS	U3 URM3	Discharge Velocity	Critical Suspension Velocity	Average Peak Cloud Height	UCS Condition	UCS Method	UCS Flag	UCS Center Flag	UCS udv Flag	UCS based on Decreasing Velocity	Sweep Increase / Decrease	UDV Height Bed	Particle Motion	Solids Level	Outer Bottom Pattern	Inner Bottom Pattern	Case ID	Test	TDP	Row Number
C	g/cm^3	fraction	fraction	fraction	s	text	m/s	m/s	m/s	m/s	m/s	m/s	in.	m/s	text	text	text	text	m/s	text	mm	text	text	text	text	text	text	text	text
T	ρ_l	ϕ_S	ϕ_P	DC	t_C	Jet	U_S	U1	U2	U3	U	U_{CS}	H_C	U_{CSR}	U_{CSM}	U_{CS}vis	U_{CS}cen	U_{CS}udv	U_{CS}_D	S_W	H_{bed}	PM	Sol	SP_O	SP_I	ID	M/DDX	TDP	MSS
21.0	0.999	0.00487	0.052	0.180	40.0	P	N/A	2.80	2.87	2.90	3.00	3.40	12.50	N/A	N/A	N/A	N/A	N/A	N/A	I	N/A	AM	N/A	N/A	N/A	34S_6p1d7Yd_1	10/31A2	TDP-WTP-042	7090382
21.0	0.999	0.00487	0.050	0.180	37.5	P	N/A	2.97	3.04	3.08	3.20	3.40	13.00	N/A	N/A	N/A	N/A	N/A	N/A	I	N/A	AM+	N/A	N/A	N/A	34S_6p1d7Yd_1	10/31A2	TDP-WTP-042	7090385
21.0	0.999	0.00487	0.050	0.180	35.0	P	N/A	3.13	3.22	3.26	3.40	3.40	13.50	3.40	vis	UCSvis	N/A	N/A	N/A	I	N/A	CS	N/A	N/A	N/A	34S_6p1d7Yd_1	10/31A2	TDP-WTP-042	7090389
21.0	0.999	0.00487	0.050	0.180	33.0	P	N/A	3.29	3.39	3.44	3.60	3.40	14.25	N/A	N/A	N/A	N/A	N/A	N/A	I	N/A	BC	N/A	N/A	N/A	34S_6p1d7Yd_1	10/31A2	TDP-WTP-042	7090391
24.0	0.999	0.00487	undefined	1.000	infinite	S	5.00	N/A	N/A	N/A	5.00	5.30	13.50	N/A	N/A	N/A	N/A	N/A	N/A	I	N/A	SS	N/A	N/A	N/A	34S_6p1d7Ya-80	11/2A1	TDP-WTP-043	7090395
24.0	0.999	0.00487	undefined	1.000	infinite	S	5.29	N/A	N/A	N/A	5.30	5.30	23.50	5.30	vis	UCSvis	N/A	N/A	N/A	I	N/A	CS	N/A	N/A	N/A	34S_6p1d7Ya-80	11/2A1	TDP-WTP-043	7090398
24.0	0.999	0.00487	0.051	0.180	30.0	P	N/A	5.05	5.40	5.55	5.90	6.60	14.25	N/A	N/A	N/A	N/A	N/A	N/A	I	N/A	SS	N/A	N/A	N/A	34S_6p1d7Yd_5	11/2A2	TDP-WTP-043	7090401
24.0	0.999	0.00487	0.051	0.180	29.0	P	N/A	5.12	5.52	5.69	6.10	6.60	15.75	N/A	N/A	N/A	N/A	N/A	N/A	I	N/A	SS+	N/A	N/A	N/A	34S_6p1d7Yd_5	11/2A2	TDP-WTP-043	7090403
24.0	0.999	0.00487	0.051	0.180	28.0	P	N/A	5.04	5.57	5.80	6.30	6.60	16.75	N/A	N/A	N/A	N/A	N/A	N/A	I	N/A	AM	N/A	N/A	N/A	34S_6p1d7Yd_5	11/2A2	TDP-WTP-043	7090406
24.0	0.999	0.00487	0.051	0.180	27.0	P	N/A	5.15	5.70	5.95	6.50	6.60	18.50	N/A	N/A	N/A	N/A	N/A	N/A	I	N/A	AM+	N/A	N/A	N/A	34S_6p1d7Yd_5	11/2A2	TDP-WTP-043	7090409
24.0	0.999	0.00487	0.051	0.180	26.5	P	N/A	5.15	5.74	6.00	6.60	6.60	19.00	6.60	vis	UCSvis	N/A	N/A	N/A	I	N/A	CS	N/A	N/A	N/A	34S_6p1d7Yd_5	11/2A2	TDP-WTP-043	7090413
20.8	0.999	0.00487	undefined	1.000	infinite	S	3.13	N/A	N/A	N/A	3.00	4.60	N/A	N/A	N/A	N/A	N/A	N/A	N/A	I	N/A	SS	N/A	N/A	N/A	34S_6p1d7Ya-44	11/5A1	TDP-WTP-044	7090416
20.9	0.999	0.00487	undefined	1.000	infinite	S	3.53	N/A	N/A	N/A	3.50	4.60	N/A	N/A	N/A	N/A	N/A	N/A	N/A	I	N/A	SS	N/A	N/A	N/A	34S_6p1d7Ya-44	11/5A1	TDP-WTP-044	7090419
20.9	0.999	0.00487	undefined	1.000	infinite	S	4.01	N/A	N/A	N/A	4.00	4.60	9.25	N/A	N/A	N/A	UCScen	N/A	N/A	I	N/A	AM	N/A	N/A	N/A	34S_6p1d7Ya-44	11/5A1	TDP-WTP-044	7090421
0.0	0.999	0.00487	undefined	1.000	infinite	S	N/A	N/A	N/A	N/A	4.40	4.60	12.25	N/A	N/A	N/A	N/A	N/A	N/A	I	N/A	AM+	N/A	N/A	N/A	34S_6p1d7Ya-44	11/5A1	TDP-WTP-044	7090424
20.9	0.999	0.00487	undefined	1.000	infinite	S	4.65	N/A	N/A	N/A	4.60	4.60	15.25	4.60	vis	UCSvis	N/A	N/A	N/A	I	N/A	CS	N/A	N/A	N/A	34S_6p1d7Ya-44	11/5A1	TDP-WTP-044	7090428
21.0	0.999	0.00487	undefined	1.000	infinite	S	4.80	N/A	N/A	N/A	4.80	4.60	18.50	N/A	N/A	N/A	N/A	N/A	N/A	I	N/A	BC	N/A	N/A	N/A	34S_6p1d7Ya-44	11/5A1	TDP-WTP-044	7090430
21.0	0.999	0.00487	0.050	0.180	42.0	P	N/A	4.04	4.12	4.16	4.00	6.30	9.00	N/A	N/A	N/A	N/A	N/A	N/A	D	N/A	SS	N/A	N/A	N/A	34S_6p1d7Yd_0	11/5A2	TDP-WTP-044	7090434
21.0	0.999	0.00487	0.051	0.180	39.5	P	N/A	4.24	4.35	4.39	4.50	6.30	9.50	N/A	N/A	N/A	N/A	N/A	N/A	I	N/A	AM	N/A	N/A	N/A	34S_6p1d7Yd_0	11/5A2	TDP-WTP-044	7090436
21.0	0.999	0.00487	0.051	0.180	36.5	P	N/A	4.60	4.72	4.78	4.90	6.30	10.25	N/A	N/A	N/A	N/A	N/A	N/A	I	N/A	AM	N/A	N/A	N/A	34S_6p1d7Yd_0	11/5A2	TDP-WTP-044	7090439
21.0	0.999	0.00487	0.051	0.180	33.5	P	N/A	4.87	5.05	5.13	5.30	6.30	12.00	N/A	N/A	N/A	N/A	N/A	N/A	I	N/A	AM	N/A	N/A	N/A	34S_6p1d7Yd_0	11/5A2	TDP-WTP-044	7090443
21.0	0.999	0.00487	0.051	0.180	32.0	P	N/A	5.09	5.25	5.33	5.50	6.30	13.00	N/A	N/A	N/A	N/A	N/A	N/A	I	N/A	AM+	N/A	N/A	N/A	34S_6p1d7Yd_0	11/5A2	TDP-WTP-044	7090445
21.0	0.999	0.00487	0.051	0.180	31.0	P	N/A	5.12	5.35	5.46	5.70	6.30	13.75	N/A	N/A	N/A	N/A	N/A	N/A	I	N/A	AM+	N/A	N/A	N/A	34S_6p1d7Yd_0	11/5A2	TDP-WTP-044	7090448
21.0	0.999	0.00487	0.051	0.180	30.0	P	N/A	5.15	5.46	5.60	5.90	6.30	14.75	N/A	N/A	N/A	N/A	N/A	N/A	I	N/A	AM+	N/A	N/A	N/A	34S_6p1d7Yd_0	11/5A2	TDP-WTP-044	7090451
21.0	0.999	0.00487	0.051	0.180	28.8	P	N/A	5.22	5.59	5.75	6.10	6.30	16.00	N/A	N/A	N/A	N/A	N/A	N/A	I	N/A	AM+	N/A	N/A	N/A	34S_6p1d7Yd_0	11/5A2	TDP-WTP-044	7090454
21.0	0.999	0.00487	0.051	0.180	27.8	P	N/A	5.23	5.67	5.86	6.30	6.30	16.50	6.30	vis	UCSvis	N/A	N/A	N/A	I	N/A	CS	N/A	N/A	N/A	34S_6p1d7Yd_0	11/5A2	TDP-WTP-044	7090458
21.3	0.999	0.00487	undefined	1.000	infinite	S	4.52	N/A	N/A	N/A	4.50	6.50	9.50	N/A	N/A	N/A	N/A	N/A	N/A	D	N/A	SS	N/A	N/A	N/A	34S_6p1d7Ya-04	11/5B1	TDP-WTP-044	7090461
21.3	0.999	0.00487	undefined	1.000	infinite	S	5.00	N/A	N/A	N/A	5.00	6.50	11.25	N/A	N/A	N/A	N/A	N/A	N/A	I	N/A	SS+	N/A	N/A	N/A	34S_6p1d7Ya-04	11/5B1	TDP-WTP-044	7090464
21.4	0.999	0.00487	undefined	1.000	infinite	S	5.57	N/A	N/A	N/A	5.50	6.50	13.75	N/A	N/A	N/A	N/A	N/A	N/A	I	N/A	AM	N/A	N/A	N/A	34S_6p1d7Ya-04	11/5B1	TDP-WTP-044	7090466
21.4	0.999	0.00487	undefined	1.000	infinite	S	6.04	N/A	N/A	N/A	6.00	6.50	16.00	N/A	N/A	N/A	N/A	N/A	N/A	I	N/A	AM+	N/A	N/A	N/A	34S_6p1d7Ya-04	11/5B1	TDP-WTP-044	7090469
21.4	0.999	0.00487	undefined	1.000	infinite	S	6.53	N/A	N/A	N/A	6.50	6.50	19.50	6.50	vis	UCSvis	N/A	N/A	N/A	I	N/A	CS	N/A	N/A	N/A	34S_6p1d7Ya-04	11/5B1	TDP-WTP-044	7090473
21.0	0.999	0.00487	0.047	0.180	62.0	P	N/A	5.51	5.59	5.63	5.50	7.80	12.50	N/A	N/A	N/A	N/A	N/A	N/A	D	N/A	SS	N/A	N/A	N/A	34S_6p1d7Yd_9	11/5B2	TDP-WTP-044	7090476
21.0	0.999	0.00487	0.052	0.180	58.5	P	N/A	5.99	6.08	6.12	6.00	7.80	14.25	N/A	N/A	N/A	N/A	N/A	N/A	I	N/A	AM-	N/A	N/A	N/A	34S_6p1d7Yd_9	11/5B2	TDP-WTP-044	7090479
21.0	0.999	0.00487	0.052	0.180	54.0	P	N/A	6.40	6.50	6.55	6.50	7.80	15.75	N/A	N/A	N/A	N/A	N/A	N/A	I	N/A	AM	N/A	N/A	N/A	34S_6p1d7Yd_9	11/5B2	TDP-WTP-044	7090481
21.0	0.999	0.00487	0.051	0.180	49.5	P	N/A	6.89	7.01	7.07	7.00	7.80	17.25	N/A	N/A	N/A	N/A	N/A	N/A	I	N/A	AM+	N/A	N/A	N/A	34S_6p1d7Yd_9	11/5B2	TDP-WTP-044	7090484
21.0	0.999	0.00487	0.050	0.180	46.5	P	N/A	7.04	7.26	7.36	7.40	7.80	19.00	N/A	N/A	N/A	N/A	N/A	N/A	I	N/A	AM+	N/A	N/A	N/A	34S_6p1d7Yd_9	11/5B2	TDP-WTP-044	7090487
21.0	0.999	0.00487	0.051	0.180	44.3	P	N/A	7.26	7.57	7.70	7.80	7.80	20.25	7.80	vis	UCSvis	N/A	N/A	N/A	I	N/A	CS	N/A	N/A	N/A	34S_6p1d7Yd_9	11/5B2	TDP-WTP-044	7090491
20.6	0.999	0.00487	undefined	1.000	infinite	S	5.48	N/A	N/A	N/A	5.50	6.40	N/A	N/A	N/A	N/A	N/A	N/A	N/A	I	N/A	SS	N/A	N/A	N/A	34S_6p1d7Ya-40	11/6A1	TDP-WTP-049	7090493
20.7	0.999	0.00487	undefined	1.000	infinite	S	5.99	N/A	N/A	N/A	6.00	6.40	10.50	N/A	N/A	N/A	N/A	N/A	N/A	I	N/A	AM	N/A	N/A	N/A	34S_6p1d7Ya-40	11/6A1	TDP-WTP-049	7090496
20.7	0.999	0.00487	undefined	1.000	infinite	S	6.20	N/A	N/A	N/A	6.20	6.40	17.00	N/A	N/A	N/A	N/A	N/A	N/A	I	N/A	AM+	N/A	N/A	N/A	34S_6p1d7Ya-40	11/6A1	TDP-WTP-049	7090499
20.8	0.999	0.00487	undefined	1.000	infinite	S	6.42	N/A	N/A	N/A	6.40	6.40	21.00	6.40	vis	UCSvis	N/A	N/A	N/A	I	N/A	CS	N/A	N/A	N/A	34S_6p1d7Ya-40	11/6A1	TDP-WTP-049	7090503

Table B.8. Data from Fall 2007 Tests in Mid-Scale Vessel with Spherical Head A.5

Row Number	Test	Case ID	Tank Diameter	Head Shape	Dish Height	Dish Volume	Tank Fill Height	Return Line Height	Nozzle Inner Diameter	Nozzle Stand-off Distance	Pulse Tube Configuration	Installed Nozzles	Outer Nozzles Operated	Inner Nozzles Operated	Pulse Tube Outer Diameter	Outer PJM Radius	Inner PJM Radius	"FIO" Outer PJM Impingement Angle	"FIO" Inner PJM Impingement Angle	Ratio Outer PJM to Tank Radius	Ratio Inner PJM to Tank Radius	Simulant	Solids Density	Particle Diameter d5	Particle Diameter d50	Particle Diameter d95	Void Fraction
text	text	text	in.	text	in.	in. ^{3}	in.	in.	in.	in.	text	number	number	number	in.	in.	in.	deg	deg	nondim	nondim	text	g/cm^3	m	m	m	fraction
MSS	M/DDX	ID	D	HS	H_{dish}	V_{dish}	H	Rtn	d	sod	PT	N	N_O	N_I	PT_{od}	R_O	R_I	θ_O	θ_I	R_O/R	R_I/R	sxdx	ρ_s	d_5	d_{50}	d_{95}	vf
7090506	11/6A1	34S_6p1d7Ya-40	33 7/8	S	9	4437.4	33 7/8	31 7/8	0.446	0.669	HLP-22	12	4	0	1.9	10.5	5.7	30.8	16.1	0.62	0.33	p1d7	2.45	0.0001213	0.0001780	0.0002606	0.4277
7090508	11/6A2	34S_6p1d7Yd_6	33 7/8	S	9	4437.4	33 7/8	31 7/8	0.446	0.669	HLP-22	12	4	0	1.9	10.5	5.7	30.8	16.1	0.62	0.33	p1d7	2.45	0.0001213	0.0001780	0.0002606	0.4277
7090511	11/6A2	34S_6p1d7Yd_6	33 7/8	S	9	4437.4	33 7/8	31 7/8	0.446	0.669	HLP-22	12	4	0	1.9	10.5	5.7	30.8	16.1	0.62	0.33	p1d7	2.45	0.0001213	0.0001780	0.0002606	0.4277
7090514	11/6A2	34S_6p1d7Yd_6	33 7/8	S	9	4437.4	33 7/8	31 7/8	0.446	0.669	HLP-22	12	4	0	1.9	10.5	5.7	30.8	16.1	0.62	0.33	p1d7	2.45	0.0001213	0.0001780	0.0002606	0.4277
7090518	11/6A2	34S_6p1d7Yd_6	33 7/8	S	9	4437.4	33 7/8	31 7/8	0.446	0.669	HLP-22	12	4	0	1.9	10.5	5.7	30.8	16.1	0.62	0.33	p1d7	2.45	0.0001213	0.0001780	0.0002606	0.4277
7090520	11/6A2	34S_6p1d7Yd_6	33 7/8	S	9	4437.4	33 7/8	31 7/8	0.446	0.669	HLP-22	12	4	0	1.9	10.5	5.7	30.8	16.1	0.62	0.33	p1d7	2.45	0.0001213	0.0001780	0.0002606	0.4277
7090523	11/7A1	34S_6p1d7Ya	33 7/8	S	9	4437.4	23 5/7	21 5/7	0.446	0.669	HLP-22	12	8	4	1.9	10.5	5.7	30.8	16.1	0.62	0.33	p1d7	2.45	0.0001213	0.0001780	0.0002606	0.4277
7090526	11/7A1	34S_6p1d7Ya	33 7/8	S	9	4437.4	23 5/7	21 5/7	0.446	0.669	HLP-22	12	8	4	1.9	10.5	5.7	30.8	16.1	0.62	0.33	p1d7	2.45	0.0001213	0.0001780	0.0002606	0.4277
7090529	11/7A1	34S_6p1d7Ya	33 7/8	S	9	4437.4	23 5/7	21 5/7	0.446	0.669	HLP-22	12	8	4	1.9	10.5	5.7	30.8	16.1	0.62	0.33	p1d7	2.45	0.0001213	0.0001780	0.0002606	0.4277
7090532	11/7A1	34S_6p1d7Ya	33 7/8	S	9	4437.4	23 5/7	21 5/7	0.446	0.669	HLP-22	12	8	4	1.9	10.5	5.7	30.8	16.1	0.62	0.33	p1d7	2.45	0.0001213	0.0001780	0.0002606	0.4277
7090536	11/7A1	34S_6p1d7Ya	33 7/8	S	9	4437.4	23 5/7	21 5/7	0.446	0.669	HLP-22	12	8	4	1.9	10.5	5.7	30.8	16.1	0.62	0.33	p1d7	2.45	0.0001213	0.0001780	0.0002606	0.4277
7090538	11/7A1	34S_6p1d7Ya	33 7/8	S	9	4437.4	23 5/7	21 5/7	0.446	0.669	HLP-22	12	8	4	1.9	10.5	5.7	30.8	16.1	0.62	0.33	p1d7	2.45	0.0001213	0.0001780	0.0002606	0.4277
7090542	11/7A2	34S_6p1d7Yd_1	33 7/8	S	9	4437.4	23 5/7	21 5/7	0.446	0.669	HLP-22	12	8	4	1.9	10.5	5.7	30.8	16.1	0.62	0.33	p1d7	2.45	0.0001213	0.0001780	0.0002606	0.4277
7090544	11/7A2	34S_6p1d7Yd_1	33 7/8	S	9	4437.4	23 5/7	21 5/7	0.446	0.669	HLP-22	12	8	4	1.9	10.5	5.7	30.8	16.1	0.62	0.33	p1d7	2.45	0.0001213	0.0001780	0.0002606	0.4277
7090547	11/7A2	34S_6p1d7Yd_1	33 7/8	S	9	4437.4	23 5/7	21 5/7	0.446	0.669	HLP-22	12	8	4	1.9	10.5	5.7	30.8	16.1	0.62	0.33	p1d7	2.45	0.0001213	0.0001780	0.0002606	0.4277
7090551	11/7A2	34S_6p1d7Yd_1	33 7/8	S	9	4437.4	23 5/7	21 5/7	0.446	0.669	HLP-22	12	8	4	1.9	10.5	5.7	30.8	16.1	0.62	0.33	p1d7	2.45	0.0001213	0.0001780	0.0002606	0.4277
7090553	11/7B1	34S_6p1d7Ya-44	33 7/8	S	9	4437.4	23 5/7	21 5/7	0.446	0.669	HLP-22	12	4	4	1.9	10.5	5.7	30.8	16.1	0.62	0.33	p1d7	2.45	0.0001213	0.0001780	0.0002606	0.4277
7090557	11/7B1	34S_6p1d7Ya-44	33 7/8	S	9	4437.4	23 5/7	21 5/7	0.446	0.669	HLP-22	12	4	4	1.9	10.5	5.7	30.8	16.1	0.62	0.33	p1d7	2.45	0.0001213	0.0001780	0.0002606	0.4277
7090560	11/7B1	34S_6p1d7Ya-44	33 7/8	S	9	4437.4	23 5/7	21 5/7	0.446	0.669	HLP-22	12	4	4	1.9	10.5	5.7	30.8	16.1	0.62	0.33	p1d7	2.45	0.0001213	0.0001780	0.0002606	0.4277
7090562	11/7B1	34S_6p1d7Ya-44	33 7/8	S	9	4437.4	23 5/7	21 5/7	0.446	0.669	HLP-22	12	4	4	1.9	10.5	5.7	30.8	16.1	0.62	0.33	p1d7	2.45	0.0001213	0.0001780	0.0002606	0.4277
7090566	11/7B1	34S_6p1d7Ya-44	33 7/8	S	9	4437.4	23 5/7	21 5/7	0.446	0.669	HLP-22	12	4	4	1.9	10.5	5.7	30.8	16.1	0.62	0.33	p1d7	2.45	0.0001213	0.0001780	0.0002606	0.4277
7090569	11/7B2	34S_6p1d7Yd_0	33 7/8	S	9	4437.4	23 5/7	21 5/7	0.446	0.669	HLP-22	12	4	4	1.9	10.5	5.7	30.8	16.1	0.62	0.33	p1d7	2.45	0.0001213	0.0001780	0.0002606	0.4277
7090571	11/7B2	34S_6p1d7Yd_0	33 7/8	S	9	4437.4	23 5/7	21 5/7	0.446	0.669	HLP-22	12	4	4	1.9	10.5	5.7	30.8	16.1	0.62	0.33	p1d7	2.45	0.0001213	0.0001780	0.0002606	0.4277
7090574	11/7B2	34S_6p1d7Yd_0	33 7/8	S	9	4437.4	23 5/7	21 5/7	0.446	0.669	HLP-22	12	4	4	1.9	10.5	5.7	30.8	16.1	0.62	0.33	p1d7	2.45	0.0001213	0.0001780	0.0002606	0.4277
7090577	11/7B2	34S_6p1d7Yd_0	33 7/8	S	9	4437.4	23 5/7	21 5/7	0.446	0.669	HLP-22	12	4	4	1.9	10.5	5.7	30.8	16.1	0.62	0.33	p1d7	2.45	0.0001213	0.0001780	0.0002606	0.4277
7090580	11/7B2	34S_6p1d7Yd_0	33 7/8	S	9	4437.4	23 5/7	21 5/7	0.446	0.669	HLP-22	12	4	4	1.9	10.5	5.7	30.8	16.1	0.62	0.33	p1d7	2.45	0.0001213	0.0001780	0.0002606	0.4277
7090583	11/7B2	34S_6p1d7Yd_0	33 7/8	S	9	4437.4	23 5/7	21 5/7	0.446	0.669	HLP-22	12	4	4	1.9	10.5	5.7	30.8	16.1	0.62	0.33	p1d7	2.45	0.0001213	0.0001780	0.0002606	0.4277
7090587	11/7B2	34S_6p1d7Yd_0	33 7/8	S	9	4437.4	23 5/7	21 5/7	0.446	0.669	HLP-22	12	4	4	1.9	10.5	5.7	30.8	16.1	0.62	0.33	p1d7	2.45	0.0001213	0.0001780	0.0002606	0.4277
7090591	11/8A2	34S_6p1d7Yd_9	33 7/8	S	9	4437.4	23 5/7	21 5/7	0.446	0.669	HLP-22	12	0	4	1.9	10.5	5.7	30.8	16.1	0.62	0.33	p1d7	2.45	0.0001213	0.0001780	0.0002606	0.4277
7090594	11/8A2	34S_6p1d7Yd_9	33 7/8	S	9	4437.4	23 5/7	21 5/7	0.446	0.669	HLP-22	12	0	4	1.9	10.5	5.7	30.8	16.1	0.62	0.33	p1d7	2.45	0.0001213	0.0001780	0.0002606	0.4277
7090596	11/8A2	34S_6p1d7Yd_9	33 7/8	S	9	4437.4	23 5/7	21 5/7	0.446	0.669	HLP-22	12	0	4	1.9	10.5	5.7	30.8	16.1	0.62	0.33	p1d7	2.45	0.0001213	0.0001780	0.0002606	0.4277
7090599	11/8A2	34S_6p1d7Yd_9	33 7/8	S	9	4437.4	23 5/7	21 5/7	0.446	0.669	HLP-22	12	0	4	1.9	10.5	5.7	30.8	16.1	0.62	0.33	p1d7	2.45	0.0001213	0.0001780	0.0002606	0.4277
7090602	11/8A2	34S_6p1d7Yd_9	33 7/8	S	9	4437.4	23 5/7	21 5/7	0.446	0.669	HLP-22	12	0	4	1.9	10.5	5.7	30.8	16.1	0.62	0.33	p1d7	2.45	0.0001213	0.0001780	0.0002606	0.4277
7090605	11/8A2	34S_6p1d7Yd_9	33 7/8	S	9	4437.4	23 5/7	21 5/7	0.446	0.669	HLP-22	12	0	4	1.9	10.5	5.7	30.8	16.1	0.62	0.33	p1d7	2.45	0.0001213	0.0001780	0.0002606	0.4277
7090608	11/8A2	34S_6p1d7Yd_9	33 7/8	S	9	4437.4	23 5/7	21 5/7	0.446	0.669	HLP-22	12	0	4	1.9	10.5	5.7	30.8	16.1	0.62	0.33	p1d7	2.45	0.0001213	0.0001780	0.0002606	0.4277
7090612	11/8A2	34S_6p1d7Yd_9	33 7/8	S	9	4437.4	23 5/7	21 5/7	0.446	0.669	HLP-22	12	0	4	1.9	10.5	5.7	30.8	16.1	0.62	0.33	p1d7	2.45	0.0001213	0.0001780	0.0002606	0.4277
7090616	11/8C1	34S_6p1d7Ya	33 7/8	S	9	4437.4	33 7/8	31 7/8	0.446	0.669	HLP-22	12	8	4	1.9	10.5	5.7	30.8	16.1	0.62	0.33	p1d7	2.45	0.0001213	0.0001780	0.0002606	0.4277
7090619	11/8C1	34S_6p1d7Ya	33 7/8	S	9	4437.4	33 7/8	31 7/8	0.446	0.669	HLP-22	12	8	4	1.9	10.5	5.7	30.8	16.1	0.62	0.33	p1d7	2.45	0.0001213	0.0001780	0.0002606	0.4277
7090622	11/8C1	34S_6p1d7Ya	33 7/8	S	9	4437.4	33 7/8	31 7/8	0.446	0.669	HLP-22	12	8	4	1.9	10.5	5.7	30.8	16.1	0.62	0.33	p1d7	2.45	0.0001213	0.0001780	0.0002606	0.4277
7090626	11/8C1	34S_6p1d7Ya	33 7/8	S	9	4437.4	33 7/8	31 7/8	0.446	0.669	HLP-22	12	8	4	1.9	10.5	5.7	30.8	16.1	0.62	0.33	p1d7	2.45	0.0001213	0.0001780	0.0002606	0.4277
7090628	11/8C2	34S_6p1d7Yd_1	33 7/8	S	9	4437.4	33 7/8	31 7/8	0.446	0.669	HLP-22	12	8	4	1.9	10.5	5.7	30.8	16.1	0.62	0.33	p1d7	2.45	0.0001213	0.0001780	0.0002606	0.4277

Table B.8. Data from Fall 2007 Tests in Mid-Scale Vessel with Spherical Head B.5

Tank Water Temperature	Water Density	Solids Fraction	Pulse Volume Fraction	Duty Cycle	Cycle Time	Pulsed or Steady Jet	Us Steady Jet	U1 Pulsing Jet	U2 URMS	U3 URM3	Discharge Velocity	Critical Suspension Velocity	Average Peak Cloud Height	UCS Condition	UCS Method	UCS Flag	UCS Center Flag	UCS udv Flag	UCS based on Decreasing Velocity	Sweep Increase / Decrease	UDV Height Bed	Particle Motion	Solids Level	Outer Bottom Pattern	Inner Bottom Pattern	Case ID	Test	TDP	Row Number
C	g/cm^3	fraction	fraction	fraction	s	text	m/s	m/s	m/s	m/s	m/s	m/s	in.	m/s	text	text	text	text	m/s	text	mm	text	text	text	text	text	text	text	text
T	ρ_l	ϕ_S	ϕ_P	DC	t_C	Jet	U_S	U1	U2	U3	U	U_{CS}	H_C	U_{CSR}	U_{CSM}	U_{CS}vis	U_{CS}cen	U_{CS}udv	U_{CS}_D	S_W	H_{bed}	PM	Sol	SP_O	SP_I	ID	M/DDX	TDP	MSS
20.7	0.999	0.00487	undefined	1.000	infinite	S	6.59	N/A	N/A	N/A	6.60	6.40	24.00	N/A	N/A	N/A	N/A	N/A	N/A	I	N/A	BC	N/A	N/A	N/A	34S_6p1d7Ya-40	11/6A1	TDP-WTP-049	7090506
21.0	0.999	0.00487	0.051	0.180	58.0	P	N/A	5.91	5.98	6.01	6.00	7.30	10.00	N/A	N/A	N/A	N/A	N/A	N/A	I	N/A	SS	N/A	N/A	N/A	34S_6p1d7Yd_6	11/6A2	TDP-WTP-049	7090508
21.0	0.999	0.00487	0.051	0.180	54.0	P	N/A	6.34	6.42	6.46	6.50	7.30	10.75	N/A	N/A	N/A	N/A	N/A	N/A	I	N/A	SS+	N/A	N/A	N/A	34S_6p1d7Yd_6	11/6A2	TDP-WTP-049	7090511
21.0	0.999	0.00487	0.051	0.180	50.0	P	N/A	6.61	6.80	6.89	7.00	7.30	11.50	N/A	N/A	N/A	N/A	N/A	N/A	I	N/A	AM	N/A	N/A	N/A	34S_6p1d7Yd_6	11/6A2	TDP-WTP-049	7090514
21.0	0.999	0.00487	0.050	0.180	47.3	P	N/A	6.84	7.07	7.17	7.30	7.30	13.50	7.30	vis	UCSvis	N/A	N/A	N/A	I	N/A	CS	N/A	N/A	N/A	34S_6p1d7Yd_6	11/6A2	TDP-WTP-049	7090518
21.0	0.999	0.00487	0.050	0.180	45.3	P	N/A	6.95	7.26	7.39	7.60	7.30	15.50	N/A	N/A	N/A	N/A	N/A	N/A	I	N/A	BC	N/A	N/A	N/A	34S_6p1d7Yd_6	11/6A2	TDP-WTP-049	7090520
20.9	0.999	0.00487	undefined	1.000	infinite	S	2.62	N/A	N/A	N/A	2.60	3.40	N/A	N/A	N/A	N/A	N/A	N/A	N/A	D	N/A	SS+	N/A	N/A	N/A	34S_6p1d7Ya	11/7A1	TDP-WTP-050	7090523
20.9	0.999	0.00487	undefined	1.000	infinite	S	2.81	N/A	N/A	N/A	2.80	3.40	9.00	N/A	N/A	N/A	N/A	N/A	N/A	I	N/A	AM	N/A	N/A	N/A	34S_6p1d7Ya	11/7A1	TDP-WTP-050	7090526
21.0	0.999	0.00487	undefined	1.000	infinite	S	3.02	N/A	N/A	N/A	3.00	3.40	9.50	N/A	N/A	N/A	N/A	N/A	N/A	I	N/A	AM	N/A	N/A	N/A	34S_6p1d7Ya	11/7A1	TDP-WTP-050	7090529
20.9	0.999	0.00487	undefined	1.000	infinite	S	3.22	N/A	N/A	N/A	3.20	3.40	10.00	N/A	N/A	N/A	N/A	N/A	N/A	I	N/A	AM+	N/A	N/A	N/A	34S_6p1d7Ya	11/7A1	TDP-WTP-050	7090532
21.0	0.999	0.00487	undefined	1.000	infinite	S	3.38	N/A	N/A	N/A	3.40	3.40	11.00	3.40	vis	UCSvis	N/A	N/A	N/A	I	N/A	CS	N/A	N/A	N/A	34S_6p1d7Ya	11/7A1	TDP-WTP-050	7090536
21.0	0.999	0.00487	undefined	1.000	infinite	S	3.60	N/A	N/A	N/A	3.60	3.40	15.00	N/A	N/A	N/A	N/A	N/A	N/A	I	N/A	BC	N/A	N/A	N/A	34S_6p1d7Ya	11/7A1	TDP-WTP-050	7090538
21.0	0.999	0.00487	0.050	0.180	39.0	P	N/A	2.83	2.92	2.96	3.00	4.20	8.75	N/A	N/A	N/A	N/A	N/A	N/A	D	N/A	SS	N/A	N/A	N/A	34S_6p1d7Yd_1	11/7A2	TDP-WTP-050	7090542
21.0	0.999	0.00487	0.051	0.180	35.3	P	N/A	3.11	3.21	3.26	3.40	4.20	10.00	N/A	N/A	N/A	N/A	N/A	N/A	I	N/A	SS+	N/A	N/A	N/A	34S_6p1d7Yd_1	11/7A2	TDP-WTP-050	7090544
21.0	0.999	0.00487	0.051	0.180	31.0	P	N/A	3.37	3.52	3.59	3.80	4.20	11.00	N/A	N/A	N/A	N/A	N/A	N/A	I	N/A	AM-	N/A	N/A	N/A	34S_6p1d7Yd_1	11/7A2	TDP-WTP-050	7090547
21.0	0.999	0.00487	0.050	0.180	28.0	P	N/A	3.49	3.76	3.88	4.20	4.20	11.75	4.20	vis	UCSvis	N/A	N/A	N/A	I	N/A	CS	N/A	N/A	N/A	34S_6p1d7Yd_1	11/7A2	TDP-WTP-050	7090551
21.1	0.999	0.00487	undefined	1.000	infinite	S	3.99	N/A	N/A	N/A	4.00	4.80	8.75	N/A	N/A	N/A	N/A	N/A	N/A	D	N/A	AM	N/A	N/A	N/A	34S_6p1d7Ya-44	11/7B1	TDP-WTP-050	7090553
21.1	0.999	0.00487	undefined	1.000	infinite	S	4.18	N/A	N/A	N/A	4.20	4.80	9.50	N/A	N/A	N/A	N/A	N/A	N/A	I	N/A	AM	N/A	N/A	N/A	34S_6p1d7Ya-44	11/7B1	TDP-WTP-050	7090557
21.2	0.999	0.00487	undefined	1.000	infinite	S	4.41	N/A	N/A	N/A	4.40	4.80	11.00	N/A	N/A	N/A	N/A	N/A	N/A	I	N/A	AM	N/A	N/A	N/A	34S_6p1d7Ya-44	11/7B1	TDP-WTP-050	7090560
21.2	0.999	0.00487	undefined	1.000	infinite	S	4.62	N/A	N/A	N/A	4.60	4.80	13.25	N/A	N/A	N/A	N/A	N/A	N/A	I	N/A	AM+	N/A	N/A	N/A	34S_6p1d7Ya-44	11/7B1	TDP-WTP-050	7090562
21.3	0.999	0.00487	undefined	1.000	infinite	S	4.81	N/A	N/A	N/A	4.80	4.80	17.75	4.80	vis	UCSvis	N/A	N/A	N/A	I	N/A	CS	N/A	N/A	N/A	34S_6p1d7Ya-44	11/7B1	TDP-WTP-050	7090566
21.0	0.999	0.00487	0.048	0.180	39.5	P	N/A	4.18	4.30	4.35	4.50	6.20	9.25	N/A	N/A	N/A	N/A	N/A	N/A	D	N/A	SS	N/A	N/A	N/A	34S_6p1d7Yd_0	11/7B2	TDP-WTP-050	7090569
21.0	0.999	0.00487	0.050	0.180	35.3	P	N/A	4.58	4.74	4.81	5.00	6.20	11.00	N/A	N/A	N/A	N/A	N/A	N/A	I	N/A	AM	N/A	N/A	N/A	34S_6p1d7Yd_0	11/7B2	TDP-WTP-050	7090571
21.0	0.999	0.00487	0.050	0.180	32.5	P	N/A	4.65	4.95	5.08	5.40	6.20	12.75	N/A	N/A	N/A	N/A	N/A	N/A	I	N/A	AM+	N/A	N/A	N/A	34S_6p1d7Yd_0	11/7B2	TDP-WTP-050	7090574
21.0	0.999	0.00487	0.050	0.180	31.5	P	N/A	4.77	5.10	5.24	5.60	6.20	14.00	N/A	N/A	N/A	N/A	N/A	N/A	I	N/A	AM+	N/A	N/A	N/A	34S_6p1d7Yd_0	11/7B2	TDP-WTP-050	7090577
21.0	0.999	0.00487	0.050	0.180	30.0	P	N/A	4.85	5.23	5.40	5.80	6.20	14.50	N/A	N/A	N/A	N/A	N/A	N/A	I	N/A	AM+	N/A	N/A	N/A	34S_6p1d7Yd_0	11/7B2	TDP-WTP-050	7090580
21.0	0.999	0.00487	0.050	0.180	29.0	P	N/A	4.96	5.37	5.55	6.00	6.20	15.75	N/A	N/A	N/A	N/A	N/A	N/A	I	N/A	AM+	N/A	N/A	N/A	34S_6p1d7Yd_0	11/7B2	TDP-WTP-050	7090583
21.0	0.999	0.00487	0.050	0.180	28.0	P	N/A	5.07	5.52	5.72	6.20	6.20	16.00	6.20	vis	UCSvis	N/A	N/A	N/A	I	N/A	CS	N/A	N/A	N/A	34S_6p1d7Yd_0	11/7B2	TDP-WTP-050	7090587
21.0	0.999	0.00487	0.046	0.180	63.0	P	N/A	5.38	5.46	5.49	5.50	8.40	12.75	N/A	N/A	N/A	N/A	N/A	N/A	D	N/A	SS	N/A	N/A	N/A	34S_6p1d7Yd_9	11/8A2	TDP-WTP-051	7090591
21.0	0.999	0.00487	0.051	0.180	58.5	P	N/A	5.85	5.92	5.95	6.00	8.40	15.00	N/A	N/A	N/A	N/A	N/A	N/A	I	N/A	SS+	N/A	N/A	N/A	34S_6p1d7Yd_9	11/8A2	TDP-WTP-051	7090594
21.0	0.999	0.00487	0.051	0.180	55.0	P	N/A	6.23	6.31	6.35	6.40	8.40	15.25	N/A	N/A	N/A	N/A	N/A	N/A	I	N/A	AM	N/A	N/A	N/A	34S_6p1d7Yd_9	11/8A2	TDP-WTP-051	7090596
21.0	0.999	0.00487	0.051	0.180	51.5	P	N/A	6.59	6.69	6.74	6.80	8.40	17.00	N/A	N/A	N/A	N/A	N/A	N/A	I	N/A	AM	N/A	N/A	N/A	34S_6p1d7Yd_9	11/8A2	TDP-WTP-051	7090599
21.0	0.999	0.00487	0.050	0.180	48.5	P	N/A	6.91	7.05	7.11	7.20	8.40	18.25	N/A	N/A	N/A	N/A	N/A	N/A	I	N/A	AM	N/A	N/A	N/A	34S_6p1d7Yd_9	11/8A2	TDP-WTP-051	7090602
21.0	0.999	0.00487	0.050	0.180	45.5	P	N/A	6.99	7.29	7.42	7.60	8.40	20.25	N/A	N/A	N/A	N/A	N/A	N/A	I	N/A	AM+	N/A	N/A	N/A	34S_6p1d7Yd_9	11/8A2	TDP-WTP-051	7090605
21.0	0.999	0.00487	0.049	0.180	43.5	P	N/A	7.20	7.56	7.71	8.00	8.40	21.00	N/A	N/A	N/A	N/A	N/A	N/A	I	N/A	AM+	N/A	N/A	N/A	34S_6p1d7Yd_9	11/8A2	TDP-WTP-051	7090608
21.0	0.999	0.00487	0.050	0.180	41.0	P	N/A	7.47	7.88	8.06	8.40	8.40	22.25	8.40	vis	UCSvis	N/A	N/A	N/A	I	N/A	CS	N/A	N/A	N/A	34S_6p1d7Yd_9	11/8A2	TDP-WTP-051	7090612
20.9	0.999	0.00487	undefined	1.000	infinite	S	2.51	N/A	N/A	N/A	2.50	2.60	N/A	N/A	N/A	N/A	N/A	N/A	N/A	I	N/A	SS	N/A	N/A	N/A	34S_6p1d7Ya	11/8C1	TDP-WTP-051	7090616
20.9	0.999	0.00487	undefined	1.000	infinite	S	3.01	N/A	N/A	N/A	3.00	3.40	9.25	N/A	N/A	N/A	N/A	N/A	N/A	I	N/A	AM	N/A	N/A	N/A	34S_6p1d7Ya	11/8C1	TDP-WTP-051	7090619
20.9	0.999	0.00487	undefined	1.000	infinite	S	3.23	N/A	N/A	N/A	3.20	3.40	9.75	N/A	N/A	N/A	N/A	N/A	N/A	I	N/A	CS-	N/A	N/A	N/A	34S_6p1d7Ya	11/8C1	TDP-WTP-051	7090622
20.9	0.999	0.00487	undefined	1.000	infinite	S	3.39	N/A	N/A	N/A	3.40	3.40	11.00	3.40	vis	UCSvis	N/A	N/A	N/A	I	N/A	CS	N/A	N/A	N/A	34S_6p1d7Ya	11/8C1	TDP-WTP-051	7090626
21.0	0.999	0.00487	0.051	0.180	34.0	P	N/A	3.18	3.30	3.36	3.50	4.40	9.75	N/A	N/A	N/A	N/A	N/A	N/A	I	N/A	SS+	N/A	N/A	N/A	34S_6p1d7Yd_1	11/8C2	TDP-WTP-051	7090628

Table B.8. Data from Fall 2007 Tests in Mid-Scale Vessel with Spherical Head A.6

Row Number	Test	Case ID	Tank Diameter	Head Shape	Dish Height	Dish Volume	Tank Fill Height	Return Line Height	Nozzle Inner Diameter	Nozzle Stand-off Distance	Pulse Tube Configuration	Installed Nozzles	Outer Nozzles Operated	Inner Nozzles Operated	Pulse Tube Outer Diameter	Outer PJM Radius	Inner PJM Radius	"FIO" Outer PJM Impingement Angle	"FIO" Inner PJM Impingement Angle	Ratio Outer PJM to Tank Radius	Ratio Inner PJM to Tank Radius	Simulant	Solids Density	Particle Diameter d5	Particle Diameter d50	Particle Diameter d95	Void Fraction
text	text	text	in.	text	in.	in. ^{3}	in.	in.	in.	in.	text	number	number	number	in.	in.	in.	deg	deg	nondim	nondim	text	g/cm^3	m	m	m	fraction
MSS	M/DDX	ID	D	HS	H_{dish}	V_{dish}	H	Rtn	d	sod	PT	N	N_O	N_I	PT_{od}	R_O	R_I	θ_O	θ_I	R_O/R	R_I/R	sxdx	ρ_s	d_5	d_{50}	d_{95}	vf
7090631	11/8C2	34S_6p1d7Yd_1	33 7/8	S	9	4437.4	33 7/8	31 7/8	0.446	0.669	HLP-22	12	8	4	1.9	10.5	5.7	30.8	16.1	0.62	0.33	p1d7	2.45	0.0001213	0.0001780	0.0002606	0.4277
7090634	11/8C2	34S_6p1d7Yd_1	33 7/8	S	9	4437.4	33 7/8	31 7/8	0.446	0.669	HLP-22	12	8	4	1.9	10.5	5.7	30.8	16.1	0.62	0.33	p1d7	2.45	0.0001213	0.0001780	0.0002606	0.4277
7090637	11/8C2	34S_6p1d7Yd_1	33 7/8	S	9	4437.4	33 7/8	31 7/8	0.446	0.669	HLP-22	12	8	4	1.9	10.5	5.7	30.8	16.1	0.62	0.33	p1d7	2.45	0.0001213	0.0001780	0.0002606	0.4277
7090641	11/8C2	34S_6p1d7Yd_1	33 7/8	S	9	4437.4	33 7/8	31 7/8	0.446	0.669	HLP-22	12	8	4	1.9	10.5	5.7	30.8	16.1	0.62	0.33	p1d7	2.45	0.0001213	0.0001780	0.0002606	0.4277
7090643	11/8C2	34S_6p1d7Yd_1	33 7/8	S	9	4437.4	33 7/8	31 7/8	0.446	0.669	HLP-22	12	8	4	1.9	10.5	5.7	30.8	16.1	0.62	0.33	p1d7	2.45	0.0001213	0.0001780	0.0002606	0.4277
7090648	11/8D2	34S_6p1d7Yd_0	33 7/8	S	9	4437.4	33 7/8	31 7/8	0.446	0.669	HLP-22	12	4	4	1.9	10.5	5.7	30.8	16.1	0.62	0.33	p1d7	2.45	0.0001213	0.0001780	0.0002606	0.4277
7090650	11/8D2	34S_6p1d7Yd_0	33 7/8	S	9	4437.4	33 7/8	31 7/8	0.446	0.669	HLP-22	12	4	4	1.9	10.5	5.7	30.8	16.1	0.62	0.33	p1d7	2.45	0.0001213	0.0001780	0.0002606	0.4277
7090653	11/8D2	34S_6p1d7Yd_0	33 7/8	S	9	4437.4	33 7/8	31 7/8	0.446	0.669	HLP-22	12	4	4	1.9	10.5	5.7	30.8	16.1	0.62	0.33	p1d7	2.45	0.0001213	0.0001780	0.0002606	0.4277
7090656	11/8D2	34S_6p1d7Yd_0	33 7/8	S	9	4437.4	33 7/8	31 7/8	0.446	0.669	HLP-22	12	4	4	1.9	10.5	5.7	30.8	16.1	0.62	0.33	p1d7	2.45	0.0001213	0.0001780	0.0002606	0.4277
7090659	11/8D2	34S_6p1d7Yd_0	33 7/8	S	9	4437.4	33 7/8	31 7/8	0.446	0.669	HLP-22	12	4	4	1.9	10.5	5.7	30.8	16.1	0.62	0.33	p1d7	2.45	0.0001213	0.0001780	0.0002606	0.4277
7090662	11/8D2	34S_6p1d7Yd_0	33 7/8	S	9	4437.4	33 7/8	31 7/8	0.446	0.669	HLP-22	12	4	4	1.9	10.5	5.7	30.8	16.1	0.62	0.33	p1d7	2.45	0.0001213	0.0001780	0.0002606	0.4277
7090665	11/8D2	34S_6p1d7Yd_0	33 7/8	S	9	4437.4	33 7/8	31 7/8	0.446	0.669	HLP-22	12	4	4	1.9	10.5	5.7	30.8	16.1	0.62	0.33	p1d7	2.45	0.0001213	0.0001780	0.0002606	0.4277
7090668	11/8D2	34S_6p1d7Yd_0	33 7/8	S	9	4437.4	33 7/8	31 7/8	0.446	0.669	HLP-22	12	4	4	1.9	10.5	5.7	30.8	16.1	0.62	0.33	p1d7	2.45	0.0001213	0.0001780	0.0002606	0.4277
7090671	11/8D2	34S_6p1d7Yd_0	33 7/8	S	9	4437.4	33 7/8	31 7/8	0.446	0.669	HLP-22	12	4	4	1.9	10.5	5.7	30.8	16.1	0.62	0.33	p1d7	2.45	0.0001213	0.0001780	0.0002606	0.4277
7090674	11/8D2	34S_6p1d7Yd_0	33 7/8	S	9	4437.4	33 7/8	31 7/8	0.446	0.669	HLP-22	12	4	4	1.9	10.5	5.7	30.8	16.1	0.62	0.33	p1d7	2.45	0.0001213	0.0001780	0.0002606	0.4277
7090678	11/8D2	34S_6p1d7Yd_0	33 7/8	S	9	4437.4	33 7/8	31 7/8	0.446	0.669	HLP-22	12	4	4	1.9	10.5	5.7	30.8	16.1	0.62	0.33	p1d7	2.45	0.0001213	0.0001780	0.0002606	0.4277
7090681	11/9A1	34S_6p1d7Ya-04	33 7/8	S	9	4437.4	33 7/8	31 7/8	0.446	0.669	HLP-22	12	0	4	1.9	10.5	5.7	30.8	16.1	0.62	0.33	p1d7	2.45	0.0001213	0.0001780	0.0002606	0.4277
7090684	11/9A1	34S_6p1d7Ya-04	33 7/8	S	9	4437.4	33 7/8	31 7/8	0.446	0.669	HLP-22	12	0	4	1.9	10.5	5.7	30.8	16.1	0.62	0.33	p1d7	2.45	0.0001213	0.0001780	0.0002606	0.4277
7090687	11/9A1	34S_6p1d7Ya-04	33 7/8	S	9	4437.4	33 7/8	31 7/8	0.446	0.669	HLP-22	12	0	4	1.9	10.5	5.7	30.8	16.1	0.62	0.33	p1d7	2.45	0.0001213	0.0001780	0.0002606	0.4277
7090690	11/9A1	34S_6p1d7Ya-04	33 7/8	S	9	4437.4	33 7/8	31 7/8	0.446	0.669	HLP-22	12	0	4	1.9	10.5	5.7	30.8	16.1	0.62	0.33	p1d7	2.45	0.0001213	0.0001780	0.0002606	0.4277
7090692	11/9A1	34S_6p1d7Ya-04	33 7/8	S	9	4437.4	33 7/8	31 7/8	0.446	0.669	HLP-22	12	0	4	1.9	10.5	5.7	30.8	16.1	0.62	0.33	p1d7	2.45	0.0001213	0.0001780	0.0002606	0.4277
7090696	11/9A1	34S_6p1d7Ya-04	33 7/8	S	9	4437.4	33 7/8	31 7/8	0.446	0.669	HLP-22	12	0	4	1.9	10.5	5.7	30.8	16.1	0.62	0.33	p1d7	2.45	0.0001213	0.0001780	0.0002606	0.4277
7090698	11/9A1	34S_6p1d7Ya-04	33 7/8	S	9	4437.4	33 7/8	31 7/8	0.446	0.669	HLP-22	12	0	4	1.9	10.5	5.7	30.8	16.1	0.62	0.33	p1d7	2.45	0.0001213	0.0001780	0.0002606	0.4277
7090702	11/9A1	34S_6p1d7Ya-04	33 7/8	S	9	4437.4	33 7/8	31 7/8	0.446	0.669	HLP-22	12	0	4	1.9	10.5	5.7	30.8	16.1	0.62	0.33	p1d7	2.45	0.0001213	0.0001780	0.0002606	0.4277
7090705	11/9A2	34S_6p1d7Yd_9	33 7/8	S	9	4437.4	33 7/8	31 7/8	0.446	0.669	HLP-22	12	0	4	1.9	10.5	5.7	30.8	16.1	0.62	0.33	p1d7	2.45	0.0001213	0.0001780	0.0002606	0.4277
7090708	11/9A2	34S_6p1d7Yd_9	33 7/8	S	9	4437.4	33 7/8	31 7/8	0.446	0.669	HLP-22	12	0	4	1.9	10.5	5.7	30.8	16.1	0.62	0.33	p1d7	2.45	0.0001213	0.0001780	0.0002606	0.4277
7090710	11/9A2	34S_6p1d7Yd_9	33 7/8	S	9	4437.4	33 7/8	31 7/8	0.446	0.669	HLP-22	12	0	4	1.9	10.5	5.7	30.8	16.1	0.62	0.33	p1d7	2.45	0.0001213	0.0001780	0.0002606	0.4277
7090713	11/9A2	34S_6p1d7Yd_9	33 7/8	S	9	4437.4	33 7/8	31 7/8	0.446	0.669	HLP-22	12	0	4	1.9	10.5	5.7	30.8	16.1	0.62	0.33	p1d7	2.45	0.0001213	0.0001780	0.0002606	0.4277
7090716	11/9A2	34S_6p1d7Yd_9	33 7/8	S	9	4437.4	33 7/8	31 7/8	0.446	0.669	HLP-22	12	0	4	1.9	10.5	5.7	30.8	16.1	0.62	0.33	p1d7	2.45	0.0001213	0.0001780	0.0002606	0.4277
7090719	11/9A2	34S_6p1d7Yd_9	33 7/8	S	9	4437.4	33 7/8	31 7/8	0.446	0.669	HLP-22	12	0	4	1.9	10.5	5.7	30.8	16.1	0.62	0.33	p1d7	2.45	0.0001213	0.0001780	0.0002606	0.4277
7090722	11/9A2	34S_6p1d7Yd_9	33 7/8	S	9	4437.4	33 7/8	31 7/8	0.446	0.669	HLP-22	12	0	4	1.9	10.5	5.7	30.8	16.1	0.62	0.33	p1d7	2.45	0.0001213	0.0001780	0.0002606	0.4277
7090725	11/9A2	34S_6p1d7Yd_9	33 7/8	S	9	4437.4	33 7/8	31 7/8	0.446	0.669	HLP-22	12	0	4	1.9	10.5	5.7	30.8	16.1	0.62	0.33	p1d7	2.45	0.0001213	0.0001780	0.0002606	0.4277
7090728	11/9A2	34S_6p1d7Yd_9	33 7/8	S	9	4437.4	33 7/8	31 7/8	0.446	0.669	HLP-22	12	0	4	1.9	10.5	5.7	30.8	16.1	0.62	0.33	p1d7	2.45	0.0001213	0.0001780	0.0002606	0.4277
7090732	11/9A2	34S_6p1d7Yd_9	33 7/8	S	9	4437.4	33 7/8	31 7/8	0.446	0.669	HLP-22	12	0	4	1.9	10.5	5.7	30.8	16.1	0.62	0.33	p1d7	2.45	0.0001213	0.0001780	0.0002606	0.4277
7090737	11/14A1	34S_6p1d7Ya-44	33 7/8	S	9	4437.4	67 3/4	65 3/4	0.446	0.669	HLP-22	12	4	4	1.9	10.5	5.7	30.8	16.1	0.62	0.33	p1d7	2.45	0.0001213	0.0001780	0.0002606	0.4277
7090740	11/14A2	34S_6p1d7Yd_0	33 7/8	S	9	4437.4	67 3/4	65 3/4	0.446	0.669	HLP-22	12	4	4	1.9	10.5	5.7	30.8	16.1	0.62	0.33	p1d7	2.45	0.0001213	0.0001780	0.0002606	0.4277
7090742	11/14A2	34S_6p1d7Yd_0	33 7/8	S	9	4437.4	67 3/4	65 3/4	0.446	0.669	HLP-22	12	4	4	1.9	10.5	5.7	30.8	16.1	0.62	0.33	p1d7	2.45	0.0001213	0.0001780	0.0002606	0.4277
7090745	11/14A2	34S_6p1d7Yd_0	33 7/8	S	9	4437.4	67 3/4	65 3/4	0.446	0.669	HLP-22	12	4	4	1.9	10.5	5.7	30.8	16.1	0.62	0.33	p1d7	2.45	0.0001213	0.0001780	0.0002606	0.4277
7090748	11/14A2	34S_6p1d7Yd_0	33 7/8	S	9	4437.4	67 3/4	65 3/4	0.446	0.669	HLP-22	12	4	4	1.9	10.5	5.7	30.8	16.1	0.62	0.33	p1d7	2.45	0.0001213	0.0001780	0.0002606	0.4277
7090751	11/14A2	34S_6p1d7Yd_0	33 7/8	S	9	4437.4	67 3/4	65 3/4	0.446	0.669	HLP-22	12	4	4	1.9	10.5	5.7	30.8	16.1	0.62	0.33	p1d7	2.45	0.0001213	0.0001780	0.0002606	0.4277
7090754	11/14A2	34S_6p1d7Yd_0	33 7/8	S	9	4437.4	67 3/4	65 3/4	0.446	0.669	HLP-22	12	4	4	1.9	10.5	5.7	30.8	16.1	0.62	0.33	p1d7	2.45	0.0001213	0.0001780	0.0002606	0.4277

Table B.8. Data from Fall 2007 Tests in Mid-Scale Vessel with Spherical Head B.6

Tank Water Temperature	Water Density	Solids Fraction	Pulse Volume Fraction	Duty Cycle	Cycle Time	Pulsed or Steady Jet	Us Steady Jet	U1 Pulsing Jet	U2 URMS	U3 URM3	Discharge Velocity	Critical Suspension Velocity	Average Peak Cloud Height	UCS Condition	UCS Method	UCS Flag	UCS Center Flag	UCS udv Flag	UCS based on Decreasing Velocity	Sweep Increase / Decrease	UDV Height Bed	Particle Motion	Solids Level	Outer Bottom Pattern	Inner Bottom Pattern	Case ID	Test	TDP	Row Number
C	g/cm³	fraction	fraction	fraction	s	text	m/s	m/s	m/s	m/s	m/s	m/s	in.	m/s	text	text	text	text	m/s	text	mm	text	text	text	text	text	text	text	text
T	ρ_l	ϕ_S	ϕ_P	DC	t_C	Jet	U_S	U1	U2	U3	U	U_{CS}	H_C	U_{CSR}	U_{CSM}	U_{CS}vis	U_{CS}cen	U_{CS}udv	U_{CS}_D	S_W	H_{bed}	PM	Sol	SP_O	SP_I	ID	M/DDX	TDP	MSS
21.0	0.999	0.00487	0.050	0.180	31.3	P	N/A	3.43	3.56	3.63	3.80	4.40	10.50	N/A	N/A	N/A	N/A	N/A	N/A	I	N/A	AM	N/A	N/A	N/A	34S_6p1d7Yd_1	11/8C2	TDP-WTP-051	7090631
21.0	0.999	0.00487	0.050	0.180	29.5	P	N/A	3.41	3.63	3.73	4.00	4.40	11.25	N/A	N/A	N/A	N/A	N/A	N/A	I	N/A	AM	N/A	N/A	N/A	34S_6p1d7Yd_1	11/8C2	TDP-WTP-051	7090634
21.0	0.999	0.00487	0.050	0.180	28.3	P	N/A	3.58	3.81	3.92	4.20	4.40	11.50	N/A	N/A	N/A	N/A	N/A	N/A	I	N/A	AM+	N/A	N/A	N/A	34S_6p1d7Yd_1	11/8C2	TDP-WTP-051	7090637
21.0	0.999	0.00487	0.050	0.180	26.8	P	N/A	3.62	3.92	4.05	4.40	4.40	12.50	4.40	vis	UCSvis	N/A	N/A	N/A	I	N/A	CS	N/A	N/A	N/A	34S_6p1d7Yd_1	11/8C2	TDP-WTP-051	7090641
21.0	0.999	0.00487	0.049	0.180	25.5	P	N/A	3.64	4.01	4.18	4.60	4.40	12.75	N/A	N/A	N/A	N/A	N/A	N/A	I	N/A	BC	N/A	N/A	N/A	34S_6p1d7Yd_1	11/8C2	TDP-WTP-051	7090643
21.0	0.999	0.00487	0.050	0.180	44.0	P	N/A	3.83	3.90	3.93	4.00	7.20	9.50	N/A	N/A	N/A	N/A	N/A	N/A	D	N/A	SS	N/A	N/A	N/A	34S_6p1d7Yd_0	11/8D2	TDP-WTP-051	7090648
21.0	0.999	0.00487	0.051	0.180	38.0	P	N/A	4.28	4.37	4.41	4.50	7.20	9.50	N/A	N/A	N/A	N/A	N/A	N/A	I	N/A	AM-	N/A	N/A	N/A	34S_6p1d7Yd_0	11/8D2	TDP-WTP-051	7090650
21.0	0.999	0.00487	0.050	0.180	36.8	P	N/A	4.49	4.60	4.65	4.80	7.20	10.50	N/A	N/A	N/A	N/A	N/A	N/A	I	N/A	AM	N/A	N/A	N/A	34S_6p1d7Yd_0	11/8D2	TDP-WTP-051	7090653
21.0	0.999	0.00487	0.050	0.180	34.5	P	N/A	4.69	4.85	4.92	5.10	7.20	11.50	N/A	N/A	N/A	N/A	N/A	N/A	I	N/A	AM	N/A	N/A	N/A	34S_6p1d7Yd_0	11/8D2	TDP-WTP-051	7090656
21.0	0.999	0.00487	0.050	0.180	32.5	P	N/A	4.71	4.99	5.11	5.40	7.20	12.25	N/A	N/A	N/A	N/A	N/A	N/A	I	N/A	AM	N/A	N/A	N/A	34S_6p1d7Yd_0	11/8D2	TDP-WTP-051	7090659
21.0	0.999	0.00487	0.050	0.180	30.8	P	N/A	4.83	5.17	5.32	5.70	7.20	13.25	N/A	N/A	N/A	N/A	N/A	N/A	I	N/A	AM	N/A	N/A	N/A	34S_6p1d7Yd_0	11/8D2	TDP-WTP-051	7090662
21.0	0.999	0.00487	0.050	0.180	29.0	P	N/A	4.96	5.38	5.56	6.00	7.20	14.75	N/A	N/A	N/A	N/A	N/A	N/A	I	N/A	AM+	N/A	N/A	N/A	34S_6p1d7Yd_0	11/8D2	TDP-WTP-051	7090665
21.0	0.999	0.00487	0.050	0.180	27.3	P	N/A	4.99	5.52	5.75	6.30	7.20	16.00	N/A	N/A	N/A	N/A	N/A	N/A	I	N/A	AM+	N/A	N/A	N/A	34S_6p1d7Yd_0	11/8D2	TDP-WTP-051	7090668
21.0	0.999	0.00487	0.050	0.180	26.0	P	N/A	4.99	5.62	5.89	6.60	7.20	17.00	N/A	N/A	N/A	N/A	N/A	N/A	I	N/A	AM+	N/A	N/A	N/A	34S_6p1d7Yd_0	11/8D2	TDP-WTP-051	7090671
21.0	0.999	0.00487	0.049	0.180	24.5	P	N/A	4.80	5.62	5.98	6.90	7.20	17.50	N/A	N/A	N/A	N/A	N/A	N/A	I	N/A	CS-	N/A	N/A	N/A	34S_6p1d7Yd_0	11/8D2	TDP-WTP-051	7090674
21.0	0.999	0.00487	0.049	0.180	23.0	P	N/A	4.57	5.57	6.03	7.20	7.20	18.00	7.20	vis	UCSvis	N/A	N/A	N/A	I	N/A	CS	N/A	N/A	N/A	34S_6p1d7Yd_0	11/8D2	TDP-WTP-051	7090678
21.4	0.999	0.00487	undefined	1.000	infinite	S	3.63	N/A	N/A	N/A	3.60	7.00	N/A	N/A	N/A	N/A	UCScen	N/A	N/A	I	N/A	SS+	N/A	N/A	N/A	34S_6p1d7Ya-04	11/9A1	TDP-WTP-052	7090681
21.5	0.999	0.00487	undefined	1.000	infinite	S	4.00	N/A	N/A	N/A	4.00	7.00	8.50	N/A	N/A	N/A	N/A	N/A	N/A	I	N/A	SS	N/A	N/A	N/A	34S_6p1d7Ya-04	11/9A1	TDP-WTP-052	7090684
21.4	0.999	0.00487	undefined	1.000	infinite	S	4.52	N/A	N/A	N/A	4.50	7.00	9.25	N/A	N/A	N/A	N/A	N/A	N/A	I	N/A	AM-	N/A	N/A	N/A	34S_6p1d7Ya-04	11/9A1	TDP-WTP-052	7090687
21.5	0.999	0.00487	undefined	1.000	infinite	S	5.02	N/A	N/A	N/A	5.00	7.00	11.00	N/A	N/A	N/A	N/A	N/A	N/A	I	N/A	AM	N/A	N/A	N/A	34S_6p1d7Ya-04	11/9A1	TDP-WTP-052	7090690
21.4	0.999	0.00487	undefined	1.000	infinite	S	5.58	N/A	N/A	N/A	5.50	7.00	13.00	N/A	N/A	N/A	N/A	N/A	N/A	I	N/A	AM	N/A	N/A	N/A	34S_6p1d7Ya-04	11/9A1	TDP-WTP-052	7090692
21.5	0.999	0.00487	undefined	1.000	infinite	S	6.03	N/A	N/A	N/A	6.00	7.00	16.00	N/A	N/A	N/A	N/A	N/A	N/A	I	N/A	AM	N/A	N/A	N/A	34S_6p1d7Ya-04	11/9A1	TDP-WTP-052	7090696
21.5	0.999	0.00487	undefined	1.000	infinite	S	6.54	N/A	N/A	N/A	6.50	7.00	19.25	N/A	N/A	N/A	N/A	N/A	N/A	I	N/A	AM+	N/A	N/A	N/A	34S_6p1d7Ya-04	11/9A1	TDP-WTP-052	7090698
21.5	0.999	0.00487	undefined	1.000	infinite	S	7.01	N/A	N/A	N/A	7.00	7.00	22.50	7.00	vis	UCSvis	N/A	N/A	N/A	I	N/A	CS	N/A	N/A	N/A	34S_6p1d7Ya-04	11/9A1	TDP-WTP-052	7090702
22.0	0.999	0.00487	0.051	0.180	91.0	P	N/A	3.80	3.83	3.84	3.80	8.50	N/A	N/A	N/A	N/A	UCScen	N/A	N/A	I	N/A	SS	N/A	N/A	N/A	34S_6p1d7Yd_9	11/9A2	TDP-WTP-052	7090705
22.0	0.999	0.00487	0.050	0.180	77.5	P	N/A	4.46	4.49	4.50	4.50	8.50	9.25	N/A	N/A	N/A	N/A	N/A	N/A	I	N/A	AM-	N/A	N/A	N/A	34S_6p1d7Yd_9	11/9A2	TDP-WTP-052	7090708
22.0	0.999	0.00487	0.049	0.180	70.0	P	N/A	4.95	4.99	5.01	5.00	8.50	11.00	N/A	N/A	N/A	N/A	N/A	N/A	I	N/A	AM	N/A	N/A	N/A	34S_6p1d7Yd_9	11/9A2	TDP-WTP-052	7090710
22.0	0.999	0.00487	0.050	0.180	63.0	P	N/A	5.44	5.49	5.52	5.50	8.50	12.75	N/A	N/A	N/A	N/A	N/A	N/A	I	N/A	AM	N/A	N/A	N/A	34S_6p1d7Yd_9	11/9A2	TDP-WTP-052	7090713
22.0	0.999	0.00487	0.050	0.180	58.0	P	N/A	5.84	5.93	5.97	6.00	8.50	14.50	N/A	N/A	N/A	N/A	N/A	N/A	I	N/A	AM	N/A	N/A	N/A	34S_6p1d7Yd_9	11/9A2	TDP-WTP-052	7090716
22.0	0.999	0.00487	0.051	0.180	53.5	P	N/A	6.32	6.42	6.47	6.50	8.50	16.50	N/A	N/A	N/A	N/A	N/A	N/A	I	N/A	AM	N/A	N/A	N/A	34S_6p1d7Yd_9	11/9A2	TDP-WTP-052	7090719
22.0	0.999	0.00487	0.050	0.180	49.5	P	N/A	6.70	6.86	6.94	7.00	8.50	17.75	N/A	N/A	N/A	N/A	N/A	N/A	I	N/A	AM	N/A	N/A	N/A	34S_6p1d7Yd_9	11/9A2	TDP-WTP-052	7090722
22.0	0.999	0.00487	0.050	0.180	46.0	P	N/A	6.71	7.07	7.22	7.50	8.50	20.00	N/A	N/A	N/A	N/A	N/A	N/A	I	N/A	AM+	N/A	N/A	N/A	34S_6p1d7Yd_9	11/9A2	TDP-WTP-052	7090725
22.0	0.999	0.00487	0.051	0.180	43.0	P	N/A	7.12	7.53	7.71	8.00	8.50	21.50	N/A	N/A	N/A	N/A	N/A	N/A	I	N/A	AM+	N/A	N/A	N/A	34S_6p1d7Yd_9	11/9A2	TDP-WTP-052	7090728
22.0	0.999	0.00487	0.051	0.180	40.5	P	N/A	7.37	7.87	8.09	8.50	8.50	22.75	8.50	vis	UCSvis	N/A	N/A	N/A	I	N/A	CS	N/A	N/A	N/A	34S_6p1d7Yd_9	11/9A2	TDP-WTP-052	7090732
22.9	0.999	0.00487	undefined	1.000	infinite	S	3.40	N/A	N/A	N/A	3.40	N/A	N/A	N/A	N/A	N/A	UCScen	N/A	N/A	I	N/A	SS	N/A	N/A	N/A	34S_6p1d7Ya-44	11/14A1	TDP-WTP-063	7090737
23.0	0.999	0.00487	0.051	0.180	44.0	P	N/A	3.82	3.90	3.94	4.00	7.00	8.50	N/A	N/A	N/A	UCScen	N/A	N/A	I	N/A	SS+	N/A	N/A	N/A	34S_6p1d7Yd_0	11/14A2	TDP-WTP-063	7090740
23.0	0.999	0.00487	0.051	0.180	39.5	P	N/A	4.18	4.30	4.35	4.50	7.00	9.25	N/A	N/A	N/A	N/A	N/A	N/A	I	N/A	AM	N/A	N/A	N/A	34S_6p1d7Yd_0	11/14A2	TDP-WTP-063	7090742
23.0	0.999	0.00487	0.051	0.180	35.3	P	N/A	4.52	4.71	4.80	5.00	7.00	10.75	N/A	N/A	N/A	N/A	N/A	N/A	I	N/A	AM	N/A	N/A	N/A	34S_6p1d7Yd_0	11/14A2	TDP-WTP-063	7090745
23.0	0.999	0.00487	0.050	0.180	32.0	P	N/A	4.69	5.01	5.15	5.50	7.00	13.00	N/A	N/A	N/A	N/A	N/A	N/A	I	N/A	AM	N/A	N/A	N/A	34S_6p1d7Yd_0	11/14A2	TDP-WTP-063	7090748
23.0	0.999	0.00487	0.051	0.180	29.0	P	N/A	4.83	5.30	5.50	6.00	7.00	15.75	N/A	N/A	N/A	N/A	N/A	N/A	I	N/A	AM+	N/A	N/A	N/A	34S_6p1d7Yd_0	11/14A2	TDP-WTP-063	7090751
23.0	0.999	0.00487	0.050	0.180	26.3	P	N/A	4.88	5.53	5.81	6.50	7.00	17.00	N/A	N/A	N/A	N/A	N/A	N/A	I	N/A	AM+	N/A	N/A	N/A	34S_6p1d7Yd_0	11/14A2	TDP-WTP-063	7090754

Table B.8. Data from Fall 2007 Tests in Mid-Scale Vessel with Spherical Head A.7

Row Number	Test	Case ID	Tank Diameter	Head Shape	Dish Height	Dish Volume	Tank Fill Height	Return Line Height	Nozzle Inner Diameter	Nozzle Stand-off Distance	Pulse Tube Configuration	Installed Nozzles	Outer Nozzles Operated	Inner Nozzles Operated	Pulse Tube Outer Diameter	Outer PJM Radius	Inner PJM Radius	"FIO" Outer PJM Impingement Angle	"FIO" Inner PJM Impingement Angle	Ratio Outer PJM to Tank Radius	Ratio Inner PJM to Tank Radius	Simulant	Solids Density	Particle Diameter d5	Particle Diameter d50	Particle Diameter d95	Void Fraction
text	text	text	in.	text	in.	in.^{3}	in.	in.	in.	in.	text	number	number	number	in.	in.	in.	deg	deg	nondim	nondim	text	g/cm^3	m	m	m	fraction
MSS	M/DDX	ID	D	HS	H_{dish}	V_{dish}	H	Rtn	d	sod	PT	N	N_O	N_I	PT_{od}	R_O	R_I	θ_O	θ_I	R_O/R	R_I/R	sxdx	ρ_s	d_5	d_{50}	d_{95}	vf
7090758MX	11/14A2	34S_6p1d7Yd_0	33 7/8	S	9	4437.4	67 3/4	65 3/4	0.446	0.669	HLP-22	12	4	4	1.9	10.5	5.7	30.8	16.1	0.62	0.33	p1d7	2.45	0.0001213	0.0001780	0.0002606	0.4277
7090761	11/14B1	34S_6p1d7Ya-44	33 7/8	S	9	4437.4	67 3/4	61 3/4	0.446	0.669	HLP-22	12	4	4	1.9	10.5	5.7	30.8	16.1	0.62	0.33	p1d7	2.45	0.0001213	0.0001780	0.0002606	0.4277
7090764	11/14B2	34S_6p1d7Yd_0	33 7/8	S	9	4437.4	67 3/4	61 3/4	0.446	0.669	HLP-22	12	4	4	1.9	10.5	5.7	30.8	16.1	0.62	0.33	p1d7	2.45	0.0001213	0.0001780	0.0002606	0.4277
7090766	11/14C1	34S_6p1d7Ya-04	33 7/8	S	9	4437.4	67 3/4	61 3/4	0.446	0.669	HLP-22	12	0	4	1.9	10.5	5.7	30.8	16.1	0.62	0.33	p1d7	2.45	0.0001213	0.0001780	0.0002606	0.4277
7090772	11/14C2	34S_6p1d7Yd_9	33 7/8	S	9	4437.4	67 3/4	61 3/4	0.446	0.669	HLP-22	12	0	4	1.9	10.5	5.7	30.8	16.1	0.62	0.33	p1d7	2.45	0.0001213	0.0001780	0.0002606	0.4277
7090776	11/14D1	34S_6p1d7Yc_1	33 7/8	S	9	4437.4	67 3/4	61 3/4	0.446	0.669	HLP-22	12	8	4	1.9	10.5	5.7	30.8	16.1	0.62	0.33	p1d7	2.45	0.0001213	0.0001780	0.0002606	0.4277
7090779M	11/14D1	34S_6p1d7Yc_1	33 7/8	S	9	4437.4	67 3/4	61 3/4	0.446	0.669	HLP-22	12	8	4	1.9	10.5	5.7	30.8	16.1	0.62	0.33	p1d7	2.45	0.0001213	0.0001780	0.0002606	0.4277
7090781M	11/14D1	34S_6p1d7Yc_1	33 7/8	S	9	4437.4	67 3/4	61 3/4	0.446	0.669	HLP-22	12	8	4	1.9	10.5	5.7	30.8	16.1	0.62	0.33	p1d7	2.45	0.0001213	0.0001780	0.0002606	0.4277
7090785	11/15A1	34S_6p1d7Yc_0	33 7/8	S	9	4437.4	67 3/4	61 3/4	0.446	0.669	HLP-22	12	4	4	1.9	10.5	5.7	30.8	16.1	0.62	0.33	p1d7	2.45	0.0001213	0.0001780	0.0002606	0.4277
7090787	11/15A1	34S_6p1d7Yc_0	33 7/8	S	9	4437.4	67 3/4	61 3/4	0.446	0.669	HLP-22	12	4	4	1.9	10.5	5.7	30.8	16.1	0.62	0.33	p1d7	2.45	0.0001213	0.0001780	0.0002606	0.4277
7090790	11/15A1	34S_6p1d7Yc_0	33 7/8	S	9	4437.4	67 3/4	61 3/4	0.446	0.669	HLP-22	12	4	4	1.9	10.5	5.7	30.8	16.1	0.62	0.33	p1d7	2.45	0.0001213	0.0001780	0.0002606	0.4277
7090793	11/15A1	34S_6p1d7Yc_0	33 7/8	S	9	4437.4	67 3/4	61 3/4	0.446	0.669	HLP-22	12	4	4	1.9	10.5	5.7	30.8	16.1	0.62	0.33	p1d7	2.45	0.0001213	0.0001780	0.0002606	0.4277
7090796	11/15A1	34S_6p1d7Yc_0	33 7/8	S	9	4437.4	67 3/4	61 3/4	0.446	0.669	HLP-22	12	4	4	1.9	10.5	5.7	30.8	16.1	0.62	0.33	p1d7	2.45	0.0001213	0.0001780	0.0002606	0.4277
7090799	11/15A1	34S_6p1d7Yc_0	33 7/8	S	9	4437.4	67 3/4	61 3/4	0.446	0.669	HLP-22	12	4	4	1.9	10.5	5.7	30.8	16.1	0.62	0.33	p1d7	2.45	0.0001213	0.0001780	0.0002606	0.4277
7090802	11/15A1	34S_6p1d7Yc_0	33 7/8	S	9	4437.4	67 3/4	61 3/4	0.446	0.669	HLP-22	12	4	4	1.9	10.5	5.7	30.8	16.1	0.62	0.33	p1d7	2.45	0.0001213	0.0001780	0.0002606	0.4277
7090806M	11/15A1	34S_6p1d7Yc_0	33 7/8	S	9	4437.4	67 3/4	61 3/4	0.446	0.669	HLP-22	12	4	4	1.9	10.5	5.7	30.8	16.1	0.62	0.33	p1d7	2.45	0.0001213	0.0001780	0.0002606	0.4277
7090808M	11/15A1	34S_6p1d7Yc_0	33 7/8	S	9	4437.4	67 3/4	61 3/4	0.446	0.669	HLP-22	12	4	4	1.9	10.5	5.7	30.8	16.1	0.62	0.33	p1d7	2.45	0.0001213	0.0001780	0.0002606	0.4277
7090812	11/15B1	34S_6p1d7Yc_9	33 7/8	S	9	4437.4	67 3/4	61 3/4	0.446	0.669	HLP-22	12	0	4	1.9	10.5	5.7	30.8	16.1	0.62	0.33	p1d7	2.45	0.0001213	0.0001780	0.0002606	0.4277
7090814	11/15B1	34S_6p1d7Yc_9	33 7/8	S	9	4437.4	67 3/4	61 3/4	0.446	0.669	HLP-22	12	0	4	1.9	10.5	5.7	30.8	16.1	0.62	0.33	p1d7	2.45	0.0001213	0.0001780	0.0002606	0.4277
7090816	11/15B1	34S_6p1d7Yc_9	33 7/8	S	9	4437.4	67 3/4	61 3/4	0.446	0.669	HLP-22	12	0	4	1.9	10.5	5.7	30.8	16.1	0.62	0.33	p1d7	2.45	0.0001213	0.0001780	0.0002606	0.4277
7090819	11/15B1	34S_6p1d7Yc_9	33 7/8	S	9	4437.4	67 3/4	61 3/4	0.446	0.669	HLP-22	12	0	4	1.9	10.5	5.7	30.8	16.1	0.62	0.33	p1d7	2.45	0.0001213	0.0001780	0.0002606	0.4277
7090822	11/15B1	34S_6p1d7Yc_9	33 7/8	S	9	4437.4	67 3/4	61 3/4	0.446	0.669	HLP-22	12	0	4	1.9	10.5	5.7	30.8	16.1	0.62	0.33	p1d7	2.45	0.0001213	0.0001780	0.0002606	0.4277
7090825	11/15B1	34S_6p1d7Yc_9	33 7/8	S	9	4437.4	67 3/4	61 3/4	0.446	0.669	HLP-22	12	0	4	1.9	10.5	5.7	30.8	16.1	0.62	0.33	p1d7	2.45	0.0001213	0.0001780	0.0002606	0.4277
7090828	11/15B1	34S_6p1d7Yc_9	33 7/8	S	9	4437.4	67 3/4	61 3/4	0.446	0.669	HLP-22	12	0	4	1.9	10.5	5.7	30.8	16.1	0.62	0.33	p1d7	2.45	0.0001213	0.0001780	0.0002606	0.4277
7090831	11/15B1	34S_6p1d7Yc_9	33 7/8	S	9	4437.4	67 3/4	61 3/4	0.446	0.669	HLP-22	12	0	4	1.9	10.5	5.7	30.8	16.1	0.62	0.33	p1d7	2.45	0.0001213	0.0001780	0.0002606	0.4277
7090835M	11/15B1	34S_6p1d7Yc_9	33 7/8	S	9	4437.4	67 3/4	61 3/4	0.446	0.669	HLP-22	12	0	4	1.9	10.5	5.7	30.8	16.1	0.62	0.33	p1d7	2.45	0.0001213	0.0001780	0.0002606	0.4277
7090837M	11/15B1	34S_6p1d7Yc_9	33 7/8	S	9	4437.4	67 3/4	61 3/4	0.446	0.669	HLP-22	12	0	4	1.9	10.5	5.7	30.8	16.1	0.62	0.33	p1d7	2.45	0.0001213	0.0001780	0.0002606	0.4277
7090840	11/15C1	34S_6p1d7Yc_6	33 7/8	S	9	4437.4	67 3/4	61 3/4	0.446	0.669	HLP-22	12	4	0	1.9	10.5	5.7	30.8	16.1	0.62	0.33	p1d7	2.45	0.0001213	0.0001780	0.0002606	0.4277
7090842	11/15C1	34S_6p1d7Yc_6	33 7/8	S	9	4437.4	67 3/4	61 3/4	0.446	0.669	HLP-22	12	4	0	1.9	10.5	5.7	30.8	16.1	0.62	0.33	p1d7	2.45	0.0001213	0.0001780	0.0002606	0.4277
7090844	11/15C1	34S_6p1d7Yc_6	33 7/8	S	9	4437.4	67 3/4	61 3/4	0.446	0.669	HLP-22	12	4	0	1.9	10.5	5.7	30.8	16.1	0.62	0.33	p1d7	2.45	0.0001213	0.0001780	0.0002606	0.4277
7090847	11/15C1	34S_6p1d7Yc_6	33 7/8	S	9	4437.4	67 3/4	61 3/4	0.446	0.669	HLP-22	12	4	0	1.9	10.5	5.7	30.8	16.1	0.62	0.33	p1d7	2.45	0.0001213	0.0001780	0.0002606	0.4277
7090850	11/15C1	34S_6p1d7Yc_6	33 7/8	S	9	4437.4	67 3/4	61 3/4	0.446	0.669	HLP-22	12	4	0	1.9	10.5	5.7	30.8	16.1	0.62	0.33	p1d7	2.45	0.0001213	0.0001780	0.0002606	0.4277
7090854M	11/15C1	34S_6p1d7Yc_6	33 7/8	S	9	4437.4	67 3/4	61 3/4	0.446	0.669	HLP-22	12	4	0	1.9	10.5	5.7	30.8	16.1	0.62	0.33	p1d7	2.45	0.0001213	0.0001780	0.0002606	0.4277
7090856M	11/15C1	34S_6p1d7Yc_6	33 7/8	S	9	4437.4	67 3/4	61 3/4	0.446	0.669	HLP-22	12	4	0	1.9	10.5	5.7	30.8	16.1	0.62	0.33	p1d7	2.45	0.0001213	0.0001780	0.0002606	0.4277
7090859	11/19A1	34S_4p1d7Ya	33 7/8	S	9	4437.4	67 3/4	61 3/4	0.297	0.446	HLP-22	12	8	4	1.9	10.5	5.7	30.8	16.1	0.62	0.33	p1d7	2.45	0.0001213	0.0001780	0.0002606	0.4277
7090863	11/19A1	34S_4p1d7Ya	33 7/8	S	9	4437.4	67 3/4	61 3/4	0.297	0.446	HLP-22	12	8	4	1.9	10.5	5.7	30.8	16.1	0.62	0.33	p1d7	2.45	0.0001213	0.0001780	0.0002606	0.4277
7090865	11/19A1	34S_4p1d7Ya	33 7/8	S	9	4437.4	67 3/4	61 3/4	0.297	0.446	HLP-22	12	8	4	1.9	10.5	5.7	30.8	16.1	0.62	0.33	p1d7	2.45	0.0001213	0.0001780	0.0002606	0.4277
7090869	11/19A2	34S_4p1d7Yd_1	33 7/8	S	9	4437.4	67 3/4	61 3/4	0.297	0.446	HLP-22	12	8	4	1.9	10.5	5.7	30.8	16.1	0.62	0.33	p1d7	2.45	0.0001213	0.0001780	0.0002606	0.4277
7090871	11/19A2	34S_4p1d7Yd_1	33 7/8	S	9	4437.4	67 3/4	61 3/4	0.297	0.446	HLP-22	12	8	4	1.9	10.5	5.7	30.8	16.1	0.62	0.33	p1d7	2.45	0.0001213	0.0001780	0.0002606	0.4277
7090875M	11/19A2	34S_4p1d7Yd_1	33 7/8	S	9	4437.4	67 3/4	61 3/4	0.297	0.446	HLP-22	12	8	4	1.9	10.5	5.7	30.8	16.1	0.62	0.33	p1d7	2.45	0.0001213	0.0001780	0.0002606	0.4277
7090877M	11/19A2	34S_4p1d7Yd_1	33 7/8	S	9	4437.4	67 3/4	61 3/4	0.297	0.446	HLP-22	12	8	4	1.9	10.5	5.7	30.8	16.1	0.62	0.33	p1d7	2.45	0.0001213	0.0001780	0.0002606	0.4277

Table B.8. Data from Fall 2007 Tests in Mid-Scale Vessel with Spherical Head B.7

Tank Water Temperature	Water Density	Solids Fraction	Pulse Volume Fraction	Duty Cycle	Cycle Time	Pulsed or Steady Jet	Us Steady Jet	U1 Pulsing Jet	U2 URMS	U3 URM3	Discharge Velocity	Critical Suspension Velocity	Average Peak Cloud Height	UCS Condition	UCS Method	UCS Flag	UCS Center Flag	UCS udv Flag	UCS based on Decreasing Velocity	Sweep Increase / Decrease	UDV Height Bed	Particle Motion	Solids Level	Outer Bottom Pattern	Inner Bottom Pattern	Case ID	Test	TDP	Row Number
C	g/cm³	fraction	fraction	fraction	s	text	m/s	m/s	m/s	m/s	m/s	m/s	in.	m/s	text	text	text	text	m/s	text	mm	text	text	text	text	text	text	text	text
T	ρ_l	ϕ_S	ϕ_P	DC	t_C	Jet	U_S	U1	U2	U3	U	U_{CS}	H_C	U_{CSR}	U_{CSM}	U_{CS}vis	U_{CS}cen	U_{CS}udv	U_{CS}_D	S_W	H_{bed}	PM	Sol	SP_O	SP_I	ID	M/DDX	TDP	MSS
23.0	0.999	0.00487	0.050	0.180	24.0	P	N/A	4.60	5.51	5.92	7.00	7.00	19.00	7.00	vis	UCSvis	N/A	N/A	N/A	I	N/A	CS	N/A	N/A	N/A	34S_6p1d7Yd_0	11/14A2	TDP-WTP-063	7090758
23.3	0.999	0.00487	undefined	1.000	infinite	S	3.63	N/A	N/A	N/A	3.60	N/A	N/A	N/A	N/A	N/A	UCScen	N/A	N/A	I	N/A	AM-	N/A	N/A	N/A	34S_6p1d7Ya-44	11/14B1	TDP-WTP-063	7090761
23.0	0.999	0.00487	0.050	0.180	45.3	P	N/A	3.71	3.78	3.81	3.90	N/A	N/A	N/A	N/A	N/A	UCScen	N/A	N/A	I	N/A	SS	N/A	N/A	N/A	34S_6p1d7Yd_0	11/14B2	TDP-WTP-063	7090764
23.1	0.999	0.00487	undefined	1.000	infinite	S	3.43	N/A	N/A	N/A	3.40	N/A	N/A	N/A	N/A	N/A	UCScen	N/A	N/A	I	N/A	SS	N/A	N/A	N/A	34S_6p1d7Ya-04	11/14C1	TDP-WTP-063	7090766
23.0	0.999	0.00487	0.050	0.180	94.5	P	N/A	3.69	3.72	3.75	3.70	N/A	N/A	N/A	center dec	N/A	UCScen	N/A	3.70	D	N/A	SS	N/A	N/A	N/A	34S_6p1d7Yd_9	11/14C2	TDP-WTP-063	7090772
23.0	0.999	0.00487	0.050	0.330	18.3	P	N/A	3.02	3.22	3.31	3.50	4.50	10.50	N/A	N/A	N/A	N/A	N/A	N/A	D	N/A	SS	N/A	N/A	N/A	34S_6p1d7Yc_1	11/14D1	TDP-WTP-063	7090776
23.0	0.999	0.00487	0.051	0.330	14.0	P	N/A	3.28	3.77	4.00	4.50	4.50	12.00	4.50	vis	UCSvis	N/A	N/A	N/A	I	N/A	CS	N/A	N/A	N/A	34S_6p1d7Yc_1	11/14D1	TDP-WTP-063	7090779
23.0	0.999	0.00487	0.052	0.330	12.5	P	N/A	2.89	3.66	4.02	5.00	4.50	12.25	N/A	N/A	N/A	N/A	N/A	N/A	I	N/A	BC	N/A	N/A	N/A	34S_6p1d7Yc_1	11/14D1	TDP-WTP-063	7090781
22.0	0.999	0.00487	0.051	0.330	23.8	P	N/A	3.78	3.88	3.92	4.00	7.00	8.50	N/A	N/A	N/A	UCScen	N/A	N/A	I	N/A	SS	N/A	N/A	N/A	34S_6p1d7Yc_0	11/15A1	TDP-WTP-053	7090785
22.0	0.999	0.00487	0.050	0.330	21.3	P	N/A	3.95	4.17	4.26	4.50	7.00	9.50	N/A	N/A	N/A	N/A	N/A	N/A	I	N/A	AM-	N/A	N/A	N/A	34S_6p1d7Yc_0	11/15A1	TDP-WTP-053	7090787
22.0	0.999	0.00487	0.051	0.330	19.0	P	N/A	4.23	4.56	4.70	5.00	7.00	11.25	N/A	N/A	N/A	N/A	N/A	N/A	I	N/A	AM	N/A	N/A	N/A	34S_6p1d7Yc_0	11/15A1	TDP-WTP-053	7090790
22.0	0.999	0.00487	0.048	0.330	16.0	P	N/A	3.47	4.30	4.66	5.50	7.00	12.75	N/A	N/A	N/A	N/A	N/A	N/A	I	N/A	AM	N/A	N/A	N/A	34S_6p1d7Yc_0	11/15A1	TDP-WTP-053	7090793
22.0	0.999	0.00487	0.050	0.330	15.5	P	N/A	4.18	4.91	5.23	6.00	7.00	13.50	N/A	N/A	N/A	N/A	N/A	N/A	I	N/A	AM	N/A	N/A	N/A	34S_6p1d7Yc_0	11/15A1	TDP-WTP-053	7090796
22.0	0.999	0.00487	0.051	0.330	14.5	P	N/A	4.60	5.32	5.65	6.40	7.00	15.00	N/A	N/A	N/A	N/A	N/A	N/A	I	N/A	AM+	N/A	N/A	N/A	34S_6p1d7Yc_0	11/15A1	TDP-WTP-053	7090799
22.0	0.999	0.00487	0.050	0.330	13.5	P	N/A	4.63	5.47	5.85	6.80	7.00	17.25	N/A	N/A	N/A	N/A	N/A	N/A	I	N/A	CS-	N/A	N/A	N/A	34S_6p1d7Yc_0	11/15A1	TDP-WTP-053	7090802
22.0	0.999	0.00487	0.049	0.330	0.0	P	N/A	4.79	5.63	6.01	7.00	7.00	18.00	7.00	vis	UCSvis	N/A	N/A	N/A	I	N/A	CS	N/A	N/A	N/A	34S_6p1d7Yc_0	11/15A1	TDP-WTP-053	7090806
22.0	0.999	0.00487	0.050	0.330	12.0	P	N/A	4.47	5.53	6.05	7.40	7.00	18.75	N/A	N/A	N/A	N/A	N/A	N/A	I	N/A	BC	N/A	N/A	N/A	34S_6p1d7Yc_0	11/15A1	TDP-WTP-053	7090808
22.0	0.999	0.00487	0.050	0.330	51.8	P	N/A	3.64	3.67	3.69	3.70	8.70	N/A	N/A	N/A	N/A	UCScen	N/A	N/A	I	N/A	SS	N/A	N/A	N/A	34S_6p1d7Yc_9	11/15B1	TDP-WTP-053	7090812
22.0	0.999	0.00487	0.050	0.330	34.5	P	N/A	5.38	5.45	5.48	5.50	8.70	12.50	N/A	N/A	N/A	N/A	N/A	N/A	I	N/A	AM-	N/A	N/A	N/A	34S_6p1d7Yc_9	11/15B1	TDP-WTP-053	7090814
22.0	0.999	0.00487	0.050	0.330	31.5	P	N/A	5.84	5.92	5.96	6.00	8.70	14.50	N/A	N/A	N/A	N/A	N/A	N/A	I	N/A	AM	N/A	N/A	N/A	34S_6p1d7Yc_9	11/15B1	TDP-WTP-053	7090816
22.0	0.999	0.00487	0.051	0.330	29.0	P	N/A	6.39	6.47	6.51	6.50	8.70	16.50	N/A	N/A	N/A	N/A	N/A	N/A	I	N/A	AM	N/A	N/A	N/A	34S_6p1d7Yc_9	11/15B1	TDP-WTP-053	7090819
22.0	0.999	0.00487	0.050	0.330	0.0	P	N/A	6.84	6.93	6.98	7.00	8.70	18.00	N/A	N/A	N/A	N/A	N/A	N/A	I	N/A	AM	N/A	N/A	N/A	34S_6p1d7Yc_9	11/15B1	TDP-WTP-053	7090822
22.0	0.999	0.00487	0.051	0.330	25.3	P	N/A	7.29	7.41	7.48	7.50	8.70	19.75	N/A	N/A	N/A	N/A	N/A	N/A	I	N/A	AM+	N/A	N/A	N/A	34S_6p1d7Yc_9	11/15B1	TDP-WTP-053	7090825
22.0	0.999	0.00487	0.051	0.330	23.5	P	N/A	7.23	7.64	7.81	8.00	8.70	21.25	N/A	N/A	N/A	N/A	N/A	N/A	I	N/A	AM+	N/A	N/A	N/A	34S_6p1d7Yc_9	11/15B1	TDP-WTP-053	7090828
22.0	0.999	0.00487	0.050	0.330	22.3	P	N/A	7.35	7.85	8.05	8.40	8.70	23.25	N/A	N/A	N/A	N/A	N/A	N/A	I	N/A	AM+	N/A	N/A	N/A	34S_6p1d7Yc_9	11/15B1	TDP-WTP-053	7090831
22.0	0.999	0.00487	0.050	0.330	21.5	P	N/A	7.43	8.02	8.26	8.70	8.70	24.00	8.70	vis	UCSvis	N/A	N/A	N/A	I	N/A	CS	N/A	N/A	N/A	34S_6p1d7Yc_9	11/15B1	TDP-WTP-053	7090835
22.0	0.999	0.00487	0.050	0.330	20.8	P	N/A	7.50	8.18	8.46	9.00	8.70	25.25	N/A	N/A	N/A	N/A	N/A	N/A	I	N/A	BC	N/A	N/A	N/A	34S_6p1d7Yc_9	11/15B1	TDP-WTP-053	7090837
22.0	0.999	0.00487	0.051	0.330	34.5	P	N/A	5.43	5.48	5.51	5.50	7.10	N/A	N/A	N/A	N/A	N/A	N/A	N/A	I	N/A	SS	N/A	N/A	N/A	34S_6p1d7Yc_6	11/15C1	TDP-WTP-053	7090840
22.0	0.999	0.00487	0.050	0.330	31.5	P	N/A	5.92	5.97	6.01	6.00	7.10	9.00	N/A	N/A	N/A	N/A	N/A	N/A	I	N/A	SS	N/A	N/A	N/A	34S_6p1d7Yc_6	11/15C1	TDP-WTP-053	7090842
22.0	0.999	0.00487	0.050	0.330	29.0	P	N/A	6.38	6.46	6.50	6.50	7.10	10.00	N/A	N/A	N/A	N/A	N/A	N/A	I	N/A	SS+	N/A	N/A	N/A	34S_6p1d7Yc_6	11/15C1	TDP-WTP-053	7090844
22.0	0.999	0.00487	0.050	0.330	28.0	P	N/A	6.50	6.61	6.67	6.70	7.10	11.50	N/A	N/A	N/A	N/A	N/A	N/A	I	N/A	SS+	N/A	N/A	N/A	34S_6p1d7Yc_6	11/15C1	TDP-WTP-053	7090847
22.0	0.999	0.00487	0.050	0.330	27.3	P	N/A	6.70	6.82	6.87	6.90	7.10	12.00	N/A	N/A	N/A	N/A	N/A	N/A	I	N/A	AM	N/A	N/A	N/A	34S_6p1d7Yc_6	11/15C1	TDP-WTP-053	7090850
22.0	0.999	0.00487	0.050	0.330	26.5	P	N/A	6.88	7.01	7.07	7.10	7.10	13.25	7.10	vis	UCSvis	N/A	N/A	N/A	I	N/A	CS	N/A	N/A	N/A	34S_6p1d7Yc_6	11/15C1	TDP-WTP-053	7090854
22.0	0.999	0.00487	0.050	0.330	25.5	P	N/A	7.11	7.27	7.34	7.40	7.10	15.50	N/A	N/A	N/A	N/A	N/A	N/A	I	N/A	BC	N/A	N/A	N/A	34S_6p1d7Yc_6	11/15C1	TDP-WTP-053	7090856
21.5	0.995	0.00487	undefined	1.000	infinite	S	5.46	N/A	N/A	N/A	5.40	5.60	8.75	N/A	N/A	N/A	UCScen	N/A	N/A	I	N/A	CS-	N/A	N/A	N/A	34S_4p1d7Ya	11/19A1	TDP-WTP-054	7090859
21.5	0.999	0.00487	undefined	1.000	infinite	S	5.64	N/A	N/A	N/A	5.60	5.60	9.25	5.60	vis	UCSvis	N/A	N/A	N/A	I	N/A	CS	N/A	N/A	N/A	34S_4p1d7Ya	11/19A1	TDP-WTP-054	7090863
21.5	0.999	0.00487	undefined	1.000	infinite	S	6.06	N/A	N/A	N/A	6.00	5.60	12.13	N/A	N/A	N/A	N/A	N/A	N/A	I	N/A	BC	N/A	N/A	N/A	34S_4p1d7Ya	11/19A1	TDP-WTP-054	7090865
22.0	0.999	0.00487	0.049	0.180	47.0	P	N/A	5.33	5.41	5.45	5.50	6.40	8.50	N/A	N/A	N/A	N/A	N/A	N/A	D	N/A	SS	N/A	N/A	N/A	34S_4p1d7Yd_1	11/19A2	TDP-WTP-054	7090869
22.0	0.999	0.00487	0.051	0.180	43.0	P	N/A	5.76	5.91	5.97	6.00	6.40	9.00	N/A	N/A	N/A	N/A	N/A	N/A	I	N/A	AM+	N/A	N/A	N/A	34S_4p1d7Yd_1	11/19A2	TDP-WTP-054	7090871
22.0	0.999	0.00487	0.053	0.180	40.0	P	N/A	6.25	6.53	6.65	6.40	6.40	9.75	6.40	vis	UCSvis	N/A	N/A	N/A	I	N/A	CS	N/A	N/A	N/A	34S_4p1d7Yd_1	11/19A2	TDP-WTP-054	7090875
22.0	0.999	0.00487	0.052	0.180	38.0	P	N/A	6.16	6.55	6.73	6.80	6.40	10.50	N/A	N/A	N/A	N/A	N/A	N/A	I	N/A	BC	N/A	N/A	N/A	34S_4p1d7Yd_1	11/19A2	TDP-WTP-054	7090877

Table B.8. Data from Fall 2007 Tests in Mid-Scale Vessel with Spherical Head A.8

Row Number	Test	Case ID	Tank Diameter	Head Shape	Dish Height	Dish Volume	Tank Fill Height	Return Line Height	Nozzle Inner Diameter	Nozzle Stand-off Distance	Pulse Tube Configuration	Installed Nozzles	Outer Nozzles Operated	Inner Nozzles Operated	Pulse Tube Outer Diameter	Outer PJM Radius	Inner PJM Radius	"FIO" Outer PJM Impingement Angle	"FIO" Inner PJM Impingement Angle	Ratio Outer PJM to Tank Radius	Ratio Inner PJM to Tank Radius	Simulant	Solids Density	Particle Diameter d5	Particle Diameter d50	Particle Diameter d95	Void Fraction
text	text	text	in.	text	in.	in. ^{3}	in.	in.	in.	in.	text	number	number	number	in.	in.	in.	deg	deg	nondim	nondim	text	g/cm^3	m	m	m	fraction
MSS	M/DDX	ID	D	HS	H_{dish}	V_{dish}	H	Rtn	d	sod	PT	N	N_O	N_I	PT_{od}	R_O	R_I	θ_O	θ_I	R_O/R	R_I/R	sxdx	ρ_s	d_5	d_{50}	d_{95}	vf
7090881	11/20A1	34S_4p1d7Ya-44	33 7/8	S	9	4437.4	67 3/4	61 3/4	0.297	0.446	HLP-22	12	4	4	1.9	10.5	5.7	30.8	16.1	0.62	0.33	p1d7	2.45	0.0001213	0.0001780	0.0002606	0.4277
7090883	11/20A1	34S_4p1d7Ya-44	33 7/8	S	9	4437.4	67 3/4	61 3/4	0.297	0.446	HLP-22	12	4	4	1.9	10.5	5.7	30.8	16.1	0.62	0.33	p1d7	2.45	0.0001213	0.0001780	0.0002606	0.4277
7090886	11/20A1	34S_4p1d7Ya-44	33 7/8	S	9	4437.4	67 3/4	61 3/4	0.297	0.446	HLP-22	12	4	4	1.9	10.5	5.7	30.8	16.1	0.62	0.33	p1d7	2.45	0.0001213	0.0001780	0.0002606	0.4277
7090889	11/20A1	34S_4p1d7Ya-44	33 7/8	S	9	4437.4	67 3/4	61 3/4	0.297	0.446	HLP-22	12	4	4	1.9	10.5	5.7	30.8	16.1	0.62	0.33	p1d7	2.45	0.0001213	0.0001780	0.0002606	0.4277
7090892	11/20A1	34S_4p1d7Ya-44	33 7/8	S	9	4437.4	67 3/4	61 3/4	0.297	0.446	HLP-22	12	4	4	1.9	10.5	5.7	30.8	16.1	0.62	0.33	p1d7	2.45	0.0001213	0.0001780	0.0002606	0.4277
7090895	11/20A1	34S_4p1d7Ya-44	33 7/8	S	9	4437.4	67 3/4	61 3/4	0.297	0.446	HLP-22	12	4	4	1.9	10.5	5.7	30.8	16.1	0.62	0.33	p1d7	2.45	0.0001213	0.0001780	0.0002606	0.4277
7090899	11/20A1	34S_4p1d7Ya-44	33 7/8	S	9	4437.4	67 3/4	61 3/4	0.297	0.446	HLP-22	12	4	4	1.9	10.5	5.7	30.8	16.1	0.62	0.33	p1d7	2.45	0.0001213	0.0001780	0.0002606	0.4277
7090901	11/20A1	34S_4p1d7Ya-44	33 7/8	S	9	4437.4	67 3/4	61 3/4	0.297	0.446	HLP-22	12	4	4	1.9	10.5	5.7	30.8	16.1	0.62	0.33	p1d7	2.45	0.0001213	0.0001780	0.0002606	0.4277
7090905	11/20A2	34S_4p1d7Yd_0	33 7/8	S	9	4437.4	67 3/4	61 3/4	0.297	0.446	HLP-22	12	4	4	1.9	10.5	5.7	30.8	16.1	0.62	0.33	p1d7	2.45	0.0001213	0.0001780	0.0002606	0.4277
7090908	11/20A2	34S_4p1d7Yd_0	33 7/8	S	9	4437.4	67 3/4	61 3/4	0.297	0.446	HLP-22	12	4	4	1.9	10.5	5.7	30.8	16.1	0.62	0.33	p1d7	2.45	0.0001213	0.0001780	0.0002606	0.4277
7090910	11/20A2	34S_4p1d7Yd_0	33 7/8	S	9	4437.4	67 3/4	61 3/4	0.297	0.446	HLP-22	12	4	4	1.9	10.5	5.7	30.8	16.1	0.62	0.33	p1d7	2.45	0.0001213	0.0001780	0.0002606	0.4277
7090913	11/20A2	34S_4p1d7Yd_0	33 7/8	S	9	4437.4	67 3/4	61 3/4	0.297	0.446	HLP-22	12	4	4	1.9	10.5	5.7	30.8	16.1	0.62	0.33	p1d7	2.45	0.0001213	0.0001780	0.0002606	0.4277
7090916	11/20A2	34S_4p1d7Yd_0	33 7/8	S	9	4437.4	67 3/4	61 3/4	0.297	0.446	HLP-22	12	4	4	1.9	10.5	5.7	30.8	16.1	0.62	0.33	p1d7	2.45	0.0001213	0.0001780	0.0002606	0.4277
7090919	11/20A2	34S_4p1d7Yd_0	33 7/8	S	9	4437.4	67 3/4	61 3/4	0.297	0.446	HLP-22	12	4	4	1.9	10.5	5.7	30.8	16.1	0.62	0.33	p1d7	2.45	0.0001213	0.0001780	0.0002606	0.4277
7090922	11/20A2	34S_4p1d7Yd_0	33 7/8	S	9	4437.4	67 3/4	61 3/4	0.297	0.446	HLP-22	12	4	4	1.9	10.5	5.7	30.8	16.1	0.62	0.33	p1d7	2.45	0.0001213	0.0001780	0.0002606	0.4277
7090925	11/20A2	34S_4p1d7Yd_0	33 7/8	S	9	4437.4	67 3/4	61 3/4	0.297	0.446	HLP-22	12	4	4	1.9	10.5	5.7	30.8	16.1	0.62	0.33	p1d7	2.45	0.0001213	0.0001780	0.0002606	0.4277
7090928	11/20A2	34S_4p1d7Yd_0	33 7/8	S	9	4437.4	67 3/4	61 3/4	0.297	0.446	HLP-22	12	4	4	1.9	10.5	5.7	30.8	16.1	0.62	0.33	p1d7	2.45	0.0001213	0.0001780	0.0002606	0.4277
7090932M	11/20A2	34S_4p1d7Yd_0	33 7/8	S	9	4437.4	67 3/4	61 3/4	0.297	0.446	HLP-22	12	4	4	1.9	10.5	5.7	30.8	16.1	0.62	0.33	p1d7	2.45	0.0001213	0.0001780	0.0002606	0.4277
7090934M	11/20A2	34S_4p1d7Yd_0	33 7/8	S	9	4437.4	67 3/4	61 3/4	0.297	0.446	HLP-22	12	4	4	1.9	10.5	5.7	30.8	16.1	0.62	0.33	p1d7	2.45	0.0001213	0.0001780	0.0002606	0.4277
7090938	11/20B1	34S_4p1d7Ya-04	33 7/8	S	9	4437.4	67 3/4	61 3/4	0.297	0.446	HLP-22	12	0	4	1.9	10.5	5.7	30.8	16.1	0.62	0.33	p1d7	2.45	0.0001213	0.0001780	0.0002606	0.4277
7090941	11/20B1	34S_4p1d7Ya-04	33 7/8	S	9	4437.4	67 3/4	61 3/4	0.297	0.446	HLP-22	12	0	4	1.9	10.5	5.7	30.8	16.1	0.62	0.33	p1d7	2.45	0.0001213	0.0001780	0.0002606	0.4277
7090943	11/20B1	34S_4p1d7Ya-04	33 7/8	S	9	4437.4	67 3/4	61 3/4	0.297	0.446	HLP-22	12	0	4	1.9	10.5	5.7	30.8	16.1	0.62	0.33	p1d7	2.45	0.0001213	0.0001780	0.0002606	0.4277
7090946	11/20B1	34S_4p1d7Ya-04	33 7/8	S	9	4437.4	67 3/4	61 3/4	0.297	0.446	HLP-22	12	0	4	1.9	10.5	5.7	30.8	16.1	0.62	0.33	p1d7	2.45	0.0001213	0.0001780	0.0002606	0.4277
7090949	11/20B1	34S_4p1d7Ya-04	33 7/8	S	9	4437.4	67 3/4	61 3/4	0.297	0.446	HLP-22	12	0	4	1.9	10.5	5.7	30.8	16.1	0.62	0.33	p1d7	2.45	0.0001213	0.0001780	0.0002606	0.4277
7090952	11/20B1	34S_4p1d7Ya-04	33 7/8	S	9	4437.4	67 3/4	61 3/4	0.297	0.446	HLP-22	12	0	4	1.9	10.5	5.7	30.8	16.1	0.62	0.33	p1d7	2.45	0.0001213	0.0001780	0.0002606	0.4277
7090956	11/20B1	34S_4p1d7Ya-04	33 7/8	S	9	4437.4	67 3/4	61 3/4	0.297	0.446	HLP-22	12	0	4	1.9	10.5	5.7	30.8	16.1	0.62	0.33	p1d7	2.45	0.0001213	0.0001780	0.0002606	0.4277
7090958	11/20B1	34S_4p1d7Ya-04	33 7/8	S	9	4437.4	67 3/4	61 3/4	0.297	0.446	HLP-22	12	0	4	1.9	10.5	5.7	30.8	16.1	0.62	0.33	p1d7	2.45	0.0001213	0.0001780	0.0002606	0.4277
7090962	11/20B2	34S_4p1d7Yd_9	33 7/8	S	9	4437.4	67 3/4	61 3/4	0.297	0.446	HLP-22	12	0	4	1.9	10.5	5.7	30.8	16.1	0.62	0.33	p1d7	2.45	0.0001213	0.0001780	0.0002606	0.4277
7090965	11/20B2	34S_4p1d7Yd_9	33 7/8	S	9	4437.4	67 3/4	61 3/4	0.297	0.446	HLP-22	12	0	4	1.9	10.5	5.7	30.8	16.1	0.62	0.33	p1d7	2.45	0.0001213	0.0001780	0.0002606	0.4277
7090967	11/20B2	34S_4p1d7Yd_9	33 7/8	S	9	4437.4	67 3/4	61 3/4	0.297	0.446	HLP-22	12	0	4	1.9	10.5	5.7	30.8	16.1	0.62	0.33	p1d7	2.45	0.0001213	0.0001780	0.0002606	0.4277
7090970	11/20B2	34S_4p1d7Yd_9	33 7/8	S	9	4437.4	67 3/4	61 3/4	0.297	0.446	HLP-22	12	0	4	1.9	10.5	5.7	30.8	16.1	0.62	0.33	p1d7	2.45	0.0001213	0.0001780	0.0002606	0.4277
7090973	11/20B2	34S_4p1d7Yd_9	33 7/8	S	9	4437.4	67 3/4	61 3/4	0.297	0.446	HLP-22	12	0	4	1.9	10.5	5.7	30.8	16.1	0.62	0.33	p1d7	2.45	0.0001213	0.0001780	0.0002606	0.4277
7090977M	11/20B2	34S_4p1d7Yd_9	33 7/8	S	9	4437.4	67 3/4	61 3/4	0.297	0.446	HLP-22	12	0	4	1.9	10.5	5.7	30.8	16.1	0.62	0.33	p1d7	2.45	0.0001213	0.0001780	0.0002606	0.4277
7090979M	11/20B2	34S_4p1d7Yd_9	33 7/8	S	9	4437.4	67 3/4	61 3/4	0.297	0.446	HLP-22	12	0	4	1.9	10.5	5.7	30.8	16.1	0.62	0.33	p1d7	2.45	0.0001213	0.0001780	0.0002606	0.4277
7090982	11/26A1	34S_4p1d7Ya-40	33 7/8	S	9	4437.4	67 3/4	61 3/4	0.297	0.446	HLP-22	12	4	0	1.9	10.5	5.7	30.8	16.1	0.62	0.33	p1d7	2.45	0.0001213	0.0001780	0.0002606	0.4277
7090985	11/26A1	34S_4p1d7Ya-40	33 7/8	S	9	4437.4	67 3/4	61 3/4	0.297	0.446	HLP-22	12	4	0	1.9	10.5	5.7	30.8	16.1	0.62	0.33	p1d7	2.45	0.0001213	0.0001780	0.0002606	0.4277
7090989	11/26A1	34S_4p1d7Ya-40	33 7/8	S	9	4437.4	67 3/4	61 3/4	0.297	0.446	HLP-22	12	4	0	1.9	10.5	5.7	30.8	16.1	0.62	0.33	p1d7	2.45	0.0001213	0.0001780	0.0002606	0.4277
7090991	11/26A1	34S_4p1d7Ya-40	33 7/8	S	9	4437.4	67 3/4	61 3/4	0.297	0.446	HLP-22	12	4	0	1.9	10.5	5.7	30.8	16.1	0.62	0.33	p1d7	2.45	0.0001213	0.0001780	0.0002606	0.4277
7090994	11/26A1	34S_4p1d7Ya-40	33 7/8	S	9	4437.4	67 3/4	61 3/4	0.297	0.446	HLP-22	12	4	0	1.9	10.5	5.7	30.8	16.1	0.62	0.33	p1d7	2.45	0.0001213	0.0001780	0.0002606	0.4277
7090996	11/26A1	34S_4p1d7Ya-40	33 7/8	S	9	4437.4	67 3/4	61 3/4	0.297	0.446	HLP-22	12	4	0	1.9	10.5	5.7	30.8	16.1	0.62	0.33	p1d7	2.45	0.0001213	0.0001780	0.0002606	0.4277
7090998	11/26A1	34S_4p1d7Ya-40	33 7/8	S	9	4437.4	67 3/4	61 3/4	0.297	0.446	HLP-22	12	4	0	1.9	10.5	5.7	30.8	16.1	0.62	0.33	p1d7	2.45	0.0001213	0.0001780	0.0002606	0.4277

Table B.8. Data from Fall 2007 Tests in Mid-Scale Vessel with Spherical Head B.8

Tank Water Temperature	Water Density	Solids Fraction	Pulse Volume Fraction	Duty Cycle	Cycle Time	Pulsed or Steady Jet	Us Steady Jet	U1 Pulsing Jet	U2 URMS	U3 URM3	Discharge Velocity	Critical Suspension Velocity	Average Peak Cloud Height	UCS Condition	UCS Method	UCS Flag	UCS Center Flag	UCS udv Flag	UCS based on Decreasing Velocity	Sweep Increase / Decrease	UDV Height Bed	Particle Motion	Solids Level	Outer Bottom Pattern	Inner Bottom Pattern	Case ID	Test	TDP	Row Number
C	g/cm³	fraction	fraction	fraction	s	text	m/s	m/s	m/s	m/s	m/s	m/s	in.	m/s	text	text	text	text	m/s	text	mm	text	text	text	text	text	text	text	text
T	ρ_l	ϕ_S	ϕ_P	DC	t_C	Jet	U_S	U1	U2	U3	U	U_{CS}	H_C	U_{CSR}	U_{CSM}	U_{CS}vis	U_{CS}cen	U_{CS}udv	U_{CS}_D	S_W	H_{bed}	PM	Sol	SP_O	SP_I	ID	M/DDX	TDP	MSS
21.4	0.999	0.00487	undefined	1.000	infinite	S	5.55	N/A	N/A	N/A	5.50	8.50	N/A	N/A	N/A	N/A	UCScen	N/A	N/A	I	N/A	SS+	N/A	N/A	N/A	34S_4p1d7Ya-44	11/20A1	TDP-WTP-055	7090881
21.4	0.999	0.00487	undefined	1.000	infinite	S	6.04	N/A	N/A	N/A	6.00	8.50	N/A	N/A	N/A	N/A	N/A	N/A	N/A	I	N/A	AM	N/A	N/A	N/A	34S_4p1d7Ya-44	11/20A1	TDP-WTP-055	7090883
21.5	0.999	0.00487	undefined	1.000	infinite	S	6.53	N/A	N/A	N/A	6.50	8.50	8.75	N/A	N/A	N/A	N/A	N/A	N/A	I	N/A	AM	N/A	N/A	N/A	34S_4p1d7Ya-44	11/20A1	TDP-WTP-055	7090886
21.5	0.999	0.00487	undefined	1.000	infinite	S	7.06	N/A	N/A	N/A	7.00	8.50	10.00	N/A	N/A	N/A	N/A	N/A	N/A	I	N/A	AM	N/A	N/A	N/A	34S_4p1d7Ya-44	11/20A1	TDP-WTP-055	7090889
21.5	0.999	0.00487	undefined	1.000	infinite	S	7.55	N/A	N/A	N/A	7.50	8.50	13.25	N/A	N/A	N/A	N/A	N/A	N/A	I	N/A	AM+	N/A	N/A	N/A	34S_4p1d7Ya-44	11/20A1	TDP-WTP-055	7090892
21.5	0.999	0.00487	undefined	1.000	infinite	S	8.05	N/A	N/A	N/A	8.00	8.50	20.50	N/A	N/A	N/A	N/A	N/A	N/A	I	N/A	AM+	N/A	N/A	N/A	34S_4p1d7Ya-44	11/20A1	TDP-WTP-055	7090895
21.5	0.999	0.00487	undefined	1.000	infinite	S	8.60	N/A	N/A	N/A	8.50	8.50	30.00	8.50	vis	UCSvis	N/A	N/A	N/A	I	N/A	CS	N/A	N/A	N/A	34S_4p1d7Ya-44	11/20A1	TDP-WTP-055	7090899
21.6	0.999	0.00487	undefined	1.000	infinite	S	9.03	N/A	N/A	N/A	9.00	8.50	36.75	N/A	N/A	N/A	N/A	N/A	N/A	I	N/A	BC-	N/A	N/A	N/A	34S_4p1d7Ya-44	11/20A1	TDP-WTP-055	7090901
22.0	0.999	0.00487	0.049	0.180	71.0	P	N/A	5.58	5.64	5.68	5.50	11.00	N/A	N/A	center dec	N/A	UCScen	N/A	5.50	D	N/A	SS	N/A	N/A	N/A	34S_4p1d7Yd_0	11/20A2	TDP-WTP-055	7090905
22.0	0.999	0.00487	0.051	0.180	64.5	P	N/A	6.10	6.18	6.23	6.00	11.00	N/A	N/A	N/A	N/A	N/A	N/A	N/A	I	N/A	AM-	N/A	N/A	N/A	34S_4p1d7Yd_0	11/20A2	TDP-WTP-055	7090908
22.0	0.999	0.00487	0.051	0.180	55.0	P	N/A	7.10	7.21	7.27	7.00	11.00	9.25	N/A	N/A	N/A	N/A	N/A	N/A	I	N/A	AM	N/A	N/A	N/A	34S_4p1d7Yd_0	11/20A2	TDP-WTP-055	7090910
22.0	0.999	0.00487	0.051	0.180	47.0	P	N/A	8.11	8.26	8.35	8.00	11.00	11.25	N/A	N/A	N/A	N/A	N/A	N/A	I	N/A	AM	N/A	N/A	N/A	34S_4p1d7Yd_0	11/20A2	TDP-WTP-055	7090913
22.0	0.999	0.00487	0.050	0.180	44.5	P	N/A	8.18	8.50	8.65	8.50	11.00	12.00	N/A	N/A	N/A	N/A	N/A	N/A	I	N/A	AM	N/A	N/A	N/A	34S_4p1d7Yd_0	11/20A2	TDP-WTP-055	7090916
22.0	0.999	0.00487	0.051	0.180	41.5	P	N/A	8.46	8.92	9.14	9.00	11.00	14.25	N/A	N/A	N/A	N/A	N/A	N/A	I	N/A	AM	N/A	N/A	N/A	34S_4p1d7Yd_0	11/20A2	TDP-WTP-055	7090919
22.0	0.999	0.00487	0.051	0.180	40.0	P	N/A	9.02	9.44	9.64	9.50	11.00	15.75	N/A	N/A	N/A	N/A	N/A	N/A	I	N/A	AM+	N/A	N/A	N/A	34S_4p1d7Yd_0	11/20A2	TDP-WTP-055	7090922
22.0	0.999	0.00487	0.051	0.180	37.5	P	N/A	9.33	9.85	10.09	10.00	11.00	16.63	N/A	N/A	N/A	N/A	N/A	N/A	I	N/A	AM+	N/A	N/A	N/A	34S_4p1d7Yd_0	11/20A2	TDP-WTP-055	7090925
22.0	0.999	0.00487	0.051	0.180	35.5	P	N/A	9.57	10.20	10.50	10.50	11.00	19.00	N/A	N/A	N/A	N/A	N/A	N/A	I	N/A	AM+	N/A	N/A	N/A	34S_4p1d7Yd_0	11/20A2	TDP-WTP-055	7090928
22.0	0.999	0.00487	0.050	0.180	33.5	P	N/A	9.80	10.56	10.92	11.00	11.00	19.50	11.00	vis	UCSvis	N/A	N/A	N/A	I	N/A	CS	N/A	N/A	N/A	34S_4p1d7Yd_0	11/20A2	TDP-WTP-055	7090932
22.0	0.999	0.00487	0.050	0.180	30.7	P	N/A	11.69	12.18	12.43	12.00	11.00	22.00	N/A	N/A	N/A	N/A	N/A	N/A	I	N/A	BC	N/A	N/A	N/A	34S_4p1d7Yd_0	11/20A2	TDP-WTP-055	7090934
22.2	0.999	0.00487	undefined	1.000	infinite	S	6.02	N/A	N/A	N/A	6.00	12.00	N/A	N/A	N/A	N/A	UCScen	N/A	N/A	I	N/A	SS	N/A	N/A	N/A	34S_4p1d7Ya-04	11/20B1	TDP-WTP-055	7090938
22.2	0.999	0.00487	undefined	1.000	infinite	S	7.01	N/A	N/A	N/A	7.00	12.00	8.75	N/A	N/A	N/A	N/A	N/A	N/A	I	N/A	SS+	N/A	N/A	N/A	34S_4p1d7Ya-04	11/20B1	TDP-WTP-055	7090941
22.3	0.999	0.00487	undefined	1.000	infinite	S	7.98	N/A	N/A	N/A	8.00	12.00	10.50	N/A	N/A	N/A	N/A	N/A	N/A	I	N/A	AM	N/A	N/A	N/A	34S_4p1d7Ya-04	11/20B1	TDP-WTP-055	7090943
22.3	0.999	0.00487	undefined	1.000	infinite	S	9.01	N/A	N/A	N/A	9.00	12.00	13.25	N/A	N/A	N/A	N/A	N/A	N/A	I	N/A	AM	N/A	N/A	N/A	34S_4p1d7Ya-04	11/20B1	TDP-WTP-055	7090946
22.3	0.999	0.00487	undefined	1.000	infinite	S	10.06	N/A	N/A	N/A	10.00	12.00	16.50	N/A	N/A	N/A	N/A	N/A	N/A	I	N/A	AM	N/A	N/A	N/A	34S_4p1d7Ya-04	11/20B1	TDP-WTP-055	7090949
22.2	0.999	0.00487	undefined	1.000	infinite	S	11.05	N/A	N/A	N/A	11.00	12.00	21.00	N/A	N/A	N/A	N/A	N/A	N/A	I	N/A	AM+	N/A	N/A	N/A	34S_4p1d7Ya-04	11/20B1	TDP-WTP-055	7090952
22.3	0.999	0.00487	undefined	1.000	infinite	S	12.11	N/A	N/A	N/A	12.00	12.00	29.50	12.00	vis	UCSvis	N/A	N/A	N/A	I	N/A	CS	N/A	N/A	N/A	34S_4p1d7Ya-04	11/20B1	TDP-WTP-055	7090956
22.3	0.999	0.00487	undefined	1.000	infinite	S	13.06	N/A	N/A	N/A	13.00	12.00	39.25	N/A	N/A	N/A	N/A	N/A	N/A	I	N/A	BC	N/A	N/A	N/A	34S_4p1d7Ya-04	11/20B1	TDP-WTP-055	7090958
22.0	0.999	0.00487	0.052	0.180	100.0	P	N/A	8.15	8.32	8.54	7.70	14.00	10.00	N/A	N/A	N/A	N/A	N/A	N/A	D	N/A	SS	N/A	N/A	N/A	34S_4p1d7Yd_9	11/20B2	TDP-WTP-055	7090962
22.0	0.999	0.00487	0.051	0.180	85.5	P	N/A	9.31	9.52	9.77	9.00	14.00	12.75	N/A	N/A	N/A	N/A	N/A	N/A	I	N/A	SS+	N/A	N/A	N/A	34S_4p1d7Yd_9	11/20B2	TDP-WTP-055	7090965
22.0	0.999	0.00487	0.052	0.180	77.0	P	N/A	10.37	10.61	10.90	10.00	14.00	15.50	N/A	N/A	N/A	N/A	N/A	N/A	I	N/A	AM	N/A	N/A	N/A	34S_4p1d7Yd_9	11/20B2	TDP-WTP-055	7090967
22.0	0.999	0.00487	0.052	0.180	63.5	P	N/A	12.50	12.81	13.16	12.00	14.00	18.75	N/A	N/A	N/A	N/A	N/A	N/A	I	N/A	AM	N/A	N/A	N/A	34S_4p1d7Yd_9	11/20B2	TDP-WTP-055	7090970
22.0	0.999	0.00487	0.051	0.180	57.5	P	N/A	13.57	13.92	14.31	13.00	14.00	20.50	N/A	N/A	N/A	N/A	N/A	N/A	I	N/A	AM+	N/A	N/A	N/A	34S_4p1d7Yd_9	11/20B2	TDP-WTP-055	7090973
22.0	0.999	0.00487	0.051	0.180	53.3	P	N/A	14.55	14.97	15.40	14.00	14.00	23.00	14.00	vis	UCSvis	N/A	N/A	N/A	I	N/A	CS	N/A	N/A	N/A	34S_4p1d7Yd_9	11/20B2	TDP-WTP-055	7090977
22.0	0.999	0.00487	0.051	0.180	48.5	P	N/A	15.90	16.35	16.84	15.00	14.00	26.25	N/A	N/A	N/A	N/A	N/A	N/A	I	N/A	BC	N/A	N/A	N/A	34S_4p1d7Yd_9	11/20B2	TDP-WTP-055	7090979
20.5	0.999	0.00487	undefined	1.000	infinite	S	9.06	N/A	N/A	N/A	9.00	9.50	N/A	N/A	N/A	N/A	N/A	N/A	N/A	I	N/A	SS+	N/A	N/A	N/A	34S_4p1d7Ya-40	11/26A1	TDP-WTP-064	7090982
20.5	0.999	0.00487	undefined	1.000	infinite	S	10.06	N/A	N/A	N/A	10.00	9.50	21.50	N/A	N/A	N/A	N/A	N/A	N/A	I	N/A	BC	N/A	N/A	N/A	34S_4p1d7Ya-40	11/26A1	TDP-WTP-064	7090985
20.5	0.999	0.00487	undefined	1.000	infinite	S	9.62	N/A	N/A	N/A	9.50	9.50	17.50	N/A	vis dec	UCSvis	N/A	N/A	9.50	D	N/A	CS	N/A	N/A	N/A	34S_4p1d7Ya-40	11/26A1	TDP-WTP-064	7090989
20.5	0.999	0.00487	undefined	1.000	infinite	S	9.03	N/A	N/A	N/A	9.00	9.50	N/A	N/A	N/A	N/A	N/A	N/A	N/A	D	N/A	SS+	N/A	N/A	N/A	34S_4p1d7Ya-40	11/26A1	TDP-WTP-064	7090991
20.6	0.999	0.00487	undefined	1.000	infinite	S	9.42	N/A	N/A	N/A	9.25	9.50	9.25	N/A	N/A	N/A	N/A	N/A	N/A	I	N/A	AM	N/A	N/A	N/A	34S_4p1d7Ya-40	11/26A1	TDP-WTP-064	7090994
20.6	0.999	0.00487	undefined	1.000	infinite	S	9.42	N/A	N/A	N/A	9.30	9.50	9.25	N/A	N/A	N/A	N/A	N/A	N/A	I	N/A	N/A	N/A	N/A	N/A	34S_4p1d7Ya-40	11/26A1	TDP-WTP-064	7090996
20.5	0.999	0.00487	undefined	1.000	infinite	S	9.60	N/A	N/A	N/A	9.50	9.50	13.75	9.50	vis	UCSvis	N/A	N/A	N/A	I	N/A	CS	N/A	N/A	N/A	34S_4p1d7Ya-40	11/26A1	TDP-WTP-064	7090998

Table B.8. Data from Fall 2007 Tests in Mid-Scale Vessel with Spherical Head A.9

Row Number	Test	Case ID	Tank Diameter	Head Shape	Dish Height	Dish Volume	Tank Fill Height	Return Line Height	Nozzle Inner Diameter	Nozzle Stand-off Distance	Pulse Tube Configuration	Installed Nozzles	Outer Nozzles Operated	Inner Nozzles Operated	Pulse Tube Outer Diameter	Outer PJM Radius	Inner PJM Radius	"FIO" Outer PJM Impingement Angle	"FIO" Inner PJM Impingement Angle	Ratio Outer PJM to Tank Radius	Ratio Inner PJM to Tank Radius	Simulant	Solids Density	Particle Diameter d5	Particle Diameter d50	Particle Diameter d95	Void Fraction
text	text	text	in.	text	in.	in. ^{3}	in.	in.	in.	in.	text	number	number	number	in.	in.	in.	deg	deg	nondim	nondim	text	g/cm^3	m	m	m	fraction
MSS	M/DDX	ID	D	HS	H_{dish}	V_{dish}	H	Rtn	d	sod	PT	N	N_O	N_I	PT_{od}	R_O	R_I	θ_O	θ_I	R_O/R	R_I/R	sxdx	ρ_s	d_5	d_{50}	d_{95}	vf
7091000	11/26A1	34S_4p1d7Ya-40	33 7/8	S	9	4437.4	67 3/4	61 3/4	0.297	0.446	HLP-22	12	4	0	1.9	10.5	5.7	30.8	16.1	0.62	0.33	p1d7	2.45	0.0001213	0.0001780	0.0002606	0.4277
7091003	11/26A2	34S_4p1d7Yd_6	33 7/8	S	9	4437.4	67 3/4	61 3/4	0.297	0.446	HLP-22	12	4	0	1.9	10.5	5.7	30.8	16.1	0.62	0.33	p1d7	2.45	0.0001213	0.0001780	0.0002606	0.4277
7091006	11/26A2	34S_4p1d7Yd_6	33 7/8	S	9	4437.4	67 3/4	61 3/4	0.297	0.446	HLP-22	12	4	0	1.9	10.5	5.7	30.8	16.1	0.62	0.33	p1d7	2.45	0.0001213	0.0001780	0.0002606	0.4277
7091010M	11/26A2	34S_4p1d7Yd_6	33 7/8	S	9	4437.4	67 3/4	61 3/4	0.297	0.446	HLP-22	12	4	0	1.9	10.5	5.7	30.8	16.1	0.62	0.33	p1d7	2.45	0.0001213	0.0001780	0.0002606	0.4277
7091012M	11/26A2	34S_4p1d7Yd_6	33 7/8	S	9	4437.4	67 3/4	61 3/4	0.297	0.446	HLP-22	12	4	0	1.9	10.5	5.7	30.8	16.1	0.62	0.33	p1d7	2.45	0.0001213	0.0001780	0.0002606	0.4277
7091015M	11/26A2	34S_4p1d7Yd_6	33 7/8	S	9	4437.4	67 3/4	61 3/4	0.297	0.446	HLP-22	12	4	0	1.9	10.5	5.7	30.8	16.1	0.62	0.33	p1d7	2.45	0.0001213	0.0001780	0.0002606	0.4277
7091018	11/26B1	34S_4p1d7Yc_1	33 7/8	S	9	4437.4	67 3/4	61 3/4	0.297	0.446	HLP-22	12	8	4	1.9	10.5	5.7	30.8	16.1	0.62	0.33	p1d7	2.45	0.0001213	0.0001780	0.0002606	0.4277
7091022	11/26B1	34S_4p1d7Yc_1	33 7/8	S	9	4437.4	67 3/4	61 3/4	0.297	0.446	HLP-22	12	8	4	1.9	10.5	5.7	30.8	16.1	0.62	0.33	p1d7	2.45	0.0001213	0.0001780	0.0002606	0.4277
7091025M	11/26B1	34S_4p1d7Yc_1	33 7/8	S	9	4437.4	67 3/4	61 3/4	0.297	0.446	HLP-22	12	8	4	1.9	10.5	5.7	30.8	16.1	0.62	0.33	p1d7	2.45	0.0001213	0.0001780	0.0002606	0.4277
7091027M	11/26B1	34S_4p1d7Yc_1	33 7/8	S	9	4437.4	67 3/4	61 3/4	0.297	0.446	HLP-22	12	8	4	1.9	10.5	5.7	30.8	16.1	0.62	0.33	p1d7	2.45	0.0001213	0.0001780	0.0002606	0.4277
7091030	11/26C1	34S_4p1d7Yc_0	33 7/8	S	9	4437.4	67 3/4	61 3/4	0.297	0.446	HLP-22	12	4	4	1.9	10.5	5.7	30.8	16.1	0.62	0.33	p1d7	2.45	0.0001213	0.0001780	0.0002606	0.4277
7091033	11/26C1	34S_4p1d7Yc_0	33 7/8	S	9	4437.4	67 3/4	61 3/4	0.297	0.446	HLP-22	12	4	4	1.9	10.5	5.7	30.8	16.1	0.62	0.33	p1d7	2.45	0.0001213	0.0001780	0.0002606	0.4277
7091036	11/26C1	34S_4p1d7Yc_0	33 7/8	S	9	4437.4	67 3/4	61 3/4	0.297	0.446	HLP-22	12	4	4	1.9	10.5	5.7	30.8	16.1	0.62	0.33	p1d7	2.45	0.0001213	0.0001780	0.0002606	0.4277
7091039	11/26C1	34S_4p1d7Yc_0	33 7/8	S	9	4437.4	67 3/4	61 3/4	0.297	0.446	HLP-22	12	4	4	1.9	10.5	5.7	30.8	16.1	0.62	0.33	p1d7	2.45	0.0001213	0.0001780	0.0002606	0.4277
7091042	11/26C1	34S_4p1d7Yc_0	33 7/8	S	9	4437.4	67 3/4	61 3/4	0.297	0.446	HLP-22	12	4	4	1.9	10.5	5.7	30.8	16.1	0.62	0.33	p1d7	2.45	0.0001213	0.0001780	0.0002606	0.4277
7091046M	11/26C1	34S_4p1d7Yc_0	33 7/8	S	9	4437.4	67 3/4	61 3/4	0.297	0.446	HLP-22	12	4	4	1.9	10.5	5.7	30.8	16.1	0.62	0.33	p1d7	2.45	0.0001213	0.0001780	0.0002606	0.4277
7091048M	11/26C1	34S_4p1d7Yc_0	33 7/8	S	9	4437.4	67 3/4	61 3/4	0.297	0.446	HLP-22	12	4	4	1.9	10.5	5.7	30.8	16.1	0.62	0.33	p1d7	2.45	0.0001213	0.0001780	0.0002606	0.4277
7091052	11/26D1	34S_4p1d7Yd_9	33 7/8	S	9	4437.4	67 3/4	61 3/4	0.297	0.446	HLP-22	12	0	4	1.9	10.5	5.7	30.8	16.1	0.62	0.33	p1d7	2.45	0.0001213	0.0001780	0.0002606	0.4277
7091055	11/26D2	34S_4p1d7Yc_9	33 7/8	S	9	4437.4	67 3/4	61 3/4	0.297	0.446	HLP-22	12	0	4	1.9	10.5	5.7	30.8	16.1	0.62	0.33	p1d7	2.45	0.0001213	0.0001780	0.0002606	0.4277
7091058	11/26D2	34S_4p1d7Yc_9	33 7/8	S	9	4437.4	67 3/4	61 3/4	0.297	0.446	HLP-22	12	0	4	1.9	10.5	5.7	30.8	16.1	0.62	0.33	p1d7	2.45	0.0001213	0.0001780	0.0002606	0.4277
7091063	11/26D2	34S_4p1d7Yc_9	33 7/8	S	9	4437.4	67 3/4	61 3/4	0.297	0.446	HLP-22	12	0	4	1.9	10.5	5.7	30.8	16.1	0.62	0.33	p1d7	2.45	0.0001213	0.0001780	0.0002606	0.4277
7091065	11/26D2	34S_4p1d7Yc_9	33 7/8	S	9	4437.4	67 3/4	61 3/4	0.297	0.446	HLP-22	12	0	4	1.9	10.5	5.7	30.8	16.1	0.62	0.33	p1d7	2.45	0.0001213	0.0001780	0.0002606	0.4277
7091070	11/26D2	34S_4p1d7Yc_9	33 7/8	S	9	4437.4	67 3/4	61 3/4	0.297	0.446	HLP-22	12	0	4	1.9	10.5	5.7	30.8	16.1	0.62	0.33	p1d7	2.45	0.0001213	0.0001780	0.0002606	0.4277
7091075M	11/26D2	34S_4p1d7Yc_9	33 7/8	S	9	4437.4	67 3/4	61 3/4	0.297	0.446	HLP-22	12	0	4	1.9	10.5	5.7	30.8	16.1	0.62	0.33	p1d7	2.45	0.0001213	0.0001780	0.0002606	0.4277
7091077M	11/26D2	34S_4p1d7Yc_9	33 7/8	S	9	4437.4	67 3/4	61 3/4	0.297	0.446	HLP-22	12	0	4	1.9	10.5	5.7	30.8	16.1	0.62	0.33	p1d7	2.45	0.0001213	0.0001780	0.0002606	0.4277
7091081M	11/26D2	34S_4p1d7Yc_9	33 7/8	S	9	4437.4	67 3/4	61 3/4	0.297	0.446	HLP-22	12	0	4	1.9	10.5	5.7	30.8	16.1	0.62	0.33	p1d7	2.45	0.0001213	0.0001780	0.0002606	0.4277
7091085	11/27A1	34S_4p1d7Yc_6	33 7/8	S	9	4437.4	67 3/4	61 3/4	0.297	0.446	HLP-22	12	4	0	1.9	10.5	5.7	30.8	16.1	0.62	0.33	p1d7	2.45	0.0001213	0.0001780	0.0002606	0.4277
7091088	11/27A1	34S_4p1d7Yc_6	33 7/8	S	9	4437.4	67 3/4	61 3/4	0.297	0.446	HLP-22	12	4	0	1.9	10.5	5.7	30.8	16.1	0.62	0.33	p1d7	2.45	0.0001213	0.0001780	0.0002606	0.4277
7091091	11/27A1	34S_4p1d7Yc_6	33 7/8	S	9	4437.4	67 3/4	61 3/4	0.297	0.446	HLP-22	12	4	0	1.9	10.5	5.7	30.8	16.1	0.62	0.33	p1d7	2.45	0.0001213	0.0001780	0.0002606	0.4277
7091095M	11/27A1	34S_4p1d7Yc_6	33 7/8	S	9	4437.4	67 3/4	61 3/4	0.297	0.446	HLP-22	12	4	0	1.9	10.5	5.7	30.8	16.1	0.62	0.33	p1d7	2.45	0.0001213	0.0001780	0.0002606	0.4277
7091097M	11/27A1	34S_4p1d7Yc_6	33 7/8	S	9	4437.4	67 3/4	61 3/4	0.297	0.446	HLP-22	12	4	0	1.9	10.5	5.7	30.8	16.1	0.62	0.33	p1d7	2.45	0.0001213	0.0001780	0.0002606	0.4277
7091100	11/27B1	34S_4p1d7Ya-80	33 7/8	S	9	4437.4	67 3/4	61 3/4	0.297	0.446	HLP-22	12	8	0	1.9	10.5	5.7	30.8	16.1	0.62	0.33	p1d7	2.45	0.0001213	0.0001780	0.0002606	0.4277
7091103	11/27B1	34S_4p1d7Ya-80	33 7/8	S	9	4437.4	67 3/4	61 3/4	0.297	0.446	HLP-22	12	8	0	1.9	10.5	5.7	30.8	16.1	0.62	0.33	p1d7	2.45	0.0001213	0.0001780	0.0002606	0.4277
7091106	11/27B1	34S_4p1d7Ya-80	33 7/8	S	9	4437.4	67 3/4	61 3/4	0.297	0.446	HLP-22	12	8	0	1.9	10.5	5.7	30.8	16.1	0.62	0.33	p1d7	2.45	0.0001213	0.0001780	0.0002606	0.4277
7091109	11/27B1	34S_4p1d7Ya-80	33 7/8	S	9	4437.4	67 3/4	61 3/4	0.297	0.446	HLP-22	12	8	0	1.9	10.5	5.7	30.8	16.1	0.62	0.33	p1d7	2.45	0.0001213	0.0001780	0.0002606	0.4277
7091113	11/27B1	34S_4p1d7Ya-80	33 7/8	S	9	4437.4	67 3/4	61 3/4	0.297	0.446	HLP-22	12	8	0	1.9	10.5	5.7	30.8	16.1	0.62	0.33	p1d7	2.45	0.0001213	0.0001780	0.0002606	0.4277
7091115	11/27B1	34S_4p1d7Ya-80	33 7/8	S	9	4437.4	67 3/4	61 3/4	0.297	0.446	HLP-22	12	8	0	1.9	10.5	5.7	30.8	16.1	0.62	0.33	p1d7	2.45	0.0001213	0.0001780	0.0002606	0.4277
7091118	11/27B2	34S_4p1d7Yd_5	33 7/8	S	9	4437.4	67 3/4	61 3/4	0.297	0.446	HLP-22	12	8	0	1.9	10.5	5.7	30.8	16.1	0.62	0.33	p1d7	2.45	0.0001213	0.0001780	0.0002606	0.4277
7091121	11/27B2	34S_4p1d7Yd_5	33 7/8	S	9	4437.4	67 3/4	61 3/4	0.297	0.446	HLP-22	12	8	0	1.9	10.5	5.7	30.8	16.1	0.62	0.33	p1d7	2.45	0.0001213	0.0001780	0.0002606	0.4277
7091124	11/27B2	34S_4p1d7Yd_5	33 7/8	S	9	4437.4	67 3/4	61 3/4	0.297	0.446	HLP-22	12	8	0	1.9	10.5	5.7	30.8	16.1	0.62	0.33	p1d7	2.45	0.0001213	0.0001780	0.0002606	0.4277
7091127	11/27B2	34S_4p1d7Yd_5	33 7/8	S	9	4437.4	67 3/4	61 3/4	0.297	0.446	HLP-22	12	8	0	1.9	10.5	5.7	30.8	16.1	0.62	0.33	p1d7	2.45	0.0001213	0.0001780	0.0002606	0.4277

Table B.8. Data from Fall 2007 Tests in Mid-Scale Vessel with Spherical Head B.9

Tank Water Temperature	Water Density	Solids Fraction	Pulse Volume Fraction	Duty Cycle	Cycle Time	Pulsed or Steady Jet	Us Steady Jet	U1 Pulsing Jet	U2 URMS	U3 URM3	Discharge Velocity	Critical Suspension Velocity	Average Peak Cloud Height	UCS Condition	UCS Method	UCS Flag	UCS Center Flag	UCS udv Flag	UCS based on Decreasing Velocity	Sweep Increase / Decrease	UDV Height Bed	Particle Motion	Solids Level	Outer Bottom Pattern	Inner Bottom Pattern	Case ID	Test	TDP	Row Number
C	g/cm³	fraction	fraction	fraction	s	text	m/s	m/s	m/s	m/s	m/s	m/s	in.	m/s	text	text	text	text	m/s	text	mm	text	text	text	text	text	text	text	text
T	ρ_l	ϕ_s	ϕ_p	DC	t_C	Jet	U_S	U1	U2	U3	U	U_{CS}	H_C	U_{CSR}	U_{CSM}	U_{CS}vis	U_{CS}cen	U_{CS}udv	U_{CS}_D	S_W	H_{bed}	PM	Sol	SP_O	SP_I	ID	M/DDX	TDP	MSS
20.5	0.999	0.00487	undefined	1.000	infinite	S	10.60	N/A	N/A	N/A	10.50	9.50	26.75	N/A	N/A	N/A	N/A	N/A	N/A	I	N/A	BC	N/A	N/A	N/A	34S_4p1d7Ya-40	11/26A1	TDP-WTP-064	7091000
21.0	0.999	0.00487	0.049	0.180	0.0	P	N/A	10.05	10.34	10.66	9.50	10.50	N/A	N/A	N/A	N/A	N/A	N/A	N/A	D	N/A	SS+	N/A	N/A	N/A	34S_4p1d7Yd_6	11/26A2	TDP-WTP-064	7091003
21.0	0.999	0.00487	0.052	0.180	0.0	P	N/A	10.59	10.86	11.17	10.00	10.50	9.50	N/A	N/A	N/A	N/A	N/A	N/A	I	N/A	AM	N/A	N/A	N/A	34S_4p1d7Yd_6	11/26A2	TDP-WTP-064	7091006
21.0	0.999	0.00487	0.052	0.180	0.0	P	N/A	11.15	11.39	11.71	10.50	10.50	12.50	10.50	vis	UCSvis	N/A	N/A	N/A	I	N/A	CS	N/A	N/A	N/A	34S_4p1d7Yd_6	11/26A2	TDP-WTP-064	7091010
21.0	0.999	0.00487	0.052	0.180	0.0	P	N/A	11.50	11.81	12.16	11.00	10.50	15.00	N/A	N/A	N/A	N/A	N/A	N/A	I	N/A	BC-	N/A	N/A	N/A	34S_4p1d7Yd_6	11/26A2	TDP-WTP-064	7091012
21.0	0.999	0.00487	0.051	0.180	0.0	P	N/A	12.21	12.55	12.94	11.50	10.50	16.50	N/A	N/A	N/A	N/A	N/A	N/A	I	N/A	BC	N/A	N/A	N/A	34S_4p1d7Yd_6	11/26A2	TDP-WTP-064	7091015
21.0	0.999	0.00487	0.046	0.330	0.0	P	N/A	4.92	5.00	5.03	5.00	6.50	N/A	N/A	N/A	N/A	N/A	N/A	N/A	D	N/A	SS	N/A	N/A	N/A	34S_4p1d7Yc_1	11/26B1	TDP-WTP-064	7091018
21.0	0.999	0.00487	0.052	0.330	0.0	P	N/A	5.90	5.99	6.03	6.00	6.50	9.25	N/A	N/A	N/A	N/A	N/A	N/A	I	N/A	AM	N/A	N/A	N/A	34S_4p1d7Yc_1	11/26B1	TDP-WTP-064	7091022
21.0	0.999	0.00487	0.051	0.330	0.0	P	N/A	6.31	6.43	6.49	6.50	6.50	9.75	6.50	vis	UCSvis	N/A	N/A	N/A	I	N/A	CS	N/A	N/A	N/A	34S_4p1d7Yc_1	11/26B1	TDP-WTP-064	7091025
21.0	0.999	0.00487	0.051	0.330	0.0	P	N/A	6.82	6.96	7.02	7.00	6.50	11.25	N/A	N/A	N/A	N/A	N/A	N/A	I	N/A	BC	N/A	N/A	N/A	34S_4p1d7Yc_1	11/26B1	TDP-WTP-064	7091027
21.0	0.999	0.00487	0.051	0.330	0.0	P	N/A	6.12	6.20	6.25	6.00	11.00	N/A	N/A	N/A	N/A	UCScen	N/A	N/A	I	N/A	AM-	N/A	N/A	N/A	34S_4p1d7Yc_0	11/26C1	TDP-WTP-064	7091030
21.0	0.999	0.00487	0.051	0.330	0.0	P	N/A	7.04	7.17	7.24	7.00	11.00	9.25	N/A	N/A	N/A	N/A	N/A	N/A	I	N/A	AM	N/A	N/A	N/A	34S_4p1d7Yc_0	11/26C1	TDP-WTP-064	7091033
21.0	0.999	0.00487	0.051	0.330	0.0	P	N/A	8.06	8.21	8.30	8.00	11.00	11.25	N/A	N/A	N/A	N/A	N/A	N/A	I	N/A	AM	N/A	N/A	N/A	34S_4p1d7Yc_0	11/26C1	TDP-WTP-064	7091036
21.0	0.999	0.00487	0.051	0.330	0.0	P	N/A	9.15	9.48	9.65	9.00	11.00	15.00	N/A	N/A	N/A	N/A	N/A	N/A	I	N/A	AM	N/A	N/A	N/A	34S_4p1d7Yc_0	11/26C1	TDP-WTP-064	7091039
21.0	0.999	0.00487	0.051	0.330	0.0	P	N/A	9.36	9.89	10.15	10.00	11.00	18.00	N/A	N/A	N/A	N/A	N/A	N/A	I	N/A	AM+	N/A	N/A	N/A	34S_4p1d7Yc_0	11/26C1	TDP-WTP-064	7091042
21.0	0.999	0.00487	0.051	0.330	0.0	P	N/A	9.83	10.60	10.97	11.00	11.00	21.25	11.00	vis	UCSvis	N/A	N/A	N/A	I	N/A	CS	N/A	N/A	N/A	34S_4p1d7Yc_0	11/26C1	TDP-WTP-064	7091046
21.0	0.999	0.00487	0.052	0.330	0.0	P	N/A	10.81	11.69	12.11	12.00	11.00	27.00	N/A	N/A	N/A	N/A	N/A	N/A	I	N/A	BC	N/A	N/A	N/A	34S_4p1d7Yc_0	11/26C1	TDP-WTP-064	7091048
22.0	0.999	0.00487	0.057	0.180	0.0	P	N/A	5.90	6.04	6.22	5.70	N/A	N/A	N/A	N/A	N/A	UCScen	N/A	N/A	N/A	N/A	SS	N/A	N/A	N/A	34S_4p1d7Yd_9	11/26D1	TDP-WTP-064	7091052
22.0	0.999	0.00487	0.051	0.330	0.0	P	N/A	6.03	6.17	6.35	5.70	13.00	N/A	N/A	N/A	N/A	UCScen	N/A	N/A	I	N/A	SS	N/A	N/A	N/A	34S_4p1d7Yc_9	11/26D2	TDP-WTP-064	7091055
22.0	0.999	0.00487	0.050	0.330	0.0	P	N/A	7.14	7.30	7.52	7.00	13.00	8.75	N/A	N/A	N/A	N/A	N/A	N/A	I	N/A	SS	N/A	N/A	N/A	34S_4p1d7Yc_9	11/26D2	TDP-WTP-064	7091058
22.0	0.999	0.00487	0.050	0.330	0.0	P	N/A	9.23	9.46	9.75	9.00	13.00	12.67	N/A	N/A	N/A	N/A	N/A	N/A	I	N/A	SS	N/A	N/A	N/A	34S_4p1d7Yc_9	11/26D2	TDP-WTP-064	7091063
22.0	0.999	0.00487	0.050	0.330	0.0	P	N/A	11.52	11.83	12.19	11.00	13.00	18.17	N/A	N/A	N/A	N/A	N/A	N/A	I	N/A	AM	N/A	N/A	N/A	34S_4p1d7Yc_9	11/26D2	TDP-WTP-064	7091065
22.0	0.999	0.00487	0.050	0.330	0.0	P	N/A	12.48	12.83	13.24	12.00	13.00	20.00	N/A	N/A	N/A	N/A	N/A	N/A	I	N/A	AM+	N/A	N/A	N/A	34S_4p1d7Yc_9	11/26D2	TDP-WTP-064	7091070
22.0	0.999	0.00487	0.050	0.330	0.0	P	N/A	13.47	13.86	14.30	13.00	13.00	21.33	13.00	vis	UCSvis	N/A	N/A	N/A	I	N/A	CS	N/A	N/A	N/A	34S_4p1d7Yc_9	11/26D2	TDP-WTP-064	7091075
22.0	0.999	0.00487	0.050	0.330	0.0	P	N/A	14.59	15.03	15.54	14.00	13.00	23.83	N/A	N/A	N/A	N/A	N/A	N/A	I	N/A	BC-	N/A	N/A	N/A	34S_4p1d7Yc_9	11/26D2	TDP-WTP-064	7091077
22.0	0.999	0.00487	0.050	0.330	0.0	P	N/A	15.48	16.07	16.67	15.00	13.00	28.83	N/A	N/A	N/A	N/A	N/A	N/A	I	N/A	BC	N/A	N/A	N/A	34S_4p1d7Yc_9	11/26D2	TDP-WTP-064	7091081
22.0	0.999	0.00487	0.052	0.330	0.0	P	N/A	9.50	9.75	10.06	9.00	11.00	8.50	N/A	N/A	N/A	N/A	N/A	N/A	I	N/A	SS	N/A	N/A	N/A	34S_4p1d7Yc_6	11/27A1	TDP-WTP-065	7091085
22.0	0.999	0.00487	0.051	0.330	0.0	P	N/A	10.63	10.89	11.24	10.00	11.00	10.00	N/A	N/A	N/A	N/A	N/A	N/A	I	N/A	AM	N/A	N/A	N/A	34S_4p1d7Yc_6	11/27A1	TDP-WTP-065	7091088
22.0	0.999	0.00487	0.051	0.330	0.0	P	N/A	11.08	11.39	11.77	10.50	11.00	11.50	N/A	N/A	N/A	UCScen	N/A	N/A	I	N/A	AM+	N/A	N/A	N/A	34S_4p1d7Yc_6	11/27A1	TDP-WTP-065	7091091
22.0	0.999	0.00487	0.051	0.330	0.0	P	N/A	11.77	12.08	12.47	11.00	11.00	14.25	11.00	vis	UCSvis	N/A	N/A	N/A	I	N/A	CS	N/A	N/A	N/A	34S_4p1d7Yc_6	11/27A1	TDP-WTP-065	7091095
22.0	0.999	0.00487	0.051	0.330	0.0	P	N/A	12.68	13.01	13.44	12.00	11.00	20.00	N/A	N/A	N/A	N/A	N/A	N/A	I	N/A	BC	N/A	N/A	N/A	34S_4p1d7Yc_6	11/27A1	TDP-WTP-065	7091097
21.9	0.999	0.00487	undefined	1.000	infinite	S	7.57	N/A	N/A	N/A	7.50	9.50	8.75	N/A	N/A	N/A	N/A	N/A	N/A	N/A	N/A	SS	N/A	N/A	N/A	34S_4p1d7Ya-80	11/27B1	TDP-WTP-065	7091100
21.8	0.999	0.00487	undefined	1.000	infinite	S	8.11	N/A	N/A	N/A	8.00	9.50	9.00	N/A	N/A	N/A	N/A	N/A	N/A	I	N/A	SS	N/A	N/A	N/A	34S_4p1d7Ya-80	11/27B1	TDP-WTP-065	7091103
21.8	0.999	0.00487	undefined	1.000	infinite	S	8.53	N/A	N/A	N/A	8.50	9.50	10.50	N/A	N/A	N/A	N/A	N/A	N/A	I	N/A	SS	N/A	N/A	N/A	34S_4p1d7Ya-80	11/27B1	TDP-WTP-065	7091106
21.9	0.999	0.00487	undefined	1.000	infinite	S	9.06	N/A	N/A	N/A	9.00	9.50	18.63	N/A	N/A	N/A	N/A	N/A	N/A	I	N/A	AM	N/A	N/A	N/A	34S_4p1d7Ya-80	11/27B1	TDP-WTP-065	7091109
21.9	0.999	0.00487	undefined	1.000	infinite	S	9.57	N/A	N/A	N/A	9.50	9.50	29.25	9.50	vis	UCSvis	N/A	N/A	N/A	I	N/A	CS	N/A	N/A	N/A	34S_4p1d7Ya-80	11/27B1	TDP-WTP-065	7091113
21.8	0.999	0.00487	undefined	1.000	infinite	S	10.01	N/A	N/A	N/A	10.00	9.50	38.50	N/A	N/A	N/A	N/A	N/A	N/A	I	N/A	BC	N/A	N/A	N/A	34S_4p1d7Ya-80	11/27B1	TDP-WTP-065	7091115
22.0	0.999	0.00487	0.053	0.180	0.0	P	N/A	7.06	7.15	7.20	7.00	10.00	9.00	N/A	N/A	N/A	N/A	N/A	N/A	N/A	N/A	SS	N/A	N/A	N/A	34S_4p1d7Yd_5	11/27B2	TDP-WTP-065	7091118
22.0	0.999	0.00487	0.051	0.180	0.0	P	N/A	8.09	8.22	8.28	8.00	10.00	11.75	N/A	N/A	N/A	N/A	N/A	N/A	I	N/A	SS	N/A	N/A	N/A	34S_4p1d7Yd_5	11/27B2	TDP-WTP-065	7091121
22.0	0.999	0.00487	0.054	0.180	0.0	P	N/A	9.72	9.88	9.96	9.00	10.00	17.00	N/A	N/A	N/A	N/A	N/A	N/A	I	N/A	SS+	N/A	N/A	N/A	34S_4p1d7Yd_5	11/27B2	TDP-WTP-065	7091124
22.0	0.999	0.00487	0.052	0.180	0.0	P	N/A	9.57	9.90	10.07	9.50	10.00	19.25	N/A	N/A	N/A	N/A	N/A	N/A	I	N/A	AM	N/A	N/A	N/A	34S_4p1d7Yd_5	11/27B2	TDP-WTP-065	7091127

Table B.8. Data from Fall 2007 Tests in Mid-Scale Vessel with Spherical Head A.10

Row Number	Test	Case ID	Tank Diameter	Head Shape	Dish Height	Dish Volume	Tank Fill Height	Return Line Height	Nozzle Inner Diameter	Nozzle Stand-off Distance	Pulse Tube Configuration	Installed Nozzles	Outer Nozzles Operated	Inner Nozzles Operated	Pulse Tube Outer Diameter	Outer PJM Radius	Inner PJM Radius	"FIO" Outer PJM Impingement Angle	"FIO" Inner PJM Impingement Angle	Ratio Outer PJM to Tank Radius	Ratio Inner PJM to Tank Radius	Simulant	Solids Density	Particle Diameter d5	Particle Diameter d50	Particle Diameter d95	Void Fraction
text	text	text	in.	text	in.	in. ^{3}	in.	in.	in.	in.	text	number	number	number	in.	in.	in.	deg	deg	nondim	nondim	text	g/cm^3	m	m	m	fraction
MSS	M/DDX	ID	D	HS	H_{dish}	V_{dish}	H	Rtn	d	sod	PT	N	N_O	N_I	PT_{od}	R_O	R_I	θ_O	θ_I	R_O/R	R_I/R	sxdx	ρ_s	d_5	d_{50}	d_{95}	vf
7091131M	11/27B2	34S_4p1d7Yd_5	33 7/8	S	9	4437.4	67 3/4	61 3/4	0.297	0.446	HLP-22	12	8	0	1.9	10.5	5.7	30.8	16.1	0.62	0.33	p1d7	2.45	0.0001213	0.0001780	0.0002606	0.4277
7091134M	11/27B2	34S_4p1d7Yd_5	33 7/8	S	9	4437.4	67 3/4	61 3/4	0.297	0.446	HLP-22	12	8	0	1.9	10.5	5.7	30.8	16.1	0.62	0.33	p1d7	2.45	0.0001213	0.0001780	0.0002606	0.4277
7091136M	11/27B2	34S_4p1d7Yd_5	33 7/8	S	9	4437.4	67 3/4	61 3/4	0.297	0.446	HLP-22	12	8	0	1.9	10.5	5.7	30.8	16.1	0.62	0.33	p1d7	2.45	0.0001213	0.0001780	0.0002606	0.4277
7091139	11/27B3	34S_4p1d7Yc_5	33 7/8	S	9	4437.4	67 3/4	61 3/4	0.297	0.446	HLP-22	12	8	0	1.9	10.5	5.7	30.8	16.1	0.62	0.33	p1d7	2.45	0.0001213	0.0001780	0.0002606	0.4277
7091142	11/27B3	34S_4p1d7Yc_5	33 7/8	S	9	4437.4	67 3/4	61 3/4	0.297	0.446	HLP-22	12	8	0	1.9	10.5	5.7	30.8	16.1	0.62	0.33	p1d7	2.45	0.0001213	0.0001780	0.0002606	0.4277
7091145	11/27B3	34S_4p1d7Yc_5	33 7/8	S	9	4437.4	67 3/4	61 3/4	0.297	0.446	HLP-22	12	8	0	1.9	10.5	5.7	30.8	16.1	0.62	0.33	p1d7	2.45	0.0001213	0.0001780	0.0002606	0.4277
7091149M	11/27B3	34S_4p1d7Yc_5	33 7/8	S	9	4437.4	67 3/4	61 3/4	0.297	0.446	HLP-22	12	8	0	1.9	10.5	5.7	30.8	16.1	0.62	0.33	p1d7	2.45	0.0001213	0.0001780	0.0002606	0.4277
7091151M	11/27B3	34S_4p1d7Yc_5	33 7/8	S	9	4437.4	67 3/4	61 3/4	0.297	0.446	HLP-22	12	8	0	1.9	10.5	5.7	30.8	16.1	0.62	0.33	p1d7	2.45	0.0001213	0.0001780	0.0002606	0.4277
7091154	11/30A1	34S_4p1d8Ya	33 7/8	S	9	4437.4	67 3/4	61 3/4	0.297	0.446	HLP-22	12	8	4	1.9	10.5	5.7	30.8	16.1	0.62	0.33	p1d8	2.45	0.0000605	0.0000895	0.0001320	0.4269
7091158	11/30A1	34S_4p1d8Ya	33 7/8	S	9	4437.4	67 3/4	61 3/4	0.297	0.446	HLP-22	12	8	4	1.9	10.5	5.7	30.8	16.1	0.62	0.33	p1d8	2.45	0.0000605	0.0000895	0.0001320	0.4269
7091161	11/30A1	34S_4p1d8Ya	33 7/8	S	9	4437.4	67 3/4	61 3/4	0.297	0.446	HLP-22	12	8	4	1.9	10.5	5.7	30.8	16.1	0.62	0.33	p1d8	2.45	0.0000605	0.0000895	0.0001320	0.4269
7091164	11/30A1	34S_4p1d8Ya	33 7/8	S	9	4437.4	67 3/4	61 3/4	0.297	0.446	HLP-22	12	8	4	1.9	10.5	5.7	30.8	16.1	0.62	0.33	p1d8	2.45	0.0000605	0.0000895	0.0001320	0.4269
7091167	11/30A1	34S_4p1d8Ya	33 7/8	S	9	4437.4	67 3/4	61 3/4	0.297	0.446	HLP-22	12	8	4	1.9	10.5	5.7	30.8	16.1	0.62	0.33	p1d8	2.45	0.0000605	0.0000895	0.0001320	0.4269
7091169	11/30A1	34S_4p1d8Ya	33 7/8	S	9	4437.4	67 3/4	61 3/4	0.297	0.446	HLP-22	12	8	4	1.9	10.5	5.7	30.8	16.1	0.62	0.33	p1d8	2.45	0.0000605	0.0000895	0.0001320	0.4269
7091172	11/30A2	34S_4p1d8Yd_1	33 7/8	S	9	4437.4	67 3/4	61 3/4	0.297	0.446	HLP-22	12	8	4	1.9	10.5	5.7	30.8	16.1	0.62	0.33	p1d8	2.45	0.0000605	0.0000895	0.0001320	0.4269
7091175	11/30A2	34S_4p1d8Yd_1	33 7/8	S	9	4437.4	67 3/4	61 3/4	0.297	0.446	HLP-22	12	8	4	1.9	10.5	5.7	30.8	16.1	0.62	0.33	p1d8	2.45	0.0000605	0.0000895	0.0001320	0.4269
7091178	11/30A2	34S_4p1d8Yd_1	33 7/8	S	9	4437.4	67 3/4	61 3/4	0.297	0.446	HLP-22	12	8	4	1.9	10.5	5.7	30.8	16.1	0.62	0.33	p1d8	2.45	0.0000605	0.0000895	0.0001320	0.4269
7091181	11/30A2	34S_4p1d8Yd_1	33 7/8	S	9	4437.4	67 3/4	61 3/4	0.297	0.446	HLP-22	12	8	4	1.9	10.5	5.7	30.8	16.1	0.62	0.33	p1d8	2.45	0.0000605	0.0000895	0.0001320	0.4269
7091185M	11/30A2	34S_4p1d8Yd_1	33 7/8	S	9	4437.4	67 3/4	61 3/4	0.297	0.446	HLP-22	12	8	4	1.9	10.5	5.7	30.8	16.1	0.62	0.33	p1d8	2.45	0.0000605	0.0000895	0.0001320	0.4269
7091187M	11/30A2	34S_4p1d8Yd_1	33 7/8	S	9	4437.4	67 3/4	61 3/4	0.297	0.446	HLP-22	12	8	4	1.9	10.5	5.7	30.8	16.1	0.62	0.33	p1d8	2.45	0.0000605	0.0000895	0.0001320	0.4269
7091191	11/30B1	34S_4p1d8Yc_1	33 7/8	S	9	4437.4	67 3/4	61 3/4	0.297	0.446	HLP-22	12	8	4	1.9	10.5	5.7	30.8	16.1	0.62	0.33	p1d8	2.45	0.0000605	0.0000895	0.0001320	0.4269
7091193	11/30B1	34S_4p1d8Yc_1	33 7/8	S	9	4437.4	67 3/4	61 3/4	0.297	0.446	HLP-22	12	8	4	1.9	10.5	5.7	30.8	16.1	0.62	0.33	p1d8	2.45	0.0000605	0.0000895	0.0001320	0.4269
7091197	11/30B1	34S_4p1d8Yc_1	33 7/8	S	9	4437.4	67 3/4	61 3/4	0.297	0.446	HLP-22	12	8	4	1.9	10.5	5.7	30.8	16.1	0.62	0.33	p1d8	2.45	0.0000605	0.0000895	0.0001320	0.4269
7091200M	11/30B1	34S_4p1d8Yc_1	33 7/8	S	9	4437.4	67 3/4	61 3/4	0.297	0.446	HLP-22	12	8	4	1.9	10.5	5.7	30.8	16.1	0.62	0.33	p1d8	2.45	0.0000605	0.0000895	0.0001320	0.4269
7091202M	11/30B1	34S_4p1d8Yc_1	33 7/8	S	9	4437.4	67 3/4	61 3/4	0.297	0.446	HLP-22	12	8	4	1.9	10.5	5.7	30.8	16.1	0.62	0.33	p1d8	2.45	0.0000605	0.0000895	0.0001320	0.4269
7091206	11/30C1	34S_4p1d8Ya-44	33 7/8	S	9	4437.4	67 3/4	61 3/4	0.297	0.446	HLP-22	12	4	4	1.9	10.5	5.7	30.8	16.1	0.62	0.33	p1d8	2.45	0.0000605	0.0000895	0.0001320	0.4269
7091209	11/30C1	34S_4p1d8Ya-44	33 7/8	S	9	4437.4	67 3/4	61 3/4	0.297	0.446	HLP-22	12	4	4	1.9	10.5	5.7	30.8	16.1	0.62	0.33	p1d8	2.45	0.0000605	0.0000895	0.0001320	0.4269
7091212	11/30C1	34S_4p1d8Ya-44	33 7/8	S	9	4437.4	67 3/4	61 3/4	0.297	0.446	HLP-22	12	4	4	1.9	10.5	5.7	30.8	16.1	0.62	0.33	p1d8	2.45	0.0000605	0.0000895	0.0001320	0.4269
7091215	11/30C1	34S_4p1d8Ya-44	33 7/8	S	9	4437.4	67 3/4	61 3/4	0.297	0.446	HLP-22	12	4	4	1.9	10.5	5.7	30.8	16.1	0.62	0.33	p1d8	2.45	0.0000605	0.0000895	0.0001320	0.4269
7091217	11/30C1	34S_4p1d8Ya-44	33 7/8	S	9	4437.4	67 3/4	61 3/4	0.297	0.446	HLP-22	12	4	4	1.9	10.5	5.7	30.8	16.1	0.62	0.33	p1d8	2.45	0.0000605	0.0000895	0.0001320	0.4269
7091221	11/30C1	34S_4p1d8Ya-44	33 7/8	S	9	4437.4	67 3/4	61 3/4	0.297	0.446	HLP-22	12	4	4	1.9	10.5	5.7	30.8	16.1	0.62	0.33	p1d8	2.45	0.0000605	0.0000895	0.0001320	0.4269
7091224	11/30C2	34S_4p1d8Yd_0	33 7/8	S	9	4437.4	67 3/4	61 3/4	0.297	0.446	HLP-22	12	4	4	1.9	10.5	5.7	30.8	16.1	0.62	0.33	p1d8	2.45	0.0000605	0.0000895	0.0001320	0.4269
7091226	11/30C2	34S_4p1d8Yd_0	33 7/8	S	9	4437.4	67 3/4	61 3/4	0.297	0.446	HLP-22	12	4	4	1.9	10.5	5.7	30.8	16.1	0.62	0.33	p1d8	2.45	0.0000605	0.0000895	0.0001320	0.4269
7091229	11/30C2	34S_4p1d8Yd_0	33 7/8	S	9	4437.4	67 3/4	61 3/4	0.297	0.446	HLP-22	12	4	4	1.9	10.5	5.7	30.8	16.1	0.62	0.33	p1d8	2.45	0.0000605	0.0000895	0.0001320	0.4269
7091232	11/30C2	34S_4p1d8Yd_0	33 7/8	S	9	4437.4	67 3/4	61 3/4	0.297	0.446	HLP-22	12	4	4	1.9	10.5	5.7	30.8	16.1	0.62	0.33	p1d8	2.45	0.0000605	0.0000895	0.0001320	0.4269
7091236	11/30C2	34S_4p1d8Yd_0	33 7/8	S	9	4437.4	67 3/4	61 3/4	0.297	0.446	HLP-22	12	4	4	1.9	10.5	5.7	30.8	16.1	0.62	0.33	p1d8	2.45	0.0000605	0.0000895	0.0001320	0.4269
7091240	11/30C2	34S_4p1d8Yd_0	33 7/8	S	9	4437.4	67 3/4	61 3/4	0.297	0.446	HLP-22	12	4	4	1.9	10.5	5.7	30.8	16.1	0.62	0.33	p1d8	2.45	0.0000605	0.0000895	0.0001320	0.4269
7091243	11/30C2	34S_4p1d8Yd_0	33 7/8	S	9	4437.4	67 3/4	61 3/4	0.297	0.446	HLP-22	12	4	4	1.9	10.5	5.7	30.8	16.1	0.62	0.33	p1d8	2.45	0.0000605	0.0000895	0.0001320	0.4269
7091246	11/30C2	34S_4p1d8Yd_0	33 7/8	S	9	4437.4	67 3/4	61 3/4	0.297	0.446	HLP-22	12	4	4	1.9	10.5	5.7	30.8	16.1	0.62	0.33	p1d8	2.45	0.0000605	0.0000895	0.0001320	0.4269
7091249	11/30C2	34S_4p1d8Yd_0	33 7/8	S	9	4437.4	67 3/4	61 3/4	0.297	0.446	HLP-22	12	4	4	1.9	10.5	5.7	30.8	16.1	0.62	0.33	p1d8	2.45	0.0000605	0.0000895	0.0001320	0.4269
7091253M	11/30C2	34S_4p1d8Yd_0	33 7/8	S	9	4437.4	67 3/4	61 3/4	0.297	0.446	HLP-22	12	4	4	1.9	10.5	5.7	30.8	16.1	0.62	0.33	p1d8	2.45	0.0000605	0.0000895	0.0001320	0.4269

Table B.8. Data from Fall 2007 Tests in Mid-Scale Vessel with Spherical Head B.10

Tank Water Temperature	Water Density	Solids Fraction	Pulse Volume Fraction	Duty Cycle	Cycle Time	Pulsed or Steady Jet	Us Steady Jet	U1 Pulsing Jet	U2 URMS	U3 URM3	Discharge Velocity	Critical Suspension Velocity	Average Peak Cloud Height	UCS Condition	UCS Method	UCS Flag	UCS Center Flag	UCS udv Flag	UCS based on Decreasing Velocity	Sweep Increase / Decrease	UDV Height Bed	Particle Motion	Solids Level	Outer Bottom Pattern	Inner Bottom Pattern	Case ID	Test	TDP	Row Number
C	g/cm³	fraction	fraction	fraction	s	text	m/s	m/s	m/s	m/s	m/s	m/s	in.	m/s	text	text	text	text	m/s	text	mm	text	text	text	text	text	text	text	text
T	ρ_l	ϕ_S	ϕ_P	DC	t_C	Jet	U_S	U1	U2	U3	U	U_{CS}	H_C	U_{CSR}	U_{CSM}	U_{CS}vis	U_{CS}cen	U_{CS}udv	U_{CS}_D	S_W	H_{bed}	PM	Sol	SP_O	SP_I	ID	M/DDX	TDP	MSS
22.0	0.999	0.00487	0.052	0.180	0.0	P	N/A	9.72	10.20	10.44	10.00	10.00	21.25	10.00	vis	UCSvis	N/A	N/A	N/A	I	N/A	CS	N/A	N/A	N/A	34S_4p1d7Yd_5	11/27B2	TDP-WTP-065	7091131
22.0	0.999	0.00487	0.051	0.180	0.0	P	N/A	9.73	10.32	10.60	10.50	10.00	21.75	N/A	N/A	N/A	N/A	N/A	N/A	I	N/A	BC-	N/A	N/A	N/A	34S_4p1d7Yd_5	11/27B2	TDP-WTP-065	7091134
22.0	0.999	0.00487	0.051	0.180	0.0	P	N/A	9.89	10.59	10.92	11.00	10.00	23.25	N/A	N/A	N/A	N/A	N/A	N/A	I	N/A	BC	N/A	N/A	N/A	34S_4p1d7Yd_5	11/27B2	TDP-WTP-065	7091136
22.0	0.999	0.00487	0.051	0.330	0.0	P	N/A	7.99	8.14	8.22	8.00	10.00	12.25	N/A	N/A	N/A	N/A	N/A	N/A	I	N/A	SS	N/A	N/A	N/A	34S_4p1d7Yc_5	11/27B3	TDP-WTP-065	7091139
22.0	0.999	0.00487	0.056	0.330	0.0	P	N/A	9.99	10.19	10.29	9.00	10.00	16.25	N/A	N/A	N/A	N/A	N/A	N/A	I	N/A	SS+	N/A	N/A	N/A	34S_4p1d7Yc_5	11/27B3	TDP-WTP-065	7091142
22.0	0.999	0.00487	0.051	0.330	0.0	P	N/A	9.45	9.70	9.84	9.50	10.00	19.50	N/A	N/A	N/A	N/A	N/A	N/A	I	N/A	AM	N/A	N/A	N/A	34S_4p1d7Yc_5	11/27B3	TDP-WTP-065	7091145
22.0	0.999	0.00487	0.050	0.330	0.0	P	N/A	9.86	10.14	10.28	10.00	10.00	21.25	10.00	vis	UCSvis	N/A	N/A	N/A	I	N/A	CS	N/A	N/A	N/A	34S_4p1d7Yc_5	11/27B3	TDP-WTP-065	7091149
22.0	0.999	0.00487	0.050	0.330	0.0	P	N/A	10.29	10.83	11.08	11.00	10.00	26.75	N/A	N/A	N/A	N/A	N/A	N/A	I	N/A	BC	N/A	N/A	N/A	34S_4p1d7Yc_5	11/27B3	TDP-WTP-065	7091151
21.0	0.999	0.00487	undefined	1.000	infinite	S	1.99	N/A	N/A	N/A	2.00	3.90	N/A	N/A	N/A	N/A	N/A	N/A	N/A	N/A	N/A	SS	N/A	N/A	N/A	34S_4p1d8Ya	11/30A1	TDP-WTP-066	7091154
20.9	0.999	0.00487	undefined	1.000	infinite	S	3.05	N/A	N/A	N/A	3.00	3.90	N/A	N/A	N/A	N/A	N/A	N/A	N/A	I	N/A	AM	N/A	N/A	N/A	34S_4p1d8Ya	11/30A1	TDP-WTP-066	7091158
20.9	0.999	0.00487	undefined	1.000	infinite	S	3.52	N/A	N/A	N/A	3.50	3.90	14.50	N/A	N/A	N/A	UCScen	N/A	N/A	I	N/A	AM	N/A	N/A	N/A	34S_4p1d8Ya	11/30A1	TDP-WTP-066	7091161
21.0	0.999	0.00487	undefined	1.000	infinite	S	3.72	N/A	N/A	N/A	3.70	3.90	24.50	N/A	N/A	N/A	N/A	N/A	N/A	I	N/A	AM+	N/A	N/A	N/A	34S_4p1d8Ya	11/30A1	TDP-WTP-066	7091164
21.0	0.999	0.00487	undefined	1.000	infinite	S	3.96	N/A	N/A	N/A	3.90	3.90	33.50	3.90	vis	UCSvis	N/A	N/A	N/A	I	N/A	CS	N/A	N/A	N/A	34S_4p1d8Ya	11/30A1	TDP-WTP-066	7091167
21.0	0.999	0.00487	undefined	1.000	infinite	S	4.12	N/A	N/A	N/A	4.10	3.90	42.50	N/A	N/A	N/A	N/A	N/A	N/A	I	N/A	BC	N/A	N/A	N/A	34S_4p1d8Ya	11/30A1	TDP-WTP-066	7091169
21.0	0.999	0.00487	0.050	0.180	0.0	P	N/A	3.91	3.95	3.97	4.00	6.00	N/A	N/A	N/A	N/A	N/A	N/A	N/A	I	N/A	SS	N/A	N/A	N/A	34S_4p1d8Yd_1	11/30A2	TDP-WTP-066	7091172
21.0	0.999	0.00487	0.050	0.180	0.0	P	N/A	4.44	4.48	4.50	4.50	6.00	9.00	N/A	N/A	N/A	N/A	N/A	N/A	I	N/A	AM-	N/A	N/A	N/A	34S_4p1d8Yd_1	11/30A2	TDP-WTP-066	7091175
21.0	0.999	0.00487	0.049	0.180	0.0	P	N/A	4.85	4.90	4.93	5.00	6.00	9.75	N/A	N/A	N/A	N/A	N/A	N/A	I	N/A	AM	N/A	N/A	N/A	34S_4p1d8Yd_1	11/30A2	TDP-WTP-066	7091178
21.0	0.999	0.00487	0.050	0.180	0.0	P	N/A	5.38	5.45	5.49	5.50	6.00	11.25	N/A	N/A	N/A	N/A	N/A	N/A	I	N/A	AM+	N/A	N/A	N/A	34S_4p1d8Yd_1	11/30A2	TDP-WTP-066	7091181
21.0	0.999	0.00487	0.050	0.180	0.0	P	N/A	5.86	5.95	5.99	6.00	6.00	12.50	6.00	vis	UCSvis	N/A	N/A	N/A	I	N/A	CS	N/A	N/A	N/A	34S_4p1d8Yd_1	11/30A2	TDP-WTP-066	7091185
21.0	0.999	0.00487	0.050	0.180	0.0	P	N/A	6.37	6.48	6.53	6.50	6.00	16.75	N/A	N/A	N/A	N/A	N/A	N/A	I	N/A	BC	N/A	N/A	N/A	34S_4p1d8Yd_1	11/30A2	TDP-WTP-066	7091187
21.0	0.999	0.00487	0.050	0.330	0.0	P	N/A	3.89	3.93	3.95	4.00	5.30	8.50	N/A	N/A	N/A	N/A	N/A	N/A	D	N/A	SS	N/A	N/A	N/A	34S_4p1d8Yc_1	11/30B1	TDP-WTP-066	7091191
21.0	0.999	0.00487	0.050	0.330	0.0	P	N/A	4.43	4.48	4.50	4.50	5.30	9.75	N/A	N/A	N/A	N/A	N/A	N/A	I	N/A	SS+	N/A	N/A	N/A	34S_4p1d8Yc_1	11/30B1	TDP-WTP-066	7091193
21.0	0.999	0.00487	0.052	0.330	0.0	P	N/A	4.87	4.94	4.97	5.00	5.30	10.75	N/A	N/A	N/A	N/A	N/A	N/A	I	N/A	AM	N/A	N/A	N/A	34S_4p1d8Yc_1	11/30B1	TDP-WTP-066	7091197
21.0	0.999	0.00487	0.050	0.330	0.0	P	N/A	5.16	5.22	5.25	5.30	5.30	12.50	5.30	vis	UCSvis	N/A	N/A	N/A	I	N/A	CS	N/A	N/A	N/A	34S_4p1d8Yc_1	11/30B1	TDP-WTP-066	7091200
21.0	0.999	0.00487	0.050	0.330	0.0	P	N/A	5.52	5.59	5.62	5.60	5.30	17.50	N/A	N/A	N/A	N/A	N/A	N/A	I	N/A	BC	N/A	N/A	N/A	34S_4p1d8Yc_1	11/30B1	TDP-WTP-066	7091202
21.3	0.999	0.00487	undefined	1.000	infinite	S	3.53	N/A	N/A	N/A	3.50	5.50	N/A	N/A	N/A	N/A	N/A	N/A	N/A	I	N/A	SS	N/A	N/A	N/A	34S_4p1d8Ya-44	11/30C1	TDP-WTP-066	7091206
21.2	0.999	0.00487	undefined	1.000	infinite	S	3.70	N/A	N/A	N/A	3.70	5.50	N/A	N/A	N/A	N/A	UCScen	N/A	N/A	I	N/A	SS	N/A	N/A	N/A	34S_4p1d8Ya-44	11/30C1	TDP-WTP-066	7091209
21.3	0.999	0.00487	undefined	1.000	infinite	S	4.04	N/A	N/A	N/A	4.00	5.50	9.50	N/A	N/A	N/A	N/A	N/A	N/A	I	N/A	AM	N/A	N/A	N/A	34S_4p1d8Ya-44	11/30C1	TDP-WTP-066	7091212
21.3	0.999	0.00487	undefined	1.000	infinite	S	4.54	N/A	N/A	N/A	4.50	5.50	14.25	N/A	N/A	N/A	N/A	N/A	N/A	I	N/A	AM	N/A	N/A	N/A	34S_4p1d8Ya-44	11/30C1	TDP-WTP-066	7091215
21.3	0.999	0.00487	undefined	1.000	infinite	S	5.03	N/A	N/A	N/A	5.00	5.50	29.25	N/A	N/A	N/A	N/A	N/A	N/A	I	N/A	AM+	N/A	N/A	N/A	34S_4p1d8Ya-44	11/30C1	TDP-WTP-066	7091217
21.3	0.999	0.00487	undefined	1.000	infinite	S	5.55	N/A	N/A	N/A	5.50	5.50	43.75	5.50	vis	UCSvis	N/A	N/A	N/A	I	N/A	CS	N/A	N/A	N/A	34S_4p1d8Ya-44	11/30C1	TDP-WTP-066	7091221
21.0	0.999	0.00487	0.051	0.180	87.0	P	N/A	4.55	4.60	4.63	4.50	9.00	N/A	N/A	N/A	N/A	UCScen	N/A	N/A	I	N/A	SS	N/A	N/A	N/A	34S_4p1d8Yd_0	11/30C2	TDP-WTP-066	7091224
21.0	0.999	0.00487	0.051	0.180	78.0	P	N/A	5.06	5.10	5.14	5.00	9.00	9.50	N/A	N/A	N/A	N/A	N/A	N/A	I	N/A	AM	N/A	N/A	N/A	34S_4p1d8Yd_0	11/30C2	TDP-WTP-066	7091226
21.0	0.999	0.00487	0.051	0.180	70.0	P	N/A	5.61	5.67	5.71	5.50	9.00	11.00	N/A	N/A	N/A	N/A	N/A	N/A	I	N/A	AM	N/A	N/A	N/A	34S_4p1d8Yd_0	11/30C2	TDP-WTP-066	7091229
21.0	0.999	0.00487	0.050	0.180	64.0	P	N/A	6.10	6.16	6.21	6.00	9.00	12.83	N/A	N/A	N/A	N/A	N/A	N/A	I	N/A	AM	N/A	N/A	N/A	34S_4p1d8Yd_0	11/30C2	TDP-WTP-066	7091232
21.0	0.999	0.00487	0.050	0.180	59.0	P	N/A	6.58	6.65	6.71	6.50	9.00	15.00	N/A	N/A	N/A	N/A	N/A	N/A	I	N/A	AM	N/A	N/A	N/A	34S_4p1d8Yd_0	11/30C2	TDP-WTP-066	7091236
21.0	0.999	0.00487	0.051	0.180	54.0	P	N/A	7.15	7.23	7.29	7.00	9.00	15.50	N/A	N/A	N/A	N/A	N/A	N/A	I	N/A	AM+	N/A	N/A	N/A	34S_4p1d8Yd_0	11/30C2	TDP-WTP-066	7091240
21.0	0.999	0.00487	0.050	0.180	50.5	P	N/A	7.55	7.66	7.74	7.50	9.00	17.63	N/A	N/A	N/A	N/A	N/A	N/A	I	N/A	AM+	N/A	N/A	N/A	34S_4p1d8Yd_0	11/30C2	TDP-WTP-066	7091243
21.0	0.999	0.00487	0.046	0.180	47.0	P	N/A	8.16	8.28	8.37	8.00	9.00	20.25	N/A	N/A	N/A	N/A	N/A	N/A	I	N/A	AM+	N/A	N/A	N/A	34S_4p1d8Yd_0	11/30C2	TDP-WTP-066	7091246
21.0	0.999	0.00487	0.050	0.180	45.0	P	N/A	8.58	8.69	8.76	8.50	9.00	22.25	N/A	N/A	N/A	N/A	N/A	N/A	I	N/A	AM+	N/A	N/A	N/A	34S_4p1d8Yd_0	11/30C2	TDP-WTP-066	7091249
21.0	0.999	0.00487	0.051	0.180	42.5	P	N/A	9.10	9.24	9.33	9.00	9.00	25.88	9.00	vis	UCSvis	N/A	N/A	N/A	I	N/A	CS	N/A	N/A	N/A	34S_4p1d8Yd_0	11/30C2	TDP-WTP-066	7091253

Table B.8. Data from Fall 2007 Tests in Mid-Scale Vessel with Spherical Head A.11

Row Number	Test	Case ID	Tank Diameter	Head Shape	Dish Height	Dish Volume	Tank Fill Height	Return Line Height	Nozzle Inner Diameter	Nozzle Stand-off Distance	Pulse Tube Configuration	Installed Nozzles	Outer Nozzles Operated	Inner Nozzles Operated	Pulse Tube Outer Diameter	Outer PJM Radius	Inner PJM Radius	"FIO" Outer PJM Impingement Angle	"FIO" Inner PJM Impingement Angle	Ratio Outer PJM to Tank Radius	Ratio Inner PJM to Tank Radius	Simulant	Solids Density	Particle Diameter d5	Particle Diameter d50	Particle Diameter d95	Void Fraction
text	text	text	in.	text	in.	in. ^{3}	in.	in.	in.	in.	text	number	number	number	in.	in.	in.	deg	deg	nondim	nondim	text	g/cm^3	m	m	m	fraction
MSS	M/DDX	ID	D	HS	H_{dish}	V_{dish}	H	Rtn	d	sod	PT	N	N_O	N_I	PT_{od}	R_O	R_I	θ_O	θ_I	R_O/R	R_I/R	sxdx	ρ_s	d_5	d_{50}	d_{95}	vf
7091256	12/3A1	34S_4p1d8Yc_0	33 7/8	S	9	4437.4	67 3/4	61 3/4	0.297	0.446	HLP-22	12	4	4	1.9	10.5	5.7	30.8	16.1	0.62	0.33	p1d8	2.45	0.0000605	0.0000895	0.0001320	0.4269
7091259	12/3A1	34S_4p1d8Yc_0	33 7/8	S	9	4437.4	67 3/4	61 3/4	0.297	0.446	HLP-22	12	4	4	1.9	10.5	5.7	30.8	16.1	0.62	0.33	p1d8	2.45	0.0000605	0.0000895	0.0001320	0.4269
7091261	12/3A1	34S_4p1d8Yc_0	33 7/8	S	9	4437.4	67 3/4	61 3/4	0.297	0.446	HLP-22	12	4	4	1.9	10.5	5.7	30.8	16.1	0.62	0.33	p1d8	2.45	0.0000605	0.0000895	0.0001320	0.4269
7091265	12/3A1	34S_4p1d8Yc_0	33 7/8	S	9	4437.4	67 3/4	61 3/4	0.297	0.446	HLP-22	12	4	4	1.9	10.5	5.7	30.8	16.1	0.62	0.33	p1d8	2.45	0.0000605	0.0000895	0.0001320	0.4269
7091268M	12/3A1	34S_4p1d8Yc_0	33 7/8	S	9	4437.4	67 3/4	61 3/4	0.297	0.446	HLP-22	12	4	4	1.9	10.5	5.7	30.8	16.1	0.62	0.33	p1d8	2.45	0.0000605	0.0000895	0.0001320	0.4269
7091270M	12/3A1	34S_4p1d8Yc_0	33 7/8	S	9	4437.4	67 3/4	61 3/4	0.297	0.446	HLP-22	12	4	4	1.9	10.5	5.7	30.8	16.1	0.62	0.33	p1d8	2.45	0.0000605	0.0000895	0.0001320	0.4269
7091274	12/3B1	34S_4p1d8Ya-04	33 7/8	S	9	4437.4	67 3/4	61 3/4	0.297	0.446	HLP-22	12	0	4	1.9	10.5	5.7	30.8	16.1	0.62	0.33	p1d8	2.45	0.0000605	0.0000895	0.0001320	0.4269
7091277	12/3B1	34S_4p1d8Ya-04	33 7/8	S	9	4437.4	67 3/4	61 3/4	0.297	0.446	HLP-22	12	0	4	1.9	10.5	5.7	30.8	16.1	0.62	0.33	p1d8	2.45	0.0000605	0.0000895	0.0001320	0.4269
7091279	12/3B1	34S_4p1d8Ya-04	33 7/8	S	9	4437.4	67 3/4	61 3/4	0.297	0.446	HLP-22	12	0	4	1.9	10.5	5.7	30.8	16.1	0.62	0.33	p1d8	2.45	0.0000605	0.0000895	0.0001320	0.4269
7091283	12/3B1	34S_4p1d8Ya-04	33 7/8	S	9	4437.4	67 3/4	61 3/4	0.297	0.446	HLP-22	12	0	4	1.9	10.5	5.7	30.8	16.1	0.62	0.33	p1d8	2.45	0.0000605	0.0000895	0.0001320	0.4269
7091286	12/3B1	34S_4p1d8Ya-04	33 7/8	S	9	4437.4	67 3/4	61 3/4	0.297	0.446	HLP-22	12	0	4	1.9	10.5	5.7	30.8	16.1	0.62	0.33	p1d8	2.45	0.0000605	0.0000895	0.0001320	0.4269
7091289	12/3B2	34S_4p1d8Yd_9	33 7/8	S	9	4437.4	67 3/4	61 3/4	0.297	0.446	HLP-22	12	0	4	1.9	10.5	5.7	30.8	16.1	0.62	0.33	p1d8	2.45	0.0000605	0.0000895	0.0001320	0.4269
7091291	12/3B2	34S_4p1d8Yd_9	33 7/8	S	9	4437.4	67 3/4	61 3/4	0.297	0.446	HLP-22	12	0	4	1.9	10.5	5.7	30.8	16.1	0.62	0.33	p1d8	2.45	0.0000605	0.0000895	0.0001320	0.4269
7091294	12/3B2	34S_4p1d8Yd_9	33 7/8	S	9	4437.4	67 3/4	61 3/4	0.297	0.446	HLP-22	12	0	4	1.9	10.5	5.7	30.8	16.1	0.62	0.33	p1d8	2.45	0.0000605	0.0000895	0.0001320	0.4269
7091297	12/3B2	34S_4p1d8Yd_9	33 7/8	S	9	4437.4	67 3/4	61 3/4	0.297	0.446	HLP-22	12	0	4	1.9	10.5	5.7	30.8	16.1	0.62	0.33	p1d8	2.45	0.0000605	0.0000895	0.0001320	0.4269
7091300	12/3B2	34S_4p1d8Yd_9	33 7/8	S	9	4437.4	67 3/4	61 3/4	0.297	0.446	HLP-22	12	0	4	1.9	10.5	5.7	30.8	16.1	0.62	0.33	p1d8	2.45	0.0000605	0.0000895	0.0001320	0.4269
7091303	12/3B2	34S_4p1d8Yd_9	33 7/8	S	9	4437.4	67 3/4	61 3/4	0.297	0.446	HLP-22	12	0	4	1.9	10.5	5.7	30.8	16.1	0.62	0.33	p1d8	2.45	0.0000605	0.0000895	0.0001320	0.4269
7091306	12/3B2	34S_4p1d8Yd_9	33 7/8	S	9	4437.4	67 3/4	61 3/4	0.297	0.446	HLP-22	12	0	4	1.9	10.5	5.7	30.8	16.1	0.62	0.33	p1d8	2.45	0.0000605	0.0000895	0.0001320	0.4269
7091310M	12/3B2	34S_4p1d8Yd_9	33 7/8	S	9	4437.4	67 3/4	61 3/4	0.297	0.446	HLP-22	12	0	4	1.9	10.5	5.7	30.8	16.1	0.62	0.33	p1d8	2.45	0.0000605	0.0000895	0.0001320	0.4269
7091312M	12/3B2	34S_4p1d8Yd_9	33 7/8	S	9	4437.4	67 3/4	61 3/4	0.297	0.446	HLP-22	12	0	4	1.9	10.5	5.7	30.8	16.1	0.62	0.33	p1d8	2.45	0.0000605	0.0000895	0.0001320	0.4269
7091316	12/3C1	34S_4p1d8Yc_9	33 7/8	S	9	4437.4	67 3/4	61 3/4	0.297	0.446	HLP-22	12	0	4	1.9	10.5	5.7	30.8	16.1	0.62	0.33	p1d8	2.45	0.0000605	0.0000895	0.0001320	0.4269
7091318	12/3C1	34S_4p1d8Yc_9	33 7/8	S	9	4437.4	67 3/4	61 3/4	0.297	0.446	HLP-22	12	0	4	1.9	10.5	5.7	30.8	16.1	0.62	0.33	p1d8	2.45	0.0000605	0.0000895	0.0001320	0.4269
7091321	12/3C1	34S_4p1d8Yc_9	33 7/8	S	9	4437.4	67 3/4	61 3/4	0.297	0.446	HLP-22	12	0	4	1.9	10.5	5.7	30.8	16.1	0.62	0.33	p1d8	2.45	0.0000605	0.0000895	0.0001320	0.4269
7091324	12/3C1	34S_4p1d8Yc_9	33 7/8	S	9	4437.4	67 3/4	61 3/4	0.297	0.446	HLP-22	12	0	4	1.9	10.5	5.7	30.8	16.1	0.62	0.33	p1d8	2.45	0.0000605	0.0000895	0.0001320	0.4269
7091328M	12/3C1	34S_4p1d8Yc_9	33 7/8	S	9	4437.4	67 3/4	61 3/4	0.297	0.446	HLP-22	12	0	4	1.9	10.5	5.7	30.8	16.1	0.62	0.33	p1d8	2.45	0.0000605	0.0000895	0.0001320	0.4269
7091330M	12/3C1	34S_4p1d8Yc_9	33 7/8	S	9	4437.4	67 3/4	61 3/4	0.297	0.446	HLP-22	12	0	4	1.9	10.5	5.7	30.8	16.1	0.62	0.33	p1d8	2.45	0.0000605	0.0000895	0.0001320	0.4269
7091333	12/4A1	34S_4p1d8Ya-40	33 7/8	S	9	4437.4	67 3/4	61 3/4	0.297	0.446	HLP-22	12	4	0	1.9	10.5	5.7	30.8	16.1	0.62	0.33	p1d8	2.45	0.0000605	0.0000895	0.0001320	0.4269
7091336	12/4A1	34S_4p1d8Ya-40	33 7/8	S	9	4437.4	67 3/4	61 3/4	0.297	0.446	HLP-22	12	4	0	1.9	10.5	5.7	30.8	16.1	0.62	0.33	p1d8	2.45	0.0000605	0.0000895	0.0001320	0.4269
7091339	12/4A1	34S_4p1d8Ya-40	33 7/8	S	9	4437.4	67 3/4	61 3/4	0.297	0.446	HLP-22	12	4	0	1.9	10.5	5.7	30.8	16.1	0.62	0.33	p1d8	2.45	0.0000605	0.0000895	0.0001320	0.4269
7091342	12/4A1	34S_4p1d8Ya-40	33 7/8	S	9	4437.4	67 3/4	61 3/4	0.297	0.446	HLP-22	12	4	0	1.9	10.5	5.7	30.8	16.1	0.62	0.33	p1d8	2.45	0.0000605	0.0000895	0.0001320	0.4269
7091346	12/4A1	34S_4p1d8Ya-40	33 7/8	S	9	4437.4	67 3/4	61 3/4	0.297	0.446	HLP-22	12	4	0	1.9	10.5	5.7	30.8	16.1	0.62	0.33	p1d8	2.45	0.0000605	0.0000895	0.0001320	0.4269
7091348	12/4A1	34S_4p1d8Ya-40	33 7/8	S	9	4437.4	67 3/4	61 3/4	0.297	0.446	HLP-22	12	4	0	1.9	10.5	5.7	30.8	16.1	0.62	0.33	p1d8	2.45	0.0000605	0.0000895	0.0001320	0.4269
7091351	12/4A2	34S_4p1d8Yd_6	33 7/8	S	9	4437.4	67 3/4	61 3/4	0.297	0.446	HLP-22	12	4	0	1.9	10.5	5.7	30.8	16.1	0.62	0.33	p1d8	2.45	0.0000605	0.0000895	0.0001320	0.4269
7091354	12/4A2	34S_4p1d8Yd_6	33 7/8	S	9	4437.4	67 3/4	61 3/4	0.297	0.446	HLP-22	12	4	0	1.9	10.5	5.7	30.8	16.1	0.62	0.33	p1d8	2.45	0.0000605	0.0000895	0.0001320	0.4269
7091357	12/4A2	34S_4p1d8Yd_6	33 7/8	S	9	4437.4	67 3/4	61 3/4	0.297	0.446	HLP-22	12	4	0	1.9	10.5	5.7	30.8	16.1	0.62	0.33	p1d8	2.45	0.0000605	0.0000895	0.0001320	0.4269
7091360	12/4A2	34S_4p1d8Yd_6	33 7/8	S	9	4437.4	67 3/4	61 3/4	0.297	0.446	HLP-22	12	4	0	1.9	10.5	5.7	30.8	16.1	0.62	0.33	p1d8	2.45	0.0000605	0.0000895	0.0001320	0.4269
7091364M	12/4A2	34S_4p1d8Yd_6	33 7/8	S	9	4437.4	67 3/4	61 3/4	0.297	0.446	HLP-22	12	4	0	1.9	10.5	5.7	30.8	16.1	0.62	0.33	p1d8	2.45	0.0000605	0.0000895	0.0001320	0.4269
7091366M	12/4A2	34S_4p1d8Yd_6	33 7/8	S	9	4437.4	67 3/4	61 3/4	0.297	0.446	HLP-22	12	4	0	1.9	10.5	5.7	30.8	16.1	0.62	0.33	p1d8	2.45	0.0000605	0.0000895	0.0001320	0.4269
7091369	12/4B1	34S_4p1d8Yc_6	33 7/8	S	9	4437.4	67 3/4	61 3/4	0.297	0.446	HLP-22	12	4	0	1.9	10.5	5.7	30.8	16.1	0.62	0.33	p1d8	2.45	0.0000605	0.0000895	0.0001320	0.4269
7091372	12/4B1	34S_4p1d8Yc_6	33 7/8	S	9	4437.4	67 3/4	61 3/4	0.297	0.446	HLP-22	12	4	0	1.9	10.5	5.7	30.8	16.1	0.62	0.33	p1d8	2.45	0.0000605	0.0000895	0.0001320	0.4269
7091375	12/4B1	34S_4p1d8Yc_6	33 7/8	S	9	4437.4	67 3/4	61 3/4	0.297	0.446	HLP-22	12	4	0	1.9	10.5	5.7	30.8	16.1	0.62	0.33	p1d8	2.45	0.0000605	0.0000895	0.0001320	0.4269

Table B.8. Data from Fall 2007 Tests in Mid-Scale Vessel with Spherical Head B.11

Tank Water Temperature	Water Density	Solids Fraction	Pulse Volume Fraction	Duty Cycle	Cycle Time	Pulsed or Steady Jet	Us Steady Jet	U1 Pulsing Jet	U2 URMS	U3 URM3	Discharge Velocity	Critical Suspension Velocity	Average Peak Cloud Height	UCS Condition	UCS Method	UCS Flag	UCS Center Flag	UCS udv Flag	UCS based on Decreasing Velocity	Sweep Increase / Decrease	UDV Height Bed	Particle Motion	Solids Level	Outer Bottom Pattern	Inner Bottom Pattern	Case ID	Test	TDP	Row Number
C	g/cm³	fraction	fraction	fraction	s	text	m/s	m/s	m/s	m/s	m/s	m/s	in.	m/s	text	text	text	text	m/s	text	mm	text	text	text	text	text	text	text	text
T	ρ_l	ϕ_S	ϕ_P	DC	t_C	Jet	U_S	U1	U2	U3	U	U_{CS}	H_C	U_{CSR}	U_{CSM}	U_{CS}vis	U_{CS}cen	U_{CS}udv	U_{CS}_D	S_W	H_{bed}	PM	Sol	SP_O	SP_I	ID	M/DDX	TDP	MSS
21.0	0.999	0.00487	0.050	0.330	47.0	P	N/A	4.53	4.58	4.62	4.50	7.30	N/A	N/A	N/A	N/A	N/A	N/A	N/A	I	N/A	SS	N/A	N/A	N/A	34S_4p1d8Yc_0	12/3A1	TDP-WTP-067	7091256
21.0	0.999	0.00487	0.051	0.330	42.0	P	N/A	5.12	5.16	5.20	5.00	7.30	9.25	N/A	N/A	N/A	UCScen	N/A	N/A	I	N/A	SS	N/A	N/A	N/A	34S_4p1d8Yc_0	12/3A1	TDP-WTP-067	7091259
21.0	0.999	0.00487	0.051	0.330	35.0	P	N/A	6.08	6.16	6.21	6.00	7.30	13.50	N/A	N/A	N/A	N/A	N/A	N/A	D	N/A	AM	N/A	N/A	N/A	34S_4p1d8Yc_0	12/3A1	TDP-WTP-067	7091261
21.0	0.999	0.00487	0.051	0.330	30.0	P	N/A	7.03	7.14	7.22	7.00	7.30	17.50	N/A	N/A	N/A	N/A	N/A	N/A	I	N/A	AM	N/A	N/A	N/A	34S_4p1d8Yc_0	12/3A1	TDP-WTP-067	7091265
21.0	0.999	0.00487	0.051	0.330	28.8	P	N/A	7.33	7.44	7.51	7.30	7.30	20.50	7.30	vis	UCSvis	N/A	N/A	N/A	I	N/A	CS	N/A	N/A	N/A	34S_4p1d8Yc_0	12/3A1	TDP-WTP-067	7091268
21.0	0.999	0.00487	0.050	0.330	26.0	P	N/A	8.08	8.22	8.31	8.00	7.30	31.25	N/A	N/A	N/A	N/A	N/A	N/A	I	N/A	BC	N/A	N/A	N/A	34S_4p1d8Yc_0	12/3A1	TDP-WTP-067	7091270
21.3	0.999	0.00487	undefined	1.000	infinite	S	4.54	N/A	N/A	N/A	4.50	8.00	N/A	N/A	N/A	N/A	UCScen	N/A	N/A	I	N/A	SS	N/A	N/A	N/A	34S_4p1d8Ya-04	12/3B1	TDP-WTP-067	7091274
21.3	0.999	0.00487	undefined	1.000	infinite	S	5.03	N/A	N/A	N/A	5.00	8.00	8.75	N/A	N/A	N/A	N/A	N/A	N/A	I	N/A	SS	N/A	N/A	N/A	34S_4p1d8Ya-04	12/3B1	TDP-WTP-067	7091277
21.3	0.999	0.00487	undefined	1.000	infinite	S	6.04	N/A	N/A	N/A	6.00	8.00	14.25	N/A	N/A	N/A	N/A	N/A	N/A	I	N/A	AM	N/A	N/A	N/A	34S_4p1d8Ya-04	12/3B1	TDP-WTP-067	7091279
21.3	0.999	0.00487	undefined	1.000	infinite	S	7.04	N/A	N/A	N/A	7.00	8.00	22.75	N/A	N/A	N/A	N/A	N/A	N/A	I	N/A	AM	N/A	N/A	N/A	34S_4p1d8Ya-04	12/3B1	TDP-WTP-067	7091283
21.3	0.999	0.00487	undefined	1.000	infinite	S	8.02	N/A	N/A	N/A	8.00	8.00	42.50	8.00	vis	UCSvis	N/A	N/A	N/A	I	N/A	CS	N/A	N/A	N/A	34S_4p1d8Ya-04	12/3B1	TDP-WTP-067	7091286
22.0	0.999	0.00487	0.049	0.180	190.0	P	N/A	4.03	4.15	4.38	4.00	12.00	N/A	N/A	center dec	N/A	UCScen	N/A	4.00	D	N/A	SS	N/A	N/A	N/A	34S_4p1d8Yd_9	12/3B2	TDP-WTP-067	7091289
22.0	0.999	0.00487	0.049	0.180	127.0	P	N/A	6.05	6.20	6.46	6.00	12.00	11.00	N/A	N/A	N/A	N/A	N/A	N/A	I	N/A	AM-	N/A	N/A	N/A	34S_4p1d8Yd_9	12/3B2	TDP-WTP-067	7091291
22.0	0.999	0.00487	0.048	0.180	105.0	P	N/A	7.17	7.37	7.67	7.00	12.00	13.50	N/A	N/A	N/A	N/A	N/A	N/A	I	N/A	AM	N/A	N/A	N/A	34S_4p1d8Yd_9	12/3B2	TDP-WTP-067	7091294
22.0	0.999	0.00487	0.049	0.180	92.8	P	N/A	8.17	8.40	8.75	8.00	12.00	16.75	N/A	N/A	N/A	N/A	N/A	N/A	I	N/A	AM	N/A	N/A	N/A	34S_4p1d8Yd_9	12/3B2	TDP-WTP-067	7091297
22.0	0.999	0.00487	0.049	0.180	80.0	P	N/A	9.29	9.57	9.96	9.00	12.00	19.75	N/A	N/A	N/A	N/A	N/A	N/A	I	N/A	AM	N/A	N/A	N/A	34S_4p1d8Yd_9	12/3B2	TDP-WTP-067	7091300
22.0	0.999	0.00487	0.048	0.180	72.5	P	N/A	10.20	10.50	10.92	10.00	12.00	20.25	N/A	N/A	N/A	N/A	N/A	N/A	I	N/A	AM+	N/A	N/A	N/A	34S_4p1d8Yd_9	12/3B2	TDP-WTP-067	7091303
22.0	0.999	0.00487	0.048	0.180	66.0	P	N/A	11.19	11.53	12.00	11.00	12.00	22.50	N/A	N/A	N/A	N/A	N/A	N/A	I	N/A	AM+	N/A	N/A	N/A	34S_4p1d8Yd_9	12/3B2	TDP-WTP-067	7091306
22.0	0.999	0.00487	0.049	0.180	60.5	P	N/A	12.31	12.73	13.27	12.00	12.00	27.25	12.00	vis	UCSvis	N/A	N/A	N/A	I	N/A	CS	N/A	N/A	N/A	34S_4p1d8Yd_9	12/3B2	TDP-WTP-067	7091310
22.0	0.999	0.00487	0.049	0.180	56.0	P	N/A	13.43	13.91	14.51	13.00	12.00	31.75	N/A	N/A	N/A	N/A	N/A	N/A	I	N/A	BC-	N/A	N/A	N/A	34S_4p1d8Yd_9	12/3B2	TDP-WTP-067	7091312
22.0	0.999	0.00487	0.047	0.330	93.0	P	N/A	4.51	4.63	4.83	4.50	10.50	N/A	N/A	N/A	N/A	UCScen	N/A	N/A	I	N/A	SS	N/A	N/A	N/A	34S_4p1d8Yc_9	12/3C1	TDP-WTP-067	7091316
22.0	0.999	0.00487	0.050	0.330	59.0	P	N/A	7.20	7.36	7.61	7.00	10.50	14.00	N/A	N/A	N/A	N/A	N/A	N/A	I	N/A	AM-	N/A	N/A	N/A	34S_4p1d8Yc_9	12/3C1	TDP-WTP-067	7091318
22.0	0.999	0.00487	0.049	0.330	51.5	P	N/A	8.12	8.32	8.59	8.00	10.50	16.00	N/A	N/A	N/A	N/A	N/A	N/A	I	N/A	AM	N/A	N/A	N/A	34S_4p1d8Yc_9	12/3C1	TDP-WTP-067	7091321
22.0	0.999	0.00487	0.050	0.330	41.0	P	N/A	10.29	10.54	10.90	10.00	10.50	22.50	N/A	N/A	N/A	N/A	N/A	N/A	I	N/A	AM+	N/A	N/A	N/A	34S_4p1d8Yc_9	12/3C1	TDP-WTP-067	7091324
22.0	0.999	0.00487	0.049	0.330	38.5	P	N/A	10.77	11.06	11.44	10.50	10.50	26.75	10.50	vis	UCSvis	N/A	N/A	N/A	I	N/A	CS	N/A	N/A	N/A	34S_4p1d8Yc_9	12/3C1	TDP-WTP-067	7091328
22.0	0.999	0.00487	0.049	0.330	35.0	P	N/A	11.78	12.14	12.57	11.50	10.50	34.50	N/A	N/A	N/A	N/A	N/A	N/A	I	N/A	BC	N/A	N/A	N/A	34S_4p1d8Yc_9	12/3C1	TDP-WTP-067	7091330
21.7	0.999	0.00487	undefined	1.000	infinite	S	5.09	N/A	N/A	N/A	5.00	7.00	N/A	N/A	N/A	N/A	N/A	N/A	N/A	D	N/A	SS	N/A	N/A	N/A	34S_4p1d8Ya-40	12/4A1	TDP-WTP-068	7091333
21.7	0.998	0.00487	undefined	1.000	infinite	S	5.56	N/A	N/A	N/A	5.50	7.00	10.00	N/A	N/A	N/A	N/A	N/A	N/A	I	N/A	SS	N/A	N/A	N/A	34S_4p1d8Ya-40	12/4A1	TDP-WTP-068	7091336
21.7	0.998	0.00487	undefined	1.000	infinite	S	6.04	N/A	N/A	N/A	6.00	7.00	13.25	N/A	N/A	N/A	N/A	N/A	N/A	I	N/A	AM	N/A	N/A	N/A	34S_4p1d8Ya-40	12/4A1	TDP-WTP-068	7091339
21.7	0.998	0.00487	undefined	1.000	infinite	S	6.54	N/A	N/A	N/A	6.50	7.00	22.50	N/A	N/A	N/A	UCScen	N/A	N/A	I	N/A	CS-	N/A	N/A	N/A	34S_4p1d8Ya-40	12/4A1	TDP-WTP-068	7091342
21.7	0.998	0.00487	undefined	1.000	infinite	S	7.04	N/A	N/A	N/A	7.00	7.00	30.00	7.00	vis	UCSvis	N/A	N/A	N/A	I	N/A	CS	N/A	N/A	N/A	34S_4p1d8Ya-40	12/4A1	TDP-WTP-068	7091346
21.7	0.998	0.00487	undefined	1.000	infinite	S	7.60	N/A	N/A	N/A	7.50	7.00	40.50	N/A	N/A	N/A	N/A	N/A	N/A	I	N/A	BC	N/A	N/A	N/A	34S_4p1d8Ya-40	12/4A1	TDP-WTP-068	7091348
22.0	0.999	0.00487	0.050	0.180	152.0	P	N/A	5.12	5.24	5.43	5.00	9.00	9.50	N/A	N/A	N/A	N/A	N/A	N/A	N/A	N/A	SS	N/A	N/A	N/A	34S_4p1d8Yd_6	12/4A2	TDP-WTP-068	7091351
22.0	0.999	0.00487	0.049	0.180	125.0	P	N/A	6.12	6.25	6.47	6.00	9.00	11.00	N/A	N/A	N/A	N/A	N/A	N/A	I	N/A	SS	N/A	N/A	N/A	34S_4p1d8Yd_6	12/4A2	TDP-WTP-068	7091354
22.0	0.999	0.00487	0.050	0.180	107.0	P	N/A	7.23	7.40	7.65	7.00	9.00	14.50	N/A	N/A	N/A	N/A	N/A	N/A	I	N/A	SS	N/A	N/A	N/A	34S_4p1d8Yd_6	12/4A2	TDP-WTP-068	7091357
22.0	0.999	0.00487	0.049	0.180	92.0	P	N/A	8.19	8.42	8.72	8.00	9.00	17.50	N/A	N/A	N/A	N/A	N/A	N/A	I	N/A	AM-	N/A	N/A	N/A	34S_4p1d8Yd_6	12/4A2	TDP-WTP-068	7091360
22.0	0.999	0.00487	0.049	0.180	82.0	P	N/A	9.30	9.52	9.83	9.00	9.00	22.00	9.00	vis	UCSvis	N/A	N/A	N/A	I	N/A	CS	N/A	N/A	N/A	34S_4p1d8Yd_6	12/4A2	TDP-WTP-068	7091364
22.0	0.999	0.00487	0.049	0.180	74.0	P	N/A	10.39	10.68	11.08	10.00	9.00	24.75	N/A	N/A	N/A	N/A	N/A	N/A	I	N/A	BC	N/A	N/A	N/A	34S_4p1d8Yd_6	12/4A2	TDP-WTP-068	7091366
22.0	0.999	0.00487	0.049	0.330	68.0	P	N/A	6.11	6.27	6.50	6.00	9.00	11.00	N/A	N/A	N/A	N/A	N/A	N/A	N/A	N/A	SS	N/A	N/A	N/A	34S_4p1d8Yc_6	12/4B1	TDP-WTP-068	7091369
22.0	0.999	0.00487	0.049	0.330	58.0	P	N/A	7.14	7.33	7.60	7.00	9.00	13.75	N/A	N/A	N/A	N/A	N/A	N/A	I	N/A	SS	N/A	N/A	N/A	34S_4p1d8Yc_6	12/4B1	TDP-WTP-068	7091372
22.0	0.999	0.00487	0.050	0.330	50.8	P	N/A	8.21	8.42	8.72	8.00	9.00	19.00	N/A	N/A	N/A	N/A	N/A	N/A	I	N/A	AM-	N/A	N/A	N/A	34S_4p1d8Yc_6	12/4B1	TDP-WTP-068	7091375

Table B.8. Data from Fall 2007 Tests in Mid-Scale Vessel with Spherical Head A.12

Row Number	Test	Case ID	Tank Diameter	Head Shape	Dish Height	Dish Volume	Tank Fill Height	Return Line Height	Nozzle Inner Diameter	Nozzle Stand-off Distance	Pulse Tube Configuration	Installed Nozzles	Outer Nozzles Operated	Inner Nozzles Operated	Pulse Tube Outer Diameter	Outer PJM Radius	Inner PJM Radius	"FIO" Outer PJM Impingement Angle	"FIO" Inner PJM Impingement Angle	Ratio Outer PJM to Tank Radius	Ratio Inner PJM to Tank Radius	Simulant	Solids Density	Particle Diameter d5	Particle Diameter d50	Particle Diameter d95	Void Fraction
text	text	text	in.	text	in.	in. ^{3}	in.	in.	in.	in.	text	number	number	number	in.	in.	in.	deg	deg	nondim	nondim	text	g/cm^3	m	m	m	fraction
MSS	M/DDX	ID	D	HS	H_{dish}	V_{dish}	H	Rtn	d	sod	PT	N	N_O	N_I	PT_{od}	R_O	R_I	θ_O	θ_I	R_O/R	R_I/R	sxdx	ρ_s	d_5	d_{50}	d_{95}	vf
7091379M	12/4B1	34S_4p1d8Yc_6	33 7/8	S	9	4437.4	67 3/4	61 3/4	0.297	0.446	HLP-22	12	4	0	1.9	10.5	5.7	30.8	16.1	0.62	0.33	p1d8	2.45	0.0000605	0.0000895	0.0001320	0.4269
7091381M	12/4B1	34S_4p1d8Yc_6	33 7/8	S	9	4437.4	67 3/4	61 3/4	0.297	0.446	HLP-22	12	4	0	1.9	10.5	5.7	30.8	16.1	0.62	0.33	p1d8	2.45	0.0000605	0.0000895	0.0001320	0.4269
7091384	12/4C1	34S_4p1d8Ya-80	33 7/8	S	9	4437.4	67 3/4	61 3/4	0.297	0.446	HLP-22	12	8	0	1.9	10.5	5.7	30.8	16.1	0.62	0.33	p1d8	2.45	0.0000605	0.0000895	0.0001320	0.4269
7091388	12/4C1	34S_4p1d8Ya-80	33 7/8	S	9	4437.4	67 3/4	61 3/4	0.297	0.446	HLP-22	12	8	0	1.9	10.5	5.7	30.8	16.1	0.62	0.33	p1d8	2.45	0.0000605	0.0000895	0.0001320	0.4269
7091391	12/4C1	34S_4p1d8Ya-80	33 7/8	S	9	4437.4	67 3/4	61 3/4	0.297	0.446	HLP-22	12	8	0	1.9	10.5	5.7	30.8	16.1	0.62	0.33	p1d8	2.45	0.0000605	0.0000895	0.0001320	0.4269
7091393	12/4C2	34S_4p1d8Yd_5	33 7/8	S	9	4437.4	67 3/4	61 3/4	0.297	0.446	HLP-22	12	8	0	1.9	10.5	5.7	30.8	16.1	0.62	0.33	p1d8	2.45	0.0000605	0.0000895	0.0001320	0.4269
7091396	12/4C2	34S_4p1d8Yd_5	33 7/8	S	9	4437.4	67 3/4	61 3/4	0.297	0.446	HLP-22	12	8	0	1.9	10.5	5.7	30.8	16.1	0.62	0.33	p1d8	2.45	0.0000605	0.0000895	0.0001320	0.4269
7091399	12/4C2	34S_4p1d8Yd_5	33 7/8	S	9	4437.4	67 3/4	61 3/4	0.297	0.446	HLP-22	12	8	0	1.9	10.5	5.7	30.8	16.1	0.62	0.33	p1d8	2.45	0.0000605	0.0000895	0.0001320	0.4269
7091402	12/4C2	34S_4p1d8Yd_5	33 7/8	S	9	4437.4	67 3/4	61 3/4	0.297	0.446	HLP-22	12	8	0	1.9	10.5	5.7	30.8	16.1	0.62	0.33	p1d8	2.45	0.0000605	0.0000895	0.0001320	0.4269
7091405	12/4C2	34S_4p1d8Yd_5	33 7/8	S	9	4437.4	67 3/4	61 3/4	0.297	0.446	HLP-22	12	8	0	1.9	10.5	5.7	30.8	16.1	0.62	0.33	p1d8	2.45	0.0000605	0.0000895	0.0001320	0.4269
7091409M	12/4C2	34S_4p1d8Yd_5	33 7/8	S	9	4437.4	67 3/4	61 3/4	0.297	0.446	HLP-22	12	8	0	1.9	10.5	5.7	30.8	16.1	0.62	0.33	p1d8	2.45	0.0000605	0.0000895	0.0001320	0.4269
7091411M	12/4C2	34S_4p1d8Yd_5	33 7/8	S	9	4437.4	67 3/4	61 3/4	0.297	0.446	HLP-22	12	8	0	1.9	10.5	5.7	30.8	16.1	0.62	0.33	p1d8	2.45	0.0000605	0.0000895	0.0001320	0.4269
7091414	12/4D1	34S_4p1d8Yc_5	33 7/8	S	9	4437.4	67 3/4	61 3/4	0.297	0.446	HLP-22	12	8	0	1.9	10.5	5.7	30.8	16.1	0.62	0.33	p1d8	2.45	0.0000605	0.0000895	0.0001320	0.4269
7091417	12/4D1	34S_4p1d8Yc_5	33 7/8	S	9	4437.4	67 3/4	61 3/4	0.297	0.446	HLP-22	12	8	0	1.9	10.5	5.7	30.8	16.1	0.62	0.33	p1d8	2.45	0.0000605	0.0000895	0.0001320	0.4269
7091421M	12/4D1	34S_4p1d8Yc_5	33 7/8	S	9	4437.4	67 3/4	61 3/4	0.297	0.446	HLP-22	12	8	0	1.9	10.5	5.7	30.8	16.1	0.62	0.33	p1d8	2.45	0.0000605	0.0000895	0.0001320	0.4269
7091423M	12/4D1	34S_4p1d8Yc_5	33 7/8	S	9	4437.4	67 3/4	61 3/4	0.297	0.446	HLP-22	12	8	0	1.9	10.5	5.7	30.8	16.1	0.62	0.33	p1d8	2.45	0.0000605	0.0000895	0.0001320	0.4269

Table B.8. Data from Fall 2007 Tests in Mid-Scale Vessel with Spherical Head B.12

Tank Water Temperature	Water Density	Solids Fraction	Pulse Volume Fraction	Duty Cycle	Cycle Time	Pulsed or Steady Jet	Us Steady Jet	U1 Pulsing Jet	U2 URMS	U3 URM3	Discharge Velocity	Critical Suspension Velocity	Average Peak Cloud Height	UCS Condition	UCS Method	UCS Flag	UCS Center Flag	UCS udv Flag	UCS based on Decreasing Velocity	Sweep Increase / Decrease	UDV Height Bed	Particle Motion	Solids Level	Outer Bottom Pattern	Inner Bottom Pattern	Case ID	Test	TDP	Row Number
C	g/cm³	fraction	fraction	fraction	s	text	m/s	m/s	m/s	m/s	m/s	m/s	in.	m/s	text	text	text	text	m/s	text	mm	text	text	text	text	text	text	text	text
T	ρ_l	ϕ_S	ϕ_p	DC	t_C	Jet	U_S	U1	U2	U3	U	U_{CS}	H_C	U_{CSR}	U_{CSM}	U_{CS}vis	U_{CS}cen	U_{CS}udv	U_{CS}_D	S_W	H_{bed}	PM	Sol	SP_O	SP_I	ID	M/DDX	TDP	MSS
22.0	0.999	0.00487	0.049	0.330	45.0	P	N/A	9.27	9.53	9.88	9.00	9.00	25.63	9.00	vis	UCSvis	N/A	N/A	N/A	I	N/A	CS	N/A	N/A	N/A	34S_4p1d8Yc_6	12/4B1	TDP-WTP-068	7091379
22.0	0.999	0.00487	0.050	0.330	41.0	P	N/A	10.29	10.57	10.97	10.00	9.00	34.00	N/A	N/A	N/A	N/A	N/A	N/A	I	N/A	BC	N/A	N/A	N/A	34S_4p1d8Yc_6	12/4B1	TDP-WTP-068	7091381
22.1	0.998	0.00487	undefined	1.000	infinite	S	4.07	N/A	N/A	N/A	4.00	5.20	17.00	N/A	N/A	N/A	N/A	N/A	N/A	N/A	N/A	SS	N/A	N/A	N/A	34S_4p1d8Ya-80	12/4C1	TDP-WTP-068	7091384
22.1	0.998	0.00487	undefined	1.000	infinite	S	5.05	N/A	N/A	N/A	5.00	5.20	42.00	N/A	N/A	N/A	N/A	N/A	N/A	I	N/A	AM	N/A	N/A	N/A	34S_4p1d8Ya-80	12/4C1	TDP-WTP-068	7091388
22.2	0.998	0.00487	undefined	1.000	infinite	S	5.30	N/A	N/A	N/A	5.20	5.20	51.00	5.20	vis	UCSvis	N/A	N/A	N/A	I	N/A	CS	N/A	N/A	N/A	34S_4p1d8Ya-80	12/4C1	TDP-WTP-068	7091391
22.0	0.999	0.00487	0.049	0.180	76.0	P	N/A	4.97	5.03	5.06	5.00	9.00	14.25	N/A	N/A	N/A	N/A	N/A	N/A	N/A	N/A	SS	N/A	N/A	N/A	34S_4p1d8Yd_5	12/4C2	TDP-WTP-068	7091393
22.0	0.999	0.00487	0.049	0.180	63.5	P	N/A	5.97	6.04	6.09	6.00	9.00	16.75	N/A	N/A	N/A	N/A	N/A	N/A	I	N/A	SS	N/A	N/A	N/A	34S_4p1d8Yd_5	12/4C2	TDP-WTP-068	7091396
22.0	0.999	0.00487	0.050	0.180	54.5	P	N/A	6.95	7.05	7.11	7.00	9.00	20.25	N/A	N/A	N/A	N/A	N/A	N/A	I	N/A	SS	N/A	N/A	N/A	34S_4p1d8Yd_5	12/4C2	TDP-WTP-068	7091399
22.0	0.999	0.00487	0.049	0.180	47.8	P	N/A	7.88	8.00	8.07	8.00	9.00	26.13	N/A	N/A	N/A	N/A	N/A	N/A	I	N/A	SS	N/A	N/A	N/A	34S_4p1d8Yd_5	12/4C2	TDP-WTP-068	7091402
22.0	0.999	0.00487	0.050	0.180	45.0	P	N/A	8.43	8.58	8.67	8.50	9.00	28.00	N/A	N/A	N/A	N/A	N/A	N/A	I	N/A	SS+	N/A	N/A	N/A	34S_4p1d8Yd_5	12/4C2	TDP-WTP-068	7091405
22.0	0.999	0.00487	0.049	0.180	41.0	P	N/A	9.00	9.12	9.21	9.00	9.00	37.50	9.00	vis	UCSvis	N/A	N/A	N/A	I	N/A	CS	N/A	N/A	N/A	34S_4p1d8Yd_5	12/4C2	TDP-WTP-068	7091409
22.0	0.999	0.00487	0.049	0.180	40.0	P	N/A	9.41	9.60	9.71	9.50	9.00	47.75	N/A	N/A	N/A	N/A	N/A	N/A	I	N/A	BC	N/A	N/A	N/A	34S_4p1d8Yd_5	12/4C2	TDP-WTP-068	7091411
22.0	0.999	0.00487	0.050	0.330	35.0	P	N/A	5.98	6.04	6.09	6.00	7.50	18.75	N/A	N/A	N/A	N/A	N/A	N/A	N/A	N/A	SS	N/A	N/A	N/A	34S_4p1d8Yc_5	12/4D1	TDP-WTP-068	7091414
22.0	0.999	0.00487	0.049	0.330	29.5	P	N/A	7.04	7.11	7.15	7.00	7.50	29.75	N/A	N/A	N/A	N/A	N/A	N/A	I	N/A	SS+	N/A	N/A	N/A	34S_4p1d8Yc_5	12/4D1	TDP-WTP-068	7091417
22.0	0.999	0.00487	0.049	0.330	27.5	P	N/A	7.51	7.61	7.67	7.50	7.50	38.00	7.50	vis	UCSvis	N/A	N/A	N/A	I	N/A	CS	N/A	N/A	N/A	34S_4p1d8Yc_5	12/4D1	TDP-WTP-068	7091421
22.0	0.999	0.00487	0.049	0.330	26.0	P	N/A	7.92	8.03	8.09	8.00	7.50	48.00	N/A	N/A	N/A	N/A	N/A	N/A	I	N/A	BC	N/A	N/A	N/A	34S_4p1d8Yc_5	12/4D1	TDP-WTP-068	7091423

Table B.9. Updated Data from Fall 2007 Tests in Mid-Scale Vessel with Spherical Head A.1

Row Number	Test	Case ID	Tank Diameter	Head Shape	Dish Height	Dish Volume	Tank Fill Height	Return Line Height	Nozzle Inner Diameter	Nozzle Stand-off Distance	Pulse Tube Configuration	Installed Nozzles	Outer Nozzles Operated	Inner Nozzles Operated	Pulse Tube Outer Diameter	Outer PJM Radius	Inner PJM Radius	"FIO" Outer PJM Impingement Angle	"FIO" Inner PJM Impingement Angle	Ratio Outer PJM to Tank Radius	Ratio Inner PJM to Tank Radius	Simulant	Solids Density	Particle Diameter d5	Particle Diameter d50	Particle Diameter d95	Void Fraction
text	text	text	in.	text	in.	in. ^{3}	in.	in.	in.	in.	text	number	number	number	in.	in.	in.	deg	deg	nondim	nondim	text	g/cm^3	m	m	m	fraction
MSS	M/DDX	ID	D	HS	H_{dish}	V_{dish}	H	Rtn	d	sod	PT	N	N_O	N_I	PT_{od}	R_O	R_I	Θ_O	Θ_I	R_O/R	R_I/R	sxdx	ρ_S	d_5	d_{50}	d_{95}	vf
7090002	10/17A1	34S_6p1d7Ya-80	33 7/8	S	9	4437.4	67 3/4	61 3/4	0.446	0.669	HLP-22	12	8	0	1.9	10.5	5.7	30.8	16.1	0.62	0.33	p1d7	2.45	0.0001213	0.0001780	0.0002606	0.4277
7090004	10/17A1	34S_6p1d7Ya-80	33 7/8	S	9	4437.4	67 3/4	61 3/4	0.446	0.669	HLP-22	12	8	0	1.9	10.5	5.7	30.8	16.1	0.62	0.33	p1d7	2.45	0.0001213	0.0001780	0.0002606	0.4277
7090006	10/17A1	34S_6p1d7Ya-80	33 7/8	S	9	4437.4	67 3/4	61 3/4	0.446	0.669	HLP-22	12	8	0	1.9	10.5	5.7	30.8	16.1	0.62	0.33	p1d7	2.45	0.0001213	0.0001780	0.0002606	0.4277
7090008	10/17A1	34S_6p1d7Ya-80	33 7/8	S	9	4437.4	67 3/4	61 3/4	0.446	0.669	HLP-22	12	8	0	1.9	10.5	5.7	30.8	16.1	0.62	0.33	p1d7	2.45	0.0001213	0.0001780	0.0002606	0.4277
7090012	10/17A1	34S_6p1d7Ya-80	33 7/8	S	9	4437.4	67 3/4	61 3/4	0.446	0.669	HLP-22	12	8	0	1.9	10.5	5.7	30.8	16.1	0.62	0.33	p1d7	2.45	0.0001213	0.0001780	0.0002606	0.4277
7090015	10/17A1	34S_6p1d7Ya-80	33 7/8	S	9	4437.4	67 3/4	61 3/4	0.446	0.669	HLP-22	12	8	0	1.9	10.5	5.7	30.8	16.1	0.62	0.33	p1d7	2.45	0.0001213	0.0001780	0.0002606	0.4277
7090019	10/17A1	34S_6p1d7Ya-80	33 7/8	S	9	4437.4	67 3/4	61 3/4	0.446	0.669	HLP-22	12	8	0	1.9	10.5	5.7	30.8	16.1	0.62	0.33	p1d7	2.45	0.0001213	0.0001780	0.0002606	0.4277
7090023	10/17A2	34S_6p1d7Yd_5	33 7/8	S	9	4437.4	67 3/4	61 3/4	0.446	0.669	HLP-22	12	8	0	1.9	10.5	5.7	30.8	16.1	0.62	0.33	p1d7	2.45	0.0001213	0.0001780	0.0002606	0.4277
7090026	10/17A2	34S_6p1d7Yd_5	33 7/8	S	9	4437.4	67 3/4	61 3/4	0.446	0.669	HLP-22	12	8	0	1.9	10.5	5.7	30.8	16.1	0.62	0.33	p1d7	2.45	0.0001213	0.0001780	0.0002606	0.4277
7090029	10/17A2	34S_6p1d7Yd_5	33 7/8	S	9	4437.4	67 3/4	61 3/4	0.446	0.669	HLP-22	12	8	0	1.9	10.5	5.7	30.8	16.1	0.62	0.33	p1d7	2.45	0.0001213	0.0001780	0.0002606	0.4277
7090032	10/17A2	34S_6p1d7Yd_5	33 7/8	S	9	4437.4	67 3/4	61 3/4	0.446	0.669	HLP-22	12	8	0	1.9	10.5	5.7	30.8	16.1	0.62	0.33	p1d7	2.45	0.0001213	0.0001780	0.0002606	0.4277
7090035	10/17A2	34S_6p1d7Yd_5	33 7/8	S	9	4437.4	67 3/4	61 3/4	0.446	0.669	HLP-22	12	8	0	1.9	10.5	5.7	30.8	16.1	0.62	0.33	p1d7	2.45	0.0001213	0.0001780	0.0002606	0.4277
7090038	10/17A2	34S_6p1d7Yd_5	33 7/8	S	9	4437.4	67 3/4	61 3/4	0.446	0.669	HLP-22	12	8	0	1.9	10.5	5.7	30.8	16.1	0.62	0.33	p1d7	2.45	0.0001213	0.0001780	0.0002606	0.4277
7090040	10/17A2	34S_6p1d7Yd_5	33 7/8	S	9	4437.4	67 3/4	61 3/4	0.446	0.669	HLP-22	12	8	0	1.9	10.5	5.7	30.8	16.1	0.62	0.33	p1d7	2.45	0.0001213	0.0001780	0.0002606	0.4277
7090043	10/17A2	34S_6p1d7Yd_5	33 7/8	S	9	4437.4	67 3/4	61 3/4	0.446	0.669	HLP-22	12	8	0	1.9	10.5	5.7	30.8	16.1	0.62	0.33	p1d7	2.45	0.0001213	0.0001780	0.0002606	0.4277
7090046	10/17A2	34S_6p1d7Yd_5	33 7/8	S	9	4437.4	67 3/4	61 3/4	0.446	0.669	HLP-22	12	8	0	1.9	10.5	5.7	30.8	16.1	0.62	0.33	p1d7	2.45	0.0001213	0.0001780	0.0002606	0.4277
7090048	10/17A2	34S_6p1d7Yd_5	33 7/8	S	9	4437.4	67 3/4	61 3/4	0.446	0.669	HLP-22	12	8	0	1.9	10.5	5.7	30.8	16.1	0.62	0.33	p1d7	2.45	0.0001213	0.0001780	0.0002606	0.4277
7090052	10/17A2	34S_6p1d7Yd_5	33 7/8	S	9	4437.4	67 3/4	61 3/4	0.446	0.669	HLP-22	12	8	0	1.9	10.5	5.7	30.8	16.1	0.62	0.33	p1d7	2.45	0.0001213	0.0001780	0.0002606	0.4277
7090054M	10/17A2	34S_6p1d7Yd_5	33 7/8	S	9	4437.4	67 3/4	61 3/4	0.446	0.669	HLP-22	12	8	0	1.9	10.5	5.7	30.8	16.1	0.62	0.33	p1d7	2.45	0.0001213	0.0001780	0.0002606	0.4277
7090056	10/18A1	34S_6p1d7Ya-44	33 7/8	S	9	4437.4	67 3/4	61 3/4	0.446	0.669	HLP-22	12	4	4	1.9	10.5	5.7	30.8	16.1	0.62	0.33	p1d7	2.45	0.0001213	0.0001780	0.0002606	0.4277
7090059	10/18A1	34S_6p1d7Ya-44	33 7/8	S	9	4437.4	67 3/4	61 3/4	0.446	0.669	HLP-22	12	4	4	1.9	10.5	5.7	30.8	16.1	0.62	0.33	p1d7	2.45	0.0001213	0.0001780	0.0002606	0.4277
7090063	10/18A1	34S_6p1d7Ya-44	33 7/8	S	9	4437.4	67 3/4	61 3/4	0.446	0.669	HLP-22	12	4	4	1.9	10.5	5.7	30.8	16.1	0.62	0.33	p1d7	2.45	0.0001213	0.0001780	0.0002606	0.4277
7090066	10/18A1	34S_6p1d7Ya-44	33 7/8	S	9	4437.4	67 3/4	61 3/4	0.446	0.669	HLP-22	12	4	4	1.9	10.5	5.7	30.8	16.1	0.62	0.33	p1d7	2.45	0.0001213	0.0001780	0.0002606	0.4277
7090068	10/18A1	34S_6p1d7Ya-44	33 7/8	S	9	4437.4	67 3/4	61 3/4	0.446	0.669	HLP-22	12	4	4	1.9	10.5	5.7	30.8	16.1	0.62	0.33	p1d7	2.45	0.0001213	0.0001780	0.0002606	0.4277
7090071	10/18A2	34S_6p1d7Yd_0	33 7/8	S	9	4437.4	67 3/4	61 3/4	0.446	0.669	HLP-22	12	4	4	1.9	10.5	5.7	30.8	16.1	0.62	0.33	p1d7	2.45	0.0001213	0.0001780	0.0002606	0.4277
7090074	10/18A2	34S_6p1d7Yd_0	33 7/8	S	9	4437.4	67 3/4	61 3/4	0.446	0.669	HLP-22	12	4	4	1.9	10.5	5.7	30.8	16.1	0.62	0.33	p1d7	2.45	0.0001213	0.0001780	0.0002606	0.4277
7090077	10/18A2	34S_6p1d7Yd_0	33 7/8	S	9	4437.4	67 3/4	61 3/4	0.446	0.669	HLP-22	12	4	4	1.9	10.5	5.7	30.8	16.1	0.62	0.33	p1d7	2.45	0.0001213	0.0001780	0.0002606	0.4277
7090081	10/18A2	34S_6p1d7Yd_0	33 7/8	S	9	4437.4	67 3/4	61 3/4	0.446	0.669	HLP-22	12	4	4	1.9	10.5	5.7	30.8	16.1	0.62	0.33	p1d7	2.45	0.0001213	0.0001780	0.0002606	0.4277
7090085	10/18A2	34S_6p1d7Yd_0	33 7/8	S	9	4437.4	67 3/4	61 3/4	0.446	0.669	HLP-22	12	4	4	1.9	10.5	5.7	30.8	16.1	0.62	0.33	p1d7	2.45	0.0001213	0.0001780	0.0002606	0.4277
7090089	10/18A2	34S_6p1d7Yd_0	33 7/8	S	9	4437.4	67 3/4	61 3/4	0.446	0.669	HLP-22	12	4	4	1.9	10.5	5.7	30.8	16.1	0.62	0.33	p1d7	2.45	0.0001213	0.0001780	0.0002606	0.4277
7090095M	10/18A2	34S_6p1d7Yd_0	33 7/8	S	9	4437.4	67 3/4	61 3/4	0.446	0.669	HLP-22	12	4	4	1.9	10.5	5.7	30.8	16.1	0.62	0.33	p1d7	2.45	0.0001213	0.0001780	0.0002606	0.4277
7090097	10/18B1	34S_6p1d7Ya-40	33 7/8	S	9	4437.4	67 3/4	61 3/4	0.446	0.669	HLP-22	12	4	0	1.9	10.5	5.7	30.8	16.1	0.62	0.33	p1d7	2.45	0.0001213	0.0001780	0.0002606	0.4277
7090101	10/18B1	34S_6p1d7Ya-40	33 7/8	S	9	4437.4	67 3/4	61 3/4	0.446	0.669	HLP-22	12	4	0	1.9	10.5	5.7	30.8	16.1	0.62	0.33	p1d7	2.45	0.0001213	0.0001780	0.0002606	0.4277
7090105	10/18B1	34S_6p1d7Ya-40	33 7/8	S	9	4437.4	67 3/4	61 3/4	0.446	0.669	HLP-22	12	4	0	1.9	10.5	5.7	30.8	16.1	0.62	0.33	p1d7	2.45	0.0001213	0.0001780	0.0002606	0.4277
7090111	10/18B1	34S_6p1d7Ya-40	33 7/8	S	9	4437.4	67 3/4	61 3/4	0.446	0.669	HLP-22	12	4	0	1.9	10.5	5.7	30.8	16.1	0.62	0.33	p1d7	2.45	0.0001213	0.0001780	0.0002606	0.4277
7090113	10/18B2	34S_6p1d7Yd_6	33 7/8	S	9	4437.4	67 3/4	61 3/4	0.446	0.669	HLP-22	12	4	0	1.9	10.5	5.7	30.8	16.1	0.62	0.33	p1d7	2.45	0.0001213	0.0001780	0.0002606	0.4277
7090116	10/18B2	34S_6p1d7Yd_6	33 7/8	S	9	4437.4	67 3/4	61 3/4	0.446	0.669	HLP-22	12	4	0	1.9	10.5	5.7	30.8	16.1	0.62	0.33	p1d7	2.45	0.0001213	0.0001780	0.0002606	0.4277
7090119	10/18B2	34S_6p1d7Yd_6	33 7/8	S	9	4437.4	67 3/4	61 3/4	0.446	0.669	HLP-22	12	4	0	1.9	10.5	5.7	30.8	16.1	0.62	0.33	p1d7	2.45	0.0001213	0.0001780	0.0002606	0.4277
7090122	10/18B2	34S_6p1d7Yd_6	33 7/8	S	9	4437.4	67 3/4	61 3/4	0.446	0.669	HLP-22	12	4	0	1.9	10.5	5.7	30.8	16.1	0.62	0.33	p1d7	2.45	0.0001213	0.0001780	0.0002606	0.4277
7090126	10/18B2	34S_6p1d7Yd_6	33 7/8	S	9	4437.4	67 3/4	61 3/4	0.446	0.669	HLP-22	12	4	0	1.9	10.5	5.7	30.8	16.1	0.62	0.33	p1d7	2.45	0.0001213	0.0001780	0.0002606	0.4277
7090130	10/18B2	34S_6p1d7Yd_6	33 7/8	S	9	4437.4	67 3/4	61 3/4	0.446	0.669	HLP-22	12	4	0	1.9	10.5	5.7	30.8	16.1	0.62	0.33	p1d7	2.45	0.0001213	0.0001780	0.0002606	0.4277

Table B.9. Updated Data from Fall 2007 Tests in Mid-Scale Vessel with Spherical Head B.1

Tank Water Temperature	Water Density	Solids Fraction	Pulse Volume Fraction	Duty Cycle	Cycle Time	Pulsed or Steady Jet	Us Steady Jet	U1 Pulsing Jet	U2 URMS	U3 URM3	Discharge Velocity	Critical Suspension Velocity	Average Peak Cloud Height	U_{CS} Condition	U_{CS} Method	U_{CS} Flag	U_{CS} Center Flag	U_{CS} udv Flag	U_{CS} based on Decreasing Velocity	Sweep Increase / Decrease	UDV Height Bed	Particle Motion	Solids Level	Outer Bottom Pattern	Inner Bottom Pattern	Case ID	Test	TDP	Row Number
C	g/cm³	fraction	fraction	fraction	s	text	m/s	m/s	m/s	m/s	m/s	m/s	in.	m/s	text	text	text	text	m/s	text	mm	text	text	text	text	text	text	text	text
T	ρ_l	ϕ_S	ϕ_P	DC	t_C	Jet	US	U1	U2	U3	U	U_{CS}	H_C	U_{CSR}	U_{CSM}	U_{CS}vis	U_{CS}cen	U_{CS}udv	U_{CS_D}	S_W	H_{bed}	PM	Sol	SP_O	SP_I	ID	M/DDX	TDP	MSS
21.2	0.999	0.00487	undefined	1.000	infinite	S	3.04	N/A	N/A	N/A	3.00	4.50	8.63	N/A	N/A	N/A	N/A	N/A	N/A	I	N/A	SS	N/A	N/A	N/A	34S_6p1d7Ya-80	10/17A1	TDP-WTP-033	7090002
21.3	0.999	0.00487	undefined	1.000	infinite	S	3.30	N/A	N/A	N/A	3.30	4.50	9.13	N/A	N/A	N/A	N/A	N/A	N/A	I	N/A	SS	N/A	N/A	N/A	34S_6p1d7Ya-80	10/17A1	TDP-WTP-033	7090004
21.2	0.999	0.00487	undefined	1.000	infinite	S	3.74	N/A	N/A	N/A	3.70	4.50	10.13	N/A	N/A	N/A	N/A	N/A	N/A	I	N/A	SS	N/A	N/A	N/A	34S_6p1d7Ya-80	10/17A1	TDP-WTP-033	7090006
21.3	0.999	0.00487	undefined	1.000	infinite	S	4.14	N/A	N/A	N/A	4.10	4.50	19.63	N/A	N/A	N/A	N/A	N/A	N/A	I	N/A	SS	SCO	BP5	N/A	34S_6p1d7Ya-80	10/17A1	TDP-WTP-033	7090008
21.3	0.999	0.00487	undefined	1.000	infinite	S	4.33	N/A	N/A	N/A	4.30	4.50	24.29	N/A	N/A	N/A	N/A	N/A	N/A	I	N/A	AM	SOO	BP6	N/A	34S_6p1d7Ya-80	10/17A1	TDP-WTP-033	7090012
21.3	0.999	0.00487	undefined	1.000	infinite	S	4.46	N/A	N/A	N/A	4.50	4.50	31.29	4.50	vis	UCSvis	N/A	N/A	N/A	I	N/A	CS	NSS	BP6	N/A	34S_6p1d7Ya-80	10/17A1	TDP-WTP-033	7090015
21.3	0.999	0.00487	undefined	1.000	infinite	S	4.40	N/A	N/A	N/A	4.40	4.50	28.29	N/A	vis dec	UCSvis	N/A	N/A	4.40	D	N/A	CS	NSS	BP6	N/A	34S_6p1d7Ya-80	10/17A1	TDP-WTP-033	7090019
21.0	0.999	0.00487	0.053	0.180	62.5	P	N/A	2.91	2.95	2.96	3.00	6.60	9.46	N/A	N/A	N/A	N/A	N/A	N/A	D	N/A	SS	N/A	N/A	N/A	34S_6p1d7Yd_5	10/17A2	TDP-WTP-033	7090023
21.0	0.999	0.00487	0.060	0.180	57.1	P	N/A	3.41	3.45	3.48	3.50	6.60	9.96	N/A	N/A	N/A	N/A	N/A	N/A	I	N/A	SS	N/A	N/A	N/A	34S_6p1d7Yd_5	10/17A2	TDP-WTP-033	7090026
21.0	0.999	0.00487	0.057	0.180	48.8	P	N/A	3.60	3.79	3.87	4.00	6.60	11.63	N/A	N/A	N/A	N/A	N/A	N/A	I	N/A	SS	N/A	N/A	N/A	34S_6p1d7Yd_5	10/17A2	TDP-WTP-033	7090029
21.0	0.999	0.00487	0.056	0.180	40.0	P	N/A	3.89	4.15	4.26	4.50	6.60	11.96	N/A	N/A	N/A	N/A	N/A	N/A	I	N/A	SS	N/A	N/A	N/A	34S_6p1d7Yd_5	10/17A2	TDP-WTP-033	7090032
21.0	0.999	0.00487	0.052	0.180	35.7	P	N/A	4.10	4.47	4.63	5.00	6.60	12.96	N/A	N/A	N/A	N/A	N/A	N/A	I	N/A	SS	N/A	N/A	N/A	34S_6p1d7Yd_5	10/17A2	TDP-WTP-033	7090035
21.0	0.999	0.00487	0.053	0.180	32.3	P	N/A	4.24	4.75	4.97	5.50	6.60	14.63	N/A	N/A	N/A	N/A	N/A	N/A	I	N/A	SS	N/A	N/A	N/A	34S_6p1d7Yd_5	10/17A2	TDP-WTP-033	7090038
21.0	0.999	0.00487	0.051	0.180	30.2	P	N/A	4.19	4.82	5.10	5.80	6.60	17.13	N/A	N/A	N/A	N/A	N/A	N/A	I	N/A	SS+	SCO	BP5	N/A	34S_6p1d7Yd_5	10/17A2	TDP-WTP-033	7090040
21.0	0.999	0.00487	0.051	0.180	29.1	P	N/A	4.18	4.88	5.20	6.00	6.60	19.13	N/A	N/A	N/A	N/A	N/A	N/A	I	N/A	AM	SCO	BP5	N/A	34S_6p1d7Yd_5	10/17A2	TDP-WTP-033	7090043
21.0	0.999	0.00487	0.053	0.180	28.7	P	N/A	4.12	4.93	5.30	6.20	6.60	21.63	N/A	N/A	N/A	N/A	N/A	N/A	I	N/A	AM	SCO	BP5	N/A	34S_6p1d7Yd_5	10/17A2	TDP-WTP-033	7090046
21.0	0.999	0.00487	0.051	0.180	27.0	P	N/A	3.97	4.88	5.30	6.40	6.60	21.63	N/A	N/A	N/A	N/A	N/A	N/A	I	N/A	AM+	SCO	BP5	N/A	34S_6p1d7Yd_5	10/17A2	TDP-WTP-033	7090048
21.0	0.999	0.00487	0.052	0.180	27.0	P	N/A	3.88	4.86	5.31	6.50	6.60	22.63	N/A	N/A	N/A	N/A	N/A	N/A	I	N/A	AM	SCO	BP5	N/A	34S_6p1d7Yd_5	10/17A2	TDP-WTP-033	7090052
21.0	0.999	0.00487	0.053	0.180	27.0	P	N/A	4.24	5.14	5.55	6.60	6.60	23.63	6.60	vis	UCSvis	N/A	N/A	N/A	I	N/A	CS	NSS	BP6	N/A	34S_6p1d7Yd_5	10/17A2	TDP-WTP-033	7090054
21.4	0.999	0.00487	undefined	1.000	infinite	S	3.52	N/A	N/A	N/A	3.50	5.50	N/A	N/A	N/A	N/A	N/A	N/A	N/A	I	N/A	SS	N/A	N/A	N/A	34S_6p1d7Ya-44	10/18A1	TDP-WTP-038	7090056
21.4	0.999	0.00487	undefined	1.000	infinite	S	4.02	N/A	N/A	N/A	4.00	5.50	10.00	N/A	N/A	N/A	N/A	N/A	N/A	I	N/A	AM	N/A	N/A	N/A	34S_6p1d7Ya-44	10/18A1	TDP-WTP-038	7090059
21.5	0.999	0.00487	undefined	1.000	infinite	S	4.51	N/A	N/A	N/A	4.50	5.50	16.00	N/A	N/A	N/A	N/A	N/A	N/A	I	N/A	AM	N/A	N/A	N/A	34S_6p1d7Ya-44	10/18A1	TDP-WTP-038	7090063
21.5	0.999	0.00487	undefined	1.000	infinite	S	5.01	N/A	N/A	N/A	5.00	5.50	31.00	N/A	N/A	N/A	N/A	N/A	N/A	I	N/A	AM	N/A	N/A	N/A	34S_6p1d7Ya-44	10/18A1	TDP-WTP-038	7090066
21.5	0.999	0.00487	undefined	1.000	infinite	S	5.52	N/A	N/A	N/A	5.50	5.50	47.50	5.50	vis	UCSvis	N/A	N/A	N/A	I	N/A	CS	N/A	N/A	N/A	34S_6p1d7Ya-44	10/18A1	TDP-WTP-038	7090068
22.0	0.999	0.00487	0.053	0.180	48.8	P	N/A	3.73	3.85	3.90	4.00	6.10	9.00	N/A	N/A	N/A	N/A	N/A	N/A	N/A	N/A	SS	N/A	N/A	N/A	34S_6p1d7Yd_0	10/18A2	TDP-WTP-038	7090071
22.0	0.999	0.00487	0.052	0.180	40.0	P	N/A	3.99	4.20	4.29	4.50	6.10	10.50	N/A	N/A	N/A	N/A	N/A	N/A	I	N/A	AM	N/A	N/A	N/A	34S_6p1d7Yd_0	10/18A2	TDP-WTP-038	7090074
22.0	0.999	0.00487	0.054	0.180	36.4	P	N/A	4.24	4.57	4.70	5.00	6.10	13.83	N/A	N/A	N/A	N/A	N/A	N/A	I	N/A	AM	N/A	N/A	N/A	34S_6p1d7Yd_0	10/18A2	TDP-WTP-038	7090077
22.0	0.999	0.00487	0.054	0.180	33.3	P	N/A	4.36	4.82	5.01	5.50	6.10	15.67	N/A	N/A	N/A	N/A	N/A	N/A	I	N/A	AM	N/A	N/A	N/A	34S_6p1d7Yd_0	10/18A2	TDP-WTP-038	7090081
22.0	0.999	0.00487	0.051	0.180	30.8	P	N/A	4.43	4.93	5.15	5.70	6.10	16.67	N/A	N/A	N/A	N/A	N/A	N/A	I	N/A	AM	N/A	N/A	N/A	34S_6p1d7Yd_0	10/18A2	TDP-WTP-038	7090085
22.0	0.999	0.00487	0.052	0.180	30.3	P	N/A	4.43	5.02	5.27	5.90	6.10	17.33	N/A	N/A	N/A	N/A	N/A	N/A	I	N/A	AM	N/A	N/A	N/A	34S_6p1d7Yd_0	10/18A2	TDP-WTP-038	7090089
22.0	0.999	0.00487	0.052	0.180	29.4	P	N/A	4.46	5.11	5.39	6.10	6.10	18.83	6.10	vis	UCSvis	N/A	N/A	N/A	I	N/A	CS	N/A	N/A	N/A	34S_6p1d7Yd_0	10/18A2	TDP-WTP-038	7090095
21.7	0.999	0.00487	undefined	1.000	infinite	S	5.05	N/A	N/A	N/A	5.00	5.90	11.00	N/A	N/A	N/A	N/A	N/A	N/A	I	N/A	SS	N/A	N/A	N/A	34S_6p1d7Ya-40	10/18B1	TDP-WTP-038	7090097
21.8	0.999	0.00487	undefined	1.000	infinite	S	5.52	N/A	N/A	N/A	5.50	5.90	13.17	N/A	N/A	N/A	N/A	N/A	N/A	I	N/A	AM	N/A	N/A	N/A	34S_6p1d7Ya-40	10/18B1	TDP-WTP-038	7090101
21.8	0.999	0.00487	undefined	1.000	infinite	S	5.72	N/A	N/A	N/A	5.70	5.90	20.33	N/A	N/A	N/A	N/A	N/A	N/A	I	N/A	AM+	N/A	N/A	N/A	34S_6p1d7Ya-40	10/18B1	TDP-WTP-038	7090105
21.8	0.999	0.00487	undefined	1.000	infinite	S	5.93	N/A	N/A	N/A	5.90	5.90	23.33	5.90	vis	UCSvis	N/A	N/A	N/A	I	N/A	CS	N/A	N/A	N/A	34S_6p1d7Ya-40	10/18B1	TDP-WTP-038	7090111
22.0	0.999	0.00487	0.037	0.180	87.0	P	N/A	3.98	4.04	4.07	4.00	6.40	9.17	N/A	N/A	N/A	N/A	N/A	N/A	D	N/A	SS	N/A	N/A	N/A	34S_6p1d7Yd_6	10/18B2	TDP-WTP-038	7090113
22.0	0.999	0.00487	0.054	0.180	80.0	P	N/A	4.41	4.45	4.47	4.50	6.40	9.33	N/A	N/A	N/A	N/A	N/A	N/A	I	N/A	SS	N/A	N/A	N/A	34S_6p1d7Yd_6	10/18B2	TDP-WTP-038	7090116
22.0	0.999	0.00487	0.054	0.180	71.4	P	N/A	4.92	4.97	4.99	5.00	6.40	9.50	N/A	N/A	N/A	N/A	N/A	N/A	I	N/A	SS	N/A	N/A	N/A	34S_6p1d7Yd_6	10/18B2	TDP-WTP-038	7090119
22.0	0.999	0.00487	0.051	0.180	64.5	P	N/A	5.38	5.44	5.46	5.50	6.40	10.33	N/A	N/A	N/A	N/A	N/A	N/A	I	N/A	SS	N/A	N/A	N/A	34S_6p1d7Yd_6	10/18B2	TDP-WTP-038	7090122
22.0	0.999	0.00487	0.052	0.180	58.8	P	N/A	5.84	5.91	5.95	6.00	6.40	11.33	N/A	N/A	N/A	N/A	N/A	N/A	I	N/A	AM	N/A	N/A	N/A	34S_6p1d7Yd_6	10/18B2	TDP-WTP-038	7090126
22.0	0.999	0.00487	0.051	0.180	57.1	P	N/A	6.01	6.09	6.13	6.20	6.40	12.00	N/A	N/A	N/A	N/A	N/A	N/A	I	N/A	AM	N/A	N/A	N/A	34S_6p1d7Yd_6	10/18B2	TDP-WTP-038	7090130

Table B.9. Updated Data from Fall 2007 Tests in Mid-Scale Vessel with Spherical Head A.2

Row Number	Test	Case ID	Tank Diameter	Head Shape	Dish Height	Dish Volume	Tank Fill Height	Return Line Height	Nozzle Inner Diameter	Nozzle Stand-off Distance	Pulse Tube Configuration	Installed Nozzles	Outer Nozzles Operated	Inner Nozzles Operated	Pulse Tube Outer Diameter	Outer PJM Radius	Inner PJM Radius	"FIO" Outer PJM Impingement Angle	"FIO" Inner PJM Impingement Angle	Ratio Outer PJM to Tank Radius	Ratio Inner PJM to Tank Radius	Simulant	Solids Density	Particle Diameter d5	Particle Diameter d50	Particle Diameter d95	Void Fraction
text	text	text	in.	text	in.	in. ^{3}	in.	in.	in.	in.	text	number	number	number	in.	in.	in.	deg	deg	nondim	nondim	text	g/cm^3	m	m	m	fraction
MSS	M/DDX	ID	D	HS	H_{dish}	V_{dish}	H	Rtn	d	sod	PT	N	N_O	N_I	PT_{od}	R_O	R_I	Θ_O	Θ_I	R_O/R	R_I/R	sxdx	ρ_S	d_5	d_{50}	d_{95}	vf
7090136M	10/18B2	34S_6p1d7Yd_6	33 7/8	S	9	4437.4	67 3/4	61 3/4	0.446	0.669	HLP-22	12	4	0	1.9	10.5	5.7	30.8	16.1	0.62	0.33	p1d7	2.45	0.0001213	0.0001780	0.0002606	0.4277
7090138M	10/18B2	34S_6p1d7Yd_6	33 7/8	S	9	4437.4	67 3/4	61 3/4	0.446	0.669	HLP-22	12	4	0	1.9	10.5	5.7	30.8	16.1	0.62	0.33	p1d7	2.45	0.0001213	0.0001780	0.0002606	0.4277
7090142	10/19A1	34S_6p1d7Ya-04	33 7/8	S	9	4437.4	67 3/4	61 3/4	0.446	0.669	HLP-22	12	0	4	1.9	10.5	5.7	30.8	16.1	0.62	0.33	p1d7	2.45	0.0001213	0.0001780	0.0002606	0.4277
7090144	10/19A1	34S_6p1d7Ya-04	33 7/8	S	9	4437.4	67 3/4	61 3/4	0.446	0.669	HLP-22	12	0	4	1.9	10.5	5.7	30.8	16.1	0.62	0.33	p1d7	2.45	0.0001213	0.0001780	0.0002606	0.4277
7090146	10/19A1	34S_6p1d7Ya-04	33 7/8	S	9	4437.4	67 3/4	61 3/4	0.446	0.669	HLP-22	12	0	4	1.9	10.5	5.7	30.8	16.1	0.62	0.33	p1d7	2.45	0.0001213	0.0001780	0.0002606	0.4277
7090149	10/19A1	34S_6p1d7Ya-04	33 7/8	S	9	4437.4	67 3/4	61 3/4	0.446	0.669	HLP-22	12	0	4	1.9	10.5	5.7	30.8	16.1	0.62	0.33	p1d7	2.45	0.0001213	0.0001780	0.0002606	0.4277
7090152	10/19A1	34S_6p1d7Ya-04	33 7/8	S	9	4437.4	67 3/4	61 3/4	0.446	0.669	HLP-22	12	0	4	1.9	10.5	5.7	30.8	16.1	0.62	0.33	p1d7	2.45	0.0001213	0.0001780	0.0002606	0.4277
7090156	10/19A1	34S_6p1d7Ya-04	33 7/8	S	9	4437.4	67 3/4	61 3/4	0.446	0.669	HLP-22	12	0	4	1.9	10.5	5.7	30.8	16.1	0.62	0.33	p1d7	2.45	0.0001213	0.0001780	0.0002606	0.4277
7090158	10/19A1	34S_6p1d7Ya-04	33 7/8	S	9	4437.4	67 3/4	61 3/4	0.446	0.669	HLP-22	12	0	4	1.9	10.5	5.7	30.8	16.1	0.62	0.33	p1d7	2.45	0.0001213	0.0001780	0.0002606	0.4277
7090161	10/19A1	34S_6p1d7Ya-04	33 7/8	S	9	4437.4	67 3/4	61 3/4	0.446	0.669	HLP-22	12	0	4	1.9	10.5	5.7	30.8	16.1	0.62	0.33	p1d7	2.45	0.0001213	0.0001780	0.0002606	0.4277
7090165	10/19A1	34S_6p1d7Ya-04	33 7/8	S	9	4437.4	67 3/4	61 3/4	0.446	0.669	HLP-22	12	0	4	1.9	10.5	5.7	30.8	16.1	0.62	0.33	p1d7	2.45	0.0001213	0.0001780	0.0002606	0.4277
7090167	10/19A2	34S_6p1d7Yd_9	33 7/8	S	9	4437.4	67 3/4	61 3/4	0.446	0.669	HLP-22	12	0	4	1.9	10.5	5.7	30.8	16.1	0.62	0.33	p1d7	2.45	0.0001213	0.0001780	0.0002606	0.4277
7090169	10/19A2	34S_6p1d7Yd_9	33 7/8	S	9	4437.4	67 3/4	61 3/4	0.446	0.669	HLP-22	12	0	4	1.9	10.5	5.7	30.8	16.1	0.62	0.33	p1d7	2.45	0.0001213	0.0001780	0.0002606	0.4277
7090172	10/19A2	34S_6p1d7Yd_9	33 7/8	S	9	4437.4	67 3/4	61 3/4	0.446	0.669	HLP-22	12	0	4	1.9	10.5	5.7	30.8	16.1	0.62	0.33	p1d7	2.45	0.0001213	0.0001780	0.0002606	0.4277
7090174	10/19A2	34S_6p1d7Yd_9	33 7/8	S	9	4437.4	67 3/4	61 3/4	0.446	0.669	HLP-22	12	0	4	1.9	10.5	5.7	30.8	16.1	0.62	0.33	p1d7	2.45	0.0001213	0.0001780	0.0002606	0.4277
7090177	10/19A2	34S_6p1d7Yd_9	33 7/8	S	9	4437.4	67 3/4	61 3/4	0.446	0.669	HLP-22	12	0	4	1.9	10.5	5.7	30.8	16.1	0.62	0.33	p1d7	2.45	0.0001213	0.0001780	0.0002606	0.4277
7090180	10/19A2	34S_6p1d7Yd_9	33 7/8	S	9	4437.4	67 3/4	61 3/4	0.446	0.669	HLP-22	12	0	4	1.9	10.5	5.7	30.8	16.1	0.62	0.33	p1d7	2.45	0.0001213	0.0001780	0.0002606	0.4277
7090184M	10/19A2	34S_6p1d7Yd_9	33 7/8	S	9	4437.4	67 3/4	61 3/4	0.446	0.669	HLP-22	12	0	4	1.9	10.5	5.7	30.8	16.1	0.62	0.33	p1d7	2.45	0.0001213	0.0001780	0.0002606	0.4277
7090186	10/26A1	34S_6p1d7Ya	33 7/8	S	9	4437.4	67 3/4	31 7/8	0.446	0.669	HLP-22	12	8	4	1.9	10.5	5.7	30.8	16.1	0.62	0.33	p1d7	2.45	0.0001213	0.0001780	0.0002606	0.4277
7090189	10/26A1	34S_6p1d7Ya	33 7/8	S	9	4437.4	67 3/4	31 7/8	0.446	0.669	HLP-22	12	8	4	1.9	10.5	5.7	30.8	16.1	0.62	0.33	p1d7	2.45	0.0001213	0.0001780	0.0002606	0.4277
7090193	10/26A1	34S_6p1d7Ya	33 7/8	S	9	4437.4	67 3/4	31 7/8	0.446	0.669	HLP-22	12	8	4	1.9	10.5	5.7	30.8	16.1	0.62	0.33	p1d7	2.45	0.0001213	0.0001780	0.0002606	0.4277
7090195	10/26A2	34S_6p1d7Yd_1	33 7/8	S	9	4437.4	67 3/4	31 7/8	0.446	0.669	HLP-22	12	8	4	1.9	10.5	5.7	30.8	16.1	0.62	0.33	p1d7	2.45	0.0001213	0.0001780	0.0002606	0.4277
7090198	10/26A2	34S_6p1d7Yd_1	33 7/8	S	9	4437.4	67 3/4	31 7/8	0.446	0.669	HLP-22	12	8	4	1.9	10.5	5.7	30.8	16.1	0.62	0.33	p1d7	2.45	0.0001213	0.0001780	0.0002606	0.4277
7090201	10/26A2	34S_6p1d7Yd_1	33 7/8	S	9	4437.4	67 3/4	31 7/8	0.446	0.669	HLP-22	12	8	4	1.9	10.5	5.7	30.8	16.1	0.62	0.33	p1d7	2.45	0.0001213	0.0001780	0.0002606	0.4277
7090204	10/26A2	34S_6p1d7Yd_1	33 7/8	S	9	4437.4	67 3/4	31 7/8	0.446	0.669	HLP-22	12	8	4	1.9	10.5	5.7	30.8	16.1	0.62	0.33	p1d7	2.45	0.0001213	0.0001780	0.0002606	0.4277
7090208MX	10/26A2	34S_6p1d7Yd_1	33 7/8	S	9	4437.4	67 3/4	31 7/8	0.446	0.669	HLP-22	12	8	4	1.9	10.5	5.7	30.8	16.1	0.62	0.33	p1d7	2.45	0.0001213	0.0001780	0.0002606	0.4277
7090210	10/26B1	34S_6p1d7Ya-44	33 7/8	S	9	4437.4	67 3/4	31 7/8	0.446	0.669	HLP-22	12	4	4	1.9	10.5	5.7	30.8	16.1	0.62	0.33	p1d7	2.45	0.0001213	0.0001780	0.0002606	0.4277
7090213	10/26B1	34S_6p1d7Ya-44	33 7/8	S	9	4437.4	67 3/4	31 7/8	0.446	0.669	HLP-22	12	4	4	1.9	10.5	5.7	30.8	16.1	0.62	0.33	p1d7	2.45	0.0001213	0.0001780	0.0002606	0.4277
7090217	10/26B1	34S_6p1d7Ya-44	33 7/8	S	9	4437.4	67 3/4	31 7/8	0.446	0.669	HLP-22	12	4	4	1.9	10.5	5.7	30.8	16.1	0.62	0.33	p1d7	2.45	0.0001213	0.0001780	0.0002606	0.4277
7090219	10/26B1	34S_6p1d7Ya-44	33 7/8	S	9	4437.4	67 3/4	31 7/8	0.446	0.669	HLP-22	12	4	4	1.9	10.5	5.7	30.8	16.1	0.62	0.33	p1d7	2.45	0.0001213	0.0001780	0.0002606	0.4277
7090223	10/26B1	34S_6p1d7Ya-44	33 7/8	S	9	4437.4	67 3/4	31 7/8	0.446	0.669	HLP-22	12	4	4	1.9	10.5	5.7	30.8	16.1	0.62	0.33	p1d7	2.45	0.0001213	0.0001780	0.0002606	0.4277
7090225	10/26B2	34S_6p1d7Yd_0	33 7/8	S	9	4437.4	67 3/4	31 7/8	0.446	0.669	HLP-22	12	4	4	1.9	10.5	5.7	30.8	16.1	0.62	0.33	p1d7	2.45	0.0001213	0.0001780	0.0002606	0.4277
7090228	10/26B2	34S_6p1d7Yd_0	33 7/8	S	9	4437.4	67 3/4	31 7/8	0.446	0.669	HLP-22	12	4	4	1.9	10.5	5.7	30.8	16.1	0.62	0.33	p1d7	2.45	0.0001213	0.0001780	0.0002606	0.4277
7090231	10/26B2	34S_6p1d7Yd_0	33 7/8	S	9	4437.4	67 3/4	31 7/8	0.446	0.669	HLP-22	12	4	4	1.9	10.5	5.7	30.8	16.1	0.62	0.33	p1d7	2.45	0.0001213	0.0001780	0.0002606	0.4277
7090234	10/26B2	34S_6p1d7Yd_0	33 7/8	S	9	4437.4	67 3/4	31 7/8	0.446	0.669	HLP-22	12	4	4	1.9	10.5	5.7	30.8	16.1	0.62	0.33	p1d7	2.45	0.0001213	0.0001780	0.0002606	0.4277
7090237	10/26B2	34S_6p1d7Yd_0	33 7/8	S	9	4437.4	67 3/4	31 7/8	0.446	0.669	HLP-22	12	4	4	1.9	10.5	5.7	30.8	16.1	0.62	0.33	p1d7	2.45	0.0001213	0.0001780	0.0002606	0.4277
7090240	10/26B2	34S_6p1d7Yd_0	33 7/8	S	9	4437.4	67 3/4	31 7/8	0.446	0.669	HLP-22	12	4	4	1.9	10.5	5.7	30.8	16.1	0.62	0.33	p1d7	2.45	0.0001213	0.0001780	0.0002606	0.4277
7090244MX	10/26B2	34S_6p1d7Yd_0	33 7/8	S	9	4437.4	67 3/4	31 7/8	0.446	0.669	HLP-22	12	4	4	1.9	10.5	5.7	30.8	16.1	0.62	0.33	p1d7	2.45	0.0001213	0.0001780	0.0002606	0.4277
7090247	10/29A1	34S_6p1d7Ya-04	33 7/8	S	9	4437.4	67 3/4	31 7/8	0.446	0.669	HLP-22	12	0	4	1.9	10.5	5.7	30.8	16.1	0.62	0.33	p1d7	2.45	0.0001213	0.0001780	0.0002606	0.4277
7090250	10/29A1	34S_6p1d7Ya-04	33 7/8	S	9	4437.4	67 3/4	31 7/8	0.446	0.669	HLP-22	12	0	4	1.9	10.5	5.7	30.8	16.1	0.62	0.33	p1d7	2.45	0.0001213	0.0001780	0.0002606	0.4277
7090252	10/29A1	34S_6p1d7Ya-04	33 7/8	S	9	4437.4	67 3/4	31 7/8	0.446	0.669	HLP-22	12	0	4	1.9	10.5	5.7	30.8	16.1	0.62	0.33	p1d7	2.45	0.0001213	0.0001780	0.0002606	0.4277

Table B.9. Updated Data from Fall 2007 Tests in Mid-Scale Vessel with Spherical Head B.2

Tank Water Temperature	Water Density	Solids Fraction	Pulse Volume Fraction	Duty Cycle	Cycle Time	Pulsed or Steady Jet	Us Steady Jet	U1 Pulsing Jet	U2 URMS	U3 URM3	Discharge Velocity	Critical Suspension Velocity	Average Peak Cloud Height	U_{CS} Condition	U_{CS} Method	U_{CS} Flag	U_{CS} Center Flag	U_{CS} udv Flag	U_{CS} based on Decreasing Velocity	Sweep Increase / Decrease	UDV Height Bed	Particle Motion	Solids Level	Outer Bottom Pattern	Inner Bottom Pattern	Case ID	Test	TDP	Row Number
C	g/cm^3	fraction	fraction	fraction	s	text	m/s	m/s	m/s	m/s	m/s	m/s	in.	m/s	text	text	text	text	m/s	text	mm	text	text	text	text	text	text	text	text
T	ρ_l	ϕ_S	ϕ_P	DC	t_C	Jet	US	U1	U2	U3	U	U_{CS}	H_C	U_{CSR}	U_{CSM}	U_{CS}vis	U_{CS}cen	U_{CS}udv	U_{CS_D}	S_W	H_{bed}	PM	Sol	SP_O	SP_I	ID	M/DDX	TDP	MSS
22.0	0.999	0.00487	0.051	0.180	54.9	P	N/A	6.22	6.31	6.35	6.40	6.40	13.00	6.40	vis	UCSvis	N/A	N/A	N/A	I	N/A	CS	N/A	N/A	N/A	34S_6p1d7Yd_6	10/18B2	TDP-WTP-038	7090136
22.0	0.999	0.00487	0.051	0.180	54.1	P	N/A	6.41	6.50	6.55	6.60	6.40	16.00	N/A	N/A	N/A	N/A	N/A	N/A	I	N/A	BC	N/A	N/A	N/A	34S_6p1d7Yd_6	10/18B2	TDP-WTP-038	7090138
21.8	0.999	0.00487	undefined	1.000	infinite	S	4.06	N/A	N/A	N/A	4.00	8.00	9.00	N/A	N/A	N/A	N/A	N/A	N/A	I	N/A	SS	N/A	N/A	N/A	34S_6p1d7Ya-04	10/19A1	TDP-WTP-034	7090142
21.7	0.999	0.00487	undefined	1.000	infinite	S	4.52	N/A	N/A	N/A	4.50	8.00	10.00	N/A	N/A	N/A	N/A	N/A	N/A	I	N/A	SS	N/A	N/A	N/A	34S_6p1d7Ya-04	10/19A1	TDP-WTP-034	7090144
21.8	0.999	0.00487	undefined	1.000	infinite	S	5.02	N/A	N/A	N/A	5.00	8.00	12.00	N/A	N/A	N/A	N/A	N/A	N/A	I	N/A	SS	N/A	BP5	N/A	34S_6p1d7Ya-04	10/19A1	TDP-WTP-034	7090146
21.8	0.999	0.00487	undefined	1.000	infinite	S	5.11	N/A	N/A	N/A	5.50	8.00	15.50	N/A	N/A	N/A	N/A	N/A	N/A	I	N/A	AM	N/A	BP5	N/A	34S_6p1d7Ya-04	10/19A1	TDP-WTP-034	7090149
21.8	0.999	0.00487	undefined	1.000	infinite	S	6.01	N/A	N/A	N/A	6.00	8.00	18.50	N/A	N/A	N/A	N/A	N/A	N/A	I	N/A	AM	N/A	BP5	N/A	34S_6p1d7Ya-04	10/19A1	TDP-WTP-034	7090152
21.8	0.999	0.00487	undefined	1.000	infinite	S	6.55	N/A	N/A	N/A	6.50	8.00	24.00	N/A	N/A	N/A	N/A	N/A	N/A	I	N/A	AM	N/A	BP5	N/A	34S_6p1d7Ya-04	10/19A1	TDP-WTP-034	7090156
21.8	0.999	0.00487	undefined	1.000	infinite	S	7.01	N/A	N/A	N/A	7.00	8.00	33.00	N/A	N/A	N/A	N/A	N/A	N/A	I	N/A	AM+	N/A	BP5	N/A	34S_6p1d7Ya-04	10/19A1	TDP-WTP-034	7090158
21.9	0.999	0.00487	undefined	1.000	infinite	S	7.51	N/A	N/A	N/A	7.50	8.00	40.00	N/A	N/A	N/A	N/A	N/A	N/A	I	N/A	AM+	N/A	BP5	N/A	34S_6p1d7Ya-04	10/19A1	TDP-WTP-034	7090161
21.9	0.999	0.00487	undefined	1.000	infinite	S	8.02	N/A	N/A	N/A	8.00	8.00	50.00	8.00	vis	UCSvis	N/A	N/A	N/A	I	N/A	CS	N/A	BP6	N/A	34S_6p1d7Ya-04	10/19A1	TDP-WTP-034	7090165
22.0	0.999	0.00487	0.049	0.180	87.0	P	N/A	4.09	4.13	4.15	4.00	8.50	9.00	N/A	N/A	N/A	N/A	N/A	N/A	I	N/A	SS	N/A	N/A	N/A	34S_6p1d7Yd_9	10/19A2	TDP-WTP-034	7090167
22.0	0.999	0.00487	0.052	0.180	71.4	P	N/A	4.95	5.00	5.02	5.00	8.50	12.50	N/A	N/A	N/A	N/A	N/A	N/A	I	N/A	SS	N/A	N/A	N/A	34S_6p1d7Yd_9	10/19A2	TDP-WTP-034	7090169
22.0	0.999	0.00487	0.053	0.180	58.8	P	N/A	5.85	5.92	5.96	6.00	8.50	16.00	N/A	N/A	N/A	N/A	N/A	N/A	I	N/A	SS	N/A	BP4	N/A	34S_6p1d7Yd_9	10/19A2	TDP-WTP-034	7090172
22.0	0.999	0.00487	0.054	0.180	51.3	P	N/A	6.23	6.58	6.72	7.00	8.50	19.50	N/A	N/A	N/A	N/A	N/A	N/A	I	N/A	AM	N/A	BP5	N/A	34S_6p1d7Yd_9	10/19A2	TDP-WTP-034	7090174
22.0	0.999	0.00487	0.051	0.180	46.5	P	N/A	6.32	6.83	7.04	7.50	8.50	23.00	N/A	N/A	N/A	N/A	N/A	N/A	I	N/A	AM+	N/A	BP5	N/A	34S_6p1d7Yd_9	10/19A2	TDP-WTP-034	7090177
22.0	0.999	0.00487	0.052	0.180	43.5	P	N/A	6.72	7.29	7.52	8.00	8.50	25.50	N/A	N/A	N/A	N/A	N/A	N/A	I	N/A	AM+	N/A	BP6	N/A	34S_6p1d7Yd_9	10/19A2	TDP-WTP-034	7090180
22.0	0.999	0.00487	0.050	0.180	40.0	P	N/A	6.76	7.51	7.83	8.50	8.50	29.00	8.50	vis	UCSvis	N/A	N/A	N/A	I	N/A	CS	N/A	BP6	N/A	34S_6p1d7Yd_9	10/19A2	TDP-WTP-034	7090184
20.8	0.999	0.00487	undefined	1.000	infinite	S	2.51	N/A	N/A	N/A	2.50	3.20	8.50	N/A	N/A	N/A	N/A	N/A	N/A	I	N/A	SS+	N/A	N/A	N/A	34S_6p1d7Ya	10/26A1	TDP-WTP-039	7090186
20.7	0.999	0.00487	undefined	1.000	infinite	S	3.02	N/A	N/A	N/A	3.00	3.20	10.00	N/A	N/A	N/A	N/A	N/A	N/A	I	N/A	AM+	N/A	N/A	N/A	34S_6p1d7Ya	10/26A1	TDP-WTP-039	7090189
20.7	0.999	0.00487	undefined	1.000	infinite	S	3.21	N/A	N/A	N/A	3.20	3.20	10.75	3.20	vis	UCSvis	N/A	N/A	N/A	I	N/A	CS	N/A	N/A	N/A	34S_6p1d7Ya	10/26A1	TDP-WTP-039	7090193
21.0	0.999	0.00487	0.045	0.180	40.0	P	N/A	2.74	2.85	2.90	3.00	4.00	9.75	N/A	N/A	N/A	N/A	N/A	N/A	D	N/A	AM	N/A	N/A	N/A	34S_6p1d7Yd_1	10/26A2	TDP-WTP-039	7090195
21.0	0.999	0.00487	0.050	0.180	37.0	P	N/A	2.92	3.02	3.07	3.20	4.00	11.00	N/A	N/A	N/A	N/A	N/A	N/A	I	N/A	AM	N/A	N/A	N/A	34S_6p1d7Yd_1	10/26A2	TDP-WTP-039	7090198
21.0	0.999	0.00487	0.051	0.180	35.5	P	N/A	3.02	3.15	3.22	3.40	4.00	11.00	N/A	N/A	N/A	N/A	N/A	N/A	I	N/A	AM+	N/A	N/A	N/A	34S_6p1d7Yd_1	10/26A2	TDP-WTP-039	7090201
21.0	0.999	0.00487	0.052	0.180	33.0	P	N/A	3.06	3.27	3.36	3.60	4.00	11.00	N/A	N/A	N/A	N/A	N/A	N/A	I	N/A	AM+	N/A	N/A	N/A	34S_6p1d7Yd_1	10/26A2	TDP-WTP-039	7090204
21.0	0.999	0.00487	0.051	0.180	29.5	P	N/A	3.23	3.53	3.67	4.00	4.00	12.00	4.00	vis	UCSvis	N/A	N/A	N/A	I	N/A	CS	N/A	N/A	N/A	34S_6p1d7Yd_1	10/26A2	TDP-WTP-039	7090208
20.8	0.999	0.00487	undefined	1.000	infinite	S	3.40	N/A	N/A	N/A	3.40	4.60	N/A	N/A	N/A	N/A	N/A	N/A	N/A	I	N/A	SS	N/A	N/A	N/A	34S_6p1d7Ya-44	10/26B1	TDP-WTP-039	7090210
20.8	0.999	0.00487	undefined	1.000	infinite	S	3.82	N/A	N/A	N/A	3.80	4.60	9.00	N/A	N/A	N/A	N/A	N/A	N/A	I	N/A	AM	N/A	N/A	N/A	34S_6p1d7Ya-44	10/26B1	TDP-WTP-039	7090213
20.8	0.999	0.00487	undefined	1.000	infinite	S	4.22	N/A	N/A	N/A	4.20	4.60	12.00	N/A	N/A	N/A	UCScen	N/A	N/A	I	N/A	AM	N/A	N/A	N/A	34S_6p1d7Ya-44	10/26B1	TDP-WTP-039	7090217
20.8	0.999	0.00487	undefined	1.000	infinite	S	4.42	N/A	N/A	N/A	4.40	4.60	17.00	N/A	N/A	N/A	N/A	N/A	N/A	I	N/A	AM+	N/A	N/A	N/A	34S_6p1d7Ya-44	10/26B1	TDP-WTP-039	7090219
20.9	0.999	0.00487	undefined	1.000	infinite	S	4.61	N/A	N/A	N/A	4.60	4.60	21.00	4.60	vis	UCSvis	N/A	N/A	N/A	I	N/A	CS	N/A	N/A	N/A	34S_6p1d7Ya-44	10/26B1	TDP-WTP-039	7090223
21.0	0.999	0.00487	0.045	0.180	45.0	P	N/A	3.69	3.79	3.84	4.00	6.10	9.00	N/A	N/A	N/A	N/A	N/A	N/A	D	N/A	SS+	N/A	N/A	N/A	34S_6p1d7Yd_0	10/26B2	TDP-WTP-039	7090225
21.0	0.999	0.00487	0.051	0.180	40.5	P	N/A	4.04	4.18	4.24	4.40	6.10	10.00	N/A	N/A	N/A	N/A	N/A	N/A	I	N/A	SS+	N/A	N/A	N/A	34S_6p1d7Yd_0	10/26B2	TDP-WTP-039	7090228
21.0	0.999	0.00487	0.051	0.180	37.5	P	N/A	4.14	4.40	4.51	4.80	6.10	12.50	N/A	N/A	N/A	N/A	N/A	N/A	I	N/A	AM	N/A	N/A	N/A	34S_6p1d7Yd_0	10/26B2	TDP-WTP-039	7090231
21.0	0.999	0.00487	0.050	0.180	34.0	P	N/A	4.41	4.72	4.86	5.20	6.10	14.00	N/A	N/A	N/A	N/A	N/A	N/A	I	N/A	AM	N/A	N/A	N/A	34S_6p1d7Yd_0	10/26B2	TDP-WTP-039	7090234
21.0	0.999	0.00487	0.050	0.180	31.5	P	N/A	4.52	4.94	5.12	5.60	6.10	14.75	N/A	N/A	N/A	N/A	N/A	N/A	I	N/A	AM+	N/A	N/A	N/A	34S_6p1d7Yd_0	10/26B2	TDP-WTP-039	7090237
21.0	0.999	0.00487	0.050	0.180	29.0	P	N/A	4.64	5.19	5.43	6.00	6.10	16.50	N/A	N/A	N/A	N/A	N/A	N/A	I	N/A	CS-	N/A	N/A	N/A	34S_6p1d7Yd_0	10/26B2	TDP-WTP-039	7090240
21.0	0.999	0.00487	0.050	0.180	28.5	P	N/A	4.66	5.23	5.47	6.10	6.10	18.00	6.10	vis	UCSvis	N/A	N/A	N/A	I	N/A	CS	N/A	N/A	N/A	34S_6p1d7Yd_0	10/26B2	TDP-WTP-039	7090244
20.9	0.999	0.00487	undefined	1.000	infinite	S	4.01	N/A	N/A	N/A	4.00	6.00	10.75	N/A	N/A	N/A	N/A	N/A	N/A	I	N/A	SS	N/A	N/A	N/A	34S_6p1d7Ya-04	10/29A1	TDP-WTP-040	7090247
20.9	0.999	0.00487	undefined	1.000	infinite	S	4.50	N/A	N/A	N/A	4.50	6.00	13.50	N/A	N/A	N/A	N/A	N/A	N/A	I	N/A	SS	N/A	N/A	N/A	34S_6p1d7Ya-04	10/29A1	TDP-WTP-040	7090250
20.9	0.999	0.00487	undefined	1.000	infinite	S	5.00	N/A	N/A	N/A	5.00	6.00	16.75	N/A	N/A	N/A	N/A	N/A	N/A	I	N/A	AM	N/A	N/A	N/A	34S_6p1d7Ya-04	10/29A1	TDP-WTP-040	7090252

Table B.9. Updated Data from Fall 2007 Tests in Mid-Scale Vessel with Spherical Head A.3

Row Number	Test	Case ID	Tank Diameter	Head Shape	Dish Height	Dish Volume	Tank Fill Height	Return Line Height	Nozzle Inner Diameter	Nozzle Stand-off Distance	Pulse Tube Configuration	Installed Nozzles	Outer Nozzles Operated	Inner Nozzles Operated	Pulse Tube Outer Diameter	Outer PJM Radius	Inner PJM Radius	"FIO" Outer PJM Impingement Angle	"FIO" Inner PJM Impingement Angle	Ratio Outer PJM to Tank Radius	Ratio Inner PJM to Tank Radius	Simulant	Solids Density	Particle Diameter d5	Particle Diameter d50	Particle Diameter d95	Void Fraction
text	text	text	in.	text	in.	in. ^{3}	in.	in.	in.	in.	text	number	number	number	in.	in.	in.	deg	deg	nondim	nondim	text	g/cm^3	m	m	m	fraction
MSS	M/DDX	ID	D	HS	H_{dish}	V_{dish}	H	Rtn	d	sod	PT	N	N_O	N_I	PT_{od}	R_O	R_I	Θ_O	Θ_I	R_O/R	R_I/R	sxdx	ρ_S	d_5	d_{50}	d_{95}	vf
7090256	10/29A1	34S_6p1d7Ya-04	33 7/8	S	9	4437.4	67 3/4	31 7/8	0.446	0.669	HLP-22	12	0	4	1.9	10.5	5.7	30.8	16.1	0.62	0.33	p1d7	2.45	0.0001213	0.0001780	0.0002606	0.4277
7090258	10/29A1	34S_6p1d7Ya-04	33 7/8	S	9	4437.4	67 3/4	31 7/8	0.446	0.669	HLP-22	12	0	4	1.9	10.5	5.7	30.8	16.1	0.62	0.33	p1d7	2.45	0.0001213	0.0001780	0.0002606	0.4277
7090261	10/29A1	34S_6p1d7Ya-04	33 7/8	S	9	4437.4	67 3/4	31 7/8	0.446	0.669	HLP-22	12	0	4	1.9	10.5	5.7	30.8	16.1	0.62	0.33	p1d7	2.45	0.0001213	0.0001780	0.0002606	0.4277
7090265	10/29A1	34S_6p1d7Ya-04	33 7/8	S	9	4437.4	67 3/4	31 7/8	0.446	0.669	HLP-22	12	0	4	1.9	10.5	5.7	30.8	16.1	0.62	0.33	p1d7	2.45	0.0001213	0.0001780	0.0002606	0.4277
7090268	10/29A2	34S_6p1d7Ym_9	33 7/8	S	9	4437.4	67 3/4	31 7/8	0.446	0.669	HLP-22	12	0	4	1.9	10.5	5.7	30.8	16.1	0.62	0.33	p1d7	2.45	0.0001213	0.0001780	0.0002606	0.4277
7090271MX	10/29A2	34S_6p1d7Ym_9	33 7/8	S	9	4437.4	67 3/4	31 7/8	0.446	0.669	HLP-22	12	0	4	1.9	10.5	5.7	30.8	16.1	0.62	0.33	p1d7	2.45	0.0001213	0.0001780	0.0002606	0.4277
7090274MX	10/29A2	34S_6p1d7Ym_9	33 7/8	S	9	4437.4	67 3/4	31 7/8	0.446	0.669	HLP-22	12	0	4	1.9	10.5	5.7	30.8	16.1	0.62	0.33	p1d7	2.45	0.0001213	0.0001780	0.0002606	0.4277
7090276	10/29B1	34S_6p1d7Ya-40	33 7/8	S	9	4437.4	67 3/4	31 7/8	0.446	0.669	HLP-22	12	4	0	1.9	10.5	5.7	30.8	16.1	0.62	0.33	p1d7	2.45	0.0001213	0.0001780	0.0002606	0.4277
7090279	10/29B1	34S_6p1d7Ya-40	33 7/8	S	9	4437.4	67 3/4	31 7/8	0.446	0.669	HLP-22	12	4	0	1.9	10.5	5.7	30.8	16.1	0.62	0.33	p1d7	2.45	0.0001213	0.0001780	0.0002606	0.4277
7090283	10/29B1	34S_6p1d7Ya-40	33 7/8	S	9	4437.4	67 3/4	31 7/8	0.446	0.669	HLP-22	12	4	0	1.9	10.5	5.7	30.8	16.1	0.62	0.33	p1d7	2.45	0.0001213	0.0001780	0.0002606	0.4277
7090285	10/29B1	34S_6p1d7Ya-40	33 7/8	S	9	4437.4	67 3/4	31 7/8	0.446	0.669	HLP-22	12	4	0	1.9	10.5	5.7	30.8	16.1	0.62	0.33	p1d7	2.45	0.0001213	0.0001780	0.0002606	0.4277
7090288	10/29B2	34S_6p1d7Yd_6	33 7/8	S	9	4437.4	67 3/4	31 7/8	0.446	0.669	HLP-22	12	4	0	1.9	10.5	5.7	30.8	16.1	0.62	0.33	p1d7	2.45	0.0001213	0.0001780	0.0002606	0.4277
7090291	10/29B2	34S_6p1d7Yd_6	33 7/8	S	9	4437.4	67 3/4	31 7/8	0.446	0.669	HLP-22	12	4	0	1.9	10.5	5.7	30.8	16.1	0.62	0.33	p1d7	2.45	0.0001213	0.0001780	0.0002606	0.4277
7090294	10/29B2	34S_6p1d7Yd_6	33 7/8	S	9	4437.4	67 3/4	31 7/8	0.446	0.669	HLP-22	12	4	0	1.9	10.5	5.7	30.8	16.1	0.62	0.33	p1d7	2.45	0.0001213	0.0001780	0.0002606	0.4277
7090298MX	10/29B2	34S_6p1d7Yd_6	33 7/8	S	9	4437.4	67 3/4	31 7/8	0.446	0.669	HLP-22	12	4	0	1.9	10.5	5.7	30.8	16.1	0.62	0.33	p1d7	2.45	0.0001213	0.0001780	0.0002606	0.4277
7090300MX	10/29B2	34S_6p1d7Yd_6	33 7/8	S	9	4437.4	67 3/4	31 7/8	0.446	0.669	HLP-22	12	4	0	1.9	10.5	5.7	30.8	16.1	0.62	0.33	p1d7	2.45	0.0001213	0.0001780	0.0002606	0.4277
7090303	10/30A1	34S_6p1d7Ya	33 7/8	S	9	4437.4	67 3/4	21 5/7	0.446	0.669	HLP-22	12	8	4	1.9	10.5	5.7	30.8	16.1	0.62	0.33	p1d7	2.45	0.0001213	0.0001780	0.0002606	0.4277
7090306	10/30A1	34S_6p1d7Ya	33 7/8	S	9	4437.4	67 3/4	21 5/7	0.446	0.669	HLP-22	12	8	4	1.9	10.5	5.7	30.8	16.1	0.62	0.33	p1d7	2.45	0.0001213	0.0001780	0.0002606	0.4277
7090310	10/30A1	34S_6p1d7Ya	33 7/8	S	9	4437.4	67 3/4	21 5/7	0.446	0.669	HLP-22	12	8	4	1.9	10.5	5.7	30.8	16.1	0.62	0.33	p1d7	2.45	0.0001213	0.0001780	0.0002606	0.4277
7090313	10/30A1	34S_6p1d7Ya	33 7/8	S	9	4437.4	67 3/4	21 5/7	0.446	0.669	HLP-22	12	8	4	1.9	10.5	5.7	30.8	16.1	0.62	0.33	p1d7	2.45	0.0001213	0.0001780	0.0002606	0.4277
7090315	10/30A2	34S_6p1d7Yd_1	33 7/8	S	9	4437.4	67 3/4	21 5/7	0.446	0.669	HLP-22	12	8	4	1.9	10.5	5.7	30.8	16.1	0.62	0.33	p1d7	2.45	0.0001213	0.0001780	0.0002606	0.4277
7090318	10/30A2	34S_6p1d7Yd_1	33 7/8	S	9	4437.4	67 3/4	21 5/7	0.446	0.669	HLP-22	12	8	4	1.9	10.5	5.7	30.8	16.1	0.62	0.33	p1d7	2.45	0.0001213	0.0001780	0.0002606	0.4277
7090321	10/30A2	34S_6p1d7Yd_1	33 7/8	S	9	4437.4	67 3/4	21 5/7	0.446	0.669	HLP-22	12	8	4	1.9	10.5	5.7	30.8	16.1	0.62	0.33	p1d7	2.45	0.0001213	0.0001780	0.0002606	0.4277
7090324	10/30A2	34S_6p1d7Yd_1	33 7/8	S	9	4437.4	67 3/4	21 5/7	0.446	0.669	HLP-22	12	8	4	1.9	10.5	5.7	30.8	16.1	0.62	0.33	p1d7	2.45	0.0001213	0.0001780	0.0002606	0.4277
7090328MX	10/30A2	34S_6p1d7Yd_1	33 7/8	S	9	4437.4	67 3/4	21 5/7	0.446	0.669	HLP-22	12	8	4	1.9	10.5	5.7	30.8	16.1	0.62	0.33	p1d7	2.45	0.0001213	0.0001780	0.0002606	0.4277
7090333	10/30C1	34S_6p1d7Ya-04	33 7/8	S	9	4437.4	67 3/4	21 5/7	0.446	0.669	HLP-22	12	0	4	1.9	10.5	5.7	30.8	16.1	0.62	0.33	p1d7	2.45	0.0001213	0.0001780	0.0002606	0.4277
7090335	10/30C1	34S_6p1d7Ya-04	33 7/8	S	9	4437.4	67 3/4	21 5/7	0.446	0.669	HLP-22	12	0	4	1.9	10.5	5.7	30.8	16.1	0.62	0.33	p1d7	2.45	0.0001213	0.0001780	0.0002606	0.4277
7090338	10/30C1	34S_6p1d7Ya-04	33 7/8	S	9	4437.4	67 3/4	21 5/7	0.446	0.669	HLP-22	12	0	4	1.9	10.5	5.7	30.8	16.1	0.62	0.33	p1d7	2.45	0.0001213	0.0001780	0.0002606	0.4277
7090341	10/30C1	34S_6p1d7Ya-04	33 7/8	S	9	4437.4	67 3/4	21 5/7	0.446	0.669	HLP-22	12	0	4	1.9	10.5	5.7	30.8	16.1	0.62	0.33	p1d7	2.45	0.0001213	0.0001780	0.0002606	0.4277
7090344	10/30C1	34S_6p1d7Ya-04	33 7/8	S	9	4437.4	67 3/4	21 5/7	0.446	0.669	HLP-22	12	0	4	1.9	10.5	5.7	30.8	16.1	0.62	0.33	p1d7	2.45	0.0001213	0.0001780	0.0002606	0.4277
7090348	10/30C2	34S_6p1d7Yd_9	33 7/8	S	9	4437.4	67 3/4	21 5/7	0.446	0.669	HLP-22	12	0	4	1.9	10.5	5.7	30.8	16.1	0.62	0.33	p1d7	2.45	0.0001213	0.0001780	0.0002606	0.4277
7090350	10/30C2	34S_6p1d7Yd_9	33 7/8	S	9	4437.4	67 3/4	21 5/7	0.446	0.669	HLP-22	12	0	4	1.9	10.5	5.7	30.8	16.1	0.62	0.33	p1d7	2.45	0.0001213	0.0001780	0.0002606	0.4277
7090353	10/30C2	34S_6p1d7Yd_9	33 7/8	S	9	4437.4	67 3/4	21 5/7	0.446	0.669	HLP-22	12	0	4	1.9	10.5	5.7	30.8	16.1	0.62	0.33	p1d7	2.45	0.0001213	0.0001780	0.0002606	0.4277
7090357	10/30C2	34S_6p1d7Yd_9	33 7/8	S	9	4437.4	67 3/4	21 5/7	0.446	0.669	HLP-22	12	0	4	1.9	10.5	5.7	30.8	16.1	0.62	0.33	p1d7	2.45	0.0001213	0.0001780	0.0002606	0.4277
7090360MX	10/30C2	34S_6p1d7Yd_9	33 7/8	S	9	4437.4	67 3/4	21 5/7	0.446	0.669	HLP-22	12	0	4	1.9	10.5	5.7	30.8	16.1	0.62	0.33	p1d7	2.45	0.0001213	0.0001780	0.0002606	0.4277
7090362MX	10/30C2	34S_6p1d7Yd_9	33 7/8	S	9	4437.4	67 3/4	21 5/7	0.446	0.669	HLP-22	12	0	4	1.9	10.5	5.7	30.8	16.1	0.62	0.33	p1d7	2.45	0.0001213	0.0001780	0.0002606	0.4277
7090368	10/31A1	34S_6p1d7Ya	33 7/8	S	9	4437.4	33 7/8	31 7/8	0.446	0.669	HLP-22	12	8	4	1.9	10.5	5.7	30.8	16.1	0.62	0.33	p1d7	2.45	0.0001213	0.0001780	0.0002606	0.4277
7090371	10/31A1	34S_6p1d7Ya	33 7/8	S	9	4437.4	33 7/8	31 7/8	0.446	0.669	HLP-22	12	8	4	1.9	10.5	5.7	30.8	16.1	0.62	0.33	p1d7	2.45	0.0001213	0.0001780	0.0002606	0.4277
7090374	10/31A1	34S_6p1d7Ya	33 7/8	S	9	4437.4	33 7/8	31 7/8	0.446	0.669	HLP-22	12	8	4	1.9	10.5	5.7	30.8	16.1	0.62	0.33	p1d7	2.45	0.0001213	0.0001780	0.0002606	0.4277
7090376	10/31A1	34S_6p1d7Ya	33 7/8	S	9	4437.4	33 7/8	31 7/8	0.446	0.669	HLP-22	12	8	4	1.9	10.5	5.7	30.8	16.1	0.62	0.33	p1d7	2.45	0.0001213	0.0001780	0.0002606	0.4277
7090379	10/31A2	34S_6p1d7Yd_1	33 7/8	S	9	4437.4	33 7/8	31 7/8	0.446	0.669	HLP-22	12	8	4	1.9	10.5	5.7	30.8	16.1	0.62	0.33	p1d7	2.45	0.0001213	0.0001780	0.0002606	0.4277

Table B.9. Updated Data from Fall 2007 Tests in Mid-Scale Vessel with Spherical Head B.3

Tank Water Temperature	Water Density	Solids Fraction	Pulse Volume Fraction	Duty Cycle	Cycle Time	Pulsed or Steady Jet	Us Steady Jet	U1 Pulsing Jet	U2 URMS	U3 URM3	Discharge Velocity	Critical Suspension Velocity	Average Peak Cloud Height	U_{CS} Condition	U_{CS} Method	U_{CS} Flag	U_{CS} Center Flag	U_{CS} udv Flag	U_{CS} based on Decreasing Velocity	Sweep Increase / Decrease	UDV Height Bed	Particle Motion	Solids Level	Outer Bottom Pattern	Inner Bottom Pattern	Case ID	Test	TDP	Row Number
C	g/cm³	fraction	fraction	fraction	s	text	m/s	m/s	m/s	m/s	m/s	m/s	in.	m/s	text	text	text	text	m/s	text	mm	text	text	text	text	text	text	text	text
T	ρ_l	ϕ_s	ϕ_p	DC	t_C	Jet	US	U1	U2	U3	U	U_{CS}	H_C	U_{CSR}	U_{CSM}	U_{CS}vis	U_{CS}cen	U_{CS}udv	U_{CS_D}	S_W	H_{bed}	PM	Sol	SP_O	SP_I	ID	M/DDX	TDP	MSS
20.9	0.999	0.00487	undefined	1.000	infinite	S	5.40	N/A	N/A	N/A	5.40	6.00	19.50	N/A	N/A	N/A	N/A	N/A	N/A	I	N/A	AM	N/A	N/A	N/A	34S_6p1d7Ya-04	10/29A1	TDP-WTP-040	7090256
20.9	0.999	0.00487	undefined	1.000	infinite	S	5.60	N/A	N/A	N/A	5.60	6.00	21.50	N/A	N/A	N/A	N/A	N/A	N/A	I	N/A	AM+	N/A	N/A	N/A	34S_6p1d7Ya-04	10/29A1	TDP-WTP-040	7090258
20.9	0.999	0.00487	undefined	1.000	infinite	S	5.80	N/A	N/A	N/A	5.80	6.00	23.00	N/A	N/A	N/A	N/A	N/A	N/A	I	N/A	CS-	N/A	N/A	N/A	34S_6p1d7Ya-04	10/29A1	TDP-WTP-040	7090261
20.9	0.999	0.00487	undefined	1.000	infinite	S	5.99	N/A	N/A	N/A	6.00	6.00	24.50	6.00	vis	UCSvis	N/A	N/A	N/A	I	N/A	CS	N/A	N/A	N/A	34S_6p1d7Ya-04	10/29A1	TDP-WTP-040	7090265
21.0	0.999	0.00487	0.046	0.196	45.0	P	N/A	6.11	6.53	6.70	7.00	7.50	24.50	N/A	N/A	N/A	N/A	N/A	N/A	I	N/A	AM	N/A	N/A	N/A	34S_6p1d7Ym_9	10/29A2	TDP-WTP-040	7090268
21.0	0.999	0.00487	0.049	0.203	45.0	P	N/A	6.44	6.92	7.12	7.50	7.50	27.00	7.50	vis	UCSvis	N/A	N/A	N/A	I	N/A	CS	N/A	N/A	N/A	34S_6p1d7Ym_9	10/29A2	TDP-WTP-040	7090271
21.0	0.999	0.00487	0.051	0.198	45.0	P	N/A	6.62	7.10	7.30	7.70	7.50	28.00	N/A	N/A	N/A	N/A	N/A	N/A	I	N/A	BC	N/A	N/A	N/A	34S_6p1d7Ym_9	10/29A2	TDP-WTP-040	7090274
21.0	0.999	0.00487	undefined	1.000	infinite	S	4.49	N/A	N/A	N/A	4.50	5.50	10.00	N/A	N/A	N/A	N/A	N/A	N/A	I	N/A	SS	N/A	N/A	N/A	34S_6p1d7Ya-40	10/29B1	TDP-WTP-040	7090276
21.0	0.999	0.00487	undefined	1.000	infinite	S	4.99	N/A	N/A	N/A	5.00	5.50	11.50	N/A	N/A	N/A	N/A	N/A	N/A	I	N/A	AM-	N/A	N/A	N/A	34S_6p1d7Ya-40	10/29B1	TDP-WTP-040	7090279
21.1	0.999	0.00487	undefined	1.000	infinite	S	5.50	N/A	N/A	N/A	5.50	5.50	21.25	5.50	vis	UCSvis	N/A	N/A	N/A	I	N/A	CS	N/A	N/A	N/A	34S_6p1d7Ya-40	10/29B1	TDP-WTP-040	7090283
21.0	0.999	0.00487	undefined	1.000	infinite	S	5.70	N/A	N/A	N/A	5.70	5.50	25.00	N/A	N/A	N/A	N/A	N/A	N/A	I	N/A	BC	N/A	N/A	N/A	34S_6p1d7Ya-40	10/29B1	TDP-WTP-040	7090285
21.0	0.999	0.00487	0.050	0.180	70.0	P	N/A	4.90	4.95	4.98	5.00	6.20	9.75	N/A	N/A	N/A	N/A	N/A	N/A	D	N/A	SS	N/A	N/A	N/A	34S_6p1d7Yd_6	10/29B2	TDP-WTP-040	7090288
21.0	0.999	0.00487	0.050	0.180	63.0	P	N/A	5.39	5.45	5.48	5.50	6.20	11.50	N/A	N/A	N/A	N/A	N/A	N/A	I	N/A	SS+	N/A	N/A	N/A	34S_6p1d7Yd_6	10/29B2	TDP-WTP-040	7090291
21.0	0.999	0.00487	0.055	0.180	58.0	P	N/A	5.83	5.90	5.93	6.00	6.20	14.00	N/A	N/A	N/A	N/A	N/A	N/A	I	N/A	AM+	N/A	N/A	N/A	34S_6p1d7Yd_6	10/29B2	TDP-WTP-040	7090294
21.0	0.999	0.00487	0.050	0.180	56.0	P	N/A	6.06	6.14	6.17	6.20	6.20	16.00	6.20	vis	UCSvis	N/A	N/A	N/A	I	N/A	CS	N/A	N/A	N/A	34S_6p1d7Yd_6	10/29B2	TDP-WTP-040	7090298
21.0	0.999	0.00487	0.050	0.180	53.0	P	N/A	6.23	6.32	6.37	6.40	6.20	17.25	N/A	N/A	N/A	N/A	N/A	N/A	I	N/A	BC	N/A	N/A	N/A	34S_6p1d7Yd_6	10/29B2	TDP-WTP-040	7090300
21.1	0.999	0.00487	undefined	1.000	infinite	S	2.02	N/A	N/A	N/A	2.00	3.20	N/A	N/A	N/A	N/A	N/A	N/A	N/A	N/A	N/A	SS	N/A	N/A	N/A	34S_6p1d7Ya	10/30A1	TDP-WTP-041	7090303
21.1	0.999	0.00487	undefined	1.000	infinite	S	2.50	N/A	N/A	N/A	2.50	3.20	9.00	N/A	N/A	N/A	N/A	N/A	N/A	I	N/A	SS+	N/A	N/A	N/A	34S_6p1d7Ya	10/30A1	TDP-WTP-041	7090306
21.1	0.999	0.00487	undefined	1.000	infinite	S	3.01	N/A	N/A	N/A	3.00	3.20	10.25	N/A	N/A	N/A	N/A	N/A	N/A	I	N/A	AM	N/A	N/A	N/A	34S_6p1d7Ya	10/30A1	TDP-WTP-041	7090310
21.1	0.999	0.00487	undefined	1.000	infinite	S	3.23	N/A	N/A	N/A	3.20	3.20	17.75	3.20	vis	UCSvis	N/A	N/A	N/A	I	N/A	CS	N/A	N/A	N/A	34S_6p1d7Ya	10/30A1	TDP-WTP-041	7090313
21.0	0.999	0.00487	0.043	0.180	48.0	P	N/A	2.30	2.36	2.39	2.50	3.60	9.50	N/A	N/A	N/A	N/A	N/A	N/A	I	N/A	SS	N/A	N/A	N/A	34S_6p1d7Yd_1	10/30A2	TDP-WTP-041	7090315
21.0	0.999	0.00487	0.050	0.180	39.5	P	N/A	2.78	2.86	2.90	3.00	3.60	11.00	N/A	N/A	N/A	N/A	N/A	N/A	I	N/A	SS+	N/A	N/A	N/A	34S_6p1d7Yd_1	10/30A2	TDP-WTP-041	7090318
21.0	0.999	0.00487	0.051	0.180	37.0	P	N/A	2.94	3.04	3.09	3.20	3.60	11.75	N/A	N/A	N/A	N/A	N/A	N/A	I	N/A	AM	N/A	N/A	N/A	34S_6p1d7Yd_1	10/30A2	TDP-WTP-041	7090321
21.0	0.999	0.00487	0.051	0.180	35.0	P	N/A	3.06	3.18	3.24	3.40	3.60	12.50	N/A	N/A	N/A	N/A	N/A	N/A	I	N/A	AM+	N/A	N/A	N/A	34S_6p1d7Yd_1	10/30A2	TDP-WTP-041	7090324
21.0	0.999	0.00487	0.051	0.180	33.0	P	N/A	3.09	3.25	3.33	3.60	3.60	12.75	3.60	vis	UCSvis	N/A	N/A	N/A	I	N/A	CS	N/A	N/A	N/A	34S_6p1d7Yd_1	10/30A2	TDP-WTP-041	7090328
21.3	0.999	0.00487	undefined	1.000	infinite	S	4.02	N/A	N/A	N/A	4.00	N/A	11.25	N/A	N/A	N/A	N/A	N/A	N/A	I	N/A	SS	N/A	N/A	N/A	34S_6p1d7Ya-04	10/30C1	TDP-WTP-041	7090333
21.3	0.999	0.00487	undefined	1.000	infinite	S	4.51	N/A	N/A	N/A	4.50	N/A	14.00	N/A	N/A	N/A	N/A	N/A	N/A	I	N/A	AM	N/A	N/A	N/A	34S_6p1d7Ya-04	10/30C1	TDP-WTP-041	7090335
21.3	0.999	0.00487	undefined	1.000	infinite	S	5.02	N/A	N/A	N/A	5.00	N/A	16.75	N/A	N/A	N/A	N/A	N/A	N/A	I	N/A	AM	N/A	N/A	N/A	34S_6p1d7Ya-04	10/30C1	TDP-WTP-041	7090338
21.4	0.999	0.00487	undefined	1.000	infinite	S	5.52	N/A	N/A	N/A	5.50	N/A	20.50	N/A	N/A	N/A	N/A	N/A	N/A	I	N/A	AM+	N/A	N/A	N/A	34S_6p1d7Ya-04	10/30C1	TDP-WTP-041	7090341
21.4	0.999	0.00487	undefined	1.000	infinite	S	5.74	N/A	N/A	N/A	5.70	N/A	23.50	N/A	N/A	N/A	N/A	N/A	N/A	I	N/A	CS-	N/A	N/A	N/A	34S_6p1d7Ya-04	10/30C1	TDP-WTP-041	7090344
21.0	0.999	0.00487	0.046	0.180	70.0	P	N/A	4.87	4.93	4.96	5.00	6.70	15.50	N/A	N/A	N/A	N/A	N/A	N/A	D	N/A	SS+	N/A	N/A	N/A	34S_6p1d7Yd_9	10/30C2	TDP-WTP-041	7090348
21.0	0.999	0.00487	0.050	0.180	63.5	P	N/A	5.37	5.44	5.48	5.50	6.70	18.25	N/A	N/A	N/A	N/A	N/A	N/A	I	N/A	AM	N/A	N/A	N/A	34S_6p1d7Yd_9	10/30C2	TDP-WTP-041	7090350
21.0	0.999	0.00487	0.050	0.180	57.5	P	N/A	5.86	5.95	5.99	6.00	6.70	20.50	N/A	N/A	N/A	N/A	N/A	N/A	I	N/A	AM	N/A	N/A	N/A	34S_6p1d7Yd_9	10/30C2	TDP-WTP-041	7090353
21.0	0.999	0.00487	0.051	0.180	54.0	P	N/A	6.25	6.38	6.44	6.50	6.70	22.25	N/A	N/A	N/A	N/A	N/A	N/A	I	N/A	AM+	N/A	N/A	N/A	34S_6p1d7Yd_9	10/30C2	TDP-WTP-041	7090357
21.0	0.999	0.00487	0.050	0.180	51.5	P	N/A	6.37	6.54	6.62	6.70	6.70	24.50	6.70	vis	UCSvis	N/A	N/A	N/A	I	N/A	CS	N/A	N/A	N/A	34S_6p1d7Yd_9	10/30C2	TDP-WTP-041	7090360
21.0	0.999	0.00487	0.051	0.180	50.5	P	N/A	6.12	6.49	6.64	6.90	6.70	25.50	N/A	N/A	N/A	N/A	N/A	N/A	I	N/A	BC	N/A	N/A	N/A	34S_6p1d7Yd_9	10/30C2	TDP-WTP-041	7090362
21.5	0.999	0.00487	undefined	1.000	infinite	S	2.81	N/A	N/A	N/A	2.80	3.00	10.50	N/A	N/A	N/A	N/A	N/A	N/A	I	N/A	AM	N/A	N/A	N/A	34S_6p1d7Ya	10/31A1	TDP-WTP-042	7090368
21.4	0.999	0.00487	undefined	1.000	infinite	S	2.42	N/A	N/A	N/A	2.40	3.00	9.50	N/A	N/A	N/A	N/A	N/A	N/A	D	N/A	SS	N/A	N/A	N/A	34S_6p1d7Ya	10/31A1	TDP-WTP-042	7090371
21.4	0.999	0.00487	undefined	1.000	infinite	S	3.01	N/A	N/A	N/A	3.00	3.00	16.50	3.00	vis	UCSvis	N/A	N/A	N/A	I	N/A	CS	N/A	N/A	N/A	34S_6p1d7Ya	10/31A1	TDP-WTP-042	7090374
21.4	0.999	0.00487	undefined	1.000	infinite	S	3.22	N/A	N/A	N/A	3.20	3.00	26.00	N/A	N/A	N/A	N/A	N/A	N/A	I	N/A	BC	N/A	N/A	N/A	34S_6p1d7Ya	10/31A1	TDP-WTP-042	7090376
21.0	0.999	0.00487	0.050	0.180	48.0	P	N/A	2.35	2.39	2.41	2.50	3.40	11.00	N/A	N/A	N/A	N/A	N/A	N/A	D	N/A	SS	N/A	N/A	N/A	34S_6p1d7Yd_1	10/31A2	TDP-WTP-042	7090379

Table B.9. Updated Data from Fall 2007 Tests in Mid-Scale Vessel with Spherical Head A.4

Row Number	Test	Case ID	Tank Diameter	Head Shape	Dish Height	Dish Volume	Tank Fill Height	Return Line Height	Nozzle Inner Diameter	Nozzle Stand-off Distance	Pulse Tube Configuration	Installed Nozzles	Outer Nozzles Operated	Inner Nozzles Operated	Pulse Tube Outer Diameter	Outer PJM Radius	Inner PJM Radius	"FIO" Outer PJM Impingement Angle	"FIO" Inner PJM Impingement Angle	Ratio Outer PJM to Tank Radius	Ratio Inner PJM to Tank Radius	Simulant	Solids Density	Particle Diameter d5	Particle Diameter d50	Particle Diameter d95	Void Fraction
text	text	text	in.	text	in.	in. ^{3}	in.	in.	in.	in.	text	number	number	number	in.	in.	in.	deg	deg	nondim	nondim	text	g/cm^3	m	m	m	fraction
MSS	M/DDX	ID	D	HS	H_{dish}	V_{dish}	H	Rtn	d	sod	PT	N	N_O	N_I	PT_{od}	R_O	R_I	Θ_O	Θ_I	R_O/R	R_I/R	sxdx	ρ_S	d_5	d_{50}	d_{95}	vf
7090382	10/31A2	34S_6p1d7Yd_1	33 7/8	S	9	4437.4	33 7/8	31 7/8	0.446	0.669	HLP-22	12	8	4	1.9	10.5	5.7	30.8	16.1	0.62	0.33	p1d7	2.45	0.0001213	0.0001780	0.0002606	0.4277
7090385	10/31A2	34S_6p1d7Yd_1	33 7/8	S	9	4437.4	33 7/8	31 7/8	0.446	0.669	HLP-22	12	8	4	1.9	10.5	5.7	30.8	16.1	0.62	0.33	p1d7	2.45	0.0001213	0.0001780	0.0002606	0.4277
7090389	10/31A2	34S_6p1d7Yd_1	33 7/8	S	9	4437.4	33 7/8	31 7/8	0.446	0.669	HLP-22	12	8	4	1.9	10.5	5.7	30.8	16.1	0.62	0.33	p1d7	2.45	0.0001213	0.0001780	0.0002606	0.4277
7090391	10/31A2	34S_6p1d7Yd_1	33 7/8	S	9	4437.4	33 7/8	31 7/8	0.446	0.669	HLP-22	12	8	4	1.9	10.5	5.7	30.8	16.1	0.62	0.33	p1d7	2.45	0.0001213	0.0001780	0.0002606	0.4277
7090395	11/2A1	34S_6p1d7Ya-80	33 7/8	S	9	4437.4	33 7/8	31 7/8	0.446	0.669	HLP-22	12	8	0	1.9	10.5	5.7	30.8	16.1	0.62	0.33	p1d7	2.45	0.0001213	0.0001780	0.0002606	0.4277
7090398	11/2A1	34S_6p1d7Ya-80	33 7/8	S	9	4437.4	33 7/8	31 7/8	0.446	0.669	HLP-22	12	8	0	1.9	10.5	5.7	30.8	16.1	0.62	0.33	p1d7	2.45	0.0001213	0.0001780	0.0002606	0.4277
7090401	11/2A2	34S_6p1d7Yd_5	33 7/8	S	9	4437.4	33 7/8	31 7/8	0.446	0.669	HLP-22	12	8	0	1.9	10.5	5.7	30.8	16.1	0.62	0.33	p1d7	2.45	0.0001213	0.0001780	0.0002606	0.4277
7090403	11/2A2	34S_6p1d7Yd_5	33 7/8	S	9	4437.4	33 7/8	31 7/8	0.446	0.669	HLP-22	12	8	0	1.9	10.5	5.7	30.8	16.1	0.62	0.33	p1d7	2.45	0.0001213	0.0001780	0.0002606	0.4277
7090406	11/2A2	34S_6p1d7Yd_5	33 7/8	S	9	4437.4	33 7/8	31 7/8	0.446	0.669	HLP-22	12	8	0	1.9	10.5	5.7	30.8	16.1	0.62	0.33	p1d7	2.45	0.0001213	0.0001780	0.0002606	0.4277
7090409	11/2A2	34S_6p1d7Yd_5	33 7/8	S	9	4437.4	33 7/8	31 7/8	0.446	0.669	HLP-22	12	8	0	1.9	10.5	5.7	30.8	16.1	0.62	0.33	p1d7	2.45	0.0001213	0.0001780	0.0002606	0.4277
7090413	11/2A2	34S_6p1d7Yd_5	33 7/8	S	9	4437.4	33 7/8	31 7/8	0.446	0.669	HLP-22	12	8	0	1.9	10.5	5.7	30.8	16.1	0.62	0.33	p1d7	2.45	0.0001213	0.0001780	0.0002606	0.4277
7090416	11/5A1	34S_6p1d7Ya-44	33 7/8	S	9	4437.4	33 7/8	31 7/8	0.446	0.669	HLP-22	12	4	4	1.9	10.5	5.7	30.8	16.1	0.62	0.33	p1d7	2.45	0.0001213	0.0001780	0.0002606	0.4277
7090419	11/5A1	34S_6p1d7Ya-44	33 7/8	S	9	4437.4	33 7/8	31 7/8	0.446	0.669	HLP-22	12	4	4	1.9	10.5	5.7	30.8	16.1	0.62	0.33	p1d7	2.45	0.0001213	0.0001780	0.0002606	0.4277
7090421	11/5A1	34S_6p1d7Ya-44	33 7/8	S	9	4437.4	33 7/8	31 7/8	0.446	0.669	HLP-22	12	4	4	1.9	10.5	5.7	30.8	16.1	0.62	0.33	p1d7	2.45	0.0001213	0.0001780	0.0002606	0.4277
7090424	11/5A1	34S_6p1d7Ya-44	33 7/8	S	9	4437.4	33 7/8	31 7/8	0.446	0.669	HLP-22	12	4	4	1.9	10.5	5.7	30.8	16.1	0.62	0.33	p1d7	2.45	0.0001213	0.0001780	0.0002606	0.4277
7090428	11/5A1	34S_6p1d7Ya-44	33 7/8	S	9	4437.4	33 7/8	31 7/8	0.446	0.669	HLP-22	12	4	4	1.9	10.5	5.7	30.8	16.1	0.62	0.33	p1d7	2.45	0.0001213	0.0001780	0.0002606	0.4277
7090430	11/5A1	34S_6p1d7Ya-44	33 7/8	S	9	4437.4	33 7/8	31 7/8	0.446	0.669	HLP-22	12	4	4	1.9	10.5	5.7	30.8	16.1	0.62	0.33	p1d7	2.45	0.0001213	0.0001780	0.0002606	0.4277
7090434	11/5A2	34S_6p1d7Yd_0	33 7/8	S	9	4437.4	33 7/8	31 7/8	0.446	0.669	HLP-22	12	4	4	1.9	10.5	5.7	30.8	16.1	0.62	0.33	p1d7	2.45	0.0001213	0.0001780	0.0002606	0.4277
7090436	11/5A2	34S_6p1d7Yd_0	33 7/8	S	9	4437.4	33 7/8	31 7/8	0.446	0.669	HLP-22	12	4	4	1.9	10.5	5.7	30.8	16.1	0.62	0.33	p1d7	2.45	0.0001213	0.0001780	0.0002606	0.4277
7090439	11/5A2	34S_6p1d7Yd_0	33 7/8	S	9	4437.4	33 7/8	31 7/8	0.446	0.669	HLP-22	12	4	4	1.9	10.5	5.7	30.8	16.1	0.62	0.33	p1d7	2.45	0.0001213	0.0001780	0.0002606	0.4277
7090443	11/5A2	34S_6p1d7Yd_0	33 7/8	S	9	4437.4	33 7/8	31 7/8	0.446	0.669	HLP-22	12	4	4	1.9	10.5	5.7	30.8	16.1	0.62	0.33	p1d7	2.45	0.0001213	0.0001780	0.0002606	0.4277
7090445	11/5A2	34S_6p1d7Yd_0	33 7/8	S	9	4437.4	33 7/8	31 7/8	0.446	0.669	HLP-22	12	4	4	1.9	10.5	5.7	30.8	16.1	0.62	0.33	p1d7	2.45	0.0001213	0.0001780	0.0002606	0.4277
7090448	11/5A2	34S_6p1d7Yd_0	33 7/8	S	9	4437.4	33 7/8	31 7/8	0.446	0.669	HLP-22	12	4	4	1.9	10.5	5.7	30.8	16.1	0.62	0.33	p1d7	2.45	0.0001213	0.0001780	0.0002606	0.4277
7090451	11/5A2	34S_6p1d7Yd_0	33 7/8	S	9	4437.4	33 7/8	31 7/8	0.446	0.669	HLP-22	12	4	4	1.9	10.5	5.7	30.8	16.1	0.62	0.33	p1d7	2.45	0.0001213	0.0001780	0.0002606	0.4277
7090454	11/5A2	34S_6p1d7Yd_0	33 7/8	S	9	4437.4	33 7/8	31 7/8	0.446	0.669	HLP-22	12	4	4	1.9	10.5	5.7	30.8	16.1	0.62	0.33	p1d7	2.45	0.0001213	0.0001780	0.0002606	0.4277
7090458	11/5A2	34S_6p1d7Yd_0	33 7/8	S	9	4437.4	33 7/8	31 7/8	0.446	0.669	HLP-22	12	4	4	1.9	10.5	5.7	30.8	16.1	0.62	0.33	p1d7	2.45	0.0001213	0.0001780	0.0002606	0.4277
7090461	11/5B1	34S_6p1d7Ya-04	33 7/8	S	9	4437.4	33 7/8	31 7/8	0.446	0.669	HLP-22	12	0	4	1.9	10.5	5.7	30.8	16.1	0.62	0.33	p1d7	2.45	0.0001213	0.0001780	0.0002606	0.4277
7090464	11/5B1	34S_6p1d7Ya-04	33 7/8	S	9	4437.4	33 7/8	31 7/8	0.446	0.669	HLP-22	12	0	4	1.9	10.5	5.7	30.8	16.1	0.62	0.33	p1d7	2.45	0.0001213	0.0001780	0.0002606	0.4277
7090466	11/5B1	34S_6p1d7Ya-04	33 7/8	S	9	4437.4	33 7/8	31 7/8	0.446	0.669	HLP-22	12	0	4	1.9	10.5	5.7	30.8	16.1	0.62	0.33	p1d7	2.45	0.0001213	0.0001780	0.0002606	0.4277
7090469	11/5B1	34S_6p1d7Ya-04	33 7/8	S	9	4437.4	33 7/8	31 7/8	0.446	0.669	HLP-22	12	0	4	1.9	10.5	5.7	30.8	16.1	0.62	0.33	p1d7	2.45	0.0001213	0.0001780	0.0002606	0.4277
7090473	11/5B1	34S_6p1d7Ya-04	33 7/8	S	9	4437.4	33 7/8	31 7/8	0.446	0.669	HLP-22	12	0	4	1.9	10.5	5.7	30.8	16.1	0.62	0.33	p1d7	2.45	0.0001213	0.0001780	0.0002606	0.4277
7090476	11/5B2	34S_6p1d7Yd_9	33 7/8	S	9	4437.4	33 7/8	31 7/8	0.446	0.669	HLP-22	12	0	4	1.9	10.5	5.7	30.8	16.1	0.62	0.33	p1d7	2.45	0.0001213	0.0001780	0.0002606	0.4277
7090479	11/5B2	34S_6p1d7Yd_9	33 7/8	S	9	4437.4	33 7/8	31 7/8	0.446	0.669	HLP-22	12	0	4	1.9	10.5	5.7	30.8	16.1	0.62	0.33	p1d7	2.45	0.0001213	0.0001780	0.0002606	0.4277
7090481	11/5B2	34S_6p1d7Yd_9	33 7/8	S	9	4437.4	33 7/8	31 7/8	0.446	0.669	HLP-22	12	0	4	1.9	10.5	5.7	30.8	16.1	0.62	0.33	p1d7	2.45	0.0001213	0.0001780	0.0002606	0.4277
7090484	11/5B2	34S_6p1d7Yd_9	33 7/8	S	9	4437.4	33 7/8	31 7/8	0.446	0.669	HLP-22	12	0	4	1.9	10.5	5.7	30.8	16.1	0.62	0.33	p1d7	2.45	0.0001213	0.0001780	0.0002606	0.4277
7090487	11/5B2	34S_6p1d7Yd_9	33 7/8	S	9	4437.4	33 7/8	31 7/8	0.446	0.669	HLP-22	12	0	4	1.9	10.5	5.7	30.8	16.1	0.62	0.33	p1d7	2.45	0.0001213	0.0001780	0.0002606	0.4277
7090491	11/5B2	34S_6p1d7Yd_9	33 7/8	S	9	4437.4	33 7/8	31 7/8	0.446	0.669	HLP-22	12	0	4	1.9	10.5	5.7	30.8	16.1	0.62	0.33	p1d7	2.45	0.0001213	0.0001780	0.0002606	0.4277
7090493	11/6A1	34S_6p1d7Ya-40	33 7/8	S	9	4437.4	33 7/8	31 7/8	0.446	0.669	HLP-22	12	4	0	1.9	10.5	5.7	30.8	16.1	0.62	0.33	p1d7	2.45	0.0001213	0.0001780	0.0002606	0.4277
7090496	11/6A1	34S_6p1d7Ya-40	33 7/8	S	9	4437.4	33 7/8	31 7/8	0.446	0.669	HLP-22	12	4	0	1.9	10.5	5.7	30.8	16.1	0.62	0.33	p1d7	2.45	0.0001213	0.0001780	0.0002606	0.4277
7090499	11/6A1	34S_6p1d7Ya-40	33 7/8	S	9	4437.4	33 7/8	31 7/8	0.446	0.669	HLP-22	12	4	0	1.9	10.5	5.7	30.8	16.1	0.62	0.33	p1d7	2.45	0.0001213	0.0001780	0.0002606	0.4277
7090503	11/6A1	34S_6p1d7Ya-40	33 7/8	S	9	4437.4	33 7/8	31 7/8	0.446	0.669	HLP-22	12	4	0	1.9	10.5	5.7	30.8	16.1	0.62	0.33	p1d7	2.45	0.0001213	0.0001780	0.0002606	0.4277

Table B.9. Updated Data from Fall 2007 Tests in Mid-Scale Vessel with Spherical Head B.4

Tank Water Temperature	Water Density	Solids Fraction	Pulse Volume Fraction	Duty Cycle	Cycle Time	Pulsed or Steady Jet	Us Steady Jet	U1 Pulsing Jet	U2 URMS	U3 URM3	Discharge Velocity	Critical Suspension Velocity	Average Peak Cloud Height	U_{CS} Condition	U_{CS} Method	U_{CS} Flag	U_{CS} Center Flag	U_{CS} udv Flag	U_{CS} based on Decreasing Velocity	Sweep Increase / Decrease	UDV Height Bed	Particle Motion	Solids Level	Outer Bottom Pattern	Inner Bottom Pattern	Case ID	Test	TDP	Row Number
C	g/cm³	fraction	fraction	fraction	s	text	m/s	m/s	m/s	m/s	m/s	m/s	in.	m/s	text	text	text	text	m/s	text	mm	text	text	text	text	text	text	text	text
T	ρ_l	ϕ_s	ϕ_p	DC	t_C	Jet	US	U1	U2	U3	U	U_{CS}	H_C	U_{CSR}	U_{CSM}	U_{CS}vis	U_{CS}cen	U_{CS}udv	U_{CS_D}	S_W	H_{bed}	PM	Sol	SP_O	SP_I	ID	M/DDX	TDP	MSS
21.0	0.999	0.00487	0.052	0.180	40.0	P	N/A	2.80	2.87	2.90	3.00	3.40	12.50	N/A	N/A	N/A	N/A	N/A	N/A	I	N/A	AM	N/A	N/A	N/A	34S_6p1d7Yd_1	10/31A2	TDP-WTP-042	7090382
21.0	0.999	0.00487	0.050	0.180	37.5	P	N/A	2.97	3.04	3.08	3.20	3.40	13.00	N/A	N/A	N/A	N/A	N/A	N/A	I	N/A	AM+	N/A	N/A	N/A	34S_6p1d7Yd_1	10/31A2	TDP-WTP-042	7090385
21.0	0.999	0.00487	0.050	0.180	35.0	P	N/A	3.13	3.22	3.26	3.40	3.40	13.50	3.40	vis	UCSvis	N/A	N/A	N/A	I	N/A	CS	N/A	N/A	N/A	34S_6p1d7Yd_1	10/31A2	TDP-WTP-042	7090389
21.0	0.999	0.00487	0.050	0.180	33.0	P	N/A	3.29	3.39	3.44	3.60	3.40	14.25	N/A	N/A	N/A	N/A	N/A	N/A	I	N/A	BC	N/A	N/A	N/A	34S_6p1d7Yd_1	10/31A2	TDP-WTP-042	7090391
24.0	0.999	0.00487	undefined	1.000	infinite	S	5.00	N/A	N/A	N/A	5.00	5.30	13.50	N/A	N/A	N/A	N/A	N/A	N/A	I	N/A	SS	N/A	N/A	N/A	34S_6p1d7Ya-80	11/2A1	TDP-WTP-043	7090395
24.0	0.999	0.00487	undefined	1.000	infinite	S	5.29	N/A	N/A	N/A	5.30	5.30	23.50	5.30	vis	UCSvis	N/A	N/A	N/A	I	N/A	CS	N/A	N/A	N/A	34S_6p1d7Ya-80	11/2A1	TDP-WTP-043	7090398
24.0	0.999	0.00487	0.051	0.180	30.0	P	N/A	5.05	5.40	5.55	5.90	6.60	14.25	N/A	N/A	N/A	N/A	N/A	N/A	I	N/A	SS	N/A	N/A	N/A	34S_6p1d7Yd_5	11/2A2	TDP-WTP-043	7090401
24.0	0.999	0.00487	0.051	0.180	29.0	P	N/A	5.12	5.52	5.69	6.10	6.60	15.75	N/A	N/A	N/A	N/A	N/A	N/A	I	N/A	SS+	N/A	N/A	N/A	34S_6p1d7Yd_5	11/2A2	TDP-WTP-043	7090403
24.0	0.999	0.00487	0.051	0.180	28.0	P	N/A	5.04	5.57	5.80	6.30	6.60	16.75	N/A	N/A	N/A	N/A	N/A	N/A	I	N/A	AM	N/A	N/A	N/A	34S_6p1d7Yd_5	11/2A2	TDP-WTP-043	7090406
24.0	0.999	0.00487	0.051	0.180	27.0	P	N/A	5.15	5.70	5.95	6.50	6.60	18.50	N/A	N/A	N/A	N/A	N/A	N/A	I	N/A	AM+	N/A	N/A	N/A	34S_6p1d7Yd_5	11/2A2	TDP-WTP-043	7090409
24.0	0.999	0.00487	0.051	0.180	26.5	P	N/A	5.15	5.74	6.00	6.60	6.60	19.00	6.60	vis	UCSvis	N/A	N/A	N/A	I	N/A	CS	N/A	N/A	N/A	34S_6p1d7Yd_5	11/2A2	TDP-WTP-043	7090413
20.8	0.999	0.00487	undefined	1.000	infinite	S	3.13	N/A	N/A	N/A	3.00	4.60	N/A	N/A	N/A	N/A	N/A	N/A	N/A	I	N/A	SS	N/A	N/A	N/A	34S_6p1d7Ya-44	11/5A1	TDP-WTP-044	7090416
20.9	0.999	0.00487	undefined	1.000	infinite	S	3.53	N/A	N/A	N/A	3.50	4.60	N/A	N/A	N/A	N/A	N/A	N/A	N/A	I	N/A	SS	N/A	N/A	N/A	34S_6p1d7Ya-44	11/5A1	TDP-WTP-044	7090419
20.9	0.999	0.00487	undefined	1.000	infinite	S	4.01	N/A	N/A	N/A	4.00	4.60	9.25	N/A	N/A	N/A	UCScen	N/A	N/A	I	N/A	AM	N/A	N/A	N/A	34S_6p1d7Ya-44	11/5A1	TDP-WTP-044	7090421
0.0	0.999	0.00487	undefined	1.000	infinite	S	N/A	N/A	N/A	N/A	4.40	4.60	12.25	N/A	N/A	N/A	N/A	N/A	N/A	I	N/A	AM+	N/A	N/A	N/A	34S_6p1d7Ya-44	11/5A1	TDP-WTP-044	7090424
20.9	0.999	0.00487	undefined	1.000	infinite	S	4.65	N/A	N/A	N/A	4.60	4.60	15.25	4.60	vis	UCSvis	N/A	N/A	N/A	I	N/A	CS	N/A	N/A	N/A	34S_6p1d7Ya-44	11/5A1	TDP-WTP-044	7090428
21.0	0.999	0.00487	undefined	1.000	infinite	S	4.80	N/A	N/A	N/A	4.80	4.60	18.50	N/A	N/A	N/A	N/A	N/A	N/A	I	N/A	BC	N/A	N/A	N/A	34S_6p1d7Ya-44	11/5A1	TDP-WTP-044	7090430
21.0	0.999	0.00487	0.050	0.180	42.0	P	N/A	4.04	4.12	4.16	4.00	6.30	9.00	N/A	N/A	N/A	N/A	N/A	N/A	D	N/A	SS	N/A	N/A	N/A	34S_6p1d7Yd_0	11/5A2	TDP-WTP-044	7090434
21.0	0.999	0.00487	0.051	0.180	39.5	P	N/A	4.24	4.35	4.39	4.50	6.30	9.50	N/A	N/A	N/A	N/A	N/A	N/A	I	N/A	AM	N/A	N/A	N/A	34S_6p1d7Yd_0	11/5A2	TDP-WTP-044	7090436
21.0	0.999	0.00487	0.051	0.180	36.5	P	N/A	4.60	4.72	4.78	4.90	6.30	10.25	N/A	N/A	N/A	N/A	N/A	N/A	I	N/A	AM	N/A	N/A	N/A	34S_6p1d7Yd_0	11/5A2	TDP-WTP-044	7090439
21.0	0.999	0.00487	0.051	0.180	33.5	P	N/A	4.87	5.05	5.13	5.30	6.30	12.00	N/A	N/A	N/A	N/A	N/A	N/A	I	N/A	AM	N/A	N/A	N/A	34S_6p1d7Yd_0	11/5A2	TDP-WTP-044	7090443
21.0	0.999	0.00487	0.051	0.180	32.0	P	N/A	5.09	5.25	5.33	5.50	6.30	13.00	N/A	N/A	N/A	N/A	N/A	N/A	I	N/A	AM+	N/A	N/A	N/A	34S_6p1d7Yd_0	11/5A2	TDP-WTP-044	7090445
21.0	0.999	0.00487	0.051	0.180	31.0	P	N/A	5.12	5.35	5.46	5.70	6.30	13.75	N/A	N/A	N/A	N/A	N/A	N/A	I	N/A	AM+	N/A	N/A	N/A	34S_6p1d7Yd_0	11/5A2	TDP-WTP-044	7090448
21.0	0.999	0.00487	0.051	0.180	30.0	P	N/A	5.15	5.46	5.60	5.90	6.30	14.75	N/A	N/A	N/A	N/A	N/A	N/A	I	N/A	AM+	N/A	N/A	N/A	34S_6p1d7Yd_0	11/5A2	TDP-WTP-044	7090451
21.0	0.999	0.00487	0.051	0.180	28.8	P	N/A	5.22	5.59	5.75	6.10	6.30	16.00	N/A	N/A	N/A	N/A	N/A	N/A	I	N/A	AM+	N/A	N/A	N/A	34S_6p1d7Yd_0	11/5A2	TDP-WTP-044	7090454
21.0	0.999	0.00487	0.051	0.180	27.8	P	N/A	5.23	5.67	5.86	6.30	6.30	16.50	6.30	vis	UCSvis	N/A	N/A	N/A	I	N/A	CS	N/A	N/A	N/A	34S_6p1d7Yd_0	11/5A2	TDP-WTP-044	7090458
21.3	0.999	0.00487	undefined	1.000	infinite	S	4.52	N/A	N/A	N/A	4.50	6.50	9.50	N/A	N/A	N/A	N/A	N/A	N/A	D	N/A	SS	N/A	N/A	N/A	34S_6p1d7Ya-04	11/5B1	TDP-WTP-044	7090461
21.3	0.999	0.00487	undefined	1.000	infinite	S	5.00	N/A	N/A	N/A	5.00	6.50	11.25	N/A	N/A	N/A	N/A	N/A	N/A	I	N/A	SS+	N/A	N/A	N/A	34S_6p1d7Ya-04	11/5B1	TDP-WTP-044	7090464
21.4	0.999	0.00487	undefined	1.000	infinite	S	5.57	N/A	N/A	N/A	5.50	6.50	13.75	N/A	N/A	N/A	N/A	N/A	N/A	I	N/A	AM	N/A	N/A	N/A	34S_6p1d7Ya-04	11/5B1	TDP-WTP-044	7090466
21.4	0.999	0.00487	undefined	1.000	infinite	S	6.04	N/A	N/A	N/A	6.00	6.50	16.00	N/A	N/A	N/A	N/A	N/A	N/A	I	N/A	AM+	N/A	N/A	N/A	34S_6p1d7Ya-04	11/5B1	TDP-WTP-044	7090469
21.4	0.999	0.00487	undefined	1.000	infinite	S	6.53	N/A	N/A	N/A	6.50	6.50	19.50	6.50	vis	UCSvis	N/A	N/A	N/A	I	N/A	CS	N/A	N/A	N/A	34S_6p1d7Ya-04	11/5B1	TDP-WTP-044	7090473
21.0	0.999	0.00487	0.047	0.180	62.0	P	N/A	5.51	5.59	5.63	5.50	7.80	12.50	N/A	N/A	N/A	N/A	N/A	N/A	D	N/A	SS	N/A	N/A	N/A	34S_6p1d7Yd_9	11/5B2	TDP-WTP-044	7090476
21.0	0.999	0.00487	0.052	0.180	58.5	P	N/A	5.99	6.08	6.12	6.00	7.80	14.25	N/A	N/A	N/A	N/A	N/A	N/A	I	N/A	AM-	N/A	N/A	N/A	34S_6p1d7Yd_9	11/5B2	TDP-WTP-044	7090479
21.0	0.999	0.00487	0.052	0.180	54.0	P	N/A	6.40	6.50	6.55	6.50	7.80	15.75	N/A	N/A	N/A	N/A	N/A	N/A	I	N/A	AM	N/A	N/A	N/A	34S_6p1d7Yd_9	11/5B2	TDP-WTP-044	7090481
21.0	0.999	0.00487	0.051	0.180	49.5	P	N/A	6.89	7.01	7.07	7.00	7.80	17.25	N/A	N/A	N/A	N/A	N/A	N/A	I	N/A	AM+	N/A	N/A	N/A	34S_6p1d7Yd_9	11/5B2	TDP-WTP-044	7090484
21.0	0.999	0.00487	0.050	0.180	46.5	P	N/A	7.04	7.26	7.36	7.40	7.80	19.00	N/A	N/A	N/A	N/A	N/A	N/A	I	N/A	AM+	N/A	N/A	N/A	34S_6p1d7Yd_9	11/5B2	TDP-WTP-044	7090487
21.0	0.999	0.00487	0.051	0.180	44.3	P	N/A	7.26	7.57	7.70	7.80	7.80	20.25	7.80	vis	UCSvis	N/A	N/A	N/A	I	N/A	CS	N/A	N/A	N/A	34S_6p1d7Yd_9	11/5B2	TDP-WTP-044	7090491
20.6	0.999	0.00487	undefined	1.000	infinite	S	5.48	N/A	N/A	N/A	5.50	6.40	N/A	N/A	N/A	N/A	N/A	N/A	N/A	I	N/A	SS	N/A	N/A	N/A	34S_6p1d7Ya-40	11/6A1	TDP-WTP-049	7090493
20.7	0.999	0.00487	undefined	1.000	infinite	S	5.99	N/A	N/A	N/A	6.00	6.40	10.50	N/A	N/A	N/A	N/A	N/A	N/A	I	N/A	AM	N/A	N/A	N/A	34S_6p1d7Ya-40	11/6A1	TDP-WTP-049	7090496
20.7	0.999	0.00487	undefined	1.000	infinite	S	6.20	N/A	N/A	N/A	6.20	6.40	17.00	N/A	N/A	N/A	N/A	N/A	N/A	I	N/A	AM+	N/A	N/A	N/A	34S_6p1d7Ya-40	11/6A1	TDP-WTP-049	7090499
20.8	0.999	0.00487	undefined	1.000	infinite	S	6.42	N/A	N/A	N/A	6.40	6.40	21.00	6.40	vis	UCSvis	N/A	N/A	N/A	I	N/A	CS	N/A	N/A	N/A	34S_6p1d7Ya-40	11/6A1	TDP-WTP-049	7090503

Table B.9. Updated Data from Fall 2007 Tests in Mid-Scale Vessel with Spherical Head A.5

Row Number	Test	Case ID	Tank Diameter	Head Shape	Dish Height	Dish Volume	Tank Fill Height	Return Line Height	Nozzle Inner Diameter	Nozzle Stand-off Distance	Pulse Tube Configuration	Installed Nozzles	Outer Nozzles Operated	Inner Nozzles Operated	Pulse Tube Outer Diameter	Outer PJM Radius	Inner PJM Radius	"FIO" Outer PJM Impingement Angle	"FIO" Inner PJM Impingement Angle	Ratio Outer PJM to Tank Radius	Ratio Inner PJM to Tank Radius	Simulant	Solids Density	Particle Diameter d5	Particle Diameter d50	Particle Diameter d95	Void Fraction
text	text	text	in.	text	in.	in. ^{3}	in.	in.	in.	in.	text	number	number	number	in.	in.	in.	deg	deg	nondim	nondim	text	g/cm^3	m	m	m	fraction
MSS	M/DDX	ID	D	HS	H_{dish}	V_{dish}	H	Rtn	d	sod	PT	N	N_O	N_I	PT_{od}	R_O	R_I	Θ_O	Θ_I	R_O/R	R_I/R	sxdx	ρ_S	d_5	d_{50}	d_{95}	vf
7090506	11/6A1	34S_6p1d7Ya-40	33 7/8	S	9	4437.4	33 7/8	31 7/8	0.446	0.669	HLP-22	12	4	0	1.9	10.5	5.7	30.8	16.1	0.62	0.33	p1d7	2.45	0.0001213	0.0001780	0.0002606	0.4277
7090508	11/6A2	34S_6p1d7Yd_6	33 7/8	S	9	4437.4	33 7/8	31 7/8	0.446	0.669	HLP-22	12	4	0	1.9	10.5	5.7	30.8	16.1	0.62	0.33	p1d7	2.45	0.0001213	0.0001780	0.0002606	0.4277
7090511	11/6A2	34S_6p1d7Yd_6	33 7/8	S	9	4437.4	33 7/8	31 7/8	0.446	0.669	HLP-22	12	4	0	1.9	10.5	5.7	30.8	16.1	0.62	0.33	p1d7	2.45	0.0001213	0.0001780	0.0002606	0.4277
7090514	11/6A2	34S_6p1d7Yd_6	33 7/8	S	9	4437.4	33 7/8	31 7/8	0.446	0.669	HLP-22	12	4	0	1.9	10.5	5.7	30.8	16.1	0.62	0.33	p1d7	2.45	0.0001213	0.0001780	0.0002606	0.4277
7090518	11/6A2	34S_6p1d7Yd_6	33 7/8	S	9	4437.4	33 7/8	31 7/8	0.446	0.669	HLP-22	12	4	0	1.9	10.5	5.7	30.8	16.1	0.62	0.33	p1d7	2.45	0.0001213	0.0001780	0.0002606	0.4277
7090520	11/6A2	34S_6p1d7Yd_6	33 7/8	S	9	4437.4	33 7/8	31 7/8	0.446	0.669	HLP-22	12	4	0	1.9	10.5	5.7	30.8	16.1	0.62	0.33	p1d7	2.45	0.0001213	0.0001780	0.0002606	0.4277
7090523	11/7A1	34S_6p1d7Ya	33 7/8	S	9	4437.4	23 5/7	21 5/7	0.446	0.669	HLP-22	12	8	4	1.9	10.5	5.7	30.8	16.1	0.62	0.33	p1d7	2.45	0.0001213	0.0001780	0.0002606	0.4277
7090526	11/7A1	34S_6p1d7Ya	33 7/8	S	9	4437.4	23 5/7	21 5/7	0.446	0.669	HLP-22	12	8	4	1.9	10.5	5.7	30.8	16.1	0.62	0.33	p1d7	2.45	0.0001213	0.0001780	0.0002606	0.4277
7090529	11/7A1	34S_6p1d7Ya	33 7/8	S	9	4437.4	23 5/7	21 5/7	0.446	0.669	HLP-22	12	8	4	1.9	10.5	5.7	30.8	16.1	0.62	0.33	p1d7	2.45	0.0001213	0.0001780	0.0002606	0.4277
7090532	11/7A1	34S_6p1d7Ya	33 7/8	S	9	4437.4	23 5/7	21 5/7	0.446	0.669	HLP-22	12	8	4	1.9	10.5	5.7	30.8	16.1	0.62	0.33	p1d7	2.45	0.0001213	0.0001780	0.0002606	0.4277
7090536	11/7A1	34S_6p1d7Ya	33 7/8	S	9	4437.4	23 5/7	21 5/7	0.446	0.669	HLP-22	12	8	4	1.9	10.5	5.7	30.8	16.1	0.62	0.33	p1d7	2.45	0.0001213	0.0001780	0.0002606	0.4277
7090538	11/7A1	34S_6p1d7Ya	33 7/8	S	9	4437.4	23 5/7	21 5/7	0.446	0.669	HLP-22	12	8	4	1.9	10.5	5.7	30.8	16.1	0.62	0.33	p1d7	2.45	0.0001213	0.0001780	0.0002606	0.4277
7090542	11/7A2	34S_6p1d7Yd_1	33 7/8	S	9	4437.4	23 5/7	21 5/7	0.446	0.669	HLP-22	12	8	4	1.9	10.5	5.7	30.8	16.1	0.62	0.33	p1d7	2.45	0.0001213	0.0001780	0.0002606	0.4277
7090544	11/7A2	34S_6p1d7Yd_1	33 7/8	S	9	4437.4	23 5/7	21 5/7	0.446	0.669	HLP-22	12	8	4	1.9	10.5	5.7	30.8	16.1	0.62	0.33	p1d7	2.45	0.0001213	0.0001780	0.0002606	0.4277
7090547	11/7A2	34S_6p1d7Yd_1	33 7/8	S	9	4437.4	23 5/7	21 5/7	0.446	0.669	HLP-22	12	8	4	1.9	10.5	5.7	30.8	16.1	0.62	0.33	p1d7	2.45	0.0001213	0.0001780	0.0002606	0.4277
7090551	11/7A2	34S_6p1d7Yd_1	33 7/8	S	9	4437.4	23 5/7	21 5/7	0.446	0.669	HLP-22	12	8	4	1.9	10.5	5.7	30.8	16.1	0.62	0.33	p1d7	2.45	0.0001213	0.0001780	0.0002606	0.4277
7090553	11/7B1	34S_6p1d7Ya-44	33 7/8	S	9	4437.4	23 5/7	21 5/7	0.446	0.669	HLP-22	12	4	4	1.9	10.5	5.7	30.8	16.1	0.62	0.33	p1d7	2.45	0.0001213	0.0001780	0.0002606	0.4277
7090557	11/7B1	34S_6p1d7Ya-44	33 7/8	S	9	4437.4	23 5/7	21 5/7	0.446	0.669	HLP-22	12	4	4	1.9	10.5	5.7	30.8	16.1	0.62	0.33	p1d7	2.45	0.0001213	0.0001780	0.0002606	0.4277
7090560	11/7B1	34S_6p1d7Ya-44	33 7/8	S	9	4437.4	23 5/7	21 5/7	0.446	0.669	HLP-22	12	4	4	1.9	10.5	5.7	30.8	16.1	0.62	0.33	p1d7	2.45	0.0001213	0.0001780	0.0002606	0.4277
7090562	11/7B1	34S_6p1d7Ya-44	33 7/8	S	9	4437.4	23 5/7	21 5/7	0.446	0.669	HLP-22	12	4	4	1.9	10.5	5.7	30.8	16.1	0.62	0.33	p1d7	2.45	0.0001213	0.0001780	0.0002606	0.4277
7090566	11/7B1	34S_6p1d7Ya-44	33 7/8	S	9	4437.4	23 5/7	21 5/7	0.446	0.669	HLP-22	12	4	4	1.9	10.5	5.7	30.8	16.1	0.62	0.33	p1d7	2.45	0.0001213	0.0001780	0.0002606	0.4277
7090569	11/7B2	34S_6p1d7Yd_0	33 7/8	S	9	4437.4	23 5/7	21 5/7	0.446	0.669	HLP-22	12	4	4	1.9	10.5	5.7	30.8	16.1	0.62	0.33	p1d7	2.45	0.0001213	0.0001780	0.0002606	0.4277
7090571	11/7B2	34S_6p1d7Yd_0	33 7/8	S	9	4437.4	23 5/7	21 5/7	0.446	0.669	HLP-22	12	4	4	1.9	10.5	5.7	30.8	16.1	0.62	0.33	p1d7	2.45	0.0001213	0.0001780	0.0002606	0.4277
7090574	11/7B2	34S_6p1d7Yd_0	33 7/8	S	9	4437.4	23 5/7	21 5/7	0.446	0.669	HLP-22	12	4	4	1.9	10.5	5.7	30.8	16.1	0.62	0.33	p1d7	2.45	0.0001213	0.0001780	0.0002606	0.4277
7090577	11/7B2	34S_6p1d7Yd_0	33 7/8	S	9	4437.4	23 5/7	21 5/7	0.446	0.669	HLP-22	12	4	4	1.9	10.5	5.7	30.8	16.1	0.62	0.33	p1d7	2.45	0.0001213	0.0001780	0.0002606	0.4277
7090580	11/7B2	34S_6p1d7Yd_0	33 7/8	S	9	4437.4	23 5/7	21 5/7	0.446	0.669	HLP-22	12	4	4	1.9	10.5	5.7	30.8	16.1	0.62	0.33	p1d7	2.45	0.0001213	0.0001780	0.0002606	0.4277
7090583	11/7B2	34S_6p1d7Yd_0	33 7/8	S	9	4437.4	23 5/7	21 5/7	0.446	0.669	HLP-22	12	4	4	1.9	10.5	5.7	30.8	16.1	0.62	0.33	p1d7	2.45	0.0001213	0.0001780	0.0002606	0.4277
7090587	11/7B2	34S_6p1d7Yd_0	33 7/8	S	9	4437.4	23 5/7	21 5/7	0.446	0.669	HLP-22	12	4	4	1.9	10.5	5.7	30.8	16.1	0.62	0.33	p1d7	2.45	0.0001213	0.0001780	0.0002606	0.4277
7090591	11/8A2	34S_6p1d7Yd_9	33 7/8	S	9	4437.4	23 5/7	21 5/7	0.446	0.669	HLP-22	12	0	4	1.9	10.5	5.7	30.8	16.1	0.62	0.33	p1d7	2.45	0.0001213	0.0001780	0.0002606	0.4277
7090594	11/8A2	34S_6p1d7Yd_9	33 7/8	S	9	4437.4	23 5/7	21 5/7	0.446	0.669	HLP-22	12	0	4	1.9	10.5	5.7	30.8	16.1	0.62	0.33	p1d7	2.45	0.0001213	0.0001780	0.0002606	0.4277
7090596	11/8A2	34S_6p1d7Yd_9	33 7/8	S	9	4437.4	23 5/7	21 5/7	0.446	0.669	HLP-22	12	0	4	1.9	10.5	5.7	30.8	16.1	0.62	0.33	p1d7	2.45	0.0001213	0.0001780	0.0002606	0.4277
7090599	11/8A2	34S_6p1d7Yd_9	33 7/8	S	9	4437.4	23 5/7	21 5/7	0.446	0.669	HLP-22	12	0	4	1.9	10.5	5.7	30.8	16.1	0.62	0.33	p1d7	2.45	0.0001213	0.0001780	0.0002606	0.4277
7090602	11/8A2	34S_6p1d7Yd_9	33 7/8	S	9	4437.4	23 5/7	21 5/7	0.446	0.669	HLP-22	12	0	4	1.9	10.5	5.7	30.8	16.1	0.62	0.33	p1d7	2.45	0.0001213	0.0001780	0.0002606	0.4277
7090605	11/8A2	34S_6p1d7Yd_9	33 7/8	S	9	4437.4	23 5/7	21 5/7	0.446	0.669	HLP-22	12	0	4	1.9	10.5	5.7	30.8	16.1	0.62	0.33	p1d7	2.45	0.0001213	0.0001780	0.0002606	0.4277
7090608	11/8A2	34S_6p1d7Yd_9	33 7/8	S	9	4437.4	23 5/7	21 5/7	0.446	0.669	HLP-22	12	0	4	1.9	10.5	5.7	30.8	16.1	0.62	0.33	p1d7	2.45	0.0001213	0.0001780	0.0002606	0.4277
7090612	11/8A2	34S_6p1d7Yd_9	33 7/8	S	9	4437.4	23 5/7	21 5/7	0.446	0.669	HLP-22	12	0	4	1.9	10.5	5.7	30.8	16.1	0.62	0.33	p1d7	2.45	0.0001213	0.0001780	0.0002606	0.4277
7090616	11/8C1	34S_6p1d7Ya	33 7/8	S	9	4437.4	33 7/8	21 5/7	0.446	0.669	HLP-22	12	8	4	1.9	10.5	5.7	30.8	16.1	0.62	0.33	p1d7	2.45	0.0001213	0.0001780	0.0002606	0.4277
7090619	11/8C1	34S_6p1d7Ya	33 7/8	S	9	4437.4	33 7/8	21 5/7	0.446	0.669	HLP-22	12	8	4	1.9	10.5	5.7	30.8	16.1	0.62	0.33	p1d7	2.45	0.0001213	0.0001780	0.0002606	0.4277
7090622	11/8C1	34S_6p1d7Ya	33 7/8	S	9	4437.4	33 7/8	21 5/7	0.446	0.669	HLP-22	12	8	4	1.9	10.5	5.7	30.8	16.1	0.62	0.33	p1d7	2.45	0.0001213	0.0001780	0.0002606	0.4277
7090626	11/8C1	34S_6p1d7Ya	33 7/8	S	9	4437.4	33 7/8	21 5/7	0.446	0.669	HLP-22	12	8	4	1.9	10.5	5.7	30.8	16.1	0.62	0.33	p1d7	2.45	0.0001213	0.0001780	0.0002606	0.4277
7090628	11/8C2	34S_6p1d7Yd_1	33 7/8	S	9	4437.4	33 7/8	21 5/7	0.446	0.669	HLP-22	12	8	4	1.9	10.5	5.7	30.8	16.1	0.62	0.33	p1d7	2.45	0.0001213	0.0001780	0.0002606	0.4277

Table B.9. Updated Data from Fall 2007 Tests in Mid-Scale Vessel with Spherical Head B.5

Tank Water Temperature	Water Density	Solids Fraction	Pulse Volume Fraction	Duty Cycle	Cycle Time	Pulsed or Steady Jet	Us Steady Jet	U1 Pulsing Jet	U2 URMS	U3 URM3	Discharge Velocity	Critical Suspension Velocity	Average Peak Cloud Height	U_{CS} Condition	U_{CS} Method	U_{CS} Flag	U_{CS} Center Flag	U_{CS} udv Flag	U_{CS} based on Decreasing Velocity	Sweep Increase / Decrease	UDV Height Bed	Particle Motion	Solids Level	Outer Bottom Pattern	Inner Bottom Pattern	Case ID	Test	TDP	Row Number
C	g/cm³	fraction	fraction	fraction	s	text	m/s	m/s	m/s	m/s	m/s	m/s	in.	m/s	text	text	text	text	m/s	text	mm	text	text	text	text	text	text	text	text
T	ρ_l	ϕ_S	ϕ_P	DC	t_C	Jet	US	U1	U2	U3	U	U_{CS}	H_C	U_{CSR}	U_{CSM}	U_{CS}vis	U_{CS}cen	U_{CS}udv	U_{CS_D}	S_W	H_{bed}	PM	Sol	SP_O	SP_I	ID	M/DDX	TDP	MSS
20.7	0.999	0.00487	undefined	1.000	infinite	S	6.59	N/A	N/A	N/A	6.60	6.40	24.00	N/A	N/A	N/A	N/A	N/A	N/A	I	N/A	BC	N/A	N/A	N/A	34S_6p1d7Ya-40	11/6A1	TDP-WTP-049	7090506
21.0	0.999	0.00487	0.051	0.180	58.0	P	N/A	5.91	5.98	6.01	6.00	7.30	10.00	N/A	N/A	N/A	N/A	N/A	N/A	I	N/A	SS	N/A	N/A	N/A	34S_6p1d7Yd_6	11/6A2	TDP-WTP-049	7090508
21.0	0.999	0.00487	0.051	0.180	54.0	P	N/A	6.34	6.42	6.46	6.50	7.30	10.75	N/A	N/A	N/A	N/A	N/A	N/A	I	N/A	SS+	N/A	N/A	N/A	34S_6p1d7Yd_6	11/6A2	TDP-WTP-049	7090511
21.0	0.999	0.00487	0.051	0.180	50.0	P	N/A	6.61	6.80	6.89	7.00	7.30	11.50	N/A	N/A	N/A	N/A	N/A	N/A	I	N/A	AM	N/A	N/A	N/A	34S_6p1d7Yd_6	11/6A2	TDP-WTP-049	7090514
21.0	0.999	0.00487	0.050	0.180	47.3	P	N/A	6.84	7.07	7.17	7.30	7.30	13.50	7.30	vis	UCSvis	N/A	N/A	N/A	I	N/A	CS	N/A	N/A	N/A	34S_6p1d7Yd_6	11/6A2	TDP-WTP-049	7090518
21.0	0.999	0.00487	0.050	0.180	45.3	P	N/A	6.95	7.26	7.39	7.60	7.30	15.50	N/A	N/A	N/A	N/A	N/A	N/A	I	N/A	BC	N/A	N/A	N/A	34S_6p1d7Yd_6	11/6A2	TDP-WTP-049	7090520
20.9	0.999	0.00487	undefined	1.000	infinite	S	2.62	N/A	N/A	N/A	2.60	3.40	N/A	N/A	N/A	N/A	N/A	N/A	N/A	D	N/A	SS+	N/A	N/A	N/A	34S_6p1d7Ya	11/7A1	TDP-WTP-050	7090523
20.9	0.999	0.00487	undefined	1.000	infinite	S	2.81	N/A	N/A	N/A	2.80	3.40	9.00	N/A	N/A	N/A	N/A	N/A	N/A	I	N/A	AM	N/A	N/A	N/A	34S_6p1d7Ya	11/7A1	TDP-WTP-050	7090526
21.0	0.999	0.00487	undefined	1.000	infinite	S	3.02	N/A	N/A	N/A	3.00	3.40	9.50	N/A	N/A	N/A	N/A	N/A	N/A	I	N/A	AM	N/A	N/A	N/A	34S_6p1d7Ya	11/7A1	TDP-WTP-050	7090529
20.9	0.999	0.00487	undefined	1.000	infinite	S	3.22	N/A	N/A	N/A	3.20	3.40	10.00	N/A	N/A	N/A	N/A	N/A	N/A	I	N/A	AM+	N/A	N/A	N/A	34S_6p1d7Ya	11/7A1	TDP-WTP-050	7090532
21.0	0.999	0.00487	undefined	1.000	infinite	S	3.38	N/A	N/A	N/A	3.40	3.40	11.00	3.40	vis	UCSvis	N/A	N/A	N/A	I	N/A	CS	N/A	N/A	N/A	34S_6p1d7Ya	11/7A1	TDP-WTP-050	7090536
21.0	0.999	0.00487	undefined	1.000	infinite	S	3.60	N/A	N/A	N/A	3.60	3.40	15.00	N/A	N/A	N/A	N/A	N/A	N/A	I	N/A	BC	N/A	N/A	N/A	34S_6p1d7Ya	11/7A1	TDP-WTP-050	7090538
21.0	0.999	0.00487	0.050	0.180	39.0	P	N/A	2.83	2.92	2.96	3.00	4.20	8.75	N/A	N/A	N/A	N/A	N/A	N/A	D	N/A	SS	N/A	N/A	N/A	34S_6p1d7Yd_1	11/7A2	TDP-WTP-050	7090542
21.0	0.999	0.00487	0.051	0.180	35.3	P	N/A	3.11	3.21	3.26	3.40	4.20	10.00	N/A	N/A	N/A	N/A	N/A	N/A	I	N/A	SS+	N/A	N/A	N/A	34S_6p1d7Yd_1	11/7A2	TDP-WTP-050	7090544
21.0	0.999	0.00487	0.051	0.180	31.0	P	N/A	3.37	3.52	3.59	3.80	4.20	11.00	N/A	N/A	N/A	N/A	N/A	N/A	I	N/A	AM-	N/A	N/A	N/A	34S_6p1d7Yd_1	11/7A2	TDP-WTP-050	7090547
21.0	0.999	0.00487	0.050	0.180	28.0	P	N/A	3.49	3.76	3.88	4.20	4.20	11.75	4.20	vis	UCSvis	N/A	N/A	N/A	I	N/A	CS	N/A	N/A	N/A	34S_6p1d7Yd_1	11/7A2	TDP-WTP-050	7090551
21.1	0.999	0.00487	undefined	1.000	infinite	S	3.99	N/A	N/A	N/A	4.00	4.80	8.75	N/A	N/A	N/A	N/A	N/A	N/A	D	N/A	AM	N/A	N/A	N/A	34S_6p1d7Ya-44	11/7B1	TDP-WTP-050	7090553
21.1	0.999	0.00487	undefined	1.000	infinite	S	4.18	N/A	N/A	N/A	4.20	4.80	9.50	N/A	N/A	N/A	N/A	N/A	N/A	I	N/A	AM	N/A	N/A	N/A	34S_6p1d7Ya-44	11/7B1	TDP-WTP-050	7090557
21.2	0.999	0.00487	undefined	1.000	infinite	S	4.41	N/A	N/A	N/A	4.40	4.80	11.00	N/A	N/A	N/A	N/A	N/A	N/A	I	N/A	AM	N/A	N/A	N/A	34S_6p1d7Ya-44	11/7B1	TDP-WTP-050	7090560
21.2	0.999	0.00487	undefined	1.000	infinite	S	4.62	N/A	N/A	N/A	4.60	4.80	13.25	N/A	N/A	N/A	N/A	N/A	N/A	I	N/A	AM+	N/A	N/A	N/A	34S_6p1d7Ya-44	11/7B1	TDP-WTP-050	7090562
21.3	0.999	0.00487	undefined	1.000	infinite	S	4.81	N/A	N/A	N/A	4.80	4.80	17.75	4.80	vis	UCSvis	N/A	N/A	N/A	I	N/A	CS	N/A	N/A	N/A	34S_6p1d7Ya-44	11/7B1	TDP-WTP-050	7090566
21.0	0.999	0.00487	0.048	0.180	39.5	P	N/A	4.18	4.30	4.35	4.50	6.20	9.25	N/A	N/A	N/A	N/A	N/A	N/A	D	N/A	SS	N/A	N/A	N/A	34S_6p1d7Yd_0	11/7B2	TDP-WTP-050	7090569
21.0	0.999	0.00487	0.050	0.180	35.3	P	N/A	4.58	4.74	4.81	5.00	6.20	11.00	N/A	N/A	N/A	N/A	N/A	N/A	I	N/A	AM	N/A	N/A	N/A	34S_6p1d7Yd_0	11/7B2	TDP-WTP-050	7090571
21.0	0.999	0.00487	0.050	0.180	32.5	P	N/A	4.65	4.95	5.08	5.40	6.20	12.75	N/A	N/A	N/A	N/A	N/A	N/A	I	N/A	AM+	N/A	N/A	N/A	34S_6p1d7Yd_0	11/7B2	TDP-WTP-050	7090574
21.0	0.999	0.00487	0.050	0.180	31.5	P	N/A	4.77	5.10	5.24	5.60	6.20	14.00	N/A	N/A	N/A	N/A	N/A	N/A	I	N/A	AM+	N/A	N/A	N/A	34S_6p1d7Yd_0	11/7B2	TDP-WTP-050	7090577
21.0	0.999	0.00487	0.050	0.180	30.0	P	N/A	4.85	5.23	5.40	5.80	6.20	14.50	N/A	N/A	N/A	N/A	N/A	N/A	I	N/A	AM+	N/A	N/A	N/A	34S_6p1d7Yd_0	11/7B2	TDP-WTP-050	7090580
21.0	0.999	0.00487	0.050	0.180	29.0	P	N/A	4.96	5.37	5.55	6.00	6.20	15.75	N/A	N/A	N/A	N/A	N/A	N/A	I	N/A	AM+	N/A	N/A	N/A	34S_6p1d7Yd_0	11/7B2	TDP-WTP-050	7090583
21.0	0.999	0.00487	0.050	0.180	28.0	P	N/A	5.07	5.52	5.72	6.20	6.20	16.00	6.20	vis	UCSvis	N/A	N/A	N/A	I	N/A	CS	N/A	N/A	N/A	34S_6p1d7Yd_0	11/7B2	TDP-WTP-050	7090587
21.0	0.999	0.00487	0.046	0.180	63.0	P	N/A	5.38	5.46	5.49	5.50	8.40	12.75	N/A	N/A	N/A	N/A	N/A	N/A	D	N/A	SS	N/A	N/A	N/A	34S_6p1d7Yd_9	11/8A2	TDP-WTP-051	7090591
21.0	0.999	0.00487	0.051	0.180	58.5	P	N/A	5.85	5.92	5.95	6.00	8.40	15.00	N/A	N/A	N/A	N/A	N/A	N/A	I	N/A	SS+	N/A	N/A	N/A	34S_6p1d7Yd_9	11/8A2	TDP-WTP-051	7090594
21.0	0.999	0.00487	0.051	0.180	55.0	P	N/A	6.23	6.31	6.35	6.40	8.40	15.25	N/A	N/A	N/A	N/A	N/A	N/A	I	N/A	AM	N/A	N/A	N/A	34S_6p1d7Yd_9	11/8A2	TDP-WTP-051	7090596
21.0	0.999	0.00487	0.051	0.180	51.5	P	N/A	6.59	6.69	6.74	6.80	8.40	17.00	N/A	N/A	N/A	N/A	N/A	N/A	I	N/A	AM	N/A	N/A	N/A	34S_6p1d7Yd_9	11/8A2	TDP-WTP-051	7090599
21.0	0.999	0.00487	0.050	0.180	48.5	P	N/A	6.91	7.05	7.11	7.20	8.40	18.25	N/A	N/A	N/A	N/A	N/A	N/A	I	N/A	AM	N/A	N/A	N/A	34S_6p1d7Yd_9	11/8A2	TDP-WTP-051	7090602
21.0	0.999	0.00487	0.050	0.180	45.5	P	N/A	6.99	7.29	7.42	7.60	8.40	20.25	N/A	N/A	N/A	N/A	N/A	N/A	I	N/A	AM+	N/A	N/A	N/A	34S_6p1d7Yd_9	11/8A2	TDP-WTP-051	7090605
21.0	0.999	0.00487	0.049	0.180	43.5	P	N/A	7.20	7.56	7.71	8.00	8.40	21.00	N/A	N/A	N/A	N/A	N/A	N/A	I	N/A	AM+	N/A	N/A	N/A	34S_6p1d7Yd_9	11/8A2	TDP-WTP-051	7090608
21.0	0.999	0.00487	0.050	0.180	41.0	P	N/A	7.47	7.88	8.06	8.40	8.40	22.25	8.40	vis	UCSvis	N/A	N/A	N/A	I	N/A	CS	N/A	N/A	N/A	34S_6p1d7Yd_9	11/8A2	TDP-WTP-051	7090612
20.9	0.999	0.00487	undefined	1.000	infinite	S	2.51	N/A	N/A	N/A	2.50	2.60	N/A	N/A	N/A	N/A	N/A	N/A	N/A	I	N/A	SS	N/A	N/A	N/A	34S_6p1d7Ya	11/8C1	TDP-WTP-051	7090616
20.9	0.999	0.00487	undefined	1.000	infinite	S	3.01	N/A	N/A	N/A	3.00	3.40	9.25	N/A	N/A	N/A	N/A	N/A	N/A	I	N/A	AM	N/A	N/A	N/A	34S_6p1d7Ya	11/8C1	TDP-WTP-051	7090619
20.9	0.999	0.00487	undefined	1.000	infinite	S	3.23	N/A	N/A	N/A	3.20	3.40	9.75	N/A	N/A	N/A	N/A	N/A	N/A	I	N/A	CS-	N/A	N/A	N/A	34S_6p1d7Ya	11/8C1	TDP-WTP-051	7090622
20.9	0.999	0.00487	undefined	1.000	infinite	S	3.39	N/A	N/A	N/A	3.40	3.40	11.00	3.40	vis	UCSvis	N/A	N/A	N/A	I	N/A	CS	N/A	N/A	N/A	34S_6p1d7Ya	11/8C1	TDP-WTP-051	7090626
21.0	0.999	0.00487	0.051	0.180	34.0	P	N/A	3.18	3.30	3.36	3.50	4.40	9.75	N/A	N/A	N/A	N/A	N/A	N/A	I	N/A	SS+	N/A	N/A	N/A	34S_6p1d7Yd_1	11/8C2	TDP-WTP-051	7090628

Table B.9. Updated Data from Fall 2007 Tests in Mid-Scale Vessel with Spherical Head A.6

Row Number	Test	Case ID	Tank Diameter	Head Shape	Dish Height	Dish Volume	Tank Fill Height	Return Line Height	Nozzle Inner Diameter	Nozzle Stand-off Distance	Pulse Tube Configuration	Installed Nozzles	Outer Nozzles Operated	Inner Nozzles Operated	Pulse Tube Outer Diameter	Outer PJM Radius	Inner PJM Radius	"FIO" Outer PJM Impingement Angle	"FIO" Inner PJM Impingement Angle	Ratio Outer PJM to Tank Radius	Ratio Inner PJM to Tank Radius	Simulant	Solids Density	Particle Diameter d5	Particle Diameter d50	Particle Diameter d95	Void Fraction
text	text	text	in.	text	in.	in. ^{3}	in.	in.	in.	in.	text	number	number	number	in.	in.	in.	deg	deg	nondim	nondim	text	g/cm^3	m	m	m	fraction
MSS	M/DDX	ID	D	HS	H_{dish}	V_{dish}	H	Rtn	d	sod	PT	N	N_O	N_I	PT_{od}	R_O	R_I	Θ_O	Θ_I	R_O/R	R_I/R	sxdx	ρ_S	d_5	d_{50}	d_{95}	vf
7090631	11/8C2	34S_6p1d7Yd_1	33 7/8	S	9	4437.4	33 7/8	21 5/7	0.446	0.669	HLP-22	12	8	4	1.9	10.5	5.7	30.8	16.1	0.62	0.33	p1d7	2.45	0.0001213	0.0001780	0.0002606	0.4277
7090634	11/8C2	34S_6p1d7Yd_1	33 7/8	S	9	4437.4	33 7/8	21 5/7	0.446	0.669	HLP-22	12	8	4	1.9	10.5	5.7	30.8	16.1	0.62	0.33	p1d7	2.45	0.0001213	0.0001780	0.0002606	0.4277
7090637	11/8C2	34S_6p1d7Yd_1	33 7/8	S	9	4437.4	33 7/8	21 5/7	0.446	0.669	HLP-22	12	8	4	1.9	10.5	5.7	30.8	16.1	0.62	0.33	p1d7	2.45	0.0001213	0.0001780	0.0002606	0.4277
7090641	11/8C2	34S_6p1d7Yd_1	33 7/8	S	9	4437.4	33 7/8	21 5/7	0.446	0.669	HLP-22	12	8	4	1.9	10.5	5.7	30.8	16.1	0.62	0.33	p1d7	2.45	0.0001213	0.0001780	0.0002606	0.4277
7090643	11/8C2	34S_6p1d7Yd_1	33 7/8	S	9	4437.4	33 7/8	21 5/7	0.446	0.669	HLP-22	12	8	4	1.9	10.5	5.7	30.8	16.1	0.62	0.33	p1d7	2.45	0.0001213	0.0001780	0.0002606	0.4277
7090648	11/8D2	34S_6p1d7Yd_0	33 7/8	S	9	4437.4	33 7/8	21 5/7	0.446	0.669	HLP-22	12	4	4	1.9	10.5	5.7	30.8	16.1	0.62	0.33	p1d7	2.45	0.0001213	0.0001780	0.0002606	0.4277
7090650	11/8D2	34S_6p1d7Yd_0	33 7/8	S	9	4437.4	33 7/8	21 5/7	0.446	0.669	HLP-22	12	4	4	1.9	10.5	5.7	30.8	16.1	0.62	0.33	p1d7	2.45	0.0001213	0.0001780	0.0002606	0.4277
7090653	11/8D2	34S_6p1d7Yd_0	33 7/8	S	9	4437.4	33 7/8	21 5/7	0.446	0.669	HLP-22	12	4	4	1.9	10.5	5.7	30.8	16.1	0.62	0.33	p1d7	2.45	0.0001213	0.0001780	0.0002606	0.4277
7090656	11/8D2	34S_6p1d7Yd_0	33 7/8	S	9	4437.4	33 7/8	21 5/7	0.446	0.669	HLP-22	12	4	4	1.9	10.5	5.7	30.8	16.1	0.62	0.33	p1d7	2.45	0.0001213	0.0001780	0.0002606	0.4277
7090659	11/8D2	34S_6p1d7Yd_0	33 7/8	S	9	4437.4	33 7/8	21 5/7	0.446	0.669	HLP-22	12	4	4	1.9	10.5	5.7	30.8	16.1	0.62	0.33	p1d7	2.45	0.0001213	0.0001780	0.0002606	0.4277
7090662	11/8D2	34S_6p1d7Yd_0	33 7/8	S	9	4437.4	33 7/8	21 5/7	0.446	0.669	HLP-22	12	4	4	1.9	10.5	5.7	30.8	16.1	0.62	0.33	p1d7	2.45	0.0001213	0.0001780	0.0002606	0.4277
7090665	11/8D2	34S_6p1d7Yd_0	33 7/8	S	9	4437.4	33 7/8	21 5/7	0.446	0.669	HLP-22	12	4	4	1.9	10.5	5.7	30.8	16.1	0.62	0.33	p1d7	2.45	0.0001213	0.0001780	0.0002606	0.4277
7090668	11/8D2	34S_6p1d7Yd_0	33 7/8	S	9	4437.4	33 7/8	21 5/7	0.446	0.669	HLP-22	12	4	4	1.9	10.5	5.7	30.8	16.1	0.62	0.33	p1d7	2.45	0.0001213	0.0001780	0.0002606	0.4277
7090671	11/8D2	34S_6p1d7Yd_0	33 7/8	S	9	4437.4	33 7/8	21 5/7	0.446	0.669	HLP-22	12	4	4	1.9	10.5	5.7	30.8	16.1	0.62	0.33	p1d7	2.45	0.0001213	0.0001780	0.0002606	0.4277
7090674	11/8D2	34S_6p1d7Yd_0	33 7/8	S	9	4437.4	33 7/8	21 5/7	0.446	0.669	HLP-22	12	4	4	1.9	10.5	5.7	30.8	16.1	0.62	0.33	p1d7	2.45	0.0001213	0.0001780	0.0002606	0.4277
7090678	11/8D2	34S_6p1d7Yd_0	33 7/8	S	9	4437.4	33 7/8	21 5/7	0.446	0.669	HLP-22	12	4	4	1.9	10.5	5.7	30.8	16.1	0.62	0.33	p1d7	2.45	0.0001213	0.0001780	0.0002606	0.4277
7090681	11/9A1	34S_6p1d7Ya-04	33 7/8	S	9	4437.4	33 7/8	21 5/7	0.446	0.669	HLP-22	12	0	4	1.9	10.5	5.7	30.8	16.1	0.62	0.33	p1d7	2.45	0.0001213	0.0001780	0.0002606	0.4277
7090684	11/9A1	34S_6p1d7Ya-04	33 7/8	S	9	4437.4	33 7/8	21 5/7	0.446	0.669	HLP-22	12	0	4	1.9	10.5	5.7	30.8	16.1	0.62	0.33	p1d7	2.45	0.0001213	0.0001780	0.0002606	0.4277
7090687	11/9A1	34S_6p1d7Ya-04	33 7/8	S	9	4437.4	33 7/8	21 5/7	0.446	0.669	HLP-22	12	0	4	1.9	10.5	5.7	30.8	16.1	0.62	0.33	p1d7	2.45	0.0001213	0.0001780	0.0002606	0.4277
7090690	11/9A1	34S_6p1d7Ya-04	33 7/8	S	9	4437.4	33 7/8	21 5/7	0.446	0.669	HLP-22	12	0	4	1.9	10.5	5.7	30.8	16.1	0.62	0.33	p1d7	2.45	0.0001213	0.0001780	0.0002606	0.4277
7090692	11/9A1	34S_6p1d7Ya-04	33 7/8	S	9	4437.4	33 7/8	21 5/7	0.446	0.669	HLP-22	12	0	4	1.9	10.5	5.7	30.8	16.1	0.62	0.33	p1d7	2.45	0.0001213	0.0001780	0.0002606	0.4277
7090696	11/9A1	34S_6p1d7Ya-04	33 7/8	S	9	4437.4	33 7/8	21 5/7	0.446	0.669	HLP-22	12	0	4	1.9	10.5	5.7	30.8	16.1	0.62	0.33	p1d7	2.45	0.0001213	0.0001780	0.0002606	0.4277
7090698	11/9A1	34S_6p1d7Ya-04	33 7/8	S	9	4437.4	33 7/8	21 5/7	0.446	0.669	HLP-22	12	0	4	1.9	10.5	5.7	30.8	16.1	0.62	0.33	p1d7	2.45	0.0001213	0.0001780	0.0002606	0.4277
7090702	11/9A1	34S_6p1d7Ya-04	33 7/8	S	9	4437.4	33 7/8	21 5/7	0.446	0.669	HLP-22	12	0	4	1.9	10.5	5.7	30.8	16.1	0.62	0.33	p1d7	2.45	0.0001213	0.0001780	0.0002606	0.4277
7090705	11/9A2	34S_6p1d7Yd_9	33 7/8	S	9	4437.4	33 7/8	21 5/7	0.446	0.669	HLP-22	12	0	4	1.9	10.5	5.7	30.8	16.1	0.62	0.33	p1d7	2.45	0.0001213	0.0001780	0.0002606	0.4277
7090708	11/9A2	34S_6p1d7Yd_9	33 7/8	S	9	4437.4	33 7/8	21 5/7	0.446	0.669	HLP-22	12	0	4	1.9	10.5	5.7	30.8	16.1	0.62	0.33	p1d7	2.45	0.0001213	0.0001780	0.0002606	0.4277
7090710	11/9A2	34S_6p1d7Yd_9	33 7/8	S	9	4437.4	33 7/8	21 5/7	0.446	0.669	HLP-22	12	0	4	1.9	10.5	5.7	30.8	16.1	0.62	0.33	p1d7	2.45	0.0001213	0.0001780	0.0002606	0.4277
7090713	11/9A2	34S_6p1d7Yd_9	33 7/8	S	9	4437.4	33 7/8	21 5/7	0.446	0.669	HLP-22	12	0	4	1.9	10.5	5.7	30.8	16.1	0.62	0.33	p1d7	2.45	0.0001213	0.0001780	0.0002606	0.4277
7090716	11/9A2	34S_6p1d7Yd_9	33 7/8	S	9	4437.4	33 7/8	21 5/7	0.446	0.669	HLP-22	12	0	4	1.9	10.5	5.7	30.8	16.1	0.62	0.33	p1d7	2.45	0.0001213	0.0001780	0.0002606	0.4277
7090719	11/9A2	34S_6p1d7Yd_9	33 7/8	S	9	4437.4	33 7/8	21 5/7	0.446	0.669	HLP-22	12	0	4	1.9	10.5	5.7	30.8	16.1	0.62	0.33	p1d7	2.45	0.0001213	0.0001780	0.0002606	0.4277
7090722	11/9A2	34S_6p1d7Yd_9	33 7/8	S	9	4437.4	33 7/8	21 5/7	0.446	0.669	HLP-22	12	0	4	1.9	10.5	5.7	30.8	16.1	0.62	0.33	p1d7	2.45	0.0001213	0.0001780	0.0002606	0.4277
7090725	11/9A2	34S_6p1d7Yd_9	33 7/8	S	9	4437.4	33 7/8	21 5/7	0.446	0.669	HLP-22	12	0	4	1.9	10.5	5.7	30.8	16.1	0.62	0.33	p1d7	2.45	0.0001213	0.0001780	0.0002606	0.4277
7090728	11/9A2	34S_6p1d7Yd_9	33 7/8	S	9	4437.4	33 7/8	21 5/7	0.446	0.669	HLP-22	12	0	4	1.9	10.5	5.7	30.8	16.1	0.62	0.33	p1d7	2.45	0.0001213	0.0001780	0.0002606	0.4277
7090732	11/9A2	34S_6p1d7Yd_9	33 7/8	S	9	4437.4	33 7/8	21 5/7	0.446	0.669	HLP-22	12	0	4	1.9	10.5	5.7	30.8	16.1	0.62	0.33	p1d7	2.45	0.0001213	0.0001780	0.0002606	0.4277
7090737	11/14A1	34S_6p1d7Ya-44	33 7/8	S	9	4437.4	67 3/4	21 5/7	0.446	0.669	HLP-22	12	4	4	1.9	10.5	5.7	30.8	16.1	0.62	0.33	p1d7	2.45	0.0001213	0.0001780	0.0002606	0.4277
7090740	11/14A2	34S_6p1d7Yd_0	33 7/8	S	9	4437.4	67 3/4	21 5/7	0.446	0.669	HLP-22	12	4	4	1.9	10.5	5.7	30.8	16.1	0.62	0.33	p1d7	2.45	0.0001213	0.0001780	0.0002606	0.4277
7090742	11/14A2	34S_6p1d7Yd_0	33 7/8	S	9	4437.4	67 3/4	21 5/7	0.446	0.669	HLP-22	12	4	4	1.9	10.5	5.7	30.8	16.1	0.62	0.33	p1d7	2.45	0.0001213	0.0001780	0.0002606	0.4277
7090745	11/14A2	34S_6p1d7Yd_0	33 7/8	S	9	4437.4	67 3/4	21 5/7	0.446	0.669	HLP-22	12	4	4	1.9	10.5	5.7	30.8	16.1	0.62	0.33	p1d7	2.45	0.0001213	0.0001780	0.0002606	0.4277
7090748	11/14A2	34S_6p1d7Yd_0	33 7/8	S	9	4437.4	67 3/4	21 5/7	0.446	0.669	HLP-22	12	4	4	1.9	10.5	5.7	30.8	16.1	0.62	0.33	p1d7	2.45	0.0001213	0.0001780	0.0002606	0.4277
7090751	11/14A2	34S_6p1d7Yd_0	33 7/8	S	9	4437.4	67 3/4	21 5/7	0.446	0.669	HLP-22	12	4	4	1.9	10.5	5.7	30.8	16.1	0.62	0.33	p1d7	2.45	0.0001213	0.0001780	0.0002606	0.4277
7090754	11/14A2	34S_6p1d7Yd_0	33 7/8	S	9	4437.4	67 3/4	21 5/7	0.446	0.669	HLP-22	12	4	4	1.9	10.5	5.7	30.8	16.1	0.62	0.33	p1d7	2.45	0.0001213	0.0001780	0.0002606	0.4277

Table B.9. Data from Fall 2007 Tests in Mid-Scale Vessel with Spherical Head B.6

Tank Water Temperature	Water Density	Solids Fraction	Pulse Volume Fraction	Duty Cycle	Cycle Time	Pulsed or Steady Jet	Us Steady Jet	U1 Pulsing Jet	U2 URMS	U3 URM3	Discharge Velocity	Critical Suspension Velocity	Average Peak Cloud Height	U_{CS} Condition	U_{CS} Method	U_{CS} Flag	U_{CS} Center Flag	U_{CS} udv Flag	U_{CS} based on Decreasing Velocity	Sweep Increase / Decrease	UDV Height Bed	Particle Motion	Solids Level	Outer Bottom Pattern	Inner Bottom Pattern	Case ID	Test	TDP	Row Number
C	g/cm³	fraction	fraction	fraction	s	text	m/s	m/s	m/s	m/s	m/s	m/s	in.	m/s	text	text	text	text	m/s	text	mm	text	text	text	text	text	text	text	text
T	ρ_l	ϕ_S	ϕ_P	DC	t_C	Jet	US	U1	U2	U3	U	U_{CS}	H_C	U_{CSR}	U_{CSM}	U_{CS}vis	U_{CS}cen	U_{CS}udv	U_{CS_D}	S_W	H_{bed}	PM	Sol	SP_O	SP_I	ID	M/DDX	TDP	MSS
21.0	0.999	0.00487	0.050	0.180	31.3	P	N/A	3.43	3.56	3.63	3.80	4.40	10.50	N/A	N/A	N/A	N/A	N/A	N/A	I	N/A	AM	N/A	N/A	N/A	34S_6p1d7Yd_1	11/8C2	TDP-WTP-051	7090631
21.0	0.999	0.00487	0.050	0.180	29.5	P	N/A	3.41	3.63	3.73	4.00	4.40	11.25	N/A	N/A	N/A	N/A	N/A	N/A	I	N/A	AM	N/A	N/A	N/A	34S_6p1d7Yd_1	11/8C2	TDP-WTP-051	7090634
21.0	0.999	0.00487	0.050	0.180	28.3	P	N/A	3.58	3.81	3.92	4.20	4.40	11.50	N/A	N/A	N/A	N/A	N/A	N/A	I	N/A	AM+	N/A	N/A	N/A	34S_6p1d7Yd_1	11/8C2	TDP-WTP-051	7090637
21.0	0.999	0.00487	0.050	0.180	26.8	P	N/A	3.62	3.92	4.05	4.40	4.40	12.50	4.40	vis	UCSvis	N/A	N/A	N/A	I	N/A	CS	N/A	N/A	N/A	34S_6p1d7Yd_1	11/8C2	TDP-WTP-051	7090641
21.0	0.999	0.00487	0.049	0.180	25.5	P	N/A	3.64	4.01	4.18	4.60	4.40	12.75	N/A	N/A	N/A	N/A	N/A	N/A	I	N/A	BC	N/A	N/A	N/A	34S_6p1d7Yd_1	11/8C2	TDP-WTP-051	7090643
21.0	0.999	0.00487	0.050	0.180	44.0	P	N/A	3.83	3.90	3.93	4.00	7.20	9.50	N/A	N/A	N/A	N/A	N/A	N/A	D	N/A	SS	N/A	N/A	N/A	34S_6p1d7Yd_0	11/8D2	TDP-WTP-051	7090648
21.0	0.999	0.00487	0.051	0.180	38.0	P	N/A	4.28	4.37	4.41	4.50	7.20	9.50	N/A	N/A	N/A	N/A	N/A	N/A	I	N/A	AM-	N/A	N/A	N/A	34S_6p1d7Yd_0	11/8D2	TDP-WTP-051	7090650
21.0	0.999	0.00487	0.050	0.180	36.8	P	N/A	4.49	4.60	4.65	4.80	7.20	10.50	N/A	N/A	N/A	N/A	N/A	N/A	I	N/A	AM	N/A	N/A	N/A	34S_6p1d7Yd_0	11/8D2	TDP-WTP-051	7090653
21.0	0.999	0.00487	0.050	0.180	34.5	P	N/A	4.69	4.85	4.92	5.10	7.20	11.50	N/A	N/A	N/A	N/A	N/A	N/A	I	N/A	AM	N/A	N/A	N/A	34S_6p1d7Yd_0	11/8D2	TDP-WTP-051	7090656
21.0	0.999	0.00487	0.050	0.180	32.5	P	N/A	4.71	4.99	5.11	5.40	7.20	12.25	N/A	N/A	N/A	N/A	N/A	N/A	I	N/A	AM	N/A	N/A	N/A	34S_6p1d7Yd_0	11/8D2	TDP-WTP-051	7090659
21.0	0.999	0.00487	0.050	0.180	30.8	P	N/A	4.83	5.17	5.32	5.70	7.20	13.25	N/A	N/A	N/A	N/A	N/A	N/A	I	N/A	AM	N/A	N/A	N/A	34S_6p1d7Yd_0	11/8D2	TDP-WTP-051	7090662
21.0	0.999	0.00487	0.050	0.180	29.0	P	N/A	4.96	5.38	5.56	6.00	7.20	14.75	N/A	N/A	N/A	N/A	N/A	N/A	I	N/A	AM+	N/A	N/A	N/A	34S_6p1d7Yd_0	11/8D2	TDP-WTP-051	7090665
21.0	0.999	0.00487	0.050	0.180	27.3	P	N/A	4.99	5.52	5.75	6.30	7.20	16.00	N/A	N/A	N/A	N/A	N/A	N/A	I	N/A	AM+	N/A	N/A	N/A	34S_6p1d7Yd_0	11/8D2	TDP-WTP-051	7090668
21.0	0.999	0.00487	0.050	0.180	26.0	P	N/A	4.99	5.62	5.89	6.60	7.20	17.00	N/A	N/A	N/A	N/A	N/A	N/A	I	N/A	AM+	N/A	N/A	N/A	34S_6p1d7Yd_0	11/8D2	TDP-WTP-051	7090671
21.0	0.999	0.00487	0.049	0.180	24.5	P	N/A	4.80	5.62	5.98	6.90	7.20	17.50	N/A	N/A	N/A	N/A	N/A	N/A	I	N/A	CS-	N/A	N/A	N/A	34S_6p1d7Yd_0	11/8D2	TDP-WTP-051	7090674
21.0	0.999	0.00487	0.049	0.180	23.0	P	N/A	4.57	5.57	6.03	7.20	7.20	18.00	7.20	vis	UCSvis	N/A	N/A	N/A	I	N/A	CS	N/A	N/A	N/A	34S_6p1d7Yd_0	11/8D2	TDP-WTP-051	7090678
21.4	0.999	0.00487	undefined	1.000	infinite	S	3.63	N/A	N/A	N/A	3.60	7.00	N/A	N/A	N/A	N/A	UCScen	N/A	N/A	I	N/A	SS+	N/A	N/A	N/A	34S_6p1d7Ya-04	11/9A1	TDP-WTP-052	7090681
21.5	0.999	0.00487	undefined	1.000	infinite	S	4.00	N/A	N/A	N/A	4.00	7.00	8.50	N/A	N/A	N/A	N/A	N/A	N/A	I	N/A	SS	N/A	N/A	N/A	34S_6p1d7Ya-04	11/9A1	TDP-WTP-052	7090684
21.4	0.999	0.00487	undefined	1.000	infinite	S	4.52	N/A	N/A	N/A	4.50	7.00	9.25	N/A	N/A	N/A	N/A	N/A	N/A	I	N/A	AM-	N/A	N/A	N/A	34S_6p1d7Ya-04	11/9A1	TDP-WTP-052	7090687
21.5	0.999	0.00487	undefined	1.000	infinite	S	5.02	N/A	N/A	N/A	5.00	7.00	11.00	N/A	N/A	N/A	N/A	N/A	N/A	I	N/A	AM	N/A	N/A	N/A	34S_6p1d7Ya-04	11/9A1	TDP-WTP-052	7090690
21.4	0.999	0.00487	undefined	1.000	infinite	S	5.58	N/A	N/A	N/A	5.50	7.00	13.00	N/A	N/A	N/A	N/A	N/A	N/A	I	N/A	AM	N/A	N/A	N/A	34S_6p1d7Ya-04	11/9A1	TDP-WTP-052	7090692
21.5	0.999	0.00487	undefined	1.000	infinite	S	6.03	N/A	N/A	N/A	6.00	7.00	16.00	N/A	N/A	N/A	N/A	N/A	N/A	I	N/A	AM	N/A	N/A	N/A	34S_6p1d7Ya-04	11/9A1	TDP-WTP-052	7090696
21.5	0.999	0.00487	undefined	1.000	infinite	S	6.54	N/A	N/A	N/A	6.50	7.00	19.25	N/A	N/A	N/A	N/A	N/A	N/A	I	N/A	AM+	N/A	N/A	N/A	34S_6p1d7Ya-04	11/9A1	TDP-WTP-052	7090698
21.5	0.999	0.00487	undefined	1.000	infinite	S	7.01	N/A	N/A	N/A	7.00	7.00	22.50	7.00	vis	UCSvis	N/A	N/A	N/A	I	N/A	CS	N/A	N/A	N/A	34S_6p1d7Ya-04	11/9A1	TDP-WTP-052	7090702
22.0	0.999	0.00487	0.051	0.180	91.0	P	N/A	3.80	3.83	3.84	3.80	8.50	N/A	N/A	N/A	N/A	UCScen	N/A	N/A	I	N/A	SS	N/A	N/A	N/A	34S_6p1d7Yd_9	11/9A2	TDP-WTP-052	7090705
22.0	0.999	0.00487	0.050	0.180	77.5	P	N/A	4.46	4.49	4.50	4.50	8.50	9.25	N/A	N/A	N/A	N/A	N/A	N/A	I	N/A	AM-	N/A	N/A	N/A	34S_6p1d7Yd_9	11/9A2	TDP-WTP-052	7090708
22.0	0.999	0.00487	0.049	0.180	70.0	P	N/A	4.95	4.99	5.01	5.00	8.50	11.00	N/A	N/A	N/A	N/A	N/A	N/A	I	N/A	AM	N/A	N/A	N/A	34S_6p1d7Yd_9	11/9A2	TDP-WTP-052	7090710
22.0	0.999	0.00487	0.050	0.180	63.0	P	N/A	5.44	5.49	5.52	5.50	8.50	12.75	N/A	N/A	N/A	N/A	N/A	N/A	I	N/A	AM	N/A	N/A	N/A	34S_6p1d7Yd_9	11/9A2	TDP-WTP-052	7090713
22.0	0.999	0.00487	0.050	0.180	58.0	P	N/A	5.84	5.93	5.97	6.00	8.50	14.50	N/A	N/A	N/A	N/A	N/A	N/A	I	N/A	AM	N/A	N/A	N/A	34S_6p1d7Yd_9	11/9A2	TDP-WTP-052	7090716
22.0	0.999	0.00487	0.051	0.180	53.5	P	N/A	6.32	6.42	6.47	6.50	8.50	16.50	N/A	N/A	N/A	N/A	N/A	N/A	I	N/A	AM	N/A	N/A	N/A	34S_6p1d7Yd_9	11/9A2	TDP-WTP-052	7090719
22.0	0.999	0.00487	0.050	0.180	49.5	P	N/A	6.70	6.86	6.94	7.00	8.50	17.75	N/A	N/A	N/A	N/A	N/A	N/A	I	N/A	AM	N/A	N/A	N/A	34S_6p1d7Yd_9	11/9A2	TDP-WTP-052	7090722
22.0	0.999	0.00487	0.050	0.180	46.0	P	N/A	6.71	7.07	7.22	7.50	8.50	20.00	N/A	N/A	N/A	N/A	N/A	N/A	I	N/A	AM+	N/A	N/A	N/A	34S_6p1d7Yd_9	11/9A2	TDP-WTP-052	7090725
22.0	0.999	0.00487	0.051	0.180	43.0	P	N/A	7.12	7.53	7.71	8.00	8.50	21.50	N/A	N/A	N/A	N/A	N/A	N/A	I	N/A	AM+	N/A	N/A	N/A	34S_6p1d7Yd_9	11/9A2	TDP-WTP-052	7090728
22.0	0.999	0.00487	0.051	0.180	40.5	P	N/A	7.37	7.87	8.09	8.50	8.50	22.75	8.50	vis	UCSvis	N/A	N/A	N/A	I	N/A	CS	N/A	N/A	N/A	34S_6p1d7Yd_9	11/9A2	TDP-WTP-052	7090732
22.9	0.999	0.00487	undefined	1.000	infinite	S	3.40	N/A	N/A	N/A	3.40	N/A	N/A	N/A	N/A	N/A	UCScen	N/A	N/A	I	N/A	SS	N/A	N/A	N/A	34S_6p1d7Ya-44	11/14A1	TDP-WTP-063	7090737
23.0	0.999	0.00487	0.051	0.180	44.0	P	N/A	3.82	3.90	3.94	4.00	7.00	8.50	N/A	N/A	N/A	UCScen	N/A	N/A	I	N/A	SS+	N/A	N/A	N/A	34S_6p1d7Yd_0	11/14A2	TDP-WTP-063	7090740
23.0	0.999	0.00487	0.051	0.180	39.5	P	N/A	4.18	4.30	4.35	4.50	7.00	9.25	N/A	N/A	N/A	N/A	N/A	N/A	I	N/A	AM	N/A	N/A	N/A	34S_6p1d7Yd_0	11/14A2	TDP-WTP-063	7090742
23.0	0.999	0.00487	0.051	0.180	35.3	P	N/A	4.52	4.71	4.80	5.00	7.00	10.75	N/A	N/A	N/A	N/A	N/A	N/A	I	N/A	AM	N/A	N/A	N/A	34S_6p1d7Yd_0	11/14A2	TDP-WTP-063	7090745
23.0	0.999	0.00487	0.050	0.180	32.0	P	N/A	4.69	5.01	5.15	5.50	7.00	13.00	N/A	N/A	N/A	N/A	N/A	N/A	I	N/A	AM	N/A	N/A	N/A	34S_6p1d7Yd_0	11/14A2	TDP-WTP-063	7090748
23.0	0.999	0.00487	0.051	0.180	29.0	P	N/A	4.83	5.30	5.50	6.00	7.00	15.75	N/A	N/A	N/A	N/A	N/A	N/A	I	N/A	AM+	N/A	N/A	N/A	34S_6p1d7Yd_0	11/14A2	TDP-WTP-063	7090751
23.0	0.999	0.00487	0.050	0.180	26.3	P	N/A	4.88	5.53	5.81	6.50	7.00	17.00	N/A	N/A	N/A	N/A	N/A	N/A	I	N/A	AM+	N/A	N/A	N/A	34S_6p1d7Yd_0	11/14A2	TDP-WTP-063	7090754

Table B.9. Updated Data from Fall 2007 Tests in Mid-Scale Vessel with Spherical Head A.7

Row Number	Test	Case ID	Tank Diameter	Head Shape	Dish Height	Dish Volume	Tank Fill Height	Return Line Height	Nozzle Inner Diameter	Nozzle Stand-off Distance	Pulse Tube Configuration	Installed Nozzles	Outer Nozzles Operated	Inner Nozzles Operated	Pulse Tube Outer Diameter	Outer PJM Radius	Inner PJM Radius	"FIO" Outer PJM Impingement Angle	"FIO" Inner PJM Impingement Angle	Ratio Outer PJM to Tank Radius	Ratio Inner PJM to Tank Radius	Simulant	Solids Density	Particle Diameter d5	Particle Diameter d50	Particle Diameter d95	Void Fraction
text	text	text	in.	text	in.	in. ^{3}	in.	in.	in.	in.	text	number	number	number	in.	in.	in.	deg	deg	nondim	nondim	text	g/cm^3	m	m	m	fraction
MSS	M/DDX	ID	D	HS	H_{dish}	V_{dish}	H	Rtn	d	sod	PT	N	N_O	N_I	PT_{od}	R_O	R_I	Θ_O	Θ_I	R_O/R	R_I/R	sxdx	ρ_S	d_5	d_{50}	d_{95}	vf
7090758MX	11/14A2	34S_6p1d7Yd_0	33 7/8	S	9	4437.4	67 3/4	21 5/7	0.446	0.669	HLP-22	12	4	4	1.9	10.5	5.7	30.8	16.1	0.62	0.33	p1d7	2.45	0.0001213	0.0001780	0.0002606	0.4277
7090761	11/14B1	34S_6p1d7Ya-44	33 7/8	S	9	4437.4	67 3/4	61 3/4	0.446	0.669	HLP-22	12	4	4	1.9	10.5	5.7	30.8	16.1	0.62	0.33	p1d7	2.45	0.0001213	0.0001780	0.0002606	0.4277
7090764	11/14B2	34S_6p1d7Yd_0	33 7/8	S	9	4437.4	67 3/4	61 3/4	0.446	0.669	HLP-22	12	4	4	1.9	10.5	5.7	30.8	16.1	0.62	0.33	p1d7	2.45	0.0001213	0.0001780	0.0002606	0.4277
7090766	11/14C1	34S_6p1d7Ya-04	33 7/8	S	9	4437.4	67 3/4	61 3/4	0.446	0.669	HLP-22	12	0	4	1.9	10.5	5.7	30.8	16.1	0.62	0.33	p1d7	2.45	0.0001213	0.0001780	0.0002606	0.4277
7090772	11/14C2	34S_6p1d7Yd_9	33 7/8	S	9	4437.4	67 3/4	61 3/4	0.446	0.669	HLP-22	12	0	4	1.9	10.5	5.7	30.8	16.1	0.62	0.33	p1d7	2.45	0.0001213	0.0001780	0.0002606	0.4277
7090776	11/14D1	34S_6p1d7Yc_1	33 7/8	S	9	4437.4	67 3/4	61 3/4	0.446	0.669	HLP-22	12	8	4	1.9	10.5	5.7	30.8	16.1	0.62	0.33	p1d7	2.45	0.0001213	0.0001780	0.0002606	0.4277
7090779M	11/14D1	34S_6p1d7Yc_1	33 7/8	S	9	4437.4	67 3/4	61 3/4	0.446	0.669	HLP-22	12	8	4	1.9	10.5	5.7	30.8	16.1	0.62	0.33	p1d7	2.45	0.0001213	0.0001780	0.0002606	0.4277
7090781M	11/14D1	34S_6p1d7Yc_1	33 7/8	S	9	4437.4	67 3/4	61 3/4	0.446	0.669	HLP-22	12	8	4	1.9	10.5	5.7	30.8	16.1	0.62	0.33	p1d7	2.45	0.0001213	0.0001780	0.0002606	0.4277
7090785	11/15A1	34S_6p1d7Yc_0	33 7/8	S	9	4437.4	67 3/4	61 3/4	0.446	0.669	HLP-22	12	4	4	1.9	10.5	5.7	30.8	16.1	0.62	0.33	p1d7	2.45	0.0001213	0.0001780	0.0002606	0.4277
7090787	11/15A1	34S_6p1d7Yc_0	33 7/8	S	9	4437.4	67 3/4	61 3/4	0.446	0.669	HLP-22	12	4	4	1.9	10.5	5.7	30.8	16.1	0.62	0.33	p1d7	2.45	0.0001213	0.0001780	0.0002606	0.4277
7090790	11/15A1	34S_6p1d7Yc_0	33 7/8	S	9	4437.4	67 3/4	61 3/4	0.446	0.669	HLP-22	12	4	4	1.9	10.5	5.7	30.8	16.1	0.62	0.33	p1d7	2.45	0.0001213	0.0001780	0.0002606	0.4277
7090793	11/15A1	34S_6p1d7Yc_0	33 7/8	S	9	4437.4	67 3/4	61 3/4	0.446	0.669	HLP-22	12	4	4	1.9	10.5	5.7	30.8	16.1	0.62	0.33	p1d7	2.45	0.0001213	0.0001780	0.0002606	0.4277
7090796	11/15A1	34S_6p1d7Yc_0	33 7/8	S	9	4437.4	67 3/4	61 3/4	0.446	0.669	HLP-22	12	4	4	1.9	10.5	5.7	30.8	16.1	0.62	0.33	p1d7	2.45	0.0001213	0.0001780	0.0002606	0.4277
7090799	11/15A1	34S_6p1d7Yc_0	33 7/8	S	9	4437.4	67 3/4	61 3/4	0.446	0.669	HLP-22	12	4	4	1.9	10.5	5.7	30.8	16.1	0.62	0.33	p1d7	2.45	0.0001213	0.0001780	0.0002606	0.4277
7090802	11/15A1	34S_6p1d7Yc_0	33 7/8	S	9	4437.4	67 3/4	61 3/4	0.446	0.669	HLP-22	12	4	4	1.9	10.5	5.7	30.8	16.1	0.62	0.33	p1d7	2.45	0.0001213	0.0001780	0.0002606	0.4277
7090806M	11/15A1	34S_6p1d7Yc_0	33 7/8	S	9	4437.4	67 3/4	61 3/4	0.446	0.669	HLP-22	12	4	4	1.9	10.5	5.7	30.8	16.1	0.62	0.33	p1d7	2.45	0.0001213	0.0001780	0.0002606	0.4277
7090808M	11/15A1	34S_6p1d7Yc_0	33 7/8	S	9	4437.4	67 3/4	61 3/4	0.446	0.669	HLP-22	12	4	4	1.9	10.5	5.7	30.8	16.1	0.62	0.33	p1d7	2.45	0.0001213	0.0001780	0.0002606	0.4277
7090812	11/15B1	34S_6p1d7Yc_9	33 7/8	S	9	4437.4	67 3/4	61 3/4	0.446	0.669	HLP-22	12	0	4	1.9	10.5	5.7	30.8	16.1	0.62	0.33	p1d7	2.45	0.0001213	0.0001780	0.0002606	0.4277
7090814	11/15B1	34S_6p1d7Yc_9	33 7/8	S	9	4437.4	67 3/4	61 3/4	0.446	0.669	HLP-22	12	0	4	1.9	10.5	5.7	30.8	16.1	0.62	0.33	p1d7	2.45	0.0001213	0.0001780	0.0002606	0.4277
7090816	11/15B1	34S_6p1d7Yc_9	33 7/8	S	9	4437.4	67 3/4	61 3/4	0.446	0.669	HLP-22	12	0	4	1.9	10.5	5.7	30.8	16.1	0.62	0.33	p1d7	2.45	0.0001213	0.0001780	0.0002606	0.4277
7090819	11/15B1	34S_6p1d7Yc_9	33 7/8	S	9	4437.4	67 3/4	61 3/4	0.446	0.669	HLP-22	12	0	4	1.9	10.5	5.7	30.8	16.1	0.62	0.33	p1d7	2.45	0.0001213	0.0001780	0.0002606	0.4277
7090822	11/15B1	34S_6p1d7Yc_9	33 7/8	S	9	4437.4	67 3/4	61 3/4	0.446	0.669	HLP-22	12	0	4	1.9	10.5	5.7	30.8	16.1	0.62	0.33	p1d7	2.45	0.0001213	0.0001780	0.0002606	0.4277
7090825	11/15B1	34S_6p1d7Yc_9	33 7/8	S	9	4437.4	67 3/4	61 3/4	0.446	0.669	HLP-22	12	0	4	1.9	10.5	5.7	30.8	16.1	0.62	0.33	p1d7	2.45	0.0001213	0.0001780	0.0002606	0.4277
7090828	11/15B1	34S_6p1d7Yc_9	33 7/8	S	9	4437.4	67 3/4	61 3/4	0.446	0.669	HLP-22	12	0	4	1.9	10.5	5.7	30.8	16.1	0.62	0.33	p1d7	2.45	0.0001213	0.0001780	0.0002606	0.4277
7090831	11/15B1	34S_6p1d7Yc_9	33 7/8	S	9	4437.4	67 3/4	61 3/4	0.446	0.669	HLP-22	12	0	4	1.9	10.5	5.7	30.8	16.1	0.62	0.33	p1d7	2.45	0.0001213	0.0001780	0.0002606	0.4277
7090835M	11/15B1	34S_6p1d7Yc_9	33 7/8	S	9	4437.4	67 3/4	61 3/4	0.446	0.669	HLP-22	12	0	4	1.9	10.5	5.7	30.8	16.1	0.62	0.33	p1d7	2.45	0.0001213	0.0001780	0.0002606	0.4277
7090837M	11/15B1	34S_6p1d7Yc_9	33 7/8	S	9	4437.4	67 3/4	61 3/4	0.446	0.669	HLP-22	12	0	4	1.9	10.5	5.7	30.8	16.1	0.62	0.33	p1d7	2.45	0.0001213	0.0001780	0.0002606	0.4277
7090840	11/15C1	34S_6p1d7Yc_6	33 7/8	S	9	4437.4	67 3/4	61 3/4	0.446	0.669	HLP-22	12	4	0	1.9	10.5	5.7	30.8	16.1	0.62	0.33	p1d7	2.45	0.0001213	0.0001780	0.0002606	0.4277
7090842	11/15C1	34S_6p1d7Yc_6	33 7/8	S	9	4437.4	67 3/4	61 3/4	0.446	0.669	HLP-22	12	4	0	1.9	10.5	5.7	30.8	16.1	0.62	0.33	p1d7	2.45	0.0001213	0.0001780	0.0002606	0.4277
7090844	11/15C1	34S_6p1d7Yc_6	33 7/8	S	9	4437.4	67 3/4	61 3/4	0.446	0.669	HLP-22	12	4	0	1.9	10.5	5.7	30.8	16.1	0.62	0.33	p1d7	2.45	0.0001213	0.0001780	0.0002606	0.4277
7090847	11/15C1	34S_6p1d7Yc_6	33 7/8	S	9	4437.4	67 3/4	61 3/4	0.446	0.669	HLP-22	12	4	0	1.9	10.5	5.7	30.8	16.1	0.62	0.33	p1d7	2.45	0.0001213	0.0001780	0.0002606	0.4277
7090850	11/15C1	34S_6p1d7Yc_6	33 7/8	S	9	4437.4	67 3/4	61 3/4	0.446	0.669	HLP-22	12	4	0	1.9	10.5	5.7	30.8	16.1	0.62	0.33	p1d7	2.45	0.0001213	0.0001780	0.0002606	0.4277
7090854M	11/15C1	34S_6p1d7Yc_6	33 7/8	S	9	4437.4	67 3/4	61 3/4	0.446	0.669	HLP-22	12	4	0	1.9	10.5	5.7	30.8	16.1	0.62	0.33	p1d7	2.45	0.0001213	0.0001780	0.0002606	0.4277
7090856M	11/15C1	34S_6p1d7Yc_6	33 7/8	S	9	4437.4	67 3/4	61 3/4	0.446	0.669	HLP-22	12	4	0	1.9	10.5	5.7	30.8	16.1	0.62	0.33	p1d7	2.45	0.0001213	0.0001780	0.0002606	0.4277
7090859	11/19A1	34S_4p1d7Ya	33 7/8	S	9	4437.4	67 3/4	61 3/4	0.297	0.446	HLP-22	12	8	4	1.9	10.5	5.7	30.8	16.1	0.62	0.33	p1d7	2.45	0.0001213	0.0001780	0.0002606	0.4277
7090863	11/19A1	34S_4p1d7Ya	33 7/8	S	9	4437.4	67 3/4	61 3/4	0.297	0.446	HLP-22	12	8	4	1.9	10.5	5.7	30.8	16.1	0.62	0.33	p1d7	2.45	0.0001213	0.0001780	0.0002606	0.4277
7090865	11/19A1	34S_4p1d7Ya	33 7/8	S	9	4437.4	67 3/4	61 3/4	0.297	0.446	HLP-22	12	8	4	1.9	10.5	5.7	30.8	16.1	0.62	0.33	p1d7	2.45	0.0001213	0.0001780	0.0002606	0.4277
7090869	11/19A2	34S_4p1d7Yd_1	33 7/8	S	9	4437.4	67 3/4	61 3/4	0.297	0.446	HLP-22	12	8	4	1.9	10.5	5.7	30.8	16.1	0.62	0.33	p1d7	2.45	0.0001213	0.0001780	0.0002606	0.4277
7090871	11/19A2	34S_4p1d7Yd_1	33 7/8	S	9	4437.4	67 3/4	61 3/4	0.297	0.446	HLP-22	12	8	4	1.9	10.5	5.7	30.8	16.1	0.62	0.33	p1d7	2.45	0.0001213	0.0001780	0.0002606	0.4277
7090875M	11/19A2	34S_4p1d7Yd_1	33 7/8	S	9	4437.4	67 3/4	61 3/4	0.297	0.446	HLP-22	12	8	4	1.9	10.5	5.7	30.8	16.1	0.62	0.33	p1d7	2.45	0.0001213	0.0001780	0.0002606	0.4277
7090877M	11/19A2	34S_4p1d7Yd_1	33 7/8	S	9	4437.4	67 3/4	61 3/4	0.297	0.446	HLP-22	12	8	4	1.9	10.5	5.7	30.8	16.1	0.62	0.33	p1d7	2.45	0.0001213	0.0001780	0.0002606	0.4277

Table B.9. Updated Data from Fall 2007 Tests in Mid-Scale Vessel with Spherical Head B.7

Tank Water Temperature	Water Density	Solids Fraction	Pulse Volume Fraction	Duty Cycle	Cycle Time	Pulsed or Steady Jet	Us Steady Jet	U1 Pulsing Jet	U2 URMS	U3 URM3	Discharge Velocity	Critical Suspension Velocity	Average Peak Cloud Height	U_{CS} Condition	U_{CS} Method	U_{CS} Flag	U_{CS} Center Flag	U_{CS} udv Flag	U_{CS} based on Decreasing Velocity	Sweep Increase / Decrease	UDV Height Bed	Particle Motion	Solids Level	Outer Bottom Pattern	Inner Bottom Pattern	Case ID	Test	TDP	Row Number
C	g/cm³	fraction	fraction	fraction	s	text	m/s	m/s	m/s	m/s	m/s	m/s	in.	m/s	text	text	text	text	m/s	text	mm	text	text	text	text	text	text	text	text
T	ρ_l	ϕ_S	ϕ_P	DC	t_C	Jet	US	U1	U2	U3	U	U_{CS}	H_C	U_{CSR}	U_{CSM}	U_{CS}vis	U_{CS}cen	U_{CS}udv	U_{CS_D}	S_W	H_{bed}	PM	Sol	SP_O	SP_I	ID	M/DDX	TDP	MSS
23.0	0.999	0.00487	0.050	0.180	24.0	P	N/A	4.60	5.51	5.92	7.00	7.00	19.00	7.00	vis	UCSvis	N/A	N/A	N/A	I	N/A	CS	N/A	N/A	N/A	34S_6p1d7Yd_0	11/14A2	TDP-WTP-063	7090758
23.3	0.999	0.00487	undefined	1.000	infinite	S	3.63	N/A	N/A	N/A	3.60	N/A	N/A	N/A	N/A	N/A	UCScen	N/A	N/A	I	N/A	AM-	N/A	N/A	N/A	34S_6p1d7Ya-44	11/14B1	TDP-WTP-063	7090761
23.0	0.999	0.00487	0.050	0.180	45.3	P	N/A	3.71	3.78	3.81	3.90	N/A	N/A	N/A	N/A	N/A	UCScen	N/A	N/A	I	N/A	SS	N/A	N/A	N/A	34S_6p1d7Yd_0	11/14B2	TDP-WTP-063	7090764
23.1	0.999	0.00487	undefined	1.000	infinite	S	3.43	N/A	N/A	N/A	3.40	N/A	N/A	N/A	N/A	N/A	UCScen	N/A	N/A	I	N/A	SS	N/A	N/A	N/A	34S_6p1d7Ya-04	11/14C1	TDP-WTP-063	7090766
23.0	0.999	0.00487	0.050	0.180	94.5	P	N/A	3.69	3.72	3.75	3.70	N/A	N/A	N/A	center dec	N/A	UCScen	N/A	3.70	D	N/A	SS	N/A	N/A	N/A	34S_6p1d7Yd_9	11/14C2	TDP-WTP-063	7090772
23.0	0.999	0.00487	0.050	0.330	18.3	P	N/A	3.02	3.22	3.31	3.50	4.50	10.50	N/A	N/A	N/A	N/A	N/A	N/A	D	N/A	SS	N/A	N/A	N/A	34S_6p1d7Yc_1	11/14D1	TDP-WTP-063	7090776
23.0	0.999	0.00487	0.051	0.330	14.0	P	N/A	3.28	3.77	4.00	4.50	4.50	12.00	4.50	vis	UCSvis	N/A	N/A	N/A	I	N/A	CS	N/A	N/A	N/A	34S_6p1d7Yc_1	11/14D1	TDP-WTP-063	7090779
23.0	0.999	0.00487	0.052	0.330	12.5	P	N/A	2.89	3.66	4.02	5.00	4.50	12.25	N/A	N/A	N/A	N/A	N/A	N/A	I	N/A	BC	N/A	N/A	N/A	34S_6p1d7Yc_1	11/14D1	TDP-WTP-063	7090781
22.0	0.999	0.00487	0.051	0.330	23.8	P	N/A	3.78	3.88	3.92	4.00	7.00	8.50	N/A	N/A	N/A	UCScen	N/A	N/A	I	N/A	SS	N/A	N/A	N/A	34S_6p1d7Yc_0	11/15A1	TDP-WTP-053	7090785
22.0	0.999	0.00487	0.050	0.330	21.3	P	N/A	3.95	4.17	4.26	4.50	7.00	9.50	N/A	N/A	N/A	N/A	N/A	N/A	I	N/A	AM-	N/A	N/A	N/A	34S_6p1d7Yc_0	11/15A1	TDP-WTP-053	7090787
22.0	0.999	0.00487	0.051	0.330	19.0	P	N/A	4.23	4.56	4.70	5.00	7.00	11.25	N/A	N/A	N/A	N/A	N/A	N/A	I	N/A	AM	N/A	N/A	N/A	34S_6p1d7Yc_0	11/15A1	TDP-WTP-053	7090790
22.0	0.999	0.00487	0.048	0.330	16.0	P	N/A	3.47	4.30	4.66	5.50	7.00	12.75	N/A	N/A	N/A	N/A	N/A	N/A	I	N/A	AM	N/A	N/A	N/A	34S_6p1d7Yc_0	11/15A1	TDP-WTP-053	7090793
22.0	0.999	0.00487	0.050	0.330	15.5	P	N/A	4.18	4.91	5.23	6.00	7.00	13.50	N/A	N/A	N/A	N/A	N/A	N/A	I	N/A	AM	N/A	N/A	N/A	34S_6p1d7Yc_0	11/15A1	TDP-WTP-053	7090796
22.0	0.999	0.00487	0.051	0.330	14.5	P	N/A	4.60	5.32	5.65	6.40	7.00	15.00	N/A	N/A	N/A	N/A	N/A	N/A	I	N/A	AM+	N/A	N/A	N/A	34S_6p1d7Yc_0	11/15A1	TDP-WTP-053	7090799
22.0	0.999	0.00487	0.050	0.330	13.5	P	N/A	4.63	5.47	5.85	6.80	7.00	17.25	N/A	N/A	N/A	N/A	N/A	N/A	I	N/A	CS-	N/A	N/A	N/A	34S_6p1d7Yc_0	11/15A1	TDP-WTP-053	7090802
22.0	0.999	0.00487	0.049	0.330	0.0	P	N/A	4.79	5.63	6.01	7.00	7.00	18.00	7.00	vis	UCSvis	N/A	N/A	N/A	I	N/A	CS	N/A	N/A	N/A	34S_6p1d7Yc_0	11/15A1	TDP-WTP-053	7090806
22.0	0.999	0.00487	0.050	0.330	12.0	P	N/A	4.47	5.53	6.05	7.40	7.00	18.75	N/A	N/A	N/A	N/A	N/A	N/A	I	N/A	BC	N/A	N/A	N/A	34S_6p1d7Yc_0	11/15A1	TDP-WTP-053	7090808
22.0	0.999	0.00487	0.050	0.330	51.8	P	N/A	3.64	3.67	3.69	3.70	8.70	N/A	N/A	N/A	N/A	UCScen	N/A	N/A	I	N/A	SS	N/A	N/A	N/A	34S_6p1d7Yc_9	11/15B1	TDP-WTP-053	7090812
22.0	0.999	0.00487	0.050	0.330	34.5	P	N/A	5.38	5.45	5.48	5.50	8.70	12.50	N/A	N/A	N/A	N/A	N/A	N/A	I	N/A	AM-	N/A	N/A	N/A	34S_6p1d7Yc_9	11/15B1	TDP-WTP-053	7090814
22.0	0.999	0.00487	0.050	0.330	31.5	P	N/A	5.84	5.92	5.96	6.00	8.70	14.50	N/A	N/A	N/A	N/A	N/A	N/A	I	N/A	AM	N/A	N/A	N/A	34S_6p1d7Yc_9	11/15B1	TDP-WTP-053	7090816
22.0	0.999	0.00487	0.051	0.330	29.0	P	N/A	6.39	6.47	6.51	6.50	8.70	16.50	N/A	N/A	N/A	N/A	N/A	N/A	I	N/A	AM	N/A	N/A	N/A	34S_6p1d7Yc_9	11/15B1	TDP-WTP-053	7090819
22.0	0.999	0.00487	0.050	0.330	0.0	P	N/A	6.84	6.93	6.98	7.00	8.70	18.00	N/A	N/A	N/A	N/A	N/A	N/A	I	N/A	AM	N/A	N/A	N/A	34S_6p1d7Yc_9	11/15B1	TDP-WTP-053	7090822
22.0	0.999	0.00487	0.051	0.330	25.3	P	N/A	7.29	7.41	7.48	7.50	8.70	19.75	N/A	N/A	N/A	N/A	N/A	N/A	I	N/A	AM+	N/A	N/A	N/A	34S_6p1d7Yc_9	11/15B1	TDP-WTP-053	7090825
22.0	0.999	0.00487	0.051	0.330	23.5	P	N/A	7.23	7.64	7.81	8.00	8.70	21.25	N/A	N/A	N/A	N/A	N/A	N/A	I	N/A	AM+	N/A	N/A	N/A	34S_6p1d7Yc_9	11/15B1	TDP-WTP-053	7090828
22.0	0.999	0.00487	0.050	0.330	22.3	P	N/A	7.35	7.85	8.05	8.40	8.70	23.25	N/A	N/A	N/A	N/A	N/A	N/A	I	N/A	AM+	N/A	N/A	N/A	34S_6p1d7Yc_9	11/15B1	TDP-WTP-053	7090831
22.0	0.999	0.00487	0.050	0.330	21.5	P	N/A	7.43	8.02	8.26	8.70	8.70	24.00	8.70	vis	UCSvis	N/A	N/A	N/A	I	N/A	CS	N/A	N/A	N/A	34S_6p1d7Yc_9	11/15B1	TDP-WTP-053	7090835
22.0	0.999	0.00487	0.050	0.330	20.8	P	N/A	7.50	8.18	8.46	9.00	8.70	25.25	N/A	N/A	N/A	N/A	N/A	N/A	I	N/A	BC	N/A	N/A	N/A	34S_6p1d7Yc_9	11/15B1	TDP-WTP-053	7090837
22.0	0.999	0.00487	0.051	0.330	34.5	P	N/A	5.43	5.48	5.51	5.50	7.10	N/A	N/A	N/A	N/A	N/A	N/A	N/A	I	N/A	SS	N/A	N/A	N/A	34S_6p1d7Yc_6	11/15C1	TDP-WTP-053	7090840
22.0	0.999	0.00487	0.050	0.330	31.5	P	N/A	5.92	5.97	6.01	6.00	7.10	9.00	N/A	N/A	N/A	N/A	N/A	N/A	I	N/A	SS	N/A	N/A	N/A	34S_6p1d7Yc_6	11/15C1	TDP-WTP-053	7090842
22.0	0.999	0.00487	0.050	0.330	29.0	P	N/A	6.38	6.46	6.50	6.50	7.10	10.00	N/A	N/A	N/A	N/A	N/A	N/A	I	N/A	SS+	N/A	N/A	N/A	34S_6p1d7Yc_6	11/15C1	TDP-WTP-053	7090844
22.0	0.999	0.00487	0.050	0.330	28.0	P	N/A	6.50	6.61	6.67	6.70	7.10	11.50	N/A	N/A	N/A	N/A	N/A	N/A	I	N/A	SS+	N/A	N/A	N/A	34S_6p1d7Yc_6	11/15C1	TDP-WTP-053	7090847
22.0	0.999	0.00487	0.050	0.330	27.3	P	N/A	6.70	6.82	6.87	6.90	7.10	12.00	N/A	N/A	N/A	N/A	N/A	N/A	I	N/A	AM	N/A	N/A	N/A	34S_6p1d7Yc_6	11/15C1	TDP-WTP-053	7090850
22.0	0.999	0.00487	0.050	0.330	26.5	P	N/A	6.88	7.01	7.07	7.10	7.10	13.25	7.10	vis	UCSvis	N/A	N/A	N/A	I	N/A	CS	N/A	N/A	N/A	34S_6p1d7Yc_6	11/15C1	TDP-WTP-053	7090854
22.0	0.999	0.00487	0.050	0.330	25.5	P	N/A	7.11	7.27	7.34	7.40	7.10	15.50	N/A	N/A	N/A	N/A	N/A	N/A	I	N/A	BC	N/A	N/A	N/A	34S_6p1d7Yc_6	11/15C1	TDP-WTP-053	7090856
21.5	0.995	0.00487	undefined	1.000	infinite	S	5.46	N/A	N/A	N/A	5.40	5.60	8.75	N/A	N/A	N/A	UCScen	N/A	N/A	I	N/A	CS-	N/A	N/A	N/A	34S_4p1d7Ya	11/19A1	TDP-WTP-054	7090859
21.5	0.999	0.00487	undefined	1.000	infinite	S	5.64	N/A	N/A	N/A	5.60	5.60	9.25	5.60	vis	UCSvis	N/A	N/A	N/A	I	N/A	CS	N/A	N/A	N/A	34S_4p1d7Ya	11/19A1	TDP-WTP-054	7090863
21.5	0.999	0.00487	undefined	1.000	infinite	S	6.06	N/A	N/A	N/A	6.00	5.60	12.13	N/A	N/A	N/A	N/A	N/A	N/A	I	N/A	BC	N/A	N/A	N/A	34S_4p1d7Ya	11/19A1	TDP-WTP-054	7090865
22.0	0.999	0.00487	0.049	0.180	47.0	P	N/A	5.33	5.41	5.45	5.50	6.40	8.50	N/A	N/A	N/A	N/A	N/A	N/A	D	N/A	SS	N/A	N/A	N/A	34S_4p1d7Yd_1	11/19A2	TDP-WTP-054	7090869
22.0	0.999	0.00487	0.051	0.180	43.0	P	N/A	5.76	5.91	5.97	6.00	6.40	9.00	N/A	N/A	N/A	N/A	N/A	N/A	I	N/A	AM+	N/A	N/A	N/A	34S_4p1d7Yd_1	11/19A2	TDP-WTP-054	7090871
22.0	0.999	0.00487	0.053	0.180	40.0	P	N/A	6.25	6.53	6.65	6.40	6.40	9.75	6.40	vis	UCSvis	N/A	N/A	N/A	I	N/A	CS	N/A	N/A	N/A	34S_4p1d7Yd_1	11/19A2	TDP-WTP-054	7090875
22.0	0.999	0.00487	0.052	0.180	38.0	P	N/A	6.16	6.55	6.73	6.80	6.40	10.50	N/A	N/A	N/A	N/A	N/A	N/A	I	N/A	BC	N/A	N/A	N/A	34S_4p1d7Yd_1	11/19A2	TDP-WTP-054	7090877

Table B.9. Updated Data from Fall 2007 Tests in Mid-Scale Vessel with Spherical Head A.8

Row Number	Test	Case ID	Tank Diameter	Head Shape	Dish Height	Dish Volume	Tank Fill Height	Return Line Height	Nozzle Inner Diameter	Nozzle Stand-off Distance	Pulse Tube Configuration	Installed Nozzles	Outer Nozzles Operated	Inner Nozzles Operated	Pulse Tube Outer Diameter	Outer PJM Radius	Inner PJM Radius	"FIO" Outer PJM Impingement Angle	"FIO" Inner PJM Impingement Angle	Ratio Outer PJM to Tank Radius	Ratio Inner PJM to Tank Radius	Simulant	Solids Density	Particle Diameter d5	Particle Diameter d50	Particle Diameter d95	Void Fraction
text	text	text	in.	text	in.	in. ^{3}	in.	in.	in.	in.	text	number	number	number	in.	in.	in.	deg	deg	nondim	nondim	text	g/cm^3	m	m	m	fraction
MSS	M/DDX	ID	D	HS	H_{dish}	V_{dish}	H	Rtn	d	sod	PT	N	N_O	N_I	PT_{od}	R_O	R_I	Θ_O	Θ_I	R_O/R	R_I/R	sxdx	ρ_S	d_5	d_{50}	d_{95}	vf
7090881	11/20A1	34S_4p1d7Ya-44	33 7/8	S	9	4437.4	67 3/4	61 3/4	0.297	0.446	HLP-22	12	4	4	1.9	10.5	5.7	30.8	16.1	0.62	0.33	p1d7	2.45	0.0001213	0.0001780	0.0002606	0.4277
7090883	11/20A1	34S_4p1d7Ya-44	33 7/8	S	9	4437.4	67 3/4	61 3/4	0.297	0.446	HLP-22	12	4	4	1.9	10.5	5.7	30.8	16.1	0.62	0.33	p1d7	2.45	0.0001213	0.0001780	0.0002606	0.4277
7090886	11/20A1	34S_4p1d7Ya-44	33 7/8	S	9	4437.4	67 3/4	61 3/4	0.297	0.446	HLP-22	12	4	4	1.9	10.5	5.7	30.8	16.1	0.62	0.33	p1d7	2.45	0.0001213	0.0001780	0.0002606	0.4277
7090889	11/20A1	34S_4p1d7Ya-44	33 7/8	S	9	4437.4	67 3/4	61 3/4	0.297	0.446	HLP-22	12	4	4	1.9	10.5	5.7	30.8	16.1	0.62	0.33	p1d7	2.45	0.0001213	0.0001780	0.0002606	0.4277
7090892	11/20A1	34S_4p1d7Ya-44	33 7/8	S	9	4437.4	67 3/4	61 3/4	0.297	0.446	HLP-22	12	4	4	1.9	10.5	5.7	30.8	16.1	0.62	0.33	p1d7	2.45	0.0001213	0.0001780	0.0002606	0.4277
7090895	11/20A1	34S_4p1d7Ya-44	33 7/8	S	9	4437.4	67 3/4	61 3/4	0.297	0.446	HLP-22	12	4	4	1.9	10.5	5.7	30.8	16.1	0.62	0.33	p1d7	2.45	0.0001213	0.0001780	0.0002606	0.4277
7090899	11/20A1	34S_4p1d7Ya-44	33 7/8	S	9	4437.4	67 3/4	61 3/4	0.297	0.446	HLP-22	12	4	4	1.9	10.5	5.7	30.8	16.1	0.62	0.33	p1d7	2.45	0.0001213	0.0001780	0.0002606	0.4277
7090901	11/20A1	34S_4p1d7Ya-44	33 7/8	S	9	4437.4	67 3/4	61 3/4	0.297	0.446	HLP-22	12	4	4	1.9	10.5	5.7	30.8	16.1	0.62	0.33	p1d7	2.45	0.0001213	0.0001780	0.0002606	0.4277
7090905	11/20A2	34S_4p1d7Yd_0	33 7/8	S	9	4437.4	67 3/4	61 3/4	0.297	0.446	HLP-22	12	4	4	1.9	10.5	5.7	30.8	16.1	0.62	0.33	p1d7	2.45	0.0001213	0.0001780	0.0002606	0.4277
7090908	11/20A2	34S_4p1d7Yd_0	33 7/8	S	9	4437.4	67 3/4	61 3/4	0.297	0.446	HLP-22	12	4	4	1.9	10.5	5.7	30.8	16.1	0.62	0.33	p1d7	2.45	0.0001213	0.0001780	0.0002606	0.4277
7090910	11/20A2	34S_4p1d7Yd_0	33 7/8	S	9	4437.4	67 3/4	61 3/4	0.297	0.446	HLP-22	12	4	4	1.9	10.5	5.7	30.8	16.1	0.62	0.33	p1d7	2.45	0.0001213	0.0001780	0.0002606	0.4277
7090913	11/20A2	34S_4p1d7Yd_0	33 7/8	S	9	4437.4	67 3/4	61 3/4	0.297	0.446	HLP-22	12	4	4	1.9	10.5	5.7	30.8	16.1	0.62	0.33	p1d7	2.45	0.0001213	0.0001780	0.0002606	0.4277
7090916	11/20A2	34S_4p1d7Yd_0	33 7/8	S	9	4437.4	67 3/4	61 3/4	0.297	0.446	HLP-22	12	4	4	1.9	10.5	5.7	30.8	16.1	0.62	0.33	p1d7	2.45	0.0001213	0.0001780	0.0002606	0.4277
7090919	11/20A2	34S_4p1d7Yd_0	33 7/8	S	9	4437.4	67 3/4	61 3/4	0.297	0.446	HLP-22	12	4	4	1.9	10.5	5.7	30.8	16.1	0.62	0.33	p1d7	2.45	0.0001213	0.0001780	0.0002606	0.4277
7090922	11/20A2	34S_4p1d7Yd_0	33 7/8	S	9	4437.4	67 3/4	61 3/4	0.297	0.446	HLP-22	12	4	4	1.9	10.5	5.7	30.8	16.1	0.62	0.33	p1d7	2.45	0.0001213	0.0001780	0.0002606	0.4277
7090925	11/20A2	34S_4p1d7Yd_0	33 7/8	S	9	4437.4	67 3/4	61 3/4	0.297	0.446	HLP-22	12	4	4	1.9	10.5	5.7	30.8	16.1	0.62	0.33	p1d7	2.45	0.0001213	0.0001780	0.0002606	0.4277
7090928	11/20A2	34S_4p1d7Yd_0	33 7/8	S	9	4437.4	67 3/4	61 3/4	0.297	0.446	HLP-22	12	4	4	1.9	10.5	5.7	30.8	16.1	0.62	0.33	p1d7	2.45	0.0001213	0.0001780	0.0002606	0.4277
7090932M	11/20A2	34S_4p1d7Yd_0	33 7/8	S	9	4437.4	67 3/4	61 3/4	0.297	0.446	HLP-22	12	4	4	1.9	10.5	5.7	30.8	16.1	0.62	0.33	p1d7	2.45	0.0001213	0.0001780	0.0002606	0.4277
7090934M	11/20A2	34S_4p1d7Yd_0	33 7/8	S	9	4437.4	67 3/4	61 3/4	0.297	0.446	HLP-22	12	4	4	1.9	10.5	5.7	30.8	16.1	0.62	0.33	p1d7	2.45	0.0001213	0.0001780	0.0002606	0.4277
7090938	11/20B1	34S_4p1d7Ya-04	33 7/8	S	9	4437.4	67 3/4	61 3/4	0.297	0.446	HLP-22	12	0	4	1.9	10.5	5.7	30.8	16.1	0.62	0.33	p1d7	2.45	0.0001213	0.0001780	0.0002606	0.4277
7090941	11/20B1	34S_4p1d7Ya-04	33 7/8	S	9	4437.4	67 3/4	61 3/4	0.297	0.446	HLP-22	12	0	4	1.9	10.5	5.7	30.8	16.1	0.62	0.33	p1d7	2.45	0.0001213	0.0001780	0.0002606	0.4277
7090943	11/20B1	34S_4p1d7Ya-04	33 7/8	S	9	4437.4	67 3/4	61 3/4	0.297	0.446	HLP-22	12	0	4	1.9	10.5	5.7	30.8	16.1	0.62	0.33	p1d7	2.45	0.0001213	0.0001780	0.0002606	0.4277
7090946	11/20B1	34S_4p1d7Ya-04	33 7/8	S	9	4437.4	67 3/4	61 3/4	0.297	0.446	HLP-22	12	0	4	1.9	10.5	5.7	30.8	16.1	0.62	0.33	p1d7	2.45	0.0001213	0.0001780	0.0002606	0.4277
7090949	11/20B1	34S_4p1d7Ya-04	33 7/8	S	9	4437.4	67 3/4	61 3/4	0.297	0.446	HLP-22	12	0	4	1.9	10.5	5.7	30.8	16.1	0.62	0.33	p1d7	2.45	0.0001213	0.0001780	0.0002606	0.4277
7090952	11/20B1	34S_4p1d7Ya-04	33 7/8	S	9	4437.4	67 3/4	61 3/4	0.297	0.446	HLP-22	12	0	4	1.9	10.5	5.7	30.8	16.1	0.62	0.33	p1d7	2.45	0.0001213	0.0001780	0.0002606	0.4277
7090956	11/20B1	34S_4p1d7Ya-04	33 7/8	S	9	4437.4	67 3/4	61 3/4	0.297	0.446	HLP-22	12	0	4	1.9	10.5	5.7	30.8	16.1	0.62	0.33	p1d7	2.45	0.0001213	0.0001780	0.0002606	0.4277
7090958	11/20B1	34S_4p1d7Ya-04	33 7/8	S	9	4437.4	67 3/4	61 3/4	0.297	0.446	HLP-22	12	0	4	1.9	10.5	5.7	30.8	16.1	0.62	0.33	p1d7	2.45	0.0001213	0.0001780	0.0002606	0.4277
7090962	11/20B2	34S_4p1d7Yd_9	33 7/8	S	9	4437.4	67 3/4	61 3/4	0.297	0.446	HLP-22	12	0	4	1.9	10.5	5.7	30.8	16.1	0.62	0.33	p1d7	2.45	0.0001213	0.0001780	0.0002606	0.4277
7090965	11/20B2	34S_4p1d7Yd_9	33 7/8	S	9	4437.4	67 3/4	61 3/4	0.297	0.446	HLP-22	12	0	4	1.9	10.5	5.7	30.8	16.1	0.62	0.33	p1d7	2.45	0.0001213	0.0001780	0.0002606	0.4277
7090967	11/20B2	34S_4p1d7Yd_9	33 7/8	S	9	4437.4	67 3/4	61 3/4	0.297	0.446	HLP-22	12	0	4	1.9	10.5	5.7	30.8	16.1	0.62	0.33	p1d7	2.45	0.0001213	0.0001780	0.0002606	0.4277
7090970	11/20B2	34S_4p1d7Yd_9	33 7/8	S	9	4437.4	67 3/4	61 3/4	0.297	0.446	HLP-22	12	0	4	1.9	10.5	5.7	30.8	16.1	0.62	0.33	p1d7	2.45	0.0001213	0.0001780	0.0002606	0.4277
7090973	11/20B2	34S_4p1d7Yd_9	33 7/8	S	9	4437.4	67 3/4	61 3/4	0.297	0.446	HLP-22	12	0	4	1.9	10.5	5.7	30.8	16.1	0.62	0.33	p1d7	2.45	0.0001213	0.0001780	0.0002606	0.4277
7090977M	11/20B2	34S_4p1d7Yd_9	33 7/8	S	9	4437.4	67 3/4	61 3/4	0.297	0.446	HLP-22	12	0	4	1.9	10.5	5.7	30.8	16.1	0.62	0.33	p1d7	2.45	0.0001213	0.0001780	0.0002606	0.4277
7090979M	11/20B2	34S_4p1d7Yd_9	33 7/8	S	9	4437.4	67 3/4	61 3/4	0.297	0.446	HLP-22	12	0	4	1.9	10.5	5.7	30.8	16.1	0.62	0.33	p1d7	2.45	0.0001213	0.0001780	0.0002606	0.4277
7090982	11/26A1	34S_4p1d7Ya-40	33 7/8	S	9	4437.4	67 3/4	61 3/4	0.297	0.446	HLP-22	12	4	0	1.9	10.5	5.7	30.8	16.1	0.62	0.33	p1d7	2.45	0.0001213	0.0001780	0.0002606	0.4277
7090985	11/26A1	34S_4p1d7Ya-40	33 7/8	S	9	4437.4	67 3/4	61 3/4	0.297	0.446	HLP-22	12	4	0	1.9	10.5	5.7	30.8	16.1	0.62	0.33	p1d7	2.45	0.0001213	0.0001780	0.0002606	0.4277
7090989	11/26A1	34S_4p1d7Ya-40	33 7/8	S	9	4437.4	67 3/4	61 3/4	0.297	0.446	HLP-22	12	4	0	1.9	10.5	5.7	30.8	16.1	0.62	0.33	p1d7	2.45	0.0001213	0.0001780	0.0002606	0.4277
7090991	11/26A1	34S_4p1d7Ya-40	33 7/8	S	9	4437.4	67 3/4	61 3/4	0.297	0.446	HLP-22	12	4	0	1.9	10.5	5.7	30.8	16.1	0.62	0.33	p1d7	2.45	0.0001213	0.0001780	0.0002606	0.4277
7090994	11/26A1	34S_4p1d7Ya-40	33 7/8	S	9	4437.4	67 3/4	61 3/4	0.297	0.446	HLP-22	12	4	0	1.9	10.5	5.7	30.8	16.1	0.62	0.33	p1d7	2.45	0.0001213	0.0001780	0.0002606	0.4277
7090996	11/26A1	34S_4p1d7Ya-40	33 7/8	S	9	4437.4	67 3/4	61 3/4	0.297	0.446	HLP-22	12	4	0	1.9	10.5	5.7	30.8	16.1	0.62	0.33	p1d7	2.45	0.0001213	0.0001780	0.0002606	0.4277
7090998	11/26A1	34S_4p1d7Ya-40	33 7/8	S	9	4437.4	67 3/4	61 3/4	0.297	0.446	HLP-22	12	4	0	1.9	10.5	5.7	30.8	16.1	0.62	0.33	p1d7	2.45	0.0001213	0.0001780	0.0002606	0.4277

Table B.9. Updated Data from Fall 2007 Tests in Mid-Scale Vessel with Spherical Head B.8

Tank Water Temperature	Water Density	Solids Fraction	Pulse Volume Fraction	Duty Cycle	Cycle Time	Pulsed or Steady Jet	Us Steady Jet	U1 Pulsing Jet	U2 URMS	U3 URM3	Discharge Velocity	Critical Suspension Velocity	Average Peak Cloud Height	U_{CS} Condition	U_{CS} Method	U_{CS} Flag	U_{CS} Center Flag	U_{CS} udv Flag	U_{CS} based on Decreasing Velocity	Sweep Increase / Decrease	UDV Height Bed	Particle Motion	Solids Level	Outer Bottom Pattern	Inner Bottom Pattern	Case ID	Test	TDP	Row Number
C	g/cm³	fraction	fraction	fraction	s	text	m/s	m/s	m/s	m/s	m/s	m/s	in.	m/s	text	text	text	text	m/s	text	mm	text	text	text	text	text	text	text	text
T	ρ_l	ϕ_S	ϕ_P	DC	t_C	Jet	US	U1	U2	U3	U	U_{CS}	H_C	U_{CSR}	U_{CSM}	U_{CS}vis	U_{CS}cen	U_{CS}udv	U_{CS_D}	S_W	H_{bed}	PM	Sol	SP_O	SP_I	ID	M/DDX	TDP	MSS
21.4	0.999	0.00487	undefined	1.000	infinite	S	5.55	N/A	N/A	N/A	5.50	8.50	N/A	N/A	N/A	N/A	UCScen	N/A	N/A	I	N/A	SS+	N/A	N/A	N/A	34S_4p1d7Ya-44	11/20A1	TDP-WTP-055	7090881
21.4	0.999	0.00487	undefined	1.000	infinite	S	6.04	N/A	N/A	N/A	6.00	8.50	N/A	N/A	N/A	N/A	N/A	N/A	N/A	I	N/A	AM	N/A	N/A	N/A	34S_4p1d7Ya-44	11/20A1	TDP-WTP-055	7090883
21.5	0.999	0.00487	undefined	1.000	infinite	S	6.53	N/A	N/A	N/A	6.50	8.50	8.75	N/A	N/A	N/A	N/A	N/A	N/A	I	N/A	AM	N/A	N/A	N/A	34S_4p1d7Ya-44	11/20A1	TDP-WTP-055	7090886
21.5	0.999	0.00487	undefined	1.000	infinite	S	7.06	N/A	N/A	N/A	7.00	8.50	10.00	N/A	N/A	N/A	N/A	N/A	N/A	I	N/A	AM	N/A	N/A	N/A	34S_4p1d7Ya-44	11/20A1	TDP-WTP-055	7090889
21.5	0.999	0.00487	undefined	1.000	infinite	S	7.55	N/A	N/A	N/A	7.50	8.50	13.25	N/A	N/A	N/A	N/A	N/A	N/A	I	N/A	AM+	N/A	N/A	N/A	34S_4p1d7Ya-44	11/20A1	TDP-WTP-055	7090892
21.5	0.999	0.00487	undefined	1.000	infinite	S	8.05	N/A	N/A	N/A	8.00	8.50	20.50	N/A	N/A	N/A	N/A	N/A	N/A	I	N/A	AM+	N/A	N/A	N/A	34S_4p1d7Ya-44	11/20A1	TDP-WTP-055	7090895
21.5	0.999	0.00487	undefined	1.000	infinite	S	8.60	N/A	N/A	N/A	8.50	8.50	30.00	8.50	vis	UCSvis	N/A	N/A	N/A	I	N/A	CS	N/A	N/A	N/A	34S_4p1d7Ya-44	11/20A1	TDP-WTP-055	7090899
21.6	0.999	0.00487	undefined	1.000	infinite	S	9.03	N/A	N/A	N/A	9.00	8.50	36.75	N/A	N/A	N/A	N/A	N/A	N/A	I	N/A	BC-	N/A	N/A	N/A	34S_4p1d7Ya-44	11/20A1	TDP-WTP-055	7090901
22.0	0.999	0.00487	0.049	0.180	71.0	P	N/A	5.58	5.64	5.68	5.50	11.00	N/A	N/A	center dec	N/A	UCScen	N/A	5.50	D	N/A	SS	N/A	N/A	N/A	34S_4p1d7Yd_0	11/20A2	TDP-WTP-055	7090905
22.0	0.999	0.00487	0.051	0.180	64.5	P	N/A	6.10	6.18	6.23	6.00	11.00	N/A	N/A	N/A	N/A	N/A	N/A	N/A	I	N/A	AM-	N/A	N/A	N/A	34S_4p1d7Yd_0	11/20A2	TDP-WTP-055	7090908
22.0	0.999	0.00487	0.051	0.180	55.0	P	N/A	7.10	7.21	7.27	7.00	11.00	9.25	N/A	N/A	N/A	N/A	N/A	N/A	I	N/A	AM	N/A	N/A	N/A	34S_4p1d7Yd_0	11/20A2	TDP-WTP-055	7090910
22.0	0.999	0.00487	0.051	0.180	47.0	P	N/A	8.11	8.26	8.35	8.00	11.00	11.25	N/A	N/A	N/A	N/A	N/A	N/A	I	N/A	AM	N/A	N/A	N/A	34S_4p1d7Yd_0	11/20A2	TDP-WTP-055	7090913
22.0	0.999	0.00487	0.050	0.180	44.5	P	N/A	8.18	8.50	8.65	8.50	11.00	12.00	N/A	N/A	N/A	N/A	N/A	N/A	I	N/A	AM	N/A	N/A	N/A	34S_4p1d7Yd_0	11/20A2	TDP-WTP-055	7090916
22.0	0.999	0.00487	0.051	0.180	41.5	P	N/A	8.46	8.92	9.14	9.00	11.00	14.25	N/A	N/A	N/A	N/A	N/A	N/A	I	N/A	AM	N/A	N/A	N/A	34S_4p1d7Yd_0	11/20A2	TDP-WTP-055	7090919
22.0	0.999	0.00487	0.051	0.180	40.0	P	N/A	9.02	9.44	9.64	9.50	11.00	15.75	N/A	N/A	N/A	N/A	N/A	N/A	I	N/A	AM+	N/A	N/A	N/A	34S_4p1d7Yd_0	11/20A2	TDP-WTP-055	7090922
22.0	0.999	0.00487	0.051	0.180	37.5	P	N/A	9.33	9.85	10.09	10.00	11.00	16.63	N/A	N/A	N/A	N/A	N/A	N/A	I	N/A	AM+	N/A	N/A	N/A	34S_4p1d7Yd_0	11/20A2	TDP-WTP-055	7090925
22.0	0.999	0.00487	0.051	0.180	35.5	P	N/A	9.57	10.20	10.50	10.50	11.00	19.00	N/A	N/A	N/A	N/A	N/A	N/A	I	N/A	AM+	N/A	N/A	N/A	34S_4p1d7Yd_0	11/20A2	TDP-WTP-055	7090928
22.0	0.999	0.00487	0.050	0.180	33.5	P	N/A	9.80	10.56	10.92	11.00	11.00	19.50	11.00	vis	UCSvis	N/A	N/A	N/A	I	N/A	CS	N/A	N/A	N/A	34S_4p1d7Yd_0	11/20A2	TDP-WTP-055	7090932
22.0	0.999	0.00487	0.050	0.180	30.7	P	N/A	11.69	12.18	12.43	12.00	11.00	22.00	N/A	N/A	N/A	N/A	N/A	N/A	I	N/A	BC	N/A	N/A	N/A	34S_4p1d7Yd_0	11/20A2	TDP-WTP-055	7090934
22.2	0.999	0.00487	undefined	1.000	infinite	S	6.02	N/A	N/A	N/A	6.00	12.00	N/A	N/A	N/A	N/A	UCScen	N/A	N/A	I	N/A	SS	N/A	N/A	N/A	34S_4p1d7Ya-04	11/20B1	TDP-WTP-055	7090938
22.2	0.999	0.00487	undefined	1.000	infinite	S	7.01	N/A	N/A	N/A	7.00	12.00	8.75	N/A	N/A	N/A	N/A	N/A	N/A	I	N/A	SS+	N/A	N/A	N/A	34S_4p1d7Ya-04	11/20B1	TDP-WTP-055	7090941
22.3	0.999	0.00487	undefined	1.000	infinite	S	7.98	N/A	N/A	N/A	8.00	12.00	10.50	N/A	N/A	N/A	N/A	N/A	N/A	I	N/A	AM	N/A	N/A	N/A	34S_4p1d7Ya-04	11/20B1	TDP-WTP-055	7090943
22.3	0.999	0.00487	undefined	1.000	infinite	S	9.01	N/A	N/A	N/A	9.00	12.00	13.25	N/A	N/A	N/A	N/A	N/A	N/A	I	N/A	AM	N/A	N/A	N/A	34S_4p1d7Ya-04	11/20B1	TDP-WTP-055	7090946
22.3	0.999	0.00487	undefined	1.000	infinite	S	10.06	N/A	N/A	N/A	10.00	12.00	16.50	N/A	N/A	N/A	N/A	N/A	N/A	I	N/A	AM	N/A	N/A	N/A	34S_4p1d7Ya-04	11/20B1	TDP-WTP-055	7090949
22.2	0.999	0.00487	undefined	1.000	infinite	S	11.05	N/A	N/A	N/A	11.00	12.00	21.00	N/A	N/A	N/A	N/A	N/A	N/A	I	N/A	AM+	N/A	N/A	N/A	34S_4p1d7Ya-04	11/20B1	TDP-WTP-055	7090952
22.3	0.999	0.00487	undefined	1.000	infinite	S	12.11	N/A	N/A	N/A	12.00	12.00	29.50	12.00	vis	UCSvis	N/A	N/A	N/A	I	N/A	CS	N/A	N/A	N/A	34S_4p1d7Ya-04	11/20B1	TDP-WTP-055	7090956
22.3	0.999	0.00487	undefined	1.000	infinite	S	13.06	N/A	N/A	N/A	13.00	12.00	39.25	N/A	N/A	N/A	N/A	N/A	N/A	I	N/A	BC	N/A	N/A	N/A	34S_4p1d7Ya-04	11/20B1	TDP-WTP-055	7090958
22.0	0.999	0.00487	0.052	0.180	100.0	P	N/A	8.15	8.32	8.54	7.70	14.00	10.00	N/A	N/A	N/A	N/A	N/A	N/A	D	N/A	SS	N/A	N/A	N/A	34S_4p1d7Yd_9	11/20B2	TDP-WTP-055	7090962
22.0	0.999	0.00487	0.051	0.180	85.5	P	N/A	9.31	9.52	9.77	9.00	14.00	12.75	N/A	N/A	N/A	N/A	N/A	N/A	I	N/A	SS+	N/A	N/A	N/A	34S_4p1d7Yd_9	11/20B2	TDP-WTP-055	7090965
22.0	0.999	0.00487	0.052	0.180	77.0	P	N/A	10.37	10.61	10.90	10.00	14.00	15.50	N/A	N/A	N/A	N/A	N/A	N/A	I	N/A	AM	N/A	N/A	N/A	34S_4p1d7Yd_9	11/20B2	TDP-WTP-055	7090967
22.0	0.999	0.00487	0.052	0.180	63.5	P	N/A	12.50	12.81	13.16	12.00	14.00	18.75	N/A	N/A	N/A	N/A	N/A	N/A	I	N/A	AM	N/A	N/A	N/A	34S_4p1d7Yd_9	11/20B2	TDP-WTP-055	7090970
22.0	0.999	0.00487	0.051	0.180	57.5	P	N/A	13.57	13.92	14.31	13.00	14.00	20.50	N/A	N/A	N/A	N/A	N/A	N/A	I	N/A	AM+	N/A	N/A	N/A	34S_4p1d7Yd_9	11/20B2	TDP-WTP-055	7090973
22.0	0.999	0.00487	0.051	0.180	53.3	P	N/A	14.55	14.97	15.40	14.00	14.00	23.00	14.00	vis	UCSvis	N/A	N/A	N/A	I	N/A	CS	N/A	N/A	N/A	34S_4p1d7Yd_9	11/20B2	TDP-WTP-055	7090977
22.0	0.999	0.00487	0.051	0.180	48.5	P	N/A	15.90	16.35	16.84	15.00	14.00	26.25	N/A	N/A	N/A	N/A	N/A	N/A	I	N/A	BC	N/A	N/A	N/A	34S_4p1d7Yd_9	11/20B2	TDP-WTP-055	7090979
20.5	0.999	0.00487	undefined	1.000	infinite	S	9.06	N/A	N/A	N/A	9.00	9.50	N/A	N/A	N/A	N/A	N/A	N/A	N/A	I	N/A	SS+	N/A	N/A	N/A	34S_4p1d7Ya-40	11/26A1	TDP-WTP-064	7090982
20.5	0.999	0.00487	undefined	1.000	infinite	S	10.06	N/A	N/A	N/A	10.00	9.50	21.50	N/A	N/A	N/A	N/A	N/A	N/A	I	N/A	BC	N/A	N/A	N/A	34S_4p1d7Ya-40	11/26A1	TDP-WTP-064	7090985
20.5	0.999	0.00487	undefined	1.000	infinite	S	9.62	N/A	N/A	N/A	9.50	9.50	17.50	N/A	vis dec	UCSvis	N/A	N/A	9.50	D	N/A	CS	N/A	N/A	N/A	34S_4p1d7Ya-40	11/26A1	TDP-WTP-064	7090989
20.5	0.999	0.00487	undefined	1.000	infinite	S	9.03	N/A	N/A	N/A	9.00	9.50	N/A	N/A	N/A	N/A	N/A	N/A	N/A	D	N/A	SS+	N/A	N/A	N/A	34S_4p1d7Ya-40	11/26A1	TDP-WTP-064	7090991
20.6	0.999	0.00487	undefined	1.000	infinite	S	9.42	N/A	N/A	N/A	9.25	9.50	9.25	N/A	N/A	N/A	N/A	N/A	N/A	I	N/A	AM	N/A	N/A	N/A	34S_4p1d7Ya-40	11/26A1	TDP-WTP-064	7090994
20.6	0.999	0.00487	undefined	1.000	infinite	S	9.42	N/A	N/A	N/A	9.30	9.50	9.25	N/A	N/A	N/A	N/A	N/A	N/A	I	N/A	N/A	N/A	N/A	N/A	34S_4p1d7Ya-40	11/26A1	TDP-WTP-064	7090996
20.5	0.999	0.00487	undefined	1.000	infinite	S	9.60	N/A	N/A	N/A	9.50	9.50	13.75	9.50	vis	UCSvis	N/A	N/A	N/A	I	N/A	CS	N/A	N/A	N/A	34S_4p1d7Ya-40	11/26A1	TDP-WTP-064	7090998

Table B.9. Update Data from Fall 2007 Tests in Mid-Scale Vessel with Spherical Head A.9

Row Number	Test	Case ID	Tank Diameter	Head Shape	Dish Height	Dish Volume	Tank Fill Height	Return Line Height	Nozzle Inner Diameter	Nozzle Stand-off Distance	Pulse Tube Configuration	Installed Nozzles	Outer Nozzles Operated	Inner Nozzles Operated	Pulse Tube Outer Diameter	Outer PJM Radius	Inner PJM Radius	"FIO" Outer PJM Impingement Angle	"FIO" Inner PJM Impingement Angle	Ratio Outer PJM to Tank Radius	Ratio Inner PJM to Tank Radius	Simulant	Solids Density	Particle Diameter d5	Particle Diameter d50	Particle Diameter d95	Void Fraction
text	text	text	in.	text	in.	in. ^{3}	in.	in.	in.	in.	text	number	number	number	in.	in.	in.	deg	deg	nondim	nondim	text	g/cm^3	m	m	m	fraction
MSS	M/DDX	ID	D	HS	H_{dish}	V_{dish}	H	Rtn	d	sod	PT	N	N_O	N_I	PT_{od}	R_O	R_I	Θ_O	Θ_I	R_O/R	R_I/R	sxdx	ρ_S	d_5	d_{50}	d_{95}	vf
7091000	11/26A1	34S_4p1d7Ya-40	33 7/8	S	9	4437.4	67 3/4	61 3/4	0.297	0.446	HLP-22	12	4	0	1.9	10.5	5.7	30.8	16.1	0.62	0.33	p1d7	2.45	0.0001213	0.0001780	0.0002606	0.4277
7091003	11/26A2	34S_4p1d7Yd_6	33 7/8	S	9	4437.4	67 3/4	61 3/4	0.297	0.446	HLP-22	12	4	0	1.9	10.5	5.7	30.8	16.1	0.62	0.33	p1d7	2.45	0.0001213	0.0001780	0.0002606	0.4277
7091006	11/26A2	34S_4p1d7Yd_6	33 7/8	S	9	4437.4	67 3/4	61 3/4	0.297	0.446	HLP-22	12	4	0	1.9	10.5	5.7	30.8	16.1	0.62	0.33	p1d7	2.45	0.0001213	0.0001780	0.0002606	0.4277
7091010M	11/26A2	34S_4p1d7Yd_6	33 7/8	S	9	4437.4	67 3/4	61 3/4	0.297	0.446	HLP-22	12	4	0	1.9	10.5	5.7	30.8	16.1	0.62	0.33	p1d7	2.45	0.0001213	0.0001780	0.0002606	0.4277
7091012M	11/26A2	34S_4p1d7Yd_6	33 7/8	S	9	4437.4	67 3/4	61 3/4	0.297	0.446	HLP-22	12	4	0	1.9	10.5	5.7	30.8	16.1	0.62	0.33	p1d7	2.45	0.0001213	0.0001780	0.0002606	0.4277
7091015M	11/26A2	34S_4p1d7Yd_6	33 7/8	S	9	4437.4	67 3/4	61 3/4	0.297	0.446	HLP-22	12	4	0	1.9	10.5	5.7	30.8	16.1	0.62	0.33	p1d7	2.45	0.0001213	0.0001780	0.0002606	0.4277
7091018	11/26B1	34S_4p1d7Yc_1	33 7/8	S	9	4437.4	67 3/4	61 3/4	0.297	0.446	HLP-22	12	8	4	1.9	10.5	5.7	30.8	16.1	0.62	0.33	p1d7	2.45	0.0001213	0.0001780	0.0002606	0.4277
7091022	11/26B1	34S_4p1d7Yc_1	33 7/8	S	9	4437.4	67 3/4	61 3/4	0.297	0.446	HLP-22	12	8	4	1.9	10.5	5.7	30.8	16.1	0.62	0.33	p1d7	2.45	0.0001213	0.0001780	0.0002606	0.4277
7091025M	11/26B1	34S_4p1d7Yc_1	33 7/8	S	9	4437.4	67 3/4	61 3/4	0.297	0.446	HLP-22	12	8	4	1.9	10.5	5.7	30.8	16.1	0.62	0.33	p1d7	2.45	0.0001213	0.0001780	0.0002606	0.4277
7091027M	11/26B1	34S_4p1d7Yc_1	33 7/8	S	9	4437.4	67 3/4	61 3/4	0.297	0.446	HLP-22	12	8	4	1.9	10.5	5.7	30.8	16.1	0.62	0.33	p1d7	2.45	0.0001213	0.0001780	0.0002606	0.4277
7091030	11/26C1	34S_4p1d7Yc_0	33 7/8	S	9	4437.4	67 3/4	61 3/4	0.297	0.446	HLP-22	12	4	4	1.9	10.5	5.7	30.8	16.1	0.62	0.33	p1d7	2.45	0.0001213	0.0001780	0.0002606	0.4277
7091033	11/26C1	34S_4p1d7Yc_0	33 7/8	S	9	4437.4	67 3/4	61 3/4	0.297	0.446	HLP-22	12	4	4	1.9	10.5	5.7	30.8	16.1	0.62	0.33	p1d7	2.45	0.0001213	0.0001780	0.0002606	0.4277
7091036	11/26C1	34S_4p1d7Yc_0	33 7/8	S	9	4437.4	67 3/4	61 3/4	0.297	0.446	HLP-22	12	4	4	1.9	10.5	5.7	30.8	16.1	0.62	0.33	p1d7	2.45	0.0001213	0.0001780	0.0002606	0.4277
7091039	11/26C1	34S_4p1d7Yc_0	33 7/8	S	9	4437.4	67 3/4	61 3/4	0.297	0.446	HLP-22	12	4	4	1.9	10.5	5.7	30.8	16.1	0.62	0.33	p1d7	2.45	0.0001213	0.0001780	0.0002606	0.4277
7091042	11/26C1	34S_4p1d7Yc_0	33 7/8	S	9	4437.4	67 3/4	61 3/4	0.297	0.446	HLP-22	12	4	4	1.9	10.5	5.7	30.8	16.1	0.62	0.33	p1d7	2.45	0.0001213	0.0001780	0.0002606	0.4277
7091046M	11/26C1	34S_4p1d7Yc_0	33 7/8	S	9	4437.4	67 3/4	61 3/4	0.297	0.446	HLP-22	12	4	4	1.9	10.5	5.7	30.8	16.1	0.62	0.33	p1d7	2.45	0.0001213	0.0001780	0.0002606	0.4277
7091048M	11/26C1	34S_4p1d7Yc_0	33 7/8	S	9	4437.4	67 3/4	61 3/4	0.297	0.446	HLP-22	12	4	4	1.9	10.5	5.7	30.8	16.1	0.62	0.33	p1d7	2.45	0.0001213	0.0001780	0.0002606	0.4277
7091052	11/26D1	34S_4p1d7Yd_9	33 7/8	S	9	4437.4	67 3/4	61 3/4	0.297	0.446	HLP-22	12	0	4	1.9	10.5	5.7	30.8	16.1	0.62	0.33	p1d7	2.45	0.0001213	0.0001780	0.0002606	0.4277
7091055	11/26D2	34S_4p1d7Yc_9	33 7/8	S	9	4437.4	67 3/4	61 3/4	0.297	0.446	HLP-22	12	0	4	1.9	10.5	5.7	30.8	16.1	0.62	0.33	p1d7	2.45	0.0001213	0.0001780	0.0002606	0.4277
7091058	11/26D2	34S_4p1d7Yc_9	33 7/8	S	9	4437.4	67 3/4	61 3/4	0.297	0.446	HLP-22	12	0	4	1.9	10.5	5.7	30.8	16.1	0.62	0.33	p1d7	2.45	0.0001213	0.0001780	0.0002606	0.4277
7091063	11/26D2	34S_4p1d7Yc_9	33 7/8	S	9	4437.4	67 3/4	61 3/4	0.297	0.446	HLP-22	12	0	4	1.9	10.5	5.7	30.8	16.1	0.62	0.33	p1d7	2.45	0.0001213	0.0001780	0.0002606	0.4277
7091065	11/26D2	34S_4p1d7Yc_9	33 7/8	S	9	4437.4	67 3/4	61 3/4	0.297	0.446	HLP-22	12	0	4	1.9	10.5	5.7	30.8	16.1	0.62	0.33	p1d7	2.45	0.0001213	0.0001780	0.0002606	0.4277
7091070	11/26D2	34S_4p1d7Yc_9	33 7/8	S	9	4437.4	67 3/4	61 3/4	0.297	0.446	HLP-22	12	0	4	1.9	10.5	5.7	30.8	16.1	0.62	0.33	p1d7	2.45	0.0001213	0.0001780	0.0002606	0.4277
7091075M	11/26D2	34S_4p1d7Yc_9	33 7/8	S	9	4437.4	67 3/4	61 3/4	0.297	0.446	HLP-22	12	0	4	1.9	10.5	5.7	30.8	16.1	0.62	0.33	p1d7	2.45	0.0001213	0.0001780	0.0002606	0.4277
7091077M	11/26D2	34S_4p1d7Yc_9	33 7/8	S	9	4437.4	67 3/4	61 3/4	0.297	0.446	HLP-22	12	0	4	1.9	10.5	5.7	30.8	16.1	0.62	0.33	p1d7	2.45	0.0001213	0.0001780	0.0002606	0.4277
7091081M	11/26D2	34S_4p1d7Yc_9	33 7/8	S	9	4437.4	67 3/4	61 3/4	0.297	0.446	HLP-22	12	0	4	1.9	10.5	5.7	30.8	16.1	0.62	0.33	p1d7	2.45	0.0001213	0.0001780	0.0002606	0.4277
7091085	11/27A1	34S_4p1d7Yc_6	33 7/8	S	9	4437.4	67 3/4	61 3/4	0.297	0.446	HLP-22	12	4	0	1.9	10.5	5.7	30.8	16.1	0.62	0.33	p1d7	2.45	0.0001213	0.0001780	0.0002606	0.4277
7091088	11/27A1	34S_4p1d7Yc_6	33 7/8	S	9	4437.4	67 3/4	61 3/4	0.297	0.446	HLP-22	12	4	0	1.9	10.5	5.7	30.8	16.1	0.62	0.33	p1d7	2.45	0.0001213	0.0001780	0.0002606	0.4277
7091091	11/27A1	34S_4p1d7Yc_6	33 7/8	S	9	4437.4	67 3/4	61 3/4	0.297	0.446	HLP-22	12	4	0	1.9	10.5	5.7	30.8	16.1	0.62	0.33	p1d7	2.45	0.0001213	0.0001780	0.0002606	0.4277
7091095M	11/27A1	34S_4p1d7Yc_6	33 7/8	S	9	4437.4	67 3/4	61 3/4	0.297	0.446	HLP-22	12	4	0	1.9	10.5	5.7	30.8	16.1	0.62	0.33	p1d7	2.45	0.0001213	0.0001780	0.0002606	0.4277
7091097M	11/27A1	34S_4p1d7Yc_6	33 7/8	S	9	4437.4	67 3/4	61 3/4	0.297	0.446	HLP-22	12	4	0	1.9	10.5	5.7	30.8	16.1	0.62	0.33	p1d7	2.45	0.0001213	0.0001780	0.0002606	0.4277
7091100	11/27B1	34S_4p1d7Ya-80	33 7/8	S	9	4437.4	67 3/4	61 3/4	0.297	0.446	HLP-22	12	8	0	1.9	10.5	5.7	30.8	16.1	0.62	0.33	p1d7	2.45	0.0001213	0.0001780	0.0002606	0.4277
7091103	11/27B1	34S_4p1d7Ya-80	33 7/8	S	9	4437.4	67 3/4	61 3/4	0.297	0.446	HLP-22	12	8	0	1.9	10.5	5.7	30.8	16.1	0.62	0.33	p1d7	2.45	0.0001213	0.0001780	0.0002606	0.4277
7091106	11/27B1	34S_4p1d7Ya-80	33 7/8	S	9	4437.4	67 3/4	61 3/4	0.297	0.446	HLP-22	12	8	0	1.9	10.5	5.7	30.8	16.1	0.62	0.33	p1d7	2.45	0.0001213	0.0001780	0.0002606	0.4277
7091109	11/27B1	34S_4p1d7Ya-80	33 7/8	S	9	4437.4	67 3/4	61 3/4	0.297	0.446	HLP-22	12	8	0	1.9	10.5	5.7	30.8	16.1	0.62	0.33	p1d7	2.45	0.0001213	0.0001780	0.0002606	0.4277
7091113	11/27B1	34S_4p1d7Ya-80	33 7/8	S	9	4437.4	67 3/4	61 3/4	0.297	0.446	HLP-22	12	8	0	1.9	10.5	5.7	30.8	16.1	0.62	0.33	p1d7	2.45	0.0001213	0.0001780	0.0002606	0.4277
7091115	11/27B1	34S_4p1d7Ya-80	33 7/8	S	9	4437.4	67 3/4	61 3/4	0.297	0.446	HLP-22	12	8	0	1.9	10.5	5.7	30.8	16.1	0.62	0.33	p1d7	2.45	0.0001213	0.0001780	0.0002606	0.4277
7091118	11/27B2	34S_4p1d7Yd_5	33 7/8	S	9	4437.4	67 3/4	61 3/4	0.297	0.446	HLP-22	12	8	0	1.9	10.5	5.7	30.8	16.1	0.62	0.33	p1d7	2.45	0.0001213	0.0001780	0.0002606	0.4277
7091121	11/27B2	34S_4p1d7Yd_5	33 7/8	S	9	4437.4	67 3/4	61 3/4	0.297	0.446	HLP-22	12	8	0	1.9	10.5	5.7	30.8	16.1	0.62	0.33	p1d7	2.45	0.0001213	0.0001780	0.0002606	0.4277
7091124	11/27B2	34S_4p1d7Yd_5	33 7/8	S	9	4437.4	67 3/4	61 3/4	0.297	0.446	HLP-22	12	8	0	1.9	10.5	5.7	30.8	16.1	0.62	0.33	p1d7	2.45	0.0001213	0.0001780	0.0002606	0.4277
7091127	11/27B2	34S_4p1d7Yd_5	33 7/8	S	9	4437.4	67 3/4	61 3/4	0.297	0.446	HLP-22	12	8	0	1.9	10.5	5.7	30.8	16.1	0.62	0.33	p1d7	2.45	0.0001213	0.0001780	0.0002606	0.4277

Table B.9. Updated Data from Fall 2007 Tests in Mid-Scale Vessel with Spherical Head B.9

Tank Water Temperature	Water Density	Solids Fraction	Pulse Volume Fraction	Duty Cycle	Cycle Time	Pulsed or Steady Jet	Us Steady Jet	U1 Pulsing Jet	U2 URMS	U3 URM3	Discharge Velocity	Critical Suspension Velocity	Average Peak Cloud Height	U_{CS} Condition	U_{CS} Method	U_{CS} Flag	U_{CS} Center Flag	U_{CS} udv Flag	U_{CS} based on Decreasing Velocity	Sweep Increase / Decrease	UDV Height Bed	Particle Motion	Solids Level	Outer Bottom Pattern	Inner Bottom Pattern	Case ID	Test	TDP	Row Number
C	g/cm³	fraction	fraction	fraction	s	text	m/s	m/s	m/s	m/s	m/s	m/s	in.	m/s	text	text	text	text	m/s	text	mm	text	text	text	text	text	text	text	text
T	ρ_l	ϕ_S	ϕ_p	DC	t_C	Jet	US	U1	U2	U3	U	U_{CS}	H_C	U_{CSR}	U_{CSM}	U_{CS}vis	U_{CS}cen	U_{CS}udv	U_{CS_D}	S_W	H_{bed}	PM	Sol	SP_O	SP_I	ID	M/DDX	TDP	MSS
20.5	0.999	0.00487	undefined	1.000	infinite	S	10.60	N/A	N/A	N/A	10.50	9.50	26.75	N/A	N/A	N/A	N/A	N/A	N/A	I	N/A	BC	N/A	N/A	N/A	34S_4p1d7Ya-40	11/26A1	TDP-WTP-064	7091000
21.0	0.999	0.00487	0.049	0.180	0.0	P	N/A	10.05	10.34	10.66	9.50	10.50	N/A	N/A	N/A	N/A	N/A	N/A	N/A	D	N/A	SS+	N/A	N/A	N/A	34S_4p1d7Yd_6	11/26A2	TDP-WTP-064	7091003
21.0	0.999	0.00487	0.052	0.180	0.0	P	N/A	10.59	10.86	11.17	10.00	10.50	9.50	N/A	N/A	N/A	N/A	N/A	N/A	I	N/A	AM	N/A	N/A	N/A	34S_4p1d7Yd_6	11/26A2	TDP-WTP-064	7091006
21.0	0.999	0.00487	0.052	0.180	0.0	P	N/A	11.15	11.39	11.71	10.50	10.50	12.50	10.50	vis	UCSvis	N/A	N/A	N/A	I	N/A	CS	N/A	N/A	N/A	34S_4p1d7Yd_6	11/26A2	TDP-WTP-064	7091010
21.0	0.999	0.00487	0.052	0.180	0.0	P	N/A	11.50	11.81	12.16	11.00	10.50	15.00	N/A	N/A	N/A	N/A	N/A	N/A	I	N/A	BC-	N/A	N/A	N/A	34S_4p1d7Yd_6	11/26A2	TDP-WTP-064	7091012
21.0	0.999	0.00487	0.051	0.180	0.0	P	N/A	12.21	12.55	12.94	11.50	10.50	16.50	N/A	N/A	N/A	N/A	N/A	N/A	I	N/A	BC	N/A	N/A	N/A	34S_4p1d7Yd_6	11/26A2	TDP-WTP-064	7091015
21.0	0.999	0.00487	0.046	0.330	0.0	P	N/A	4.92	5.00	5.03	5.00	6.50	N/A	N/A	N/A	N/A	N/A	N/A	N/A	D	N/A	SS	N/A	N/A	N/A	34S_4p1d7Yc_1	11/26B1	TDP-WTP-064	7091018
21.0	0.999	0.00487	0.052	0.330	0.0	P	N/A	5.90	5.99	6.03	6.00	6.50	9.25	N/A	N/A	N/A	N/A	N/A	N/A	I	N/A	AM	N/A	N/A	N/A	34S_4p1d7Yc_1	11/26B1	TDP-WTP-064	7091022
21.0	0.999	0.00487	0.051	0.330	0.0	P	N/A	6.31	6.43	6.49	6.50	6.50	9.75	6.50	vis	UCSvis	N/A	N/A	N/A	I	N/A	CS	N/A	N/A	N/A	34S_4p1d7Yc_1	11/26B1	TDP-WTP-064	7091025
21.0	0.999	0.00487	0.051	0.330	0.0	P	N/A	6.82	6.96	7.02	7.00	6.50	11.25	N/A	N/A	N/A	N/A	N/A	N/A	I	N/A	BC	N/A	N/A	N/A	34S_4p1d7Yc_1	11/26B1	TDP-WTP-064	7091027
21.0	0.999	0.00487	0.051	0.330	0.0	P	N/A	6.12	6.20	6.25	6.00	11.00	N/A	N/A	N/A	N/A	UCScen	N/A	N/A	I	N/A	AM-	N/A	N/A	N/A	34S_4p1d7Yc_0	11/26C1	TDP-WTP-064	7091030
21.0	0.999	0.00487	0.051	0.330	0.0	P	N/A	7.04	7.17	7.24	7.00	11.00	9.25	N/A	N/A	N/A	N/A	N/A	N/A	I	N/A	AM	N/A	N/A	N/A	34S_4p1d7Yc_0	11/26C1	TDP-WTP-064	7091033
21.0	0.999	0.00487	0.051	0.330	0.0	P	N/A	8.06	8.21	8.30	8.00	11.00	11.25	N/A	N/A	N/A	N/A	N/A	N/A	I	N/A	AM	N/A	N/A	N/A	34S_4p1d7Yc_0	11/26C1	TDP-WTP-064	7091036
21.0	0.999	0.00487	0.051	0.330	0.0	P	N/A	9.15	9.48	9.65	9.00	11.00	15.00	N/A	N/A	N/A	N/A	N/A	N/A	I	N/A	AM	N/A	N/A	N/A	34S_4p1d7Yc_0	11/26C1	TDP-WTP-064	7091039
21.0	0.999	0.00487	0.051	0.330	0.0	P	N/A	9.36	9.89	10.15	10.00	11.00	18.00	N/A	N/A	N/A	N/A	N/A	N/A	I	N/A	AM+	N/A	N/A	N/A	34S_4p1d7Yc_0	11/26C1	TDP-WTP-064	7091042
21.0	0.999	0.00487	0.051	0.330	0.0	P	N/A	9.83	10.60	10.97	11.00	11.00	21.25	11.00	vis	UCSvis	N/A	N/A	N/A	I	N/A	CS	N/A	N/A	N/A	34S_4p1d7Yc_0	11/26C1	TDP-WTP-064	7091046
21.0	0.999	0.00487	0.052	0.330	0.0	P	N/A	10.81	11.69	12.11	12.00	11.00	27.00	N/A	N/A	N/A	N/A	N/A	N/A	I	N/A	BC	N/A	N/A	N/A	34S_4p1d7Yc_0	11/26C1	TDP-WTP-064	7091048
22.0	0.999	0.00487	0.057	0.180	0.0	P	N/A	5.90	6.04	6.22	5.70	N/A	N/A	N/A	N/A	N/A	UCScen	N/A	N/A	N/A	N/A	SS	N/A	N/A	N/A	34S_4p1d7Yd_9	11/26D1	TDP-WTP-064	7091052
22.0	0.999	0.00487	0.051	0.330	0.0	P	N/A	6.03	6.17	6.35	5.70	13.00	N/A	N/A	N/A	N/A	UCScen	N/A	N/A	I	N/A	SS	N/A	N/A	N/A	34S_4p1d7Yc_9	11/26D2	TDP-WTP-064	7091055
22.0	0.999	0.00487	0.050	0.330	0.0	P	N/A	7.14	7.30	7.52	7.00	13.00	8.75	N/A	N/A	N/A	N/A	N/A	N/A	I	N/A	SS	N/A	N/A	N/A	34S_4p1d7Yc_9	11/26D2	TDP-WTP-064	7091058
22.0	0.999	0.00487	0.050	0.330	0.0	P	N/A	9.23	9.46	9.75	9.00	13.00	12.67	N/A	N/A	N/A	N/A	N/A	N/A	I	N/A	SS	N/A	N/A	N/A	34S_4p1d7Yc_9	11/26D2	TDP-WTP-064	7091063
22.0	0.999	0.00487	0.050	0.330	0.0	P	N/A	11.52	11.83	12.19	11.00	13.00	18.17	N/A	N/A	N/A	N/A	N/A	N/A	I	N/A	AM	N/A	N/A	N/A	34S_4p1d7Yc_9	11/26D2	TDP-WTP-064	7091065
22.0	0.999	0.00487	0.050	0.330	0.0	P	N/A	12.48	12.83	13.24	12.00	13.00	20.00	N/A	N/A	N/A	N/A	N/A	N/A	I	N/A	AM+	N/A	N/A	N/A	34S_4p1d7Yc_9	11/26D2	TDP-WTP-064	7091070
22.0	0.999	0.00487	0.050	0.330	0.0	P	N/A	13.47	13.86	14.30	13.00	13.00	21.33	13.00	vis	UCSvis	N/A	N/A	N/A	I	N/A	CS	N/A	N/A	N/A	34S_4p1d7Yc_9	11/26D2	TDP-WTP-064	7091075
22.0	0.999	0.00487	0.050	0.330	0.0	P	N/A	14.59	15.03	15.54	14.00	13.00	23.83	N/A	N/A	N/A	N/A	N/A	N/A	I	N/A	BC-	N/A	N/A	N/A	34S_4p1d7Yc_9	11/26D2	TDP-WTP-064	7091077
22.0	0.999	0.00487	0.050	0.330	0.0	P	N/A	15.48	16.07	16.67	15.00	13.00	28.83	N/A	N/A	N/A	N/A	N/A	N/A	I	N/A	BC	N/A	N/A	N/A	34S_4p1d7Yc_9	11/26D2	TDP-WTP-064	7091081
22.0	0.999	0.00487	0.052	0.330	0.0	P	N/A	9.50	9.75	10.06	9.00	11.00	8.50	N/A	N/A	N/A	N/A	N/A	N/A	I	N/A	SS	N/A	N/A	N/A	34S_4p1d7Yc_6	11/27A1	TDP-WTP-065	7091085
22.0	0.999	0.00487	0.051	0.330	0.0	P	N/A	10.63	10.89	11.24	10.00	11.00	10.00	N/A	N/A	N/A	N/A	N/A	N/A	I	N/A	AM	N/A	N/A	N/A	34S_4p1d7Yc_6	11/27A1	TDP-WTP-065	7091088
22.0	0.999	0.00487	0.051	0.330	0.0	P	N/A	11.08	11.39	11.77	10.50	11.00	11.50	N/A	N/A	N/A	UCScen	N/A	N/A	I	N/A	AM+	N/A	N/A	N/A	34S_4p1d7Yc_6	11/27A1	TDP-WTP-065	7091091
22.0	0.999	0.00487	0.051	0.330	0.0	P	N/A	11.77	12.08	12.47	11.00	11.00	14.25	11.00	vis	UCSvis	N/A	N/A	N/A	I	N/A	CS	N/A	N/A	N/A	34S_4p1d7Yc_6	11/27A1	TDP-WTP-065	7091095
22.0	0.999	0.00487	0.051	0.330	0.0	P	N/A	12.68	13.01	13.44	12.00	11.00	20.00	N/A	N/A	N/A	N/A	N/A	N/A	I	N/A	BC	N/A	N/A	N/A	34S_4p1d7Yc_6	11/27A1	TDP-WTP-065	7091097
21.9	0.999	0.00487	undefined	1.000	infinite	S	7.57	N/A	N/A	N/A	7.50	9.50	8.75	N/A	N/A	N/A	N/A	N/A	N/A	N/A	N/A	SS	N/A	N/A	N/A	34S_4p1d7Ya-80	11/27B1	TDP-WTP-065	7091100
21.8	0.999	0.00487	undefined	1.000	infinite	S	8.11	N/A	N/A	N/A	8.00	9.50	9.00	N/A	N/A	N/A	N/A	N/A	N/A	I	N/A	SS	N/A	N/A	N/A	34S_4p1d7Ya-80	11/27B1	TDP-WTP-065	7091103
21.8	0.999	0.00487	undefined	1.000	infinite	S	8.53	N/A	N/A	N/A	8.50	9.50	10.50	N/A	N/A	N/A	N/A	N/A	N/A	I	N/A	SS	N/A	N/A	N/A	34S_4p1d7Ya-80	11/27B1	TDP-WTP-065	7091106
21.9	0.999	0.00487	undefined	1.000	infinite	S	9.06	N/A	N/A	N/A	9.00	9.50	18.63	N/A	N/A	N/A	N/A	N/A	N/A	I	N/A	AM	N/A	N/A	N/A	34S_4p1d7Ya-80	11/27B1	TDP-WTP-065	7091109
21.9	0.999	0.00487	undefined	1.000	infinite	S	9.57	N/A	N/A	N/A	9.50	9.50	29.25	9.50	vis	UCSvis	N/A	N/A	N/A	I	N/A	CS	N/A	N/A	N/A	34S_4p1d7Ya-80	11/27B1	TDP-WTP-065	7091113
21.8	0.999	0.00487	undefined	1.000	infinite	S	10.01	N/A	N/A	N/A	10.00	9.50	38.50	N/A	N/A	N/A	N/A	N/A	N/A	I	N/A	BC	N/A	N/A	N/A	34S_4p1d7Ya-80	11/27B1	TDP-WTP-065	7091115
22.0	0.999	0.00487	0.053	0.180	0.0	P	N/A	7.06	7.15	7.20	7.00	10.00	9.00	N/A	N/A	N/A	N/A	N/A	N/A	N/A	N/A	SS	N/A	N/A	N/A	34S_4p1d7Yd_5	11/27B2	TDP-WTP-065	7091118
22.0	0.999	0.00487	0.051	0.180	0.0	P	N/A	8.09	8.22	8.28	8.00	10.00	11.75	N/A	N/A	N/A	N/A	N/A	N/A	I	N/A	SS	N/A	N/A	N/A	34S_4p1d7Yd_5	11/27B2	TDP-WTP-065	7091121
22.0	0.999	0.00487	0.054	0.180	0.0	P	N/A	9.72	9.88	9.96	9.00	10.00	17.00	N/A	N/A	N/A	N/A	N/A	N/A	I	N/A	SS+	N/A	N/A	N/A	34S_4p1d7Yd_5	11/27B2	TDP-WTP-065	7091124
22.0	0.999	0.00487	0.052	0.180	0.0	P	N/A	9.57	9.90	10.07	9.50	10.00	19.25	N/A	N/A	N/A	N/A	N/A	N/A	I	N/A	AM	N/A	N/A	N/A	34S_4p1d7Yd_5	11/27B2	TDP-WTP-065	7091127

Table B.9. Updated Data from Fall 2007 Tests in Mid-Scale Vessel with Spherical Head A.10

Row Number	Test	Case ID	Tank Diameter	Head Shape	Dish Height	Dish Volume	Tank Fill Height	Return Line Height	Nozzle Inner Diameter	Nozzle Stand-off Distance	Pulse Tube Configuration	Installed Nozzles	Outer Nozzles Operated	Inner Nozzles Operated	Pulse Tube Outer Diameter	Outer PJM Radius	Inner PJM Radius	"FIO" Outer PJM Impingement Angle	"FIO" Inner PJM Impingement Angle	Ratio Outer PJM to Tank Radius	Ratio Inner PJM to Tank Radius	Simulant	Solids Density	Particle Diameter d5	Particle Diameter d50	Particle Diameter d95	Void Fraction
text	text	text	in.	text	in.	in. ^{3}	in.	in.	in.	in.	text	number	number	number	in.	in.	in.	deg	deg	nondim	nondim	text	g/cm^3	m	m	m	fraction
MSS	M/DDX	ID	D	HS	H_{dish}	V_{dish}	H	Rtn	d	sod	PT	N	N_O	N_I	PT_{od}	R_O	R_I	Θ_O	Θ_I	R_O/R	R_I/R	sxdx	ρ_S	d_5	d_{50}	d_{95}	vf
7091131M	11/27B2	34S_4p1d7Yd_5	33 7/8	S	9	4437.4	67 3/4	61 3/4	0.297	0.446	HLP-22	12	8	0	1.9	10.5	5.7	30.8	16.1	0.62	0.33	p1d7	2.45	0.0001213	0.0001780	0.0002606	0.4277
7091134M	11/27B2	34S_4p1d7Yd_5	33 7/8	S	9	4437.4	67 3/4	61 3/4	0.297	0.446	HLP-22	12	8	0	1.9	10.5	5.7	30.8	16.1	0.62	0.33	p1d7	2.45	0.0001213	0.0001780	0.0002606	0.4277
7091136M	11/27B2	34S_4p1d7Yd_5	33 7/8	S	9	4437.4	67 3/4	61 3/4	0.297	0.446	HLP-22	12	8	0	1.9	10.5	5.7	30.8	16.1	0.62	0.33	p1d7	2.45	0.0001213	0.0001780	0.0002606	0.4277
7091139	11/27B3	34S_4p1d7Yc_5	33 7/8	S	9	4437.4	67 3/4	61 3/4	0.297	0.446	HLP-22	12	8	0	1.9	10.5	5.7	30.8	16.1	0.62	0.33	p1d7	2.45	0.0001213	0.0001780	0.0002606	0.4277
7091142	11/27B3	34S_4p1d7Yc_5	33 7/8	S	9	4437.4	67 3/4	61 3/4	0.297	0.446	HLP-22	12	8	0	1.9	10.5	5.7	30.8	16.1	0.62	0.33	p1d7	2.45	0.0001213	0.0001780	0.0002606	0.4277
7091145	11/27B3	34S_4p1d7Yc_5	33 7/8	S	9	4437.4	67 3/4	61 3/4	0.297	0.446	HLP-22	12	8	0	1.9	10.5	5.7	30.8	16.1	0.62	0.33	p1d7	2.45	0.0001213	0.0001780	0.0002606	0.4277
7091149M	11/27B3	34S_4p1d7Yc_5	33 7/8	S	9	4437.4	67 3/4	61 3/4	0.297	0.446	HLP-22	12	8	0	1.9	10.5	5.7	30.8	16.1	0.62	0.33	p1d7	2.45	0.0001213	0.0001780	0.0002606	0.4277
7091151M	11/27B3	34S_4p1d7Yc_5	33 7/8	S	9	4437.4	67 3/4	61 3/4	0.297	0.446	HLP-22	12	8	0	1.9	10.5	5.7	30.8	16.1	0.62	0.33	p1d7	2.45	0.0001213	0.0001780	0.0002606	0.4277
7091154	11/30A1	34S_4p1d8Ya	33 7/8	S	9	4437.4	67 3/4	61 3/4	0.297	0.446	HLP-22	12	8	4	1.9	10.5	5.7	30.8	16.1	0.62	0.33	p1d8	2.45	0.0000605	0.0000895	0.0001320	0.4269
7091158	11/30A1	34S_4p1d8Ya	33 7/8	S	9	4437.4	67 3/4	61 3/4	0.297	0.446	HLP-22	12	8	4	1.9	10.5	5.7	30.8	16.1	0.62	0.33	p1d8	2.45	0.0000605	0.0000895	0.0001320	0.4269
7091161	11/30A1	34S_4p1d8Ya	33 7/8	S	9	4437.4	67 3/4	61 3/4	0.297	0.446	HLP-22	12	8	4	1.9	10.5	5.7	30.8	16.1	0.62	0.33	p1d8	2.45	0.0000605	0.0000895	0.0001320	0.4269
7091164	11/30A1	34S_4p1d8Ya	33 7/8	S	9	4437.4	67 3/4	61 3/4	0.297	0.446	HLP-22	12	8	4	1.9	10.5	5.7	30.8	16.1	0.62	0.33	p1d8	2.45	0.0000605	0.0000895	0.0001320	0.4269
7091167	11/30A1	34S_4p1d8Ya	33 7/8	S	9	4437.4	67 3/4	61 3/4	0.297	0.446	HLP-22	12	8	4	1.9	10.5	5.7	30.8	16.1	0.62	0.33	p1d8	2.45	0.0000605	0.0000895	0.0001320	0.4269
7091169	11/30A1	34S_4p1d8Ya	33 7/8	S	9	4437.4	67 3/4	61 3/4	0.297	0.446	HLP-22	12	8	4	1.9	10.5	5.7	30.8	16.1	0.62	0.33	p1d8	2.45	0.0000605	0.0000895	0.0001320	0.4269
7091172	11/30A2	34S_4p1d8Yd_1	33 7/8	S	9	4437.4	67 3/4	61 3/4	0.297	0.446	HLP-22	12	8	4	1.9	10.5	5.7	30.8	16.1	0.62	0.33	p1d8	2.45	0.0000605	0.0000895	0.0001320	0.4269
7091175	11/30A2	34S_4p1d8Yd_1	33 7/8	S	9	4437.4	67 3/4	61 3/4	0.297	0.446	HLP-22	12	8	4	1.9	10.5	5.7	30.8	16.1	0.62	0.33	p1d8	2.45	0.0000605	0.0000895	0.0001320	0.4269
7091178	11/30A2	34S_4p1d8Yd_1	33 7/8	S	9	4437.4	67 3/4	61 3/4	0.297	0.446	HLP-22	12	8	4	1.9	10.5	5.7	30.8	16.1	0.62	0.33	p1d8	2.45	0.0000605	0.0000895	0.0001320	0.4269
7091181	11/30A2	34S_4p1d8Yd_1	33 7/8	S	9	4437.4	67 3/4	61 3/4	0.297	0.446	HLP-22	12	8	4	1.9	10.5	5.7	30.8	16.1	0.62	0.33	p1d8	2.45	0.0000605	0.0000895	0.0001320	0.4269
7091185M	11/30A2	34S_4p1d8Yd_1	33 7/8	S	9	4437.4	67 3/4	61 3/4	0.297	0.446	HLP-22	12	8	4	1.9	10.5	5.7	30.8	16.1	0.62	0.33	p1d8	2.45	0.0000605	0.0000895	0.0001320	0.4269
7091187M	11/30A2	34S_4p1d8Yd_1	33 7/8	S	9	4437.4	67 3/4	61 3/4	0.297	0.446	HLP-22	12	8	4	1.9	10.5	5.7	30.8	16.1	0.62	0.33	p1d8	2.45	0.0000605	0.0000895	0.0001320	0.4269
7091191	11/30B1	34S_4p1d8Yc_1	33 7/8	S	9	4437.4	67 3/4	61 3/4	0.297	0.446	HLP-22	12	8	4	1.9	10.5	5.7	30.8	16.1	0.62	0.33	p1d8	2.45	0.0000605	0.0000895	0.0001320	0.4269
7091193	11/30B1	34S_4p1d8Yc_1	33 7/8	S	9	4437.4	67 3/4	61 3/4	0.297	0.446	HLP-22	12	8	4	1.9	10.5	5.7	30.8	16.1	0.62	0.33	p1d8	2.45	0.0000605	0.0000895	0.0001320	0.4269
7091197	11/30B1	34S_4p1d8Yc_1	33 7/8	S	9	4437.4	67 3/4	61 3/4	0.297	0.446	HLP-22	12	8	4	1.9	10.5	5.7	30.8	16.1	0.62	0.33	p1d8	2.45	0.0000605	0.0000895	0.0001320	0.4269
7091200M	11/30B1	34S_4p1d8Yc_1	33 7/8	S	9	4437.4	67 3/4	61 3/4	0.297	0.446	HLP-22	12	8	4	1.9	10.5	5.7	30.8	16.1	0.62	0.33	p1d8	2.45	0.0000605	0.0000895	0.0001320	0.4269
7091202M	11/30B1	34S_4p1d8Yc_1	33 7/8	S	9	4437.4	67 3/4	61 3/4	0.297	0.446	HLP-22	12	8	4	1.9	10.5	5.7	30.8	16.1	0.62	0.33	p1d8	2.45	0.0000605	0.0000895	0.0001320	0.4269
7091206	11/30C1	34S_4p1d8Ya-44	33 7/8	S	9	4437.4	67 3/4	61 3/4	0.297	0.446	HLP-22	12	4	4	1.9	10.5	5.7	30.8	16.1	0.62	0.33	p1d8	2.45	0.0000605	0.0000895	0.0001320	0.4269
7091209	11/30C1	34S_4p1d8Ya-44	33 7/8	S	9	4437.4	67 3/4	61 3/4	0.297	0.446	HLP-22	12	4	4	1.9	10.5	5.7	30.8	16.1	0.62	0.33	p1d8	2.45	0.0000605	0.0000895	0.0001320	0.4269
7091212	11/30C1	34S_4p1d8Ya-44	33 7/8	S	9	4437.4	67 3/4	61 3/4	0.297	0.446	HLP-22	12	4	4	1.9	10.5	5.7	30.8	16.1	0.62	0.33	p1d8	2.45	0.0000605	0.0000895	0.0001320	0.4269
7091215	11/30C1	34S_4p1d8Ya-44	33 7/8	S	9	4437.4	67 3/4	61 3/4	0.297	0.446	HLP-22	12	4	4	1.9	10.5	5.7	30.8	16.1	0.62	0.33	p1d8	2.45	0.0000605	0.0000895	0.0001320	0.4269
7091217	11/30C1	34S_4p1d8Ya-44	33 7/8	S	9	4437.4	67 3/4	61 3/4	0.297	0.446	HLP-22	12	4	4	1.9	10.5	5.7	30.8	16.1	0.62	0.33	p1d8	2.45	0.0000605	0.0000895	0.0001320	0.4269
7091221	11/30C1	34S_4p1d8Ya-44	33 7/8	S	9	4437.4	67 3/4	61 3/4	0.297	0.446	HLP-22	12	4	4	1.9	10.5	5.7	30.8	16.1	0.62	0.33	p1d8	2.45	0.0000605	0.0000895	0.0001320	0.4269
7091224	11/30C2	34S_4p1d8Yd_0	33 7/8	S	9	4437.4	67 3/4	61 3/4	0.297	0.446	HLP-22	12	4	4	1.9	10.5	5.7	30.8	16.1	0.62	0.33	p1d8	2.45	0.0000605	0.0000895	0.0001320	0.4269
7091226	11/30C2	34S_4p1d8Yd_0	33 7/8	S	9	4437.4	67 3/4	61 3/4	0.297	0.446	HLP-22	12	4	4	1.9	10.5	5.7	30.8	16.1	0.62	0.33	p1d8	2.45	0.0000605	0.0000895	0.0001320	0.4269
7091229	11/30C2	34S_4p1d8Yd_0	33 7/8	S	9	4437.4	67 3/4	61 3/4	0.297	0.446	HLP-22	12	4	4	1.9	10.5	5.7	30.8	16.1	0.62	0.33	p1d8	2.45	0.0000605	0.0000895	0.0001320	0.4269
7091232	11/30C2	34S_4p1d8Yd_0	33 7/8	S	9	4437.4	67 3/4	61 3/4	0.297	0.446	HLP-22	12	4	4	1.9	10.5	5.7	30.8	16.1	0.62	0.33	p1d8	2.45	0.0000605	0.0000895	0.0001320	0.4269
7091236	11/30C2	34S_4p1d8Yd_0	33 7/8	S	9	4437.4	67 3/4	61 3/4	0.297	0.446	HLP-22	12	4	4	1.9	10.5	5.7	30.8	16.1	0.62	0.33	p1d8	2.45	0.0000605	0.0000895	0.0001320	0.4269
7091240	11/30C2	34S_4p1d8Yd_0	33 7/8	S	9	4437.4	67 3/4	61 3/4	0.297	0.446	HLP-22	12	4	4	1.9	10.5	5.7	30.8	16.1	0.62	0.33	p1d8	2.45	0.0000605	0.0000895	0.0001320	0.4269
7091243	11/30C2	34S_4p1d8Yd_0	33 7/8	S	9	4437.4	67 3/4	61 3/4	0.297	0.446	HLP-22	12	4	4	1.9	10.5	5.7	30.8	16.1	0.62	0.33	p1d8	2.45	0.0000605	0.0000895	0.0001320	0.4269
7091246	11/30C2	34S_4p1d8Yd_0	33 7/8	S	9	4437.4	67 3/4	61 3/4	0.297	0.446	HLP-22	12	4	4	1.9	10.5	5.7	30.8	16.1	0.62	0.33	p1d8	2.45	0.0000605	0.0000895	0.0001320	0.4269
7091249	11/30C2	34S_4p1d8Yd_0	33 7/8	S	9	4437.4	67 3/4	61 3/4	0.297	0.446	HLP-22	12	4	4	1.9	10.5	5.7	30.8	16.1	0.62	0.33	p1d8	2.45	0.0000605	0.0000895	0.0001320	0.4269
7091253M	11/30C2	34S_4p1d8Yd_0	33 7/8	S	9	4437.4	67 3/4	61 3/4	0.297	0.446	HLP-22	12	4	4	1.9	10.5	5.7	30.8	16.1	0.62	0.33	p1d8	2.45	0.0000605	0.0000895	0.0001320	0.4269

Table B.9. Updated Data from Fall 2007 Tests in Mid-Scale Vessel with Spherical Head B.10

Tank Water Temperature	Water Density	Solids Fraction	Pulse Volume Fraction	Duty Cycle	Cycle Time	Pulsed or Steady Jet	Us Steady Jet	U1 Pulsing Jet	U2 URMS	U3 URM3	Discharge Velocity	Critical Suspension Velocity	Average Peak Cloud Height	UCS Condition	UCS Method	UCS Flag	UCS Center Flag	UCS udv Flag	UCS based on Decreasing Velocity	Sweep Increase / Decrease	UDV Height Bed	Particle Motion	Solids Level	Outer Bottom Pattern	Inner Bottom Pattern	Case ID	Test	TDP	Row Number
C	g/cm3	fraction	fraction	fraction	s	text	m/s	m/s	m/s	m/s	m/s	m/s	in.	m/s	text	text	text	text	m/s	text	mm	text	text	text	text	text	text	text	text
T	rl	fS	fp	DC	tC	Jet	US	U1	U2	U3	U	UCS	HC	UCSR	UCSM	UCSvis	UCScen	UCSudv	UCS_D	SW	Hbed	PM	Sol	SPO	SPI	ID	M/DDX	TDP	MSS
22.0	0.999	0.00487	0.052	0.180	0.0	P	N/A	9.72	10.20	10.44	10.00	10.00	21.25	10.00	vis	UCSvis	N/A	N/A	N/A	I	N/A	CS	N/A	N/A	N/A	34S_4p1d7Yd_5	11/27B2	TDP-WTP-065	7091131
22.0	0.999	0.00487	0.051	0.180	0.0	P	N/A	9.73	10.32	10.60	10.50	10.00	21.75	N/A	N/A	N/A	N/A	N/A	N/A	I	N/A	BC-	N/A	N/A	N/A	34S_4p1d7Yd_5	11/27B2	TDP-WTP-065	7091134
22.0	0.999	0.00487	0.051	0.180	0.0	P	N/A	9.89	10.59	10.92	11.00	10.00	23.25	N/A	N/A	N/A	N/A	N/A	N/A	I	N/A	BC	N/A	N/A	N/A	34S_4p1d7Yd_5	11/27B2	TDP-WTP-065	7091136
22.0	0.999	0.00487	0.051	0.330	0.0	P	N/A	7.99	8.14	8.22	8.00	10.00	12.25	N/A	N/A	N/A	N/A	N/A	N/A	I	N/A	SS	N/A	N/A	N/A	34S_4p1d7Yc_5	11/27B3	TDP-WTP-065	7091139
22.0	0.999	0.00487	0.056	0.330	0.0	P	N/A	9.99	10.19	10.29	9.00	10.00	16.25	N/A	N/A	N/A	N/A	N/A	N/A	I	N/A	SS+	N/A	N/A	N/A	34S_4p1d7Yc_5	11/27B3	TDP-WTP-065	7091142
22.0	0.999	0.00487	0.051	0.330	0.0	P	N/A	9.45	9.70	9.84	9.50	10.00	19.50	N/A	N/A	N/A	N/A	N/A	N/A	I	N/A	AM	N/A	N/A	N/A	34S_4p1d7Yc_5	11/27B3	TDP-WTP-065	7091145
22.0	0.999	0.00487	0.050	0.330	0.0	P	N/A	9.86	10.14	10.28	10.00	10.00	21.25	10.00	vis	UCSvis	N/A	N/A	N/A	I	N/A	CS	N/A	N/A	N/A	34S_4p1d7Yc_5	11/27B3	TDP-WTP-065	7091149
22.0	0.999	0.00487	0.050	0.330	0.0	P	N/A	10.29	10.83	11.08	11.00	10.00	26.75	N/A	N/A	N/A	N/A	N/A	N/A	I	N/A	BC	N/A	N/A	N/A	34S_4p1d7Yc_5	11/27B3	TDP-WTP-065	7091151
21.0	0.999	0.00487	undefined	1.000	infinite	S	1.99	N/A	N/A	N/A	2.00	3.90	N/A	N/A	N/A	N/A	N/A	N/A	N/A	N/A	N/A	SS	N/A	N/A	N/A	34S_4p1d8Ya	11/30A1	TDP-WTP-066	7091154
20.9	0.999	0.00487	undefined	1.000	infinite	S	3.05	N/A	N/A	N/A	3.00	3.90	N/A	N/A	N/A	N/A	N/A	N/A	N/A	I	N/A	AM	N/A	N/A	N/A	34S_4p1d8Ya	11/30A1	TDP-WTP-066	7091158
20.9	0.999	0.00487	undefined	1.000	infinite	S	3.52	N/A	N/A	N/A	3.50	3.90	14.50	N/A	N/A	N/A	UCScen	N/A	N/A	I	N/A	AM	N/A	N/A	N/A	34S_4p1d8Ya	11/30A1	TDP-WTP-066	7091161
21.0	0.999	0.00487	undefined	1.000	infinite	S	3.72	N/A	N/A	N/A	3.70	3.90	24.50	N/A	N/A	N/A	N/A	N/A	N/A	I	N/A	AM+	N/A	N/A	N/A	34S_4p1d8Ya	11/30A1	TDP-WTP-066	7091164
21.0	0.999	0.00487	undefined	1.000	infinite	S	3.96	N/A	N/A	N/A	3.90	3.90	33.50	3.90	vis	UCSvis	N/A	N/A	N/A	I	N/A	CS	N/A	N/A	N/A	34S_4p1d8Ya	11/30A1	TDP-WTP-066	7091167
21.0	0.999	0.00487	undefined	1.000	infinite	S	4.12	N/A	N/A	N/A	4.10	3.90	42.50	N/A	N/A	N/A	N/A	N/A	N/A	I	N/A	BC	N/A	N/A	N/A	34S_4p1d8Ya	11/30A1	TDP-WTP-066	7091169
21.0	0.999	0.00487	0.050	0.180	0.0	P	N/A	3.91	3.95	3.97	4.00	6.00	N/A	N/A	N/A	N/A	N/A	N/A	N/A	I	N/A	SS	N/A	N/A	N/A	34S_4p1d8Yd_1	11/30A2	TDP-WTP-066	7091172
21.0	0.999	0.00487	0.050	0.180	0.0	P	N/A	4.44	4.48	4.50	4.50	6.00	9.00	N/A	N/A	N/A	N/A	N/A	N/A	I	N/A	AM-	N/A	N/A	N/A	34S_4p1d8Yd_1	11/30A2	TDP-WTP-066	7091175
21.0	0.999	0.00487	0.049	0.180	0.0	P	N/A	4.85	4.90	4.93	5.00	6.00	9.75	N/A	N/A	N/A	N/A	N/A	N/A	I	N/A	AM	N/A	N/A	N/A	34S_4p1d8Yd_1	11/30A2	TDP-WTP-066	7091178
21.0	0.999	0.00487	0.050	0.180	0.0	P	N/A	5.38	5.45	5.49	5.50	6.00	11.25	N/A	N/A	N/A	N/A	N/A	N/A	I	N/A	AM+	N/A	N/A	N/A	34S_4p1d8Yd_1	11/30A2	TDP-WTP-066	7091181
21.0	0.999	0.00487	0.050	0.180	0.0	P	N/A	5.86	5.95	5.99	6.00	6.00	12.50	6.00	vis	UCSvis	N/A	N/A	N/A	I	N/A	CS	N/A	N/A	N/A	34S_4p1d8Yd_1	11/30A2	TDP-WTP-066	7091185
21.0	0.999	0.00487	0.050	0.180	0.0	P	N/A	6.37	6.48	6.53	6.50	6.00	16.75	N/A	N/A	N/A	N/A	N/A	N/A	I	N/A	BC	N/A	N/A	N/A	34S_4p1d8Yd_1	11/30A2	TDP-WTP-066	7091187
21.0	0.999	0.00487	0.050	0.330	0.0	P	N/A	3.89	3.93	3.95	4.00	5.30	8.50	N/A	N/A	N/A	N/A	N/A	N/A	D	N/A	SS	N/A	N/A	N/A	34S_4p1d8Yc_1	11/30B1	TDP-WTP-066	7091191
21.0	0.999	0.00487	0.050	0.330	0.0	P	N/A	4.43	4.48	4.50	4.50	5.30	9.75	N/A	N/A	N/A	N/A	N/A	N/A	I	N/A	SS+	N/A	N/A	N/A	34S_4p1d8Yc_1	11/30B1	TDP-WTP-066	7091193
21.0	0.999	0.00487	0.052	0.330	0.0	P	N/A	4.87	4.94	4.97	5.00	5.30	10.75	N/A	N/A	N/A	N/A	N/A	N/A	I	N/A	AM	N/A	N/A	N/A	34S_4p1d8Yc_1	11/30B1	TDP-WTP-066	7091197
21.0	0.999	0.00487	0.050	0.330	0.0	P	N/A	5.16	5.22	5.25	5.30	5.30	12.50	5.30	vis	UCSvis	N/A	N/A	N/A	I	N/A	CS	N/A	N/A	N/A	34S_4p1d8Yc_1	11/30B1	TDP-WTP-066	7091200
21.0	0.999	0.00487	0.050	0.330	0.0	P	N/A	5.52	5.59	5.62	5.60	5.30	17.50	N/A	N/A	N/A	N/A	N/A	N/A	I	N/A	BC	N/A	N/A	N/A	34S_4p1d8Yc_1	11/30B1	TDP-WTP-066	7091202
21.3	0.999	0.00487	undefined	1.000	infinite	S	3.53	N/A	N/A	N/A	3.50	5.50	N/A	N/A	N/A	N/A	N/A	N/A	N/A	I	N/A	SS	N/A	N/A	N/A	34S_4p1d8Ya-44	11/30C1	TDP-WTP-066	7091206
21.2	0.999	0.00487	undefined	1.000	infinite	S	3.70	N/A	N/A	N/A	3.70	5.50	N/A	N/A	N/A	N/A	UCScen	N/A	N/A	I	N/A	SS	N/A	N/A	N/A	34S_4p1d8Ya-44	11/30C1	TDP-WTP-066	7091209
21.3	0.999	0.00487	undefined	1.000	infinite	S	4.04	N/A	N/A	N/A	4.00	5.50	9.50	N/A	N/A	N/A	N/A	N/A	N/A	I	N/A	AM	N/A	N/A	N/A	34S_4p1d8Ya-44	11/30C1	TDP-WTP-066	7091212
21.3	0.999	0.00487	undefined	1.000	infinite	S	4.54	N/A	N/A	N/A	4.50	5.50	14.25	N/A	N/A	N/A	N/A	N/A	N/A	I	N/A	AM	N/A	N/A	N/A	34S_4p1d8Ya-44	11/30C1	TDP-WTP-066	7091215
21.3	0.999	0.00487	undefined	1.000	infinite	S	5.03	N/A	N/A	N/A	5.00	5.50	29.25	N/A	N/A	N/A	N/A	N/A	N/A	I	N/A	AM+	N/A	N/A	N/A	34S_4p1d8Ya-44	11/30C1	TDP-WTP-066	7091217
21.3	0.999	0.00487	undefined	1.000	infinite	S	5.55	N/A	N/A	N/A	5.50	5.50	43.75	5.50	vis	UCSvis	N/A	N/A	N/A	I	N/A	CS	N/A	N/A	N/A	34S_4p1d8Ya-44	11/30C1	TDP-WTP-066	7091221
21.0	0.999	0.00487	0.051	0.180	87.0	P	N/A	4.55	4.60	4.63	4.50	9.00	N/A	N/A	N/A	N/A	UCScen	N/A	N/A	I	N/A	SS	N/A	N/A	N/A	34S_4p1d8Yd_0	11/30C2	TDP-WTP-066	7091224
21.0	0.999	0.00487	0.051	0.180	78.0	P	N/A	5.06	5.10	5.14	5.00	9.00	9.50	N/A	N/A	N/A	N/A	N/A	N/A	I	N/A	AM	N/A	N/A	N/A	34S_4p1d8Yd_0	11/30C2	TDP-WTP-066	7091226
21.0	0.999	0.00487	0.051	0.180	70.0	P	N/A	5.61	5.67	5.71	5.50	9.00	11.00	N/A	N/A	N/A	N/A	N/A	N/A	I	N/A	AM	N/A	N/A	N/A	34S_4p1d8Yd_0	11/30C2	TDP-WTP-066	7091229
21.0	0.999	0.00487	0.050	0.180	64.0	P	N/A	6.10	6.16	6.21	6.00	9.00	12.83	N/A	N/A	N/A	N/A	N/A	N/A	I	N/A	AM	N/A	N/A	N/A	34S_4p1d8Yd_0	11/30C2	TDP-WTP-066	7091232
21.0	0.999	0.00487	0.050	0.180	59.0	P	N/A	6.58	6.65	6.71	6.50	9.00	15.00	N/A	N/A	N/A	N/A	N/A	N/A	I	N/A	AM	N/A	N/A	N/A	34S_4p1d8Yd_0	11/30C2	TDP-WTP-066	7091236
21.0	0.999	0.00487	0.051	0.180	54.0	P	N/A	7.15	7.23	7.29	7.00	9.00	15.50	N/A	N/A	N/A	N/A	N/A	N/A	I	N/A	AM+	N/A	N/A	N/A	34S_4p1d8Yd_0	11/30C2	TDP-WTP-066	7091240
21.0	0.999	0.00487	0.050	0.180	50.5	P	N/A	7.55	7.66	7.74	7.50	9.00	17.63	N/A	N/A	N/A	N/A	N/A	N/A	I	N/A	AM+	N/A	N/A	N/A	34S_4p1d8Yd_0	11/30C2	TDP-WTP-066	7091243
21.0	0.999	0.00487	0.046	0.180	47.0	P	N/A	8.16	8.28	8.37	8.00	9.00	20.25	N/A	N/A	N/A	N/A	N/A	N/A	I	N/A	AM+	N/A	N/A	N/A	34S_4p1d8Yd_0	11/30C2	TDP-WTP-066	7091246
21.0	0.999	0.00487	0.050	0.180	45.0	P	N/A	8.58	8.69	8.76	8.50	9.00	22.25	N/A	N/A	N/A	N/A	N/A	N/A	I	N/A	AM+	N/A	N/A	N/A	34S_4p1d8Yd_0	11/30C2	TDP-WTP-066	7091249
21.0	0.999	0.00487	0.051	0.180	42.5	P	N/A	9.10	9.24	9.33	9.00	9.00	25.88	9.00	vis	UCSvis	N/A	N/A	N/A	I	N/A	CS	N/A	N/A	N/A	34S_4p1d8Yd_0	11/30C2	TDP-WTP-066	7091253

Table B.9. Updated Data from Fall 2007 Tests in Mid-Scale Vessel with Spherical Head A.11

Row Number	Test	Case ID	Tank Diameter	Head Shape	Dish Height	Dish Volume	Tank Fill Height	Return Line Height	Nozzle Inner Diameter	Nozzle Stand-off Distance	Pulse Tube Configuration	Installed Nozzles	Outer Nozzles Operated	Inner Nozzles Operated	Pulse Tube Outer Diameter	Outer PJM Radius	Inner PJM Radius	"FIO" Outer PJM Impingement Angle	"FIO" Inner PJM Impingement Angle	Ratio Outer PJM to Tank Radius	Ratio Inner PJM to Tank Radius	Simulant	Solids Density	Particle Diameter d5	Particle Diameter d50	Particle Diameter d95	Void Fraction
text	text	text	in.	text	in.	in. ^{3}	in.	in.	in.	in.	text	number	number	number	in.	in.	in.	deg	deg	nondim	nondim	text	g/cm^3	m	m	m	fraction
MSS	M/DDX	ID	D	HS	H_{dish}	V_{dish}	H	Rtn	d	sod	PT	N	N_O	N_I	PT_{od}	R_O	R_I	Θ_O	Θ_I	R_O/R	R_I/R	sxdx	ρ_S	d_5	d_{50}	d_{95}	vf
7091256	12/3A1	34S_4p1d8Yc_0	33 7/8	S	9	4437.4	67 3/4	61 3/4	0.297	0.446	HLP-22	12	4	4	1.9	10.5	5.7	30.8	16.1	0.62	0.33	p1d8	2.45	0.0000605	0.0000895	0.0001320	0.4269
7091259	12/3A1	34S_4p1d8Yc_0	33 7/8	S	9	4437.4	67 3/4	61 3/4	0.297	0.446	HLP-22	12	4	4	1.9	10.5	5.7	30.8	16.1	0.62	0.33	p1d8	2.45	0.0000605	0.0000895	0.0001320	0.4269
7091261	12/3A1	34S_4p1d8Yc_0	33 7/8	S	9	4437.4	67 3/4	61 3/4	0.297	0.446	HLP-22	12	4	4	1.9	10.5	5.7	30.8	16.1	0.62	0.33	p1d8	2.45	0.0000605	0.0000895	0.0001320	0.4269
7091265	12/3A1	34S_4p1d8Yc_0	33 7/8	S	9	4437.4	67 3/4	61 3/4	0.297	0.446	HLP-22	12	4	4	1.9	10.5	5.7	30.8	16.1	0.62	0.33	p1d8	2.45	0.0000605	0.0000895	0.0001320	0.4269
7091268M	12/3A1	34S_4p1d8Yc_0	33 7/8	S	9	4437.4	67 3/4	61 3/4	0.297	0.446	HLP-22	12	4	4	1.9	10.5	5.7	30.8	16.1	0.62	0.33	p1d8	2.45	0.0000605	0.0000895	0.0001320	0.4269
7091270M	12/3A1	34S_4p1d8Yc_0	33 7/8	S	9	4437.4	67 3/4	61 3/4	0.297	0.446	HLP-22	12	4	4	1.9	10.5	5.7	30.8	16.1	0.62	0.33	p1d8	2.45	0.0000605	0.0000895	0.0001320	0.4269
7091274	12/3B1	34S_4p1d8Ya-04	33 7/8	S	9	4437.4	67 3/4	61 3/4	0.297	0.446	HLP-22	12	0	4	1.9	10.5	5.7	30.8	16.1	0.62	0.33	p1d8	2.45	0.0000605	0.0000895	0.0001320	0.4269
7091277	12/3B1	34S_4p1d8Ya-04	33 7/8	S	9	4437.4	67 3/4	61 3/4	0.297	0.446	HLP-22	12	0	4	1.9	10.5	5.7	30.8	16.1	0.62	0.33	p1d8	2.45	0.0000605	0.0000895	0.0001320	0.4269
7091279	12/3B1	34S_4p1d8Ya-04	33 7/8	S	9	4437.4	67 3/4	61 3/4	0.297	0.446	HLP-22	12	0	4	1.9	10.5	5.7	30.8	16.1	0.62	0.33	p1d8	2.45	0.0000605	0.0000895	0.0001320	0.4269
7091283	12/3B1	34S_4p1d8Ya-04	33 7/8	S	9	4437.4	67 3/4	61 3/4	0.297	0.446	HLP-22	12	0	4	1.9	10.5	5.7	30.8	16.1	0.62	0.33	p1d8	2.45	0.0000605	0.0000895	0.0001320	0.4269
7091286	12/3B1	34S_4p1d8Ya-04	33 7/8	S	9	4437.4	67 3/4	61 3/4	0.297	0.446	HLP-22	12	0	4	1.9	10.5	5.7	30.8	16.1	0.62	0.33	p1d8	2.45	0.0000605	0.0000895	0.0001320	0.4269
7091289	12/3B2	34S_4p1d8Yd_9	33 7/8	S	9	4437.4	67 3/4	61 3/4	0.297	0.446	HLP-22	12	0	4	1.9	10.5	5.7	30.8	16.1	0.62	0.33	p1d8	2.45	0.0000605	0.0000895	0.0001320	0.4269
7091291	12/3B2	34S_4p1d8Yd_9	33 7/8	S	9	4437.4	67 3/4	61 3/4	0.297	0.446	HLP-22	12	0	4	1.9	10.5	5.7	30.8	16.1	0.62	0.33	p1d8	2.45	0.0000605	0.0000895	0.0001320	0.4269
7091294	12/3B2	34S_4p1d8Yd_9	33 7/8	S	9	4437.4	67 3/4	61 3/4	0.297	0.446	HLP-22	12	0	4	1.9	10.5	5.7	30.8	16.1	0.62	0.33	p1d8	2.45	0.0000605	0.0000895	0.0001320	0.4269
7091297	12/3B2	34S_4p1d8Yd_9	33 7/8	S	9	4437.4	67 3/4	61 3/4	0.297	0.446	HLP-22	12	0	4	1.9	10.5	5.7	30.8	16.1	0.62	0.33	p1d8	2.45	0.0000605	0.0000895	0.0001320	0.4269
7091300	12/3B2	34S_4p1d8Yd_9	33 7/8	S	9	4437.4	67 3/4	61 3/4	0.297	0.446	HLP-22	12	0	4	1.9	10.5	5.7	30.8	16.1	0.62	0.33	p1d8	2.45	0.0000605	0.0000895	0.0001320	0.4269
7091303	12/3B2	34S_4p1d8Yd_9	33 7/8	S	9	4437.4	67 3/4	61 3/4	0.297	0.446	HLP-22	12	0	4	1.9	10.5	5.7	30.8	16.1	0.62	0.33	p1d8	2.45	0.0000605	0.0000895	0.0001320	0.4269
7091306	12/3B2	34S_4p1d8Yd_9	33 7/8	S	9	4437.4	67 3/4	61 3/4	0.297	0.446	HLP-22	12	0	4	1.9	10.5	5.7	30.8	16.1	0.62	0.33	p1d8	2.45	0.0000605	0.0000895	0.0001320	0.4269
7091310M	12/3B2	34S_4p1d8Yd_9	33 7/8	S	9	4437.4	67 3/4	61 3/4	0.297	0.446	HLP-22	12	0	4	1.9	10.5	5.7	30.8	16.1	0.62	0.33	p1d8	2.45	0.0000605	0.0000895	0.0001320	0.4269
7091312M	12/3B2	34S_4p1d8Yd_9	33 7/8	S	9	4437.4	67 3/4	61 3/4	0.297	0.446	HLP-22	12	0	4	1.9	10.5	5.7	30.8	16.1	0.62	0.33	p1d8	2.45	0.0000605	0.0000895	0.0001320	0.4269
7091316	12/3C1	34S_4p1d8Yc_9	33 7/8	S	9	4437.4	67 3/4	61 3/4	0.297	0.446	HLP-22	12	0	4	1.9	10.5	5.7	30.8	16.1	0.62	0.33	p1d8	2.45	0.0000605	0.0000895	0.0001320	0.4269
7091318	12/3C1	34S_4p1d8Yc_9	33 7/8	S	9	4437.4	67 3/4	61 3/4	0.297	0.446	HLP-22	12	0	4	1.9	10.5	5.7	30.8	16.1	0.62	0.33	p1d8	2.45	0.0000605	0.0000895	0.0001320	0.4269
7091321	12/3C1	34S_4p1d8Yc_9	33 7/8	S	9	4437.4	67 3/4	61 3/4	0.297	0.446	HLP-22	12	0	4	1.9	10.5	5.7	30.8	16.1	0.62	0.33	p1d8	2.45	0.0000605	0.0000895	0.0001320	0.4269
7091324	12/3C1	34S_4p1d8Yc_9	33 7/8	S	9	4437.4	67 3/4	61 3/4	0.297	0.446	HLP-22	12	0	4	1.9	10.5	5.7	30.8	16.1	0.62	0.33	p1d8	2.45	0.0000605	0.0000895	0.0001320	0.4269
7091328M	12/3C1	34S_4p1d8Yc_9	33 7/8	S	9	4437.4	67 3/4	61 3/4	0.297	0.446	HLP-22	12	0	4	1.9	10.5	5.7	30.8	16.1	0.62	0.33	p1d8	2.45	0.0000605	0.0000895	0.0001320	0.4269
7091330M	12/3C1	34S_4p1d8Yc_9	33 7/8	S	9	4437.4	67 3/4	61 3/4	0.297	0.446	HLP-22	12	0	4	1.9	10.5	5.7	30.8	16.1	0.62	0.33	p1d8	2.45	0.0000605	0.0000895	0.0001320	0.4269
7091333	12/4A1	34S_4p1d8Ya-40	33 7/8	S	9	4437.4	67 3/4	61 3/4	0.297	0.446	HLP-22	12	4	0	1.9	10.5	5.7	30.8	16.1	0.62	0.33	p1d8	2.45	0.0000605	0.0000895	0.0001320	0.4269
7091336	12/4A1	34S_4p1d8Ya-40	33 7/8	S	9	4437.4	67 3/4	61 3/4	0.297	0.446	HLP-22	12	4	0	1.9	10.5	5.7	30.8	16.1	0.62	0.33	p1d8	2.45	0.0000605	0.0000895	0.0001320	0.4269
7091339	12/4A1	34S_4p1d8Ya-40	33 7/8	S	9	4437.4	67 3/4	61 3/4	0.297	0.446	HLP-22	12	4	0	1.9	10.5	5.7	30.8	16.1	0.62	0.33	p1d8	2.45	0.0000605	0.0000895	0.0001320	0.4269
7091342	12/4A1	34S_4p1d8Ya-40	33 7/8	S	9	4437.4	67 3/4	61 3/4	0.297	0.446	HLP-22	12	4	0	1.9	10.5	5.7	30.8	16.1	0.62	0.33	p1d8	2.45	0.0000605	0.0000895	0.0001320	0.4269
7091346	12/4A1	34S_4p1d8Ya-40	33 7/8	S	9	4437.4	67 3/4	61 3/4	0.297	0.446	HLP-22	12	4	0	1.9	10.5	5.7	30.8	16.1	0.62	0.33	p1d8	2.45	0.0000605	0.0000895	0.0001320	0.4269
7091348	12/4A1	34S_4p1d8Ya-40	33 7/8	S	9	4437.4	67 3/4	61 3/4	0.297	0.446	HLP-22	12	4	0	1.9	10.5	5.7	30.8	16.1	0.62	0.33	p1d8	2.45	0.0000605	0.0000895	0.0001320	0.4269
7091351	12/4A2	34S_4p1d8Yd_6	33 7/8	S	9	4437.4	67 3/4	61 3/4	0.297	0.446	HLP-22	12	4	0	1.9	10.5	5.7	30.8	16.1	0.62	0.33	p1d8	2.45	0.0000605	0.0000895	0.0001320	0.4269
7091354	12/4A2	34S_4p1d8Yd_6	33 7/8	S	9	4437.4	67 3/4	61 3/4	0.297	0.446	HLP-22	12	4	0	1.9	10.5	5.7	30.8	16.1	0.62	0.33	p1d8	2.45	0.0000605	0.0000895	0.0001320	0.4269
7091357	12/4A2	34S_4p1d8Yd_6	33 7/8	S	9	4437.4	67 3/4	61 3/4	0.297	0.446	HLP-22	12	4	0	1.9	10.5	5.7	30.8	16.1	0.62	0.33	p1d8	2.45	0.0000605	0.0000895	0.0001320	0.4269
7091360	12/4A2	34S_4p1d8Yd_6	33 7/8	S	9	4437.4	67 3/4	61 3/4	0.297	0.446	HLP-22	12	4	0	1.9	10.5	5.7	30.8	16.1	0.62	0.33	p1d8	2.45	0.0000605	0.0000895	0.0001320	0.4269
7091364M	12/4A2	34S_4p1d8Yd_6	33 7/8	S	9	4437.4	67 3/4	61 3/4	0.297	0.446	HLP-22	12	4	0	1.9	10.5	5.7	30.8	16.1	0.62	0.33	p1d8	2.45	0.0000605	0.0000895	0.0001320	0.4269
7091366M	12/4A2	34S_4p1d8Yd_6	33 7/8	S	9	4437.4	67 3/4	61 3/4	0.297	0.446	HLP-22	12	4	0	1.9	10.5	5.7	30.8	16.1	0.62	0.33	p1d8	2.45	0.0000605	0.0000895	0.0001320	0.4269
7091369	12/4B1	34S_4p1d8Yc_6	33 7/8	S	9	4437.4	67 3/4	61 3/4	0.297	0.446	HLP-22	12	4	0	1.9	10.5	5.7	30.8	16.1	0.62	0.33	p1d8	2.45	0.0000605	0.0000895	0.0001320	0.4269
7091372	12/4B1	34S_4p1d8Yc_6	33 7/8	S	9	4437.4	67 3/4	61 3/4	0.297	0.446	HLP-22	12	4	0	1.9	10.5	5.7	30.8	16.1	0.62	0.33	p1d8	2.45	0.0000605	0.0000895	0.0001320	0.4269
7091375	12/4B1	34S_4p1d8Yc_6	33 7/8	S	9	4437.4	67 3/4	61 3/4	0.297	0.446	HLP-22	12	4	0	1.9	10.5	5.7	30.8	16.1	0.62	0.33	p1d8	2.45	0.0000605	0.0000895	0.0001320	0.4269

Table B.9. Updated Data from Fall 2007 Tests in Mid-Scale Vessel with Spherical Head B.11

Tank Water Temperature	Water Density	Solids Fraction	Pulse Volume Fraction	Duty Cycle	Cycle Time	Pulsed or Steady Jet	Us Steady Jet	U1 Pulsing Jet	U2 URMS	U3 URM3	Discharge Velocity	Critical Suspension Velocity	Average Peak Cloud Height	U_{CS} Condition	U_{CS} Method	U_{CS} Flag	U_{CS} Center Flag	U_{CS} udv Flag	U_{CS} based on Decreasing Velocity	Sweep Increase / Decrease	UDV Height Bed	Particle Motion	Solids Level	Outer Bottom Pattern	Inner Bottom Pattern	Case ID	Test	TDP	Row Number
C	g/cm³	fraction	fraction	fraction	s	text	m/s	m/s	m/s	m/s	m/s	m/s	in.	m/s	text	text	text	text	m/s	text	mm	text	text	text	text	text	text	text	text
T	ρ_l	ϕ_S	ϕ_P	DC	t_C	Jet	US	U1	U2	U3	U	U_{CS}	H_C	U_{CSR}	U_{CSM}	U_{CS}vis	U_{CS}cen	U_{CS}udv	U_{CS_D}	S_W	H_{bed}	PM	Sol	SP_O	SP_I	ID	M/DDX	TDP	MSS
21.0	0.999	0.00487	0.050	0.330	47.0	P	N/A	4.53	4.58	4.62	4.50	7.30	N/A	N/A	N/A	N/A	N/A	N/A	N/A	I	N/A	SS	N/A	N/A	N/A	34S_4p1d8Yc_0	12/3A1	TDP-WTP-067	7091256
21.0	0.999	0.00487	0.051	0.330	42.0	P	N/A	5.12	5.16	5.20	5.00	7.30	9.25	N/A	N/A	N/A	UCScen	N/A	N/A	I	N/A	SS	N/A	N/A	N/A	34S_4p1d8Yc_0	12/3A1	TDP-WTP-067	7091259
21.0	0.999	0.00487	0.051	0.330	35.0	P	N/A	6.08	6.16	6.21	6.00	7.30	13.50	N/A	N/A	N/A	N/A	N/A	N/A	D	N/A	AM	N/A	N/A	N/A	34S_4p1d8Yc_0	12/3A1	TDP-WTP-067	7091261
21.0	0.999	0.00487	0.051	0.330	30.0	P	N/A	7.03	7.14	7.22	7.00	7.30	17.50	N/A	N/A	N/A	N/A	N/A	N/A	I	N/A	AM	N/A	N/A	N/A	34S_4p1d8Yc_0	12/3A1	TDP-WTP-067	7091265
21.0	0.999	0.00487	0.051	0.330	28.8	P	N/A	7.33	7.44	7.51	7.30	7.30	20.50	7.30	vis	UCSvis	N/A	N/A	N/A	I	N/A	CS	N/A	N/A	N/A	34S_4p1d8Yc_0	12/3A1	TDP-WTP-067	7091268
21.0	0.999	0.00487	0.050	0.330	26.0	P	N/A	8.08	8.22	8.31	8.00	7.30	31.25	N/A	N/A	N/A	N/A	N/A	N/A	I	N/A	BC	N/A	N/A	N/A	34S_4p1d8Yc_0	12/3A1	TDP-WTP-067	7091270
21.3	0.999	0.00487	undefined	1.000	infinite	S	4.54	N/A	N/A	N/A	4.50	8.00	N/A	N/A	N/A	N/A	UCScen	N/A	N/A	I	N/A	SS	N/A	N/A	N/A	34S_4p1d8Ya-04	12/3B1	TDP-WTP-067	7091274
21.3	0.999	0.00487	undefined	1.000	infinite	S	5.03	N/A	N/A	N/A	5.00	8.00	8.75	N/A	N/A	N/A	N/A	N/A	N/A	I	N/A	SS	N/A	N/A	N/A	34S_4p1d8Ya-04	12/3B1	TDP-WTP-067	7091277
21.3	0.999	0.00487	undefined	1.000	infinite	S	6.04	N/A	N/A	N/A	6.00	8.00	14.25	N/A	N/A	N/A	N/A	N/A	N/A	I	N/A	AM	N/A	N/A	N/A	34S_4p1d8Ya-04	12/3B1	TDP-WTP-067	7091279
21.3	0.999	0.00487	undefined	1.000	infinite	S	7.04	N/A	N/A	N/A	7.00	8.00	22.75	N/A	N/A	N/A	N/A	N/A	N/A	I	N/A	AM	N/A	N/A	N/A	34S_4p1d8Ya-04	12/3B1	TDP-WTP-067	7091283
21.3	0.999	0.00487	undefined	1.000	infinite	S	8.02	N/A	N/A	N/A	8.00	8.00	42.50	8.00	vis	UCSvis	N/A	N/A	N/A	I	N/A	CS	N/A	N/A	N/A	34S_4p1d8Ya-04	12/3B1	TDP-WTP-067	7091286
22.0	0.999	0.00487	0.049	0.180	190.0	P	N/A	4.03	4.15	4.38	4.00	12.00	N/A	N/A	center dec	N/A	UCScen	N/A	4.00	D	N/A	SS	N/A	N/A	N/A	34S_4p1d8Yd_9	12/3B2	TDP-WTP-067	7091289
22.0	0.999	0.00487	0.049	0.180	127.0	P	N/A	6.05	6.20	6.46	6.00	12.00	11.00	N/A	N/A	N/A	N/A	N/A	N/A	I	N/A	AM-	N/A	N/A	N/A	34S_4p1d8Yd_9	12/3B2	TDP-WTP-067	7091291
22.0	0.999	0.00487	0.048	0.180	105.0	P	N/A	7.17	7.37	7.67	7.00	12.00	13.50	N/A	N/A	N/A	N/A	N/A	N/A	I	N/A	AM	N/A	N/A	N/A	34S_4p1d8Yd_9	12/3B2	TDP-WTP-067	7091294
22.0	0.999	0.00487	0.049	0.180	92.8	P	N/A	8.17	8.40	8.75	8.00	12.00	16.75	N/A	N/A	N/A	N/A	N/A	N/A	I	N/A	AM	N/A	N/A	N/A	34S_4p1d8Yd_9	12/3B2	TDP-WTP-067	7091297
22.0	0.999	0.00487	0.049	0.180	80.0	P	N/A	9.29	9.57	9.96	9.00	12.00	19.75	N/A	N/A	N/A	N/A	N/A	N/A	I	N/A	AM	N/A	N/A	N/A	34S_4p1d8Yd_9	12/3B2	TDP-WTP-067	7091300
22.0	0.999	0.00487	0.048	0.180	72.5	P	N/A	10.20	10.50	10.92	10.00	12.00	20.25	N/A	N/A	N/A	N/A	N/A	N/A	I	N/A	AM+	N/A	N/A	N/A	34S_4p1d8Yd_9	12/3B2	TDP-WTP-067	7091303
22.0	0.999	0.00487	0.048	0.180	66.0	P	N/A	11.19	11.53	12.00	11.00	12.00	22.50	N/A	N/A	N/A	N/A	N/A	N/A	I	N/A	AM+	N/A	N/A	N/A	34S_4p1d8Yd_9	12/3B2	TDP-WTP-067	7091306
22.0	0.999	0.00487	0.049	0.180	60.5	P	N/A	12.31	12.73	13.27	12.00	12.00	27.25	12.00	vis	UCSvis	N/A	N/A	N/A	I	N/A	CS	N/A	N/A	N/A	34S_4p1d8Yd_9	12/3B2	TDP-WTP-067	7091310
22.0	0.999	0.00487	0.049	0.180	56.0	P	N/A	13.43	13.91	14.51	13.00	12.00	31.75	N/A	N/A	N/A	N/A	N/A	N/A	I	N/A	BC-	N/A	N/A	N/A	34S_4p1d8Yd_9	12/3B2	TDP-WTP-067	7091312
22.0	0.999	0.00487	0.047	0.330	93.0	P	N/A	4.51	4.63	4.83	4.50	10.50	N/A	N/A	N/A	N/A	UCScen	N/A	N/A	I	N/A	SS	N/A	N/A	N/A	34S_4p1d8Yc_9	12/3C1	TDP-WTP-067	7091316
22.0	0.999	0.00487	0.050	0.330	59.0	P	N/A	7.20	7.36	7.61	7.00	10.50	14.00	N/A	N/A	N/A	N/A	N/A	N/A	I	N/A	AM-	N/A	N/A	N/A	34S_4p1d8Yc_9	12/3C1	TDP-WTP-067	7091318
22.0	0.999	0.00487	0.049	0.330	51.5	P	N/A	8.12	8.32	8.59	8.00	10.50	16.00	N/A	N/A	N/A	N/A	N/A	N/A	I	N/A	AM	N/A	N/A	N/A	34S_4p1d8Yc_9	12/3C1	TDP-WTP-067	7091321
22.0	0.999	0.00487	0.050	0.330	41.0	P	N/A	10.29	10.54	10.90	10.00	10.50	22.50	N/A	N/A	N/A	N/A	N/A	N/A	I	N/A	AM+	N/A	N/A	N/A	34S_4p1d8Yc_9	12/3C1	TDP-WTP-067	7091324
22.0	0.999	0.00487	0.049	0.330	38.5	P	N/A	10.77	11.06	11.44	10.50	10.50	26.75	10.50	vis	UCSvis	N/A	N/A	N/A	I	N/A	CS	N/A	N/A	N/A	34S_4p1d8Yc_9	12/3C1	TDP-WTP-067	7091328
22.0	0.999	0.00487	0.049	0.330	35.0	P	N/A	11.78	12.14	12.57	11.50	10.50	34.50	N/A	N/A	N/A	N/A	N/A	N/A	I	N/A	BC	N/A	N/A	N/A	34S_4p1d8Yc_9	12/3C1	TDP-WTP-067	7091330
21.7	0.999	0.00487	undefined	1.000	infinite	S	5.09	N/A	N/A	N/A	5.00	7.00	N/A	N/A	N/A	N/A	N/A	N/A	N/A	D	N/A	SS	N/A	N/A	N/A	34S_4p1d8Ya-40	12/4A1	TDP-WTP-068	7091333
21.7	0.998	0.00487	undefined	1.000	infinite	S	5.56	N/A	N/A	N/A	5.50	7.00	10.00	N/A	N/A	N/A	N/A	N/A	N/A	I	N/A	SS	N/A	N/A	N/A	34S_4p1d8Ya-40	12/4A1	TDP-WTP-068	7091336
21.7	0.998	0.00487	undefined	1.000	infinite	S	6.04	N/A	N/A	N/A	6.00	7.00	13.25	N/A	N/A	N/A	N/A	N/A	N/A	I	N/A	AM	N/A	N/A	N/A	34S_4p1d8Ya-40	12/4A1	TDP-WTP-068	7091339
21.7	0.998	0.00487	undefined	1.000	infinite	S	6.54	N/A	N/A	N/A	6.50	7.00	22.50	N/A	N/A	N/A	UCScen	N/A	N/A	I	N/A	CS-	N/A	N/A	N/A	34S_4p1d8Ya-40	12/4A1	TDP-WTP-068	7091342
21.7	0.998	0.00487	undefined	1.000	infinite	S	7.04	N/A	N/A	N/A	7.00	7.00	30.00	7.00	vis	UCSvis	N/A	N/A	N/A	I	N/A	CS	N/A	N/A	N/A	34S_4p1d8Ya-40	12/4A1	TDP-WTP-068	7091346
21.7	0.998	0.00487	undefined	1.000	infinite	S	7.60	N/A	N/A	N/A	7.50	7.00	40.50	N/A	N/A	N/A	N/A	N/A	N/A	I	N/A	BC	N/A	N/A	N/A	34S_4p1d8Ya-40	12/4A1	TDP-WTP-068	7091348
22.0	0.999	0.00487	0.050	0.180	152.0	P	N/A	5.12	5.24	5.43	5.00	9.00	9.50	N/A	N/A	N/A	N/A	N/A	N/A	N/A	N/A	SS	N/A	N/A	N/A	34S_4p1d8Yd_6	12/4A2	TDP-WTP-068	7091351
22.0	0.999	0.00487	0.049	0.180	125.0	P	N/A	6.12	6.25	6.47	6.00	9.00	11.00	N/A	N/A	N/A	N/A	N/A	N/A	I	N/A	SS	N/A	N/A	N/A	34S_4p1d8Yd_6	12/4A2	TDP-WTP-068	7091354
22.0	0.999	0.00487	0.050	0.180	107.0	P	N/A	7.23	7.40	7.65	7.00	9.00	14.50	N/A	N/A	N/A	N/A	N/A	N/A	I	N/A	SS	N/A	N/A	N/A	34S_4p1d8Yd_6	12/4A2	TDP-WTP-068	7091357
22.0	0.999	0.00487	0.049	0.180	92.0	P	N/A	8.19	8.42	8.72	8.00	9.00	17.50	N/A	N/A	N/A	N/A	N/A	N/A	I	N/A	AM-	N/A	N/A	N/A	34S_4p1d8Yd_6	12/4A2	TDP-WTP-068	7091360
22.0	0.999	0.00487	0.049	0.180	82.0	P	N/A	9.30	9.52	9.83	9.00	9.00	22.00	9.00	vis	UCSvis	N/A	N/A	N/A	I	N/A	CS	N/A	N/A	N/A	34S_4p1d8Yd_6	12/4A2	TDP-WTP-068	7091364
22.0	0.999	0.00487	0.049	0.180	74.0	P	N/A	10.39	10.68	11.08	10.00	9.00	24.75	N/A	N/A	N/A	N/A	N/A	N/A	I	N/A	BC	N/A	N/A	N/A	34S_4p1d8Yd_6	12/4A2	TDP-WTP-068	7091366
22.0	0.999	0.00487	0.049	0.330	68.0	P	N/A	6.11	6.27	6.50	6.00	9.00	11.00	N/A	N/A	N/A	N/A	N/A	N/A	N/A	N/A	SS	N/A	N/A	N/A	34S_4p1d8Yc_6	12/4B1	TDP-WTP-068	7091369
22.0	0.999	0.00487	0.049	0.330	58.0	P	N/A	7.14	7.33	7.60	7.00	9.00	13.75	N/A	N/A	N/A	N/A	N/A	N/A	I	N/A	SS	N/A	N/A	N/A	34S_4p1d8Yc_6	12/4B1	TDP-WTP-068	7091372
22.0	0.999	0.00487	0.050	0.330	50.8	P	N/A	8.21	8.42	8.72	8.00	9.00	19.00	N/A	N/A	N/A	N/A	N/A	N/A	I	N/A	AM-	N/A	N/A	N/A	34S_4p1d8Yc_6	12/4B1	TDP-WTP-068	7091375

Table B.9. Updated Data from Fall 2007 Tests in Mid-Scale Vessel with Spherical Head A.12

Row Number	Test	Case ID	Tank Diameter	Head Shape	Dish Height	Dish Volume	Tank Fill Height	Return Line Height	Nozzle Inner Diameter	Nozzle Stand-off Distance	Pulse Tube Configuration	Installed Nozzles	Outer Nozzles Operated	Inner Nozzles Operated	Pulse Tube Outer Diameter	Outer PJM Radius	Inner PJM Radius	"FIO" Outer PJM Impingement Angle	"FIO" Inner PJM Impingement Angle	Ratio Outer PJM to Tank Radius	Ratio Inner PJM to Tank Radius	Simulant	Solids Density	Particle Diameter d5	Particle Diameter d50	Particle Diameter d95	Void Fraction
text	text	text	in.	text	in.	in. ^{3}	in.	in.	in.	in.	text	number	number	number	in.	in.	in.	deg	deg	nondim	nondim	text	g/cm^3	m	m	m	fraction
MSS	M/DDX	ID	D	HS	H_{dish}	V_{dish}	H	Rtn	d	sod	PT	N	N_O	N_I	PT_{od}	R_O	R_I	Θ_O	Θ_I	R_O/R	R_I/R	sxdx	ρ_S	d_5	d_{50}	d_{95}	vf
7091379	12/4B1	34S_4p1d8Yc_6	33 7/8	S	9	4437.4	67 3/4	61 3/4	0.297	0.446	HLP-22	12	4	0	1.9	10.5	5.7	30.8	16.1	0.62	0.33	p1d8	2.45	0.0000605	0.0000895	0.0001320	0.4269
7091381	12/4B1	34S_4p1d8Yc_6	33 7/8	S	9	4437.4	67 3/4	61 3/4	0.297	0.446	HLP-22	12	4	0	1.9	10.5	5.7	30.8	16.1	0.62	0.33	p1d8	2.45	0.0000605	0.0000895	0.0001320	0.4269
7091384	12/4C1	34S_4p1d8Ya-80	33 7/8	S	9	4437.4	67 3/4	61 3/4	0.297	0.446	HLP-22	12	8	0	1.9	10.5	5.7	30.8	16.1	0.62	0.33	p1d8	2.45	0.0000605	0.0000895	0.0001320	0.4269
7091388	12/4C1	34S_4p1d8Ya-80	33 7/8	S	9	4437.4	67 3/4	61 3/4	0.297	0.446	HLP-22	12	8	0	1.9	10.5	5.7	30.8	16.1	0.62	0.33	p1d8	2.45	0.0000605	0.0000895	0.0001320	0.4269
7091391	12/4C1	34S_4p1d8Ya-80	33 7/8	S	9	4437.4	67 3/4	61 3/4	0.297	0.446	HLP-22	12	8	0	1.9	10.5	5.7	30.8	16.1	0.62	0.33	p1d8	2.45	0.0000605	0.0000895	0.0001320	0.4269
7091393	12/4C2	34S_4p1d8Yd_5	33 7/8	S	9	4437.4	67 3/4	61 3/4	0.297	0.446	HLP-22	12	8	0	1.9	10.5	5.7	30.8	16.1	0.62	0.33	p1d8	2.45	0.0000605	0.0000895	0.0001320	0.4269
7091396	12/4C2	34S_4p1d8Yd_5	33 7/8	S	9	4437.4	67 3/4	61 3/4	0.297	0.446	HLP-22	12	8	0	1.9	10.5	5.7	30.8	16.1	0.62	0.33	p1d8	2.45	0.0000605	0.0000895	0.0001320	0.4269
7091399	12/4C2	34S_4p1d8Yd_5	33 7/8	S	9	4437.4	67 3/4	61 3/4	0.297	0.446	HLP-22	12	8	0	1.9	10.5	5.7	30.8	16.1	0.62	0.33	p1d8	2.45	0.0000605	0.0000895	0.0001320	0.4269
7091402	12/4C2	34S_4p1d8Yd_5	33 7/8	S	9	4437.4	67 3/4	61 3/4	0.297	0.446	HLP-22	12	8	0	1.9	10.5	5.7	30.8	16.1	0.62	0.33	p1d8	2.45	0.0000605	0.0000895	0.0001320	0.4269
7091405	12/4C2	34S_4p1d8Yd_5	33 7/8	S	9	4437.4	67 3/4	61 3/4	0.297	0.446	HLP-22	12	8	0	1.9	10.5	5.7	30.8	16.1	0.62	0.33	p1d8	2.45	0.0000605	0.0000895	0.0001320	0.4269
7091409	12/4C2	34S_4p1d8Yd_5	33 7/8	S	9	4437.4	67 3/4	61 3/4	0.297	0.446	HLP-22	12	8	0	1.9	10.5	5.7	30.8	16.1	0.62	0.33	p1d8	2.45	0.0000605	0.0000895	0.0001320	0.4269
7091411	12/4C2	34S_4p1d8Yd_5	33 7/8	S	9	4437.4	67 3/4	61 3/4	0.297	0.446	HLP-22	12	8	0	1.9	10.5	5.7	30.8	16.1	0.62	0.33	p1d8	2.45	0.0000605	0.0000895	0.0001320	0.4269
7091414	12/4D1	34S_4p1d8Yc_5	33 7/8	S	9	4437.4	67 3/4	61 3/4	0.297	0.446	HLP-22	12	8	0	1.9	10.5	5.7	30.8	16.1	0.62	0.33	p1d8	2.45	0.0000605	0.0000895	0.0001320	0.4269
7091417	12/4D1	34S_4p1d8Yc_5	33 7/8	S	9	4437.4	67 3/4	61 3/4	0.297	0.446	HLP-22	12	8	0	1.9	10.5	5.7	30.8	16.1	0.62	0.33	p1d8	2.45	0.0000605	0.0000895	0.0001320	0.4269
7091421	12/4D1	34S_4p1d8Yc_5	33 7/8	S	9	4437.4	67 3/4	61 3/4	0.297	0.446	HLP-22	12	8	0	1.9	10.5	5.7	30.8	16.1	0.62	0.33	p1d8	2.45	0.0000605	0.0000895	0.0001320	0.4269
7091423	12/4D1	34S_4p1d8Yc_5	33 7/8	S	9	4437.4	67 3/4	61 3/4	0.297	0.446	HLP-22	12	8	0	1.9	10.5	5.7	30.8	16.1	0.62	0.33	p1d8	2.45	0.0000605	0.0000895	0.0001320	0.4269

Table B.9. Updated Data from Fall 2007 Tests in Mid-Scale Vessel with Spherical Head B.12

Tank Water Temperature	Water Density	Solids Fraction	Pulse Volume Fraction	Duty Cycle	Cycle Time	Pulsed or Steady Jet	Us Steady Jet	U1 Pulsing Jet	U2 URMS	U3 URM3	Discharge Velocity	Critical Suspension Velocity	Average Peak Cloud Height	U_{CS} Condition	U_{CS} Method	U_{CS} Flag	U_{CS} Center Flag	U_{CS} udv Flag	U_{CS} based on Decreasing Velocity	Sweep Increase / Decrease	UDV Height Bed	Particle Motion	Solids Level	Outer Bottom Pattern	Inner Bottom Pattern	Case ID	Test	TDP	Row Number
C	g/cm³	fraction	fraction	fraction	s	text	m/s	m/s	m/s	m/s	m/s	m/s	in.	m/s	text	text	text	text	m/s	text	mm	text	text	text	text	text	text	text	text
T	ρ_l	ϕ_S	ϕ_p	DC	t_C	Jet	US	U1	U2	U3	U	U_{CS}	H_C	U_{CSR}	U_{CSM}	U_{CS}vis	U_{CS}cen	U_{CS}udv	U_{CS_D}	S_W	H_{bed}	PM	Sol	SP_O	SP_I	ID	M/DDX	TDP	MSS
22.0	0.999	0.00487	0.049	0.330	45.0	P	N/A	9.27	9.53	9.88	9.00	9.00	25.63	9.00	vis	UCSvis	N/A	N/A	N/A	I	N/A	CS	N/A	N/A	N/A	34S_4p1d8Yc_6	12/4B1	TDP-WTP-068	7091379
22.0	0.999	0.00487	0.050	0.330	41.0	P	N/A	10.29	10.57	10.97	10.00	9.00	34.00	N/A	N/A	N/A	N/A	N/A	N/A	I	N/A	BC	N/A	N/A	N/A	34S_4p1d8Yc_6	12/4B1	TDP-WTP-068	7091381
22.1	0.998	0.00487	undefined	1.000	infinite	S	4.07	N/A	N/A	N/A	4.00	5.20	17.00	N/A	N/A	N/A	N/A	N/A	N/A	N/A	N/A	SS	N/A	N/A	N/A	34S_4p1d8Ya-80	12/4C1	TDP-WTP-068	7091384
22.1	0.998	0.00487	undefined	1.000	infinite	S	5.05	N/A	N/A	N/A	5.00	5.20	42.00	N/A	N/A	N/A	N/A	N/A	N/A	I	N/A	AM	N/A	N/A	N/A	34S_4p1d8Ya-80	12/4C1	TDP-WTP-068	7091388
22.2	0.998	0.00487	undefined	1.000	infinite	S	5.30	N/A	N/A	N/A	5.20	5.20	51.00	5.20	vis	UCSvis	N/A	N/A	N/A	I	N/A	CS	N/A	N/A	N/A	34S_4p1d8Ya-80	12/4C1	TDP-WTP-068	7091391
22.0	0.999	0.00487	0.049	0.180	76.0	P	N/A	4.97	5.03	5.06	5.00	9.00	14.25	N/A	N/A	N/A	N/A	N/A	N/A	N/A	N/A	SS	N/A	N/A	N/A	34S_4p1d8Yd_5	12/4C2	TDP-WTP-068	7091393
22.0	0.999	0.00487	0.049	0.180	63.5	P	N/A	5.97	6.04	6.09	6.00	9.00	16.75	N/A	N/A	N/A	N/A	N/A	N/A	I	N/A	SS	N/A	N/A	N/A	34S_4p1d8Yd_5	12/4C2	TDP-WTP-068	7091396
22.0	0.999	0.00487	0.050	0.180	54.5	P	N/A	6.95	7.05	7.11	7.00	9.00	20.25	N/A	N/A	N/A	N/A	N/A	N/A	I	N/A	SS	N/A	N/A	N/A	34S_4p1d8Yd_5	12/4C2	TDP-WTP-068	7091399
22.0	0.999	0.00487	0.049	0.180	47.8	P	N/A	7.88	8.00	8.07	8.00	9.00	26.13	N/A	N/A	N/A	N/A	N/A	N/A	I	N/A	SS	N/A	N/A	N/A	34S_4p1d8Yd_5	12/4C2	TDP-WTP-068	7091402
22.0	0.999	0.00487	0.050	0.180	45.0	P	N/A	8.43	8.58	8.67	8.50	9.00	28.00	N/A	N/A	N/A	N/A	N/A	N/A	I	N/A	SS+	N/A	N/A	N/A	34S_4p1d8Yd_5	12/4C2	TDP-WTP-068	7091405
22.0	0.999	0.00487	0.049	0.180	41.0	P	N/A	9.00	9.12	9.21	9.00	9.00	37.50	9.00	vis	UCSvis	N/A	N/A	N/A	I	N/A	CS	N/A	N/A	N/A	34S_4p1d8Yd_5	12/4C2	TDP-WTP-068	7091409
22.0	0.999	0.00487	0.049	0.180	40.0	P	N/A	9.41	9.60	9.71	9.50	9.00	47.75	N/A	N/A	N/A	N/A	N/A	N/A	I	N/A	BC	N/A	N/A	N/A	34S_4p1d8Yd_5	12/4C2	TDP-WTP-068	7091411
22.0	0.999	0.00487	0.050	0.330	35.0	P	N/A	5.98	6.04	6.09	6.00	7.50	18.75	N/A	N/A	N/A	N/A	N/A	N/A	N/A	N/A	SS	N/A	N/A	N/A	34S_4p1d8Yc_5	12/4D1	TDP-WTP-068	7091414
22.0	0.999	0.00487	0.049	0.330	29.5	P	N/A	7.04	7.11	7.15	7.00	7.50	29.75	N/A	N/A	N/A	N/A	N/A	N/A	I	N/A	SS+	N/A	N/A	N/A	34S_4p1d8Yc_5	12/4D1	TDP-WTP-068	7091417
22.0	0.999	0.00487	0.049	0.330	27.5	P	N/A	7.51	7.61	7.67	7.50	7.50	38.00	7.50	vis	UCSvis	N/A	N/A	N/A	I	N/A	CS	N/A	N/A	N/A	34S_4p1d8Yc_5	12/4D1	TDP-WTP-068	7091421
22.0	0.999	0.00487	0.049	0.330	26.0	P	N/A	7.92	8.03	8.09	8.00	7.50	48.00	N/A	N/A	N/A	N/A	N/A	N/A	I	N/A	BC	N/A	N/A	N/A	34S_4p1d8Yc_5	12/4D1	TDP-WTP-068	7091423

Appendix C

Concentration Profile Data

Appendix C

Figures

C.1 0.367-m- (14 7/16-in.-) diameter tank, 0.320-cm- (0.126-in.-) diameter nozzle; solids nominal diameter 69.3 μm, 2.48 g/cm^3 density; 0.00155 nominal solids fraction; 33.2% duty cycle, cycle time 22.0 s, pulse volume fraction 0.050, U_{CS} velocity 2.8 m/s, target nozzle exit velocity 2.8 m/s; peak cloud height upper bound 0.184 m (7.25 in.). Case ID 15E_4s1d2Zc_1. ..... C.7

C.2 0.367-m- (14 7/16-in.-) diameter tank, 0.320-cm- (0.126-in.-) diameter nozzle; solids nominal diameter 69.3 μm, 2.48 g/cm^3 density, 0.005 nominal solids fraction, 33.0% duty cycle, cycle time 15.0 s, pulse volume fraction 0.050, U_{CS} velocity 4.3 m/s, target nozzle exit velocity 4.2 m/s; peak cloud height upper bound 0.140 m (5.5 in.). Case ID 15E_4s1d2Yc_1. ..... C.9

C.3 0.367-m- (14 7/16-in.-) diameter tank, 0.320-cm- (0.126-in.-) diameter nozzle, solids nominal diameter 69.3 μm, 2.48 g/cm^3 density; 0.015 nominal solids fraction, 18.4% duty cycle, cycle time 16.0 s, pulse volume fraction 0.050, U_{CS} velocity 7.2 m/s, target nozzle exit velocity 7.2 m/s; peak cloud height upper bound 0.152 m (6 in.). Case ID 15E_4s1d2Xd_1. ..... C.11

C.4 0.367-m- (14 7/16-in.-) diameter tank, 0.320-cm- (0.126-in.-) diameter nozzle; solids nominal diameter 69.3 μm, 2.48 g/cm^3 density; 0.015 nominal solids fraction, 33.0% duty cycle, cycle time 11.0 s, pulse volume fraction 0.050; U_{CS} velocity 5.8 m/s, target nozzle exit velocity 5.8 m/s; peak cloud height upper bound 0.178 m (7 in.). Case ID 15E_4s1d2Xc_1. ..... C.13

C.5 0.367-m- (14 7/16-in.-) diameter tank, 0.320-cm- (0.126-in.-) diameter nozzle; solids nominal diameter 69.3 μm, 2.48 g/cm^3 density; 0.015 nominal solids fraction, 66.7% duty cycle, cycle time 8.0 s, pulse volume fraction 0.050, U_{CS} velocity 3.9 m/s, target nozzle exit velocity 3.9 m/s; peak cloud height upper bound 0.191 m (7.5 in.). Case ID 15E_4s1d2Xe_1. ..... C.15

C.6 0.367-m- (14 7/16-in.-) diameter tank, 0.320-cm- (0.126-in.-) diameter nozzle; solids nominal diameter 69.3 μm, 2.48 g/cm^3 density, 0.045 nominal solids fraction; 18.8% duty cycle, cycle time 15.8 s, pulse volume fraction 0.050, U_{CS} velocity 7.2 m/s, target nozzle exit velocity 7.2 m/s; peak cloud height upper bound 0.152 m (6 in.). Case ID 15E_4s1d2Wd_1. ..... C.17

C.7 0.367-m- (14 7/16-in.-) diameter tank, 0.320-cm- (0.126-in.-) diameter nozzle; solids nominal diameter 69.3 μm, 2.48 g/cm^3 density; 0.045 nominal solids fraction; 33.2% duty cycle, cycle time 9.8 s, pulse volume fraction 0.050; U_{CS} velocity 6.5 m/s, target nozzle exit velocity 6.5 m/s; peak cloud height upper bound 0.203 m (8 in.). Case ID 15E_4s1d2Wc_1. ..... C.19

C.8 0.367-m- (14 7/16-in.-) diameter tank, 0.320-cm- (0.126-in.-) diameter nozzle; solids nominal diameter 69.3 μm, 2.48 g/cm^3 density; 0.045 nominal solids fraction; 100.0% duty cycle, cycle time infinite, pulse volume fraction undefined, U_{CS} velocity 3 m/s, target nozzle exit velocity 3 m/s; peak cloud height upper bound 0.381 m (15 in.). Case ID 15E_4s1d2Wa. C.21

C.9 0.367-m- (14 7/16-in.-) diameter tank, 0.320-cm- (0.126-in.-) diameter nozzle; solids nominal diameter 69.3 µm, 2.48 g/cm^3 density; 0.045 nominal solids fraction; 33.7% duty cycle, cycle time 8.0 s, pulse volume fraction 0.050, U_{CS} velocity 6.5 m/s, target nozzle exit velocity 8 m/s; peak cloud height upper bound 0.381 m (15 in.). Case ID 15E_4s1d2Wc_1. ..... C.23

C.10 0.367-m- (14 7/16-in.-) diameter tank, 0.320-cm- (0.126-in.-) diameter nozzle; solids nominal diameter 69.3 µm, 2.48 g/cm^3 density; 0.06 nominal solids fraction; 33.6% duty cycle, cycle time 10.2 s, pulse volume fraction 0.050, U_{CS} velocity 6.2 m/s, target nozzle exit velocity 6.2 m/s; peak cloud height upper bound 0.241 m (9.5 in.). Case ID 15E_4s1d2Pc_1 ..... C.25

C.11 0.367-m- (14 7/16-in.-) diameter tank, 0.320-cm- (0.126-in.-) diameter nozzle; solids nominal diameter 75.6 µm, 4.18 g/cm^3 density; 0.00155 nominal solids fraction; 33.5% duty cycle, cycle time 12.0 s, pulse volume fraction 0.050, U_{CS} velocity 5.2 m/s, target nozzle exit velocity 5.2 m/s; peak cloud height upper bound 0.191 m (7.5 in.). Case ID 15E_4s2d2Zc_1. ..... C.27

C.12 0.367-m- (14 7/16-in.-) diameter tank, 0.320-cm- (0.126-in.-) diameter nozzle; solids nominal diameter 75.6 µm, 4.18 g/cm^3 density; 0.015 nominal solids fraction; 33.4% duty cycle, cycle time 5.5 s, pulse volume fraction 0.050, U_{CS} velocity 11.8 m/s, target nozzle exit velocity 11.8 m/s; peak cloud height upper bound 0.165 m (6.5 in.). Case ID 15E_4s2d2Xc_1. ..... C.29

C.13 0.367-m- (14 7/16-in.-) diameter tank, 0.320-cm- (0.126-in.-) diameter nozzle; solids nominal diameter 75.6 µm, 4.18 g/cm^3 density; 0.005 nominal solids fraction; 33.4% duty cycle, cycle time 8.4 s, pulse volume fraction 0.050, U_{CS} velocity 7.6 m/s, target nozzle exit velocity 7.6 m/s; peak cloud height upper bound 0.165 m (6.5 in.). Case ID 15E_4s2d2Yc_1. ..... C.31

C.14 0.367-m- (14 7/16-in.-) diameter tank, 0.320-cm- (0.126-in.-) diameter nozzle; solids nominal diameter 166.4 µm, 2.46 g/cm^3 density; 0.00155 nominal solids fraction; 33.4% duty cycle, cycle time 14.6 s, pulse volume fraction 0.050, U_{CS} velocity 4.2m/s, target nozzle exit velocity 4.2 m/s; peak cloud height upper bound 0.165 m (6.5 in.). Case ID 15E_4s1d1Zc_1 ..... C.33

C.15 0.367-m- (14 7/16-in.-) diameter tank, 0.320-cm- (0.126-in.-) diameter nozzle; solids nominal diameter 166.4 µm, 2.46 g/cm^3 density; 0.015 nominal solids fraction; 33.5% duty cycle, cycle time 7.4 s, pulse volume fraction 0.050, U_{CS} velocity 8.6 m/s, target nozzle exit velocity 8.6 m/s; peak cloud height upper bound 0.152 m (6 in.). Case ID 15E_4s1d1Xc_1. ..... C.35

C.16 0.367-m- (14 7/16-in.-) diameter tank, 0.320-cm- (0.126-in.-) diameter nozzle; solids nominal diameter 43.9 µm, 2.5 g/cm^3 density; 0.005 nominal solids fraction; 33.2% duty cycle, cycle time 17.6 s, pulse volume fraction 0.050, U_{CS} velocity 3.7 m/s, target nozzle exit velocity 3.5 m/s; peak cloud height upper bound 0.229 m (9 in.). Case ID 15E_4s1d5Yc_1. ..... C.37

C.17 0.367-m- (14 7/16-in.-) diameter tank, 0.320-cm- (0.126-in.-) diameter nozzle; solids nominal diameter 164.2 µm, 4.17 g/cm^3 density; 0.00155 nominal solids fraction; 32.8% duty cycle, cycle time 9.4 s, pulse volume fraction 0.050, U_{CS} velocity 6.8 m/s, target nozzle exit velocity 6.8 m/s; peak cloud height upper bound 0.216 m (8.5 in.). Case ID 15E_4s2d1Zc_1 ..... C.39

C.18 0.367-m- (14 7/16-in.-) diameter tank, 0.485-cm- (0.191-in.-) diameter nozzle; solids nominal diameter 69.3 µm, 2.48 g/cm^3 density; 0.0143 nominal solids fraction; 33.3% duty cycle, cycle time 8.8 s, pulse volume fraction 0.050, U_{CS} velocity 4.8 m/s, target nozzle exit velocity 4.8 m/s; peak cloud height upper bound 0.254 (10 in.). Case ID 15E_6s1d2Vc_1. ..... C.41

C.19 0.367-m- (14 7/16-in.-) diameter tank, 0.485-cm- (0.191-in.-) diameter nozzle; solids nominal diameter 69.3 µm, 2.48 g/cm^3 density; 0.015 nominal solids fraction; 33.3% duty cycle, cycle time 9.3 s, pulse volume fraction 0.050, U_{CS} velocity 4.6 m/s, target nozzle exit velocity 4.6 m/s; peak cloud height upper bound 0.229 m (9 in.). Case ID 15E_6s1d2Xc_1. ..... C.43

C.20 0.367-m- (14 7/16-in.-) diameter tank, 0.485-cm- (0.191-in.-) diameter nozzle; solids nominal diameter 69.3 µm, 2.48 g/cm^3 density; 0.015 nominal solids fraction, 32.9% duty cycle, cycle time 18.8 s, pulse volume fraction 0.100, U_{CS} velocity 4.4 m/s, target nozzle exit velocity 4.4 m/s; peak cloud height upper bound 0.229 m (9 in.). Case ID 15E_6s1d2Xc_2. ..... C.45

C.21 0.367-m- (14 7/16-in.-) diameter tank, 0.681-cm- (0.268-in.-) diameter nozzle; solids nominal diameter 69.3 µm, 2.48 g/cm^3 density; 0.0143 nominal solids fraction; 33.0% duty cycle, cycle time 7.6 s, pulse volume fraction 0.050, U_{CS} velocity 2.9 m/s, target nozzle exit velocity 2.9 m/s; peak cloud height upper bound 0.229 m (9 in.). Case ID 15E_Ms1d2Vc_1. ..... C.47

C.22 0.367-m- (14 7/16-in.-) diameter tank, 0.953-cm- (0.375-in.-) diameter nozzle; solids nominal diameter 69.3 µm, 2.48 g/cm^3 density; 0.0143 nominal solids fraction; 33.7% duty cycle, cycle time 5.8 s, pulse volume fraction 0.050, U_{CS} velocity 1.9 m/s, target nozzle exit velocity 1.9 m/s; peak cloud height upper bound 0.254 m (10 in.). Case ID 15E_Ls1d2Vc_1. ..... C.49

C.23 0.367-m- (14 7/16-in.-) diameter tank, 0.953-cm- (0.375-in.-) diameter nozzle; solids nominal diameter 69.3 µm, 2.48 g/cm^3 density; 0.0143 nominal solids fraction; 33.5% duty cycle, cycle time 11.4 s, pulse volume fraction 0.101, U_{CS} velocity 1.9 m/s, target nozzle exit velocity 1.9 m/s; peak cloud height upper bound 0.305 m (12 in.). Case ID 15E_Ls1d2Vc_2. ..... C.51

C.24 0.367-m- (14 7/16-in.-) diameter tank, 0.953-cm- (0.375-in.-) diameter nozzle; solids nominal diameter 69.3 µm, 2.48 g/cm^3 density; 0.0143 nominal solids fraction; 33.5% duty cycle, cycle time 17.0 s, pulse volume fraction 0.100, U_{CS} velocity 2.5 m/s, target nozzle exit velocity 2.5 m/s; peak cloud height upper bound 0.305 m (12 in.). Case ID 15E_Ls1d2Vc_7. ..... C.53

C.25 0.860-m- (33 7/8-in.-) diameter tank, 0.754-cm- (0.297-in.-) diameter nozzle; solids nominal diameter 166.4 µm, 2.46 g/cm^3 density; 0.00155 nominal solids fraction; 33.8% duty cycle, cycle time 32.0 s, pulse volume fraction 0.050, U_{CS} velocity 4.5 m/s, target nozzle exit velocity 4.5 m/s; peak cloud height upper bound 0.356 m (14 in.). Case ID 34S_4s1d1Zc_1 (shown as 34E on plots). C.55

C.26 0.860-m- (33 7/8-in.-) diameter tank, 0.754-cm- (0.297-in.-) diameter nozzle; solids nominal diameter 69.3 µm, 2.48 g/cm^3 density; 0.0015 nominal solids fraction; 33.6% duty cycle, cycle time 39.0 s, pulse volume fraction 0.050, U_{CS} velocity 3.7 m/s, target nozzle exit velocity 3.7 m/s; peak cloud height upper bound 0.533 m (21 in.). Case ID 34S_4s1d2Sc_1 (shown as 34E on plots). C.57

C.27 0.860-m- (33 7/8-in.-) diameter tank, 0.754-cm- (0.297-in.-) diameter nozzle; solids nominal diameter 69.3 µm, 2.48 g/cm^3 density; 0.005 nominal solids fraction; 33.6% duty cycle, cycle time 28.4 s, pulse volume fraction 0.050, U_{CS} velocity 5.1 m/s, target nozzle exit velocity 5.1 m/s; peak cloud height upper bound 0.508 m (20 in.). Case ID 34S_4s1d2Yc_1 (shown as 34E on plots).....C.59

C.28 0.860-m- (33 7/8-in.-) diameter tank, 0.754-cm- (0.297-in.-) diameter nozzle; solids nominal diameter 69.3 µm, 2.48 g/cm^3 density; 0.005 nominal solids fraction; 18.6% duty cycle, cycle time 42.4 s, pulse volume fraction 0.050, U_{CS} velocity 6 m/s, target nozzle exit velocity 6.2 m/s; peak cloud height upper bound 0.559 m (22 in.). Case ID 34S_4s1d2Yd_1 (shown as 34E on plots). C.61

C.29 0.860-m- (33 7/8-in.-) diameter tank, 0.754-cm- (0.297-in.-) diameter nozzle; solids nominal diameter 75.6 µm, 4.18 g/cm^3 density; 0.00155 nominal solids fraction; 33.5% duty cycle, cycle time 24.9 s, pulse volume fraction 0.050, U_{CS} velocity 5.6 m/s, target nozzle exit velocity 5.6 m/s; peak cloud height upper bound 0.368 m (14.5 in.). Case ID 34S_4s2d2Zc_1 (shown as 34E on plots). C.63

C.30 0.860-m- (33 7/8-in.-) diameter tank, 0.754-cm- (0.297-in.-) diameter nozzle; solids nominal diameter 75.6 µm, 4.18 g/cm^3 density; 0.015 nominal solids fraction; 33.9% duty cycle, cycle time 14.8 s, pulse volume fraction 0.050, U_{CS} velocity 9.8 m/s, target nozzle exit velocity 10 m/s; peak cloud height upper bound 0.279 m (11 in.). Case ID 34S_4s2d2Xc_1 (shown as 34E on plots).....C.65

C.31 0.860-m- (33 7/8-in.-) diameter tank, 0.754-cm- (0.297-in.-) diameter nozzle; solids nominal diameter 75.6 µm, 4.18 g/cm^3 density; 0.005 nominal solids fraction; 33.6% duty cycle, cycle time 17.0 s, pulse volume fraction 0.050, U_{CS} velocity 8.6 m/s, target nozzle exit velocity 8.6 m/s; peak cloud height upper bound 0.483 m (19 in.). Case ID 34S_4s2d2Yc_1 (shown as 34E on plots).....C.67

C.32 1.778-m- (70-in.-) diameter tank, 1.557-cm- (0.613-in.-) diameter nozzle; solids nominal diameter 166.4 µm, 2.46 g/cm^3 density; 0.00155 nominal solids fraction; 33.2% duty cycle, cycle time 45.4 s, pulse volume fraction 0.050, U_{CS} velocity 6.7 m/s, target nozzle exit velocity 6.7 m/s; peak cloud height upper bound 0.660 m (26 in.). Case ID 70F_4s1d1Zc_1. .....C.69

C.33 1.778-m- (70-in.-) diameter tank, 1.557-cm- (0.613-in.-) diameter nozzle; solids nominal diameter 166.4 µm, 2.46 g/cm^3 density; 0.00155 nominal solids fraction; 33.5% duty cycle, cycle time 100.8 s, pulse volume fraction 0.101, U_{CS} velocity 5.8 m/s, target nozzle exit velocity 5.8 m/s; peak cloud height upper bound 0.660 m (26 in.). Case ID 70F_4s1d1Zc_2. .....C.71

C.34 1.778-m- (70-in.-) diameter tank, 1.557-cm- (0.613-in.-) diameter nozzle; solids nominal diameter 69.3 µm, 2.48 g/cm^3 density; 0.00155 nominal solids fraction; 33.6% duty cycle, cycle time 67.4 s, pulse volume fraction 0.050, U_{CS} velocity 4.4 m/s, target nozzle exit velocity 4.4 m/s; peak cloud height upper bound 0.749 m (29.5 in.). Case ID 70F_4s1d2Zc_1.....C.73

C.35 1.778-m- (70-in.-) diameter tank, 1.557-cm- (0.613-in.-) diameter nozzle; solids nominal diameter 69.3 µm, 2.48 g/cm^3 density; 0.01 nominal solids fraction; 33.9% duty cycle, cycle time 44.6 s, pulse volume fraction 0.050, U_{CS} velocity 6.6 m/s, target nozzle exit velocity 6.6 m/s; peak cloud height upper bound 0.610 m (24 in.). Case ID 70F_4s1d2Rc_1. .....C.75

C.36 1.778-m- (70-in.-) diameter tank, 1.557-cm- (0.613-in.-) diameter nozzle; solids nominal diameter 69.3 µm, 2.48 g/cm^3 density; 0.005 nominal solids fraction; 33.5% duty cycle, cycle time 51.0 s, pulse volume fraction 0.050, U_{CS} velocity 5.8 m/s, target nozzle exit velocity 5.8 m/s; peak cloud height upper bound 0.597 m (23.5 in.). Case ID 70F_4s1d2Yc_1. ..... C.77

C.37 1.778-m- (70-in.-) diameter tank, 1.557-cm- (0.613-in.-) diameter nozzle; solids nominal diameter 69.3 µm, 2.48 g/cm^3 density; 0.0143 nominal solids fraction; 33.6% duty cycle, cycle time 42.2 s, pulse volume fraction 0.050, U_{CS} velocity 7.1 m/s, target nozzle exit velocity 7.1 m/s; peak cloud height upper bound 0.787 m (31 in.). Case ID 70F_4s1d2Vc_1. ..... C.79

C.38 1.778-m- (70-in.-) diameter tank, 1.557-cm- (0.613-in.-) diameter nozzle; solids nominal diameter 69.3 µm, 2.48 g/cm^3 density; 0.0143 nominal solids fraction; 33.6% duty cycle, cycle time 42.2 s, pulse volume fraction 0.050, U_{CS} velocity 7.1 m/s, target nozzle exit velocity 7.1 m/s; peak cloud height upper bound 0.787 m (31 in.). Case ID 70F_4s1d2Vc_1. ..... C.81

C.39 1.778-m- (70-in.-) diameter tank, 1.557-cm- (0.613-in.-) diameter nozzle; solids nominal diameter 69.3 µm, 2.48 g/cm^3 density; 0.0143 nominal solids fraction; 33.6% duty cycle, cycle time 42.2 s, pulse volume fraction 0.050, U_{CS} velocity 7.1 m/s, target nozzle exit velocity 7.1 m/s; peak cloud height upper bound 0.787 m (31 in.). Case ID 70F_4s1d2Vc_1. ..... C.83

C.40 1.778-m- (70-in.-) diameter tank, 1.557-cm- (0.613-in.-) diameter nozzle; solids nominal diameter 69.3 µm, 2.48 g/cm^3 density; 0.0143 nominal solids fraction; 18.7% duty cycle, cycle time 56.4 s, pulse volume fraction 0.050, U_{CS} velocity 9.8 m/s, target nozzle exit velocity 9.6 m/s; peak cloud height upper bound 0.673 m (26.5 in.). Case ID 70F_4s1d2Vd_1. ..... C.85

C.41 1.778-m- (70-in.-) diameter tank, 1.557-cm- (0.613-in.-) diameter nozzle; solids nominal diameter 69.3 µm, 2.48 g/cm^3 density; 0.0143 nominal solids fraction; 18.7% duty cycle, cycle time 55.6 s, pulse volume fraction 0.050, U_{CS} condition 9.8 m/s, target nozzle exit velocity 9.8 m/s; peak cloud height upper bound 0.724 m (28.5 in.). Case ID 70F_4s1d2Vd_1. ..... C.87

C.42 1.778-m- (70-in.-) diameter tank, 1.557-cm- (0.613-in.-) diameter nozzle; solids nominal diameter 69.3 µm, 2.48 g/cm^3 density; 0.0143 nominal solids fraction; 18.5% duty cycle, cycle time 54.8 s, pulse volume fraction 0.050, U_{CS} velocity 9.9 m/s, target nozzle exit velocity 9.9 m/s; peak cloud height upper bound 0.711 m (28 in.). Case ID 70F_4s1d2Vd_1. ..... C.89

C.43 1.778-m- (70-in.-) diameter tank, 1.557-cm- (0.613-in.-) diameter nozzle; solids nominal diameter 69.3 µm, 2.48 g/cm^3 density; 0.0143 nominal solids fraction; 33.6% duty cycle, cycle time 41.2 s, pulse volume fraction 0.050, U_{CS} velocity 7.3 m/s, target nozzle exit velocity 7.3 m/s; peak cloud height upper bound 0.813 m (32 in.). Case ID 70F_4s1d2Vc_1. ..... C.91

C.44 1.778-m- (70-in.-) diameter tank, 1.557-cm- (0.613-in.-) diameter nozzle; solids nominal diameter 69.3 µm, 2.48 g/cm^3 density; 0.0143 nominal solids fraction; 66.6% duty cycle, cycle time 31.2 s, pulse volume fraction 0.050, U_{CS} velocity 4.8 m/s, target nozzle exit velocity 4.8 m/s; peak cloud height upper bound 0.927 m (36.5 in.). Case ID 70F_4s1d2Ve_1. ..... C.93

C.45 1.778-m- (70-in.-) diameter tank, 1.557-cm- (0.613-in.-) diameter nozzle; solids nominal diameter 69.3 μm, 2.48 g/cm^3 density; 0.0143 nominal solids fraction; 32.7% duty cycle, cycle time 90.0 s, pulse volume fraction 0.100, U_{CS} velocity 6.6 m/s, target nozzle exit velocity 6.6 m/s; peak cloud height upper bound 0.749 m (29.5 in.). Case ID 70F_4s1d2Vc_2. ..... C.95

C.46 1.778-m- (70-in.-) diameter tank, 1.557-cm- (0.613-in.-) diameter nozzle; solids nominal diameter 69.3 μm, 2.48 g/cm^3 density; 0.00155 nominal solids fraction; 33.7% duty cycle, cycle time 63.6 s, pulse volume fraction 0.050; U_{CS} velocity 4.6 m/s, target nozzle exit velocity 4.6 m/s; peak cloud height upper bound 0.787 m (31 in.). Case ID 70E_4s1d2Zc_1. ..... C.97

C.47 1.778-m- (70-in.-) diameter tank, 1.557-cm- (0.613-in.-) diameter nozzle; solids nominal diameter 69.3 μm, 2.48 g/cm^3 density; 0.005 nominal solids fraction; 33.5% duty cycle, cycle time 49.6 s, pulse volume fraction 0.050, U_{CS} velocity 6 m/s, target nozzle exit velocity 6 m/s; peak cloud height upper bound 0.724 m (28.5 in.). Case ID 70E_4s1d2Yc_1. ..... C.99

C.48 1.778-m- (70-in.-) diameter tank, 1.557-cm- (0.613-in.-) diameter nozzle; solids nominal diameter 69.3 μm, 2.48 g/cm^3 density; 0.0143 nominal solids fraction; 18.9% duty cycle, cycle time 48.6 s, pulse volume fraction 0.050, U_{CS} velocity 10.9 m/s, target nozzle exit velocity 11.2 m/s; peak cloud height upper bound 1.168 m (46 in.). Case ID 70E_4s1d2Vd_1. ..... C.101

C.49 1.778-m- (70-in.-) diameter tank, 1.557-cm- (0.613-in.-) diameter nozzle; solids nominal diameter 69.3 μm, 2.48 g/cm^3 density; 0.0143 nominal solids fraction; 18.9% duty cycle, cycle time 48.6 s, pulse volume fraction 0.050, U_{CS} velocity 10.9 m/s, target nozzle exit velocity 11.2 m/s; peak cloud height upper bound 1.168 m (46 in.). Case ID 70E_4s1d2Vd_1. ..... C.103

C.50 1.778-m- (70-in.-) diameter tank, 1.557-cm- (0.613-in.-) diameter nozzle; solids nominal diameter 69.3 μm, 2.48 g/cm^3 density; 0.0143 nominal solids fraction; 18.9% duty cycle, cycle time 48.6 s, pulse volume fraction 0.050, U_{CS} velocity 10.9 m/s, target nozzle exit velocity 11.2 m/s; peak cloud height upper bound 1.168 m (46 in.). Case ID 70E_4s1d2Vd_1. ..... C.105

C.51 1.778-m- (70-in.-) diameter tank, 1.557-cm- (0.613-in.-) diameter nozzle; solids nominal diameter 69.3 μm, 2.48 g/cm^3 density; 0.0143 nominal solids fraction; 33.3% duty cycle, cycle time 38.8 s, pulse volume fraction 0.050, U_{CS} velocity 7.8 m/s, target nozzle exit velocity 7.8 m/s; peak cloud height upper bound 1.041 m (41 in.). Case ID 70E_4s1d2Vc_1. ..... C.107

C.52 1.778-m- (70-in.-) diameter tank, 1.557-cm- (0.613-in.-) diameter nozzle; solids nominal diameter 69.3 μm, 2.48 g/cm^3 density; 0.0143 nominal solids fraction; 33.3% duty cycle, cycle time 38.8 s, pulse volume fraction 0.050, U_{CS} velocity 7.8 m/s, target nozzle exit velocity 7.8 m/s; peak cloud height upper bound 1.041 m (41 in.). Case ID 70E_4s1d2Vc_1. ..... C.109

C.53 1.778-m- (70-in.-) diameter tank, 1.557-cm- (0.613-in.-) diameter nozzle; solids nominal diameter 69.3 μm, 2.48 g/cm^3 density; 0.0143 nominal solids fraction; 33.3% duty cycle, cycle time 38.8 s, pulse volume fraction 0.050, U_{CS} velocity 7.8 m/s, target nozzle exit velocity 7.8 m/s; peak cloud height upper bound 1.041 m (41 in.). Case ID 70E_4s1d2Vc_1. ..... C.111

C.54 1.778-m- (70-in.-) diameter tank, 1.557-cm- (0.613-in.-) diameter nozzle; solids nominal diameter 69.3 μm, 2.48 g/cm^3 density; 0.015 nominal solids fraction; 32.9% duty cycle, cycle time 44.6 s, pulse volume fraction 0.050, U_{CS} velocity 8.5 m/s, target nozzle exit velocity 6.8 m/s; peak cloud height upper bound 0.572 m (22.5 in.). Case ID 70E_4s1d2Xc_1. ..... C.113

C.55 1.778-m- (70-in.-) diameter tank, 1.557-cm- (0.613-in.-) diameter nozzle; solids nominal diameter 69.3 μm, 2.48 g/cm^3 density; 0.015 nominal solids fraction; 33.7% duty cycle, cycle time 35.4 s, pulse volume fraction 0.050, U_{CS} velocity 8.5 m/s, target nozzle exit velocity 8.5 m/s; peak cloud height upper bound 1.067 m (42 in.). Case ID 70E_4s1d2Xc_1. ..... C.115

C.56 1.778-m- (70-in.-) diameter tank, 1.557-cm- (0.613-in.-) diameter nozzle; solids nominal diameter 69.3 μm, 2.48 g/cm^3 density; 0.015 nominal solids fraction; 33.7% duty cycle, cycle time 35.4 s, pulse volume fraction 0.050, U_{CS} velocity 8.5 m/s, target nozzle exit velocity 8.5 m/s; peak cloud height upper bound 1.067 m (42 in.). Case ID 70E_4s1d2Xc_1. ..... C.117

C.57 1.778-m- (70-in.-) diameter tank, 1.557-cm- (0.613-in.-) diameter nozzle; solids nominal diameter 69.3 μm, 2.48 g/cm^3 density; 0.015 nominal solids fraction; 33.7% duty cycle, cycle time 35.4 s, pulse volume fraction 0.050, U_{CS} velocity 8.5 m/s, target nozzle exit velocity 8.5 m/s; peak cloud height upper bound 1.067 m (42 in.). Case ID 70E_4s1d2Xc_1. ..... C.119

C.58 1.778-m- (70-in.-) diameter tank, 1.557-cm- (0.613-in.-) diameter nozzle; solids nominal diameter 75.6 μm, 4.18 g/cm^3 density; 0.00155 nominal solids fraction; 33.9% duty cycle, cycle time 35.6 s, pulse volume fraction 0.050, U_{CS} velocity 8.4 m/s, target nozzle exit velocity 8.4 m/s; peak cloud height upper bound 0.737 m (29 in.). Case ID 70E_4s2d2Zc_1. ..... C.121

C.59 1.778-m- (70-in.-) diameter tank, 1.557-cm- (0.613-in.-) diameter nozzle; solids nominal diameter 75.6 μm, 4.18 g/cm^3 density; 0.005 nominal solids fraction; 32.8% duty cycle, cycle time 26.0 s, pulse volume fraction 0.050, U_{CS} velocity 12.5 m/s, target nozzle exit velocity 12 m/s; peak cloud height upper bound 0.660 m (26 in.). Case ID 70E_4s2d2Yc_1. ..... C.123

C.60 1.778-m- (70-in.-) diameter tank, 1.557-cm- (0.613-in.-) diameter nozzle; solids nominal diameter 75.6 μm, 4.18 g/cm^3 density; 0.005 nominal solids fraction, 32.8% duty cycle, cycle time 26.0 s, pulse volume fraction 0.050, U_{CS} velocity 12.5 m/s, target nozzle exit velocity 12 m/s; peak cloud height upper bound 0.660 m (26 in.). Case ID 70E_4s2d2Yc_1. ..... C.125

C.61 1.778-m- (70-in.-) diameter tank, 1.557-cm- (0.613-in.-) diameter nozzle; solids nominal diameter 75.6 μm, 4.18 g/cm^3 density; 0.005 nominal solids fraction; 32.8% duty cycle, cycle time 26.0 s, pulse volume fraction 0.050, U_{CS} velocity 12.5 m/s, target nozzle exit velocity 12 m/s; peak cloud height upper bound 0.660 m (26 in.). Case ID 70E_4s2d2Yc_1. ..... C.127

C.62 1.778-m- (70-in.-) diameter tank, 1.557-cm- (0.613-in.-) diameter nozzle; solids nominal diameter 166.4 μm, 2.46 g/cm^3 density; 0.00155 nominal solids fraction; 33.4% duty cycle, cycle time 42.6 s, pulse volume fraction 0.050, U_{CS} velocity 7.1 m/s, target nozzle exit velocity 7.1 m/s; peak cloud height upper bound 0.800 m (31.5 in.). Case ID 70E_4s1d1Zc_1. ..... C.129

C.63 1.778-m- (70-in.-) diameter tank, 1.557-cm- (0.613-in.-) diameter nozzle; solids nominal diameter 166.4 μm, 2.46 g/cm^3 density; 0.00155 nominal solids fraction; 33.4% duty cycle, cycle time 42.6 s, pulse volume fraction 0.050, U_{CS} velocity 7.1 m/s, target nozzle exit velocity 7.1 m/s; peak cloud height upper bound 0.800 m (31.5 in.). Case ID 70E_4s1d1Zc_1. ....C.131

C.64 1.778-m- (70-in.-) diameter tank, 1.557-cm- (0.613-in.-) diameter nozzle; solids nominal diameter 166.4 μm, 2.46 g/cm^3 density; 0.00155 nominal solids fraction; 33.4% duty cycle, cycle time 42.6 s, pulse volume fraction 0.050, U_{CS} velocity 7.1 m/s, target nozzle exit velocity 7.1 m/s; peak cloud height upper bound 0.800 m (31.5 in.). Case ID 70E_4s1d1Zc_1. ....C.133

C.65 1.778-m- (70-in.-) diameter tank, 2.337-cm- (0.92-in.-) diameter nozzle; solids nominal diameter 69.3 μm, 2.48 g/cm^3 density; 0.0143 nominal solids fraction; 33.5% duty cycle, cycle time 29.6 s, pulse volume fraction 0.050, U_{CS} velocity 6.8 m/s, target nozzle exit velocity 6.8 m/s; peak cloud height upper bound 1.829 m (72 in.). Case ID 70E_6s1d2Vc_1. ....C.135

C.66 1.778-m- (70-in.-) diameter tank, 2.337-cm- (0.92-in.-) diameter nozzle; solids nominal diameter 69.3 μm, 2.48 g/cm^3 density; 0.0143 nominal solids fraction; 33.1% duty cycle, cycle time 61.8 s, pulse volume fraction 0.100, U_{CS} velocity 6.4 m/s, target nozzle exit velocity 6.4 m/s; peak cloud height upper bound 1.626 m (64 in.). Case ID 70E_6s1d2Vc_2. ....C.137

Tables

C.1 Summary of Concentration Profile Cases C.2

Symbols

D	diameter of tank
DC	duty cycle
d	diameter of jet nozzle
d_{50}	mean particle diameter
H	fluid height, normal fill level
H_C	average peak cloud height
HS	head shape
N_I	number of jets operating in the inner ring
N_O	number of jets operating in the outer ring
R	tank radius
sxdx	simulant designator (density#particle#)
U	jet velocity
U_{CS}	critical-suspension velocity
V_P	volume of pulse
V_{REF}	reference volume based on the volume of a right circular cylinder of diameter D where height equals diameter, $V_{REF} = (\pi D^3)/4$
V_S	volume of solid particulate
Z	elevation

Greek Symbols

ϕ_p	pulse volume fraction = $(N_I+N_O)\ V_P/\ V_{REF}$
ϕ_S	solids volume fraction: ratio of volume of solid particulate to reference volume = $V_S/(\pi D^3)/4$
ρ_s	solids density

Appendix C

Concentration Profile Data

Solid concentration by volume profile measurements in the cloud of suspended particles were obtained using the ultrasonic concentration probe described in Appendix A. The probe was inserted into the tank at a radial location and elevation. At this position, the probe measured the ultrasonic signal attenuation in real time during the pulse jet mixer cycle. The attenuation measurement was made on the fluid in the volume between the probe ultrasonic transducers. The signal attenuation was used to determine the concentration between the transducers of the probe at that location.

A list of the profiles measured, the test operating conditions, and the velocity and cloud height data for each profile is provided in Table C.1. The table shows the test parameters and radial position of the probe. The first column lists the Appendix C figure number for each profile. The second column lists the test Case ID. The Case ID provides a quick summary of major test conditions, and the components of the Case ID are described in Table B.2. The next ten columns list the operating parameters for the test. For some tests in the large-scale tank, profiles were obtained at three radial locations: tank center [0R], halfway between the center and the wall [0.5R], and near the wall [0.9R], where R is the tank radius. Table C.1 lists the elevation of the "highest concentration test measurement location" associated with the measurement at that radial location. This is the highest nondimensional elevation within the cloud where a measurement was taken. Above this elevation the cloud was not visible. This information is followed by the jet velocity, the critical suspension velocity, and the average peak cloud height associated with the profile. The last column lists the test which shows the date of the measurement followed by the sequence during the day. If the entry in the velocity column is shown in italics, the profile was taken at a velocity below U_{CS}; if the entry in the velocity column is shown in bold, the profile was taken at a velocity above U_{CS}. Most measurements were taken at the critical suspension velocity.

Concentration profiles taken in the small-scale tank with elliptical bottom are shown in Figures C.1 through C.24. Concentration profiles taken in the mid-scale tank with spherical bottom are shown in Figures C.25 through C.31. Concentration profiles taken in the large-scale tank with the flange and dish bottom are shown in Figures C.32 through C.45, and concentration profiles taken in the large-scale tank with the elliptical bottom are shown in Figures C.46 through C.66. When profiles were taken at multiple radii the profile at the tank center [0R] is listed in the first figure for that group, the profile half way between the center and the wall [0.5R] is listed in the next figure, and the profile near the wall [0.9R] is listed in the last figure for that group (where R is the tank radius).

Table C.1. Summary of Concentration Profile Cases

Figure	Case ID	Tank Diameter D	Head Shape HS	Nozzle Diameter d	Number of Nozzles Operated		Density ρ_s	Particle Diameter	Concentration ϕ_S	Duty Cycle DC	Pulse Volume ϕ_p	Elevation of Highest Positive Concentration Measurement			Velocity U	Velocity at U_{CS}	Average Peak Cloud Height H_C	Test
					Outer N_O	Inner N_I		d_{50}				at 0 R	at 0.5 R	at 0.9 R				
text	text	in.	text	in.	integer	integer	g/cm^3	μm	volume fraction	fraction	fraction	Z/D	Z/D	Z/D	m/s	m/s	In.	text
C.1	15E_4s1d2Zc_1	14 7/16	E	0.126	8	4	2.48	69.3	0.00155	0.33	0.05	0.5	n/a	n/a	2.8	2.8	6.88	6/6A
C.2	15E_4s1d2Yc_1	14 7/16	E	0.126	8	4	2.48	69.3	0.005	0.33	0.05	0.4	n/a	n/a	*4.2*	4.3	5	6/9A
C.3	15E_4s1d2Xd_1	14 7/16	E	0.126	8	4	2.48	69.3	0.015	0.18	0.05	0.4	n/a	n/a	7.2	7.2	5.75	6/11A
C.4	15E_4s1d2Xc_1	14 7/16	E	0.126	8	4	2.48	69.3	0.015	0.33	0.05	0.45	n/a	n/a	5.8	5.8	6.62	6/10B
C.5	15E_4s1d2Xe_1	14 7/16	E	0.126	8	4	2.48	69.3	0.015	0.67	0.05	0.55	n/a	n/a	3.9	3.9	7.25	6/12A
C.6	15E_4s1d2Wd_1	14 7/16	E	0.126	8	4	2.48	69.3	0.045	0.19	0.05	0.45	n/a	n/a	7.2	7.2	5.75	6/17A
C.7	15E_4s1d2Wc_1	14 7/16	E	0.126	8	4	2.48	69.3	0.045	0.33	0.05	0.55	n/a	n/a	6.5	6.5	7.5	6/16B
C.8	15E_4s1d2Wa	14 7/16	E	0.126	8	4	2.48	69.3	0.045	1.00	undefined	1.1	n/a	n/a	3	3	14.5	6/17B
C.9	15E_4s1d2Wc_1	14 7/16	E	0.126	8	4	2.48	69.3	0.045	0.34	0.05	1	n/a	n/a	**8**	6.5	14.5	6/17C
C.10	15E_4s1d2Pc_1	14 7/16	E	0.126	8	4	2.48	69.3	0.06	0.34	0.05	0.7	n/a	n/a	6.2	6.2	9.5	6/18A
C.11	15E_4s2d2Zc_1	14 7/16	E	0.126	8	4	4.18	75.6	0.00155	0.34	0.05	0.4	n/a	n/a	5.2	5.2	7	6/19A
C.12	15E_4s2d2Xc_1	14 7/16	E	0.126	8	4	4.18	75.6	0.015	0.33	0.05	0.35	n/a	n/a	11.8	11.8	6	6/20B
C.13	15E_4s2d2Yc_1	14 7/16	E	0.126	8	4	4.18	75.6	0.005	0.33	0.05	0.4	n/a	n/a	7.6	7.6	6	6/20A
C.14	15E_4s1d1Zc_1	14 7/16	E	0.126	8	4	2.46	166.4	0.00155	0.33	0.05	0.45	n/a	n/a	4.2	4.2	6.25	6/26A
C.15	15E_4s1d1Xc_1	14 7/16	E	0.126	8	4	2.46	166.4	0.015	0.34	0.05	0.3	n/a	n/a	8.6	8.6	5.5	6/30A
C.16	15E_4s1d5Yc_1	14 7/16	E	0.126	8	4	2.5	43.9	0.005	0.33	0.05	0.6	n/a	n/a	*3.5*	3.7	8.5	7/1B
C.17	15E_4s2d1Zc_1	14 7/16	E	0.126	8	4	4.17	164.2	0.00155	0.33	0.05	0.6	n/a	n/a	6.8	6.8	8	7/2B
C.18	15E_6s1d2Vc_1	14 7/16	E	0.191	4	4	2.48	69.3	0.0143	0.33	0.05	0.7	n/a	n/a	4.8	4.8	9.5	7/8C
C.19	15E_6s1d2Xc_1	14 7/16	E	0.191	4	4	2.48	69.3	0.015	0.33	0.05	0.6	n/a	n/a	4.6	4.6	8.5	7/9B
C.20	15E_6s1d2Xc_2	14 7/16	E	0.191	4	4	2.48	69.3	0.015	0.33	0.10	0.7	n/a	n/a	4.4	4.4	8.5	7/9C
C.21	15E_Ms1d2Vc_1	14 7/16	E	0.268	4	4	2.48	69.3	0.0143	0.33	0.05	0.8	n/a	n/a	2.9	2.9	8.5	7/11A
C.22	15E_Ls1d2Vc_1	14 7/16	E	0.375	4	4	2.48	69.3	0.0143	0.34	0.05	0.7	n/a	n/a	1.9	1.9	9.5	7/14B
C.23	15E_Ls1d2Vc_2	14 7/16	E	0.375	4	4	2.48	69.3	0.0143	0.33	0.10	0.9	n/a	n/a	1.9	1.9	11.5	7/15B
C.24	15E_Ls1d2Vc_7	14 7/16	E	0.375	4	0	2.48	69.3	0.0143	0.34	0.10	0.9	n/a	n/a	2.5	2.5	11.5	7/15A
C.25	34S_4s1d1Zc_1	33 7/8	S	0.297	8	4	2.46	166.4	0.00155	0.34	0.05	0.4	n/a	n/a	4.5	4.5	13.75	3/5A
C.26	34S_4s1d2Sc_1	33 7/8	S	0.297	8	4	2.48	69.3	0.0015	0.34	0.05	0.6	n/a	n/a	3.7	3.7	19.75	3/7C
C.27	34S_4s1d2Yc_1	33 7/8	S	0.297	8	4	2.48	69.3	0.005	0.34	0.05	0.7	n/a	n/a	5.1	5.1	19.5	3/9A
C.28	34S_4s1d2Yd_1	33 7/8	S	0.297	8	4	2.48	69.3	0.005	0.19	0.05	0.5	n/a	n/a	**6.2**	6	21	3/9B
C.29	34S_4s2d2Zc_1	33 7/8	S	0.297	8	4	4.18	75.6	0.00155	0.33	0.05	0.4	n/a	n/a	5.6	5.6	14	3/11B
C.30	34S_4s2d2Xc_1	33 7/8	S	0.297	8	4	4.18	75.6	0.015	0.34	0.05	0.35	n/a	n/a	**10**	9.8	10.5	3/12C
C.31	34S_4s2d2Yc_1	33 7/8	S	0.297	8	4	4.18	75.6	0.005	0.34	0.05	0.5	n/a	n/a	8.6	8.6	18.5	3/12A

Table C.1. Summary of Concentration Profile Cases (continued)

Figure	Case ID	Tank Diameter D	Head Shape HS	Nozzle Diameter d	Number of Nozzles Operated		Density ρ_s	Particle Diameter	Concentration ϕ_S	Duty Cycle DC	Pulse Volume ϕ_p	Elevation of Highest Positive Concentration Measurement			Velocity U	Velocity at U_{CS}	Average Peak Cloud Height H_C	Test
					Outer N_O	Inner N_I		d_{50}				at 0 R	at 0.5 R	at 0.9 R				
text	text	in.	text	in.	integer	integer	g/cm^3	μm	volume fraction	fraction	fraction	Z/D	Z/D	Z/D	m/s	m/s	m	text
C.32	70F_4s1d1Zc_1	70	FD	0.613	8	4	2.46	166.4	0.00155	0.33	0.05	0.4	n/a	n/a	6.7	6.7	25.5	4/14A
C.33	70F_4s1d1Zc_2	70	FD	0.613	8	4	2.46	166.4	0.00155	0.33	0.10	0.5	n/a	n/a	5.8	5.8	26	4/15C
C.34	70F_4s1d2Zc_1	70	FD	0.613	8	4	2.48	69.3	0.00155	0.34	0.05	0.45	n/a	n/a	4.4	4.4	28.25	4/17A
C.35	70F_4s1d2Rc_1	70	FD	0.613	8	4	2.48	69.3	0.01	0.34	0.05	0.4	n/a	n/a	6.6	6.6	23	4/18B
C.36	70F_4s1d2Yc_1	70	FD	0.613	8	4	2.48	69.3	0.005	0.33	0.05	0.35	n/a	n/a	5.8	5.8	23	4/18A
C.37	70F_4s1d2Vc_1	70	FD	0.613	8	4	2.48	69.3	0.0143	0.34	0.05	0.45	n/a	n/a	7.1	7.1	30	4/21A
C.38	70F_4s1d2Vc_1	70	FD	0.613	8	4	2.48	69.3	0.0143	0.34	0.05	n/a	0.35	n/a	7.1	7.1	30	4/21A
C.39	70F_4s1d2Vc_1	70	FD	0.613	8	4	2.48	69.3	0.0143	0.34	0.05	n/a	n/a	0.35	7.1	7.1	30	4/21A
C.40	70F_4s1d2Vd_1	70	FD	0.613	8	4	2.48	69.3	0.0143	0.19	0.05	0.4	n/a	n/a	*9.6*	9.8	26.25	4/28A
C.41	70F_4s1d2Vd_1	70	FD	0.613	8	4	2.48	69.3	0.0143	0.19	0.05	0.4	n/a	n/a	9.8	9.8	28	4/28A
C.42	70F_4s1d2Vd_1	70	FD	0.613	8	4	2.48	69.3	0.0143	0.19	0.05	0.45	n/a	n/a	9.9	9.9	27.5	4/22A
C.43	70F_4s1d2Vc_1	70	FD	0.613	8	4	2.48	69.3	0.0143	0.34	0.05	0.45	n/a	n/a	7.3	7.3	31	4/29A
C.44	70F_4s1d2Ve_1	70	FD	0.613	8	4	2.48	69.3	0.0143	0.67	0.05	0.6	n/a	n/a	4.8	4.8	35.75	4/25B
C.45	70F_4s1d2Vc_2	70	FD	0.613	8	4	2.48	69.3	0.0143	0.33	0.10	0.45	n/a	n/a	6.6	6.6	28.5	4/25C
C.46	70E_4s1d2Zc_1	70	E	0.613	8	4	2.48	69.3	0.00155	0.34	0.05	0.45	n/a	n/a	4.6	4.6	30.5	5/9A
C.47	70E_4s1d2Yc_1	70	E	0.613	8	4	2.48	69.3	0.005	0.34	0.05	0.45	n/a	n/a	6	6	27.75	5/12A
C.48	70E_4s1d2Vd_1	70	E	0.613	8	4	2.48	69.3	0.0143	0.19	0.05	0.6	n/a	n/a	**11.2**	10.9	45	5/15A
C.49	70E_4s1d2Vd_1	70	E	0.613	8	4	2.48	69.3	0.0143	0.19	0.05	n/a	0.6	n/a	**11.2**	10.9	45	5/15A
C.50	70E_4s1d2Vd_1	70	E	0.613	8	4	2.48	69.3	0.0143	0.19	0.05	n/a	n/a	0.6	**11.2**	10.9	45	5/15A
C.51	70E_4s1d2Vc_1	70	E	0.613	8	4	2.48	69.3	0.0143	0.33	0.05	0.6	n/a	n/a	7.8	7.8	41	5/14A
C.52	70E_4s1d2Vc_1	70	E	0.613	8	4	2.48	69.3	0.0143	0.33	0.05	n/a	0.6	n/a	7.8	7.8	41	5/14A
C.53	70E_4s1d2Vc_1	70	E	0.613	8	4	2.48	69.3	0.0143	0.33	0.05	n/a	n/a	0.6	7.8	7.8	41	5/14A
C.54	70E_4s1d2Xc_1	70	E	0.613	8	4	2.48	69.3	0.015	0.33	0.05	0.35	n/a	n/a	*6.8*	8.5	22	5/20A
C.55	70E_4s1d2Xc_1	70	E	0.613	8	4	2.48	69.3	0.015	0.34	0.05	0.7	n/a	n/a	8.5	8.5	41	5/20A
C.56	70E_4s1d2Xc_1	70	E	0.613	8	4	2.48	69.3	0.015	0.34	0.05	n/a	0.7	n/a	8.5	8.5	41	5/20A
C.57	70E_4s1d2Xc_1	70	E	0.613	8	4	2.48	69.3	0.015	0.34	0.05	n/a	n/a	0.7	8.5	8.5	41	5/20A
C.58	70E_4s2d2Zc_1	70	E	0.613	8	4	4.18	75.6	0.00155	0.34	0.05	0.5	n/a	n/a	8.4	8.4	28.5	5/27A
C.59	70E_4s2d2Yc_1	70	E	0.613	8	4	4.18	75.6	0.005	0.33	0.05	0.35	n/a	n/a	*12*	12.5	25.5	5/28A
C.60	70E_4s2d2Yc_1	70	E	0.613	8	4	4.18	75.6	0.005	0.33	0.05	n/a	0.35	n/a	*12*	12.5	25.5	5/28A
C.61	70E_4s2d2Yc_1	70	E	0.613	8	4	4.18	75.6	0.005	0.33	0.05	n/a	n/a	0.35	*12*	12.5	25.5	5/28A
C.62	70E_4s1d1Zc_1	70	E	0.613	8	4	2.46	166.4	0.00155	0.33	0.05	0.4	n/a	n/a	7.1	7.1	30.75	5/30A
C.63	70E_4s1d1Zc_1	70	E	0.613	8	4	2.46	166.4	0.00155	0.33	0.05	n/a	0.35	n/a	7.1	7.1	30.75	5/30A
C.64	70E_4s1d1Zc_1	70	E	0.613	8	4	2.46	166.4	0.00155	0.33	0.05	n/a	n/a	0.35	7.1	7.1	30.75	5/30A
C.65	70E_6s1d2Vc_1	70	E	0.92	4	4	2.48	69.3	0.0143	0.34	0.05	1.0	n/a	n/a	6.8	6.8	70	7/18A
C.66	70E_6s1d2Vc_2	70	E	0.92	4	4	2.48	69.3	0.0143	0.33	0.10	0.8	n/a	n/a	6.4	6.4	63	7/18B

In the small-scale tank, 24 concentration profiles were measured and are shown in Figures C.1 through C.24. This test platform provided the broadest range of test conditions, which are listed below grouped by simulant:

- s1d2
  - 10 profiles were obtained in the HLP-22 12 tube array vessel configuration[8/4]
  - 3 profiles were obtained in the 8TA (eight tube array) configuration [4/4] with a 6-in. full-scale nozzle
  - 1 profile was obtained in the 8TA configuration [4/4] using an 8.5 in. full-scale nozzle (M in the Case ID)
  - 2 profiles were obtained in the 8TA configuration [4/4] using an 11.8-in. full-scale nozzle (L in the Case ID)
  - 1 profile was obtained in the 8TA configuration using an 11.8-in. full-scale nozzle with only the four outer tubes operating [4/0]
- s2d2
  - 3 profiles were obtained in the HLP-22 vessel configuration
- s1d1
  - 2 profiles were obtained in the HLP-22 vessel configuration
- s1d5
  - 1 profile was obtained in the HLP-22 vessel configuration
- s2d1
  - 1 profile was obtained in the HLP-22 vessel configuration

In the mid-scale tank seven concentration profiles were measured, which are shown in Figures C.25 through C.31. The profiles were all conducted in the HLP-22 vessel configuration and are grouped by simulant.

- s1d2
  - 3 profiles
- s1d1
  - 1 profile
- s2d2
  - 3 profiles

In the large-scale tank with the flange and dish bottom, 14 concentration profiles were measured and are shown in Figures C.32 through C.45. The profiles were all conducted in the HLP-22 vessel configuration and are grouped by simulant.

- s1d2
  - 10 profiles at R=0; 1 profile at R=0.5; 1 profile at R=0.9
- s1d1
  - 2 profiles at R=0

In the large-scale tank with the elliptical bottom, 21 concentration profiles were measured and are shown in Figures C.46 through C.66.

- s1d2
  - 6 profiles at R = 0; 3 profile at R = 0.5; 3 profile at R = 0.9 in the HLP-22 vessel configuration
  - 2 profiles at R = 0 were obtained in the 8TA configuration using a 6 in. full-scale nozzle
- s1d1
  - 1 profile at R = 0; 1 profile at R = 0.5; 1 profile at R = 0.9 were obtained in the HLP-22 vessel configuration
- s2d2
  - 2 profiles at R = 0; 1 profile at R = 0.5; 1 profile at R = 0.9 were obtained in the HLP-22 vessel configuration

The first solid concentration by volume profile shown in Figure C.1 for Case ID 15E_4s1d2Zc-1 is used to describe the types of information provided for each profile. For each profile the data are plotted dimensionally in the upper row of five plots and nondimensionally in the lower row of five plots. For pulsating flow, each data set consists of a series of 10 plots. The first plot shows the minimum (diamond symbol), average (triangle symbol), and maximum (square symbol) concentration at each elevation throughout the entire pulse cycle. The second plot shows the minimum, average, and maximum concentration at each elevation during the drive portion of the cycle, when fluid is flowing through the pulse tubes. The third plot shows the minimum, average, and maximum concentration at each elevation through the non-drive portion of the cycle, when there is no flow through the pulse tubes. The fourth plot shows the average concentration at each elevation at fractional cycle time increments (slices) during the drive portion of the cycle corresponding to 0.00 (the profile at the start of the pulse), 0.25 (the profile one-quarter of the way through the pulse, 0.50 (the profile half-way through the pulse), 0.75 (the profile three-quarters of the way through the pulse) and 1.00 (the profile at the end of the pulse). The fifth plot shows similar fractional cycle time increments (slices) during the non-drive portion of the cycle. Time 0.00 corresponds to the beginning of the non-drive portion of the pulse and is equivalent to time 1.00 shown in the drive portion of the pulse in the fourth plot. Time 1.00 corresponds to the end of the non-drive portion of the pulse and is equivalent to the time 0.00 at the start of the next pulse.

The accompanying Figure C.1A shows the concentration transient during the pulse cycle at each elevation. Each profile measurement at a specified location captured the concentration transient over duration of one cycle. The measurement started at the beginning of the pulse and ended at the completion of the cycle. Data obtained for up to five pulses were averaged to obtain the transient plots shown in Figure C.1A. The number of pulses in the average is shown in parenthesis as the last number in each plot heading. For example in Figure C.1A the heading of the first plot is 15E_4s1d2Zc_1 H 0.1D R 0R 15_06_06_2008_10_31 (5). 15E_4s1d2Zc_1 is the Case ID. H 0.1D shows the probe elevation [H = 0.1D]. R 0R shows the probe radial location [R = 0R], the center of the tank. 15_06_06_2008_10_31 shows the vessel diameter (15) followed by the date (06-06-2008) followed by the time (10:31), and (5) shows the number of pulses averaged for this plot. At each elevation the averaged data were analyzed to determine the average minimum concentration, average maximum concentration, and average concentration, which are shown in C.1 plots where diamond symbols denote minimum concentration, triangle symbols denote average concentration, and square symbols denote maximum concentration.

If photographs of the side of the tank were taken at this velocity they are shown “for information only” above the first row of figures. The photos are arranged in the following order: The first photo shows the maximum cloud height observed during the pulse. The second photo shows the cloud at the start of the drive portion of the pulse. The third photo shows the cloud at the middle of the drive portion of the pulse. The fourth photo shows the cloud at the end of the drive portion of the pulse. The fifth photo shows the cloud at the middle of the non-drive portion of the pulse.

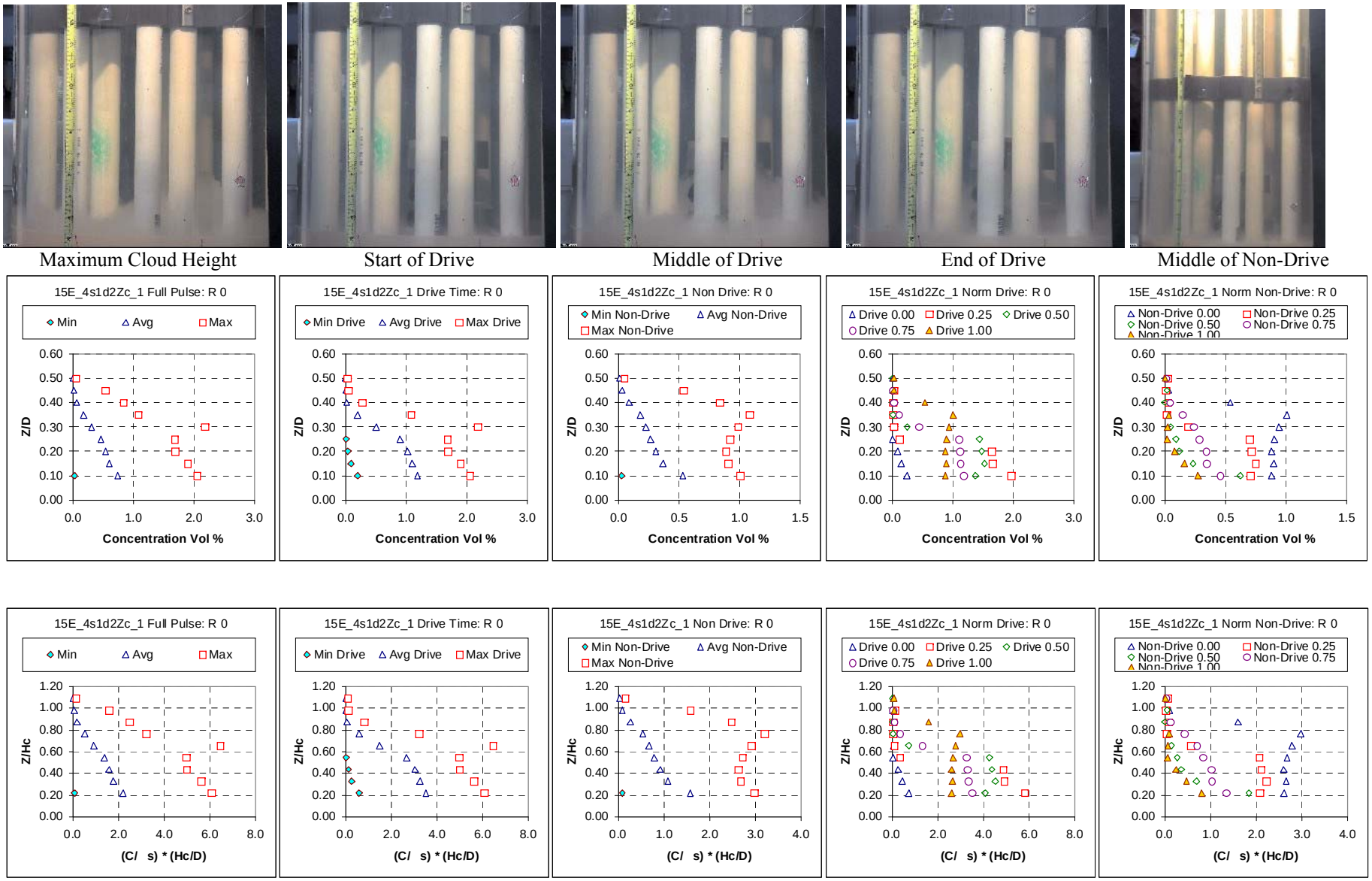

Figure C.1. 0.367-m- (14 7/16-in.-) diameter tank, 0.320-cm- (0.126-in.-) diameter nozzle; solids nominal diameter 69.3 µm, 2.48 g/cm^3 density; 0.00155 nominal solids fraction; 33.2% duty cycle, cycle time 22.0 s, pulse volume fraction 0.050, U_{CS} velocity 2.8 m/s, target nozzle exit velocity 2.8 m/s; peak cloud height upper bound 0.184 m (7.25 in.). Case ID 15E_4s1d2Zc_1.

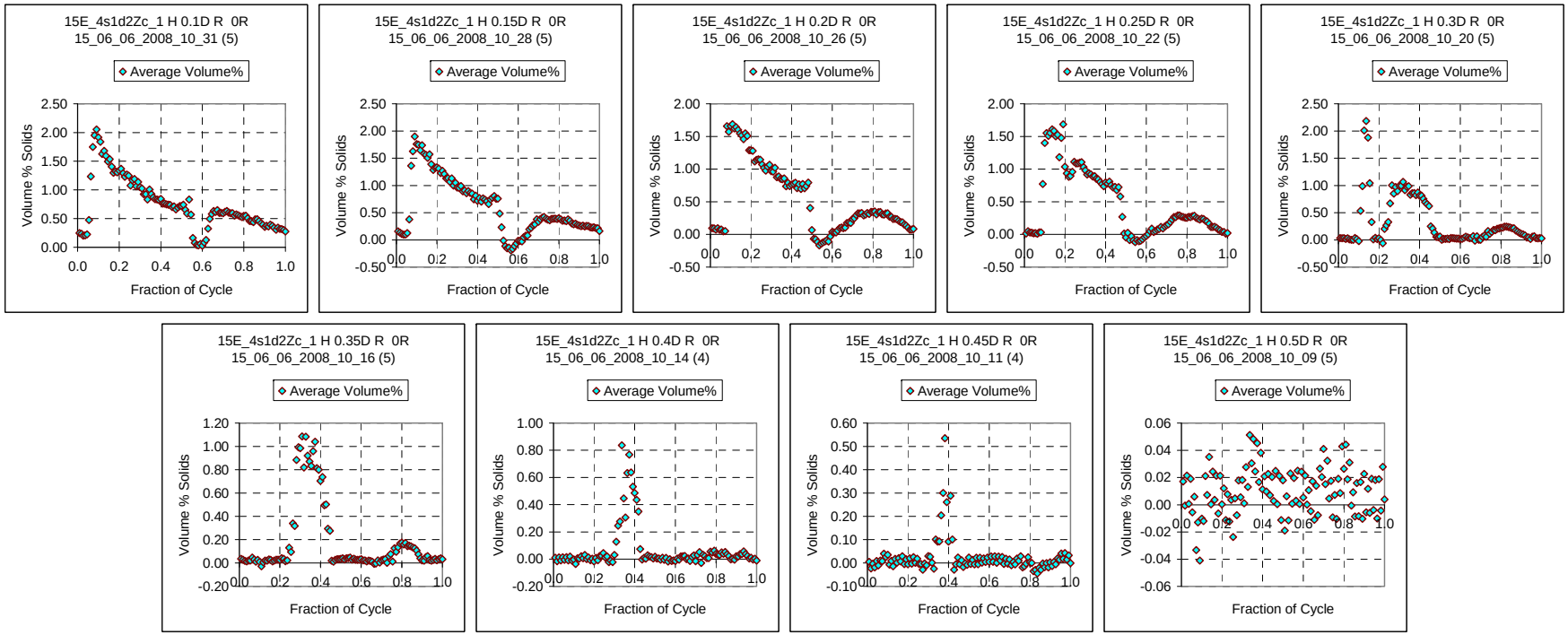

Figure C.1A. Case ID 15E_4s1d2Zc_1 Concentration Variation During the Cycle

The plots in Figure C.1 show the first profile using simulant s1d2 in the small-scale tank. The solids fraction was 0.00155. The U_{CS} velocity was 2.8 m/s. The data in Figure C.1 show that the cloud height rose to an elevation of ~ half the tank diameter. The peak cloud height upper bound was 7.25 in. The transient data in Figure C.1A shows that at H = 0.1D, the maximum concentration occurred at ~0.1 cycle. The maximum concentration at H = 0.45D occurred at ~0.4 cycle. This time lag shows the effect of the pulse upon the solids concentration at that elevation. The concentration in the cloud at 0.1 Z/D was on average <1 vol% solids and at the maximum >2 vol% solids.

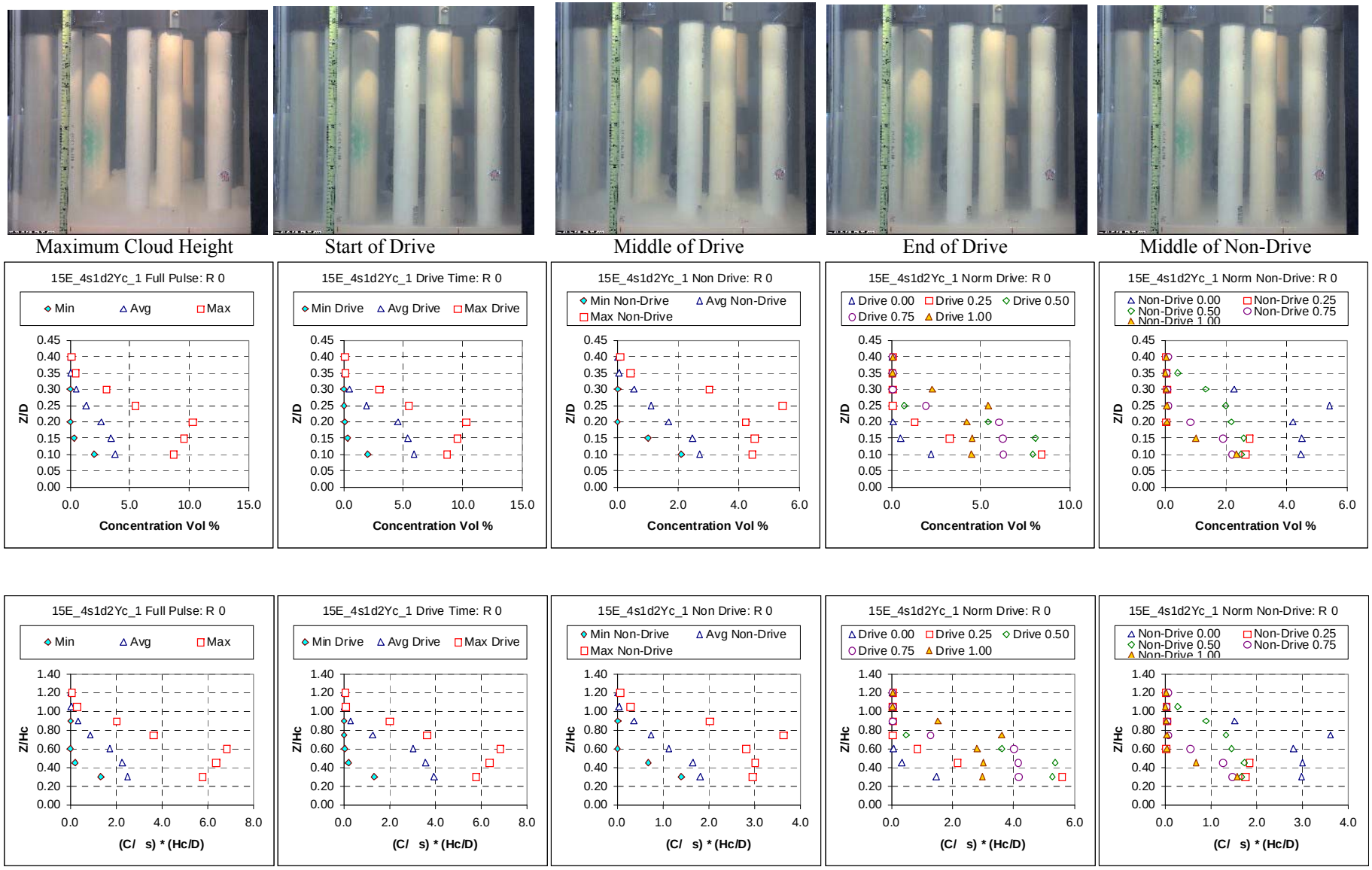

Figure C.2. 0.367-m- (14 7/16-in.-) diameter tank, 0.320-cm- (0.126-in.-) diameter nozzle; solids nominal diameter 69.3 µm, 2.48 g/cm^3 density, 0.005 nominal solids fraction, 33.0% duty cycle, cycle time 15.0 s, pulse volume fraction 0.050, U_{CS} velocity 4.3 m/s, target nozzle exit velocity 4.2 m/s; peak cloud height upper bound 0.140 m (5.5 in.). Case ID 15E_4s1d2Yc_1.

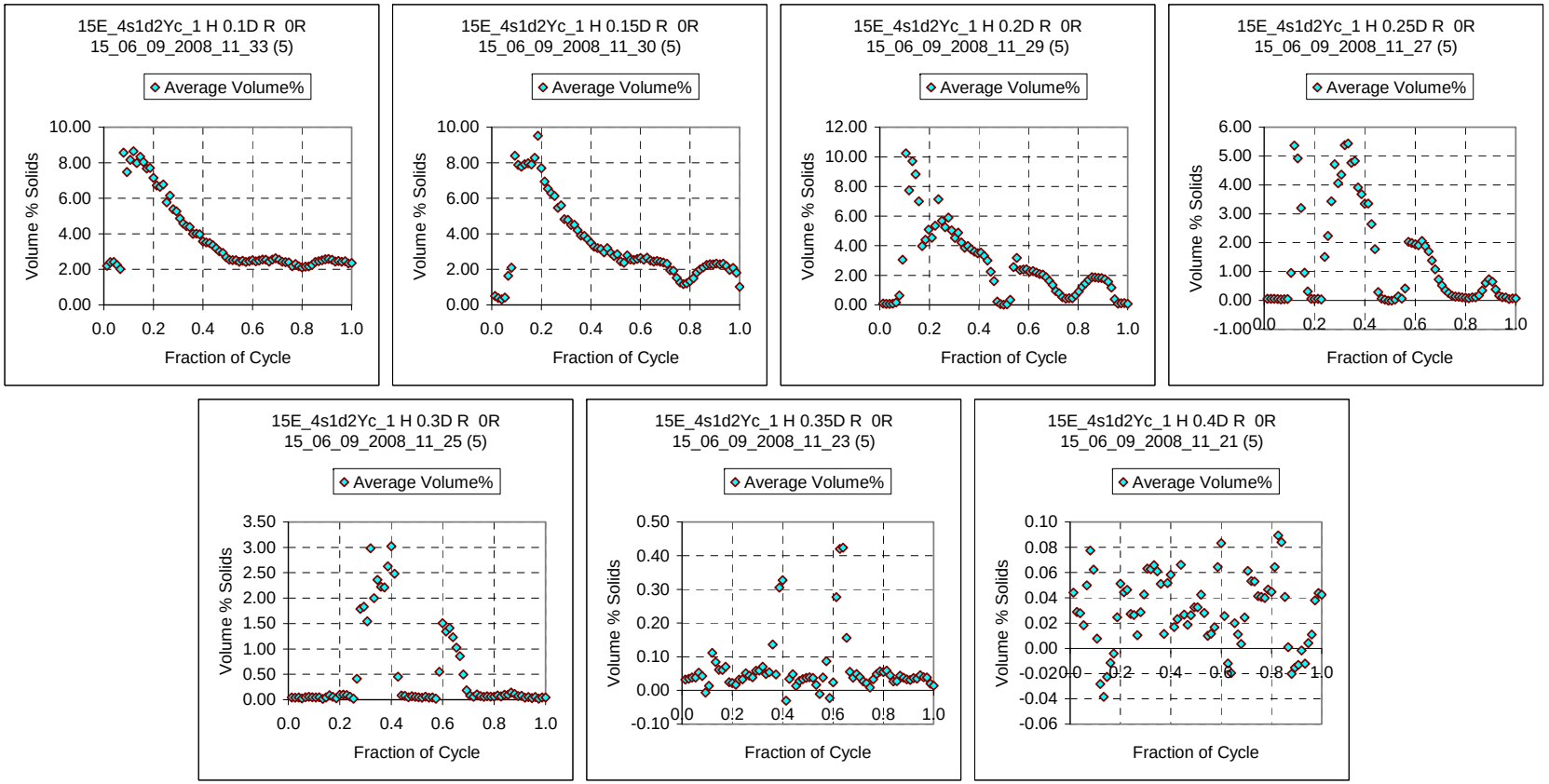

Figure C.2A. Case ID 15E_4s1d2Yc_1 Concentration Variation During the Cycle

This is the second profile shown using simulant s1d2 in the small-scale tank. The solids fraction has increased ~5 times, from 0.00155 in Figure C.1 to 0.005 in Figure C.2. The U_{CS} velocity was higher at 4.3 m/s having increased from 2.8 m/s in the prior test. The peak cloud height upper bound was also lower at 5.5 in. compared to 7.25 in. in the prior test. The transient data in Figure C.2A shows that at H = 0.1D, the maximum concentration occurred at 0.1 cycle as in the prior test. The maximum concentration at H = 0.3D occurred at 0.4 cycle with a second smaller peak observed at 0.6 cycle. The maximum concentration transient of 10 vol% occurred at H = 0.2D at 0.1 cycle.

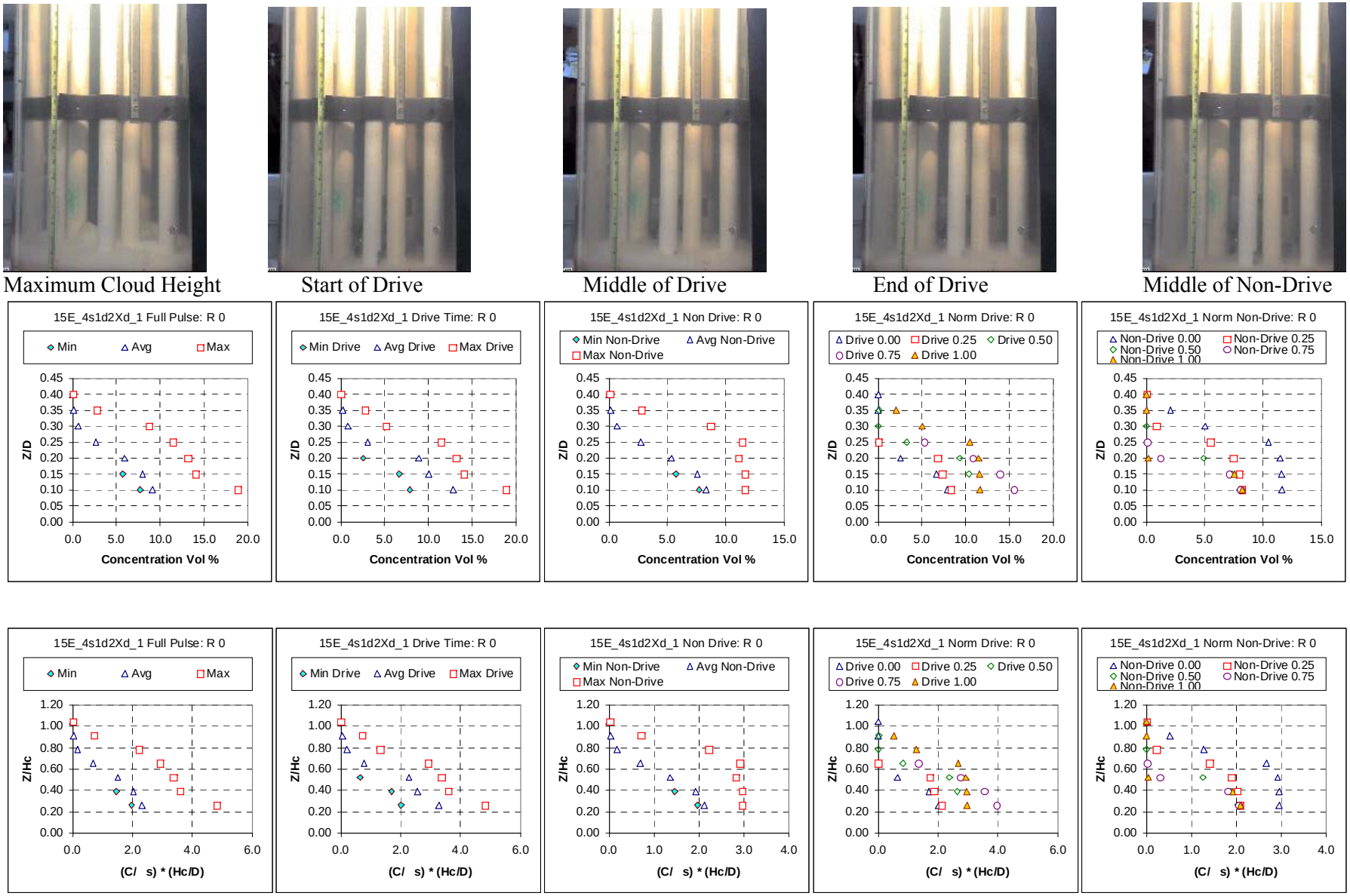

Figure C.3. 0.367-m- (14 7/16-in.-) diameter tank, 0.320-cm- (0.126-in.-) diameter nozzle, solids nominal diameter 69.3 µm, 2.48 g/cm^3 density; 0.015 nominal solids fraction, 18.4% duty cycle, cycle time 16.0 s, pulse volume fraction 0.050, U_{CS} velocity 7.2 m/s, target nozzle exit velocity 7.2 m/s; peak cloud height upper bound 0.152 m (6 in.). Case ID 15E_4s1d2Xd_1.

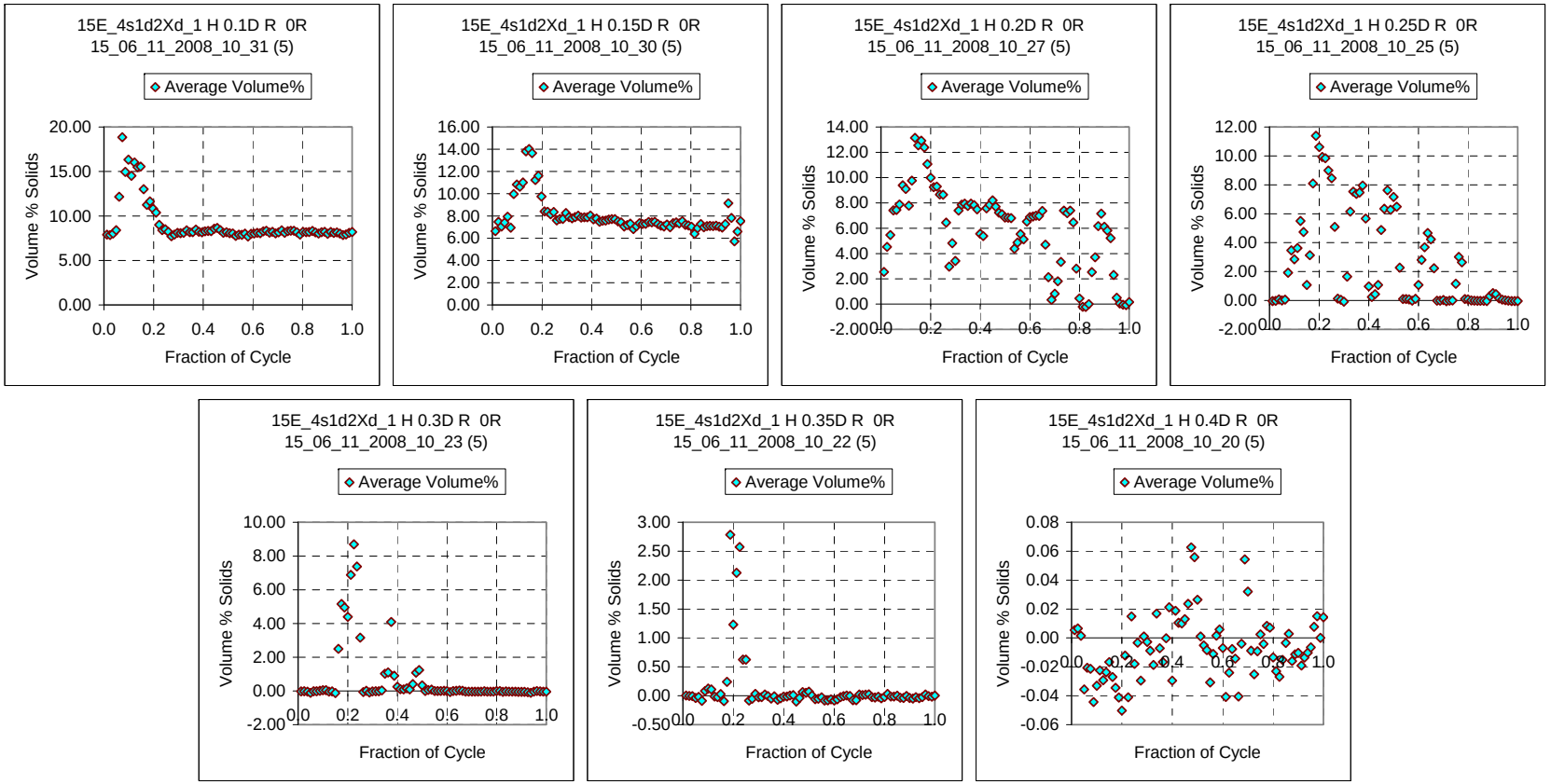

Figure C.3A. Case ID 15E_4s1d2Xd_1 Concentration Variation During the Cycle

This is the third profile shown using simulant s1d2 in the small-scale tank. The solids fraction has increased ~3 times, from 0.005 in Figure C.2 to 0.015 in Figure C.3. The U_{CS} velocity was higher at 7.2 m/s having increased from 4.3 m/s in the prior test. The cloud height was slightly higher at 6.0 in. instead of 5.5 in. in the prior test. In addition, the duty cycle has changed to 18.4% from 33.0% in the prior test. The transient data in Figure C.3A shows that at H = 0.1D, the maximum concentration occurred at ~0.1 cycle as in the prior two tests. The maximum concentration at H = 0.35D occurred at 0.2 cycle. In the prior test with a DC of 33.0 this peak was observed at ~0.4 cycle. The maximum concentration transient of 19 vol% occurred at H = 0.1D at ~0.1 cycle.

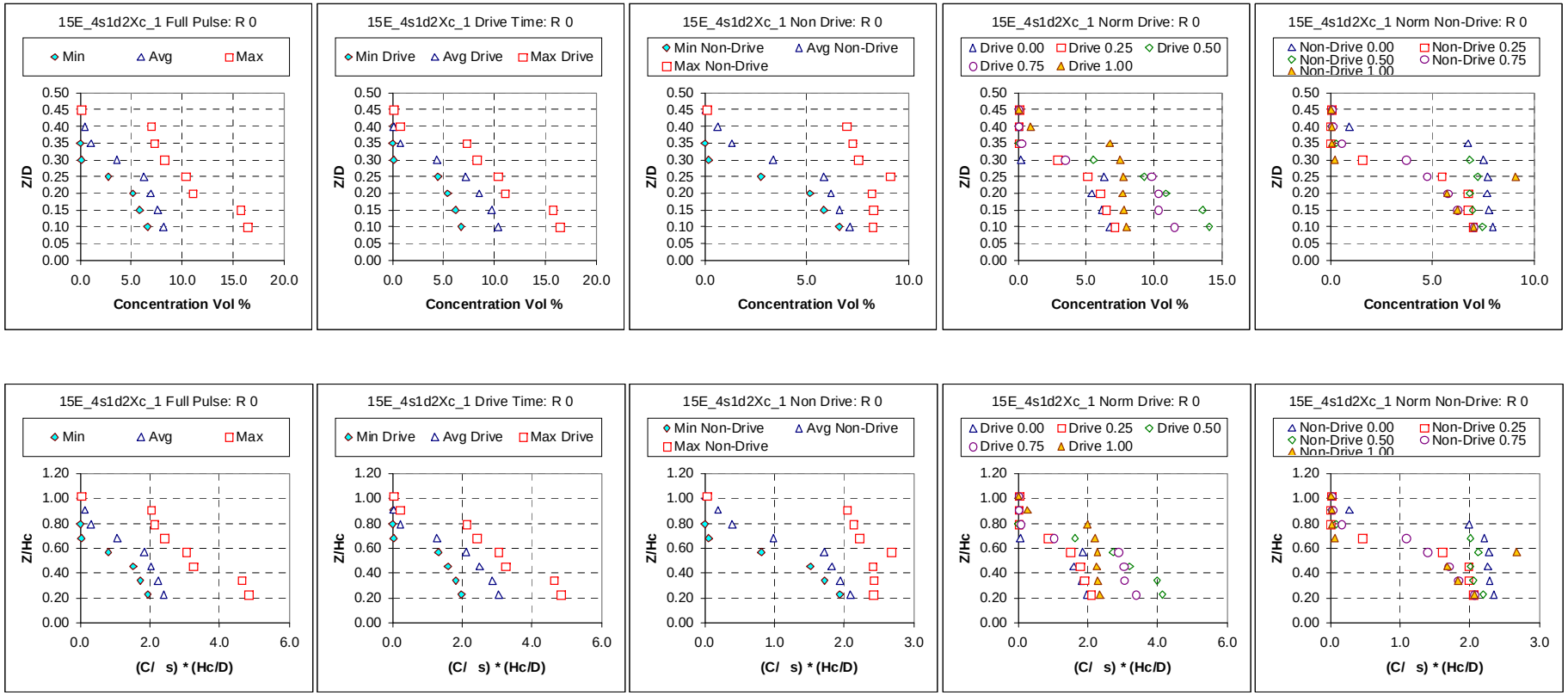

Figure C.4. 0.367-m- (14 7/16-in.-) diameter tank, 0.320-cm- (0.126-in.-) diameter nozzle; solids nominal diameter 69.3 µm, 2.48 g/cm^3 density; 0.015 nominal solids fraction, 33.0% duty cycle, cycle time 11.0 s, pulse volume fraction 0.050; U_{CS} velocity 5.8 m/s, target nozzle exit velocity 5.8 m/s; peak cloud height upper bound 0.178 m (7 in.). Case ID 15E_4s1d2Xc_1.

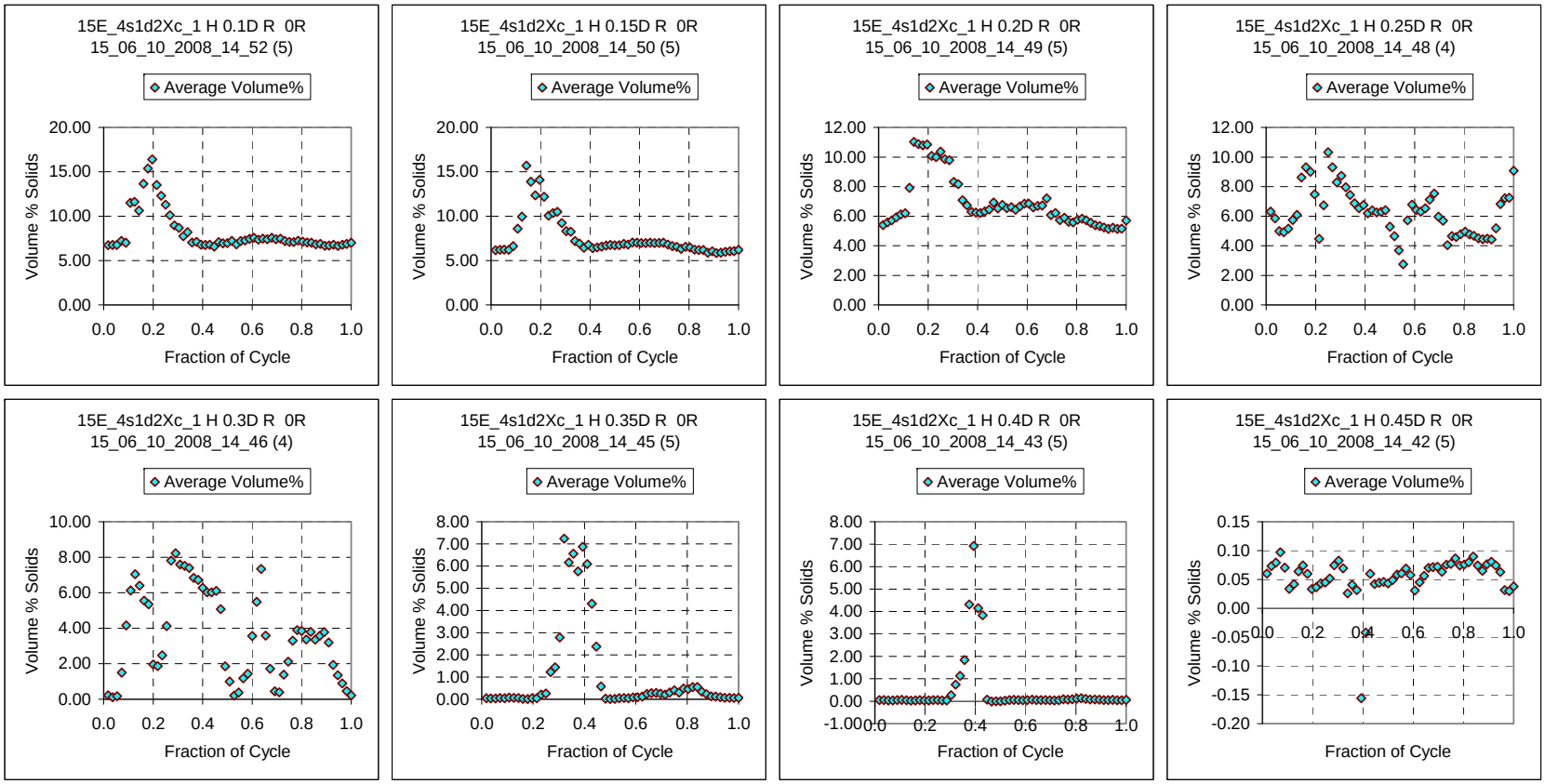

Figure C.4A. Case ID 15E_4s1d2Xc_1 Concentration Variation During the Cycle

This is the fourth profile shown using simulant s1d2 in the small-scale tank. The solids fraction remains at 0.015, the same as in the prior test shown in Figure C.3. The duty cycle has changed to 33.0% from 18.4% in the prior test. The U_{CS} velocity was lower at 5.8 m/s having decreased from 7.2 m/s in the prior test. The peak cloud height upper bound was slightly higher at 7.0 in. instead of 6.0 in. in the prior test. The transient data in Figure C.4A shows that at H = 0.1D, the maximum concentration occurred at 0.2 cycle, later than in the prior two tests. The maximum concentration at H = 0.4D occurred at 0.4 cycle. The maximum concentration transient of 16 vol% occurred at H = 0.1D at 0.2 cycle. Some additional peaks perhaps due to simulant sloshing were observed at elevations of H = 0.25D and 0.3D.

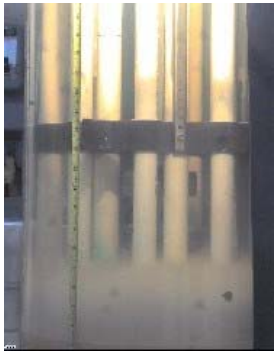

Maximum Cloud Height

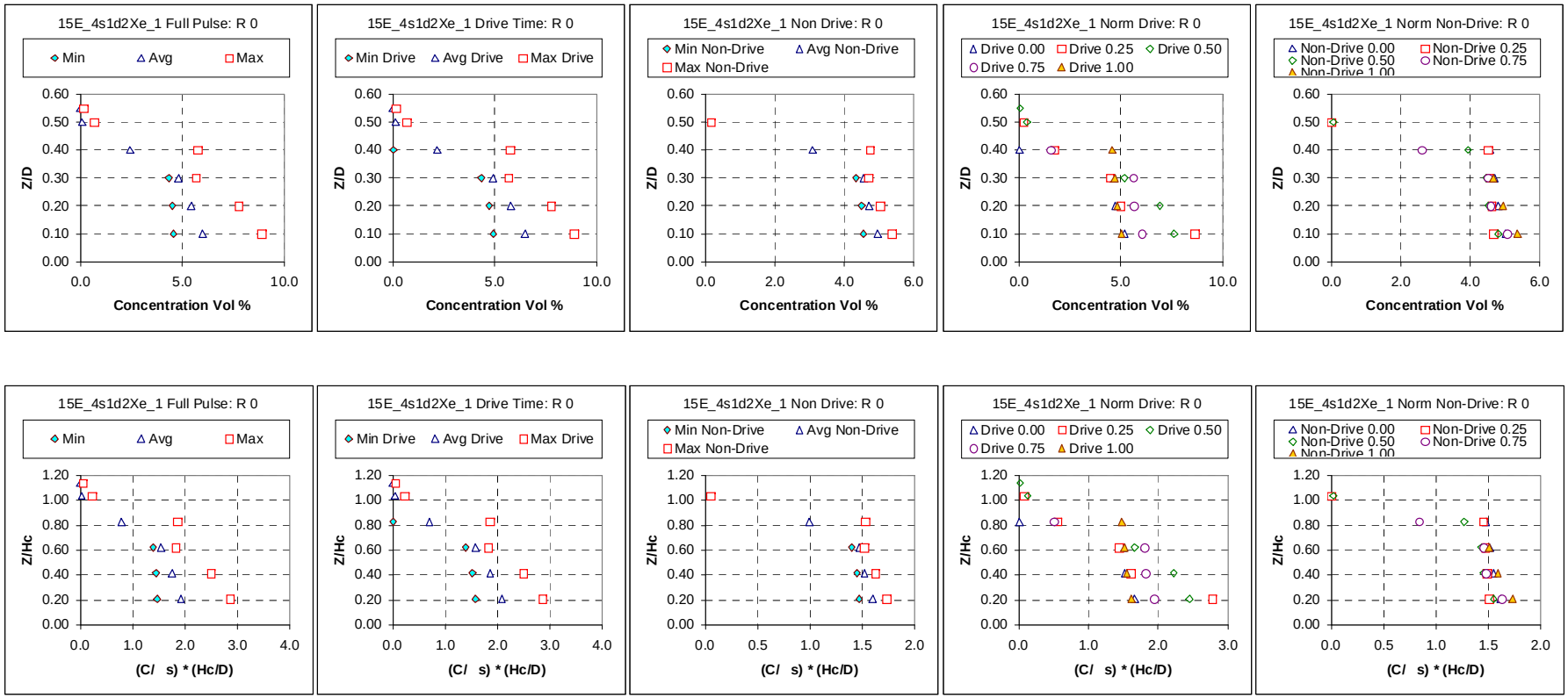

Figure C.5. 0.367-m- (14 7/16-in.-) diameter tank, 0.320-cm- (0.126-in.-) diameter nozzle; solids nominal diameter 69.3 µm, 2.48 g/cm^3 density; 0.015 nominal solids fraction, 66.7% duty cycle, cycle time 8.0 s, pulse volume fraction 0.050, U_{CS} velocity 3.9 m/s, target nozzle exit velocity 3.9 m/s; peak cloud height upper bound 0.191 m (7.5 in.). Case ID 15E_4s1d2Xe_1.

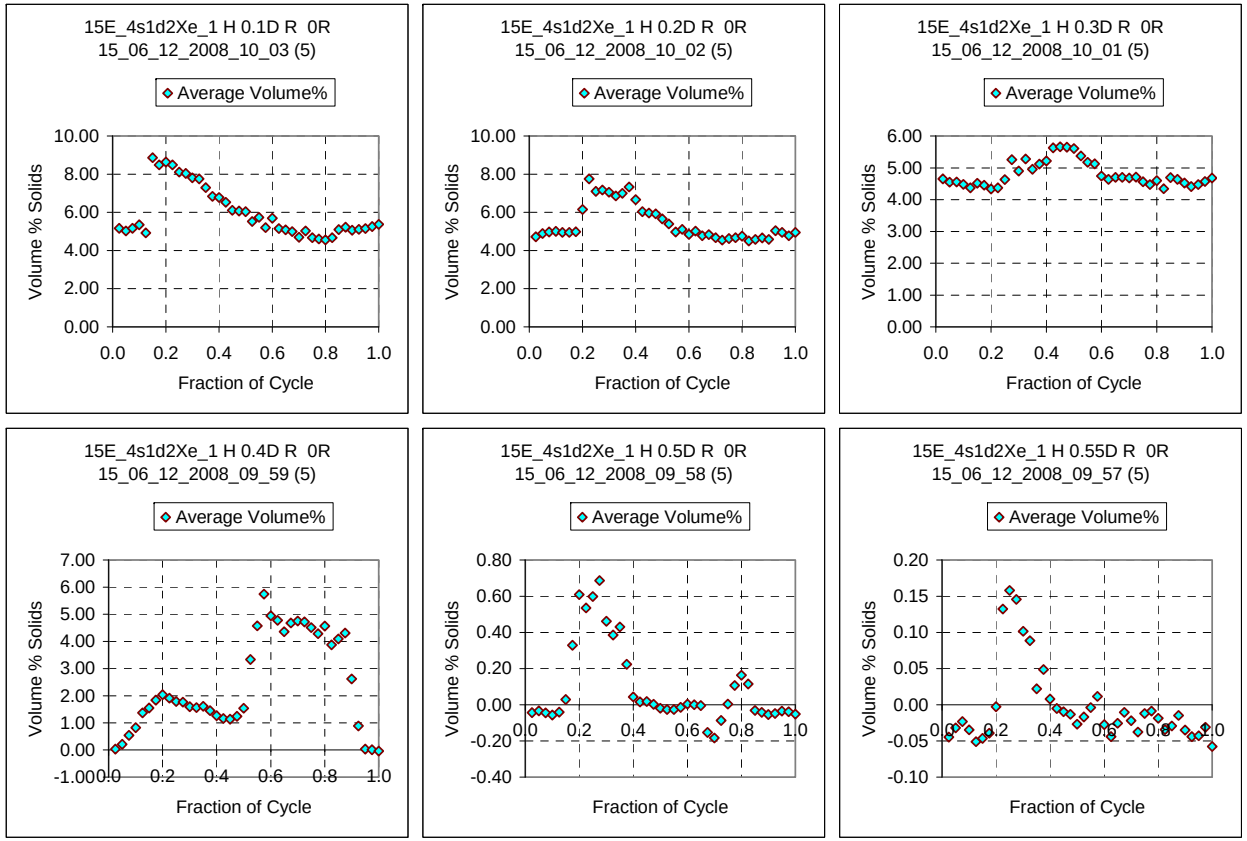

Figure C.5A. Case ID 15E_4s1d2Xe_1 Concentration Variation During the Cycle

This is the fifth profile shown using simulant s1d2 in the small-scale tank. The solids fraction remains at 0.015, the same as in the prior two tests shown in Figures C.3 and C.4. The U_{CS} velocity was lower at 3.9 m/s, having decreased from 5.8 m/s in Figure C.4 and 7.2 m/s in Figure C.3. The peak cloud height upper bound was slightly higher at 7.5 in. instead of 7.0 in. in Figure C.4 and 6.0 in. in Figure C.3. In addition, the duty cycle has changed to 66.7% from 33.0% in Figure C.4 and 18.4% in Figure C.3. The pulse jet was approaching a steady jet. In Figure C.5, the average concentration profile was relatively uniform up to an elevation of Z = 0.3D. The transient data in Figure C.5A shows that at H = 0.1D, the maximum concentration occurred at 0.15 cycle, with a broader peak than in the prior two tests. The maximum concentration at H = 0.5D occurred at ~0.3 cycle. The maximum concentration transient of 9 vol% occurred at H = 0.1D at ~0.15 cycle.

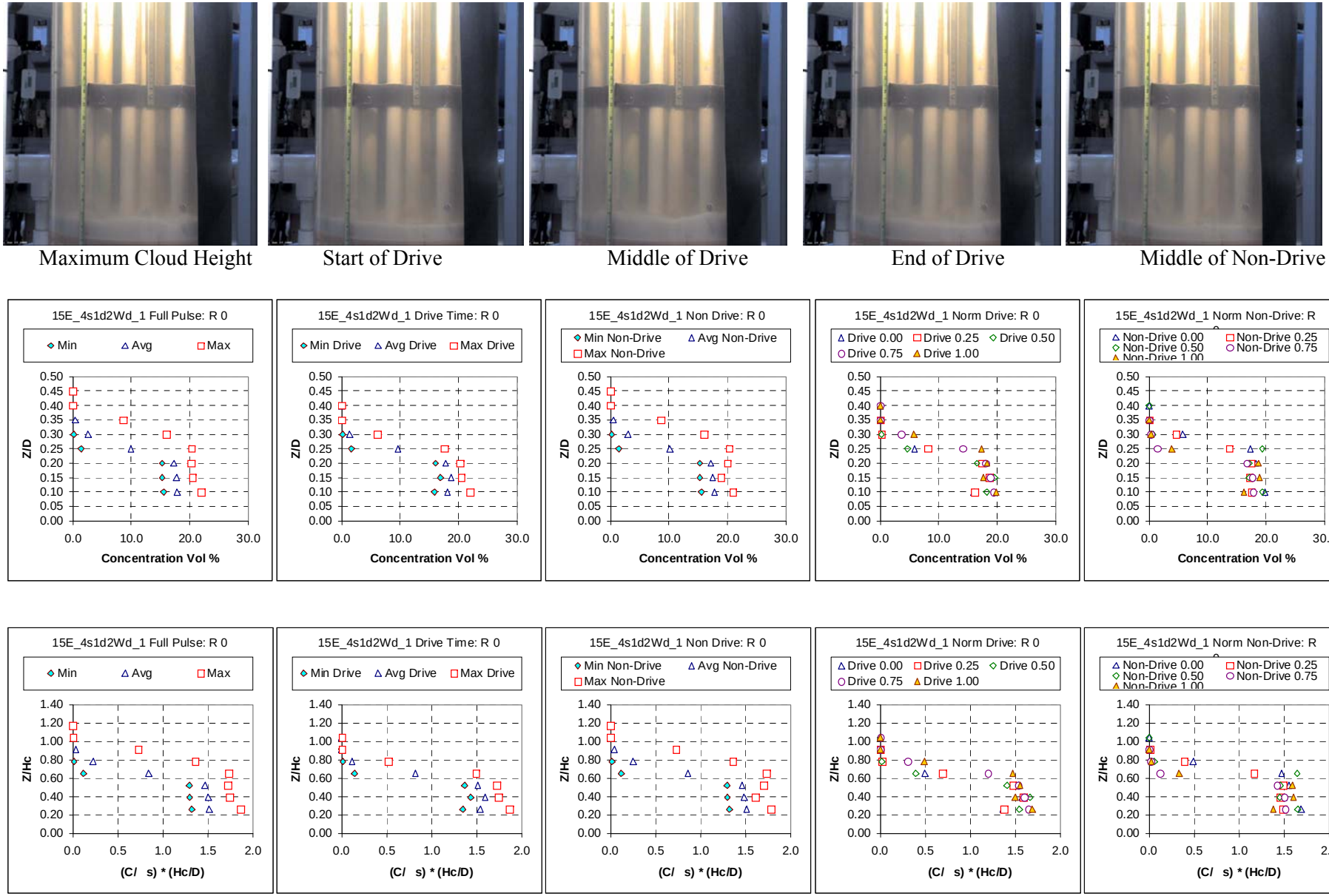

Figure C.6. 0.367-m- (14 7/16-in.-) diameter tank, 0.320-cm- (0.126-in.-) diameter nozzle; solids nominal diameter 69.3 µm, 2.48 g/cm^3 density, 0.045 nominal solids fraction; 18.8% duty cycle, cycle time 15.8 s, pulse volume fraction 0.050, U_{CS} velocity 7.2 m/s, target nozzle exit velocity 7.2 m/s; peak cloud height upper bound 0.152 m (6 in.). Case ID 15E_4s1d2Wd_1.

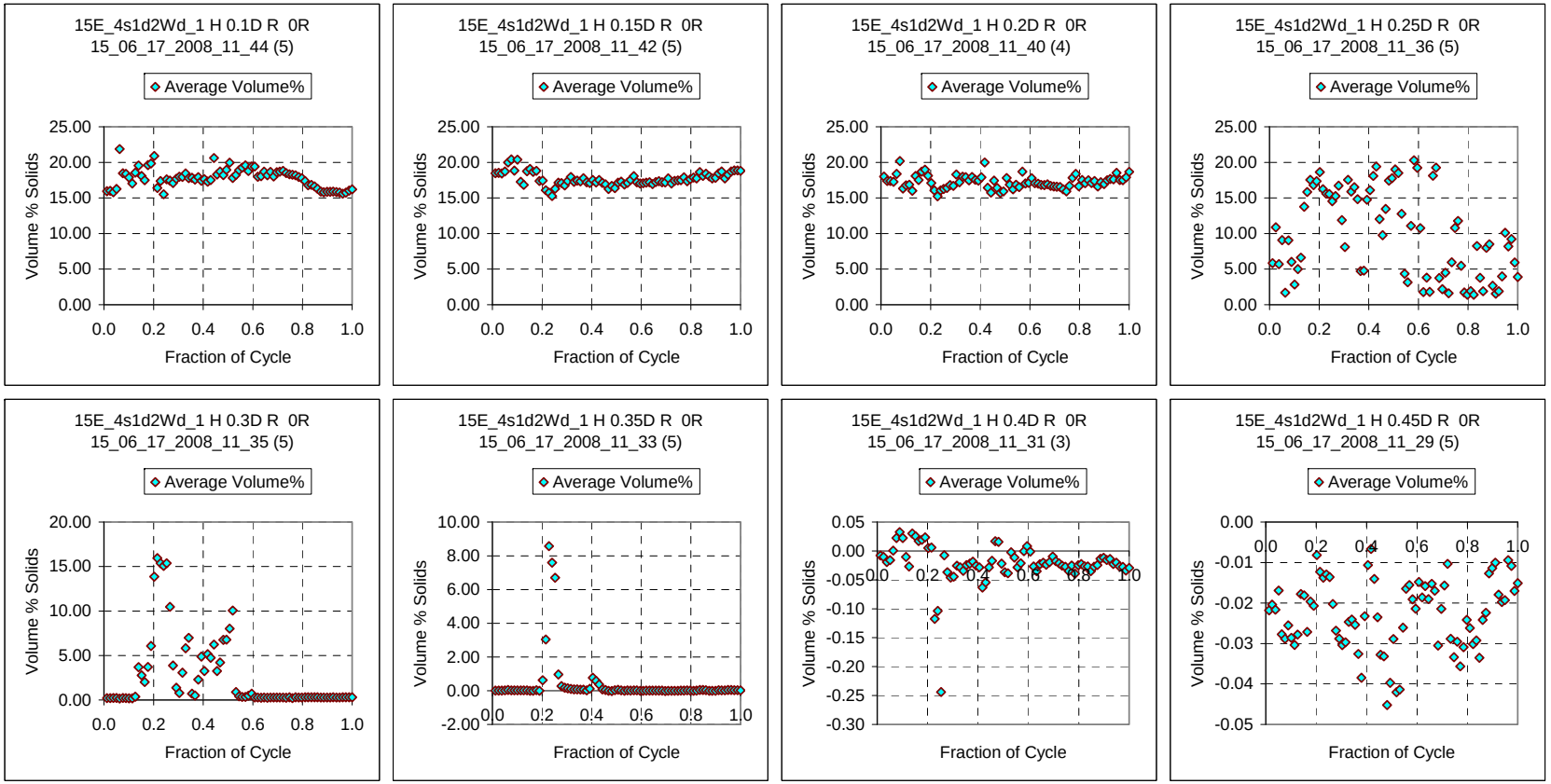

Figure C.6A. Case ID 15E_4s1d2Wd_1 Concentration Variation During the Cycle

This is the sixth profile shown using simulant s1d2 in the small-scale tank. The solids fraction increased ~3 times, to 0.045 from 0.015 in the prior three tests shown in Figures C.3, C.4 and C.5. The U_{CS} velocity occurs 7.2 m/s, the same as was observed in Figure C.3. The peak cloud height upper bound was 6.0 in., also the same as was observed in Figure C.3. In addition the duty cycle was 18.8%, essentially the same as the 18.4% in Figure C.3. In Figure C.6 the average concentration profile was relatively uniform up to an elevation of Z = 0.2D. The transient data in Figure C.6A shows that in the range of H = 0.1D to H = 0.2D concentration was relatively constant throughout the cycle. At the higher elevation of H = 0.35D, the maximum concentration transient of 9 vol% occurred at 0.25 cycle.

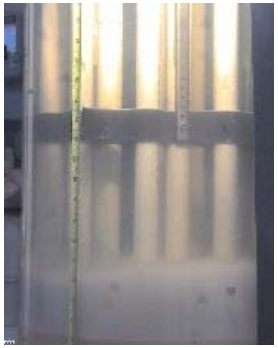

Maximum Cloud Height

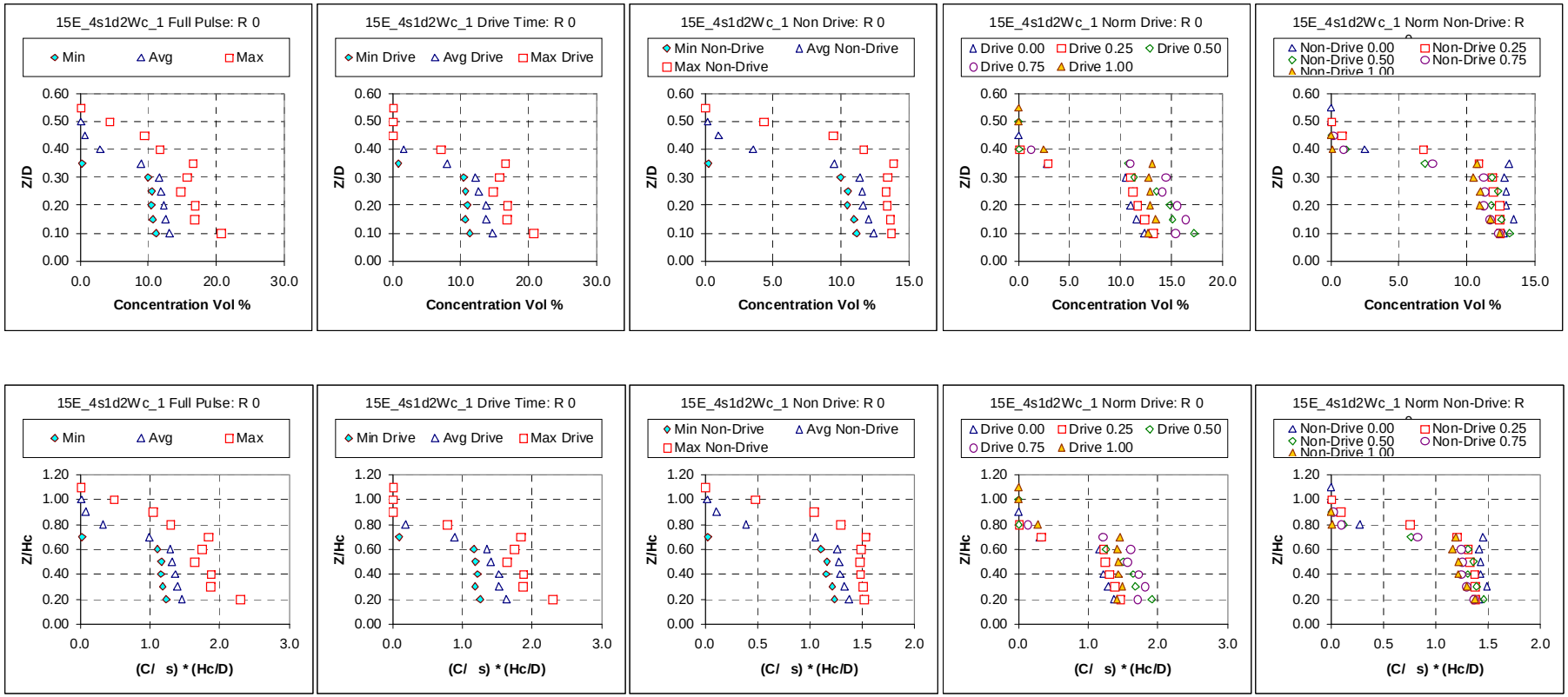

Figure C.7. 0.367-m- (14 7/16-in.-) diameter tank, 0.320-cm- (0.126-in.-) diameter nozzle; solids nominal diameter 69.3 µm, 2.48 g/cm^3 density; 0.045 nominal solids fraction; 33.2% duty cycle, cycle time 9.8 s, pulse volume fraction 0.050; U_{CS} velocity 6.5 m/s, target nozzle exit velocity 6.5 m/s; peak cloud height upper bound 0.203 m (8 in.). Case ID 15E_4s1d2Wc_1.

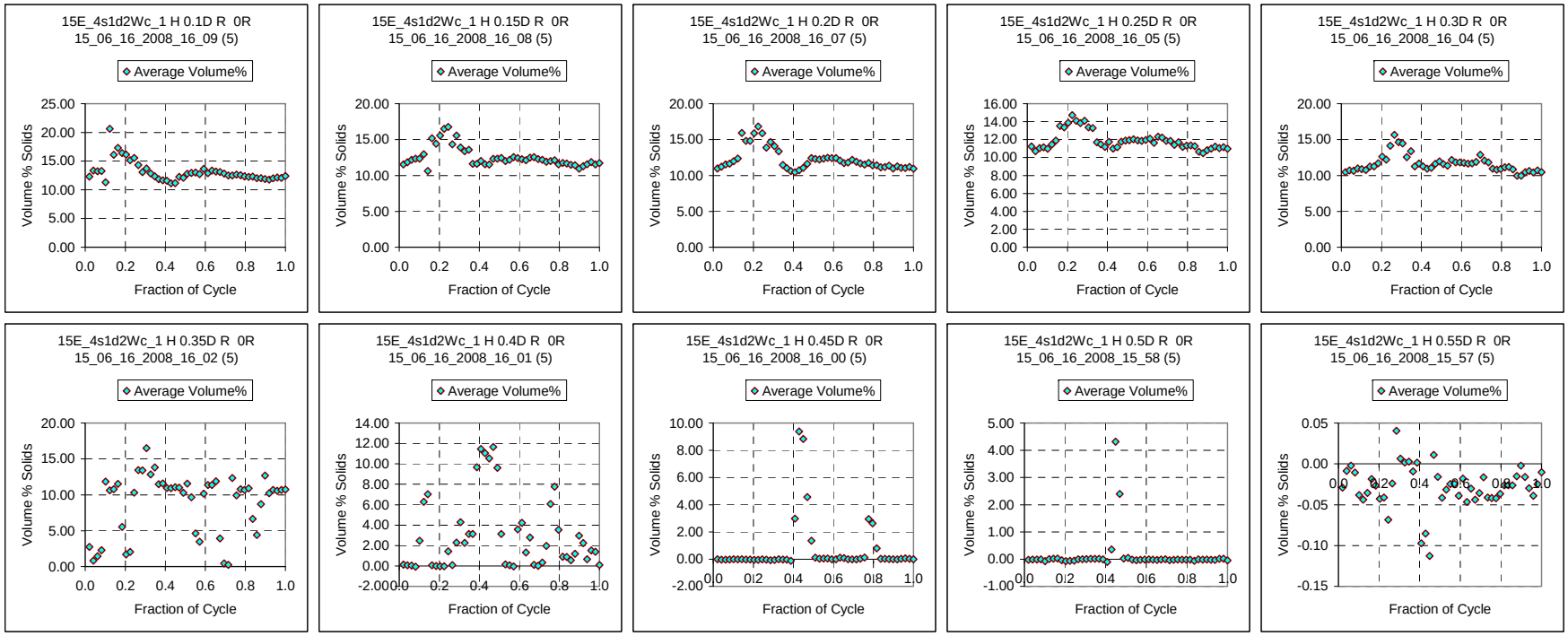

Figure C.7A. Case ID 15E_4s1d2Wc_1 Concentration Variation During the Cycle

This is the seventh profile shown using simulant s1d2 in the small-scale tank. The solids fraction remained constant at 0.045; however, the duty cycle increased to 33.2% from 18.8% in Figure C.6. The U_{CS} velocity occurred 6.5 m/s, slightly less than 7.2 m/s that was observed in Figure C.6. The peak cloud height upper bound was 8.0 in., slightly higher than the 6 in. observed in Figure C.6. In Figure C.7, the average concentration profile was relatively uniform up to an elevation of Z = 0.3D. The transient data in Figure C.5A show that at in the range of H = 0.1D to H = 0.3D concentration was relatively constant throughout the cycle. At the higher elevation of H = 0.45D, the maximum concentration transient of 9 vol% occurred at 0.45 cycle.

The eighth profile shown using simulant s1d2 is shown in Figure C.8. The solids fraction remained constant at 0.045; however, the system was operated as a steady jet. In this case, the concentration was uniform to an elevation of Z = 0.8D.

Maximum Cloud Height

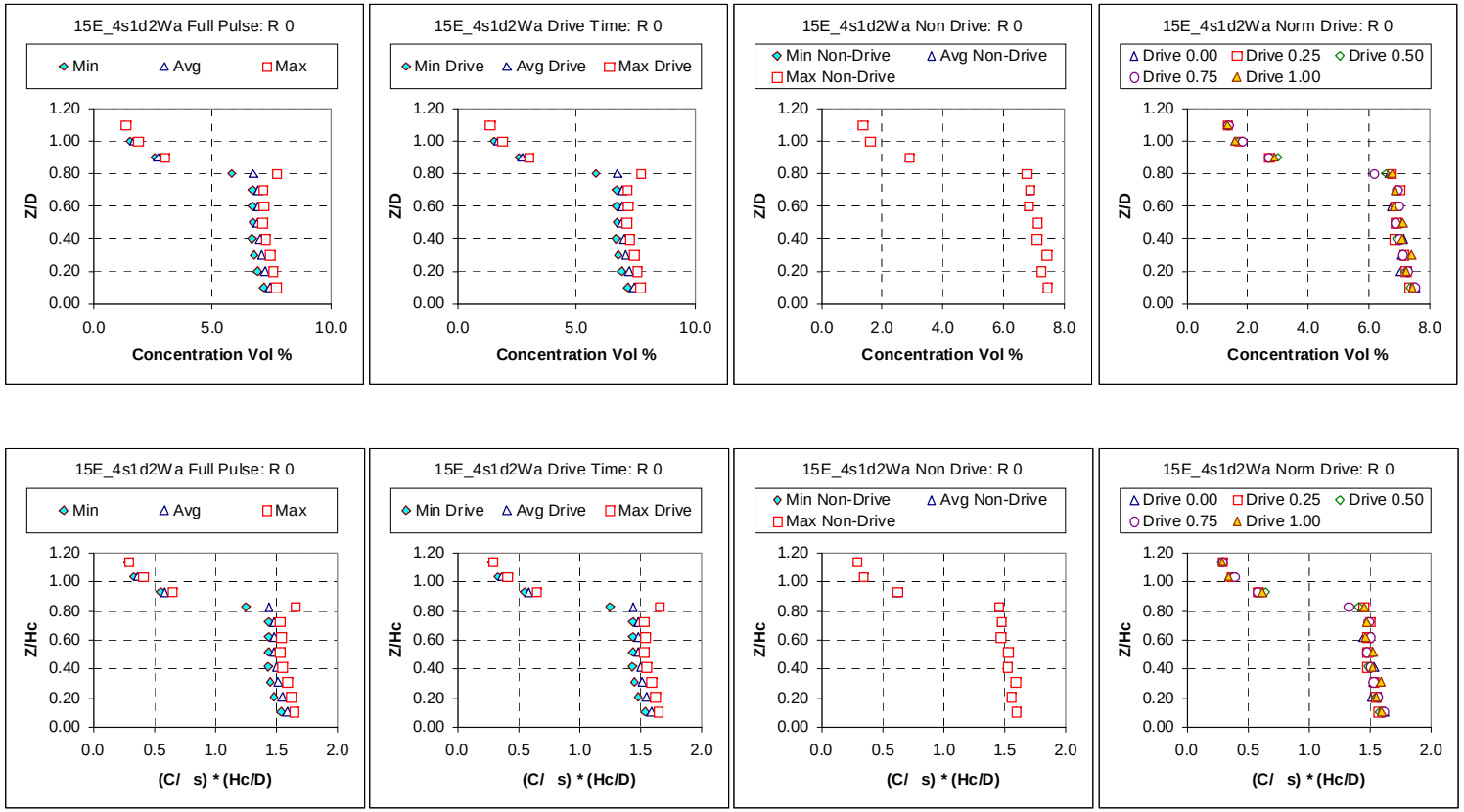

Figure C.8. 0.367-m- (14 7/16-in.-) diameter tank, 0.320-cm- (0.126-in.-) diameter nozzle; solids nominal diameter 69.3 µm, 2.48 g/cm^3 density; 0.045 nominal solids fraction; 100.0% duty cycle, cycle time infinite, pulse volume fraction undefined, U_{CS} velocity 3 m/s, target nozzle exit velocity 3 m/s; peak cloud height upper bound 0.381 m (15 in.). Case ID 15E_4s1d2Wa.

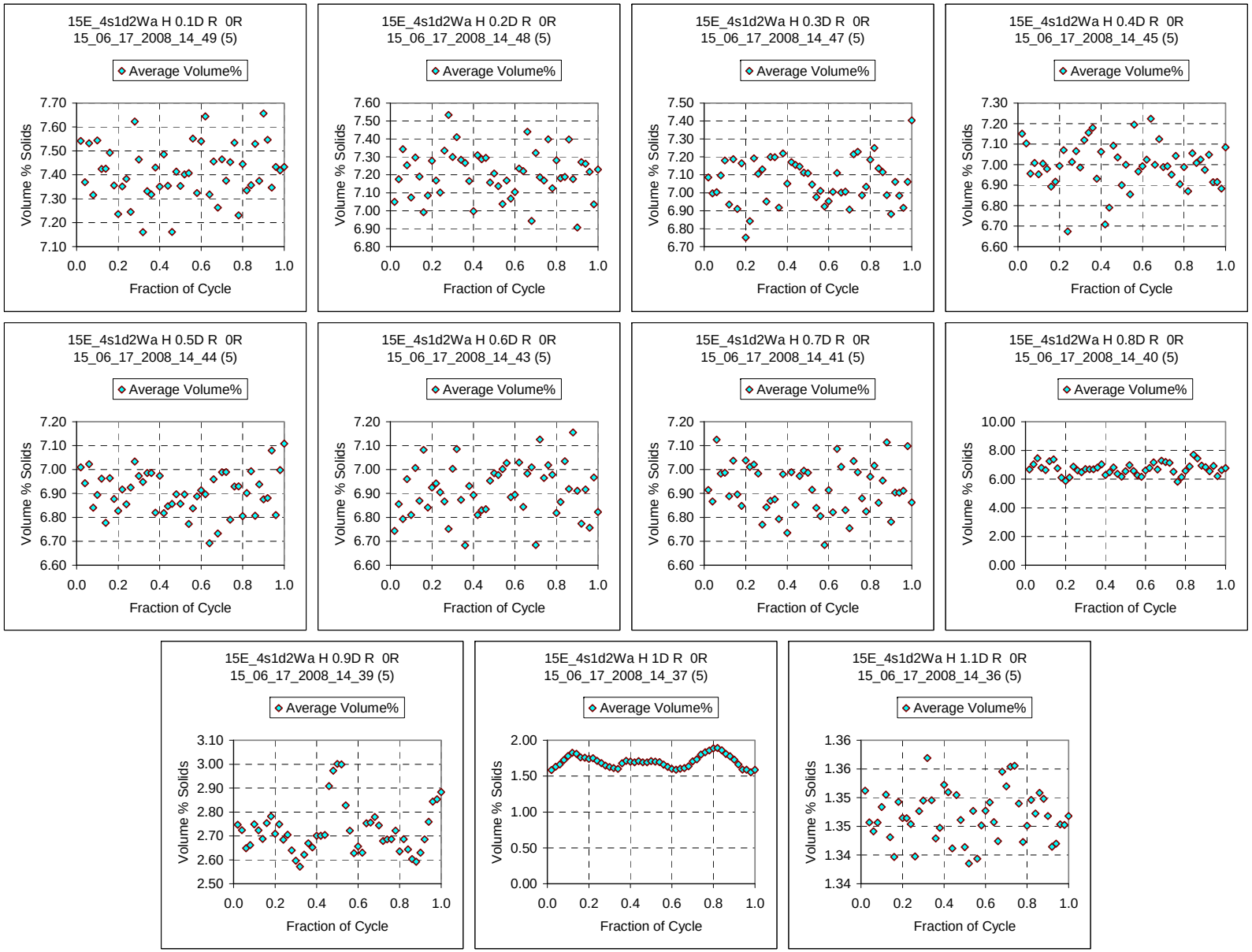

Figure C.8A. Case ID 15E_4s1d2Wa Concentration Variation During the Cycle

Maximum Cloud Height

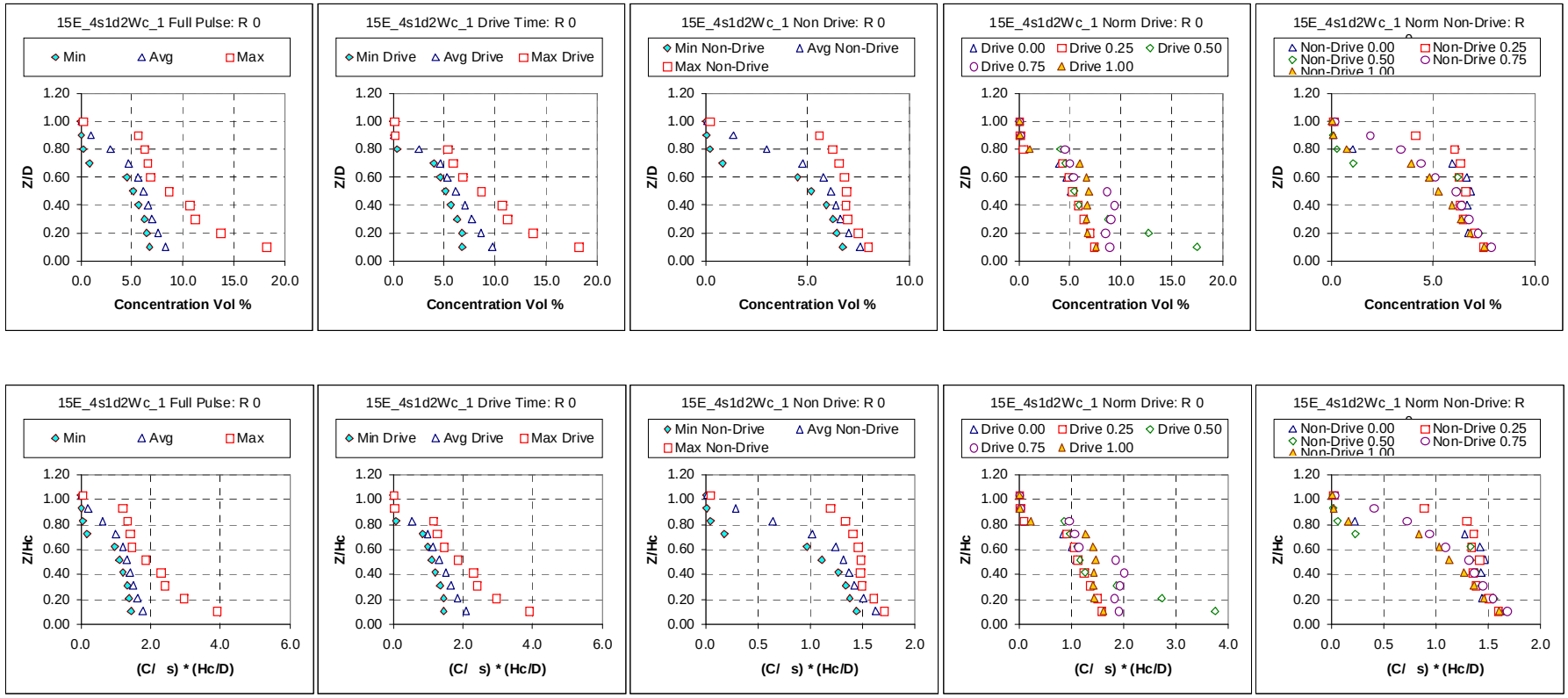

Figure C.9. 0.367-m- (14 7/16-in.-) diameter tank, 0.320-cm- (0.126-in.-) diameter nozzle; solids nominal diameter 69.3 µm, 2.48 g/cm^3 density; 0.045 nominal solids fraction; 33.7% duty cycle, cycle time 8.0 s, pulse volume fraction 0.050, U_{CS} velocity 6.5 m/s, target nozzle exit velocity 8 m/s; peak cloud height upper bound 0.381 m (15 in.). Case ID 15E_4s1d2Wc_1.

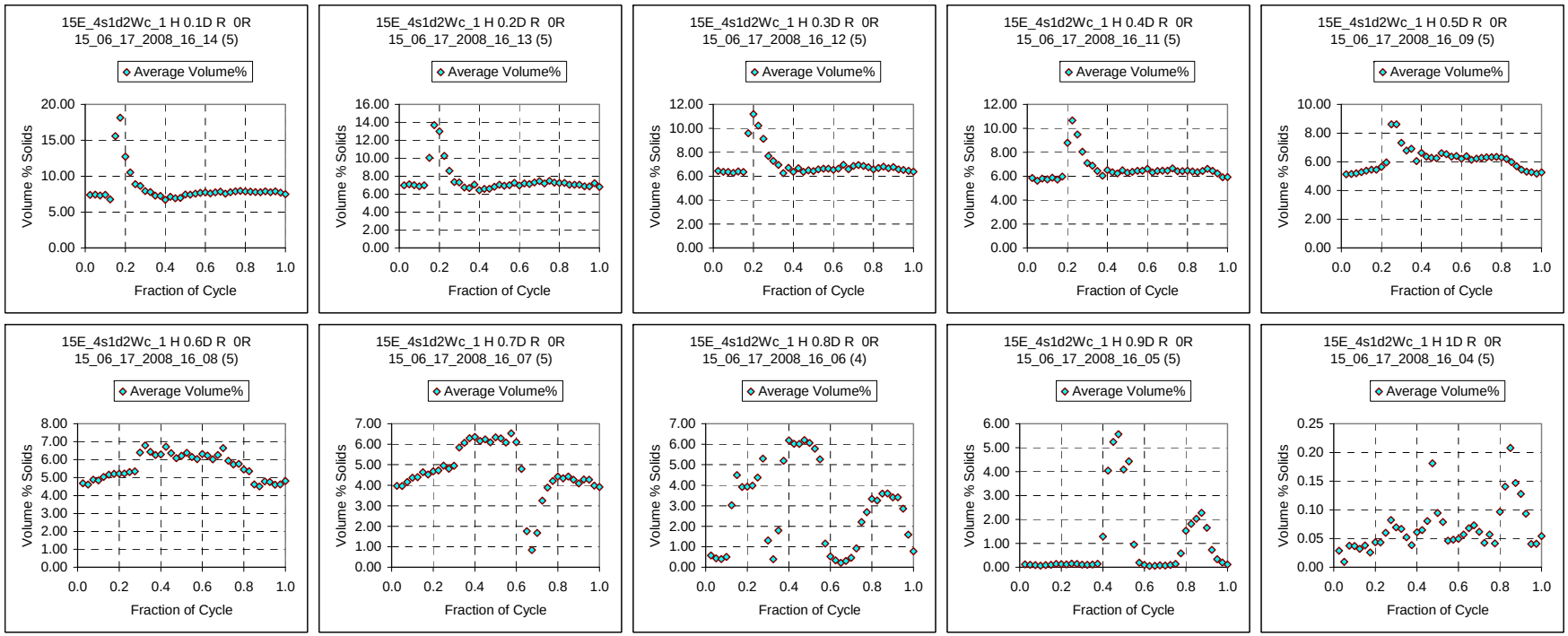

Figure C.9A. Case ID 15E_4s1d2Wc_1 Concentration Variation During the Cycle

This is the ninth profile shown using simulant s1d2 in the small-scale tank. This was the first test with a velocity above U_{CS}. The conditions match those in Figure C.7 except for nozzle exit velocity. The solids fraction remained constant at 0.045; the duty cycle remained essentially constant at 33.7% from 33.2% in Figure C.7. The nozzle exit velocity of 8 m/s was $>U_{CS}$ velocity which occurred at 6.5 m/s. The peak cloud height upper bound of 15.0 in. was much higher than the 8 in. observed in Figure C.7. In Figure C.9, the average concentration profile was relatively uniform up to an elevation of Z = 0.7D – more than twice the height obtained at U_{CS} in Figure C.7. This change shows the benefit in concentration uniformity obtained when operating at velocities above U_{CS}.

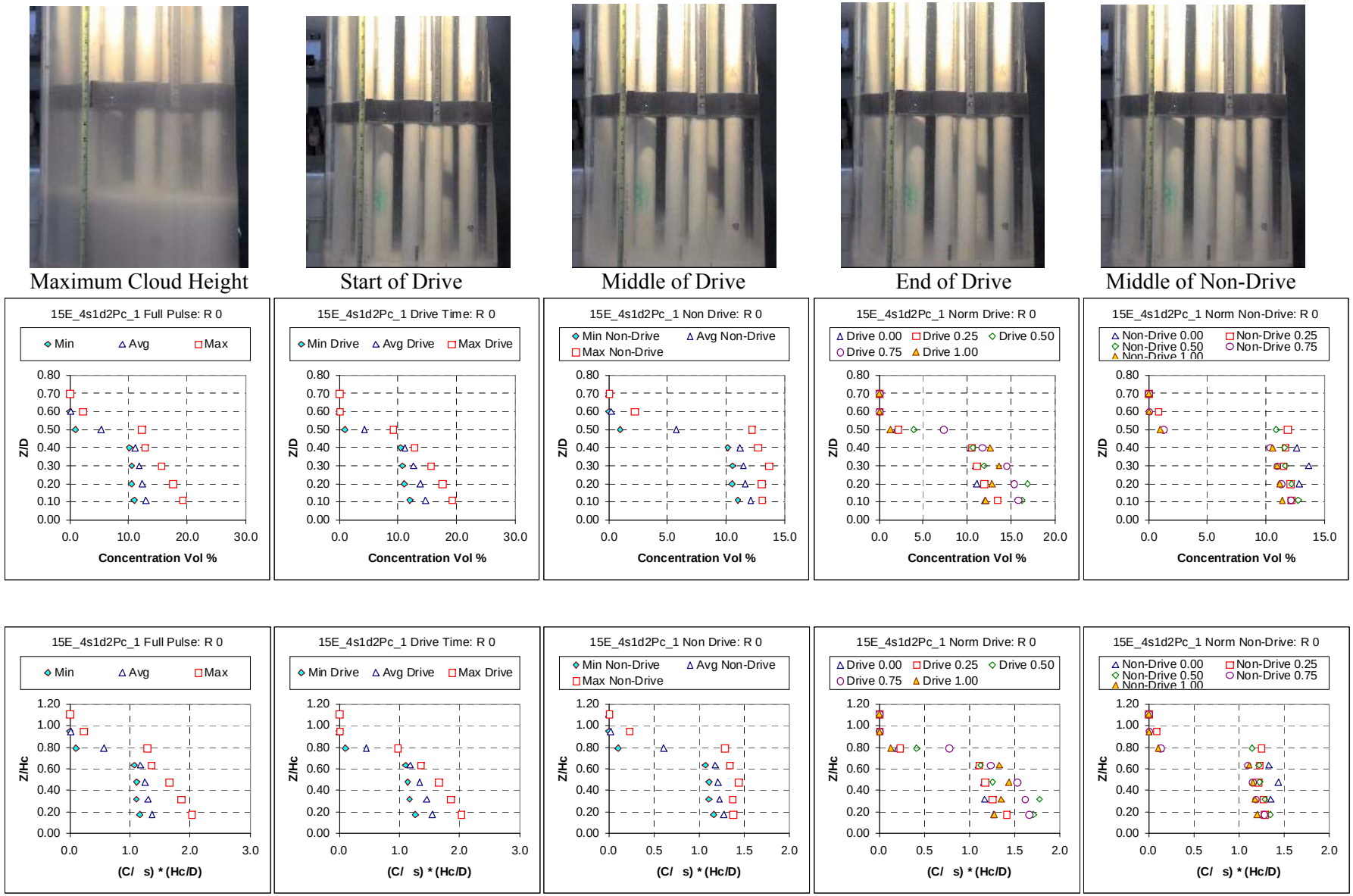

Figure C.10. 0.367-m- (14 7/16-in.-) diameter tank, 0.320-cm- (0.126-in.-) diameter nozzle; solids nominal diameter 69.3 µm, 2.48 g/cm^3 density; 0.06 nominal solids fraction; 33.6% duty cycle, cycle time 10.2 s, pulse volume fraction 0.050, U_{CS} velocity 6.2 m/s, target nozzle exit velocity 6.2 m/s; peak cloud height upper bound 0.241 m (9.5 in.). Case ID 15E_4s1d2Pc_1.

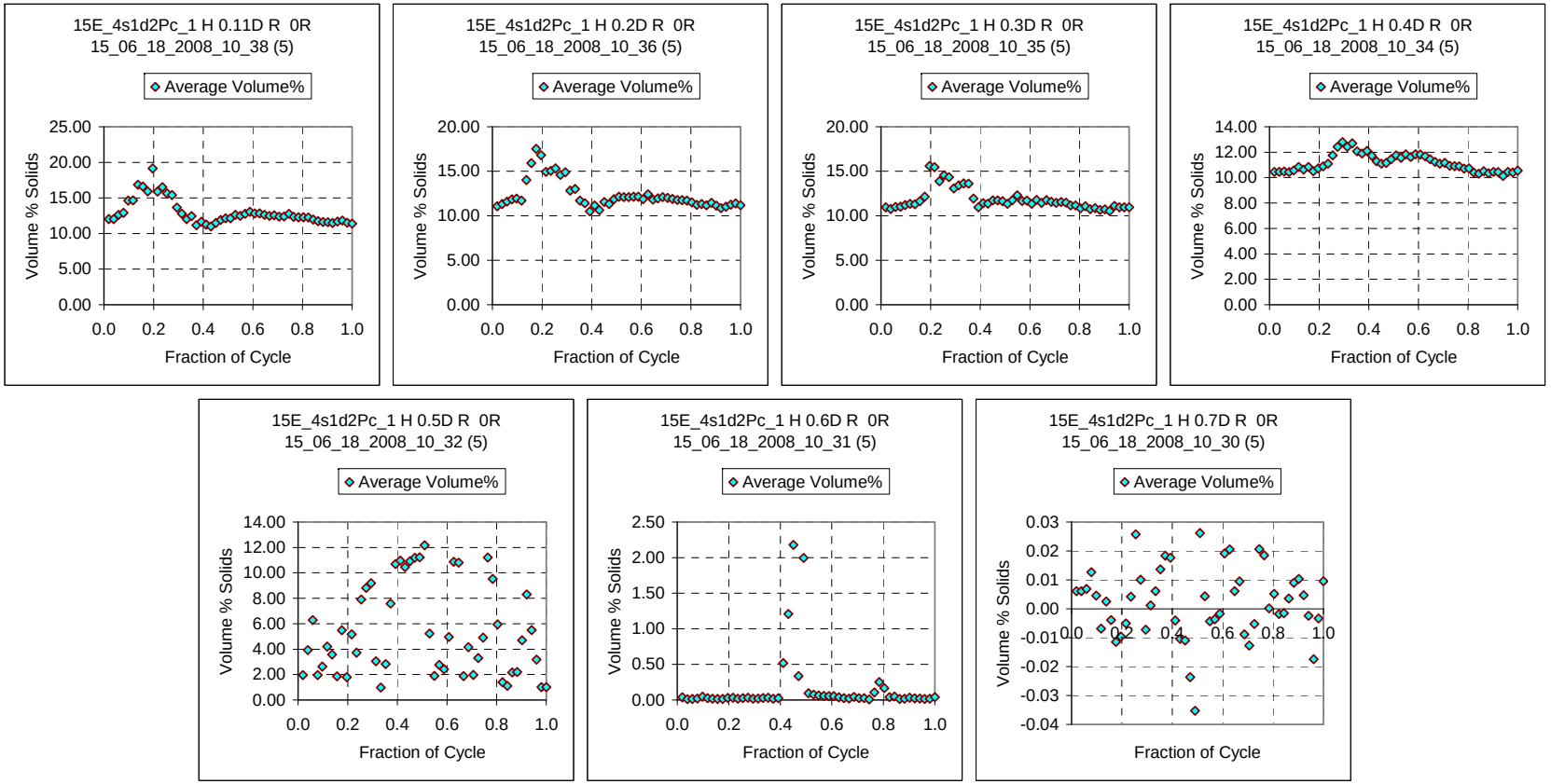

Figure C.10A. Case ID 15E_4s1d2Pc_1 Concentration Variation During the Cycle

This is the tenth profile shown using simulant s1d2 in the small-scale tank. This was highest solids concentration tested. The solids fraction increased to 0.06 from 0.045 in the prior four tests; the duty cycle remained essentially constant at 33.6% from 33.2% in Figure C.7. The U_{CS} velocity occurred at 6.2 m/s slightly less than 6.5 m/s that was observed in Figure C.7. The peak cloud height upper bound was 9.5 in. slightly higher than the 8 in. observed in Figure C.7. In Figure C.10, the average concentration profile was relatively uniform up to an elevation of Z = 0.4D. The transient data in Figure C.10A shows that at H = 0.1D, the maximum concentration of ~20 vol% solids occurred at 0.2 cycle.

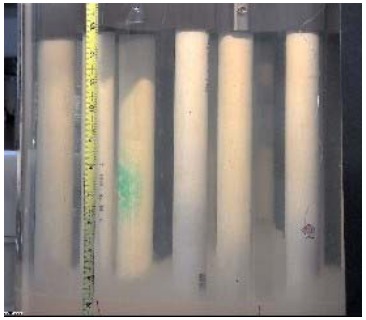

Maximum Cloud Height

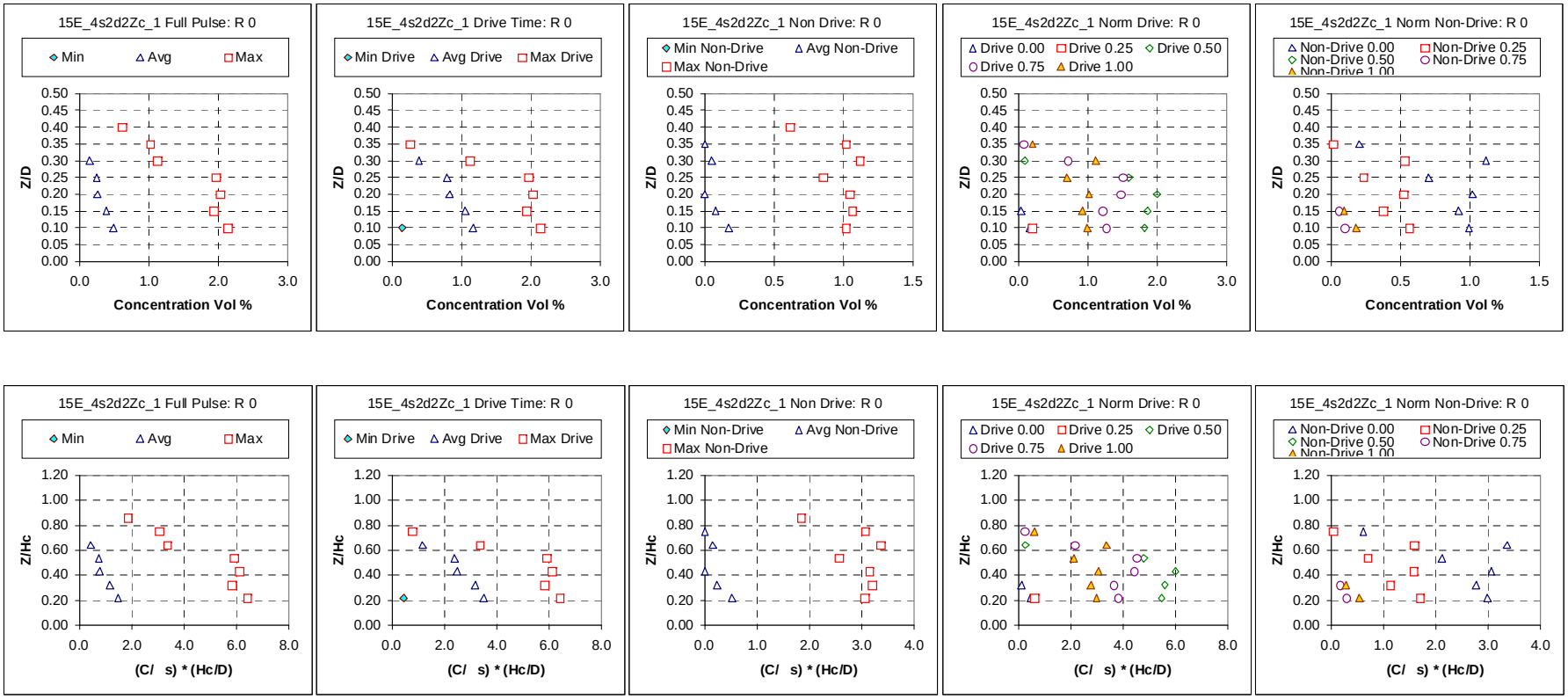

Figure C.11. 0.367-m- (14 7/16-in.-) diameter tank, 0.320-cm- (0.126-in.-) diameter nozzle; solids nominal diameter 75.6 µm, 4.18 g/cm^3 density; 0.00155 nominal solids fraction; 33.5% duty cycle, cycle time 12.0 s, pulse volume fraction 0.050, U_{CS} velocity 5.2 m/s, target nozzle exit velocity 5.2 m/s; peak cloud height upper bound 0.191 m (7.5 in.). Case ID 15E_4s2d2Zc_1.

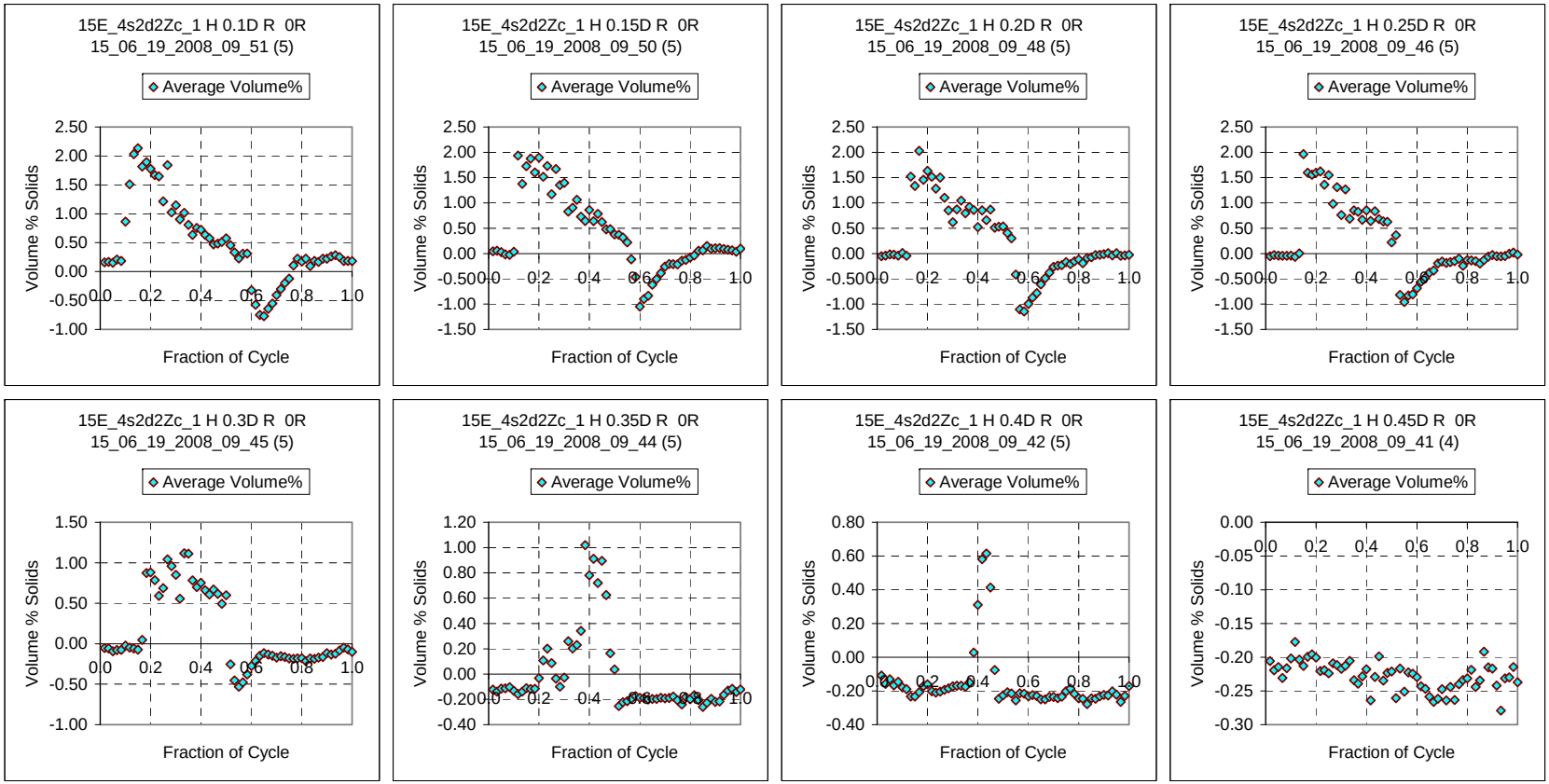

Figure C.11A. Case ID 15E_4s2d2Zc_1 Concentration Variation During the Cycle

This is the first of three profiles using simulant s2d2 in the small-scale tank. During these three tests, the duty cycle remained essentially constant at 33.5% and the pulse volume fraction was constant at 0.050. The results in Figure C.11 were taken at a solids concentration of 0.00155, which was the lowest value tested. The process conditions for this profile match those shown in Figure C.1, which used simulant s1d2, which has a lower density than s2d2 and similar particle size. Here, the U_{CS} velocity occurred at 5.2 m/s. The peak cloud height upper bound was 7.5 in. With simulant s1d2, the U_{CS} velocity was 2.8 m/s. The peak cloud height upper bound using s1d2 was 7.25 in. With the denser particulate, the U_{CS} velocity occurred at a higher velocity; however, the peak cloud height upper bound was essentially the same in both profiles.

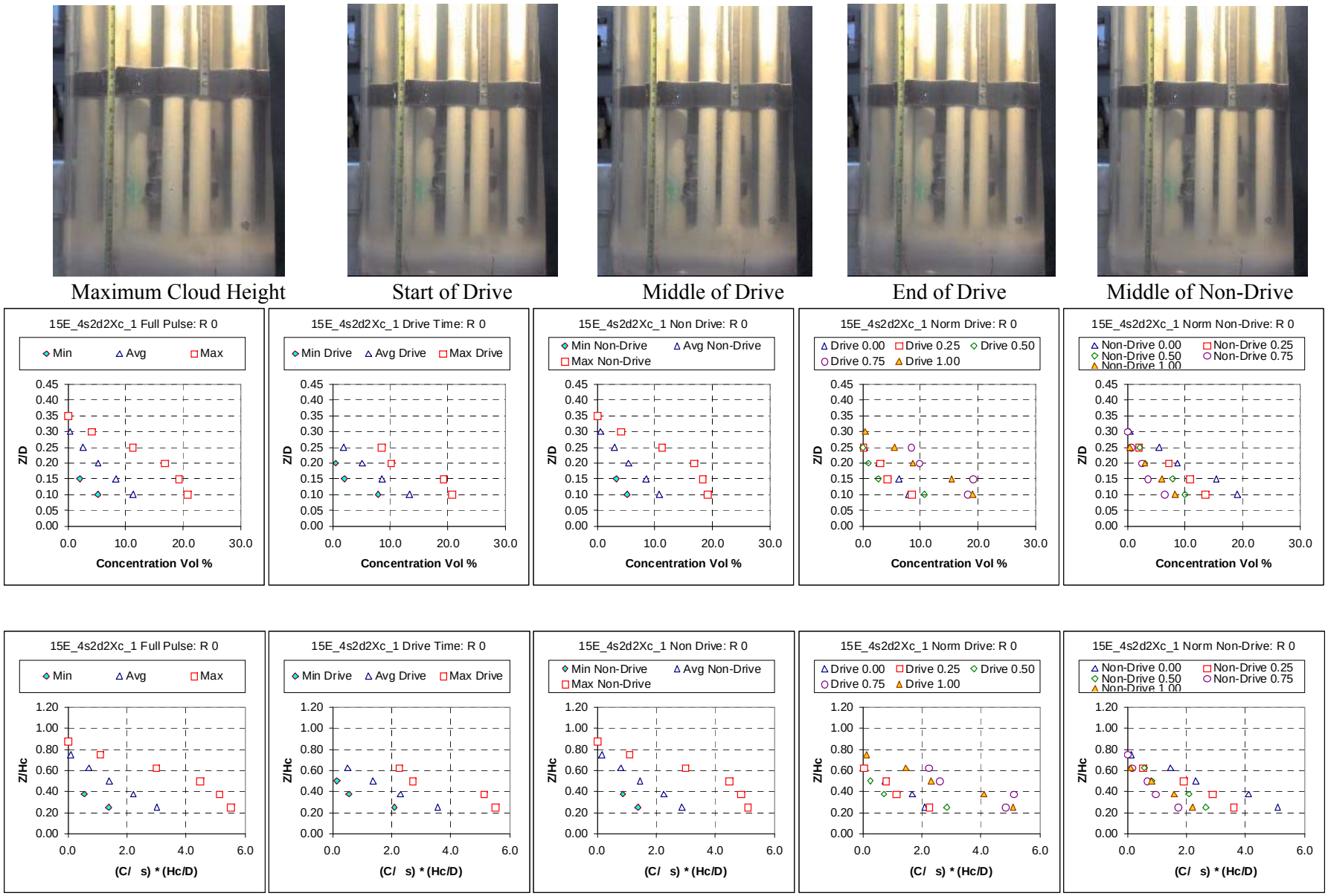

Figure C.12. 0.367-m- (14 7/16-in.-) diameter tank, 0.320-cm- (0.126-in.-) diameter nozzle; solids nominal diameter 75.6 µm, 4.18 g/cm^3 density; 0.015 nominal solids fraction; 33.4% duty cycle, cycle time 5.5 s, pulse volume fraction 0.050, U_{CS} velocity 11.8 m/s, target nozzle exit velocity 11.8 m/s; peak cloud height upper bound 0.165 m (6.5 in.). Case ID 15E_4s2d2Xc_1.

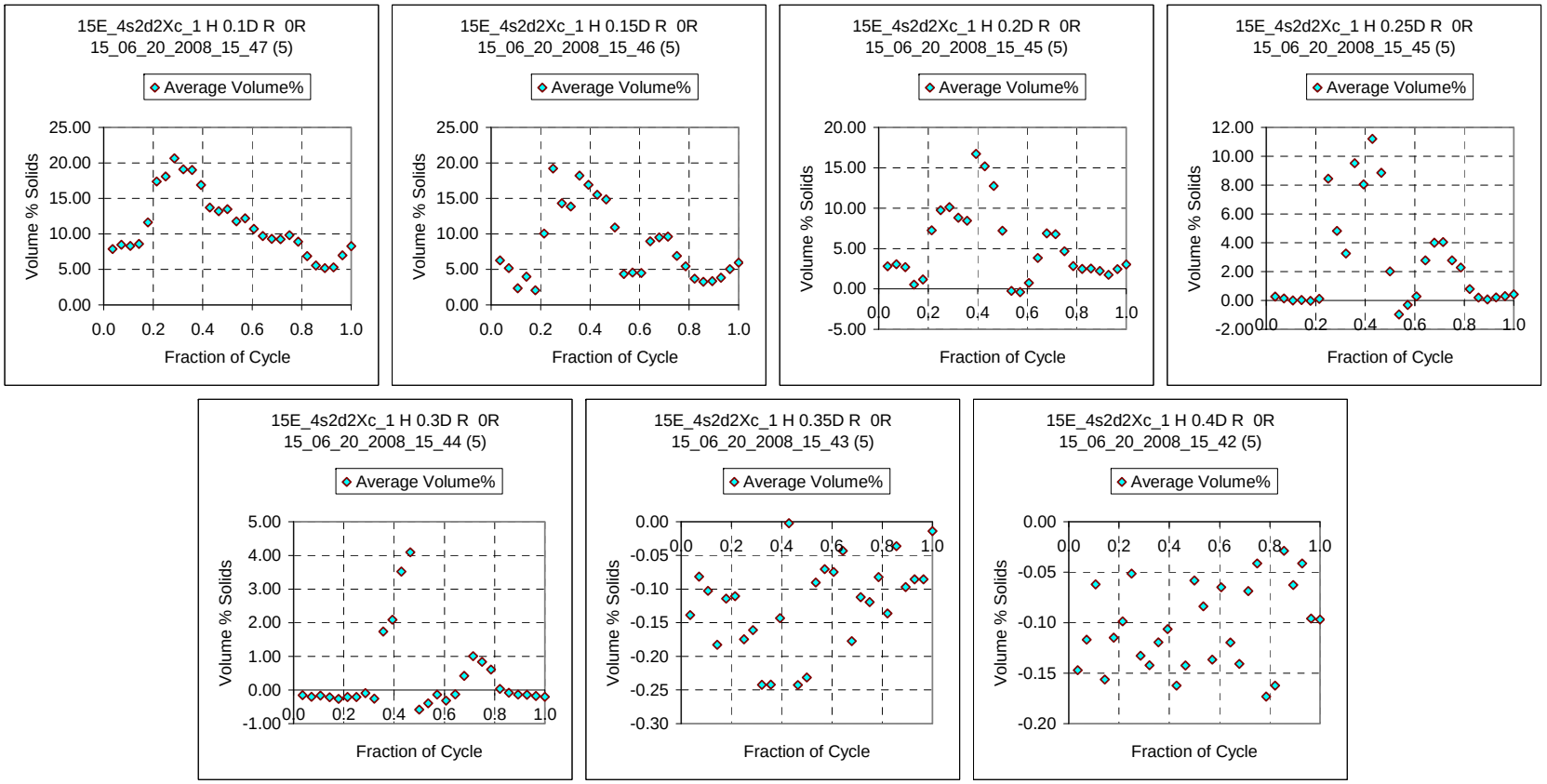

Figure C.12A. Case ID 15E_4s2d2Xc_1 Concentration Variation During the Cycle

This is the second of three profiles using simulant s2d2 in the small-scale tank. This solids fraction increased ~10 times to 0.015 from 0.00155. The duty cycle remained at 33.4% and the pulse volume fraction remained at 0.050. The U_{CS} velocity occurred at 11.8 m/s – an increase from the prior test, which was 5.2 m/s. The peak cloud height upper bound was 6.5 in. – a decrease from 7.5 in. of the prior test. The process conditions during this profile match those shown in Figure C.4, which used simulant s1d2, which has a lower density than s2d2. For the latter case, the U_{CS} velocity was 5.8 m/s. The peak cloud height upper bound was 7 in. With the denser particulate, the U_{CS} velocity occurred at a higher velocity; however, the peak cloud height upper bound was essentially the same.

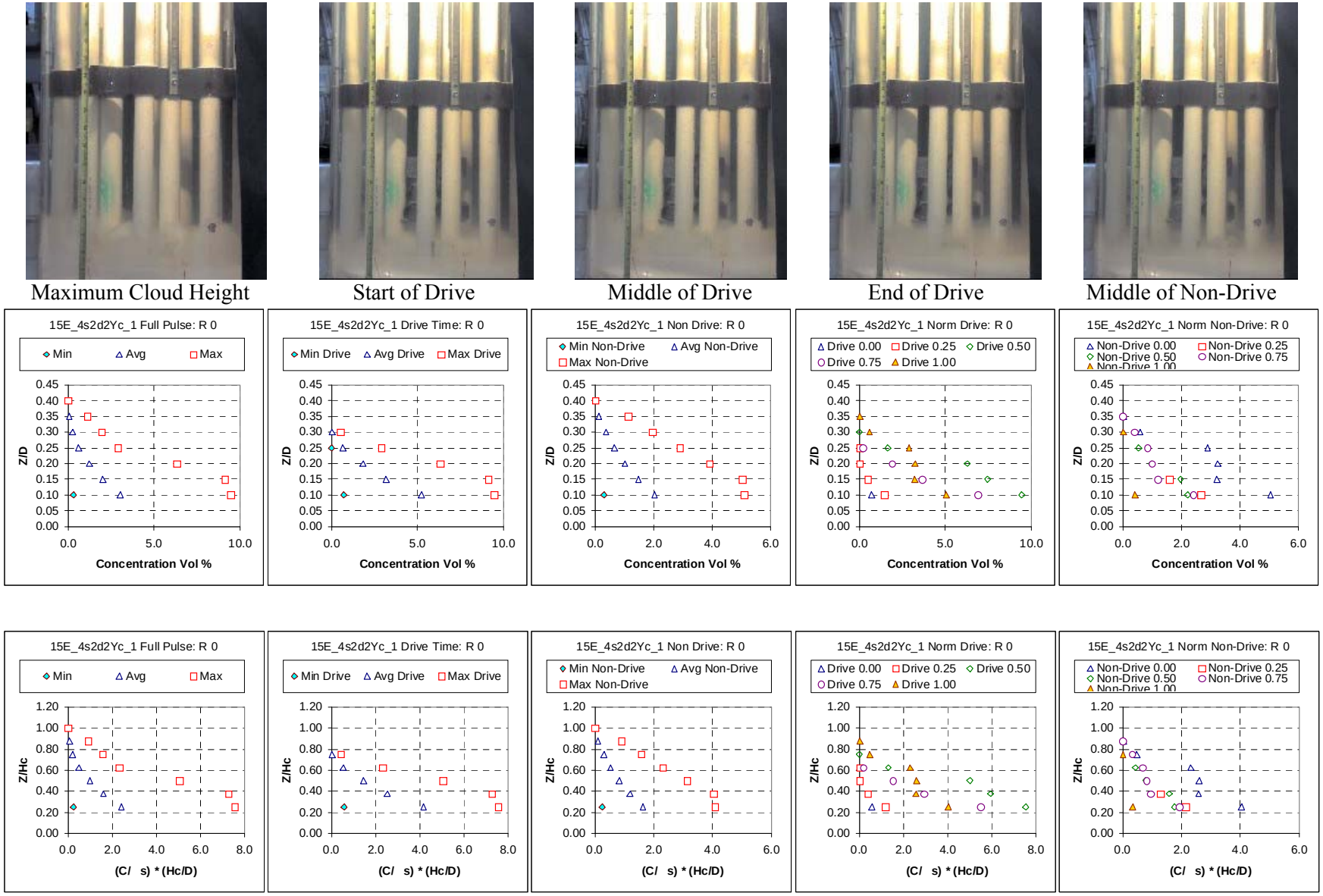

Figure C.13. 0.367-m- (14 7/16-in.-) diameter tank, 0.320-cm- (0.126-in.-) diameter nozzle; solids nominal diameter 75.6 µm, 4.18 g/cm^3 density; 0.005 nominal solids fraction; 33.4% duty cycle, cycle time 8.4 s, pulse volume fraction 0.050, U_{CS} velocity 7.6 m/s, target nozzle exit velocity 7.6 m/s; peak cloud height upper bound 0.165 m (6.5 in.). Case ID 15E_4s2d2Yc_1.

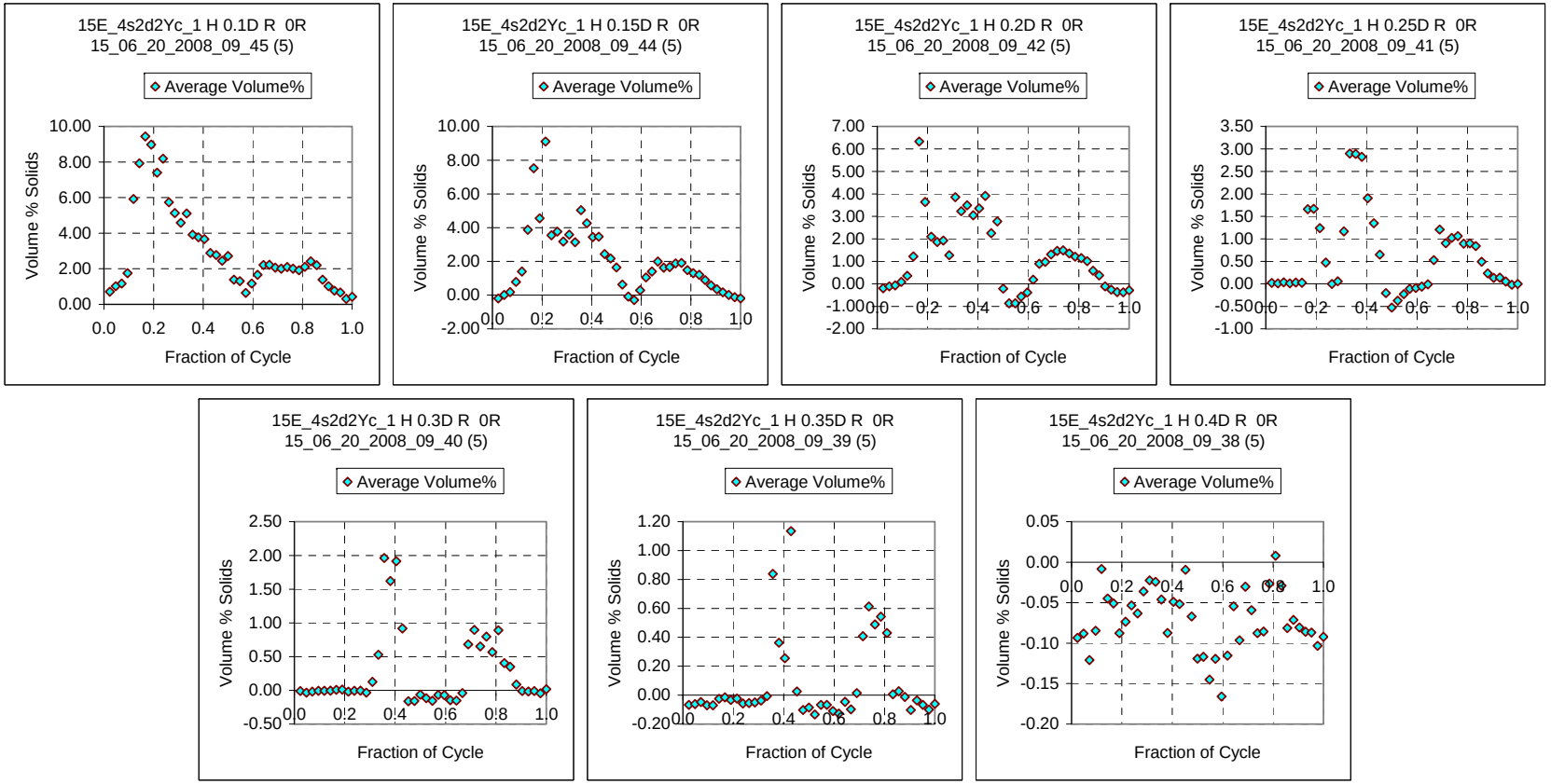

Figure C.13A. Case ID 15E_4s2d2Yc_1 Concentration Variation During the Cycle

This is the third of three profiles using simulant s2d2 in the small-scale tank. The solids fraction decreased to 0.005 from 0.015. Once again, the duty cycle remained at 33.4% and the pulse volume fraction remained at 0.050. The U_{CS} velocity occurred at 7.6 m/s – a decrease from the prior test, which was 11.8 m/s. The peak cloud height upper bound was 6.5 in. – the same as the prior test. The conditions during this profile match those shown in Figure C.2, which used simulant s1d2, which has a lower density than s2d2. There the U_{CS} velocity was 4.3 m/s and the peak cloud height upper bound was 5.5 in. With the denser particulate, the U_{CS} velocity occurred at a higher velocity; the peak cloud height upper bound was slightly higher.

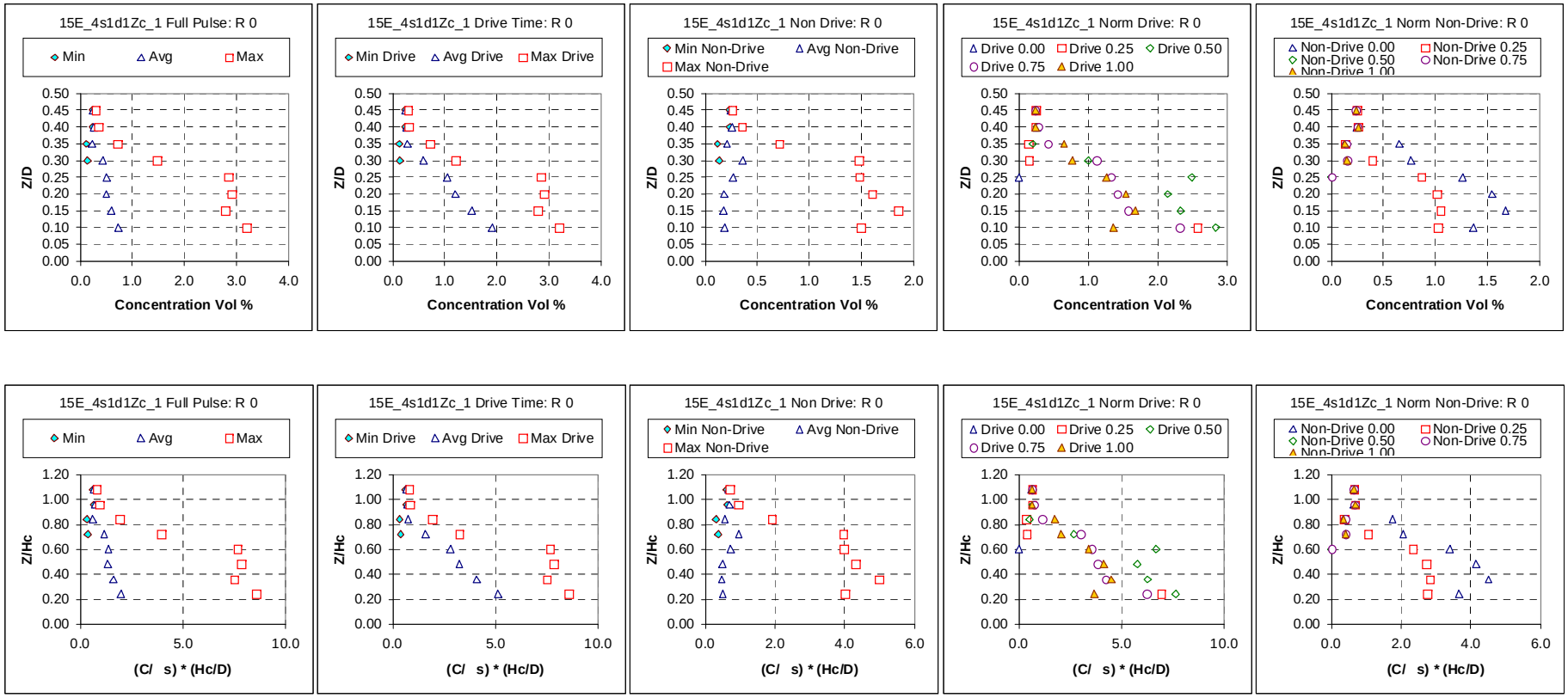

Figure C.14. 0.367-m- (14 7/16-in.-) diameter tank, 0.320-cm- (0.126-in.-) diameter nozzle; solids nominal diameter 166.4 µm, 2.46 g/cm^3 density; 0.00155 nominal solids fraction; 33.4% duty cycle, cycle time 14.6 s, pulse volume fraction 0.050, U_{CS} velocity 4.2 m/s, target nozzle exit velocity 4.2 m/s; peak cloud height upper bound 0.165 m (6.5 in.). Case ID 15E_4s1d1Zc_1.

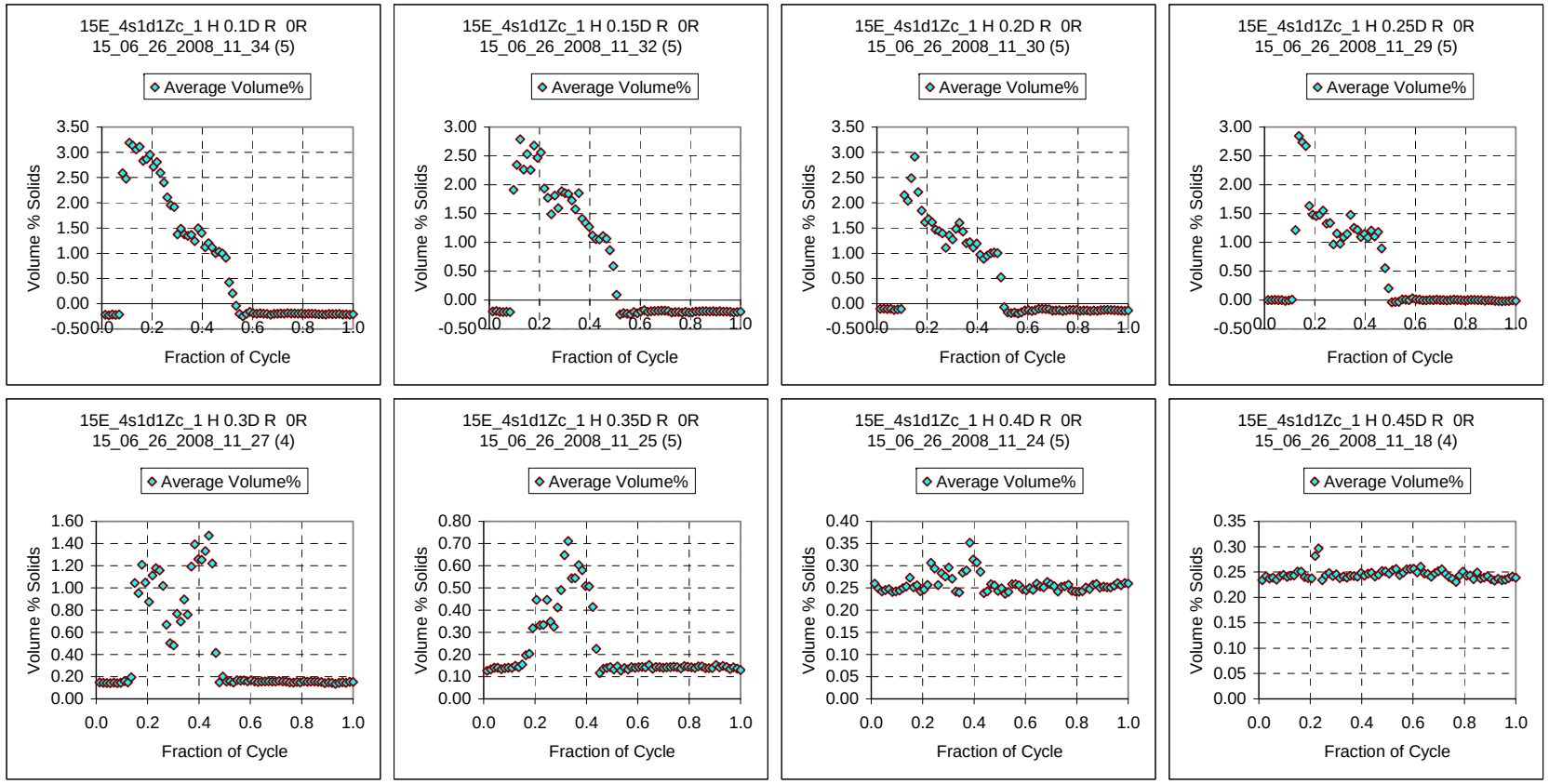

Figure C.14A. Case ID 15E_4s1d1Zc_1 Concentration Variation During the Cycle

This is the first of two profiles using simulant s1d1 in the small-scale tank. During the two tests, the duty cycle remained essentially constant at 33.4% and the pulse volume fraction was constant at 0.050. For this test, the solids fraction was 0.00155. The U_{CS} velocity occurred at 4.2 m/s. The peak cloud height upper bound is 6.5 in. The operating conditions during this profile match those shown in Figure C.1, which used simulant s1d2, which has a smaller diameter particle than s1d1. There the U_{CS} velocity was 2.8 m/s and the peak cloud height upper bound was 7.25 in. With the larger particulate, the U_{CS} velocity occurred at a higher velocity; the peak cloud height upper bound was slightly lower.

Maximum Cloud Height

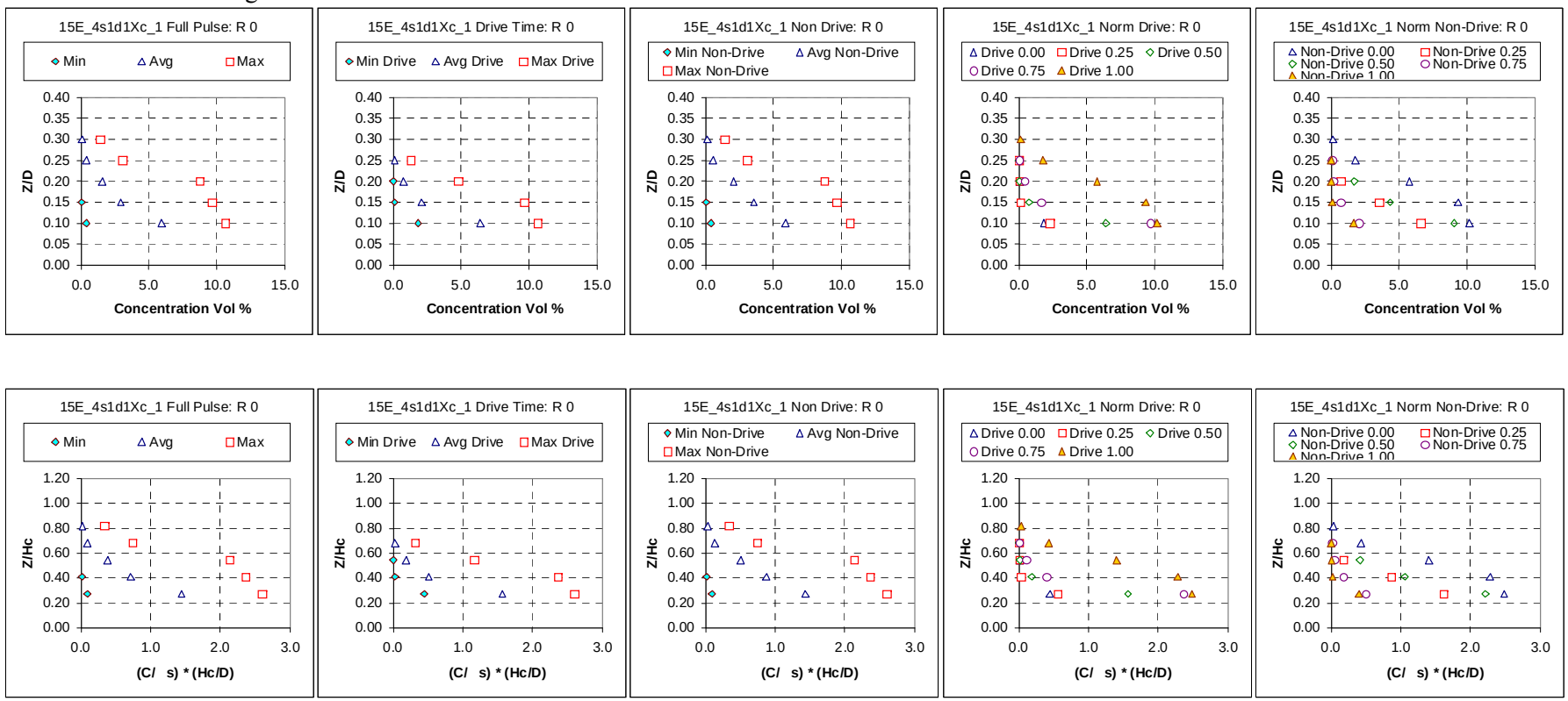

Figure C.15. 0.367-m- (14 7/16-in.-) diameter tank, 0.320-cm- (0.126-in.-) diameter nozzle; solids nominal diameter 166.4 µm, 2.46 g/cm^3 density; 0.015 nominal solids fraction; 33.5% duty cycle, cycle time 7.4 s, pulse volume fraction 0.050, U_{CS} velocity 8.6 m/s, target nozzle exit velocity 8.6 m/s; peak cloud height upper bound 0.152 m (6 in.). Case ID 15E_4s1d1Xc_1.

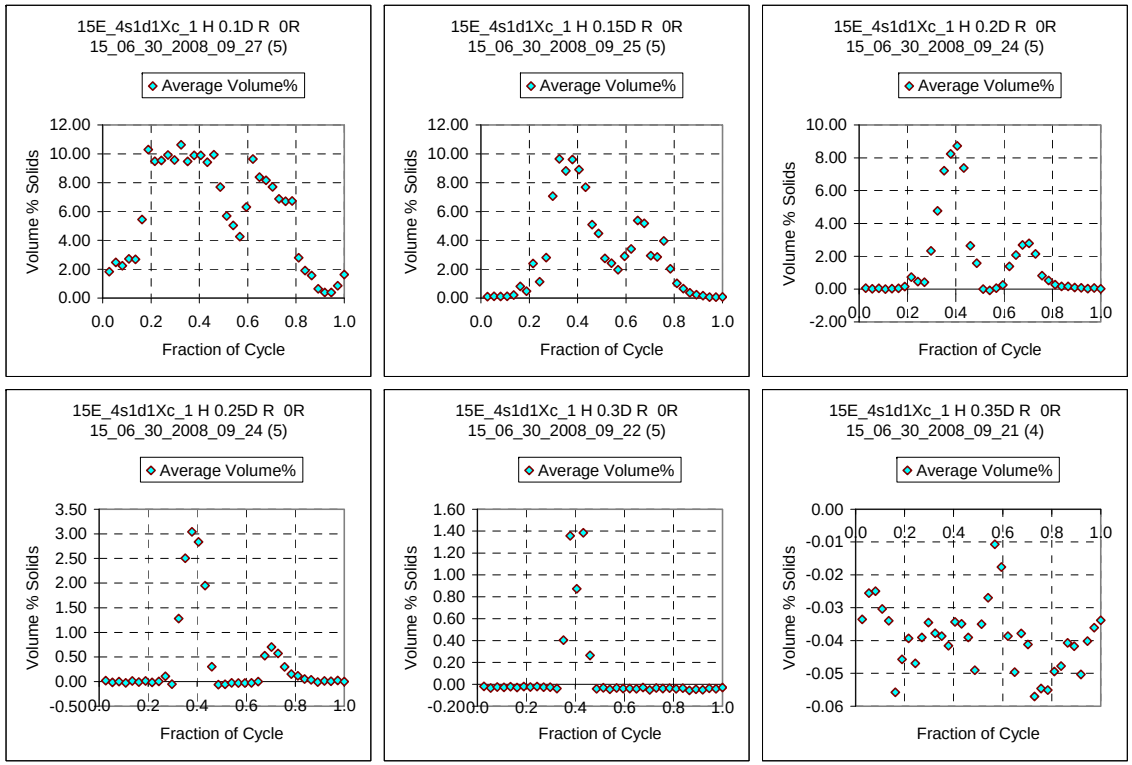

Figure C.15A. Case ID 15E_4s1d1Xc_1 Concentration Variation During the Cycle

This is the second of two profiles using simulant s1d1 in the small-scale tank. The duty cycle remained at 33.5% and the pulse volume fraction remained at 0.050. The solids fraction was increased ~10 times to 0.015 from 0.00155. The U_{CS} velocity occurred at 8.6 m/s an increase from the prior test, which was 4.2 m/s. The peak cloud height upper bound was 6.0 in. – slightly lower than the 6.5 in. from the prior test. The conditions during this profile match those shown in Figure C.3, which used simulant s1d2, which has a smaller diameter particle than s1d1. There the U_{CS} velocity was 7.2 m/s and the peak cloud height upper bound was 6.0 in. With the larger particulate, the U_{CS} velocity occurred at a higher velocity; the peak cloud height upper bound was essentially the same.

Maximum Cloud Height

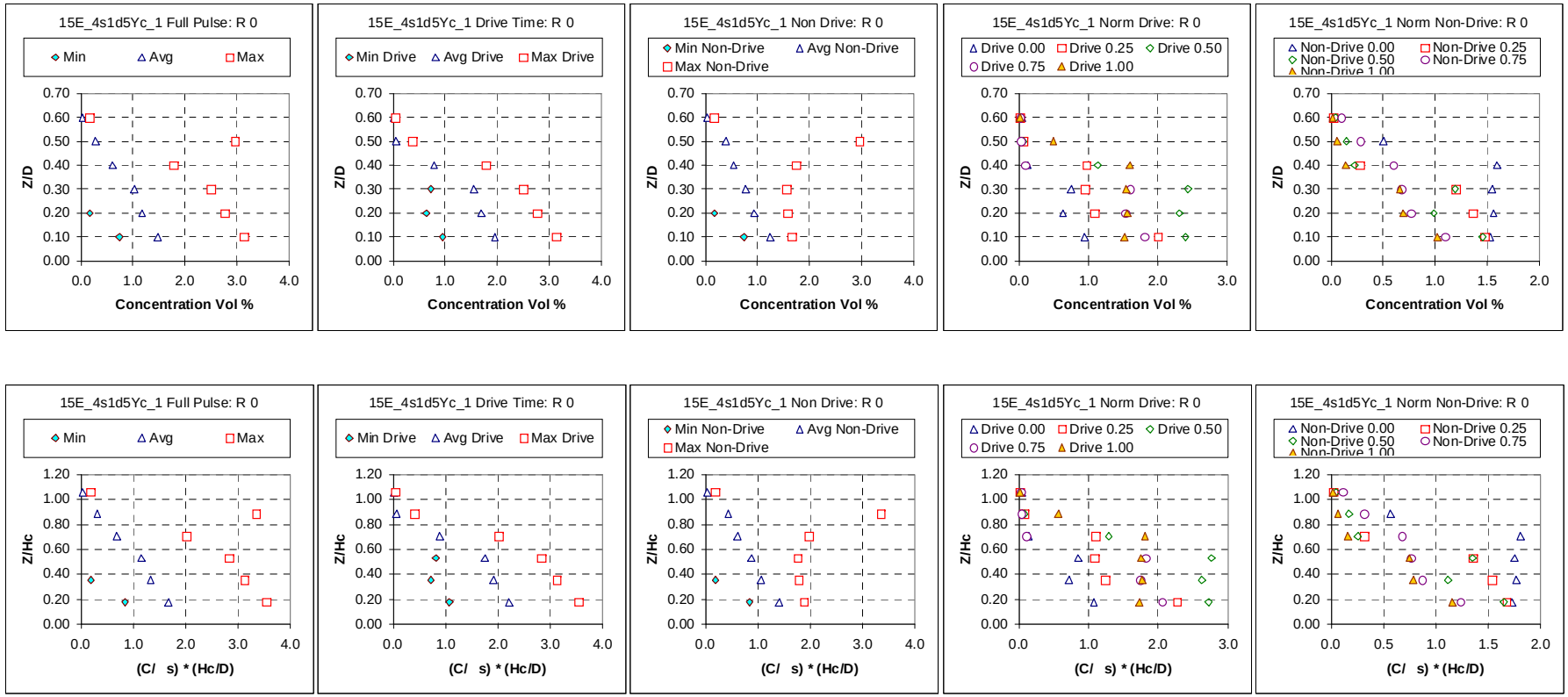

Figure C.16. 0.367-m- (14 7/16-in.-) diameter tank, 0.320-cm- (0.126-in.-) diameter nozzle; solids nominal diameter 43.9 µm, 2.5 g/cm^3 density; 0.005 nominal solids fraction; 33.2% duty cycle, cycle time 17.6 s, pulse volume fraction 0.050, U_{CS} velocity 3.7 m/s, target nozzle exit velocity 3.5 m/s; peak cloud height upper bound 0.229 m (9 in.). Case ID 15E_4s1d5Yc_1.

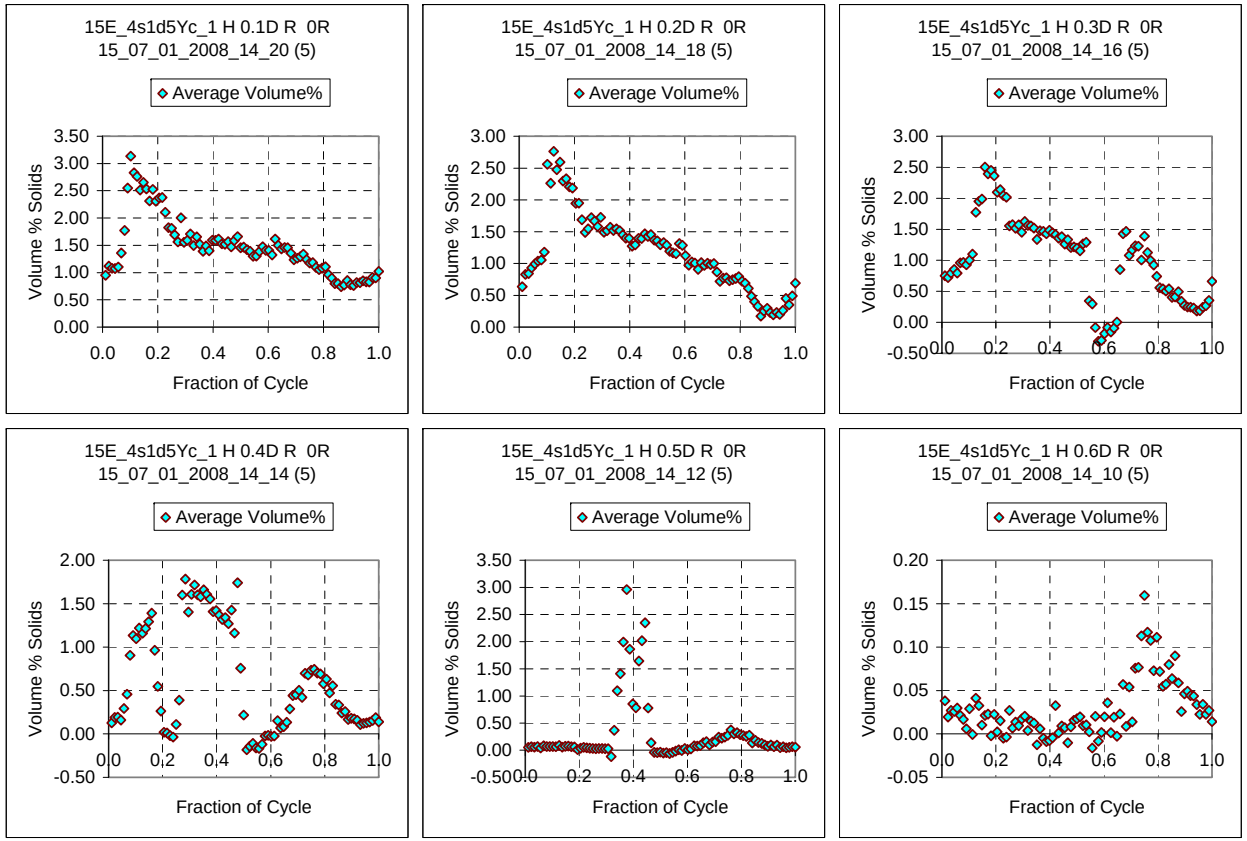

Figure C.16A. Case ID 15E_4s1d5Yc_1 Concentration Variation During the Cycle

Figure C.16 is the only profile shown using simulant s1d5 in the small-scale tank. This solids fraction was 0.005. During the test, the duty cycle was 33.2% and the pulse volume fraction was constant at 0.050. The U_{CS} velocity occurred at 3.7 m/s. The peak cloud height upper bound was 9 in. The conditions during this profile match those shown in Figure C.2, which used simulant s1d2, which has a larger diameter particle than s1d5 and similar density. There the U_{CS} velocity was 4.3 m/s and the peak cloud height upper bound was 5.5 in. With the smaller particulate, the U_{CS} velocity occurred at a lower velocity; the peak cloud height upper bound was much higher, too.

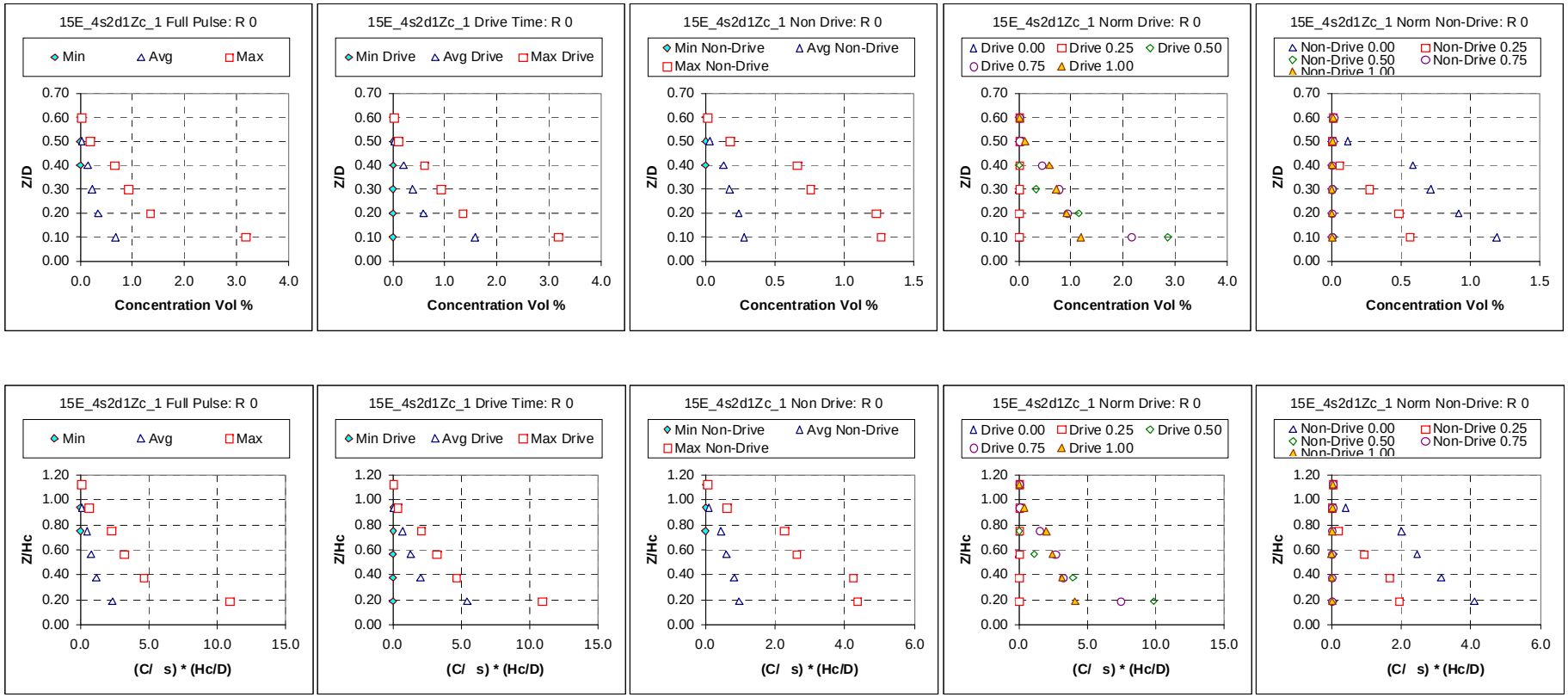

Figure C.17. 0.367-m- (14 7/16-in.-) diameter tank, 0.320-cm- (0.126-in.-) diameter nozzle; solids nominal diameter 164.2 µm, 4.17 g/cm^3 density; 0.00155 nominal solids fraction; 32.8% duty cycle, cycle time 9.4 s, pulse volume fraction 0.050, U_{CS} velocity 6.8 m/s, target nozzle exit velocity 6.8 m/s; peak cloud height upper bound 0.216 m (8.5 in.). Case ID 15E_4s2d1Zc_1.

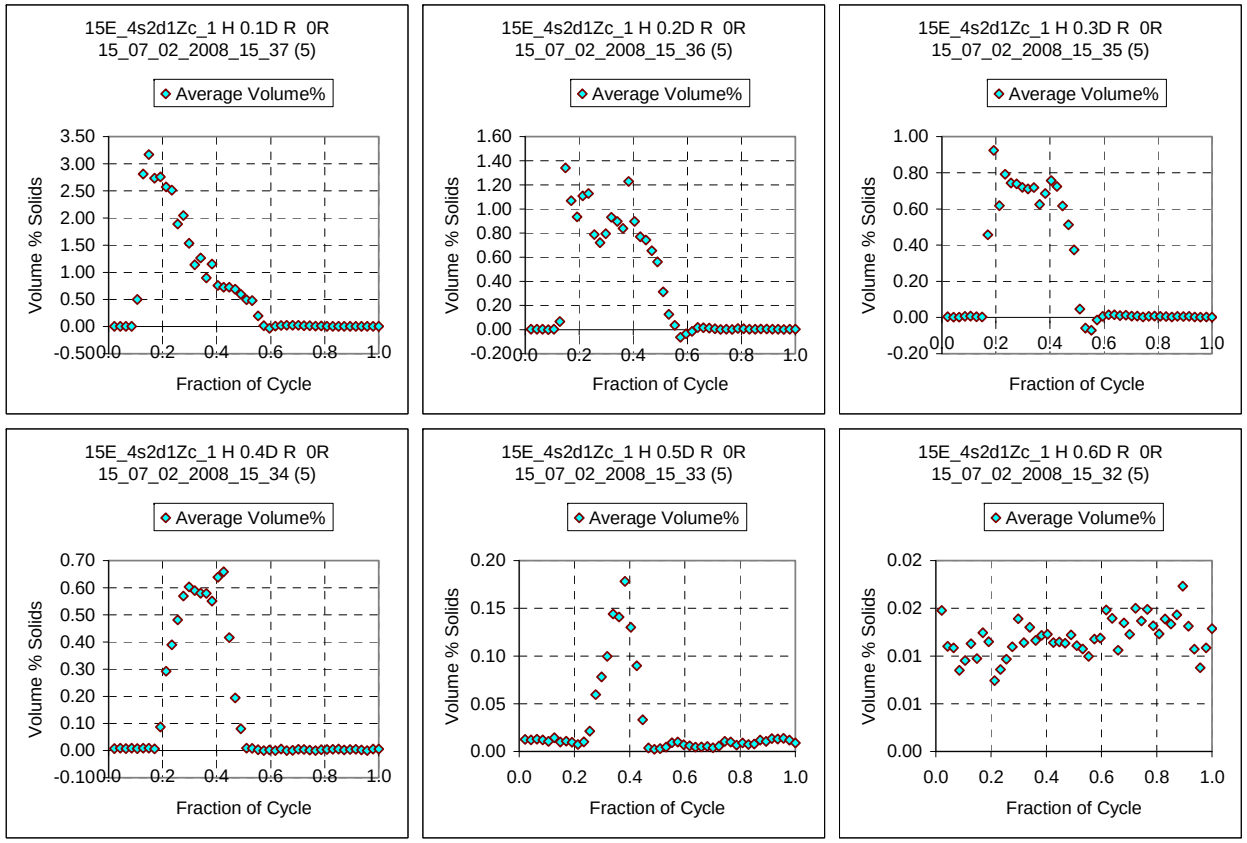

Figure C.17A. Case ID 15E_4s2d1Zc_1 Concentration Variation During the Cycle

Figure C.17 is the only profile shown using simulant s2d1 in the small-scale tank. This solids fraction was 0.00155. The duty cycle was 32.8% and the pulse volume fraction was 0.050. The U_{CS} velocity occurred at 6.8 m/s. The peak cloud height upper bound was 8.5 in. The conditions during this profile match those shown in Figure C.11 which used simulant s2d2 which has a smaller diameter particle than s2d1 and a similar density. Using simulant s2d2 the U_{CS} velocity was 5.2 m/s and the peak cloud height upper bound was 7.5 in. With the larger particulate the U_{CS} velocity occurred at a higher velocity; the peak cloud height upper bound was slightly higher too.

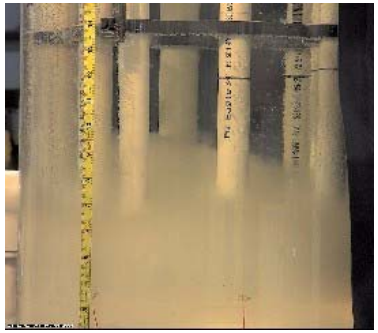

Maximum Cloud Height

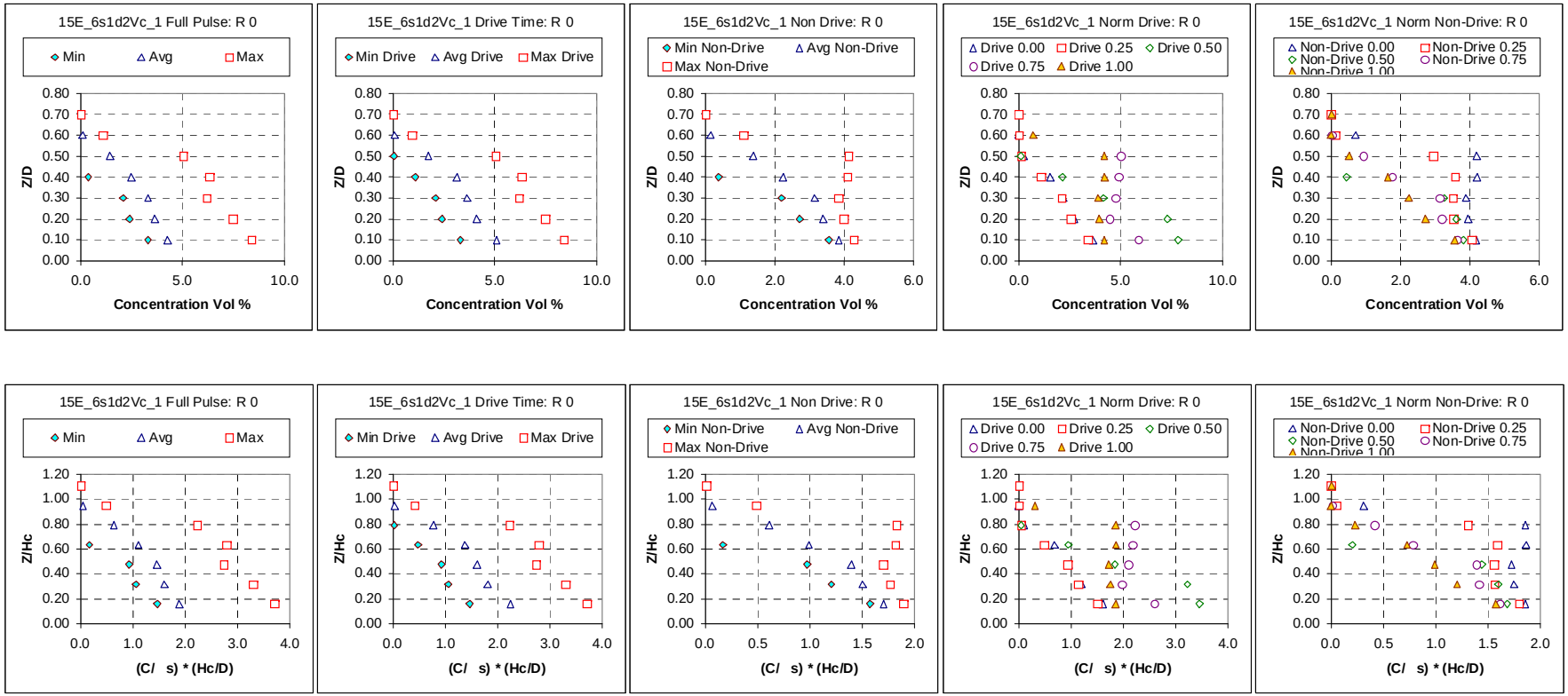

Figure C.18. 0.367-m- (14 7/16-in.-) diameter tank, 0.485-cm- (0.191-in.-) diameter nozzle; solids nominal diameter 69.3 µm, 2.48 g/cm^3 density; 0.0143 nominal solids fraction; 33.3% duty cycle, cycle time 8.8 s, pulse volume fraction 0.050, U_{CS} velocity 4.8 m/s, target nozzle exit velocity 4.8 m/s; peak cloud height upper bound 0.254 (10 in.). Case ID 15E_6s1d2Vc_1.

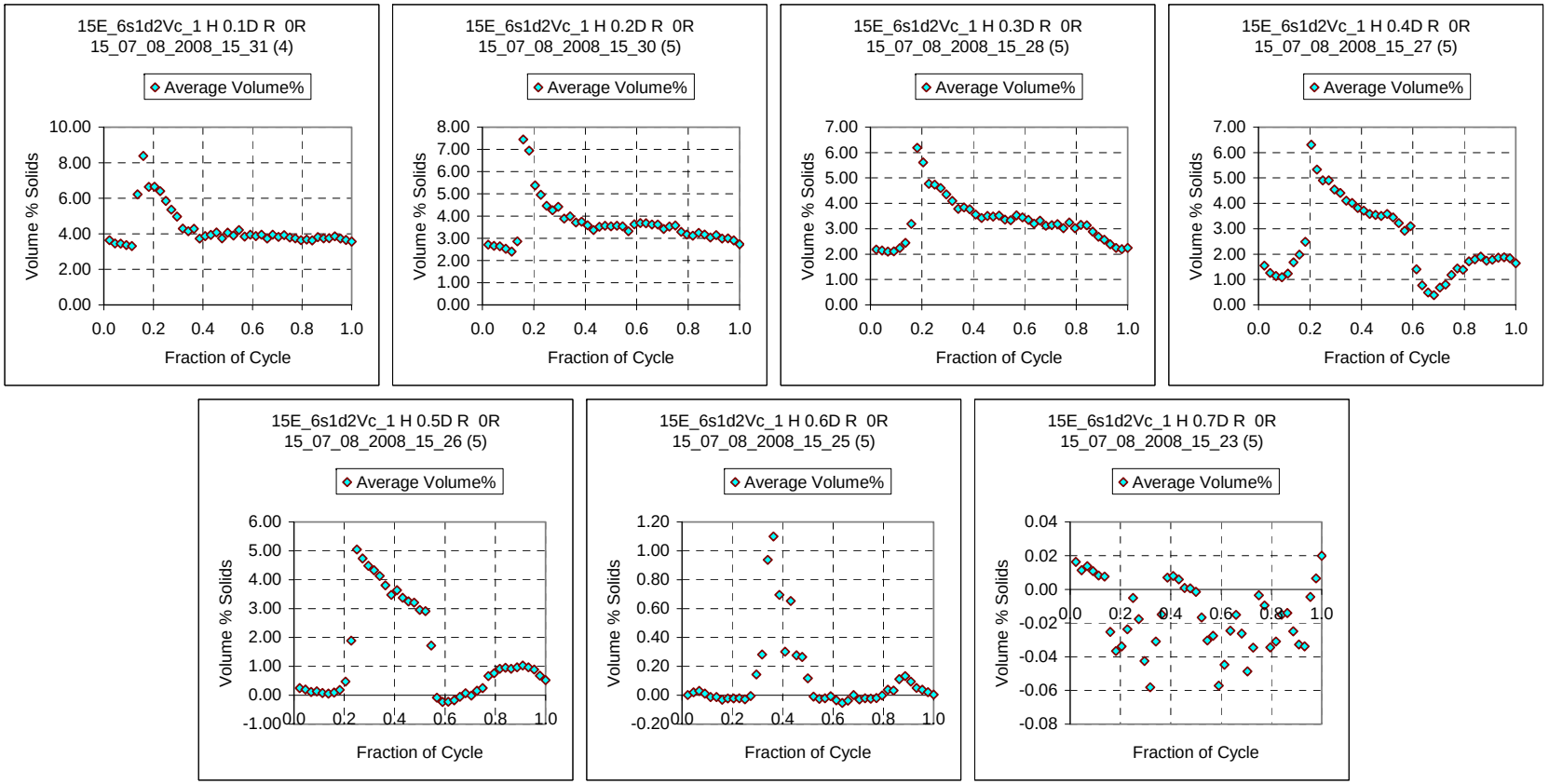

Figure C.18A. Case ID 15E_6s1d2Vc_1 Concentration Variation During the Cycle

Figure C.18 is the first of three profiles shown using simulant s1d2 in the small-scale tank using the 8TA vessel configuration with four pulse tubes in the outer ring and four in the inner ring and a nozzle diameter of 6 in. full scale. The solids fraction was 0.0143. The duty cycle was 33.3% and the pulse volume fraction was 0.050. The U_{CS} velocity occurred at 4.8 m/s. The peak cloud height upper bound was 10 in.

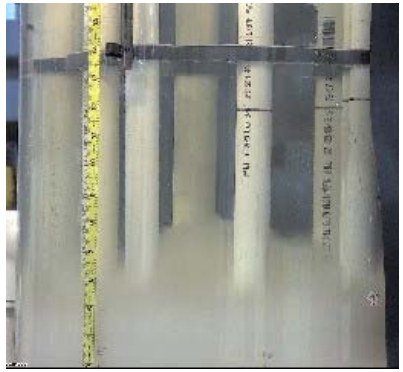

Maximum Cloud Height

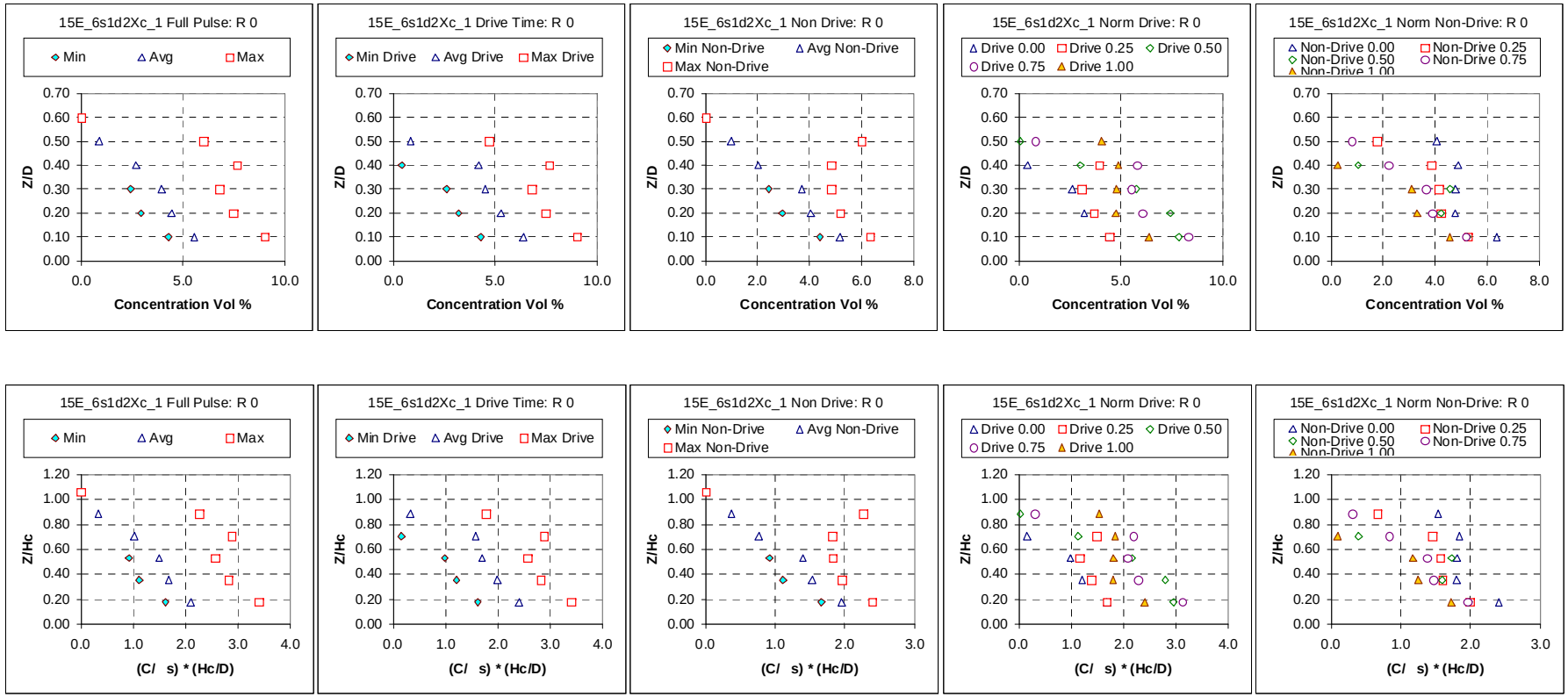

Figure C.19. 0.367-m- (14 7/16-in.-) diameter tank, 0.485-cm- (0.191-in.-) diameter nozzle; solids nominal diameter 69.3 µm, 2.48 g/cm^3 density; 0.015 nominal solids fraction; 33.3% duty cycle, cycle time 9.3 s, pulse volume fraction 0.050, U_{CS} velocity 4.6 m/s, target nozzle exit velocity 4.6 m/s; peak cloud height upper bound 0.229 m (9 in.). Case ID 15E_6s1d2Xc_1.

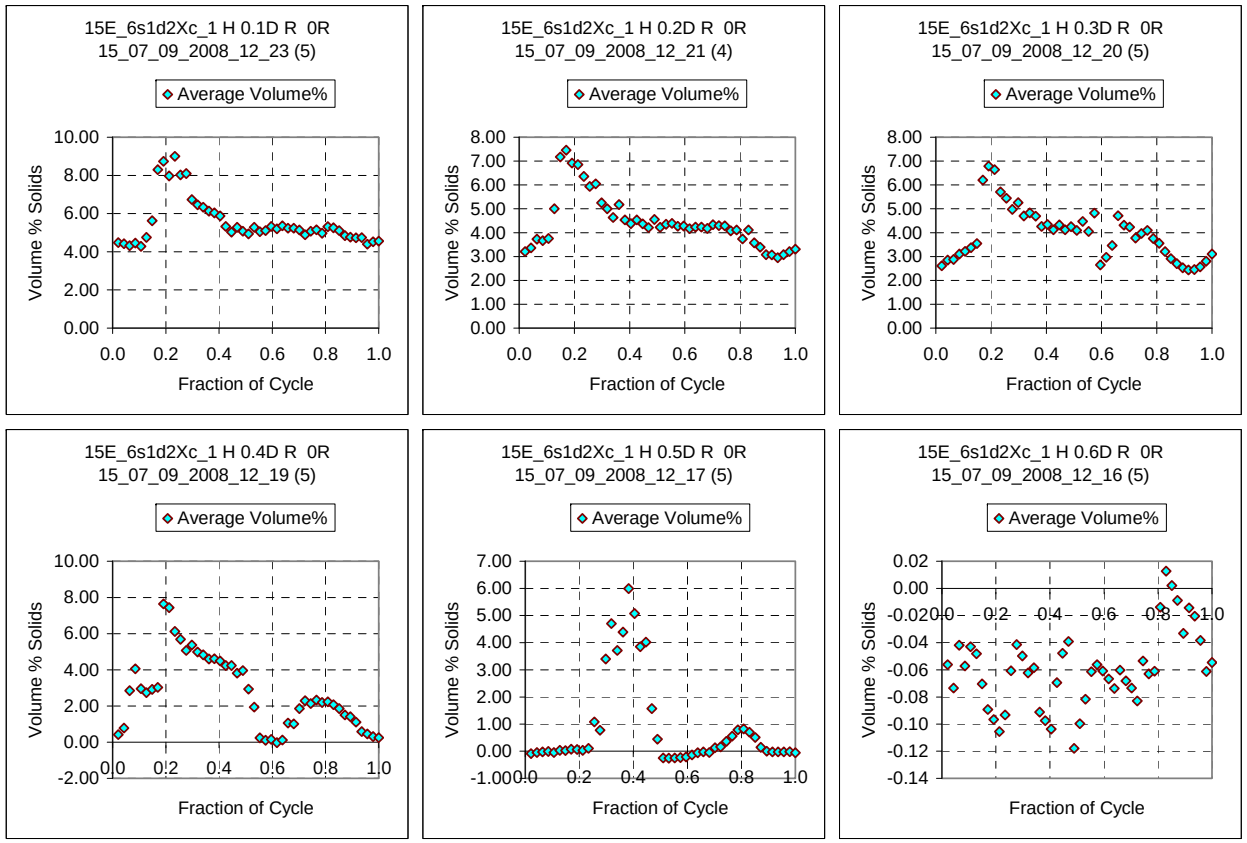

Figure C.19A. Case ID 15E_6s1d2Xc_1 Concentration Variation During the Cycle

Figure C.19 is the second of three profiles shown using simulant s1d2 in the small-scale tank using the 8TA vessel configuration with a 6-in. full-scale nozzle. The solids fraction increased slightly to 0.015 from 0.0143 during the prior test. The duty cycle was 33.3% and the pulse volume fraction was 0.050. The U_{CS} velocity occurred at 4.6 m/s, slightly lower than 4.8 m/s for the prior test. The peak cloud height upper bound was 9 in., slightly lower than 10 in. for the prior test.

Maximum Cloud Height

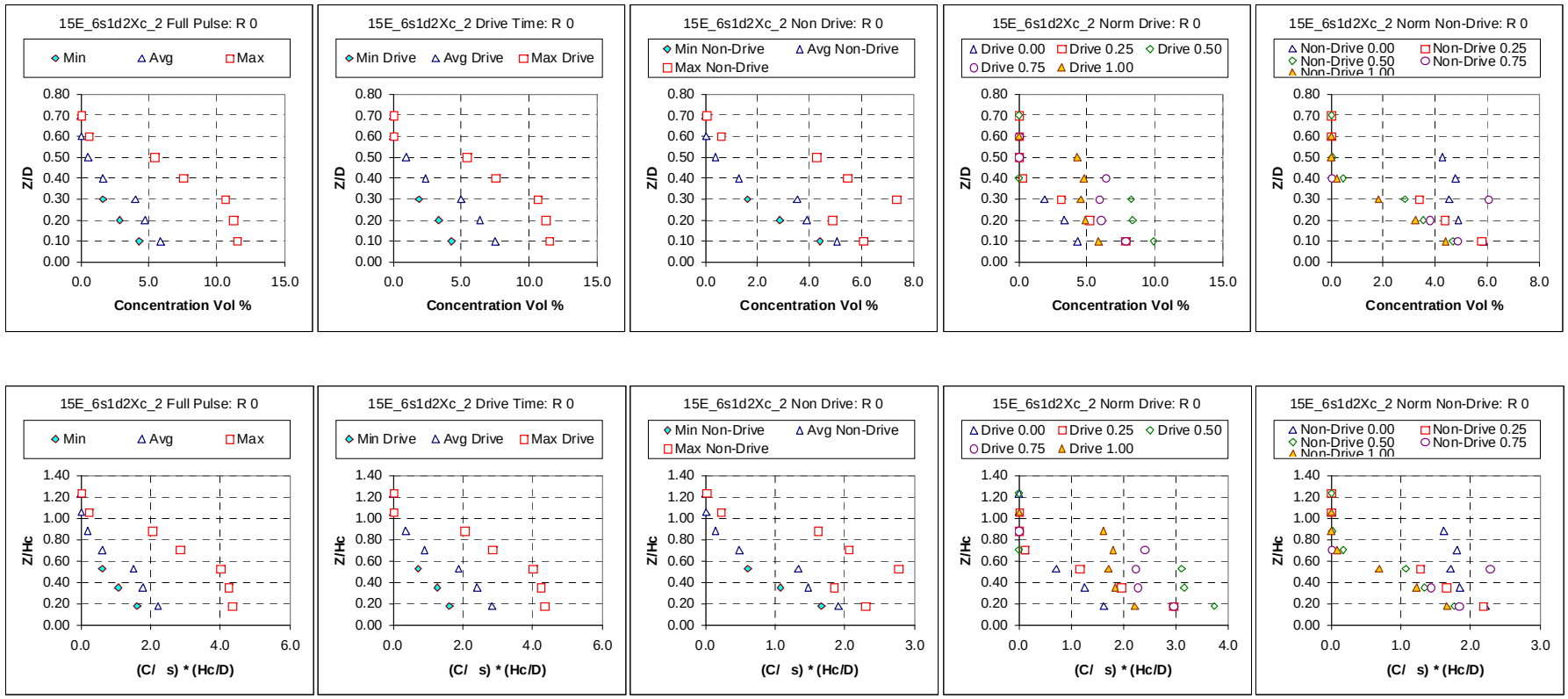

Figure C.20. 0.367-m- (14 7/16-in.-) diameter tank, 0.485-cm- (0.191-in.-) diameter nozzle; solids nominal diameter 69.3 µm, 2.48 g/cm^3 density; 0.015 nominal solids fraction, 32.9% duty cycle, cycle time 18.8 s, pulse volume fraction 0.100, U_{CS} velocity 4.4 m/s, target nozzle exit velocity 4.4 m/s; peak cloud height upper bound 0.229 m (9 in.). Case ID 15E_6s1d2Xc_2.

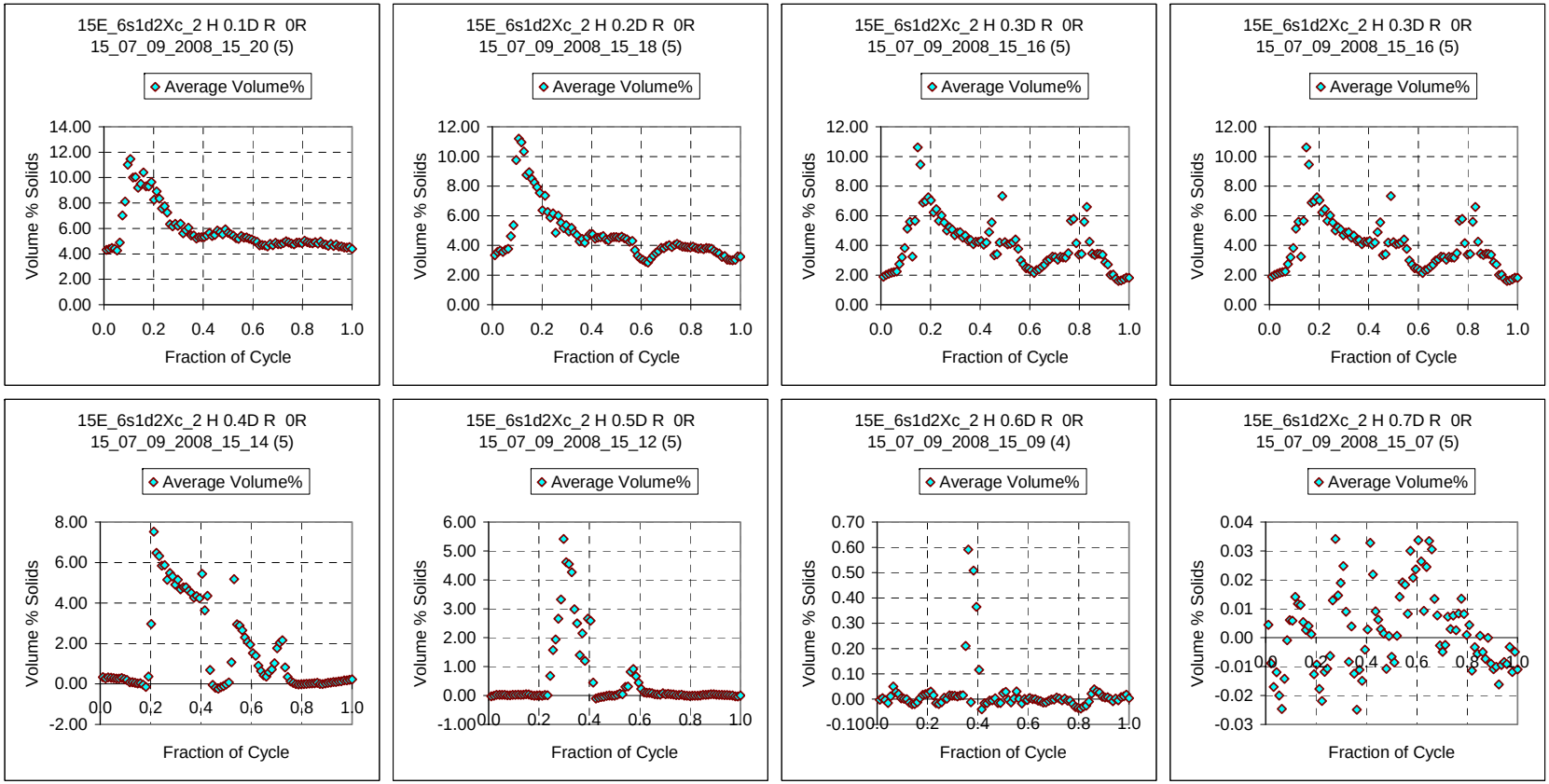

Figure C.20A. Case ID 15E_6s1d2Xc_2 Concentration Variation During the Cycle

Figure C.20 is the third of three profiles shown using simulant s1d2 in the small-scale tank using the 8TA vessel configuration with a 6-in. full-scale nozzle. The solids fraction was unchanged from the prior test at 0.015. The duty cycle was 32.9% and the pulse volume fraction was 0.1, an increase from 0.050 from the prior test. The U_{CS} velocity occurred at 4.4 m/s, slightly lower than 4.6 m/s for the prior test. The peak cloud height upper bound was 9 in. – no change from the prior test.

Maximum Cloud Height

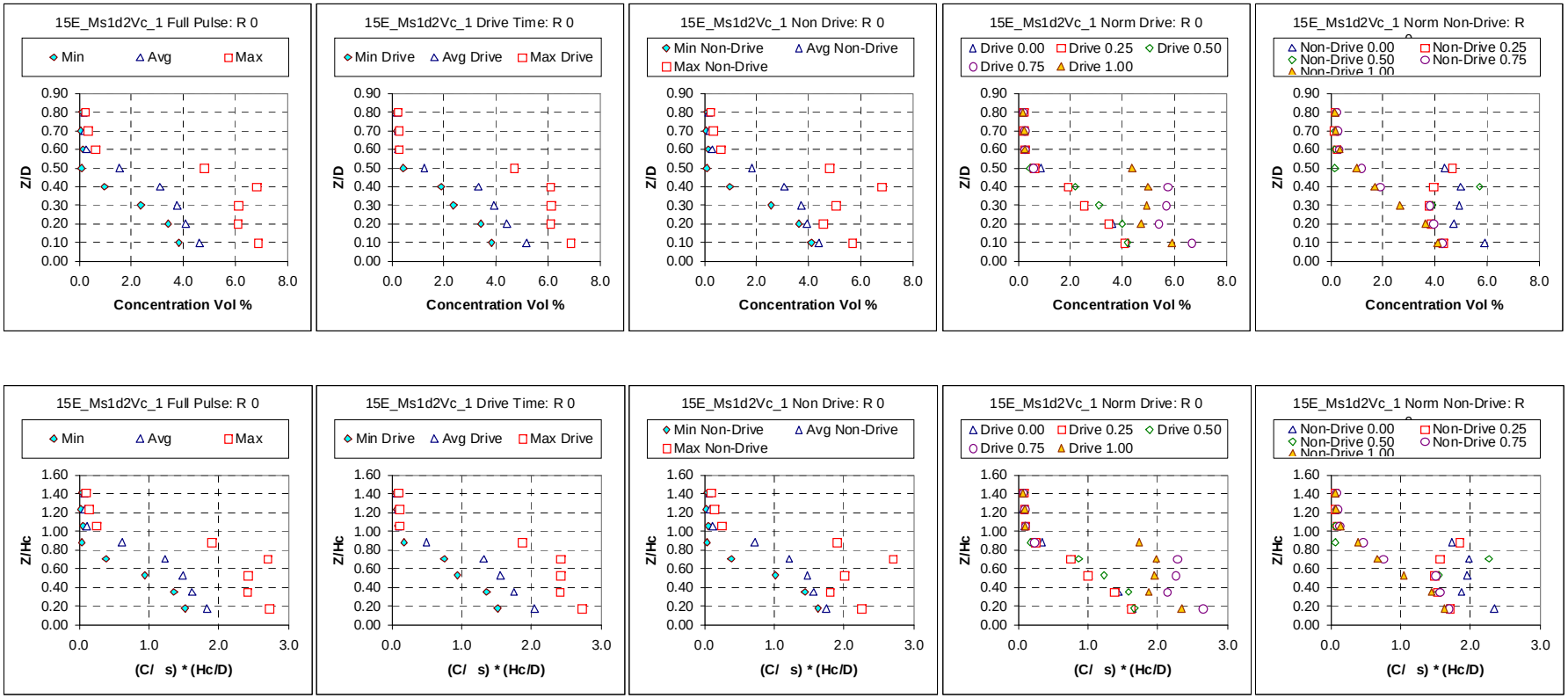

Figure C.21. 0.367-m- (14 7/16-in.-) diameter tank, 0.681-cm- (0.268-in.-) diameter nozzle; solids nominal diameter 69.3 µm, 2.48 g/cm^3 density; 0.0143 nominal solids fraction; 33.0% duty cycle, cycle time 7.6 s, pulse volume fraction 0.050, U_{CS} velocity 2.9 m/s, target nozzle exit velocity 2.9 m/s; peak cloud height upper bound 0.229 m (9 in.). Case ID 15E_Ms1d2Vc_1.

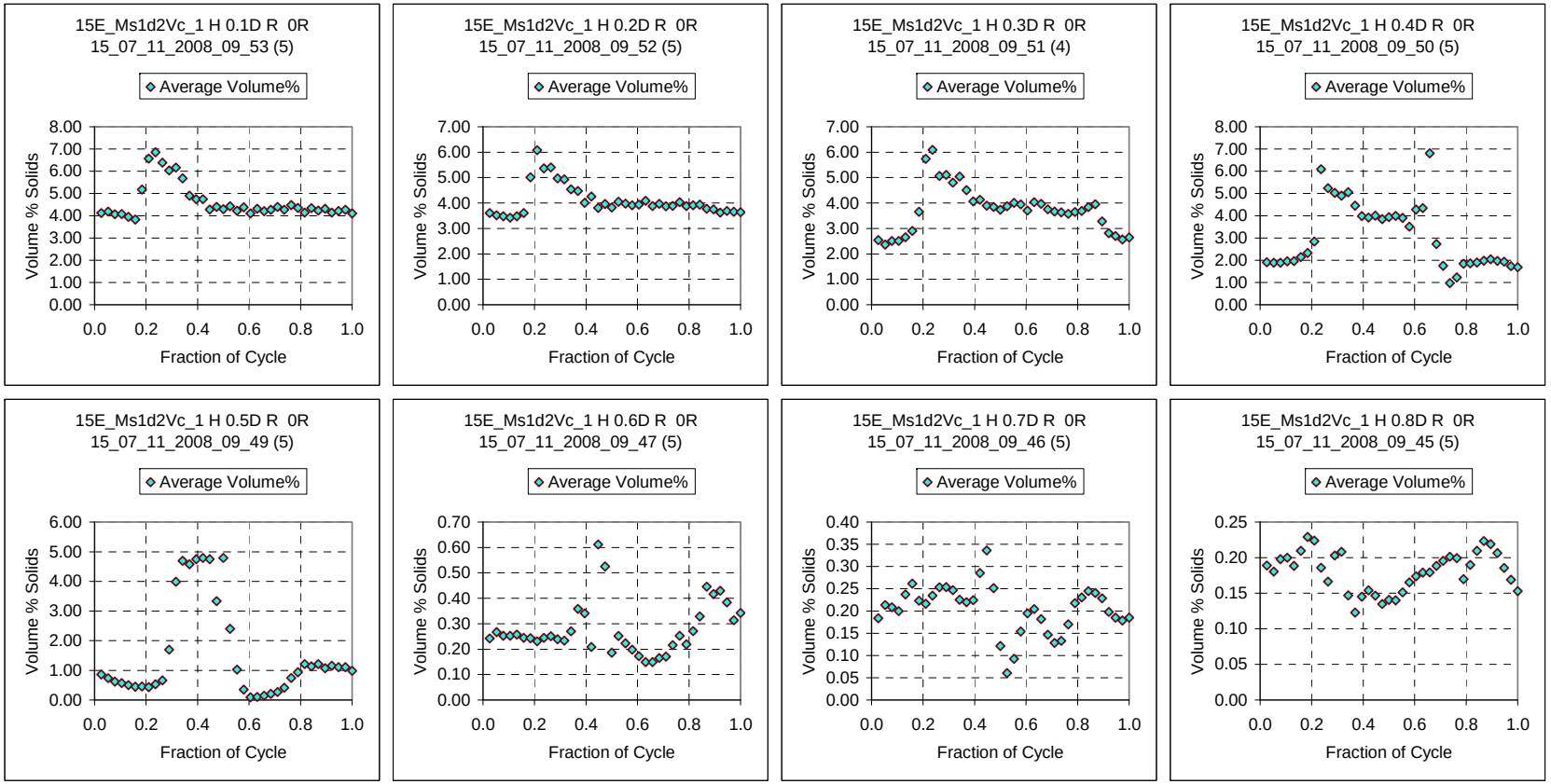

Figure C.21A. Case ID 15E_Ms1d2Vc_1 Concentration Variation During the Cycle

Figure C.21 is the only profile shown using simulant s1d2 in the small-scale tank using the 8TA vessel configuration with a nozzle diameter of 0.268 in., a full-scale nozzle diameter of 8.5 in. The solids fraction was 0.0143. The duty cycle was 33.0% and the pulse volume fraction was 0.050. This profile can be compared with that shown in Figure C.18 with similar conditions but using a smaller 0.191-in. nozzle, a full-scale nozzle diameter of 6 in. The U_{CS} velocity with the larger nozzle occurred at 2.9 m/s, which was lower than the 4.8 m/s value obtained with the smaller nozzle. The peak cloud height upper bound with the larger nozzle was 9 in. while the peak cloud height upper bound with the smaller was 10 in.

Maximum Cloud Height

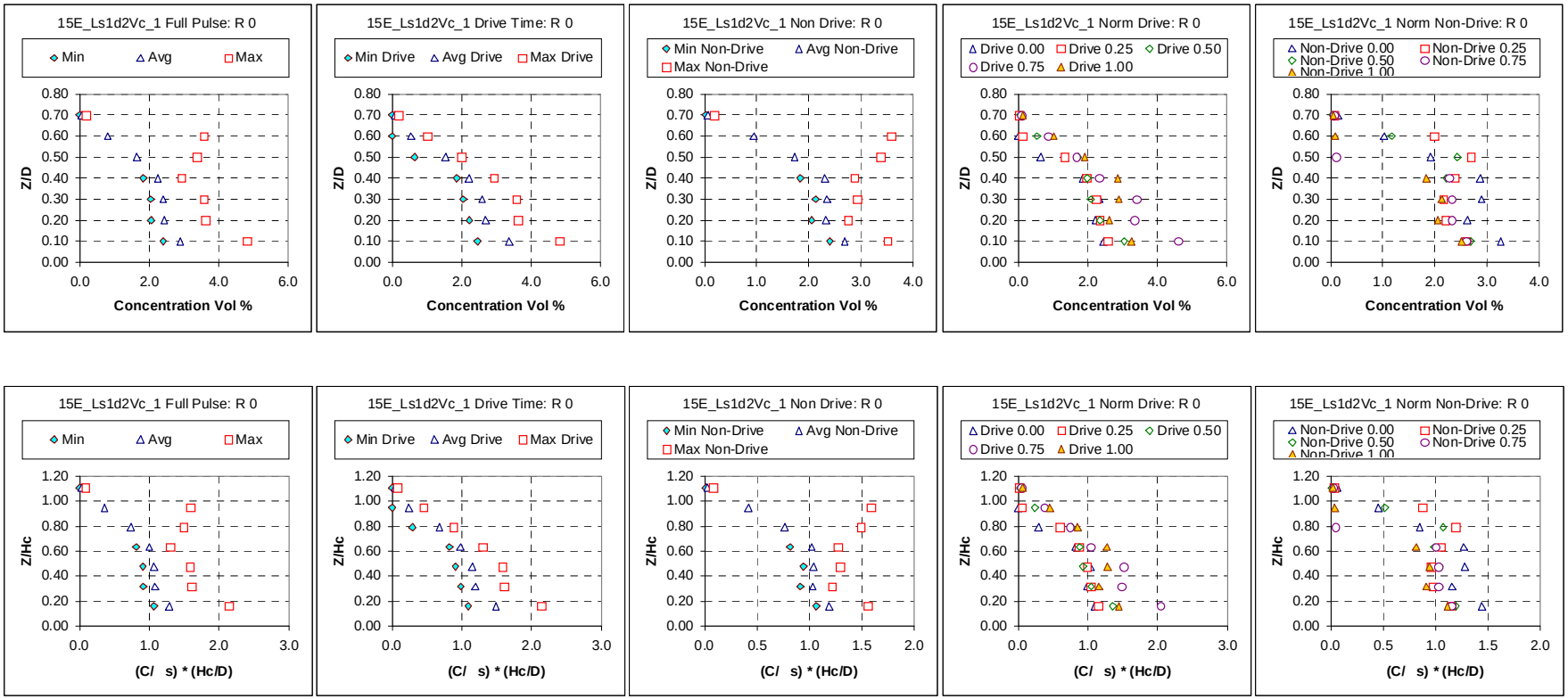

Figure C.22. 0.367-m- (14 7/16-in.-) diameter tank, 0.953-cm- (0.375-in.-) diameter nozzle; solids nominal diameter 69.3 µm, 2.48 g/cm^3 density; 0.0143 nominal solids fraction; 33.7% duty cycle, cycle time 5.8 s, pulse volume fraction 0.050, U_{CS} velocity 1.9 m/s, target nozzle exit velocity 1.9 m/s; peak cloud height upper bound 0.254 m (10 in.). Case ID 15E_Ls1d2Vc_1.

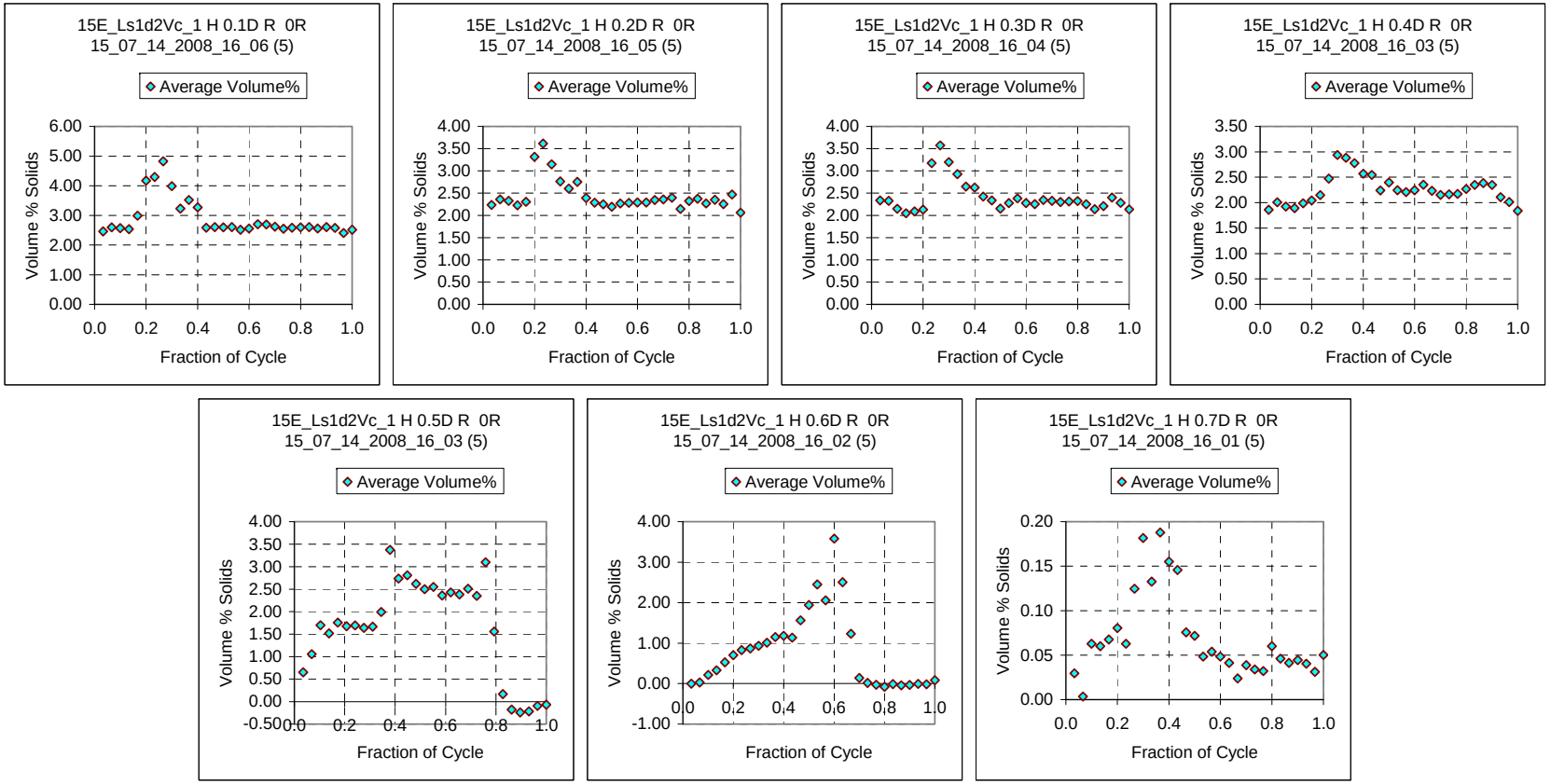

Figure C.22A. Case ID 15E_Ls1d2Vc_1 Concentration Variation During the Cycle

Figure C.22 is the first of three profiles shown using simulant s1d2 in the small-scale tank using the 8TA vessel configuration with a nozzle diameter of 0.375 in., a full-scale nozzle diameter of 11.8 in. The solids fraction was 0.0143. The duty cycle was 33.7% and the pulse volume fraction was 0.050. The U_{CS} velocity occurred at 1.9 m/s. The peak cloud height upper bound was 10 in.

Maximum Cloud Height

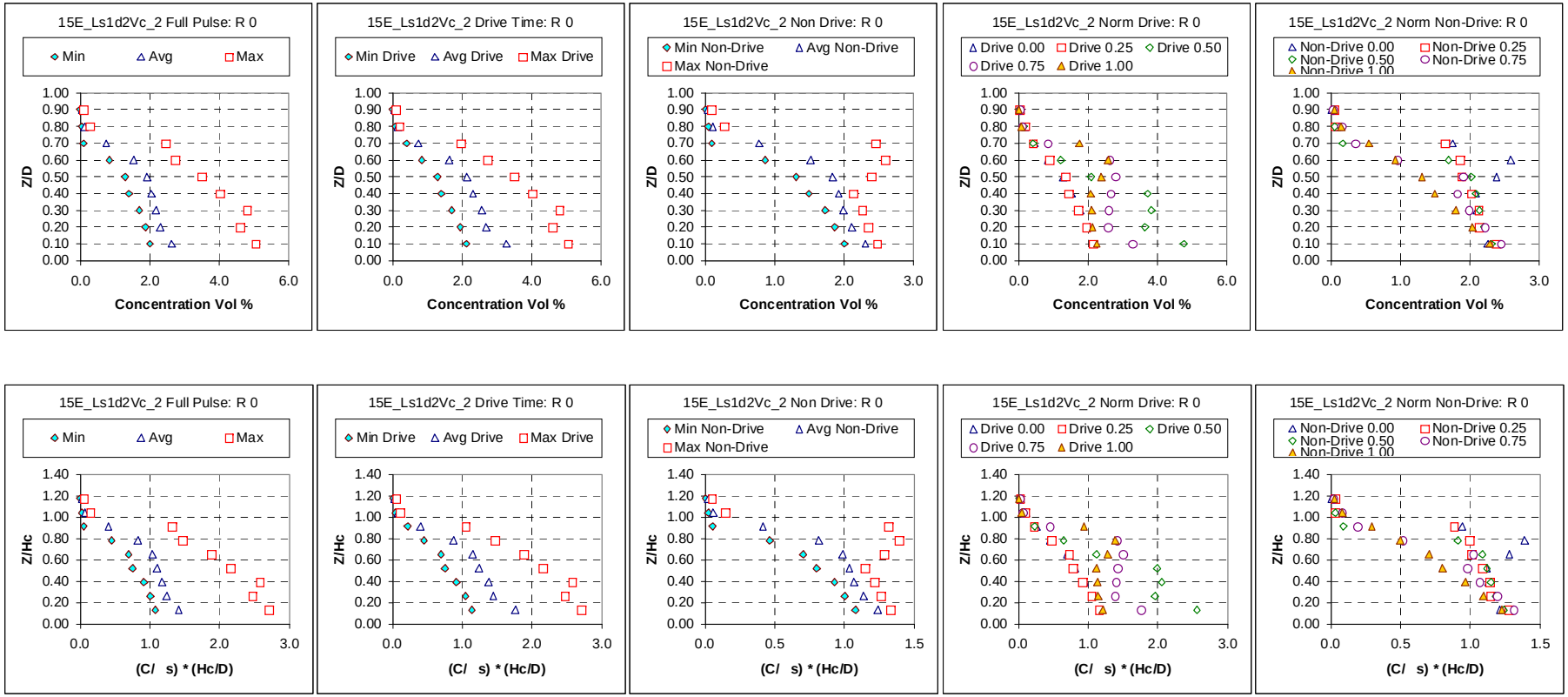

Figure C.23. 0.367-m- (14 7/16-in.-) diameter tank, 0.953-cm- (0.375-in.-) diameter nozzle; solids nominal diameter 69.3 µm, 2.48 g/cm^3 density; 0.0143 nominal solids fraction; 33.5% duty cycle, cycle time 11.4 s, pulse volume fraction 0.101, U_{CS} velocity 1.9 m/s, target nozzle exit velocity 1.9 m/s; peak cloud height upper bound 0.305 m (12 in.). Case ID 15E_Ls1d2Vc_2.

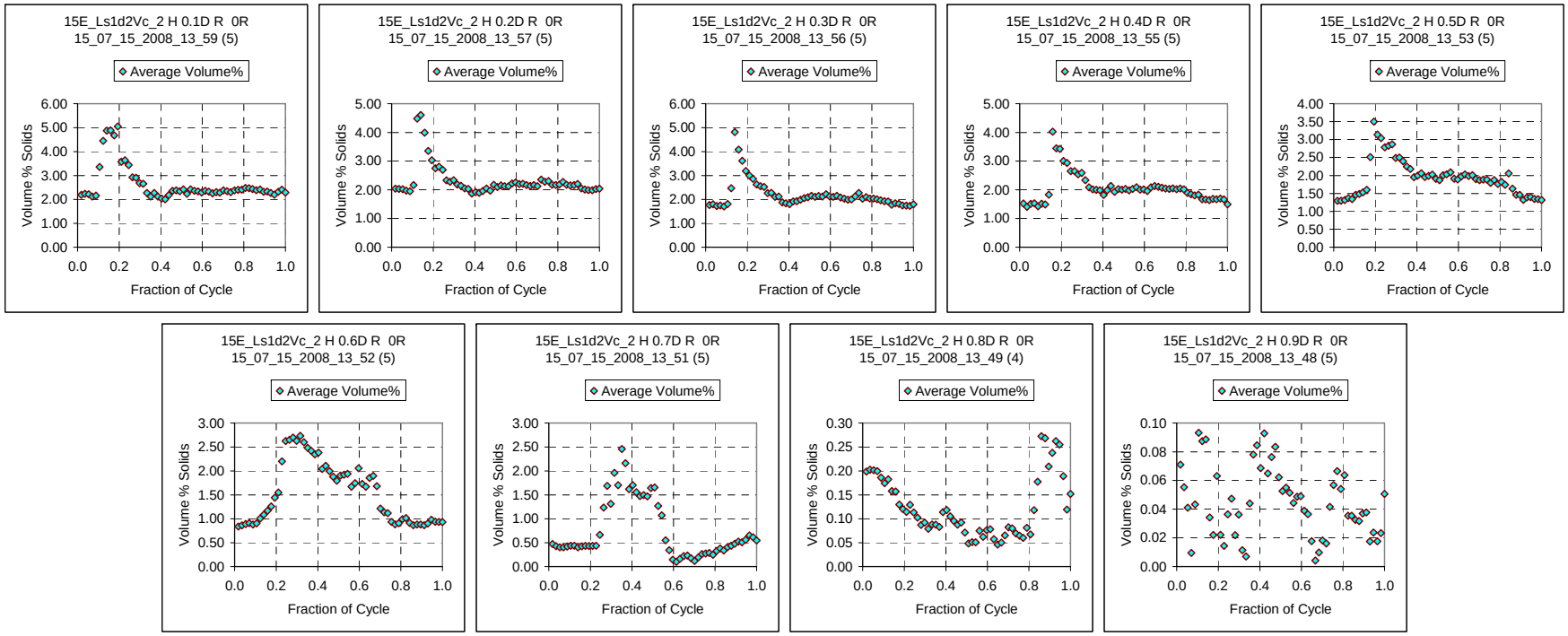

Figure C.23A. Case ID 15E_Ls1d2Vc_2 Concentration Variation During the Cycle

Figure C.23 is the second of three profiles shown using simulant s1d2 in the small-scale tank using the 8TA vessel configuration with a nozzle diameter of 0.375 in., a full-scale nozzle diameter of 11.8 in. The solids fraction was 0.0143. The duty cycle was 33.5% and the pulse volume fraction was 0.10 – a change from the pulse volume of 0.050 in the prior test. The U_{CS} velocity occurred at 1.9 m/s, which was the same as for the prior test. The peak cloud height upper bound was 12 in. while the peak cloud height upper bound for the prior test was 10 in.

Maximum Cloud Height

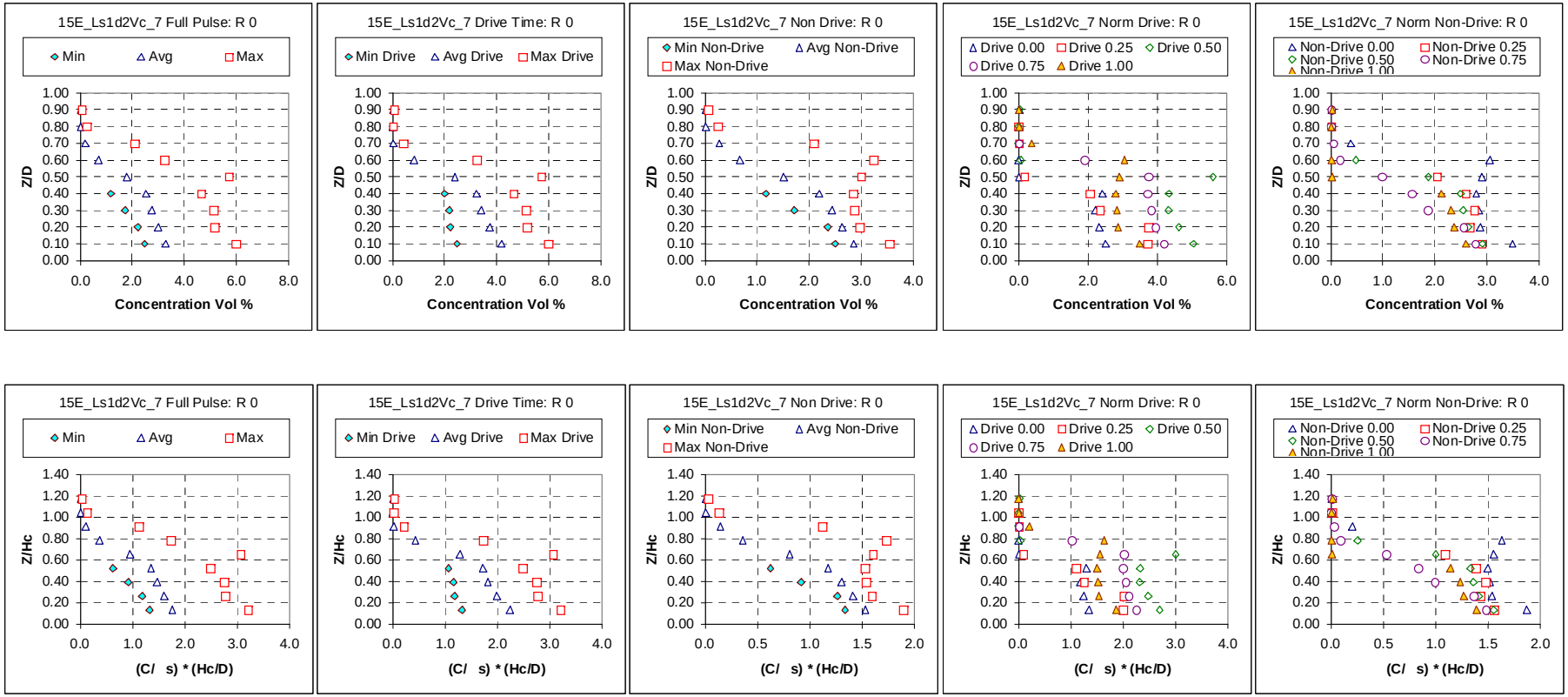

Figure C.24. 0.367-m- (14 7/16-in.-) diameter tank, 0.953-cm- (0.375-in.-) diameter nozzle; solids nominal diameter 69.3 µm, 2.48 g/cm^3 density; 0.0143 nominal solids fraction; 33.5% duty cycle, cycle time 17.0 s, pulse volume fraction 0.100, U_{CS} velocity 2.5 m/s, target nozzle exit velocity 2.5 m/s; peak cloud height upper bound 0.305 m (12 in.). Case ID 15E_Ls1d2Vc_7.

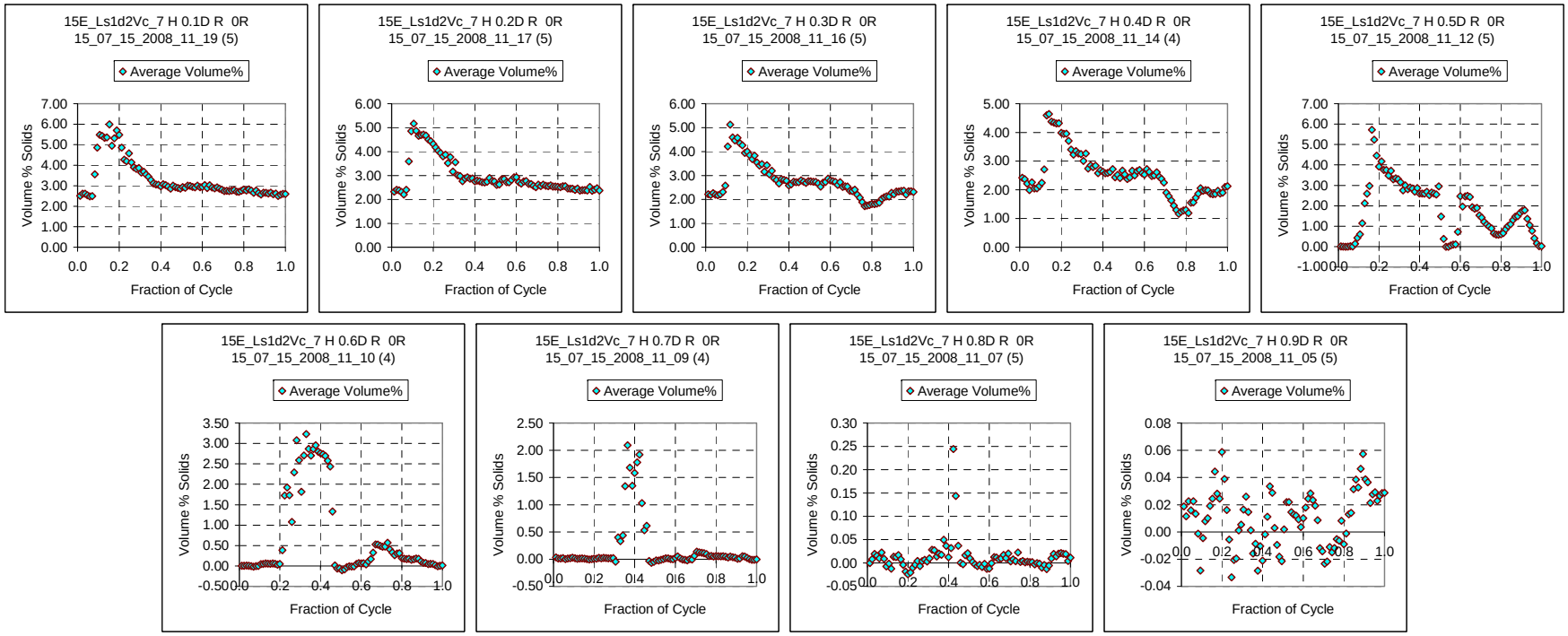

Figure C.24A. Case ID 15E_Ls1d2Vc_7 Concentration Variation During the Cycle

Figure C.24 is the third of three profiles shown using simulant s1d2 in the small-scale tank using the 8TA vessel configuration with a nozzle diameter of 0.375 in., a full-scale nozzle diameter of 11.8 in. The solids fraction was 0.0143. The duty cycle was 33.5% and the pulse volume fraction was 0.10, no change from the prior test. In this test, only the four outer pulse tubes were operated. The U_{CS} velocity occurred at 2.5 m/s, which was an increase from the 1.9-m/s value obtained in the prior test when all eight pulse tubes were operating. The peak cloud height upper bound of 12 in. was unchanged from the prior test.

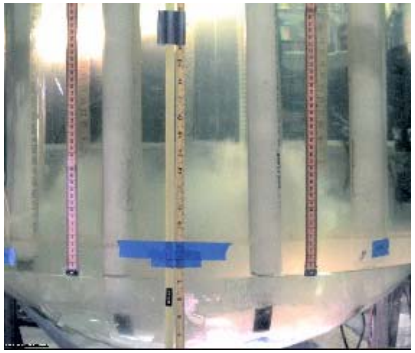

Maximum Cloud Height

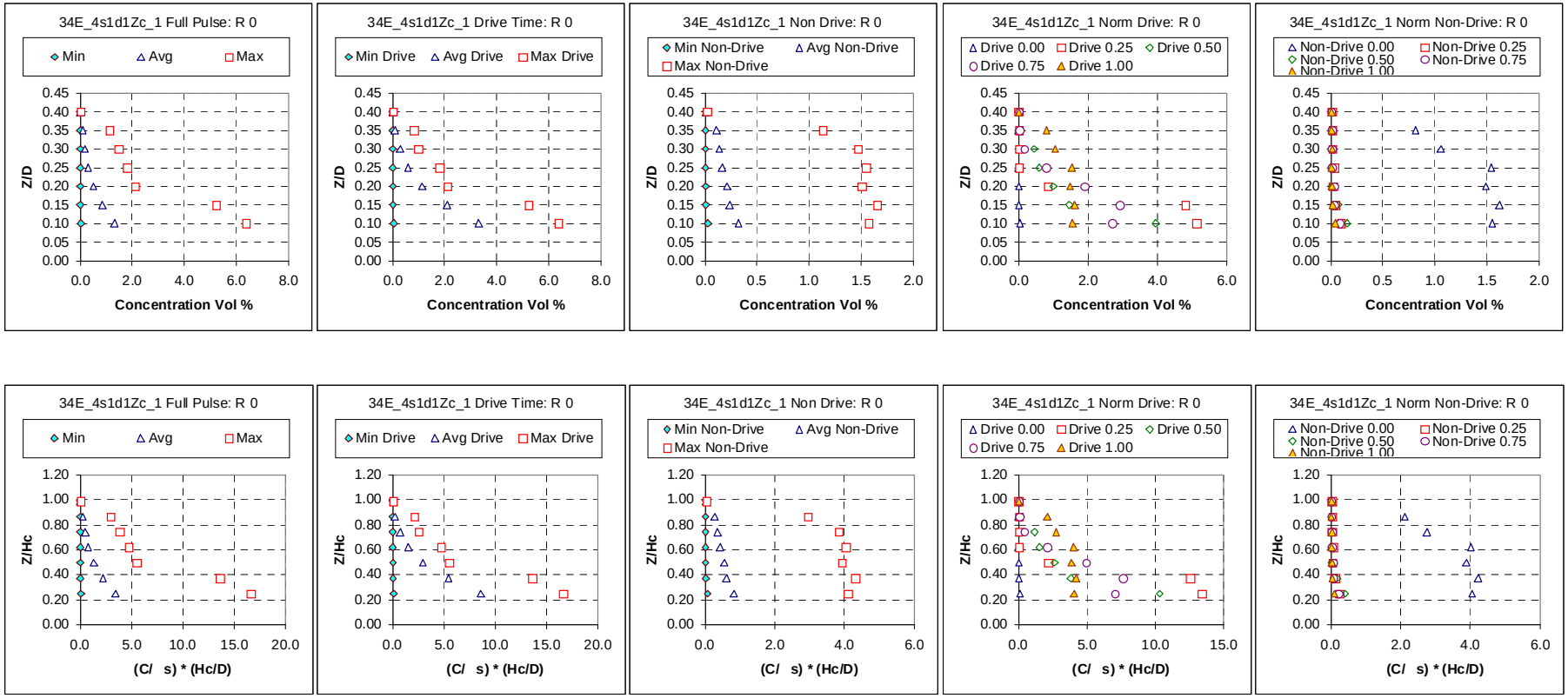

Figure C.25. 0.860-m- (33 7/8-in.-) diameter tank, 0.754-cm- (0.297-in.-) diameter nozzle; solids nominal diameter 166.4 µm, 2.46 g/cm^3 density; 0.00155 nominal solids fraction; 33.8% duty cycle, cycle time 32.0 s, pulse volume fraction 0.050, U_{CS} velocity 4.5 m/s, target nozzle exit velocity 4.5 m/s; peak cloud height upper bound 0.356 m (14 in.). Case ID 34S_4s1d1Zc_1 (shown as 34E on plots).

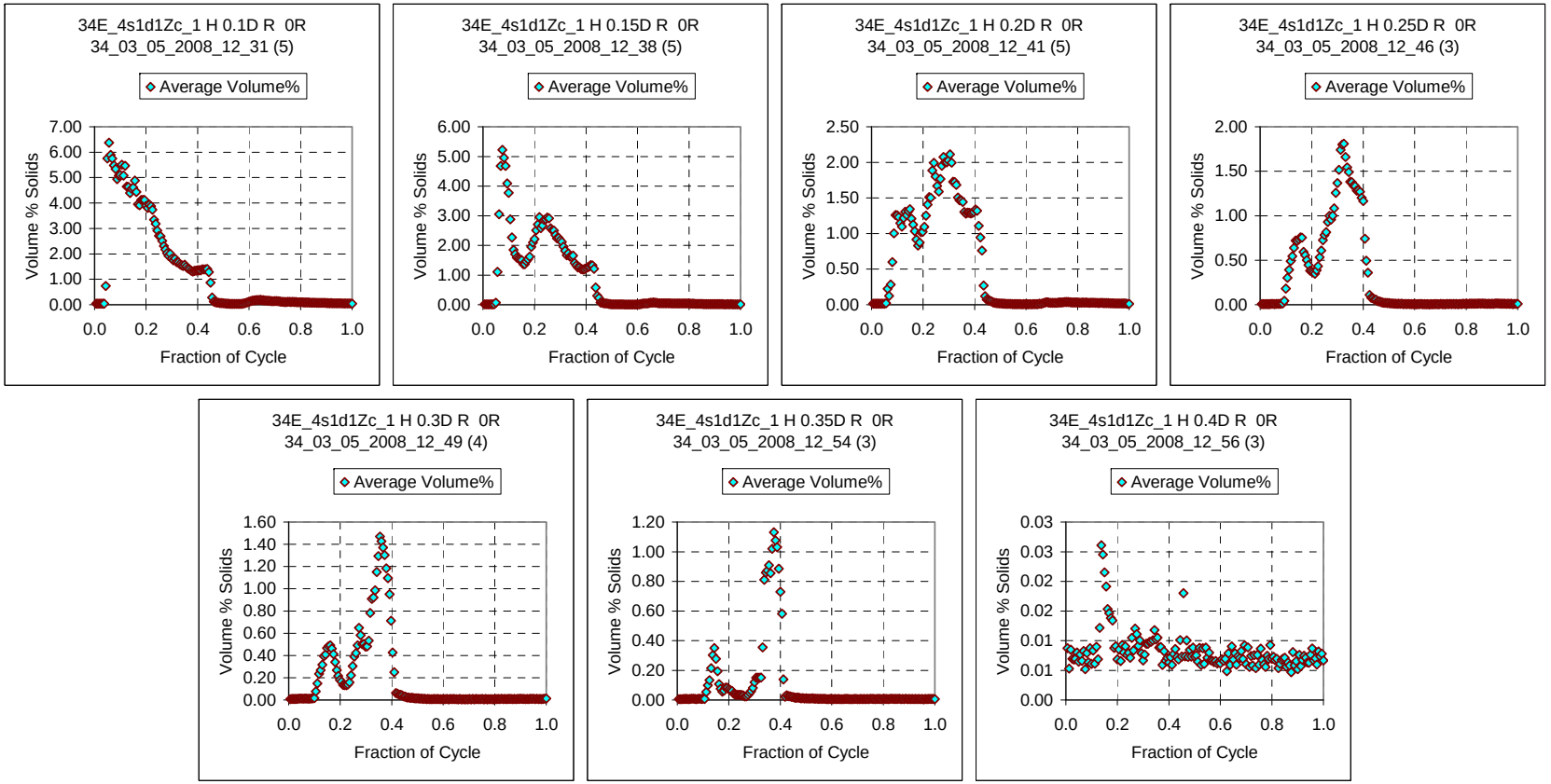

Figure C.25A. Case ID 34S_4s1d1Zc_1 Concentration Variation During the Cycle

Figure C.25 is the only profile shown using simulant s1d1 in the mid-scale tank. The solids fraction was 0.00155. The duty cycle was 33.8% and the pulse volume fraction was 0.050. The U_{CS} velocity occurred at 4.5 m/s. The peak cloud height upper bound was 14 in.

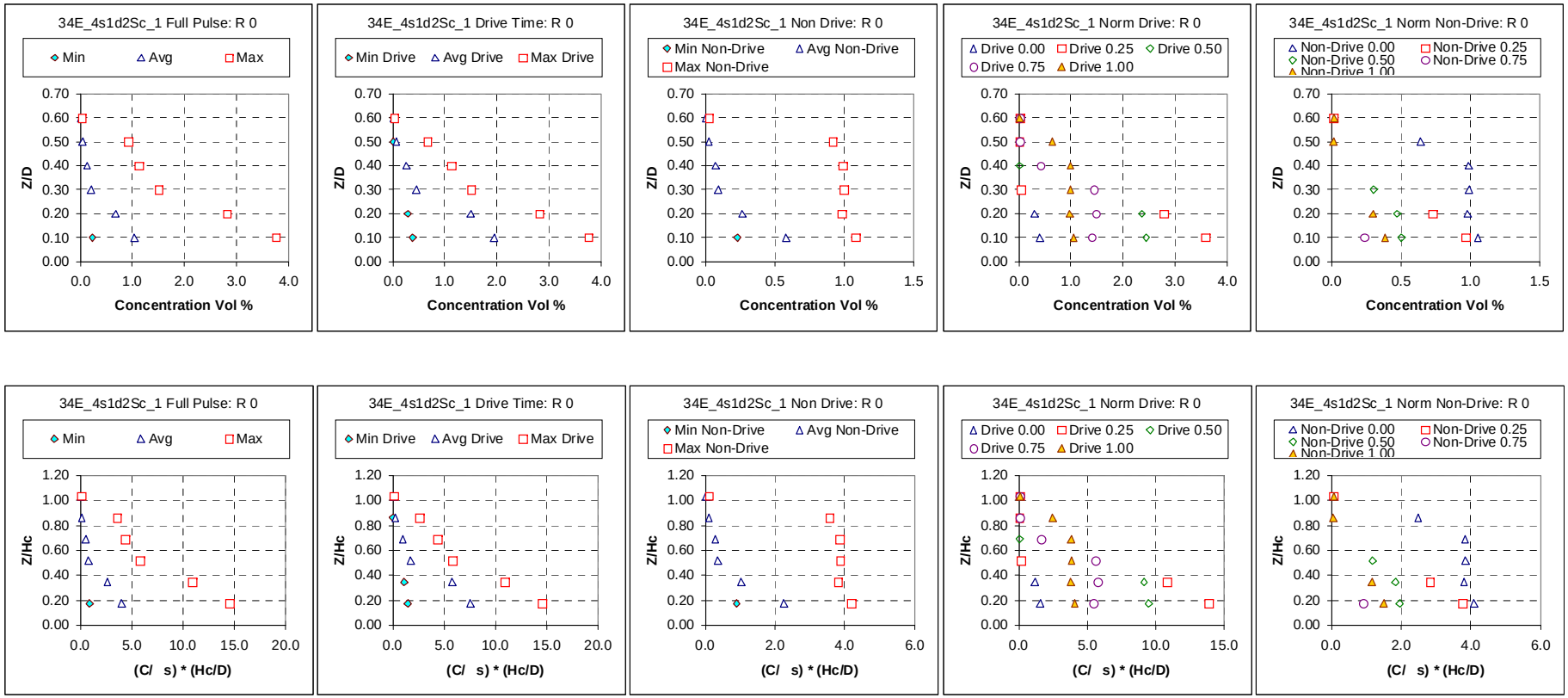

Figure C.26. 0.860-m- (33 7/8-in.-) diameter tank, 0.754-cm- (0.297-in.-) diameter nozzle; solids nominal diameter 69.3 µm, 2.48 g/cm^3 density; 0.0015 nominal solids fraction; 33.6% duty cycle, cycle time 39.0 s, pulse volume fraction 0.050, U_{CS} velocity 3.7 m/s, target nozzle exit velocity 3.7 m/s; peak cloud height upper bound 0.533 m (21 in.). Case ID 34S_4s1d2Sc_1 (shown as 34E on plots).

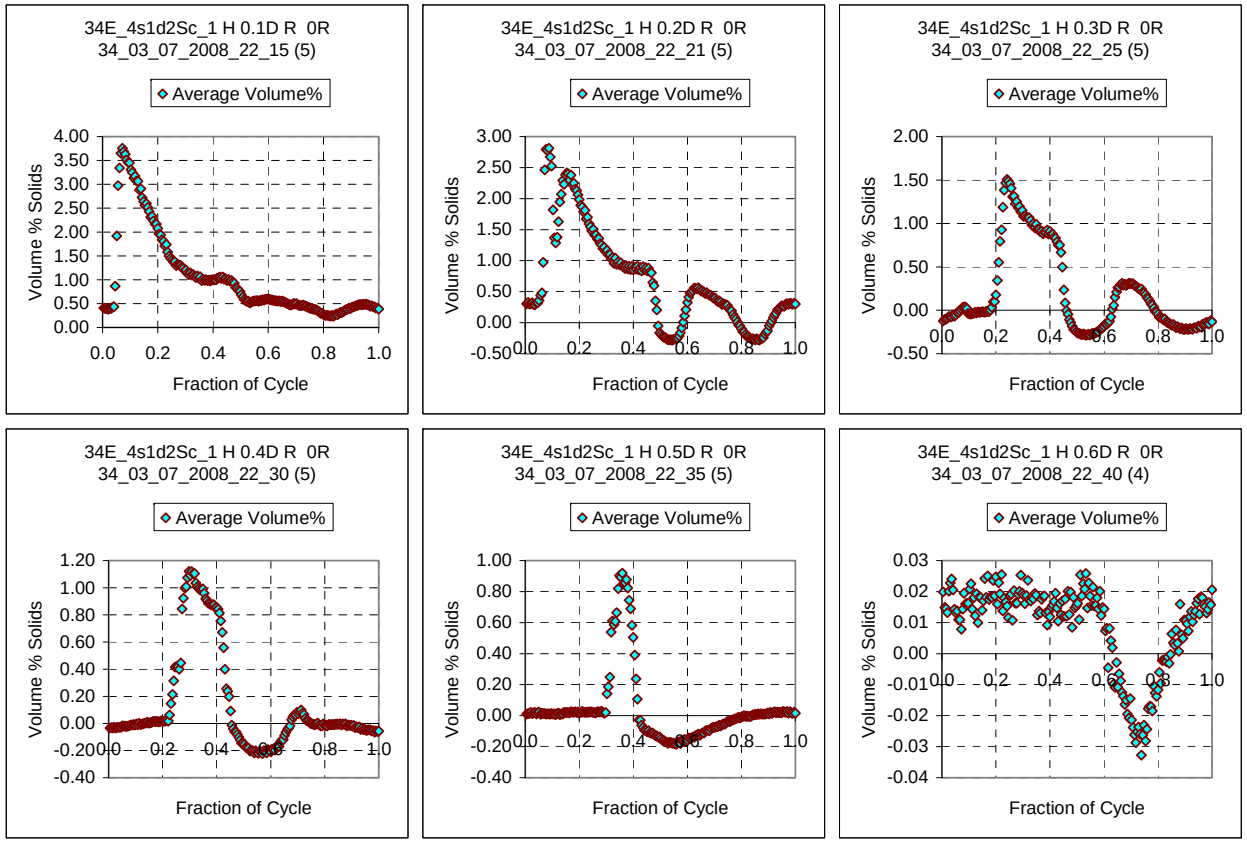

Figure C.26A. Case ID 34S_4s1d2Sc_1 Concentration Variation During the Cycle

Figure C.26 is the first of three profiles shown using simulant s1d2 in the mid-scale tank. The solids fraction was 0.0015. The duty cycle was 33.6% and the pulse volume fraction was 0.050. The U_{CS} velocity occurred at 3.7 m/s. The peak cloud height upper bound was 21 in.

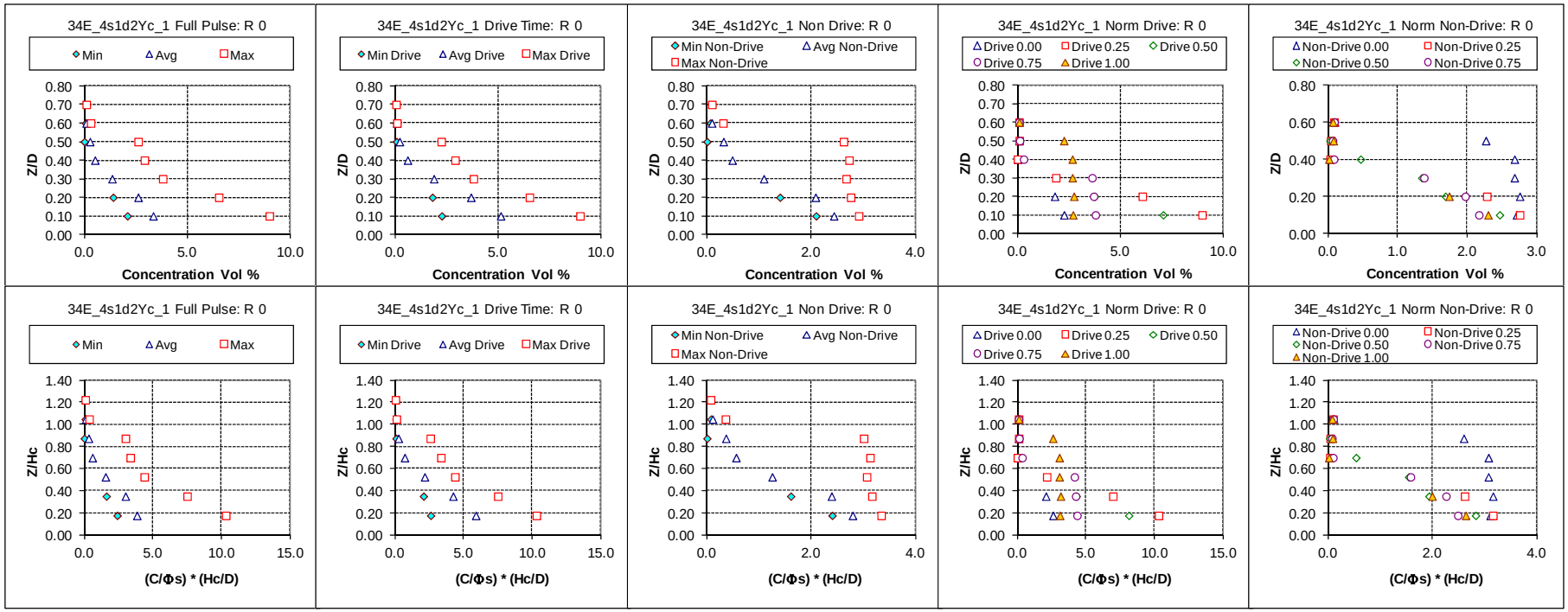

Figure C.27. 0.860-m- (33 7/8-in.-) diameter tank, 0.754-cm- (0.297-in.-) diameter nozzle; solids nominal diameter 69.3 µm, 2.48 g/cm^3 density; 0.005 nominal solids fraction; 33.6% duty cycle, cycle time 28.4 s, pulse volume fraction 0.050, U_{CS} velocity 5.1 m/s, target nozzle exit velocity 5.1 m/s; peak cloud height upper bound 0.508 m (20 in.). Case ID 34S_4s1d2Yc_1 (shown as 34E on plots).

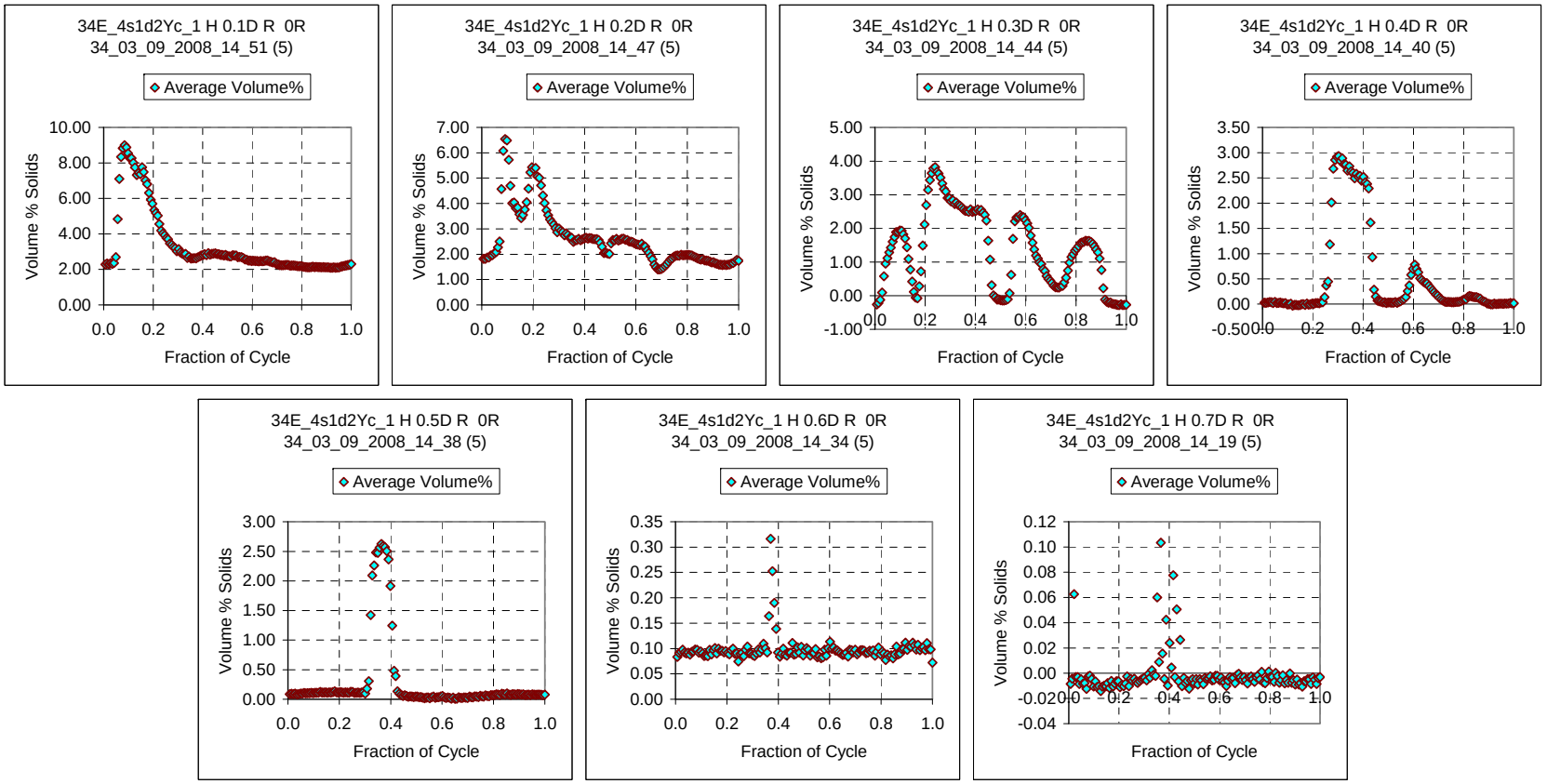

Figure C.27A. Case ID 34S_4s1d2Yc_1 Concentration Variation During the Cycle

Figure C.27 is the second of three profiles shown using simulant s1d2 in the mid-scale tank. The solids fraction was 0.005, an increase from 0.0015 in the prior test. The duty cycle was 33.6% and the pulse volume fraction was 0.050. The U_{CS} velocity occurred at 5.1, an increase from 3.7 m/s from the prior test. The peak cloud height upper bound was 20 in., a slight decrease from 21 in. in the prior test.

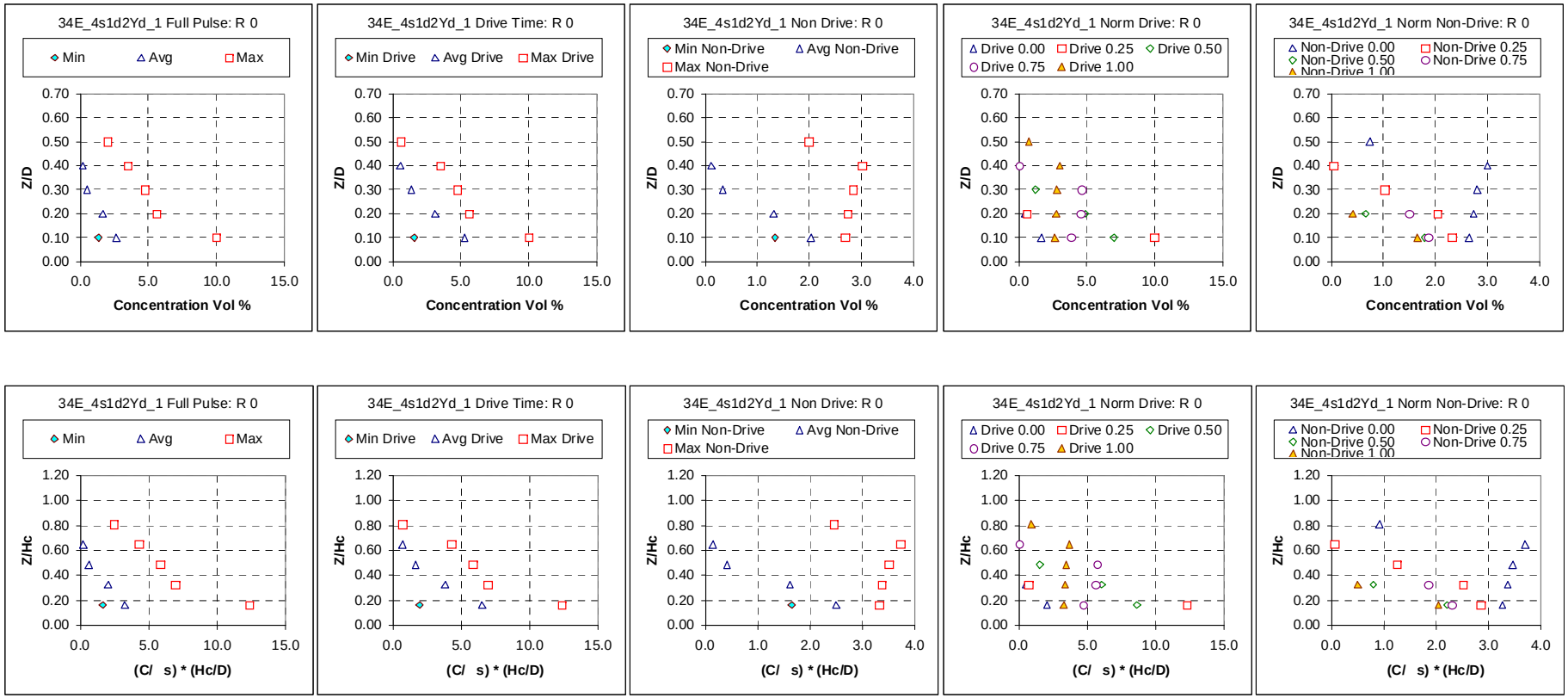

Figure C.28. 0.860-m- (33 7/8-in.-) diameter tank, 0.754-cm- (0.297-in.-) diameter nozzle; solids nominal diameter 69.3 µm, 2.48 g/cm^3 density; 0.005 nominal solids fraction; 18.6% duty cycle, cycle time 42.4 s, pulse volume fraction 0.050, U_{CS} velocity 6 m/s, target nozzle exit velocity 6.2 m/s; peak cloud height upper bound 0.559 m (22 in.). Case ID 34S_4s1d2Yd_1 (shown as 34E on plots).

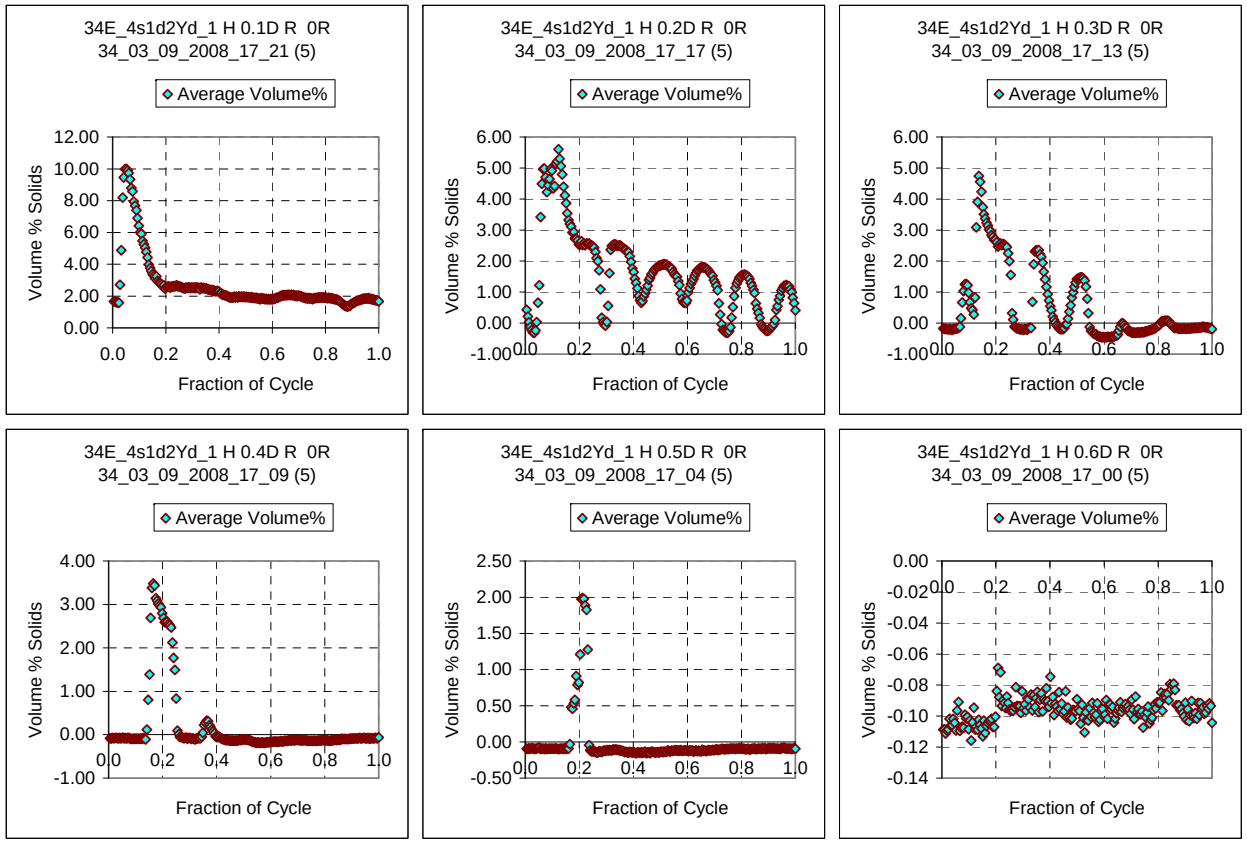

Figure C.28A. Case ID 34S_4s1d2Yd_1 Concentration Variation During the Cycle

Figure C.28 is the third of three profiles shown using simulant s1d2 in the mid-scale tank. The solids fraction was 0.005 unchanged from the prior test. The duty cycle was 18.6% changed from 33.6% in the prior test and the pulse volume fraction was 0.050, no change from the prior test. The U_{CS} velocity occurred at 6 m/s, but the test was conducted at a nozzle exit velocity of 6.2 m/s, slightly above U_{CS}. The prior test was conducted at UCS of 5.1 m/s. The peak cloud height upper bound was 22 in., a slight increase from 20 in. in the prior test.

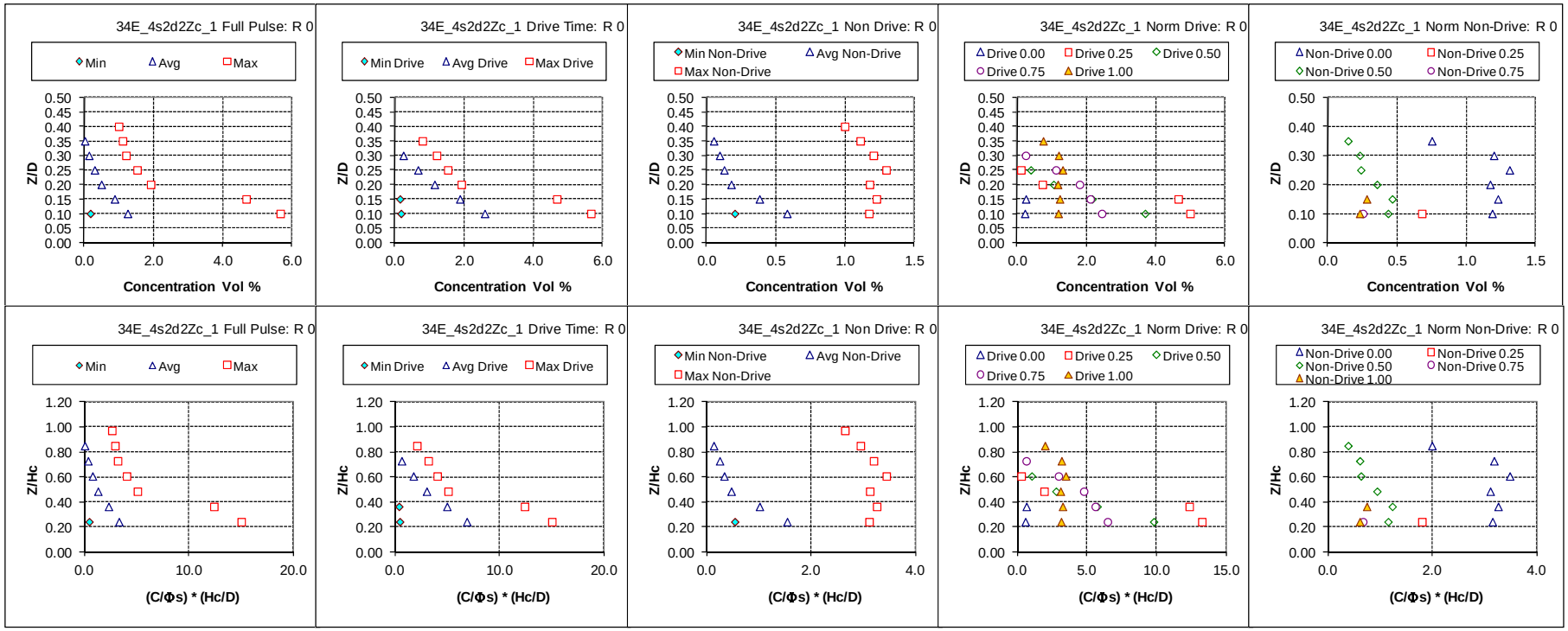

Figure C.29. 0.860-m- (33 7/8-in.-) diameter tank, 0.754-cm- (0.297-in.-) diameter nozzle; solids nominal diameter 75.6 µm, 4.18 g/cm^3 density; 0.00155 nominal solids fraction; 33.5% duty cycle, cycle time 24.9 s, pulse volume fraction 0.050, U_{CS} velocity 5.6 m/s, target nozzle exit velocity 5.6 m/s; peak cloud height upper bound 0.368 m (14.5 in.). Case ID 34S_4s2d2Zc_1 (shown as 34E on plots).

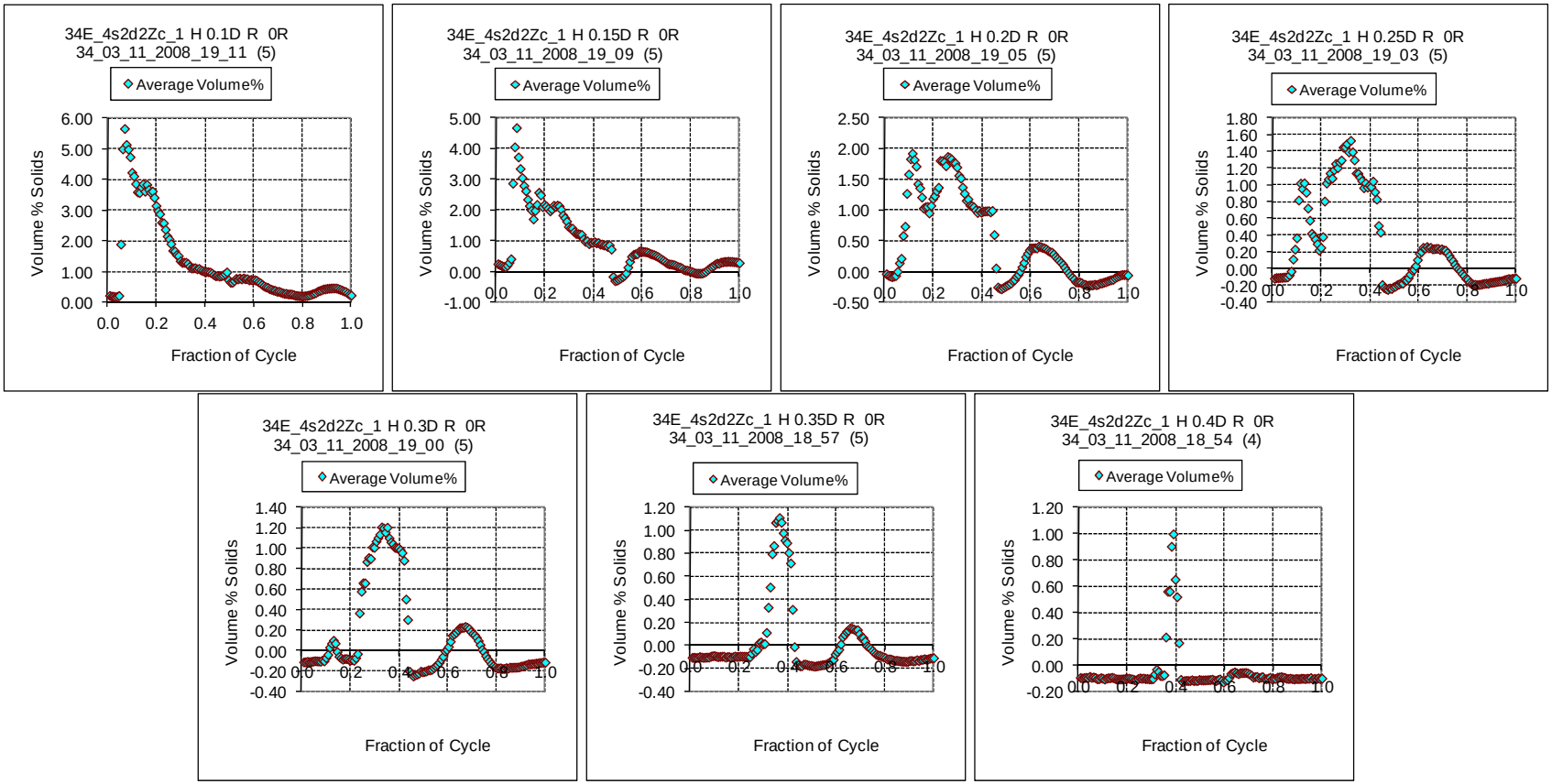

Figure C.29A. Case ID 34S_4s2d2Zc_1 Concentration Variation During the Cycle

Figure C.29 is the first of three profiles shown using simulant s2d2 in the mid-scale tank. The solids fraction was 0.00155. The duty cycle was 33.5%, and the pulse volume fraction was 0.050. The U_{CS} velocity occurred at 5.6 m/s. The peak cloud height upper bound was 14.5 in. This test can be compared with Figure C.25, which was conducted with the same conditions except for simulant (s1d1 was used for the data in Figure C.25). In the prior test, the particle diameter was larger and the particles were less dense. In Figure C.25, the U_{CS} velocity occurred at 4.5 m/s and the peak cloud height upper bound was 14 in. As expected, the denser, smaller particles had a higher critical-suspension velocity.

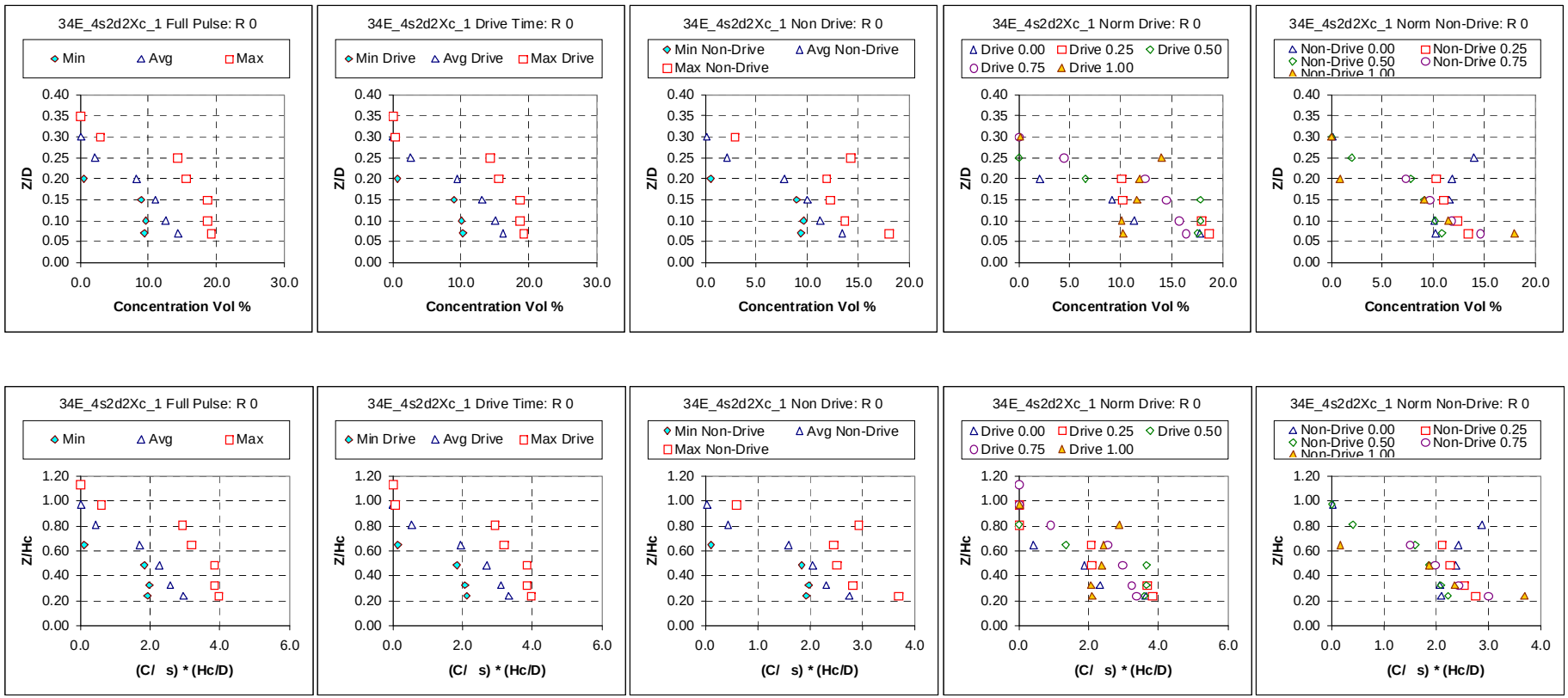

Figure C.30. 0.860-m- (33 7/8-in.-) diameter tank, 0.754-cm- (0.297-in.-) diameter nozzle; solids nominal diameter 75.6 µm, 4.18 g/cm^3 density; 0.015 nominal solids fraction; 33.9% duty cycle, cycle time 14.8 s, pulse volume fraction 0.050, U_{CS} velocity 9.8 m/s, target nozzle exit velocity 10 m/s; peak cloud height upper bound 0.279 m (11 in.). Case ID 34S_4s2d2Xc_1 (shown as 34E on plots).

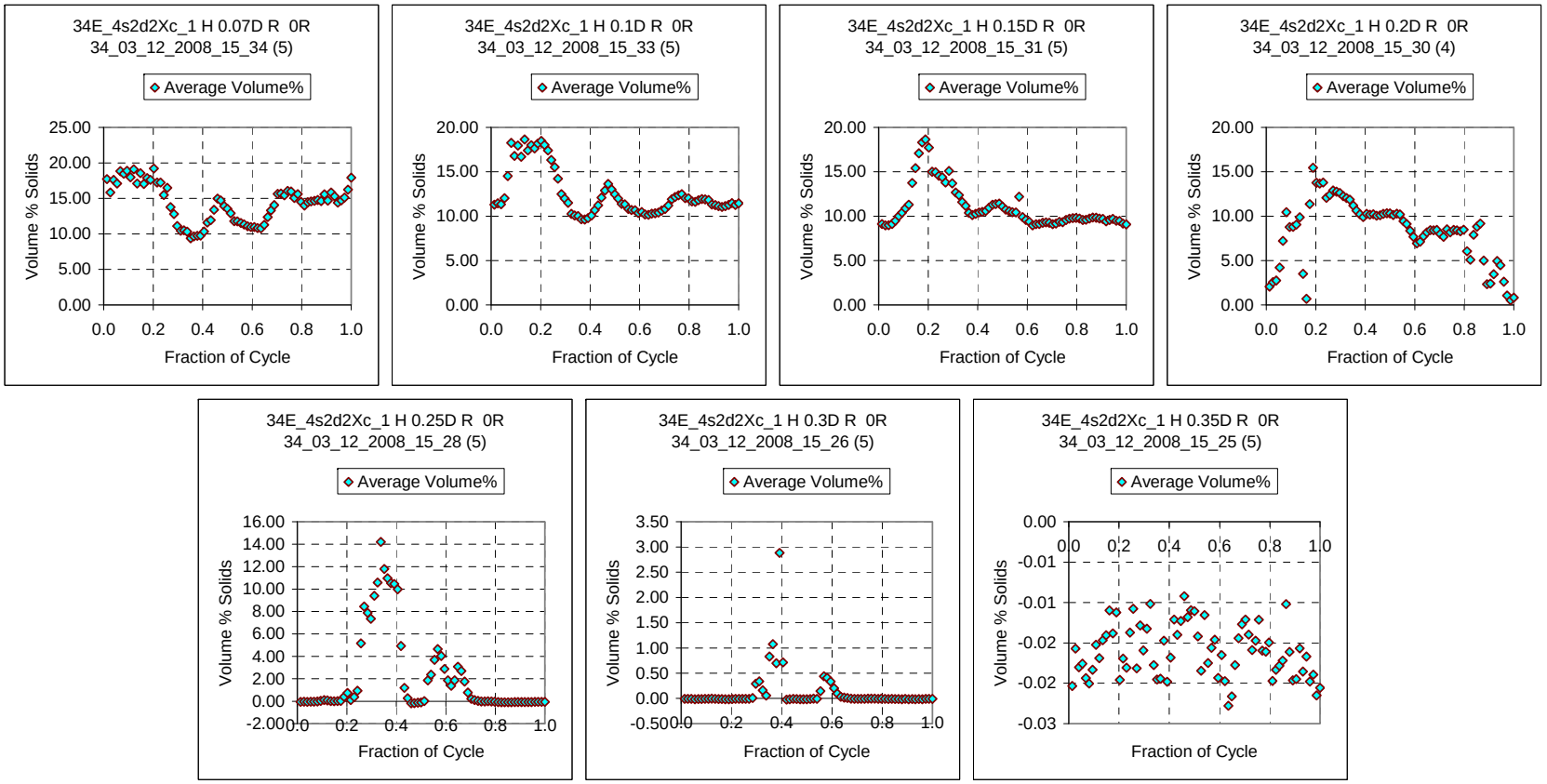

Figure C.30A. Case ID 34S_4s2d2Xc_1 Concentration Variation During the Cycle

Figure C.30 is the second of three profiles shown using simulant s2d2 in the mid-scale tank. The solids fraction was 0.015, an increase from 0.00155 in the prior test. The duty cycle was 33.9%, a slight increase from the value of 33.5% in the prior test. The pulse volume fraction was 0.050 (no change from the prior test). The U_{CS} velocity occurred at 9.8 m/s, which was an increase from 5.6 m/s in the prior test. The peak cloud height upper bound was 11.0 in. which was a decrease from 14.5 in the prior test.

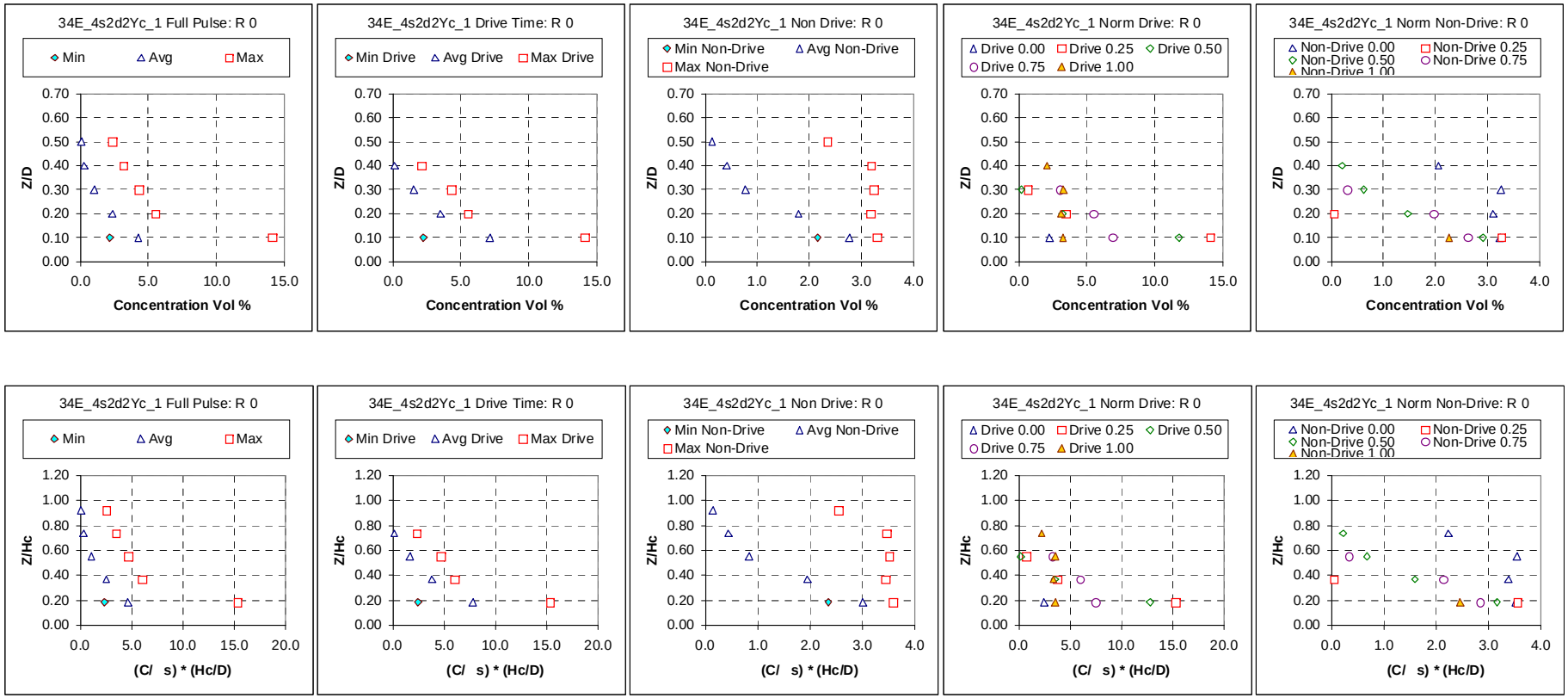

Figure C.31. 0.860-m- (33 7/8-in.-) diameter tank, 0.754-cm- (0.297-in.-) diameter nozzle; solids nominal diameter 75.6 µm, 4.18 g/cm^3 density; 0.005 nominal solids fraction; 33.6% duty cycle, cycle time 17.0 s, pulse volume fraction 0.050, U_{CS} velocity 8.6 m/s, target nozzle exit velocity 8.6 m/s; peak cloud height upper bound 0.483 m (19 in.). Case ID 34S_4s2d2Yc_1 (shown as 34E on plots).

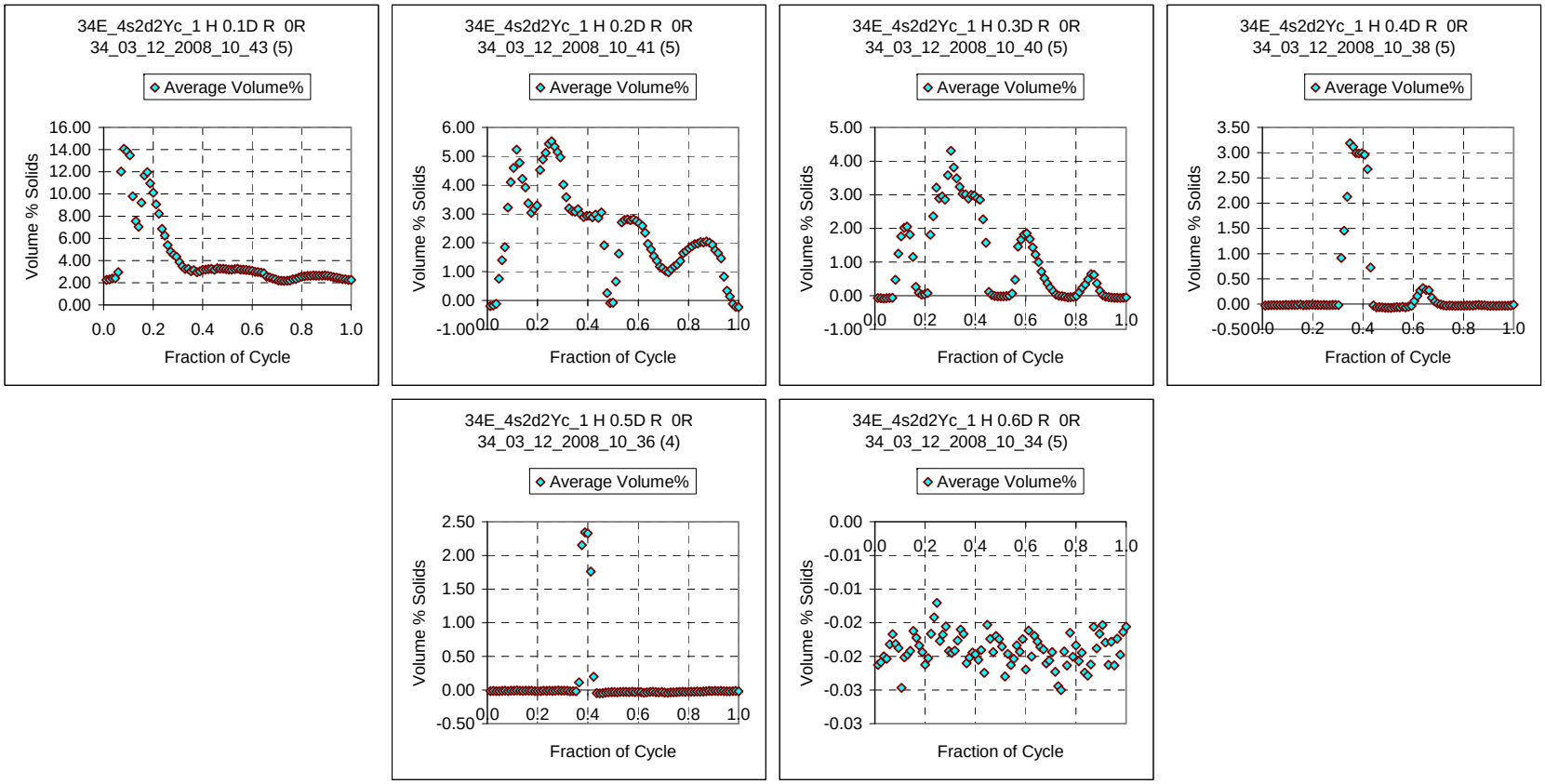

Figure C.31A. Case ID 34S_4s2d2Yc_1 Concentration Variation During the Cycle

Figure C.31 is the third of three profiles shown using simulant s2d2 in the mid-scale tank. The solids fraction was 0.005, which was a decrease from 0.015 in the prior test. The duty cycle was 33.6%, reduced from 33.9% in the prior test. The pulse volume fraction was 0.050 (no change from the prior test). The U_{CS} velocity occurred at 8.6 m/s, which was a decrease from 9.8 m/s obtained in the prior test. The peak cloud height upper bound was 19.0 in., which was an increase from the 11.0 in. value in the prior test.

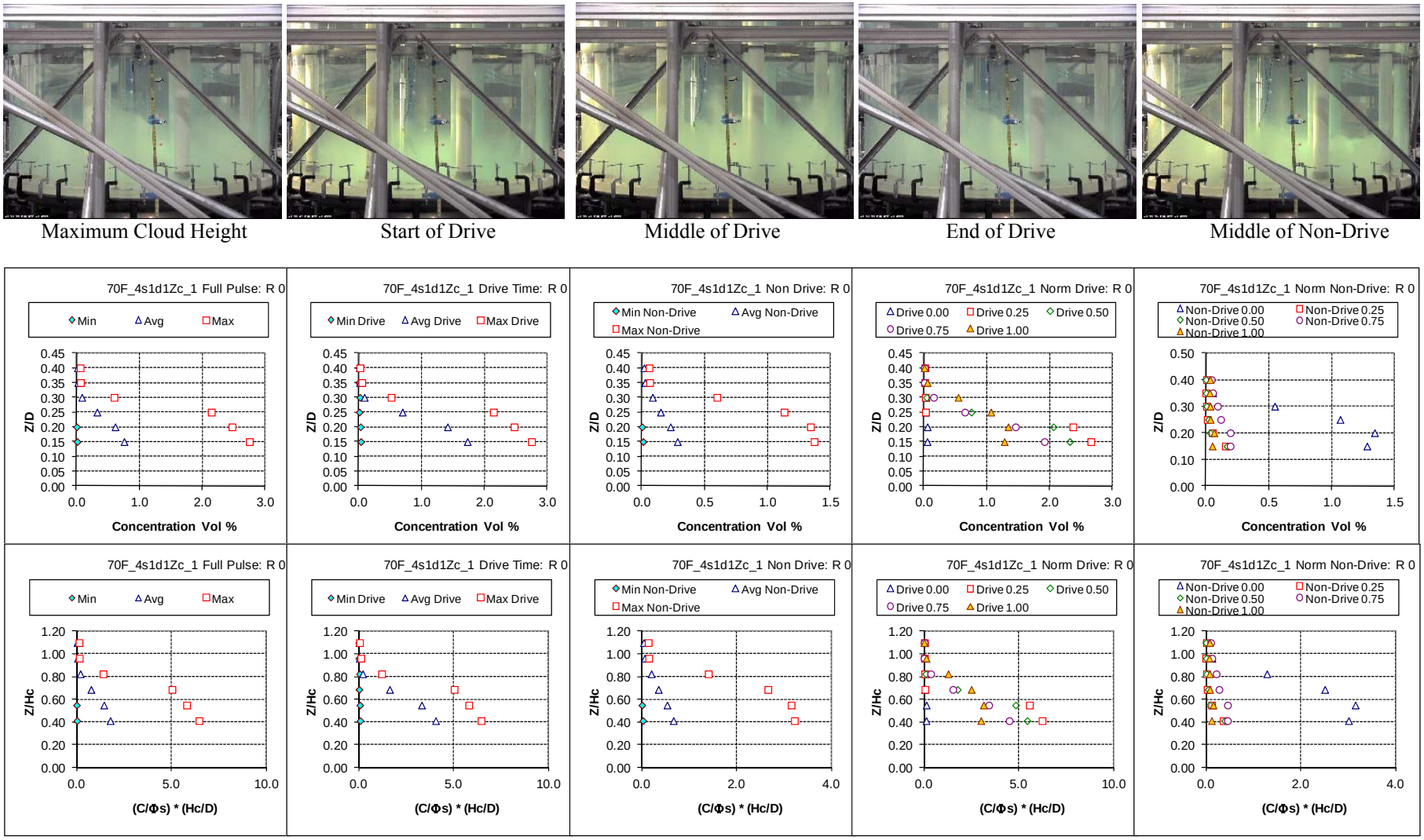

Figure C.32. 1.778-m- (70-in.-) diameter tank, 1.557-cm- (0.613-in.-) diameter nozzle; solids nominal diameter 166.4 µm, 2.46 g/cm^3 density; 0.00155 nominal solids fraction; 33.2% duty cycle, cycle time 45.4 s, pulse volume fraction 0.050, U_{CS} velocity 6.7 m/s, target nozzle exit velocity 6.7 m/s; peak cloud height upper bound 0.660 m (26 in.). Case ID 70F_4s1d1Zc_1.

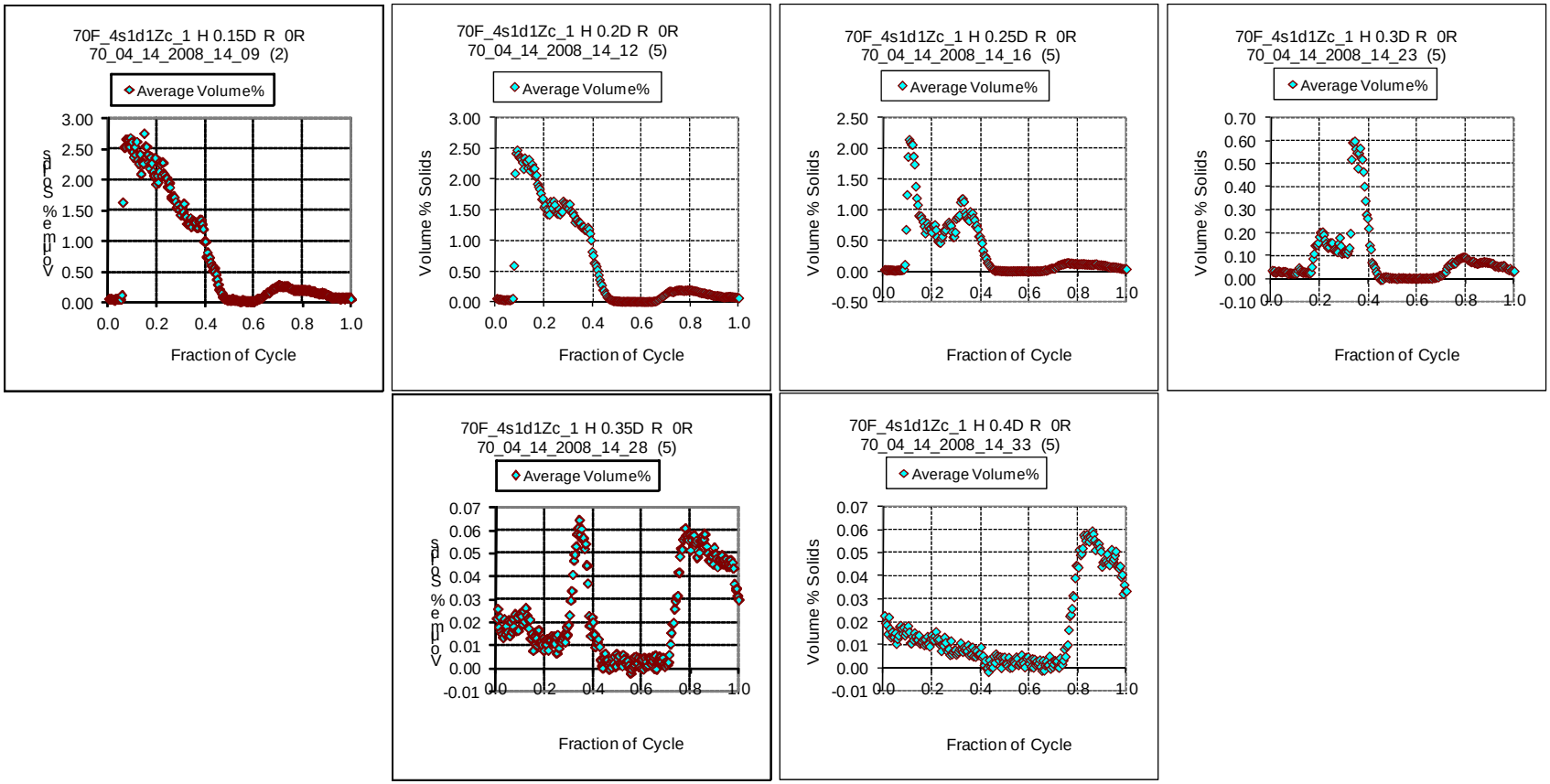

Figure C.32A. Case ID 70F_4s1d1Zc_1 Concentration Variation During the Cycle

Figure C.32 is the first of two profiles shown using simulant s1d1 in the large-scale tank with the flange and dish bottom. The solids fraction was 0.00155. The duty cycle was 33.2% and the pulse volume fraction was 0.050. The U_{CS} velocity occurred at 6.7 m/s. The peak cloud height upper bound was 26 in. Data were obtained at six elevations during this profile.

Maximum Cloud Height

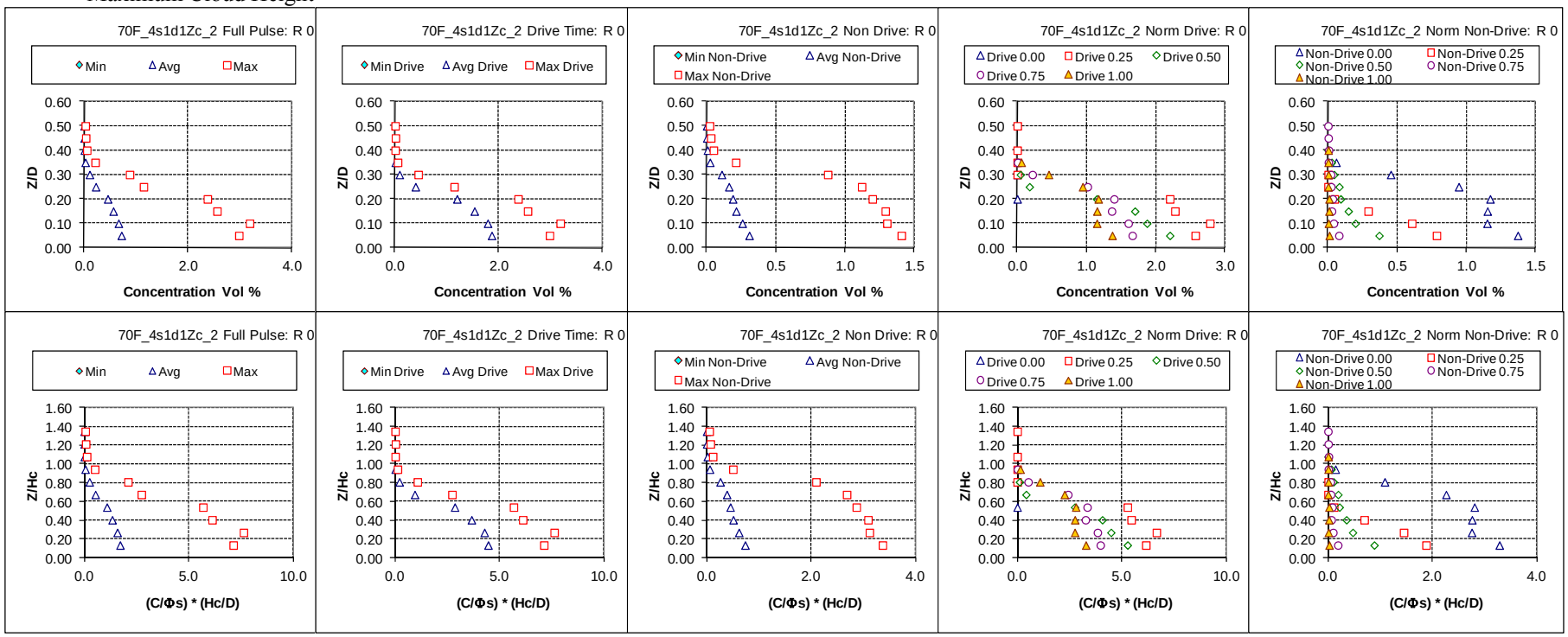

Figure C.33. 1.778-m- (70-in.-) diameter tank, 1.557-cm- (0.613-in.-) diameter nozzle; solids nominal diameter 166.4 µm, 2.46 g/cm^3 density; 0.00155 nominal solids fraction; 33.5% duty cycle, cycle time 100.8 s, pulse volume fraction 0.101, U_{CS} velocity 5.8 m/s, target nozzle exit velocity 5.8 m/s; peak cloud height upper bound 0.660 m (26 in.). Case ID 70F_4s1d1Zc_2.

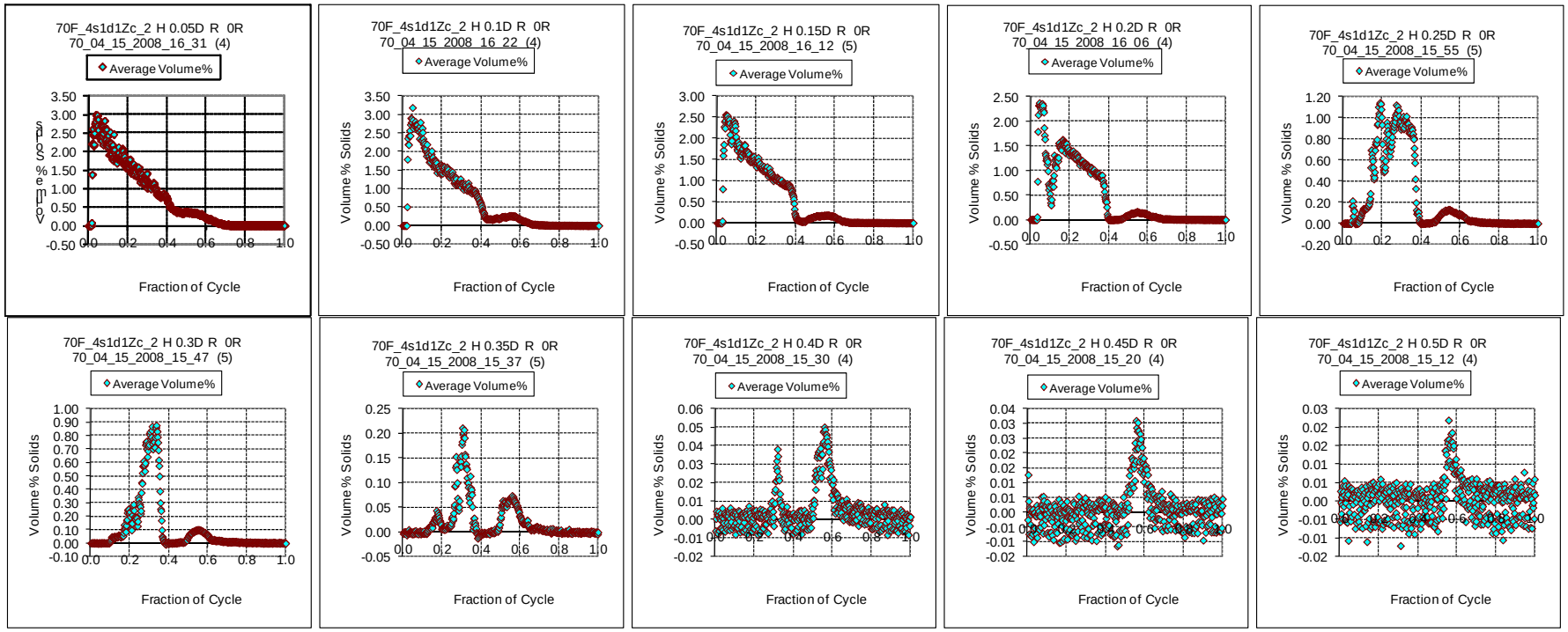

Figure C.33A. Case ID 70F_4s1d1Zc_2 Concentration Variation During the Cycle

Figure C.33 is the second of two profiles shown using simulant s1d1 in the large-scale tank with the flange and dish bottom. The solids fraction was 0.00155, the same as in the prior test. The duty cycle was 33.5%, unchanged from 33.2% in the prior test. The pulse volume fraction was 0.10, which was an increase from 0.050 in the prior test. The U_{CS} velocity occurred at 5.8 m/s, a decrease from 6.7 m/s in the prior test. The peak cloud height upper bound was 26 in., the same as in the prior test. The increased pulse volume fraction caused the U_{CS} to decrease; however, the peak cloud height upper bound remained unchanged.

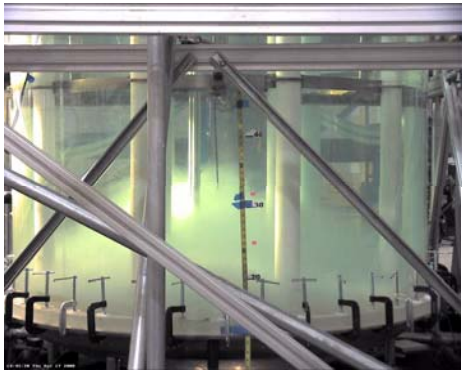

Maximum Cloud Height

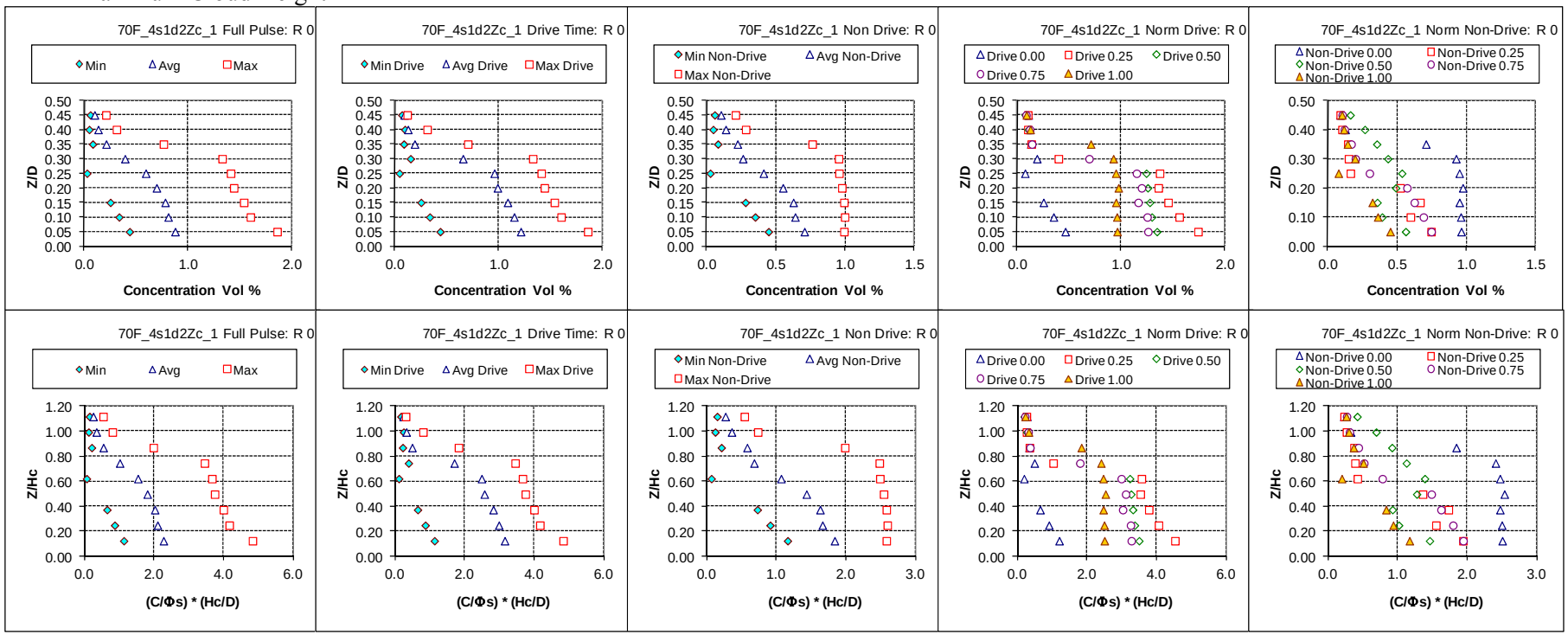

Figure C.34. 1.778-m- (70-in.-) diameter tank, 1.557-cm- (0.613-in.-) diameter nozzle; solids nominal diameter 69.3 µm, 2.48 g/cm^3 density; 0.00155 nominal solids fraction; 33.6% duty cycle, cycle time 67.4 s, pulse volume fraction 0.050, U_{CS} velocity 4.4 m/s, target nozzle exit velocity 4.4 m/s; peak cloud height upper bound 0.749 m (29.5 in.). Case ID 70F_4s1d2Zc_1.

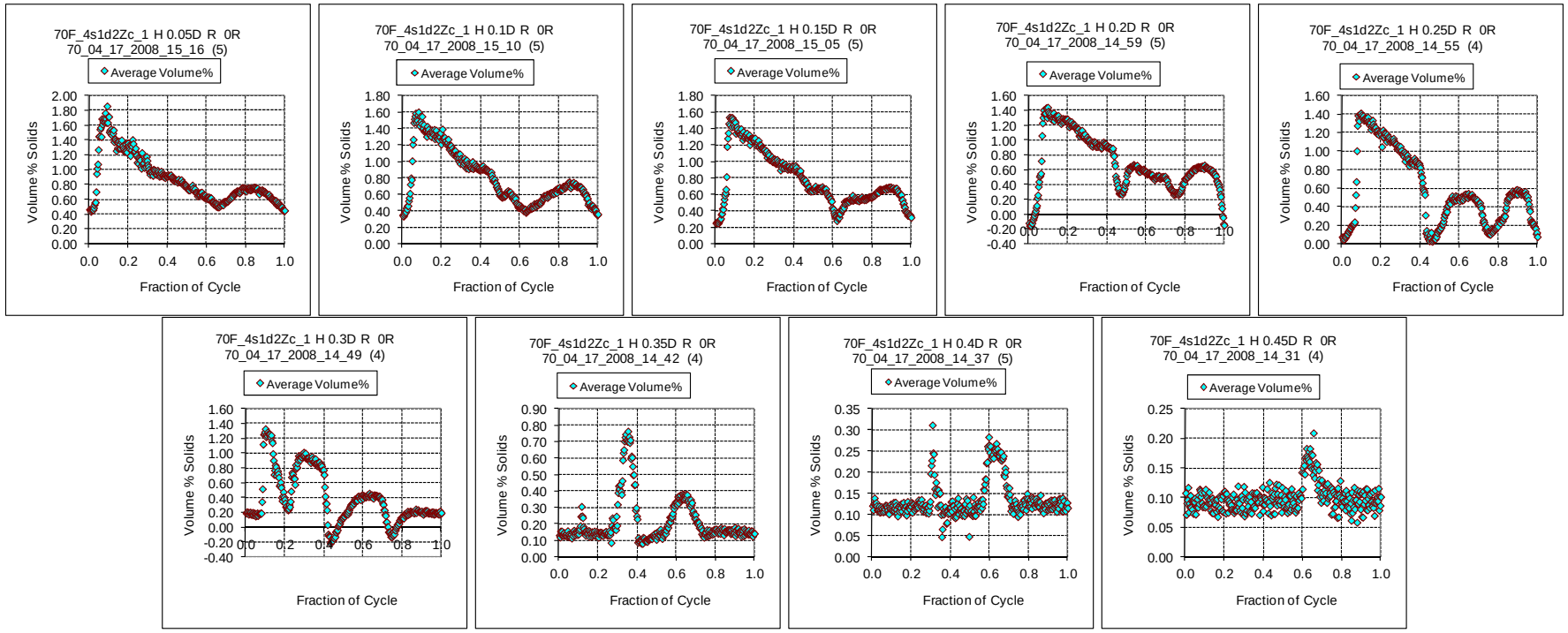

Figure C.34A. Case ID 70F_4s1d2Zc_1 Concentration Variation During the Cycle

Figure C.34 is the first of 12 profiles shown using simulant s1d2 in the large-scale tank with the flange and dish bottom. The solids fraction was 0.00155, the same as in the prior test. The duty cycle was 33.6%, essentially unchanged from 33.5% in the prior test. The pulse volume fraction was 0.05, which was a decrease from the value of 0.10 in the prior test. The U_{CS} velocity occurred at 4.4 m/s, which was a decrease from 5.8 m/s in the prior test. The peak cloud height upper bound was 29.5 in., which was an increase over the value of 26 in. obtained in the prior test.

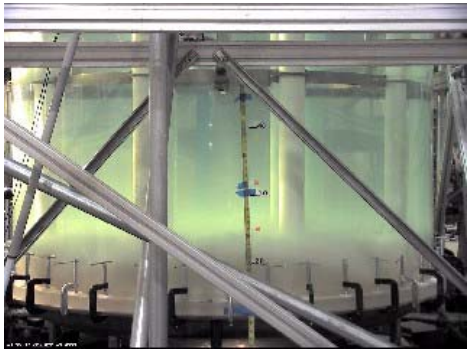

Maximum Cloud Height

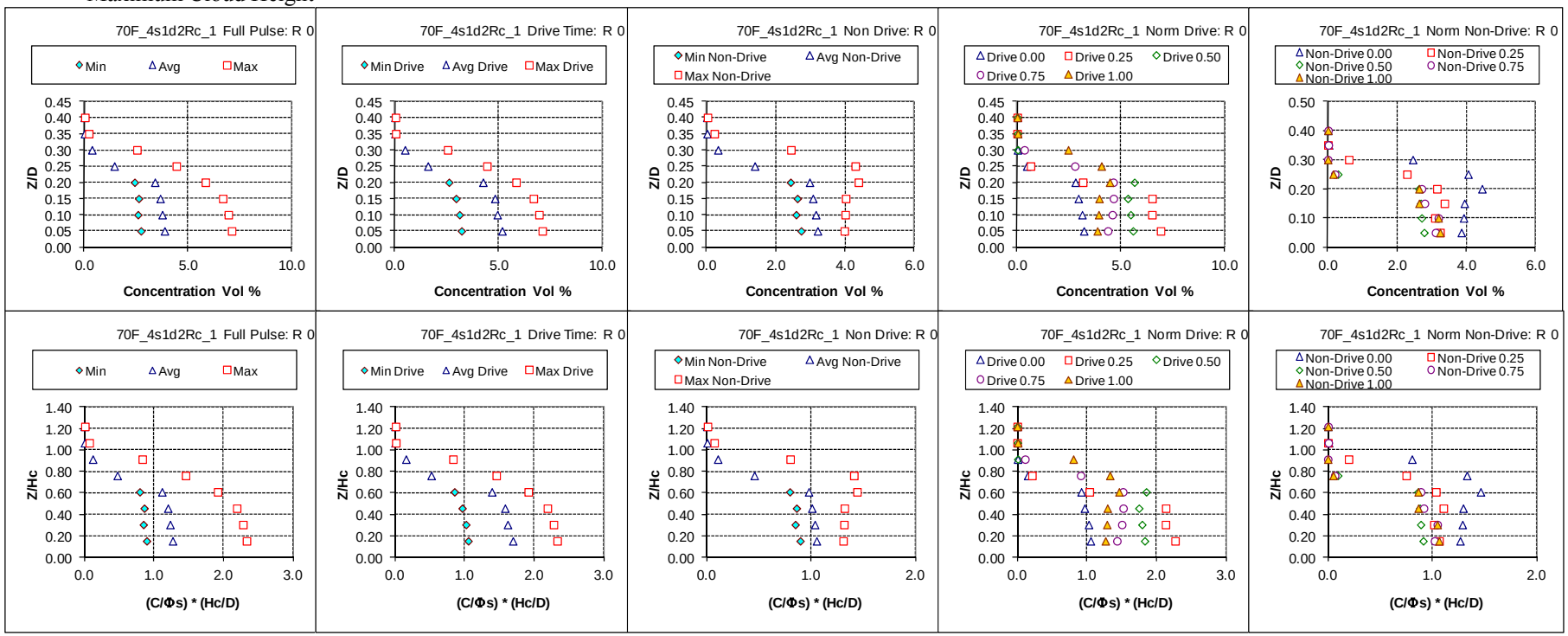

Figure C.35. 1.778-m- (70-in.-) diameter tank, 1.557-cm- (0.613-in.-) diameter nozzle; solids nominal diameter 69.3 µm, 2.48 g/cm^3 density; 0.01 nominal solids fraction; 33.9% duty cycle, cycle time 44.6 s, pulse volume fraction 0.050, U_{CS} velocity 6.6 m/s, target nozzle exit velocity 6.6 m/s; peak cloud height upper bound 0.610 m (24 in.). Case ID 70F_4s1d2Rc_1.

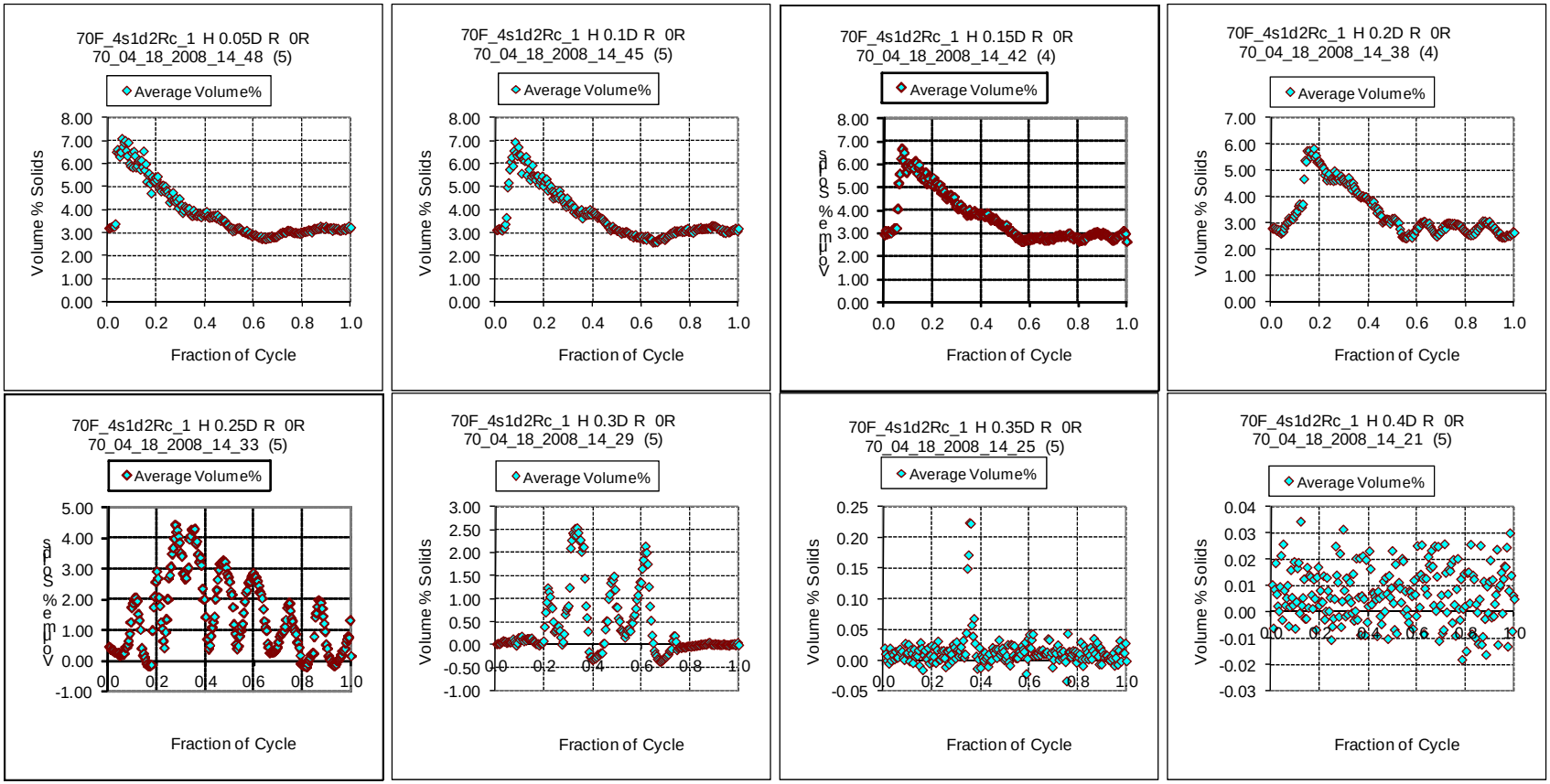

Figure C.35A. Case ID 70F_4s1d2Rc_1 Concentration Variation During the Cycle

Figure C.35 is the second of 12 profiles shown using simulant s1d2 in the large-scale tank with the flange and dish bottom. The solids fraction was 0.01, an increase over the value of 0.00155 in the prior test. The duty cycle was 33.9%, essentially unchanged from 33.6% in the prior test. The pulse volume fraction was 0.050 (the same as in the prior test). The U_{CS} velocity occurred at 6.6 m/s, which was an increase from 4.4 m/s in the prior test. The peak cloud height upper bound was 24 in, which was a decrease from the value of 29.5 in. in the prior test. The increased concentration caused the U_{CS} to increase; however, the peak cloud height upper bound remained unchanged.

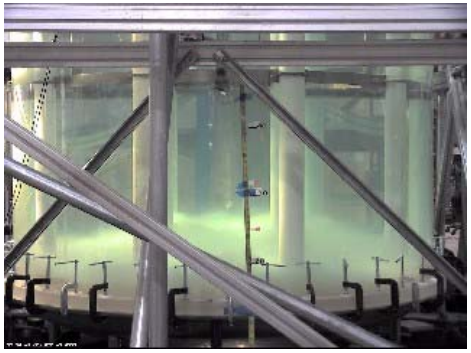

Maximum Cloud Height

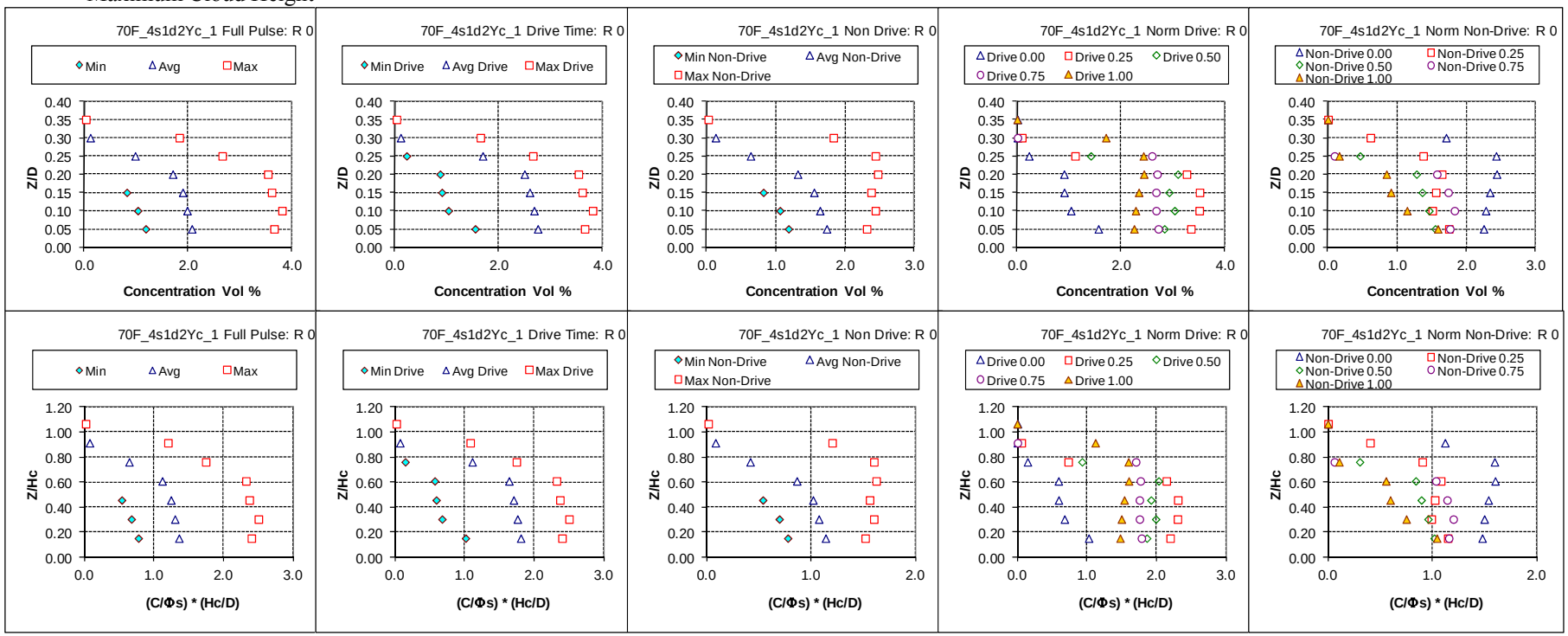

Figure C.36. 1.778-m- (70-in.-) diameter tank, 1.557-cm- (0.613-in.-) diameter nozzle; solids nominal diameter 69.3 µm, 2.48 g/cm^3 density; 0.005 nominal solids fraction; 33.5% duty cycle, cycle time 51.0 s, pulse volume fraction 0.050, U_{CS} velocity 5.8 m/s, target nozzle exit velocity 5.8 m/s; peak cloud height upper bound 0.597 m (23.5 in.). Case ID 70F_4s1d2Yc_1.

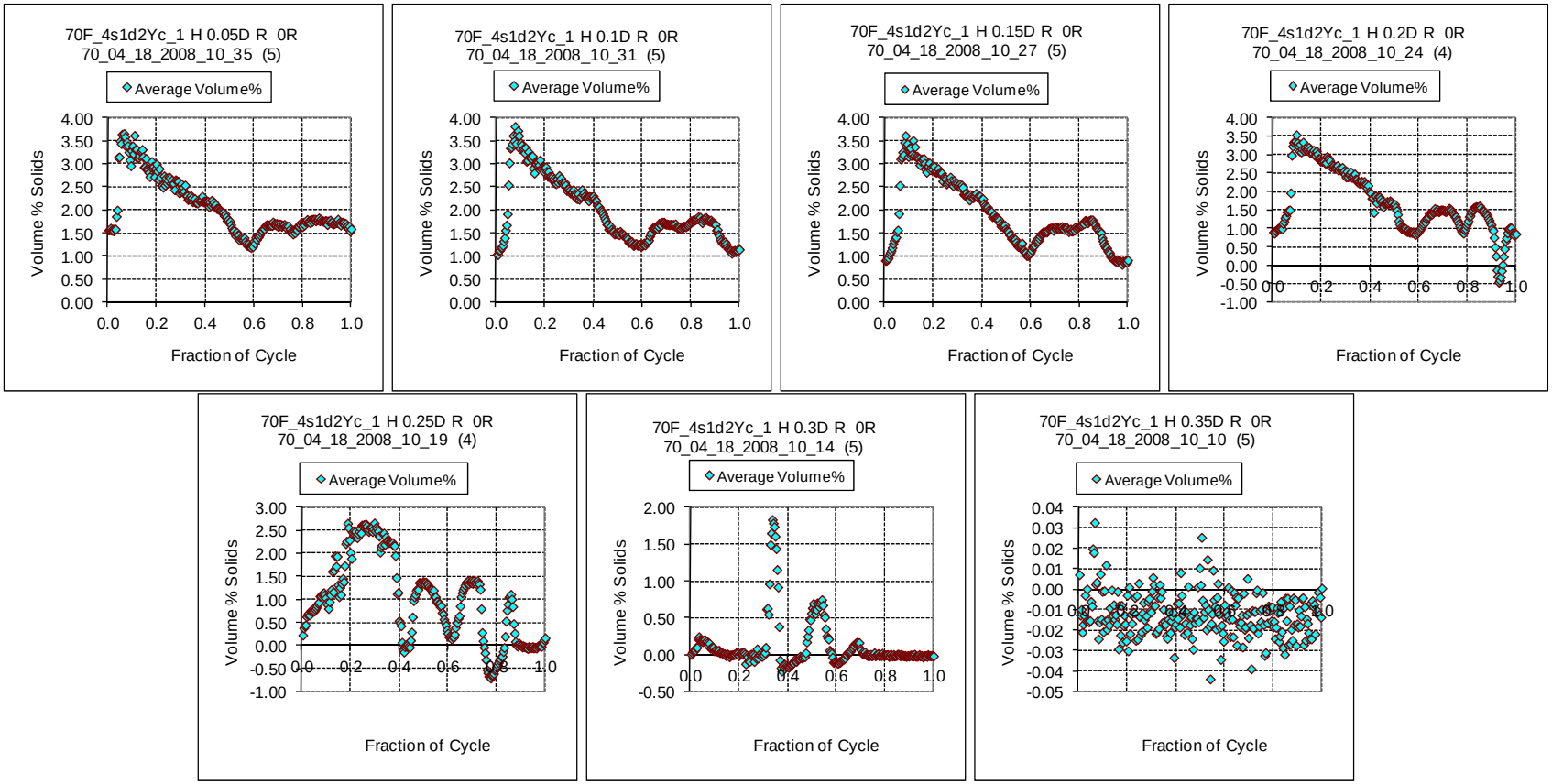

Figure C.36A. Case ID 70F_4s1d2Yc_1 Concentration Variation During the Cycle

Figure C.36 is the third of 12 profiles shown using simulant s1d2 in the large-scale tank with the flange and dish bottom. The solids fraction was 0.005, reduced by half from the prior test. The duty cycle was 33.5%, essentially unchanged from 33.9% in the prior test. The pulse volume fraction was 0.050 (the same as in the prior test). The U_{CS} velocity occurred at 5.8 m/s, which was a decrease from 6.6 m/s in the prior test. The peak cloud height upper bound was 23.5 in., a slight decrease from 24 in. in the prior test. The decreased concentration caused the U_{CS} to decrease; however, the peak cloud height upper bound remained relatively constant.

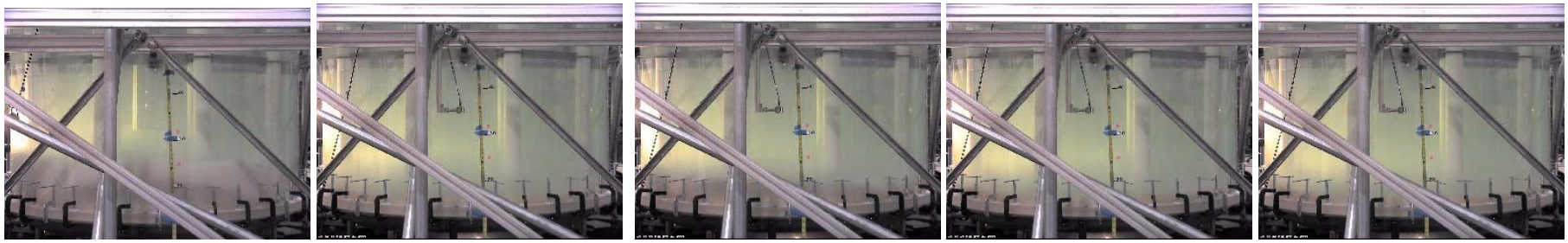

Maximum Cloud Height | Start of Drive | Middle of Drive | End of Drive | Middle of Non-Drive

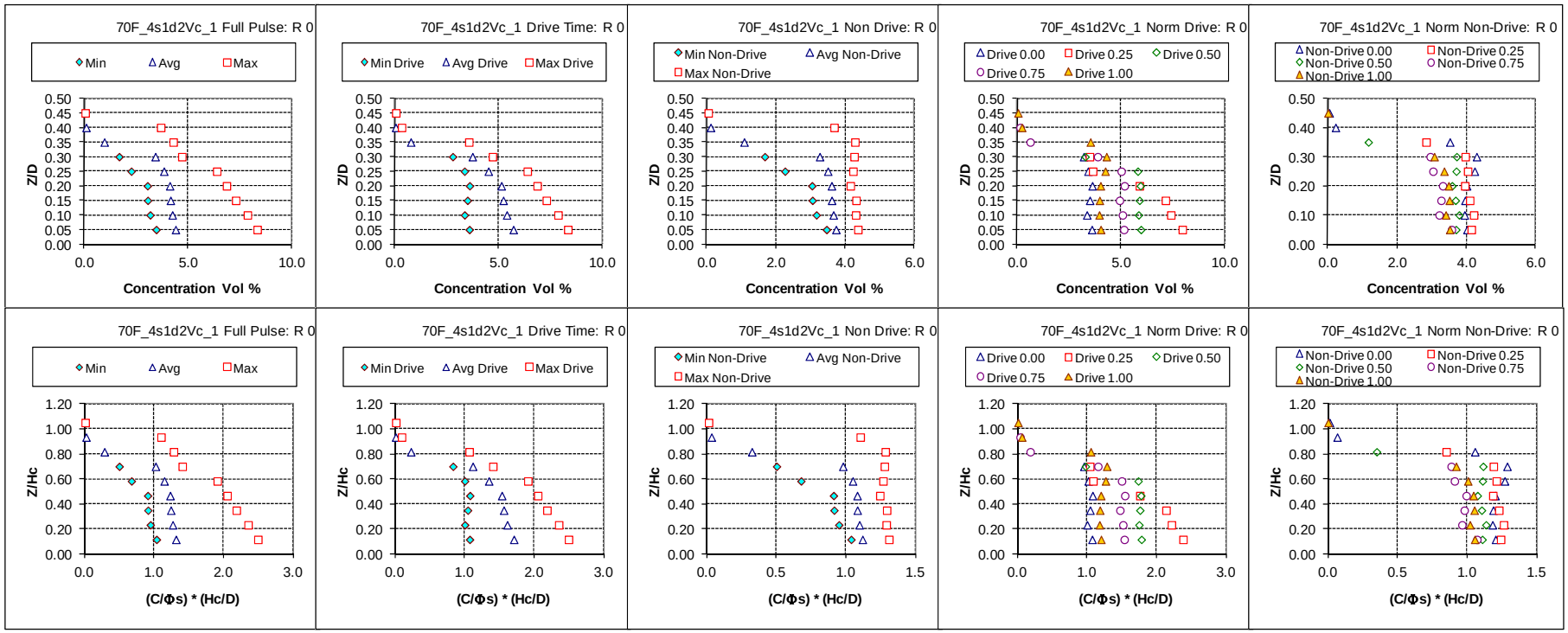

Figure C.37. 1.778-m- (70-in.-) diameter tank, 1.557-cm- (0.613-in.-) diameter nozzle; solids nominal diameter 69.3 µm, 2.48 g/cm^3 density; 0.0143 nominal solids fraction; 33.6% duty cycle, cycle time 42.2 s, pulse volume fraction 0.050, U_{CS} velocity 7.1 m/s, target nozzle exit velocity 7.1 m/s; peak cloud height upper bound 0.787 m (31 in.). Case ID 70F_4s1d2Vc_1.

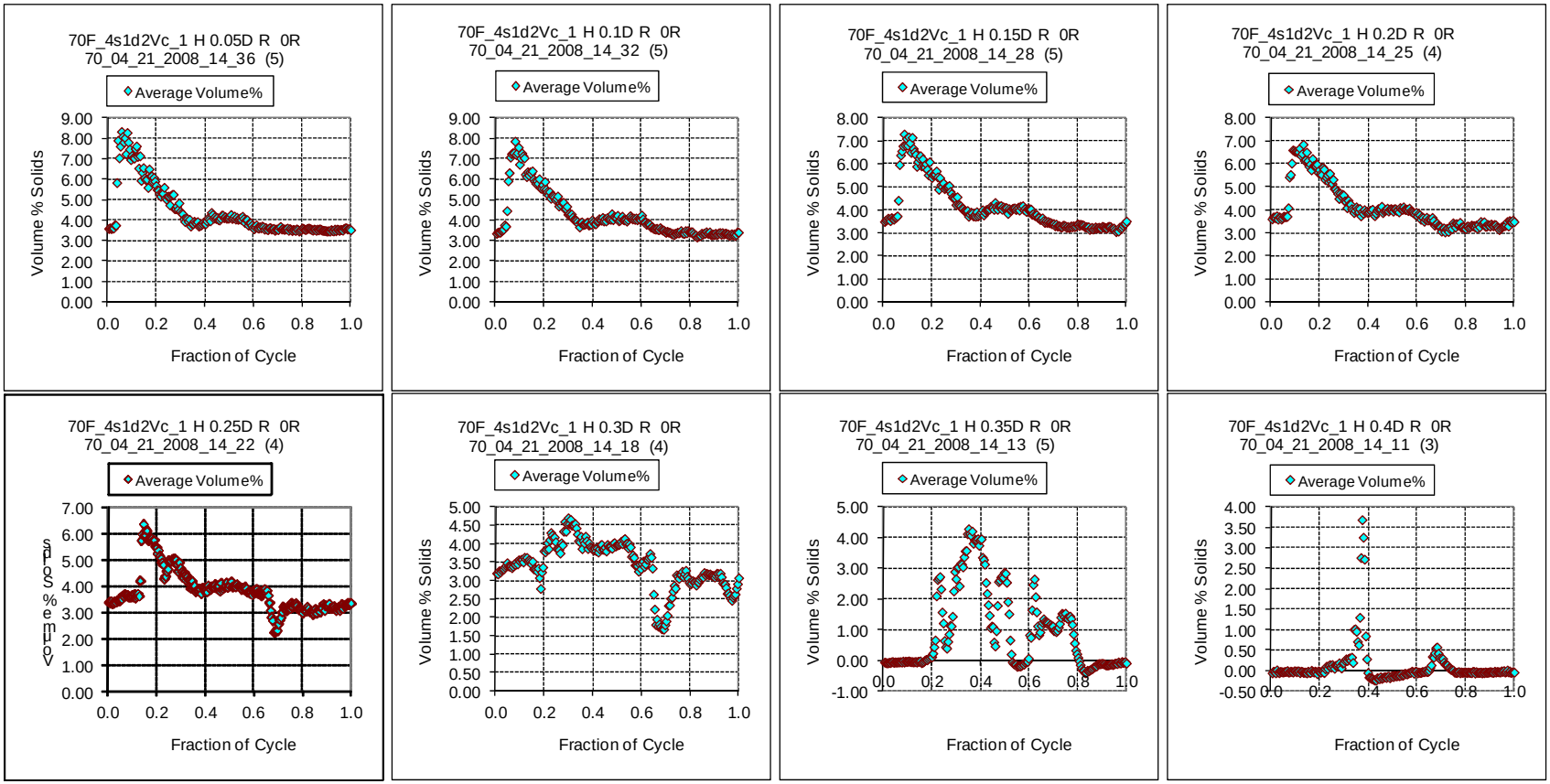

Figure C.37A. Case ID 70F_4s1d2Vc_1 Concentration Variation During the Cycle

Figure C.37 is the fourth of 12 profiles shown using simulant s1d2 in the large-scale tank with the flange and dish bottom. Figures C.37, C.38, and C.39 are a group of three profiles taken at the same flow conditions and differing radial locations. Figure C.37 shows a profile at the center of the tank at R=0. The solids fraction was 0.0143. The duty cycle was 33.6%. The pulse volume fraction was 0.050. The U_{CS} velocity occurred at 7.1 m/s. The peak cloud height upper bound was 31 in. When the radial profiles are compared, the concentrations are relatively constant in the radial direction at a height of Z/D = 0.3 with concentrations of ~4 vol% solids at R = 0 and R = 0.5 and ~3.5 vol% solids at R = 0.9. This shows that the concentration in the tank was relatively constant in these three radial locations.

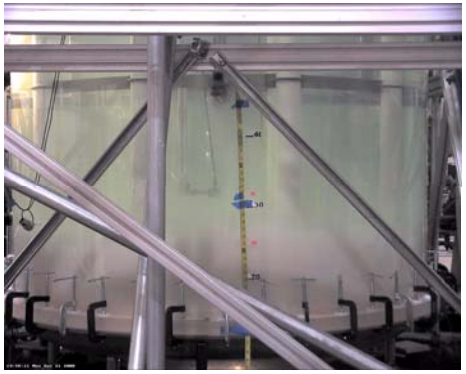

Maximum Cloud Height

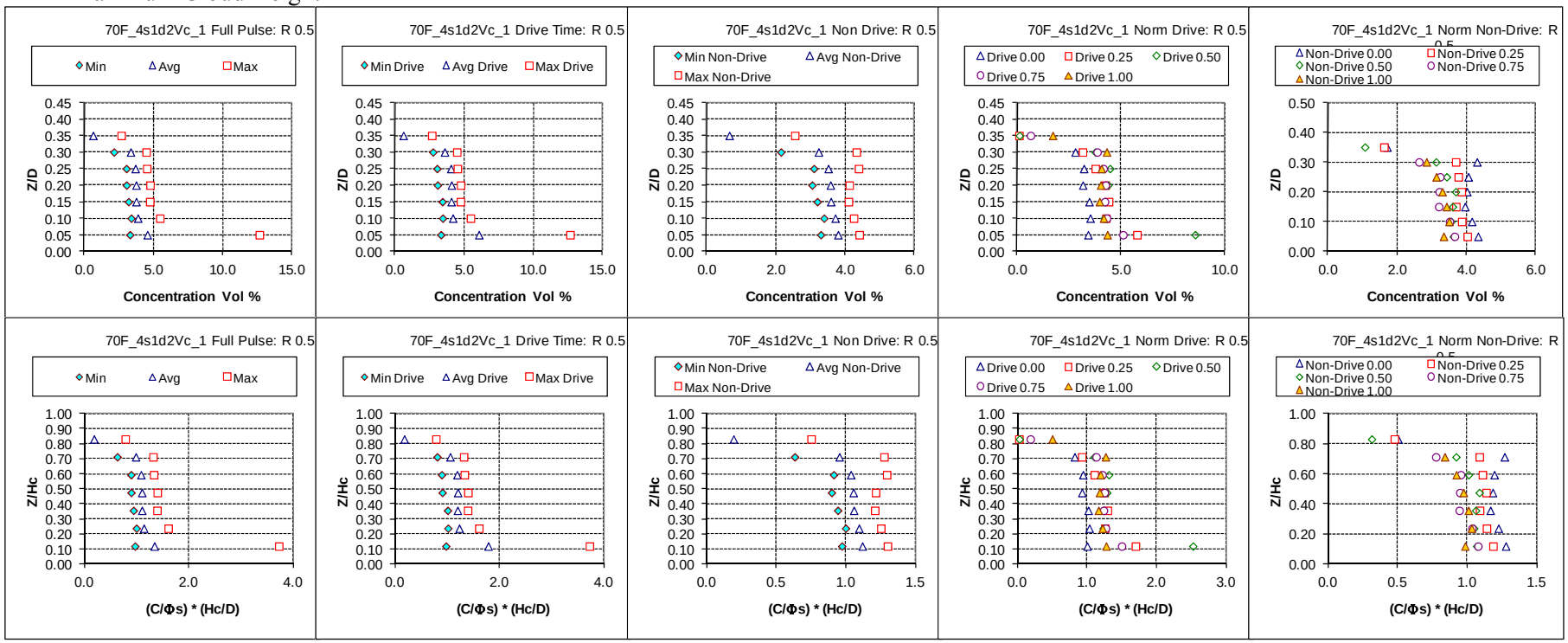

Figure C.38. 1.778-m- (70-in.-) diameter tank, 1.557-cm- (0.613-in.-) diameter nozzle; solids nominal diameter 69.3 µm, 2.48 g/cm^3 density; 0.0143 nominal solids fraction; 33.6% duty cycle, cycle time 42.2 s, pulse volume fraction 0.050, U_{CS} velocity 7.1 m/s, target nozzle exit velocity 7.1 m/s; peak cloud height upper bound 0.787 m (31 in.). Case ID 70F_4s1d2Vc_1.

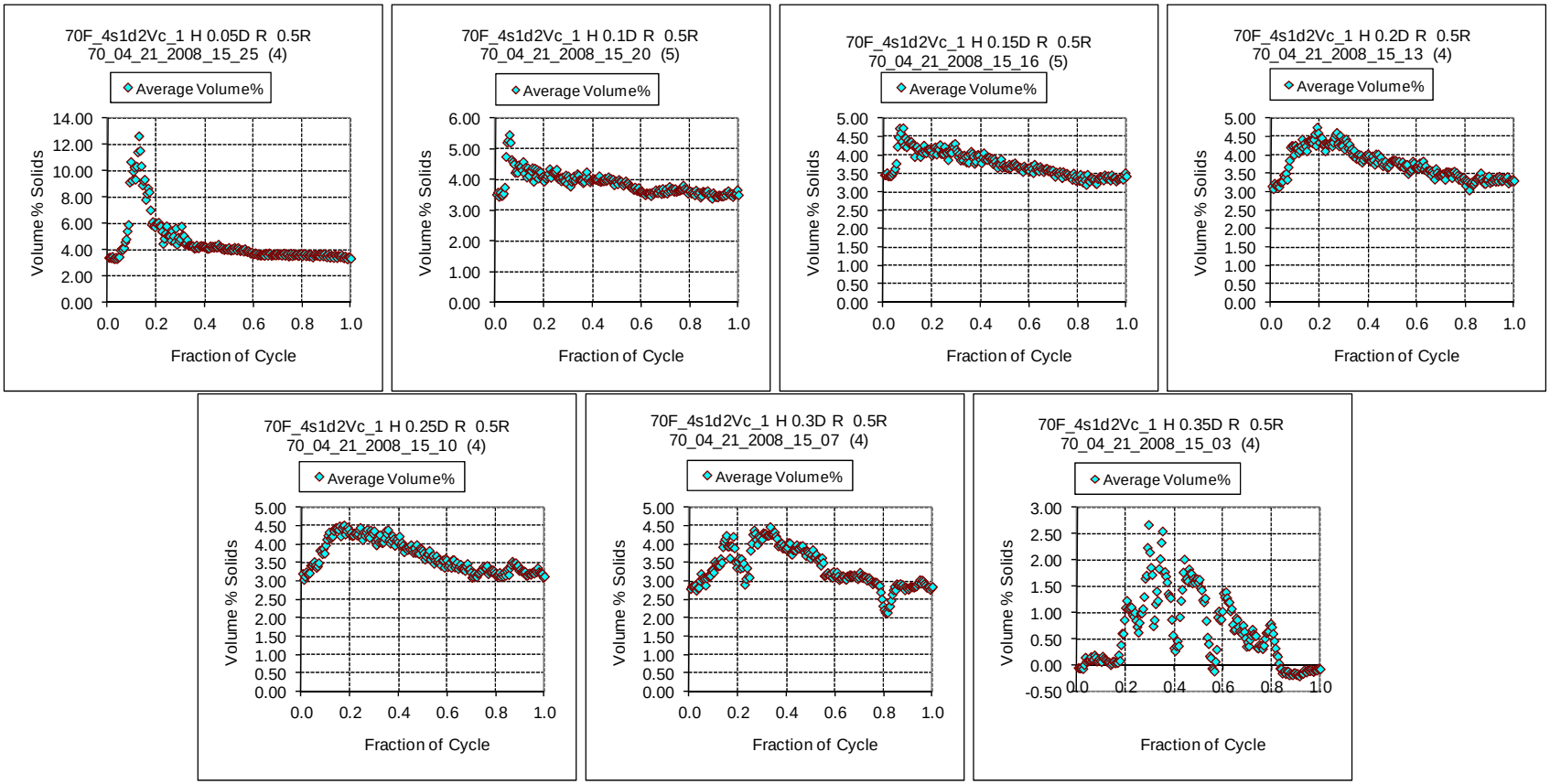

Figure C.38A. Case ID 70F_4s1d2Vc_1 Concentration Variation During the Cycle

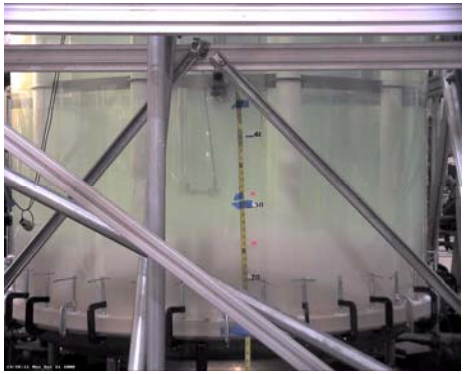

Maximum Cloud Height

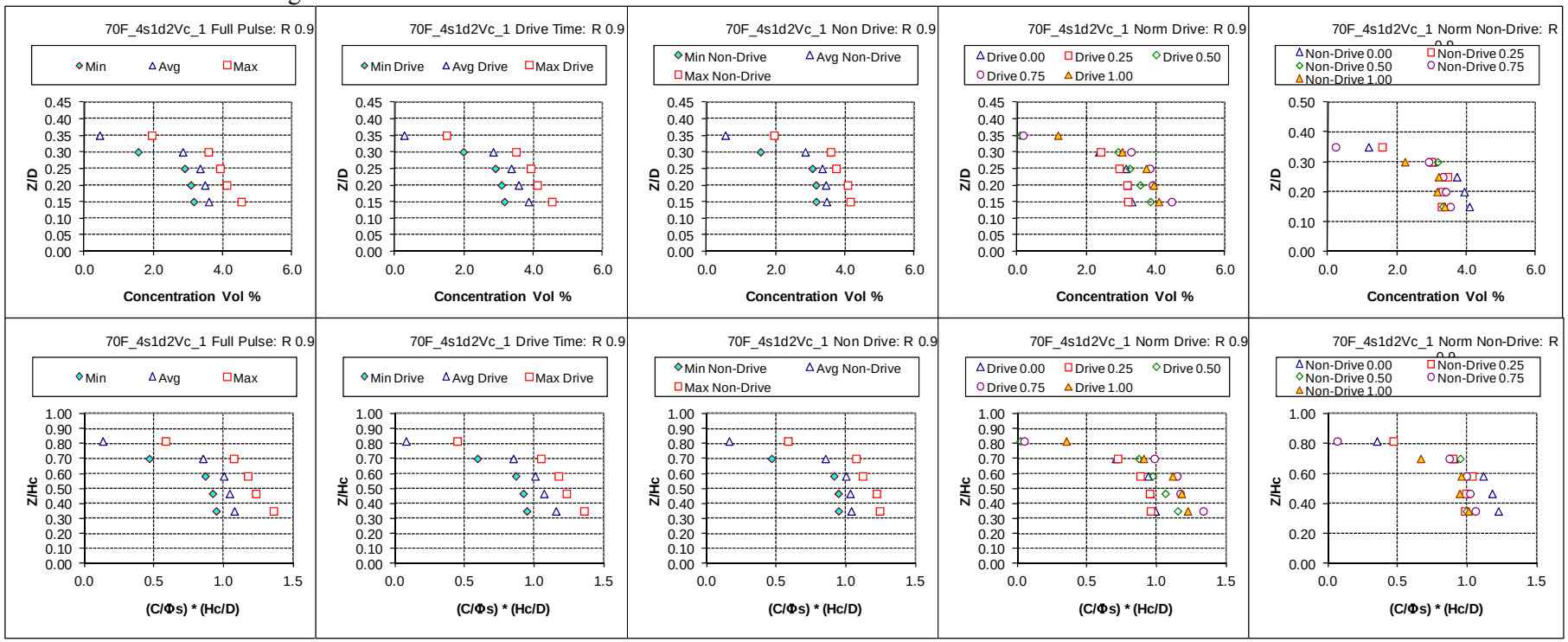

Figure C.39. 1.778-m- (70-in.-) diameter tank, 1.557-cm- (0.613-in.-) diameter nozzle; solids nominal diameter 69.3 µm, 2.48 g/cm^3 density; 0.0143 nominal solids fraction; 33.6% duty cycle, cycle time 42.2 s, pulse volume fraction 0.050, U_{CS} velocity 7.1 m/s, target nozzle exit velocity 7.1 m/s; peak cloud height upper bound 0.787 m (31 in.). Case ID 70F_4s1d2Vc_1.

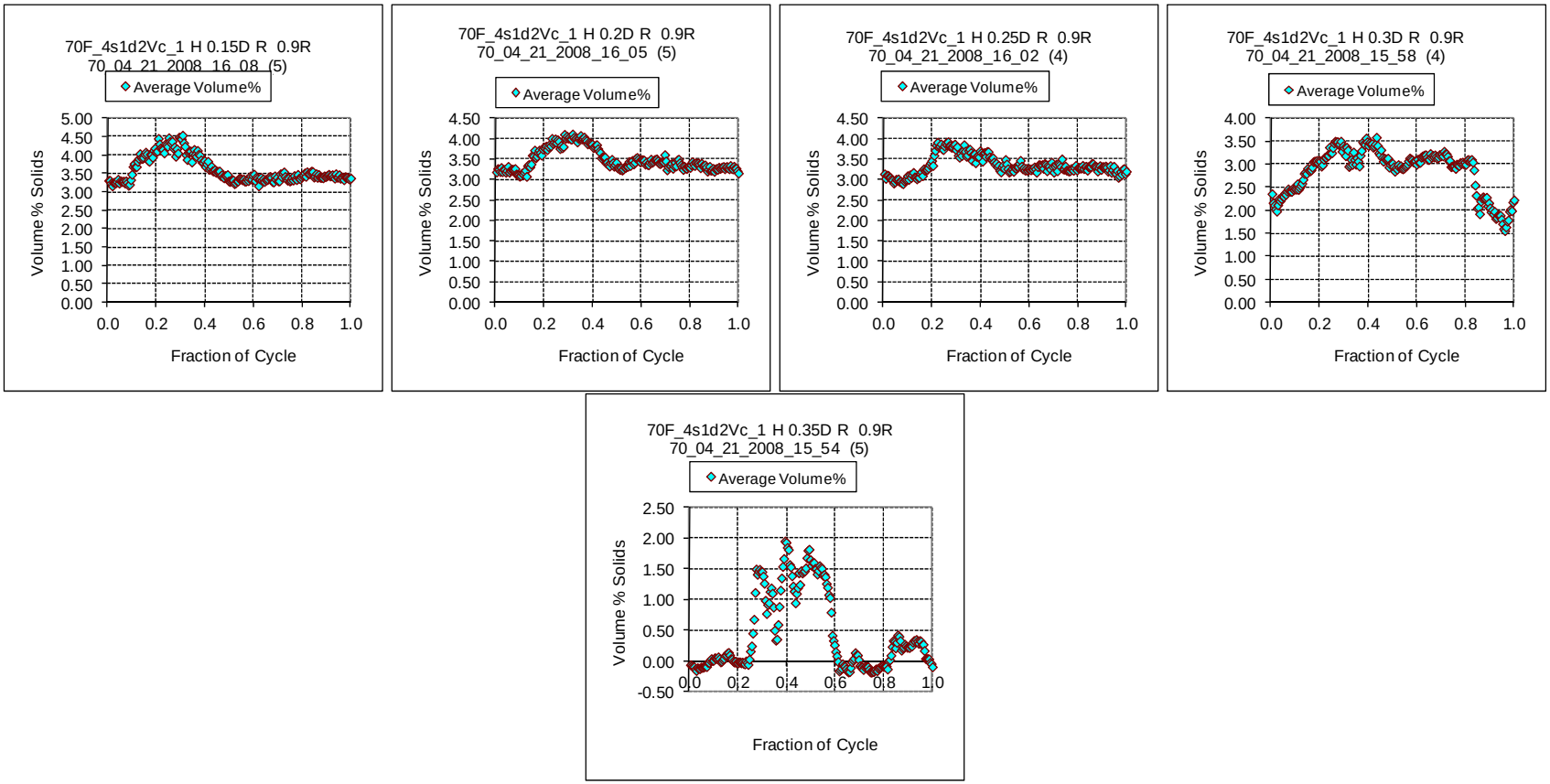

Figure C.39A. Case ID 70F_4s1d2Vc_1 Concentration Variation During the Cycle

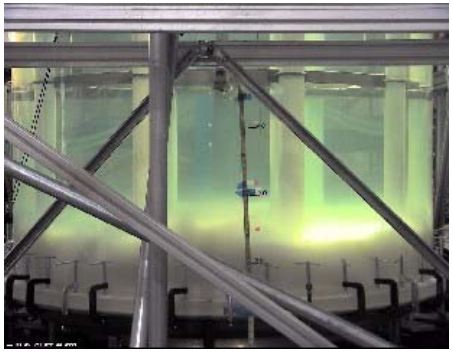

Maximum Cloud Height

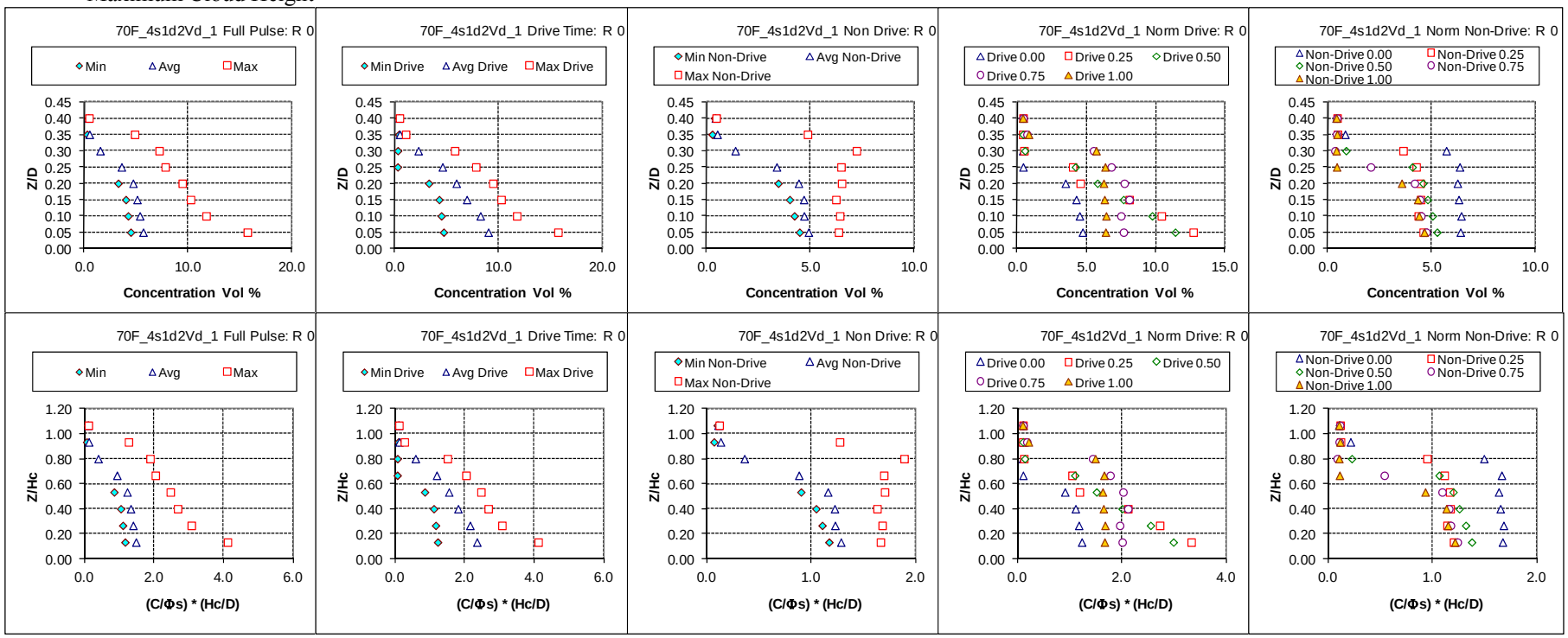

Figure C.40. 1.778-m- (70-in.-) diameter tank, 1.557-cm- (0.613-in.-) diameter nozzle; solids nominal diameter 69.3 µm, 2.48 g/cm^3 density; 0.0143 nominal solids fraction; 18.7% duty cycle, cycle time 56.4 s, pulse volume fraction 0.050, U_{CS} velocity 9.8 m/s, target nozzle exit velocity 9.6 m/s; peak cloud height upper bound 0.673 m (26.5 in.). Case ID 70F_4s1d2Vd_1.

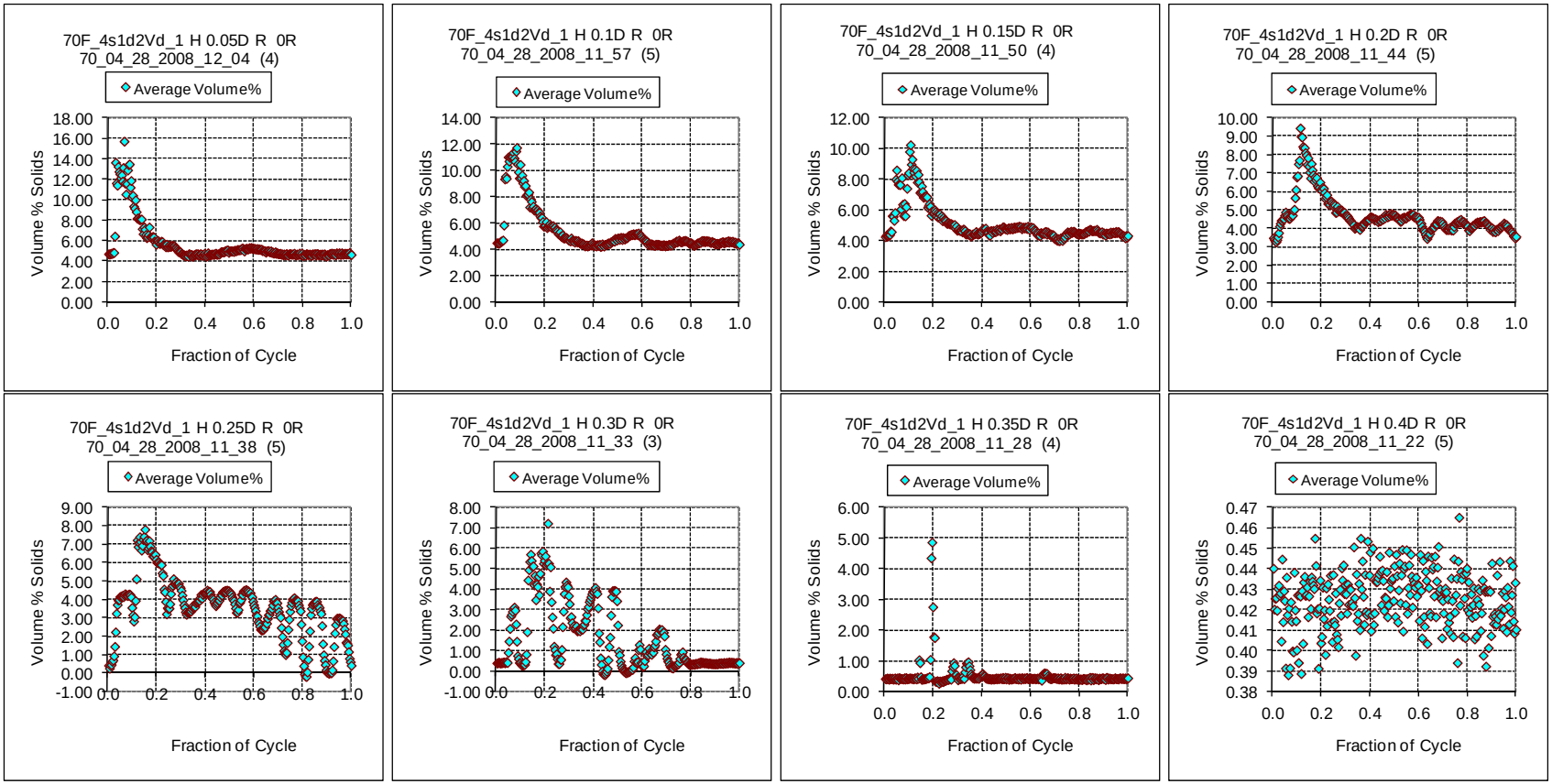

Figure C.40A. Case ID 70F_4s1d2Vd_1 Concentration Variation During the Cycle

Figure C.40 is the seventh of 12 profiles shown using simulant s1d2 in the large-scale tank with the flange and dish bottom. The solids fraction was 0.0143. The duty cycle was 18.7%. The pulse volume fraction was 0.050. The U_{CS} velocity occurred at 9.8 m/s. The measurements were taken at a velocity of 9.6 m/s, which was slightly below U_{CS}. The peak cloud height upper bound was 26.5 in. The concentration profile plots illustrate that the average concentration as a function of elevation and the minimum concentration as a function of elevation are quite similar.

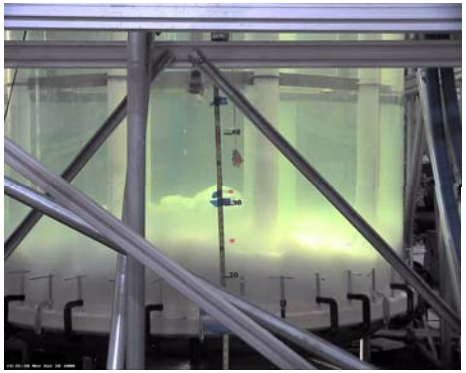

Maximum Cloud Height

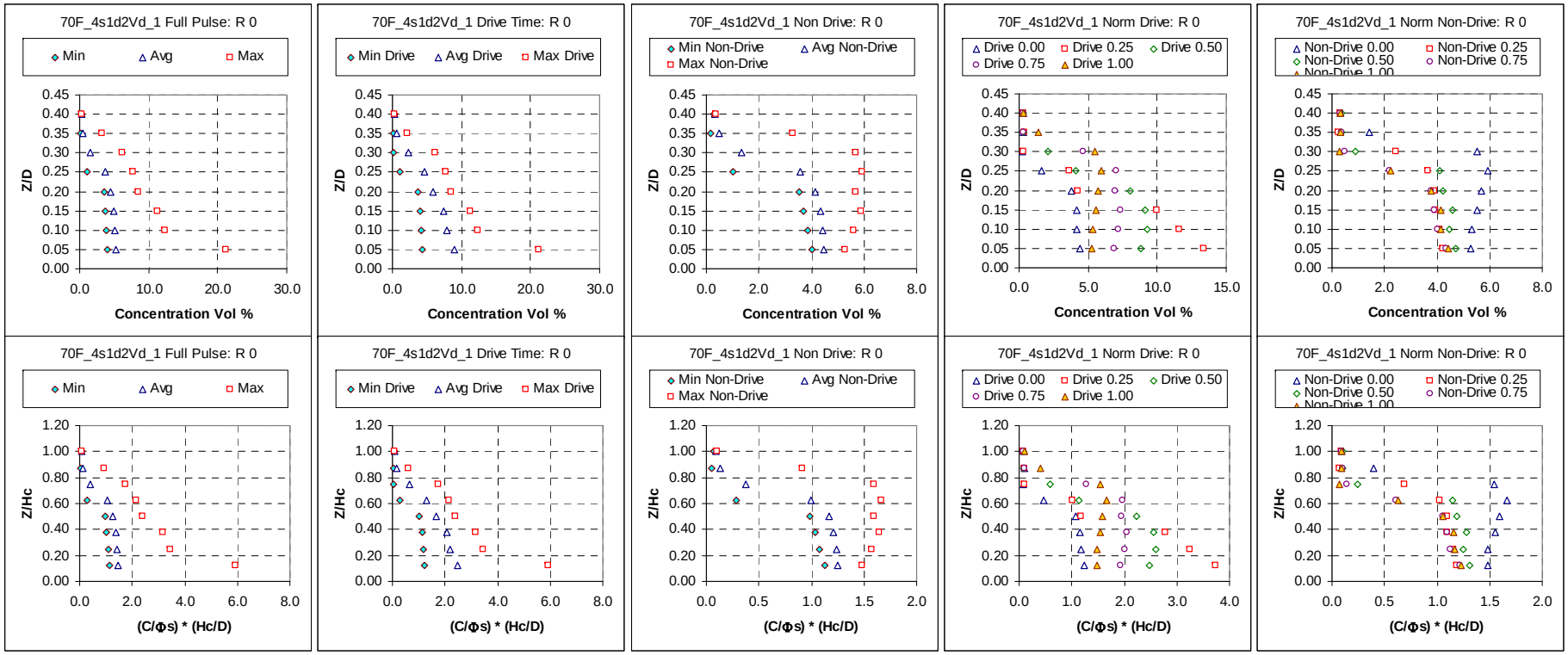

Figure C.41. 1.778-m- (70-in.-) diameter tank, 1.557-cm- (0.613-in.-) diameter nozzle; solids nominal diameter 69.3 µm, 2.48 g/cm^3 density; 0.0143 nominal solids fraction; 18.7% duty cycle, cycle time 55.6 s, pulse volume fraction 0.050, U_{CS} condition 9.8 m/s, target nozzle exit velocity 9.8 m/s; peak cloud height upper bound 0.724 m (28.5 in.). Case ID 70F_4s1d2Vd_1.

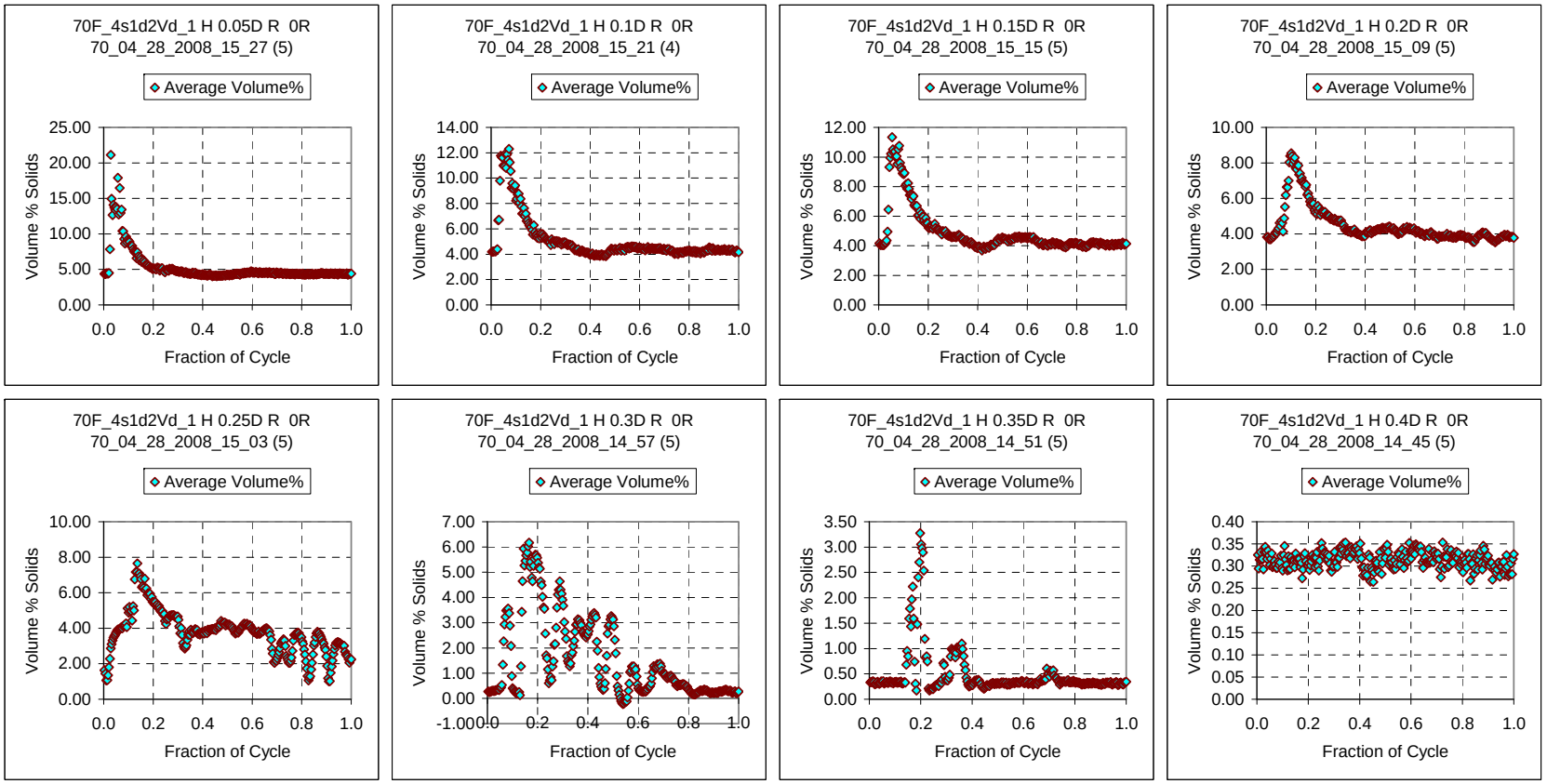

Figure C.41A. Case ID 70F_4s1d2Vd_1 Concentration Variation During the Cycle

Figure C.41 is the eighth of 12 profiles shown using simulant s1d2 in the large-scale tank with the flange and dish bottom. The solids fraction was 0.0143. The duty cycle was 18.7%. The pulse volume fraction was 0.050. The U_{CS} velocity occurred at 9.8 m/s. The peak cloud height upper bound was 28.5 in., which was an increase from 26.5 in. in the prior test. As in the prior test, the average concentration as a function of elevation and the minimum concentration as a function of elevation were quite similar.

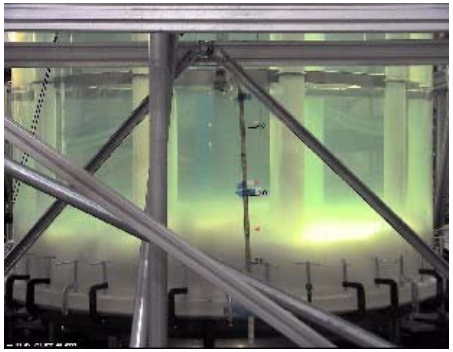

Maximum Cloud Height

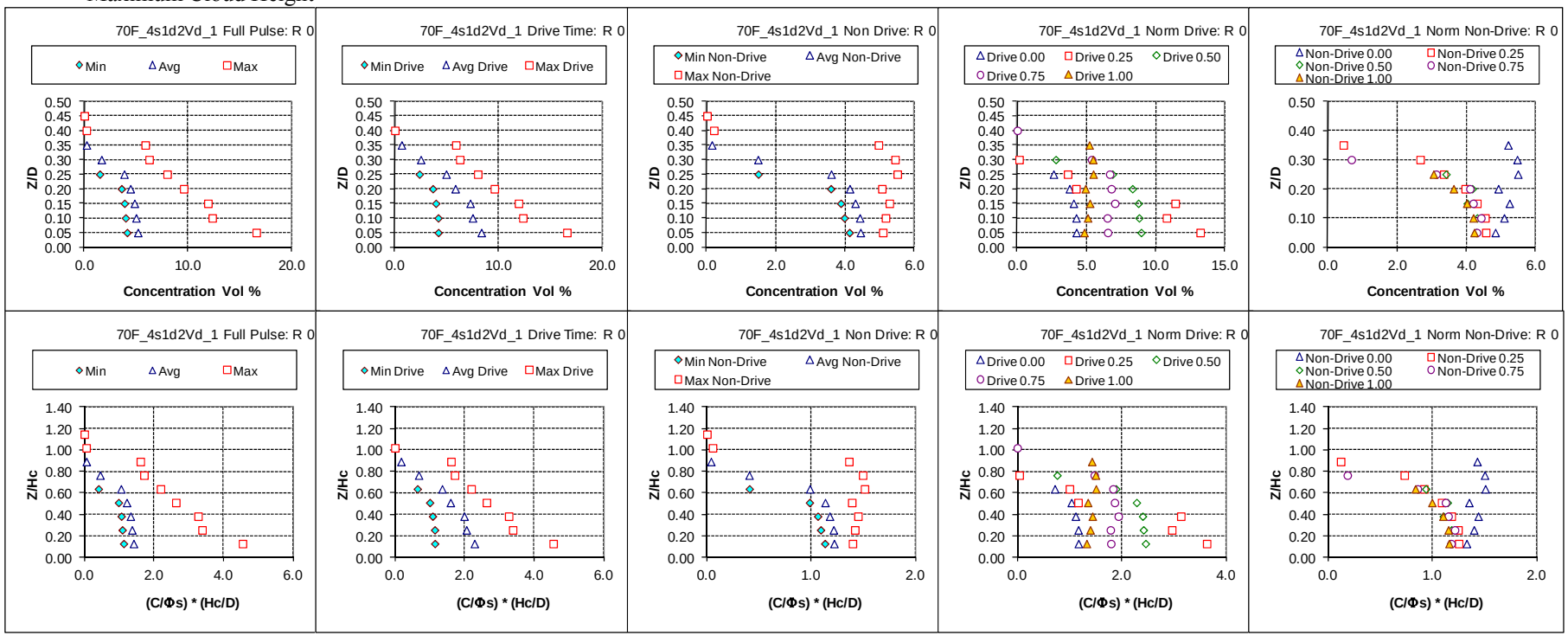

Figure C.42. 1.778-m- (70-in.-) diameter tank, 1.557-cm- (0.613-in.-) diameter nozzle; solids nominal diameter 69.3 µm, 2.48 g/cm^3 density; 0.0143 nominal solids fraction; 18.5% duty cycle, cycle time 54.8 s, pulse volume fraction 0.050, U_{CS} velocity 9.9 m/s, target nozzle exit velocity 9.9 m/s; peak cloud height upper bound 0.711 m (28 in.). Case ID 70F_4s1d2Vd_1.

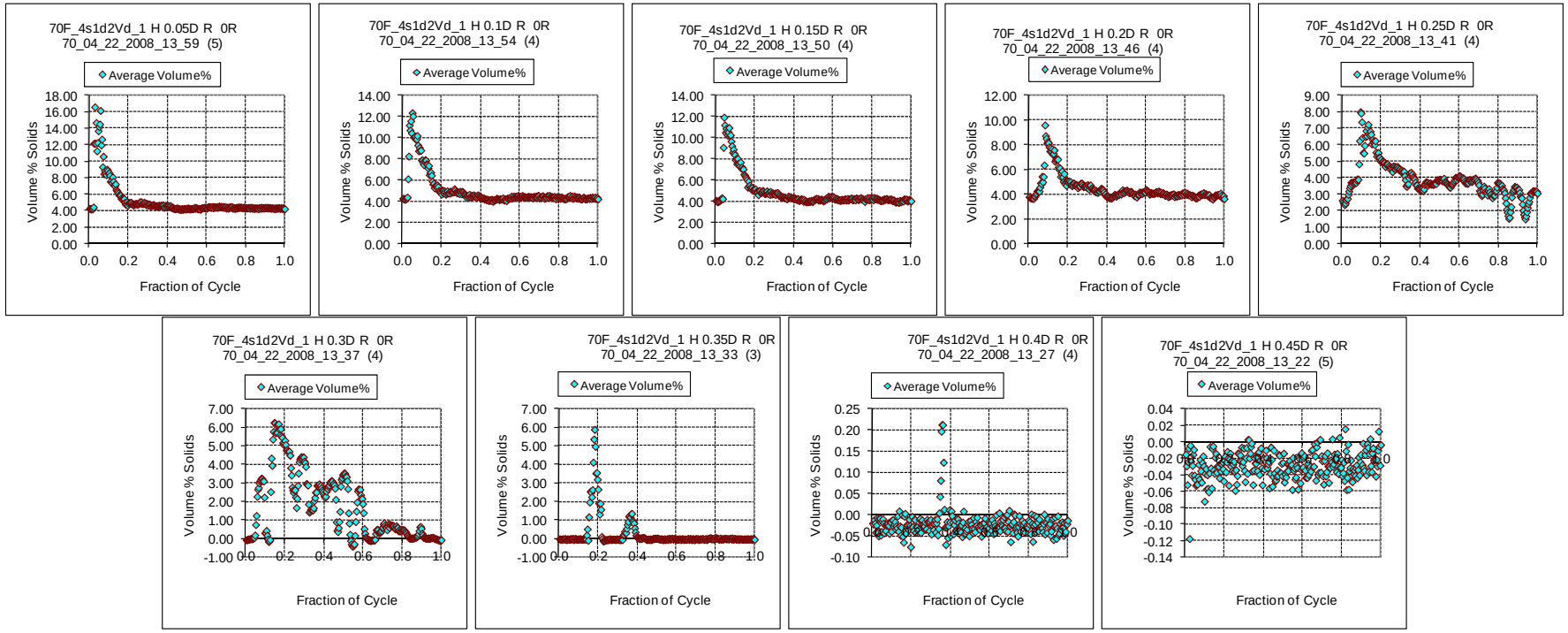

Figure C.42A. Case ID 70F_4s1d2Vd_1 Concentration Variation During the Cycle

Figure C.42 is the ninth of 12 profiles shown using simulant s1d2 in the large-scale tank with the flange and dish bottom. The solids fraction was 0.0143. The duty cycle was 18.5%. The pulse volume fraction was 0.050. The U_{CS} velocity occurred at 9.9 m/s. This profile and the one shown in Figure C.41 are for the same test condition both operating at a velocity equal to the corresponding U_{CS}. The profiles both show similar features.

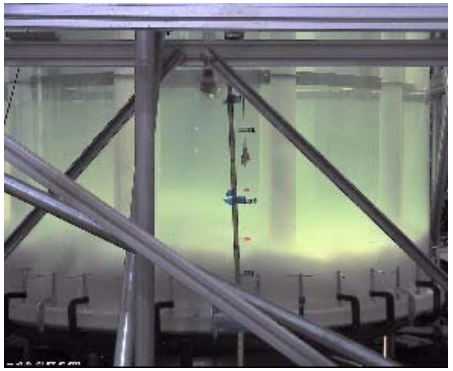

Maximum Cloud Height

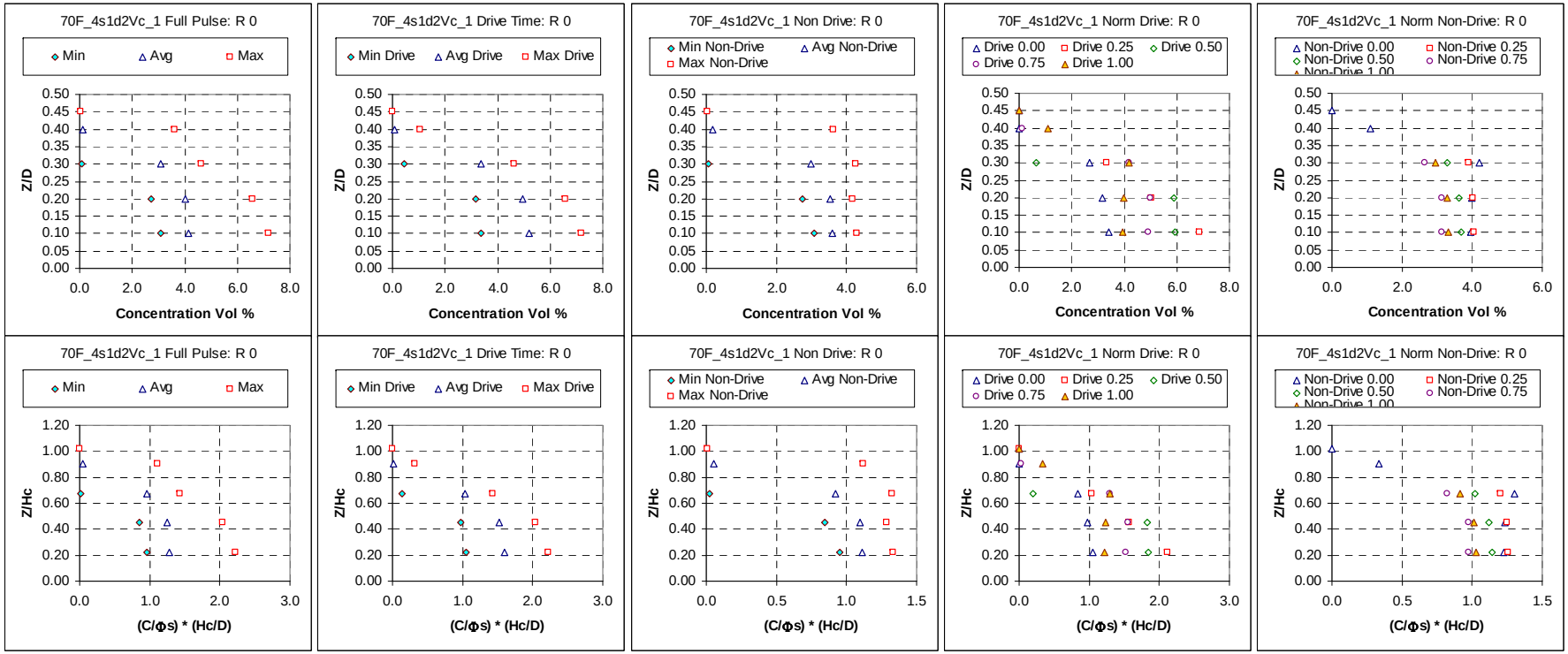

Figure C.43. 1.778-m- (70-in.-) diameter tank, 1.557-cm- (0.613-in.-) diameter nozzle; solids nominal diameter 69.3 µm, 2.48 g/cm^3 density; 0.0143 nominal solids fraction; 33.6% duty cycle, cycle time 41.2 s, pulse volume fraction 0.050, U_{CS} velocity 7.3 m/s, target nozzle exit velocity 7.3 m/s; peak cloud height upper bound 0.813 m (32 in.). Case ID 70F_4s1d2Vc_1.

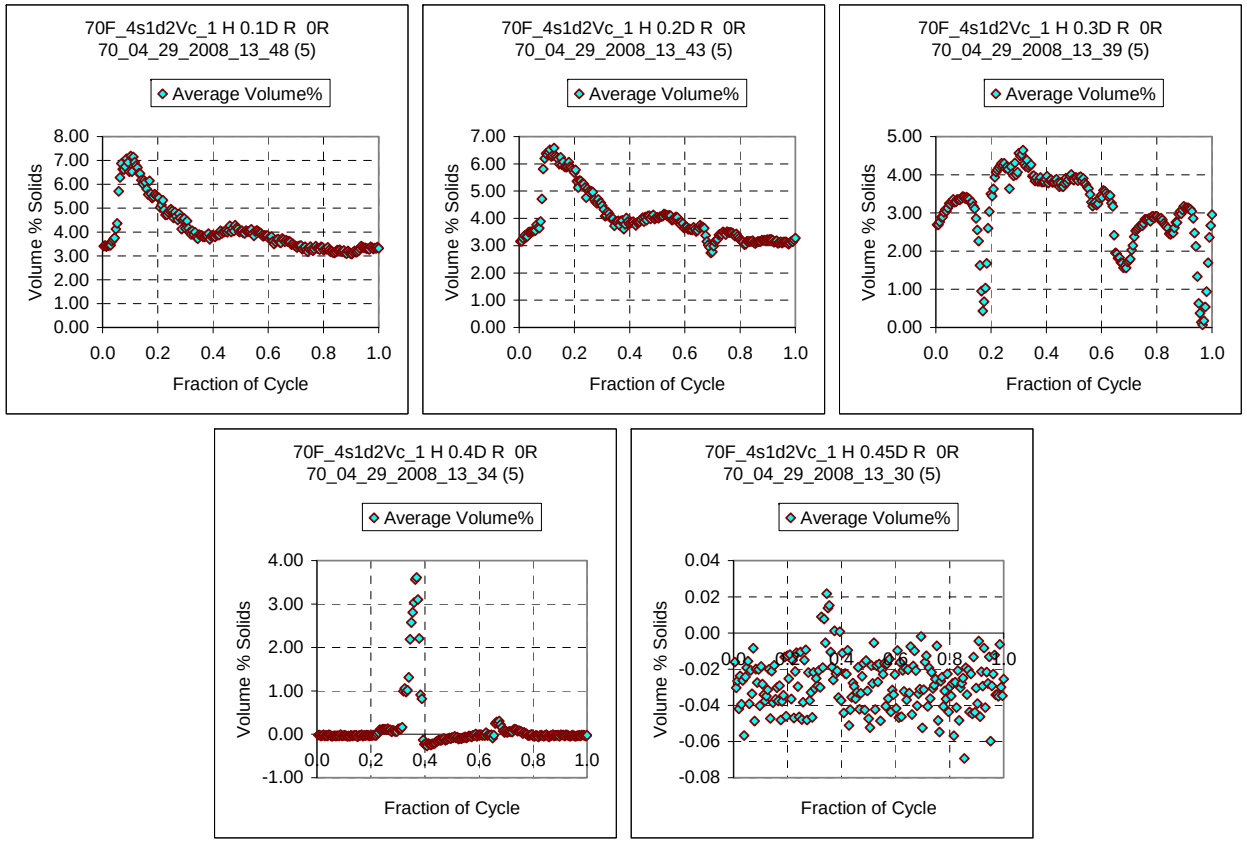

Figure C.43A. Case ID 70F_4s1d2Vc_1 Concentration Variation During the Cycle

Figure C.43 is the tenth of 12 profiles shown using simulant s1d2 in the large-scale tank with the flange and dish bottom. The solids fraction was 0.0143. The duty cycle was 33.6% increased from 18.5% shown in the prior profile. The pulse volume fraction was unchanged at 0.050. The U_{CS} velocity occurred at 7.3 m/s, a decrease from 9.9 m/s shown in the prior profile.

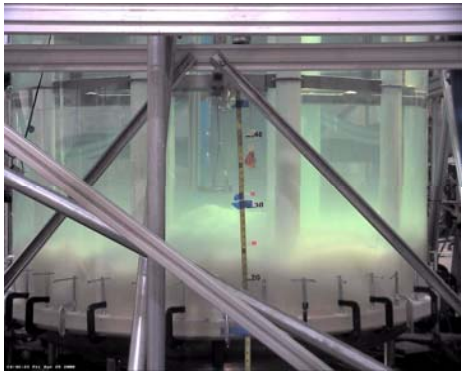

Maximum Cloud Height

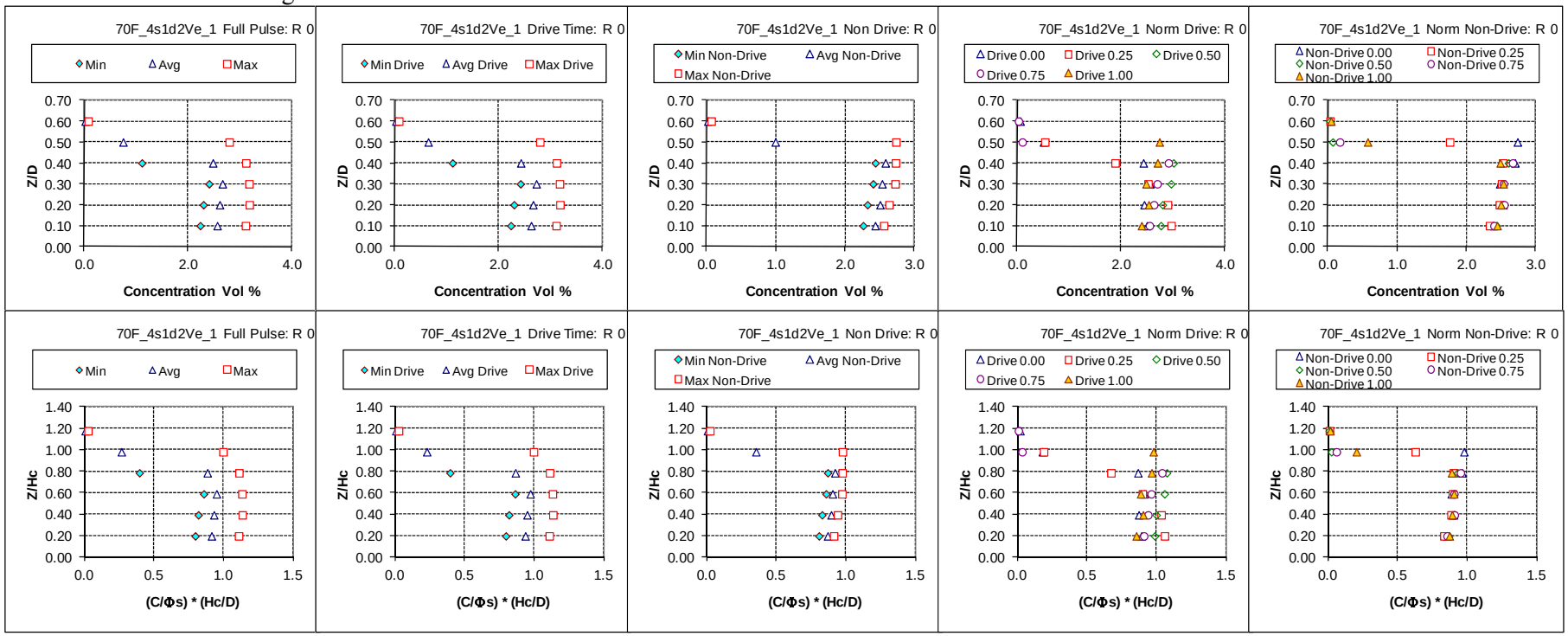

Figure C.44. 1.778-m- (70-in.-) diameter tank, 1.557-cm- (0.613-in.-) diameter nozzle; solids nominal diameter 69.3 µm, 2.48 g/cm^3 density; 0.0143 nominal solids fraction; 66.6% duty cycle, cycle time 31.2 s, pulse volume fraction 0.050, U_{CS} velocity 4.8 m/s, target nozzle exit velocity 4.8 m/s; peak cloud height upper bound 0.927 m (36.5 in.). Case ID 70F_4s1d2Ve_1.

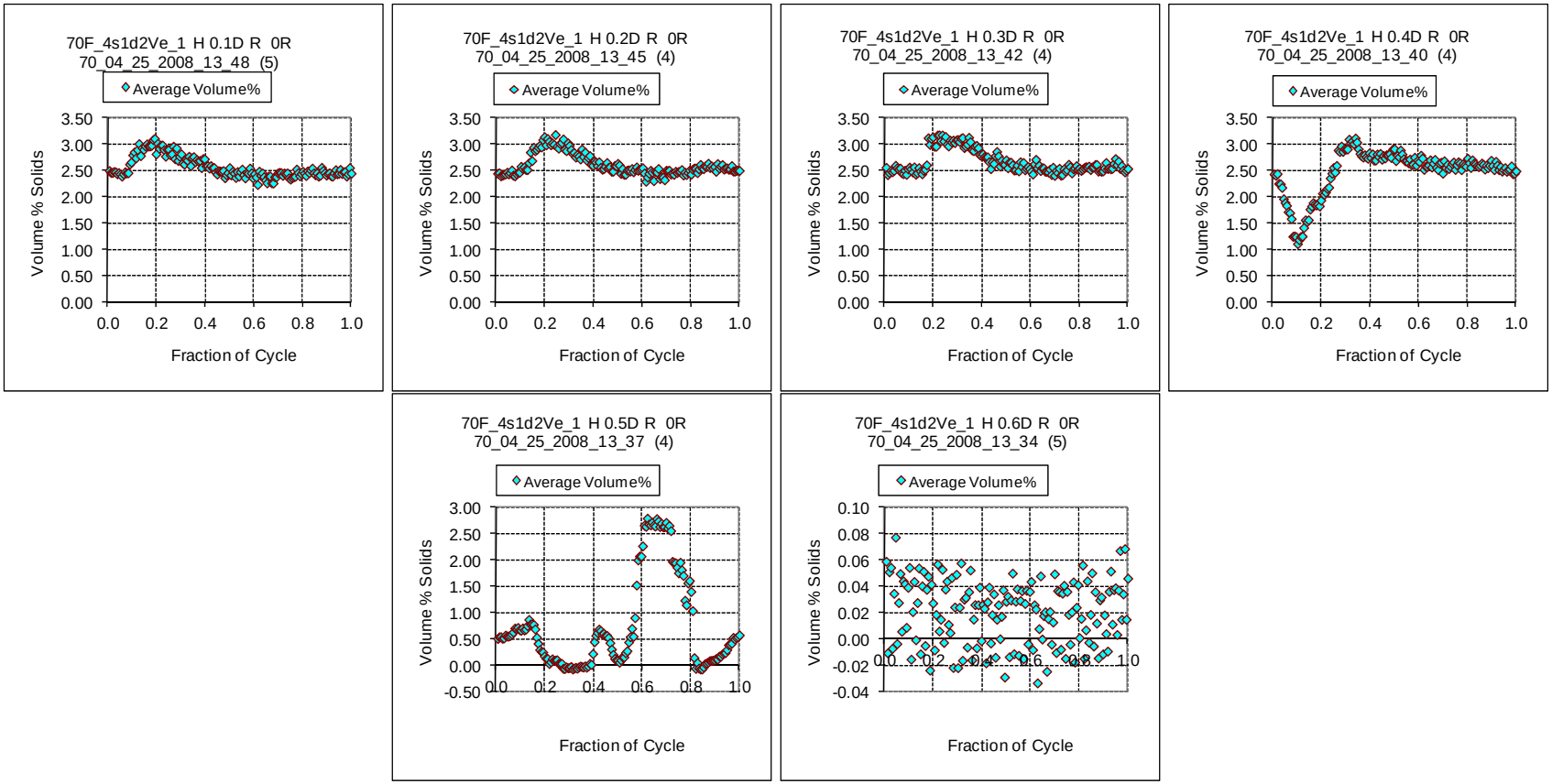

Figure C.44A. Case ID 70F_4s1d2Ve_1 Concentration Variation During the Cycle

Figure C.44 is the eleventh of 12 profiles shown using simulant s1d2 in the large-scale tank with the flange and dish bottom. The solids fraction was 0.0143. The duty cycle was 66.6%, increased from 33.6% in the prior profile and from 18.5% shown in Figure C.42. The pulse volume fraction was unchanged at 0.050. The UCS velocity occurred at 4.8 m/s, a decrease from 7.3 m/s shown in the prior profile and a decrease from 9.9 m/s shown in Figure C.42. The average concentration profile was essentially uniform at ~2.5 vol% to an elevation of Z/D = 0.4. This was an increase in the region of uniform concentration from the prior two profiles.

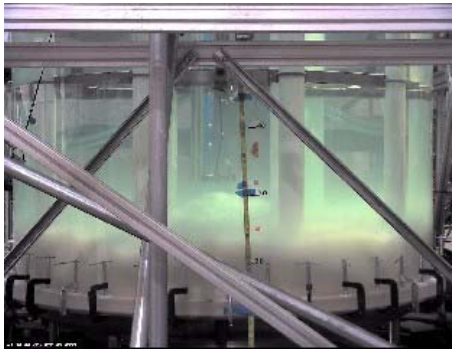

Maximum Cloud Height

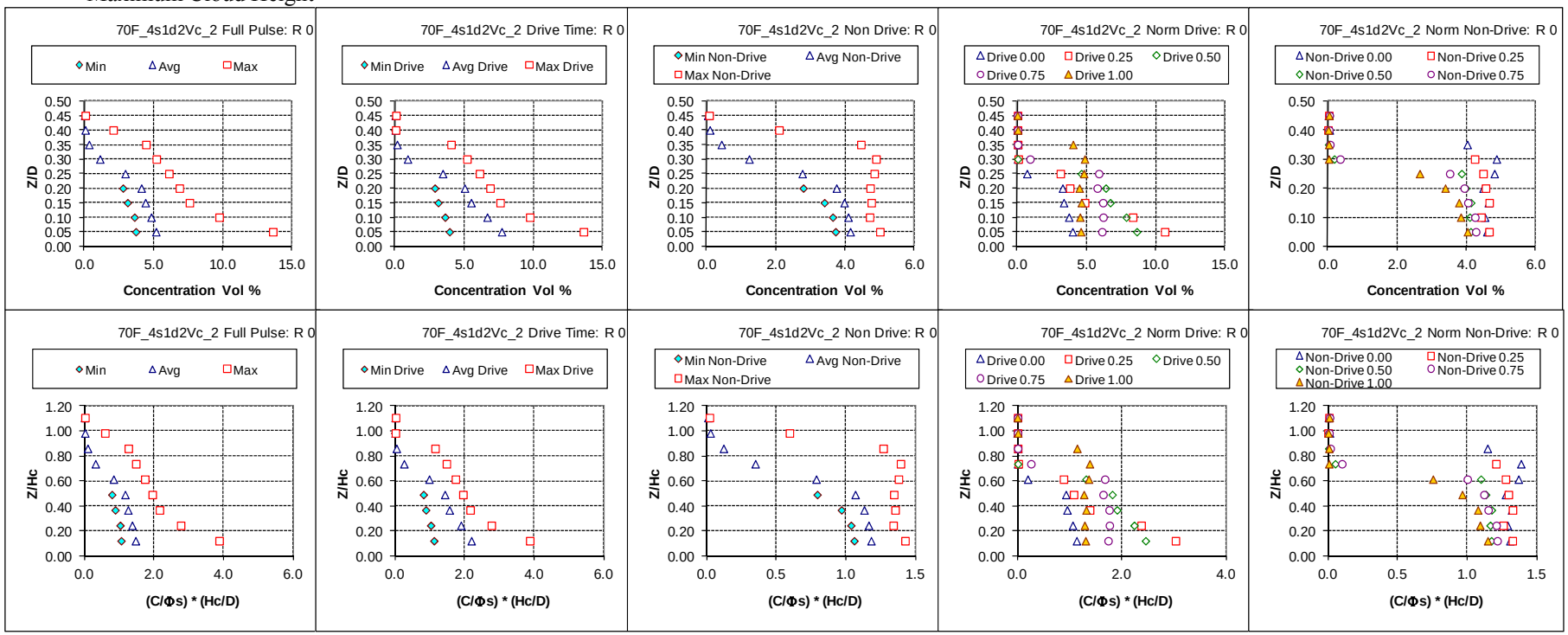

Figure C.45. 1.778-m- (70-in.-) diameter tank, 1.557-cm- (0.613-in.-) diameter nozzle; solids nominal diameter 69.3 µm, 2.48 g/cm^3 density; 0.0143 nominal solids fraction; 32.7% duty cycle, cycle time 90.0 s, pulse volume fraction 0.100, U_{CS} velocity 6.6 m/s, target nozzle exit velocity 6.6 m/s; peak cloud height upper bound 0.749 m (29.5 in.). Case ID 70F_4s1d2Vc_2.

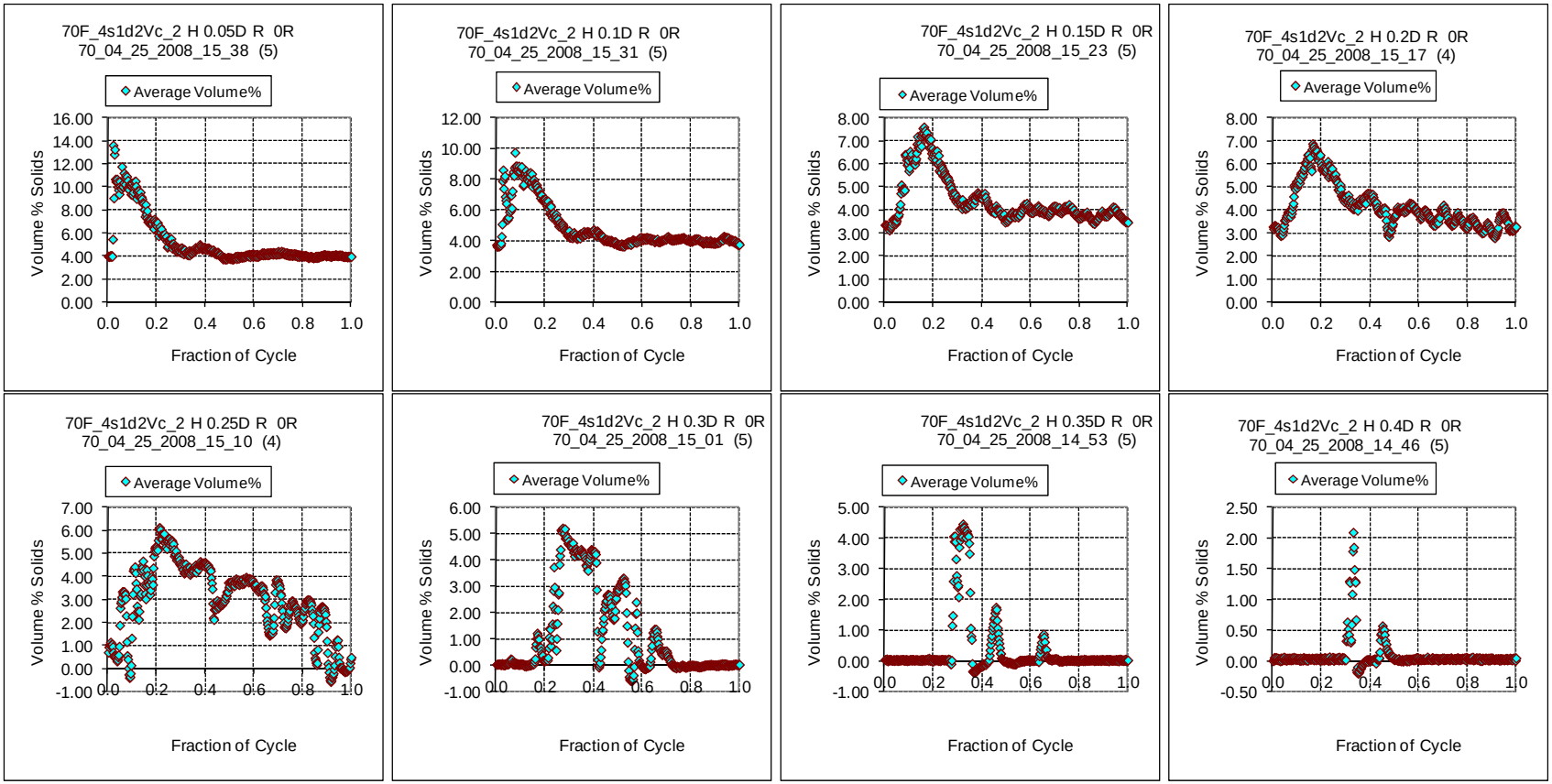

Figure C.45A. Case ID 70F_4s1d2Vc_2 Concentration Variation During the Cycle

Figure C.45 is the last of 12 profiles shown using simulant s1d2 in the large-scale tank with the flange and dish bottom. The solids fraction was 0.0143. The duty cycle was 32.7%, similar to that shown in Figure C.43 of 33.6%. The pulse volume fraction was increased to 0.10 from 0.050 shown in Figure C.43. The U_{CS} velocity occurred at 6.6 m/s, a decrease from 7.3 m/s shown in Figure C.43. The average concentration at Z/D = 0.05 starts at ~5 vol% and decreases with elevation to ~0 vol% at Z/D = 0.4. In comparison, the profile shown in Figure C.42 starts at ~4 vol% at Z/D = 0.05 and decreases with elevation to ~0 vol% at Z/D = 0.4.

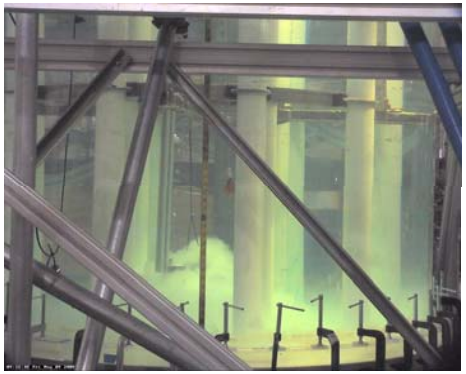

Maximum Cloud Height

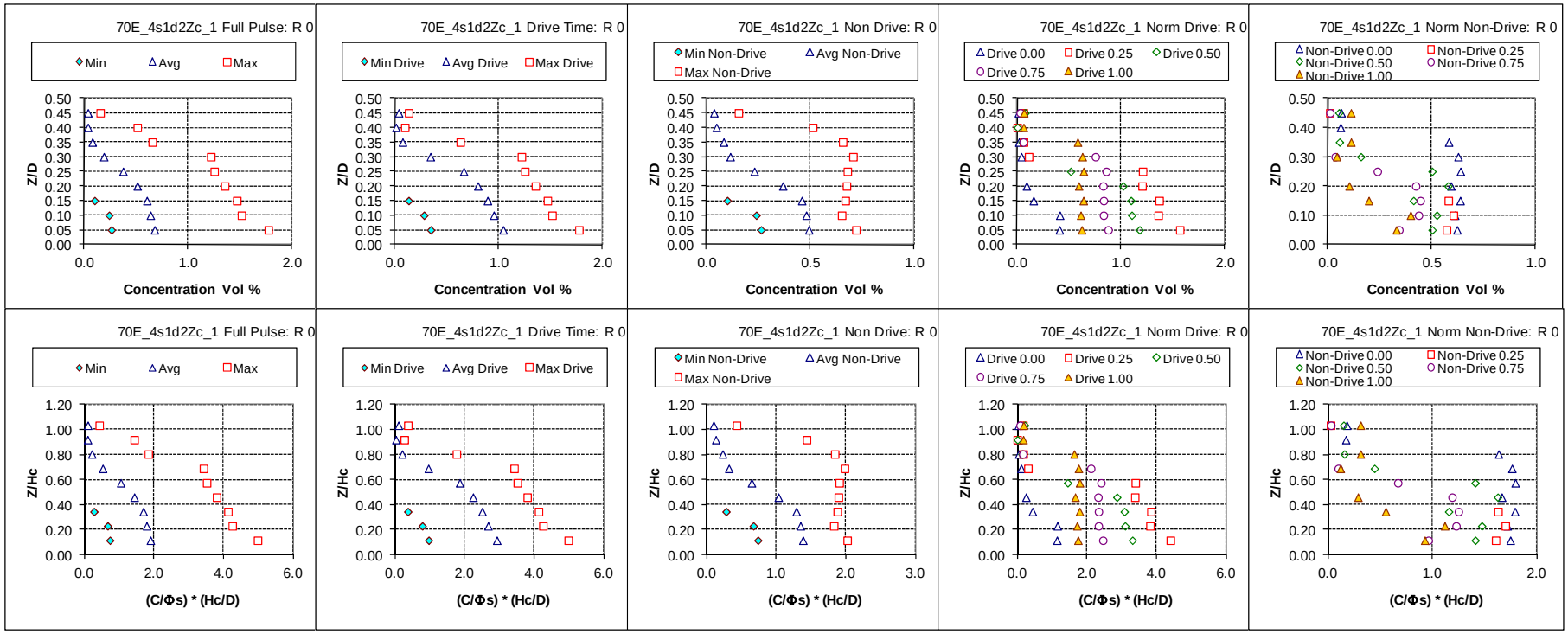

Figure C.46. 1.778-m- (70-in.-) diameter tank, 1.557-cm- (0.613-in.-) diameter nozzle; solids nominal diameter 69.3 µm, 2.48 g/cm^3 density; 0.00155 nominal solids fraction; 33.7% duty cycle, cycle time 63.6 s, pulse volume fraction 0.050; U_{CS} velocity 4.6 m/s, target nozzle exit velocity 4.6 m/s; peak cloud height upper bound 0.787 m (31 in.). Case ID 70E_4s1d2Zc_1.

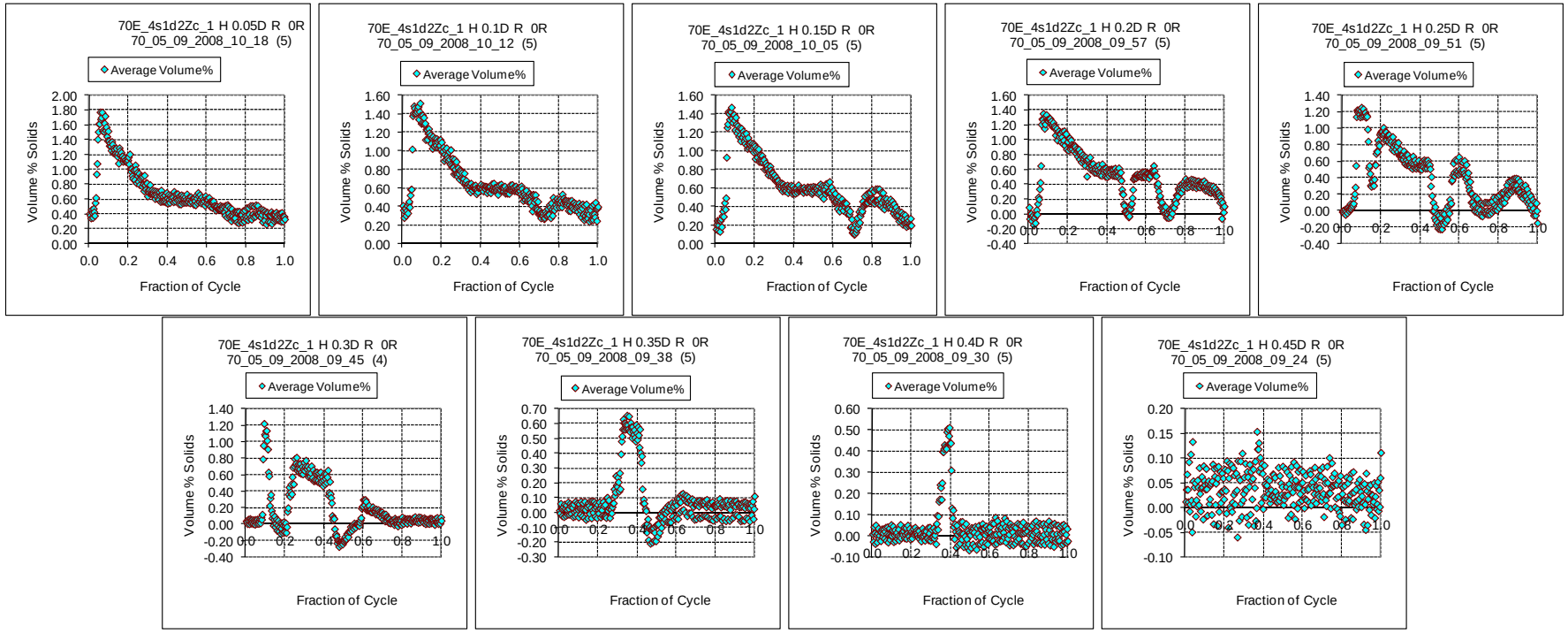

Figure C.46A. Case ID 70E_4s1d2Zc_1 Concentration Variation During the Cycle

Figure C.46 was the first of 12 profiles shown using simulant s1d2 in the large-scale tank with the elliptical bottom. The solids fraction was 0.00155. The duty cycle was 33.7% and the pulse volume fraction was 0.050. The U_{CS} velocity occurred at 4.6 m/s. The peak cloud height upper bound was 31 in. This profile can be compared with that shown in Figure C.34, which was conducted at similar conditions in the large-scale tank with the flanged and dished bottom. The profiles are very similar with the one with the elliptical bottom showing slightly reduced average concentrations as a function of elevation.

Maximum Cloud Height

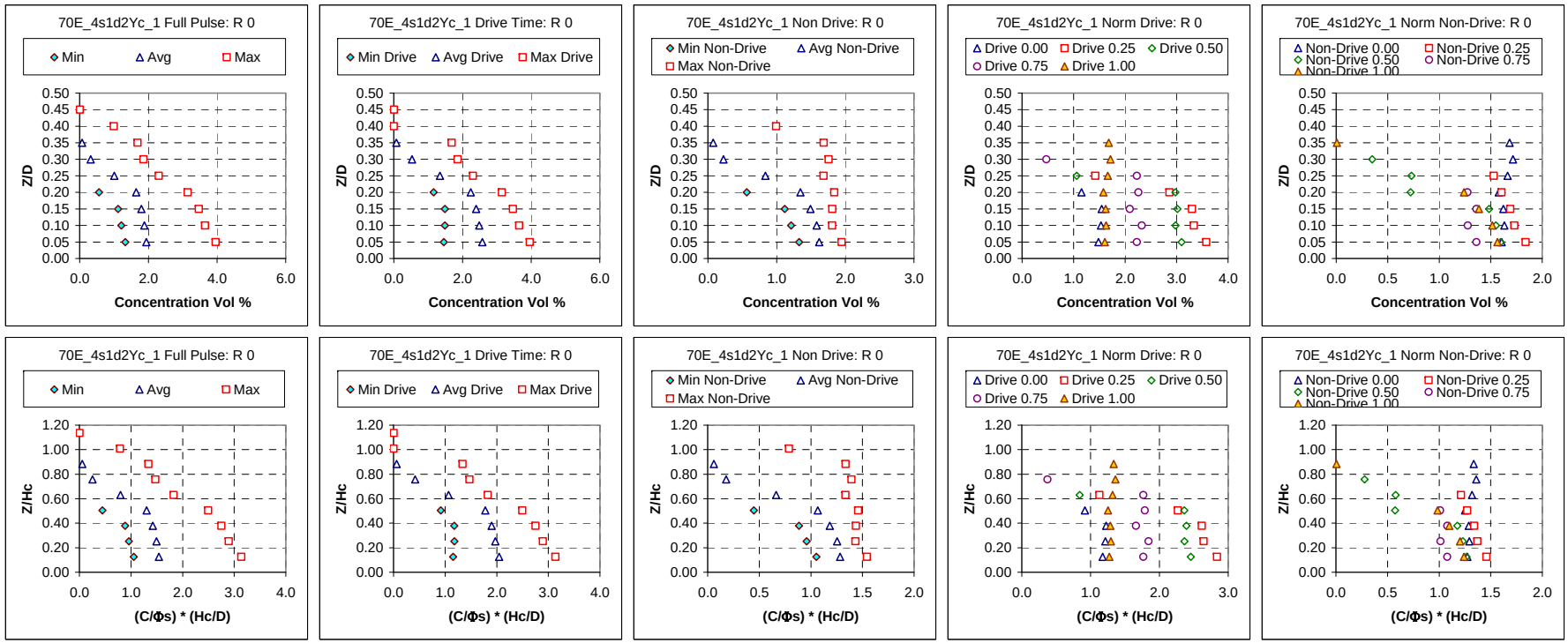

Figure C.47. 1.778-m- (70-in.-) diameter tank, 1.557-cm- (0.613-in.-) diameter nozzle; solids nominal diameter 69.3 µm, 2.48 g/cm^3 density; 0.005 nominal solids fraction; 33.5% duty cycle, cycle time 49.6 s, pulse volume fraction 0.050, U_{CS} velocity 6 m/s, target nozzle exit velocity 6 m/s; peak cloud height upper bound 0.724 m (28.5 in.). Case ID 70E_4s1d2Yc_1.

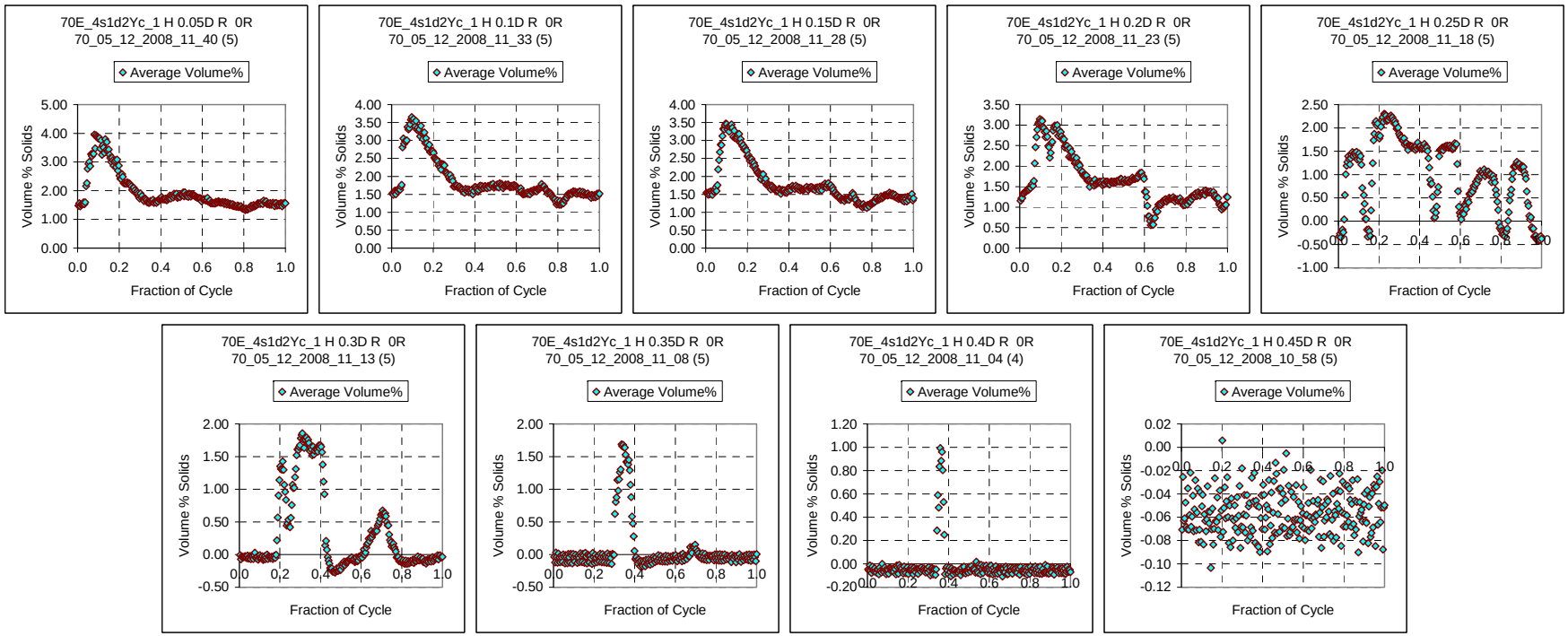

Figure C.47A. Case ID 70E_4s1d2Yc_1 Concentration Variation During the Cycle

Figure C.47 is the second of 12 profiles shown using simulant s1d2 in the large-scale tank with the elliptical bottom. The solids fraction was 0.005, an increase from 0.00155 shown in Figure C.46. The duty cycle was 33.5% and the pulse volume fraction was 0.050. The U_{CS} velocity occurred at 6 m/s, which was an increase from 4.6 m/s from the prior test. The peak cloud height upper bound was 28.5 in., which was a decrease from 31 in. in the prior test. This vertical profile was relatively constant at slightly below 2 vol% solids over the range from Z/D = 0.5 to Z/D = 0.2.

Maximum Cloud Height

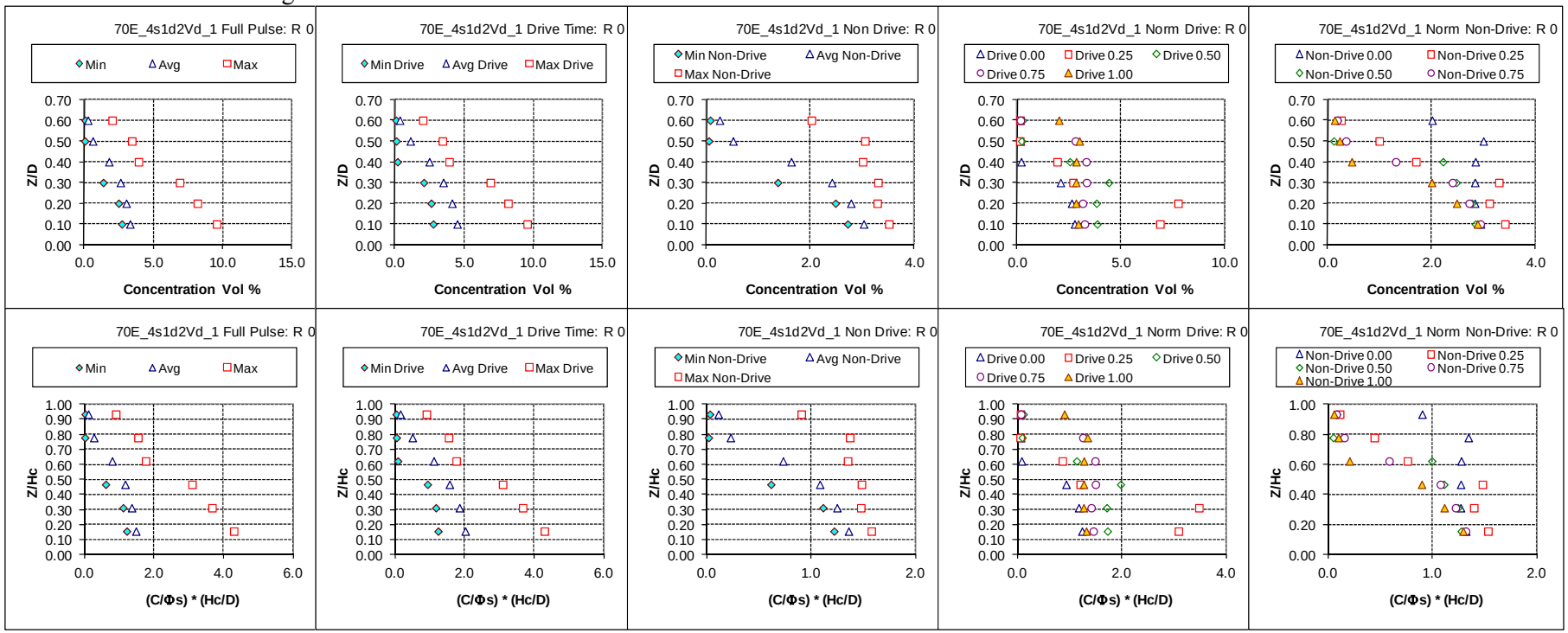

Figure C.48. 1.778-m- (70-in.-) diameter tank, 1.557-cm- (0.613-in.-) diameter nozzle; solids nominal diameter 69.3 µm, 2.48 g/cm^3 density; 0.0143 nominal solids fraction; 18.9% duty cycle, cycle time 48.6 s, pulse volume fraction 0.050, U_{CS} velocity 10.9 m/s, target nozzle exit velocity 11.2 m/s; peak cloud height upper bound 1.168 m (46 in.). Case ID 70E_4s1d2Vd_1.

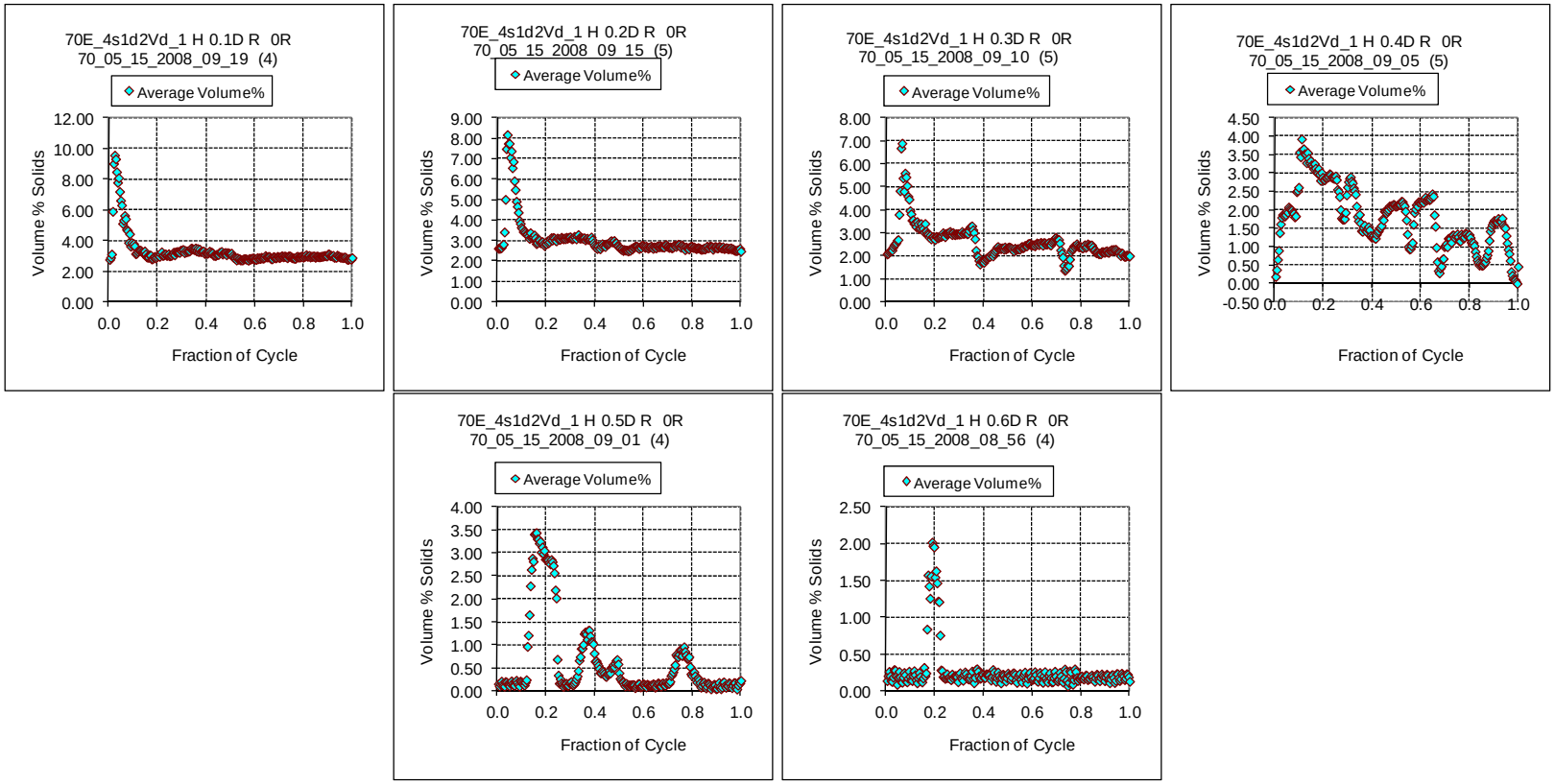

Figure C.48A. Case ID 70E_4s1d2Vd_1 R 0 Concentration Variation During the Cycle

Figure C.48 is the third of 12 profiles shown using simulant s1d2 in the large-scale tank with the elliptical bottom. Figures C.48, C.49, and C.50 are a group of three profiles taken at the same flow conditions and differing radial locations. The solids fraction was 0.0143. The duty cycle was 18.9%. The peak cloud height upper bound was 46 in. The U_{CS} velocity occurred at 10.9 m/s. In each of the three figures, the velocity was above the U_{CS} velocity of 11.2 m/s. Figure C.48 shows a profile at the center of the tank with R = 0. When the radial profiles in the set of three figures are compared, the concentrations are shown to decline slightly with increasing radius. The concentration decreases with elevation in all three radial locations. Since the velocity was greater than the critical suspension velocity, a more constant concentration with height was expected; however, instead of maintaining a more constant profile, the additional velocity above the critical suspension velocity may have produced a higher peak cloud height upper bound.

Maximum Cloud Height

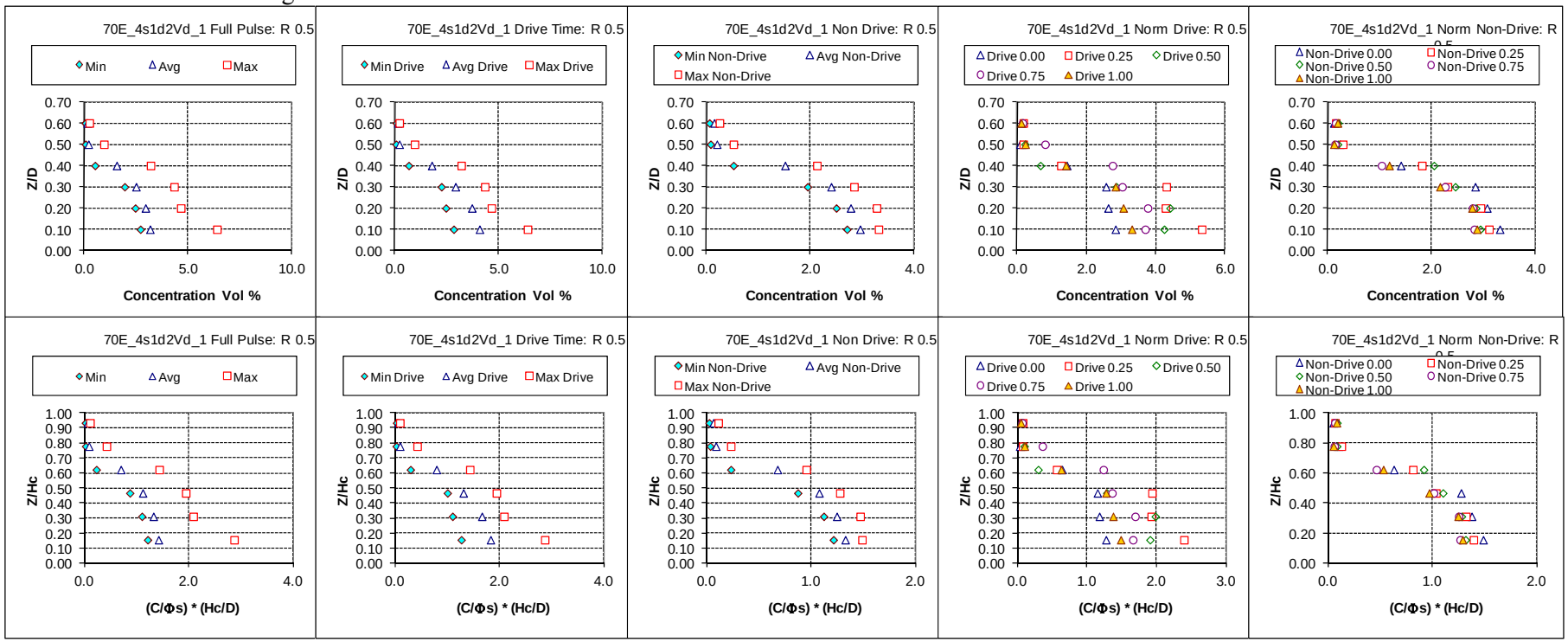

Figure C.49. 1.778-m- (70-in.-) diameter tank, 1.557-cm- (0.613-in.-) diameter nozzle; solids nominal diameter 69.3 µm, 2.48 g/cm^3 density; 0.0143 nominal solids fraction; 18.9% duty cycle, cycle time 48.6 s, pulse volume fraction 0.050, U_{CS} velocity 10.9 m/s, target nozzle exit velocity 11.2 m/s; peak cloud height upper bound 1.168 m (46 in.). Case ID 70E_4s1d2Vd_1.

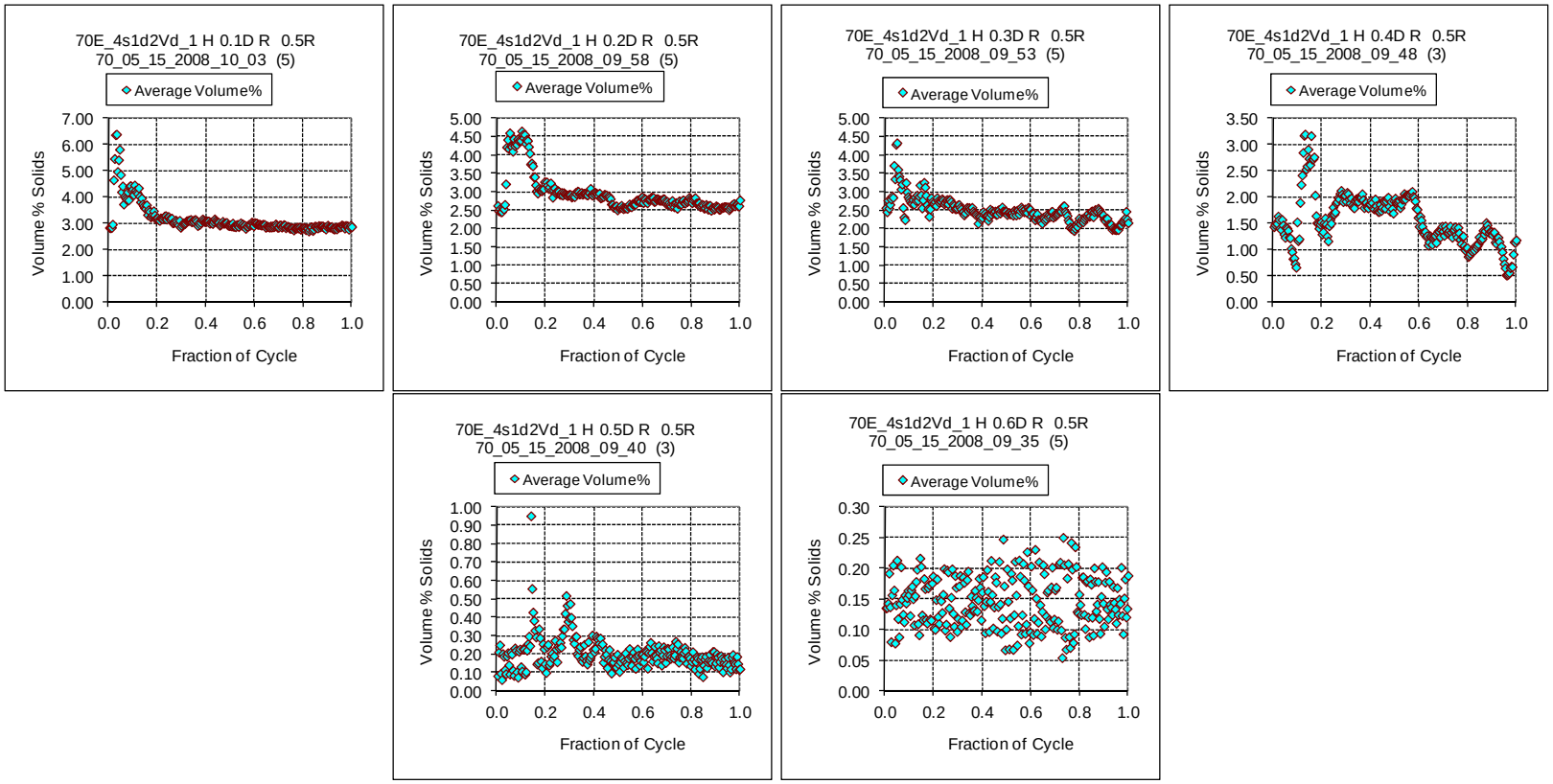

Figure C.49A. Case ID 70E_4s1d2Vd_1 R 0.5 Concentration Variation During the Cycle

Maximum Cloud Height

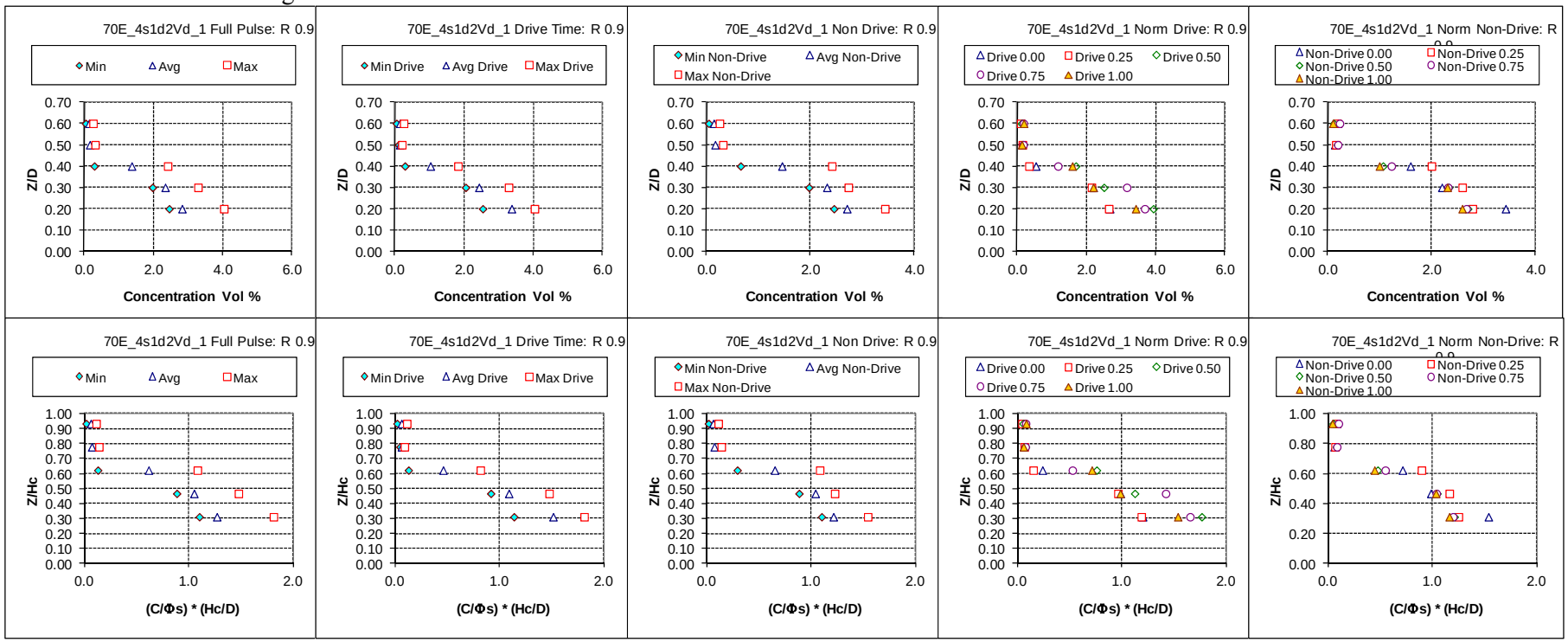

Figure C.50. 1.778-m- (70-in.-) diameter tank, 1.557-cm- (0.613-in.-) diameter nozzle; solids nominal diameter 69.3 µm, 2.48 g/cm^3 density; 0.0143 nominal solids fraction; 18.9% duty cycle, cycle time 48.6 s, pulse volume fraction 0.050, U_{CS} velocity 10.9 m/s, target nozzle exit velocity 11.2 m/s; peak cloud height upper bound 1.168 m (46 in.). Case ID 70E_4s1d2Vd_1.

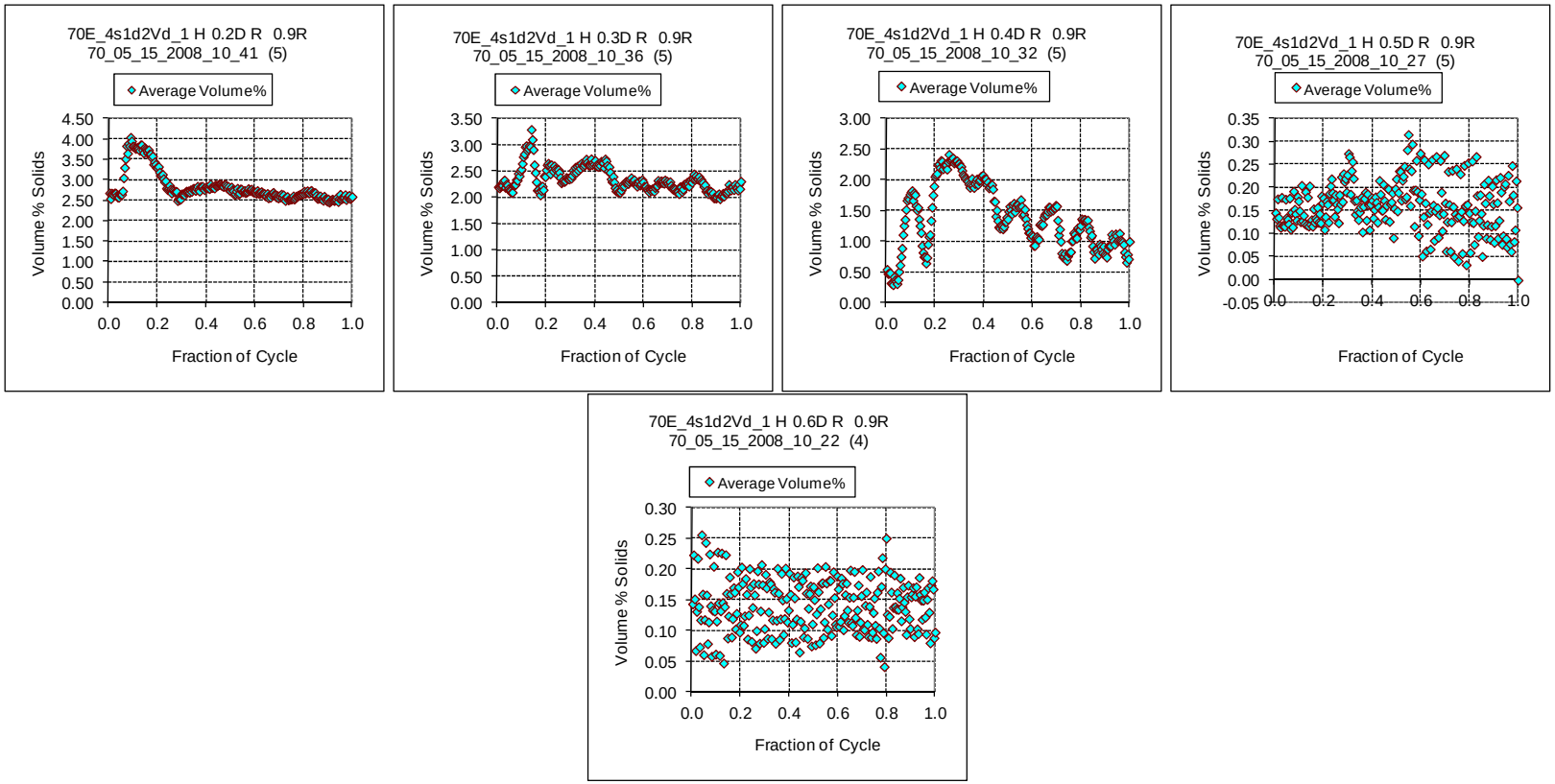

Figure C.50A. Case ID 70E_4s1d2Vd_1 R 0.9 Concentration Variation During the Cycle

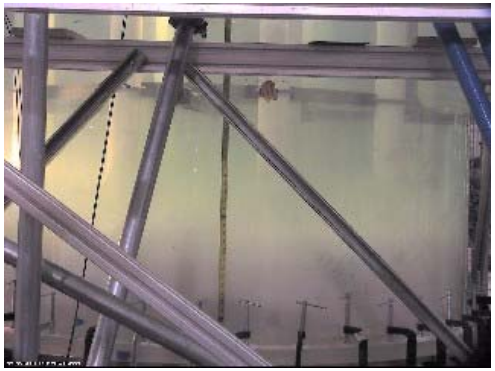

Maximum Cloud Height

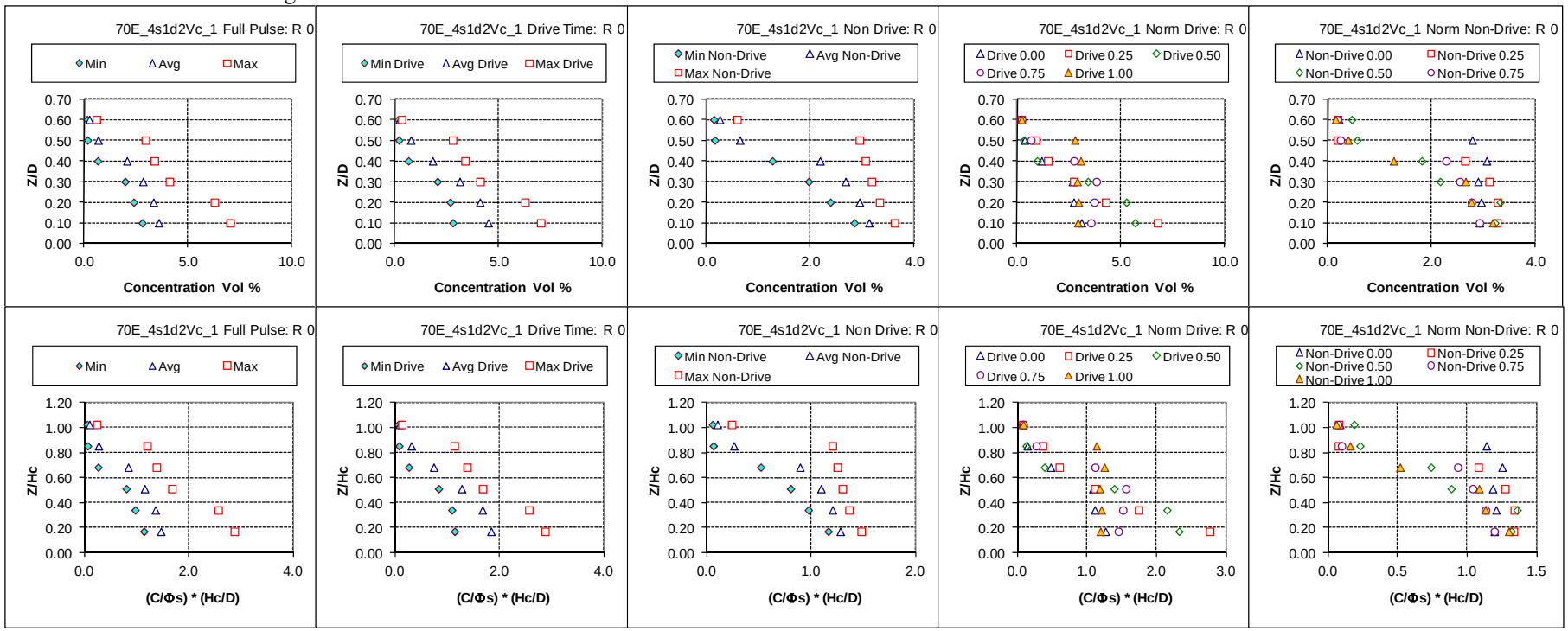

Figure C.51. 1.778-m- (70-in.-) diameter tank, 1.557-cm- (0.613-in.-) diameter nozzle; solids nominal diameter 69.3 µm, 2.48 g/cm^3 density; 0.0143 nominal solids fraction; 33.3% duty cycle, cycle time 38.8 s, pulse volume fraction 0.050, U_{CS} velocity 7.8 m/s, target nozzle exit velocity 7.8 m/s; peak cloud height upper bound 1.041 m (41 in.). Case ID 70E_4s1d2Vc_1.

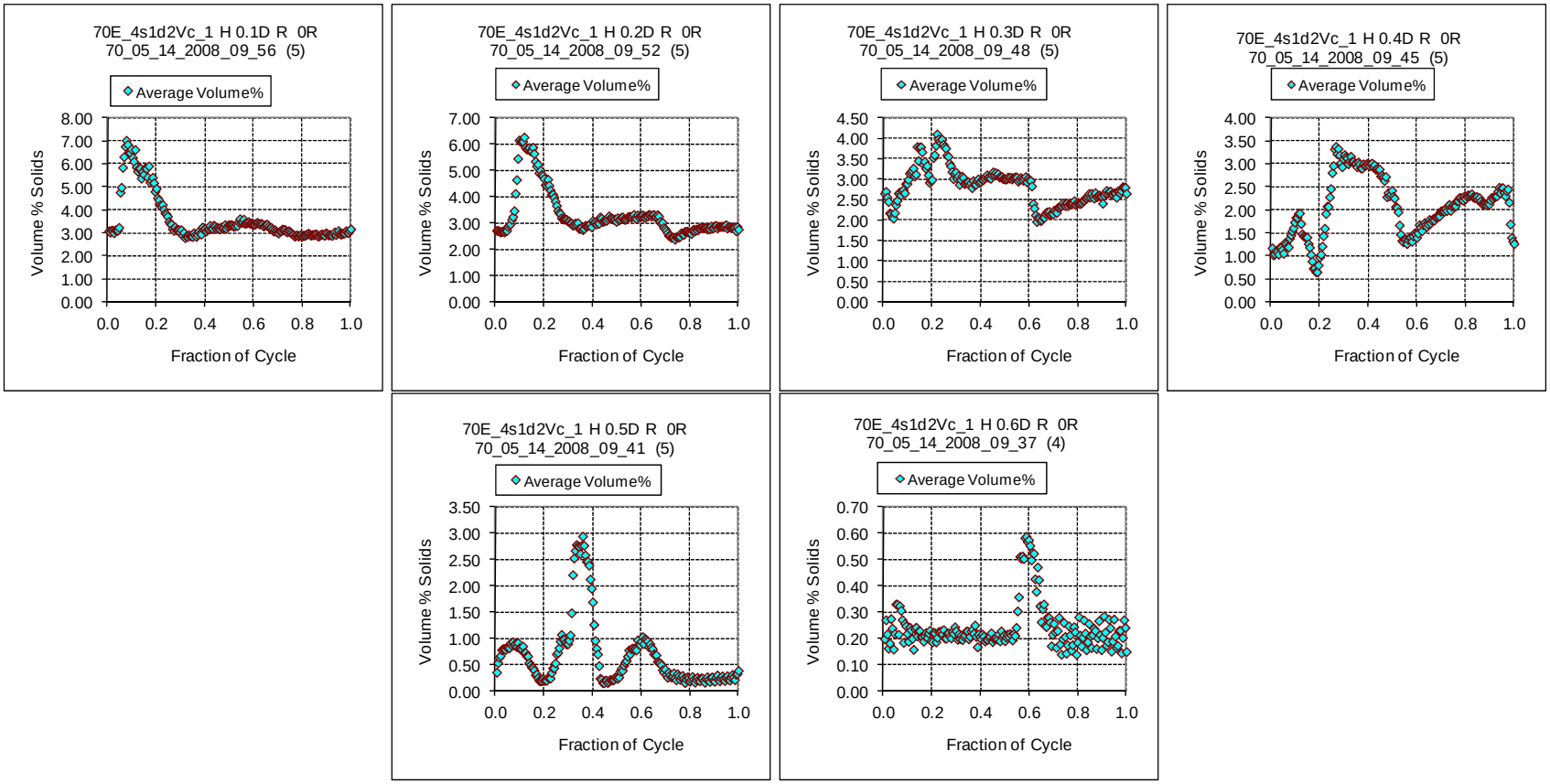

Figure C.51A. Case ID 70E_4s1d2Vc_1 Concentration Variation During the Cycle

Figure C.51 is the sixth of 12 profiles shown using simulant s1d2 in the large-scale tank with the elliptical bottom. Figures C.51, C.52, and C.53 are a group of three profiles taken at the same flow conditions and differing radial locations. The solids fraction in each case was 0.0143. The peak cloud height upper bound was 41 in. The duty cycle was 33.3%, which was an increase from 18.9% shown in Figures C.48, C.49, and C.50. In Figures C.51, C.52, and C.53, the U_{CS} velocity occurred at 7.8 m/s, which was a decrease from 10.9 m/s shown in the earlier series of three. Unlike the other series, these measurements were taken at U_{CS}. Figure C.51 shows a profile at the center of the tank with R = 0. When the radial profiles in the current set of three figures are compared, the concentrations are shown to decline slightly with increasing radius. The profiles show the same trends exhibited in the prior three profiles. The profiles at R = 0, R = 0.5, and R = 0.9 all reach Z/D = 0.6. The concentration decreases with elevation in all three radial locations.

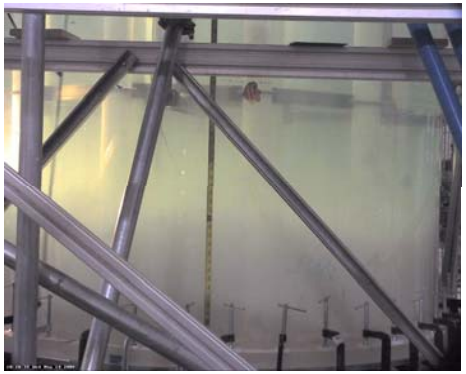

Maximum Cloud Height

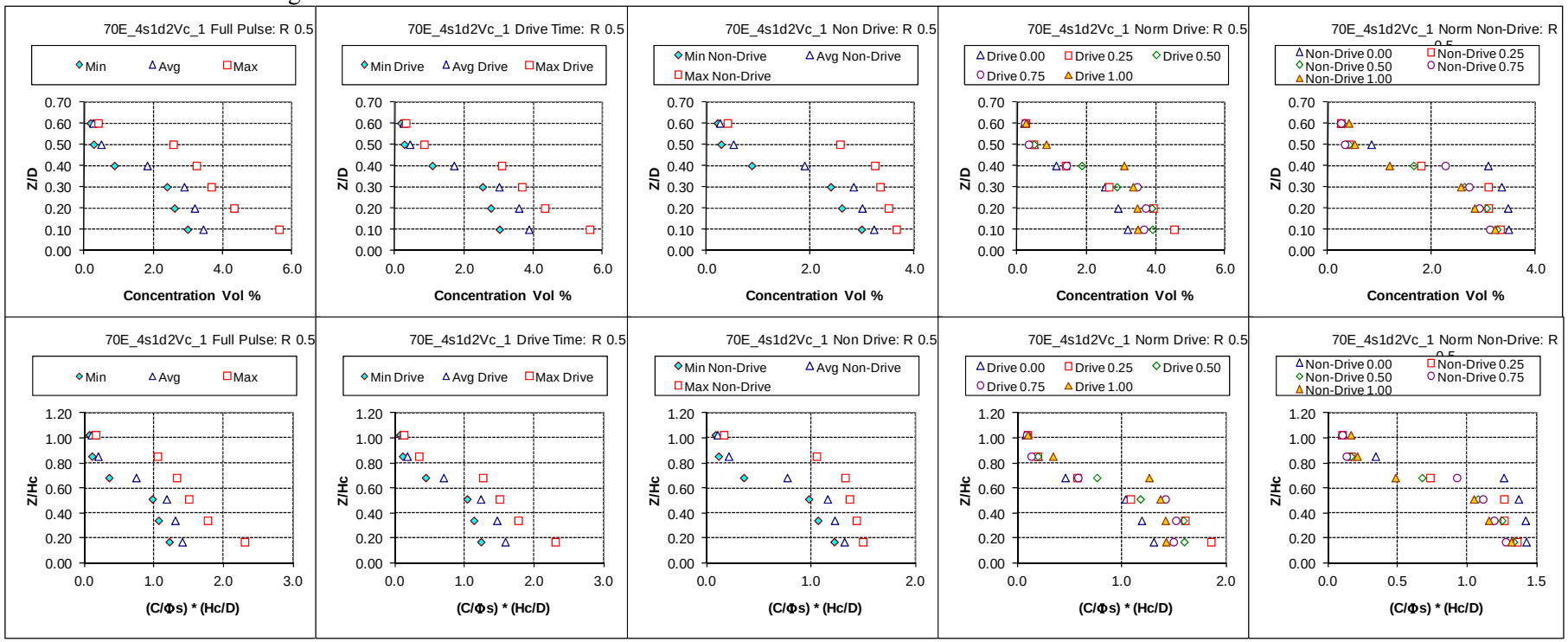

Figure C.52. 1.778-m- (70-in.-) diameter tank, 1.557-cm- (0.613-in.-) diameter nozzle; solids nominal diameter 69.3 µm, 2.48 g/cm^3 density; 0.0143 nominal solids fraction; 33.3% duty cycle, cycle time 38.8 s, pulse volume fraction 0.050, U_{CS} velocity 7.8 m/s, target nozzle exit velocity 7.8 m/s; peak cloud height upper bound 1.041 m (41 in.). Case ID 70E_4s1d2Vc_1.

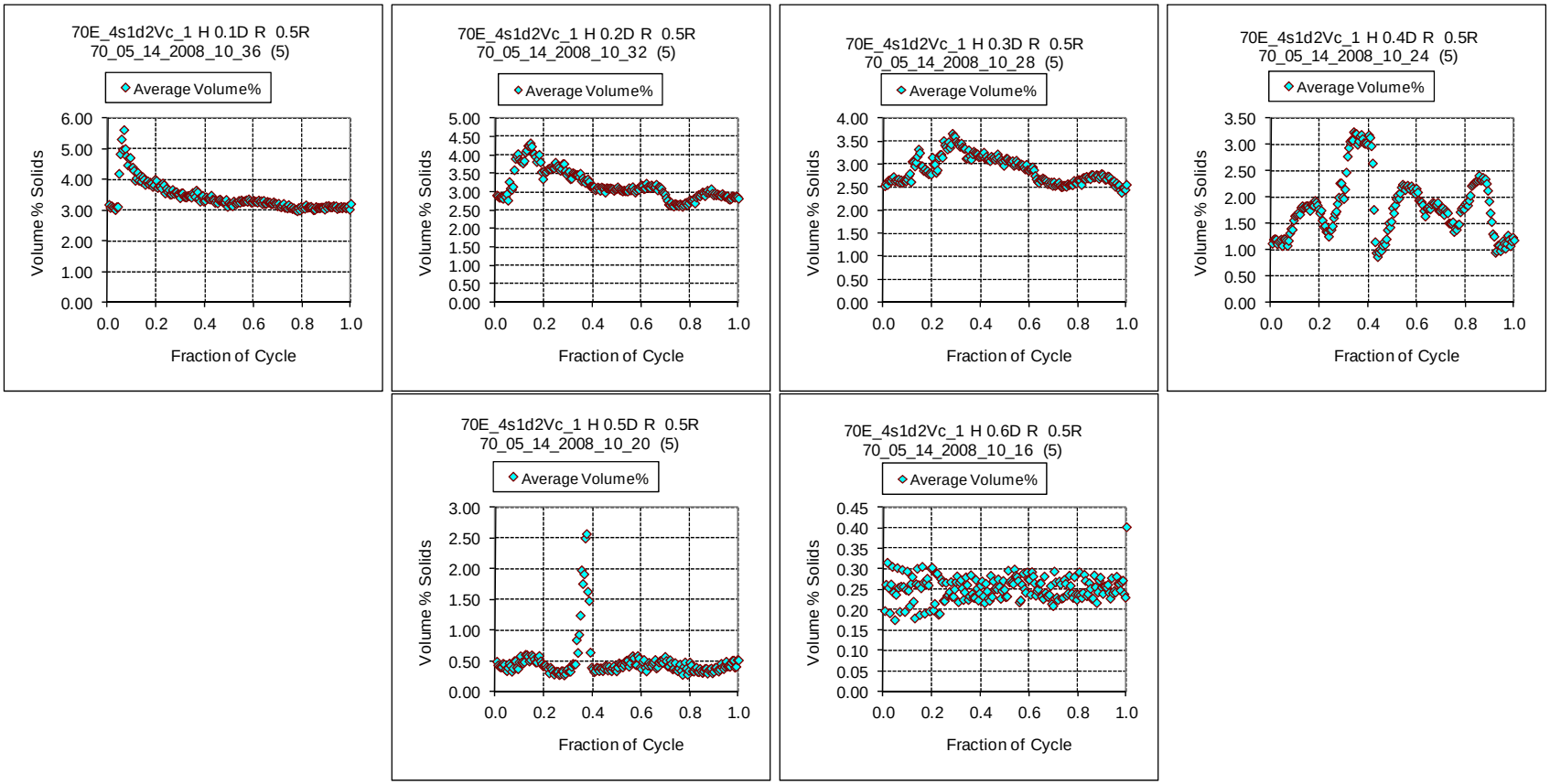

Figure C.52A. Case ID 70E_4s1d2Vc_1 Concentration Variation During the Cycle

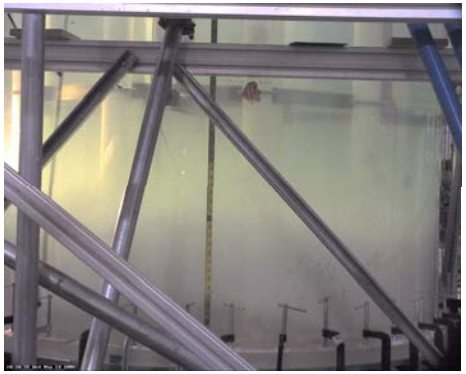

Maximum Cloud Height

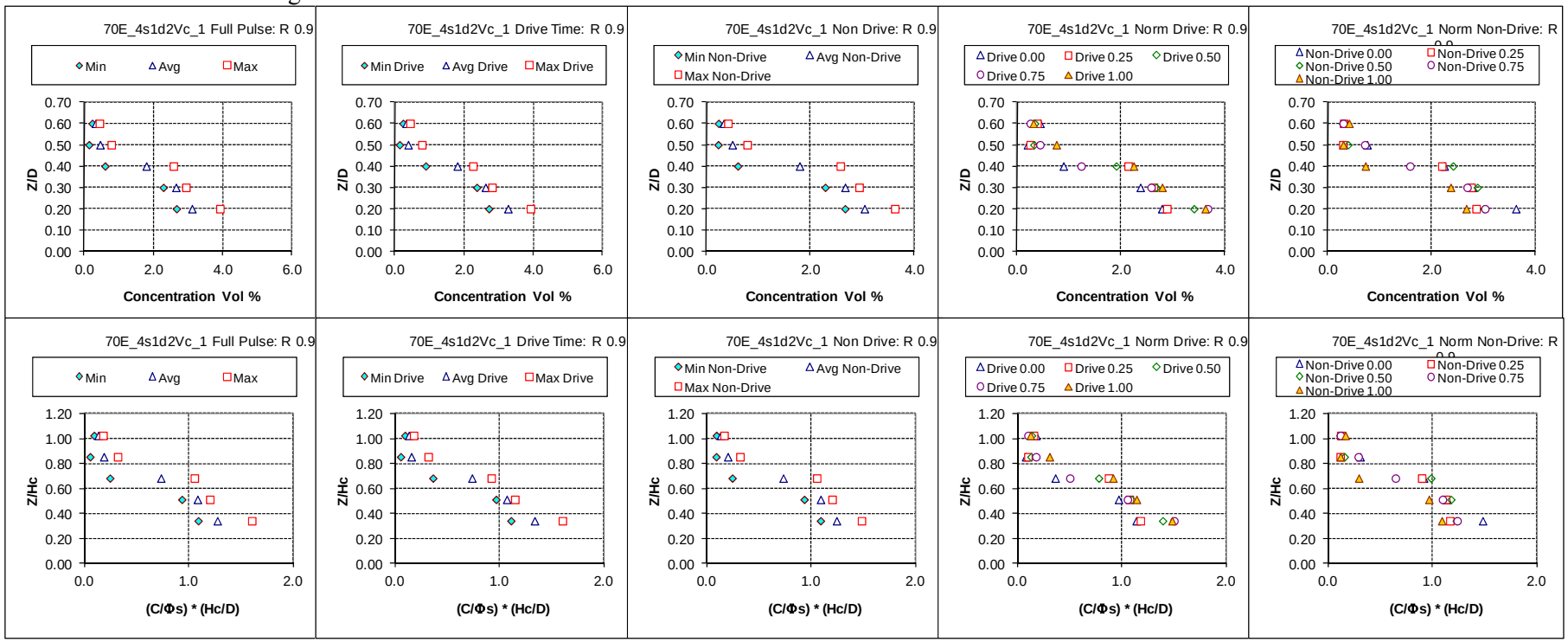

Figure C.53. 1.778-m- (70-in.-) diameter tank, 1.557-cm- (0.613-in.-) diameter nozzle; solids nominal diameter 69.3 µm, 2.48 g/cm^3 density; 0.0143 nominal solids fraction; 33.3% duty cycle, cycle time 38.8 s, pulse volume fraction 0.050, U_{CS} velocity 7.8 m/s, target nozzle exit velocity 7.8 m/s; peak cloud height upper bound 1.041 m (41 in.). Case ID 70E_4s1d2Vc_1.

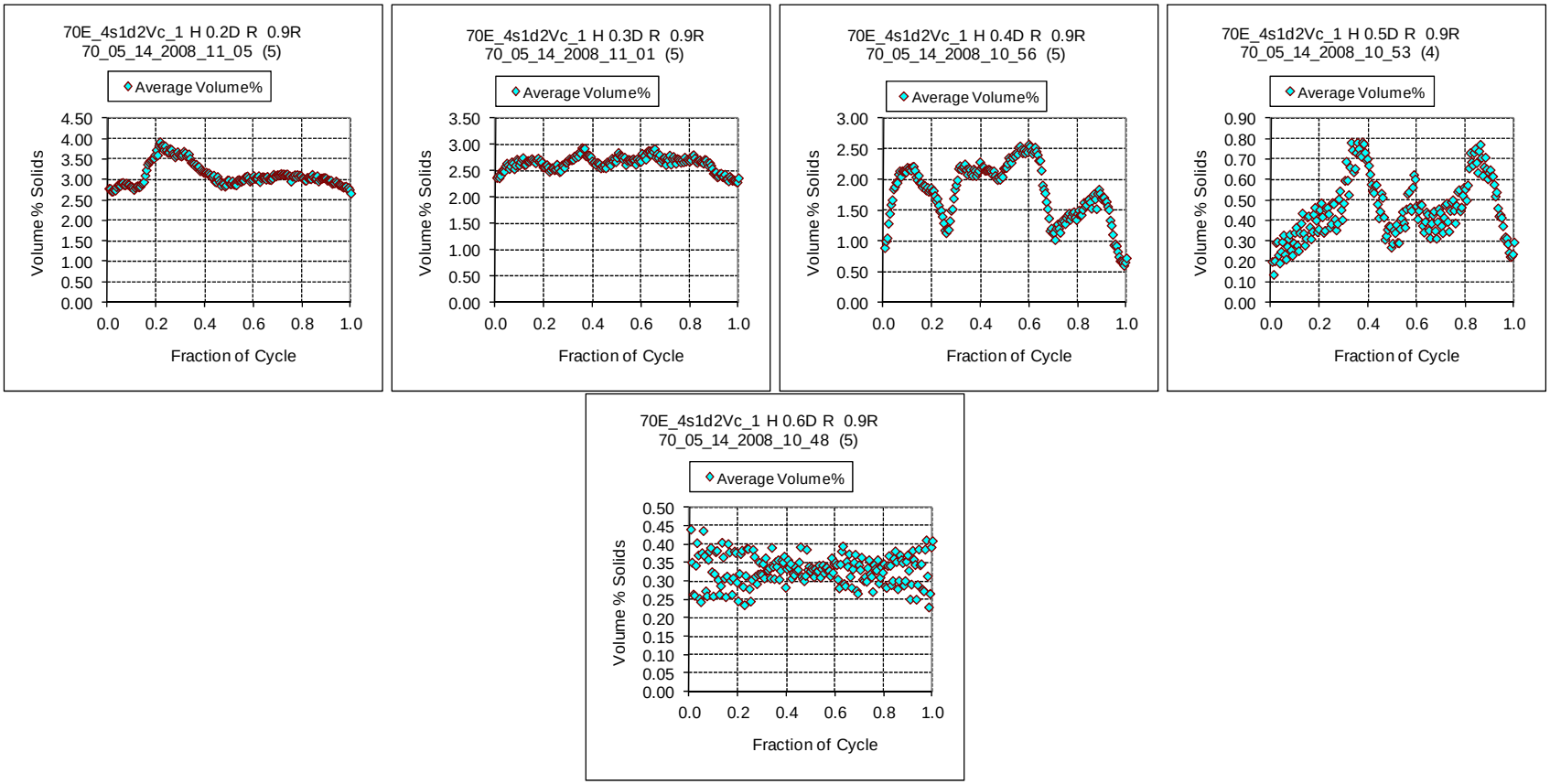

Figure C.53A. Case ID 70E_4s1d2Vc_1 Concentration Variation During the Cycle

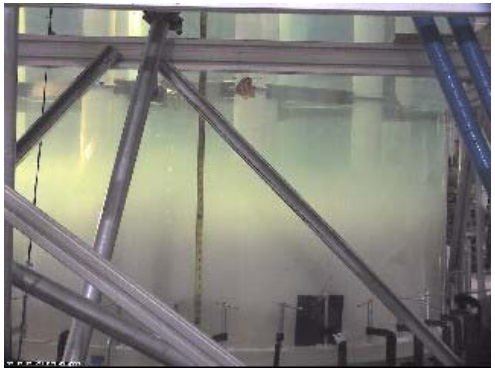

Maximum Cloud Height

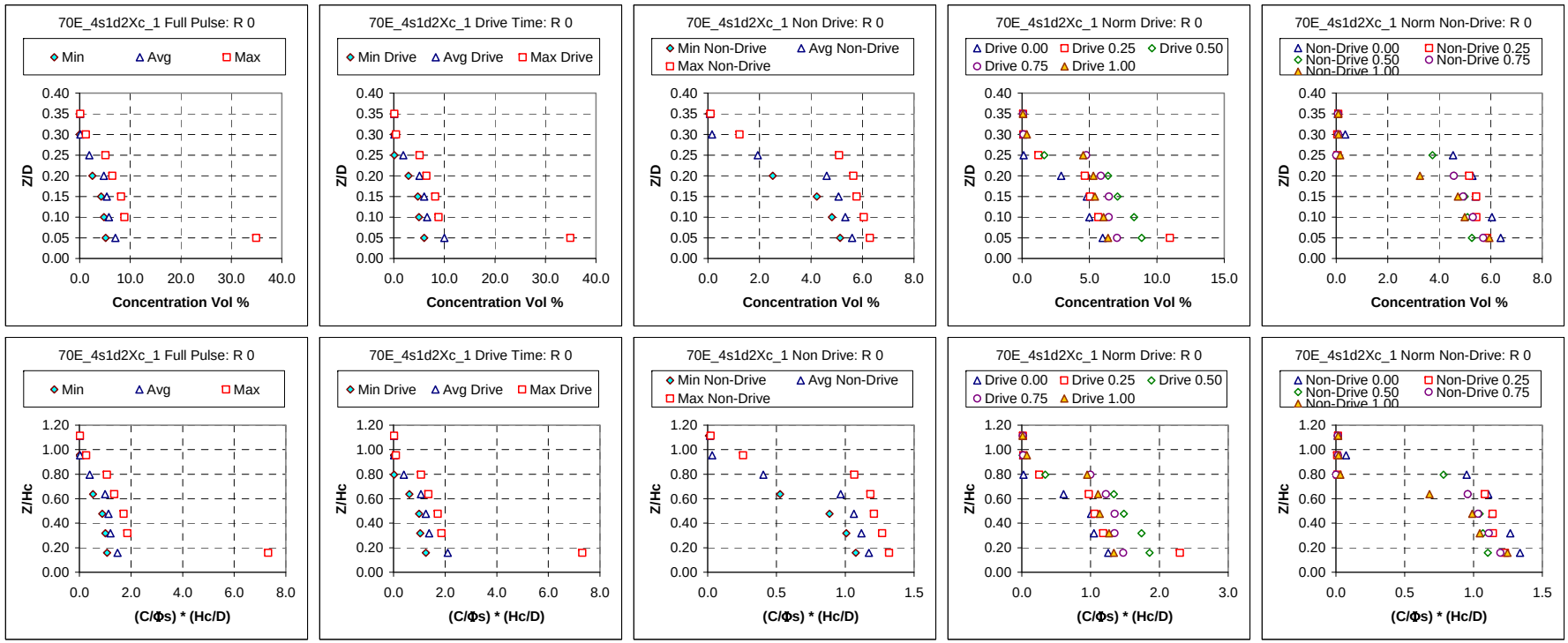

Figure C.54. 1.778-m- (70-in.-) diameter tank, 1.557-cm- (0.613-in.-) diameter nozzle; solids nominal diameter 69.3 µm, 2.48 g/cm^3 density; 0.015 nominal solids fraction; 32.9% duty cycle, cycle time 44.6 s, pulse volume fraction 0.050, U_{CS} velocity 8.5 m/s, target nozzle exit velocity 6.8 m/s; peak cloud height upper bound 0.572 m (22.5 in.). Case ID 70E_4s1d2Xc_1.

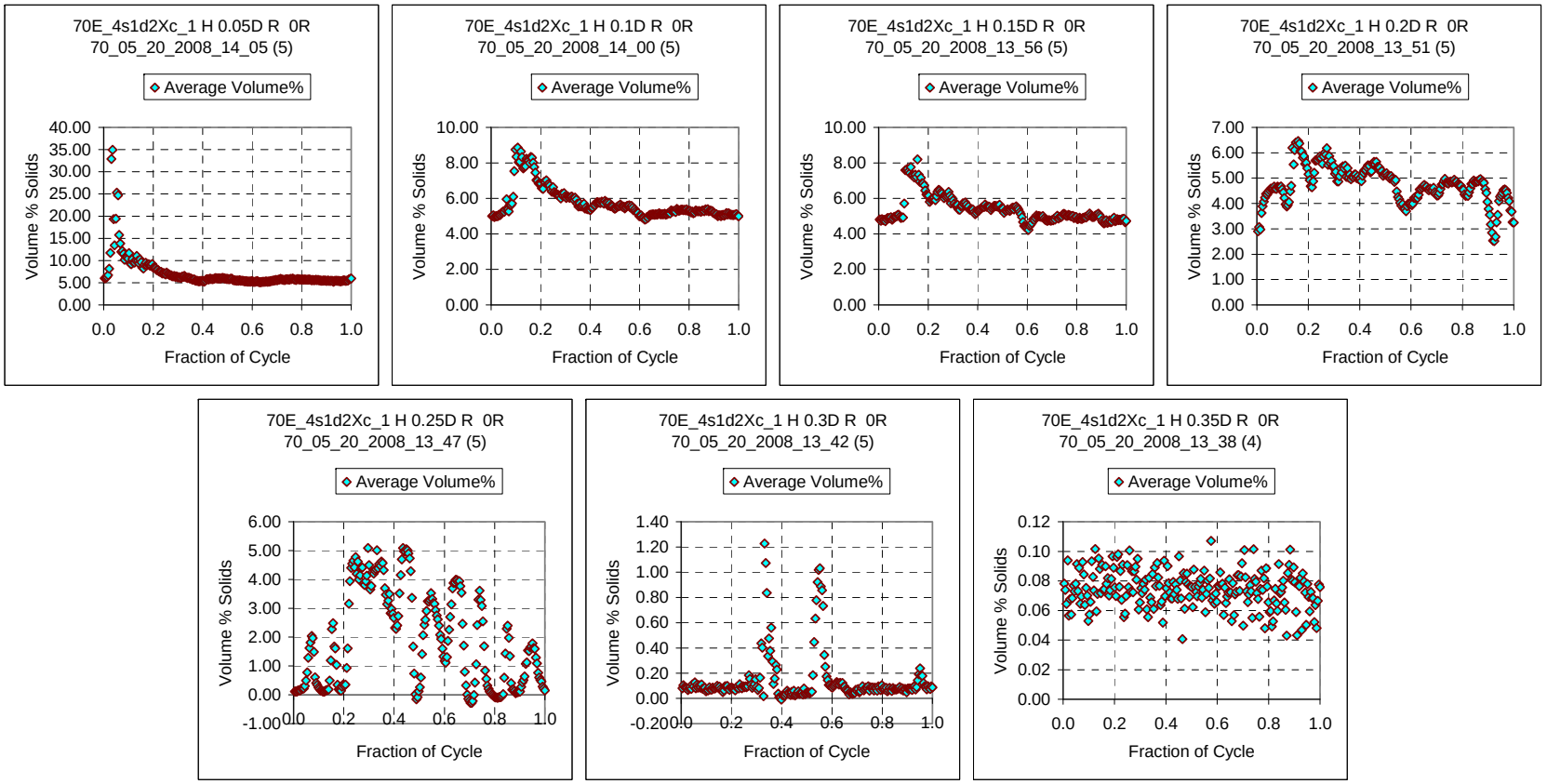

Figure C.54A. Case ID 70E_4s1d2Xc_1 Concentration Variation During the Cycle

Figure C.54 is the ninth of 12 profiles shown using simulant s1d2 in the large-scale tank with the elliptical bottom. This profile occurs at a velocity of 6.8 m/s, which is below the U_{CS} velocity of 8.5 m/s. The solids fraction was 0.015. The duty cycle was 32.9%. Figures C.55, C.56, and C.57 are a group of three similar profiles taken at the same conditions but at a higher velocity equal to the U_{CS} velocity. In the latter three figures, the duty cycle is 33.7%. For the lower velocity condition of Figure C.54, the peak cloud height upper bound was 22.5 in. This value was below the 42 in. obtained with the operating velocity equal to the velocity at U_{CS}.

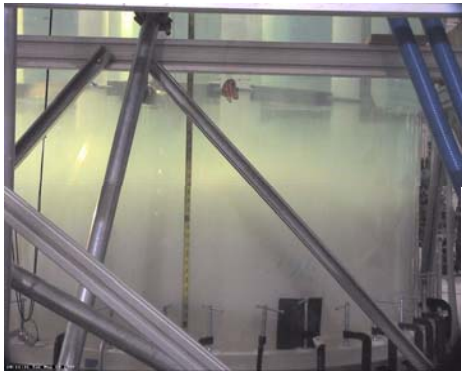

Maximum Cloud Height

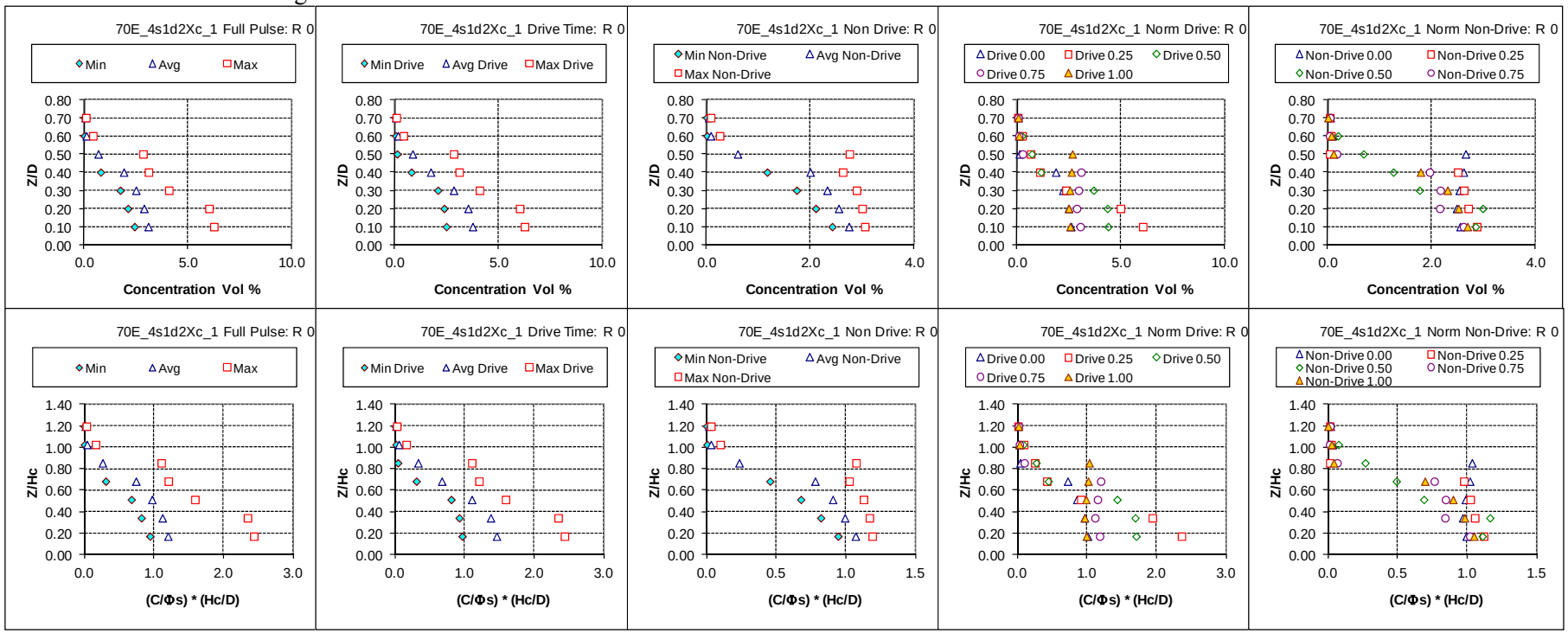

Figure C.55. 1.778-m- (70-in.-) diameter tank, 1.557-cm- (0.613-in.-) diameter nozzle; solids nominal diameter 69.3 µm, 2.48 g/cm^3 density; 0.015 nominal solids fraction; 33.7% duty cycle, cycle time 35.4 s, pulse volume fraction 0.050, U_{CS} velocity 8.5 m/s, target nozzle exit velocity 8.5 m/s; peak cloud height upper bound 1.067 m (42 in.). Case ID 70E_4s1d2Xc_1.

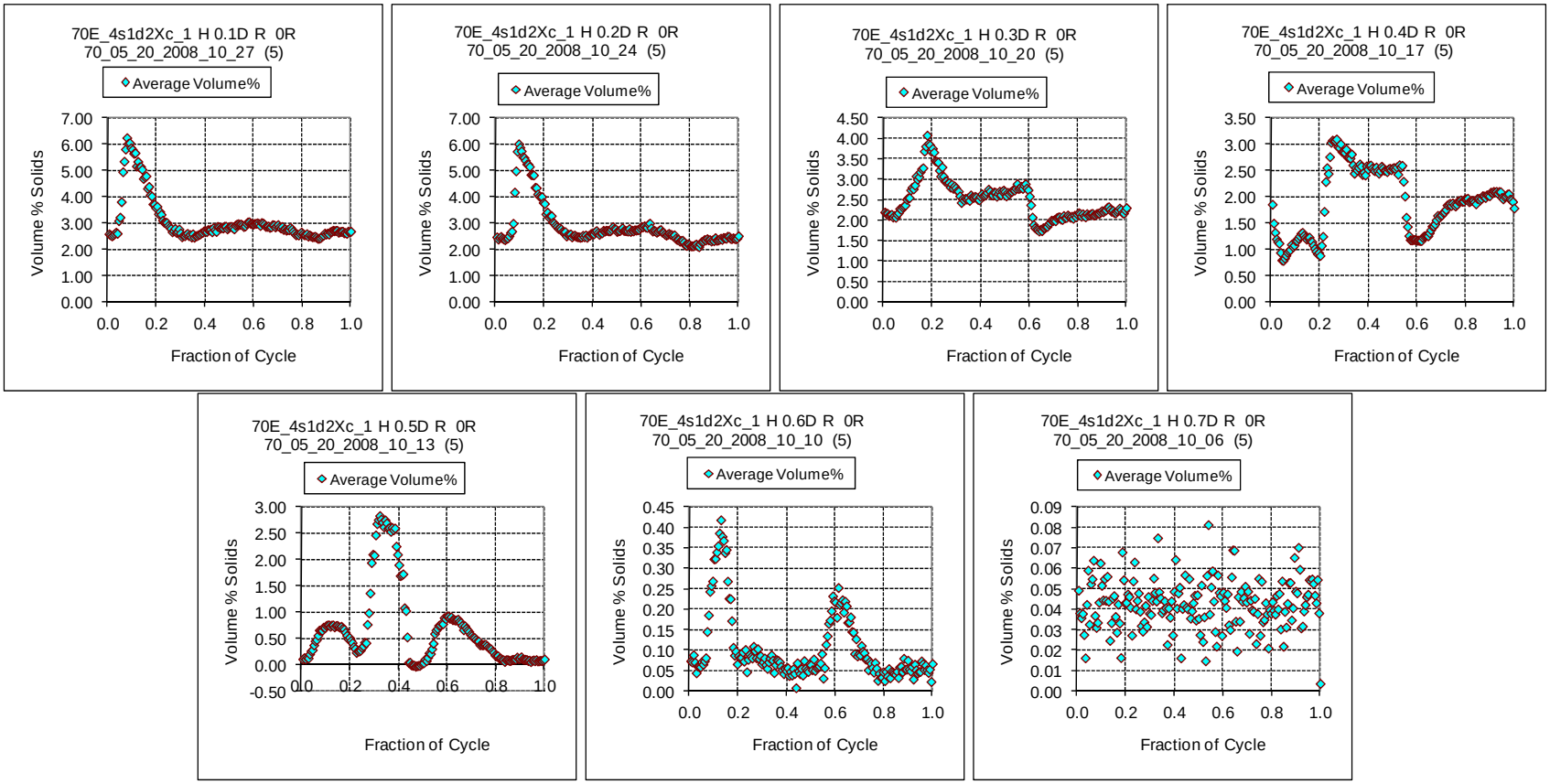

Figure C.55A. Case ID 70E_4s1d2Xc_1 R 0 Concentration Variation During the Cycle

Figure C.55 is the tenth of 12 profiles shown using simulant s1d2 in the large-scale tank with the elliptical bottom. Figures C.55, C.56, and C.57 are a group of three profiles taken at the same flow conditions and differing radial locations. The solids fraction was 0.015, a slight increase from 0.0143 shown in the prior profile groups. The duty cycle was 33.7%, similar to the 33.3% shown in Figures C.51, C.52, and C.53, also a set of three radial profiles. The U_{CS} velocity occurred at 8.5 m/s, a slight increase from 7.8 m/s shown for the prior three profiles. These measurements were taken at U_{CS}. The peak cloud height upper bound was 42 in. Figure C.55 shows a profile at the center of the tank with R = 0. When the radial profiles in Figures C.55 through C.57 are compared, the concentrations are shown to decline slightly with radius. The concentration decreases with elevation in all three radial locations. The concentration at radial location R = 0.9 was lower than at R = 0.5, which was in turn lower than at R = 0 when compared at equal elevations.

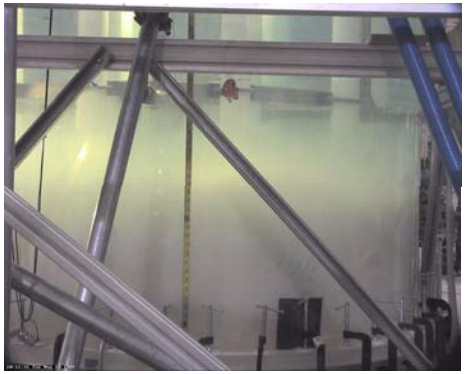

Maximum Cloud Height

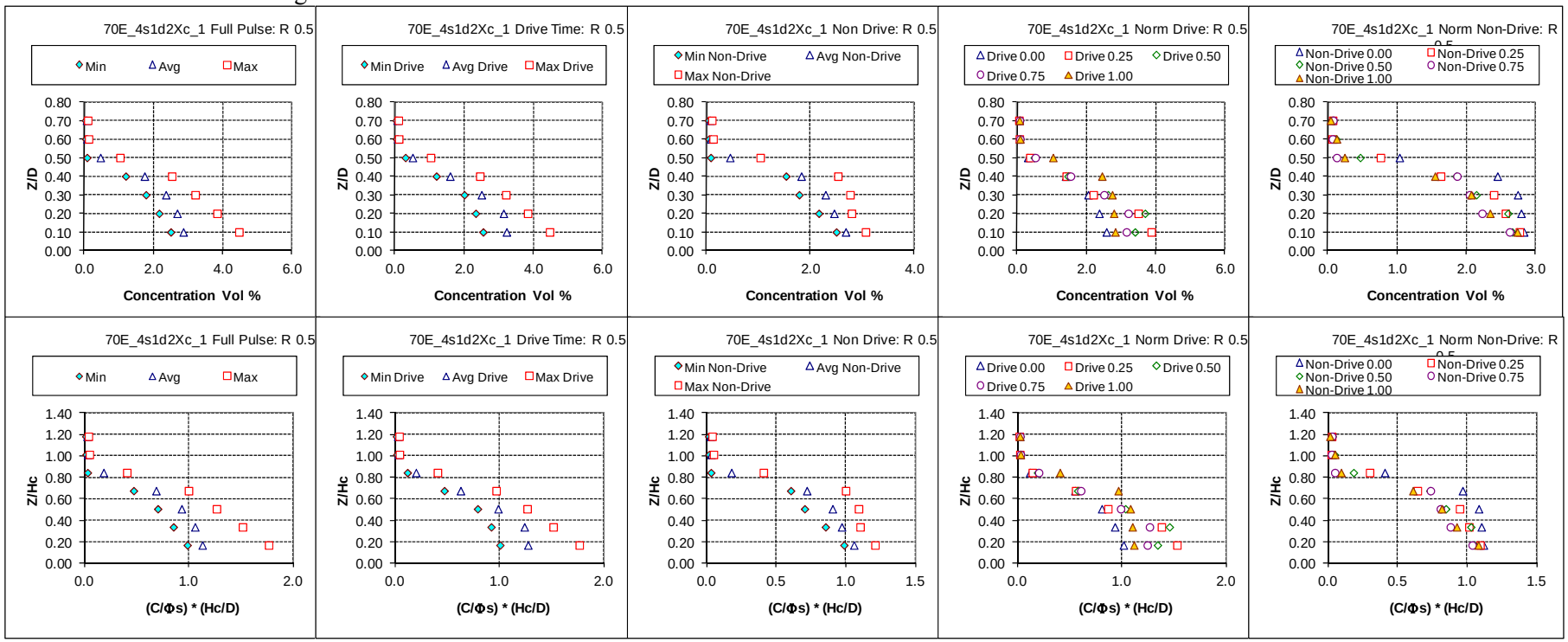

Figure C.56. 1.778-m- (70-in.-) diameter tank, 1.557-cm- (0.613-in.-) diameter nozzle; solids nominal diameter 69.3 µm, 2.48 g/cm^3 density; 0.015 nominal solids fraction; 33.7% duty cycle, cycle time 35.4 s, pulse volume fraction 0.050, U_{CS} velocity 8.5 m/s, target nozzle exit velocity 8.5 m/s; peak cloud height upper bound 1.067 m (42 in.). Case ID 70E_4s1d2Xc_1.

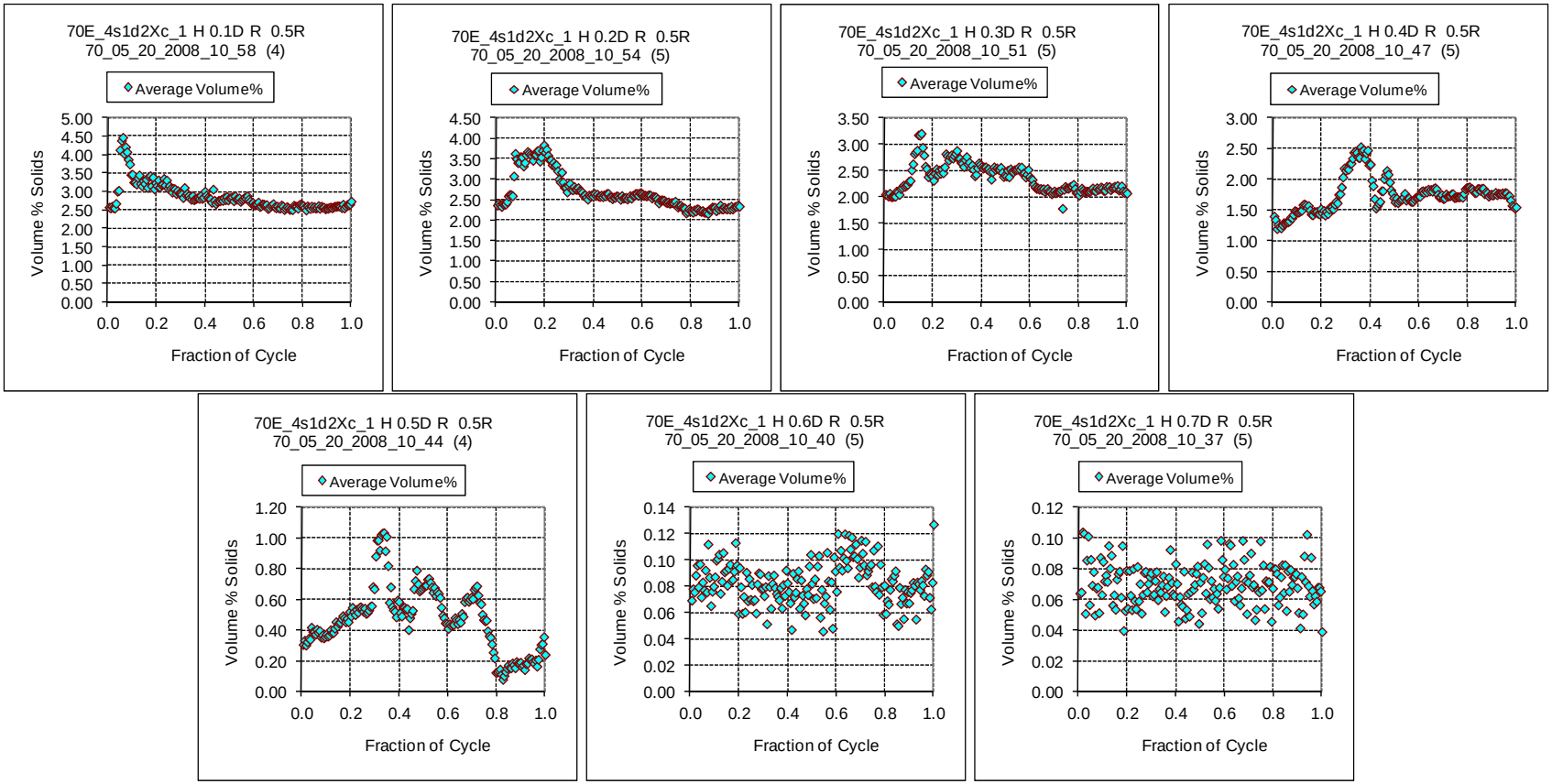

Figure C.56A. Case ID 70E_4s1d2Xc_1 R 0.5 Concentration Variation During the Cycle

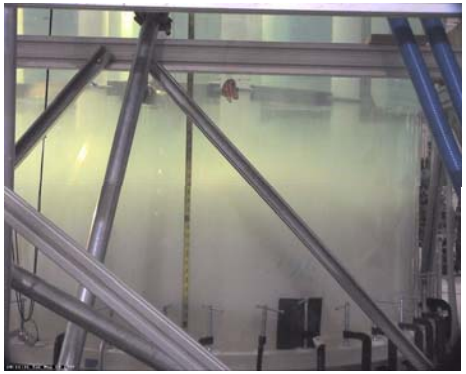

Maximum Cloud Height

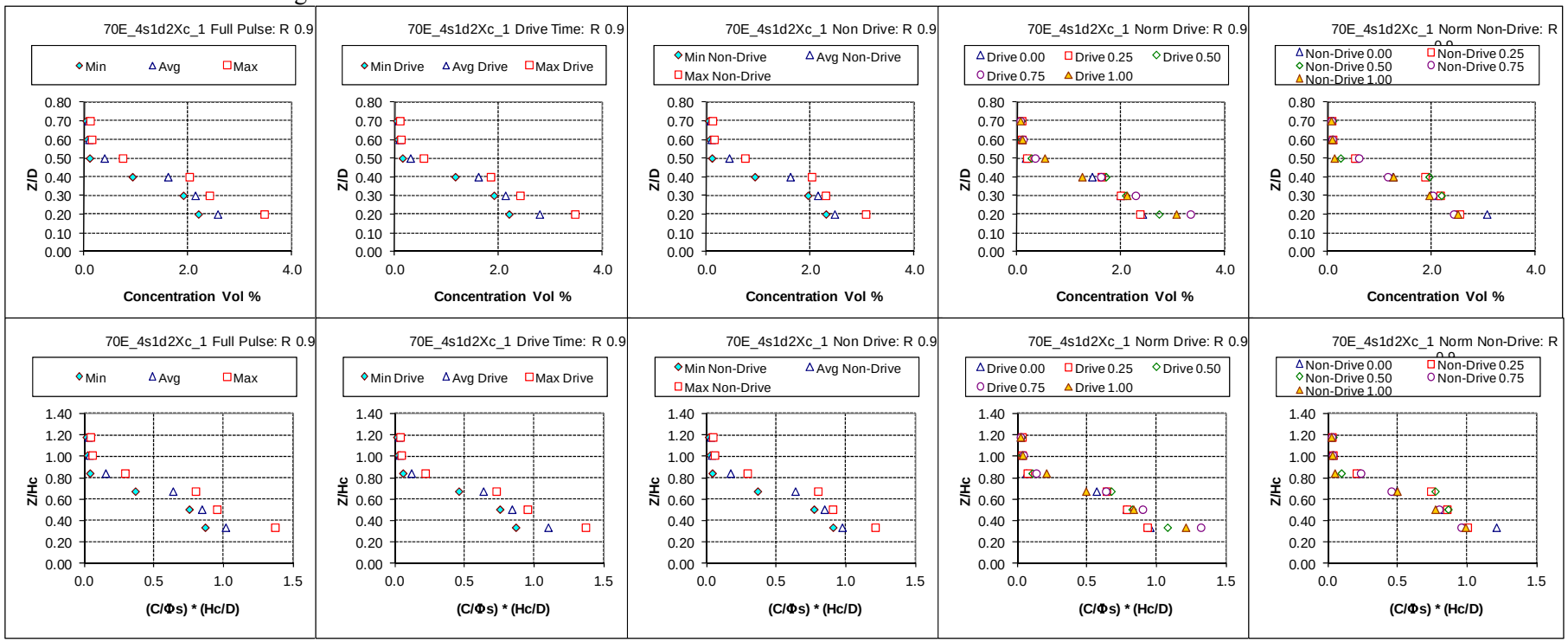

Figure C.57. 1.778-m- (70-in.-) diameter tank, 1.557-cm- (0.613-in.-) diameter nozzle; solids nominal diameter 69.3 µm, 2.48 g/cm^3 density; 0.015 nominal solids fraction; 33.7% duty cycle, cycle time 35.4 s, pulse volume fraction 0.050, U_{CS} velocity 8.5 m/s, target nozzle exit velocity 8.5 m/s; peak cloud height upper bound 1.067 m (42 in.). Case ID 70E_4s1d2Xc_1.

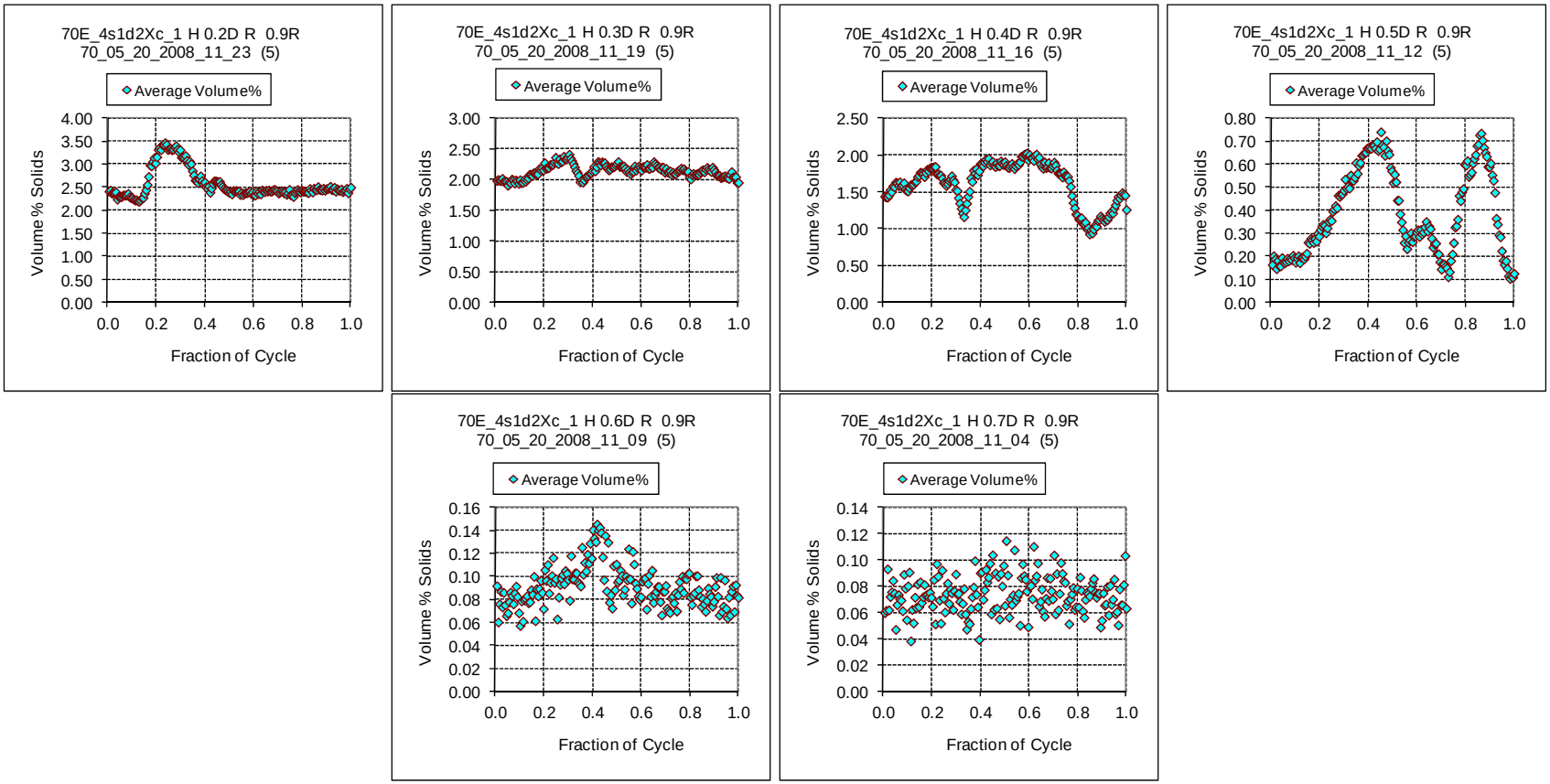

Figure C.57A. Case ID 70E_4s1d2Xc_1 R 0.9 Concentration Variation During the Cycle

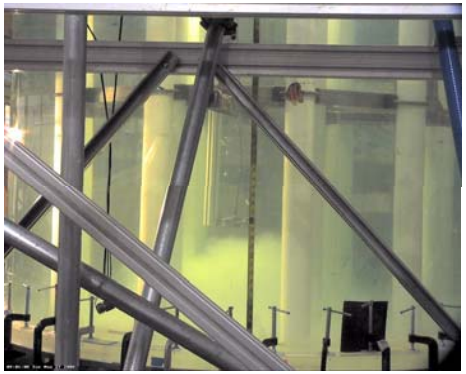

Maximum Cloud Height

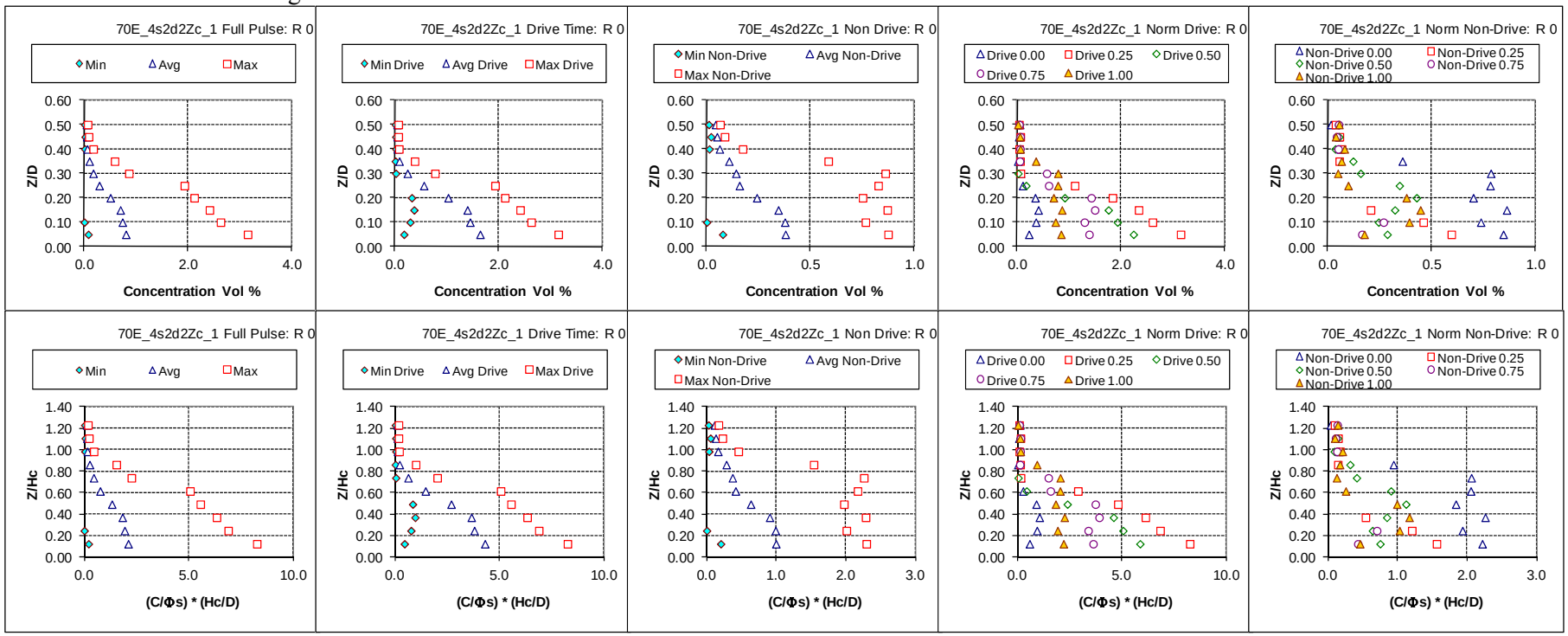

Figure C.58. 1.778-m- (70-in.-) diameter tank, 1.557-cm- (0.613-in.-) diameter nozzle; solids nominal diameter 75.6 µm, 4.18 g/cm^3 density; 0.00155 nominal solids fraction; 33.9% duty cycle, cycle time 35.6 s, pulse volume fraction 0.050, U_{CS} velocity 8.4 m/s, target nozzle exit velocity 8.4 m/s; peak cloud height upper bound 0.737 m (29 in.). Case ID 70E_4s2d2Zc_1.

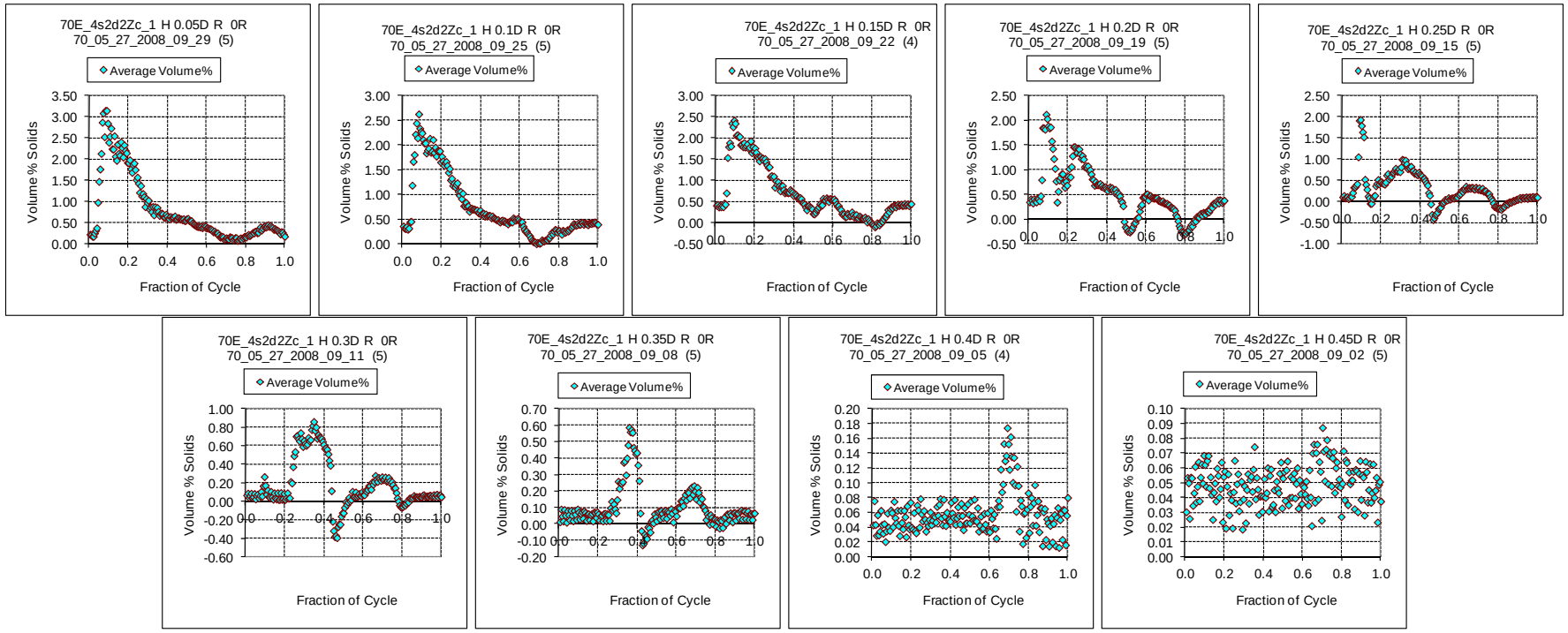

Figure C.58A. Case ID 70E_4s2d2Zc_1 Concentration Variation During the Cycle

Figure C.58 is the first of four profiles shown using simulant s2d2 in the large-scale tank with the elliptical bottom. Figure C.58 shows a profile at the center of the tank with R = 0. The solids fraction was 0.00155. The duty cycle was 33.9%. The pulse volume fraction was 0.050. The U_{CS} velocity occurred at 8.4 m/s, the velocity at which the profile was taken. The peak cloud height upper bound was 29 in. This profile can be compared with Figure C.46, which had similar conditions using simulant s1d2. There the U_{CS} velocity was 4.6 m/s, the target nozzle exit velocity was 4.6 m/s, and the peak cloud height upper bound was 31 in. The profiles for the two cases are very similar.

Maximum Cloud Height

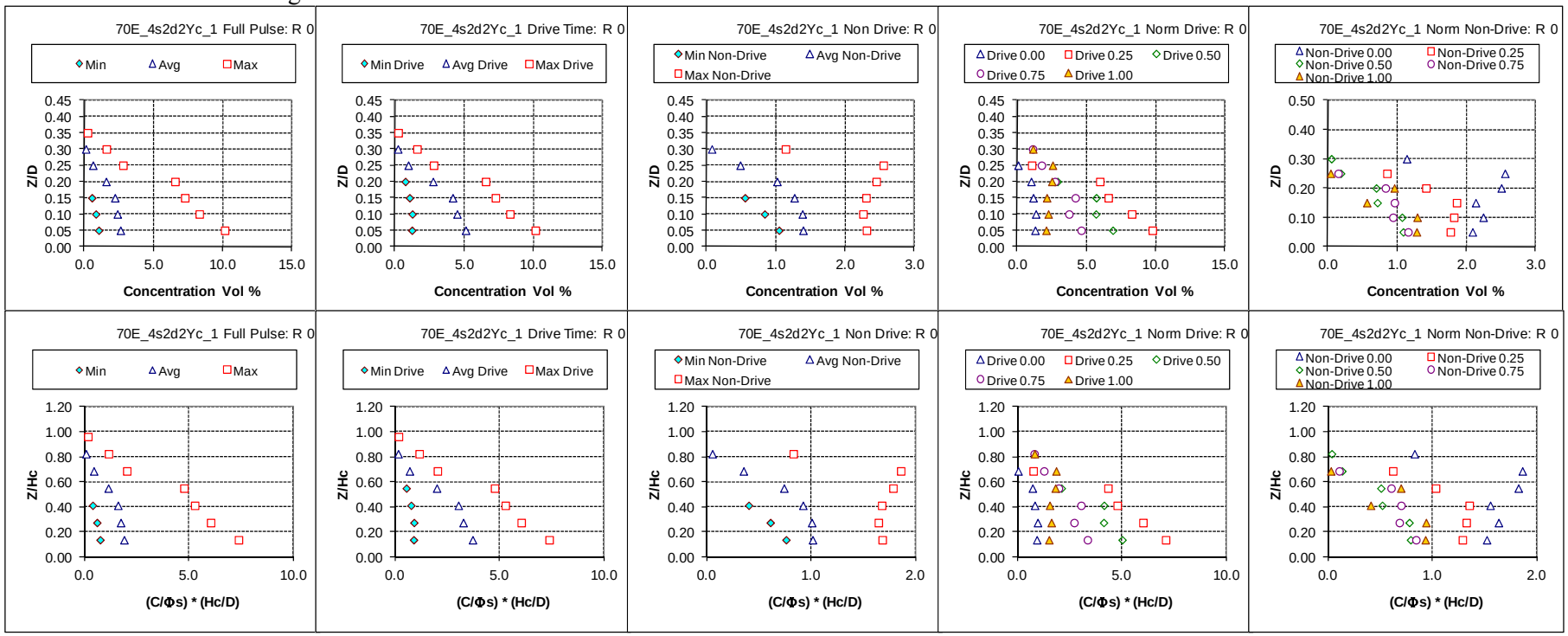

Figure C.59. 1.778-m- (70-in.-) diameter tank, 1.557-cm- (0.613-in.-) diameter nozzle; solids nominal diameter 75.6 µm, 4.18 g/cm^3 density; 0.005 nominal solids fraction; 32.8% duty cycle, cycle time 26.0 s, pulse volume fraction 0.050, U_{CS} velocity 12.5 m/s, target nozzle exit velocity 12 m/s; peak cloud height upper bound 0.660 m (26 in.). Case ID 70E_4s2d2Yc_1.

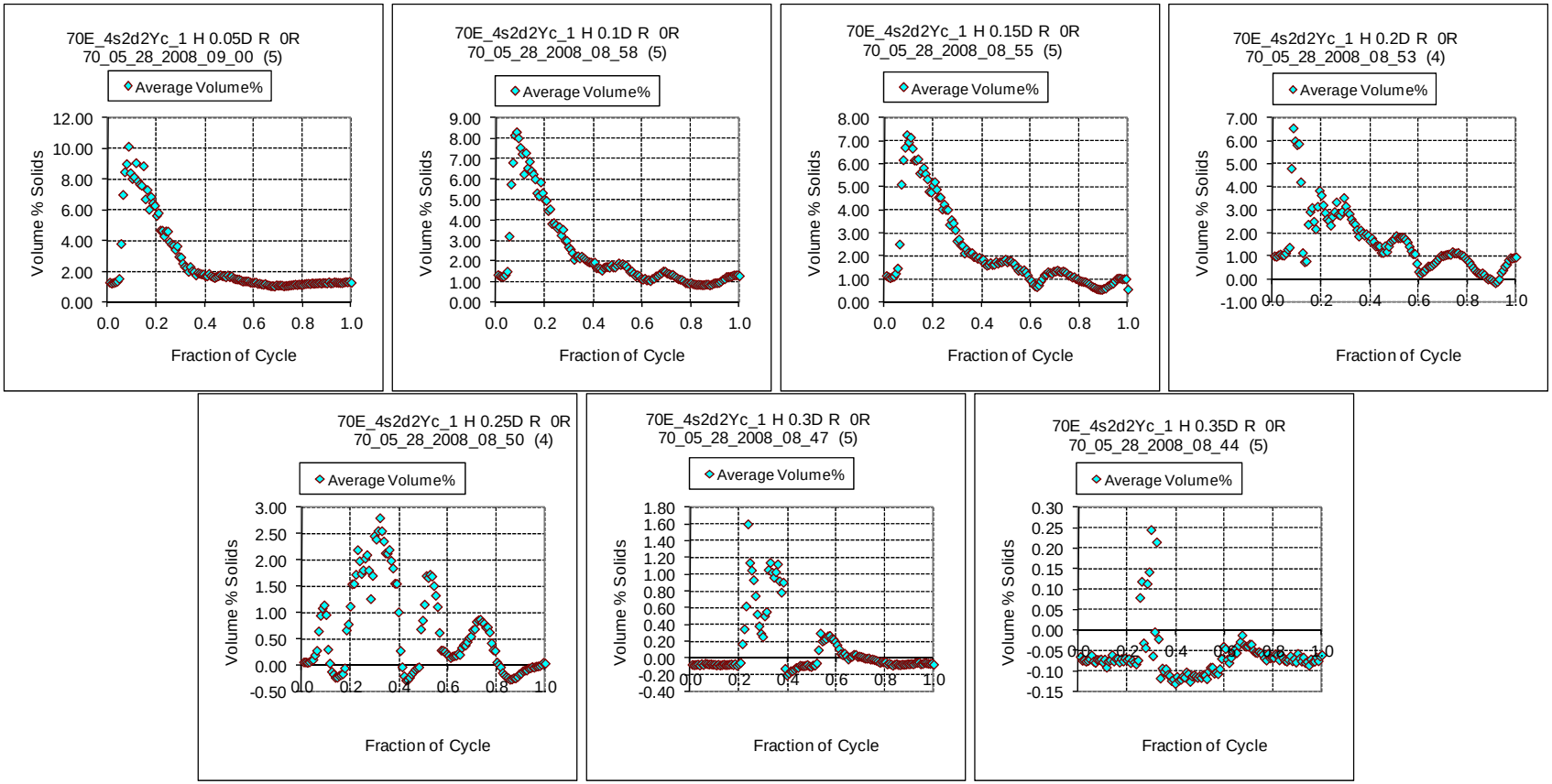

Figure C.59A. Case ID 70E_4s2d2Yc_1 R 0 Concentration Variation During the Cycle

Figure C.59 is the second of four profiles shown using simulant s2d2 in the large-scale tank with the elliptical bottom. Figures C.59, C.60, and C.61 are a group of three profiles taken at the same flow conditions and differing radial locations. For these cases, the solids fraction was 0.005. The duty cycle was 32.8%. The U_{CS} velocity occurred at 12.5 m/s; however, the velocity for these profiles was slightly below U_{CS} at 12 m/s. The peak cloud height upper bound was 26 in. Figure C.50 shows a profile at the center of the tank with R = 0. When the radial profiles are compared, the concentration was seen to decrease as radius increases.

Maximum Cloud Height

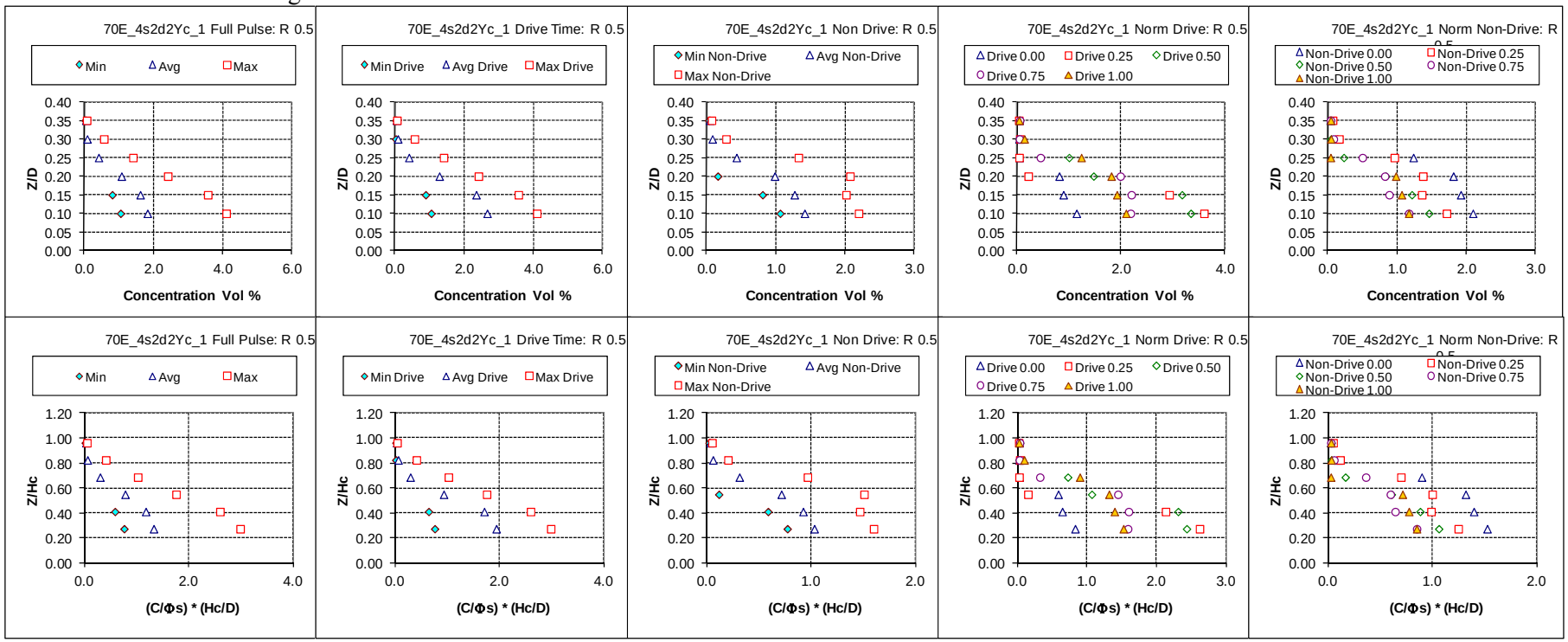

Figure C.60. 1.778-m- (70-in.-) diameter tank, 1.557-cm- (0.613-in.-) diameter nozzle; solids nominal diameter 75.6 µm, 4.18 g/cm^3 density; 0.005 nominal solids fraction, 32.8% duty cycle, cycle time 26.0 s, pulse volume fraction 0.050, U_{CS} velocity 12.5 m/s, target nozzle exit velocity 12 m/s; peak cloud height upper bound 0.660 m (26 in.). Case ID 70E_4s2d2Yc_1.

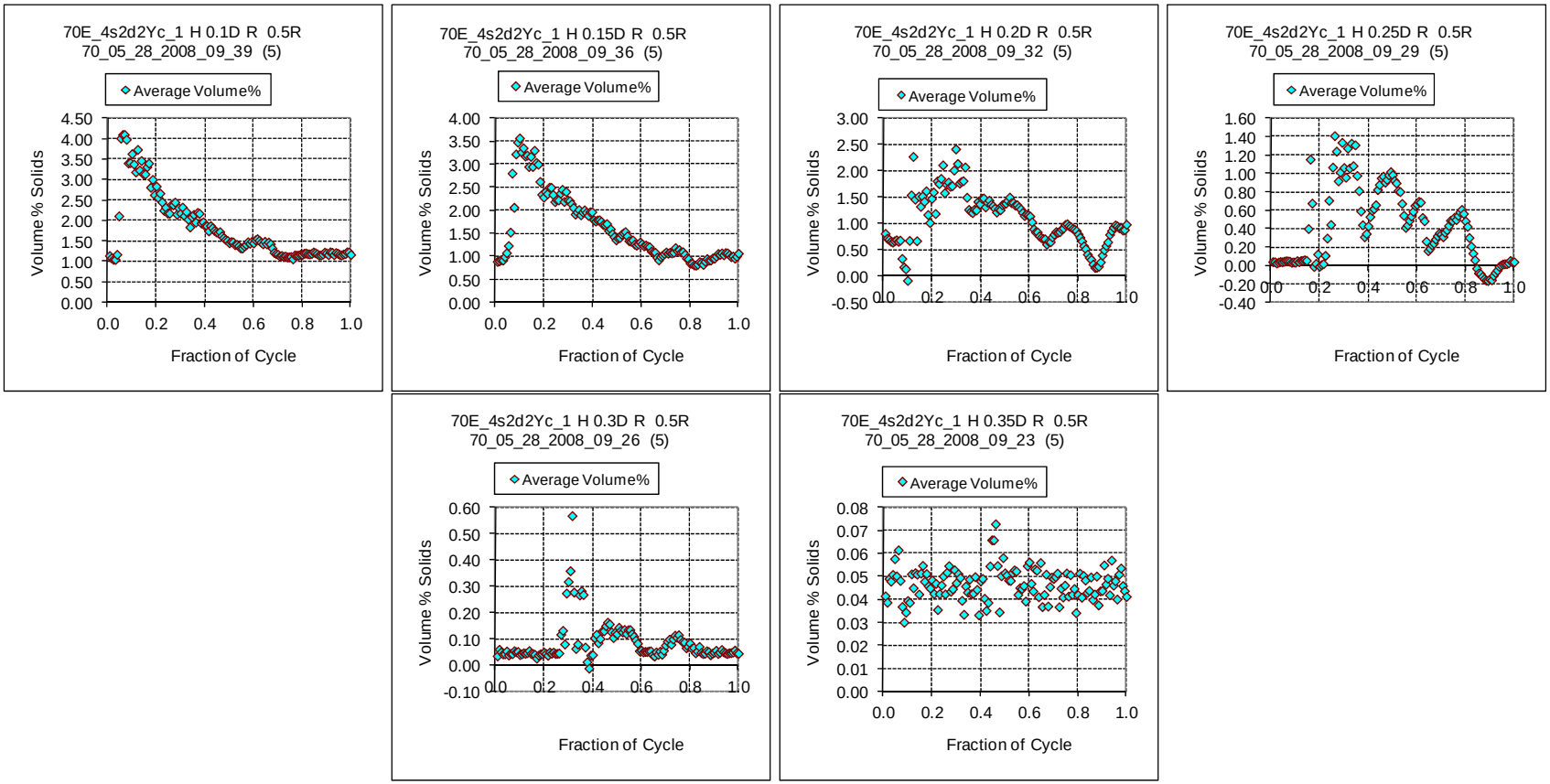

Figure C.60A. Case ID 70E_4s2d2Yc_1 R 0.5 Concentration Variation During the Cycle

Maximum Cloud Height

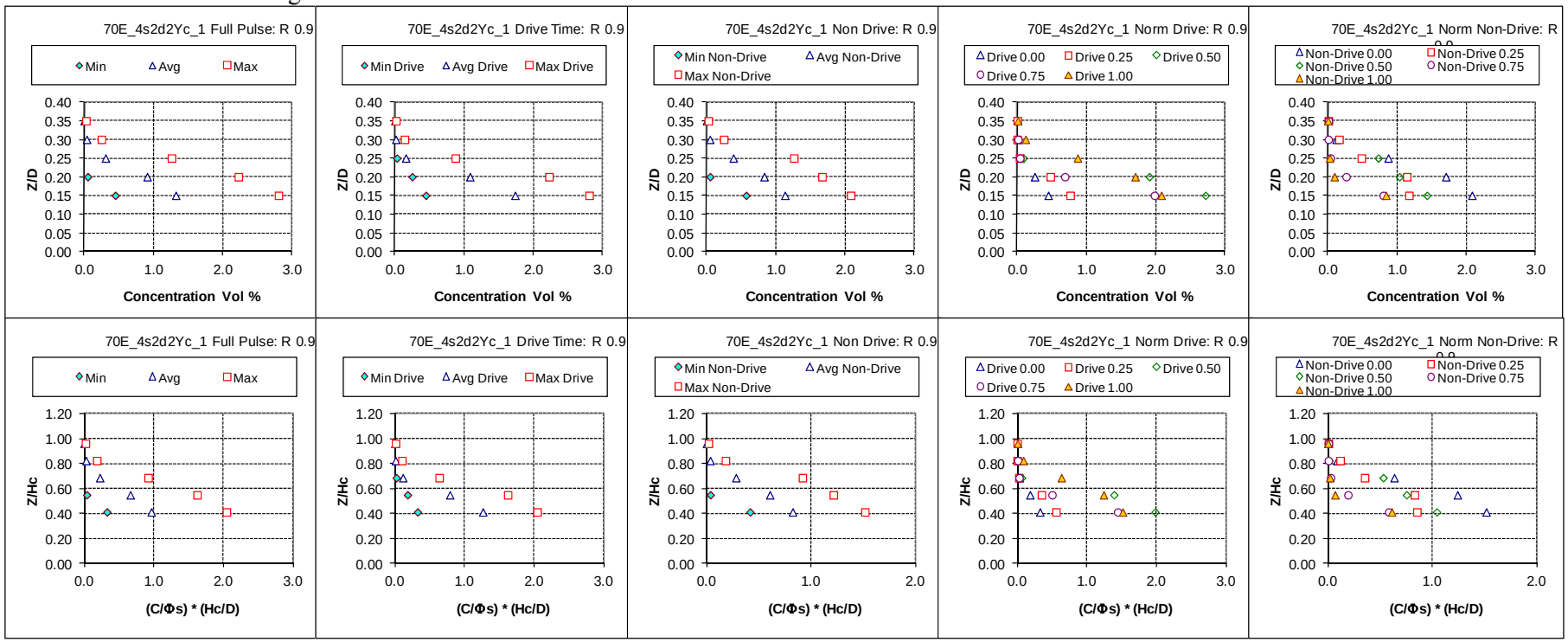

Figure C.61. 1.778-m- (70-in.-) diameter tank, 1.557-cm- (0.613-in.-) diameter nozzle; solids nominal diameter 75.6 µm, 4.18 g/cm^3 density; 0.005 nominal solids fraction; 32.8% duty cycle, cycle time 26.0 s, pulse volume fraction 0.050, U_{CS} velocity 12.5 m/s, target nozzle exit velocity 12 m/s; peak cloud height upper bound 0.660 m (26 in.). Case ID 70E_4s2d2Yc_1.

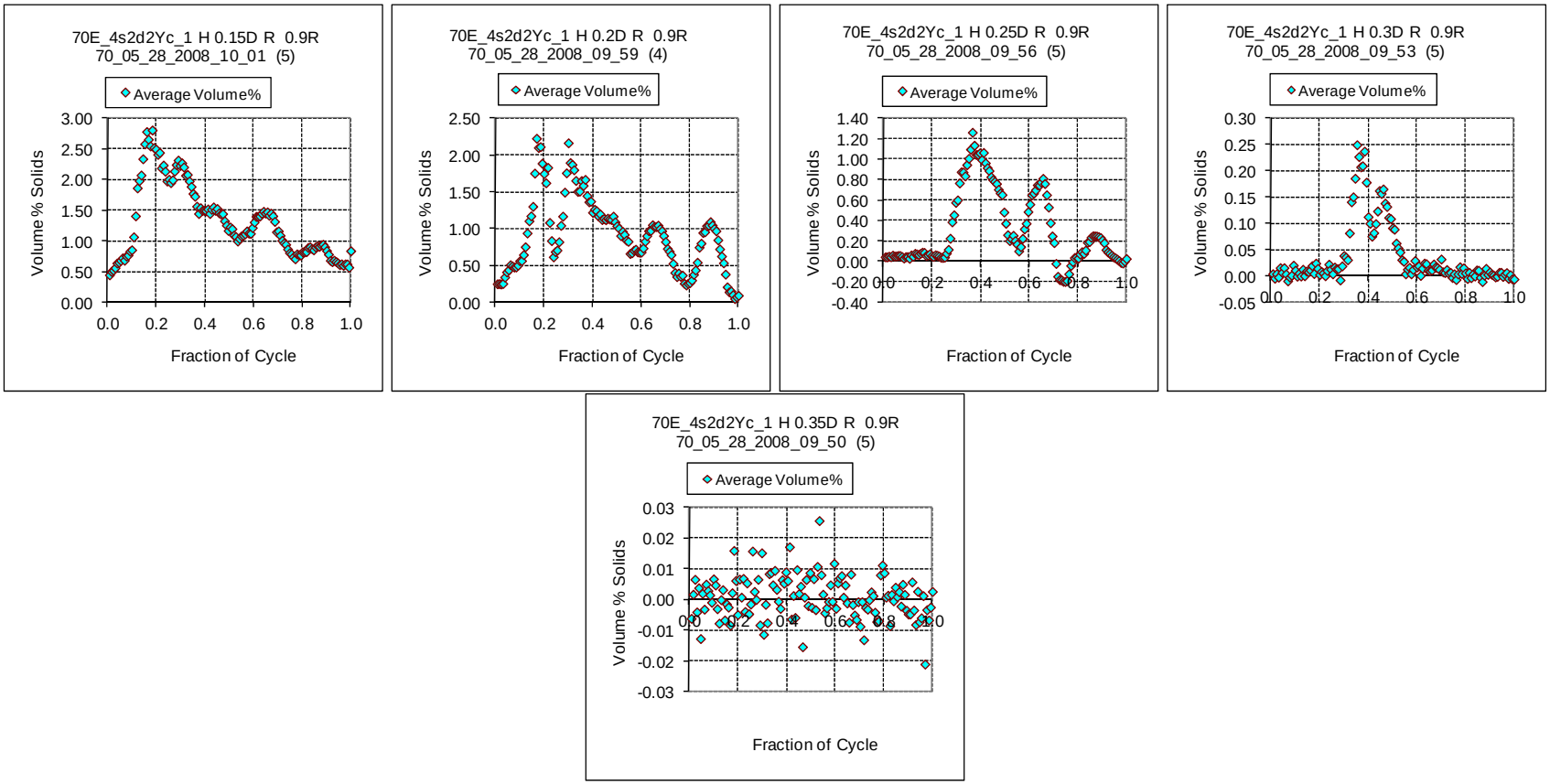

Figure C.61A. Case ID 70E_4s2d2Yc_1 R 0.9 Concentration Variation During the Cycle

Maximum Cloud Height

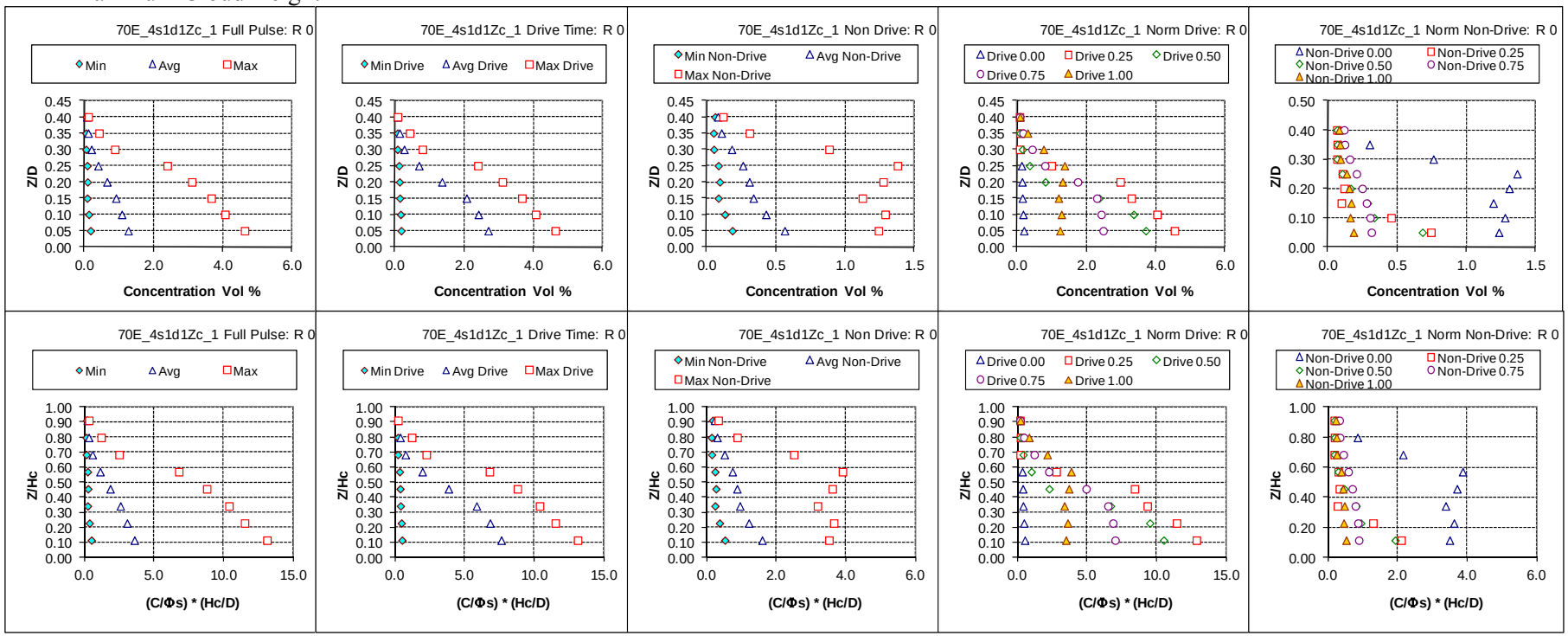

Figure C.62. 1.778-m- (70-in.-) diameter tank, 1.557-cm- (0.613-in.-) diameter nozzle; solids nominal diameter 166.4 µm, 2.46 g/cm^3 density; 0.00155 nominal solids fraction; 33.4% duty cycle, cycle time 42.6 s, pulse volume fraction 0.050, U_{CS} velocity 7.1 m/s, target nozzle exit velocity 7.1 m/s; peak cloud height upper bound 0.800 m (31.5 in.). Case ID 70E_4s1d1Zc_1.

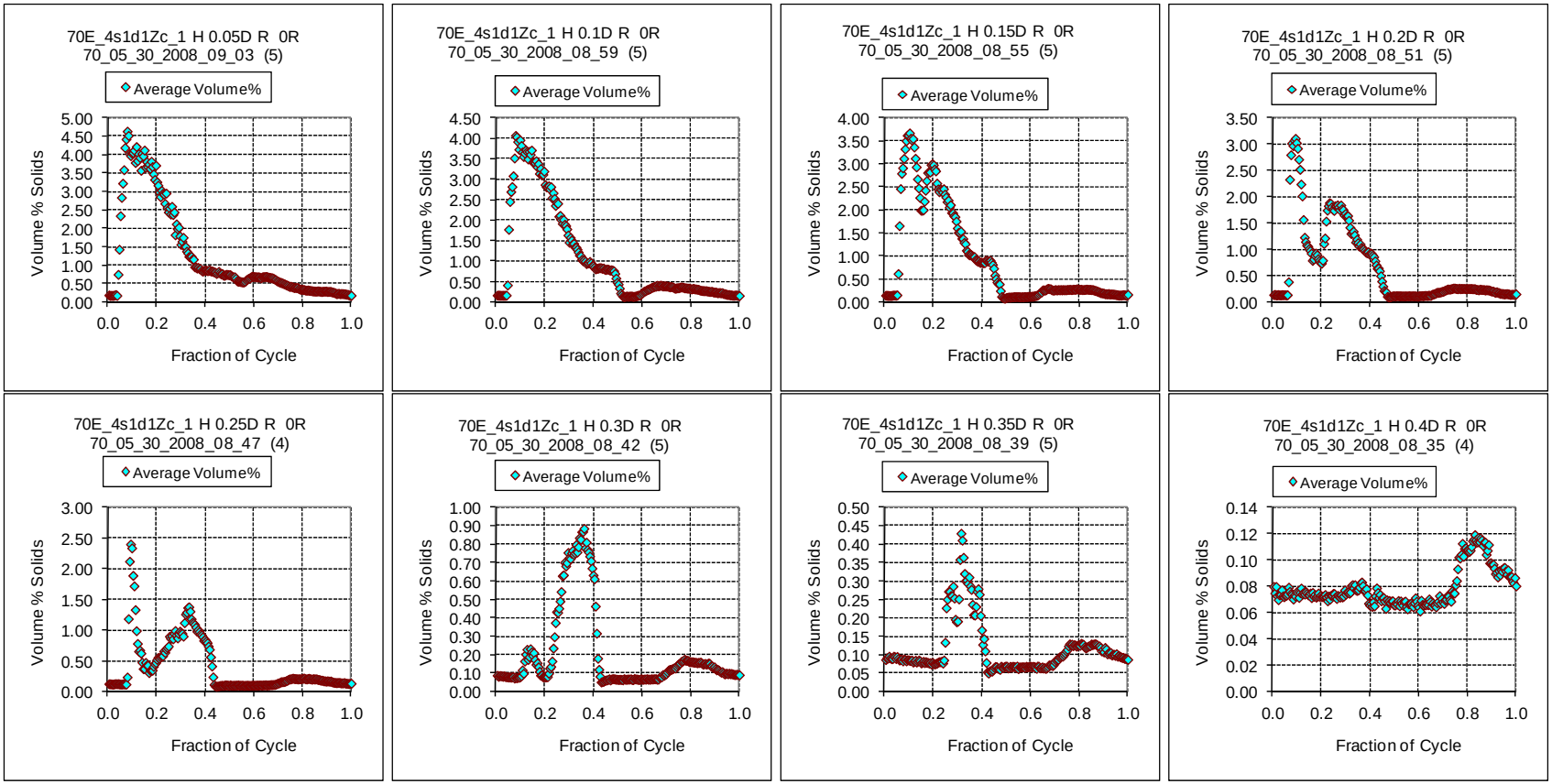

Figure C.62A. Case ID 70E_4s1d1Zc_1 R 0 Concentration Variation During the Cycle

Figure C.62 is the first of three profiles shown using simulant s1d1 in the large-scale tank with the elliptical bottom. Figures C.62, C.63, and C.64 are a group of three profiles taken at the same flow conditions and differing radial locations. For these cases, the solids fraction was 0.00155. The duty cycle was 33.4%. The U_{CS} velocity occurred at 7.1 m/s and these measurements were made at the U_{CS} velocity. The peak cloud height upper bound was 31.5 in. Figure C.62 shows a profile at the center of the tank with R = 0. When the radial profiles are compared, the concentration was seen to decrease as radius increases.

Maximum Cloud Height

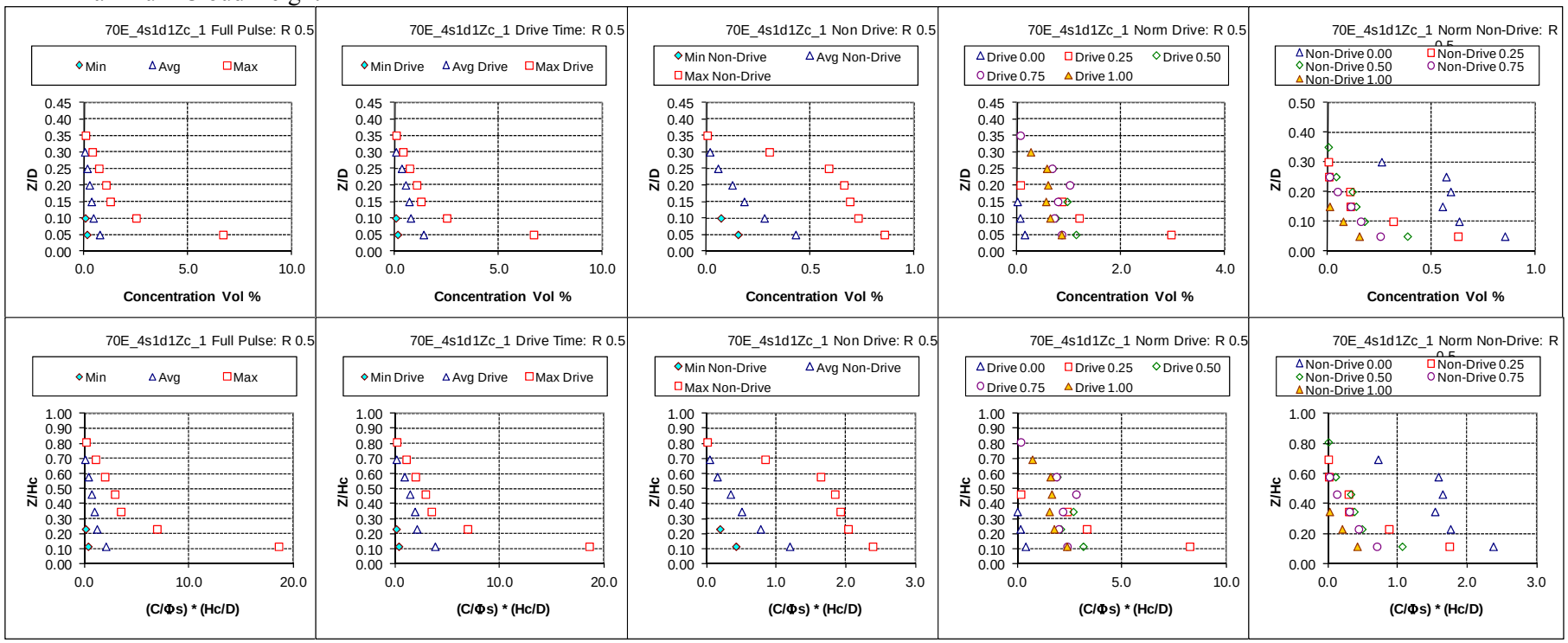

Figure C.63. 1.778-m- (70-in.-) diameter tank, 1.557-cm- (0.613-in.-) diameter nozzle; solids nominal diameter 166.4 µm, 2.46 g/cm^3 density; 0.00155 nominal solids fraction; 33.4% duty cycle, cycle time 42.6 s, pulse volume fraction 0.050, U_{CS} velocity 7.1 m/s, target nozzle exit velocity 7.1 m/s; peak cloud height upper bound 0.800 m (31.5 in.). Case ID 70E_4s1d1Zc_1.

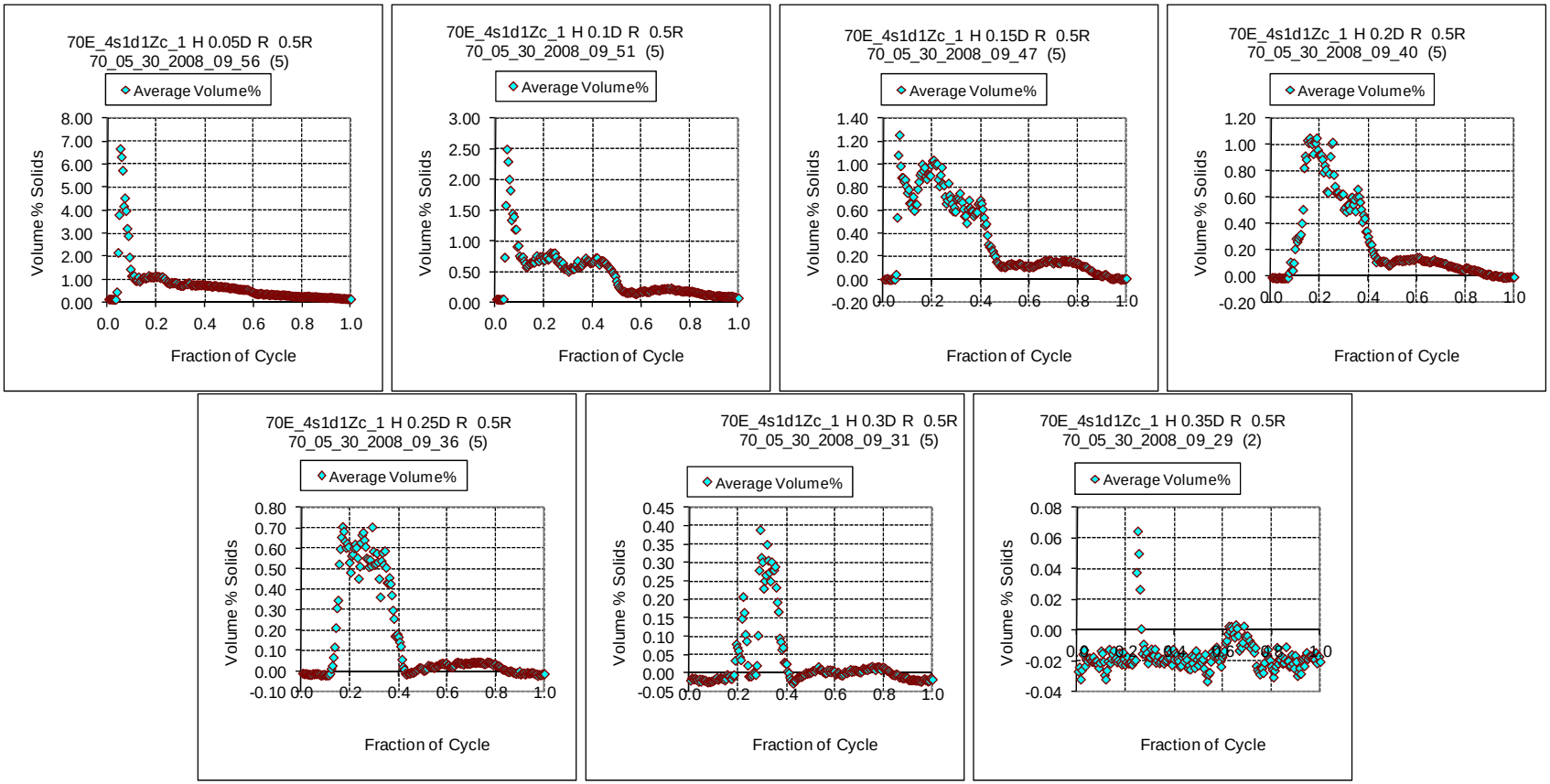

Figure C.63A. Case ID 70E_4s1d1Zc_1 R 0.5 Concentration Variation During the Cycle

Maximum Cloud Height

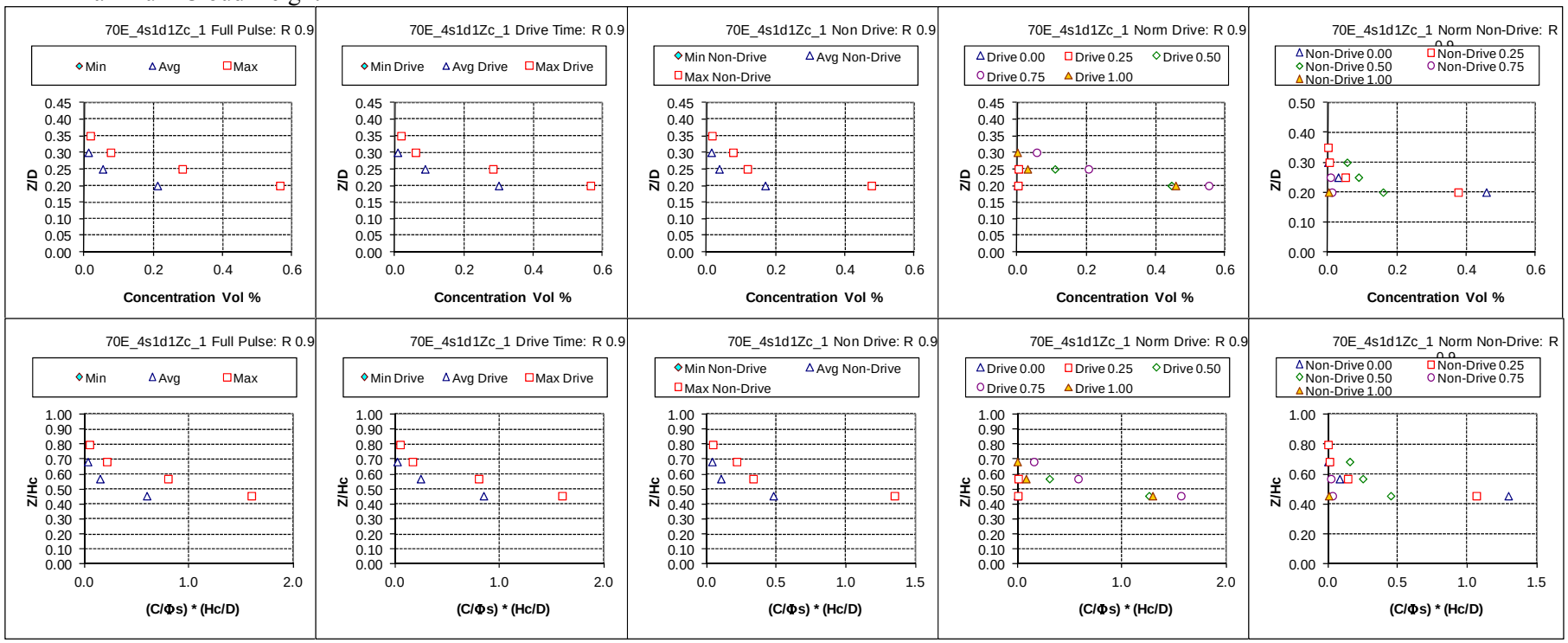

Figure C.64. 1.778-m- (70-in.-) diameter tank, 1.557-cm- (0.613-in.-) diameter nozzle; solids nominal diameter 166.4 µm, 2.46 g/cm^3 density; 0.00155 nominal solids fraction; 33.4% duty cycle, cycle time 42.6 s, pulse volume fraction 0.050, U_{CS} velocity 7.1 m/s, target nozzle exit velocity 7.1 m/s; peak cloud height upper bound 0.800 m (31.5 in.). Case ID 70E_4s1d1Zc_1.

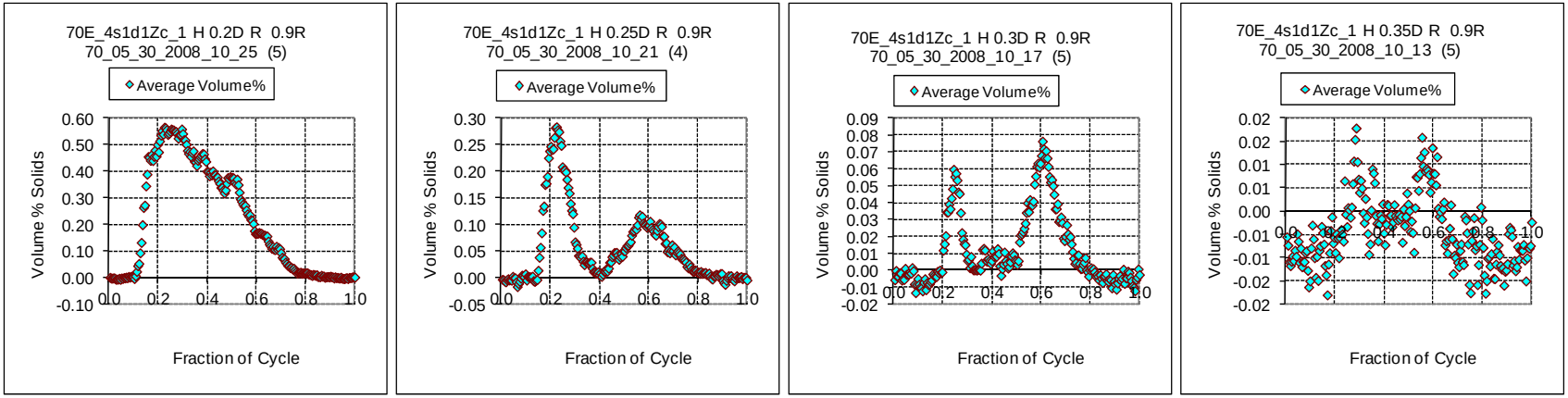

Figure C.64A. Case ID 70E_4s1d1Zc_1 R 0.9 Concentration Variation During the Cycle

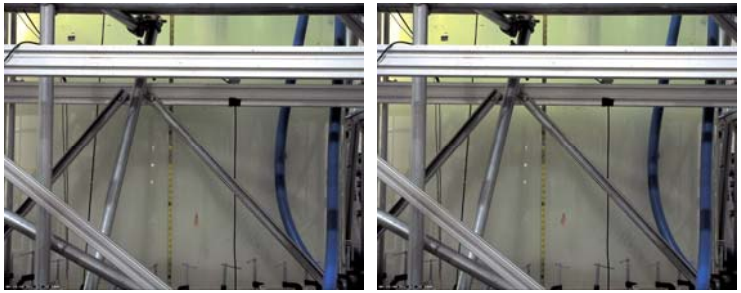

Maximum Cloud Height Minimum Cloud Height

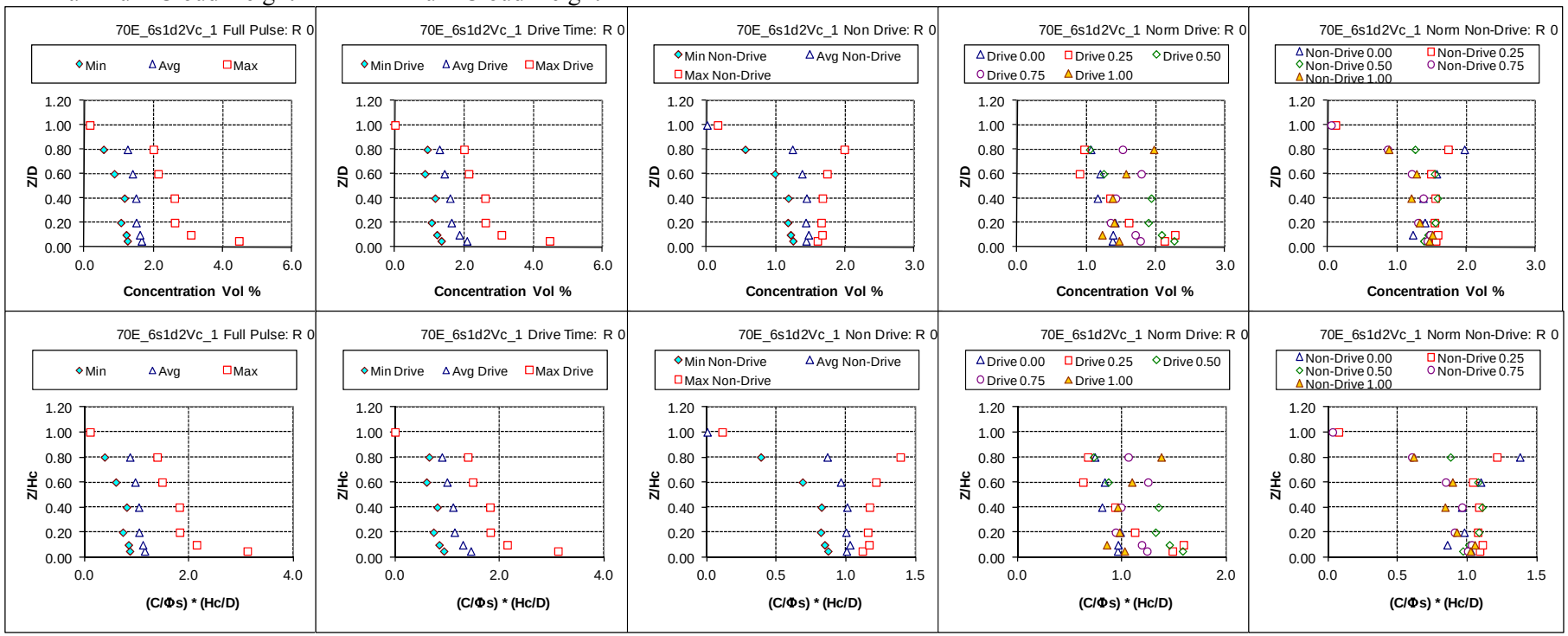

Figure C.65. 1.778-m- (70-in.-) diameter tank, 2.337-cm- (0.92-in.-) diameter nozzle; solids nominal diameter 69.3 µm, 2.48 g/cm^3 density; 0.0143 nominal solids fraction; 33.5% duty cycle, cycle time 29.6 s, pulse volume fraction 0.050, U_{CS} velocity 6.8 m/s, target nozzle exit velocity 6.8 m/s; peak cloud height upper bound 1.829 m (72 in.). Case ID 70E_6s1d2Vc_1.

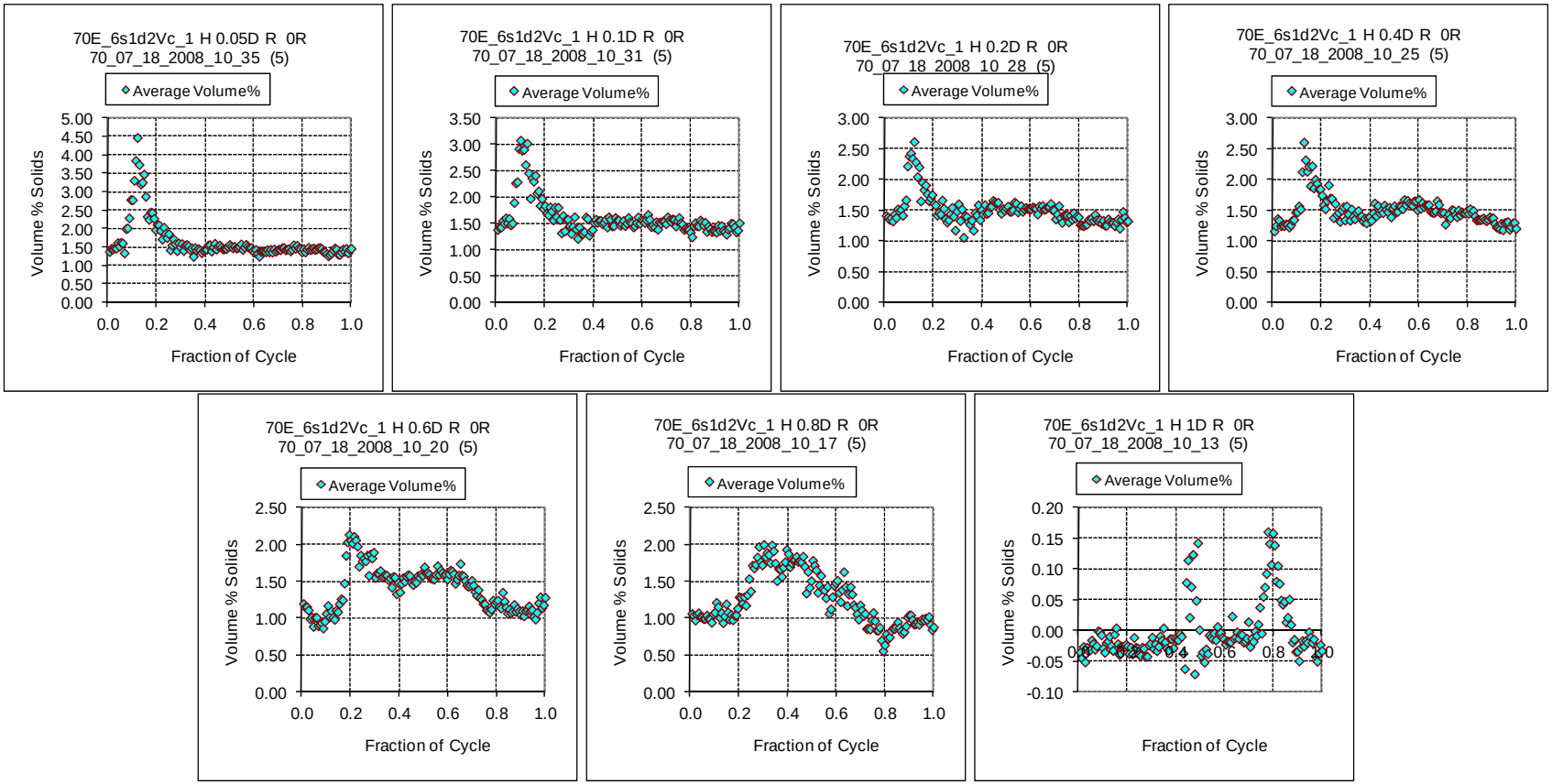

Figure C.65A. Case ID 70E_6s1d2Vc_1 Concentration Variation During the Cycle

Figure C.65 is the first of two profiles shown using simulant s1d2 in the large-scale tank with the elliptical bottom configured with the 8TA pulse tube design, with four pulse tubes in the outer ring and four pulse tubes in the inner and a nozzle diameter of 0.92 in. (equivalent to 6 in. at full scale). For these cases, the solids fraction was 0.0143. The duty cycle was 33.5% and the pulse volume fraction was 0.050. The U_{CS} velocity occurred at 6.8 m/s and the profile was conducted at a velocity equal to the U_{CS} velocity. The peak cloud height upper bound was 72 in. This profile can be compared with the profile shown in Figure C. 51, configured for the HLP-22 pulse tube design with eight pulse tubes in the outer ring and four pulse tubes in the inner ring and a nozzle diameter of 0.613 in. (equivalent to 4 in. full scale). In the 8TA test, the solids concentration at R = 0 was nearly constant at ~1.8 vol% solids up to an elevation of Z/D = 0.8. The profile shown in Figure C.51 does not show quite the same vertical behavior. In the latter case, the solids concentration at R = 0 was ~3.6 vol% solids at Z/D = 0.05 and drops to ~2 vol% solids at Z/D = 0.4 and it approaches 0 vol% solids at Z/D = 0.6.

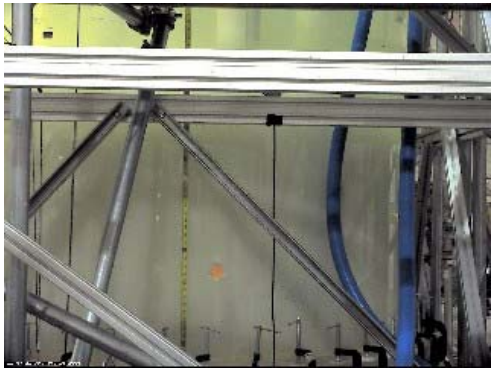

Maximum Cloud Height

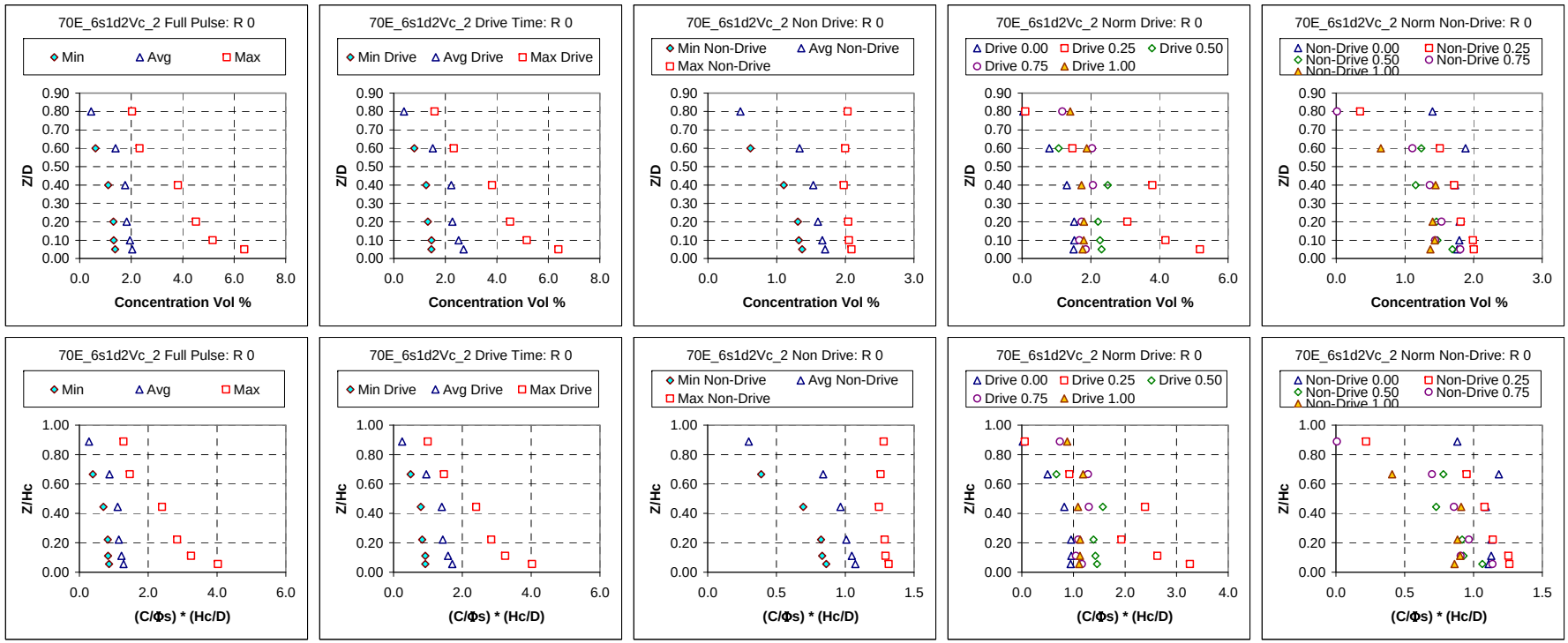

Figure C.66. 1.778-m- (70-in.-) diameter tank, 2.337-cm- (0.92-in.-) diameter nozzle; solids nominal diameter 69.3 µm, 2.48 g/cm^3 density; 0.0143 nominal solids fraction; 33.1% duty cycle, cycle time 61.8 s, pulse volume fraction 0.100, U_{CS} velocity 6.4 m/s, target nozzle exit velocity 6.4 m/s; peak cloud height upper bound 1.626 m (64 in.). Case ID 70E_6s1d2Vc_2.

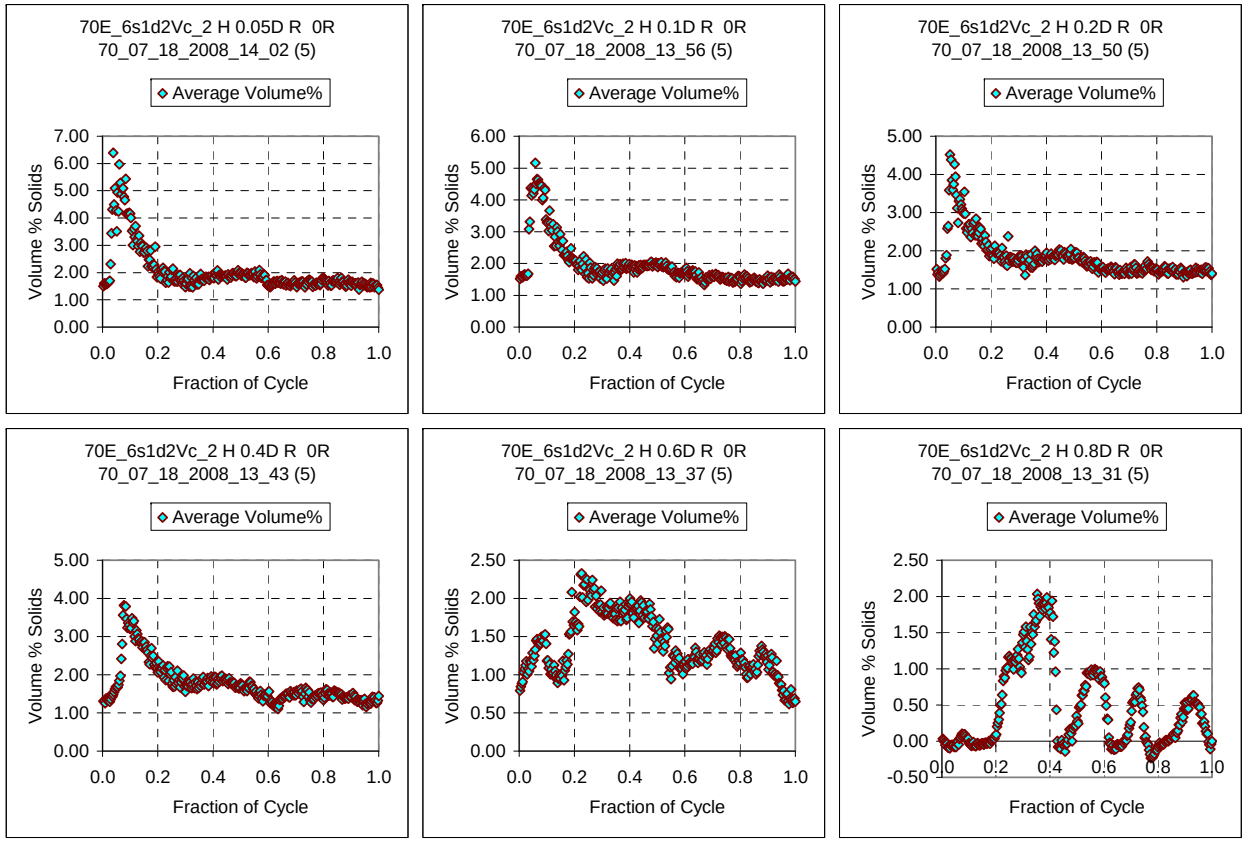

Figure C.66A. Case ID 70E_6s1d2Vc_2 Concentration Variation During the Cycle

Figure C.66 is the second of two profiles shown using simulant s1d2 in the large-scale tank with the elliptical bottom configured with the 8TA pulse tube design with four pulse tubes in the outer ring and four pulse tubes in the inner and a nozzle diameter of 0.92 in. (equivalent to 6 in. full scale). The solids fraction was 0.0143. The duty cycle was 33.1%. The pulse volume fraction was increased to 0.1, up from 0.05 from the prior test. The U_{CS} velocity occurred at 6.4 m/s, which was a decrease from 6.8 m/s in the prior test. The peak cloud height upper bound was 64 in., a decrease from 72 in. in the prior test. The solids concentration at R = 0 was not quite as constant as the profile in the prior test (which showed a constant concentration of ~1.8 vol% solids up to an elevation of Z/D = 0.8). In the current case, the solids concentration at R = 0 was ~2 vol% solids at Z/D = 0.05, drops to ~1.4 vol% solids at Z/D = 0.6, and drops to ~0.5 vol% solids at Z/D = 0.8.

Appendix D

Statistical Methods Used to Develop, Evaluate, and Validate Multiple-Regression Models

GF Piepel

Appendix D

Contents

D.1 Model Forms D.1

D.1.1 Nondimensional Models D.1

D.1.2 Multiple-Regression Model Forms D.2

D.1.3 Spurious Correlation D.3

D.2 Linear and Nonlinear Least-Squares Regression Methods and Assumptions for Fitting Models D.3

D.2.1 Linear and Nonlinear Regression D.4

D.2.2 Ordinary and Weighted Least Squares Regression D.5

D.3 Statistical Methods for Model Evaluation D.7

D.3.1 Notation for Regression Model Evaluation and Validation D.7

D.3.2 Methods for Evaluating Regression Models Fit to Experimental Data D.8

D.3.3 Formulas for Three R^2 Statistics D.11

D.4 Statistical Methods for Model Reduction and Augmentation D.13

D.4.1 Statistical Methods for Reducing Regression Models D.13

D.4.2 Statistical Methods for Adding Terms to Models D.13

D.5 Statistical Methods for Model Validation D.14

D.5.1 Validation R^2 ..... D.15

D.5.2 Validation RMSE D.15

D.5.3 Predicted Versus Measured Plots for Validation D.16

D.6 Statistical Intervals for Quantifying Uncertainties in Model Predictions D.16

D.6.1 One-Sided Confidence Intervals D.17

D.6.2 Two-Sided Confidence Interval D.18

D.6.3 Two-Sided Prediction Interval D.19

D.6.4 Simultaneous Confidence Intervals D.20

D.6.5 Statistical Intervals in Transformed and Untransformed Units D.20

D.7 References D.21

Acronyms

CV	coefficient of variation
GLS	generalized least squares
H_C	cloud height
LOF	lack-of-fit
LR	linear regression
MR	multiple regression
MSE	mean squared error
NLR	nonlinear regression
OLS	ordinary (unweighted) least squares
PI	prediction interval
PvM	predicted-versus-measured
RMSE	root-mean-squared error
SCI	simultaneous confidence interval
SSE	sum of squares error
SSPE	sum of squares pure error
UCI	upper confidence interval
U_{CS}	critical suspension velocity
WLS	weighted least squares
Y	nondimensional response variable

Symbols

$\mathbf{a}^T$	transpose of the vector **x** of predictor-variable values expanded in the form of the model
$\mathbf{A}^T$	transpose of data matrix of predictor-variable values, expanded in the form of the model
C_U	estimated variance-covariance matrix for the estimated coefficients of model fit by OLS regression
C_W	estimated variance-covariance matrix for the estimated coefficients of model fit by WLS regression
f( )	function of predictor variables inside the parentheses, which may include constant coefficients and unknown coefficients to be estimated using experimental data
g( )	function of variables inside the parentheses, which may include constant coefficients
h( )	function of variables inside the parentheses, which may include constant coefficients and unknown coefficients to be estimated using experimental data
k	multiplicative coefficient
n	number of data points used to fit a model
p	number of parameters (coefficients) in a model form estimated via regression on the data

r_i	residual for the ith data point = $y_i - \hat{y}_i$
$t_{1-\alpha}(n-p)$	$100(1-\alpha)$-percentile of the Student's t-distribution with $n - p$ degrees of freedom
$t(y)$	mathematical transformation of the response variable y, which could be the identity transformation, a logarithmic transformation, or some other transformation
$\mathbf{W}$	an $n \times n$ diagonal weight matrix with entries w_i, $i = 1, 2, \ldots, n$
w_i	weight applied to i^{th} data point in cases where WLS regression is used
x_j	j^{th} nondimensional or dimensional predictor variable, $j = 1, 2, \ldots, p$
X_j	j^{th} nondimensional predictor variable
$\{X_j\}_{j \in A}$	subset A of the nondimensional predictor variables
$\{X_j\}_{j \in B}$	set B (which could be all or a subset) of the nondimensional predictor variables
y	response variable
y_i	measured response for the ith data point
$\hat{y}_i$	predicted response value for i^{th} data point made using the model fit to all data points
$\hat{y}_{(i)}$	predicted response value for the ith data point, made using a model fit to all n data points except the ith data point
$\bar{y}$	unweighted average (mean) of the n measured response values (mathematically transformed if appropriate for the model form used)
$\bar{y}_w$	weighted average (mean) of the n measured response values (mathematically transformed if appropriate for the model form used)
$\hat{y}(\mathbf{x})$	model predicted value at a set of predictor-variable values $\mathbf{x}$

Greek Symbols

α_j	coefficient of the jth term in the model
ε	random experimental and measurement error
δ	multiplicative random experimental and measurement error assumed to be normally distributed with mean 0 and standard deviation $y\sigma$

Appendix D

Statistical Methods Used to Develop, Evaluate, and Validate Multiple Regression Models

This appendix summarizes statistical methods used for developing, evaluating, and validating empirical or semi-empirical models obtained using multiple regression. The text was adapted from Appendix C of Piepel et al. (2007), so much of it is written in a general manner. Applications of the methods discussed in this appendix to develop, evaluate, and validate models for predicting slurry mixing response variables as functions of mixing test variables are discussed in Appendix F.

Section D.1 discusses terminology, mathematical forms of models, and issues related to the form of the model. Section D.2 discusses the least-squares regression methods used to fit models to data and the corresponding assumptions. Section D.3 discusses the statistical methods and summary statistics used to evaluate a model based on the data used to fit it. Section D.4 discusses statistical methods for model augmentation (i.e., adding terms to a model) and model reduction (i.e., removing unneeded terms from a model). Section D.5 discusses the statistical methods and summary statistics used for model validation based on data not used to fit a model. Section D.6 discusses several statistical intervals used to quantify uncertainties in model predictions.

D.1 Model Forms

In many areas of application, experimental data are used to develop an equation relating a response variable to one or more predictor variables. Such an equation enables making predictions of the response variable for combinations of the predictor variables not tested in experiments. Statistical methods for developing these equations provide for quantifying the uncertainty in predicted response values.

When experimental data are used to develop this type of equation, it is referred to as a correlation in many disciplines. In statistics and other disciplines, these equations are referred to as empirical or semi-empirical models. The term semi-empirical model is used when the mathematical form of the equation is based on subject-matter theory or first principles, and the coefficients of the equation are estimated using experimental data. The term empirical model is used when the general mathematical form (e.g., power-law, polynomial, etc.) is provided or assumed, while the specific form and coefficients of the equation are determined using experimental data. In statistics, the term "correlation" has a specific meaning with specific formulas to measure its magnitude, which is why statisticians prefer the empirical or semi-empirical model terms. Correlation is sometimes uses in the slurry mixing field and other disciplines. However, in this appendix, the general term "model" is used to avoid confusion with statistical uses of the word correlation. The term model includes both empirical and semi-empirical models.

D.1.1 Nondimensional Models

It is traditional in some disciplines to develop models using nondimensional variables as the response variable and predictor variables. This is common in engineering models because 1) they must be dimensionally consistent to represent physical relationships, 2) it is common to derive theoretical forms

for models from dimensionless forms of the controlling physical laws, and 3) it is always possible to reduce a set of dimensional variables to a physically equivalent set of fewer dimensionless groups. Formulating such models in terms of dimensionless groups both ensures dimensional consistency and provides a model with coefficients with magnitudes that are independent of the choice of dimensional units. Often the response variable consequently is combined with one or more predictor variables in a dimensionless group. In such cases, one or more nondimensional predictor variables appear on both sides of the equation. This is denoted by

$$g(Y, \{X_j\}_{j \in A}) = h(\{X_j\}_{j \in B}) \tag{D.1}$$

where

- Y = nondimensional response variable
- X_j = j^{th} nondimensional predictor variable
- $g(\ )$ = function (i.e., mathematical expression) of the variables inside the parentheses, which may include constant coefficients
- $h(\ )$ = function (i.e., mathematical expression) of the variables inside the parentheses, which may include constant coefficients and unknown coefficients to be estimated (fit) using experimental data
- $\{X_j\}_{j \in A}$ = subset A of the nondimensional predictor variables
- $\{X_j\}_{j \in B}$ = set B (which could be all or a subset) of the nondimensional predictor variables.

In Eq. (D.1), typically only a subset of the full set of predictor variables appears on the left side of the equation, but the full set or a subset of the predictor variables can appear on the right side of the equation.

D.1.2 Multiple-Regression Model Forms

In many disciplines, it is traditional to develop models with only the response variable on the left side of the equation, and all predictor variables on the right side of the equation. These are often called multiple-regression (MR) models and are denoted in general by

$$t(y) = f(x_j, j = 1, 2, \ldots, p) \tag{D.2}$$

where

- $t(y)$ = mathematical transformation of the response variable y, which could be the identity transformation, a logarithmic transformation, or some other transformation
- x_j = j^{th} nondimensional or dimensional predictor variable, j = 1, 2, …, p
- $f(\ )$ = function (i.e., mathematical expression) of the predictor variables inside the parentheses, which may include constant coefficients and unknown coefficients to be estimated (fit) using experimental data.

The predictor variables could be dimensional or nondimensional variables that are functions of dimensional predictor variables. Having the same dimensional predictor variable appear in more than one nondimensional predictor variable can induce correlations among nondimensional predictor variables. This makes it harder for regression (model fitting) routines to separate the effects of the variables and can

also inflate the uncertainties of model predictions. Hence, it can be worthwhile to gather predictor variables together in separate terms to the extent possible. This also makes it easier to investigate interactive effects among predictor variables.

For many nondimensional models of the form in Eq. (D.1), it is possible to move all predictor variables from the left to the right side to obtain a mathematically equivalent model of the form in Eq. (D.2). This form of model is consistent with least-squares regression methods, as discussed in Section D.2. Models of the form in Eq. (D.2) also have the advantage of not being affected by spurious correlation (see Section D.1.3).

D.1.3 Spurious Correlation

If one or more nondimensional predictor variables, X_i, appear on both the left and right sides of a model such as that represented by Eq. (D.1), a phenomenon known as spurious self-correlation (or spurious correlation) can occur. Including the same predictor variables on both sides of an equation can artificially inflate the apparent relationship and measures of relationship (such as R^2, see Section D.3.3). Research in the literature using randomly generated (and thus unrelated) values for the predictor variables and response variable has shown it is possible to obtain very strong correlations (R^2 approaching 1.0) despite the lack of relationship between the response and predictor variables (Kenney 1982, Brett 2004).

The degree of spurious correlation in a nondimensional model depends on 1) the true strength of relationship between the response variable and predictor variables and 2) the magnitudes of the coefficients of variation (CV)[1] of predictor variables that appear on both sides of the equation (common variables) relative to the CV of the response variable. If the CV of one or more common variables is large relative to the CV of the response variable, some degree of spurious correlation will occur and will increase if more of the common predictor variables have large CVs relative to the CV of the response variable. However, an otherwise very strong correlation may have little spurious correlation resulting from including the same predictor variables on both sides of the model equation.

D.2 Linear and Nonlinear Least-Squares Regression Methods and Assumptions for Fitting Models

Empirical or semi-empirical models (models, for simplicity) are typically fit to data sets using least-squares regression methods. Depending on whether the mathematical form of the model being fit is linear or nonlinear in the model coefficients, linear regression (LR) or nonlinear regression (NLR) methods and software can be used. LR methods give a one-step solution to estimating the model coefficients, whereas NLR methods involve an iterative algorithm that must converge to a solution for the estimated model coefficients. Depending on the structure of uncertainties in the response variable being regressed against predictor variables, ordinary (unweighted) least squares (OLS) regression or weighted least squares (WLS) regression methods can be applied with both the LR and NLR. Section D.2.1 discusses LR and NLR, while Section D.2.2 discusses OLS and WLS regression. Draper and Smith (1998) and Montgomery et al. (2001) provide additional discussion of LR and NLR, implemented via OLS or WLS.

[1] The CV of a variable is defined as its standard deviation divided by its mean.

D.2.1 Linear and Nonlinear Regression

Different methods are required to fit regression models to data depending on whether the model form is linear or nonlinear in the coefficients to be estimated (fit) using the data. A linear regression model has the general form

$$t(y) = \sum_{j=1}^{p} \alpha_j x_j + \varepsilon \tag{D.3}$$

where

- $t(y)$ = a mathematical transformation of the response variable y, which could be the identity transformation, a logarithmic transformation, or some other transformation
- x_j = j^{th} predictor variable in the model, j = 1, 2, …, p. An x_j could be one (1) so the model includes a constant term; a test variable that was changed in experimental work; a transformation of a test variable [e.g., $\ln(x_j)$ or x_j^2], or a function of two or more test variables (e.g., $x_j\, x_k$)
- α_j = coefficient of the jth term in the model
- ε = random experimental and measurement error. The n-dimensional vector of these errors for the n data points used to fit the model is assumed to be normally distributed with mean vector 0 and n × n variance-covariance matrix **V**. If $\mathbf{V} = \sigma^2\mathbf{I}$ (where **I** is an n × n matrix with ones on the diagonal and zeros off-diagonal), then OLS is applicable. If **V** is a diagonal matrix with σ_i^2 in the ith diagonal position, then WLS is applicable. The OLS and WLS assumptions are further discussed in Section D.2.2.

A linear regression model can include nonlinear functions of the predictor variables but is linear in its coefficients.

A nonlinear regression model is any equation that is not linear in at least one coefficient. In this report, power-law models are an example of a nonlinear regression model. A basic power-law model with multiplicative error structure has the general form

$$y = k \prod_{j=1}^{p} x_j^{a_j}\ \delta \tag{D.4}$$

where

- y = response variable
- k = multiplicative coefficient
- x_j = j^{th} predictor variable in the model, j = 1, 2, …, p. An x_j could be one so that the model includes a constant term, a test variable changed in experimental work, a transformation of a test variable [e.g., $\ln(x_j)$ or x_j^2], or a function of two or more test variables (e.g., $x_j\, x_k$)
- α_j = exponent coefficient of the jth term in the model
- δ = multiplicative random experimental and measurement error assumed to be normally distributed with mean 0 and standard deviation $y\sigma$. Hence, the magnitude of experimental and measurement uncertainties increases in proportion to the magnitude of the response variable. This error structure requires the use of WLS regression (see Section D.2.2).

Some nonlinear regression models can be linearized by transforming both sides of the model. For example, taking the natural logarithm of both sides of the power-law model in Eq. (D.4) yields

$$\ln(y) = \ln(k) + \sum_{i=1}^{p} a_i \ln(z_i) + \ln(\delta) = a_0 + \sum_{i=1}^{p} a_i \ln(z_i) + \varepsilon \qquad \text{(D.5)}$$

which is linear in the coefficients $a_0 = \ln(k)$ and $a_1, a_2, \ldots, a_p$. Taking the natural logarithm of both sides also transforms the multiplicative random error term in Eq. (D.4), which was dependent on the magnitude of y, to an additive random error term that is independent of the magnitude of y. This enables OLS linear regression to be used for Eq. (D.5) instead of WLS nonlinear regression for Eq. (D.4).

D.2.2 Ordinary and Weighted Least Squares Regression

The underlying assumptions of OLS and WLS regression are:

1) The predictor-variable values are known or measured without uncertainty or the uncertainty is small relative to the uncertainty in response-variable values.
2) The testing and/or measurement errors in a response variable over a model development data set are independently distributed (i.e., the errors are not correlated). For OLS regression, the additional assumption is made that the errors are identically distributed (i.e., with zero mean and the same variance). For WLS regression, the errors are also assumed to have zero mean, but the variance can be different for different data points.
3) The errors from (2) are normally (Gaussian) distributed.

Regarding assumption (1), the true values of predictor variables in an experimental data set for developing models for mixing response variables are generally not known. Target values or measured values of the predictor variables are typically used. However, the uncertainties in these values were judged to be small enough that use of least-squares regression methods is acceptable.

The portion of assumption (2) that has to do with the independence of errors in testing and measuring response variables may not be completely satisfied when model development data sets comprise subsets of data generated at different times or locations. There is a potential for errors in testing and measuring response variables to vary for different subsets of data and be more alike within the same subset of data. Data were generated at different times or locations for the M3 mixing work conducted in the three experimental campaigns: July 2007, Fall 2007, and 2008.

The portion of assumption (2) having to do with independence of errors can also be violated if experimental data are collected with a restricted order of experimental tests rather than a randomized order of tests. Restricted order of testing typically occurs when one or more test variables are harder to change than other test variables (Myers and Montgomery 1995). In the M3 mixing tests, all tests with a given tank size had to be performed in the same block of days. Other test variables (e.g., simulant) also had restrictions on the order of testing. These types of restrictions in the order of testing can have two effects: different uncertainties in response variables for different subsets of data and correlated uncertainties for different subsets of data. Experiments with restrictions on the order of testing are referred to as split-plot, split-split-plot, etc., experiments in the statistics literature. Generalized least squares (GLS) methods exist to account for different uncertainties and correlation structure for different subsets of data (Myers and Montgomery 1995). However, it was beyond the scope of the data analysis effort to (i) determine whether the uncertainty structure actually confounds regression analyses of any of

the data, or (ii) develop models for mixing response variables that account for the complicated uncertainty structure corresponding to the way the mixing data were collected in the different test campaigns (July 2007, Fall 2007, and 2008).

The identically distributed portion of assumption (2) for OLS regression is not valid for any response variable where the variance of errors in testing and measurement depends on the value of the response variable. For example, the variances of critical suspension velocity (U_{CS}) and cloud height (H_C) tend to increase as the values of these responses increase. In such cases where the identically distributed (equal variance) assumption is violated, it can often be remedied by applying an appropriate mathematical transformation to the values of the response values (e.g., a logarithmic transformation). The Box-Cox family of transformations contains transformations (including the logarithmic transformation) appropriate for many models (see Draper and Smith 1998). Such transformations also often yield better-fitting models. In some cases, a response-variable transformation used in a particular model form may be preferred for some reason (e.g., provides a better fit), but does not satisfy the constant variance assumption of (2). Or it may be that the difference in variances across response values in the data set cannot be rectified by a response transformation. In such cases, other regression methods such as WLS regression or generalized linear models (Myers et al. 2002) could be applied.

The assumption of normally distributed measurement and testing errors in the measured response variable values allows the use of normal-theory significance tests and uncertainty equations associated with the fitted regression model. For example, confidence intervals and prediction intervals based on normal-distribution theory can be used (see Section D.6).

As discussed, OLS regression requires that all response values for the model development data have constant variance (i.e., uncertainty). WLS regression accounts for response values having different variances by using a weight for each data point (w_i). Often, w_i is chosen to be proportional to the reciprocal of the variance (squared standard deviation) of the response for the ith data point (y_i):

$$w_i = \frac{\lambda}{\mathrm{Var}(y_i)} = \frac{\lambda}{[\mathrm{SD}(y_i)]^2} \tag{D.6}$$

where λ is a proportionality constant (which could be 1). In such a WLS regression the weighted response values $\sqrt{w_i}\, y_i$ then have equal variance. However, other methods for selecting weights can be applicable for various situations.

In summary, assumptions of OLS regression may not be completely satisfied for a given mixing response variable and corresponding data set. Violations of the constant-variance assumption for response values over a data set can sometimes be addressed by appropriate response transformations so that OLS regression may be used. Other violations may be small enough that OLS regression methods can still be used without significant consequence. However, if there are large enough differences in variances of response values across a modeling data set that cannot be addressed by a response transformation, WLS regression methods should be used. If there are correlations among uncertainties for response values in a regression data set, GLS methods could be used.

D.3 Statistical Methods for Model Evaluation

There are many statistical methods (both numerical and graphical) for assessing models. Evaluation methods assess a model with the data used to develop the model. Such data are referred to as model-development data and are used to assess 1) how well a model fits the data used to develop it, 2) how well the least-squares or other regression method assumptions are satisfied (see Section D.2), and 3) whether there are any outlying or influential data points that significantly affect the fitted model. Problems detected by model evaluation such as violation of assumptions, detection of outlying data points, or detection of model inadequacy require implementing various remedies in the model development process until the problem(s) are corrected. When the model being evaluated acceptably fits the data used to develop it, model-validation methods should be applied using data not used to develop the model. Such data are referred to as model-validation data. If model-validation data are not available, cross-validation methods can be applied using the model-development data. Cross-validation methods leave out one or more data points at a time, so some of the data are used for model fitting and some for model validation. Such methods are also referred to as data-splitting validation methods, where part of the data is used for model fitting and evaluation, while the other part is used for model validation. Draper and Smith (1998) and Montgomery et al. (2001) discuss statistical methods for evaluating and validating regression models.

Model evaluation techniques include predicted-versus-measured (PvM) plots for a response variable, standardized residual plots, outlier diagnostics, three R^2 statistics, root-mean-squared error (RMSE), and statistical lack-of-fit (LOF) tests. Each of these is explained briefly in Section D.3.2. First, the relevant notation used in the subsequent descriptions and definitions is defined in Section D.3.1.

D.3.1 Notation for Regression Model Evaluation and Validation

The following notation is used subsequently in this appendix in formulas for methods to evaluate regression models fit to experimental data.

n = number of data points used to fit a model

p = number of parameters (coefficients) in a model form estimated via regression on the data

y_i = measured response value (mathematically transformed, if appropriate for the model form used) for the ith data point

$\hat{y}_i$ = predicted response value (mathematically transformed, if appropriate for the model form used) for the ith data point made, using the model fit to all n data points

r_i = residual for the ith data point = $y_i - \hat{y}_i$

$\hat{y}_{(i)}$ = predicted response value (mathematically transformed, if appropriate for the model form used) for the ith data point, made using a model fit to all n data points except the ith data point

w_i = weight applied to the ith data point in cases where WLS regression is used. Typically, w_i is proportional to the reciprocal of the variance of the response variable for the ith data point

$\bar{y}$ = unweighted average (mean) of the n measured response values (mathematically transformed, if appropriate for the model form used)

$\bar{y}_w$ = weighted average (mean) of the n measured response values (mathematically transformed if appropriate for the model form used)

$$\bar{y}_w = \frac{\sum_{i=1}^{n} w_i y_i}{\sum_{i=1}^{n} w_i} \tag{D.7}$$

D.3.2 Methods for Evaluating Regression Models Fit to Experimental Data

Methods for evaluating models fit to experimental data using least-squares regression are briefly described in the following:

- Predicted-versus-measured (PvM) plots show how well model predicted values $\hat{y}_i$ compare to the measured values y_i for the data points in the model-development data set. Predicted response values $\hat{y}_i$ are plotted on the y-axis and measured response values y_i are plotted on the x-axis. A line with a slope of one is included in the plot for reference purposes, and represents the ideal of predicted response values equaling measured response values. Plotted points falling above this line correspond to data points for which the model over-predicts the response, while plotted points falling below this line represent data points for which the model under-predicts the response. A preponderance of plotted points in a portion of the PvM plot falling above or below the line indicates that the model tends to yield biased predictions for that range of response values. Plotted points far from the line are outlying or potentially influential data points.

  For WLS regression, an ordinary (unweighted) PvM plot of $\hat{y}_i$ versus y_i could be viewed as is done for OLS regression. Or a weighted PvM plot of $\sqrt{w_i}\,\hat{y}_i$ versus $\sqrt{w_i}\,y_i$ could be viewed. The ordinary (unweighted) PvM plot has the advantage of retaining the units of the response (or its transformation), but the disadvantage that points with smaller weights (i.e., higher uncertainties) may appear farther from the line with slope one. However, rather than considering this a disadvantage, it may be better thought of as showing the penalty paid in obtaining predictions having more uncertainty for modeling data points with smaller weights (i.e., higher uncertainty). The weighted PvM plot would show the model predictive performance for the modeling data points after accounting for (i.e., removing the scatter due to) the differing weights (i.e., uncertainties).

- RMSE for OLS regression is given by

$$\mathrm{RMSE}_U = \sqrt{\frac{\sum_{i=1}^{n} (\hat{y}_i - y_i)^2}{n-p}} \tag{D.8a}$$

  and for WLS regression by

$$\mathrm{RMSE}_W = \sqrt{\frac{\sum_{i=1}^{n} w_i (\hat{y}_i - y_i)^2}{n-p}}\,, \tag{D.8b}$$

where the subscripts on $RMSE_U$ and $RMSE_W$ denote "unweighted" and "weighted" least squares (i.e., OLS and WLS). If the fitted model is adequate and does not have a statistically significant lack-of-fit, this statistic provides an estimate of the experimental and measurement uncertainty standard deviation associated with performing a test and measuring the associated response. The statistic RMSE is included as standard output in most regression software, and has units the same as the response values y_i (including any mathematical transformation of the response in the model form) for OLS regression and the units of $\sqrt{w_i}\, y_i$ for WLS regression.

- Standardized residual plots display standardized residuals (s_i, differences in predicted and measured response values divided by their standard deviations) versus various quantities, such as predictor variables (x_i) or predicted response values ($\hat{y}_i$). The formula for a standardized residual is given by

$$s_i = \frac{r_i}{RMSE_U \left[1 - \mathbf{a}_i^T \left(\mathbf{A}^T \mathbf{A} \right)^{-1} \mathbf{a}_i \right]^{0.5}} \tag{D.9a}$$

for OLS regression and by

$$s_i = \frac{\sqrt{w_i}\, r_i}{RMSE_W \left[1 - w_i \mathbf{a}_i^T \left(\mathbf{A}^T \mathbf{W} \mathbf{A} \right)^{-1} \mathbf{a}_i \right]^{0.5}} \tag{D.9b}$$

for WLS regression. In Eqs. (D.9a), (D.9b): s_i, w_i, and r_i are as previously described; $RMSE_U$ and $RMSE_W$ are given respectively by Eqs. (D.8a) and (D.8b); $\mathbf{a}_i$ is the column vector of predictor-variable values for the ith modeling data point expanded in the form of the model; $\mathbf{A}$ is an $n \times p$ matrix of the predictor-variable values in the modeling data set expanded in the form of the model; $\mathbf{W}$ is an $n \times n$ matrix with the weights w_i along the main diagonal, and zeros elsewhere.

Patterns in the s_i versus $\hat{y}_i$ plot can indicate a violation of the least squares regression assumptions and suggest a response transformation to remedy the situation. Patterns in the s_i versus x_i plots can indicate inadequacies of the model or least-squares assumptions. Patterns in s_i versus data indices can indicate subsets of the data for which a model may be inadequate (e.g., yield biased predictions). Standardized residuals are typically used in residual plots because the majority should fall within the range of ±2.0 and almost all should fall within ±3.0. Comparing standardized residuals to such a range provides an easy criterion for judging whether a data point is outlying.

- Normality plots display normal scores versus the ordered (from smallest to largest) standardized residuals (from Eqs. (D.9a) and (D.9b) for OLS and WLS regression, respectively) for the n data points used to fit the model being assessed. Normal scores are the expected values of a sample of size n from standard normal distribution (with mean 0 and standard deviation 1). The plotted points are compared to the ideal of a straight line corresponding to a normal distribution. A straight middle portion of the plot with curved "tails" on each end of the plot indicate the presence of outlying data points, which cause a heavier-tailed distribution than the normal distribution.

- Outlier diagnostics and plots indicate data points that are outlying or influential with respect to response-variable or predictor-variable values. There are too many of these diagnostics and plots to discuss here, but several produced by the R software (Ihaka and Gentleman 1996, R Development Core Team 2006) were considered in this work. Draper and Smith (1998) and Montgomery et al.

(2001) discuss outlier diagnostics and plots for OLS regression, but software such as R produces the appropriate versions of diagnostics and plots for WLS regression as well.

- R^2 statistics quantify the proportion of variation in the response values y_i (for OLS regression) or weighted response values $\sqrt{w_i}\, y_i$ (for WLS regression) accounted for by the fitted model. Three R^2 statistics are used, as discussed later in this section.
- An LOF test checks whether the differences (for OLS regression) or weighted differences (for WLS regression) between measured and predicted response values from a fitted model are larger than expected based on the experimental and measurement uncertainty in the data. If the predicted-versus-measured differences are larger than data uncertainty at a high enough statistical confidence (greater than 90%), the model is said to have a statistically significant LOF. Replicate data points containing all applicable sources of experimental and measurement uncertainty[1] are required to perform

statistical LOF tests. This process is conducted using a LOF F-test given by

$$F = \frac{(SSE - SSPE)/(n - p - f)}{SSPE/f} = \frac{\left[\left(\sum_{i=1}^{n}(\hat{y}_i - y_i)^2 - \sum_{k=1}^{K}\sum_{j=1}^{m_k}(y_{kj} - \bar{y}_k)^2\right)\Big/(n-p-f)\right]}{\sum_{k=1}^{K}\sum_{j=1}^{m_k}(y_{kj} - \bar{y}_k)^2 \Big/ f} \tag{D.10a}$$

for OLS regression and by

$$F = \frac{(SSE - SSPE)/(n - p - f)}{SSPE/f} = \frac{\left[\left(\sum_{i=1}^{n} w_i(\hat{y}_i - y_i)^2 - \sum_{k=1}^{K}\sum_{j=1}^{m_k} w_j(y_{kj} - \bar{y}_k)^2\right)\Big/(n-p-f)\right]}{\sum_{k=1}^{K}\sum_{j=1}^{m_k} w_j(y_{kj} - \bar{y}_k)^2 \Big/ f} \tag{D.10b}$$

for WLS regression. In Eqs. (D.10a) and D.10b), SSE = sum of squares error; SSPE = sum of squared pure error (i.e., from replicates); n and p are as described previously such that n – p is the degrees of freedom for SSE; and the degrees of freedom for pure error is given by $f = \sum_{k=1}^{K}(m_k - 1)$, where m_k is the number of replicate data points in the kth replicate set, k = 1, 2, …, K. In practice, if the F-test is statistically significant at a significance level (often referred to as a p-value) of 0.05 or smaller (i.e., 95% confidence or higher), then it is concluded that the fitted model has a statistically significant

[1] To be appropriate replicate data points, two or more tests with exactly the same test variables must be tested and the corresponding response variables measured at different times. It is insufficient, for example, to set up a mixing test once, and run it and measure its responses several times (because uncertainties in setting up and performing the test at different times are not included in the data). Similarly, replicate samples should not be measured at the same time (or close in time) because all sources of measurement uncertainty will not be included in the data.

LOF for the modeling data set. See Draper and Smith (1998) or Montgomery et al. (2001) for additional discussion of the statistical test for model LOF.

Even when a fitted model has a statistically significant LOF, the LOF may not be practically significant. An example of such a situation is when a fitted model yields biased predictions for higher and/or lower values of a response or in a particular subregion of predictor-variable space, but the model will not be applied to such areas in practice. Another example is when the model fits the data very well (e.g., $R^2 > 0.95$) without bias over the model's region of validity, but the LOF is statistically significant because the experimental and measurement uncertainty is very small (e.g., because experimental tests are very reproducible). Finally, a statistically significant LOF may not be practically significant if the uncertainty in model predictions is considerably smaller than uncertainty that can be tolerated and still satisfy requirements.

The model evaluation techniques discussed in the preceding bullets are included in or can be obtained from the output of the R software (Ihaka and Gentleman 1996, R Development Core Team 2006). See Draper and Smith (1998) or Montgomery et al. (2001) for further discussion of the concepts.

D.3.3 Formulas for Three R^2 Statistics

Three different R^2 statistics are useful in evaluating models fit to experimental data. These are denoted as R^2, R_A^2, and R_P^2, which are discussed subsequently. Formulas for these statistics are given when models are fit by OLS or WLS.

The (ordinary) R^2 statistic is given by

$$R^2 = 1 - \frac{\sum_{i=1}^{n} (\hat{y}_i - y_i)^2}{\sum_{i=1}^{n} (y_i - \bar{y})^2} \tag{D.11a}$$

for OLS regression and by

$$R^2 = 1 - \frac{\sum_{i=1}^{n} w_i (\hat{y}_i - y_i)^2}{\sum_{i=1}^{n} w_i (y_i - \bar{y}_w)^2} \tag{D.11b}$$

for WLS regression, where $\bar{y}_w$ in Eq. (D.11b) is the weighted mean whose formula is given in Eq. (D.7). R^2 is interpreted as the fraction of variability in the unweighted (for OLS regression) or weighted (for WLS regression) response data (transformed if appropriate) accounted for by the fit model. The adjusted R^2 statistic is given by

$$R_A^2 = 1 - \frac{\sum_{i=1}^{n} (\hat{y}_i - y_i)^2 \Big/ (n-p)}{\sum_{i=1}^{n} (y_i - \bar{y})^2 \Big/ (n-1)} \tag{D.12a}$$

for OLS regression and by

$$R_A^2 = 1 - \frac{\sum_{i=1}^{n} w_i (\hat{y}_i - y_i)^2 \Big/ (n-p)}{\sum_{i=1}^{n} w_i (y_i - \bar{y}_w)^2 \Big/ (n-1)} \tag{D.12b}$$

for WLS regression. R_A^2 is interpreted as the adjusted fraction of variability in the unweighted or weighted response data (transformed if appropriate) accounted for by the fitted model. The adjustment is for the number of coefficients (p) and number of data points (n) used in fitting the model.

The predicted-R^2 statistic is given by

$$R_P^2 = 1 - \frac{\sum_{i=1}^{n} (\hat{y}_{(i)} - y_i)^2}{\sum_{i=1}^{n} (y_i - \bar{y})^2} \tag{D.13a}$$

for OLS regression and by

$$R_P^2 = 1 - \frac{\sum_{i=1}^{n} w_i (\hat{y}_{(i)} - y_i)^2}{\sum_{i=1}^{n} w_i (y_i - \bar{y}_w)^2} \tag{D.13b}$$

for WLS regression. R_P^2 is interpreted as the leave-one-out cross-validation fraction of variability in the unweighted or weighted response data (transformed if appropriate) accounted for by the fitted model. This statistic is calculated by a method equivalent to leaving each data point out of the model fit and then evaluating how well the model predicts the response for that data point. R_P^2 estimates the fraction of variability that would be explained in predicting new observations drawn from the same predictor-variable space. However, computational simplifications for OLS and WLS regression do not require refitting a model with each data point removed.

Generally R^2 statistics take values between 0 and 1. However, R_A^2 and R_P^2 can take negative values for a poor-fitting model, a model that contains many more terms than needed to fit the data, or a model fit to data with one or more very influential data points. Among the three R^2 statistics, typically $R^2 > R_A^2 > R_P^2$. More than a minor difference between R^2 and R_A^2 indicates that the model may contain more terms than needed to achieve the same goodness of fit. A substantial difference between R^2 and R_P^2 is indicative of one or more data points being very influential in determining the fit of the model. Some reduction from R^2 to R_P^2 is expected because R^2 corresponds to using all data to fit the model, whereas R_P^2 corresponds to leaving each data point out of the fit when evaluating the performance of the model for that point. In general, a model will tend to predict better for data used to fit it than for data not used to fit it. R_P^2 is a cross-validation evaluation method.

D.4 Statistical Methods for Model Reduction and Augmentation

Section D.4.1 discusses methods for identifying and removing unnecessary terms from models fit to experimental data. Section D.4.2 discusses methods for augmenting initial models with additional terms.

D.4.1 Statistical Methods for Reducing Regression Models

In evaluating a fitted regression model, it may often be determined that there are unnecessary terms in the model. Such terms may not improve and can even degrade the predictive performance of the model in applications to data not used to develop the model.

The most basic statistical method for identifying unnecessary terms in a model is a t-test, which corresponds to a hypothesis test of whether a particular model term has a significant effect. Depending on the nature of the term, a nonsignificant effect could correspond to a hypothesis of its coefficient being zero (for a coefficient on an additive term) or one (a coefficient that is an exponent, such as in a power-law model). The t-test computes a t-statistic equal to

$$\text{t} - \text{statistic} = \frac{\text{coefficient} - \text{hypothesized value}}{\text{standard deviation of coefficient}} \tag{D.14}$$

The t-statistic is then compared to the Student-t probability distribution to determine the probability of getting a t-statistic at least that large. The resulting probability is referred to as a p-value and represents the probability of incorrectly deciding a coefficient is significantly different from its hypothesized value. Most regression software outputs estimated model coefficients, coefficient standard deviations, t-statistics, and p-values when the hypothesized value of the coefficient is zero. However, the more general form of t-test in Eq. (D.14) can also be implemented. Typically, practitioners require a p-value to be smaller than 0.05 or 0.01 as strong evidence that the coefficient is significantly different from its hypothesized value, and thus that the corresponding model term is needed. If there are not too many potentially unnecessary terms in a model, a practitioner can assess the t-statistics and p-values for the coefficients in a "full" model, and remove the model term whose coefficient is least statistically significant. Then the model would be refit without that term, and the t-statistics and p-values again considered, deleting the model term with the least statistically significant coefficient. This process continues until all terms in the model have p-values lower than 0.05. This process, known as backward elimination (Draper and Smith 1998, Montgomery et al. 2001), is a widely used statistical method for removing unneeded terms from a model. This method basically automates the process just described, where the practitioner sets a stopping criterion.

D.4.2 Statistical Methods for Adding Terms to Models

It is often desirable to add additional terms to a starting model in the hopes of improving its predictive performance. For example, a model linear in the predictor variables, or a power-law model, may be considered a starting model. If it has a significant LOF, adding interaction terms may be considered to improve the predictive performance of the model. Stepwise regression is the most commonly used method to add terms to an existing starting model. In stepwise regression, certain terms can be forced into the model, and a candidate list of possible terms to add is identified. The procedure identifies the term from the candidate list that, if added to the model, would yield the greatest reduction in the error sum of squares (i.e., the sum of squared differences in measured and model-predicted values across the

modeling data set). If the reduction is statistically significant, that term is added to the model. Stepwise regression proceeds in stages, with one additional term being added at each stage unless the user-selected stopping criterion is reached. After adding a term, stepwise regression checks all other terms in the model to assess whether they are still statistically significant. If not, a term can be removed during a stage.

The stepwise-regression algorithm requires that a significance level be specified for terms to enter the model and that a significance level be specified for terms to remain in the model. In each iteration of a stepwise-regression application, t-tests are conducted for each term already in the model and for terms being considered for inclusion in the model. To describe the results of these t-tests, a p-value is calculated for each of the terms. Loosely speaking, the p-values represent the probability that the respective model terms do not make a significant contribution to the predictive ability of the model. Terms whose corresponding p-values are small (often <0.05 is considered sufficiently small) are deemed important in the model. The significance levels specified for the stepwise-regression algorithm indicate how small p-values must be for the corresponding terms to be included in the model. The statistical literature generally indicates that the stepwise algorithm is somewhat liberal in allowing terms into models (i.e., may over-fit the data and add too many terms). However, models containing unnecessary terms are undesirable because they tend to have inflated prediction variance. Thus, it is typically advisable to use tight significance levels such as 0.05 or 0.01 when applying the stepwise-regression algorithm. Draper and Smith (1998) and Montgomery et al. (2001) have further discussion and details on stepwise regression.

D.5 Statistical Methods for Model Validation

Model validation methods assess how well a fitted model predicts response values for data not used in fitting the model. A validation data set could be separate from the modeling data set or could be a subset obtained by splitting or partitioning the modeling data set into modeling and validation subsets.

The data used for validation ideally should be in the same predictor-variable region as the data used to fit the model being validated. This is because, in general, fitted empirical and semi-empirical models should not be used to extrapolate much beyond the region covered by the modeling data. Also, ideally the validation data should be evenly distributed over the region of model validity[1] to properly assess predictive ability over the region. These ideals can generally be achieved when splitting or partitioning the modeling data set into modeling and validation subsets. However, they can be difficult to achieve in practice for a separate validation data set because such data are typically not designed but often consist of whatever extra or older data are available.

Validation generally consists of using a fitted model to predict response values for a set of validation data, and then comparing the predicted response values to the measured values from the validation database. The following subsections describe several methods for comparing predicted and measured values of response variables.

[1] A model validity region is the region of predictor-variable combinations where a model has been determined to be valid.

D.5.1 Validation R^2

Statistical summary comparisons of predicted and measured response values are also useful to see whether differences are larger than their expected uncertainties. One such comparison is the validation R^2 (R_V^2) statistic, which in general is given by

$$R_V^2 = 1 - \frac{\sum_{i=1}^{n}(\hat{y}_i - y_i)^2}{\sum_{i=1}^{n}(y_i - \bar{y})^2} \tag{D.15a}$$

However, in cases where WLS regression is used to fit the model and corresponding weights are available for the validation data set, a weighted version of the validation R^2 statistics is given by

$$R_V^2 = 1 - \frac{\sum_{i=1}^{n} w_i(\hat{y}_i - y_i)^2}{\sum_{i=1}^{n} w_i(y_i - \bar{y}_w)^2} \tag{D.15b}$$

If weights are not available for the validation data set in the WLS case, weights $w_i = 1$ can be used, which is equivalent to using Eq. (D.15a) instead of Eq. (D.15b). R_V^2 is interpreted as the fraction of variability in the unweighted or weighted response values (transformed if appropriate) in the validation data accounted for by the fitted model. Note that R_V^2 is defined exactly the same as the ordinary R^2 defined in Eqs. (D.11a) and (D.11b), except that model-validation data are used to assess model predictive performance instead of the model-development data. Hence, the y_i, $\hat{y}_i$, $\bar{y}$, w_i, and $\bar{y}_w$ values in Eqs. (D.15a) and (D.15b) correspond to the model validation data.

Generally, $R_V^2 \le R_P^2 \le R_A^2 \le R^2 \le 1$. However, R_V^2 can take negative values (when a model predicts a validation set very poorly) and can take values larger than R_P^2, R_A^2, or R^2 (when a model predicts a particular validation data set better than estimated by these statistics based on the modeling data).

D.5.2 Validation RMSE

Another useful summary statistic for model validation is validation RMSE ($RMSE_V$). This statistic is calculated by

$$RMSE_V = \sqrt{\frac{\sum_{i=1}^{n}(\hat{y}_i - y_i)^2}{n_V}} \tag{D.16a}$$

for OLS-fitted models and by

$$\mathrm{RMSE}_V = \sqrt{\frac{\sum_{i=1}^{n} w_i (\hat{y}_i - y_i)^2}{n_V}} \tag{D.16b}$$

for WLS-fitted models. For the WLS case, if weights are not available for the validation data set, weights $w_i = 1$ are used. This is equivalent to using Eq. (D.16a) instead of Eq. (D.16b).

In Eqs. (D.16a) and (D.16b), the denominator n_V is the number of observations in the validation data set. The denominator is different from the $n - p$ denominator for the modeling RMSE given in Eqs. (D.8a) and (D.8b), where n is the number of observations in the modeling data set and p is the number of model coefficients estimated using the modeling data set. In Eqs. (D.8a) and (D.8b), the $n - p$ denominator accounts for estimating the p model coefficients using the n observations in the modeling data set. However, because no model coefficients are estimated from a validation data set, the denominator in Eqs. (D.16a) and (D.16b) is n_V rather than $n - p$.

In general, RMSE_V calculated by Eqs. (D.16a) and (D.16b) is expected to be larger than RMSE calculated by Eqs. (D.8a) and (D.8b) because the validation subset was not used to fit the model. The difference can be larger when the validation data set is small relative to the modeling data set, so that n_V is much smaller than $n - p$. The difference between RMSE and RMSE_V depends not only on how well a model predicts for the validation data set, but also on the distribution of points in the validation data set relative to the distribution in the modeling data set. The non-representativeness of a smaller validation data set can thus cause a larger difference between RMSE and RMSE_V.

D.5.3 Predicted Versus Measured Plots for Validation

Predicted and measured values for a model validation data set can be compared by plotting the predicted versus the measured response values for each data point. Such predicted versus measured plots are the same as described in Section D.3.2, except model validation data are used instead of model development data. Also, similarly as described in Section D.3.2, unweighted or weighted PvM plots may be produced and viewed to validate models fit by WLS regression.

Optionally, error bars consisting of 95% two-sided prediction intervals (PIs) on the predicted values can be included in the predicted-versus-measured plot for validation. Then, if the error bar for a given validation data point overlaps a line with slope one superimposed on the PvM plot, the model is validated for that data point. Draper and Smith (1998) and Montgomery et al. (2001) provide additional discussion of 95% PIs for regression models. The formulas for a 95% two-sided PI in the OLS and WLS cases are given in Section D.6.3.

D.6 Statistical Intervals for Quantifying Uncertainties in Model Predictions

Several types of statistical intervals are available to describe the uncertainty associated with model predictions. Each type of statistical interval has a particular interpretation. A common assumption for all statistical intervals based on regression models is that the model represents the true underlying response surface without a statistically significant lack of fit.

The following subsections present the formulas for one-sided upper (or lower) confidence intervals (Section D.6.1), two-sided confidence intervals (Section D.6.2), and two-sided prediction intervals (Section D.6.3). These types of statistical intervals are used to describe the uncertainty associated with model predictions at a single, specific set of predictor-variable values. Section D.6.4 presents the formulas for simultaneous confidence intervals, which are used to describe the uncertainty associated with model predictions at many different sets of predictor-variable values. The formulas for these types of statistical intervals are given in each subsection for the OLS and WLS cases. Section D.6.5 discusses aspects of using the statistical intervals.

D.6.1 One-Sided Confidence Intervals

Formulas for one-sided upper and one-sided lower confidence intervals are presented in subsections D.6.1.1 and D.6.1.2, respectively.

D.6.1.1 One-Sided Upper Confidence Interval

A 100(1−α)% upper confidence interval (UCI) for the true <u>mean</u> response value for a given set of predictor-variable values $\mathbf{x} = (x_1, x_2, \ldots, x_q)$ is given by

$$\begin{aligned}\hat{y}(\mathbf{x}) + t_{1-\alpha}(n-p)\sqrt{\mathbf{a}^T\mathbf{C}_U\,\mathbf{a}} &= \hat{y}(\mathbf{x}) + t_{1-\alpha}(n-p)\sqrt{\mathbf{a}^T[(\mathbf{A}^T\mathbf{A})^{-1}\mathrm{MSE}_U]\,\mathbf{a}} \\ &= \hat{y}(\mathbf{x}) + t_{1-\alpha}(n-p)\mathrm{RMSE}_U\sqrt{\mathbf{a}^T(\mathbf{A}^T\mathbf{A})^{-1}\mathbf{a}}\end{aligned} \tag{D.17a}$$

for OLS regression and by

$$\begin{aligned}\hat{y}(\mathbf{x}) + t_{1-\alpha}(n-p)\sqrt{\mathbf{a}^T\mathbf{C}_W\,\mathbf{a}} &= \hat{y}(\mathbf{x}) + t_{1-\alpha}(n-p)\sqrt{\mathbf{a}^T[(\mathbf{A}^T\mathbf{W}\mathbf{A})^{-1}\mathrm{MSE}_W]\,\mathbf{a}} \\ &= \hat{y}(\mathbf{x}) + t_{1-\alpha}(n-p)\mathrm{RMSE}_W\sqrt{\mathbf{a}^T(\mathbf{A}^T\mathbf{W}\mathbf{A})^{-1}\mathbf{a}}\end{aligned} \tag{D.17b}$$

for WLS regression. The notations in Eqs. (D.17a) and (D.17b) are defined as follows:

$\hat{y}(\mathbf{x})$	=	model predicted value at a set of predictor-variable values x
$100(1-\alpha)$	=	desired confidence (e.g., 90%) for the confidence interval, where α denotes the significance level (e.g., α = 0.10 for 90% confidence)
$t_{1-\alpha}(n-p)$	=	100(1−α)-percentile of the Student's t-distribution with n − p degrees of freedom
n	=	number of data points used to fit the model
p	=	number of coefficients estimated in the model
C_U	=	estimated variance-covariance matrix for the estimated coefficients of a model fit by OLS regression $(\mathbf{A}^T\mathbf{A})^{-1}\mathrm{MSE}_U$
C_W	=	estimated variance-covariance matrix for the estimated coefficients of a model fit by WLS regression = $(\mathbf{A}^T\mathbf{W}\mathbf{A})^{-1}\mathrm{MSE}_W$
$\mathbf{a}^T$	=	transpose of the vector **x** of predictor-variable values expanded in the form of the model

$\mathbf{A}^T$ = transpose of the data matrix of predictor-variable values, expanded in the form of the model

$\mathbf{W}$ = an $n \times n$ diagonal weight matrix with entries w_i, $i = 1, 2, \ldots, n$ (i.e., the weights associated with the model-development set of n data points)

MSE = mean squared error, which is obtained from the OLS (MSE_U) or WLS (MSE_W) regression fit of the model

RMSE = the root mean squared error = $\sqrt{MSE}$, with $RMSE_U$ and $RMSE_W$ resulting from OLS and WLS regression fits of a model, respectively.

A $100(1-\alpha)\%$ UCI, as given by Eqs. (D.17a) and (D.17b), is appropriate when an uncertainty statement is desired about the true mean response for a given set of predictor-variable values $\mathbf{x}$.

D.6.1.2 One-Sided Lower Confidence Interval

The formulas for a one-sided lower confidence interval are the same as in Eqs. (D.17a) and (D.17b) except the plus signs following $\hat{y}(\mathbf{x})$ are changed to minus signs. Thus, a $100(1-\alpha)\%$ lower confidence interval (LCI) for the true <u>mean</u> response value for a given set of predictor-variable values $\mathbf{x} = (x_1, x_2, \ldots, x_q)$ is given by

$$\begin{aligned}\hat{y}(\mathbf{x}) - t_{1-\alpha}(n-p)\sqrt{\mathbf{a}^T\mathbf{C}_U\,\mathbf{a}} &= \hat{y}(\mathbf{x}) - t_{1-\alpha}(n-p)\sqrt{\mathbf{a}^T[(\mathbf{A}^T\mathbf{A})^{-1}MSE_U]\,\mathbf{a}} \\ &= \hat{y}(\mathbf{x}) - t_{1-\alpha}(n-p)RMSE_U\sqrt{\mathbf{a}^T(\mathbf{A}^T\mathbf{A})^{-1}\mathbf{a}}\end{aligned} \tag{D.18a}$$

for OLS regression and by

$$\begin{aligned}\hat{y}(\mathbf{x}) - t_{1-\alpha}(n-p)\sqrt{\mathbf{a}^T\mathbf{C}_W\,\mathbf{a}} &= \hat{y}(\mathbf{x}) - t_{1-\alpha}(n-p)\sqrt{\mathbf{a}^T[(\mathbf{A}^T\mathbf{W}\mathbf{A})^{-1}MSE_W]\,\mathbf{a}} \\ &= \hat{y}(\mathbf{x}) - t_{1-\alpha}(n-p)RMSE_W\sqrt{\mathbf{a}^T(\mathbf{A}^T\mathbf{W}\mathbf{A})^{-1}\mathbf{a}}\end{aligned} \tag{D.18b}$$

for WLS regression. The notation is as previously defined.

D.6.2 Two-Sided Confidence Interval

A $100(1-\alpha)\%$ two-sided confidence interval (CI) for the true <u>mean</u> response value for a given set of predictor variables $\mathbf{x} = (x_1, x_2, \ldots, x_q)$ is given by

$$\begin{aligned}\hat{y}(\mathbf{x}) \mp t_{1-\alpha/2}(n-p)\sqrt{\mathbf{a}^T\mathbf{C}_U\,\mathbf{a}} &= \hat{y}(\mathbf{x}) \mp t_{1-\alpha/2}(n-p)\sqrt{\mathbf{a}^T[(\mathbf{A}^T\mathbf{A})^{-1}MSE_U]\,\mathbf{a}} \\ &= \hat{y}(\mathbf{x}) \mp t_{1-\alpha/2}(n-p)RMSE_U\sqrt{\mathbf{a}^T(\mathbf{A}^T\mathbf{A})^{-1}\mathbf{a}}\end{aligned} \tag{D.19a}$$

for OLS regression and by

$$\hat{y}(\mathbf{x}) \mp t_{1-\alpha/2}(n-p)\sqrt{\mathbf{a}^T \mathbf{C}_W\ \mathbf{a}} = \hat{y}(\mathbf{x}) \mp t_{1-\alpha/2}(n-p)\sqrt{\mathbf{a}^T[(\mathbf{A}^T\mathbf{W}\mathbf{A})^{-1}\mathrm{MSE}_W]\,\mathbf{a}}$$
$$= \hat{y}(\mathbf{x}) \mp t_{1-\alpha/2}(n-p)\mathrm{RMSE}_W\sqrt{\mathbf{a}^T(\mathbf{A}^T\mathbf{W}\mathbf{A})^{-1}\mathbf{a}} \tag{D.19b}$$

for WLS regression. In Eqs. (D.19a) and (D.19b), the notation is all the same as described in Section D.6.1 except that $t_{1-\alpha/2}(n-p)$ denotes the 100(1−α/2)-percentile of the Student t-distribution with n − p degrees of freedom.

D.6.3 Two-Sided Prediction Interval

A 100(1−α)% two-sided prediction interval (PI) for an <u>individual</u> response value for a given set of predictor-variable values **x** is given by

$$\hat{y}(\mathbf{x}) \mp t_{1-\alpha/2}(n-p)\sqrt{\mathrm{MSE}_U + \mathbf{a}^T\mathbf{C}_U\ \mathbf{a}}$$
$$= \hat{y}(\mathbf{x}) \mp t_{1-\alpha/2}(n-p)\mathrm{RMSE}_U\sqrt{1+\mathbf{a}^T(\mathbf{A}^T\mathbf{A})^{-1}\mathbf{a}} \tag{D.20a}$$

for OLS regression and by

$$\hat{y}(\mathbf{x}) \mp t_{1-\alpha/2}(n-p)\sqrt{\frac{\mathrm{MSE}_W}{w_i} + \mathbf{a}^T\mathbf{C}_W\ \mathbf{a}}$$
$$= \hat{y}(\mathbf{x}) \mp t_{1-\alpha/2}(n-p)\mathrm{RMSE}_W\sqrt{\frac{1}{w_i} + \mathbf{a}^T(\mathbf{A}^T\mathbf{W}\mathbf{A})^{-1}\mathbf{a}} \tag{D.20b}$$

for WLS regression. The notations in Eqs. (D.20a) and (D.20b) are defined as given following the UCI formulas in Section D.6.1.

The preceding equations for 100(1−α)% two-sided PIs are easily converted to 100(1−α)% one-sided PIs by replacing "∓" with "−" or "+", replacing $t_{1-\alpha/2}(n-p)$ with $t_{1-\alpha}(n-p)$, and replacing $t_{1-\alpha/2}(n_g-p_g)$ with $t_{1-\alpha}(n_g-p_g)$.

In Eq. (D.20b) the w_i under the square root applies when PIs are calculated for modeling data, validation data, or application data (i.e., data used in applying the models and PIs) with weights. In situations where validation or application data do not have weights, w_i should be set to 1.

A 100(1−α)% PI is appropriately used when comparing a model predicted response value for a given set of predictor-variable values to an individual measurement of the response for that same set of predictor-variable values. This type of application arises in validating the predictive performance of a model for one or more sets of predictor-variable values not used to fit the model. Specifically, Eqs. (D.20a) and (D.20b) can be used to produce 95% PIs displayed as error bars in PvM plots for validation data, as described in Section D.5.3.

D.6.4 Simultaneous Confidence Intervals

At times it is desirable to describe the uncertainty associated with predictions obtained for many sets of predictor-variable values. For example, a statement may be desired that indicates with high confidence that the predicted response value for every set of predictor-variable values **x** in a specified region meets requirements. A simultaneous confidence interval provides such a statistical statement. The formula for a 100(1−α)% simultaneous confidence interval (SCI) associated with predictions on an unlimited number of sets of predictor variables **x** is given by

$$\begin{aligned}\hat{y}(\mathbf{x}) &\pm \sqrt{pF_{1-\alpha}(p, n-p)}\sqrt{\mathbf{a}^T\mathbf{C}_U\,\mathbf{a}} \\ &= \hat{y}(\mathbf{x}) \pm \mathrm{RMSE}_U\sqrt{pF_{1-\alpha}(p, n-p)}\sqrt{\mathbf{a}^T(\mathbf{A}^T\mathbf{A})^{-1}\mathbf{a}}\end{aligned} \tag{D.21a}$$

for OLS regression and by

$$\begin{aligned}\hat{y}(\mathbf{x}) &\pm \sqrt{pF_{1-\alpha}(p, n-p)}\sqrt{\mathbf{a}^T\mathbf{C}_W\,\mathbf{a}} \\ &= \hat{y}(\mathbf{x}) \pm \mathrm{RMSE}_W\sqrt{pF_{1-\alpha}(p, n-p)}\sqrt{\mathbf{a}^T(\mathbf{A}^T\mathbf{W}\mathbf{A})^{-1}\mathbf{a}}\end{aligned} \tag{D.21b}$$

for WLS regression. In Eqs. (D.21a) and (D.21b), $F_{1-\alpha}$ (p, n − p) = 100(1−α)-percentile of the statistical F-distribution with p and n – p degrees of freedom. The remaining notations were defined previously.

D.6.5 Statistical Intervals in Transformed and Untransformed Units

Eqs. (D.17) to (D.21) yield statistical intervals in transformed units when a transformed response is modeled. For example, a natural logarithm transformation of a response y [i.e., ln(y)] is often used for models of responses with experimental and measurement uncertainty proportional to the magnitude of the response. In such cases, the statistical intervals calculated using the preceding equations would be in ln(y) units. The statistical intervals can be transformed back to the original units of y by exponentiating the endpoint(s) of the statistical interval. However, the process of back-transforming (exponentiating) a statistical interval can change its interpretation. For example, if a 90% UCI in ln(y) units has the value v, the back-transformed 90% UCI in the original units of y is given by e^v. The 90% UCI in units of ln(y) is a statement about the true <u>mean</u> response in ln(y) units for a given set of predictor-variable values **x**. However, the resulting back-transformed interval is a 90% UCI on the true <u>median</u> response value for the given set of predictor-variable values **x** under the assumption that experimental errors in the data used to develop the model are lognormally distributed. This assumption corresponds to the assumption of the natural-log-transformed response data being normally distributed. This change in interpretation occurs because the mean and median of a normal distribution are the same, but the mean of a lognormal distribution is larger than the median of a lognormal distribution.

Hence, back-transforming a 100(1−α)% UCI on a mean response (in ln-units) for a given set of predictor-variable values **x** (see Section D.6.1) yields a 100(1−α)% UCI on the median response (in original units) for the given set of predictor-variable values **x**. This then underestimates a 100(1−α)% UCI on the mean response (in original units) for a given set of predictor-variable values **x**. Similar interpretations hold for 100(1−α)% LCIs (see Section D.6.1) and CIs (see Section D.6.2). Back-transforming 100(1−α)% SCIs (see Section D.6.4) given in ln-transformed units has a similar

change in interpretation. Whereas the original 100(1−α)% SCIs are statements about the true mean values of responses in ln-transformed response units for multiple sets of predictor-variable values **x**, the back-transformed 100(1−α)% SCIs are statements about the true median values of responses in original response units for multiple sets of predictor-variable values **x**. However, a 100(1−α)% PI (Section D.6.3) in ln-transformed units does not have a change in interpretation when back-transforming because the original statement (in ln-transformed units) and the back-transformed statement (in original units) are both about a true individual response value.

Alternatives exist to using normal-theory-based Eqs. (D.17) to (D.21) and back-transforming them when a transformed response variable is modeled. One alternative is to modify the statistical interval equations so the statistical statement is about the true mean response value in the original units for a given set of predictor-variable values **x** (e.g., Eq. D.17 for an UCI) or multiple sets of predictor-variable values **x** (e.g., Eq. D.21 for a SCI). Although this type of alternative is discussed in the literature for non-regression problems (e.g., Gilbert 1987), no references were found for the regression context. Another alternative, the generalized linear model regression approach (Myers et al. 2002), avoids directly transforming the response variable and instead uses the transformation indirectly. These alternative approaches were not pursued in this work, but the interested reader may refer to the references given.

Note that Eqs. (D.17) to (D.21) require knowledge of the variance-covariance matrix of the regression coefficients, denoted $\mathbf{C_U} = \mathrm{MSE_U}(\mathbf{A}^T\mathbf{A})^{-1}$ for OLS regression and $\mathbf{C_W} = \mathrm{MSE_W}(\mathbf{A}^T\mathbf{W}\mathbf{A})^{-1}$ for WLS regression. The $\mathrm{MSE_U}$ and $\mathrm{MSE_W}$ are mean-squared errors equal to the squares of $\mathrm{RMSE_U}$ and $\mathrm{RMSE_W}$ given by Eqs. (D.8a) and (D.8b). This information is included in the OLS or WLS regression software output that comes with the estimates of the p model coefficients. A variance-covariance matrix is a p × p matrix with coefficient variances along the diagonal and covariances between coefficient pairs in the off-diagonal entries.

D.7 References

Brett MT. 2004. "When is a Correlation Between Non-Independent Variables 'Spurious'?" *Oikos* 105(3):647-656.

Draper NR and H Smith. 1998. *Applied Regression Analysis*, Third Edition. John Wiley and Sons, New York.

Gilbert RO. 1987. *Statistical Methods for Environmental Pollution Monitoring.* Van Nostrand Reinhold, New York.

Ihaka R and R Gentleman. 1996. "R: A Language for Data Analysis and Graphics." *Journal of Computational and Graphical Statistics* 5:299-314.

Kenney BC. 1982. "Beware of Spurious Self-Correlations!" *Water Resources Research* 18(4):1041-1048.

Montgomery DC, EA Peck, and GG Vining. 2001. *Introduction to Linear Regression Analysis*, Third Edition. John Wiley and Sons, New York.

Myers RH and DC Montgomery. 1995. *Response Surface Methodology: Process and Product Optimization Using Designed Experiments*, John Wiley and Sons, New York.

Myers RH, DC Montgomery, and GG Vining. 2002. *Generalized Linear Models: With Applications in Engineering and the Sciences.* John Wiley and Sons, New York.

Piepel GF, SK Cooley, I Muller, H Gan, I Joseph, and IL Pegg. June 2007. *ILAW PCT, VHT, Viscosity and Electrical Conductivity Model Development*. VSL-07R1230-1, Vitreous State Laboratory, The Catholic University of America, Washington, D.C.

R Development Core Team. 2006. *R: A Language and Environment for Statistical Computing.* R Foundation for Statistical Computing, Vienna. http://www.R-project.org.

Appendix E

Data Assessment and Analysis to Support Developing Multiple Regression Models for Mixing Responses

GF Piepel
BG Amidan
A Heredia-Langner

Contents

E.1 Assessment of Data for Developing Mixing Models....E.1
E.2 Functionality Investigations....E.14
E.3 Replicate and Repeat Tests....E.50

Figures

E.1 Dot Plots Showing Distributions of Potential Predictor Variables for U_{CS} and H_C Mixing Models Over the Full Set of 2007 and 2008 Experimental Data....E.3
E.2 Dot Plots Showing Distributions of Potential Predictor Variables for U_{CS} and H_C Mixing Models Over the Trimmed Set of July 2007, Fall 2007, and 2008 Experimental Data....E.8
E.3 Scatterplot Matrix Plot of Pairwise Distributions of Predictor Variable Values for U_{CS} and H_C Mixing Models Over the Full Set of July 2007 (o), Fall 2007 (Δ), and 2008 (×) Experimental Data....E.11
E.4 Scatterplot Matrix Plot of Pairwise Distributions of Predictor Variable Values for U_{CS} and H_C Mixing Models Over the Trimmed Set of July 2007 (o), Fall 2007 (Δ), and 2008 (×) Experimental Data....E.12
E.5 Scatterplots of Pairwise Distributions of U_{TH} and U_T Values for U_{CS} and H_C Mixing Models Over the Full and Trimmed Sets of July 2007 (o), Fall 2007 (Δ), and 2008 (×) Experimental Data....E.13
E.6 Log-Log Plot of the Functional Relationship Between Critical Suspension Velocity (U_{CS}) and Tank Diameter (D) for Constant Sets of Values of Other Test Variables....E.17
E.7 Log-Log Plot of the Functional Relationship Between Critical Suspension Velocity (U_{CS}) and Number of Pulse Jets (N_J) for Constant Sets of Values of Other Test Variables....E.17
E.8 Log-Log Plot of the Functional Relationship Between Critical Suspension Velocity (U_{CS}) and Jet Nozzle Diameter (d) for Constant Sets of Values of Other Test Variables....E.18
E.9 Log-Log Plot of the Functional Relationship Between Critical Suspension Velocity (U_{CS}) and Jet Density (ϕ_J) for Constant Sets of Values of Other Test Variables....E.18
E.10 Log-Log Plot of the Functional Relationship Between Critical Suspension Velocity (U_{CS}) and Pulse Volume Fraction (ϕ_p) for Constant Sets of Values of Other Test Variables....E.19
E.11 Log-Log Plot of the Functional Relationship Between Critical Suspension Velocity (U_{CS}) and Duty Cycle (DC) for Constant Sets of Values of Other Test Variables....E.20
E.12 Log-Log Plot of the Functional Relationship Between Critical Suspension Velocity (U_{CS}) and Solids Volume Fraction (ϕ_S) for Constant Sets of Values of Other Test Variables....E.21
E.13 Log-Log Plot of the Functional Relationship Between Critical Suspension Velocity (U_{CS}) and Solids Particle Diameter ($d_S = d_{50}$) for Constant Sets of Values of Other Test Variables....E.22
E.14 Log-Log Plot of the Functional Relationship Between Critical Suspension Velocity (U_{CS}) and Density Ratio (s) for Constant Sets of Values of Other Test Variables....E.23

E.15 Log-Categorical Plot of Functional Relationship Between Critical Suspension Velocity (U_{CS}) and Head Shape (HS) for Constant Sets of Values of Other Test Variables E.23

E.16 Log-Log Plot of the Functional Relationship Between Critical Suspension Velocity (U_{CS}) and Unhindered Terminal Settling Velocity (U_T) for Constant Sets of Values of Other Test Variables E.24

E.17 Log-Log Plot of the Functional Relationship Between Cloud Height (H_C) and Velocity (U) for Each Set of Test Conditions in the July 2007 Data Set E.27

E.18 Log-Log Plot of the Functional Relationship Between Cloud Height (H_C) and Velocity (U) for Each Set of Test Conditions in the Fall 2007 Data Set E.28

E.19 Log-Log Plot of the Functional Relationship Between Cloud Height (H_C) and Velocity (U) for Each Set of 15-in. Tank Test Conditions in the 2008 Data Set E.29

E.20 Log-Log Plot of the Functional Relationship Between Cloud Height (H_C) and Velocity (U) for Each Set of D = 0.860 m (~ 34-in.) Tank Test Conditions in the 2008 Data Set E.30

E.21 Log-Log Plot of the Functional Relationship Between Cloud Height (H_C) and Velocity (U) for Each Set of 70-in. Tank Test Conditions in the 2008 Data Set E.31

E.22 Log-Log Plot of Functional Relationship Between Cloud Height at Critical Suspension Velocity (H_{CS}) and Tank Diameter (D) for Constant Sets of Values of Other Test Variables E.33

E.23 Log-Log Plot of Functional Relationship Between Cloud Height at Critical Suspension Velocity (H_{CS}) and Number of Pulse Jets (N_J) for Constant Sets of Values of Other Test Variables E.33

E.24 Log-Log Plot of Functional Relationship Between Cloud Height at Critical Suspension Velocity (H_{CS}) and Jet Nozzle Diameter (d) for Constant Sets of Values of Other Test Variables E.34

E.25 Log-Log Plot of the Functional Relationship Between Cloud Height at Critical Suspension Velocity (H_{CS}) and Jet Density (ϕ_J) for Constant Sets of Values of Other Test Variables E.34

E.26 Log-Log Plot of Functional Relationship Between Cloud Height at Critical Suspension Velocity (H_{CS}) and Pulse Volume Fraction (ϕ_p) for Constant Sets of Values of Other Test Variables E.35

E.27 Log-Log Plot of the Functional Relationship Between Cloud Height at Critical Suspension Velocity (H_{CS}) and Duty Cycle (DC) for Constant Sets of Values of Other Test Variables E.36

E.28 Log-Log Plot of Functional Relationship Between Cloud Height at Critical Suspension Velocity (H_{CS}) and Solids Volume Fraction (ϕ_S) for Constant Sets of Values of Other Test Variables E.37

E.29 Log-Log Plot of Functional Relationship Between Cloud Height at Critical Suspension Velocity (H_{CS}) and Solids Particle Diameter ($d_S = d_{50}$) for Constant Sets of Values of Other Test Variables E.38

E.30 Log-Log Plot of Functional Relationship Between Cloud Height at Critical Suspension Velocity (H_{CS}) and Density Ratio (s) for Constant Sets of Values of Other Test Variables E.39

E.31 Log-Categorical Plot of the Functional Relationship Between Cloud Height at Critical Suspension Velocity (H_{CS}) and Head Shape (HS) for Constant Sets of Values of Other Test Variables E.39

E.32 Log-Log Plot of Functional Relationship Between Cloud Height at Critical Suspension Velocity (H_{CS}) and Unhindered Terminal Settling Velocity (U_T) for Constant Sets of Values of Other Test Variables E.40
E.33 Cloud Height (H_C) Versus Target Velocity (U) Values for the 70E and 70F Head Shapes with s = 2.48, $d_{50} = 6.93\times10^{-5}$, $\phi_p = 0.05$, $\phi_S = 0.00155$ and DC = 0.33 ..... E.43
E.34 Cloud Height (H_C) Versus Target Velocity (U) Values for the 70E and 70F Head Shapes with s = 2.48, $d_{50} = 6.93\times10^{-5}$, $\phi_p = 0.05$, $\phi_S = 0.005$ and DC = 0.33 ..... E.43
E.35 Cloud Height (H_C) Versus Target Velocity (U) Values for the 70E and 70F Head Shapes with s = 2.48, $d_{50} = 6.93\times10^{-5}$, $\phi_p = 0.05$, $\phi_S = 0.01$ and DC = 0.33 ..... E.44
E.36 Cloud Height (H_C) Versus Target Velocity (U) Values for the 70E and 70F Head Shapes with s = 2.48, $d_{50} = 6.93\times10^{-5}$, $\phi_p = 0.05$, $\phi_S = 0.0143$ and DC = 0.18 ..... E.44
E.37 Cloud Height (H_C) Versus Target Velocity (U) Values for the 70E and 70F Head Shapes with s = 2.48, $d_{50} = 6.93\times10^{-5}$, $\phi_p = 0.05$, $\phi_S = 0.0143$ and DC = 0.33 ..... E.45
E.38 Cloud Height (H_C) Versus Target Velocity (U) Values for the 70E and 70F Head Shapes with s = 2.48, $d_{50} = 6.93\times10^{-5}$, $\phi_p = 0.05$, $\phi_S = 0.0143$ and DC = 0.66 ..... E.45
E.39 Cloud Height (H_C) Versus Target Velocity (U) Values for the 70E and 70F Head Shapes with s = 2.48, $d_{50} = 6.93\times10^{-5}$, $\phi_p = 0.10$, $\phi_S = 0.0143$ and DC = 0.18 ..... E.46
E.40 Cloud Height (H_C) Versus Target Velocity (U) Values for the 70E and 70F Head Shapes with s = 2.48, $d_{50} = 6.93\times10^{-5}$, $\phi_p = 0.10$, $\phi_S = 0.0143$ and DC = 0.33 ..... E.46
E.41 Cloud Height (H_C) Versus Target Velocity (U) Values for the 70E and 70F Head Shapes with s = 2.48, $d_{50} = 6.93\times10^{-5}$, $\phi_p = 0.10$, $\phi_S = 0.0143$ and DC = 0.66 ..... E.47
E.42 Cloud Height (H_C) Versus Target Velocity (U) Values for the 70E and 70F Head Shapes with s = 2.48, $d_{50} = 6.93\times10^{-5}$, $\phi_p = 0.15$, $\phi_S = 0.0143$ and DC = 0.18 ..... E.47
E.43 Cloud Height (H_C) Versus Target Velocity (U) Values for the 70E and 70F Head Shapes with s = 2.48, $d_{50} = 6.93\times10^{-5}$, $\phi_p = 0.15$, $\phi_S = 0.0143$ and DC = 0.33 ..... E.48
E.44 Cloud Height (H_C) Versus Target Velocity (U) Values for the 70E and 70F Head Shapes with s = 2.46, $d_{50} = 1.664\times10^{-4}$, $\phi_p = 0.05$, $\phi_S = 0.00155$ and DC = 0.33 ..... E.48
E.45 Cloud Height (H_C) Versus Target Velocity (U) Values for the 70E and 70F Head Shapes with s = 4.18, $d_{50} = 7.56\times10^{-5}$, $\phi_p = 0.05$, $\phi_S = 0.005$ and DC = 0.18 ..... E.49
E.46 Cloud Height (H_C) Versus Target Velocity (U) Values for the 70E and 70F Head Shapes with s = 4.18, $d_{50} = 7.56\times10^{-5}$, $\phi_p = 0.05$, $\phi_S = 0.005$ and DC = 0.33 ..... E.49

Tables

E.1 Potential Predictor Variables for Developing Models of UCS and HC Response Variables E.1
E.2 Comparison of U_{CS} and H_{CS} Data from 2008 Tests with Two Head Shapes (E and FD) on 70-in. Tanks E.42
E.3 Near-Replicate and Near-Repeat Tests at Critical Suspension Conditions E.51
E.4 U_{CS} and H_{CS} Values, SDs, and %RSDs for Near-Replicate Sets of M3 Mixing Tests E.53
E.5 U_{CS} and H_{CS} Values, %RSDs, and Standard Deviations for Near-Repeat Sets of M3 Mixing Tests E.54

Appendix E

Data Assessment and Analysis to Support Developing Multiple Regression Models for Mixing Responses

This appendix discusses the data assessments and analyses performed to support development of empirical and semi-empirical models between key mixing variables (response variables) and nondimensional or dimensional explanatory variables (predictor variables). The response variables of interest include critical suspension velocity (U_{CS}) and cloud height (H_C). The predictor variables are generally test variables or functions of test variables.

Section E.1 presents and discusses plots to assess how well the data support developing empirical or semi-empirical models (henceforth, models) for mixing response variables. Section E.2 presents the results of investigations to understand the functionality between mixing response variables and test variables. Section E.3 briefly discusses uncertainty estimates based on limited near-replicate and near-repeat sets of test data.

E.1 Assessment of Data for Developing Mixing Models

This section presents and discusses plots of the data available for developing models for the mixing response variables U_{CS} and H_C. The intent of these plots is to assess the degree of support the data provide for including potential predictor variables or interactions of predictor variables in models. One- and two-dimensional plots of the potential predictor variables (listed in Table E.1) are presented and discussed in Sections E.1.1 and E.1.2, respectively.

Table E.1. Potential Predictor Variables for Developing Models of UCS and HC Response Variables

Variable	Definition
D	tank diameter (m)
N_O	number of operating pulse jets on outer ring
N_I	number of operating pulse jets on inner ring
N_J	$N_J = N_O + N_I$ = number of operating pulse jets (number)
d	jet nozzle diameter (m)
ϕ_J	phiJ = jet density = $N_J(d/D)^2$ (nondimensional)
ϕ_p	phiP = pulse volume fraction = $N_J V_P / V_{REF}$ (nondimensional)
DC	duty cycle (nondimensional)
s	density ratio of solids to liquid (nondimensional)
ϕ_S	phiS = solids volume fraction = $V_S/V_{REF} = V_S/(\square D^3/4)$ (nondimensional)
d_S	solids particle diameter = d_{50} = median particle diameter (m)
HS	head shape (E = elliptical, FD = flange and dish, S = spherical)
U_T	unhindered terminal settling velocity (m/s)
U_{TH}	hindered terminal settling velocity (m/s)

In Sections E.1.1 and E.1.2, the predictor variable values are plotted using data from the U_{CS} data set combined from the July 2007, Fall 2007, and 2008 test campaigns. Only the pulsed data (i.e., DC < 1) were used for the plots in this section because the mixing models discussed in Appendix F were only developed for pulsed data. Insufficient steady-state (DC = 1) data were collected to include for model development purposes.

The U_{CS} data set was used for the plots in this section because the H_C data set would contain multiples of predictor-variable combinations, corresponding to measuring H_C at each of several target velocities (U) for each set of test conditions. However, the distribution and scatter plots in this section apply to both U_{CS} and H_C. The functionality plots for H_C versus U (in Section E.2.3) show the distribution of target velocity values for each set of test conditions. Hence, U is not included in the plots in Section E.1.

E.1.1 One-Dimensional Dot Plots of Potential Predictor Variables

One-dimensional dot plots are used to assess the distribution of values for each potential predictor variable over its data range. Plots showing outlying values or limited data in a subrange of a predictor variable suggest caution in using such data to develop models. Outlying data, or sparse data over a subrange of the predictor variable, can be very influential when fitting a model to data. Further, the functional relationship between a response variable and a predictor variable can change over a wider range of the predictor variable. In addition, interactive effects between two (or more) predictor variables are more likely to be significant over wider ranges of the predictor variables. Thus, it can be difficult to develop and fit more complicated relationships over wider ranges of predictor variables when there are outlying or sparse data in subranges of one or more predictor variables. Model fits over wider ranges of predictor variables when there are outlying or sparse values may be degraded or have much higher uncertainty compared with model fits over subranges where predictor-variable values are better distributed.

However, when models must be used to extrapolate, the existence of few data that lie closer to the state to which one must extrapolate represent particularly useful information. Consider the hypothetical situation where numerous experimental data exist from scaled experiments at several closely-distributed length scales, and a few data exist for the actual, full-scale system of interest. In a statistical sense, these latter data are outliers that can unduly influence the fit to the data that ultimately is used to predict the behavior of the actual system. But in an engineering sense, the few data available for the actual system ought to be highly influential in predicting the behavior of the system because they are the only measurements made that require no extrapolation. Then if the few data are not at the actual scale but at a scale significantly closer to actual scale than for the majority of the data, their high influence on a fitted model used for extrapolation might be beneficial.

Figure E.1 shows dot plots for the potential predictor variables listed in Table E.1, using the combined July 2007, Fall 2007, and 2008 data described at the end of Section E.1. The number of data points represented by a dot is shown on the right of each dot plot in Figure E.1. Fractional-size dots are used to represent fewer than the number of data points indicated for full-size dots. The following observations are made regarding distributions of values of potential model predictor variables over their experimental ranges. Although not shown in the dot plots, the observations include information on the number of data points from each of the three test campaigns.

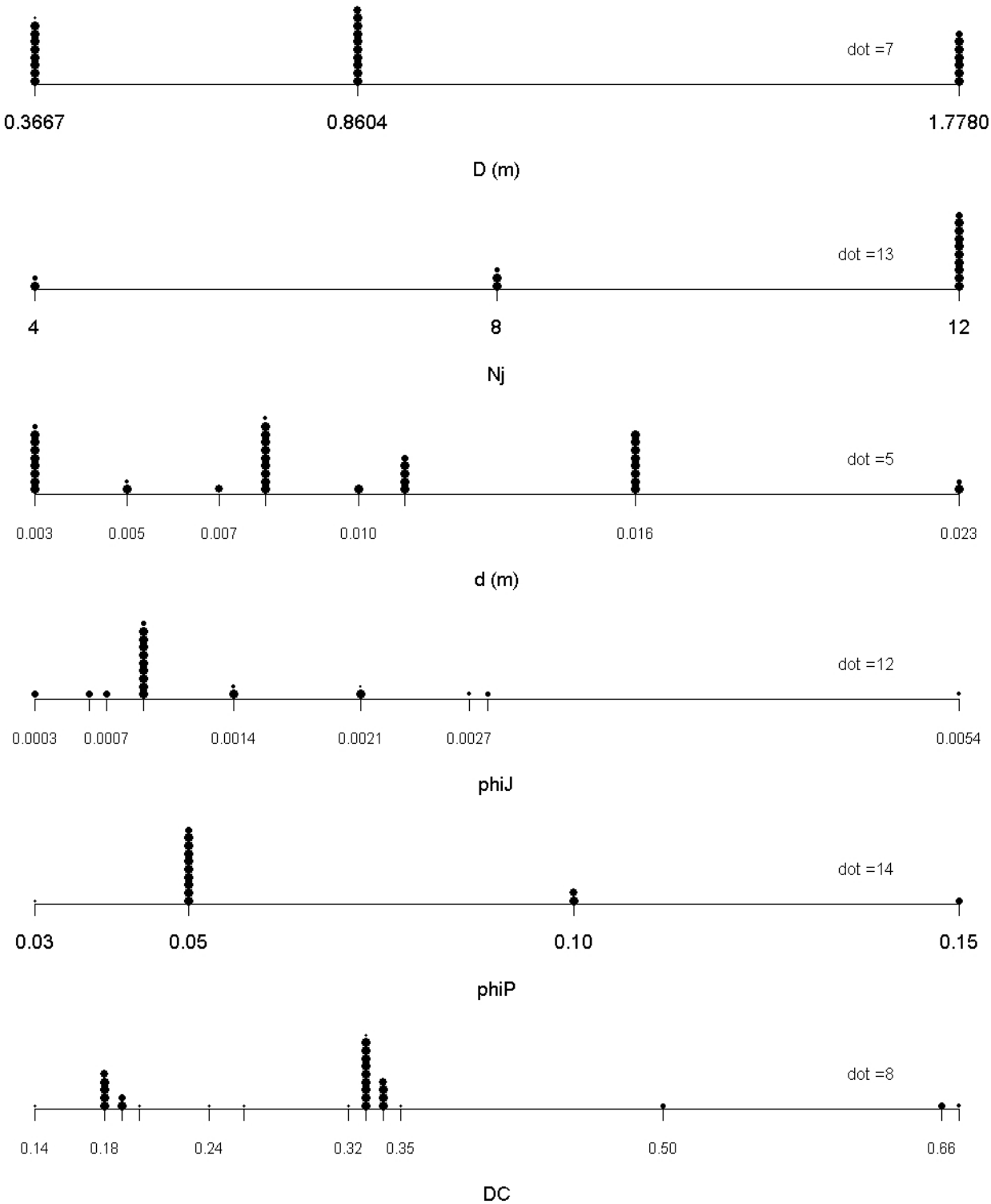

Figure E.1. Dot Plots Showing Distributions of Potential Predictor Variables for U_{CS} and H_C Mixing Models Over the Full Set of 2007 and 2008 Experimental Data. The number of data points represented by a dot is shown on the right of each dot plot. Fractional-size dots represent fewer than the indicated number of data points.

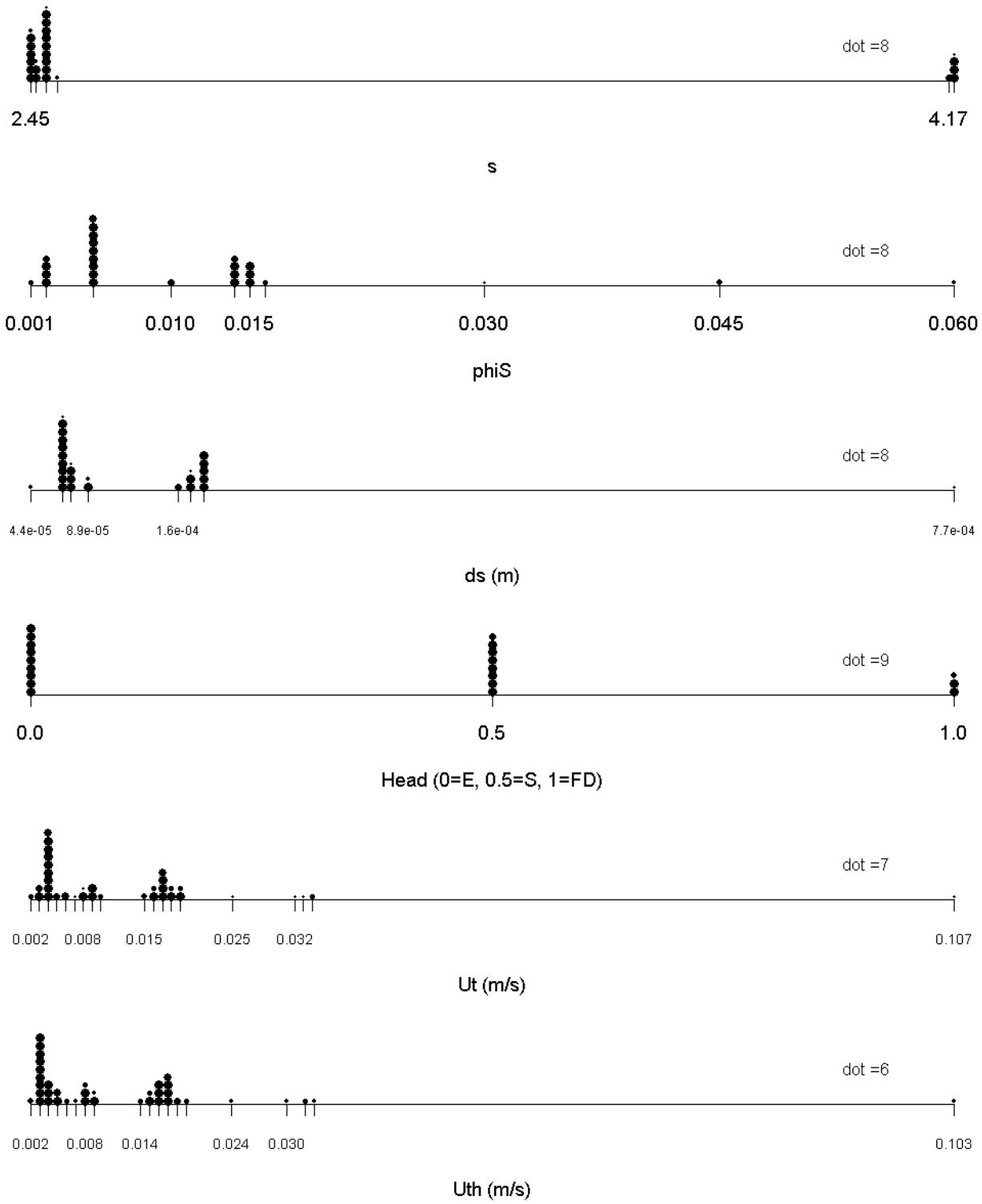

Figure E.1. (contd) Dot Plots Showing Distributions of Potential Predictor Variables for U_{CS} and H_C Mixing Models Over the Full Set of 2007 and 2008 Experimental Data. The number of data points represented by a dot is shown on the right of each dot plot. Fractional-size dots represent fewer than the indicated number of data points.

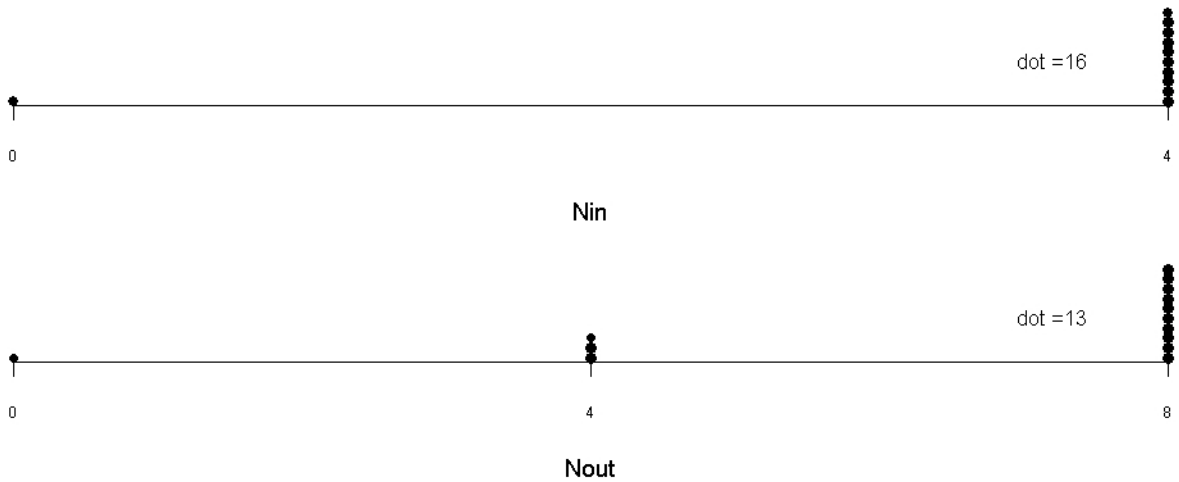

Figure E.1. (contd) Dot Plots Showing Distributions of Potential Predictor Variables for U_{CS} and H_C Mixing Models Over the Full Set of 2007 and 2008 Experimental Data. The number of data points represented by a dot is shown on the right of each dot plot. Fractional-size dots represent fewer than the indicated number of data points.

The U_{CS} data set contained 186 rows after the steady-state (DC = 1) data were removed, as discussed in Section E.1. In addition, 11 rows were removed because the return-line height was less than D; these included the limited Fall 2007 data in which fill height was varied. Finally, two rows were removed because of questionable U_{CS} values (the U_{CS} values were greater than the target velocity for the row). These changes resulted in a full data set of 173 rows, which is the same data set used to develop the physical-based models for U_{CS} in Section 7.3.2.

1. Diameter of tank, D (m)

a. 57 of 173 values are 14.44 in. (0.367 m), all from 2008
b. 69 of 173 values are 33.88 in. (0.860 m), 16 from July 2007, 35 from Fall 2007, and 18 from 2008
c. 47 of 173 values are 70 in. (1.778 m), all from 2008.

2. Number of operating pulse jets, N_J

a. 18 of 173 values are 4 (15 from Fall 2007, 3 from 2008)
b. 30 of 173 values are 8 (13 from Fall 2007, 17 from 2008)
c. 125 of 173 values are 12 (16 from July 2007, 7 from Fall 2007, and 102 from 2008).

3. Jet nozzle diameter, d (m)

a. Values range from 0.0032 to 0.0234 m
b. There are 7 values at 0.0234 m, and the rest are ≤ 0.0156 m.

4. Jet density, ϕ_J (nondimensional)

a. Values range from approximately 0.0003 to 0.0054
b. There are 3 values ~ 0.0054 and 6 values ~ 0.0027 or 0.0028 (all 2008)
c. 164 of the 173 values are ≤ 0.0021 approximately.

5. Pulse Volume Fraction, ϕ_p (nondimensional)

d. 2 of 173 values are ~ 0.03 (all from July 2007)
b. 136 of 173 values are ~ 0.05 (10 from July 2007, 35 from Fall 2007, 91 from 2008)
c. 26 of 173 values are ~ 0.10 (4 from July 2007, 22 from 2008)
d. 9 of 173 values are ~ 0.15 (all from 2008).

6. Duty Cycle, DC (nondimensional)

a. 162 of 173 values are ≤ 0.40
b. 3 of 173 range from ~ 0.47 to 0.54 (2 from July 2007, 1 from 2008)
c. 8 of 173 ~ 0.66 (all from 2008).

7. Density Ratio, s (nondimensional)

a. 143 of 173 have s ~ 2.45 − 2.50 (15 from July 2007, 46 from Fall 2007, 92 from 2008)
b. 30 of 173 have s ~ 4.17 or 4.18 (all from 2008).

8. Solids Volume Fraction, ϕ_S (nondimensional)

a. 166 of 173 values are ≤ 0.016 (16 from July 2007, 35 from Fall 2007, 115 from 2008)
e. 1 of 173 values = 0.03 (2008)
f. 4 of 173 values = 0.045 (all from 2008)
g. 2 of 173 values = 0.06 (all from 2008).

9. Median particle size diameter, $d_S = d_{50}$ (m)

a. 110 of 173 values range from ~ 4.4E-05 to 8.9E-05 (10 from Fall 2007, 100 from 2008)
b. 62 of 173 values range from ~ 1.4E-04 to 1.8E-04 (15 from July 2007, 25 from Fall 2007, 22 from 2008)
c. 1 of 173 values ~ 7.7E-04 (July 2007).

10. Head Shape, HS (E, S, or FD)

a. 81 of 173 are "E" (all from 2008)
b. 69 of 173 are "S" (16 from July 2007, 35 from Fall 2007, 18 from 2008)
c. 23 of 173 are "FD" (all for tests in 70-in. tank in 2008).

11. Unhindered terminal settling velocity, U_T (m/s)

a. 167 of 173 values are ≤ 0.017 approximately (15 from July 2007, 35 from Fall 2007,
b. 117 from 2008)
c. 5 of 173 ~ 0.028 (all 2008)
d. 1 of 173 ~ 0.102 (July 2007).

12. Hindered terminal settling velocity, U_{TH} (m/s)

a. 167 of 173 values are ≤ 0.019 approximately (15 from July 2007, 35 from Fall 2007, 117 from 2008)
b. 5 of 173 range from ~ 0.024 to 0.033 (all 2008)
c. 1 of 173 ~ 0.103 (Fall 2007).

Several of the preceding observations show that some test variables have outlying or limited data that significantly expand the ranges of those variables. As is noted in Section E.1.1, such data can be very influential when developing empirical or semi-empirical models, yielding model coefficients that are very uncertain because of being mostly determined by the outlying or limited data. Hence, in addition to the full data set, it was decided to form a "trimmed" data set that eliminates these outlying data points in

predictor-variable space. Specifically, the ranges of predictor variables eliminated in forming the trimmed data set include:

- DC > 0.41 (eliminates 11 of 173 test conditions)
- ϕ_S > 0.016 (eliminates 7 of 173 test conditions)
- d_S (d_{50}) > 1.8E-04 (eliminates 1 of 173 test conditions).

Hence, the trimmed data set for U_{CS} consists of 154 rows of data.

However, as is noted in Section E.1.1, these trimmed data lie in the direction of the expected values for the system to which models developed from the data must be extrapolated. Hence, models for mixing responses (U_{CS} and H_C) were developed for both the full and trimmed data sets (see Appendix F). In the case of models fit to the full data set, caution will need to be exercised regarding the limited number and influential nature of the outlying data.

Note that the test condition eliminated by the d_S (d_{50}) > 1.8E-04 constraint is the same test condition with extreme values of U_T and U_{TH}. It was decided not to eliminate the five data points with ϕ_J ~ 0.0054, even though they roughly double the range of that variable (the next closest values are ~ 0.0027). The values of N_J, d, and D used to calculate ϕ_J (the formula is given in Table E.1) for these three data points are not extreme within their ranges. Hence, they were not eliminated in forming the trimmed data set.

Figure E.2 shows another set of dot plots for the trimmed data set, which provides for visualizing the distribution of predictor variable values over the ranges where the vast majority of data points fall. The trimmed data set also provides a more stable basis for developing models for mixing response variables.

E.1.2 Two-Dimensional Scatterplots of Potential Predictor Variables

Two-dimensional scatterplots are used to assess the bivariate distributions of two predictor variables over the rectangular space determined by their respective ranges. Scatterplot matrix plots display in a single figure all possible pairwise scatterplots for a set of predictor variables. The size of individual scatterplots of pairs of predictor variables are reduced in such plots, but are sufficient for the intended purpose. Specifically, scatterplot matrix plots are useful for identifying 1) highly correlated predictor variables, and 2) subregions of predictor-variable combinations that are not represented, or are only sparsely represented, in the data.

When two predictor variables are very highly correlated, it will usually be inappropriate to include both in a model. Rather, only one of the predictor variables should be included in the model, and it should be kept in mind that the one predictor variable is representing the combined effects of the highly-correlated pair of variables.

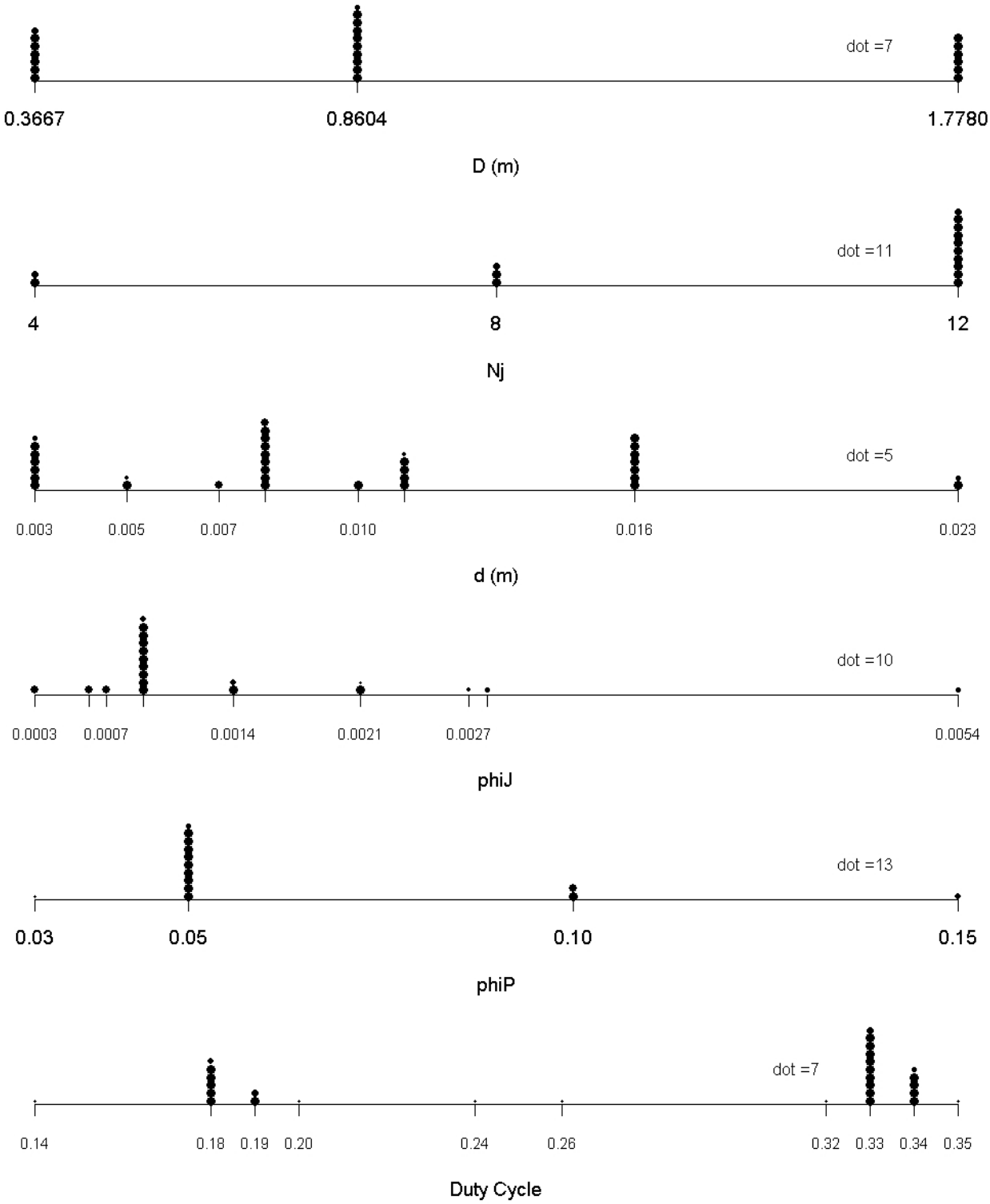

Figure E.2. Dot Plots Showing Distributions of Potential Predictor Variables for U_{CS} and H_C Mixing Models Over the Trimmed Set of July 2007, Fall 2007, and 2008 Experimental Data. The number of data points represented by a dot is shown on the right of each dot plot. Fractional-size dots represent fewer than the indicated number of data points.

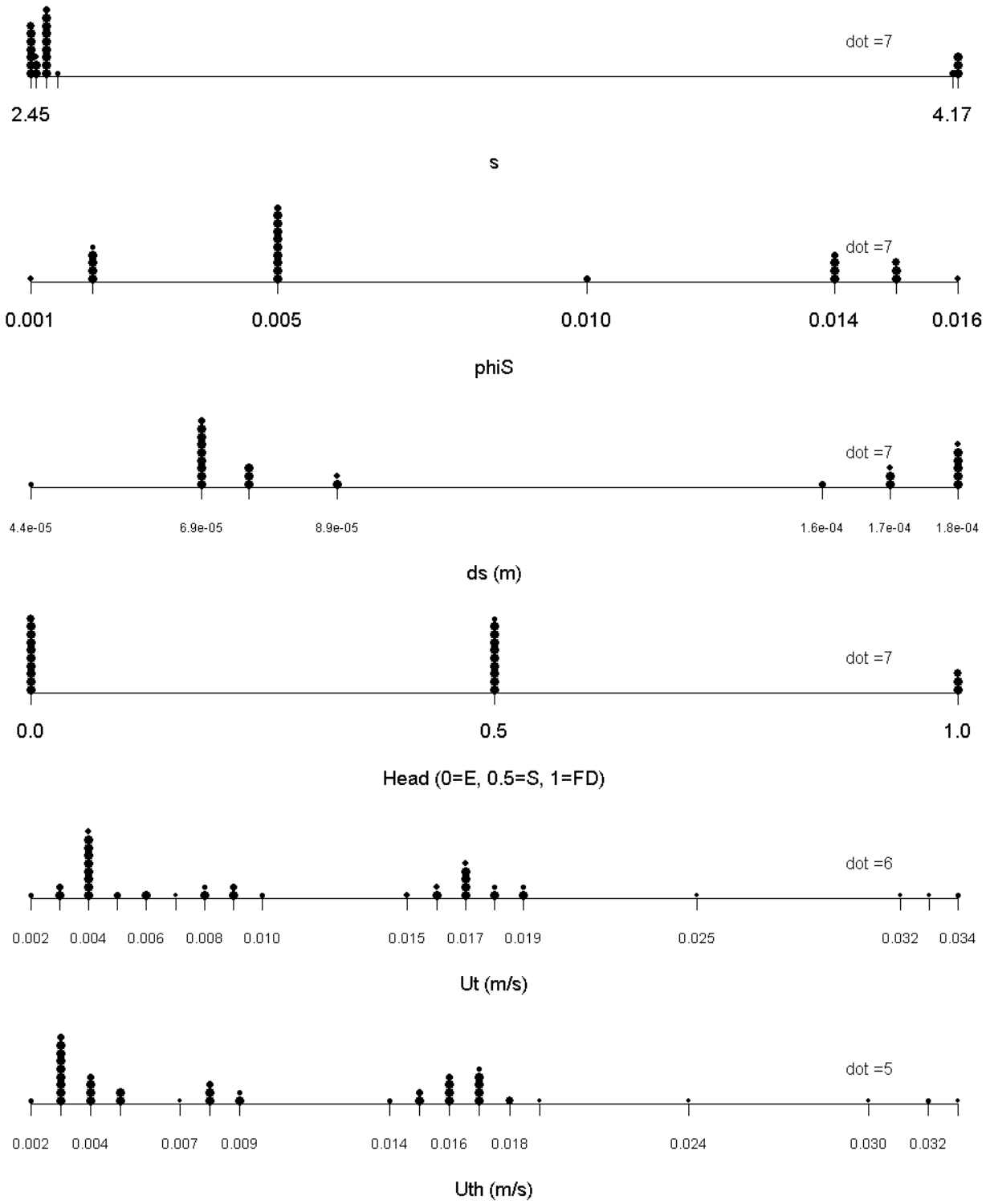

Figure E.2. (contd) Dot Plots Showing Distributions of Potential Predictor Variables for U_{CS} and H_C Mixing Models Over the Trimmed Set of July 2007, Fall 2007, and 2008 Experimental Data. The number of data points represented by a dot is shown on the right of each dot plot. Fractional-size dots represent fewer than the indicated number of data points.

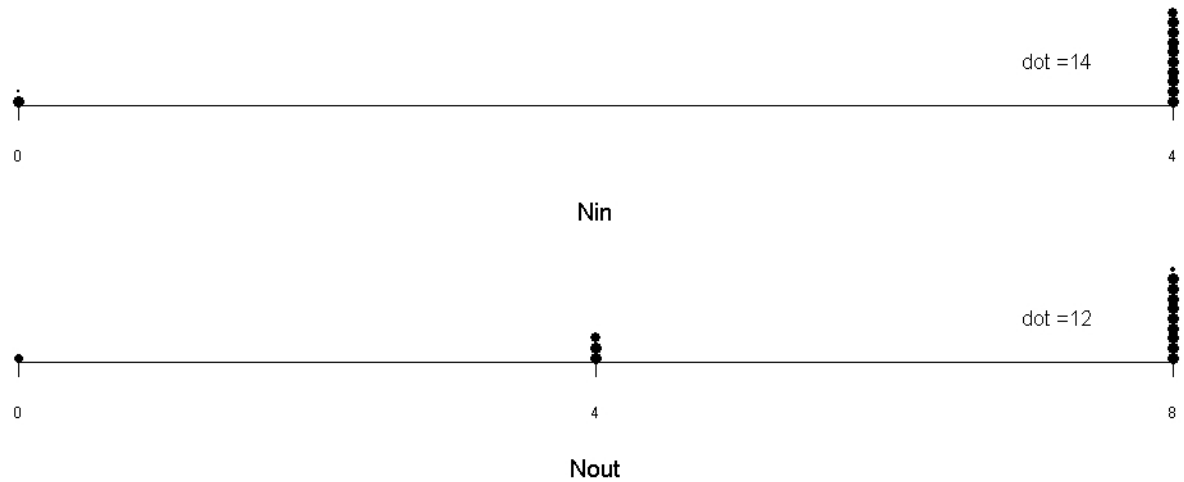

Figure E.2. (contd) Dot Plots Showing Distributions of Potential Predictor Variables for U_{CS} and H_C Mixing Models Over the Trimmed Set of July 2007, Fall 2007, and 2008 Experimental Data. The number of data points represented by a dot is shown on the right of each dot plot. Fractional-size dots represent fewer than the indicated number of data points.

A scatterplot of two predictor variables should ideally have data points well distributed over the rectangle representing combinations of values of the two variables over their ranges. Patterns in the shape of an "L" (in any orientation) or "+" indicate that each variable was only varied at a single value (or a small range of similar values) of the other variable. Data with such patterns do not support assessing whether there is an interactive effect of the two variables. A corner of a scatterplot (e.g., both variables at their highest values at the same time) with no data indicates that the corresponding variable combinations were not investigated in the testing. Such data patterns can limit the ability to assess interactive effects of the pair of variables.

Figure E.3 displays the scatterplot matrix for the variables listed in Table E.1 using the full data set of 173 points described at the end of Section E.1 and Section E.1.1. Figure E.4 shows the scatterplot matrix for the trimmed data set of 154 points discussed in Section E.1.1. Although the individual scatterplots in these figures are small, they are sufficient for the intended purpose of seeing strong correlations, outliers, or untested combinations of pairs of predictor variables. Figure E.5 displays a separate scatterplot of U_{TH} versus U_T. The following observations are made based on Figures E.3 to E.5.

- D and d are strongly positively correlated for the full (Figure E.3) and trimmed (Figure E.4) data sets. This suggests that it may not be appropriate to include both in a model for U_{CS} or H_C. Also, because $\phi_J = N_J (d/D)^2$, the strong correlation between D and d means that the resulting value of ϕ_J will be strongly determined by N_J. Further, on a log-log basis ϕ_J would be redundant given N_J, d, and D.
- Terminal settling velocity (U_T) and hindered terminal settling velocity (U_{TH}) are strongly correlated for the full and trimmed data sets (Figure E.5). Figure E.5 shows some differences for U_{TH} versus U_T for the outlying data points dropped from the full data set to form the trimmed data set. However, there may not be enough of those data points to show the merit of using U_{TH} instead of U_T in U_{CS} and H_C modeling work (in Appendix F). Hence, it is not clear whether there is any advantage (for these data sets) to use U_{TH} instead of U_T in developing multiple-regression models for mixing response

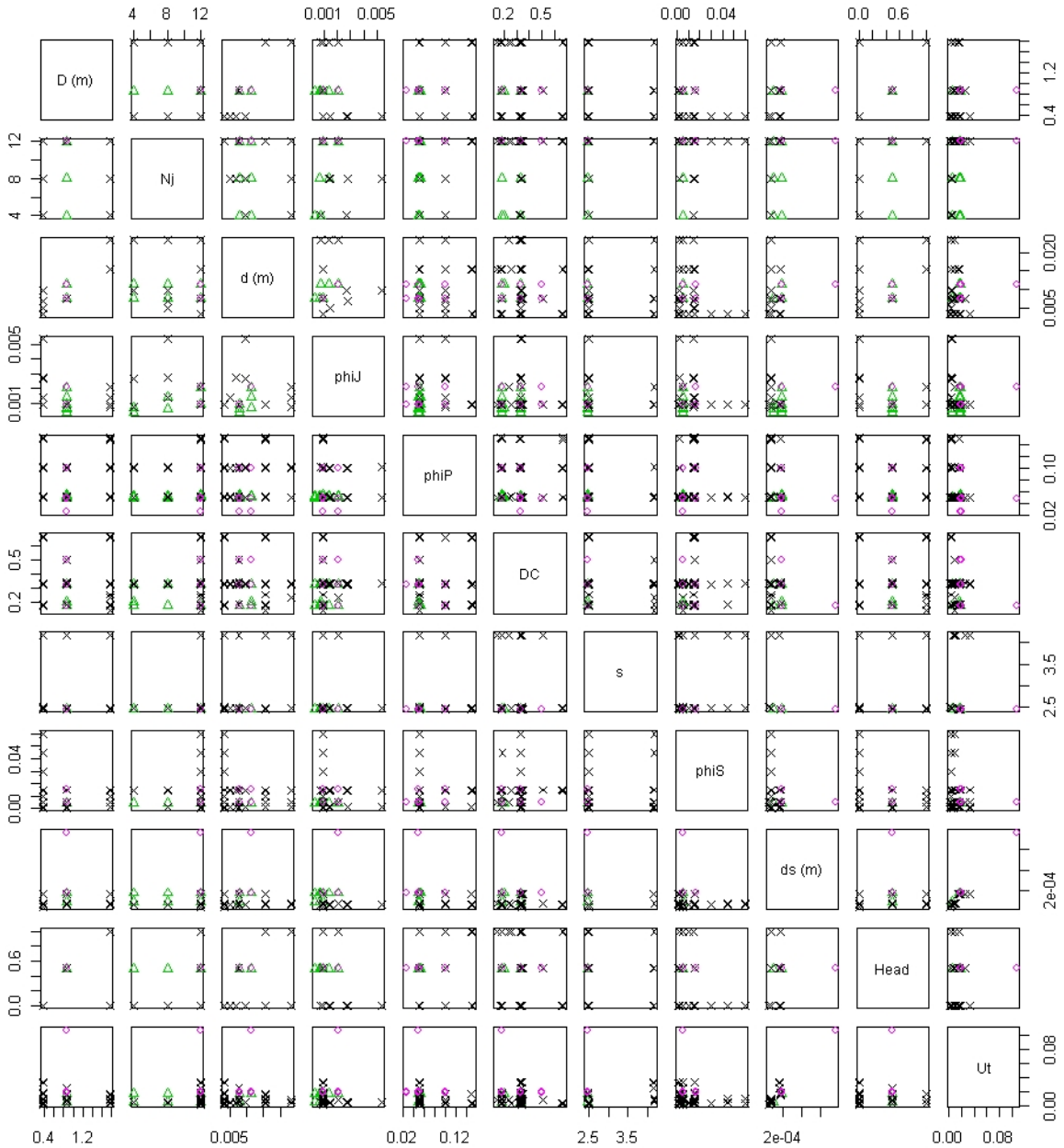

Figure E.3. Scatterplot Matrix Plot of Pairwise Distributions of Predictor Variable Values for U_{CS} and H_C Mixing Models Over the Full Set of July 2007 (o), Fall 2007 (Δ), and 2008 (×) Experimental Data. Note that for HS (Head), 0 = E and 1 = FD.

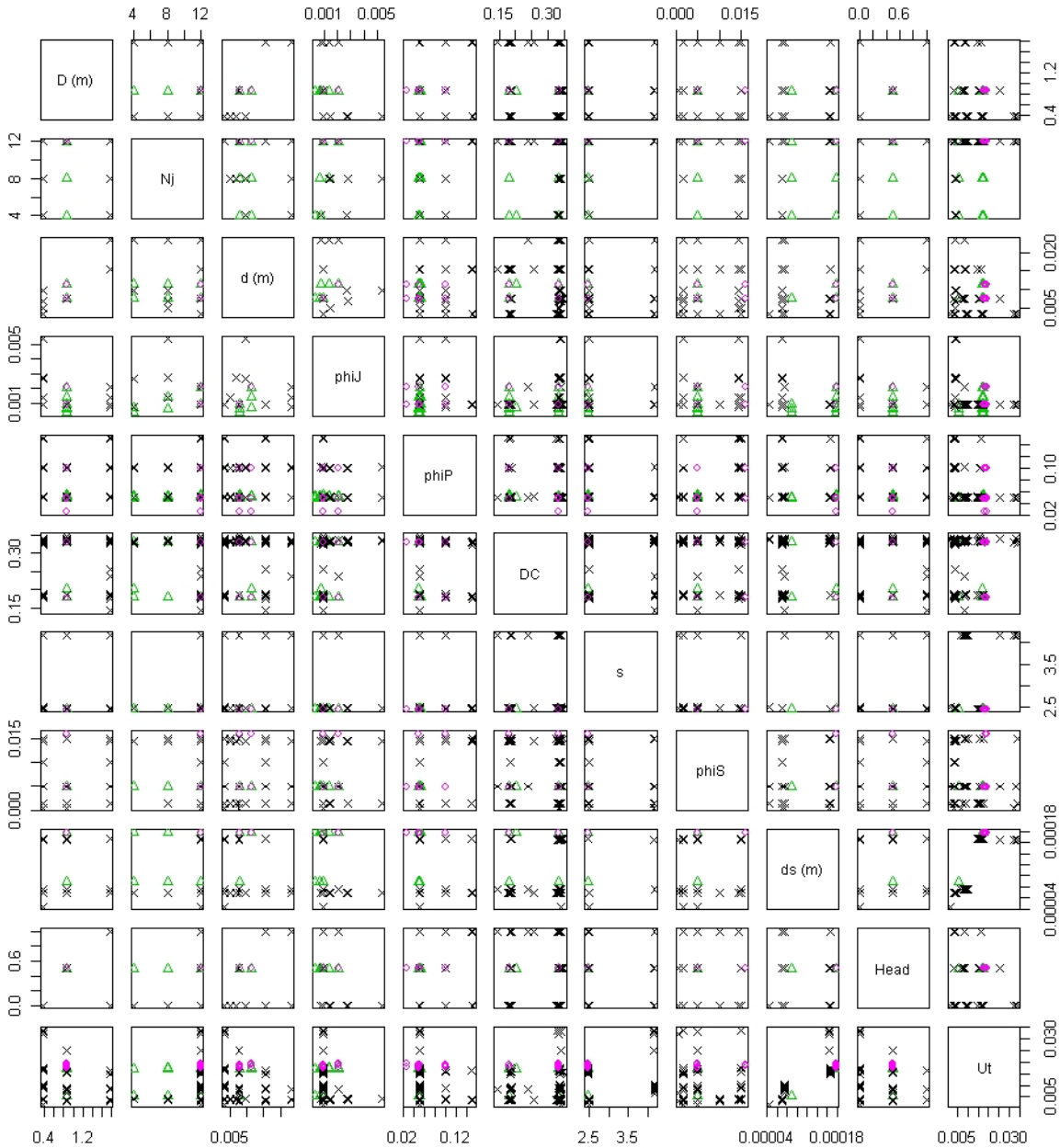

Figure E.4. Scatterplot Matrix Plot of Pairwise Distributions of Predictor Variable Values for U_{CS} and H_C Mixing Models Over the Trimmed Set of July 2007 (o), Fall 2007 (Δ), and 2008 (×) Experimental Data. Note that for HS (Head), 0 = E and 1 = FD.

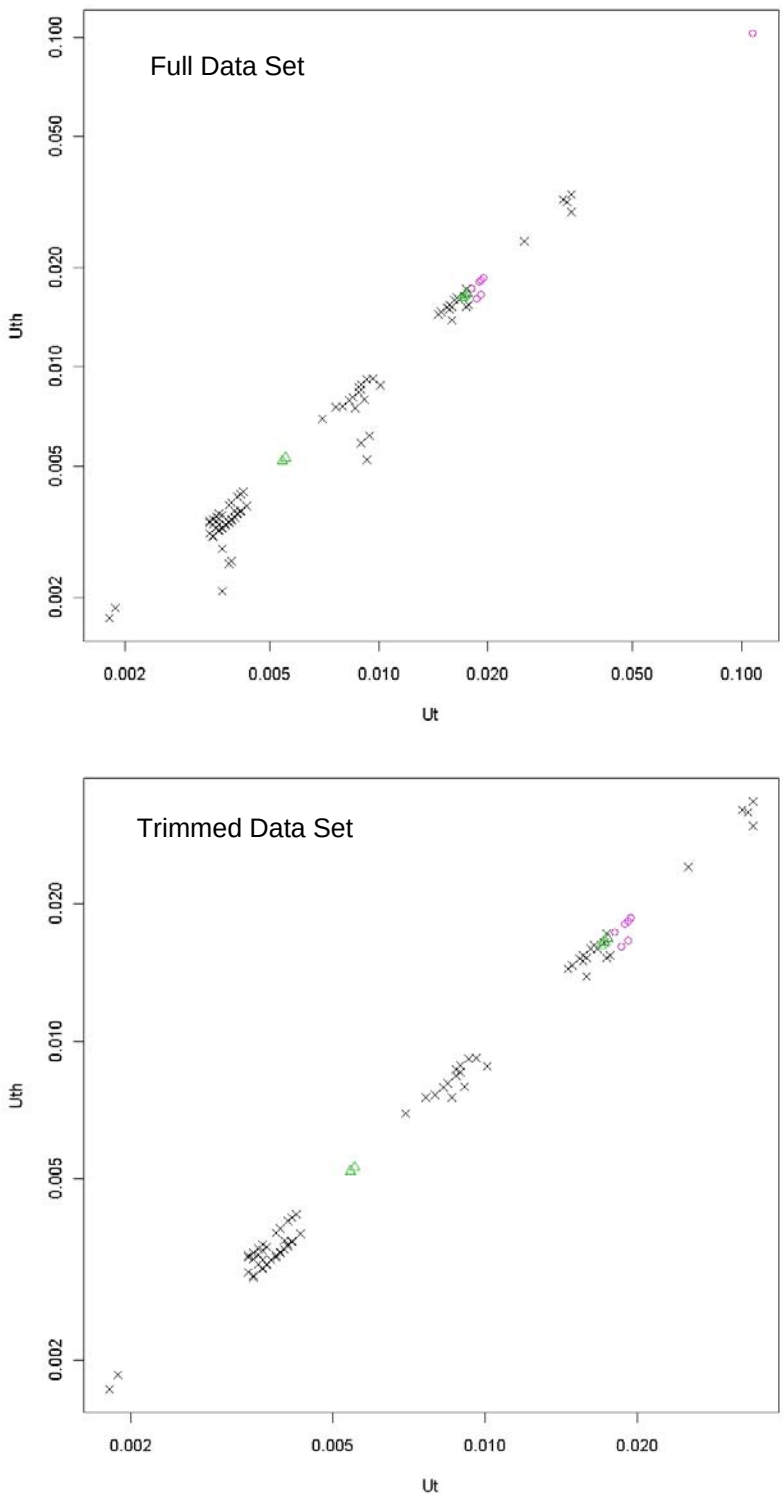

Figure E.5. Scatterplots of Pairwise Distributions of U_{TH} and U_T Values for U_{CS} and H_C Mixing Models Over the Full and Trimmed Sets of July 2007 (o), Fall 2007 (Δ), and 2008 (×) Experimental Data

variables. Further, U_T is associated physically with only the materials used in a test (the particles and the liquid in which they settle). However, U_{TH} also depends strongly on the local particle concentration, which varies profoundly over space and time during a pulse cycle. Consequently it may be difficult to physically interpret any apparent correlation of the response variables with U_{TH} compared to (or in addition to) the correlation with U_T.

- The variable d_S (d_{50}) is very strongly correlated with U_T for the full data set (Figure E.3), and still strongly correlated for the trimmed data set (Figure E.4). The latter correlation is very strong except for a few data points (seen in the upper right portions of the d_S vs. U_T scatterplot), which weakened the overall correlation somewhat. This observation suggests that it may be of limited benefit to include both d_S and U_T (or U_{TH}) in a multiple-regression model for mixing response variables. Further, the only anticipated effect of d_S on the behavior of the system is through its effect on U_T. Hence, a priori there is a physical reason not to include d_S in addition to U_T.
- The ϕ_J vs. s, ϕ_J vs. d_S, and ϕ_J vs. HS scatterplots in Figures E.3 and E.4 have less than complete rectangular distributions of points, indicating somewhat limited bases for assessing interactive effects of those pairs of predictor variables.
- The s vs. N_J scatterplots in Figures E.3 and E.4 show that tests with the high value of s (~4.17) were only performed with 12-jet configurations. Hence, there is no basis for assessing whether s and N_J have an interactive effect.
- Several scatterplots of ϕ_S with other variables in Figure E.3 (full data set) have less than complete rectangular distributions of points, indicating a lack of support for quantifying interactive effects of these variables over the full range of ϕ_S. The issue is resolved in Figure E.4 for the trimmed data set.
- Several scatterplots of HS with other variables in Figures E.3 and E.4 have less than complete rectangular distributions of points. This is because tests with HS = FD were only performed in the 70-inch tank (D = 1.778 m) with 12-jet (N_J = 12) configurations, and with only partial ranges of some other test variables. These observations indicate a lack of support for quantifying interactive effects of D and N_J with HS, and limited support for interactive effects of some other variables with HS.
- The scatterplots of U_T with other variables in Figure E.3 show limited or no support for interactive effects because of the outlying value of U_T (d_S). The situation is improved for the trimmed data set in Figure E.4, although there is still less than complete rectangular distributions of points in the scatterplots of some variables with U_T. This indicates some limitations on support for interactive effects of some other variables with U_T (or U_{TH}).

These observations were factored into the process of developing and confirming multiple-regression models for U_{CS} and H_C, as discussed in Appendix F.

E.2 Functionality Investigations

This section presents plots that provide information on the functional relationships between the mixing response variables and test variables. Such plots are referred to simply as *functionality plots*. Several test variables were varied in the test runs, with each one potentially impacting the value of a given mixing response variable observed for a given set of test variable values. Hence, plots of all the data with a response variable on the y-axis and each test variable on the x-axis typically are not very informative.

The reason for this is that the effect on the response variable of the test variable on the x-axis is obscured by the effects of the many other test variables. Thus, functionality plots described in more detail in the subsequent subsection were investigated.

E.2.1 Functionality Plots

In subsequent subsections, functionality plots are shown for a response variable (y-axis) versus each test variable (x-axis) for subsets of the data. All test runs with two or more values of the test variable on the x-axis, and a set of constant values for the remaining test variables, are included in a given functionality plot. For each set of constant values of the remaining test variables, a different plotting symbol is used. The same plotting symbols for the two or more values of the test variable on the x-axis are joined by line segments to aid in visualizing how the relationship between a response variable and the test variable on the x-axis depends on the different sets of constant values for the other test variables.

A challenge in constructing functionality plots is that several test variables have close but not exactly the same values for different tests. This makes it difficult for the functionality plot of a given variable to obtain sets of constant values for the remaining test variables. Thus, it was necessary to do some rounding and grouping of test variable values to be able to obtain sets of constant values for the remaining test variables. The following adjustments were made to the test variable values to yield the functionality plots presented in Sections E.2.2 and E.2.3.

- d values were not used in determining sets of constant values because of the larger number of values it has, and also because there is a strong correlation between d and D (see Figures E.3 and E.4).
- ϕ_p values close to 0.05, 0.10, and 0.15 were rounded to these values.
- DC values close to 0.18, 0.33, and 0.66 were grouped at these values.
- s values close to 2.48 and 4.18 were rounded to these values.
- $d_S = d_{50}$ values ~ 0.00006 and ~ 0.00007 were grouped as 0.00007, values ~ 0.00008 and 0.00009 were grouped as 0.00008, and values around 0.00016 were grouped at this value.

However, these adjustments to test variable values were only used for obtaining sets of constant values of the remaining variables for the functionality plot of a given variable. The actual values of a variable were used on the x-axis for that variable's functionality plot.

The x-y functionality plots in this section are presented with logarithmic scales on each axis, corresponding to the belief that many relationships between the mixing response variables and a test variable may be represented (or adequately approximated) by a power-law equation:

$$y = a\ x^b \tag{E.1}$$

On a log-log plot, the power-law model in Eq. (E.1) is represented by a line

$$\log(y) = \log(a) + b\ \log(x) \tag{E.2}$$

with intercept log(a) and slope b. Other forms of plots (original-original, log-original, and original-log) corresponding to other functional relationships were also investigated. While there were some indications

other functional relationships besides the power-law might be appropriate for some variables, the power-law relationships were best for a substantial majority of cases.

Curvature in a log-log plot indicates a departure from a power-law relationship between the mixing response variable y and the test variable x. Non-parallelism in the x-y relationship for different sets of constant values of the remaining test variables indicates that one or more of the other test variables and the test variable on the x-axis of a functionality plot have an interactive effect on the mixing response variable y. Non-parallelism in a log-log plot corresponds to different values of the slope b for different values of the interacting test variable(s). In turn, this means that the exponent b in the power-law model in Eq. (E.1) is a function of one or more other test variables.

Note that interactions identified by statistical methods do not necessarily indicate physically meaningful interactions between the involved variables. This can occur when a set of variables are correlated, so that correlated variables are identified as interacting rather than variables having physically meaningful interactions. However, this is not an issue in the subsequent functionality plots because all data points in a given plot have approximately constant values for all other variables. Statistical methods might also identify variable interactions that are not physically meaningful if the form of the model [e.g., power-law in Eqs. (E.1) and (E.2)] is incorrect. However, this possibility was addressed in this appendix by considering other forms of functionality plots (as discussed previously). Ultimately, interactions identified as statistically significant during model development work should be assessed as to whether they are physically meaningful by subject-matter experts. This topic is addressed in Appendix F.

Finally, it must be recognized that the functionality plots presented subsequently display only a fraction of the test data. This is because the functionality plot of a given variable displays only groups of data points with constant values for the remaining test variables. Many of the test combinations performed in the M3 mixing study did not have corresponding tests meeting this condition. This is a result of the large number of possible combinations of many test variables varied at two or more levels in the M3 mixing study. Ultimately, the functionality plots displayed subsequently should be considered with caution, since the relationships shown may or may not hold for other combinations of test variables where there were insufficient data for those data to appear in the plots.

E.2.2 Functionality Plots for Critical Suspension Velocity

Figures E.6 to E.16 show functionality plots using the full set of July 2007, Fall 2007, and 2008 data for critical suspension velocity (U_{CS}) versus D, N_J, d, ϕ_J, ϕ_p, DC, s, ϕ_S, d_S, HS, and U_T, where these variables are defined in Table E.1. The following observations are made regarding linearity and parallelism in the relationships for different sets of constant values of the remaining variables in each U_{CS} functionality plot.

- D (Figure E.6): Increasing D tends to increase U_{CS}. The relationships are roughly linear with weak to moderate curvature in a few cases. Some non-parallelism is apparent, suggesting some interactive effects of D with other variables. The effects of D and HS are confounded in this plot because including HS as a variable to define the groups would result in no D = 0.860 data being plotted.

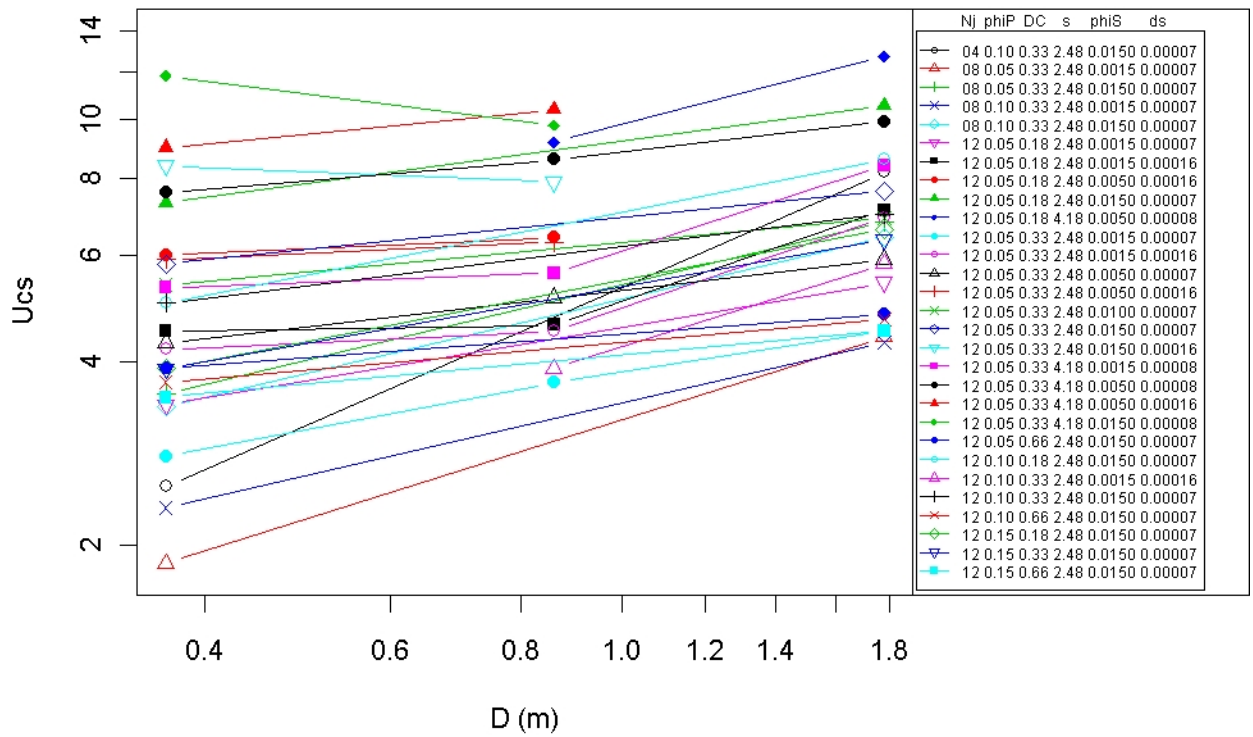

Figure E.6. Log-Log Plot of the Functional Relationship Between Critical Suspension Velocity (U_{CS}) and Tank Diameter (D) for Constant Sets of Values of Other Test Variables. The head shape (HS) variable was not used to define the groups, otherwise no D = 0.860 data would have plotted (since that was the only test tank with a spherical head shape). Hence, the effect of head shape as well as tank diameter is shown in the plot.

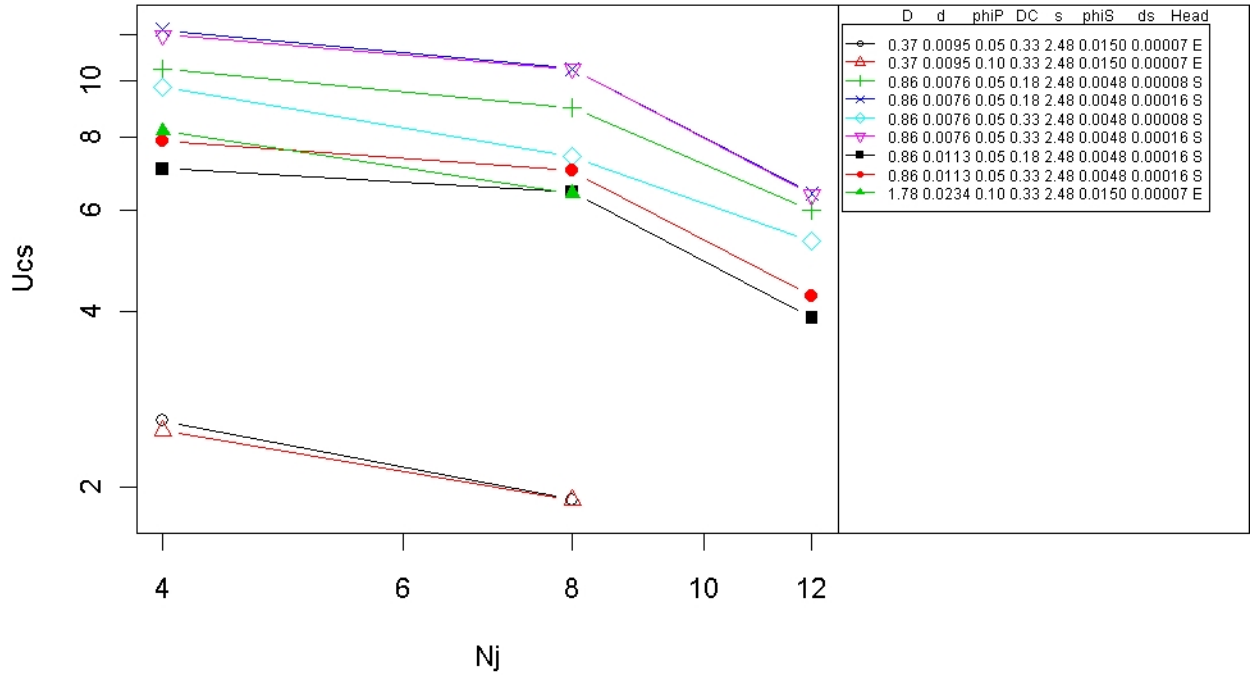

Figure E.7. Log-Log Plot of the Functional Relationship Between Critical Suspension Velocity (U_{CS}) and Number of Pulse Jets (N_J) for Constant Sets of Values of Other Test Variables

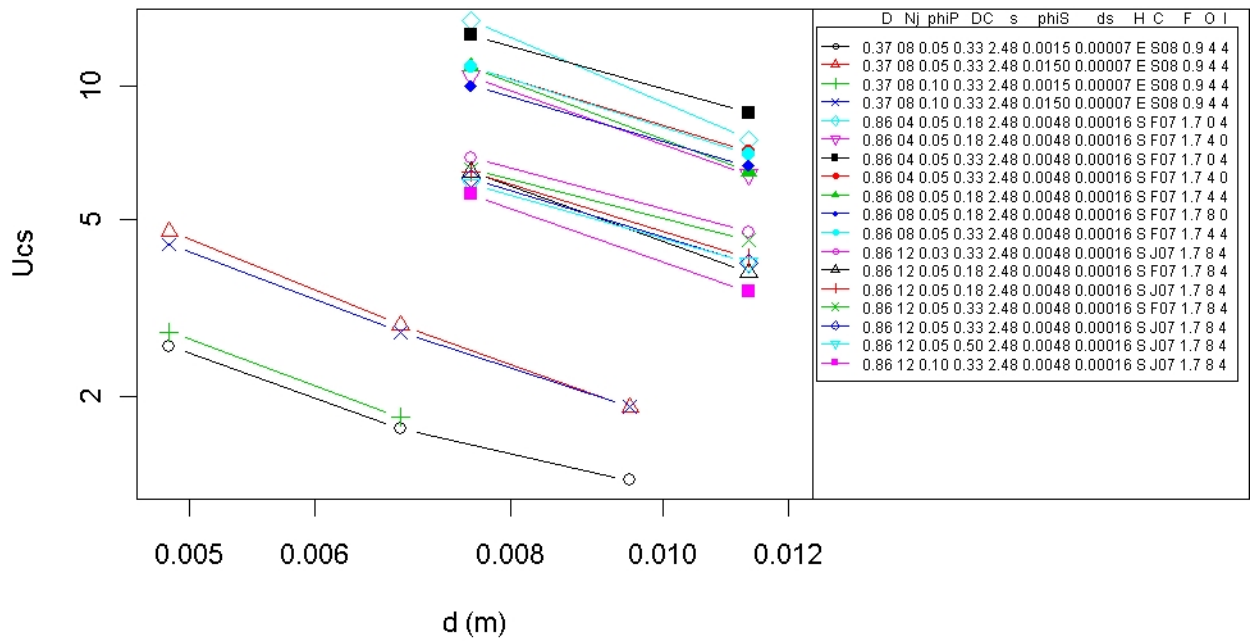

Figure E.8. Log-Log Plot of the Functional Relationship Between Critical Suspension Velocity (U_{CS}) and Jet Nozzle Diameter (d) for Constant Sets of Values of Other Test Variables. Variables in the legend include H = head, C = test campaign, F = vessel fill height (m), O = number of outer nozzles operating, and I = number of inner nozzles operating.

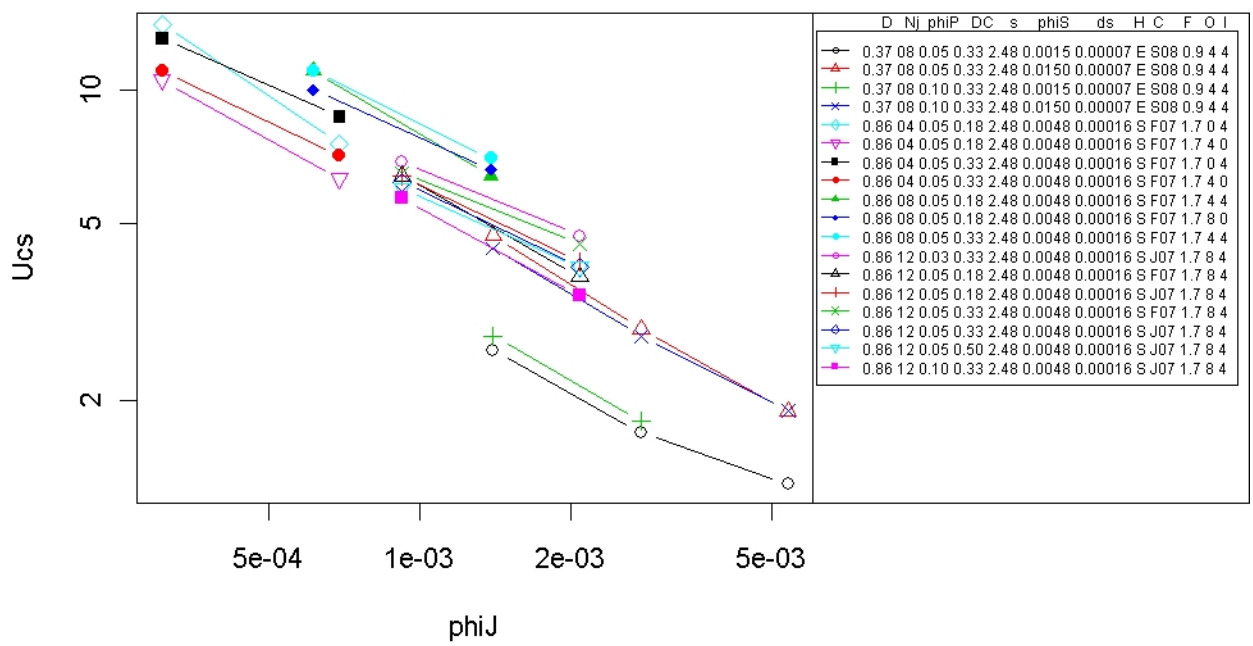

Figure E.9. Log-Log Plot of the Functional Relationship Between Critical Suspension Velocity (U_{CS}) and Jet Density (ϕ_J) for Constant Sets of Values of Other Test Variables. Variables in the legend include H = head, C = test campaign, F = vessel fill height (m), O = number of outer nozzles operating, and I = number of inner nozzles operating.

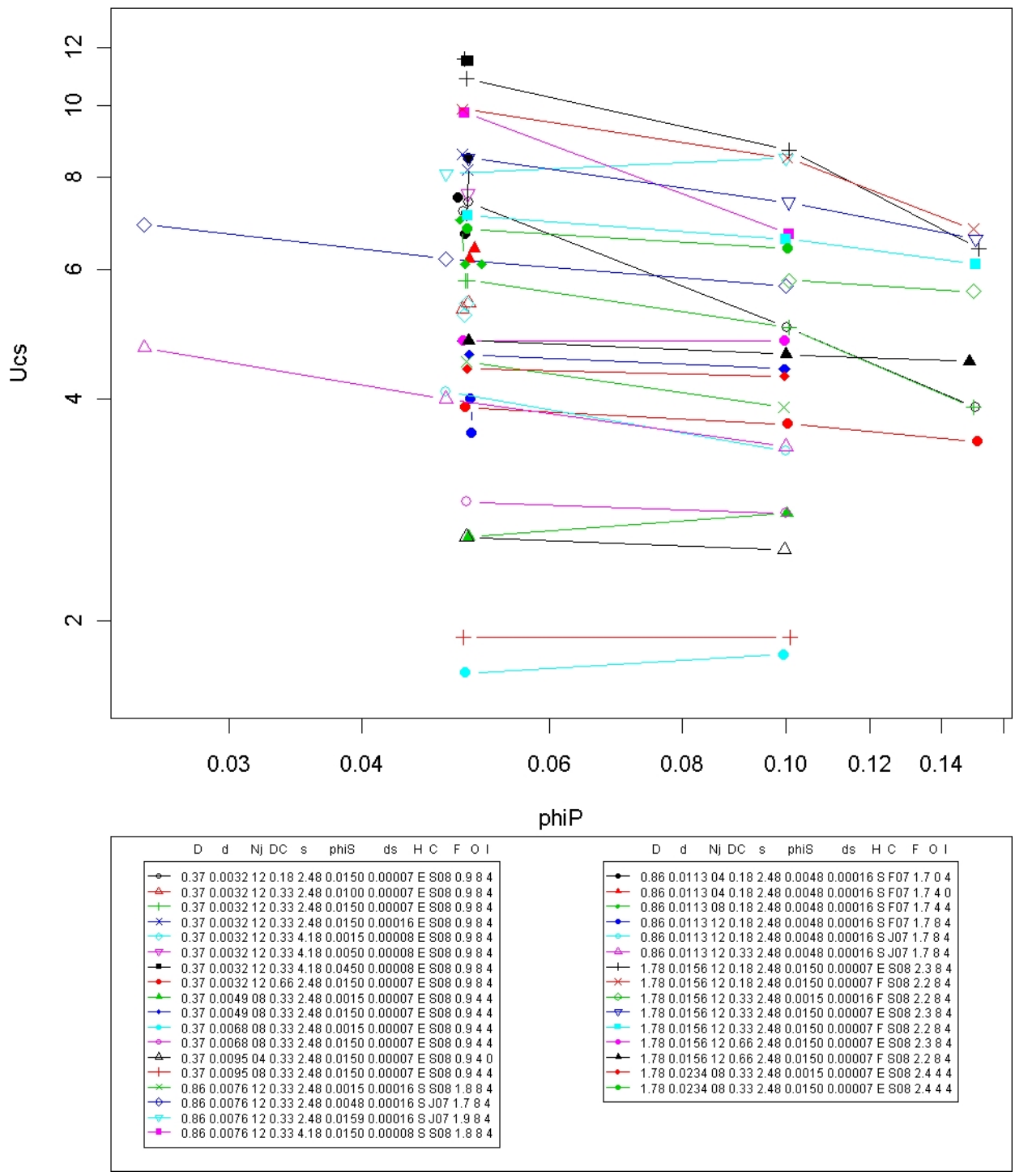

Figure E.10. Log-Log Plot of the Functional Relationship Between Critical Suspension Velocity (U_{CS}) and Pulse Volume Fraction (ϕ_p) for Constant Sets of Values of Other Test Variables.

Variables in the legend include H = head, C = test campaign, F = vessel fill height (m), O = number of outer nozzles operating, and I = number of inner nozzles operating.

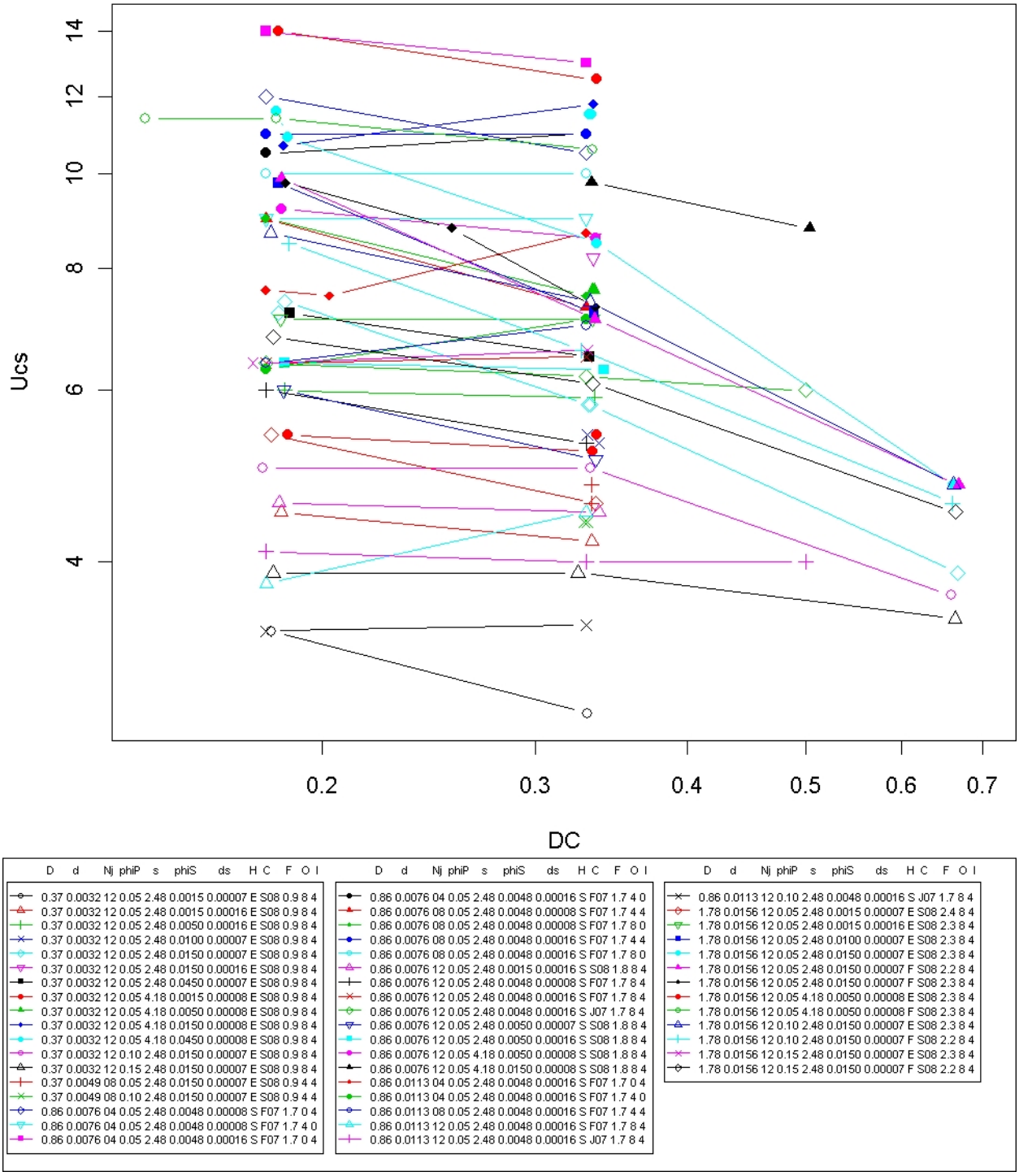

Figure E.11. Log-Log Plot of the Functional Relationship Between Critical Suspension Velocity (U_{CS}) and Duty Cycle (DC) for Constant Sets of Values of Other Test Variables. Variables in the legend include H = head, C = test campaign, F = vessel fill height (m), O = number of outer nozzles operating, and I = number of inner nozzles operating.

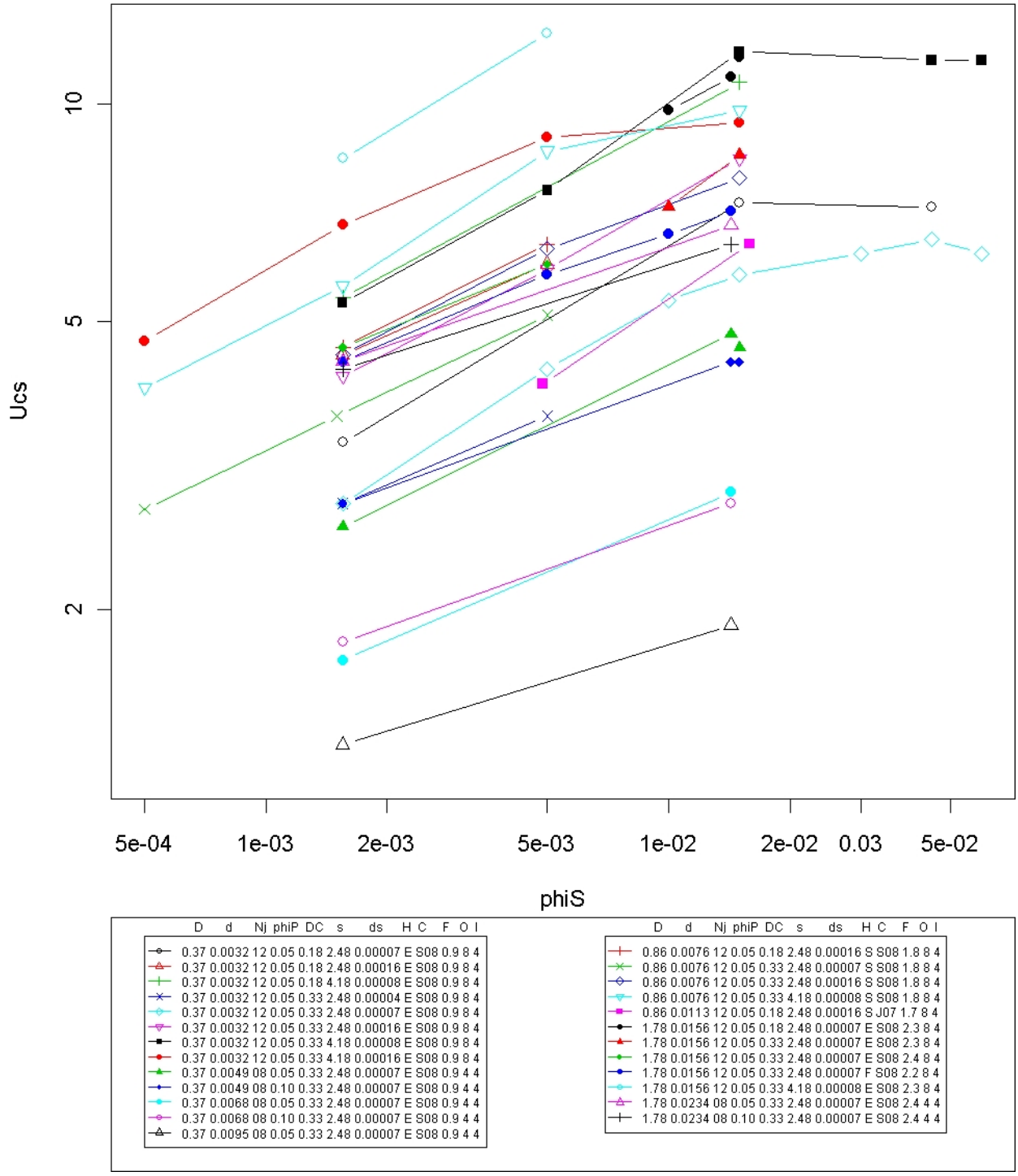

Figure E.12. Log-Log Plot of the Functional Relationship Between Critical Suspension Velocity (U_{CS}) and Solids Volume Fraction (ϕ_S) for Constant Sets of Values of Other Test Variables. Variables in the legend include H = head, C = test campaign, F = vessel fill height (m), O = number of outer nozzles operating, and I = number of inner nozzles operating.

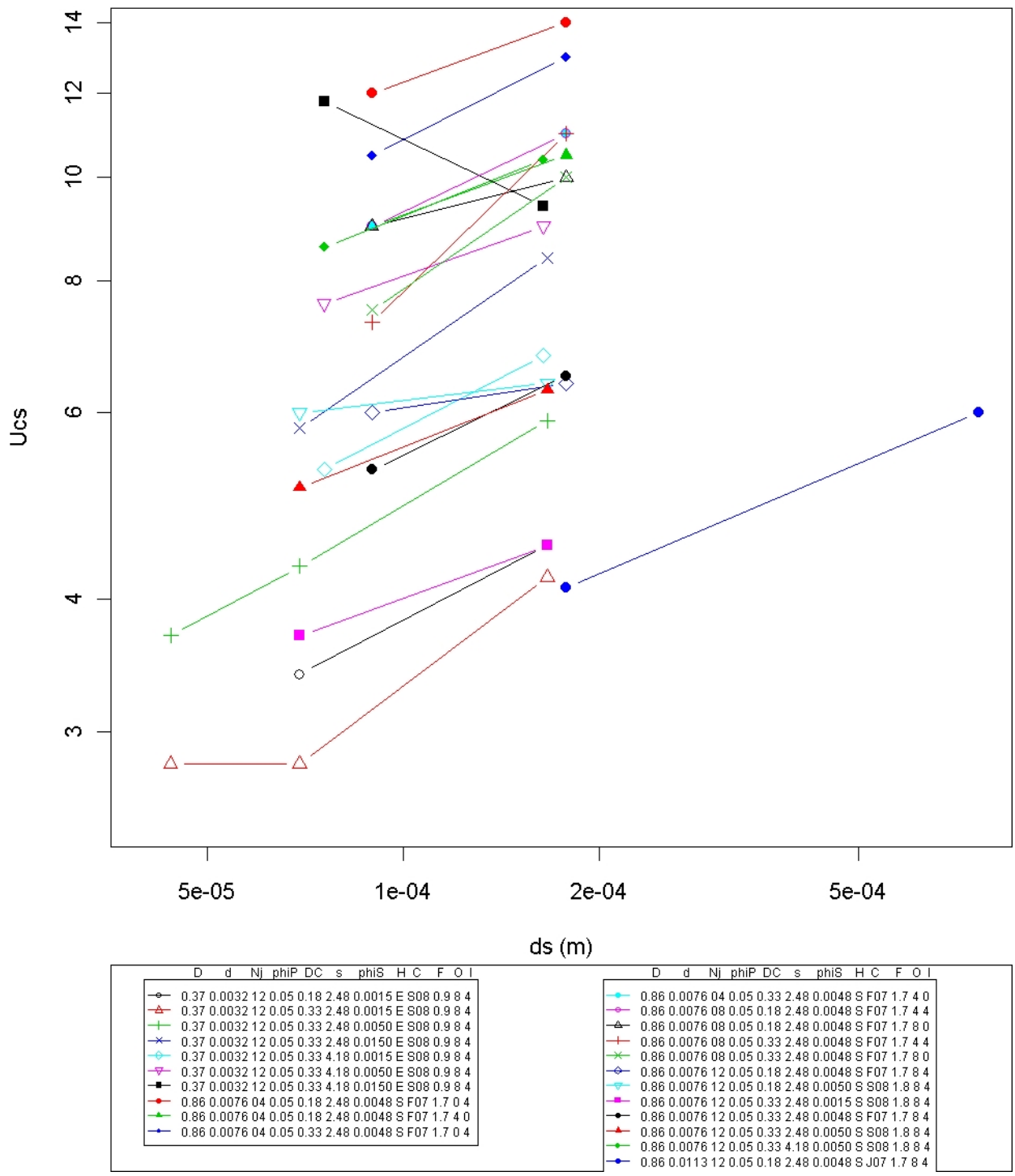

Figure E.13. Log-Log Plot of the Functional Relationship Between Critical Suspension Velocity (U_{CS}) and Solids Particle Diameter ($d_S = d_{50}$) for Constant Sets of Values of Other Test Variables. Variables in the legend include H = head, C = test campaign, F = vessel fill height (m), O = number of outer nozzles operating, and I = number of inner nozzles operating.

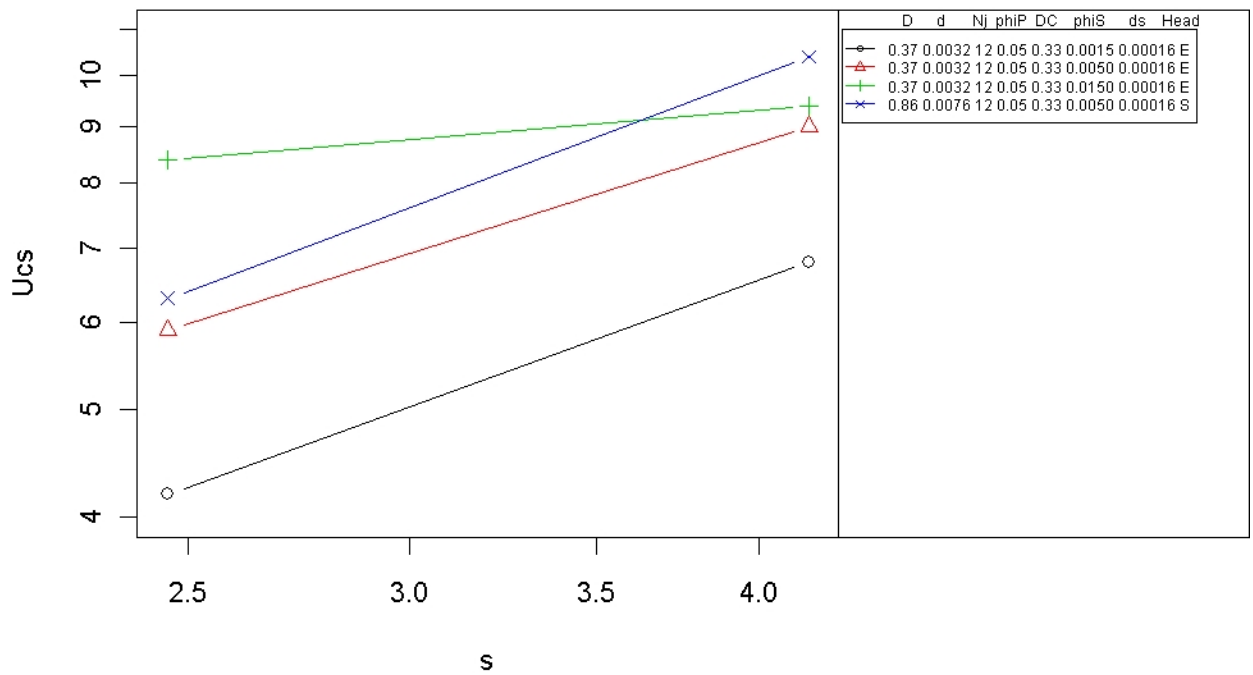

Figure E.14. Log-Log Plot of the Functional Relationship Between Critical Suspension Velocity (U_{CS}) and Density Ratio (s) for Constant Sets of Values of Other Test Variables

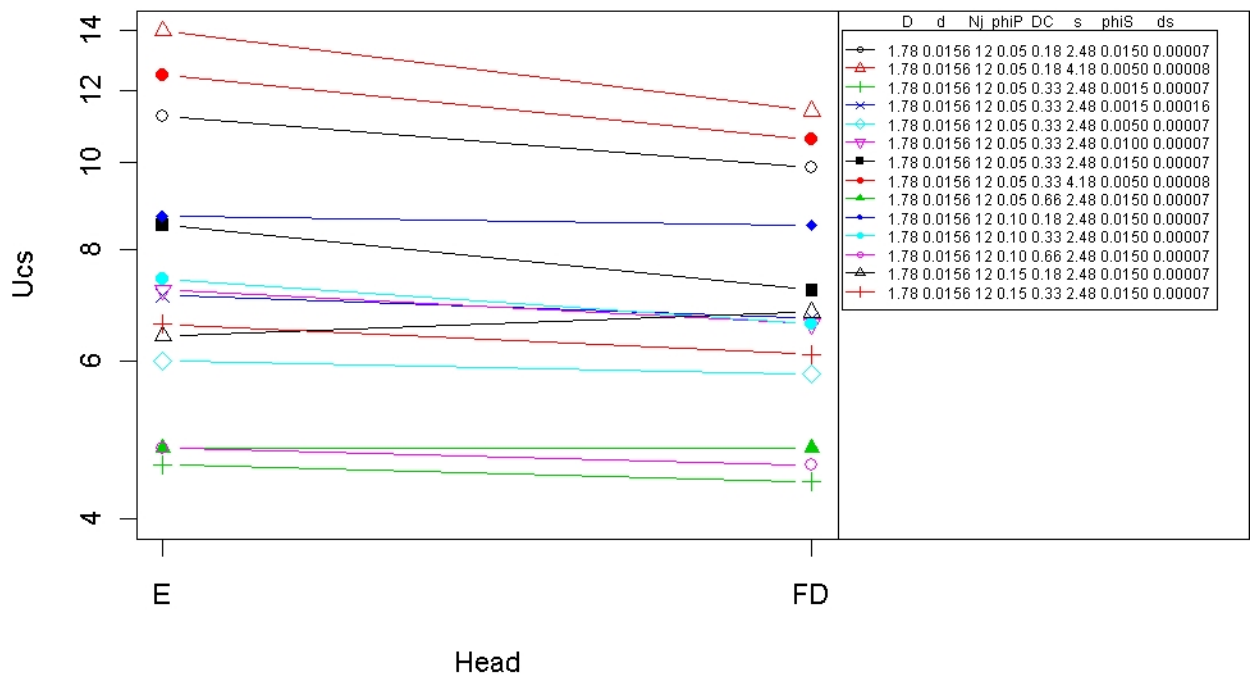

Figure E.15. Log-Categorical Plot of Functional Relationship Between Critical Suspension Velocity (U_{CS}) and Head Shape (HS) for Constant Sets of Values of Other Test Variables. No data are plotted for the spherical head shape (S), because it was only used in the D = 0.860 m tank.

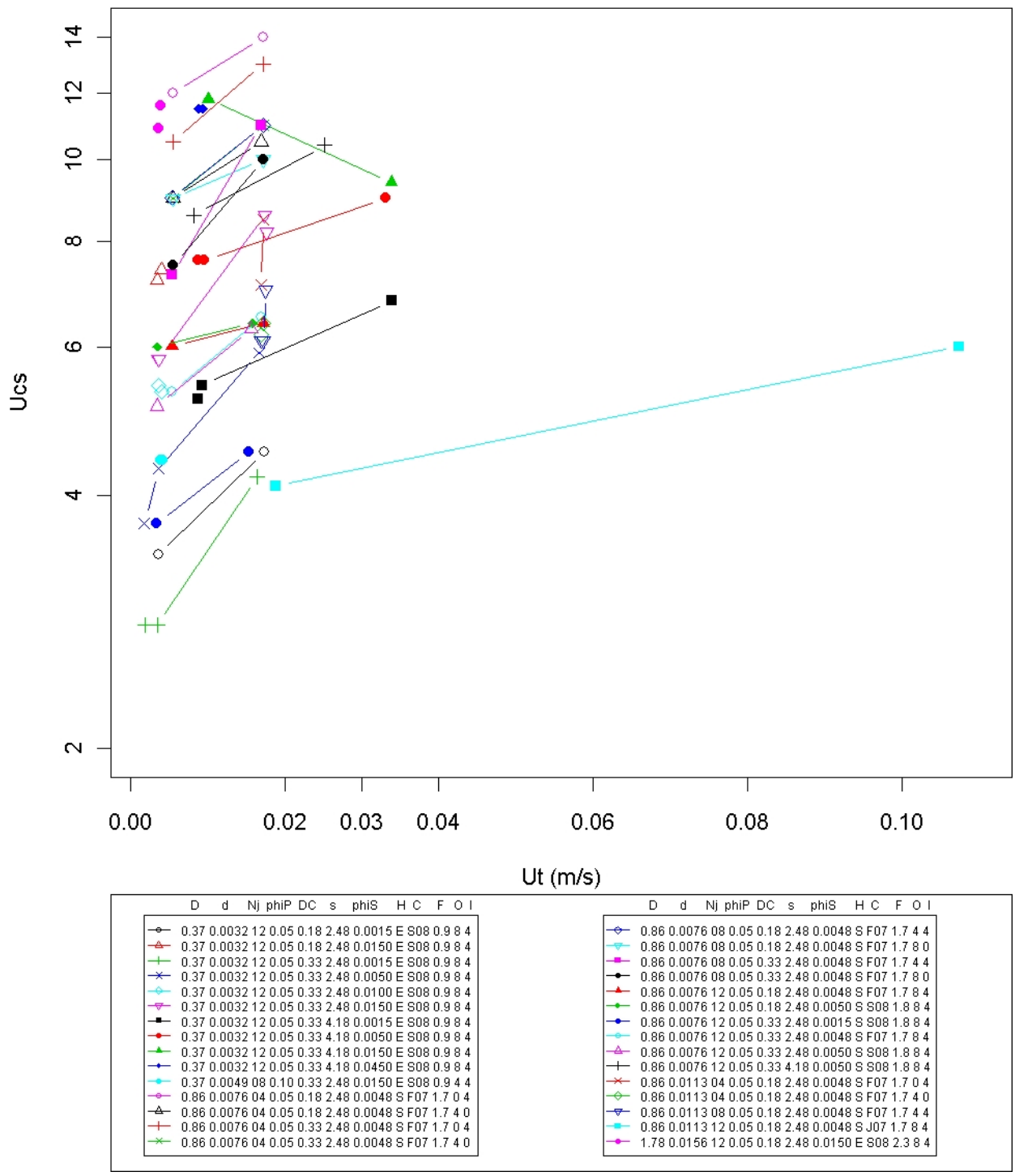

Figure E.16. Log-Log Plot of the Functional Relationship Between Critical Suspension Velocity (U_{CS}) and Unhindered Terminal Settling Velocity (U_T) for Constant Sets of Values of Other Test Variables. Because U_T is calculated as a function of d_S and (s−1), d_S was not used to define the plotting sets in the legend. Hence, the effects of U_T and d_S are confounded in the plot.

- N_J (Figure E.7): Increasing the number of operating jets decreases U_{CS} with the increase from 8 to 12 jets, causing a larger decrease in U_{CS} than from 4 to 8 jets. Curvature is apparent in several relationships with similar patterns. For these conditions, there is no strong indication of interactive effects with N_J.
- d (Figure E.8): Increasing d tends to decrease U_{CS}. In the three cases where there are sufficient data to assess curvature, the relationships are roughly linear. Although there are some differences in slopes (indicating some possible interactive effects), the slopes tend to vary around an average slope.
- ϕ_J (Figure E.9): Increasing ϕ_J tends to decrease U_{CS}. In the three cases where there are sufficient data to assess curvature, the relationships are roughly linear. Although there are some differences in slopes (indicating some possible interactive effects of other variables with ϕ_J), the slopes tend to have limited variation around an average slope.
- ϕ_p (Figure E.10): For $\phi_p \geq 0.05$, increasing ϕ_p has effects ranging from weakly increasing U_{CS} to significantly decreasing U_{CS}. The relationships are roughly linear, with weak curvature for two cases. Non-parallelism is apparent, indicating some interactive effects of ϕ_p with other variables.
- DC (Figure E.11): U_{CS} tends to decrease with DC, although some cases show increases (indicating interactive effects). Some relationships display slight to moderate curvature, as a result of U_{CS} generally decreasing as DC increases from ~ 0.33 to ~ 0.66.
- ϕ_S (Figure E.12): The relationships are roughly linear for $\phi_S \leq 0.015$, with U_{CS} increasing as ϕ_S increases. However, there is a flattening-out of the three relationships that have data for $\phi_S > 0.015$. This flattening-out behavior starts at lower ϕ_S values for one case.
- d_S (Figure E.13): Increasing the median solids particle size from ~ 0.00007 to ~ 0.00016 increases U_{CS} for many cases, but U_{CS} decreases for one case. There are noticeable differences in slope, indicating possible interactive effects. For the two cases with data for d_S increasing from ~ 0.00004 to ~ 0.00007, U_{CS} increased (one case) or had a negligible change (other case). Only the latter case showed curvature over the tested range of d_S. For the one case where d_S ranged from ~ 0.00018 to ~0.00077, the positive slope was within the range of slopes for the other cases with smaller d_S values.
- s (Figure E.14): Increasing s tends to increase U_{CS}. The slope of the relationship is similar for several cases, but there is one different slope indicating possible interactive effects. Only having data for four conditions in this plot limits the general conclusions that can be made.
- HS (Figure E.15): The flange and dish (FD) head shape tends to yield smaller U_{CS} values than the elliptical (E) head shape. See Section E.2.4 for additional discussion. No data are plotted for the spherical (S) head shape, because that shape was only used in tests with the D = 0.860 m (~ 34-in.) tank, and thus there are no sets of conditions with values for E, FD, and S head shapes.
- U_T (Figure E.16): Increasing U_T tends to increase U_{CS}, except for one case. The rate of increase in U_{CS} appears to decrease as U_T increases. For U_T up to ~ 0.035, the slopes vary enough to suggest possible interactive effects with other variables. However, because U_T is calculated as a function of d_S and s – 1, the d_S variable was not used in the plotting groups shown in the legend of the figure. Hence, the effects of U_T and d_S on U_{CS} are confounded, and any statements made here may be as much due to d_S effects as U_T effects on U_{CS}.

These observations and the functionality plots they are based on serve as a basis for assessing multiple-regression models developed for U_{CS} in Section F.2, Appendix F.

E.2.3 Functionality Plots for Cloud Height

Figures E.17 to E.21 show the functionality plots of cloud height (H_C) versus target velocity (U) for each set of test conditions in the "full" set of July 2007, Fall 2007, and 2008 data. Each plot is shown with logarithmic scales on both axes. Only target velocity values greater than or equal to the critical suspension velocity (i.e., $U \geq U_{CS}$) are shown in the plots.

For the 2008 data (Figures E.19 to E.21), the relationships between H_C and $U \geq U_{CS}$ are generally linear for most sets of conditions displayed, with H_C increasing as U increases (as expected). There is weak curvature in the relationship for a few cases. The slopes of the roughly linear relationships are generally similar within a given figure, but with noticeable differences (especially for 2008 15-in. tank data in Figure E.19). Differences in slopes of the relationships correspond to possible interactive effects on H_C of U with other variables.

For the July 2007 (Figure E.17) and Fall 2007 data (Figure E.18), in some cases the HC versus U relationships are flat or negative for low velocities. This suggests that U_{CS} may have been determined as too low a velocity in some cases (which may be because those test campaigns were earlier in the learning curve of performing these kinds of tests). Still, the relationships are generally linear, though curvature is apparent for some cases. Slopes are notably different, indicating possible interactive effects of other variables with U.

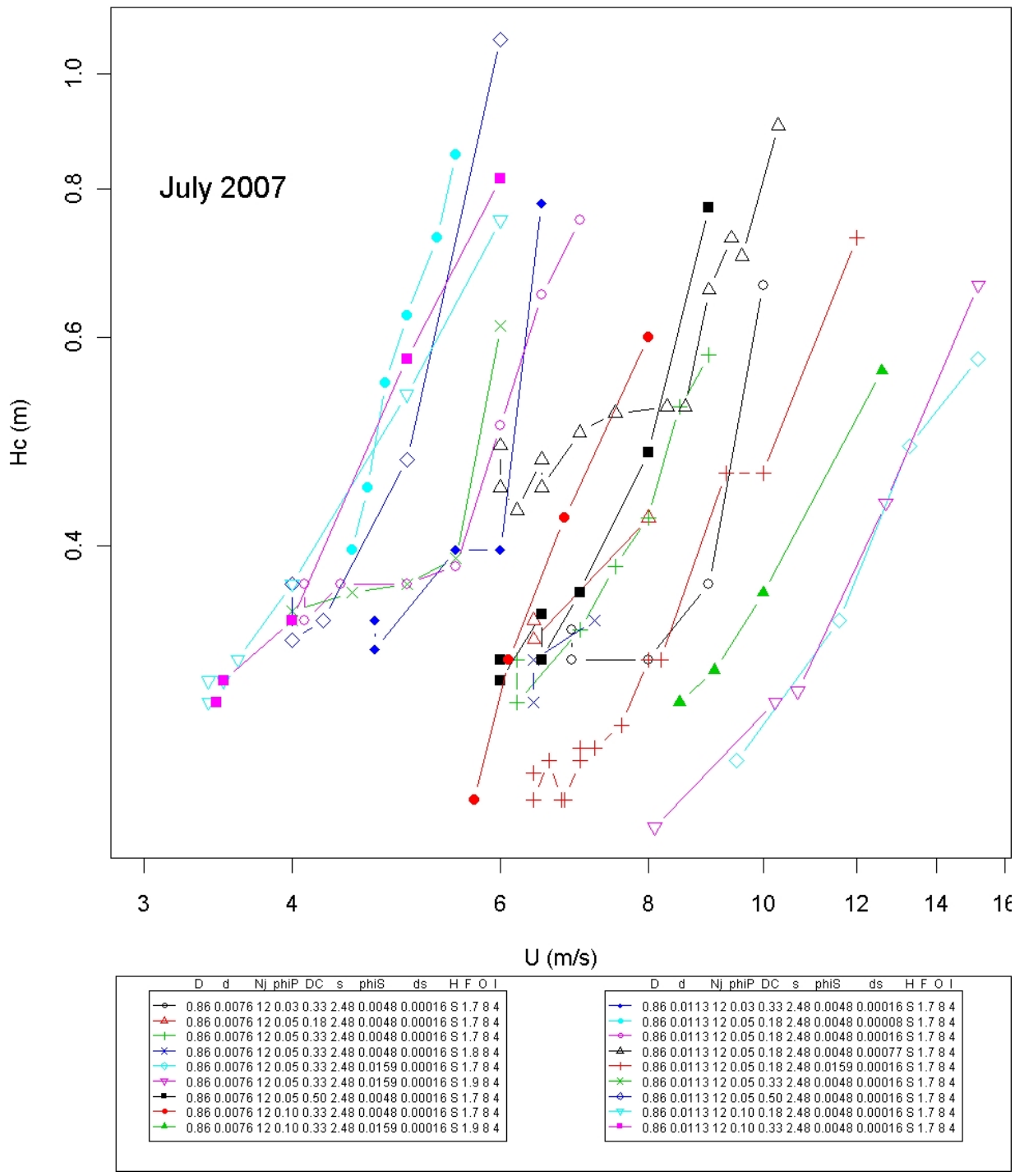

Figure E.17. Log-Log Plot of the Functional Relationship Between Cloud Height (H_C) and Velocity (U) for Each Set of Test Conditions in the July 2007 Data Set. Only velocities greater than or equal to the critical suspension velocity ($U \geq U_{CS}$) are shown. Variables in the legend include H = head, F = vessel fill height (m), O = number of outer nozzles operating, and I = number of inner nozzles operating.

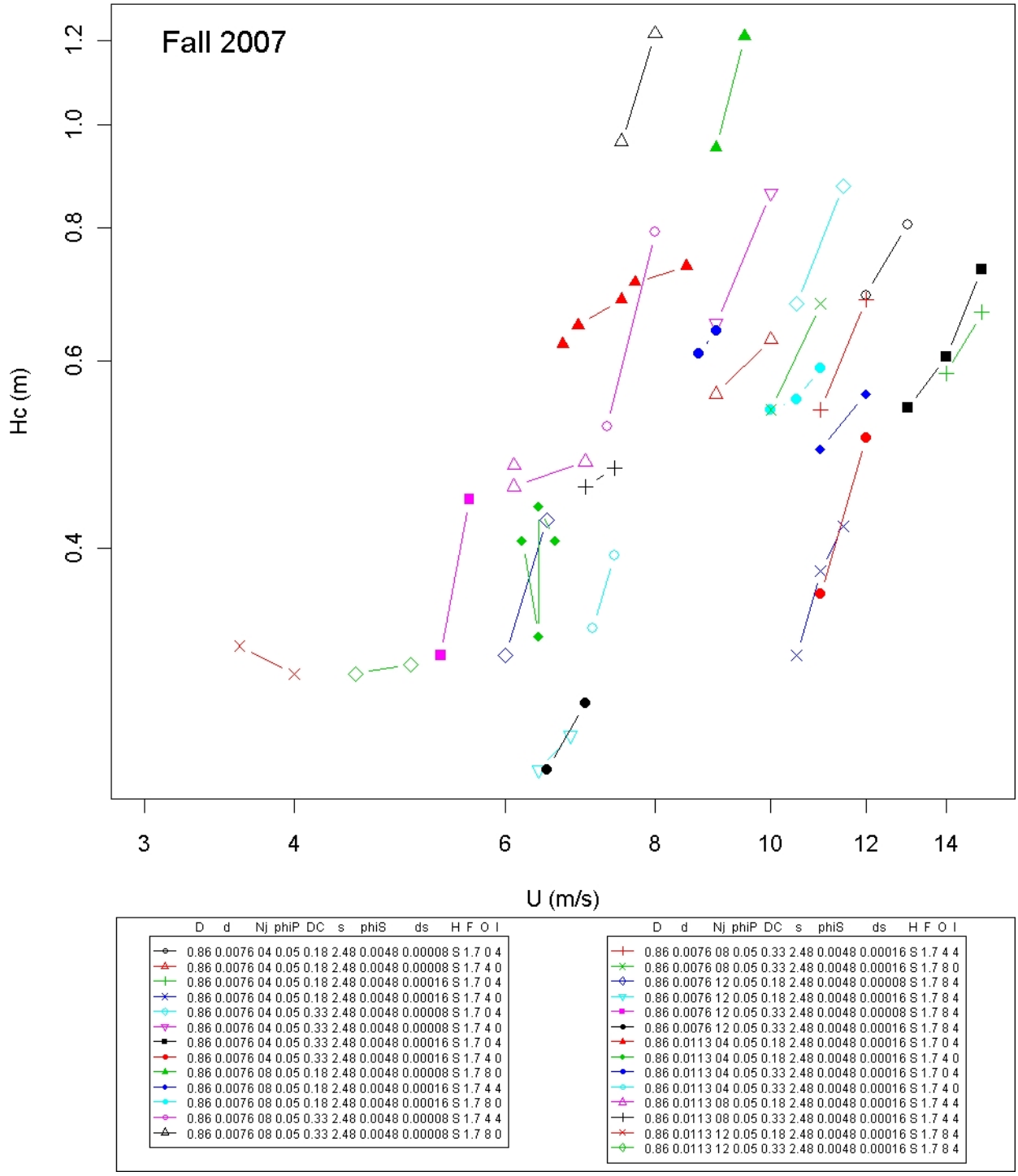

Figure E.18. Log-Log Plot of the Functional Relationship Between Cloud Height (H_C) and Velocity (U) for Each Set of Test Conditions in the Fall 2007 Data Set. Only velocities greater than or equal to the critical suspension velocity ($U \geq U_{CS}$) are shown. Variables in the legend include H = head, F = vessel fill height (m), O = number of outer nozzles operating, and I = number of inner nozzles operating.

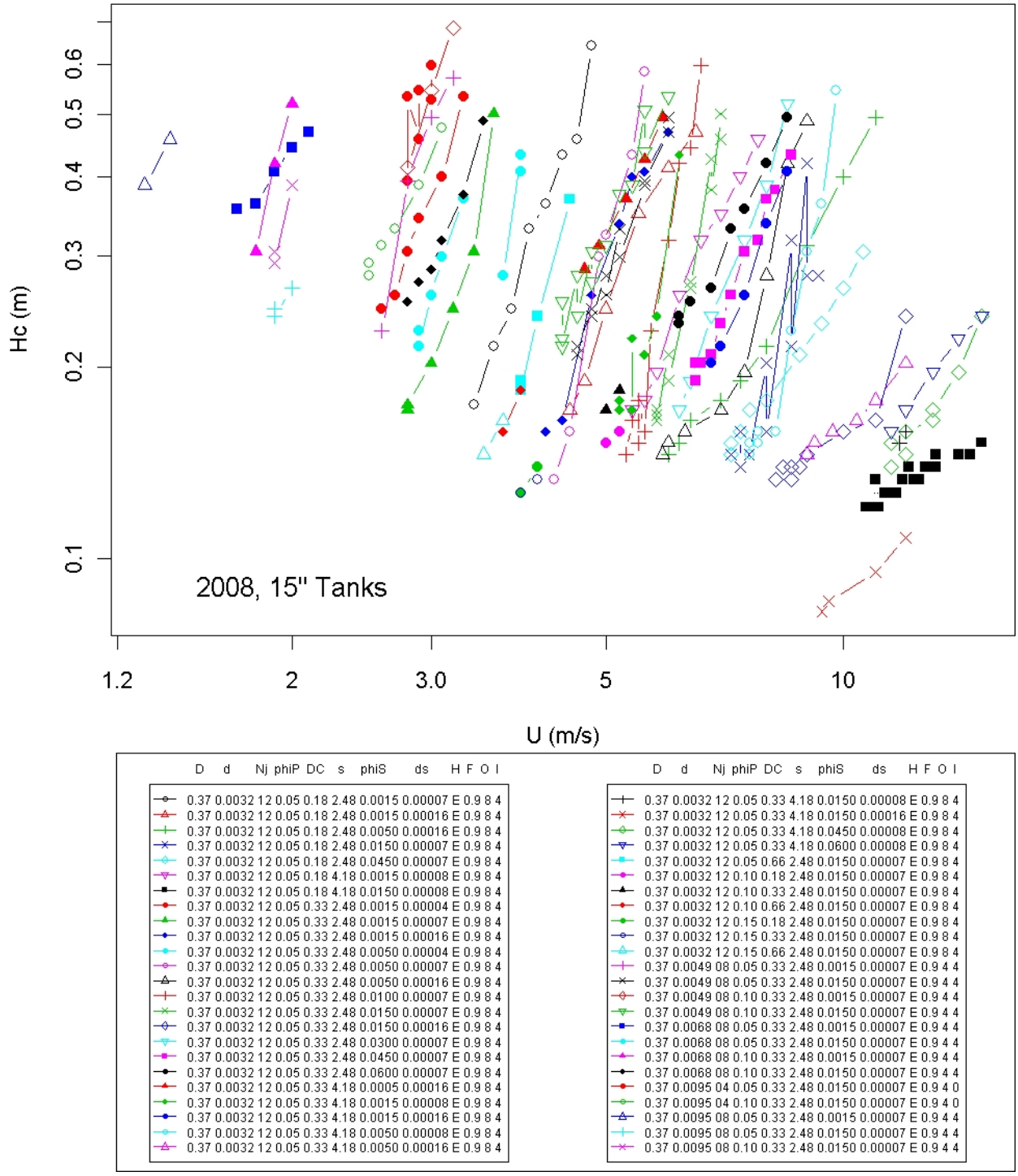

Figure E.19. Log-Log Plot of the Functional Relationship Between Cloud Height (H_C) and Velocity (U) for Each Set of 15-in. Tank Test Conditions in the 2008 Data Set. Only velocities greater than or equal to the critical suspension velocity ($U \geq U_{CS}$) are shown. Variables in the legend include H = head, F = vessel fill height (m), O = number of outer nozzles operating, and I = number of inner nozzles operating.

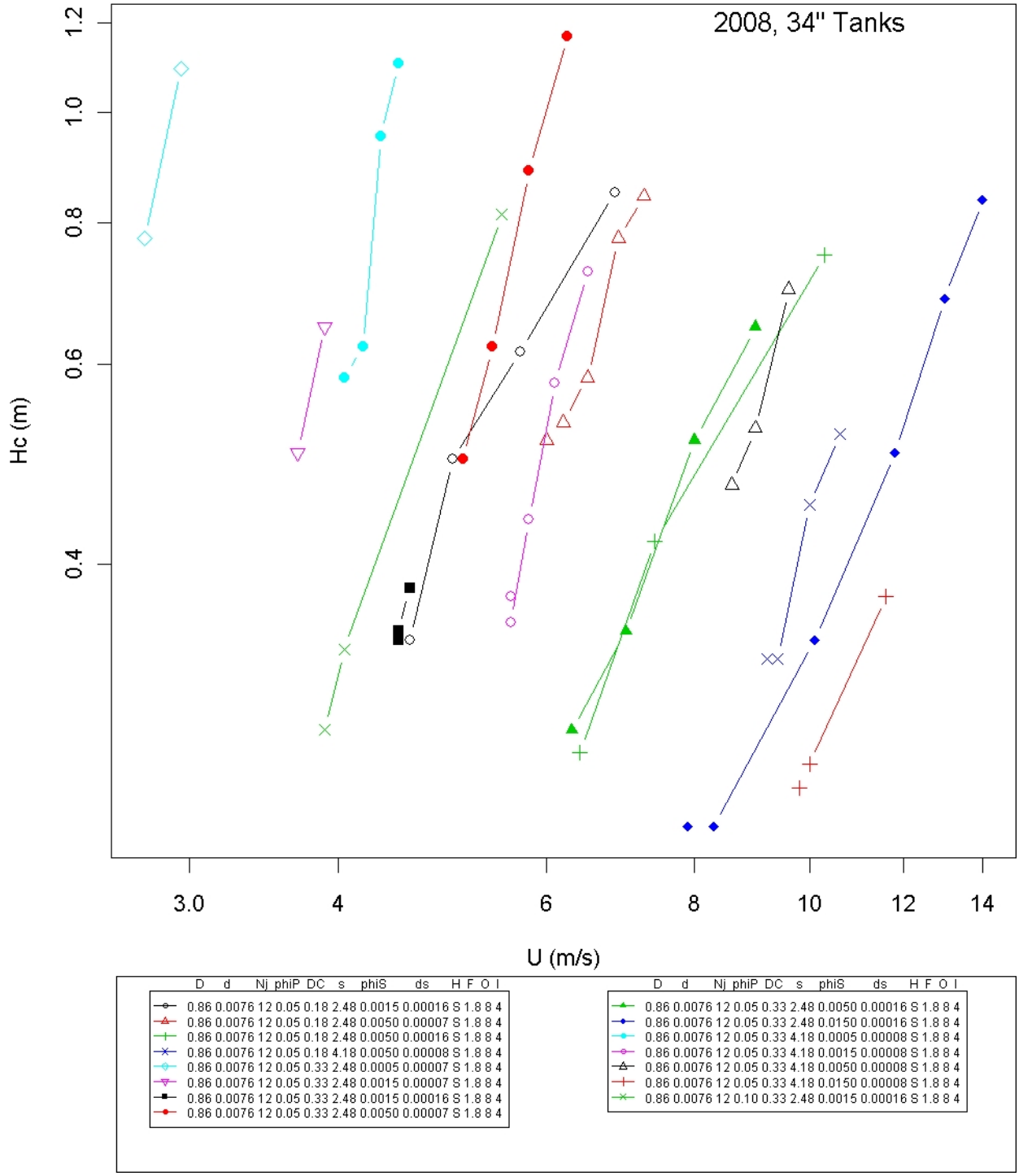

Figure E.20. Log-Log Plot of the Functional Relationship Between Cloud Height (H_C) and Velocity (U) for Each Set of D = 0.860 m (~ 34-in.) Tank Test Conditions in the 2008 Data Set. Only velocities greater than or equal to the critical suspension velocity ($U \geq U_{CS}$) are shown. Variables in the legend include H = head, F = vessel fill height (m), O = number of outer nozzles operating, and I = number of inner nozzles operating.

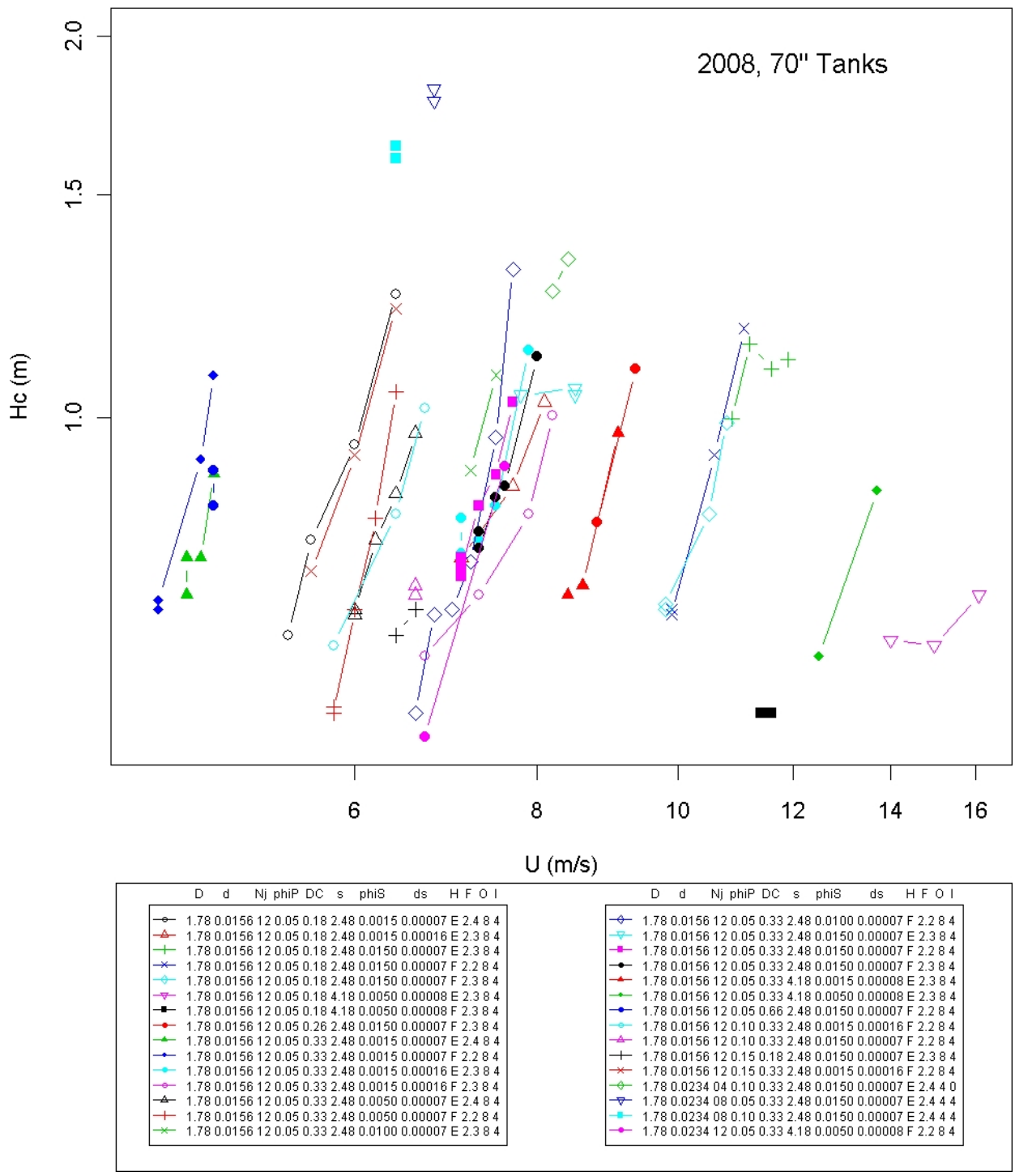

Figure E.21. Log-Log Plot of the Functional Relationship Between Cloud Height (H_C) and Velocity (U) for Each Set of 70-in. Tank Test Conditions in the 2008 Data Set. Only velocities greater than or equal to the critical suspension velocity ($U \geq U_{CS}$) are shown. Variables in the legend include H = head, F = vessel fill height (m), O = number of outer nozzles operating, and I = number of inner nozzles operating.

Figures E.22 to E.32 show functionality plots for cloud height at the critical suspension velocity (H_{CS}) versus D, N_J, d, ϕ_J, ϕ_p, DC, S, ϕ_S, d_S, HS, and U_T where these variables are defined in Table E.1. It was not possible to produce functionality plots for H_C versus these test variables because cloud height observations were not made for specific velocity values for all tests. Thus there are no sets of variables (velocity and other test variables) with different sets of constant values for a given test variable on the x-axis, and it was necessary to focus on functionality plots for H_{CS} rather than H_C for the test variables other than U.

The following observations are made regarding linearity and parallelism in the relationships for different sets of constant values of the remaining variables in each H_{CS} functionality plot. The observations apply to the sets of conditions shown in each plot, and may or may not hold for other sets of conditions where there were not at least two data points to form a line segment.

- D (Figure E.22): Increasing D strongly increases H_{CS} as expected. Most of the relationships are linear with similar slopes. However, significant curvature and differences in slope are seen for some cases. Note that the effects of D and HS are confounded in this plot, since including HS as a variable to define the groups would have resulted in no D = 0.860 data being plotted.
- N_J (Figure E.23): Increasing from 4 to 8 jets generally maintains or slightly increases H_{CS}, while increasing from 8 to 12 jets decreases H_{CS}. Curvature is apparent for several cases. Non-parallelism of slopes is also apparent, suggesting possible interactions with other variables.
- d (Figure E.24): The effect of d on H_{CS} is relatively small, varying from weakly-positive to weakly-negative slopes. Curvature is weak for the three sets of conditions where it can be assessed.
- ϕ_J (Figure E.25): The effect of ϕ_J on H_{CS} is relatively small, varying from weakly-positive to weakly-negative slopes. Curvature is weak for the three sets of conditions where it can be assessed.
- ϕ_p (Figure E.26): The effect of ϕ_p on H_{CS} is relatively small for $\phi_p \geq 0.05$, varying from weakly-negative to moderately-positive slopes. The relationships are roughly linear, having weak slopes varying around zero. However, two cases show weak curvature. There are only two cases with data for ϕ_p increasing from 0.03 to 0.05, with negligible effects on H_{CS}.
- DC (Figure E.27): When DC increases from ~ 0.18 to ~ 0.33, H_{CS} generally has slopes that range from slightly negative to moderately positive. Hence, there is evidence of interactive effects of DC and other variables on H_{CS}. There are less data in the approximate range of $0.33 < DC \leq 0.66$, with H_{CS} decreasing or increasing slightly over this range.
- ϕ_S (Figure E.28): The majority of test data are for $\phi_S \leq 0.015$, where increasing ϕ_S moderately decreases H_{CS} for most cases. For the three cases with data $\phi_S > 0.015$, the relationship with H_{CS} flattens out or increases. For two cases, this tendency to increase H_{CS} begins at $\phi_S \sim 0.005$.
- d_S (Figure E.29): Increasing the median solids particle size from ~ 0.00007 to ~ 0.00016 sometimes increases and sometimes decreases H_{CS}. Hence, there may be an interactive effect between d_S and at least one other variable. For the two cases with data for d_S increasing from ~ 0.00004 to ~ 0.00007, H_{CS} decreased significantly. These two cases had strong curvature over the tested range of d_S. For the one case where d_S ranged from ~ 0.00018 to ~0.00077, the positive slope was within the range of slopes for the other cases with smaller d_S values.

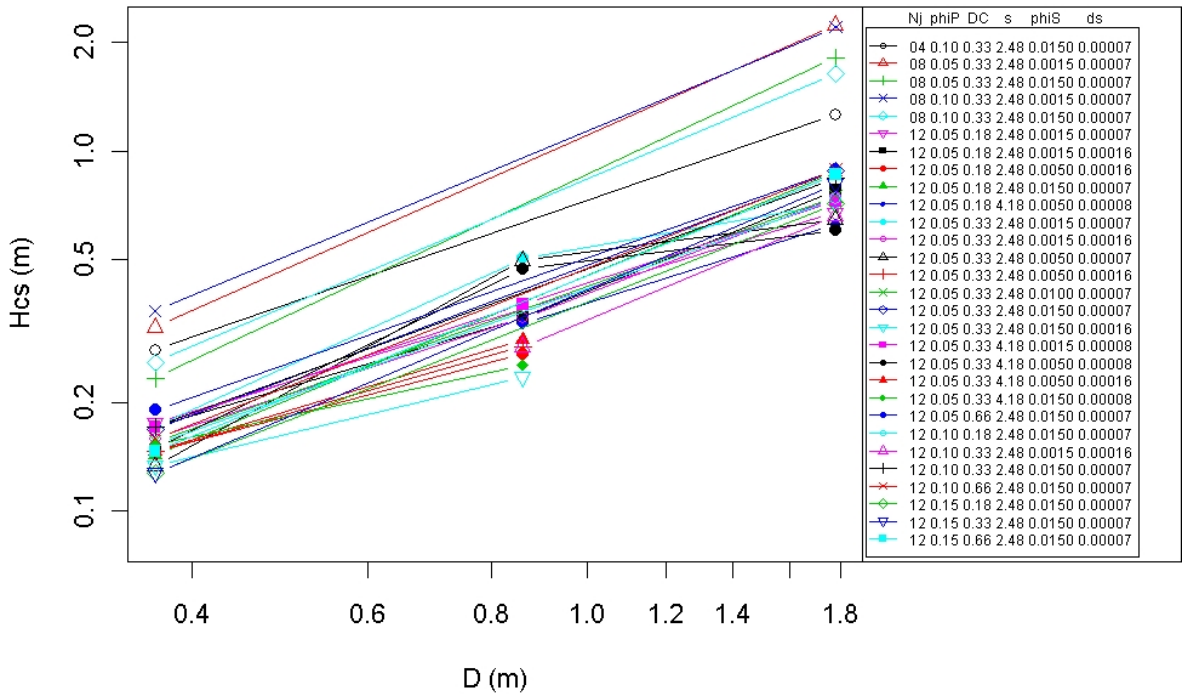

Figure E.22. Log-Log Plot of Functional Relationship Between Cloud Height at Critical Suspension Velocity (H_{CS}) and Tank Diameter (D) for Constant Sets of Values of Other Test Variables. The head shape (HS) variable was not used to define the groups, otherwise no D = 0.860 data would have plotted (since that was the only test tank with a spherical head shape). Hence, the effect of head shape as well as tank diameter is shown in the plot.

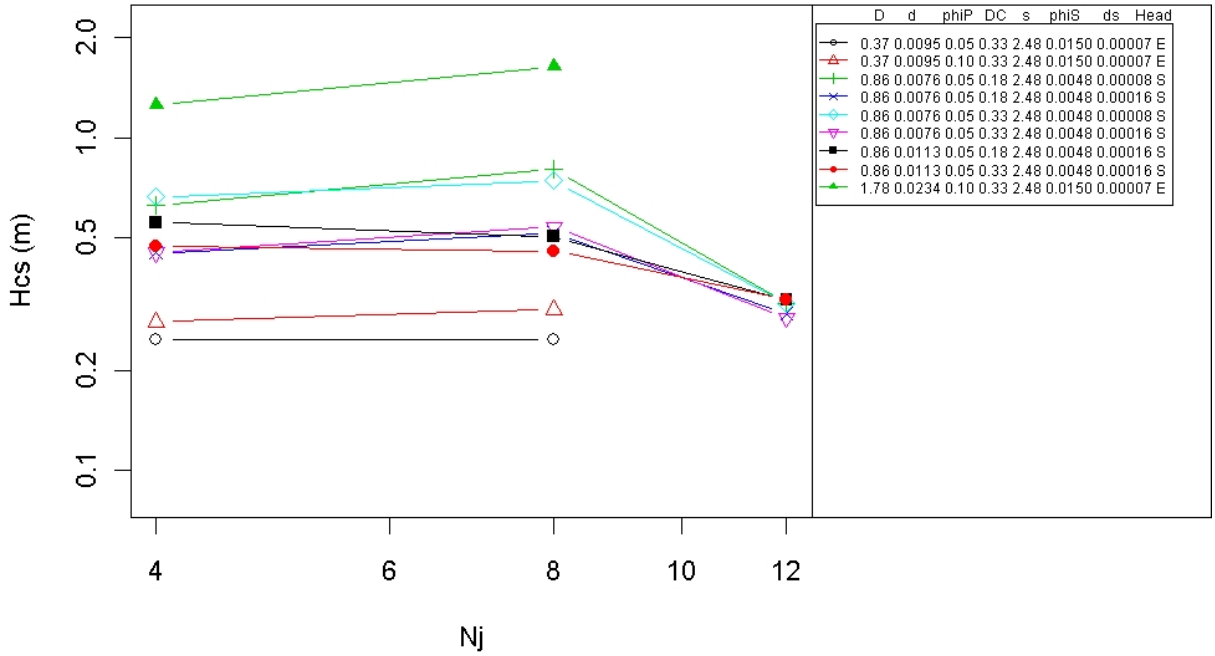

Figure E.23. Log-Log Plot of Functional Relationship Between Cloud Height at Critical Suspension Velocity (H_{CS}) and Number of Pulse Jets (N_J) for Constant Sets of Values of Other Test Variables

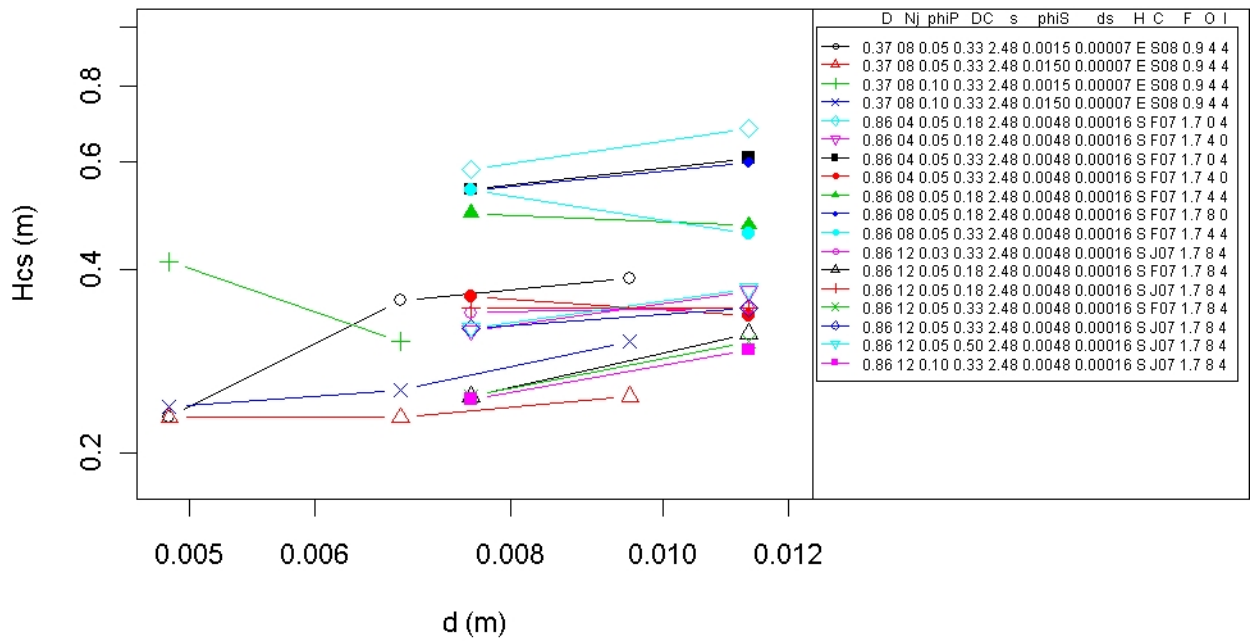

Figure E.24. Log-Log Plot of Functional Relationship Between Cloud Height at Critical Suspension Velocity (H_{CS}) and Jet Nozzle Diameter (d) for Constant Sets of Values of Other Test Variables. Variables in the legend include H = head, C = test campaign, F = vessel fill height (m), O = number of outer nozzles operating, and I = number of inner nozzles operating.

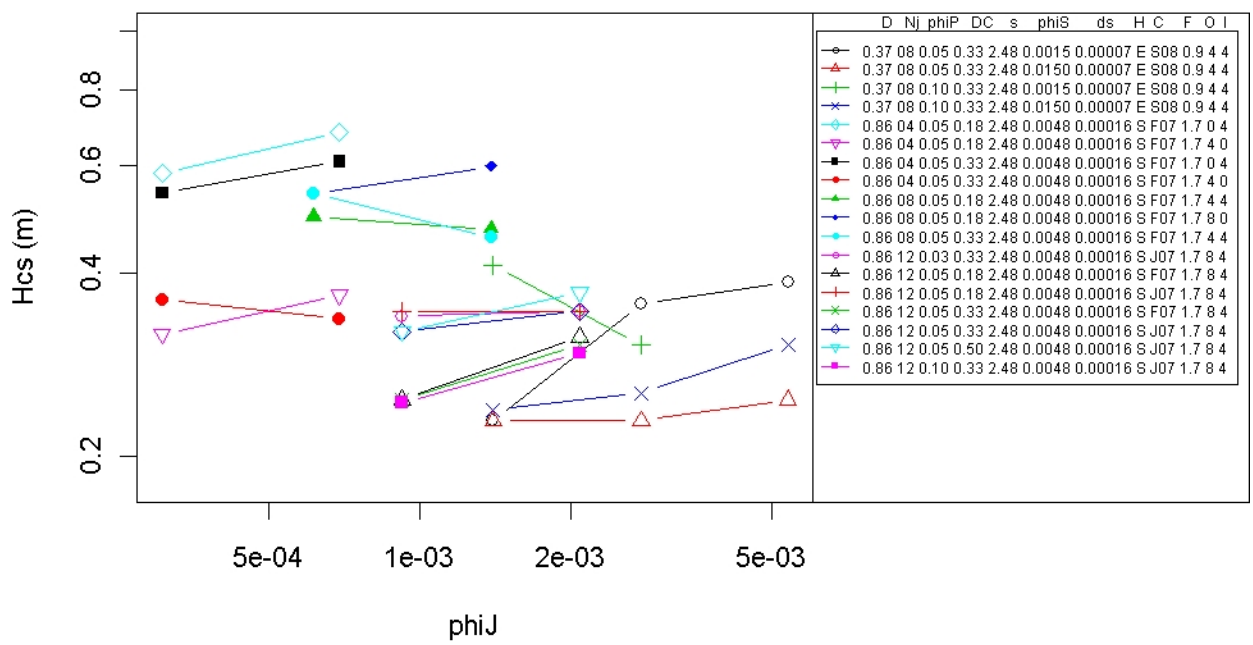

Figure E.25. Log-Log Plot of the Functional Relationship Between Cloud Height at Critical Suspension Velocity (H_{CS}) and Jet Density (ϕ_J) for Constant Sets of Values of Other Test Variables. Variables in the legend include H = head, C = test campaign, F = vessel fill height (m), O = number of outer nozzles operating, and I = number of inner nozzles operating.

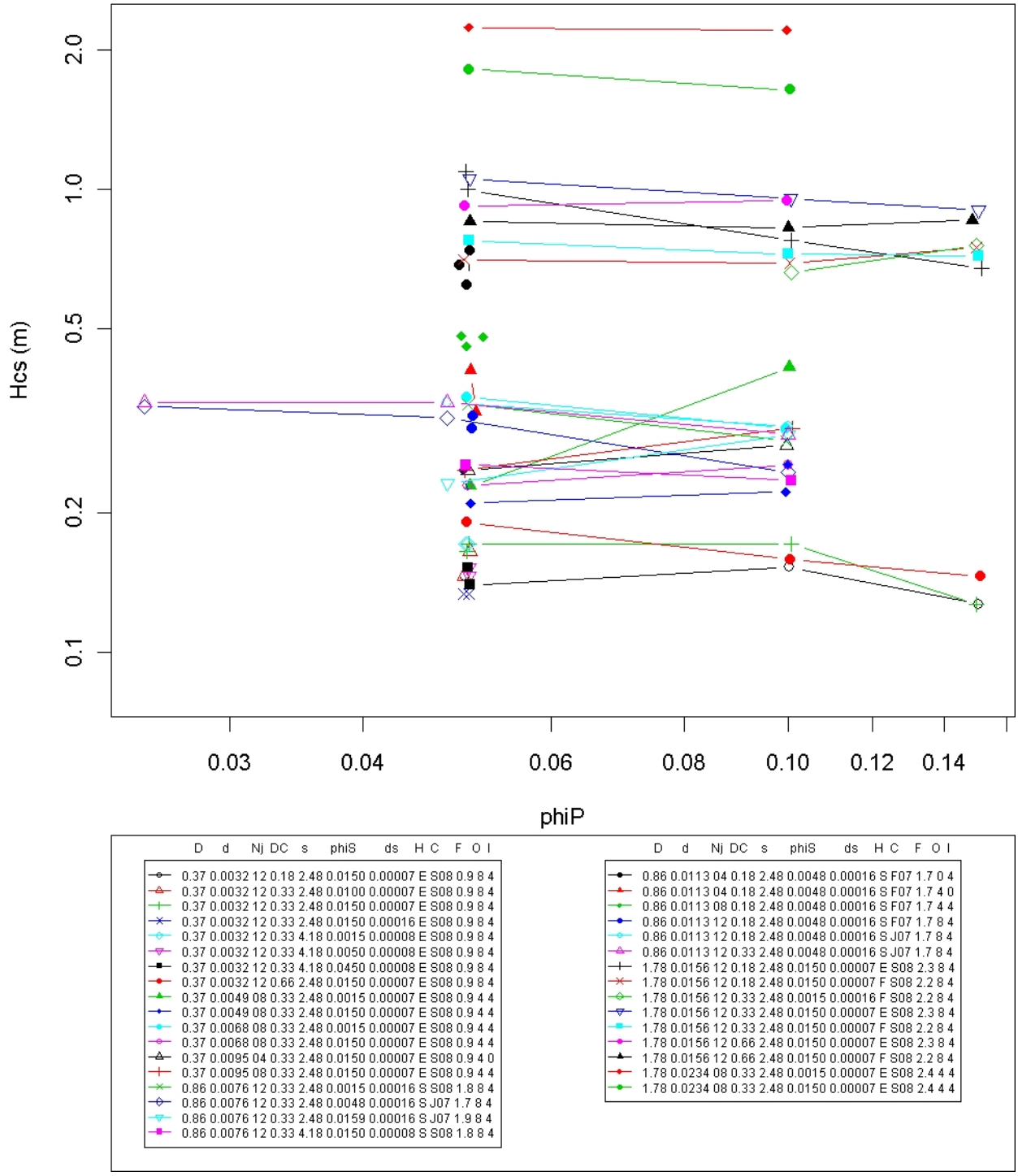

Figure E.26. Log-Log Plot of Functional Relationship Between Cloud Height at Critical Suspension Velocity (H_{CS}) and Pulse Volume Fraction (ϕ_p) for Constant Sets of Values of Other Test Variables. Variables in the legend include H = head, C = test campaign, F = vessel fill height (m), O = number of outer nozzles operating, and I = number of inner nozzles operating.

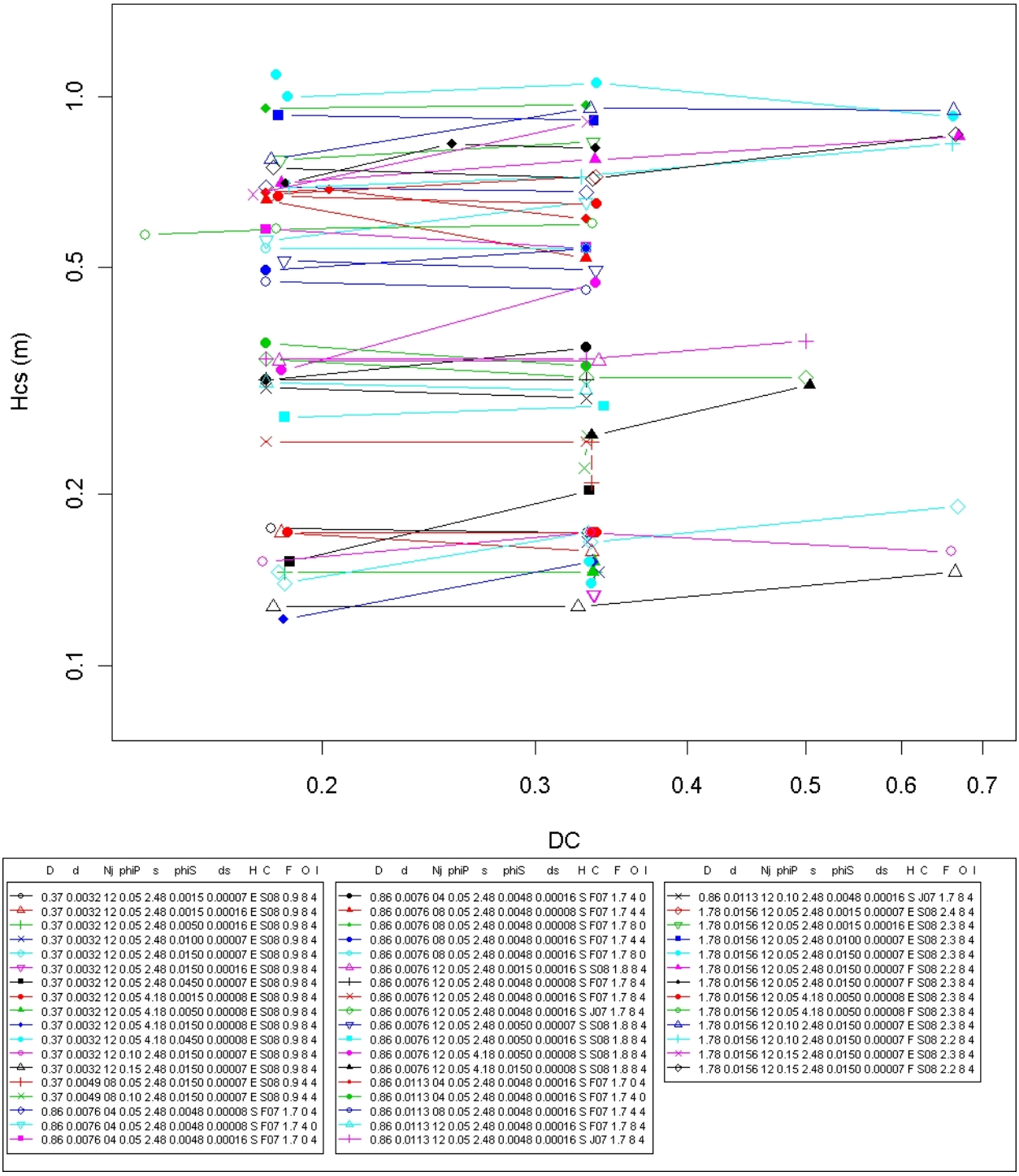

Figure E.27. Log-Log Plot of the Functional Relationship Between Cloud Height at Critical Suspension Velocity (H_{CS}) and Duty Cycle (DC) for Constant Sets of Values of Other Test Variables. Variables in the legend include H = head, C = test campaign, F = vessel fill height (m), O = number of outer nozzles operating, and I = number of inner nozzles operating.

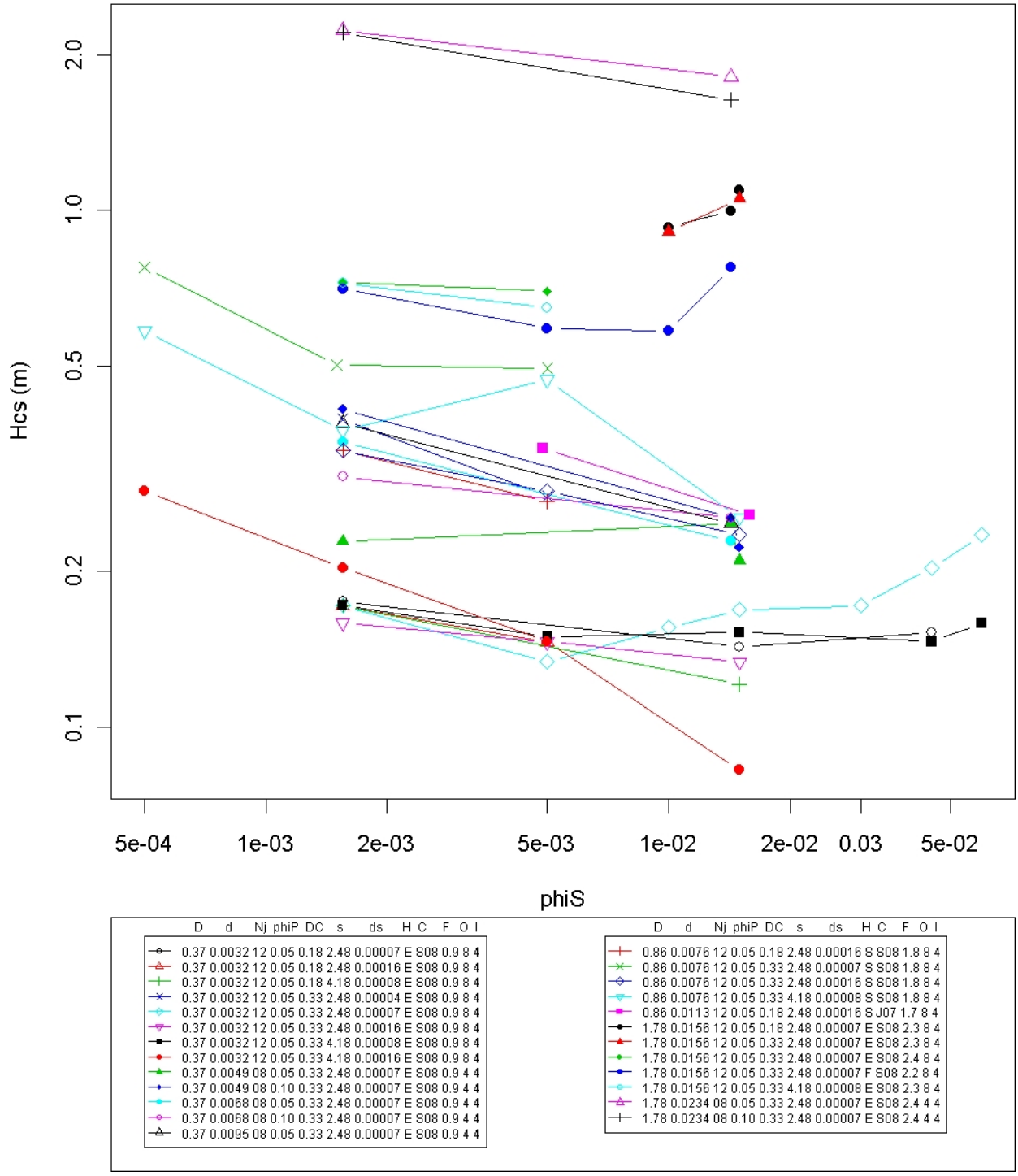

Figure E.28. Log-Log Plot of Functional Relationship Between Cloud Height at Critical Suspension Velocity (H_{CS}) and Solids Volume Fraction (ϕ_S) for Constant Sets of Values of Other Test Variables. Variables in the legend include H = head, C = test campaign, F = vessel fill height (m), O = number of outer nozzles operating, and I = number of inner nozzles operating.

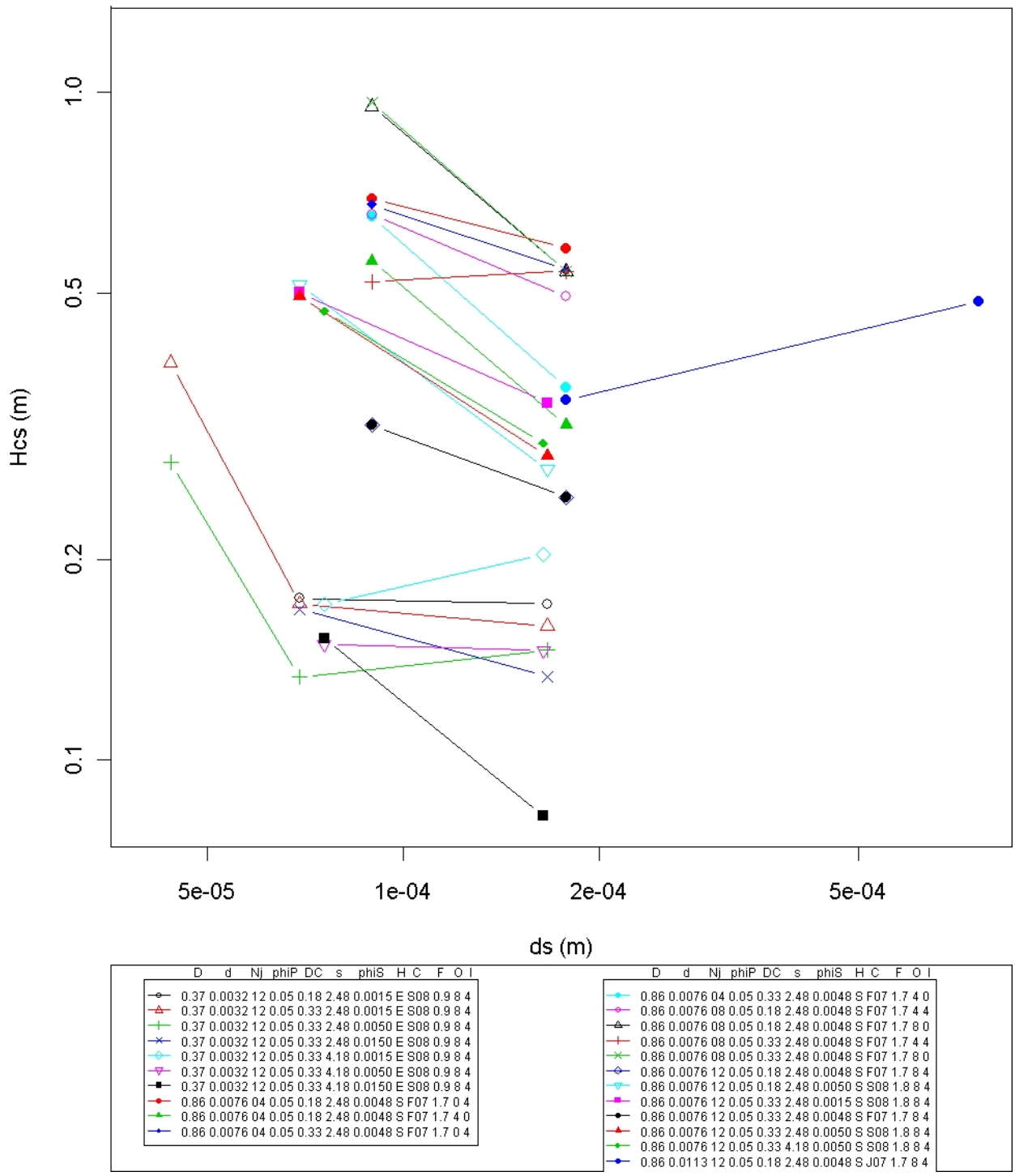

Figure E.29. Log-Log Plot of Functional Relationship Between Cloud Height at Critical Suspension Velocity (H_{CS}) and Solids Particle Diameter ($d_S = d_{50}$) for Constant Sets of Values of Other Test Variables. Variables in the legend include H = head, C = test campaign, F = vessel fill height (m), O = number of outer nozzles operating, and I = number of inner nozzles operating.

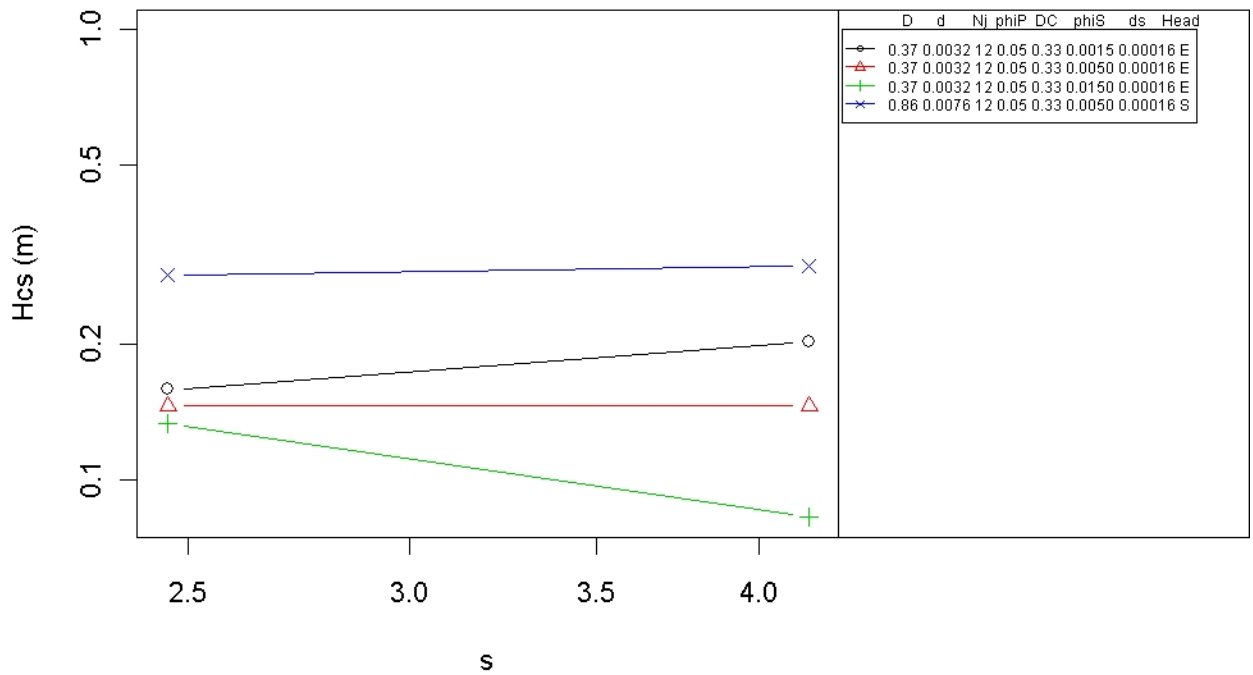

Figure E.30. Log-Log Plot of Functional Relationship Between Cloud Height at Critical Suspension Velocity (H_{CS}) and Density Ratio (s) for Constant Sets of Values of Other Test Variables

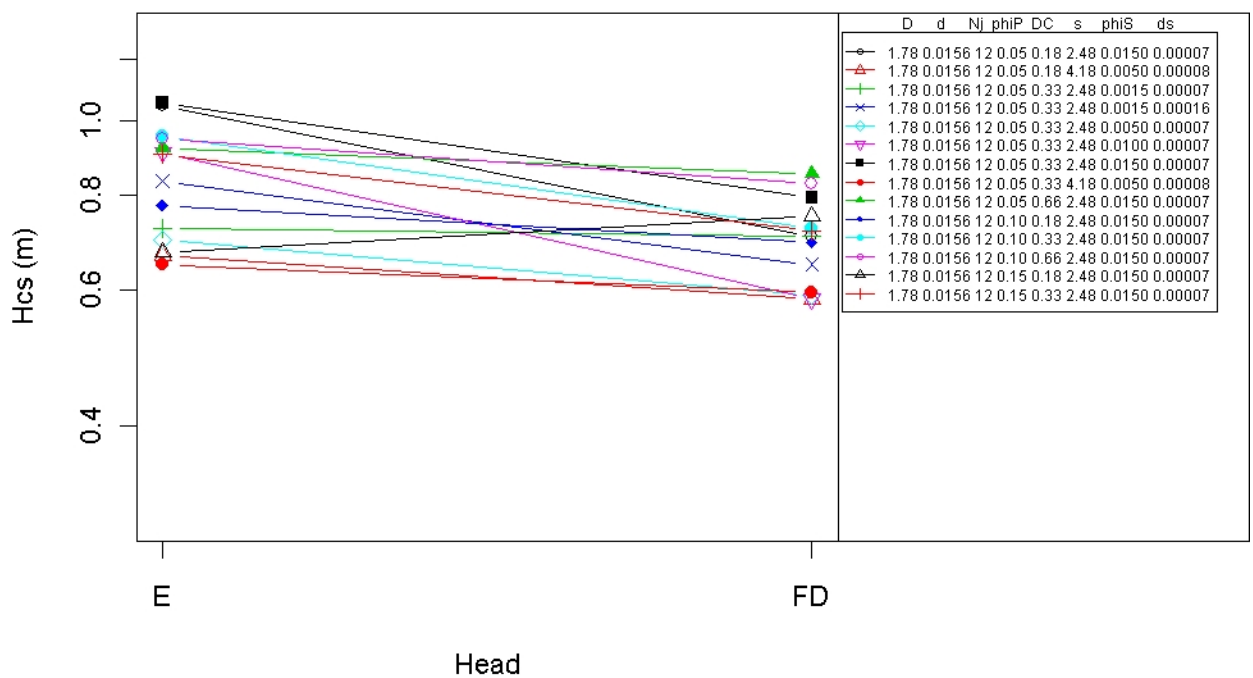

Figure E.31. Log-Categorical Plot of the Functional Relationship Between Cloud Height at Critical Suspension Velocity (H_{CS}) and Head Shape (HS) for Constant Sets of Values of Other Test Variables. No data are plotted for the spherical head shape (S) because it was only used in the D = 0.860 m (~ 34-in.) tank.

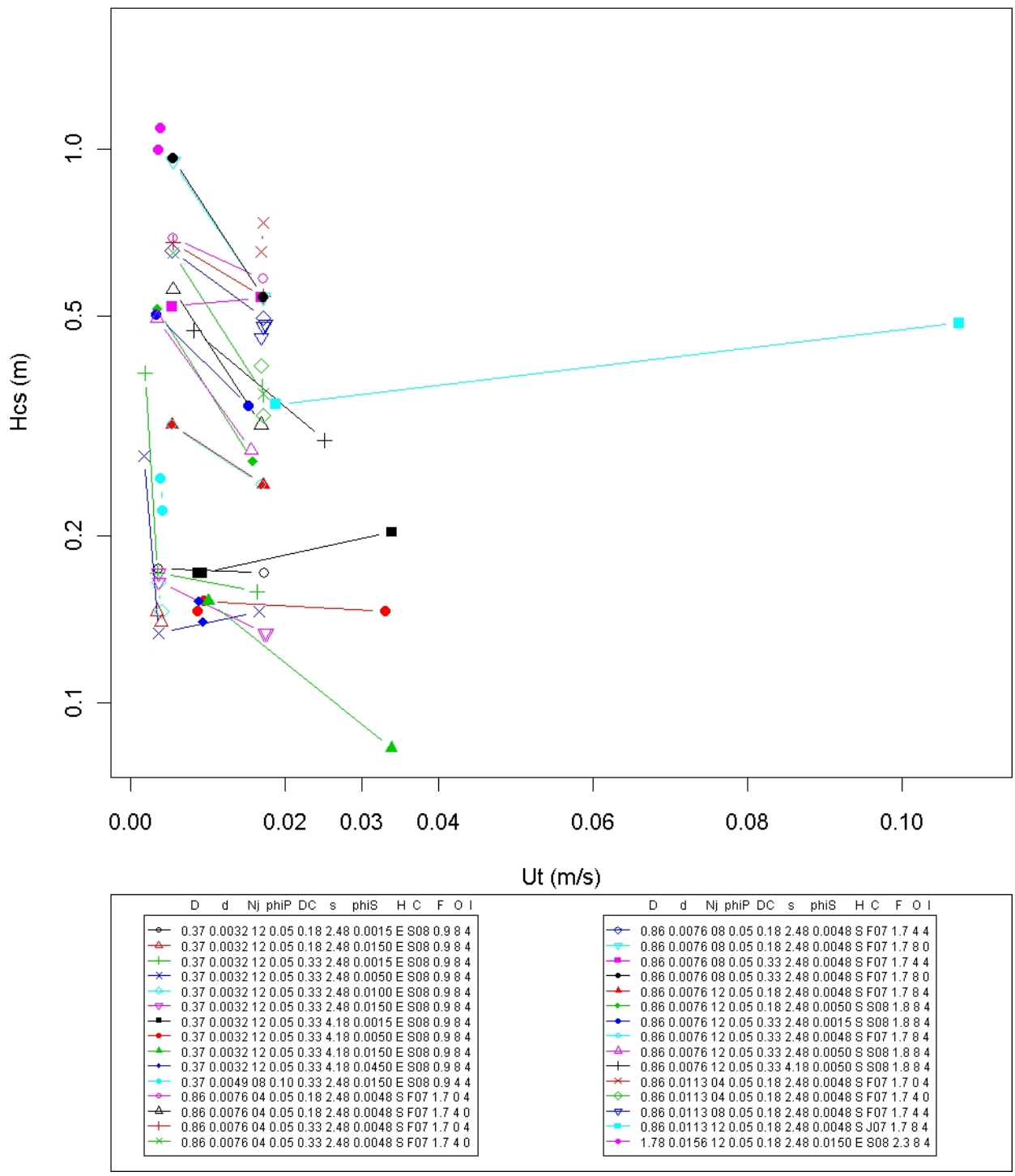

Figure E.32. Log-Log Plot of Functional Relationship Between Cloud Height at Critical Suspension Velocity (H_{CS}) and Unhindered Terminal Settling Velocity (U_T) for Constant Sets of Values of Other Test Variables. Because U_T is calculated as a function of d_S and (s−1), d_S was not used to define the plotting sets in the legend. Hence, the effects of U_T and d_S are confounded in the plot.

- s (Figure E.30): Increasing s tends to weakly affect H_{CS}, with slopes ranging from slightly positive to moderately negative. Hence, there is an indication of possible interactive effects of s and other variables on H_{CS}. Only having data for four conditions in this plot limits the general conclusions that can be made.
- HS (Figure E.31): The flange-and-dish (FD) head shape tends to yield smaller H_{CS} values than the elliptical (E) head shape. See Section E.2.4 for additional discussion. No data are plotted for the spherical (S) head shape, because that shape was only used in tests with the D = 0.860 m (~ 34-in.) tank, and thus there are no sets of conditions with values for E, FD, and S head shapes.

U_T (Figure E.32): Increasing U_T tends to decrease H_{CS}, except for a couple of cases. The rate of decrease in H_{CS} appears to decrease as U_T increases, with even the possibility of H_{CS} increasing after initial decreases with increasing U_T. For U_T up to ~ 0.035, the slopes vary enough to suggest possible interactive effects with other variables. However, because U_T is calculated as a function of d_S and (s – 1, the d_S variable was not used in the plotting groups shown in the legend of the figure. Hence, the effects of U_T and d_S on H_{CS} are confounded, and any statements made here may be as much due to d_S effects as U_T effects on H_{CS}.

These observations and the functionality plots on which they are based serve as a basis for assessing multiple-regression models developed for H_C in Section F.3, Appendix F.

E.2.4 Additional Investigation of Head Shape Effect

The functionality plots for U_{CS} versus HS and H_{CS} versus HS suggest that U_{CS} and H_{CS} values tended to be smaller for FD heads than for E heads in 70-in. tank tests. However, it was only in 70-in. tank tests that the two head shapes were tested. Preliminary model development work with the 2008 data indicated that HS did not have statistically significant effects in predicting U_{CS} or H_{CS}. Hence, additional investigations were undertaken. However, the results (tables and figures) in this subsection are for information purposes only.

Table E.2 summarizes the U_{CS} and H_{CS} data values from 2008 testing with the 70-in. tank having E and FD heads. Ratios of FD to E results for U_{CS} and H_{CS} are shown in the last two columns of Table E.2. For U_{CS}, all FD/E ratios are less than one except for Row #8 (= 1.00) and Row #12 (1.06). For H_{CS}, all FD/E ratios are less than one except for Row #12 (= 1.11). The FD/E ratios for U_{CS} appear to possibly depend on the simulant, with the two lowest ratios (0.81 and 0.85) for simulant s2d2, and ratios ranging from 0.88 to 1.06 for simulants s1d2 and s1d1. However, no such dependence is apparent for FD/E ratios for H_{CS}.

Figures E.33 to E.46 contain plots showing values of cloud height (H_C, in meters) against target velocity (U, m/s) for cases where U is greater than or equal to the corresponding U_{CS} value. The plots were created for the 14 cases in Table E.2 that contain H_C and U data for 70-in.-diameter tanks with both E and FD head shapes. In each plot, all other test variables in the 2008 testing campaign remained constant. The plots are useful in assessing the differences that exist in H_C as a function of U for the two different head shapes if all other variables were kept constant. Many of the plots lack sufficient data to make any clear determination if or how the H_C versus U data differ for E and FD head shapes over the 14 cases.

The objective of creating the plots in Figures E.33 to E.46 was to help determine if a simple empirical model or a single summary statistic (a ratio or difference) could be found that explained the difference in H_C results for E and FD head shapes as a function of the other test variables. The lack of data, however, makes it difficult to visualize a consistent pattern and thus difficult to summarize the H_C results for E vs. FD heads in a simple manner. For example, U_{CS} and H_{CS} values for 70F tests tended to be less than the values for 70E tests, as shown in Table E.2. However, Figures E.33, E.34 and E.46 show H_C results that are smaller for 70E than 70F tests, and this is order is suggested by other figures with less data. On the other hand, Figures E.35 and E.44 show H_C results that are smaller for 70F tests than 70E tests. This is also suggested by other figures with fewer data. Hence, no clear conclusions can be made about the effect of E versus FD differences in tank-head shape on H_C results.

Table E.2. Comparison of U_{CS} and H_{CS} Data from 2008 Tests with Two Head Shapes (E and FD) on 70-in. Tanks. The values for d = 0.613 m (ϕ_J = 0.0009203) were constant for all data in the table.

Row #	Simulant	s	$d_S = d_{50}$ (m)	ϕ_p [(a)]	ϕ_S	DC[(a)]	U_{CS} E (m/s)	U_{CS} FD (m/s)	H_{CS} E (in.)	H_{CS} FD (in.)	Ratio FD/E U_{CS}	Ratio FD/E H_{CS}
1	s1d2	2.48	0.0000693	0.05	0.00155	0.18	5.40	– [(b)]	26.50	–	–	–
2	s1d2	2.48	0.0000693	0.05	0.00155	0.33	4.60	4.40	28.50	27.75	0.96	0.97
3	s1d2	2.48	0.0000693	0.05	0.00500	0.33	6.00	5.80	23.25	27.50	0.97	0.85
4	s1d2	2.48	0.0000693	0.05	0.01000	0.33	7.13[(c)]	6.60	34.92[(c)]	23.00	0.93	0.66
5	s1d2	2.48	0.0000693	0.05	0.01430	0.18	10.90	9.85[(c)]	39.25	27.75	0.90	0.71
6	s1d2	2.48	0.0000693	0.05	0.01430	0.26	–	8.80	–	32.50	–	–
7	s1d2	2.48	0.0000693	0.05	0.01430	0.33	7.80	7.18[(c)]	41.00	31.13[(c)]	0.92	0.76
8	s1d2	2.48	0.0000693	0.05	0.01430	0.66	4.80	4.80	36.25	33.50	1.00	0.92
9	s1d2	2.48	0.0000693	0.10	0.01430	0.18	8.70	8.50	30.50	27.25	0.98	0.89
10	s1d2	2.48	0.0000693	0.10	0.01430	0.33	7.40	6.60	37.50	28.50	0.89	0.76
11	s1d2	2.48	0.0000693	0.10	0.01430	0.66	4.80	4.60	37.25	32.50	0.96	0.87
12	s1d2	2.48	0.0000693	0.15	0.01430	0.18	6.40	6.80	26.50	29.50	1.06	1.11
13	s1d2	2.48	0.0000693	0.15	0.01430	0.33	6.60	6.10	35.50	28.25	0.92	0.80
14	s1d2	2.48	0.0000693	0.15	0.01430	0.66	–	4.50	–	33.75	–	–
15	s1d2	2.48	0.0000693	0.05	0.01500	0.18	11.60	–	43.00	–	–	–
16	s1d2	2.48	0.0000693	0.05	0.01500	0.33	8.50	–	41.50	–	–	–
17	s1d1	2.46	0.0001664	0.05	0.00155	0.18	7.10	–	30.50	–	–	–
18	s1d1	2.46	0.0001664	0.05	0.00155	0.33	7.10	6.70	32.75	25.50	0.94	0.78
19	s1d1	2.46	0.0001664	0.10	0.00155	0.33	–	5.80	–	26.00	–	–
20	s1d1	2.46	0.0001664	0.15	0.00155	0.33	–	5.60	–	29.75	–	–
21	s2d2	4.18	0.0000756	0.05	0.00155	0.33	8.40	–	28.50	–	–	–
22	s2d2	4.18	0.0000756	0.05	0.00500	0.18	14.00	11.40	26.25	23.00	0.81	0.88
23	s2d2	4.18	0.0000756	0.05	0.00500	0.14	–	11.40	–	22.50	–	–
24	s2d2	4.18	0.0000756	0.05	0.00500	0.33	12 .50	10.60	25.50	23.50	0.85	0.92

(a) Rounded.
(b) A dash (–) denotes the test was not performed.
(c) These are average values.

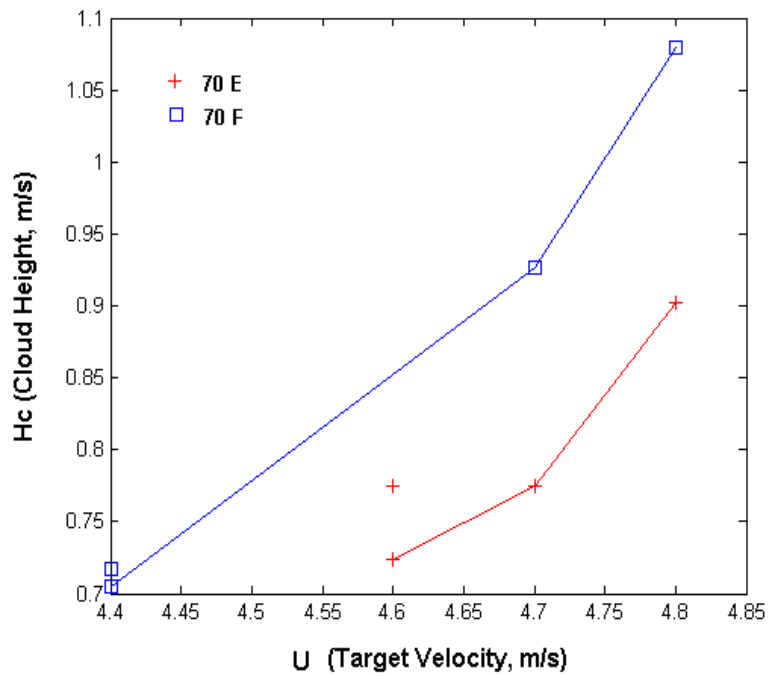

Figure E.33. Cloud Height (H_C) Versus Target Velocity (U) Values for the 70E and 70F Head Shapes with s = 2.48, $d_{50} = 6.93\times10^{-5}$, $\phi_p = 0.05$, $\phi_S = 0.00155$ and DC = 0.33

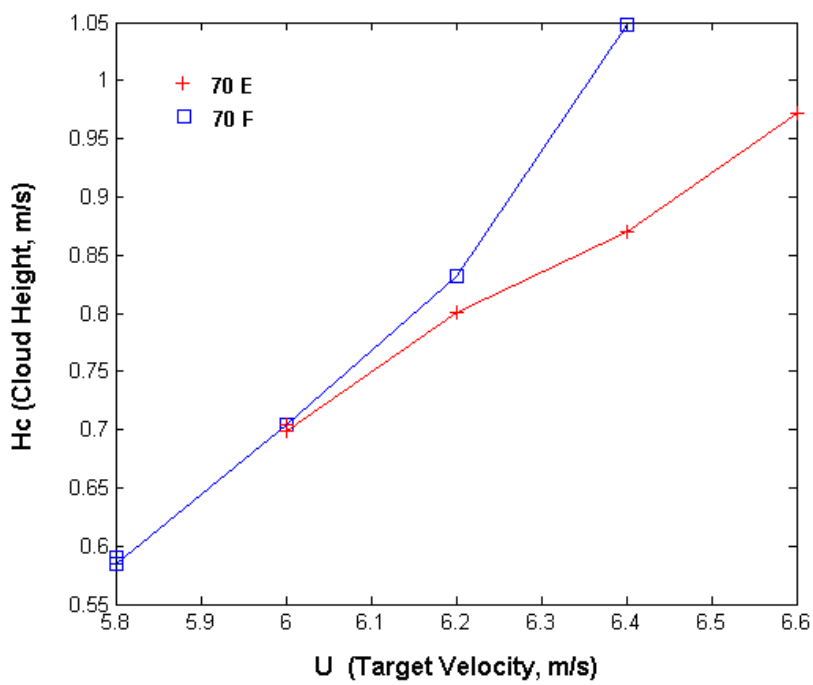

Figure E.34. Cloud Height (H_C) Versus Target Velocity (U) Values for the 70E and 70F Head Shapes with s = 2.48, $d_{50} = 6.93\times10^{-5}$, $\phi_p = 0.05$, $\phi_S = 0.005$ and DC = 0.33

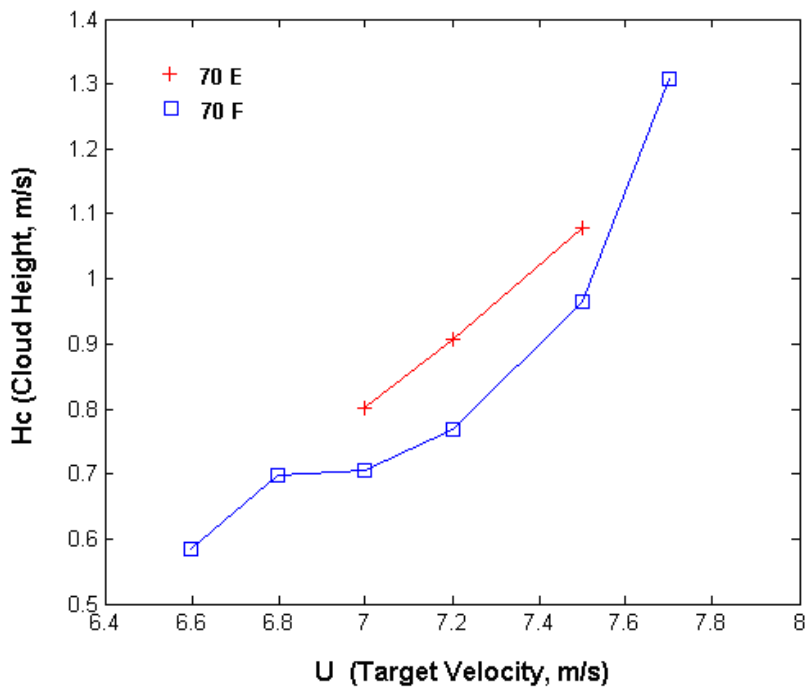

Figure E.35. Cloud Height (H_C) Versus Target Velocity (U) Values for the 70E and 70F Head Shapes with s = 2.48, $d_{50} = 6.93\times10^{-5}$, $\phi_p = 0.05$, $\phi_S = 0.01$ and DC = 0.33

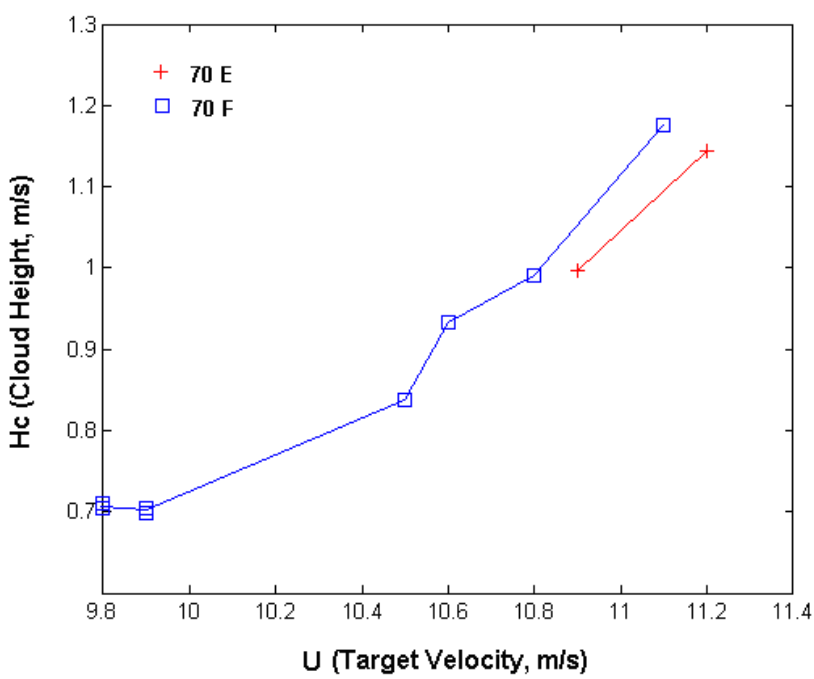

Figure E.36. Cloud Height (H_C) Versus Target Velocity (U) Values for the 70E and 70F Head Shapes with s = 2.48, $d_{50} = 6.93\times10^{-5}$, $\phi_p = 0.05$, $\phi_S = 0.0143$ and DC = 0.18

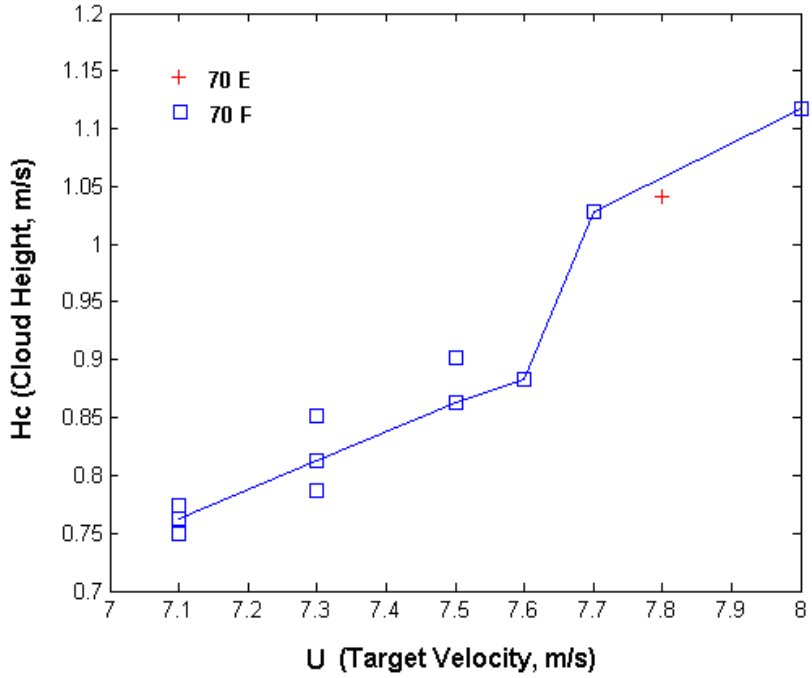

Figure E.37. Cloud Height (H_C) Versus Target Velocity (U) Values for the 70E and 70F Head Shapes with s = 2.48, $d_{50} = 6.93\times10^{-5}$, $\phi_p = 0.05$, $\phi_S = 0.0143$ and DC = 0.33

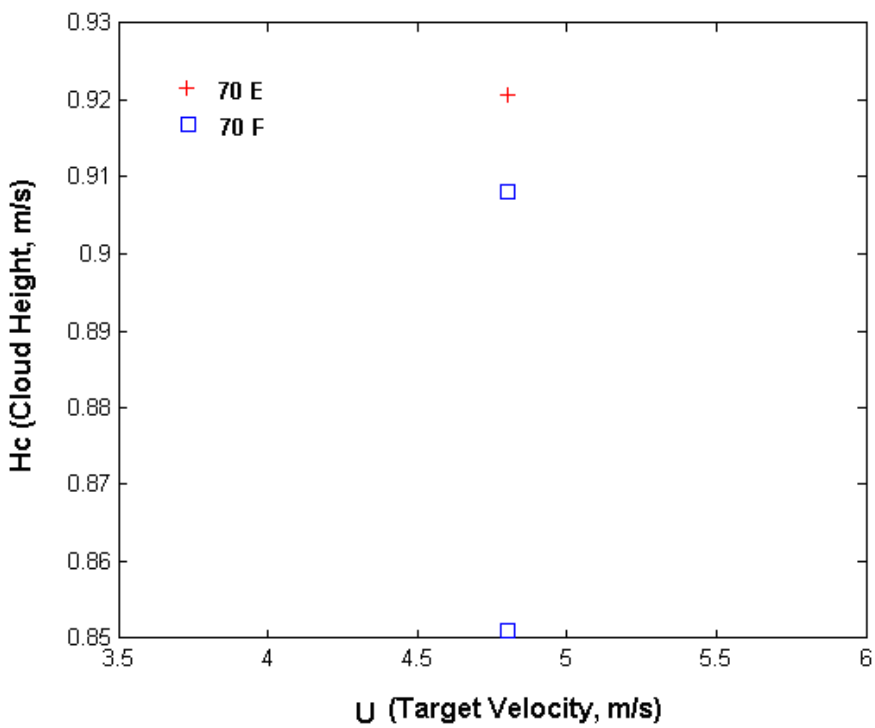

Figure E.38. Cloud Height (H_C) Versus Target Velocity (U) Values for the 70E and 70F Head Shapes with s = 2.48, $d_{50} = 6.93\times10^{-5}$, $\phi_p = 0.05$, $\phi_S = 0.0143$ and DC = 0.66

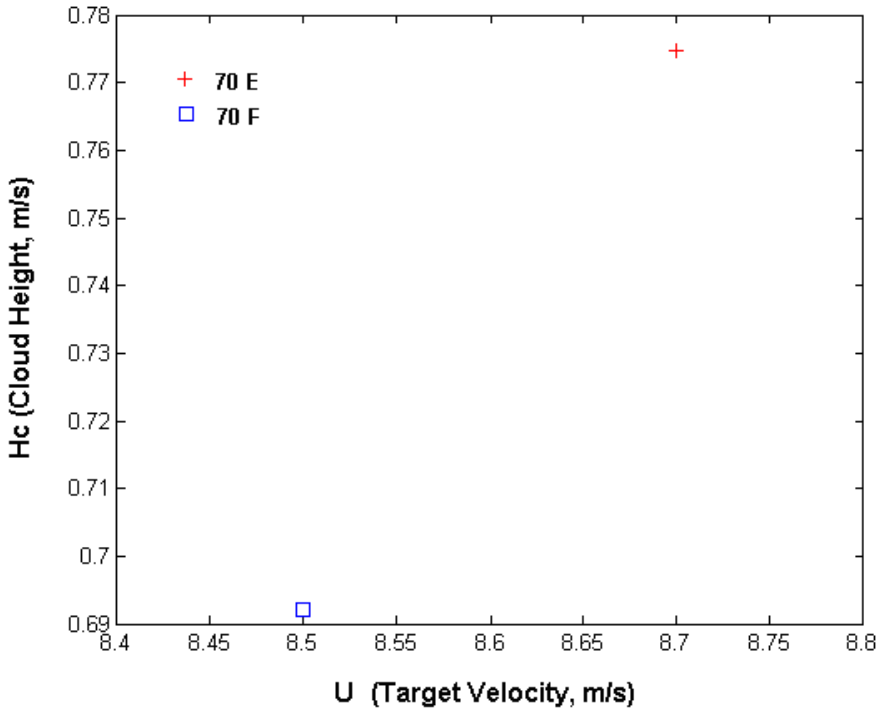

Figure E.39. Cloud Height (H_C) Versus Target Velocity (U) Values for the 70E and 70F Head Shapes with s = 2.48, $d_{50} = 6.93\times10^{-5}$, $\phi_p = 0.10$, $\phi_S = 0.0143$ and DC = 0.18

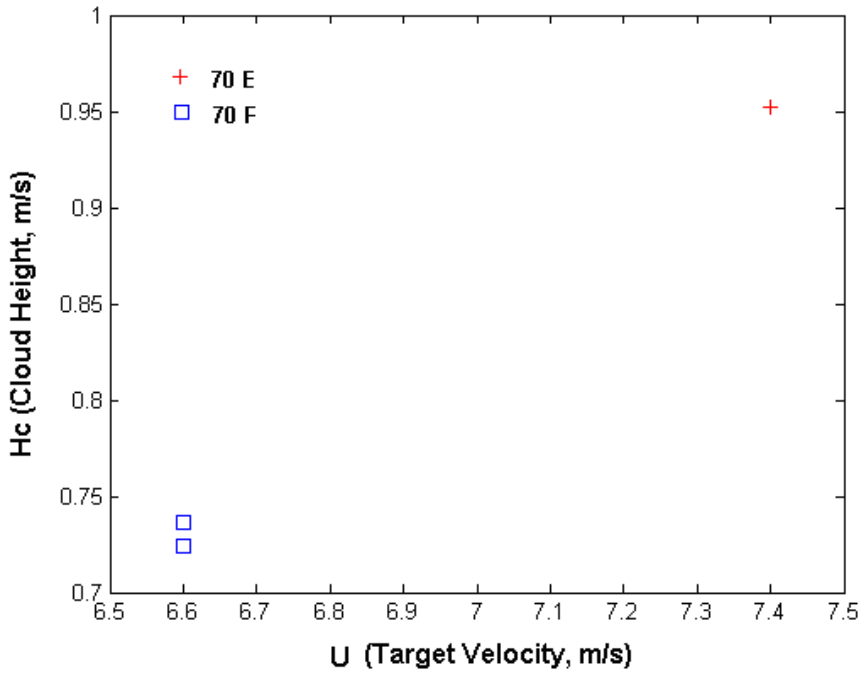

Figure E.40. Cloud Height (H_C) Versus Target Velocity (U) Values for the 70E and 70F Head Shapes with s = 2.48, $d_{50} = 6.93\times10^{-5}$, $\phi_p = 0.10$, $\phi_S = 0.0143$ and DC = 0.33

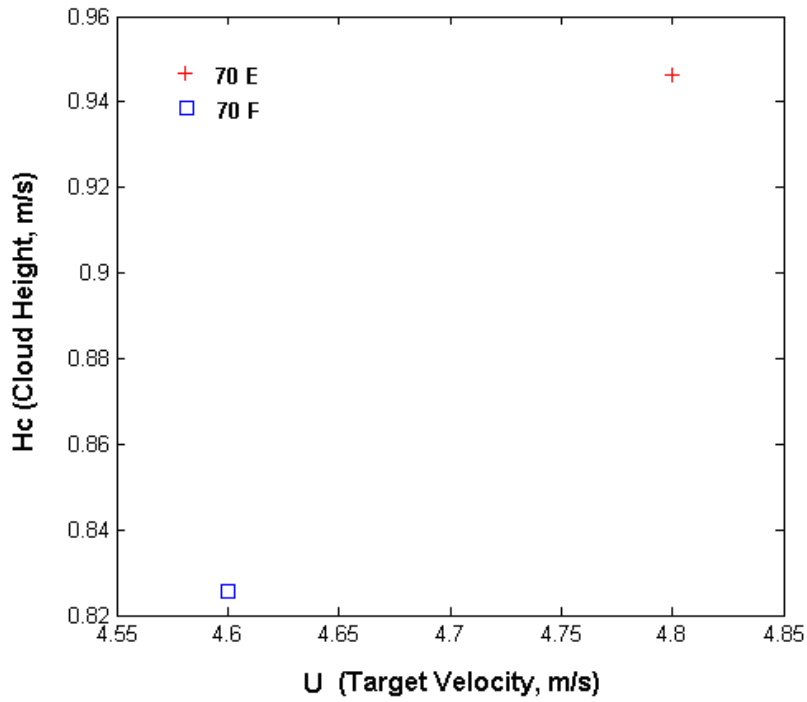

Figure E.41. Cloud Height (H_C) Versus Target Velocity (U) Values for the 70E and 70F Head Shapes with s = 2.48, $d_{50} = 6.93\times10^{-5}$, $\phi_p = 0.10$, $\phi_S = 0.0143$ and DC = 0.66

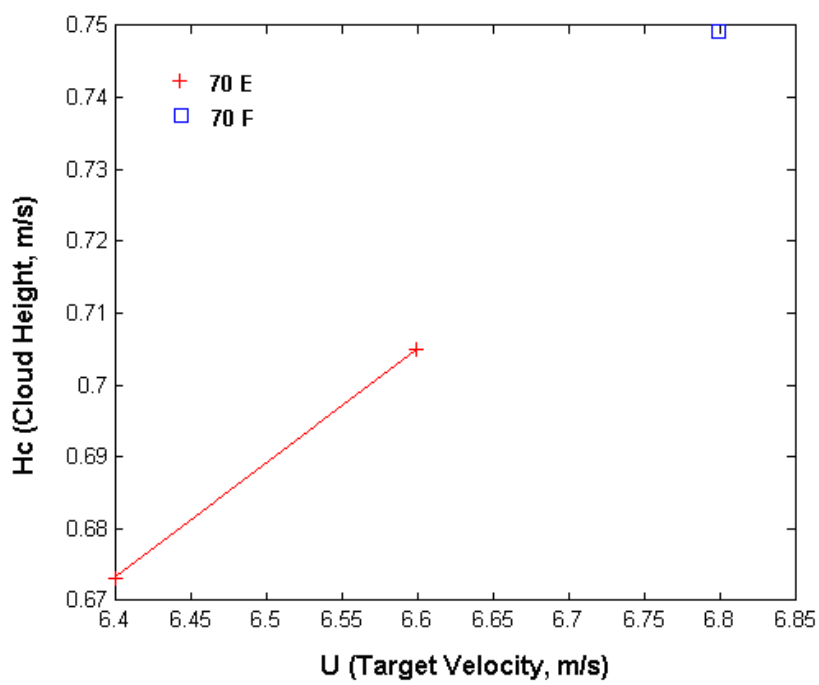

Figure E.42. Cloud Height (H_C) Versus Target Velocity (U) Values for the 70E and 70F Head Shapes with s = 2.48, $d_{50} = 6.93\times10^{-5}$, $\phi_p = 0.15$, $\phi_S = 0.0143$ and DC = 0.18

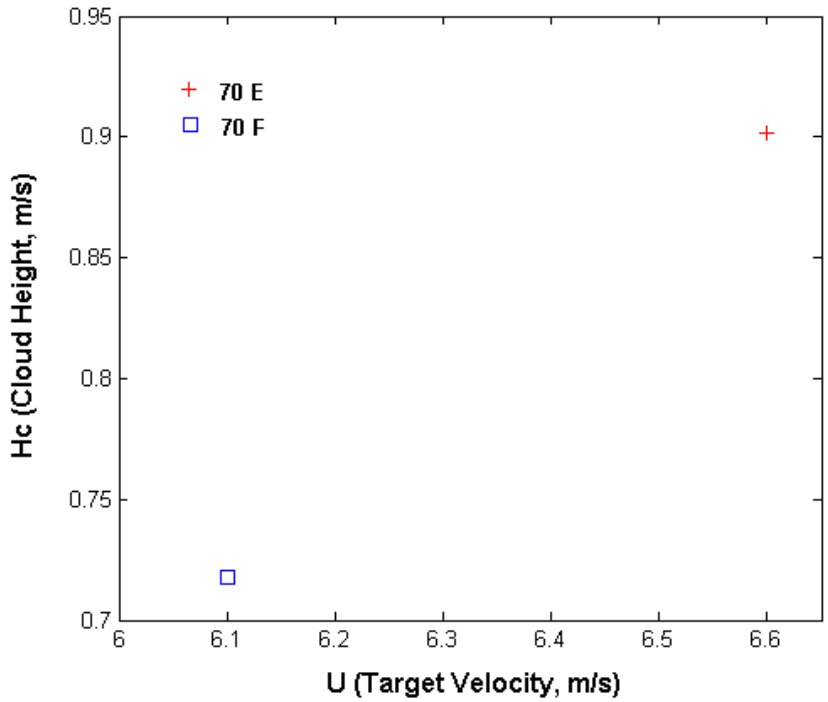

Figure E.43. Cloud Height (H_C) Versus Target Velocity (U) Values for the 70E and 70F Head Shapes with s = 2.48, $d_{50} = 6.93\times10^{-5}$, $\phi_p = 0.15$, $\phi_S = 0.0143$ and DC = 0.33

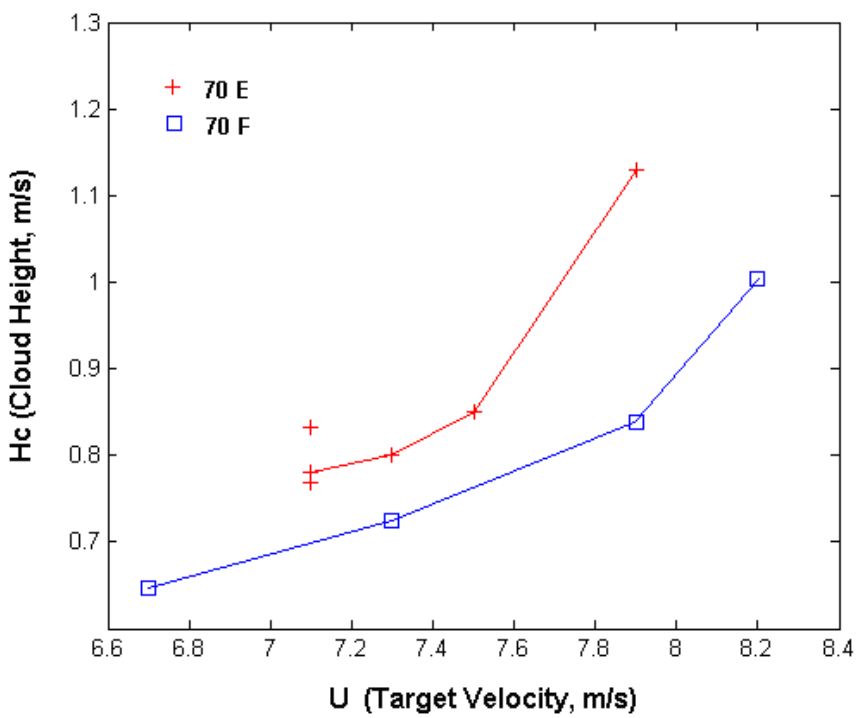

Figure E.44. Cloud Height (H_C) Versus Target Velocity (U) Values for the 70E and 70F Head Shapes with s = 2.46, $d_{50} = 1.664\times10^{-4}$, $\phi_p = 0.05$, $\phi_S = 0.00155$ and DC = 0.33

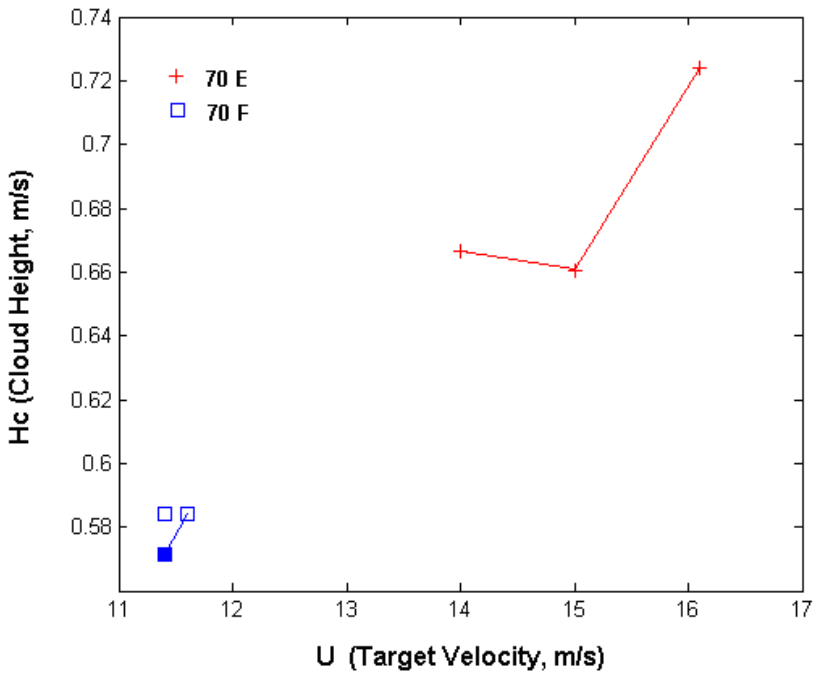

Figure E.45. Cloud Height (H_C) Versus Target Velocity (U) Values for the 70E and 70F Head Shapes with s = 4.18, $d_{50} = 7.56\times10^{-5}$, $\phi_p = 0.05$, $\phi_S = 0.005$ and DC = 0.18. The solid square has DC = 0.14.

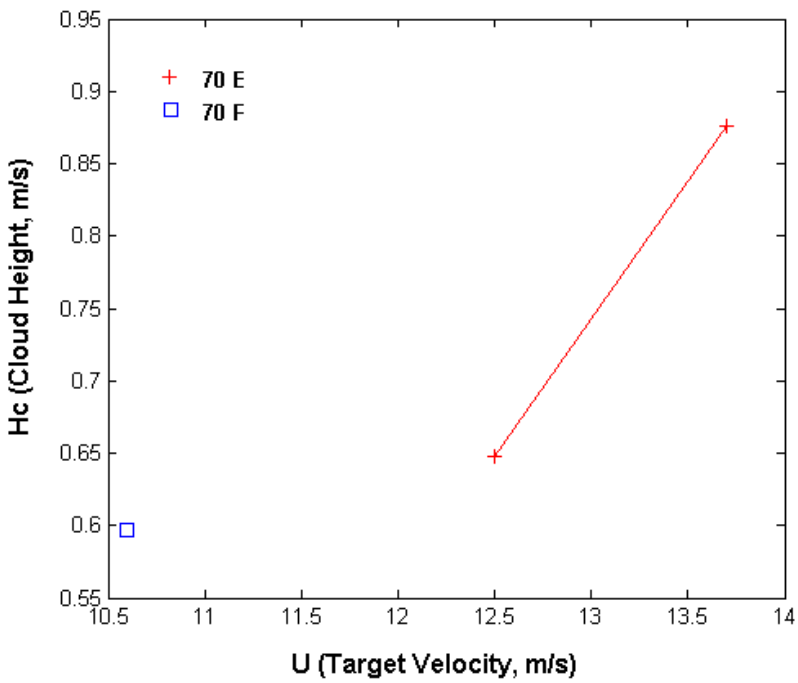

Figure E.46. Cloud Height (H_C) Versus Target Velocity (U) Values for the 70E and 70F Head Shapes with s = 4.18, $d_{50} = 7.56\times10^{-5}$, $\phi_p = 0.05$, $\phi_S = 0.005$ and DC = 0.33

E.3 Replicate and Repeat Tests

In performing experimental work, replicate tests of several test conditions should be included in each testing campaign to provide a basis for quantifying the experimental and measurement uncertainty in the response variables of interest. By *replicate tests* we mean tests performed at the same set of conditions but at different times, with tests at other sets of conditions intervening. Replicate tests performed in this way provide data subject to all of the sources of experimental and measurement variation/uncertainty. However, only limited replicate tests involving the July 2007 and Fall 2007 test campaigns were performed. In addition to replicate tests, some repeat testing was performed within the July 2007, Fall 2007 and 2008 test campaigns. By *repeat tests*, we mean tests performed at the same conditions one after another (or close in time), without a change of simulant. Repeat testing only captures information about short-term testing and measurement uncertainties, which are typically much smaller than longer-term testing variations/uncertainties that would be captured by replicate testing. Table E.3 lists the test conditions investigated with near-replicate and near-repeat testing. The terms *near-replicate* and *near-repeat* are used because the test conditions are close but not exactly the same for some test variables.

Table E.4 shows the five sets of near-replicate test results for U_{CS} and H_{CS} responses. Table E.4 lists the standard deviation (SD) and percent relative standard deviation (%RSD) for U_{CS} and H_{CS} for each near-replicate set. Also listed are pooled (combined) values of SD and %RSD for each of U_{CS} and H_{CS} over the five near-replicate sets. For U_{CS}, the pooled SD = 0.224 m/s and the pooled %RSD = 5.29 for near-replicate experimental uncertainty. For H_{CS}, the pooled SD = 0.040 m and the pooled %RSD = 13.34 for near-replicate experimental uncertainty. Although not apparent from this small number of near-replicate sets, the uncertainties in U_{CS} and H_{CS} are expected to increase with the values of these responses. Hence, the pooled %RSD values are the more appropriate summary measure of near-replicate testing and measurement uncertainty.

Table E.5 shows the 13 sets of tests with near-repeat conditions, as well as SD and %RSD values for each near-repeat set and pooled over the sets. Because near-repeat set #11 has large values of SD and %RSD for U_{CS}, pooled SD and %RSD values were calculated across all near-repeat sets with and without set #11. For U_{CS} without set #11, the pooled SD = 0.247 m/s and the pooled %RSD = 4.12 for near-repeat uncertainty. For H_{CS}, the pooled SD = 0.019 m and the pooled %RSD = 5.54 for near-repeat uncertainty. Although not apparent from this relatively small number of near-repeat sets, the uncertainties in U_{CS} and H_{CS} are expected to increase with the values of these responses. Hence, the pooled %RSD values are the more appropriate summary measure of near-repeat testing and measurement uncertainty.

Time and budget limitations did not permit processing the H_C data set to identify near-replicate and near-repeat sets. The H_{CS} near-replicate and near-repeat sets of data would be a subset of those sets of data for H_C. If the uncertainty in H_C increases proportionally to the magnitude of H_C as expected, then the pooled %RSDs from near-replicate and near-repeat sets for H_{CS} should be reasonable estimates of the %RSDs for uncertainties in H_C.

As expected, uncertainties from the near-replicate sets are larger than from the near-repeat sets. Hence, uncertainties from the near-replicate sets should be used as estimates of uncertainties in U_{CS}, H_{CS}, and H_C results. However, the limited nature of these estimates should be kept in mind. Also, the results indicate that the relative uncertainty in experimentally determining H_{CS} (and presumably H_C) values is notably larger than the relative uncertainty in experimentally determining H_C values.

Table E.3. Near-Replicate and Near-Repeat Tests at Critical Suspension Conditions

Row Number	Case ID	Test	Tank Diameter	Solids Density	Solids Fraction	Particle Size	Duty Cycle	Pulse Volume Fraction	Number Installed Tubes	# Operating Tubes	# Outer -Layer Tubes	# Inner -Layer Tubes	Nozzle Inner Diameter	Head Shape	Discharge Velocity	Near-Repeat Set	Near-Replicate Set
text	text	text	in	g/cm^3	fraction	m	fraction	fraction	#	#	#	#	in	text	m/s		
MSS	ID	M/DDX	D	S	f_S	d_{50} (d_S)	DC	ϕ_P	N	N_J	N_O	N_I	d	HS	U		
9150506	15E_4s1d1Xc_1	6/27C	14.4375	2.46	0.015	0.00017	0.334	0.050	12	12	8	4	0.126	E	8.2	1	–[(a)]
9150516	15E_4s1d1Xc_1	6/30A	14.4375	2.46	0.015	0.00017	0.335	0.050	12	12	8	4	0.126	E	8.6	1	–
9150048	15E_4s1d2Rc_1	6/9B	14.4375	2.48	0.01	6.9E-05	0.338	0.050	12	12	8	4	0.126	E	5.3	2	–
9150053	15E_4s1d2Rc_1	6/10A	14.4375	2.48	0.01	6.9E-05	0.331	0.050	12	12	8	4	0.126	E	5.4	2	–
9150063	15E_4s1d2Xc_1	6/10B	14.4375	2.48	0.015	6.9E-05	0.331	0.050	12	12	8	4	0.126	E	5.8	3	–
9150108	15E_4s1d2Xc_1	6/11C	14.4375	2.48	0.015	6.9E-05	0.333	0.050	12	12	8	4	0.126	E	5.8	3	–
9150083	15E_4s1d2Xd_1	6/11A	14.4375	2.48	0.015	6.9E-05	0.184	0.050	12	12	8	4	0.126	E	7.2	4	–
9150174	15E_4s1d2Xd_1	6/13C	14.4375	2.48	0.015	6.9E-05	0.186	0.050	12	12	8	4	0.126	E	7.4	4	–
9150412	15E_4s2d2Wc_1	6/24B	14.4375	4.18	0.045	7.6E-05	0.333	0.050	12	12	8	4	0.126	E	11.5	5	–
9150419	15E_4s2d2Wc_1	6/25A	14.4375	4.18	0.045	7.6E-05	0.332	0.050	12	12	8	4	0.126	E	11.5	5	–
9150345	15E_4s2d2Yc_1	6/19C	14.4375	4.18	0.005	7.6E-05	0.335	0.050	12	12	8	4	0.126	E	7.6	6	–
9150347	15E_4s2d2Yc_1	6/20A	14.4375	4.18	0.005	7.6E-05	0.334	0.050	12	12	8	4	0.126	E	7.6	6	–
9150307	15E_4s2d2Zc_1	6/18B	14.4375	4.18	0.00155	7.6E-05	0.337	0.050	12	12	8	4	0.126	E	5.4	7	–
9150312	15E_4s2d2Zc_1	6/19A	14.4375	4.18	0.00155	7.6E-05	0.334	0.050	12	12	8	4	0.126	E	5.2	7	–
7091025	34S_4p1d7Yc_1	11/26B1	33.875	2.45	0.00487	0.00018	0.330	0.05105	12	12	8	4	0.297	S	6.5	–	1
20070105	34S_4p1d7Yc_8	7/16 A2	33.875	2.45	0.00487	0.00018	0.330	0.05	12	12	8	4	0.297	S	6.4	–	1
20070387	34S_4p1d7Yc_8	7/19 A1	33.875	2.45	0.00487	0.00018	0.330	0.048	12	12	8	4	0.297	S	6.2	–	1
7090875	34S_4p1d7Yd_1	11/19A2	33.875	2.45	0.00487	0.00018	0.180	0.05325	12	12	8	4	0.297	S	6.4	–	2
20070441	34S_4p1d7Yd_8	7/19 A4	33.875	2.45	0.00487	0.00018	0.180	0.048	12	12	8	4	0.297	S	6.4	–	2
7090779	34S_6p1d7Yc_1	11/14D1	33.875	2.45	0.00487	0.00018	0.330	0.05109	12	12	8	4	0.446	S	4.5	–	3
20070627	34S_6p1d7Yc_8	7/21 A2	33.875	2.45	0.00487	0.00018	0.330	0.048	12	12	8	4	0.446	S	4.0	–	3
7090095	34S_6p1d7Yd_0	10/18A2	33.875	2.45	0.00487	0.00018	0.180	0.052	12	8	4	4	0.446	S	6.1	8	–
7090244	34S_6p1d7Yd_0	10/26B2	33.875	2.45	0.00487	0.00018	0.180	0.050	12	8	4	4	0.446	S	6.1	8	–
7090758	34S_6p1d7Yd_0	11/14A2	33.875	2.45	0.00487	0.00018	0.180	0.050	12	8	4	4	0.446	S	7.0	8	–
7090136	34S_6p1d7Yd_6	10/18B2	33.875	2.45	0.00487	0.00018	0.180	0.051	12	4	4	0	0.446	S	6.4	9	–
7090298	34S_6p1d7Yd_6	10/29B2	33.875	2.45	0.00487	0.00018	0.180	0.050	12	4	4	0	0.446	S	6.2	9	–

(a) A dash (–) indicates the test condition is not included in a near-replicate or near-repeat set.

Table E.3. Near-Replicate and Near-Repeat Tests at Critical Suspension Conditions (contd)

Row Number	Case ID	Test	Tank Diameter	Solids Density	Solids Fraction	Particle Size	Duty Cycle	Pulse Volume Fraction	Number Installed Tubes	# Operating Tubes	# Outer -Layer Tubes	# Inner -Layer Tubes	Nozzle Inner Diameter	Head Shape	Discharge Velocity	Near-Repeat Set	Near-Replicate Set
text	text	text	in	g/cm^3	fraction	m	fraction	fraction	#	#	#	#	in	text	m/s		
MSS	ID	M/DDX	D	S	f_S	d_{50} (d_S)	DC	ϕ_P	N	N_J	N_O	N_I	d	HS	U		
7090208	34S_6p1d7Yd_1	10/26A2	33.875	2.45	0.00487	0.00018	0.180	0.051	12	12	8	4	0.446	S	4.0	10	4a
7090328	34S_6p1d7Yd_1	10/30A2	33.875	2.45	0.00487	0.00018	0.180	0.051	12	12	8	4	0.446	S	3.6	10	4b
20070750	34S_6p1d7Yd_8	7/23 A1	33.875	2.45	0.00487	0.00018	0.180	0.048	12	12	8	4	0.446	S	4.1	−	4a, 4b
7090184	34S_6p1d7Yd_9	10/19A2	33.875	2.45	0.00487	0.00018	0.180	0.050	12	4	0	4	0.446	S	8.5	11	−
7090360	34S_6p1d7Yd_9	10/30C2	33.875	2.45	0.00487	0.00018	0.180	0.050	12	4	0	4	0.446	S	6.7	11	−
700319	70F_4s1d2Vc_1	4/21A	70	2.48	0.0143	6.9E-05	0.336	0.050	12	12	8	4	0.613	FD	7.1	12	−
700430	70F_4s1d2Vc_1	4/29A	70	2.48	0.0143	6.9E-05	0.336	0.050	12	12	8	4	0.613	FD	7.3	12	−
700356	70F_4s1d2Vd_1	4/22A	70	2.48	0.0143	6.9E-05	0.185	0.050	12	12	8	4	0.613	FD	9.9	13	−
700415	70F_4s1d2Vd_1	4/28A	70	2.48	0.0143	6.9E-05	0.187	0.050	12	12	8	4	0.613	FD	9.8	13	−

(a) A dash (−) indicates the test condition is not included in a near-replicate or near-repeat set.

Table E.4. U_{CS} and H_{CS} Values, SDs, and %RSDs for Near-Replicate Sets of M3 Mixing Tests

Near-Replicate Set	MSS#[a] of Near-Replicate Set	Case ID of Near-Replicate Set	Test Number	U_{CS} m/s	U_{CS} SD[b] (m/s)	U_{CS} %RSD[c]	H_{CS} in.	H_{CS} m	H_{CS} SD[b] (m)	H_{CS} %RSD[c]
1	7091025	34S_4p1d7Yc_1	11/26B1	6.5	0.153	2.40	9.75	0.2477	0.037	12.88
	20070105	34S_4p1d7Yc_8	7/16 A2	6.4			11.625	0.2954		
	20070387	34S_4p1d7Yc_8	7/19 A1	6.2			12.625	0.3208		
2	7090875	34S_4p1d7Yd_1	11/19A2	6.4	0.000	0.00	9.75	0.2477	0.070	23.44
	20070441	34S_4p1d7Yd_8	7/19 A4	6.4			13.625	0.3462		
3	7090779	34S_6p1d7Yc_1	11/14D1	4.5	0.354	8.32	12.00	0.3048	0.029	8.97
	20070627	34S_6p1d7Yc_8	7/21 A2	4.0			13.625	0.3462		
4a	7090208	34S_6p1d7Yd_1	10/26A2	4.0	0.071	1.75	12.00	0.3048	0.029	8.97
	20070750	34S_6p1d7Yd_8	7/23 A1	4.1			13.625	0.3462		
4b	7090328	34S_6p1d7Yd_1	10/30A2	3.6	0.354	9.18	12.75	0.3239	0.016	4.69
	20070750	34S_6p1d7Yd_8	7/23 A1	4.1			13.625	0.3462		
Pooled Over All 5 Near-Replicate Sets					**0.224**	**5.29**			**0.040**	**13.32**

(a) MSS# = Master Spreadsheet Number.
(b) SD = standard deviation.
(c) %RSD = percent relative standard deviation = 100(SD/mean).

Table E.5. U_{CS} and H_{CS} Values, %RSDs, and Standard Deviations for Near-Repeat Sets of M3 Mixing Tests

Near-Repeat Set	MSS#[a] of Near-Repeat Set	Case ID of Near-Repeat Set	Test Number	U_{CS} m/s	U_{CS} SD[b] (m/s)	U_{CS} %RSD[c]	H_{CS} in.	H_{CS} m	H_{CS} SD[b] (m)	H_{CS} %RSD[c]
1	9150506	15E_4s1d1Xc_1	6/27C	8.2	0.283	3.37	5.25	0.1334	0.000	0.00
	9150516	15E_4s1d1Xc_1	6/30A	8.6			5.25	0.1334		
2	9150048	15E_4s1d2Rc_1	6/9B	5.3	0.071	1.32	5.75	0.1461	0.013	8.66
	9150053	15E_4s1d2Rc_1	6/10A	5.4			6.50	0.1651		
3	9150063	15E_4s1d2Xc_1	6/10B	5.8	0.000	0.00	6.75	0.1715	0.004	2.67
	9150108	15E_4s1d2Xc_1	6/11C	5.8			6.50	0.1651		
4	9150083	15E_4s1d2Xd_1	6/11A	7.2	0.141	1.94	5.75	0.1461	0.004	3.14
	9150174	15E_4s1d2Xd_1	6/13C	7.4			5.50	0.1397		
5	9150412	15E_4s2d2Wc_1	6/24B	11.5	0.000	0.00	5.50	0.1397	0.009	6.15
	9150419	15E_4s2d2Wc_1	6/25A	11.5			6.00	0.1524		
6	9150345	15E_4s2d2Yc_1	6/19C	7.6	0.000	0.00	6.00	0.1524	0.004	3.01
	9150347	15E_4s2d2Yc_1	6/20A	7.6			5.75	0.1461		
7	9150307	15E_4s2d2Zc_1	6/18B	5.4	0.141	2.67	6.75	0.1715	0.000	0.00
	9150312	15E_4s2d2Zc_1	6/19A	5.2			6.75	0.1715		
8	7090095	34S_6p1d7Yd_0	10/18A2	6.1	0.520	8.12	18.83	0.4783	0.014	2.88
	7090244	34S_6p1d7Yd_0	10/26B2	6.1			18.00	0.4572		
	7090758	34S_6p1d7Yd_0	11/14A2	7.0			19.00	0.4826		
9	7090136	34S_6p1d7Yd_6	10/18B2	6.4	0.141	2.24	13.00	0.3302	0.054	14.63
	7090298	34S_6p1d7Yd_6	10/29B2	6.2			16.00	0.4064		
10	7090208	34S_6p1d7Yd_1	10/26A2	4.0	0.283	7.44	12.00	0.3048	0.013	4.29
	7090328	34S_6p1d7Yd_1	10/30A2	3.6			12.75	0.3239		
11	7090184	34S_6p1d7Yd_9	10/19A2	8.5	1.273	16.75	(d)	(d)	(d)	(d)
	7090360	34S_6p1d7Yd_9	10/30C2	6.7			(d)	(d)		
12	700319	70F_4s1d2Vc_1	4/21A	7.1	0.141	1.96	30.50	0.7747	0.027	3.39
	700430	70F_4s1d2Vc_1	4/29A	7.3			32.00	0.8128		
13	700356	70F_4s1d2Vd_1	4/22A	9.9	0.071	0.72	27.75	0.7049	0.000	0.00
	700415	70F_4s1d2Vd_1	4/28A	9.8			27.75	0.7049		
Pooled Over All 13 Near-Repeat Sets					**0.415**	**5.98**			N/A[e]	N/A
Pooled w/o Near-Repeat Set # 11					**0.247**	**4.12**			**0.019**	**5.54**

(a) MSS# = Master Spreadsheet Number.
(b) SD = standard deviation.
(c) %RSD = percent relative standard deviation = 100(SD/mean).
(d) Velocity (U) values differ too much to be considered near-repeat values for determining near-repeat sets of test conditions for H_C.
(e) N/A = not applicable.

Appendix F

Multiple Regression Modeling of Mixing Data

GF Piepel
BG Amidan
A Heredia-Langner

Contents

F.1 Data Used to Develop U_{CS} and H_C Models F.1
F.1.1 Data Sets Used to Fit U_{CS} and H_C Models F.1
F.1.2 Aspects of Experimental Data Collection F.2
F.2 Models for Critical-Suspension Velocity (U_{CS}) F.3
F.2.1 U_{CS} Model Forms F.3
F.2.2 U_{CS} Power-Law Model Forms F.4
F.2.3 U_{CS} Power-Law Models with Interaction Terms F.6
F.2.4 Results for U_{CS} Power-Law Models F.7
F.2.5 Results for U_{CS} Power-Law Models with Interaction Terms F.16
F.2.6 Comparison of U_{CS} Models F.20
F.3 Cloud Height (H_C) Models F.21
F.3.1 H_C Model Forms F.21
F.3.2 H_C Power-Law Model Forms F.22
F.3.3 H_C Power-Law Models with Interaction Terms F.24
F.3.4 Results for H_C Power-Law Models F.24
F.3.5 Results for H_C Power-Law Models with Interaction Terms F.33
F.3.6 Comparison of H_C Models F.37
F.4 Illustration of U_{CS} and H_C Model Application and Uncertainty Calculations F.39
F.5 Model Validity Region F.47
F.6 Possible Future Activities F.47
F.6.1 Experimental Design F.47
F.6.2 Other Data/Modeling Analyses F.48
F.7 References F.49

Figures

F.1 Performance of a Power-Law Equation to Relate Unhindered Terminal Settling Velocity (U_T) to s − 1 and $d_S = d_{50}$ for the Full Data Set F.8

F.2 Log-Log Plot of Predicted Versus Measured U_{CS} (m/s) Values for the 9-Term Dimensional Model in Table F.1 Fit to the Full Data Set F.13

F.3 Log-Log Plot of Predicted Versus Measured U_{CS} (m/s) Values for the 9-Term Dimensional Model in Table F.2 Fit to the Trimmed Data Set F.13

F.4 Log-Log Plot of Predicted Versus Measured U_{CS} (m/s) Values for the 9-Term Dimensionally Consistent Model in Table F.3 with 8 Coefficients Fit to the Full Data Set F.14

F.5 Log-Log Plot of Predicted Versus Measured U_{CS} (m/s) Values for the 9-Term Dimensionally Consistent Model in Table F.4 with 8 Coefficients Fit to Trimmed Data Set F.15

F.6 Log-Log Plot of Predicted Versus Measured U_{CS} (in m/s) Values for the 12-Term Dimensional Model with Interactions in Table F.3 Fit to the Full Data Set F.17

F.7 Log-Log Plot of Predicted Versus Measured U_{CS} (m/s) Values for the 11-Term Dimensional Model with Interactions in Table F.4 Fit to the Trimmed Data Set F.18

F.8 Log-Log Plot of Predicted Versus Measured U_{CS} (m/s) Values for the Nondimensional Model From Section 7.3.2 Developed Using the Full Data Set F.20

F.9 Log-Log Plot of Predicted Versus Measured H_C Values for the 11-Term Dimensional Model in Table F.8 Fit to the Full Data Set F.29

F.10 Log-Log Plot of Predicted Versus Measured H_C Values for the 10-Term Dimensional Model in Table F.9 Fit to the Trimmed Data Set F.29

F.11 Log-Log Plot of Predicted Versus Measured H_C (m) Values for 11-Term Dimensionally Consistent Model in Table F.10 with 10 Coefficients Fit to Full Data Set F.31

F.12 Log-Log Plot of Predicted Versus Measured H_C (m) Values for 10-Term Dimensionally Consistent Model in Table F.11 with 9 Coefficients Fit to Trimmed Data Set F.32

F.13 Log-Log Plot of Predicted Versus Measured H_C Values for the 13-Term Dimensional Model with Interactions in Table F.12 Fit to the Full Data Set F.34

F.14 Log-Log Plot of Predicted Versus Measured H_C Values for the 12-Term Dimensional Model with Interactions in Table F.13 Fit to the Trimmed Data Set F.35

F.15 Log-Log Plot of Predicted Versus Measured H_C (m/s) Values for the Nondimensional Model from Section 7.3.2 Developed Using the Full Data Set F.37

Tables

F.1 Coefficients and Performance Summary for the 9-Term Linearized Power-Law Model on the Natural Logarithm of U_{CS} Fit to the Full Data Set F.11

F.2 Coefficients and Performance Summary for the 9-Term Linearized Power-Law Model on the Natural Logarithm of U_{CS} Fit to the Trimmed Data Set F.11

F.3 Coefficients and Performance Summary for the Linearized Version of 9-Term Dimensionally Consistent Model on the Natural Logarithm of U_{CS} with 8 Coefficients Fit to the Full Data Set F.14

F.4 Coefficients and Performance Summary for the Linearized Version of 9-Term Dimensionally Consistent Model on Natural Logarithm of U_{CS} with 8 Coefficients Fit to the Trimmed Data Set F.15

F.5 Coefficients and Performance Summary for the 12-Term Dimensional Model with Interactions for the Natural Logarithm of U_{CS} Fit to the Full Data Set F.17

F.6 Coefficients and Performance Summary for the 11-Term Dimensional Model with Interactions for the Natural Logarithm of U_{CS} Fit to the Trimmed Data Set F.18

F.7. Coefficients of U_{CS} Models Expressed in the Dimensional Form of Equation (F.8a) F.21

F.8 Coefficients and Performance Summary for the 11-Term Linearized Power-Law Model on the Natural Logarithm of H_C Fit to the Full Data Set F.27

F.9 Coefficients and Performance Summary for the 10-Term Linearized Power-Law Model on the Natural Logarithm of H_C Fit to the Trimmed Data Set F.27

F.10 Coefficients and Performance Summary for Linearized Version of 11-Term Dimensionally Consistent Model on Natural Logarithm of H_C with 10 Coefficients Fit to the Full Data Set F.31

F.11 Coefficients and Performance Summary for the Linearized Version of the 10-Term Dimensionally Consistent Model on the Natural Logarithm of H_C with 9 Coefficients Fit to the Trimmed Data Set F.32

F.12 Coefficients and Performance Summary for the 13-Term Dimensional Model with Interactions on the Natural Logarithm of H_C Fit to the Full Data Set F.34

F.13 Coefficients and Performance Summary for the 12-Term Dimensional Model with Interactions on the Natural Logarithm of H_C Fit to the Trimmed Data Set F.35

F.14 Coefficients of H_C Models Fit to Full Data Set Expressed in the Dimensional Form of Equation (F.21a) F.38

F.15 Values of Predictor Variables Selected to Illustrate Application of Models Fit to the Full Data Sets for U_{CS} and H_C F.39

F.16 Predictor Variable Values in Formats Needed to Illustrate Use of Models Fit to the Full Data Sets for U_{CS} and H_C F.40

F.17 Predicted U_{CS} and Corresponding 95% CIs and 95% SCIs Using Models Fit to the Full Data Set Applied to the Experimental Set of Conditions Shown in Tables F.15 and F.16 ..... F.43

F.18 Predicted H_C and Corresponding 95% CIs and 95% SCIs Using Models Fit to the Full Data Set Applied to the Experimental Set of Conditions Shown in Tables F.15 and F.16 ..... F.43

F.19 Variance-Covariance Matrix for the 9-Term $\ln(U_{CS})$ Model in F.1 ..... F.44

F.20 Variance-Covariance Matrix for 12-Term $\ln(U_{CS})$ Model in F.5 ..... F.44

F.21 Variance-Covariance Matrix for 11-Term $\ln(H_C)$ Model in F.8 ..... F.45

F.22 Variance-Covariance Matrix for 13-Term $\ln(H_C)$ Model in F.12 ..... F.46

F.23 Ranges of Predictor Variables in the Full and Trimmed Data Sets Used to Develop U_{CS} and H_C Multiple-Regression Models F.47

Acronyms

CI	confidence intervals
CL	confidence level
D	tank diameter (scale)
DC	duty cycle
E	elliptical head
F&D	flange and dish head
H_C	cloud height
HS	head shape
LR	linear regression
MR	multiple regression
NLR	nonlinear regression
OLS	ordinary least squares
P	pulsed
RMSE	root-mean-square-error
RSM	response surface methodology
S	steady state
SCI	simultaneous confidence intervals
SD	standard deviation
U	target velocity
U_{CS}	critical-suspension velocity
WLS	weighted least squares

Symbols

a_i	model coefficients to be estimated using experimental data
a_0	multiplicative coefficient
b_i	model coefficients to be estimated using experimental data (nondimensional)
b_0	multiplicative coefficient (nondimensional)
d	jet nozzle diameter (m)
D	tank diameter (m)
DC	duty cycle (nondimensional)
$\frac{d}{D}$	nondimensional pulse-jet diameter
d_S	solid s particle diameter = d_{50} = median particle diameter (m)

$\frac{U^2}{D(s-1)g}$	Froude number (nondimensional)
g	gravity constant (9.80665 m/s^2)
ln( )	natural logarithm of the variable in parentheses
N_J	number of operating jets
s	density ratio of solids to liquid (nondimensional)
U_{CS}	critical-suspension velocity (m/s)
U_T	unhindered terminal settling velocity (m/s)
$\frac{U_T}{U}$	kinematic ratio (nondimensional)
U_{TH}	hindered terminal settling velocity
ν	kinematic viscosity
x_j	predictor variables

Greek Symbols

ϕ_S	solids volume fraction (nondimensional)
ϕ_p	pulse volume fraction (nondimensional)
ϕ_J	jet density = $N_J (d/D)^2$ (nondimensional)
δ	multiplicative random error term
	additive random error term

Appendix F

Multiple Regression Modeling of Mixing Data

This appendix discusses the results from applying statistical methods for multiple regression (MR) to develop, evaluate, validate, and quantify prediction uncertainties of empirical models using the July 2007, Fall 2007, and 2008 mixing experimental data. Models are presented that relate two key mixing response variables to nondimensional and dimensional predictor variables. The key mixing response variables are critical-suspension velocity (U_{CS}) and cloud height (H_C). The predictor variables are generally test variables or functions of test variables. The statistical MR methods and formulas that were applied are discussed in Appendix D. References to specific sections of that appendix are cited where appropriate.

Section F.1 discusses the data used to develop MR models for U_{CS} and H_C. Section F.2 presents the MR model results for U_{CS}. Section F.3 presents the MR model results for H_C. Sections F.2 and F.3 discuss how the starting form of each model was obtained and how the starting model form was generalized and/or extended. Model forms were extended by applying stepwise regression methods (see Section D.4.2 of Appendix D) to identify two variable interaction terms that improved the fits of the models to the experimental data. The interaction terms selected were verified as being reasonable based on subject-matter knowledge and experience, as well as the functionality plots of the data (see Section E.2 of Appendix E). Section F.4 illustrates how the models developed in Sections F.2 and F.3 can be applied, using one set of experimental conditions as an example. Section F.4 also illustrates how confidence intervals around predicted values of either U_{CS} or H_C can be obtained. Section F.5 discusses the validity regions for the U_{CS} and H_C models presented. Section F.6 briefly mentions other analyses that were not possible to perform as part of this work but may be useful to perform in the future.

The results of fitting the U_{CS} and H_C model forms to experimental data are presented in tables and figures of Sections F.2 and F.3. The results tables contain the fitted coefficients of the models, standard deviations of the fitted coefficients, and goodness-of-fit summary statistics. Graphical displays that show how well the models fit the experimental data are also provided and discussed.

F.1 Data Used to Develop U_{CS} and H_C Models

Section F.1.1 discusses two data sets used to fit U_{CS} and H_C models. Section F.1.2 discusses aspects of the experimental collection of data that affect modeling and other data analyses.

F.1.1 Data Sets Used to Fit U_{CS} and H_C Models

Two sets of combined July 2007, Fall 2007, and 2008 data were used to fit U_{CS} and H_C models. The sets are generally referred to as "full" or "trimmed," as described below:

- Full Data Set: This data set contains the pulsed (i.e., not steady state) data from the July 2007, Fall 2007, and 2008 testing campaigns that met technical, data quality, and quality assurance requirements. Data with a return-line height less than D were removed, as were data with questionable U_{CS} values (see Section E.1.1).
  - For U_{CS}, this data set contains 173 data points.

– For H_C, this data set contains 669 data points with target velocity (U) values greater than or equal to the corresponding critical-suspension velocity values (i.e., $U \geq U_{CS}$).

- Trimmed Data Set: This data set is a trimmed version of the full data set. It excludes data with duty cycle (DC) > 0.41 (which eliminates 11 of 173 test conditions), $\phi_S > 0.016$ (which eliminates 7 of 173 test conditions), and d_S (d_{50}) > 1.8E-04 (which eliminates 1 of 173 test conditions). Functionality plots for U_{CS} and H_{CS} versus DC (see Figures E.11 and E.26 in Appendix E) show a significant change in relationship when DC reaches ~ 0.66. Because there are limited data in the range $0.41 \leq DC \leq 0.67$ to support modeling the more complicated relationship, it was decided to trim those data to obtain less complicated model forms that fit the experimental data better. Similarly, functionality plots for U_{CS} and H_{CS} versus ϕ_S (see Figures E.12 and E.27 in Appendix E) show a significant change in relationship for $\phi_S \geq \sim 0.016$. Because there are limited data (7 test conditions) in the range $0.016 \leq \phi_S \leq 0.06$ to support modeling the more complicated relationship, it was decided to trim those data to obtain less complicated model forms that fit the experimental data better. The full data set contains only one test condition with $d_S \sim$ 7.7E-04, whereas the remaining conditions have $d_S <$ 1.8E-04.

  However, as noted in Section E.1.1, where these trimmed data lie in the direction of the expected actual values for the system to which the data are extrapolated when they are being extrapolated, it may be beneficial to include them in spite of the potential for statistically undue influence on the fit.

  – For U_{CS}, this data set contains 154 data points.

  – For H_C, this data set contains 581 data points with $U \geq U_{CS}$.

In both the full and trimmed data sets for H_C, only data with $U \geq U_{CS}$ are included because the relationship between H_C and U changes significantly for velocities below U_{CS}. This portion of the H_C versus U relationship is not relevant to understanding how well tanks are mixed. Thus, only data with $U \geq U_{CS}$ were retained in both the full and trimmed data sets for H_C.

Figures E.1 and E.3 in Appendix E contain dot and scatterplot matrix plots, respectively, for the predictor variables using the full data set. Figures E.2 and E.4 in Appendix E contain dot and scatterplot matrix plots, respectively, for the predictor variables using the trimmed data set.

F.1.2 Aspects of Experimental Data Collection

As discussed in Section D.2.2 of Appendix D, a restricted order of performing experimental tests rather than a randomized order likely causes groups of data to have different uncertainties and to be correlated, thus violating assumptions for ordinary least squares (OLS) regression methods. Several restrictions in the order of testing occurred for the M3 mixing tests. First, there were some differences between the July 2007, Fall 2007, and 2008 test campaigns, which were each performed in contiguous periods of time. Also, tests with a given scaled tank size were performed together. Once a given simulant was put in a tank, all tests with that simulant were performed. Other restrictions on the order of testing were also used in collecting the M3 mixing experimental data. These included collecting H_C data at several velocities for a given set of test conditions.

The restrictions in the order of performing M3 mixing tests were substantial and likely result in a very complicated variance-covariance (i.e., uncertainty) structure for the resulting data. Rather than one magnitude of uncertainty in response variables (U_{CS} and H_C), there are several different magnitudes of

uncertainties. There are also complicated covariances among subgroups of data. There are additional possible complications by not performing tests at a given "restriction level" in a randomized order but rather in an increasing or decreasing order according to the magnitude of a test variable. This can cause the effects of any uncontrolled variables, trends, etc., to be confounded with the effect of the test variable.

So the order in which M3 mixing tests were performed likely imposes a very complicated uncertainty structure on the resulting data and could have led to confounding of effects of uncontrolled variables with the effects of test variables. Sufficient replicate tests scattered throughout the testing would have provided some basis to investigate these concerns and to assess whether resulting multiple-regression models have a significant lack-of-fit (see Section D.3.2 of Appendix D). However, the number of replicate tests performed as part of the M3 testing work (see Section E.3 of Appendix E) were not sufficient for this purpose.

Ultimately, it was not possible, given existing limitations, to account in modeling efforts for the order in which the data were collected and the associated complicated uncertainty structure of the data. Hence, OLS regression methods (as discussed in Appendix D) were applied to obtain the results presented in Sections F.2 and F.3.

F.2 Models for Critical-Suspension Velocity (U_{CS})

This section discusses the development, results, and uncertainties of U_{CS} models fit to the full and trimmed data sets described in Section F.1.

F.2.1 U_{CS} Model Forms

To develop a model form for U_{CS}, various functionality plots of U_{CS} vs. x_i (test variables) were investigated. Specifically, plots of

- U_{CS} versus x_i
- U_{CS} versus $\ln(x_i)$
- $\ln(U_{CS})$ versus $\ln(x_i)$
- $\ln(U_{CS})$ versus x_i

were considered. The goal was to identify the plot for each x_i that gave linear or nearly-linear relationships for various combinations of other test variables. This would then provide the simplest relationship for that x_i, which would be more likely to support extrapolation (if needed). Each of the above types of functionality plots provided the "most linear" relationships for at least one x_i. Unfortunately, that greatly complicates the development of a model form relating U_{CS} to all of the x_i. There was insufficient time and budget to develop and fit more complicated model forms that would be fully consistent with the results of the functionality-plot investigation for U_{CS}. Also, there was concern about placing too much emphasis on the functionality plots, which only showed results for a fraction of the data (as discussed at the end of Section E.2.1).

Ultimately, the $\ln(U_{CS})$ versus $\ln(x_i)$ plots (which are shown in Figures E.6 to E.16 of Appendix E as log-log plots of U_{CS} versus x_i) had linear or not too curvilinear relationships for all of the test variables. Hence, it was concluded that the corresponding power-law model form would be an adequate

"first-order" approximation of the true, unknown relationships between U_{CS} and the x_i. It was recognized that adopting the power-law model form would result in some model lack-of-fit for some test variables. Based on the plots in Figures E.6 to E.16, these test variables are N_J (the number of operating jets), DC (duty cycle) > 0.33 for some conditions, and $\phi_S > 0.015$. However, this situation was judged acceptable given the goal of using the models to perform coarse ratings of the mixing designs of WTP vessels. Also, fitting models to both "full" and "trimmed" data sets, as described in Section F.1.1, addresses some of these issues. More accurate U_{CS} models could be developed in the future from the M3 mixing-test data, but they would have more complicated forms, require more time to develop, and require more advanced statistical fitting and uncertainty methods.

A statistical *response surface methodology* (RSM) approach to developing empirical models (Myers and Montgomery 1995) was also investigated in a preliminary manner. Specifically, model forms relating U_{CS} [or $\ln(U_{CS})$] to first- and second-degree polynomial functions of the test variables x_i were investigated. First- and second-order polynomials adequately approximate many functional forms based on Taylor-series approximation theory. Hence, the RSM approach has been widely and successfully used in many scientific, business, and industrial applications. However, the first-order polynomial model

$$\ln(U_{CS}) = b_0 + \sum_{i=1}^{K} b_i x_i$$

using the same predictor variables x_i (I = 1, 2, …, K) as in Eqs. (F.4a) and (F.4b) did not perform as well as power-law based models. Adding statistically significant quadratic [squared $(x_i)^2$ or interaction $x_i x_j$] terms via stepwise regression methods (see Section D.4.2 of Appendix D)

$$\ln(U_{CS}) = b_0 + \sum_{i=1}^{K} b_i x_i + \text{Selected}\left\{ \sum_{i=1}^{K} b_{ii} x_i^2 + \sum_{i=1}^{K-1} \sum_{j>i}^{K} b_{ij} x_i x_j \right\}$$

yielded a second-order model that fit the U_{CS} modeling data better than the first-order model. However, that model still did not perform as well as the power-law based models discussed subsequently. Also, an issue with RSM-type polynomial models is that they are generally not appropriate for extrapolation. Hence, the results of the first- and second-order polynomial modeling efforts for U_{CS} are not discussed in this report.

F.2.2 U_{CS} Power-Law Model Forms

The initial U_{CS} model form considered was developed by generalizing the *physical model* for U_{CS} discussed in Sections 7.3.2 and 7.3.4 of the report. Taking that form of the model, moving the predictor variables to the right side of the equation, expanding variables calculated as functions of other variables, and collecting similar terms yields the statistical model form:

$$U_{CS} = a_0 (D)^{a12} (s-1)^{a2} (\phi_S)^{a3} (U_{TH})^{a4} (DC)^{a7} (\phi_p)^{a8} (d_S)^{a9} (\phi_J)^{a10} \ \delta \qquad \text{(F.1a)}$$

where

U_{CS} = critical-suspension velocity (m/s)

a_0 = multiplicative coefficient

a_i = model coefficients to be estimated using experimental data

D = tank diameter (m)

s = density ratio of solids to liquid (nondimensional)

ϕ_S = solids volume fraction (nondimensional)

U_{TH} = hindered terminal settling velocity (m/s)

DC = duty cycle (nondimensional)

ϕ_p = pulse volume fraction (nondimensional)

d_S = solid s particle diameter = d_{50} = median particle diameter (m)

ϕ_J = jet density = $N_J (d/D)^2$ (nondimensional)

N_J = number of operating jets

d = jet nozzle diameter (m)

δ = multiplicative random error term, as discussed in Section D.2.1, Appendix D.

Note that Eq. (F.1a) is a power-law model form, which was judged as adequate for first-order approximation and predictive purposes, as discussed above.

Because Eq. (F.1a) is nonlinear in its coefficients and has a multiplicative error structure, it can be converted to a model linear in its coefficients with an additive error structure by taking the natural logarithm of both sides, as discussed in Section D.2.1 of Appendix D. This yields the model

$$\begin{aligned}\ln(U_{CS}) = \ln(a_0) + a_{12}\ln(D) + a_2\ln(s-1) + a_3\ln(\phi_S) + a_4\ln(U_{TH}) + a_7\ln(DC) \\ + a_8\ln(\phi_p) + a_9\ln(d_S) + a_{10}\ln(\phi_J) + \varepsilon\,,\end{aligned} \tag{F.1b}$$

where

ln( ) = natural logarithm of the variable in parentheses

ε = additive random error term, as discussed in Section D.2.1 of Appendix D

and the remaining notation is as previously defined. The model form in Eq. (F.1b) can be fit by OLS linear regression (LR), whereas the model form in Eq. (F.1a) must be fit by weighted least squares (WLS) nonlinear regression (NLR). See Section D.2, Appendix D for more discussion of these issues.

Equations (F.1a) and (F.1b) can be expanded by substituting into them a generalization of the equation for U_{TH} given by

$$U_{TH} = U_T\left(1 - \frac{\phi_S}{0.5}\right)^{4.5} \tag{F.2}$$

This yields the model forms

$$U_{CS} = a_0\,(D)^{a12}\,(s-1)^{a2}\,(\phi_S)^{a3}\left(1 - \frac{\phi_S}{0.5}\right)^{a5}(U_T)^{a6}\,(DC)^{a7}\,(\phi_p)^{a8}\,(d_S)^{a9}\,(\phi_J)^{a10}\;\delta \tag{F.3a}$$

and

$$\ln(U_{CS}) = \ln(a_0) + a_{12}\ln(D) + a_2\ln(s-1) + a_3\ln(\phi_S) + a_5\ln(1-\frac{\phi_S}{0.5}) + a_6\ln(U_T) + a_7\ln(DC) + a_8\ln(\phi_p) + a_9\ln(d_S) + a_{10}\ln(\phi_J) + \varepsilon, \quad \text{(F.3b)}$$

where

a_i = model coefficients to be estimated using experimental data

U_T = unhindered terminal settling velocity (m/s)

and the other notation is as previously defined. The a_6 and a_5 coefficients in Eqs. (F.3a) and (F.3b) generalize, respectively, the 1.0 exponent (implied) on U_T and the 4.5 exponent on $(1 - \phi_S/0.5)$ in Eq. (F.2).

Using a generalization of the formula $\phi_J = N_J\,(d/D)^2$ where N_J and d are allowed to have their own coefficients and D is absorbed into the existing D term, the model forms in Eqs. (F.3a) and (F.3b) can be further generalized as

$$U_{CS} = a_0\,(D)^{a_1}(s-1)^{a_2}(\phi_S)^{a_3}(1-\frac{\phi_S}{0.5})^{a_5}(U_T)^{a_6}(DC)^{a_7}(\phi_p)^{a_8}(d_S)^{a_9}(N_J)^{a_{10}}(d)^{a_{11}}\,\delta \quad \text{(F.4a)}$$

and

$$\ln(U_{CS}) = \ln(a_0) + a_1\ln(D) + a_2\ln(s-1) + a_3\ln(\phi_S) + a_5\ln(1-\frac{\phi_S}{0.5}) + a_6\ln(U_T) + a_7\ln(DC) + a_8\ln(\phi_p) + a_9\ln(d_S) + a_{10}\ln(N_J) + a_{11}\ln(d) + \varepsilon, \quad \text{(F.4b)}$$

where all notation is as previously defined.

In summary, Eqs. (F.4a) and (F.4b) are generalizations of the model forms in Eqs. (F.1a) and (F.1b), where the latter are obtained from the former using the coefficient constraints $a_6 = a_4$, $a_5 = 4.5a_4$, $a_{11} = 2a_{10}$, and $a_1 = a_{12} - 2a_{10}$.

The model form for U_{CS} in Sections 7.3.2 and 7.3.4 and the generalization of that model form in Eqs. (F.4a) and (F.4b) do not contain a head shape (HS) term. The reason is that the data do not sufficiently support quantifying the effect of HS over the three tank sizes used in M3 testing. The spherical head (HS = S) was used only in the 34-in. tank, which was used during all three test campaigns. The elliptical head (HS = E) was used only in the 15- and 70-in. tanks in 2008. The flange and dish head (HS = FD) was used only for some 70-in. tank tests in 2008. Section E.2.4 in Appendix E discusses differences in U_{CS}, H_{CS}, and H_C data from tests in the 70-in. tank with elliptical (E) and FD head shapes. There is no way to know how these differences would translate to the 15-in., 34-in., or full-scale tanks.

F.2.3 U_{CS} Power-Law Models with Interaction Terms

Stepwise regression methods (see Section D.4.2, Appendix D) were used to augment U_{CS} models of the form in Eq. (F.4b) with interaction terms of the form

$$a_{ij}x_j\ln(x_i) \quad \text{(F.5a)}$$

This corresponds to augmenting models of the form in Eq. (F.4a) with interaction terms of the form

$$x_i^{a_{ij}x_j} \tag{F.5b}$$

Allowing such interaction terms provides for models with power-law terms of the form

$$x_i^{a_i + a_{ij}x_j} \tag{F.6}$$

so the exponent [slope of the relationship between ln(y) and ln(x_i)] can depend on other predictor variables (x_j). The log-log functionality plots of U_{CS} versus each test variable (see Section E.2.2 of Appendix E) show differences in slopes of relationships as other test variables change. Hence, there is strong evidence that suggests interaction terms of the above form may improve the predictive performance of mixing models, at least within the experimental region of the data. However, models with interaction terms can yield inaccurate predictions when extrapolated significantly outside the experimental region of data used to develop them. Hence, unless U_{CS} models with interaction terms have been well validated for extrapolative use, it is recommended that only U_{CS} models without interaction terms be used for extrapolative predictions.

F.2.4 Results for U_{CS} Power-Law Models

The dimensional and corresponding dimensionally consistent model forms investigated for U_{CS} are presented in Section F.2.4.1. The results of fitting the dimensional models for U_{CS} to the full and trimmed data sets are presented in Section F.2.4.2. The results of fitting the dimensionally consistent models for U_{CS} are presented in Section F.2.4.3.

F.2.4.1 Dimensional and Dimensionally Consistent Power-Law Model Forms for U_{CS}

To begin, models of the form in Eq. (F.4b) were fit to the full and trimmed data sets described in Section F.1. For both data sets, the coefficients for the $s - 1$, $(1 - \phi_S/0.5)$, U_T, and d_S terms are statistically nonsignificant. There are two reasons for these results:

- The hindered terminal settling velocity (U_{TH}) and unhindered terminal settling velocity (U_T) are highly correlated for the full and trimmed data sets, as seen in Figure E.5 of Appendix E. This suggests that there may not be any additional value (within the region of test conditions investigated) to using U_{TH} instead of U_T in mixing response (U_{CS} or H_C) models. Because $(1 - \phi_S/0.5)$ is the term involved in converting U_T to U_{TH}, the statistical nonsignificance of that term is understandable.
- U_T is a complicated function of $s - 1$ and d_S, given by the equation

$$U_T = \frac{\nu}{d_S}\left[\sqrt{15 + \frac{(s-1)gd_S^3/\nu^2}{0.3}} - \sqrt{15}\right]^2 \tag{F.7}$$

  where ν is the kinematic viscosity, g is the gravity constant, and all other notation is as defined previously. However, over the variable space covered by the full and trimmed data sets, U_T, is represented extremely well by a power-law model in $s - 1$ and d_S. This is shown in Figure F.1 for the full data set. Because the model of the form in Eq. (F.4a) already contains power-law terms for $s - 1$

and d_S, it is essentially redundant to have a power-law term for U_T in models used to fit the full and trimmed data sets.

These two observations are conditional in the full and trimmed data sets described in Section F.1. Under other test conditions, unhindered or hindered terminal settling velocity may be useful in improving predictions of mixing responses such as U_{CS} and H_C.

The two preceding observations, along with statistical methods for reducing terms in models (see Section D.4.1, Appendix D), led to dropping the $(1 - \phi_S/0.5)$ and d_S terms from the model form in Eq. (F.4). It may seem more natural to drop U_T than d_S because U_T is calculated using d_S and $s - 1$. However, U_T is more physically meaningful as a predictor variable than d_S. Further, there was little difference in the goodness-of-fit of a model that retained U_T instead of d_S. Models with $(1 - \phi_S)$ instead of $(1 - \phi_S/0.5)$ were also investigated, but that term was statistically nonsignificant for both the full and trimmed data sets.

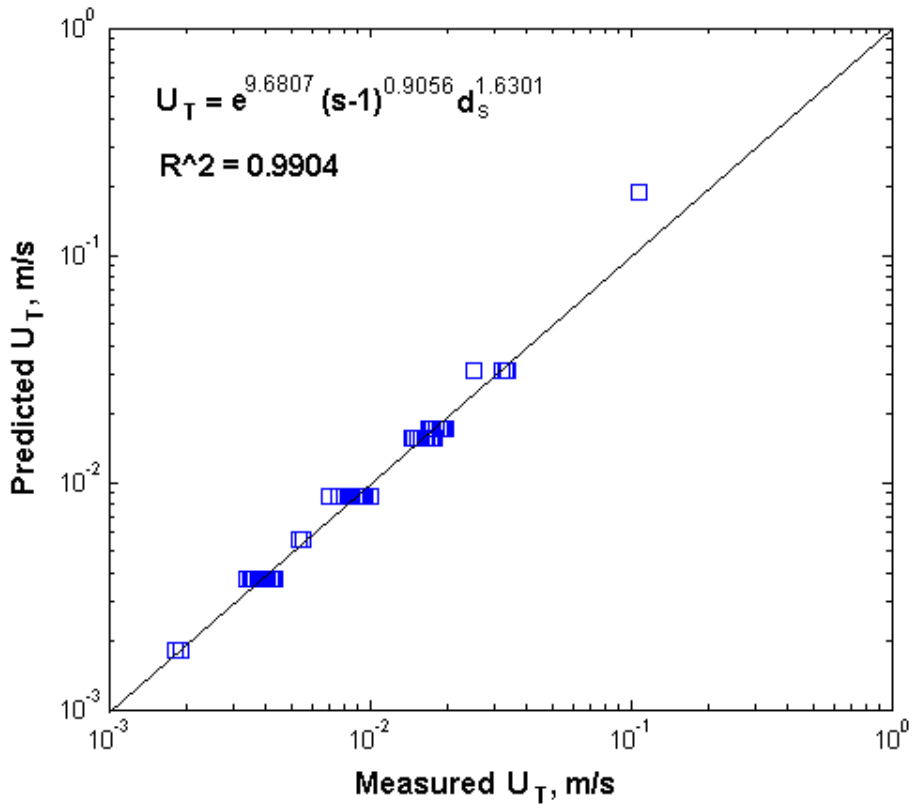

Figure F.1. Performance of a Power-Law Equation to Relate Unhindered Terminal Settling Velocity (U_T) to $s - 1$ and $d_S = d_{50}$ for the Full Data Set

The reduced forms of the models in Eqs. (F.4a) and (F.4b) that resulted from dropping the $(1 - \phi_S/0.5)$ and d_S terms are

$$U_{CS} = a_0 \, (D)^{a1} (s-1)^{a2} (\phi_S)^{a3} (U_T)^{a6} (DC)^{a7} (\phi_p)^{a8} (N_J)^{a10} (d)^{a11} \, \delta \qquad \text{(F.8a)}$$

and

$$\ln(U_{CS}) = \ln(a_0) + a_1\ln(D) + a_2\ln(s-1) + a_3\ln(\phi_S) + a_6\ln(U_T) + a_7\ln(DC) + a_8\ln(\phi_p) + a_{10}\ln(N_J) + a_{11}\ln(d) + \varepsilon, \tag{F.8b}$$

All notation in Eqs. (F.8a) and (F.8b) is as previously defined.

The coefficients estimated by fitting Eq. (F.8b) to the full or trimmed data sets by OLS MR may subsequently be written in the form of Eq. (F.8a). However, this will result in a dimensional constant a_0 with units that may differ from those of subsumed physical constants (e.g., g) and dropped model terms. Unfortunately, there is not a unique set of dimensional consistency constraints that can be applied by fitting Eq. (F.8b) using restricted least squares (Section 9.5, Draper and Smith 1998) to impose dimensional consistency. Instead, a dimensionally consistent model form was developed starting from Eq. (F.8a), with the goal of retaining as much as possible of the generalizations added in Section F.2.2. The dimensionally consistent model for U_{CS} that resulted from this process is

$$U_{CS} = b_0 U_T \left(\frac{D(s-1)g}{U_T^2}\right)^{b_1} \left(\frac{d}{D}\right)^{b_2} (s-1)^{b_3} DC^{b_4} \phi_S^{b_5} \phi_p^{b_6} N_J^{b_7}\ \delta \tag{F.9a}$$

where

b_0 = multiplicative coefficient (nondimensional)

b_i = model coefficients (i = 1, …, 7) to be estimated using experimental data (nondimensional)

$\frac{D(s-1)g}{U_T^2}$ = reciprocal of a Froude number based on unhindered terminal settling velocity (nondimensional)

g = 9.80665 (m/s^2) is the gravity constant

$\frac{d}{D}$ = nondimensional pulse-jet diameter

and all remaining notation is as defined previously. Because Eq. (F.9a) is nonlinear in its coefficients and has a multiplicative error structure, it can be converted to a model linear in its coefficients with an additive error structure by taking the natural logarithm of both sides, as discussed in Section D.2.1 of Appendix D. This yields the model

$$\ln(U_{CS}) = \ln(b_0) + \ln(U_T) + b_1 \ln\left(\frac{D(s-1)g}{U_T^2}\right) + b_2 \ln\left(\frac{d}{D}\right) + b_3 \ln(s-1) + b_4 \ln(DC) + b_5 \ln(\phi_S) + b_6 \ln(\phi_p) + b_7 \ln(N_J) + \varepsilon \tag{F.9b}$$

The dimensionally consistent models in Eqs. (F.9a) and (F.9b) can be considered as reduced forms of the dimensional models in Eqs. (F.8a) and (F.8b), with the relationships among the coefficients given by

$$
\begin{aligned}
a_0 &= b_0\, g^{b_1} \quad \text{or} \quad \ln(a_0) = \ln(b_0) + b_1 \ln(g) \\
a_1 &= b_1 - b_2 \\
a_2 &= b_1 + b_3 \\
a_3 &= b_5 \\
a_6 &= 1 - 2b_1 \\
a_7 &= b_4 \\
a_8 &= b_6 \\
a_{10} &= b_7 \\
a_{11} &= b_2
\end{aligned}
\tag{F.10}
$$

Note that the U_{CS} dimensional models in Eqs. (F.8a) and (F.8b) have 9 coefficients to be estimated using the data, whereas the dimensionally consistent models in Eqs. (F.9a) and (F.9b) have only 8 coefficients to be estimated using the data. The difference exists because the leading U_T term (after the constant term) in Eqs. (F.9a) and (F.9b) has an exponent/coefficient equal to 1. Suppose the U_T term was given a separate exponent, b_8. That would give $a_6 = b_8 - 2b_1$. The model form in Eqs. (F.9a) and (F.9b) extended in this way would be mathematically equivalent to the model form in Eqs. (F.8a) and (F.8b). In other words, they would fit a given data set exactly the same, and predictions of U_{CS} would be exactly the same.

The dimensionless group $D(s\text{-}1)g/U_T^2$ in Eqs. (E.9a) and (E.9b) has the form of inverse Froude number, which would seem to invite a physical interpretation. However, the group was constructed only to infuse dimensional consistency into the resulting empirical model and is not necessarily physically meaningful. For example, this form ostensibly corresponds to the ratio of potential energy associated with the tank length scale and the kinetic energy associated with terminal velocity of particles relative to the fluid in which they are embedded. We would not anticipate this would correlate with U_{CS} based on physical reasoning. Of course, once a dimensionally consistent empirical correlation is obtained, ultimately such dimensionless groups can be combined with other groups to form groups that can provide important physical insights about the correlation.

F.2.4.2 Results of Fitting Dimensional Power-Law Model Forms for U_{CS} to Full and Trimmed Data Sets

The results of fitting the dimensional model form in Eq. (F.8b) to the full and trimmed data sets are given in Tables F.1 and F.2, respectively. Included in these tables are estimates of the model coefficients and their standard deviations. Also shown for each coefficient is its t-value (coefficient divided by its standard deviation) and p-value (statistical significance level). Traditionally, p-values lower than 0.05 indicate coefficients that are statistically significant (different from zero) with greater than 95% confidence. Further, p-values lower than 0.01 indicate high statistical significance (greater than 99% confidence), while values lower than 0.0001 indicate extremely high statistical significance (greater than 99.99% confidence). All model terms in Table F.1 are statistically significant at a p-value of < 0.0001. Model terms in Table F.2 are statistically significant at a p-value of < 0.0001, except for ln(DC) with p-value = 0.0004 and the constant term.

Table F.1. Coefficients and Performance Summary for the 9-Term Linearized Power-Law Model on the Natural Logarithm of U_{CS} Fit to the Full Data Set

$\ln(U_{CS})$ Model Term	Coefficient Estimate	Coefficient Standard Deviation	t-value = Coeff/SD	p-value[(a)]	Full Data, 173 Tests[(b)] Modeling Data Statistic [$\ln(U_{CS})$]	Value
$\ln(a_0)$	-1.173	0.236	-4.96	< 0.0001	R^2	0.913
ln(D)	1.321	0.046	28.72	< 0.0001	R^2 Adjusted (R^2_A)	0.908
ln(s−1)	0.471	0.038	12.55	< 0.0001	R^2 Predicted (R^2_P)	0.903
$\ln(\phi_S)$	0.222	0.011	19.31	< 0.0001	RMSE	0.134
$\ln(U_T)$	0.148	0.015	9.94	< 0.0001		
ln(DC)	-0.247	0.031	-7.96	< 0.0001		
$\ln(\phi_p)$	-0.211	0.032	-6.60	< 0.0001		
$\ln(N_J)$	-0.525	0.034	-15.37	< 0.0001		
ln(d)	-1.072	0.046	-23.12	< 0.0001		

(a) Probability that the coefficient is not statistically significant (different from 0). Values less than 0.05, 0.01, and 0.0001 indicate strong, very strong, and extremely strong statistical significance of the coefficient and corresponding model term.
(b) Model evaluation and validation statistics are defined, respectively, in Sections D.3 and D.5 of Appendix D.

Table F.2. Coefficients and Performance Summary for the 9-Term Linearized Power-Law Model on the Natural Logarithm of U_{CS} Fit to the Trimmed Data Set

$\ln(U_{CS})$ Model Term	Coefficient Estimate	Coefficient Standard Deviation	t-value = Coeff/SD	p-value[(a)]	Trimmed Data, 154 Tests[(b)] Modeling Data Statistic [$\ln(U_{CS})$]	Value
$\ln(a_0)$	-1.093	0.232	-4.72	< 0.0001	R^2	0.926
ln(D)	1.369	0.045	30.63	< 0.0001	R^2 Adjusted (R^2_A)	0.922
ln(s−1)	0.454	0.038	11.95	< 0.0001	R^2 Predicted (R^2_P)	0.916
$\ln(\phi_S)$	0.245	0.013	19.56	< 0.0001	RMSE	0.126
$\ln(U_T)$	0.145	0.015	9.68	< 0.0001		
ln(DC)	-0.132	0.037	-3.60	0.0004		
$\ln(\phi_p)$	-0.220	0.032	-6.78	< 0.0001		
$\ln(N_J)$	-0.522	0.033	-15.91	< 0.0001		
ln(d)	-1.108	0.045	-24.47	< 0.0001		

(a) Probability that the coefficient is not statistically significant (different from 0). Values less than 0.05, 0.01, and 0.0001 indicate strong, very strong, and extremely strong statistical significance of the coefficient and corresponding model term.
(b) Model evaluation and validation statistics are defined, respectively, in Sections D.3 and D.5 of Appendix D.

The right sides of Tables F.1 and F.2 list various summary statistics that provide measures of how well the 9-term models in Eqs. (F.8a) and (F.8b) fit the full and trimmed data sets, respectively. These statistics are defined and discussed in Sections D.3.2 and D.3.3 of Appendix D. The summary statistics in Tables F.1 and F.2 indicate that the 9-term linearized power-law models fit the available data well. For example, R^2 statistics show the 9-term model accounts for 91.3% of the variability in $\ln(U_{CS})$ values for the full data and 92.6% for the trimmed data. As expected, this model form fits somewhat better for the trimmed data than for the full data. Because the differences between R^2 and R^2_A are small, there are no indications that the data have been over-fitted. Because the differences between R^2_A and R^2_P are small, there are no indications of highly influential data affecting the model fits.

Figures F.2 and F.3 show predicted-versus-measured plots, which provide a graphical view of how well the 9-term model form fits the full and trimmed data sets. In each plot, the predicted value of U_{CS} is plotted on the y-axis (in log scale) and the measured (actual) values of U_{CS} are plotted on the x-axis (also in log scale). The 45-degree line represents perfect prediction, where predicted U_{CS} values would exactly equal measured U_{CS} values. Section D.3.2 of Appendix D has further discussion of using predicted-versus-measured plots to evaluate how well a model fits a data set.

Figures F.2 and F.3 show no obvious problems with the U_{CS} predictions made using the models in Tables F.1 and F.2, respectively. However, only the 2008 data spans most of the range of the U_{CS} response. Both models tend to slightly overpredict the July 2007 data (most of those data are plotted above the 45° line). This could be due to the relatively small number of July 2007 data points available.

In summary, inserting the coefficients from the U_{CS} dimensional models without interactions fit to the full data set (Table F.1) into Eqs. (F.8a) and (F.8b) results in the models

$$\begin{aligned} U_{CS} &= 0.309\,(D)^{1.321}(s-1)^{0.471}(\phi_S)^{0.222}(U_T)^{0.148}(DC)^{-0.247}(\phi_p)^{-0.211} \\ &\quad \times (N_J)^{-0.525}(d)^{-1.072} \end{aligned} \tag{F.11a}$$

and

$$\begin{aligned} \ln(U_{CS}) &= -1.173 + 1.321\ln(D) + 0.471\ln(s-1) + 0.222\ln(\phi_S) + 0.148\ln(U_T) \\ &\quad - 0.247\ln(DC) - 0.211\ln(\phi_p) - 0.525\ln(N_J) - 1.072\ln(d), \end{aligned} \tag{F.11b}$$

where all notation is as previously defined. Inserting the coefficients from the U_{CS} dimensional models without interactions fit to the trimmed data set (Table F.2) into Eqs. (F.8a) and (F.8b) results in the models

$$U_{CS} = 0.335\,(D)^{1.369}(s-1)^{0.454}(\phi_S)^{0.245}(U_T)^{0.145}(DC)^{-0.132}(\phi_p)^{-0.220}(N_J)^{-0.522}(d)^{-1.108} \tag{F.12a}$$

and

$$\begin{aligned} \ln(U_{CS}) &= -1.093 + 1.369\ln(D) + 0.454\ln(s-1) + 0.245\ln(\phi_S) + 0.145\ln(U_T) \\ &\quad - 0.132\ln(DC) - 0.220\ln(\phi_p) - 0.522\ln(N_J) - 1.108\ln(d), \end{aligned} \tag{F.12b}$$

where all notation is as previously defined.

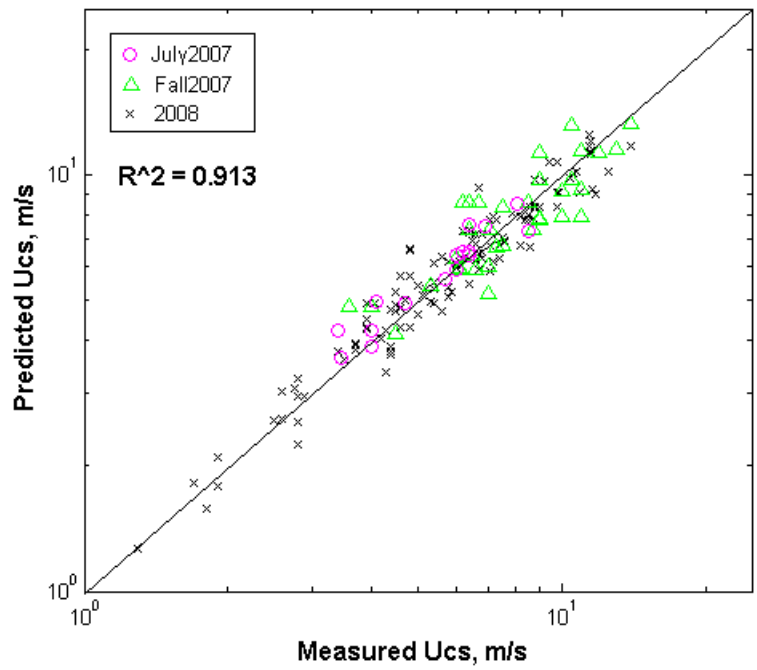

Figure F.2. Log-Log Plot of Predicted Versus Measured U_{CS} (m/s) Values for the 9-Term Dimensional Model in Table F.1 Fit to the Full Data Set. The 45-degree line represents perfect prediction where predicted U_{CS} values equal measured U_{CS} values.

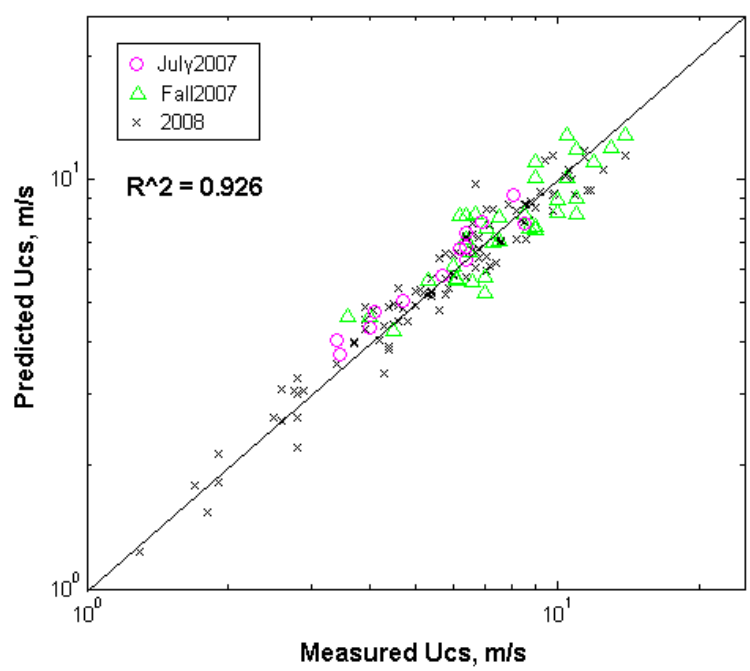

Figure F.3. Log-Log Plot of Predicted Versus Measured U_{CS} (m/s) Values for the 9-Term Dimensional Model in Table F.2 Fit to the Trimmed Data Set. The 45-degree line represents perfect prediction where predicted U_{CS} values equal measured U_{CS} values.

F.2.4.3 Results of Fitting Dimensionally Consistent Power-Law Model Forms for U_{CS} to Full and Trimmed Data Sets

The dimensionally consistent model form in Eq. (F.9b) was fit to the full and trimmed data sets using restricted least squares (Draper and Smith 1998). The results for the full data set are given in Table F.3 and Figure F.4, while the results for the trimmed data set are given in Table F.4 and Figure F.5.

Table F.3. Coefficients and Performance Summary for the Linearized Version of 9-Term Dimensionally Consistent Model on the Natural Logarithm of U_{CS} with 8 Coefficients Fit to the Full Data Set

$\ln(U_{CS})$ Model Term	Coefficient Estimate	Coefficient Standard Deviation	t-value = Coeff/SD	p-value[a]	Full Data, 173 Tests[b] Modeling Data Statistic [$\ln(U_{CS})$]	Value
$\ln(b_0)$	-1.297	–[c]	–	–	R^2	0.867
$\ln(U_T)$	1.0	N/A	N/A	N/A	R^2 Adjusted (R^2_A)	0.861
$\ln[D(s-1)g/U_T^2]$	0.397	–	–	–	R^2 Predicted (R^2_P)	–[c]
$\ln(d/D)$	-0.991	–	–	–	RMSE	0.165
$\ln(s-1)$	0.086	–	–	–		
$\ln(DC)$	-0.205	–	–	–		
$\ln(\phi_S)$	0.243	–	–	–		
$\ln(\phi_p)$	-0.221	–	–	–		
$\ln(N_J)$	-0.511	–	–	–		

(a) Probability that the coefficient is not statistically significant (different from 0). Values less than 0.05, 0.01, and 0.0001 indicate strong, very strong, and extremely strong statistical significance of the coefficient and corresponding model term.
(b) Model evaluation and validation statistics are defined, respectively, in Sections D.3 and D.5 of Appendix D.
(c) Not available from software used to fit the model via restricted least squares. These could be obtained with additional work.

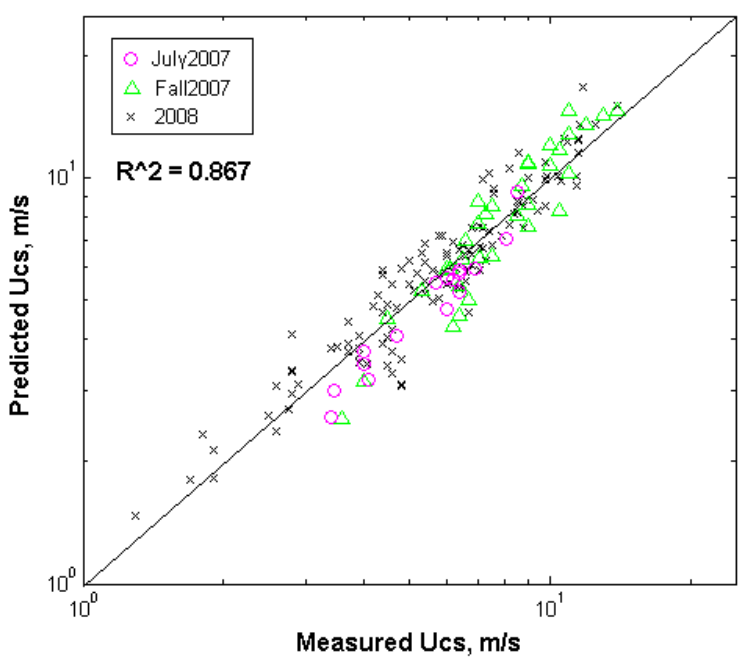

Figure F.4. Log-Log Plot of Predicted Versus Measured U_{CS} (m/s) Values for the 9-Term Dimensionally Consistent Model in Table F.3 with 8 Coefficients Fit to the Full Data Set. The 45-degree line represents perfect prediction where predicted U_{CS} values equal measured U_{CS} values.

Table F.4. Coefficients and Performance Summary for the Linearized Version of 9-Term Dimensionally Consistent Model on Natural Logarithm of U_{CS} with 8 Coefficients Fit to the Trimmed Data Set

$\ln(U_{CS})$ Model Term	Coefficient Estimate	Coefficient Standard Deviation	t-value = Coeff/SD	p-value[a]	Full Data, 154 Tests[b] Modeling Data Statistic [$\ln(U_{CS})$]	Value
$\ln(b_0)$	-1.242	–[c]	–	–	R^2	0.889
$\ln(U_T)$	1.0	N/A	N/A	N/A	R^2 Adjusted (R^2_A)	0.883
$\ln[D(s-1)g/U_T^2]$	0.400	–	–	–	R^2 Predicted (R^2_P)	–[c]
$\ln(d/D)$	-1.022	–	–	–	RMSE	0.154
$\ln(s-1)$	0.055	–	–	–		
$\ln(DC)$	-0.079	–	–	–		
$\ln(\phi_S)$	0.254	–	–	–		
$\ln(\phi_p)$	-0.223	–	–	–		
$\ln(N_J)$	-0.505	–	–	–		

(a) Probability that the coefficient is not statistically significant (different from 0). Values less than 0.05, 0.01, and 0.0001 indicate strong, very strong, and extremely strong statistical significance of the coefficient and corresponding model term.
(b) Model evaluation and validation statistics are defined, respectively, in Sections D.3 and D.5 of Appendix D.
(c) Not available from software used to fit the model via restricted least squares. These could be obtained with additional work.

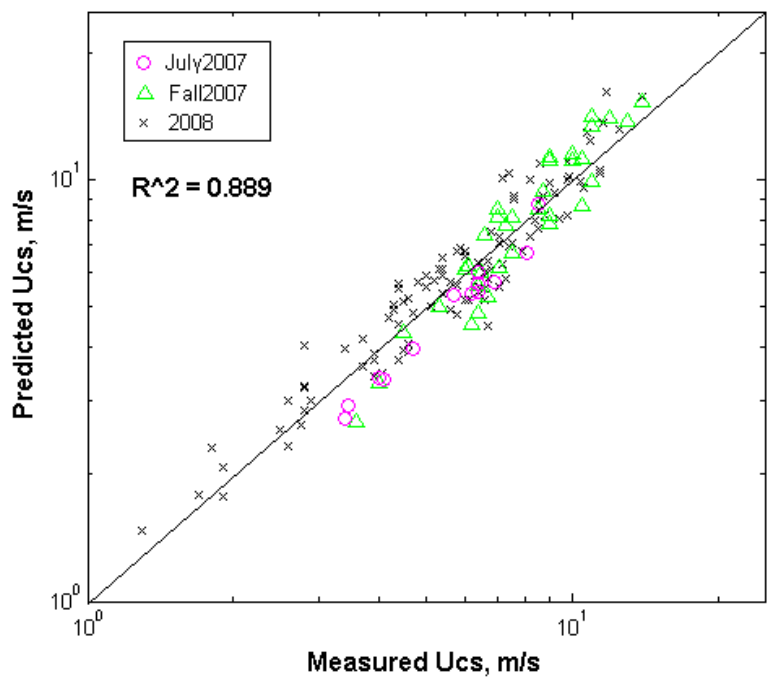

Figure F.5. Log-Log Plot of Predicted Versus Measured U_{CS} (m/s) Values for the 9-Term Dimensionally Consistent Model in Table F.4 with 8 Coefficients Fit to Trimmed Data Set. The 45-degree line represents perfect prediction where predicted U_{CS} values equal measured U_{CS} values.

The U_{CS} dimensionally consistent models in Tables F.3 and F.4 have R^2 values somewhat lower than for the dimensional models in Tables F.1 and F.2. For the full data set, $R^2 = 0.867$ for the dimensionally consistent model versus $R^2 = 0.913$ for the dimensional model. For the trimmed data set, $R^2 = 0.889$ for the dimensionally consistent model versus $R^2 = 0.926$ for the dimensional model. As noted at the end of Section F.2.4.1, adding an exponent to the U_T term would make the dimensionally consistent model mathematically equivalent to the dimensional model. This suggests the decrease in R^2 (goodness of fit)

for the dimensionally consistent model could be as a result of that model not capturing the effect of U_T as well as the dimensional model.

Figures F.4 and F.5 for the full and trimmed data sets, respectively, show tendencies for the U_{CS} dimensionally consistent models to 1) overpredict U_{CS} < ~2.0 m/s, 2) possibly overpredict U_{CS} > ~10 m/s, and 3) slightly underpredict July 2007 data. The dimensional models tend to correct the first two issues (see Figures F.2 and F.3), but in turn have a tendency to slightly overpredict the July 2007 data. Ultimately, the dimensional model form fits the full and trimmed data sets better than the dimensionally consistent model form, but the differences are not major.

In summary, inserting the coefficients from the U_{CS} dimensionally consistent models fit to the full data set (Table F.3) into Eqs. (F.9a) and (F.9b) results in the models

$$U_{CS} = 0.273\, U_T \left(\frac{D(s-1)g}{U_T^2}\right)^{0.397} \left(\frac{d}{D}\right)^{-0.991} (s-1)^{0.086}\, DC^{-0.205}\, \phi_S^{0.243}\, \phi_p^{-0.221}\, N_J^{-0.511} \tag{F.13a}$$

and

$$\begin{aligned} \ln(U_{CS}) = {} & -1.297 + \ln(U_T) + 0.397 \ln\left(\frac{D(s-1)g}{U_T^2}\right) - 0.991 \ln\left(\frac{d}{D}\right) + 0.086 \ln(s-1) \\ & - 0.205 \ln(DC) + 0.243 \ln(\phi_S) - 0.221 \ln(\phi_p) - 0.511 \ln(N_J) \end{aligned} \tag{F.13b}$$

where all notation is as previously defined. Inserting the coefficients from the U_{CS} dimensionally consistent models fit to the trimmed data set (Table F.4) into Eqs. (F.9a) and (F.9b) results in the models

$$U_{CS} = 0.289\, U_T \left(\frac{D(s-1)g}{U_T^2}\right)^{0.400} \left(\frac{d}{D}\right)^{-1.022} (s-1)^{0.055}\, DC^{-0.079}\, \phi_S^{0.254}\, \phi_p^{-0.223}\, N_J^{-0.505} \tag{F.14a}$$

and

$$\begin{aligned} \ln(U_{CS}) = {} & -1.242 + \ln(U_T) + 0.400 \ln\left(\frac{D(s-1)g}{U_T^2}\right) - 1.022 \ln\left(\frac{d}{D}\right) + 0.055 \ln(s-1) \\ & - 0.079 \ln(DC) + 0.254 \ln(\phi_S) - 0.223 \ln(\phi_p) - 0.505 \ln(N_J) \end{aligned} \tag{F.14b}$$

where all notation is as previously defined.

F.2.5 Results for U_{CS} Power-Law Models with Interaction Terms

As discussed in Section F.2.3, stepwise regression methods were used to add statistically significant interaction terms to the U_{CS} models shown in Tables F.1 and F.2. The results are shown in Table F.5 and Figure F.6 for the full data set and in Table F.6 and Figure F.7 for the trimmed data set. Three interaction terms were added to the model for the full data set and only two to the model for the trimmed data set. Only one of the interaction terms added to each model is common to both, but that is likely because of the smaller test-variable space for the model fit to the trimmed data set. All of the model terms shown in Tables F.5 and F.6 are highly statistically significant, except for two linear terms for the trimmed data set

that are included in the models because they are part of significant interactions. The constant term is not statistically significant for either the model of Table F.5 or the model of Table F.6.

Table F.5. Coefficients and Performance Summary for the 12-Term Dimensional Model with Interactions for the Natural Logarithm of U_{CS} Fit to the Full Data Set

$\ln(U_{CS})$ Model Term	Coefficient Estimate	Coefficient Standard Deviation	t-value = Coeff/SD	p-value[(a)]	Full Data, 173 Tests[(b)] Modeling Data Statistic [$\ln(U_{CS})$]	Value
$\ln(a_0)$	-0.428	0.229	-1.87	0.0635	R^2	0.939
ln(D)	1.186	0.053	22.32	< 0.0001	R^2 Adjusted (R^2_A)	0.935
ln(s−1)	0.421	0.033	12.83	< 0.0001	R^2 Predicted (R^2_P)	0.930
$\ln(\phi_S)$	0.264	0.017	15.79	< 0.0001	RMSE	0.113
$\ln(U_T)$	0.082	0.020	4.02	< 0.0001		
ln(DC)	0.366	0.081	4.51	< 0.0001		
$\ln(\phi_p)$	-0.210	0.027	-7.69	< 0.0001		
$\ln(N_J)$	-0.545	0.030	-18.48	< 0.0001		
ln(d)	-1.116	0.040	-28.19	< 0.0001		
DC $\ln(U_T)$	0.276	0.047	5.87	< 0.0001		
D ln(DC)	-0.170	0.039	-4.38	< 0.0001		
$\phi_S \ln(U_T)$	0.897	0.327	2.74	0.0068		

(a) Probability that the coefficient is not statistically significant (different from 0). Values less than 0.05, 0.01, and 0.0001 indicate strong, very strong, and extremely strong statistical significance of the coefficient and corresponding model term.
(b) Model evaluation and validation statistics are defined, respectively, in Sections D.3 and D.5 of Appendix D.

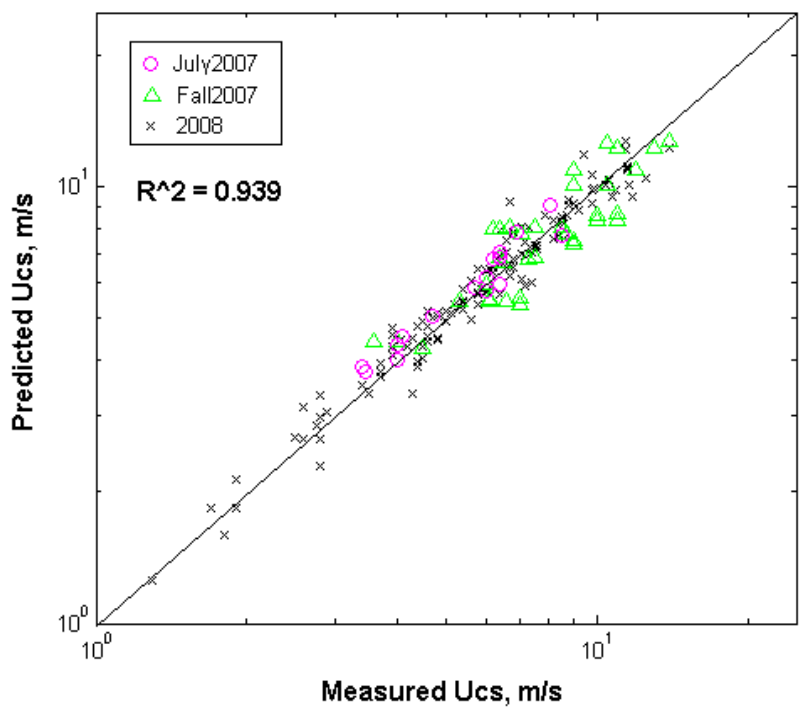

Figure F.6. Log-Log Plot of Predicted Versus Measured U_{CS} (in m/s) Values for the 12-Term Dimensional Model with Interactions in Table F.3 Fit to the Full Data Set. The 45-degree line represents perfect prediction where predicted U_{CS} values equal measured U_{CS} values.

Table F.6. Coefficients and Performance Summary for the 11-Term Dimensional Model with Interactions for the Natural Logarithm of U_{CS} Fit to the Trimmed Data Set

$\ln(U_{CS})$ Model Term	Coefficient Estimate	Coefficient Standard Deviation	t-value = Coeff/SD	p-value [(a)]	Trimmed Data, 154 Tests[(b)]	
					Modeling Data Statistic [$\ln(U_{CS})$]	Value
$\ln(a_0)$	-0.143	0.329	-0.43	0.66	R^2	0.939
ln(D)	1.221	0.062	19.83	< 0.0001	R^2 Adjusted (R^2_A)	0.935
ln(s−1)	0.952	0.146	6.52	< 0.0001	R^2 Predicted (R^2_P)	0.929
$\ln(\phi_S)$	0.247	0.012	21.26	< 0.0001	RMSE	0.115
$\ln(U_T)$	0.170	0.015	11.29	< 0.0001		
ln(DC)	0.038	0.057	0.67	0.50		
$\ln(\phi_p)$	0.094	0.091	1.04	0.30		
$\ln(N_J)$	-0.543	0.031	-17.63	< 0.0001		
ln(d)	-1.143	0.042	-27.26	< 0.0001		
D ln(DC)	-0.167	0.047	-3.55	0.0005		
ϕ_p ln(s−1)	-10.302	2.714	-3.80	0.0002		

(a) Probability that the coefficient is not statistically significant (different from 0). Values less than 0.05, 0.01, and 0.0001 indicate strong, very strong, and extremely strong statistical significance of the coefficient and corresponding model term.
(b) Model evaluation and validation statistics are defined, respectively, in Sections D.3 and D.5 of Appendix D.

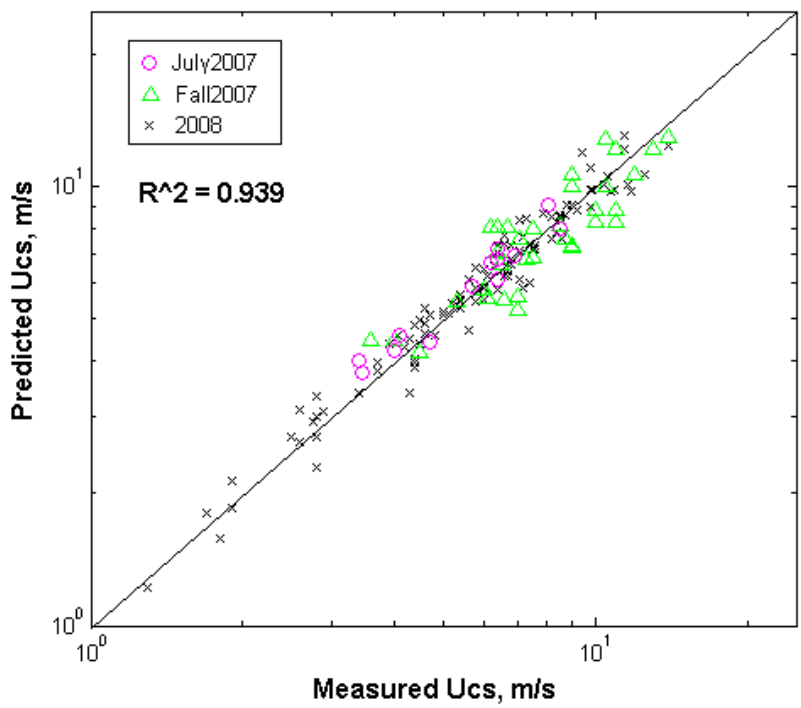

Figure F.7. Log-Log Plot of Predicted Versus Measured U_{CS} (m/s) Values for the 11-Term Dimensional Model with Interactions in Table F.4 Fit to the Trimmed Data Set. The 45-degree line represents perfect prediction where predicted U_{CS} values equal measured U_{CS} values.

All of the summary statistics for the dimensional models with interactions for U_{CS} in Tables F.5 and F.6 show improvement over the corresponding results for dimensional models without interactions in Tables F.1 and F.2. The R^2 statistics in Table F.5 ($R^2 = 0.939$) and Table F.6 ($R^2 = 0.939$) indicate that the U_{CS} dimensional models with interactions developed by stepwise selection fit the full and trimmed data sets very well. Because the values of R^2_A and R^2_p in Tables F.5 and F.6 do not differ markedly from the corresponding R^2 values, there are no indications that the U_{CS} models with interaction terms over-fit the data or that there are any highly influential data.

Figure F.6 shows a predicted-versus-measured plot for the performance of the 12-term U_{CS} dimensional model with interactions in Table F.5. In Figure F.6, the scatter around the perfect prediction (45°) line has been slightly reduced from that in Figure F.2 for the 9-term U_{CS} dimensional model without interactions in Table F.1. Figure F.7 shows that predictions made for the trimmed data set are also improved when using the 11-term dimensional model with interactions compared to the 9-term dimensional model without interactions (Table F.2 and Figure F.3).

Based on Table F.5, the U_{CS} dimensional models with interaction terms fit to the full data are

$$\begin{aligned} U_{CS} &= 0.652\,(D)^{1.186}(s-1)^{0.421}(\phi_S)^{0.264}(U_T)^{0.082+0.276(DC)+0.897(\phi_S)} \\ &\quad \times (DC)^{0.366-0.170(D)}(\phi_p)^{-0.210}(N_J)^{-0.545}(d)^{-1.116} \end{aligned} \tag{F.15a}$$

and

$$\begin{aligned} \ln(U_{CS}) &= -0.428 + 1.186\ln(D) + 0.421\ln(s-1) + 0.264\ln(\phi_S) \\ &\quad + [0.082 + 0.276(DC) + 0.897(\phi_s)]\ln(U_T) + [0.366 - 0.170(D)]\ln(DC) \\ &\quad - 0.210\ln(\phi_p) - 0.545\ln(N_J) - 1.116\ln(d)\,, \end{aligned} \tag{F.15b}$$

where all notation is as previously defined. Based on Table F.6, the U_{CS} dimensional models with interaction terms fit to the trimmed data set are

$$\begin{aligned} U_{CS} &= 0.867\,(D)^{1.221}(s-1)^{0.952-10.302\,(\phi_p)}(\phi_S)^{0.247}(U_T)^{0.170} \\ &\quad \times (DC)^{0.038-0.167(D)}(\phi_p)^{0.094}(N_J)^{-0.543}(d)^{-1.143} \end{aligned} \tag{F.16a}$$

and

$$\begin{aligned} \ln(U_{CS}) &= -0.143 + 1.221\ln(D) + [0.952 - 10.302(\phi_p)]\ln(s-1) \\ &\quad + 0.247\ln(\phi_S) + 0.170\ln(U_T) + [0.038 - 0.167(D)]\ln(DC) \\ &\quad + 0.094\ln(\phi_p) - 0.543\ln(N_J) - 1.143\ln(d)\,, \end{aligned} \tag{F.16b}$$

where all notation is as previously defined.

As discussed at the end of Section F.2.3, the U_{CS} models with interaction terms may yield inaccurate predictions when extrapolated outside the experimental region of data used to develop them. Hence, unless additional work is performed to thoroughly validate these U_{CS} models for extrapolative use, it is recommended that they only be used for interpolative use.

F.2.6 Comparison of U_{CS} Models

In this section the results for three U_{CS} models presented in Section F.2, namely the

- dimensional model without interactions (Section F.2.4.2)
- corresponding dimensionally consistent model (Section F.2.4.3)
- dimensional model with interactions (Section F.2.5)

are compared with the results of the nondimensional model for U_{CS} from Sections 7.3.2 and 7.3.4. Because the latter model was only fit using the full data set, the comparisons are based on that data.

Figure F.8 shows the predicted-versus-measured (PvM) plot and R^2 [calculated using $\ln(U_{CS})$ values] for the nondimensional U_{CS} model from Sections 7.3.2 and 7.3.4. The goodness-of-fit of the nondimensional model (Figure F.8, $R^2 = 0.896$) can be compared with the dimensional model without interactions (Figure F.2, $R^2 = 0.913$), the dimensionally consistent model (Figure F.4, $R^2 = 0.867$), and the dimensional model with interactions (Figure F.6, $R^2 = 0.939$). Based on R^2 values, the dimensional models with and without interactions provide the best fits to the full data set, followed by the nondimensional model and the dimensionally consistent model. The PvM plots for dimensional models without and with interactions (Figures F.2 and F.5) have less scatter for U_{CS} values in the middle of the range tested than the PvM plot for the nondimensional model (Figure F.8). However, the latter plot looks very good. This suggests that some of the generalizations made in constructing the dimensional model form (see Section F.2.2) may be unneeded. If so, there may be a way to reduce the number of coefficients in the dimensional models and retain the improved fit to the data. However, it was not possible in the time available to pursue this idea.

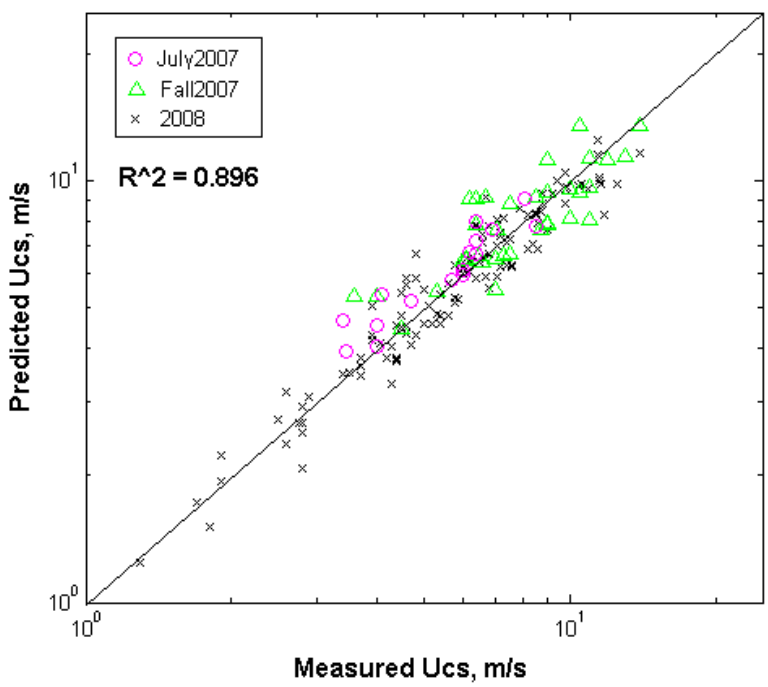

Figure F.8. Log-Log Plot of Predicted Versus Measured U_{CS} (m/s) Values for the Nondimensional Model From Section 7.3.2 Developed Using the Full Data Set. The 45-degree line represents perfect prediction where predicted U_{CS} values equal measured U_{CS} values.

Table F.7 compares the coefficients of several U_{CS} models fitted using the full data set when those models are expressed in the dimensional form of Eq. (F.8a). The U_{CS} models compared in this way include the 9-term dimensional model without interactions, the 8-term dimensionally consistent model, and the nondimensional model from Sections 7.3.2 and 7.3.4. Some variables in the nondimensional model cannot be expressed in power-law form; thus it was impossible to calculate all coefficients in the form of Eq. (F.8a) for that model. The 12-term dimensional model with interactions is not included in Table F.7 because the values of coefficients involving interactions depend on the variables involved in the interactions.

It is seen from Table F.7 that the coefficients of the three U_{CS} models expressed in dimensional form are similar for most of the predictor variables. It is of particular note that all three models have a similar coefficient for D, which controls the scale effect. The most noticeable difference is the coefficient for U_T in the nondimensional model, which is significantly larger than the U_T coefficient in the other two models. However, the nondimensional model has a $(1-\phi_S/0.5)^{1.944}$ term that offsets the impact of the larger U_T coefficient.

Table F.7. Coefficients of U_{CS} Models Expressed in the Dimensional Form of Equation (F.8a)

Model Terms	Dimensional U_{CS} Model w/o Interactions [Eq. (F.11a)]	Dimensionally Consistent U_{CS} Model w/o Interactions [Eqs. (F.10) & (F.13a)]	Nondimensional U_{CS} Model from Section 7.3.2
a_0	0.309	0.273	(a)
D (a_1)	1.321	1.388	1.363
s−1 (a_2)	0.471	0.483	(a)
ϕ_S (a_3)	0.222	0.243	0.284
$1-\phi_S$ (a_{14})	–[(b)]	–	–
U_T (a_6)	0.148	0.206	0.432
DC (a_7)	-0.247	-0.205	-0.284
ϕ_p (a_8)	-0.211	-0.221	-0.198
N_J (a_{10})	-0.525	-0.511	-0.487
d (a_{11})	-1.072	-0.991	-0.974
$1-\phi_S/0.5$	–	–	1.944
R^2	0.913	0.867	0.896

(a) Not expressible as a term in a power-law model.
(b) A dash (–) indicates the term is not included in the model.

F.3 Cloud Height (H_C) Models

This section discusses the development, results, and uncertainties of H_C models fit to the full and trimmed data sets described in Section F.1.

F.3.1 H_C Model Forms

To develop a model from for H_C, it would be desirable to investigate functionality plots for H_C vs. x_i (test variables), similar to the discussion for U_{CS} at the start of Section F.2.1. Such functionality plots would require plotting H_C versus each x_i, with lines connecting groups of data points with constant values of the remaining test variables. Jet velocity (U) is one of the test variables that strongly affects H_C, but

the values of U tested and even the ranges tested are not the same from test to test. Hence, it is not possible to produce functionality plots for other test variables with values of U constant. In lieu of this, functionality plots of H_{CS} [or $\ln(H_{CS})$] versus the other x_i [or $\ln(x_i)$] were investigated. Along with those functionality plots, functionality plots of H_C [or $\ln(H_C)$] versus U [or ln(U)] were also investigated. The same kinds of investigations were performed as described for U_{CS} at the start of Section F.2.1, so that discussion is not repeated here.

Ultimately, the $\ln(H_C)$ versus ln(U) plots (which are shown in Figures E.17 to E.21 of Appendix E as log-log plots of H_C versus U) were strongly linear, although with some curvature for U values slightly above U_{CS}. Also, the $\ln(H_{CS})$ versus $\ln(x_i)$ plots (which are shown in Figures E.22 to E.32 of Appendix E as log-log plots of H_{CS} versus x_i) had linear or not too curvilinear relationships for all of the test variables. Hence, it was concluded that the corresponding power-law model form would be an adequate "first-order" approximation of the true, unknown relationships between H_C and the x_i. It was recognized that adopting the power-law model form would result in some model lack-of-fit for some test variables. Based on the plots in Figures E.17 to E.32, these test variables are N_J (the number of operating jets), $\phi_S > 0.015$, and the smallest and largest values of d_S and U_T (for which there were very few tests performed). However, this situation was judged acceptable given the goal of using the models to perform coarse ratings of the mixing designs of WTP vessels. Also, fitting models to both "full" and "trimmed" data sets, as described in Section F.1.1, addresses some of these issues. More accurate H_C models could be developed in the future from the M3 mixing-test data, but they would have more complicated forms, require more time to develop, and require more advanced statistical fitting and uncertainty methods.

The RSM modeling approach of using first- and second-order polynomial models to approximate the relationship between a response variable and multiple predictor variables was discussed for U_{CS} at the end of Section F.2.1. Because the RSM approach did not perform as well for the easier-to-model U_{CS} data, it was decided not to investigate the RSM approach for the more-difficult-to-model H_C data. Another reason for not pursuing the RSM approach for modeling H_C is the same as for U_{CS}, namely that polynomial models are generally not appropriate for extrapolative use.

F.3.2 H_C Power-Law Model Forms

The initial H_C model form considered was developed by generalizing the *physical model* for H_C discussed in Section 7.3.2. Starting with that form of the model, the natural logarithm of the left side is removed because of its small effect and the expectation of capturing that effect in another way. Then, moving the predictor variables on the left side to the right side of the equation, expanding variables calculated as functions of other variables, and collecting similar terms yields the statistical model form

$$H_C = a_0 (D)^{a_{13}} (s-1)^{a_2} (\phi_S)^{a_3} (U_{TH})^{a_4} (DC)^{a_7} (\phi_p)^{a_8} (d_S)^{a_9} (\phi_J)^{a_{10}} (U)^{a_{12}} \ \delta \qquad \text{(F.17a)}$$

where notation is as described previously. Equation (F.17a) was generalized to include a term involving D, which does not appear in the H_C model form discussed in Section 7.3.2. Note that Eq. (F.17a) is a power-law model form, which was judged as adequate for first-order approximation and predictive purposes, as discussed above.

Because Eq. (F.17a) is nonlinear in its coefficients and has a multiplicative error structure, it can be converted to a model linear in its coefficients with an additive error structure by taking the natural logarithm of both sides, as discussed in Section D.2.1 of Appendix D. This yields the model

$$\begin{aligned}\ln(H_C) = \ln(a_0) + a_{13}\ln(D) + a_2\ln(s-1) + a_3\ln(\phi_S) + a_4\ln(U_{TH}) + a_7\ln(DC) \\ + a_8\ln(\phi_p) + a_9\ln(d_S) + a_{10}\ln(\phi_J) + a_{12}\ln(U) + \varepsilon\,,\end{aligned} \tag{F.17b}$$

where the notation is as previously defined. The model form in Eq. (F.17b) can be fit by OLS LR, whereas the model form in Eq. (F.17a) must be fit by WLS NLR. See Section D.2 of Appendix D for more discussion of these issues.

Equations (F.17a) and (F.17b) can be expanded by substituting into them a generalization of the equation for U_{TH} given by

$$U_{TH} = U_T\,(1 - \frac{\phi_S}{0.5})^{4.5} \tag{F.18}$$

This yields the model forms

$$H_C = a_0\,(D)^{a13}\,(s-1)^{a2}\,(\phi_S)^{a3}\,(1 - \frac{\phi_S}{0.5})^{a5}\,(U_T)^{a6}\,(DC)^{a7}\,(\phi_p)^{a8}\,(d_S)^{a9}\,(\phi_J)^{a10}\,(U)^{a12}\;\delta \tag{F.19a}$$

and

$$\begin{aligned}\ln(H_C) = \ln(a_0) + a_{13}\ln(D) + a_2\ln(s-1) + a_3\ln(\phi_S) + a_5\,\ln(1 - \frac{\phi_S}{0.5}) + a_6\ln(U_T) \\ + a_7\ln(DC) + a_8\ln(\phi_p) + a_9\ln(d_S) + a_{10}\ln(\phi_J) + a_{12}\ln(U) + \varepsilon\,,\end{aligned} \tag{F.19b}$$

where the notation is as previously defined. The a_6 and a_5 coefficients in Eqs. (F.19a) and (F.19b) generalize, respectively, the 1.0 exponent (implied) on U_T and the 4.5 exponent on $(1 - \phi_S/0.5)$ in Eq. (F.18).

Using a generalization of the formula $\phi_J = N_J(d/D)^2$ where N_J and d are allowed to have their own coefficients and D is absorbed into the existing D term, the model forms in Eqs. (F.19a) and (F.19b) can be further generalized as

$$\begin{aligned}H_C = a_0\,(D)^{a1}\,(s-1)^{a2}\,(\phi_S)^{a3}\,(1 - \frac{\phi_S}{0.5})^{a5}\,(U_T)^{a6}\,(DC)^{a7}\,(\phi_p)^{a8}\,(d_S)^{a9} \\ \times (N_J)^{a10}\,(d)^{a11}\,(U)^{a12}\;\delta\end{aligned} \tag{F.20a}$$

and

$$\begin{aligned}\ln(H_C) = \ln(a_0) + a_1\ln(D) + a_2\ln(s-1) + a_3\ln(\phi_S) + a_5\,\ln(1 - \frac{\phi_S}{0.5}) + a_6\ln(U_T) \\ + a_7\ln(DC) + a_8\ln(\phi_p) + a_9\ln(d_S) + a_{10}\ln(N_J) + a_{11}\ln(d) + a_{12}\ln(U) + \varepsilon\,,\end{aligned} \tag{F.20b}$$

where all notation is as previously defined.

As discussed, Eqs. (F.20a) and (F.20b) are generalizations of the model forms in Eqs. (F.17a) and (F.17b), where the latter are obtained from the former using the coefficient constraints $a_6 = a_4$, $a_5 = 4.5a_4$, $a_{11} = 2a_{10}$, and $a_1 = a_{13} - 2a_{10}$.

Finally, note that none of the model forms discussed for H_C contains an HS (head shape) term, for the same reasons discussed for U_{CS} model forms at the end of Section F.2.2.

F.3.3 H_C Power-Law Models with Interaction Terms

Stepwise regression methods (see Section D.4.2, Appendix D) were used to augment H_C models of the form in Eqs. (F.20a) and (F.20b) with interaction terms of the same form as discussed for U_{CS} in Section F.2.3. Functionality plots of H_C and H_{CS} versus test variables in Section E.2.3 of Appendix E indicate the interaction terms of the form shown in Section F.2.3 may improve the predictive performance of mixing models, at least within the experimental region of the data. However, models with interaction terms can yield inaccurate predictions when extrapolated significantly outside the experimental region of data used to develop them. Hence, unless H_C models with interaction terms have been well validated for extrapolative use, it is recommended that only H_C models without interaction terms be used for extrapolative predictions.

F.3.4 Results for H_C Power-Law Models

The dimensional and corresponding dimensionally consistent model forms investigated for H_C are presented in Section F.3.4.1. The results of fitting the dimensional models for H_C to the full and trimmed data sets are presented in Section F.3.4.2. The results of fitting the dimensionally consistent models for H_C are presented in Section F.3.4.3.

F.3.4.1 Dimensional and Dimensionally Consistent Power-Law Model Forms for H_C

To begin, models of the form in Eq. (F.20b) were fit to the full and trimmed data sets described in Section F.1. For the full data set, the $s - 1$ term was statistically nonsignificant. For the trimmed data set, the $s - 1$ and $(1 - \phi_S/0.5)$ terms were statistically nonsignificant.

The statistical nonsignificance of the $s - 1$ term for both the full and trimmed data sets was a result of the model form in Eq. (F.20b) including all three of the highly correlated terms $s - 1$, d_S, and U_T (as discussed in Section F.2.4). It was decided to drop d_S from the model to rectify this problem. It may seem more natural to drop U_T than d_S, because U_T is calculated using d_S and $s - 1$; however, U_T is more physically meaningful as a predictor variable than d_S. Further, there was little difference in the goodness-of-fit of a model that retained U_T instead of d_S.

In addition, for reasons discussed in Section F.3.3, it was decided to delete the $(1 - \phi_S/0.5)$ term from the model. However, it was discovered in preliminary H_C modeling work that a power-law term of the form $1 - \phi_S$ (in addition to a power-law term for ϕ_S) helped account for the H_C dependence on the larger values of ϕ_S in the full data set. Hence, models of the form

$$H_C = a_0 (D)^{a_1} (s-1)^{a_2} (\phi_S)^{a_3} (1-\phi_S)^{a_{14}} (U_T)^{a_6} (DC)^{a_7} (\phi_p)^{a_8} \times (N_J)^{a_{10}} (d)^{a_{11}} (U)^{a_{12}} \delta \tag{F.21a}$$

and

$$\ln(H_C) = \ln(a_0) + a_1\ln(D) + a_2\ln(s-1) + a_3\ln(\phi_S) + a_{14}\ln(1-\phi_S) + a_6\ln(U_T) \\ + a_7\ln(DC) + a_8\ln(\phi_p) + a_{10}\ln(N_J) + a_{11}\ln(d) + a_{12}\ln(U) + \varepsilon, \tag{F.21b}$$

were considered, where all notation is as previously defined.

The coefficients estimated by fitting Eq. (F.21b) to the full or trimmed data sets by OLS MR may subsequently be written in the form of Eq. (F.21a). However, this will result in a dimensional constant a_0 having units that may differ from those of subsumed physical constants (e.g., g) and dropped model terms. Unfortunately, there is not a unique set of dimensional-consistency constraints that can be applied by fitting Eq. (F.21b) using restricted-least-squares (Draper and Smith 1998, Section 9.5) to impose dimensional consistency. Instead, a dimensionally consistent model form was developed starting from Eq. (F.21a), with the goal of retaining as much as possible of the generalizations added in Section F.3.2. The dimensionally consistent model for H_C that resulted from this process is

$$H_C = b_0 D\left(\frac{U^2}{D(s-1)g}\right)^{b_1}\left(\frac{d}{D}\right)^{b_2}(s-1)^{b_3}\left(\frac{U_T}{U}\right)^{b_4} DC^{b_5}\phi_S^{b_6}(1-\phi_S)^{b_7}\phi_p^{b_8}N_J^{b_9}\,\delta \tag{F.22a}$$

where

b_i = model coefficients (i = 0, 1, …, 9) to be estimated using experimental data (nondimensional)

$\frac{U^2}{D(s-1)g}$ = Froude number (nondimensional)

g = 9.80665 (m/s^2) is the gravity constant

$\frac{U_T}{U}$ = kinematic ratio (nondimensional)

and remaining notation is as defined previously. Because Eq. (F.22a) is nonlinear in its coefficients and has a multiplicative error structure, it can be converted to a model linear in its coefficients with an additive error structure by taking the natural logarithm of both sides, as discussed in Section D.2.1 of Appendix D. This yields the model:

$$\ln(H_C) = \ln(b_0) + \ln(D) + b_1\ln\left(\frac{U^2}{D(s-1)g}\right) + b_2\ln\left(\frac{d}{D}\right) + b_3\ln(s-1) + b_4\left(\frac{U_T}{U}\right) \\ + b_5\ln(DC) + b_6\ln(\phi_S) + b_7\ln(1-\phi_S) + b_8\ln(\phi_p) + b_9\ln(N_J) + \varepsilon \tag{F.22b}$$

The dimensionally consistent models in Eqs. (F.22a) and (F.22b) can be considered as reduced forms of the dimensional models in Eqs. (F.21a) and (F.21b), with the relationships among the coefficients given by

$$
\begin{aligned}
a_0 &= b_0\, g^{-b_1} \quad \text{or} \quad \ln(a_0) = \ln(b_0) - b_1 \ln(g) \\
a_1 &= 1 - b_1 - b_2 \\
a_2 &= b_3 - b_1 \\
a_3 &= b_6 \\
a_{14} &= b_7 \\
a_6 &= b_4 \\
a_7 &= b_5 \\
a_8 &= b_8 \\
a_{10} &= b_9 \\
a_{11} &= b_2 \\
a_{12} &= 2b_1 - b_4
\end{aligned}
\tag{F.23}
$$

Note that the H_C dimensional models in Eqs. (F.21a) and (F.21b) have 11 coefficients to be estimated using the data, whereas the dimensionally consistent models in Eqs. (F.22a) and (F.22b) have only 10. The difference is because the leading D term (after the constant term) in Eqs. (F.21a) and (F.21b) has an exponent/coefficient equal to 1. If the D term were given a separate exponent, for instance, b10, that would give $a_1 = b_{10} - b_1 - b_2$. The model form in Eqs. (F.22a) and (F.22b) extended in this way would be mathematically equivalent to the model form in Eqs. (F.21a) and (F.21b). In other words, they would fit a given data set exactly the same, and predictions of H_C would be exactly the same.

F.3.4.2 Results of Fitting Dimensional Power-Law Model Forms for H_C to Full and Trimmed Data Sets

The results of fitting the dimensional model form in Eq. (F.21b) to the full and trimmed data sets are given in Tables F.8 and F.9, respectively. Included in these tables are estimates of the model coefficients and their standard deviations. Also shown for each coefficient is its t-value (coefficient divided by its standard deviation) and p-value (statistical significance level). Traditionally, p-values lower than 0.05 indicate statistically significant coefficients (different from zero) with greater than 95% confidence; p-values lower than 0.01 indicate high statistical significance (greater than 99% confidence), while values lower than 0.0001 indicate extremely high statistical significance (more than 99.99% confidence).

In Table F.8 for the full data set, all model terms except the constant [$\ln(a_0)$] are statistically significant at a p-value of < 0.0001. For the trimmed data, 10 of the 11 terms in Eq. (F.21b) were statistically significant. The $(1 - \phi_S)$ term was not statistically significant, so it was removed from the 10-term model shown in Table F.9. The statistical nonsignificance of this term is reasonable because the trimmed data set removed data with values $\phi_s > 0.015$. It was for those data that the $(1 - \phi_S)$ term improved the fit to the full data set. Table F.9 shows that the other terms (except the constant) are statistically significant, with p-values of < 0.0001.

The large negative coefficient of -17.502 on the $(1-\phi_S)$ term in Table F.8 requires some additional explanation because it "stands out" compared to other coefficients. As seen in Table F.8, this term in the

H_C model is highly statistically significant. Having both ϕ_S and $(1-\phi_S)$ terms in the model serves to represent the curvature effect of ϕ_S on H_C. This curvature can be seen in the functionality plot of ϕ_S for H_{CS} in Figure E.28 of Appendix E. A model like the one in Table F.8, but fit without the $(1-\phi_S)$ term, shows biased predictions of H_C for $\phi_S > 0.015$. Finally, when the coefficient -17.502 is combined with $(1-\phi_S)$ values in the M3 test data set (ranging from 0.94 to 0.9995), the range of contributions of this term to model predictions is smaller than for several other model terms. Hence, the model in Table F.8 with the $(1-\phi_S)$ term having coefficient -17.502 is appropriate for the range of ϕ_S studied in M3 testing. Because WTP vessels require only interpolating within the range of ϕ_S studied in M3 testing, the H_C model containing the $-17.502\ln(1-\phi_S)$ term is appropriate for use.

Table F.8. Coefficients and Performance Summary for the 11-Term Linearized Power-Law Model on the Natural Logarithm of H_C Fit to the Full Data Set

$\ln(H_C)$ Model Term	Coefficient Estimate	Coefficient Standard Deviation	t-value = Coeff/SD	p-value[(a)]	Full Data, 669 Data Points[(b)] Modeling Data Statistic [$\ln(H_C)$]	Value
$\ln(a_0)$	0.076	0.229	0.33	0.739	R^2	0.830
$\ln(D)$	-1.191	0.097	-12.31	< 0.0001	R^2 Adjusted (R^2_A)	0.828
$\ln(s-1)$	-0.836	0.046	-18.32	< 0.0001	R^2 Predicted (R^2_P)	0.825
$\ln(\phi_S)$	-0.623	0.026	-24.24	< 0.0001	RMSE	0.258
$\ln(1-\phi_S)$	-17.502	1.622	-10.79	< 0.0001		
$\ln(U_T)$	-0.412	0.018	-22.46	< 0.0001		
$\ln(DC)$	0.371	0.036	10.32	< 0.0001		
$\ln(\phi_p)$	0.218	0.039	5.63	< 0.0001		
$\ln(N_J)$	0.330	0.050	6.66	< 0.0001		
$\ln(d)$	1.722	0.086	19.95	< 0.0001		
$\ln(U)$	1.378	0.066	20.98	< 0.0001		

(a) Probability that the coefficient is not statistically significant (different from 0). Values less than 0.05, 0.01, and 0.0001 indicate strong, very strong, and extremely strong statistical significance of the coefficient and corresponding model term.
(b) Model evaluation and validation statistics are defined, respectively, in Sections D.3 and D.5 of Appendix D.

Table F.9. Coefficients and Performance Summary for the 10-Term Linearized Power-Law Model on the Natural Logarithm of H_C Fit to the Trimmed Data Set

$\ln(H_C)$ Model Term	Coefficient Estimate	Coefficient Standard Deviation	t-value = Coeff/SD	p-value [(a)]	Trimmed Data, 581 Data Points[(b)] Modeling Data Statistic [$\ln(H_C)$]	Value
$\ln(a_0)$	0.349	0.228	1.53	0.127	R^2	0.852
$\ln(D)$	-1.327	0.101	-13.13	< 0.0001	R^2 Adjusted (R^2_A)	0.850
$\ln(s-1)$	-0.804	0.046	-17.66	< 0.0001	R^2 Predicted (R^2_P)	0.847
$\ln(\phi_S)$	-0.572	0.021	-26.76	< 0.0001	RMSE	0.242
$\ln(U_T)$	-0.491	0.019	-25.39	< 0.0001		
$\ln(DC)$	0.348	0.038	9.12	< 0.0001		
$\ln(\phi_p)$	0.276	0.038	7.23	< 0.0001		
$\ln(N_J)$	0.340	0.049	7.00	< 0.0001		
$\ln(d)$	1.812	0.090	20.14	< 0.0001		
$\ln(U)$	1.501	0.068	21.99	< 0.0001		

(a) Probability that the coefficient is not statistically significant (different from 0). Values less than 0.05, 0.01, and 0.0001 indicate strong, very strong, and extremely strong statistical significance of the coefficient and corresponding model term.
(b) Model evaluation and validation statistics are defined, respectively, in Sections D.3 and D.5 of Appendix D.

The right sides of Tables F.8 and F.9 list various summary statistics that provide measures of how well the 11- and 10-term models based on Eq. (F.21b) fit the full and trimmed data sets, respectively. These summary statistics are defined and discussed in Sections D.3.2 and D.3.3 of Appendix D. The summary statistics in Tables F.8 and F.9 indicate that the linearized power-law models fit the available data reasonably well.

The 11-term model accounts for 83% of the variability in $\ln(H_C)$ values for the full data. The 10-term model accounts for 85.2% of the variability in $\ln(H_C)$ values for the trimmed data. The linearized power-law model form fits slightly better for the trimmed data set than for the full data set. In Tables F.8 and F.9 the differences between R^2 and R^2_A are small, so there are no indications that the full and trimmed data sets, respectively, have been over-fitted. Because the differences between R^2_A and R^2_P are small in both tables, there are no indications of highly influential data affecting the model fits.

Figures F.9 and F.10 show predicted-versus-measured plots, which provide a graphical view of how well the 11- and 10-term model forms fit the full and trimmed data sets, respectively. In each plot, the predicted value of H_C is plotted on the y-axis (in log scale) and the measured values of H_C are plotted on the x-axis (also in log scale). The 45-degree line represents perfect prediction, where predicted H_C values would exactly equal measured H_C values. See Section D.3.2 of Appendix D for further discussion of using predicted-versus-measured plots to evaluate how well a model fits a data set.

From Figures F.9 and F.10, it is seen that only the 2008 data span the range of the H_C response. The figures also show tendencies for the corresponding models in Tables F.8 and F.9 to overpredict H_C below ~ 0.2 m. The models have a slight tendency to underpredict H_C values between ~ 0.3 to 0.6 m.

In summary, inserting the coefficients from the H_C dimensional models without interactions fit to the full data set (Table F.8) into Eqs. (F.21a) and (F.21b) results in the models

$$\begin{aligned} H_C &= 1.079\,(D)^{-1.191}(s-1)^{-0.836}(\phi_S)^{-0.623}(1-\phi_S)^{-17.502}(U_T)^{-0.412}(DC)^{0.371} \\ &\quad \times (\phi_p)^{0.218}(N_J)^{0.330}(d)^{1.722}(U)^{1.378} \end{aligned} \tag{F.24a}$$

and

$$\begin{aligned} \ln(H_C) &= 0.076 - 1.191\ln(D) - 0.836\ln(s-1) - 0.623\ln(\phi_S) - 17.502\ln(1-\phi_S) \\ &\quad - 0.412\ln(U_T) + 0.371\ln(DC) + 0.218\ln(\phi_p) + 0.330\ln(N_J) + 1.722\ln(d) \\ &\quad + 1.378\ln(U) \end{aligned} \tag{F.24b}$$

where all notation is as previously defined. The $(1-\phi_S)^{-17.502}$ and $-17.502\ln(1-\phi_S)$ terms in Eqs. (F.24a) and (F.24b) are appropriate for the range of ϕ_S studied in M3 testing (0.0005 − 0.06). However, caution is advised if these H_C models must be extrapolated to ϕ_S values outside that range.

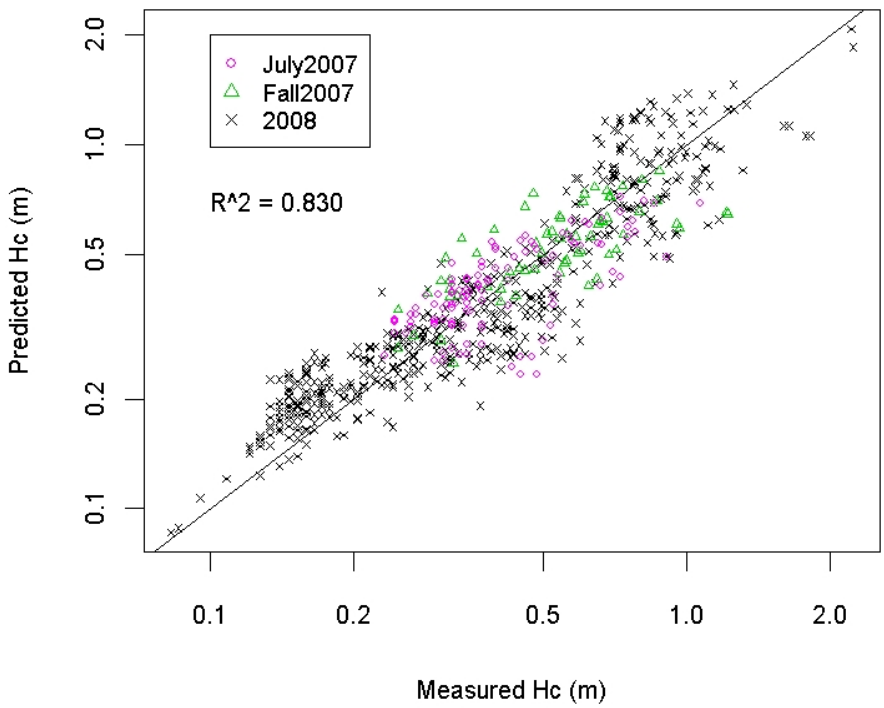

Figure F.9. Log-Log Plot of Predicted Versus Measured H_C Values for the 11-Term Dimensional Model in Table F.8 Fit to the Full Data Set. The 45-degree line represents perfect prediction where predicted H_C values equal measured H_C values.

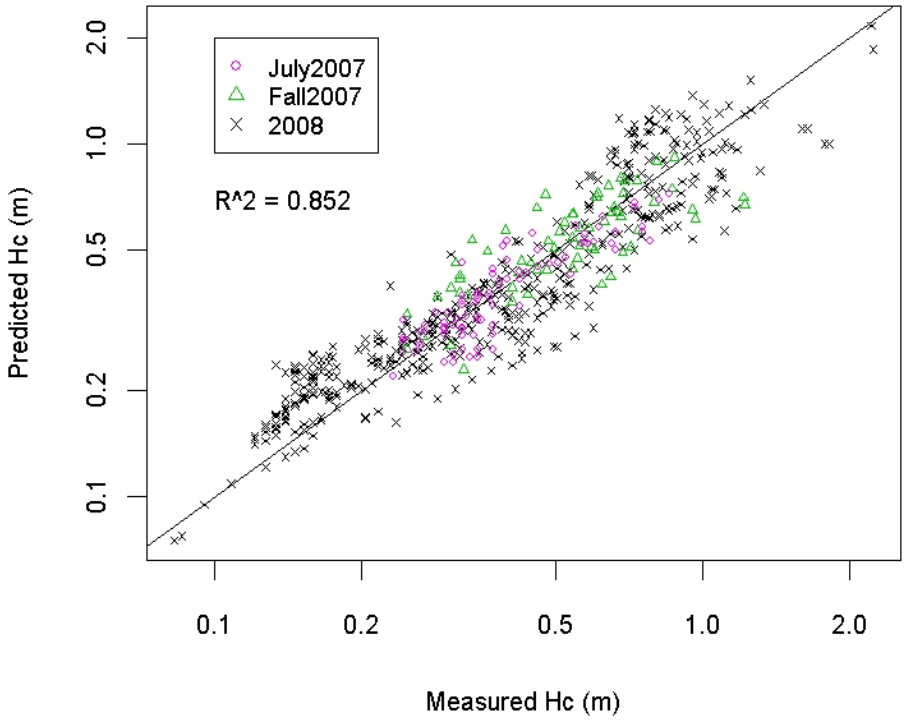

Figure F.10. Log-Log Plot of Predicted Versus Measured H_C Values for the 10-Term Dimensional Model in Table F.9 Fit to the Trimmed Data Set. The 45-degree line represents perfect prediction where predicted H_C values equal measured H_C values.

Inserting the coefficients from the H_C dimensional models without interactions fit to the trimmed data set (Table F.9) into Eqs. (F.21a) and (F.21b) results in models:

$$H_C = 1.418\,(D)^{-1.327}(s-1)^{-0.804}(\phi_S)^{-0.572}(U_T)^{-0.491}(DC)^{0.348}(\phi_p)^{0.276} \times (N_J)^{0.340}(d)^{1.812}(U)^{1.501} \tag{F.25a}$$

and

$$\ln(H_C) = 0.349 - 1.327\ln(D) - 0.804\ln(s-1) - 0.572\ln(\phi_S) - 0.491\ln(U_T) + 0.348\ln(DC) + 0.276\ln(\phi_p) + 0.340\ln(N_J) + 1.812\ln(d) + 1.501\ln(U)\,, \tag{F.25b}$$

where all notation is as previously defined.

F.3.4.3 Results of Fitting Dimensionally Consistent Power-Law Model Forms for H_C to Full and Trimmed Data Sets

The dimensionally consistent model form in Eq. (F.22b) was fit to the full and trimmed data sets using restricted least squares (Draper and Smith 1998). The results for the full data set are given in Table F.10 and Figure F.11; the results for the trimmed data set are given in Table F.11 and Figure F.12.

The H_C dimensionally consistent models in Tables F.10 and F.11 have the same R^2 values as the dimensional models in Tables F.8 and F.9. For the full data set $R^2 = 0.830$ for each model, while for the trimmed data set $R^2 = 0.852$ for each model. As noted at the end of Section F.3.4.1, adding an exponent to the D term would make the dimensionally consistent model mathematically equivalent to the dimensional model. However, that yielded an exponent close to 1. Hence, the dimensional models for H_C fit to the full and trimmed data sets are very close to being dimensionally consistent, which explains why the R^2 values for the dimensional and dimensionally consistent H_C models are the same to three decimal places.

The large negative coefficient of -17.206 on the $(1-\phi_S)$ term in Table F.10 requires some additional explanation because it "stands out" compared to other coefficients. As seen in Table F.10, this term in the H_C model is highly statistically significant. The remaining explanation of why this is an appropriate model term and cautions in using the model are the same as discussed in Section F.3.4.2, so that discussion is not repeated here.

Figures F.11 and F.12 for the full and trimmed data sets, respectively, show tendencies for the H_C dimensionally-consistent models to overpredict H_C < ~0.2 m, and slight tendencies to under-predict H_C from ~0.3 to 0.7 m. Figures F.11 and F.12 are nearly identical to the corresponding plots for the dimensional models in Figures F.9 and F.10, respectively. This is a result of the dimensional and dimensionally consistent models for H_C being nearly equivalent.

Table F.10. Coefficients and Performance Summary for Linearized Version of 11-Term Dimensionally Consistent Model on Natural Logarithm of H_C with 10 Coefficients Fit to the Full Data Set

$\ln(H_C)$ Model Term	Coefficient Estimate	Coefficient Standard Deviation	t-value = Coeff/SD	p-value[a]	Full Data, 669 Tests[b] Modeling Data Statistic [$\ln(H_C)$]	Value
$\ln(b_0)$	1.112	–[c]	–	–	R^2	0.830
$\ln(D)$[d]	1.0	N/A	N/A	N/A	R^2 Adjusted (R^2_A)	0.828
$\ln[U^2/D(s-1)g]$	0.473	–	–	–	R^2 Predicted (R^2_P)	–[c]
$\ln(d/D)$	1.693	–	–	–	RMSE	0.257
$\ln(s-1)$	-0.356	–	–	–		
$\ln(U_T/U)$	-0.410	–	–	–		
$\ln(DC)$	0.364	–	–	–		
$\ln(\phi_S)$	-0.616	–	–	–		
$\ln(1-\phi_S)$	-17.206	–	–	–		
$\ln(\phi_p)$	0.213	–	–	–		
$\ln(N_J)$	0.320	–	–	–		

(a) Probability that the coefficient is not statistically significant (different from 0). Values less than 0.05, 0.01, and 0.0001 indicate strong, very strong, and extremely strong statistical significance of the coefficient and corresponding model term.
(b) Model evaluation and validation statistics are defined, respectively, in Sections D.3 and D.5 of Appendix D.
(c) Not available from software used to fit model using restricted least squares; could be determined with additional work.
(d) Restricted least squares was used to fit this model, with the coefficient of ln(D) restricted to be 1.0.

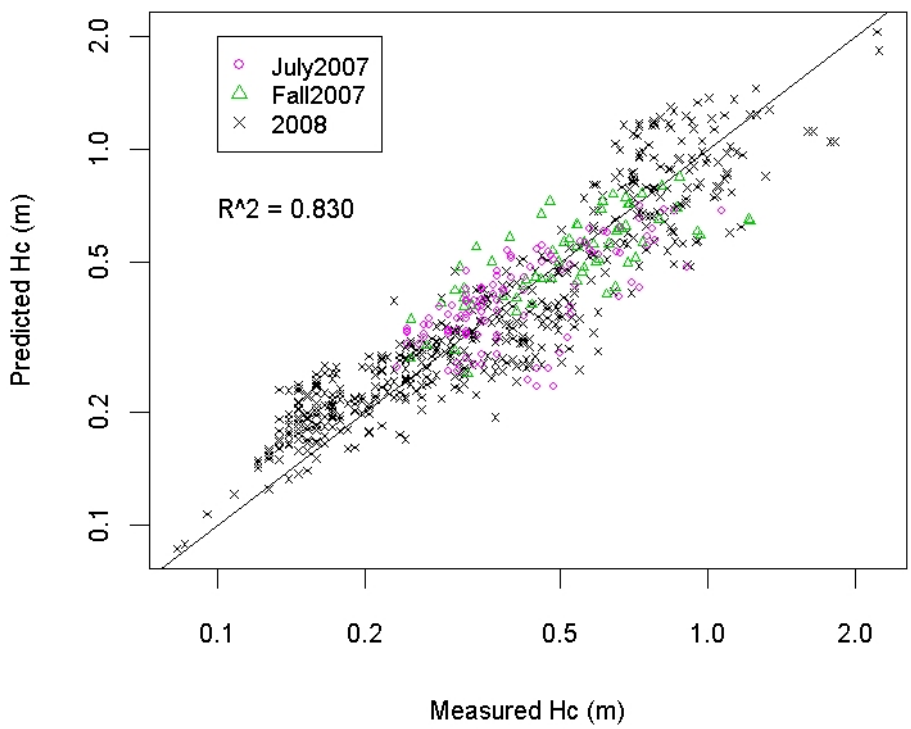

Figure F.11. Log-Log Plot of Predicted Versus Measured H_C (m) Values for 11-Term Dimensionally Consistent Model in Table F.10 with 10 Coefficients Fit to Full Data Set. The 45-degree line represents perfect prediction where predicted H_C values equal measured H_C values.

Table F.11. Coefficients and Performance Summary for the Linearized Version of the 10-Term Dimensionally Consistent Model on the Natural Logarithm of H_C with 9 Coefficients Fit to the Trimmed Data Set

$\ln(H_C)$ Model Term	Coefficient Estimate	Coefficient Standard Deviation	t-value = Coeff/SD	p-value[a]	Full Data, 581 Tests[b] Modeling Data Statistic [$\ln(H_C)$]	Value
$\ln(b_0)$	1.566	–[c]	–	–	R^2	0.852
$\ln(D)$[c]	1.0	N/A	N/A	N/A	R^2 Adjusted (R^2_A)	0.850
$\ln[U^2/D(s-1)g]$	0.513	–	–	–	R^2 Predicted (R^2_P)	–[c]
$\ln(d/D)$	1.835	–	–	–	RMSE	0.242
$\ln(s-1)$	-0.296	–	–	–		
$\ln(U_T/U)$	-0.493	–	–	–		
$\ln(DC)$	0.352	–	–	–		
$\ln(\phi_S)$	-0.576	–	–	–		
$\ln(\phi_p)$	0.280	–	–	–		
$\ln(N_J)$	0.348	–	–	–		

(a) Probability that the coefficient is not statistically significant (different from 0). Values less than 0.05, 0.01, and 0.0001 indicate strong, very strong, and extremely strong statistical significance of the coefficient and corresponding model term.
(b) Model evaluation and validation statistics are defined, respectively, in Sections D.3 and D.5 of Appendix D.
(c) Not available from output of software used to fit the model using restricted least squares. These could be determined with additional work.
(d) Restricted least squares was used to fit this model, with the coefficient of ln(D) restricted to be 1.0.

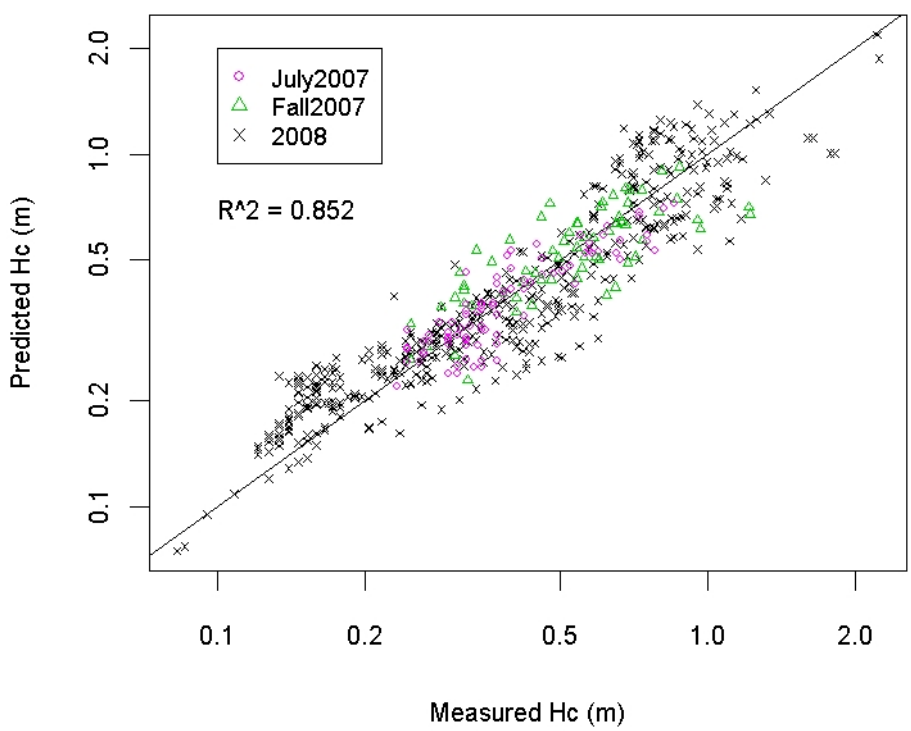

Figure F.12. Log-Log Plot of Predicted Versus Measured H_C (m) Values for 10-Term Dimensionally Consistent Model in Table F.11 with 9 Coefficients Fit to Trimmed Data Set. The 45-degree line represents perfect prediction where predicted H_C values equal measured H_C values.

In summary, inserting the coefficients from the H_C dimensionally consistent models fit to the full data set (Table F.10) into Eqs. (F.22a) and (F.22b) results in the models

$$H_C = 3.040\, D \left(\frac{U^2}{D(s-1)g}\right)^{0.473} \left(\frac{d}{D}\right)^{1.693} (s-1)^{-0.356} \left(\frac{U_T}{U}\right)^{-0.410} DC^{0.364} \times \phi_S^{-0.616} (1-\phi_s)^{-17.206}\, \phi_p^{0.213}\, N_J^{0.320} \tag{F.26a}$$

and

$$\ln(H_C) = 1.112 + \ln(D) + 0.473 \ln\left(\frac{U^2}{D(s-1)g}\right) + 1.693 \ln\left(\frac{d}{D}\right) - 0.356 \ln(s-1) - 0.410 \ln\left(\frac{U_T}{U}\right) + 0.364 \ln(DC) - 0.616 \ln(\phi_S) - 17.206 \ln(1-\phi_S) + 0.213 \ln(\phi_p) + 0.320 \ln(N_J) \tag{F.26b}$$

where all notation is as previously defined. The $(1-\phi_S)^{-17.206}$ and $-17.206 \ln(1-\phi_S)$ terms in Eqs. (F.26a) and (F.26b) are appropriate for the range of ϕ_S studied in M3 testing (0.0005 − 0.06). However, caution is advised if these H_C models must be extrapolated to ϕ_S values outside that range.

Inserting the coefficients from the H_C dimensionally consistent models fit to the trimmed data set (Table F.11) into Eqs. (F.22a) and (F.22b) results in the models

$$H_C = 4.787\, D \left(\frac{U^2}{D(s-1)g}\right)^{0.513} \left(\frac{d}{D}\right)^{1.835} (s-1)^{-0.296} \left(\frac{U_T}{U}\right)^{-0.493} DC^{0.352} \times \phi_S^{-0.576}\, \phi_p^{0.280}\, N_J^{0.348} \tag{F.27a}$$

and

$$\ln(H_C) = 1.566 + \ln(D) + 0.513 \ln\left(\frac{U^2}{D(s-1)g}\right) + 1.835 \ln\left(\frac{d}{D}\right) - 0.296 \ln(s-1) - 0.493 \ln\left(\frac{U_T}{U}\right) + 0.352 \ln(DC) - 0.576 \ln(\phi_S) + 0.280 \ln(\phi_p) + 0.348 \ln(N_J) \tag{F.27b}$$

where all notation is as previously defined.

F.3.5 Results for H_C Power-Law Models with Interaction Terms

As discussed in Section F.3.3, stepwise regression methods were used to add statistically significant interaction terms to the H_C models shown in Tables F.8 and F.9. The results are shown in Table F.12 and Figure F.13 for the full data set and in Table F.13 and Figure F.14 for the trimmed data set. Two interaction terms were added to each model, with both of them being highly statistically significant. The first interaction term added was the same for each model, but the second one is different. The difference is a result of the smaller test-variable space for the model fit to the trimmed data. All of the model terms shown in Tables F.12 and F.13 (except for the constant term in Table F.12) are highly statistically significant.

Table F.12. Coefficients and Performance Summary for the 13-Term Dimensional Model with Interactions on the Natural Logarithm of H_C Fit to the Full Data Set

$\ln(H_C)$ Model Term	Coefficient Estimate	Coefficient SD	t-value = Coeff/SD	p-value[(a)]	Full Data, 669 Data Points[(b)] Modeling Data Statistic [$\ln(H_C)$]	Value
$\ln(a_0)$	-0.467	0.228	-2.05	0.0409	R^2	0.861
$\ln(D)$	-0.820	0.095	-8.60	< 0.0001	R^2 Adjusted (R^2_A)	0.858
$\ln(s-1)$	-0.833	0.041	-20.13	< 0.0001	R^2 Predicted (R^2_P)	0.856
$\ln(\phi_S)$	-0.880	0.032	-27.76	< 0.0001	RMSE	0.234
$\ln(1-\phi_S)$	-59.975	6.098	-9.84	< 0.0001		
$\ln(U_T)$	-0.505	0.018	-27.49	< 0.0001		
$\ln(DC)$	0.434	0.033	13.13	< 0.0001		
$\ln(\phi_p)$	0.292	0.036	8.18	< 0.0001		
$\ln(N_J)$	0.497	0.047	10.53	< 0.0001		
$\ln(d)$	1.979	0.081	24.39	< 0.0001		
$\ln(U)$	1.731	0.070	24.79	< 0.0001		
$D \ln(\phi_S)$	0.153	0.013	11.42	< 0.0001		
$\phi_S \ln(U)$	-16.176	2.571	-6.29	< 0.0001		

(a) Probability that the coefficient is not statistically significant (different from 0). Values less than 0.05, 0.01, and 0.0001 indicate strong, very strong, and extremely strong statistical significance of the coefficient and corresponding model term.
(b) Model evaluation and validation statistics are defined, respectively, in Sections D.3 and D.5 of Appendix D.

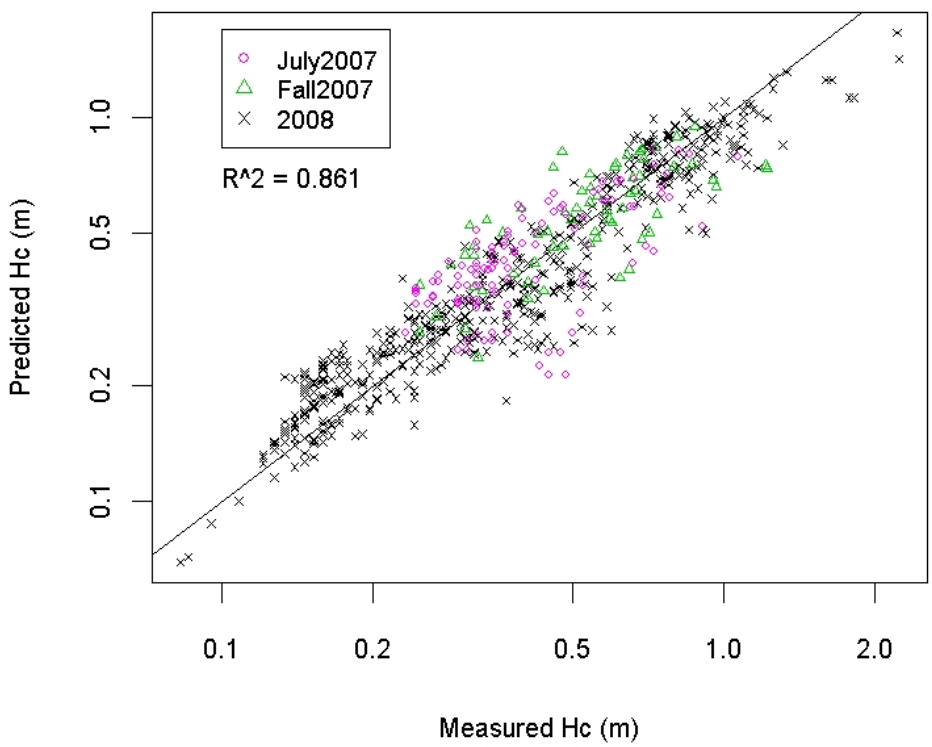

Figure F.13. Log-Log Plot of Predicted Versus Measured H_C Values for the 13-Term Dimensional Model with Interactions in Table F.12 Fit to the Full Data Set. The 45-degree line represents perfect prediction where predicted H_C values equal measured H_C values.

Table F.13. Coefficients and Performance Summary for the 12-Term Dimensional Model with Interactions on the Natural Logarithm of H_C Fit to the Trimmed Data Set

$\ln(H_C)$ Model Term	Coefficient Estimate	Coefficient SD	t-value = Coeff/SD	p-value[a]	Trimmed Data, 581 Data Points[b] Modeling Data Statistic [$\ln(H_C)$]	Value
$\ln(a_0)$	0.546	0.205	2.66	0.0080	R^2	0.884
ln(D)	-1.100	0.099	-11.07	< 0.0001	R^2 Adjusted (R^2_A)	0.882
ln(s−1)	-0.362	0.090	-4.01	< 0.0001	R^2 Predicted (R^2_P)	0.880
$\ln(\phi_S)$	-0.707	0.023	-30.39	< 0.0001	RMSE	0.214
$\ln(U_T)$	-0.579	0.019	-31.10	< 0.0001		
ln(DC)	0.402	0.035	11.55	< 0.0001		
$\ln(\phi_p)$	0.356	0.035	10.29	< 0.0001		
$\ln(N_J)$	0.470	0.044	10.59	< 0.0001		
ln(d)	2.088	0.083	25.16	< 0.0001		
ln(U)	1.848	0.071	25.99	< 0.0001		
D $\ln(\phi_S)$	0.124	0.012	10.10	< 0.0001		
U ln(s−1)	-0.050	0.009	-5.46	< 0.0001		

(a) Probability that the coefficient is not statistically significant (different from 0). Values less than 0.05, 0.01, and 0.0001 indicate strong, very strong, and extremely strong statistical significance of the coefficient and corresponding model term.
(b) Model evaluation and validation statistics are defined, respectively, in Sections D.3 and D.5 of Appendix D.

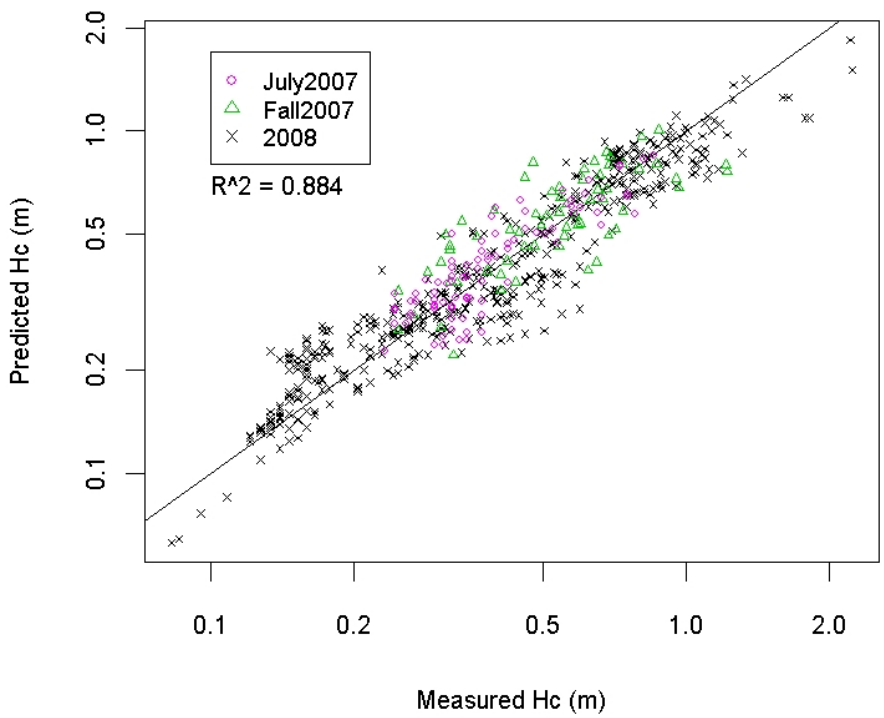

Figure F.14. Log-Log Plot of Predicted Versus Measured H_C Values for the 12-Term Dimensional Model with Interactions in Table F.13 Fit to the Trimmed Data Set. The 45-degree line represents perfect prediction where predicted H_C values equal measured H_C values.

All of the summary statistics for the dimensional models with interactions for H_C in Tables F.12 and F.13 show improvement over the corresponding results for dimensional models without interactions in Tables F.8 and F.9. The R^2 statistics in Table F.12 ($R^2 = 0.861$) and Table F.13 ($R^2 = 0.884$) indicate that the H_C dimensional models with interactions developed by stepwise selection fit the full and trimmed data sets reasonably well. Because the values of R^2_A and R^2_p in Tables F.12 and F.13 do not differ markedly from the corresponding R^2 values, there are no indications that the H_C models over-fit the data or that there are any highly influential data.

Figure F.13 shows a predicted-versus-measured plot for the performance of the 13-term H_C dimensional model with interactions in Table F.12. In Figure F.13, the scatter around the perfect prediction (45°) line has been slightly reduced from that in Figure F.9 for the 11-term H_C dimensional model without interactions in Table F.8. Figure F.14 shows that the predictions made for the trimmed data set are also improved when using the 12-term dimensional model with interactions compared to the 10-term dimensional model without interactions (Table F.9 and Figure F.10). The 12-term H_C dimensional models with interaction terms in Tables F.12 and F.13 have partially corrected the tendencies to overpredict H_C below ~ 0.2 and to underpredict in the approximate H_C range of 0.3 to 0.6 m, compared to the 11-term and 10-term H_C dimensional models without interaction terms in Tables F.8 and F.9. However, the dimensional models with interactions increase the tendency to underpredict H_C values above ~ 1 m.

Based on Table F.12, the H_C dimensional models with interactions fit to the full data set are

$$\begin{aligned} H_C &= 0.627\,(D)^{-0.820}(s-1)^{-0.833}(\phi_S)^{-0.880+0.153(D)}(1-\phi_S)^{-59.975}(U_T)^{-0.505} \\ &\quad \times (DC)^{0.434}(\phi_p)^{0.292}(N_J)^{0.497}(d)^{1.979}(U)^{1.731-16.176(\phi_S)} \end{aligned} \tag{F.28a}$$

and

$$\begin{aligned} \ln(H_C) &= -0.467 - 0.820\ln(D) - 0.833\ln(s-1) + [-0.880 + 0.153(D)]\ln(\phi_S) \\ &\quad - 59.975\ln(1-\phi_S) - 0.505\ln(U_T) + 0.434\ln(DC) + 0.292\ln(\phi_p) \\ &\quad + 0.497\ln(N_J) + 1.979\ln(d) + [1.731 - 16.176(\phi_S)]\ln(U)\,, \end{aligned} \tag{F.28b}$$

where all notation is as previously defined. Based on Table F.13, the H_C dimensional models with interactions fit to the trimmed data set are

$$\begin{aligned} H_C &= 1.726\,(D)^{-1.100}(s-1)^{-0.362-0.050\,(U)}(\phi_S)^{-0.707+0.124\,(D)}(U_T)^{-0.579} \\ &\quad \times (DC)^{0.402}(\phi_p)^{0.356}(N_J)^{0.470}(d)^{2.088}(U)^{1.848} \end{aligned} \tag{F.29a}$$

and

$$\begin{aligned} \ln(H_C) &= 0.546 - 1.100\ln(D) + [-0.362 - 0.050\,U]\ln(s-1) \\ &\quad + [-0.707 + 0.124(D)]\ln(\phi_S) - 0.579\ln(U_T) + 0.402\ln(DC) \\ &\quad + 0.356\ln(\phi_p) + 0.470\ln(N_J) + 2.088\ln(d) + 1.848\ln(U)\,, \end{aligned} \tag{F.29b}$$

where all notation is as previously defined.

Similarly as discussed for U_{CS} at the end of Section F.2.3, the H_C models with interaction terms may yield inaccurate predictions when extrapolated outside the experimental region of data used to develop them. Hence, unless additional work is performed to thoroughly validate these H_C models for extrapolative use, it is recommended that they only be used for interpolative use.

F.3.6 Comparison of H_C Models

In this section the results for three H_C models presented in Section F.3, namely the

- dimensional model without interactions (Section F.3.4.2)

- corresponding dimensionally consistent model (Section F.3.4.3)
- dimensional model with interactions (Section F.3.5)

are compared to the results of the nondimensional model for H_C from Section 7.3.2. Because the latter model was only fit using the full data set, the comparisons are based on that data.

Figure F.15 shows the predicted-versus-measured plot and R^2 [calculating using $\ln(H_C)$ values] for the nondimensional H_C model from Section 7.3.2. Figure F.15 shows that the nondimensional model tends to underpredict H_C (sometimes significantly) for the Fall 2007 data. The model also tends to underpredict $H_C < \sim 0.35$ m for the July 2007 data.

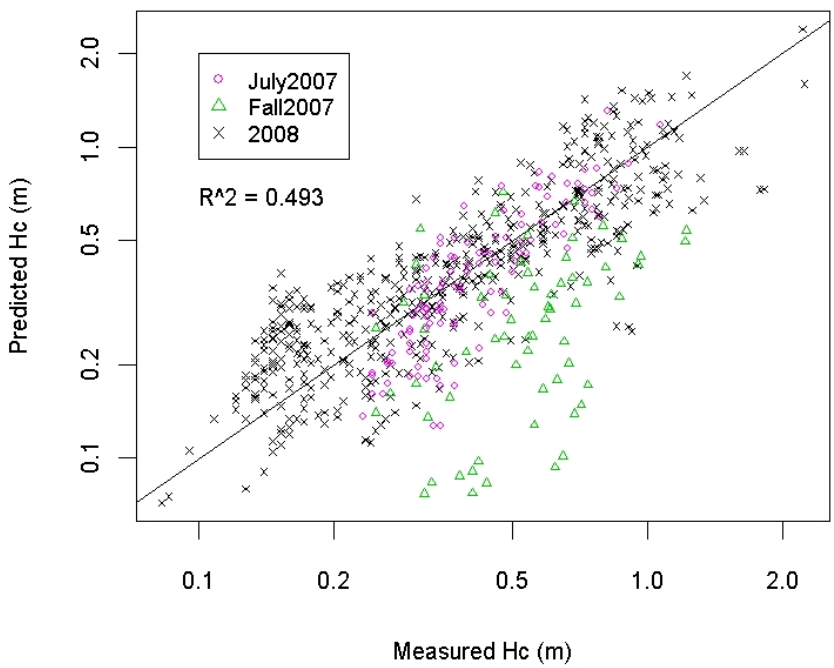

Figure F.15. Log-Log Plot of Predicted Versus Measured H_C (m/s) Values for the Nondimensional Model from Section 7.3.2 Developed Using the Full Data Set. The 45-degree line represents perfect prediction where predicted H_C values equal measured H_C values.

The goodness-of-fit of the nondimensional model (Figure F.15, $R^2 = 0.493$) can be compared to the dimensional model without interactions (Figure F.9, $R^2 = 0.830$), the dimensionally consistent model (Figure F.11, $R^2 = 0.830$), and the dimensional model with interactions (Figure F.13, $R^2 = 0.861$). The nondimensional model (from Section 7.3.2) is seen to predict significantly worse for the full data set than the other models (discussed in Section F.3). In addition to the observations made in the last paragraph, it is also noted that the nondimensional model produces considerably more scatter around the line of perfect prediction (Figure F.15) compared to the plots for the Appendix F.3 models (Figures F.9, F.11, and F.13).

Table F.14 compares the coefficients of several H_C models fitted using the full data set when the models are expressed in the dimensional form of Eq. (F.21a). The H_C models compared this way include:

- 11-term dimensional model without interactions, with 11 fitted coefficients
- 11-term dimensionally consistent model, with 10 fitted coefficients
- nondimensional model from Section 7.3.2, with 4 fitted coefficients.

Some variables in the nondimensional model cannot be expressed in power-law form, and hence it was not possible to calculate all coefficients in the form of Eq. (F.21a) for that model. The 13-term dimensional model with interactions (with 13 fitted coefficients) is not included in Table F.14, because the values of coefficients containing interactions depend on the variables involved in the interactions.

Table F.14 shows that the coefficients of the dimensional and dimensionally consistent H_C models expressed in dimensional form are very similar because the dimensional model is very close to dimensionally consistent without being forced to be so. Because of the mathematical form of the nondimensional model in Section 7.3.2, it was not possible to express several of its terms in power-law form and calculate coefficients for an equivalent model written in dimensional form. For the predictor variables where possible, the coefficients in the nondimensional model are noticeably different than these for the other two models. The coefficient for D (which controls the scale effect) in the nondimensional model is much different than the other two models, likely because the nondimensional model for H_C does not explicitly include a D term with a separately estimable coefficient (i.e., D appeared only within a nondimensional variable expressed as a function of several test variables, with only one coefficient for the nondimensional variable).

Table F.14. Coefficients of H_C Models Fit to Full Data Set Expressed in the Dimensional Form of Equation (F.21a)

Model Terms	Dimensional H_C Model w/o Interactions [Eq. (F.24a)]	Dimensionally Consistent H_C Model w/o Interactions [Eqs. (F.23) & (F.26a)]	Nondimensional H_C Model from Section 7.3.2
a_0	1.079	1.033	(a)
D (a_1)	-1.191	-1.166	-3.428
s−1 (a_2)	-0.836	-0.829	(a)
ϕ_S (a_3)	-0.623	-0.616	(a)
$1-\phi_S$ (a_{14})	-17.502	-17.206	–[(b)]
U_T (a_6)	-0.412	-0.410	(a)
DC (a_7)	0.371	0.364	1
ϕ_p (a_8)	0.218	0.213	0.698
N_J (a_{10})	0.330	0.320	1.714
d (a_{11})	1.722	1.693	3.428
U (a_{12})	1.378	1.356	(a)
$1-\phi_S$ /0.5	–	–	(a)
R^2	0.830	0.830	0.493

(a) Not expressible as a term in a power-law model.
(b) A dash (–) indicates the term is not included in the model.

F.4 Illustration of U_{CS} and H_C Model Application and Uncertainty Calculations

This section contains examples to illustrate applying selected models to obtain predicted U_{CS} and H_C values for a specific set of the eight predictor variables D, s, ϕ_S, U_T, DC, ϕ_p, N_J, d (for U_{CS} and H_C models) and a ninth predictor variable U (for H_C models). The examples also illustrate the application of statistical intervals to calculate uncertainties of predicted U_{CS} and H_C values. The formulas for calculating several kinds of statistical intervals are given in Section D.6 of Appendix D. In this section, the formulas for two-sided 95% confidence intervals (CIs) and 95% simultaneous confidence intervals (SCIs) are

illustrated. The 95% confidence level was chosen for illustrative purposes only. Other appropriate confidence levels, or other kinds of statistical intervals (e.g., prediction intervals), can be used depending on the application of the U_{CS} and H_C models.

The U_{CS} models selected to illustrate prediction and uncertainty calculations are the 1) 9-term dimensional model without interactions presented in Eq. (F.11b) and Table F.1, and 2) 12-term dimensional model with interactions shown in Eq. (F.15b) and Table F.5. These models were developed using the full data set for U_{CS}. The H_C models selected to illustrate prediction and uncertainty calculations are the 1) 11-term dimensional model without interactions presented in Eq. (F.24b) and Table F.8, and 2) 13-term dimensional model with interactions shown in Eq. (F.28b) and Table F.12. These models were developed using the full data set for H_C. The dimensionally consistent models for U_{CS} and H_C are not included in the example calculations because the more complicated equations for calculating prediction uncertainty and statistical intervals were not available in the software used. There was insufficient time to find and program these equations into special-purpose software.

Values for the predictor variables chosen to illustrate the application of the U_{CS} and H_C models are shown in Table F.15. To apply the U_{CS} and H_C models to this set of predictor variable values, the relevant values of the predictor variables must be used to form the terms of the particular models. These values are shown in Table F.16 for each of the models.

Table F.15. Values of Predictor Variables Selected to Illustrate Application of Models Fit to the Full Data Sets for U_{CS} and H_C

Variable	Measured Value	Natural Log of Measured Value
D	1.7780	0.5755
(s − 1)	3.18	1.1569
ϕ_S	0.005	-5.2983
U_T	0.0085	-4.7725
DC	0.2367	-1.4408
ϕ_P	0.0501	-2.9942
N_J	12	2.4849
d	0.0234	-3.7564
U	7.5	2.0149

For each of the U_{CS} and H_C models, predicted $\ln(U_{CS})$ and $\ln(H_C)$ values are obtained by multiplying the predictor variable values in the format needed for the specific model (from Table F.16) by the coefficients for that model, then summing the results. The coefficients for the 9- and 12-term U_{CS} dimensional models without and with interactions are given in Tables F.1 and F.5, respectively. The coefficients for the 11- and the 13-term H_C models without and with interaction are given in Tables F.8 and F.12, respectively. Using vector notation, the predicted values are calculated by

$$\hat{y}\,(\mathbf{a}) = \mathbf{a}^T\mathbf{b} \tag{F.30}$$

where $\hat{y}\,(\mathbf{a})$ is the predicted value of $\ln(U_{CS})$ or $\ln(H_C)$, **a** is a vector of values from Table F.16 chosen to match the terms in a given model, the superscript T represents a vector transpose, and **b** is the vector of coefficients for a given model.

Table F.16. Predictor Variable Values in Formats Needed to Illustrate Use of Models Fit to the Full Data Sets for U_{CS} and H_C

	Values Needed for Model			
Model Term	9-Term U_{CS} Eq. (F.11b) Table F.1	12-Term U_{CS} Eq. (F.15b) Table F.5	11-Term H_C Eq. (F.24b) Table F.8	13-Term H_C Eq. (F.28b) Table F.12
ln(D)	0.5755	0.5755	0.5755	0.5755
ln(s−1)	1.1569	1.1569	1.1569	1.1569
$\ln(\phi_S)$	-5.2983	-5.2983	-5.2983	-5.2983
$\ln(1-\phi_S)$	–[(a)]	–	-0.0050	-0.0050
$\ln(U_T)$	-4.7725	-4.7725	-4.7725	-4.7725
ln(DC)	-1.4408	-1.4408	-1.4408	-1.4408
$\ln(\phi_p)$	-2.9937	-2.9937	-2.9937	-2.9937
$\ln(N_J)$	2.4849	2.4849	2.4849	2.4849
ln(d)	-3.7564	-3.7564	-3.7564	-3.7564
ln(U)	–	–	2.0149	2.0149
D ln(DC)	–	-2.5617	–	–
DC $\ln(U_T)$	–	-1.1297	–	–
$\phi_S \ln(U_T)$	–	-0.0239	–	–
D $\ln(\phi_S)$	–	–	–	-9.4204
$\phi_S \ln(U)$	–	–	–	0.0101

(a) A "–" indicates the term is not included in the model.

The predicted $\ln(U_{CS})$ and $\ln(H_C)$ values from each model are listed in the third columns of Tables F.17 and F.18, respectively. The predicted $\ln(U_{CS})$ in ln(m/s) units are easily converted to U_{CS} units of m/s by exponentiation. Similarly, the predicted $\ln(H_C)$ in ln(m) units can be converted to H_C units of m by exponentiation. Column 4 of Tables F.17 and F.18 contain the predicted U_{CS} value in m/s and the predicted H_C value in m, respectively, for the selected set of predictor variable values. As discussed in Section D.6.5 of Appendix D, these back-transformed U_{CS} and H_C predictions in m/s and m units, respectively, have a particular interpretation. They should be considered estimates of the true medians (not the true means) of the distributions of U_{CS} and H_C values that would result if the test were repeated multiple times by independently resetting the values of the predictor variables (in Table F.15) each time.

Equation (D.19a) in Appendix D can be used to calculate a two-sided CL% CI for the true mean of $\ln(U_{CS})$ or $\ln(H_C)$ employing the predictor variable values selected for this example. For the illustrations to follow, we use CL% = 95%. In the notation of Eq. (D.19a),

- CL% = $100(1-\alpha)\%$ = 95%, so $\alpha = 0.05$
- Vector **a** contains entries corresponding to the terms in a given U_{CS} or H_C model, which are calculated using the set of predictor variable values in Tables F.15 and F.16
- Matrix **A** is formed from the data matrix used in the regression that generated a given U_{CS} or H_C model. Matrix **A** has the number of rows in the U_{CS} or H_C full modeling data set (173 and 669, respectively) and the number of columns corresponding to the number of terms in a given U_{CS} dimensional model (9 or 12) or H_C dimensional model (11 and 13). Each column is calculated according to the corresponding term in the model using the U_{CS} or H_C full data sets.

To simplify the calculations, the first expression in Equation (D.19a) is used to calculate a 95% CI on $\ln(U_{CS})$ in units of ln(m/s) or $\ln(H_C)$ in units of ln(m). The $\mathbf{C}_U$ portion of Eq. (D.19a) is the variance-covariance matrix for the estimated model coefficients. The variance-covariance matrices for the 9- and 12-term U_{CS} dimensional models without and with interactions used in the illustrative example are listed in Tables F.19 and F.20, respectively. The variance-covariance matrices for the 11- and 13-term H_C dimensional models without and with interactions used in the illustrative example are listed in Tables F.21 and F.22, respectively. The quantity $\sqrt{\mathbf{a}^T\mathbf{C}_U\mathbf{a}}$ is the standard deviation of a model prediction considered as a mean value. The value of this quantity for each model applied to the set of predictor variable values in Table F.16 is given in the fifth column of Table F.17 for U_{CS} and the fifth column of Table F.18 for H_C.

The 95% CI values for the true mean $\ln(U_{CS})$ in units of ln(m/s) for the set of predictor-variable values in Table F.15, based on the 9- and 12-term $\ln(U_{CS})$ models, are given in the sixth column of Table F.17. Similarly, the 95% CI values for the true mean $\ln(H_C)$ in units of ln(m) for the set of predictor-variable values in Table F.15, based on the 11- and 13-term $\ln(H_C)$ models, are given in the sixth column of Table F.18. Exponentiating the resulting 95% CIs on the true mean value in ln(m/s) or ln(m) units yields 95% CIs for the true median in m/s or m, respectively. For example, the 12-term model for U_{CS} has 2.0536 ln(m/s) as the upper limit of the 95% CI on the true mean $\ln(U_{CS})$ for the predictor-variable values shown in Table F.15. Then $e^{2.0536} = 7.796$ m/s is the upper limit of the 95% CI on the true median U_{CS} value at the set of predictor-variable values in Table F.15. The seventh column of Table F.17 contains 95% CIs for the true median U_{CS} value for the set of predictor-variable values selected. Similarly, the seventh column in Table F.18 contains 95% CIs for the true median H_C value for the set of predictor-variable values selected.

As discussed in Section D.6.4 of Appendix D, there are times when a CL% simultaneous confidence interval (CL% SCI) may be preferred rather than a CL% CI. This is particularly true when a regression model (U_{CS} or H_C) is to be used a large number of times for various sets of predictor-variable values from the model validity region. Equation (D.21a) in Appendix D can be used to calculate a 95% SCI for the true mean of $\ln(U_{CS})$ or the true mean of $\ln(H_C)$ for multiple sets of predictor-variable values in the model validity region. The resulting 95% SCIs for those sets of predictor-variable values simultaneously have 95% confidence for containing their true mean values.

The 95% SCI values for the true mean $\ln(U_{CS})$ in units of ln(m/s) for the set of predictor-variable values in Table F.15, based on the 9- and 12-term $\ln(U_{CS})$ models, are given in the eighth column of Table F.17. Similarly, the 95% SCI values for the true mean $\ln(H_C)$ in units of ln(m) for the set of predictor-variable values in Table F.15, based on the 11- and 13-term $\ln(H_C)$ models, are given in the eighth column of Table F.18. Exponentiating the resulting 95% SCIs for the mean in ln(m/s) and ln(m) units yields 95% SCIs for the median in m/s (for U_{CS}) or m (for H_C) units. Column nine of Table F.17 contains 95% SCIs for the true median U_{CS} value for the set of predictor-variable values using the two $\ln(U_{CS})$ models. Similarly, column nine of Table F.18 contains 95% SCIs for the true median H_C value for the set of predictor-variable values based on the two $\ln(H_C)$ models chosen for illustration. The 95% SCIs are larger than the corresponding 95% CIs because of the simultaneous-confidence protection for multiple uses of the same model.

The uncertainties in model predictions of U_{CS} and H_C illustrated in Tables F.17 and F.18 include only the uncertainties associated with fitting measured U_{CS} and H_C values in the full data set to the U_{CS} and H_C

models considered. The calculations for the 95% CIs and 95% SCIs do not include the uncertainties associated with the predictor-variable values (in Tables F.15 and F.16) substituted into the models. Predictor-variable uncertainties can be propagated through the models, and combined with model uncertainties, to obtain combined estimates of uncertainties (referred to as combined-confidence intervals) for U_{CS} and H_C predictions. This work was beyond the current scope, but could be performed in the future if desired. In the meantime, the interested reader is referred to Piepel et al. (2005) for extensive discussion, formulas, and applications of combined-confidence intervals.

The uncertainties in model predictions of U_{CS} and H_C models illustrated in Tables F.17 and F.18 do not include any additional uncertainties associated with extrapolating. The statistical formulas for CIs and SCIs include larger uncertainties when models are extrapolated, under the assumption the model form is correct both within the experimental region and outside that region where extrapolation is required. Thus, the extent to which a model form may be inappropriate for extrapolation is not accounted for in the statistical formulas for CIs and SCIs. Additional uncertainties or "margins" based on subject-matter knowledge and judgment must be used to account for uncertainties associated with any possible inadequacy of models for extrapolation.

As noted previously, it was not possible at this time to include in Tables F.17 and F.18 the example calculations for the dimensionally consistent models fitted to the full data set for U_{CS} (Table F.3) and H_C (Table F.10). However, the fits of those models to the full data sets are close (U_{CS}) and very close (H_C) to the fits of the corresponding dimensional models. Hence, the uncertainty calculations (i.e., predicted standard deviations and statistical intervals) for the dimensionally consistent models should be similar to the uncertainties for the dimensional models.

Table F.17. Predicted U_{CS} and Corresponding 95% CIs and 95% SCIs Using Models Fit to the Full Data Set Applied to the Experimental Set of Conditions Shown in Tables F.15 and F.16

Response	Model	Predicted $\ln(U_{VS})$ [ln(m/s)]	Predicted U_{CS}[a] [m/s]	SD of Predicted $\ln(U_{CS})$[b] [ln(m/s)]	95% CI on Mean $\ln(U_{CS})$ [ln(m/s)]	95% CI on Median U_{CS} [m/s]	95% SCI on Mean $\ln(U_{CS})$ [ln(m/s)]	95% SCI on Median U_{CS} [m/s]
U_{CS}	9-Term Model Table F.1	1.9594[c]	7.095	0.0367	[1.8869, 2.0319]	[6.599, 7.628]	[1.8062, 2.1126]	[6.087, 8.270]
	12-Term Model Table F.5	1.9930	7.338	0.0317	[1.9304, 2.0556]	[6.892, 7.812]	[1.8452, 2.1408]	[6.329, 8.507]

(a) For comparison purposes, the measured U_{CS} (in m/s) for the selected experiment is 7.5 m/s.
(b) The standard deviations are for the $\ln(U_{CS})$ predictions considered to be the mean of such values for the experimental conditions selected.
(c) All calculations were performed using the experimental conditions, model coefficients, and variance-covariance matrix values given in tables of this report. The calculated ln(m/s) values were rounded to four decimal places in this table. The m/s values were calculated by exponentiating the corresponding ln(m/s) values before rounding, then rounding the resulting values to three decimal places in this table.

Table F.18. Predicted H_C and Corresponding 95% CIs and 95% SCIs Using Models Fit to the Full Data Set Applied to the Experimental Set of Conditions Shown in Tables F.15 and F.16

Response	Model	Predicted $\ln(H_C)$ [ln(m)]	Predicted H_C[a] [m]	SD of Predicted $\ln(H_C)$[b] [ln(m)]	95% CI on Mean $\ln(H_C)$ [ln(m)]	95% CI on Median H_C [m]	95% SCI on Mean $\ln(H_C)$ [ln(m)]	95% SCI on Median H_C [m]
H_C	11-Term Model Table F.8	-0.2811[c]	0.755	0.0391	[-0.3579, -0.2043]	[0.699, 0.815]	[-0.4552, -0.1070]	[0.634, 0.899]
	13-Term Model Table F.12	-0.3454	0.708	0.0366	[-0.4173, -0.2735]	[0.659, 0.761]	[-0.5192, -0.1716]	[0.595, 0.842]

(a) For comparison purposes, the measured H_C for the selected experiment is 0.610 m.
(b) The standard deviations are for the $\ln(H_C)$ predictions considered to be the mean of such values for the experimental conditions selected.
(c) All calculations were performed using the experimental conditions, model coefficients, and variance-covariance matrix values given in tables of this report. The calculated ln(m) values were rounded to four decimal places in this table. The m values were calculated by exponentiating the corresponding ln(m) values before rounding, then rounding the resulting values to three decimal places in this table.

Table F.19. Variance-Covariance Matrix for the 9-Term $\ln(U_{CS})$ Model in Table F.1. The form of the variance-covariance matrix is presented in Eq. (D.17a) of Appendix D.

Term	$\ln(a_0)$	ln(D)	ln(s−1)	$\ln(\phi_S)$	$\ln(U_T)$	ln(DC)	$\ln(\phi_p)$	$\ln(N_J)$	ln(d)
$\ln(a_0)$	5.5867E-02	-7.0942E-03	6.1780E-04	7.9473E-04	1.5499E-03	1.3256E-03	2.3676E-03	2.5754E-04	7.9282E-03
ln(D)	-7.0942E-03	2.1144E-03	-1.0798E-04	4.4413E-06	1.3907E-05	1.0371E-04	8.0392E-05	-6.5097E-04	-1.9821E-03
ln(s − 1)	6.1780E-04	-1.0798E-04	1.4103E-03	1.0675E-05	-9.3703E-05	-7.5404E-05	1.3929E-04	-2.6554E-04	1.7822E-04
$\ln(\phi_S)$	7.9473E-04	4.4413E-06	1.0675E-05	1.3212E-04	3.7488E-05	-6.9818E-06	-5.4548E-05	-5.5424E-06	1.9858E-05
$\ln(U_T)$	1.5499E-03	1.3907E-05	-9.3703E-05	3.7488E-05	2.2314E-04	7.2970E-05	8.8712E-05	3.9990E-05	-6.2132E-06
ln(DC)	1.3256E-03	1.0371E-04	-7.5404E-05	-6.9818E-06	7.2970E-05	9.6501E-04	-1.0773E-04	-1.3120E-04	-5.4146E-05
$\ln(\phi_p)$	2.3676E-03	8.0392E-05	1.3929E-04	-5.4548E-05	8.8712E-05	-1.0773E-04	1.0249E-03	-8.2807E-05	-1.4503E-04
$\ln(N_J)$	2.5754E-04	-6.5097E-04	-2.6554E-04	-5.5424E-06	3.9990E-05	-1.3120E-04	-8.2807E-05	1.1684E-03	6.5999E-04
ln(d)	7.9282E-03	-1.9821E-03	1.7822E-04	1.9858E-05	-6.2132E-06	-5.4146E-05	-1.4503E-04	6.5999E-04	2.1518E-03

Table F.20. Variance-Covariance Matrix for 12-Term $\ln(U_{CS})$ Model in Table F.5. The form of the variance-covariance matrix is presented in Eq. (D.17a) of Appendix D.

Term	$\ln(a_0)$	ln(D)	ln(s−1)	$\ln(\phi_S)$	$\ln(U_T)$	ln(DC)	$\ln(\phi_p)$	$\ln(N_J)$	ln(d)	DC $\ln(U_T)$	D ln(DC)	$\phi_S \ln(U_T)$
$\ln(a_0)$	5.2513E-02	-4.2318E-03	2.5304E-04	1.3569E-03	-5.6816E-04	8.1916E-03	1.9385E-03	3.5809E-04	5.3144E-03	4.9797E-03	4.8354E-04	1.5924E-02
ln(D)	-4.2318E-03	2.8229E-03	1.5716E-04	1.1272E-05	-3.1212E-04	-6.5651E-04	1.7774E-04	-2.5884E-04	-1.2435E-03	4.9876E-04	1.4026E-03	-5.8419E-04
ln(s−1)	2.5304E-04	1.5716E-04	1.0771E-03	4.6349E-05	-8.0130E-05	-5.2108E-04	1.0700E-04	-1.3913E-04	1.5817E-04	-1.1637E-04	2.6922E-04	9.2838E-04
$\ln(\phi_S)$	1.3569E-03	1.1272E-05	4.6349E-05	2.7926E-04	-5.9619E-05	1.7355E-04	-4.5854E-05	3.4862E-05	-3.1679E-05	1.1604E-04	1.0074E-05	4.4313E-03
$\ln(U_T)$	-5.6816E-04	-3.1212E-04	-8.0130E-05	-5.9619E-05	4.1342E-04	-7.1097E-04	1.0375E-05	-2.4799E-05	3.9267E-06	-6.9289E-04	-2.9545E-04	-1.5566E-03
ln(DC)	8.1916E-03	-6.5651E-04	-5.2108E-04	1.7355E-04	-7.1097E-04	6.5950E-03	1.5480E-05	-2.5241E-04	-3.4425E-04	3.0644E-03	-1.0665E-03	2.7320E-03
$\ln(\phi_p)$	1.9385E-03	1.7774E-04	1.0700E-04	-4.5854E-05	1.0375E-05	1.5480E-05	7.4459E-04	-4.4438E-05	-9.1289E-05	1.4167E-04	1.1888E-04	-3.0264E-04
$\ln(N_J)$	3.5809E-04	-2.5884E-04	-1.3913E-04	3.4862E-05	-2.4799E-05	-2.5241E-04	-4.4438E-05	8.7029E-04	4.8734E-04	4.8972E-05	2.2106E-04	8.3928E-04
ln(d)	5.3144E-03	-1.2435E-03	1.5817E-04	-3.1679E-05	3.9267E-06	-3.4425E-04	-9.1289E-05	4.8734E-04	1.5661E-03	-6.8671E-05	1.8356E-04	-1.1300E-03
DC $\ln(U_T)$	4.9797E-03	4.9876E-04	-1.1637E-04	1.1604E-04	-6.9289E-04	3.0644E-03	1.4167E-04	4.8972E-05	-6.8671E-05	2.2146E-03	3.5311E-04	1.2884E-03
D ln(DC)	4.8354E-04	1.4026E-03	2.6922E-04	1.0074E-05	-2.9545E-04	-1.0665E-03	1.1888E-04	2.2106E-04	1.8356E-04	3.5311E-04	1.5054E-03	-4.7733E-04
$\phi_S \ln(U_T)$	1.5924E-02	-5.8419E-04	9.2838E-04	4.4313E-03	-1.5566E-03	2.7320E-03	-3.0264E-04	8.3928E-04	-1.1300E-03	1.2884E-03	-4.7733E-04	1.0709E-01

Table F.21. Variance-Covariance Matrix for 11-Term $\ln(H_C)$ Model in Table F.8. The form of the variance-covariance matrix is presented in Eq. (D.17a) of Appendix D.

Term	$\ln(a_0)$	ln(D)	ln(s−1)	$\ln(\phi_S)$	$\ln(1-\phi_S)$	$\ln(U_T)$	ln(DC)	$\ln(\phi_p)$	$\ln(N_J)$	ln(d)	ln(U)
$\ln(a_0)$	5.2319E-02	-1.0373E-02	-2.5070E-04	2.6905E-04	5.1104E-02	3.2619E-04	2.4156E-03	3.1577E-03	1.8299E-03	1.0274E-02	3.4980E-03
ln(D)	-1.0373E-02	9.3579E-03	2.1857E-03	1.6053E-03	2.6539E-02	1.1292E-03	-1.2832E-03	-8.8770E-04	-3.3652E-03	-8.1657E-03	-5.5499E-03
ln(s−1)	-2.5070E-04	2.1857E-03	2.0823E-03	5.9219E-04	1.4325E-02	2.7879E-04	-4.3658E-04	-3.1116E-04	-9.2726E-04	-1.7203E-03	-1.8048E-03
$\ln(\phi_S)$	2.6905E-04	1.6053E-03	5.9219E-04	6.6120E-04	2.9032E-02	2.3849E-04	-2.5030E-04	-2.9795E-04	-5.0207E-04	-1.4151E-03	-1.1953E-03
$\ln(1-\phi_S)$	5.1104E-02	2.6539E-02	1.4325E-02	2.9032E-02	2.6307E+00	1.1036E-03	-1.7228E-03	-7.5786E-03	-3.2093E-03	-2.9932E-02	-1.8609E-02
$\ln(U_T)$	3.2619E-04	1.1292E-03	2.7879E-04	2.3849E-04	1.1036E-03	3.3690E-04	-1.3124E-04	-9.8969E-05	-4.1674E-04	-9.7981E-04	-8.3773E-04
ln(DC)	2.4156E-03	-1.2832E-03	-4.3658E-04	-2.5030E-04	-1.7228E-03	-1.3124E-04	1.2902E-03	1.0281E-04	4.1621E-04	1.1149E-03	1.0281E-03
$\ln(\phi_p)$	3.1577E-03	-8.8770E-04	-3.1116E-04	-2.9795E-04	-7.5786E-03	-9.8969E-05	1.0281E-04	1.4940E-03	3.9853E-04	7.0285E-04	8.7819E-04
$\ln(N_J)$	1.8299E-03	-3.3652E-03	-9.2726E-04	-5.0207E-04	-3.2093E-03	-4.1674E-04	4.1621E-04	3.9853E-04	2.4521E-03	2.9864E-03	1.9229E-03
ln(d)	1.0274E-02	-8.1657E-03	-1.7203E-03	-1.4151E-03	-2.9932E-02	-9.7981E-04	1.1149E-03	7.0285E-04	2.9864E-03	7.4437E-03	4.7467E-03
ln(U)	3.4980E-03	-5.5499E-03	-1.8048E-03	-1.1953E-03	-1.8609E-02	-8.3773E-04	1.0281E-03	8.7819E-04	1.9229E-03	4.7467E-03	4.3154E-03

Table F.22. Variance-Covariance Matrix for 13-Term $\ln(H_C)$ Model in Table F.12. The form of variance-covariance matrix is presented in Eq. (D.17a) of Appendix D.

Term	$\ln(a_0)$	$\ln(D)$	$\ln(s-1)$	$\ln(\phi_S)$	$\ln(1-\phi_S)$	$\ln(U_T)$	$\ln(DC)$	$\ln(\phi_p)$
$\ln(a_0)$	5.2051E-02	-8.0973E-03	-3.2772E-04	1.3978E-03	5.9953E-01	5.2256E-04	1.8925E-03	2.5316E-03
$\ln(D)$	-8.0973E-03	9.1078E-03	1.7744E-03	7.1523E-04	1.6117E-02	6.6759E-04	-8.5565E-04	-4.8328E-04
$\ln(s-1)$	-3.2772E-04	1.7744E-03	1.7127E-03	4.7812E-04	4.6373E-03	2.2869E-04	-3.5974E-04	-2.5760E-04
$\ln(\phi_S)$	1.3978E-03	7.1523E-04	4.7812E-04	1.0064E-03	1.1125E-01	3.5717E-04	-3.1322E-04	-3.7026E-04
$\ln(1-\phi_S)$	5.9953E-01	1.6117E-02	4.6373E-03	1.1125E-01	3.7183E+01	2.2764E-02	-1.1710E-02	-1.5768E-02
$\ln(U_T)$	5.2256E-04	6.6759E-04	2.2869E-04	3.5717E-04	2.2764E-02	3.3689E-04	-1.4990E-04	-1.3152E-04
$\ln(DC)$	1.8925E-03	-8.5565E-04	-3.5974E-04	-3.1322E-04	-1.1710E-02	-1.4990E-04	1.0905E-03	1.2123E-04
$\ln(\phi_p)$	2.5316E-03	-4.8328E-04	-2.5760E-04	-3.7026E-04	-1.5768E-02	-1.3152E-04	1.2123E-04	1.2723E-03
$\ln(N_J)$	5.1907E-04	-2.4291E-03	-7.5291E-04	-7.2028E-04	-7.1897E-02	-4.4437E-04	4.0741E-04	4.0229E-04
$\ln(d)$	7.2169E-03	-6.1183E-03	-1.4043E-03	-1.6271E-03	-1.1470E-01	-9.6555E-04	1.0225E-03	7.0139E-04
$\ln(U)$	-2.7550E-04	-4.1280E-03	-1.4470E-03	-1.6641E-03	-2.2223E-01	-8.8954E-04	9.6086E-04	8.4660E-04
$D \ln(\phi_S)$	-2.1991E-04	4.8177E-04	-2.5513E-06	-2.6032E-04	-2.4736E-02	-1.0189E-04	7.3623E-05	8.9114E-05
$\phi_S \ln(U)$	2.4443E-01	6.1376E-03	-3.2233E-03	3.4247E-02	1.5157E+01	7.9033E-03	-3.2611E-03	-2.6466E-03

Term	$\ln(N_J)$	$\ln(d)$	$\ln(U)$	$D \ln(\phi_S)$	$\phi_S \ln(U)$
$\ln(a_0)$	5.1907E-04	7.2169E-03	-2.7550E-04	-2.1991E-04	2.4443E-01
$\ln(D)$	-2.4291E-03	-6.1183E-03	-4.1280E-03	4.8177E-04	6.1376E-03
$\ln(s-1)$	-7.5291E-04	-1.4043E-03	-1.4470E-03	-2.5513E-06	-3.2233E-03
$\ln(\phi_S)$	-7.2028E-04	-1.6271E-03	-1.6641E-03	-2.6032E-04	3.4247E-02
$\ln(1-\phi_S)$	-7.1897E-02	-1.1470E-01	-2.2223E-01	-2.4736E-02	1.5157E+01
$\ln(U_T)$	-4.4437E-04	-9.6555E-04	-8.8954E-04	-1.0189E-04	7.9033E-03
$\ln(DC)$	4.0741E-04	1.0225E-03	9.6086E-04	7.3623E-05	-3.2611E-03
$\ln(\phi_p)$	4.0229E-04	7.0139E-04	8.4660E-04	8.9114E-05	-2.6466E-03
$\ln(N_J)$	2.2260E-03	2.7638E-03	2.0803E-03	1.5828E-04	-2.8007E-02
$\ln(d)$	2.7638E-03	6.5819E-03	4.5943E-03	2.5777E-04	-3.5504E-02
$\ln(U)$	2.0803E-03	4.5943E-03	4.8804E-03	2.8035E-04	-8.7147E-02
$D \ln(\phi_S)$	1.5828E-04	2.5777E-04	2.8035E-04	1.7841E-04	-7.8087E-03
$\phi_S \ln(U)$	-2.8007E-02	-3.5504E-02	-8.7147E-02	-7.8087E-03	6.6119E+00

F.5 Model Validity Region

Multiple-regression models of the forms developed for U_{CS} and H_C in Sections F.2 and F.3 are typically restricted to use over the predictor-variable region covered by the data used to develop and fit the models. Table F.23 summarizes the ranges of the predictor variables represented in the full and trimmed data sets used to develop U_{CS} and H_C models in this appendix. However, it may be possible to extrapolate such models for predictor variables [e.g., D = tank diameter (scale)] where the underlying power-law relationship (without or with interactions) is considered appropriate for extrapolation.

Table F.23. Ranges of Predictor Variables in the Full and Trimmed Data Sets Used to Develop U_{CS} and H_C Multiple-Regression Models

Variable	Units	Data Set Used for Modeling	
		Full	Trimmed
D	m	0.3667 − 1.7780	0.3667 − 1.7780
N_J	number	4 − 12	4 − 12
d	m	0.0032 − 0.0234	0.0032 − 0.0234
ϕ_p	none	0.0250 − 0.1523	0.0250 − 0.1523
U_T	m/s	0.0017 – 0.1074	0.0017 – 0.0343
DC	none	0.1432 − 0.6692	0.1432 − 0.3957
s	m	2.45 − 4.18	2.45 − 4.18
ϕ_s	none	0.0005 − 0.06	0.0005 − 0.0159
$d_S = d_{50}$[(a)]	m	0.000044 − 0.000766	0.000044 − 0.000178
U (> U_{CS})[(b)]	m/s	1.30 – 16.10	1.30 – 16.10
HS	E, FD, S[(c)]	All	All
Jet Operation	P, S[(d)]	P	P
# Data Points, U_{CS}		173	154
# Data Points, H_C		669	581

(a) Even though d_S was omitted from U_{CS} and H_C models in favor of U_T, its range is still given here.
(b) The ranges of U > U_{CS} are over all test conditions. The range of U varies for different test conditions, with some conditions having zero range (i.e., one U = U_{CS}) or a small range.
(c) E = elliptical, FD = flange & dish, S = spherical.
(d) P = pulsed (i.e., DC < 1), S = steady state (i.e., DC = 1).

F.6 Possible Future Activities

Section F.6.1 discusses experimental design activities suggested for any future mixing experimental work. Section F.6.2 discusses other data/modeling analyses that were not possible to perform for this work but are suggested in the future.

F.6.1 Experimental Design

The ability to develop models relating U_{CS} and H_C to test (predictor) variables was limited by the distribution of combinations of test variables over the multivariate test-variable region. Many of the tests focused on test variables at design values, which increase model prediction uncertainties in other parts of the predictor-variable region, compared with what it could have been if a better distribution of test-variable combinations were selected. In the future, it is suggested that statistical experimental design methods be applied to help select the combinations of test variables to investigate. These methods provide for covering the relevant test-variable region, including irregularly-shaped regions that occur when some combinations of test variables are inappropriate or otherwise not of interest. Statistical

experimental design methods also provide for selecting combinations of test variables (test matrix) to provide good support for estimating their individual and interactive effects. These methods thus can provide good support for developing accurate and precise models, for the same number or fewer tests that might otherwise be selected by non-statistical approaches. Of course, the statistical approach must be informed by mixing knowledge and experience, as well as the WTP mixing situations of interest. Thus, it is recommended that a combined approach using both statistical and subject-matter aspects be used to select test combinations for any future testing of tank mixing.

As discussed in Section F.1.2 (and Section D.2.2, Appendix D), the order in which test runs from a test matrix are performed can significantly affect the uncertainty and covariance structure of the resulting data set. The order that tests will be performed should be planned as part of the experimental design, so that the data structure obtained is no more complicated than necessary. Further, the experimental design process can also develop the test matrix so that appropriate statistical methods can be applied to account for the more complicated data structure resulting from necessary (or desirable) restrictions on randomization.

Finally, any future experimental mixing testing should include at least two to three replicates each of several test-variable combinations. Replicates involve testing the same set of test conditions at different times, interspersed with the other sets of test conditions in the test matrix. Replicates are contrasted to repeats, where the same set of test conditions is performed multiple times without different sets of test conditions intervening. In general, repeat tests significantly underestimate experimental uncertainty compared with accurate estimates that would be obtained using replicates. Replicates provide for quantifying experimental as well as measurement uncertainty in the data. Experimental uncertainty is generally much larger than measurement uncertainty, so it is important to quantify it properly using replicate tests and not repeat tests or repeat measurements. However, averaging repeat measurements to effectively reduce measurement uncertainty is a very good idea. If repeat measurements are averaged, the number averaged should always be the same. Otherwise, averaging different numbers of repeat values will violate the assumption of "constant variance" for least squares regression (see Section D.2.2 of Appendix D).

F.6.2 Other Data/Modeling Analyses

Several data/modeling analyses that weren't possible to perform as part of this work, but may be useful to perform in the future, are briefly mentioned.

- Other Model Forms: The work in this appendix was based on power-law forms of models (without and with interaction terms) for U_{CS} and H_C. These forms of models fit the July 2007, Fall 2007, and 2008 data for U_{CS} very well, and for H_C reasonably well. However, there were indications in the functionality plots displayed in Section E.2 of Appendix E that other (non-power-law) functional relationships for some variables may yield better model forms. That is, there may be other model forms that better match the relationships in the data and yield more accurate and precise predictions. It can sometimes involve considerable work to develop model forms that include different functional relationship forms for different predictor variables and their interactions. However, such work may yield models that make more accurate predictions of mixing response variables with less uncertainty, especially when model extrapolation is necessary.
- Model Validation: MR models developed using a given data set should be validated using data not used to develop them.

- One way to do this is to split the data in the model development set, say with 80% in the modeling subset and 20% in the validation subset. This can be done in such a way that the full data set is split five times into five modeling subsets and five corresponding validation subsets, with the validation subsets being mutually exclusive. Then the average validation performance over the five validation subsets serves as a very good basis to assess validation performance.
- Validation can also be performed using one or more separate sets of validation data (e.g., from previous testing). Ideally such data would support model performance assessment within the model region of validity (interpolation) as well as outside it (extrapolation). The dimensionally consistent models presented in this appendix were validated using the benchmarking data, as discussed in Section 8.0 of the main report. However, it would be valuable to validate the models using any other separate data that becomes available.

Regardless of the way validation is performed, statistical prediction intervals (see Section D.6.3, Appendix D) can be used to assess with a specified confidence level whether model predictions are within statistical uncertainty of the measured values from the validation data set.

- Comparison of Multiple Regression Models with Models Develop by Physics-Based Approach: As discussed in Sections F.2.2 and F.3.2, the U_{CS} and H_C dimensional model forms investigated in Appendix F are generalizations of physics-based model forms developed in Section 7.0. Dimensionally consistent versions of the dimensional models were also investigated in Appendix F. It was possible in the time available only to perform a limited comparison of the U_{CS} and H_C models in Appendix F with those in Section 7.3.2. In the future, it would be worthwhile to further compare the results of the multiple-regression and physics-based approaches and obtain improved model forms based on a synthesis of these approaches.
- Uncertainties in Model Predictions: As discussed at the end of Section F.4, methods for quantifying and combining all uncertainties associated with mixing response models should be pursued. Statistical uncertainty intervals for quantifying model fitting uncertainty are presented in Section D.6 of Appendix D, and illustrated in Section F.4. Statistical intervals should be developed that combine model-fitting uncertainty with the uncertainty from propagating uncertainties in the predictor variables of a model. Methods for quantifying possible uncertainties associated with the form of the model should also be investigated. Or, operating margins should be developed that will protect against such uncertainties.

F.7 References

Draper NR and H Smith. 1998. *Applied Regression Analysis*, Third Edition. John Wiley and Sons, New York.

Myers RH, and DC Montgomery. 1995. *Response Surface Methodology: Process and Product Optimization Using Designed Experiments*, John Wiley and Sons, New York.

Piepel GF, BG Amidan, A Heredia-Langner, DR Weier, and SK Cooley. June 2005. *Statistical Methods and Results for WTP IHLW and ILAW Compliance*. PNWD-3568, WTP-RPT-072 Rev. 1, Battelle - Pacific Northwest Division, Richland, Washington.

Distribution*

No. of Copies

OFFSITE

1 Perry A Meyer
Defense Nuclear Facilities Safety Board
625 Indiana Ave NW Suite 700
Washington, DC 20004

1 SK Sundaram
Alfred University
Matls Science & Engineering
1 Saxon Drive
Alfred, NY 14802

No. of Copies

ONSITE

2 **U.S. Department of Energy**

LK Holton
JA Reddick

3 **Bechtel National, Inc.**

F. Damerow
P. Keuhlen
R&T Document Control

19 Pacific Northwest National Laboratory

BG Amidan
EBK Baer
JA Bamberger
CA Burns
KM Denslow
CW Enderlin
JA Fort
PA Gauglitz
MS Greenwood
BK Hatchell
A Heredia-Langner
WL Kuhn
MJ Minette
GP Morgen
GF Piepel
GL Smith
SF Snyder
BE Wells
Project Office

*All distribution will be made electronically.

Pacific Northwest
NATIONAL LABORATORY

Proudly Operated by Battelle *Since 1965*

U.S. DEPARTMENT OF
ENERGY

902 Battelle Boulevard
P.O. Box 999
Richland, WA 99352
1-888-375-PNNL (7665)
www.pnnl.gov